2010 HyspIRI Science Workshop

Objectives and Update

Woody Turner and John LaBrecque

HyspIRI Program Scientists

Earth Science Division

NASA Headquarters

August 24, 2010

Workshop Objectives

- Update Community on HyspIRI Status
- Explore relevance of HyspIRI to Climate Science
- Explore relevance of HyspIRI to Carbon Cycle Science
- Present new Technologies, Tools, and Products supporting or arising from a HyspIRI Mission
- Explore new Applications for HyspIRI Data
- Vet Domestic and International Partnership Opportunities
- Discuss options for a HyspIRI mission’s going forward

Workshop Overview

- Updates regarding HyspIRI Mission Concepts and Level 1 Requirements
- Science Focus: HyspIRI’s Importance to Climate and Carbon Science
- Reports from Initiatives at last year’s Workshop
  - Sun Glint Subgroup: characterization, scientific impacts, mitigation options, and recommendations (2 talks)
  - Hot Target Saturation Subgroup: Analysis Report
- HyspIRI and the Gulf Oil Spill
- *HyspIRI Preparatory Activities Using Existing Imagery* Project Talks
- New Science, Applications, Techniques and Tools
- Domestic and Foreign Partnerships
- Precursor Science Campaign

Since the Last Workshop

- ROSES 2009 *HyspIRI Preparatory Activities Using Existing Imagery*
  - proposals reviewed and 6 funded
- 2 Subgroups formed to address issues raised in 2009 Workshop
  - Sun Glint
  - Hot Target Saturation
  - Both reporting out at this workshop
- HyspIRI Science Symposium on Ecosystem Data Products
  - May 4-5, NASA GSFC
- Presentations to Mike Freilich, NASA Earth Science Division Director
- Iceland Volcano and Gulf Oil Spill point to the importance of HyspIRI data
- SSG discussions of HyspIRI High-level Objectives for Non-Specialists and Critical Climate Contributions
- Release of NASA Climate Plan
  - June 2010, *Responding to the Challenge of Climate & Environmental Change*
- ROSES 2010 *HyspIRI Preparatory Activities Using Existing Imagery*
  - Review panel last week

NASA Climate Plan: Missions

NASA's FY2011 Budget Accelerates:

- Tier 1 SMAP launch to 11/2014
- Tier 1 ICESAT-2 launch to 10/2015
- Tier 1 CLARREO-1 launch to 11/2017 & CLARREO-2 launch to 2020
- Tier 1 DESDynI launch to 10/2017
- Tier 2 ASCENDS launch to 2019
- Tier 2 SWOT launch to 2020

Also:

- OCO-2 launch in 2/2013; OCO-3 ready for flight as early as 2015
- Expanded Venture-class program
- SAGE-III on Space Station in 2014
- GRACE Follow-on Mission launch in 2016
- Ocean Color and Clouds/Aerosols Polarimetry Mission launch in 2018
- **Other Tier 2 missions launched at rate of ~ 1 per year starting 2021**
  – Based on scientific priorities, Administration objectives, technical maturity & partnership opportunities, NASA will work with USGCRP to determine order for remaining Tier 2 missions.

Accelerated ESD Missions

Missions	Launch Readiness Date		
SMAP	+7 mos	FY10	2015
		FY11	2014
DESDynI Radar	+2 yrs	FY10	2019
		FY11	2017
DESDynI Lidar	+2 yrs	FY10	2019
		FY11	2017
CLARREO-1	+2 yrs	FY10	2019
		FY11	2017
Venture (Satellite EV2)	+4 yrs	FY10	NET 2022
		FY11	2017
ASCENDS	+4 yrs	FY10	NET 2023
		FY11	2019
CLARREO-2	-1 yrs	FY10	2019
		FY11	2020
SWOT	+5 yrs	FY10	NET 2025
		FY11	2020

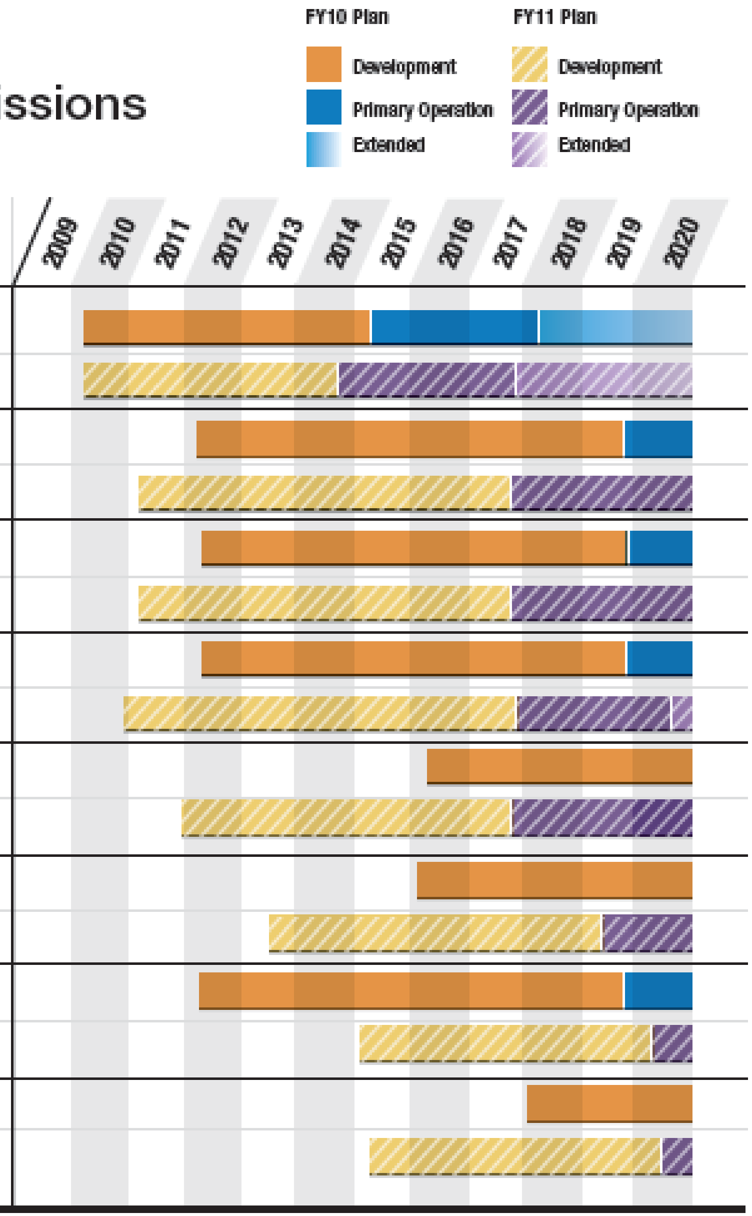

FIGURE 2: Accelerated Missions—This figure compares the timelines for mission development associated with the FY2010 and FY2011 budgets. The FY11 budget request substantially accelerates the development and launch of Decadal Survey-recommended missions.

HyspIRI Next Steps

- Remember what we are:
  - A *<u>global</u>* mission providing VSWIR imaging spectrometry (380 to 2500nm) and multispectral day/night thermal imaging in 8 bands at 60m spatial resolution for global lands and waters <50m depth, with a 19-day repeat for the VSWIR and 5-day repeat for the TIR, and ice sheets and open oceans averaged to 1km
- Build HyspIRI scientific case, with a focus on climate and the carbon cycle
- Mature mission technologies and reduce costs
- Develop precursor scientific opportunities using existing and planned airborne and complementary satellite platforms
- Seek partnerships with domestic and international partners
  - Joint Scientific Campaigns—precursor and flight
  - Calibration/Validation
  - Data Product Development and Use
  - Spacecraft
  - Launch
- Work with other NASA missions, e.g.: DESDynI and PACE
- Be Ready!

2010 HyspIRI Science Workshop
Objectives and Update

Woody Turner and John LaBrecque
HyspIRI Program Scientists
Earth Science Division
NASA Headquarters

August 24, 2010

Workshop Objectives

- Update Community on HyspIRI Status
- Explore relevance of HyspIRI to Climate Science
- Explore relevance of HyspIRI to Carbon Cycle Science
- Present new Technologies, Tools, and Products supporting or arising from a HyspIRI Mission
- Explore new Applications for HyspIRI Data
- Vet Domestic and International Partnership Opportunities
- Discuss options for a HyspIRI mission's going forward

Workshop Overview

- Updates regarding HyspIRI Mission Concepts and Level 1 Requirements
- Science Focus: HyspIRI's Importance to Climate and Carbon Science
- Reports from Initiatives at last year's Workshop
  - Sun Glint Subgroup: characterization, scientific impacts, mitigation options, and recommendations (2 talks)
  - Hot Target Saturation Subgroup: Analysis Report
- HyspIRI and the Gulf Oil Spill
- *HyspIRI Preparatory Activities Using Existing Imagery* Project Talks
- New Science, Applications, Techniques and Tools
- Domestic and Foreign Partnerships
- Precursor Science Campaign

Since the Last Workshop

- ROSES 2009 *HyspIRI Preparatory Activities Using Existing Imagery*
  - proposals reviewed and 6 funded
- 2 Subgroups formed to address issues raised in 2009 Workshop
  - Sun Glint
  - Hot Target Saturation
  - Both reporting out at this workshop
- HyspIRI Science Symposium on Ecosystem Data Products
  - May 4-5, NASA GSFC
- Presentations to Mike Freilich, NASA Earth Science Division Director
- Iceland Volcano and Gulf Oil Spill point to the importance of HyspIRI data
- SSG discussions of HyspIRI High-level Objectives for Non-Specialists and Critical Climate Contributions
- Release of NASA Climate Plan
  - June 2010, *Responding to the Challenge of Climate & Environmental Change*
- ROSES 2010 *HyspIRI Preparatory Activities Using Existing Imagery*
  - Review panel last week

NASA Climate Plan: Missions

NASA's FY2011 Budget Accelerates:

- Tier 1 SMAP launch to 11/2014
- Tier 1 ICESAT-2 launch to 10/2015
- Tier 1 CLARREO-1 launch to 11/2017 & CLARREO-2 launch to 2020
- Tier 1 DESDynI launch to 10/2017
- Tier 2 ASCENDS launch to 2019
- Tier 2 SWOT launch to 2020

Also:

- OCO-2 launch in 2/2013; OCO-3 ready for flight as early as 2015
- Expanded Venture-class program
- SAGE-III on Space Station in 2014
- GRACE Follow-on Mission launch in 2016
- Ocean Color and Clouds/Aerosols Polarimetry Mission launch in 2018
- **Other Tier 2 missions launched at rate of ~ 1 per year starting 2021**
  - Based on scientific priorities, Administration objectives, technical maturity & partnership opportunities, NASA will work with USGCRP to determine order for remaining Tier 2 missions.

Accelerated ESD Missions

FY10 Plan: Development, Primary Operation, Extended

FY11 Plan: Development, Primary Operation, Extended

Missions	Launch Readiness Date		
SMAP	+7 mos	FY10	2015
		FY11	2014
DESDynI Radar	+2 yrs	FY10	2019
		FY11	2017
DESDynI Lidar	+2 yrs	FY10	2019
		FY11	2017
CLARREO-1	+2 yrs	FY10	2019
		FY11	2017
Venture (Satellite EV2)	+4 yrs	FY10	NET 2022
		FY11	2017
ASCENDS	+4 yrs	FY10	NET 2023
		FY11	2019
CLARREO-2	-1 yrs	FY10	2019
		FY11	2020
SWOT	+5 yrs	FY10	NET 2025
		FY11	2020

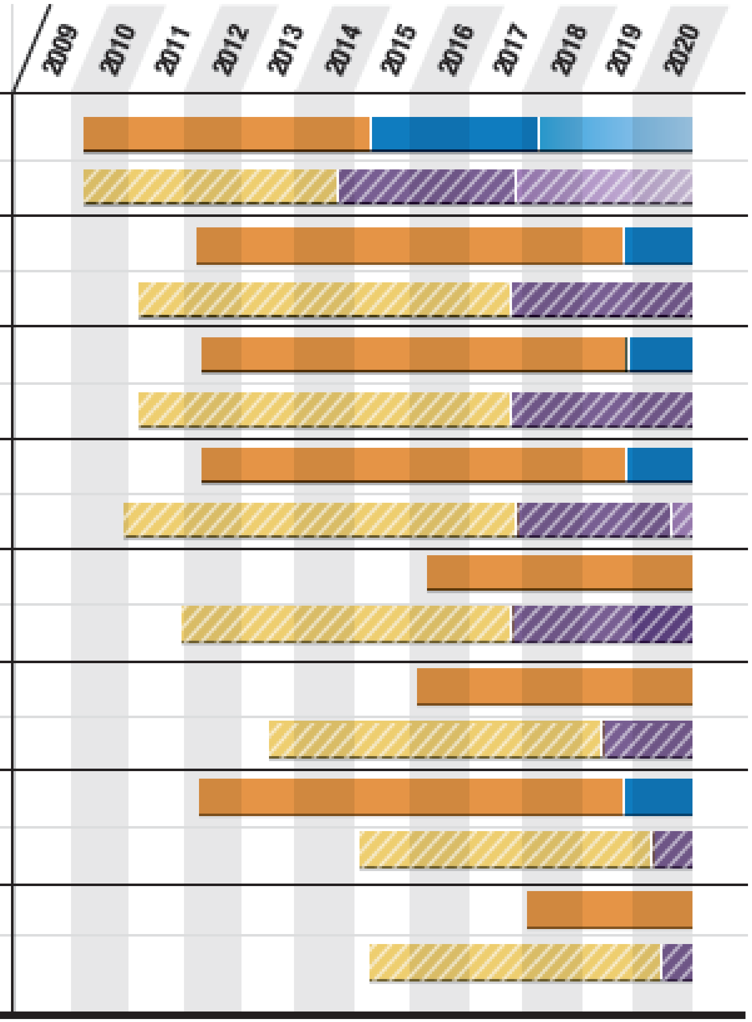

FIGURE 2: Accelerated Missions—This figure compares the timelines for mission development associated with the FY2010 and FY2011 budgets. The FY11 budget request substantially accelerates the development and launch of Decadal Survey-recommended missions.

HyspIRI Next Steps

- Remember what we are:
  - A *global* mission providing VSWIR imaging spectrometry (380 to 2500nm) and multispectral day/night thermal imaging in 8 bands at 60m spatial resolution for global lands and waters <50m depth, with a 19-day repeat for the VSWIR and 5-day repeat for the TIR, and ice sheets and open oceans averaged to 1km
- Build HyspIRI scientific case, with a focus on climate and the carbon cycle
- Mature mission technologies and reduce costs
- Develop precursor scientific opportunities using existing and planned airborne and complementary satellite platforms
- Seek partnerships with domestic and international partners
  - Joint Scientific Campaigns—precursor and flight
  - Calibration/Validation
  - Data Product Development and Use
  - Spacecraft
  - Launch
- Work with other NASA missions, e.g.: DESDynI and PACE
- Be Ready!

HyspIRI

VSWIR Science Measurement Baseline

NASA Earth Science and Applications Decadal Survey

Robert O. Green and HyspIRI Team

HyspIRI Decadal Survey Climate Science

HyspIRI: “A hyperspectral sensor (e.g., FLORA) combined with a multispectral thermal sensor (e.g., SAVII) in low Earth orbit (LEO) **is part of an integrated mission concept** [described in Parts I and II] that is relevant to several panels, <u>**especially the climate variability panel**</u>.”

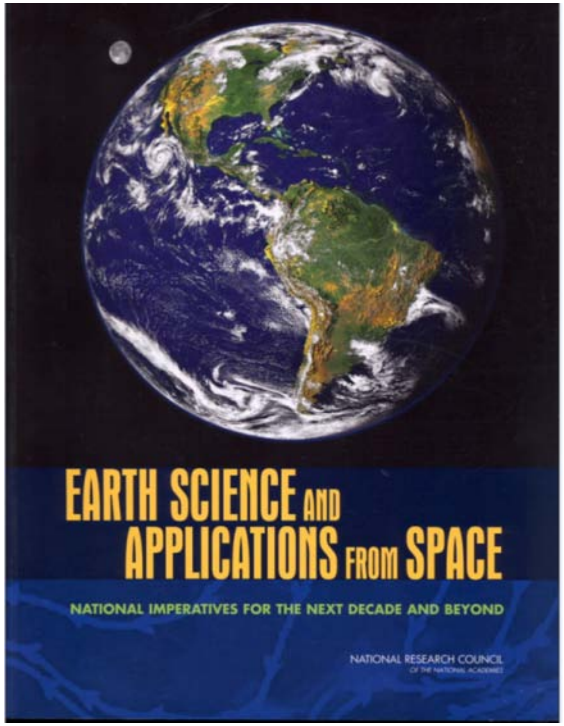

NRC Decadal Survey - HyspIRI

Global vegetation species-type and physiological condition, including agricultural lands, for biosphere feedback and land-atmosphere interactions; Spectroscopically derived terrestrial land cover composition/albedo including snow, ice, dust climate interaction; Fire: fuel, occurrence, intensity and recovery globally, as well as volcano emissions; Fine spatial & temporal scale measures of surface temperature and energy balance, including urban heat Islands.

Visible ShortWave InfraRed (VSWIR) Imaging Spectrometer

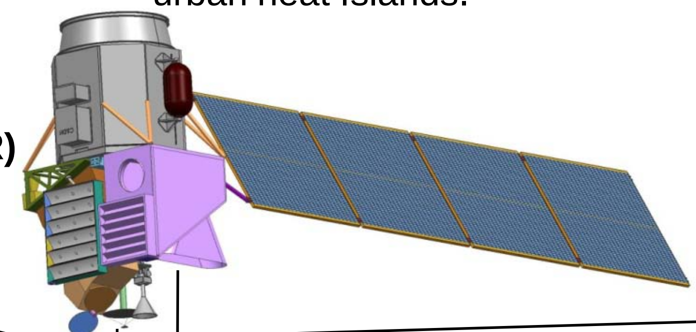

Multispectral Thermal InfraRed (TIR) Scanner

Map of dominant tree species, Bartlett Forest, NH

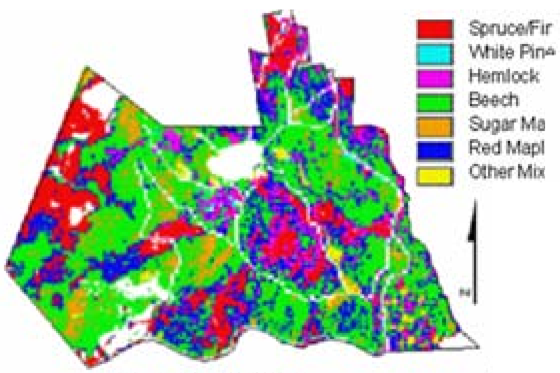

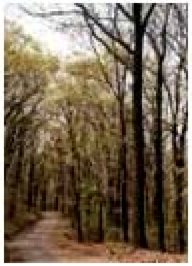

Soil C:N Ratio

White Mountain National Forest, NH

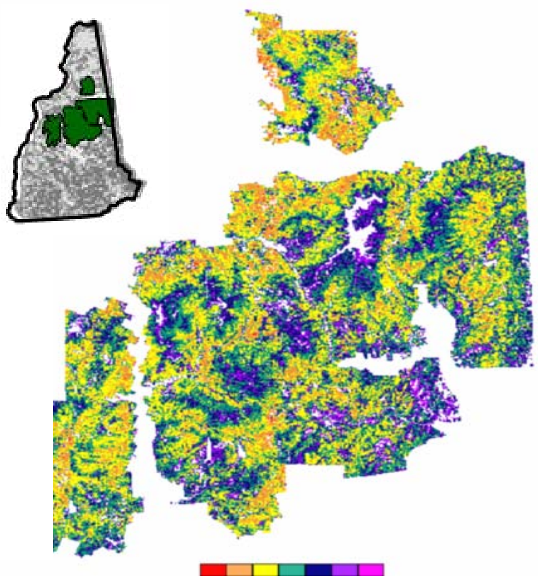

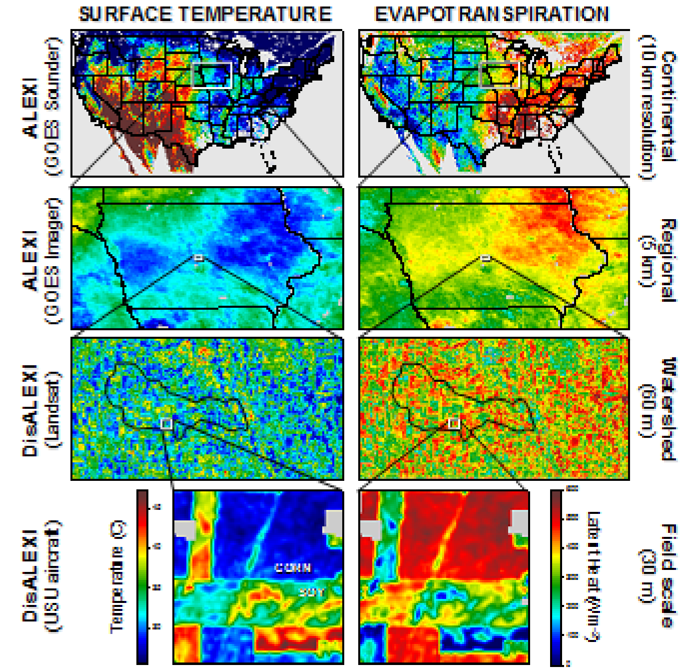

HyspIRI - Imaging Spectroscopy (VSWIR) Science Measurements

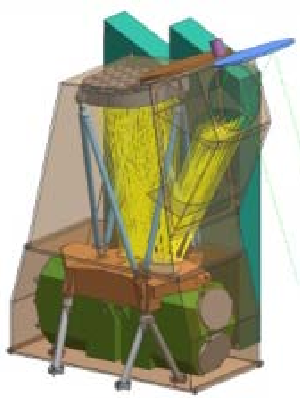

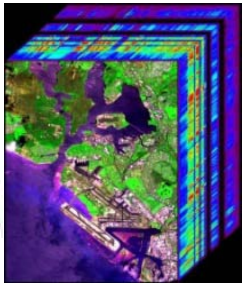

Mature Instrument concept: All components have flown in space.

Imaging spectrometer: 55kg / 41W

Schedule: 4 year phase A-D, 3 years operations (5 years consumables)

Full terrestrial coverage downlinked every 19 days

VQ1. Pattern and Spatial Distribution of Ecosystems and their Components.
What is the global spatial pattern of ecosystems and diversity distributions and how do ecosystems differ in their composition or biodiversity? [DS 195]

VQ2. Ecosystem Function, Physiology and Seasonal Activity.
What are the seasonal expressions and cycles for terrestrial and aquatic ecosystems, functional groups, and diagnostic species? How are these being altered by changes in climate, land use, and disturbance?[DS 191, 195, 203]

VQ3. Biogeochemical Cycles.
How are the biogeochemical cycles that sustain life on Earth being altered/disrupted by natural and human-induced environmental change? How do these changes affect the composition and health of ecosystems, and what are the feedbacks with other components of the Earth system?

VQ4. Changes in and Responses to Disturbance.
How are disturbance regimes changing, and how do these changes affect the ecosystem processes that support life on Earth?

VQ5. Ecosystem and Human Health.
How do changes in ecosystem composition and function affect human health, resource use, and resource management?

VQ6. Earth Surface and Shallow-Water Benthic Composition.
What are the land surface soil/rock /cryosphere and shallow-water benthic compositions,?

Measurement:

- 380 to 2500 nm at 10 nm
- Accurate 60 m resolution
- 19 days equatorial revisit
- Global land and shallow water

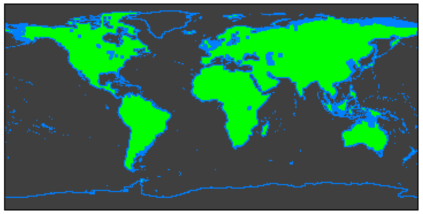

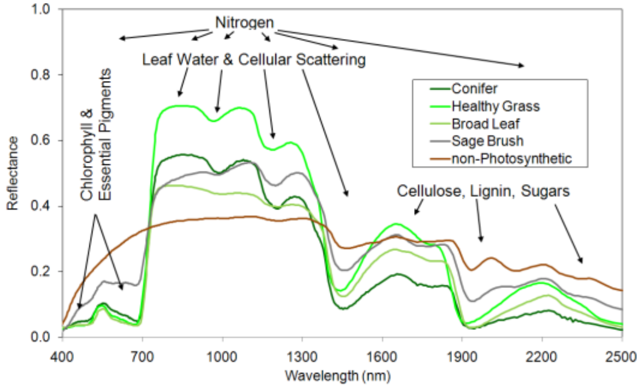

Map of dominant tree species, Bartlett Forest, NH

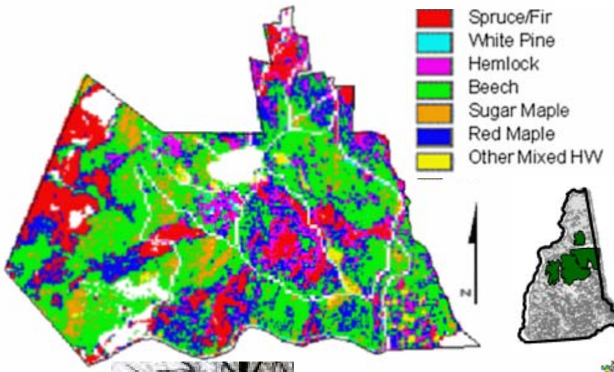

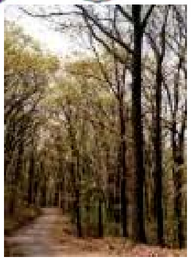

Soil C:N Ratio

White Mountain National Forest, NH

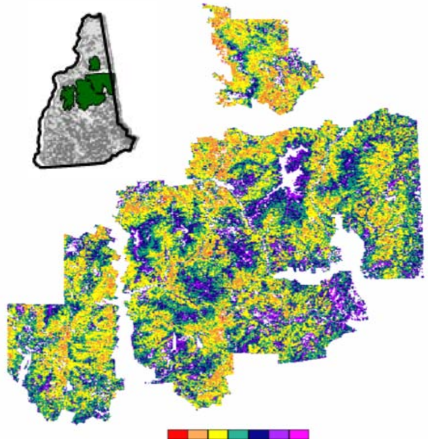

Basis for Continuous Spectral Measurement

- Plant functional types and species have biochemical and biophysical properties that are expressed as reflectance and absorption <u>features</u> spanning the spectral region from 380 to 2500 nm.
- Individual bands do not capture the diversity of biochemical and biophysical signatures of plant functional types or species.
- Changes in the chemical and physical configuration of ecosystems are often expressed as changes in the contiguous spectral signatures that relate directly to plant functional types, vegetation health, and species distribution.
- Other constituents of the Earth system (Minerals, Soils, Snow, etc) have spectral characteristics allowing use of this spectroscopic measurement approach for corresponding science questions.
- Important atmospheric correction information and calibration feedback is contained within the spectral measurement.

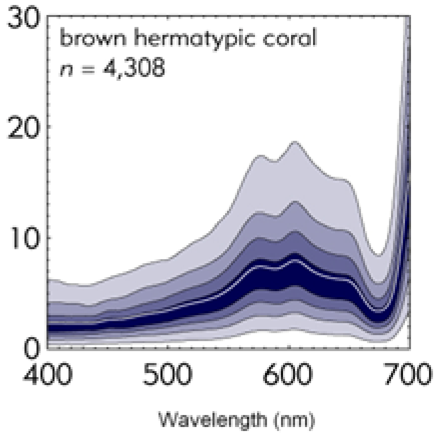

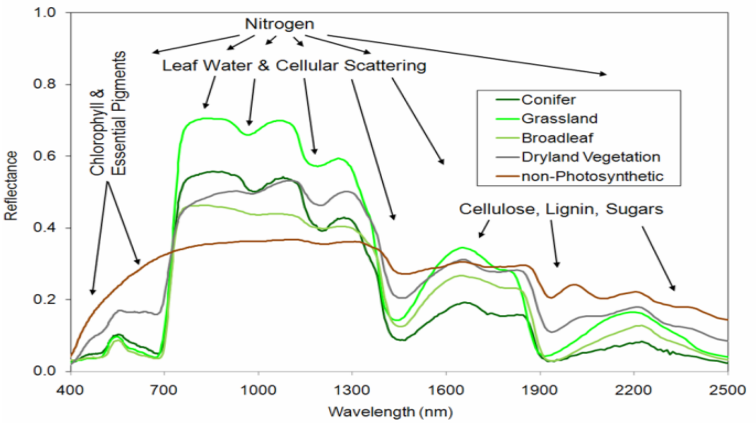

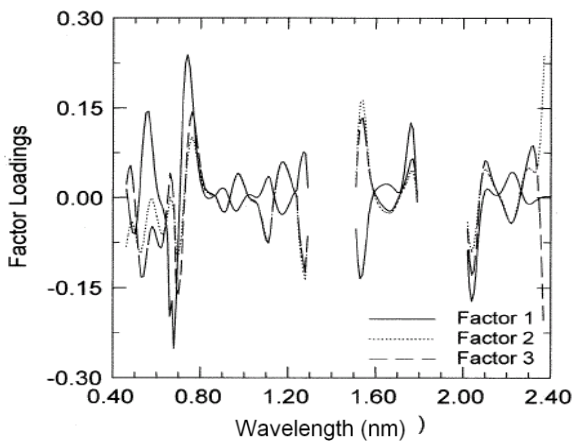

Vegetation Species/Functional-type & Fractional Cover

Santa Barbara, CA Coast Range

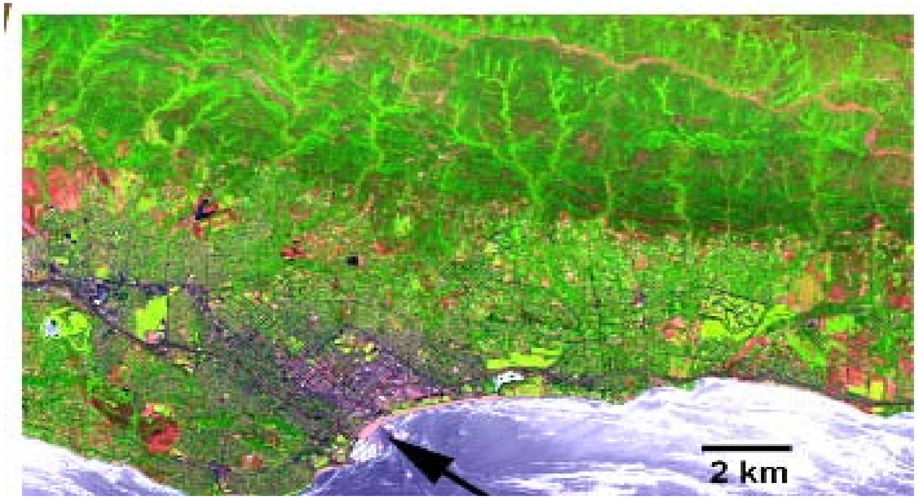

Species Type 90% accurate

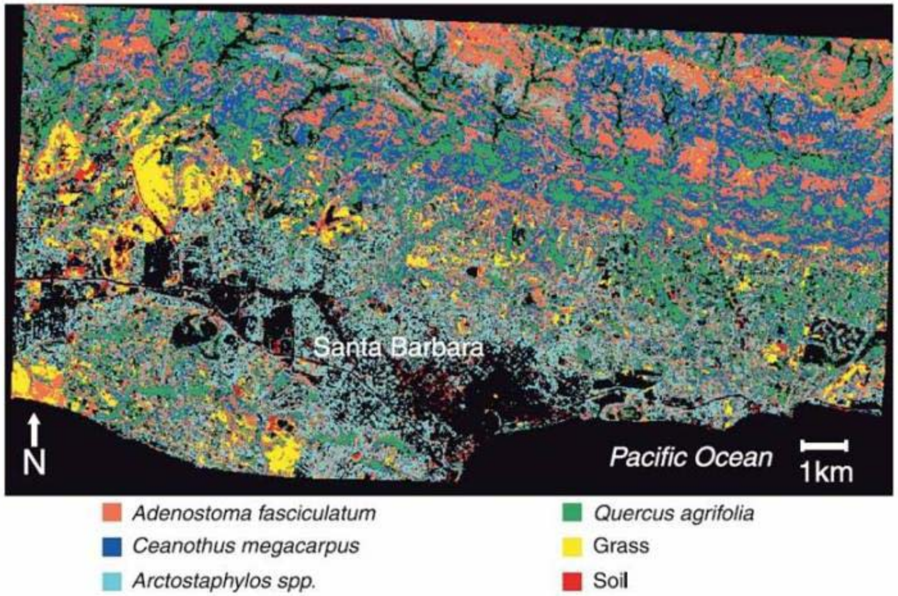

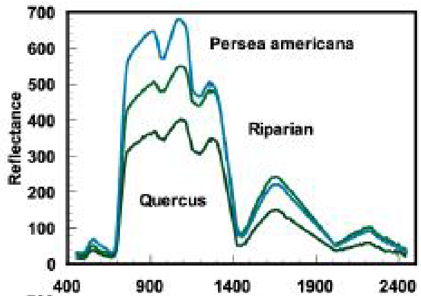

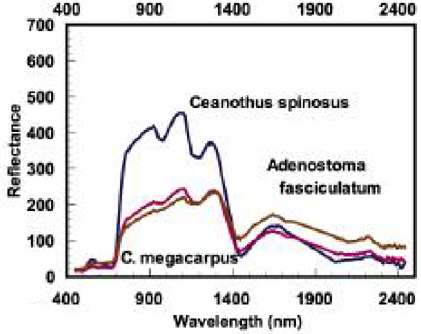

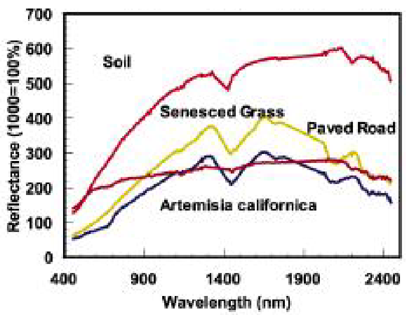

Species Fractional Cover (Quercus agrifolia)

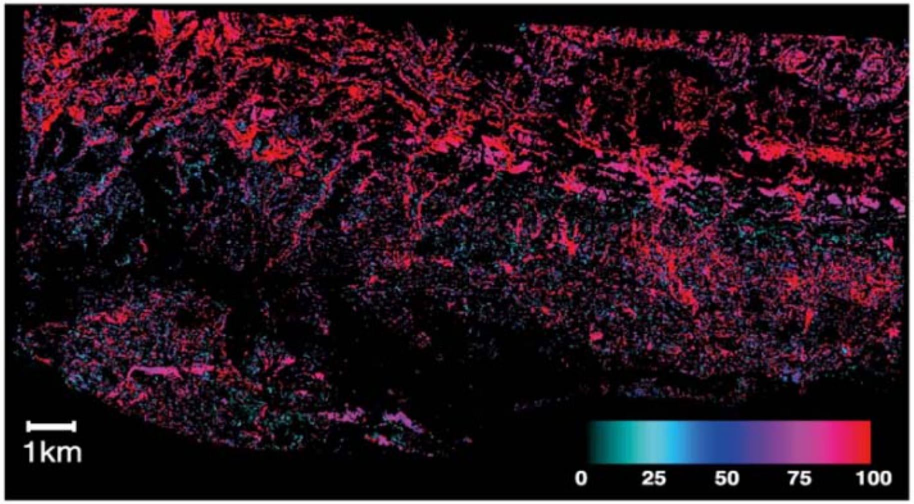

Ecosystem Species-type, Chemistry & Condition

Fractional material cover

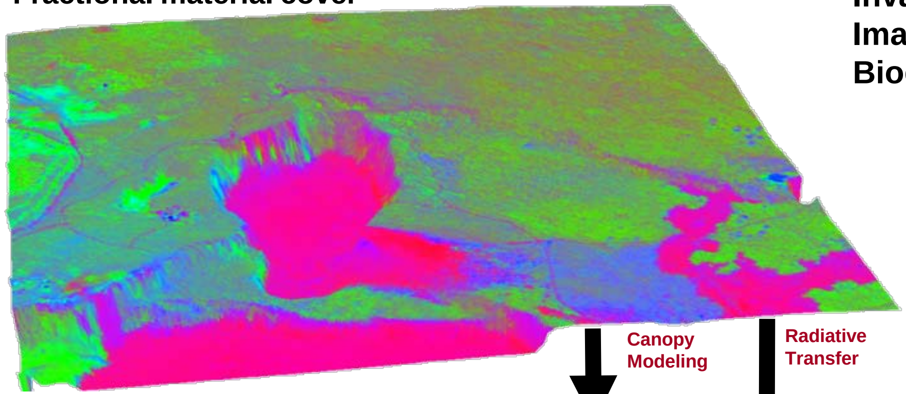

Canopy Modeling

Radiative Transfer

Leaf nitrogen concentration

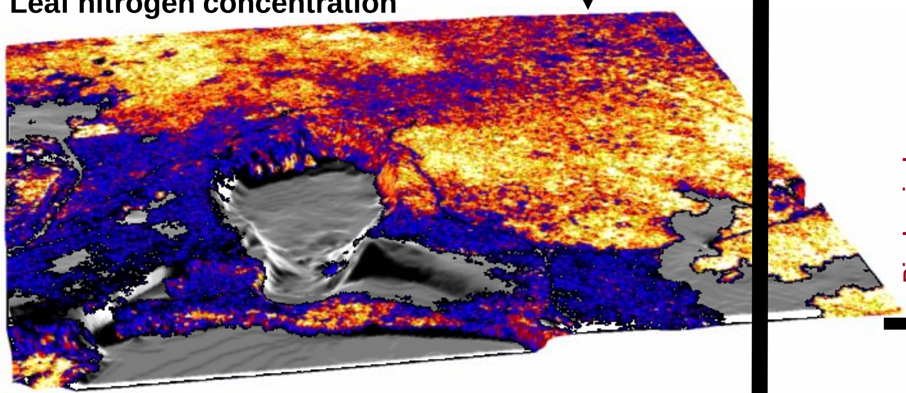

Canopy water content

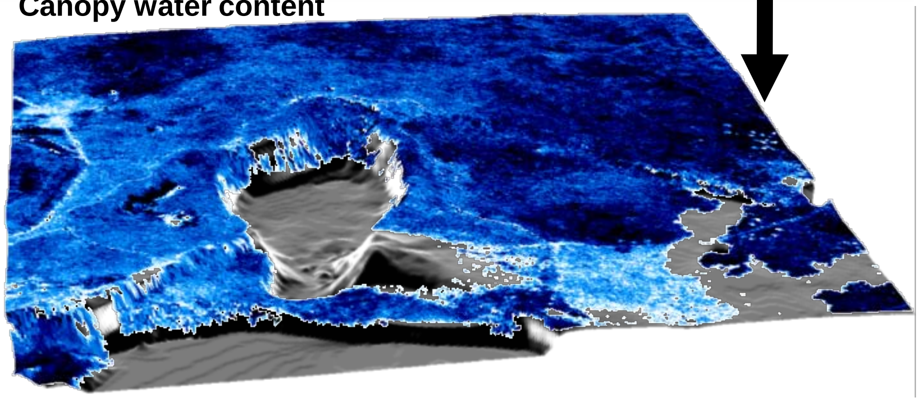

Invasive Species in the Hawaiian Rainforest from Airborne Imaging Spectrometer data: Patterns of Invasion and Biogeochemical Consequences

Biochemical Fingerprinting

Invasive species and nitrogen-fixing PFT

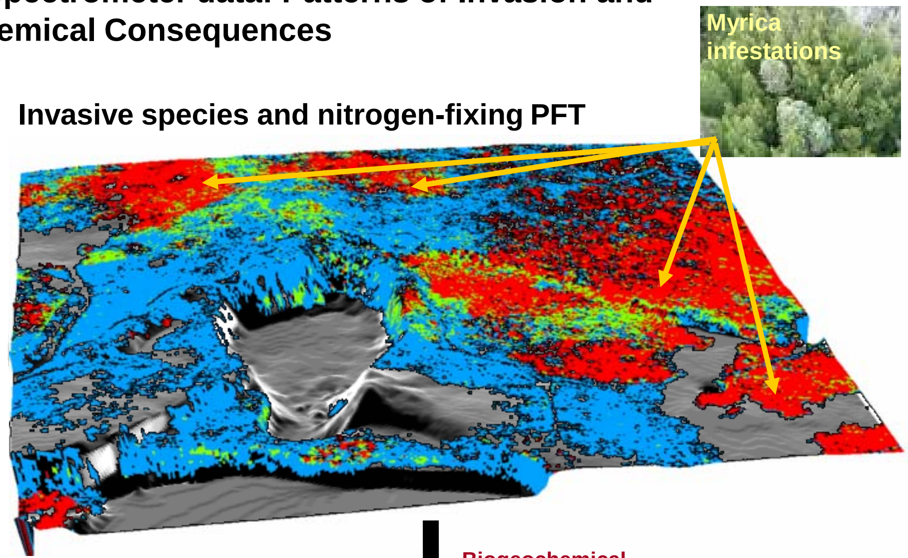

Biogeochemical Analysis

Soil nitrogen trace gas emissions

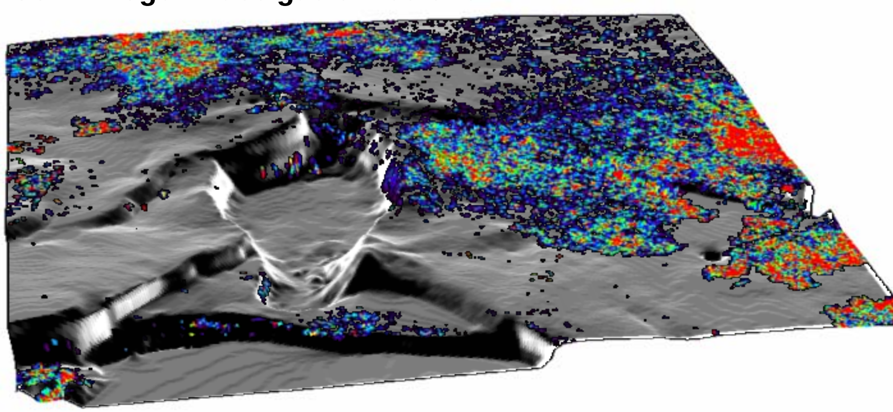

Asner and Vitousek, Proceeding of the National Academy of Sciences
Hall and Asner, Global Change Biology

Imaging Spectrometer Measurement

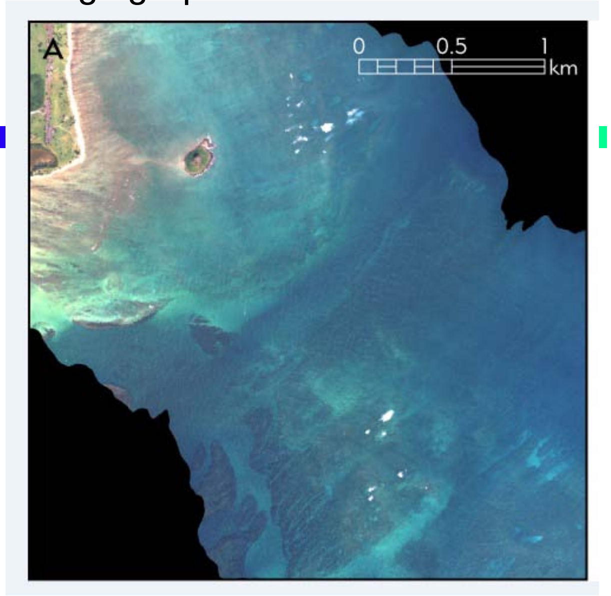

Benthic Compositional Mapping

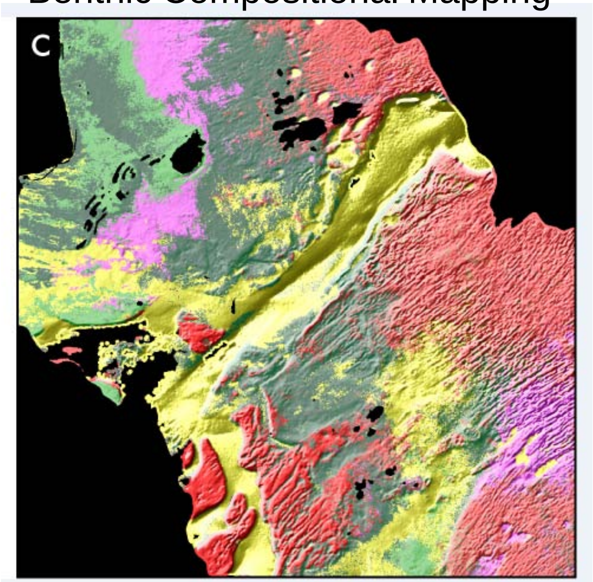

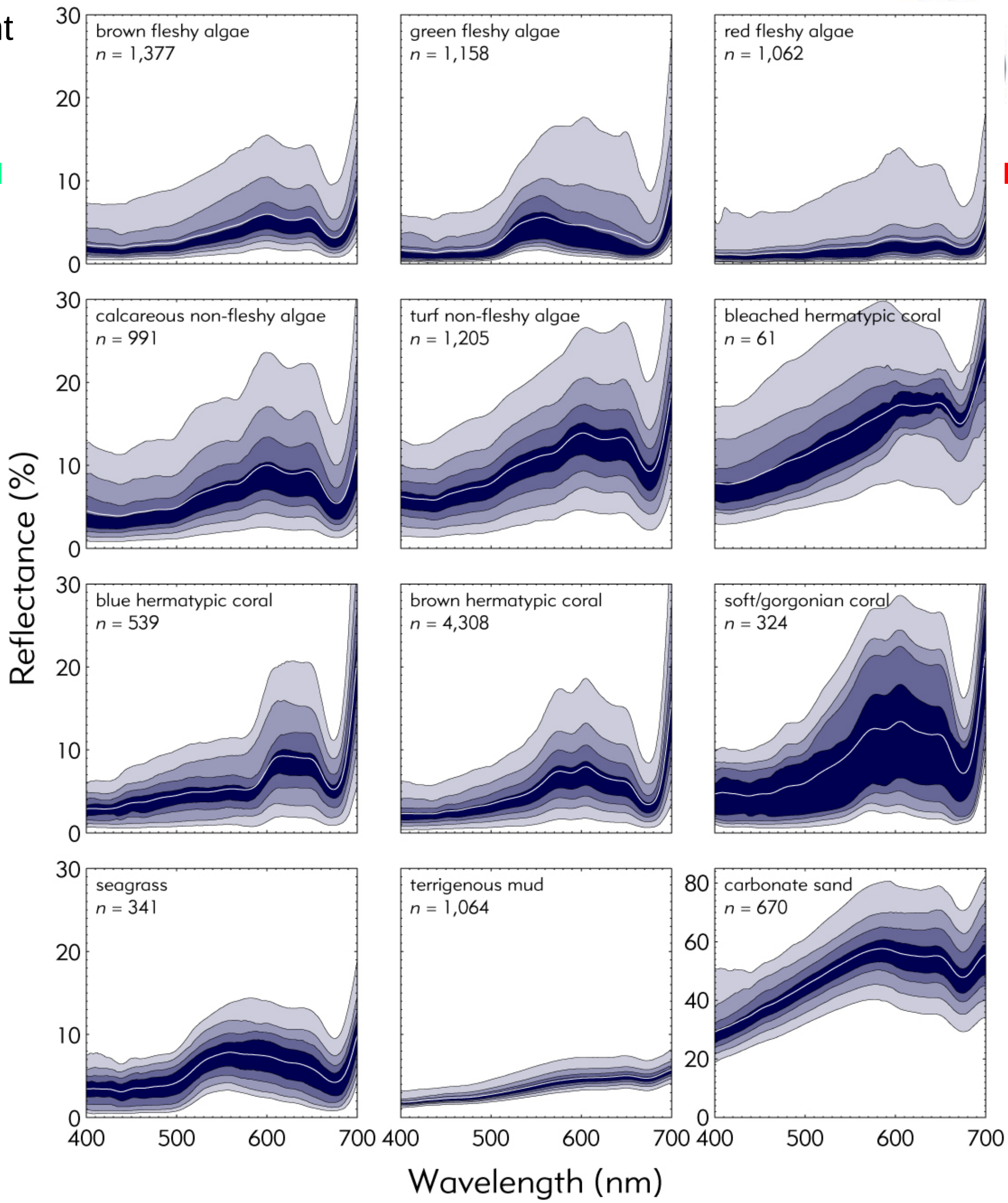

Spectral Measurements of Shallow Water Benthic Composition (E. Hochberg, Nova Southeastern University, FL)

To achieve the HyspIRI VSWIR climate contribution, global coverage is required with revisit <20 days

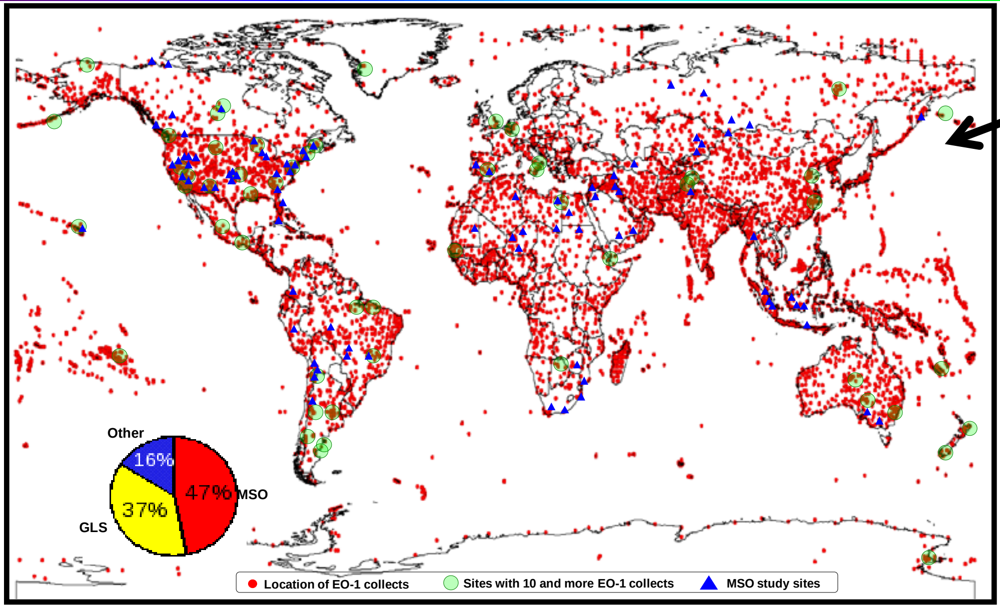

- EO-1 Hyperion acquisitions in 10 years.

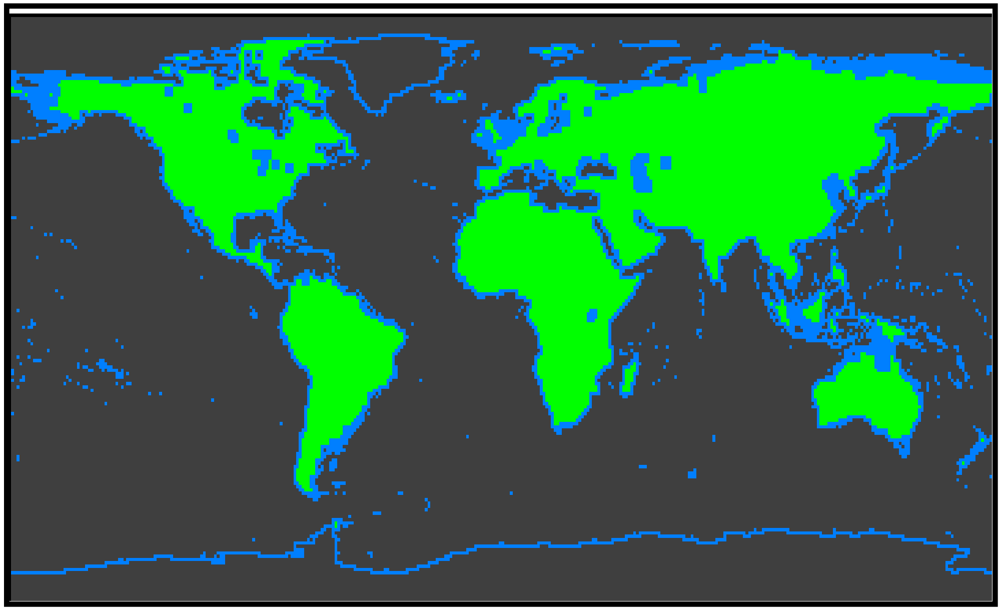

- HyspIRI provides complete terrestrial and shallow water coverage every 19 days.

- **<u>It would take Hyperion 100 years to acquire what HyspIRI measures in 1 year.</u>**

HyspIRI VSWIR
Imaging Spectrometer
Measurement Characteristics

HyspIRI VSWIR Science Measurements

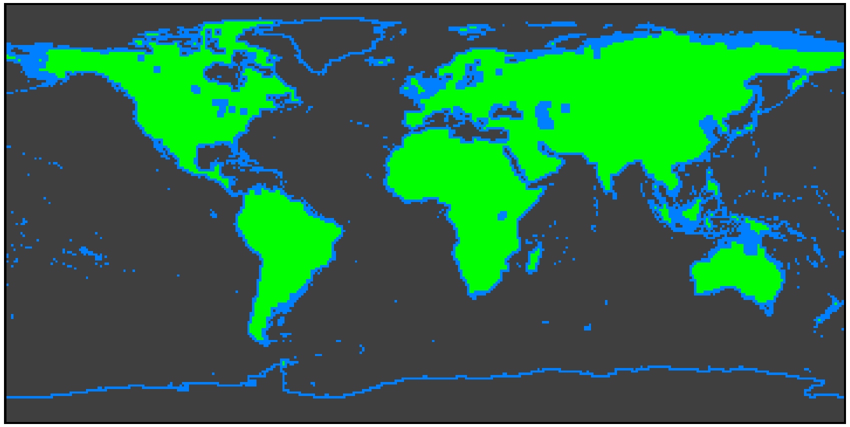

- Measure the **global** land and coastal/shallow water (> -50m).
- 19 day equatorial revisit to generate seasonal and annual products.

- Measure the molecular absorption and constituent scattering signatures in the spectral range from 380 to 2500 nm at 10 nm, and at 60 m spatial sampling.

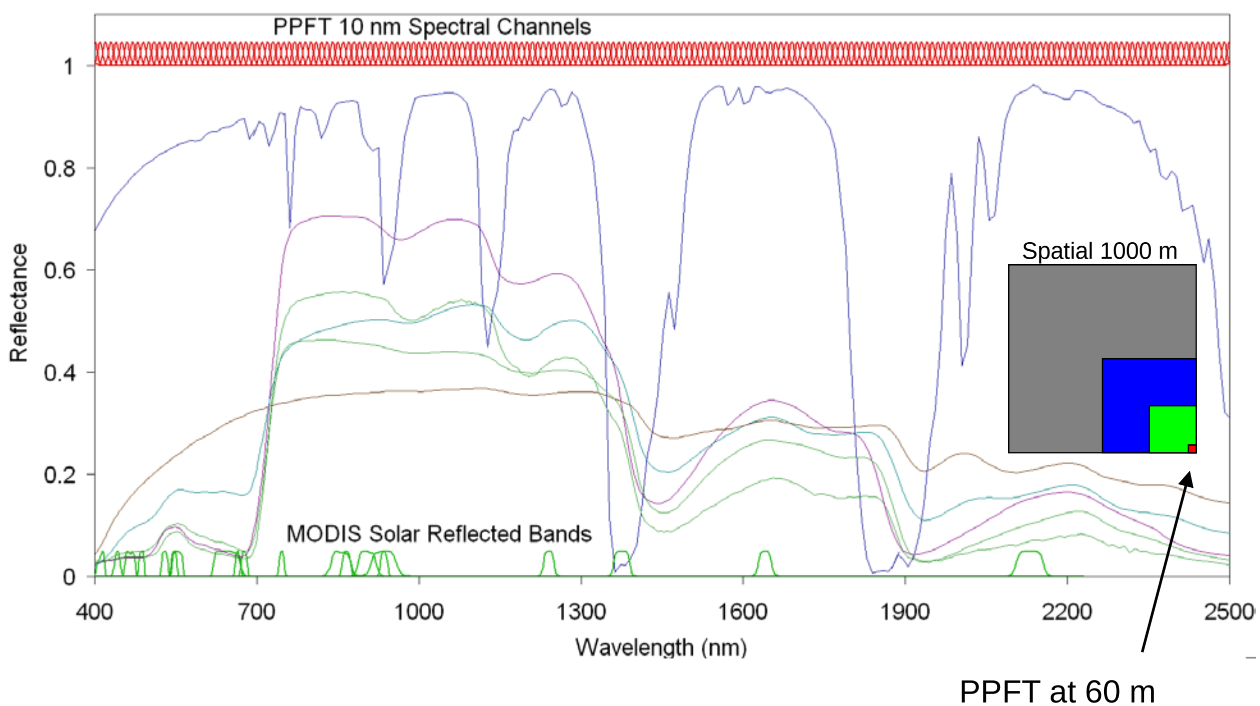

HyspIRI VSWIR
Science Measurement Characteristics

Spectral	
Range	380 to 2500 nm in the solar reflected spectrum
Sampling	<= 10 nm {uniform over range}
Response	<= 1.2 X sampling (FWHM) {uniform over range}
Accuracy	<0.5 nm
Radiometric	
Range & Sampling	0 to 1.5 X max benchmark radiance, 14 bits measured
Accuracy	>95% absolute radiometric, 98% on-orbit reflectance, 99.5% stability
Precision (SNR)	See spectral plots at benchmark radiances
Linearity	>99% characterized to 0.1 %
Polarization	<2% sensitivity, characterized to 0.5 %
Scattered Light	<1:200 characterized to 0.1%
Spatial	
Range	>150 km
Cross-Track Samples	>2500
Sampling	<=60 m
Response	<=1.2 X sampling (FWHM)
Uniformity	
Spectral Cross-Track	>95% cross-track uniformity {<0.5 nm min-max over swath}
Spectral-IFOV-Variation	>95% spectral IFOV uniformity {<5% variation over spectral range}

HyspIRI VSWIR Science Measurements Characteristics

Temporal	
Orbit Crossing	10:30 am sun synchronous descending
Global Land Coast Repeat	19 days at equator
Rapid Response Revisit	3 days (cross-track pointing)
Sunglint Reduction	
Cross Track Pointing	4 degrees in backscatter direction
OnOrbit Calibration	
Lunar View	1 per month {radiometric}
Solar Cover Views	1 per day {radiometric}
Dark signal measurements	1 per orbit and edge detector tracking
Surface Cal Experiments	5 per year {spectral & radiometric}
Data Collection	
Land Coverage	Land surface above sea level excluding ice sheets
Water Coverage	Coastal zone -50 m and shallower
Solar Elevation	20° or greater (10° Trade study)
Open Ocean/Ice Sheets	Averaged to ~1 km spatial sampling
Compression	>=3.0 lossless

HyspIRI VSWIR Science Measurements
Key SNR and Uniformity Requirements

Benchmark Radiances

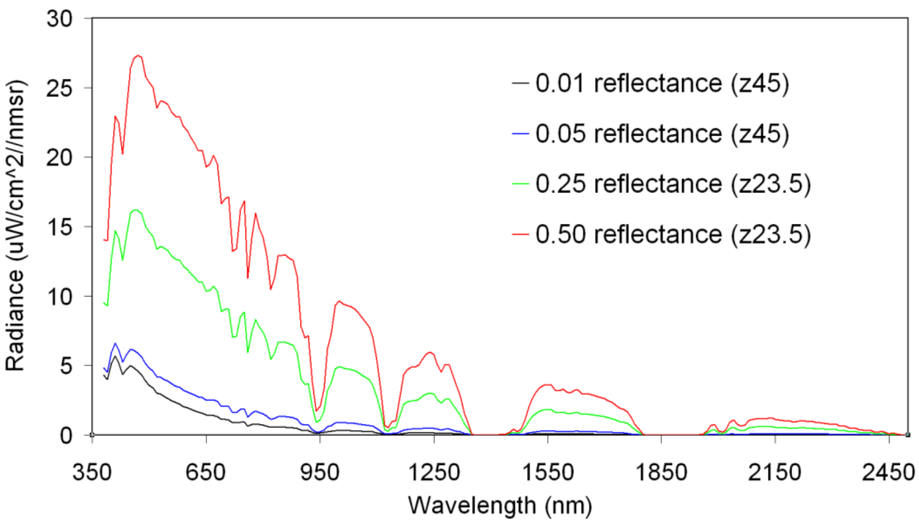

Required SNR

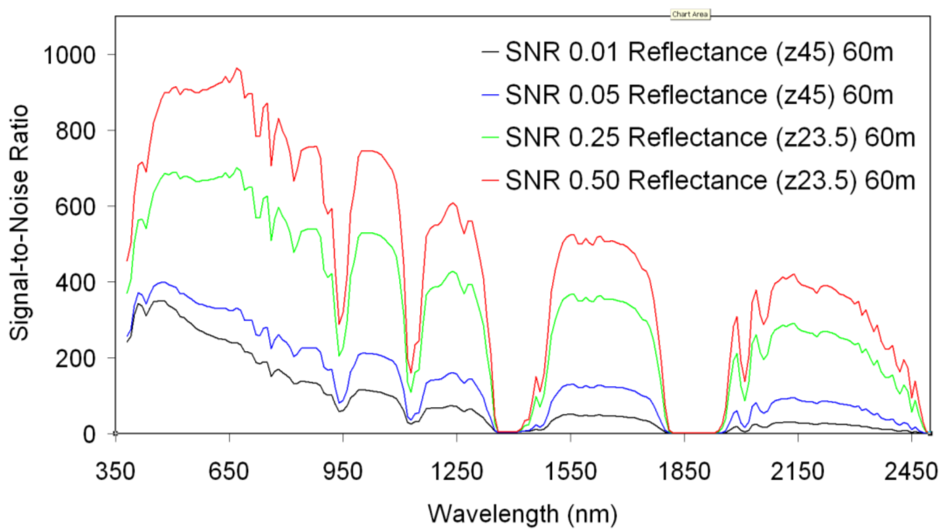

Uniformity Requirement

Cross Track Sample

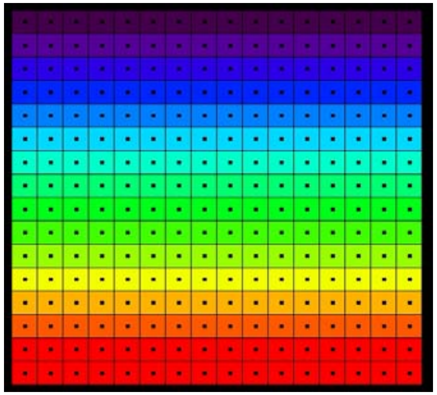

Wavelength

Depiction

-Grids are the detectors

-Dots are the IFOV centers

-Colors are the wavelengths

Requirement

Spectral Cross-Track	>95% cross-track uniformity {<0.5 nm min-max over swath}
Spectral-IFOV-Variation	>95% spectral IFOV uniformity {<5% variation over spectral range}

HyspIRI: Building on NASA Hyperion Technology Demonstration

SNR > 10X

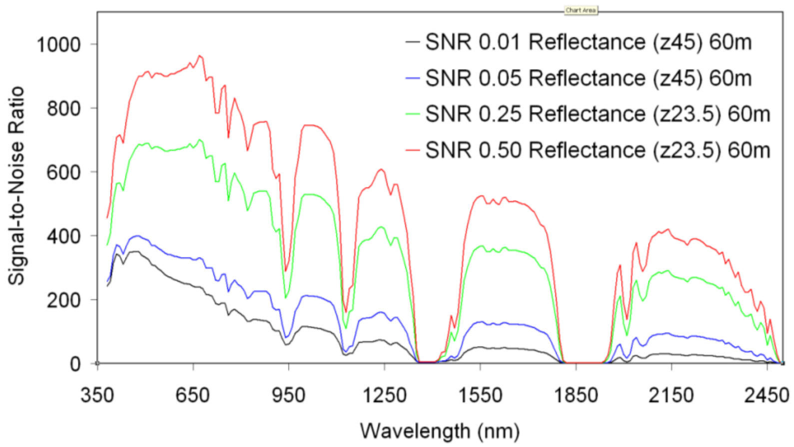

Uniformity > 10X

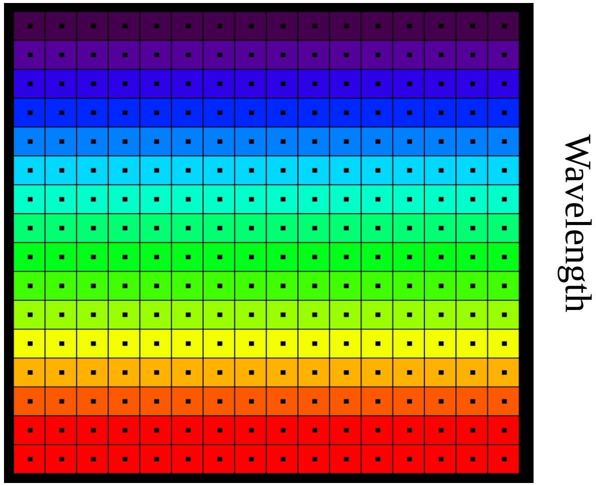

Cross Track Sample

Swath > 10X

Soil C:N Ratio

White Mountain National Forest, NH

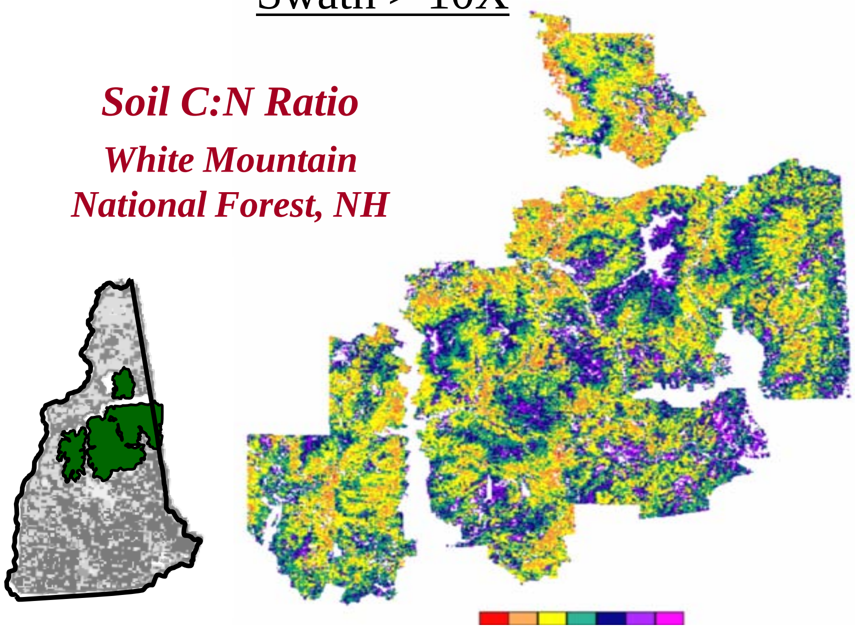

Global Coverage >> 10X

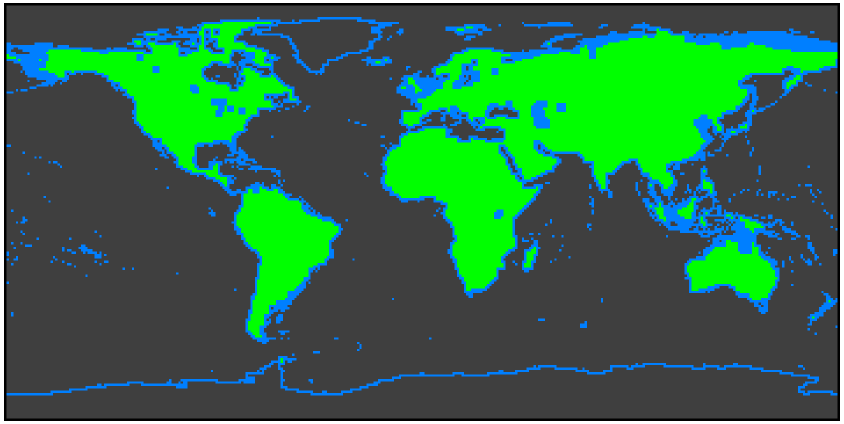

Example Heritage Imaging Spectrometer

8 Kg, 15 watts, 24 Month Build

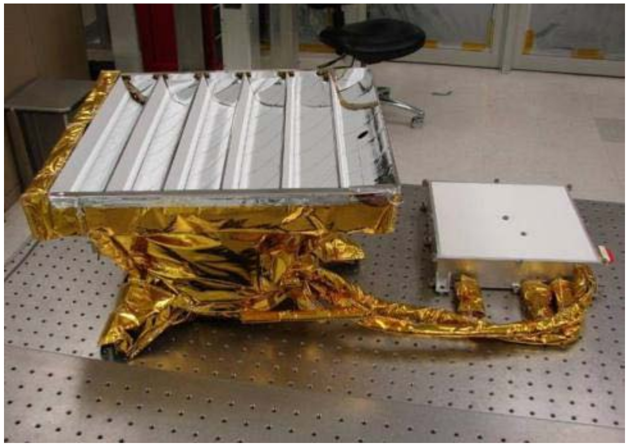

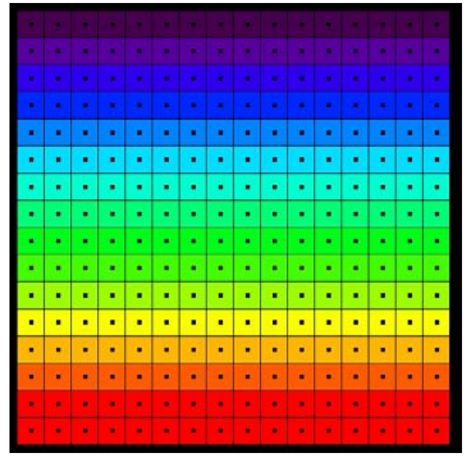

High uniformity and high SNR design by P. Mouroulis

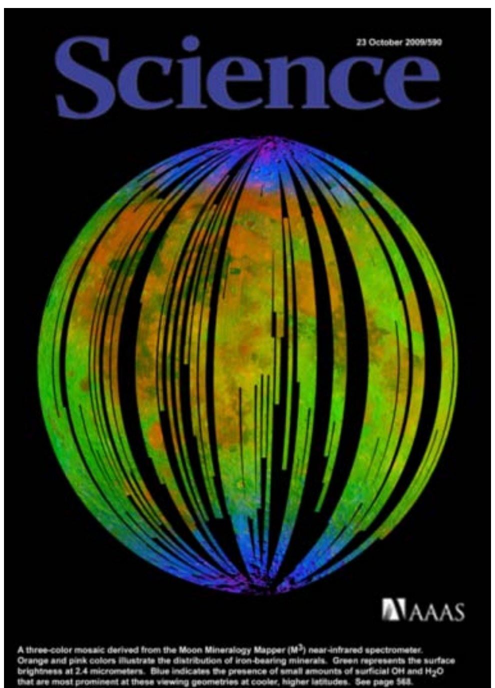

Offner
Spectro-
meter
Spherical
Mirror

Baffles

Baffle

Fold Mirror

TM-1

TM2

TM-3

Uniform
Slit

Convex Multi Facet
Blazed Grating

Order Sorting Filter
and Focal Plane
Detector Array

Baffle

M^3 Measurement of Earth

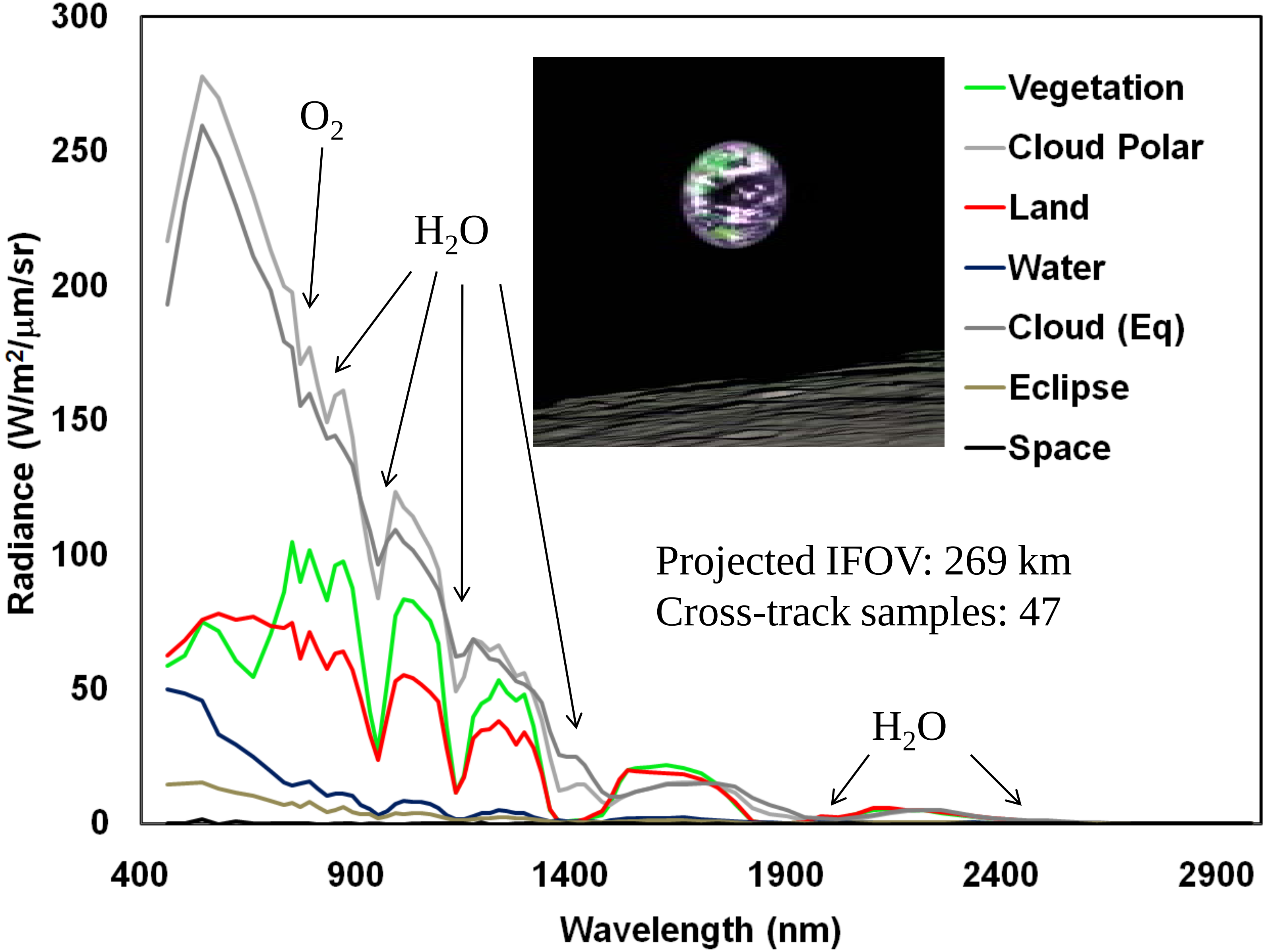

AVIRIS Next Generation

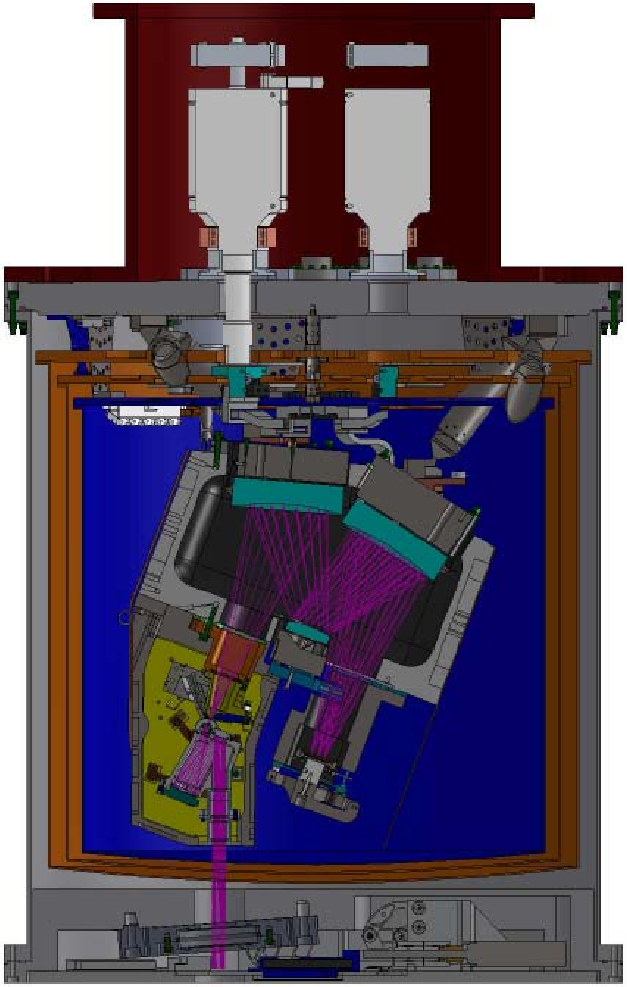

- Spectral
  - Range — 380 to 2500 nm
  - Position — 5 nm
  - Response — 1 to 1.5 X sampling
  - Calibration — +-0.1 nm
- Radiometric
  - Range — 0 to specified saturation radiance
  - Precision — >2000 @ 600 nm
    >1000 @ 2200 nm
  - Accuracy — 95% (<5% uncertainty)
  - Linearity — >=99% characterization
- Spatial (at 100km)
  - Range — 36 degree field-of-view
  - Sampling — 1 milliradian
  - Response — 1 to 1.5 X sampling
  - Slit Projection3 Axes cosines projected slit
- Uniformity
  - Spectral Cross-Track — >95% cross-track non-uniformity
  - Spectral-IFOV-Variation — >95% spectral IFOV non-uniformity

Imaging Spectrometer Instrument Innovation for NASA Science and Discovery

- Two decades of integrated investment
  - Designs, electron-beam lithography gratings & slits, mounts, alignment/calibration
- Advanced spectrometer designs are enabled by curved multi-blaze e-beam grating.

Offner Design

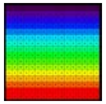

E-Beam Grating

Atomic Force Micrograph of Grating

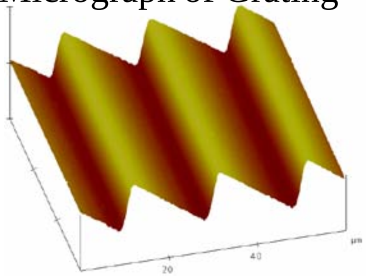

- In 1989, the proposed HIRIS Imaging Spectrometer was **970 Kg, 879 W** and the size of small car.
- Today, the HyspIRI Earth Decadal Survey instrument is **55 Kg and 41 W**, compact and provides a superior science measurement.

Imaging Spectroscopy Science

2009 Discovery of water/OH on the Illuminated Surface of the Moon

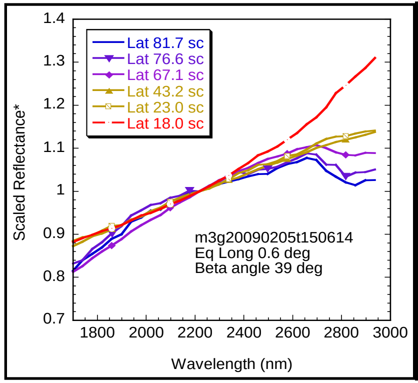

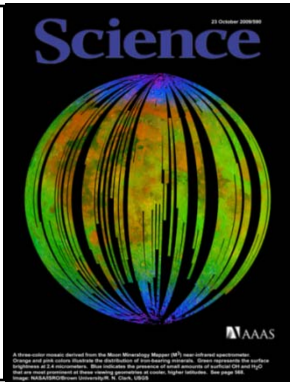

2010 Gulf Spill Volume Estimates of Surface Oil with NOAA and USGS

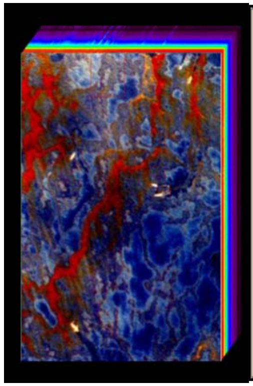

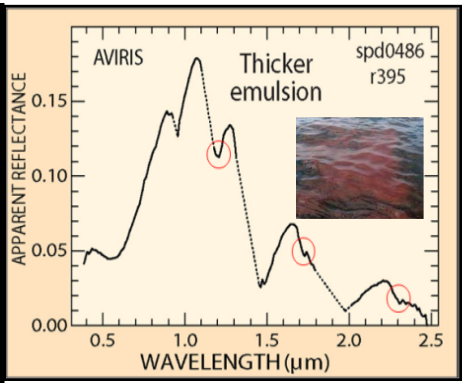

HyspIRI is Required to Reduce Uncertainties in the Land Carbon Fluxes

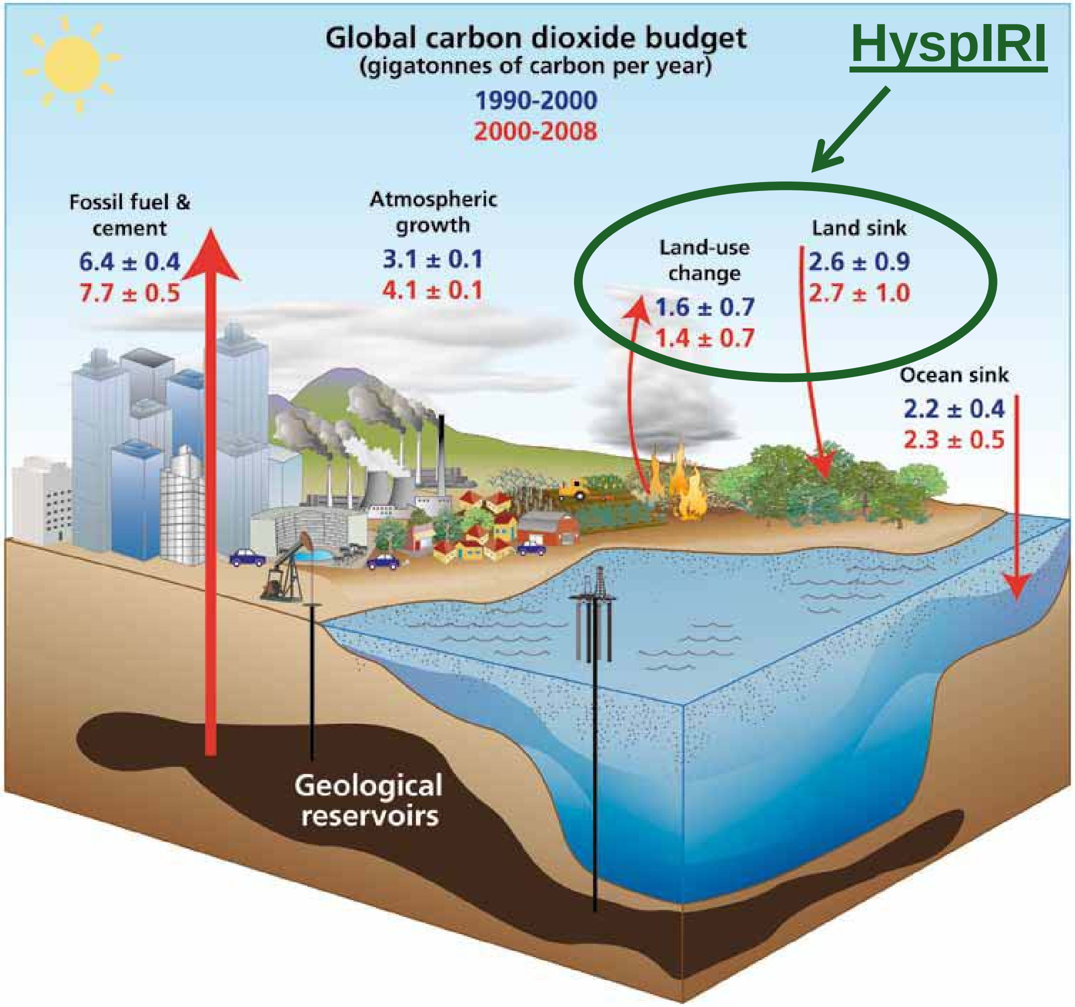

Accurate constraint of Carbon fluxes associated with land-use and terrestrial vegetation are important missing elements today for closing the carbon budget.

The HyspIRI based improvement is essential for sound policy decision making.

Global CO2 budget for 1990-2000(blue) and 2000-2008 (red) (GtC per year). Emissions from fossil-fuel and landuse change are based on economic and deforestation statistics. Atmospheric CO2 growth is measured directly. The land and ocean CO2 sinks are estimated using observations for 1990-2000 (Denman *et al.* IPCC 2007). For 2000-2008, the ocean CO2 sink is estimated using an average of several models, while the land CO2 sink is estimated from the balance of the other terms.

Summary

We have developed a set of VSWIR science questions that are carefully aligned with the HyspIRI Mission called for in the NASA Earth Science and Applications Decadal Survey.

We have reviewed and refined these questions that relate to both science and applications objectives and developed traceability to a set of science measurements.

We have addressed the roles of the HyspIRI mission in climate, global change, societal impact and adaptation.

In preparation for a NASA HyspIRI mission we have established a high heritage and low risk approach for acquiring the HyspIRI VSWIR science measurements

HyspIRI Decadal Survey Climate Science

HyspIRI: "A hyperspectral sensor (e.g., FLORA) combined with a multispectral thermal sensor (e.g., SAVII) in low Earth orbit (LEO) **is part of an integrated mission concept** [described in Parts I and II] that is relevant to several panels, ***especially the climate variability panel***."

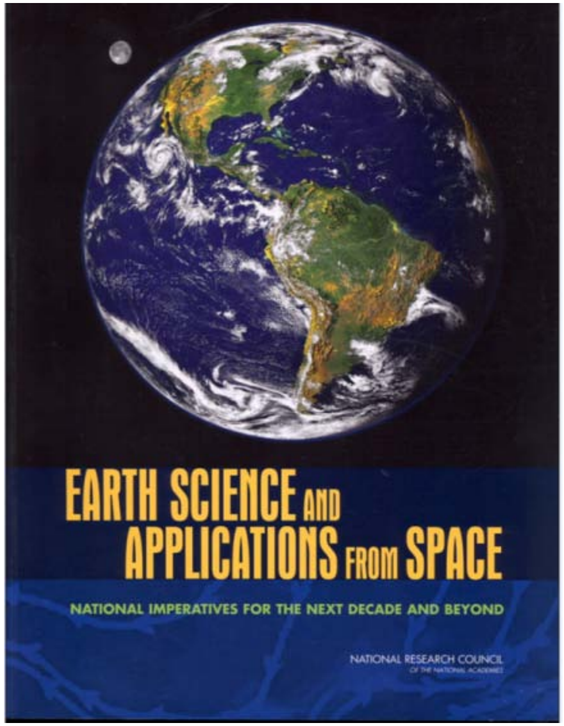

HyspIRI

TIR Science Measurement Baseline

NASA Earth Science and Applications Decadal Survey

Simon J. Hook and HyspIRI Team

NRC Decadal Survey HyspIRI

Visible ShortWave InfraRed (VSWIR) Imaging Spectrometer
+
Multispectral Thermal InfraRed (TIR) Scanner

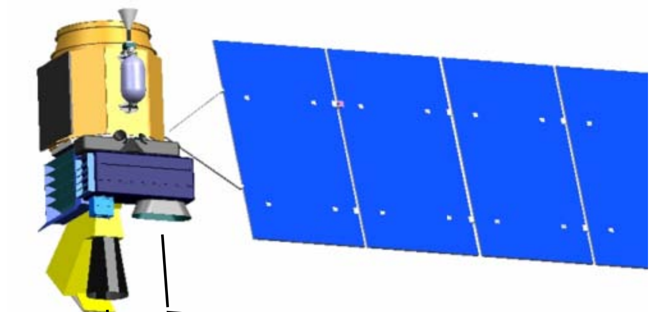

VSWIR: Plant Physiology and Function Types (PPFT)

Multispectral TIR Scanner

Map of dominant tree species, Bartlett Forest, NH

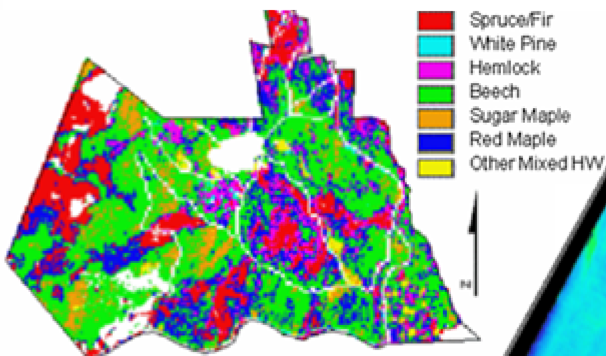

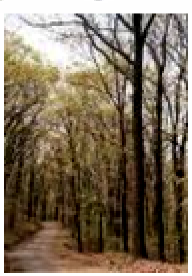

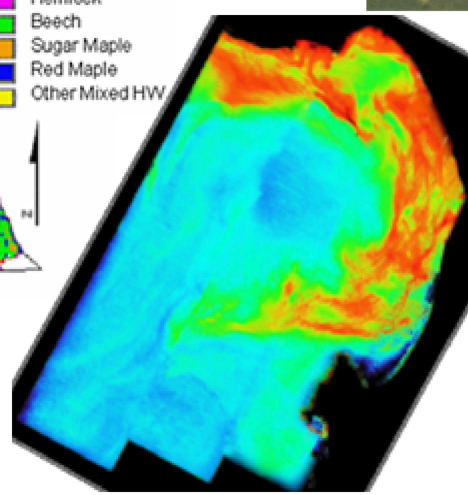

Red tide algal bloom in Monterey Bay, CA

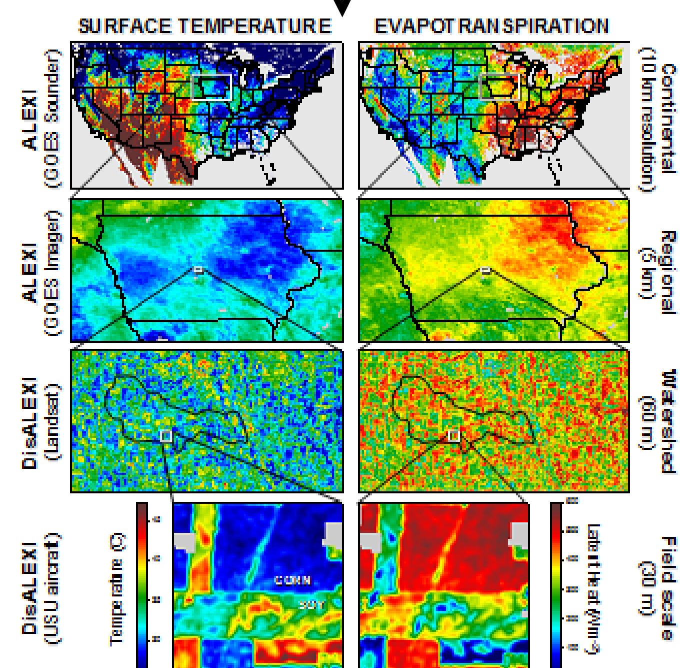

HyspIRI Thermal Infrared Multispectral (TIR) Science Measurements

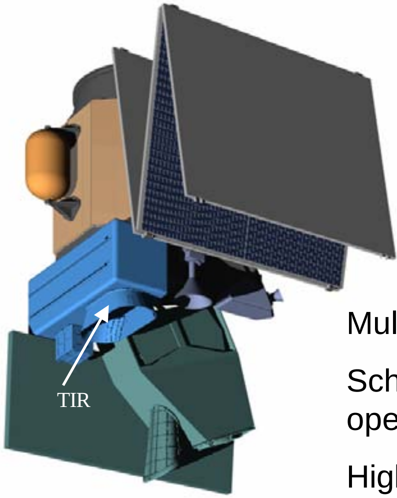

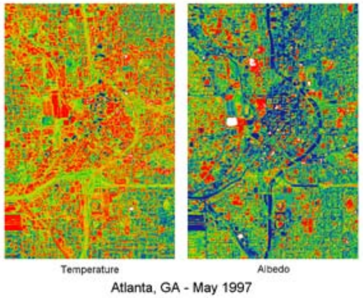

Multispectral Scanner

Schedule: 4 year phase A-D, 3 years operations

High Heritage

Science Questions:

TQ1. Volcanoes/Earthquakes (MA,FF)

– How can we help predict and mitigate earthquake and volcanic hazards through detection of transient thermal phenomena?

• TQ2. Wildfires (LG,DR)

– What is the impact of global biomass burning on the terrestrial biosphere and atmosphere, and how is this impact changing over time?

• TQ3. Water Use and Availability, (MA,RA)

– How is consumptive use of global freshwater supplies responding to changes in climate and demand, and what are the implications for sustainable management of water resources?

• TQ4. Urbanization/Human Health, (DQ,GG)

– How does urbanization affect the local, regional and global environment? Can we characterize this effect to help mitigate its impact on human health and welfare?

• TQ5. Earth surface composition and change, (AP,JC)

– What is the composition and temperature of the exposed surface of the Earth? How do these factors change over time and affect land use and habitability?

Measurement:

- 7 bands between 7.5-12 µm and 1 band at 4 µm
- 60 m resolution, 5 days revisit
- Global land and shallow water

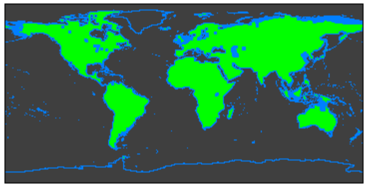

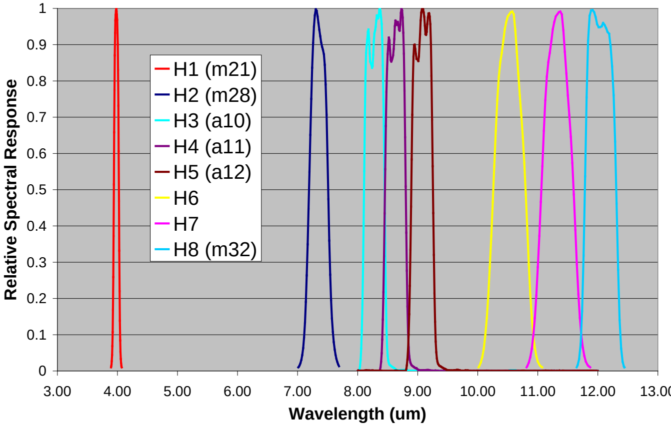

Andean volcano heats up

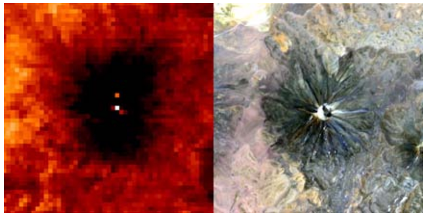

Urbanization

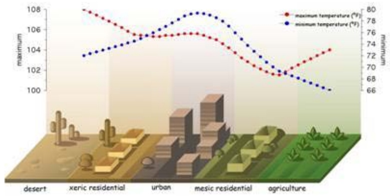

Volcanoes

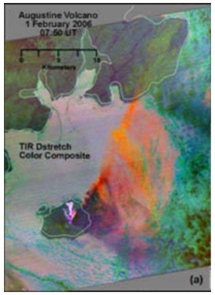

Water Use and Availability

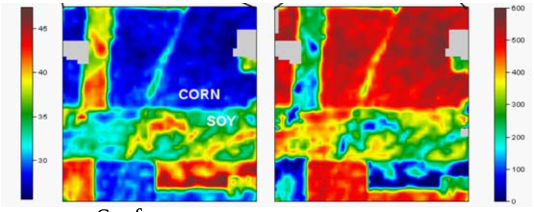

Surface Temperature

Evapotranspiration

TIR Overarching Science Questions

- **TQ1. Volcanoes/Earthquakes (MA,FF)**
  - How can we help predict and mitigate earthquake and volcanic hazards through detection of transient thermal phenomena?
- **TQ2. Wildfires (LG,DR)**
  - What is the impact of global biomass burning on the terrestrial biosphere and atmosphere, and how is this impact changing over time?
- **TQ3. Water Use and Availability, (MA,RA)**
  - How is consumptive use of global freshwater supplies responding to changes in climate and demand, and what are the implications for sustainable management of water resources?
- **TQ4. Urbanization/Human Health, (DQ,GG)**
  - How does urbanization affect the local, regional and global environment? Can we characterize this effect to help mitigate its impact on human health and welfare?
- **TQ5. Earth surface composition and change, (AP,JC)**
  - What is the composition and temperature of the exposed surface of the Earth? How do these factors change over time and affect land use and habitability?

Gas and thermal anomalies, plume composition
including SO2 and ash content on weekly basis

Characterizing and Understanding Volcanic Eruptions

"Likewise, the Tier 2 **Hyperspectral Infrared Imager (HyspIRI)** mission would include measurements over a range of optical and infrared wavelengths useful for detecting volcanic eruptions, determining the ash content of volcanic plumes, and identifying the occurrence and effects of associated landslides."

Source: Dr Jack Kaye, Presented to
Subcommittee on Space and Aeronautics
Committee on Science and Technology
United States House of Representatives,
May 5, 2010

Characterizing and Understanding Volcanic Eruptions

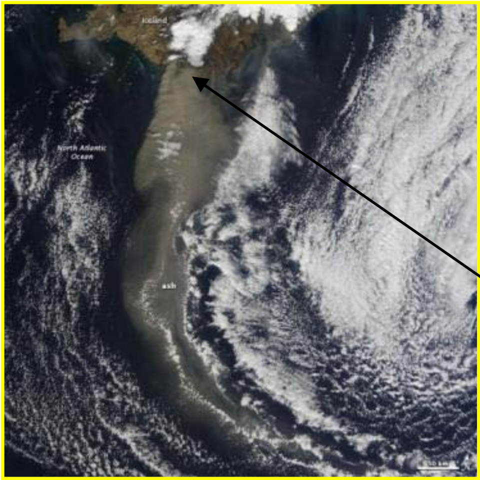

Eyjafjallajökull Iceland Volcano Eruption

April 19 2010 MODIS image of ash plume.

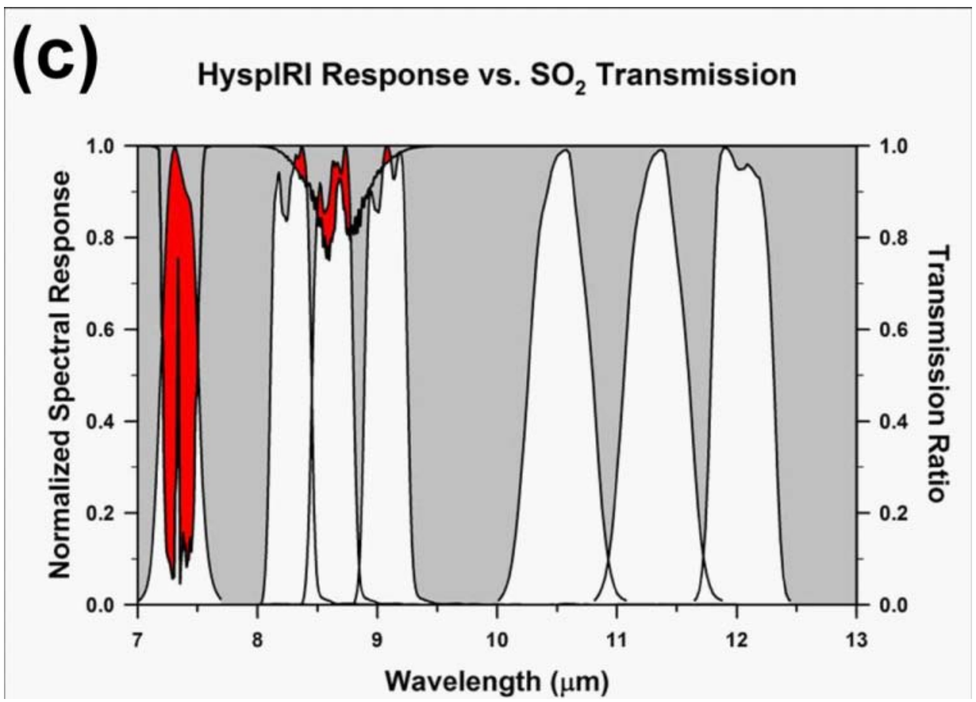

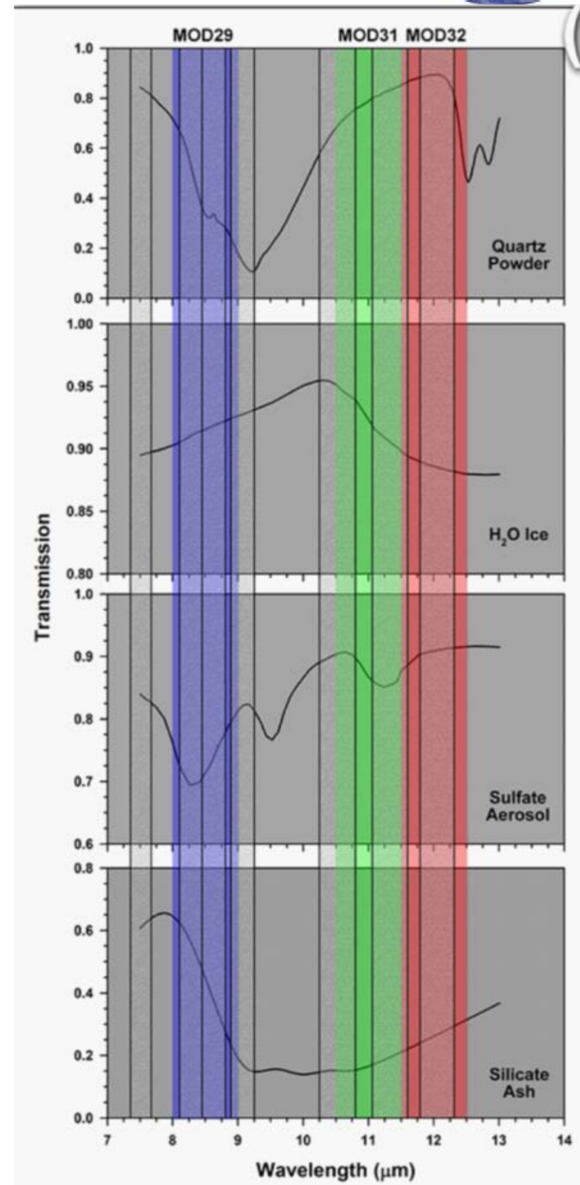

Characterizing and Understanding Volcanic Eruptions

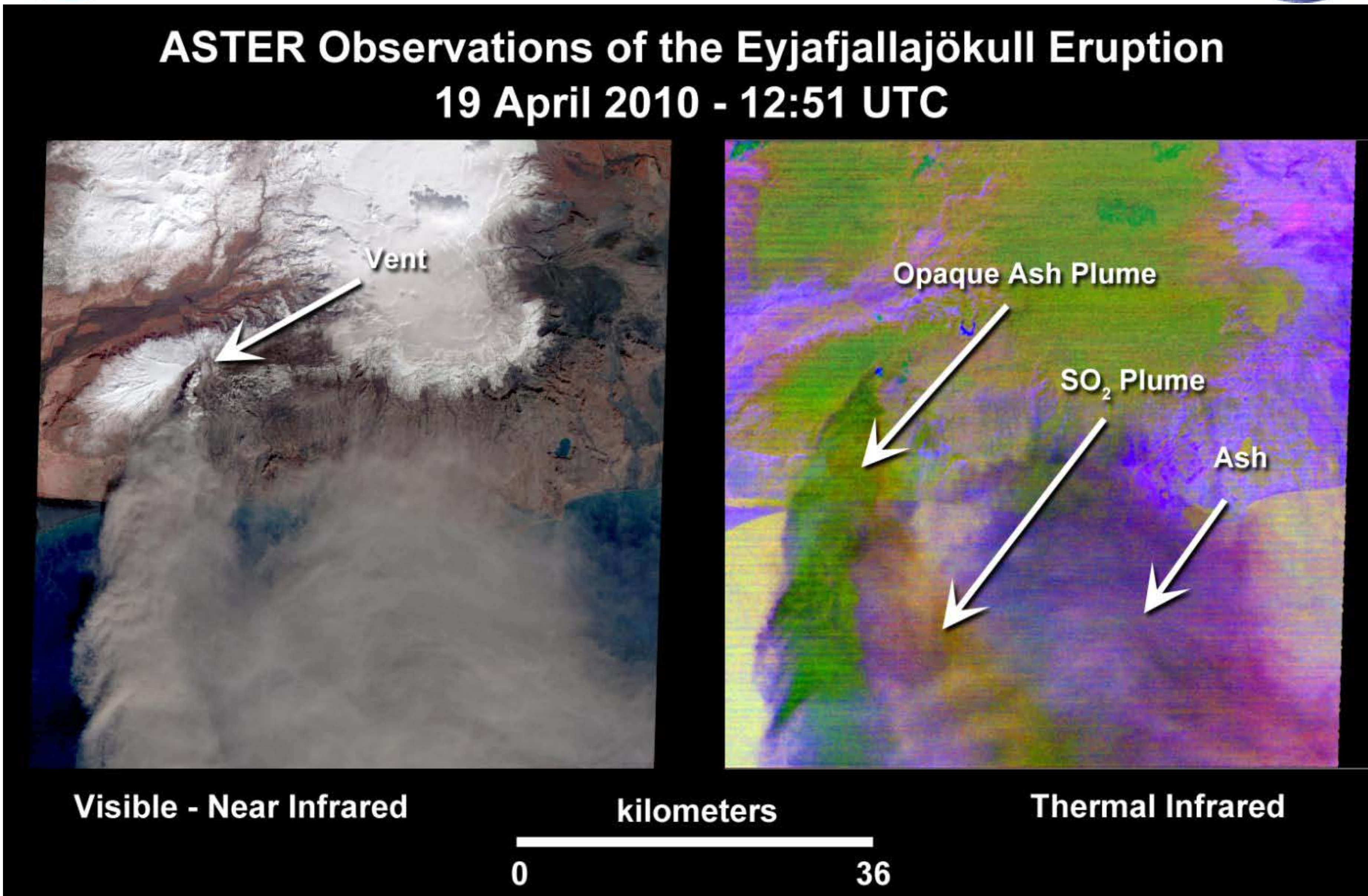

Carbon Release from Biomass Burning

Global Characterization of Fire Emission Sources

Biomass burning and fossil fuel emissions release ~10^{15} g of carbon (C) to the atmosphere each year. <u>Biomass burning constitutes ~36% of all global C emissions.</u>

Region	Fire emissions 1997-2001 average (10^15g C yr^{-1})
Central and northern South America	0.27
Southern South America	0.80
Northern Africa	0.80
Southern Africa	1.02
Southeast Asia	0.37
Boreal (north of 38°N)	0.14
Other	0.13
Global	3.53

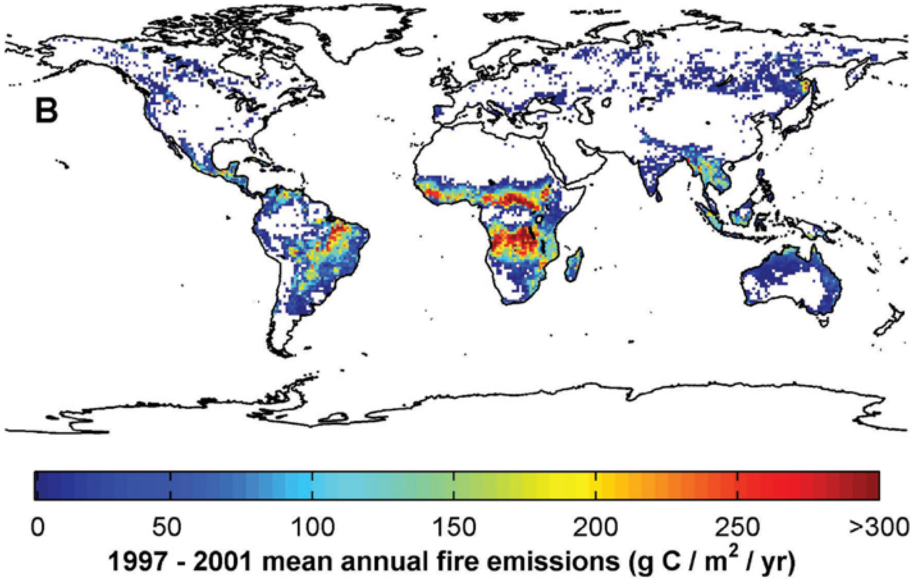

Van der Werf et al., 2004

Carbon Release from Biomass Burning

Fire Radiative Energy

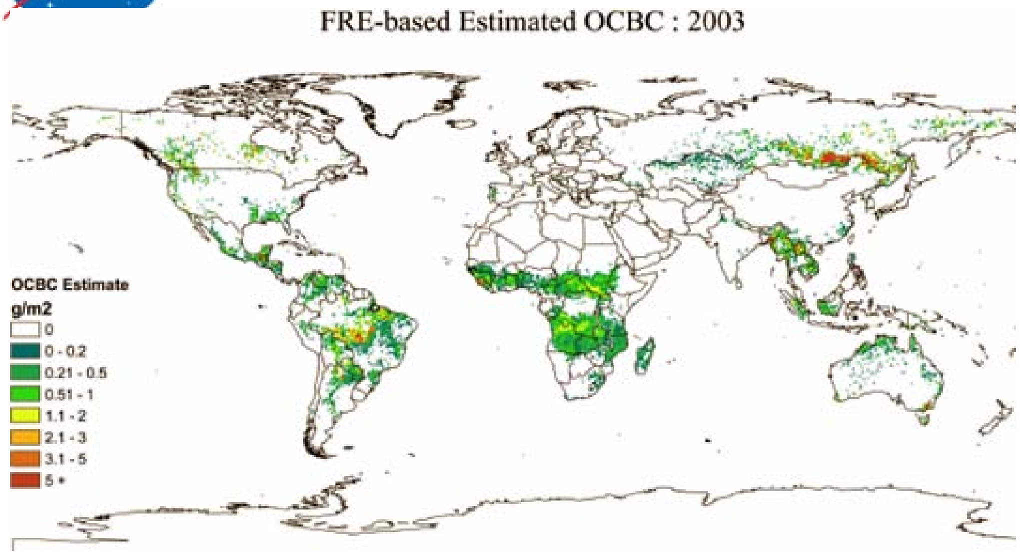

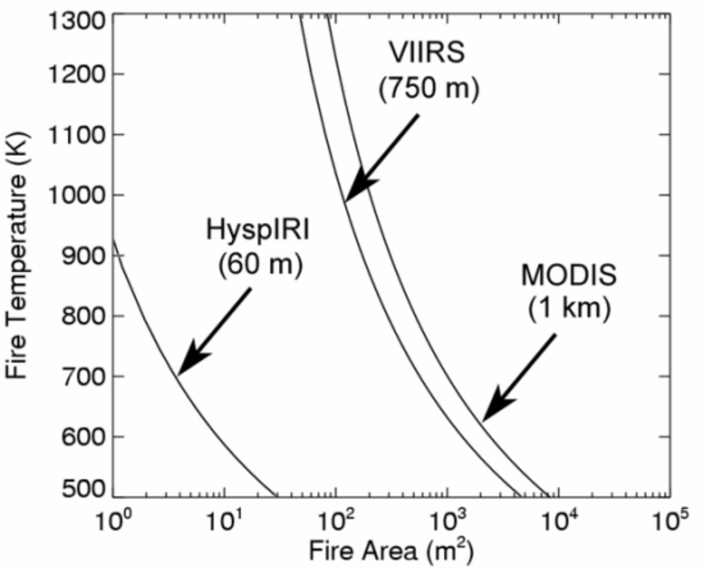

90% probability of detection; boreal forest; nadir view

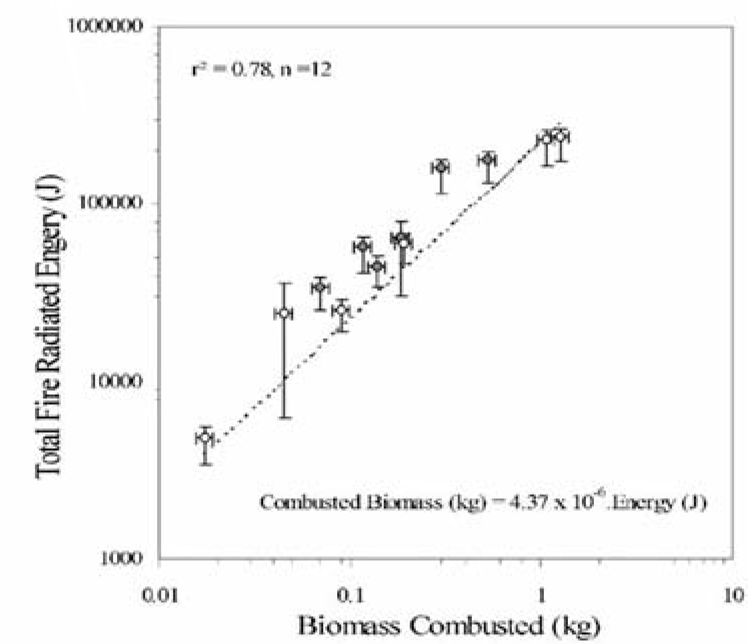

Use Fire Radiative Energy to estimate combusted biomass: Need 3-5 um data

Ellicott et al 2009

Wooster et al 2002 and 2003

Carbon Release from Biomass Burning

How are global fire regimes changing? (patterns of fire occurrences, frequency, size, severity)

High resolution thermal instrument can distinguish between the forest and non-forest parts of the flaming front allowing the fire type, intensity, etc., to be determined which indicates fire regime.

White squares show fire pixels detected by MODIS. Insufficient information to detect fire type

MIR band provides radiant flux to estimate rate at which biomass combusted and instantaneous emission estimate

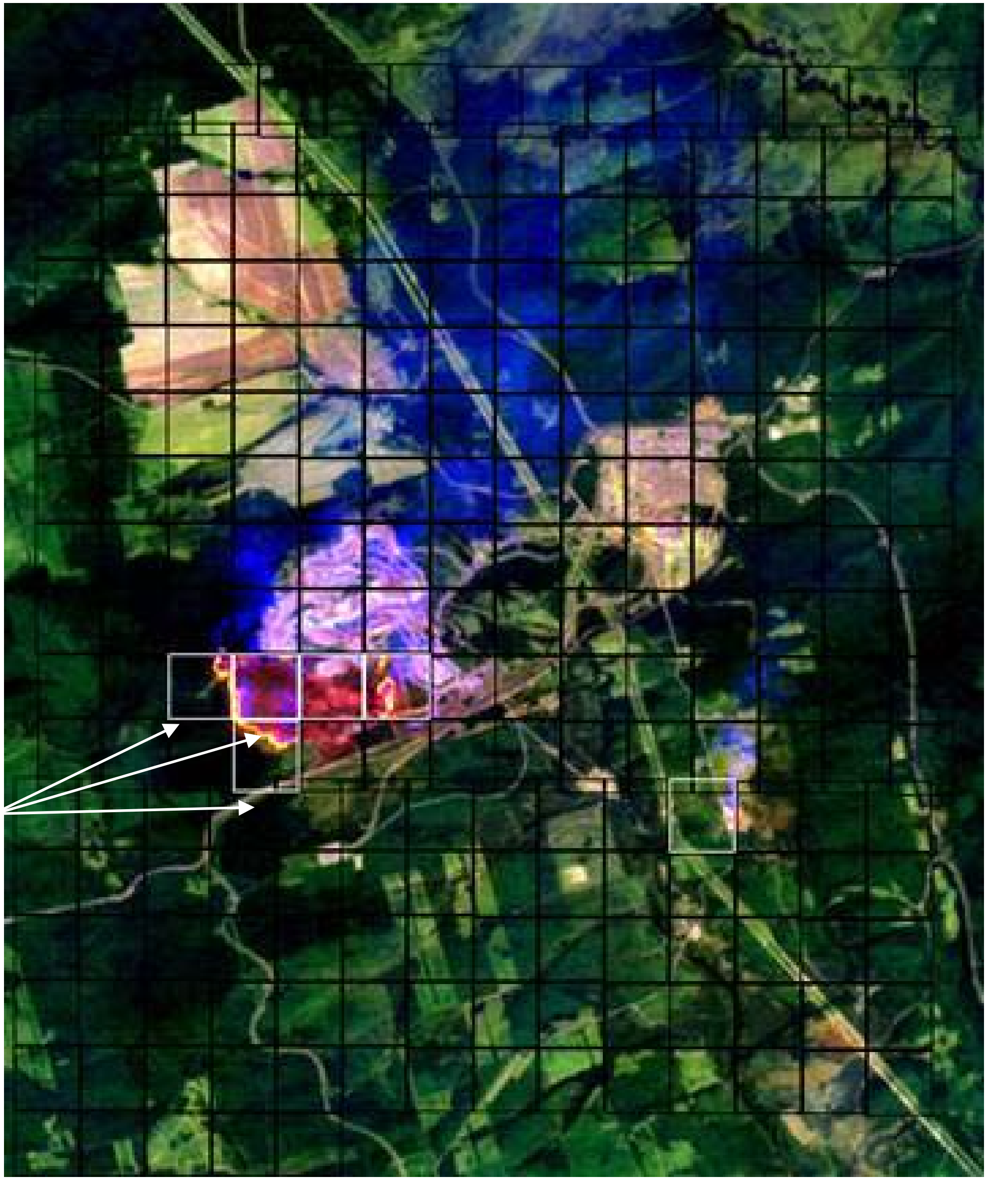

30 m ASTER scene with MODIS pixels superimposed (black squares)

Central Siberia

30 May 2001

Science Measurements

Summary Measurement Characteristics

Spectral	
Bands (8) µm	3.98 µm, 7.35 µm, 8.28 µm, 8.63 µm, 9.07 µm, 10.53 µm, 11.33 µm, 12.05
Bandwidth	0.084 µm, 0.32 µm, 0.34 µm, 0.35 µm, 0.36 µm, 0.54 µm, 0.54 µm, 0.52 µm
Accuracy	<0.01 µm
Radiometric	
Range	Bands 2-8= 200K – 500K; Band 1= 1400K
Resolution	< 0.05 K, Linear Quantization to 14 bits
Accuracy	< 0.5 K 3-sigma at 250K
Precision (NEdT)	< 0.2K
Linearity	>99% characterized to 0.1 %
Spatial	
IFOV	60 m
MTF	>0.65 at FNy
Scan Type	Push-Whisk
Swath Width	600 km (±25.5° at 623 km altitude)
Cross-Track Samples	10,000
Swath Length	15.4 km (+/- 0.7-degrees at 623km altitude)
Down-Track Samples	256
Band-to-Band Co-registraion	0.2 pixels (12 m)
Pointing Knowledge	1.5 arcsec (0.1 pixels)

Science Measurements

Characteristics Continued

Temporal	
Orbit Crossing	10:30 am sun synchronous descending
Global Land Repeat	5 days at equator
OnOrbit Calibration	
Lunar View	1 per month {radiometric}
Blackbody Views	1 per scan {radiometric}
Deep Space Views	1 per scan {radiometric}
Surface Cal Experiments	2 (d/n) every 5 days {radiometric}
Spectral Surface Cal Experiments	1 per year
Data Collection	
Time Coverage	Day and Night
Land Coverage	Land surface above sea level
Water Coverage	Coastal zone -50 m and shallower
Open Ocean	Averaged to 1km spatial sampling
Compression	2:1 lossless

Mission Concept
Operational Scenario

- Following arrival at science orbit, the baseline data acquisition plan is established. Collect data for entire land surface excluding sea ice (Arctic and Antarctic) every 5 days at 60 m spatial resolution in 8 spectral bands
- Data are downlinked and transferred to the science data processing center where calibration and baseline processing algorithms are applied.
- Level 1, 2 products are delivered to the scientific community and general users to pursue the science questions
  - With appropriate cloud screening, compositing, spatial, and temporal subsetting

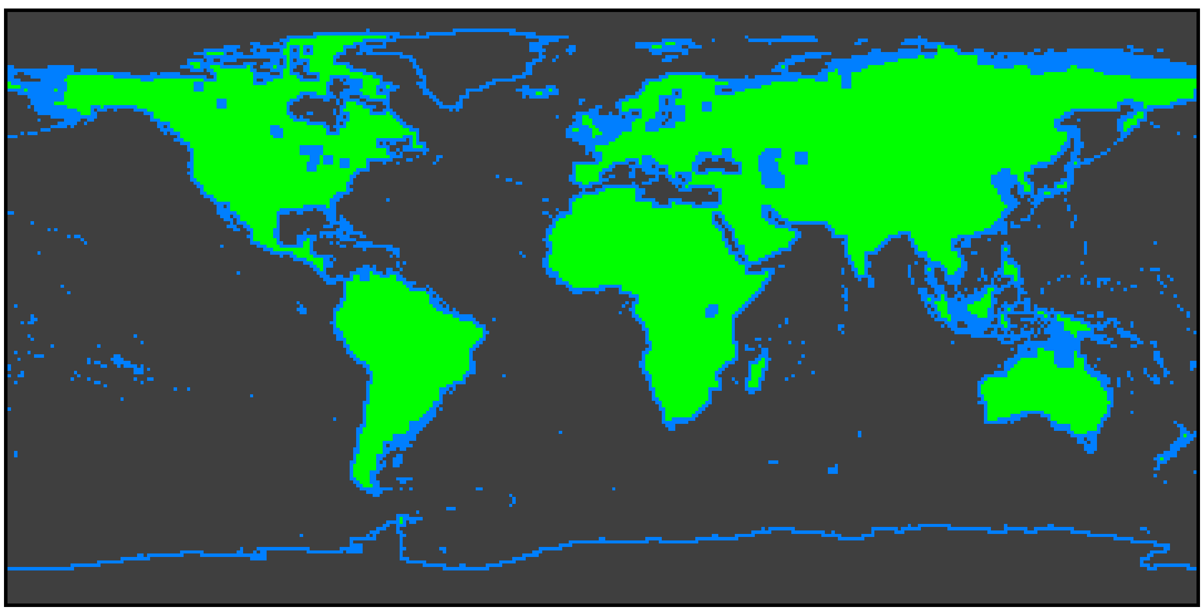

Land and coastal acquisition

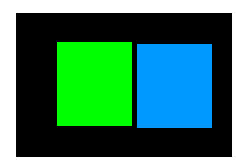

Annual TIR imaging opportunities in a 5-day near-repeating orbit, 1 yr. simulation

Oceans average to 1 km

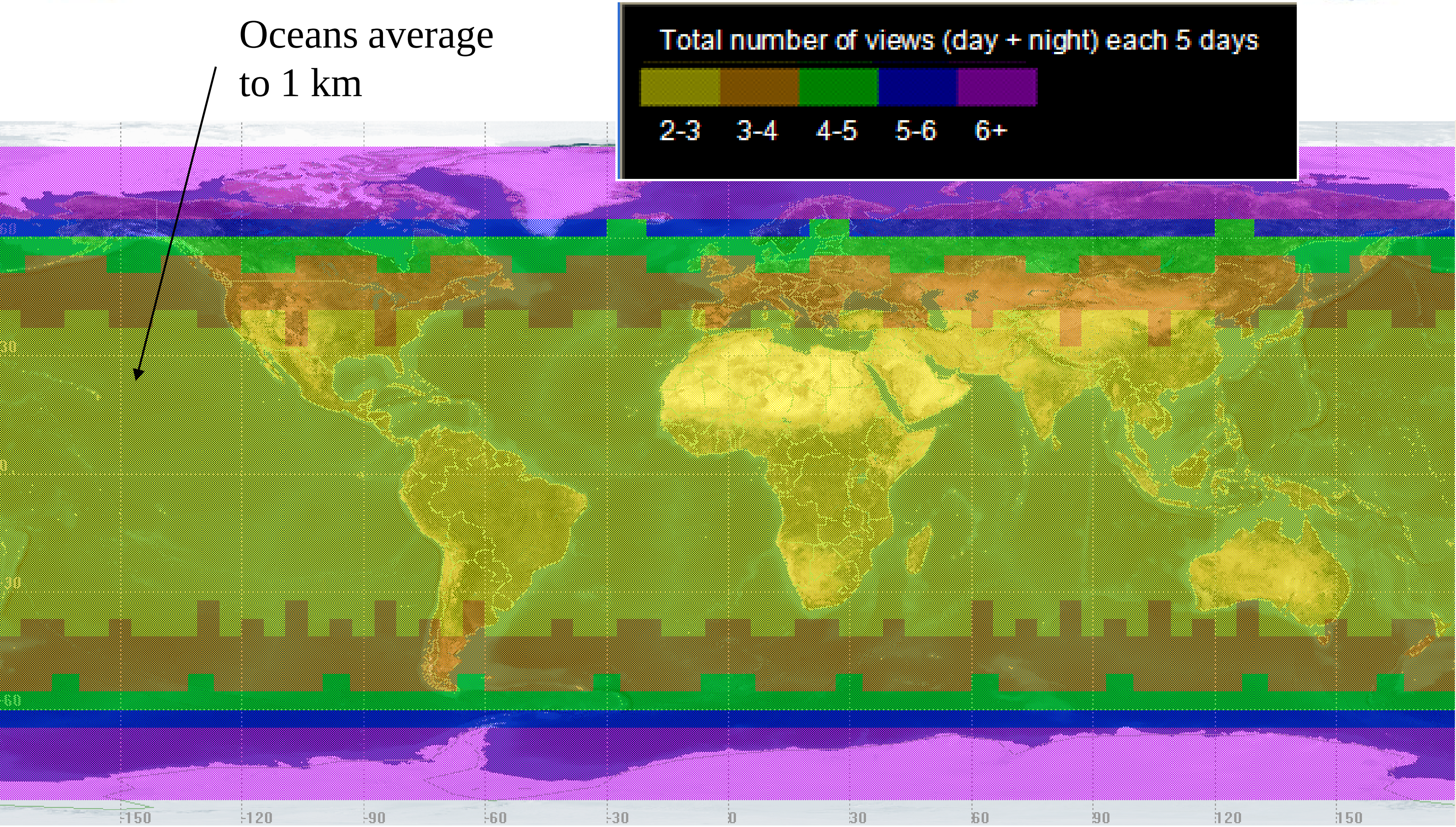

Nominal orbit: average alt. 626.8 km, inclination 97.8°. TIR imager FOV: +/- 25.46° (60 m pixel GSD at nadir, 9272 cross-track pixels).

TIR Instrument Concept

Scanning and Data Rate

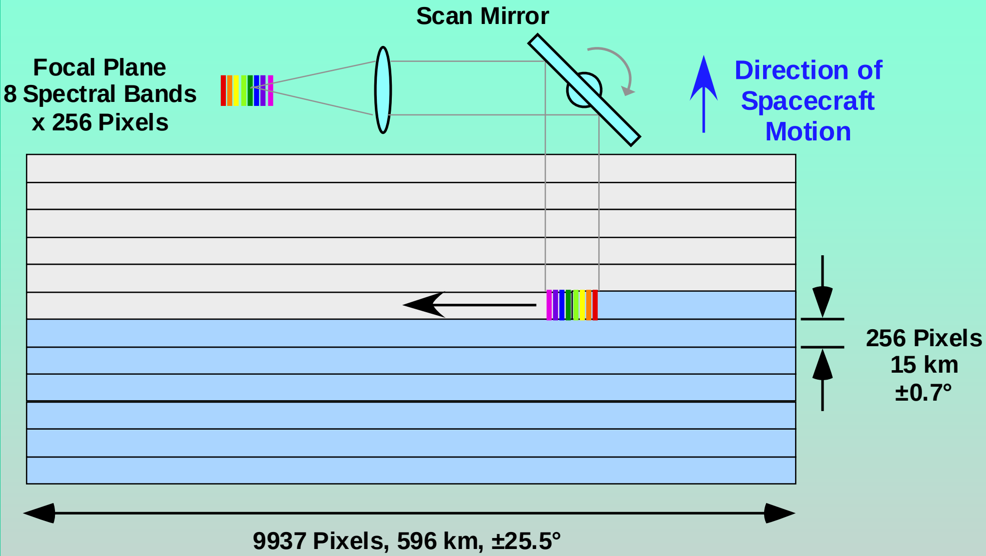

- 60 m Pixel Footprint
- Time-Averaged Science Data Rate 0.024 Gbps
- Assuming 14 bits, 2:1 Compression
- Scan Mirror Rotation Rate 13 RPM
- Pixel Dwell Time 32 microseconds

Mass and Power (JPL Team X)

- Mass CBE 60 kg
- Power CBE 109 W

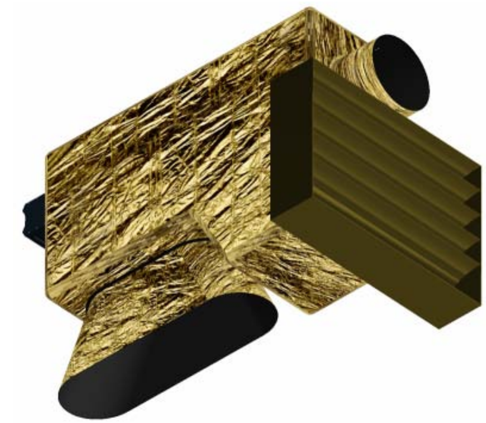

Spectral Bands

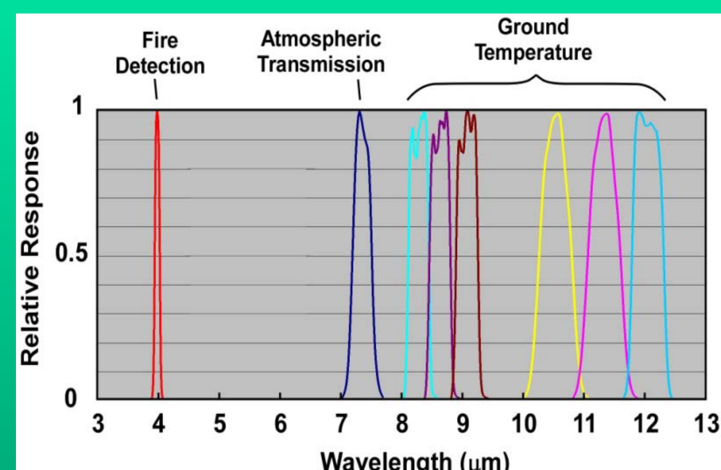

Mission Concept
TIR Overview

- Duration: 4 years development, 3 years science
- Coverage: Global land every 5 days
- Day and Night imaging (1 day and night image at a given location obtained every 5 days)
- Data download using dual-polarization X-band at high-latitude stations
- Spacecraft: LEO RSDO bus (SA-200HP)
- Launch: Taurus-class launch vehicle

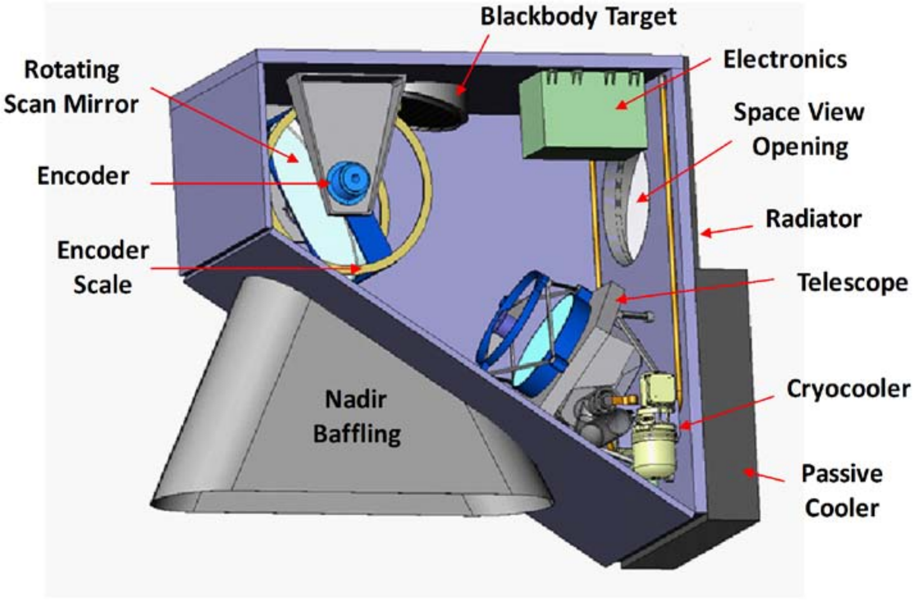

Summary

We have developed a sets of science questions that are well aligned with the HyspIRI Mission called for in the NASA Earth Science and Applications Decadal Survey. The mission has strong relevance to both climate and society.

We have reviewed and refined these questions that relate to both science and applications objectives and developed traceability to a set of science measurements.

We have established a high heritage and low risk approach for acquiring the HyspIRI VSWIR and TIR science measurements

Hyperspectral – Infrared Imager (HyspIRI) Mission

Mission Concept Review

HyspIRI VSWIR Instrument

Carl Bruce
with contributions from the HyspIRI Team

National Aeronautics and
Space Administration

Jet Propulsion Laboratory
California Institute of Technology
Pasadena, California

National Aeronautics and
Space Administration

Jet Propulsion Laboratory
California Institute of Technology
Pasadena, California

VSWIR - Instrument Concept

- *Outline*

  1. *Introduction*
  2. *Key Requirements & Performance*
  3. *Key Trades and Results*
  4. *Technology Readiness & Heritage*

HyspIRI – VSWIR '10

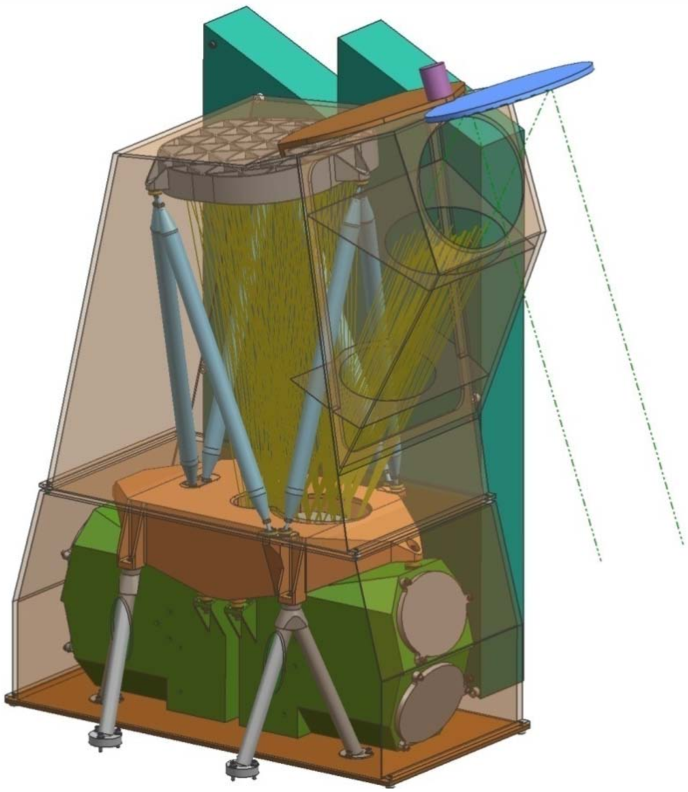

Mass (CBE)	***55Kg***
Power (Ave.)	***41Watts***

Key VSWIR Requirements

Radiometric	Requirement	Status
Range & Sampling	0 to 1.5 x benchmark radiance, 14 bits	Demonstrated via analysis and 14 bit ADC bread board electronics
Accuracy	>95% absolute radiometric, 98% on-orbit reflectance, 99.5% stability	Demonstrated – AVIRIS, MaRS
Precision (SNR)	See spectral plots at benchmark radiances	Demonstrated via analysis
Linearity	>99% characterized to 0.1 %	Demonstrated via test, MaRS and M3
Polarization	<2% sensitivity, characterized to 0.5 %	Demonstrated via analysis of design and test data on the grating
Scattered Light	<1:200 characterized to 0.1%	Demonstrated in MaRS and M3

Spectral	Requirement	Status
Range	380 to 2500 nm (solar reflected spectrum)	Demonstrated – AVRIS, MaRS, M3
Sampling	<= 10 nm {uniform over range}	Demonstrated – MaRS, M3
Response	<= 1.3 X sampling (FWHM) {uniform over range}	Demonstrated – MaRS, M3
Accuracy	<0.5 nm	Demonstrated – MaRS, M3

HyspIRI Mission

Key VSWIR Requirements

Spatial	Requirement	Status
Range	>145 km	Demonstrated by design and analysis (150 km)
X-track Sampling	>2400	Demonstrated by design and analysis (2500)
Sampling	<= 60m (Nadir)	Demonstrated by design and analysis
Response	<= 1.2X sampling (FWHM)	Demonstrated by MaRS and M3
Uniformity		
Spectral Cross-Track	>95% cross-track uniformity {<0.5 nm min-max over swath}	Demonstrated by MaRS and M3
Spectral-IFOV-Variation	>95% spectral IFOV uniformity {<5% variation over spectral range}	Demonstrated by MaRS and M3

Other Key	Requirement	Status
Data rate	~ 300 Mbits per second	Met by preliminary architecture and parts selection – all required parts are at or above TRL 6
Compression	3:1 lossless	Met by algorithm test on MaRS data. Algorithms implemented in breadboard electronics and flight FPGA
Pointing Knowledge	30m radius (3σ) ~ 9 arcsec (3σ) = 3 arcsec (1σ) reconstructed	Met by analysis and the use of ground tie points
Mass	<55 kg	Met by current design with 30% margin – working to increase margin

Instrument Approach

Spectroscopy in the range 400 to 2500 nm at 10 nm with high uniformity and high precision (SNR) is required to capture the molecular absorption and constituent scattering signatures for this mission. The following instrument options have been considered to achieve this objective.

- **Selected: Offner spectrometer (Hyperion, CRISM, ARTEMIS, M3, COMPASS^{air} TB^{air})**
  - Full range from 380 to 2500 nm demonstrated. Efficiency for high SNR optimized with multiple blaze grating demonstrated. Uniformity from design through alignment demonstrated. Snapshot acquisition detector. Dispersion efficiency tunable to optimize use of detector.
- Prism dispersion spectrometer
  - Dispersion is non-uniform. Cross-track and spectral-IFOV uniformity not inherent in optical design. Dispersion efficiency not tunable in detail to optimize use of detector full well.
- Wedge/Linear-variable filter spectrometer
  - Full spectral range coverage from 380 to 2500 nm has not been demonstrated maintaining 10 nm spectral sampling and response function. Filter uniformity is a concern over wide spectral and spatial domain. Fast, high throughput, beams interplay with filter spectral bandpass undermines uniformity.
- Fourier Transform Spectrometer
  - Dispersion is non constant with wavelength. Not typically built to operate below 1 micron. Detector dynamic range and photon shot noise concern. Architecture for > 2000 cross track elements and >200 spectral channels not identified. Not well suited for wide or moderate field of view. Requires IMC.
- Liquid Crystal Tunable & Acousto-Optical Tunable
  - Time sequential acquisition undermines uniformity. Low TRL, polarization sensitive. Limited spectral range. Requires IMC.

National Aeronautics and Space Administration

Jet Propulsion Laboratory
California Institute of Technology
Pasadena, California

HyspIRI Mission

VSWIR Concept '10

Optics

- Front End Telescope consists of a primary spherical mirror and a secondary aspherical mirror
- Back End Spectrometers consist of 2 optimized Offner spectrometers

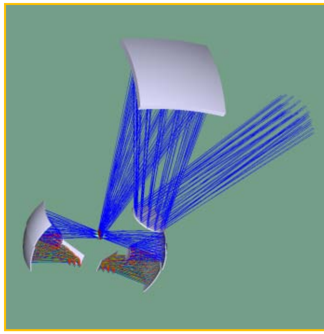

Radiator

- Area 0.6m²
- M3 technology heritage

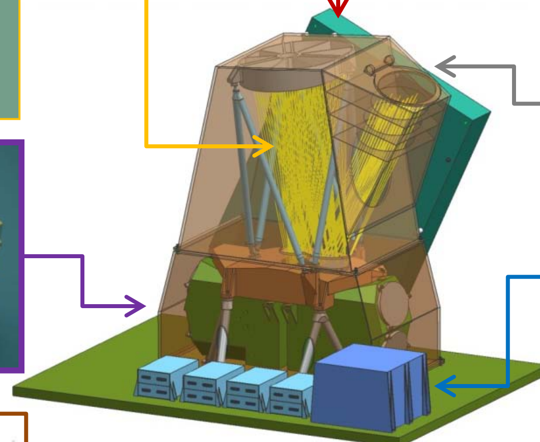

Baffle/Cover/Cal Panel

- *Launch cover*
- *Used as a solar reflectance calibration target*

Spectrometers (2x)

- 2 identical Offner spectrometers
- Each contains:
  - E-Beam grating
  - Si air slits
  - FPA assembly

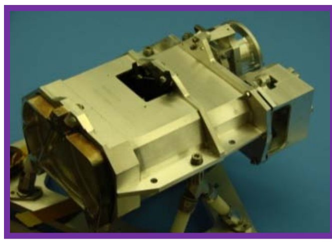

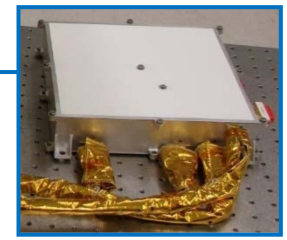

Electronics

- M3 Derivative 4x
- Electronic concept is based upon available flight approved parts
- Ins. control, Data Compression, mode control

FP A (2x)

- Mount is adjustable in 6 DOF
- Thermal strap connects mount to radiator
- Each assembly contains two Teledyne 6604a detector arrays
- Includes integral OSF

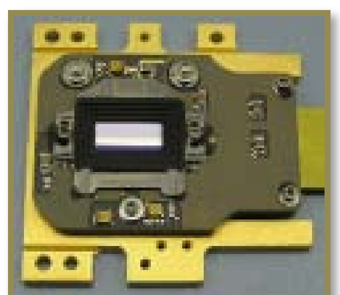

Detectors (4x)

- Teledyne 6604a detectors; full flight heritage from M3.
- Analog I/O
- Each spectrum readout as snapshot, so that there is no time delay, yaw, or jitter impact to the spectral-IFOV-uniformity.

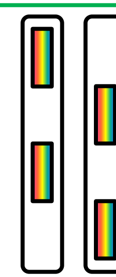

VSWIR Concept '10

Changes

a) Optical bench
b) CG Bipods
c) Telescope Bipods
d) Thermal enclosure
e) Optimized radiator
f) Cal. Cover

Results

a) Mass is reduced
b) Structure is mechanically sound (120Hz)
c) Improved thermal isolation
d) Smaller radiator
e) Electronic parts =>TRL6

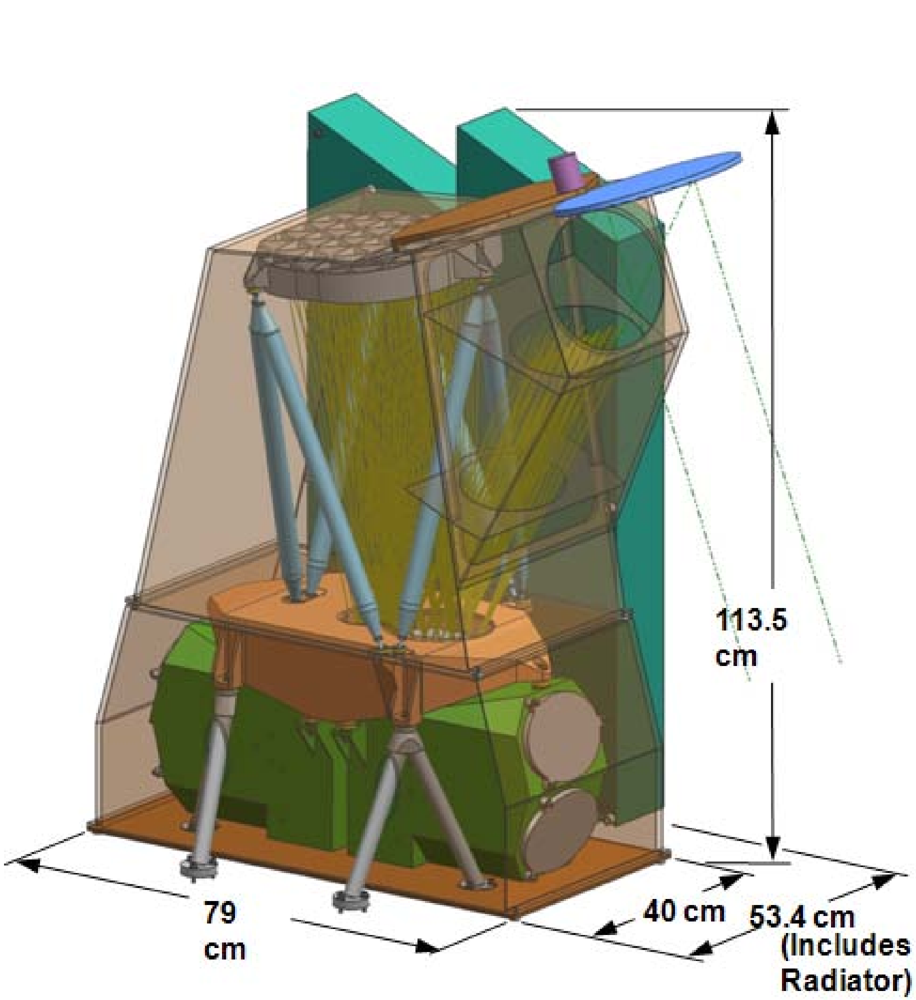

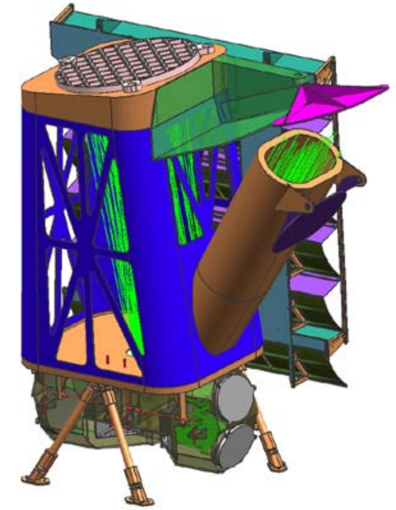

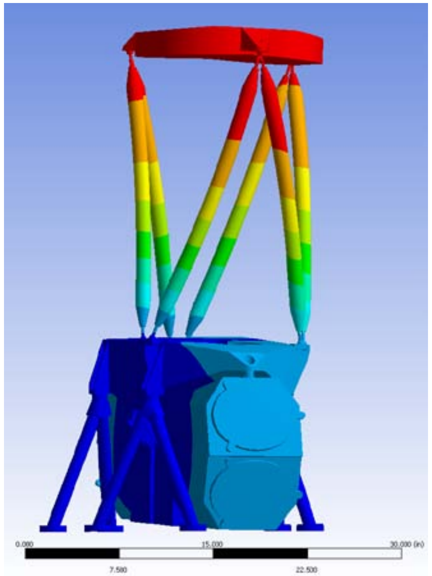

TRL & Heritage

No new technology is required for HyspIRI – VSWIR

M3 Spectrometer

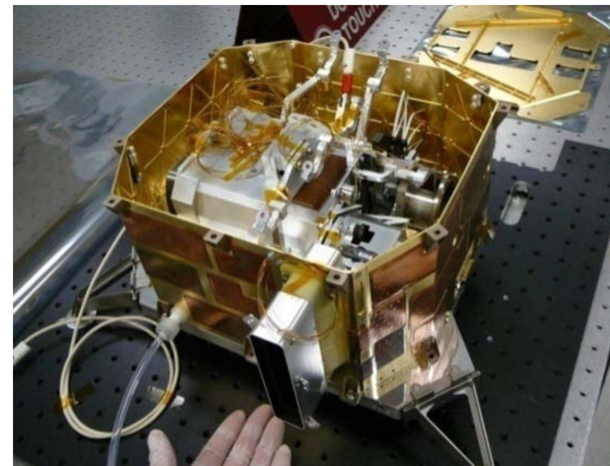

Technology Readiness Highlights

Key Technology	TRL	Comments
Spectrometer	9	Offner design flown on Hyperion, CRISM and M3
Grating	9	Flown on Hyperion, CRISM, M3
Detector array	9	Flown on M3
Opto-Mechanical (alignment & stability)	9	Flown on M3

VSWIR has high heritage in instrument architecture, requirements, manufacturing, vendors, management and engineering staff

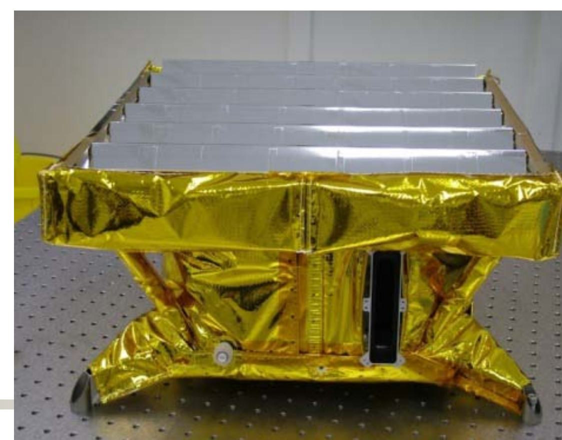

Key Technologies are Proven

1. Uniform Offner spectrometer (Mouroulis Design)

2. Finely adjustable optics and detector mounts that can be locked within fraction of a micron (0.1 microns)

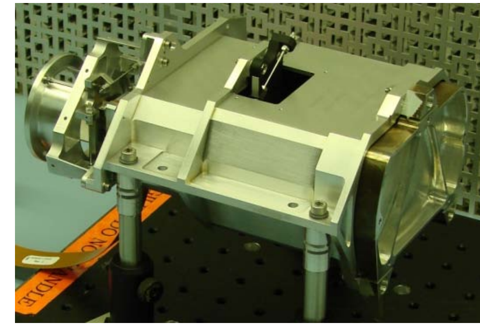

3. Electron beam fabricated gratings (large ruling period)

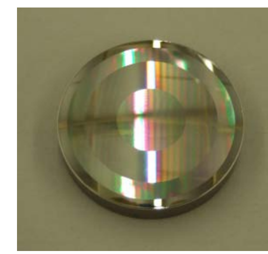

1. Electron beam fabricated air slits(non-uniformity < .05 microns)

2. Alignment and calibration sources and methodologies to achieve and verify requirements.

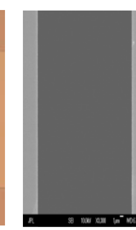

HyspIRI Thermal Infrared Radiometer (TIR) Instrument Conceptual Design

Marc Foote, William Johnson, Simon Hook
Jet Propulsion Laboratory
California Institute of Technology
HyspIRI Workshop August 24, 2010

National Aeronautics and Space Administration

Jet Propulsion Laboratory
California Institute of Technology
Pasadena, California

TIR Instrument Concept

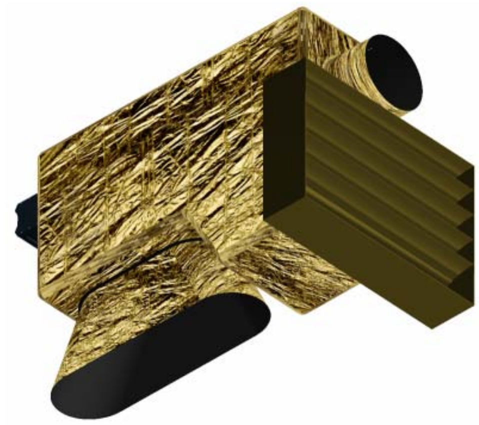

Scanning and Data Rate

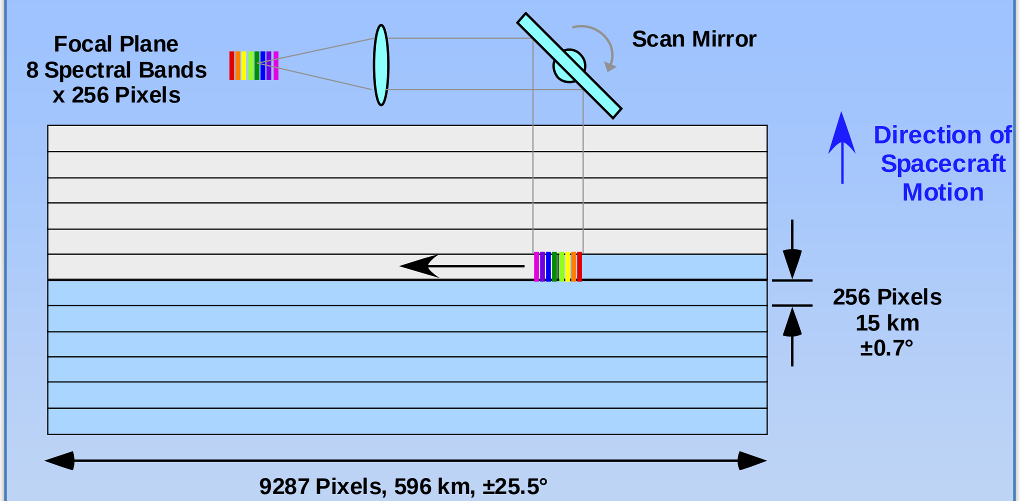

- 60 m Pixel Footprint at Nadir
- Time-Averaged Science Data Rate 0.024 Gbps
- Assuming 14 bits, 2:1 Compression, 40% Land
- Scan Mirror Rotation Rate 14.2 RPM
- Pixel Dwell Time 32 microseconds

Spectral Bands

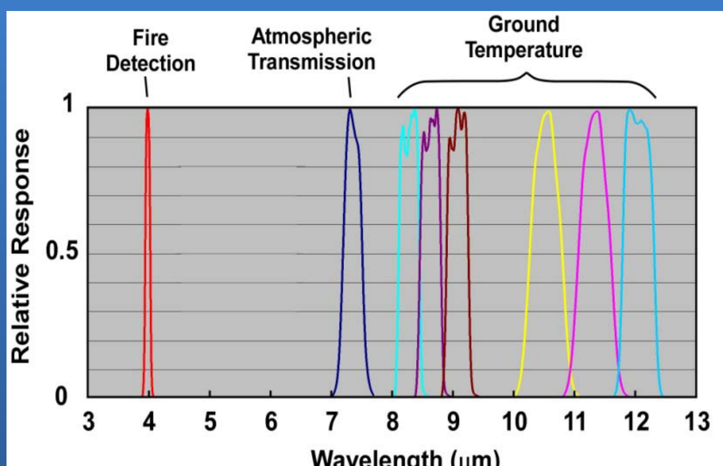

Mass and Power (JPL Team X)

- Mass CBE 60 kg
- Power CBE 109 W

National Aeronautics and
Space Administration

Jet Propulsion Laboratory
California Institute of Technology
Pasadena, California

Conceptual TIR Layout

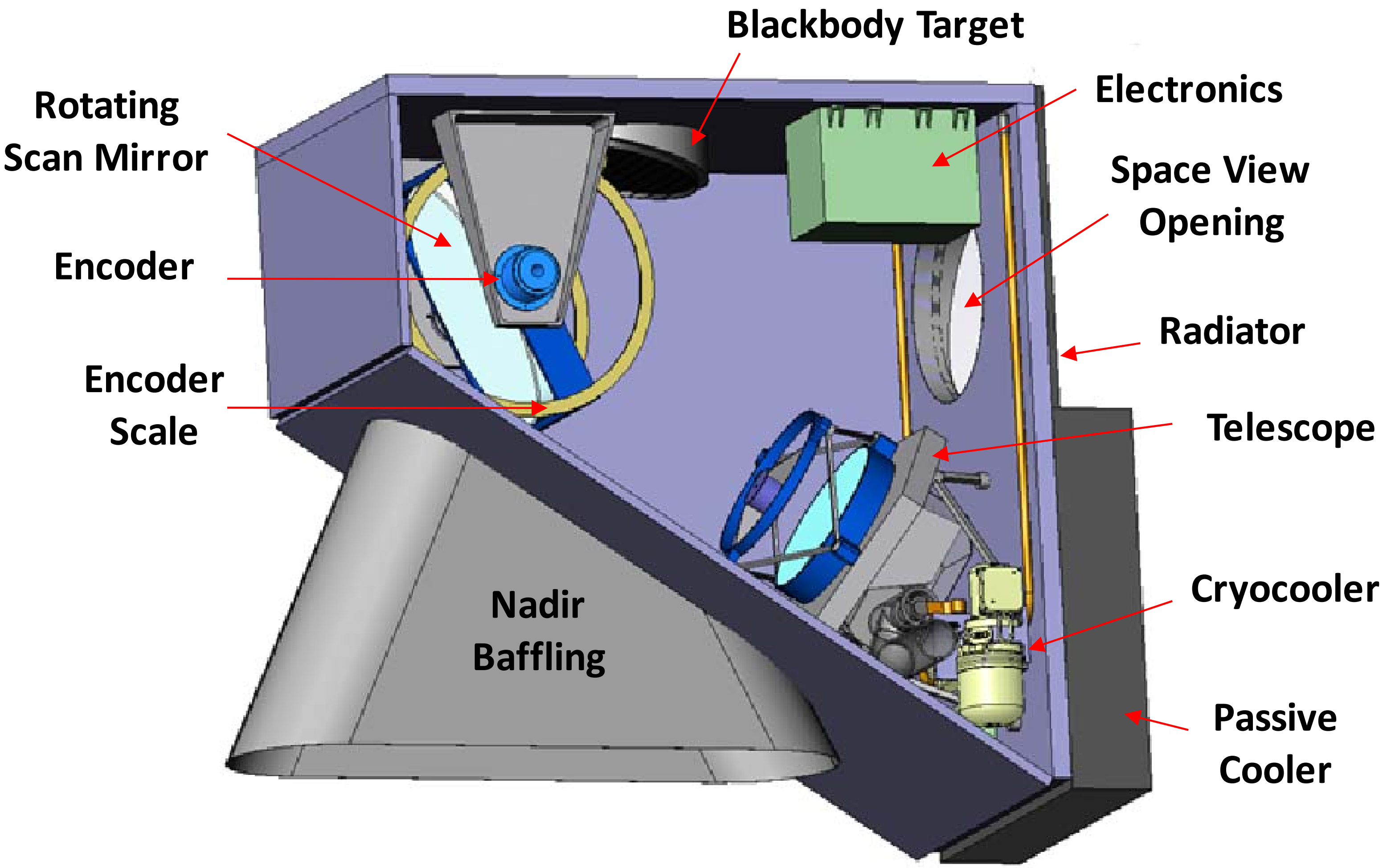

Conceptual TIR Telescope

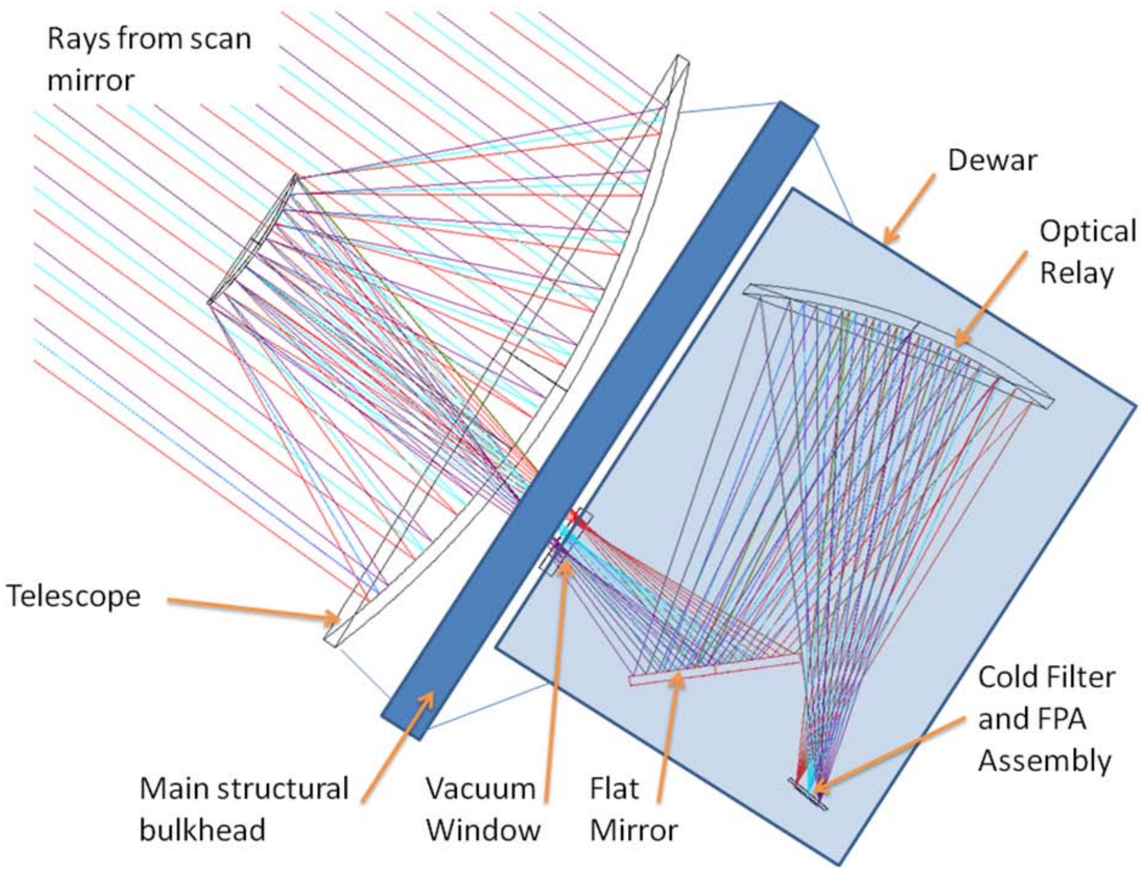

HyspIRI-TIR optics consists of a 3-mirror off axis Cassegrain.

Optical Parameters

Parameter	Value
Aperture Size	208 mm
f/#	2.0
Focal Length	416 mm

HyspIRI-TIR Polychromatic Modulation Transfer Function

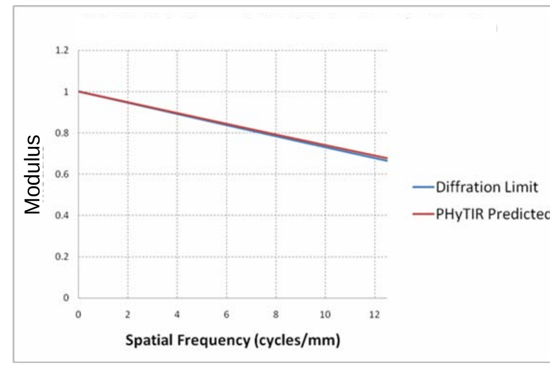

HyspIRI-TIR Polychromatic Ensquared Energy Function

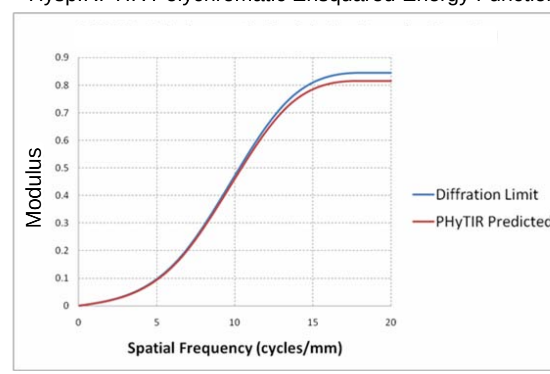

Conceptual TIR Layout

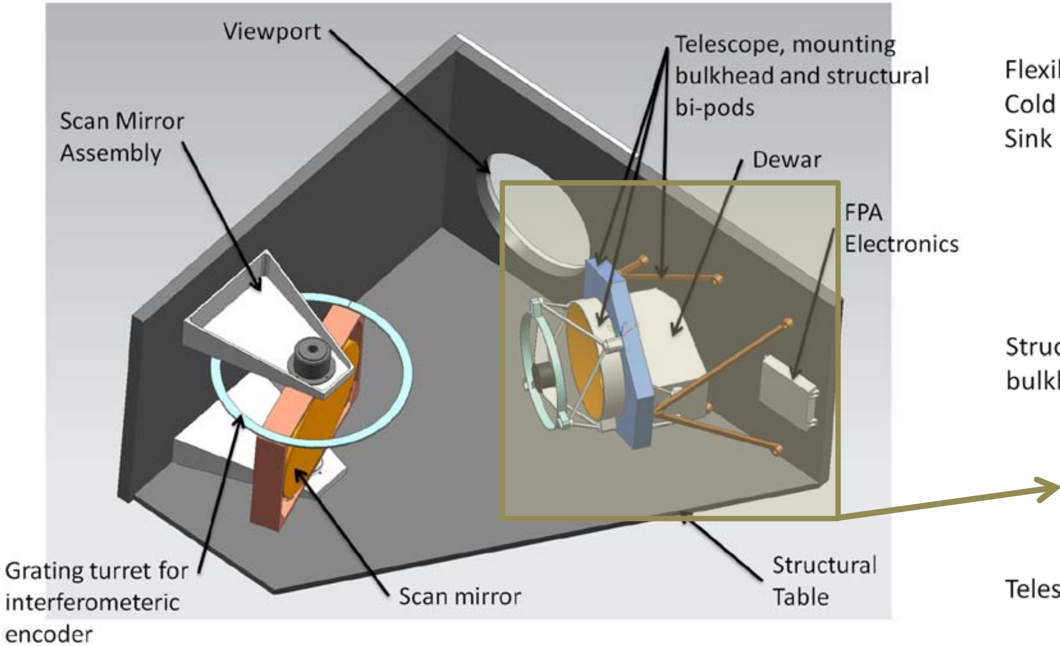

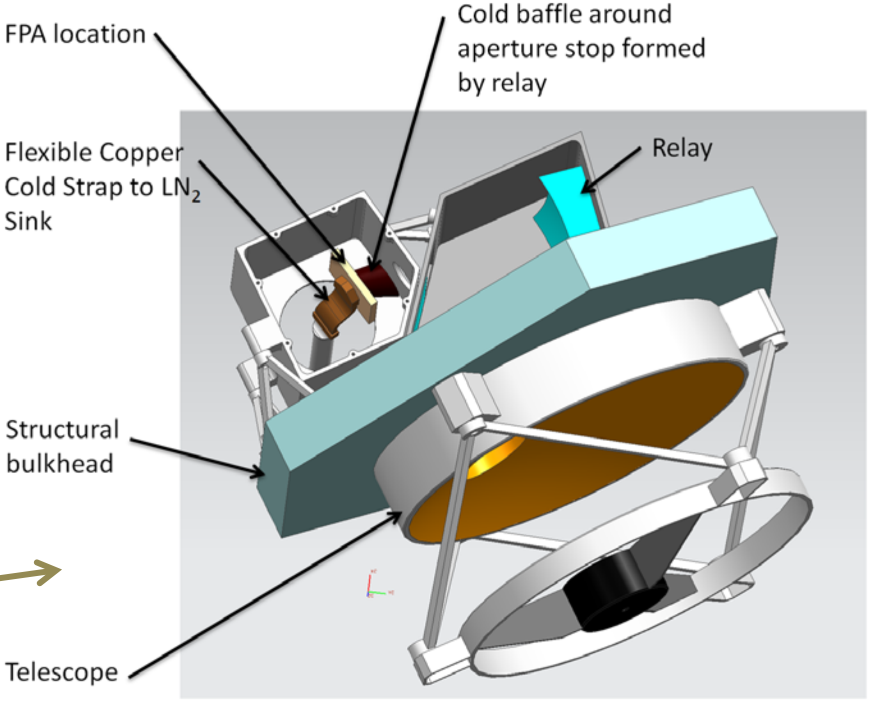

Dewar removed to show internal components

TIR Focal Plane Concept

- Butcher-Block Filter Assembly
- Baffles to Prevent Crosstalk Between Spectral Channels

- MCT Detector Array – 256 elements cross-sweep
- 1 Bandgap to Cover Full Spectral Range
- ≥ 4 Detector Columns per Spectral Channel to Allow Time Delay and Integration (TDI)

- CMOS Read-Out Integrated Circuit (ROIC)
- Multiple Output Signals to Enable Necessary Pixel Read Rate
- On-Chip Digitization Under Study

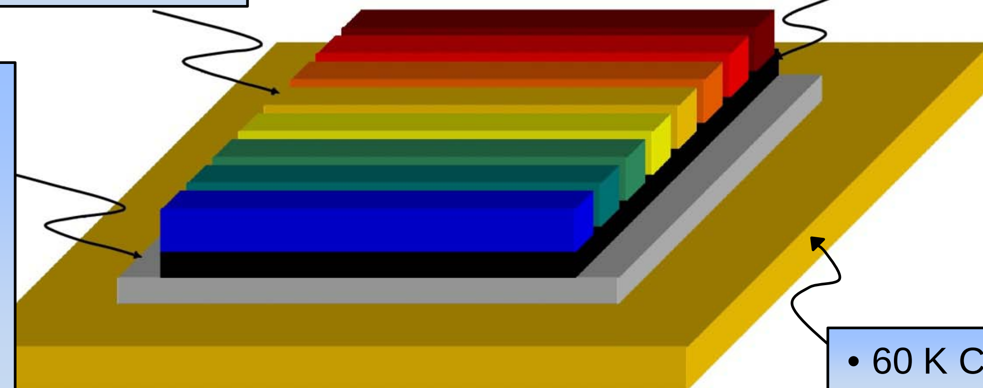

- 60 K Cold Tip of Cryocooler

➢ Peak Data Rate = 256 Mpixels/sec (256 detectors cross-sweep, x4 for TDI, x8 spectral bands every 32 µs).
  - 32 analog output lines, each operating at >10 MHz
  - Digitization in off-chip ADCs – for example, 4 Teledyne ADP 14x8 ASICs (standard Teledyne product)
  - TDI performed by FPGA after digitization

Teledyne Focal Plane Readout Architecture

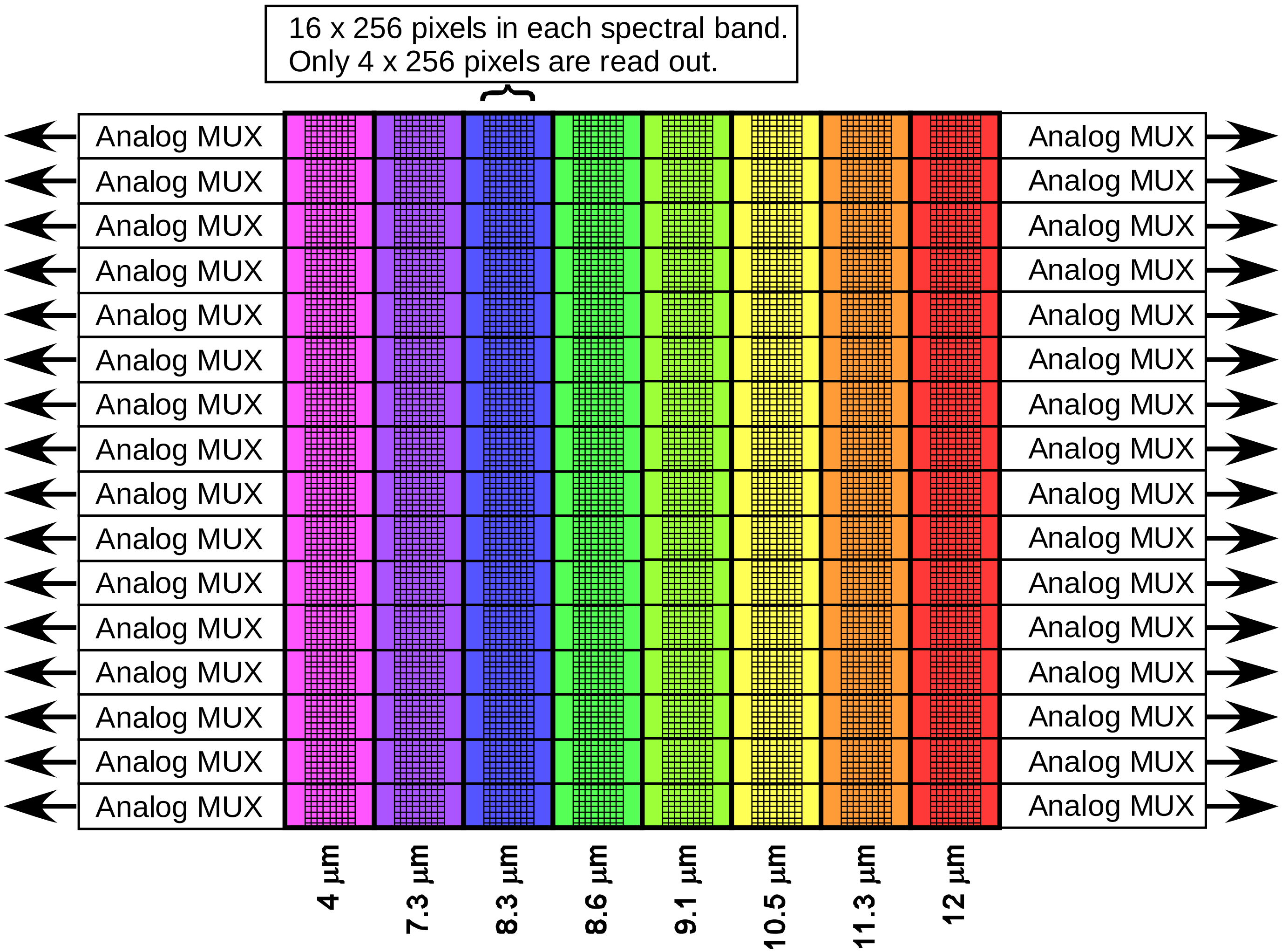

Teledyne ROIC Warm Probe Testing

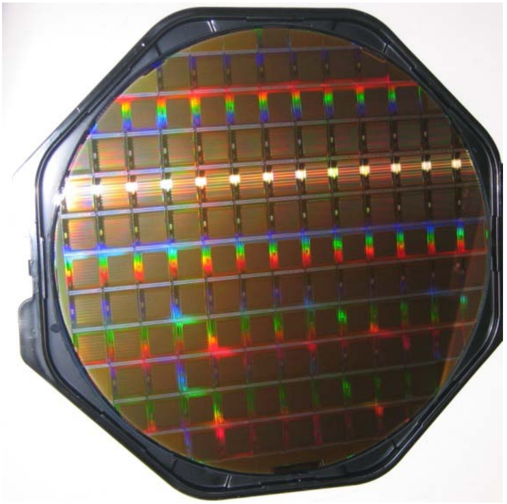

HyspIRI-TIR eight inch wafer with over 100 dies. 6 wafers are at the vendor.

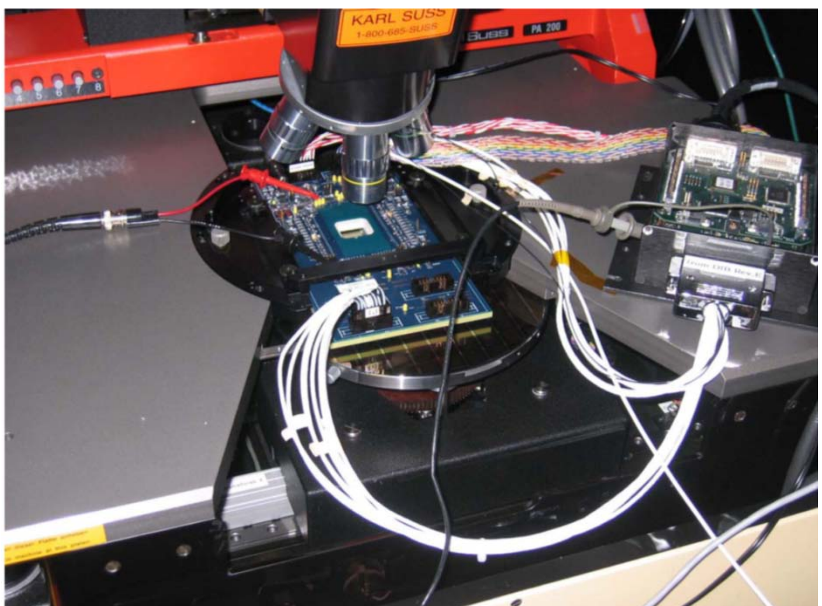

Wafer probe station. Wafer is currently being testing at nearly the required readout speed and shows as-expected noise and power performance as well as register functionality.

TIR Estimated Performance

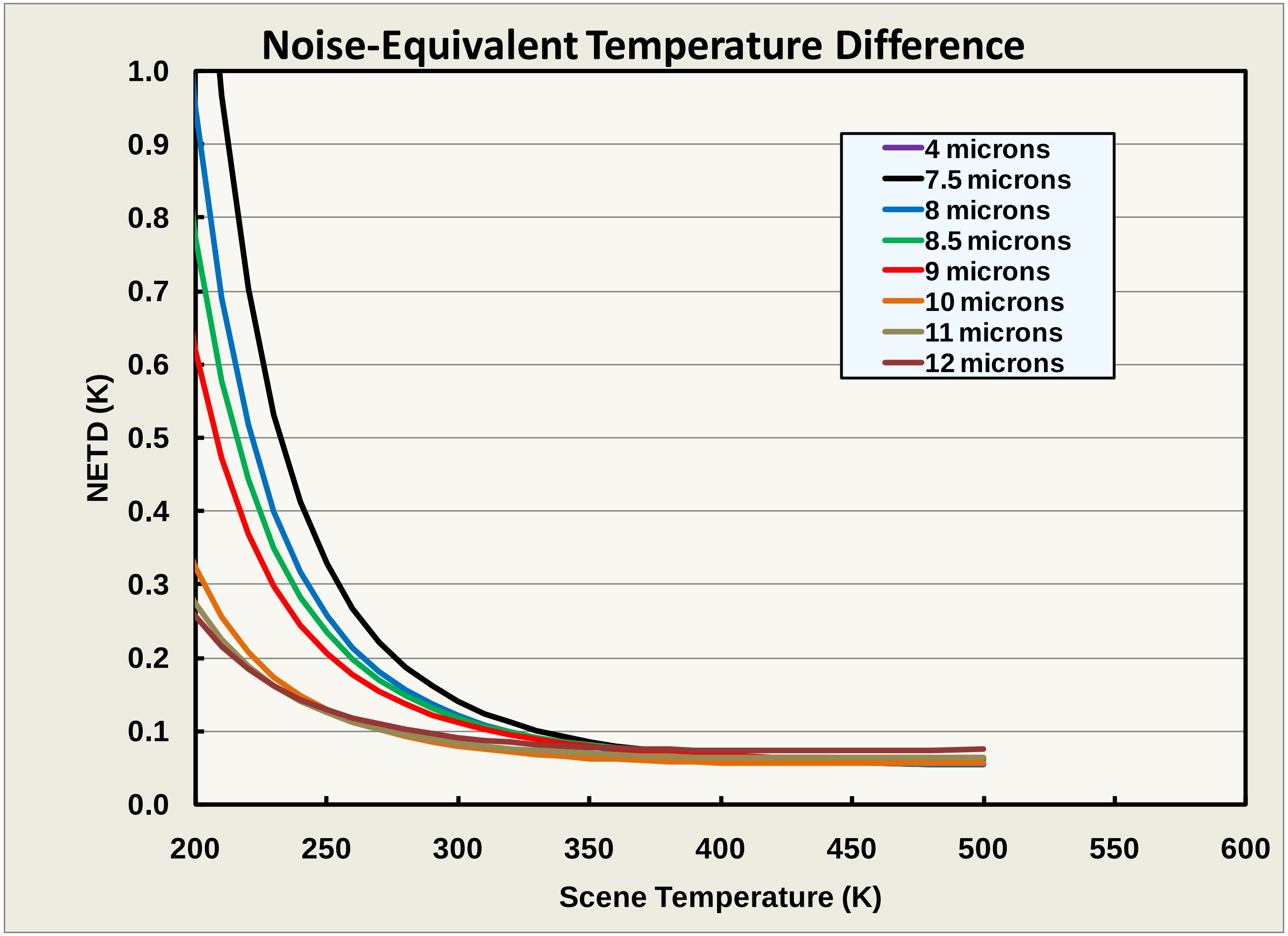

Baseline TIR Cryocooler

- Baseline is NGST HEC (High-Efficiency Compressor)
- Compressor space qualified for MIRI on JWST
- Compressor with two cold heads is being qualified for Advanced Baseline Imager (ABI) on GOES-R. This configuration could be used build-to-print for HyspIRI TIR instrument.
- Other vendors have appropriate coolers that have similar maturity

NGST ABI (GOES-R) Cooler

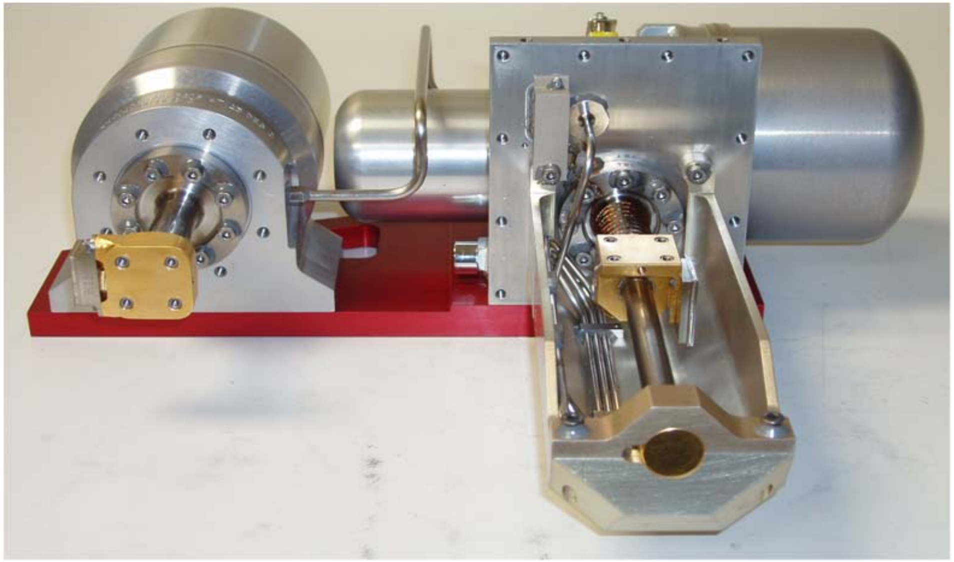

HyspIRI Low Latency Concept & Benchmarks

Dan Mandl
August 24, 2010

HyspIRI Science Workshop
August 24-26, 2010
Pasadena, CA

HyspIRI Low Latency Data Ops Concept

132 Mbps
Multispectral
Thermal InfraRed
(TIR) Scanner

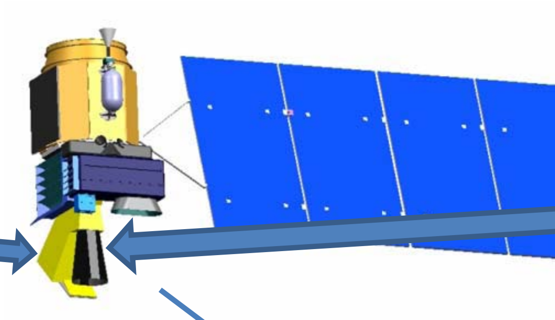

804 Mbps
Hyperspectral Visible
ShortWave InfraRed
(VSWIR) Imaging
Spectrometer

Spectral
Bands (8) 3.98 µm, 7.35 µm, 8.28 µm, 8.63 µm, 9.07 µm, 10.53 µm, 11.33 µm, 12.05
Spatial
IFOV 60 m
Range 600 km (±25.3° at 626 km)

Direct
Broadcast

Spectral
Range 380 to 2500 nm
10 nm bands
Spatial
Range ~146 km
(13.2 deg. at 626km)
Cross-Track Samples >2560
Sampling 60 m

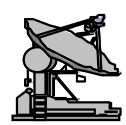

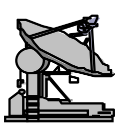

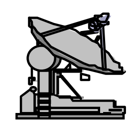

- 20 Mbps Direct Broadcast (10Mbps data throughput)
- Downlink Select Spectral Bands
- Select L-2 Products
- Continuous Earth-view Broadcast

HyspIRI Data Flow

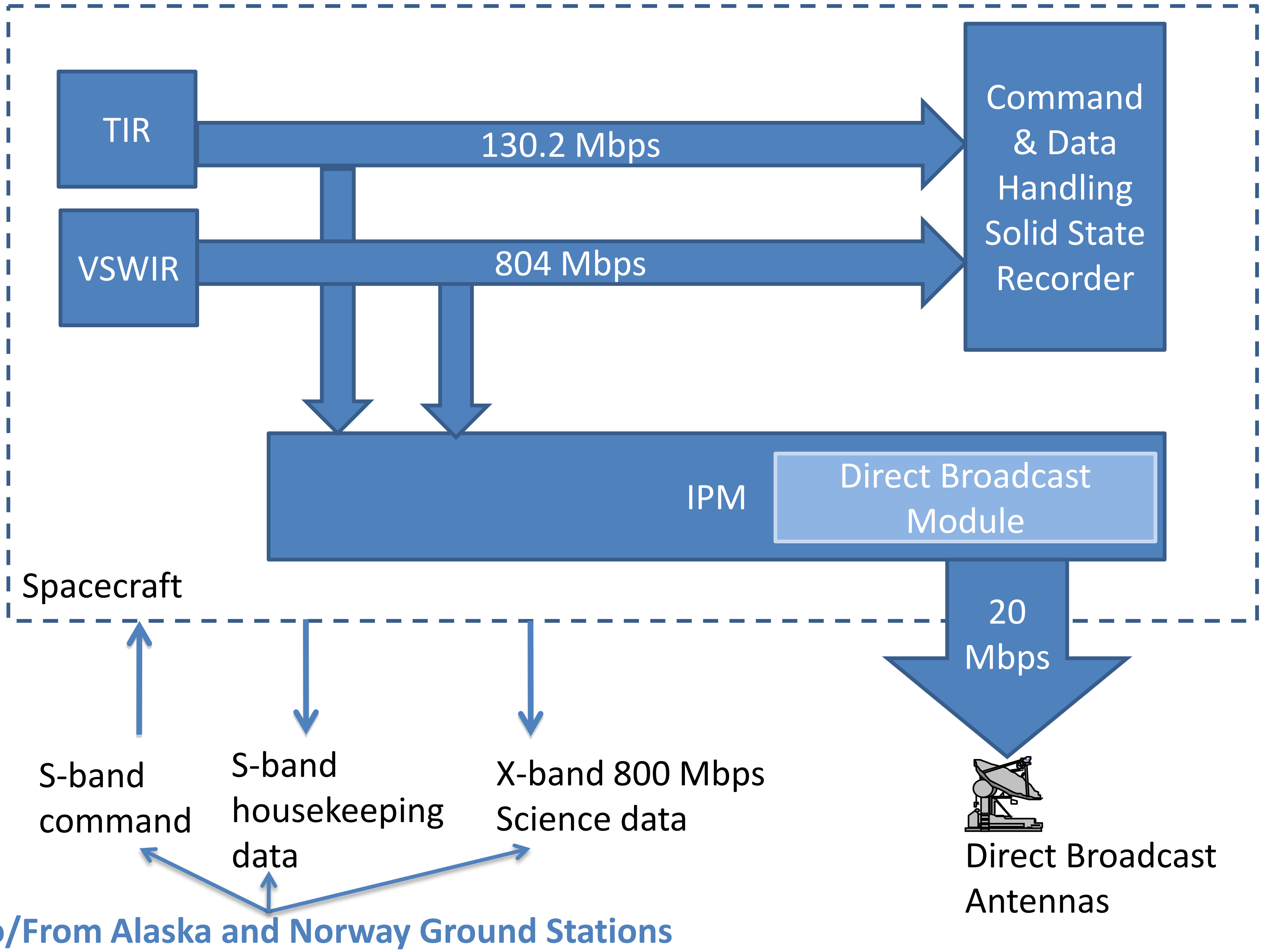

Ongoing Efforts

- Baseline detailed operations concept used to derive cost estimate to be presented by Steve Chien
- Web Coverage Processing Service (WCPS)
  - Allows scientists to define algorithms that can be dynamically loaded onboard satellite or execute as part of the ground processing
- Open Science Data Elastic Cloud
  - Many custom products generated in parallel by many virtual machines
  - Complex products generated in concurrent steps (parallel processing)
  - Elastic response to unanticipated user demand
  - Quick user access (multi-gigabit access)
  - Easy expandability of cloud as needed
- Benchmarking of CPU's for Intelligent Payload Module
  - SpaceCube (initial results presented at previous workshop)
  - Other CPU's (future workshops)
  - Onboard processing
- Delay Tolerant Network Communication Connectivity
  - Upload of algorithms and download of data with fault and delay tolerant connection

Experiment with Web Coverage Processing Service (WCPS) Approach to Injecting New Algorithms into SensorWeb

Mobile Bay Oil Spill Detection Using EO-1 Advance Land Imager Data

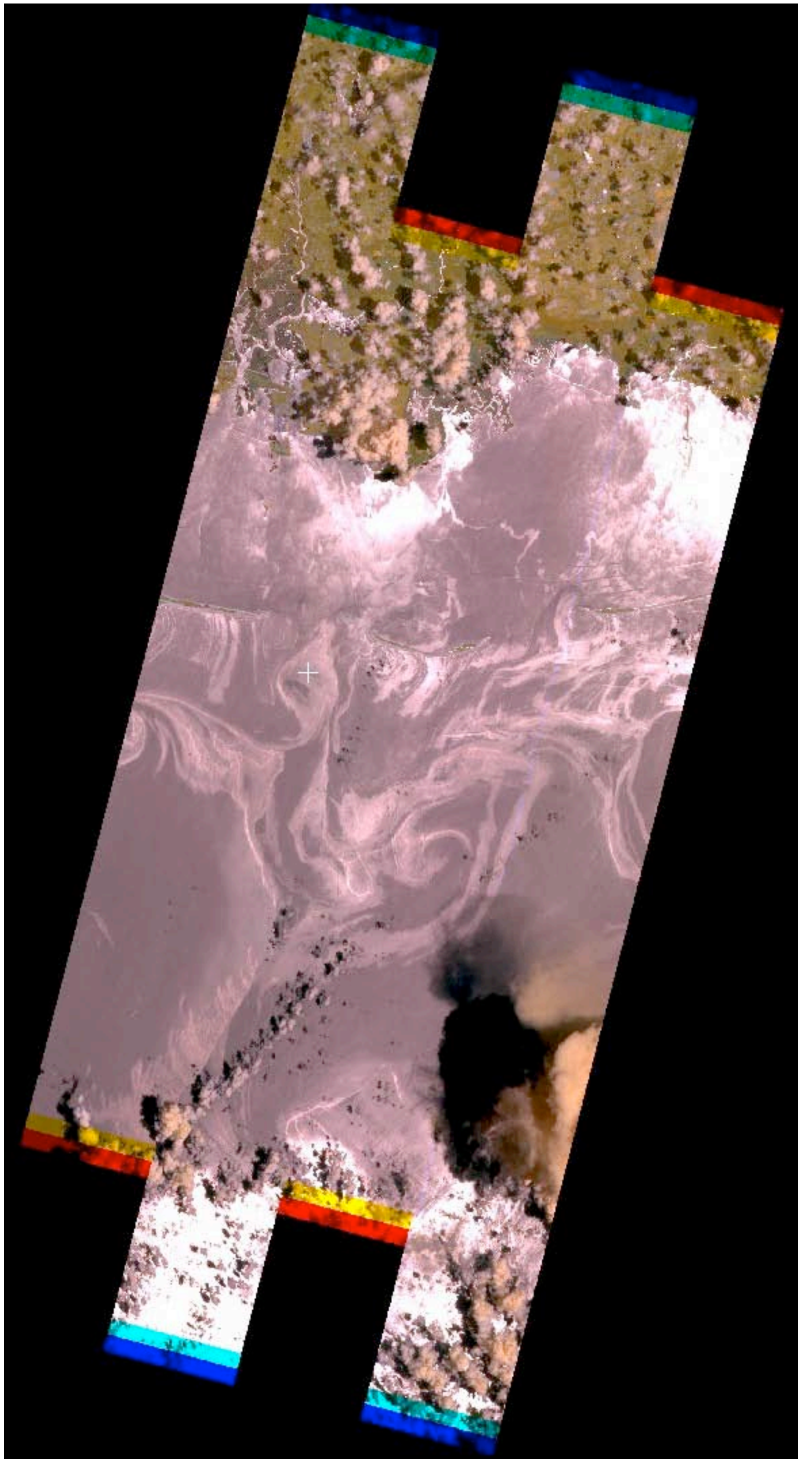

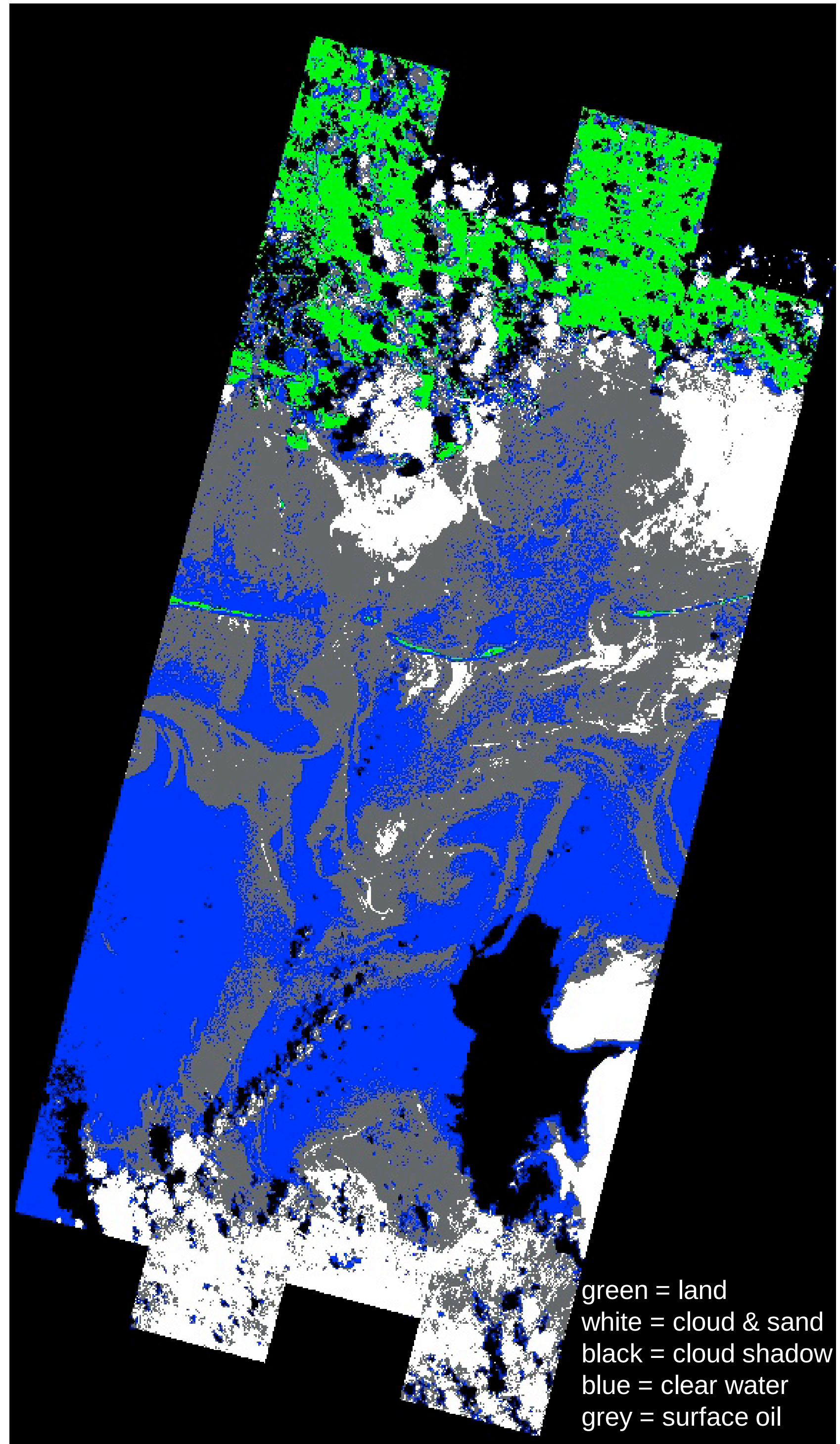

Low Fidelity HyspIRI IPM Testbed

NETGEAR Gigabit Switch
- Allows the board and the data generator workstation to connect at Gigabit speed.

Data Generator Workstation
- Generates test data and streams it to the board at rate up to 800Mbps.

Compact Flash
- Ext3 formatted file system with Linux libraries and tools

Platform Cable USB
- Provides an easy method for debugging software running on the board

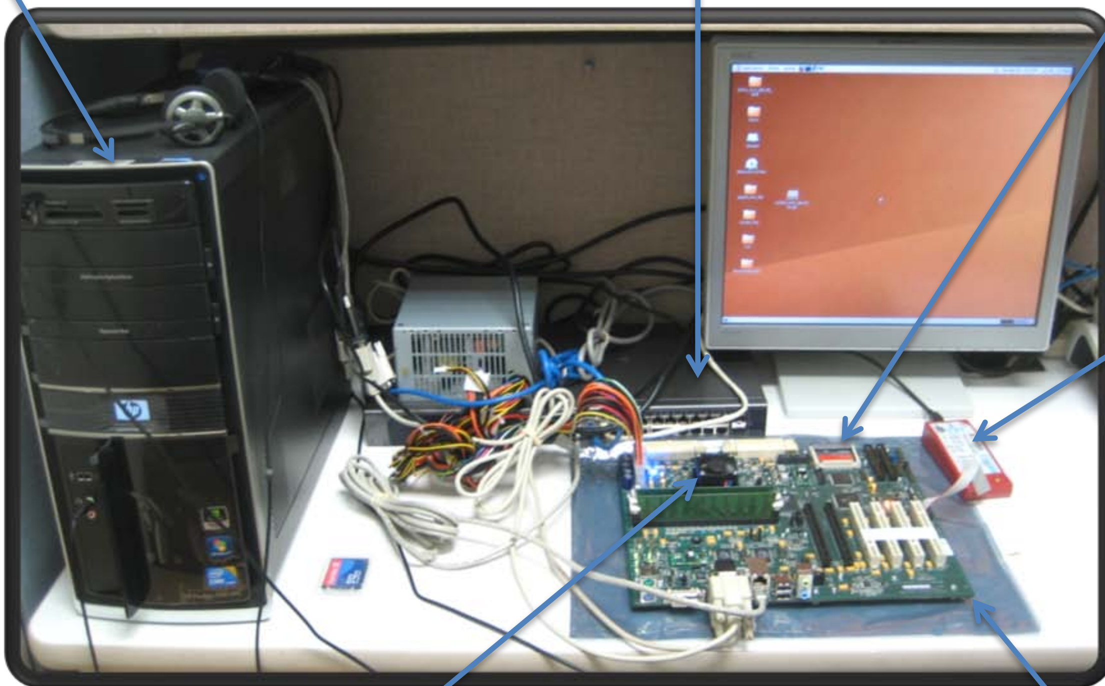

Virtex-5 FPGA
- GSFC SpaceCube 2 core FPGA
- Configured as dual 400MHz PPC design
- Capable of running with Linux or in a standalone mode

Xilinx ML510 Development Board
- Enables the development team to verify the Virtex-5 while the GSFC SpaceCube 2 is finalizing the design

Compute Cloud Testbed

- Open Cloud Consortium (OCC) providing rack with 120 Tbytes usable, 1 – 10 Gbps fiber interface connected to GSFC and Ames and 320 core to support hundreds of virtual machines (part of larger expandable infrastructure consisting of 20 racks)
  - System admin support
  - Funded by multiple sources including National Science Foundation
  - Will stand up 100 Gbps interface wide area cloud (future)
  - Expect to be there at least 5+ years
- Created account on BioNimbus cloud for NASA use
  - Demonstrated performing EO-1 ALI Level 1R and Level 1G processing in cloud
- Will receive dedicated cloud compute rack in August 2010 donated by Open Cloud Consortium
  - Plan to port automated atmospheric correction using ATREM on Hyperion Level 1R to cloud (presently running on GSFC server)
  - In process of integrating FLAASH atmospheric correction into an automated process for Hyperion for Level 1R and then porting to cloud
  - Plan to demonstrate Hyperion level 1R and Level 1G processing in cloud
  - Plan to demonstrate multiple simultaneous automated higher level data products maximizing clouds ability to handle parallel processing
  - Make use of software agent-based architecture for intelligent parallel data processing for multiple data products
  - Experiment with security in open cloud (Open ID/OAuth)

Open Cloud Testbed Environment

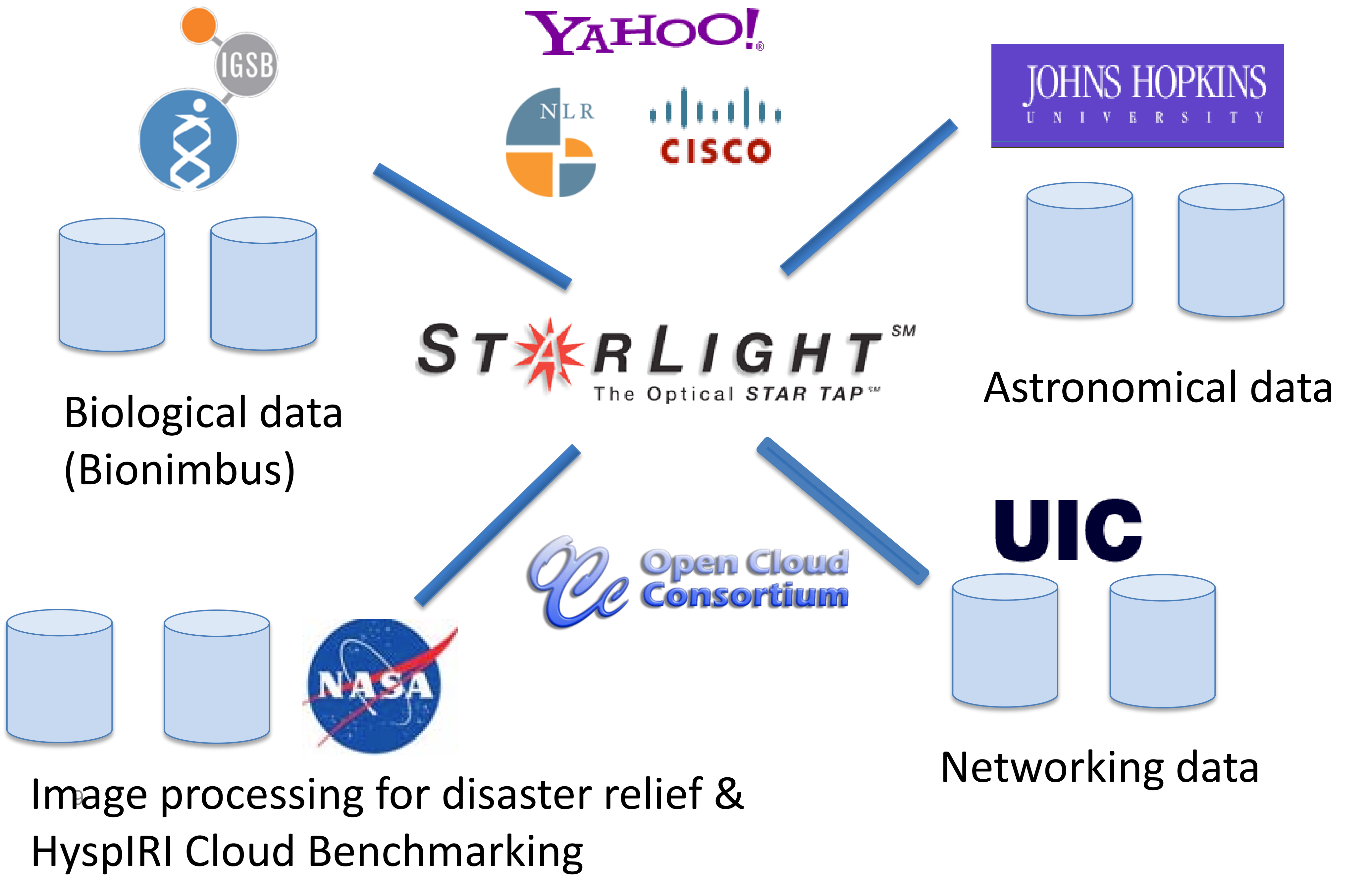

Global Lambda Integrated Facility (GLIF)
OCC Collaboration with Starlight (part of GLIF)

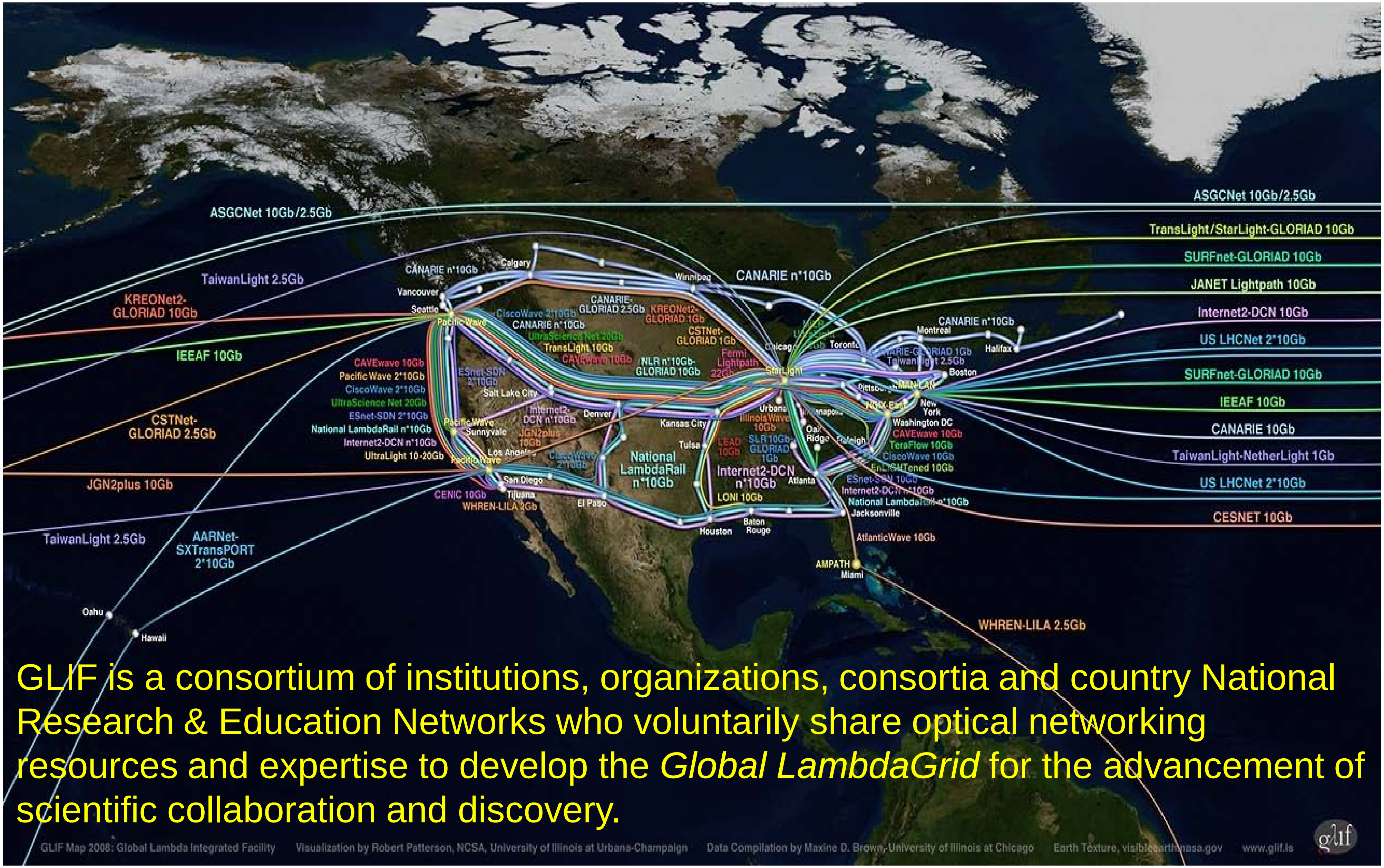

GLIF is a consortium of institutions, organizations, consortia and country National Research & Education Networks who voluntarily share optical networking resources and expertise to develop the *Global LambdaGrid* for the advancement of scientific collaboration and discovery.

Delay Tolerant Network (DTN) Protocol Benchmarking

- Prototype being funded by NASA HQ / SCAN
  - Purpose is to provide space network that is delay/disruption tolerant
  - Using EO-1 in FY 11 to demonstrate various scenarios (Hengemihle)
  - Trying to demonstrate how it is applicable to low earth observing missions
- HyspIRI applicability
  - Upload new data processing algorithms for IPM
    - Can send algorithm to DTN node without regard to when contact with satellite occurs
    - DTN node handles uplink when there is contact and send confirmation back to originator
  - Examining scenarios during Direct Broadcast to handle delays during downlink
    - E.g. data product ready but DB station not in view, DB node onboard receives data product and waits for contact to handle downlink and confirmation

EO-1 Configuration for Preliminary Delay Tolerant Network (DTN) Prototype

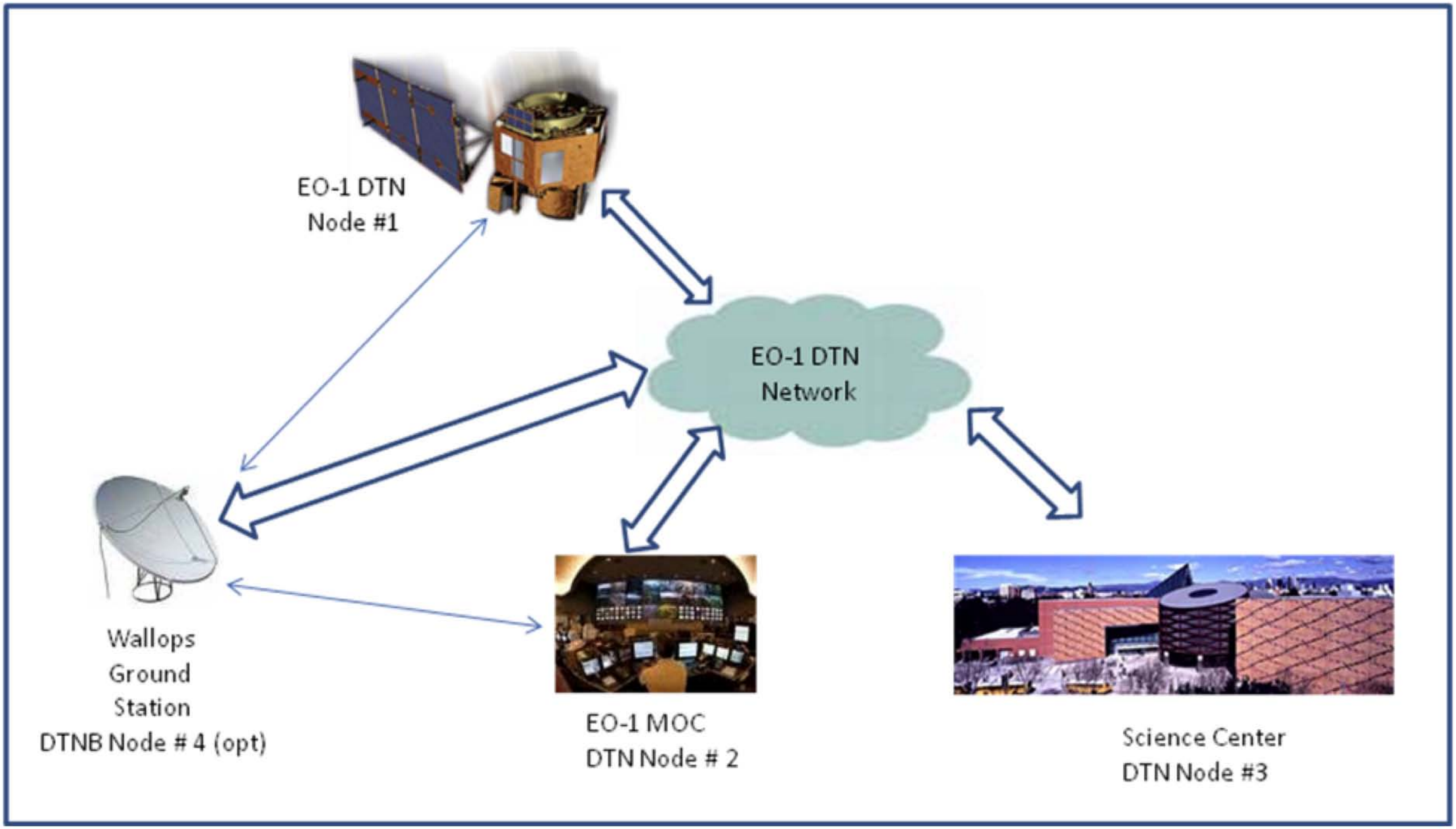

Lead: Jane Marquart Implementers: Rick Mason, Jerry Hengemihle/Microtel

Conclusion

- Experimenting with various bottlenecks for end-to-end data flow for low latency users of HyspIRI
- Leveraging other funds and using HyspIRI funds to tailor for the HyspIRI mission
- Results applicable to other high data volume Decadal missions

HyspIRI Mission Concept

Bogdan Oaida,
with contributions from
Michael Mercury [JPL]

[bogdan.oaida@jpl.nasa.gov]

Jet Propulsion Laboratory
California Institute of Technology

National Aeronautics and
Space Administration

Jet Propulsion Laboratory
California Institute of Technology
Pasadena, California

HyspIRI Mission Concept

Orbit Selection

- Key Orbit Design Considerations
  - Local time of observations
    - Sun-synchronous
    - 10:30 AM LTDN
  - Altitude
    - Low Earth Orbit
    - Repeating Ground track
  - Global coverage in a minimum number of days given the swath-width of each instrument.
    - VSWIR: 19 days revisit at the equator
    - TIR: 5 day revisit at the equator (1 day + 1 night)
- 626 km altitude at equator suits the needs of both instruments

Orbit selection and operations concept meet science requirements with infrequent ground commanding or maintenance.

Operations Concept

- Systematic mapping vs. pointing capability
- Target map driven - No need for uploading acquisition sequences
- High resolution mode and Low resolution mode
- Direct Broadcast capability
  - Uses Intelligent Payload Module
  - Applications-driven

Operational Requirement	VSWIR	TIR
10:30 am sun-sync orbit	✓	✓
626 km altitude at equator	✓	✓
19 days revisit at the equator	✓	
5 day revisit at the equator		✓
Day Observation	✓	✓
Night Observation		✓
Pointing strategy to reduce sun glint	✓	
Surface reflectance in the solar reflected spectrum for elevation angles >20	✓	
Avoid terrestrial hot spot	✓	
Monthly Lunar View calibration	✓	✓
Weekly Solar View Calibration	✓	
Blackbody View Calibration		✓
Deep Space View Calibration		✓

National Aeronautics and Space Administration

Jet Propulsion Laboratory
California Institute of Technology
Pasadena, California

HyspIRI Global Coverage

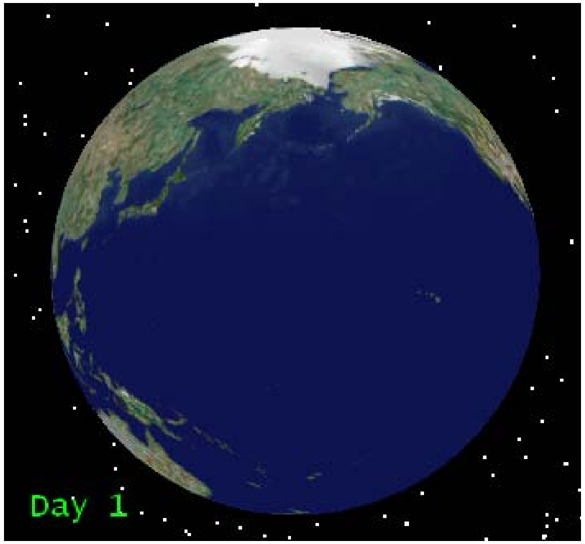

TIR Coverage after 5 days

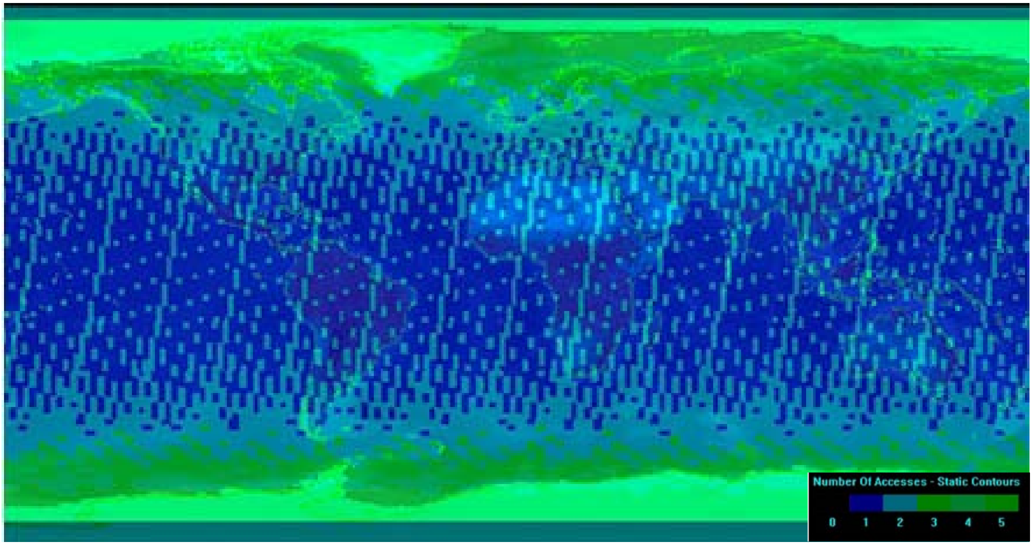

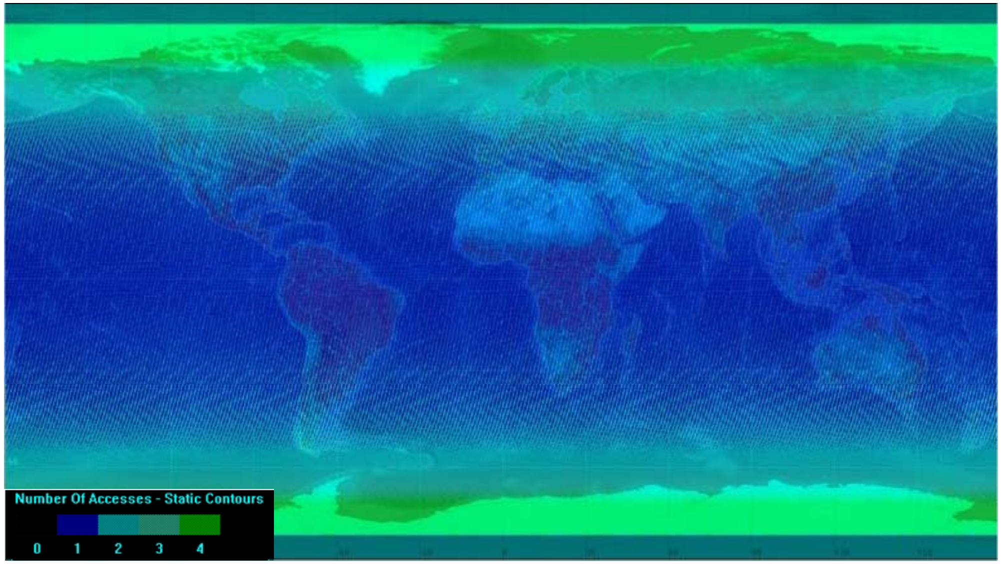

Due to the min 20 deg Sun elevation angle constraint on the VSWIR acquisition, the latitudes covered change with the seasons

VSWIR Coverage after 19 days

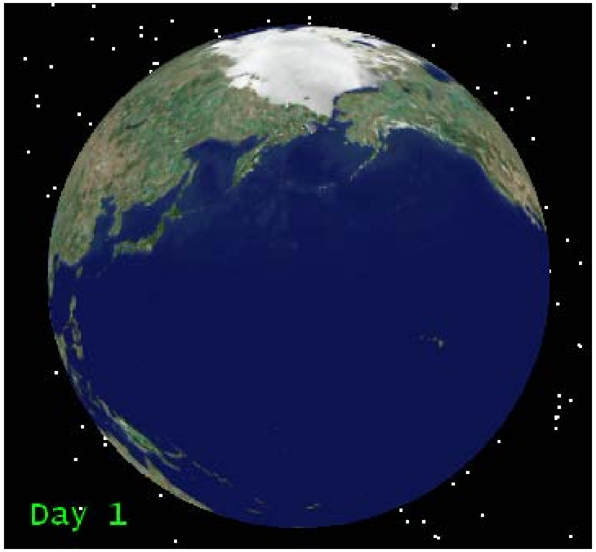

Data Acquisition Scenario

- Systematic mapping vs. pointing capability
- Target map driven - No need for uploading acquisition sequences
- Data acquisition driven by land and coastal aquatic (<50m depth) coverage
  - Impact by low resolution modes on data volume is relatively small
- Both instruments on 24/7, but VSWIR not acquiring data at 100% duty cycle
- Low-latency products available via Direct Broadcast system
  - Applications (not science) driven

Imaging Mode

Instrument	Land	Coastal	Deep Ocean	Greenland	Antarctica
VSWIR	60 m	60 m	1 km	1 km	1 km
TIR	60 m	60 m	1 km	1 km	1 km

Target Map

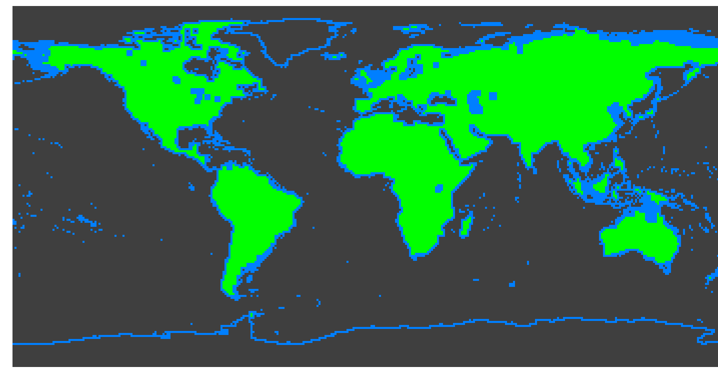

Duty Cycle

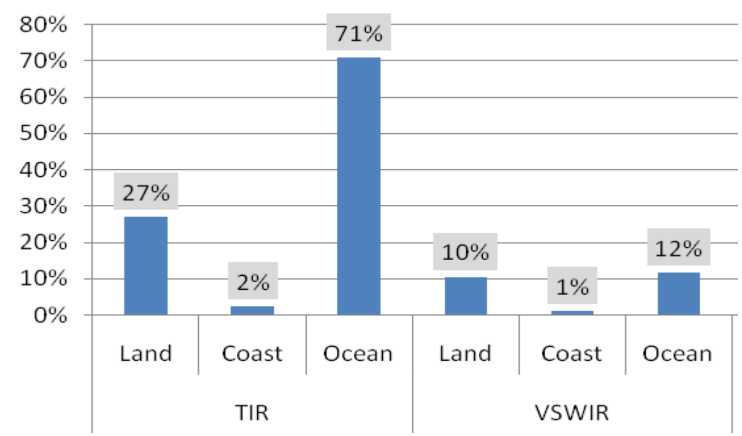

Flight System Concept

- Industry procured spacecraft bus
  - SA-200HP used as an example for the study to identify and cost needed modifications
- HyspIRI specific
  - Payload integrated on the top plate (TIR, VSWIR) and inside the S/C
  - Configuration chosen to minimize/eliminate thermal impacts on the payload radiators
  - Spacecraft Dry Mass (CBE): 520 kg
  - Launch Mass: 681 kg
  - JPL DP Margin: 31%
  - Required Power (CBE): 620W
  - Available Power: 965W, 7.2 m^2 array

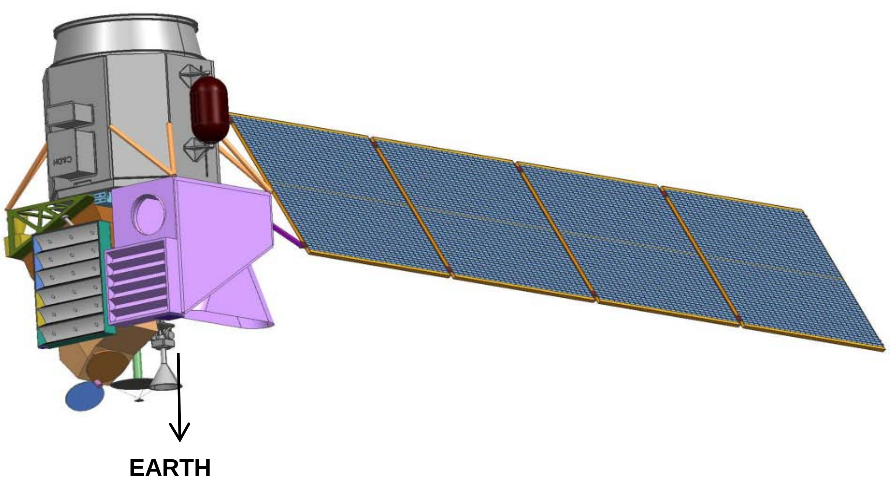

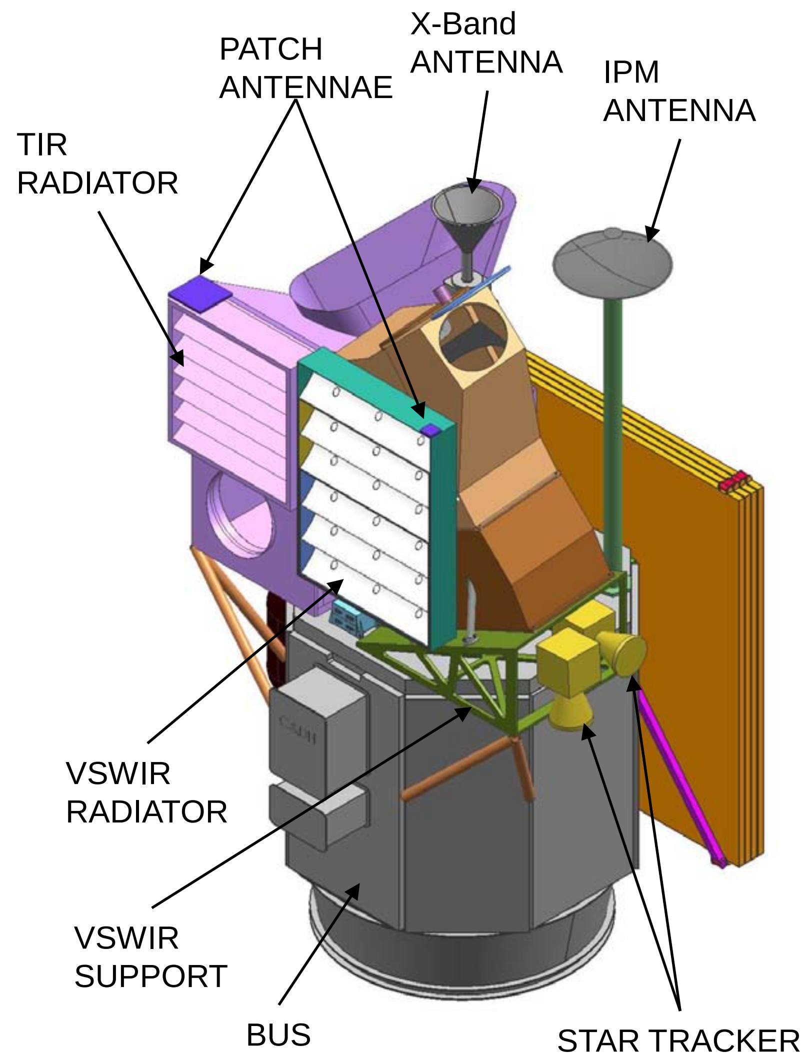

Key Bus Performance Range Summary

	Requirements	RSDO SA-200HP	HyspIRI SA-200HP	Modifications
Orbit	626 km 10:30 LTDN	✓	✓	-
Mission duration	3 years, selective redundancy	4 years, selective redundancy	3 years, single string	Remove redundancy to reduce cost
Thermal	Passive architecture	✓	✓	-
Downlink	800 Mbps	80Mbps	800 Mbps	Dual-pol X-band
Propellant	75 m/s 37 kg	131 m/s 67 kg tank	131 m/s 67 kg tank	-
Onboard recorder	1 Tbit	134 Gbits	1Tbit	SEAKR SSP-R
Payload mass	126kg	666 kg	666 kg	Support structure for Instuments
Payload Power	885 W	650 W	965 W	Single wing configuration, add one panel
Pointing Knowledge	See table below	0.5 arcsec (3σ)	<=0.5 arcsec (3σ)	Replaced one of two coarse Ball CT-602 star tracker with one fine Lockheed Martin AST-301 star tracker.
Pointing Accuracy		16 arcsec (3σ)	<=16 arcsec (3σ)	
Pointing Stability		0.1 arcsec/sec (3σ)	<=0.1 arcsec/sec (3σ)	

Pointing	VSWIR Requirement	TIR Requirement	Rationale	Driver
Knowledge	< 48 μrad (3σ/axis)	< 48 μrad (3σ/axis)	<30m (3σ) post-reconstruction orthorectification knowledge at 626km altitude	TIR
Accuracy	<4.5 mrad (3σ/axis)	<4.5 mrad (3σ/axis)	VSWIR: Limits cross-track error to < 3 km on the surface	VSWIR
Stability	±0.1 mrad/sec (3σ)	±24.7 mrad/sec (3σ)	VSWIR: Limit smear to < 0.6 meters as one pixel crosses a spot on the surface in 8.8 msec TIR: Time for 6 pixels in TDI string to cross a point on the surface at nadir is 0.39 msec.	VSWIR

Science Payload Accommodation and System Margins

Accommodations	VSWIR	TIR
Mass (CBE)	55 kg	60 kg
Volume	1.1 x 0.5 x 0.8 m	1.2 x 1.1 x 0.6 m
Power	41 W	103 W
FOV (crosstrack)	13.62 deg	50.7 deg
FOV (alongtrack)	95.9 microrad	95.9 microrad
Orientation	4 deg to starboard	nadir

	Required	Design	Margin (D-R)/D
Swath width VSWIR	141km	151 km	6%
Swath width TIR	536km	600 km	11%
Recorder capacity	0.8 Tb	1.0 Tb	20%
Power	620 W (CBE)	965 W	36%
LV mass capability	520 (CBE, dry)	790 kg	34%

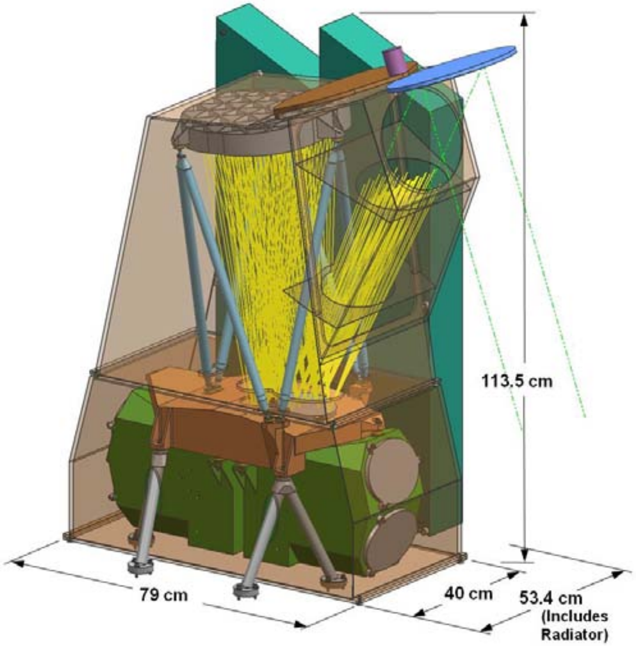

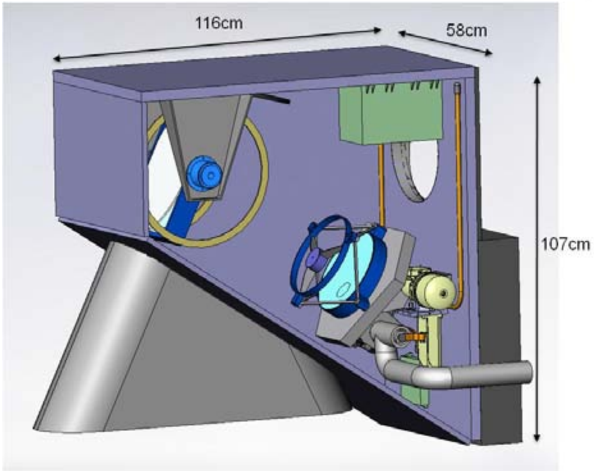

Launch Vehicle Concept

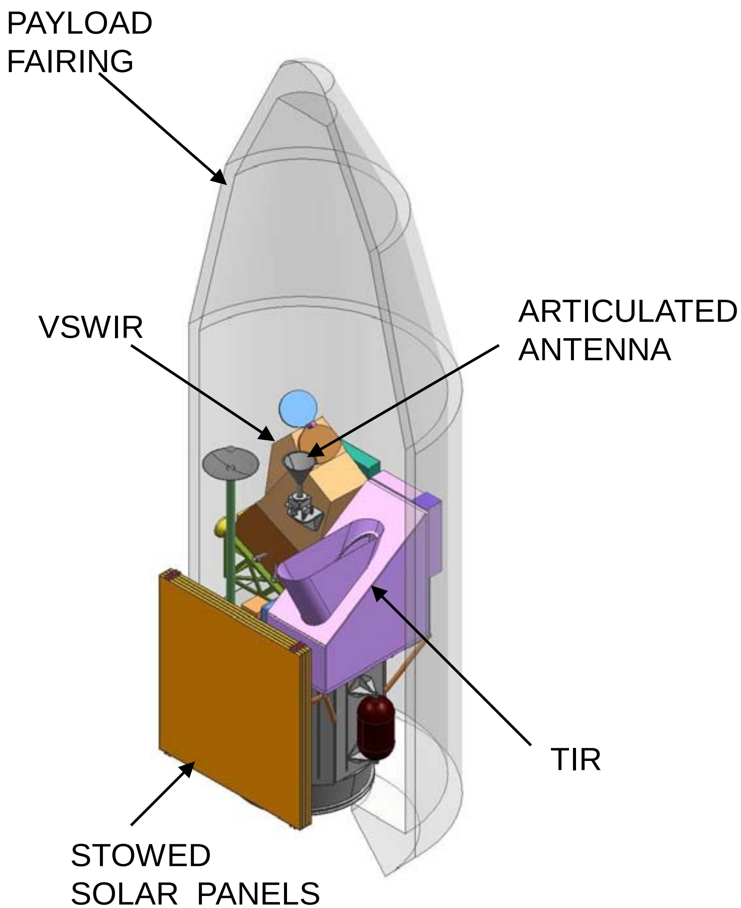

- Taurus 3210 can meet the mission needs
  - Closest fit among currently NASA approved launchers
  - 31% margin (per JPL Design Principles) with a Taurus-class launch vehicle
  - Fits dynamic volume envelope
  - 790 Kg launch capacity for HyspIRI Orbit
- Launch window
  - Mapping orbit reachable once per day

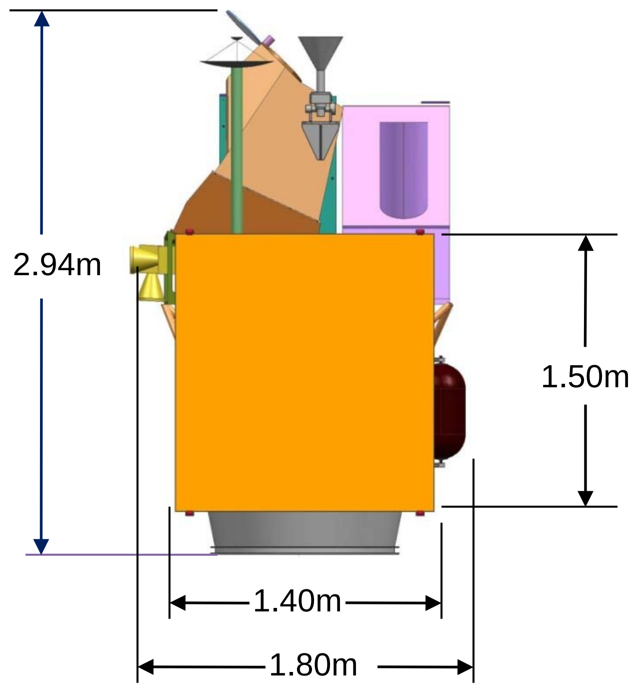

Ground System Concept

- Data Downlink
  - KSAT Ground network
    - Svalbard @ 800 Mbps Dual-pole X-Band (existing)
    - Poker Flats @ 800 Mbps Dual-pole X-Band (in development)
    - Other stations available
  - Almost 100% data return with 1 Tbit SSR on spacecraft
- Data Processing
  - SDS sized to process L0 through L2 data for both instruments
  - Deliver L2 data products to DAAC
  - L3 data products produced by users

HyspIRI will utilize existing infrastructure with proven capability to downlink and process all science data

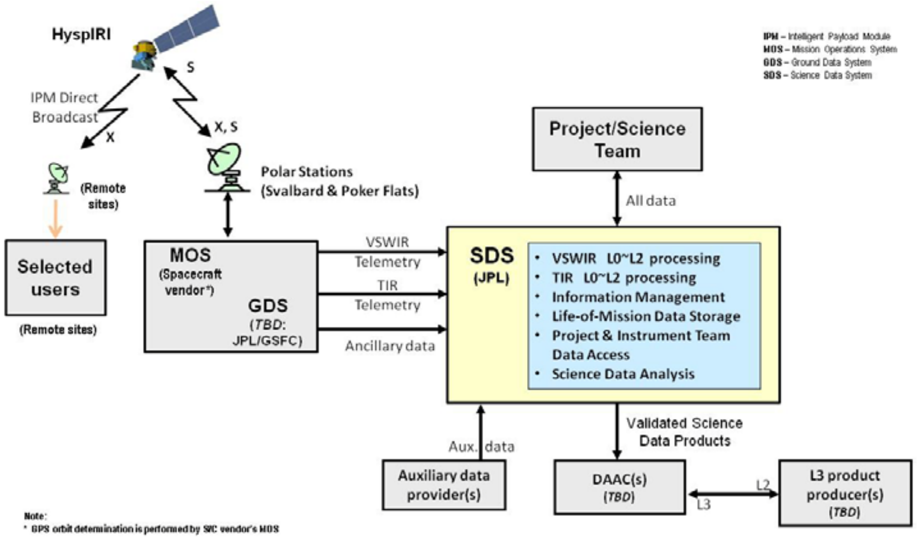

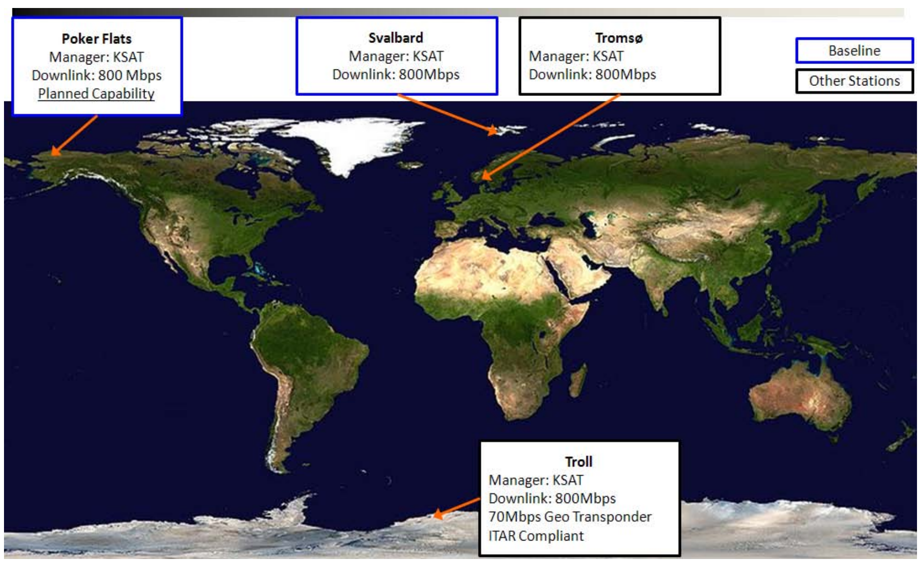

BACKUP

National Aeronautics and Space Administration

Jet Propulsion Laboratory
California Institute of Technology
Pasadena, California

Low Latency Data – Direct Broadcast

- Direct Broadcast Capability
- Low latency data (<6hrs)
- Applications Driven, Targeted Science
  - Non-stop data acquisition
  - Decision making capability
- Not tech development
- Design taken from NPP's high rate data (HRD) broadcast system
- Baseline design
  - 20 Mbps X-band
  - An Earth-coverage dish estimated at 0.5 m diameter
    - Reflector is shaped to provide peak gain at ~60 degrees off boresight
- Any user should be able to receive data when S/C is above 5 degrees

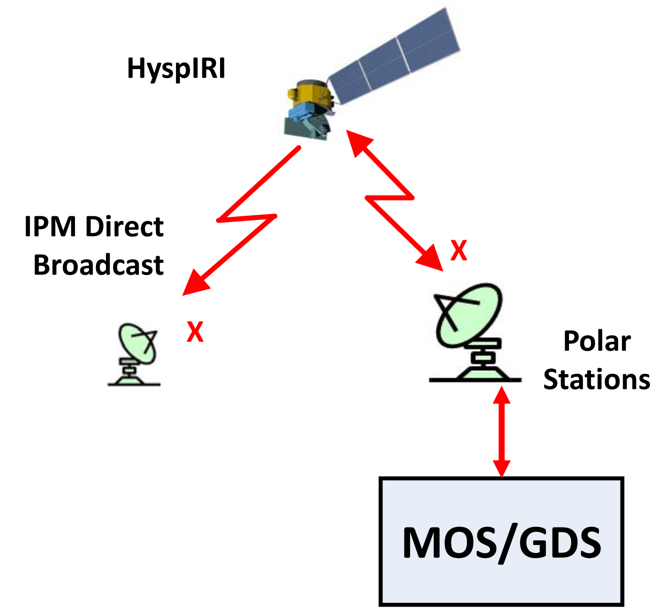

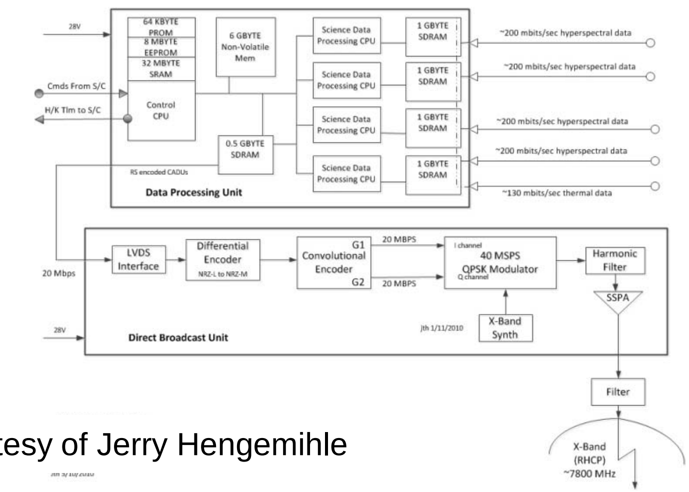

Courtesy of Jerry Hengemihle

The DB capability will make use of high heritage technology and existing algorithms to enable the development of low latency data products and applications.

Key Driving SDS Design Requirements

- Data Downlink Volumes: 5.3 Tb/day Max. (4.6 Tb/day Mean)
- Data Product Types: 2 Level 0's, 2 Level 1's, 2 Level 2's, *tbd* L3
- Data Product Availability:

Product Application	Nominal Latency From Receipt of Required L0a Data at Processing Node	Comments
Routine Science	1 week – 2 weeks	Products meet science/calibration specifications
Priority Target Events	1 day	Data acquisitions are not routinely planned but event-driven Products are L1 and L2/3 in limited quantity Products may not meet science/calibration specifications
Intelligent Payload Module Direct Broadcast	No latency requirement for SDS	Data broadcast via the IPM will not end up at the SDS

- **Total Mission Data Volume***: 47.2 Tbits (6.2 Tb L0B's, 18.6 Tb L1B's, 22.5 Tb L2's) per day
  58.2 Pb over mission life
- **Processing Loading:** Sized to meet respective product latency requirements (no backlog and with margin to include *one* reprocessing campaign
- **SDS sized for 5.2 Tb/day**
  - 98.1% of the time, less than 5.2 Tb is downlinked per day

Notes: * Mission data volume based on maximum L0A downlink volume; exclusive of data from Direct Broadcast;
Assumes all L0 processed to L1 & L2; all in 16-bit per sample;
Assumes data compression ratios of 3:1 for all VSWIR and 2:1 for all TIR image bands; assumes no compression for ancillary bands;
Tb – Terabits (10^12 bits); Pb – Petabits (10^15 bits)

HyspIRI

DRAFT PRELIMINARY

Level 1 Requirements and Mission Success Criteria

NASA Earth Science and Applications Decadal Survey

Robert O. Green, Simon Hook, Betsy Middleton, Stephen Ungar, Bob Knox, Woody Turner, John LaBrecque and the HyspIRI Team

Overview

Beginning in January 2007 a Mission Concept effort for HyspIRI Mission has been under way with involvement of NASA HQ, JPL, GSFC, and a broad Science Study Group and the 2008 workshop, 2009 workshop, 2010 symposium.

Beginning with the call of the NASA Earth Science and Applications Decadal Survey this team has worked to develop a end-to-end concept for implementation of the HyspIRI Mission.

Based on this effort and with input from SSG and the relevant communities a set of Level 1 Requirements and Success Criteria have been develop in accordance with the required NASA process.

In this presentation we are going to review key elements of the HyspIRI draft preliminary Level 1 Requirements and Success Criteria.

This is a required and enabling document for HyspIRI to proceed to the next step in the NASA Mission process.

Note: The HyspIRI Mission must remain appropriately aligned with the Decadal Survey.

HyspIRI Science Study Group

Mike Abrams	JPL	michael.j.abrams@jpl.nasa.gov	818-354-0937
Rick Allen	UID	rallen@kimberly.uidaho.edu	208-423-6601
Martha Anderson	USDA	Martha.Anderson@ars.usda.gov	301-504-6616
Greg Asner	Stanford	gpa@stanford.edu	650-462-1047
David Meyer	USGS EROS	dmeyer@usgs.gov	605-594-6046
Paul Bissett	FERI	pbissett@flenvironmental.org	813-866-3374 x102
Alex Chekalyuk	Lamont-Doh.	chekaluk@ldeo.columbia.edu	845-365-8552
James Crowley	USGS	jcrowley@usgs.gov	703-648-6356
Ivan Csiszar	UMD	icsiszar@hermes.geog.umd.edu	301-405-8696
Heidi Dierssen	U Conn.	heidi.dierssen@uconn.edu	860-405-9239
Friedmann Freund	Ames	friedemann.t.freund@nasa.gov	650 604-5183
John Gamon	U A	gamon@gmail.com	780-965-0345
Louis Giglio	UMD	louis_giglio@ssaihq.com	301 867-2030
Greg Glass	JHU	gglass@jhsph.edu	410-955-3708
Robert Green	JPL	rog@jpl.nasa.gov	818 354-9136
Simon Hook	JPL	simon.j.hook@jpl.nasa.gov	818-354-0974
James Irons	GSFC	James.R.Irons@nasa.gov	301-614-6657
Bob Knox	GSFC	Robert.G.Knox@nasa.gov	301-614-6656
John Mars	USGS	jmars@usgs.gov	703-648-6302
Betsy Middleton	GSFC	elizabeth.m.middleton@nasa.gov	301-614-6670
Peter Minnett	U. Miami	pminnett@rsmas.miami.edu	305-361-4104
Frank Muller Karger	U. MA Dart.	carib@marine.usf.edu	727-553-3335
Scott Ollinger	UNH	scott.ollinger@unh.edu	508 999 8193
Thomas Painter	U. of Utah	painter@geog.utah.edu	303.888.7119
Anupma Prakash	UAF	prakash@gi.alaska.edu	907-474-1897
Dale Quattrochi	MSFC	dale.quattrochi@nasa.gov	256-961-7887
Vince Realmuto	JPL	Vincent.J.Realmuto@jpl.nasa.gov	818-354-1824
Dar Roberts	UCSB	dar@geog.ucsb.edu	805-893-2276
Dave Siegel	UCSB	davey@icess.ucsb.edu	805-893-4547
Phil Townsend	U of Wisc.	ptownsend@wisc.edu	608-262-1669
Kevin Turpie	GSFC	kevin.r.turpie@nasa.gov	301-286-9996
Steve Ungar	GSFC	stephen.g.ungar@nasa.gov	301-614-6674
Susan Ustin	UC Davis	susan@cstars.ucdavis.edu	530-752-0621
Rob Wright	UHI	wright@higp.hawaii.edu	808-956 9194

Level 1 Requirements and Mission Success Criteria

Contents

Level 1 Requirements and Mission Success Criteria

4. Performance Requirements

4.1 Science Requirements

The science objectives in Section 2.2 can be achieved by either the baseline or minimum science mission requirements listed here, but the baseline mission provides substantially more value to NASA and the Earth Science Community.

- **4.1.1 Requirement: Baseline Science Mission**
- a) To address the Decadal Survey and community identified science and application questions related to terrestrial and coastal ocean ecosystem composition, function, and change as well as surface composition (DS113-115), the baseline science mission shall provide global mapping measurements of the surface reflectance or remote sensing reflectance for shallow water regions across the solar reflected spectrum from 380 to 2500 nm at ≤10 nm sampling at the specified signal-to-noise ratio and accuracy with >95% spectral/spatial uniformity at ≤60 m nadir spatial sampling with <20 day revisit to provide >60% seasonal and >80% annual coverage of the terrestrial and shallow water regions of the Earth for at least three years with a subset of measurements available near-real-time for designated science and applications.

Level 1 Requirements and Mission Success Criteria
VSWIR Benchmark Radiances

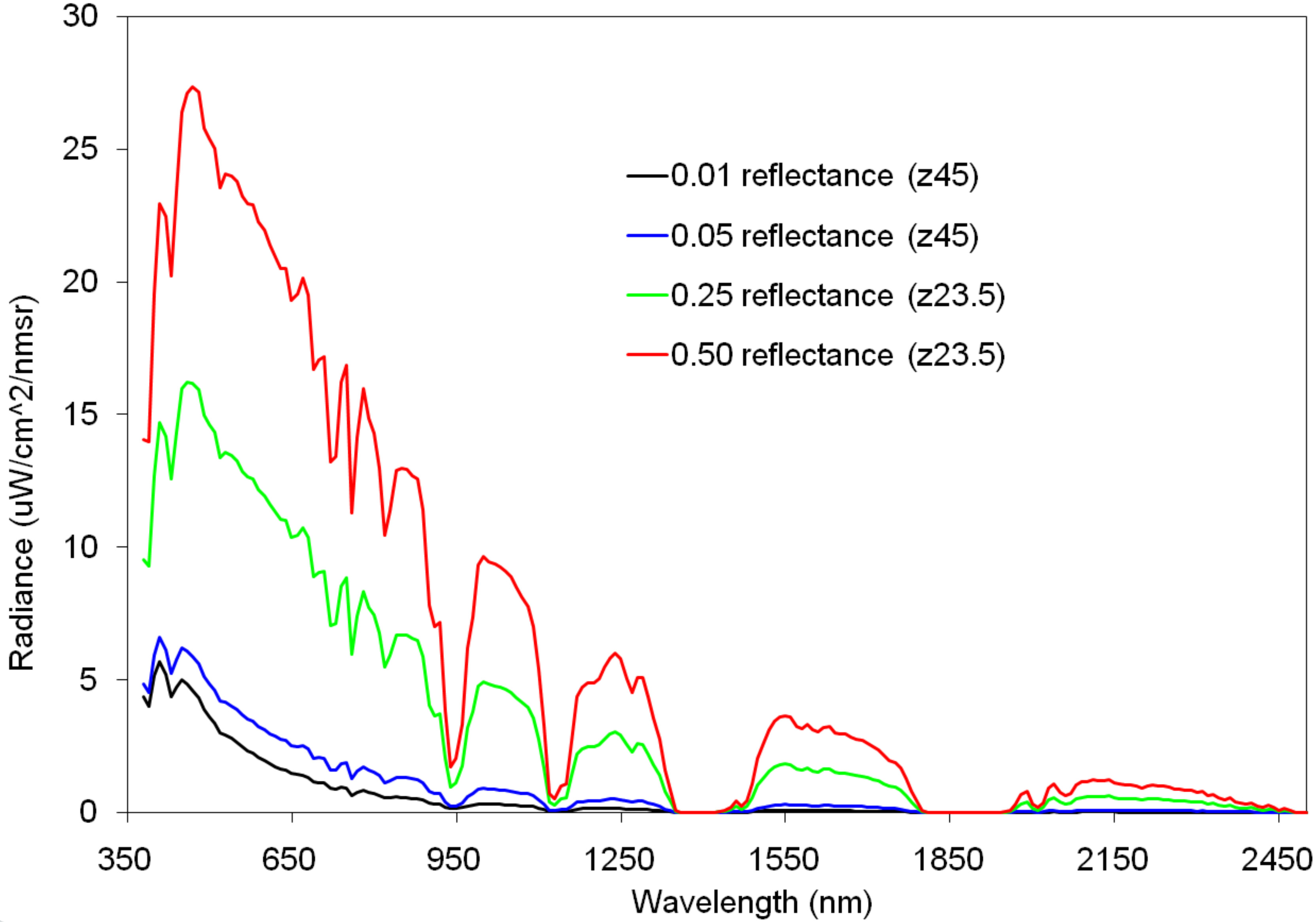

Level 1 Requirements and Mission Success Criteria VSWIR SNR

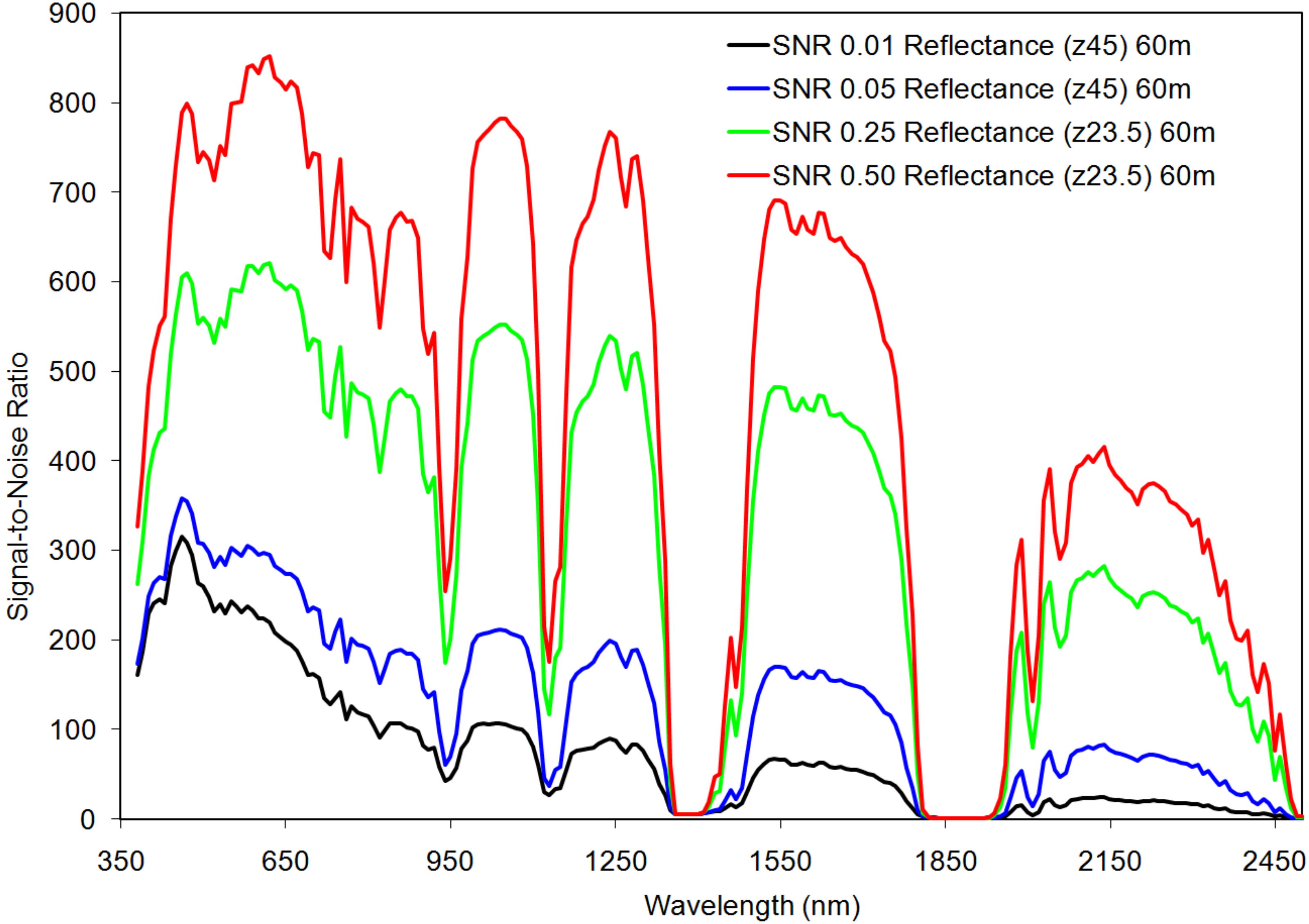

Level 1 Requirements and Mission Success Criteria (VSWIR Performance)

wavelength	0.01 reflectance (z45)	0.05 reflectance (z45)	0.25 reflectance (z23.5)	0.50 reflectance (z23.5)	wavelength	SNR 0.01 Reflectance (z45) 60m	SNR 0.05 Reflectance (z45) 60m	SNR 0.25 Reflectance (z23.5) 60m	SNR 0.50 Reflectance (z23.5) 60m	wavelength	Digitization Radiance (uW/ cm^2/nm/sr)
380	4.34E+00	4.84E+00	9.54E+00	1.41E+01	380	1.61E+02	1.73E+02	2.62E+02	3.27E+02	380	1.68E-02
390	3.99E+00	4.51E+00	9.28E+00	1.40E+01	390	1.87E+02	2.02E+02	3.09E+02	3.89E+02	390	1.22E-02
400	5.17E+00	5.93E+00	1.27E+01	1.95E+01	400	2.29E+02	2.49E+02	3.83E+02	4.83E+02	400	1.14E-02
410	5.69E+00	6.61E+00	1.47E+01	2.29E+01	410	2.41E+02	2.63E+02	4.12E+02	5.23E+02	410	1.15E-02
420	5.20E+00	6.14E+00	1.42E+01	2.25E+01	420	2.45E+02	2.70E+02	4.31E+02	5.51E+02	420	1.02E-02
430	4.37E+00	5.24E+00	1.26E+01	2.02E+01	430	2.40E+02	2.67E+02	4.36E+02	5.62E+02	430	8.88E-03
440	4.74E+00	5.77E+00	1.44E+01	2.34E+01	440	2.82E+02	3.16E+02	5.19E+02	6.70E+02	440	7.33E-03
450	5.01E+00	6.20E+00	1.60E+01	2.64E+01	450	2.99E+02	3.38E+02	5.63E+02	7.31E+02	450	6.99E-03
460	4.84E+00	6.09E+00	1.62E+01	2.71E+01	460	3.15E+02	3.58E+02	6.05E+02	7.89E+02	460	6.18E-03
470	4.60E+00	5.88E+00	1.62E+01	2.73E+01	470	3.08E+02	3.54E+02	6.09E+02	7.99E+02	470	6.09E-03
480	4.31E+00	5.61E+00	1.59E+01	2.72E+01	480	2.94E+02	3.41E+02	5.98E+02	7.88E+02	480	6.21E-03
490	3.87E+00	5.12E+00	1.50E+01	2.58E+01	490	2.63E+02	3.09E+02	5.53E+02	7.34E+02	490	6.77E-03
500	3.61E+00	4.86E+00	1.46E+01	2.54E+01	500	2.59E+02	3.07E+02	5.60E+02	7.45E+02	500	6.47E-03
510	3.38E+00	4.62E+00	1.43E+01	2.50E+01	510	2.47E+02	2.97E+02	5.50E+02	7.36E+02	510	6.54E-03
520	3.02E+00	4.20E+00	1.34E+01	2.35E+01	520	2.32E+02	2.81E+02	5.31E+02	7.13E+02	520	6.53E-03
530	2.94E+00	4.16E+00	1.36E+01	2.41E+01	530	2.39E+02	2.93E+02	5.59E+02	7.52E+02	530	6.02E-03
540	2.79E+00	4.02E+00	1.34E+01	2.40E+01	540	2.29E+02	2.84E+02	5.49E+02	7.42E+02	540	6.16E-03
550	2.65E+00	3.87E+00	1.33E+01	2.38E+01	550	2.43E+02	3.03E+02	5.91E+02	8.00E+02	550	5.28E-03
560	2.47E+00	3.67E+00	1.29E+01	2.32E+01	560	2.37E+02	2.98E+02	5.90E+02	8.00E+02	560	5.15E-03
570	2.33E+00	3.53E+00	1.27E+01	2.29E+01	570	2.31E+02	2.94E+02	5.89E+02	8.01E+02	570	5.07E-03
580	2.23E+00	3.43E+00	1.26E+01	2.29E+01	580	2.37E+02	3.05E+02	6.17E+02	8.40E+02	580	4.62E-03
590	2.08E+00	3.25E+00	1.22E+01	2.22E+01	590	2.32E+02	3.02E+02	6.17E+02	8.42E+02	590	4.47E-03
600	1.96E+00	3.13E+00	1.19E+01	2.19E+01	600	2.24E+02	2.94E+02	6.09E+02	8.33E+02	600	4.50E-03
610	1.84E+00	2.99E+00	1.16E+01	2.14E+01	610	2.23E+02	2.97E+02	6.19E+02	8.48E+02	610	4.23E-03
[illegible]	[illegible]	[illegible]	[illegible]	[illegible]	[illegible]	[illegible]	[illegible]	[illegible]	[illegible]	[illegible]	[illegible]
2200	1.72E-02	7.31E-02	4.71E-01	9.37E-01	2200	1.81E+01	6.44E+01	2.36E+02	3.51E+02	2200	9.85E-04
2210	1.87E-02	8.00E-02	5.10E-01	1.02E+00	2210	1.96E+01	6.96E+01	2.49E+02	3.68E+02	2210	9.79E-04
2220	1.89E-02	8.11E-02	5.16E-01	1.03E+00	2220	2.01E+01	7.12E+01	2.52E+02	3.74E+02	2220	9.65E-04
2230	1.88E-02	8.05E-02	5.12E-01	1.02E+00	2230	2.02E+01	7.15E+01	2.53E+02	3.75E+02	2230	9.52E-04
2240	1.82E-02	7.79E-02	4.97E-01	9.90E-01	2240	1.98E+01	7.05E+01	2.51E+02	3.72E+02	2240	9.39E-04
2250	1.74E-02	7.47E-02	4.78E-01	9.52E-01	2250	1.92E+01	6.87E+01	2.47E+02	3.66E+02	2250	9.30E-04
2260	1.64E-02	7.03E-02	4.52E-01	9.00E-01	2260	1.82E+01	6.55E+01	2.39E+02	3.55E+02	2260	9.28E-04
2270	1.60E-02	6.89E-02	4.43E-01	8.83E-01	2270	1.79E+01	6.45E+01	2.36E+02	3.51E+02	2270	9.26E-04
2280	1.55E-02	6.67E-02	4.30E-01	8.56E-01	2280	1.74E+01	6.31E+01	2.32E+02	3.46E+02	2280	9.23E-04
2290	1.50E-02	6.43E-02	4.15E-01	8.28E-01	2290	1.69E+01	6.14E+01	2.28E+02	3.41E+02	2290	9.19E-04
2300	1.39E-02	5.94E-02	3.87E-01	7.70E-01	2300	1.58E+01	5.79E+01	2.19E+02	3.28E+02	2300	9.14E-04
2310	1.44E-02	6.17E-02	3.98E-01	7.94E-01	2310	1.65E+01	5.99E+01	2.24E+02	3.35E+02	2310	9.09E-04
2320	1.16E-02	4.92E-02	3.23E-01	6.43E-01	2320	1.35E+01	4.98E+01	1.97E+02	2.98E+02	2320	9.06E-04
2330	1.26E-02	5.39E-02	3.51E-01	6.99E-01	2330	1.46E+01	5.37E+01	2.08E+02	3.12E+02	2330	9.07E-04
2340	1.04E-02	4.39E-02	2.90E-01	5.78E-01	2340	1.21E+01	4.50E+01	1.84E+02	2.79E+02	2340	9.11E-04
2350	8.65E-03	3.61E-02	2.42E-01	4.82E-01	2350	1.00E+01	3.77E+01	1.63E+02	2.50E+02	2350	9.18E-04
2360	9.78E-03	4.11E-02	2.72E-01	5.41E-01	2360	1.12E+01	4.19E+01	1.74E+02	2.66E+02	2360	9.27E-04
2370	7.28E-03	3.01E-02	2.02E-01	4.03E-01	2370	8.36E+00	3.16E+01	1.43E+02	2.22E+02	2370	9.33E-04
2380	6.32E-03	2.56E-02	1.74E-01	3.46E-01	2380	7.26E+00	2.72E+01	1.28E+02	2.02E+02	2380	9.36E-04
2390	6.21E-03	2.50E-02	1.71E-01	3.40E-01	2390	7.15E+00	2.68E+01	1.27E+02	2.00E+02	2390	9.36E-04
2400	6.71E-03	2.72E-02	1.85E-01	3.67E-01	2400	7.76E+00	2.91E+01	1.35E+02	2.11E+02	2400	9.29E-04
2410	4.50E-03	1.74E-02	1.20E-01	2.39E-01	2410	5.30E+00	1.94E+01	9.96E+01	1.61E+02	2410	9.21E-04
2420	3.75E-03	1.41E-02	9.89E-02	1.96E-01	2420	4.45E+00	1.60E+01	8.65E+01	1.42E+02	2420	9.16E-04
2430	4.95E-03	1.93E-02	1.34E-01	2.66E-01	2430	5.87E+00	2.16E+01	1.09E+02	1.74E+02	2430	9.12E-04
2440	4.13E-03	1.58E-02	1.10E-01	2.18E-01	2440	4.90E+00	1.78E+01	9.37E+01	1.52E+02	2440	9.14E-04
2450	1.85E-03	6.03E-03	4.28E-02	8.47E-02	2450	2.21E+00	7.07E+00	4.37E+01	7.65E+01	2450	9.19E-04
2460	3.00E-03	1.06E-02	7.60E-02	1.51E-01	2460	3.53E+00	1.21E+01	6.98E+01	1.17E+02	2460	9.27E-04
2470	1.58E-03	4.68E-03	3.39E-02	6.69E-02	2470	1.84E+00	5.38E+00	3.49E+01	6.21E+01	2470	9.43E-04
2480	7.80E-04	1.65E-03	1.07E-02	2.08E-02	2480	8.99E-01	1.89E+00	1.18E+01	2.21E+01	2480	9.57E-04
2490	4.00E-04	4.60E-04	1.39E-03	2.34E-03	2490	4.56E-01	5.24E-01	1.58E+00	2.64E+00	2490	9.69E-04
2500	4.30E-04	5.10E-04	1.68E-03	2.90E-03	2500	4.80E-01	5.70E-01	1.87E+00	3.21E+00	2500	9.88E-04

Level 1 Requirements and Mission Success Criteria

b) To address the Decadal Survey and community-identified science and application questions related to volcanoes, wild fires, water usage, urbanization and surface composition (DS113-115), the baseline science mission shall provide global mapping measurements of the surface radiance, temperature and emissivity with 8 spectral bands from the 3-5 micron and 8-12 micron regions of the spectrum at the specified noise-equivalent-delta-temperature and accuracy at ≤60 m nadir spatial sampling with ≤5 day revisit to provide >60% Monthly, >70% seasonal and >85% annual coverage of the terrestrial and shallow water regions of the Earth for at least three years with a subset of measurements available near-real-time for designated science and applications.

Specified NEdT

	Wavelength	Spectral Bandwidth	Min Nominal Radiance and Temperature	Max Nominal Radiance and Temperature	NEdT at Min nominal Temperature	NEdT at Max Nominal Temperature	NEdT at 300 K
	(microns)	(microns)	(W/m^2/micron/sr)	(W/m^2/micron/sr)	Kelvin	Kelvin	Kelvin
Band 1	3.98	0.08	14 (400 K)	9600 (1400 K)	1	0.12	11.2
Band 2	7.35	0.32	0.34 (200 K)	110 (500 K)	2.8	0.22	0.28
Band 3	8.28	0.34	0.45 (200 K)	100 (500 K)	2	0.22	0.24
Band 4	8.63	0.35	0.57 (200 K)	94 (560 K)	1.6	0.24	0.24
Band 5	9.07	0.36	0.68 (200 K)	86 (500 K)	1.2	0.24	0.22
Band 6	10.53	0.54	0.89 (200 K)	71 (500 K)	0.64	0.22	0.16
Band 7	11.33	0.54	1.1 (200 K)	58 (500 K)	0.56	0.26	0.16
Band 8	12.05	0.52	1.2 (200 K)	48 (500 K)	0.52	0.3	0.18

Digitization @ min radiance	Digitization @ max radiance	Digitization @ 300 K
(W/m^2/micron/sr)	(W/m^2/micron/sr)	(W/m^2/micron/sr)
4.0e-2 (0.12 K)	4.0e-2 (0.01 K)	5.0e-2 (1.4 K)
5.6e-3 (0.30 K)	5.6e-3 (0.009 K)	5.6e-3 (0.03 K)
4.8e-3 (0.23 K)	4.8e-3 (0.009 K)	4.8e-3 (0.03 K)
4.5e-3 (0.19 K)	4.5e-3 (0.009 K)	4.5e-3 (0.03 K)
4.1e-3 (0.15 K)	4.1e-3 (0.010 K)	4.1e-3 (0.03 K)
2.5e-3 (0.08 K)	2.5e-3 (0.008 K)	2.5e-3 (0.02 K)
2.2e-3 (0.07 K)	2.2e-3 (0.010 K)	2.2e-3 (0.02 K)
2.1e-3 (0.06 K)	2.1e-3 (0.012 K)	2.1e-3 (0.02 K)

Notes

Center wavelength is the average of the max and min wavelengths at the FWHM
Spectral bandwidth is the FWHM
Minimum nominal radiance is 200K except for 4 um band where it is 400K
Maximum nominal radiance is 500K except for 4 um band where it is 1400K

Level 1 Requirements and Mission Success Criteria

c) To address Decadal Survey and community-identified science and application questions (DS113-115), requiring combined reflectance, emissivity and temperature measurements, the baseline mission shall provide combined global mapping data sets.

Level 1 Requirements and Mission Success Criteria

<u>A termination review will be called if these requirements cannot be met</u>

4.1.2 Requirement: Minimum Science Mission

a) To address the Decadal Survey and community identified science and application questions related to terrestrial and coastal ocean ecosystem composition, function, and change as well as surface composition (DS113-115), the baseline science mission shall provide global global mapping measurements of the surface reflectance or remote sensing reflectance for shallow water regions across the solar reflected spectrum from 380 to 2500 nm at ≤10 nm sampling at >80% of the specified signal-to-noise ratio and accuracy with > 90% spectral/spatial uniformity at ≤60 m nadir spatial sampling with <20 day revisit to provide > 50% seasonal and >70% annual coverage of the terrestrial and shallow water regions of the Earth for at least two years.

Level 1 Requirements and Mission Success Criteria

b) To address the Decadal Survey and community identified science and application questions related to volcanoes, wild fires, water usage, urbanization and surface composition (DS113-115), the baseline science mission shall provide global mapping measurements of the surface temperature as well as emissivity and surface radiance in 8 spectral bands from the 3-5 micron and 8-12 micron regions of the spectrum at >80% the specified noise-equivalent-delta-temperature and accuracy at ≤60 m nadir spatial sampling with ≤5 day revisit to provide > 40% Monthly, > 60% seasonal and >70% annual coverage of the terrestrial and shallow water regions of the Earth for at least two years.

c) To address Decadal Survey and community identified science and application questions requiring combined reflectance, emissivity and temperature measurements, the threshold mission shall provide combined global mapping data sets.

Summary

Please keep these Level 1 Requirements and Success Criteria in mind as we proceed through the workshop.

We will review these Level 1 Requirements and Success Criteria at the end of the workshop.

Note: The HyspIRI Mission must remain appropriately aligned with the Decadal Survey.

NRC Decadal Survey - HyspIRI

Global vegetation species-type and physiological condition, including agricultural lands, for biosphere feedback and land-atmosphere interactions; Spectroscopically derived terrestrial land cover composition/albedo including snow, ice, dust climate interaction; Fire: fuel, occurrence, intensity and recovery globally, as well as volcano emissions; Fine spatial & temporal scale measures of surface temperature and energy balance, including urban heat Islands.

Visible ShortWave InfraRed (VSWIR) Imaging Spectrometer

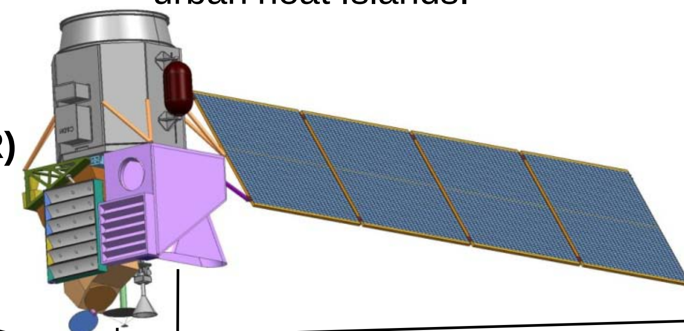

Multispectral Thermal InfraRed (TIR) Scanner

Map of dominant tree species, Bartlett Forest, NH

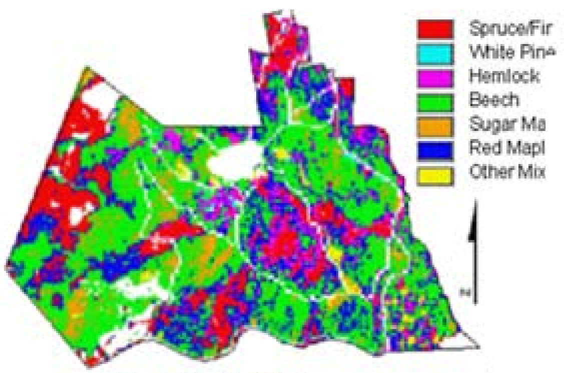

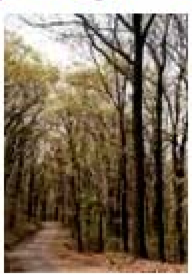

Soil C:N Ratio

White Mountain National Forest, NH

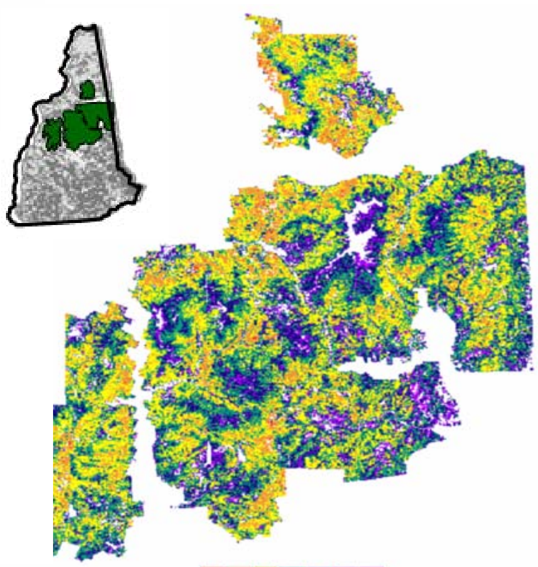

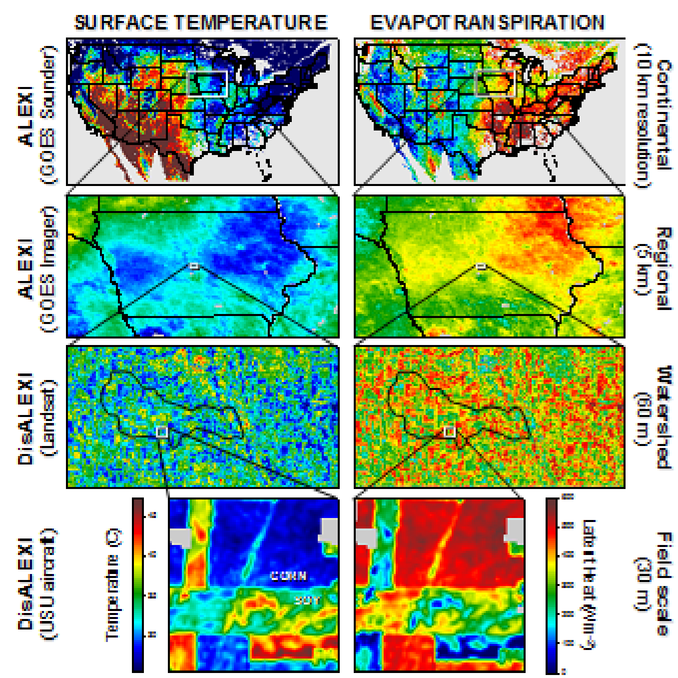

Why the HyspIRI Mission is Critical to the Future of Global Climate Science

Greg Asner
Carnegie Institution for Science

With special thanks to Tom Painter, Susan Ustin
and the HyspIRI community

Key Issues

- The big uncertainties in predicting future climate
- The biospheric feedback
- The cryospheric feedback
- Why HyspIRI and not something else

- **Imaging spectroscopy has literally hundreds of applications**. I could put up slide after slide collected from our community showing an astounding array of applications, **from agriculture to volcanoes**.

- Our community has articulated this kaleidoscope of applications time after time, from HIRIS to HyspIRI, and all mission concepts in between.

- Many of the applications are **directly linked to regional climate and, if integrated over space and time, global climate**. But this comes off as contrived to mission decision-makers, and thus our message about the climate relevance of HyspIRI has been confused and unheard.

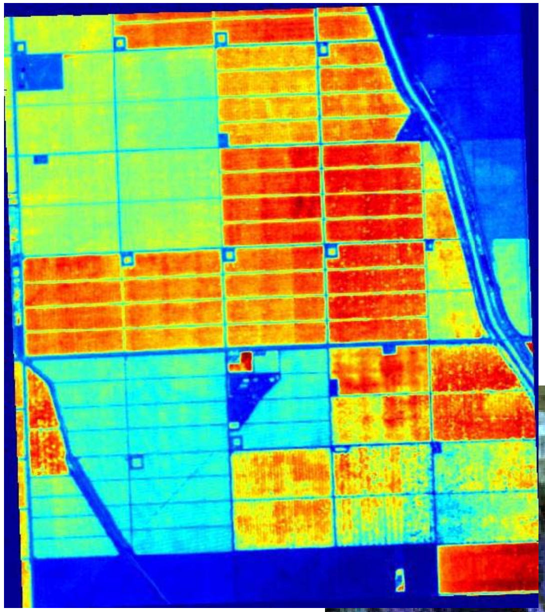

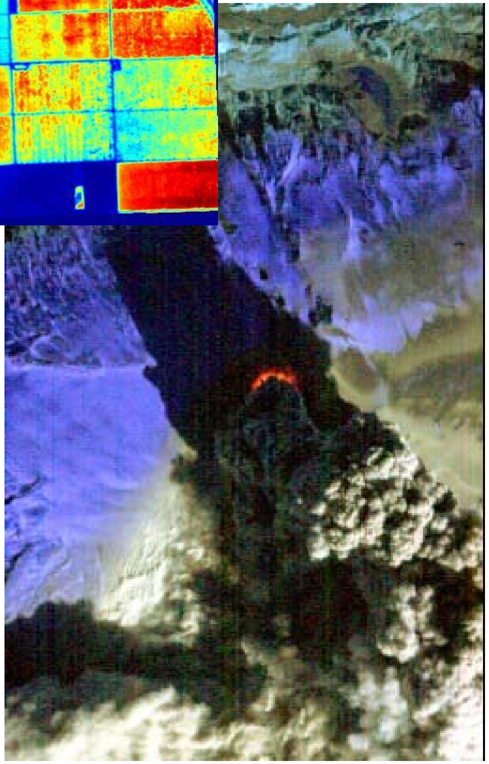

What are the big climate issues calling for the HyspIRI mission?

The biospheric feedback

1. A major uncertainty in predicting future climate lies in a biospheric feedback to a rapidly evolving climate.

2. This biospheric feedback interacts with changes in temperature, precipitation, CO_2, radiation, nutrients, ecological disturbance and plant (autotroph) distributions.

3. CRITICALLY: Although we understand many of the processes underpinning the biospheric feedback, we do not know the relative strength of these processes, spatially or temporally.

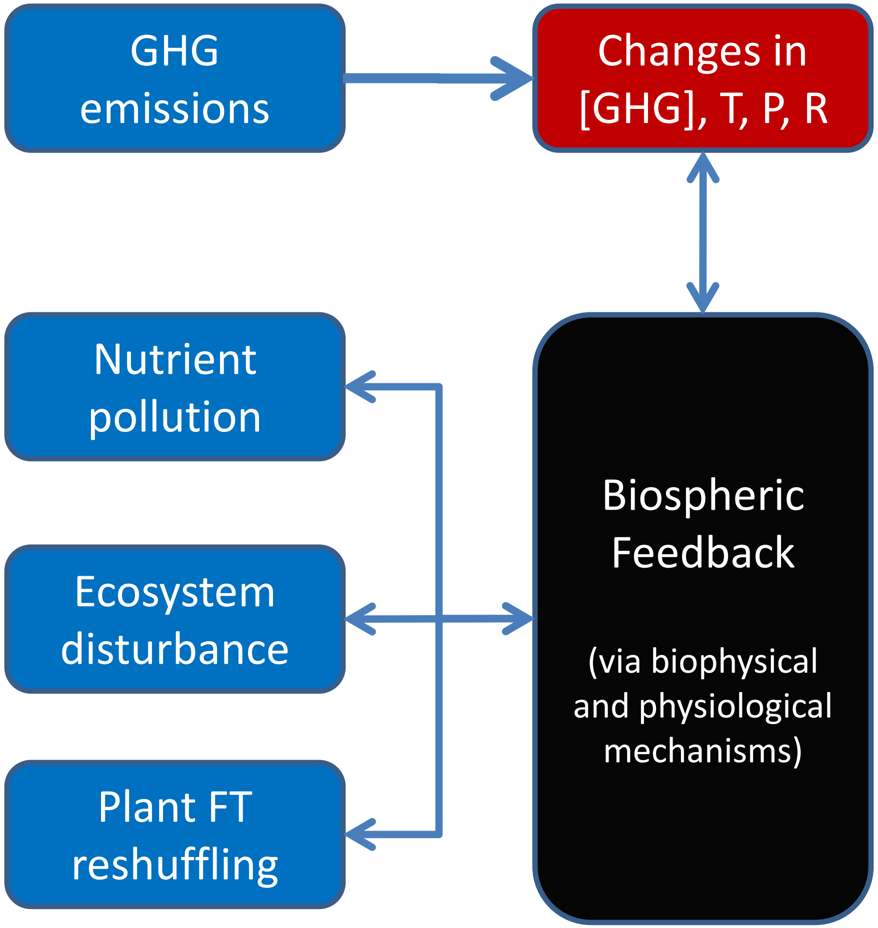

A hands-on example of a biospheric feedback

Background

Since 1950, we have witnessed a non-linear increase in the coverage of a nitrogen-fixing invasive tree in Hawaiian forests. The spread of this tree (*Morella faya*) is just a tiny example of the global reshuffling of species caused by people.

At the same time, atmospheric [GHG] has increased non-linearly, with a measureable increase in solar radiation and temperature in Hawaiian forests.

GHG emissions

Plant FT reshuffling

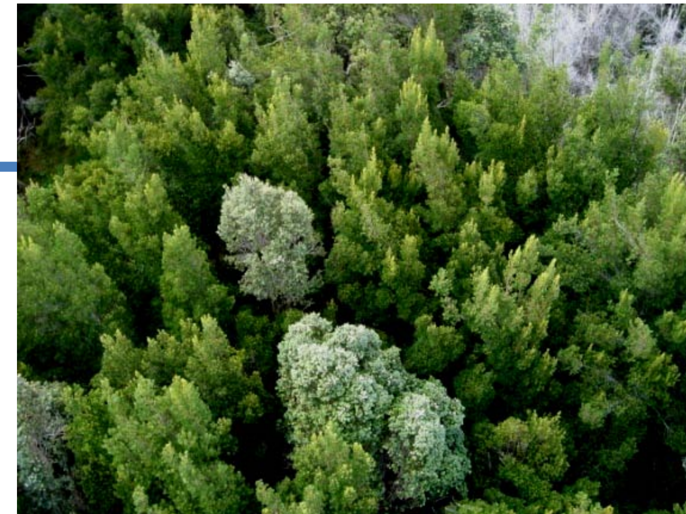

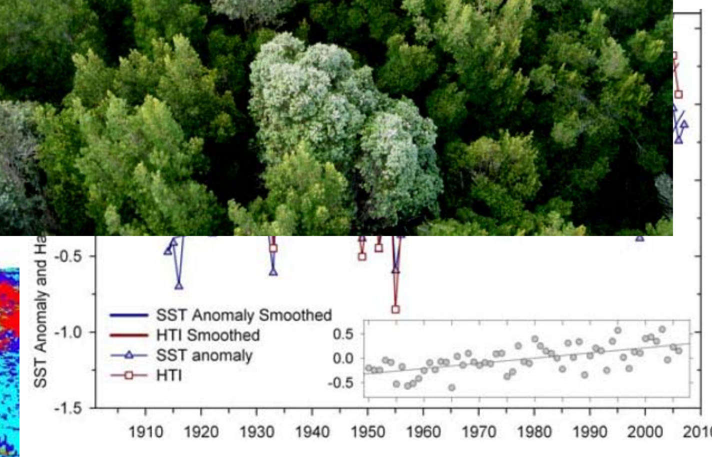

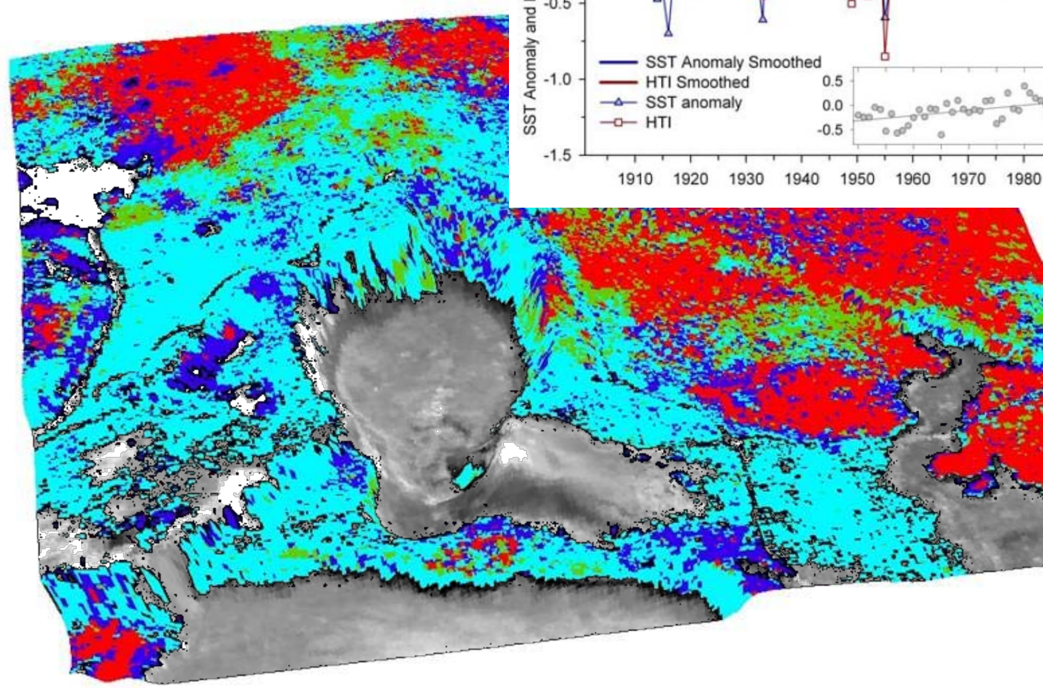

Vitousek et al. 1988, Giambelluca 2009

Four components of this biospheric feedback:

1. PFT switch → more invasion during warming/drying
2. Nutrient pollution → more GHG
3. Forest carbon loss → more GHG
4. Increased albedo → cooling

Here's how:

1. The invasive PFT grows faster and spreads more widely than all of the native PFTs combined, but only during periods of anomalously high radiation and temperature levels associated with climate change.

2. The invasive tree outcompetes native trees for light, eliminating the natives, and changing the entire makeup of the forest (a major change in PFT has occurred).

3. The new PFT increases nitrogen oxide gas emissions from soils by 16-times over background levels. This includes the super-GHG N_2O.

4. The physiological factors that allow the invader PFT to win, also cause it to store less carbon than the natives it replaces. This increases net GHG emissions.

5. The physiological factors that allow the invader to steal light also cause a 40% increase in forest albedo. This has a gross cooling effect on climate.

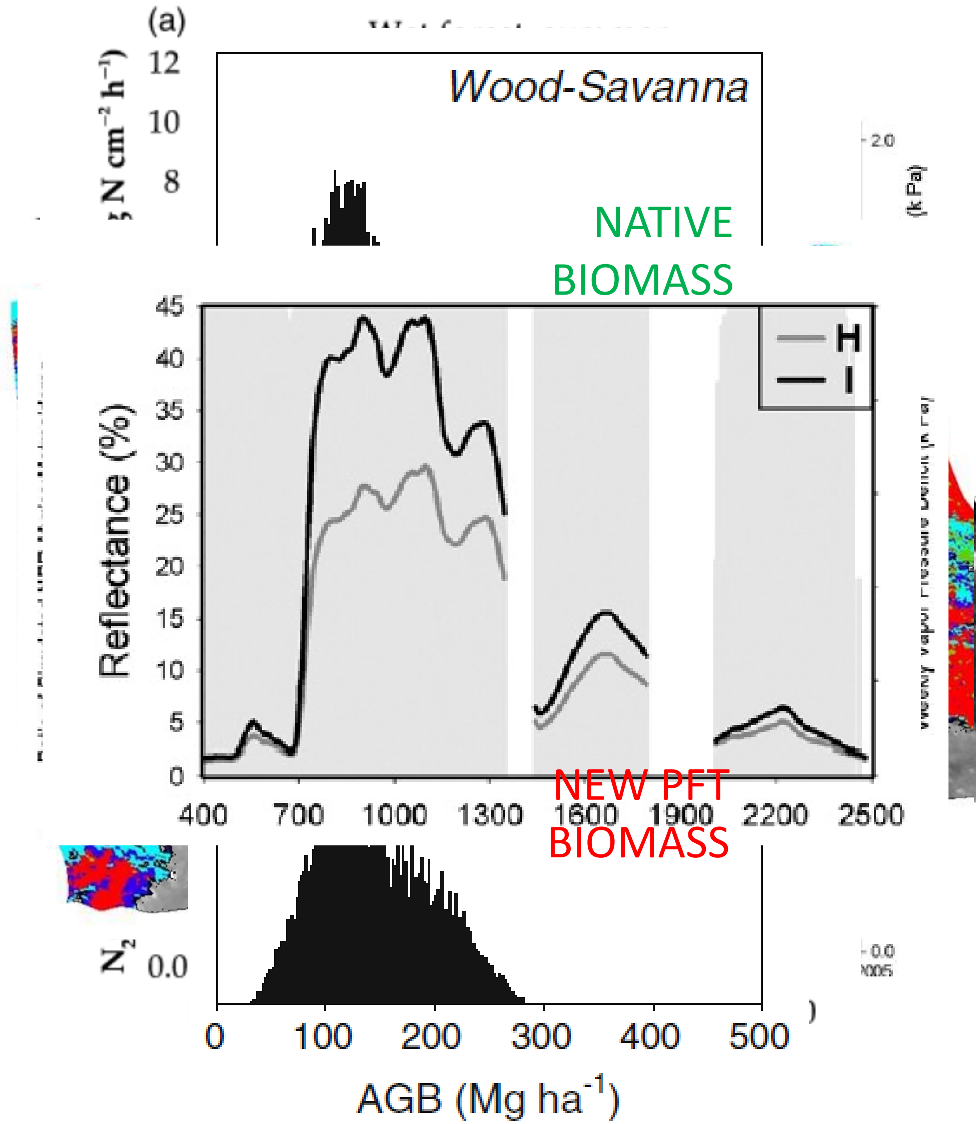

Asner et al. 2006, 2008
Asner & Vitousek 2005, Hall & Asner 2007

How did we figure this out?

(Hint: Not in 15 years of intensive field study.)

1. PFT switch → more invasion during warming and drying events
2. Nutrient pollution → more GHG
3. Forest carbon loss → more GHG
4. Increased albedo → cooling

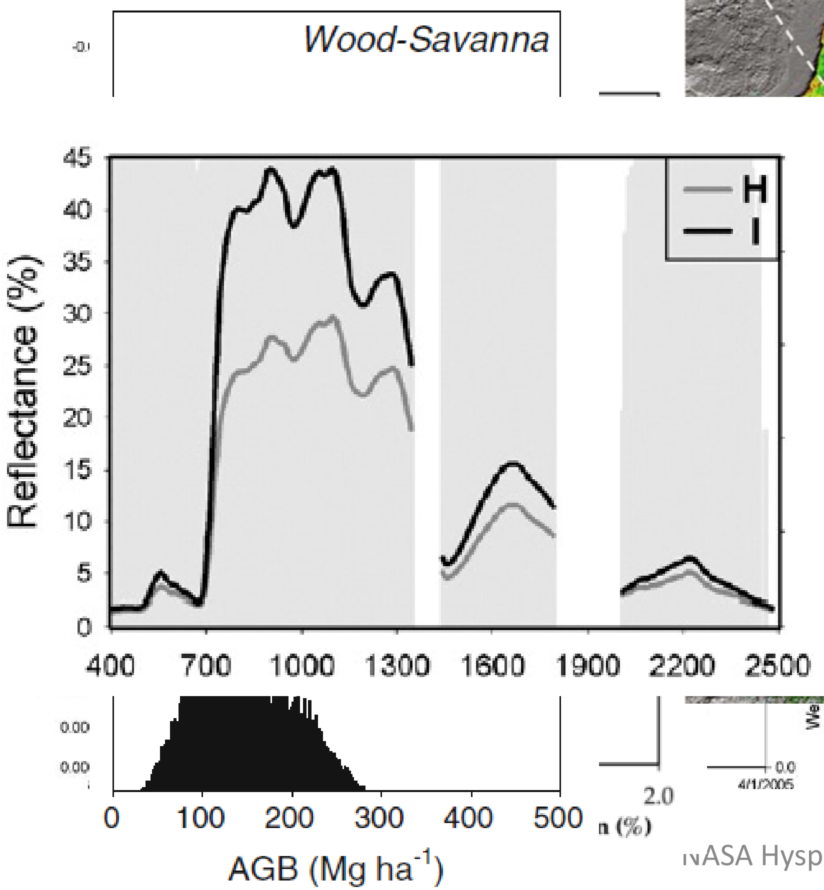

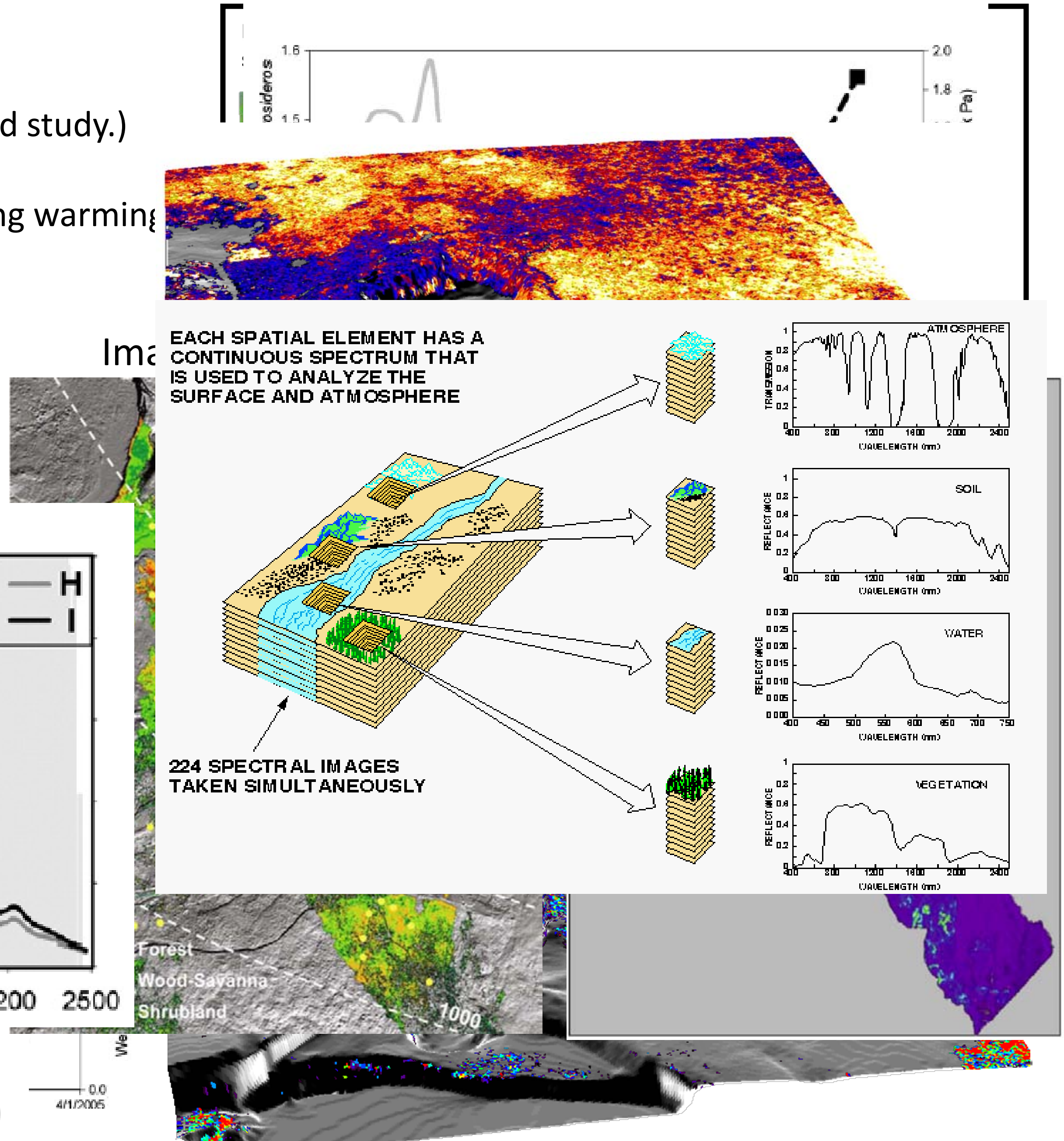

Can it be done with other technologies?

Observation	Approach	Method	Other attempts	Report card
PFT change	Chemo-spectral analysis	Spectroscopic RT inversion, PLSR, and SMA with AVIRIS	MODIS-500, Landsat veg. indices and SMA (CLASlite)	MODIS: D (spatial/spectral) Landsat: C (spectral)
Growth response to climate change	Physiological analysis	Narrowband indices with Hyperion	ALI veg. Indices	D (weak greenness effect, no other pattern)
Nitrogen increase	Chemo-spectral analysis	Spectroscopic RT inversion, PLSR with AVIRIS	Hyperion	D (way too noisy)
Carbon decrease	Species detection, then 3-D structure	AVIRIS-guided LiDAR	Landsat veg. indices	D (vague pattern in forests)
Albedo increase	Spectral	Spectral BRDF with AVIRIS	MODIS and Landsat NIR	MODIS: D (spatial) Landsat: B (11% diff in spectral)

Do biospheric feedbacks matter at the global climate scale?

The Amazon story…without an ending

Climate is changing. We are seeing an increasing in nighttime temperatures and a 0.3% per year decrease in mean annual precipitation.

A major climate change effect is drought, both ENSO and non-ENSO related. Take the 2005 Amazon mega-drought as an example.

Saleska et al. 2007 (Science) used the MODIS EVI to assess biospheric response. They observed apparent "green up". If true, then CO_2 uptake is a negative feedback response to drought and to climate warming. Was it true?

Samanta et al. 2009 (GRL) shows that a reprocessir of the MODIS data yield no apparent green up response to drought. MODIS is not the technology for quantitative detection of biospheric feedback in this case.

Meanwhile, all field indications were that mortality actually increased enormously across the Amazon (Phillips et al. Science)

Are there other feedbacks? (Chambers et al. 2009)

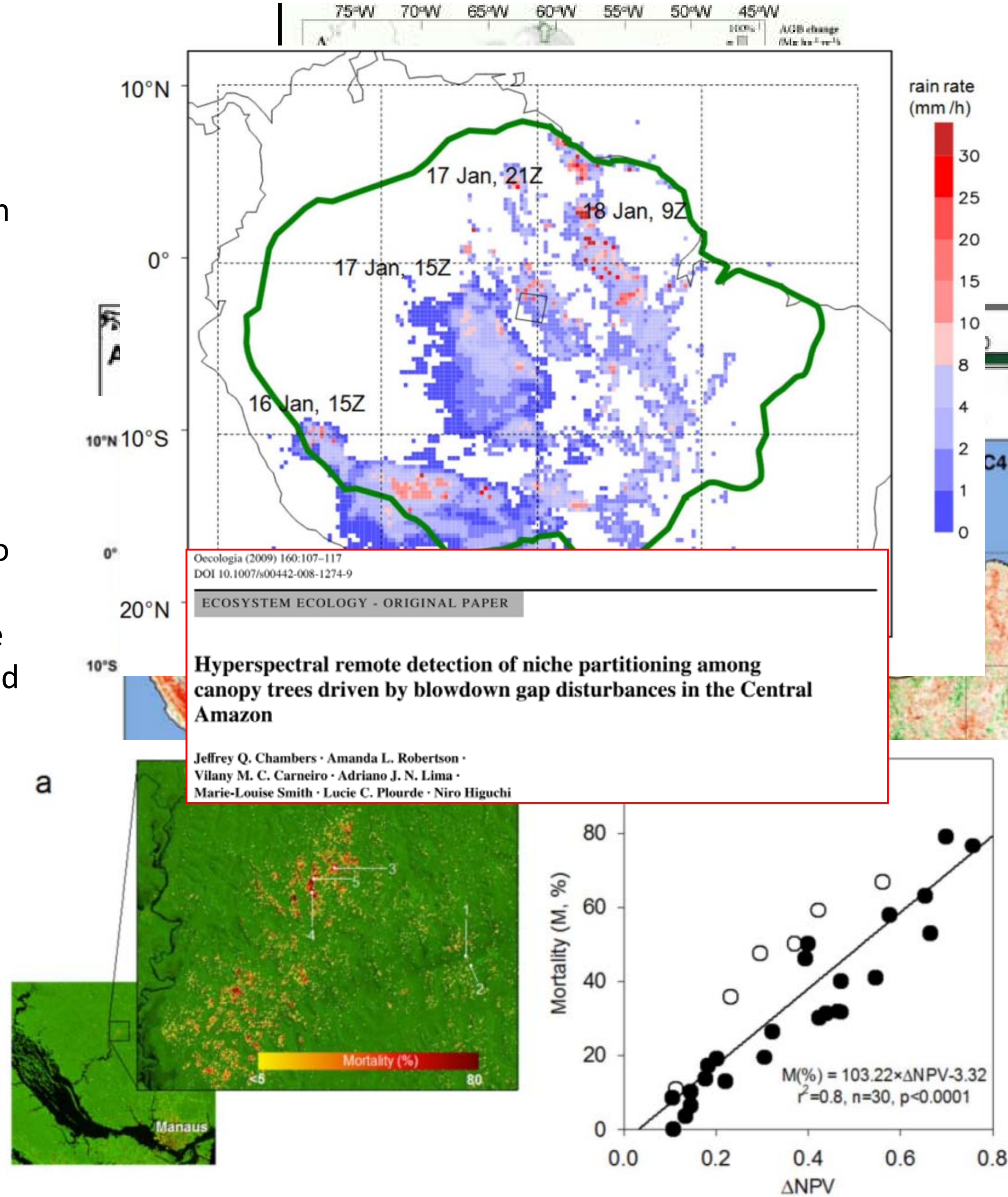

Oecologia (2009) 160:107–117
DOI 10.1007/s00442-008-1274-9

ECOSYSTEM ECOLOGY - ORIGINAL PAPER

Hyperspectral remote detection of niche partitioning among canopy trees driven by blowdown gap disturbances in the Central Amazon

Jeffrey Q. Chambers · Amanda L. Robertson · Vilany M. C. Carneiro · Adriano J. N. Lima · Marie-Louise Smith · Lucie C. Plourde · Niro Higuchi

So what can HyspIRI do to address the Amazon (and global) tropical feedback challenge?

1. Physiological response to drought – whether positive or negative – is a HUGE uncertainty in the biospheric feedback to climate variability and change. HyspIRI is the only technology to deliver **global quantitative physiological measurements** needed to constrain estimates of GHG fluxes and the models used to simulate them.

2. Diffuse disturbance patterns are the spatially dominant type of change that occurs in global ecosystems (not deforestation). HyspIRI offers both **quantitative disturbance detection and physiological response globally**.

3. PFT changes underpin CO_2 and other GHG fluxes in the biospheric feedback. HyspIRI offers **quantitative mapping of PFT changes globally**.

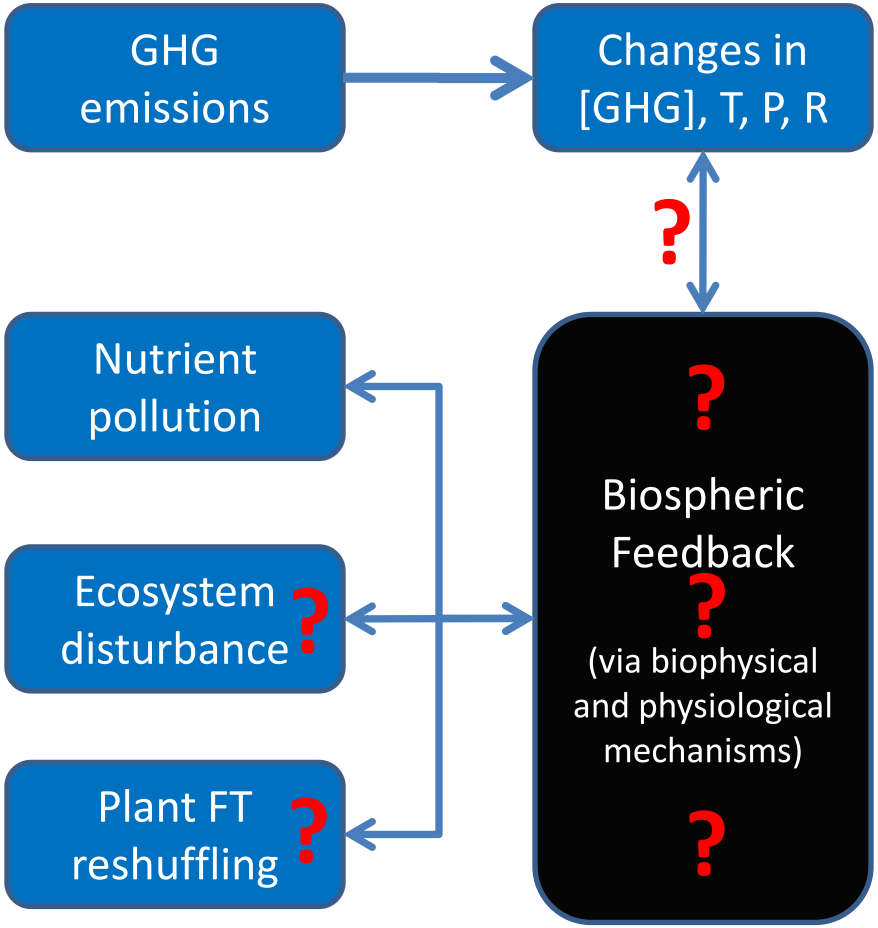

What are the big climate issues calling for the HyspIRI mission?

The cryospheric feedback

1. Another major uncertainty in predicting future climate rests in the cryospheric feedback (IPCC 2007).

2. The cryospheric feedback is determined by changes in albedo caused by changes in temperature (melt), precipitation (accumulation), and dust and black carbon deposition.

3. The cryospheric feedback is linked to the biospheric feedback.

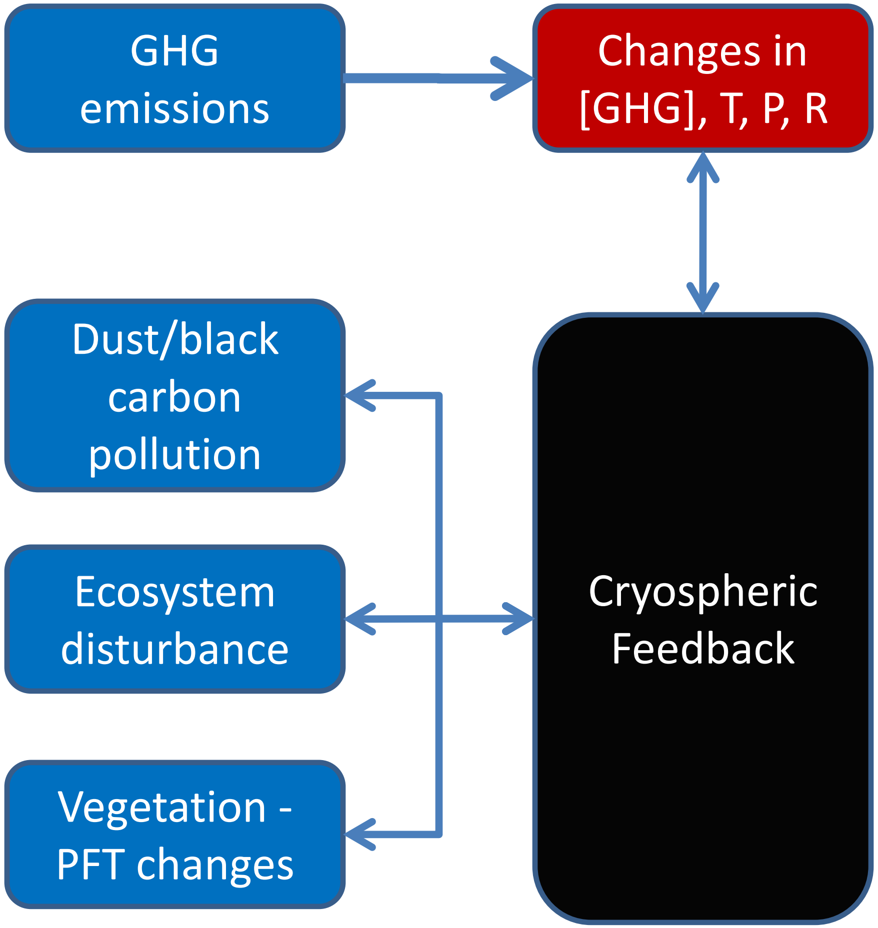

2.9.1 Uncertainties in Radiative Forcing

< >

The TAR assessed uncertainties in global mean RF by attaching an error bar to each RF term that was 'guided by the range of published values and physical understanding'. It also quoted a level of scientific understanding (LOSU) for each RF, which was a subjective judgment of the estimate's reliability.

	Evidence	Consensus	LOSU	Certainties	Uncertainties	Basis of RF range
LLGHGs	A	1	High	Past and present concentrations; spectroscopy	Pre-industrial concentrations of some species; vertical profile in stratosphere; spectroscopic strength of minor gases	Uncertainty assessment of measured trends from different observed data sets and differences between radiative transfer models
Surface albedo (land use)	A	2 to 3	Medium to Low	Some quantification of deforestation and desertification	Separation of anthropogenic changes from natural	Based on range of published estimates and published uncertainty analyses
Surface albedo (BC aerosol on snow)	B	3	Low	Estimates of BC aerosol on snow; some model studies suggest link	Separation of anthropogenic changes from natural; mixing of snow and BC aerosol; quantification of RF	Estimates based on a few published model studies

*level of scientific understanding" (*LOSU)*

Climate sensitivity of the Earth system is modulated by the response of the cryosphere to radiative forcings – primarily through the *snow-albedo feedback*

Hansen and Nazarenko 2004, *PNAS*
Ramanathan and Carmichael 2008, *Nature Geosci*
Flanner et al 2009, *ACP*

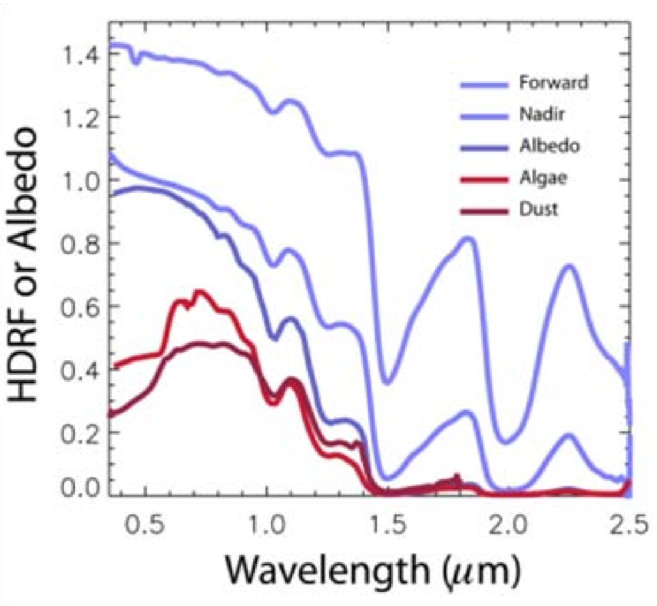

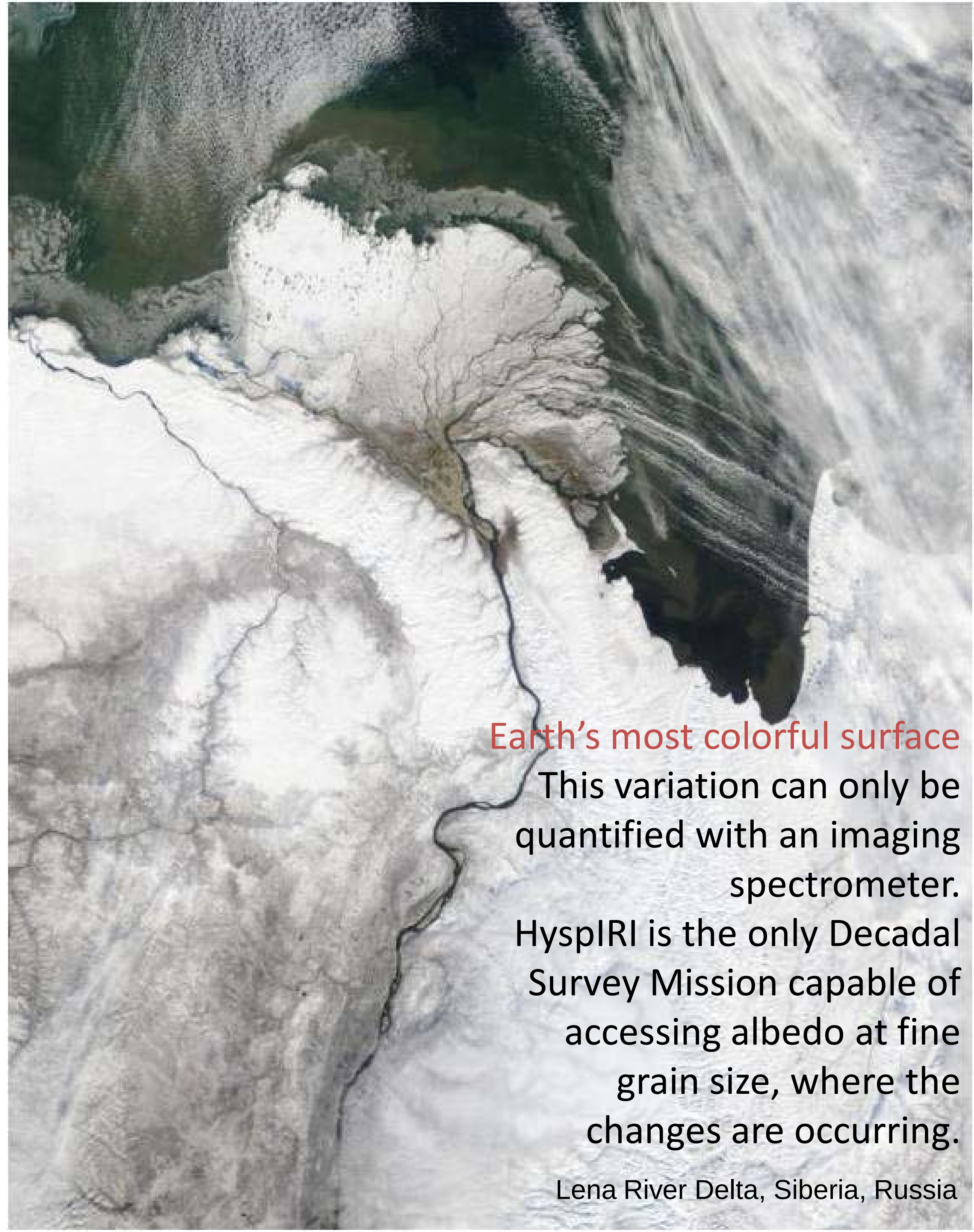

Earth's most colorful surface

This variation can only be quantified with an imaging spectrometer.

HyspIRI is the only Decadal Survey Mission capable of accessing albedo at fine grain size, where the changes are occurring.

Lena River Delta, Siberia, Russia

What is causing the downwasting and retreat of Himalayan glaciers?

Increasing temperatures and increasing dust and soot combine in unknown proportions to accelerate melt through changes in albedo. HyspIRI is the only sensor that allows us to attribute changes in albedo into effects from temperature and dust/black carbon and at a fine enough spatial resolution that heterogeneous terrain can be resolved. Multi-band sensors such as NPOESS VIIRS have neither capacity.

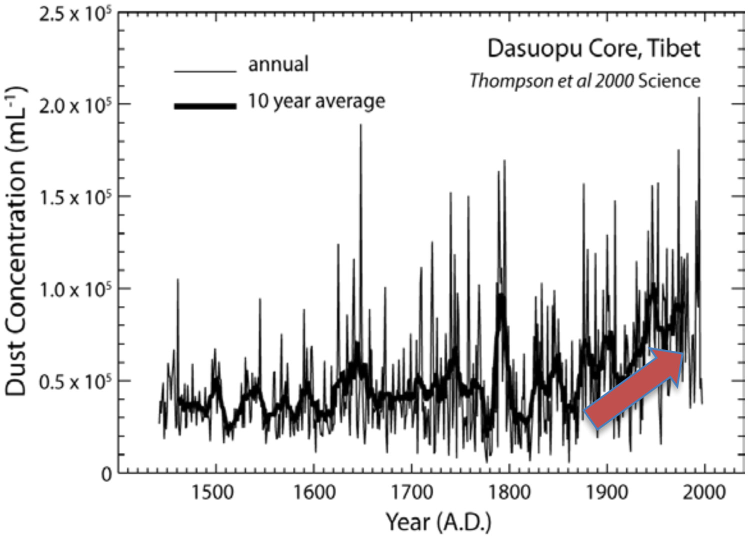

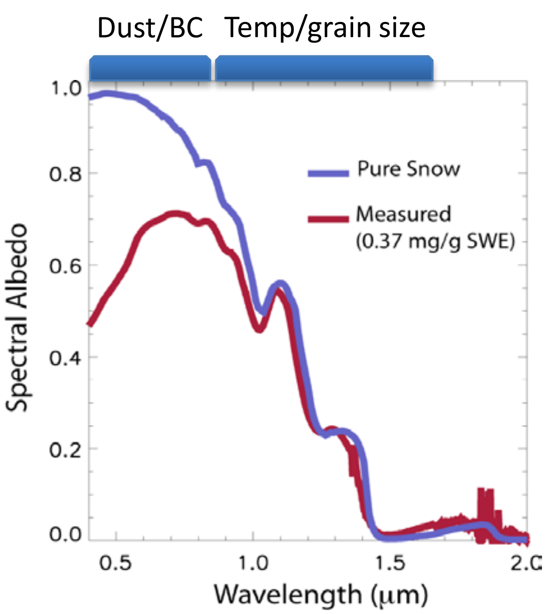

Impact of dust radiative forcing on snowpack

Land use and vegetation changes in globe's arid and semi-arid lands in the mid to late 1800s has led to 5-fold increase in dust loading to mountain snow cover in the Colorado River Basin (CRB) and other ranges of the globe. In the CRB, radiative forcing by this increased dust shortens snow cover duration by 3-5 weeks, intensifies spring runoff, and reduces total runoff. **Painter et al 2010, *PNAS***

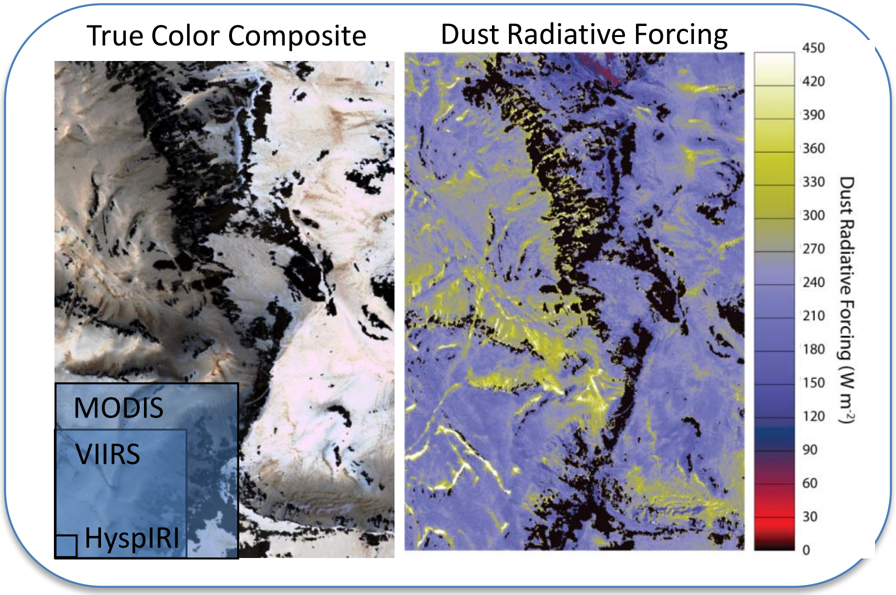

The spectral sampling of an imaging spectrometer is required to move beyond detection to quantification and attribution. The proposed spatial sampling of HyspIRI accesses entirely snow covered slopes whereas the spatial sampling of multispectral sensors MODIS and VIIRS most often is contaminated by spatial/spectral mixing of rock cliffs.

Painter et al. 2010, PNAS

Many other feedbacks are mediated by many other processes that HyspIRI uniquely measures or vastly improves measurement for:

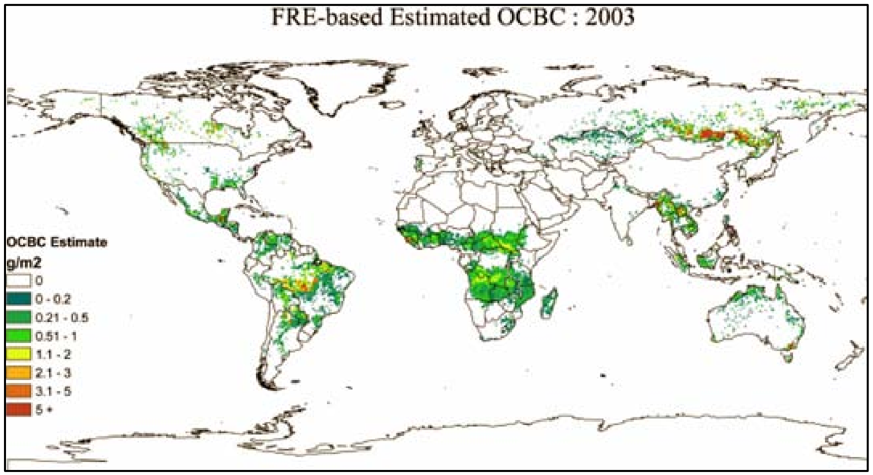

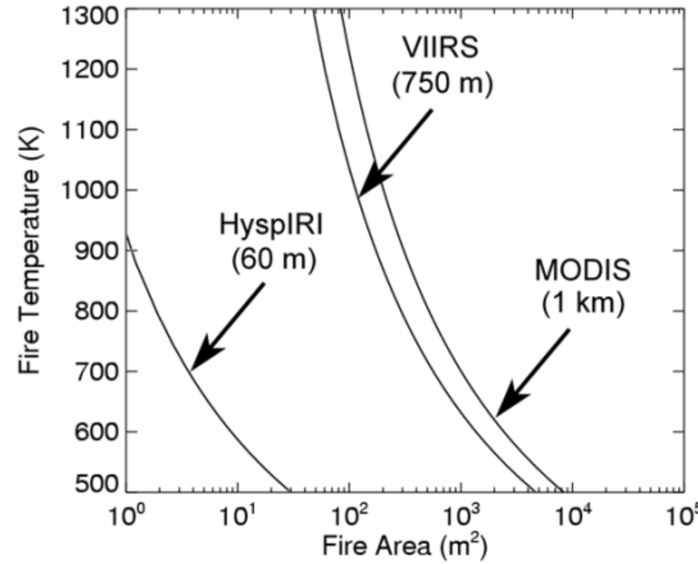

90% probability of detection; boreal forest; nadir view

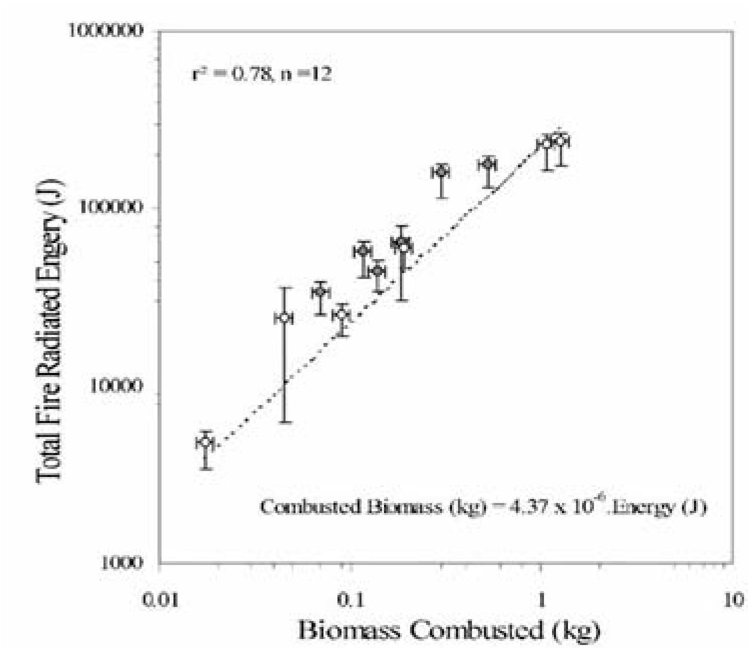

Fire Radiative Energy to estimate combusted biomass: Need 3-5 um data

Ellicott et al 2009
Wooster et al 2002 and 2003

Latent/sensible heat flux: Evapotranspiration

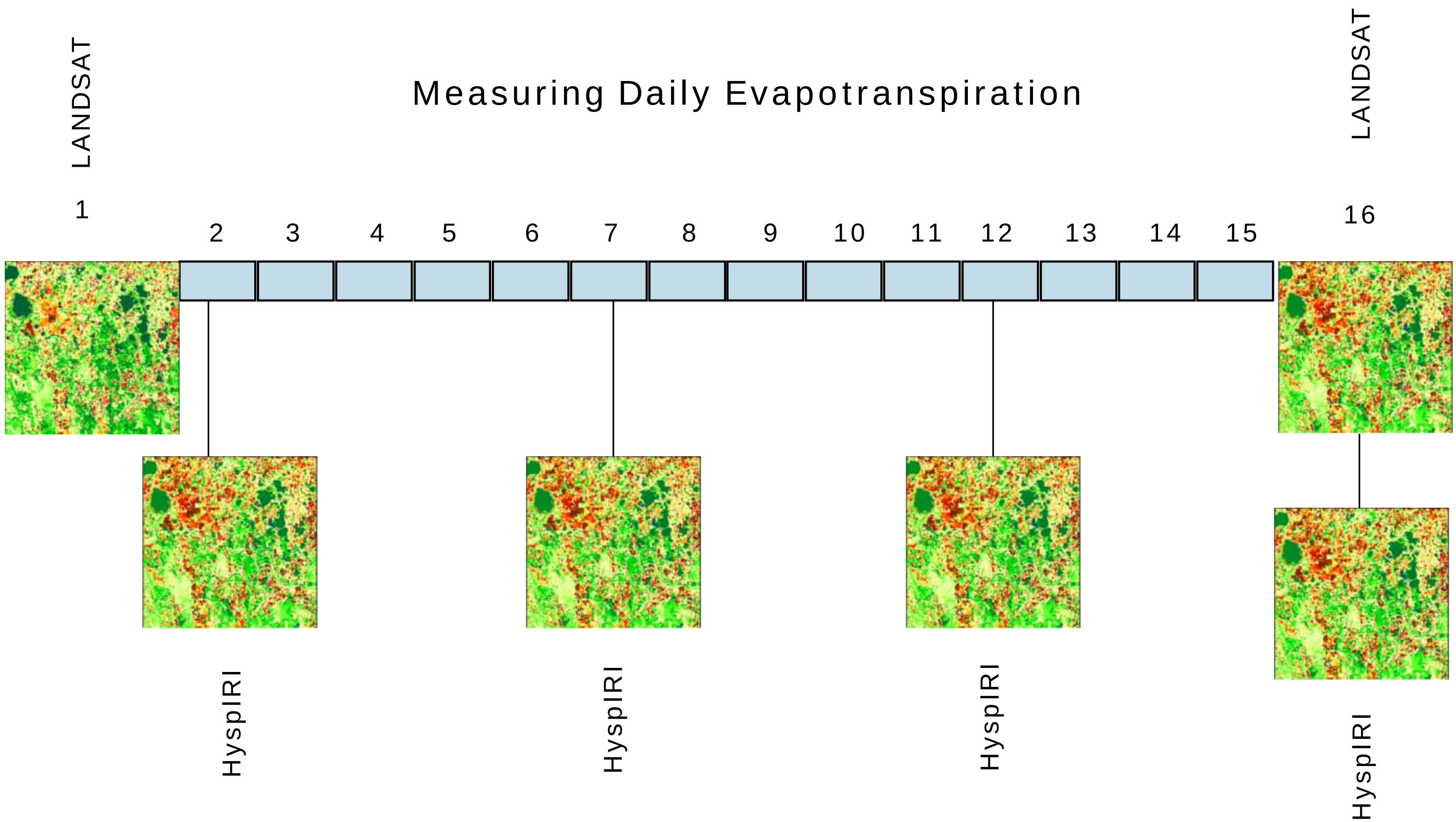

Radiative forcing: Volcanic eruptions

Eyjafjallajökull Iceland Volcano Eruption

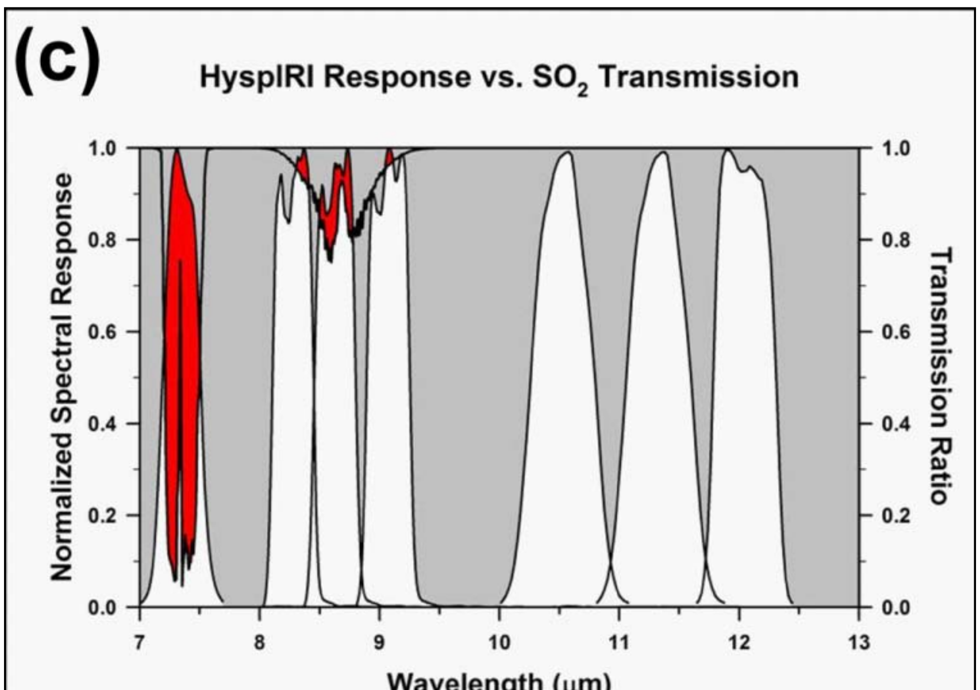

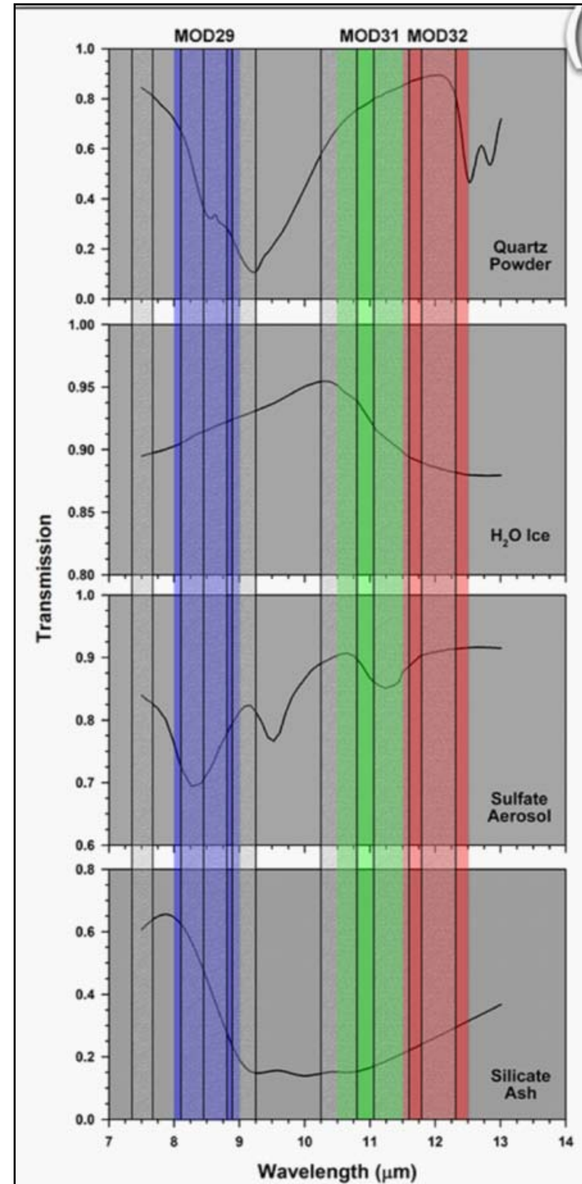

Are these "just" regional phenomena, or are these truly global, climate-relevant processes?

Footprint of the biospheric feedback in the humid tropics

Table 2 Percentage of the humid tropical forest biome with current major land use (LU) as expressed by deforestation and selective logging, predicted major climate change causing a reshuffling of vegetation types (C), a combination of climate change and land use (C+LU), and neither climate change nor land use (N)

Region	C	LU	C + LU	N
C. America	66	2	15	16
S. America	63	3	24	9
Africa	51	6	14	29
Asia-Oceania	37	19	21	23

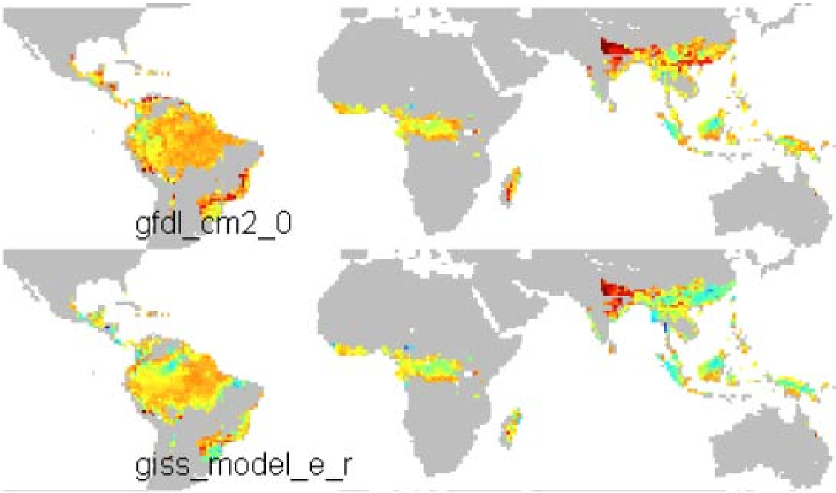

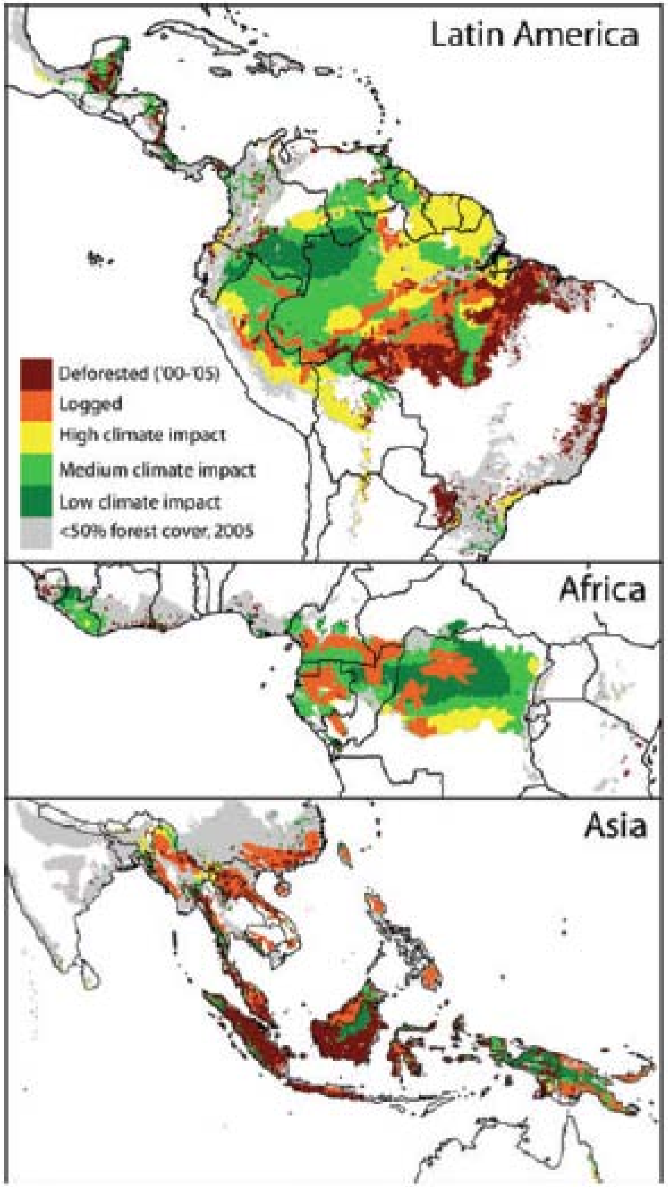

Figure 6 The footprint of deforestation, selective logging, and climate change in the humid tropical forest biome.

Asner et al. 2010

Footprint of the cryospheric feedback

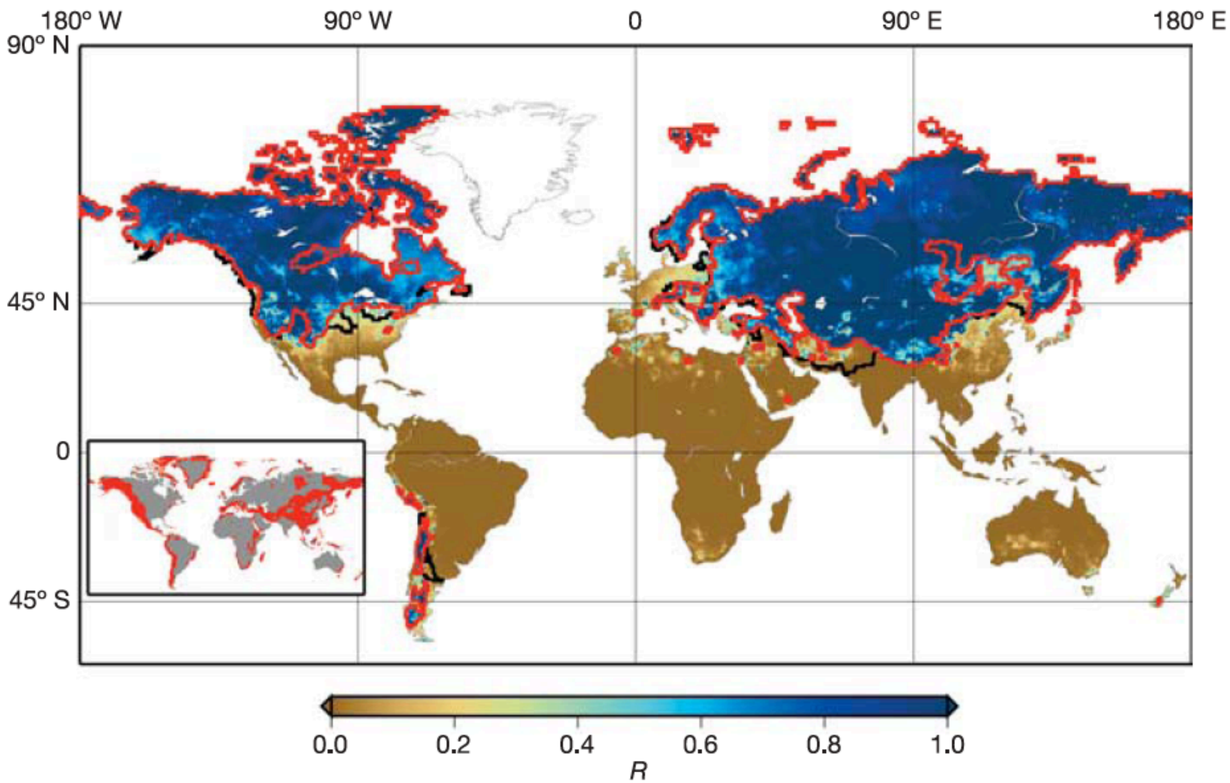

Figure 1 | Accumulated annual snowfall divided by annual runoff over the global land regions. The value of this dimensionless ratio lies between 0 and 1 and is given by the colour scale, *R*. The red lines indicate the regions where streamflow is snowmelt-dominated, and where there is not adequate reservoir storage capacity to buffer shifts in the seasonal hydrograph. The black lines indicate additional areas where water availability is predominantly influenced by snowmelt generated upstream (but runoff generated within these areas is not snowmelt-dominated). The inset shows regions of the globe that have complex topography using the criterion of ref. 17.

304

Barnett et al. 2005

Can HyspIRI deliver?

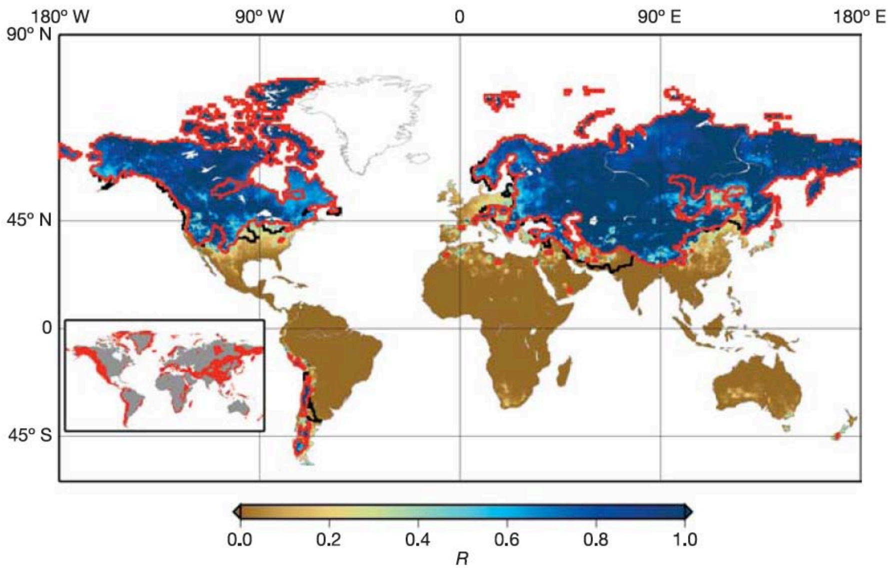

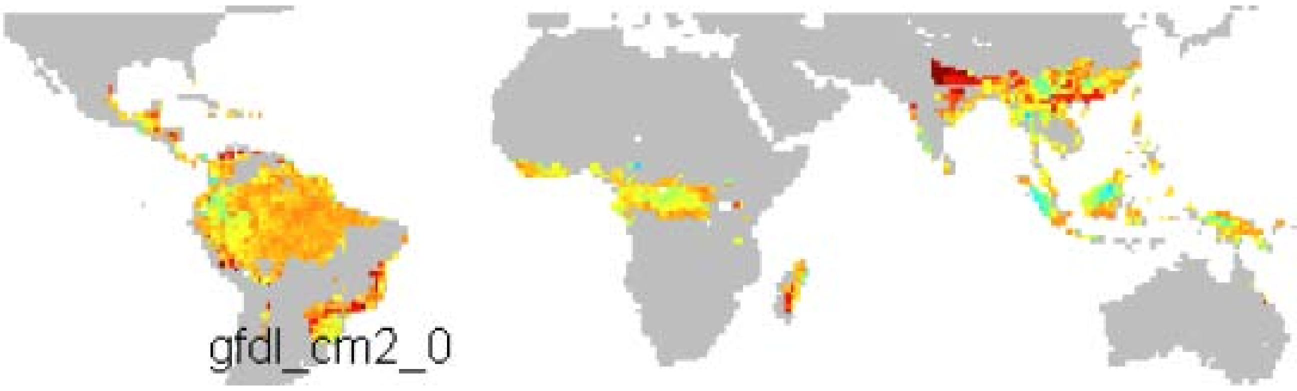

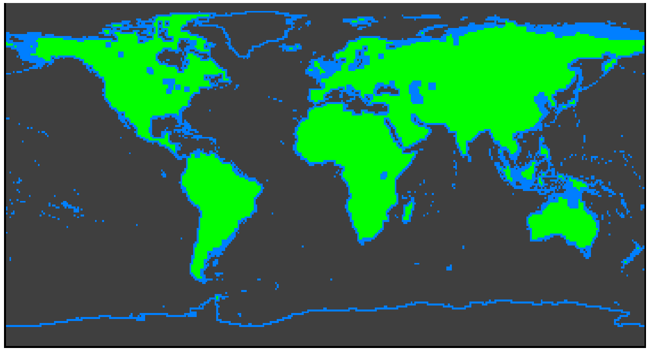

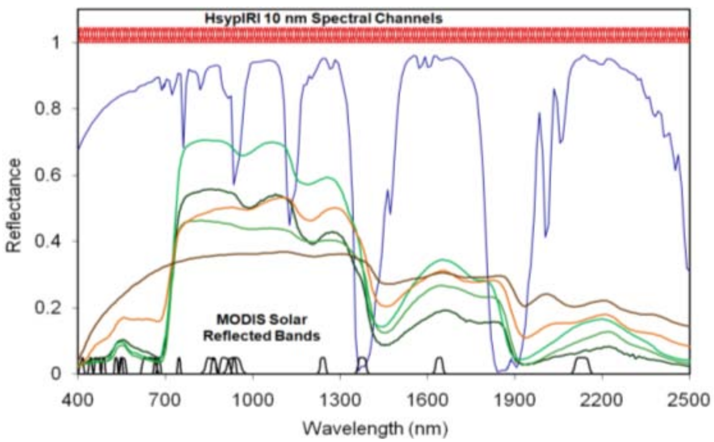

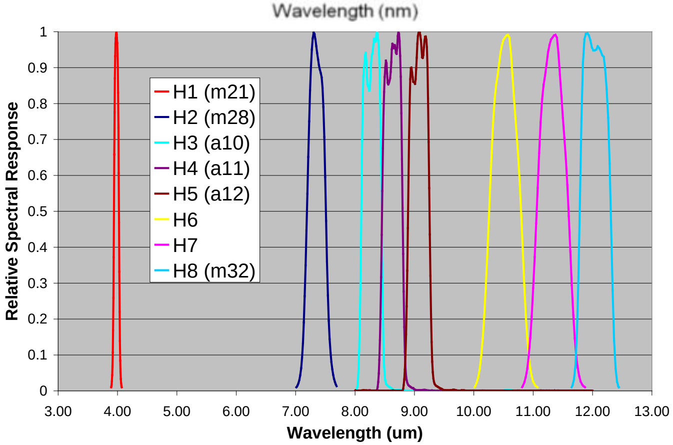

HyspIRI is a global mission, measuring land and shallow aquatic habitats at 60m and deep oceans at 1km every 5 days (TIR) and every 19 days (VSWIR)

HyspIRI's VSWIR imaging spectrometer directly measures the full solar reflected spectrum of the Earth from 380 – 2500nm at 10 nm.

HyspIRI's TIR directly samples the Earth's emitted thermal energy in 7 bands between 7.5-12 µm, & 1 band between 3-5 µm

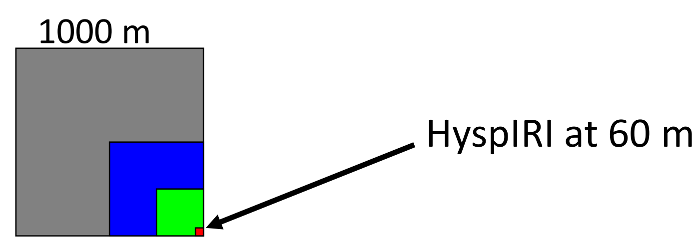

Why HyspIRI and not something else?

Country	Instrument	Swath km	~Dates	Terrestrial Coverage in 19 days	Mission Type	Repeat interval, days	TIR capability
USA	Hyperion	7.5	2000-	<0.5%	Demo/Sampling/Application	--	none
USA	HyspIRI	150	TBD	100%	Global/Climate	19	8 TIR bands
Germany	EnMAP	30	2014	<1%	Sampling/Application/Process	--	none
Italy	PRISMA	30	2013	~1%	Demo/Sampling/Application/Process	--	none
Japan	ALOS3	30	2014	~1%	Sampling/Application/Process	--	none
India	IMS Resource Sat-3	25	2013	~1%	Sampling/Application/Process	--	1 TIR band

HyspIRI Global Climate Science – Biosphere Component

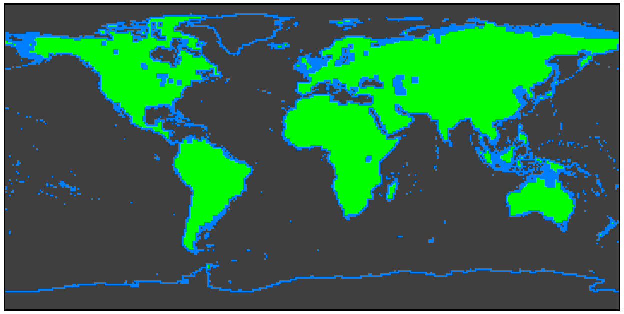

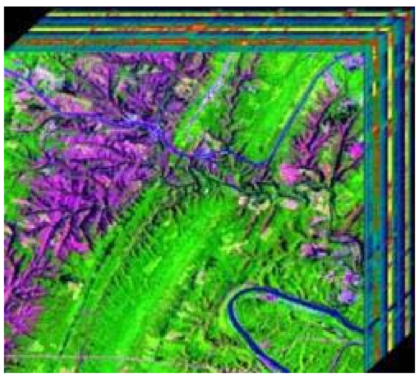

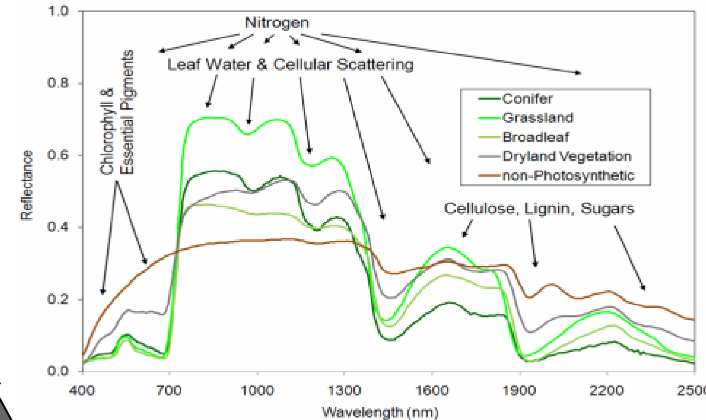

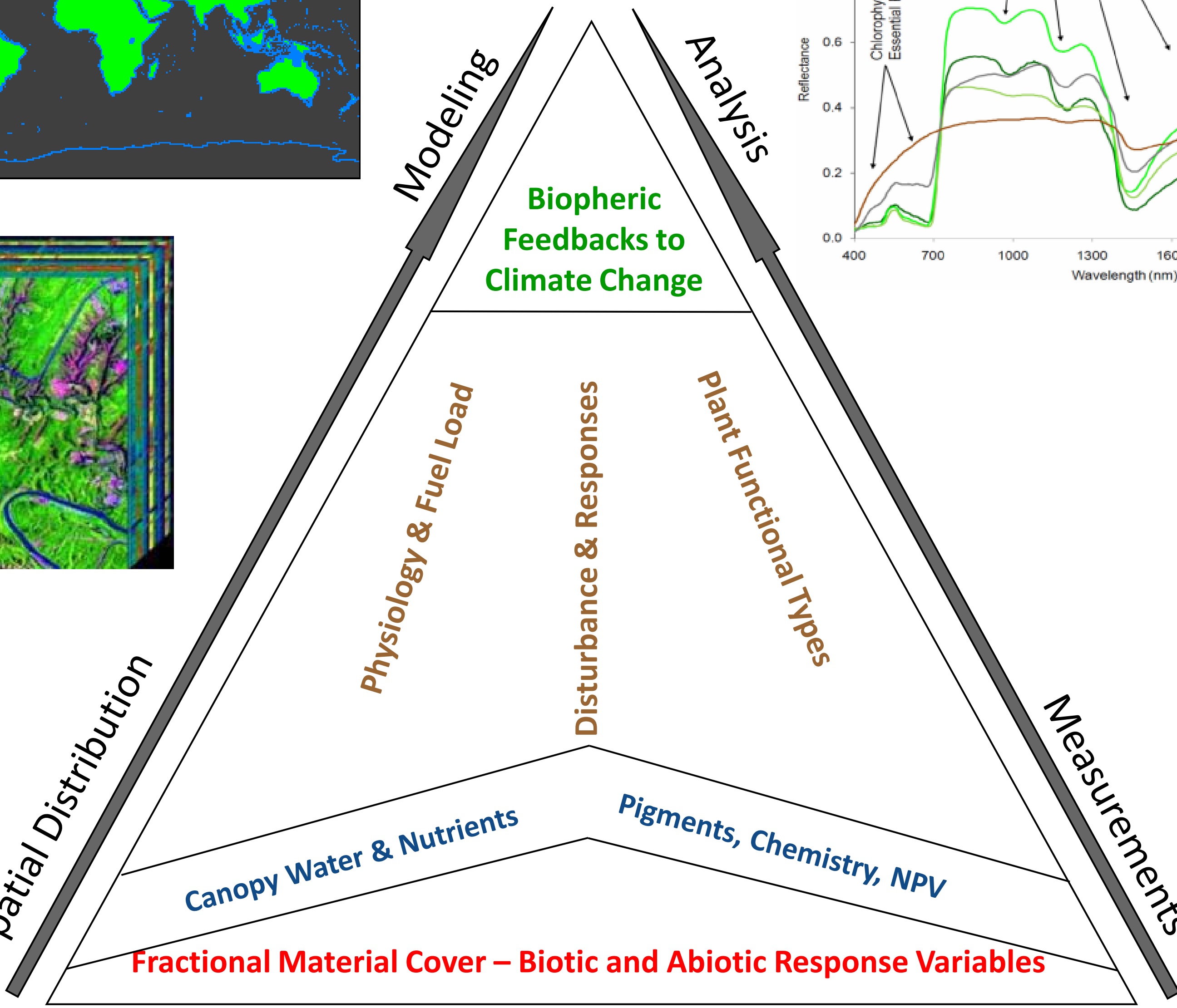

Three top land models serving as the lower boundary for GCM work

Major Model Inputs	**CASA-3D**	**SiB3**	**Ecosystem Demography**
Vegetation Type	General Land Cover	General Land Cover	Prescribed
Plant Functional Types	Prescribed	Prescribed	Prescribed
Fractional Carbon Cover	---	---	---
Vegetation Greenness	NDVI	NDVI	NDVI
Fractional PAR Absorption	NDVI	NDVI	NDVI
Leaf Area Index (0-4 LAI units)	NDVI	NDVI	NDVI
Leaf Area Index (4-10 LAI units)	---	---	---
Canopy Gap Frequency and Size	Prescribed	---	Prescribed
Light-use Efficiency (leaf water, N)	Prescribed	Prescribed	Prescribed
Live vs. Senescent Biomass	---	---	Prescribed
Woody vs. Leaf Biomass	Prescribed	Prescribed	Prescribed
Canopy Allometry	Prescribed	Prescribed	Prescribed
Disturbance Type and Intensity	Landsat-SMA	---	Prescribed

Improvements with HyspIRI

Major Model Inputs	CASA	SiB3	Ecosystem Demography
Vegetation Type	HyspIRI	HyspIRI	HyspIRI
Plant Functional Types	HyspIRI	HyspIRI	HyspIRI
Fractional Carbon Cover	HyspIRI	HyspIRI	HyspIRI
Vegetation Greenness	HyspIRI	HyspIRI	HyspIRI
Fractional PAR Absorption	HyspIRI	HyspIRI	HyspIRI
Leaf Area Index (0-4 LAI units)	HyspIRI	HyspIRI	HyspIRI
Leaf Area Index (4-10 LAI units)	HyspIRI	HyspIRI	HyspIRI
Canopy Gap Frequency and Size	HyspIRI	HyspIRI	HyspIRI
Light-use Efficiency (leaf water, N)	HyspIRI	HyspIRI	HyspIRI
Live vs. Senescent Biomass	DesdynI	DesdynI	DesdynI
Woody vs. Leaf Biomass	DesdynI	DesdynI	DesdynI
Canopy Allometry	Prescribed	Prescribed	Prescribed
Disturbance Type and Intensity	HyspIRI	HyspIRI	HyspIRI

Final Notes

- We need to articulate the precise reasons HyspIRI is a highly relevant climate mission.

- The biospheric feedback (on land and in the sea) is central to understanding current climate and especially to predicting future climate.

- The cryospheric feedback is also critical at a very fundamental level to climate prediction.

- HyspIRI is the only global mission that can serve these and other climate-relevant observations.

Acknowledgements

Amazonia: LBA colleagues

Hawaii: Tom Giambelluca, Sharon Hall, Robin Martin, Peter Vitousek

Cryosphere: Tom Painter

Remote sensing: AVIRIS, Hyperion and HyspIRI teams

Funding: NASA Terrestrial Ecology/Biodiversity, MacArthur Foundation, Moore Foundation

HyspIRI Measurement of Fire Parameters for Climate Change and Carbon Budgets: Fuel, Occurrence, Intensity and Recovery

Louis Giglio (University of Maryland)
*Ivan Csiszar (NOAA/NESDIS)
Wilfrid Schroeder (University of Maryland)
Many others (noted on slides)

August 2010

*presenter

Need for improved global and regional fire monitoring – in plain language

- Societal issues
  - long-term or permanent land cover changes
  - significant contribution to greenhouse gas and particulate emissions
  - smoke from fires is a major health hazard
  - human-fire-climate interactions

- Scientific Issues
  - need to be able to monitor fires and their impacts
  - what vegetation burned
  - how intense and severe was the burning was
  - how much material was emitted into the atmosphere
  - process of vegetation recovery over the burned areas
  - carbon exchange between the land surface and the atmosphere

Needs from the management community – an example

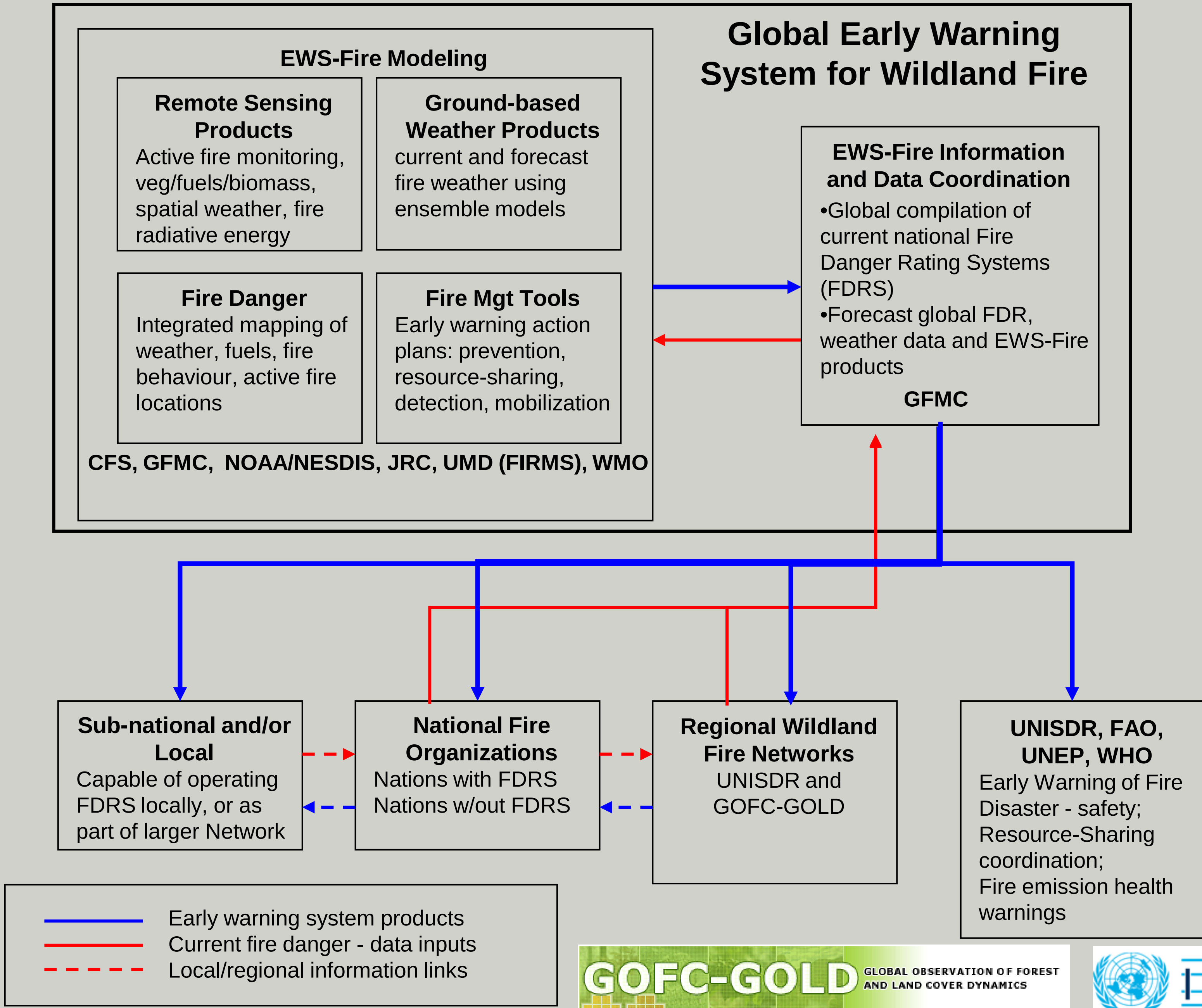

GOFC-GOLD GLOBAL OBSERVATION OF FOREST AND LAND COVER DYNAMICS

ISDR

CSIRO PUBLISHING

Review

www.publish.csiro.au/journals/ijwf

International Journal of Wildland Fire **2009**, *18*, 483–507

Implications of changing climate for global wildland fire

Mike D. Flannigan[A,C], *Meg A. Krawchuk*[B], *William J. de Groot*[A],
B. Mike Wotton[A] *and Lynn M. Gowman*[A]

[A]Natural Resources Canada, Canadian Forest Service, Great Lakes Forestry Centre, 1219 Queen Street-East, Sault Ste. Marie, ON, P6A 2E5, Canada.
[B]University of California, Berkeley, Department of Environmental Science, Policy and Management, 335 Mulford Hall, Berkeley, CA 94720, USA.
[C]Corresponding author. Email: mike.flannigan@nrcan.gc.ca

Abstract. Wildland fire is a global phenomenon, and a result of interactions between climate–weather, fuels and people. Our climate is changing rapidly primarily through the release of greenhouse gases that may have profound and possibly unexpected impacts on global fire activity. The present paper reviews the current understanding of what the future may bring with respect to wildland fire and discusses future options for research and management. To date, research suggests a general increase in area burned and fire occurrence but there is a lot of spatial variability, with some areas of no change or even decreases in area burned and occurrence. Fire seasons are lengthening for temperate and boreal regions and this trend should continue in a warmer world. Future trends of fire severity and intensity are difficult to determine owing to the complex and non-linear interactions between weather, vegetation and people. Improved fire data are required along with continued global studies that dynamically include weather, vegetation, people, and other disturbances. Lastly, we need more research on the role of policy, practices and human behaviour because most of the global fire activity is directly attributable to people.

Needs from the fire and climate community – an example

Flannigan et al., 2009

"To date, research suggests a <u>general increase in area burned and fire occurrence</u> but there is a <u>lot of spatial variability</u>, with some areas of no change or even decreases in area burned and occurrence. <u>Fire seasons are lengthening for temperate and boreal regions</u> and this trend should continue in a warmer world. Future trends of fire severity and intensity are difficult to determine owing to the <u>complex and non-linear interactions between weather, vegetation and people</u>. <u>Improved fire data are required</u> along with continued global studies that dynamically include <u>weather, vegetation, people, and other disturbances.</u> Lastly, we need more research on the role of <u>policy, practices and human behavior</u> because most of the global fire activity is directly attributable to people."

Changing fire regimes – complex interactions between climate and society

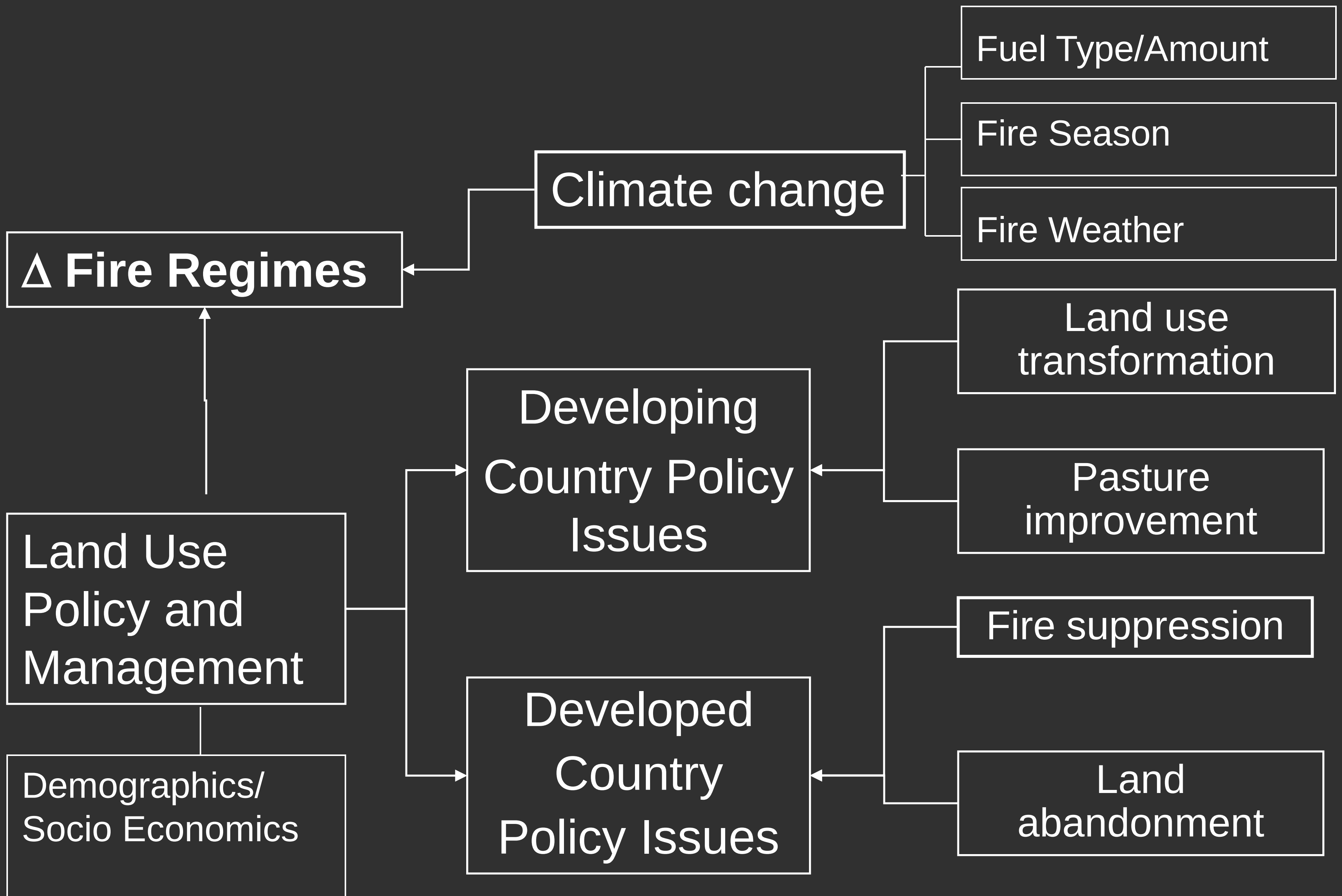

TQ2. Wildfires

- How are global fire regimes changing in response to, and driven by, changing climate, vegetation, and land use practices? [DS 198]
- Is regional and local scale fire frequency changing? [DS 196]
- What is the role of fire in global biogeochemical cycling, particularly trace gas emissions? [DS 195]
- Are there regional feedbacks between fire and climate change?

CQ2. Wildfires

- How does the timing, temperature and frequency of fires affect long-term ecosystem health?
- How does vegetation composition and fire temperature impact trace gas emissions?
- How do fires in coastal biomes affect terrestrial biogeochemical fluxes into estuarine and coastal waters and what is the subsequent biological response? [DS 198]
- What are the feedbacks between fire temperature and frequency and vegetation composition and recovery?
- How does vegetation composition influence wildfire severity?
- On a watershed scale, what is the relationship of vegetation cover, soil type, and slope to frequency of debris flows?
- How does invasive vegetation cope with fire in comparison to native species?

HyspIRI and fire – unprecedented measurement capabilities

- Pre-fire fuel properties, fire weather
  - fuel types, fuel loads
  - live fuel moisture, vegetation stress etc.
  - surface temperature, ET

A prime example for the complementarities between HyspIRI and DESDynI !

- Detection/characterization of the combustion process
  - improved fire characterization
  - improved characterization of smoke emission

- Post-fire impacts
  - fire affected area
  - burn severity
  - amount of material burned
  - hydrophobicity
  - types of ash
  - land cover change
  - nutrient transport

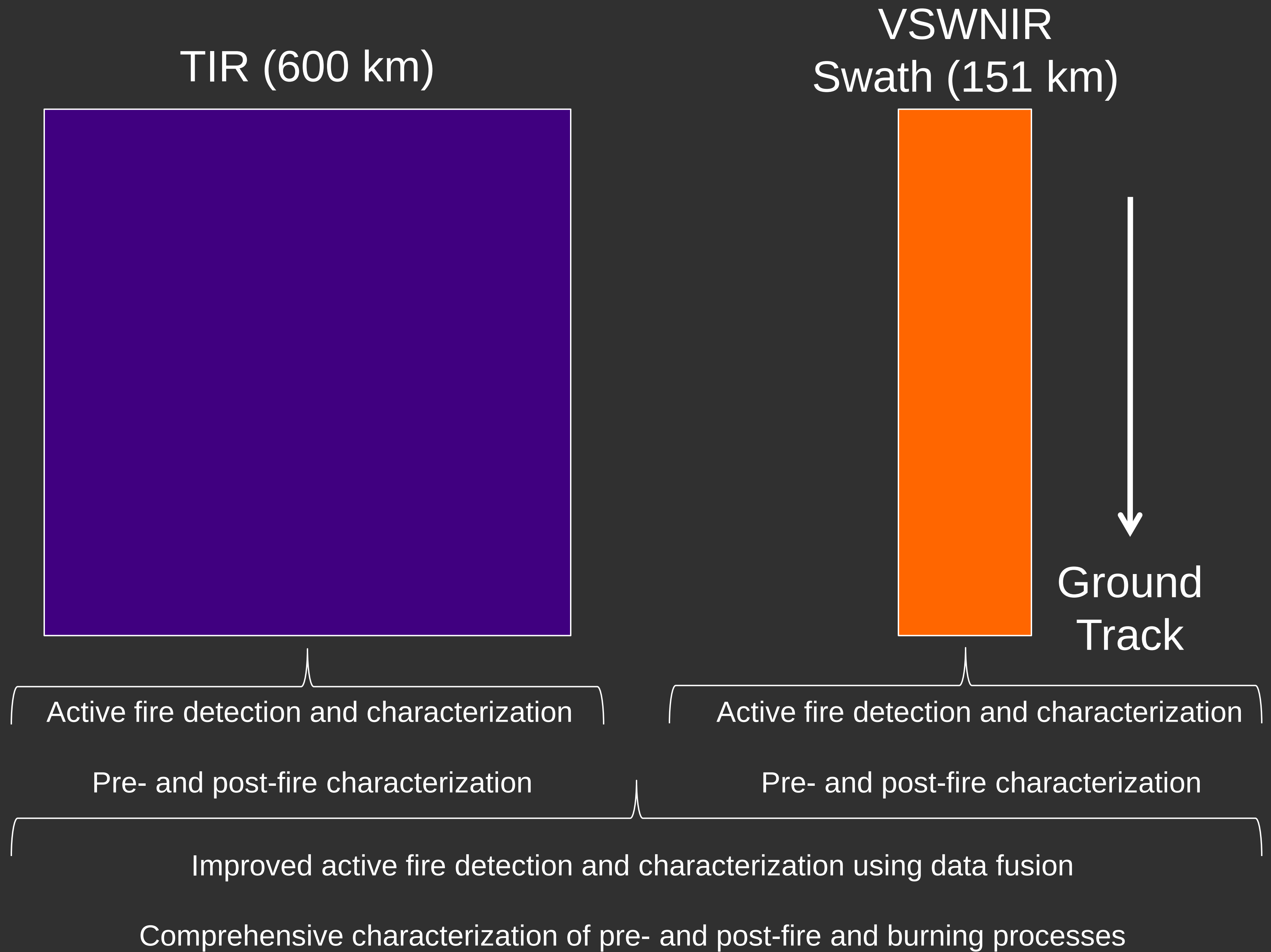
TIR (600 km)
VSWNIR
Swath (151 km)
Ground
Track
Active fire detection and characterization
Active fire detection and characterization
Pre- and post-fire characterization
Pre- and post-fire characterization
Improved active fire detection and characterization using data fusion
Comprehensive characterization of pre- and post-fire and burning processes

Fire Disturbance is an Essential Climate Variable (ECV) of the Global Climate Observing System (GCOS)

For climate-related science questions:

decades-long time series

coarse resolution fire observations
(MODIS, VIIRS, etc.)

+

better understand observations and processes

high resolution fire & fuel observations

HyspIRI

start of a new, improved data record?

Current and expected capabilities from medium an coarse resolution sensors

- Long-term monitoring of large-scale fire dynamics from medium and coarse resolution sensors
  - fire occurrence
  - Fire Radiative Power and Energy
  - burned areas
- Gradual improvement, but no quantum leap is expected from operational systems

Global fire dynamics from MODIS

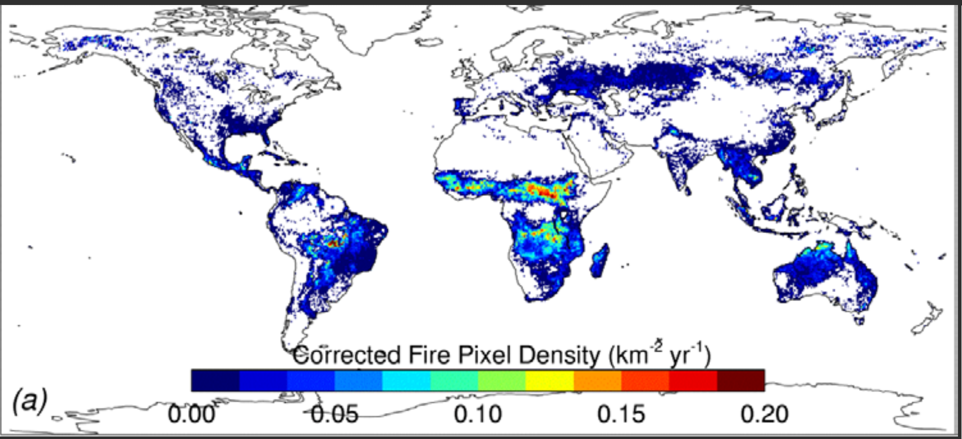

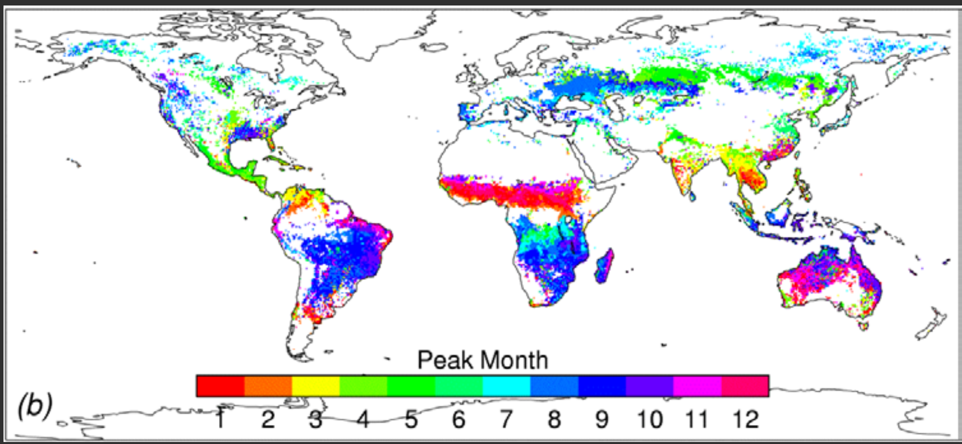

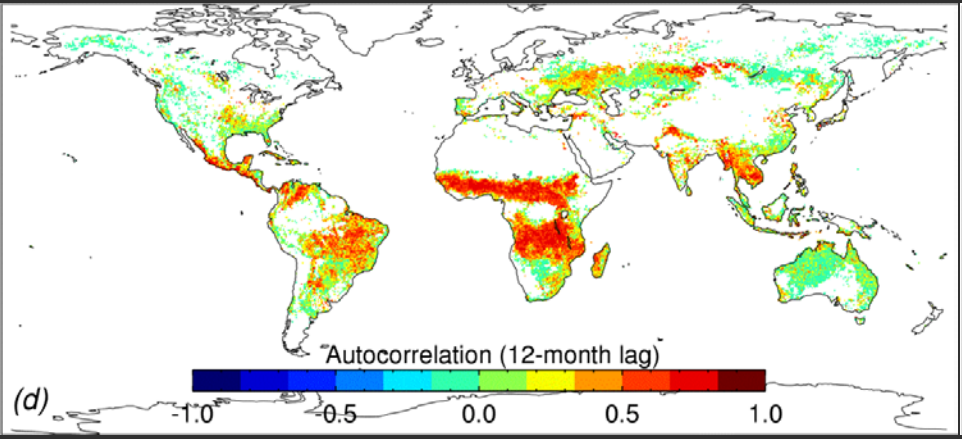

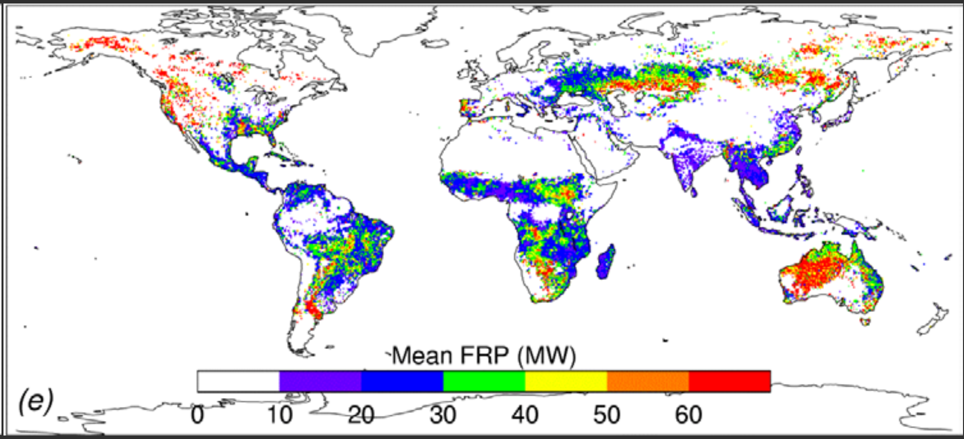

Continuity of Polar Operational Satellite Programs

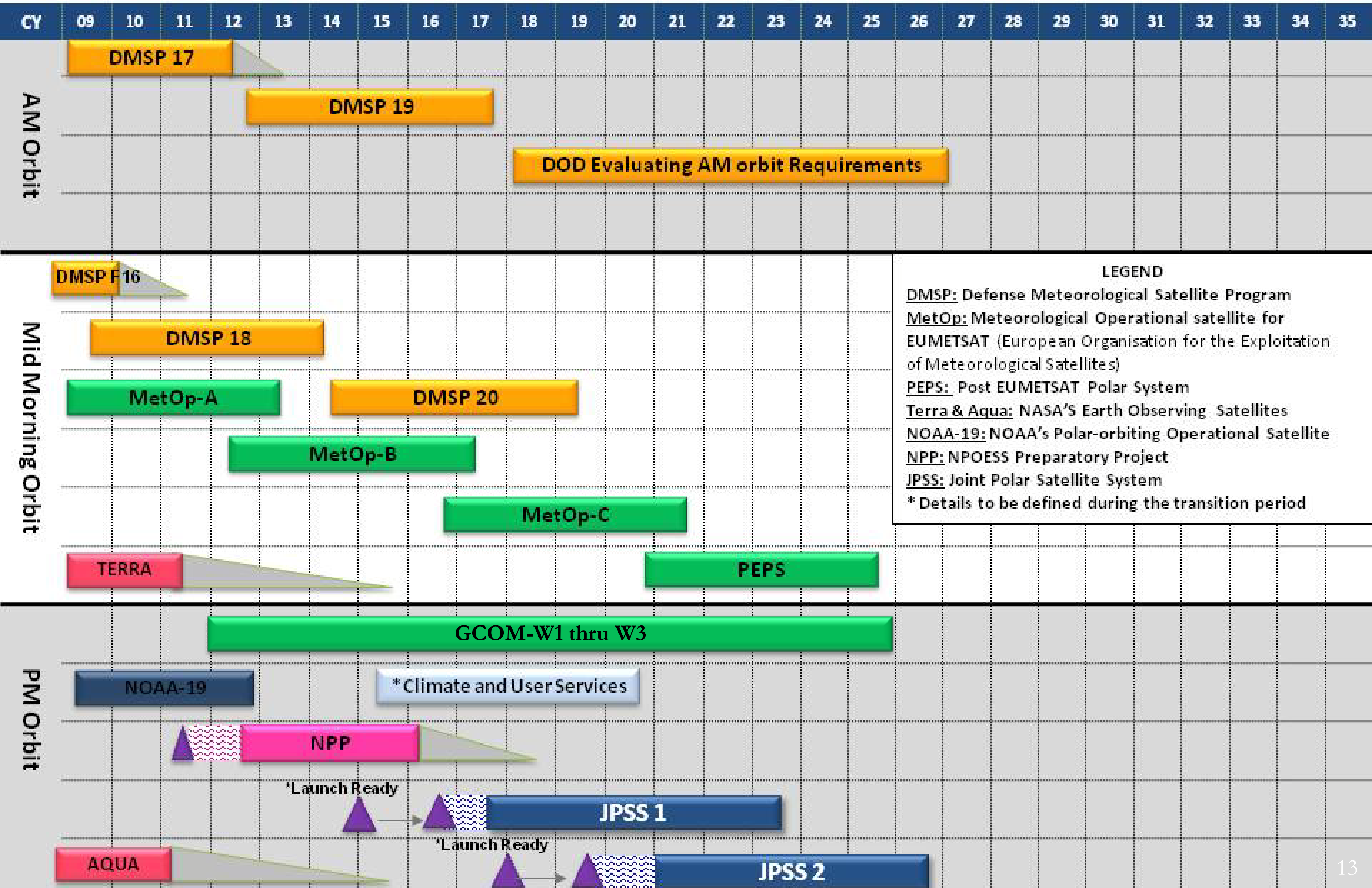

Fire occurrence in South America from GOES data (JAS)

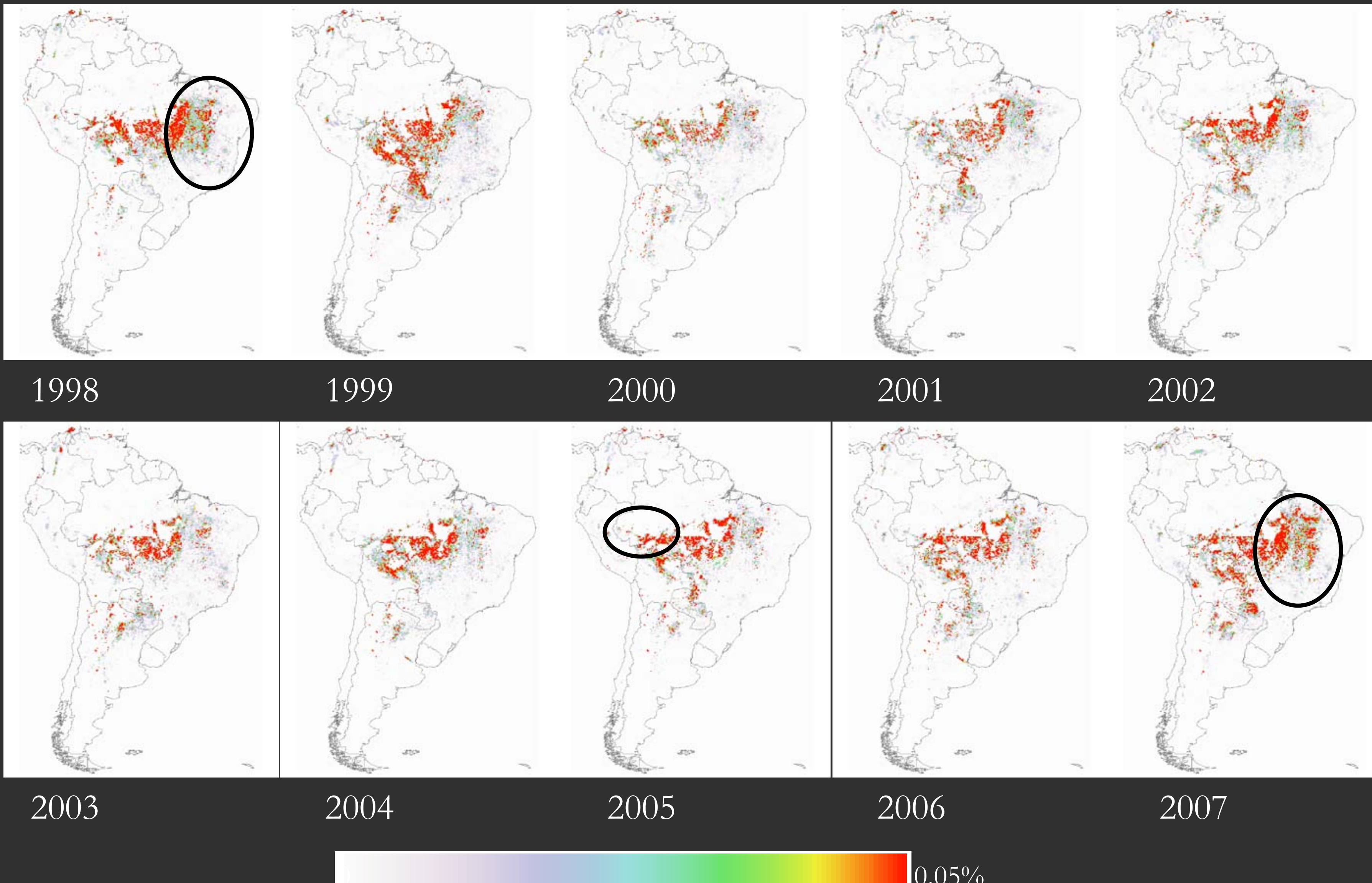

Global Geostationary Active Fire Monitoring Capabilities

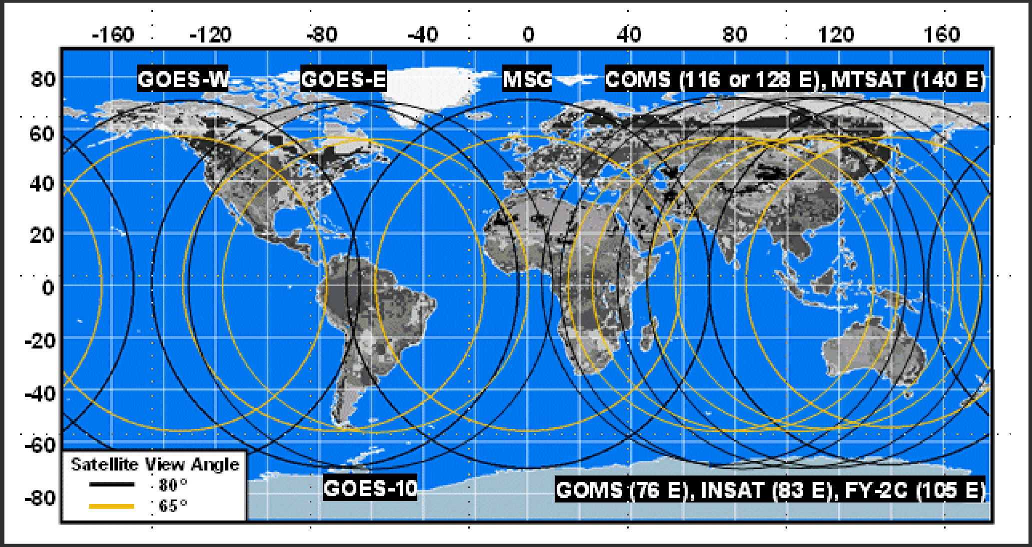

Satellite View Angle
80°
65°

Satellite	Active Fire Spectral Bands	Resolution IGFOV (km)	SSR (km)	Full Disk Coverage	3.9 µm Saturation Temperature (K)	Minimum Fire Size at Equator (at 750 K) (hectares)
GOES-E/-W Imager (75°W / 135°W)	1 visible 3.9 and 10.7 µm	1.0 4.0	0.57 2.3	3 hours (30 min NHE and SHE)	>335 K (G-11) >335 K (G-12)	0.15
GOES-10 Imager (60°W) (Ceased operation December 2009, replaced with GOES-12 in May 2010)	1 visible 3.9 and 10.7 µm	1.0 4.0	0.57 2.3	3 hours (Full Disk) 15 min (SA)	~322 K (G-10) >335 K (G-12)	0.15
Met-8/-9 SEVIRI (9.5 °E, 0°)	1 HRV 2 visible 1.6, 3.9 and 10.8 µm	1.6 4.8 4.8	1.0 3.0 3.0	15 minutes	~335 K	0.22
FY-2C/2D SVISSR (105 °E / 86.5°E)	1 visible, 3.75 and 10.8 µm	1.25 5.0		30 minutes	~330 K	
MTSAT-1R JAMI (140°E) MTSAT-2 (HRIT) (145°E) Operational 2010	1 visible 3.7 and 10.8 µm	1.0 4.0		1 hour	~320 K (MTSAT-1R) ~320 K (MTSAT-2)	0.15
INSAT-3D (83 °E ?, TBD) (Launch 2010)	1 vis, 1.6 µm 3.9 and 10.7 µm	1.0 4.0	0.57 2.3	30 minutes	?	
GOMS Elektro-L N1 (76 °E) (2010) GOMS Elektro-L N2 (14.5 °E) (2011?)	3 visible 1.6, 3.75 and 10.7 µm	1.0 km 4.0 km		30 minutes	?	
COMS (128 °E) (Launch 2010)	1 visible 3.9 and 10.7 µm	1.0 km 4.0 km		30 minutes	~350 K	

Evolving MIR/TIR fire detection capability

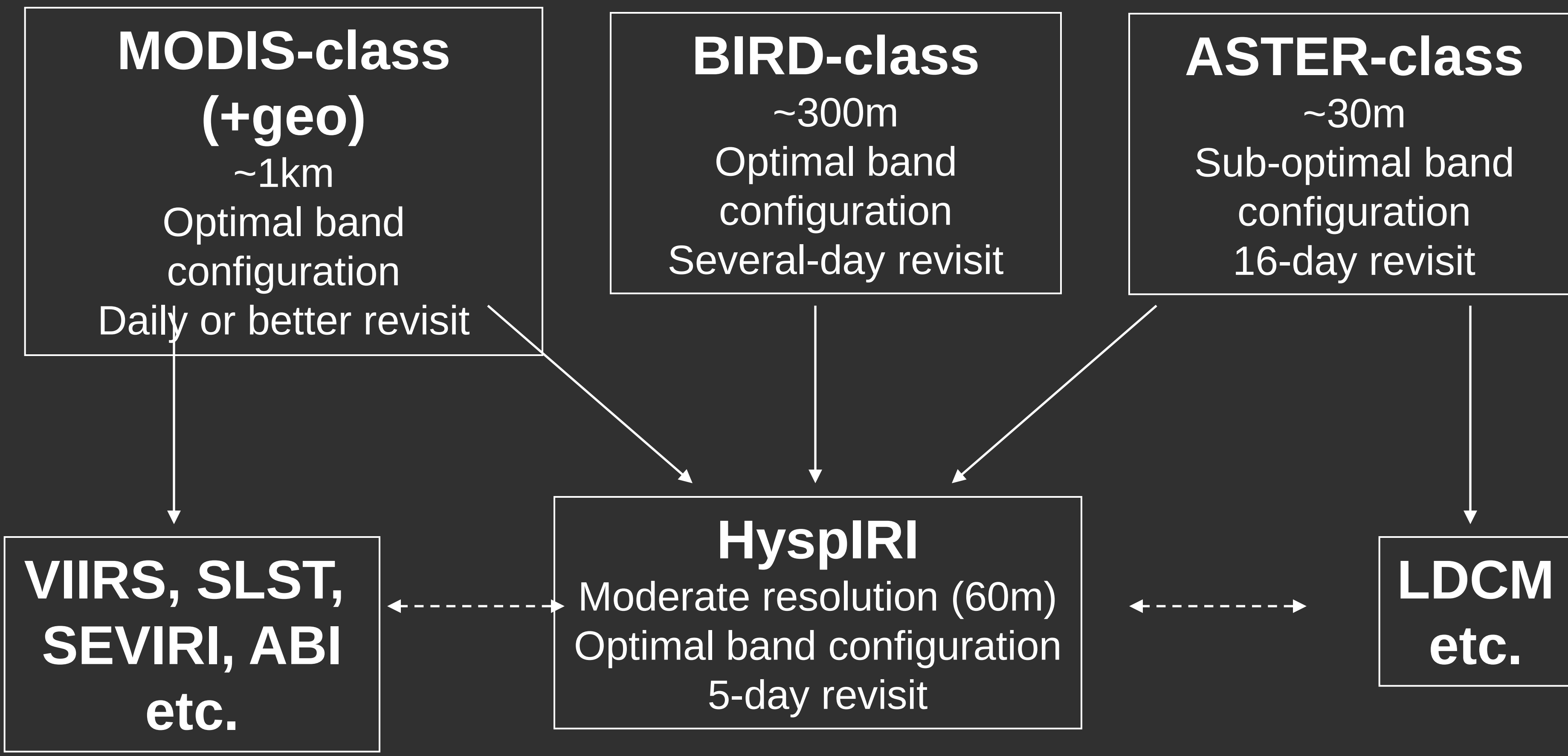

Detection envelopes

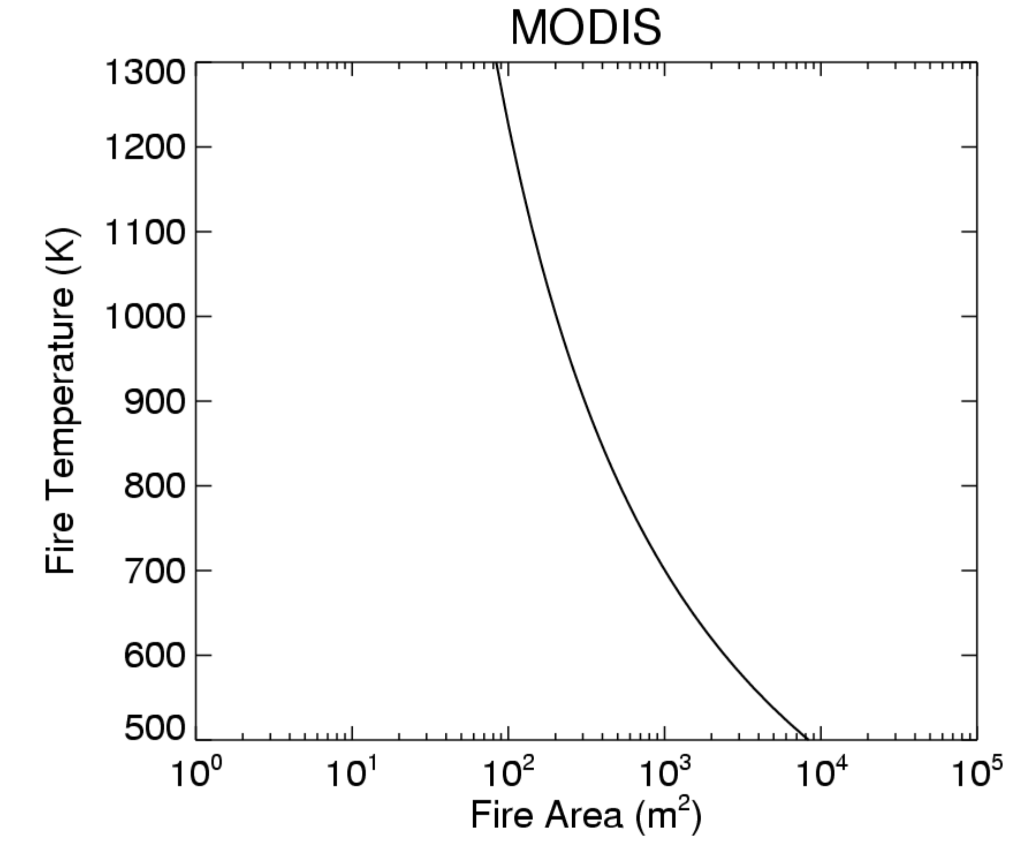

1000 m

90% probability of detection; boreal forest; nadir view

L. Giglio

Detection envelopes

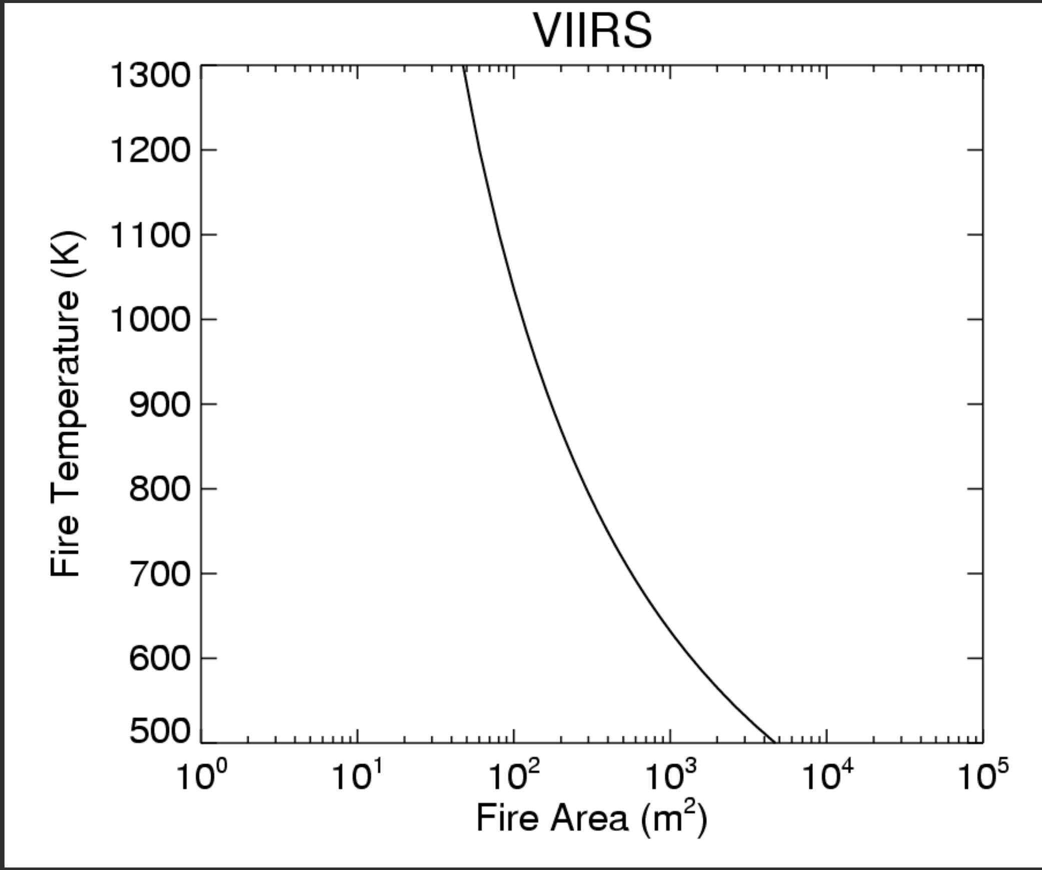

750 m

90% probability of detection; boreal forest; nadir view

L. Giglio

Detection envelopes

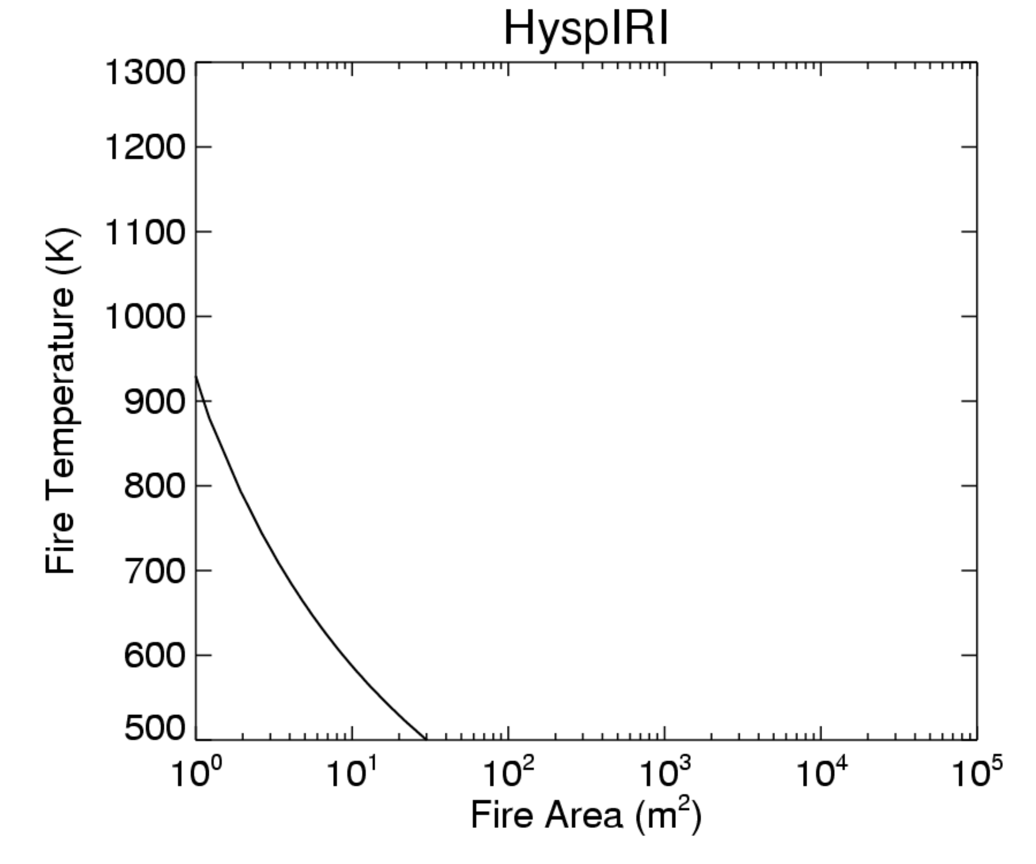

60 m

90% probability of detection; boreal forest; nadir view

L. Giglio

HyspIRI: a changing paradigm

- MODIS-class: multiple sub-pixel fires within footprint, systematic, global observations
  - "fire" often means a fire pixel

- ASTER: detect (but characterize only over a limited range) individual fires on an opportunistic basis
  - cluster size, spatial variability

- HyspIRI: detect and characterize individual fires on a more routine basis
  - cluster size, fire temperature, spatial and temporal variability, size distribution, flaming/smoldering
  - helps us understand what is within the coarse or moderate resolution fire pixel

Global fire emission estimate: 2004

Biomass burning and fossil fuel emissions release ~10^{15} g of carbon (C) to the atmosphere each year. Biomass burning constitutes <u>~36%</u> of all global C emissions.

Region	Fire emissions 1997-2001 average (10^15g C yr^{-1})
Central and northern South America	0.27
Southern South America	0.80
Northern Africa	0.80
Southern Africa	1.02
Southeast Asia	0.37
Boreal (north of 38ºN)	0.14
Other	0.13
Global	3.53

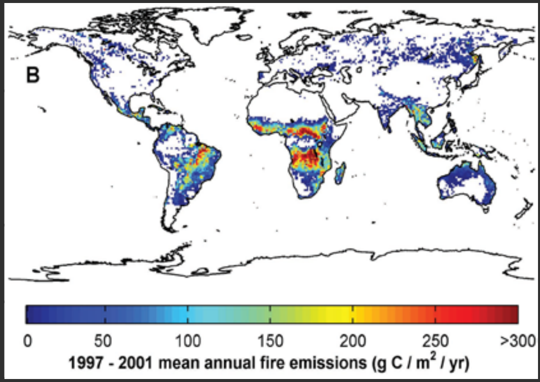

Van der Werf et al., 2004

Global fire emission estimate: 2010

Biomass burning and fossil fuel emissions release ~10^{15} g of carbon (C) to the atmosphere each year. Biomass burning constitutes <u>~25%</u> of all global C emissions.

Region	Fire emissions 1997-2009 average (10^{15} g C yr^{-1})
Central and northern South America	0.04
Southern South America	0.27
Northern Africa	0.48
Southern Africa	0.27
Southeast Asia	0.04
Boreal (north of 38°N)	0.18
Other	0.73
Global	2.01

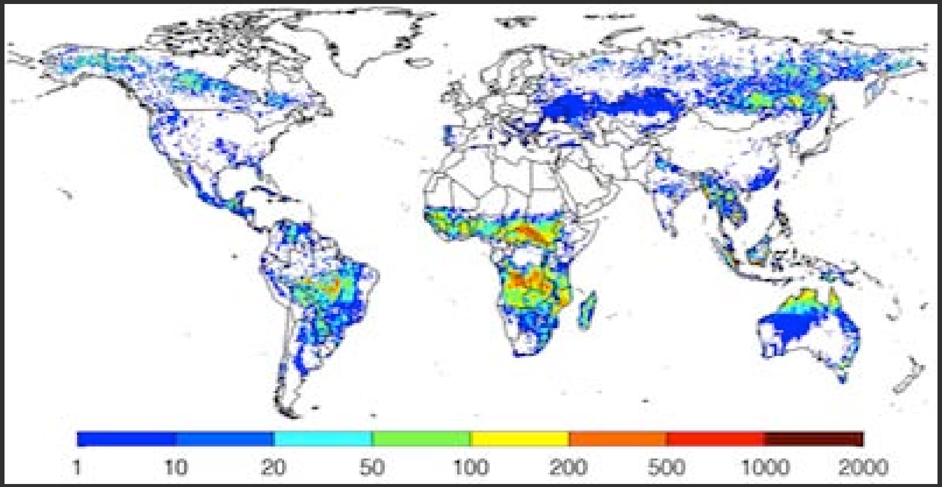

Van der Werf et al., 2010

Where does the difference in emission estimates come from?

- Longer time period (El Niño/La Niña in 1997/98)
- Updated fuel loads – HyspIRI can help further refine this!
  - Peat is important, but difficult!
- Updated burned area estimates
  - HyspIRI can help only where signal is persistent
  - HyspIRI can help over small scale, fragmented burned areas
- HyspIRI can also help better characterize the combustion, consumption and recovery processes

HyspIRI Burn Mapping Product

- Level 3
- Derived from VSWIR observations
  - Potentially use active-fire observations from TIR sensor to improve fidelity
- Generally requires coincident image pair
  - Large number (but small fraction) of global fires
- Sub-pixel area burned, combustion completeness
  - Mixture modeling (heavily underdetermined system for multi-spectral sensors)
  - Important for pyrogenic emissions estimation

Fire Radiative Energy

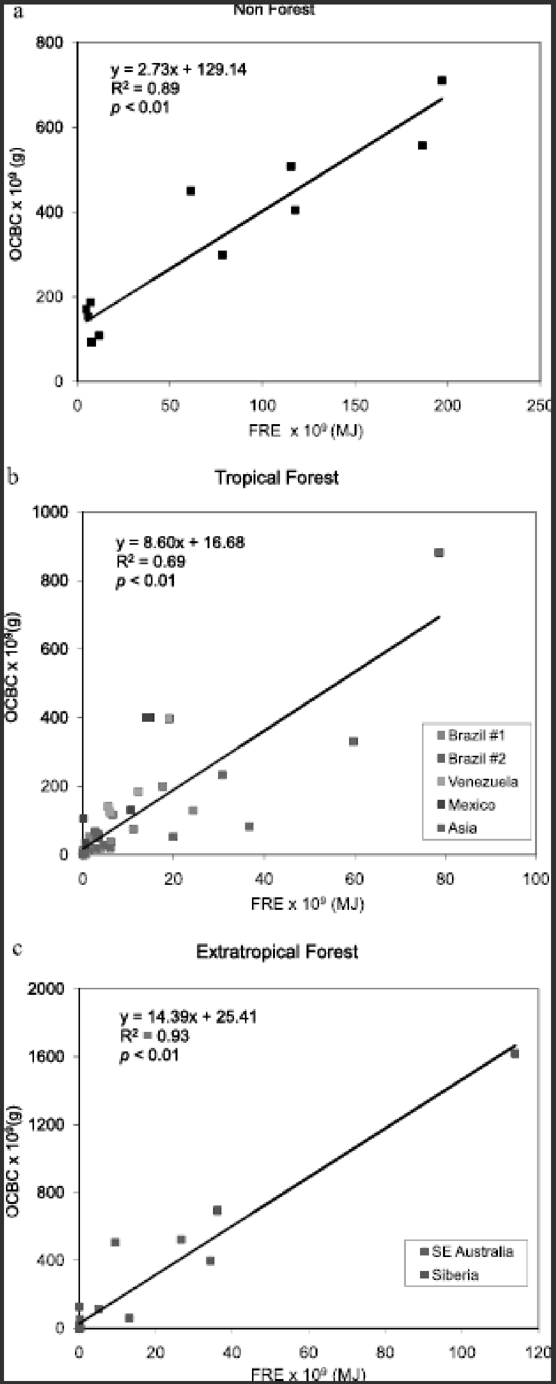

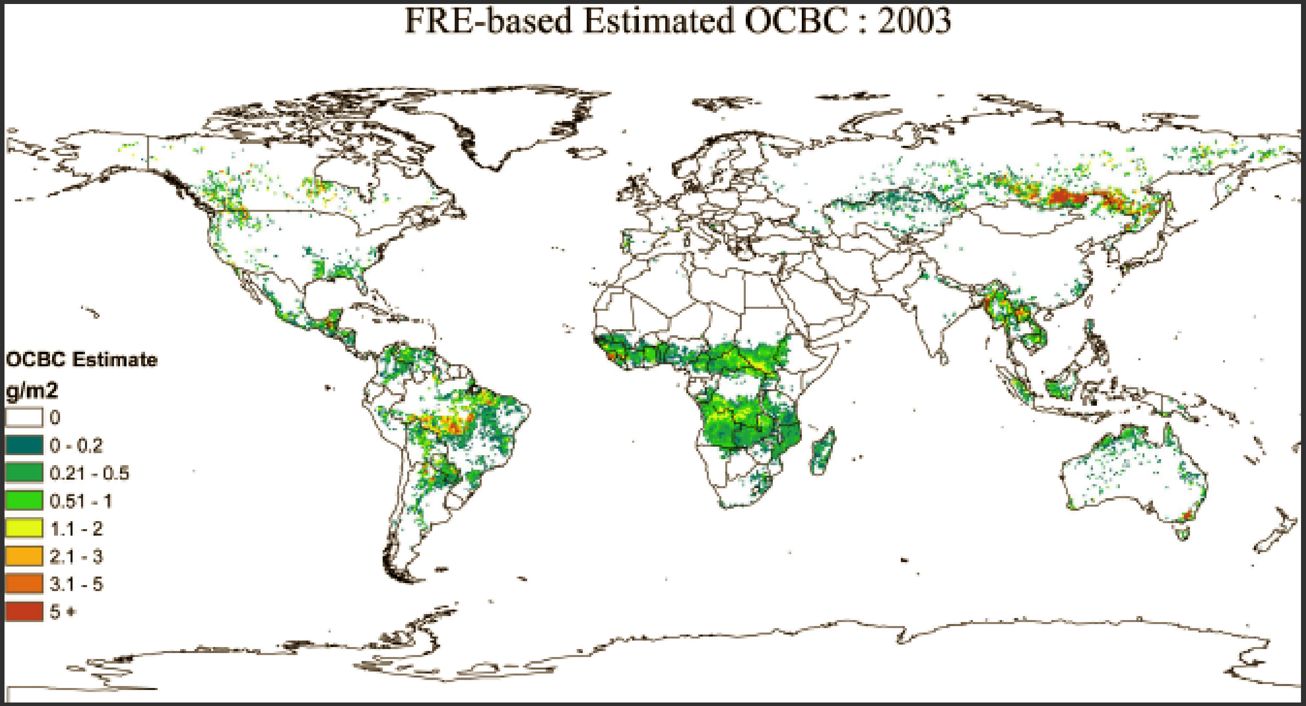

Ellicott et al 2009

HyspIRI Active Fire Product

- Level 2
- Fire mask + fire radiative power (FRP)
  - Produced across 600-km TIR swath
- Improved fire mask + detailed fire characterization
    - Produced within 151-km hyperspectral swath
    - Sub-pixel temperature(s) and area
      - Minimum of flaming + smoldering + background

Example Fire Mask from ASTER

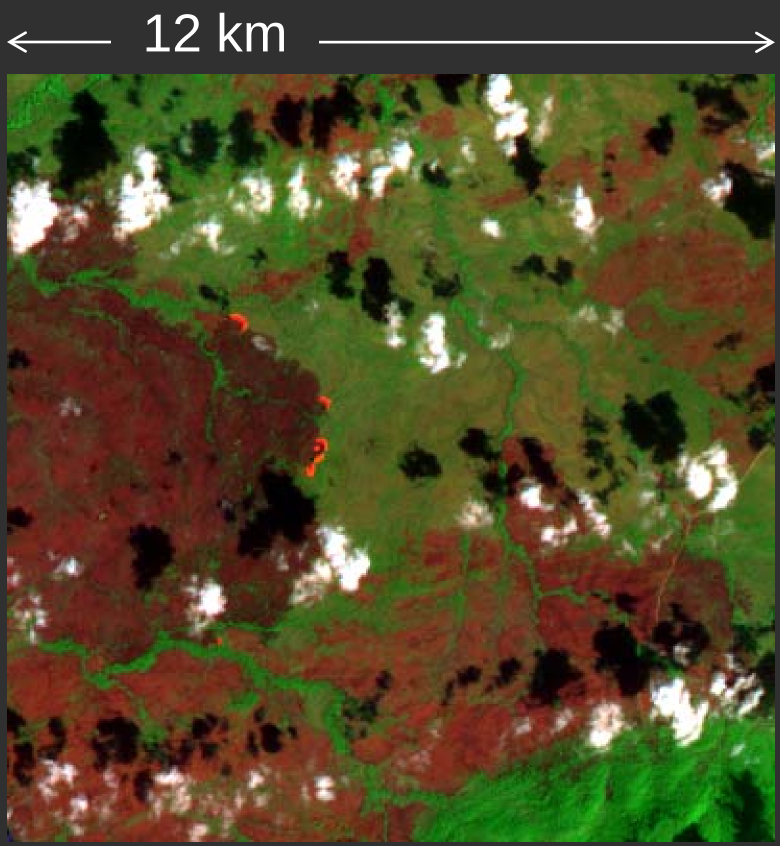

ASTER Bands 8 (2.33 µm), 3N (0.82 µm), 1 (0.56 µm)

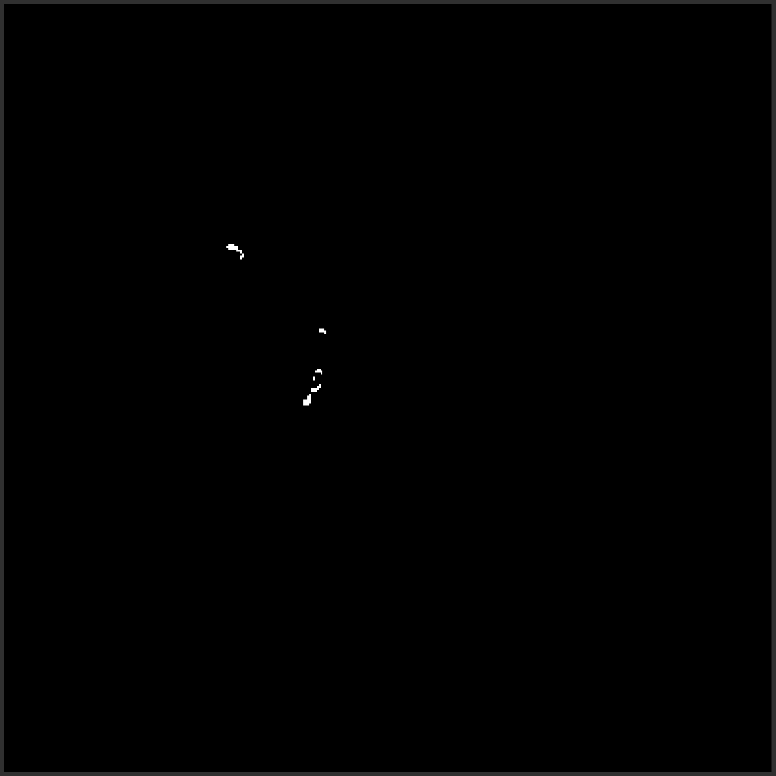

Active Fire Mask

ASTER saturates for many fires – HyspIRI will allow the “coloring” of the fire mask

HyspIRI MWIR Saturation

- Select TIR MWIR dynamic range so that saturation is extremely rare when observing fires
  - valid radiance measurement essential for fire characterization
    - FRP, sub-pixel temperature and area estimates
  - detailed characterization using hyperspectral sensor possible for only 25% of fires detectable with TIR sensor

MWIR Dynamic Range Comparison

- MODIS (1 km pixels): 500 K
  - based on theoretical worst case
- VIIRS (247 m pre.-agg.): 634 K
  - based on theoretical worst case
- BIRD (370 m): 600 K
- GOES-R ABI (2 km): 400 K
- HyspIRI (60 m): TBD

Defining HyspIRI MWIR saturation level - need for regional analysis

- Gao et al. (2007) MODIS Study – statistical analysis
  - Only 0.4% of fire pixels have $T_{\mathrm{MWIR}} > 450$ K
  - Only 1.7% of fire pixels have $T_{\mathrm{MWIR}} > 400$ K
  - For 1-km pixels saturation "*…should be specified at about 450 K or even lower to 400 K in order to make the channels more useful for quantitative remote sensing of fires.*"
- Our own independent analysis shows that from 2003-2009 only 0.02% of all fire pixels saturated MODIS MWIR band 21 (~500K saturation)

Percentage of saturated fire pixels: the Land Surface Temperature analogy

- LST retrieval not possible for saturated land pixels
  - Fire characterization not possible for saturated fire pixels
- Depict Gao et al. (2007) suggested fire-pixel saturation rates as equivalent saturated land surface area confounding hypothetical LST retrieval

1.7% 400 K saturation analog
0.4% 450 K saturation analog
0.02% 500 K saturation analog

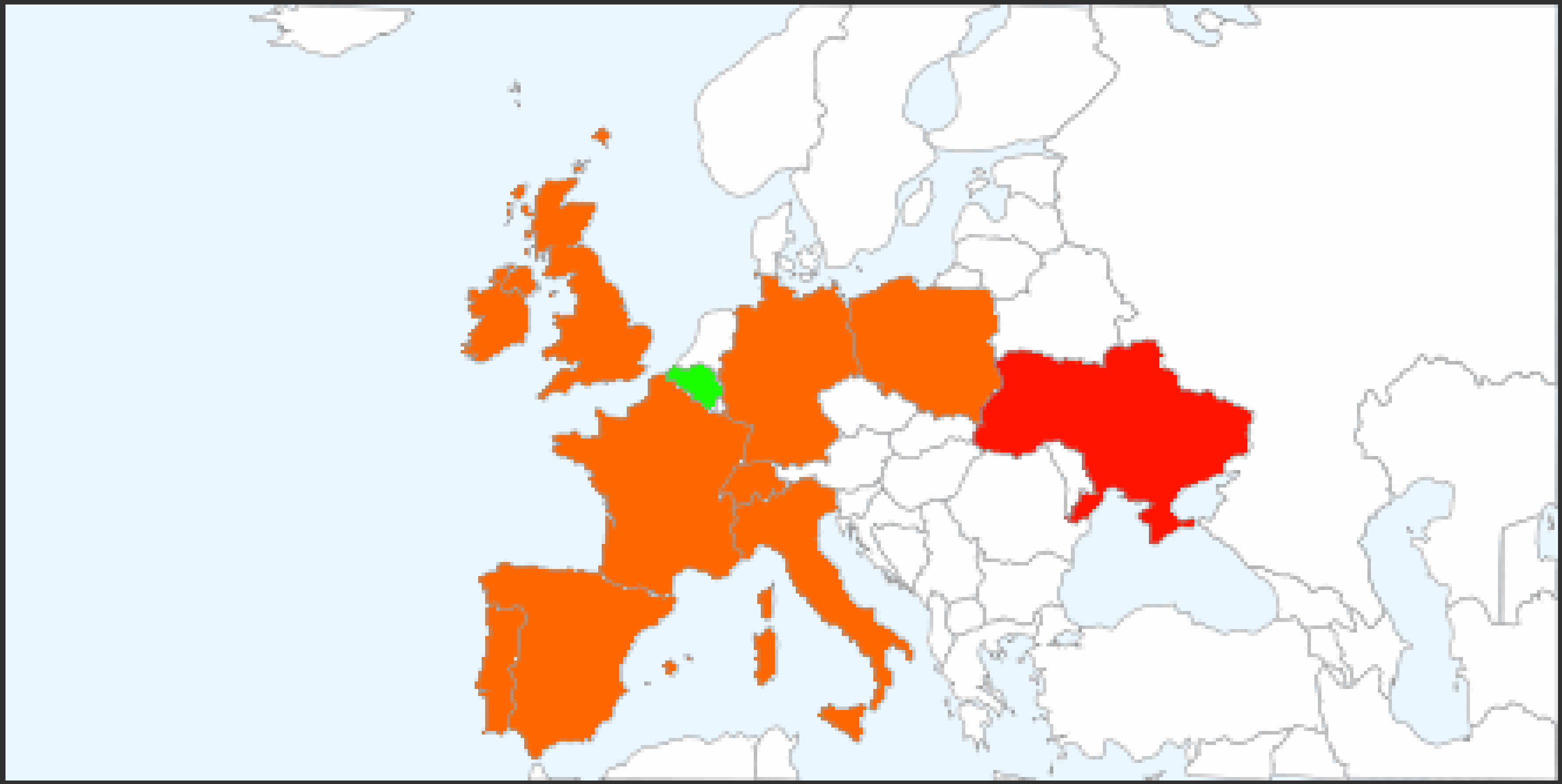

1.7% 400 K saturation analog
0.4% 450 K saturation analog
0.02% 500 K saturation analog

Saturation issues

- What is the expected uncertainty in emission estimates?
- What is the frequency of saturated pixels on a regional basis?
- What are the realistic “extreme” fire characteristics?
  - Up to ~1800K flaming temperature possible for forest (Ward et al., 1992, Lobert et al., 1993)
    - 1200 is a realistic upper end
  - Crown fires on a slope can cover the entire HyspIRI pixel

Fire characteristics in Roraima, Brazil

Maintenance

Conversion

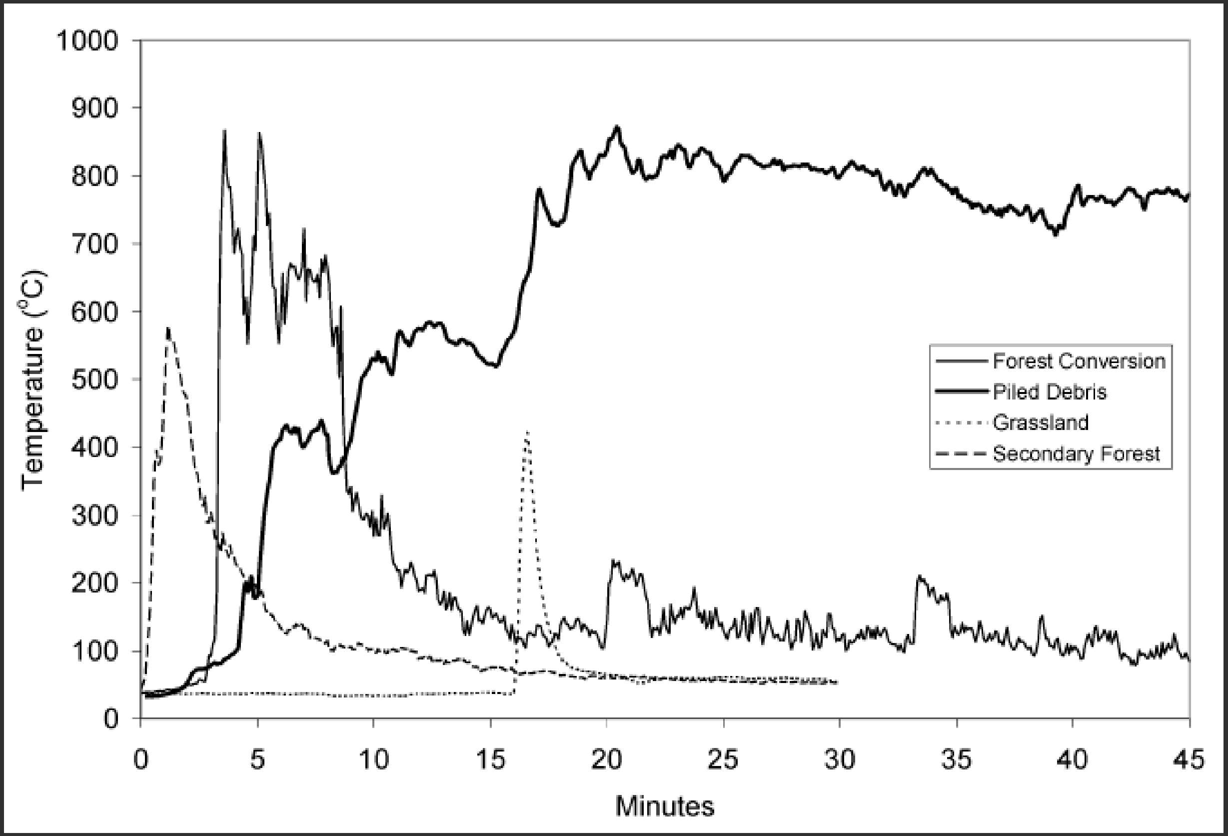

Retrieved Temperature Endmembers

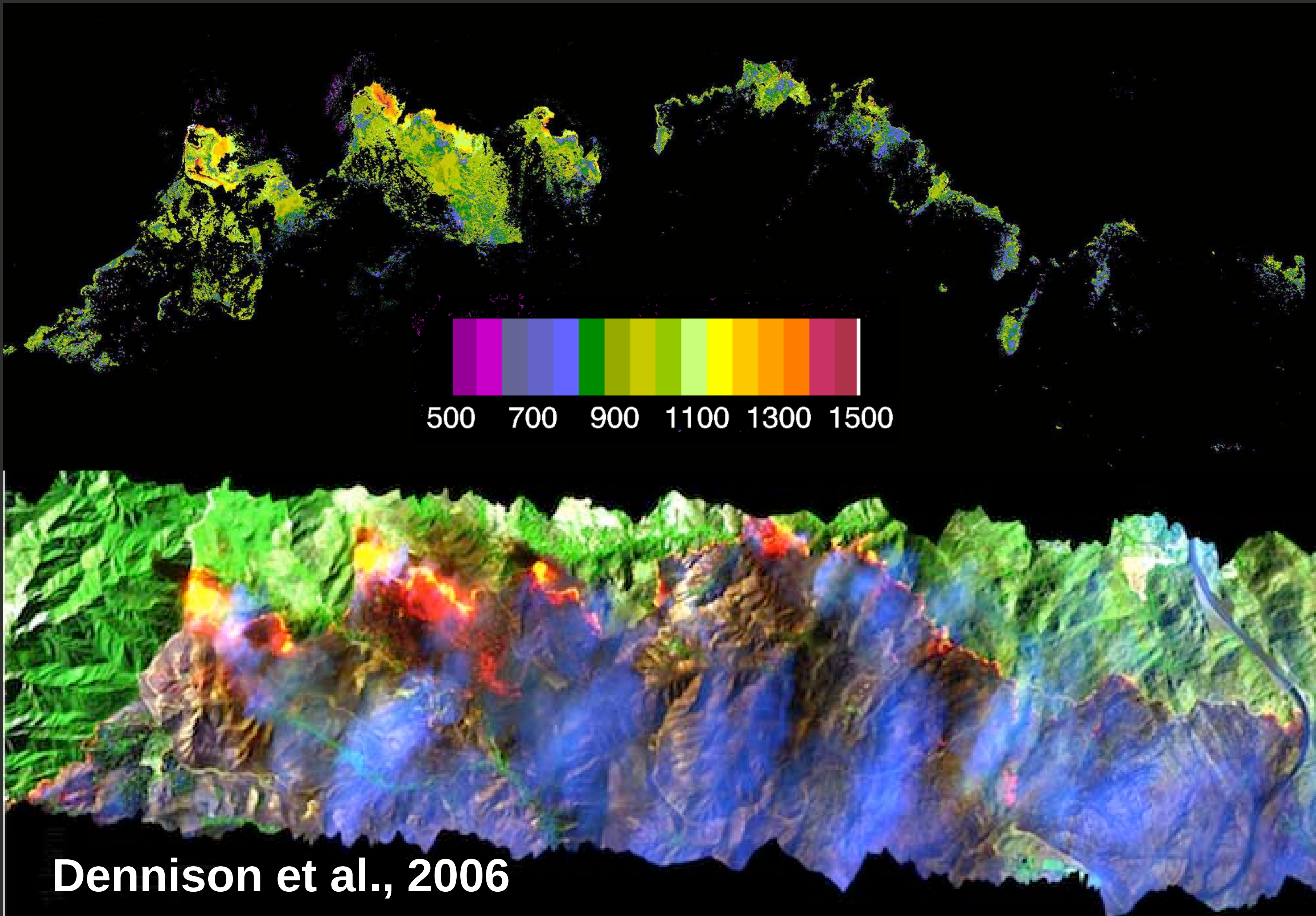

Simulated MWIR brightness temperatures

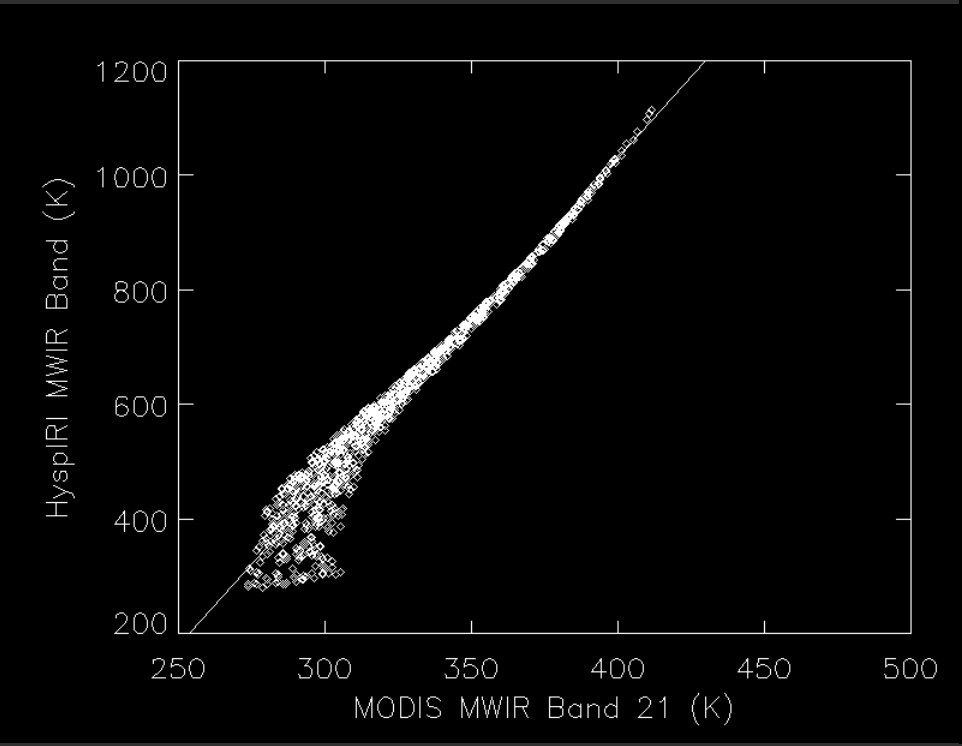

Up to 1200K, up to 100% fractional area within the HyspIRI pixel

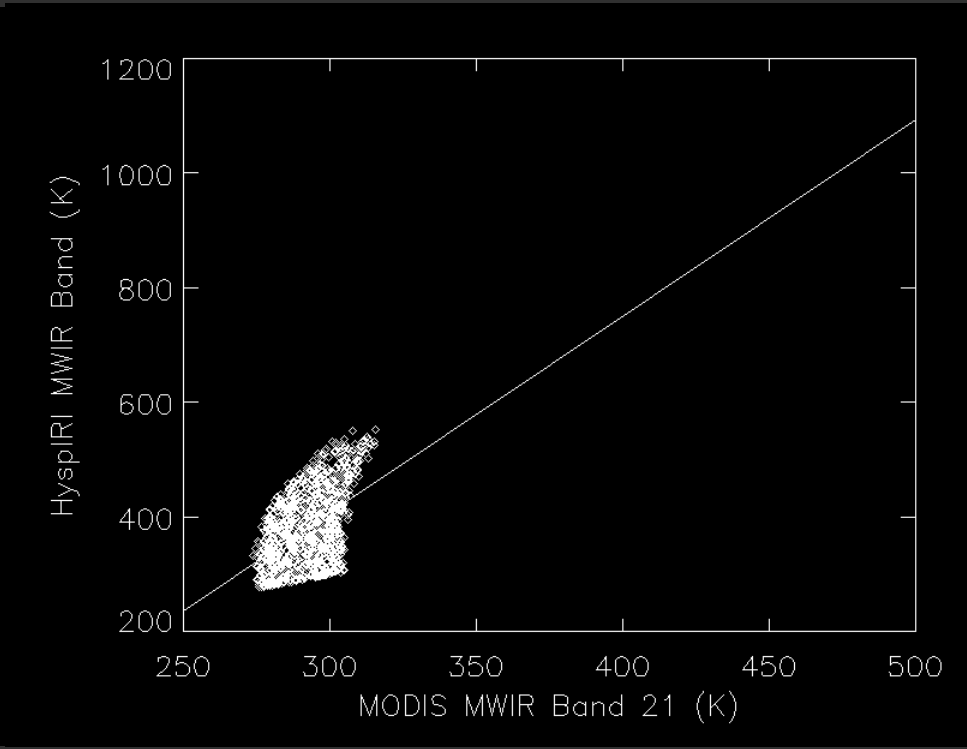

Up to 1200K, up to 20% fractional area within the HyspIRI pixel

Global dataset of ASTER fire masks

- Use of equidistant grid (circular - 900km diameter)
  - 642 cells
  - ~370 over land
  - ~210 in areas with some fire activity (deserts and poles automatically excluded in the process)
- Six years of data represented
  - 2001-2002; 2003-2004; 2005-2006
  - ASTER SWIR data quality issues beginning May 2007
- ~2500 ASTER scenes selected
  - 4 scenes for each grid cell - 2 year period
  - up to 3 scenes represensing highest number of MOD14 fire pixels
  - at least one random scene per cell/period containing fire, no fire, water, clouds, etc.
  - 140 nighttime scenes

$\Longrightarrow$ 16K daytime MOD14 fire pixels sampled

$\Longrightarrow$ 700 nighttime MOD14 fire pixels sampled

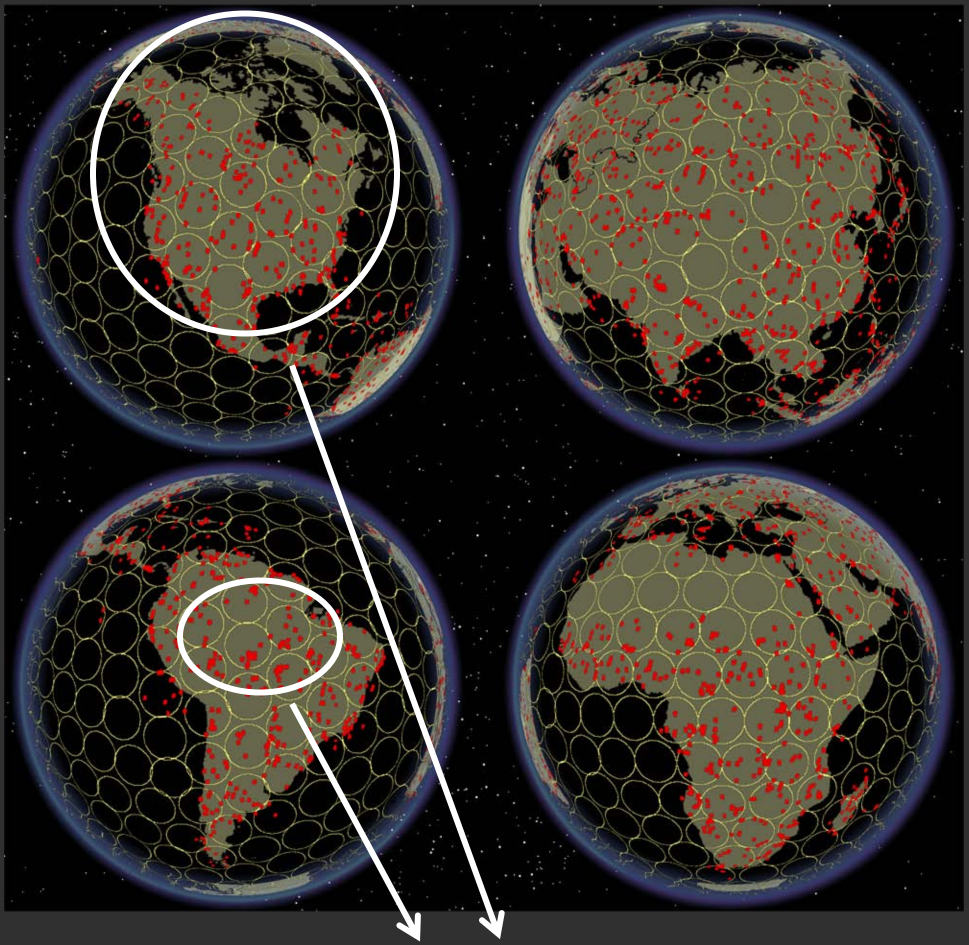

~30% of fire clusters consist of more than 10 ASTER fire pixels

The Case of Central Mato Grosso State in Brazilian Amazonia

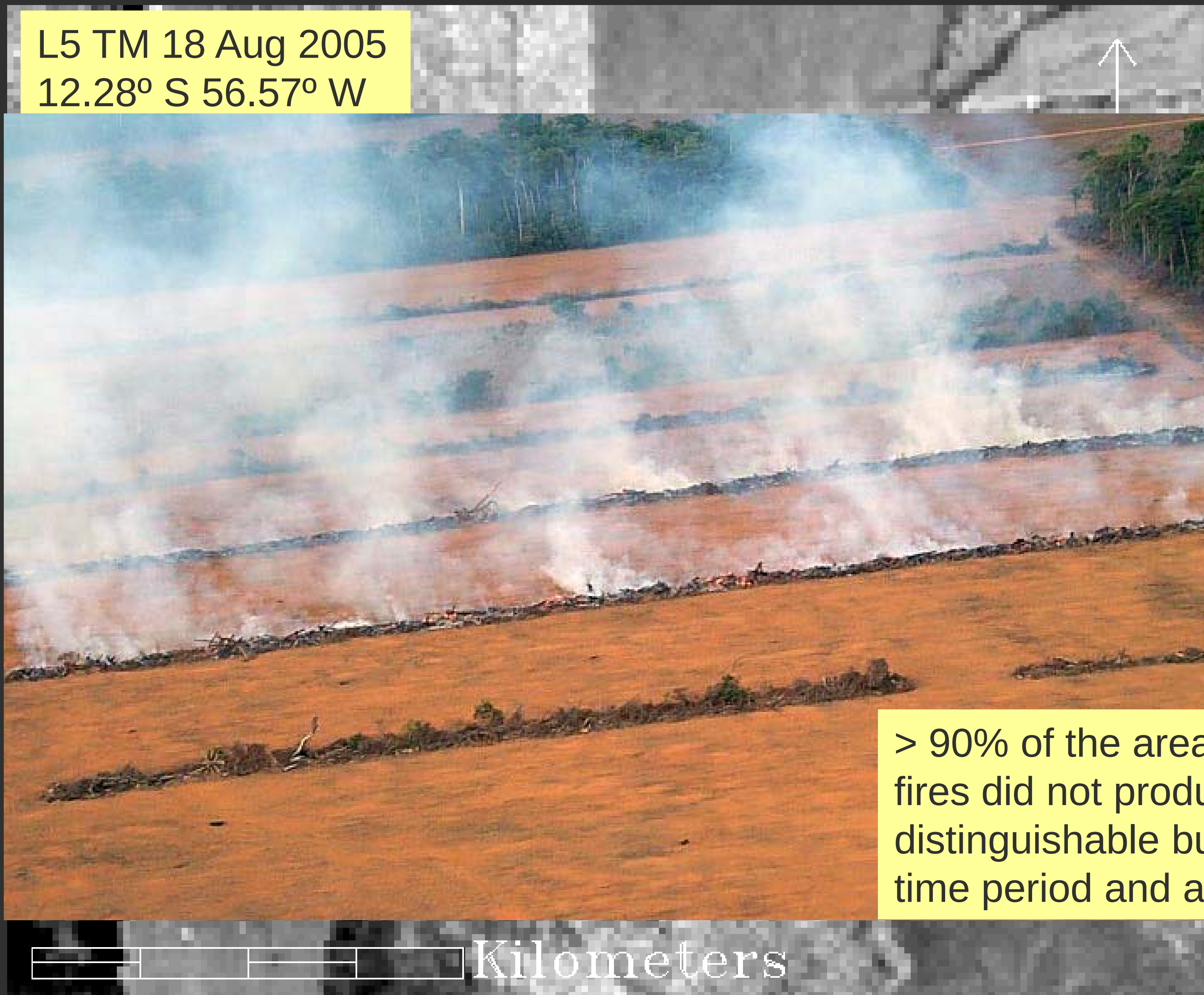

Example of piled debri burning

> 90% of the areas with active fires did not produce a distinguishable burn scar for the time period and area analyzed

Percentage of MODIS fire pixels with MWIR brightness temperature above the indicated value

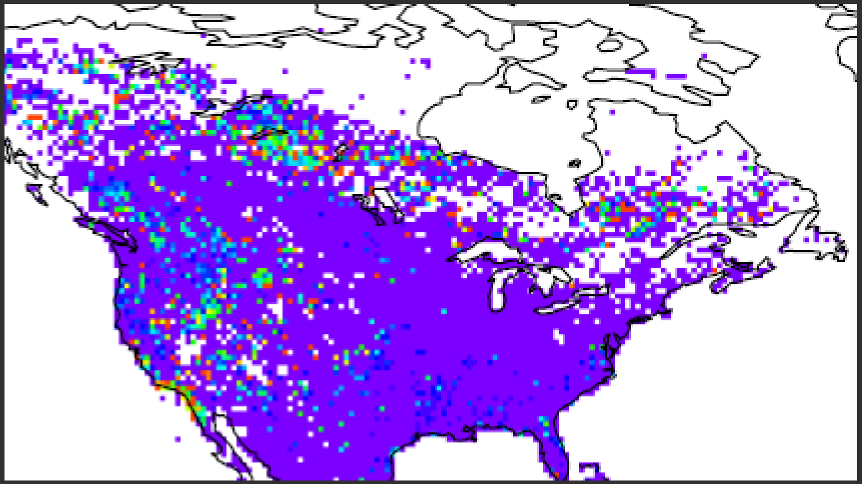

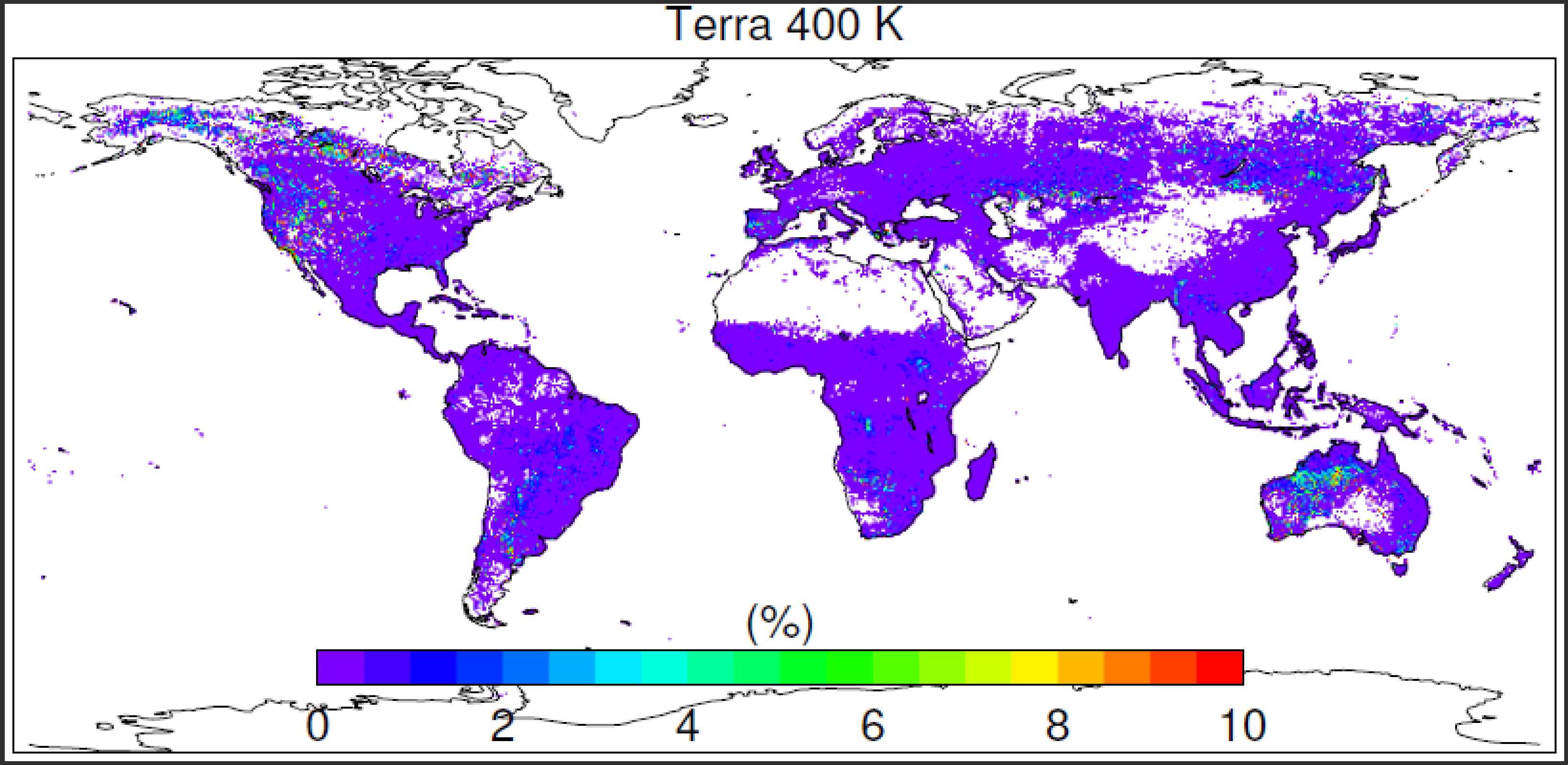

Percentage of MODIS fire pixels with MWIR brightness temperature above the indicated value

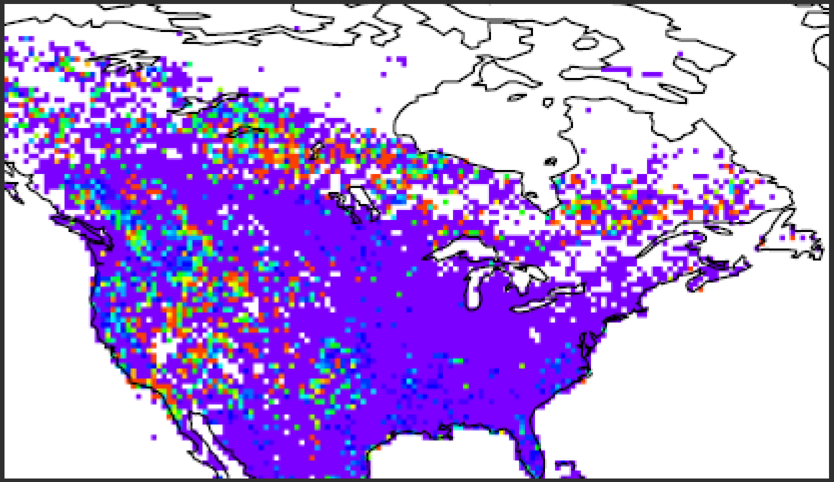

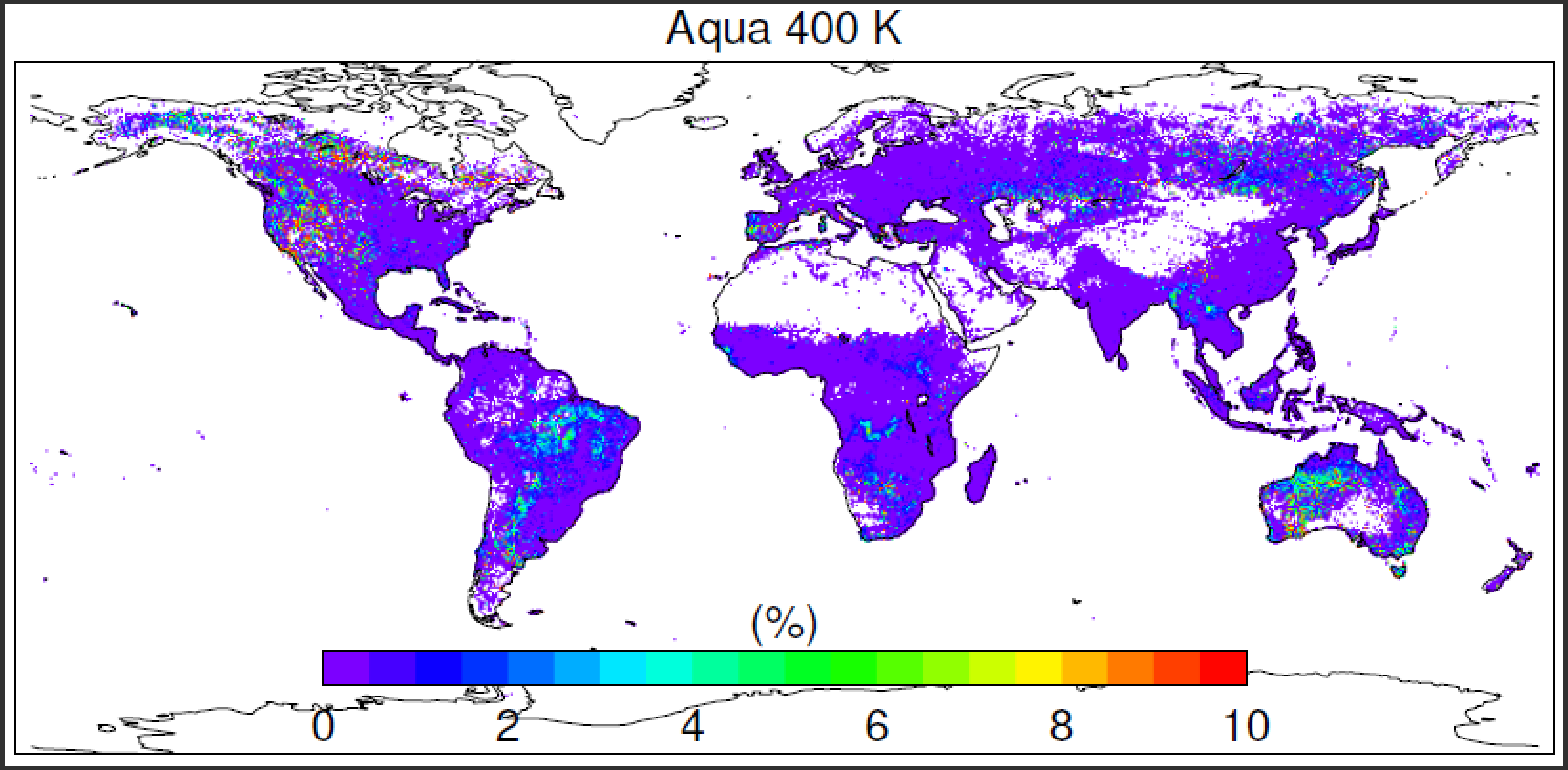

Percentage of MODIS fire pixels with MWIR brightness temperature above the indicated value

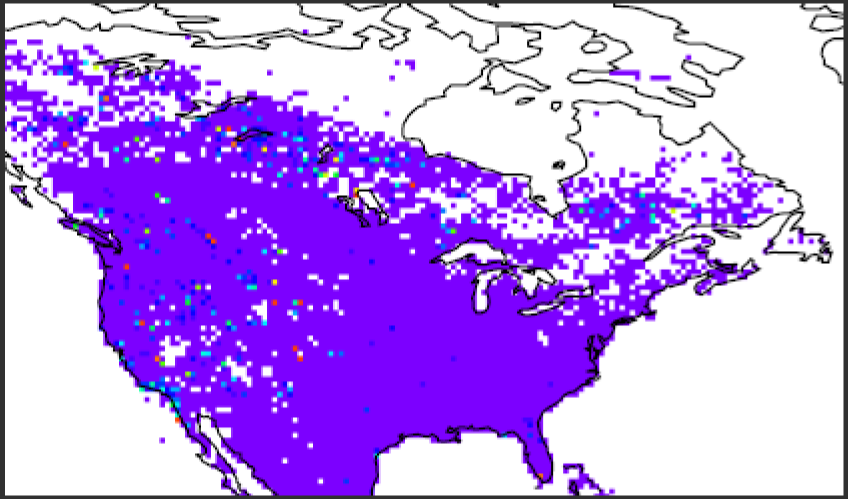

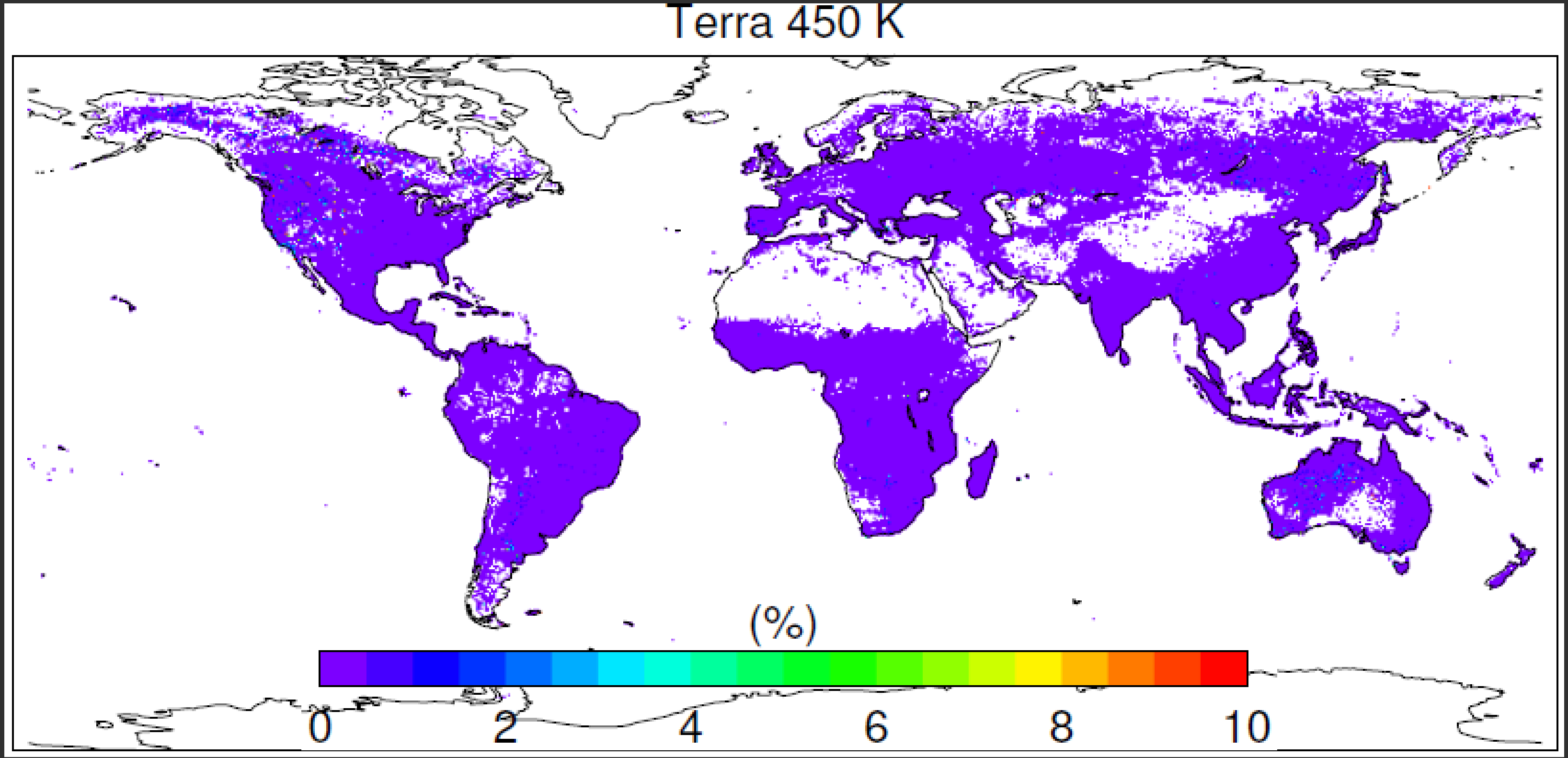

Percentage of MODIS fire pixels with MWIR brightness temperature above the indicated value

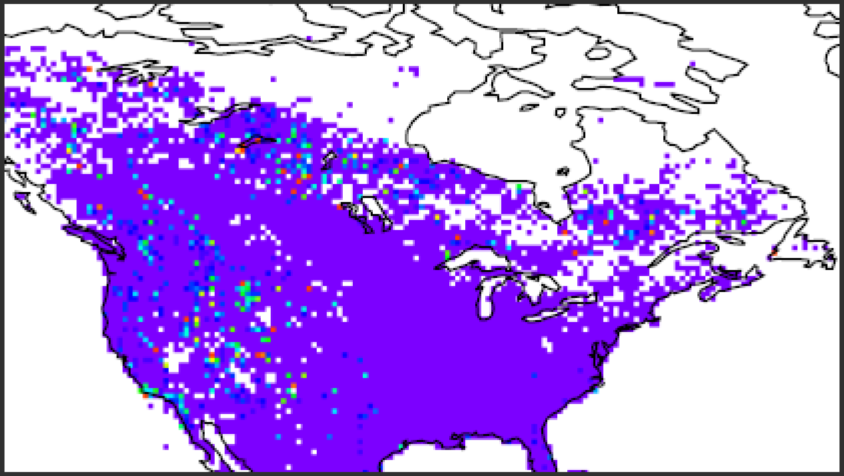

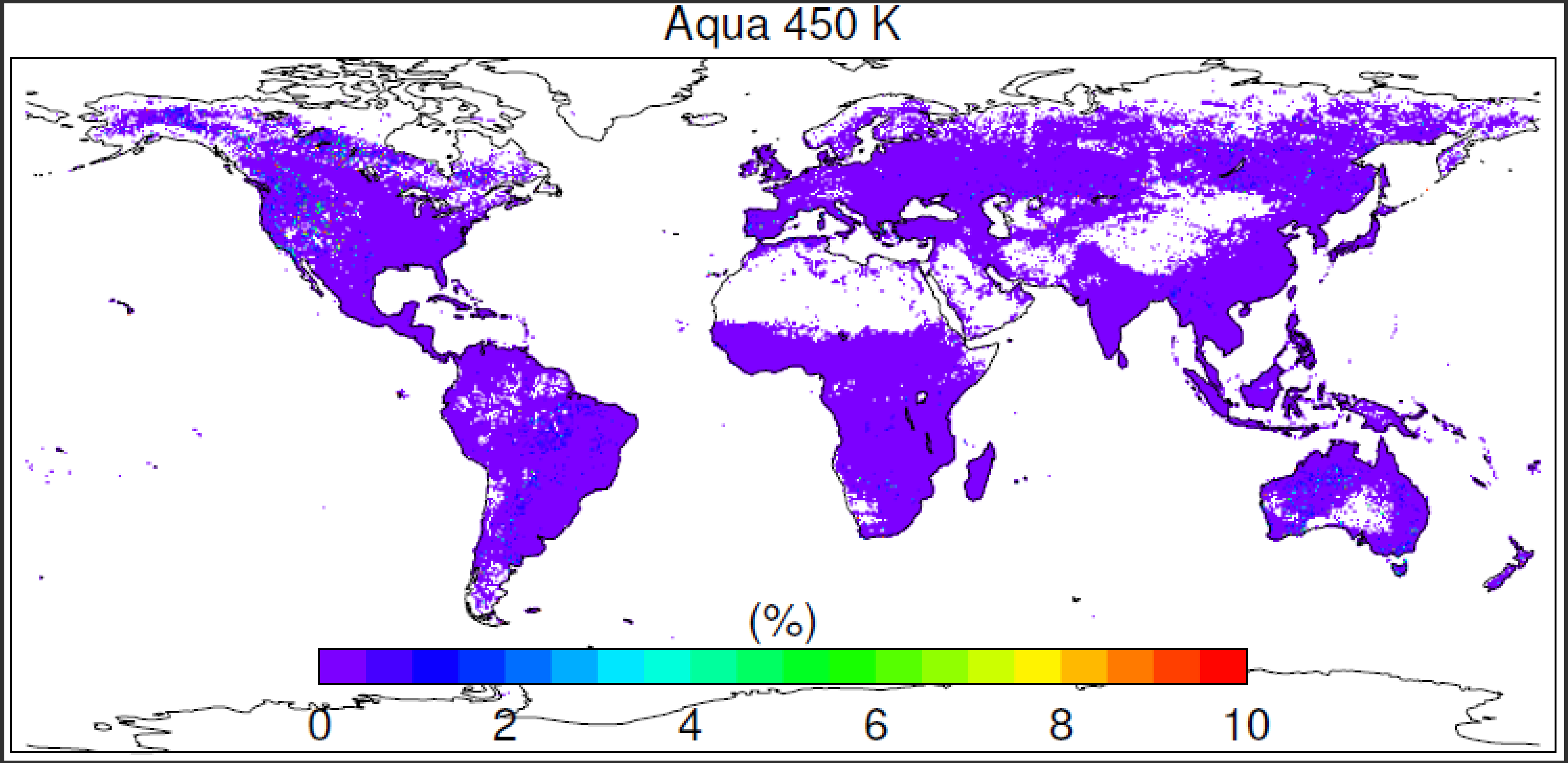

Major benefits of HyspIRI for fire

- Unprecedented capability of global fuel mapping and characterization of the recovery process
- Unprecedented sensitivity to active flaming and smoldering fires
  - can easily detect small agricultural fires (difficult with coarser resolution sensors)
  - fewer false alarms in fire detection
  - straightforward retrieval of fire radiative power
    - single band vs. three or more bands with existing sensors
- Greatly expanded spatial and temporal coverage
  - large samples of detailed fire characteristics useful for statistically modeling fires and their behavior
- Interpretation, calibration and validation of fire observations derived from coarser resolution data

Integration of GOES, MODIS, and HyspIRI Thermal Satellite Imagery for Mapping Daily ET at the Sub-field Scale

M.C. Anderson, W.P. Kustas
USDA-ARS, Hydrology and Remote Sensing Laboratory

C. Hain, J.R. Mecikalski
U Alabama-Huntsville, Atmospheric Science

Why global remotely sensed ET?

Climate Change

- **GEO: Essential Climate Variable**
- **Link between global energy and water cycles**
- **Adaptation to climate change**
    - *water availability, soil salinization*
- **Diagnostic check on GCMs/LSMs**
    - *bridge between observation and model grid scales*

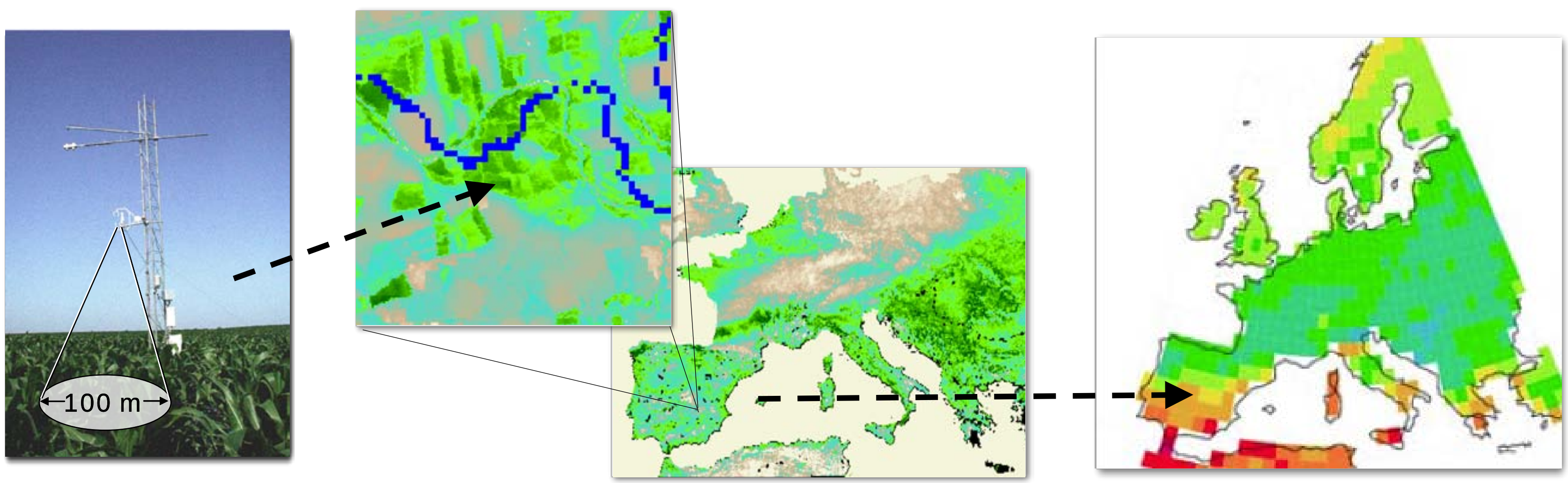

Tower flux   Remote sensing   GCM

Why global remotely sensed ET?

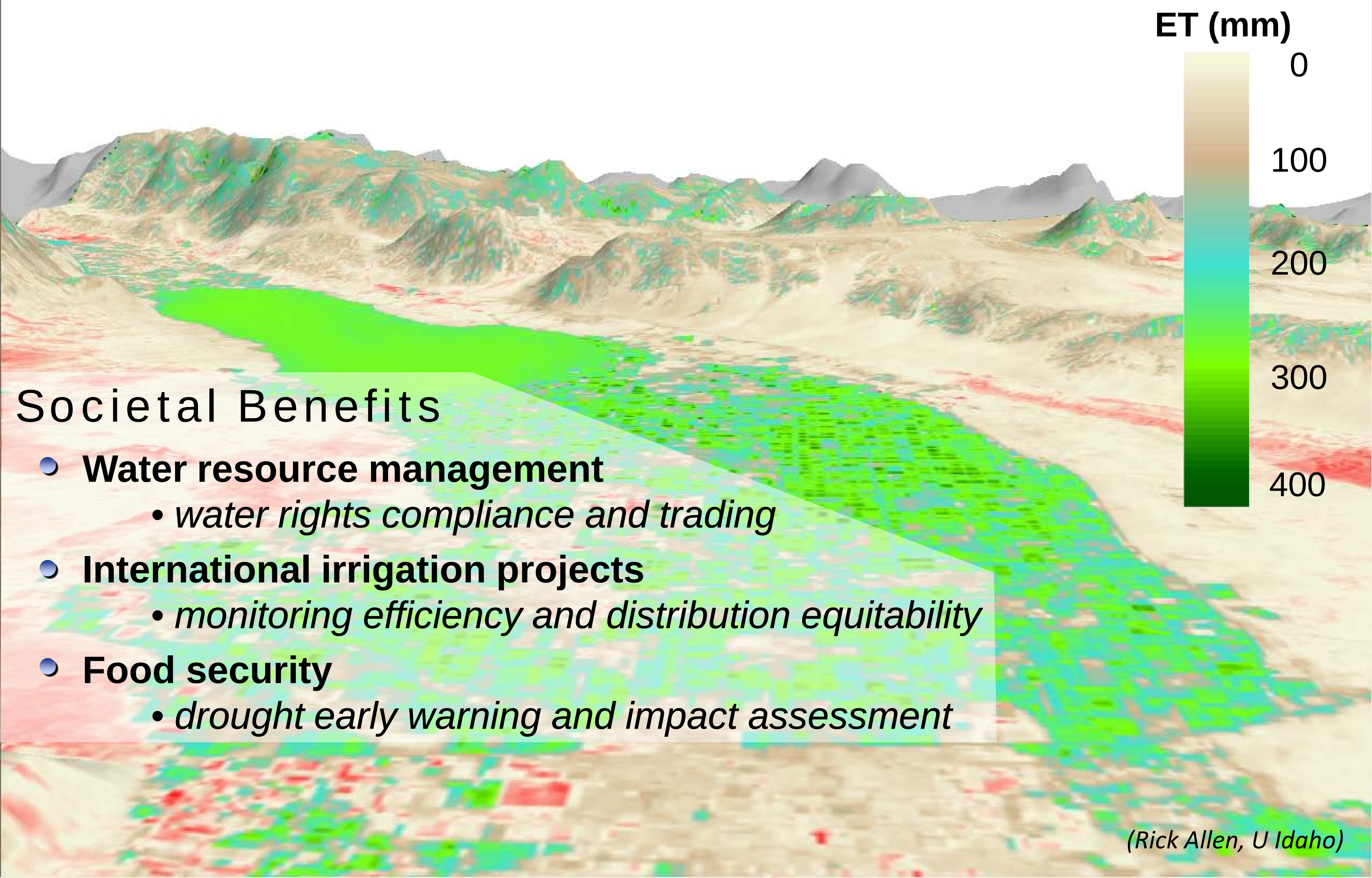

Societal Benefits

- **Water resource management**
    - *water rights compliance and trading*
- **International irrigation projects**
    - *monitoring efficiency and distribution equitability*
- **Food security**
    - *drought early warning and impact assessment*

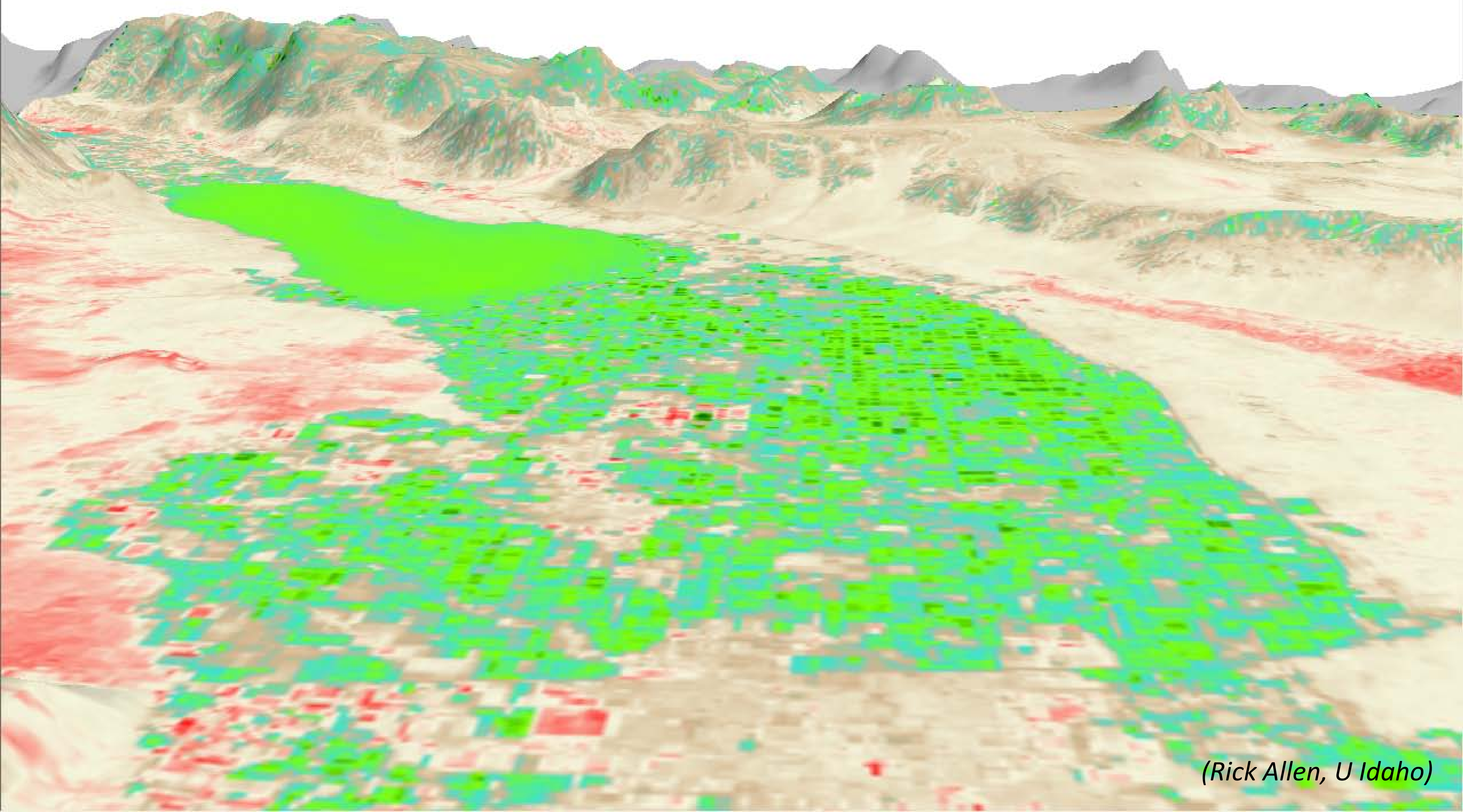

(Rick Allen, U Idaho)

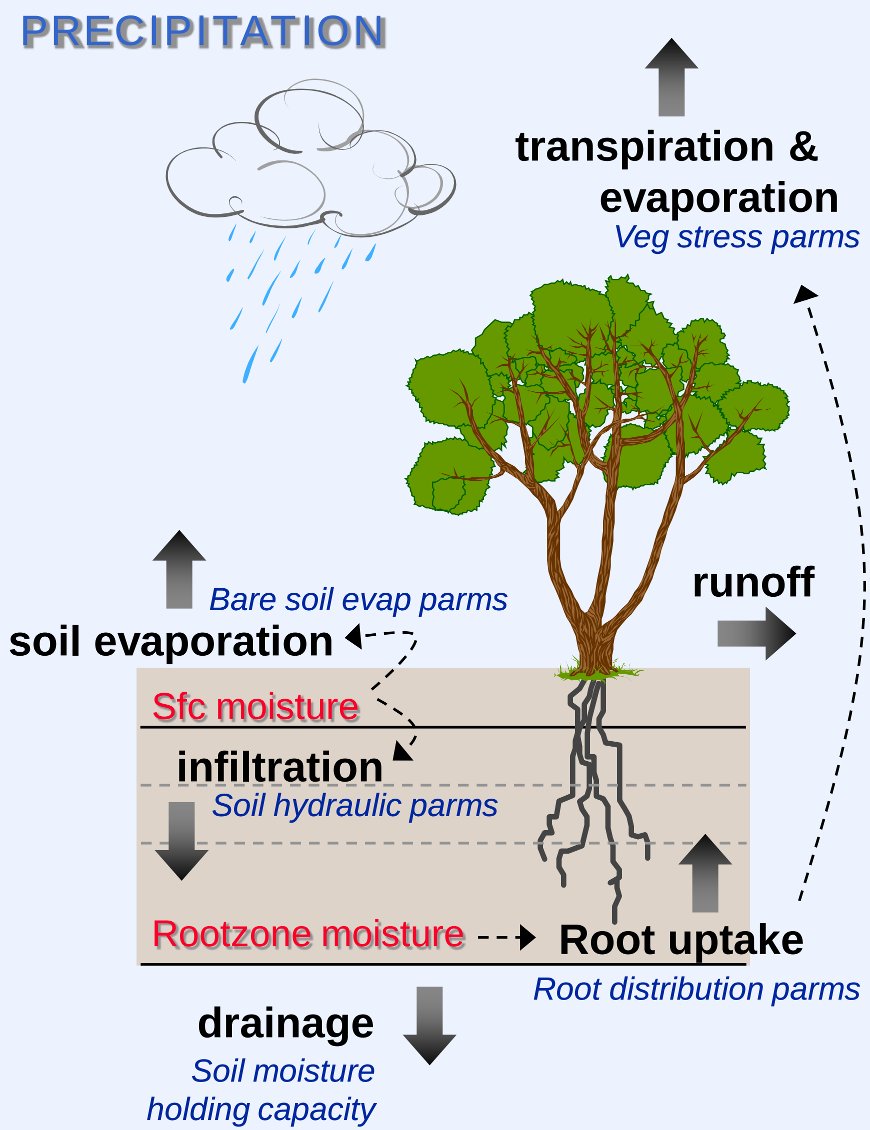

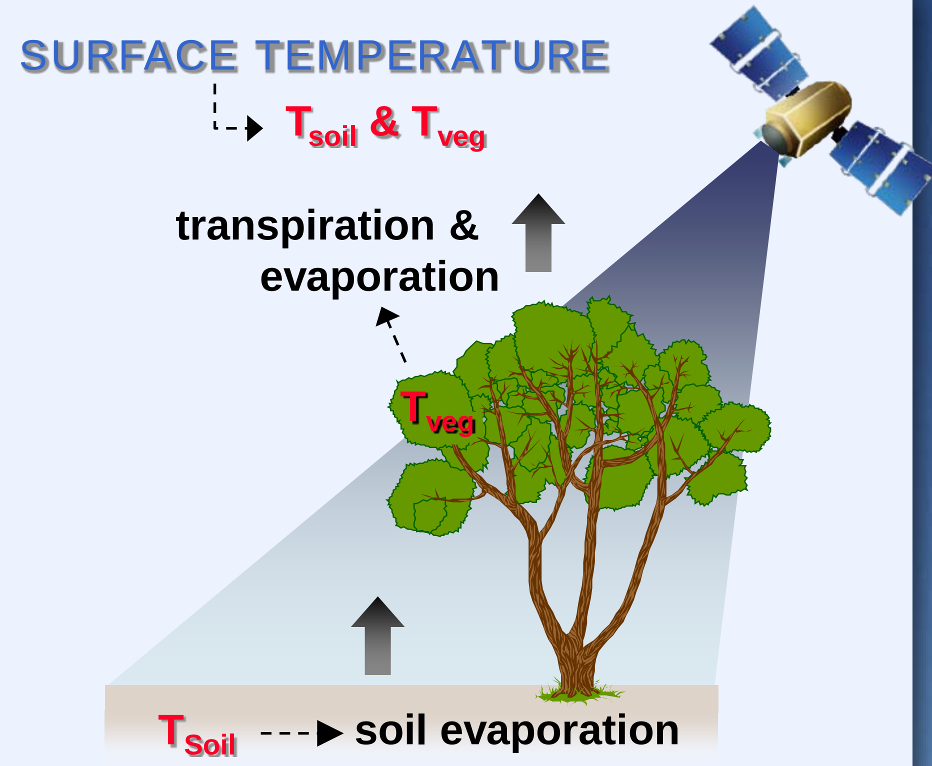

Given known radiative energy inputs, how much water loss is required to keep the soil and vegetation at the observed temperatures?

WATER BALANCE APPROACH
(“forward modeling”)

REMOTE SENSING APPROACH
(“inverse modeling”)

Sensitivity to irrigation

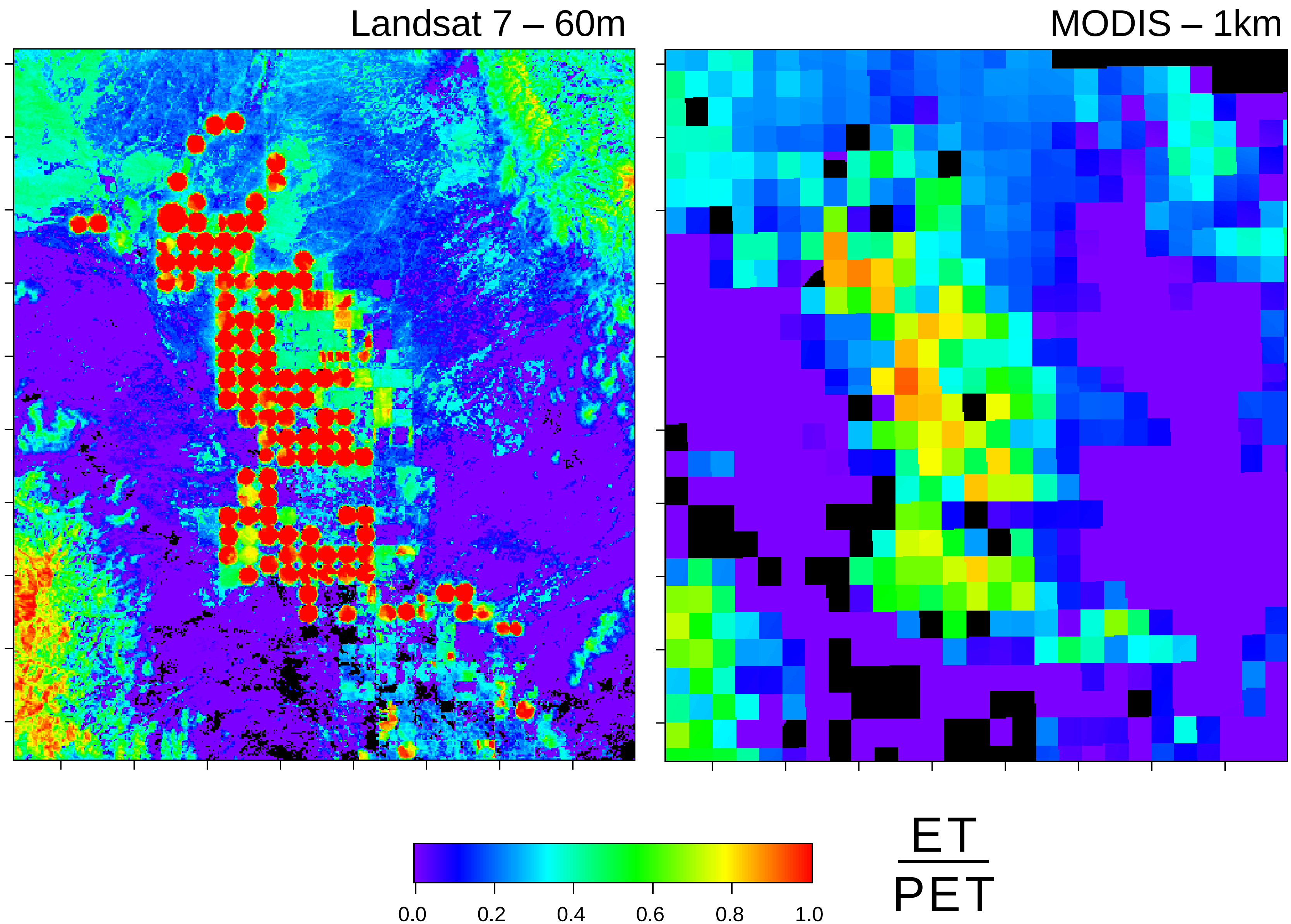

Satellite Thermal Imaging Systems

Pixel Scale	Spatial Resolution	Temporal Resolution	Current Sources	Future Sources
Coarse	5-20 km	15 min	AIRS GOES MSG	CrIS GOES MSG
Moderate	1 km	~Daily	MODIS AVHRR ATSR	VIIRS AVHRR ATSR
Fine	60–120 m	Once every 8-16 days	ASTER Landsat	LDCM HyspIRI

Table from S. Hook

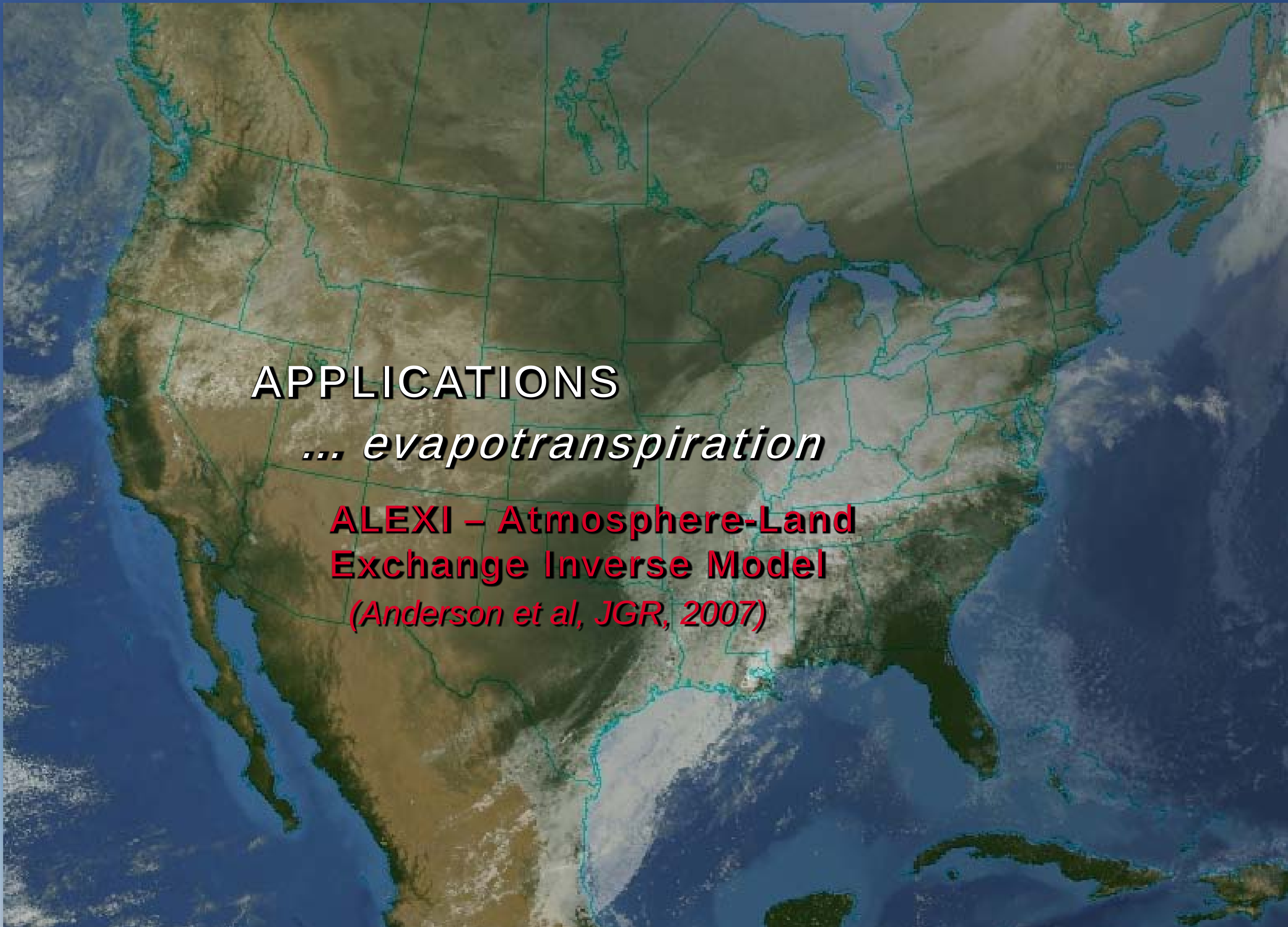
APPLICATIONS
... evapotranspiration
ALEXI – Atmosphere-Land
Exchange Inverse Model
(Anderson et al, JGR, 2007)

Atmosphere-Land Exchange Inverse (ALEXI)

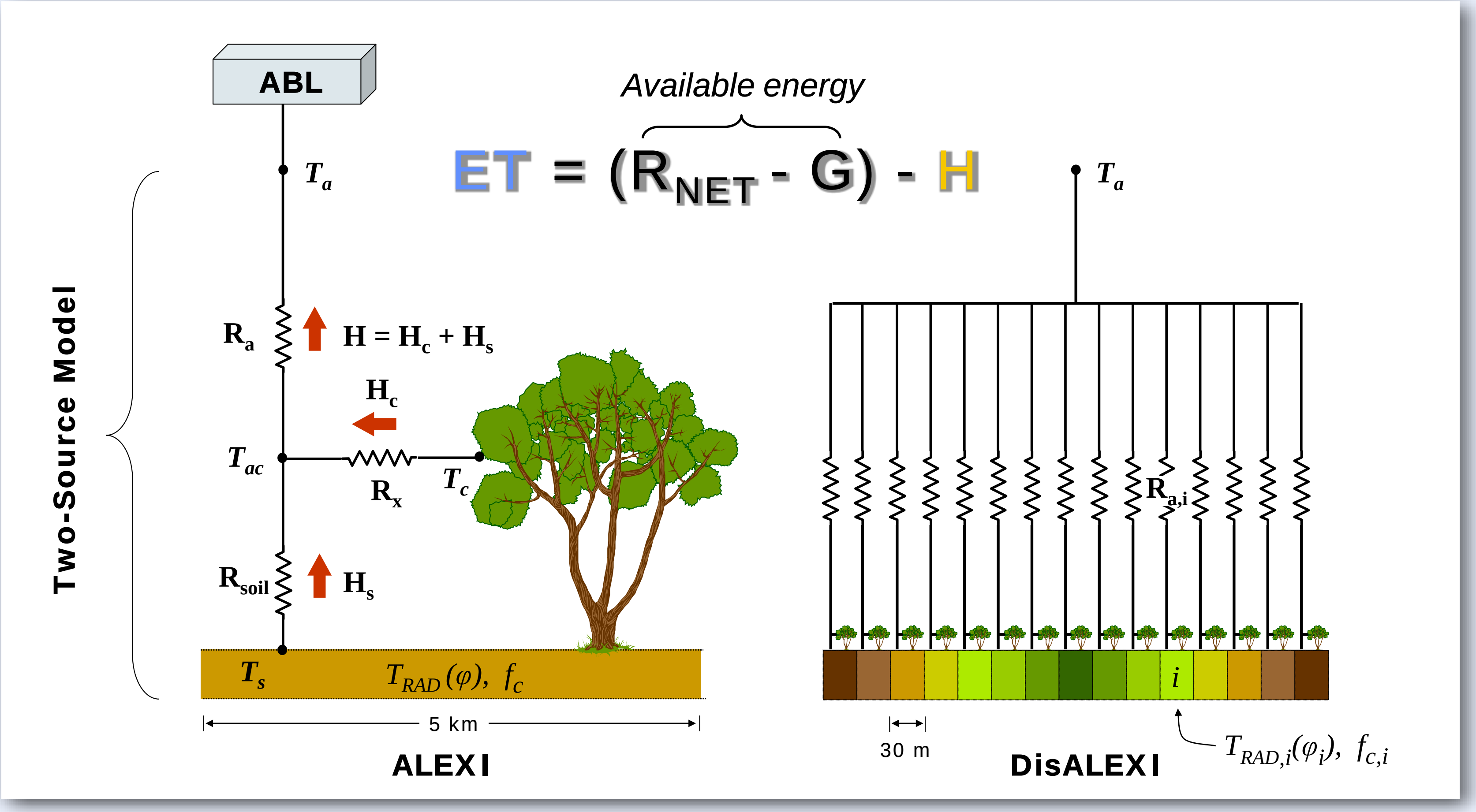

	Regional scale	Landscape scale
Surface temp:	ΔT_{RAD} - GOES	T_{RAD} - TM, MODIS, HyspIRI
Air temp:	T_a - ABL model	T_a - ALEXI

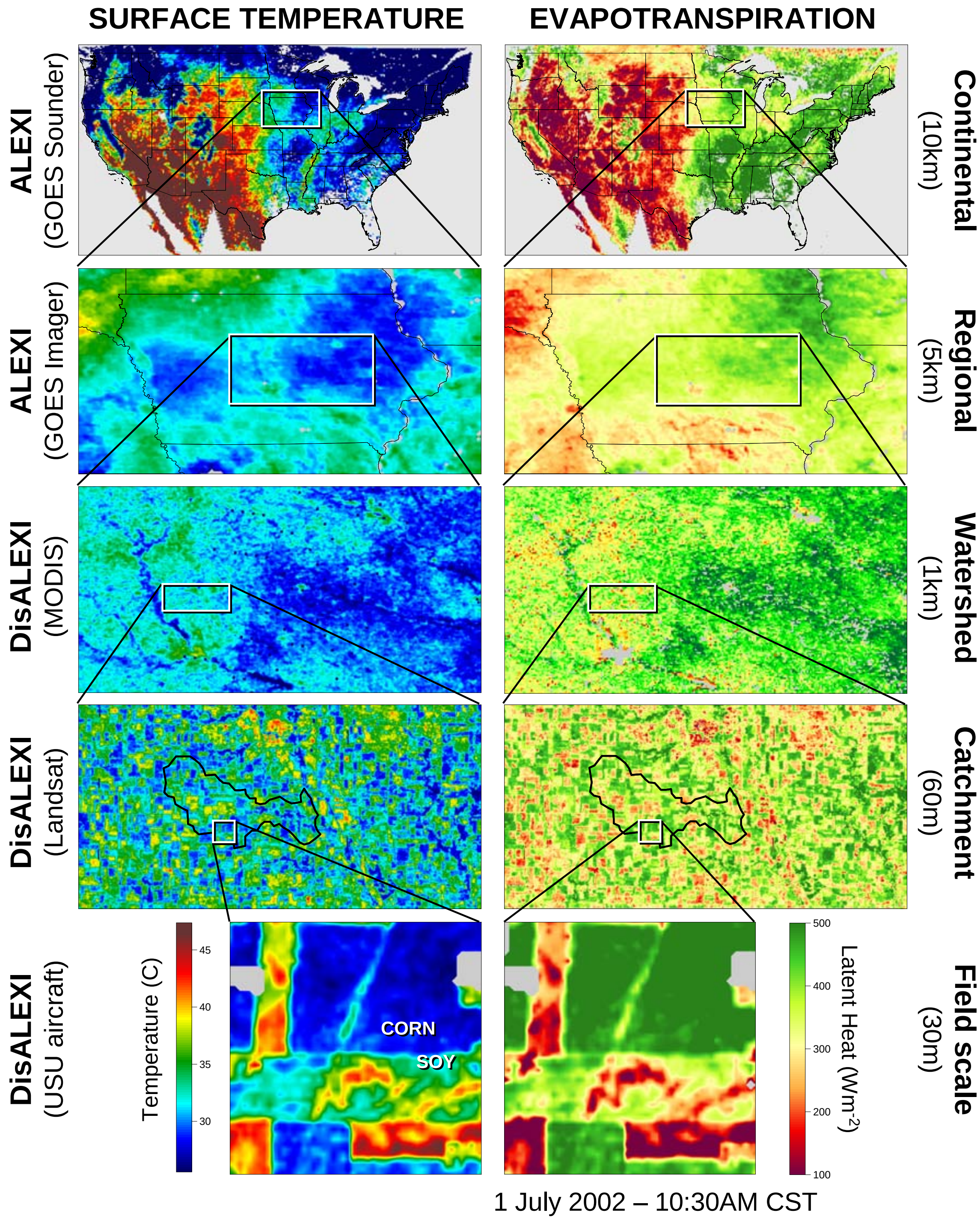

SURFACE TEMPERATURE
EVAPOTRANSPIRATION
ALEXI
(GOES Sounder)
Continental
(10km)
ALEXI
(GOES Imager)
Regional
(5km)
DisALEXI
(MODIS)
Watershed
(1km)
DisALEXI
(Landsat)
Catchment
(60m)
DisALEXI
(USU aircraft)
Field scale
(30m)
Temperature (C)
45
40
35
30
CORN
SOY
Latent Heat (Wm-2)
500
400
300
200
100
1 July 2002 – 10:30AM CST

FORT PECK, MONTANA

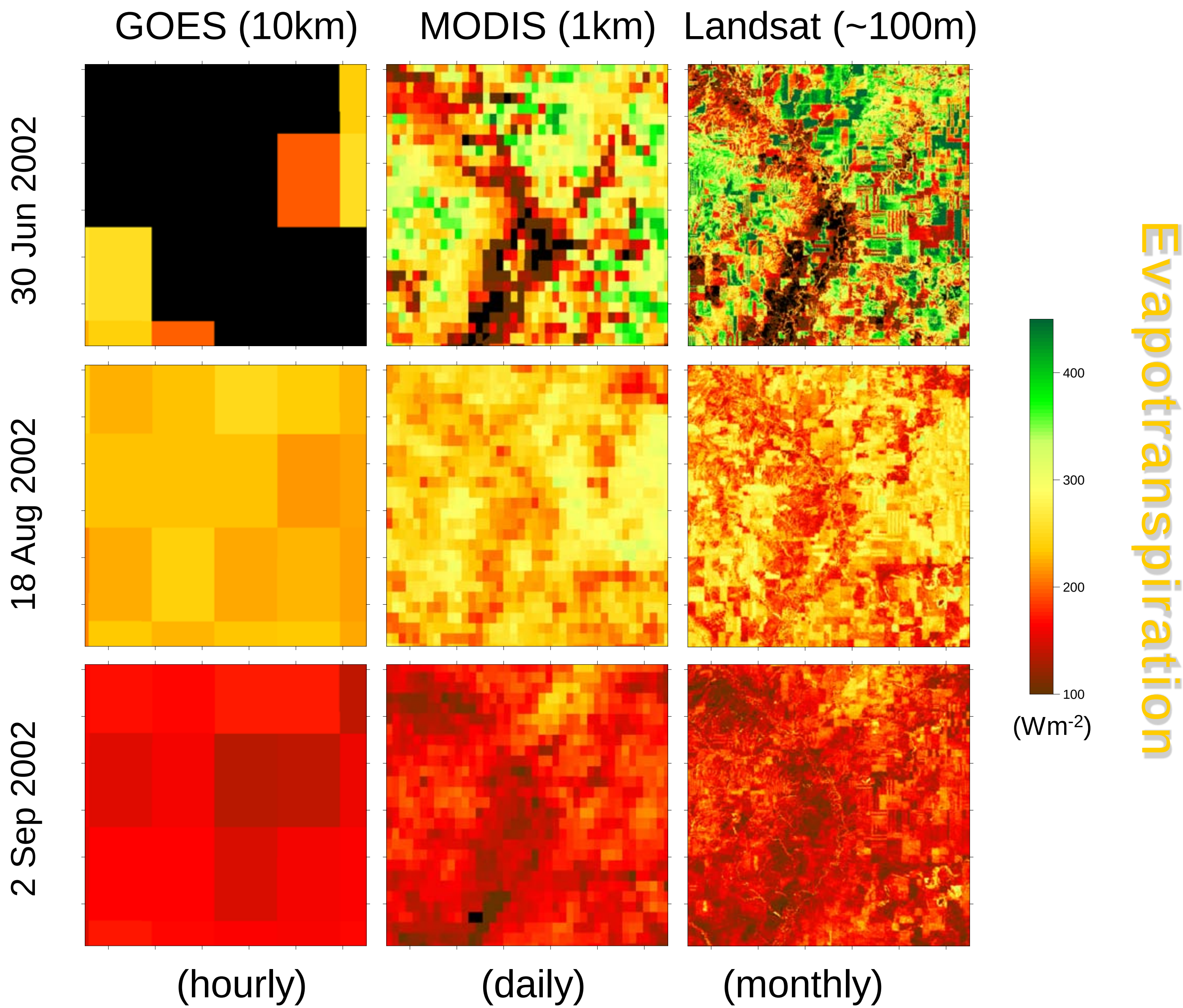

SAN PEDRO RIVER, ARIZONA

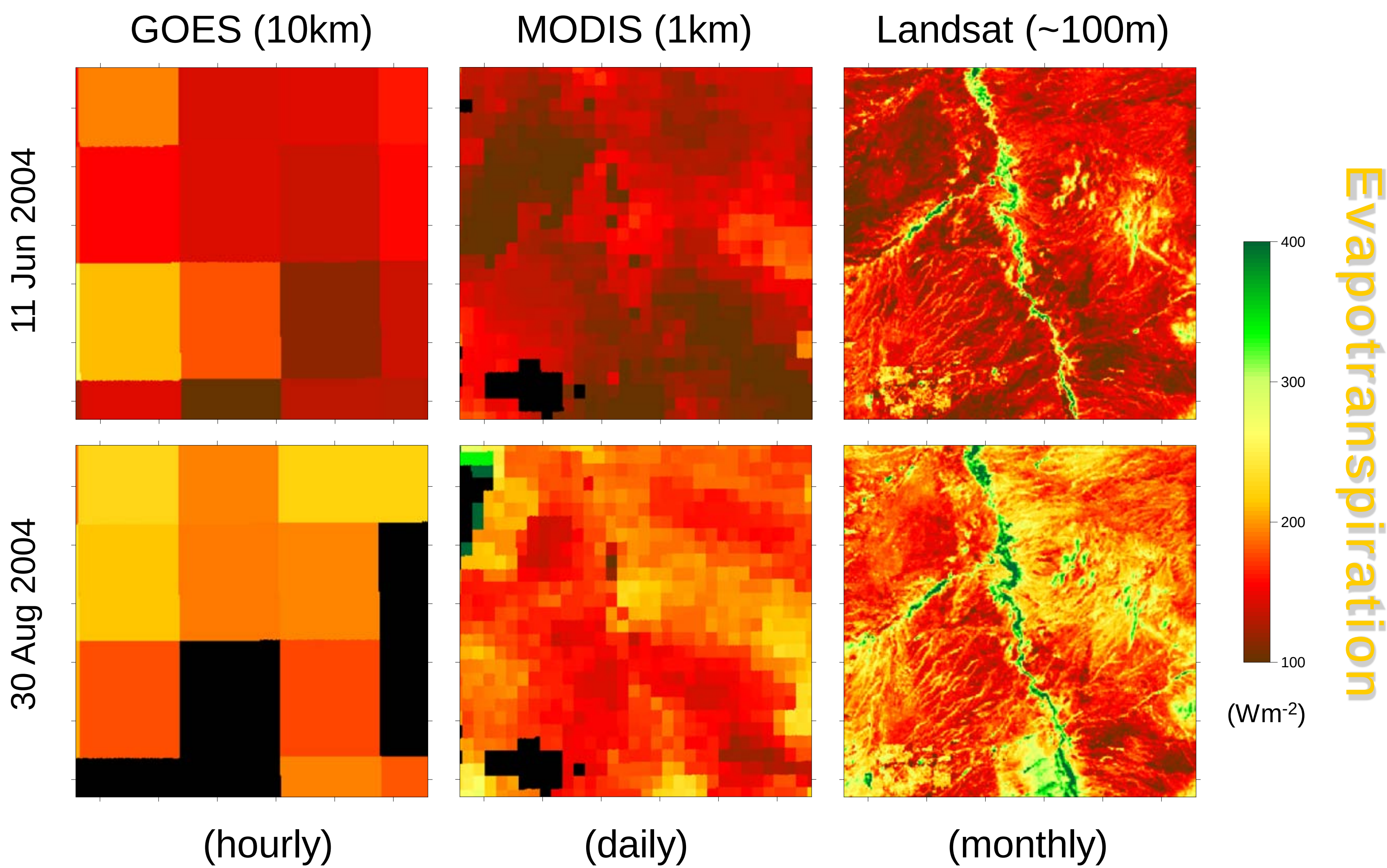

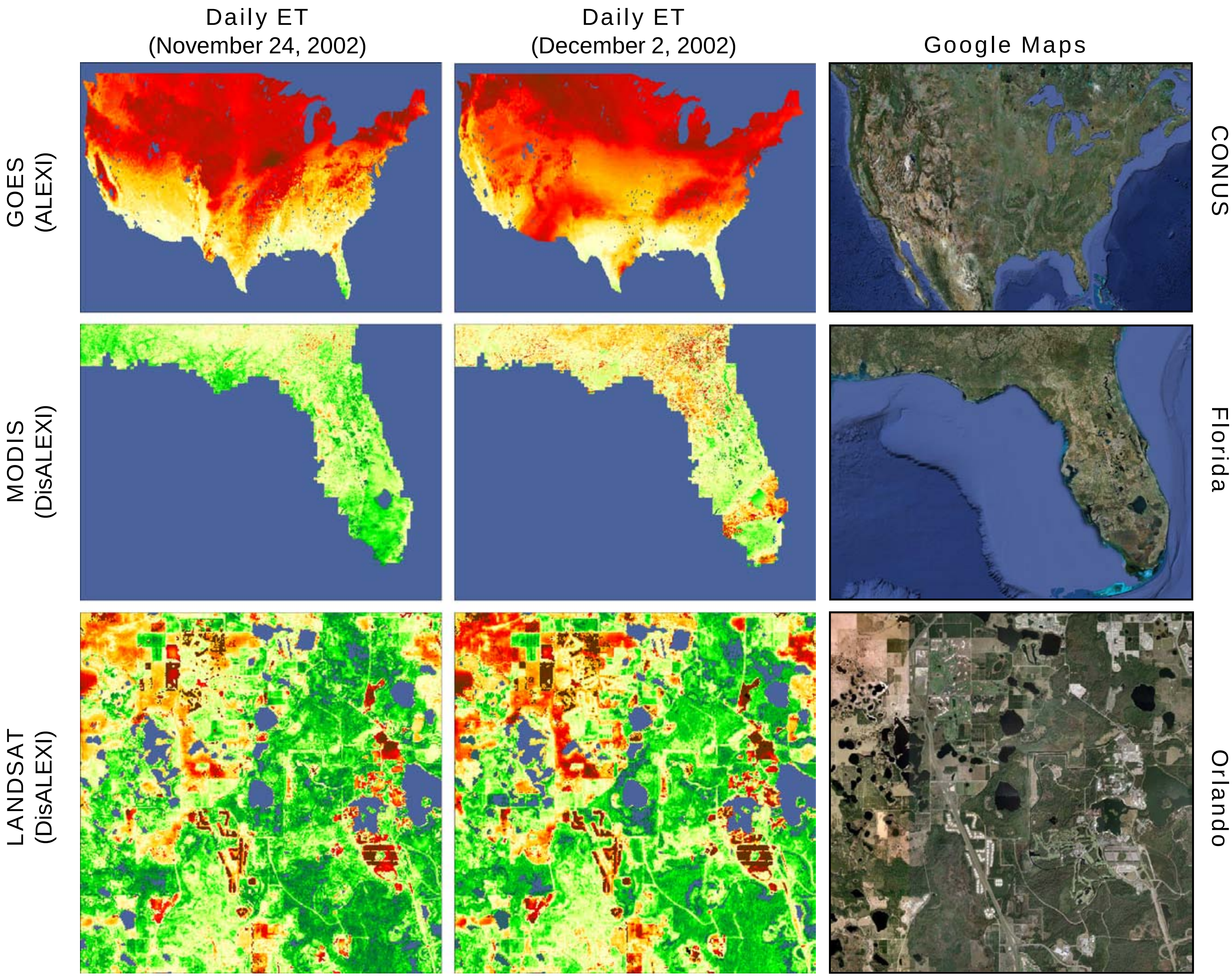
Daily ET
(November 24, 2002)
Daily ET
(December 2, 2002)
Google Maps
GOES
(ALEXI)
MODIS
(DisALEXI)
LANDSAT
(DisALEXI)
CONUS
Florida
Orlando

HIGH-RESOLUTION INTERPOLATION

Daily Evapotranspiration – Orlando, FL, 2002

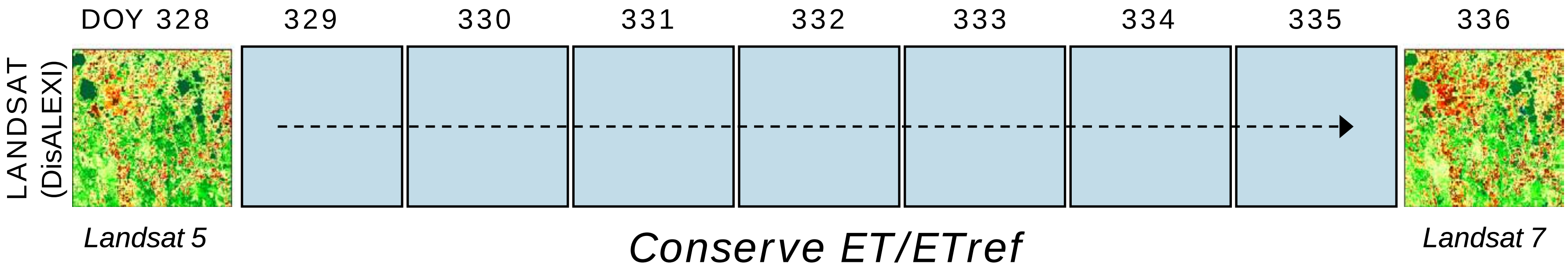

GOES/MODIS/Landsat FUSION

Daily Evapotranspiration – Orlando, FL, 2002

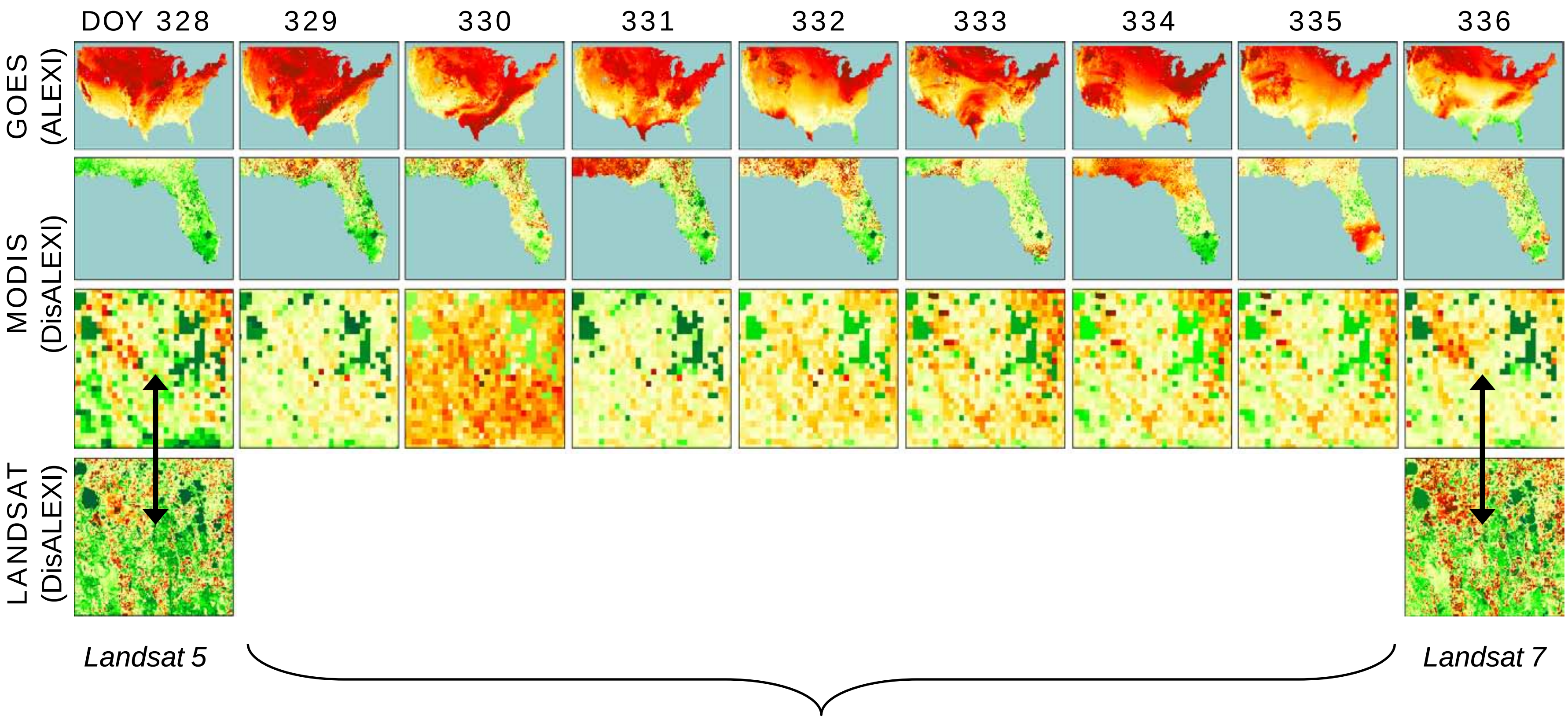

Spatial Temporal Adaptive Reflectance Fusion Model (STARFM) *(Gao et al, 2006)*

GOES/MODIS/Landsat FUSION

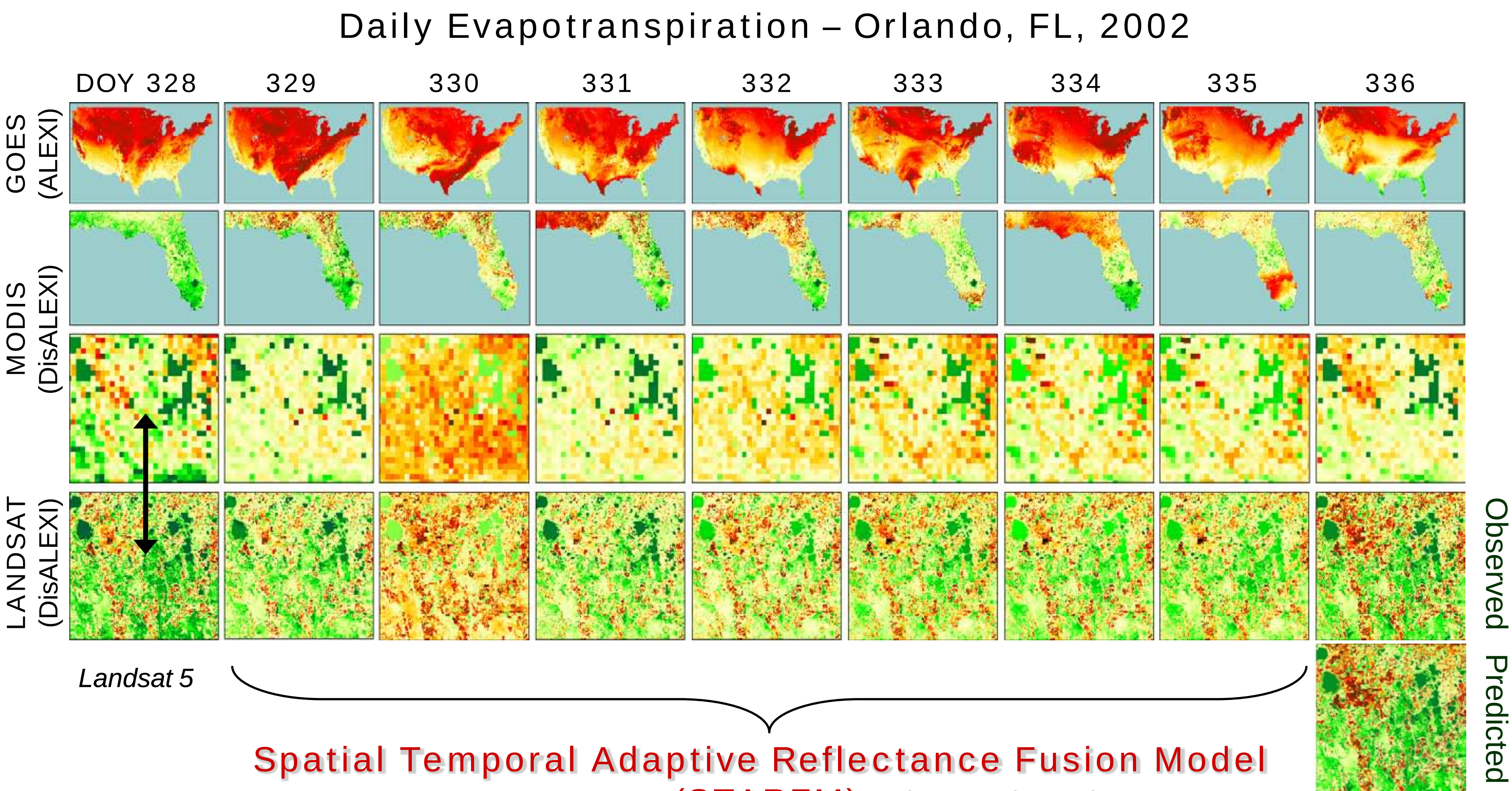

Spatial Temporal Adaptive Reflectance Fusion Model (STARFM) *(Gao et al, 2006)*

R^2: 0.83 (9% error)


APPLICATIONS
... monitoring drought
Anomalies in $\frac{AET}{PET}$
Evaporative Stress Index

MONTHLY ANOMALIES

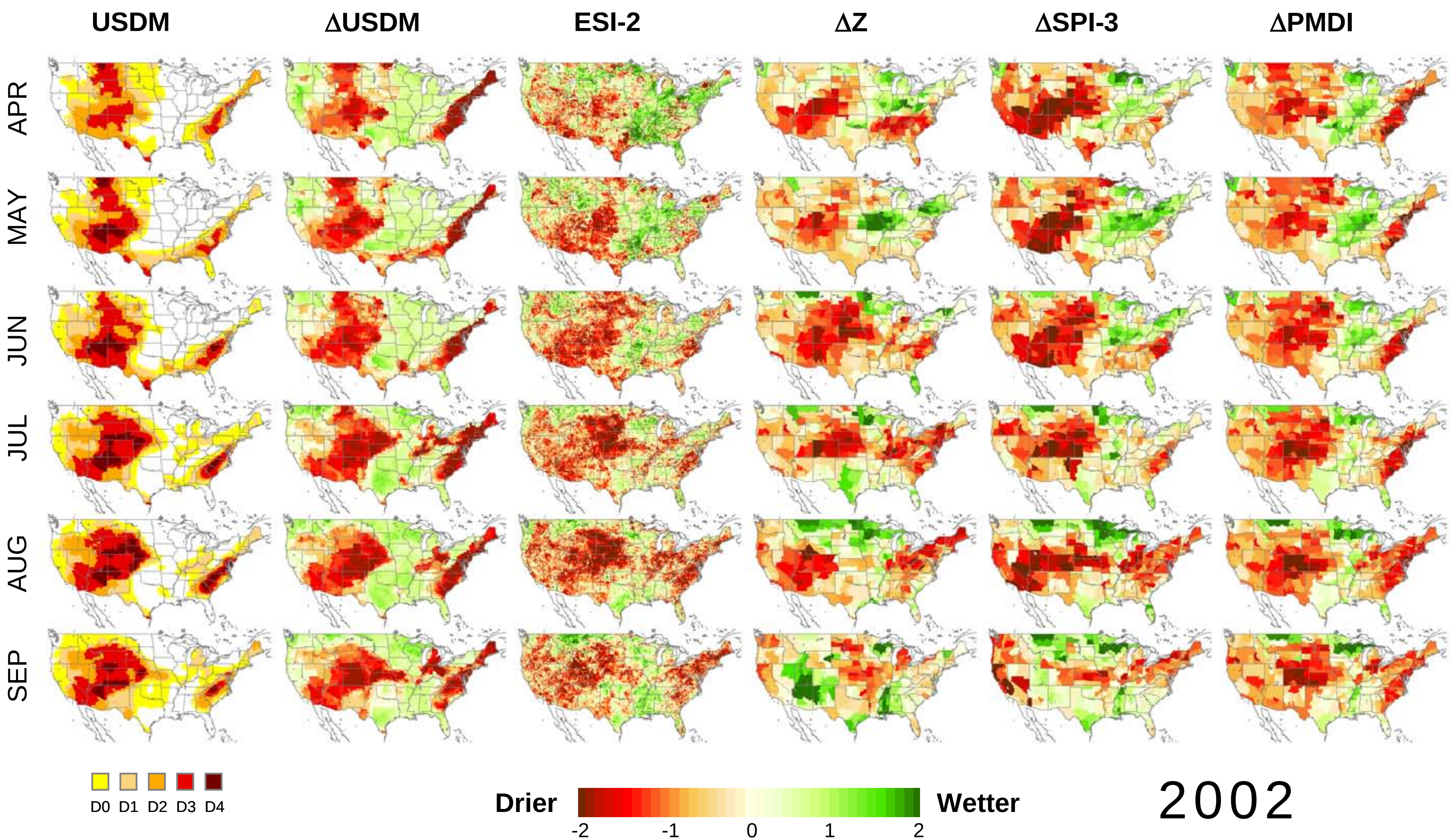

MONTHLY ANOMALIES

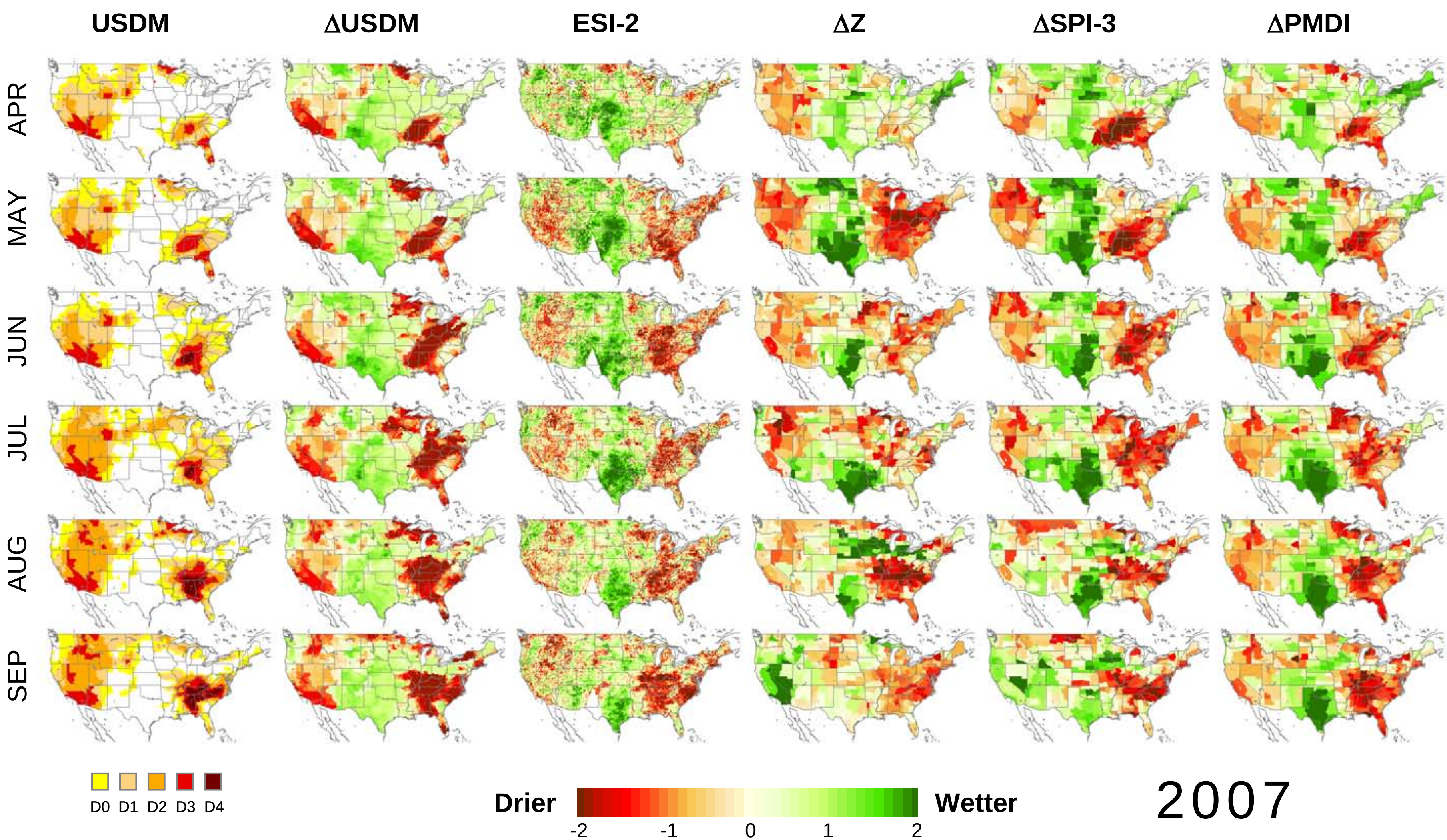

2007 SEASONAL ANOMALIES

USDM

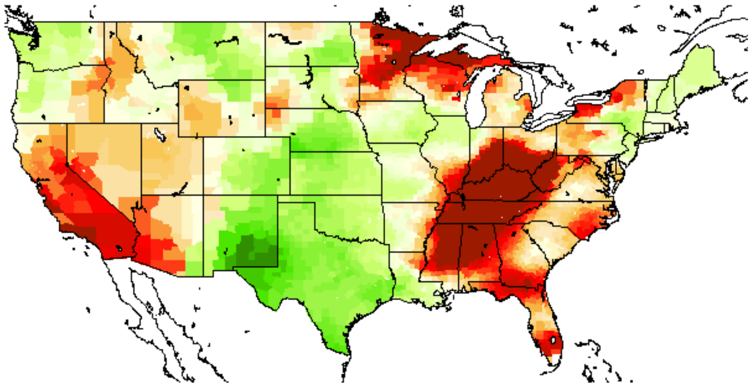

LIS - NOAH

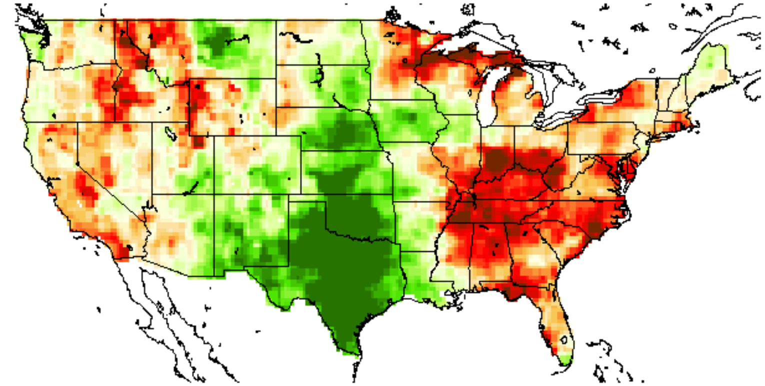

USDA AMSR-E MICROWAVE

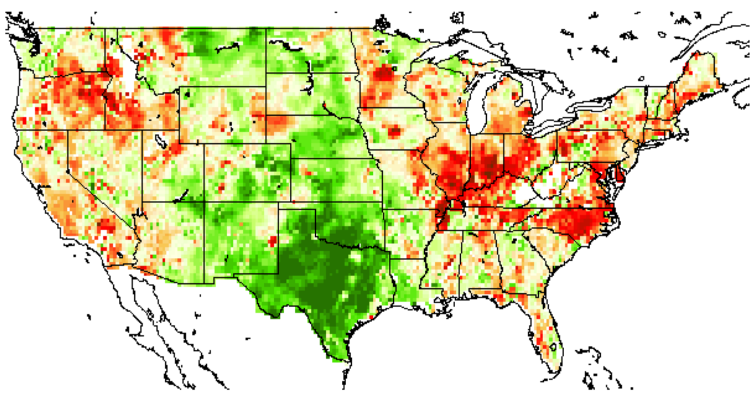

ALEXI GOES THERMAL

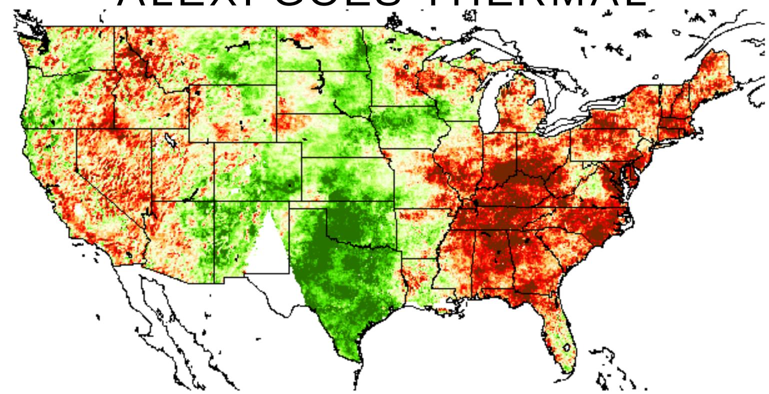

- **samples 5cm layer**
- **50km pixels (AMSR)**
- **~2-day coverage**
- **light vegetation cover**

- **samples ~1-2m layer**
- **60m - 5km pixels (L7, GOES)**
- **~15-day coverage (90%)**
- **low to high vegetation cover**

Multi-scale Drought Monitoring

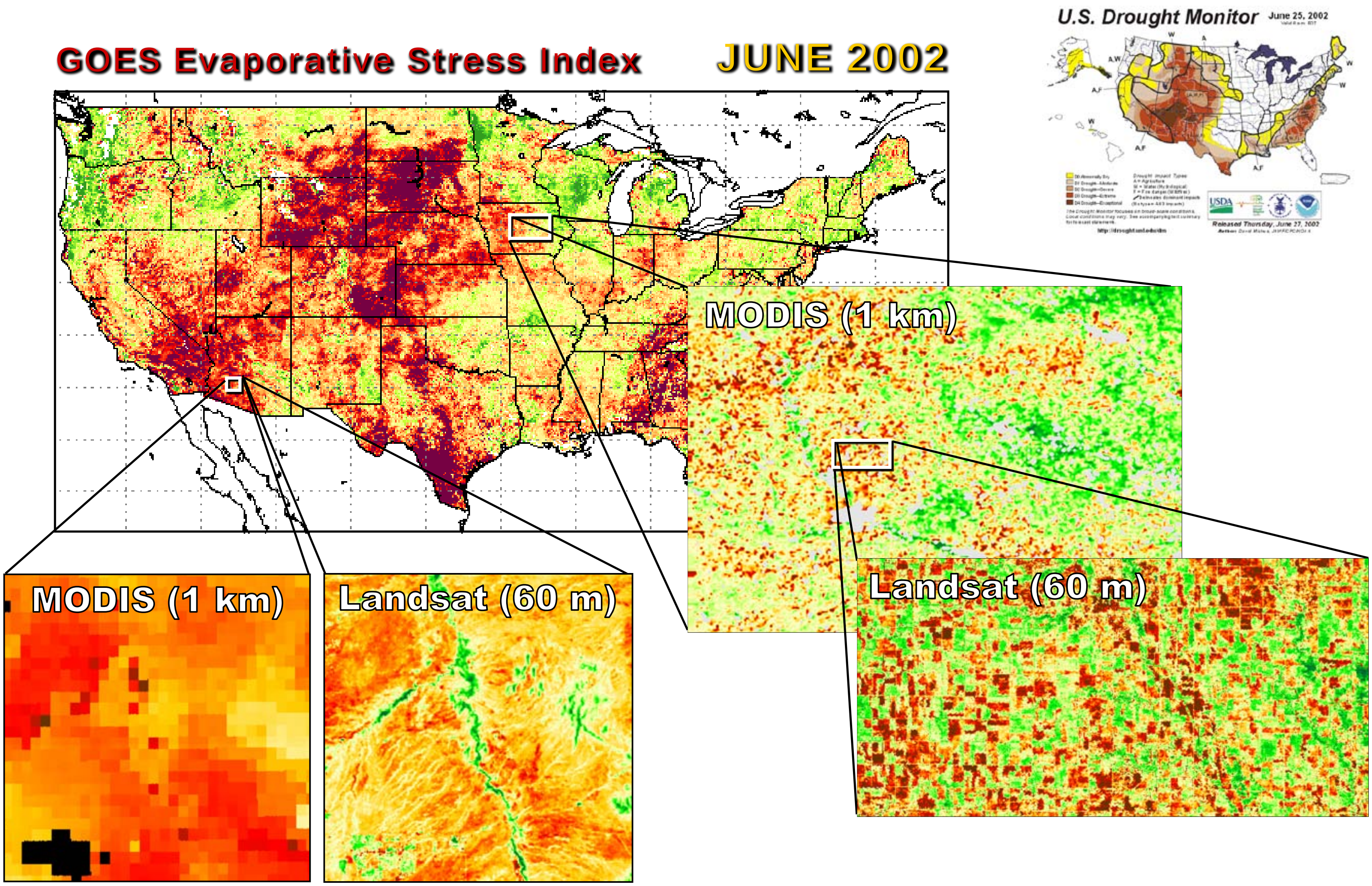


GLOBAL APPLICATIONS
... Improve ALEXI domain coverage and resolution

Geostationary Satellite Coverage

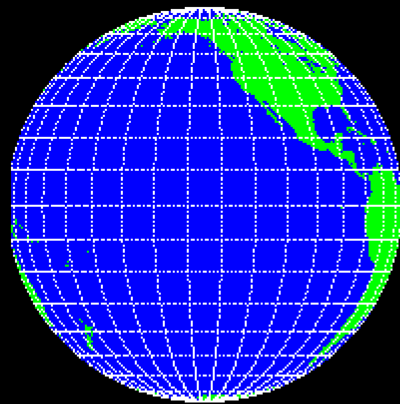

GOES W 135^{o}W
NOAA (US)

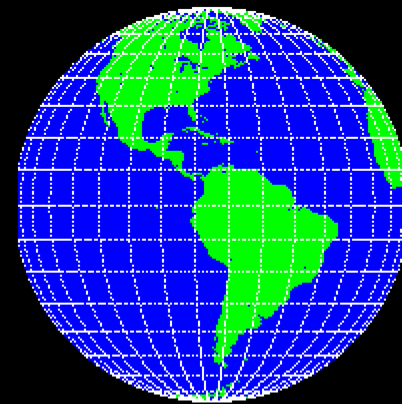

GOES E 75^{o}W
NOAA (US)

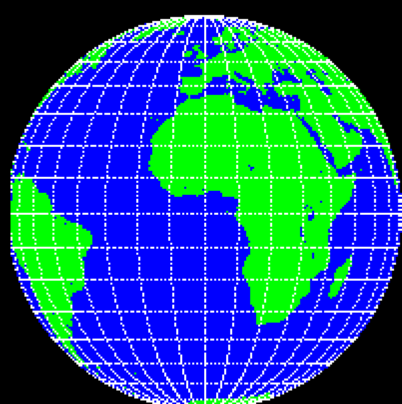

Meteosat 0^{o}
Eumetsat (EU)

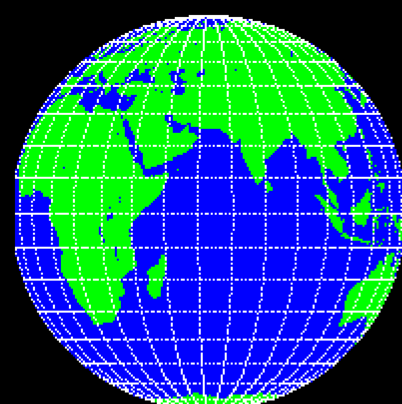

Meteosat 63^{o}E
Eumetsat (EU)

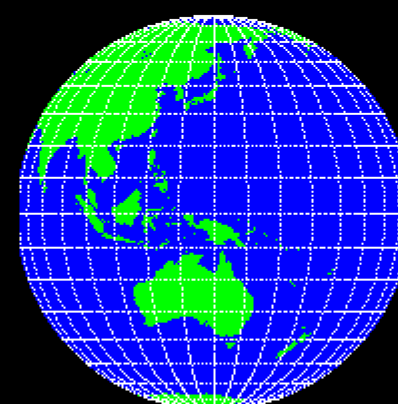

GMS 140^{o}E
JAXA (Japan)

Nile Basin Initiative Decision Support

METEOSAT COVERAGE

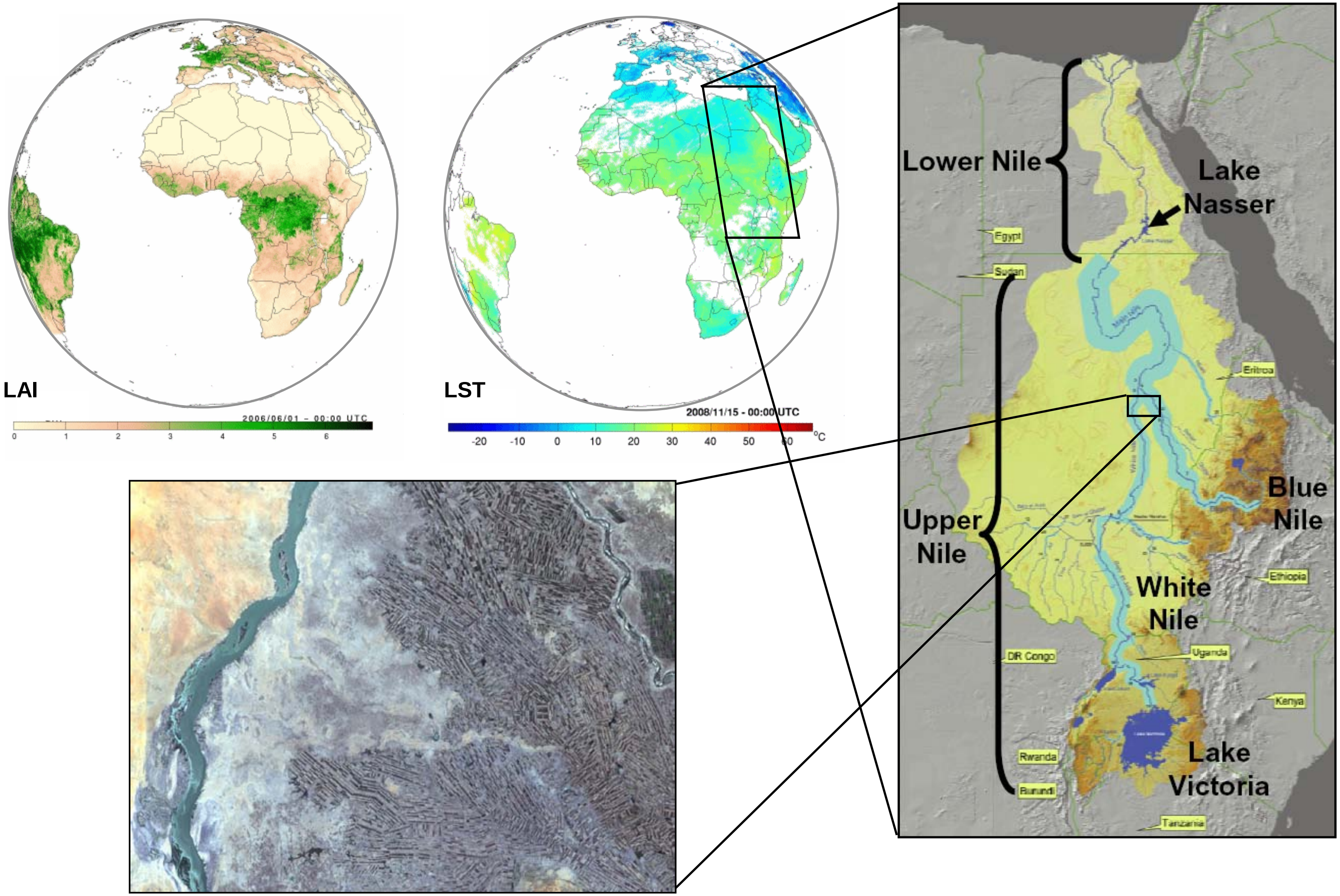

L7-ETM+ 1/12/02 USGS Image Gallery

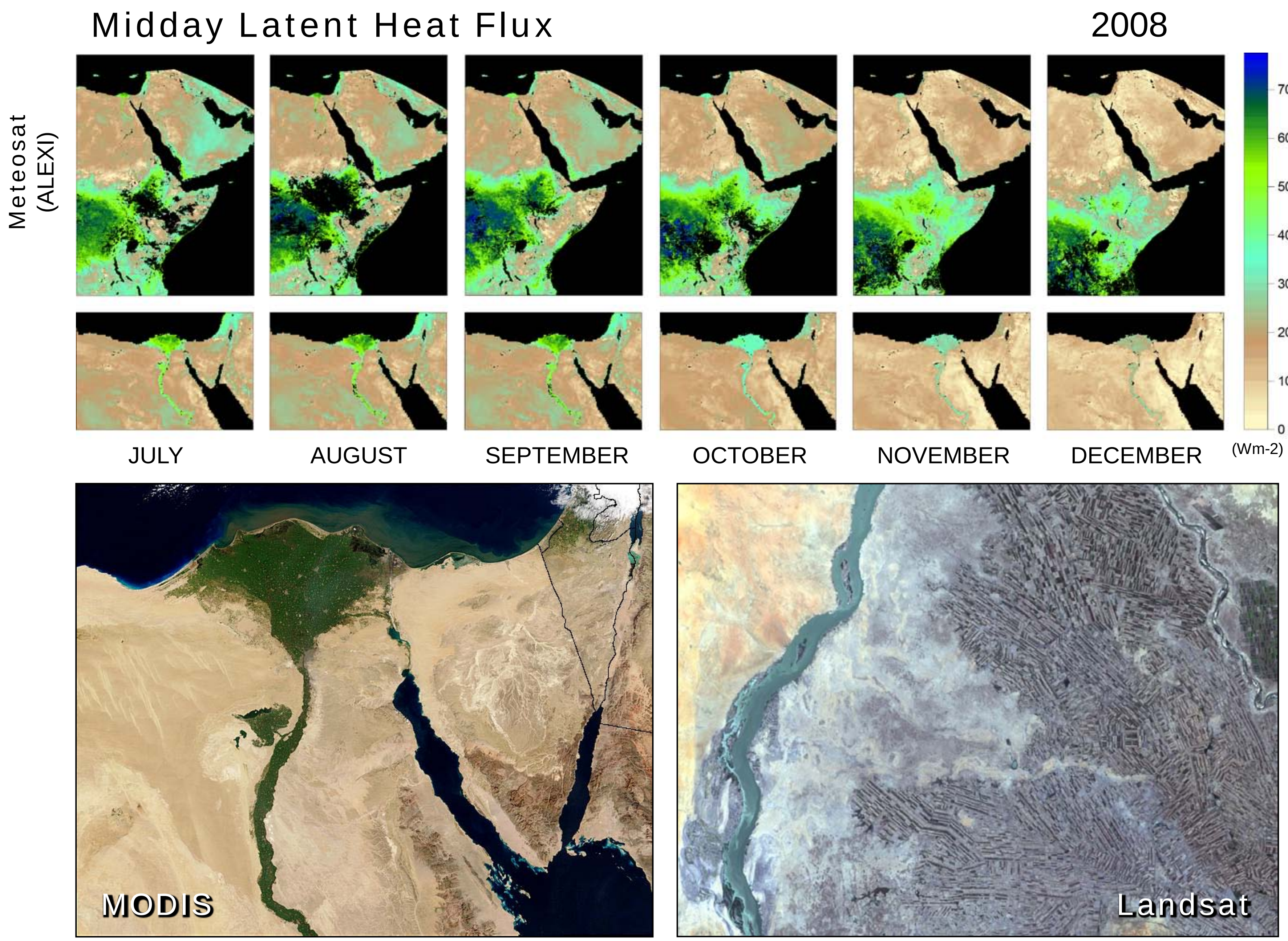

Midday Latent Heat Flux
2008
Meteosat
(ALEXI)
700
600
500
400
300
200
100
0
(Wm-2)
JULY
AUGUST
SEPTEMBER
OCTOBER
NOVEMBER
DECEMBER
MODIS
Landsat

ALEXI – Europe (Meteosat 10km)

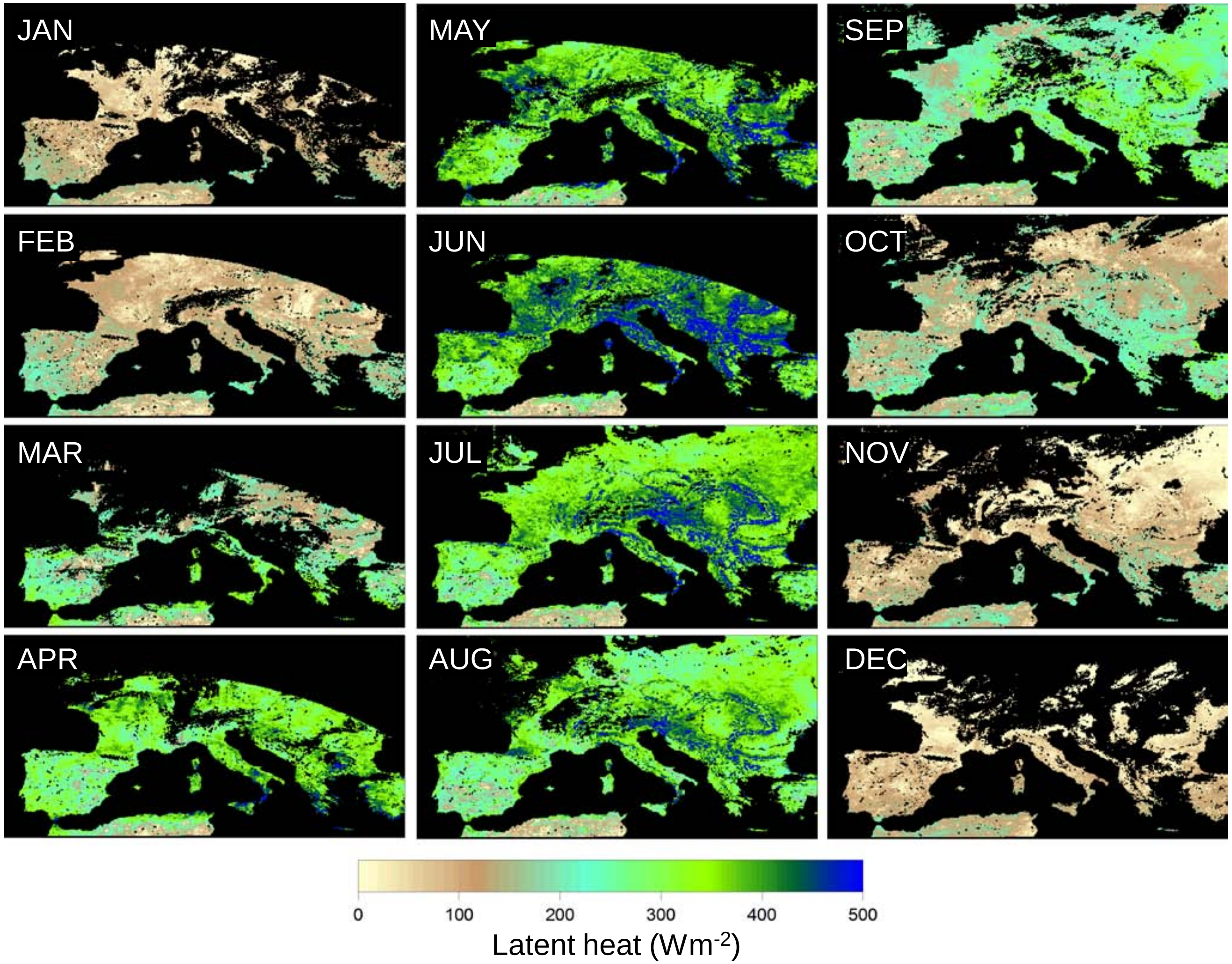

Spain (Irrigation District)

LEBRIJA, SPAIN May 15 2005

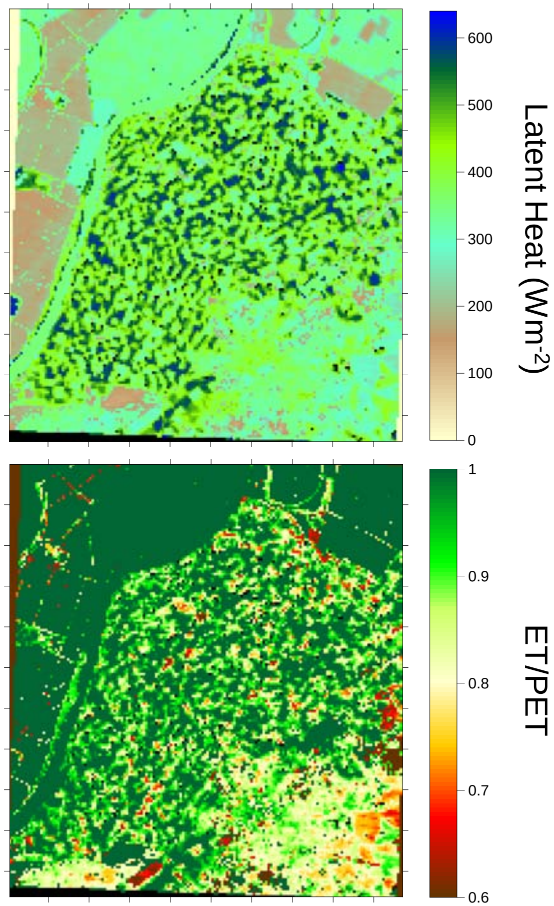

Landsat 5 (120m)

CONCLUSIONS

- HyspIRI is uniquely suited for global water use applications:

  ... wall-to-wall coverage

  ... 5-day revisit (TIR)

  ... sub-field scale resolution (60m)

  ... hyperspectral stress signals

HYSPIRI ADDS SIGNIFICANT VALUE TO OPERATIONAL TIR IMAGING SYSTEMS

Martha.Anderson@ars.usda.gov

ALEXI validation sites

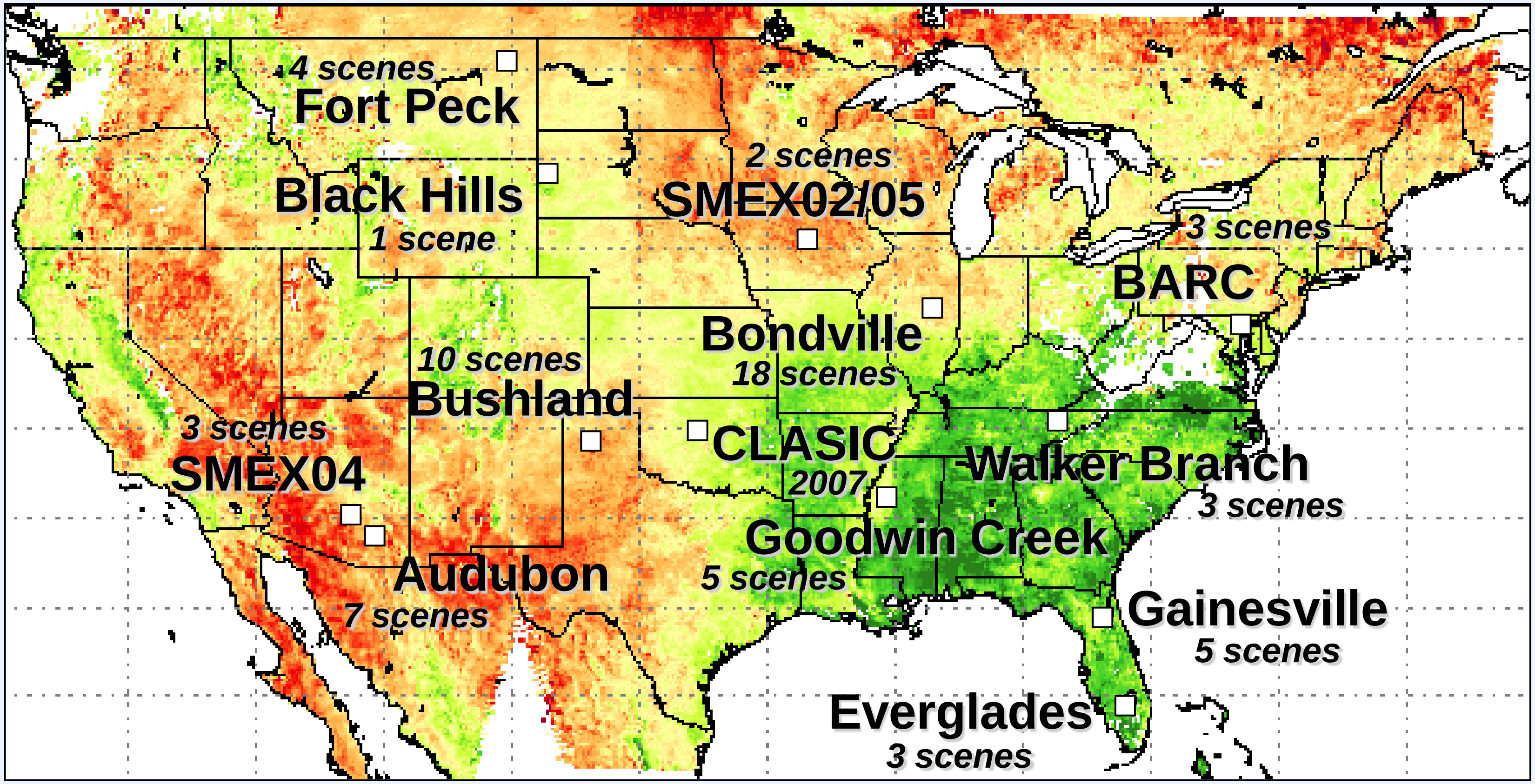

Clear-sky fluxes using Landsat TIR (~100m)

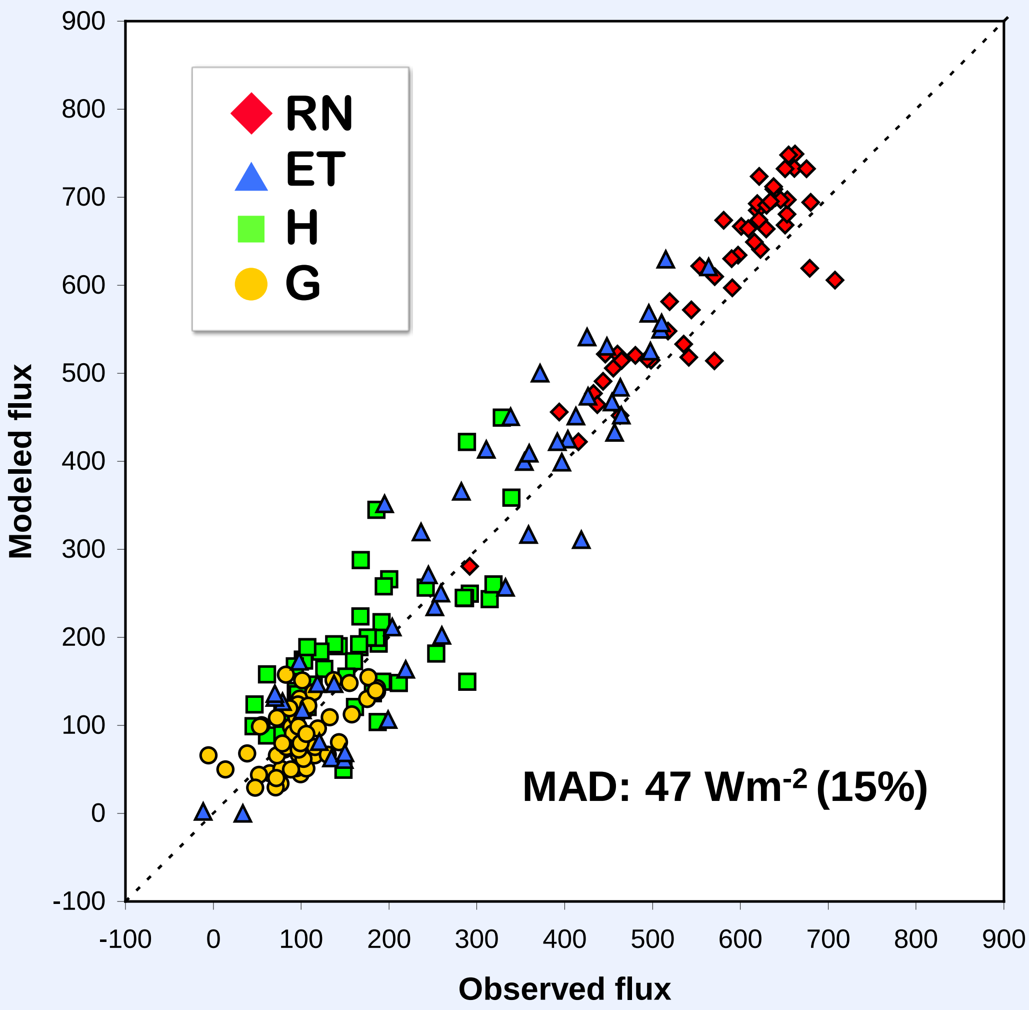

Sensitivity to shallow water tables

Simulated climatological water table*

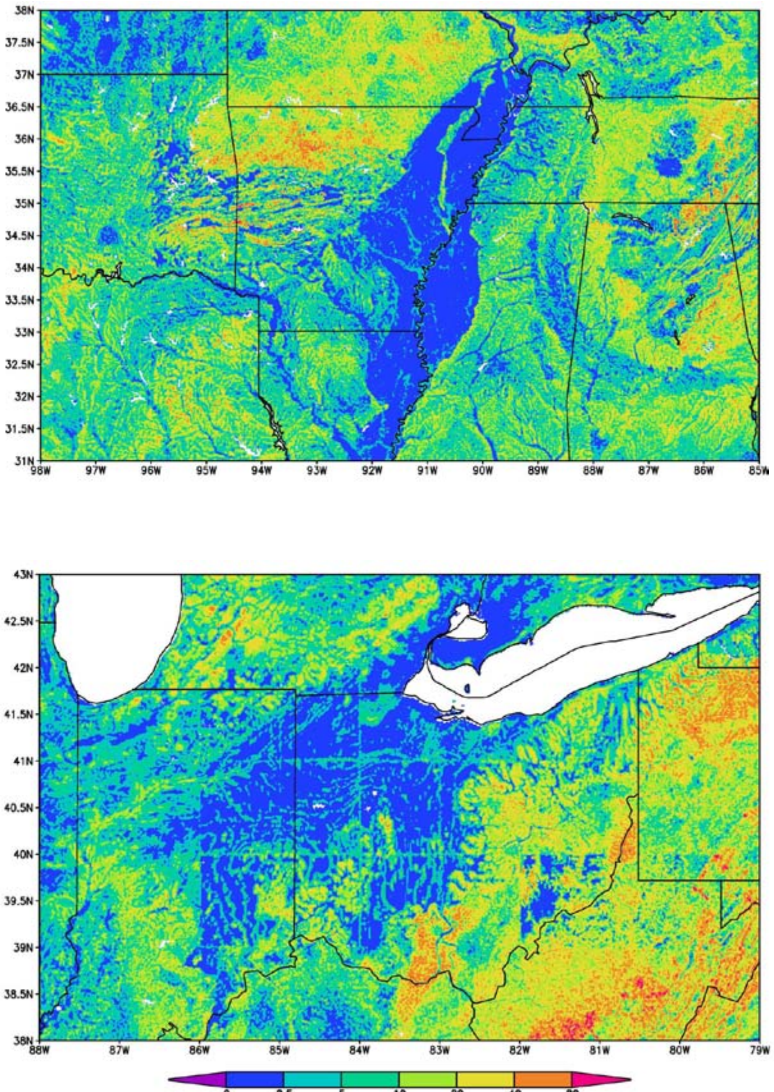

shallow deep

Temporal variability in ET/PET

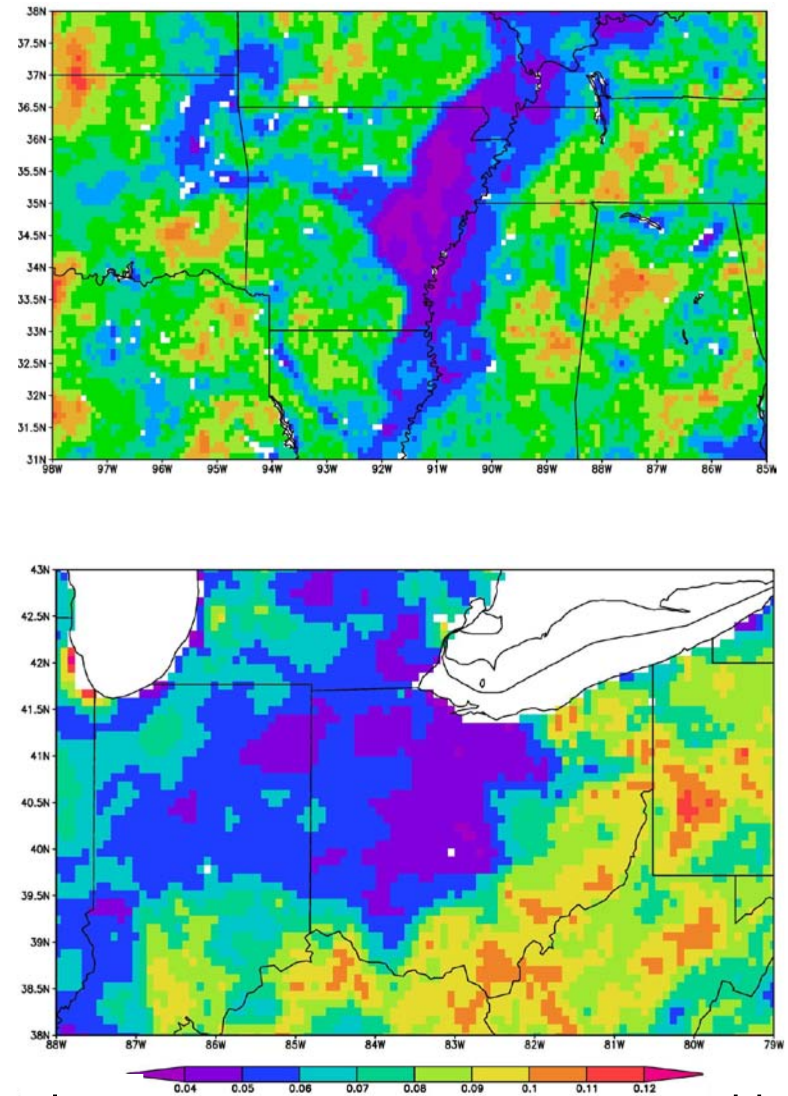

low high

* Miquez-Macho et al, BAMS, 90, 663-672

HyspIRI: Imaging Spectroscopy of Plant Metabolic and Ecological Function

Phil Townsend, Shawn Serbin, Aditya Singh, Dylan Dillaway, Brenden McNeil and Eric Kruger

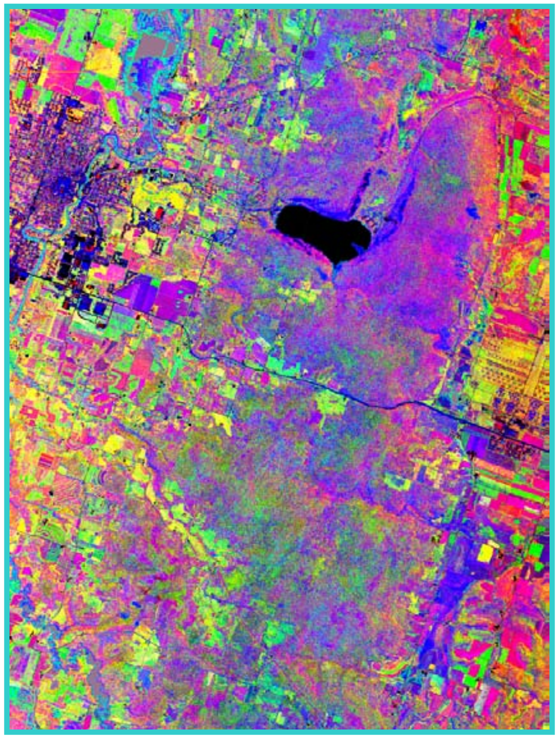

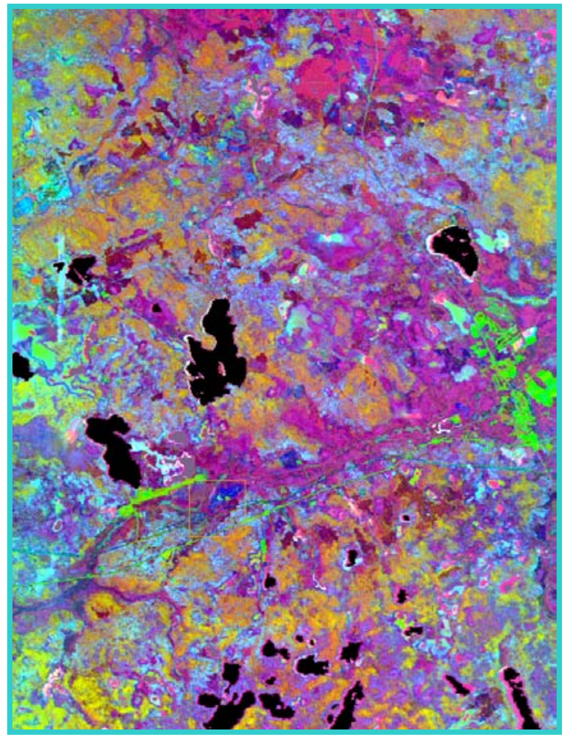

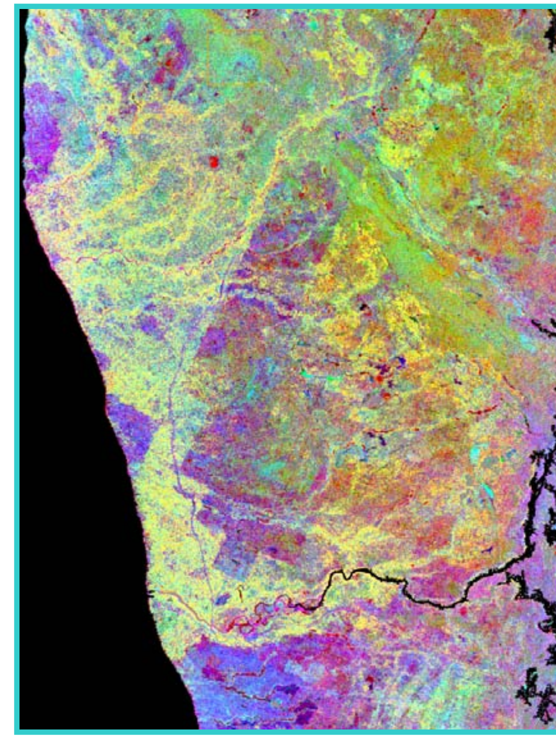

Photosynthesis:
A temperature-mediated photochemical reaction

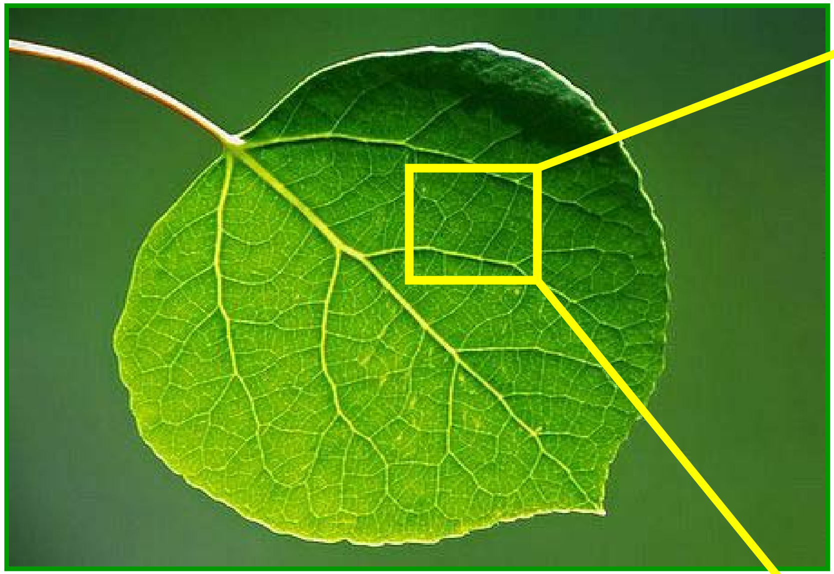

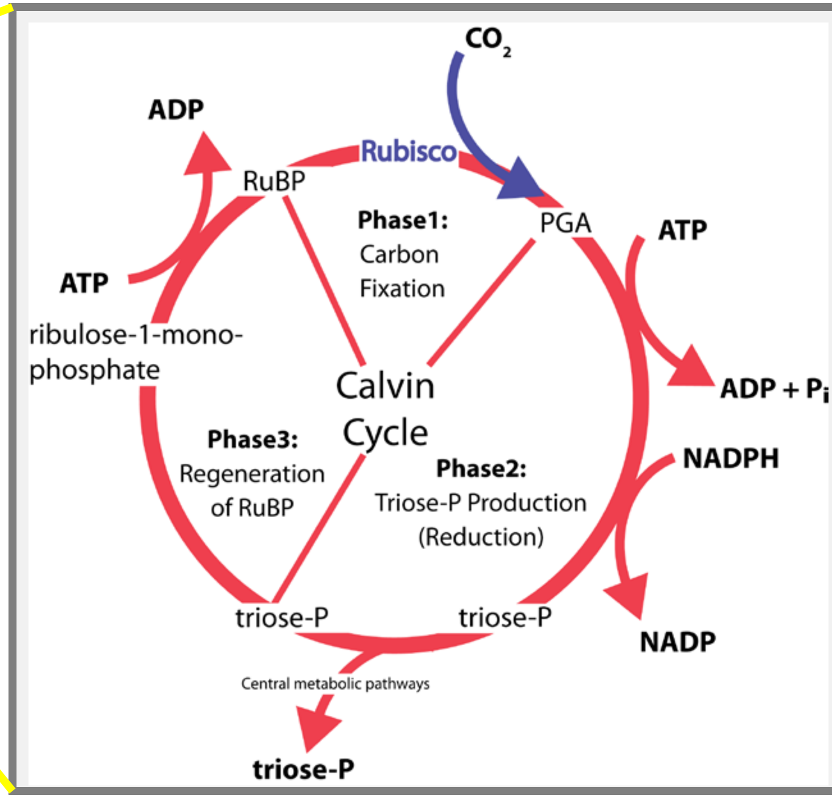

Climate is key to photo-synthetic potential.

Nutrient dynamics:
Plant allocation and use of resources

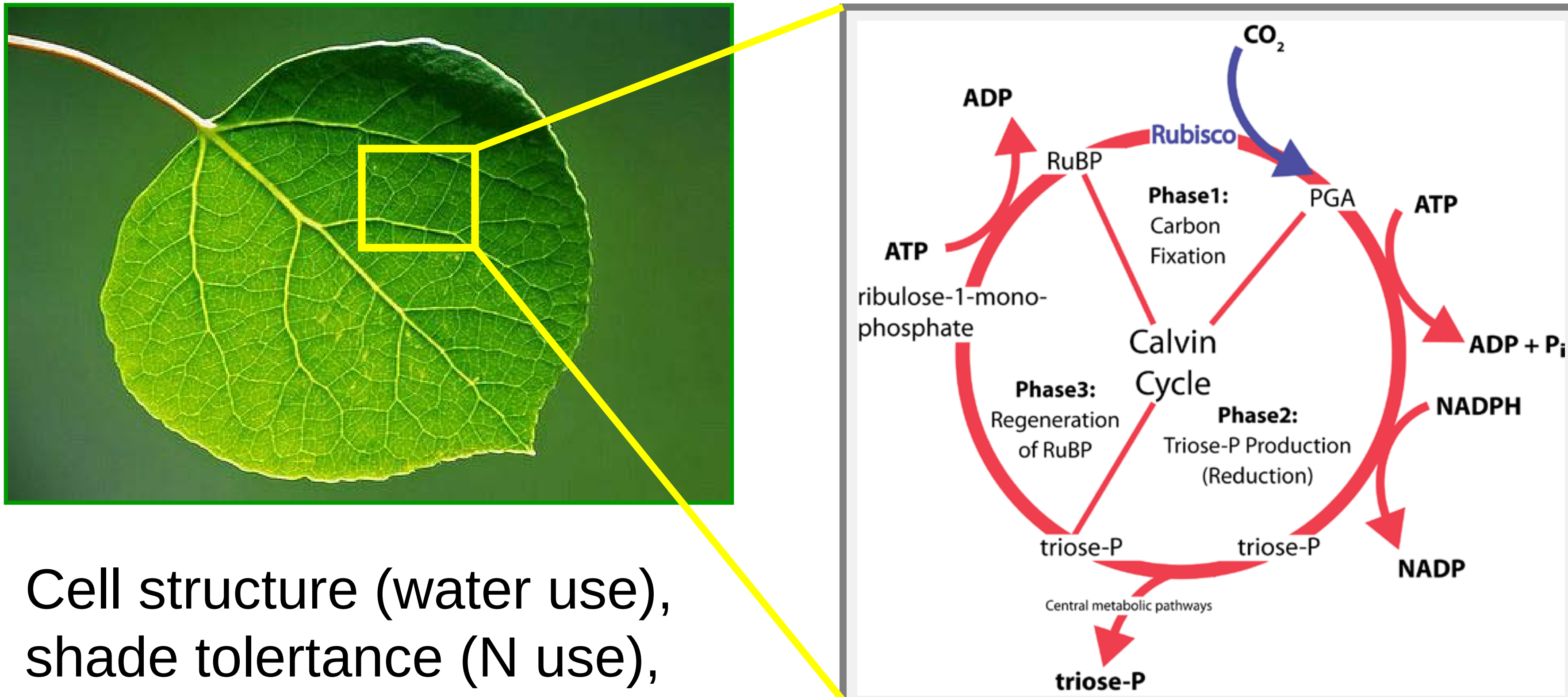

Cell structure (water use),
shade toltertance (N use),
recalcitrance (decomposition)

Key concepts for climate change research:

Photosynthesis is driven by light, temperature, water availability, nutrients, etc.

If we can measure specific processes of photosynthesis using imaging spectroscopy and thermal (temperature) measurements, then:

• We can measure changes in photosynthetic rates, and:
• Assess changes in carbon assimilation by vegetation and changes in vegetation function associated with ΔT.
• *Global mission necessary to evaluate changes in photosynthesis that occur over large areas.*

Definition: V(c)max – maximum rate of carboxylation

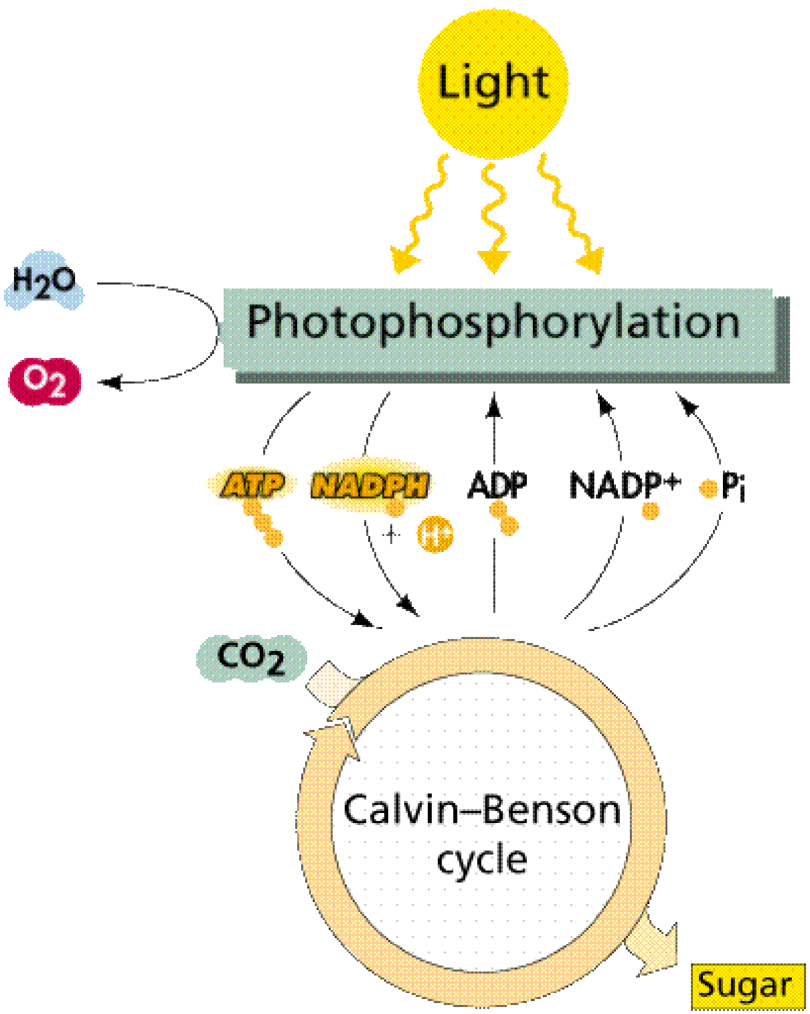

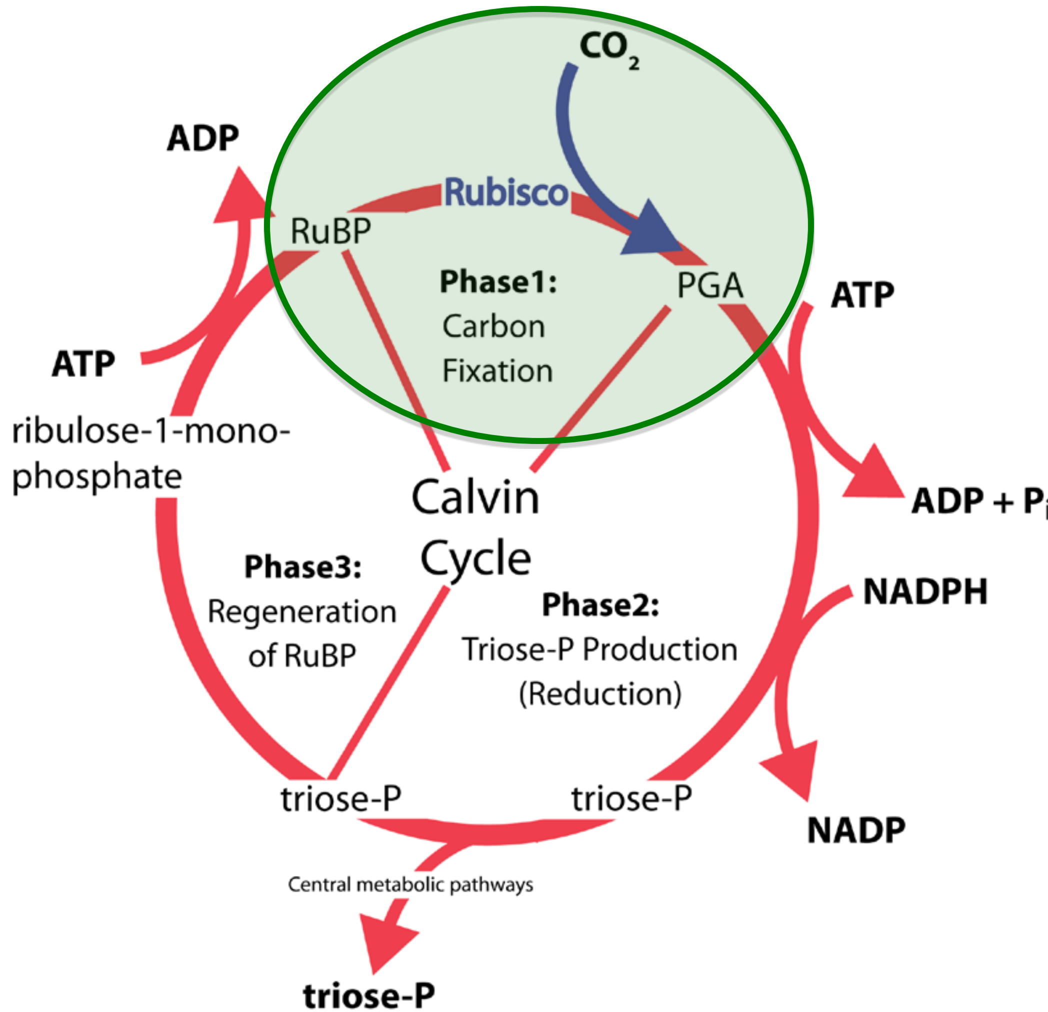

Carboxylation – initial addition of CO_2 to RuBP (catalyzed by RuBisCO). Addition of ATP and NADPH → triose phosphate

Photosynthesis – The Chloroplast

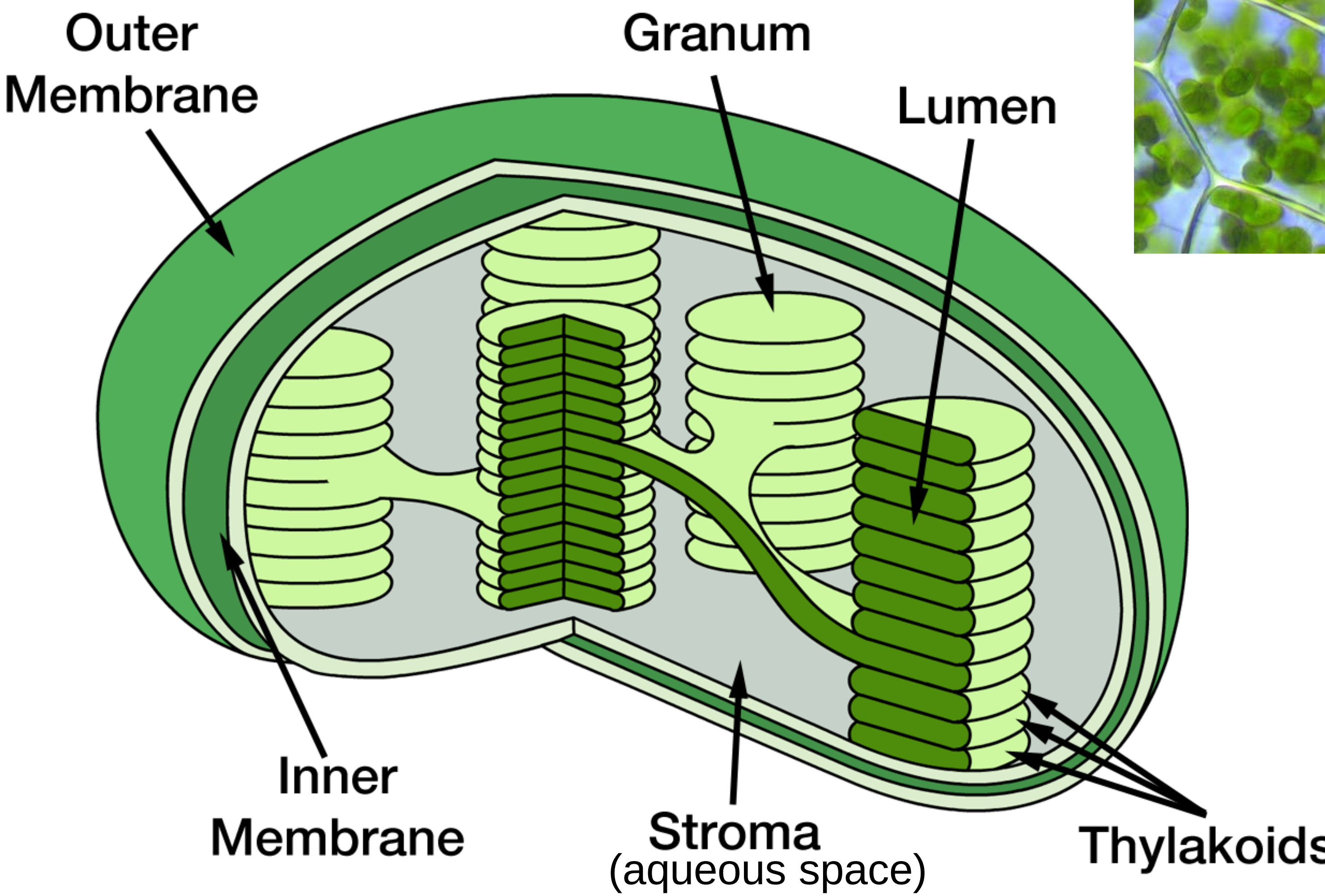

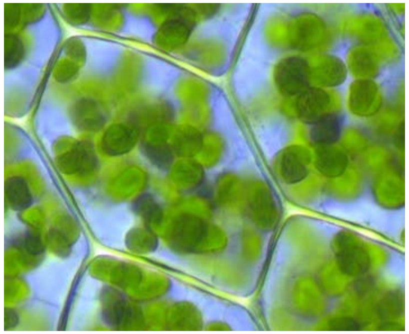

http://photoprotection.clinuvel.com/custom/uploads/LUV_fig4_chloroplast_v(1).gif

Definition: Jmax – electron transport rate

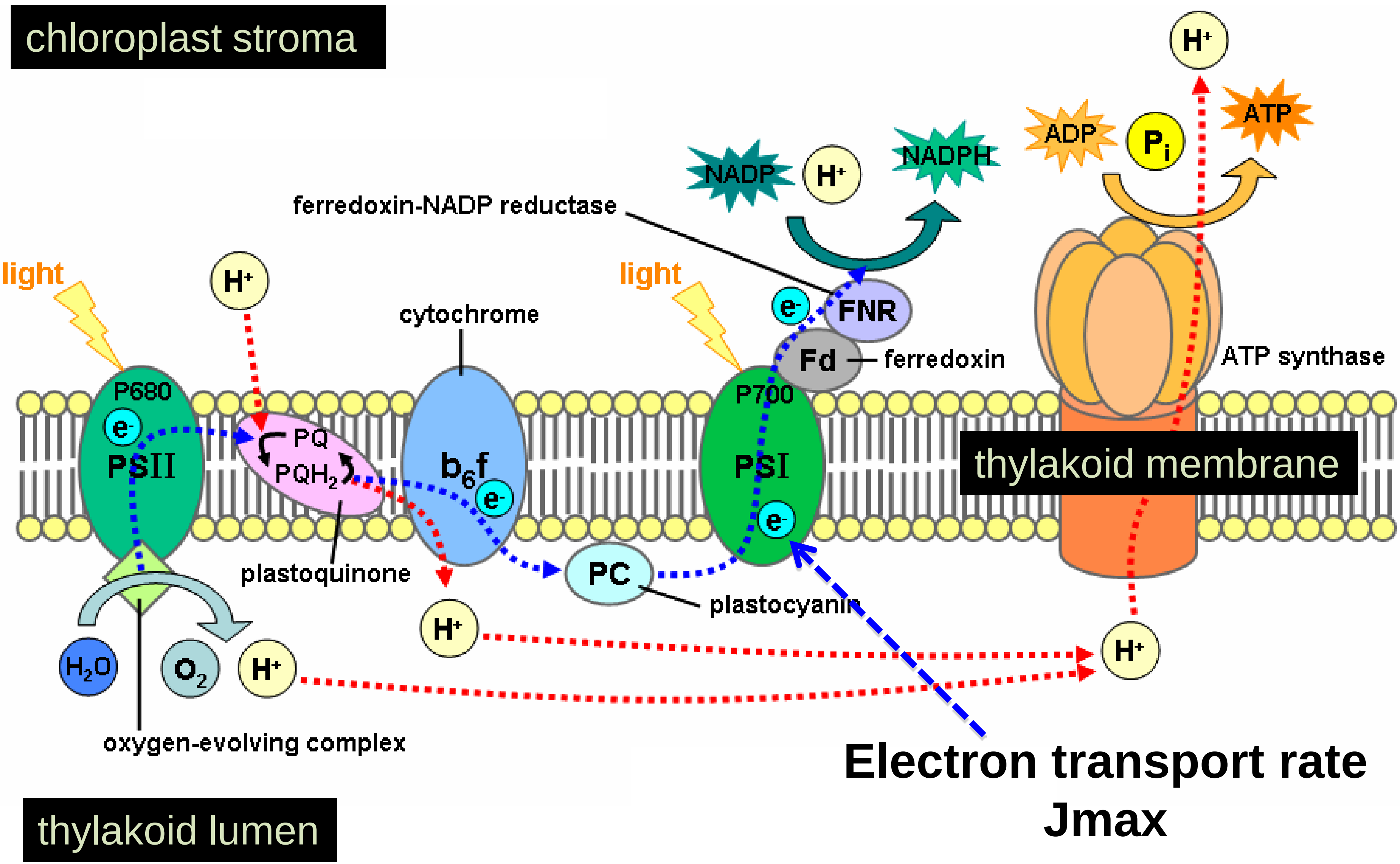

Electron transport rate
Jmax

Diagram from wikipedia commons

Background:

$V_{(c)max}$: Measurement of process by which Rubisco catalyzes RuBP with CO_2 to produce the carbon compounds that eventually become triose phosphates (G3P, PGAL)

Triose phosphates are the building block for sugars and starches.

J_{max}: Transport of electrons through the thylakoid membrane is critical to producing NADPH and ATP, which provide the metabolic energy necessary to produce triose phosphates.

Biochemical modeling of photosynthesis

$$A_n = \min(A_c, A_j, A_p) - R_d$$

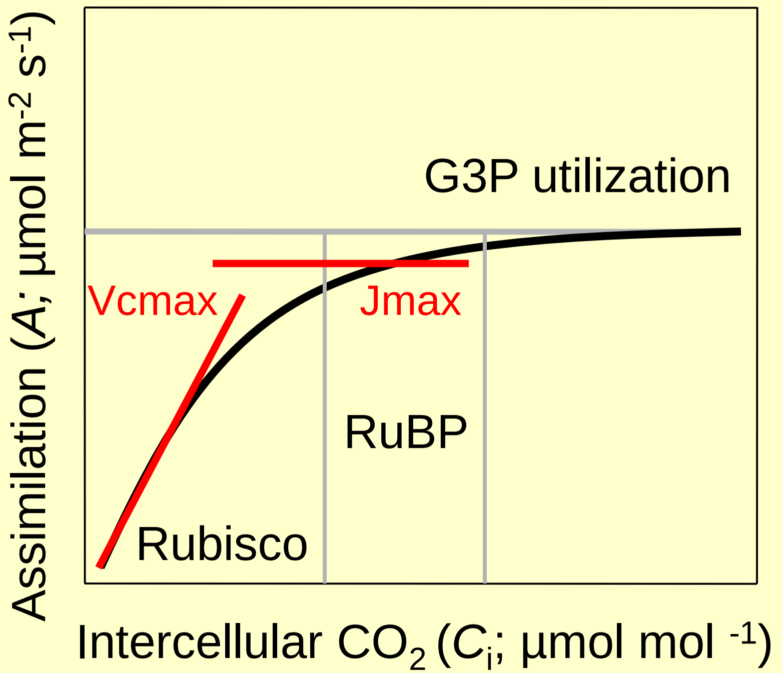

- Limited by
  - Rubisco
  - RuBP regeneration
  - triose phosphate utilization
- Determine key metabolic variables
  - **Vcmax**: Rubisco activity
  - **Jmax**: Electron transport

How will climate change affect composition and metabolism?

- Across the range of a species**
- Photosynthetic capacity varies according to climate
- Changes in climate should be expressed in changes in rates (Vcmax, Jmax)

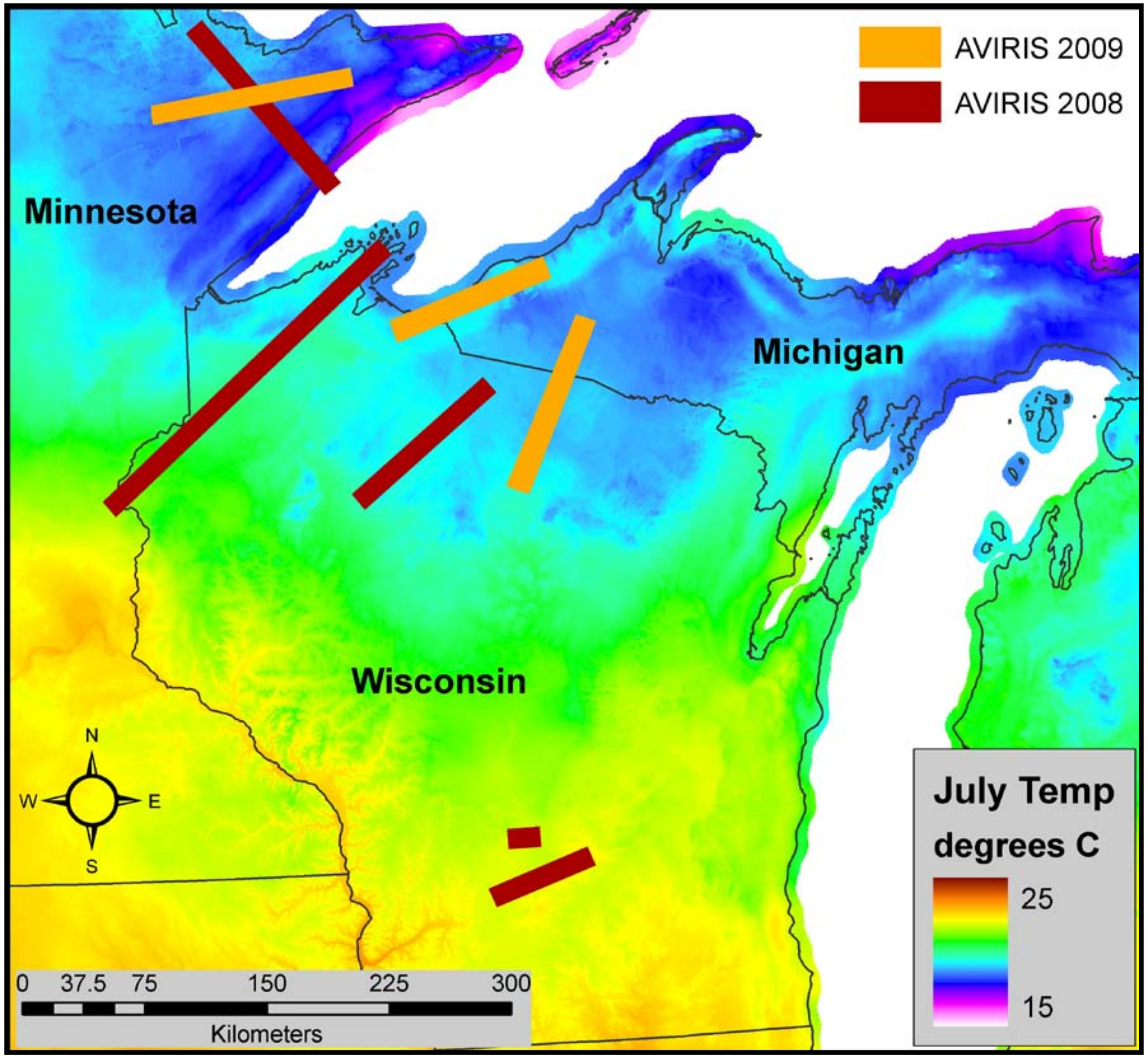

PRISM Data: http://www.prism.oregonstate.edu/

How will climate change affect composition and metabolism?

- **Hyperspectral imagery**
- Field collection
  - Gas exchange
  - Spectra
  - **Canopy temperature**
- Examine regional trends
  - Lat/Long variation

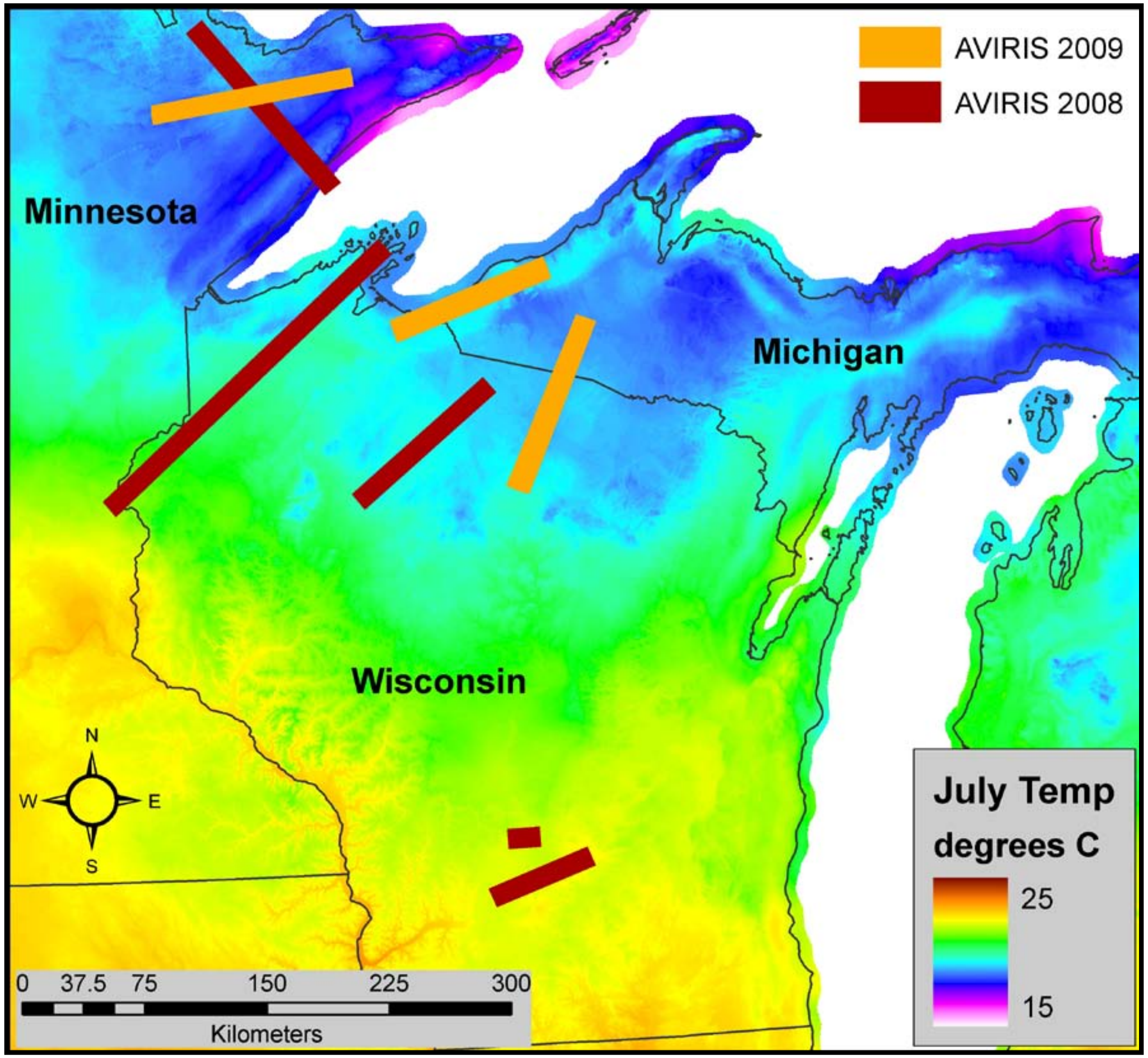

PRISM Data: http://www.prism.oregonstate.edu/

Where does HyspIRI fit in?

HyspIRI spectral and thermal measurements provide the opportunity to directly measure the photochemical processes associated with carbon assimilation (e.g., A_{max}) and respiration ***by plants across the ranges of species***.

These HyspIRI products provide the potential to identify changes in photosynthetic processes associated with climate change (e.g., temperature) across species.

Detection of leaf metabolic rates using spectroscopy

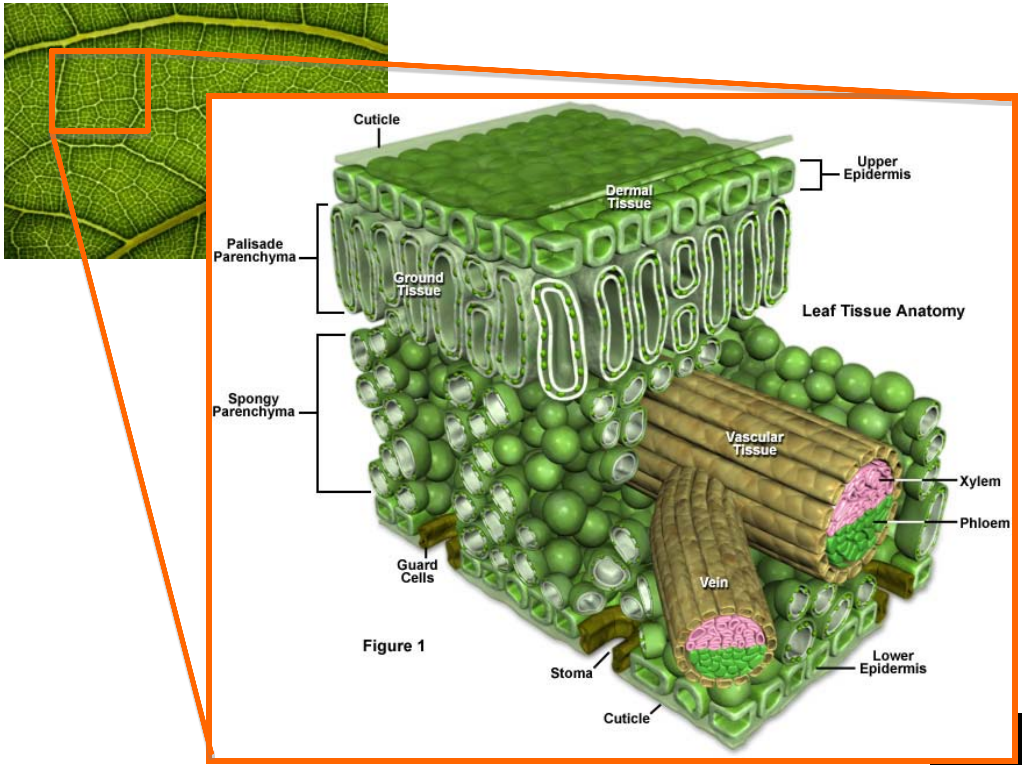

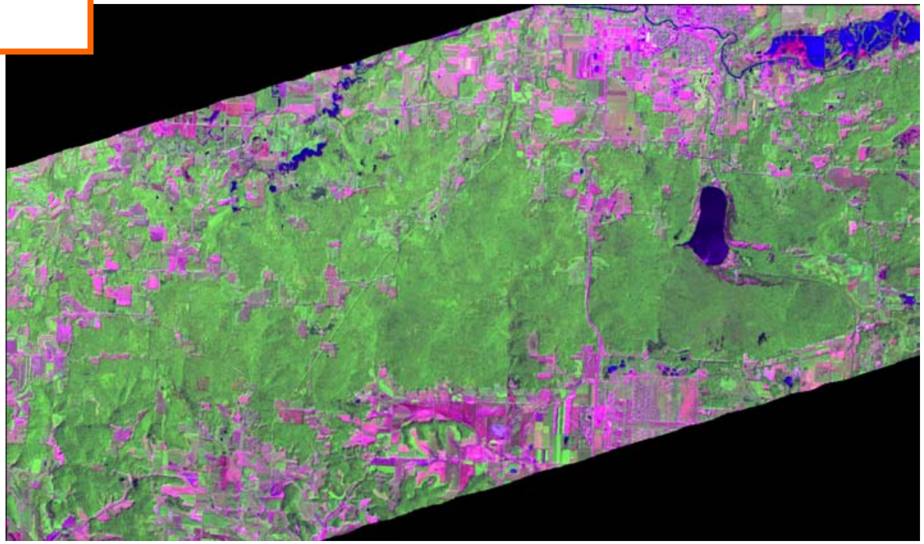

Physiological data in glasshouse study

- Three temperature regimes
  - 13/20 °C, 18/25 °C, 23/30 °C
- Leaf gas exchange
  - Vcmax, Jmax, A_{mass}, A_{area}
- Morphology and nutrition
  - SLA, Leaf N
- Leaf optical properties (350-2500 nm)

Empirical evidence: Cottonwood and Aspen

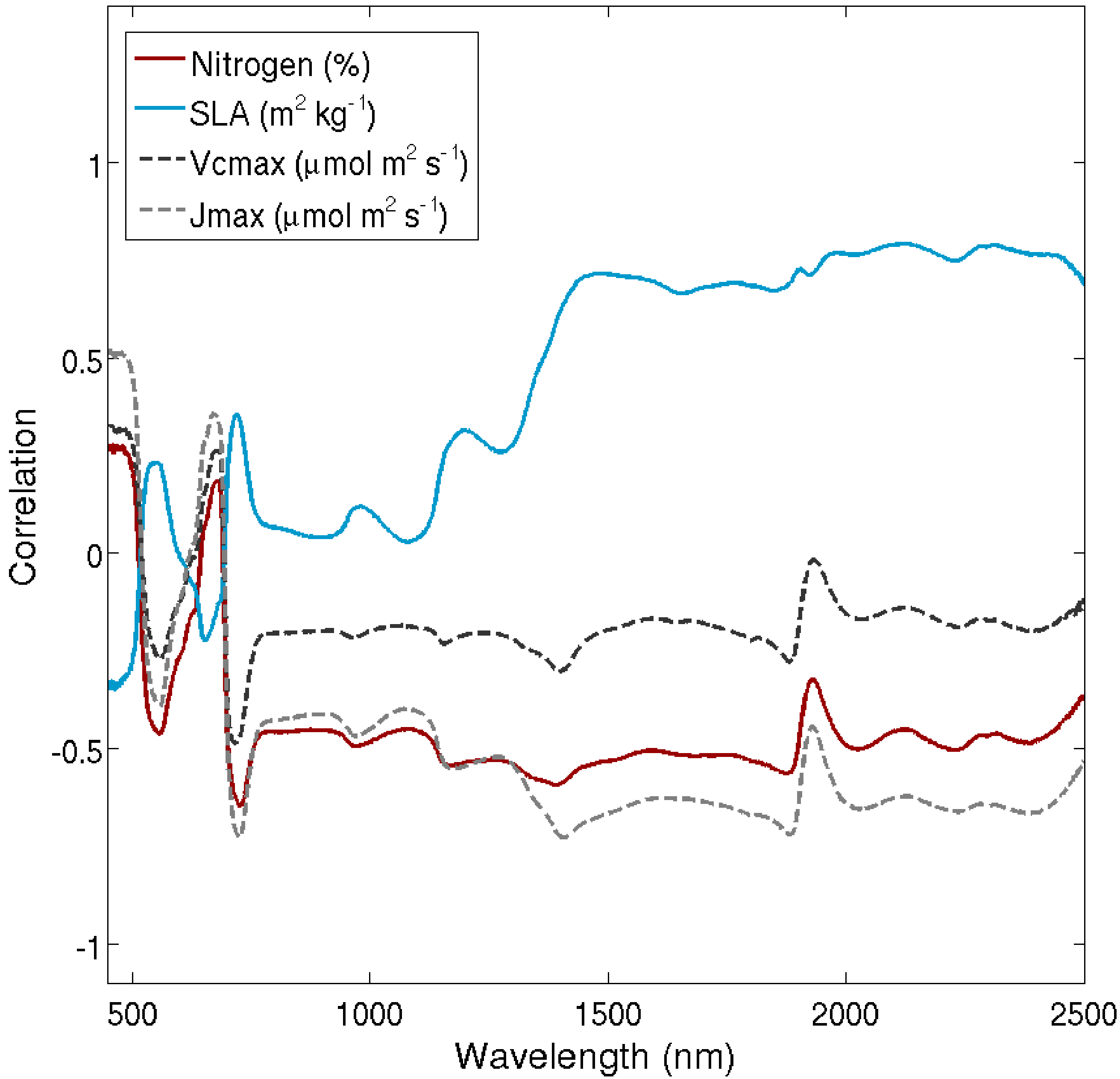

Physiological measurements across temperature regimes

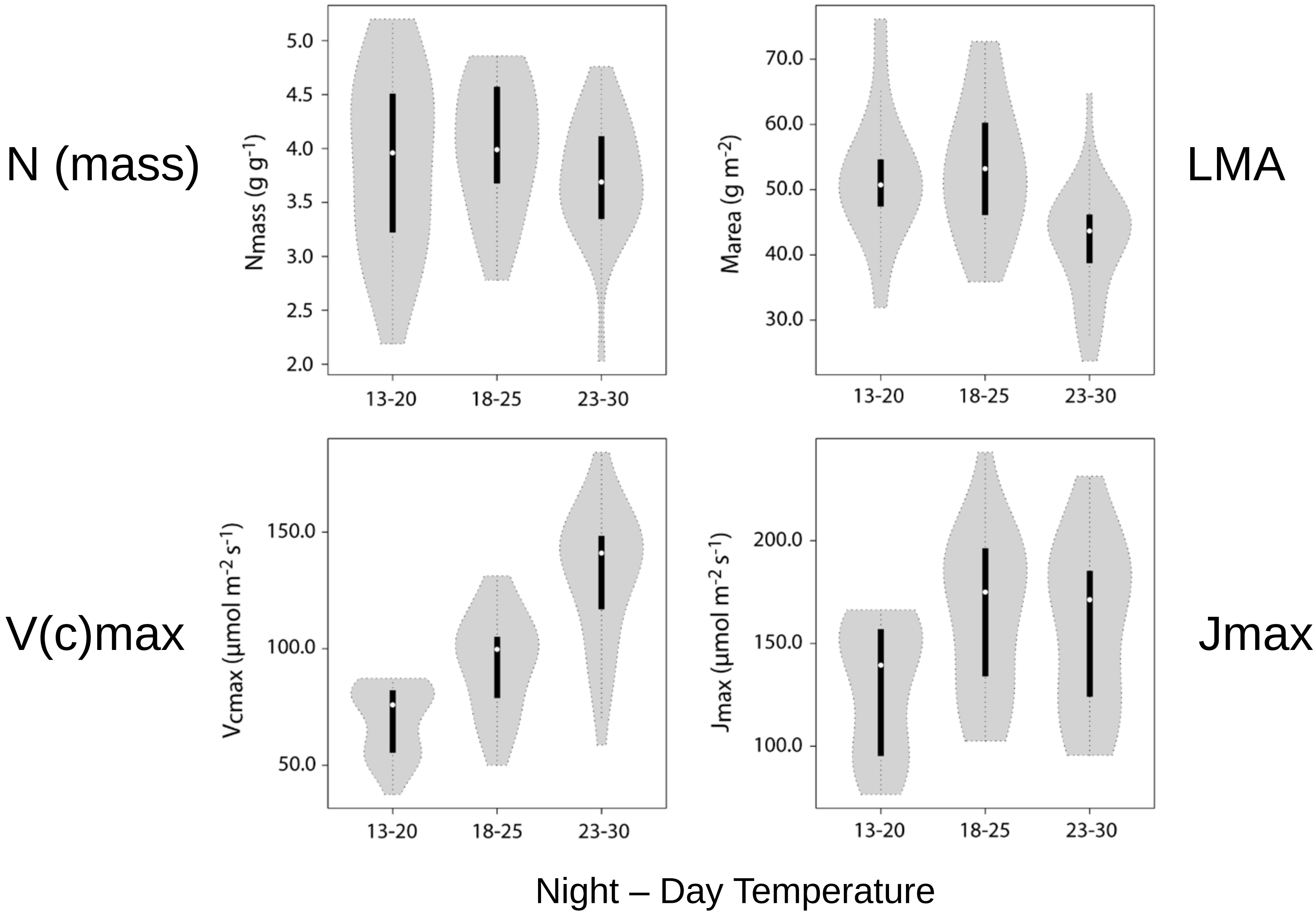

Predictions using leaf spectra and PLSR (%N example)

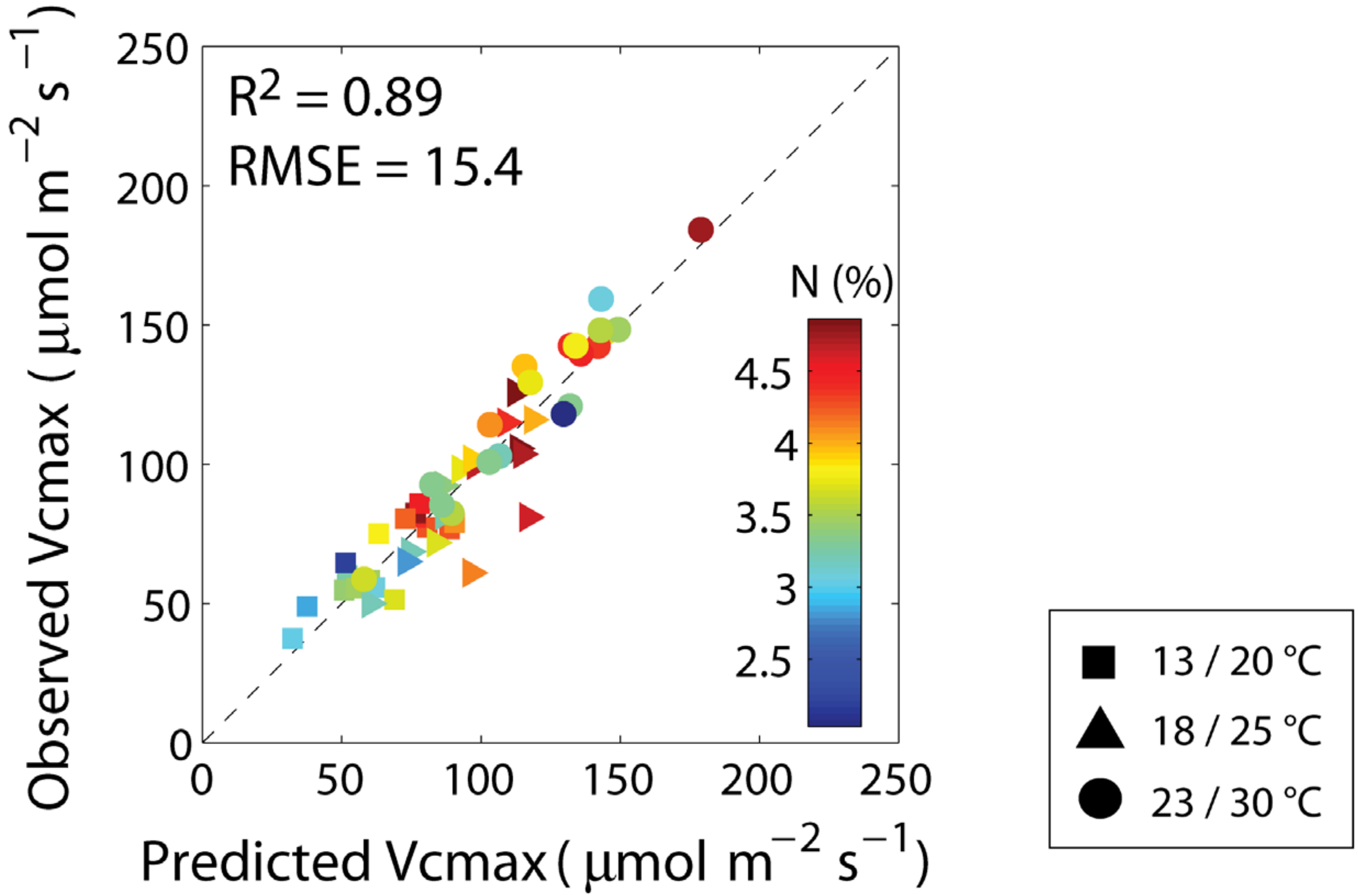

Biotron measurements show thermal effects on leaf metabolism

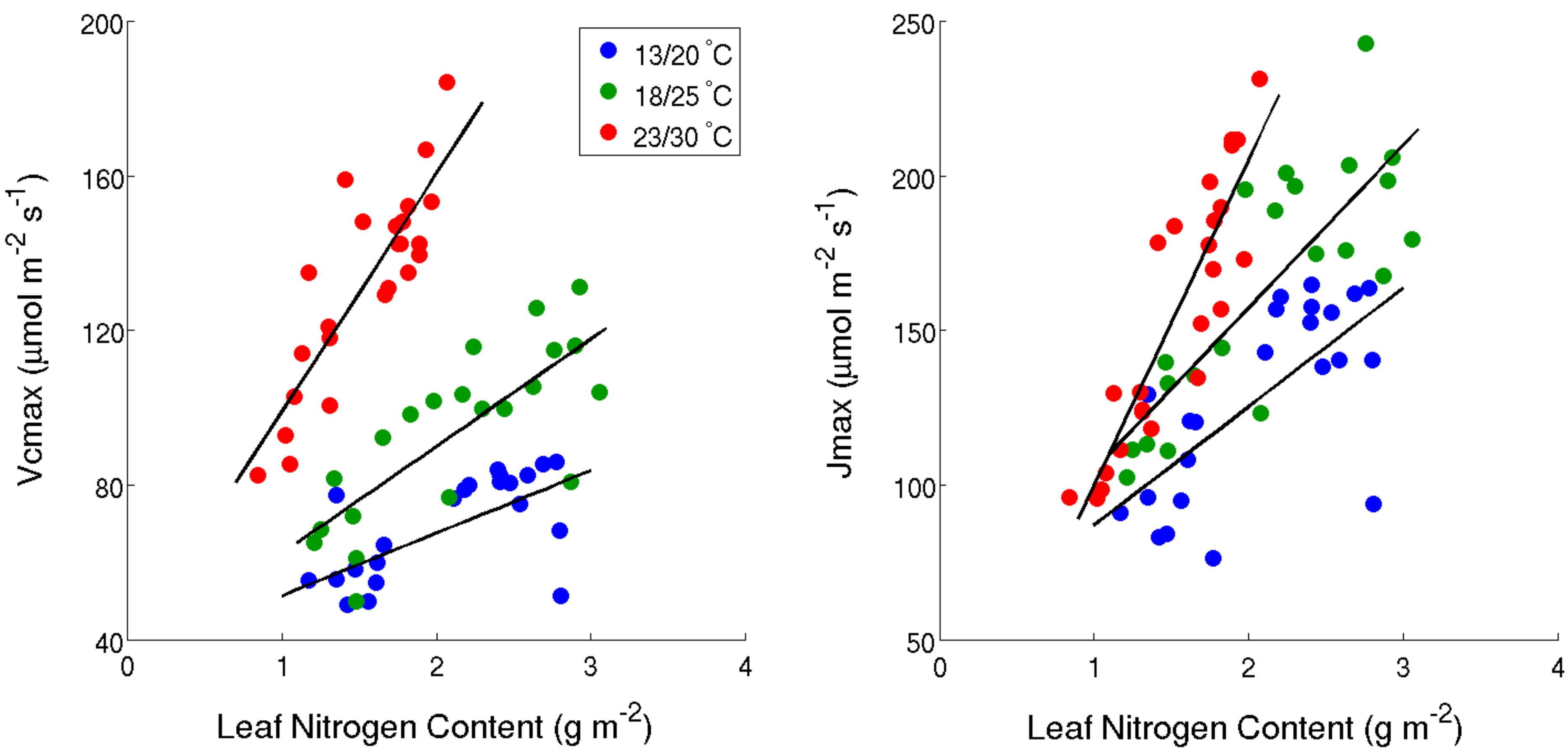

$R^2 = 0.003$ $R^2 = 0.33$

Pooled R^2 between spectra-predicted V(c)max/Jmax and leaf N

Spectra are responsive to temp.-driven variations in metabolism

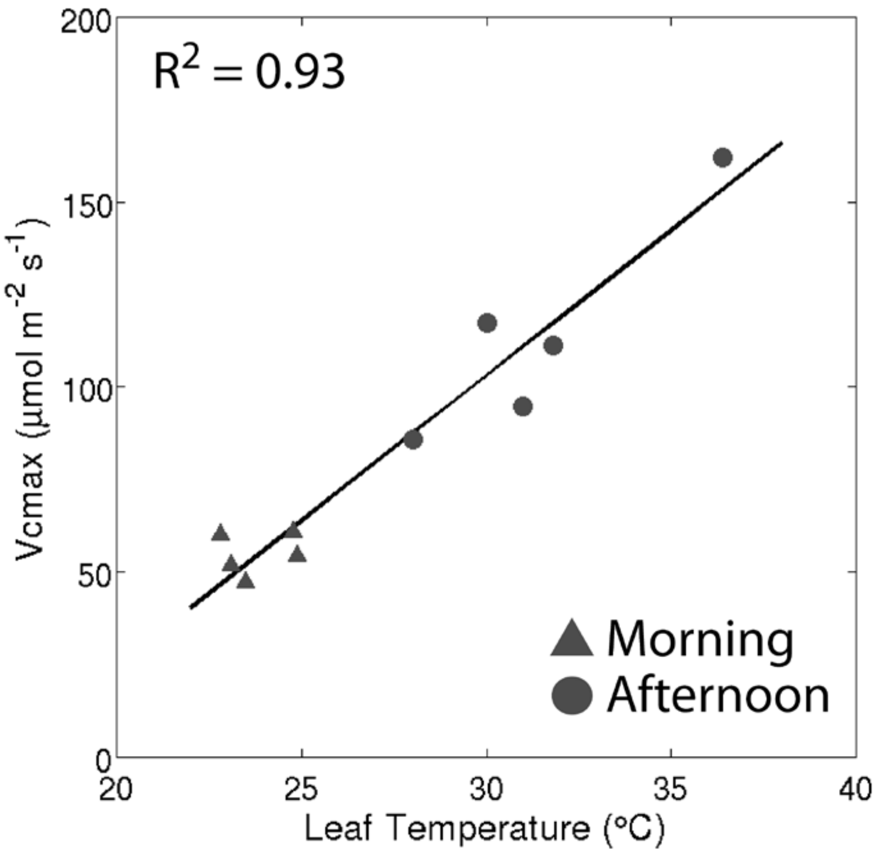

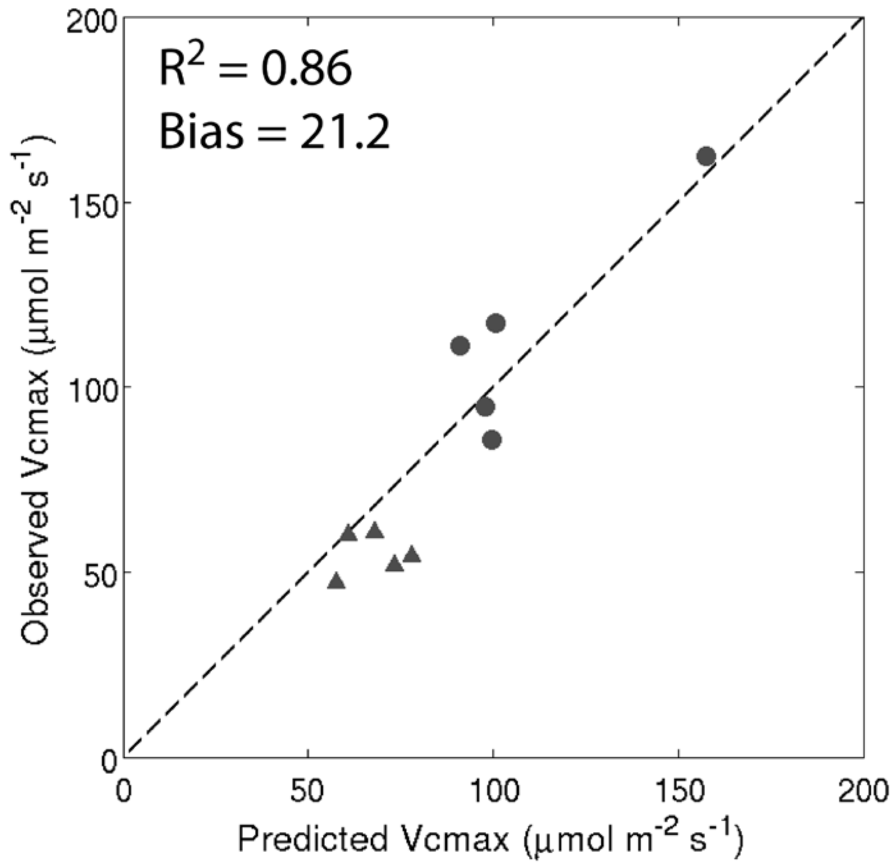

Time	Tleaf (° C)	Vcmax
Morning	23.8	54.8
Afternoon	31.4	114.3

Examples: AVIRIS imagery from the Upper Midwest

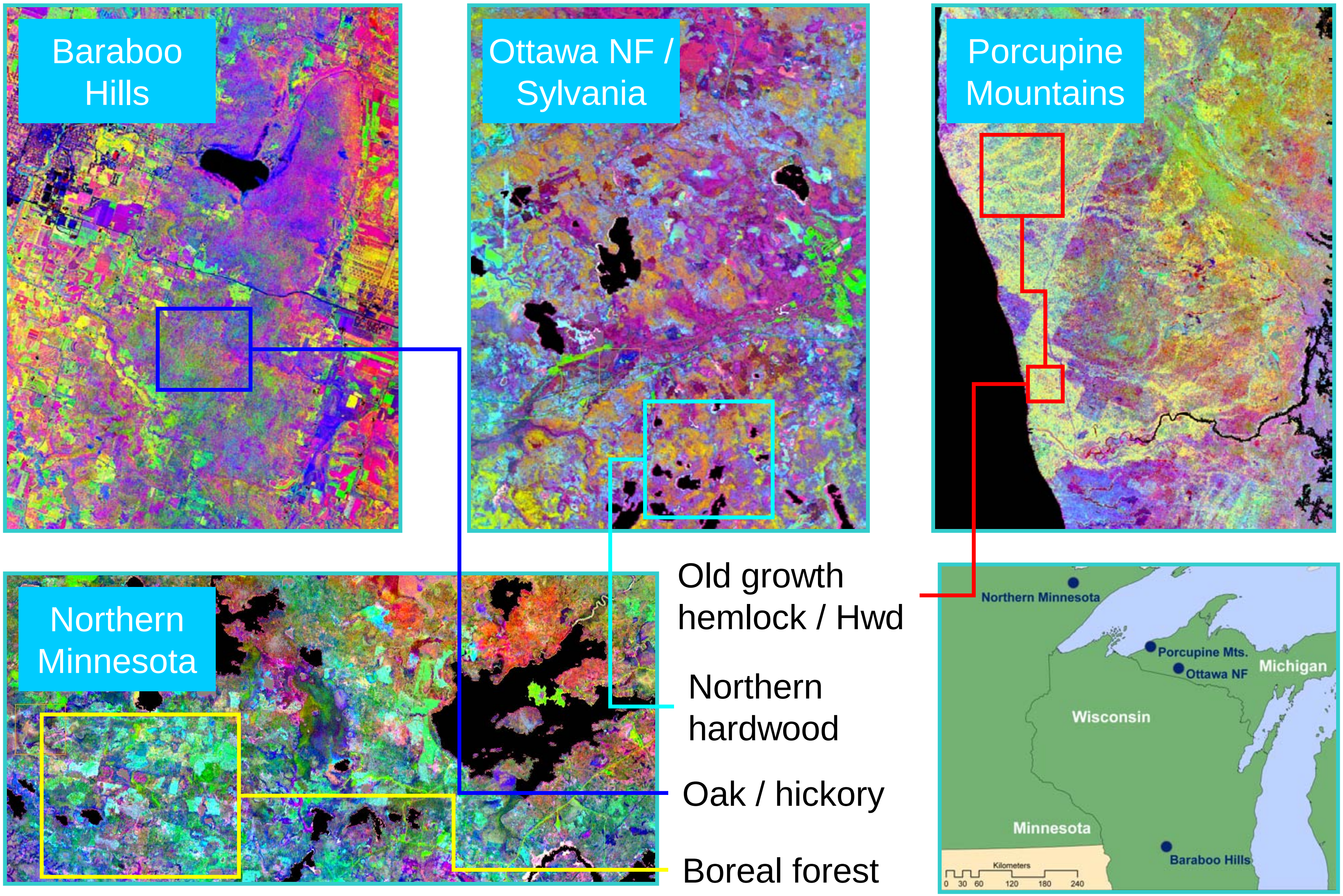

Examples: LMA – based on hypothesized relationships

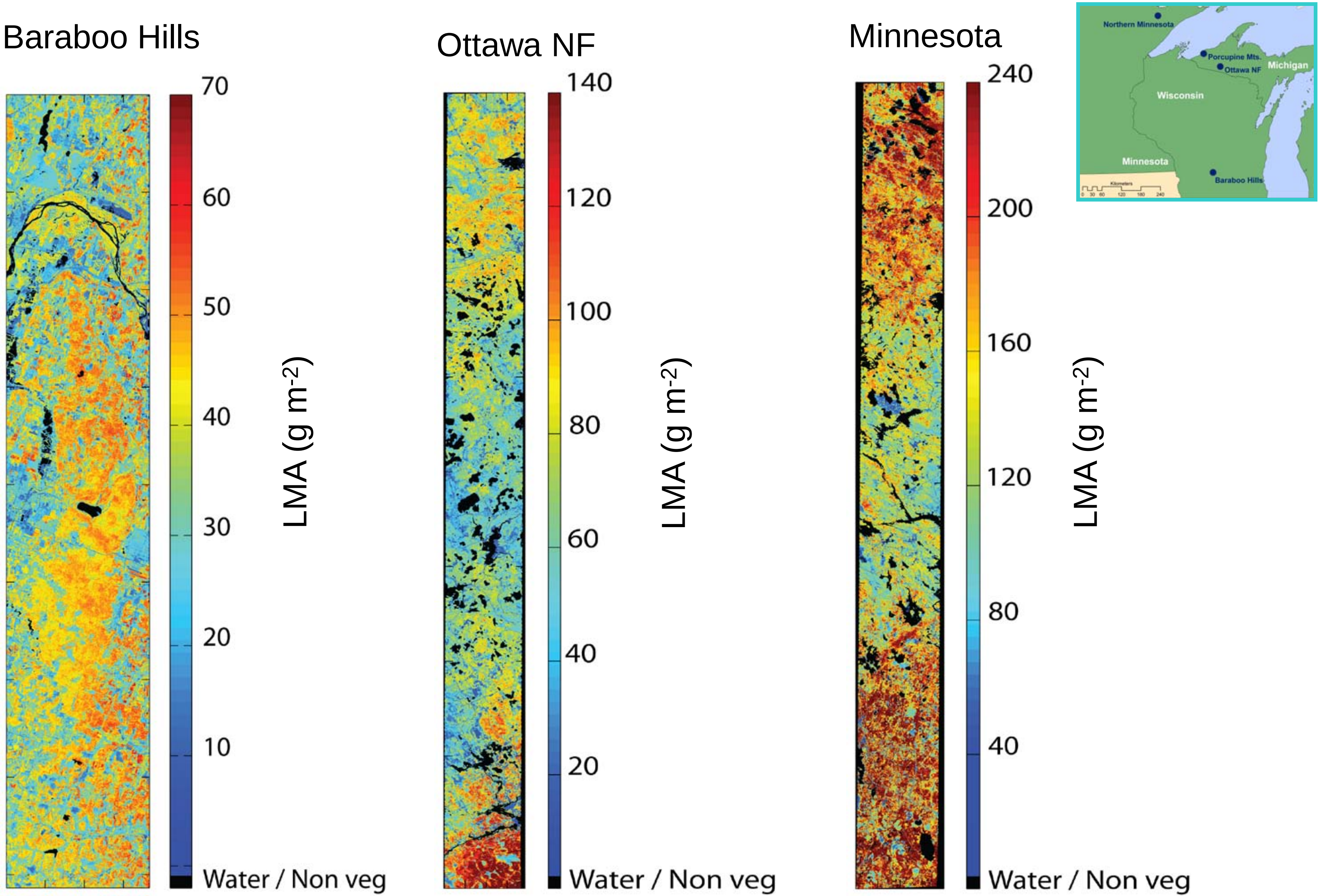

Examples: V(c)max – based on hypothesized relationships

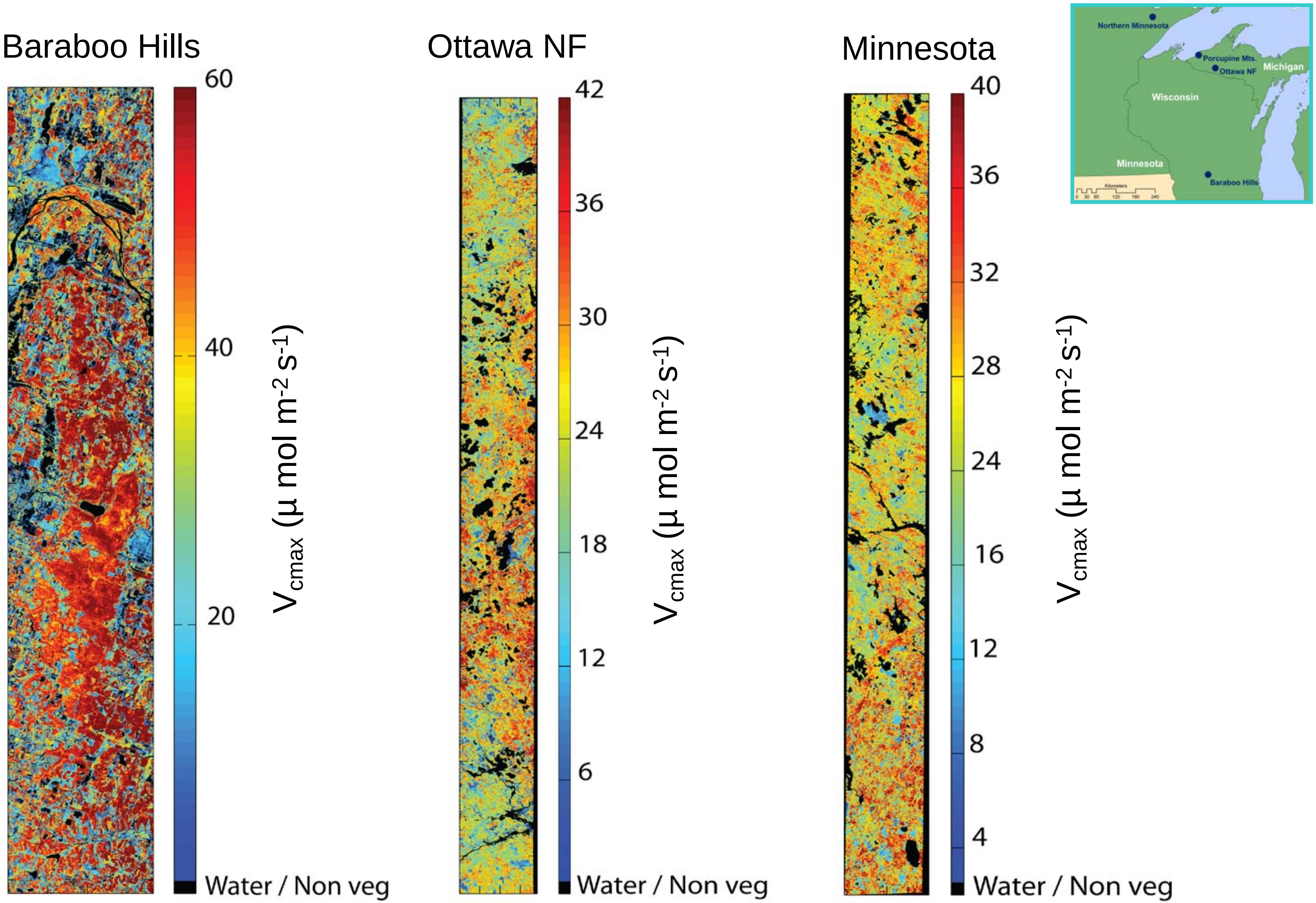

Examples: Jmax – based on hypothesized relationships

Baraboo Hills Ottawa NF Minnesota

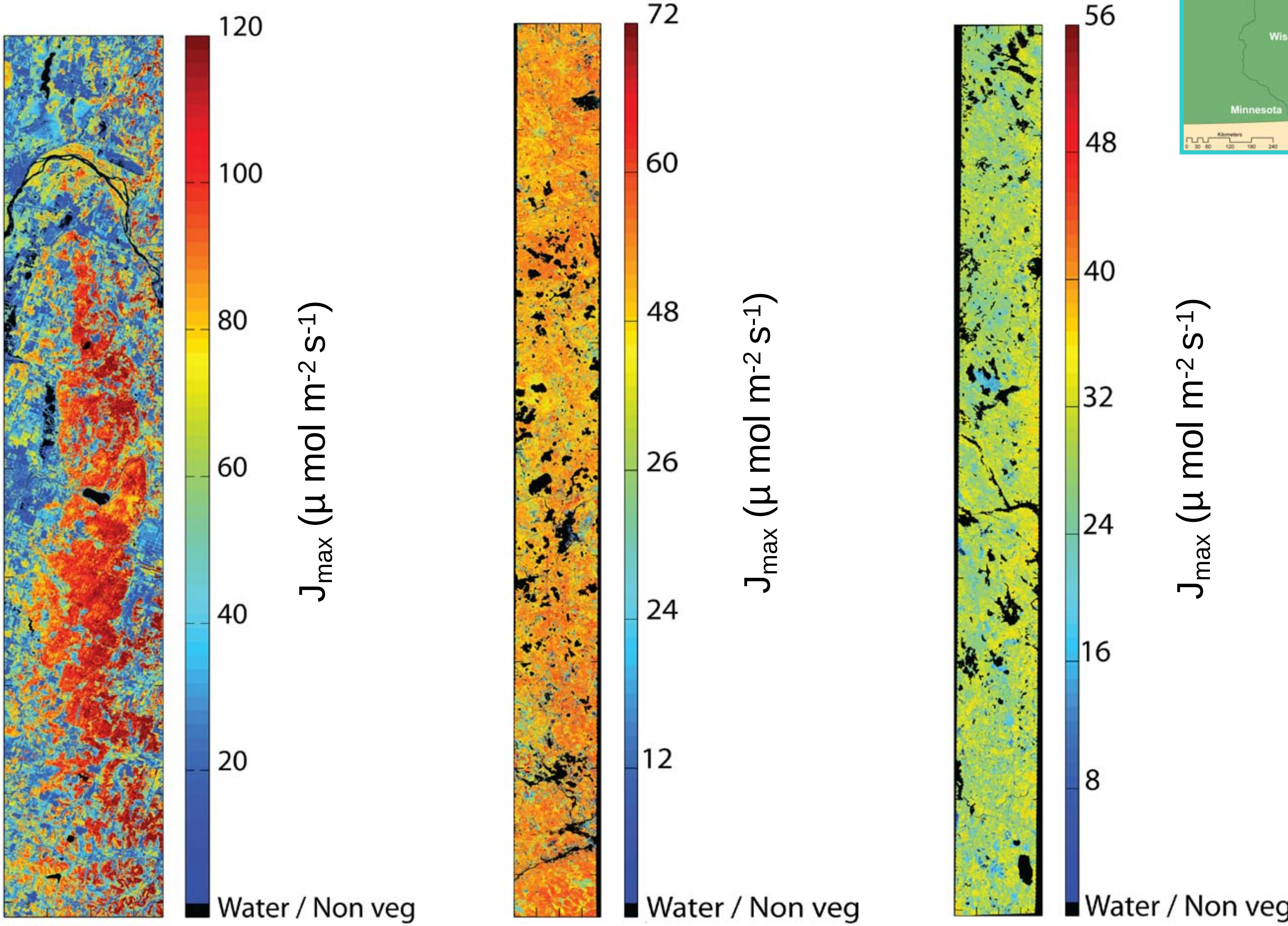

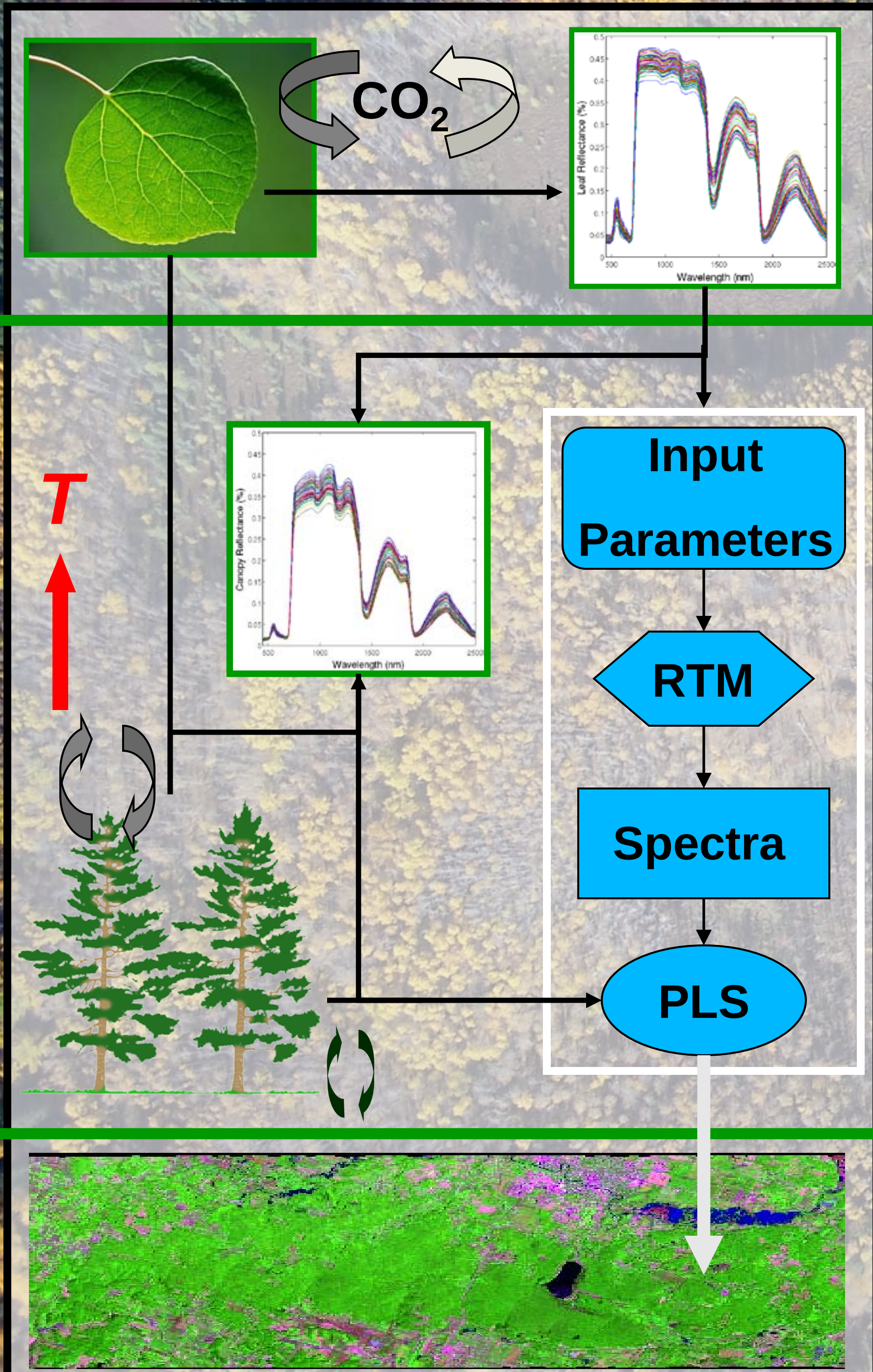

Now working on scaling leaf → canopy → sensor

Using HyspIRI-like data (AVIRIS + ASTER/MASTER), we are looking at forest acclimation to T and CO_2.

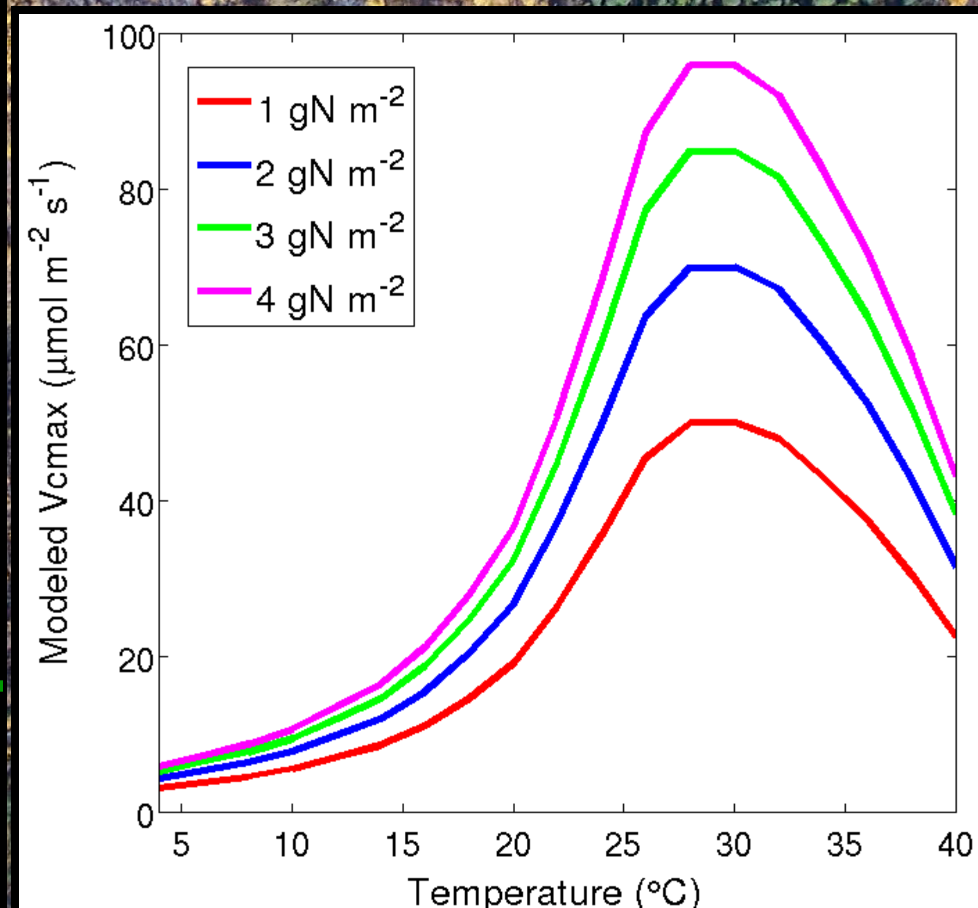

Remote sensing of genetic diversity in aspen:
Directly associated with vegetation response to climate change

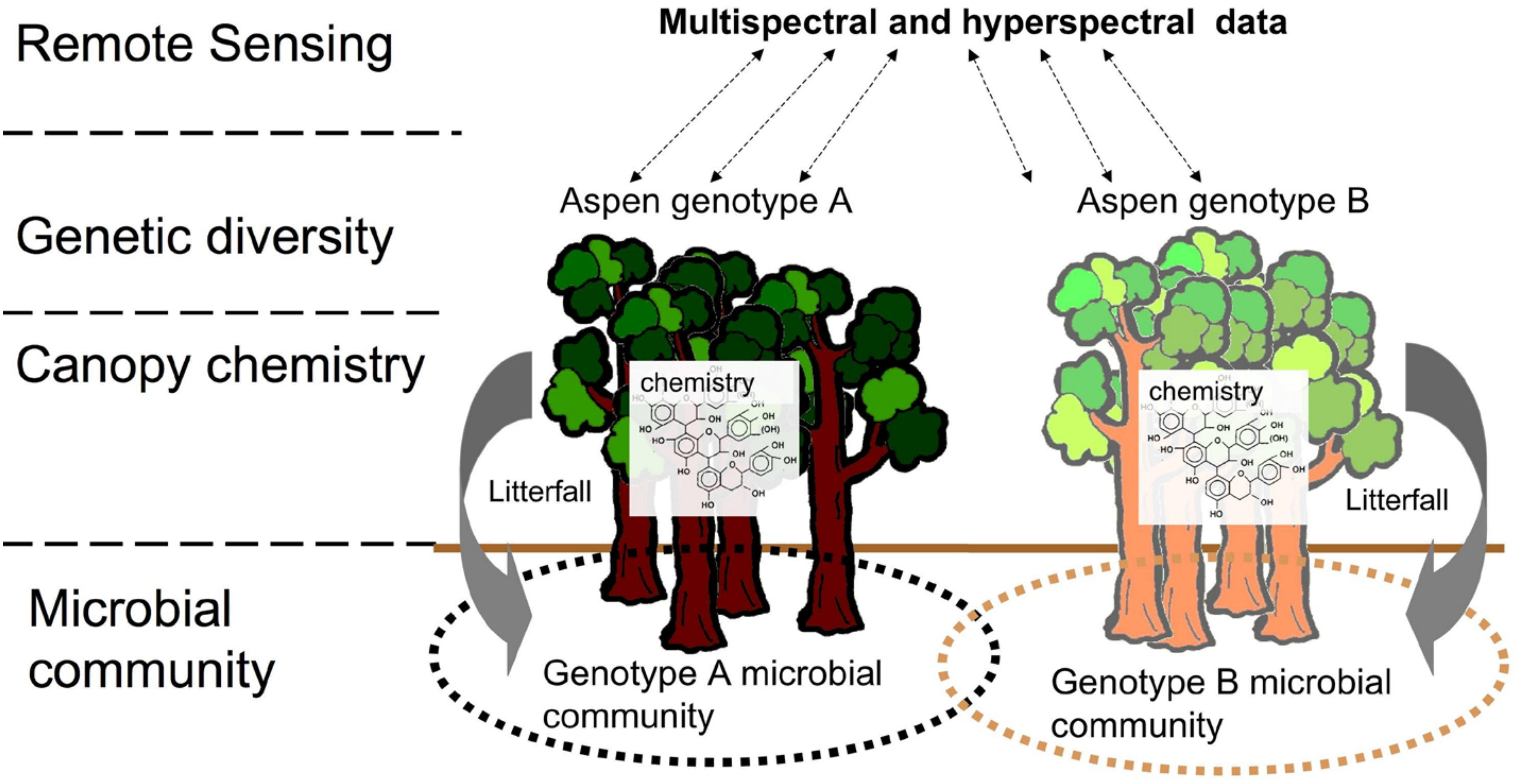

Acknowledgments

- Terrestrial Ecology and Biodiversity Program
- Earth & Space Science Fellowship
- HyspIRI Preparatory Activities

NASA

JPL

Jet Propulsion Laboratory
California Institute of Technology

AVIRIS

2010 HyspIRI Science Workshop, JPL, August 24-26

Climate Change, Urban Heat Island, and Human Health: Needs for HyspIRI-like Data Products in Urban Climate/Environmental Studies

Qihao Weng, Mahesh Rajasekar, Indiana State University

Dale A. Quattrochi, NASA MSFC, Huntsville, AL

Hua Liu, Old Dominion University, Norfolk, VA

Xuefei Hu, Emory University, Atlanta, GA

Contact: qweng@indstate.edu

CENTER FOR URBAN AND ENVIRONMENTAL CHANGE

UEC

INDIANA STATE UNIVERSITY

Urbanization and Global Change

- The extent and rate of global changes largely driven by rapid population growth.
- Half world population living in urban areas. First “Urban Century”. 100 megacities by 2025 as compared to 20 today.
- Urbanization is one of the most profound examples of human modification of the Earth’s surface.
  - Impacts on local energy, water and carbon exchanges; affect climate, ecosystems, human health, and human systems.
  - The impacts may be of local, regional, or global scale, depending on the size of the area affected.

Los Angeles

Hong Kong

Bird’s Nest, Beijing, before Olympia

Most impact are invisible.

Figure I.3. Percentage of the population in urban areas, 2007, 2025 and 2050

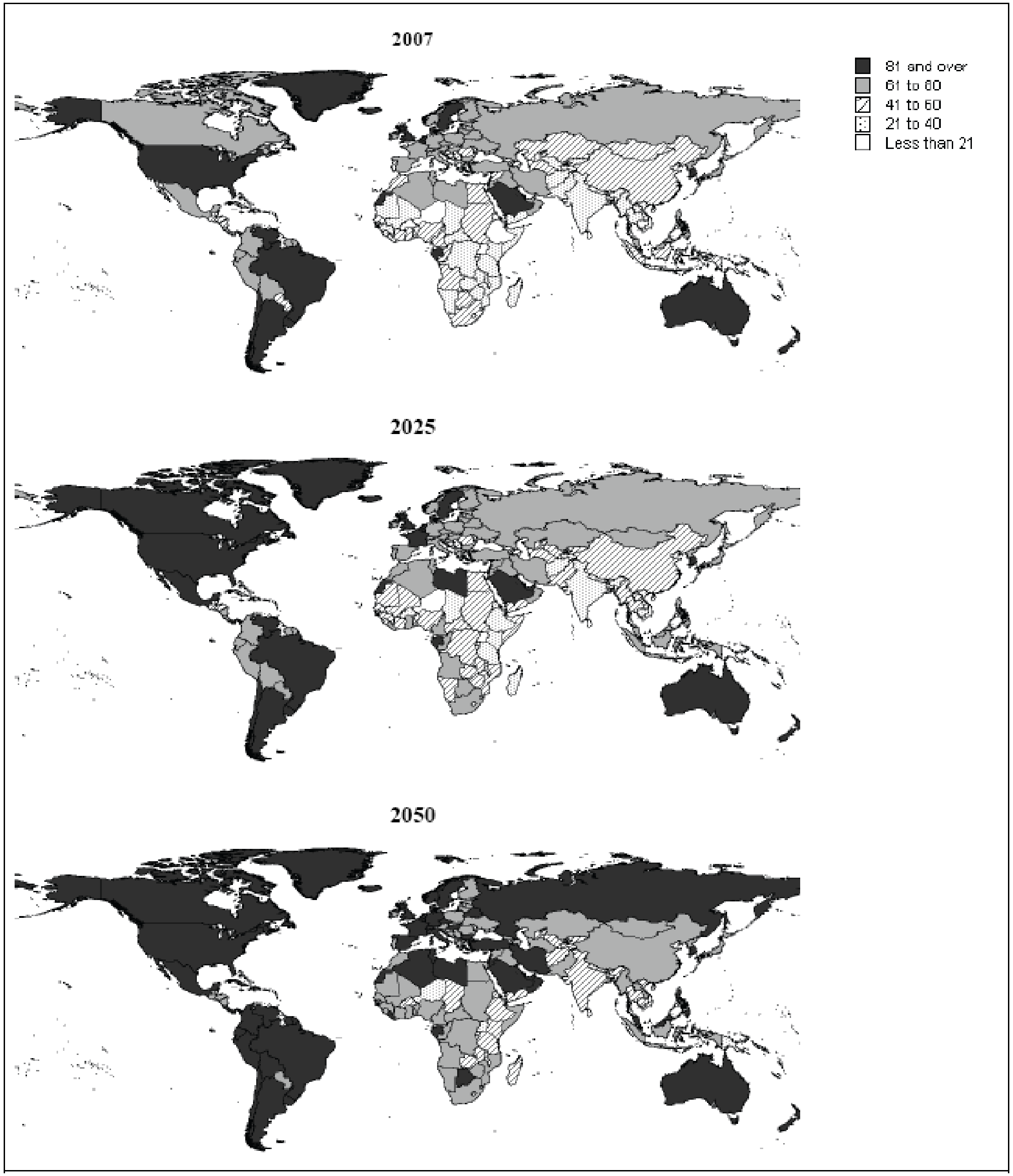

Source: United Nations, Department of Economic and Social Affairs, Population Division: World Population Prospects DEMOBASE extract. 2007.

NOTE: The boundaries shown on the present map do not imply official endorsement or acceptance by the United Nations.

Urban Population Percentage

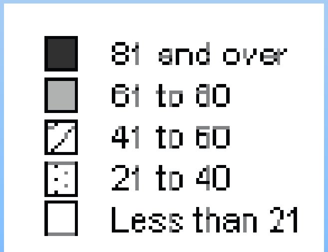

UN Department of Economics and Social Affairs, 2007

HyspIRI Urban Imaging
Weng et al. 2010

Urbanization and Global Change

- Urbanization research is uniquely suited to answer some key science questions in addressing global change, including:

- *How does urbanization affect the local, regional, and global environment?*
- *How do changes in land cover and land use from urbanization affect the sustainability and productivity of natural and human ecosystems?*
- *How do the patterns of human environmental and infectious diseases respond to urban growth and associated impacts?*
- *Can we characterize this effect to help mitigate its impacts?*

REGI

Region
Metro NE
Larger NE
Mid-Atlantic
Coastal SE
Inland SE
Upper Midwest
Inner Midwest
Appalachians
Great Plains
Mountain West
Arid Southwest
California
Northwest
Alaska
Hawaii

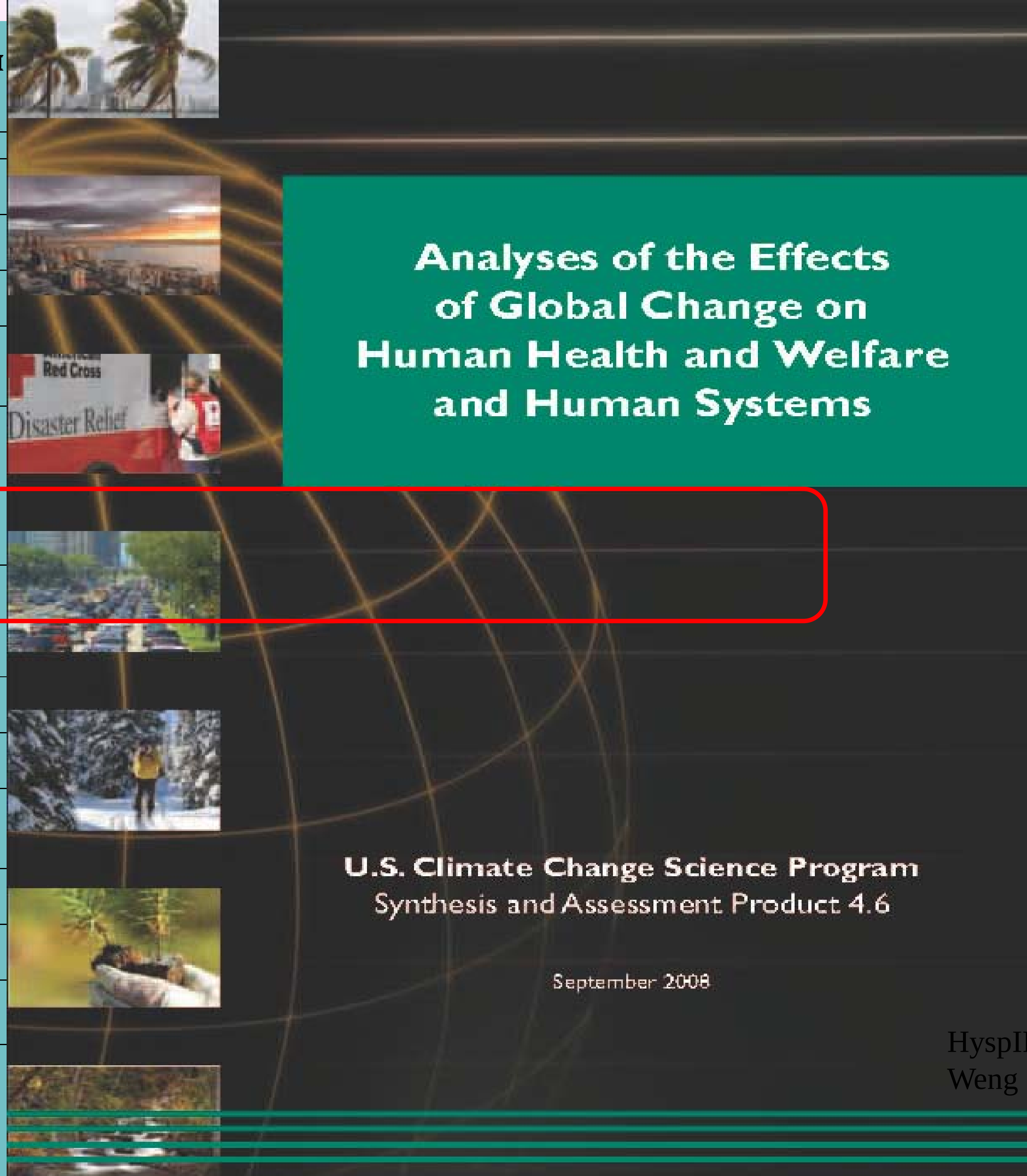

Some Recommendations Based on the Preliminary Assessment

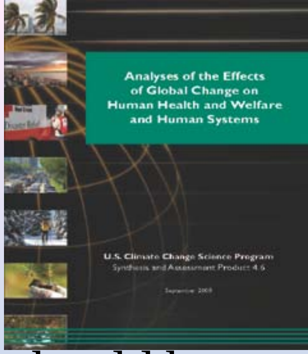

1. Research on climate change effects on human settlements in the U.S should be given a much higher priority in order to provide better metropolitan-area scale decision-making
2. In-depth case studies of selected urban area impacts and responses should be performed as soon as possible, especially for:
   - ►coastal areas in the Southeast
   - ►arid areas of the Southwest
   - ►coastal areas of the Northwest
   - ►Great Lakes region of the Midwest
6. A structure and process needs to be established for informing U.S. decision-makers about climate change effects, how to integrate climate change considerations into what they do with building codes, zoning, etc.

Climate Change and Urban Heat Island

- The UHI phenomenon is an analog of global climate change. Useful for studies on the responses of urban ecosystems and human systems to warming.
- The UHI effect: more than heat, air quality (pollution and ozone), health, and energy consumption.
- Emerging research trend includes:
  - (1) the impact of UHI on urban biogeochemical cycles and CO_2 dome;
  - (2) the dynamic interactions among UHI, earth system science, and global climate change; and
  - (3) global and regional mitigation simulation, negative radiative forcing, and GHG offset.

Guangzhou, southern China, experienced rapid urbanization since 1980s. (Weng and Yang, 2006, Env. Mon. Asse.)

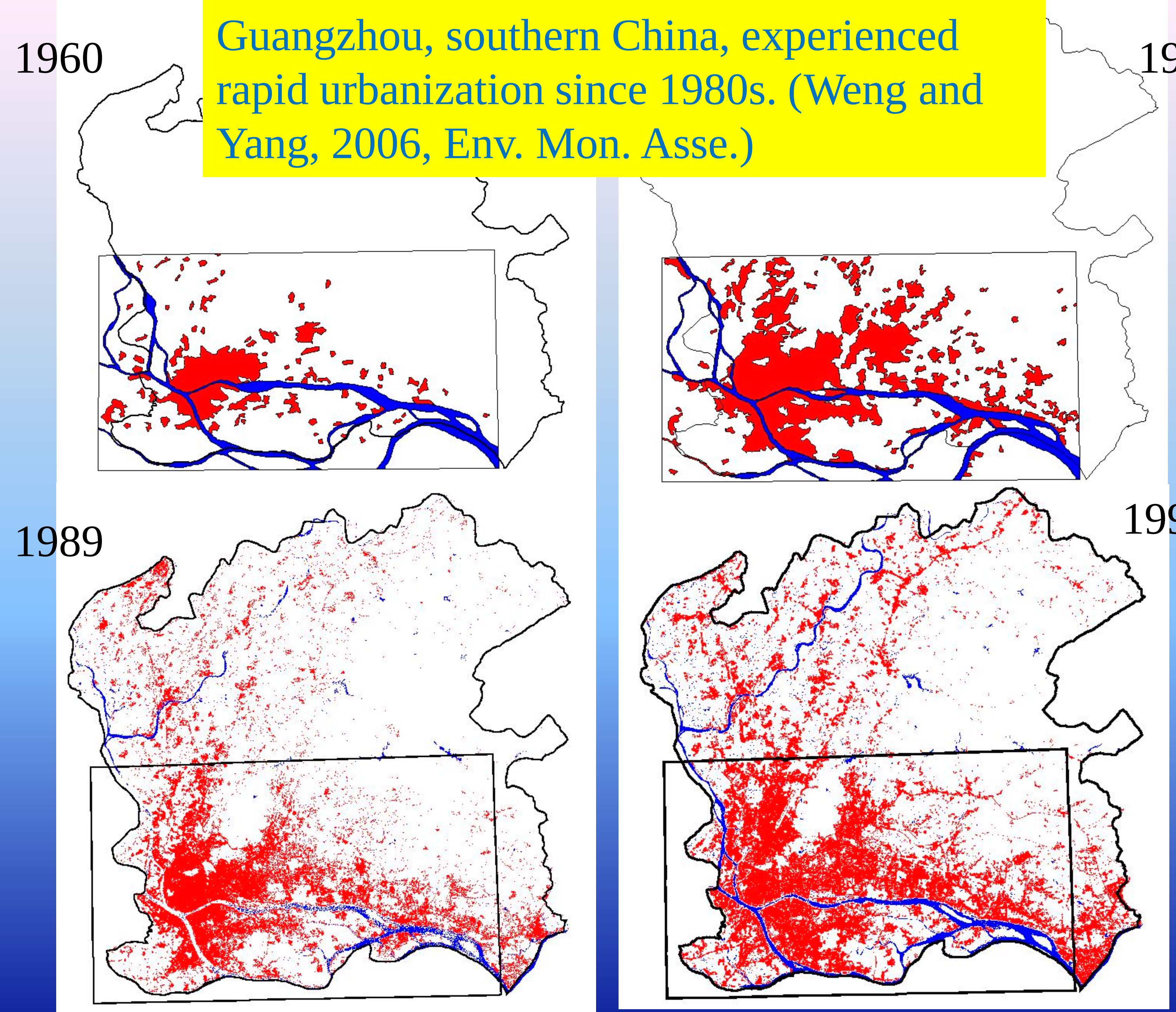

Sulfur Dioxide (mg/m^3)

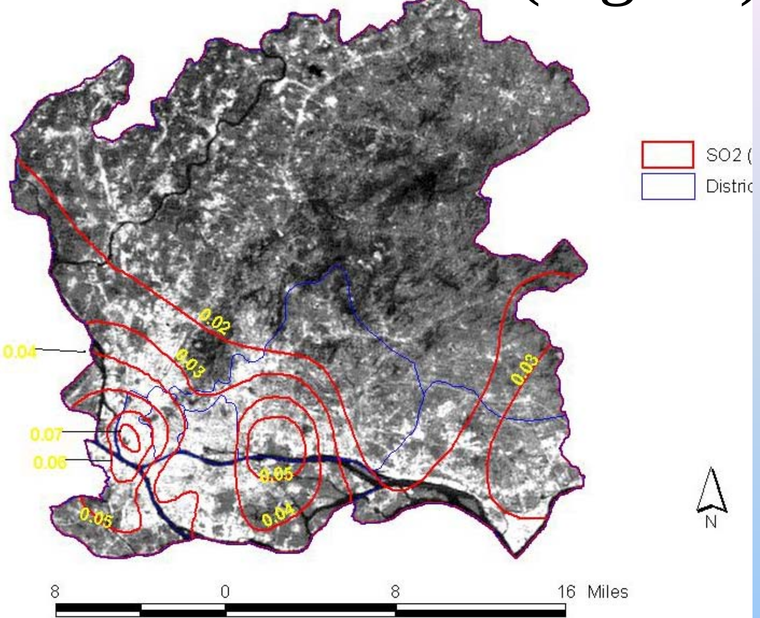

Annual Total Hours of Sunshine, 1960-1999

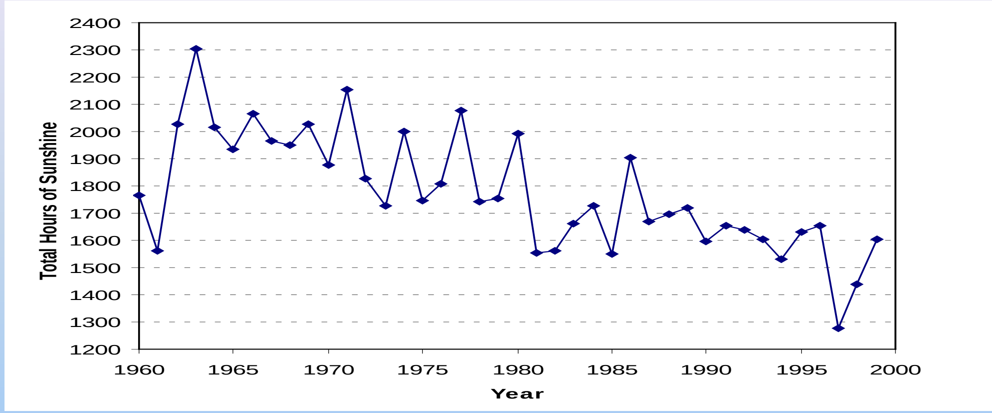

Dust (ton/km^2, month)

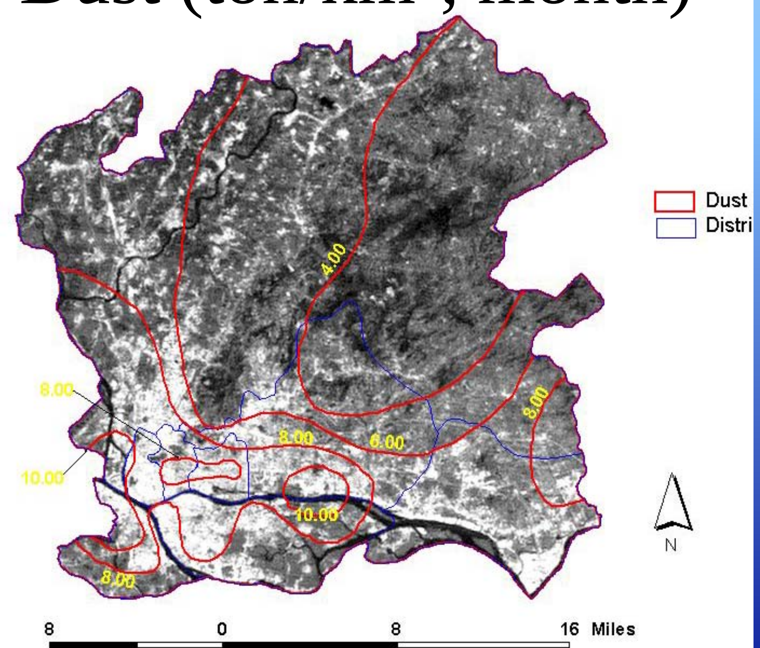

Annual Mean Air Temperature

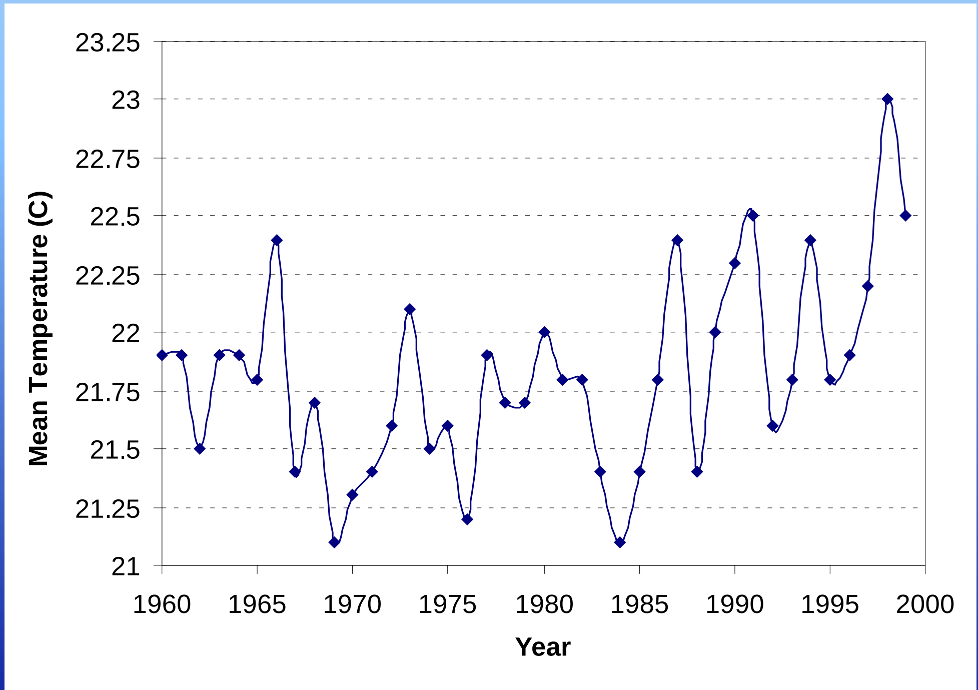

Why HyspIRI-like TIR Data Needed in UHI Studies?

- No system currently provides data combining both high spatial resolution and revisit capabilities.
  - ➢ High revisit/low resolution (AVHRR, MODIS, Meteosat, GOES)
  - ➢ High resolution/low revisit (ASTER, Landsat ETM+).
- HyspIRI will enhance resolutions and revisit simultaneously: 60-m resolution, 7 spectral bands, 5-day revisit, day and night imaging.
- HyspIRI data, in conjunction with other NASA data such as MODIS, will help provide further information on urban heat, air quality, ozone, and CO_2 “domes”.

UHI of Indianapolis as detected by Landsat ETM+, June 22, 2000

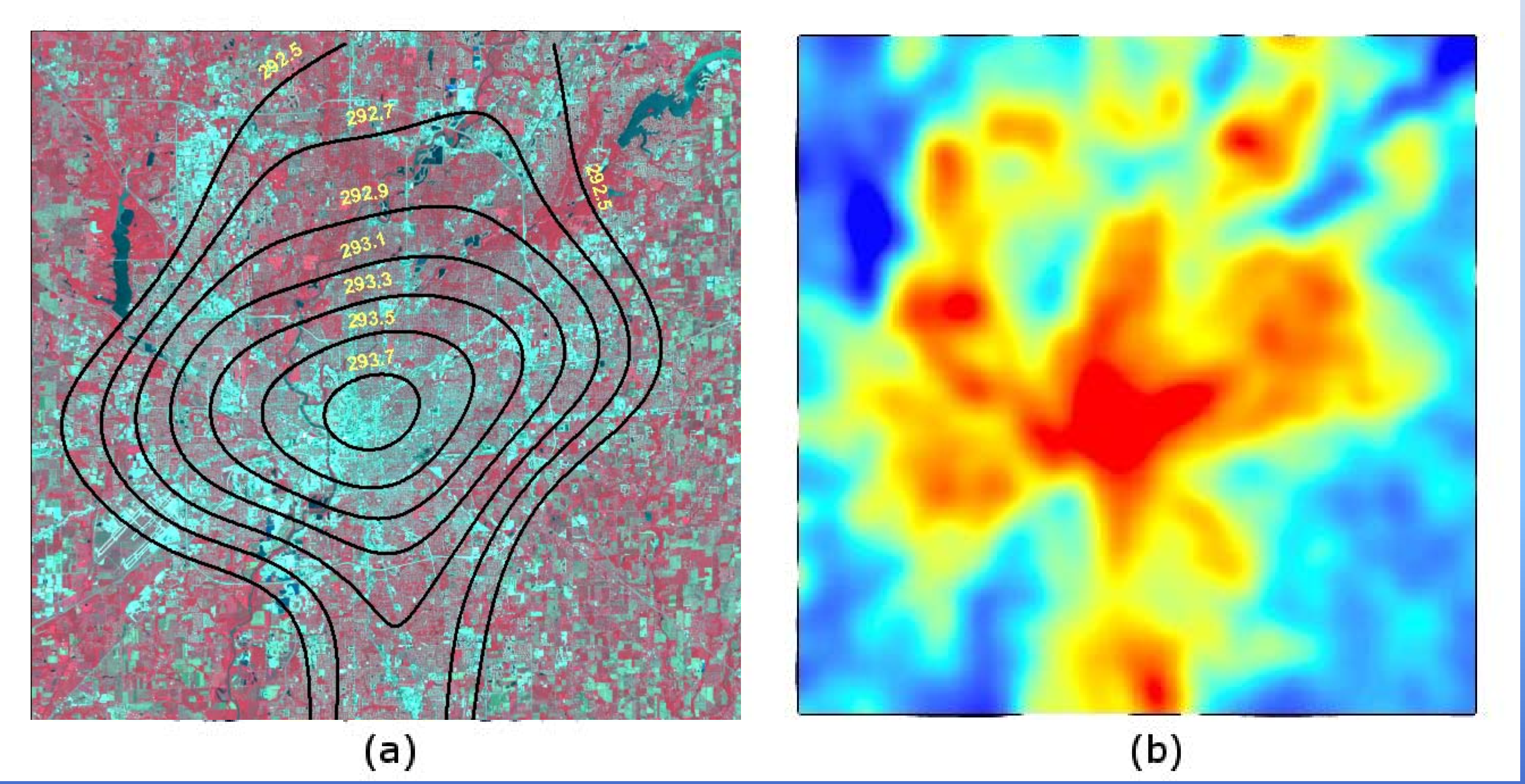

(a) FCC overlaid with temperature contour; (b) UHIs detected by Gaussian process model

(Rajasekar and Weng, 2009, *IJRS*)

3-D Models of Daytime UHIs of Indianapolis by Using MODIS LST Data

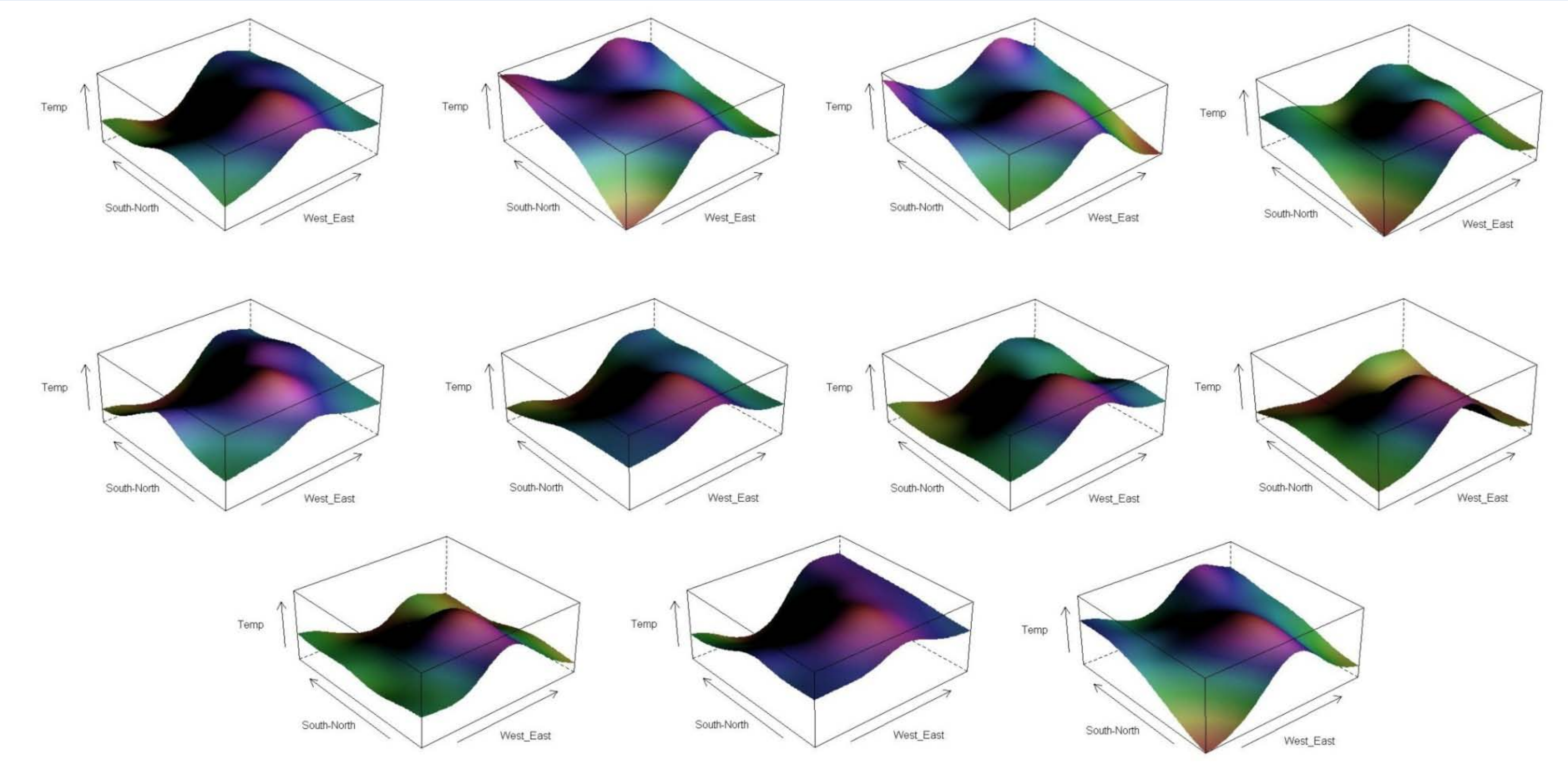

(Rajasekar and Weng, 2009, *ISPRS J.*)

3-D Models of Nighttime UHIs of Indianapolis by Using MODIS LST Data

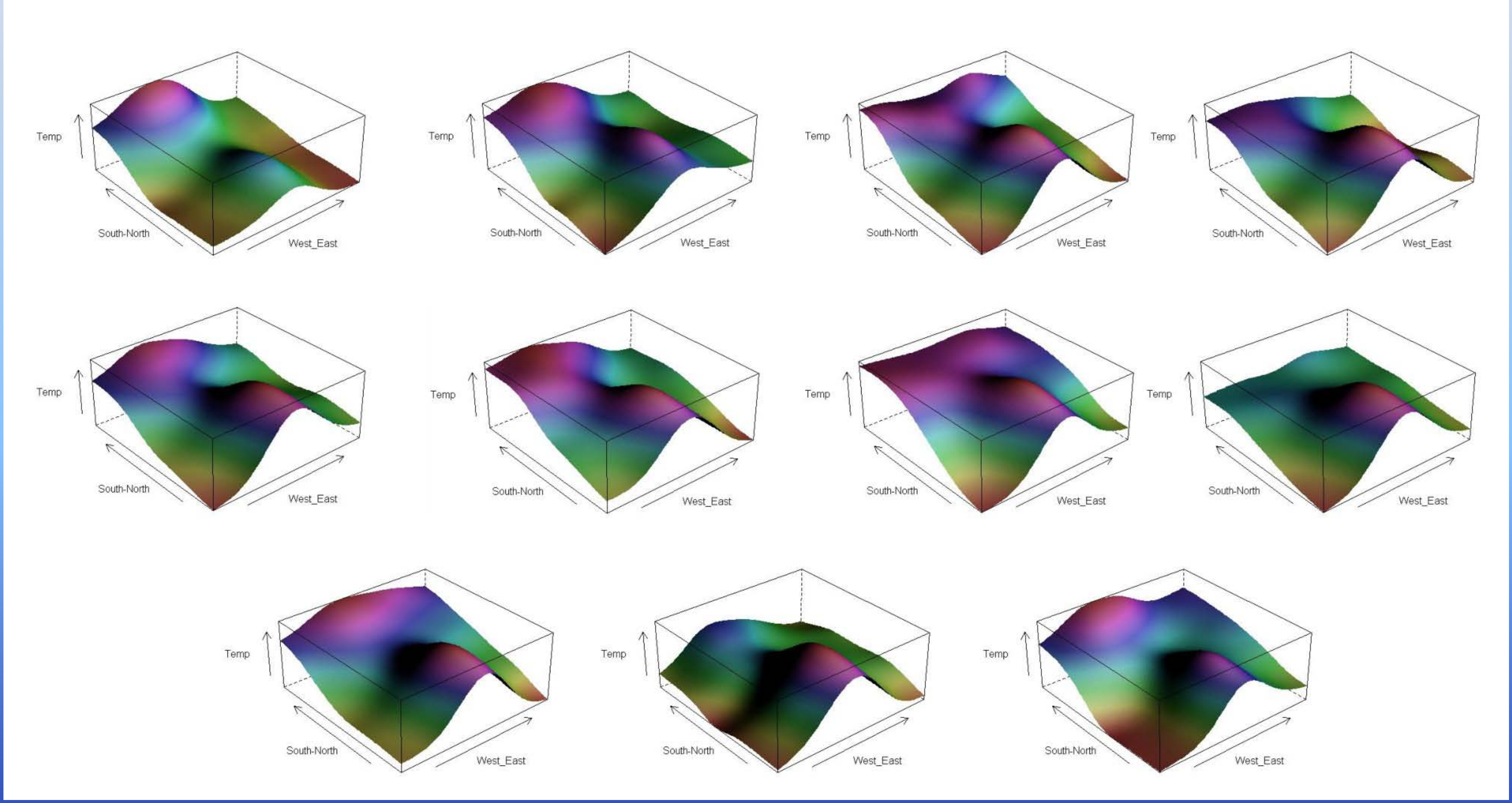

(Rajasekar and Weng, 2009, *ISPRS J.*)

UHI as an Moving Object over the Space and Time

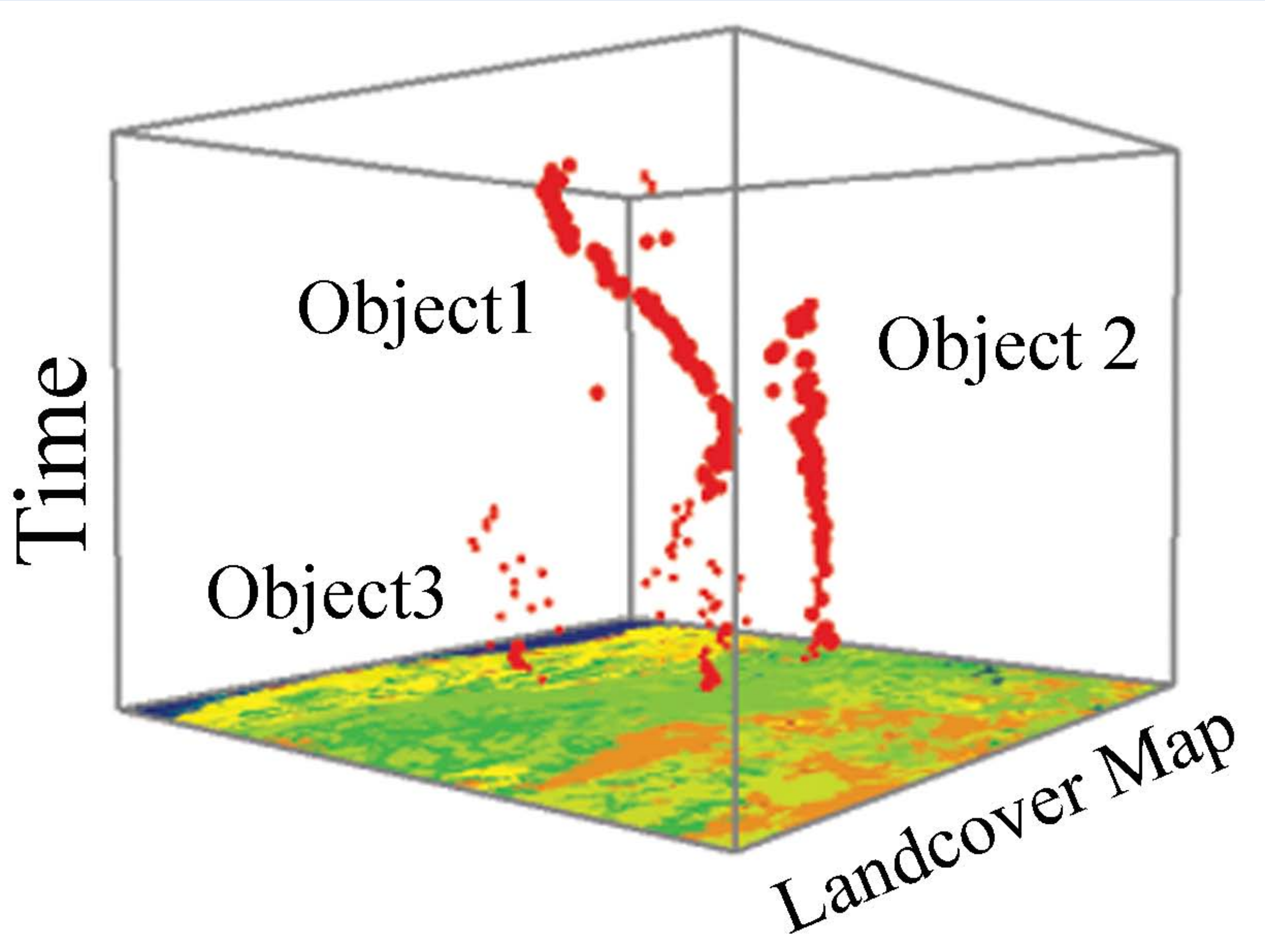

Weng et al. 2010

UHI Magnitude/Intensity in 2006

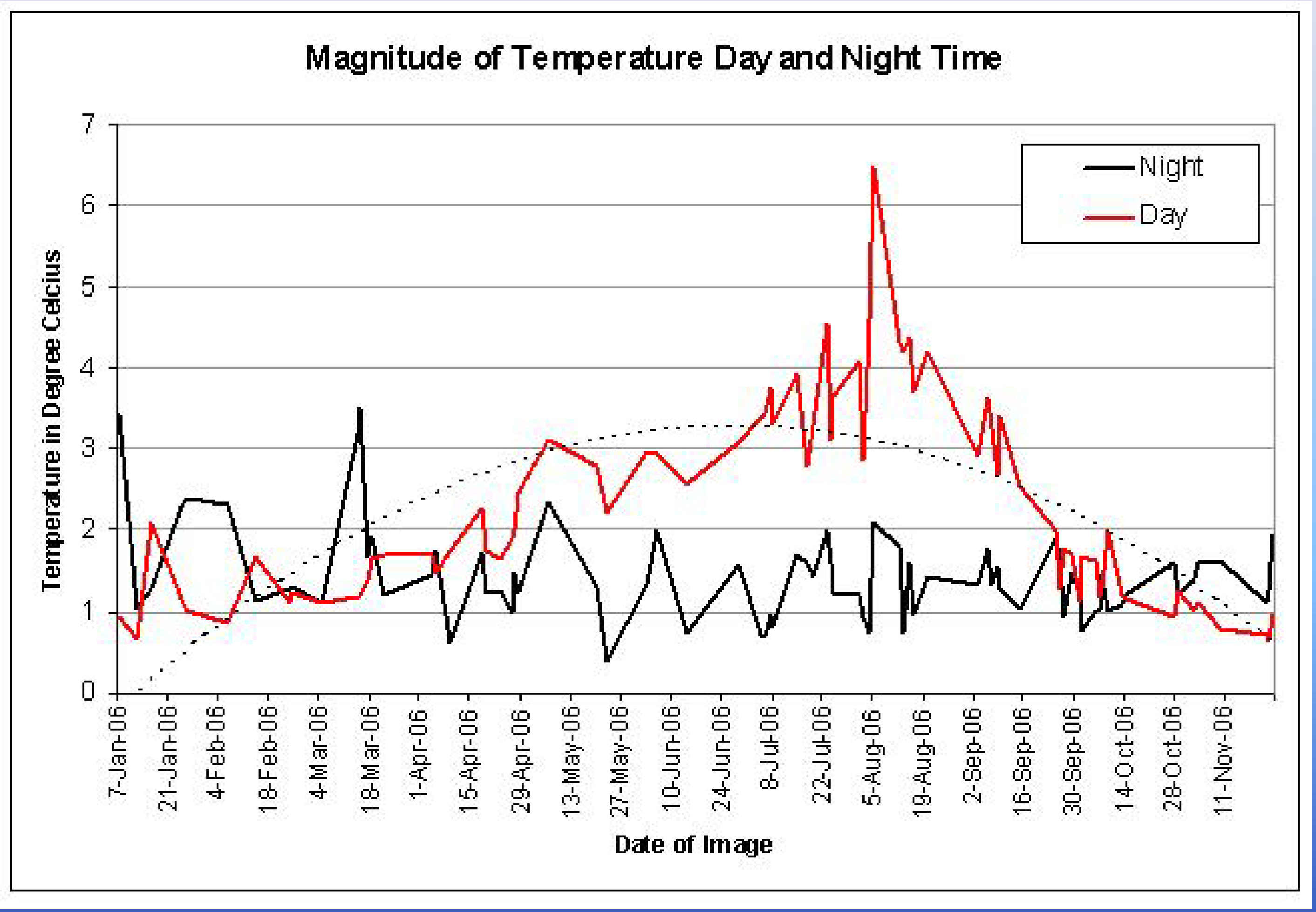

Day Mean: 2.28C (Std Dev: 1.22); Night Mean: 1.47C (Std Dev: 0.59)

(Rajasekar and Weng, 2009, *ISPRS J.*)

Needs for HyspIRI VSWIR Data in Urban Studies

- Needs for global urban morphological data in urban climate and environmental studies.
- Hyperspectral Imaging: potential to derive detailed information on the nature and properties of different urban surface materials.
- EO-1 Hyperion - very small swath width (7.7 km).
- HyspIRI's spectral, spatial and orbit characteristics will make it very attractive for producing advanced image/data products that can provide more precise and accurate data on various aspects of urban environments for use in analysis and modeling.

Urban Canopy Parameters Required for MM5 (Dupont, 2001; Lacser and Otte, 2002)

- Building height (mean, std. dev, histograms)
- Vegetation height
- Area-weighted mean building height
- Area-weighted mean vegetation height
- Surface area of walls
- Plan area fraction
- Frontal area index
- Height-to width ratio
- Sky view factor
- Mean orientation of streets
- Roughness length
- Displacement height
- Surface fraction of vegetation, roads, and rooftops
- Impervious areas directly connected to the draining network

Impervious surface map derived from EO-1 ALI image of April 12, 2003

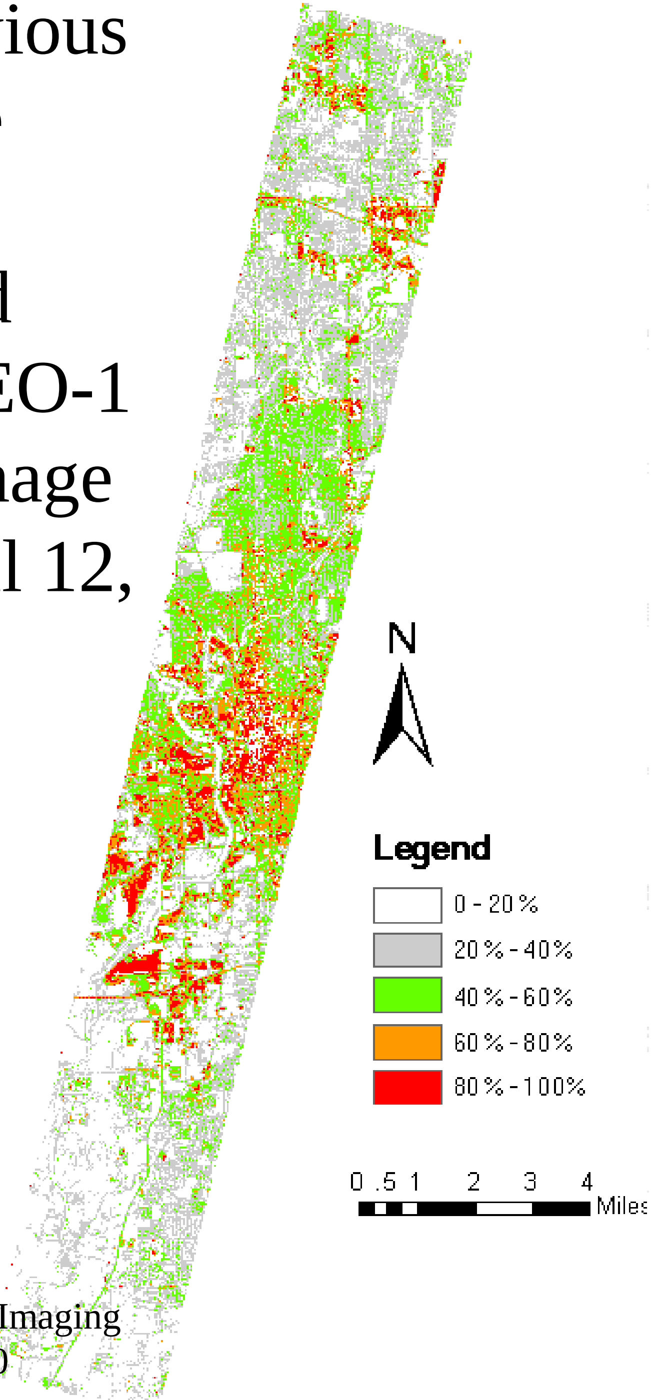

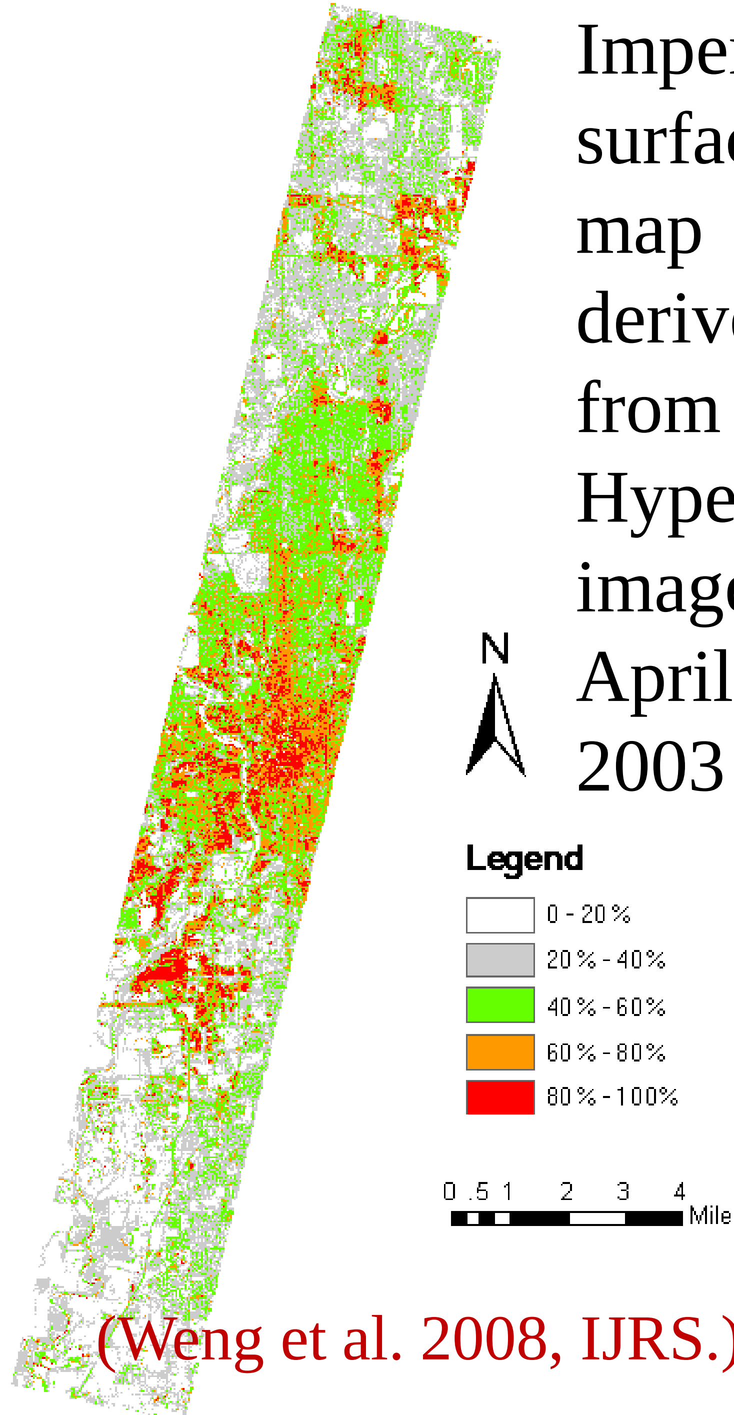

Impervious surface map derived from EO-1 Hyperion image of April 12, 2003

(Weng et al. 2008, IJRS.)

Hyperspectral vs. Multispectral Imaging

• Hyperion image was more powerful in discerning low-albedo surface materials.

• The improvement mainly came from additional bands in the mid-infrared region (Bands 7, 8, and 9 of ALI sensor).

• Implications for HyspIRI: Combined use of VNIR, SWIR, and TIR data for estimation improvement.

HyspIRI Combined with other RS/GIS data to generate Urban Morphological Datasets

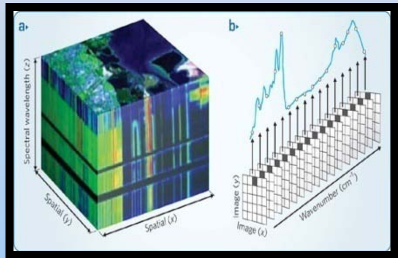

HyspIRI VSWIR data Products

Urban morphological datasets

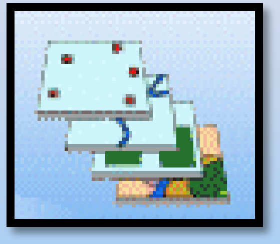

GIS datasets

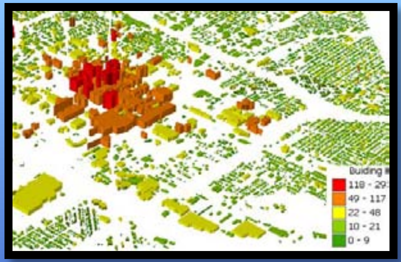

Lidar

Digital photogrammetry

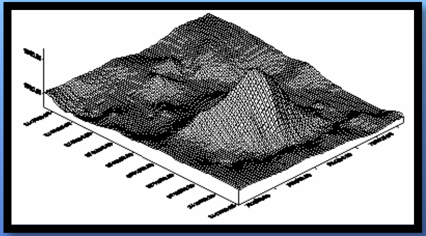

Digital elevation model

More Detailed, Morphology-Based LULC Data

- Mesoscale modeling use LULC classes as surrogates to define surface parameters (e.g., roughness lengths, displacement height)
- More detailed and morphology-based LULC classes are needed in urban climate modeling and environmental studies.
- USGS NLCD drawbacks: accuracy; update; urban heterogeneity; CIT as a single category)

- A solution is to use morphological characteristics (e.g., building density, mean building height, **vegetative cover, impervious surface fraction**) to subdivide a generalized first level of land use/cover.

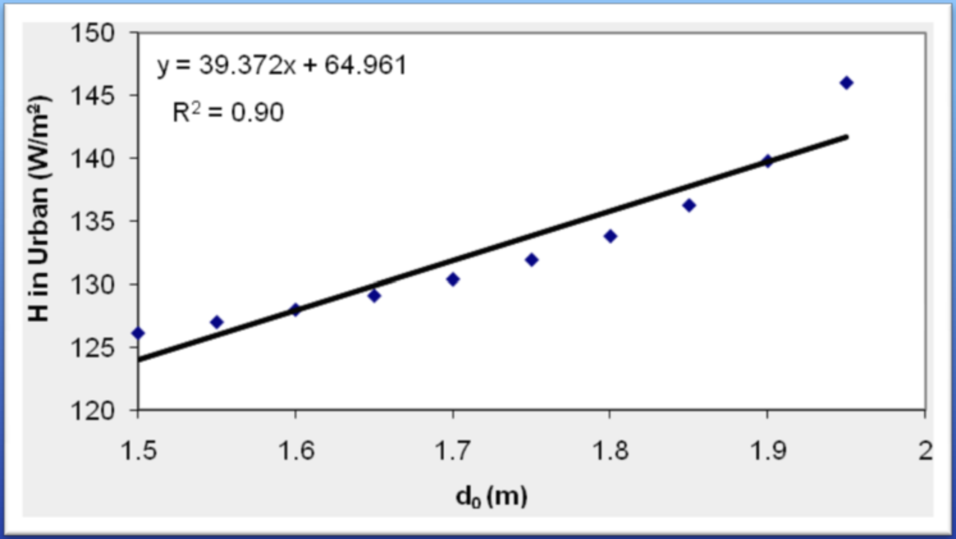

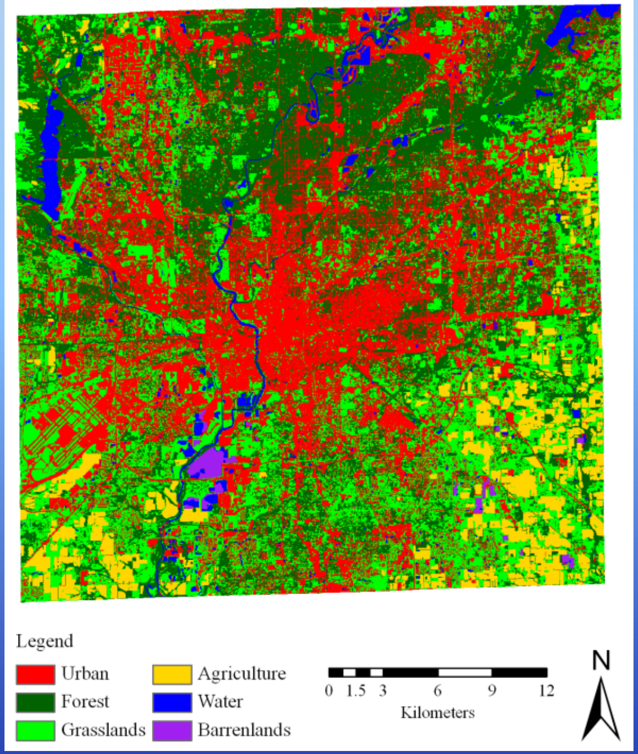

HyspIRI Urban Imaging
Weng et al. 2010

Changes in Surface Heat Fluxes due to Urbanization

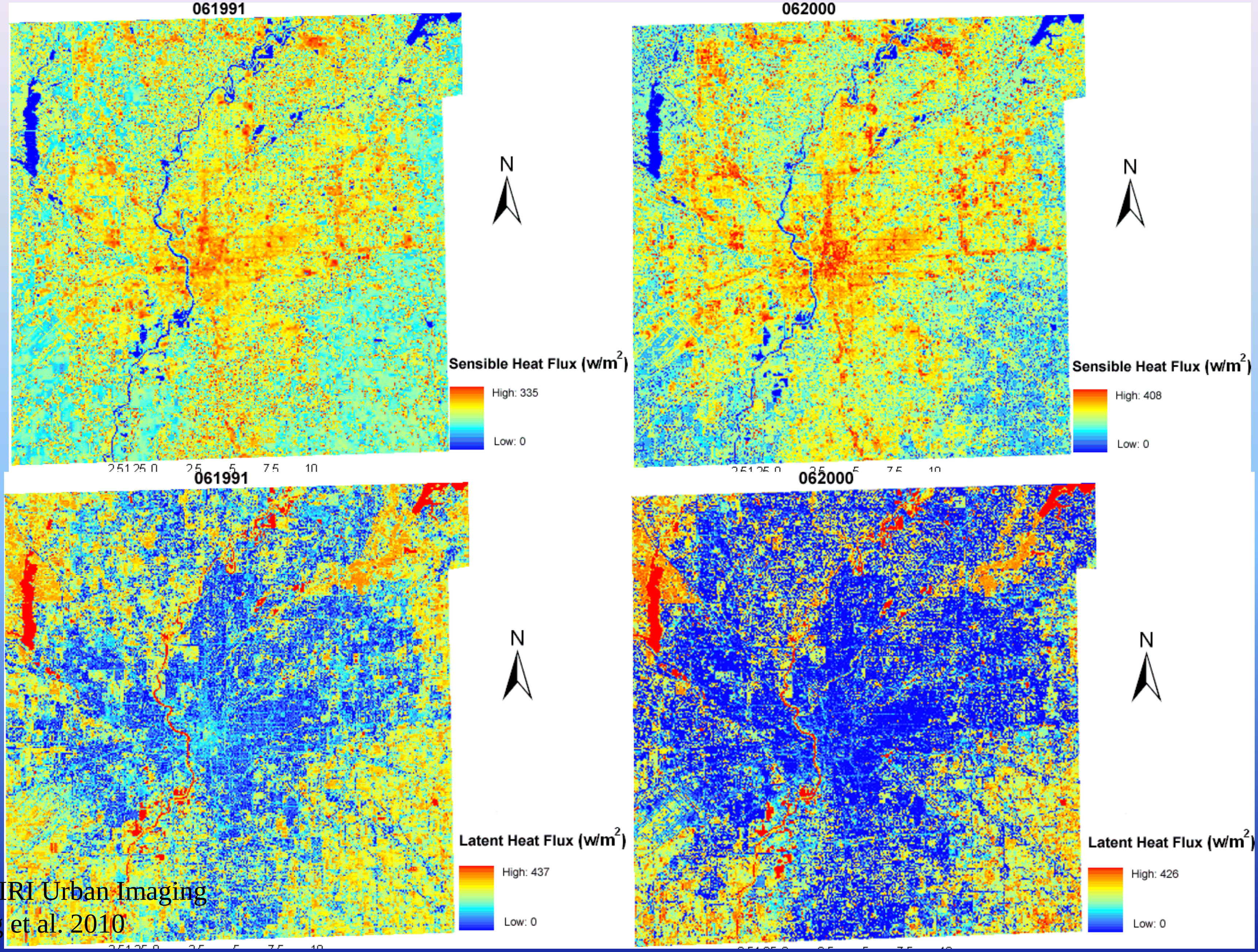

Weng et al. 2010

Sensible and Latent Heat Fluxes in Indianapolis (June 6, 1991 *vs.* June 22, 2000) (unit: W/m^2)

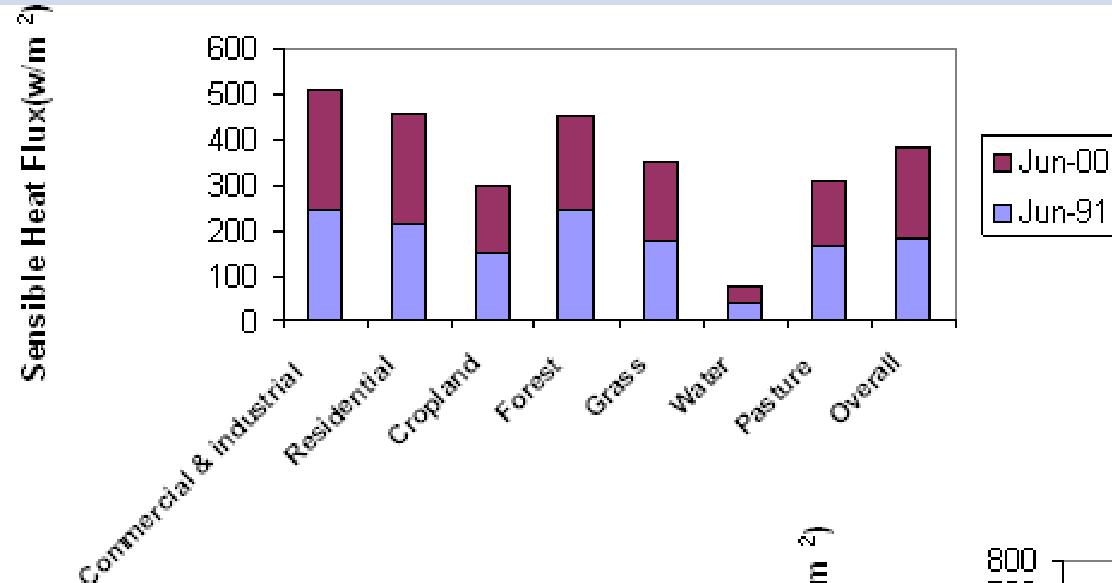

Sensible Heat Flux	1991	182.14
	2000	200.29
Latent Heat Flux	1991	151.31
	2000	94.33

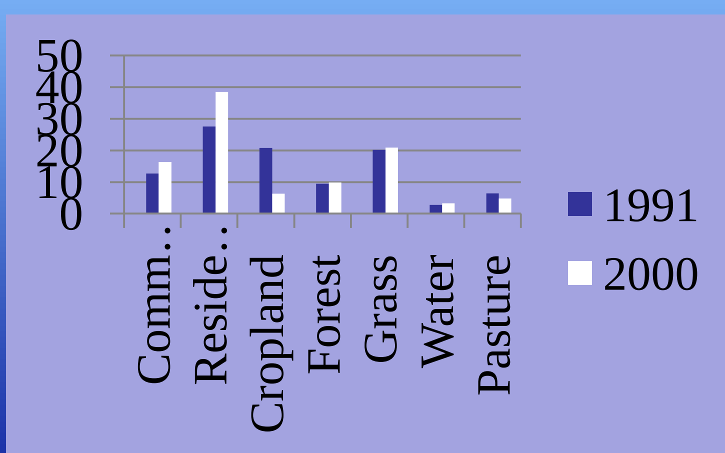

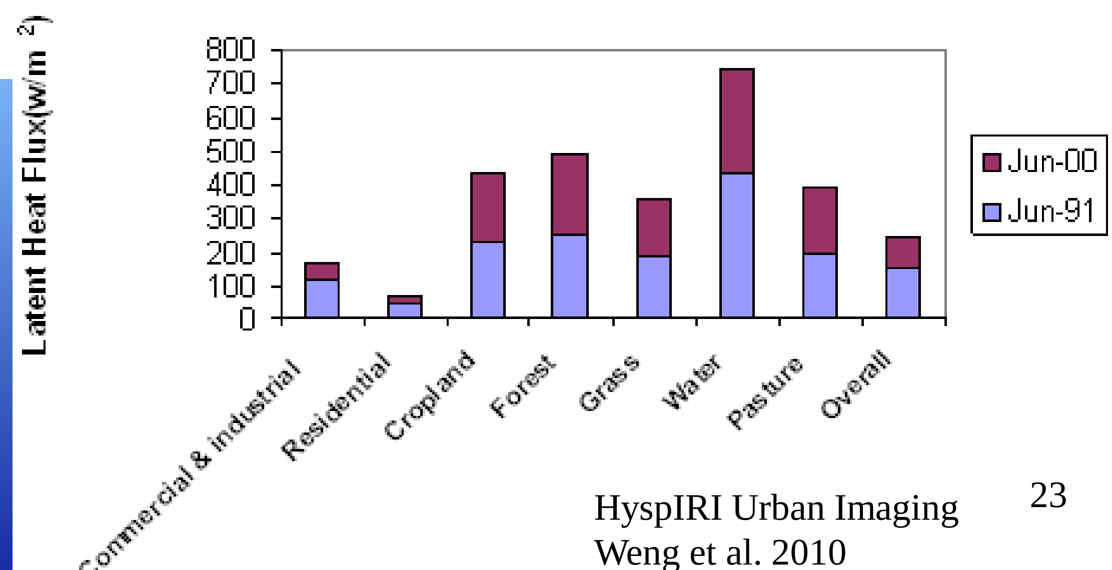

HyspIRI Urban Imaging
Weng et al. 2010

2002 West Nile Virus (WNV) Activity in the United States

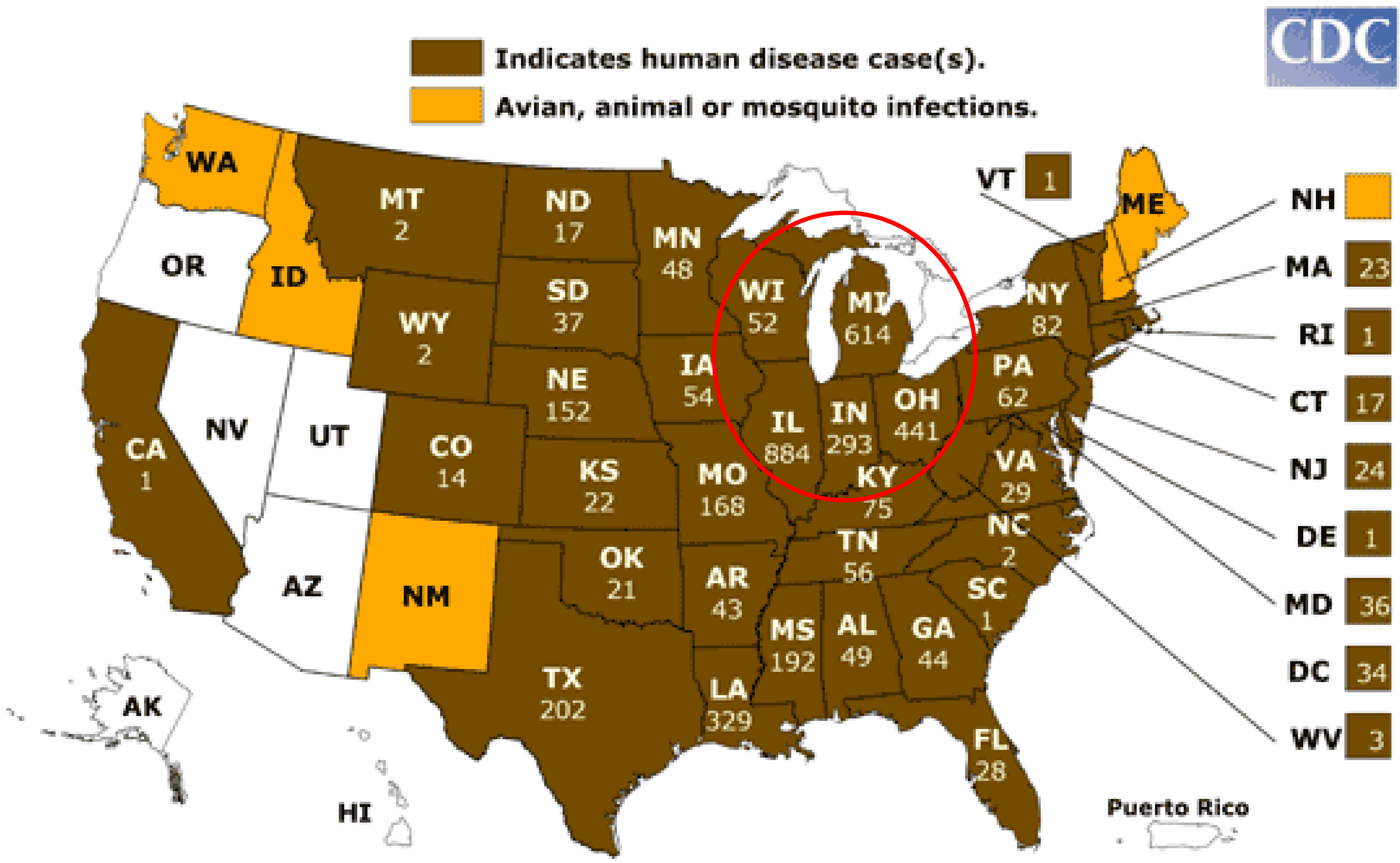

http://www.cdc.gov/ncidod/dvbid/westnile/surv&control.htm

In Indianapolis, the occurrence of WNV was found negatively correlated with sensible heat flux, but positively with evapotranspiration (ET).

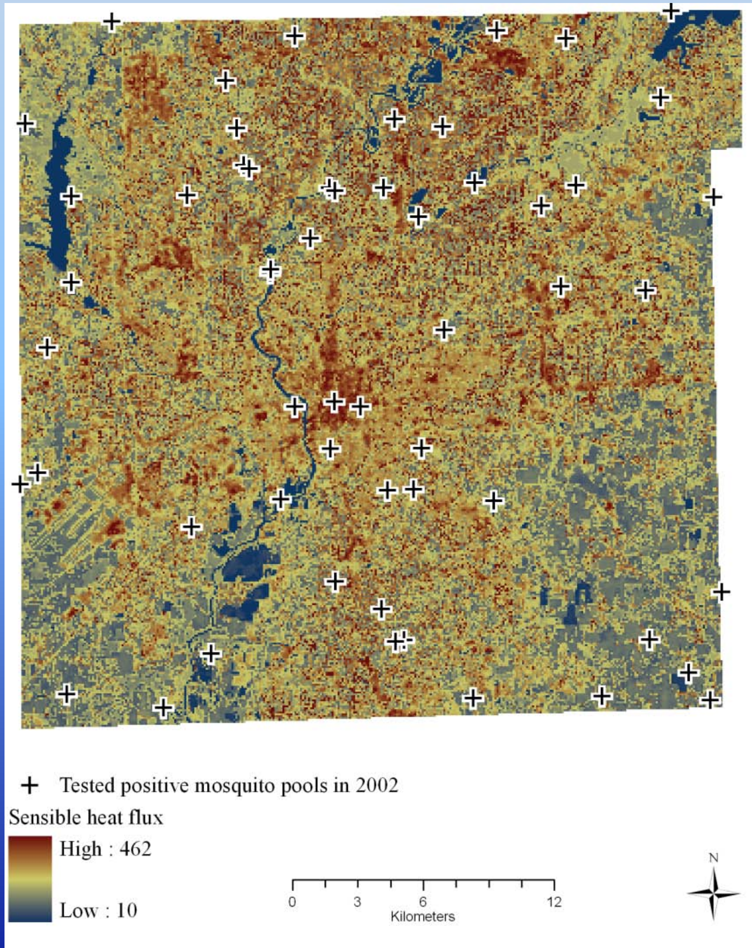

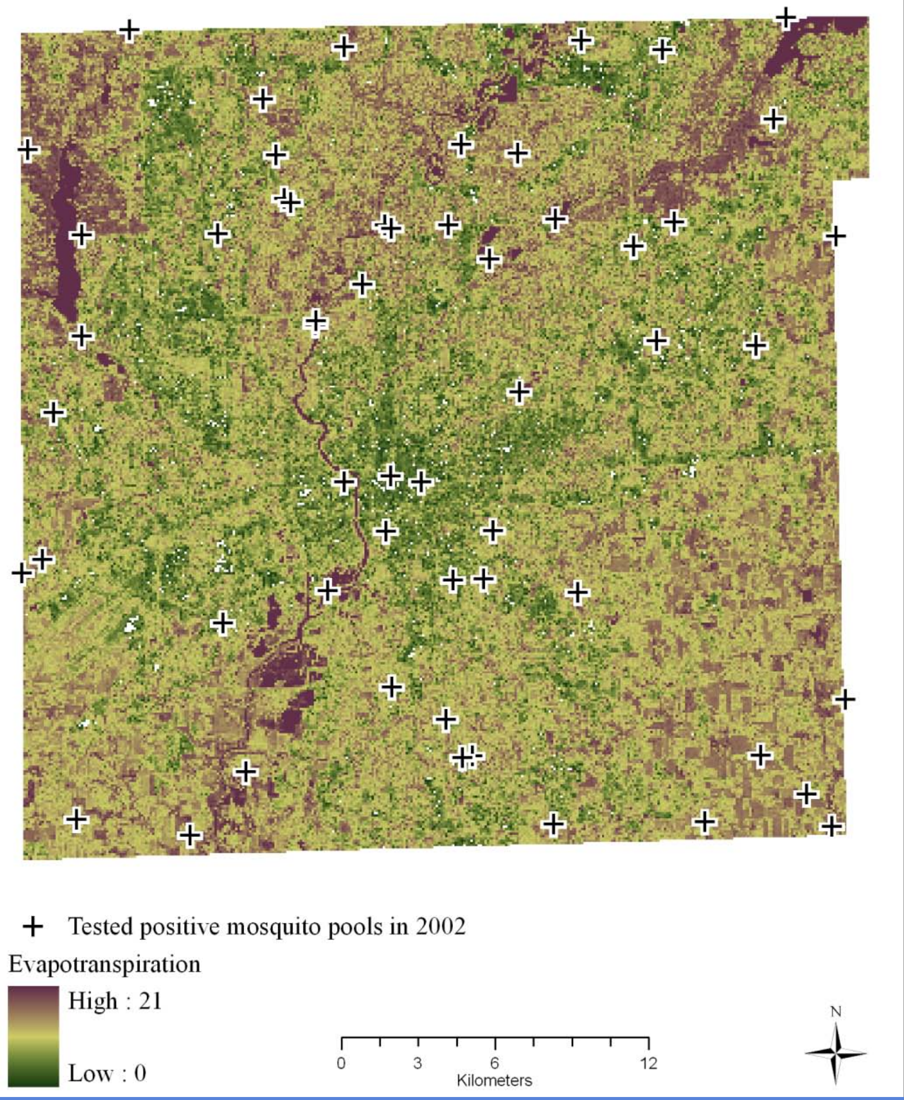

Temporal mismatch: Aster LST data was acquired June 16, 2001, but WNV data in 2002.

Weng et al. 2010

Identification of Health Hazard Risk Areas

- Mahalanobis distance analysis
  - a distance index based on correlations between variables by which different patterns can be analyzed
  - used to identify favorable habitats of WNV
  - model inputs: pertinent environmental variables retained by the Discriminant analysis
- Distance values: small – more favorable; large - less favorable.

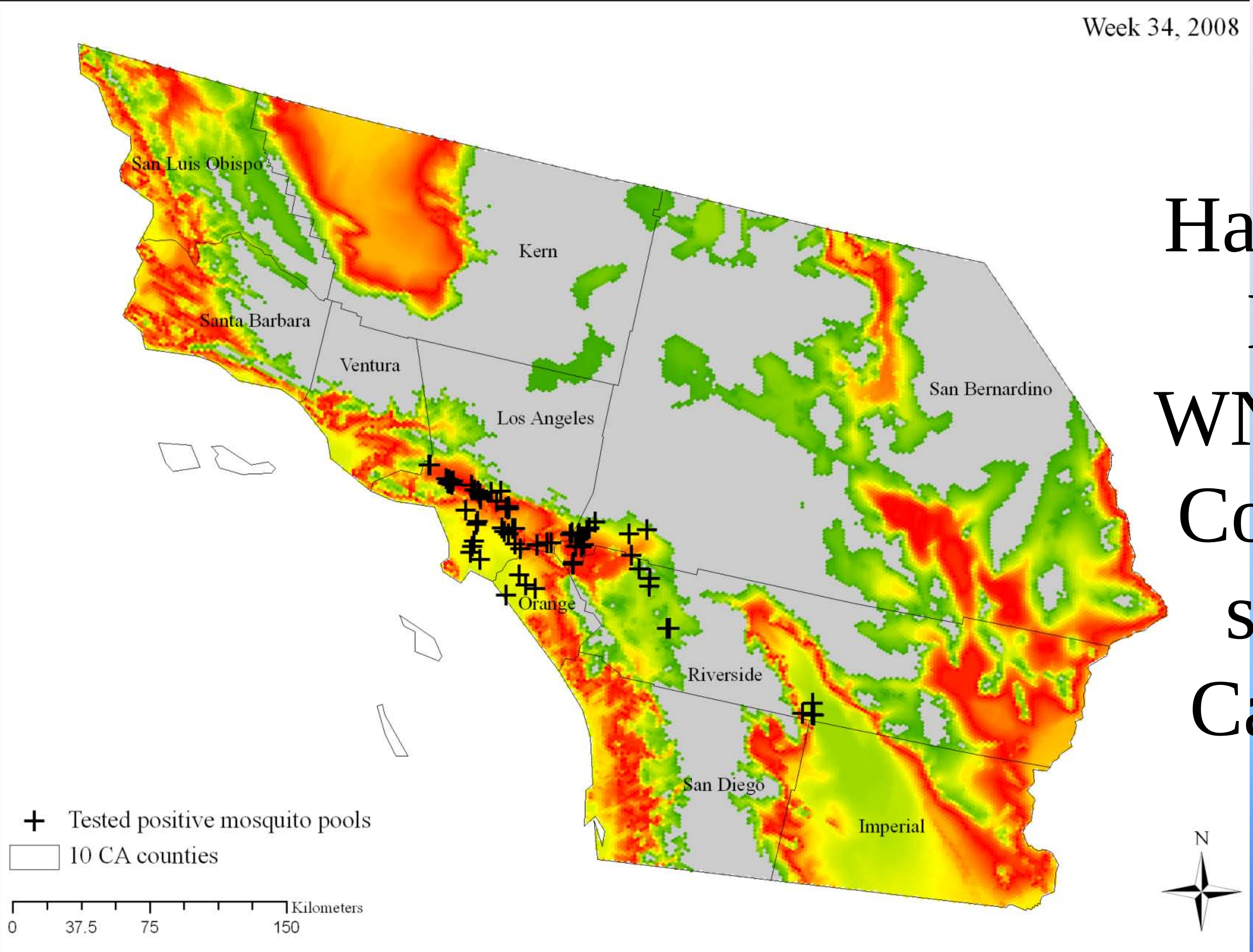

Health Hazard Risk Map of WNV in Ten Counties of southern California:

High Risk → low risk: red, yellow, green, and gray.

HyspIRI Data for WNV Studies

- TIR instrument 5-day revisit:
  - Potential one-two observations per epidemic week. Rapid detection and tracking of events.
- TIR 60-m spatial resolution:
  - Better health hazard risk maps of WNV. Targeted interventions to reduce the vulnerability of humans.
- VSWIR Data: Higher temporal resolution, spectral (7 bands) and spatial (60-m) resolution:
  - Precise spatiotemporal variations of envi. variables.
  - Better prediction of disease outbreaks.

Conclusions

- HyspIRI TIR data are essential for improving knowledge on urban heat island and related climate characteristics, air quality, ozone, and CO2 “domes”.
- The combined VSWIR and TIR data: Rapid detection and tracking of diseases, targeted interventions, better prediction of disease outbreaks.
- VSWIR data in conjunction with other NASA satellite and ancillary data: potential to provide detailed, global urban morphological datasets, key to climate modeling and characterization/quantification of urban surface heat fluxes and urban environments.

Simulated HyspIRI Volcanology Data Sets

Michael Abrams, Dave Pieri, Vince Realmuto,
NASA/Jet Propulsion Laboratory
Robert Wright, University Hawaii

Goals of Project

The primary objective of this proposal is to create precursor HyspIRI-like data sets to address several important volcanological questions:

1 What do changes in SO_2 emissions tell us about a volcano's activity?

2 How do we use measurements of lava flow temperatures and volume to predict advances of the flow front?

3 What do changes in lava lake temperatures and energy emissions tell us about possible eruptive behavior?

A second objective is to determine the saturation temperature for the Mid-IR band

ETNA

Why Mt. Etna?

- Europe's most active volcano
- Explosive and effusive eruptions
- Massive SO_2 emitter
- Extraordinarily frequent remote sensing data acquisitions
- Very well monitored by INGV
- Co-I at INGV will provide all ancillary data needed

Characteristics of Input Data Sets

	MIVIS	EO-1 Hyperion	ASTER TIR
Bands	92 in VSWIR, 10 TIR	196 unique in 0.4-2.5 micron region	5 in 8-12 micron region
Spatial resolution	6-12 m	30 m	90 m
Swath	4-9 km	7.5 km	60 km
Quantization	12 bit	16 bit	12 bit

Ancillary Data Sets

	COSPEC SO_2	Flow field Topography	Eruption chronology
Eruptions and gas emissions	X		X
Lava flow modeling		X	X
Lava lake energy release			X

ASTER Daytime Scenes (1 2 3)

2000	2001	2002	2003	2004	2005	2006	2007	2008	2009	2010
7 May	29 July	5 June	15 Jan	7 Apr	26 Apr	3 Aug	19 Jun	21 Jun	7 Oct	26 May
		7 July	13 Mar	10 June		12 Aug	21 Jun	8 Aug		7 Aug
		23 July	19 July	26 June		7 Nov	14 Jul	21 Nov		
		3 Nov	11 Aug	6 Aug			21 Jul			
		30 Dec		13 Aug			30 Jul			
				22 Aug			2 Oct			

Multispectral TIR from Daytime ASTER (1 2 3)

VNIR image: plume is gray; flows are not incandescent

TIR image: plume composition is mostly ash; flows are obvious

Multispectral Daytime ASTER (2 3)

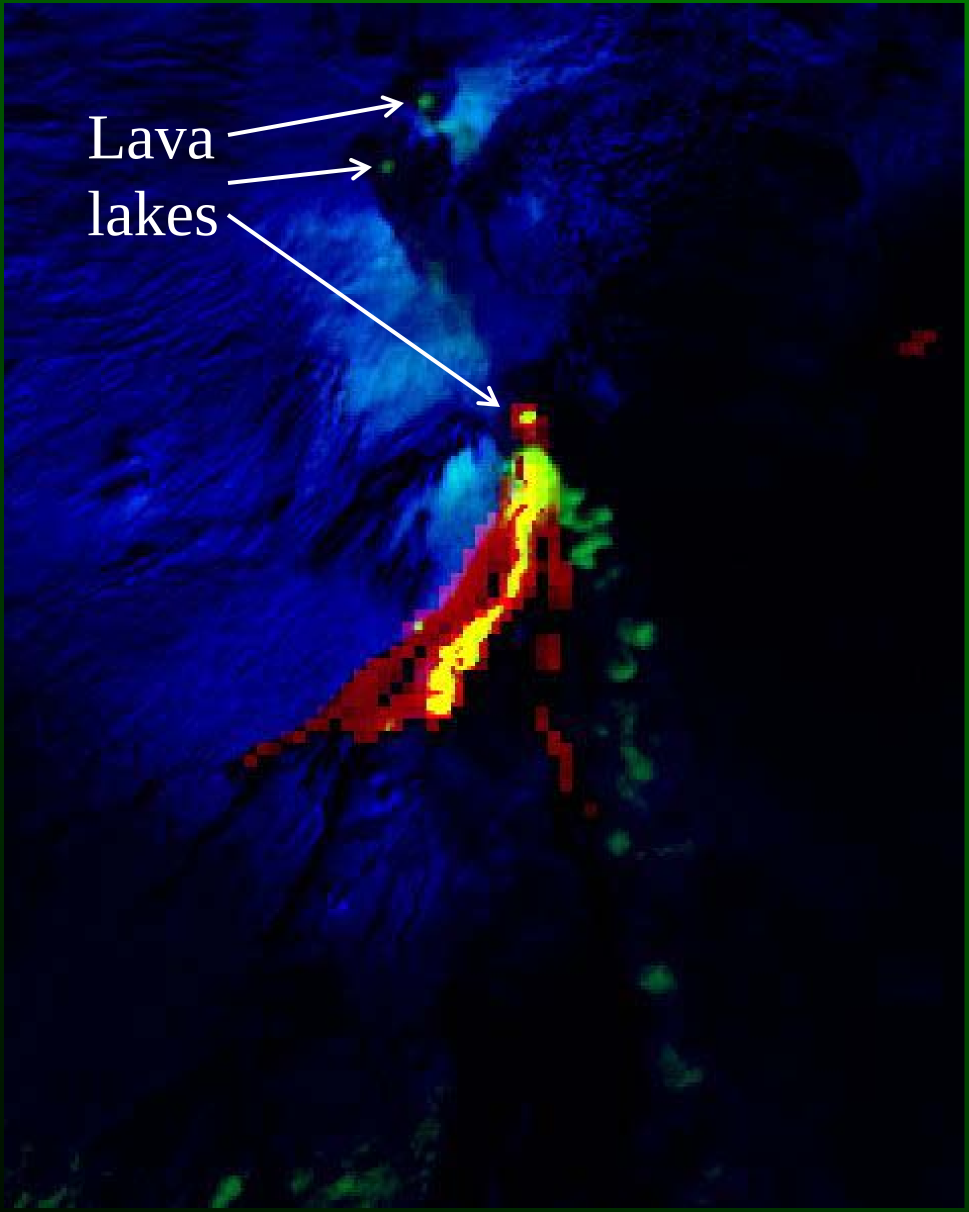

R=11um G=1.5um B=0.84um

Lava flows vary in temperature; multispectral data allow better estimation of temperatures than TIR alone.

ASTER Nighttime TIR Scenes (1 2 3)

2000	2001	2002	2003	2004	2005	2006	2007	2008	2009	2010
6-Jun	9-Jan	19-Jan	7-Feb	13-Mar	5-Feb	29-Apr	15-Mar	21-Jun	6-Jan	2-Jan
22-Jun	25-Jun	22-Jan	20-Mar	15-Jun	4-Nov	31-May	18-May	11-Oct	15-Jun	3-Feb
8-Jul	11-Jul	28-Jan	14-May	26-Jun	11-Nov	2-Jul	19-Jun	5-Dec	24-Jun	1-May
24-Jul	15-Oct	4-Feb	17-Jul	3-Jul	27-Nov	25-Jul	26-Jun		10-Jul	10-May
10-Sep	24-Oct	12-Jan	26-Jul	14-Sep		3-Aug	12-Jul		2-Aug	
28-Oct		11-May	18-Aug			10-Aug	12-Dec		15-Nov	
		20-May				4-Sep				
		28-Jun				13-Oct				
		23-Jul				7-Nov				
		16-Sep								
		18-Oct								
		27-Oct								
		19-Nov								
		28-Nov								

Selected <u>2002</u> ASTER Night TIR (1 2 3)

January 19

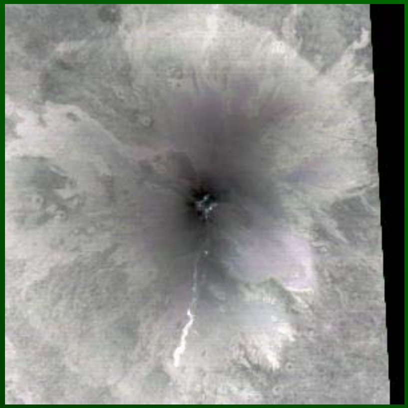

January 28

May 11

May 20

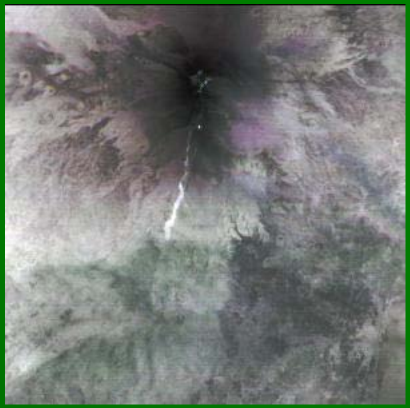

June 28

July 23

October 27

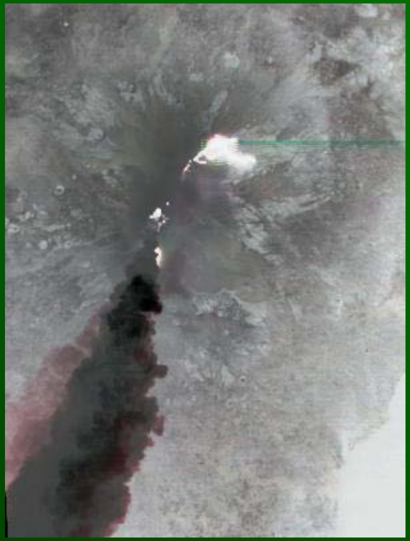

EO-1 Hyperion Daytime Scenes (2 3)

EO1H1880342009281110pf_sgs_01
EO1H1880342008206110kf_sgs_01
EO1H1880342008152110kf_sgs_01
EO1H18803420071901110kf_sgs_01
EO1H1880342007134110kf_sgs_01
EO1H1880342006303110pf_sgs_01
EO1H1880342006298110pf_sgs_01
EO1H1880342005316110kf_sgs
EO1H1880342005302110kf_sgs
EO1H1880342005205110pf_hgs
EO1H1880342004283110pw_sgs
EO1H1880342004260110kw_pf1
EO1H1880342003223110kf_sgs
EO1H1880342003207110kx_hgs
EO1H1880342003177110ky_sgs
EO1H1880342001267110kp_sgs
EO1H1880342001242110po_sgs
EO1H1880342001203110kp_sgs
EO1H1880342001194110po_sgs

October 26, 2006 Hyperion Etna Data (2 3)

0.65-0.55-0.44 0.87-0.65-0.55 2.20-1.65-0.87

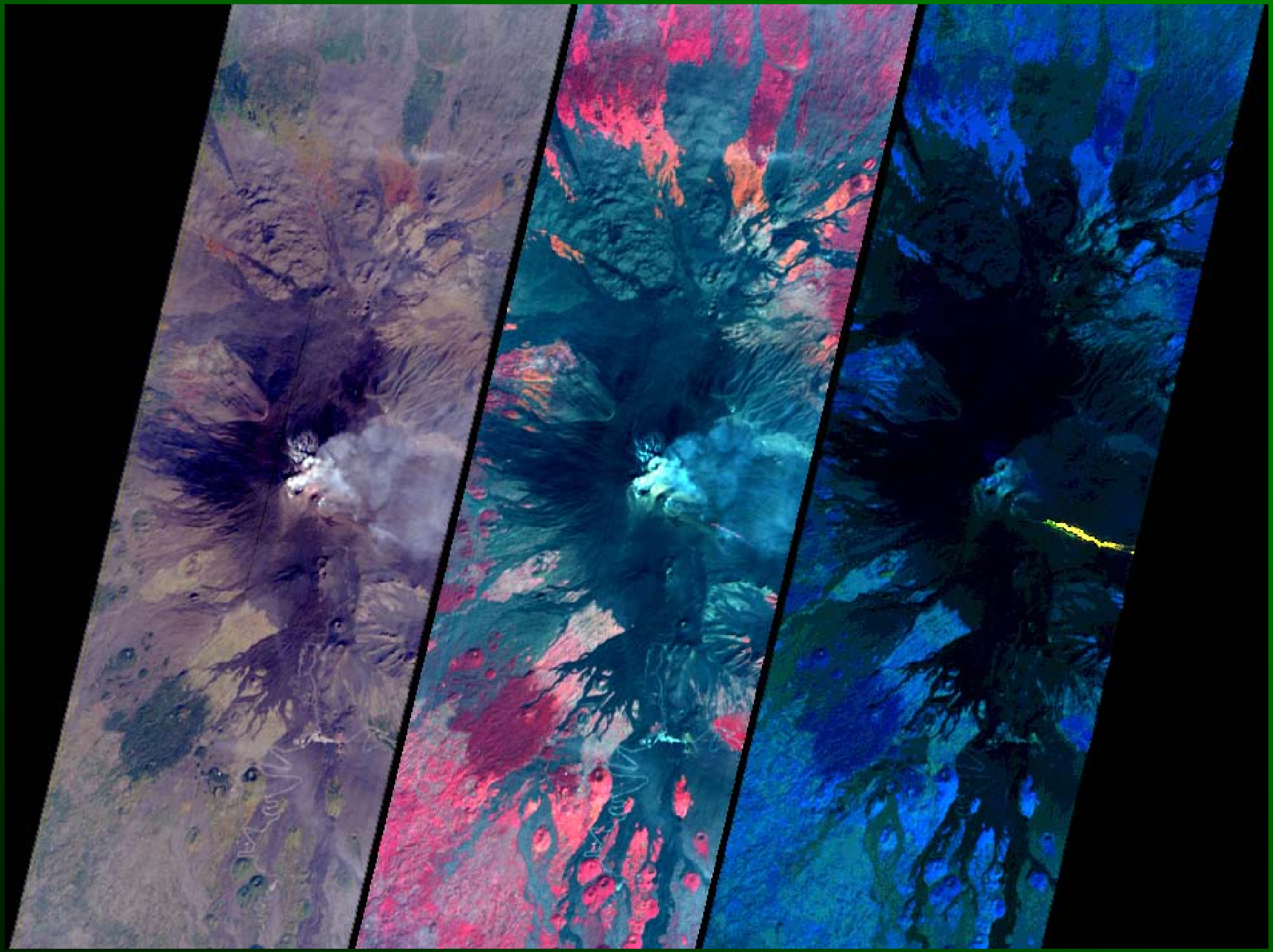

July 22, 2001 Hyperion Etna Data (2 3)

0.65-0.55-0.44 0.87-0.65-0.55 1.65-0.87-0.65

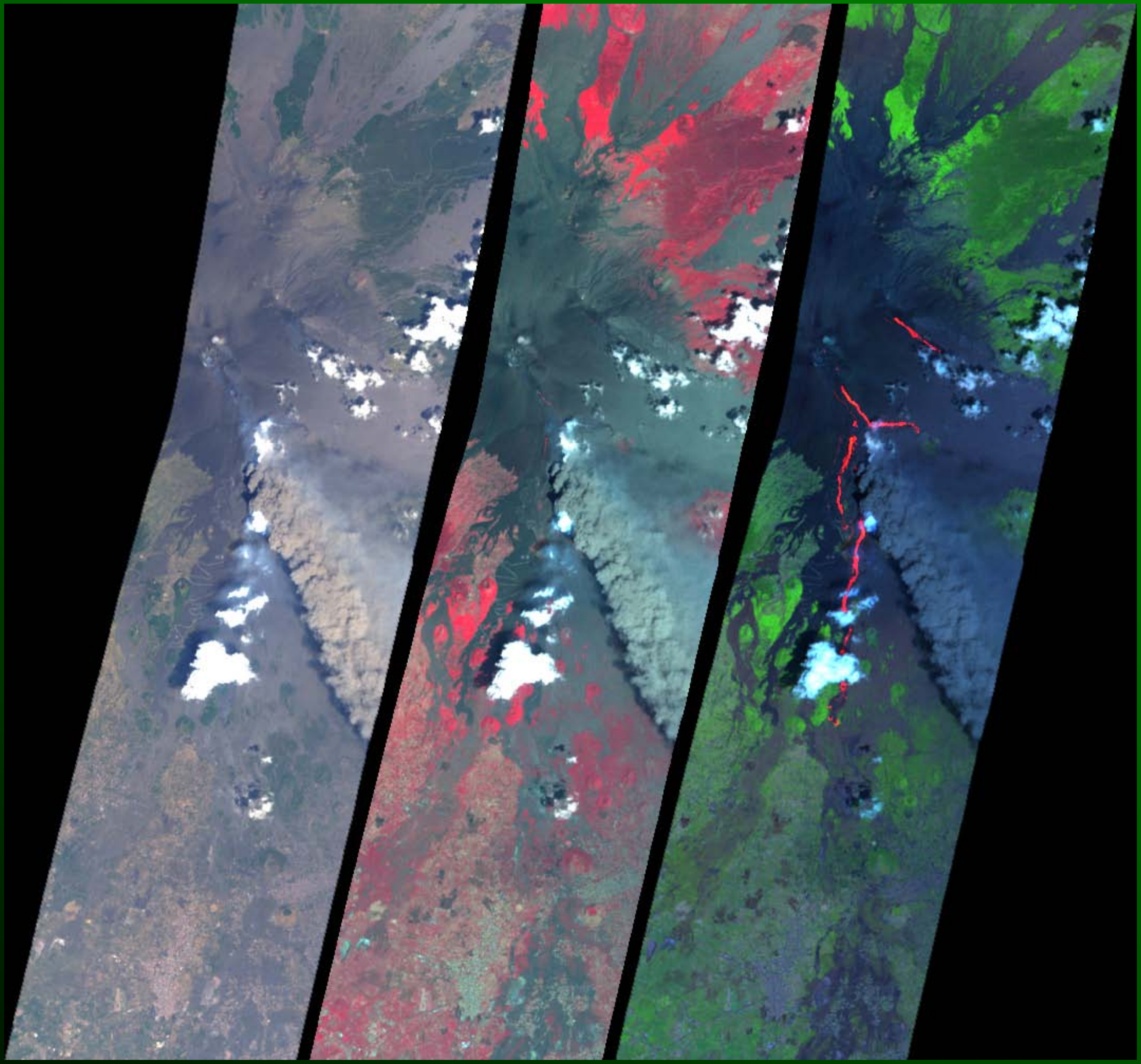

SO_2 Determination with ASTER TIR(1)

Multispectral TIR allows determination of SO_2 column abundance. With wind speed estimate, a total flux can be estimated.

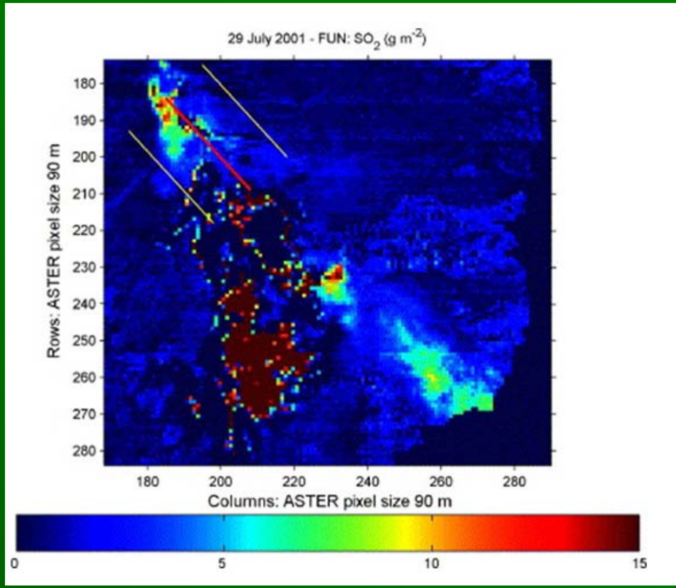

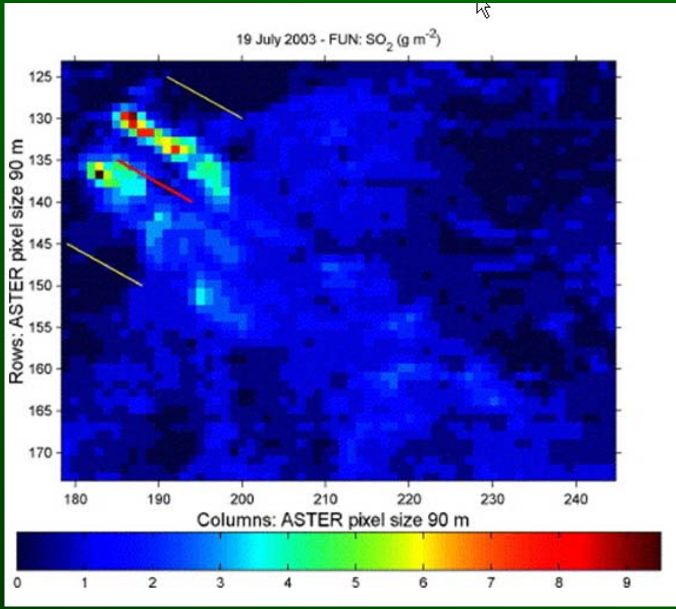

Pugnaghi et al., 2005

Lava Flows, Energy Radiated, Extent (2)

Lava flow models require DEM data, effusion rates, and Temperature distributions

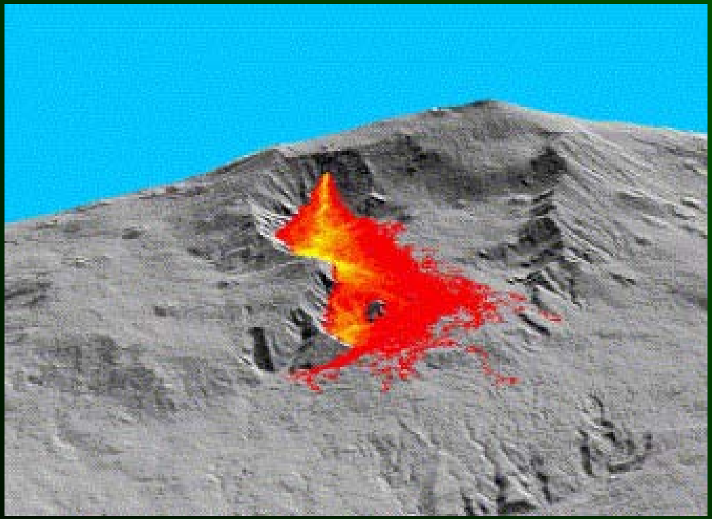

Damiani et al., 2006

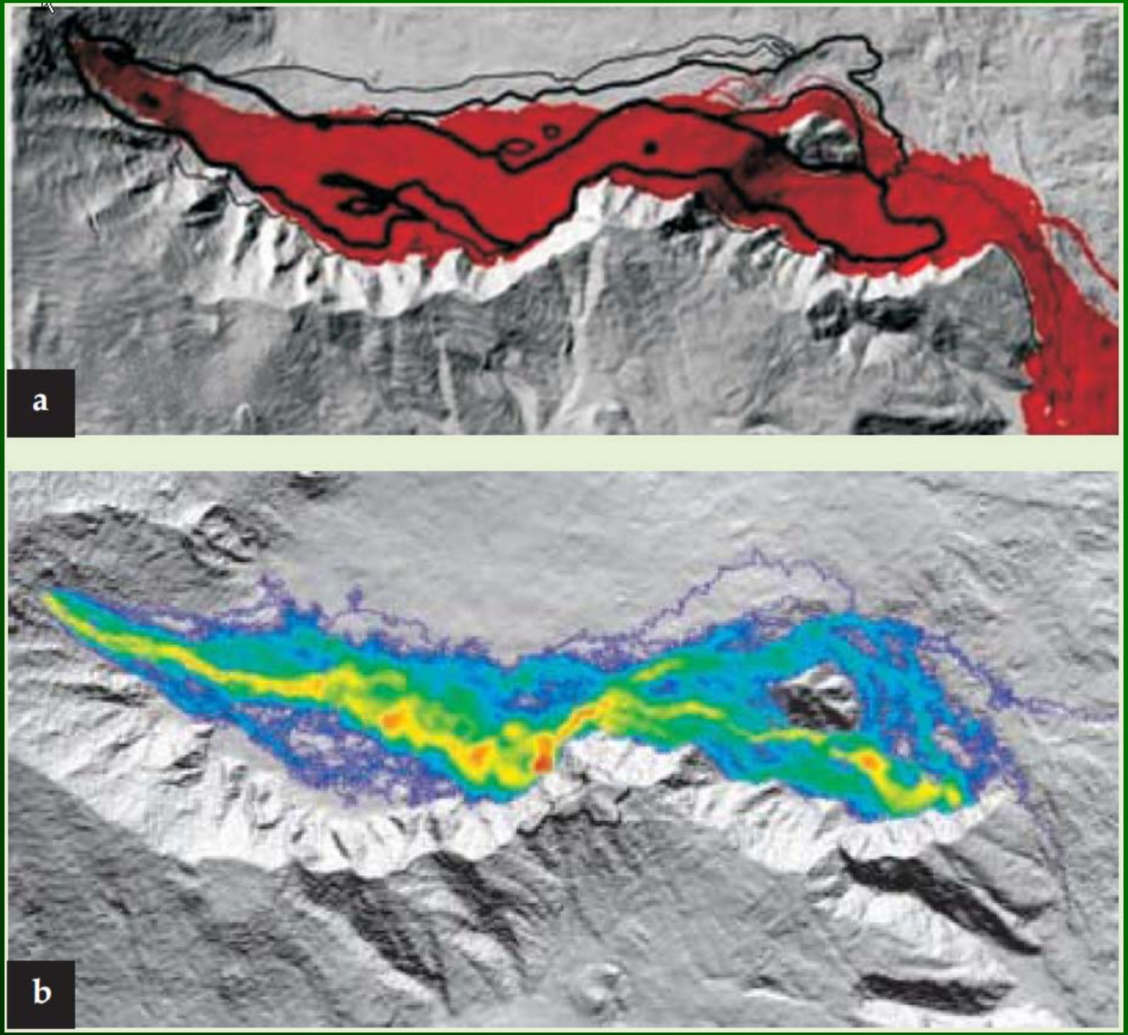

Wright et al., 2008

Lava Lakes, Energy Fluxes (3)

Radiant flux vs time for Lascar volcano:Landsat TM bands 5 & 7

OPPENHEIMER ET AL.: ANALYSIS OF VOLCANIC THERMAL FEATURES

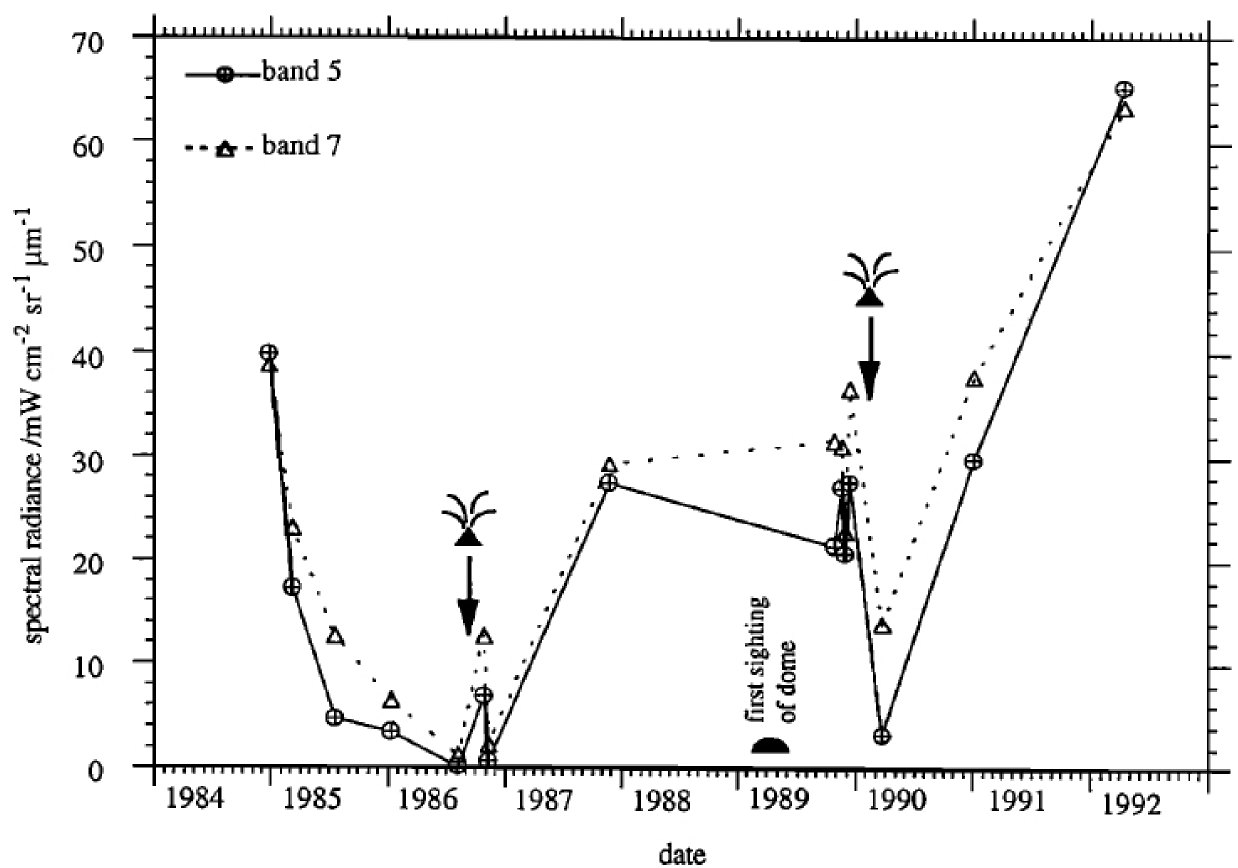

Fig.18. Bands 5 and 7 spectral radiance through time for each TM image. All $DN_{\lambda,\mathrm{thermal}}$ greater than or equal to 10 were summed, except when band 5 anomalies lacked corresponding radiance in band 7, since such pixels had most probably beel inadequately corrected for reflected sunlight. Volcano symbols mark September 16, 1986, and February 20, 1990, eruptions.

Lava Lakes, Energy Fluxes, Mass Losses (3)

Mass fluxes to sustain estimated energy losses

Radiant Fluxes

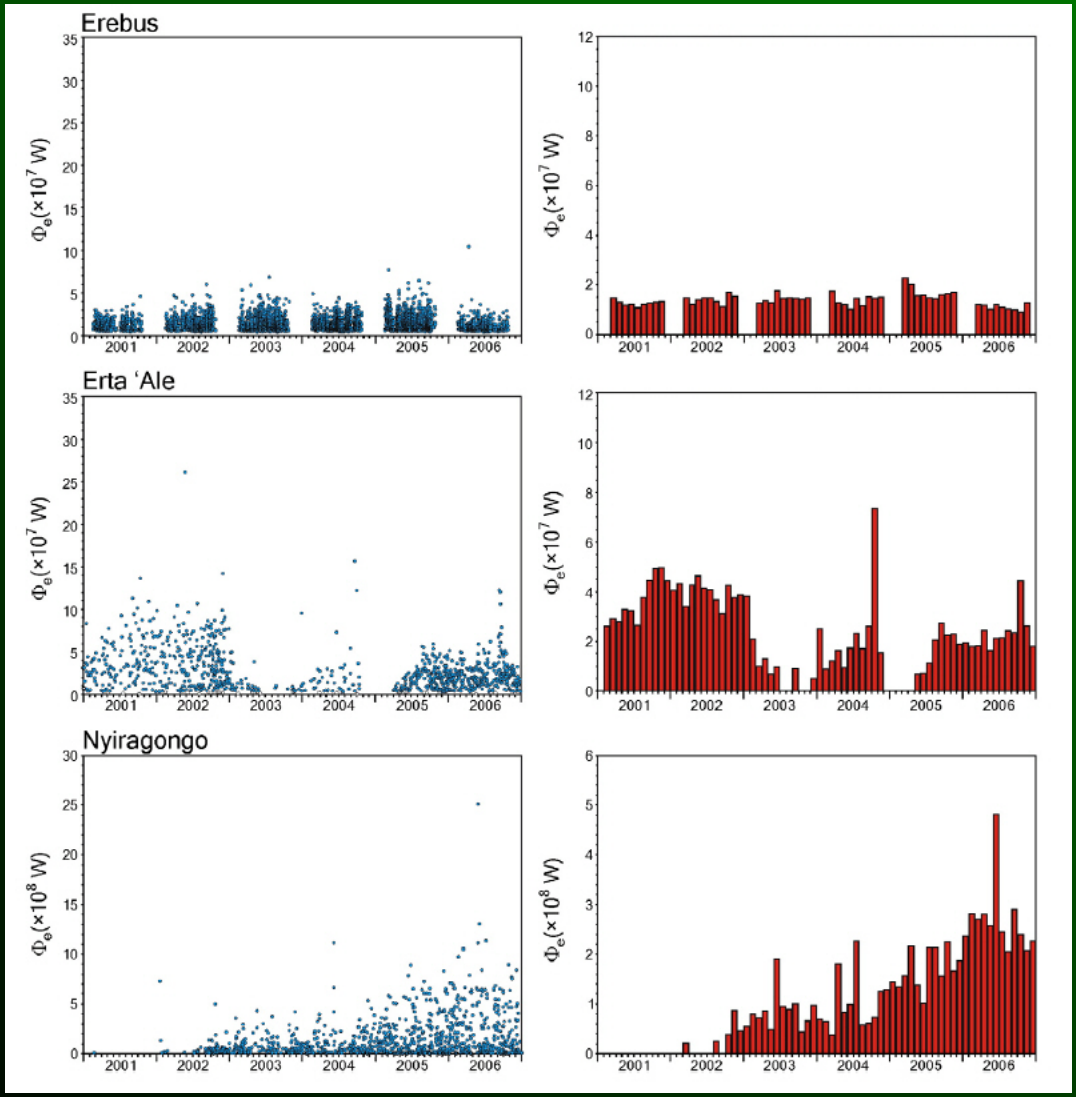

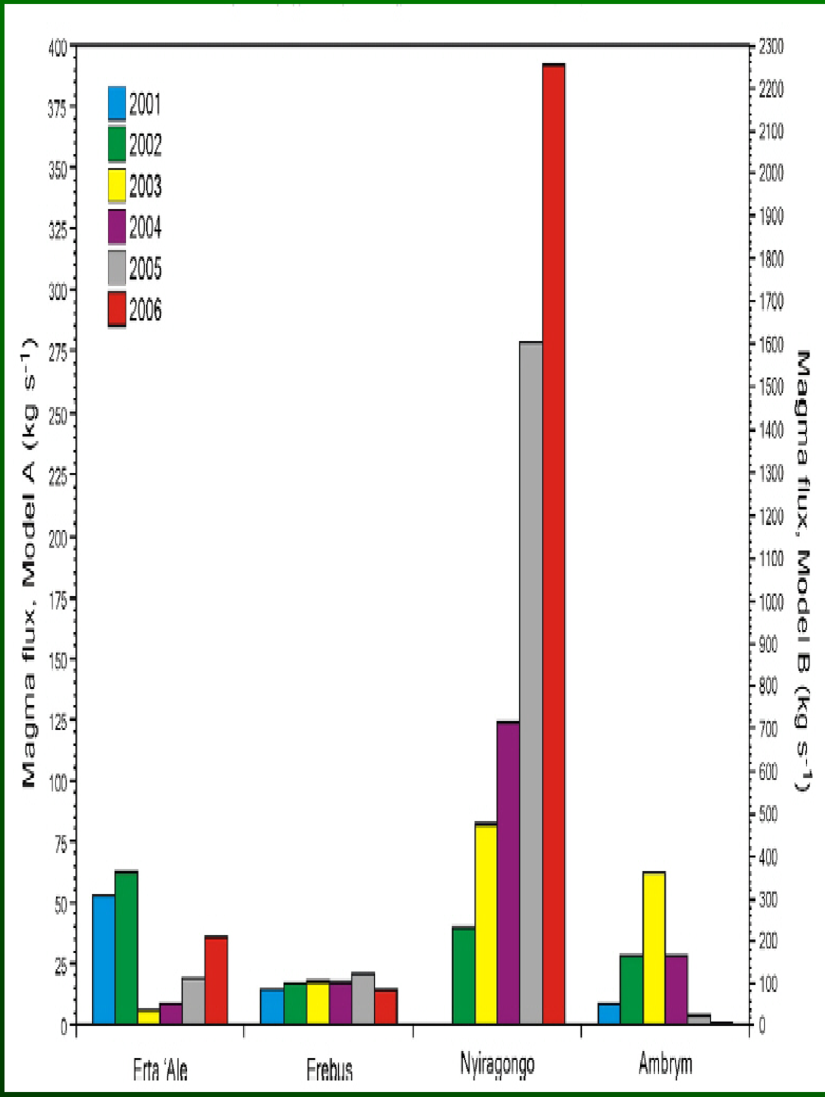

Saturation of 3-5 um Channel

- ❖ Extensive work by Co-I Rob Wright will be reported later in the workshop covering volcanoes.
- ❖ More complete report will be given by Vince Realmuto later in workshop covering volcanoes and fires.
- ❖ Recent (yesterday) discovery of China’s HJ-1B IRS sensor

China’s HJ-1B IRS Instrument

	Spectral range	Pixel size	Swath, km
1	0.75-1.0	150	720
2	1.55-1.75	150	720
3	3.5-3.9	150	720
4	10.5-12.5	300	720

China's HJ-1B IRS Instrument

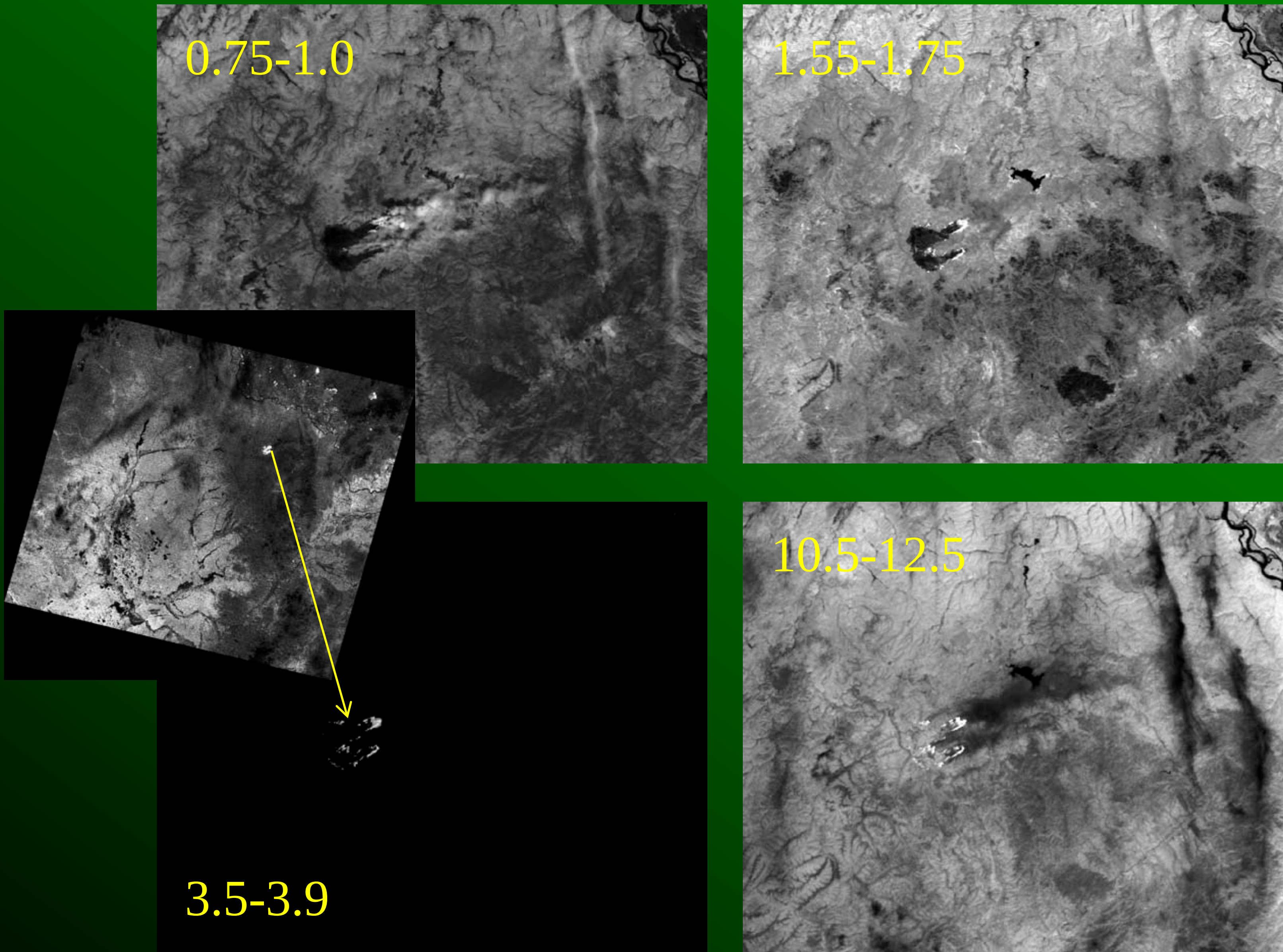

China's HJ-1B IRS Instrument

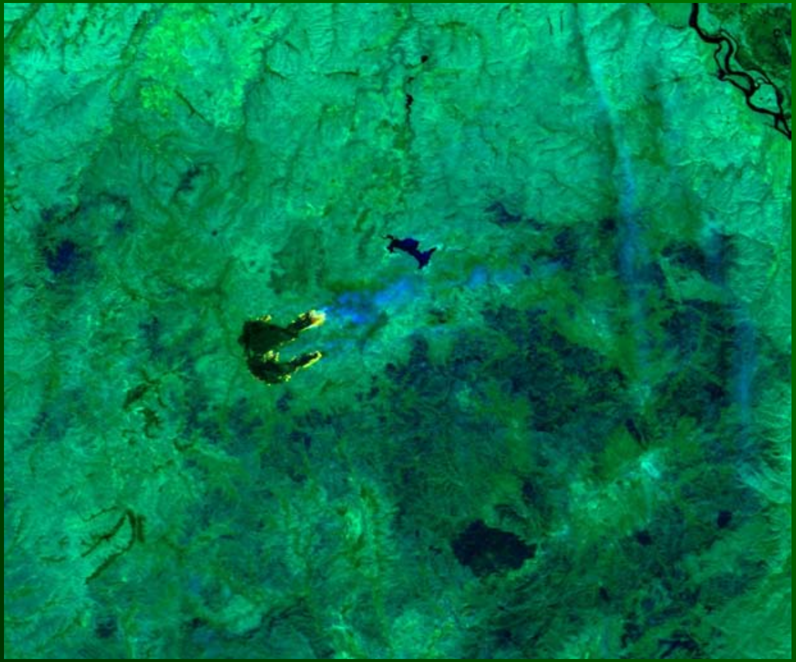

3.7, 1.65, .87

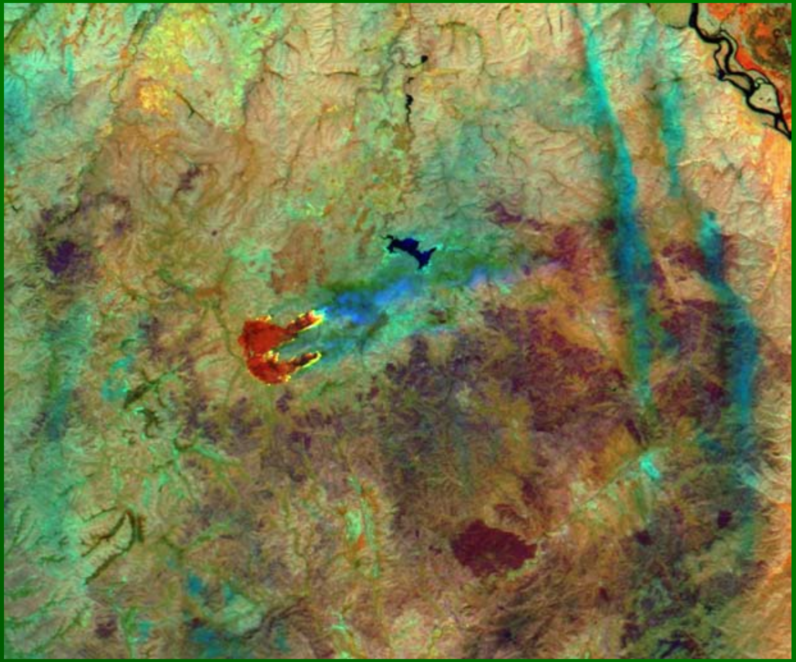

11.5, 1.65, .87

China's HJ-1B IRS Instrument

.87

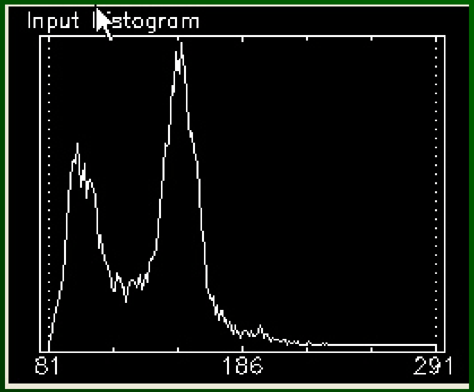

1.65

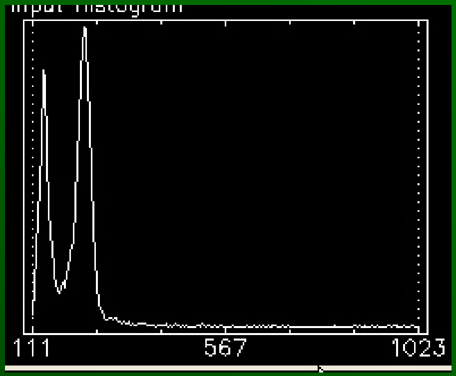

3.7

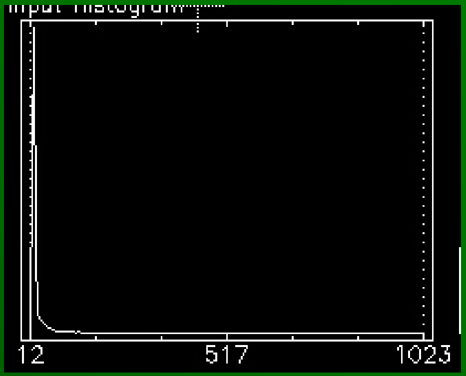

11.5

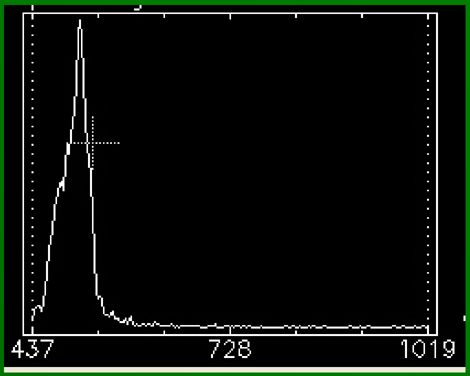

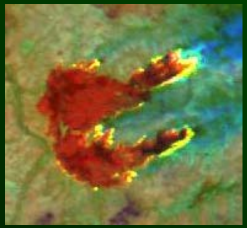

	Low DN	High DN	W/m2*sr*um (low)	W/m2*sr*um (high)
1: .75-1.0	81	291	18.9	67.9
2: 1.55-1.75	111	1023	5.98	55.1
3: 3.5-3.9	12	1023	0	80.3
4: 10.5-12.5	437	1019	7.8	17.3

China’s HJ-1B IRS Instrument

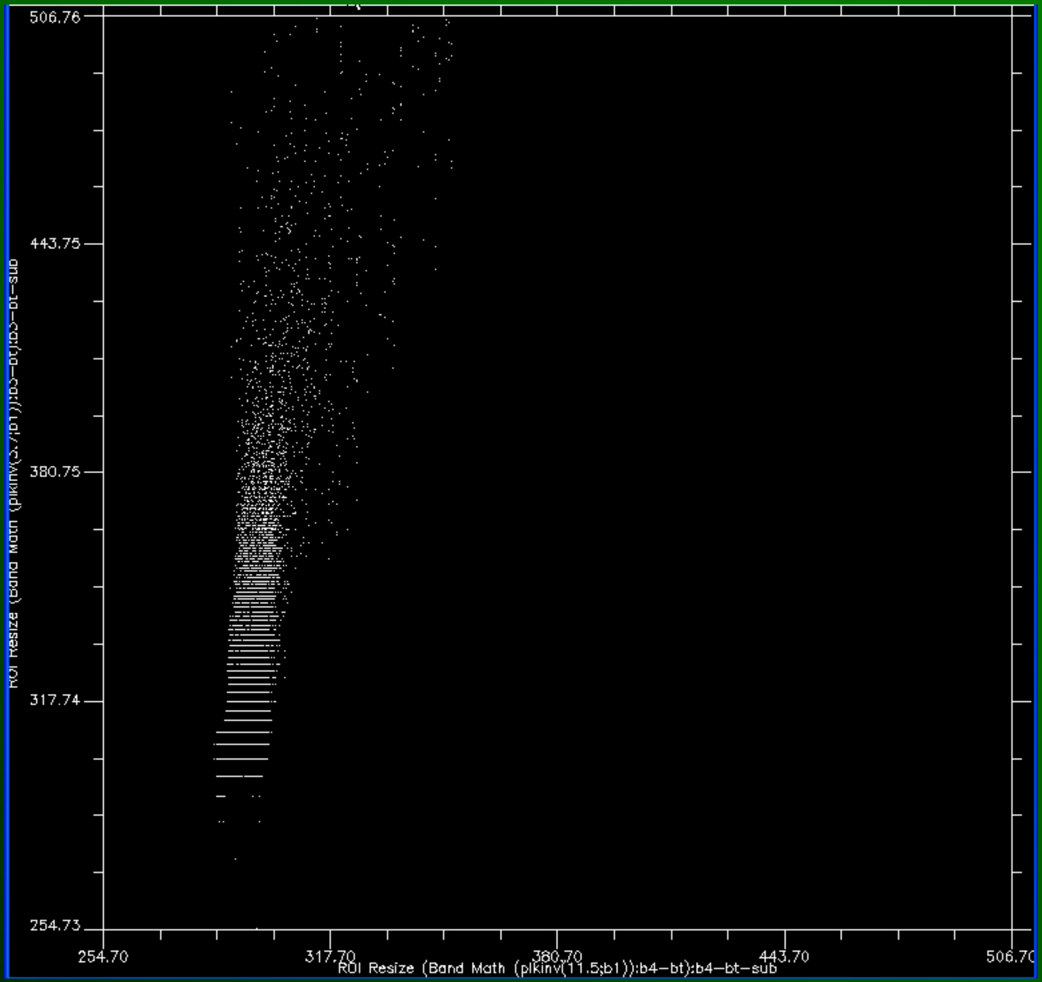

Brightness temperature: B4-xaxis, B3-yaxis

Pakistan Flood

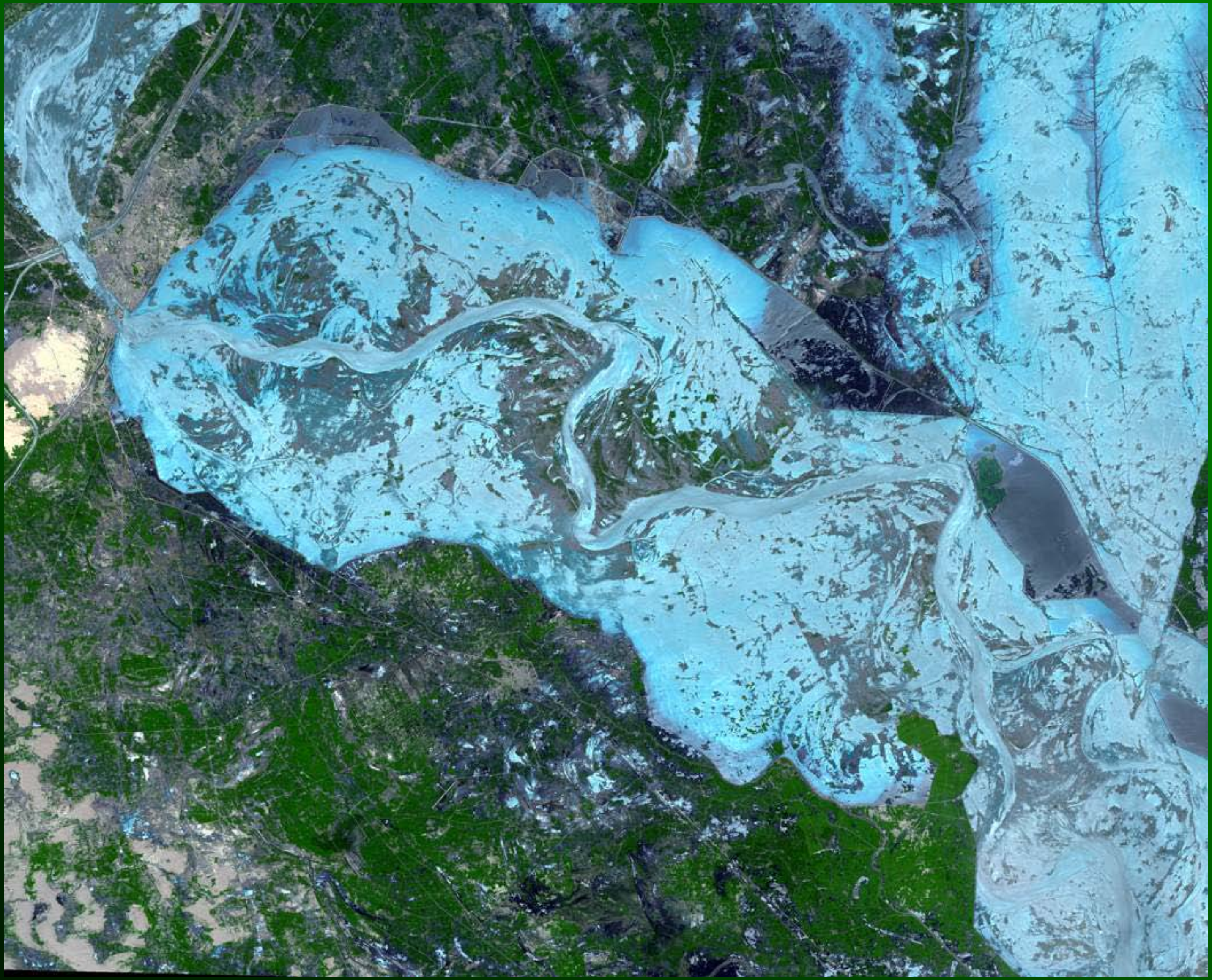

Making the connection between imaging spectroscopy and direct measures of ecosystem function

HyspIRI Workshop
August 24th, 2010

Shawn P. Serbin, Aditya Singh, Huan Gu, Eric L. Kruger, and Philip A. Townsend

THE UNIVERSITY of WISCONSIN MADISON

FERST
FOREST ECOSYSTEM REMOTE SENSING TEAM
DEPARTMENT OF FOREST AND WILDLIFE ECOLOGY
UNIVERSITY OF WISCONSIN - MADISON

Linking spectroscopy to ecosystem function

- Field data
- Lab measurements
- Scaling-up
- Link to imaging spectroscopy

Study areas

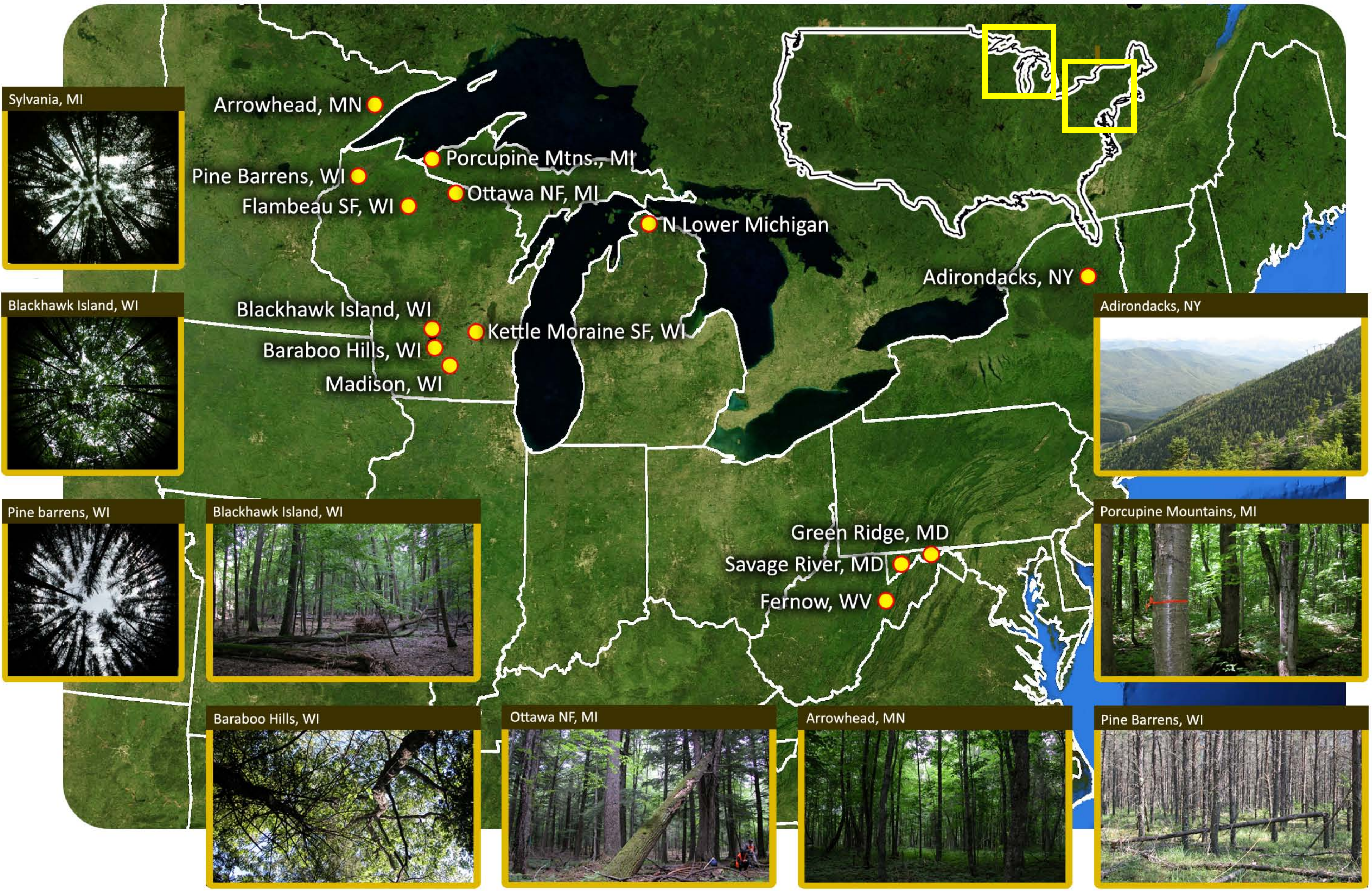
Arrowhead, MN
Porcupine Mtns., MI
Pine Barrens, WI
Ottawa NF, MI
Flambeau SF, WI
N Lower Michigan
Adirondacks, NY
Blackhawk Island, WI
Kettle Moraine SF, WI
Baraboo Hills, WI
Madison, WI
Green Ridge, MD
Savage River, MD
Fernow, WV
Sylvania, MI
Blackhawk Island, WI
Pine barrens, WI
Blackhawk Island, WI
Adirondacks, NY
Porcupine Mountains, MI
Baraboo Hills, WI
Ottawa NF, MI
Arrowhead, MN
Pine Barrens, WI

Field / lab measurements

Morphology / Nutrition

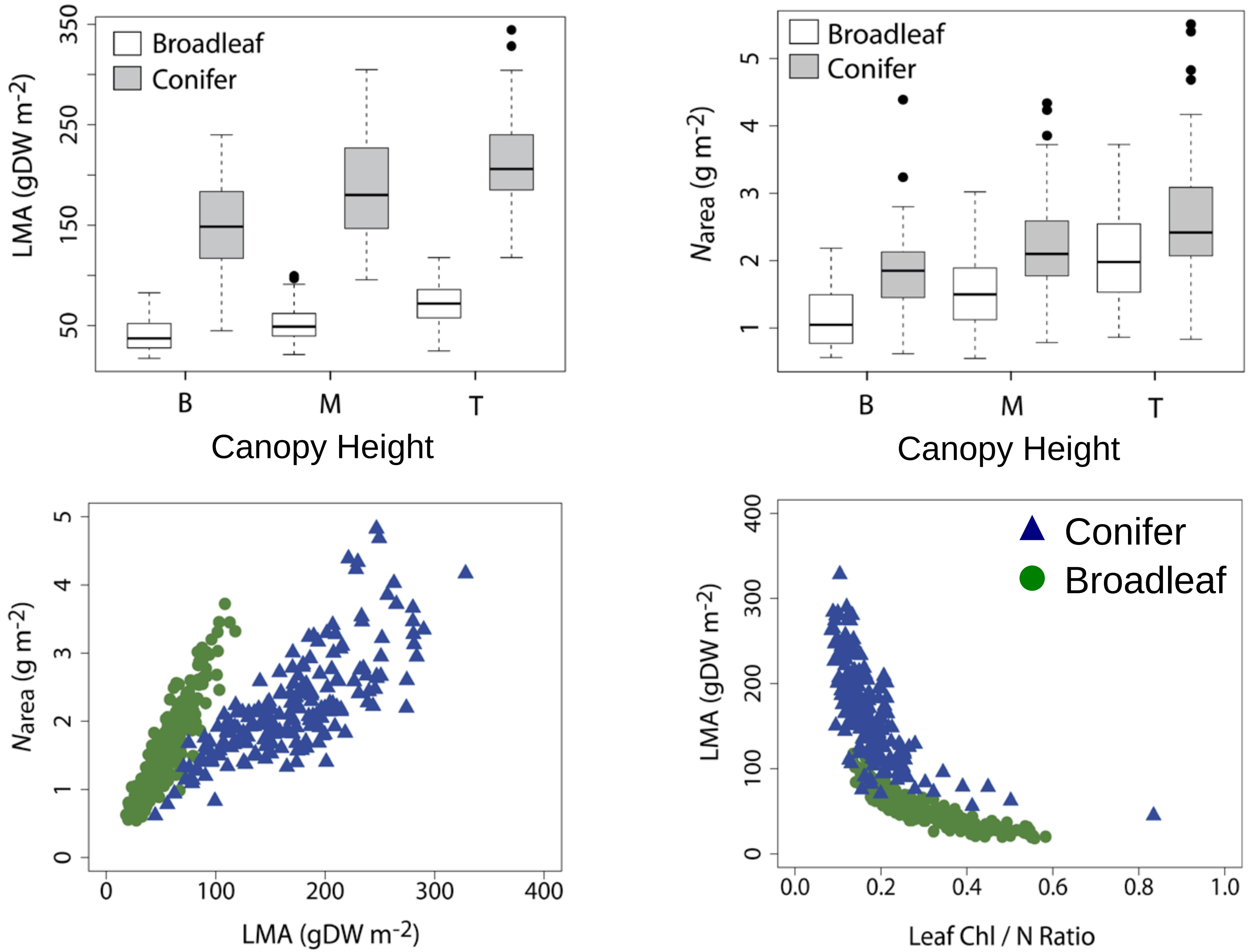

Recalcitrance / Nutrient Cycling

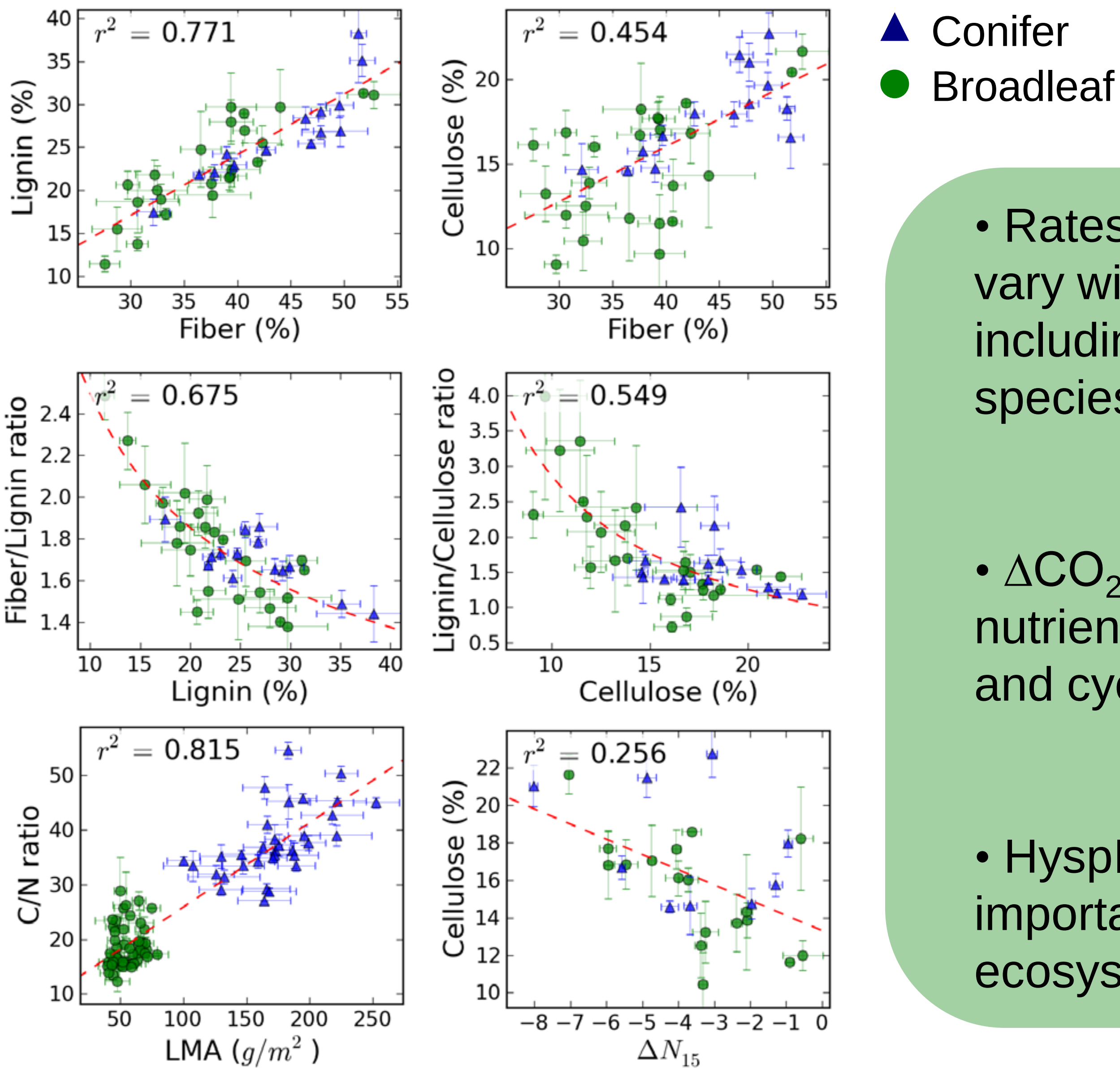

- Rates of nutrient cycling vary with many factors including climate and species

- ΔCO_2 and ΔT may alter nutrient allocation,retention, and cycling

- HyspIRI mission will be important for monitoring ecosystem changes

Leaf-level predictions

FERST

FOREST ECOSYSTEM REMOTE SENSING TEAM
DEPARTMENT OF FOREST AND WILDLIFE ECOLOGY
UNIVERSITY OF WISCONSIN - MADISON

Leaf-level predictions

Fresh-leaf spectra

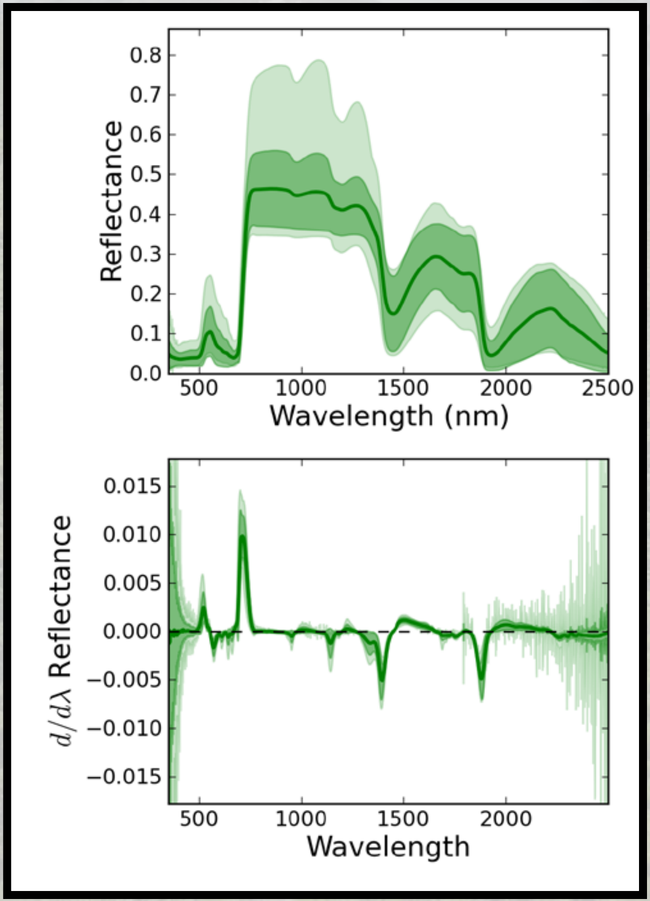

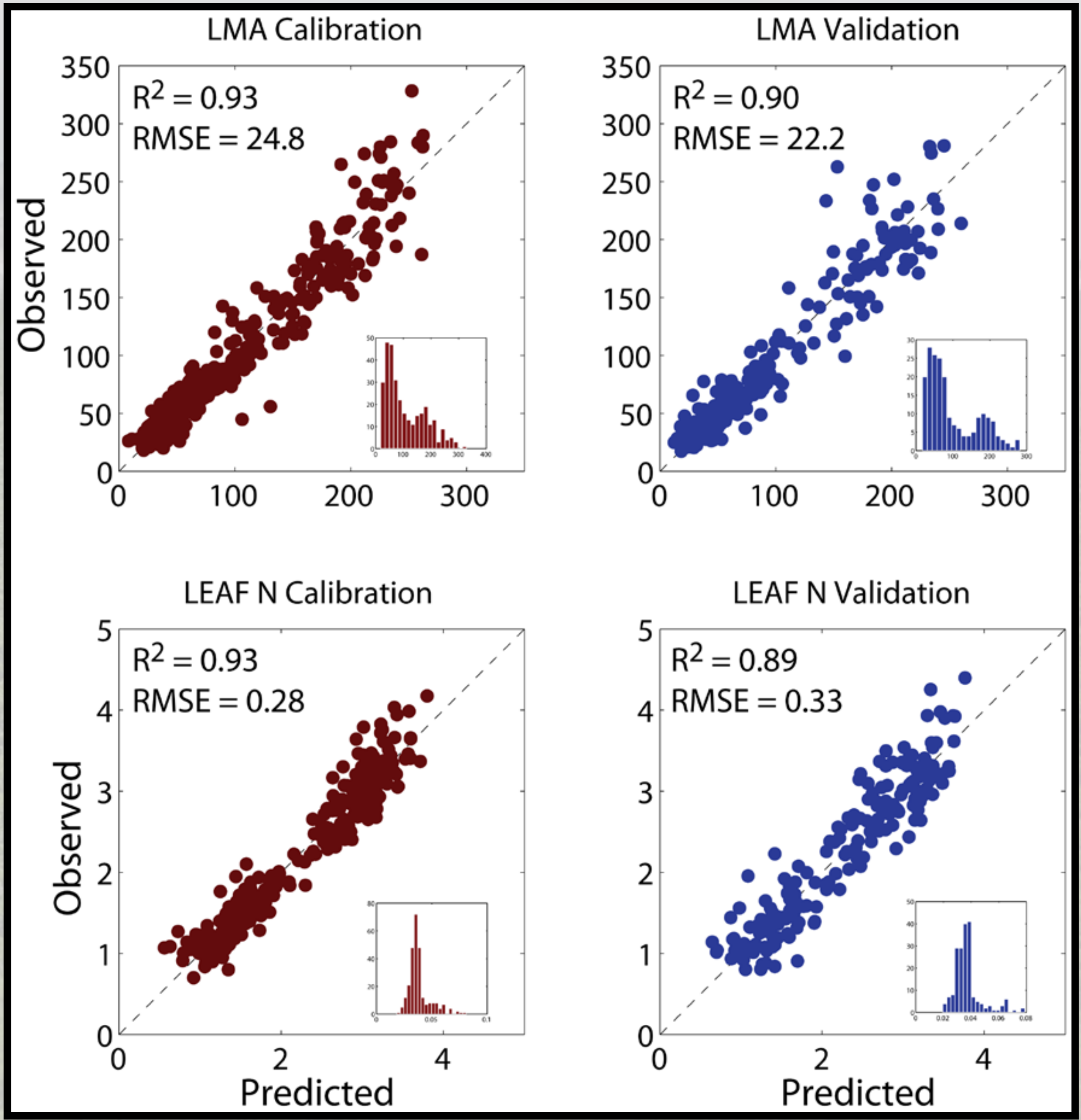

Leaf-level predictions

Dry-leaf spectra

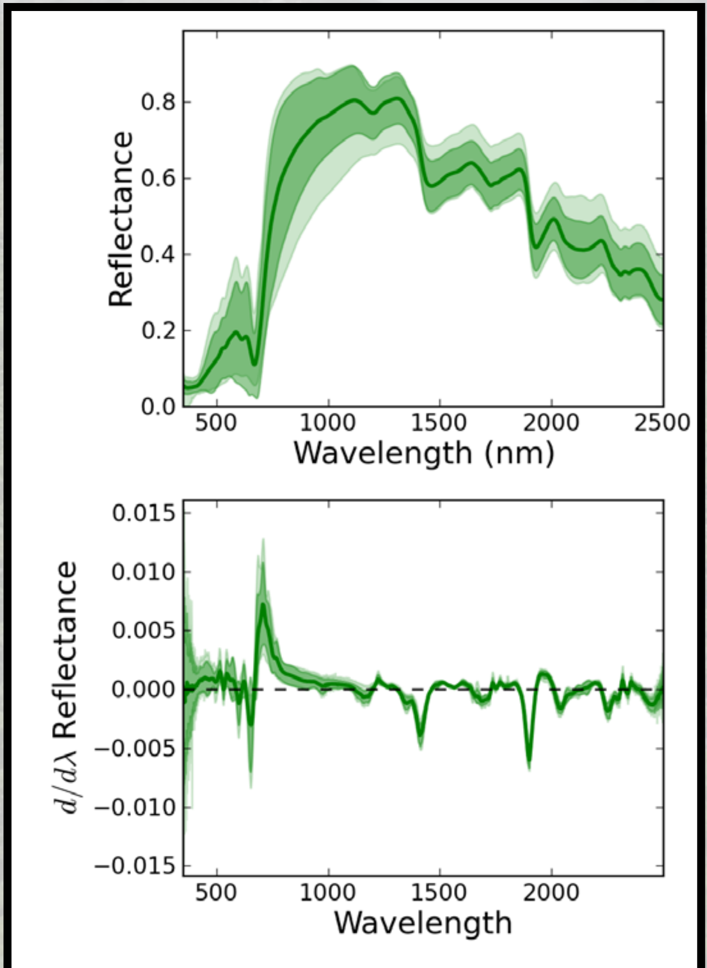

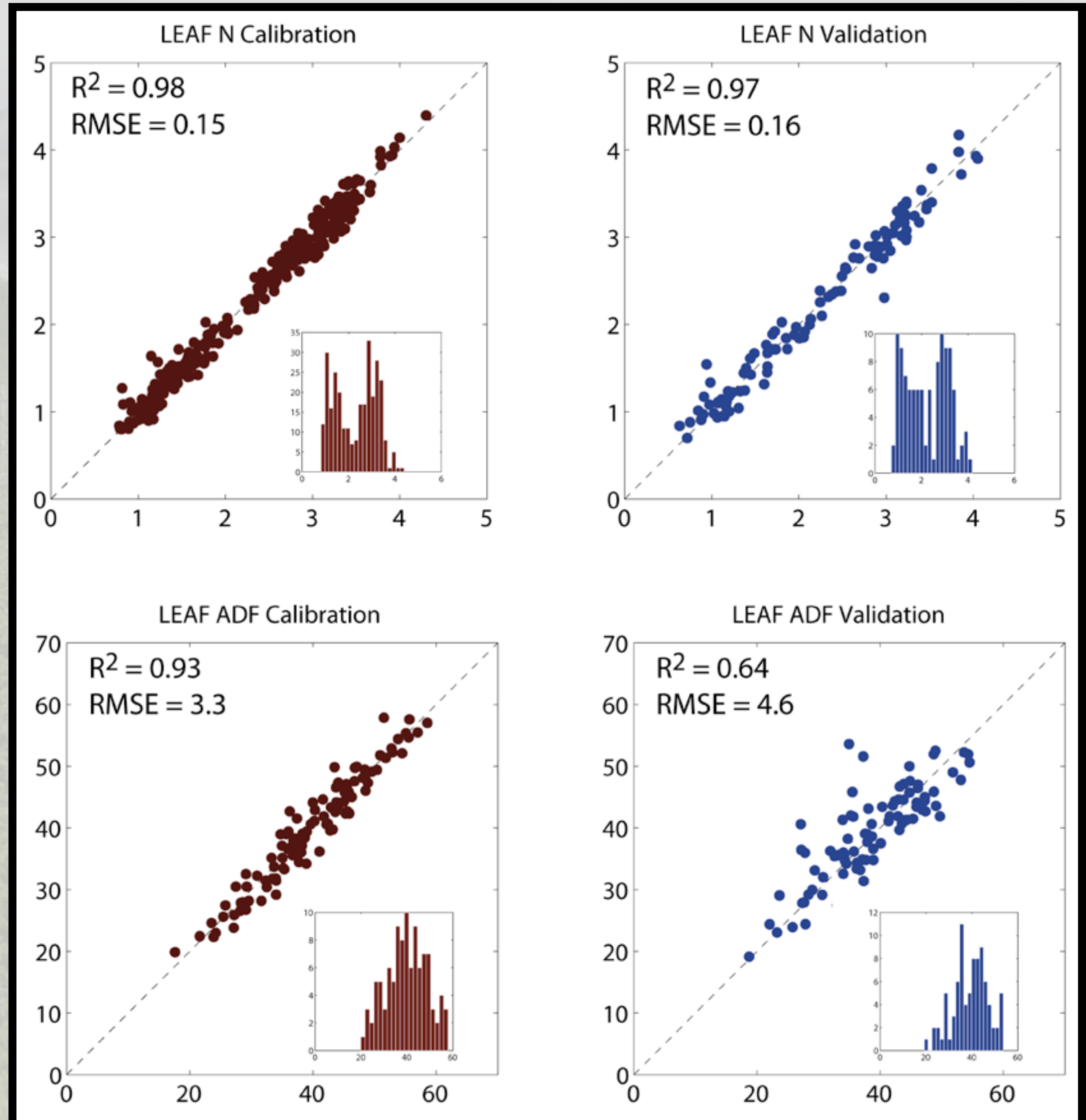

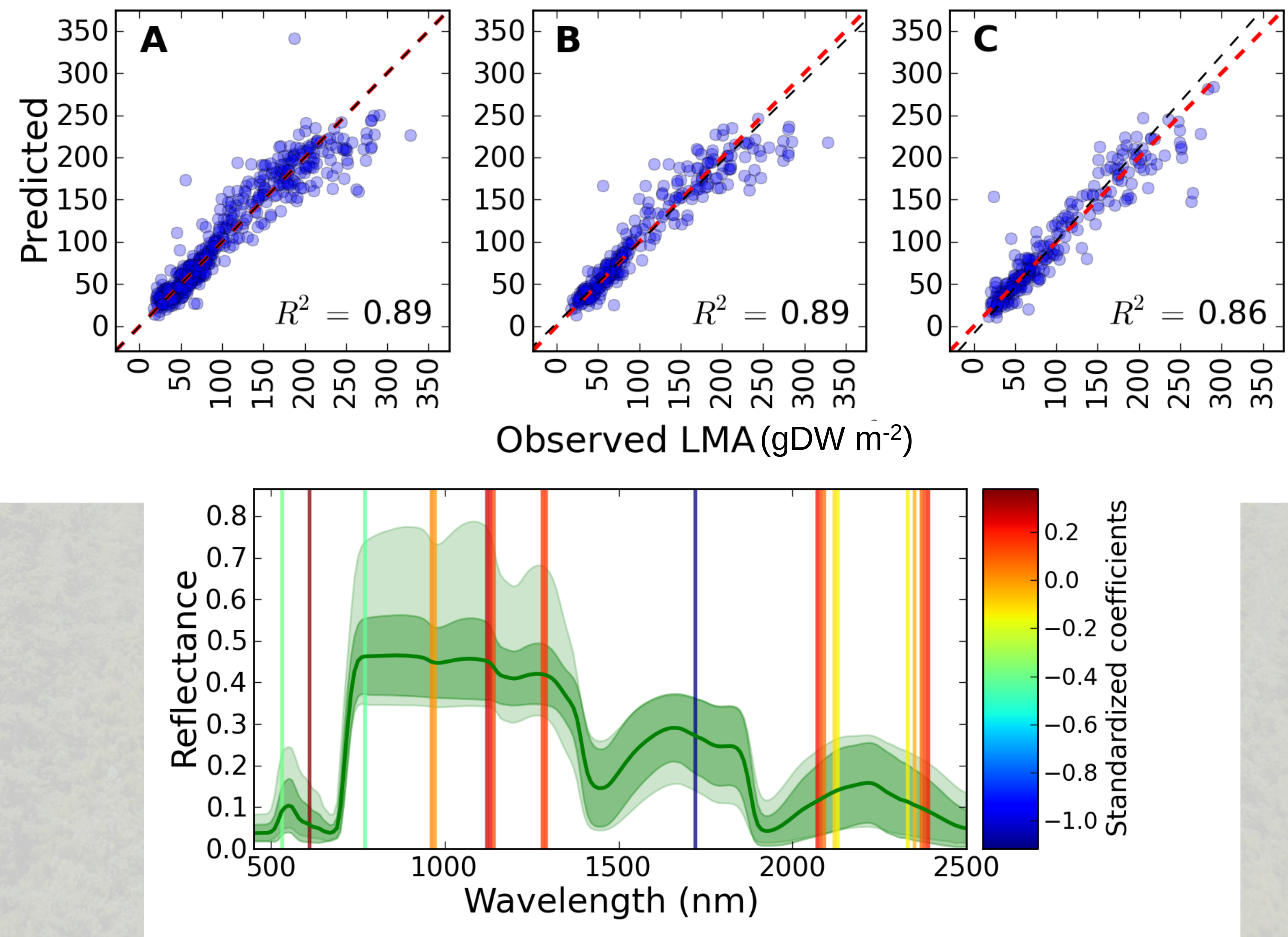
A
B
C
Predicted
$R^2 = 0.89$
$R^2 = 0.89$
$R^2 = 0.86$
Observed LMA (gDW m-2)
Reflectance
Wavelength (nm)
Standardized coefficients

AVIRIS processing

FERST

Forest Ecosystem Remote Sensing Team
Department of Forest and Wildlife Ecology
University of Wisconsin - Madison

AVIRIS Pre-processing: Steps

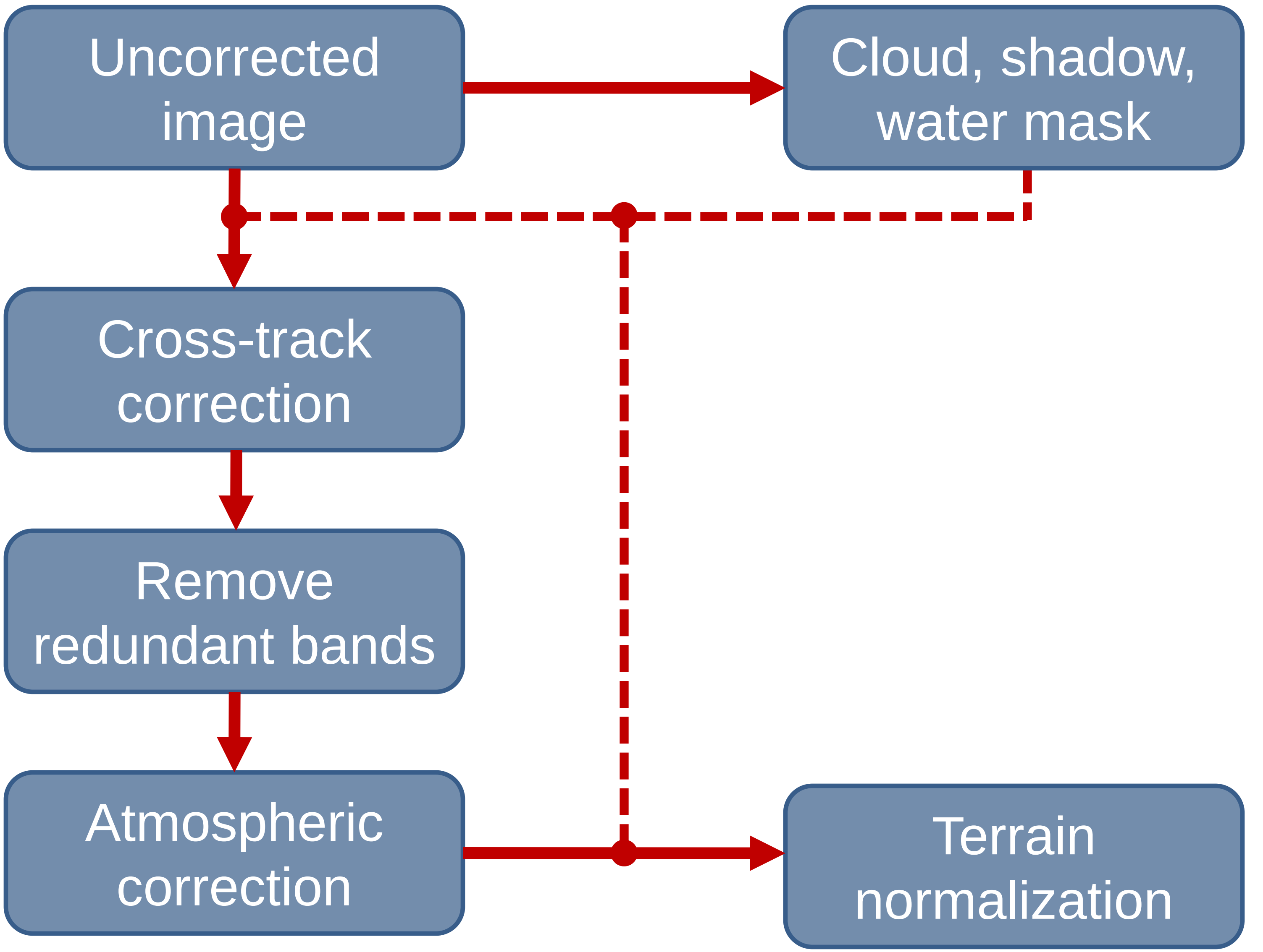

AVIRIS Pre-processing: Mask development

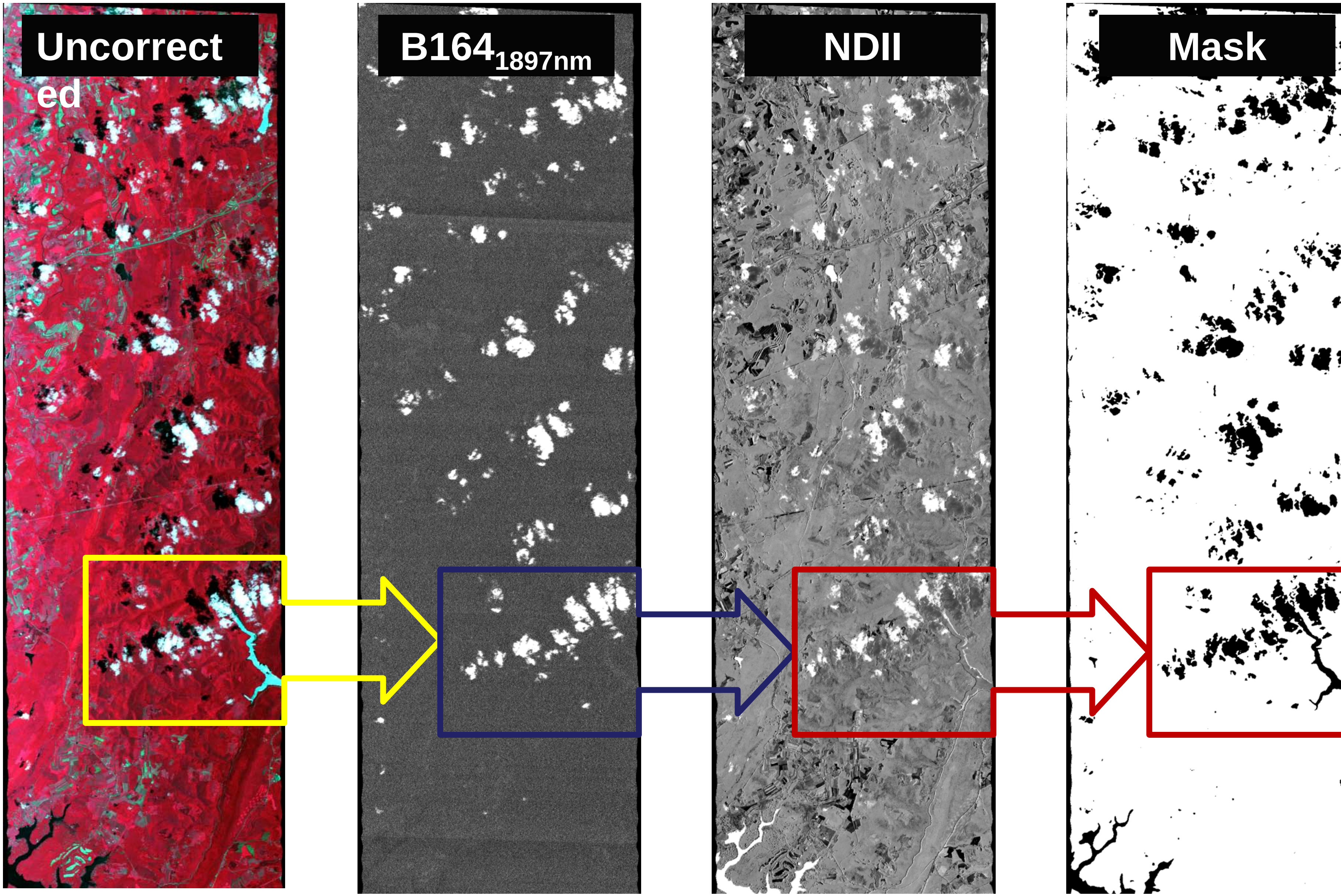

AVIRIS Pre-processing: C-factor terrain normalization

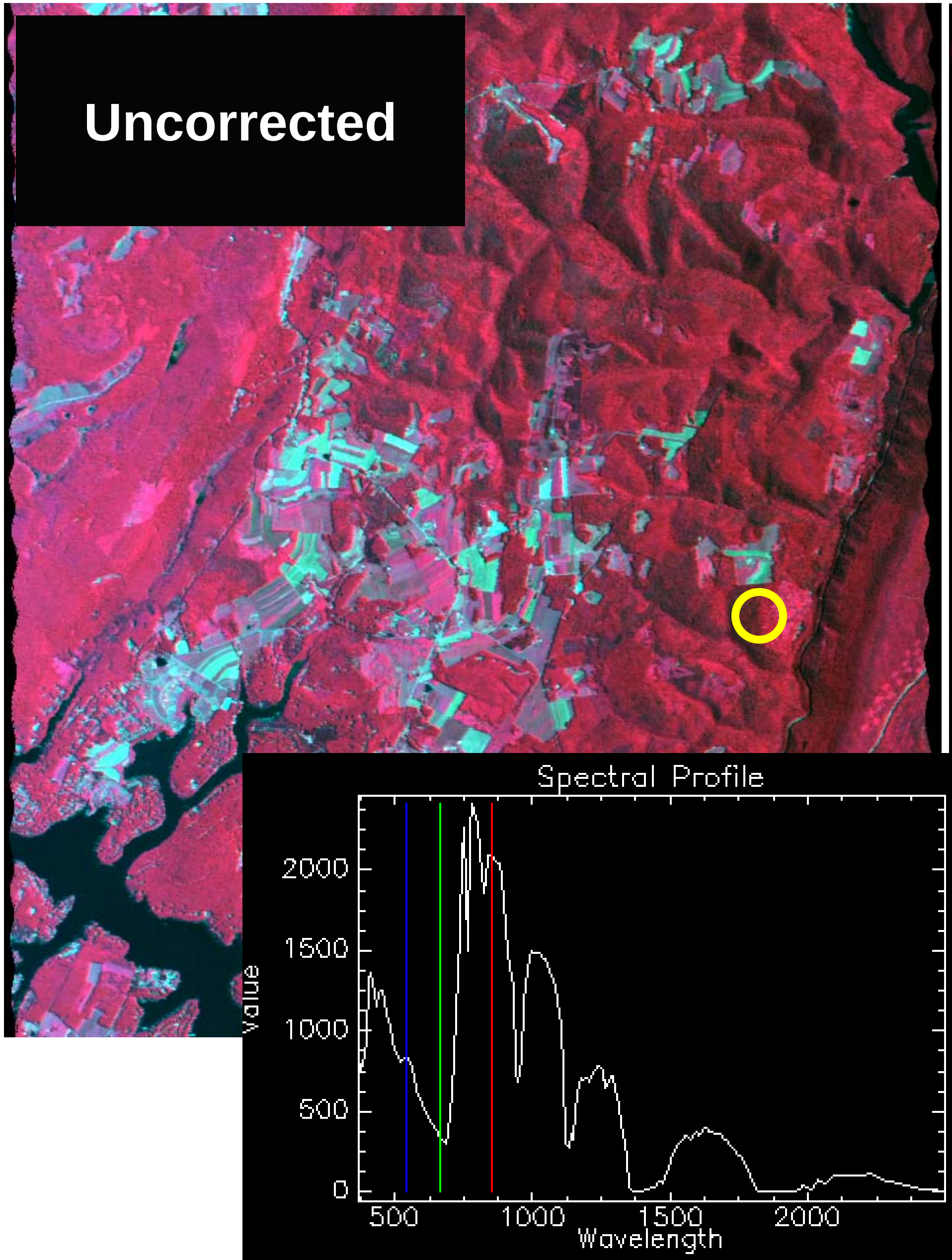

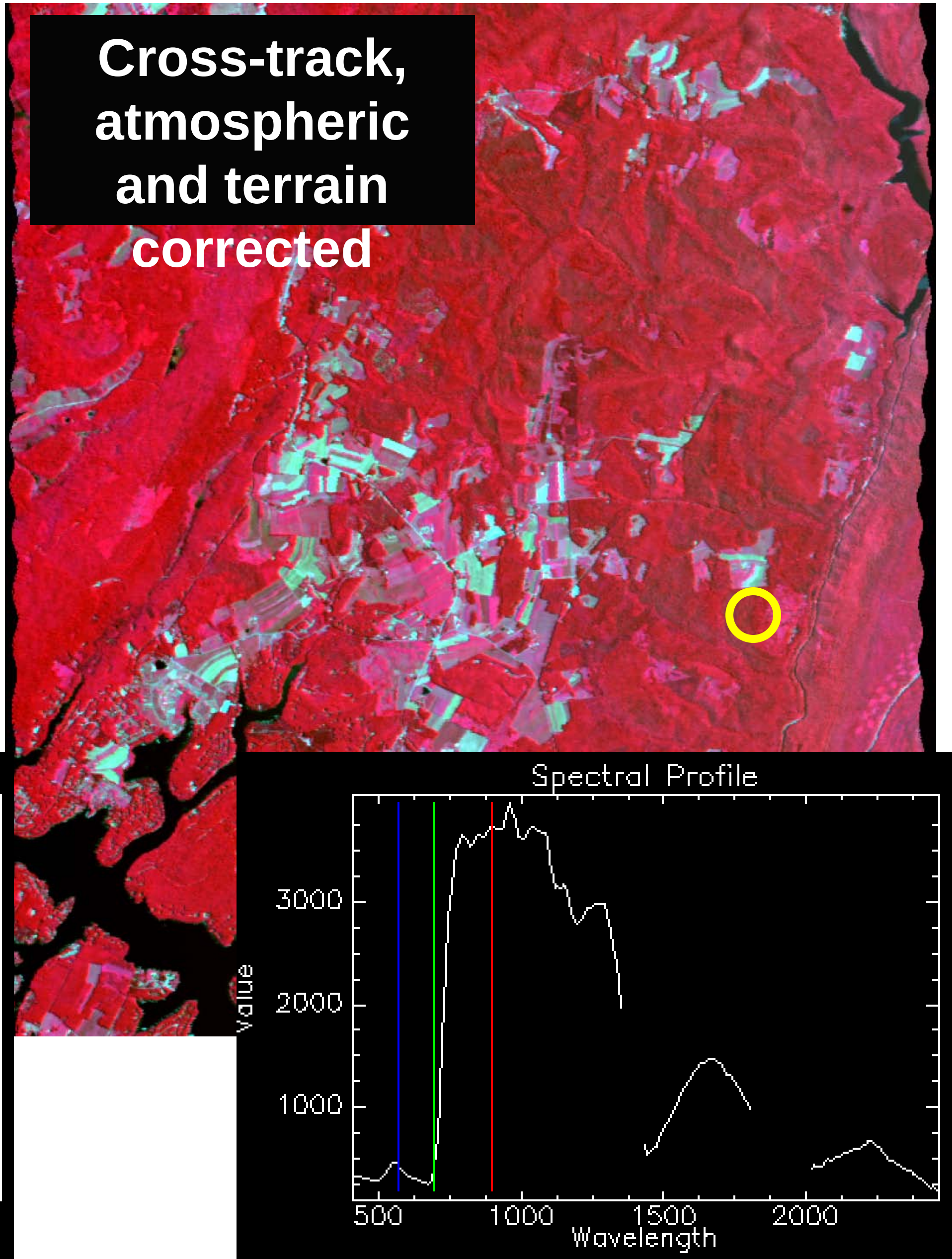

Scaling

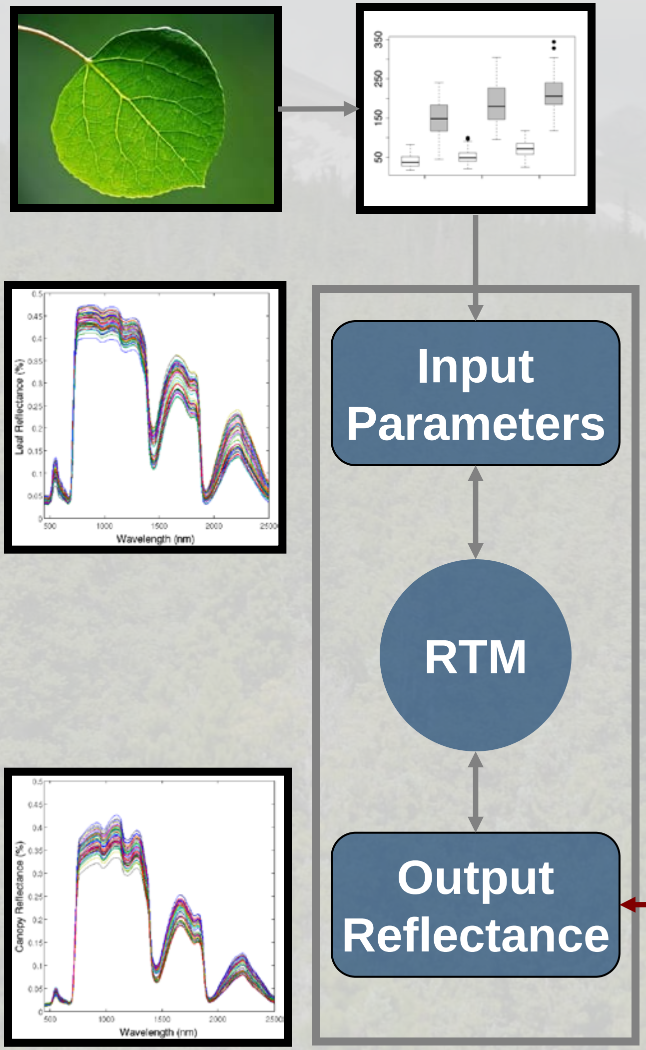

- Field-based scaling
  - LAI, Basal area
- RTM scaling
  - PROSAIL, PROFLIGHT
- Generate universal calibrations

Canopy-scale predictions

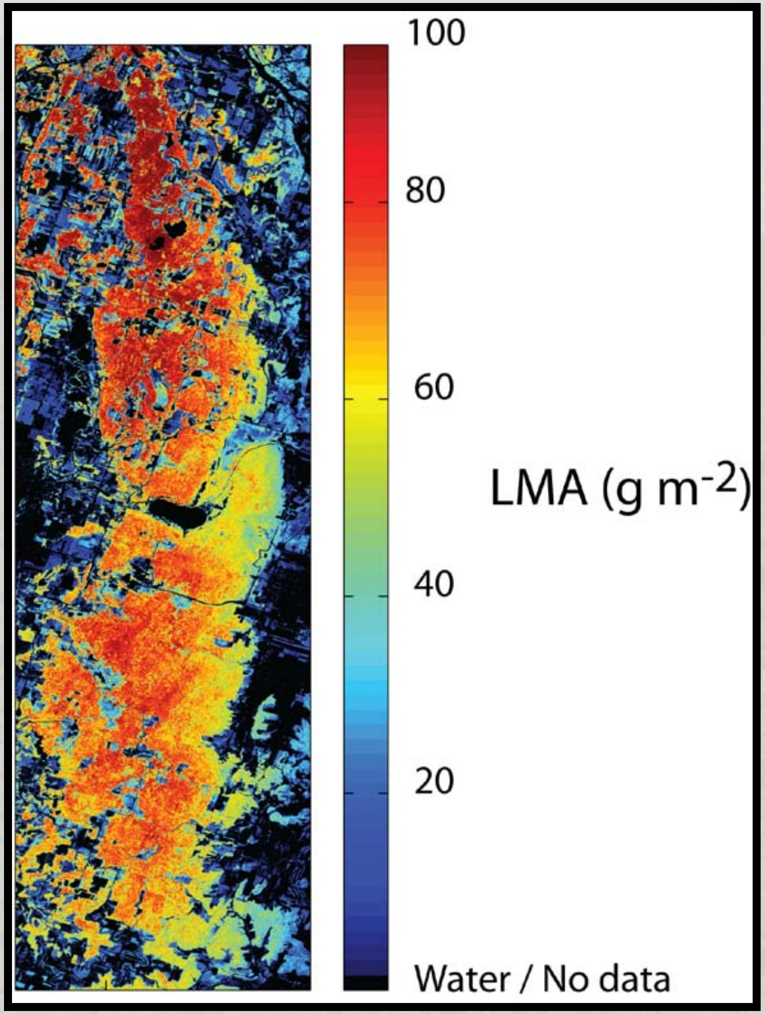

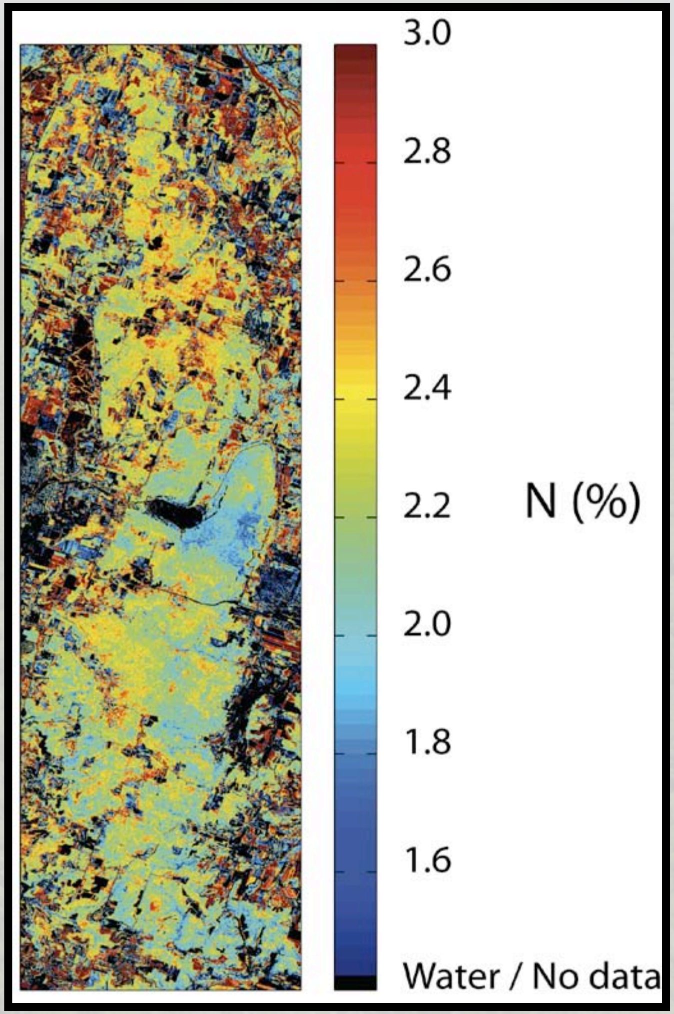

Forest metabolism

FERST

FOREST ECOSYSTEM REMOTE SENSING TEAM
DEPARTMENT OF FOREST AND WILDLIFE ECOLOGY
UNIVERSITY OF WISCONSIN - MADISON

Forest metabolism

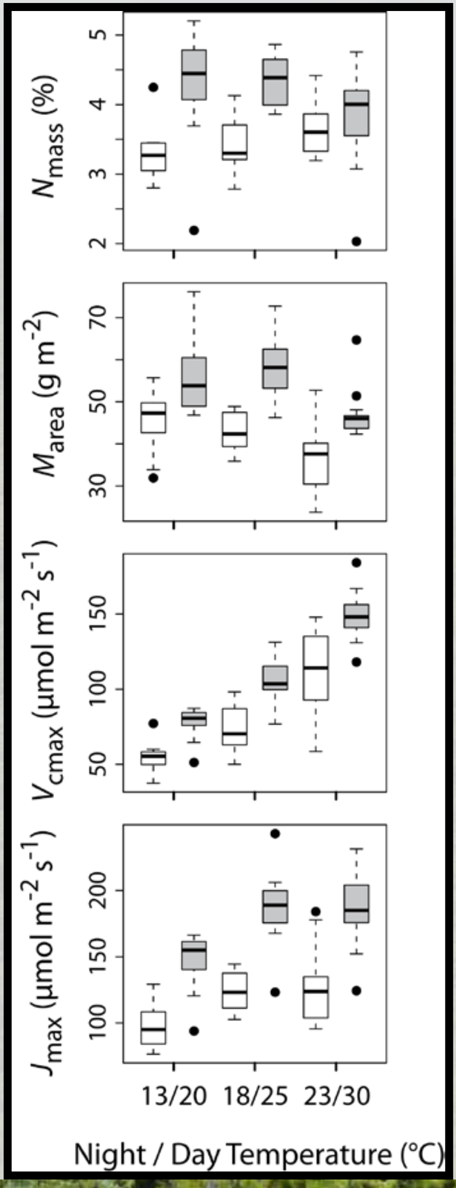

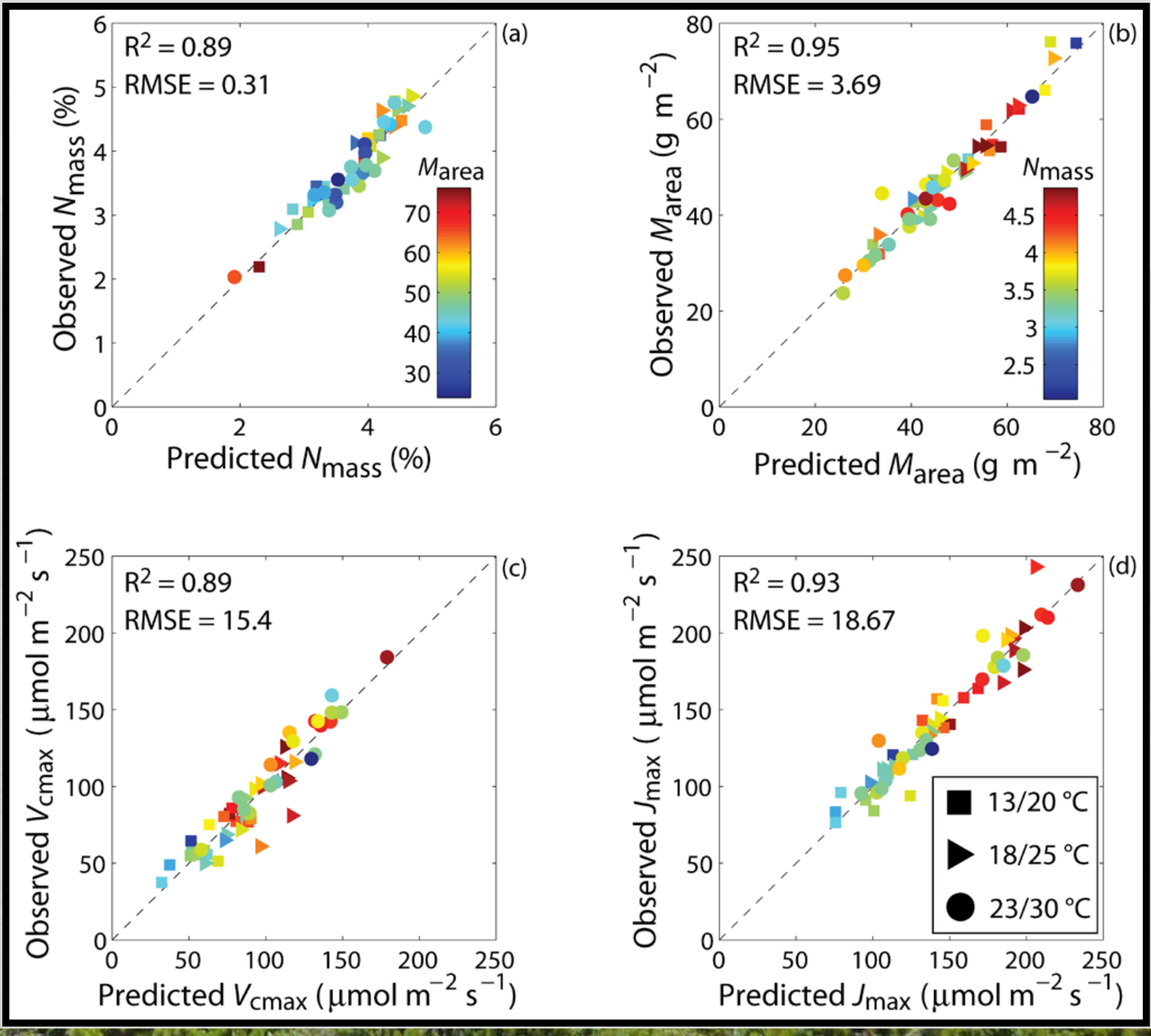

Forest metabolism

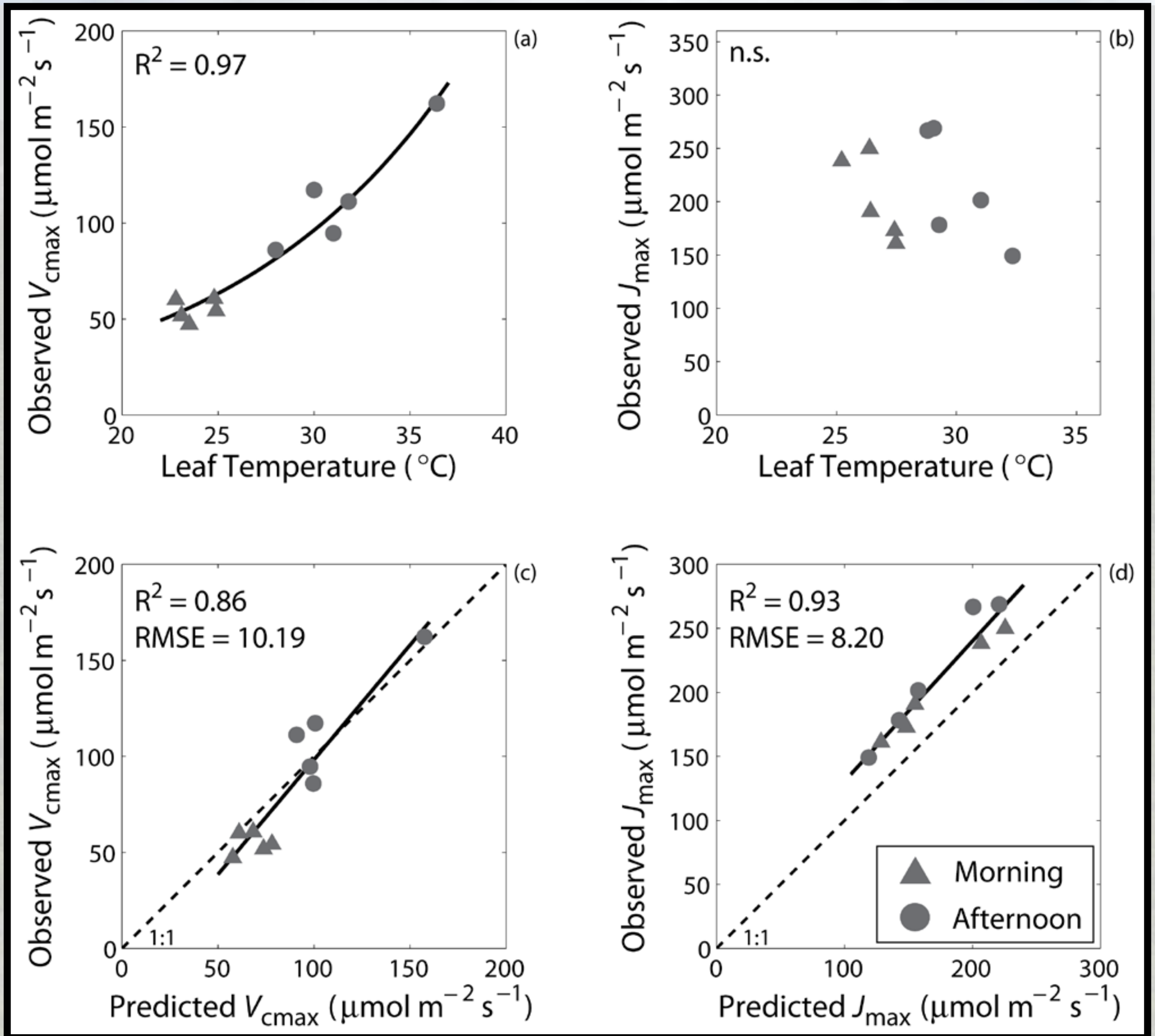

Ecosystem metabolism

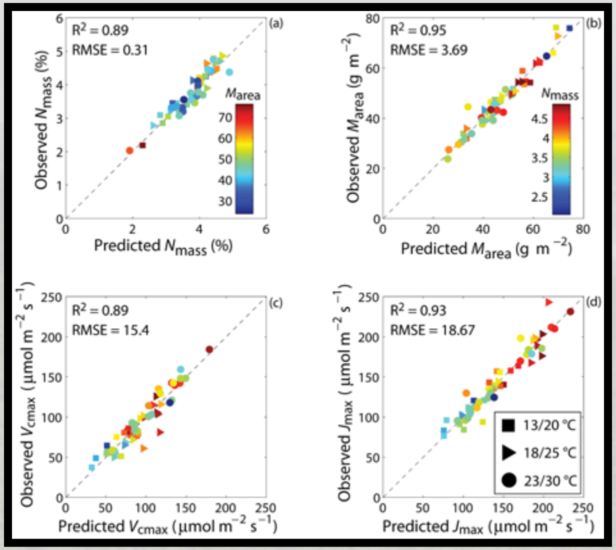

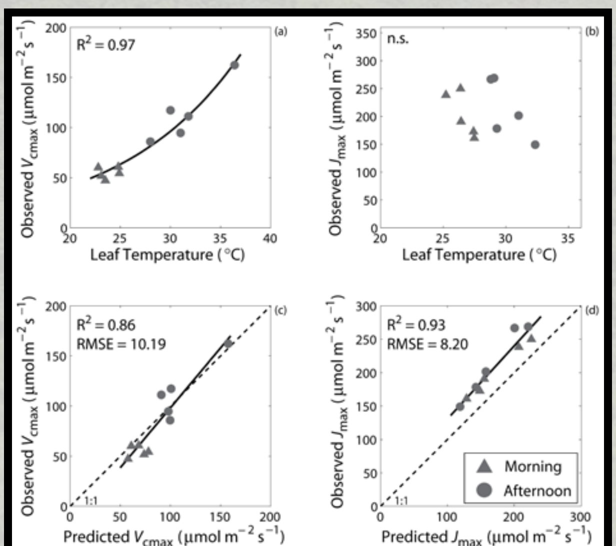

- Changes in the biosphere will broadly impact vegetation dynamics
  - e.g. Phenology, physiology, nutrient content / retention, productivity
- VSWIR / TIR sensors can provide key information for monitoring vegetation function
  - e.g. Pigments, LUE, stress
- HyspIRI will provide the means for broad-scale monitoring of the changes in ecosystem metabolism

Sensor fusion

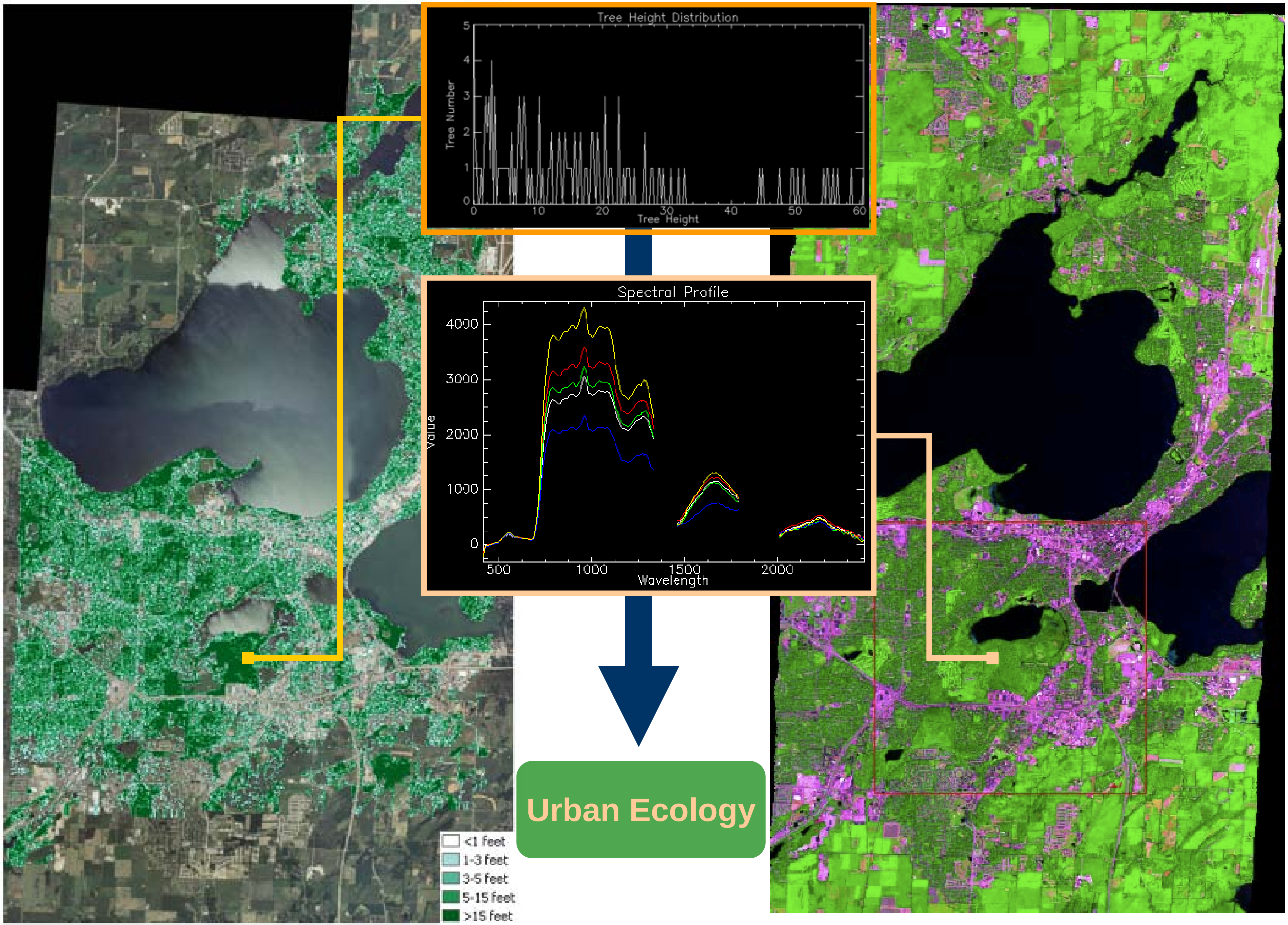

Tree Height Distribution
Tree Number
Tree Height
Spectral Profile
Value
Wavelength
<1 feet
1-3 feet
3-5 feet
5-15 feet
>15 feet
Urban Ecology

Thank you

Funding:

NASA Terrestrial Ecology

NASA HyspIRI Preparatory Activities

NASA Earth and Space Sciences Fellowship

Dr. Laurel Saulton Clark WSGC Fellowship

HyspIRI Sunglint Subgroup: Glint Characterization, Determination of Impacts on Science, and Potential Mitigation Approaches

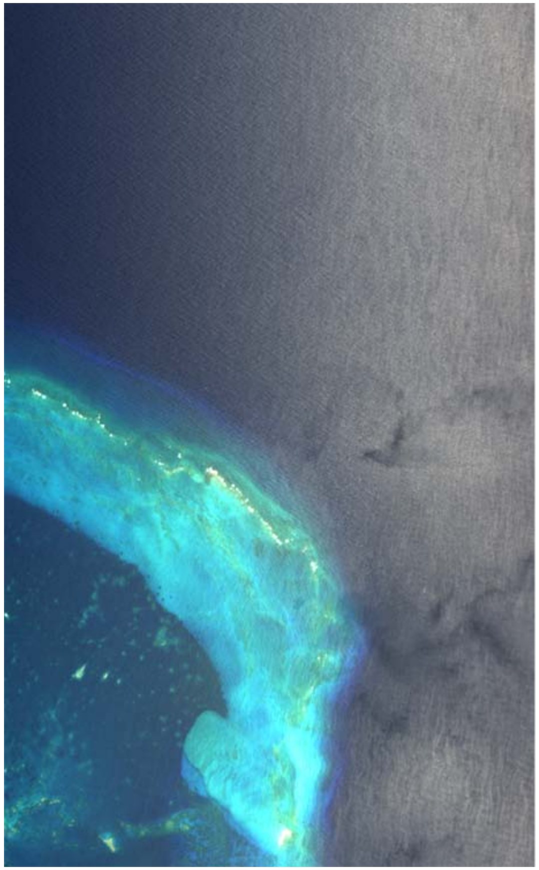

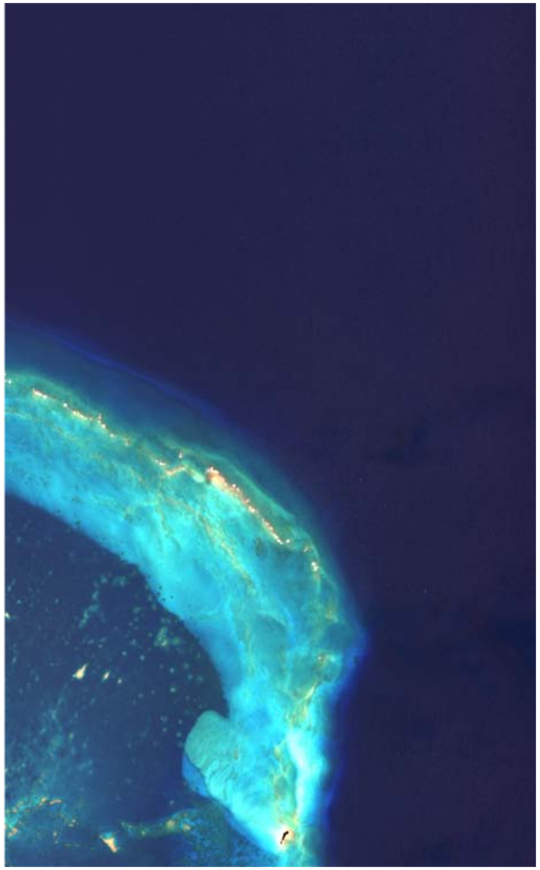

Contributors

Eric J. Hochberg, Curtis D. Mobley, Youngje Park, James Goodman, Kevin R. Turpie, Bo-Cai Gao, Carl F. Bruce, Robert O. Green, Robert G. Knox, Frank E. Muller-Karger, Elizabeth M. Middleton, Peter J. Minnet, Chelle Gentemann, Bogdan V. Oaida, Richard C. Zimmerman

Sources of light contributing to the remotely sensed signal

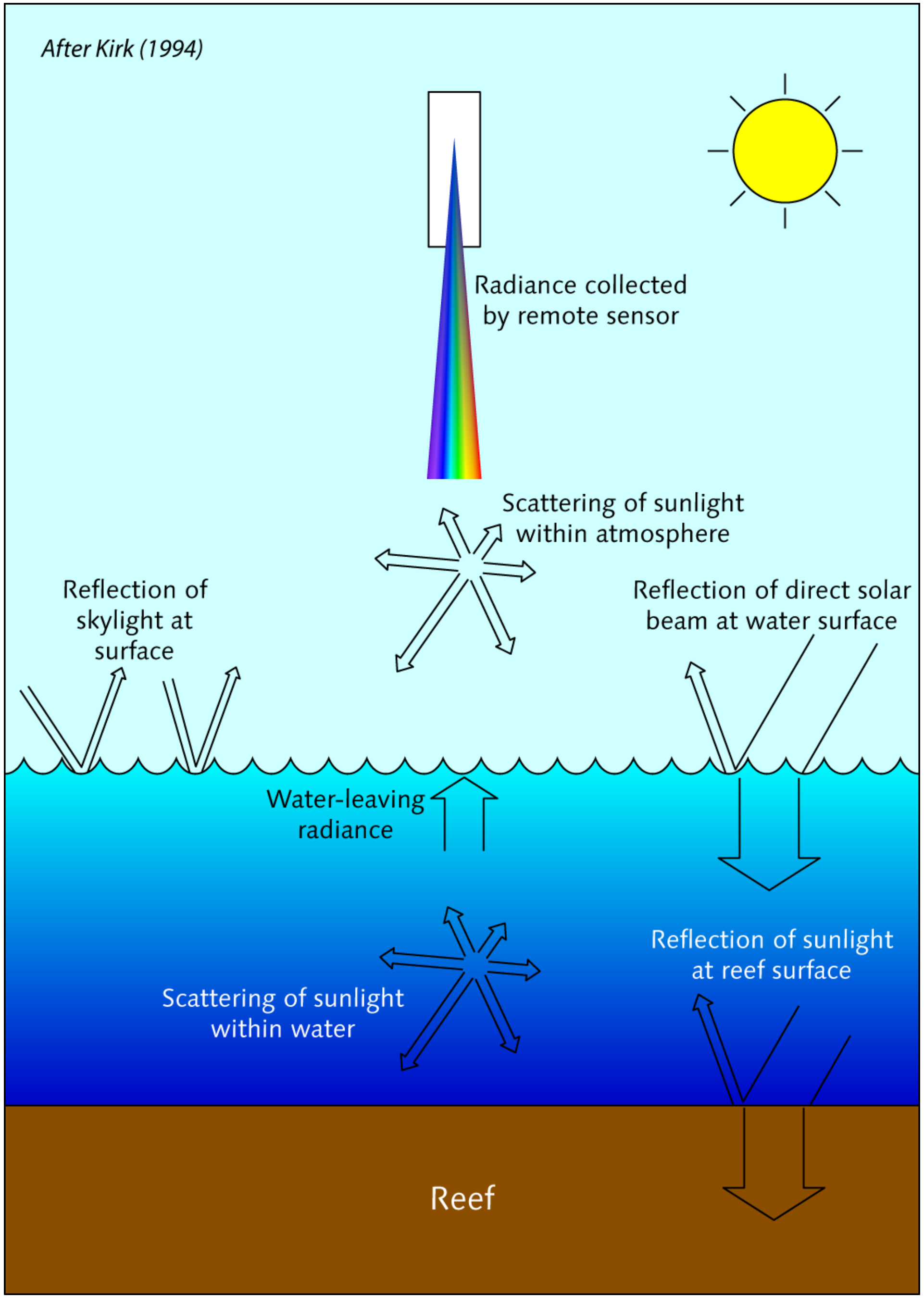

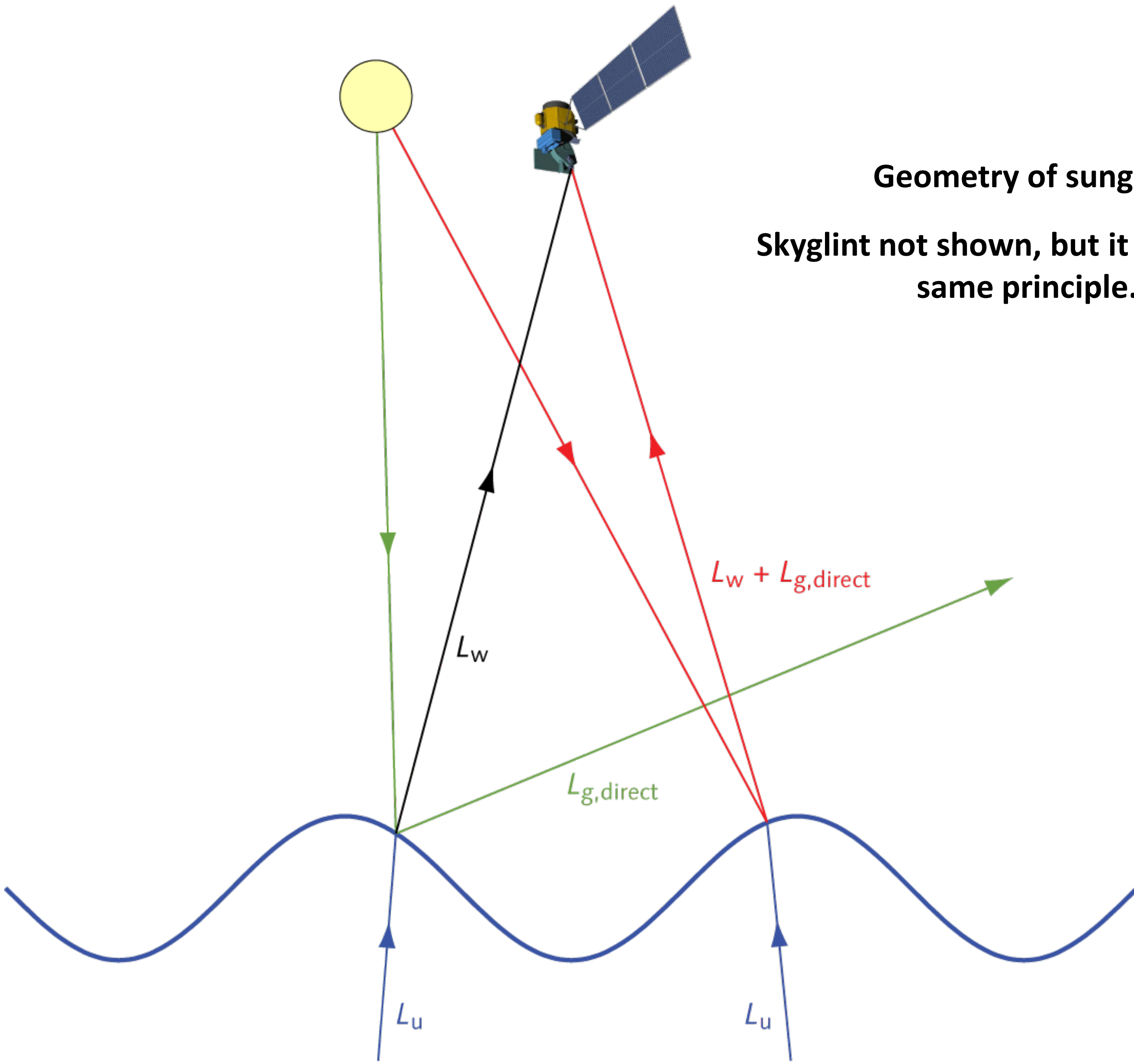

Geometry of sunglint

Skyglint not shown, but it follows the same principle.

Quickbird Example: Tampa Bay, Florida
Very calm water. No apparent sunglint, only skyglint.

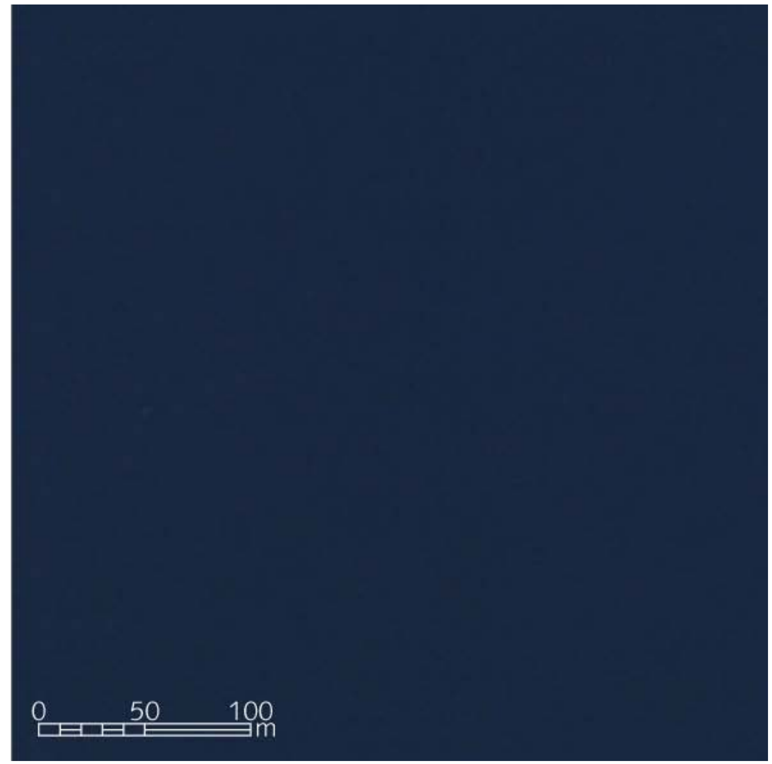

Quickbird Example: Kaneohe Bay, Oahu, Hawaii
Slight wind. Capillary waves engender some sunglint, skyglint implicit.

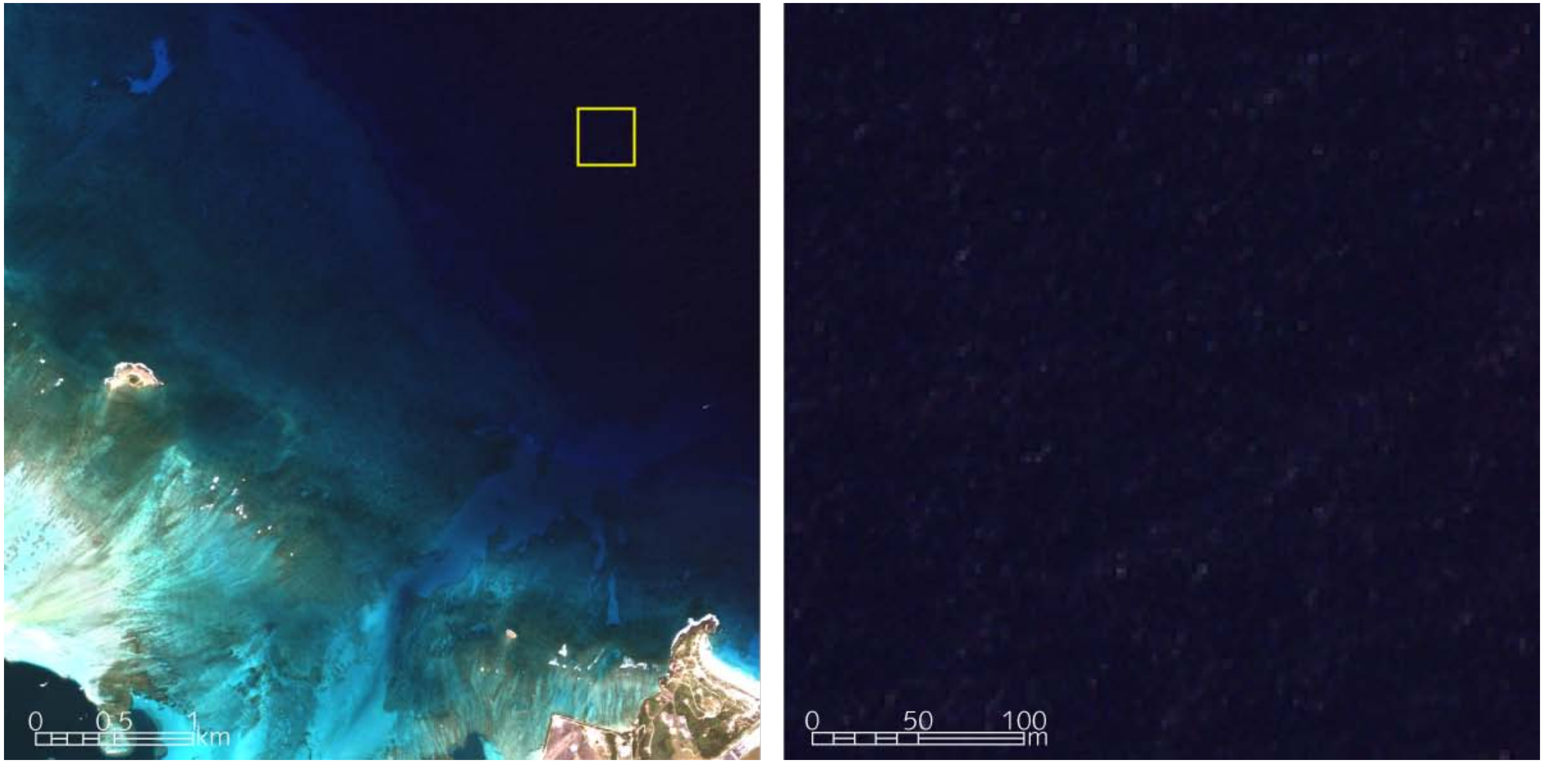

Quickbird Example: Punaluu, Oahu, Hawaii
Trade wind swell. Sunglint on wave faces, skyglint implicit.

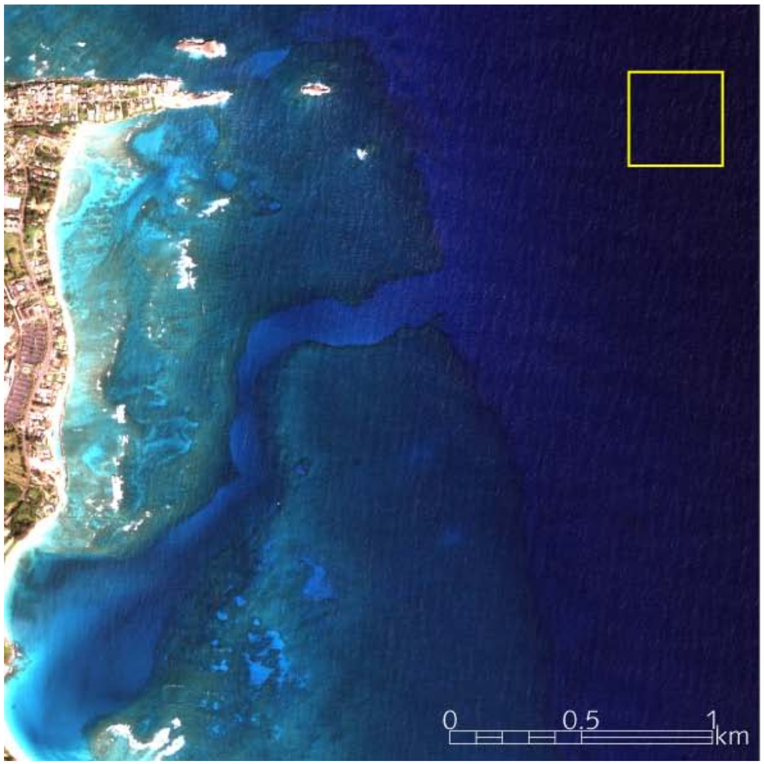

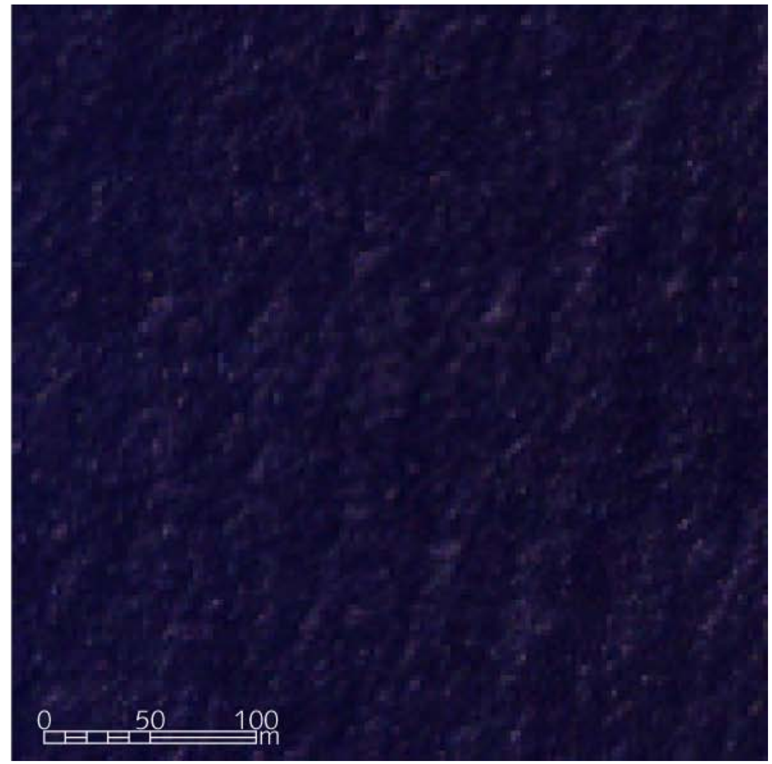

Quickbird Example: Bermuda
Fairly confused sea state. Sunglint on wave faces, skyglint implicit.

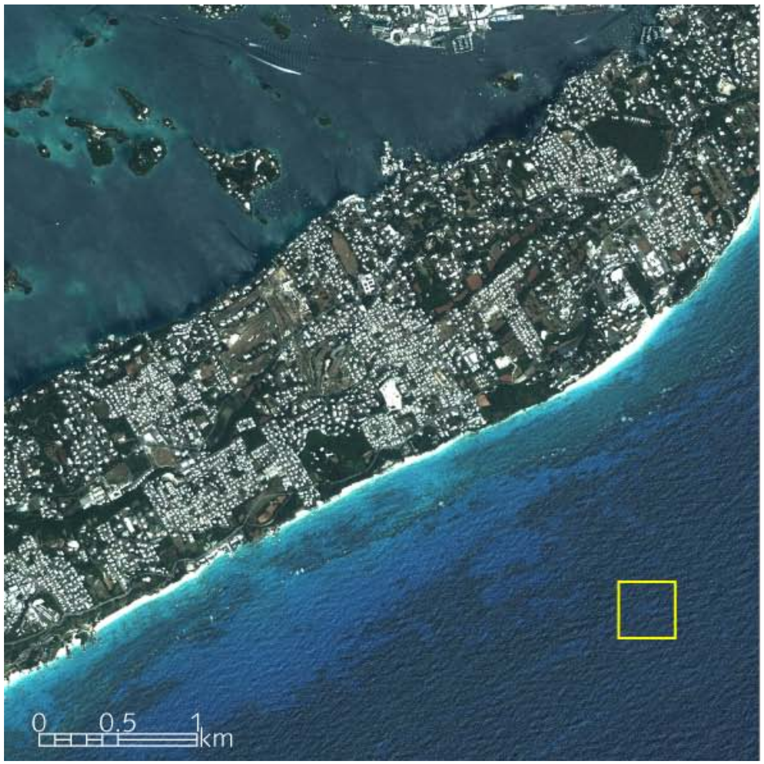

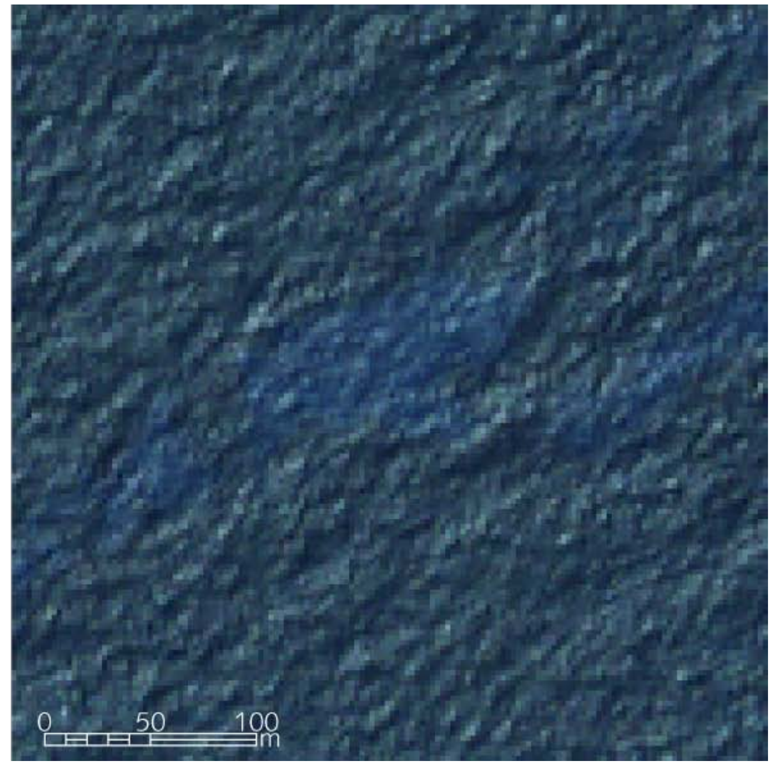

HyspIRI observation geometry. The satellite is moving south (outward from the page).

These view angles, coupled with sun angles, may lead to glint in HyspIRI aquatic scenes.

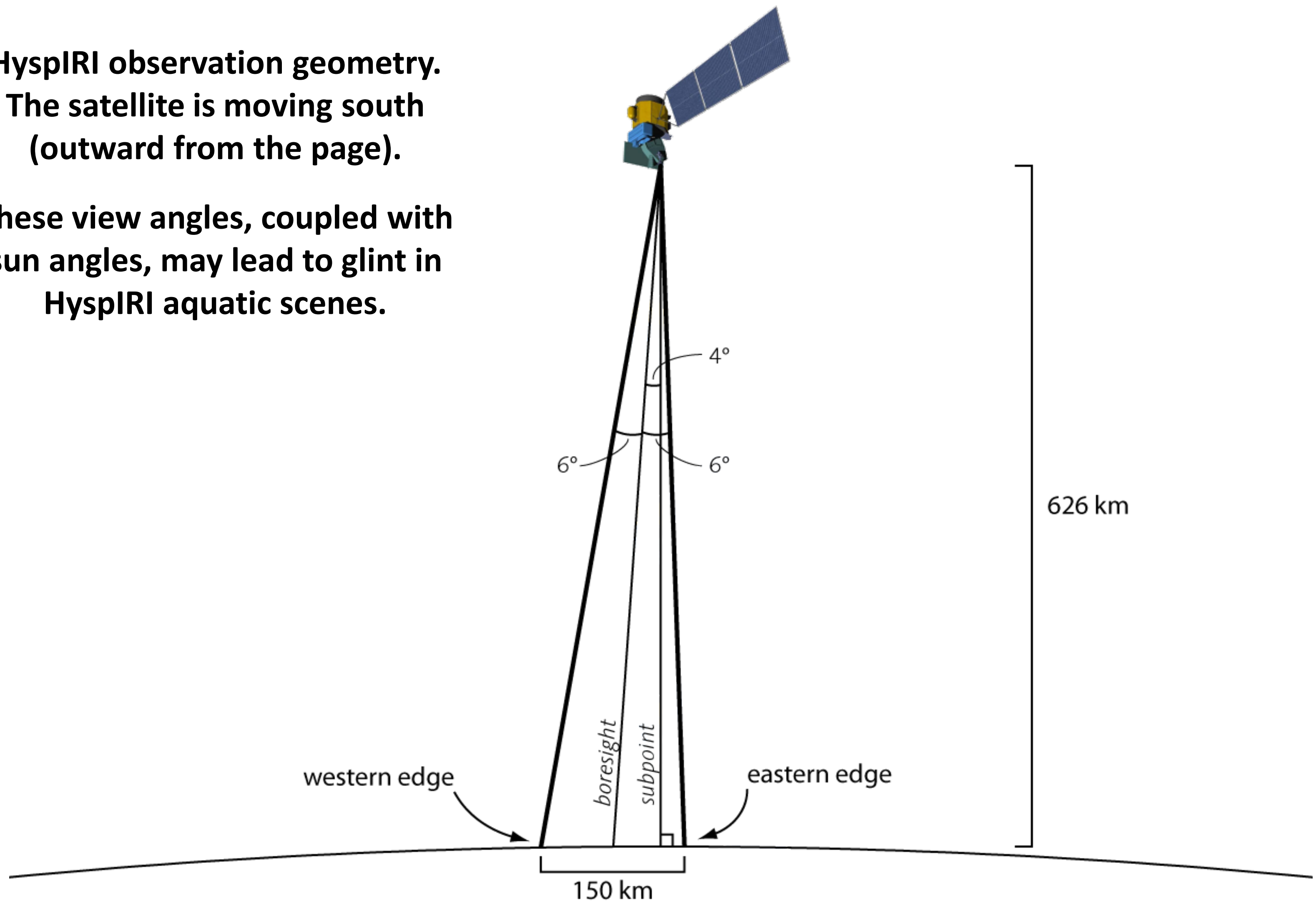

HyspIRI Sunglint Subgroup organization of activities

- Glint Defined
- Quantitative Characterization of Glint
  - Model Analysis
    - Geographic Location, Date & Wind
    - Sun/View Angles, Atmosphere & Wind
  - Image Analysis
- Glint Impact on HyspIRI Science
  - Coral Reefs: Hydrolight modeling —> classification
  - Seagrass: Hydrolight modeling —> classification
  - Ocean Color: HydroMod modeling —> inversion —> chl estimation
  - Emergent Vegetation: Examples & Challenges
- Mitigation Options
  - Discussion & Examples
- Recommendations

Source: James Goodman

- Glint has been recognized as a potentially confounding factor from the outset of ocean remote sensing.
- There is a fair amount of research on the subject.
- Review of glint and some mitigation strategies:

Kay S, Hedley JD, Lavender S (2009) Sun glint correction of high and low spatial resolution images of aquatic scenes: a review of methods for visible and near-infrared wavelengths. *Remote Sensing* 1:697-730

Approaches to glint mitigation

(A) Avoidance

- Physically pointing the remote sensor toward the ocean at an angle that minimizes specular reflection at the sea surface

- Pointing angle is determined by the position of the sensor relative to the position of the sun, generally assuming the ocean is smooth

(B) Correction

- Even in cases where the bulk of direct specular reflection can be avoided, skyglint contamination remains, as does sunglint that arises due to deviations from the level-surface ocean, i.e., waves

Two basic approaches to glint correction

(1) Statistical modeling of sea surface state to infer glint contribution

- Traced to Cox and Munk (1954), who analyzed aerial photographs of sun glint to infer statistics of the sea surface wave slope distribution as a function of wind speed

- Basis for modern ocean color glint correction

(2) Direct estimation of glint from remote sensing image data

- Based on common assumption that there is no water-leaving radiance in the NIR, especially at l > 900 nm: after atmosphere corrections, remaining NIR signals must originate from the sea surface, i.e., glint

Literature Review

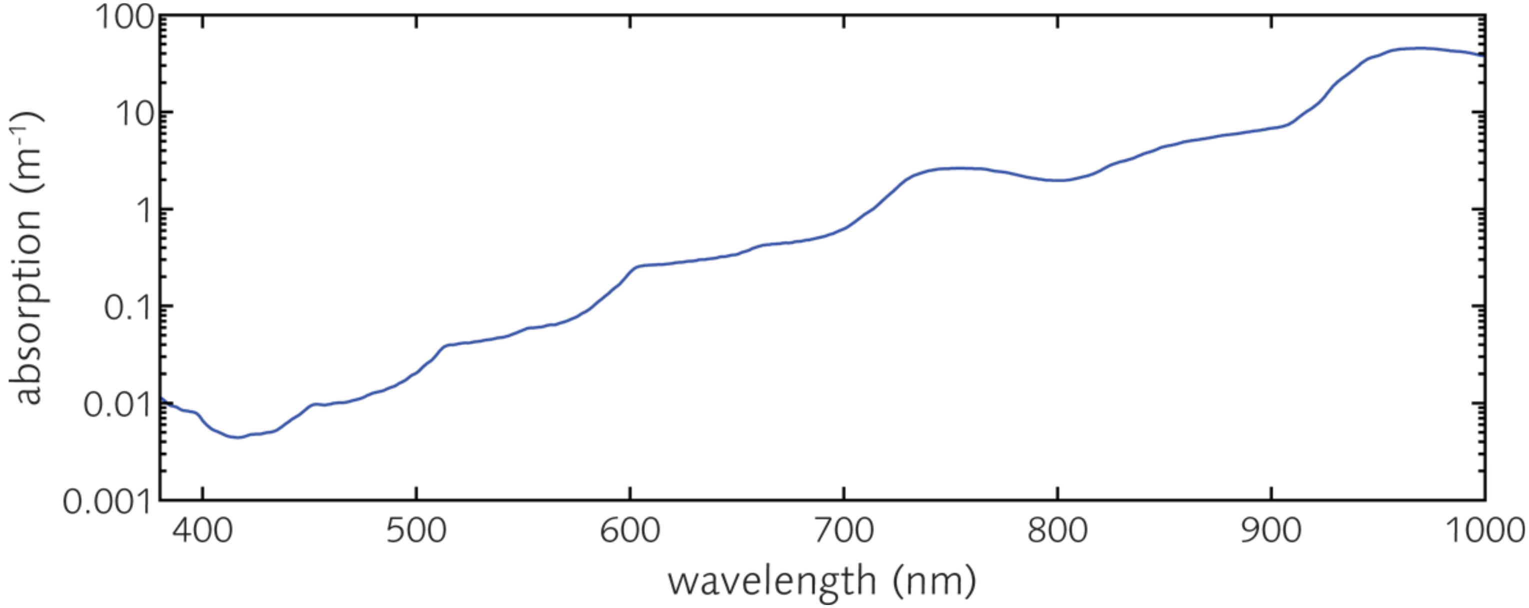

Water absorbs light very strongly at NIR wavelengths, especially >900 nm. Water-leaving radiance at these wavelengths is negligible. VIS data from Pope and Fry (1997); NIR data from Kou et al. (1993).

Direct estimation of glint from remote sensing image data

- There is a linear relationship between glint radiances in VIS and NIR.

- Enables interactive, empirical approaches to glint correction (e.g., Tassan 1994; Hochberg et al. 2003; Hedley et al. 2005; Lyzenga et al. 2006)

- The linear relationship between VIS and NIR glint radiances has a physical basis: the index of refraction of seawater is (nearly) the same at VIS and NIR wavelengths.

- Thus, the reflectance of the water surface is (nearly) spectrally flat, i.e., glint has the same reflectance at VIS and NIR wavelengths.

- The basis for an empirical correction that does not require human interaction (Gao et al. 2000): after atmospheric correction, any remaining NIR reflectance is due to glint. This glint reflectance can simply be subtracted from VIS wavelengths, leaving only water-leaving reflectance.

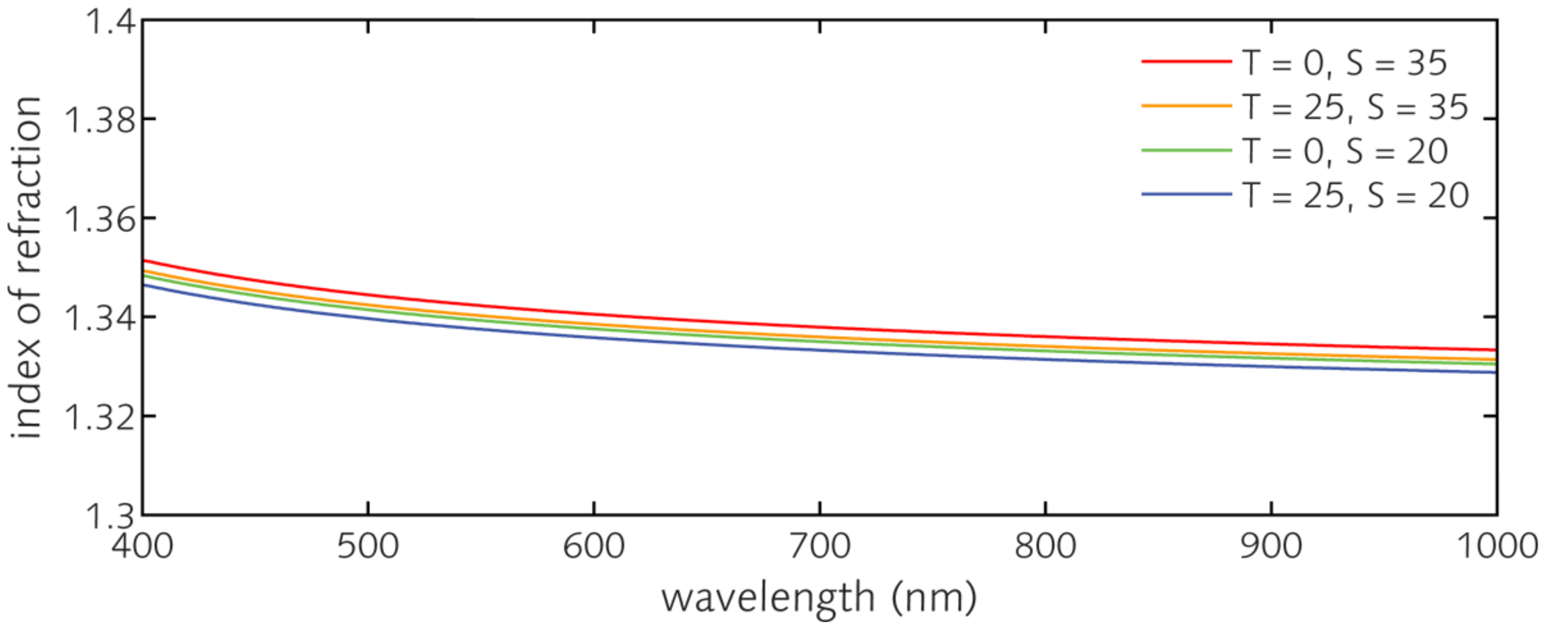

Index of refraction of water. Values are calculated following empirical model of Quan and Fry (1995). Values are modeled for four combinations of temperature (T, °C) and salinity (S, ‰).

Quantitative Characterization of Glint:
Modeling Based on Latitude, Date, and Wind

Global longitudinal variability of sea-surface sun glint reflectance for the HyspIRI orbit for (a) three levels of wind speed, which were used to compute sea-surface glint at (b) the west edge, (c) the middle point, and (d) the east edge of the HyspIRI field of view.

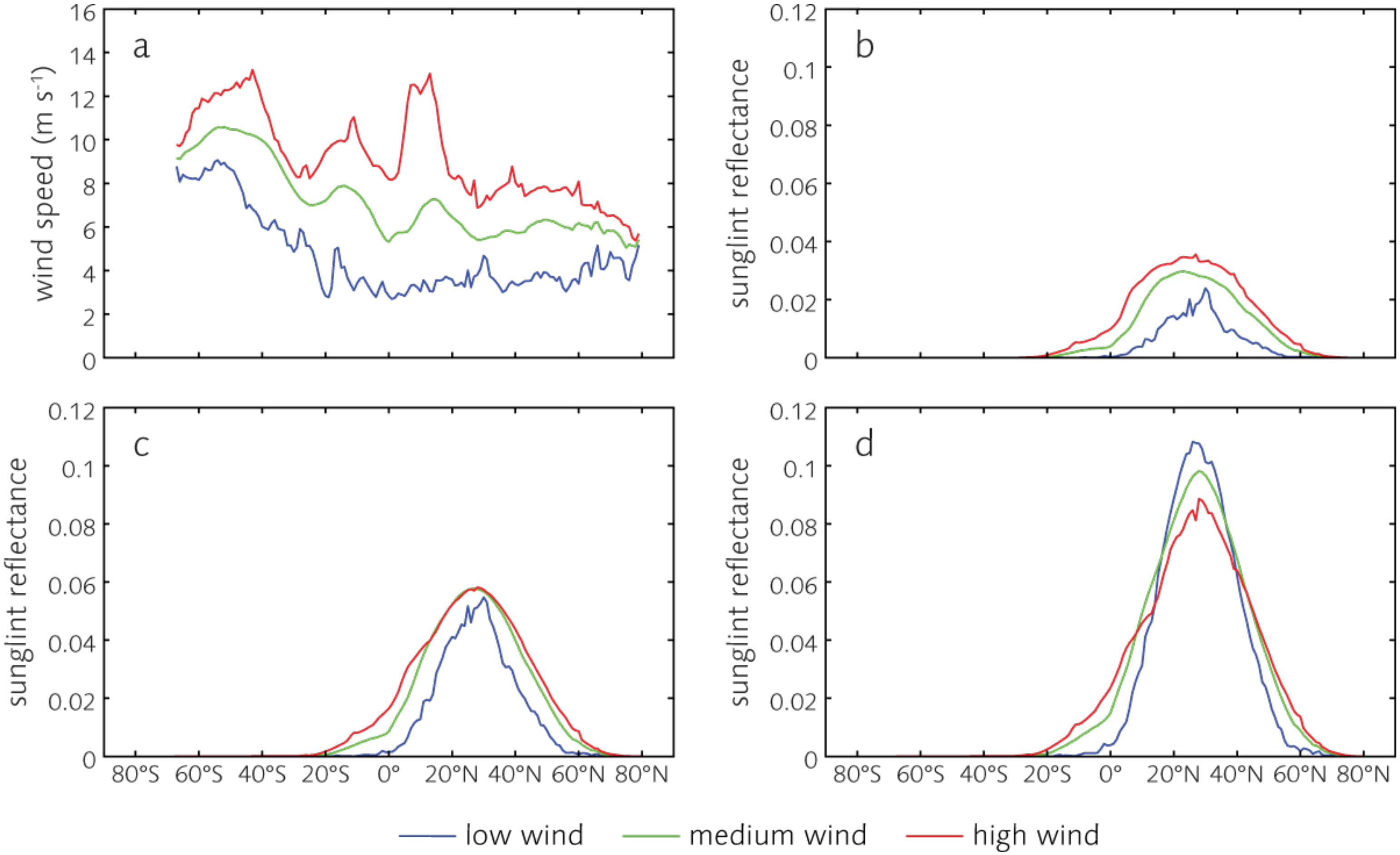

21 June

Source: Youngje Park

Quantitative Characterization of Glint:
Modeling Based on Latitude, Date, and Wind

Sea-surface sun glint reflectance variability in a 15° longitudal band (165°W–150°W) for the HyspIRI orbit at (a) three levels of wind speed, which were used to compute sea-surface glint at (b) the west edge, (c) the middle point, and (d) the east edge of the HyspIRI field of view.

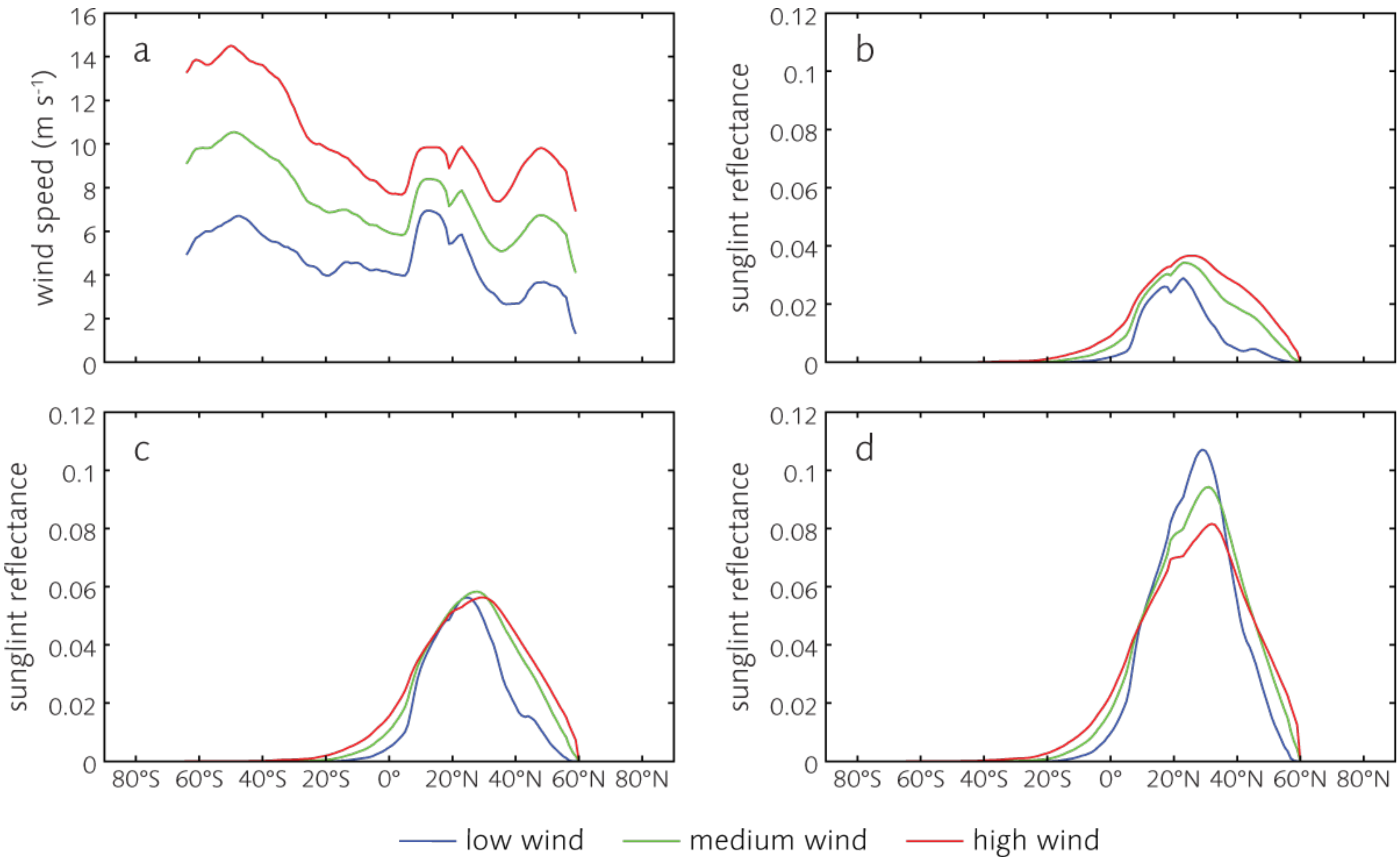

21 June

Source: Youngje Park

Glint Impact on HyspIRI Science:
Modeling Based on Sun/View Angles, Atmosphere and Wind

Example Hydrolight/HydroMod discretized output. Radiance travels outward from center of hemispheres.

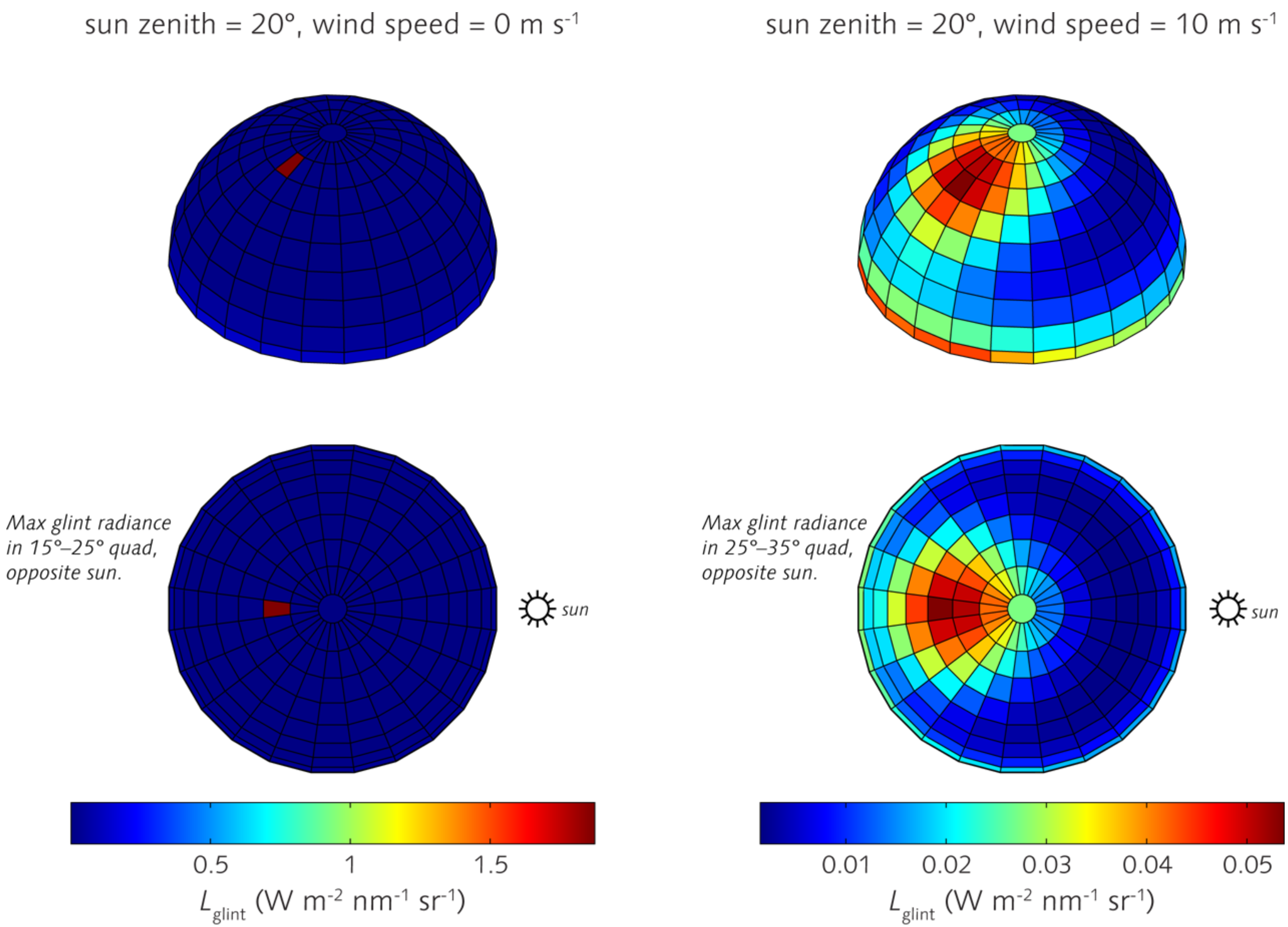

Note difference in radiance scales.

Quantitative Characterization of Glint:
Modeling Based on Sun/View Angles, Atmosphere and Wind

HydroMod simulation of shallow water, mixed bottom spectrum, case 1 inherent optical properties, and comparing east vs. west side of HyspIRI field of view

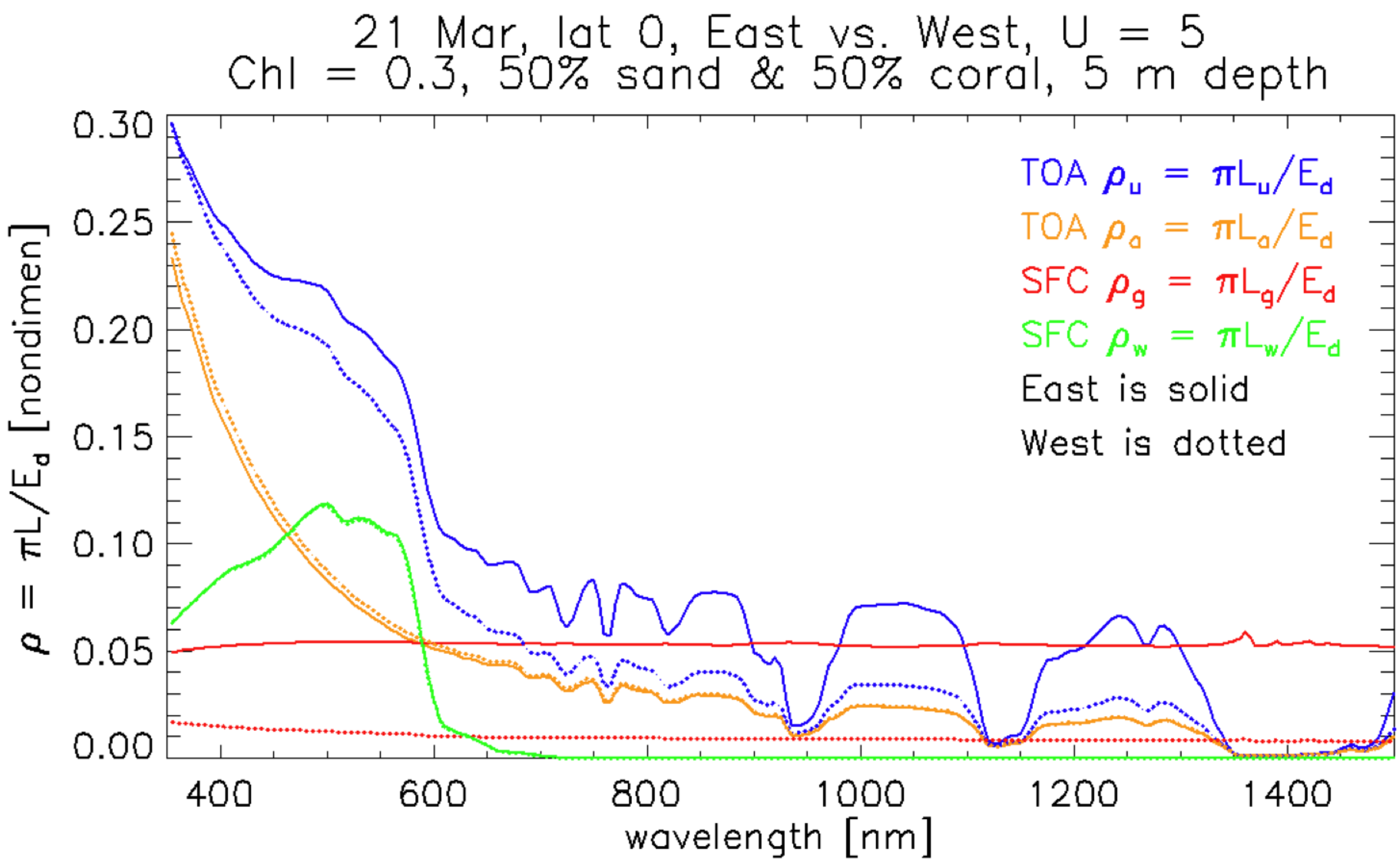

Source: Curtis Mobley

Quantitative Characterization of Glint:
Modeling Based on Sun/View Angles, Atmosphere and Wind

HydroMod simulation of east side of HyspIRI field of view, comparison between shallow water with low chlorophyll and deep water with high chlorophyll

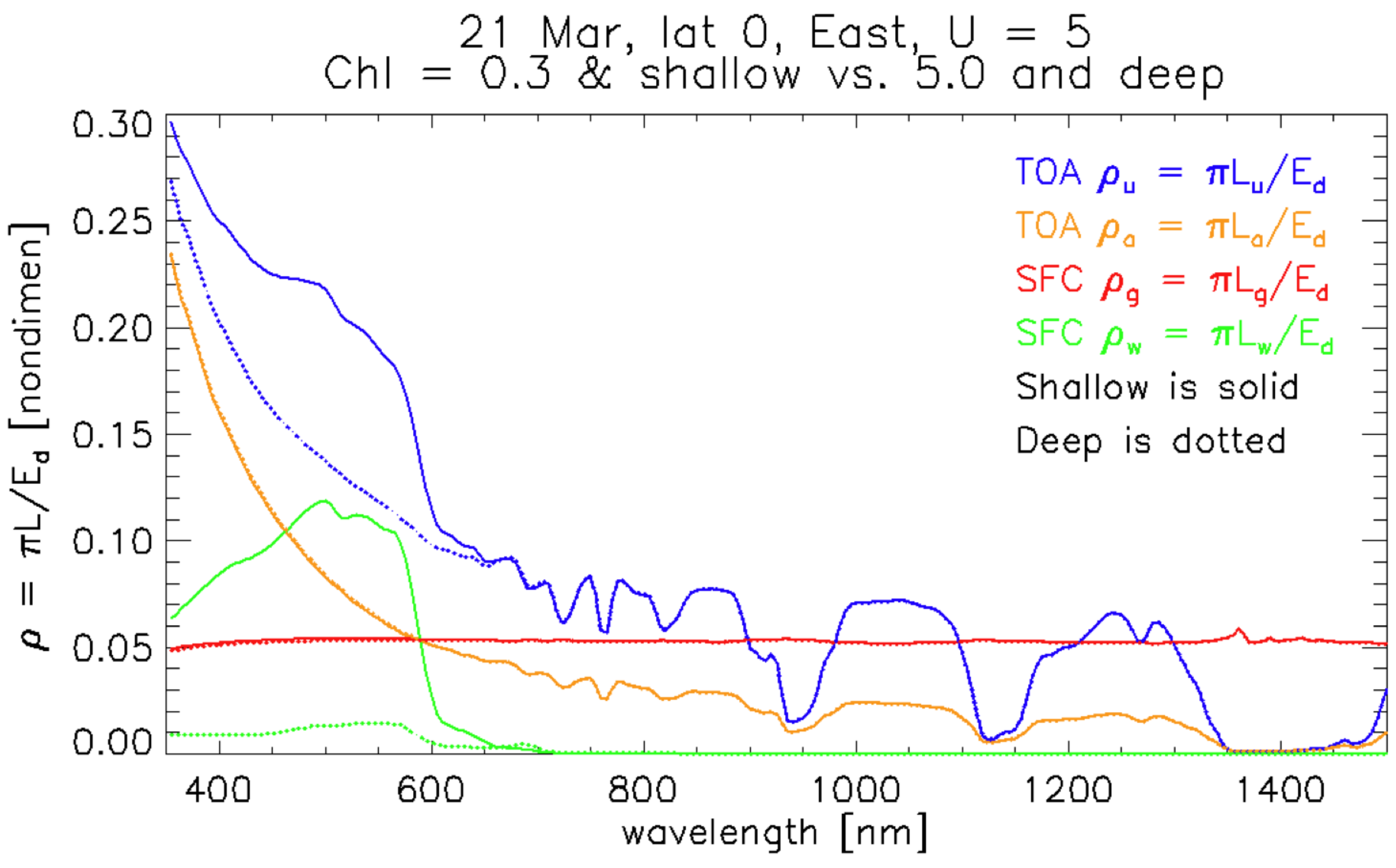

Source: Curtis Mobley

Quantitative Characterization of Glint:
Deriving Glint Statistics from AVIRIS Imagery

AVIRIS scenes used to estimate glint reflectance for comparison with modeled values. Yellow regions are deep-water areas used to extract glint statistics.

f000411t01p03_r01

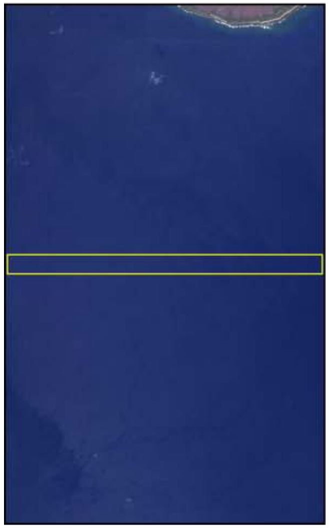

f000412t01p03_r08

f000416t01p03_r02

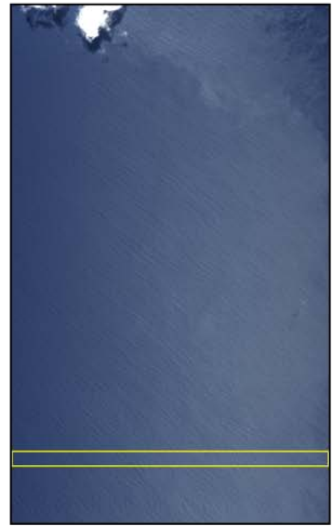

f000416t01p03_r03

f000418t01p03_r01

f000424t01p03_r09

f000425t01p03_r07

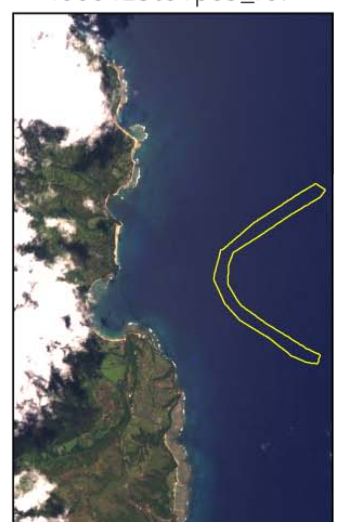

Quantitative Characterization of Glint:
Deriving Glint Statistics from AVIRIS Imagery

Estimated TOA maximum glint reflectances for seven AVIRIS scenes. These values are comparable to modeled values.

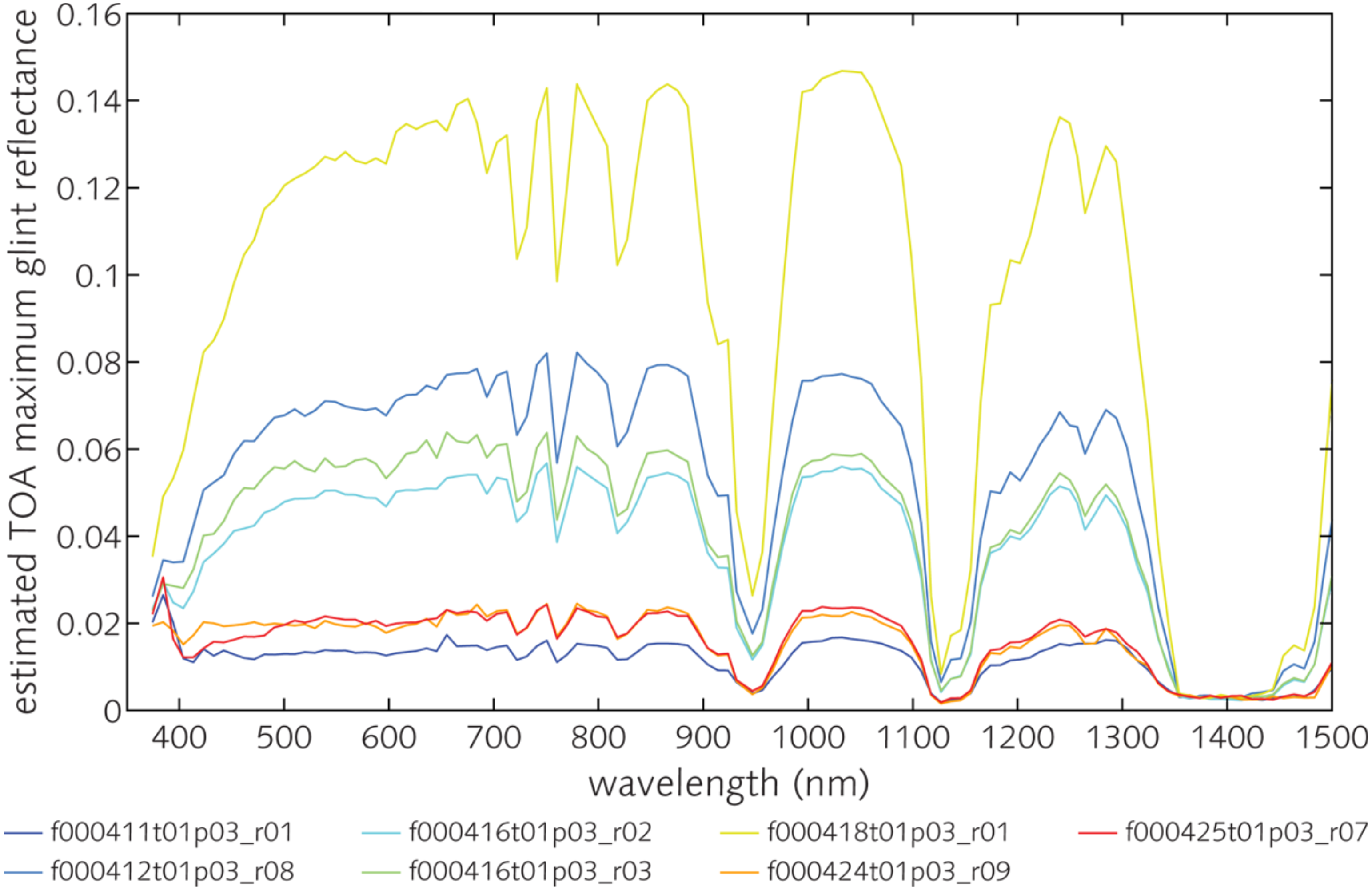

Quantitative Characterization of Glint:
Deriving Glint Statistics from AVIRIS Imagery

AVIRIS scene f000418t01p03_r01 for demonstration of glint-aerosol discimination
Yellow line shows location of cross-track sample in analysis

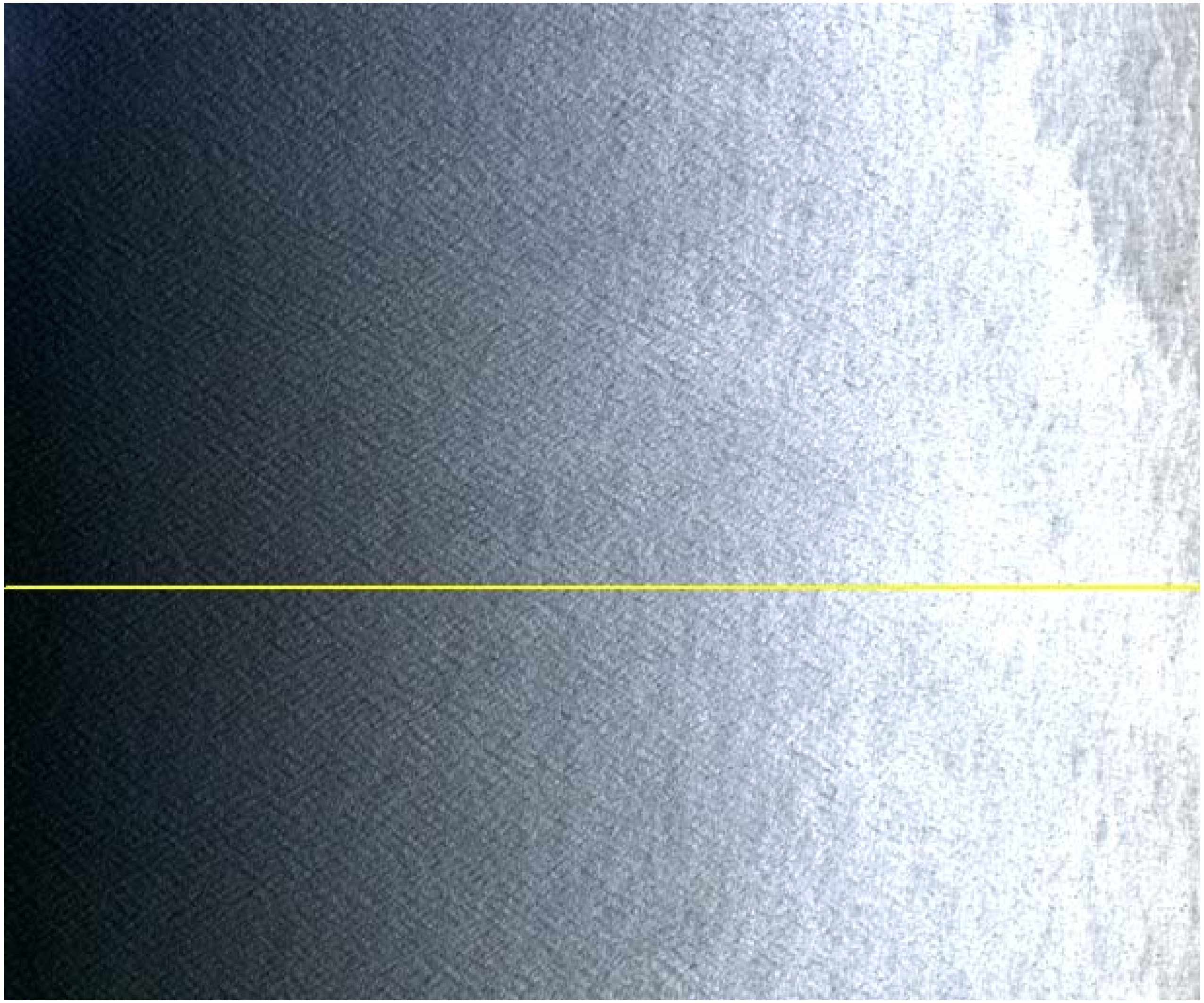

Source: Youngje Park

Quantitative Characterization of Glint:
Deriving Glint Statistics from AVIRIS Imagery

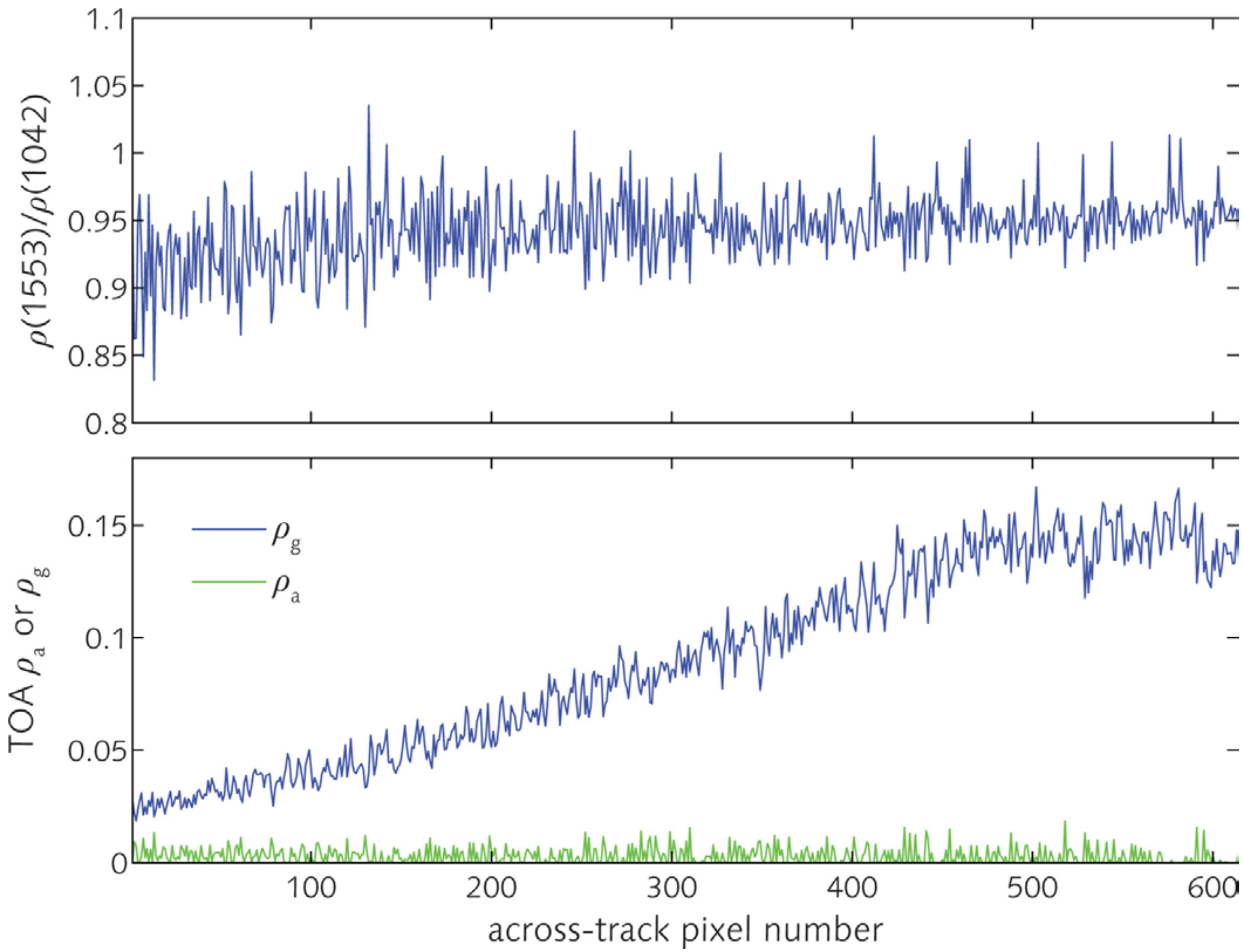

Source: Youngje Park

Quantitative Characterization of Glint: Summary

Several summary observations can be made from model and image analysis:

- The effect of latitude is very clear. Sun glint is stronger where the sun is high, because HyspIRI looks almost straight down. Sun glint effects are apparent across a latitude band of 50° to 100° (i.e., 25° S–25° N to 50° S–50° N), depending on wind speed and the across-track pixel location.
- Sun glint is sensitive to wind speed for low to moderate glint strength and less sensitive for high glint.
- Sun glint at the east edge of the HyspIRI field of view is consistently stronger (a factor of two) than at the west edge.
- Sun glint is high in summer due to high sun and low in winter due to low sun. At the equator in the middle point of the swath, sun glint reflectance takes values of 0.025, 0.01, 0.04 to 0.01 for March, June, September and December respectively.
- Regional temporal variability appears similar to global longitudinal variability in magnitude.
- Large differences in glint reflectance than can occur from the east to the west edges of the HyspIRI field of view for moderate wind speeds in equatorial regions.
- Glint intensity can surpass that of water-leaving radiance.
- Glint radiance is function of incident irradiance.
- Glint reflectance is a function of the index of refraction of the water body.
- *Glint reflectance at the sea surface, to first order, is spectrally flat.* This is particularly important, because it is the basis for virtually all glint correction strategies.

Glint Impact on HyspIRI Science:
Coral Reefs: Hydrolight Modeling & Classification

Scenario 1: Clear reef water, sun zenith 20° , wind 5 m s^{-1}

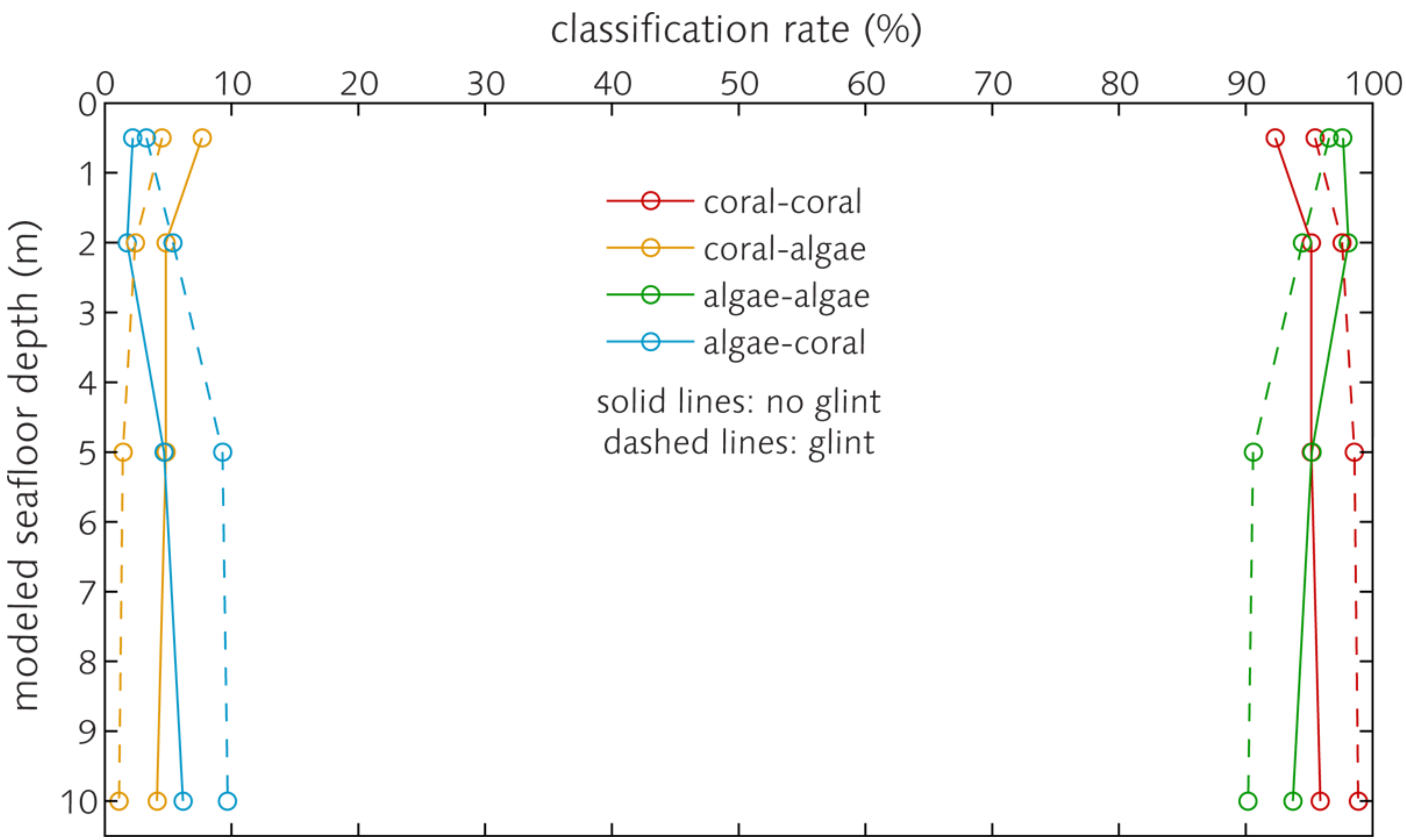

Values indicate classification rates for specific bottom-type/depth combinations classified as bottom-type at any depth. Solid lines show results of R_{rs} modeled without glint; dashed lines show results of R_{rs} modeled with full glint. Under the given water column and view conditions, glint actually increases the correct classification rate of coral at all depths, but it also increases the misclassification of algae as coral at all depths.

Glint Impact on HyspIRI Science:

Coral Reefs: Hydrolight Modeling & Classification

Scenario 2: Turbid reef water, sun zenith 40° , wind 10 m s^{-1}

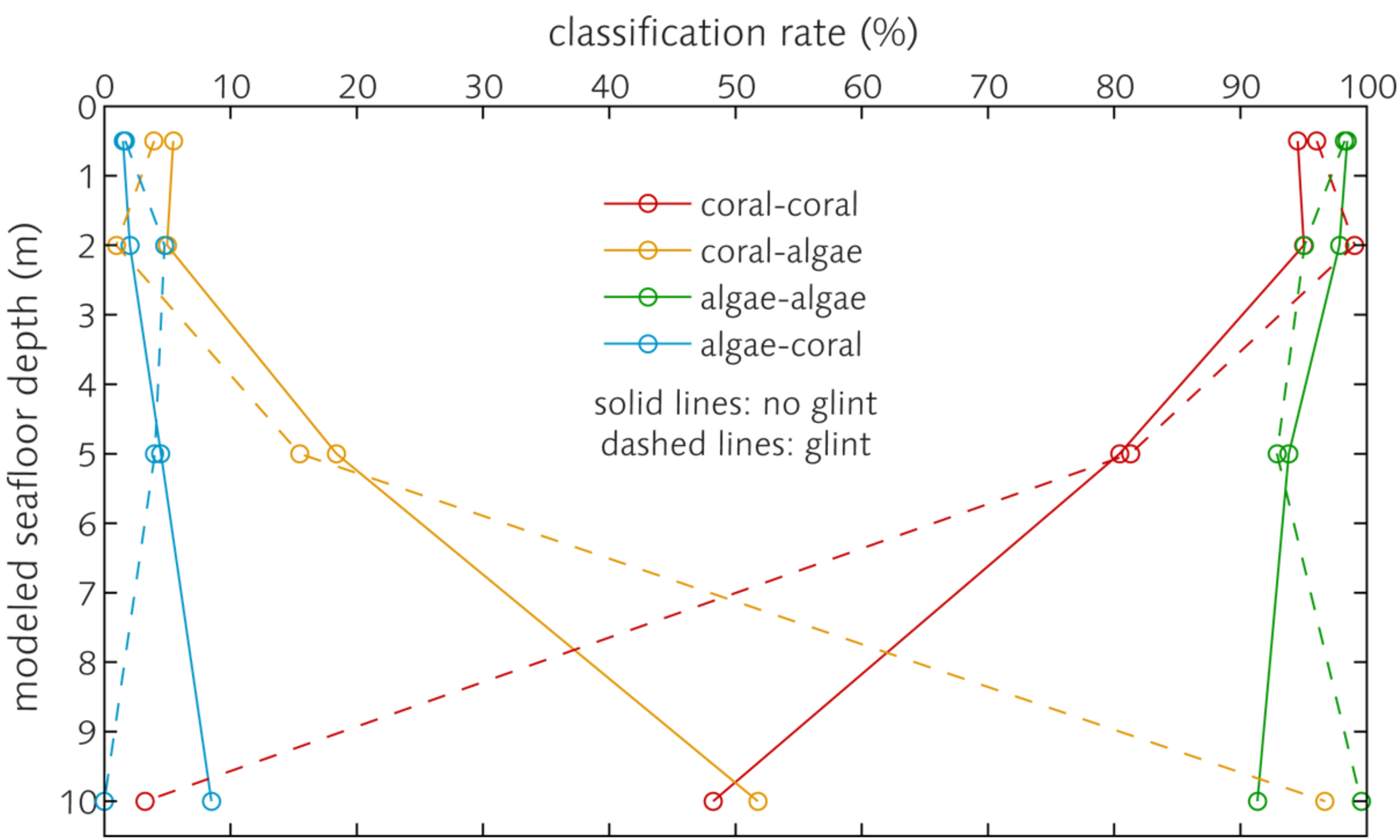

Under these conditions, glint increases the correct classification rate of coral at 0.5 and 2 m, but but greatly reduces correct coral classifications at 10 m.

Glint Impact on HyspIRI Science:
Ocean Color: HydroMod Modeling, Inversion & Analysis

HydroMod parameterization

Location:	Station ALOHA, 22° 45'N, 158° W
Date:	21 June
Sun Azimuth wrt Along Track:	107.78°
Sun Zeinth:	17.99°
Suspended Chlorophyll:	0.05 µg l^{-1}
Wind Speed:	two values modeled, 0 and 10 m s^{-1}
Atmosphere Conditions:	Clear sky with marine aerosols
Bottom Boundary:	Infinitely deep ocean

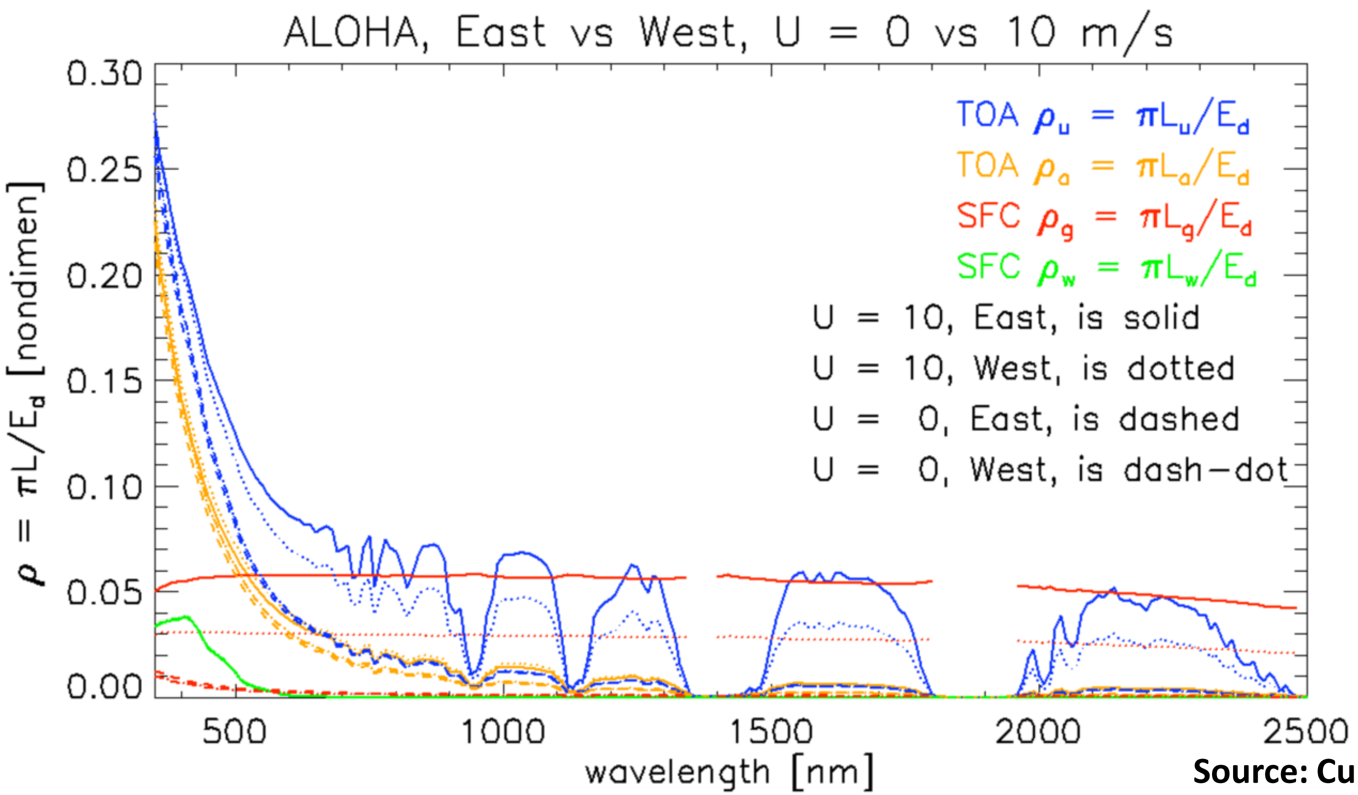

Source: Curtis D. Mobley

Glint Impact on HyspIRI Science:
Ocean Color: HydroMod Modeling, Inversion & Analysis

Radiometrically inverted water-leaving reflectance spectra for Station ALOHA 21 June simulation. (A) West edge of HyspIRI field of view, *U* = 0 m s^{-1}, (B) east edge, *U* = 0 m s^{-1}, (C) west edge, *U* = 10 m s^{-1}, (D) east edge, *U* = 10 m s^{-1}.

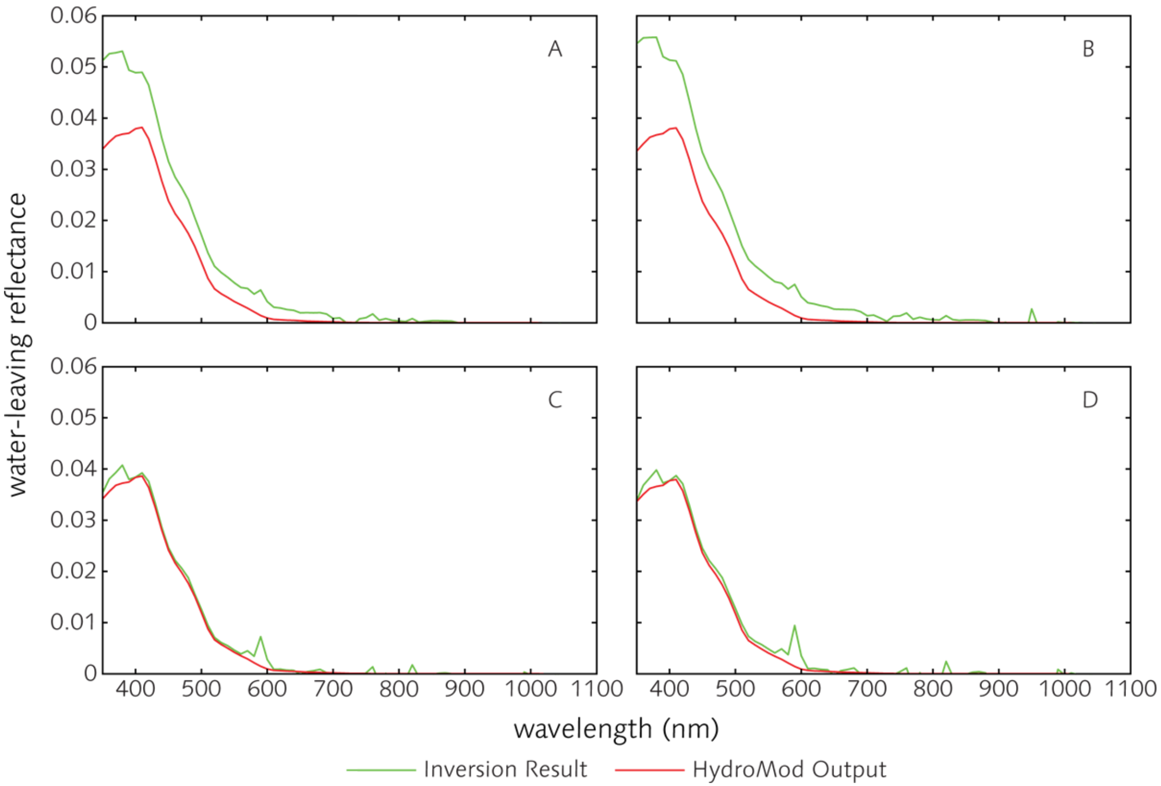

Chlorophyll values (mg m^{-3}) retrieved using OC4 and OC3M algorithms applied to R_{rs} data derived from Figure 4.3.3-2. "Edge" refers to position in HyspIRI field of view. "*U*" refers to wind speed. Actual chlorophyll concentration used in HydroMod biooptical model is 0.05 mg m^{-3}.

Edge	U (m s^{-1})	Algorithm	
		OC4	OC3M
West	0	0.12	0.12
East	0	0.14	0.13
West	10	0.08	0.07
East	10	0.08	0.08

Source: Youngje Park

Glint Impact on HyspIRI Science:
Emergent Vegetation: Examples & Challenges

Multi-angle CHRIS/Proba images of Fishing Bay Wildlife Management Area, Maryland. (a) At 0° nominal view zenith angle glint is visually apparent on water bodies interspersed amongst subaerial vegetation. (b) At 55° nominal view zenith angle glint is much less apparent. Boxes cover same ground area in (a) and (b).

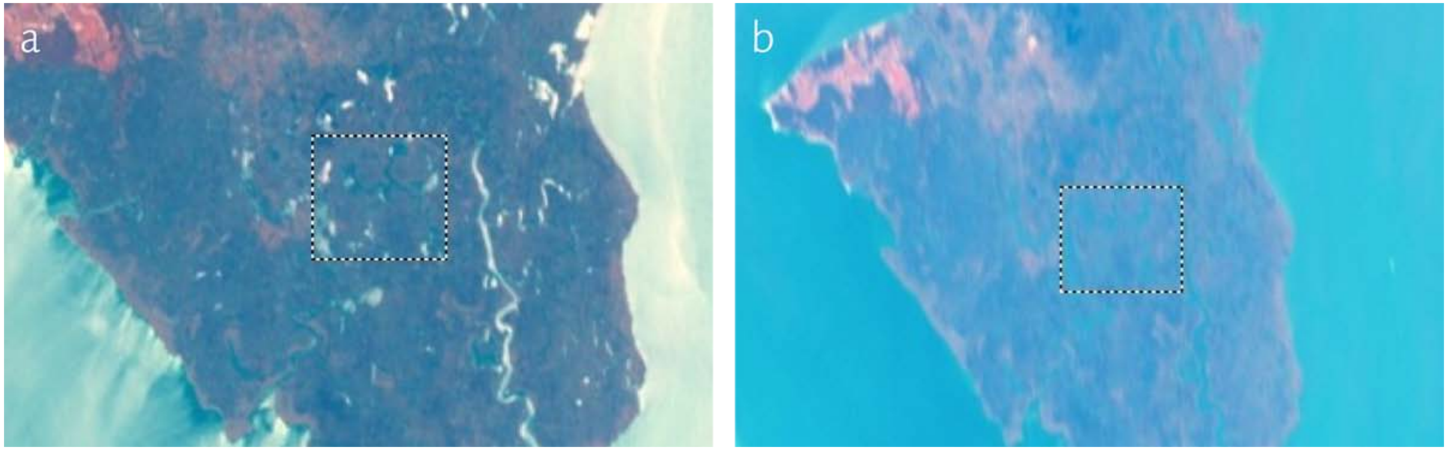

Spectra extracted from regions highlighted by boxes above. (a) At 0° nominal view zenith angle, glint produces very high values across the spectrum, evidenced by the maximum spectral curve. (b) At 55° nominal view zenith angle, the glint effect is greatly reduced.

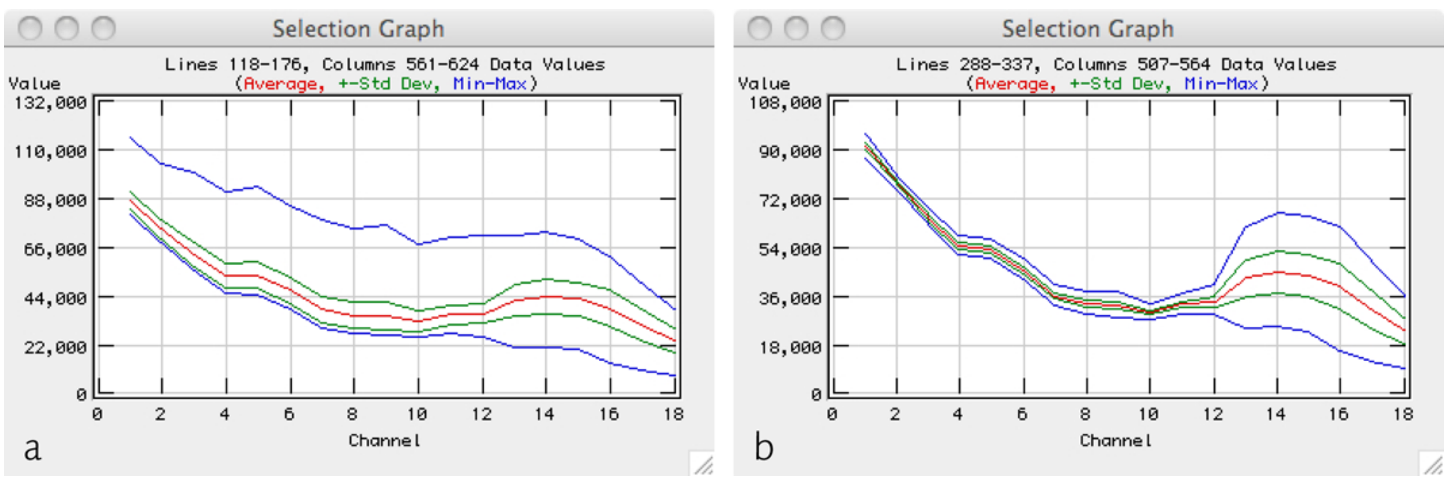

Source: Kevin Turpie

Glint Impact on HyspIRI Science: Summary

- For two basic HyspIRI science objectives, coral reefs and seagrass, expected levels of glint do not appear to dramatically impact classification retrievals.
- Glint has the greatest impact when retrieval conditions are already marginal, for example when water column optical properties limit penetration depth.
- Potential for improvement via mitigation for glint was not investigated.

- For the open ocean, with very low suspended chlorophyll levels, it is clear that glint correction must be tied to correction for atmospheric aerosols.
- Thus, both are fundamental requirements for accurate retrieval of spectral remote sensing reflectance.

- The situation is less clear for glint effects in emergent vegetation.
- Measurement and modeling capabilities for these systems lag those for shallow and deep oceans.
- At the same time, emergent vegetation has the benefit of usefully observable NIR and SWIR spectral features.

Mitigation Options
Avoidance

- Avoidance is the simplest method for mitigation of glint impacts, and it is the method of choice in operational ocean color.

- Any portions of imagery that exhibit significant glint can merely be ignored, then re-imaged on subsequent satellite overpasses.

- Nearshore and benthic applications typically require higher spatial resolution, i.e., 1–100 m vs. 1 km.

- The higher spatial resolution required closer to shore is offset by narrower fields of view and longer revisit times.

- The data rate for a given area of Earth surface is much lower, and it is generally not possible to ignore image data that exhibit glint effects.

- Thus, glint avoidance is a luxury not often afforded to nearshore and benthic applications.

Mitigation Options
NIR-VIS Empirical Linear Relationships

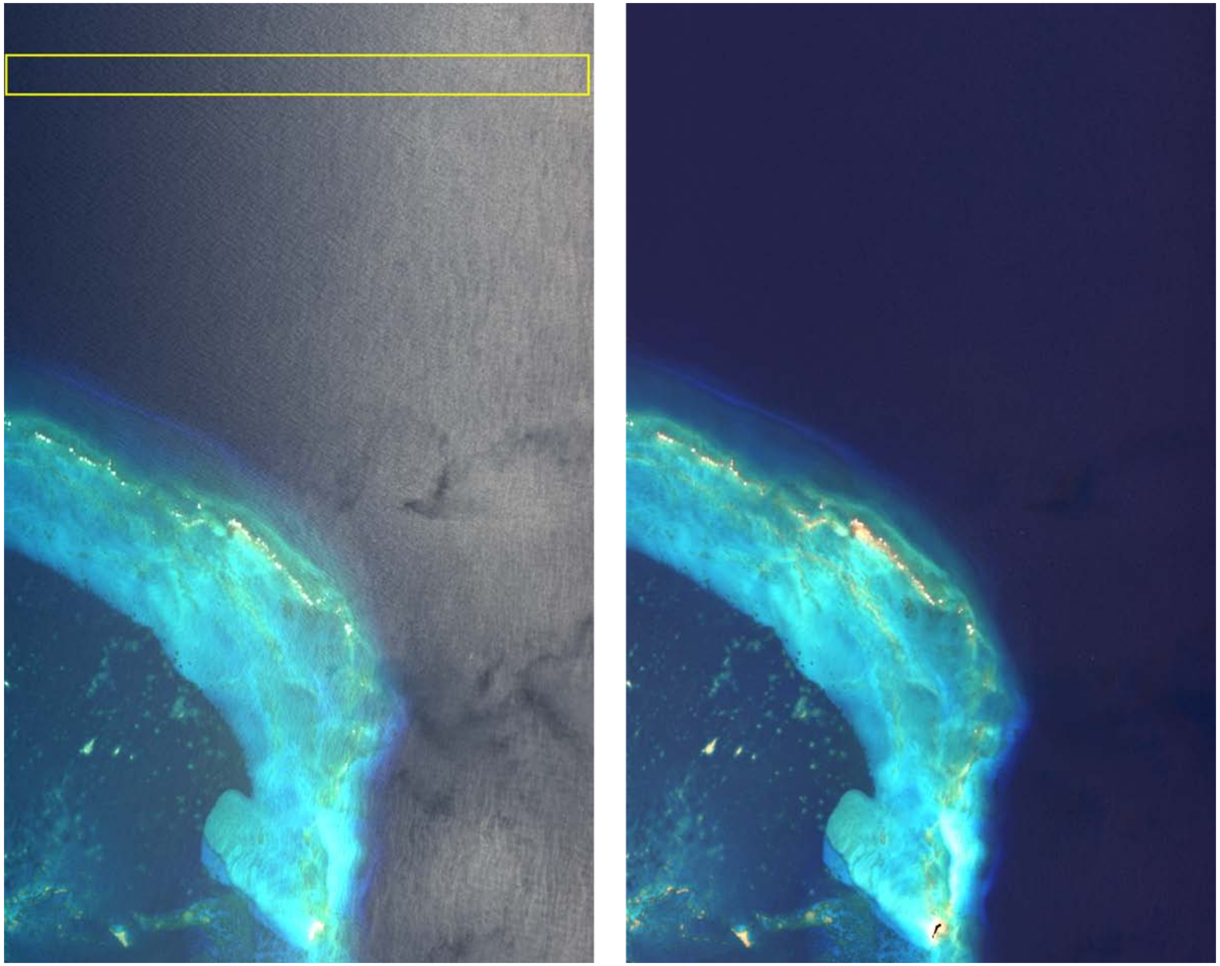

AVIRIS scene f000418t01p03_r01 covering the southeast portion of French Frigate Shoals, Hawaii and surrounding deep ocean. Image is rotated so that north is to the left of the scene. (Left) Original scene shows very strong glint effects. Yellow box highlights region from which empirical linear relationships are derived. (Right) The scene after application of glint correction. Glint effects are very effectively removed.

Mitigation Options
Subtraction of NIR Reflectance

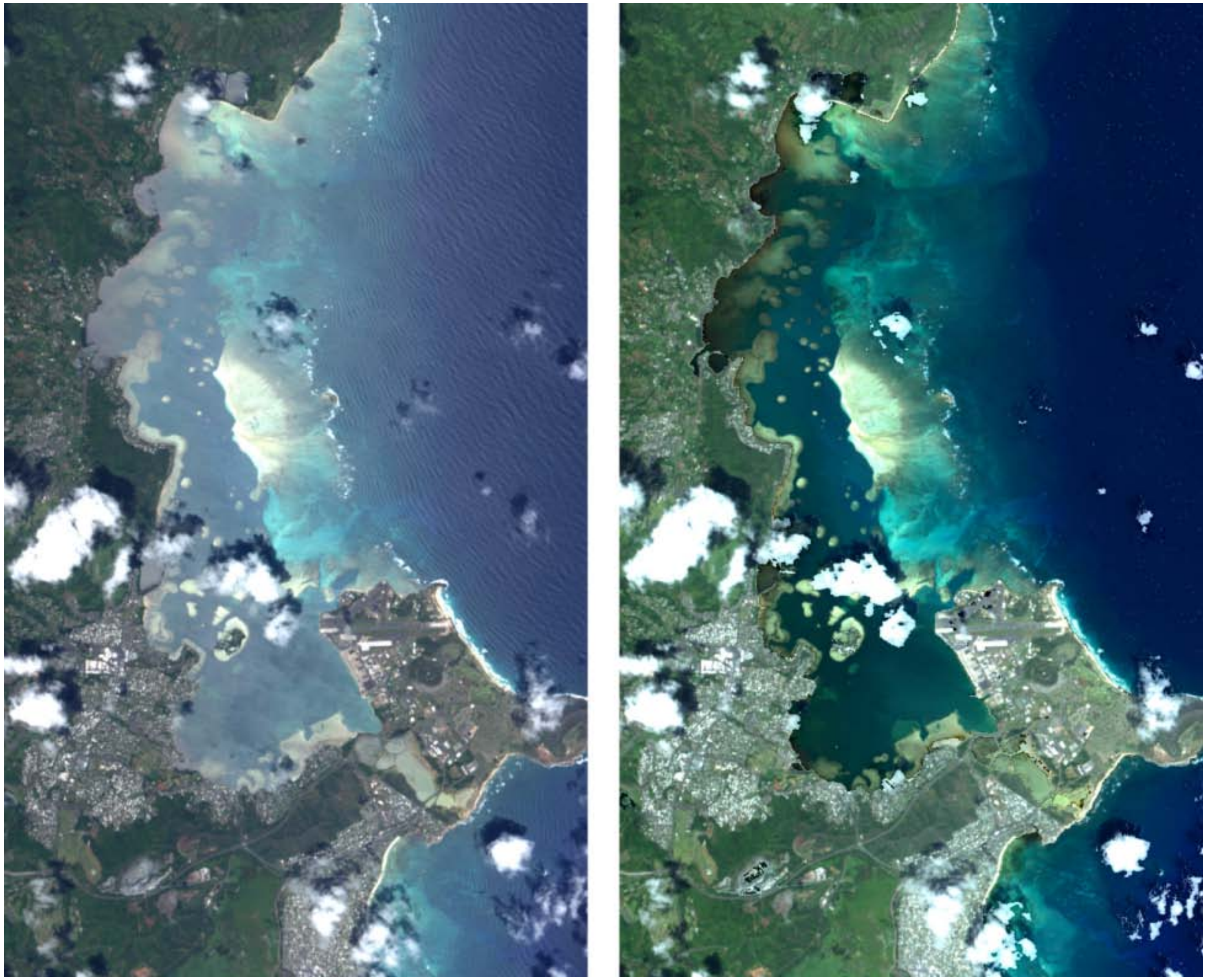

Example of glint correction using subtraction of NIR reflectance. (Left) Original AVIRIS scene of Kaneohe Bay, Hawaii (f000412t01p03_r08). (Right) The scene after atmosphere and glint correction. Clouds and some sea surface features remain; this is due to automated masking. Overall, glint correction performs quite well.

Source: Bo-Cai Gao

Mitigation Options

Uniform Spectral Offset

$$R_{rs}(\lambda) = R_{rs}^*(\lambda) - R_{rs}(750) + \Delta,$$

where

$$\Delta = 0.00019 + 0.1[R_{rs}^*(640) - R_{rs}^*(750)]$$

Source: James Goodman

Glint-Aerosol Discrimination

At-sensor reflectance

$$\rho_t = \rho_r + \rho_a + \rho_{sky}^{TOA} + \rho_g^{TOA} + \frac{\rho_w^{SFC} \cdot T_{gas} \cdot t_d \cdot t_u}{1 - s \cdot \rho_w^{SFC}}$$

For $\lambda > 1000$ nm, this reduces to

$$\rho_t - \rho_r - \rho_{sky}^{TOA} = \rho_a + \rho_g^{TOA}$$

Spectral decomposition relies on glint and aerosol spectral shapes

$$\rho_a(\lambda) = \rho_{a0} \cdot A(\lambda) \qquad \text{and} \qquad \rho_g^{TOA}(\lambda) = \rho_{g0} \cdot A(\lambda)$$

$A(\lambda)$ and $G(\lambda)$ are obtained using raditive transfer simulations.

Solve for ρ_{a0} and ρ_{g0}, then extrapolate to VIS.

Source: Youngje Park

Conclusions and Recommendations

Conclusions

- The literature and present examples demonstrate that glint correction is feasible.
- Present examples further demonstrate that key HyspIRI science objectives are achievable even in the presence of glint.
- Therefore, it is very reasonable that active glint correction can be a part of a successful HyspIRI processing flow.

Near-Term Recommendations

- The glint correction procedures described here each demonstrate strong potential. Each also requires further refinement.
- The presented analyses have touched on some key points about glint and its impact on remote sensing retrievals of certain biophysical parameters. These issues could certainly benefit from deeper investigation.
- It would be very desirable to perform field validation for model results of selected, important HyspIRI science objectives.

Long-Term Recommendations

- Environmental optics would be greatly advanced by the collection of a few comprehensive data sets that provide all inputs and outputs to the RTE.
- As glint correction procedures become codified, it would be useful to have a glint toolbox utility from which a user could select among a suite of glint correction techniques.

Using HyspIRI Derived Parameters in Climate Related Models

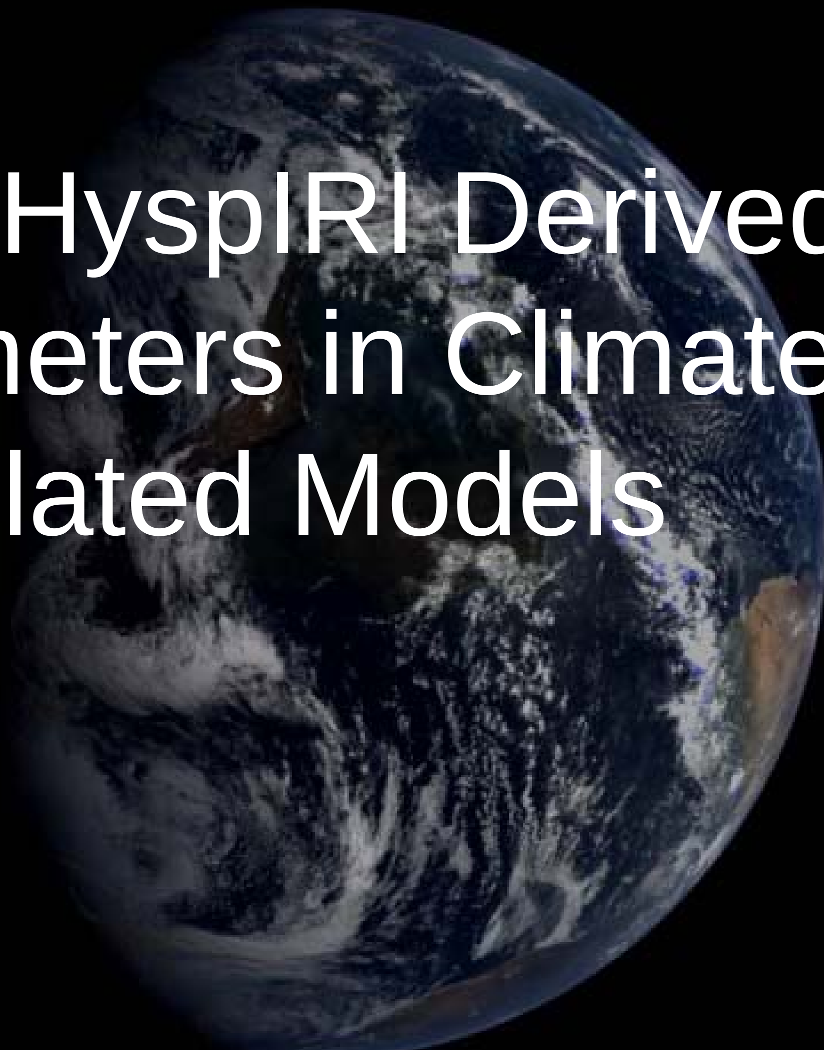

K. Fred Huemmrich
3rd HyspIRI Science Workshop
August 24, 2010

Climate – Ecosystem Feedbacks

- May be very large
- Represent a significant unknown
  - both in strength and even sign
- Need to understand
  - Ecosystem responses to climate change
  - Climate forcing from ecosystem change

Land-Atmosphere Interactions

- Include feedbacks between surface radiation, the vegetation-soil system, and the atmosphere
- These interactions produce complex exchanges of energy and water that influence climate
- There are wide disparities among current climate models in characterizing land-atmosphere interactions
- Further understanding and improving representation of the processes governing land-atmosphere interactions are important for climate predictions and projections

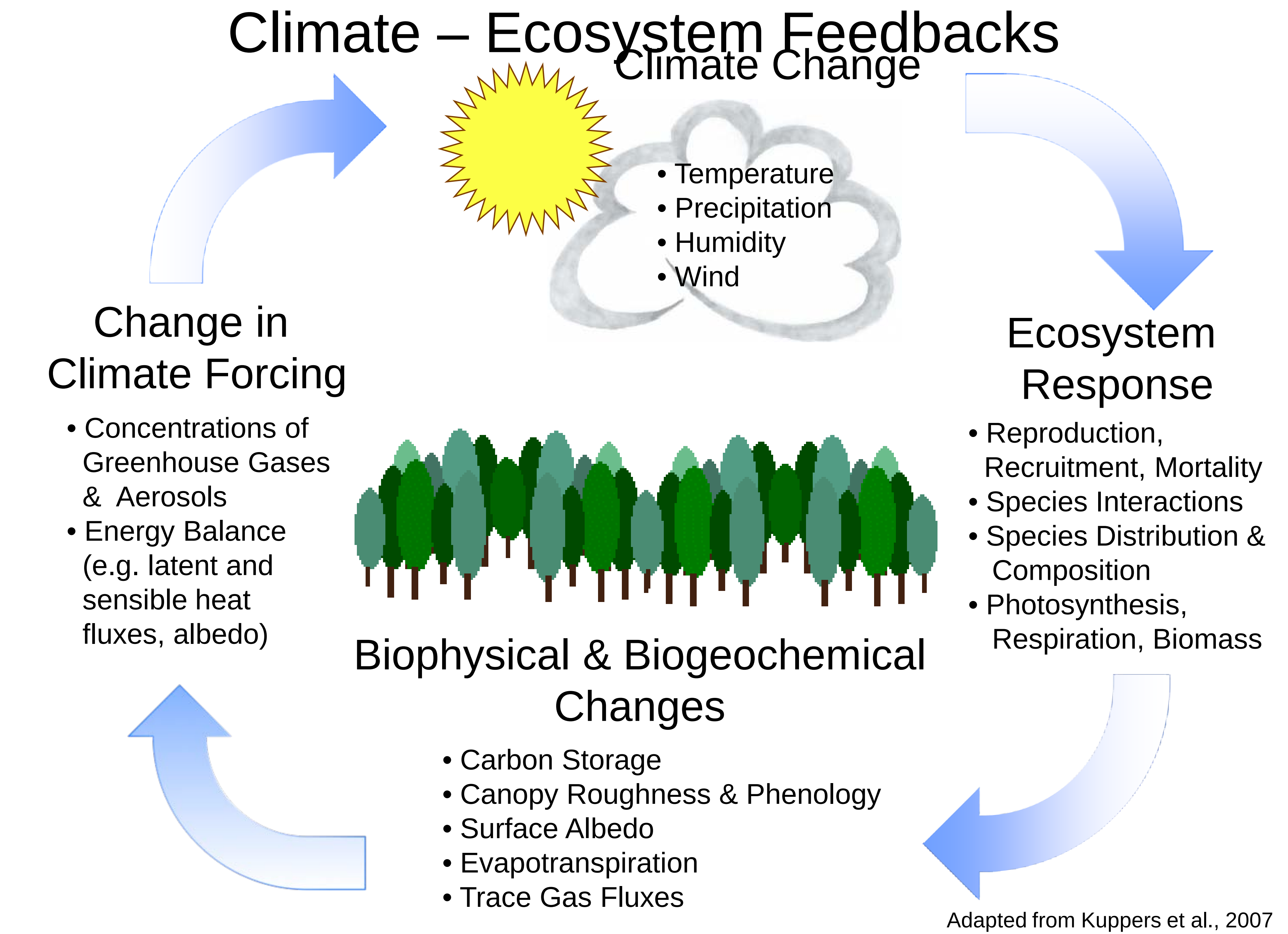

Climate – Ecosystem Feedbacks
Climate Change
• Temperature
• Precipitation
• Humidity
• Wind
Ecosystem Response
• Reproduction, Recruitment, Mortality
• Species Interactions
• Species Distribution & Composition
• Photosynthesis, Respiration, Biomass
Biophysical & Biogeochemical Changes
• Carbon Storage
• Canopy Roughness & Phenology
• Surface Albedo
• Evapotranspiration
• Trace Gas Fluxes
Change in Climate Forcing
• Concentrations of Greenhouse Gases & Aerosols
• Energy Balance (e.g. latent and sensible heat fluxes, albedo)
Adapted from Kuppers et al., 2007

Ecosystem Responses

- Productivity
  - CO_2 Fertilization effects
- Leaf area
- Phenology
- Canopy roughness
- Rooting depth
- Respiration
- Soil water holding capacity
- Changes in disturbance regimes
  - e.g. fire frequency, insect outbreaks
- Nutrient cycling
- Species composition

Climate – Ecosystem Feedbacks

- Feedbacks act through
  - Biophysical pathways that alter energy and water exchange
    - Alters albedo, evapotranspiration rates, vegetation structure, and phenology
    - Directly altering temperature, humidity, precip, convection, and wind
  - Biogeochemical pathways that alter carbon and nutrient cycles affecting uptake and release of greenhouse gasses and aerosols
    - CO_2
    - CH_4
    - N_2O
    - Black carbon
    - Aerosols
    - Volatile Organic Compounds

Climate – Ecosystem Feedbacks

- Some unknowns
  - Geographic shifts in species and plant functional types (PFT)
    - May create non-analog communities,
    - with potentially unique functional consequences
  - CO_2 fertilization
    - Effects water and energy balance
    - Constrained by N and P
  - non-CO_2 greenhouse gas release
    - CH_4
    - N_2O

Conceptual Ecosystem Flux Model

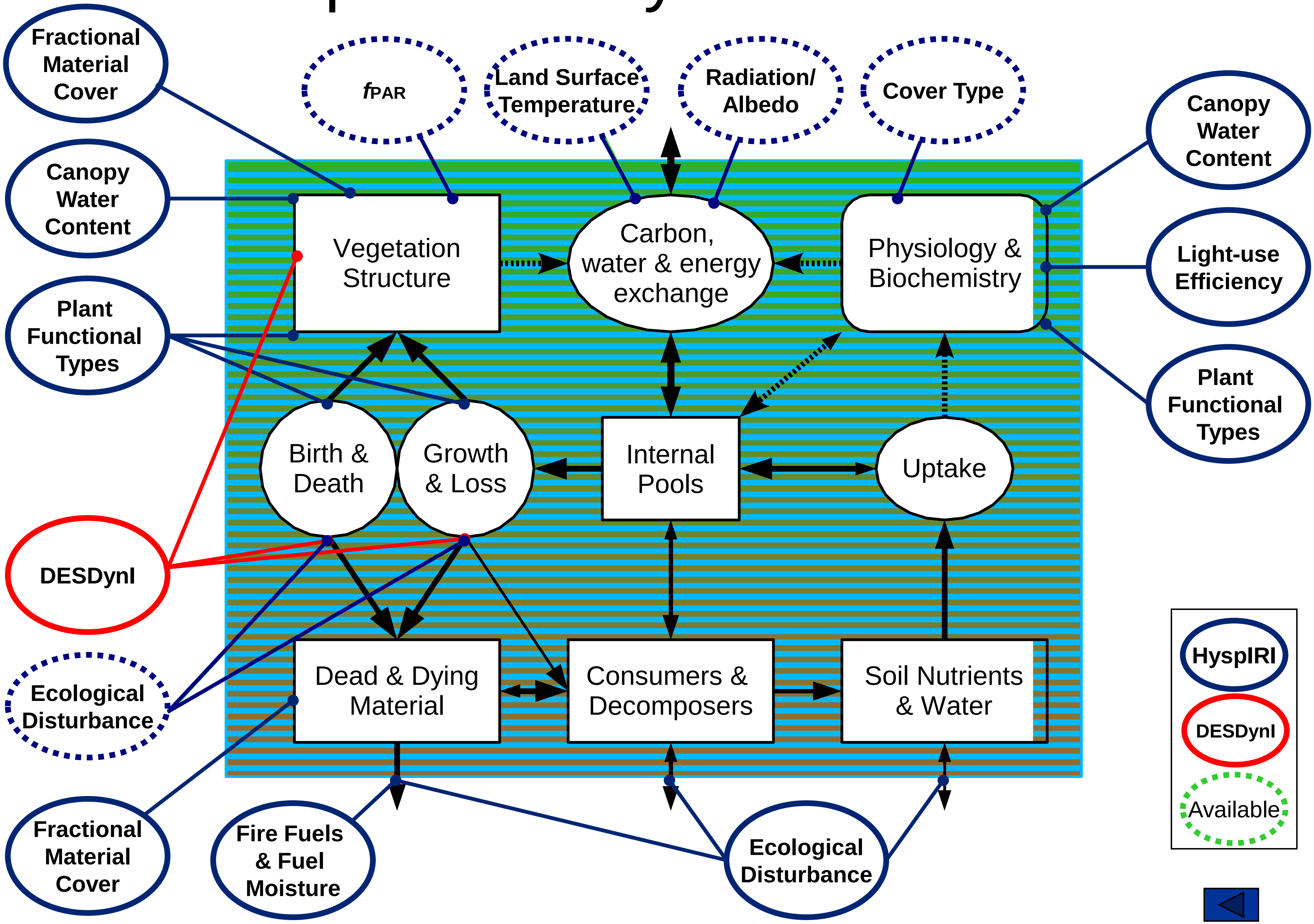

Modeling Approaches

- Diagnostic models
  - Describes fluxes, e.g. Light Use Efficiency models

  - Inputs from HyspIRI include
    - PRI
    - Chlorophyll concentrations
    - Canopy water content
    - *f*PAR
    - Albedo
    - Radiometric surface temperature

Diagnostic Models

- Diagnostic models and HyspIRI
  - HyspIRI will provide an unprecedented seasonally varying global description of vegetation type and status
    - Large-scale data use in synthesis studies
  - Output at spatial scale appropriate for land management
    - Model output will be important for applications such as carbon monitoring
  - VSWIR will not provide a dense time series
    - Merge with temporally frequent broadband data to improve temporal resolution

Diagnostic Models

- Mission too short to directly observe climate change effects
  - Provides validation data sets for prognostic models
  - Use to develop and test algorithms that can feed into prognostic models
    - e.g. examining effect of foliage N content on photosynthetic stress responses in different plant functional types

Modeling Approaches

- Prognostic models
  - Can be utilized to provide predictions and projections
  - Can be extrapolated to describe different conditions
- HyspIRI produced input data fields
  - New types of data for inputs, e.g. better descriptions of Plant Functional Types
  - Provide seasonally changing input values
  - Higher spatial resolution and improved classification provide better understanding of mixtures and disturbance

HyspIRI Model Inputs

- Leaf nitrogen
  - photosynthetic rates
- Disturbances
  - Thinning and diffuse disturbances
  - May have important effects on carbon balance
- Species distributions (functional biodiversity)
- Biomass in low stature ecosystems (grasslands, shrublands, etc.)
  - Cover types with the largest areas
  - May be significant biomass changes with increased shrubs

Plant Functional Types

- In models PFT are often defined based on landcover classification
  - HyspIRI will produce improved landcover classifications
  - Improved descriptions of complex mosaic of anthropogenic landscapes
- Different ways of grouping species into PFT for climate studies
  - By response to climate change (functional response group)
  - By role in climate forcing (functional effects group)
  - May need to detect differences in populations in terms of responses

Plant Functional Types

- PFT often used to define values for a number of variables in models
- PFT can be defined by direct measurement of a suite of variables or continuous fields of these variables could be determined from HyspIRI
- Variables such as:
  - Green/nongreen fractions, green leaf area
  - Maximum photosynthetic rate, Photosynthetic efficiency
  - Specific leaf area
  - Foliage Nitrogen, Pigment concentrations
  - Leaf water content
  - Albedo
  - Sensitivity to climate change (e.g., inferring rooting depth from stress responses)
  - Canopy roughness
  - Seasonality

Conclusions/Issues

- Model improvements occur through
  - Improved algorithms
  - Utilization of new types of information
  - Improved accuracy of input data fields
  - More and better data for validation

Conclusions/Issues

- How do we facilitate using HyspIRI data to improve models?
  - Development of ways to organize and manage the huge data volumes from HyspIRI
    - Ability to extract level 2+ data for study sites
    - Standardized gridding of global products
      - Cloud-free composites
    - Tools to make it easy to link HyspIRI data with other data products in synthesis studies

Contribution of HyspIRI measurements to improving the quality of satellite-derived Climate Data Records

Peter J. Minnett

Meteorology and Physical Oceanography
Rosenstiel School of Marine and Atmospheric Science
University of Miami
Miami, USA

pminnett@rsmas.miami.edu

UNIVERSITY OF MIAMI
ROSENSTIEL
SCHOOL of MARINE &
ATMOSPHERIC SCIENCE

Outline

- Scales of variability in the ocean and atmosphere
- Potential of higher spatial resolution measurements
- Current limitations on CDRs imposed by medium resolution data
- Overcoming the combined geophysical and instrumental effects in CDRs

Turbulent Energy Cascade

- Energy is input to the climate system on large spatial scales and "cascades" through a sequence of turbulent processes to microscales.
- Satellite remote sensing offers a unique perspective of these processes: prime example is mesoscale oceanic variability.
- "Big whorls have little whorls that feed on their velocity, and little whorls have smaller whorls and so on to viscosity." - L.F. Richardson.

Scales of atmospheric variability

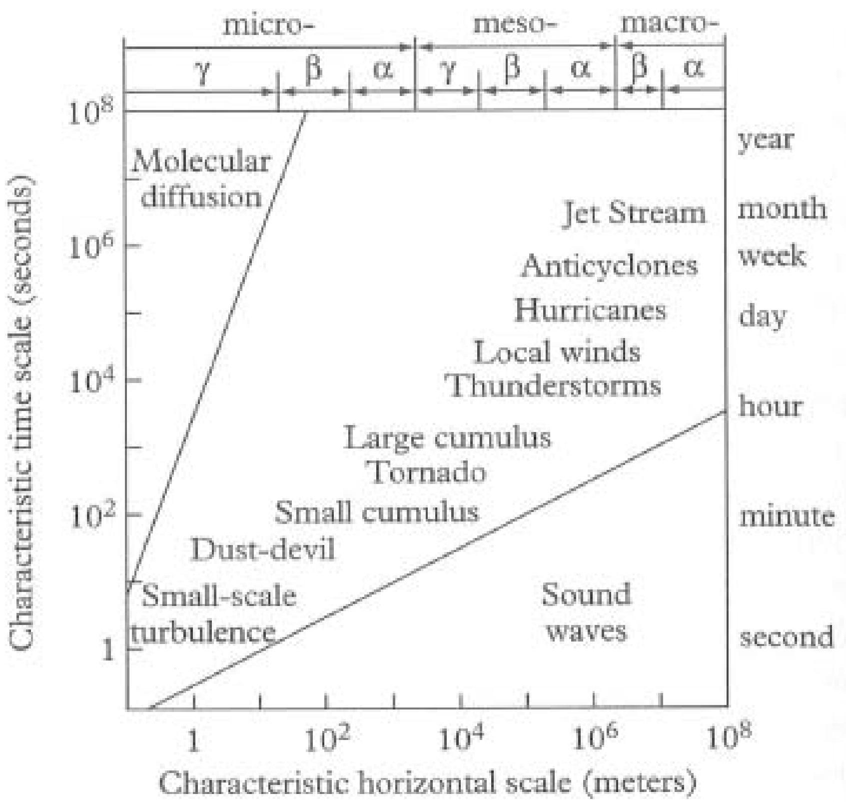

SCALES. Figure 1. *Scale definitions and different processes with characteristic time and horizontal scales.* (Adapted from Orlanski, 1975, and Oke, 1987.)

Scales of ocean variability

Sub-mesoscale variability is not limited to shelf and estuarine processes.

From Robinson, I. S. (2004), *Measuring the Oceans from Space. The principles and methods of satellite oceanography*, 515 pp., Springer Verlag - Praxis Publishing, Chichester, UK.

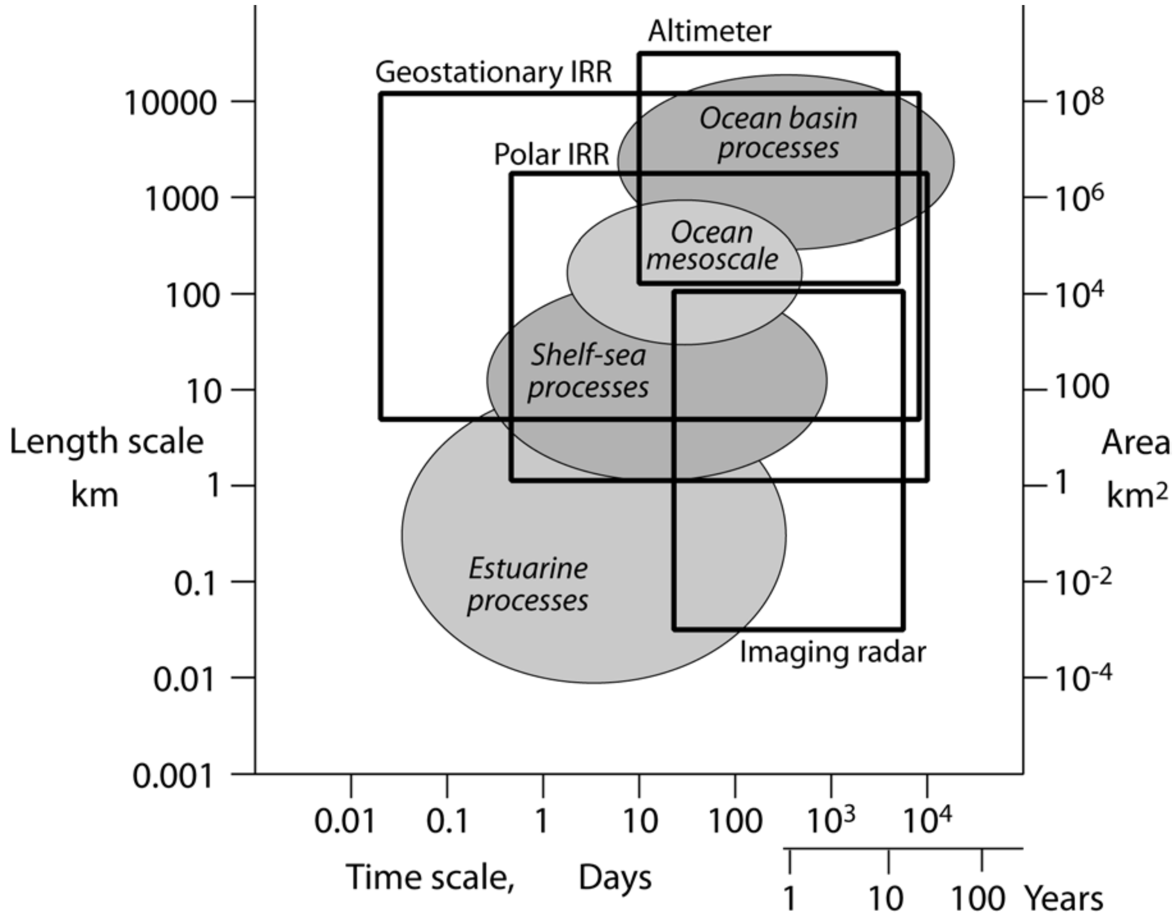

UNIVERSITY OF MIAMI
ROSENSTIEL SCHOOL of MARINE & ATMOSPHERIC SCIENCE

SST images reveal mesoscale variability.

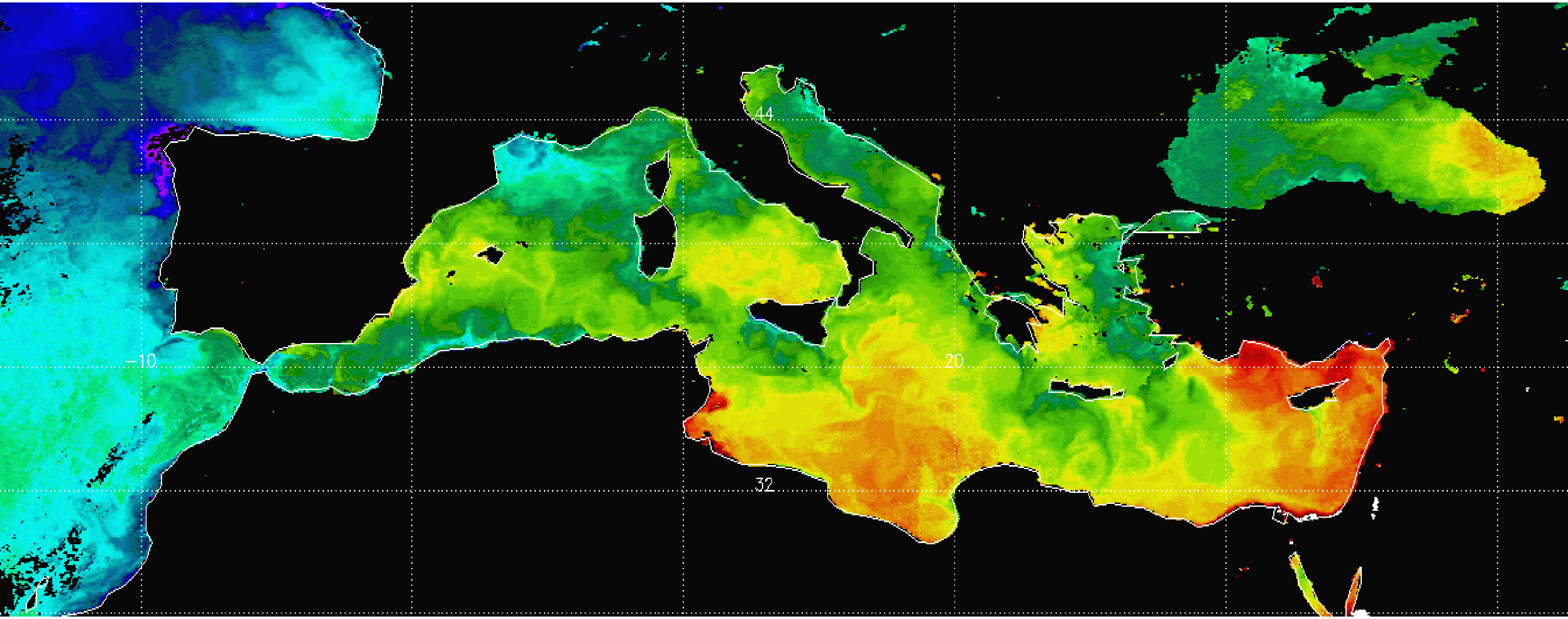

Ocean Color

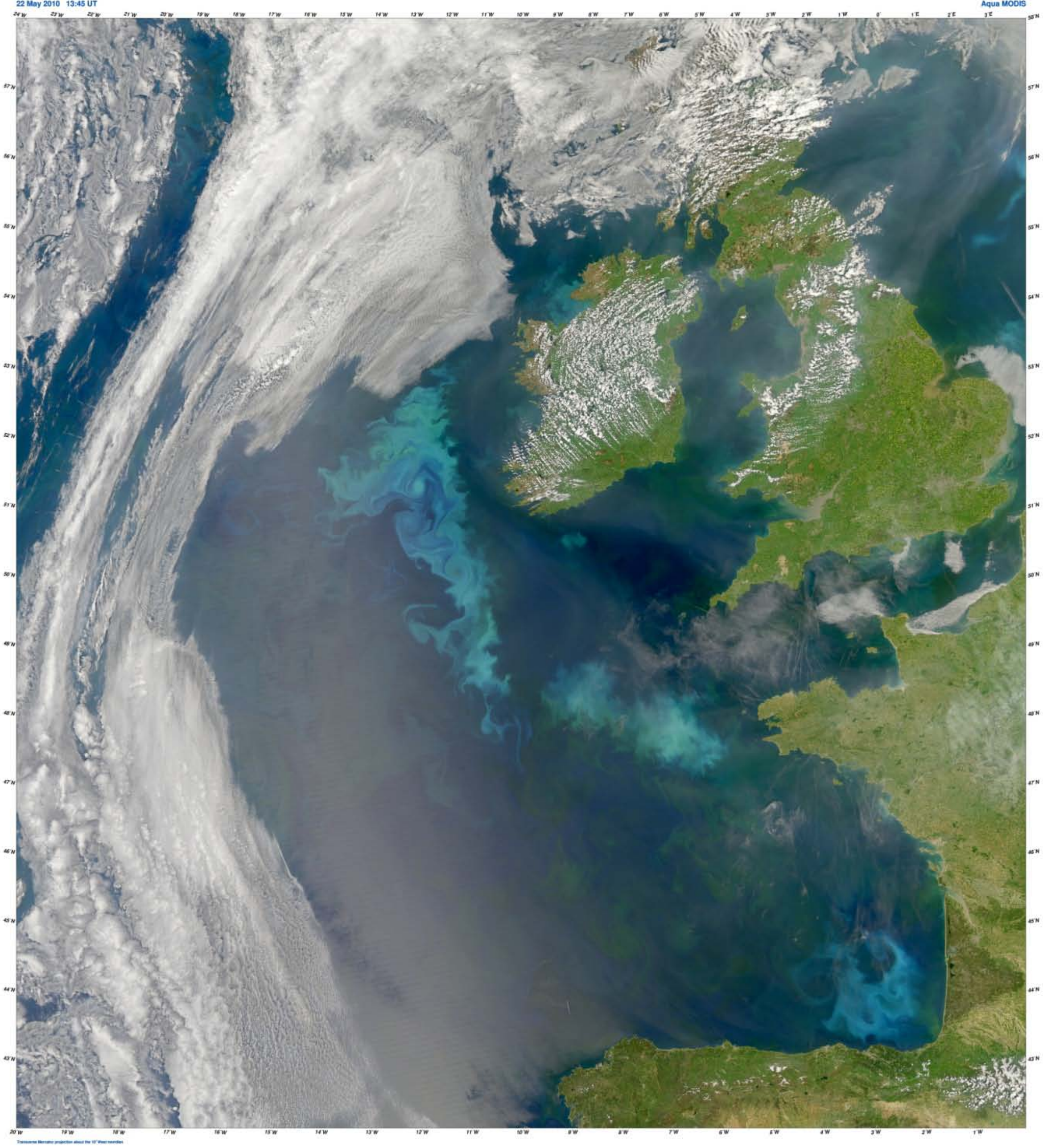

UNIVERSITY OF MIAMI
ROSENSTIEL
SCHOOL of MARINE &
ATMOSPHERIC SCIENCE

Clouds

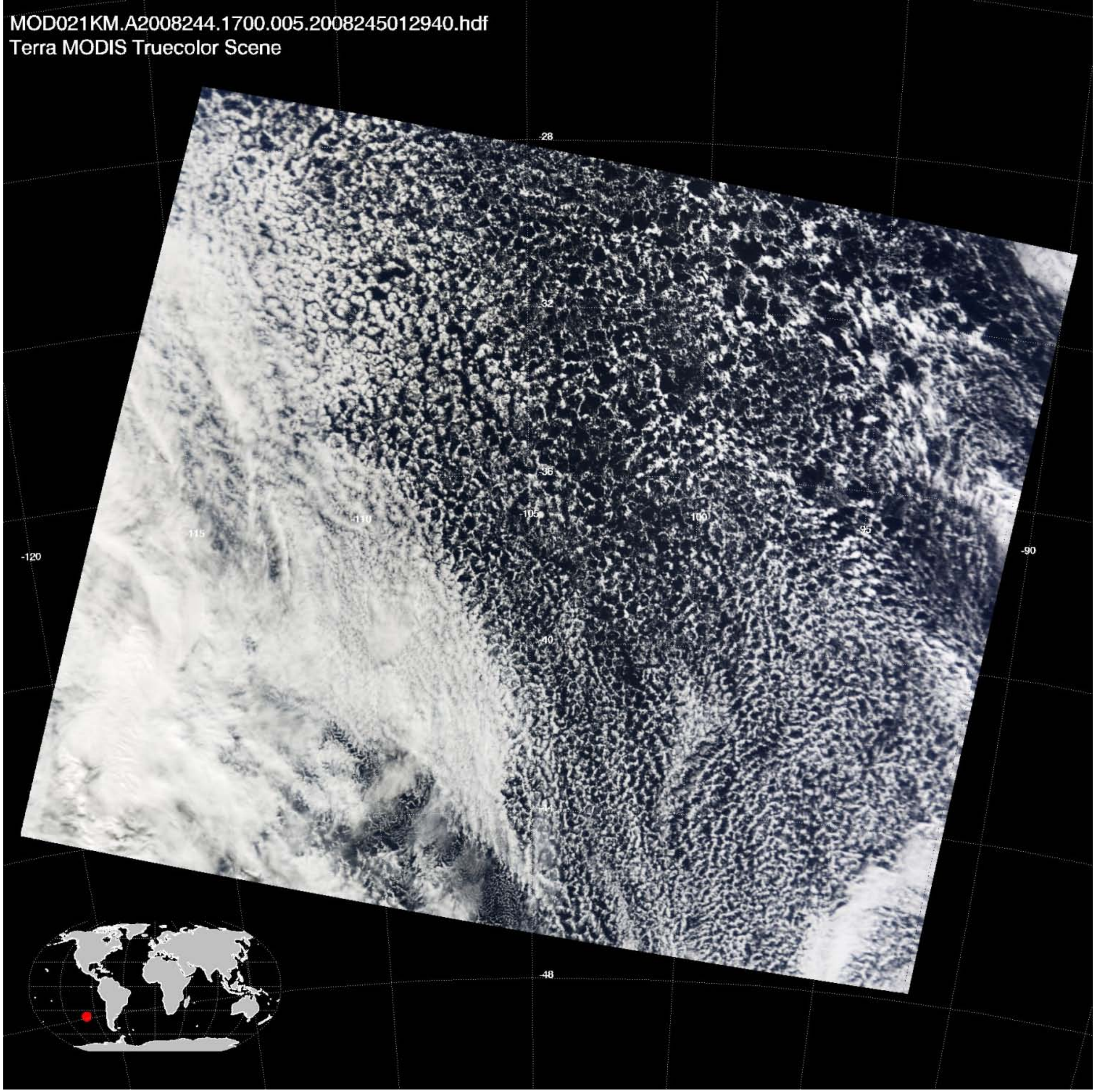

UNIVERSITY OF MIAMI
ROSENSTIEL
SCHOOL of MARINE &
ATMOSPHERIC SCIENCE

How is progress made?

- In recent decades, progress in oceanic and atmospheric science has often followed the measurements of improved instrumentation:
  - Swallow floats & satellite images of oceanic mesoscale features.
  - Radars, aircraft and satellite measurements of cloud processes.
- But now, modeling has moved beyond measurement capabilities.

High resolution simulations

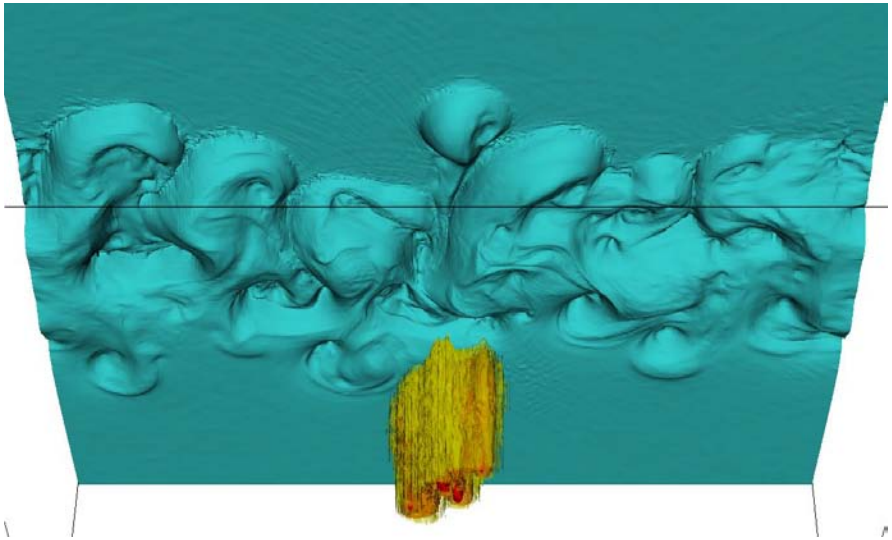

From below

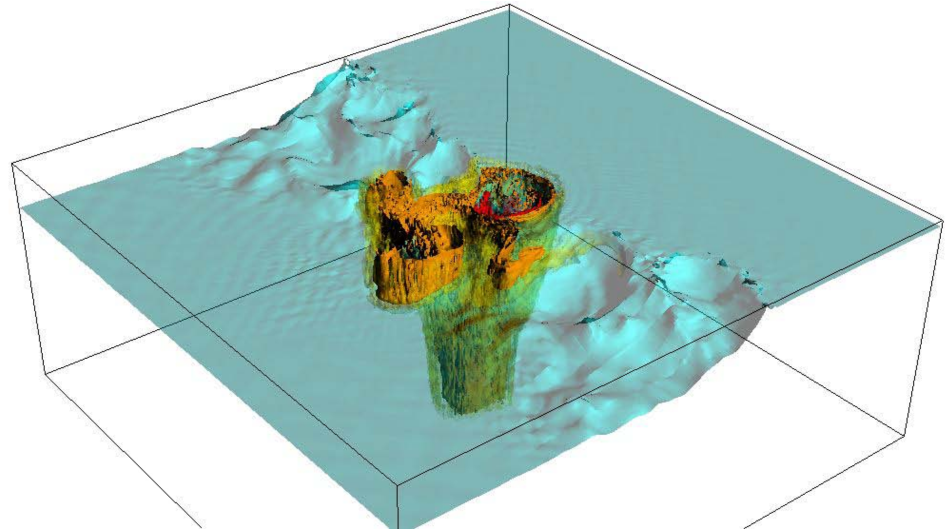

From above

Domain dimensions: 25x25 km
Blue: a density interface surface near the ocean surface
Orange: buoyant plume

Courtesy: Tamay Özgökmen, RSMAS - MPO

Simulations of ocean mixing

Domain dimensions: 10x10 km
A density interface surface intersecting the ocean surface.

Courtesy: Tamay Özgökmen, RSMAS - MPO

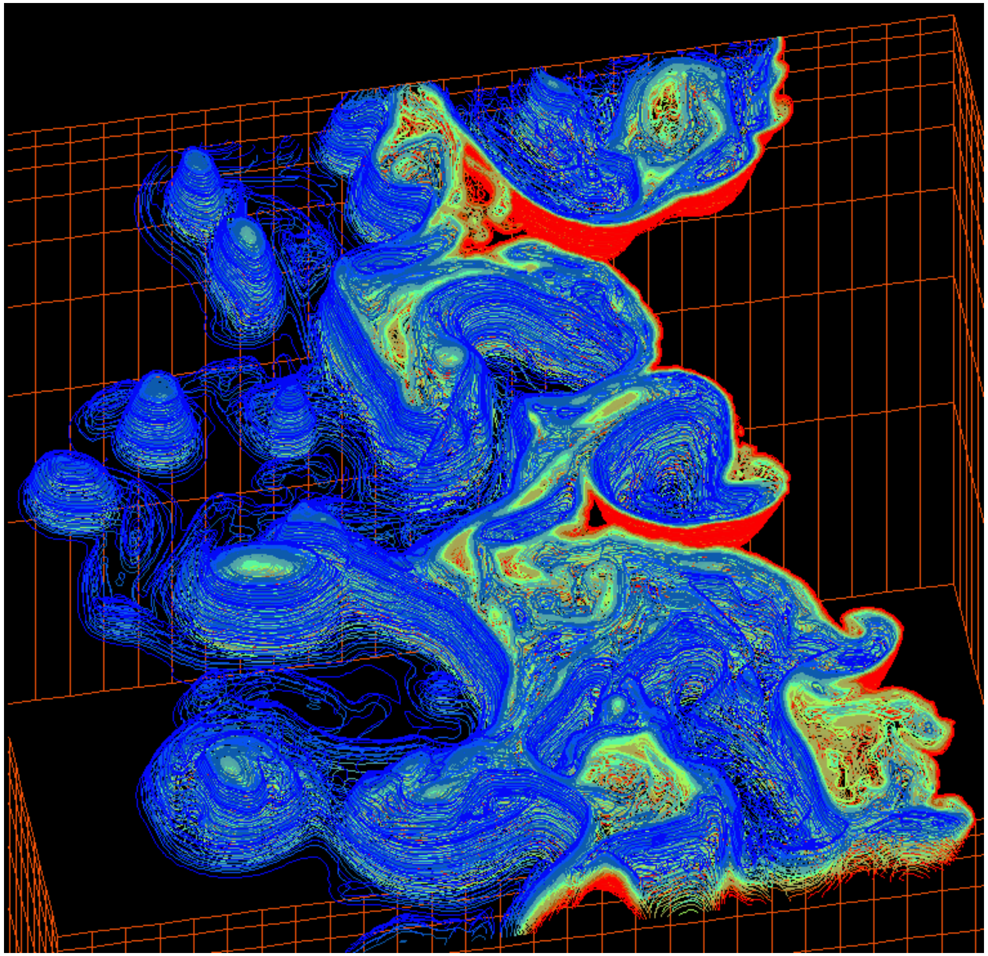

UNIVERSITY OF MIAMI
ROSENSTIEL SCHOOL of MARINE & ATMOSPHERIC SCIENCE

Modeled SST – Florida Keys

Grid size: 700m

Courtesy:
Dr Laurent Cherubin,
RSMAS-MPO

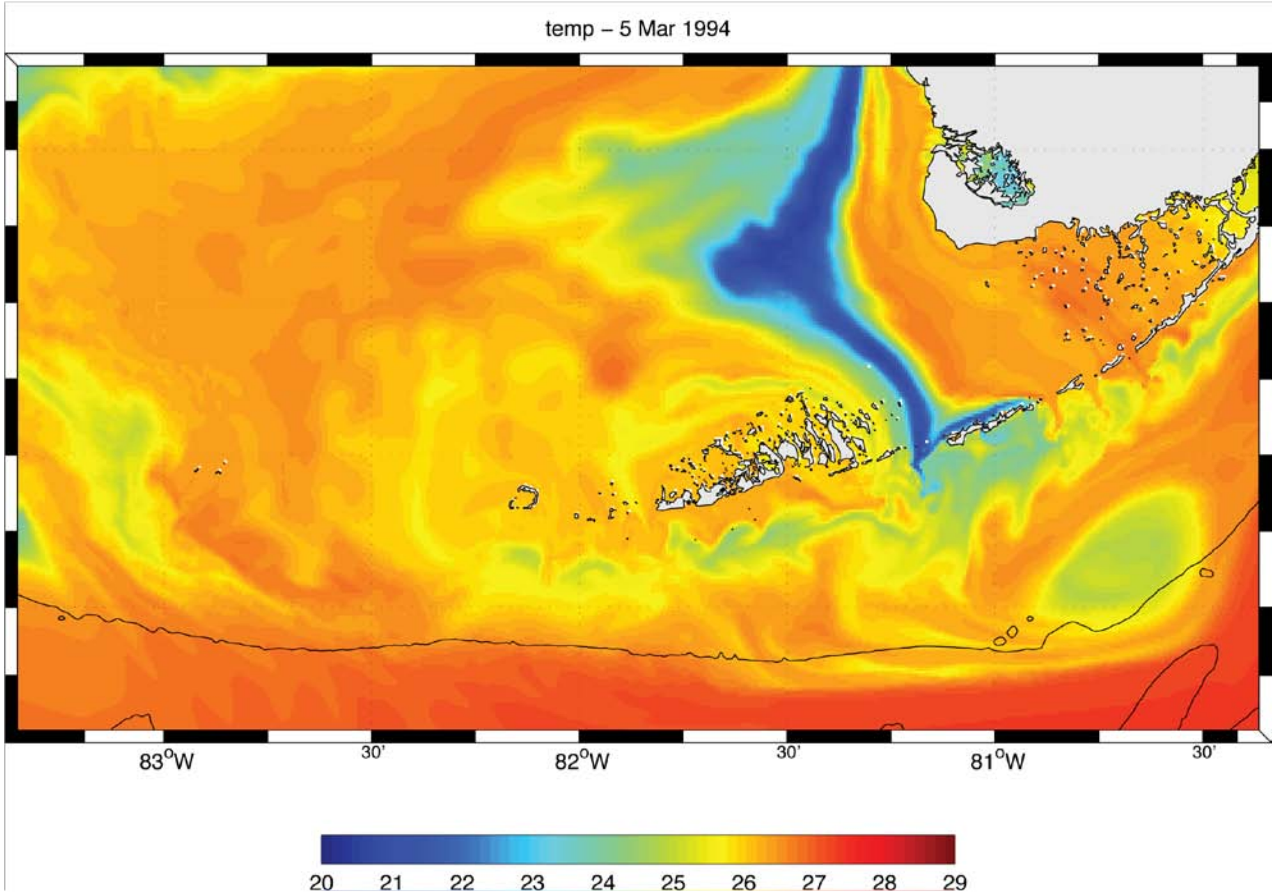

UNIVERSITY OF MIAMI
ROSENSTIEL
SCHOOL of MARINE &
ATMOSPHERIC SCIENCE

Nested Modeled SST - Belize

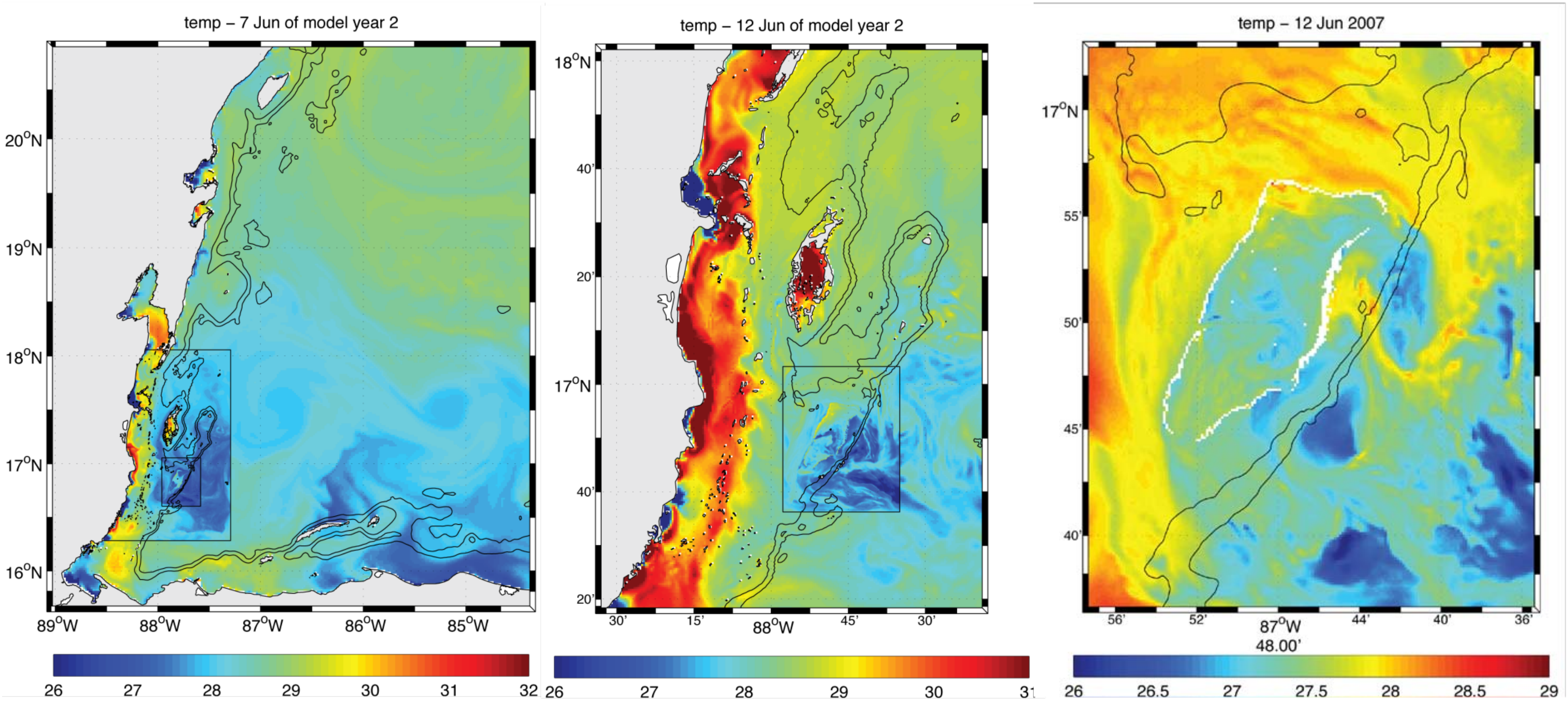

Nested grid resolutions: 2km → 690m → 230m

UNIVERSITY OF MIAMI
ROSENSTIEL SCHOOL of MARINE & ATMOSPHERIC SCIENCE

Courtesy:
Dr Laurent Cherubin, RSMAS-MPO

How to measure sub-mesoscale variability?

- Ship-based: cannot provide synoptic sampling, even using multiple ships; traditional instruments are good for vertical sections, but not for horizontal.
- Tracers: difficult to capture by ship tracking; airborne laser tracking is promising and under development. Overall, total tracer amount is too small and too short-lived to provide insight.
- Gliders: these are in vogue, but expensive (so not too many), and have major post-processing challenges due to aliasing by time along the path.
- Drifters: feasible, but need O(100) in a concentrated deployment, which is large enough to create environmental concerns.
- VHF radar: good, but limited to coastal zones.
- High resolution satellite imagers (SARs, VIS, IR) – a very feasible option.

Essential Climate Variables

GCOS
Global Climate Observing System
News Contact Publications Calendar Site map

- News
- About GCOS
- Climate Observation Needs
  - UNFCCC and GCOS
  - UNFCCC Guidelines
  - GCOS Reports to UNFCCC
  - Essential Climate Variables
  - Climate Monitoring Principles
- Observing Systems and Data
- Activities
- Partners
- Outreach
- Contact

GCOS Essential Climate Variables

The Essential Climate Variables (ECVs;) are required to support the work of the UNFCCC and the IPCC. All ECVs are technically and economically feasible for systematic observation. It is these variables for which international exchange is required for both current and historical observations. Additional variables required for research purposes are not included in this table. It is emphasized that the ordering within the table is simply for convenience and is not an indicator of relative priority. Currently, there are 44 ECVs plus soil moisture recognized as an emerging ECV.

Domain	Essential Climate Variables
Atmospheric (over land, sea and ice)	**Surface:** Air temperature, Precipitation, Air pressure, Surface radiation budget, Wind speed and direction, Water vapour. **Upper-air:** Earth radiation budget (including solar irradiance), Upper-air temperature (including MSU radiances), Wind speed and direction, Water vapour, Cloud properties. **Composition:** Carbon dioxide, Methane, Ozone, Other long-lived greenhouse gases[1], Aerosol properties.
Oceanic	**Surface:** Sea-surface temperature, Sea-surface salinity, Sea level, Sea state, Sea ice, Current, Ocean colour (for biological activity), Carbon dioxide partial pressure. **Sub-surface:** Temperature, Salinity, Current, Nutrients, Carbon, Ocean tracers, Phytoplankton.
Terrestrial[2]	River discharge, Water use, Ground water, Lake levels, Snow cover, Glaciers and ice caps, Permafrost and seasonally-frozen ground, Albedo, Land cover (including vegetation type), Fraction of absorbed photosynthetically active radiation (fAPAR), Leaf area index (LAI), Biomass, Fire disturbance, Soil moisture[3].

UNIVERSITY OF MIAMI
ROSENSTIEL SCHOOL of MARINE & ATMOSPHERIC SCIENCE

Essential Climate Variables

The Essential Climate Variables (ECVs;) are required to support the work of the UNFCCC and the IPCC. All ECVs are technically and economically feasible for systematic observation. It is these variables for which international exchange is required for both current and historical observations. Additional variables required for research purposes are not included in this

- News
- About GCOS
- Climate Observation Needs
  - UNFCCC and GCOS
  - UNFCCC Guidelines
  - GCOS Reports to UNFCCC
  - Essential Climate Variables
  - Climate Monitoring Principles
- Outreach
- Contact

GCOS Essential Climate Variables

The Essential Climate Variables (ECVs;) are required to support the work of the UNFCCC and the IPCC. All ECVs are technically and economically feasible for systematic observation. It is these variables for which international exchange is required for both current and historical observations. Additional variables required for research purposes are not included in this table. It is emphasized that the ordering within the table is simply for convenience and is not an indicator of relative priority. Currently, there are 44 ECVs plus soil moisture recognized as an emerging ECV.

Domain	Essential Climate Variables
(over land, sea and ice)	**Surface:** Air temperature, Precipitation, Air pressure, Surface radiation Wind speed and direction, Water vapour. **er-air:** Earth radiation budget (including solar irradiance), Upper-air temperature (including MSU radiances), Wind speed and direction, Water vapour, Cloud properties. **Composition:** Carbon dioxide, Methane, Ozone, Other long-lived greenhouse gases[1], Aerosol properties.
Oceanic	**Surface:** Sea-surface temperature, Sea-surface salinity, Sea level, Sea state, Sea ice, Current, Ocean colour (for biological activity), Carbon dioxide partial pressure. **Sub-surface:** Temperature, Salinity, Current, Nutrients, Carbon, Ocean tracers, Phytoplankton.
Terrestrial[2]	River discharge, Water use, Ground water, Lake levels, Snow cover, Glaciers and ice caps, Permafrost and seasonally-frozen ground, Albedo, Land cover (including vegetation type), Fraction of absorbed photosynthetically active radiation (fAPAR), Leaf area index (LAI), Biomass, Fire disturbance, Soil moisture[3].

Cloud properties.

Sea-surface temperature.

Sea ice.

River discharge.

Ocean colour (for biological activity).

Satellite-derived CDRs

- National Academy of Sciences Report (*NRC, 2000)*: "*a data set designed to enable study and assessment of long-term climate change, with 'long-term' meaning year-to-year and decade-to-decade change. Climate research often involves the detection of small changes against a background of intense, short-term variations.*"
- *"Calibration and validation should be considered as a process that encompasses the entire system, from the sensor performance to the derivation of the data products. The process can be considered to consist of five steps:*
  - *instrument characterization,*
  - *sensor calibration,*
  - *calibration verification,*
  - *data quality assessment, and*
  - *data product validation."*

Desired SST CDR uncertainties

- The useful application of all satellite-derived variables depends on a confident determination of uncertainties.
- CDRs of SSTs require most stringent knowledge of the uncertainties:
  - Target accuracies: 0.1K over large areas, stability 0.04K/decade - Ohring et al. (2005) Satellite Instrument Calibration for Measuring Global Climate Change: Report of a Workshop. Bulletin of the American Meteorological Society 86:1303-1313

Sources of uncertainty in satellite-derived SSTs

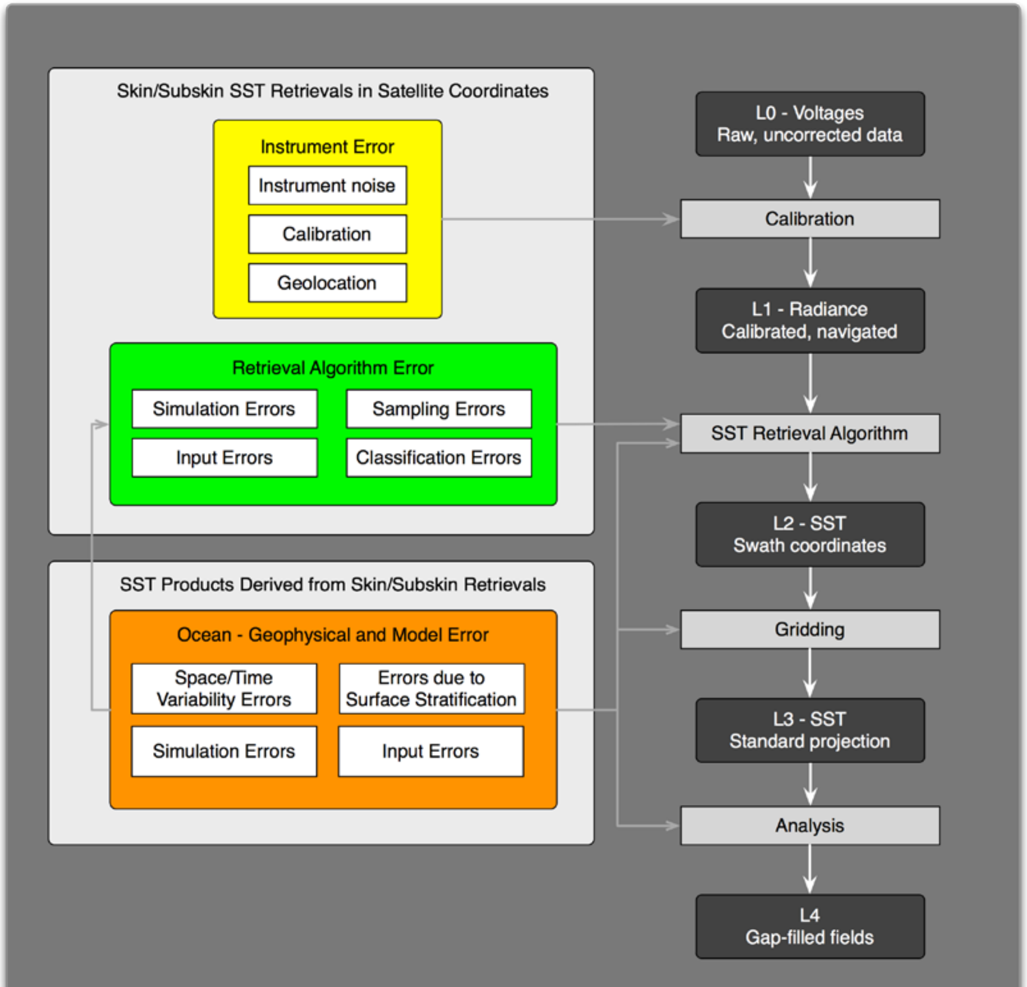

Many sources of retrieval algorithm errors (green box) and geophysical and model errors (orange box) are dependent on the spatial resolution of the satellite data.

SST retrievals: identifying clouds

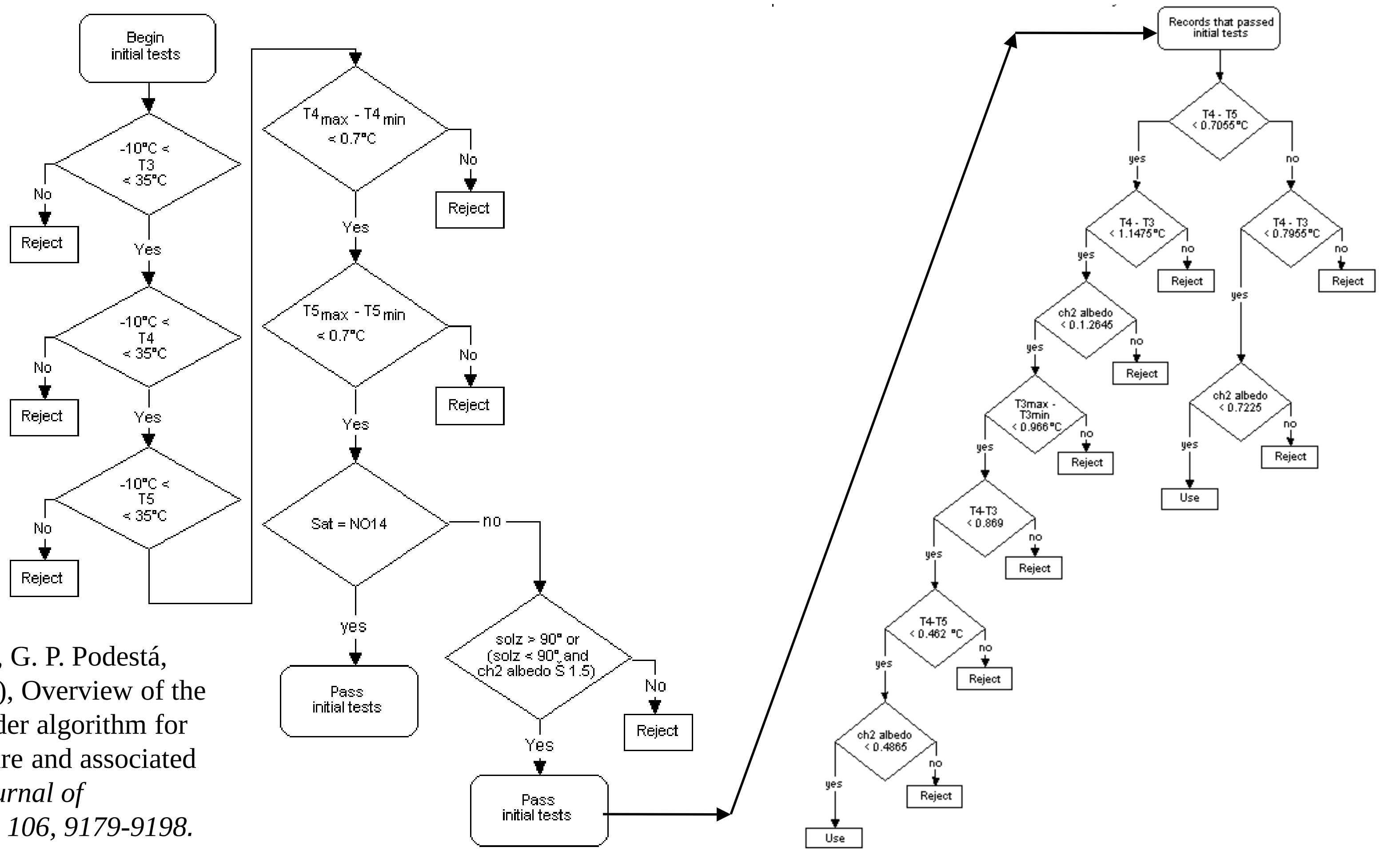

After Kilpatrick, K. A., G. P. Podestá, and R. H. Evans (2001), Overview of the NOAA/NASA Pathfinder algorithm for Sea Surface Temperature and associated Matchup Database, *Journal of Geophysical Research, 106, 9179-9198.*

UNIVERSITY OF MIAMI
ROSENSTIEL SCHOOL of MARINE & ATMOSPHERIC SCIENCE

SST retrievals: identifying clouds

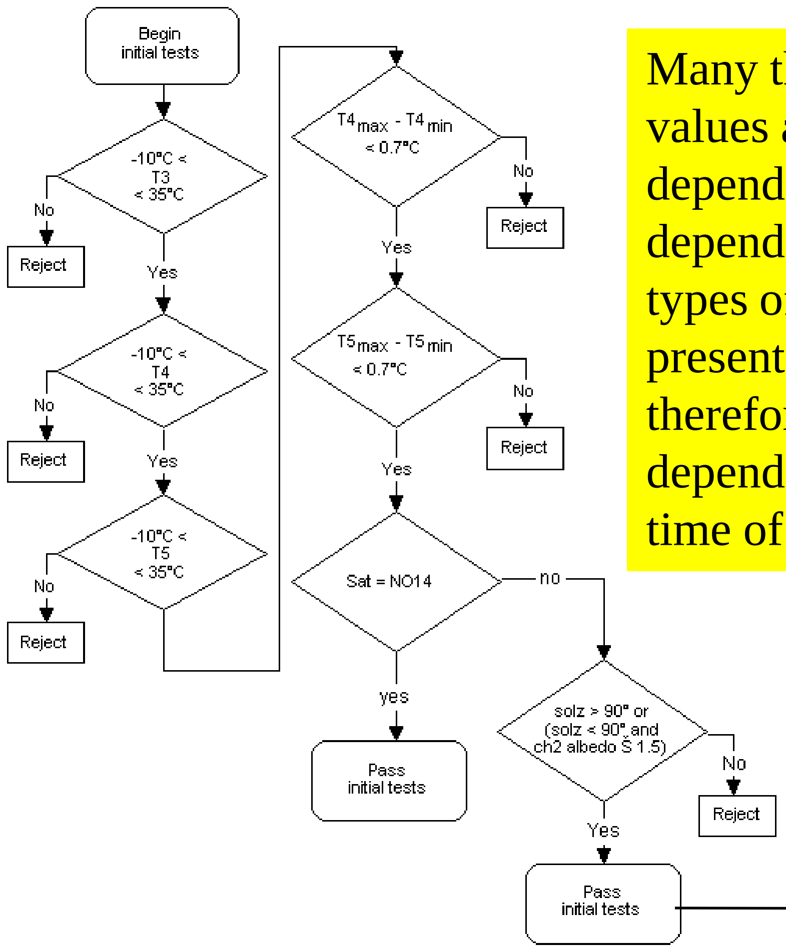

Many threshold values are scale dependent, and dependent on types of clouds present, and therefore dependent on time of day.

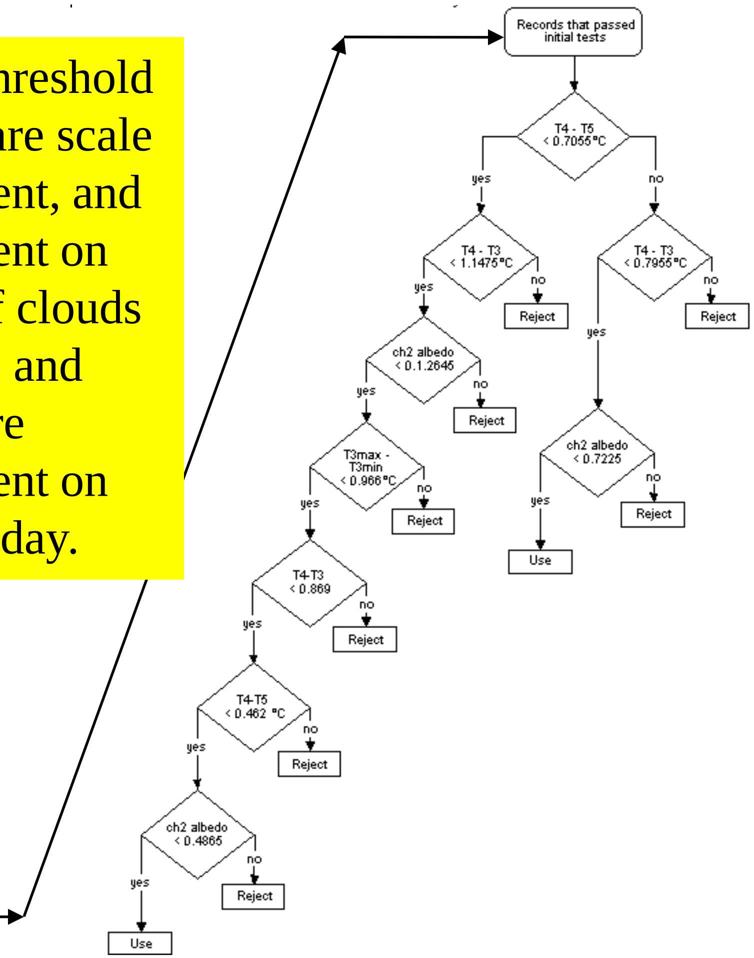

UNIVERSITY OF MIAMI
ROSENSTIEL SCHOOL of MARINE & ATMOSPHERIC SCIENCE

Why worry about sub-pixel variability?

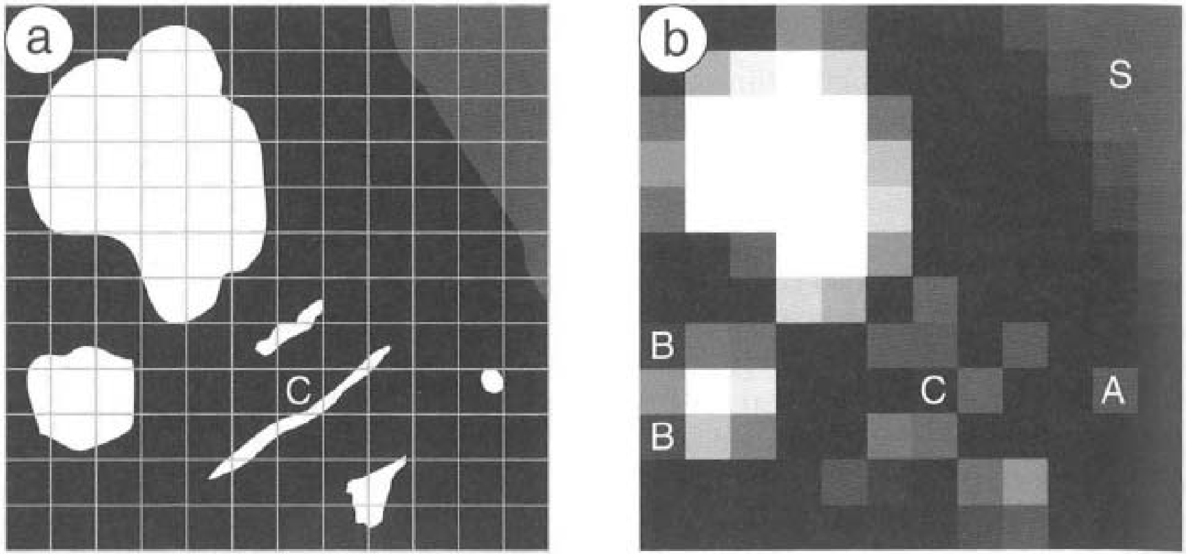

Figure 7.10. Schematic of the visible waveband view reflected from a region of partially cloudy sea. (a) As seen by a very fine resolution detector, with a coarse grid of 12 × 12 cells superimposed. (b) As it appears in the coarse pixels image.

Mixture modeling of radiances should give sub-pixel information:

$$R = \sum_{i=1}^{c} r_i a_i + e$$

From Robinson, I. S. (2004), *Measuring the Oceans from Space. The principles and methods of satellite oceanography,* 515 pp., Springer Verlag - Praxis Publishing, Chichester, UK.

Beware……

INT. J. REMOTE SENSING, 2000, VOL. 21, NO. 4, 839–843

Beware of per-pixel characterization of land cover

J. R. G. TOWNSHEND†*, C. HUANG, S. N. V. KALLURI, R. S. DEFRIES, S. LIANG

2181 LeFrak Hall, Department of Geography, University of Maryland, College Park, MD 20742, USA; e-mail: jt59@umail.umd.edu

and K. YANG

Science Systems and Applications, Inc., Code 922, NASA-GSFC, Greenbelt MD 20771, USA

Failure to account for the MTF (Modulation Transfer Function) can lead to >10% errors in classifications

MTF of MODIS

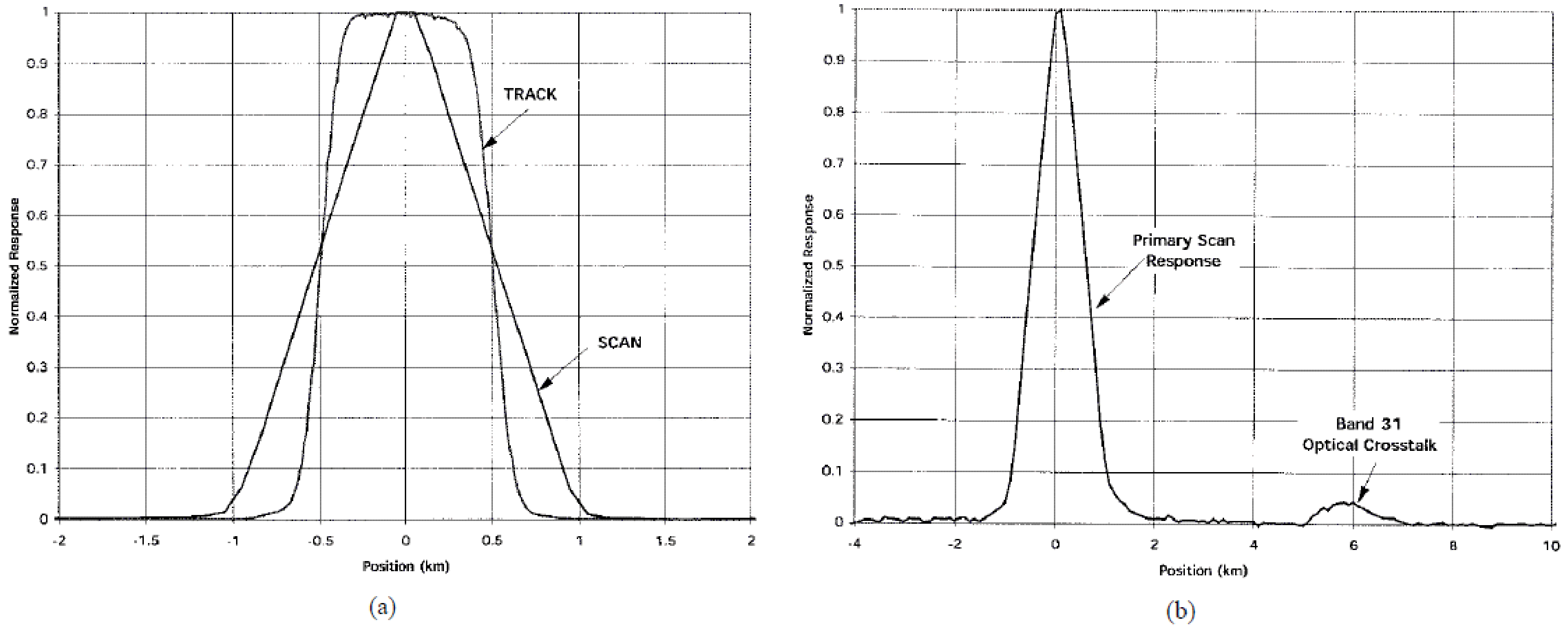

Fig. 3. Typical LSF's for MODIS. (a) Band 10, channel 6. Scan-direction LSF's are triangular due to the integration blur of the pixels in the scanning direction. Track-direction LSF's are more rectangular. (b) Band 35 has a ≈5% leak in the region of band 31 in the scan direction.

From Barnes, W. L., T. S. Pagano, and V. V. Salomonson (1998), Prelaunch characteristics of the moderate resolution imaging spectroradiometer (MODIS) on EOS-AM1, *IEEE Transactions on Geoscience and Remote Sensing, 36, 1088-1110.*

Pixel spatial response function

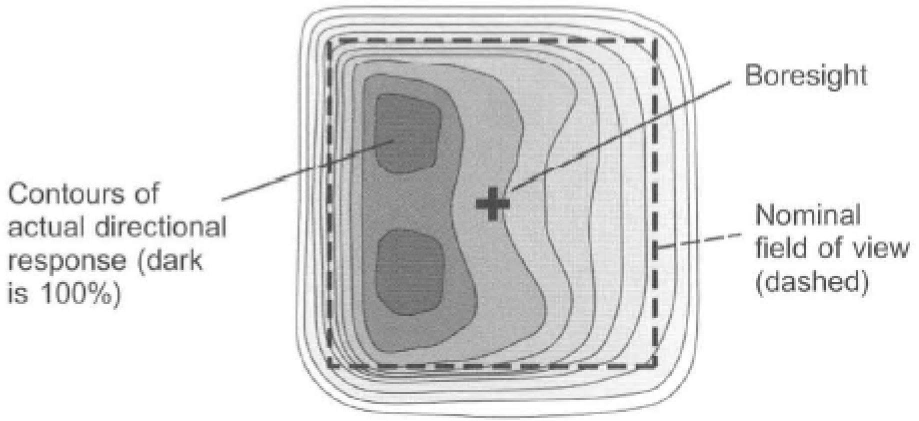

Figure 4.2. Example of a typical actual sensor 2-D response function for a sensor having a nominally square.

- Instantaneous spatial responses of detectors are not uniform.
- This compounds the MTF effect and increases errors in retrievals at the pixel scale.

From Robinson, I. S. (2004), *Measuring the Oceans from Space. The principles and methods of satellite oceanography*, 515 pp., Springer Verlag - Praxis Publishing, Chichester, UK.

HyspIRI spatial resolution

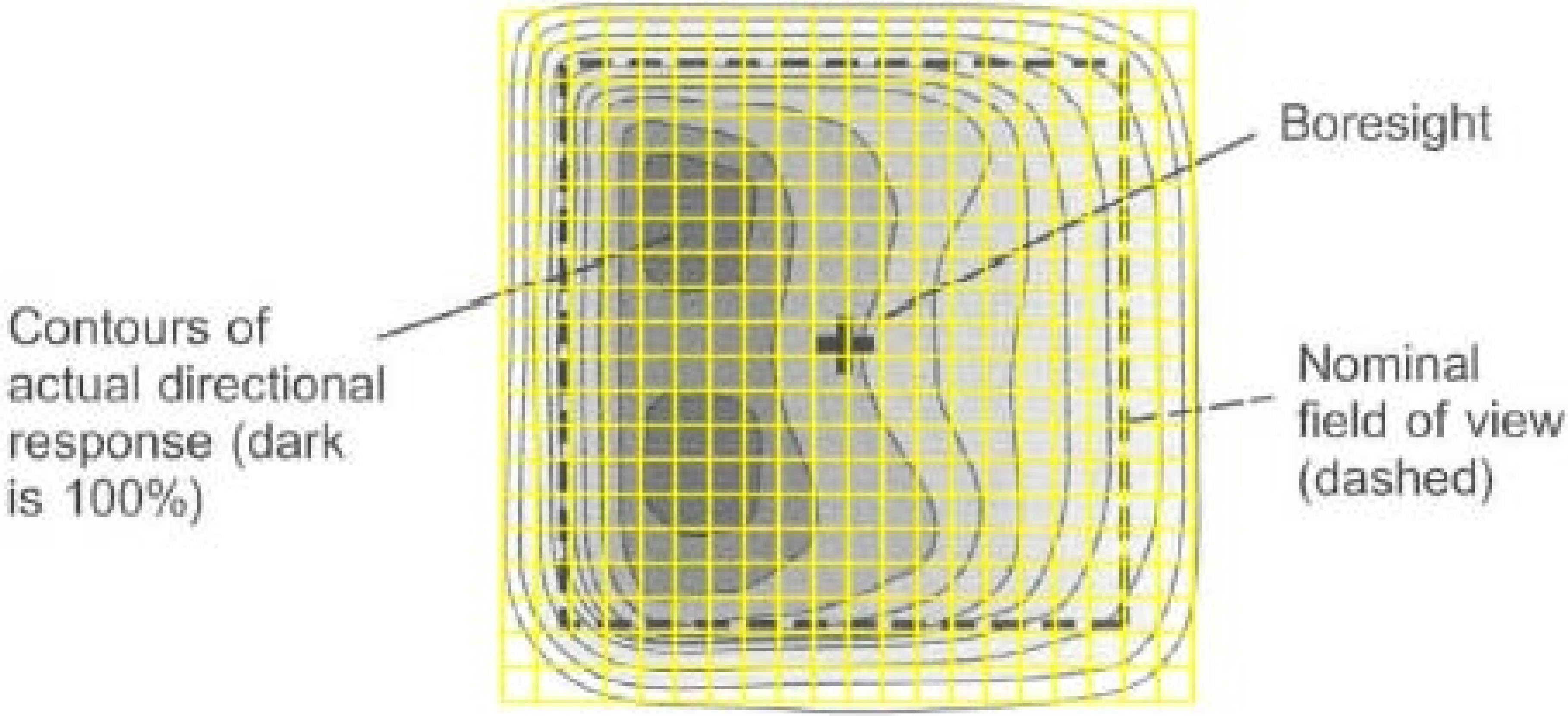

Summary

- Natural variability covers a very wide range of scales, and is not truncated at the ~1km resolution of conventional oceanic and atmospheric imagers.
- High-resolution HyspIRI data over the oceans will provide new insight into oceanic and atmospheric processes relevant to climate studies.
- Many CDRs are derived from moderate-resolution data; high-resolution HyspIRI data can provide unique data with which to test, improve, and establish the limitations on accuracies imposed by sub-pixel variability. This would guide reprocessing algorithms to improve the accuracy of CDRs.
- Improved CDRs provide a better basis for decision-makers to make hard choices… and to justify them.

One-liner….

Global HyspIRI mission **can** make a unique contribution to the climate monitoring and climate research communities.

Acknowledgements

- Colleagues at RSMAS and elsewhere
- Support from NASA PO program, Dr Eric Lindstrom

One-liner….

Global HyspIRI mission **can** make a unique contribution to the climate monitoring and climate research communities.

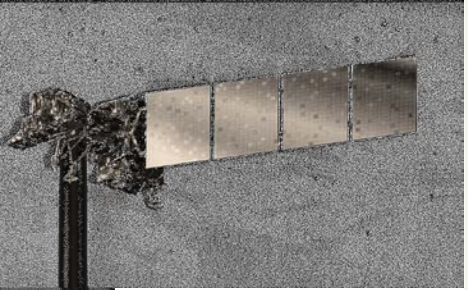

What Unique HyspIRI Products Relevant to Climate Change Science can be Produced at the Global Scale?

Susan L. Ustin
University of California Davis

Workshop on Climate Modeling and HyspIRI

Global Science Products

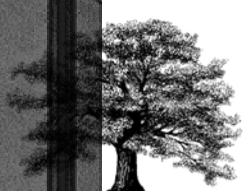

Future Workshop on global HyspIRI Products

Plan to hold workshop near end of year at Carnegie Institution at Stanford with modeling community

Sponsored by: Mike Freilich, NASA HQ, Decadal Survey
Hosted by: Chris Field and Susan Ustin

Goal: White Paper on Global Products Relevant for Climate Research
Ecosystem and Climate Modeling Communities

Request for HyspIRI Community Input:

Send ideas, papers, comments to me by email: slustin@ucdavis.edu

We must get HyspIRI products incorporated into the next generation Ecosystem Models

NEP = Annual GPP - Respiration (Auto+ Hetero)

$$NEP = \sum GPP - (R_m + R_g + R_h)$$

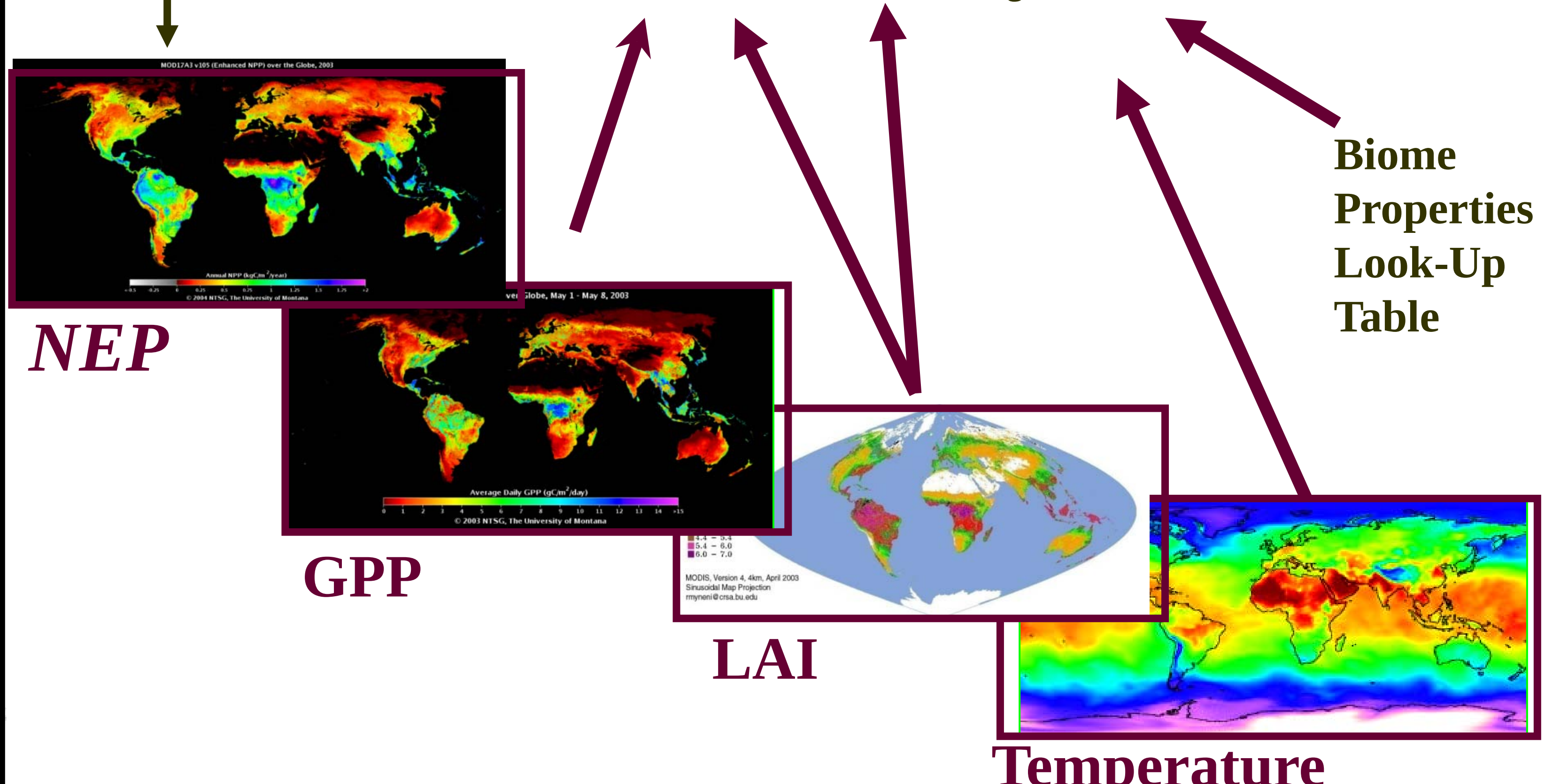

Many Possible HyspIRI Indexes:

PVI Index tracks Carbon and Water Fluxes

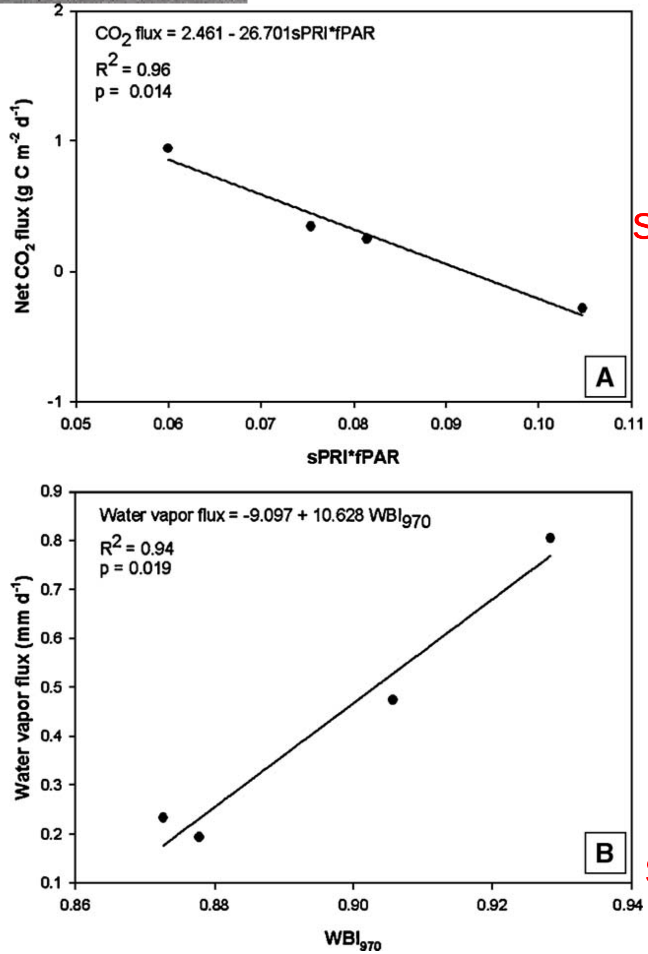

sink

source

sink

sink

source

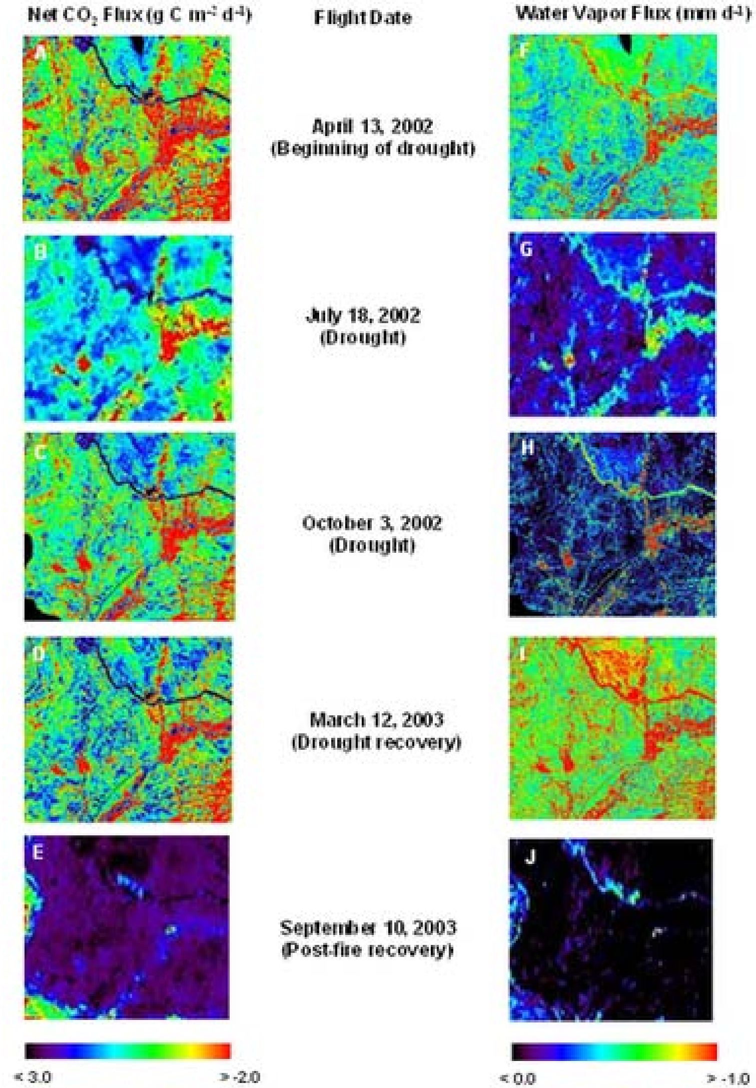

Fuentes et al. 2006

An operational PRI product could improve ecosystem carbon flux estimates, capturing physological change under disturbance, stress, and changing vegetation composition

Combined VNIR-SWIR Physiological/Thermal Stress Indicators: Unique HyspIRI Measurements

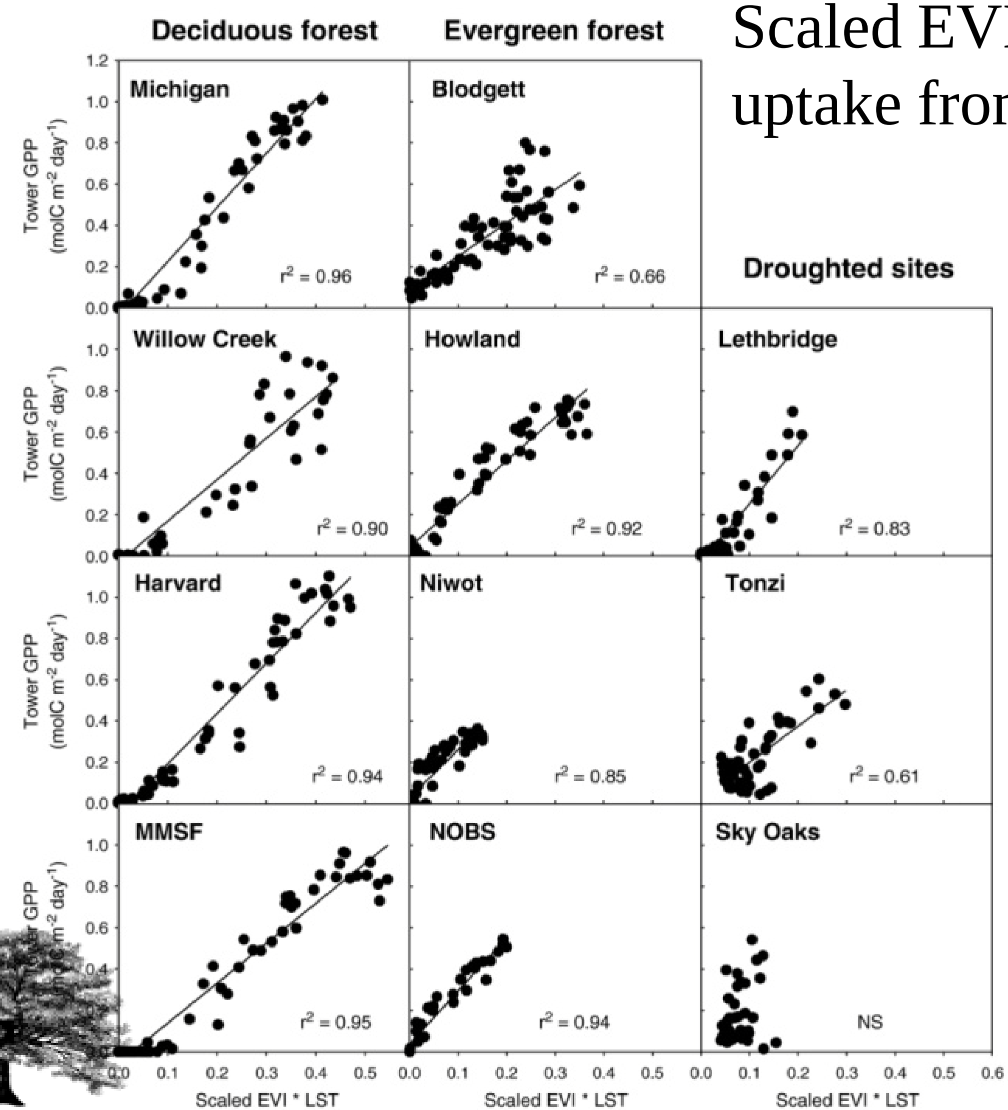

Scaled EVI*LST compared to carbon uptake from flux towers.

Improved estimates of carbon uptake using PRI established using flux data and AVIRIS

MODIS estimates of carbon uptake improved using LST, vegetation index and 60m pixels (from Sims et al., 2008)

Develop Robust Algorithms to Quantitatively Predict Photosynthetic Processes: Spectroscopy Provides Quantitative Measurements of OpticalProperties

PLSR waveband selection

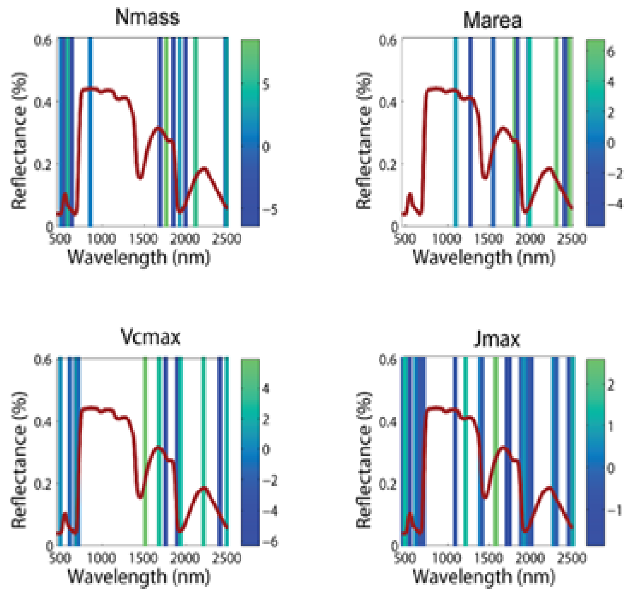

PLSR waveband selection and the state of knowledge

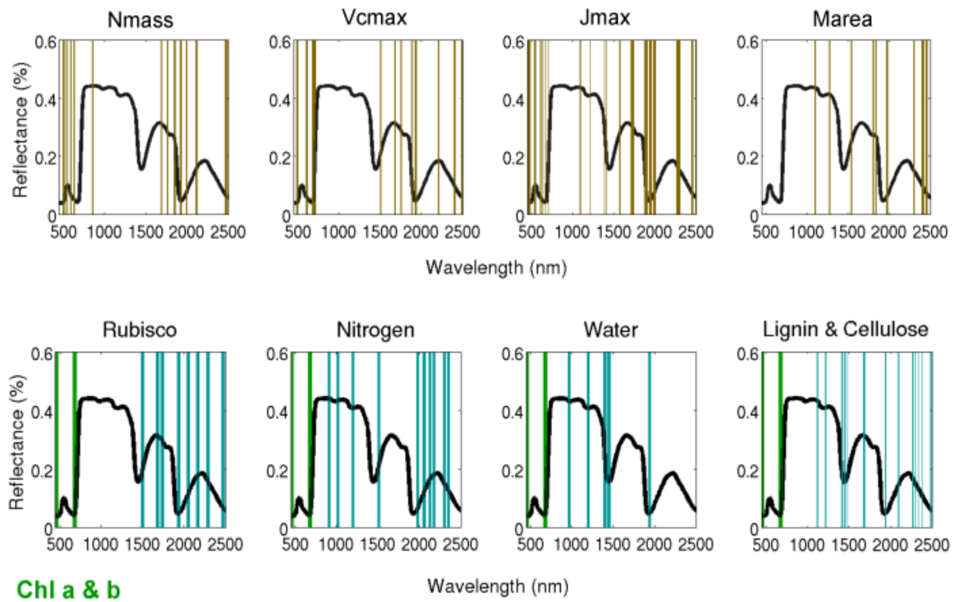

Nmass = nitrogen concentration
Marea= mass area^{-1}
Vcmax = Assimilation limit by Rubisco
Jmax = Assimilation limit by e^- transport

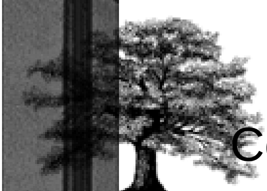

Continuing large uncertainty in flux of CO_2 due to land use change.

Global Monitoring of Physiological Processes using HyspIRI Thermal-based Flux Mapping

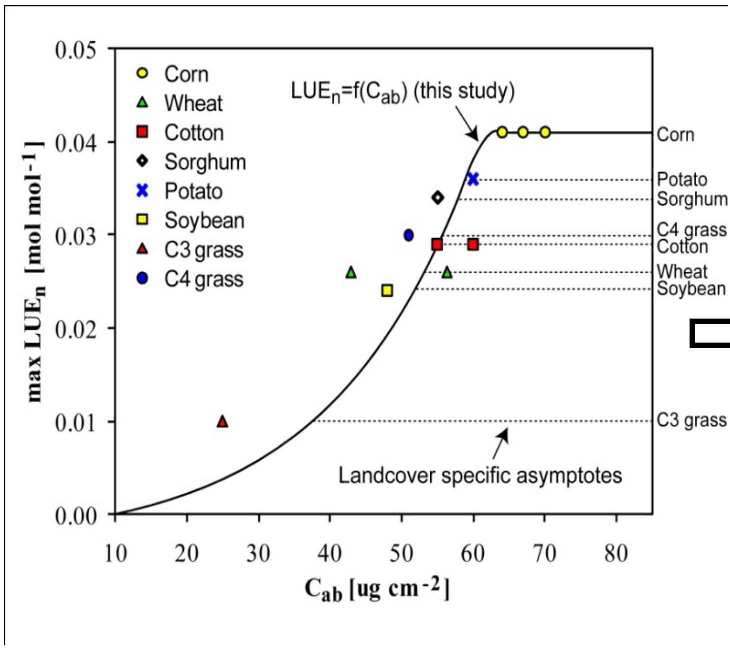

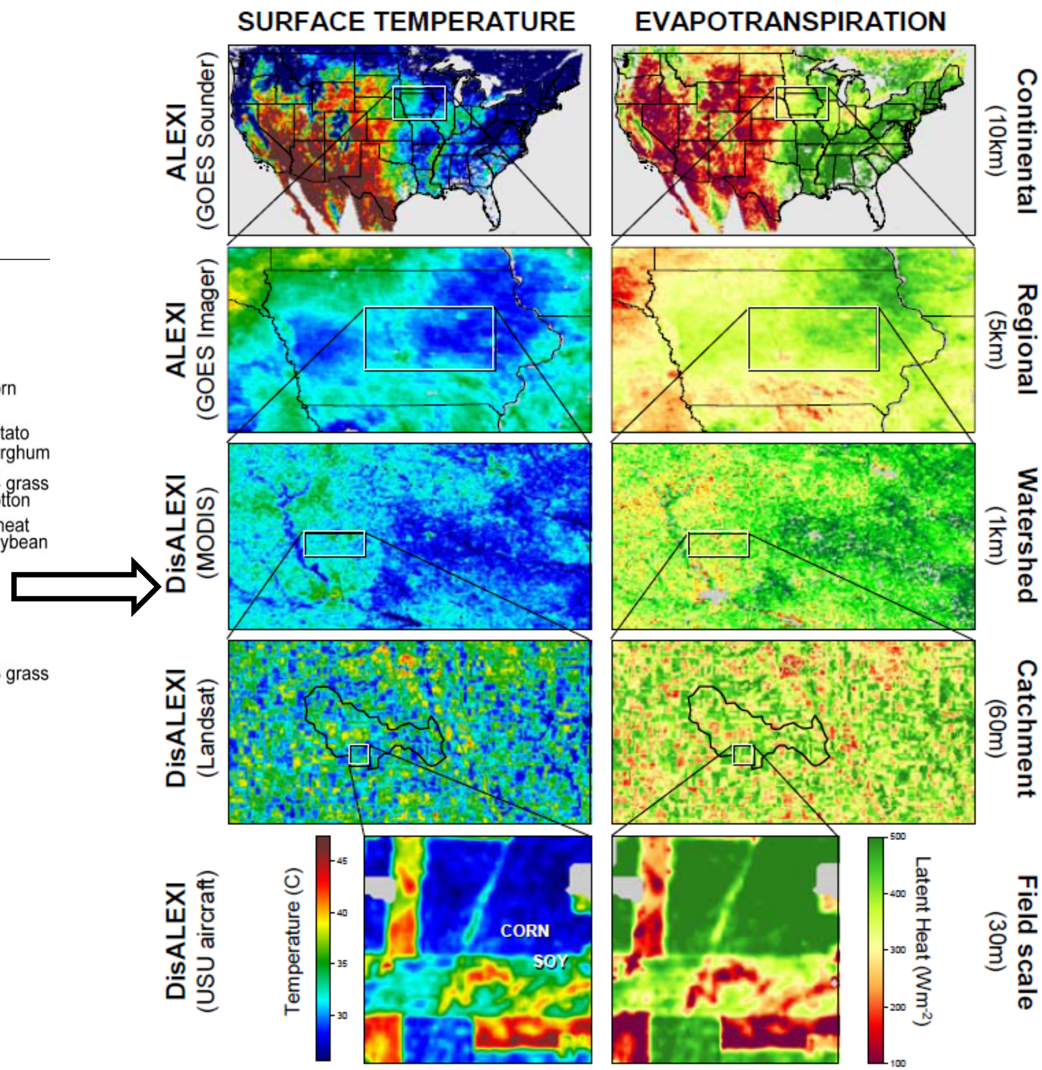

USDA Beltsville

Identifying Disruption of the Carbon, Water, and Nitrogen Cycles

Carbon budgets are sensitive to:

1. Land cover characteristics
2. Disturbance period & Successional stages
3. Species composition
4. Land use history/management
5. Variable weather & climate
6. Nutrient status, LAI

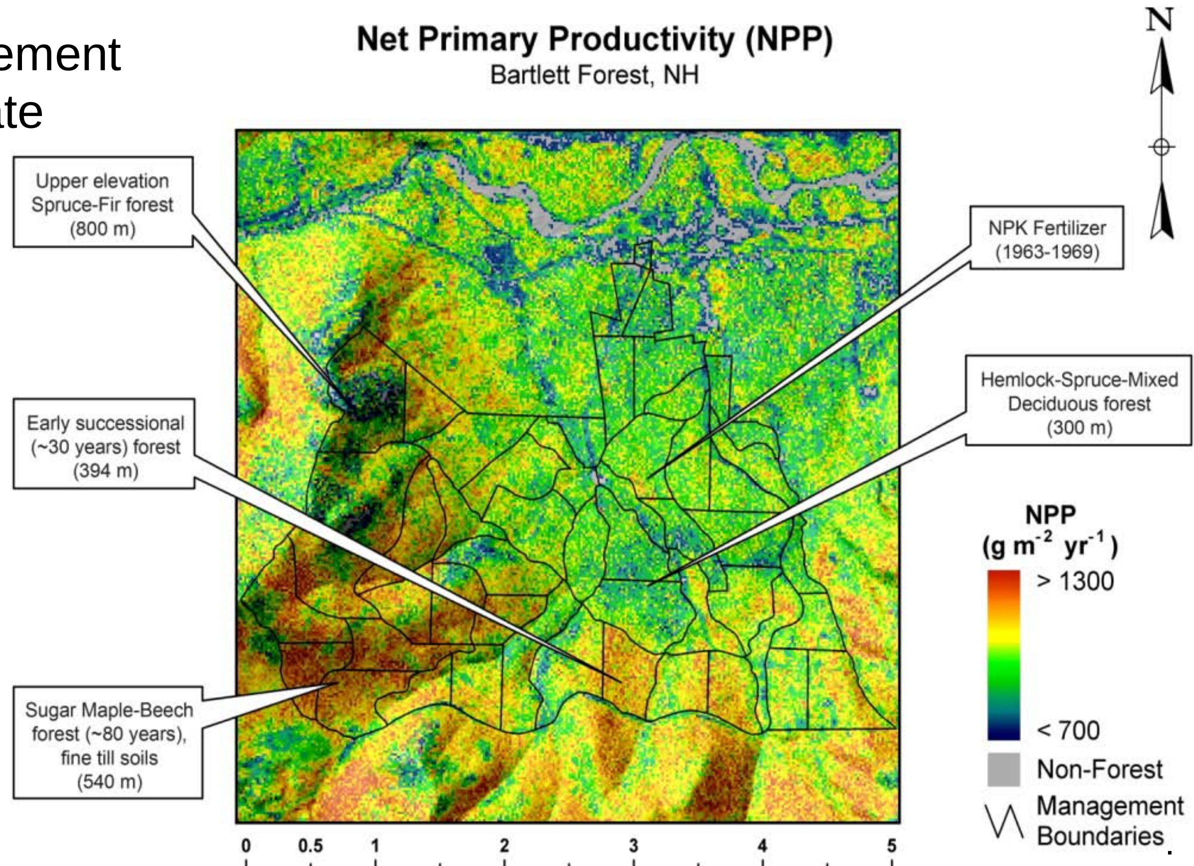

Figure from S.V. Ollinger and M.L. Smith, (2005)

What HyspIRI products can be produced routinely at the global scale?
Relevant for Climate Research? Identified as Climate Relevant?

- Plant Functional Types
- Spectral Endmember Composition & Changes in Endmembers over time
- All commonly used spectral indexes (>50 for plants, soil, snow, etc.)
- Types of disturbance, frequency & land use change
- Quantify snow/water partitioning & extent

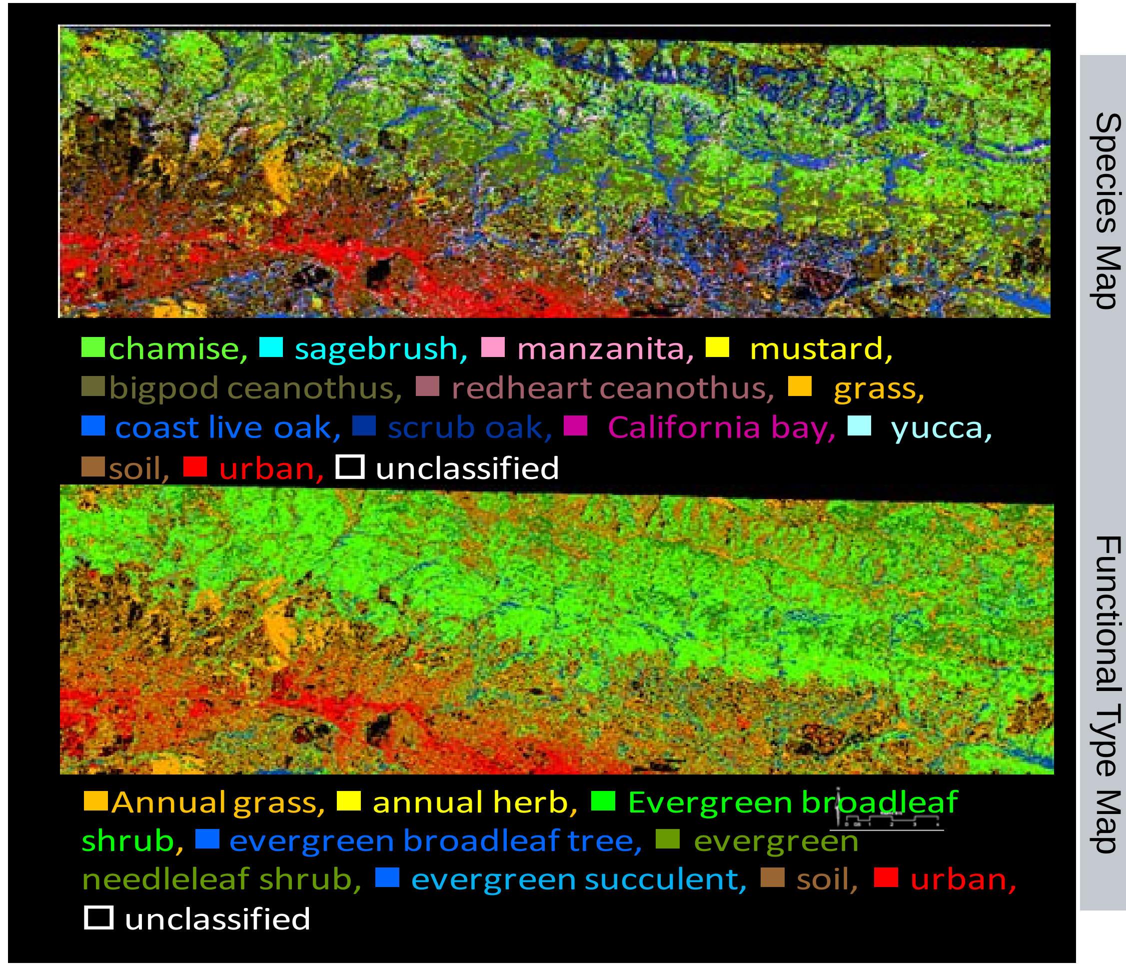

Santa Barbara Front Range Species Distribution
(AVIRIS 07/06/2004; Dar Roberts)

Vegetation Mapping at local scales is well established.
Can HyspIRI improve global vegetation maps?
Can we demonstrate or develop a path to do this?

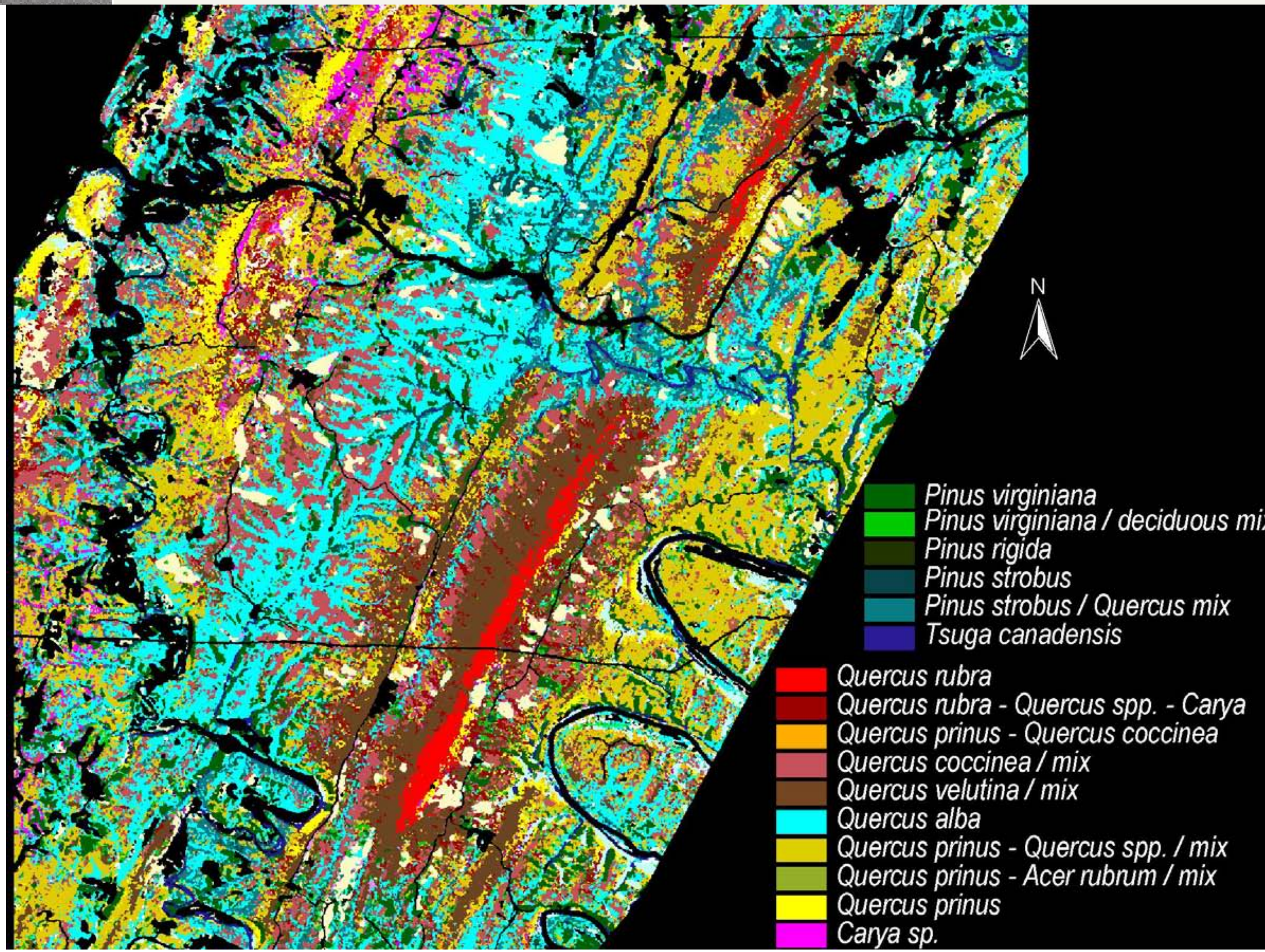

Changing Land Cover Causes Major Uncertainty in Carbon Budgets: HyspIRI can Monitor and Quantify Land Use Change and Changing Disturbance Regimes

Increased Wildfire Frequency and Extent will lead to net increased CO_2 emissions

Sub-Pixel Fire Fraction

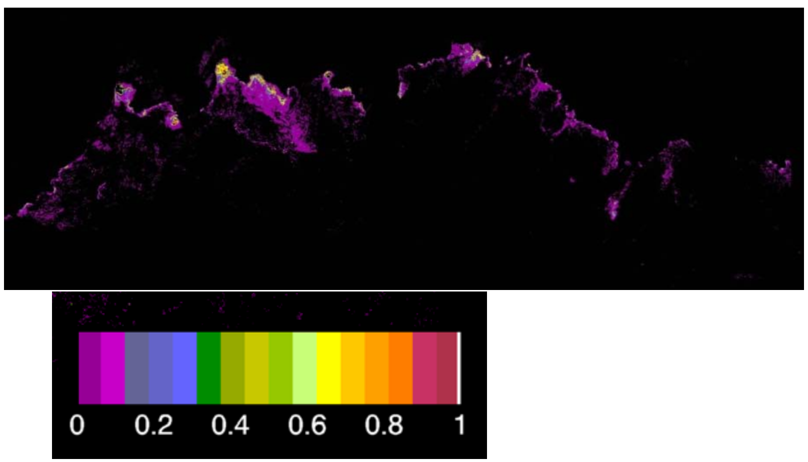

Sub-Pixel Fire Temperature

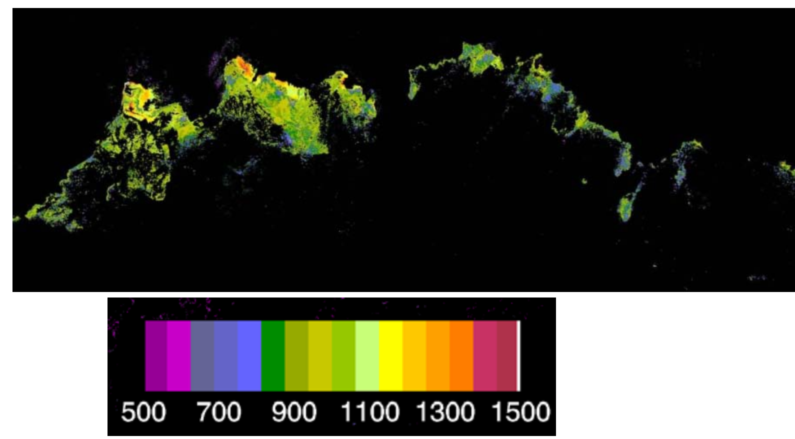

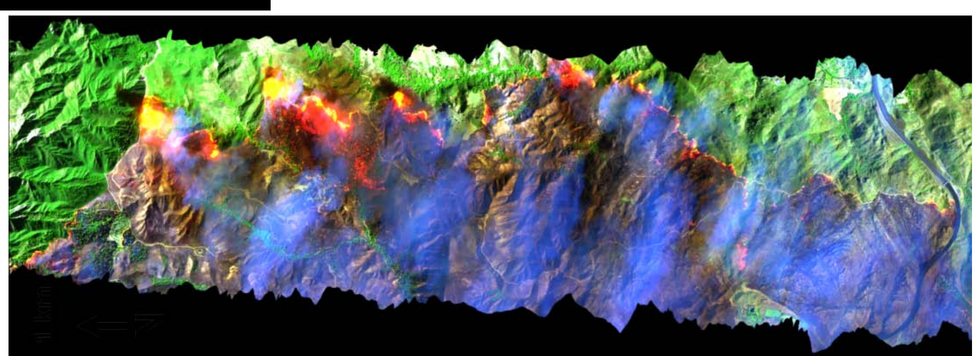

AVIRIS 2003
Dennison et al. 2006

Radiative and Hydrologic Forcing in Snow

Can we develop robust estimates of dust concentration on snow?

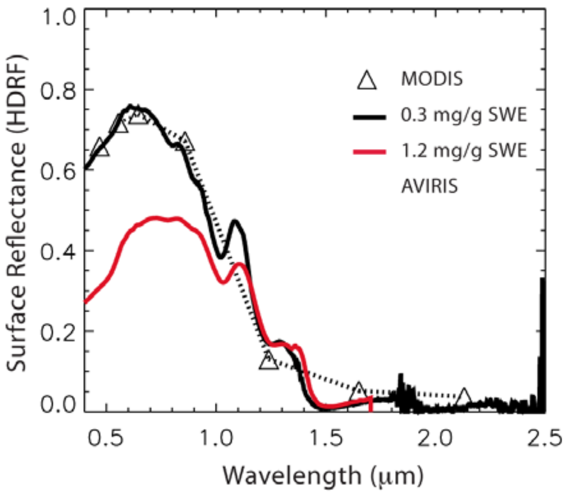

True Color Composite

Dust Radiative Forcing

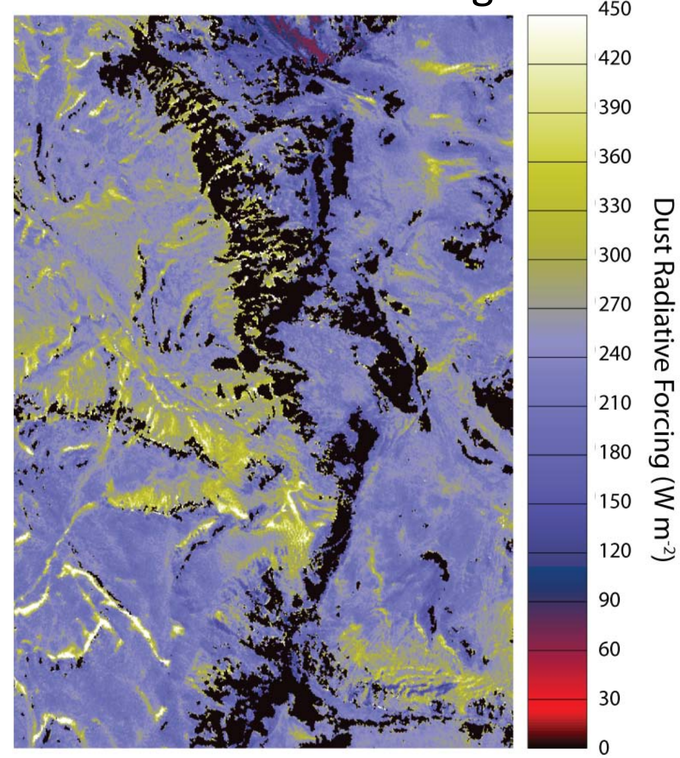

AVIRIS, Senator Beck Basin, CO May 19, 2004 – AVI-DRFS model *Painter et al 2010*

Societal Applications: Monitoring Global Environmental Disasters and Conditions

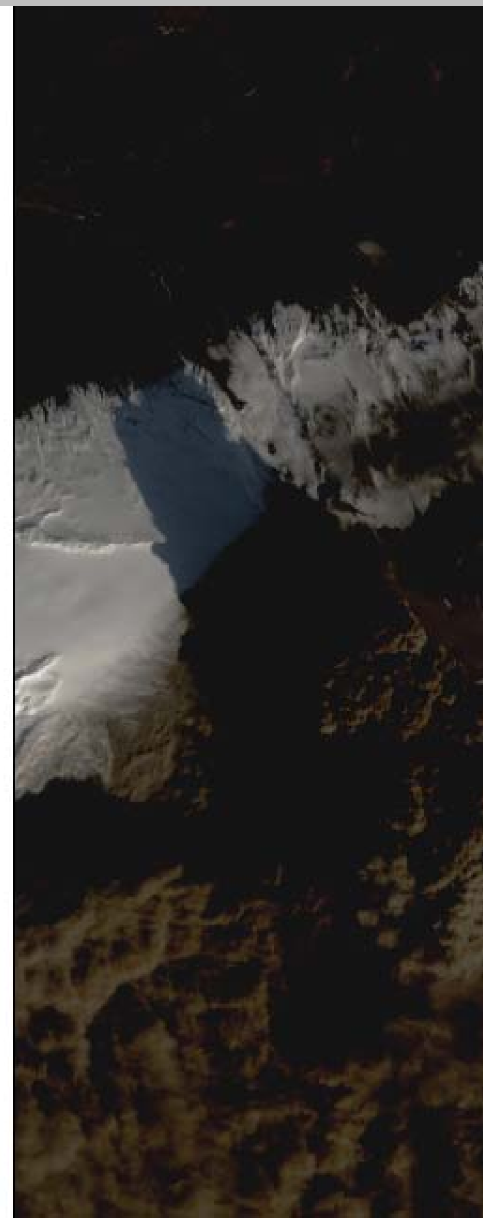

Imaging of Eyjafjallajökull Volcano Eruption 17 April 2010

VIS -plumes coating everything to the South-East making the ice brown/gray

TIR imager will make daily passes at latitude of Iceland

Responding to Environmental Disasters: Deepwater Oil Spill

AVIRIS Oil Flight 100506r17

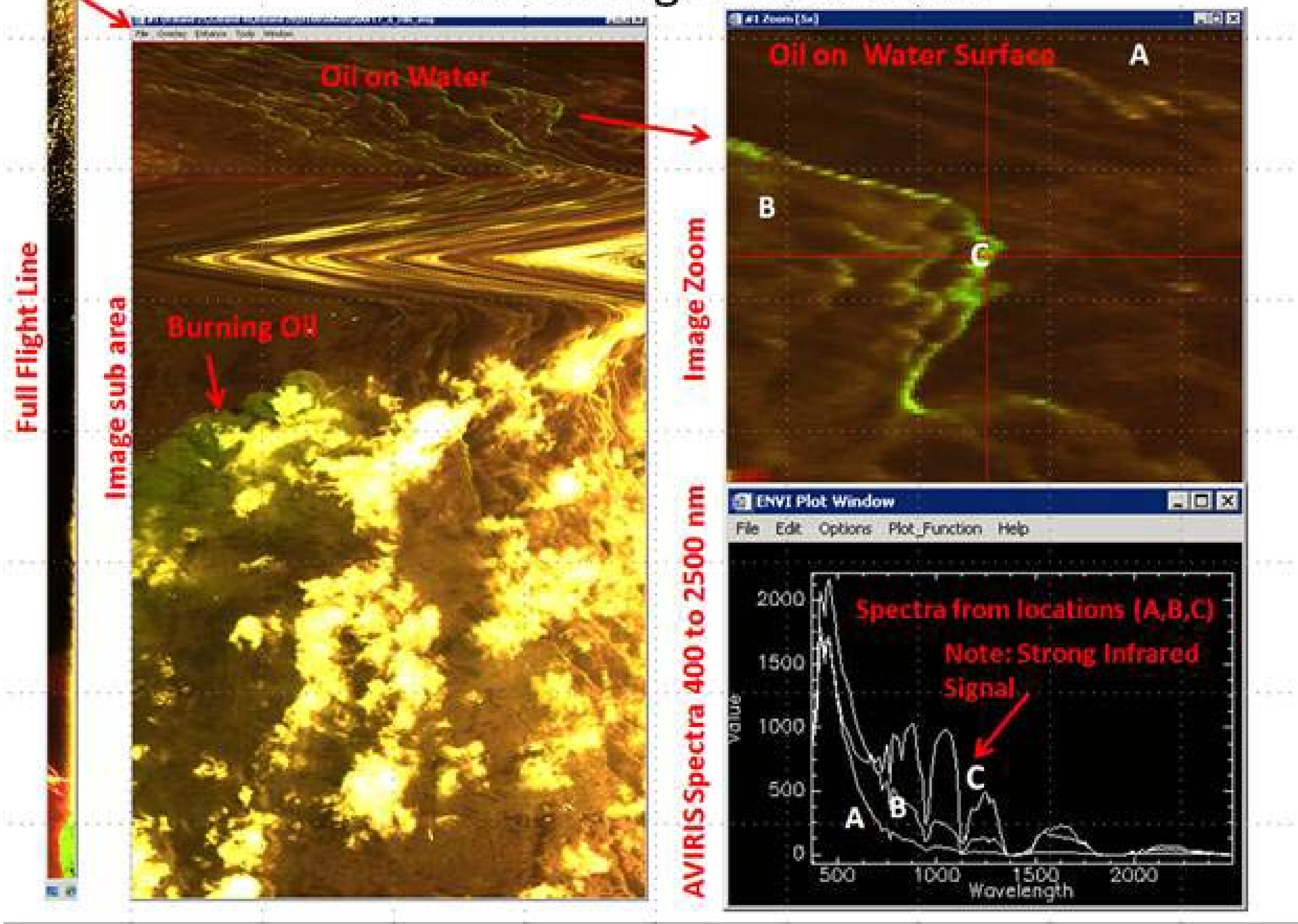

Decadal Survey: HyspIRI Recommendation, by Ecosystem, Climate and Land Use Change Panels

"A hyperspectral sensor combined with a multispectral thermal sensor in low Earth orbit **is part of an integrated mission concept** that is relevant to several panels, ***especially the climate variability panel***." p. 368.

HyspIRI Concept

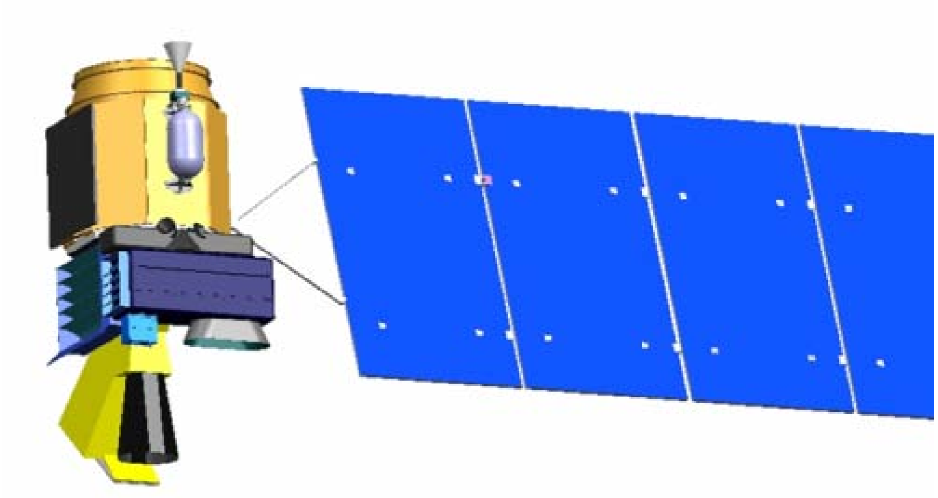

Visible ShortWave InfraRed (VSWIR) Imaging Spectrometer
+
Multispectral Thermal InfraRed (TIR) Scanner

Spectral Bands Identified As Useful by Discipline

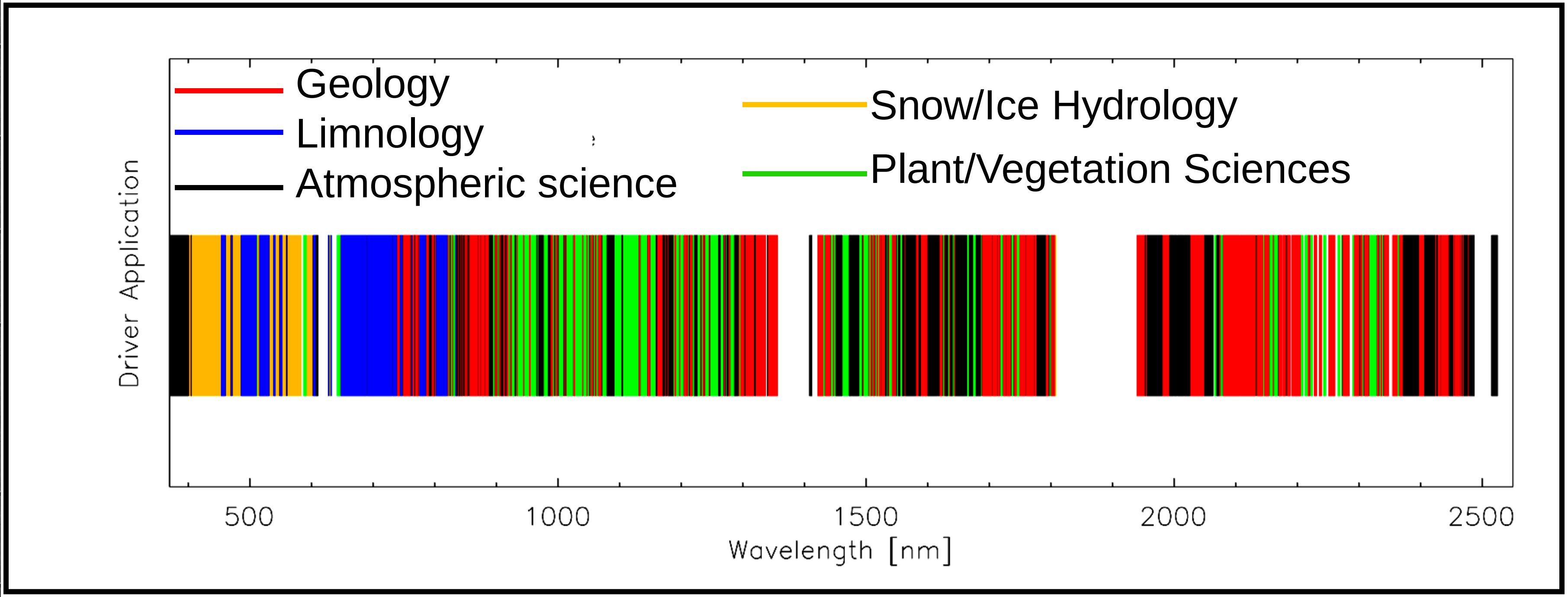

All Bands Seem Relevant to Some Discipline:
Can we prioritize development of global climate relevant products?

Schläpfer, D., & Schaepman, M.E. (2002). Modeling the noise equivalent radiance requirements of imaging spectrometers based on scientific applications. *Applied Optics, 41, 5691-5701*

FUGITIVE EMISSION FROM FOSSIL FUEL PRODUCTION WITH IMAGING SPECTROSCOPY MEASUREMENTS

Ira Leifer[1], Heinrich Bovensmann[2], Eliza Bradley[1], Michael Buchwitz[2], Daniel Culling[1], Philip Dennison, Konstantin Gerilowski[2], Bruce Luyendyk[1], Jack Margolis, Dar Roberts, Oliver Schneising[2], David Tratt

HyspIRI workshop Pasadena, CA, 24-26 Aug 2010

THANKS TO THE ENABLING SUPPORT

1 University of California, Santa Barbara
2 Jet Propulsion Laboratory
3 NASA HQ
4 US Geologic Survey
5 University of Utah
6 NOAA
8 University of California, Davis

And critical enabling support from

Methane – Stable until 1700s

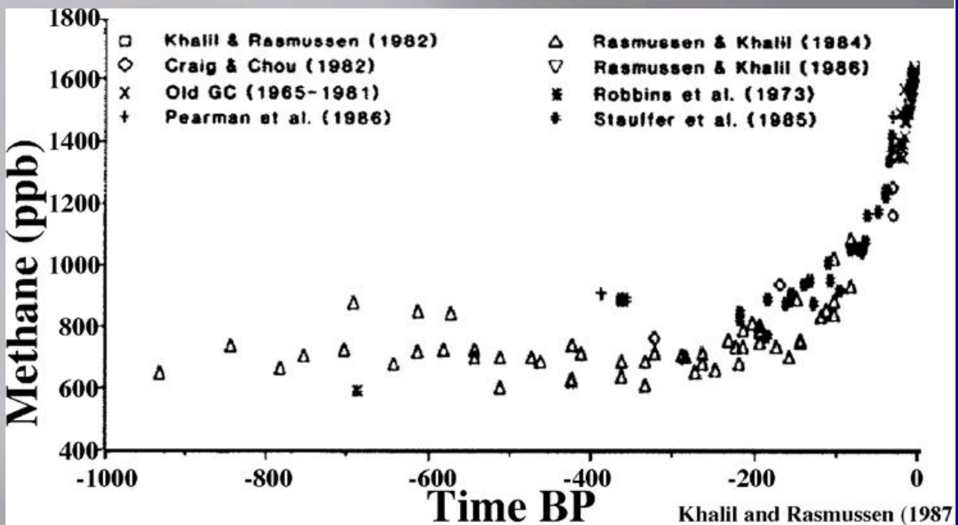

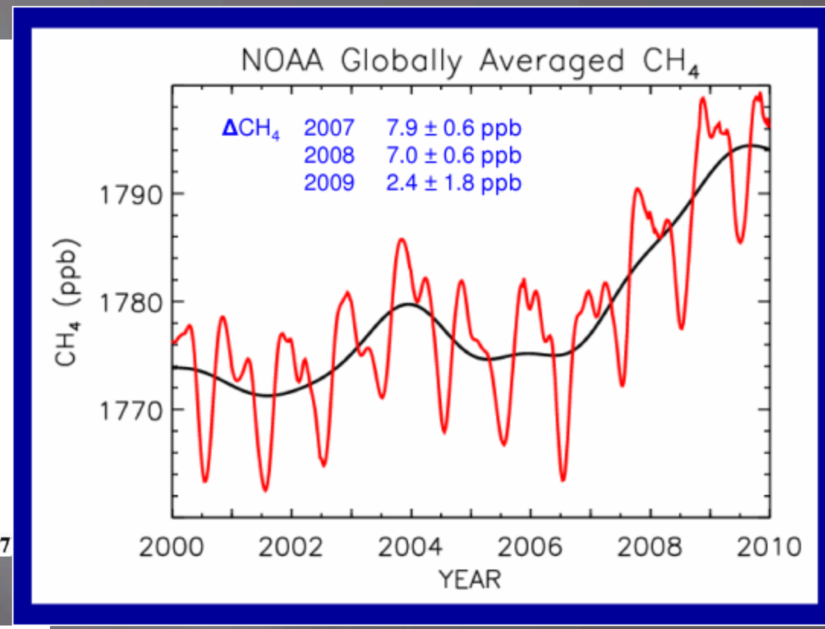

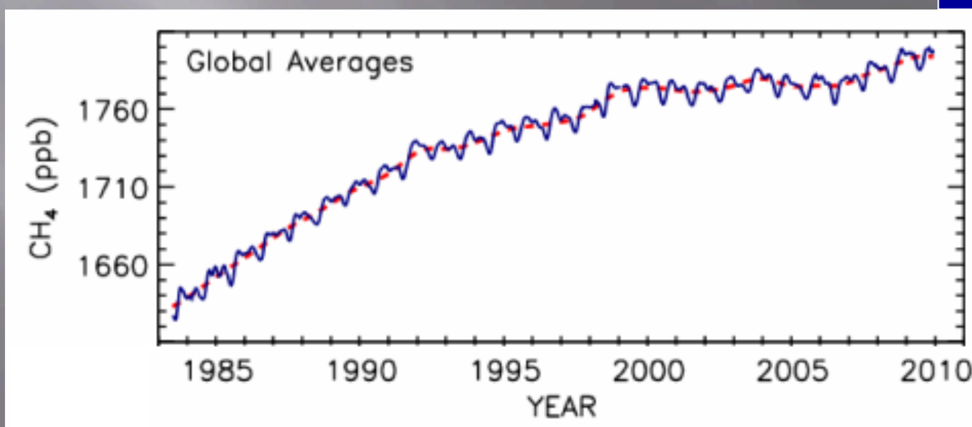

Dlugokencky et al. A Long-term Perspective on Recent Increases in Atmospheric CH4 Abundance, Global Monitoring annual Conference, 18-19 May 2020, Boulder CO.

Why methane? 20 yr time scale

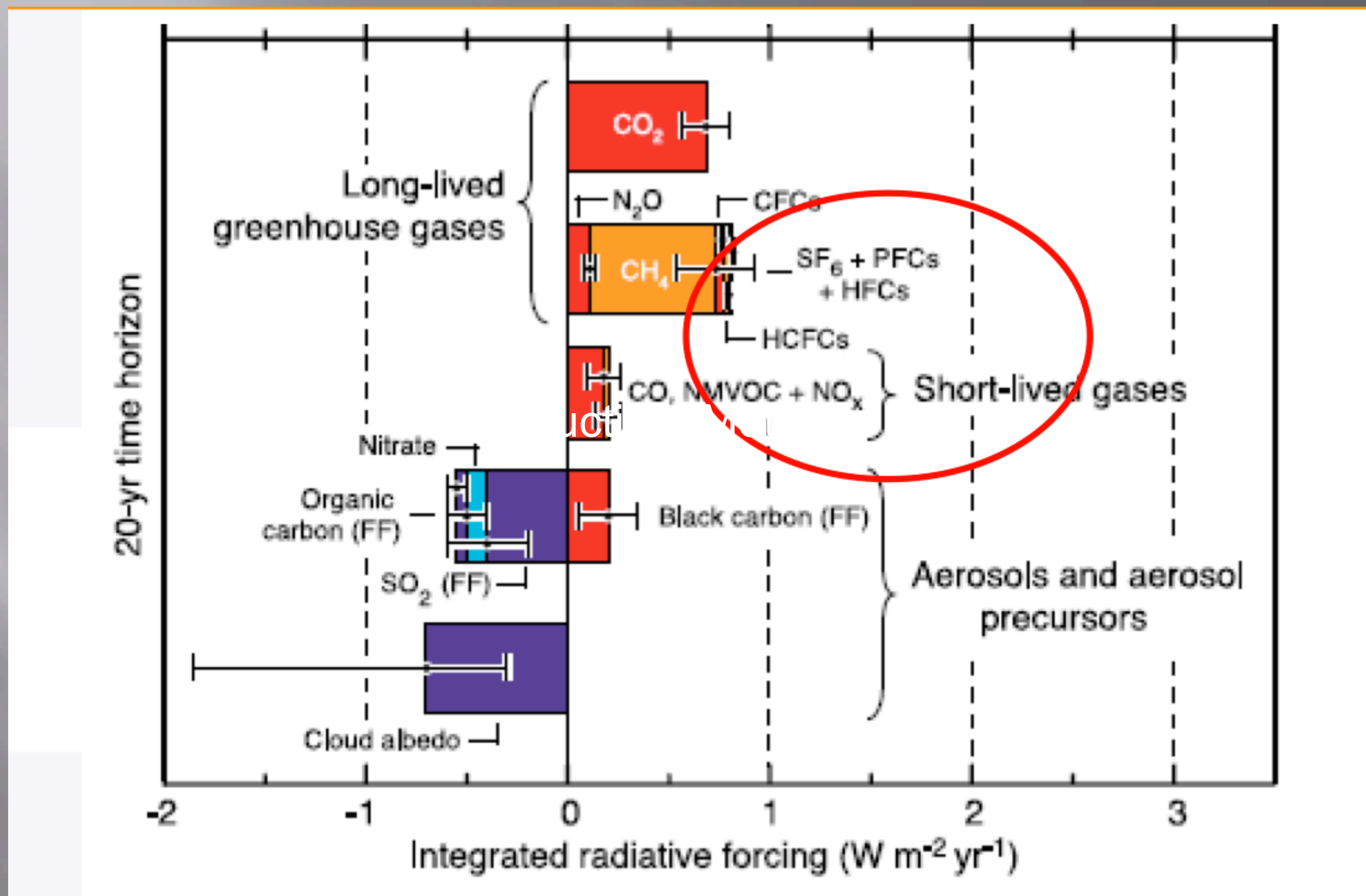

Methane is a greenhouse gas with **72 times the Global Warming Potential of carbon dioxide on a 20-year time horizon. (IPCC4, Ch2, Fig.2.22, 2007)**

Why methane? 100 yr time scale

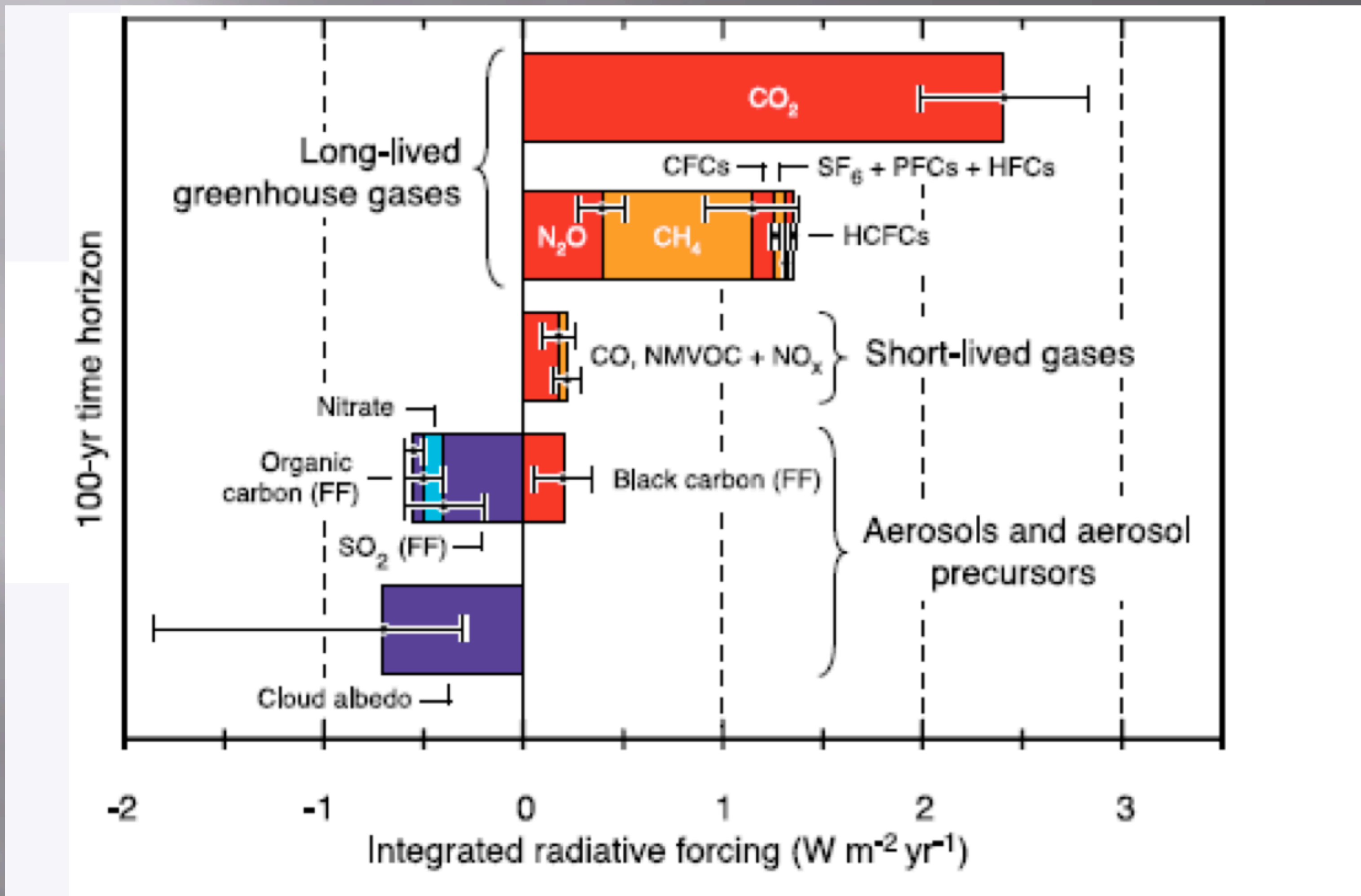

Methane is a greenhouse gas with **26 times the Global Warming Potential of carbon dioxide on a 100-year time horizon. (IPCC4, Ch2, Fig.2.21, 2007)**

Methane – Human Sources

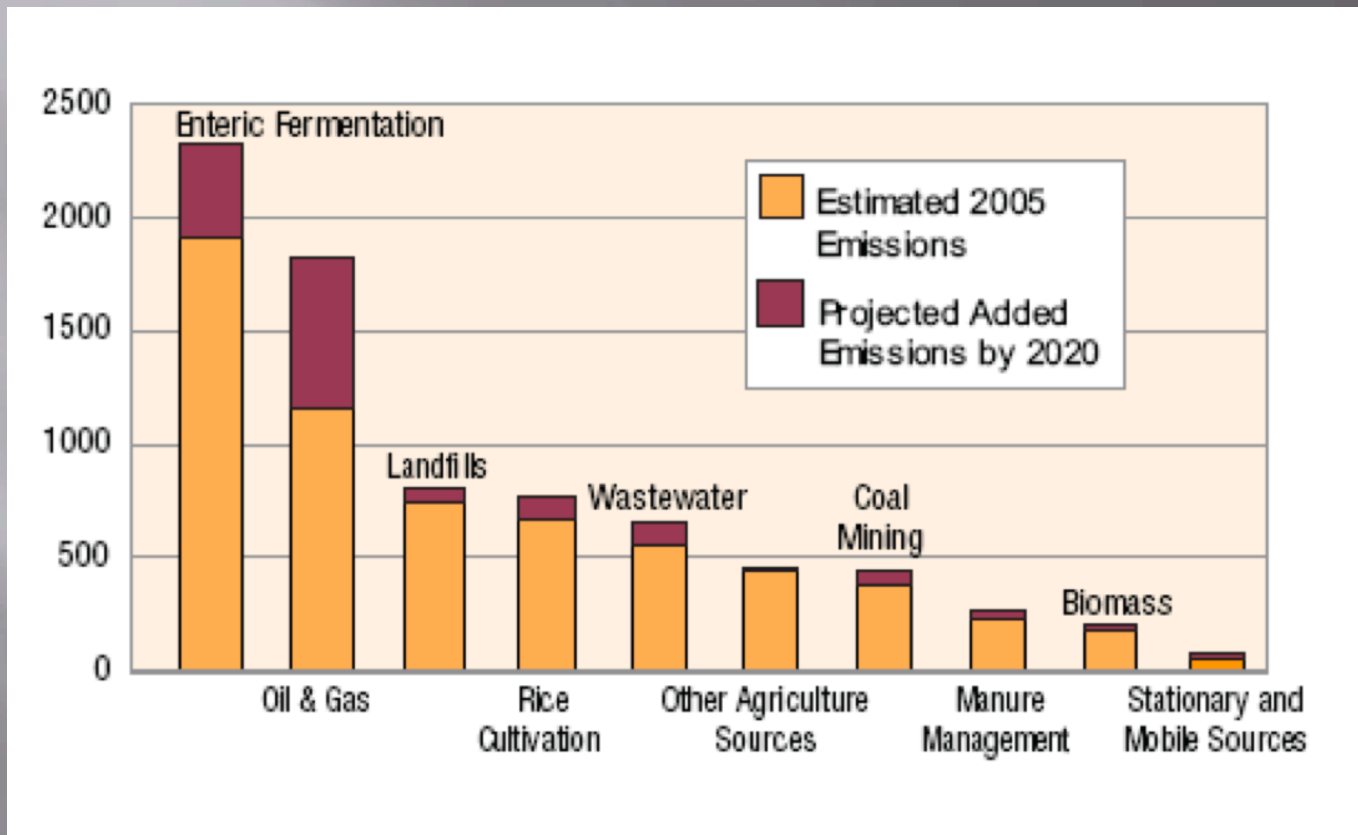

http://www.asiapacificpartnership.org/pdf/CFE/meeting_seoul/workshop_presentations/09_M2M-APP_CFETF.pdf

Figure 1 a) Showing absorption coefficients for methane (blue) and carbon dioxide (red) calculated from
HITRAN 2004 (Rothman et al., 2005)
Figure 1 b) Transmission spectra of methane and carbon dioxide calculated using MODTRAN 4.3 (Berk et al., 1999) for one airmass and concentrations of 1.8 and 380 ppm for methane and carbon dioxide, respectively

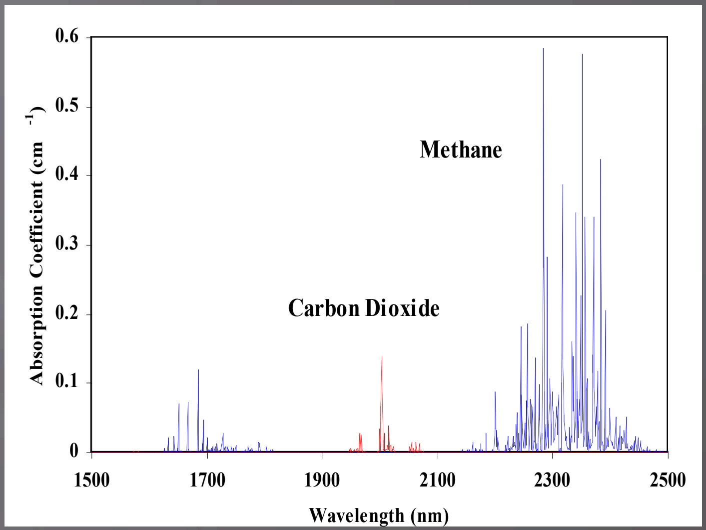

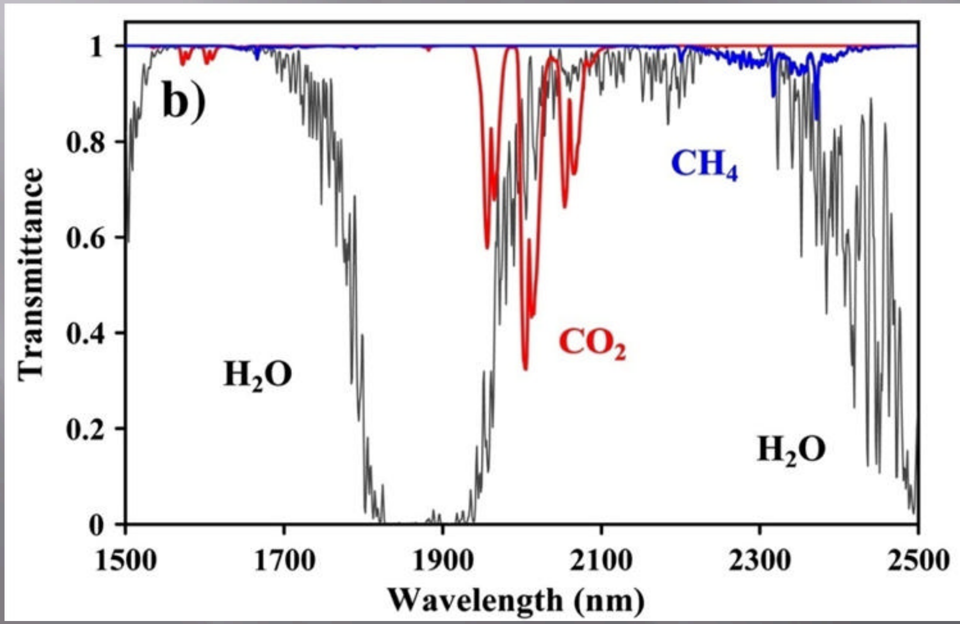

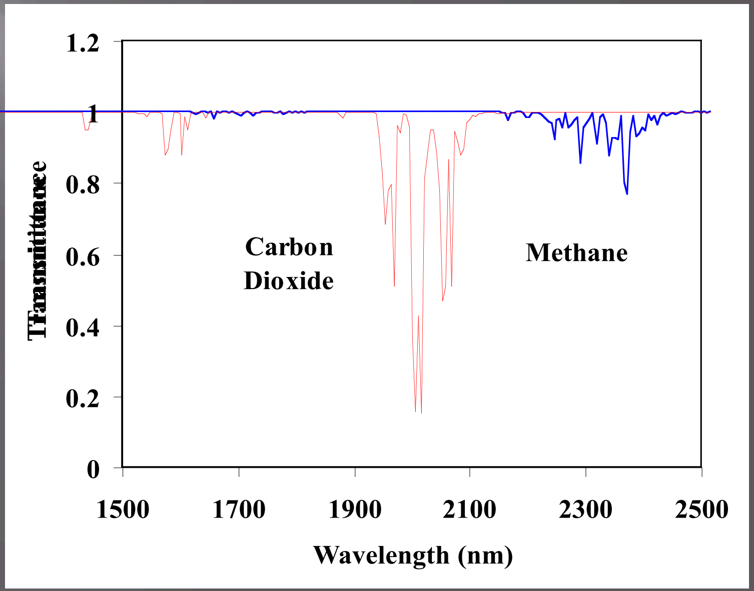

AVIRIS Modtran Simulations

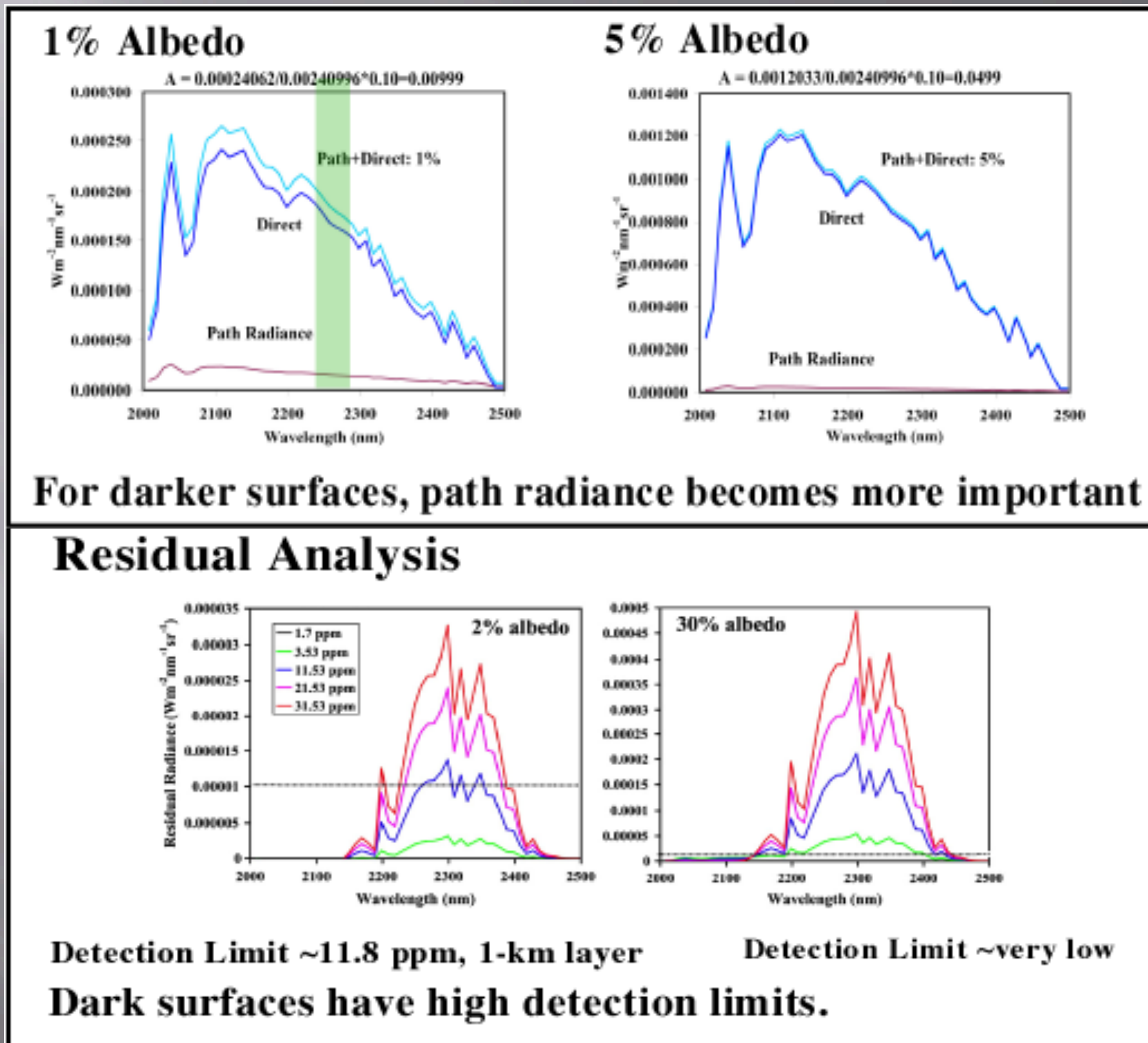

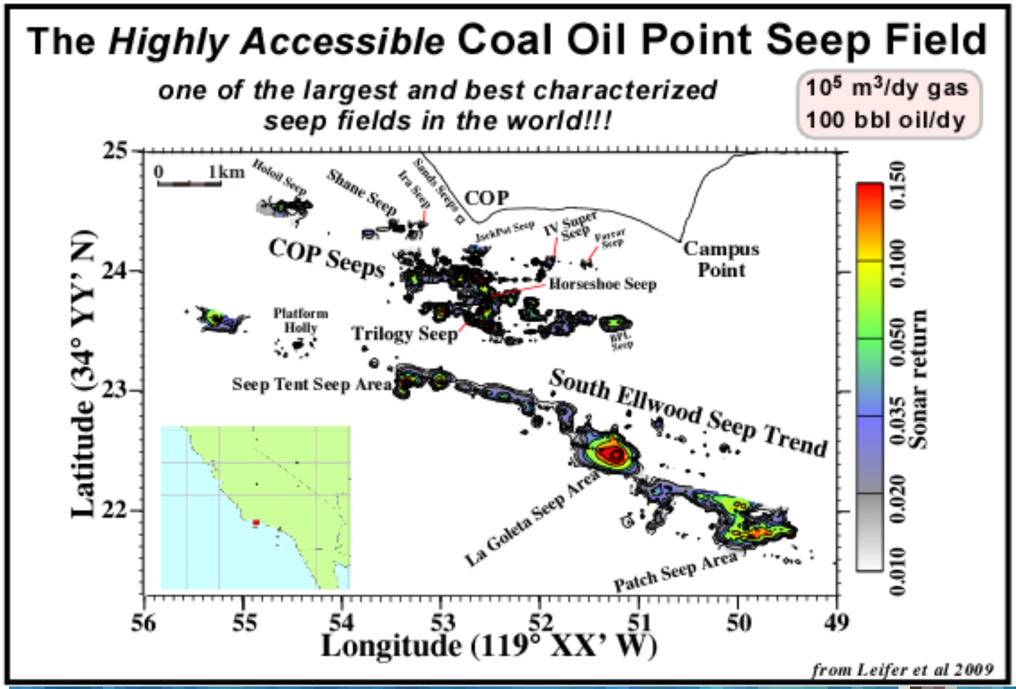

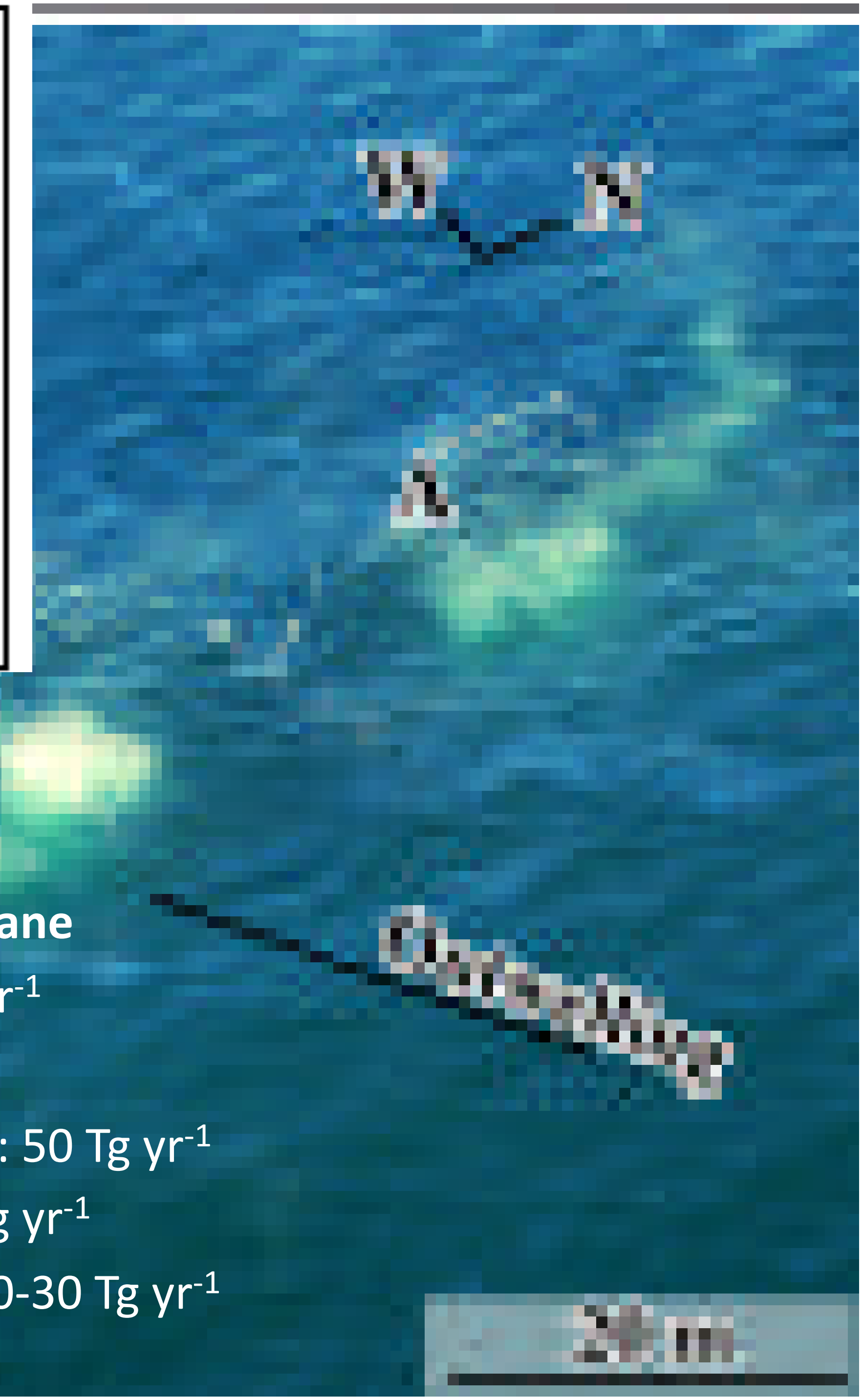

Methane

- Total: 580 ± 50 Tg yr^{-1}
- Ancient: 104 Tg yr^{-1}
- Fossil Fuel Industry: 50 Tg yr^{-1}
- Seepage: 50 – 85 Tg yr^{-1}
- Marine Seepage: 20-30 Tg yr^{-1}

Total Hydrocarbon Plume from Trilogy Seep

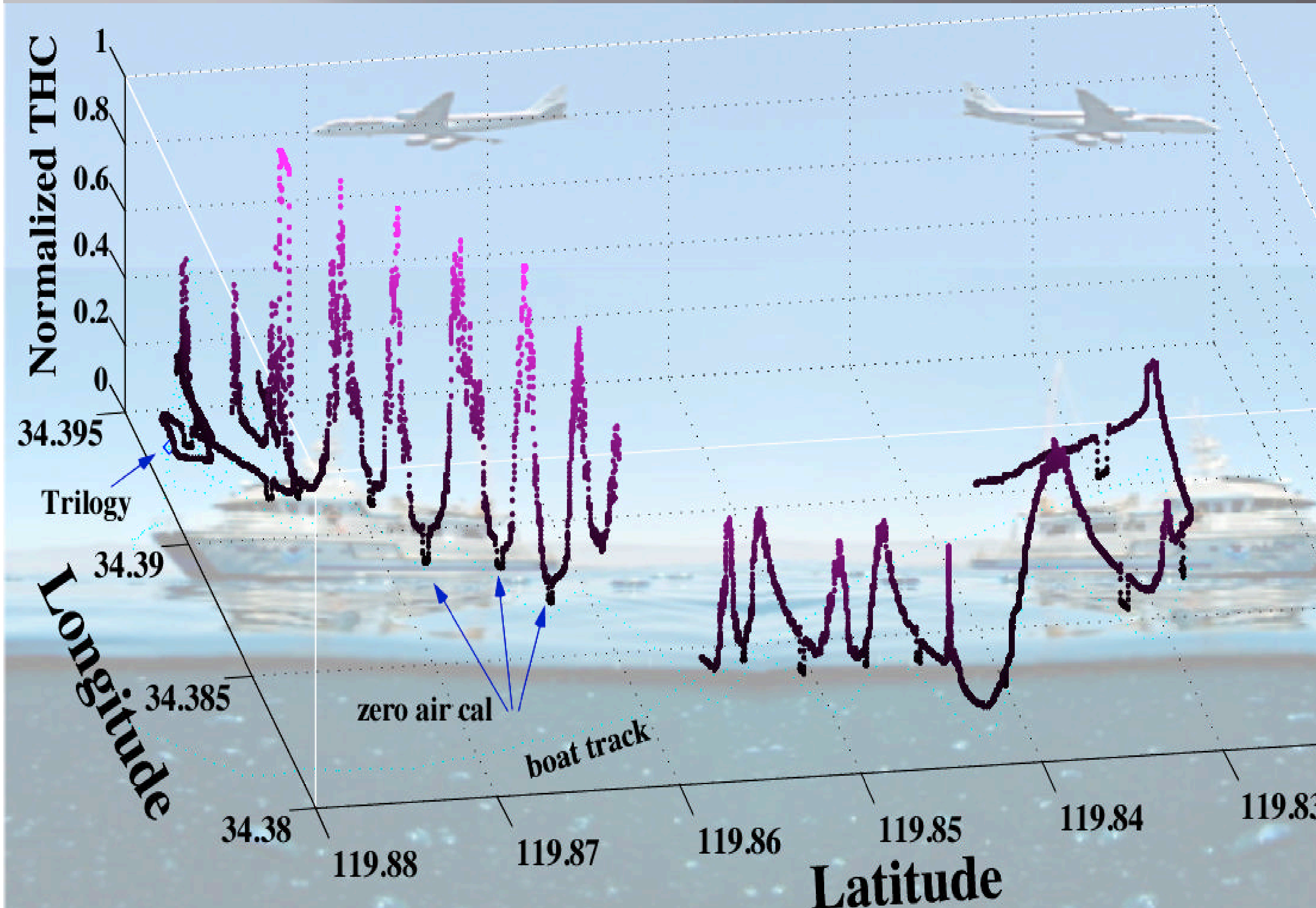

METHANE AVIRIS REMOTE SENSING

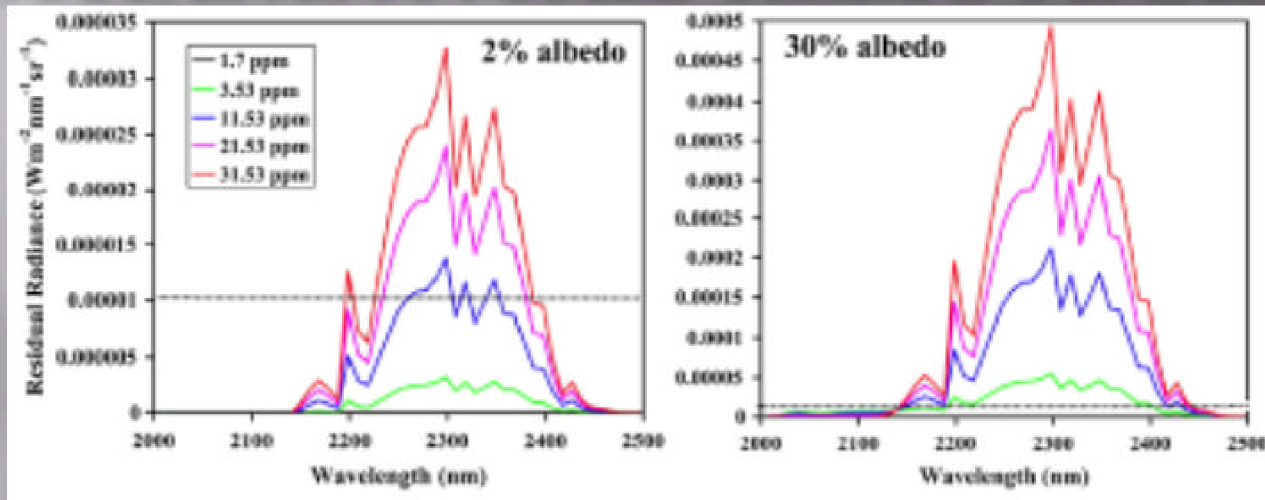

MODTRAN calculated residuals show AVIRIS can observe methane for typical Coal Oil Point seep field emissions and sea surface albedos.

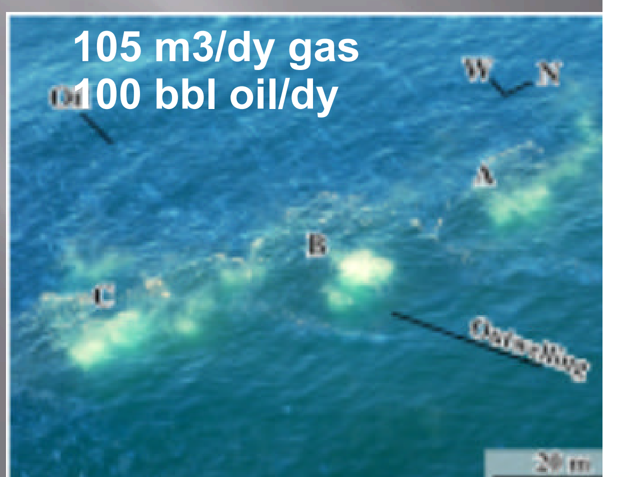

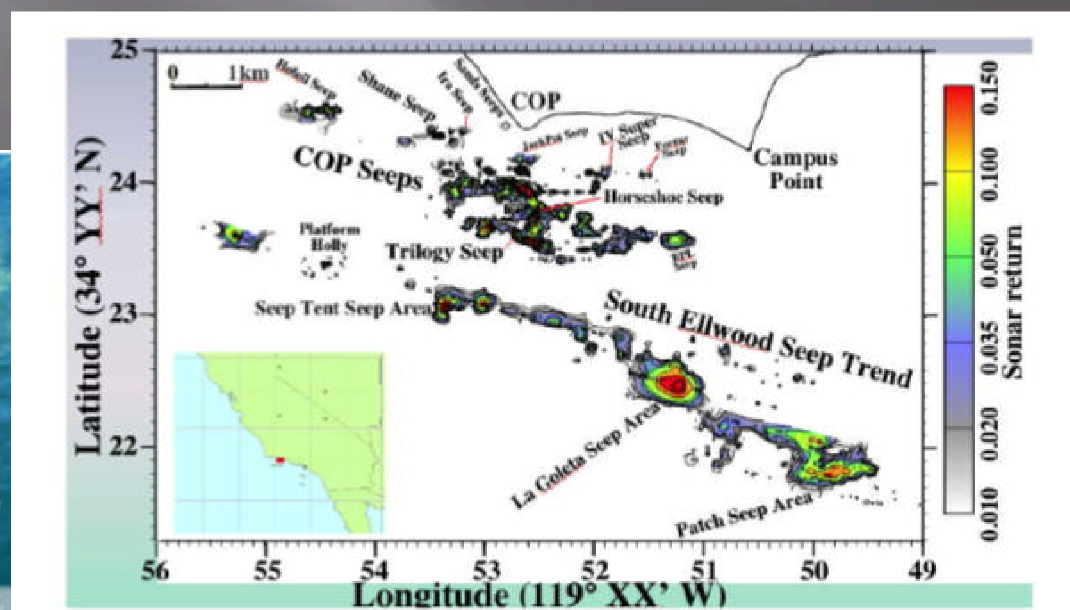

All strong methane signatures located downwind of known seep locations

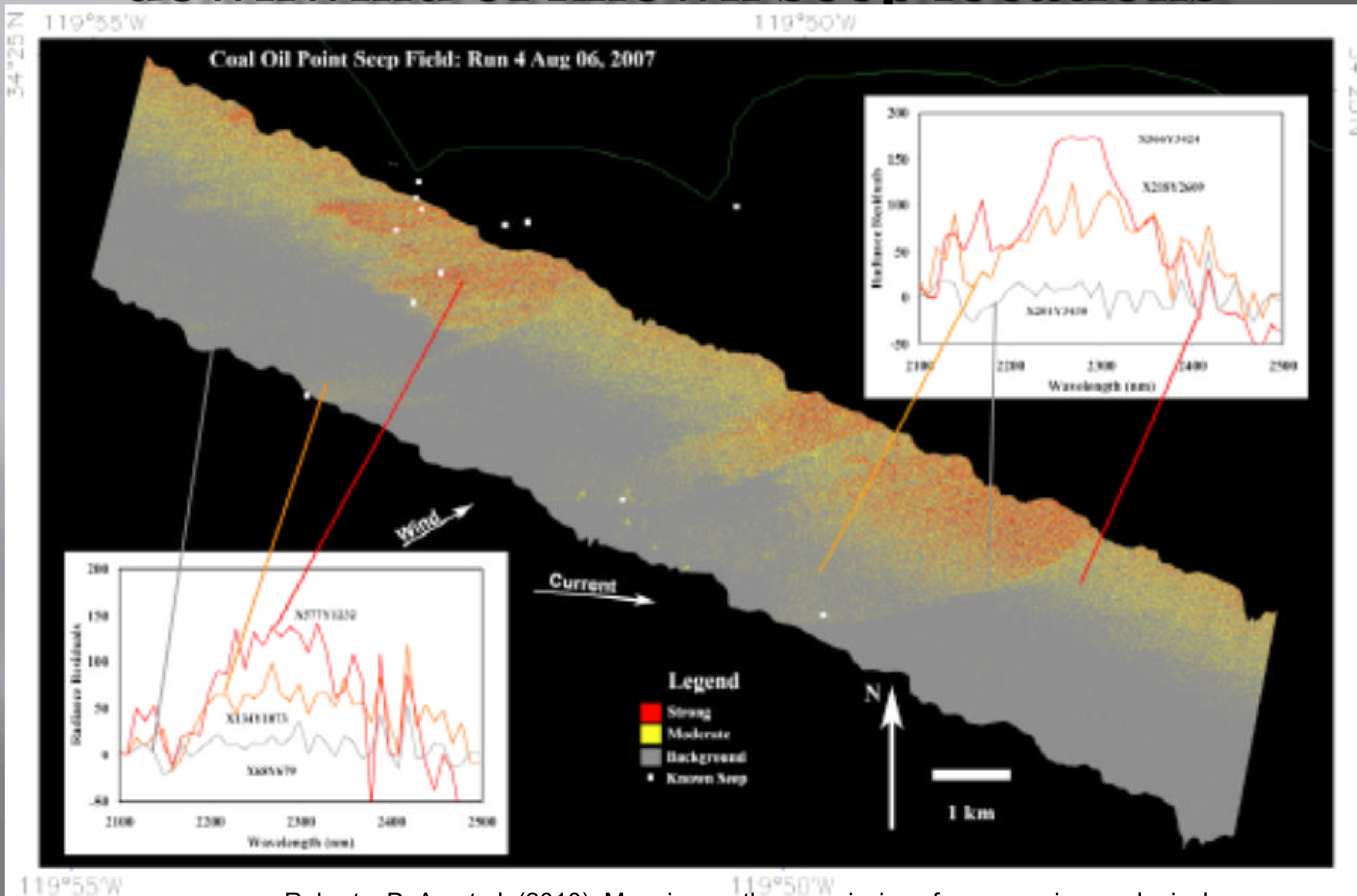

Roberts, D. A., et al. (2010), Mapping methane emissions from a marine geological seep source using imaging spectrometry, *Remote Sensing Environments*, *114*(3), 592-606

*

AVIRIS methane residual approach
(Roberts et al. 2010)

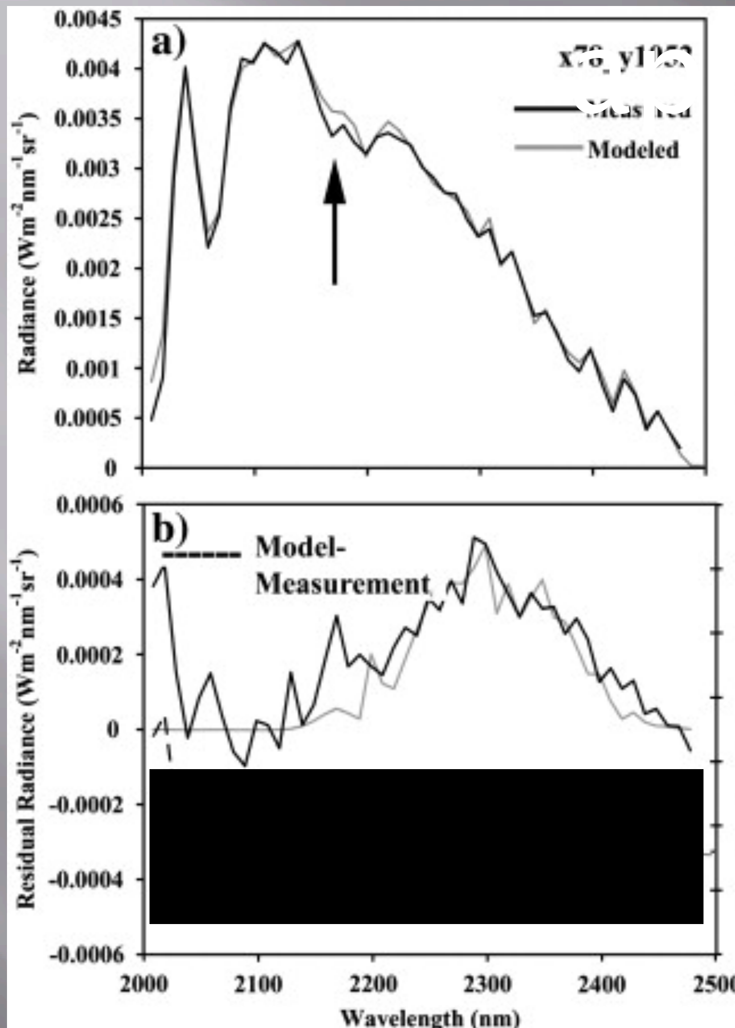

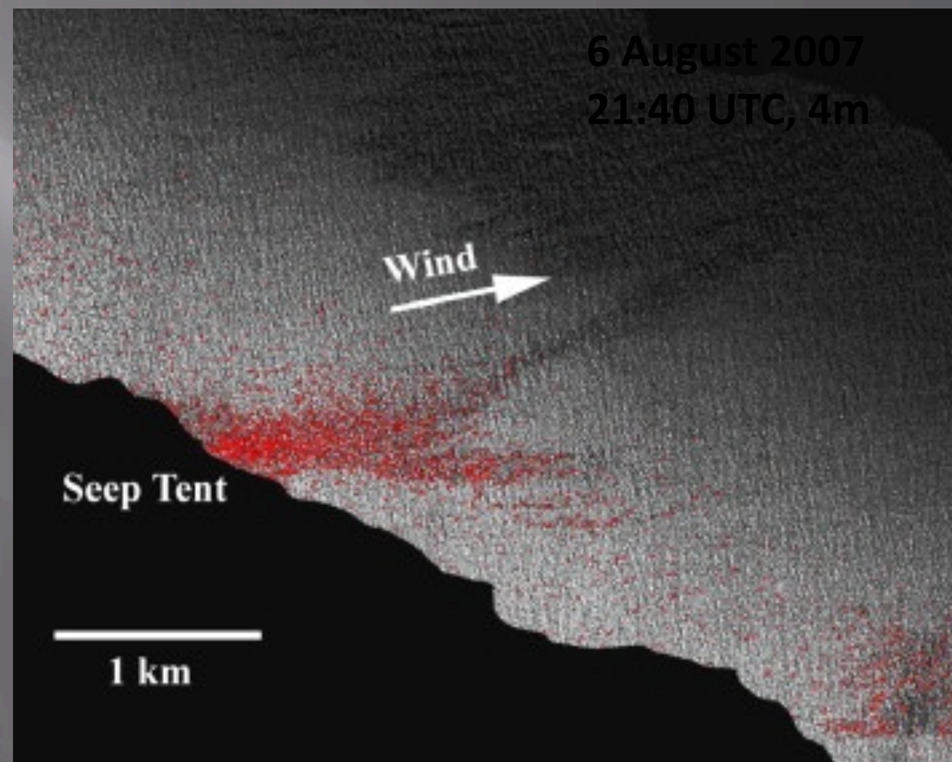

-Imagery complications (clouds, surface patterns, etc.)
-Assumes fixed path length

Equinox (June 19), solar noon, ER2

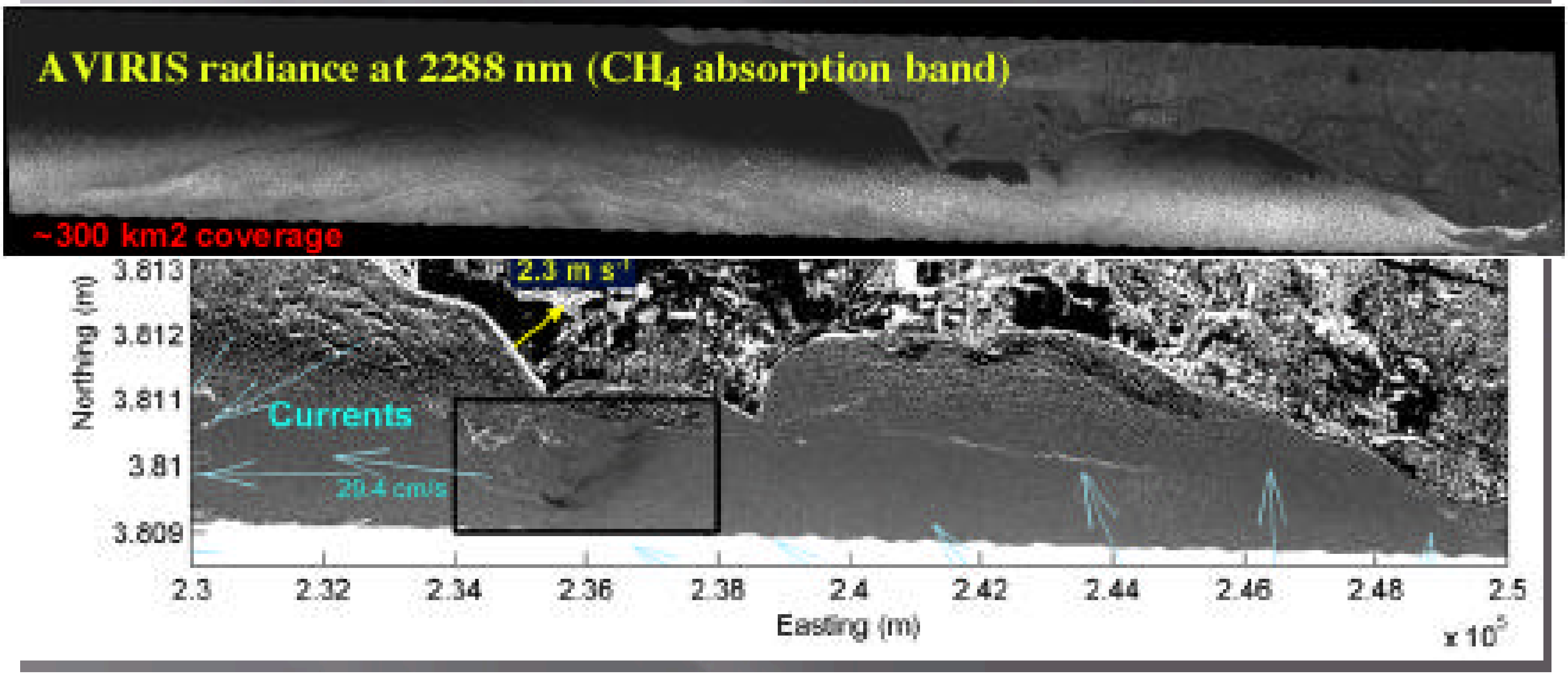

BAND RATIO ANALYSIS OF METHANE PLUMES

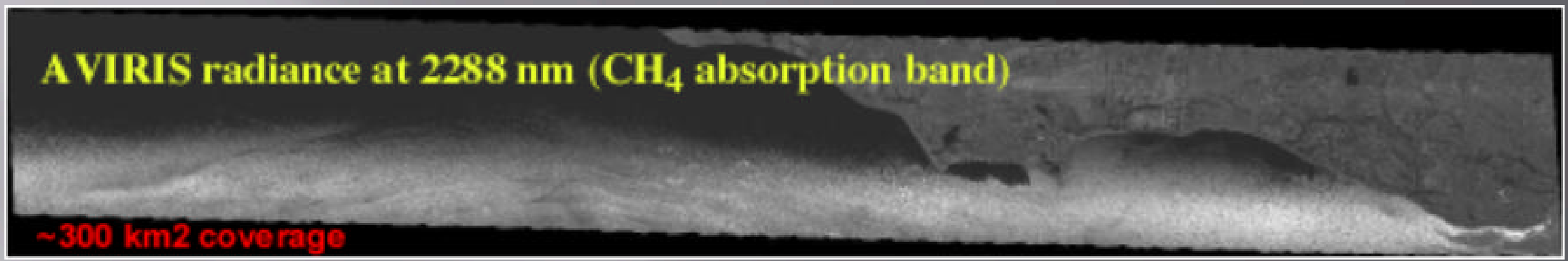

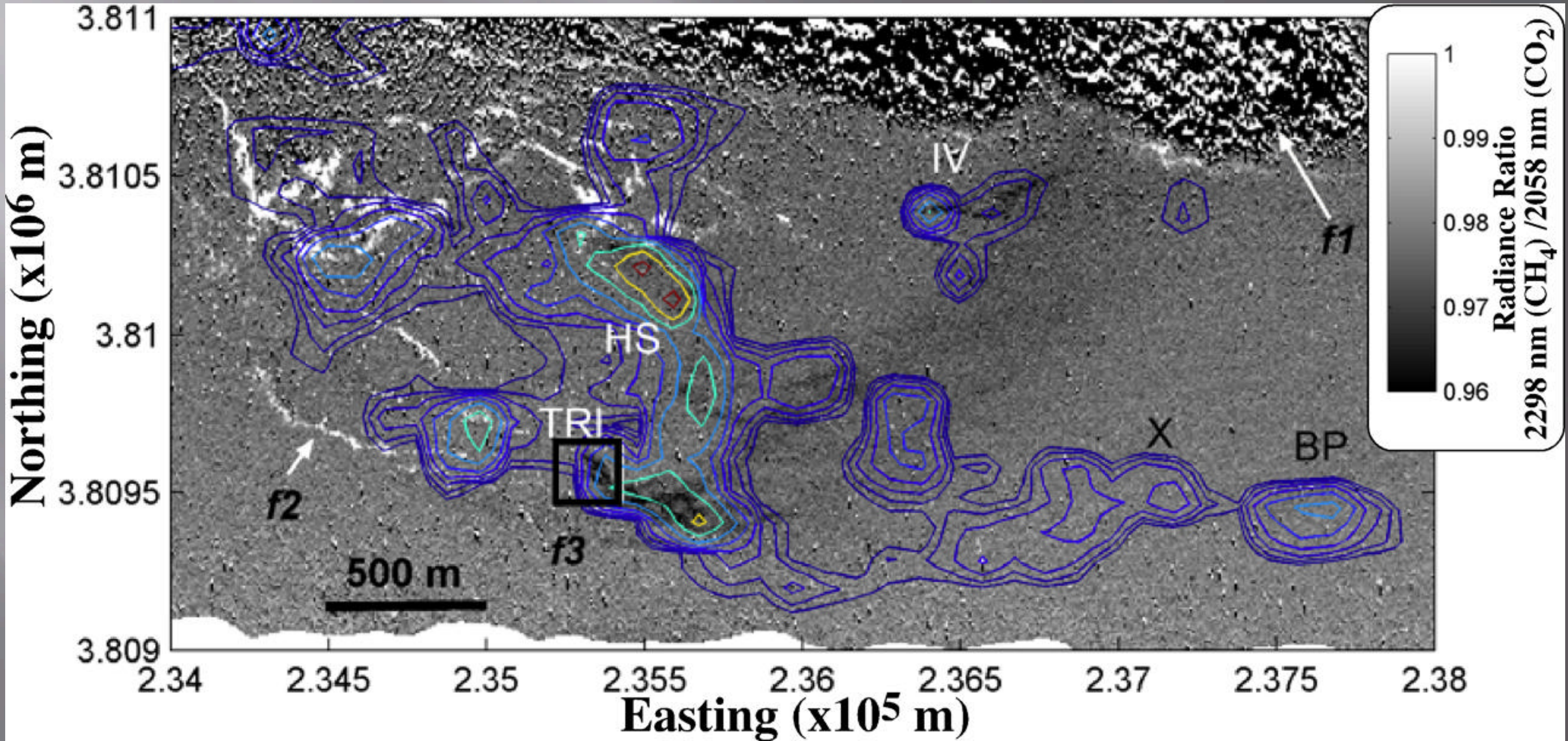

Bradley, E.B.., et al. (2010) *in progress*

Band ratio plume

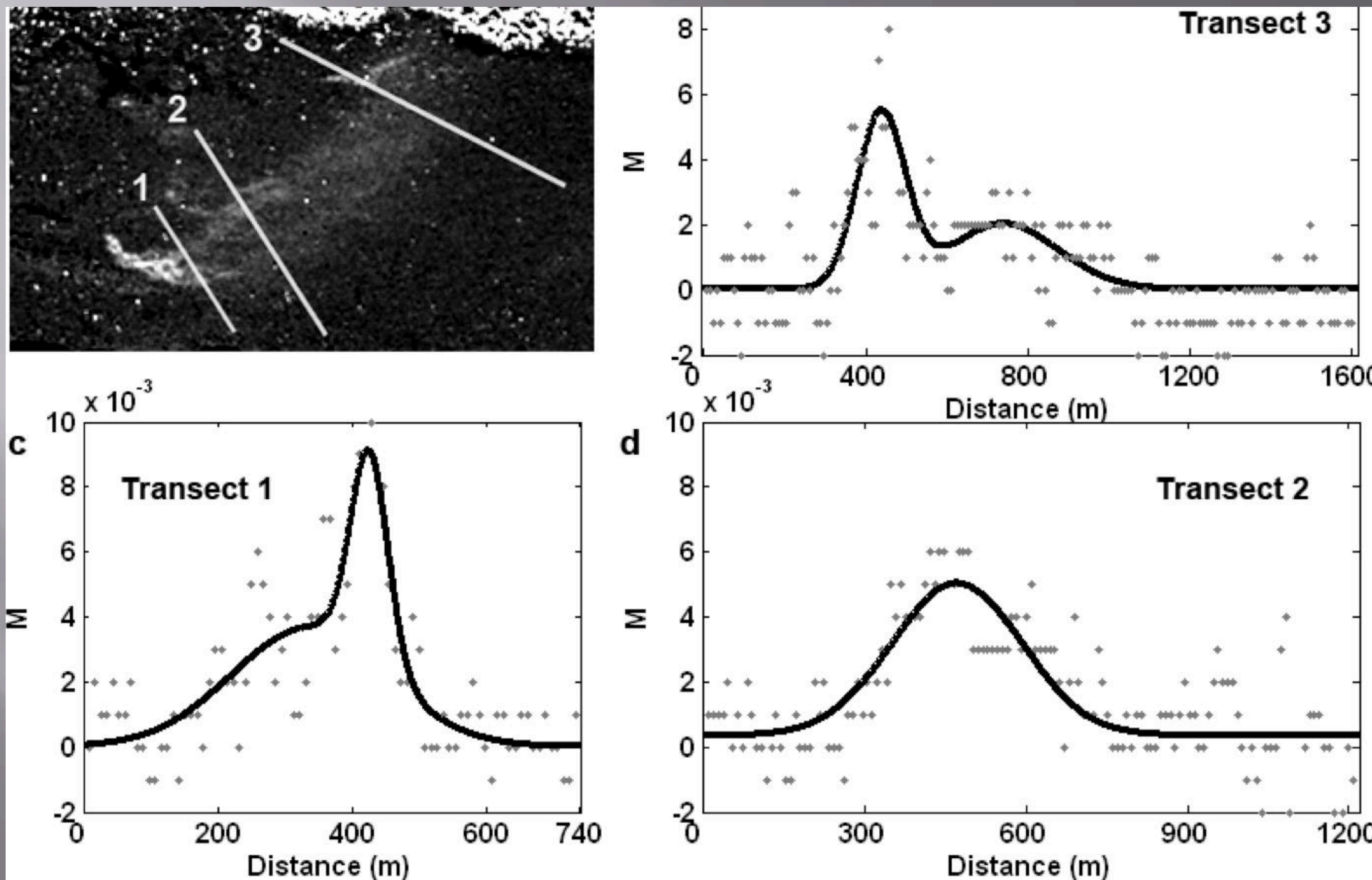

Bradley, E.B.., et al. (2010) *in progress*

Platform Habitat; 4/7/2010

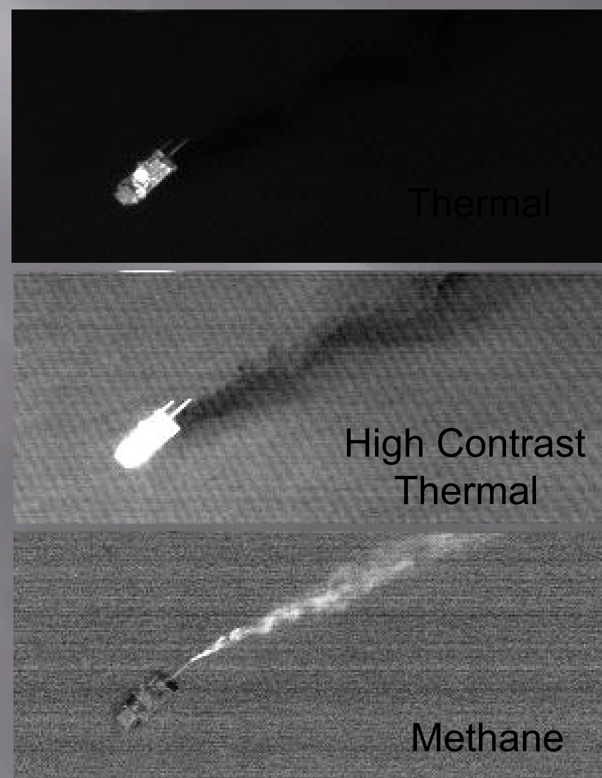

Cold water outflow
from platform

Prudhoe Bay

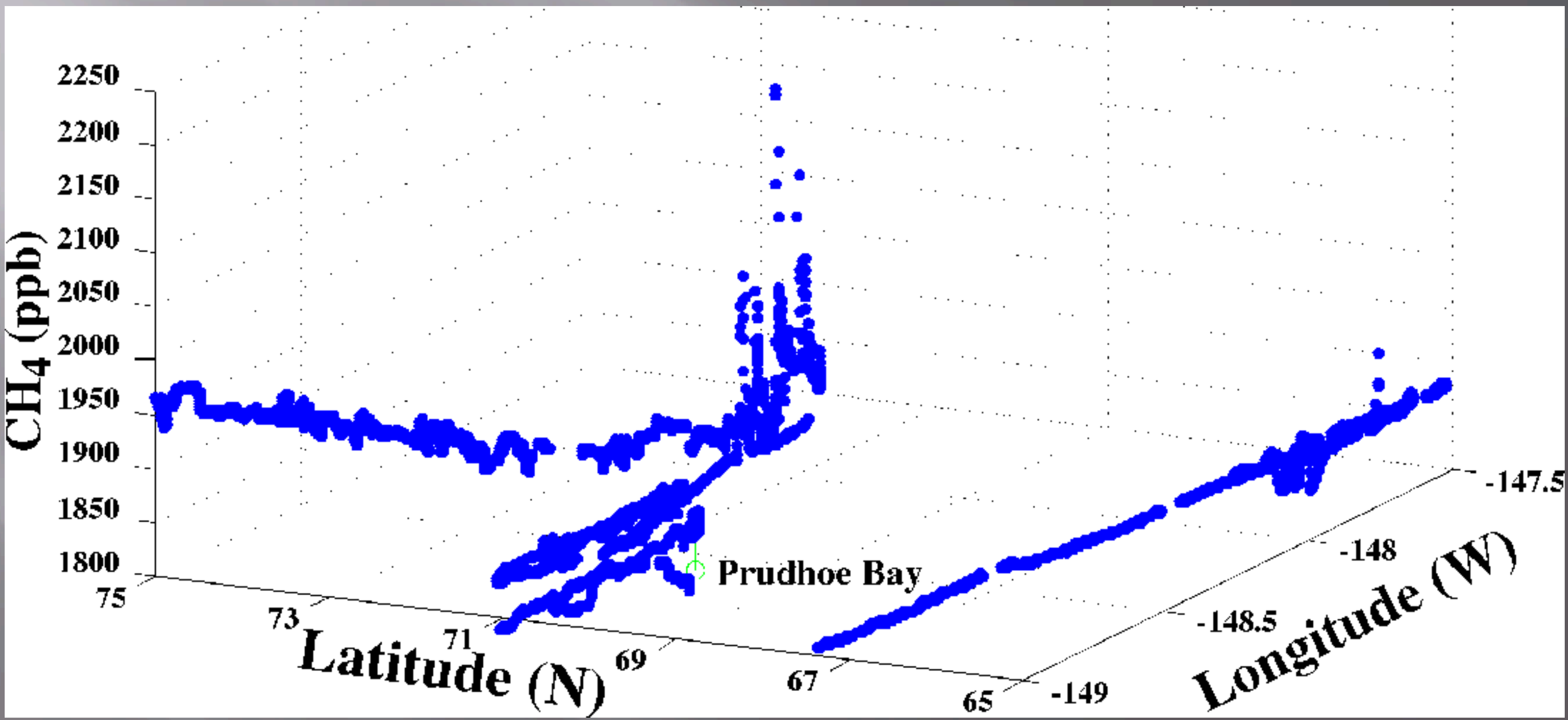

Courtesy Glenn Diskin, NASA Langley

Gulf offshore oil facilities and pipelines

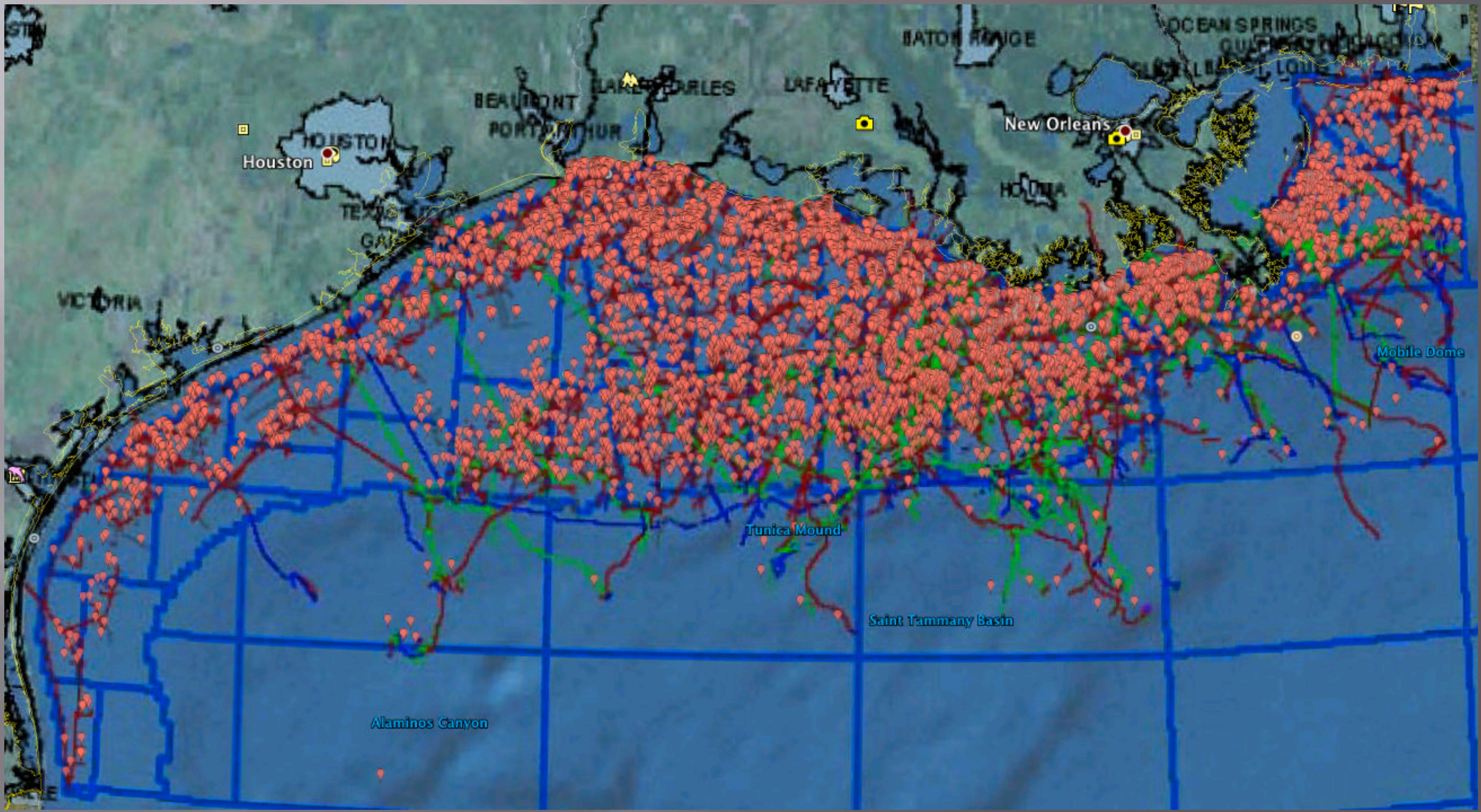

Platform Holly

F070812r3 (3.4m pixels): flare at Platform Holly (x419,y7065 unrotated)

RGB (SWIR-G-B)

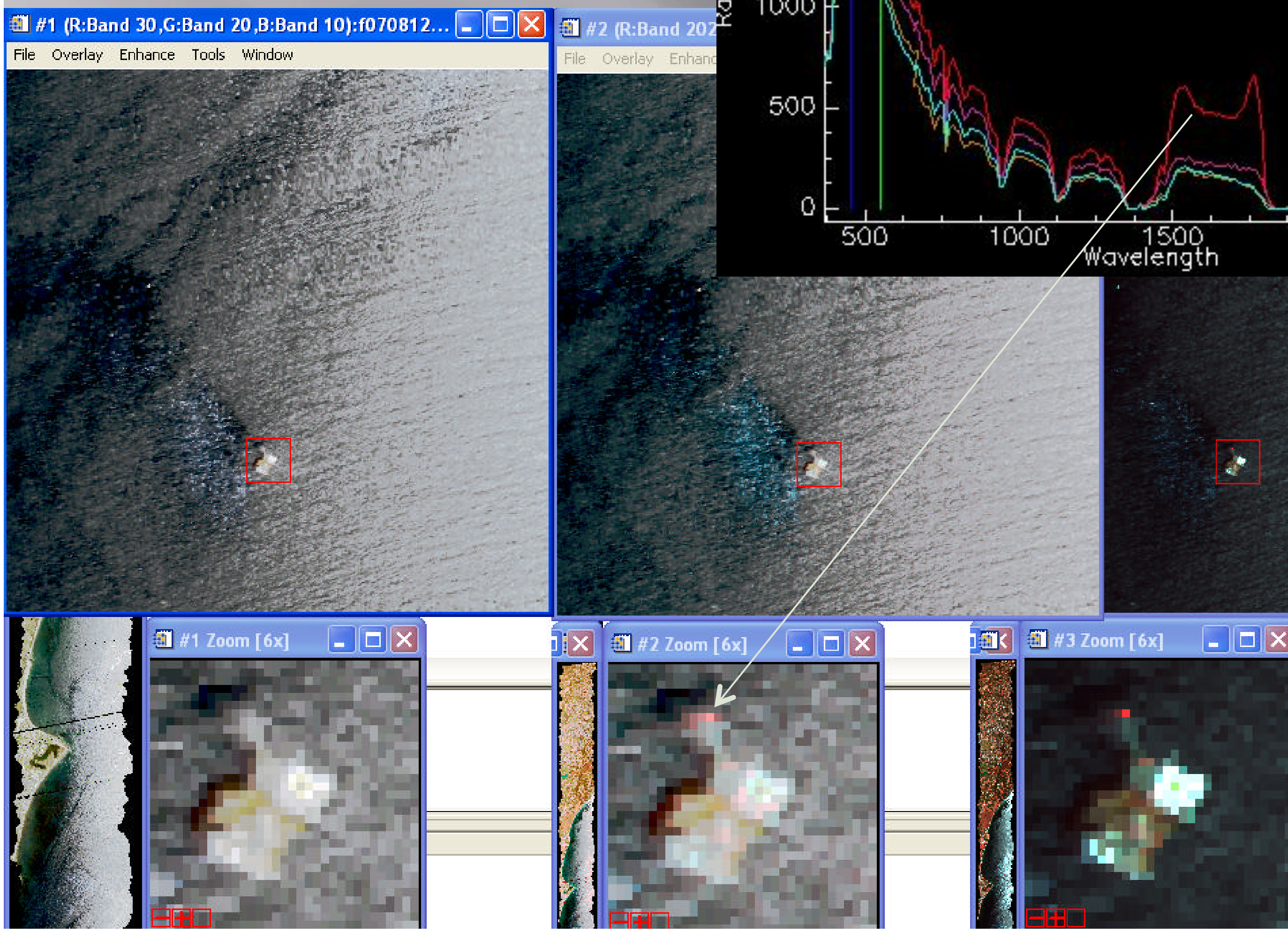

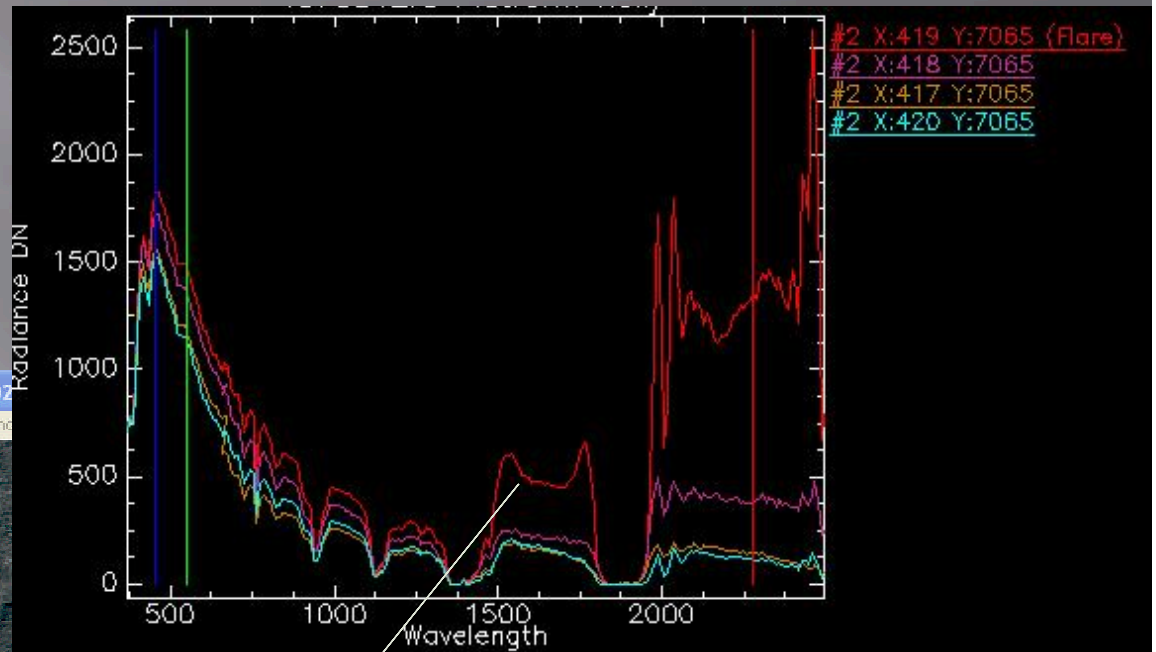

F070812r11_sc01 (4.3m pixels): flare at Platform Holly (x491,y7875 **unrotated**)

Platform Holly

RGB (SWIR-G-B)

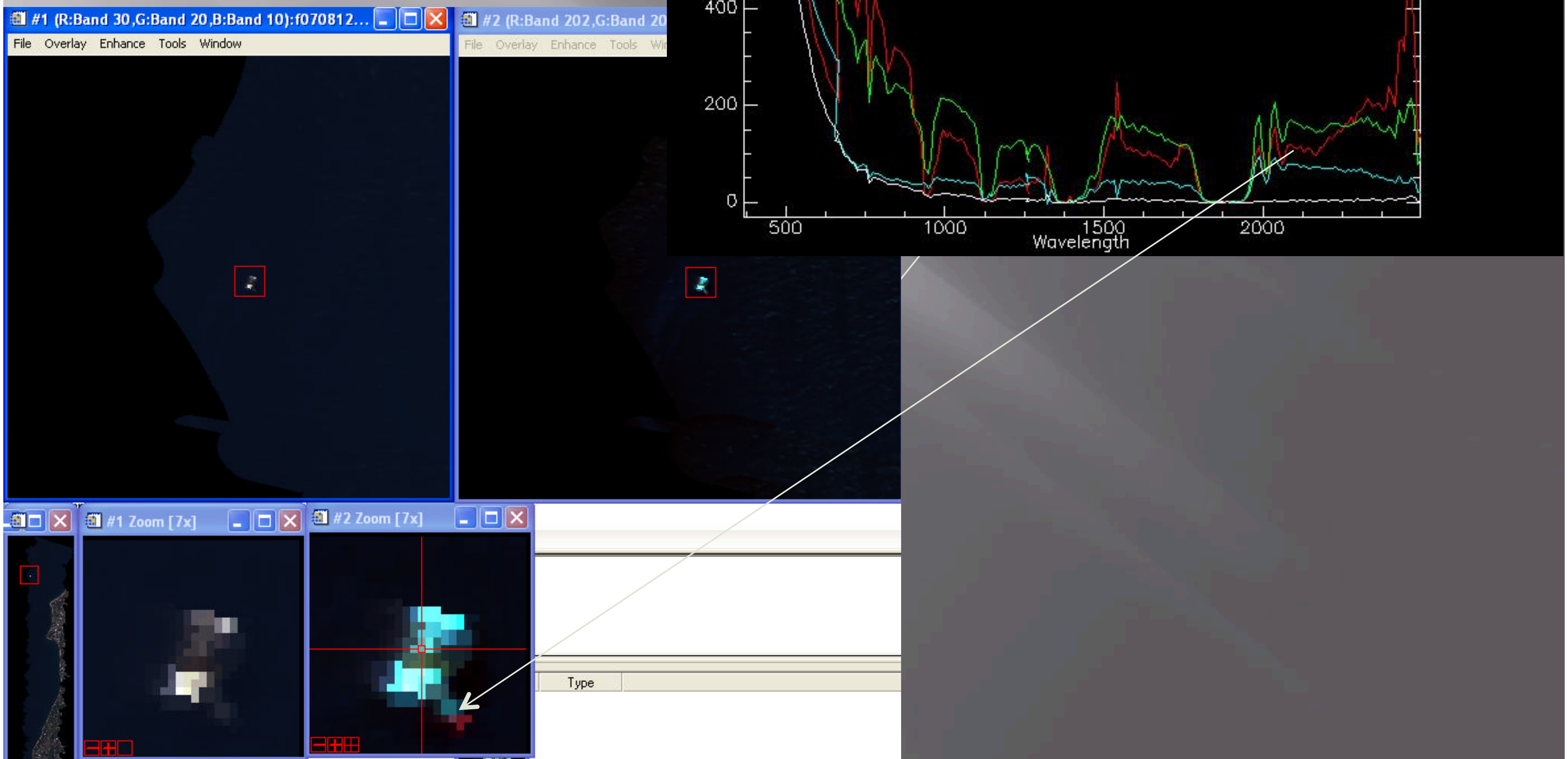

US Fossil Fuel Production

Red- Gas, Green – oil, Yelllow- both

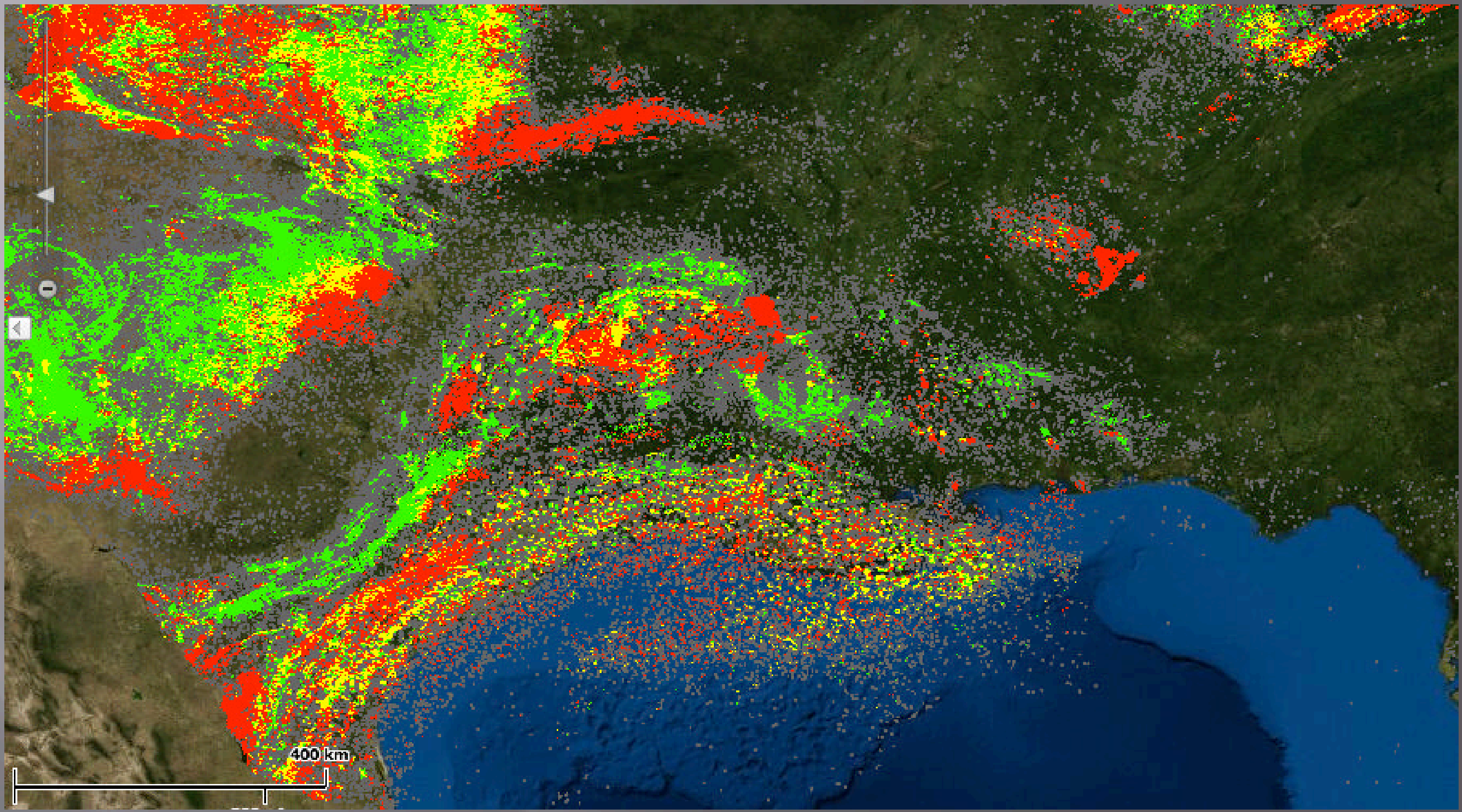

Strong Methane Anomalies co-located with production

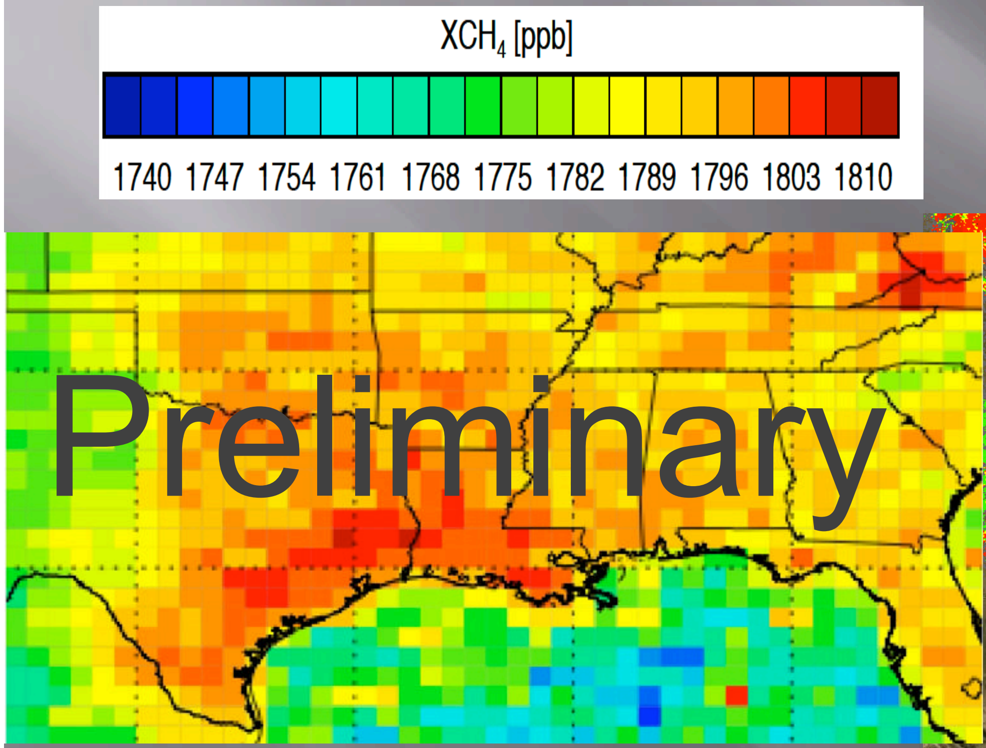

Prevailing Gulf winds from east

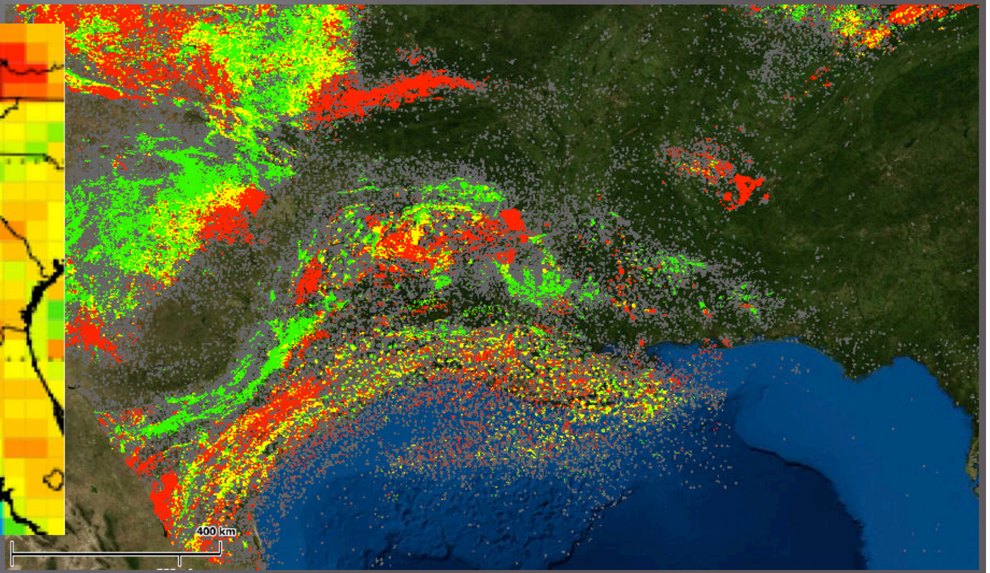

Conclusion

Marine hydrocarbon seep fields provide an ideal natural laboratory to understand, investigate, and validate petroleum related processes.

Mapping Plant Species and Plant Functional Types from the West Coast to the Gulf

D. A. Roberts[1], Keely L. Roth[1], Philip E. Dennison[2], Ray Kokaly[3], Michael Toomey[1], Seth Peterson[1], Susan Ustin[4]

1. UC Santa Barbara
2. University of Utah
3. USGS Denver
4. UC Davis

Additional thanks go to the Gulf AVIRIS flight team (i.e., Bradley, Clark, McCubbin), USGS Baton Rouge (Brady Couvillion, Sarai Piazza, David Heckman & Greg Steyer)

Funded by NASA Terrestrial Ecology program

Research Questions

- **How separable are plants at the species and plant functional type (PFT) level using imaging spectrometry?**
- **How does the ability to discriminate species/PFTS vary as a function of**
  - **Spatial resolution (4 to 60m)?**
  - **Spectral sampling (Broad band to imaging spectrometry)?**
  - **Seasonality?**
- **How does separability vary across multiple ecosystems?**

Terrestrial Ecology Study Sites

Additional sites include Sierra Nevada and Jasper Ridge

How do you Quantify Spectral Separability?

- **Spectral distance measures**
  - **Jeffries-Matsusita**
  - **Bhattacharyya distance**

$$B = \frac{1}{8}[\mu_1 - \mu_2]^T \left[\frac{\Sigma_1 + \Sigma_2}{2}\right]^{-1} [\mu_1 - \mu_2] + \frac{1}{2} \mathrm{Ln} \frac{\left|\frac{1}{2}[\Sigma_1 + \Sigma_2]\right|}{\sqrt{|\Sigma_1||\Sigma_2|}}$$

(μ - mean value | ∑ - Covariance)

- **Statistical**
  - **t-test**
- **Classification**
  - **Least Squares Analysis of Absorption Features (MICA)**
  - **Linear Discriminant Analysis**
  - **Spectral Angle Mapper**
  - **Multiple Endmember Spectral Mixture Analysis**
    - **Extension of simple mixing model**
    - **Number and type vary per pixel**
    - **2 em case**

Selecting Optimal Endmembers for MESMA

- **Objective**
  - **Select the smallest subset of spectra that has the least confusion between classes**
- **Approaches**
  - **Count-Based Endmember Selection (COB)**
  - **Endmember Average RMS (EAR)**

$$\mathrm{EAR}_{A_i,B} = \frac{\sum_{j-1}^{n} \mathrm{RMSE}_{A_i,B_j}}{n-1}$$

  - **Minimum Average Spectral Angle (MASA)**

$$\bar{\theta}_{A_i,B} = \frac{\sum_{j-1}^{n} \theta_{A_i,B_j}}{n-1}$$

- **Limitations**
  - **Difficult to evaluate relative merits of each approach and standardize**
  - **May not capture important em variability**
  - **Does not evaluate relative merits of individual ems or optimize accuracy**

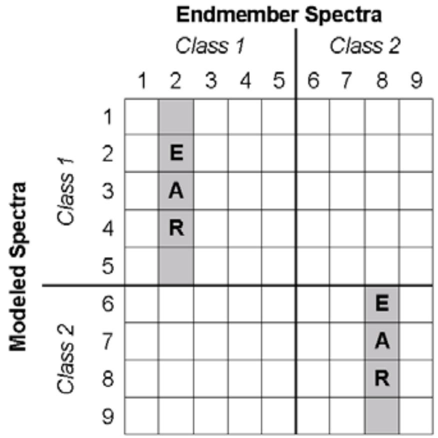

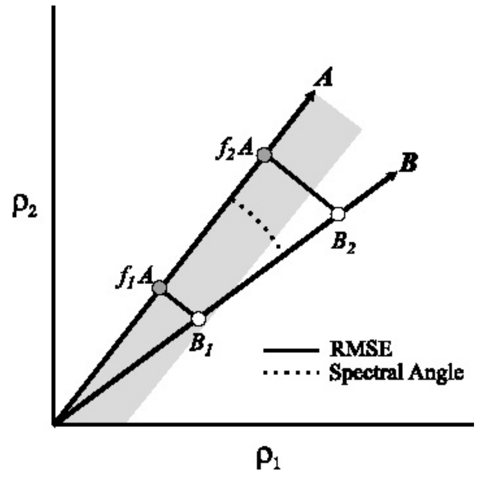

Iterative Endmember Selection and Random Selection

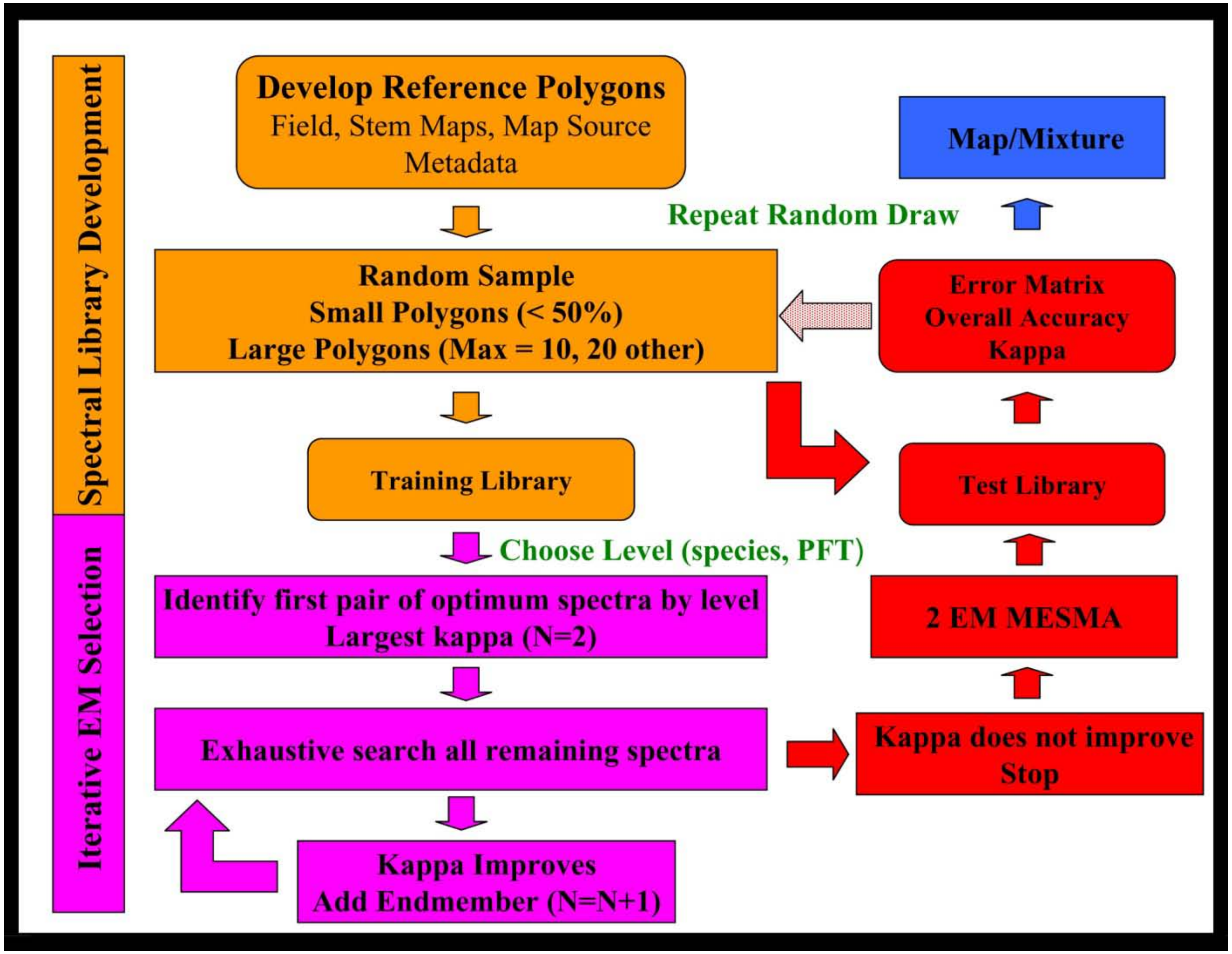

Gulf Study Site: In Detail

Louisiana Gulf (modified from Google Earth)

Coarse Resolution AVIRIS
May 6, 2010

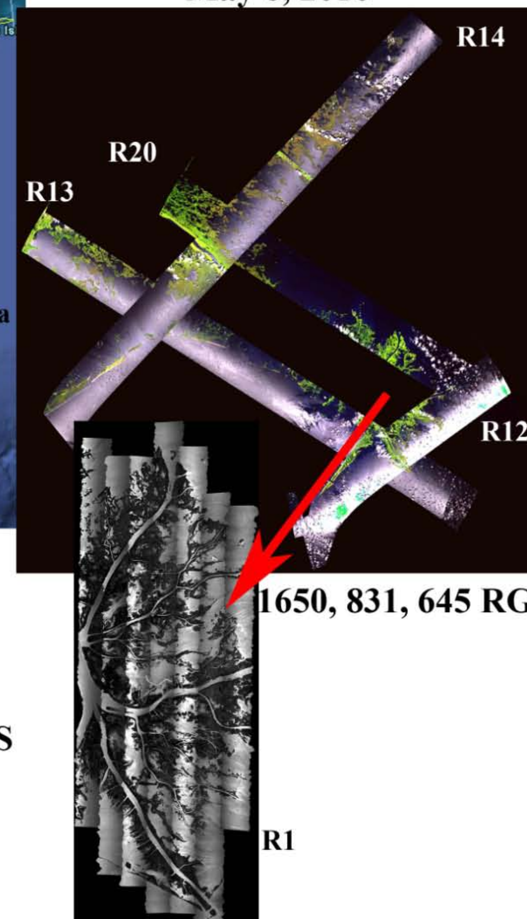

1650, 831, 645 RGB

High Resolution AVIRIS
July 10, 2010

645 nm

Building a Spectral Library: Examples from the Gulf

- **Identify suitable reference data for training and validation**
  - **CRMS (Coastal Reference Monitoring System)**
  - **NWRC (National Wetland Research Center)**
- **Extract spectra, construct metadata, sample training and test libraries**
- **Select optimum spectra**

Challenges:
•Clouds, water, glint, tides
•Limited sites
•Limited species sampled

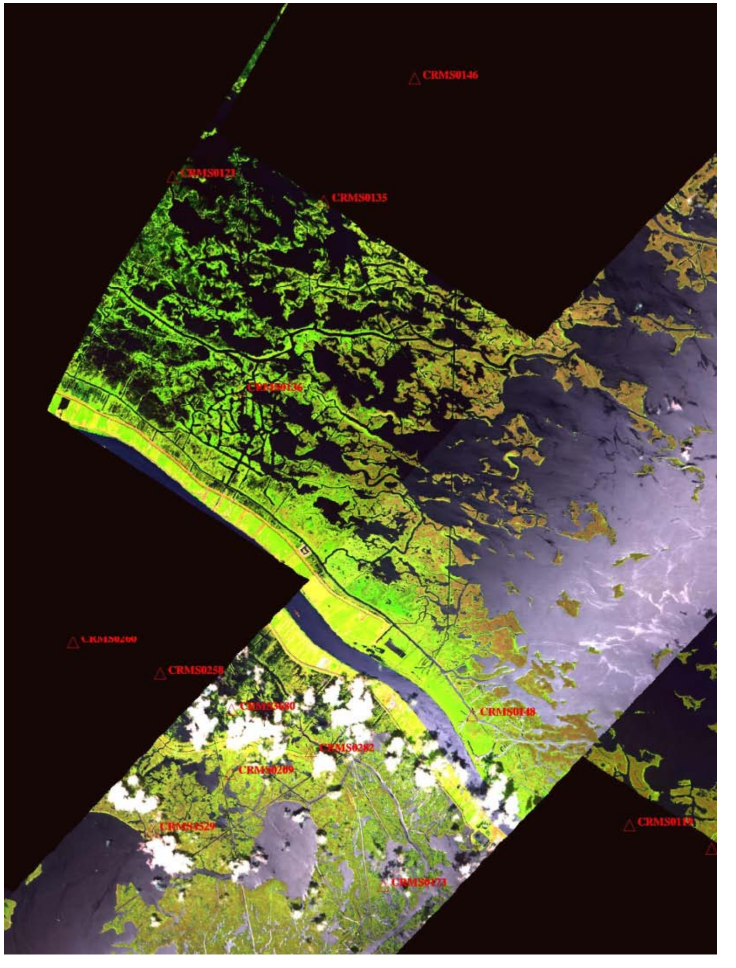

May 6, 2010

Endmember Selection: EAR, MASA, COB

- **Spectra selected from complete library**
- **Classification accuracy evaluated with test library**

	disp	dwtr	glint	juro	mwtr	phau	spal	sppa	vilu	users
disp	4	0	0	0	0	5	14	1	0	16.67%
dwtr	0	39	0	0	0	0	0	0	0	100.00%
glint	0	0	53	0	0	0	0	0	0	100.00%
juro	0	0	0	1	0	0	40	1	0	2.38%
mwtr	0	31	0	0	48	0	0	0	0	60.76%
phau	0	0	0	0	0	80	47	8	6	56.74%
spal	0	0	0	1	0	12	178	9	2	88.12%
sppa	1	0	0	0	0	26	36	17	1	20.99%
vilu	0	0	0	0	0	0	0	0	0	0.00%
Producer	80.00%	55.71%	100.00%	50.00%	100.00%	65.04%	56.51%	47.22%	0.00%	63.54%
Kappa	0.536									
Kappa v	0.00052									

- **26 spectra selected, including 1 disp (*Distichlis spicata*), 4 water, 3 glint, 1 juro (*Juncus roemerianus*), 5 phau (*Phragmites australis*), 6 spal (*Spartina alterniflora*), 3 sppa (*S. patens*) and 3 vilu (*Vigna luteola*)**
- **Classification accuracy is reasonable, but certain classes (juro,sppa and vilu) were poor**
- **Two classes (disp and juro) are poorly represented**

Iterative Endmember Selection

- Spectra selected from one training library
- Classification accuracy evaluated with remaining spectra (test library)

	disp	dwtr	glint	juro	mwtr	phau	spal	sppa	vilu	users
disp	0	0	0	0	0	0	0	0	0	0.00%
dwtr	0	70	0	0	0	0	0	0	0	100.00%
glint	0	0	53	0	0	0	1	0	0	98.15%
juro	0	0	0	0	0	0	0	0	0	0.00%
mwtr	0	0	0	0	48	0	0	0	0	100.00%
phau	0	0	0	0	0	121	26	9	6	74.69%
spal	5	0	0	2	0	15	303	20	3	87.07%
sppa	0	0	0	0	0	4	6	11	0	52.38%
vilu	0	0	0	0	0	1	1	8	7	41.18%
Producers	0.00%	100.00%	100.00%	0.00%	100.00%	85.82%	89.91%	22.92%	43.75%	85.14%
Kappa	0.79									
Kappa v	0.000336									

- *31 spectra selected, including 3 water, 2 glint, 6 phau, 9 spal, 5 sppa and 6 vilu
- Classification accuracy was significantly higher than EMC
- Two classes (disp and juro) were not selected because of low sample numbers
  - Reduced errors of commission

Wetland Spectra: Vol. I

- **Water spectra included dark water, muddy water and glint**
  - **This list was not comprehensive**
- ***Phragmites* is defined by a "classic" spectrum varying primarily in brightness**
  - **Some mixed water spectra occurred**

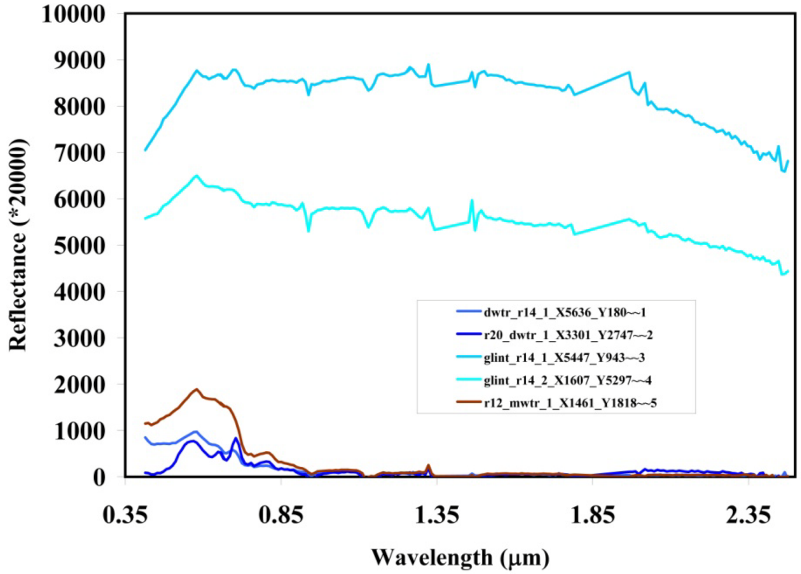

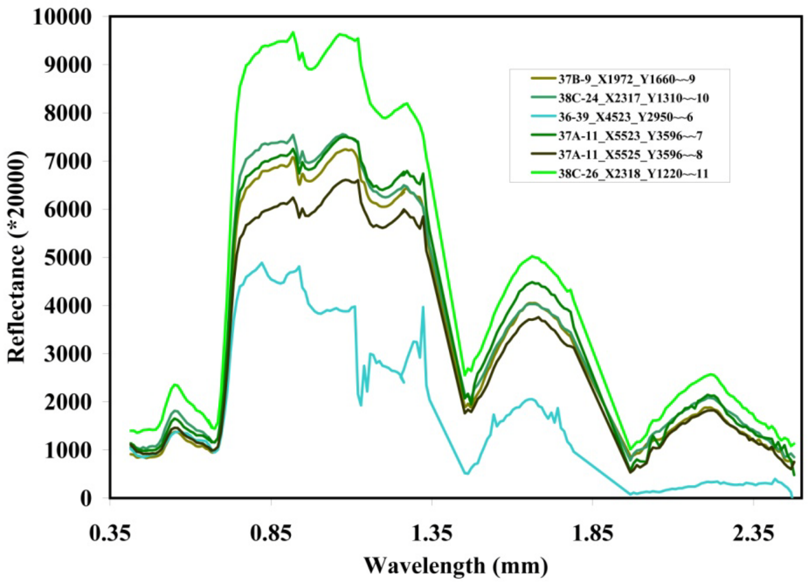

Photo source:http://plants.usda.gov/java/profile?symbol=PHAU7&photoID=phau7_002_avp.tif

Wetland Spectra: Vol. II

- ***Spartina alterniflora*** **is highly variable, generally dark due to structure**

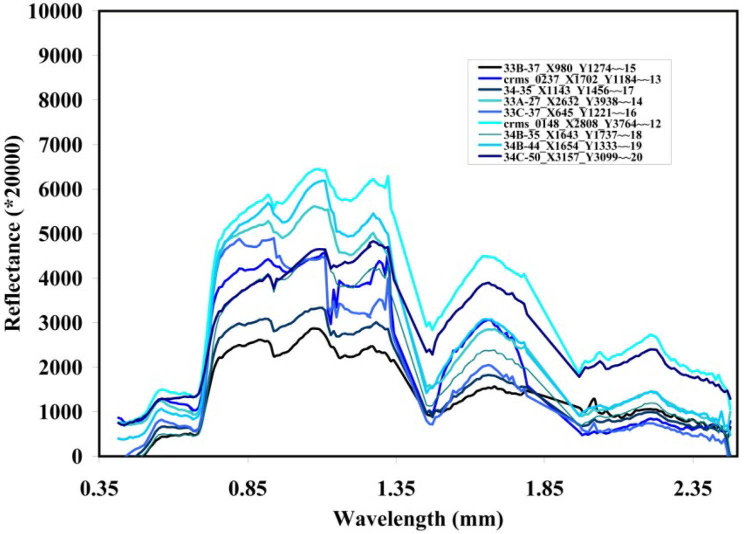

Source:http://plants.usda.gov/java/largeImage?imageID=spal_002_ahp.tif

- ***Spartina patens*** **is less variable and brighter**

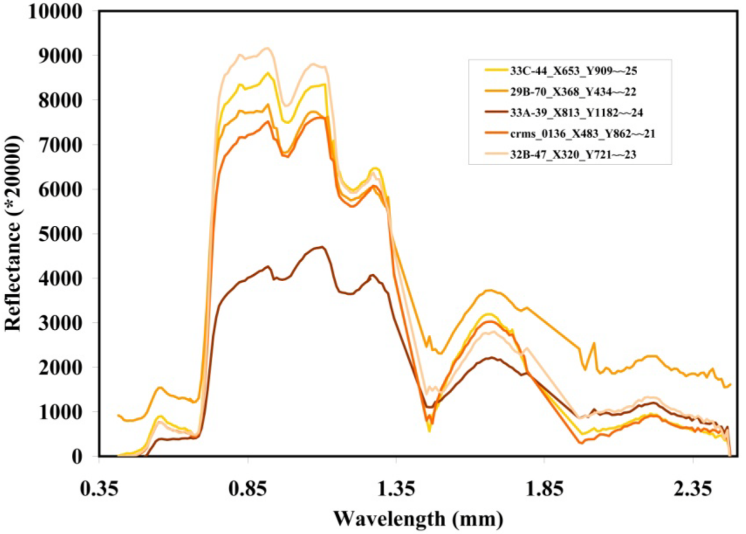

Source: http://www.google.com/imgres?imgurl=http://siera104.com/images/bio/ecology/saltmeadow.jpg

Wetland Spectra: Vol. III

- *Vigna luteola* is defined by a bimodal reflectance between bright (unflooded) and dark (flooded?) spectra
  - sppa is included for comparison

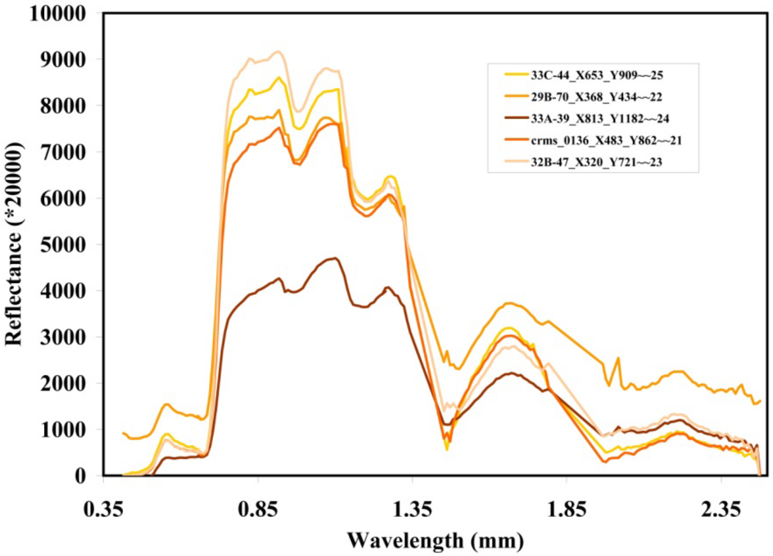

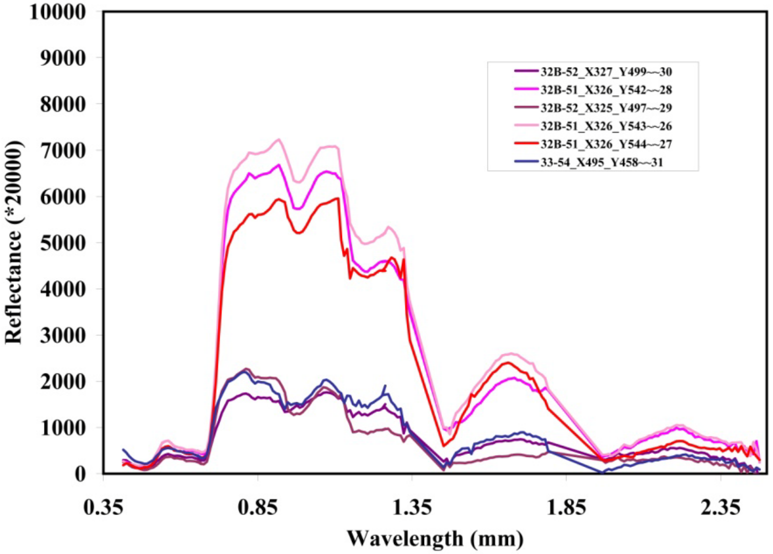

Photo source:http://plants.usda.gov/java/largeImage?imageID=vilu3_001_avp.tif

Mapping Wetland Dominants

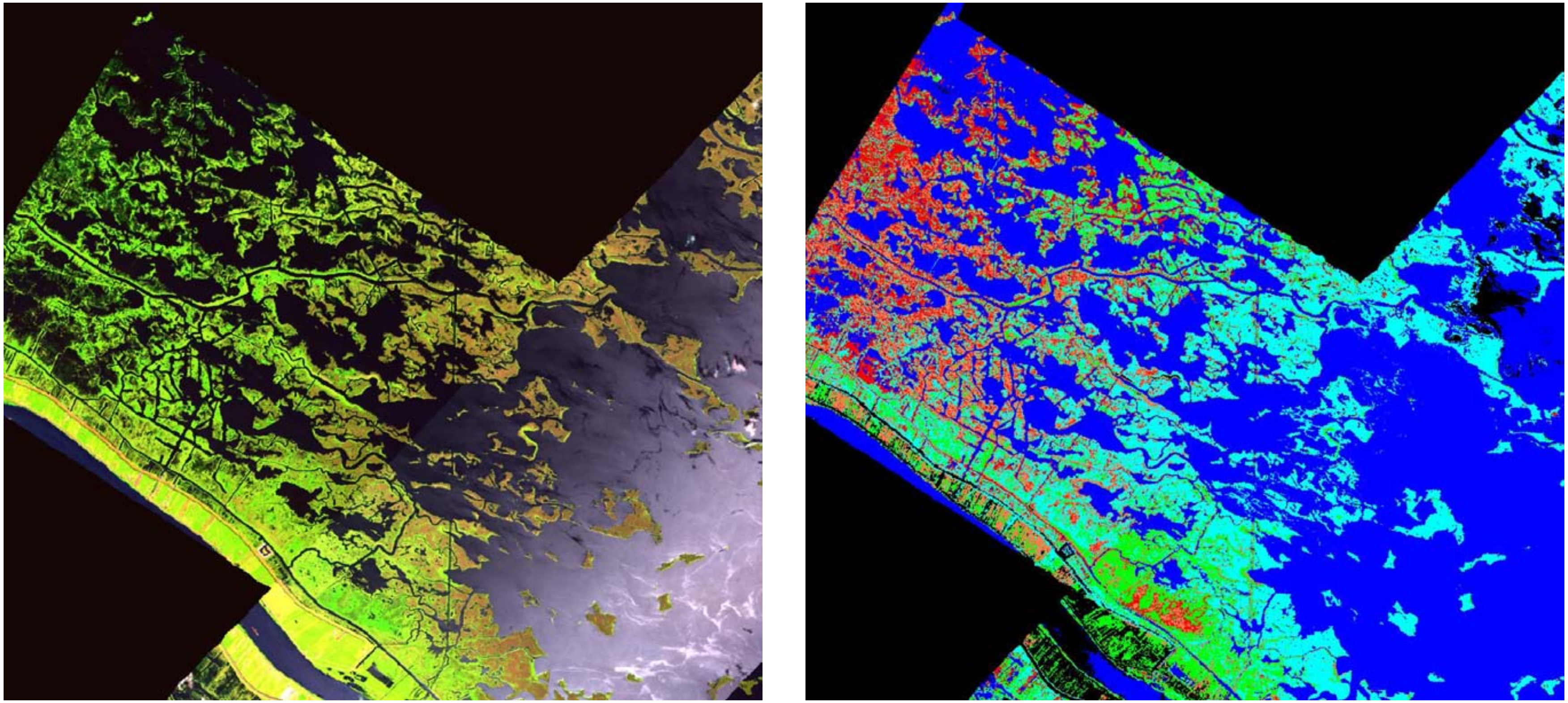

Water/glint | phau | spal | sppa | vilu | Unclass

- Vegetation mapped cleanly across scene boundaries
- Accuracy appears higher than reported using the test library due to mixed species in the NWRC sites

Mapping Wetland Dominants

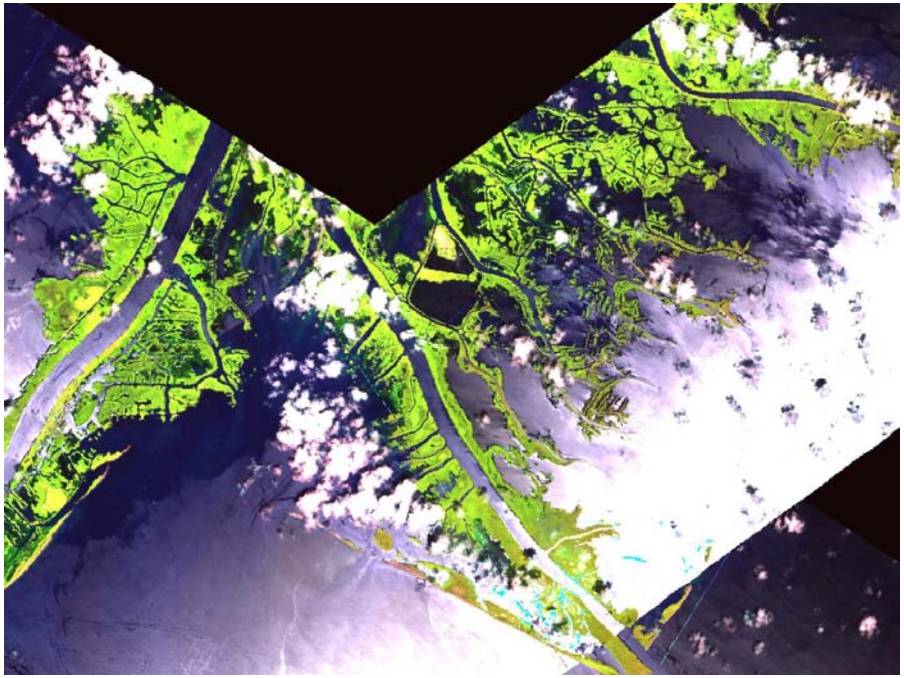

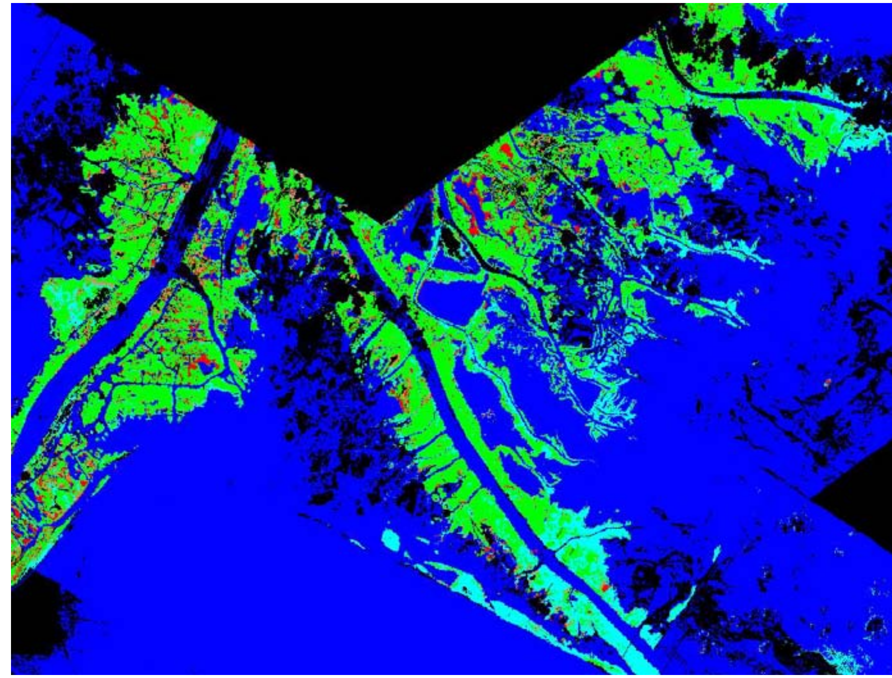

Water/ glint | phau | spal | sppa | vilu | Unclass

- Vegetation mapped cleanly across scene boundaries
- Phragmites dominates farther south along the delta

Wind River

- **Species-level accuracy of 72.7% for 10 species and 63 endmembers**
- **PFT accuracy of 96.8% for 4 PFTs**
  - **Vertical height information would remove ambiguity between herbs and broadleaf plants**

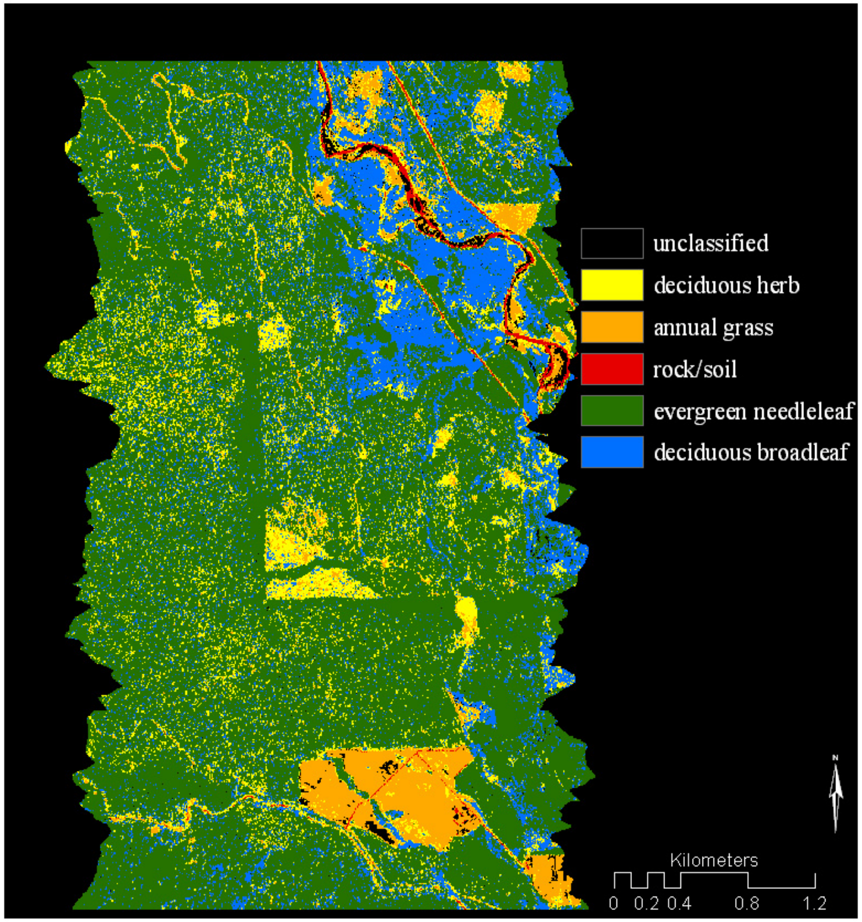

	broadleaf	grass	herb	needleleaf	soil	unmodelec	users_acc
broadleaf	2286	0	18	416	0	0	84.0441
grass	0	3475	1	5	1	0	99.799
herb	17	38	22	51	0	0	17.1875
needleleaf	86	60	4	16816	0	0	99.1159
soil	0	9	0	0	39	0	81.25
unmodelec	0	28	0	7	0	0	
prod_acc	95.68857	96.26039	48.88889	97.23041	97.5	0	
kappa		0.92599					
overall accuracy		96.8305					

Santa Barbara Front Range

- 13 species, 9 other categories (i.e., soil, rock, orchards) totaling 115 ems
- Species accuracy of 68.6%
- PFT level (8 PFT + 6 other), 103 ems, 81% accuracy

	ag	gc	adfa	arca	argl	dbrni	burn	cecu	ceme	cesp	quag	qudu	rock	soil	umca	yuwh	urban	dgrass	riparian	sycamore	orchard_sc	orchard_lo	unmodeled	User's Accu
ag	0	0	0	0	0	0	0	0	0	0	0	0	0	0	0	0	0	0	0	0	0	0	0	0
gc	13	2442	43	2	240	0	0	2	53	3	20	49	0	0	1	0	1	0	31	1	167	216	0	74.36
adfa	0	0	565	2	209	0	0	10	151	5	4	1	0	0	1	6	0	2	0	0	0	0	0	59.1
arca	0	0	1	16	0	0	0	0	1	0	0	0	0	0	0	0	0	0	0	0	0	0	0	88.89
argl	0	0	17	0	6	0	0	0	6	0	5	0	0	0	1	0	6	0	0	0	0	0	0	14.63
dbrni	0	0	0	1	0	6	0	0	0	0	0	0	0	0	0	0	0	13	0	0	0	0	0	30
burn	0	0	0	0	0	0	2353	0	0	0	0	0	0	0	0	0	0	0	0	0	0	0	0	100
cecu	0	0	0	0	0	0	0	0	0	0	0	0	0	0	0	0	0	0	0	0	0	0	0	0
ceme	0	1	90	0	64	0	0	0	675	107	119	7	0	0	3	1	0	0	1	0	4	0	0	62.97
cesp	0	2	3	0	1	0	0	0	15	16	3	0	0	1	0	0	2	0	0	0	0	0	0	37.21
quag	0	24	6	0	5	0	0	0	58	41	487	7	0	0	42	3	0	0	18	3	6	0	0	69.57
qudu	0	0	0	0	0	0	0	0	0	0	0	0	0	0	0	0	0	0	0	0	0	0	0	0
rock	0	0	0	0	0	0	0	0	0	0	0	0	35	11	0	0	1	0	0	0	0	0	0	74.47
soil	0	11	0	0	3	0	18	0	1	0	0	0	0	256	0	1	24	14	0	0	3	0	0	77.34
umca	0	0	0	0	0	0	0	0	0	0	0	0	0	0	0	0	0	0	0	0	0	0	0	0
yuwh	0	1	6	0	3	0	0	0	3	3	1	0	0	0	0	7	2	0	0	0	0	0	0	26.92
urban	0	5	0	0	0	0	4	0	0	0	0	0	0	9	0	0	405	0	0	0	0	0	0	95.74
dgrass	0	9	1	4	0	2	4	0	1	2	0	0	0	10	0	0	0	625	0	0	0	0	0	94.98
riparian	0	2	1	0	2	0	0	0	0	2	13	40	0	0	10	0	0	0	185	4	6	6	0	68.27
sycamore	0	0	0	0	0	0	0	0	0	0	0	0	0	0	0	0	0	0	0	0	0	0	0	0
orchard_sc	0	290	35	2	67	0	0	4	13	3	0	4	0	0	0	5	6	0	0	0	2341	18	0	83.97
orchard_lo	0	53	0	0	2	0	0	0	0	0	6	6	0	0	1	0	0	0	64	0	118	507	0	66.97
unmodeled	51	1529	20	0	36	0	12	0	28	1	16	6	0	11	1	0	10	1	2	0	252	160	0	
Producer's	0	55.89	71.7	59.26	0.94	75	98.41	0	67.16	8.74	72.26	0	100	85.91	0	30.43	88.62	95.42	61.46	0	80.81	55.9		
kappa	0.64107																							
kappa	1.67E-05																							
overall acc	68.6197																							
#EMs	115																							

- Highly accurate (>70%) classes include adfa, dbrni, burn, quag, rock, soil, urban, dead grass, orchard+soil)
- Intermediate (50-70%) include golf courses, arca, ceme, riparian, except argl &cesp)

Santa Barbara Front Range

Santa Barbara Front Range: Species

68.6%

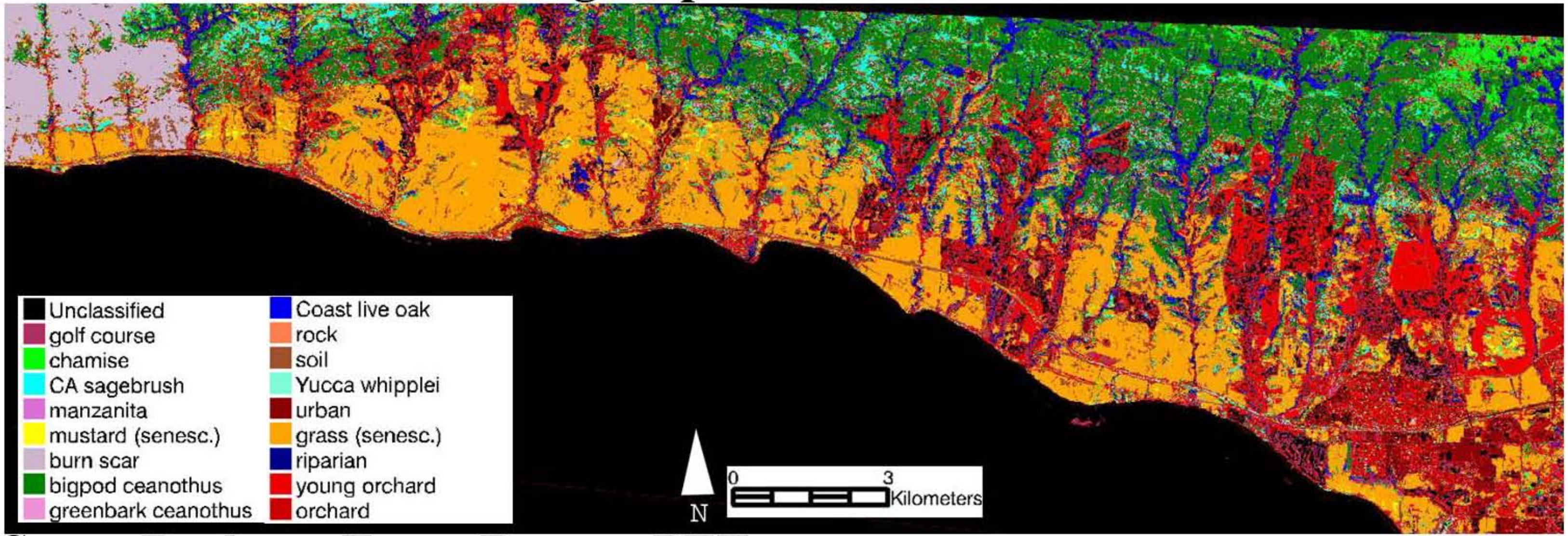

Santa Barbara Front Range: PFT

81%

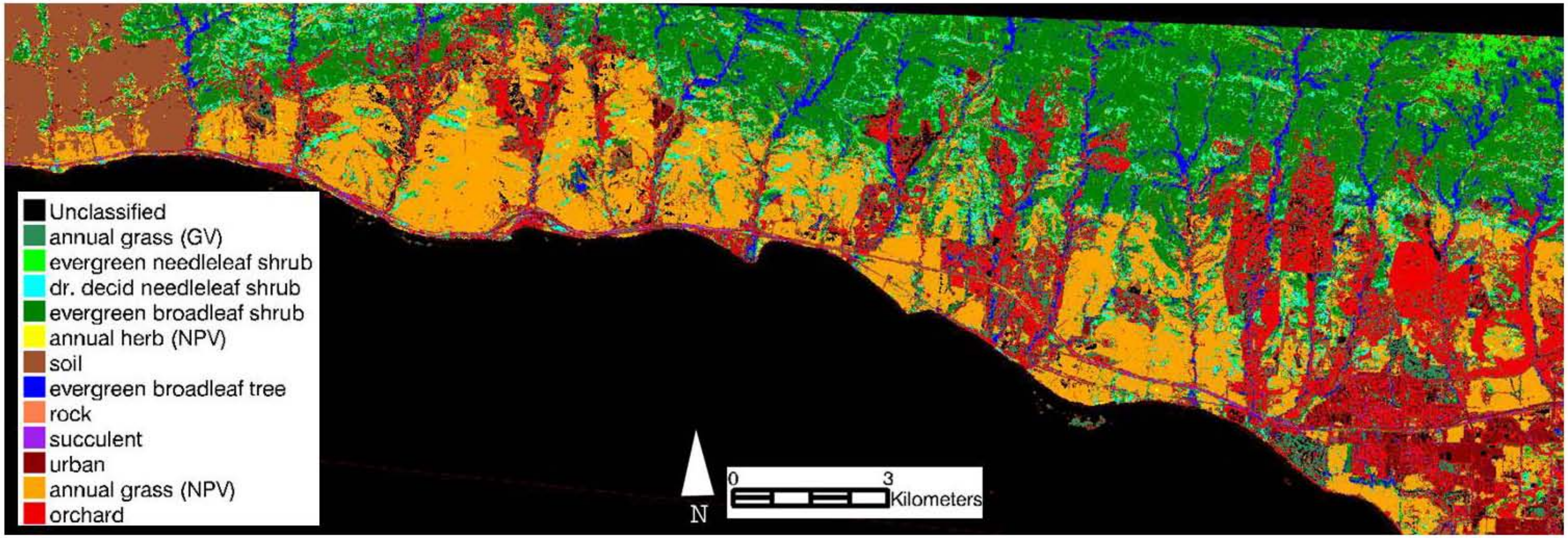

*** High Accuracy extends to the northern line with opposite viewing geometry**

Other Experiments with Iterative Endmember Selection

- **Impact of degraded spatial resolution (4-60 m)**
  - **On-going, all sites: See Dennison**
- **Impact of degraded spectral resolution (native resolution)**
  - **On-going,**

Kappa Statistic

	AVIRIS	IKONOS	MODIS	SPOT5	TM5
SERC	0.37	0.088	0.23	-0.092	-0.067
SBFR species	0.60	0.31	0.49	0.34	0.39
SBFR PFTs	0.63	0.52	0.56	0.45	0.51
WR species	0.62	0.28	0.39	0.31	0.36
WR PFTs	0.93	0.45	0.84	0.82	0.77

Keely Roth

- **Impact of random sampling**
  - **100 runs:**
    - **Accuracy varies substantially between models**
    - **Do you choose the best of 100 or build an ensemble of models?**

On-going Research in the Gulf

- **Improve spectral library to include missing species**
  - ***Juncus roemerianus, Distichlis spicata*, Mangroves**
- **Export analysis to July Twin Otter data sets**
  - **Understory glint appears to have drastically changed the spectral shape of some wetlands**
  - **Differences in tidal heights may have modified NIR reflectance**
- **Expand to three+ endmember models to map senescence and oil coated vegetation**
- **Calculate additional stress measures**
- **Image oil impacted vegetation**

Questions?

Mapping Vegetation Across Spatial and Spectral Scales Using Multiple Endmember Spectral Mixture Analysis

Philip E. Dennison[1], Abigail N. Schaaf[2], Gregory K. Fryer[1], Keely L. Roth[3], and Dar A. Roberts[3]

[1] University of Utah

[2] Forest Service Remote Sensing Applications Center

[3] University of California Santa Barbara

Utah Remote Sensing Applications Lab
University of Utah

Vegetation Mapping

- Past research has shown imaging spectroscopy is capable of mapping vegetation species and functional types at 4-30 m spatial resolutions
- Little work on mapping vegetation using coarser resolution imaging spectrometer data

Santa Barbara Front Range, 20 m AVIRIS

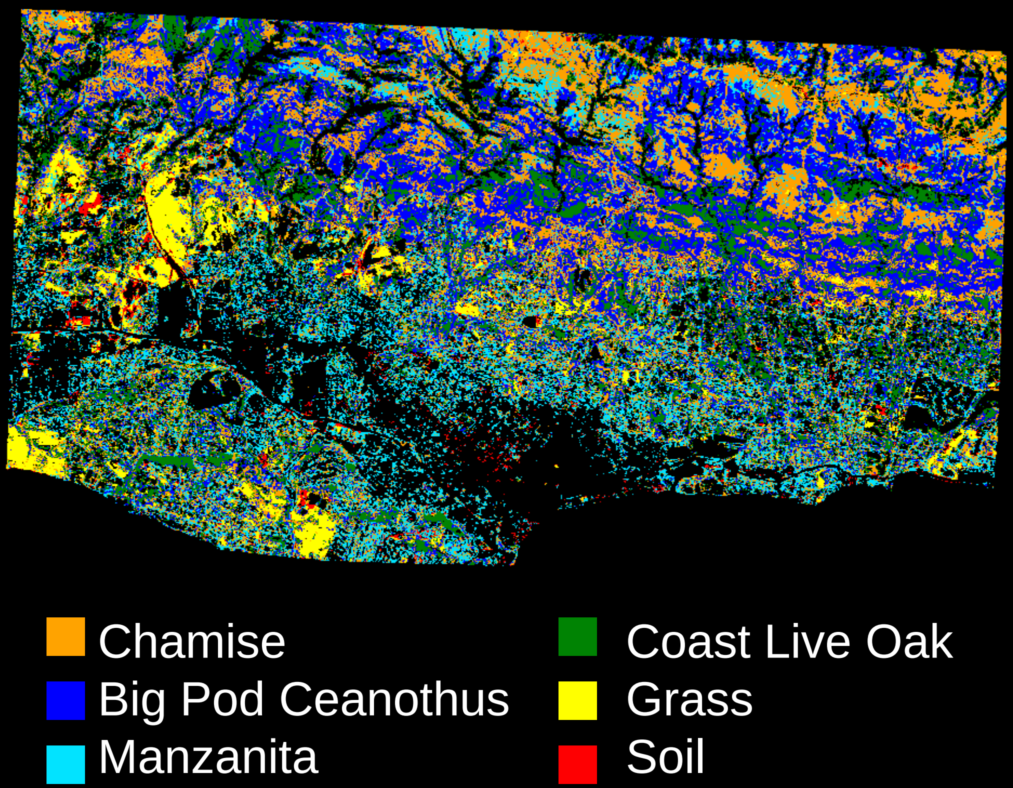

Dennison and Roberts, 2003

Mapping Vegetation in Montane Ecosystems

- Mapping vegetation in montane ecosystems can be particularly challenging
  - Spatial variation in elevation, slope, aspect, precipitation, and insolation produce spatial variation in vegetation type
  - Cloud cover, shorter summer season at higher elevation can limit remote sensing opportunities

Little Cottonwood Canyon, Wasatch Mtns

Mapping Vegetation in Montane Ecosystems

- Montane ecosystems are vulnerable to climate change
  - Favorable climates for individual species may move hundreds of meters upslope with a few degrees warming
  - Earlier snowmelt
  - Increased threat of insect outbreak (e.g. mountain pine beetle)
  - Increased summer evapotranspiration may not be offset by increased precipitation
- Vegetation mapping is essential for understanding impacts of climate change, human activity, and other disturbance on montane ecosystems

Lodgepole pine, Medicine Bow Mtns.

Mapping Vegetation in Montane Ecosystems

- How does vegetation mapping accuracy change with spatial and spectral resolution?
  - Can VNIR/SWIR imaging spectrometer data accurately map plant functional types at 60 m resolution in montane ecosystems?

Big Cottonwood Canyon, Wasatch Mtns

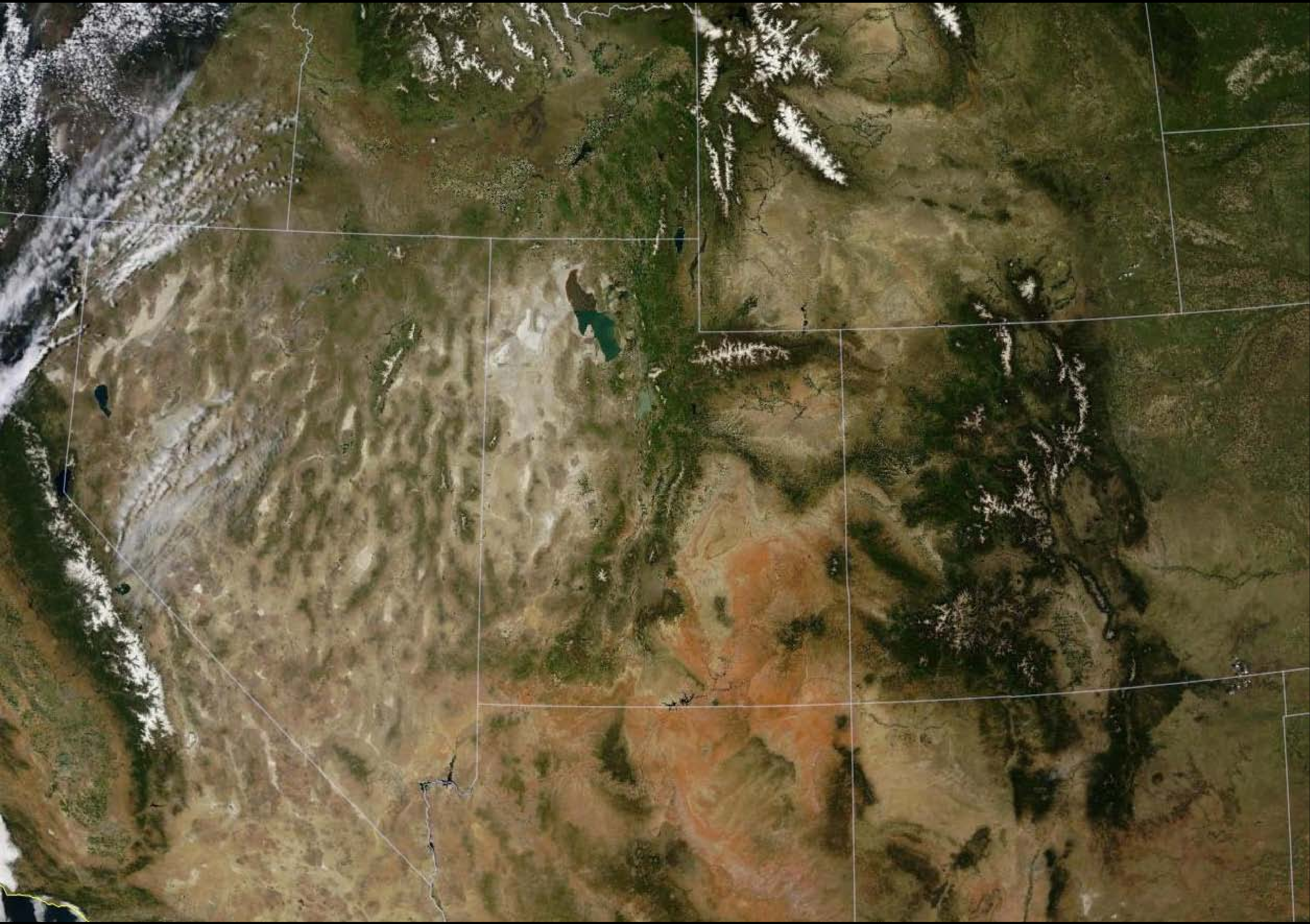

AVIRIS Data

- Acquired August 5, 1998
- 20 m IFOV
- Covers 28 km by 11 km study area within the Wasatch Range east of the Salt Lake Valley

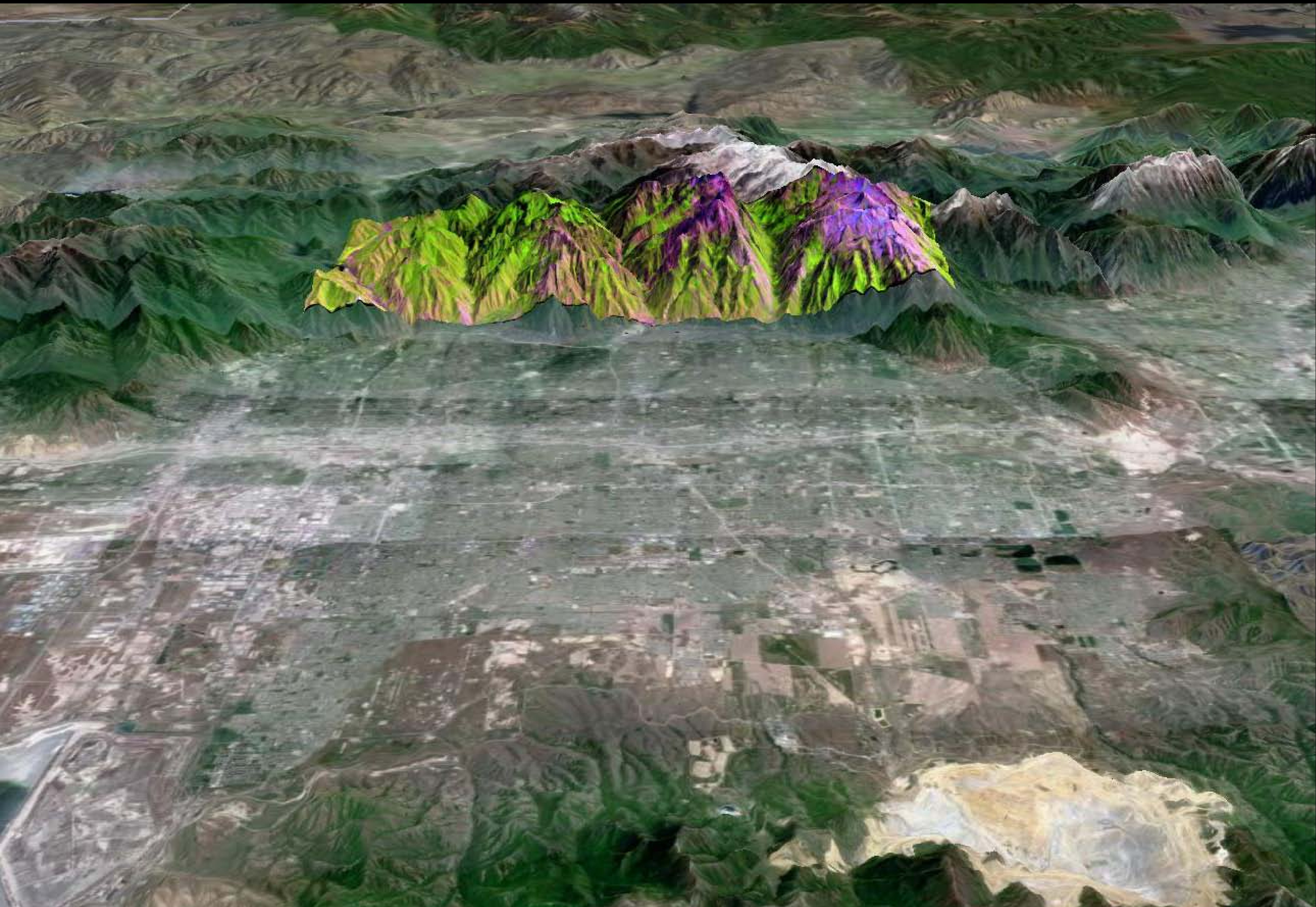

Elevation (1300-3400 m)

Hillshade (illuminated from N)

SWIR/NIR/red composite

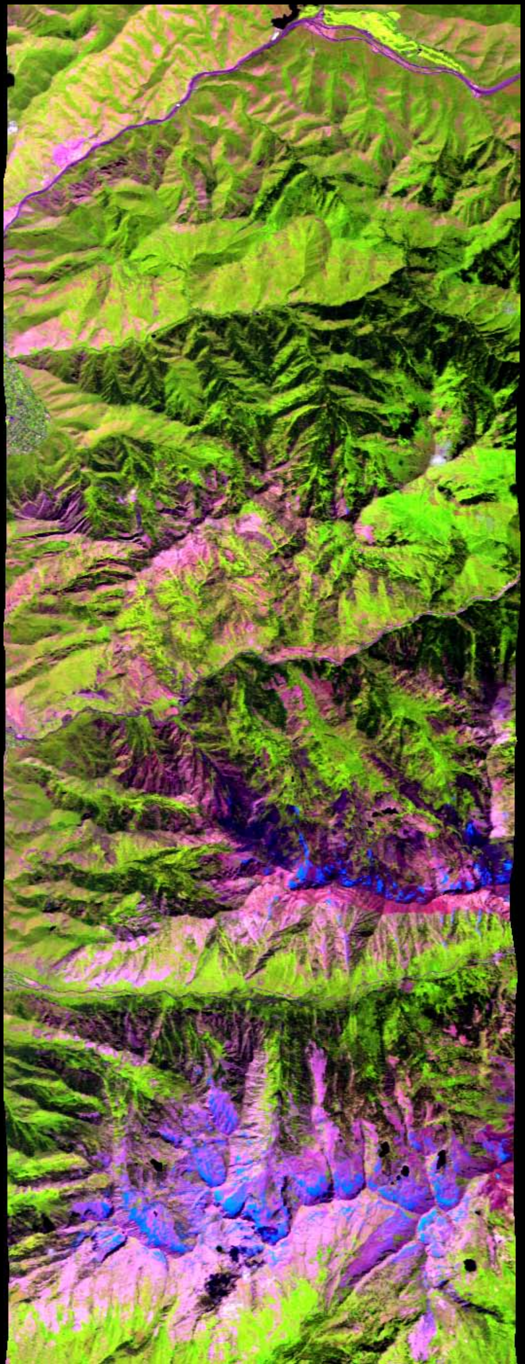

Wasatch Plant Functional Types

- 4 broad PFTs were defined based on leaf type and lifeform
  - broadleaf deciduous shrub (Gambel oak)
  - broadleaf deciduous tree (aspen)
  - needleleaf evergreen tree (white and subalpine fir, Douglas fir, and Engelmann spruce)
  - grass/herbaceous (meadows)
- A fifth rock/soil class was also mapped

Ground Reference Data

- Training and accuracy assessment polygons were derived from 1 m National Agriculture Imagery Program (NAIP) orthophotos
  - Polygons were created using image segmentation (eCognition)
  - Polygons were assigned a PFT identity in the field
  - Polygons were required to be at least 60 m by 60 m and at least 75% dominated by one PFT
  - 221 polygons were randomly partitioned into training and accuracy sets

Needleleaf evergreen tree polygon

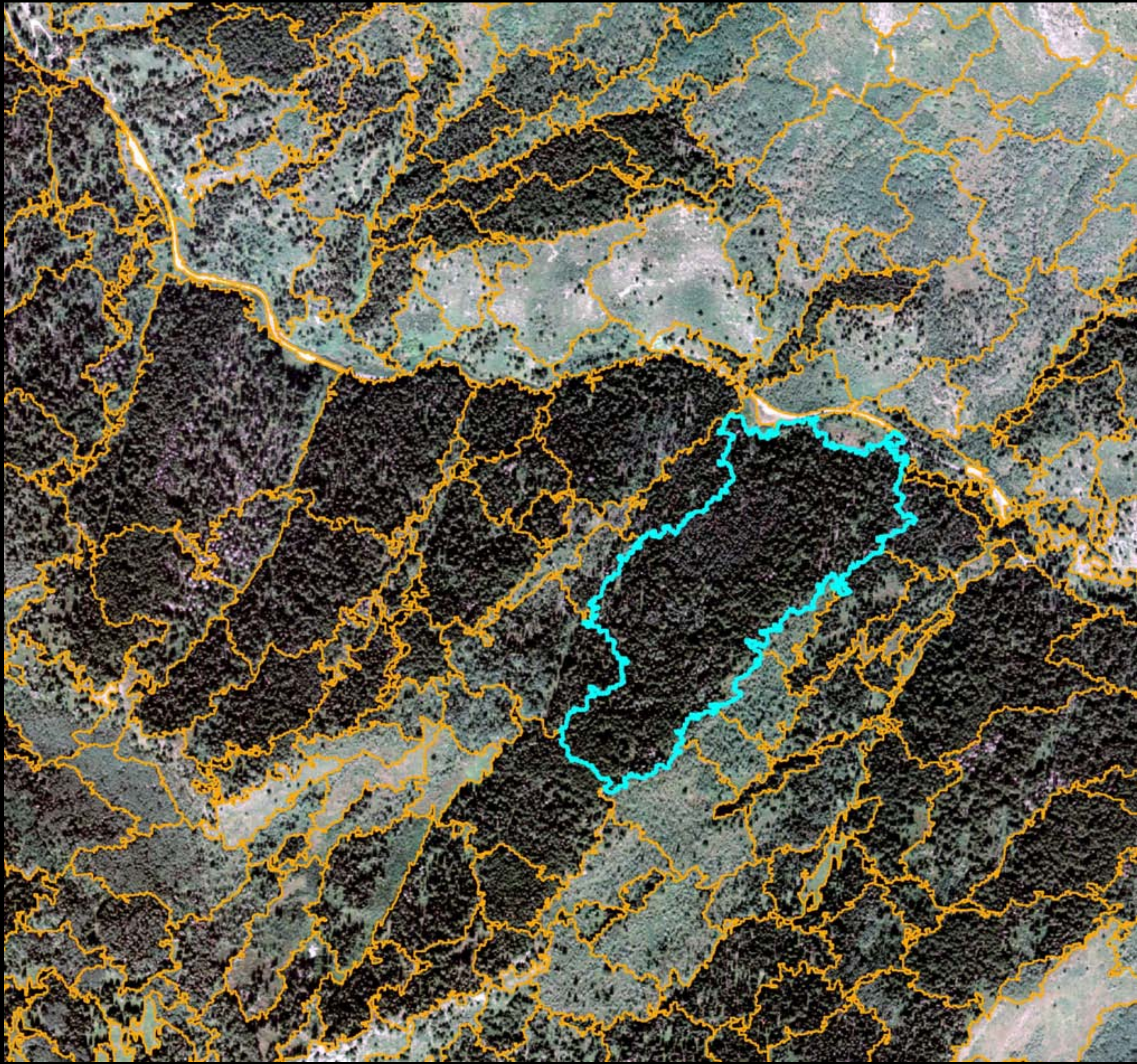

Spatial and Spectral Resampling

- The 20 m AVIRIS radiance image was spatially resampled to 40 m and 60 m resolutions
- These 3 images were separately run through FLAASH to retrieve apparent surface reflectance
- AVIRIS reflectance images were also spectrally resampled to match the spectral response function of Landsat 5 TM

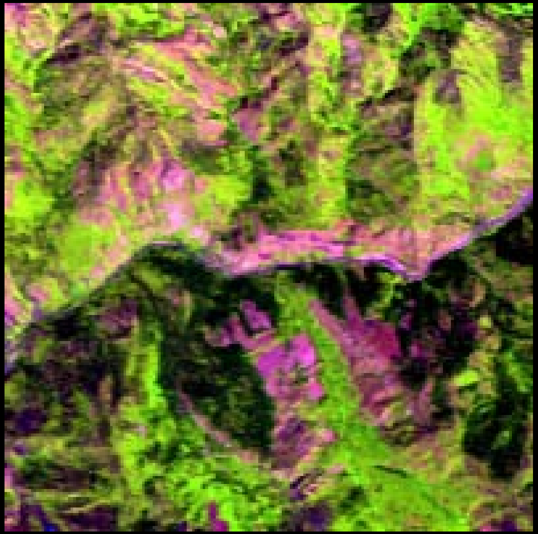

20 m

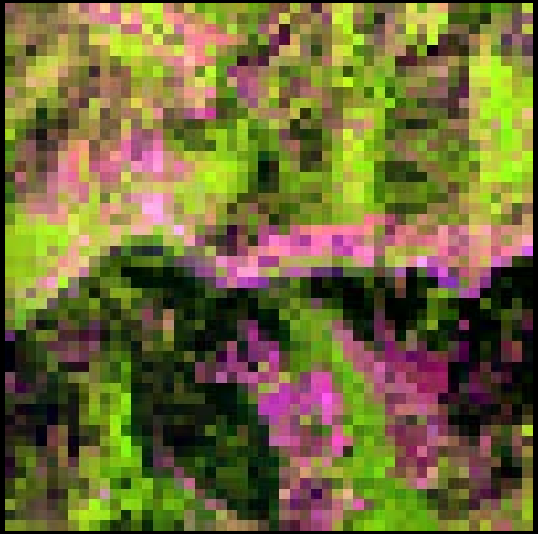

60 m

Image Classification

- Multiple Endmember Spectral Mixture Analysis
  - Models image spectra as a linear combination of endmembers
  - MESMA allows endmembers to vary on a per pixel basis
  - Endmembers were extracted from the training polygons
  - A 2-endmember model was used to classify the image
    - The best fit PFT (or rock/soil) endmember + shade

Endmember Selection

- Spectra extracted from polygons were run through an automated iterative endmember selection program
- The program models a spectral library using 2 endmember MESMA and iteratively adds and subtracts endmembers to maximize the accuracy of the classification

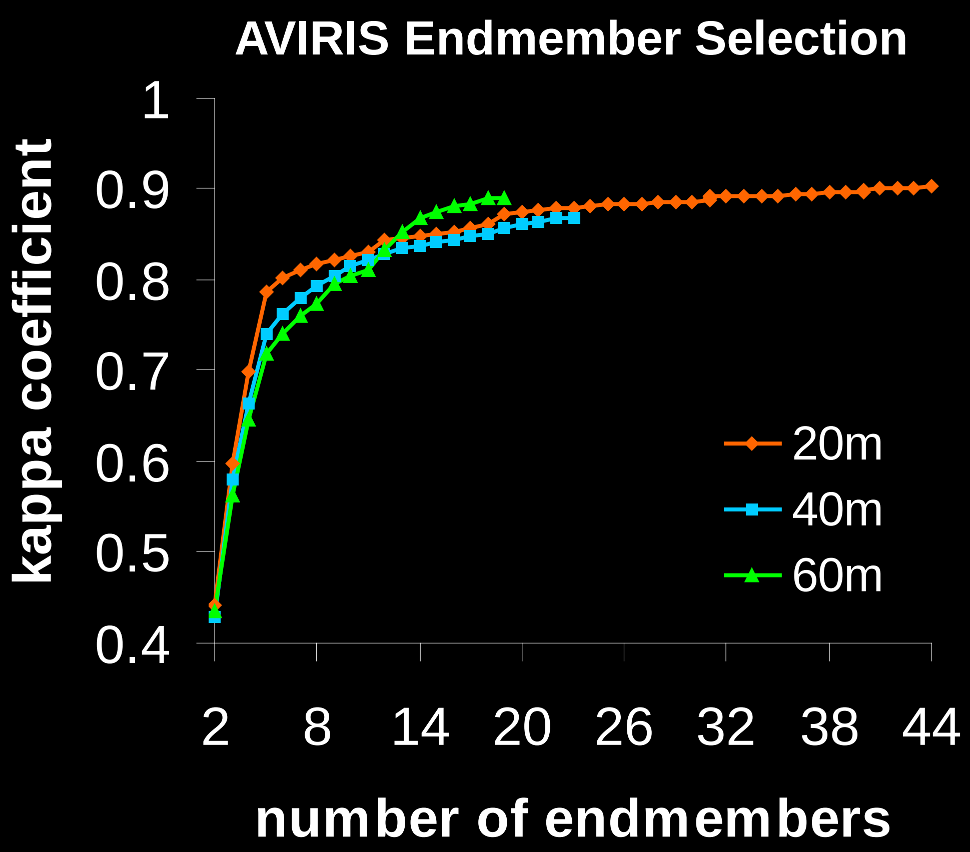

MESMA Classification

Endmembers	Used to Classify: 20 m	40 m	60 m
AVIRIS 20 m	X	X	X
AVIRIS 40 m		X	
AVIRIS 60 m			X
TM 20 m	X	X	X
TM 40 m		X	
TM 60 m			X

20m AVIRIS, 20m em

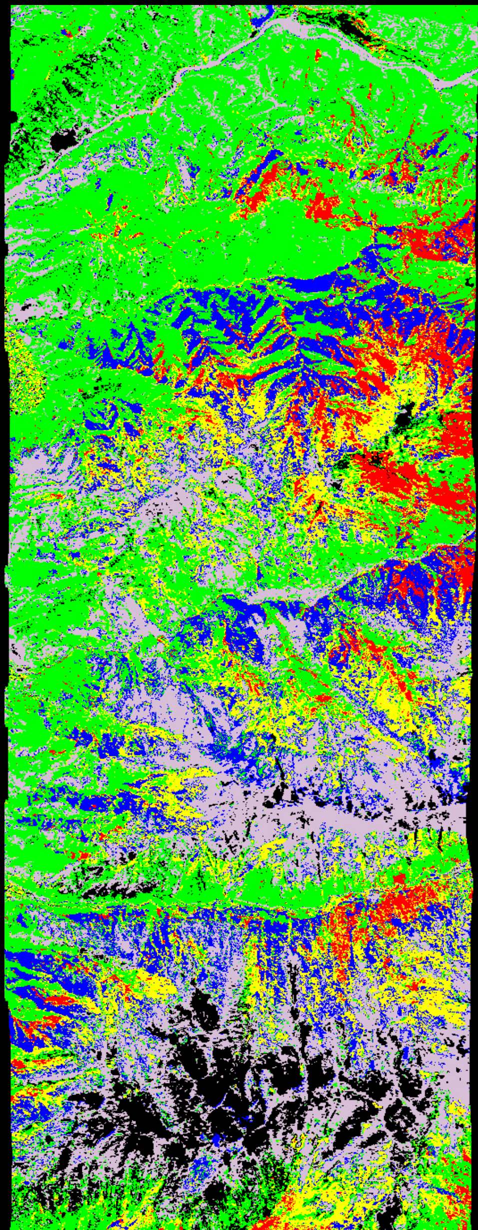

Accuracy
87.6%

Kappa
.838

SWIR/NIR/red composite

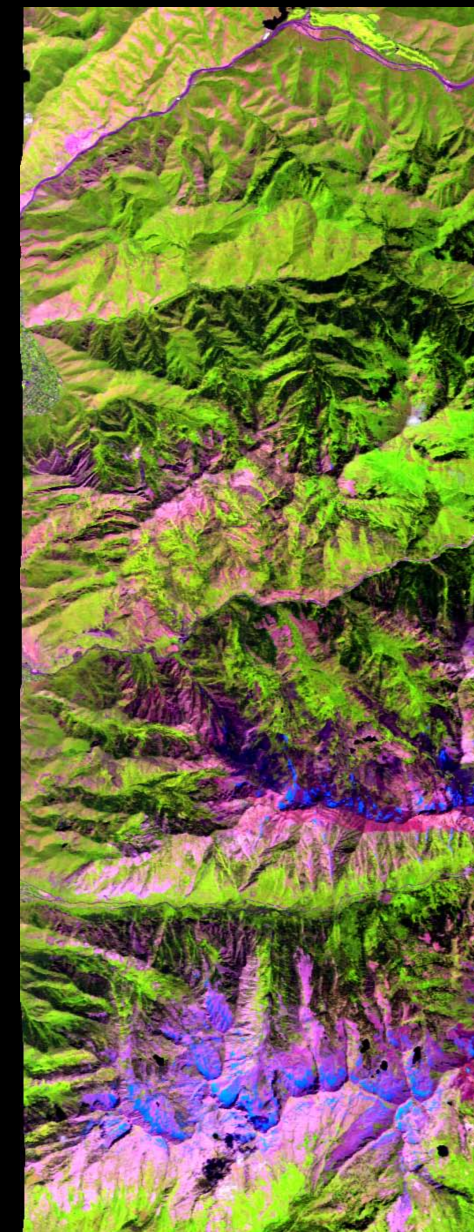

20m AVIRIS, 20m em

60m AVIRIS, 60m em

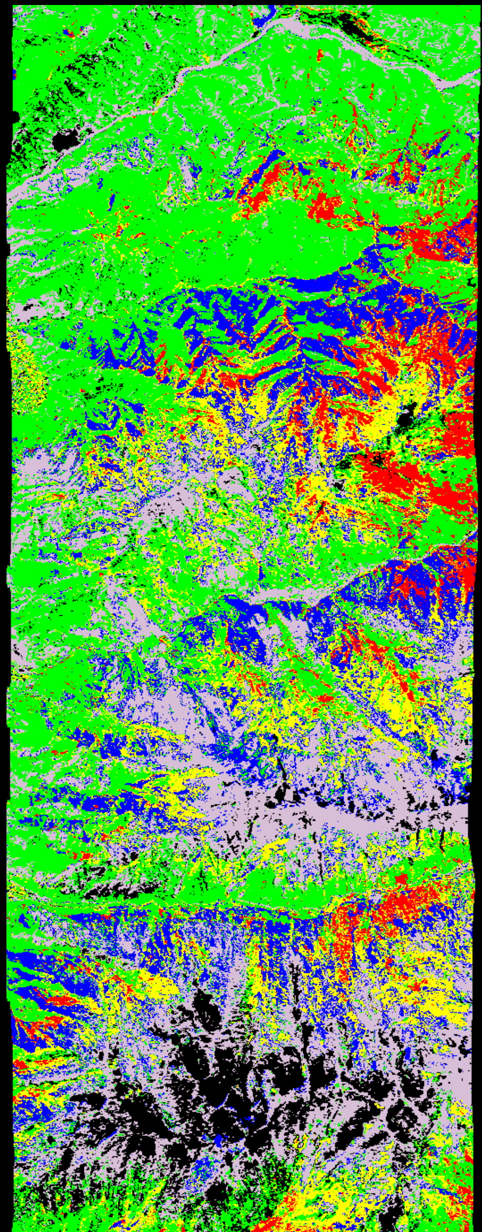

- Broadleaf Deciduous Tree
- Needleleaf Evergreen Tree
- Broadleaf Deciduous Shrub
- Grass/Herbaceous
- Soil/Rock

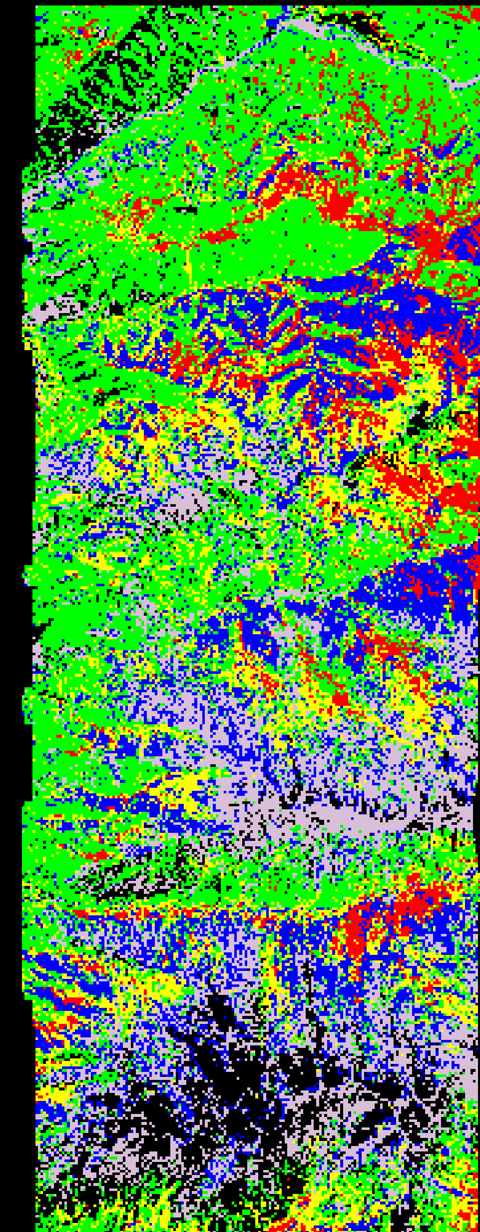

20m AVIRIS, 20m em	60m AVIRIS, 60m em
Accuracy 87.6%	Accuracy 78.8%
Kappa .838	Kappa .730

20m AVIRIS, 20m em

60m AVIRIS, 20m em

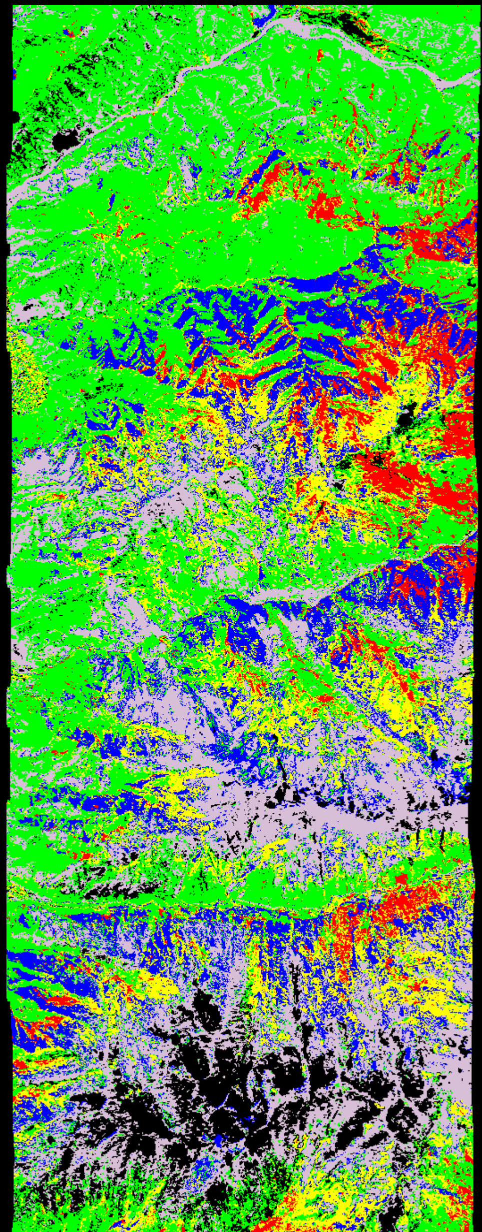

Broadleaf Deciduous Tree
Needleleaf Evergreen Tree
Broadleaf Deciduous Shrub
Grass/Herbaceous
Soil/Rock

Accuracy	Accuracy
87.6%	83.3%
Kappa	Kappa
.838	.782

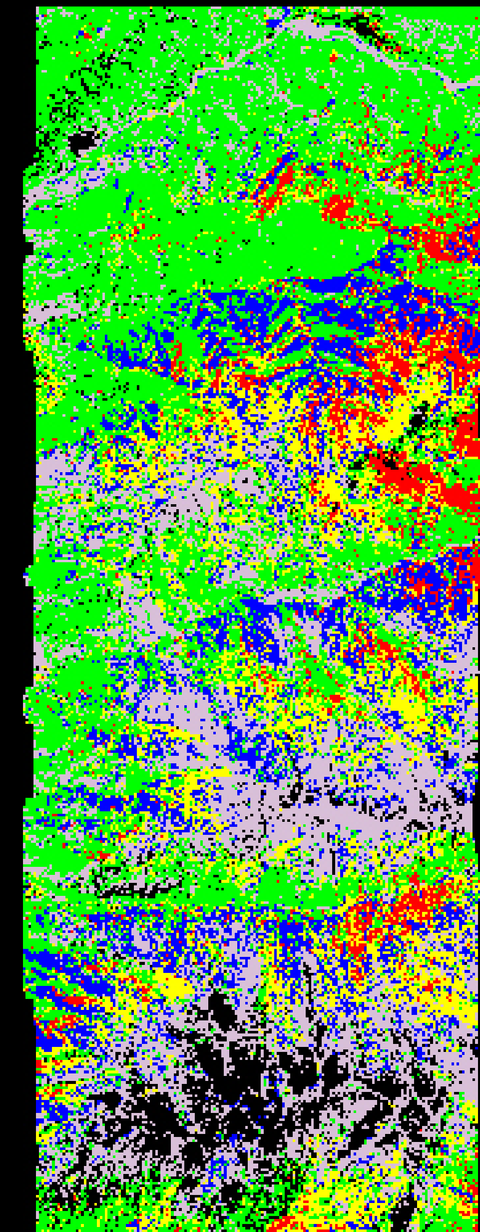

20m AVIRIS, 20m em

20m TM5, 20m em

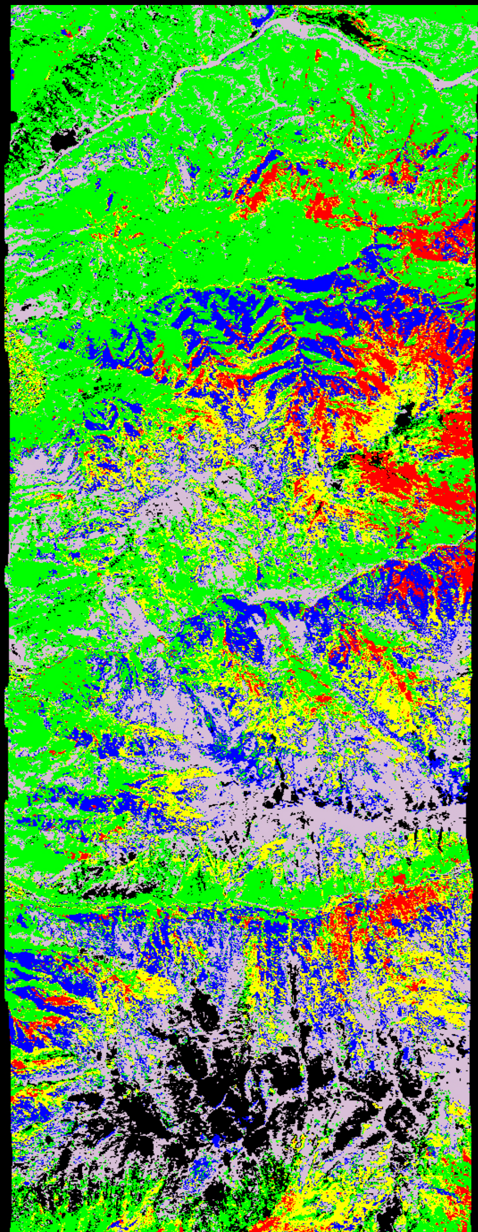

Broadleaf Deciduous Tree
Needleleaf Evergreen Tree
Broadleaf Deciduous Shrub
Grass/Herbaceous
Soil/Rock

Accuracy
87.6%

Kappa
.838

Accuracy
81.0%

Kappa
.754

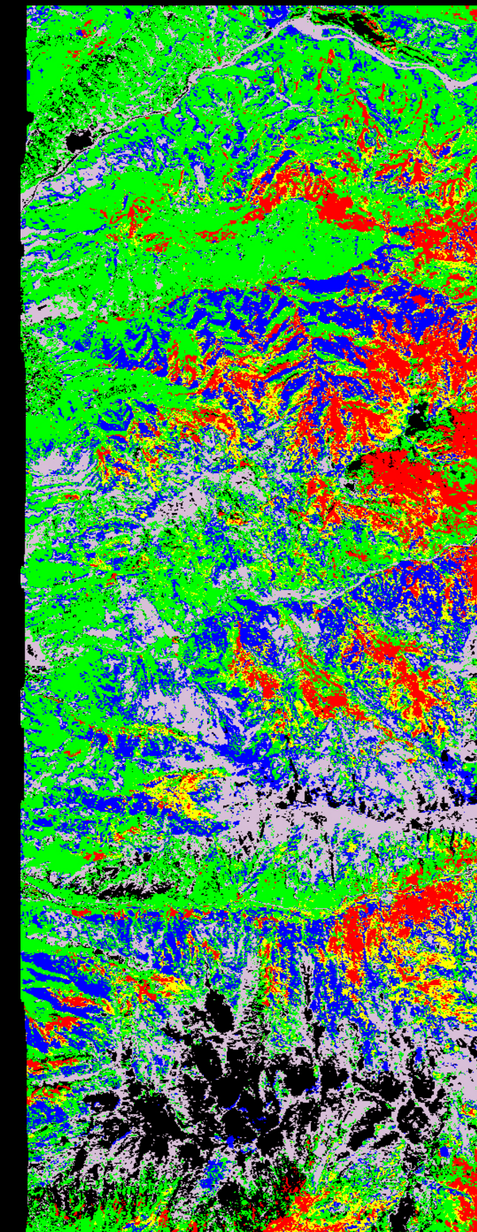

20m AVIRIS, 20m em

60m TM5, 60m em

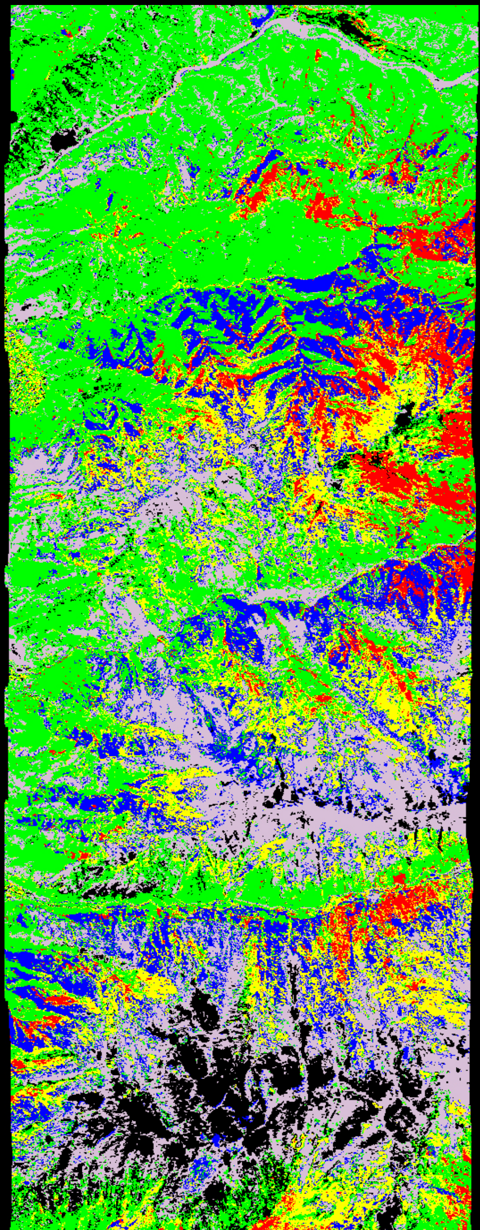

Broadleaf Deciduous Tree
Needleleaf Evergreen Tree
Broadleaf Deciduous Shrub
Grass/Herbaceous
Soil/Rock

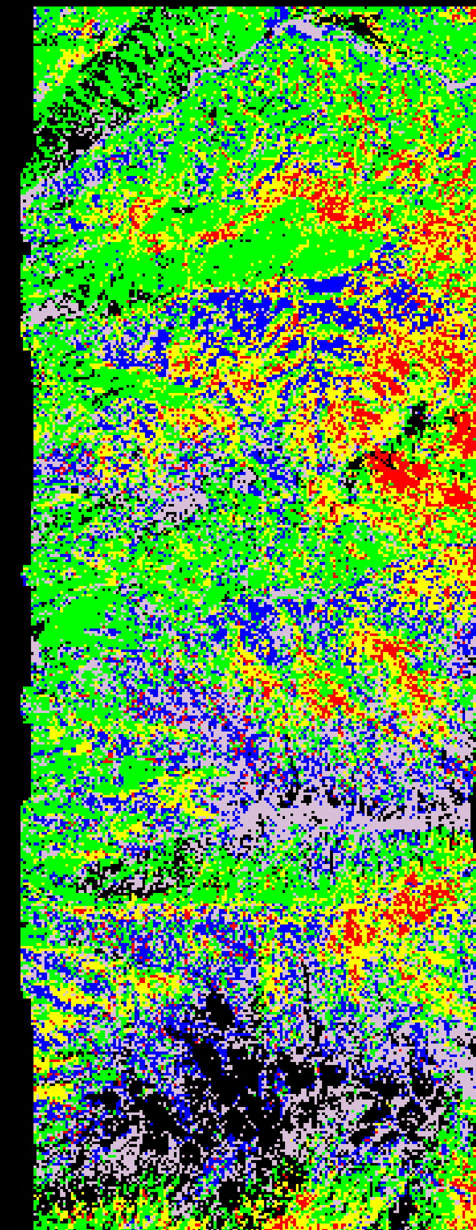

	Accuracy	Kappa
20m AVIRIS, 20m em	87.6%	.838
60m TM5, 60m em	74.5%	.607

20m AVIRIS, 20m em

60m TM5, 20m em

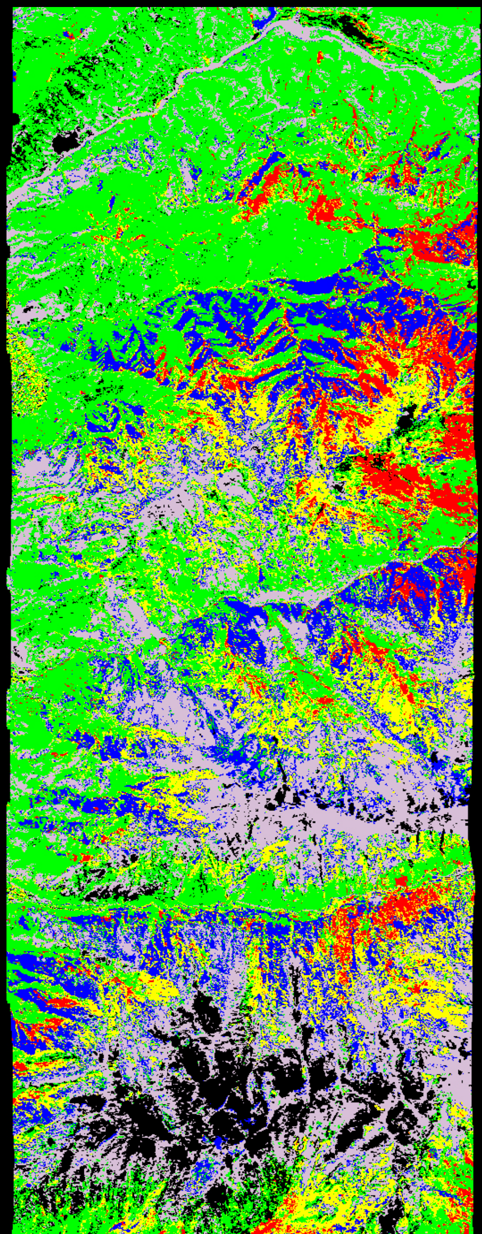

Accuracy
87.6%

Kappa
.838

Accuracy
78.6%

Kappa
.722

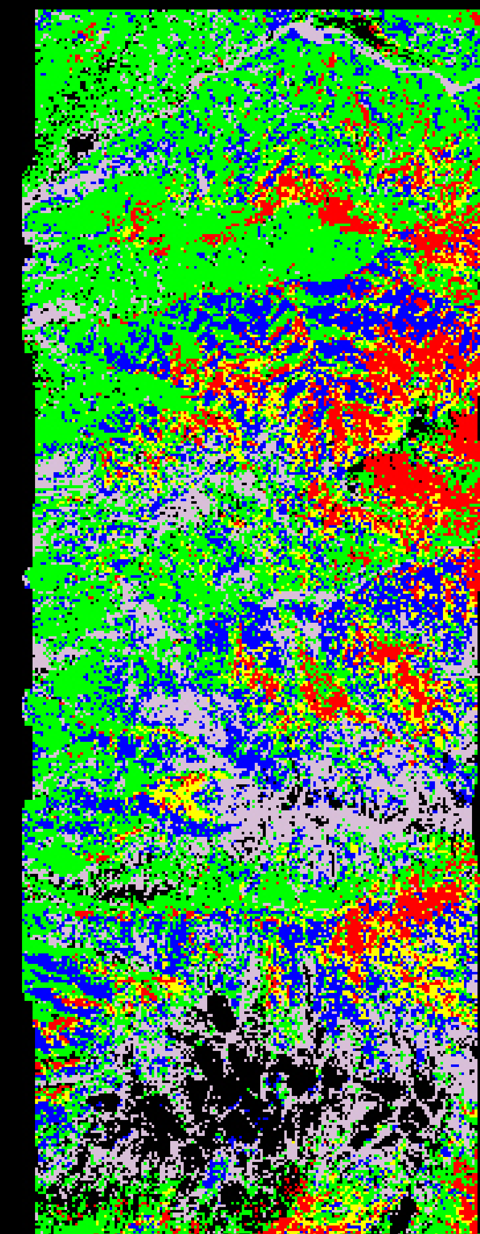

Accuracy Comparison

Spectral Resolution	Image Resolution	Em Resolution	Overall Accuracy	Kappa
AVIRIS	20	20	87.6%	0.84
AVIRIS	40	20	86.1%	0.82
AVIRIS	60	20	83.3%	0.78
TM5	20	20	81.0%	0.75
TM5	40	20	81.0%	0.75
AVIRIS	60	60	78.8%	0.73
TM5	60	20	78.6%	0.72
AVIRIS	40	40	77.8%	0.72
TM5	40	40	76.5%	0.70
TM5	60	60	74.5%	0.61

User’s Accuracy (%)

Spectral Res.	Image Res.	Em Res.	Broadleaf Deciduous Tree	Needleleaf Evergreen Tree	Broadleaf Deciduous Shrub	Grass/ Herbaceous	Soil/Rock
AVIRIS	20	20	75.6	99.1	87.1	80.2	98.2
AVIRIS	40	40	57.5	99.0	82.4	62.4	91.4
AVIRIS	40	20	76.9	97.8	84.4	78.1	95.8
AVIRIS	60	60	59.7	97.5	90.2	53.2	96.0
AVIRIS	60	20	72.1	98.3	82.0	78.1	91.1
TM5	20	20	58.3	98.6	84.3	46.1	97.5
TM5	40	40	65.5	99.6	86.7	44.3	91.5
TM5	40	20	61.0	98.2	84.4	46.6	95.3
TM5	60	60	74.6	89.5	84.4	41.2	87.6
TM5	60	20	55.7	97.5	82.6	45.5	91.1

Producer's Accuracy (%)

Spectral Res.	Image Res.	Em Res.	Broadleaf Deciduous Tree	Needleleaf Evergreen Tree	Broadleaf Deciduous Shrub	Grass/ Herbaceous	Soil/Rock
AVIRIS	20	20	91.0	83.0	97.1	85.6	80.6
AVIRIS	40	40	92.0	60.9	90.5	70.8	80.9
AVIRIS	40	20	92.0	78.8	97.9	84.3	78.3
AVIRIS	60	60	86.0	76.1	84.5	80.5	70.6
AVIRIS	60	20	88.0	72.9	96.5	78.1	80.4
TM5	20	20	93.9	82.1	93.4	27.0	78.2
TM5	40	40	84.8	74.7	80.0	56.2	77.9
TM5	40	20	96.4	77.9	94.8	30.3	78.3
TM5	60	60	88.0	60.7	80.3	85.4	76.5
TM5	60	20	88.0	74.8	93.7	24.4	80.4

Results

- Accuracy is higher at finer spatial and spectral resolutions
- Accuracy is higher when endmembers were selected from the 20 m image
  - Purer endmembers at 20 m
  - Spectral mixing at edges of polygons at coarser spatial resolution
- While finer resolution TM bands have similar overall accuracies to coarser resolution AVIRIS, accuracy can be very low for poorly discriminated classes

Limitations

- Polygons were required to have a minimum size and PFT dominance
  - Accuracy would be lower at coarser spatial resolutions if smaller, more heterogeneous polygons were included
- Our PFTs have broad structural and spectral differences
  - More spectrally similar PFTs will be more difficult to map
  - Analysis of additional spatial/spectral resampled datasets is underway for Wind River, Sierra Nevada, Santa Barbara
- Spatial average of 9 20 m pixels is not equivalent to 60 m HyspIRI point spread function

Conclusions

- Finer spatial and spectral resolutions increased PFT mapping accuracy
- High classification accuracies are possible at 60 m (for contiguous vegetation patches > 60 m)
- Finer spatial resolution airborne or spaceborne sensors may have a role creating training data for HyspIRI classification

Acknowledgements

- JPL: Rob Green, Sarah Lundeen
- Seminar students: Bob Benton, Annie Bryant, McKenzie Skiles, Jamie Turrin, Yuan Zhang

20m AVIRIS, 20m em

SWIR/NIR/red composite

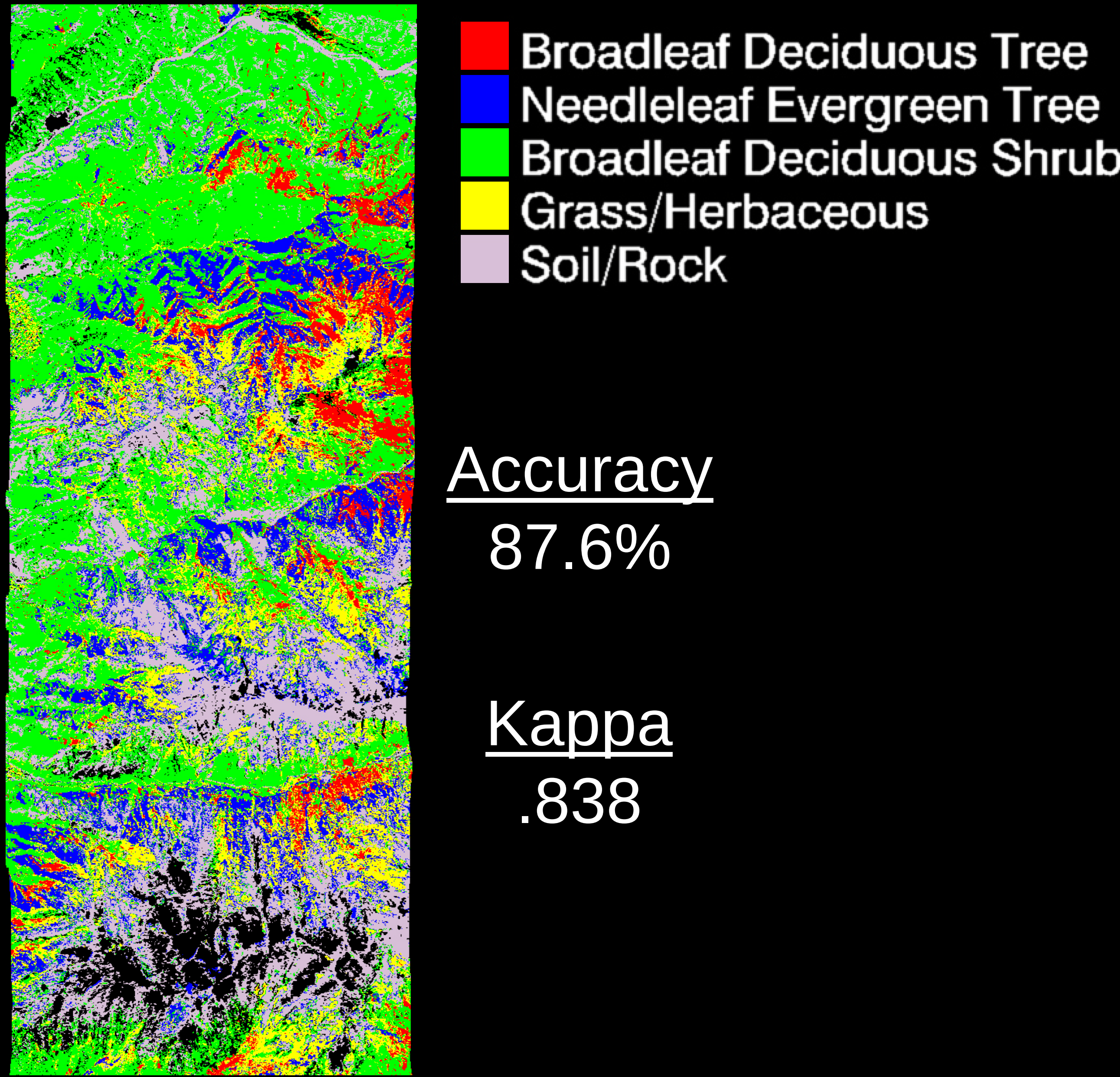

<u>Accuracy</u>
87.6%

<u>Kappa</u>
.838

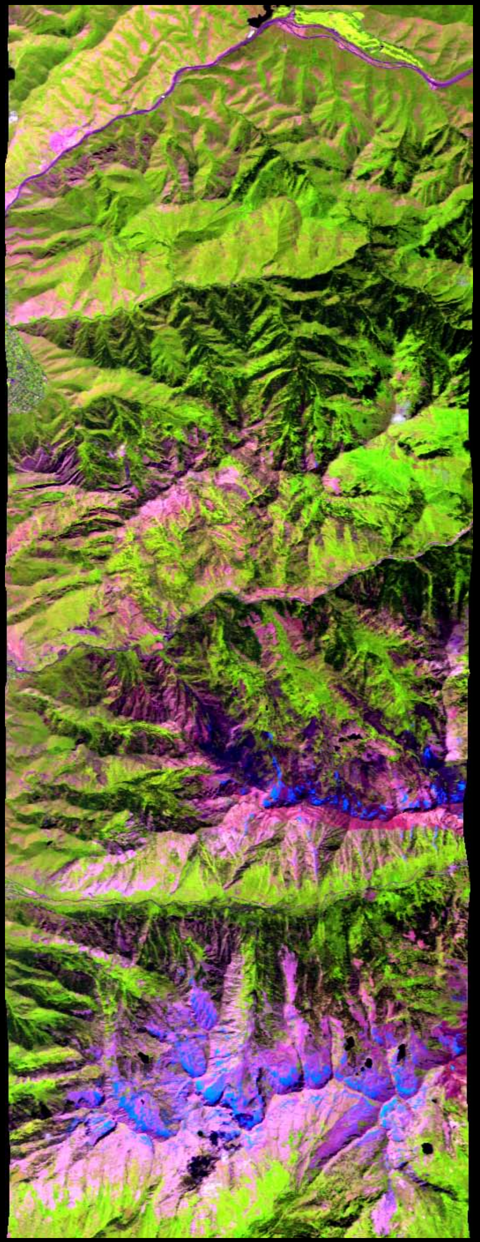

20m AVIRIS, 20m em

40 m AVIRIS, 40 m em

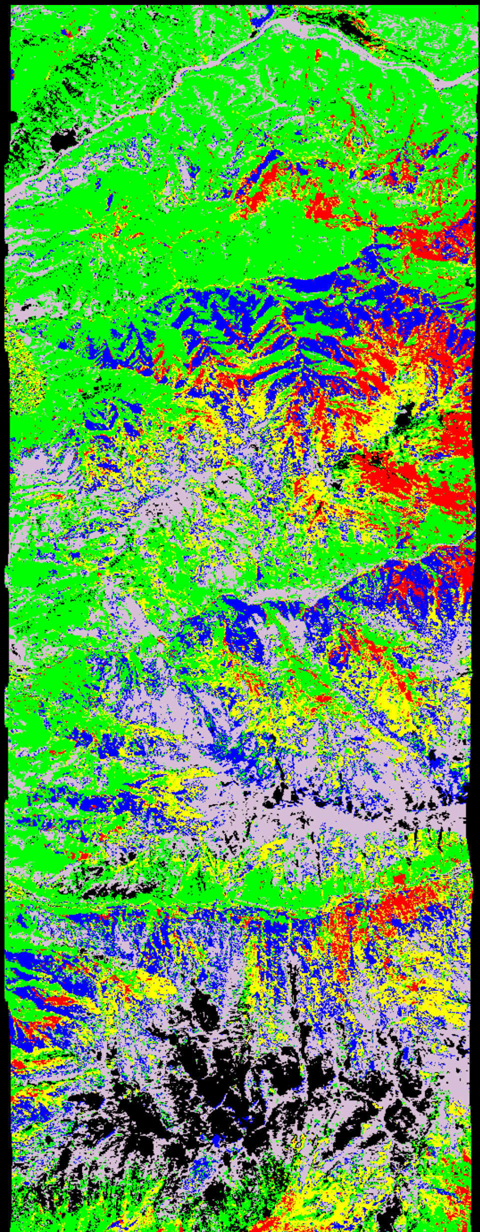

Broadleaf Deciduous Tree
Needleleaf Evergreen Tree
Broadleaf Deciduous Shrub
Grass/Herbaceous
Soil/Rock

Accuracy
87.6%

Kappa
.838

Accuracy
77.8%

Kappa
.716

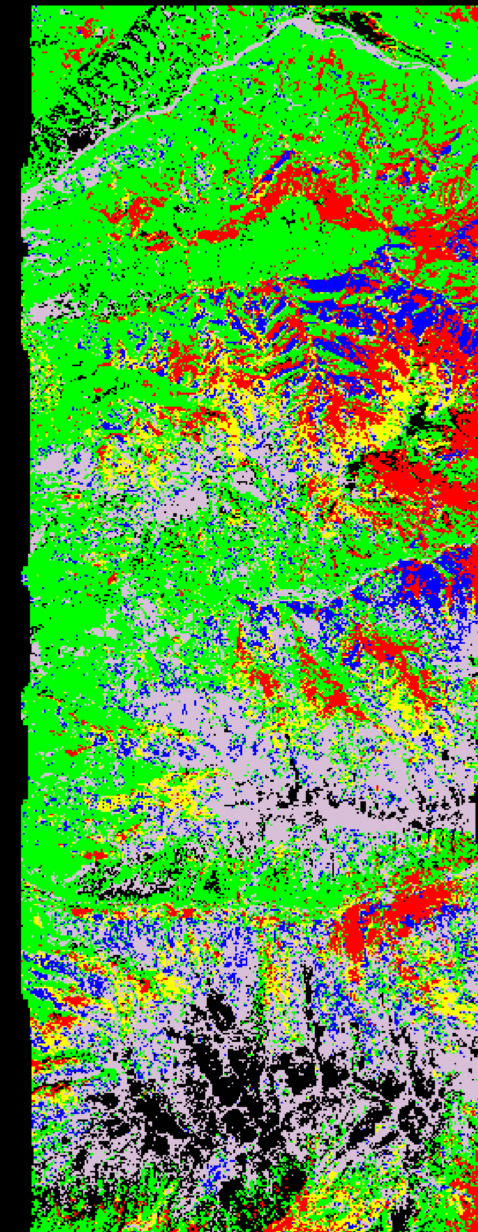

20m AVIRIS, 20m em

60m AVIRIS, 60m em

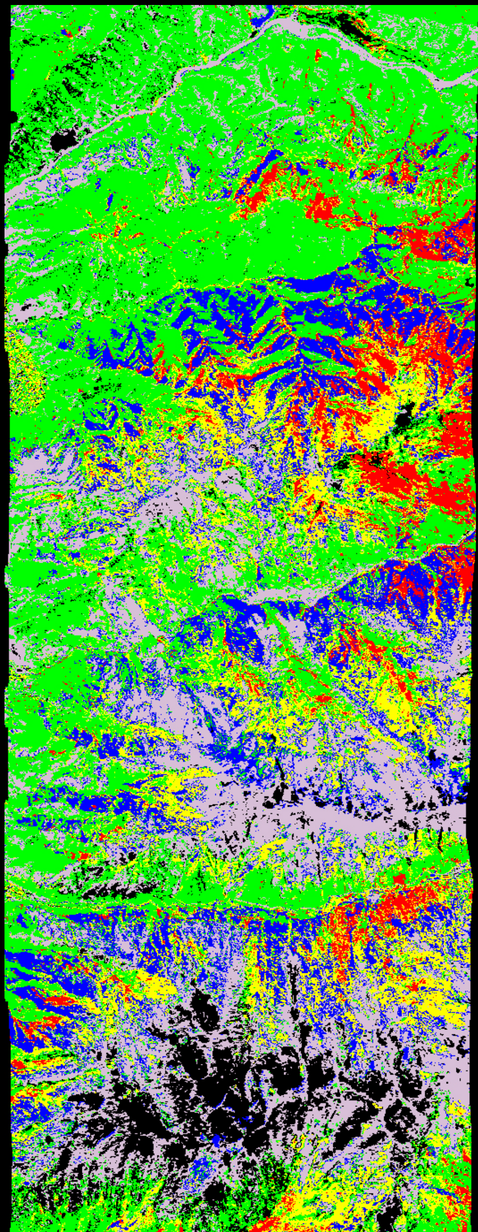

Broadleaf Deciduous Tree
Needleleaf Evergreen Tree
Broadleaf Deciduous Shrub
Grass/Herbaceous
Soil/Rock

Accuracy
87.6%

Kappa
.838

Accuracy
78.8%

Kappa
.730

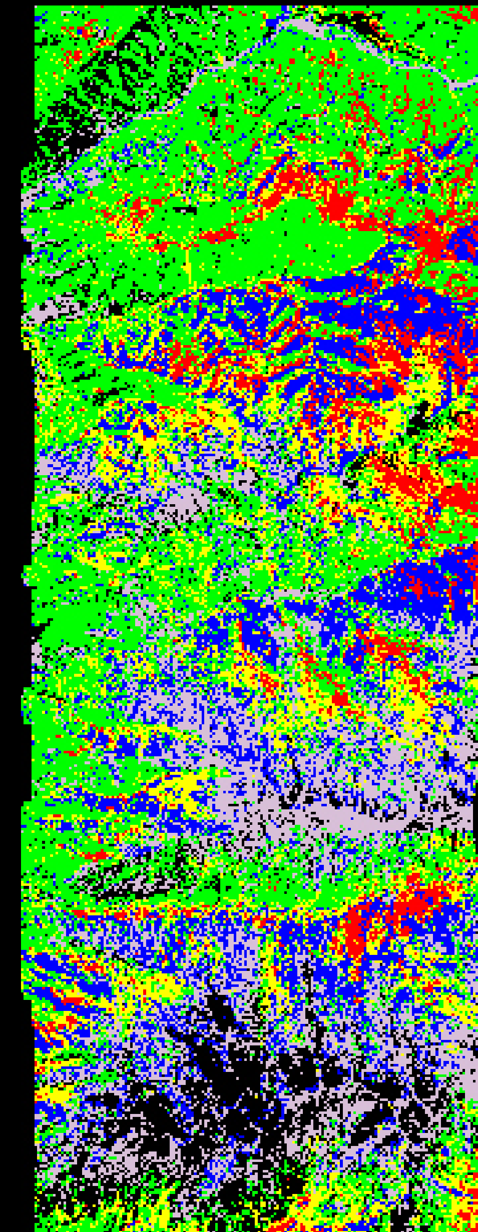

20m AVIRIS, 20m em

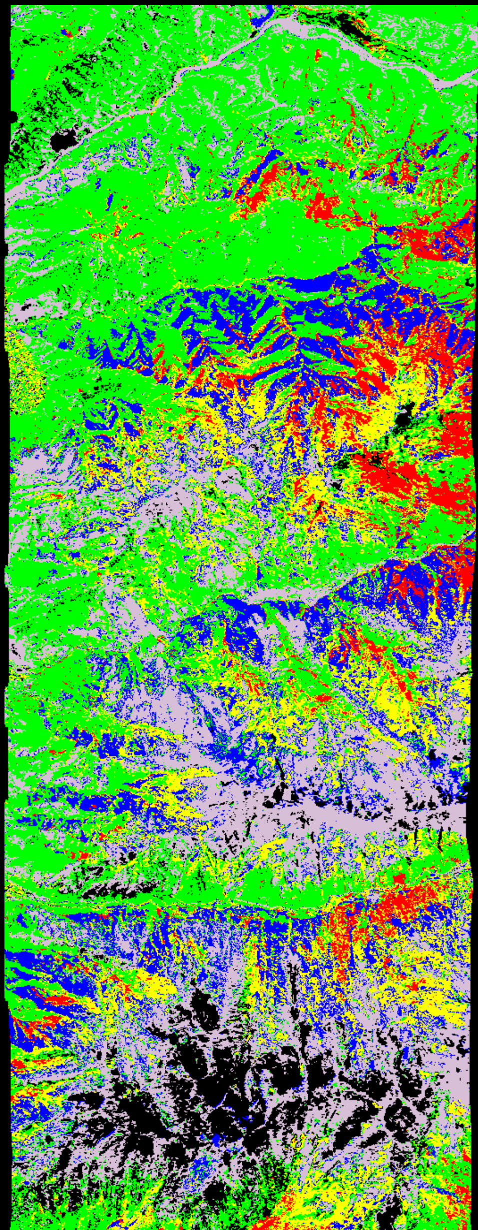

40m AVIRIS, 20m em

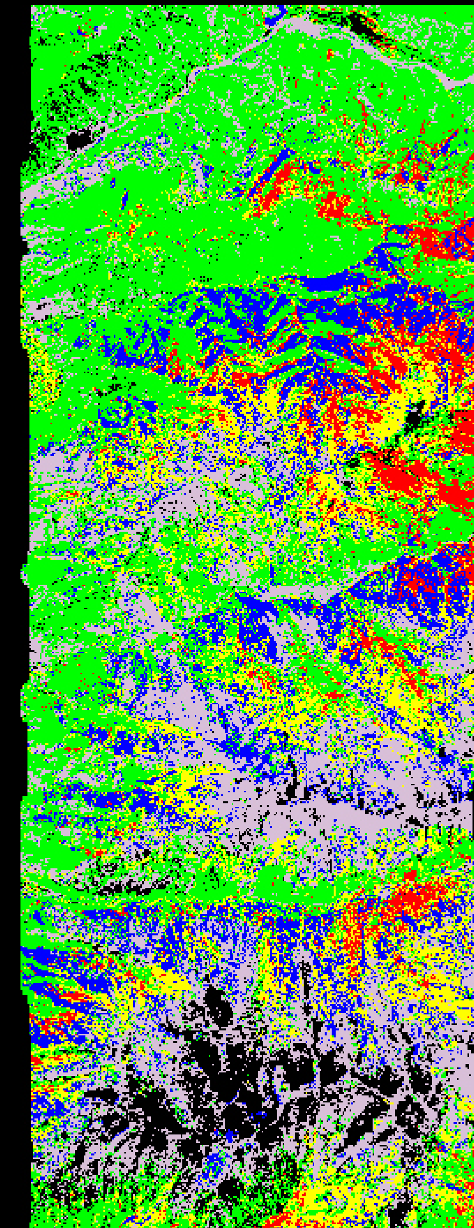

- Broadleaf Deciduous Tree
- Needleleaf Evergreen Tree
- Broadleaf Deciduous Shrub
- Grass/Herbaceous
- Soil/Rock

20m AVIRIS, 20m em	40m AVIRIS, 20m em
Accuracy 87.6%	**Accuracy** 86.1%
Kappa .838	**Kappa** .818

20m AVIRIS, 20m em

60m AVIRIS, 20m em

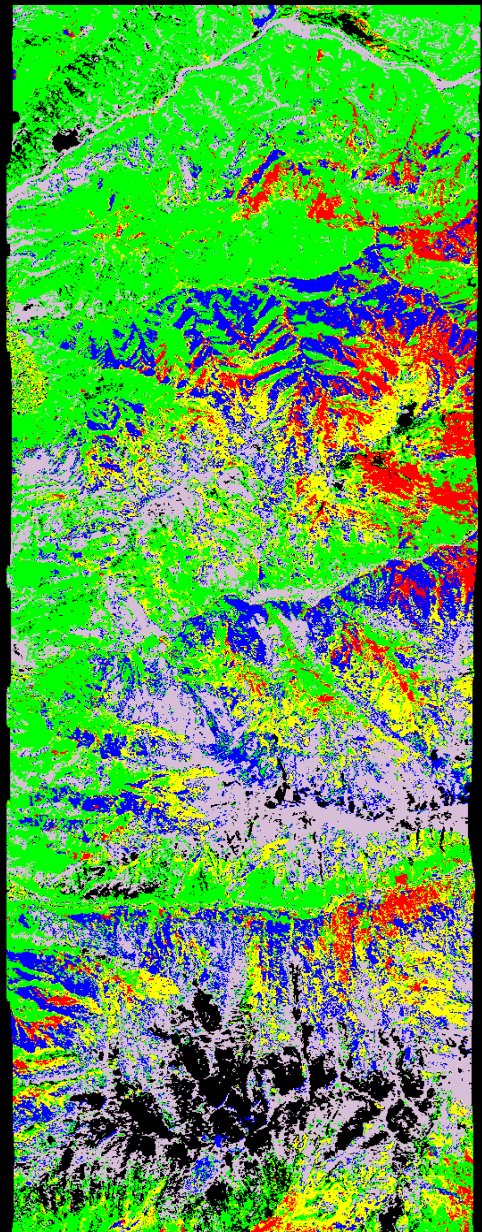

- Broadleaf Deciduous Tree
- Needleleaf Evergreen Tree
- Broadleaf Deciduous Shrub
- Grass/Herbaceous
- Soil/Rock

<u>Accuracy</u>
87.6%

<u>Kappa</u>
.838

<u>Accuracy</u>
83.3%

<u>Kappa</u>
.782

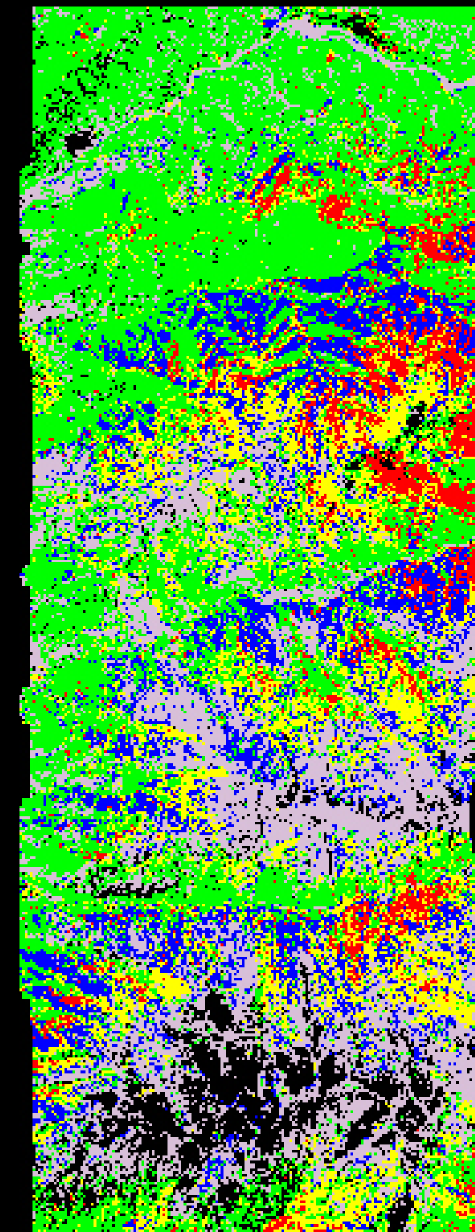

20m AVIRIS, 20m em

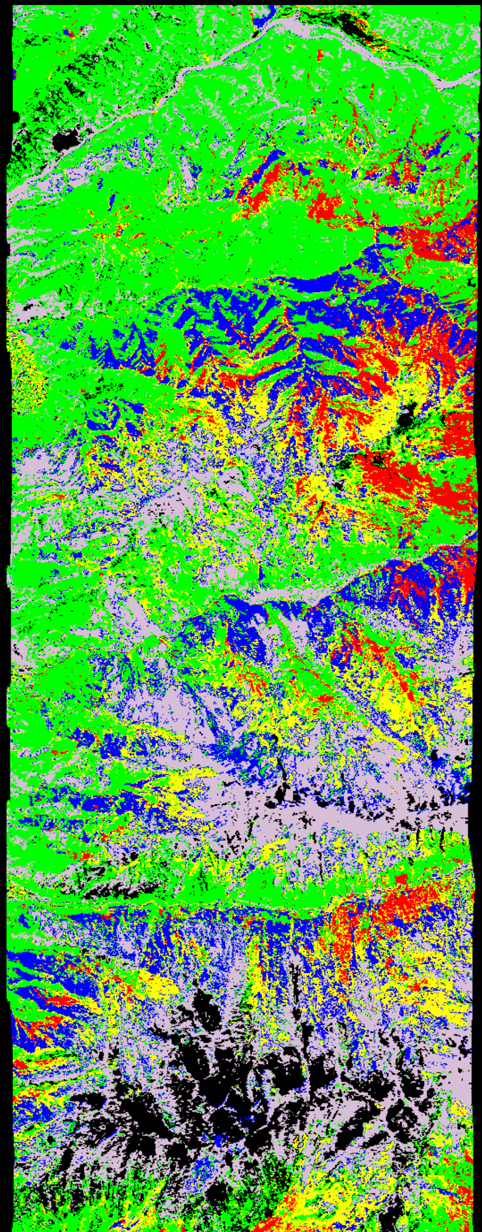

Broadleaf Deciduous Tree
Needleleaf Evergreen Tree
Broadleaf Deciduous Shrub
Grass/Herbaceous
Soil/Rock

Accuracy
87.6%

Kappa
.838

20m TM5, 20m em

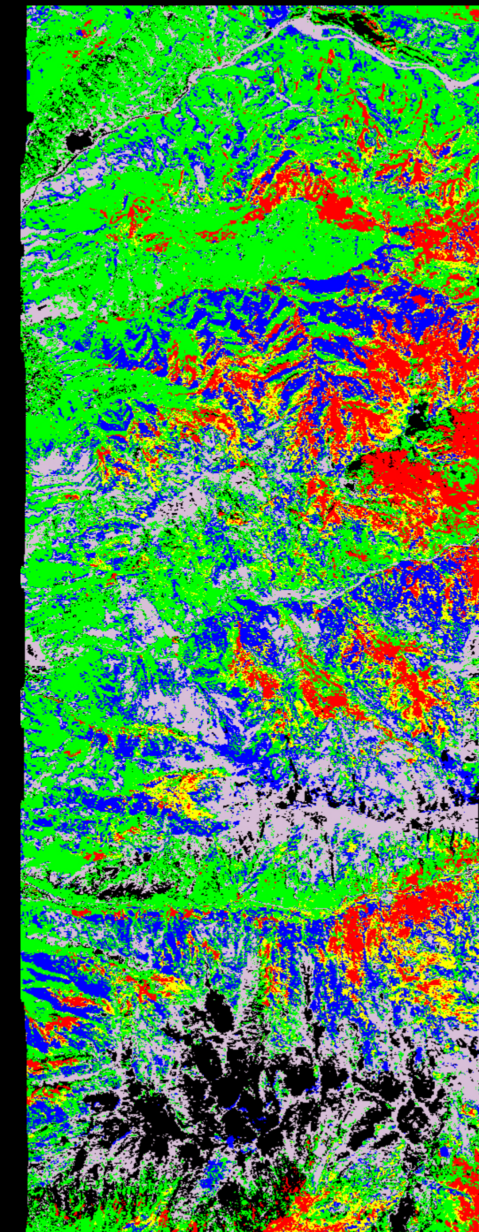

Accuracy
81.0%

Kappa
.754

20m AVIRIS, 20m em

40m TM5, 40m em

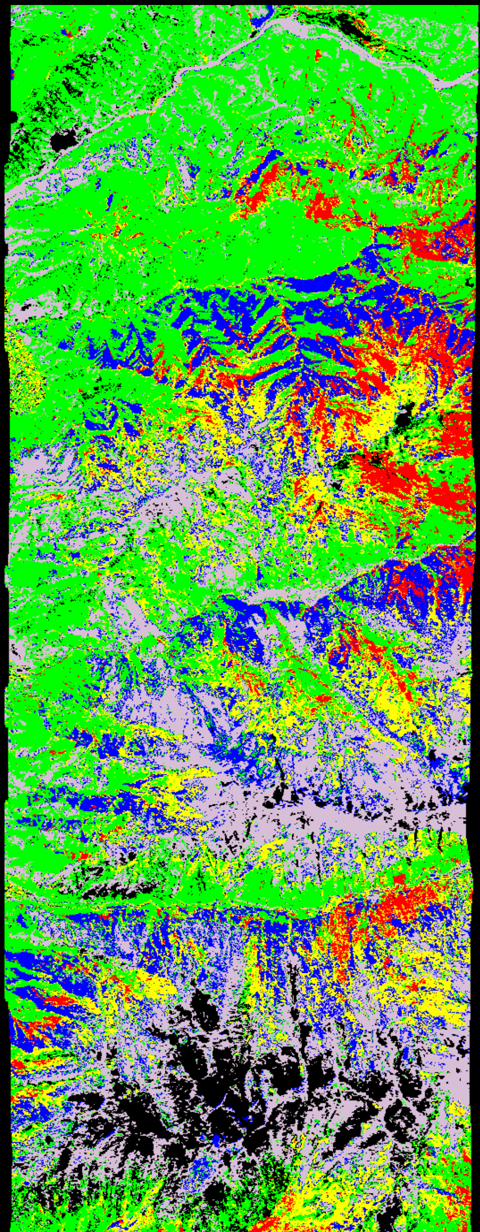

Broadleaf Deciduous Tree
Needleleaf Evergreen Tree
Broadleaf Deciduous Shrub
Grass/Herbaceous
Soil/Rock

<u>Accuracy</u>
87.6%

<u>Kappa</u>
.838

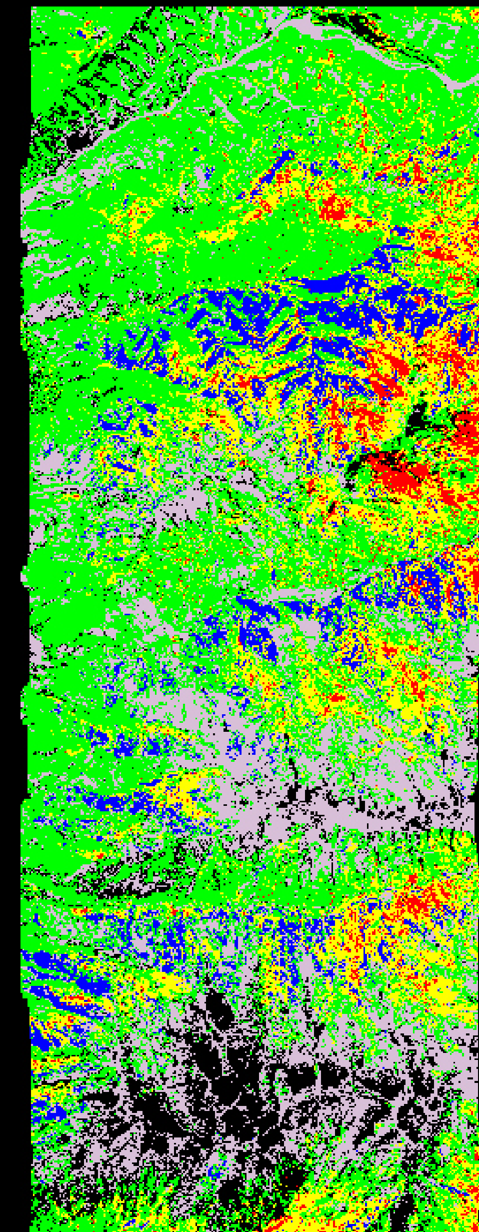

<u>Accuracy</u>
76.5%

<u>Kappa</u>
.701

20m AVIRIS, 20m em

60m TM5, 60m em

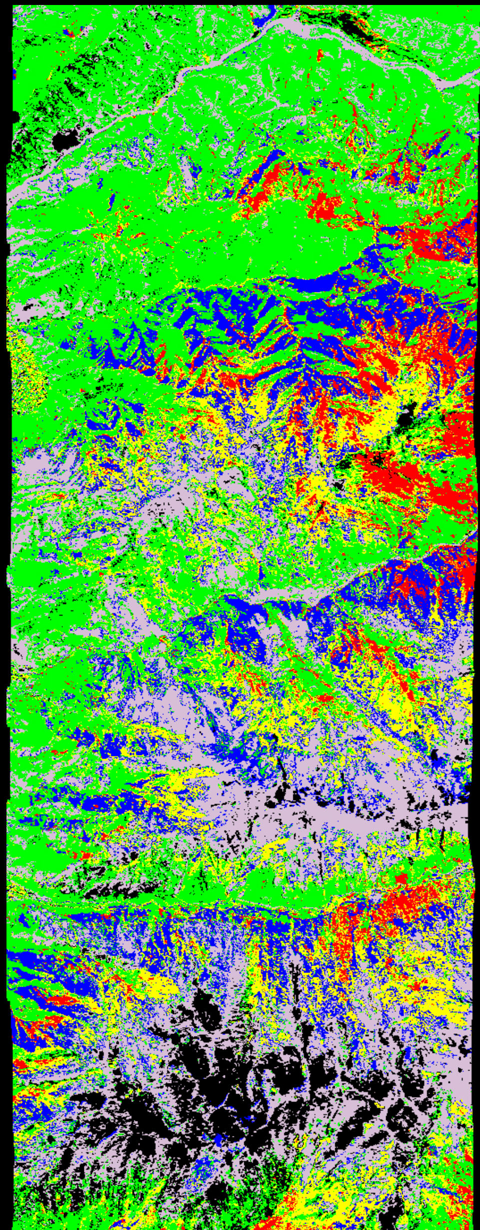

Broadleaf Deciduous Tree
Needleleaf Evergreen Tree
Broadleaf Deciduous Shrub
Grass/Herbaceous
Soil/Rock

Accuracy
87.6%

Kappa
.838

Accuracy
68.6%

Kappa
.607

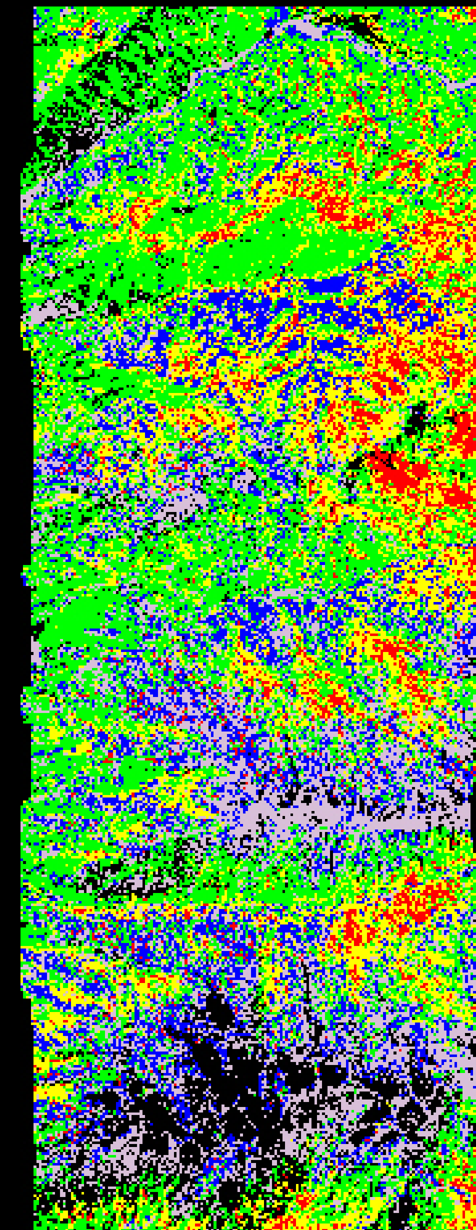

20m AVIRIS, 20m em

40m TM5, 20m em

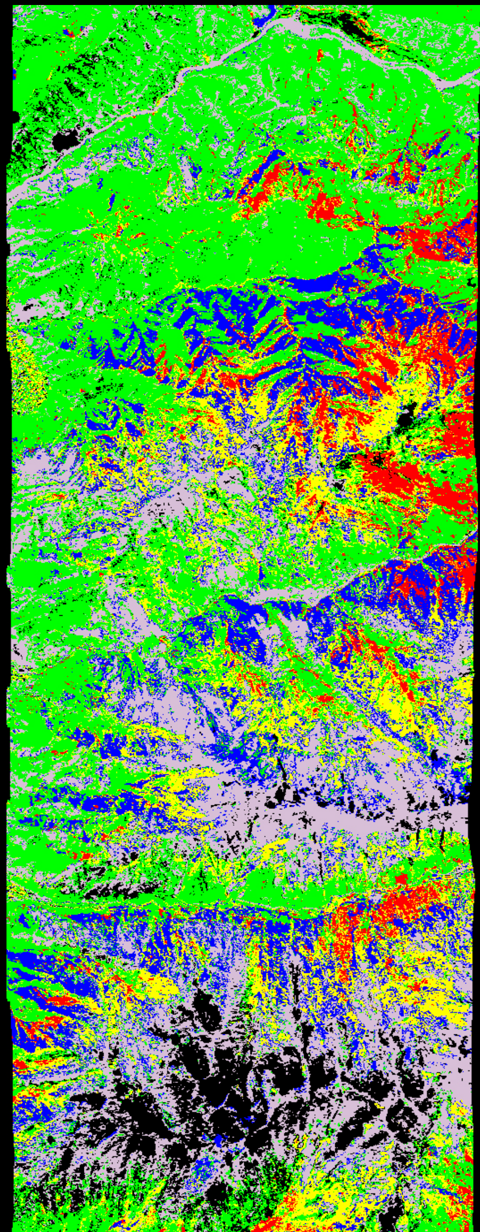

- Broadleaf Deciduous Tree
- Needleleaf Evergreen Tree
- Broadleaf Deciduous Shrub
- Grass/Herbaceous
- Soil/Rock

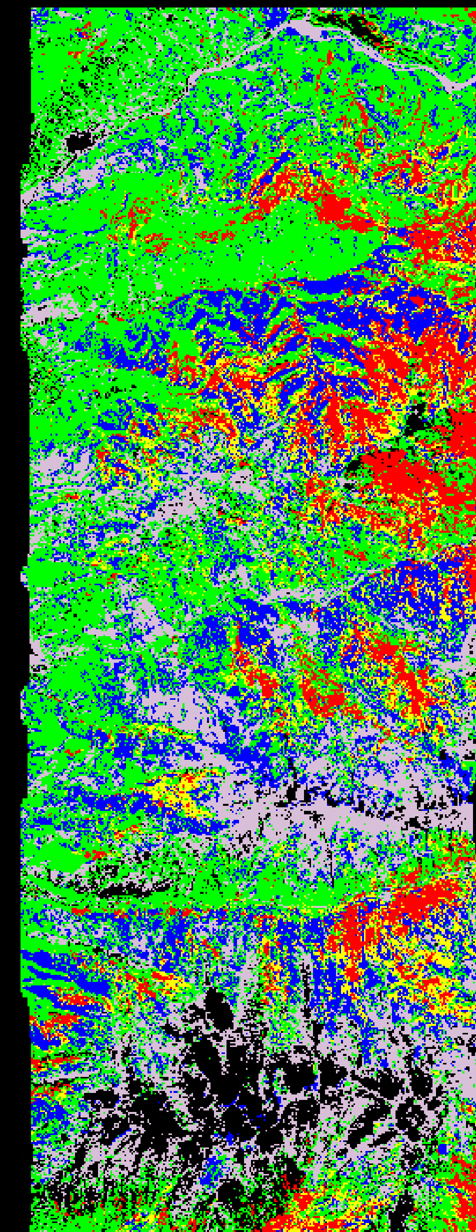

20m AVIRIS, 20m em	40m TM5, 20m em
Accuracy 87.6%	Accuracy 81.0%
Kappa .838	Kappa .753

20m AVIRIS, 20m em

60m TM5, 20m em

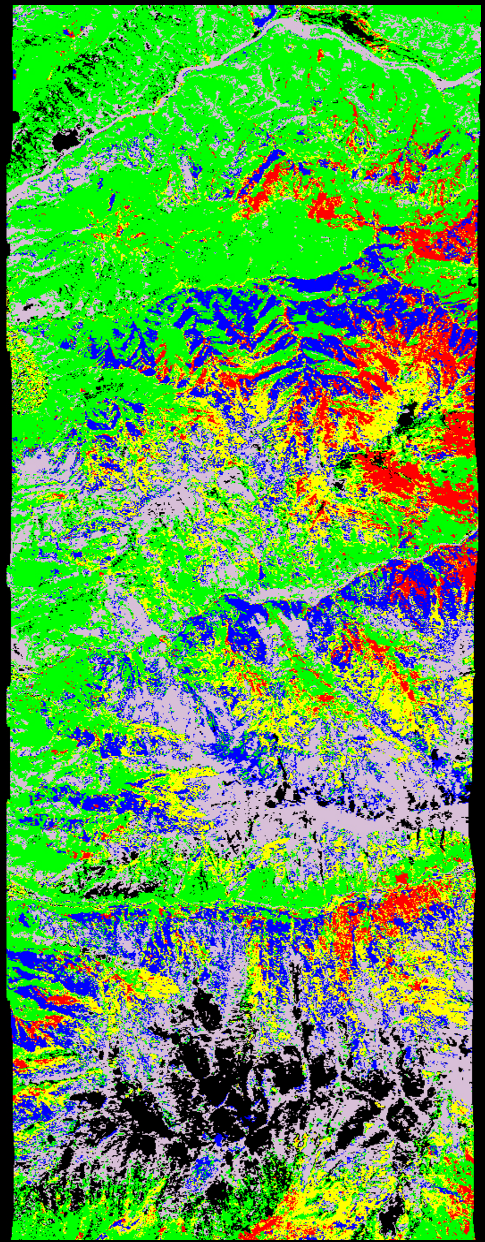

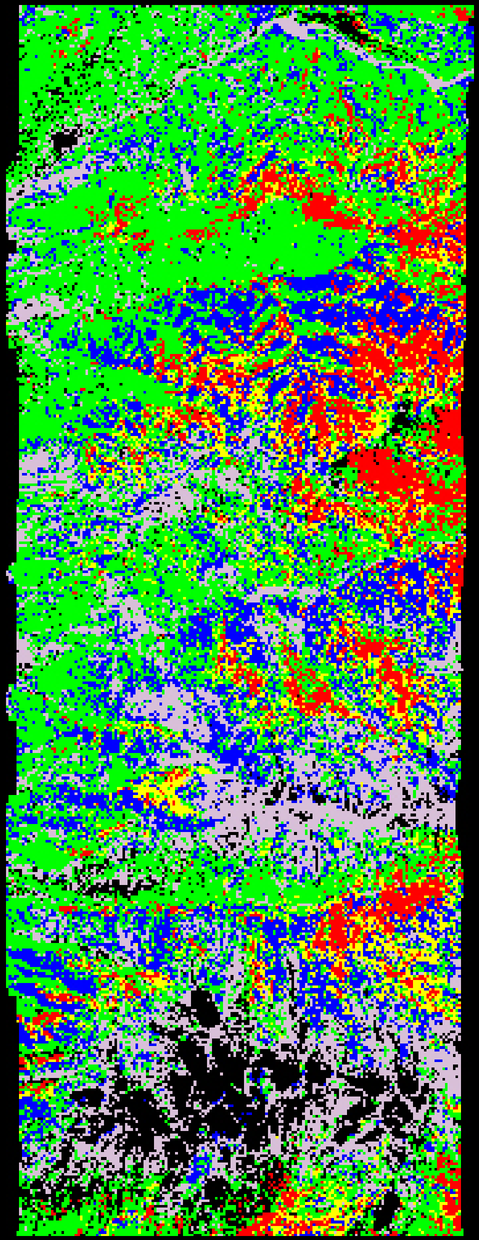

Broadleaf Deciduous Tree
Needleleaf Evergreen Tree
Broadleaf Deciduous Shrub
Grass/Herbaceous
Soil/Rock

20m AVIRIS, 20m em	60m TM5, 20m em
Accuracy 87.6%	Accuracy 78.6%
Kappa .838	Kappa .722

Broadleaf deciduous shrub Training polygon

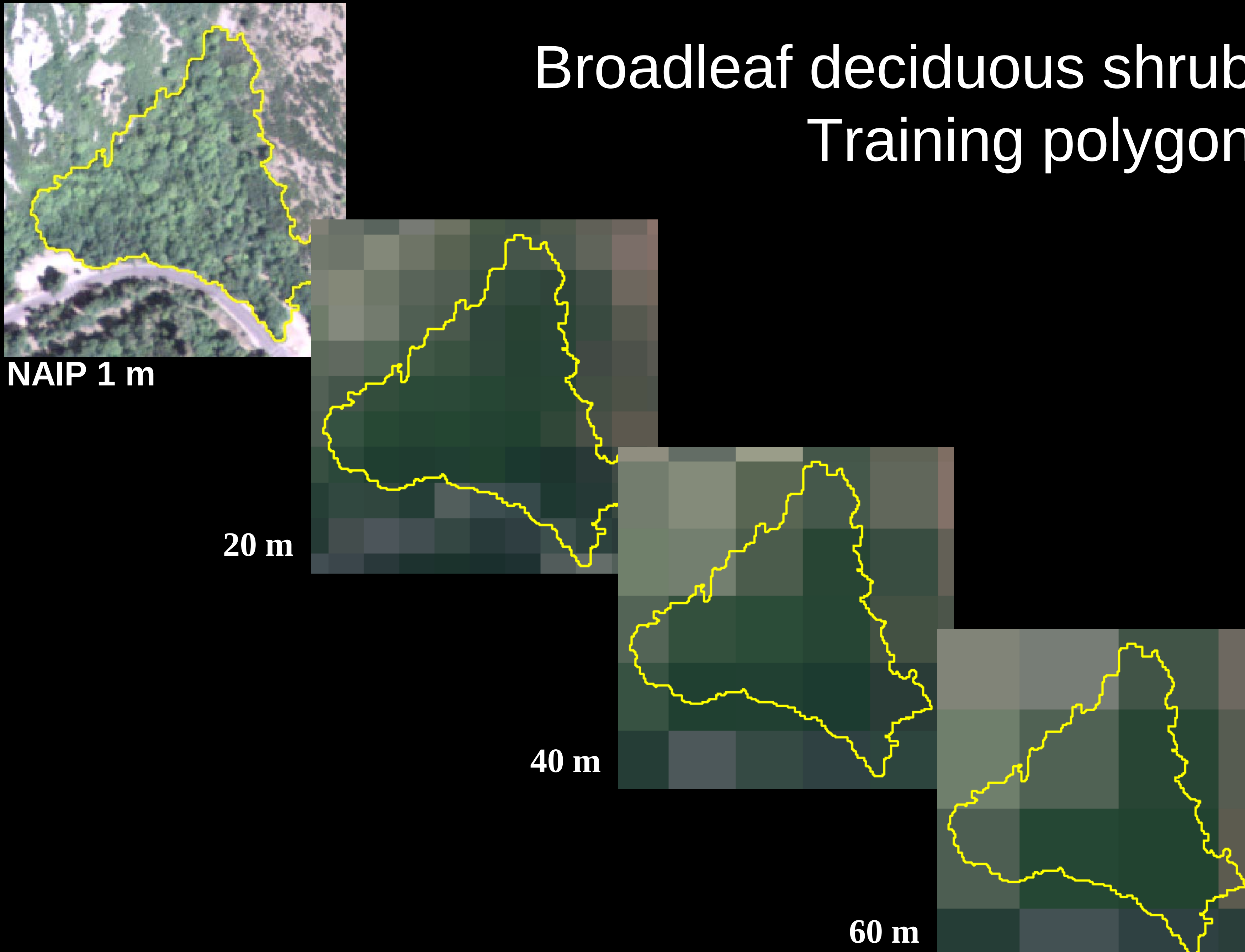

Broadleaf deciduous tree polygon

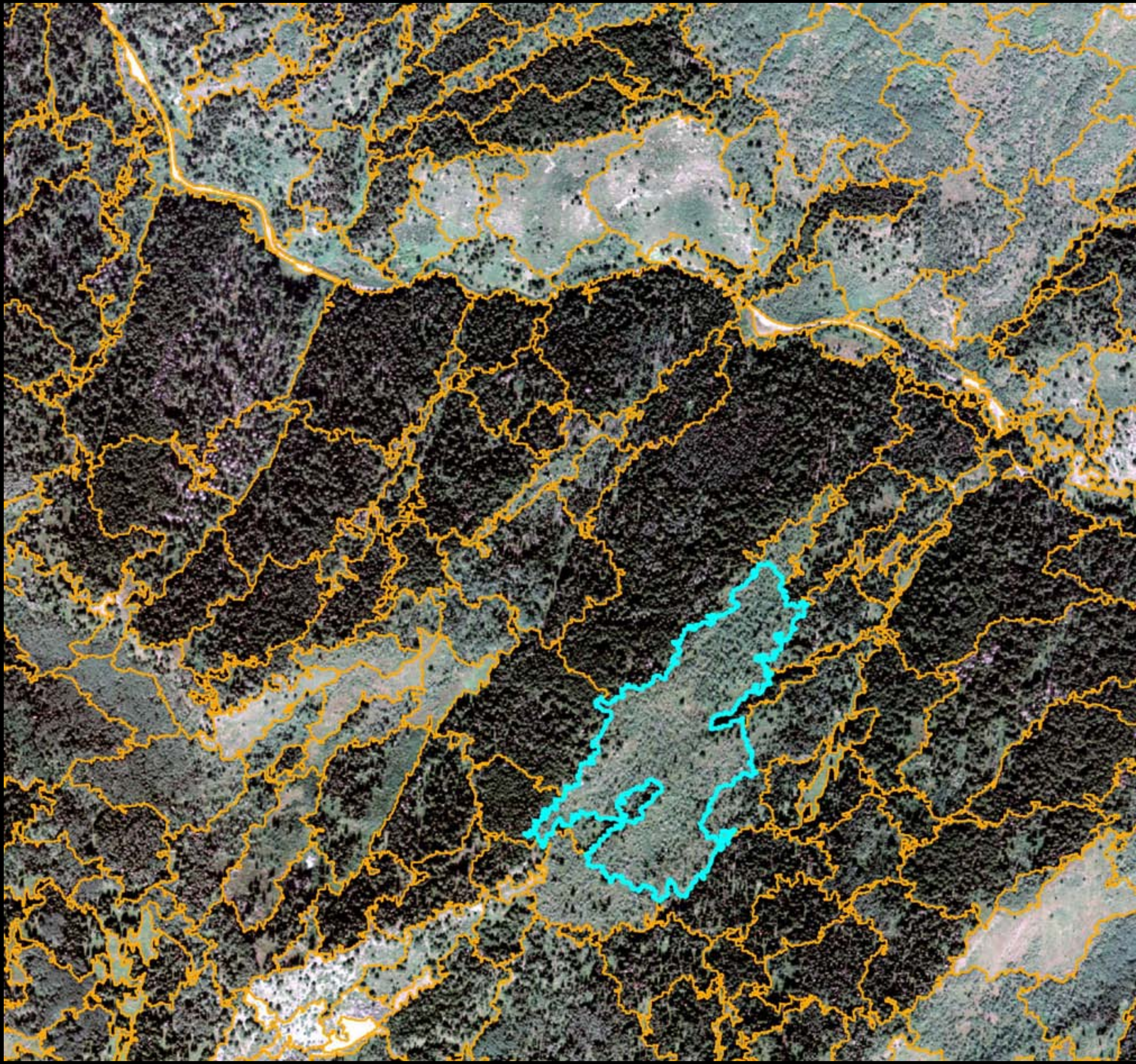

A radiometrically-accurate HyspIRI dataset created for arid land surfaces using combined ASTER and AVIRIS data

Michael Ramsey, Christopher Hughes & Steve Scheidt
Dept. of Geology and Planetary Science, University of Pittsburgh, Pittsburgh, PA

Outline

- **Arid land measurements**
  - climate relevance and importance of HyspIRI
    - dust composition, radiative cooling impact
    - thermal inertia → soil moisture → sediment mobility
- **Data analysis**
  - simple resampling vs. super-resolution
- **Target: Lunar Lake, NV**
  - site description, data sets
- **Preliminary results and future possibilities**

Overarching Questions

- **Can HyspIRI be used effectively to monitor trends for arid lands?**
  - *example:* *soil composition, soil moisture, albedo, dust properties → impact on local/regional climate, ...*

- **Will the proposed spatial and spectral resolution of HyspIRI be adequate for these studies?**
  - *can we accurately (and quantitatively) simulate HyspIRI's spatial/spectral resolution pre-launch??*

- **Conclusion:** ***yes***

Why Focus on Arid Lands?

- **Climate and geologic relevance**
  - <u>shorter-term:</u> radiative forcings of dust?, soil moisture
    - *<u>example:</u> at the last HyspIRI workshop I presented the work using thermal inertia → soil moisture → sediment mobility*
      - using ASTER, one of the driest periods at White Sands was captured two days prior to one of the largest dust plumes in the region
  - <u>longer-term:</u> movement of dunes as indicators
- **Excellent conditions for VSWIR/TIR data**
- **Large database of global sites over the decadal time scale**
    - ASTER, Landsat TM, AVIRIS, MASTER, etc.

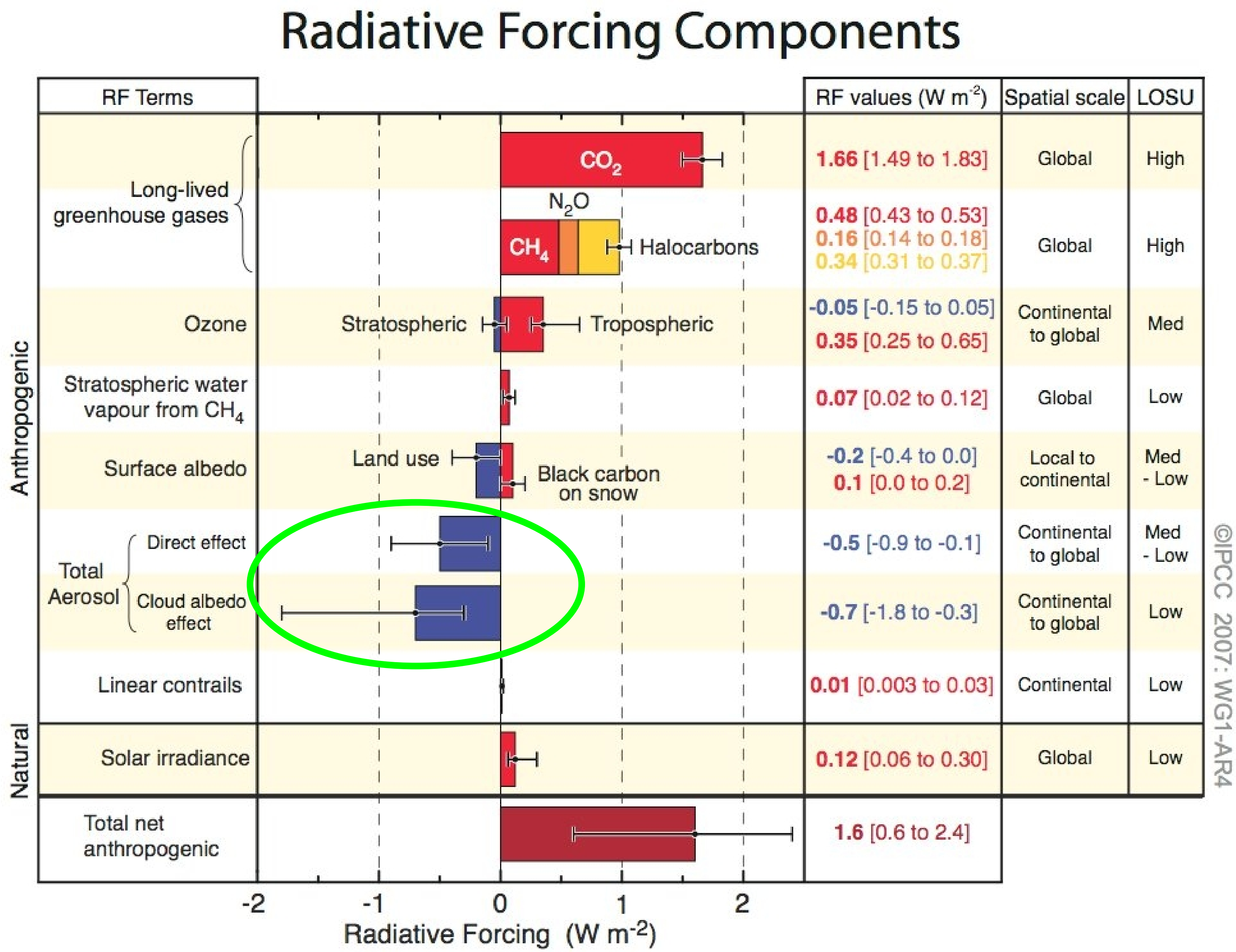

Radiative Forcing Components
RF Terms
RF values (W m-2)
Spatial scale
LOSU
Anthropogenic
Long-lived greenhouse gases
CO2
1.66 [1.49 to 1.83]
Global
High
N2O
CH4
Halocarbons
0.48 [0.43 to 0.53]
0.16 [0.14 to 0.18]
0.34 [0.31 to 0.37]
Global
High
Ozone
Stratospheric
Tropospheric
-0.05 [-0.15 to 0.05]
0.35 [0.25 to 0.65]
Continental to global
Med
Stratospheric water vapour from CH4
0.07 [0.02 to 0.12]
Global
Low
Surface albedo
Land use
Black carbon on snow
-0.2 [-0.4 to 0.0]
0.1 [0.0 to 0.2]
Local to continental
Med - Low
Total Aerosol
Direct effect
-0.5 [-0.9 to -0.1]
Continental to global
Med - Low
Cloud albedo effect
-0.7 [-1.8 to -0.3]
Continental to global
Low
Linear contrails
0.01 [0.003 to 0.03]
Continental
Low
Natural
Solar irradiance
0.12 [0.06 to 0.30]
Global
Low
Total net anthropogenic
1.6 [0.6 to 2.4]
-2
-1
0
1
2
Radiative Forcing (W m-2)
©IPCC 2007: WG1-AR4

Previous Work: *ASTER & GOES*

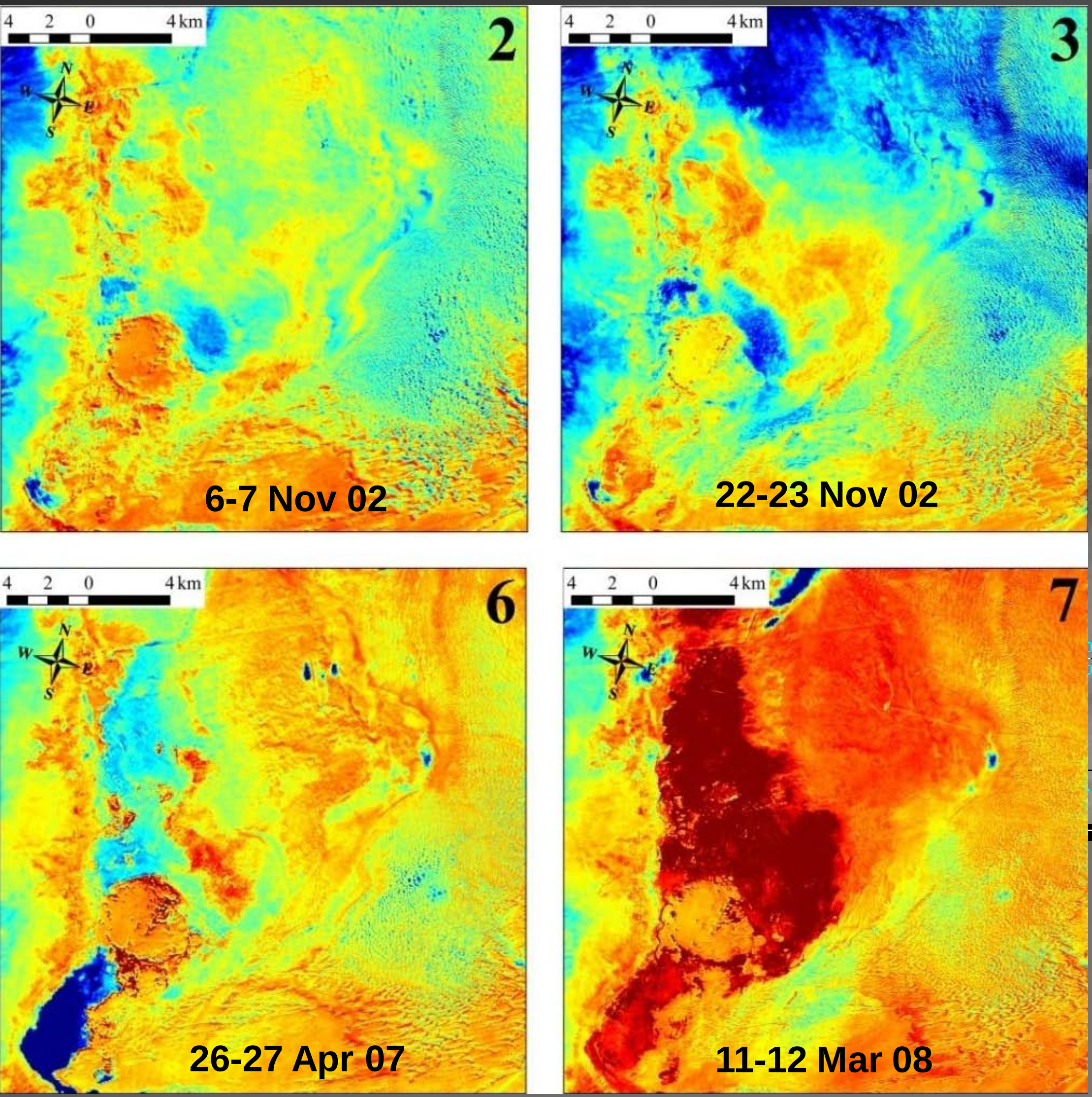

soil moisture (9% - 25%)

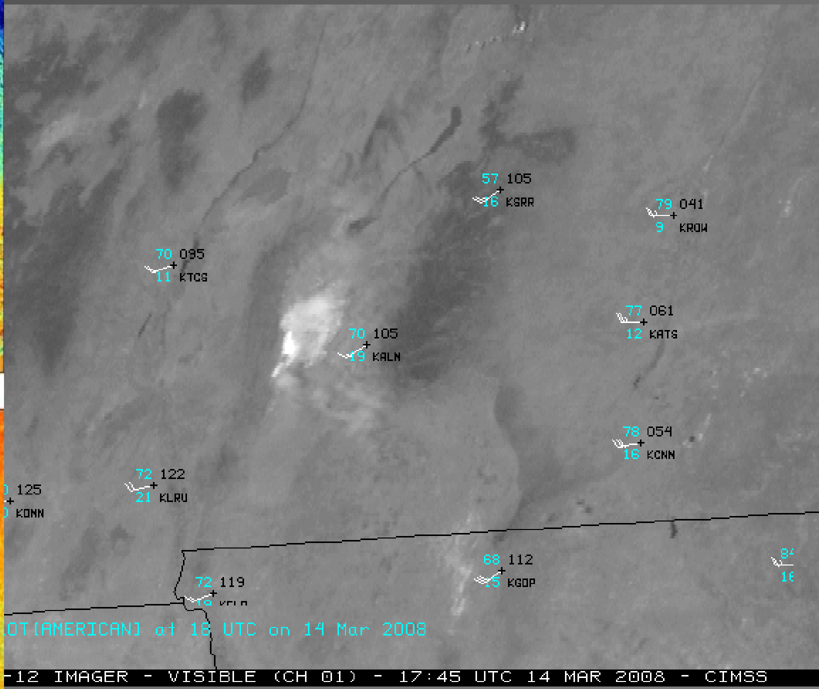

14 Mar 08

[Scheidt et al., 2010]

Larger Scale Dust Emissions?

- **Uncertainty**
  - direct vs. indirect radiative impact of dust loading
  - direct:
    - aerosols directly affect radiance
  - indirect:
    - aerosols affect clouds that affect radiance

  - what is the mineralogical composition of dust and dust source areas?
  - how does this affect local/region climate variations?

Eyjafjallajökull Volcano (*MODIS*)

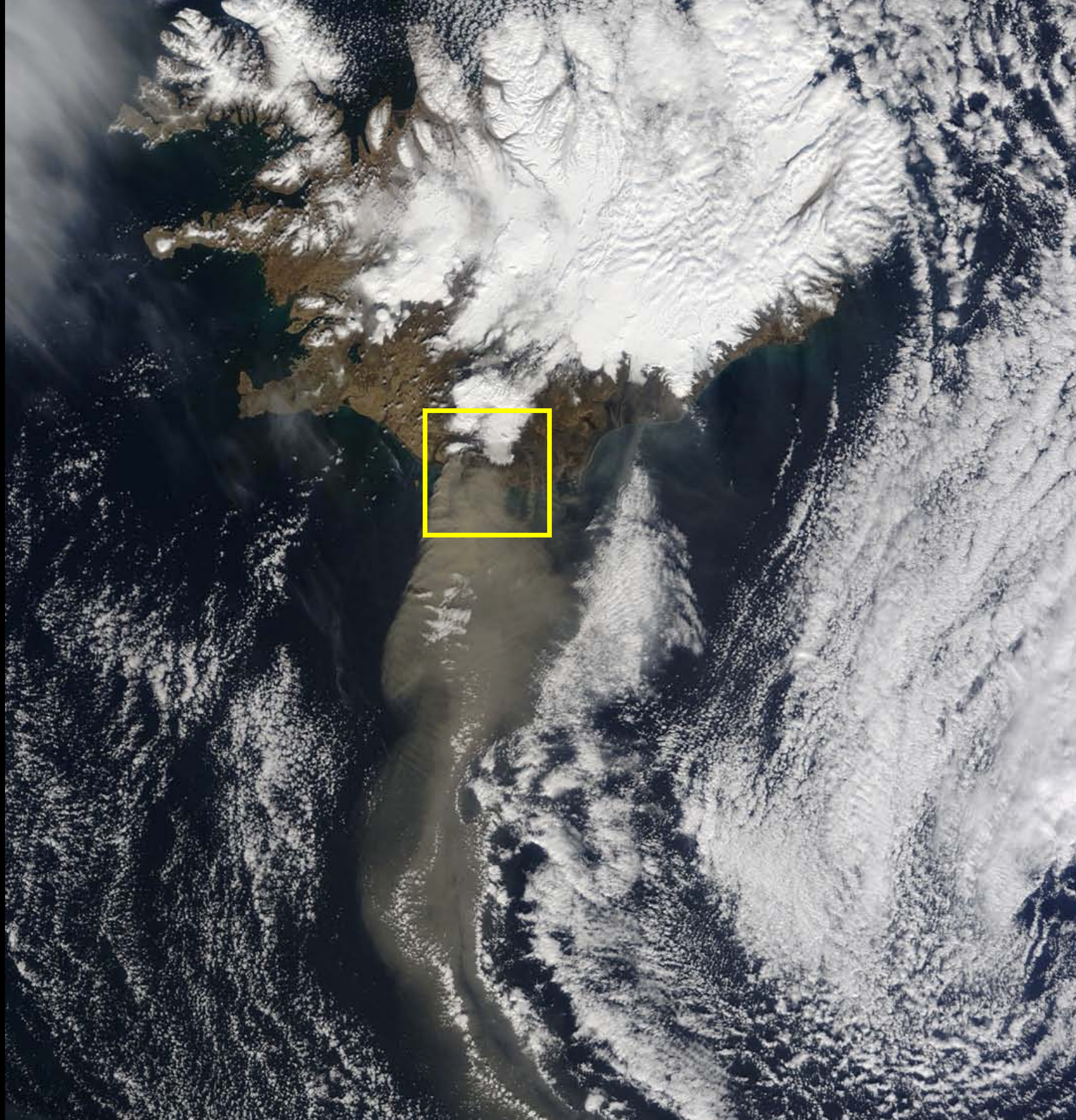

Eyjafjallajökull Volcano (*ASTER*)

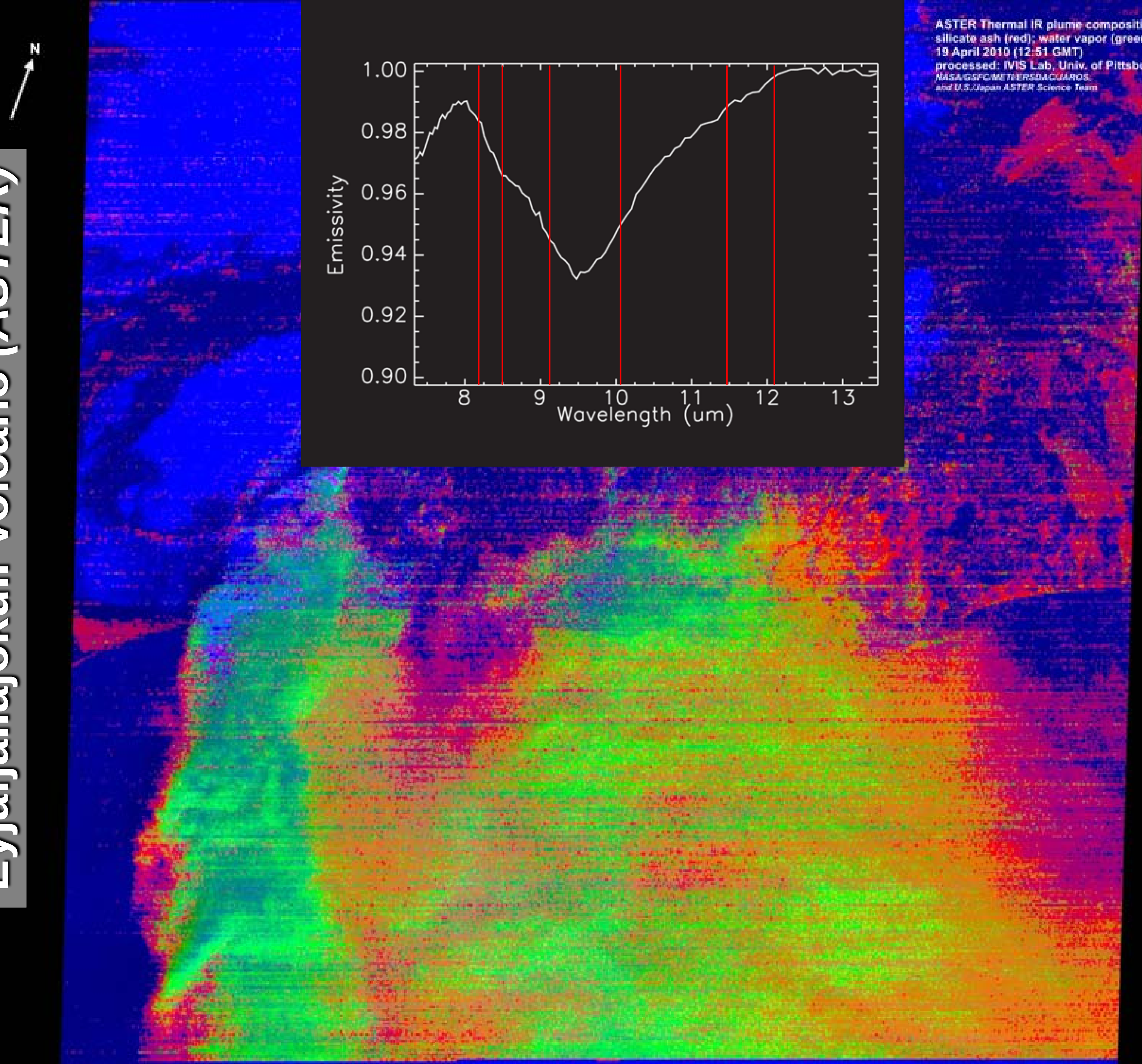

Quantitative Simulation of HyspIRI

- **Super-Resolution Approach/Assumptions:**
  - surfaces in a scene are covered by similar materials
  - and similar setting *(e.g., atmosphere, lighting, temp.)*

- **Therefore, radiance spectra are assumed similar across a wide spectral area**
  - if two regions are dissimilar in one spectral range (i.e. VNIR), they are probably different in another (i.e. TIR)
  - take advantage of the higher spatial resolution data
    - use the PSF to create radiometrically-accurate data at the higher spatial resolution
      - manipulate that data at different spatial/spectral resolutions

[Tonooka, 2005; Hughes and Ramsey, 2010]

Super-Resolution

- **What is not**
  - *not* spectral component substitution
    - *i.e., pan resolution sharpening*
  - *not* simple pixel resampling
    - *leads to averaging inaccuracies/biases*
  - steps *(greatly simplified)*:
    - resample high resolution data to same scale as low resolution bands using the instrument PSF
    - determine homogeneity of re-sampled pixels
      - calculate average standard deviation across all bands for the spectral range

Super-Resolution

- **What is it?**
  - steps (con't):
    - create a cluster tree of re-sampled pixels using ISODATA classification
      - Mahalanobis distance (MD) calculated for each class
    - generate the super-resolved image by remapping TIR spectra to each new higher resolution pixel
    - radiometrically correct super-resolved image
      - compared to original image
      - assure that it is fully-reversible

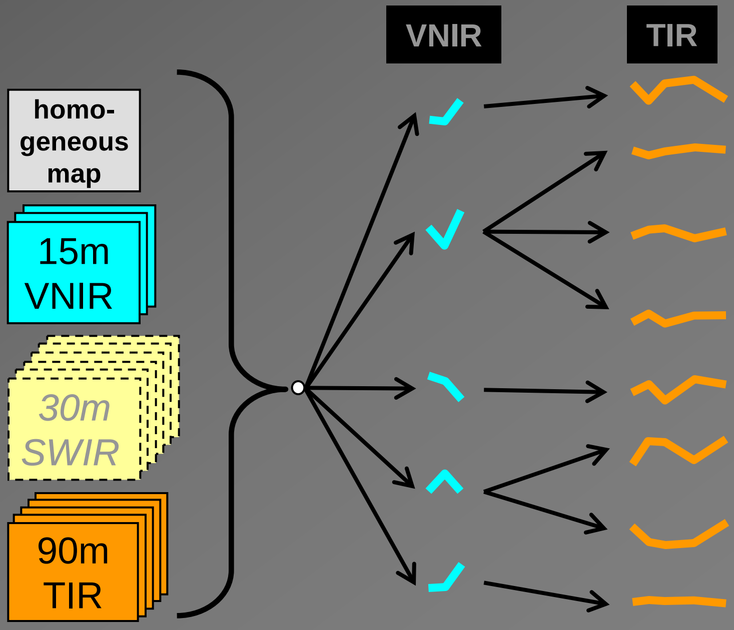

Mono Craters, Long Valley, CA

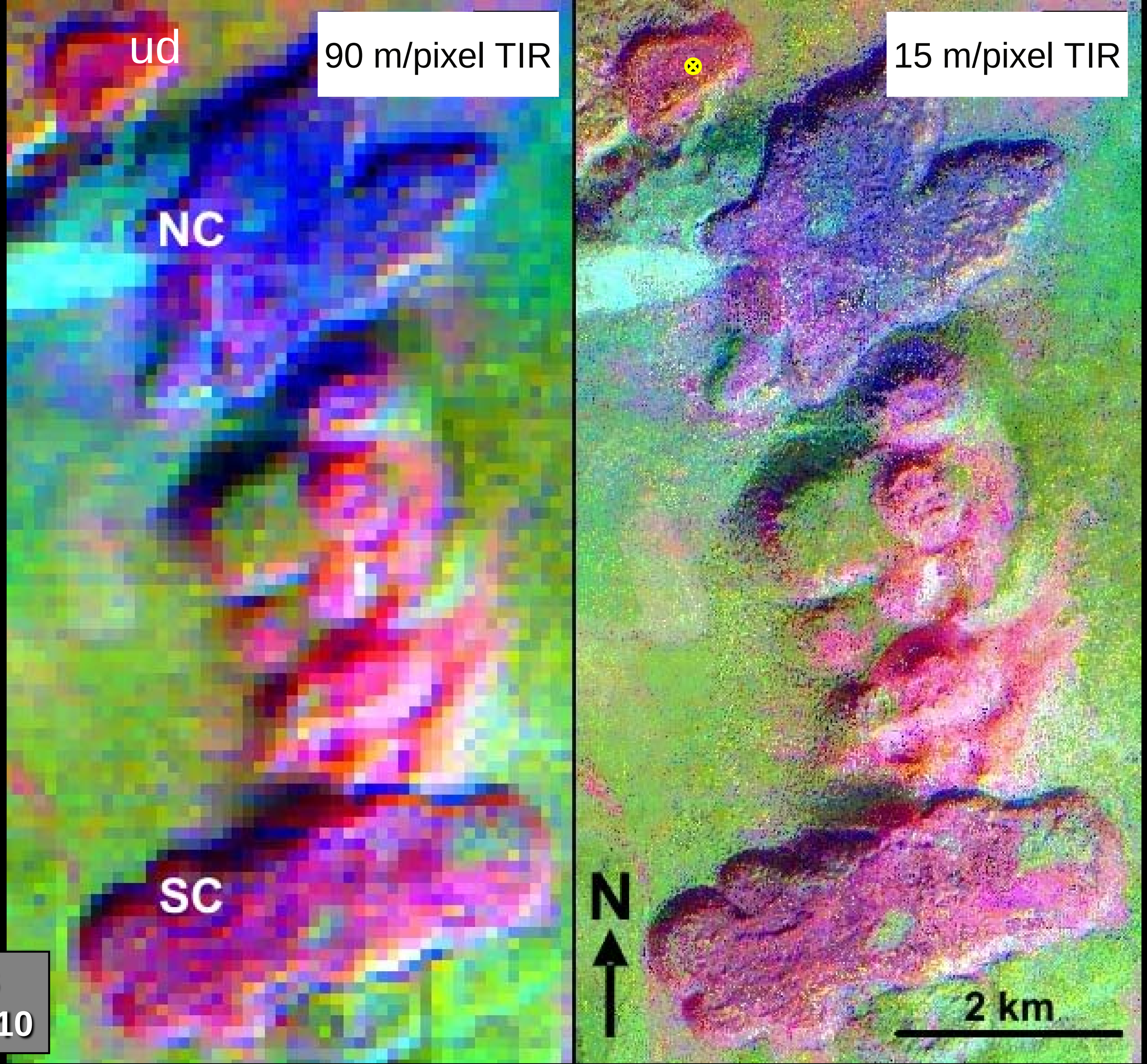

ASTER DCS
bands: 13,12,10

Results: upper dome

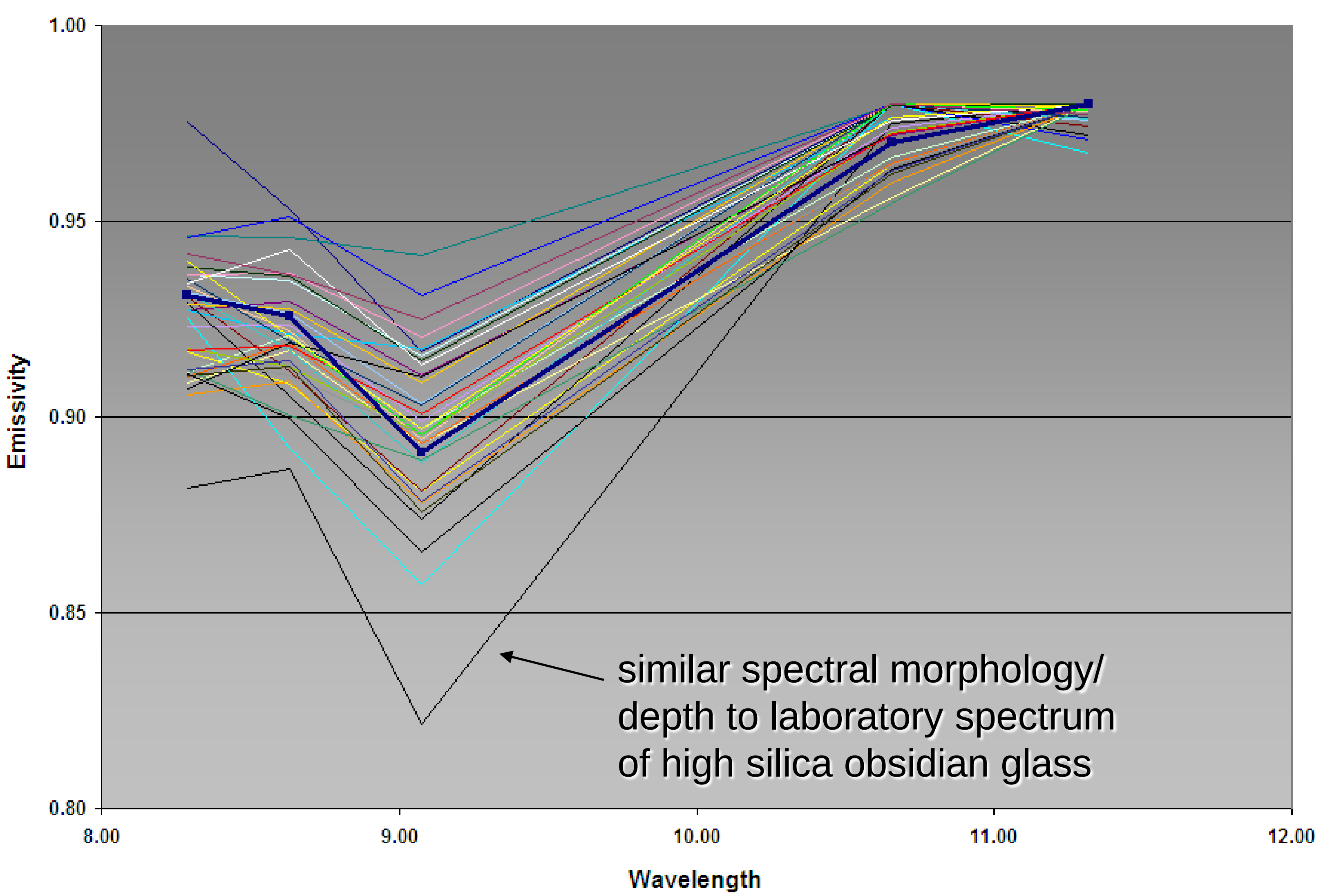

Test Site: Lunar Lake Playa, NV

- **Setting:**
  - 2km x 4km playa
  - radiometric cal/val target
  - low topography
    - spatially uniform
  - high reflectance > 0.7 μm
    - variations of < 0.5% reflectance
  - surrounded by basalt rich hills
    - mixing gradient at boundary
  - AERONET site

Test Site: Lunar Lake Playa, NV

- **Data:**
  - ASTER
    - 2003-06-27 18:44:40
    - 15/30/90 m/pixel

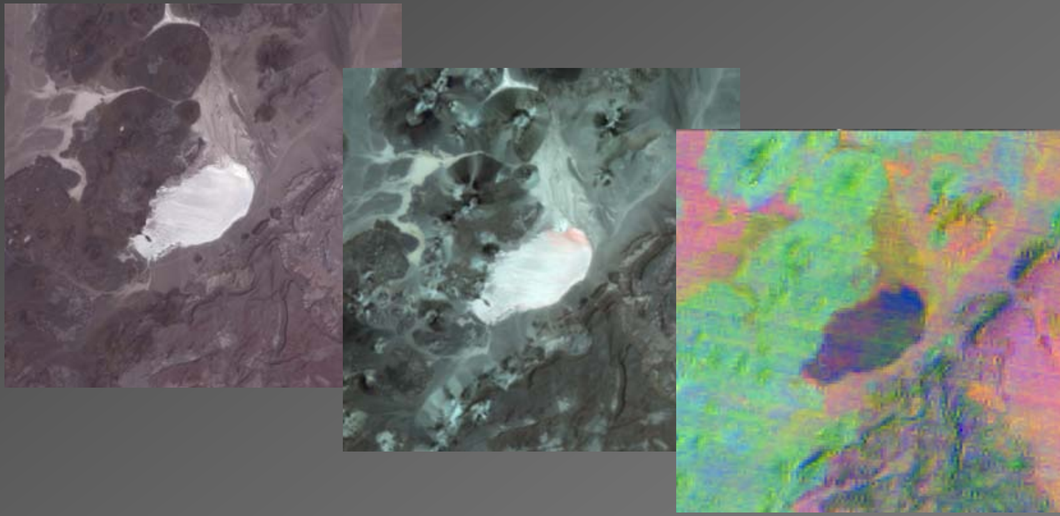

  - AVIRIS:
    - 1997-06-23 18:31:04
    - ~ 20 m/pixel
  - super-resolved area
    - 9.1 km^2
      - 151 x 151 60m pixels

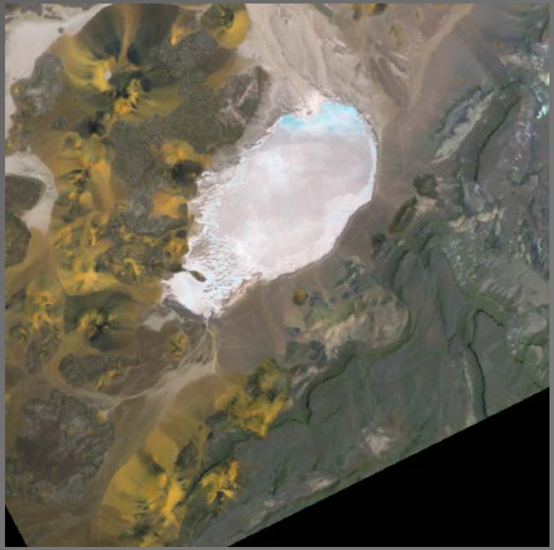

Results: ASTER + AVIRIS

- **ASTER VNIR**
  - used to super-resolve ASTER SWIR & TIR data to 15 m/pixel
- **ASTER TIR & AVIRIS data**
  - then super-resolved to 60 m/pixel HyspIRI resolution

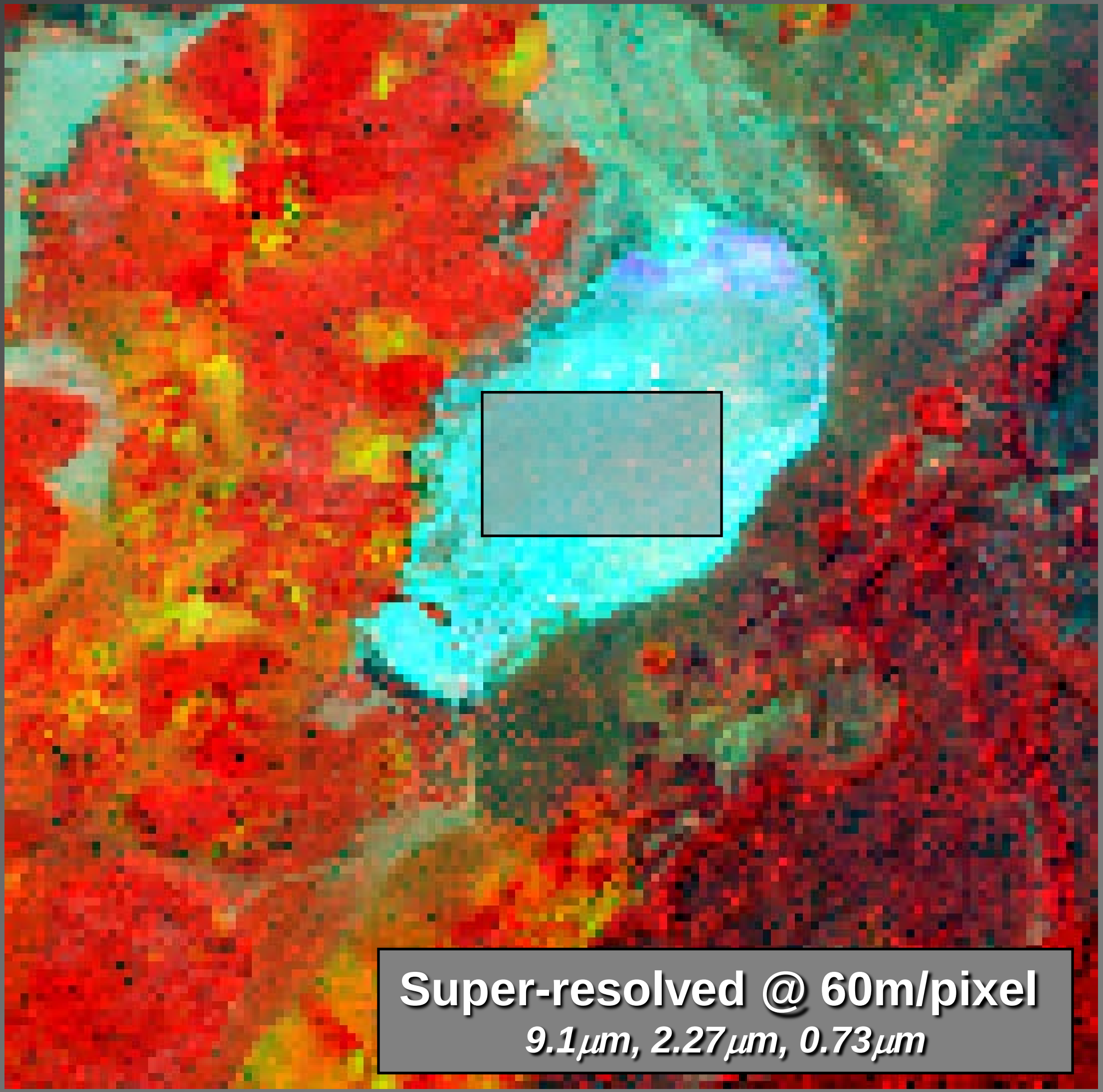

Spectral Variance: Playa

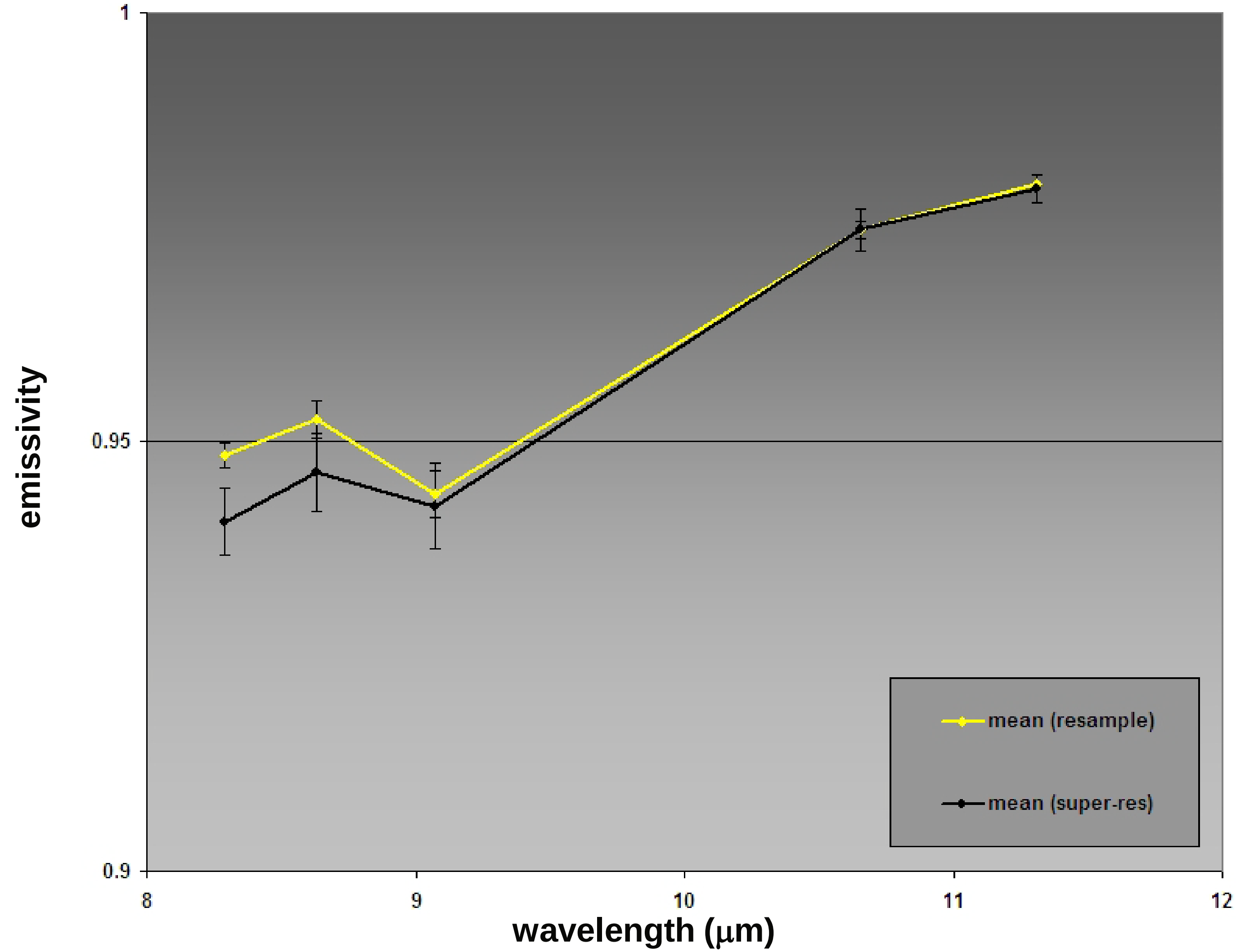

Spectral Variance: Playa

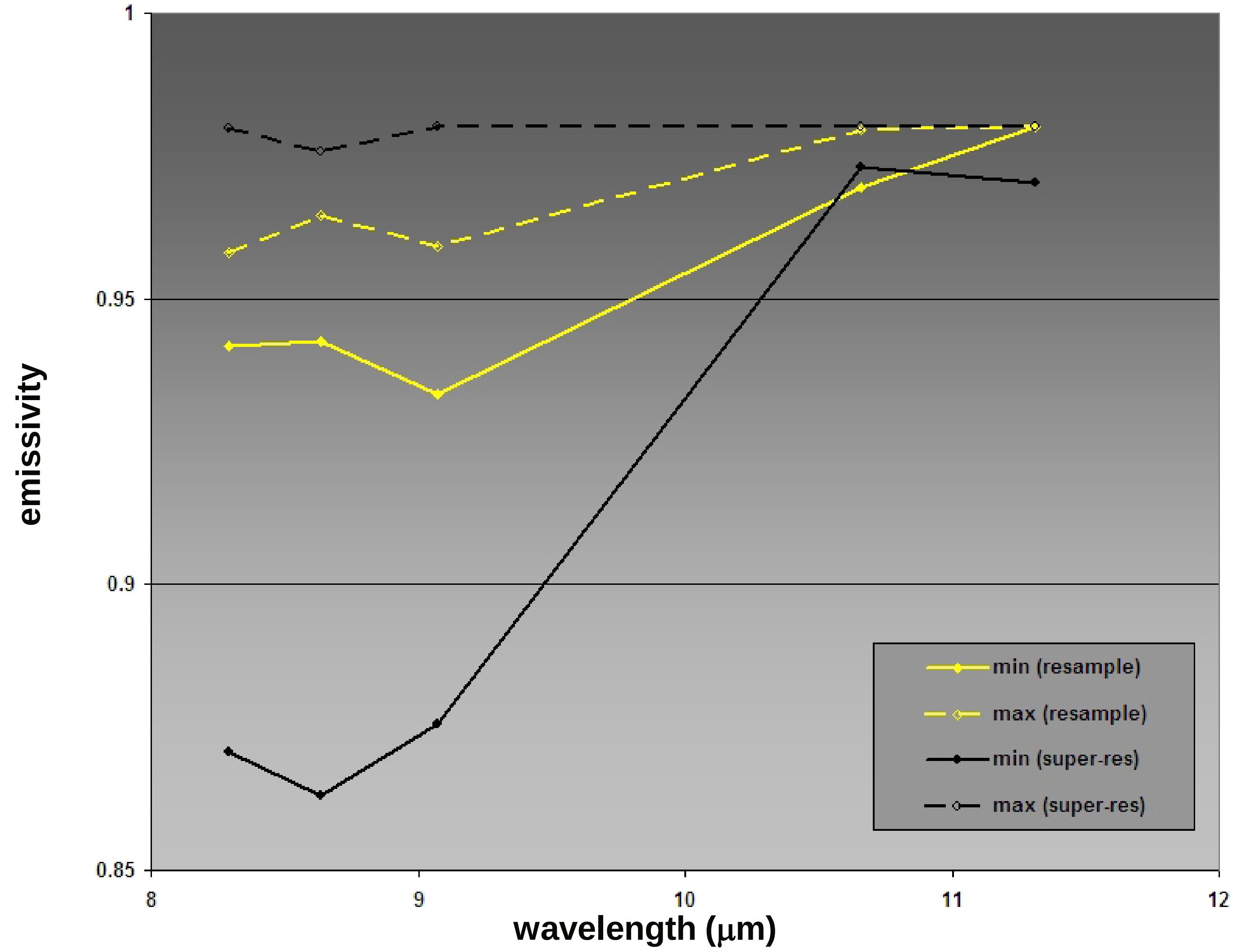

Conclusions & Future Work

- **Arid land surfaces**
  - provide an excellent target for HyspIRI validation
    - global significance, climate/geologic/natural hazard implications
      - estimate aerosol composition, soil moisture, albedo
      - excellent monitoring potential at a high spatial/temporal resolutions
- **Quantitative datasets are critical**
  - preliminary results for the super-resolution approach
  - further validation needed
    - ongoing after two field campaigns to Lunar Lake, NV
    - expand the approach to fully integrate AVIRIS (and MASTER) in the super-resolution process
      - assess the spectral leveraging against the time difference between data acquisitions

Preliminary Results
Characterization of Hydrothermal Systems Using Simulated HyspIRI Data

Supported by NASA Grant NNX10AF99G
(HyspIRI Preparatory Research Activities)

F. A. Kruse, M. Coolbaugh, J. Taranik, W. Calvin, E. Littlefield, J. Michaels
Dept of Geological Sciences and Engineering
Arthur Brant Laboratory for Exploration Geophysics
University of Nevada, Reno

B. Martini
Ormat, Reno, NV

F. A. Kruse ♦ 303-499-9471 ♦ fkruse@unr.edu ♦ http://www/unr.edu/mines/able

Why Remote Sensing of Hydrothermal/Geothermal Systems?

- **High beneficial impact: Ore deposits provide raw materials for industrialized society, while geothermal systems provide abundant energy without many of the problems of fossil fuels**
- **These two are highly related. Surface mineral assemblages and distributions often provide key information about their origin and nature. Many can be mapped using HSI and MSI VNIR/SWIR and LWIR approaches**

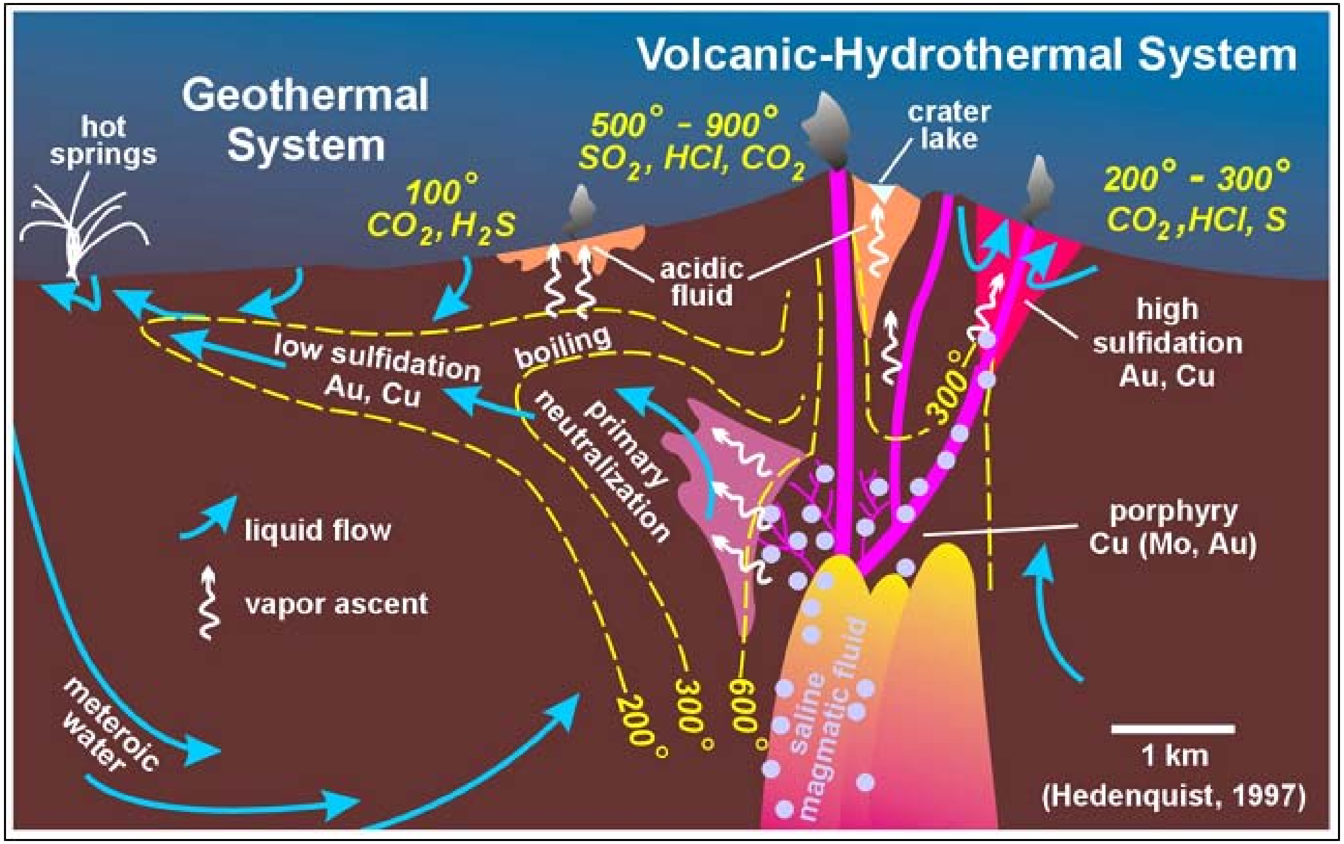

- **VNIR/SWIR spectrometry has clearly demonstrated its capability to identify minerals based on molecular physics**
- **LWIR spectrometry has unique capabilities based on fundamental molecular vibrations**

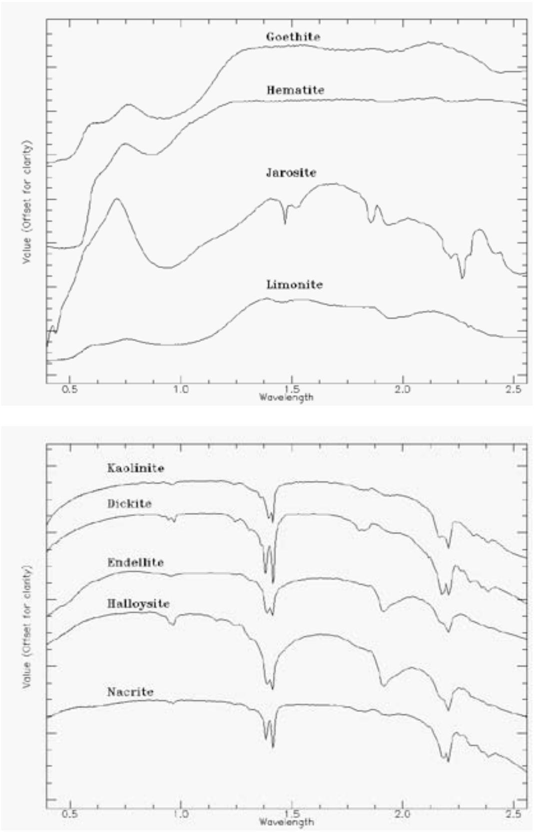

USGS Spectral Library

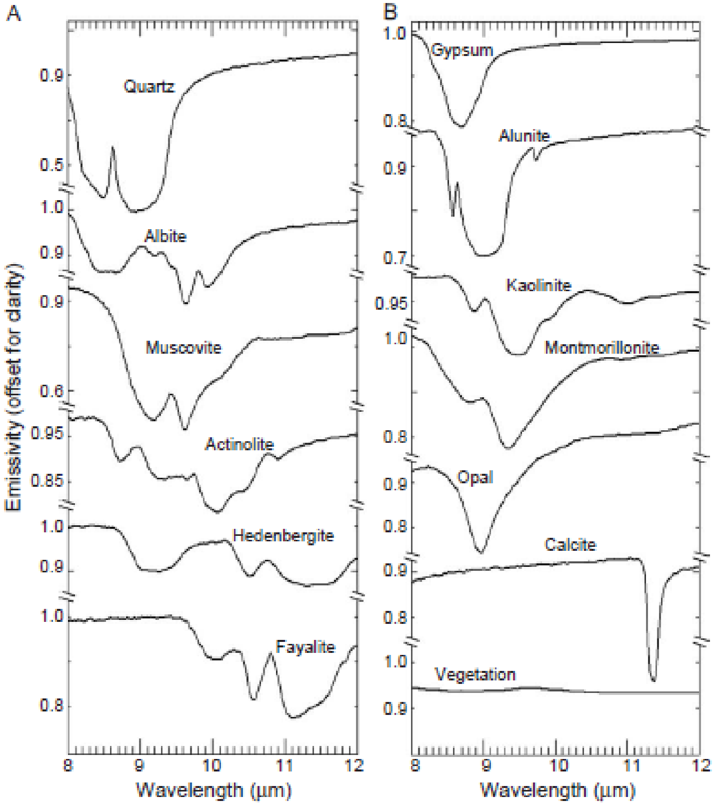

Vaughan et al., 2005

Surface Temperature Mapping at Geothermal Systems

- **LWIR Multispectral data provide the additional capability to estimate surface temperature**
- **Improved understanding of known systems by detecting/mapping**
  - **Distribution of heat anomalies and links to subsurface**
  - **Structural control**
  - **Outflow areas**
- **Provide new exploration tools**
  - **Temperature anomalies and magnitudes**
  - **"Blind" Systems**
- **Develop Methods for Monitoring**
  - **System characteristics and Natural variability**
  - **Exploitation Changes**

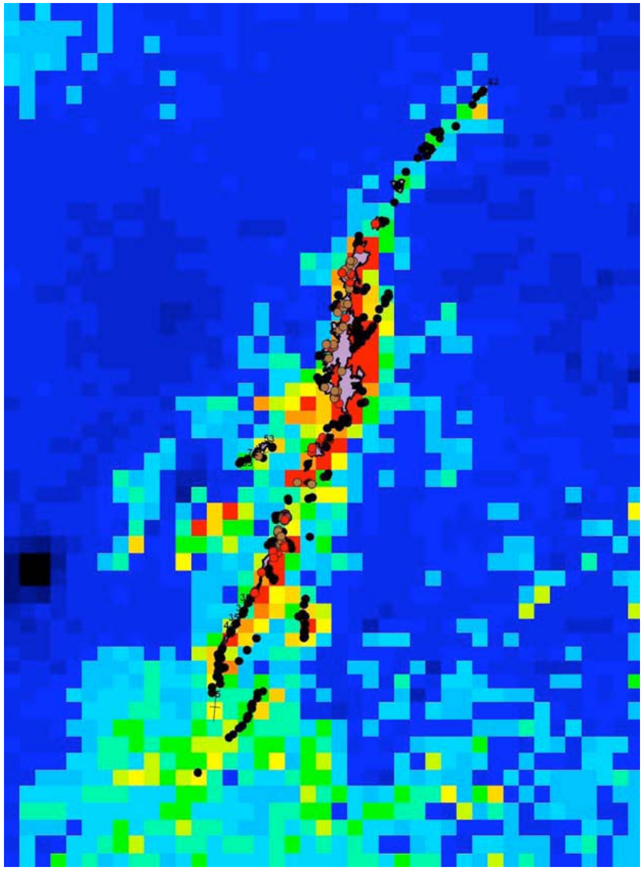

Coolbaugh, 2007 – Temperature Anomalies at Brady Hot Springs Using ASTER. Small black and brown points indicate field located steam vents or surface hot spots.

HyspIRI Precursor Project Objectives

Generate HyspIRI-like remote sensing datasets from existing NASA HSI and MSI remote sensing data, and utilize these to:

1. **Identify, characterize, and map mineral assemblages associated with surface exposures of active and fossil hydrothermal systems**
2. **Measure surface temperatures and temperature variability associated with active geothermal systems**
3. **Detect, characterize, and monitor surface changes associated with geothermal resources**

Hydrothermal Systems - Some Science Questions

- **How are surface mineral assemblages of hydrothermal systems tied to underlying geologic constraints (lithology, alteration, water chemistry, temperature regimes)? (VQ6, TQ5a, CQ5)**
- **What can surface mineralogy tell us about the morphology and evolution of hydrothermal systems and the link between active geothermal systems and ore deposits? (VQ6, TQ5a)**
- **What surface changes are taking place at active geothermal systems as the result of human activities such as recreation, geothermal energy exploration and drilling, and energy production? (TQ5b, CQ5)**
- **What is the magnitude of surface temperatures at active hot springs and geothermal areas? How do temperatures vary naturally? What can surface temperatures tell us about the morphology and evolution of these systems and temperature at-depth? How does surface temperature respond to geothermal production? (TQ5c)**

Hydrothermal Systems - Some HyspIRI Questions

- What is the effect of the proposed HyspIRI spatial and spectral resolution, and SNR or NEΔT on detection, identification, and characterization of key rocks, minerals, vegetation, and other materials associated with active and fossil geothermal systems utilizing spectral signatures?
- What is the spatial scale of temperature features that can be detected at the proposed HyspIRI 60m spatial resolution?
- What is the temperature contrast required for detection and characterization of geothermal systems at various scales?
- How does spatial mixing affect mineral identification and measurement of temperatures at geothermal systems. What is the magnitude and nature of these mixing effects?

HyspIRI Research Approach

- **Build on previous experience with epithermal mineral deposits, geothermal systems, and remote sensing data to try to improve understanding of active and fossil geothermal systems**
  - **Determination of mineral assemblages (not just the predominant mineral)**
  - **Detect and map detailed within-species variability (eg: muscovites, chalcedony vs opal, etc.)**
  - **Map additional rocks and minerals with LWIR**
  - **Use temperature mapping to quantify surface indicators of active geothermal systems**
  - **Development of comprehensive system models**

Approach (continued)

- **Create Simulated HyspIRI Data for 5 Sites (Detailed analysis of at least 3 sites)**
  - **Steamboat Springs, NV**
  - **Long Valley, CA**
  - **Fish Lake Valley, CA (Not shown)**
  - **Yellowstone, WY (Pending)**
  - **Cuprite, NV**
- **Focus on refining mineral mapping and temperature measurement capabilities using merged VSWIR and TIR data Simulation/Analysis Approach**

Simulation/Analysis Approach

- **Use existing HSI data (AVIRIS, Hyperion, HyMap, SpecTIR) to simulate the VNIR/SWIR component of HyspIRI (~210+ spectral bands 0.38 – 2.52 micrometers with approximately 10nm spectral resolution and 60 m spatial resolution)**
  - **Atmospheric Correction**
  - **Spectral Resampling**
  - **Warp to ASTER Ortho**
  - **Spatial Resampling**
  - **SNR Modeling**
  - **Spectral mapping using Refl. Spectra**

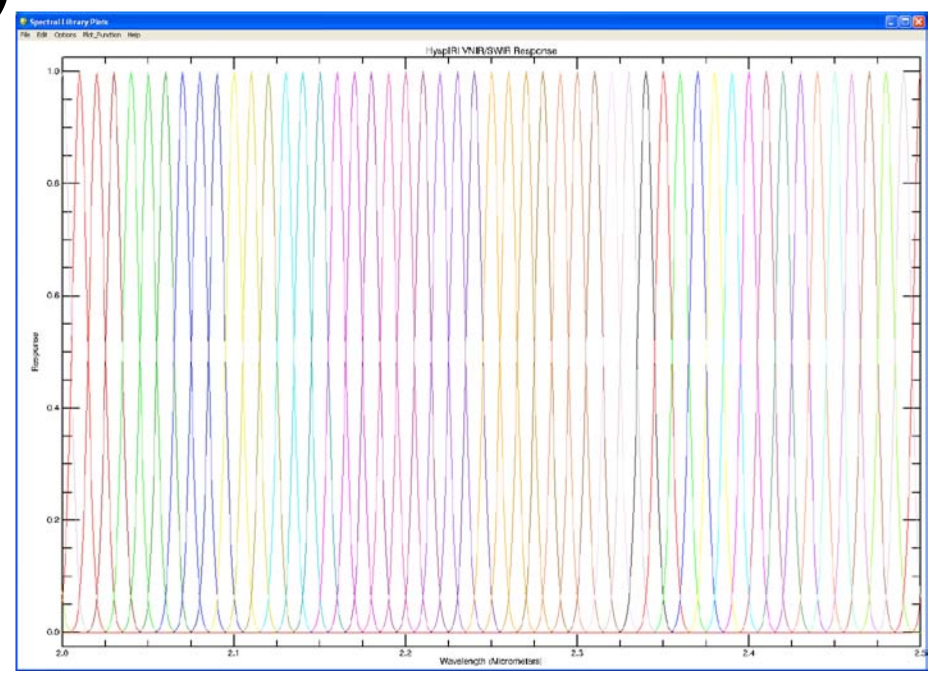

Simulation/Analysis Approach

- **Use existing TIR data (TIMS, MASTER, MAS, ASTER, SEBASS) to simulate the TIR component of HyspIRI (1 MWIR band ~4 micrometers and 7 LWIR spectral bands from ~7.3-12.0 micrometers.**
  - Atmospheric Correction
  - Temperature-Emissivity Separation
  - Warp to ASTER Ortho
  - Spatial and Spectral Resampling
  - Spectral Mapping using Emissivity Spectra
  - Additional T corrections (albedo, topo)
  - Temperature mapping and characterization

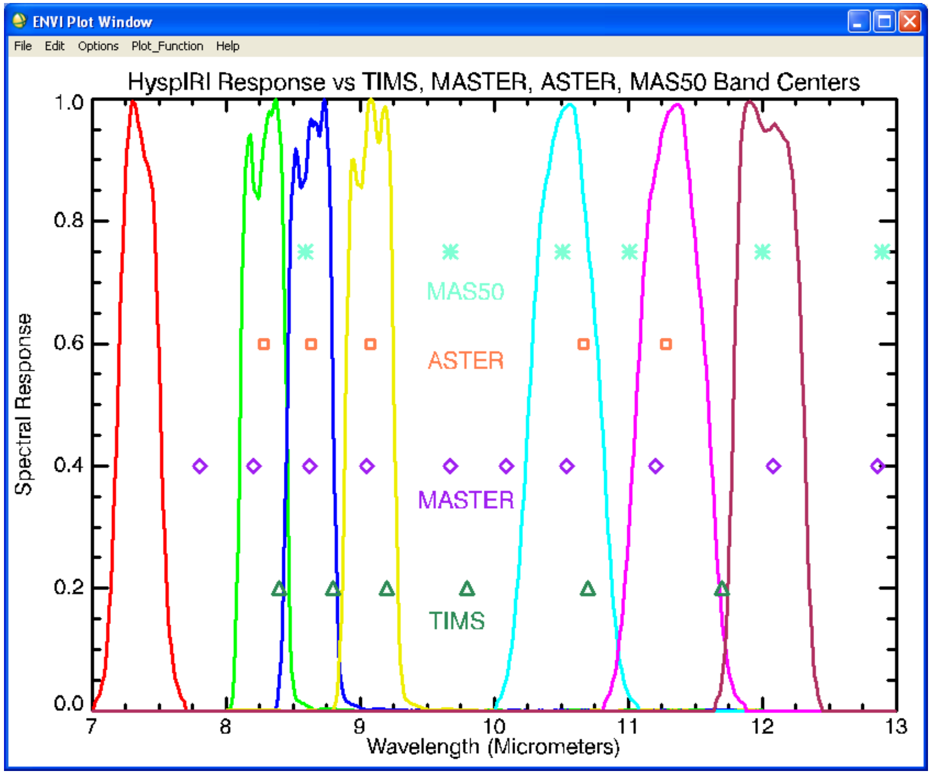

Initial Selected Data Matrix

- Cuprite, NV
  - 2007 ASTER
  - 2006 AVIRIS (16m)
  - 2006 MASTER (34m)
- Steamboat Springs, NV
  - 2006 ASTER (day-night)
  - 1995 AVIRIS (16m)
  - 1999 MASTER (8.8m)
- Fish Lake Valley, CA
  - 2004 ASTER
  - 2003 AVIRIS (3m)
  - 2006 MASTER (11m)
- Long Valley, CA
  - 2002 ASTER
  - 2000 AVIRIS (16m)
  - 2001 MASTER (33m)
  - 2006 MASTER (34m, Day-Night)
- Yellowstone, WY
  - 2004 ASTER
  - 1996 AVIRIS (16m), 1996 MAS (33m)
  - 1996 AVIRIS (16m), 2006 MASTER (3.5m)

F. A. Kruse ♦ 303-499-9471 ♦ fkruse@unr.edu ♦ http://www/unr.edu/mines/able

Steamboat Springs, NV Simulation

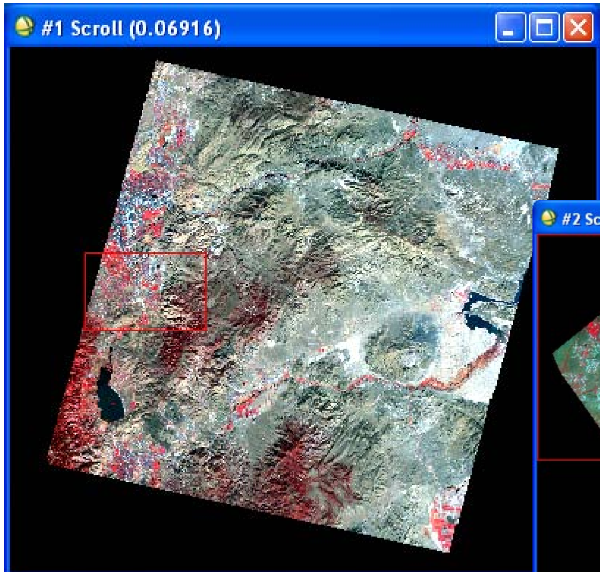

**ASTER VNIR (15m)
10-23-2006 Ortho**

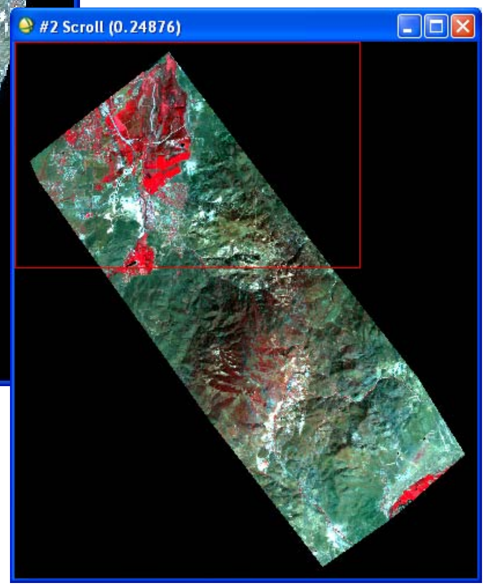

**AVIRIS VNIR (15m)
07-22-1995, Warped
to ASTER Ortho**

**MASTER VNIR (15m), 09-19-1999
GLT-Corrected, Warped to Ortho ASTER**

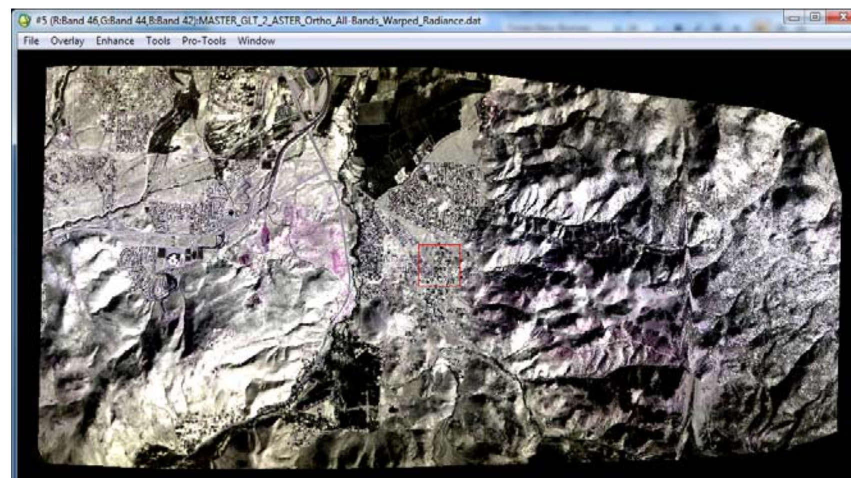

**MASTER LWIR (15m), GLT-Cor
09-19-1999, Warped to ASTER Ortho**

Steamboat Springs, NV Simulation

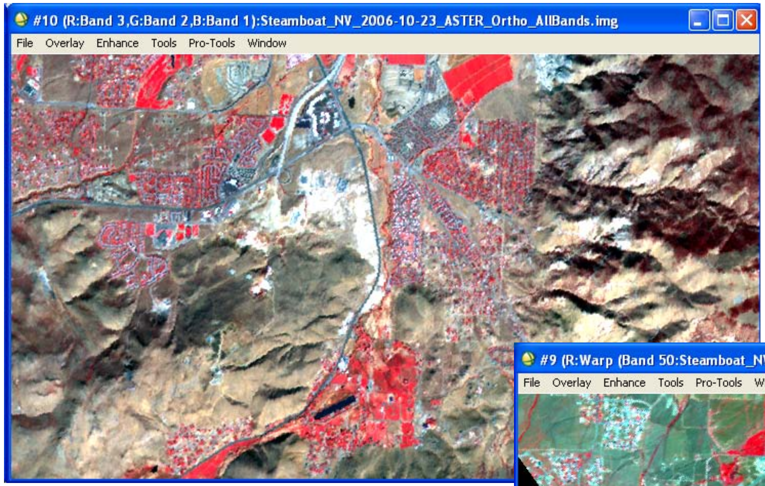

ASTER VNIR (15m)

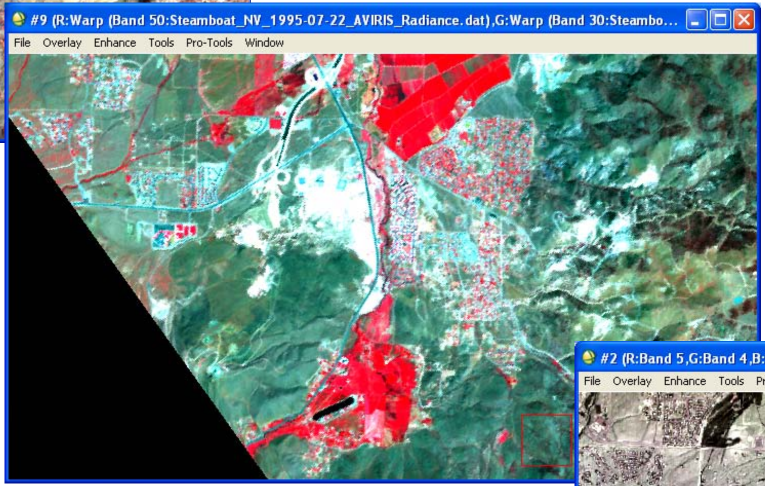

AVIRIS VNIR

MASTER LWIR

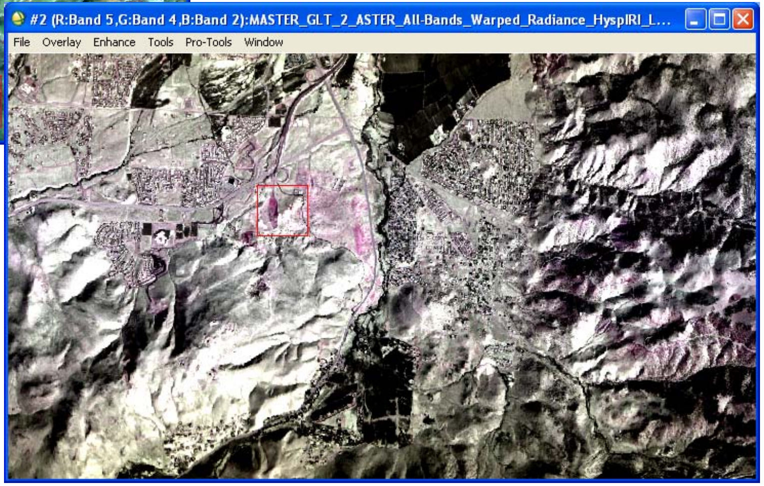

F. A. Kruse ♦ 303-499-9471 ♦ fkruse@unr.edu ♦ http://www/unr.edu/mines/able

Steamboat Springs, NV Simulation

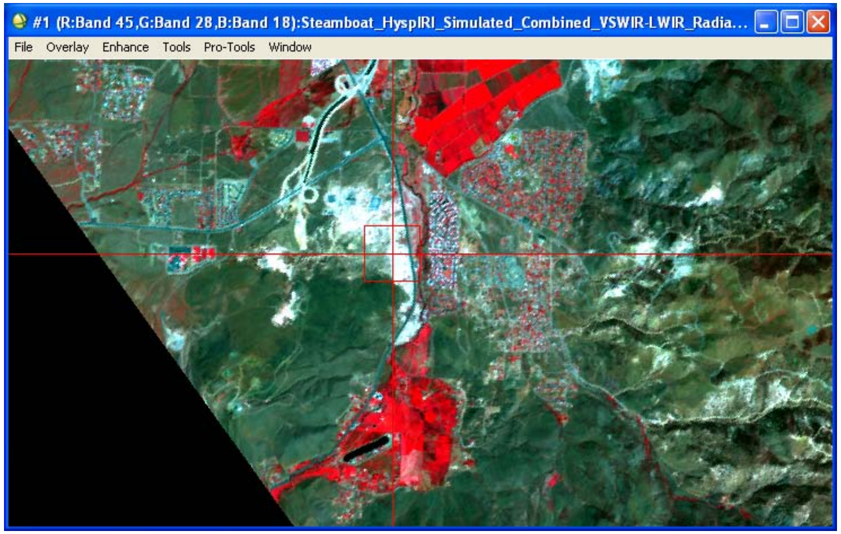

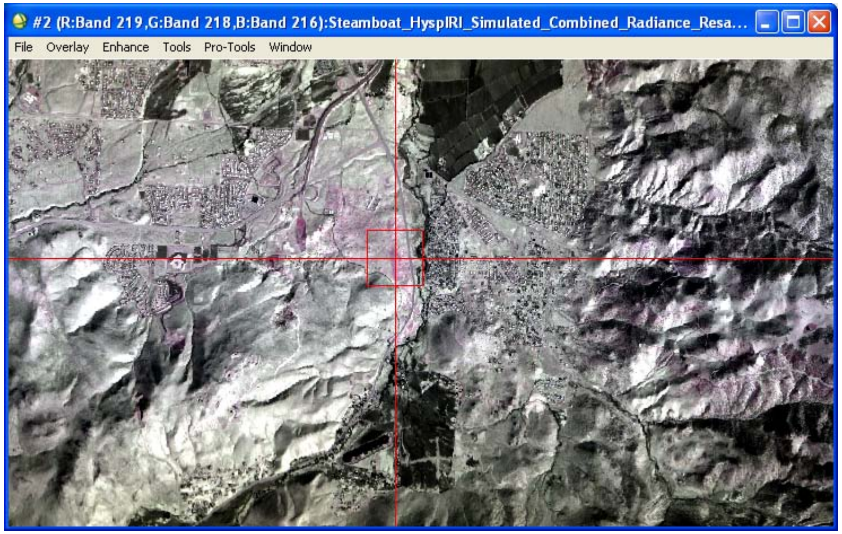

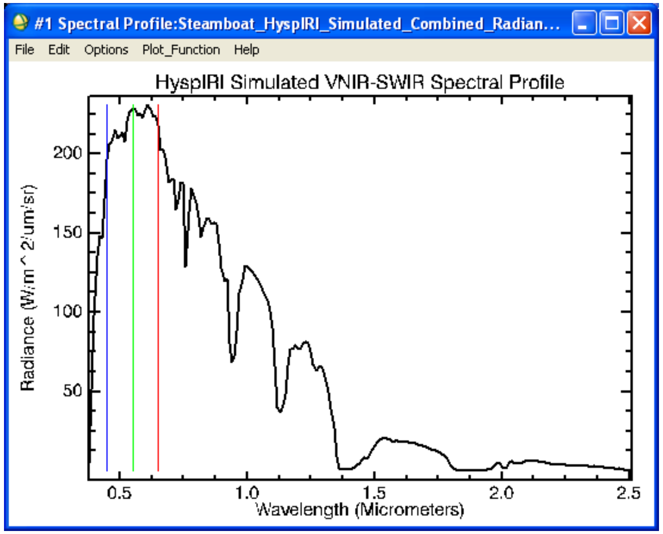

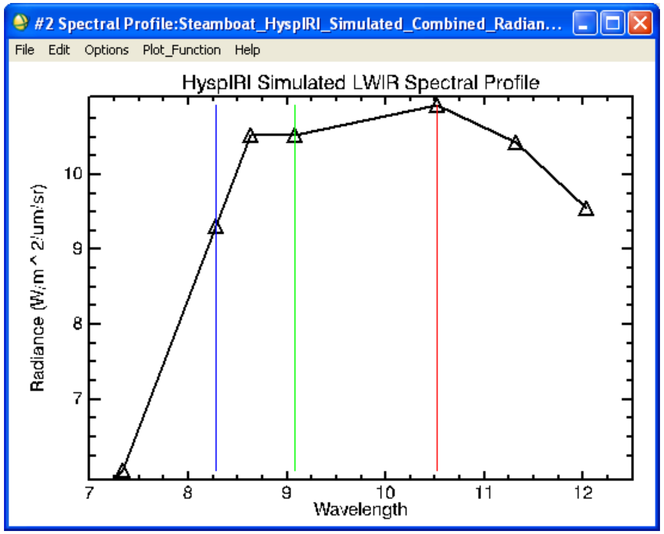

HyspIRI-Simulated VSWIR Radiance (15m)

HyspIRI-Simulated LWIR Radiance (15m)

Steamboat Springs, NV Simulation

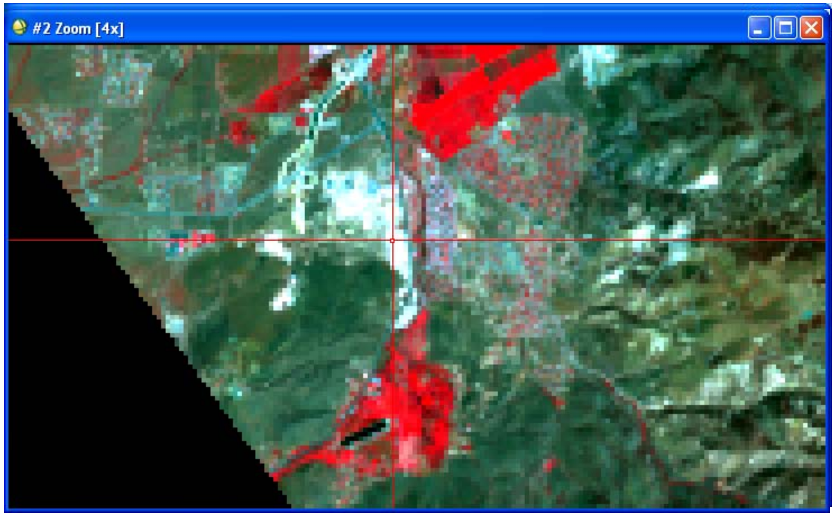

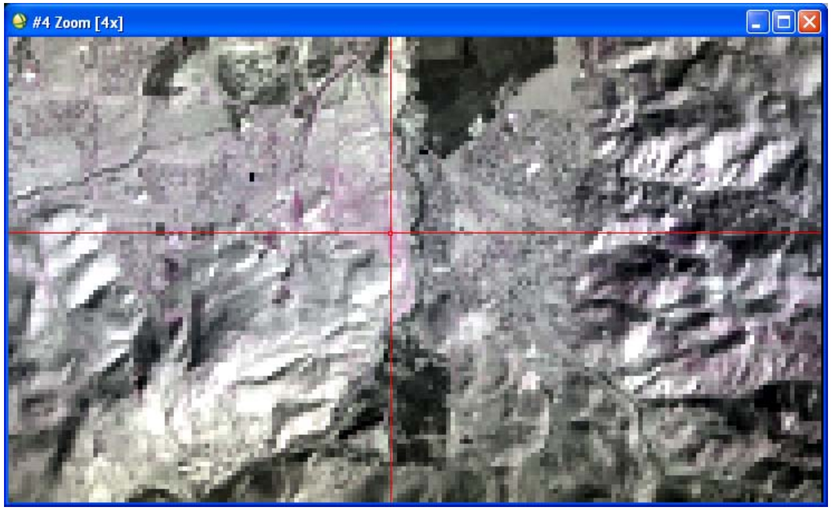

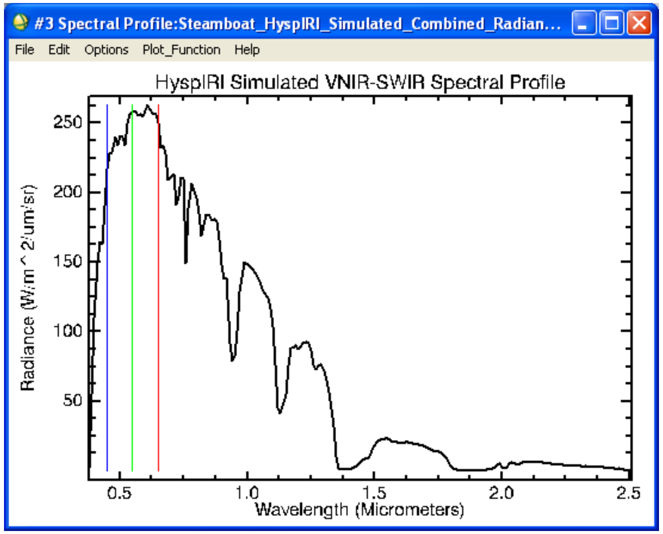

HyspIRI-Simulated VSWIR Radiance (60m)

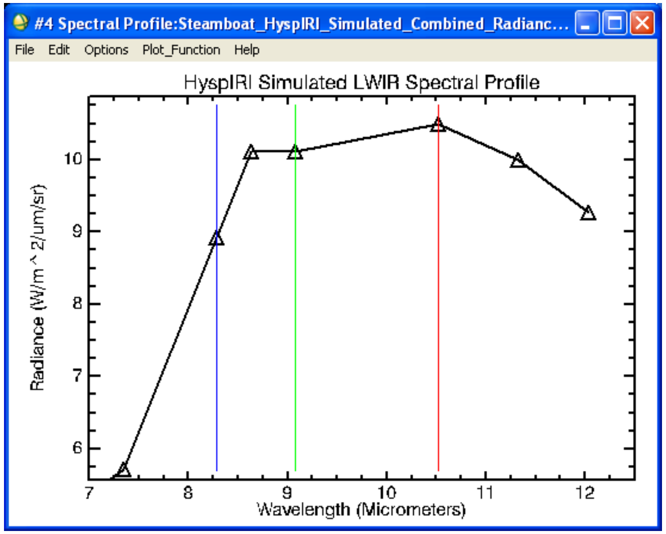

HyspIRI-Simulated LWIR Radiance (60m)

Steamboat Springs, NV Simulation (15m)

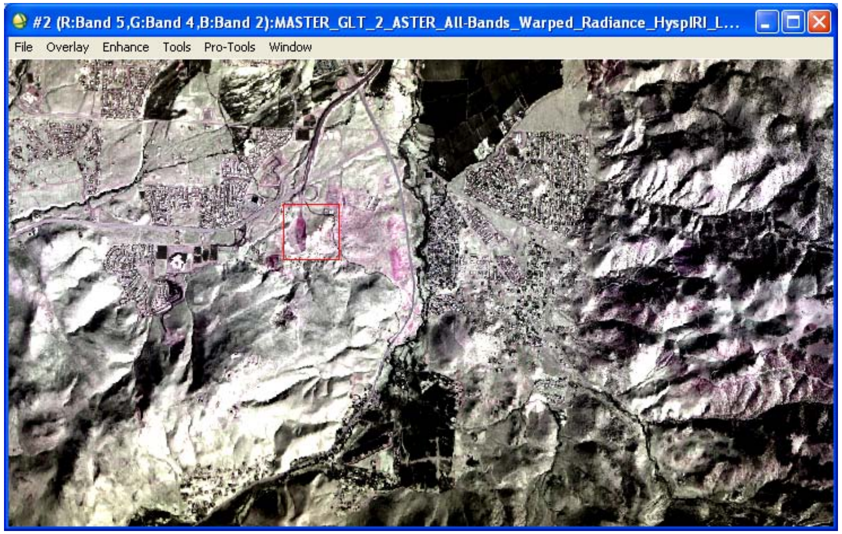

LWIR (10.0, 9.0, 8.2 μm RGB)

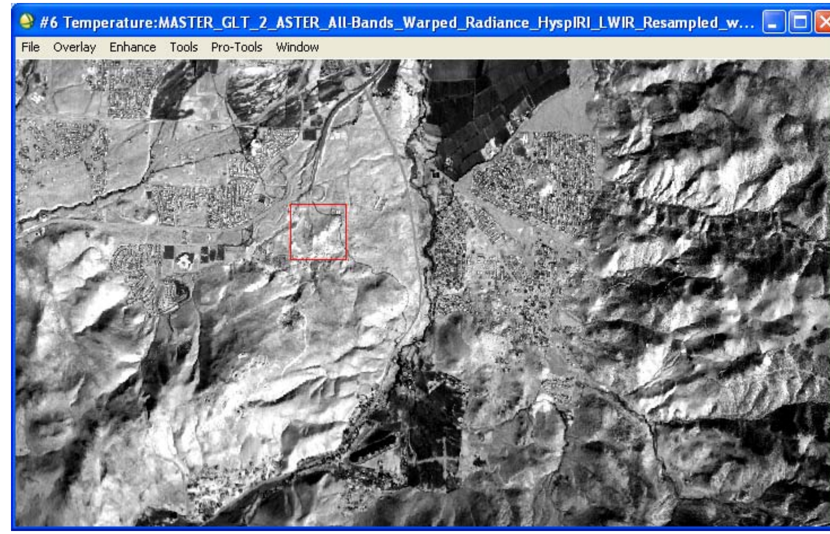

Temperature

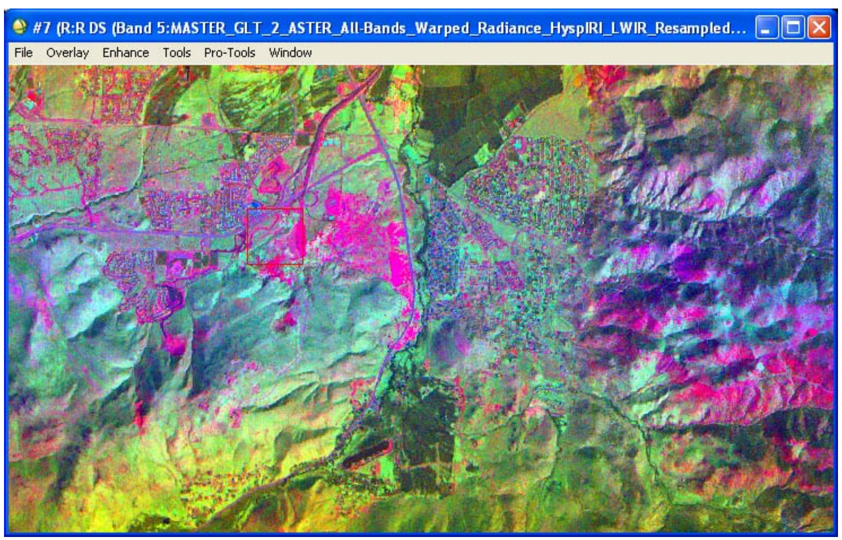

Decorellation Stretch

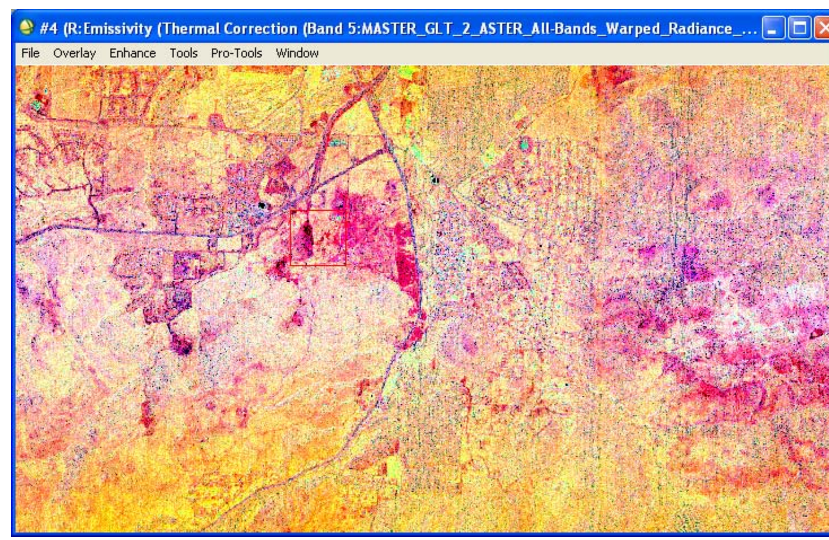

Normalized Emissivity

F. A. Kruse ♦ 303-499-9471 ♦ fkruse@unr.edu ♦ http://www/unr.edu/mines/able

Steamboat Springs, NV Simulation

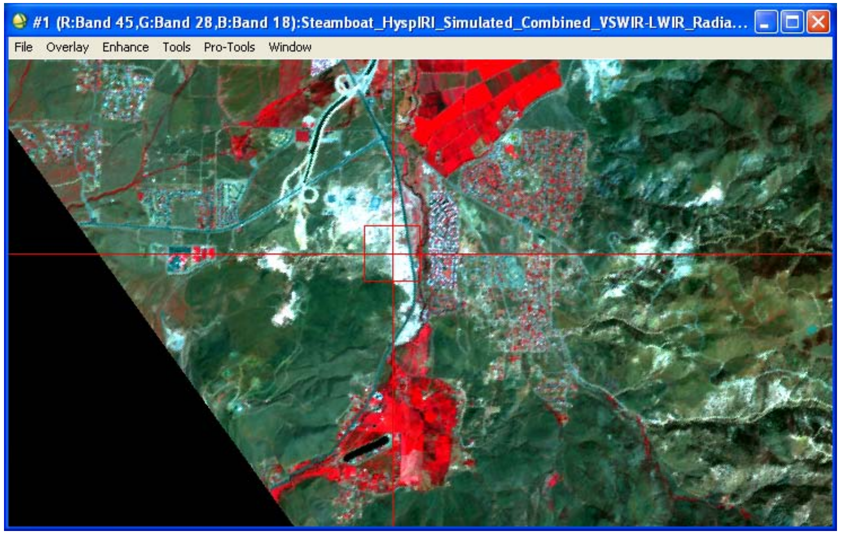

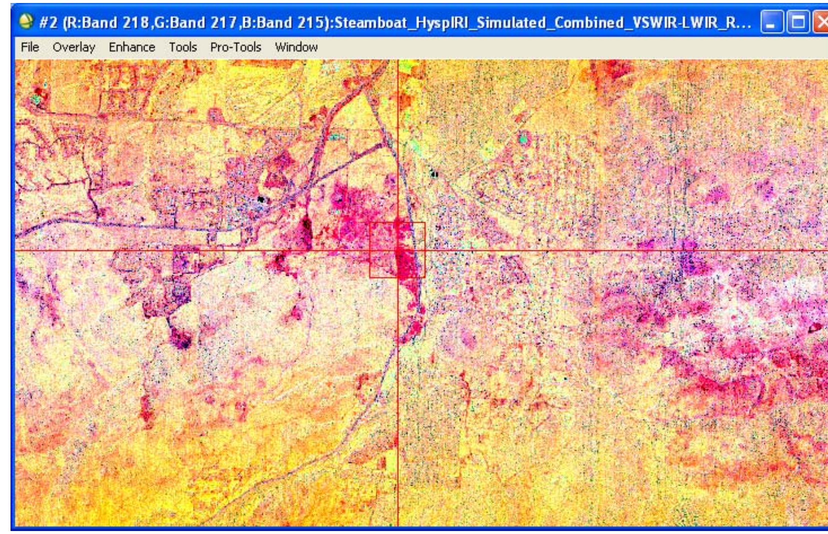

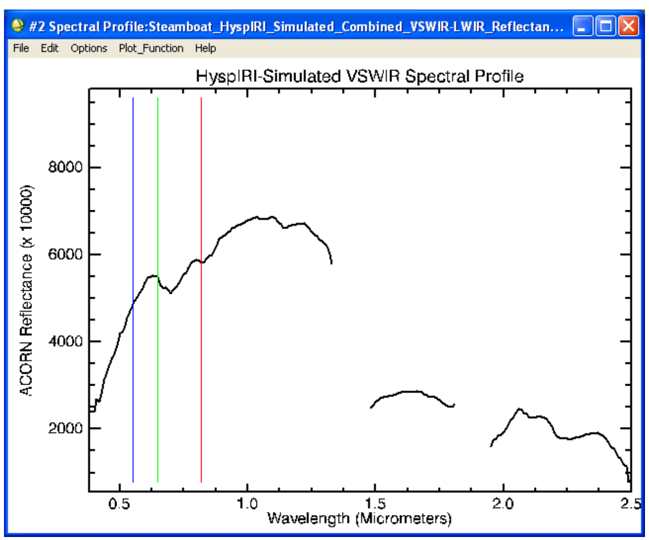

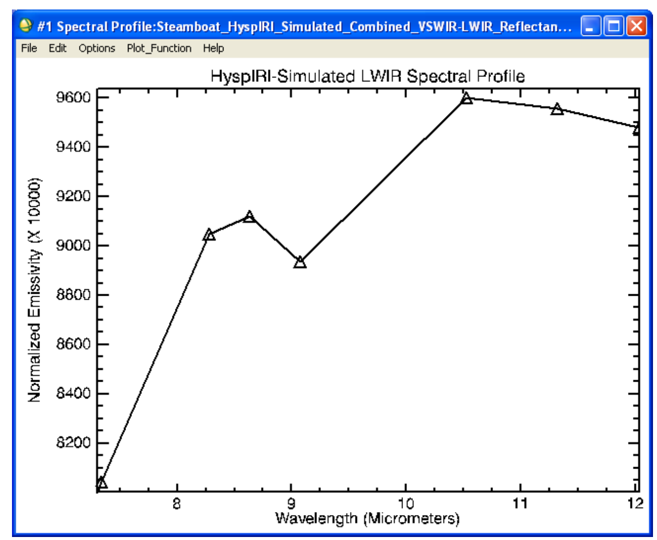

HyspIRI-Simulated VSWIR Reflectance (15m) **HyspIRI-Simulated LWIR Emissivity (15m)**

F. A. Kruse ♦ 303-499-9471 ♦ fkruse@unr.edu ♦ http://www/unr.edu/mines/able

Steamboat Springs, NV Simulation

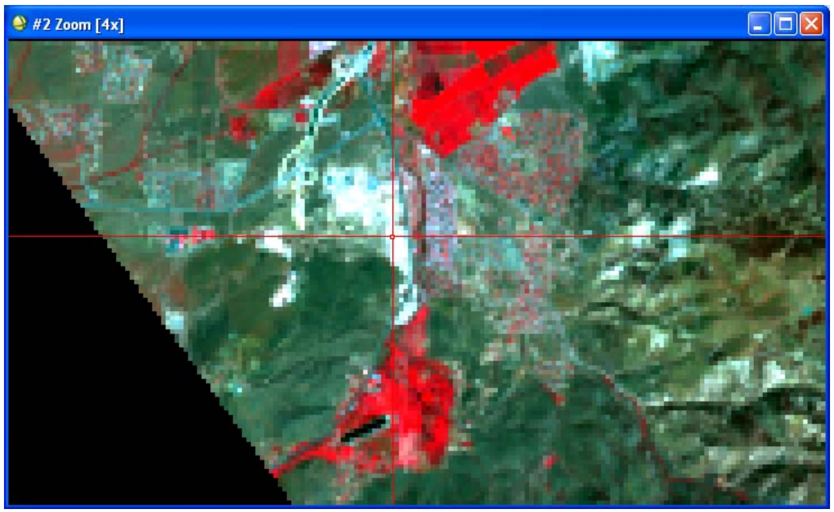

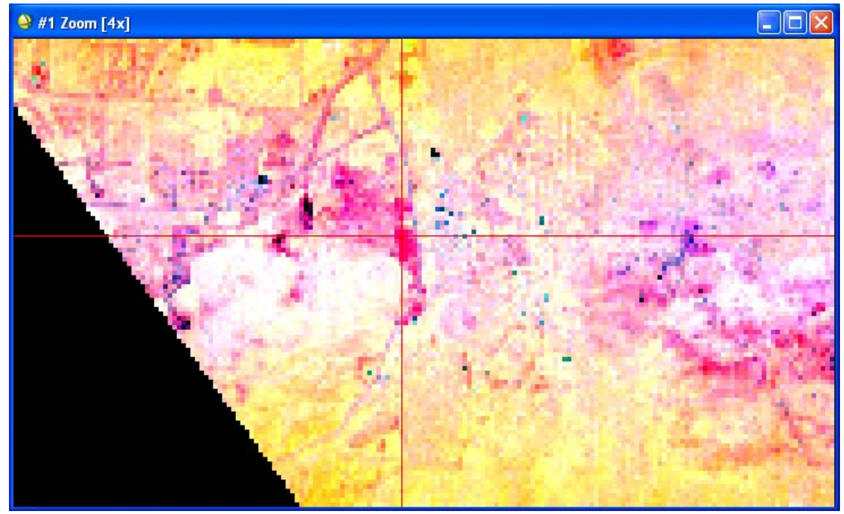

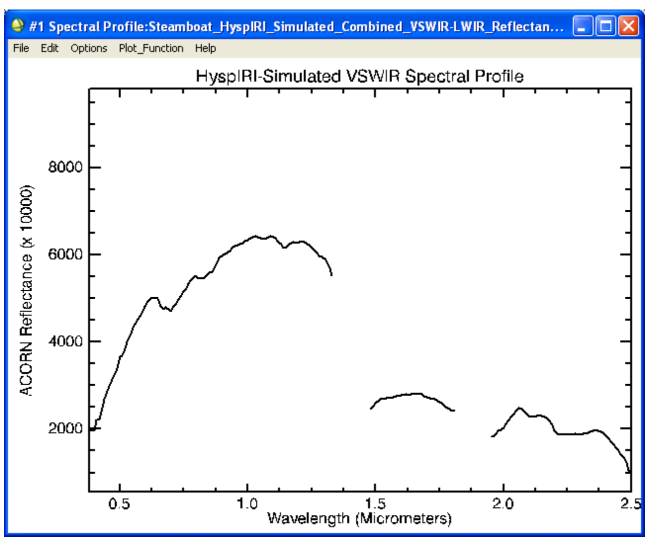

HyspIRI-Simulated VSWIR Radiance (60m)

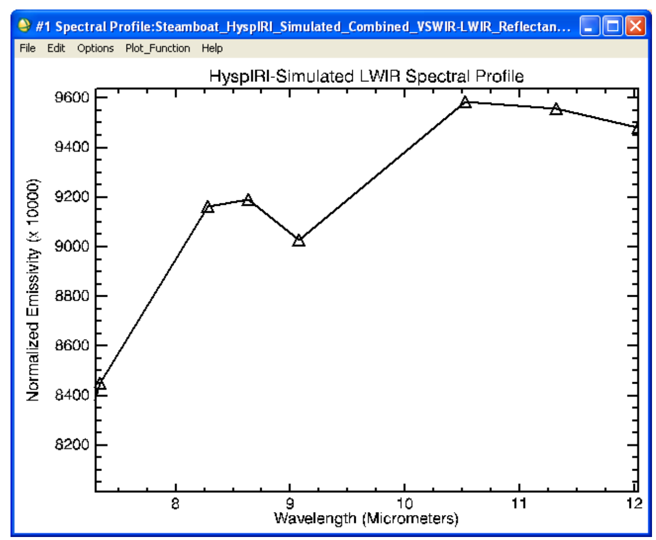

HyspIRI-Simulated LWIR Radiance (60m)

Steamboat Springs, NV ASTER Day-Night (10-23-2006 and 10-24-2006)

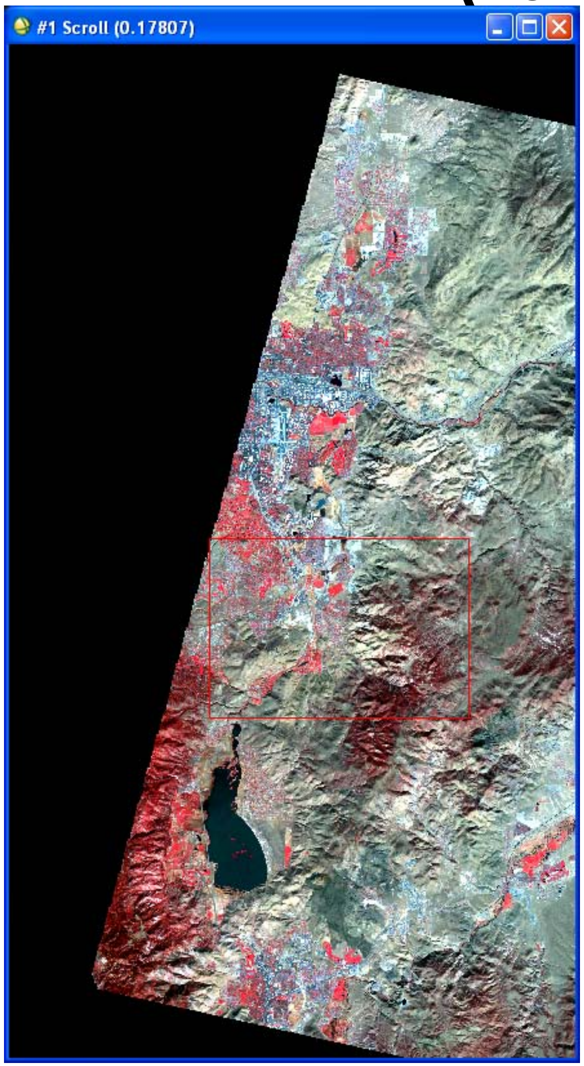

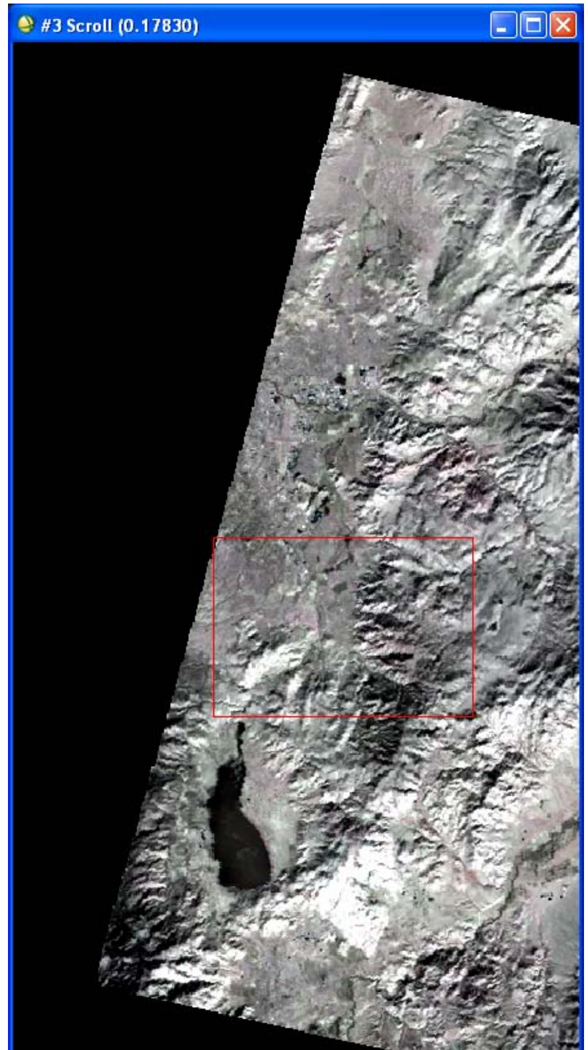

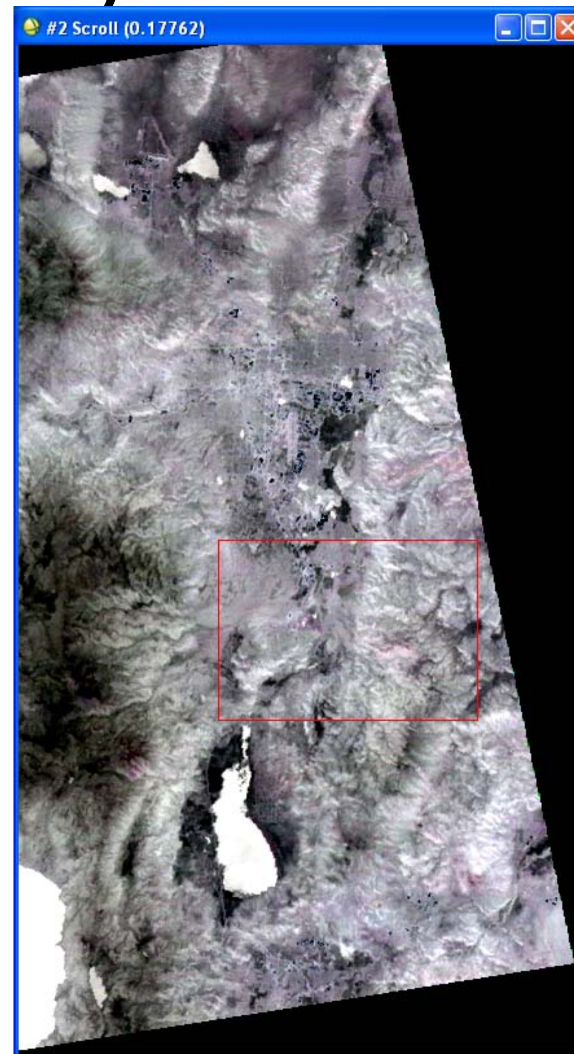

ASTER VSWIR (CIR)
0.81, 0.66, 0.56 μm (RGB)

ASTER LWIR (Day)
10.7, 9.1, 8.3 μm (RGB)

ASTER LWIR (Night)
10.7, 9.1, 8.3 μm (RGB)

F. A. Kruse ♦ 303-499-9471 ♦ fkruse@unr.edu ♦ http://www/unr.edu/mines/able

Steamboat Next Steps

- **HyspIRI Simulation**
  - **HyspIRI SNR model vs Sim-Data SNR**
  - **Mineral mapping**
- **ASTER Calibration/Corrections and Temperature**
  - **ASTER Radiance Corrections using “Unit Conversion Coefficients” from HDF**
  - **ACORN Reflectance (Day)**
  - **ISAC Atmospheric Correction (Day-Night)**
  - **Normalized Emissivity (Day-Night)**
  - **Coolbaugh Day-Night Temperature corrections setup and test**

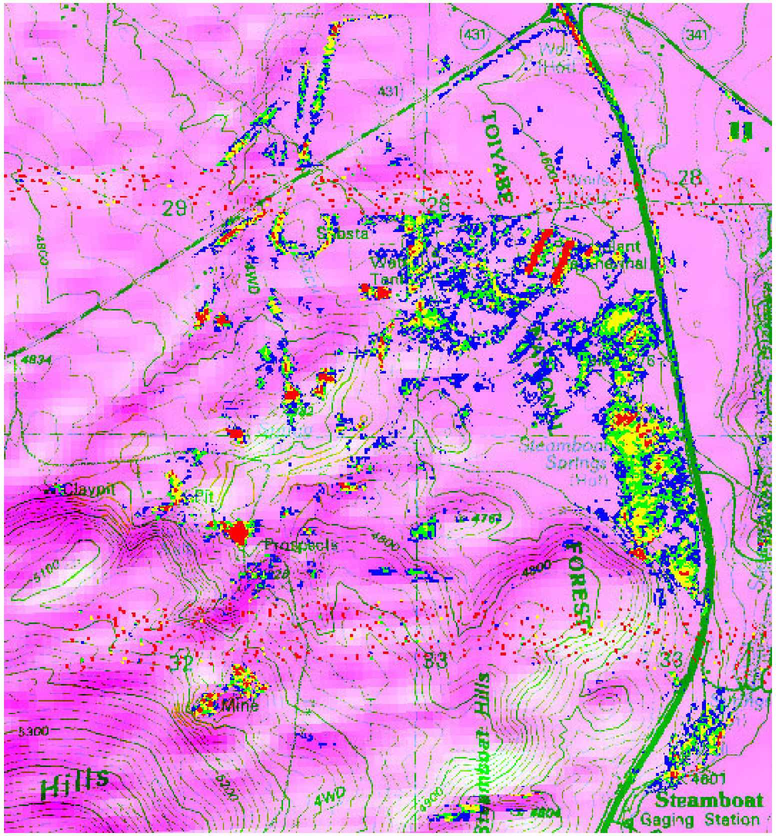

Coolbaugh et al., 2000 – Temperature Anomalies at Steamboat Springs

Long Valley, CA Simulation

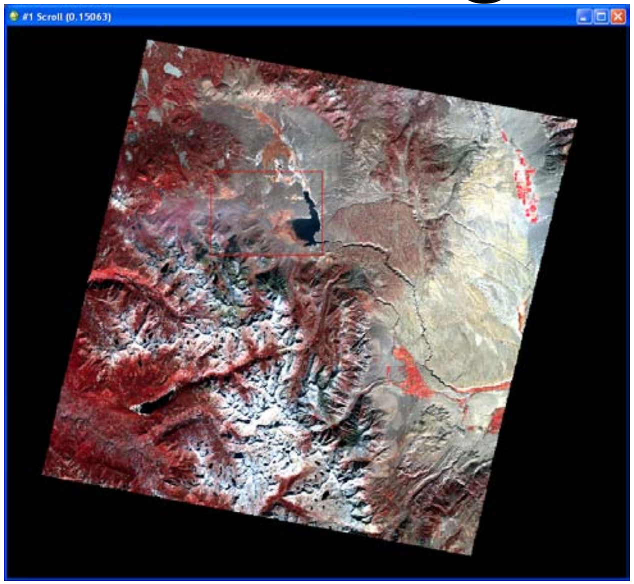

ASTER VNIR (15m) 10-30-2002 Ortho

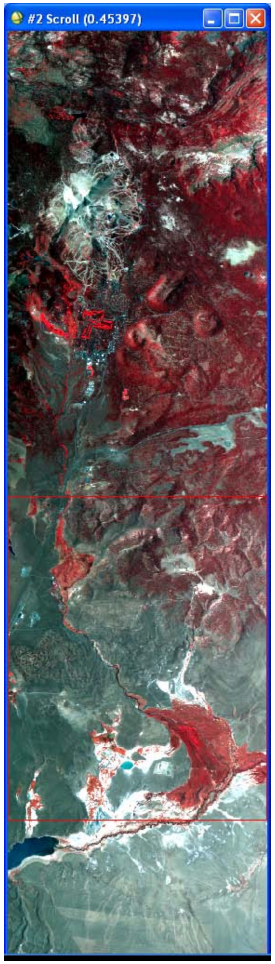

AVIRIS VNIR (15m) 09-15-2000 (no Geo)

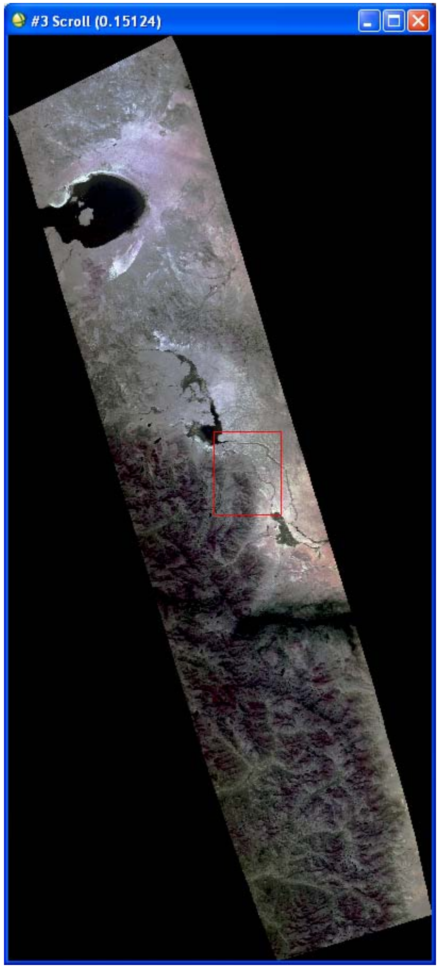

MASTER LWIR (33m), 08-18-2001 GLT-Corrected

Long Valley, CA Simulation

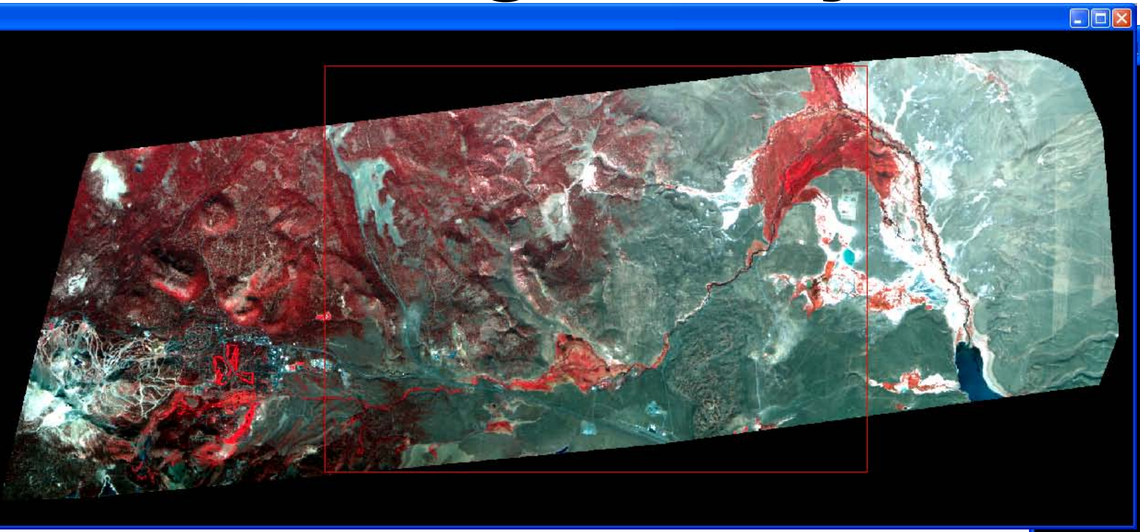

AVIRIS VNIR (15m)
09-15-2000 (warp to ortho ASTER)

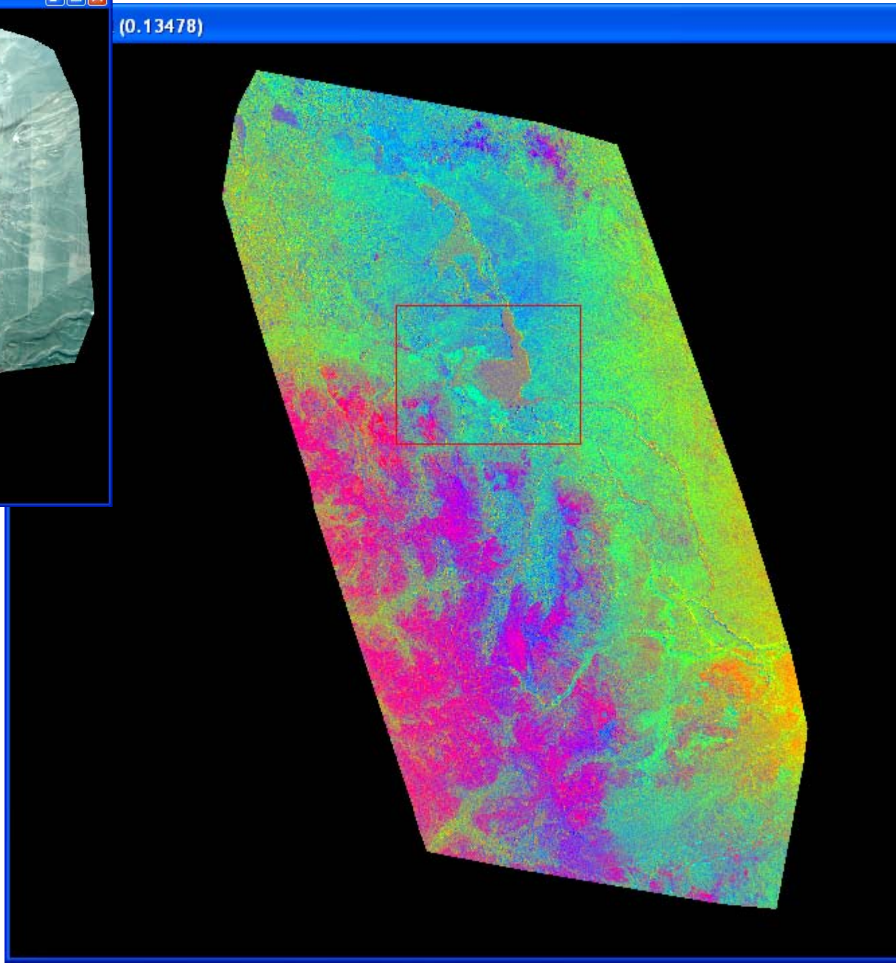

VSWIR Reflectance
+ LWIR Emissivity
= lithology and mineralogy

MASTER LWIR (33m), 08-18-2001 GLT-Corrected, ASTER Ortho, decor stretch

Long Valley, CA Simulation

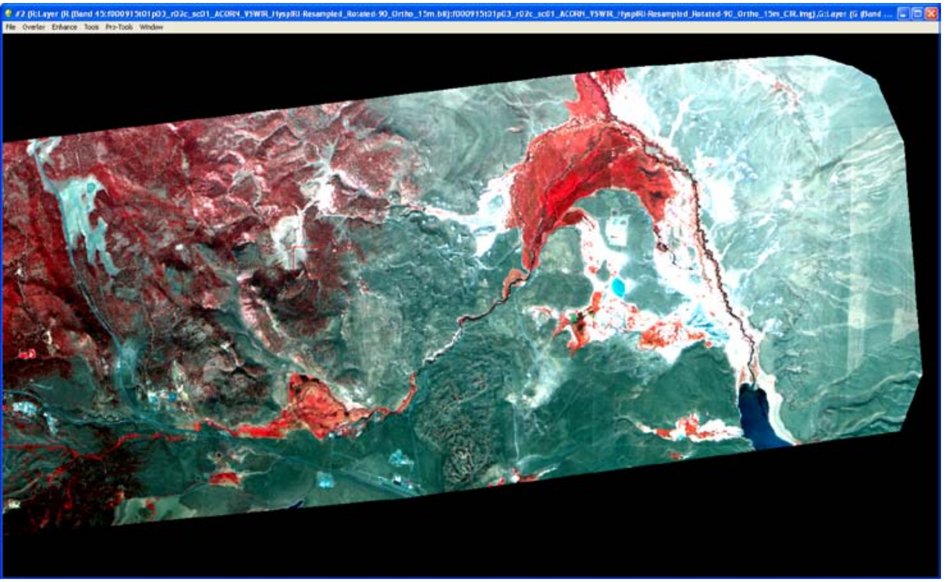

AVIRIS VNIR (15m) 09-15-2000 (Overlap)

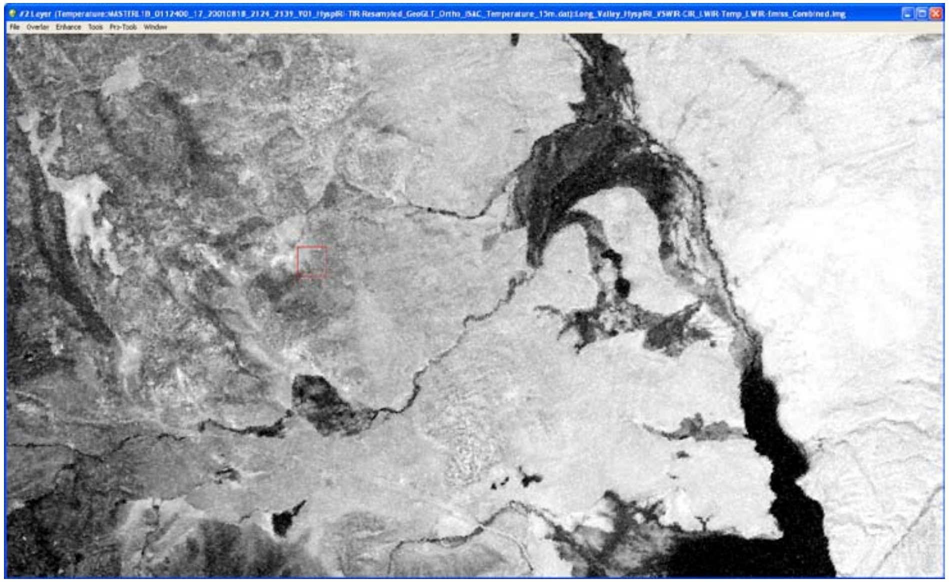

MASTER LWIR (33m), 08-18-2001 Temperature (Overlap)

MASTER LWIR (33m), 08-18-2001 Emissivity 6, 5, 3 (Overlap)

Long Valley MASTER Temperature (night), 16 June 2002

- 3.4m MASTER
- Scene Temperature Variability
- 300 – 305K: 3943 Pixels
- 305 – 310K: 192 Pixels
- 310 – 315K: 94 Pixels
- 315 – 320K: 67 Pixels
- 320 – 325K: 39 Pixels
- 325 – 330K: 14 Pixels
- 330 – 334K: 0 Pixels
- >334K: 4 Pixels
- Geothermal Outflows

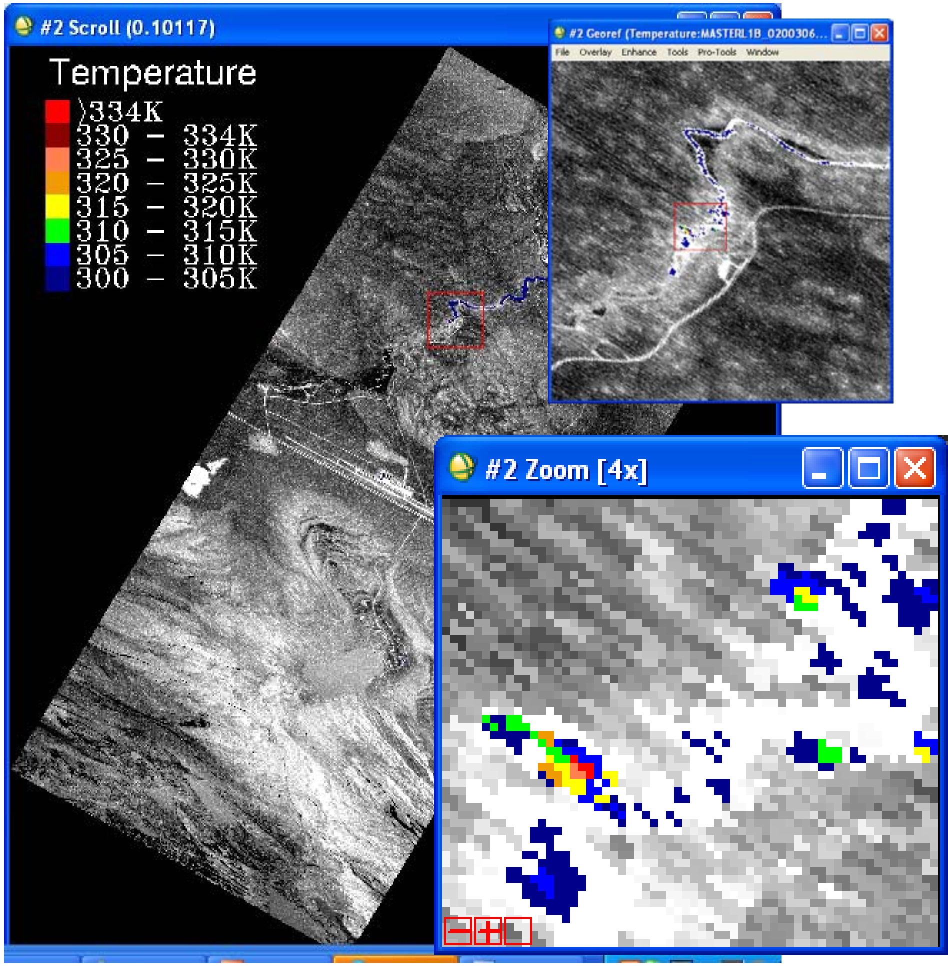

TES-Extracted Temperature, Night-Time MASTER, (Hot Creek), Long Valley, CA

F. A. Kruse ♦ 303-499-9471 ♦ fkruse@unr.edu ♦ http://www/unr.edu/mines/able

Long Valley 60m HyspIRI TIR Simulation (night), 16 June 2002

- 60m HyspIRI Simulation using MASTER, Temperatures >290K
- Scene Temperature Variability
  - 290 – 291K: 4486 Pixels
  - 291 – 292K: 2438 Pixels
  - 292 – 293K: 950 Pixels
  - 293 – 294K: 323 Pixels
  - 294 – 295K: 87 Pixels
  - 296 – 297K: 12 Pixels
  - 297 – 298K: 8 Pixels
  - >298K: 1 Pixel
- "Hot" Spots
  - Water
  - Residual Solar (Topographic) Effects
  - Albedo effects
  - Geothermal Effects

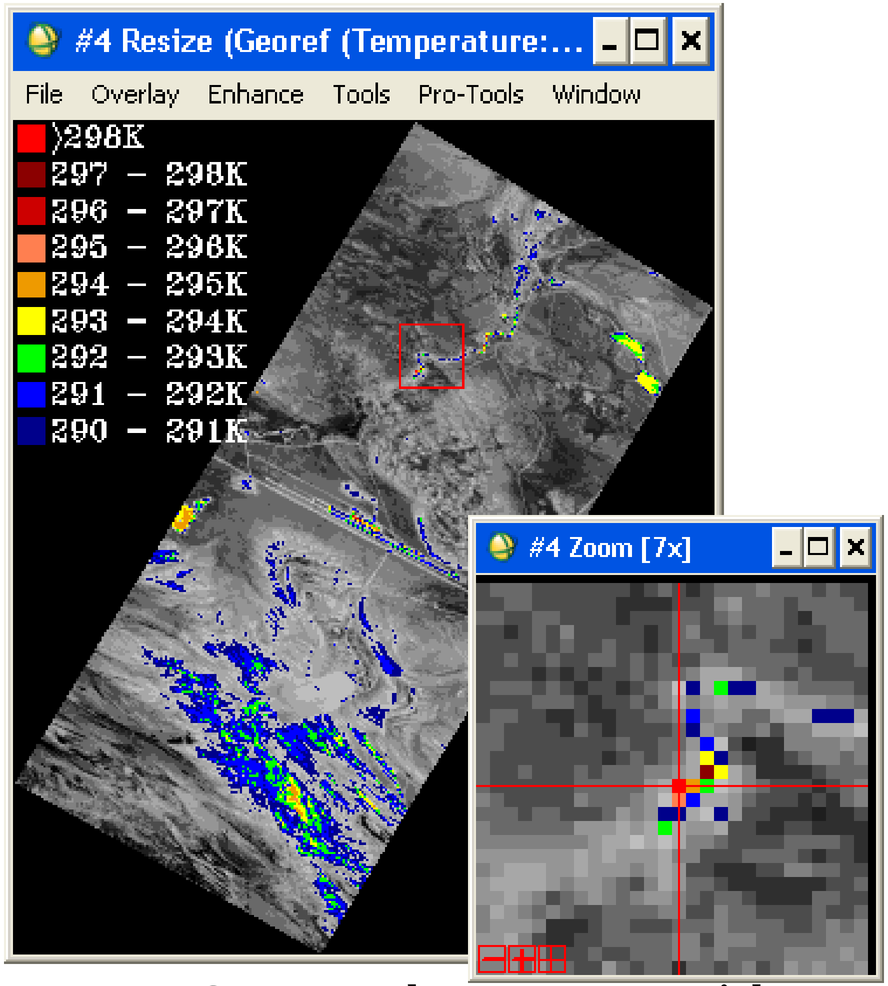

HyspIRI TES-Extracted Temperature, Night-Time MASTER, (Hot Creek), Long Valley, CA

F. A. Kruse ♦ 303-499-9471 ♦ fkruse@unr.edu ♦ http://www/unr.edu/mines/able

Long Valley, CA Synergy (eg: DESdynI):
Structural Elements from InSAR

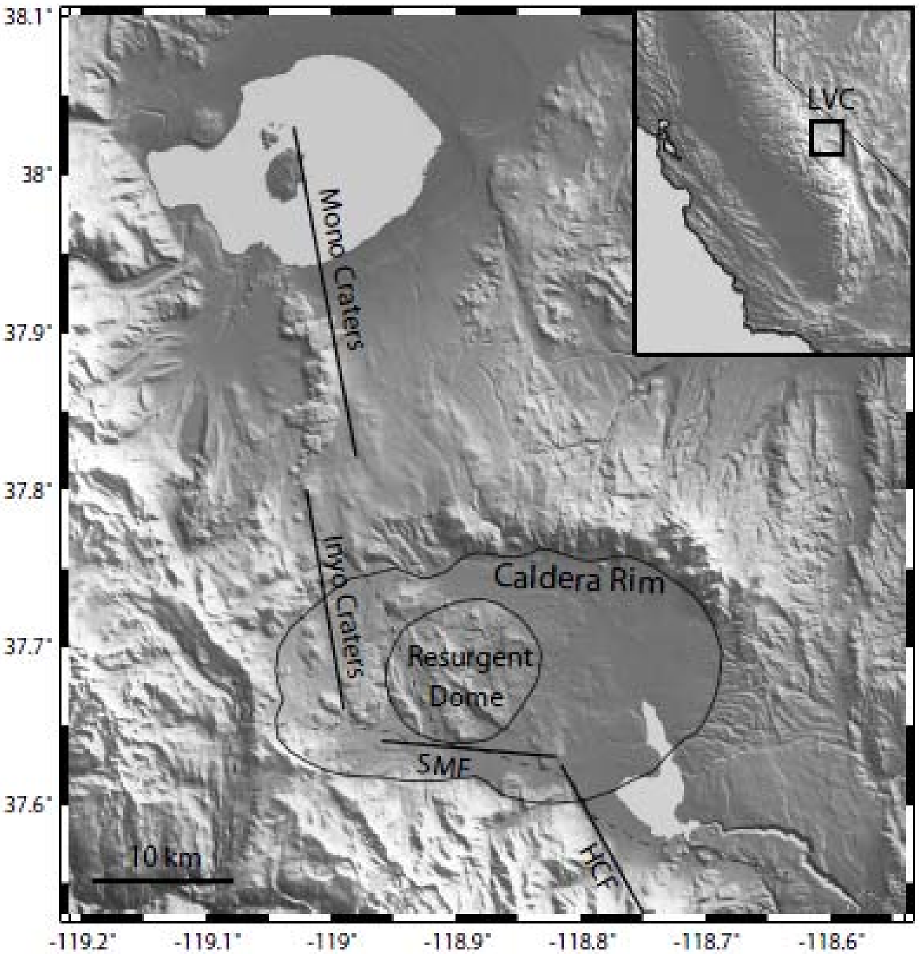

South Moat Fault (SMF) and Hilton Creek Fault (HCF)

(Newman et. al., 2005)

Inflation and deflation associated with Magma activity under “resurgent dome”

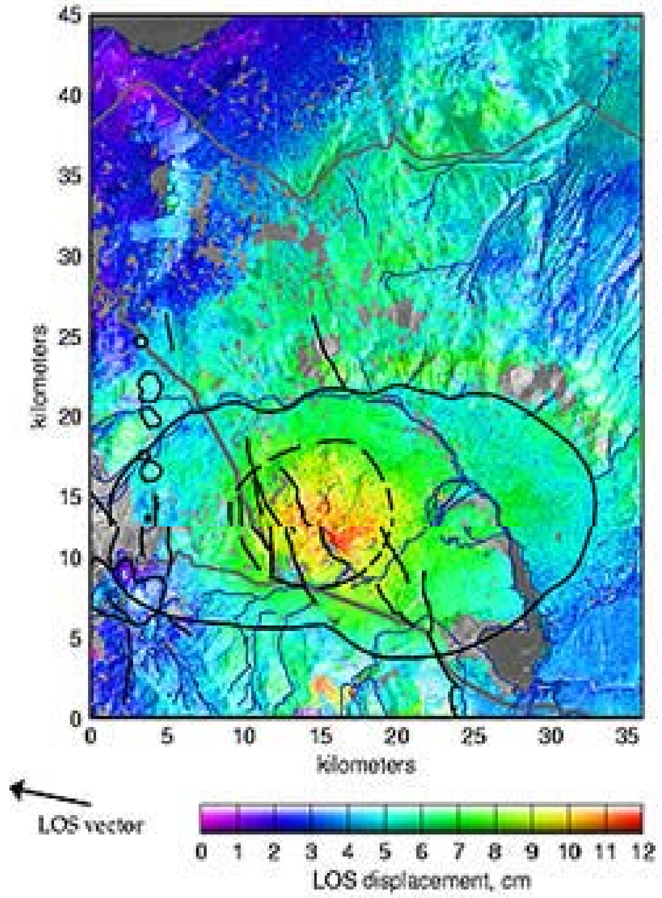

1992 - 1995

Long Valley, CA Synergy (eg: DESdynI): Structural Elements from InSAR

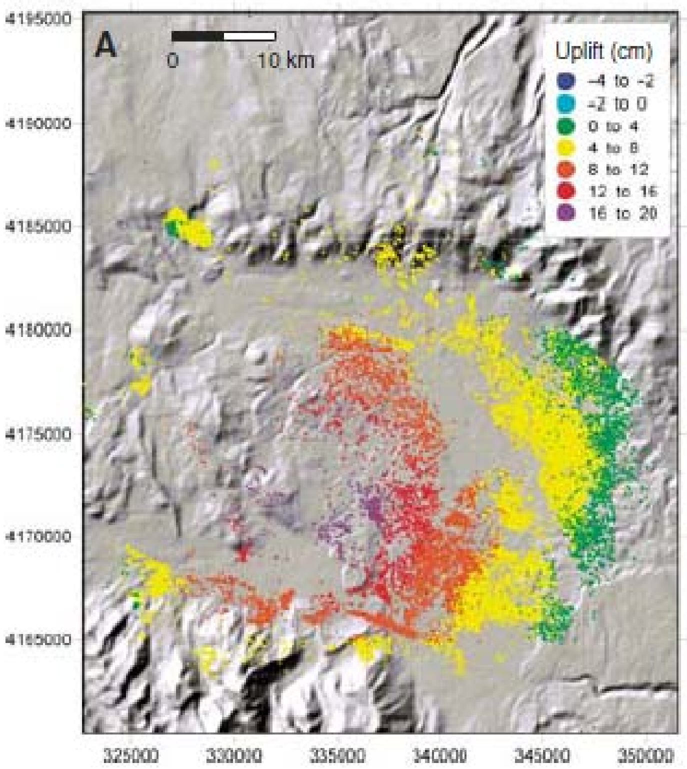

Inflation and deflation associated with magma activity under “resurgent dome”

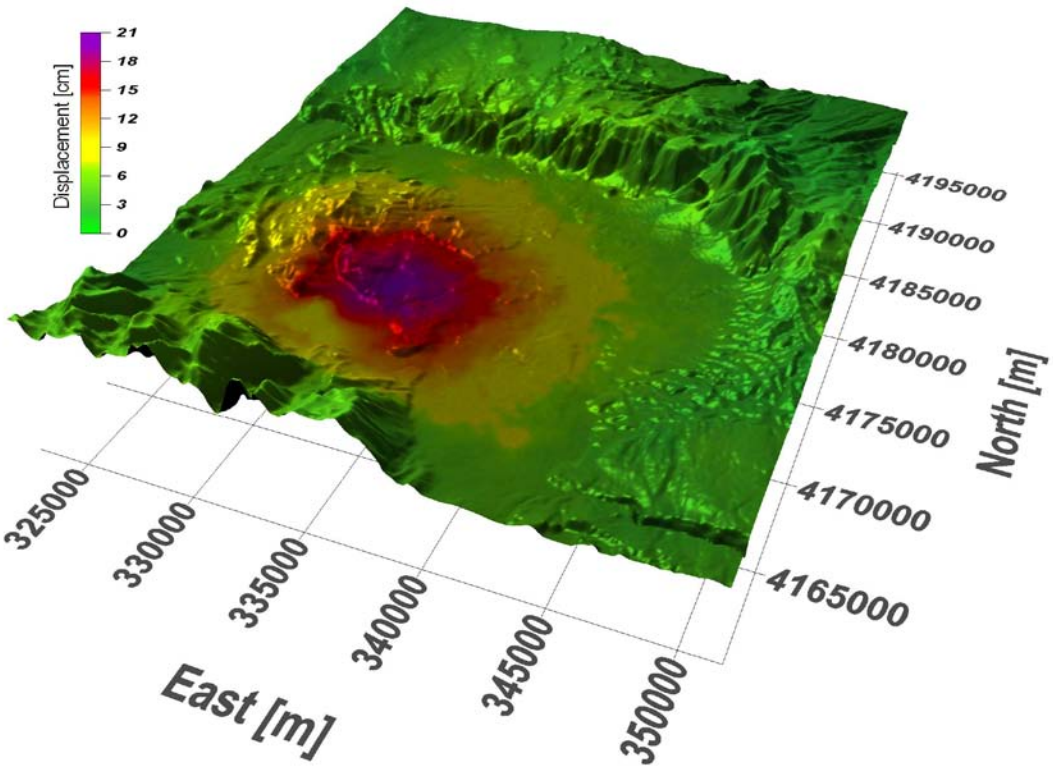

1992–1999 ERS Data: SAR interferometry (InSAR

Tizzani et al., Geology, 2009

http://eopi.esa.int/esa/

F. A. Kruse ♦ 303-499-9471 ♦ fkruse@unr.edu ♦ http://www/unr.edu/mines/able

Yellowstone, WY Simulation

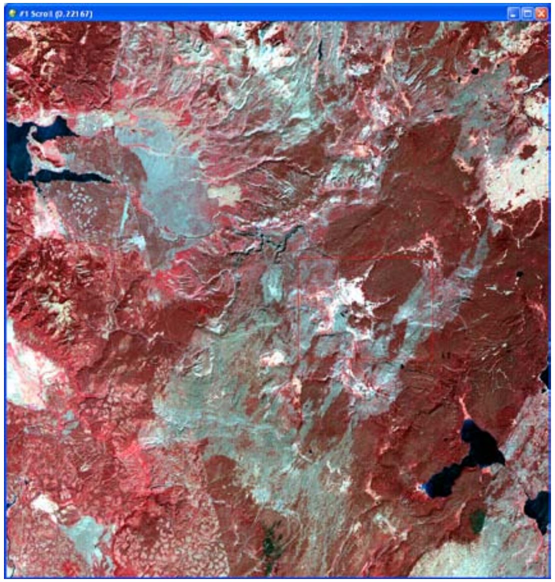

ASTER VNIR (15m)
08-06-2004 Ortho

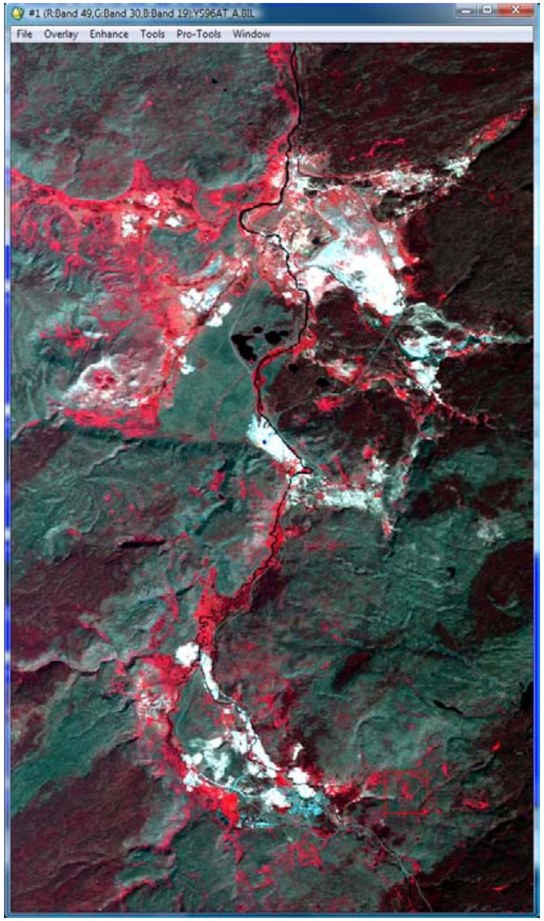

AVIRIS VNIR (15m)
08-06-1996 no geo

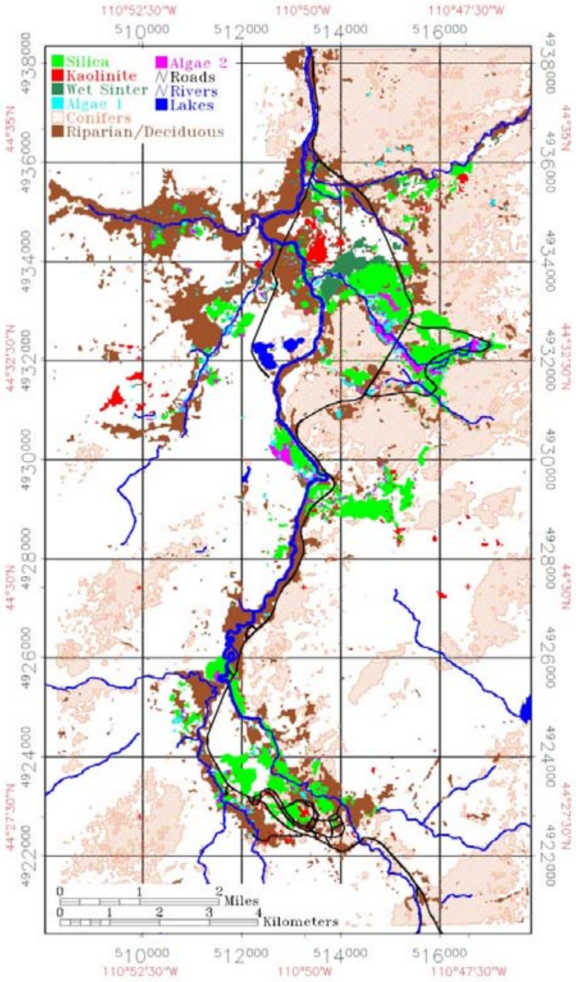

Mineral Mapping Results

F. A. Kruse ♦ 303-499-9471 ♦ fkruse@unr.edu ♦ http://www/unr.edu/mines/able

MAS data (33m) were acquired of portions of the park in 1996 (Midway Geyser Basin at center)

True Color

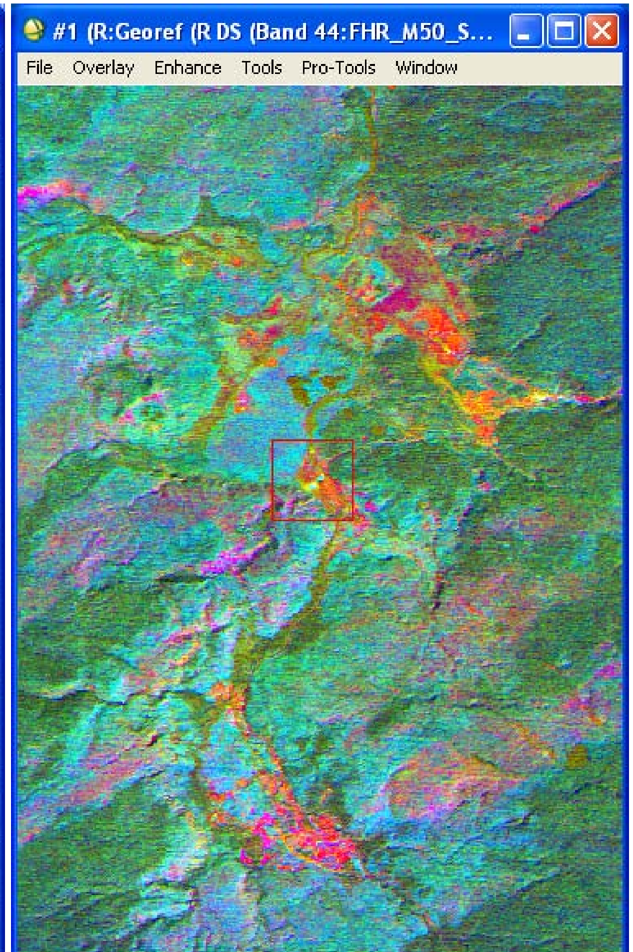

Decor 5, 3, 1

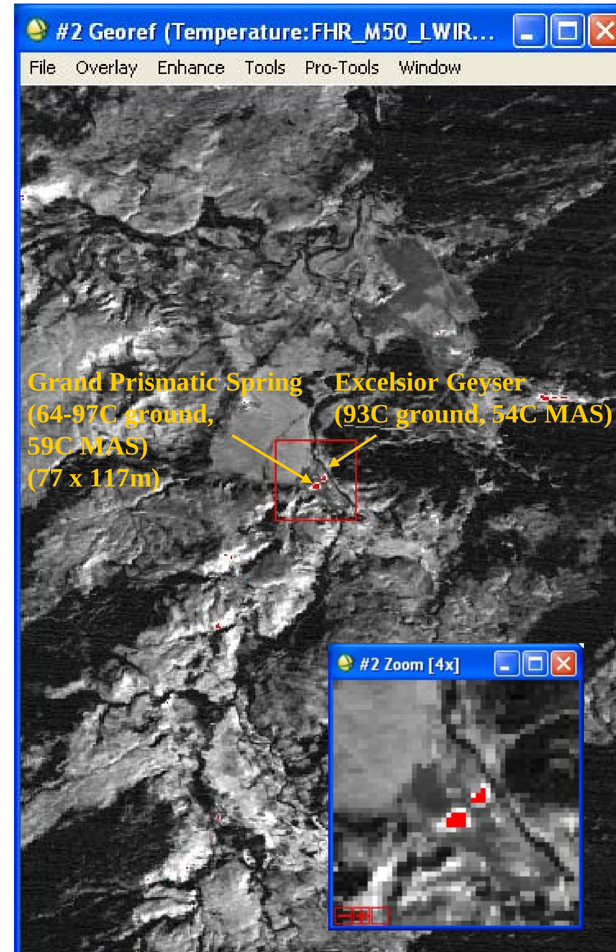

Temperature

HyspIRI Simulation using MAS data @60m)

True Color

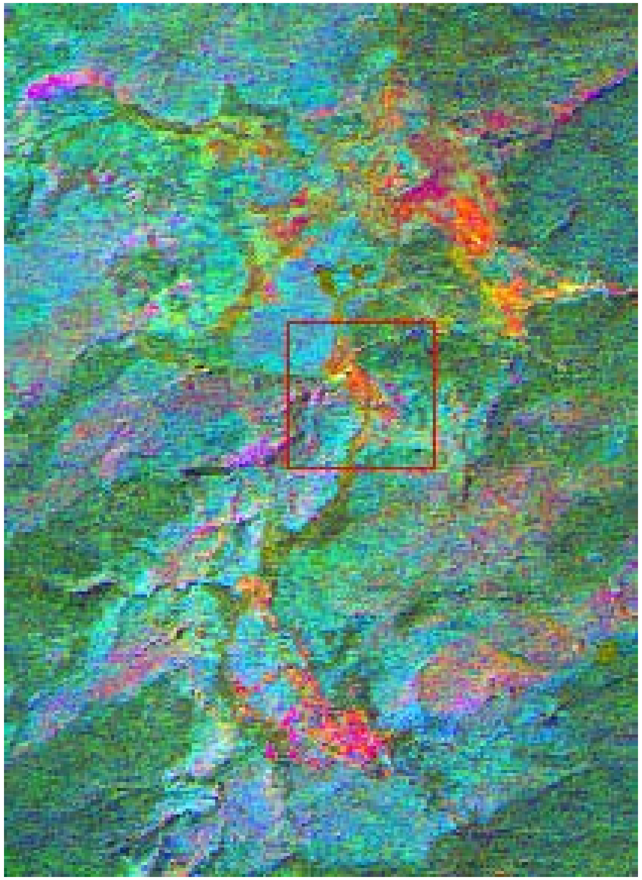

Decor 5, 3, 1

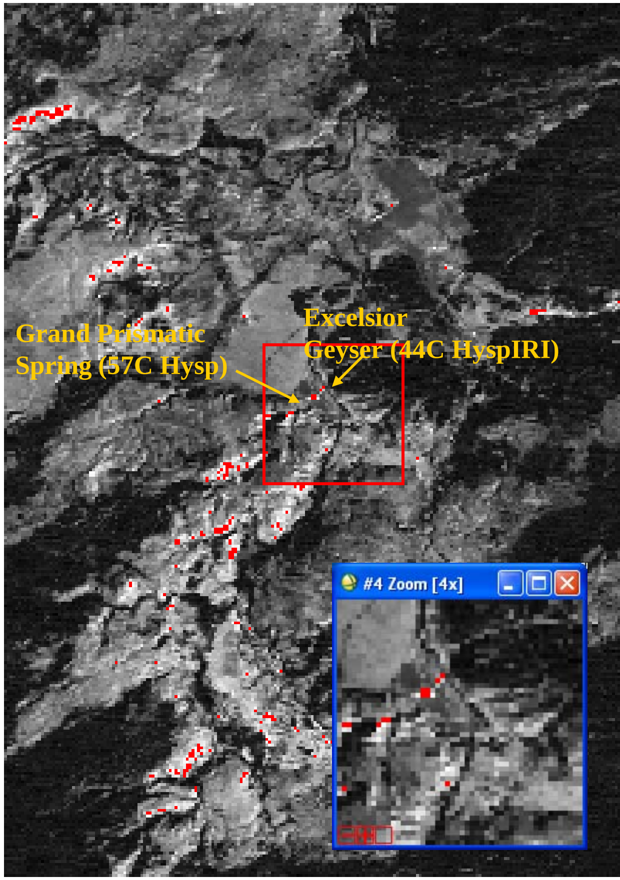

Temperature

F. A. Kruse ♦ 303-499-9471 ♦ fkruse@unr.edu ♦ http://www/unr.edu/mines/able

Cuprite, NV Simulation

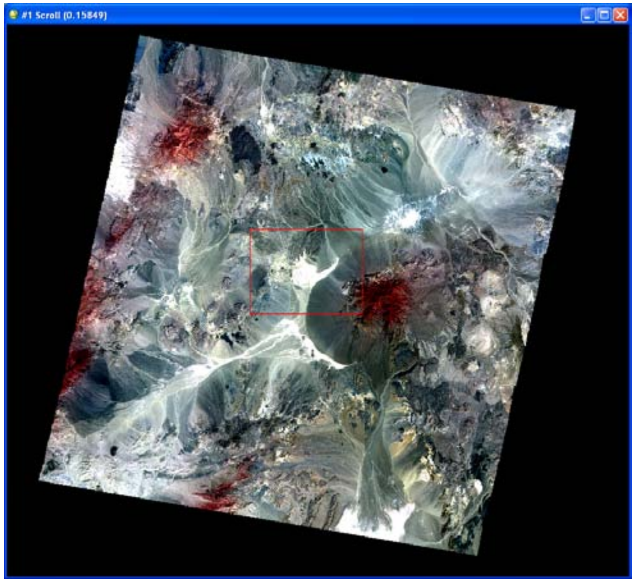

ASTER VNIR (15m)
04-28-2007 Ortho

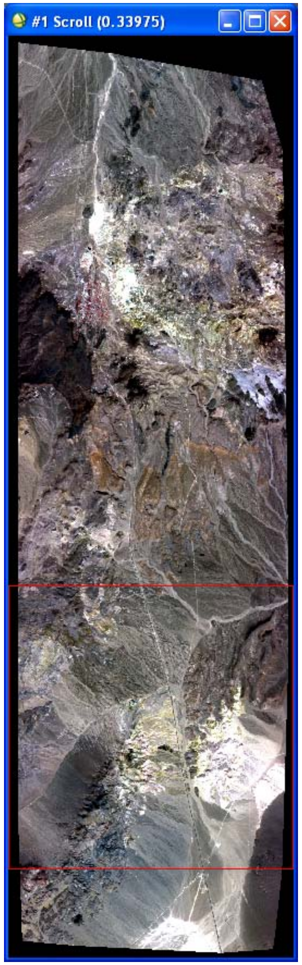

AVIRIS VNIR (15m)
09-20-2006 Ortho
Warped to ASTER Ortho

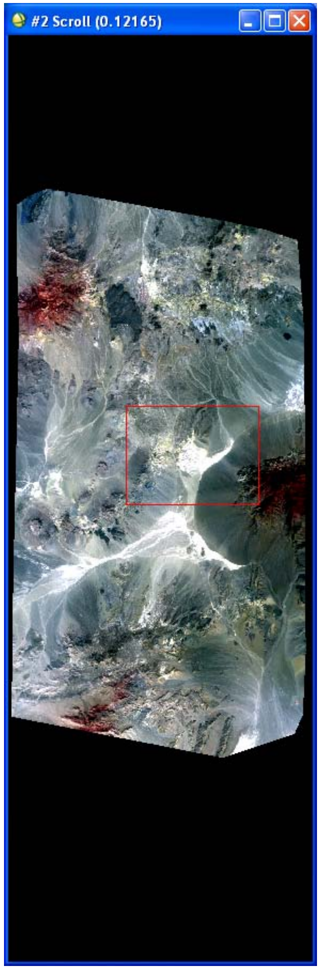

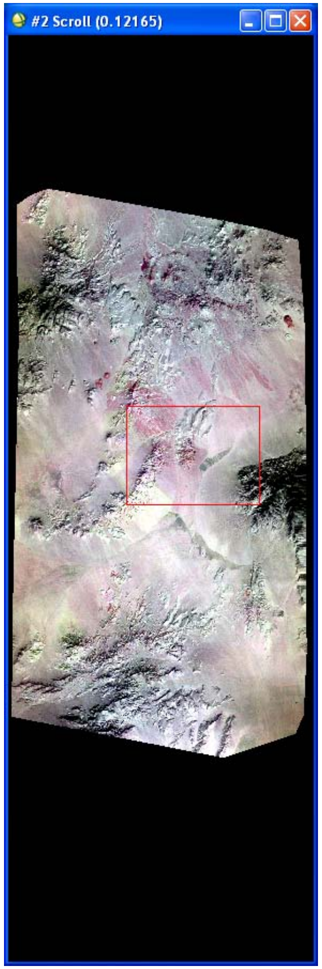

MASTER VNIR and LWIR, 09-20-2006 GLT-Corrected Warped to ASTER Ortho

Cuprite, NV Simulation: We end up with several small simulated datasets !

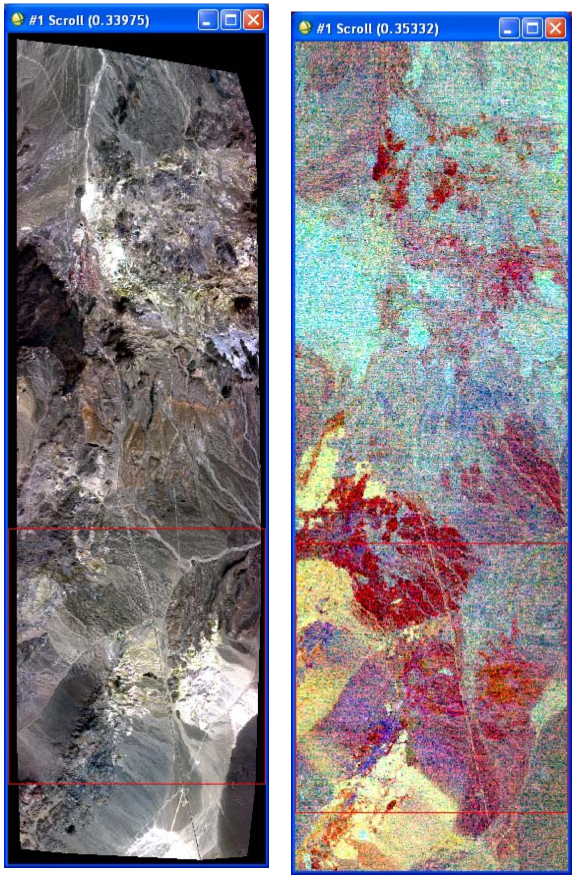

772 x 2493 Left: AVIRIS VNIR (15m) 09-20-2006 Ortho Warped to ASTER Ortho at 60m spatial resolution; Right Master Emissivity @HyspIRI bands

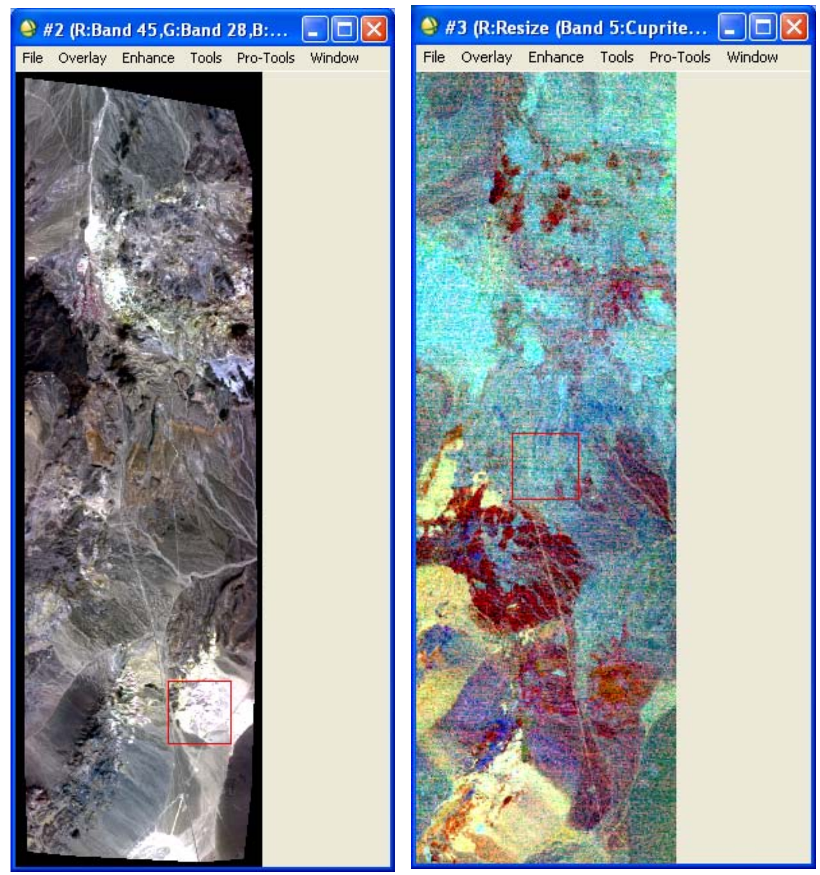

193 x 623 Left: HyspIRI simulated dataset from AVIRIS VNIR (15m) 09-20-2006 Ortho Warped to ASTER Ortho at 60m spatial resolution. Right: MASTER Emissivity @HyspIRI bands and 60m

Cuprite, NV 2002 AVIRIS versus HyspIRI-Simulated 60m SWIR MTMF Mineral Map (Kruse, Unpublished)

AVIRIS (16m)

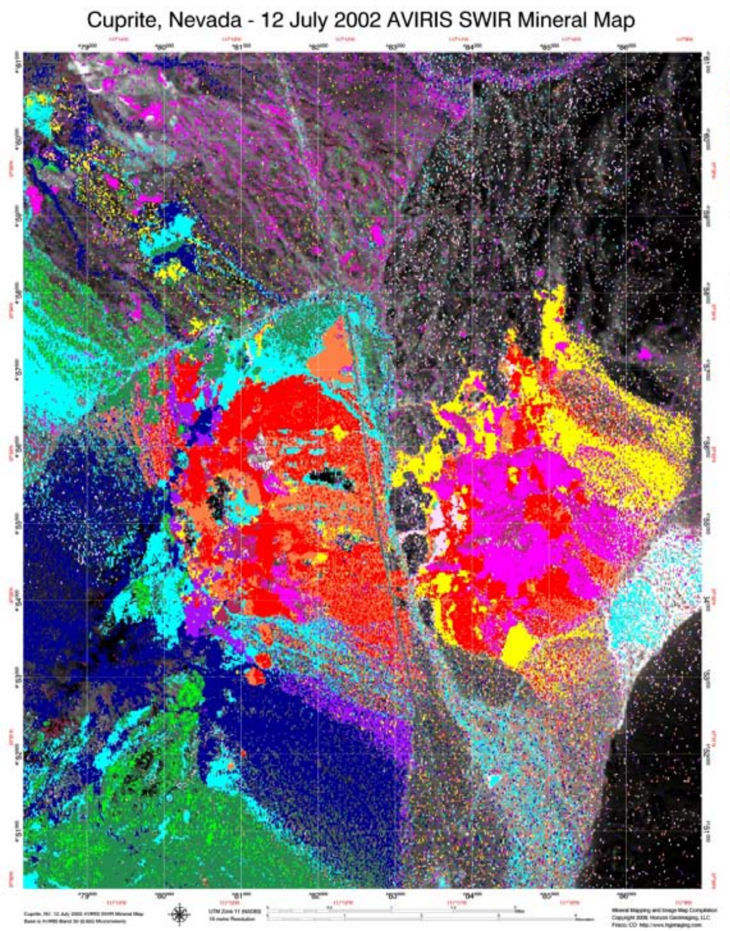

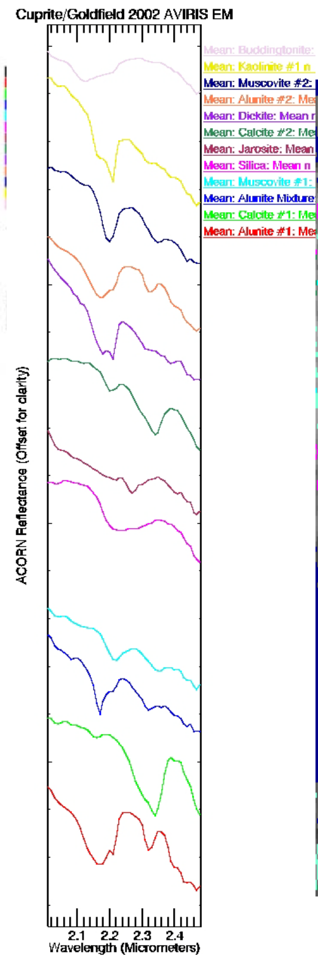

Simulated HyspIRI 60m

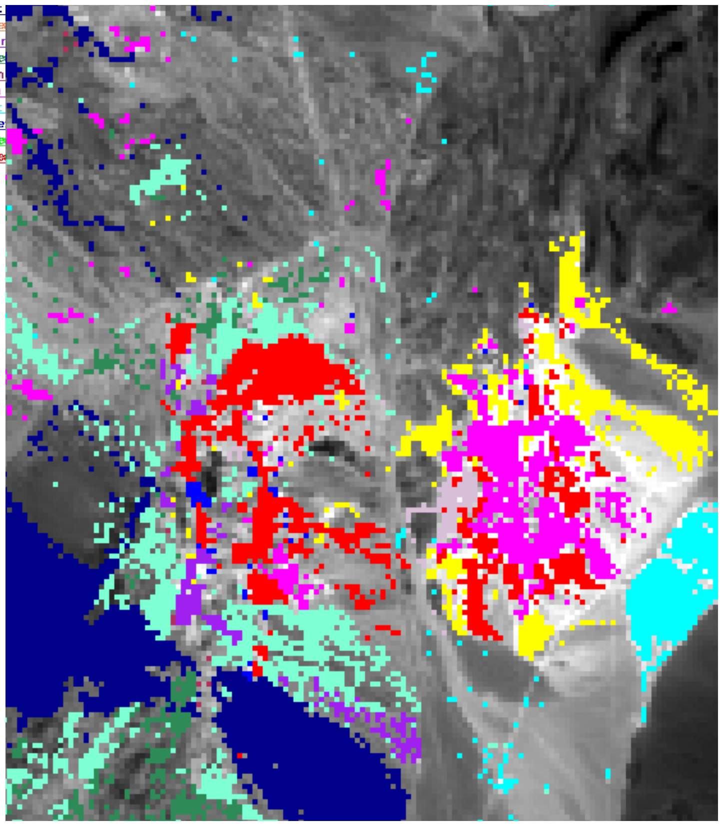

Cuprite, NV 1999 MASTER 6, 5, 3 (RGB) Decorellation Stretch versus HyspIRI-Simulated 60m

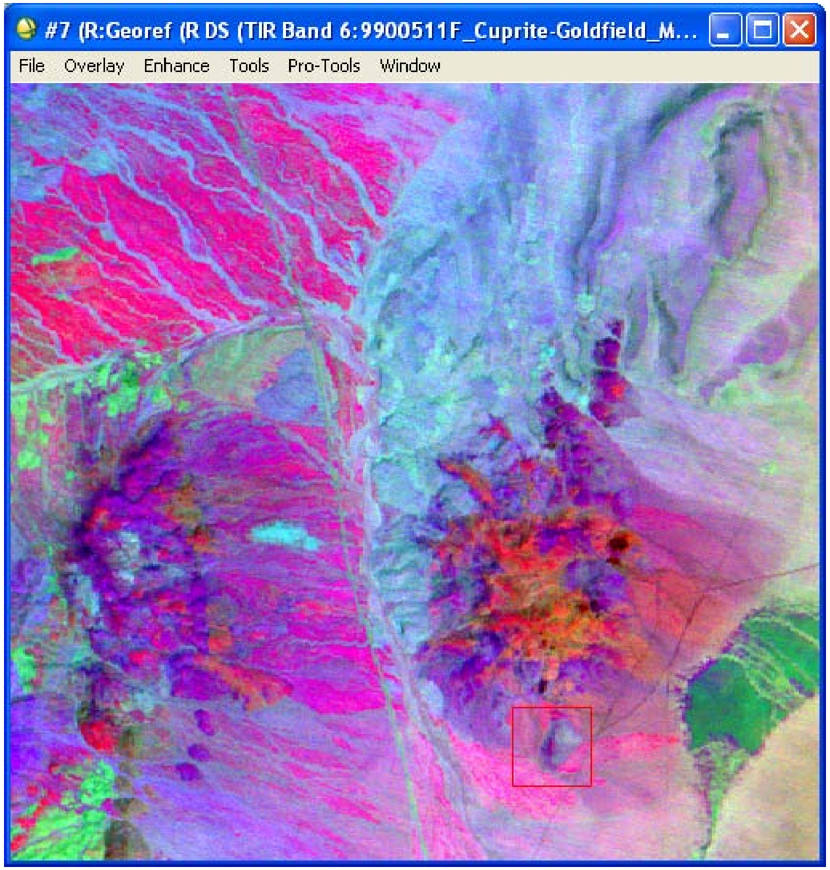

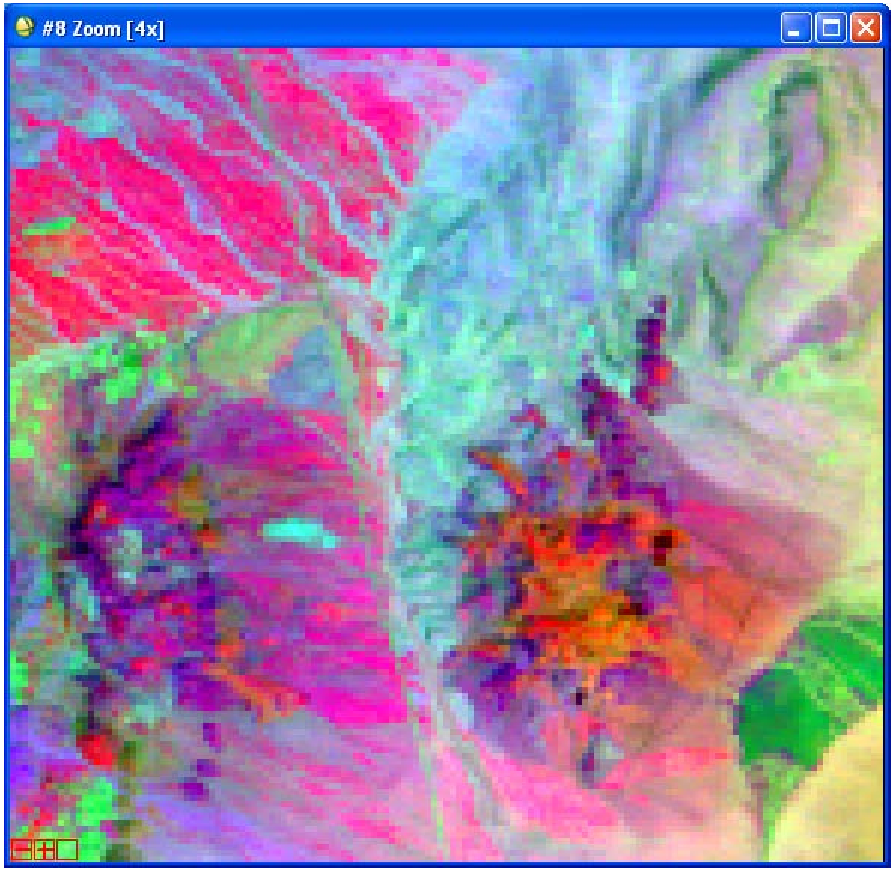

Proposed: Use spectral unmixing and modeling to create spatially extended simulated HSI data

- Geocorrect and co-register nested multispectral (ASTER) and HSI (AVIRIS) datasets (Cuprite, NV example – 2 scenes to start, 13 scenes total to get to ~HyspIRI VSWIR spatial scene
- Correct both datasets to reflectance
- Resample AVIRIS data to HyspIRI spectral response
- Extract HSI “endmember” signatures and model to ASTER wavelength centers and response
- Unmix ASTER modeled endmembers using ASTER reflectance data
- Use ASTER mixture fraction images and HSI endmember spectra to model full-resolution HSI signature for each ASTER pixel based on mixture analysis
  - Result is simulated HSI dataset with ASTER spatial coverage
  - Signature at each pixel has full HSI spectral resolution
  - Validate with other nested HSI datasets
  - Model to 60m HyspIRI spatial resolution

Extended HyspIRI Simulation Using Nested Datasets, Spectral Unmixing, and Spectral Modeling

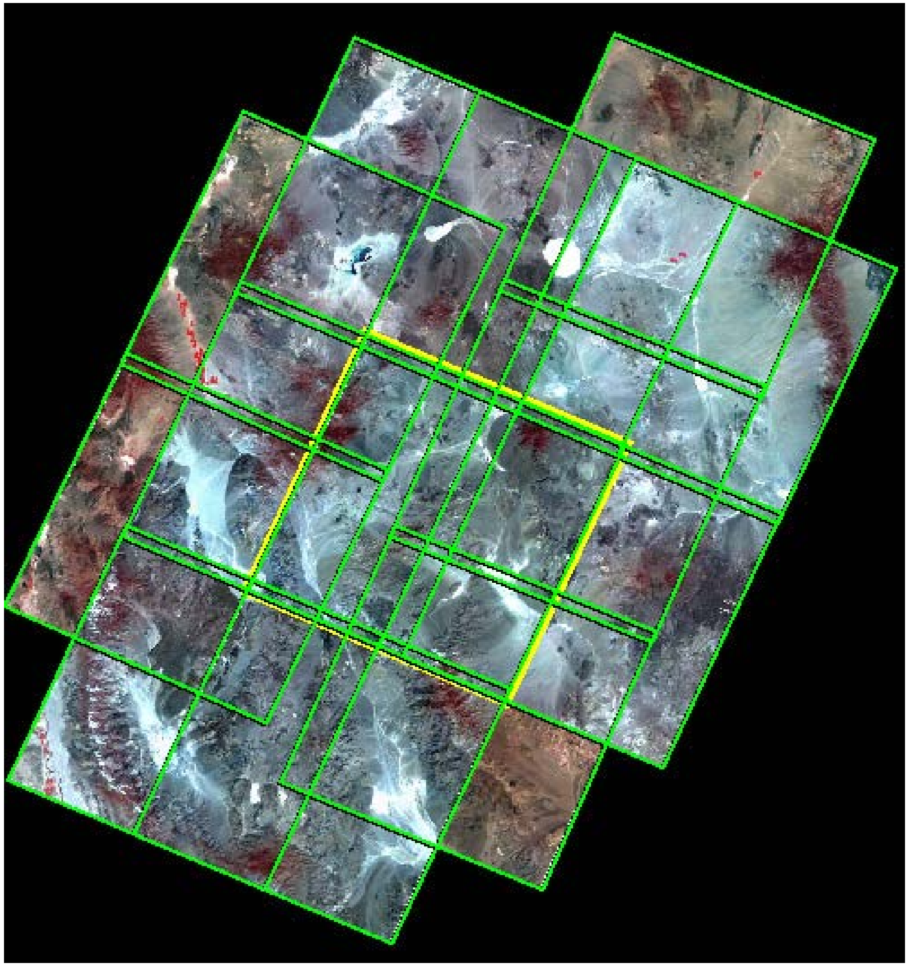

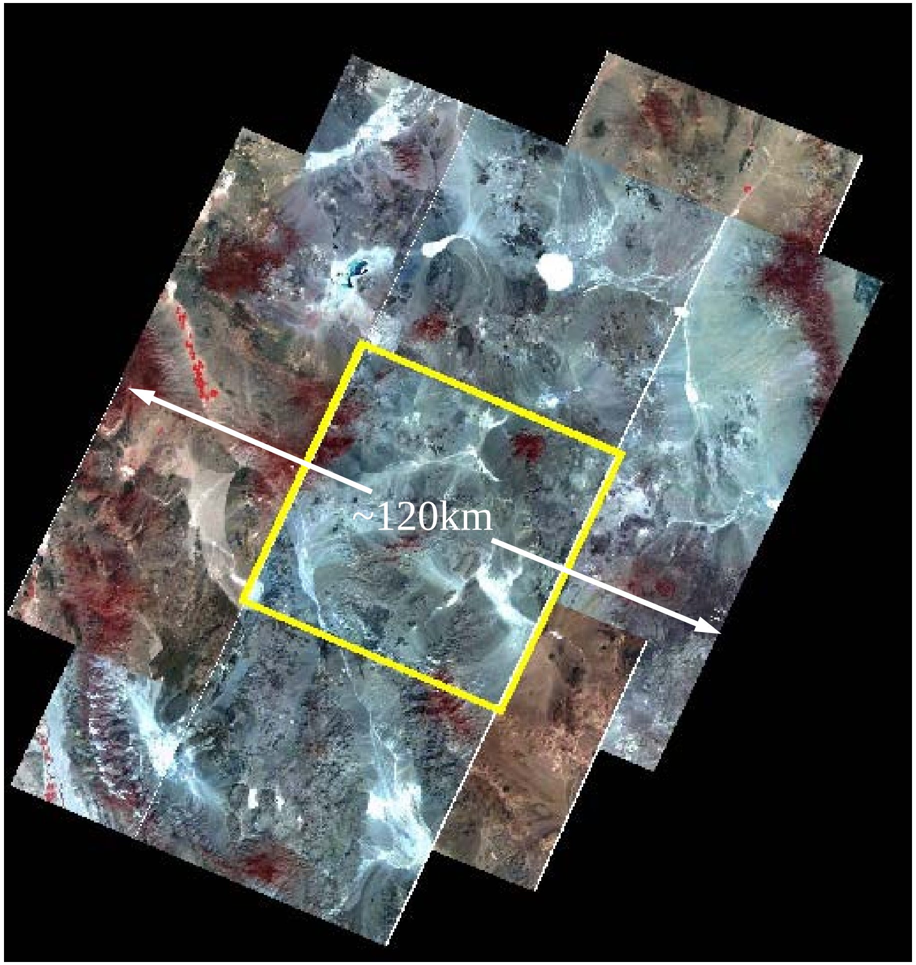

Extended ASTER Mineral Mapping (Combined AVIRIS Endmembers)

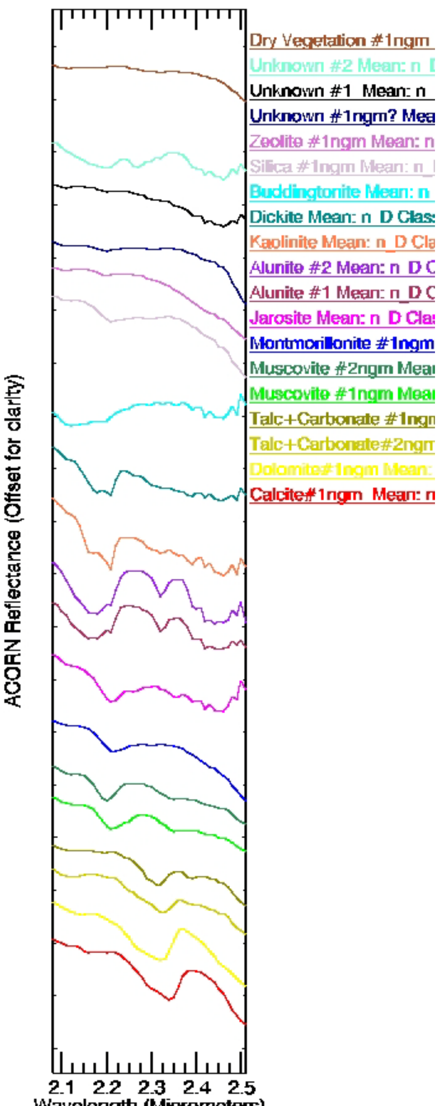

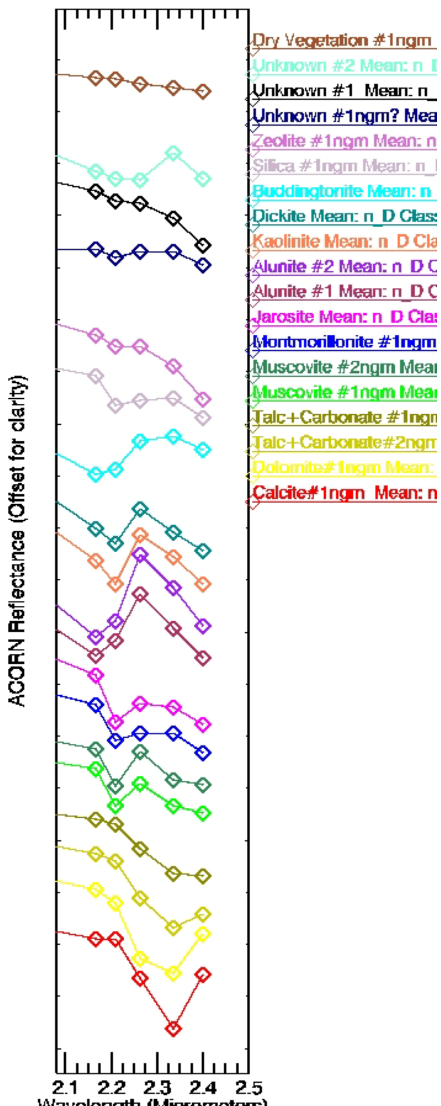

From Kruse and Perry, 2009

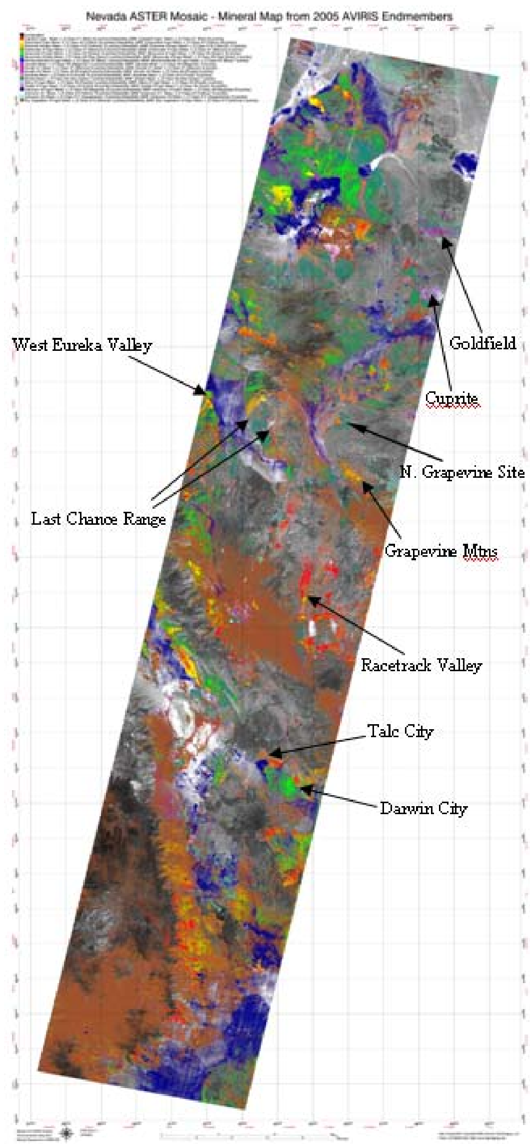

- **(1) N. Grapevine Mtns, NV: Calcite vs Dolomite vs muscovite**
- **(2) Goldfield, NV: Alunite vs kaolinite vs muscovite/illite**
- **(3) Cuprite, NV: kaolinite vs alunite vs muscovite**
- **(4) Grapevine Mtns, NV: Calcite vs Dolomite, muscovite**
- **(5) Talc City, CA: Calcite vs dolomite vs Talc vs 2 varieties of muscovite**
- **(6) Darwin City, CA: Calcite vs dolomite vs muscovite**
- **(7) Racetrack Valley, CA: Calcite vs Dolomite vs altered (sericite-rich) granite**
- **(8) Last Chance Range, CA: Calcite vs Dolomite**
- **9) West Eureka Valley, CA: Two varieties of muscovite**

AVIRIS Endmembers and Mineral Mapping

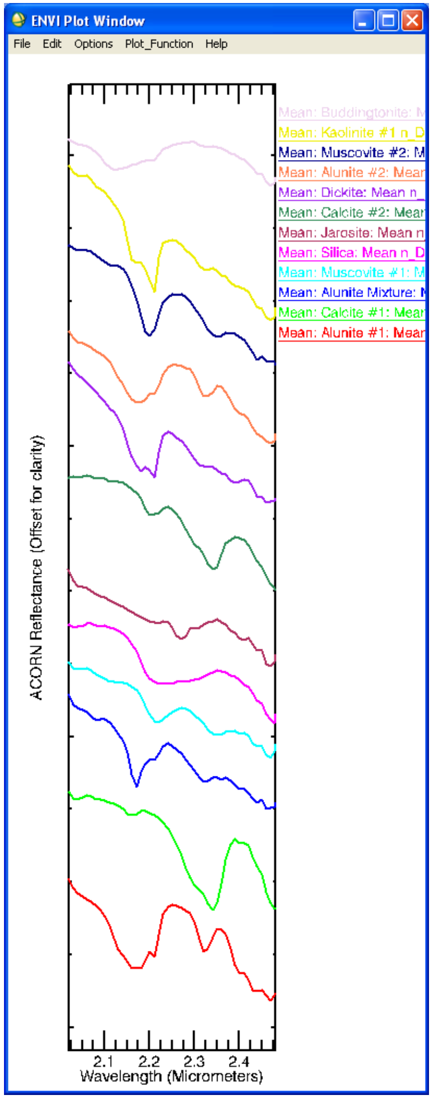

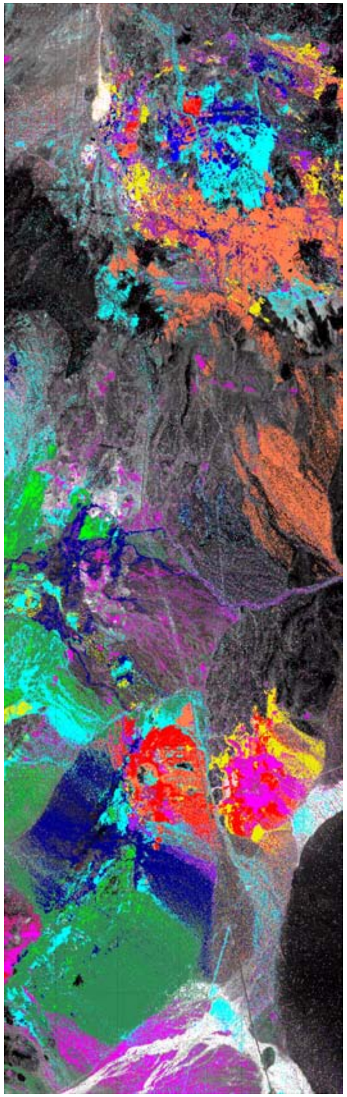

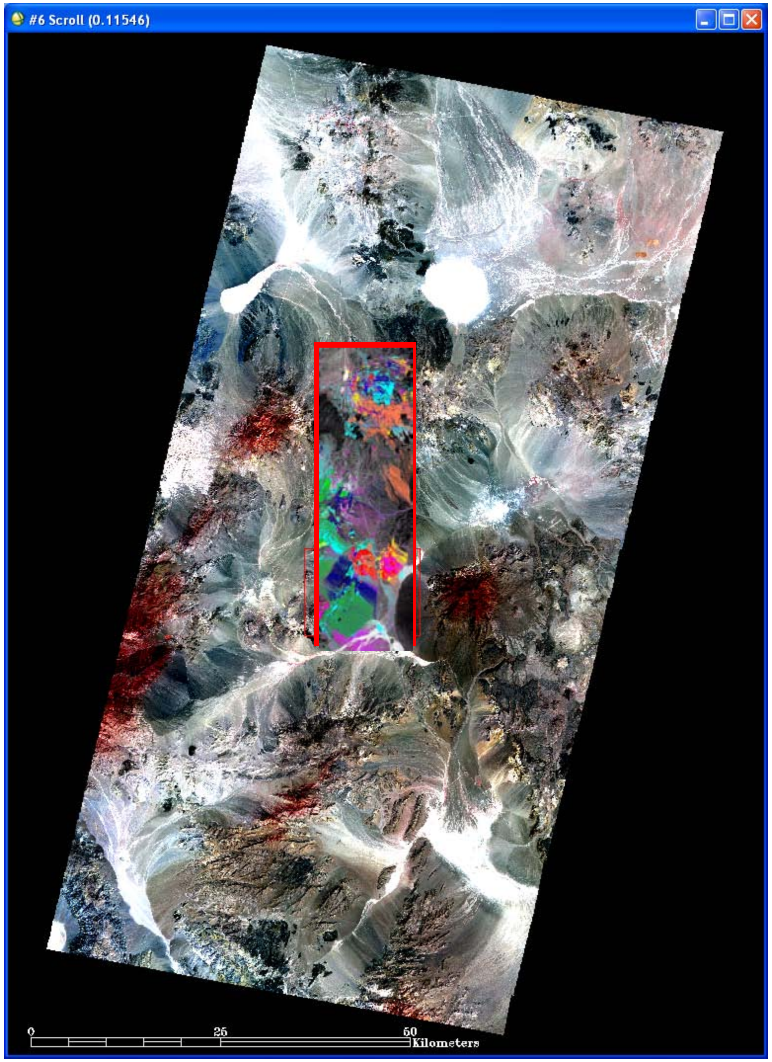

ASTER (2 scene test case)

ASTER vs AVIRIS Reflectance

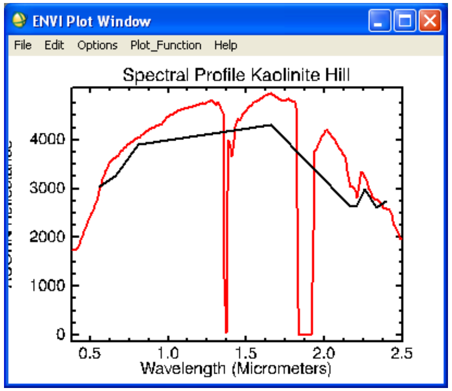

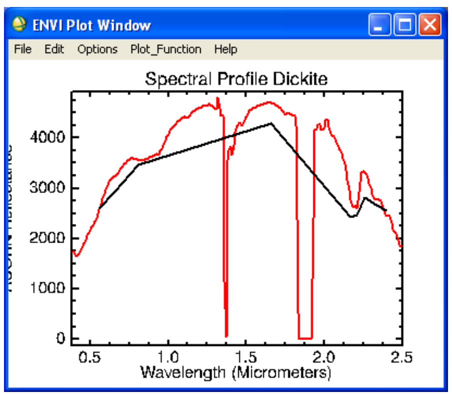

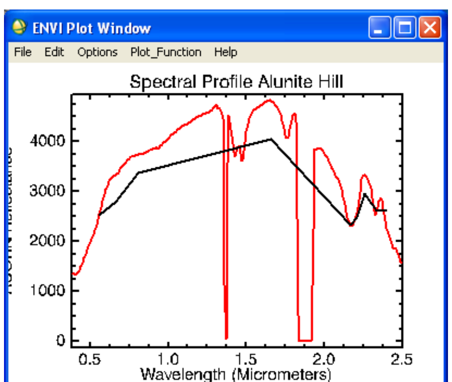

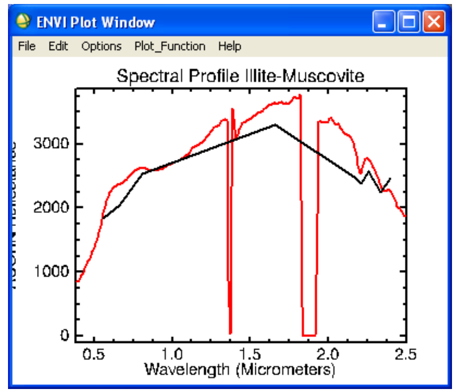

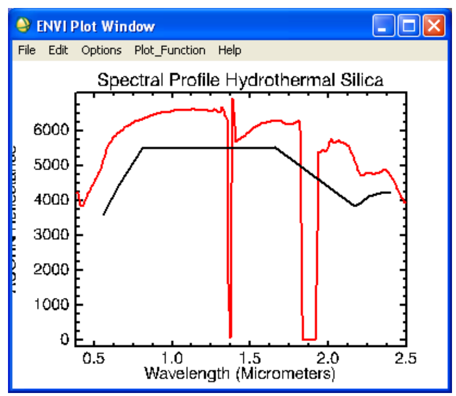

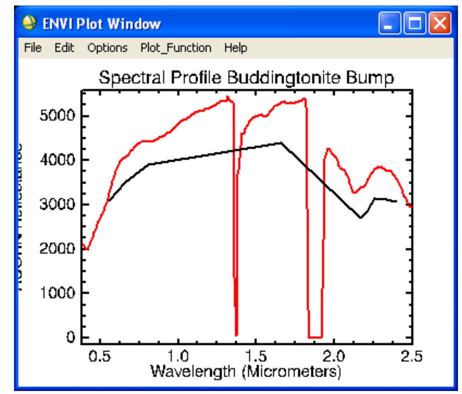

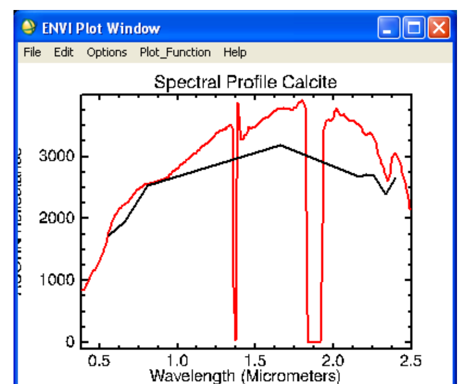

ASTER vs AVIRIS Reflectance

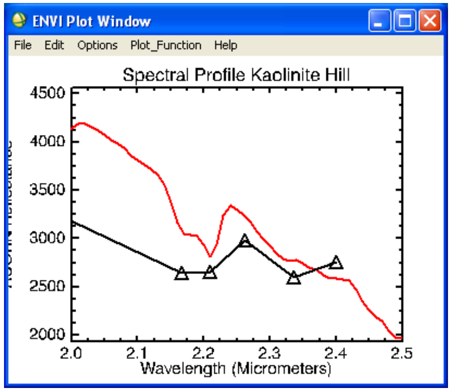

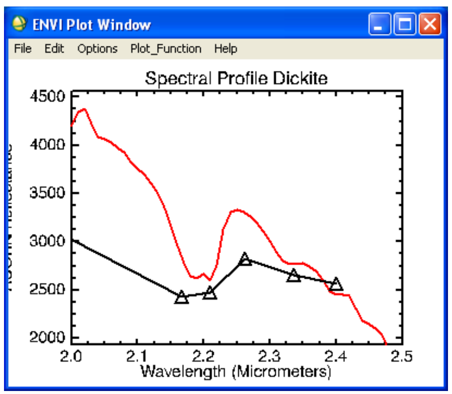

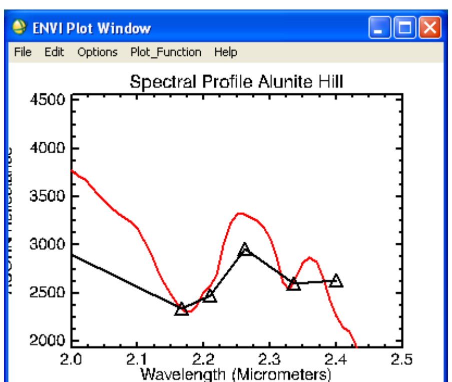

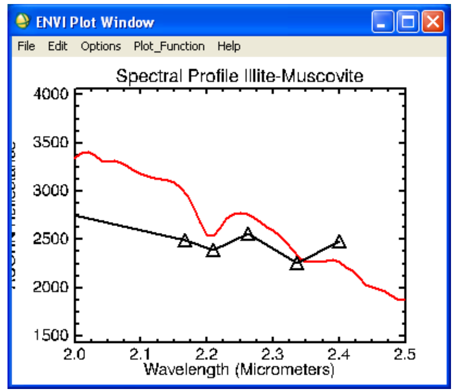

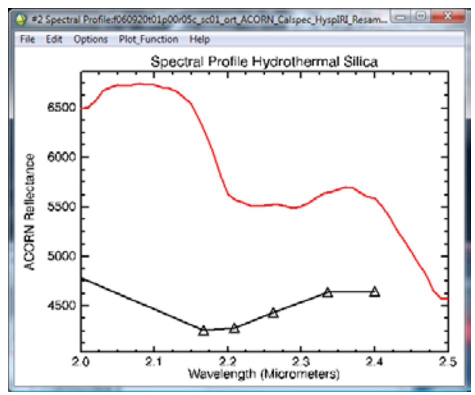

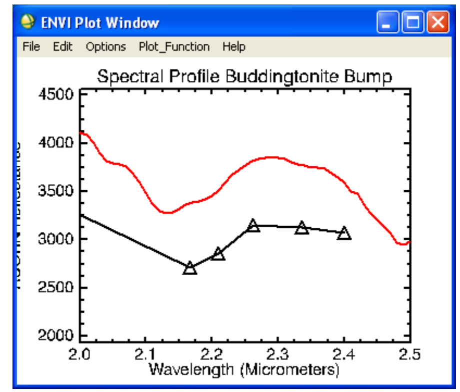

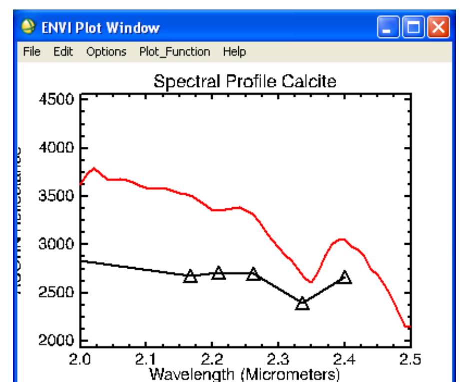

ASTER, HSI Modeling Next Steps

- Unmix ASTER modeled endmembers using ASTER reflectance data
- Use ASTER mixture fraction images and HSI endmember spectra to model full-resolution HSI signature for each ASTER pixel based on mixture analysis
  - Result is simulated HSI dataset with ASTER spatial coverage
  - Signature at each pixel has full HSI spectral resolution
  - Validate with other nested HSI datasets and field spectra (Goldfield, N. Grapevine Mtns)
  - Model to 60m HyspIRI spatial resolution

HyspIRI Simulation Status

- **All datasets in-hand**
- **ASTER orthorectifiction completed for all sites**
- **VSWIR and TIR registration to ASTER completed for all but Yellowstone and some day-night datasets**
- **HyspIRI spectral response modeling and spatial resolution modeling in progress**
- **SNR modeling pending**
- **Selected SWIR and LWIR spectral analysis performed**
- **Combined analysis pending**
- **Day/Night temperature analysis pending**

Last Words

- **What does HyspIRI give us for "classical" geology that we can't get by other means?**
  - **Global remote sensing coverage at scale that will allow development of an "inventory" – a geographic database of hydrothermal systems**
  - **Worldwide simultaneous VSWIR hyperspectral and TIR multispectral at 60m spatial resolution**
  - **Large-scale multi-band LWIR Temperature determination at 60m spatial resolution**
  - **Temporal monitoring (of active geothermal systems and other dynamic geologic systems) on a timescale of days**
  - **Possibility of global synergism with NRC decadal survey instruments and others**

Performance of the proposed HyspIRI TIR bands for accurate compositional identification of eolian dust, ash and sand

[1,3]Scheidt, S.P., [2]Ramsey, M.S., [2]Mohummad, R., [2]Mercurio, E., and [1]Lancaster, N.

1. Desert Research Institute, Reno, NV
2. University of Pittsburgh, Pittsburgh, PA
3. Smithsonian, Center for Earth and Planetary Studies (CEPS)

Presentation Outline

- Explore previous ASTER TIR work used to study eolian systems and dust with respect to HyspIRI science
- Demonstrate how HyspIRI TIR data are suited to map surface composition relevant to dust source mapping (TQ1) and volcanic ash (TQ5)
- Demonstrate the relevance of HyspIRI thermal infrared data to climate science
- How is the identification of mineral composition affected by the choice of band positions?
- How are TIR data are affect the spectral signature of dust and sand?

Previous Work: ASTER TIR Spectral Mapping

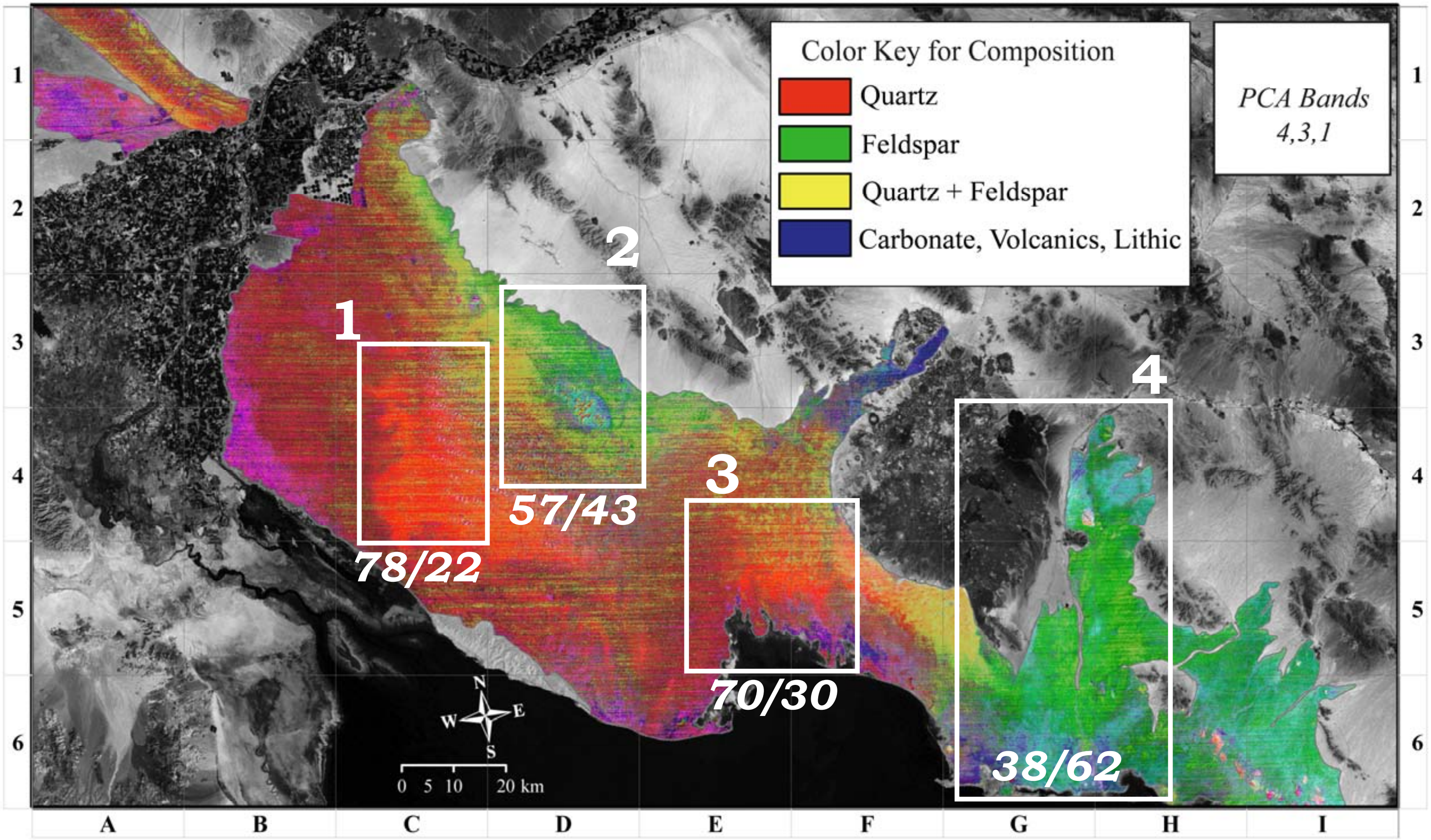

Ratio of Quartz to Feldspar

Scheidt et al. 2010 (submitted)

Previous Work: ASTER TIR Spectral Mapping

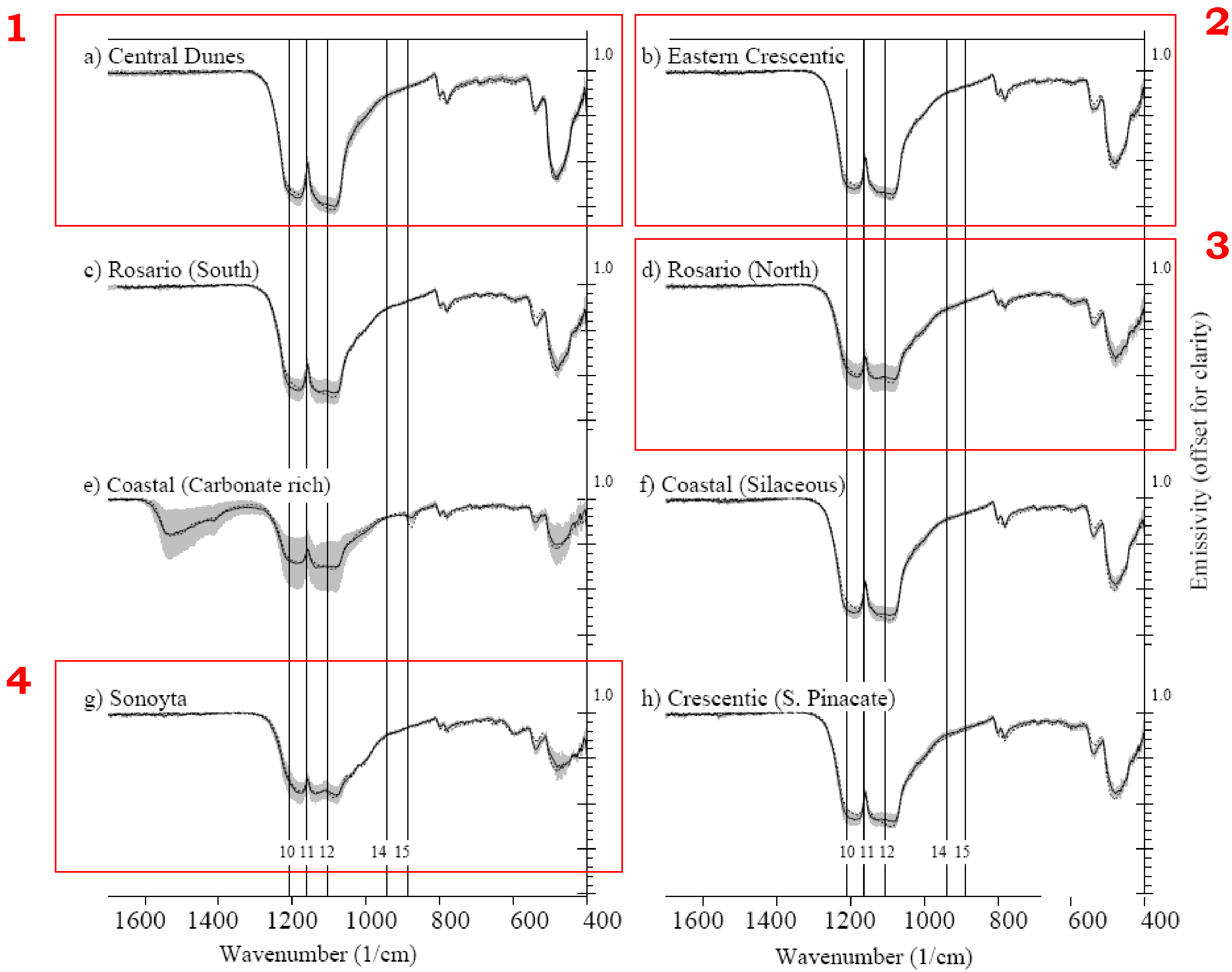

Scheidt et al. 2010 (submitted)

Previous Work: ASTER TIR Spectral Mapping

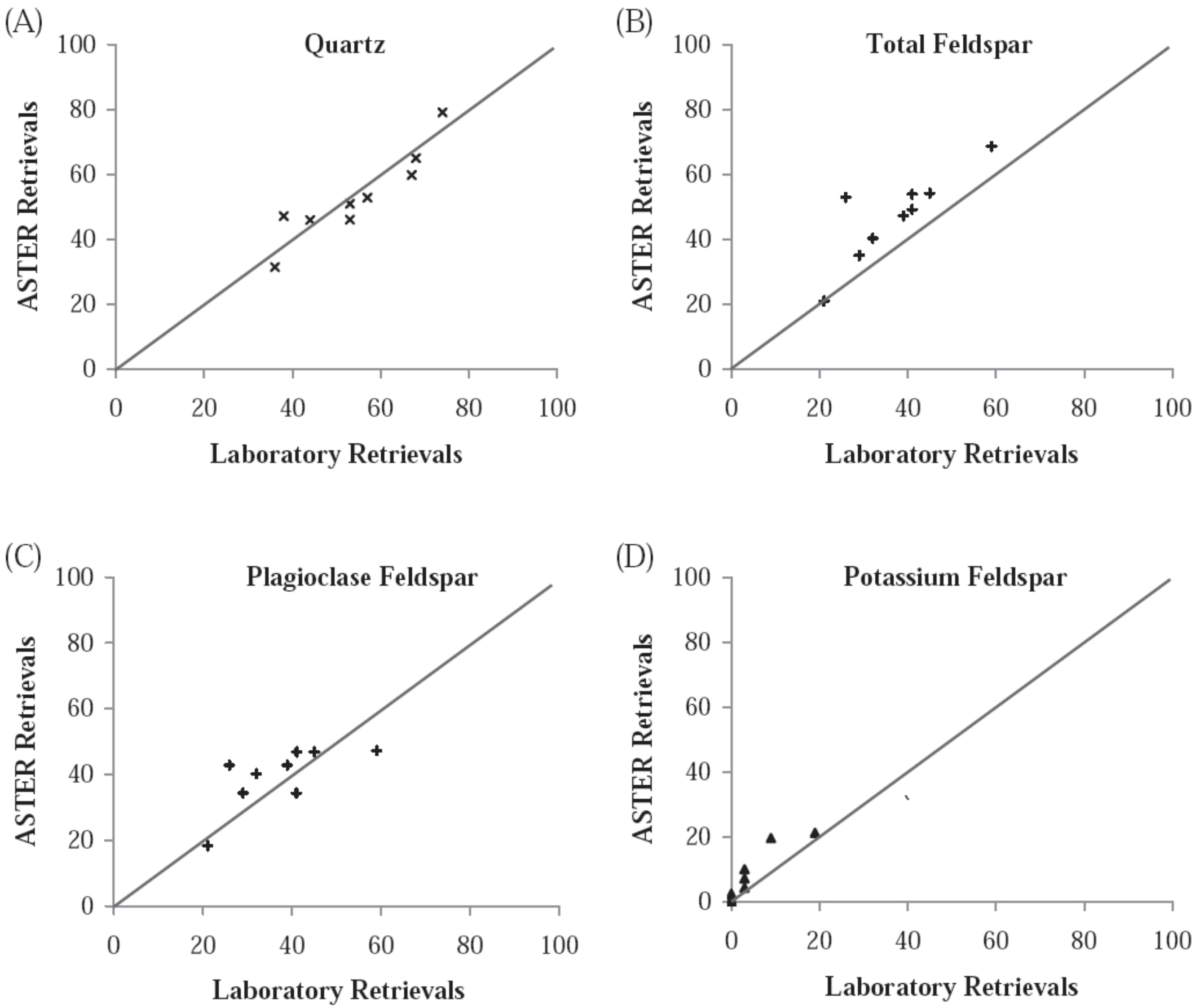

Scheidt et al. 2010 (submitted)

Previous HyspIRI Work: Kelso Dunes

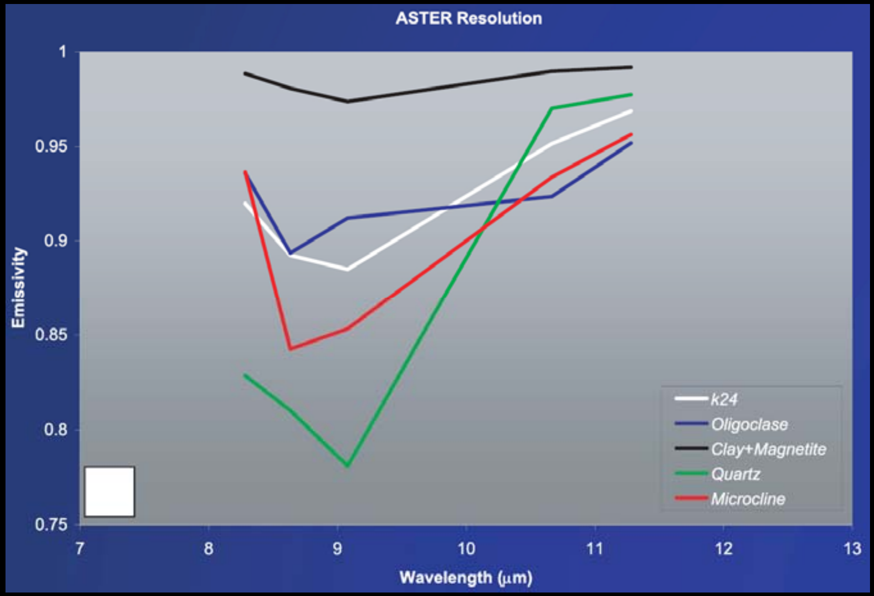

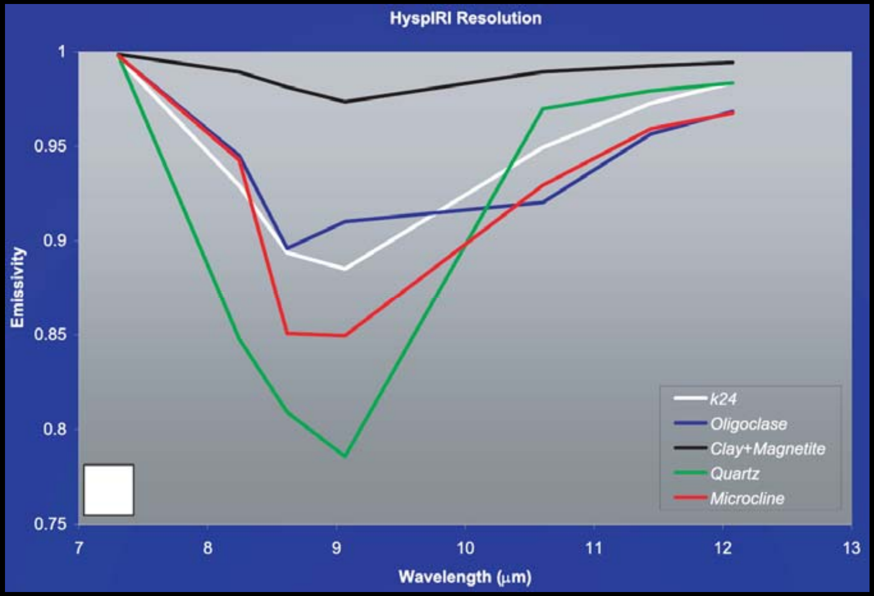

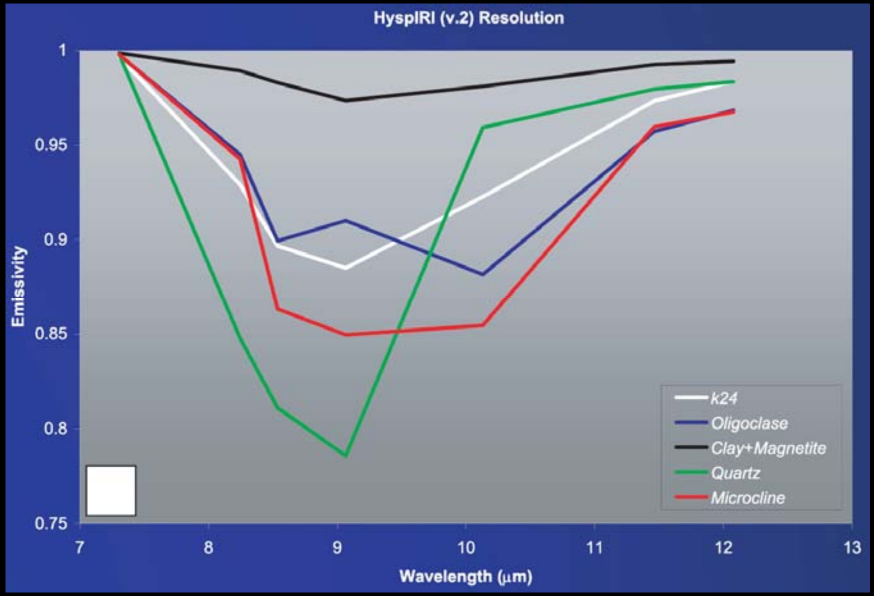

Using resampled MASTER data to HyspIRI v.2 greatly improved spectral mapping results

Presented at the last HyspIRI Workshop by M. Ramsey

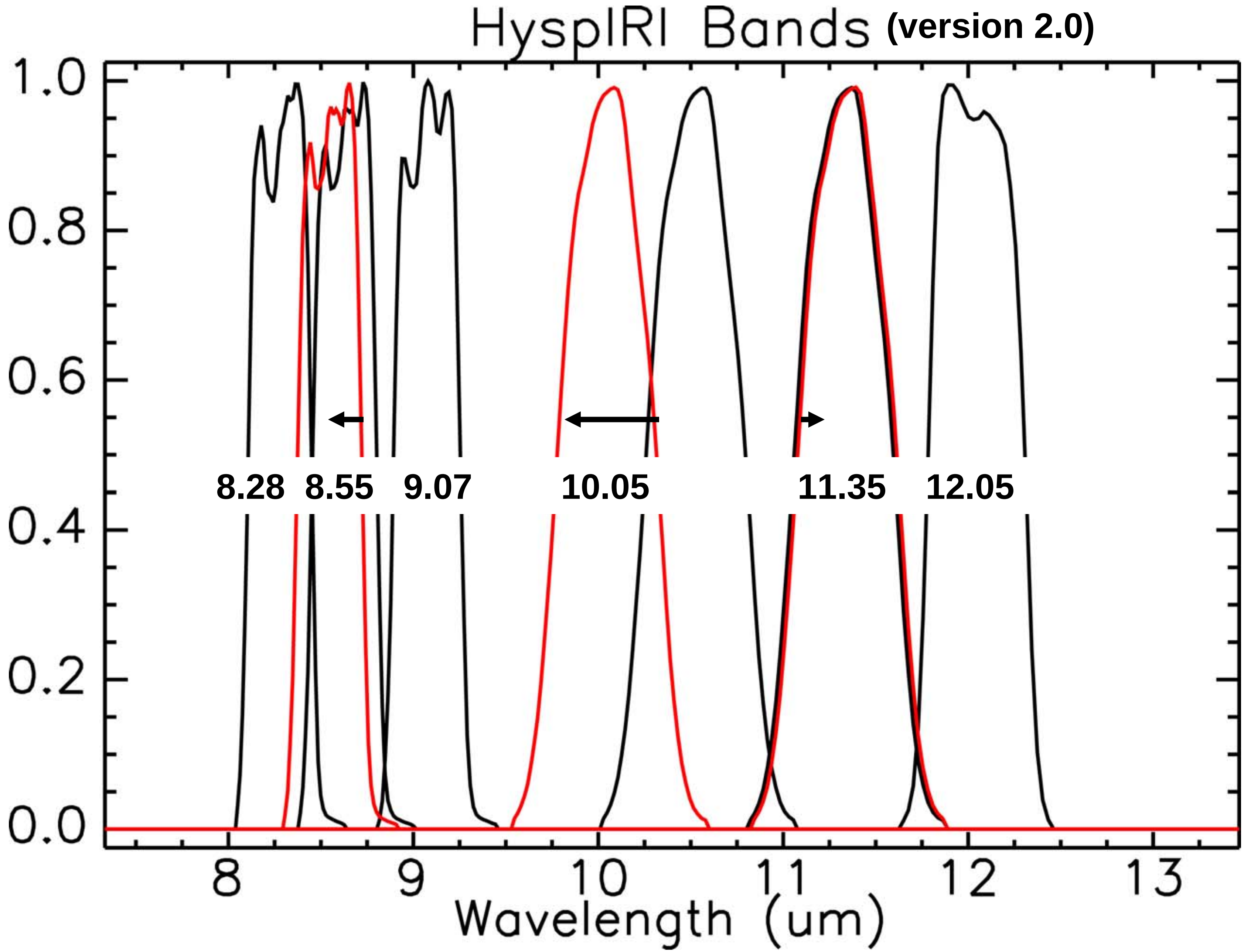
HyspIRI Bands (version 2.0)
1.0
0.8
0.6
0.4
0.2
0.0
8.28
8.55
9.07
10.05
11.35
12.05
8
9
10
11
12
13
Wavelength (um)

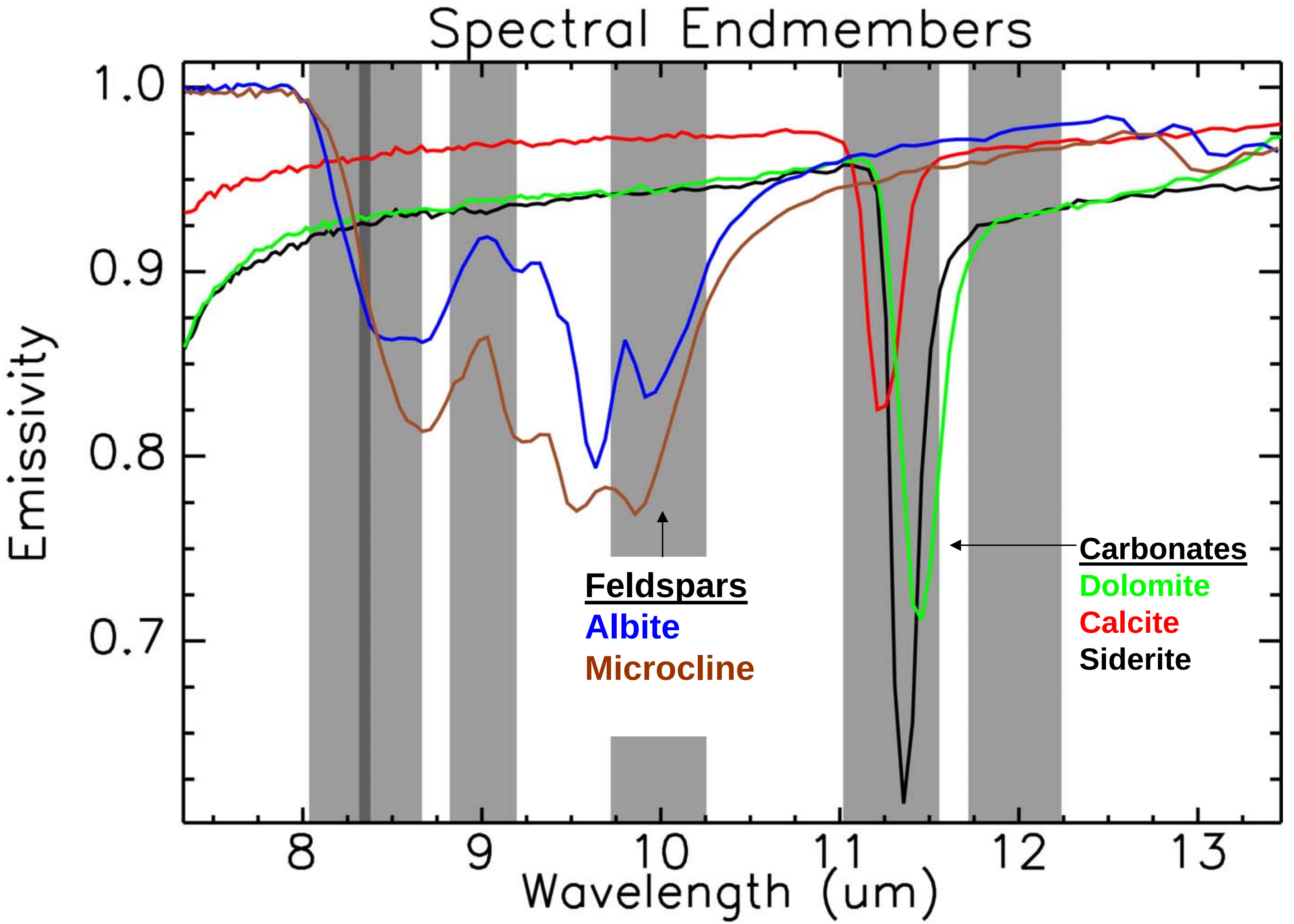

Spectral Endmembers
Emissivity
1.0
0.9
0.8
0.7
8
9
10
11
12
13
Wavelength (um)
Feldspars
Albite
Microcline
Carbonates
Dolomite
Calcite
Siderite

Preliminary Results of Hyspiri Resampling

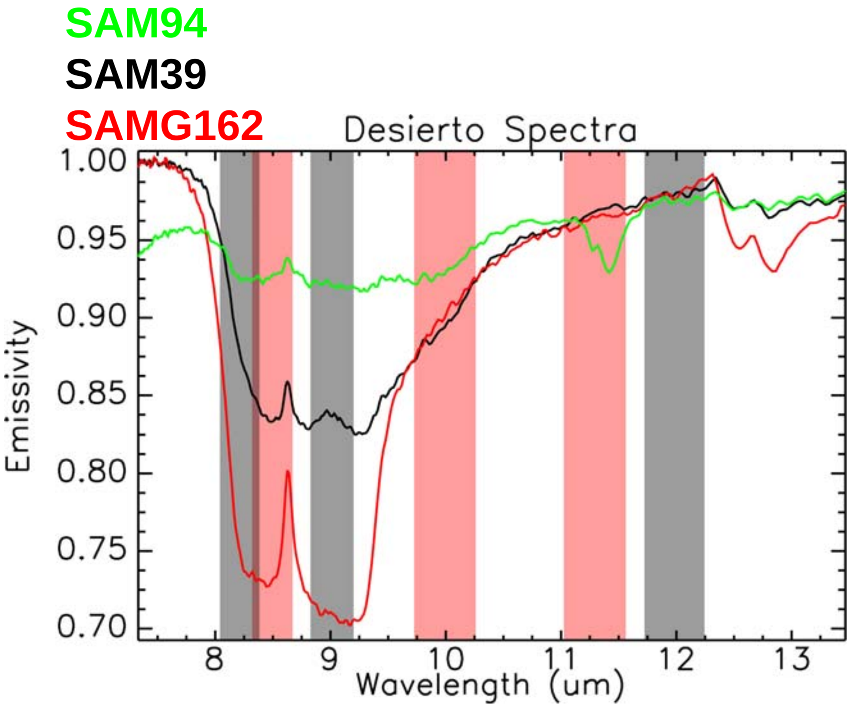

SAM94	LAB	ASTER	HYSP 1.0	HYSP 2.0
Carbonate	45.9	42.9	44.2	42.3
Feldspar	32.0	17.7	28.4	33.8
Quartz	22.1	39.4	27.3	23.9
RMS	0.0026	0.0017	0.0020	0.0022

SAM39	LAB	ASTER	HYSP 1.0	HYSP 2.0
Feldspar	64.1	74.0	72.4	65.9
Quartz	35.9	26.0	27.6	34.1
RMS	0.0038	0.0000	0.0011	0.0021

samG162	LAB	ASTER	HYSP 1.0	HYSP 2.0
Quartz	67.9	64.8	62.4	62.0
Feldspar	32.1	35.2	37.6	38.0
RMS	0.0026	0.0063	0.0037	0.0036

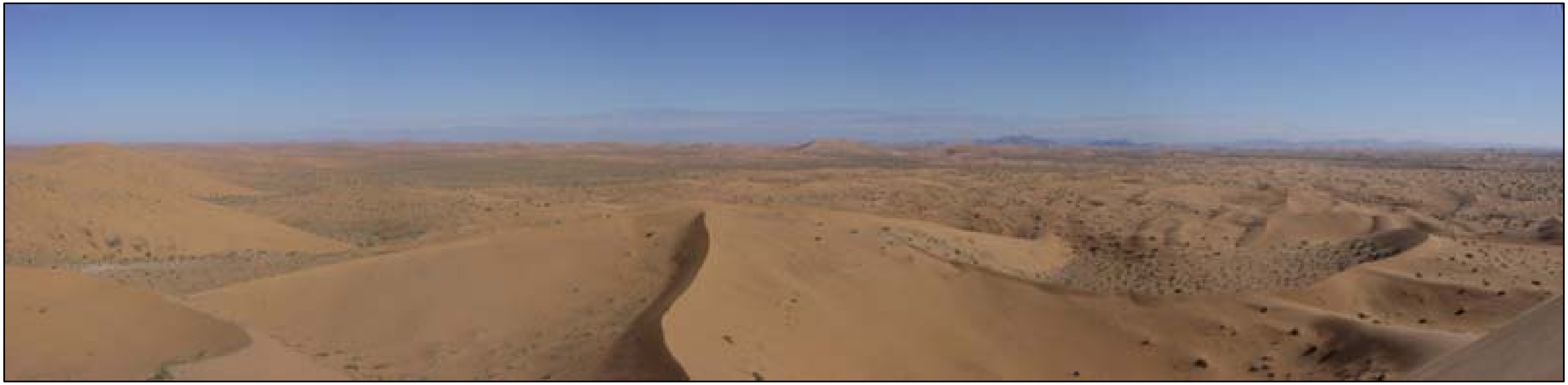

HyspIRI Advantage: Capture Large Dust Storms

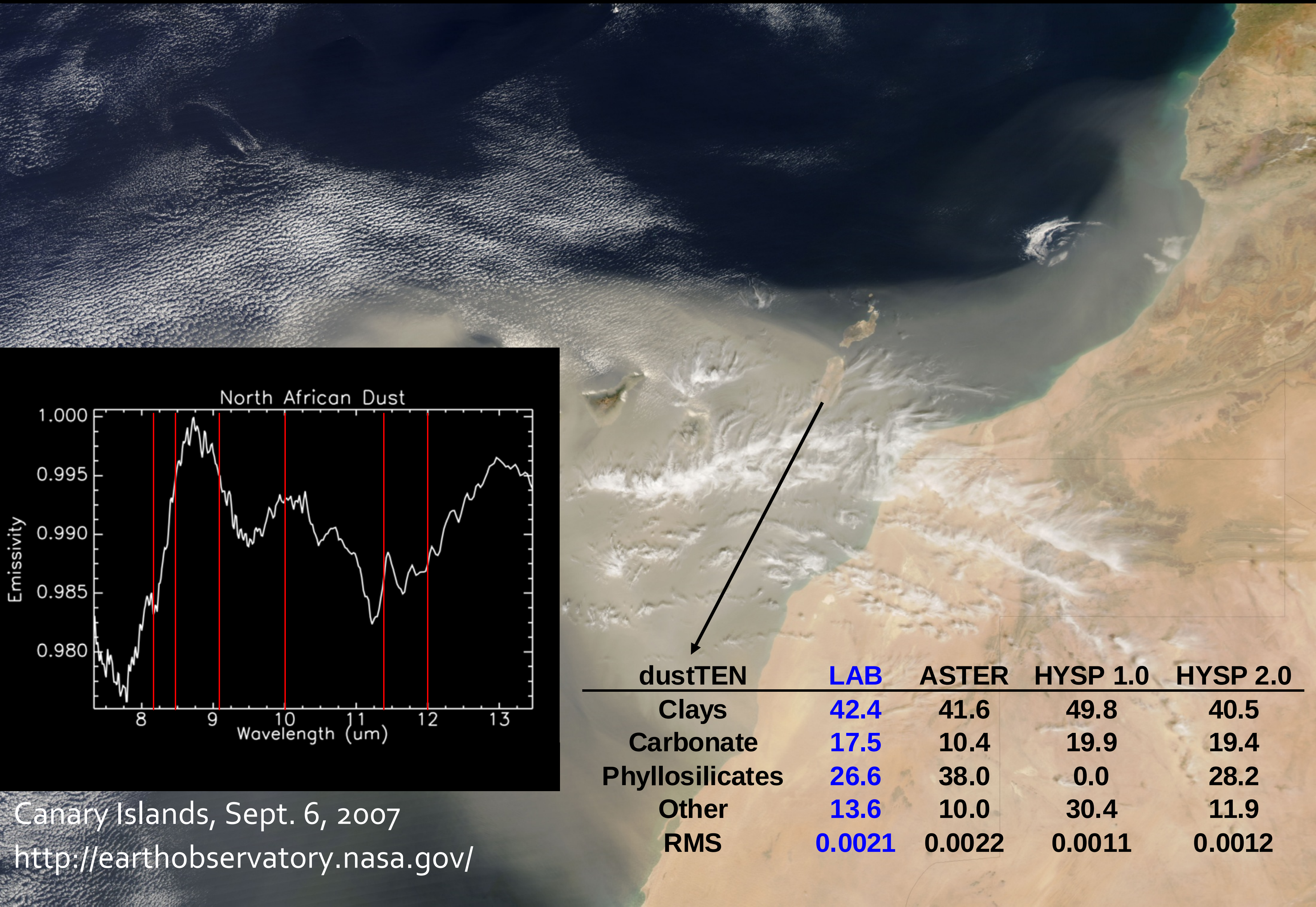

dustTEN	LAB	ASTER	HYSP 1.0	HYSP 2.0
Clays	42.4	41.6	49.8	40.5
Carbonate	17.5	10.4	19.9	19.4
Phyllosilicates	26.6	38.0	0.0	28.2
Other	13.6	10.0	30.4	11.9
RMS	0.0021	0.0022	0.0011	0.0012

Canary Islands, Sept. 6, 2007
http://earthobservatory.nasa.gov/

Dust Spectral Unmixing

CH9	LAB	ASTER	HYSP 1.0	HYSP 2.0
Phyllosilicates	61.7	58.7	34.6	55.9
Carbonate	11.4	0.0	17.8	6.6
Sulphates	14.4	0.0	47.6	37.5
Other	12.6	41.3	0.0	0.0
RMS	0.0034	0.0006	0.0024	0.0023

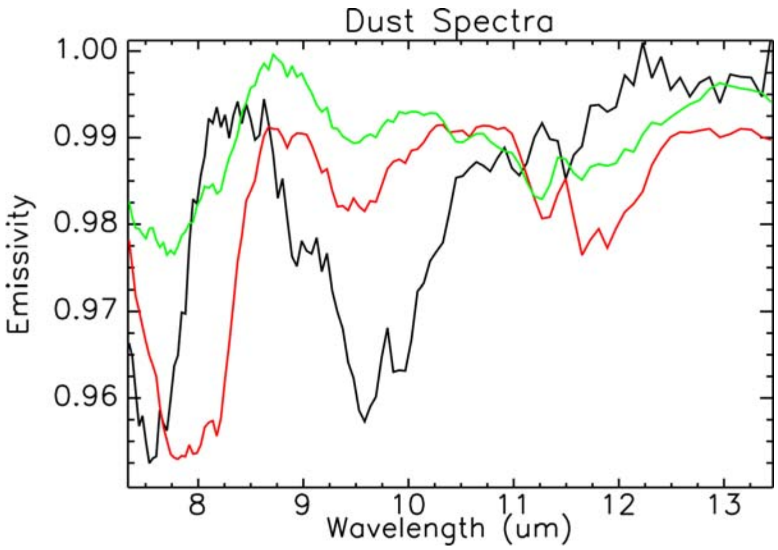

dustKW1	LAB	ASTER	HYSP 1.0	HYSP 2.0
Clays	54.2	51.8	50.5	50.8
Carbonate	23.1	19.7	24.6	32.8
Phyllosilicates	22.7	28.5	24.9	16.4
RMS	0.0027	0.0017	0.0023	0.0024

dustTEN	LAB	ASTER	HYSP 1.0	HYSP 2.0
Clays	42.4	41.6	49.8	40.5
Carbonate	17.5	10.4	19.9	19.4
Phyllosilicates	26.6	38.0	0.0	28.2
Other	13.6	10.0	30.4	11.9
RMS	0.0021	0.0022	0.0011	0.0012

Dust Affects on ASTER Spectra

Affect of Dust on ASTER Emissivity

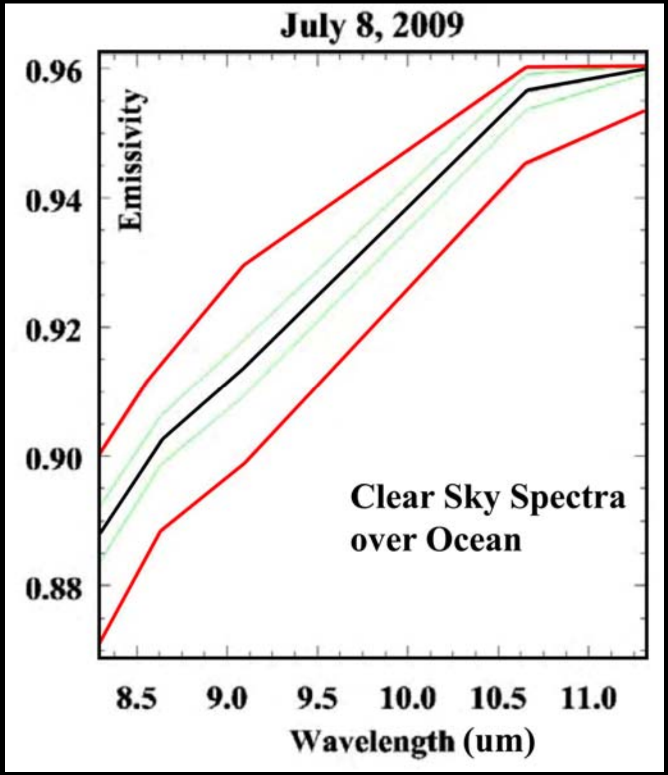

Field Validation of ASTER data

- Collecting measurements of LW sky-radiance with ground-based FLIR camera (7-14 µm)
- Coincident downward-looking MODIS, AIRS, ASTER and other A-Train instruments
- Site of AERONET Station at Izaña Atmospheric Observatory, Tenerife, Spain from July 4 – August 4, 2009

Dust Affects on ASTER Spectra

Affect of Dust on ASTER Emissivity

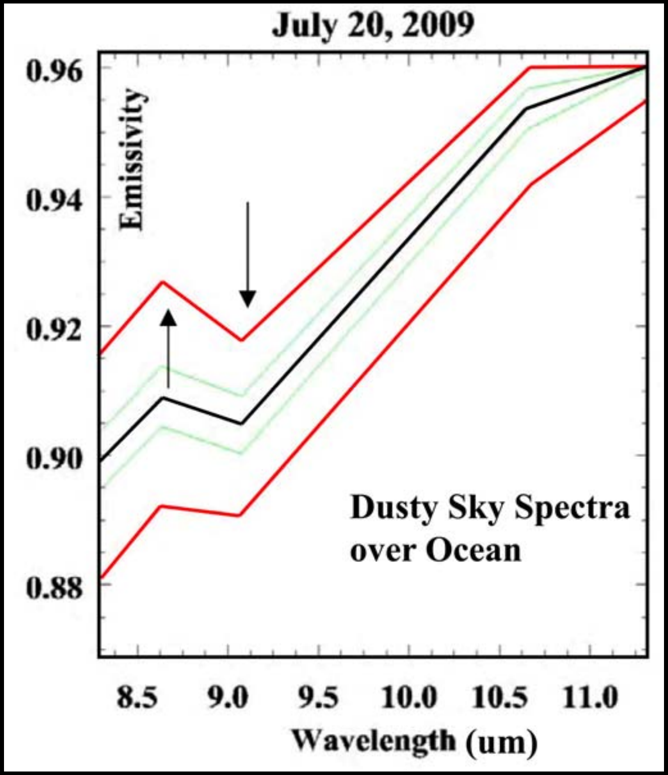

Field Validation of ASTER data

- Collecting measurements of LW sky-radiance with ground-based FLIR camera (7-14 µm)
- Coincident downward-looking MODIS, AIRS, ASTER and other A-Train instruments
- Site of AERONET Station at Izaña Atmospheric Observatory, Tenerife, Spain from July 4 – August 4, 2009

Dust Enhancement Algorithm in TIR Imagery

- Use brightness temperature differences in the TIR wavelength regions to enhance the appearance of dust.

- <u>SEVIRI Band Stretch</u>

		MIN	MAX (K)
– Red:	BT(12.0 um) – BT(10.8 um)	-4	+2
– Green:	BT(10.8 um) – BT(98.7 um)	0	+15
– Blue:	BT(10.8 um)	261	289

- <u>ASTER Band Stretch</u>

		MIN	MAX (K)
– Red:	BT(11.32 um) – BT(10.65 um)	-4	+1
– Green:	BT(10.65 um) – BT(8.63 um)	-3	+5
– Blue:	BT (10.65 um)	260	289

ASTER Dust Enhancement Example

<u>ASTER Direct Radiative Forcing</u>

Dust – Clear =
-11 W/m^2

Cloud – Clear =
- 164 W/m^2

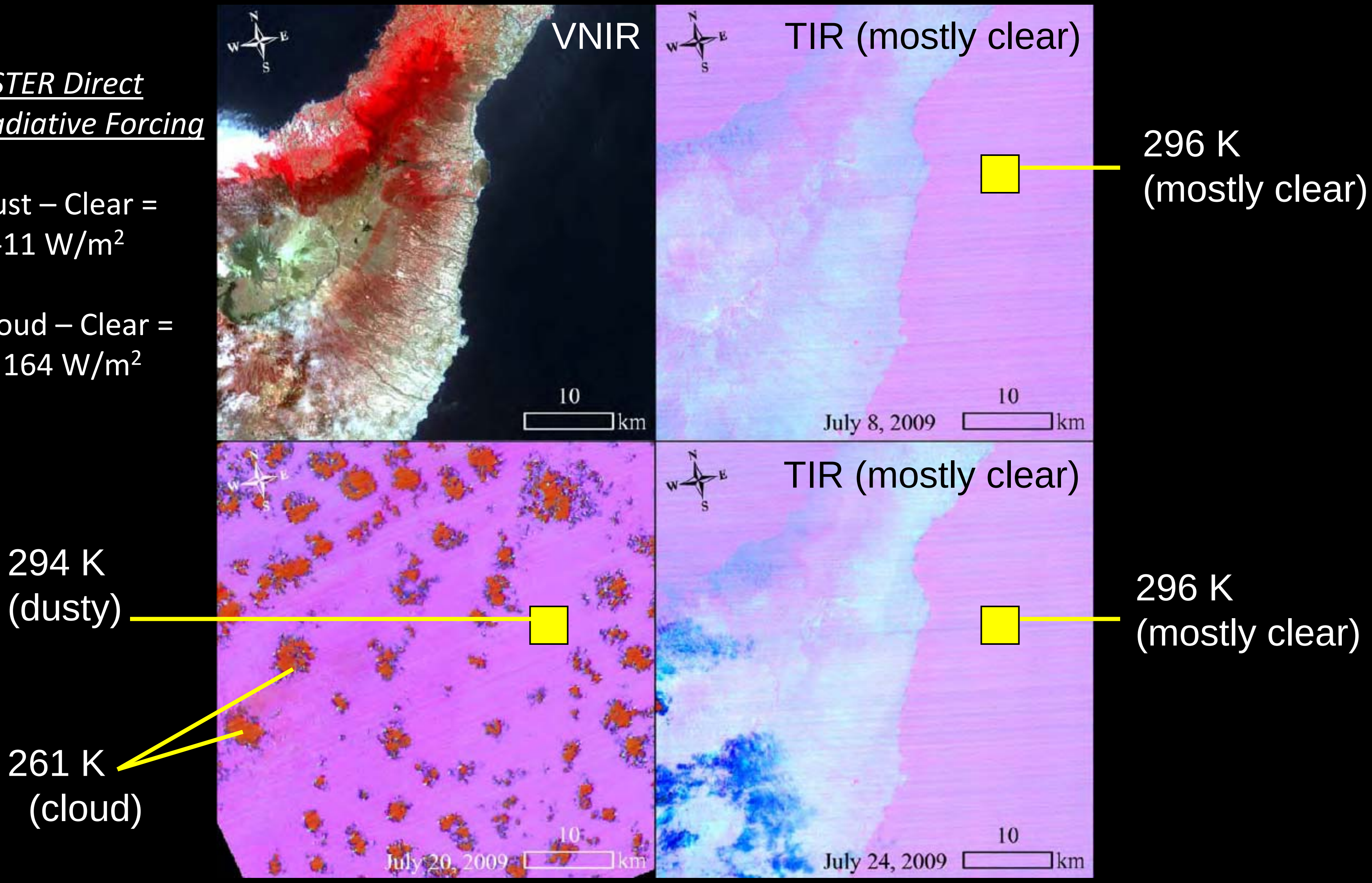

SEVIRI Dust Enhancement Product

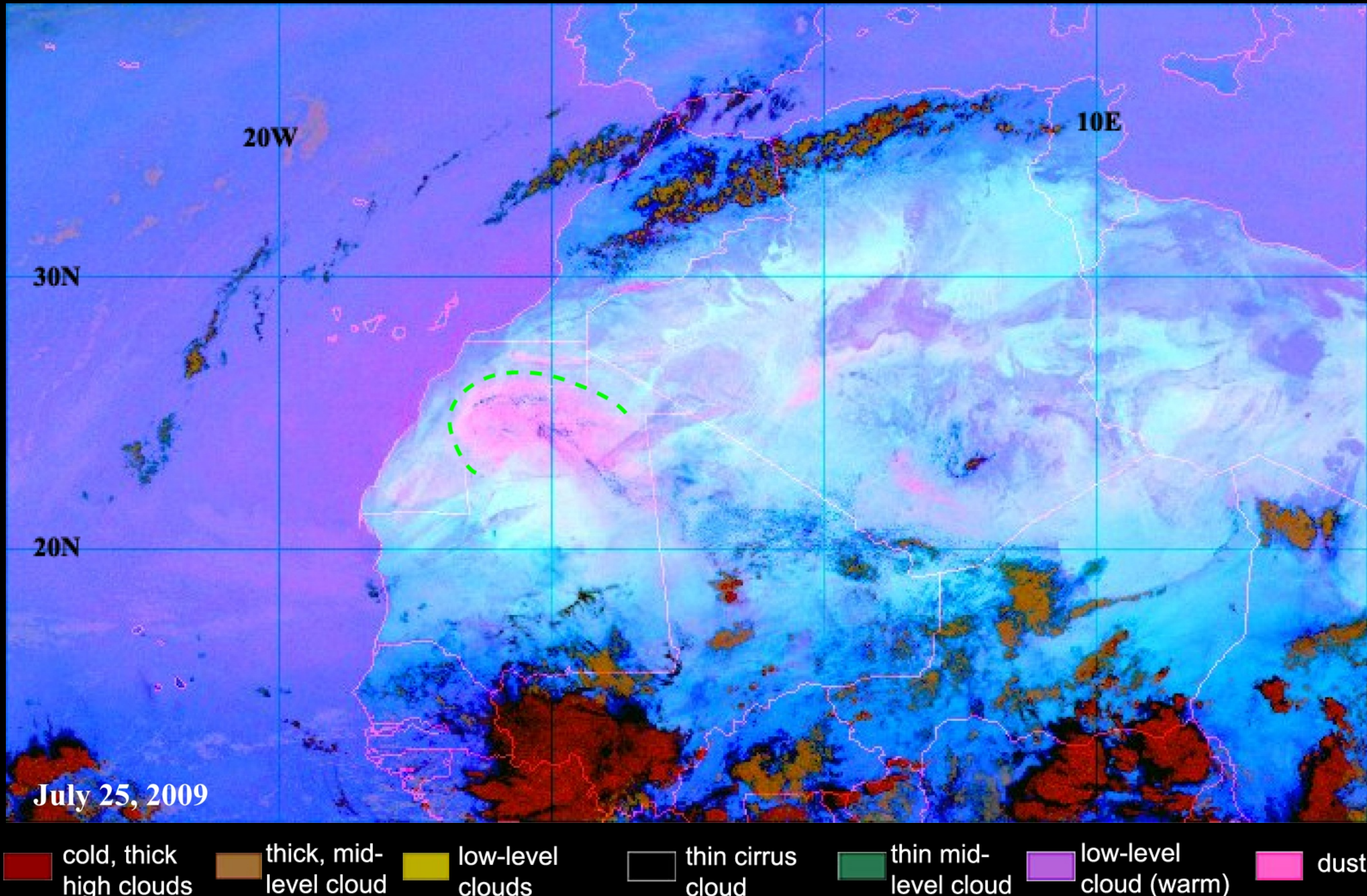

SEVIRI Dust Enhancement Product

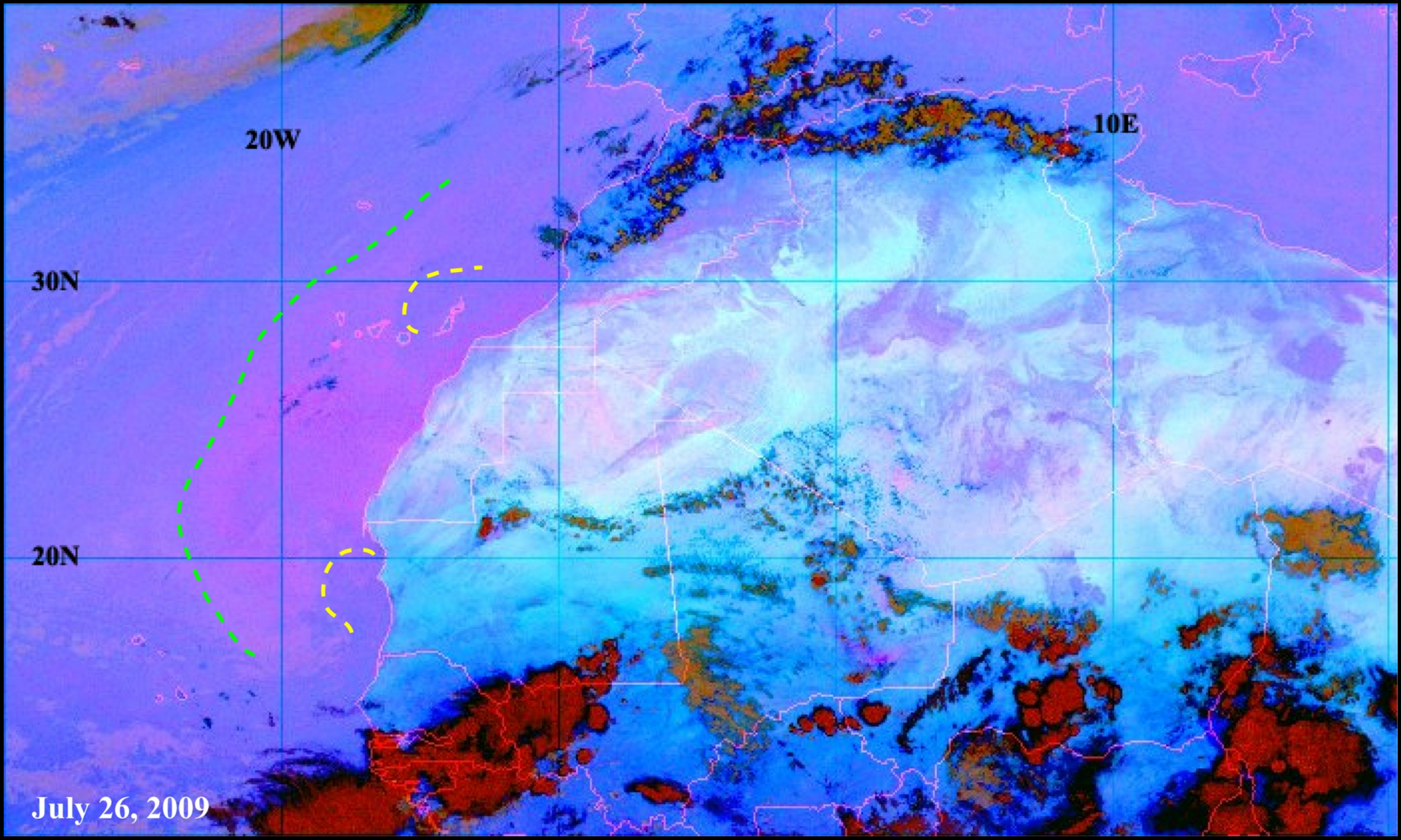

cold, thick high clouds | thick, mid-level cloud | low-level clouds | thin cirrus cloud | thin mid-level cloud | low-level cloud (warm) | dust

Conclusions

- HyspIRI's swath width, spatial, spectral and temporal resolutions are highly suited for imaging global eolian processes.

- Mapping dust source composition and imaging dust plumes in the TIR addresses the following:

  - The effects of dust on climate and the uncertainty of dust's radiative effects.

  - ecosystem responses to dust, which may be either beneficial or adverse.

- New band positions appear to improve linear spectral unmixing results.

…further rigorous analysis of spectral data is needed to determine the best band positions for mapping the widest array of compositions.

Extra Slides

Validation of TIR Remote Sensing of Dust

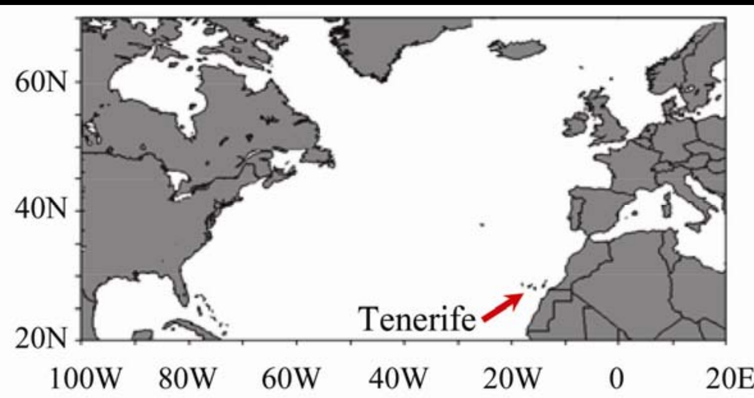

- Collaboration with
  Meteorological State Agency (AEMET)
- Sergio Rodriguez
  Head of Aerosol Program

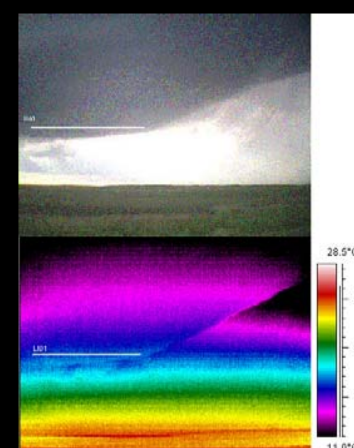

Tanamachi et al. 2006

Eyjafjallajökull Ashfall

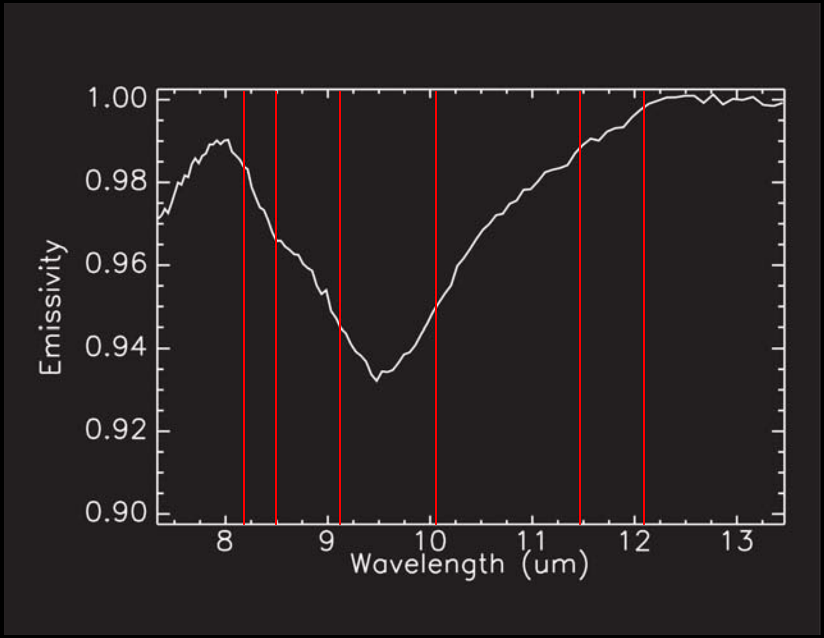

April 19, 2010 Eruption, NASA Earth Observatory

E. Mercurio

E. Mercurio

Ash samples were collected in August 2010 at Markarfljót, a glacial outwash plain that drained the April-May Eyjafjallajökull eruption materials.

E. Mercurio, Iceland sample contributor at Markarfljót waterfall.

Improved Accuracy for Spectral Unmixing

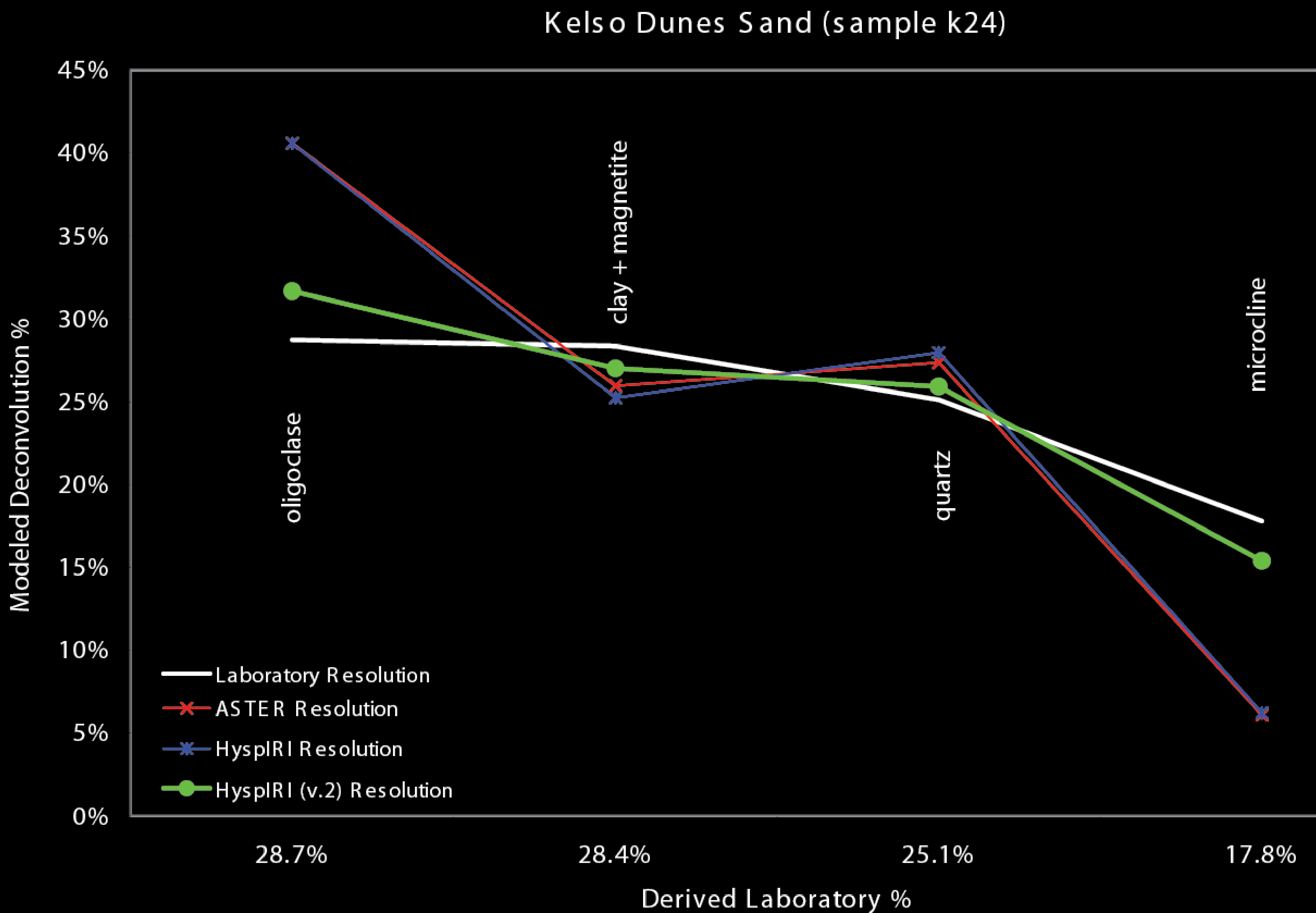

Improved Spectral Mapping using Resampled MASTER TIR Data

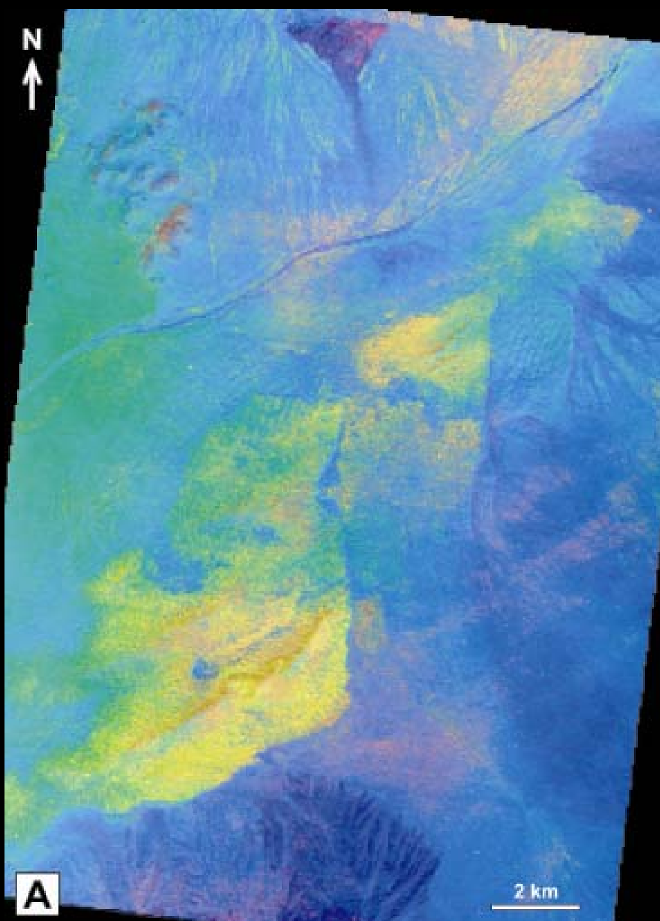

Resampled Data to HyspIRI

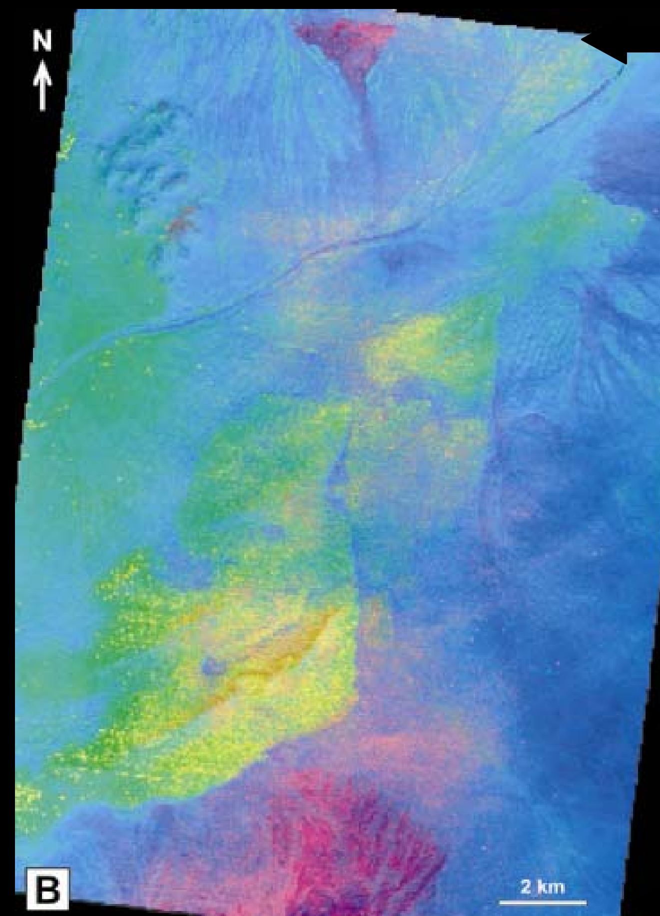

Resampled Data to HyspIRI v2

M. Ramsey 2010

White Sands Gypsum Dune Field

Decorrelation Stretch
(Bands 14,12,10), April 27, 2008

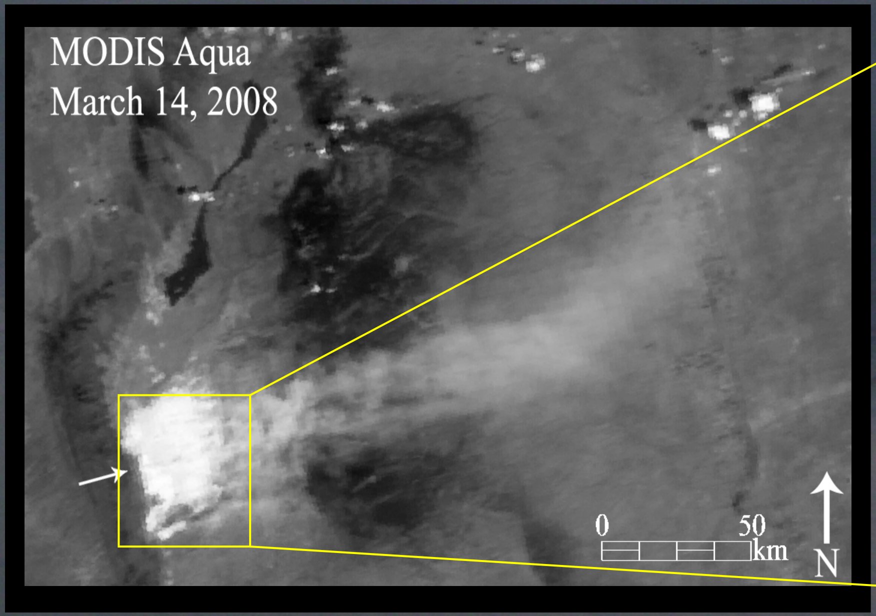

Dust storm from White Sands

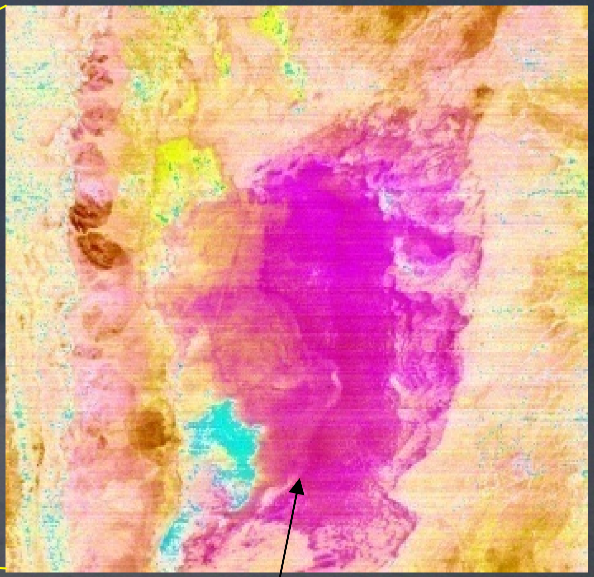

Fairly uniform composition

Ash Meadows National Wildlife Refuge

Amargosa Dunes, NV

- Dunes are under study by Nicholas Lancaster, Desert Research Institute
- Geomorphic analysis of small dunes using GPS
- Using TIR spectral analysis
- Validation using XRD and XRF geochemical measurements
- Highly varied sand composition

Decorrelation Stretch of ASTER Bands 14, 12 and 10

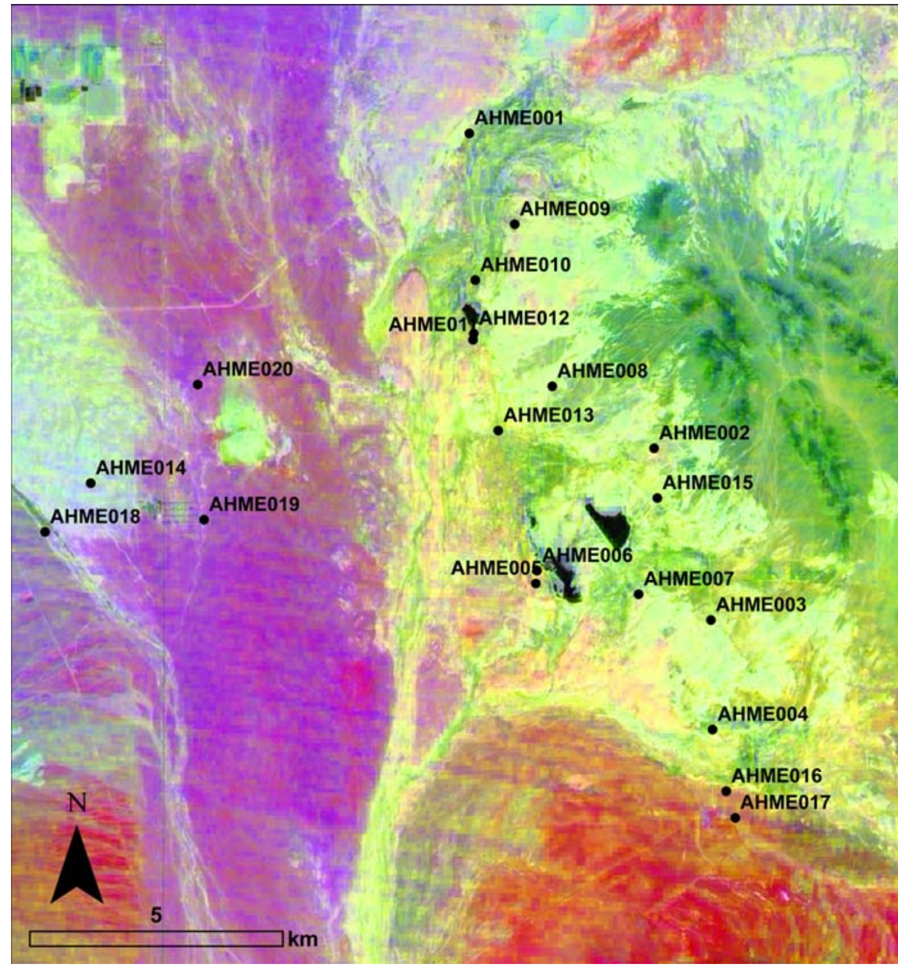

Preliminary Results of Hyspiri Resampling

Ash Meadows

AHME008	LAB	ASTER	HYSP 1.0	HYSP 2.0
Feldspar	44.8	42.9	45.3	41.0
Carbonate	37.2	41.4	40.7	43.5
Quartz	18.1	15.7	14.0	15.5
RMS	0.0029	0.0008	0.0012	0.0010

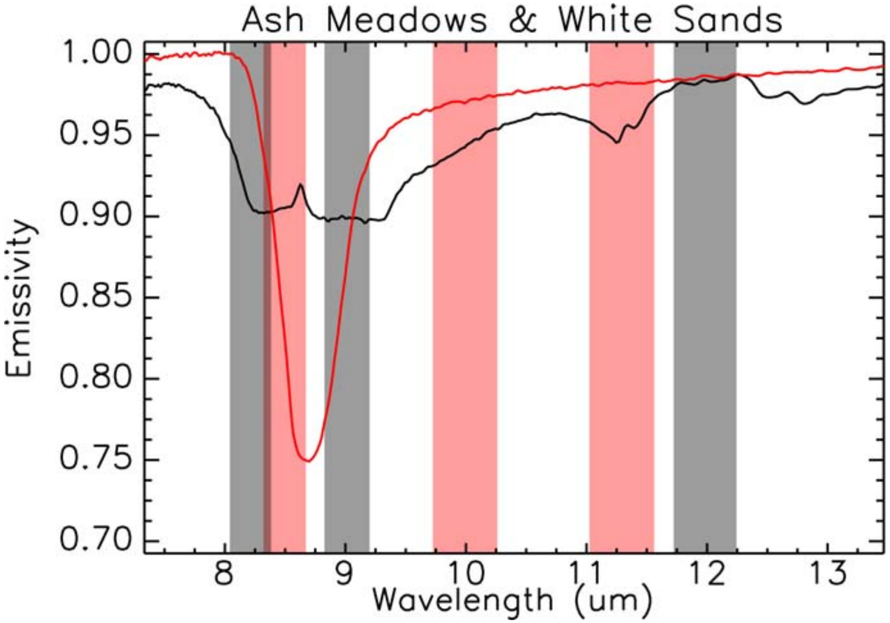

White Sands

WHSA001	LAB	ASTER	HYSP 1.0	HYSP 2.0
Sulphates	89.6	88.4	88.6	88.2
Other	9.7	11.6	9.6	11.8
Carbonate	0.7	0.0	1.8	0.0
RMS	0.0034	0.0074	0.0022	0.0015

HyspIRI Advantage: Capture Large Dust Storms

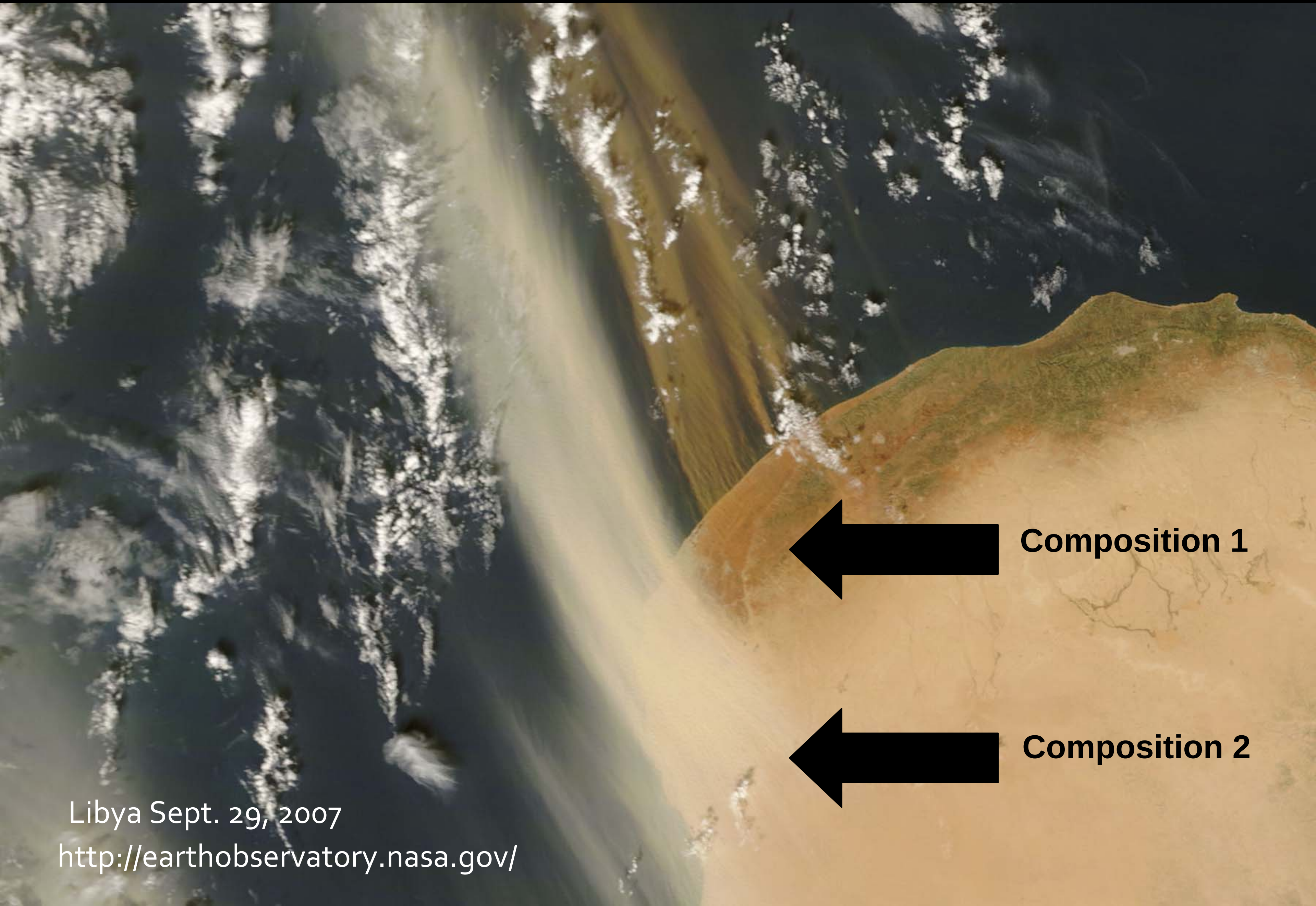

Onboard Instrument Processing Operations Concepts for the HyspIRI Mission

Steve Chien, David Mclaren
Jet Propulsion Laboratory, California Institute of Technology

Daniel Mandl, Goddard Space Flight Center

Jerry Hengemihle, Microtel LLC

Direct Broadcast Heritage

- Direct Broadcast is a technology which enables downlink of instrument data during acquisition (e.g., MODIS)

- In current use, DB downlinks all of the data acquired by the instrument

HyspIRI Direct Broadcast

- HyspIRI TIR + VSWIR will produce 900×10^6 bits per second (raw uncompressed)

- In order to use heritage technology groundstations HyspIRI DB will have an effective rate of 10×10^6 bits per second (uncompressed)
  - Even assuming 2:1 compression we have a 45x oversubscription

HyspIRI DB Concept

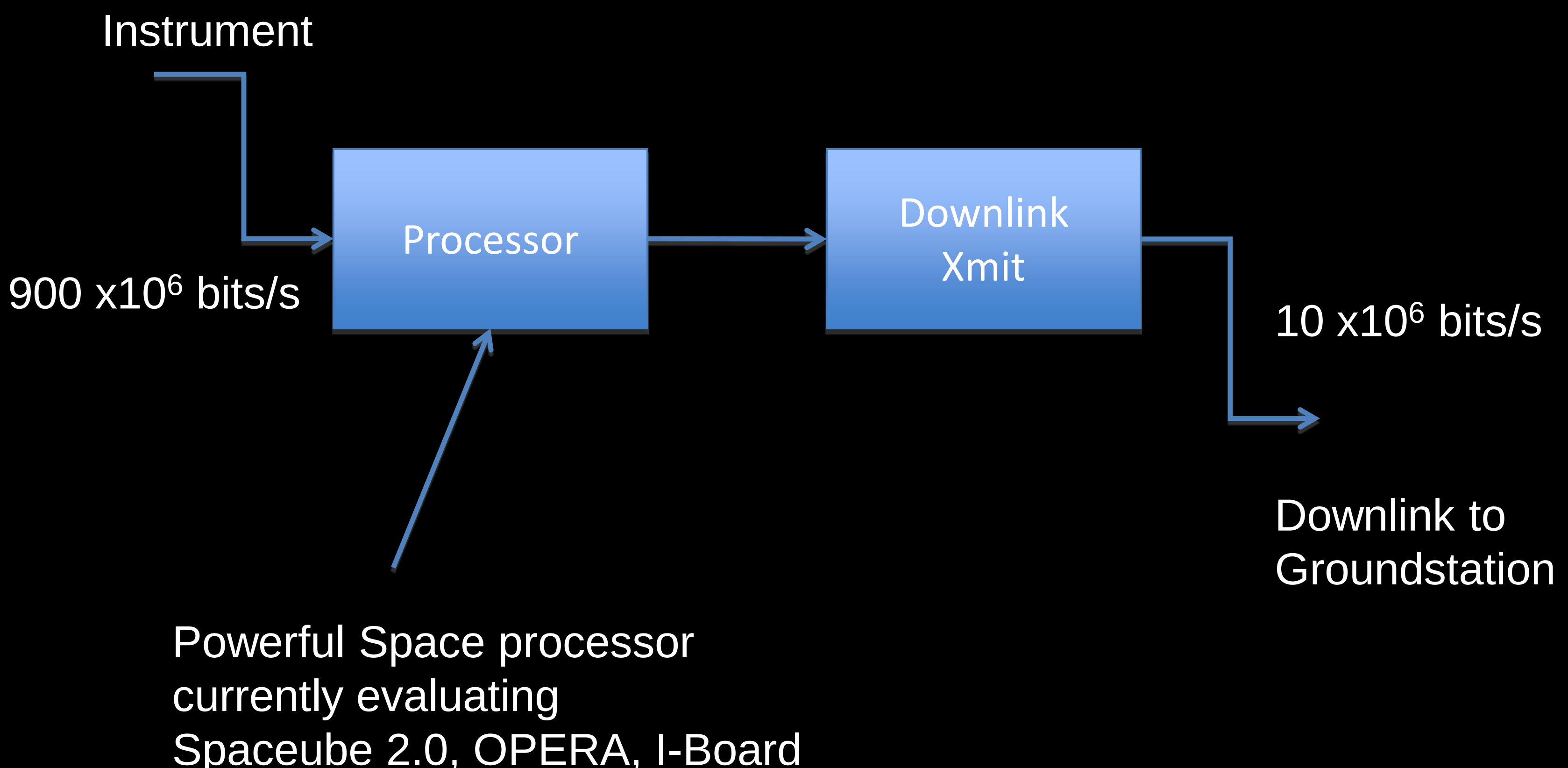

Operations for HyspIRI DB

- Users specify “areas of interest” which are
  - geographical regions (polygon on surface of Earth)
  - product, (e.g. normalized burn index)
  - priority, (e.g. 50 on 1-100 scale)
  - Constraint (sun must be at least 20 degrees above horizon)
- For each product, consider:dl bands, dl product
- In generic tool (e.g. Google Earth)

Instrument Swaths

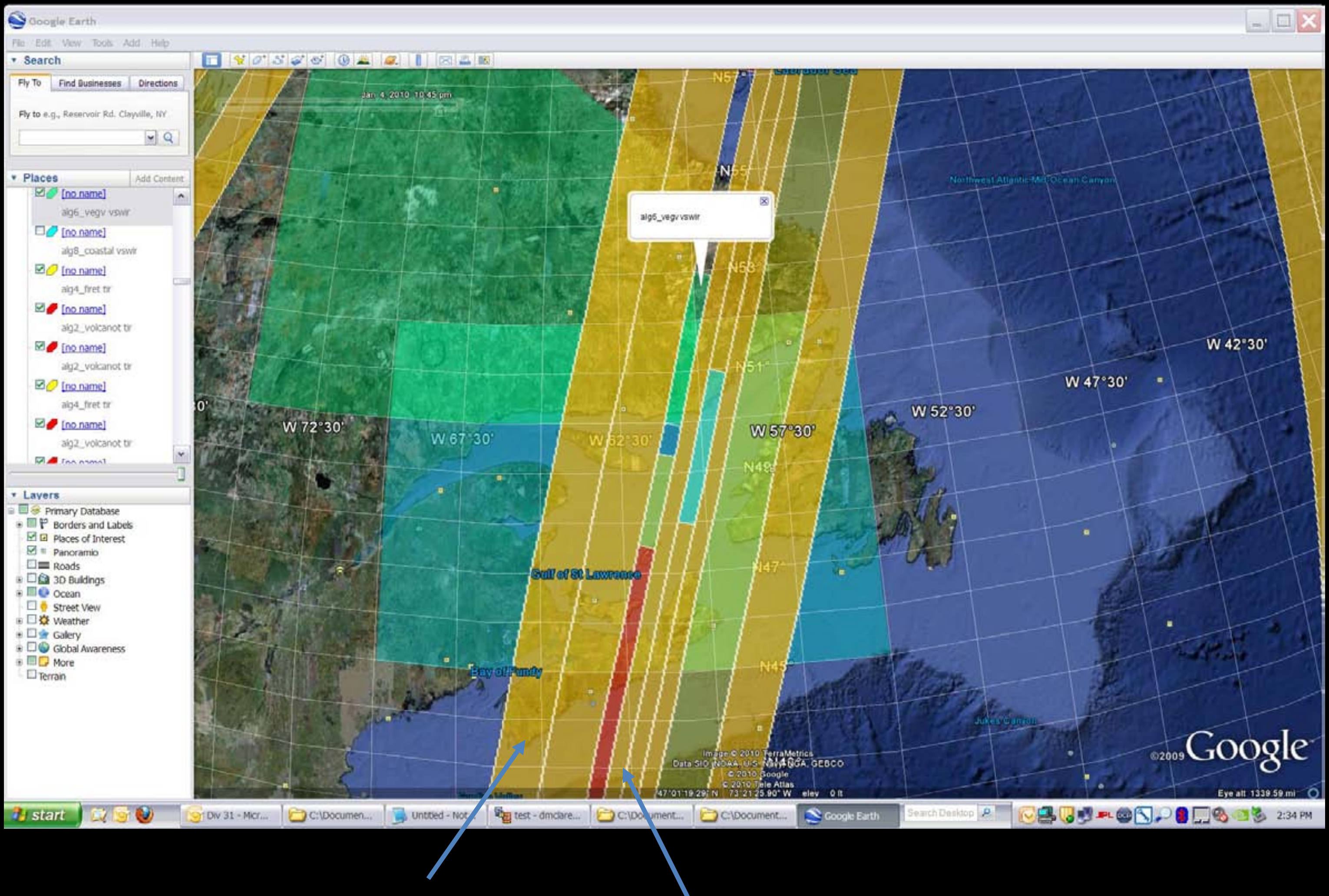

4 x 112.5.5 km wide –TIR only

4 x 37.5 km wide – VSWIR + TIR

How much can we get down DB?

- 10 x 10^6 bits/s DB downlink = ?
- 1 band @ 14 bits (uncompressed) =
  - 3.2 x 10^6 bits/s 1 band 112.5km (unc)
  - 1.0 x 10^6 bits/s 1 band 37.5km (unc)
- Assuming 2:1 lossless comp
- ~20 small swaths bands or ~6 large
- Can also downsample spatially
- Considerable leverage from products

Automated Operations Planning

- Automated Planning tool selects highest priority products while respecting
  - Visibility (instrument swaths)
  - Onboard CPU limits
  - Downlink data limits

- Result is a time ordered sequence of commands to process instrument data from each of 8 instrument swaths

Sample Plans

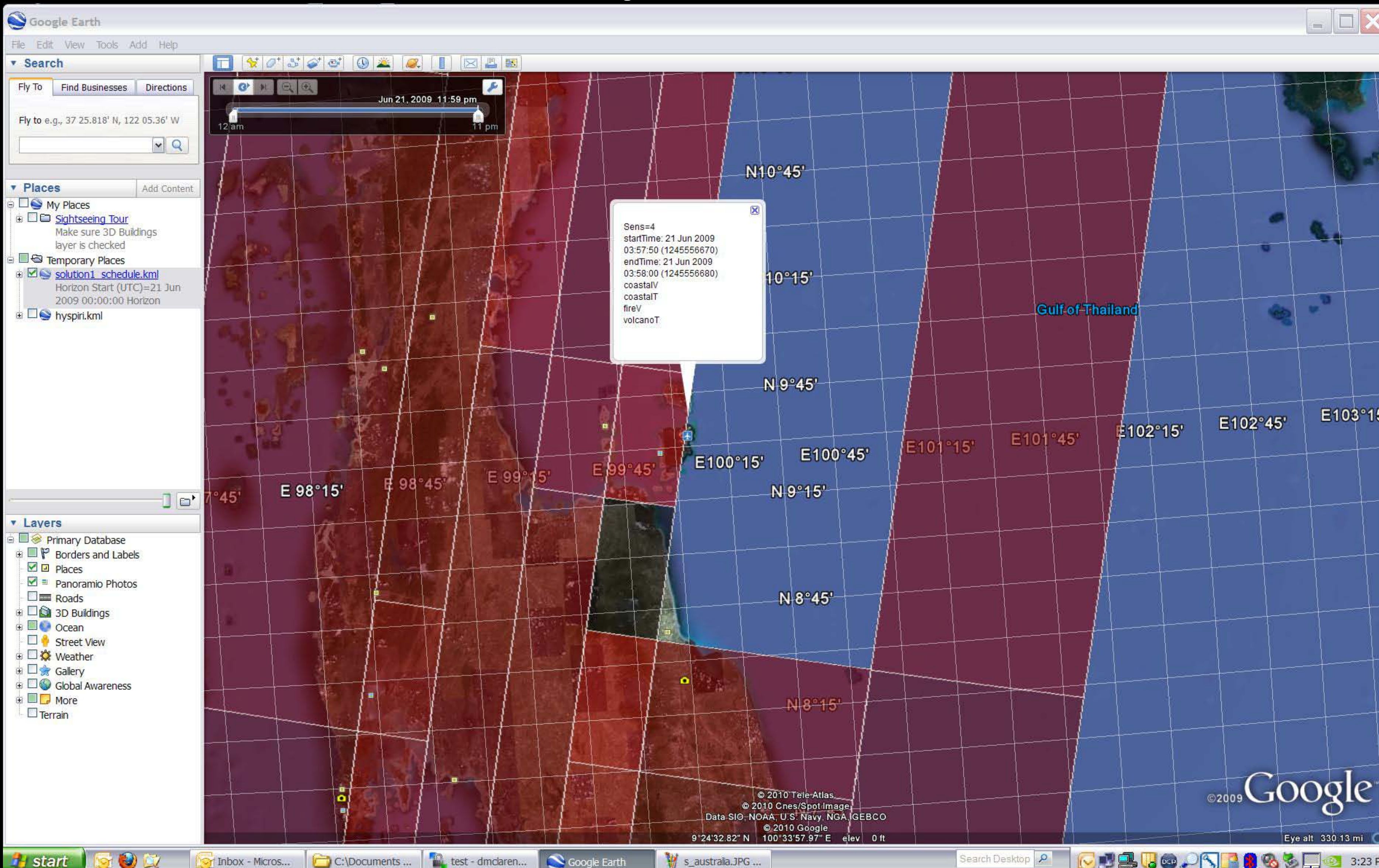

More Plans

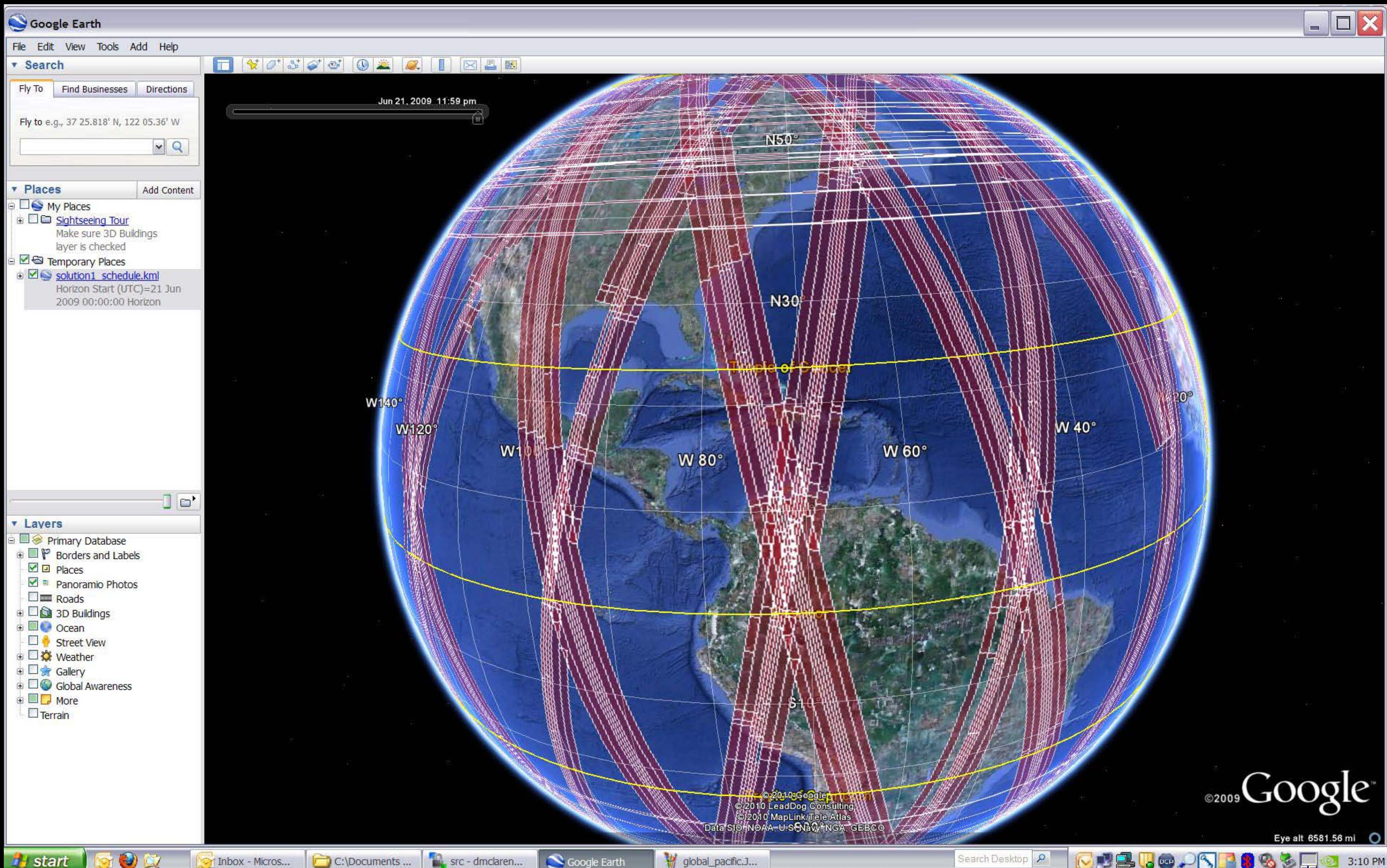

Google Earth
File Edit View Tools Add Help
Search
Fly To
Find Businesses
Directions
Fly to e.g., 37 25.818' N, 122 05.36' W
Places
Add Content
My Places
Sightseeing Tour
Make sure 3D Buildings layer is checked
Temporary Places
solution1_schedule.kml
Horizon Start (UTC)=21 Jun 2009 00:00:00 Horizon
Layers
Primary Database
Borders and Labels
Places
Panoramio Photos
Roads
3D Buildings
Ocean
Street View
Weather
Gallery
Global Awareness
More
Terrain
Jun 21, 2009 11:59 pm
N50°
N30°
W140°
W120°
W 80°
W 60°
W 40°
©2010 LeadDog Consulting
©2010 MapLink/Tele Atlas
©2009 Google
Eye alt 6581.56 mi
start
Inbox - Micros...
C:\Documents ...
src - dmclaren...
Google Earth
global_pacific.J...
Search Desktop
3:10 PM

HyspIRI DB Applications

- Volcanos
- Fires
- Flooding
- Cryosphere
- Ocean

- Applications allows spatial and spectral subsampling (bands and products) to reduce needed downlink volume

Heritage (onboard) – EO-1/ASE Thermal Detection

- EO-1
  - Onboard thermal event detection in use since 2004 using onboard Hyperion spectral signature
  - Uses spectral slope in 1.65-2.28μ (HyspIRI VSWIR)
  - Onboard event detection can trigger:
    - Subsequent imaging
    - Alert Notices
    - Generation of thermal summary and quicklook context images
    - Ground-based automatic data product generation and distribution

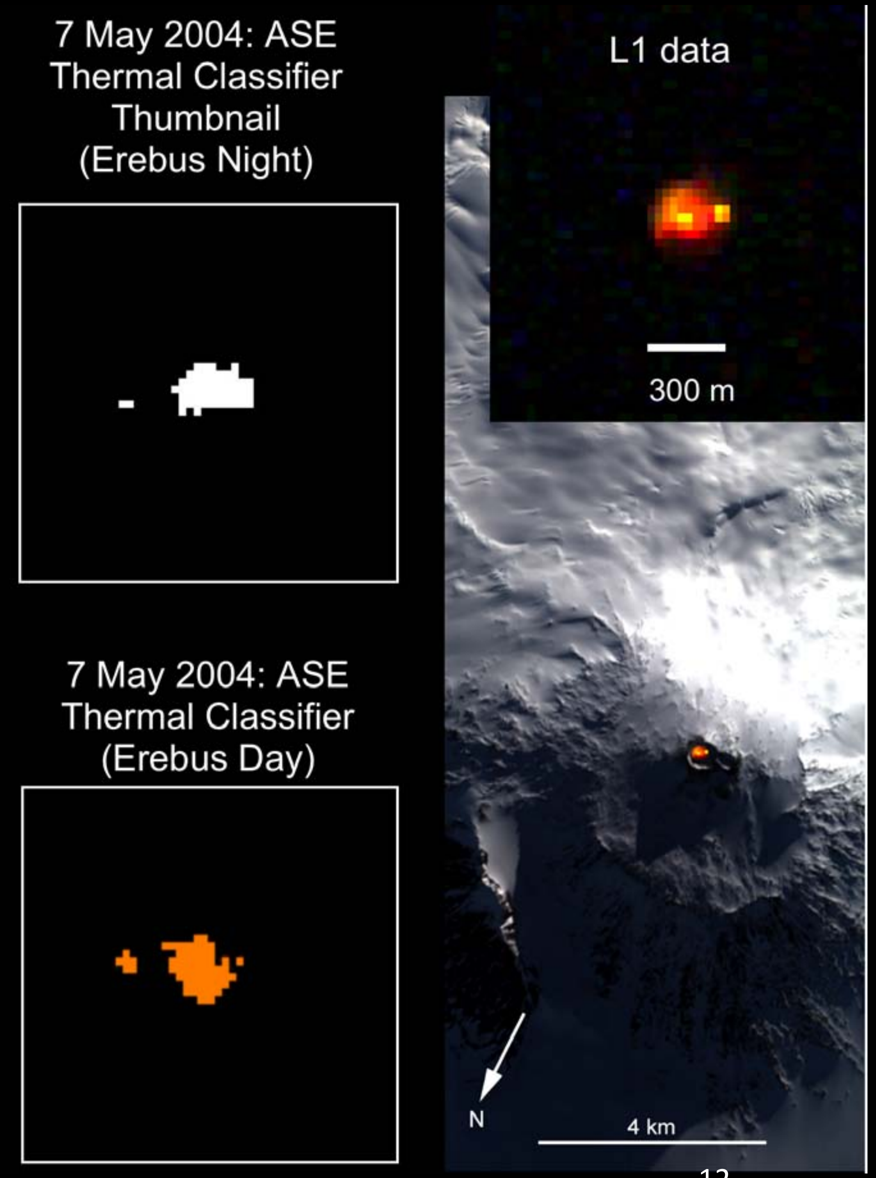

Courtesy [Davies et al. 2006]

Iceland Imagery

Eyafallajökull

2 Giga Watt Thermal emission

Left – thermal false color
Right – True color

17 April 2010
Image credit: NASA/JPL/EO-1 Mission/GSFC/Volcano Sensorweb/Ashley Davies

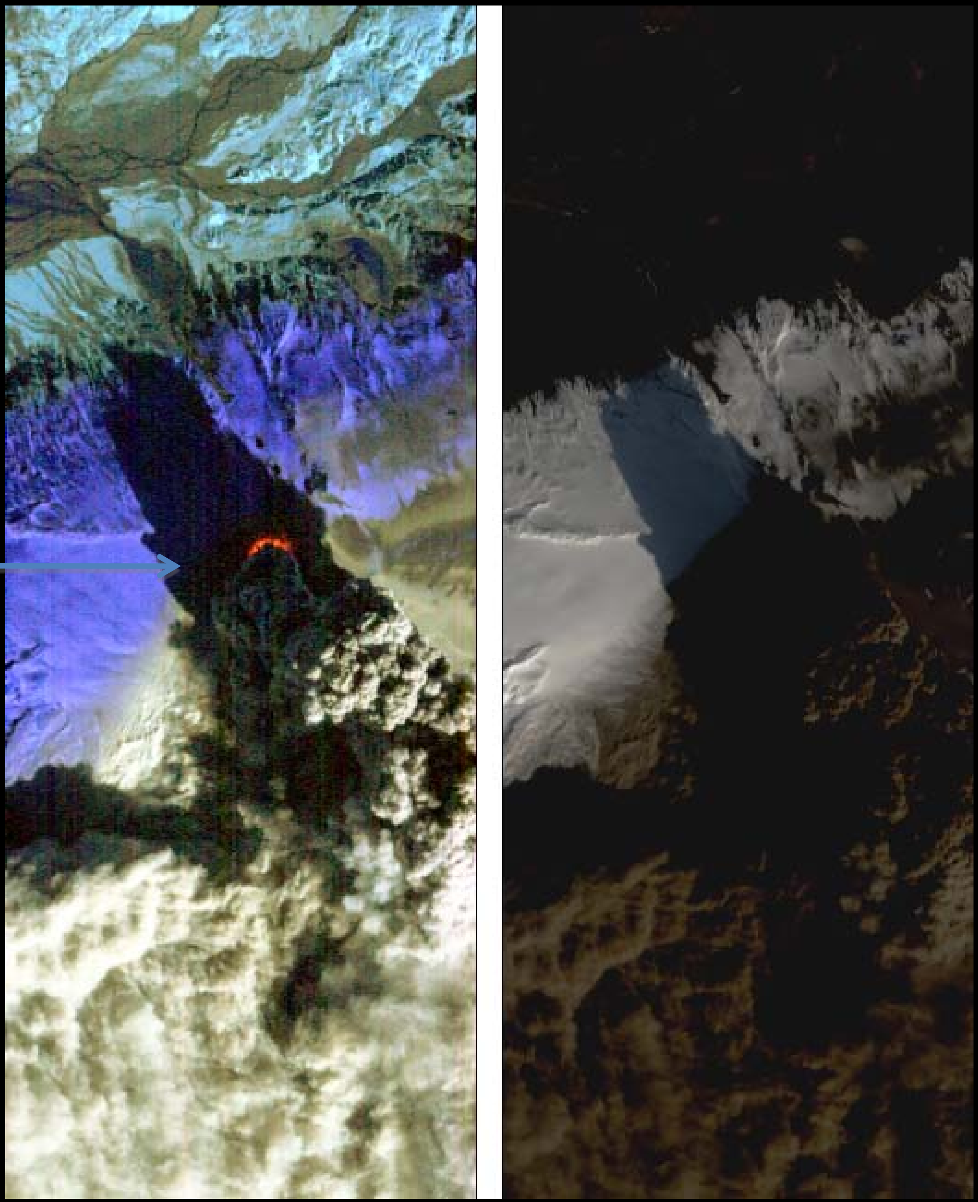

Heritage – ground-based MODIS Active Fire Detection

- Detects hotspots using
  - absolute threshold
    - T_4>360K, 330K(night) or
    - T_4>330K, 315K(night) and T_4-T_{11}>25K(10K @ night)
  - and relative threshold
    - T_4 > mean(T_4)+ 3stddev(T_4) and T_4 - T_{11} > median(T_4-T_{11})+ 3stddev(T_4-T_{11})
  - 4μ and 11 μ available on HyspIRI TIR

Looks for areas significantly hotter than surrounding area (requires 6 surrounding pixels cloud, water, fire free → 21x21)

C. Justice et al.

Fires – Burn Scar

Visible and burn scar enhanced images from ALI instrument on EO-1 of Station Fire near Los Angeles 03 September 2009

Images courtesy EO-1 Mission NASA GSFC

Burn scar:
0.76-0.90μm,
2.08-2.35μm
Both VSWIR

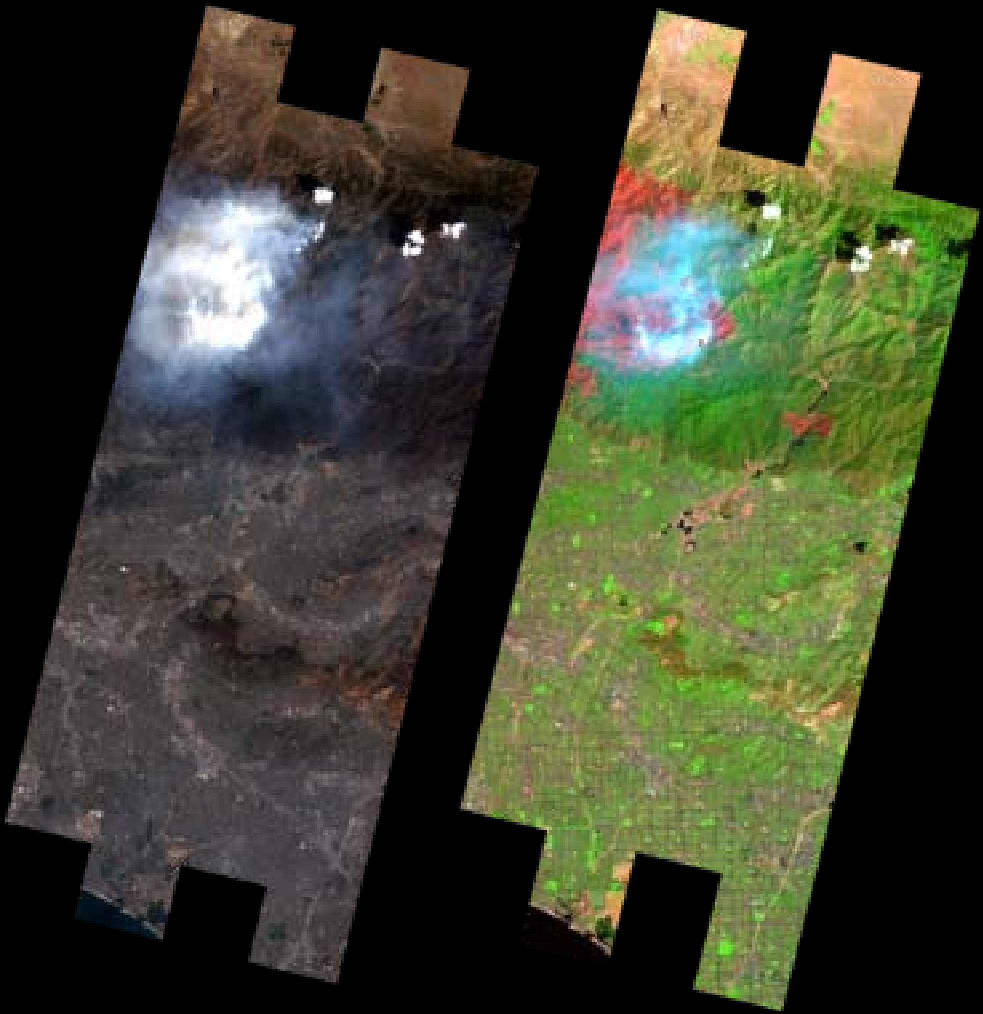

Flooding – Heritage (Ground) MODIS/UMD

- UMD Flood tracking of Myanmar using MODIS bands 1,2,5,7 (620-2155 nm avail. on VSWIR)

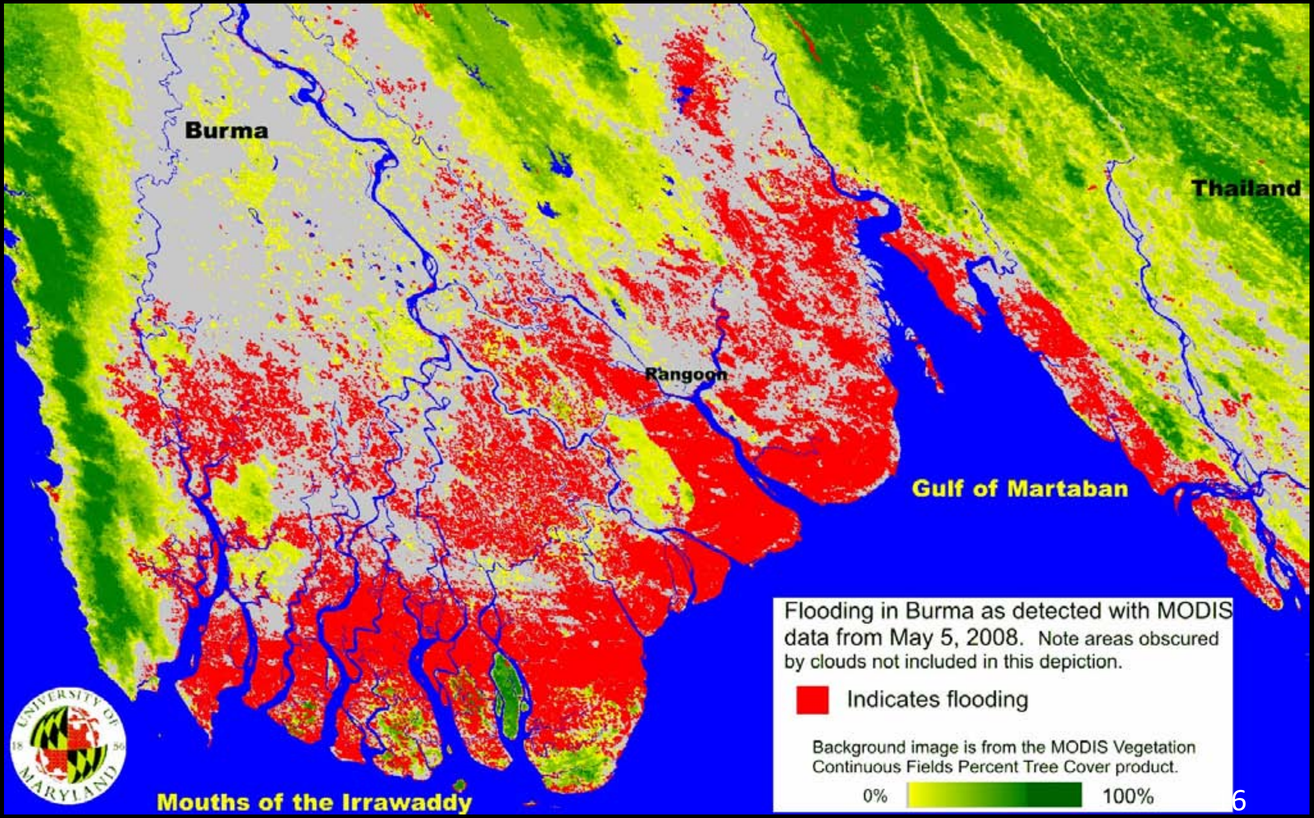

M. Carroll et al.

Flooding - Heritage (Flight) – EO-1/ASE

Onboard Detection of a Rare Major Flood on Australia's Diamantina River

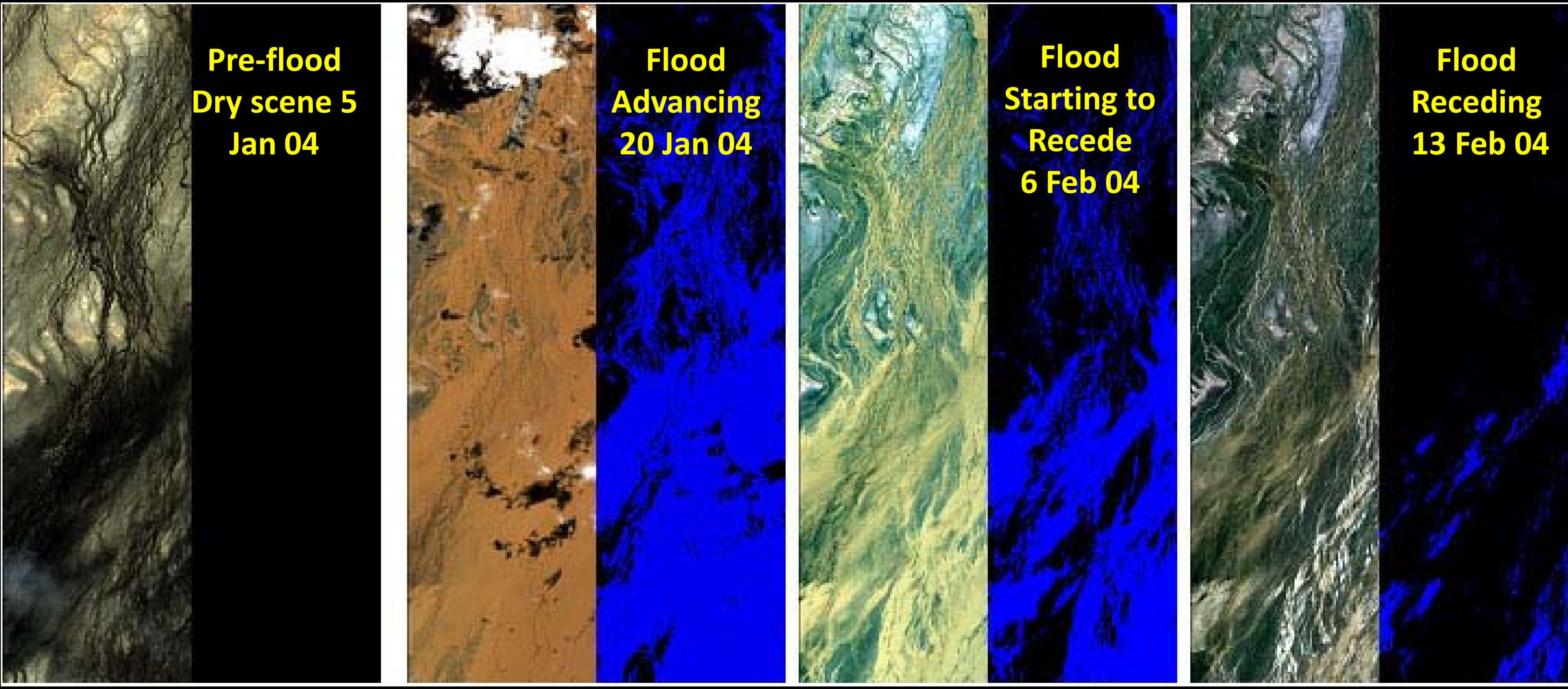

Cause of flooding: Monsoonal rain

EO-1 Hyperion. Wavelengths used: 0.86 µm and 0.99 µm (also 0.55 µm, 0.86 µm) available on VSWIR

F. Ip, V. Baker, et al., University of Arizona

Cryosphere (Ground)

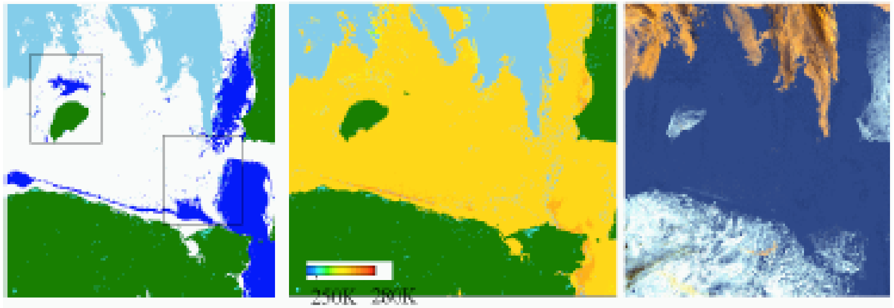

Figure 4: MODIS sea ice product by NDSI method (left), IST method calculated temperatures (center), and a composite image made from MODIS Bands 20 (3.7μm), 22 (3.9μm) and 23 (4.0μm) to highlight clouds (right).

Image courtesy of [Scharfen and Kalsa 2003]

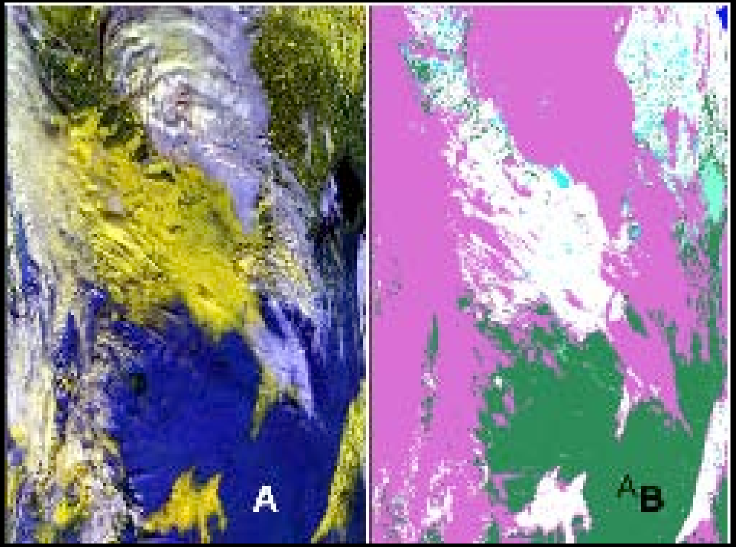

- Snow
- Land
- Water
- Lake Ice
- Cloud
- Ocean
- Night
- No Decision

Figure 1 MODIS at-satellite reflectance image from swath of MOD02HKM for 3 January 2003 (A). Snow cover appears as yellow in this display of bands 1, 4 and 6. Snow cover map of the swath (B) and the snow cover map in sinusoidal projection (C).

Courtesy of *MODIS Snow Products User Guide*

MODIS Snow product algorithms will require both VSWIR and TIR

Heritage (onboard) EO-1/ASE Hyperion Cryosphere Classifier

Deadhorse (Prudhoe Bay), Alaska

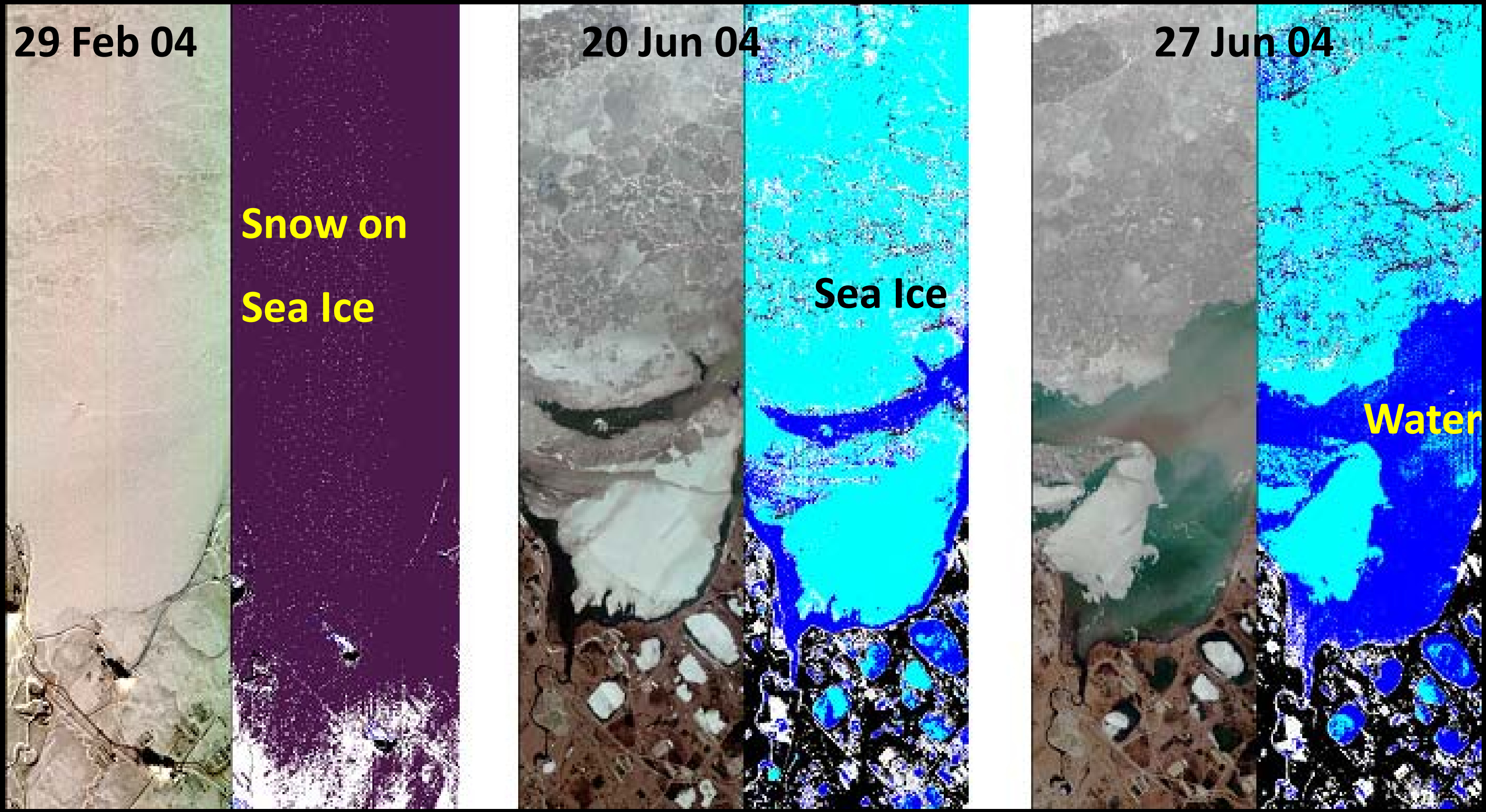

EO1/Hyperion data
Wavelengths used in classifier:
0.43, 0.56, 0.66, 0.86 and 1.65 µm (all avail. VSWIR)

Arizona State University
Planetary Geology Group

Coastal

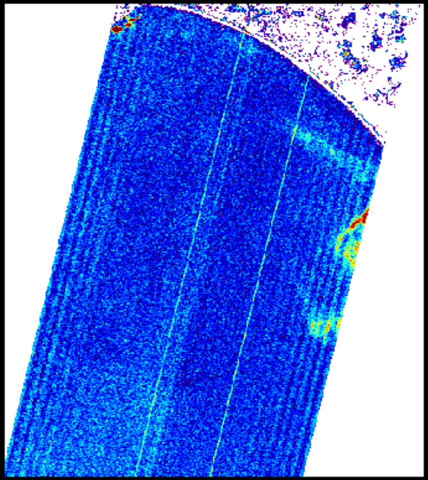

Maximum Chlorophyll Index derived from Hyperion imagery acquired 21 October 2008 of Monterey Bay [Chien et al. 2009] using 660, 681, 711, 752, nm. (ack J. Ryan/MBARI) These bands avail. VSWIR

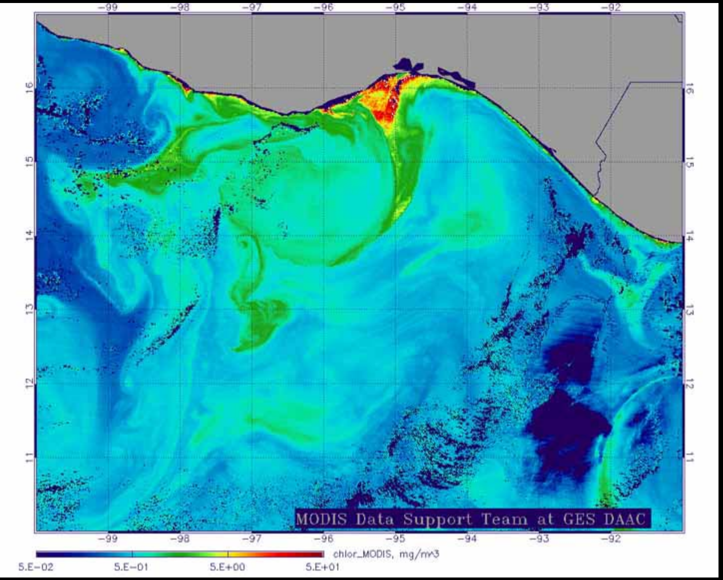

Uses 490nm/555nm or 490nm/565 nm MODIS reflectance data Courtesy GSFC DAAC

Again avail. VSWIR.

Dust

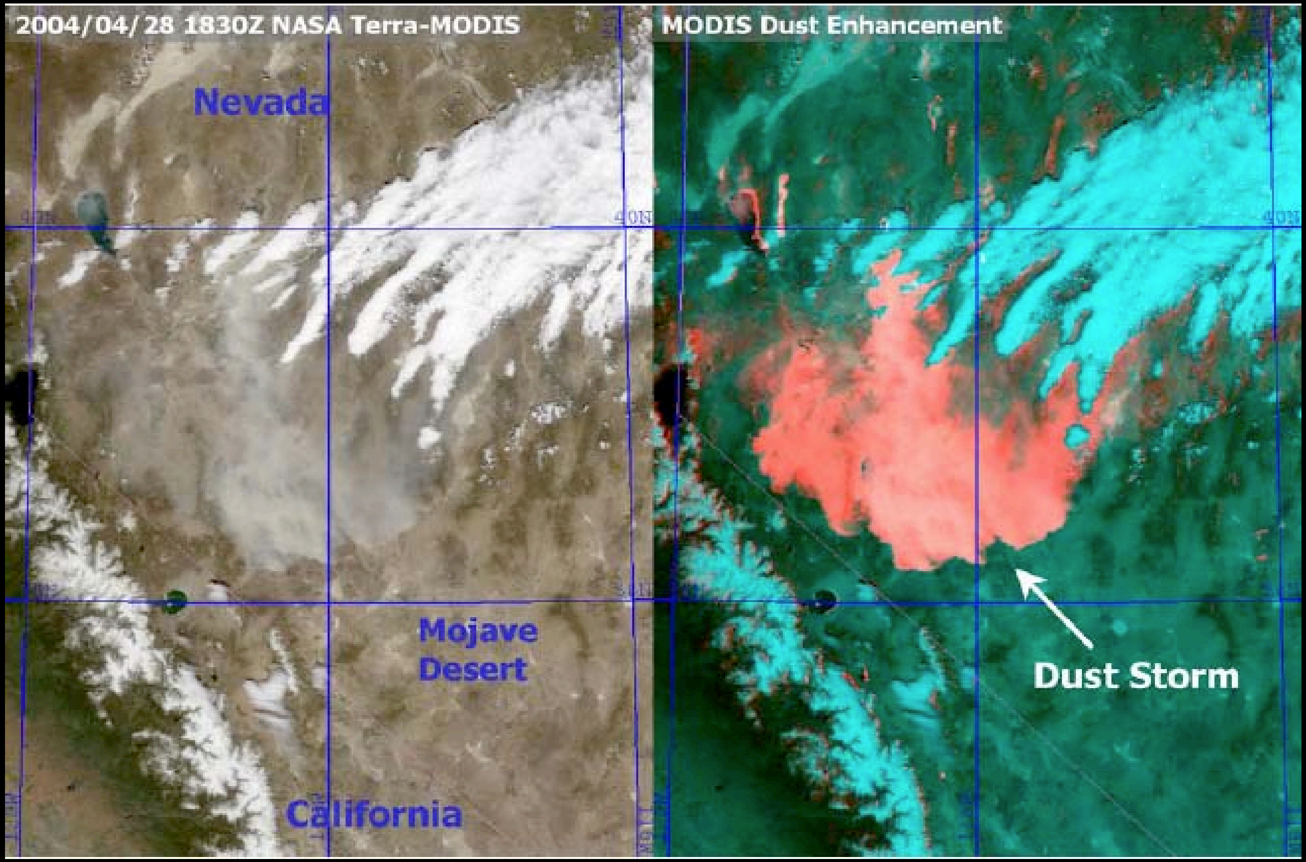

Image (processed MODIS) courtesy of *Satellite Product Tutorials: Desert Dust Storms, S. Miller et al.*
Algorithms would require both VSWIR and TIR bands.

Vegetation

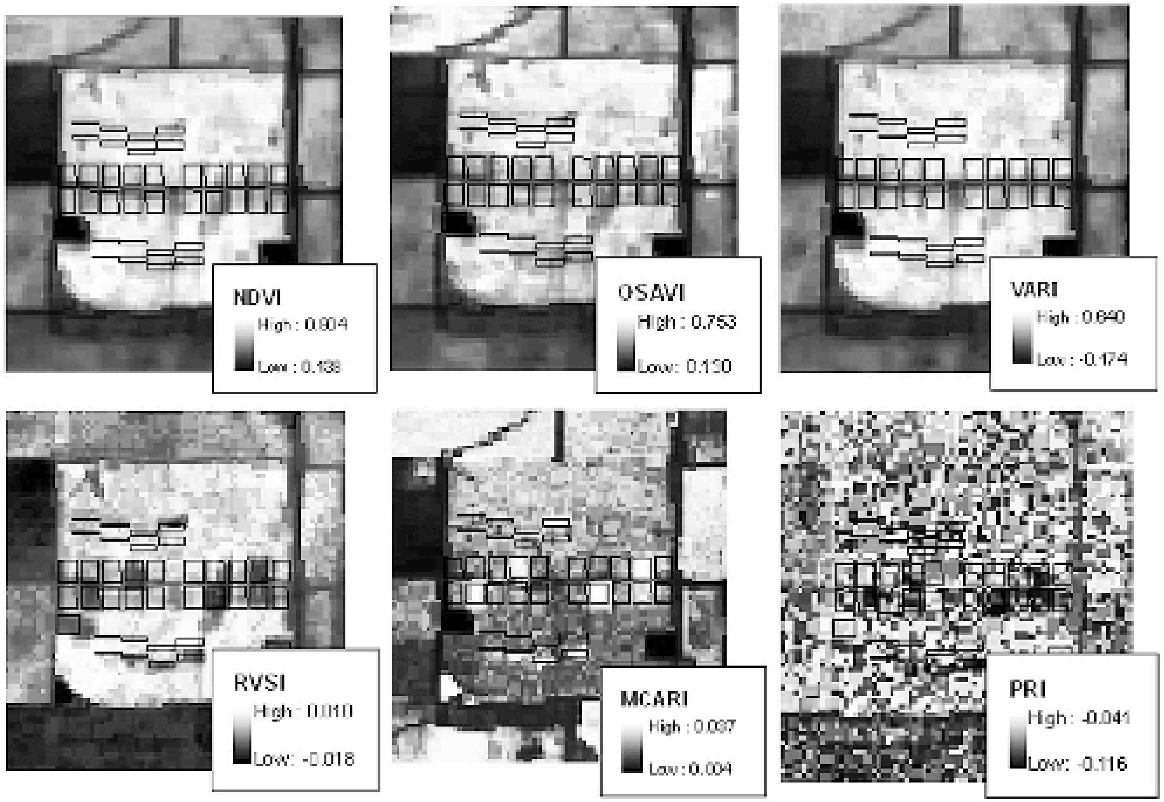

Fig. 3. Comparison of selected indices derived from 6 July Airborne Visible/Infrared Imaging Spectrometer (AVIRIS) imagery (18-m spatial resolution) with locations of N trial plots and subpixel plots shown. The corresponding classification accuracies are shown in Table 7. Note the differences between the appearance of the subpixel areas and the classification accuracies. For example, the subpixel stressed areas for the Normalized Difference Vegetation Index (NDVI) and the Modified Chlorophyll Absorption in Reflectance Index (MCARI) are quite apparent, although the classification accuracies (Table 7) for the Photochemical Reflectance Index (PRI) are generally higher.

Aviris measurement of plant stress using NDVI, MCARI, and PRI
[Perry & Roberts 2008] describes 22 measures using 500-1200 nm.
These bands are available in VSWIR data.

Conclusions

- Direct broadcast can provide key data at low latency
- Onboard computing can address issues to downselect and process data to fit within reduced downlink
- Operations can be simple and automated

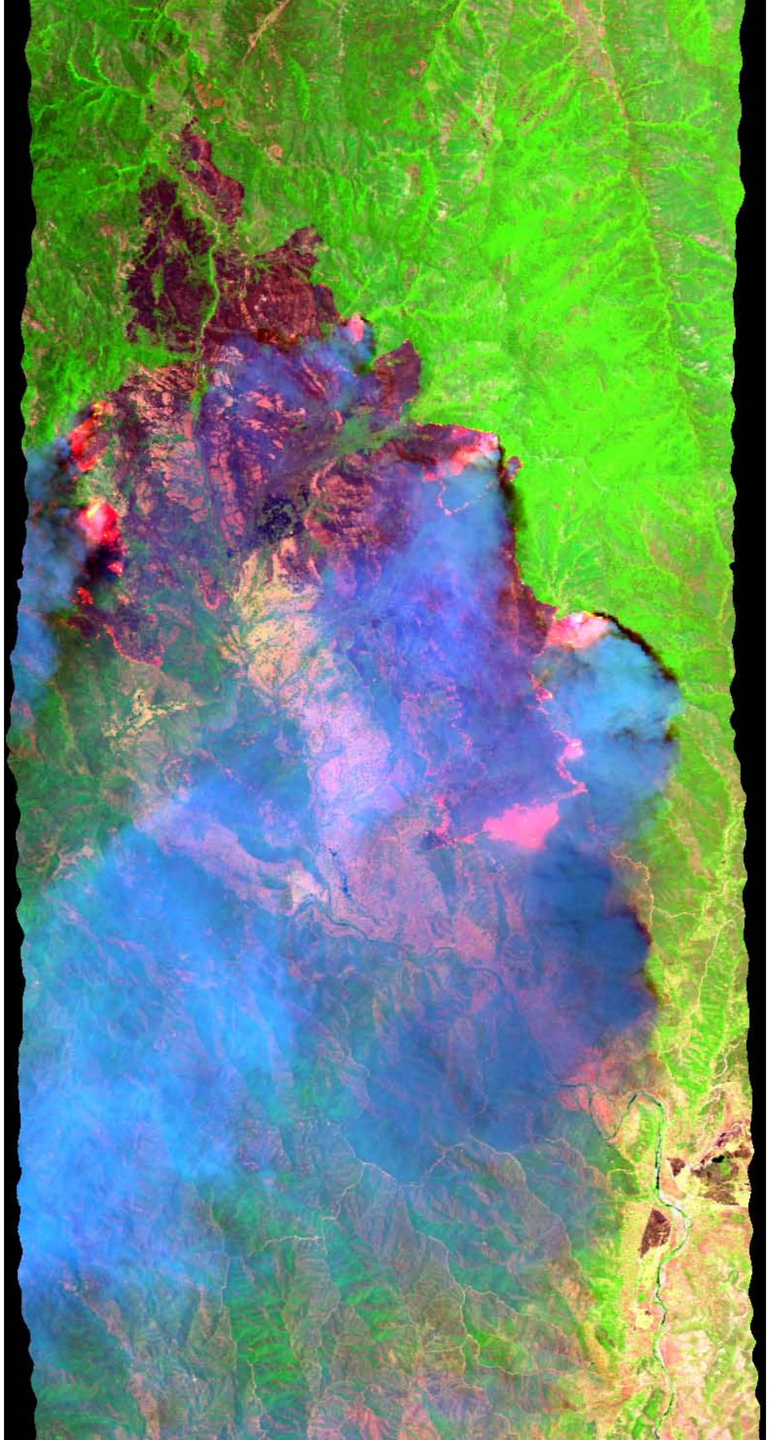

Mapping Effective Fire Temperature Using AVIRIS and MASTER

Philip E. Dennison

D. Scott Matheson

University of Utah

Utah Remote Sensing Applications Lab University of Utah

HyspIRI and Fire

- Fire is an important process
  - Major disturbance in many terrestrial ecosystems
  - Source of CO_2, CO, trace gasses and aerosols
- Fire is relevant to multiple HyspIRI science questions
  - How are fires and vegetation composition coupled? (CQ2)
  - What is the impact of global biomass burning on the terrestrial biosphere and atmosphere, and how is this impact changing over time? (TQ2)
  - How are the biogeochemical cycles that sustain life on Earth being altered/disrupted by natural and human-induced environmental change? (VQ3)
  - How are disturbance regimes changing and how do these changes affect the ecosystem processes that support life on Earth? (VQ4)

HyspIRI and Fire

- Depending on sensitivity and saturation, HyspIRI should provide excellent data for mapping fire
  - Multiple bands covering spectral regions with strong emitted radiance (SWIR, MIR, TIR)
  - 60 m spatial resolution will allow some separation of flaming and smoldering combustion within active fires
- Current approaches for characterizing fire (i.e. MODIS fire radiative power) won't take advantage of the spectral information provided by HyspIRI
  - We need to explore fire characterization methods that can

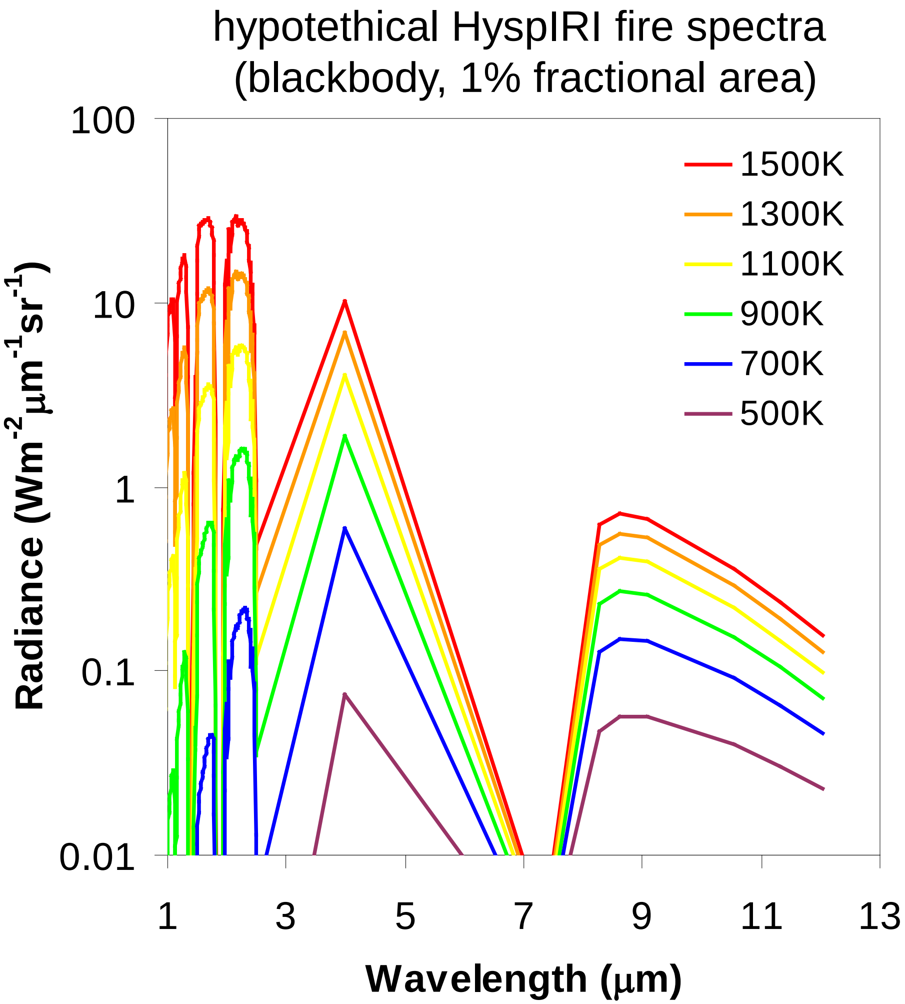

Fire Temperature Retrieval

- Fire temperature retrieval commonly relies on linear mixing models
  - Dozier (1981)
  - $L_{\lambda sensor} = L_{\lambda Ef} + L_{\lambda Eb} = f_f\,\beta(\lambda, T_f) + f_b\beta(\lambda, T_b)$
- More complex models can include atmospheric transmittance and scattering, reflected solar radiance
- Mixing model-based temperature retrievals have been applied to data from AVIRIS, AVHRR, ASTER, BIRD, and MODIS

Fire Temperature Retrieval

- Mixing models often assume a <u>single temperature blackbody</u> emitted radiance endmember
  - Emissivity of flames does approach 1, but only over meter-scale distances

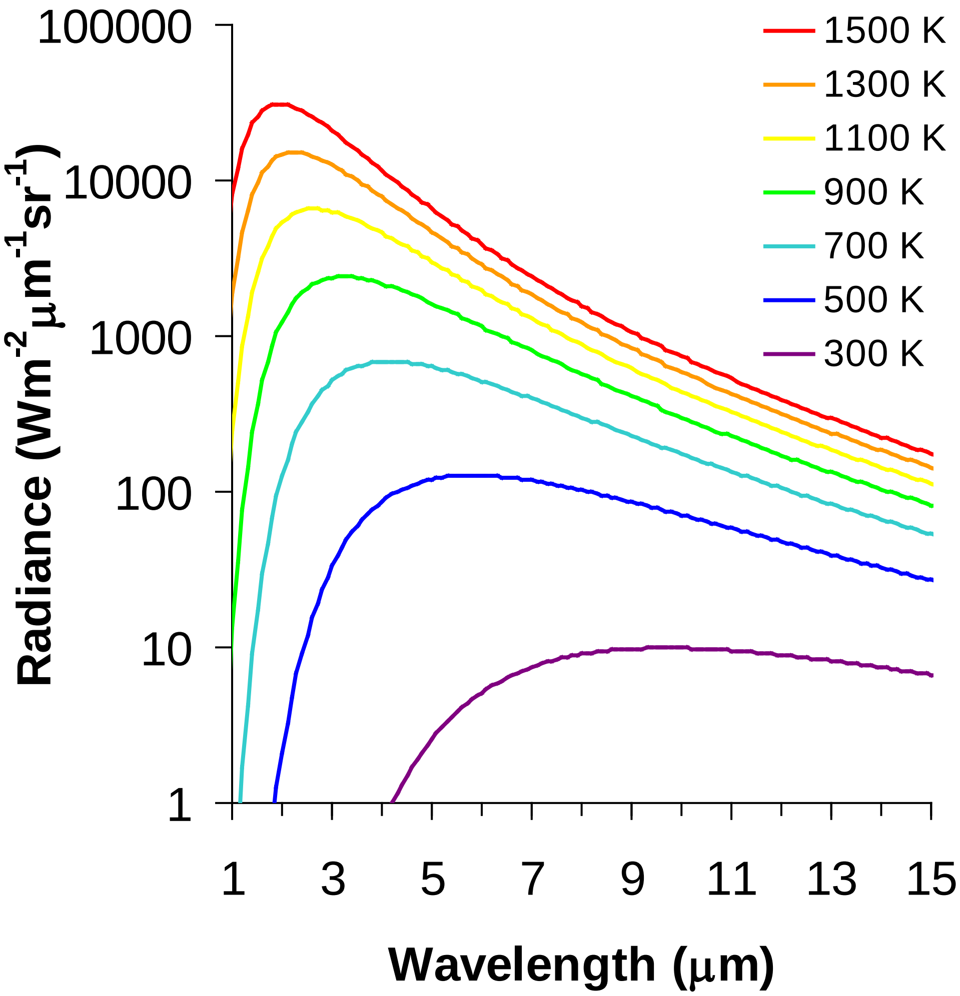

Questions

- Is single temperature blackbody emission a valid assumption?
  - Difficult to test directly because of lack of *in situ* data
  - With many discrete areas of combustion within a single pixel, common sense says emitted radiance is a lot more complex
- Can we at least test whether temperature retrieval is consistent across spectral and spatial scales?
  - Fire temperature retrieved from different regions of the spectrum should return consistent temperatures
  - Fire temperature may scale poorly because of contributions from multiple areas of combustion with different temperatures

Indians Fire Data

- June 11, 2008: NASA ER-2 acquired AVIRIS and MASTER data over the Indians Fire in central California
- AVIRIS
  - 16 m spatial resolution
  - 224 bands, 0.4-2.5 μm
- MASTER
  - 40 m spatial resolution
  - 50 bands, 0.4-12 μm

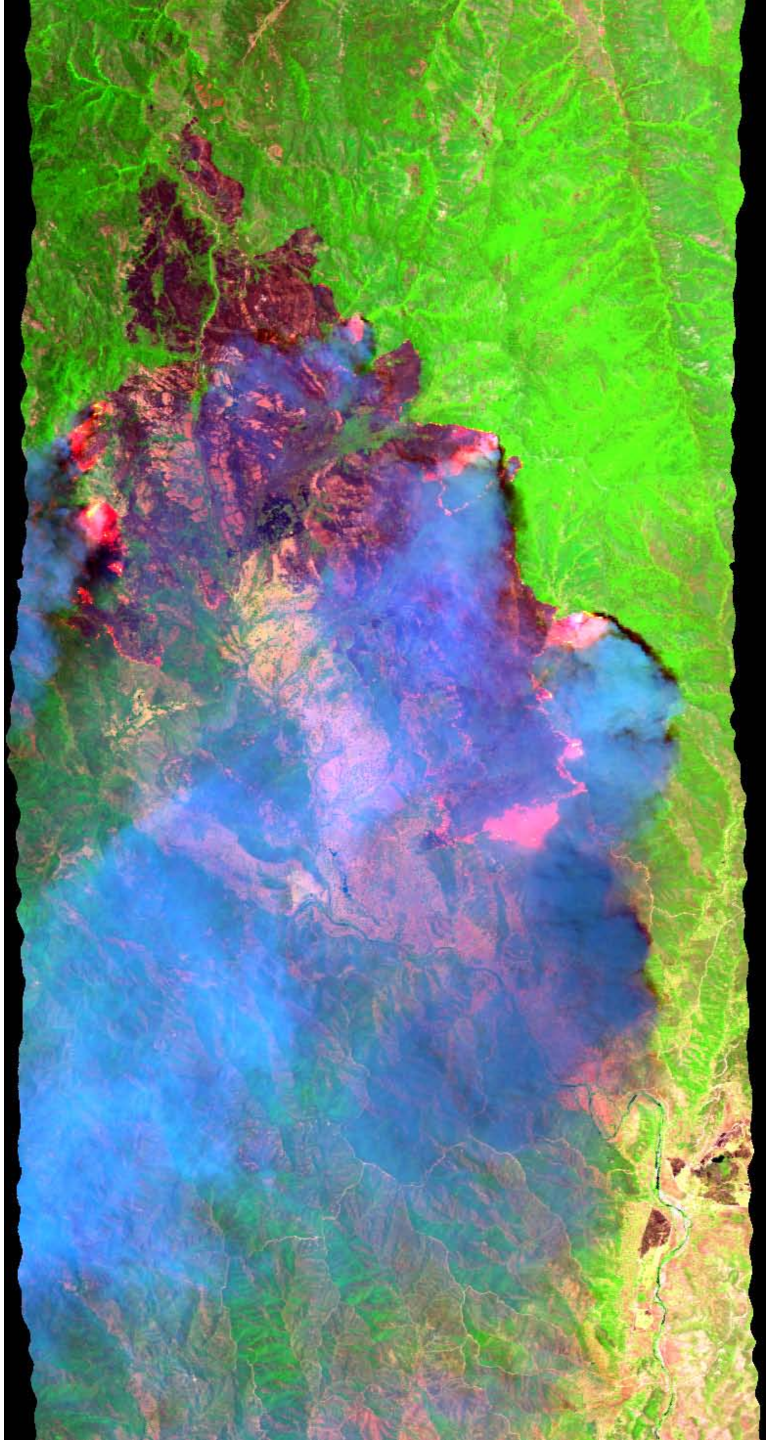

Radiance Modeling

- A multiple endmember, linear mixing model was used to model radiance measured by AVIRIS and MASTER
- Burning pixels were modeled using a three endmember linear mixing model
  1. Fire emitted radiance (MODTRAN, 300-1500K blackbody emission at 10 K interval)
  2. Background emitted and reflected radiance (selected from non-burning areas of images)
  3. Atmospheric emitted radiance and scattering (MODTRAN, 10 K blackbody; equivalent to “shade” endmember)
- Non-burning pixels were modeled using a two endmember model
  1. Background emitted and reflected radiance
  2. Atmospheric emitted radiance and scattering

4 model runs using different band combinations:

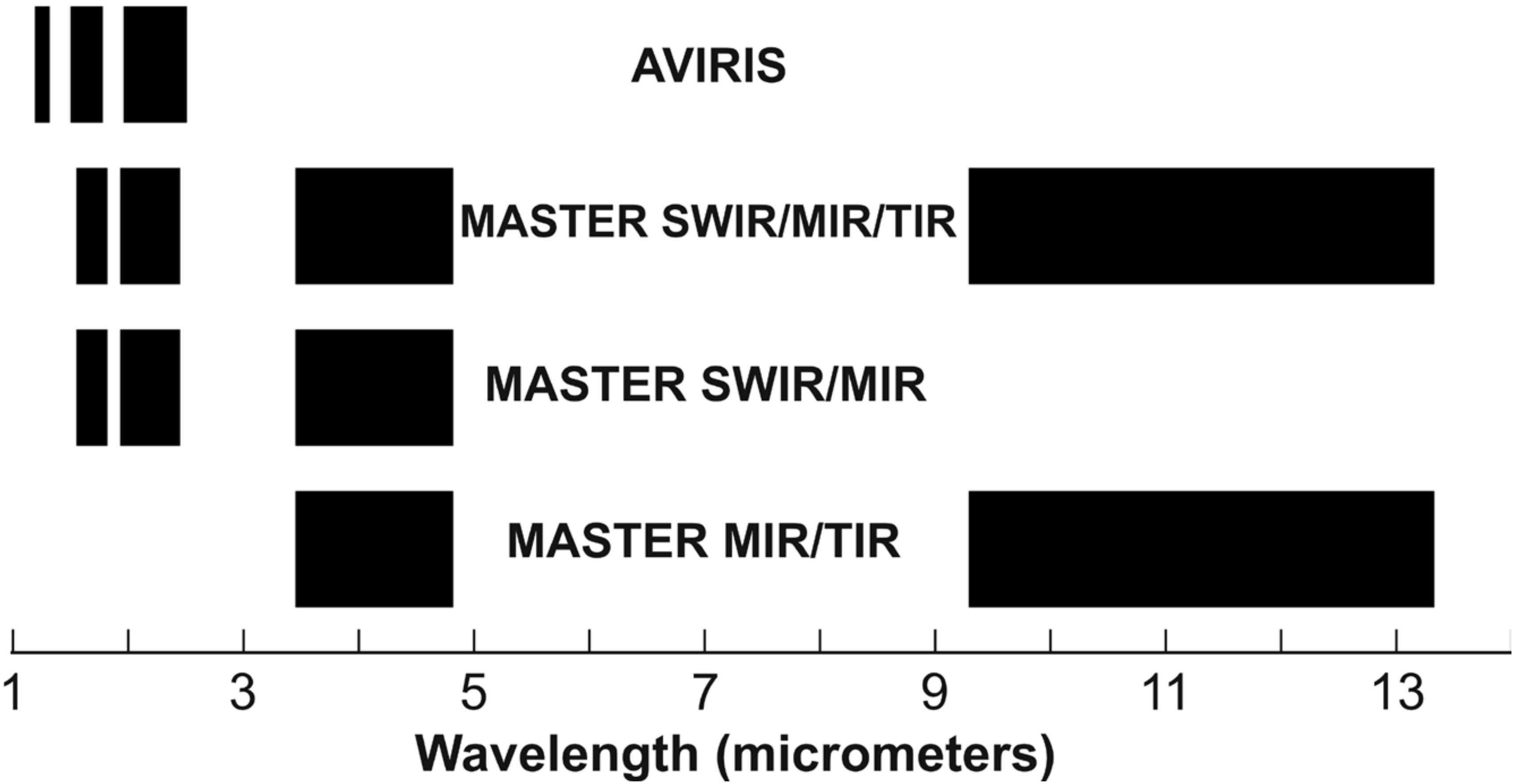

- Bands in major atmospheric water vapor absorption features were discarded

Example Temperature Retrieval (MASTER)

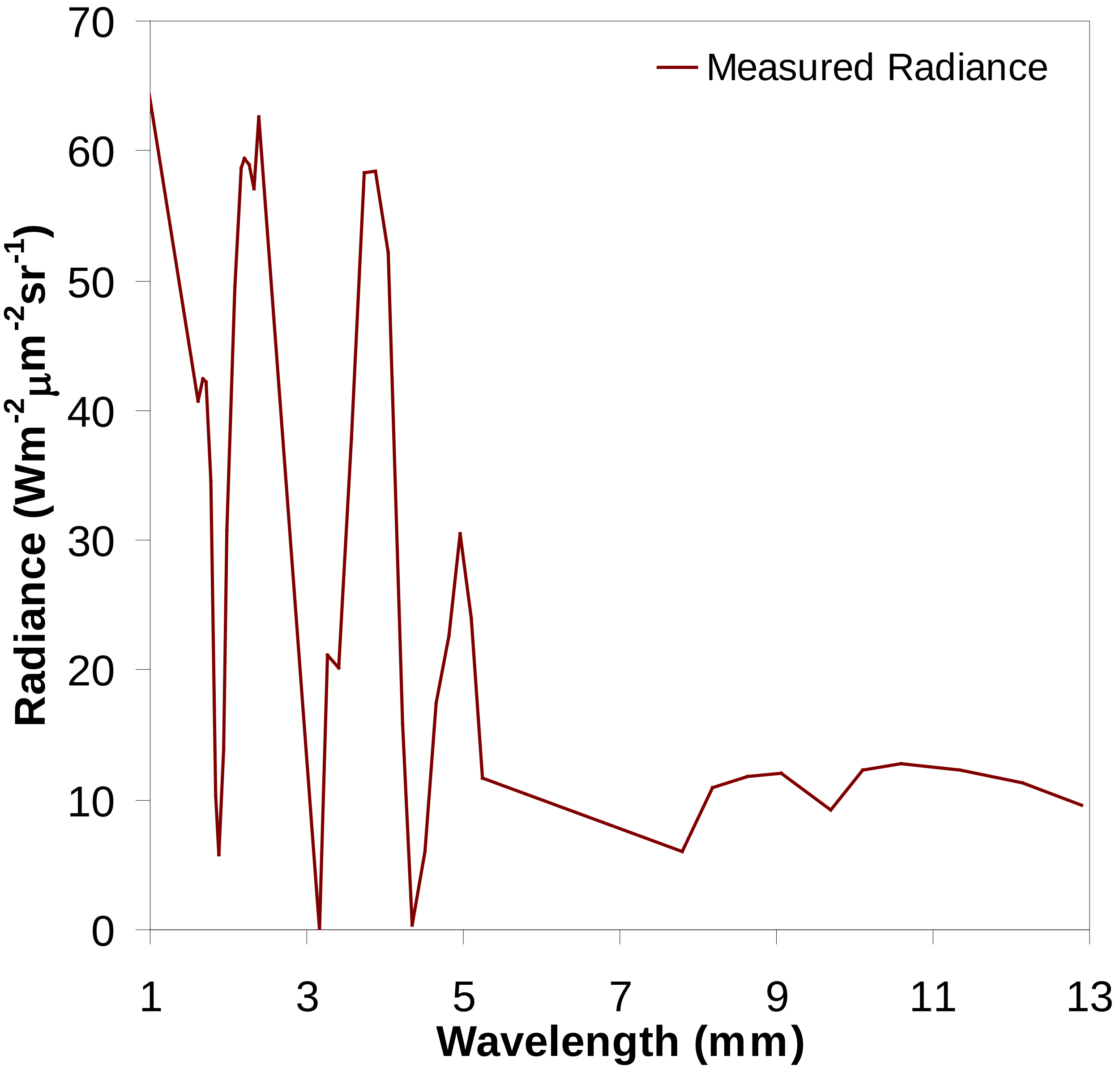

Example Temperature Retrieval (MASTER)

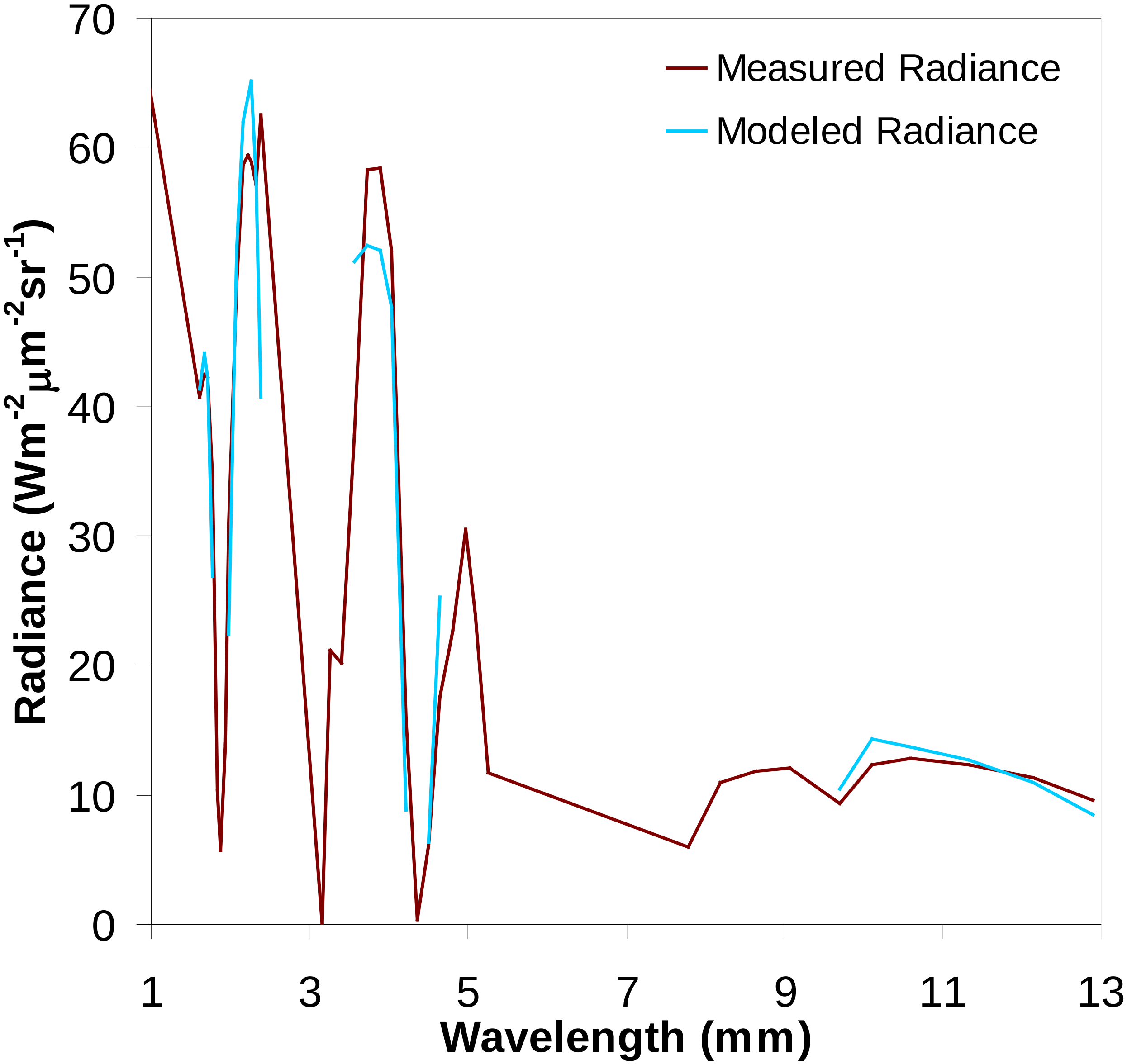

Example Temperature Retrieval (MASTER)

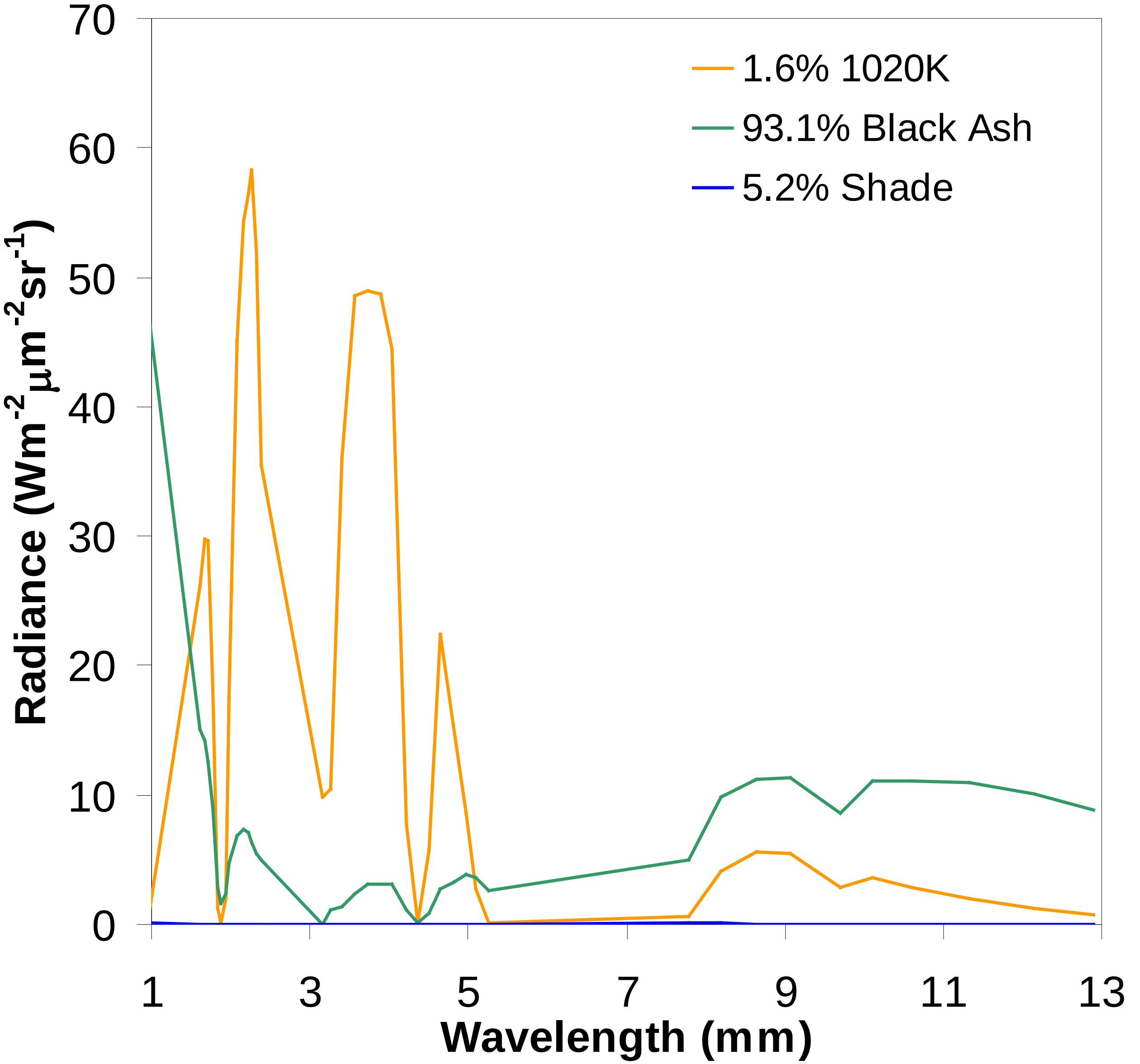

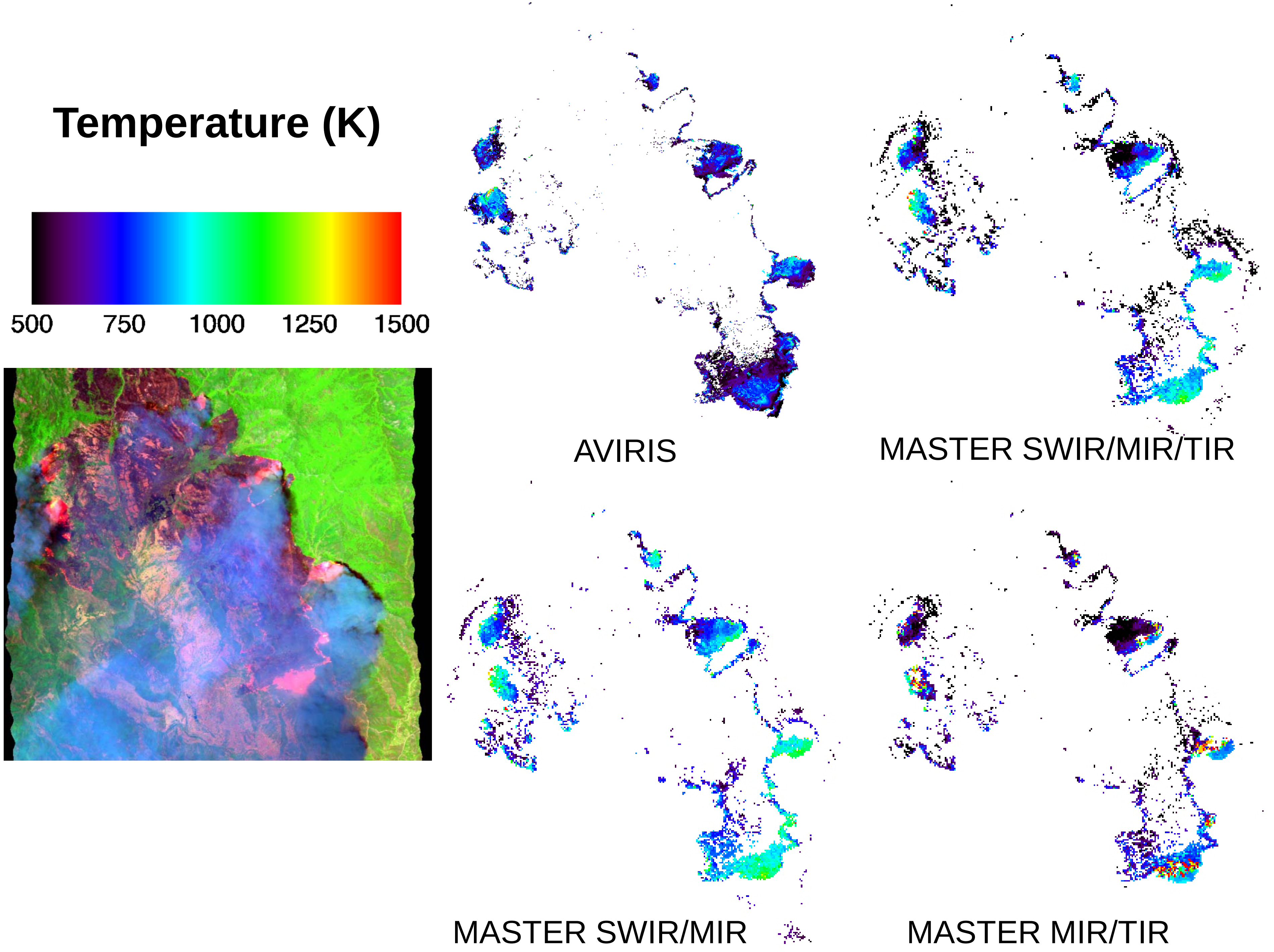
Temperature (K)
500
750
1000
1250
1500
AVIRIS
MASTER SWIR/MIR/TIR
MASTER SWIR/MIR
MASTER MIR/TIR

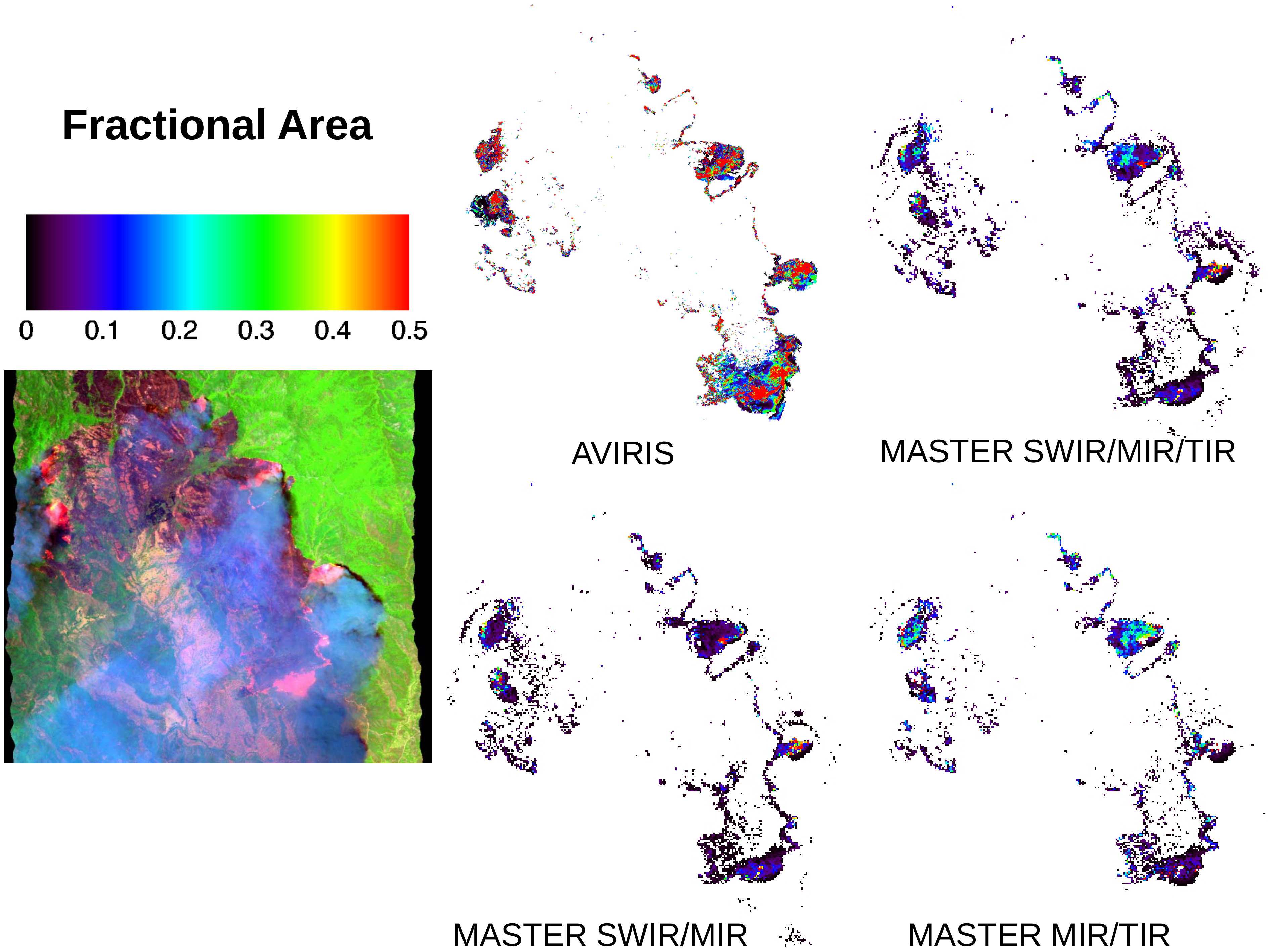
Fractional Area
0
0.1
0.2
0.3
0.4
0.5
AVIRIS
MASTER SWIR/MIR/TIR
MASTER SWIR/MIR
MASTER MIR/TIR

Histogram Comparison

- Temperatures from different spatial resolutions can not be compared directly
- Total area (m^2) at each temperature can be calculated by multiplying pixel area by fire fractional area and summing

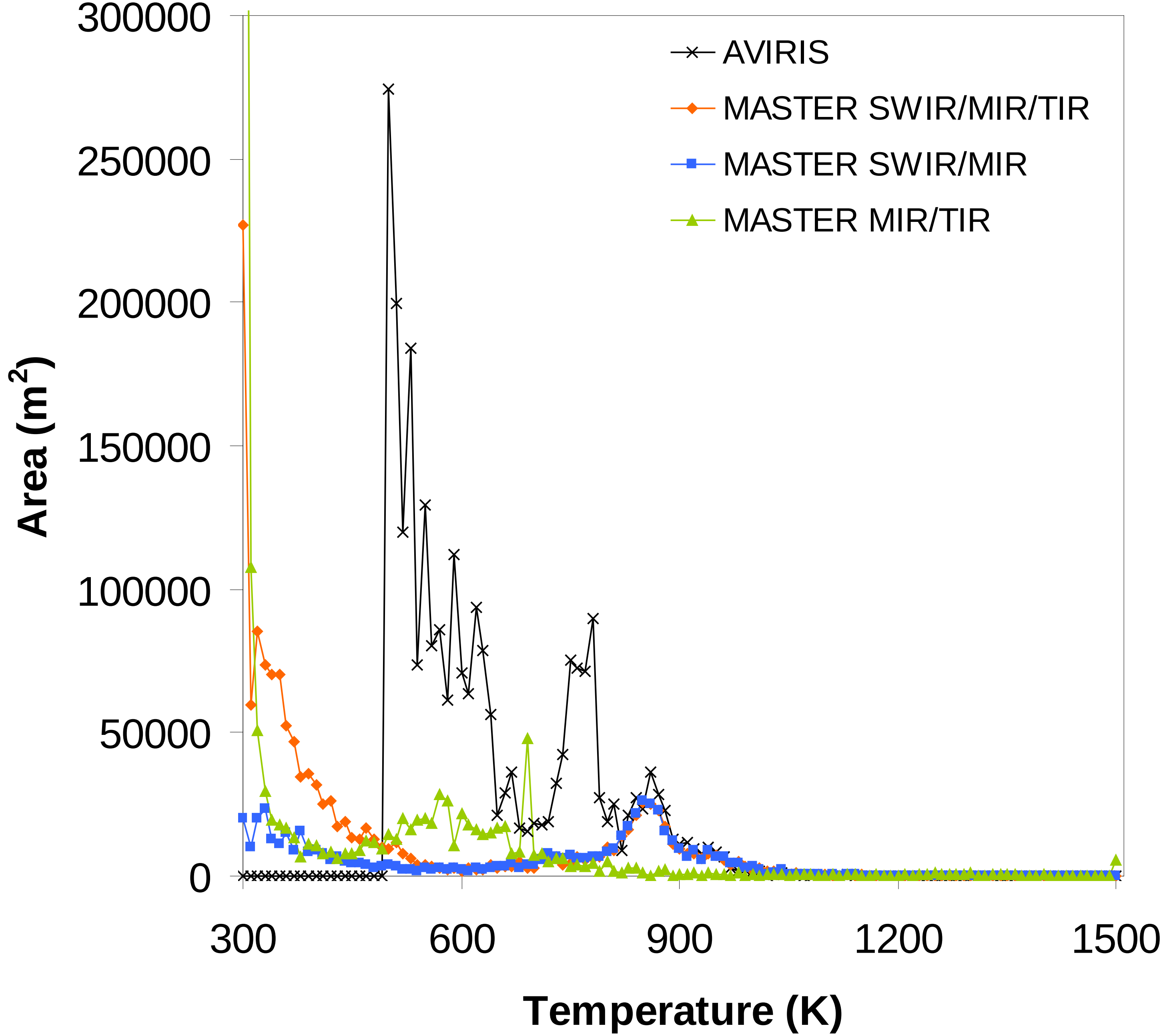

300000
250000
200000
150000
100000
50000
0
Area (m²)
300
600
900
1200
1500
Temperature (K)
AVIRIS
MASTER SWIR/MIR/TIR
MASTER SWIR/MIR
MASTER MIR/TIR

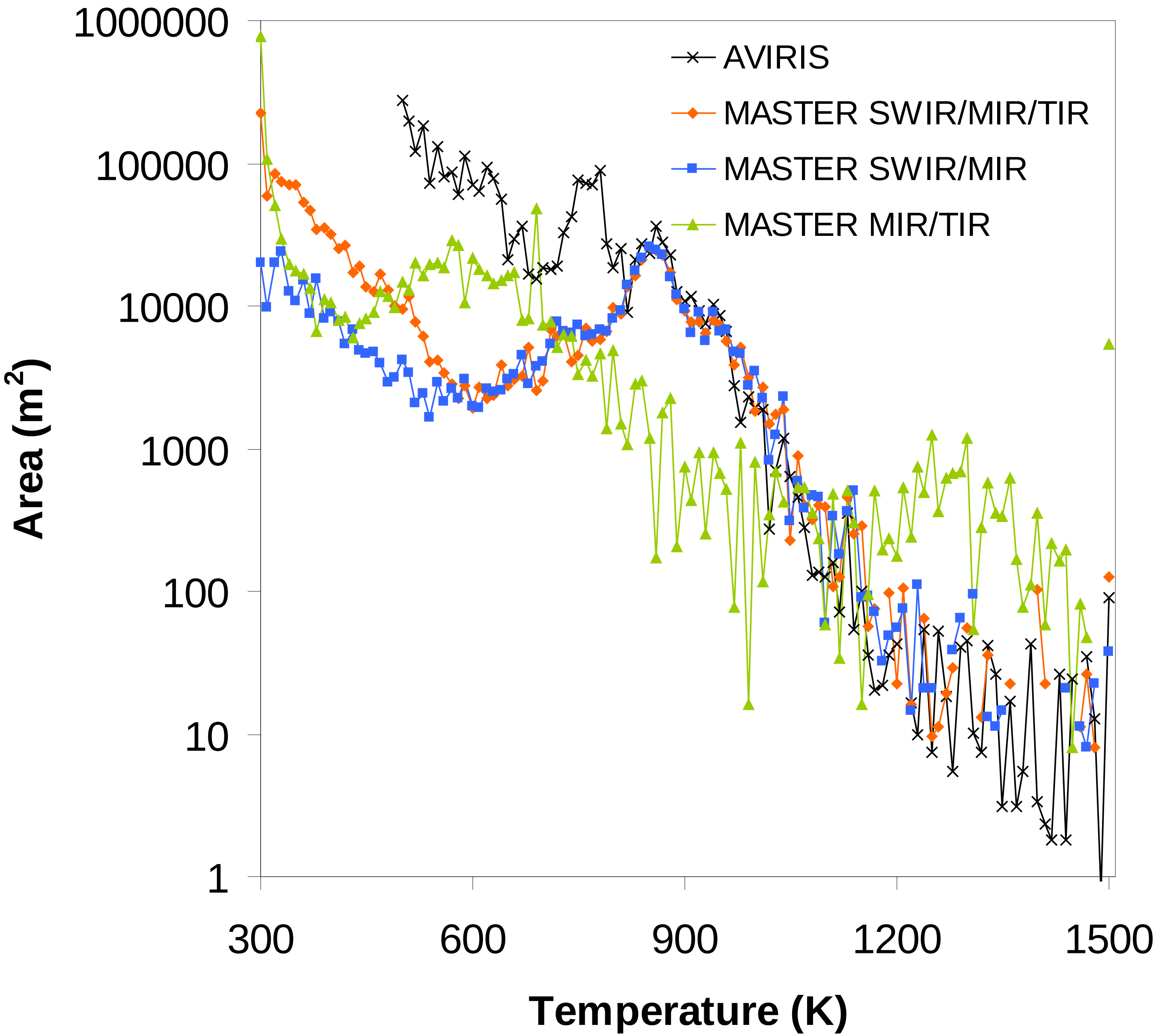

AVIRIS
MASTER SWIR/MIR/TIR
MASTER SWIR/MIR
MASTER MIR/TIR
Area (m^2)
1000000
100000
10000
1000
100
10
1
300
600
900
1200
1500
Temperature (K)

MASTER Modeled Temperatures

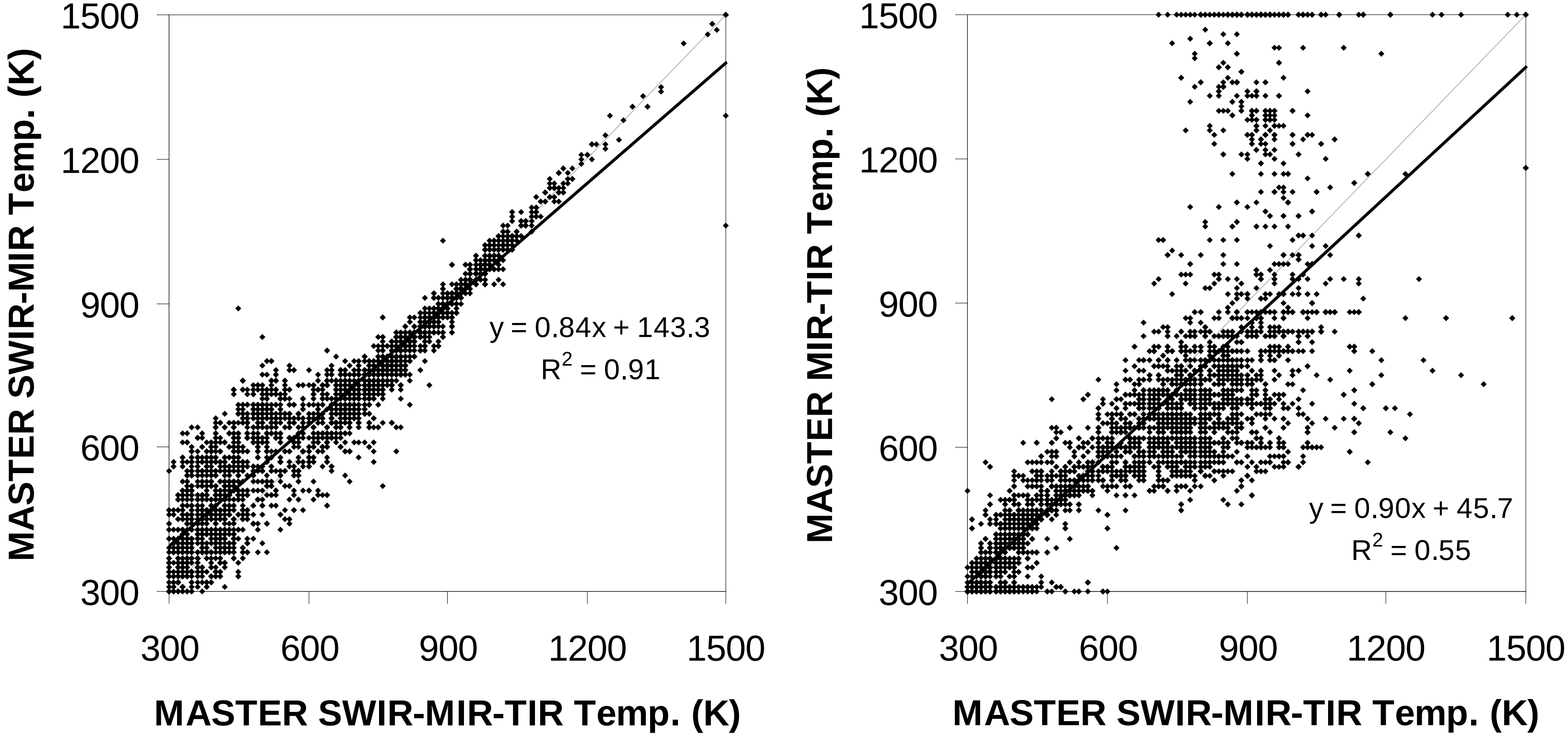

MASTER Modeled Fraction

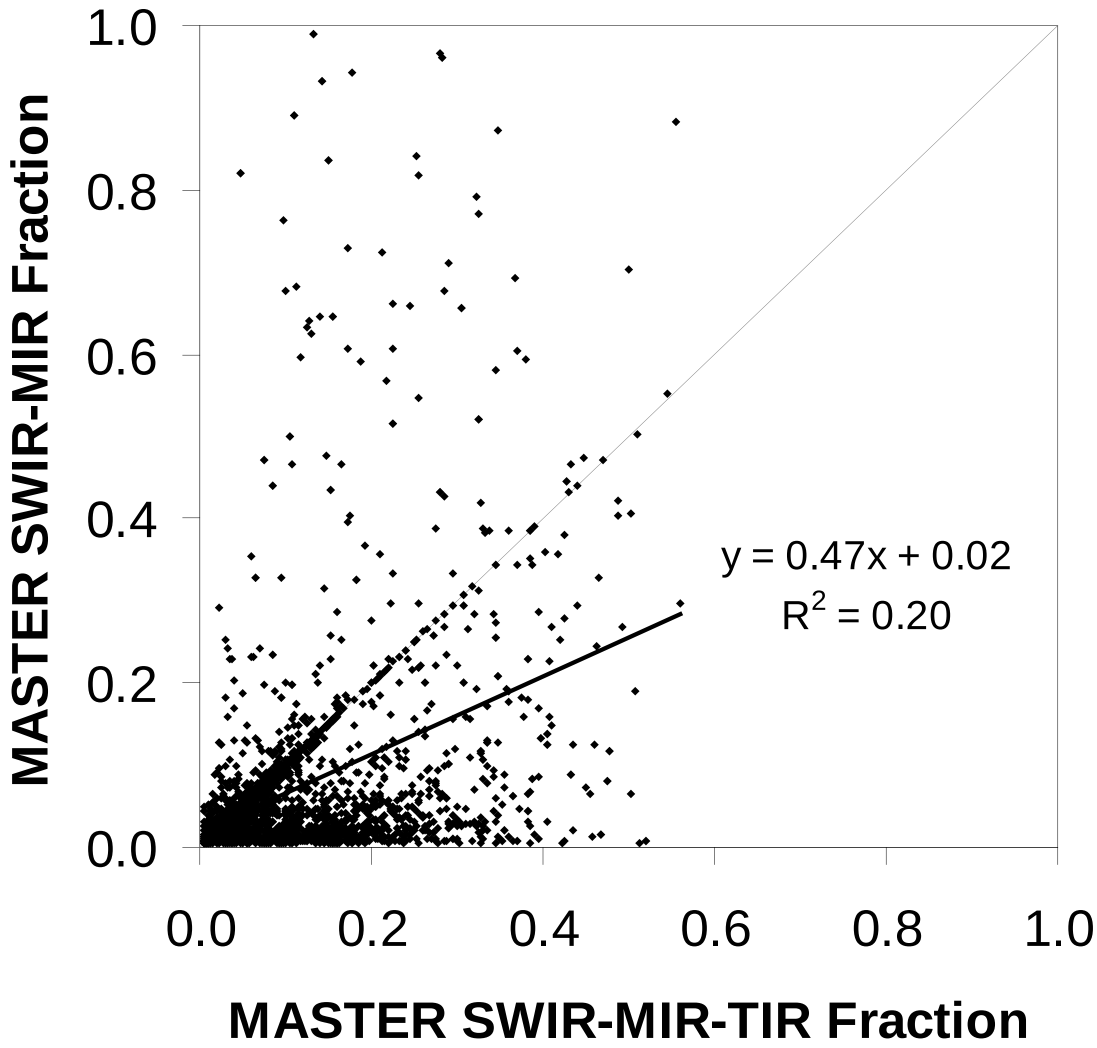

Spectral Comparison Results

- When different spectral regions are used, there is only moderate agreement in modeled fire temperature
- There is poor agreement in modeled fire fractional area

Spatial Scaling

- Averaging pixel radiance to create a coarser resolution image should result in altered radiance curves
- As a result, modeled temperature may change with spatial resolution
- We can aggregate the AVIRIS image from 16 m to 32 m and 64 m resolution and see how modeled temperature changes with spatial resolution

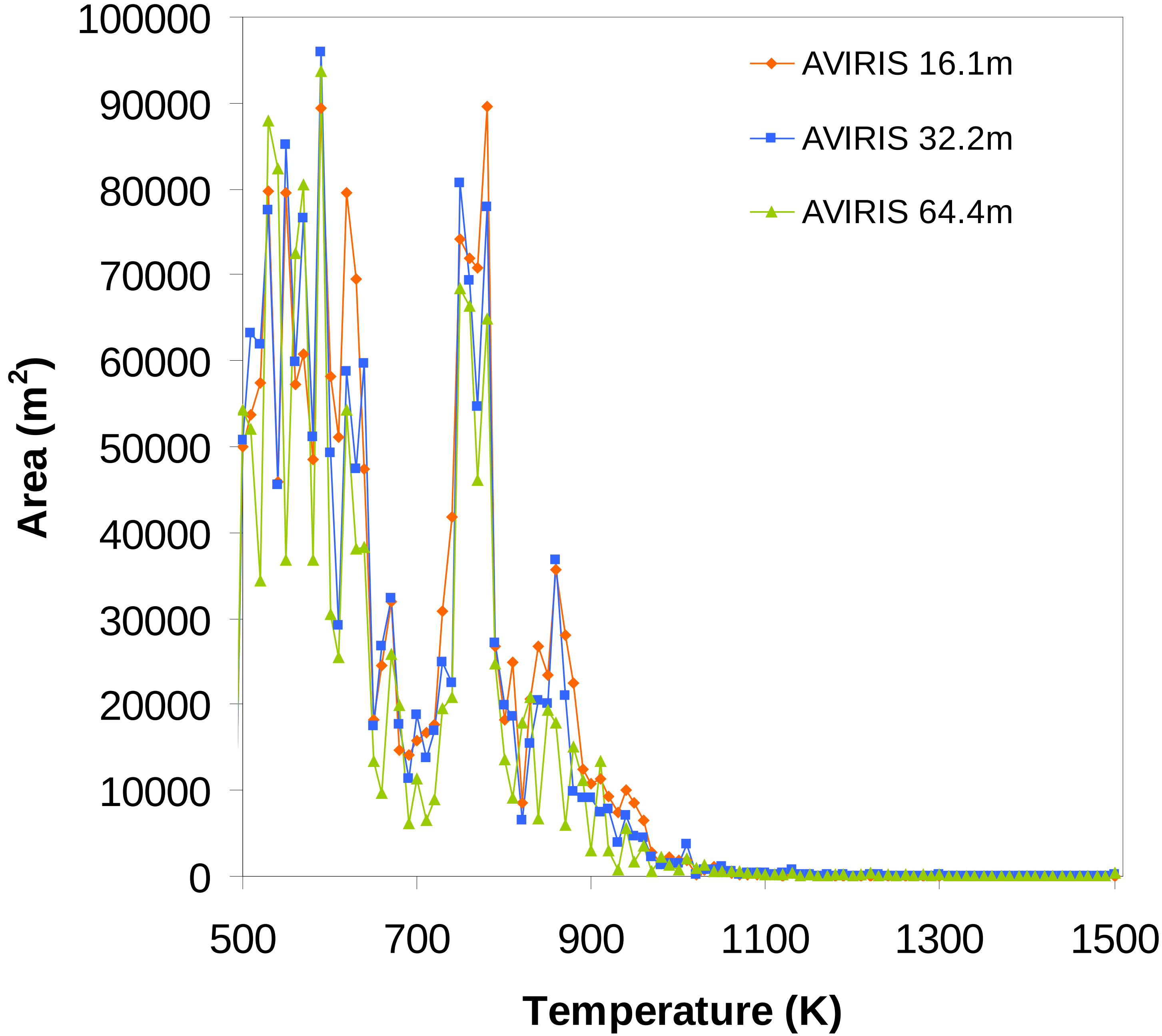

AVIRIS 16.1m
AVIRIS 32.2m
AVIRIS 64.4m
Area (m^2)
Temperature (K)
0
10000
20000
30000
40000
50000
60000
70000
80000
90000
100000
500
700
900
1100
1300
1500

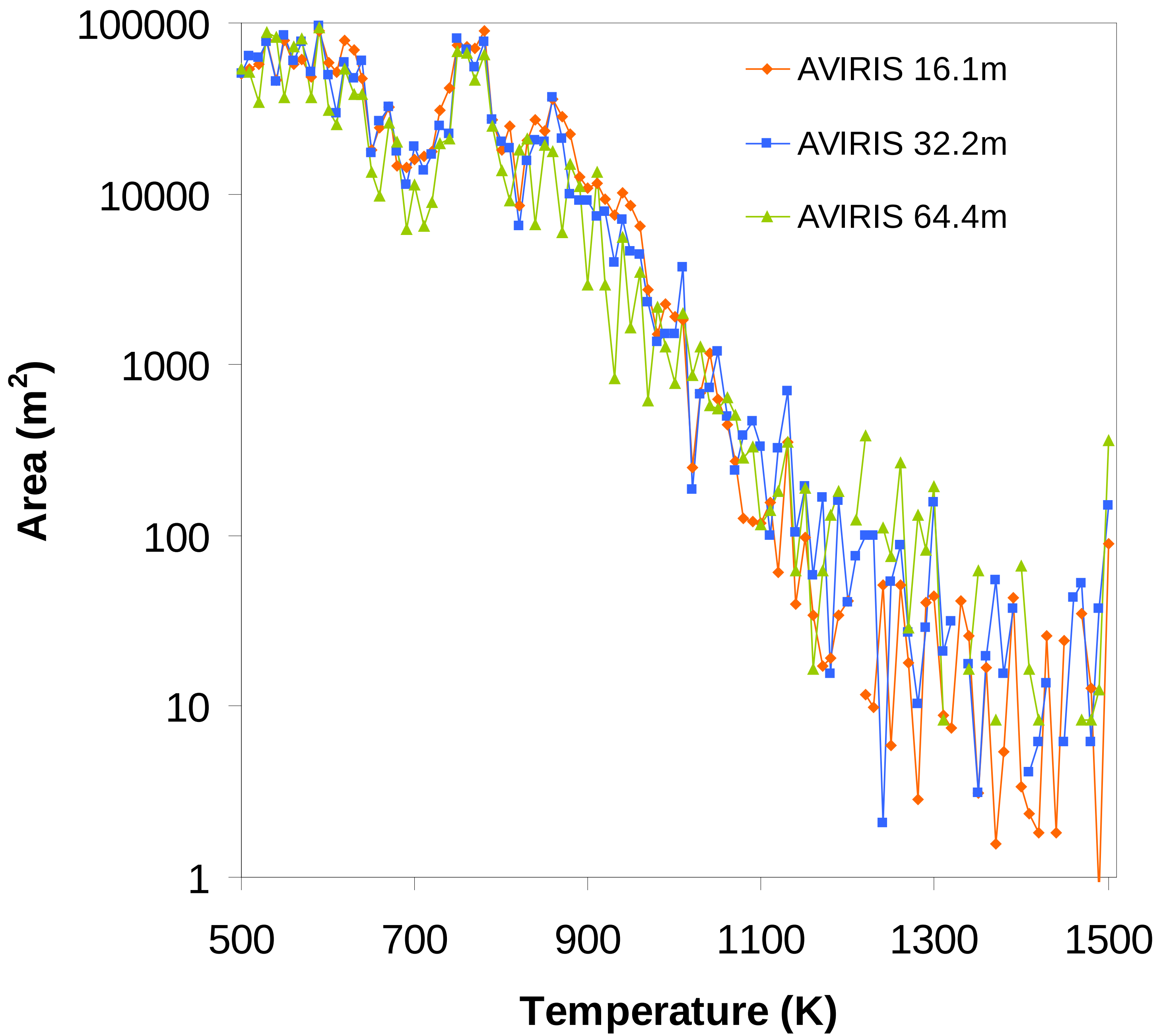

100000
10000
1000
100
10
1
500
700
900
1100
1300
1500
Area (m^2)
Temperature (K)
AVIRIS 16.1m
AVIRIS 32.2m
AVIRIS 64.4m

Other Results

- Residuals were largest at the edges of atmospheric water vapor absorption bands
  - Increased concentration and water vapor emission in fires?
- AVIRIS modeled background land cover much more accurately than MASTER

Conclusions

- What we are really modeling is “effective temperature” assuming a single temperature blackbody
  - This assumption does not hold across different wavelength regions
- High effective temperatures do correspond with the most active, highest radiance areas of fire
- Effective temperature is surprisingly stable with spatial resolution from 16 to 64 m

Conclusions

- We need better *in situ* data that allow us to compare emitted radiance across spatial scales
  - From scale of combusting fuel elements to areas covering hundreds of m^2
- We need better measures of fire that can take advantage of the spectral detail provided by imaging spectrometer data and account for radiance characteristics of actual fires
- Spectral information provided by HyspIRI can potentially help us find better/more accurate measures of fire characteristics for coarser spatial resolution sensors

AVIRIS Oil Spill Data, May 6, 2010

True Color Composite
638, 550, 462 nm

AVIRIS Oil Spill Data, May 6, 2010

Shortwave/Near Infrared
2277, 1682, 724 nm

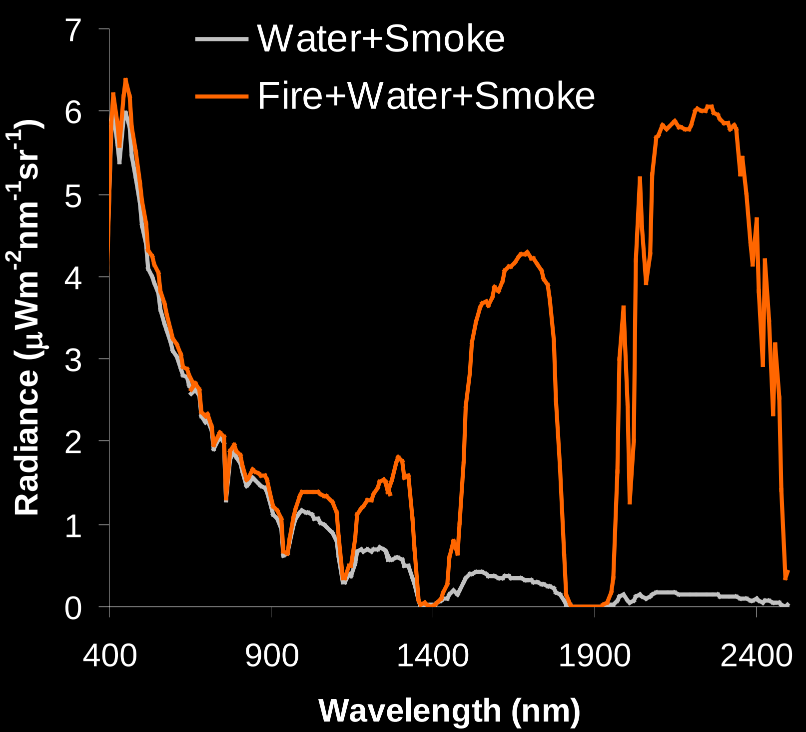

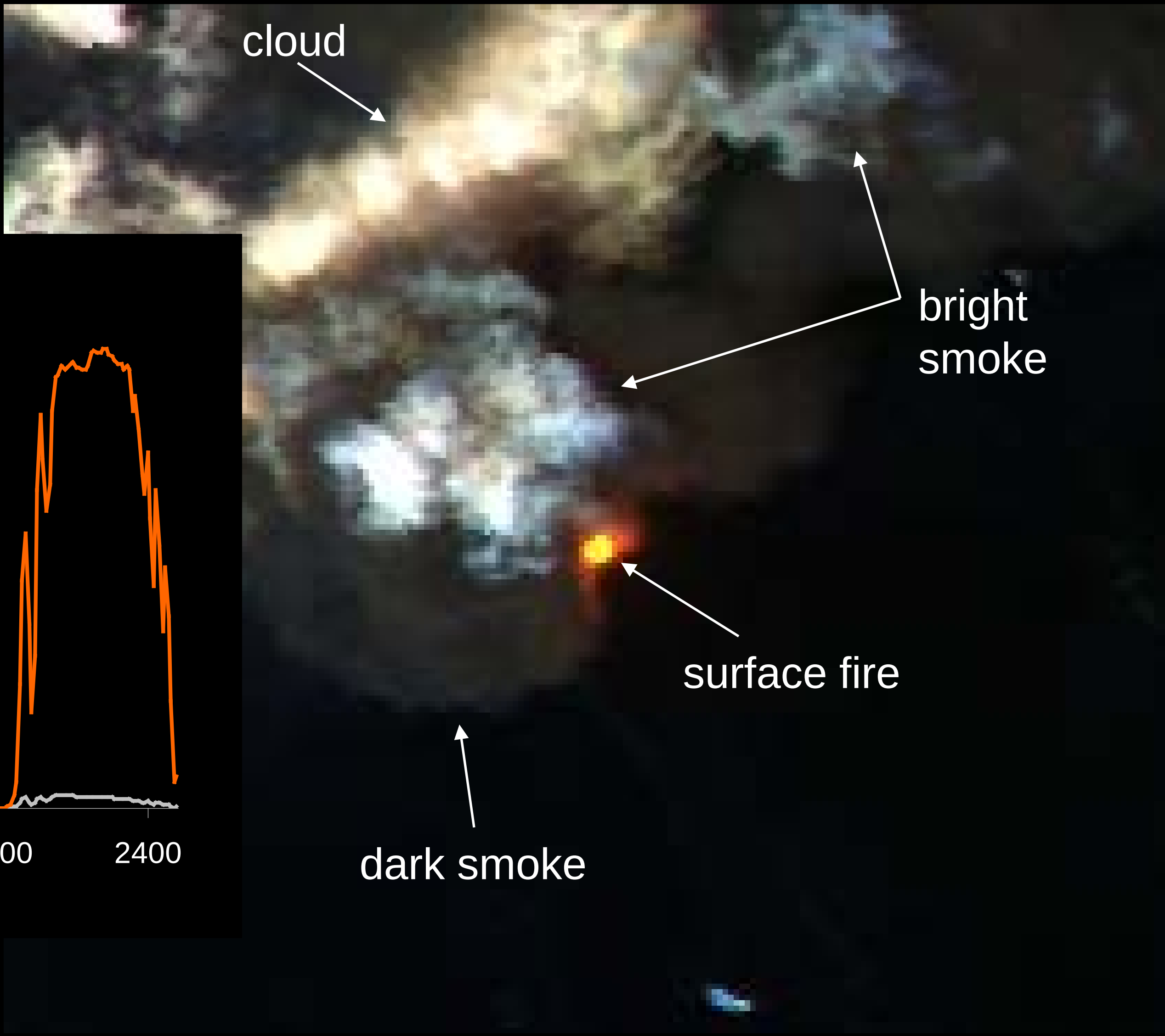

Temperature Modeling

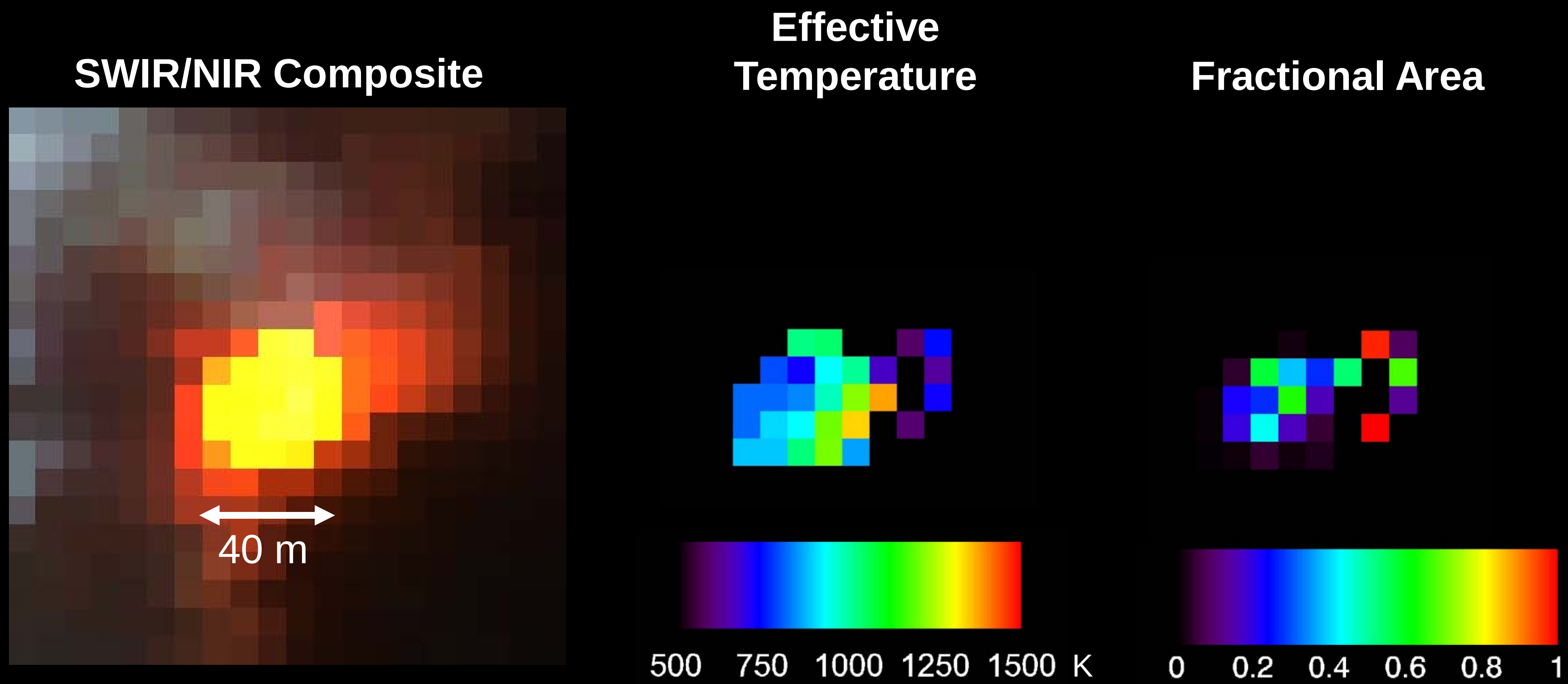

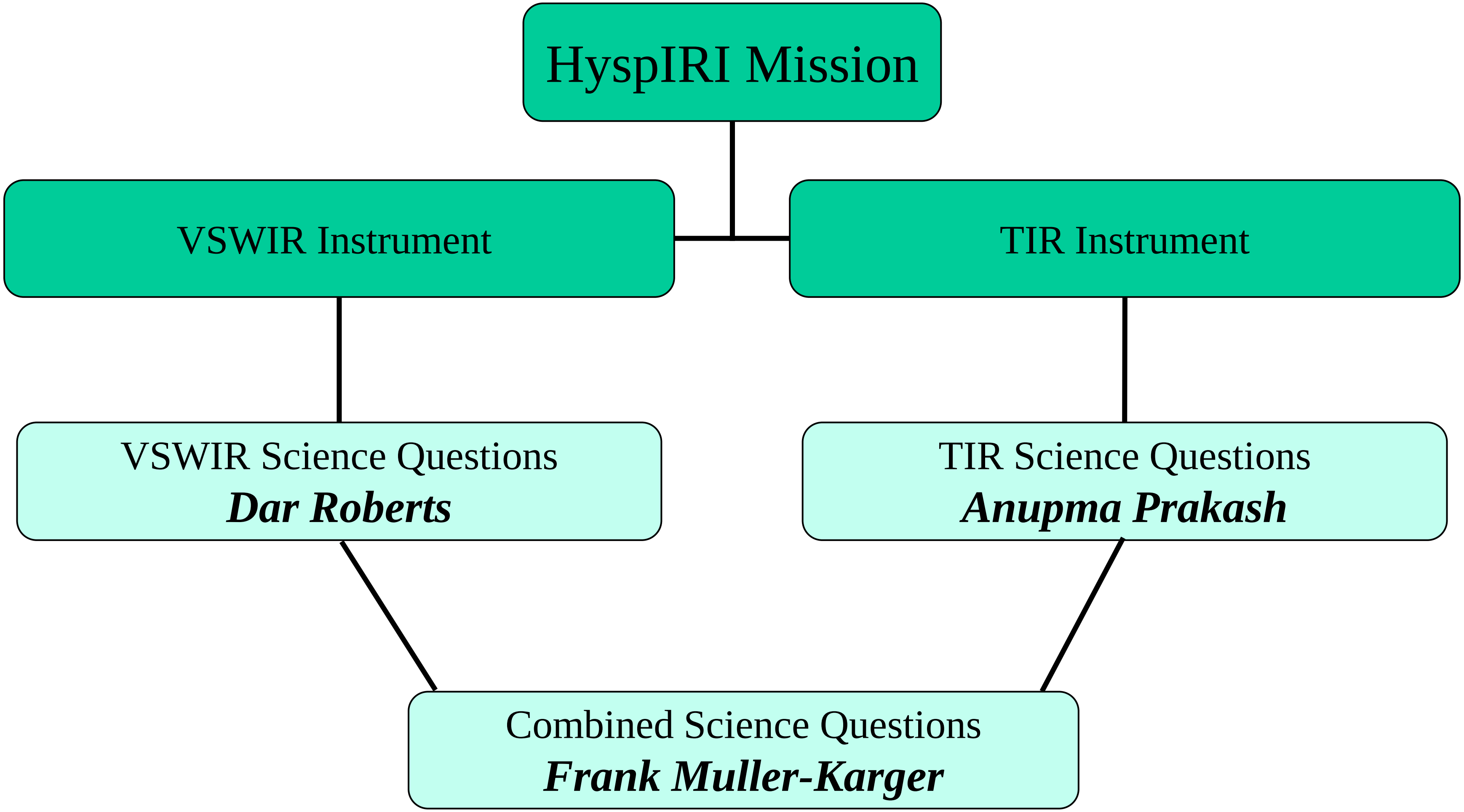
HyspIRI Mission
VSWIR Instrument
TIR Instrument
VSWIR Science Questions
Dar Roberts
TIR Science Questions
Anupma Prakash
Combined Science Questions
Frank Muller-Karger

Activities which Address Science Questions

NEON AOP
Tom Kampe

SOCO Concept
Chuck Rice

BREAK

Glint-Aerosol Discrimination
Youngje Park

Predicting Total **P**
Kaishan Song

Coastal Applications/Studies

Giant Kelp Forests
Kyle Cavanaugh

Changes in Coastal Community
Structure and Productivity
Frank Muller-Karger

Hot Target Saturation Analysis Report
Vince Realmuto

HyspIRI Decadal Survey VSWIR Science Questions

Dar A. Roberts (and a cast of thousands)

Over Arching Science Questions

- **VQ1 (Roberts/Middleton): Pattern and Spatial Distribution of Ecosystems and their Components**
  - **What is the global spatial pattern of ecosystems and diversity distributions and how do ecosystems differ in their composition or biodiversity?**
- **VQ2 (Gamon): Ecosystem Function, Physiology, and Seasonal Activity**
  - **What are the seasonal expressions and cycles for terrestrial and shallow aquatic ecosystems, functional groups, and diagnostic species? How are these being altered by changes in climate, land use, and disturbance?**
- **VQ3 (Ollinger): Biogeochemical Cycles**
  - **How are the biogeochemical cycles that sustain life on Earth being altered/disrupted by natural and human-induced environmental change? How do these changes affect the composition and health of ecosystems, and what are the feedbacks with other components of the Earth system?**
- **VQ4 (Asner/Knox): Changes in Disturbance Activity**
  - **How are disturbance regimes changing, and how do these changes affect the ecosystem processes that support life on Earth?**
- **VQ5 (Townsend/Glass): Ecosystem and Human Health**
  - **How do changes in ecosystem composition and function affect human health, resource use, and resource management?**
- **VQ6 (Green/Dierssen): Earth Surface and Shallow-Water Benthic Composition**
  - **What are the land surface soil/rock and shallow-water benthic compositions?**

VQ1: Subquestions

- **VQ1a: How are ecosystems organized within different biomes associated with temperate, tropical, and boreal zones, and how are these changing? [DS 191, 203]**
- **VQ1b: How do similar ecosystems differ in size, species composition, fractional cover and biodiversity across terrestrial and shallow aquatic biomes? [DS 195]**
- **VQ1c: What is the current spatial distribution of ecosystems, functional groups, or key species within major biomes including agriculture, and how are these being altered by climate variability, human uses, and other factors? [DS 191, 203]**
- **VQ1d: What are the extent and impact of invasive species in terrestrial and shallow aquatic ecosystems? [DS 192, 194, 196, 203, 204, 214]**
- **VQ1e: What is the spatial structure and species distribution in observable phytoplankton blooms? [DS 201, 208]**
- **VQ1f: How do changes in coastal morphology and surface composition impact coastal ecosystem composition, diversity and function [DS 41]?**

VQ1a: How are ecosystems organized within different biomes associated with temperate, tropical, and boreal zones, and how are these changing? [DS 191, 203]

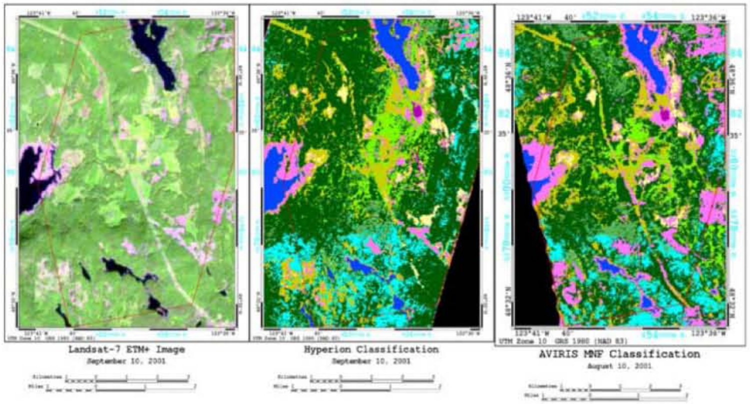

Classification of dominant plant functional types in the Pacific Northwest using Landsat, Hyperion and AVIRIS. From Goodenough et al., 2003.

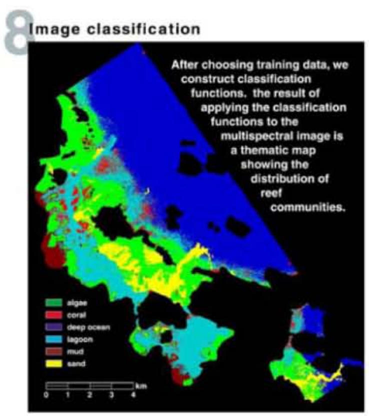

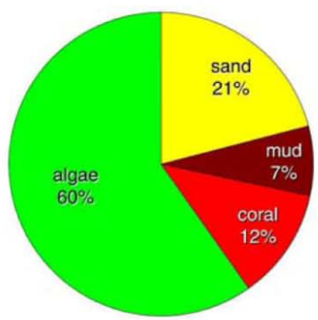

Map of the distribution of important reef communities. From Hochberg.

Science Issue:

•Ecosystems play a critical role in the cycling of water, carbon, nitrogen and nutrients and by providing critical habitats to many organisms. While our knowledge of the large scale distribution of ecosystems is good, knowledge of their distributions at finer scales is generally poorer. Furthermore, the rate at which they are changing in response to multiple stressors, including anthropogenic disturbance and climate change is insufficient.

•Tools:

•Satellite observations from HyspIRI. Requires fine spectral sampling (~ 10 nm) from the ultra-violet to Short-Wave-Infrared (380-2500 nm) to discriminate functional types and species in terrestrial and aquatic ecosystems, correct for atmospheric impacts and retrieve bi-directional reflectance. Requires high signal to noise for aquatic systems (300:1 at 45Z, 0.01 reflectance target) and fine spatial resolution (at least 60 m) to map uniform patches in the landscape. Requires high frequency repeat sampling (19 days) to provide a minimum of one acquisition per season globally and improve discrimination of species through phenology.

•Requires radiometric stability for multi-year monitoring.

•Requires supplemental spectral libraries to inform mapping.

•Approach:

•Retrieve bi-directional reflectance and surface spectral radiance using atmospheric radiative transfer

•Develop seasonal compositing approaches to generate a seamless global product for terrestrial systems and coastal waters.

•Apply standard and developed classification algorithms for mapping ecosystems in terrestrial and coastal aquatic or inland water systems.

•Utilize mixing algorithms to estimate sub-pixel fractions of ecosystems

•Link to well established calibration/validation sites for validation

•Develop products that are readily assimilated in to models.

VQ1b: How do similar ecosystems differ in size, species composition, fractional cover and biodiversity across terrestrial and aquatic biomes and on different continents? [DS 195]

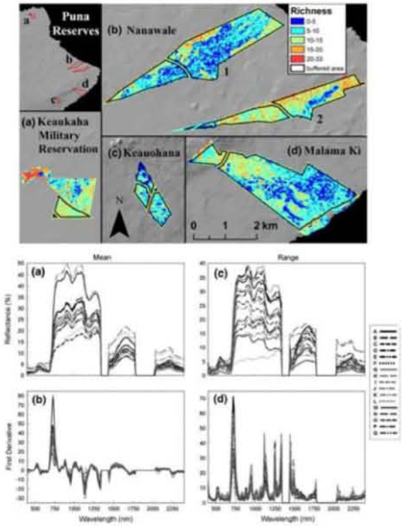

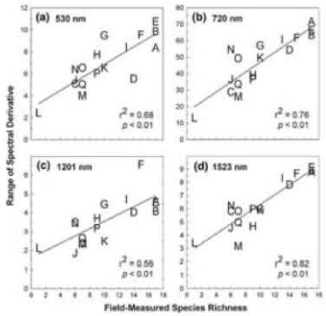

Spectral variability is directly related to canopy species diversity
From Carlson et al., 2007

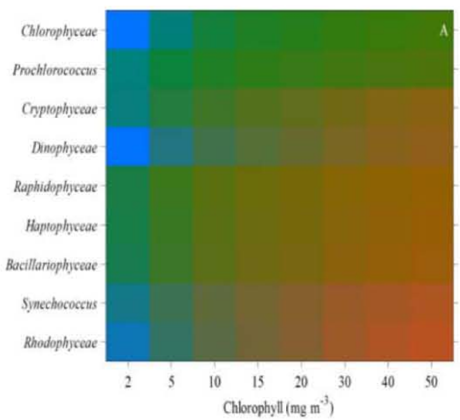

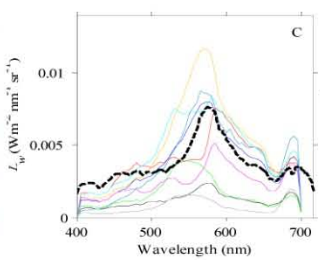

Phytoplankton functional groups can be discriminated based on spectroscopic differences due to pigments.
From Dierssen et al., 2006.

Science Issue:

•Ecosystems differ in spatial extent, biophysical properties and in the types of organisms within them. The manner in which an ecosystem responds to changing environmental conditions and disturbance is, in part, dependent upon the organisms within the ecosystem. The resilience of an ecosystem to external stressors is also dependent upon organisms within the ecosystem. Biophysical attributes, such as fractional cover, and biodiversity measures are critical elements that quantify ecosystem function and response to environmental change.

•*Tools:*

•Satellite observations from HyspIRI. Requires fine spectral sampling (~ 10 nm) from the ultra-violet to Short-Wave-Infrared (380-2500 nm) to discriminate functional types and species in terrestrial and aquatic ecosystems, correct for atmospheric impacts and retrieve bi-directional reflectance. Requires high signal to noise for aquatic systems (300:1 at 45Z, 0.01 reflectance target) and fine spatial resolution (at least 60 m) to map uniform patches in the landscape. Requires high frequency repeat sampling (~19 days) to provide at least one acquisition per season globally, with preferably multiple acquisitions within a season.
•Requires radiometric stability for multi-year monitoring.
•Requires supplemental spectral libraries to inform mapping.

•*Approach:*

•Retrieve bi-directional reflectance and surface spectral radiance using atmospheric radiative transfer
•Develop seasonal compositing approaches to generate a seamless global product for terrestrial systems and coastal waters.
•Utilize mixing algorithms to estimate sub-pixel fractions of cover, including exposed soil, photosynthetic and non-photosynthetic components
•Develop spectroscopic means for quantifying biodiversity
•Link to well established calibration/validation sites for validation

VQ2: Subquestions

- **VQ2a: How does the seasonal activity of ecosystems and functional types vary across biomes (terrestrial and aquatic), geographic zones, or environmental gradients between the equator and the poles? How are seasonal patterns of ecosystem function being affected by climate change? [DS 205, 206, 210]**
- **VQ2b: How do seasonal changes affect productivity, carbon sequestration, and hydrological processes across ecosystems and agriculture? [DS 195, 205, 210]**
- **VQ2c: How do environmental stresses affect the physiological function of water and carbon exchanges at the seasonal time scale within ecosystems (including agriculture)? [DS 203, 206, 210]**
- **VQ2d: What is the environmental impact of aquatic plants and coral in inland and coastal water environments at the seasonal time scale? [DS 201, 208]**

How do environmental stresses affect the seasonality of physiological function of water and carbon exchanges within ecosystems? [DS 203, 206, 210]

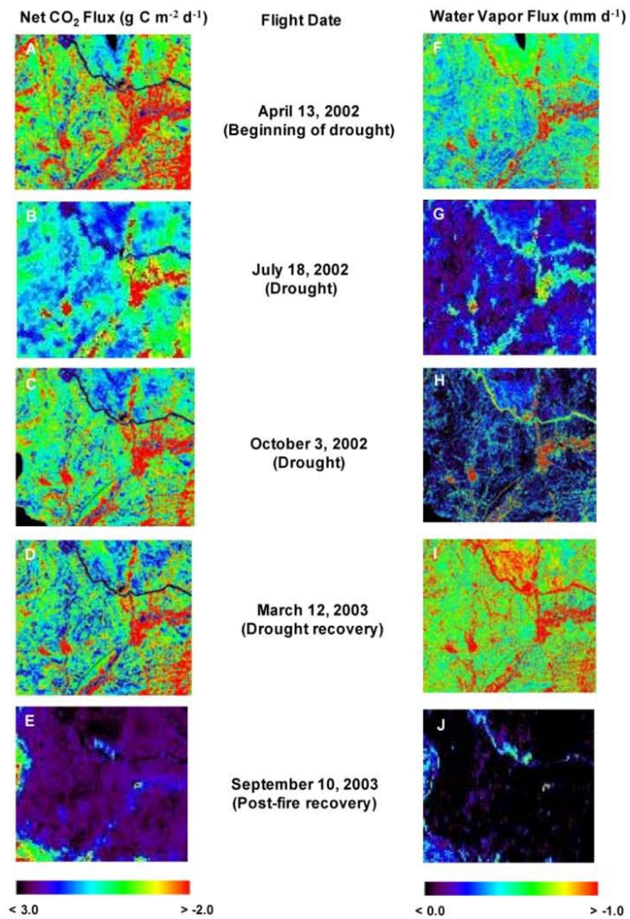

Impacts of drought and fire on carbon and water vapor fluxes (Fuentes et al. 2006)(

Science Issue:

Changing disturbance patterns (drought, fire…) alter surface-atmosphere exchanges.

Tools:

Repeat sampling in key spectral bands providing input to flux models.

Approach:

Use time series to evaluate changing biosphere-atmosphere gas exchange.

VQ3: Subquestions

- VQ3a: How do changes in climate and atmospheric processes affect the physiology and biogeochemistry of ecosystems? [DS 194, 201]
- VQ3b: What are the consequences of uses of land and coastal systems, such as urbanization and resource extraction, for the carbon cycle, hydrological cycle, nutrient fluxes and biodiversity functional composition? [DS 196, 197]
- VQ3c: What are the consequences of increasing nitrogen deposition for carbon cycling and biodiversity in terrestrial and coastal ecosystems? [DS 195, 196]
- VQ3d: How do changes in hydrology, pollutant inputs and sediment transport affect freshwater and coastal marine ecosystems? [DS 196]
- VQ3e: How do changing water balances affect carbon storage by terrestrial ecosystems? [DS 196]
- VQ3f: What are the key interactions between biogeochemical cycles and the composition and diversity of ecosystems? [195, 196]
- VQ3g: How do changes in biogeochemical processes feed back to climate and other components of the Earth system? [DS 190, 192, 195]

VQ3a: How do changes in climate and atmospheric processes affect the physiology and biogeochemistry of ecosystems? [DS 194, 201]

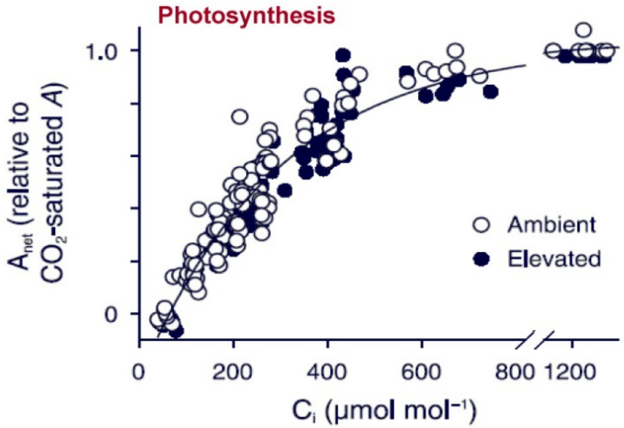

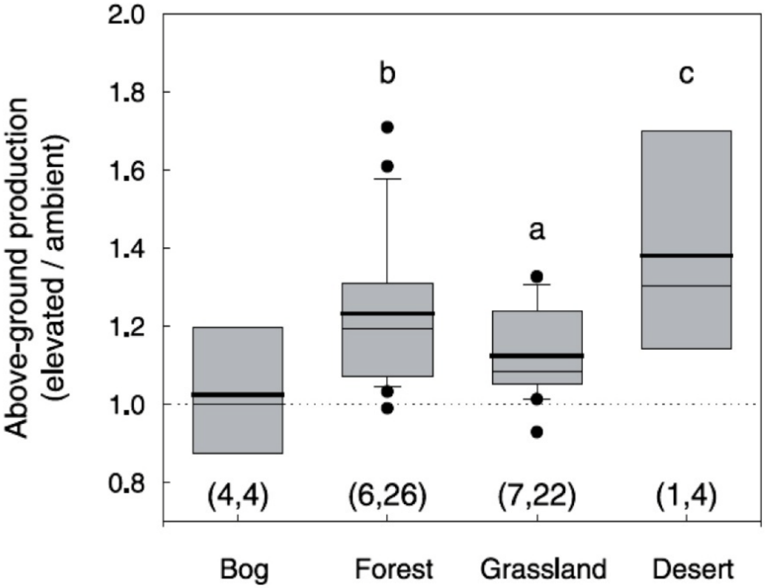

Nowack et al. 2004

Science Issue:

Changes in climate, CO2 and other atmospheric processes can influence ecosystem function through a variety of mechanisms. These include temperature and CO2-induced changes in photosynthesis, altered rates of decomposition and nutrient cycling and changes in species composition and plant tissue chemistry resulting from a combination of the above. HyspIRI will greatly enhance our ability to predict, quantify and detect changes in these factors through a combination of approaches involving the composition, seasonality and canopy chemistry of ecosystems.

Tools:

A wide variety of HyspIRI spectral bands used to along with ecosystem models and ancillary climate data.

Approach:

HyspIRI-derived estimates of physiological properties and plant functional types combined with models designed to simulate long-term effects of changing climate and CO2.

VQ3f: What are the key interactions between biogeochemical cycles and the composition and diversity of ecosystems? [195, 196]

Species Composition and Biogeochemistry: Effects of Sugar Maple on the Nitrogen Cycle

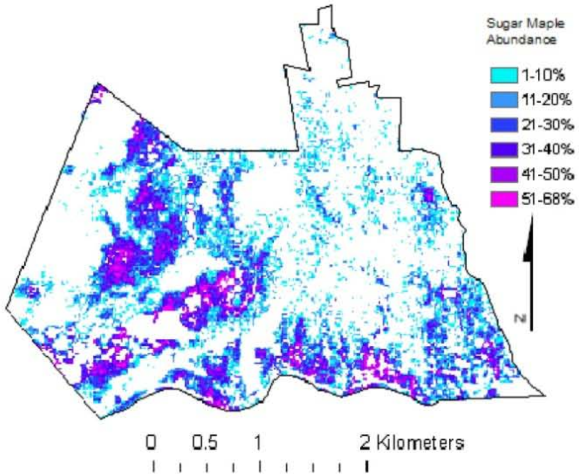

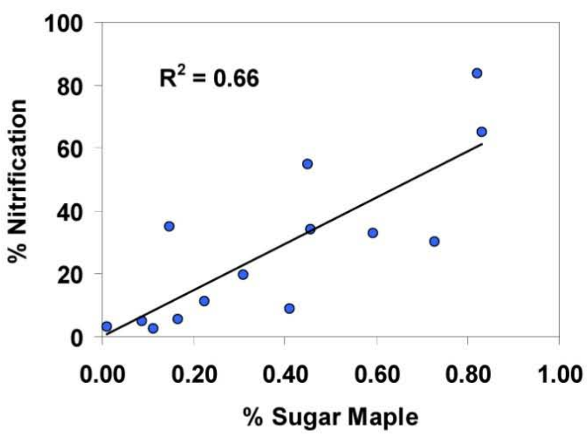

Plourde et al. 2007

Science Issue:

Because plant species and functional groups often have distinct nutrient requirements and tissue chemistries, species composition and diversity are integral components of biogeochemical cycles. Plant species distribution and abundance have become vital to studies in biogeochemistry, where there is increasing evidence that changes in health and distribution of individual tree species have implications to C and N cycling.

Tools:

•HyspIRI's VSWIR sensor data, as well as data from airborne hyperspectral sensors and multispectral satellite data, such as Landsat.

•Ecosystem models such as PnET.

Approach:

By identifying the distribution of species and functional groups, patterns in nutrient cycling can be identified and changes monitored over time. Species distribution data can also serve to better parameterize ecosystem models, resulting in improved predictions of numerous biogeochemical transformations.

VQ3g: How do changes in biogeochemical processes feed back to climate and other components of the Earth system? [DS 190, 192, 195]

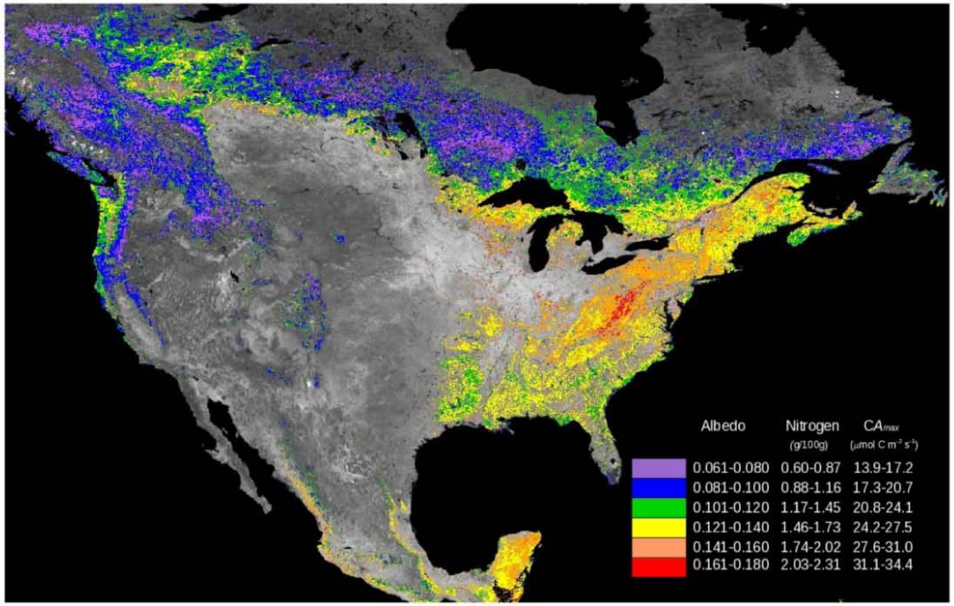

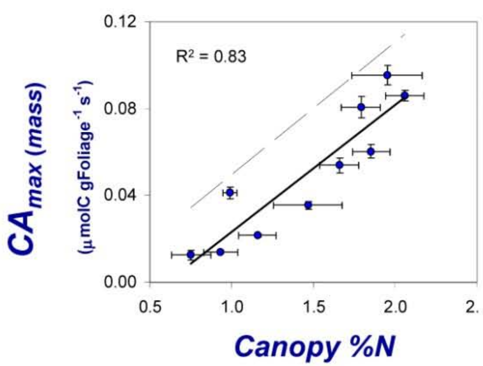

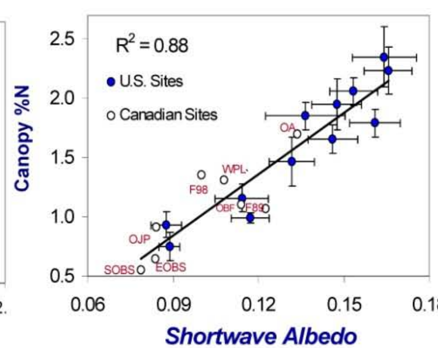

Ollinger et al. 2008

Science Issue:

Because ecosystems are an integral component of the Earth's climate system, changes in composition and biogeochemistry can have important consequences for regional and global patterns of climate. Ecosystem-climate feedbacks can take place through alterations to the carbon cycle, which influences atmospheric CO2, or through changes in vegetation surface properties such as albedo.

Tools:

The high resolution and full spectral coverage of HyspIRI's VSWIR bands allows simultaneous detection of physiological properties that control C assimilation such as the the photochemical reflectance index (PRI) and foliar %N as well as vegetation albedo and other surface properties.

Approach:

Improved detection of vegetation physiology and surface properties to **(a)** provide input for land surface-climate models and (b) provide a baseline for future change detection analyses.

VQ4: Subquestions

- **VQ4a: How do patterns of abrupt (pulse) disturbance vary and change over time within and across ecosystems?**
- **VQ4b: How do climate changes affect disturbances such as fire and insect damage? [DS 196]**
- **VQ4c: What are the interactions between invasive species and other types of disturbance?**
- **VQ4d: How are human-caused and natural disturbances changing the biodiversity composition of ecosystems, e.g.: through changes in the distribution and abundance of organisms, communities, and ecosystems?**
- **VQ4e: How do climate change, pollution and disturbance augment the vulnerability of ecosystems to invasive species? [DS 114,196]**
- **VQ4f: What are the effects of disturbances on productivity, water resources, and other ecosystem functions and services? [DS 196]**
- **VQ4g: How do changes in human uses of ecosystems affect their vulnerability to disturbance and extreme events? [DS 196]**

VQ4a: How do patterns of abrupt (pulse) disturbance vary and change over time within and across ecosystems?

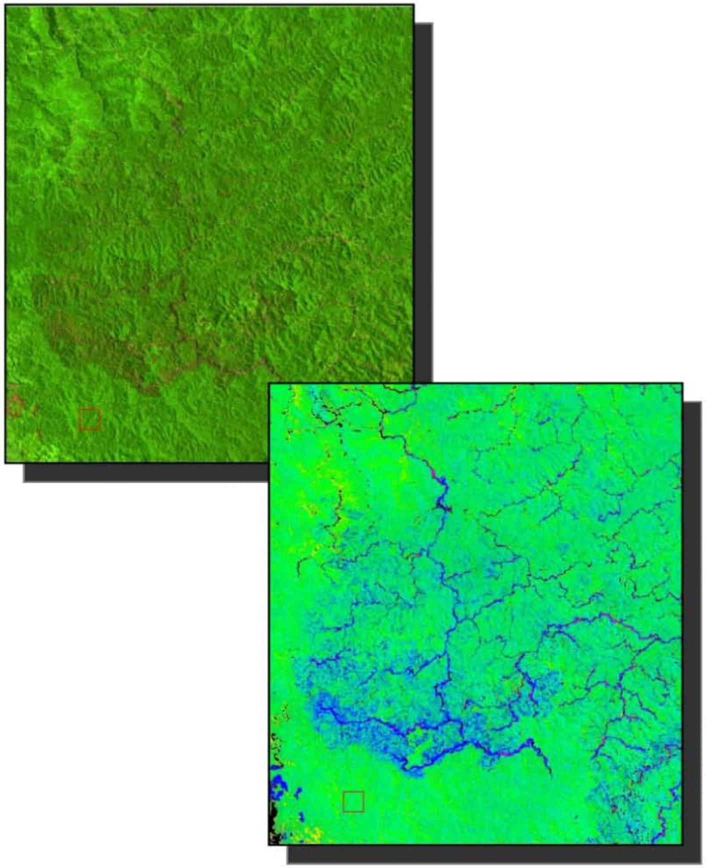

Hyperion's spectral measurements from the NASA EO-1 technology demonstration mission reveal rainforest disturbance caused by logging and fire.

Science Issue:

Natural and human-driven disturbances are not rare occurrences in ecosystems; they are the norm. Disturbances such as storms, mud slides, water spouts, fire and insect outbreaks shape ecosystems and the flow of materials between terrestrial and aquatic realms, yet it remains difficult to resolve the responses of ecosystems to these and many other types of disturbance. Biophysical and chemical attributes of ecosystems change with and respond to disturbance, thus large-scale measurements of key parameters such as fractional material cover, nutrients and water properties can reveal changing disturbance patterns over time.

Tools :

Spectral measurements from HyspIRI covering the 400 to 2500 nm wavelength range at 10 nm intervals (terrestrial); 380 to 900 nm at 10nm intervals (aquatic)

- 95% spectral cal uniformity
- SNR 600 VNIR, 300 SWIR (23.5ZA 0.25R)
- 14 bit precision: >95% abs cal: > 98% on-orbit stability
- no saturation of ecosystem targets
- < 2% polarization sensitivity 380 to 700 nm
- > 99% linearity 2 to 98% saturation
- ≤ 60 m spatial sampling
- ≥ 95% spectral IFOV uniformity
- < 20 day revisit to minimize cloud obscuration

Approach:

- Measure the spectral properties of ecosystems over time.
- Use spectral signature-based algorithms and modeling approaches to convert spectra to structural and chemical properties of ecosystems.
- Accurate atmospheric characterization and correction is a critical enable requirement.

VQ4c: What are the interactions between invasive species and other types of disturbance?

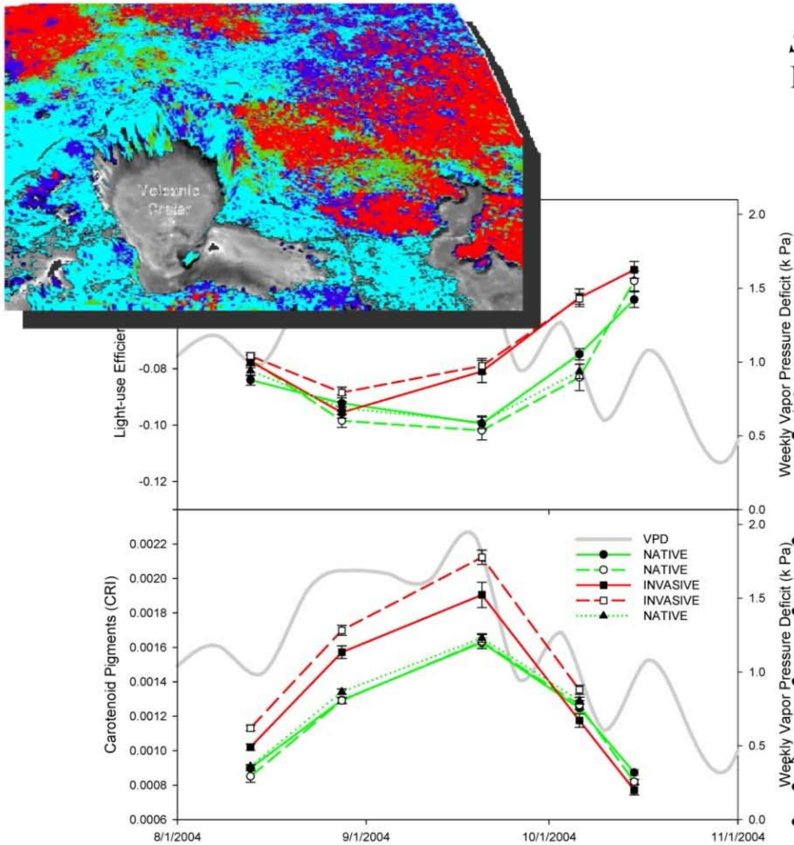

Combining NASA AVIRIS (top) and multi-temporal Hyperion (graphs) revealed that invasive trees (red lines) out-grow native trees (green lines) during periods of climate stress (gray line)

Science Issue:

Invasive species are both a cause and consequence of ecological disturbance. Climate change, air and water pollution, and physical disturbance can alter the vulnerability of ecosystems to the introduction and proliferation of invasive species. Spatially extensive, multi-temporal information is required to quantify, track and understand how human activities change the distribution of invasive species at regional and global scales.

Tools :

- Multi-temporal measurements from HyspIRI covering the 400 to 2500 nm wavelength range at 10 nm intervals (terrestrial); 380 to 900 nm at 10nm intervals (aquatic)
- Ground network and atmospheric measurements of climate variables, pollutant concentrations, winds, etc.
- Spectral libraries of plant functional types and key invasive species
- Regional (mesoscale) climate models

Approach:

- Measure the spectral properties of ecosystems over time.
- Use spectral signature-based algorithms and modeling approaches to convert spectra to plant functional types (often species) and spectral-biochemical metrics of vegetation growth and mortality.
- Combine data derived from HyspIRI with data from climate sensors, ground observation networks, and models.

VQ5: Subquestions

- **VQ5a: How do changes in ecosystem composition and function affect the spread of infectious diseases and the organisms that transmit them[DS155, 160, 161]? For Example, tracking malaria by water fraction, Hantavirus**
- **VQ5b: How will changes in pollution and biogeochemical cycling alter coastal and inland water quality?**
- **VQ5c: How are changes in ecosystem distribution and productivity linked to resource use, and resource management? Forestry management, fire effects, biofuels, agricultural management**
- **VQ5d: How will changes in climate and pollution affect the health and productivity of aquatic and agricultural resources?**
- **VQ5e: What are the economic and human health consequences associated with the spread of invasive species?**
- **VQ5f: How does the spatial pattern of policy, environmental management, and economic conditions correlate with the state and changes in ecosystem function and composition? (DS 155 [5-5]?, 230 [8-7])**
- **VQ5g: What are the impacts of flooding and sea-level rise on ecosystems, human health, and security? [DS 195, 224, 227, 348, 357]**

VQ5b: How will changes in pollution and biogeochemical cycling alter coastal and inland water quality?

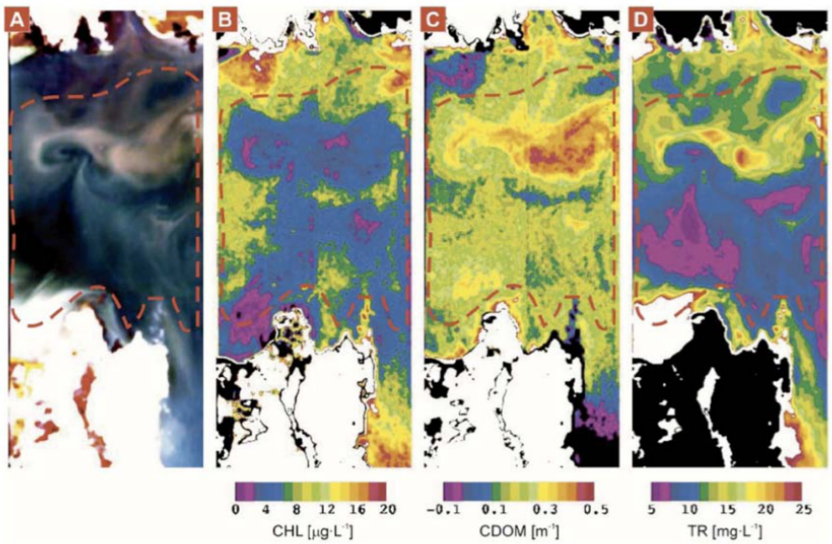

(a) Image derived from filtered Hyperion scene over Deception Bay and processed to estimate concentrations of (b) Chlorophyll, (c) Chromophoric Dissolved Organic Material (CDOM), and (d) tripton (TR). The dashed red line delimits the clear-sky, optically deep water pixels in this scene.

- Science Issue
  - Characterize conditions associated with microorganisms as well as suspended inorganic materials in areas at water/land interface
- Tools
  - Contiguous spectral measurement from 400 to 2500 nm at 10 nm spatial sampling at 60 m with high signal-to-noise ratio and with excellent spectral and IFOV uniformity.
- Approach
  - Measure and monitor
    - Chlorophyll concentration (related to eutrophication)
    - CDOM
    - Particulate matter
    - Harmful algae blooms
  - Ability to capture seasonal variations is critical

VQ6: Subquestions

- **VQ6a: What is the distribution of the primary minerals and mineral groups on the exposed terrestrial surface? [DS 218]**
- **VQ6b: What is the bottom composition (sand, rock, mud, coral, algae, SAV, etc) of the shallow water regions of the Earth?**
- **VQ6c: What fundamentally new concepts for mineral and hydrocarbon research will arise from uniform and detailed global geochemistry of the exposed rock/soil surface [DS227]**
- **VQ6d: What changes in bottom substrate occur in shallow coastal and inland aquatic environments? [DS 25]**
- **VQ6e: How can measurements of rock and soil composition be used to understand and mitigate hazards? [DS 114,227]**

VQ6a: What is the distribution of the primary minerals and mineral groups on the exposed terrestrial surface? [DS 218]

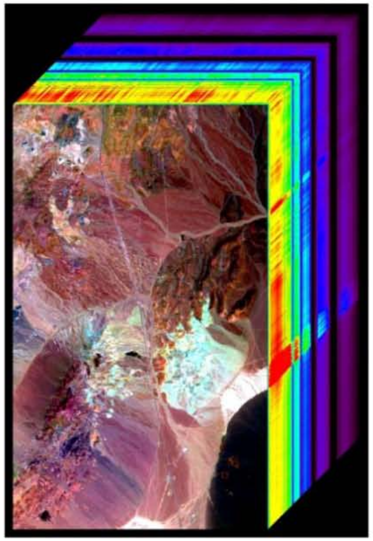

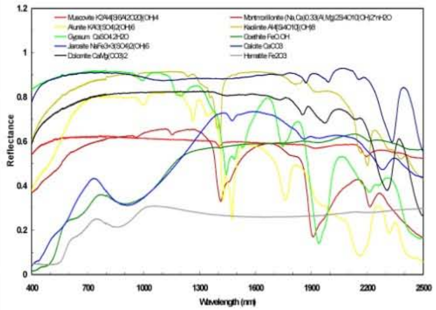

Left: Imaging spectrometer measurements of exposed rock and soil. Above: Spectral signatures of select rock and soil forming minerals.

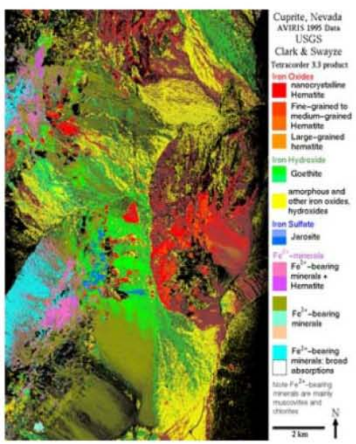

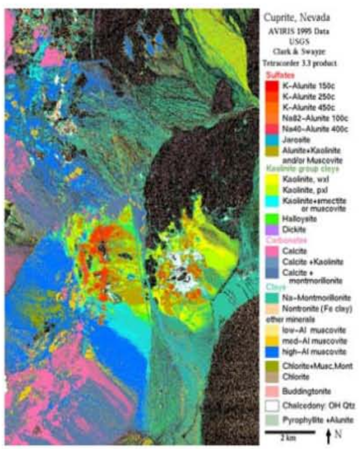

Above left and right: Spectroscopically derived maps of minerals in the 400 to 1500 nm and 1500 to 2500 nm spectral regions.

•

cience Issue

–

he composition and distribution of the exposed rock and soil substrate of the terrestrial surface is not accurately known globally. Surface rock and soil composition is closely linked to an understanding of resources, hazards and is a major critical element of the Earth system.

•

ools

–

ontiguous spectral measurement from 400 to 2500 nm at 10 nm spatial sampling at 60 m with high signal-to-noise ratio and with excellent spectral and IFOV uniformity.

•

pproach

–

easure the exposed surface rock and soil compostions globally.

–

easure the available rock forming and

VQ6b: What is the bottom composition (sand, rock, mud, coral, algae, SAV, etc) of the shallow water regions of the Earth?

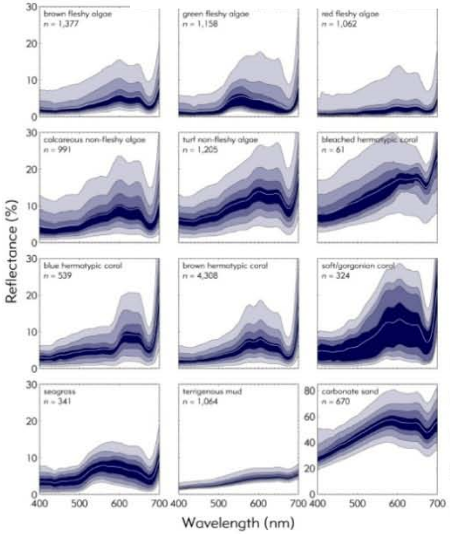

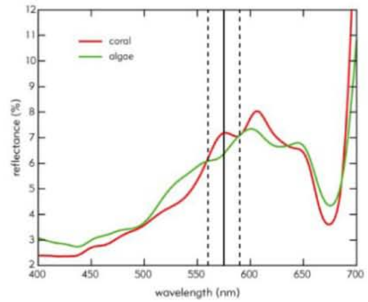

Left: In situ spectral measurements of benthic materials. Above: Example spectral descrimination of algae and coral .

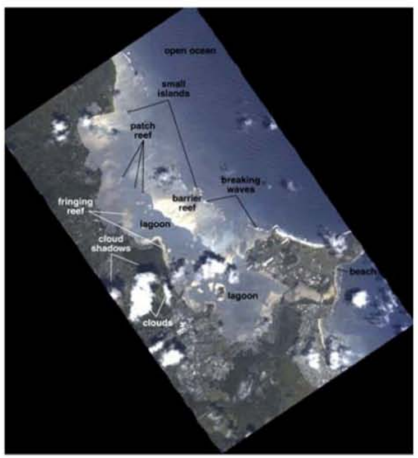

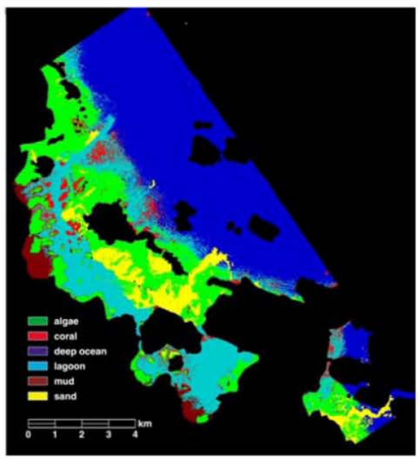

Above left: Imaging spectrometer measurements of Kaneoe Bay, Hawaii. Right: Shallow water bottom composition derived from spectral measurements

•

cience Issue

–

he composition, distribution and seasonal variability of the materials in the observable shallow water coastal regions are poorly understood globally. The habits and resources of the coastal zone is close tied to the composition and structure of the substrate.

•

ools

–

easonal measurement of the contiguous spectral signature from 400 to 800 nm at 10 nm spatial sampling at 60 m with high signal-to-noise ratio and with excellent spectral and IFOV uniformity.

•

pproach

–

easure the optically available spectral signature of the coastal zone globally through several seasons

–

se spectral signature based algorithms and forward inversion approach to measure and

Climate Relevance

- Climate plays the central role in controlling the distribution of organisms and their function and plays a major role in weathering, soils and biogeochemical inputs
- Climate-surface feedbacks represent some of the greatest uncertainties in our knowledge of the consequences and drivers of climate change
  - Biospheric feedbacks
  - Ice-albedo feedbacks
- Improved compositional and biogeochemical mapping and physiological monitoring is critical to establish a baseline for global ecosystems and quantify change in response to climate variability
  - HyspIRI provides the most comprehensive set of measurements to quantify these
    - HyspIRI VSWIR will measure and return data for the entire terrestrial surface every 19 days
      - Other planned missions return 1-2%
    - HyspIRI is a third generation, high fidelity heritage instrument with very high SNR and uniformity

Questions?

HyspIRI

TIR Science Questions

Presented by: Anupma Prakash

Contributors:

Michael Abrams; Friedemann Freund; Vince Realmuto; Rob Wright; Lyle Mars; Louis Giglio; Martha Anderson; Richard Allen; James Irons, Dale Quattrochi; Gregory Glass; Jim Crowley; Simon Hook; Fred Kruse; Ivan Csiszar; Rob Green.

TIR Measurements

Spectral	
Bands (8) µm	3.98 µm, 7.35 µm, 8.28 µm, 8.63 µm, 9.07 µm, 10.53 µm, 11.33 µm, 12.05
Bandwidth	0.084 µm, 0.32 µm, 0.34 µm, 0.35 µm, 0.36 µm, 0.54 µm, 0.54 µm, 0.52 µm
Accuracy	<0.01 µm
Radiometric	
Range	Bands 2-8= 200K – 400K; Band 1= 1400K
Resolution	< 0.05 K, Linear Quantization to 14 bits
Accuracy	< 0.5 K 3-sigma at 250K
Precision (NEdT)	< 0.2K
Linearity	>99% characterized to 0.1 %
Spatial	
IFOV	60 m
MTF	>0.65 at FNy
Scan Type	Push-Whisk
Swath Width	600 km (±25.5° at 623 km altitude)
Cross-Track Samples	10,000
Swath Length	15.4 km (+/- 0.7-degrees at 623km altitude)
Down-Track Samples	256
Band-to-Band Co-registraion	0.2 pixels (12 m)
Pointing Knowledge	1.5 arcsec (0.1 pixels)

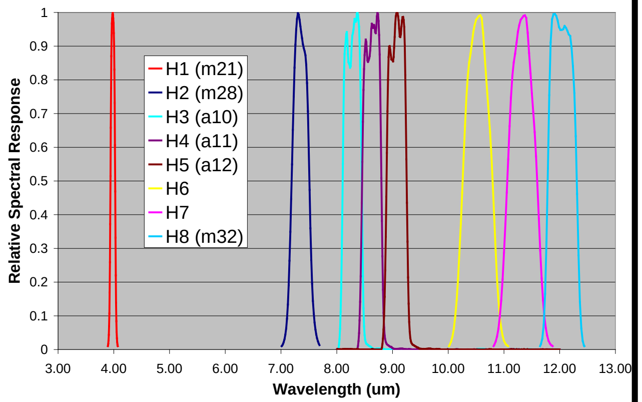

TIR Measurements

Temporal	
Orbit Crossing	11 am sun synchronous descending
Global Land Repeat	5 days at equator
OnOrbit Calibration	
Lunar View	1 per month {radiometric}
Blackbody Views	1 per scan {radiometric}
Deep Space Views	1 per scan {radiometric}
Surface Cal Experiments	2 (d/n) every 5 days {radiometric}
Spectral Surface Cal Experiments	1 per year
Data Collection	
Time Coverage	Day and Night
Land Coverage	Land surface above sea level
Water Coverage	Coastal zone -50 m and shallower
Open Ocean	Averaged to 1km spatial sampling
Compression	2:1 lossless

HyspIRI thermal measurements provide critical information on land surface temperature, which is a fundamental climate variable

HyspIRI measurements will:

- **produce fundamental climate temperature variables**
- **essential societal information on thermal phenomena**

Critical thermal information provided by HyspIRI includes:

- **The burning temperatures of fires**
- **The temperatures of cities**
- **Thermal stress and evapotranspiration of natural vegetation and croplands**
- **The temperature and evaporative rates of small inland water bodies**

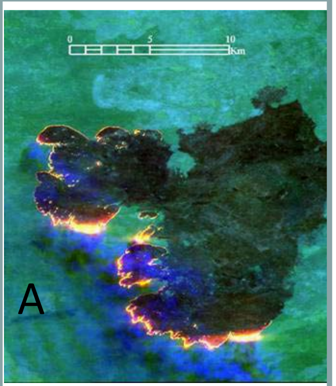

The narrow fire front, determines the temperature and carbon emission rate of fires

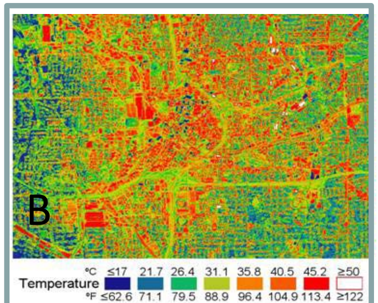

Heat island effect of cities: High resolution thermal image of downtown Atlanta,

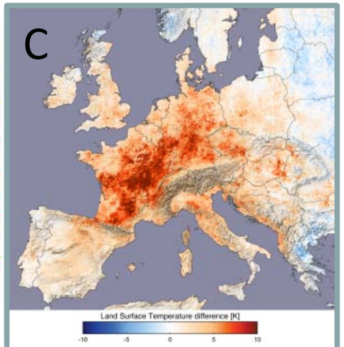

2003 European heatwave compared to 2000, 2001, 2002, 2004 (IPCC 2007c)

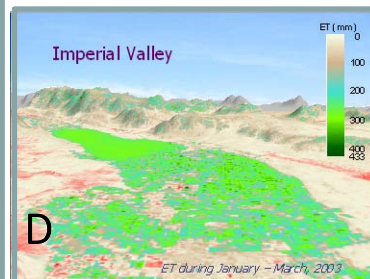

Managing water resources: evapotranspiration in the Imperial Valley, California

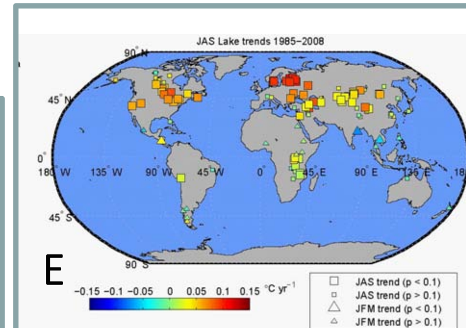

Increase in summer temperatures of large inland water bodies show warming in the northern latitudes

HyspIRI multispectral thermal measurements provide < 5 day daytime and nighttime mapping of land surface temperature, a fundamental climate variable, at high resolutions (60 m).

TIR Overarching Science Questions

- **TQ1. Volcanoes/Earthquakes (MA,FF)**
  - How can we help predict and mitigate earthquake and volcanic hazards through detection of transient thermal phenomena?
- **TQ2. Wildfires (LG,DR)**
  - What is the impact of global biomass burning on the terrestrial biosphere and atmosphere, and how is this impact changing over time?
- **TQ3. Water Use and Availability, (MA,RA)**
  - How is consumptive use of global freshwater supplies responding to changes in climate and demand, and what are the implications for sustainable management of water resources?
- **TQ4. Urbanization/Human Health, (DQ,GG)**
  - How does urbanization affect the local, regional and global environment? Can we characterize this effect to help mitigate its impact on human health and welfare?
- **TQ5. Earth surface composition and change, (AP,JC)**
  - What is the composition and temperature of the exposed surface of the Earth? How do these factors change over time and affect land use and habitability?

TQ1: Volcanoes and Earthquakes (MA,FF)

- Do volcanoes signal impending eruptions through changes in surface temperature or gas emission rates and are such changes unique to specific types of eruptions? [DS 227]
- What do changes in the rate of lava effusion tell us about the maximum lengths that lava flows can attain, and the likely duration of lava flow-forming eruptions? [DS 226]
- What are the characteristic dispersal patterns and residence times for volcanic ash clouds and how long do such clouds remain a threat to aviation? [DS 224]
- What do the transient thermal anomalies that may precede earthquakes tell us about changes in the geophysical properties of the crust? [DS 227, 229]
- Can the energy released by the periodic recharge of magma chambers be used to predict future eruptions? [DS 227]

TQ1: Volcanoes and Earthquakes

What do changes in the rate of lava effusion tell us about the maximum lengths that lava flows can attain, and the likely duration of lava flow-forming eruptions? [DS 226]

Mount Etna, Sicily
ATSR, 3 January 1992

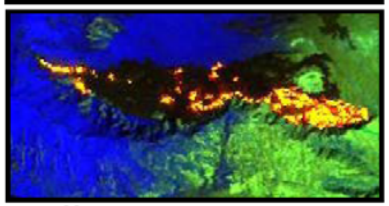

Mount Etna, Sicily
Landsat TM, 22 March 1992

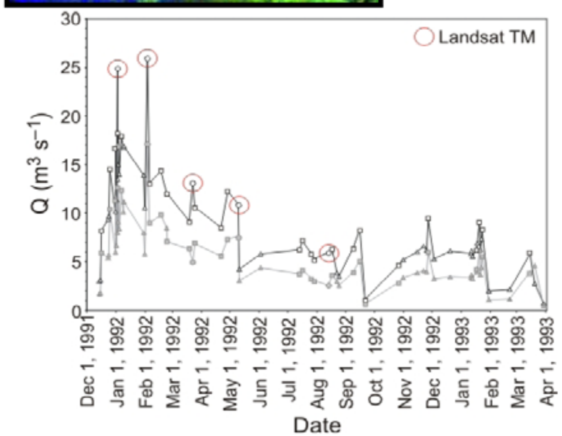

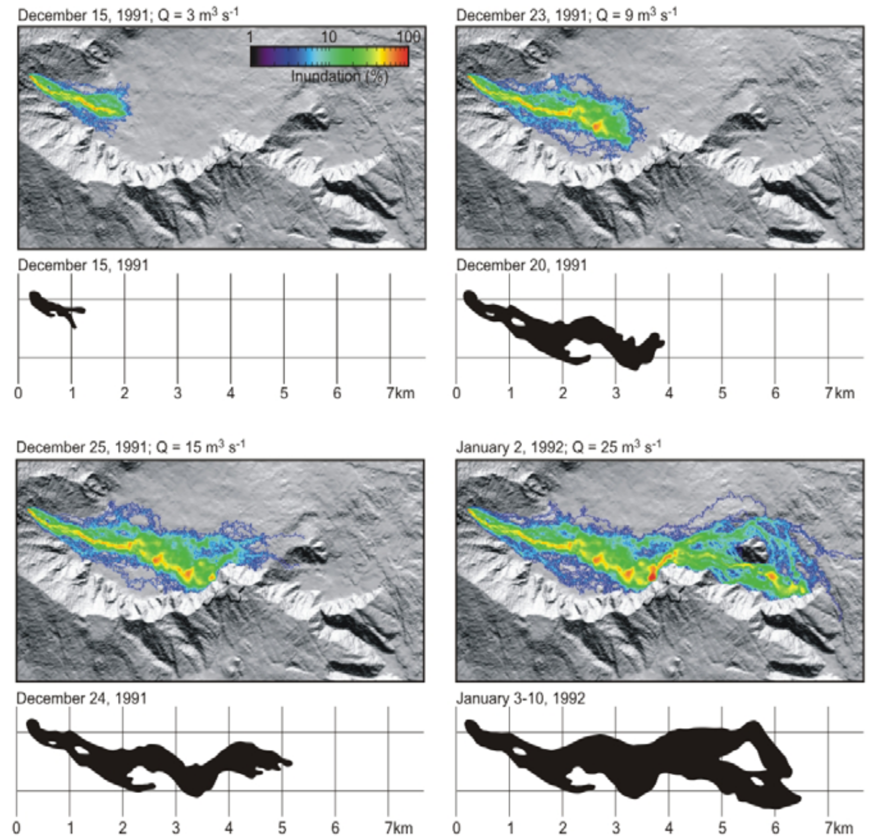

1. The length a lava flow can attain is governed by the effusion rate
2. The thermally active flow area as a function of time is proportional to the effusion rate
3. HyspIRI will allow us to determine the effusion rate twice in each 5 day period

TQ1: Volcanoes and Earthquakes

What do the transient thermal infrared anomalies that may precede earthquakes tell us about changes in the geophysical properties of the crust

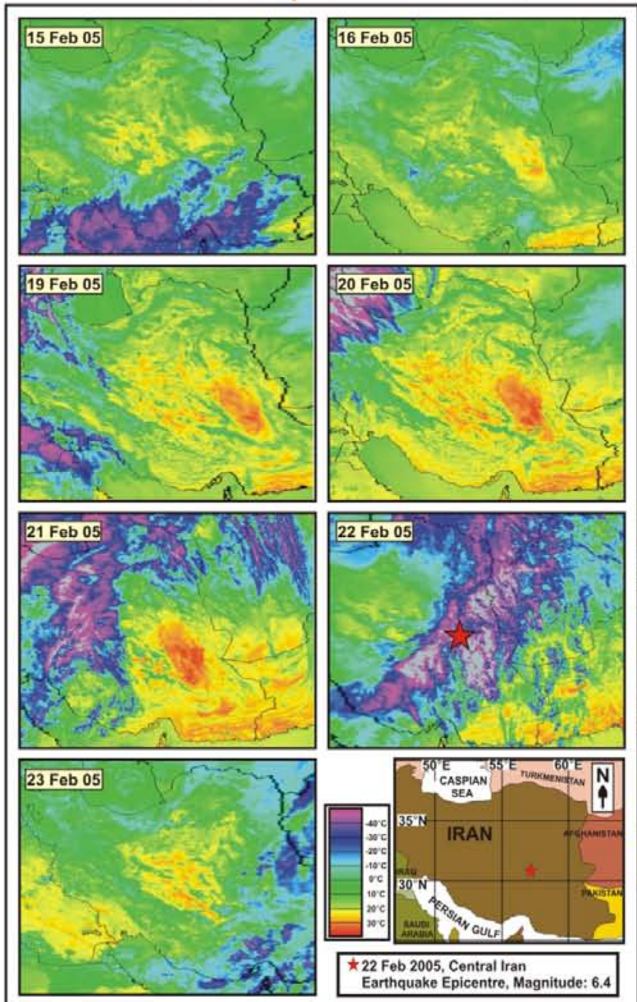

M=6.4 earthquake
in Iran 22 Feb. 2005
Good viewing conditions

IR Emission comes from region of maximum uplift/subsidence

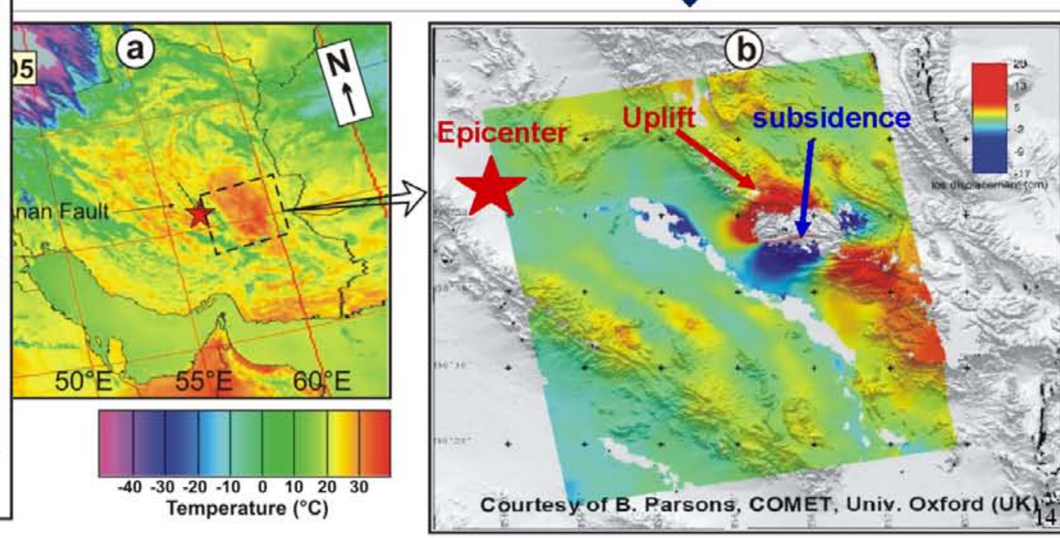

TQ2: Wildfires (LG)

- How are global fire regimes changing in response to, and driven by, changing climate, vegetation, and land use practices? [DS 198]
- Is regional and local scale fire frequency changing? [DS 196]
- What is the role of fire in global biogeochemical cycling, particularly trace gas emissions? [DS 195]
- Are there regional feedbacks between fire and climate change?

TQ2a: How are global fire regimes (fire location, type, frequency, and intensity) changing in response to changing climate and land use practices? [DS 198]

MODIS active fire detections 2000-2006 for Southern California

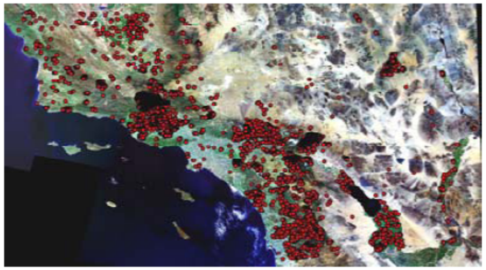

2001-2004 mean annual burned area derived from Terra MODIS active fire observations (top) and accompanying one-sigma uncertainties (bottom), expressed as fraction of grid cell that burns each year. From Giglio et al. (2005), *Atmos. Chem. Phys. Discuss.*, 5, 11091-11141

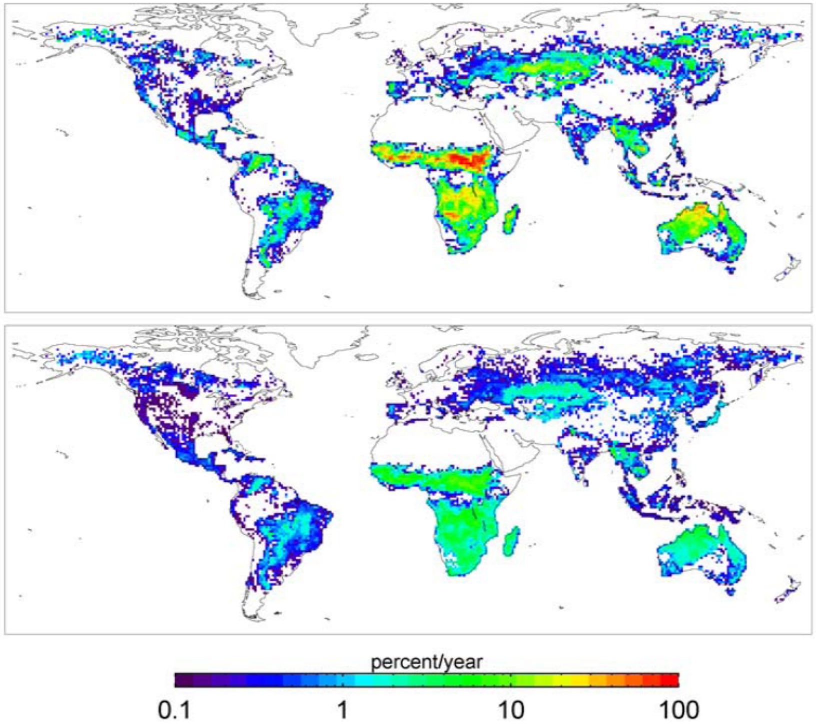

- Science issue
  Fire regimes vary considerably on a regional and global scale. Mapping fire location, type, frequency, and intensity at different times can contribute to an understanding of how they are affected by a changing climate and land use patterns.

- Tools
  Requires long-term regional or global data sets of thermal infrared imagery (low and normal gain channels at 4 and 11 µm). HyspIRI TIR data has a significantly improved capability of mapping flaming and smoldering fires. HyspIRIs greatly expanded spatial and temporal coverage can provide large sample sizes. Requires further pre-fire and post-fire thematic maps of climate variables and land use.

- Approach
  The HyspIRI thermal infrared data will provide large samples of detailed fire characteristics that are useful for statistical modeling of fires and their behavior. The database of fire detections can be analyzed in conjunction with thematic data sets of climate and land use.

Fire Regimes and Climate

GEOPHYSICAL RESEARCH LETTERS, VOL. 33, L09703, doi:10.1029/2006GL025677, 2006

Recent changes in the fire regime across the North American boreal region—Spatial and temporal patterns of burning across Canada and Alaska

Eric S. Kasischke[1] and Merritt R. Turetsky[2]

Received 16 January 2005; accepted 29 March 2006; published 3 May 2006.

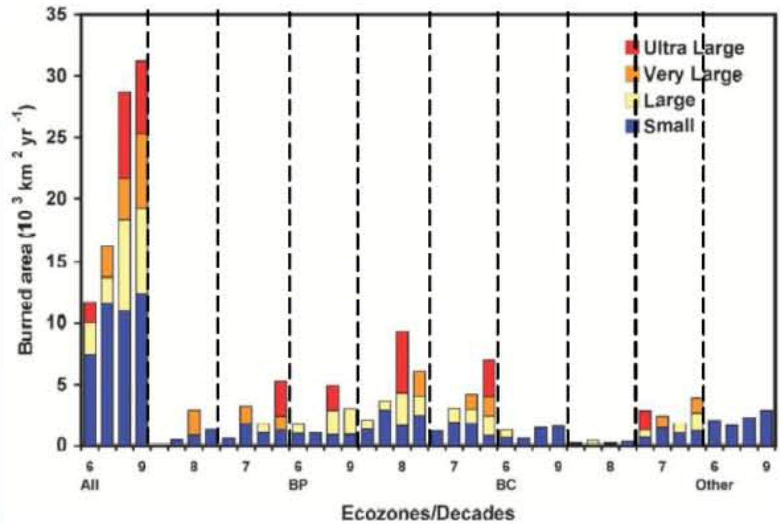

Figure 1. Decadal patterns in burned area across the NABR and in individual ecozones (on the x-axis, 6 = 1960s, 7 = 1970s, etc.; see Table 2 for the key to the ecozones).

Doubling of Annual Burned Area and increase in frequency of large fire events

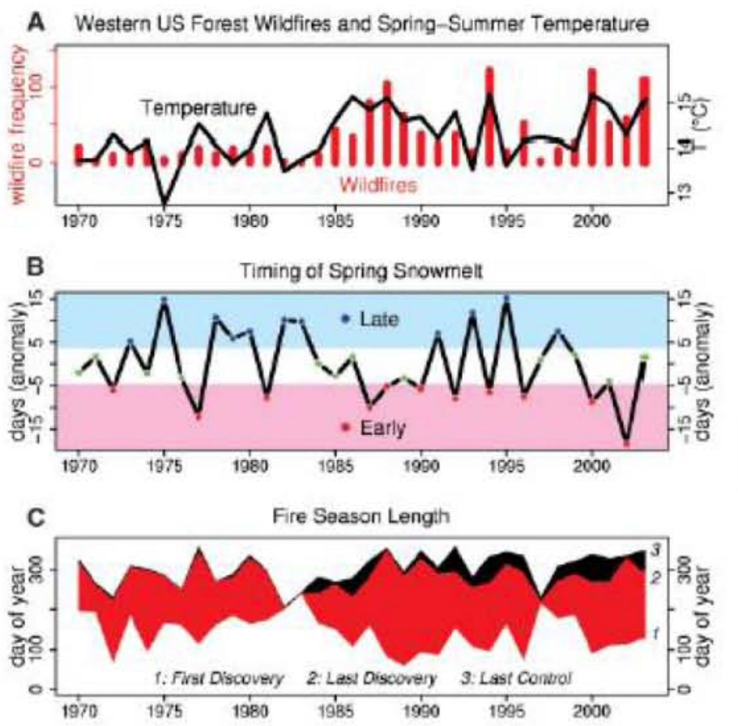

18 AUGUST 2006 VOL 313 SCIENCE www.sciencemag.org

Warming and Earlier Spring Increase Western U.S. Forest Wildfire Activity

A. L. Westerling,[1,2*] H. G. Hidalgo,[1] D. R. Cayan,[1,3] T. W. Swetnam[4]

TQ3: Water Use and Availability (MA,RA)

- How is climate variability (and ENSO) impacting the evaporative component of the global water cycle over natural and managed landscapes? [DS 166, 196, 203, 257, 368]
- What are relationships between spatial and temporal variation in evapotranspiration and land-use/land-cover and freshwater resource management? [DS 196, 203, 368]
- Can we improve early detection, mitigation, and impact assessment of droughts at local to regional scales anywhere on the globe? [DS 166, 196, 203, 368]; How does the partitioning of Precipitation into ET, surface runoff and ground-water recharge change during drought?
- What areas of Earth have water consumption by irrigated agriculture that is out of balance with sustainable water availability? [DS 196, 368]
- Can we increase food production in water-scarce agricultural regions while improving or sustaining quality and quantity of water for ecosystem function and other human uses? [DS 196, 368]

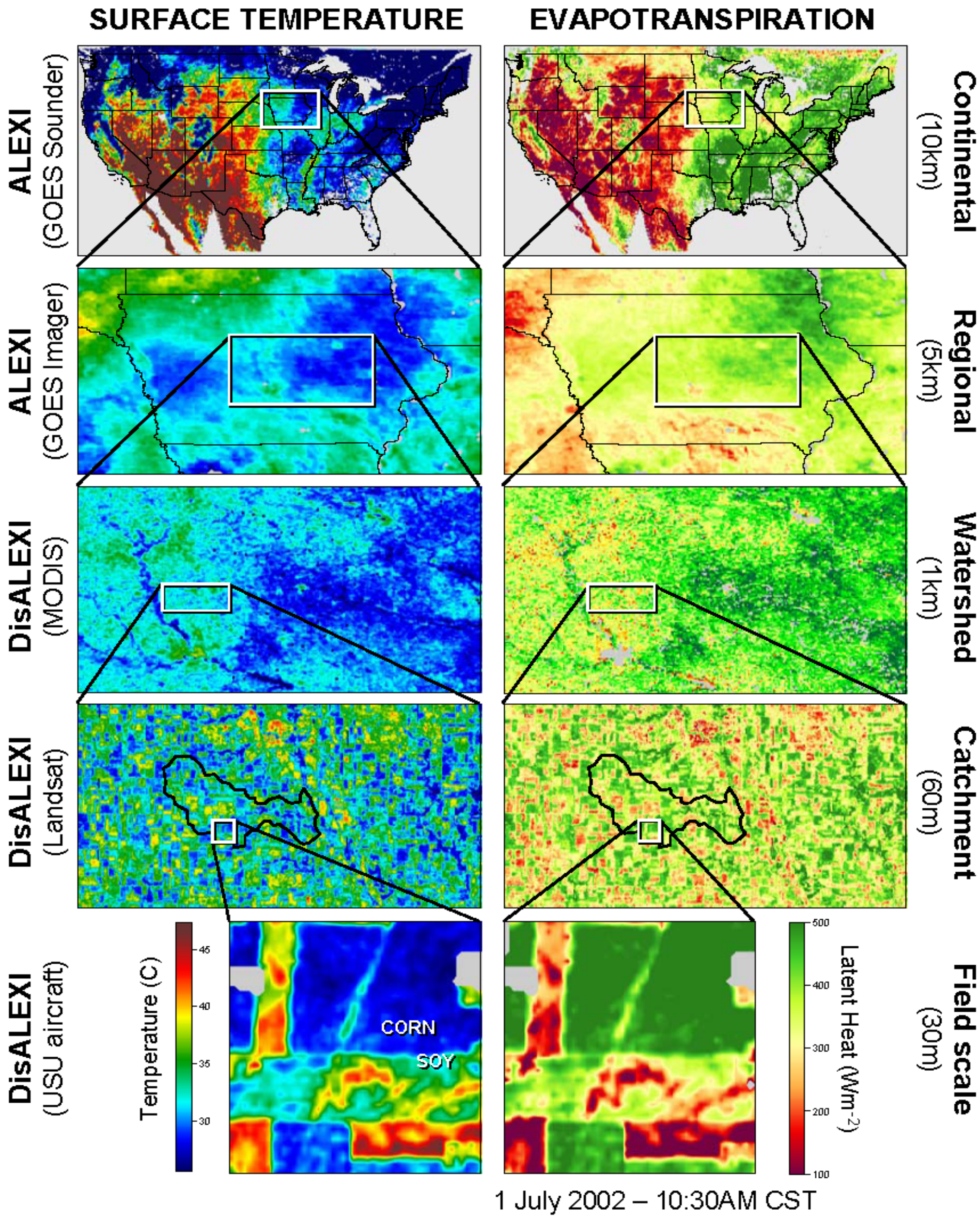
SURFACE TEMPERATURE
EVAPOTRANSPIRATION
ALEXI
(GOES Sounder)
Continental
(10km)
ALEXI
(GOES Imager)
Regional
(5km)
DisALEXI
(MODIS)
Watershed
(1km)
DisALEXI
(Landsat)
Catchment
(60m)
DisALEXI
(USU aircraft)
Temperature (C)
45
40
35
30
CORN
SOY
500
400
300
200
100
Latent Heat (Wm-2)
Field scale
(30m)
1 July 2002 – 10:30AM CST

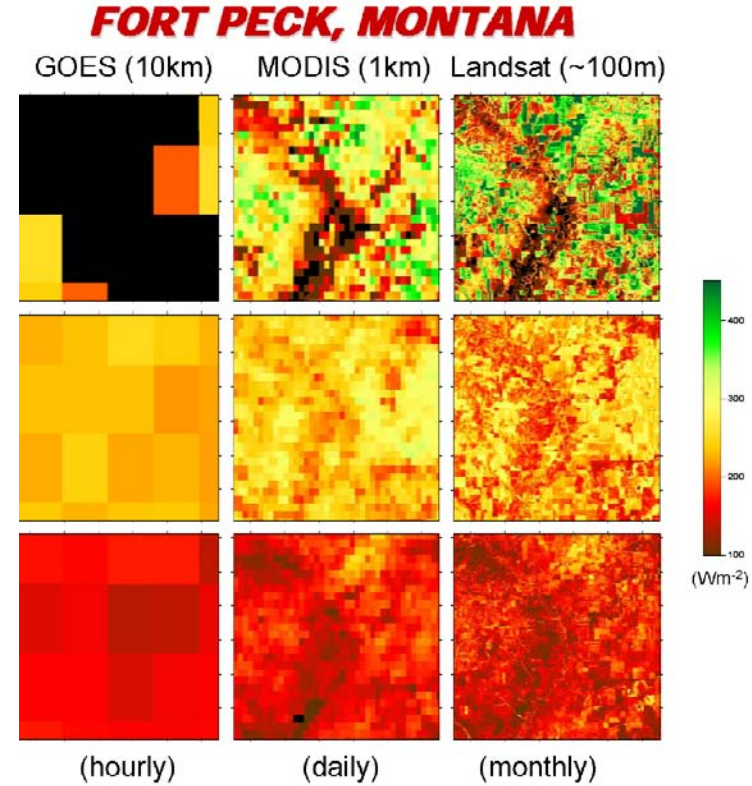
FORT PECK, MONTANA
GOES (10km)
MODIS (1km)
Landsat (~100m)
400
300
200
100
(Wm-2)
(hourly)
(daily)
(monthly)

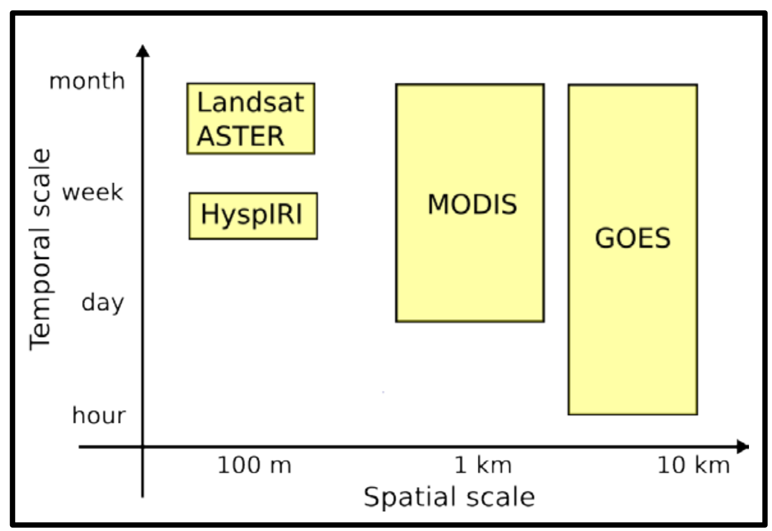
month
week
day
hour
Temporal scale
Landsat
ASTER
HyspIRI
MODIS
GOES
100 m
1 km
10 km
Spatial scale

TQ4: Human Health and Urbanization (DQ,GG)

- How do changes in local and regional land cover and land use, in particular urbanization affect surface energy balance characteristics that impact human welfare [DS: 160-161, 166-167, 196, 198]
- What are the dynamics, magnitude, and spatial form of the urban heat island effect (UHI), how does it change from city to city, what are its temporal, diurnal, and nocturnal characteristics, and what are the regional impacts of the UHI on biophysical, climatic, and environmental processes? [DS: 158, 166-168]
- How can the factors influencing heat stress on humans be better resolved and measured. [DS: 156, 158, 160, 183-184]
- How can the characteristics associated with environmentally related health effects, that affect vector-borne and animal-borne diseases, be better resolved and measured? [DS: 156, 158, 160, 183-184]
- How do horizontal and temporal scales of variation in heat flux and mixing relate to human health, human ecosystems, and urbanization? [DS: 156, 160-161, 166-167, 179,184]

TQ4b: What are the dynamics, magnitude, and spatial form of the urban heat island effect (UHI), how does it change from city to city, what are its temporal, diurnal, and nocturnal characteristics, and what are the regional impacts of the UHI on biophysical, climatic, and environmental processes? (DS 158, 166-168)

Landsat ETM+ images of the Atlanta, Georgia metropolitan area and elevated surface temperatures related to urbanization

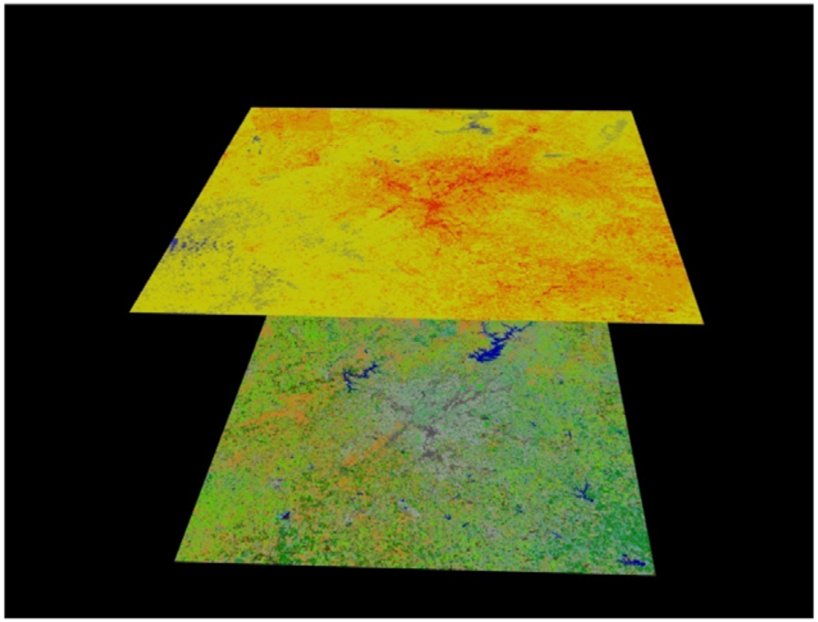

The Atlanta urbanized area is shown in gray on the bottom image. The top image shows increased surface temperatures for the corresponding urbanized area as derived from the Landsat thermal band

Science Issue:

•The UHI is a well-known effect, but there are inadequate measurements of its diurnal, temporal, and nocturnal characteristics as they vary from city to city around the globe. HyspIRI measurements can be used to collect more in-depth data on the UHI and help assess what its impacts are on biophysical, climatic, and environmental processes for urban areas around the world.

Tools:

•Satellite observations for measurement of urban surface temperature spatial extent for different sizes of cities and in different geographic and climatic domains around the globe

•Daytime and nighttime satellite thermal measurement of urban surface to assess fluxes attributable to the UHI

•Seasonal observations of urban surface temperatures to evaluate impacts on variations in the UHI

•Integration of urban surface temperatures derived from to generate global UHI models for cities around the globe

Approach:

•Use HyspIRI TIR data to evaluate the size, form, and dynamics of the UHI for cities around the world to better understand how the UHI varies in different climatic zones and geographic locales globally

•Use high spatial/temporal resolution, multispectral thermal HyspIRI data to measure and model the effects of the UHI on global biophysical, climatic, and environmental processes

Results:

The UHI has been attributed to excess deaths during heat waves on days with higher-than-average temperatures. Current satellite systems do not have adequate revisit times or multiple thermal spectral bands to provide the information to model UHI dynamics and its impact on humans and adjacent environments. HyspIRI will have a return time, spectral characteristics and nighttime viewing to greatly enhance our knowledge of UHI thermal characteristics around the world.

TQ5: Earth Surface Composition and Change (AP,LM)

- What is the spectrally observable mineralogy of the Earth's surface and how does this relate to geochemical and surficial processes? [DS 114]
- What is the nature and extent of man-made disturbance of the Earth's surface associated with exploitation of non-renewable resources (oil & gas, mining)? How do these vary over time? [DS 227]
- How do surface temperature anomalies (hot spots) relate to deeper thermal sources, such as buried lava tubes, underground coal fires and engineering structures? How do changes in the surface temperatures relate to changing nature of the deep seated hot source? [DS 243]
- What is the spatial distribution pattern of surface temperatures and emissivities of various land surfaces and how do these influence the Earth’s heat budget?
- What are the water surface temperature distributions in coastal, ocean, and inland water bodies. How do they change, and how do they influence aquatic ecosystems? [DS 378]

TQ5a: What is the spectrally observable mineralogy of the Earth's surface and how does this relate to geochemical and surficial processes? (DS 114)

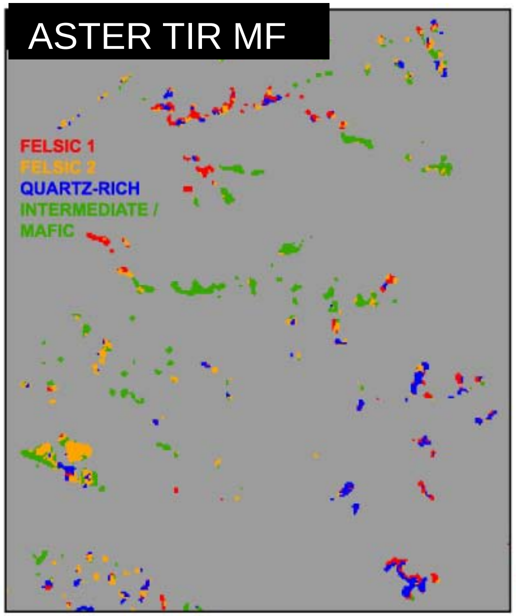

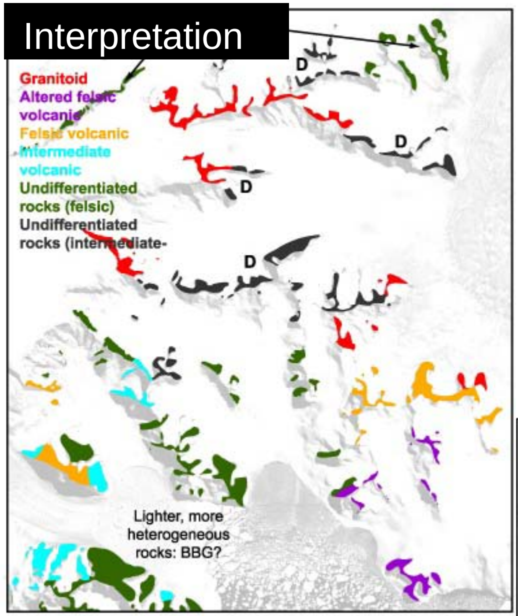

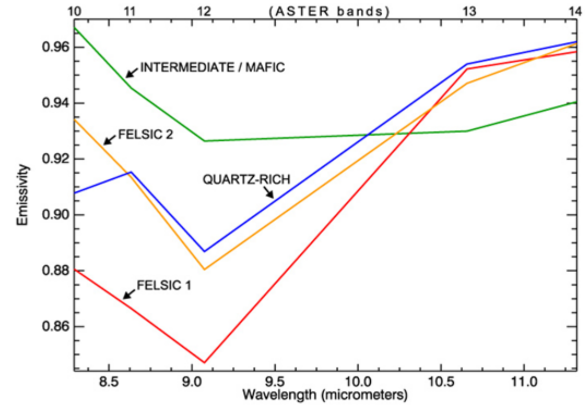

ASTER TIR image end-members

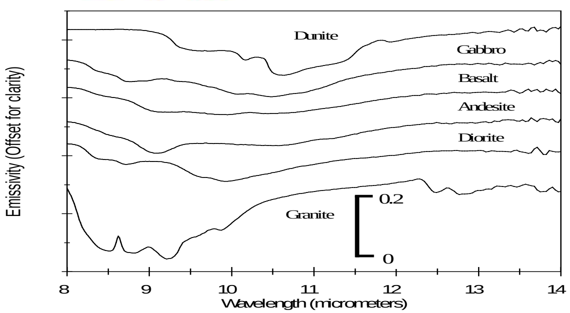

Haselwimmer et al., (2010)

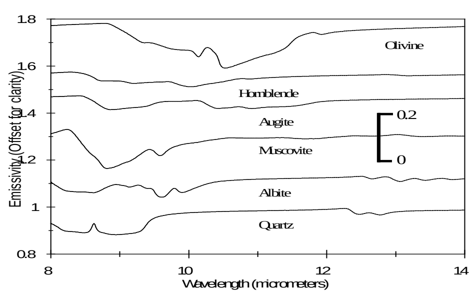

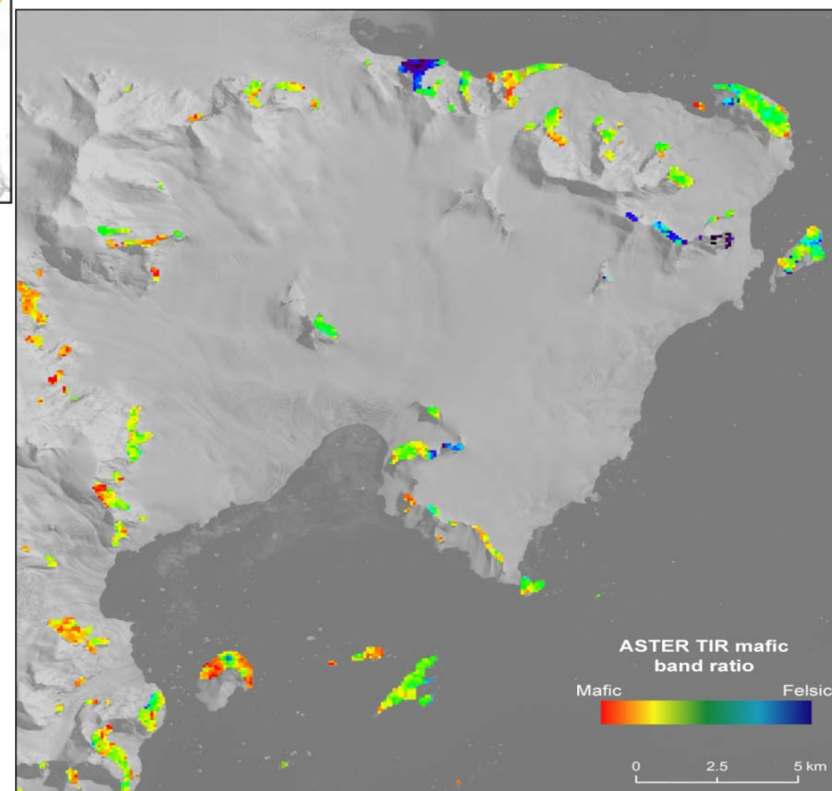

TQ5e: What are the water surface temperature distributions in coastal, ocean, and inland water bodies, how do they change, and how do they influence aquatic ecosystems? (DS 378)

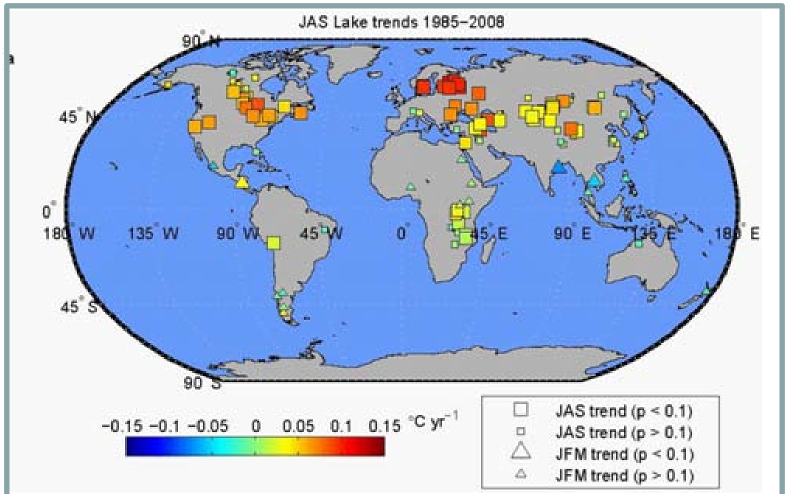

Increase in summer temperatures of large inland water bodies show warming in the northern latitudes

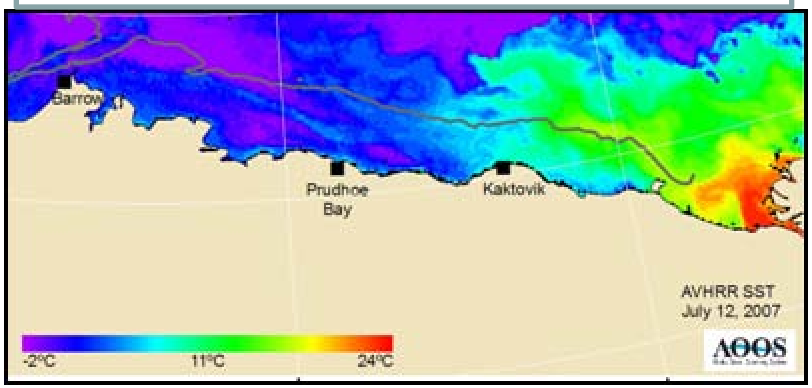

Processed AVHRR TIR image of the coast of the Arctic Alaska coast. Outflow from the Mackenzie River influences temperatures in coastal waters, breakup of sea ice, and thermal habitats of a variety of flora and fauna. Okkonen et al, 2009 (submitted to JGR)

Science Issue:

- Aquatic habitats are subject of dynamic temperature regimes, eg. coastal water temperatures vary due to temperatures of the neighboring land surface, outflow from rivers, general ocean circulation patterns, and local wind conditions.
- Flora and fauna in aquatic environments are sensitive to the water temperatures.
- They dynamics of the water temperatures and the controlling processes are not well understood.

Tools:

- HyspIRI TIR data with NEΔT < 0.2 K and weekly temporal repeat.
- Ancillary data such as high-resolution hydrography and acoustic Doppler current profiler measured currents, bathymetric information, when possible.

Approach:

- Derive water surface temperature images from HyspIRI TIR bands using established temperature estimation algorithm.
- Relate spatial temperature distribution pattern to local conditions (wind, riverine outflow, etc.)
- Relate surface temperature to bulk water temperature where ancillary data is available.

Fore more details…..

- http://hyspiri.jpl.nasa.gov/science
- http://hyspiri.jpl.nasa.gov/documents/2008-workshop/presentations
- http://hyspiri.jpl.nasa.gov/documents/2009-workshop/2009-workshop-agenda-and-presentations

HyspIRI Combined Questions (CQ)

Multi- and Inter-disciplinary Science

Requiring combined VIS, SWIR and TIR

http://HyspIRI.jpl.nasa.gov

Primary Science Justification

The combined use of HyspIRI TIR and VIS/SWIR will provide significant insight on biological and biogeochemical controls by small-scale physical processes and how these translate into small-scale ecosystem changes, globally

HyspIRI Combined (CQ) Science Questions

To answer these questions, <u>combined</u> multispectral TIR and hyperspectral VIS/ SWIR data are required

CQ1 – Coastal, ocean, and inland aquatic environments (Frank Muller-Karger)

CQ2 – Wildfires (Louis Giglio)

CQ3 – Volcanos (Robert Wright, Vince Realmuto)

CQ4 – Ecosystem Function and Diversity (Dar Roberts, Martha Anderson)

CQ5 – Earth surface composition and change (Lyle Mars, Anupma Prakash)

CQ6 – Human Health and Urbanization (Dale Quattrochi, Greg Glass)

Combined Overarching Questions

- CQ1. Coastal, ocean, and inland aquatic environments, FM-K
  - What is the status of inland and coastal aquatic ecosystems in the context of local and regional thermal climate, land-use change, and other environmental factors?
- CQ2. Wildfires, LG
  - How are fires and vegetation composition coupled?
- CQ3. Volcanoes, RW, VR
  - Do volcanoes signal impending eruptions through changes in the temperature of the ground, rates of gas and aerosol emission, temperature and composition of crater lakes, or health and extent of vegetation cover?
- CQ4. Ecosystem Function and Diversity, DR, MA
  - How do species, functional type, and biodiversity composition within ecosystems influence the energy, water and biogeochemical cycles under varying climatic conditions?
- CQ5. Earth surface composition and change, JM, AP
  - What is the composition of exposed terrestrial surface of the Earth and how does it respond to anthropogenic and non anthropogenic drivers?
- CQ6 Human Health and Urbanization, DQ, GG
  - How do patterns of human environmental and infectious diseases respond to leading environmental changes, particularly to urban growth and change and the associated impacts of urbanization?

CQ1. Coastal, ocean, and inland environments

- What are the feedbacks between climate and habitat structure, biogeochemical cycling, biodiversity, and ecosystem productivity of shallow aquatic habitats?
- What are the ecological linkages of landscape-scale ocean-atmosphere interactions including the hydrologic cycle, aerosol production and transport, and cloud radiative forcing?
- How are small-scale processes in shallow benthic habitats related to changes in functional community types (coral reefs, submerged aquatic vegetation and floating aquatic vegetation), productivity, and biogeochemical cycling including material fluxes and water quality?
- How can these observations be used to guide the management and utilization of resources in the shallow aquatic environment?
- What are the seasonal expressions and cycles for terrestrial and shallow aquatic ecosystems, functional groups and diagnostic species? What is the susceptibility and likely response in the context of changes in climate, land use, and disturbance? [DS 191, 195, 203]

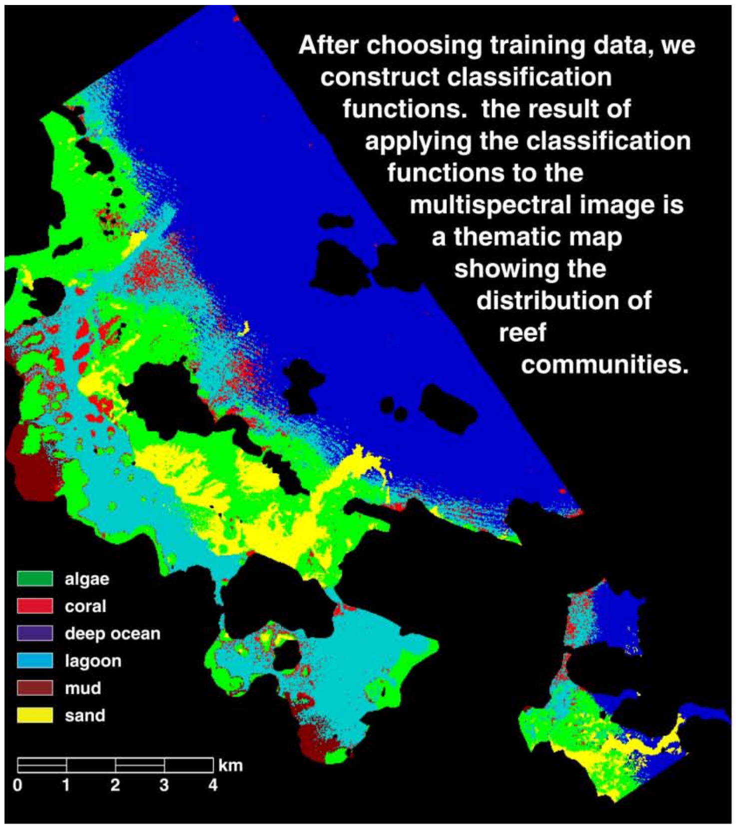

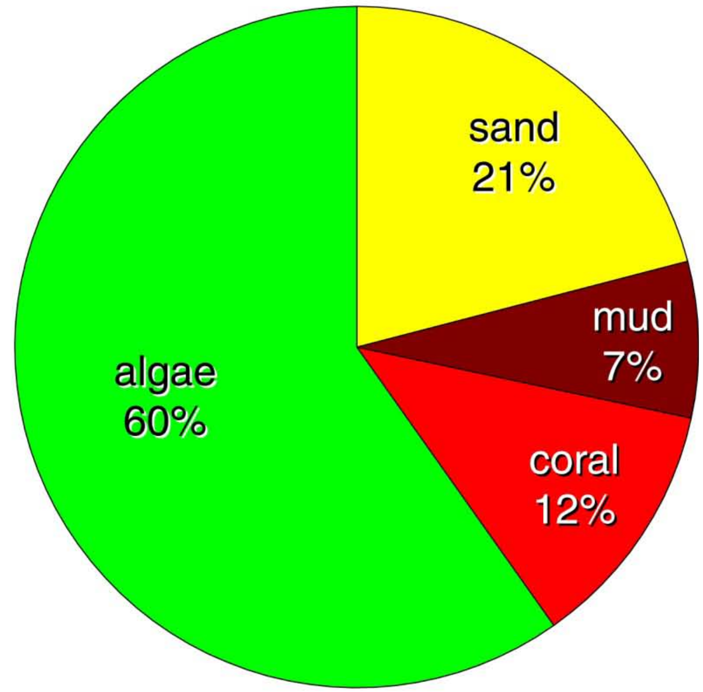

Fractional cover of bottom types derived from AVIRIS imagery of Kaneohe bay, Hawaii. (Courtesy: Eric Hochberg)

CQ2. Wildfires (LG)

- How does the timing, temperature and frequency of fires affect long-term ecosystem health?
- How does vegetation composition and fire temperature impact trace gas emissions?
- How do fires in coastal biomes affect terrestrial biogeochemical fluxes into estuarine and coastal waters and what is the subsequent biological response? [DS 198]
- What are the feedbacks between fire temperature and frequency and vegetation composition and recovery?
- How does vegetation composition influence wildfire severity?
- On a watershed scale, what is the relationship of vegetation cover, soil type, and slope to frequency of debris flows?
- How does invasive vegetation cope with fire in comparison to native species?

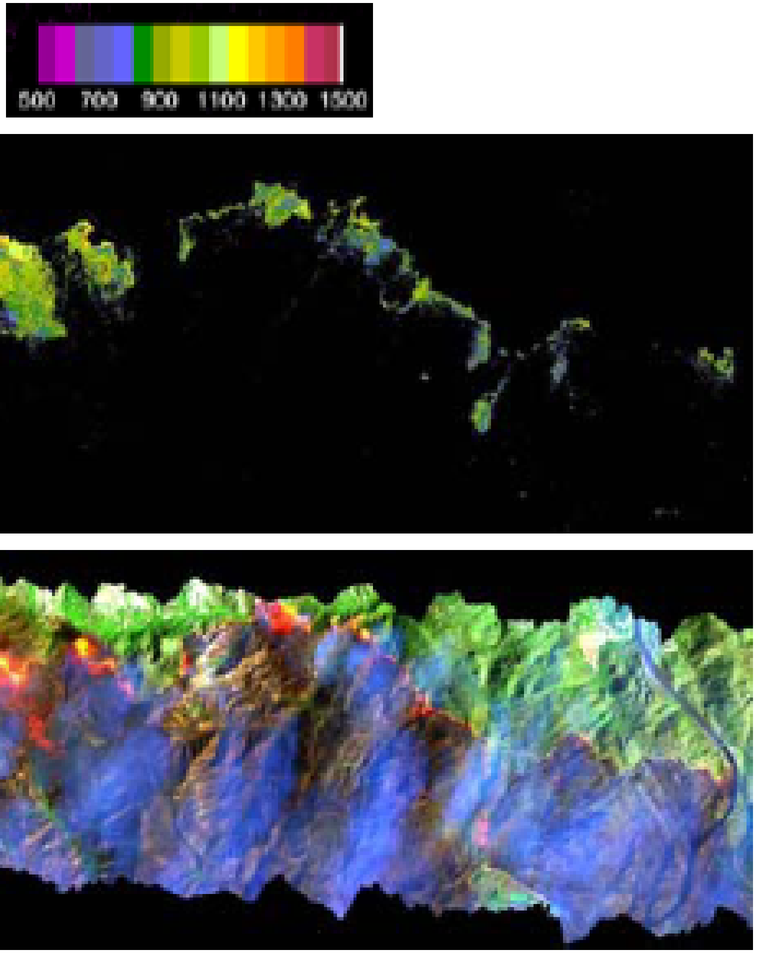

Top panel: Retrieved fire temperature (in kelvins) from an AVIRIS scene spanning a portion of the large Southern California Fire Complex from October 2003. Bottom panel: False color SWIR-NIR-red composite of the original AVIRIS scene. (Dennison et al. 2006).

CQ3. Volcanos (RW, VR)

- What do comparisons of thermal flux and SO2 emission rates tell us about the volcanic mass fluxes and the dynamics of magma ascent? [DS 227; 230]
- Does pressurization of the shallow conduit produce periodic variations in SO2 flux and lava dome surface temperature patterns that may act as precursors to explosive eruptions? [DS 50; 227; 230]
- Can measurements of the rate at which lava flows cool allow us to improve forecasts of lava flow hazards? [DS 50; 226]
- Does the temperature and composition of volcanic crater lakes change prior to eruptions? [DS 226; 227].
- Do changes in the health and extent of vegetation cover indicate changes in the release of heat and gas from crater regions? [DS 230; 231]

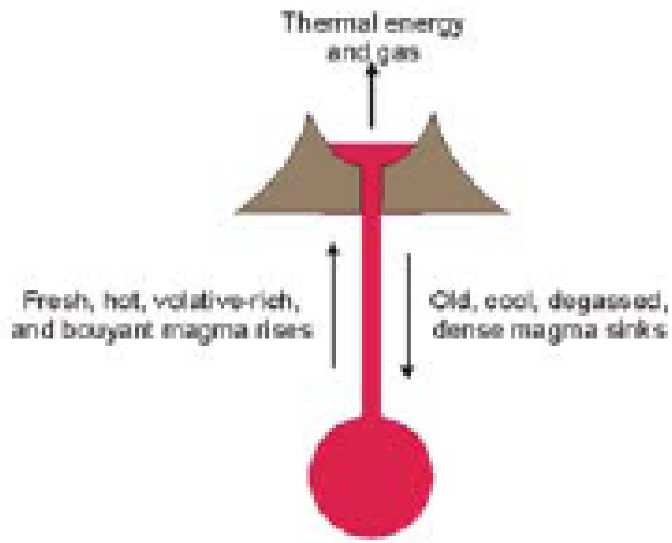

Hyperion SWIR image of Erta Ale volcano, Ethiopia, showing the active lava lake. Hyperspectral VSWIR and TIR data will allow the cooling rate and gas flux from the lake to be determined. Right: model of cooling and degassing-driven magma convection within an open system volcano. The heat and gas flux data are important boundary conditions for determining magma ascent dynamics and circulation within the conduit (adapted from Frances et al. 1993).

CQ4. Ecosystem Function and Diversity, (DR, MA)

- How can we enhance phenological & stress characterization through synergy between reflective and emitted radiation with higher frequency temporal sampling? [DS194, 195]
- How is energy partitioned between latent and sensible heat fluxes as a function of different plant types and fractional cover and how does this impact hydrology? [DS 203]
- How is physiological function affecting water and carbon exchange expressed at the ecosystem scale, especially seasonal down-regulation due to environmental stress factors? [DS 166, 196, 203, 206, 368]
- What is the vegetation phenological response to seasonal and interannual changes in temperature and moisture due to climate change and how does this response vary at the community/species level? [DS 196, 203, 206]
- What are the feedbacks between changes in canopy composition, mortality and retrieved canopy temperatures resulting from disturbances (e.g., disease, moisture deficiency, insect attack, fire, land degradation, fragmentation) in natural and managed ecosystems? [DS 166, 196, 203, 206]
- How do climate-induced temperature and moisture changes impact the distribution and spread of invasive and native species? [DS 196, 203]

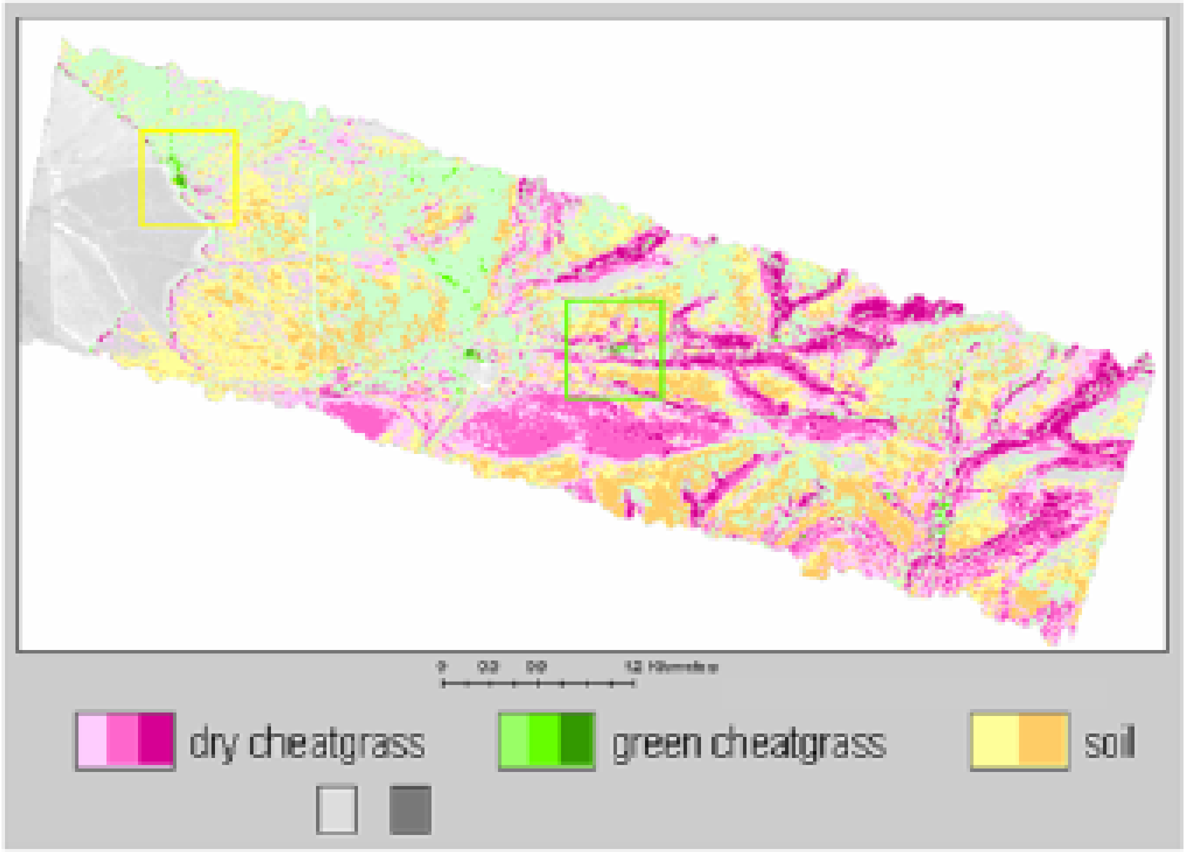

Map of *Bromus tectorum* (Cheatgrass) generated using imaging spectrometry. Cheatgrass spreads through a combination of disturbance and strategic use of soil moisture. It alters fire regimes, promoting its spread while early germination of Cheatgrass enables it to produce seed in advance of native plants while reducing available water for competitors. (Noujdina and Ustin 2008).

CQ5. Surface Composition and Change (JM,AP)

- What is the composition of the exposed terrestrial surface of the Earth? [DS 220]
- How does the surface mineralogy and soil composition relate to the plant physiology and function on the terrestrial surface of the Earth? (DS 114)
- How is the composition of exposed terrestrial surface responding to anthropogenic and non anthropogenic drivers (desertification, weathering, disturbance e.g. logging, mining)? (DS 114)
- How do types and distributions of altered rocks define regional trends in hydrothermal fluid flow for magmatic arcs and tectonic basins, better define hydrothermal deposit models, and assist in the discovery of new economic deposits? (DS 227)
- How do regional trends of minerals and shale thermal maturity within basins better define depositional models and assist in the discovery of new hydrocarbon reserves? (DS 235)

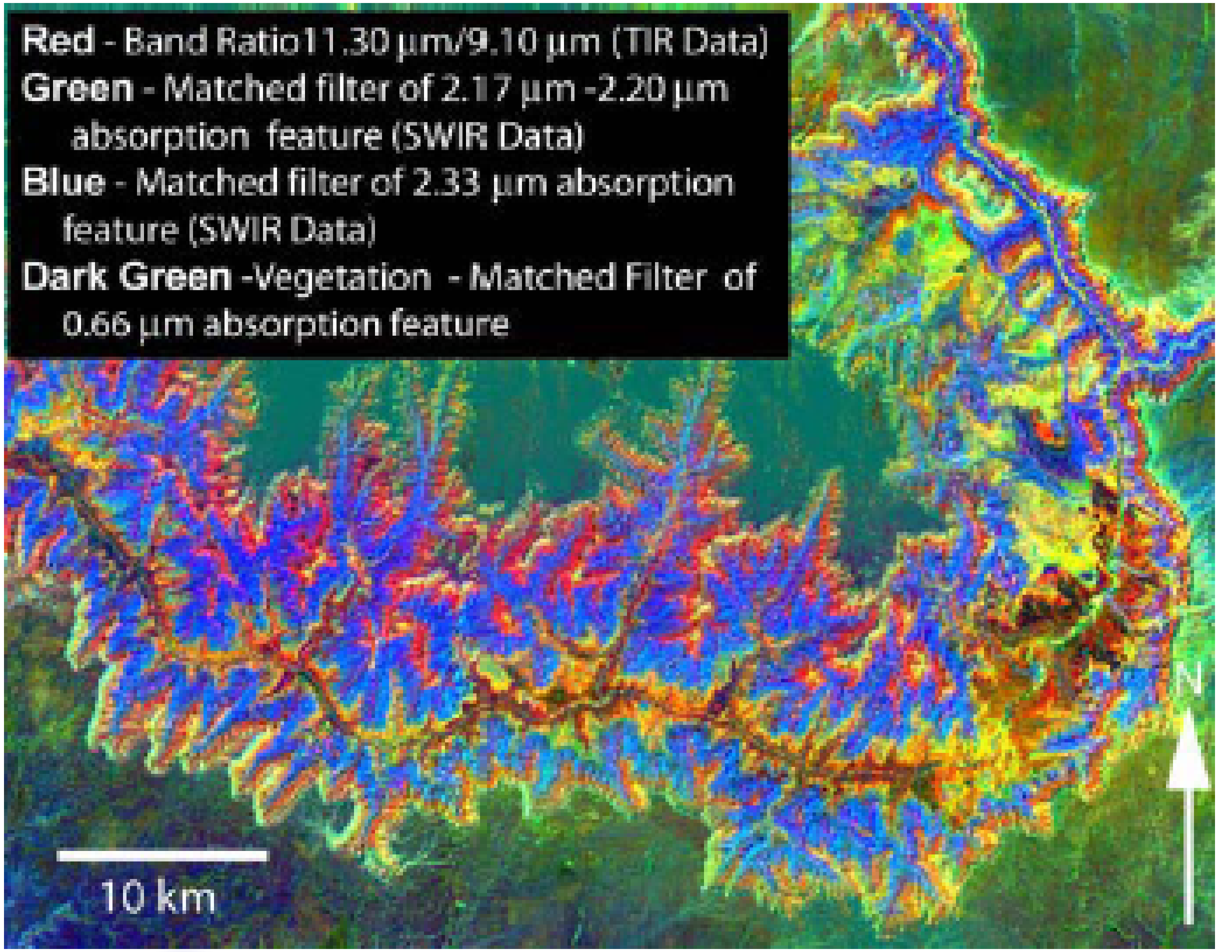

False color composite HyspIRI simulated image of Grand Canyon, Arizona derived from TIR (red band - quartz-rich rocks), SWIR (green band - clay and muscovite-rich rocks; blue band - carbonate-rich rocks), and VNIR (dark green - green vegetation) data.

CQ6. Human Health and Urbanization (DQ, GG)

- How do land surface characteristics such as vegetation state, soil moisture, temperature, and land cover composition affect heat and drought, and vector- and animal-borne diseases? (DS 156, 158, 160, 183-184, 198)
- What changes can be observed and measured in emissivities of urban surfaces and how do emissivities change for different cities around the world as they impact the urban heat island and associated land-atmosphere energy balance characteristics? (DS 167-168)
- How does the distribution of urban and peri-urban impervious surfaces affect regional energy balance fluxes, hydrologic processes, biogeochemical fluxes, and what is the response of ecosystems to these changes? (DS 167-168, 198, 203)

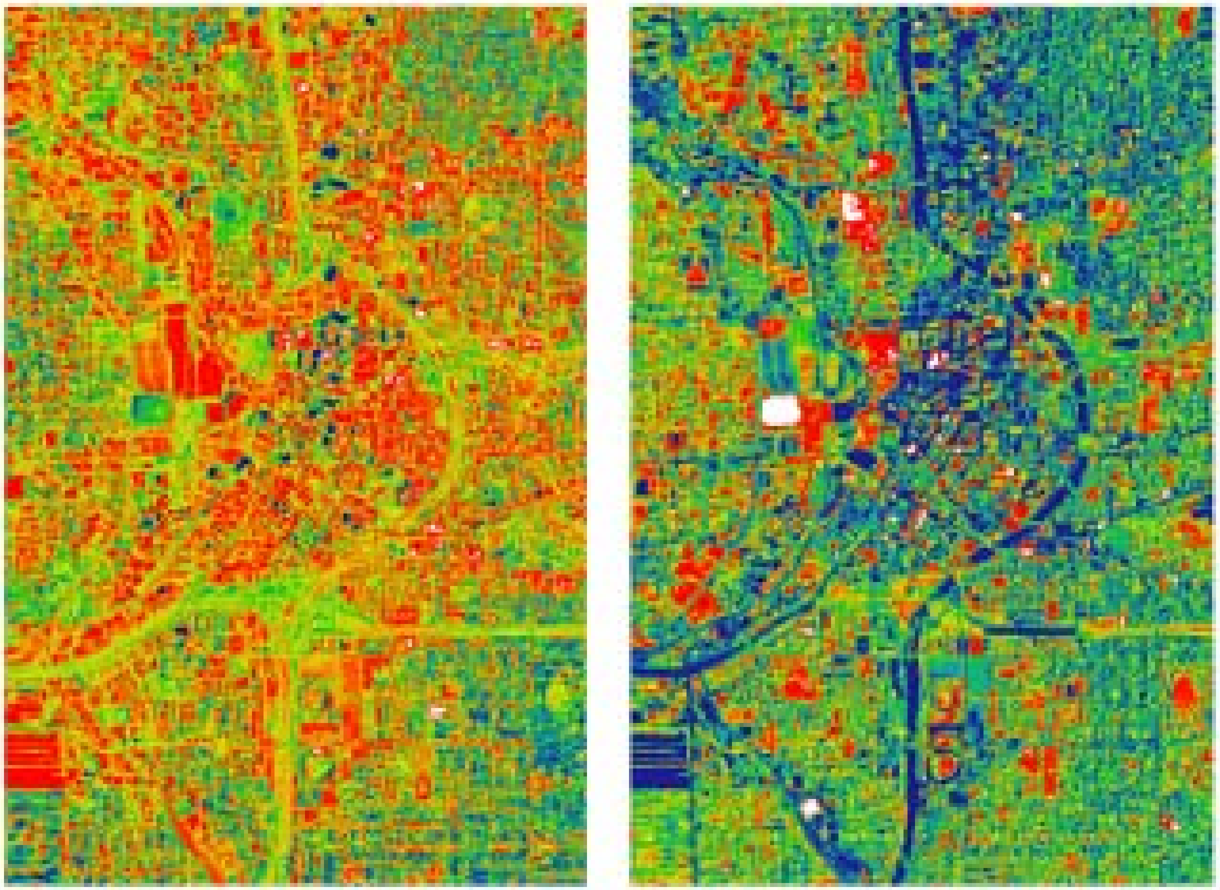

Temperature Albedo

Atlanta, GA - May 1997

Temperature and albedo measurements for the Atlanta, GA central business district as derived from multispectral aircraft data (Quattrochi et al. 2009)

TASKS TO ACCOMPLISH

- Measurement requirements have been incorporated into the Science Traceability Matrix
- Alignment with Decadal Survey has been confirmed and documented
- Identify the precursor science needed
- Level 3 products (spatial, temporal res., etc.)
  - Being defined
- Validation approach for Level 0-3+ products
  - To be defined
    - Coordinate with NPP, ACE, Geo-Cape, other teams

Soil Organic Carbon Observatory:

Combined Imaging Spectrometry, Modeling and Ground Measurement for Assessing Changes in Soil Organic C

Charles W. Rice

University Distinguished Professor

Department of Agronomy

K-State Research and Extension

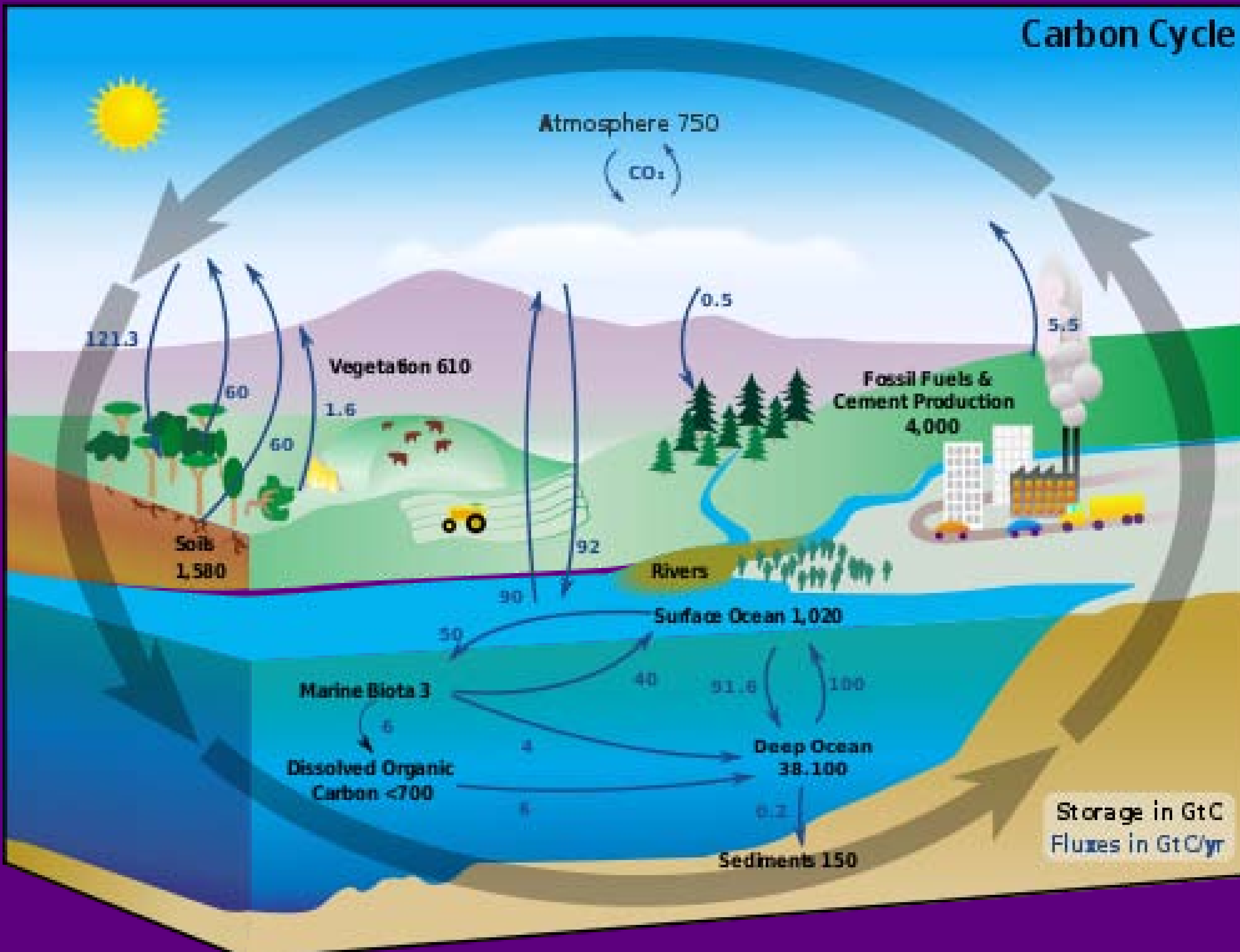
Carbon Cycle
Atmosphere 750
CO_2
121.3
60
60
1.6
Vegetation 610
Soils
1,580
92
90
0.5
5.5
Fossil Fuels &
Cement Production
4,000
Rivers
Surface Ocean 1,020
50
40
91.6
100
Marine Biota 3
6
4
Dissolved Organic
Carbon <700
6
Deep Ocean
38,100
0.2
Sediments 150
Storage in GtC
Fluxes in GtC/yr

Global economic mitigation potential for different sectors at different carbon prices

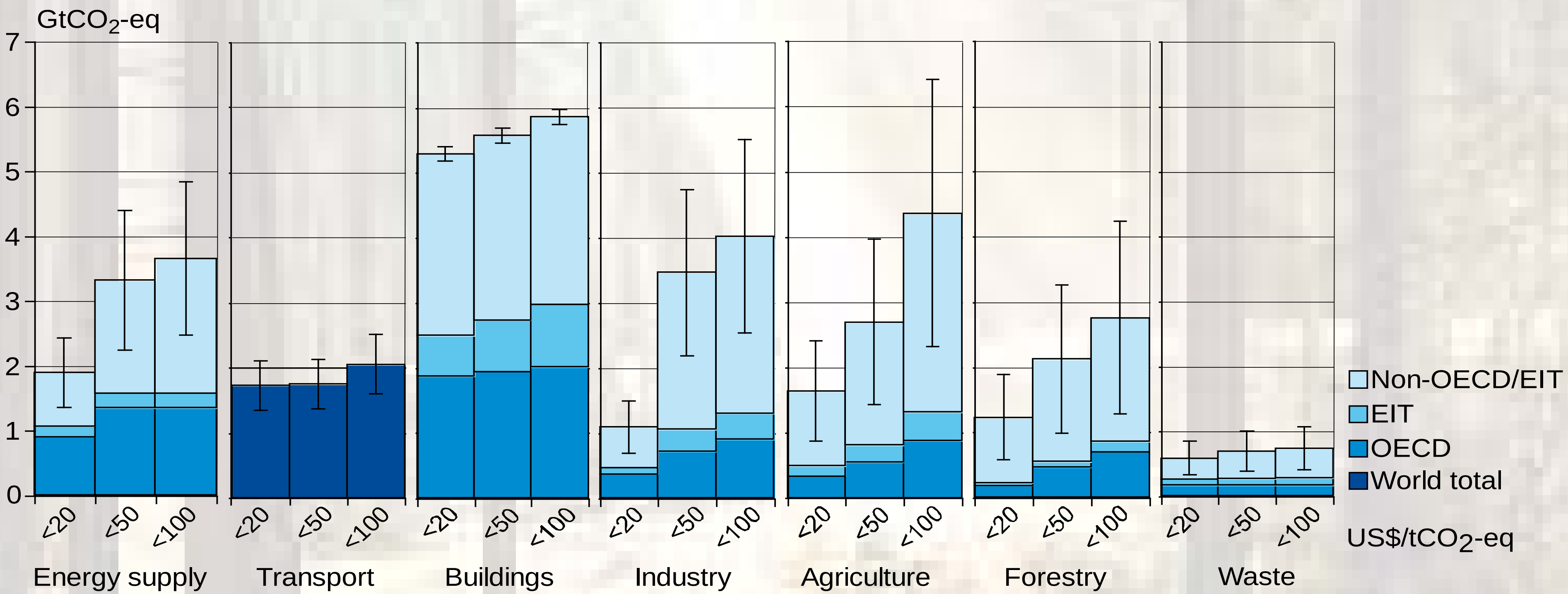

IPCC, 2007

Agriculture

- A large proportion of the mitigation potential of agriculture (excluding bioenergy) arises from soil C sequestration, which has strong synergies with sustainable agriculture and generally reduces vulnerability to climate change.

- Agricultural practices collectively can make a significant contribution at low cost
  – By increasing soil carbon sinks,
  – By reducing GHG emissions,
  – By contributing biomass feedstocks for energy use

- ***There is no universally applicable list of mitigation practices; practices need to be evaluated for individual agricultural systems and settings***

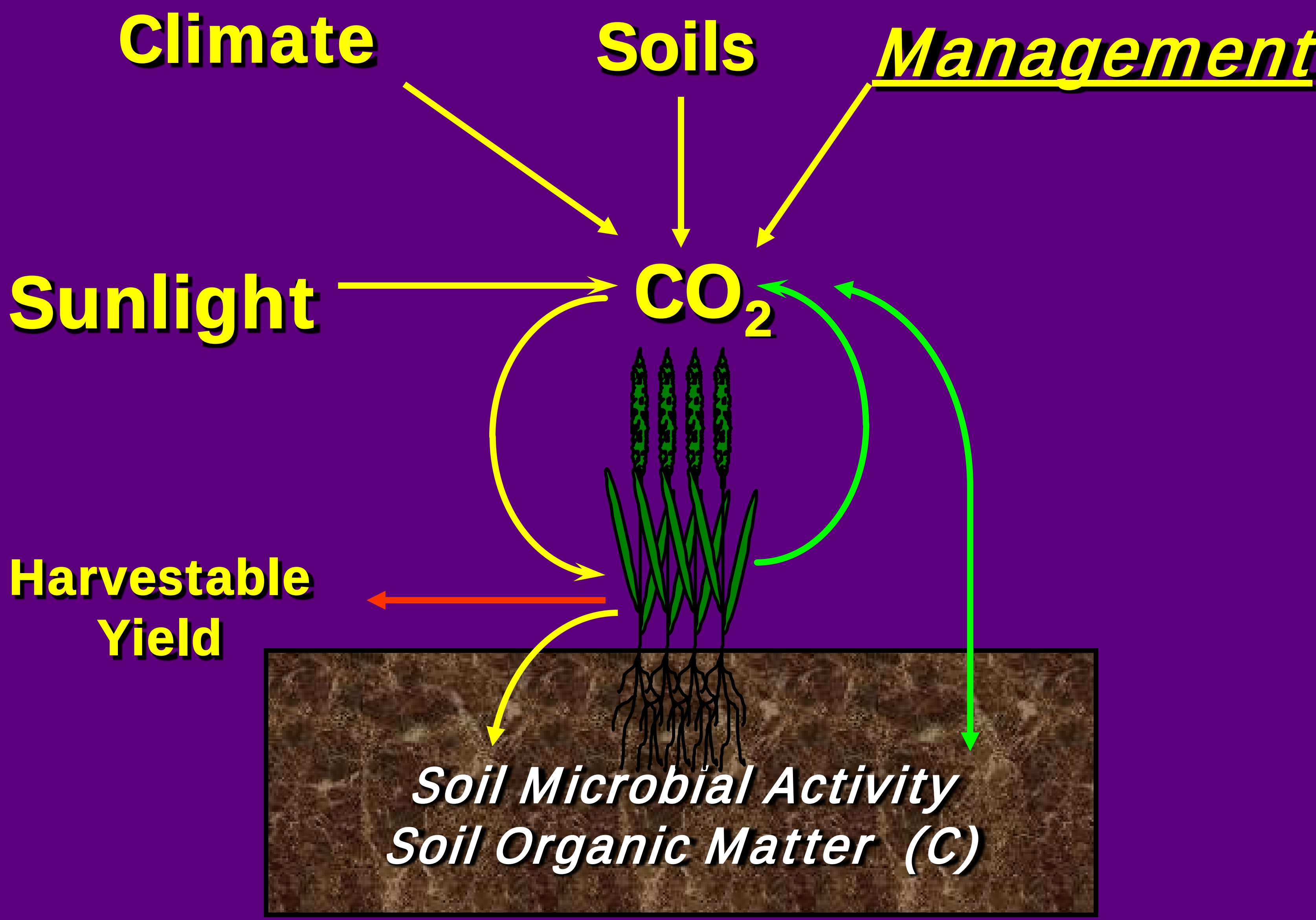
Climate
Soils
Management
Sunlight
CO_2
Harvestable Yield
Soil Microbial Activity
Soil Organic Matter (C)

<u>Many</u> opportunities for GHG mitigation!

<u>Cropland</u>

- Reduced tillage
- Rotations
  - Reduced bare fallow
  - Increased intensity
- Cover crops
- Fertility management
  - Nitrogen use efficiency
- Water management
  - Irrigation management

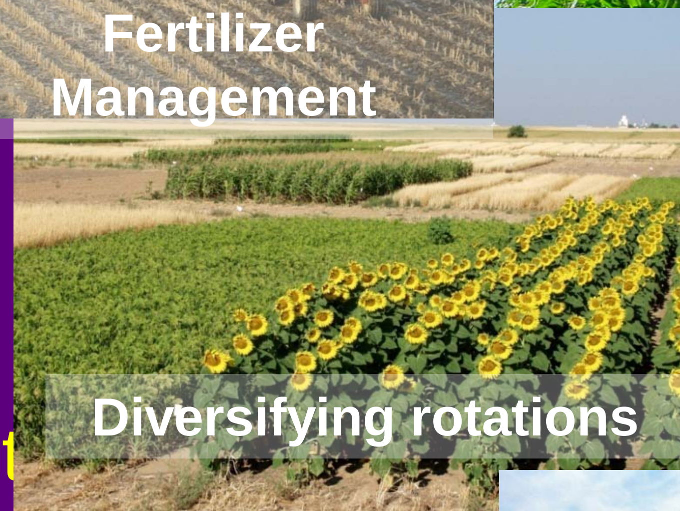

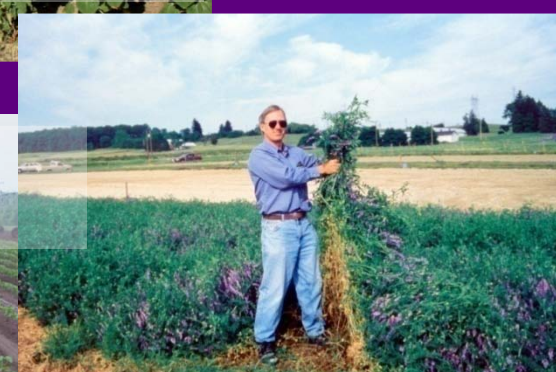

Traditional Assessment of Soil C

- Soil C analysis accurate
- Soil Sampling
  - Labor intensive
  - Time consuming
  - Landscape variation
  - Scaling issues
- Bulk density measurements highly variable

Sampling strategies: account for variable landscapes

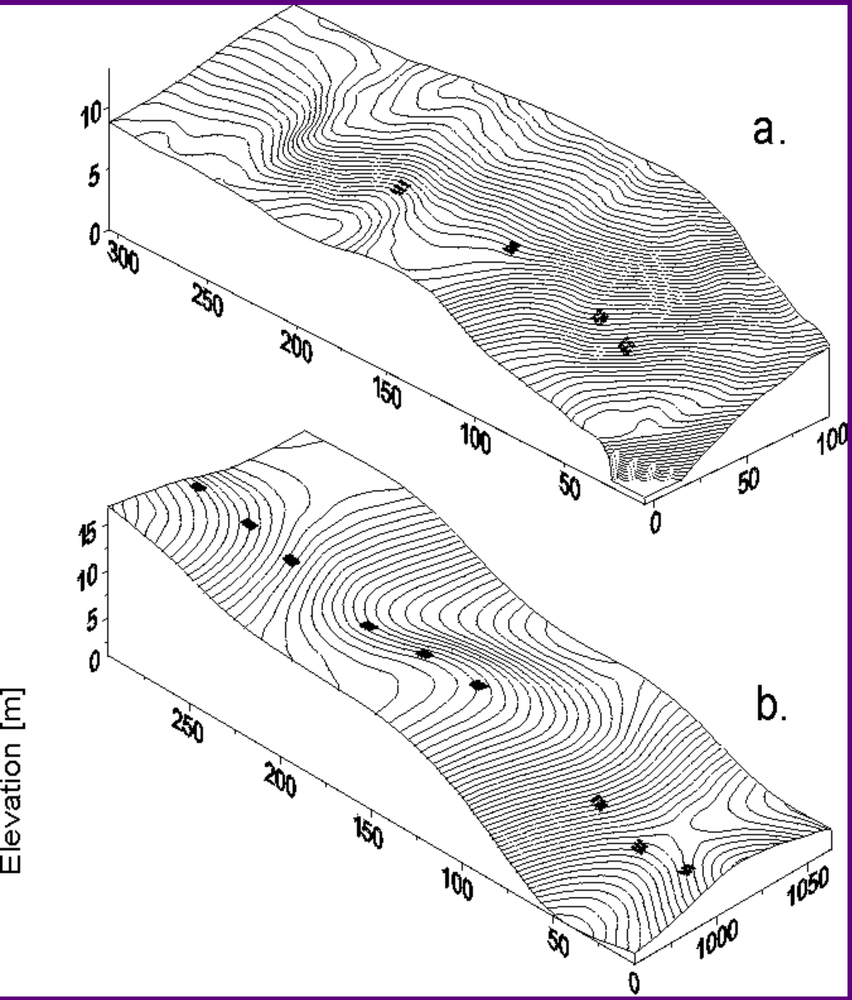

- Landscape modifications affect many processes
  - Cycling of water, carbon and nitrogen
  - Heat exchange between the land and the atmosphere
  - Lateral transport of soil by wind and water
  - Rate and extent of physical, chemical, and biological soil reactions

Upscaling from sites to regions across time

Time arrow

Databases, remote observations

Experiments

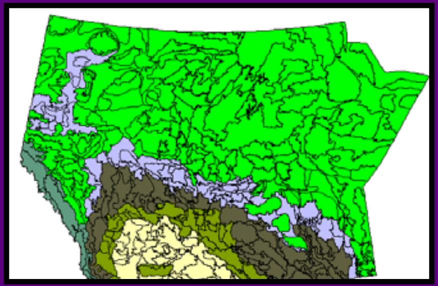

10^{12} m^2

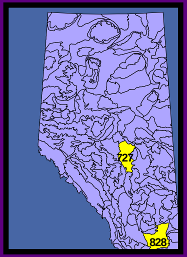

10^{9} m^2

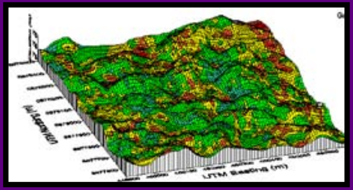

10^{6} m^2

10^{3} m^2

10^{1} m^2

10^{-6} m^2

Simpler models, metamodels?

Process models, landscape models

Measurement, Monitoring and Verification

- Methods for detecting and projecting soil C changes
  - Direct methods
    - Field measurements
  - Indirect methods
    - Accounting
      - Stratified accounting
      - Remote sensing
      - Models

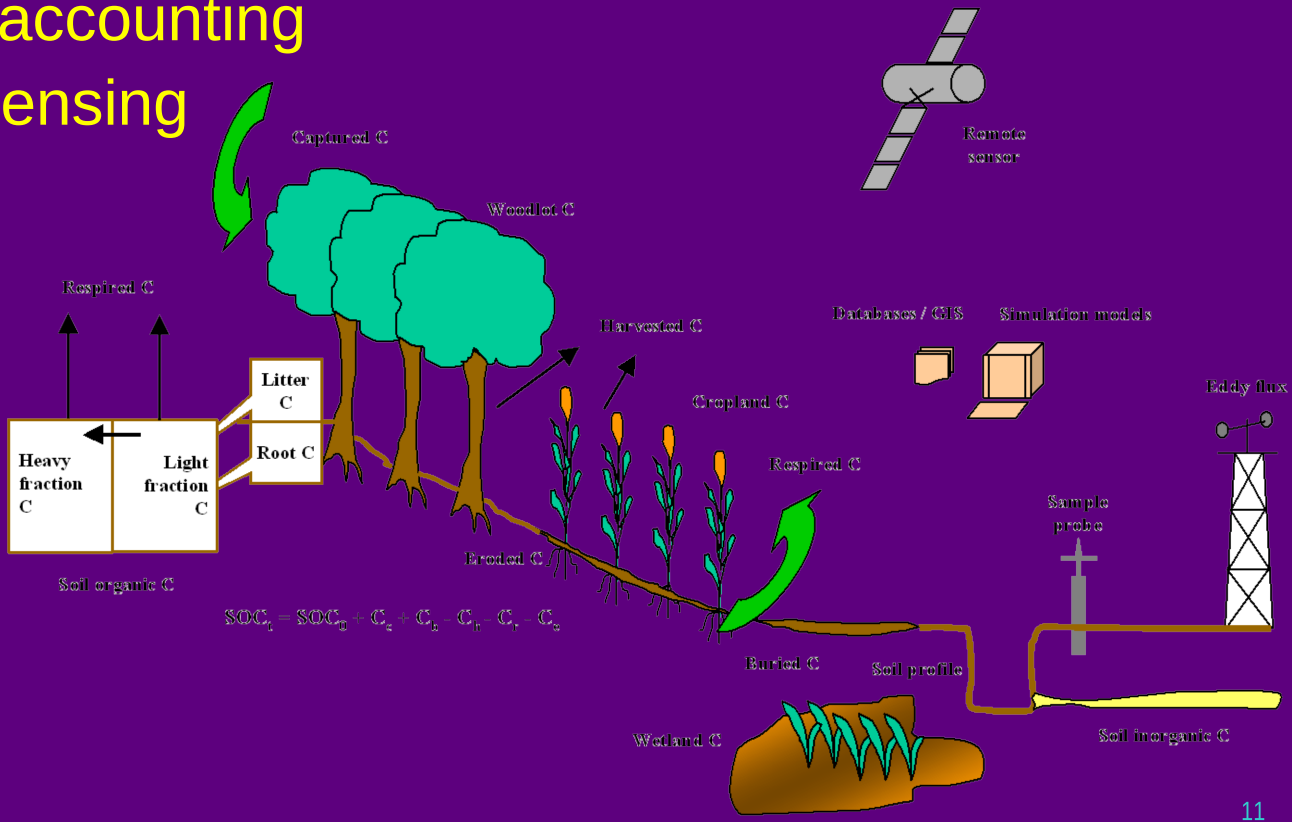

Post et al. (2001)

Soil Organic Carbon Observatory

- Quantify regional SOC changes at the resolution of individual agricultural management units for diverse environmental conditions and cropping systems.

- Evaluate the relative contributions of management factors, environmental conditions, and cropping systems for SOC changes.

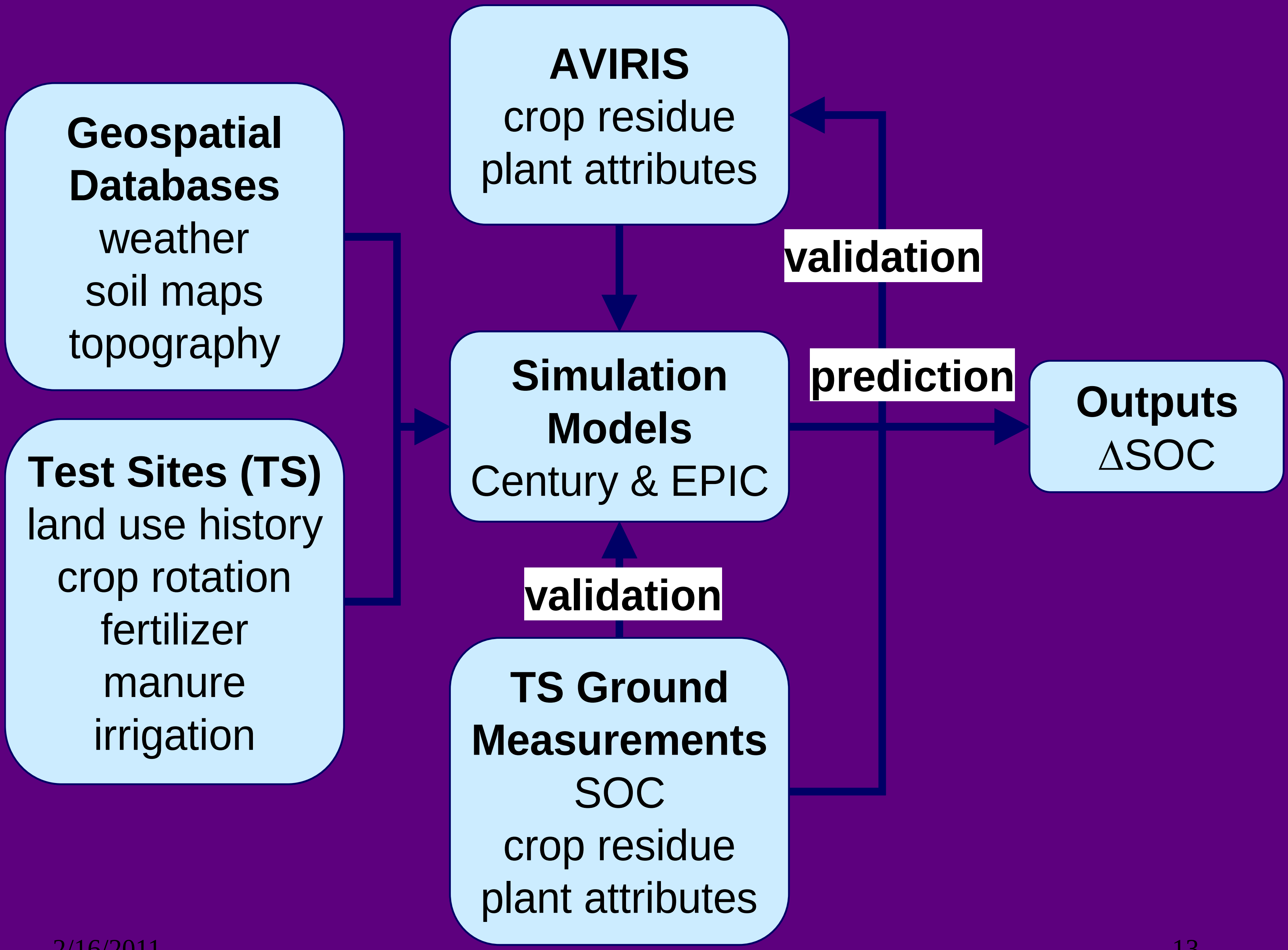
AVIRIS
crop residue
plant attributes
Geospatial Databases
weather
soil maps
topography
validation
Simulation Models
Century & EPIC
prediction
Outputs
ΔSOC
Test Sites (TS)
land use history
crop rotation
fertilizer
manure
irrigation
validation
TS Ground Measurements
SOC
crop residue
plant attributes

Geo-reference microsites

- Microsites reduces spatial variability
- Simple and inexpensive
- Used to improve models
- Used to adopt new technology
- Soil C changes detected in 3 yr
  - 0.71 Mg C ha^{-1} – semiarid
  - 1.25 Mg C ha^{-1} – subhumid

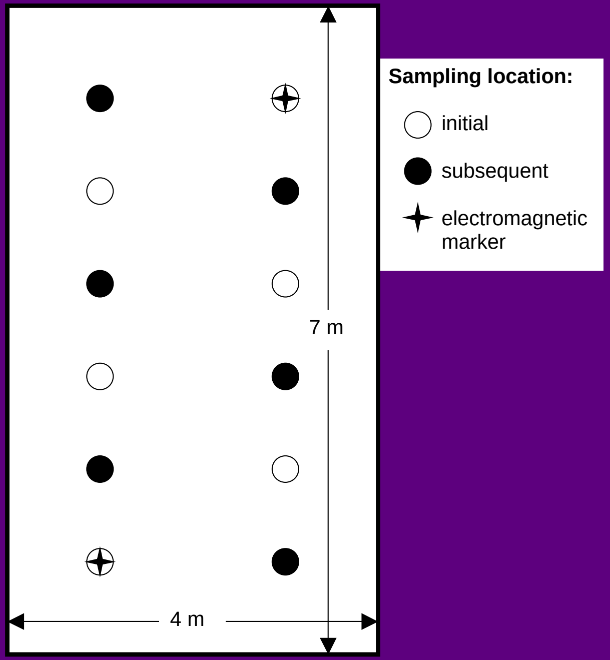

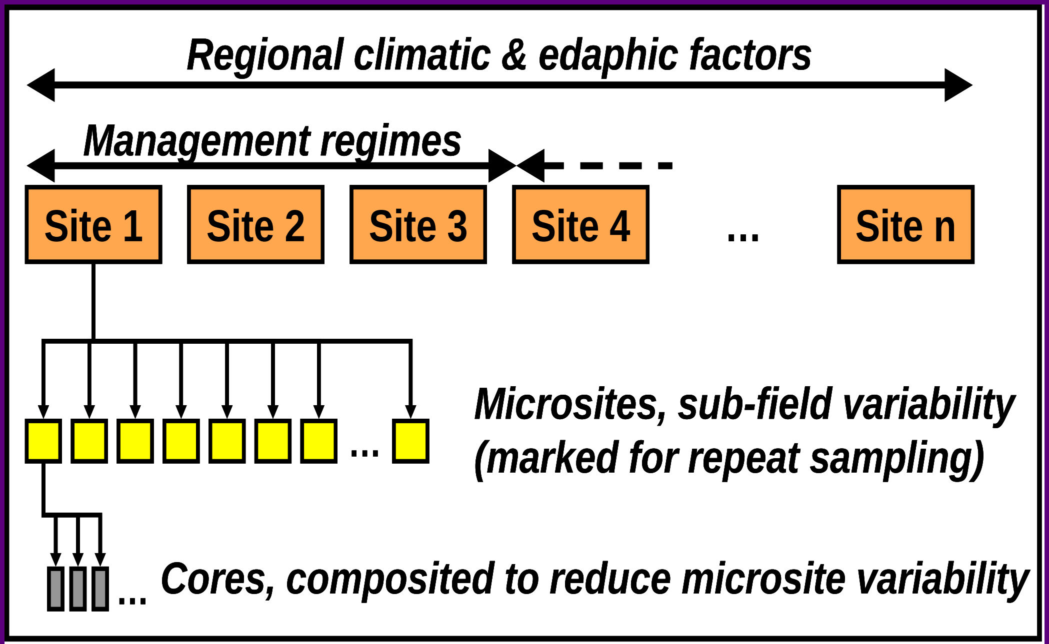

Ellert et al. (2001)

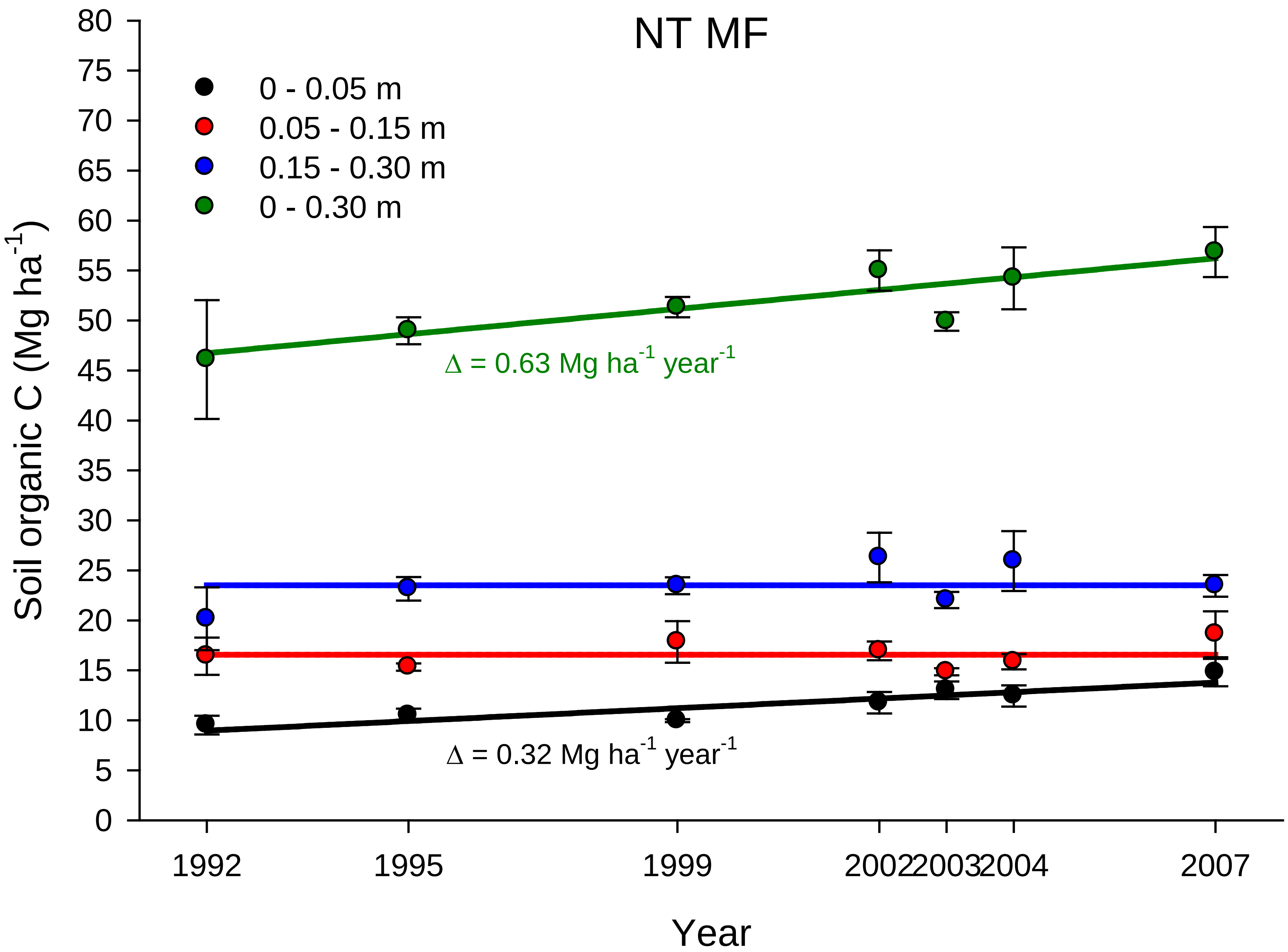

NT MF
0 - 0.05 m
0.05 - 0.15 m
0.15 - 0.30 m
0 - 0.30 m
Δ = 0.63 Mg ha-1 year-1
Δ = 0.32 Mg ha-1 year-1
Soil organic C (Mg ha-1)
Year
0
5
10
15
20
25
30
35
40
45
50
55
60
65
70
75
80
1992
1995
1999
2002
2003
2004
2007

Remote Sensing and Carbon Sequestration

- Remote sensing cannot be used to measure soil C directly unless soil is bare.
- Remote sensing useful for assessing:
  - Vegetation
    - Type
    - Cover
    - Productivity
  - Water, soil temperature
  - Tillage intensity

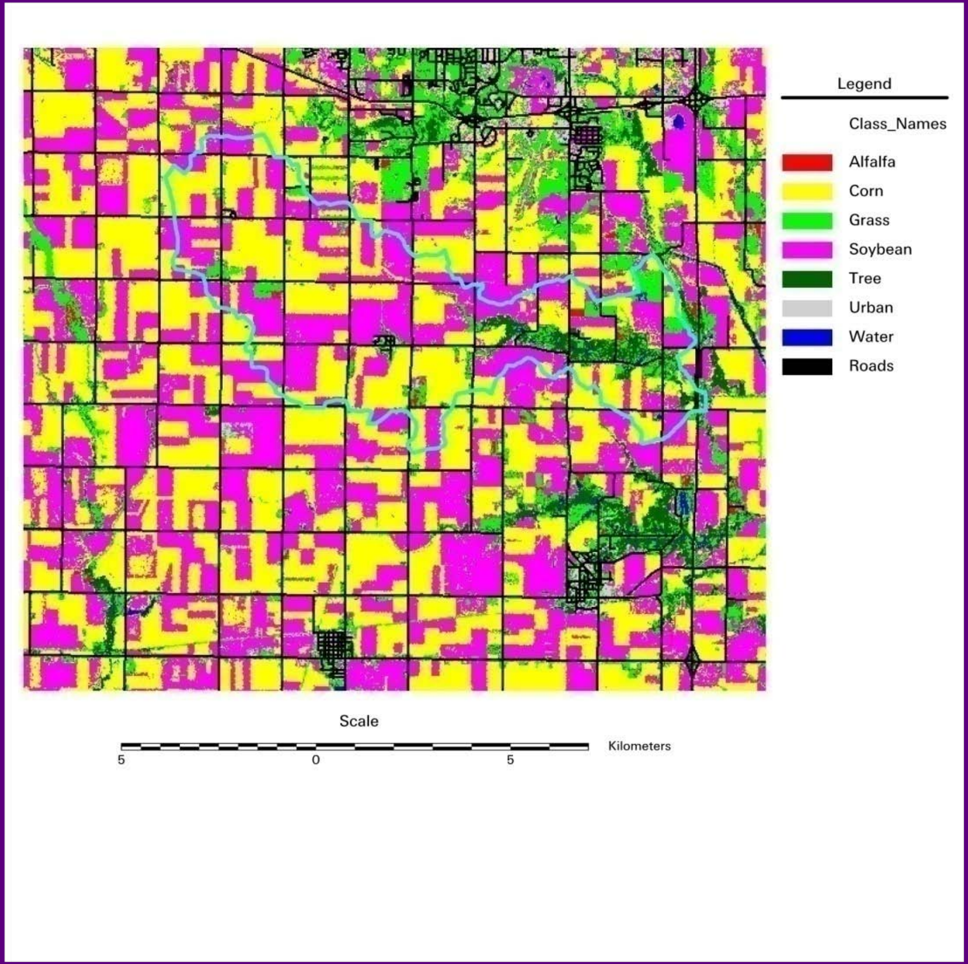

Crop identification for spatial modeling. Courtesy: P Doraiswamy, USDA-ARS, Beltsville, MD

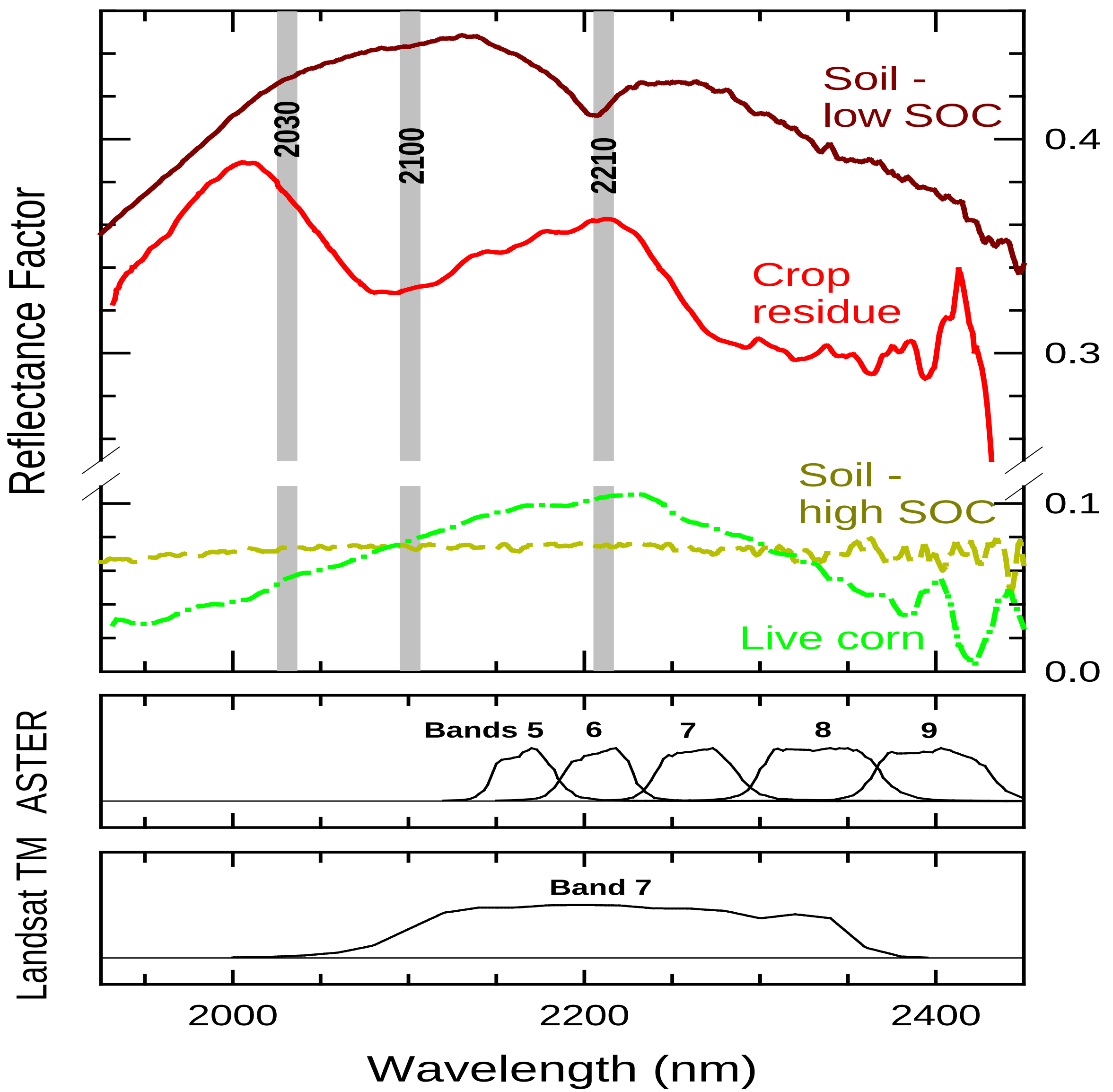

Reflectance spectra of corn, low- and high-SOC soils, and crop residue in the shortwave infrared region showing the cellulose absorption feature at 2100 nm wavelength. Shown in the bottom two panels are the wavebands for NASA ASTER and Landsat Thematic Mapper indicating these sensors can not be used to estimate crop residue. Serbin, *et al.* (in press).

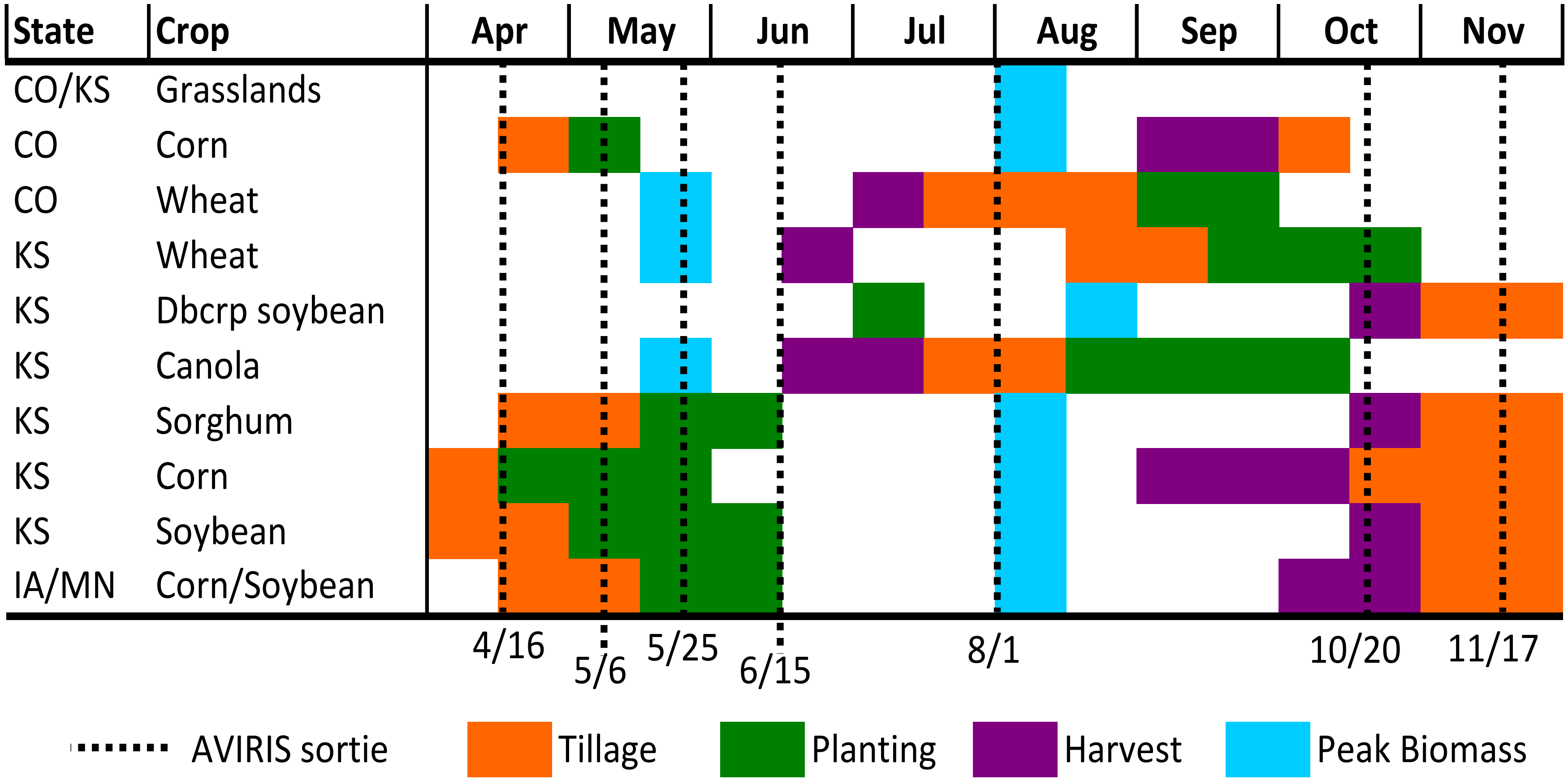

Figure 2.1-2. Key crop growth and management events are captured with seven targeted AVIRIS surveys per year. Critical times include: (a) post spring tillage or spring residue if no tillage; (b) post crop emergence, after planting; (c) peak biomass; (d) post harvest; and (e) post following fall tillage.

Terrestrial ecosystem models

- Century
  - Century
  - DayCent
  - C-STORE
- EPIC
  - EPIC
  - APEX

Processes and drivers

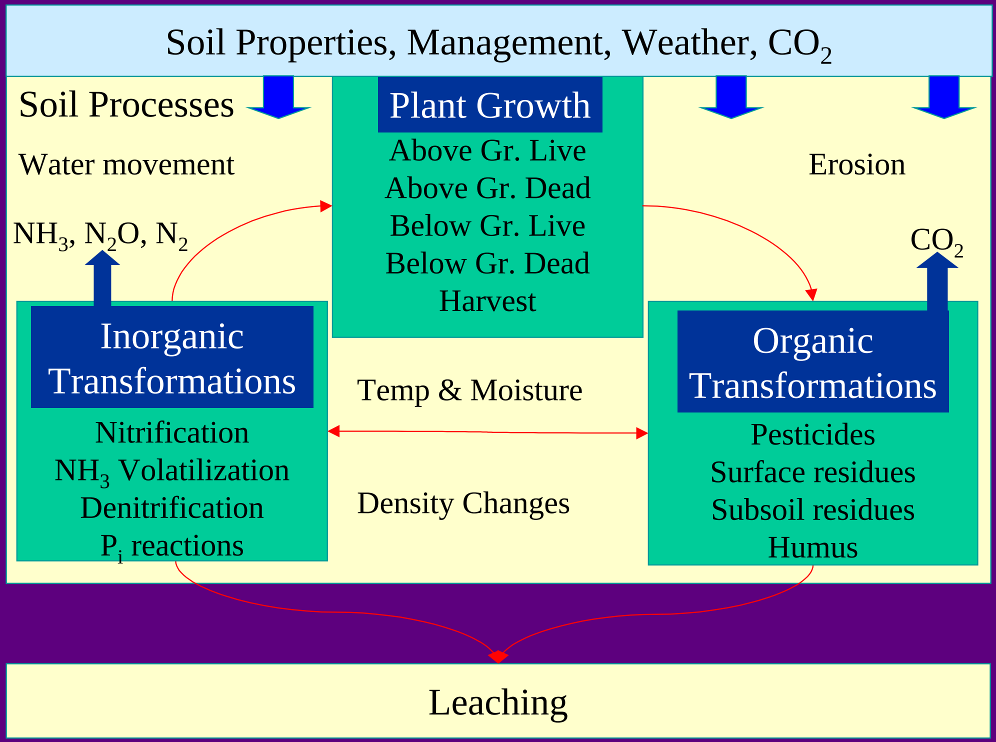

Carbon and nitrogen flows

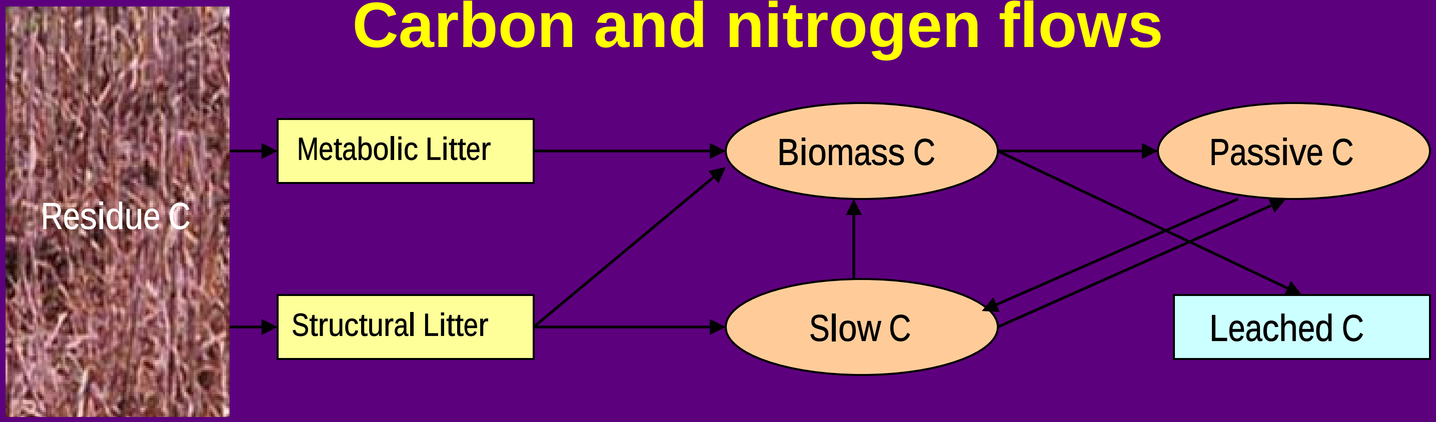

Summary

- Provides template to quantify changes in soil C that support implementation of agricultural GHG mitigation strategies.
- Provides methodology for operational GIS and carbon models functional at field to regional scales.
- Provides a framework useful to land managers and policymakers on how to manage agro-ecosystems for maximum profitability at the farm level, maintaining food security, protecting natural resources and mitigating GHG emissions

SOCO Team

- Management
  - Charles W. Rice, KSU
  - David I. Brown, JPL
  - Keith Paustian, CSU
  - Oh-ig Kwoun, JPL
  - Rob Green, JPL
  - Michael Eastwood, JPL
  - Bonny L. Schumaker, JPL
- Science Team
  - Charles Rice, Kansas State University
  - Keith Paustian, Colorado State University
  - Robert O. Green, JPL
  - Douglas Archibald, Penn State University
  - David J. Brown, Washington State University
  - E. Raymond Hunt, USDA Agricultural Research Service
  - Cesar Izaurralde, DOE Pacific Northwest National Laboratory
  - Kyle McDonald, JPL
  - Heather McNairn, Agriculture and Agri-Food Canada
  - Stephen Ogle, Colorado State University
  - Alain Plante, University of Pennsylvania
  - Kevin Price, Kansas State University
  - Guy Serbin, USDA Foreign Agricultural Service
  - Tristram West, DOE Pacific Northwest National Laboratory

Chuck Rice
Phone: 785-532-7217
Cell: 785-587-7215
cwrice@ksu.edu

- Websites

www.soilcarboncenter.k-state.edu/

K-State Research and Extension

Predicting Total Phosphorus (TP) through Spectroscopic Analysis

Kaishan Song, Lin Li, Shuai Li, Linhai Li, Tingting Zhang

Lenore Tedesco and Bob Hall

Department of Earth Sciences, Indiana University Purdue University Indianapolis

HyspIRI Science Workshop
August 24-26, 2010

Outline

1. Introduction
2. Study Sites
3. Data Sets
4. Methods
5. Results and Discussion
   - In situ data inversion
   - Image data inversion
6. Conclusions

I. Introduction-Impacts of Cyanobacteria

- Public Health
  - Toxins
    - Microcystin
    - Cylindrospermopsin
    - Anatoxin-a
  - Alter taste and odor of drinking water
    - MIB
    - Geosmin
- Ecological Effects
  - Fish kills
  - Additional effects

(Chorus and Bartram, 1999; Falconer, 2005)

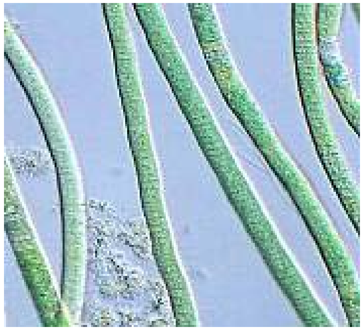

I. Introduction-TP vs. Cyanobacteria

- Ecologically, TP is a key factor for development of cyanobacterial blooms
  - Very likely if TP concentration above 25-30 ug/L
  - Rare if TN:TP ratios above 30 (16:1, according to Jorgensen)

- However, TP has no diagnostic spectral signatures, how can TP be retrieved from remote sensing data?

1. Introduction-remotely estimation TP

- Optically Active Constituents
  - Phytoplankton: pigments
    - TP->Cyanobacteria-> Chl-a and PC
  - Tripton: suspended inorganic particles
    - TP carrier
  - CDOM: colored dissolved organic matter
    - Somehow, CDOM has no direct relation to TP
- Physical properties
  - Closely associated with Secchi Disk Depth or Transparency (SDD or SDT)
  - And water turbidity

1. Introduction-Objectives

- Investigate the possibility of estimating TP from *in situ* spectral data
- Explore the underlying basis for TP inversion from image data
- Assess trophic status of drinking water resources with derived water quality data

2. Study Sites

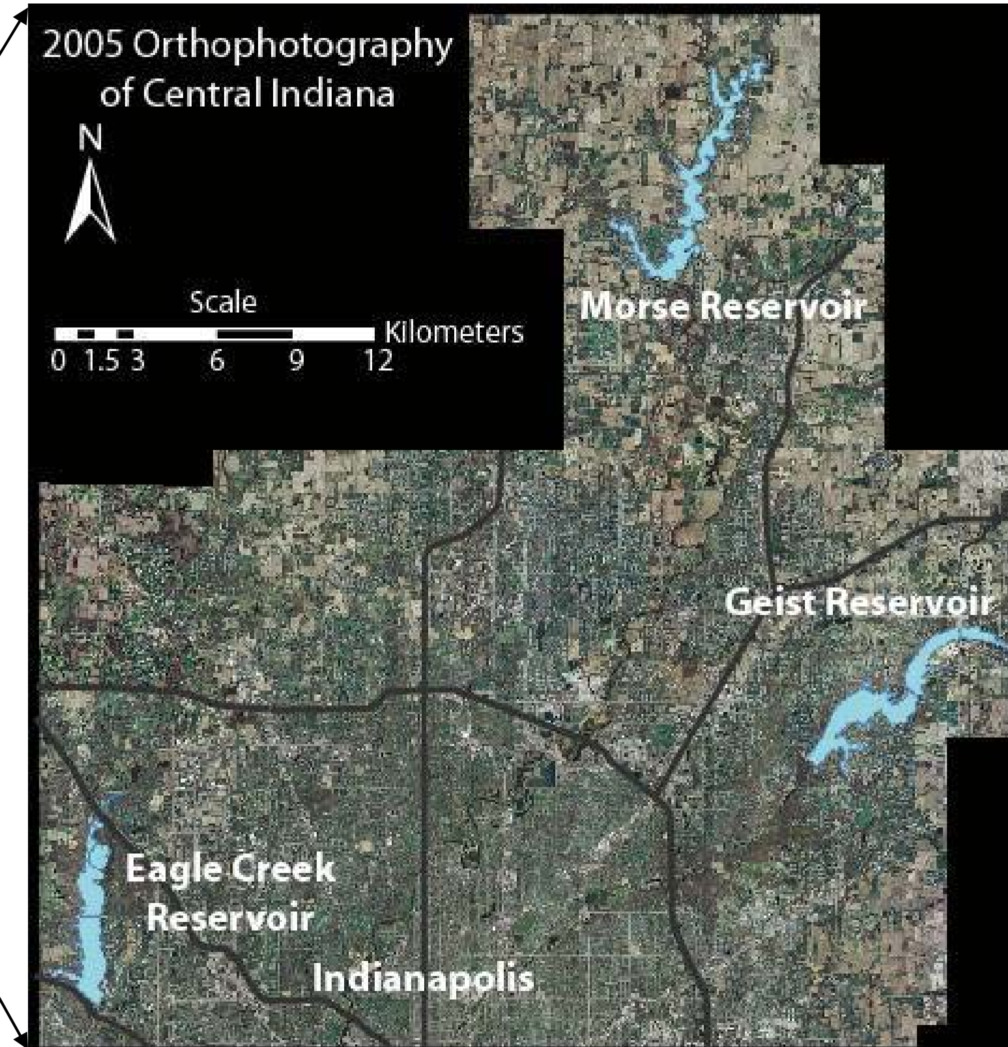

3. Data Sets- Sampling period: 2005-2008, 2010

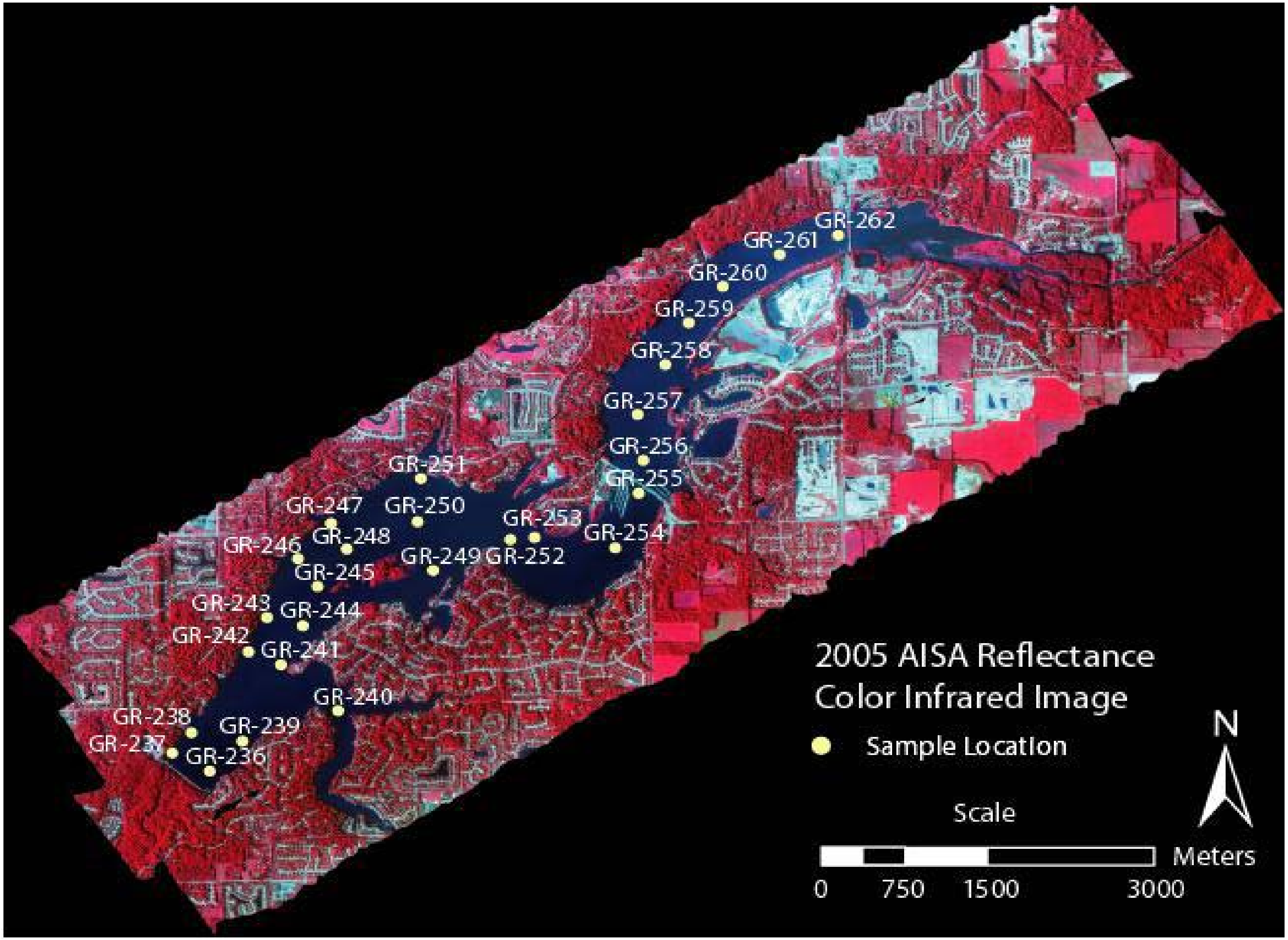

3. Datasets-Chl-a, TP, TN, turbidity, TSS and SDT (2005)

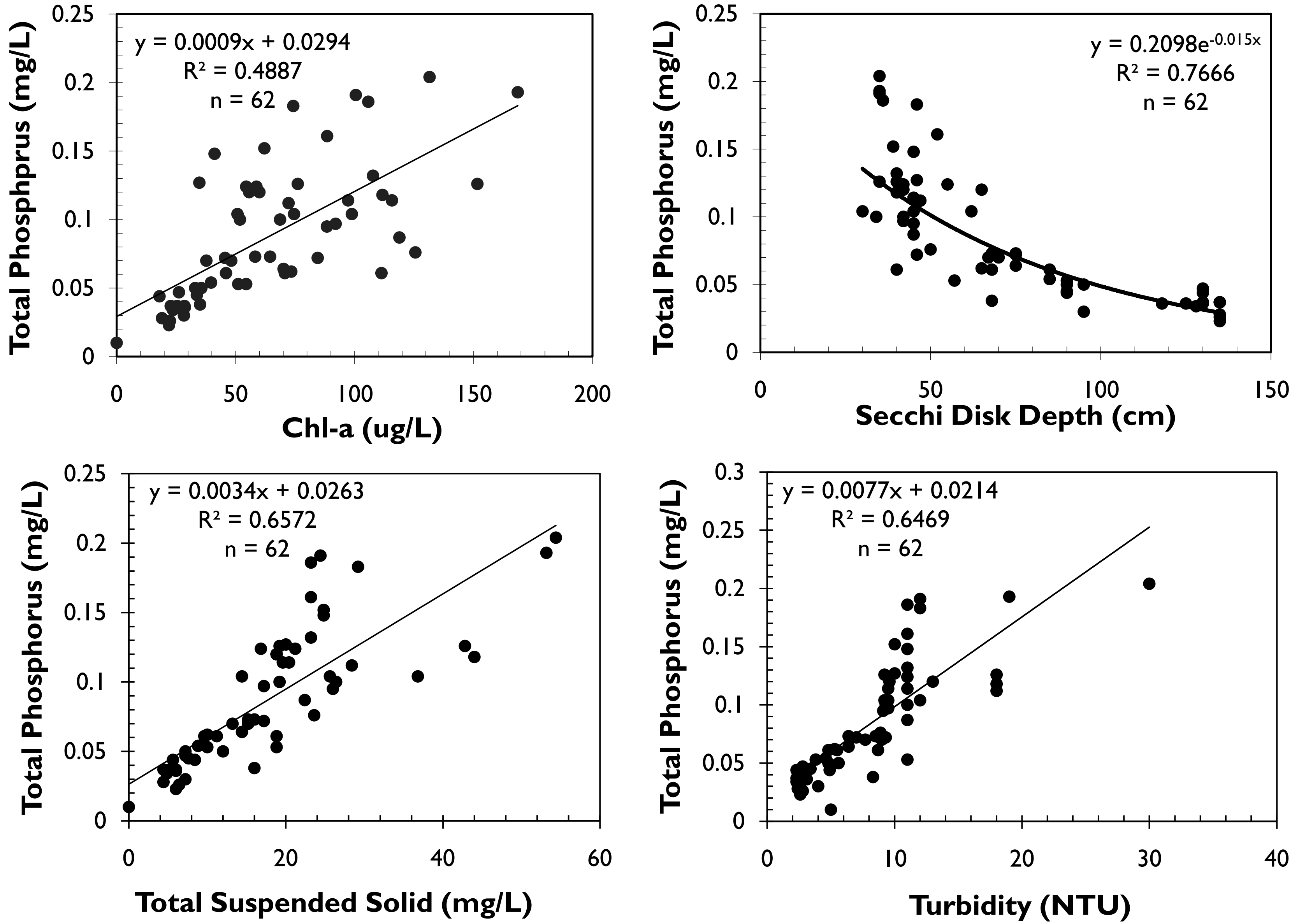

3. Datasets-Chl-a, TP, TN, turbidity, TSS and SDT (2006)

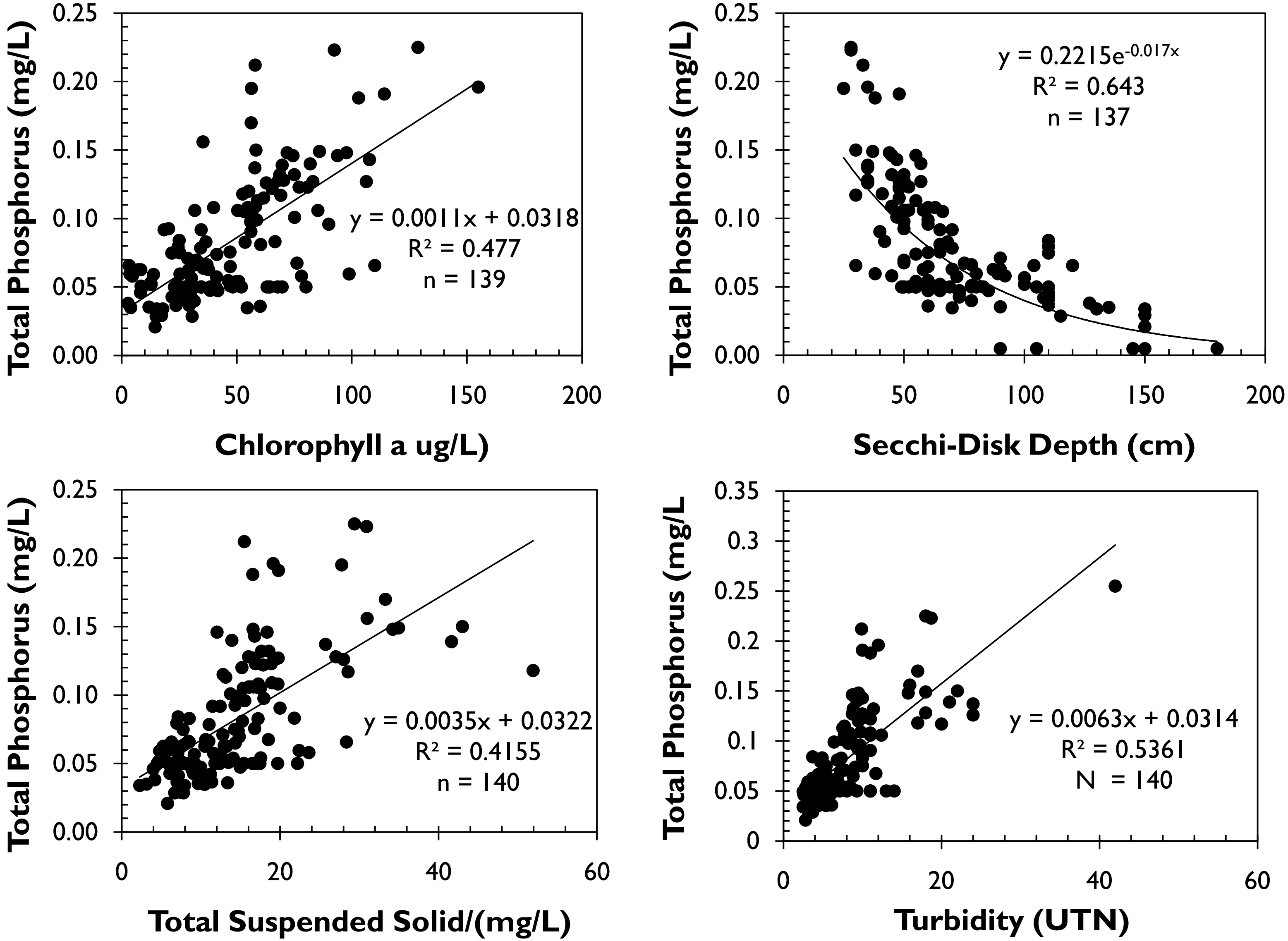

3. Datasets-spectra and images

- In situ
  - ASD, Ocean Optics, Secchi Disk
    - 2005-Morese and Geist Reservoir (ASD)
    - 2006-Morese, Eagle Creek and Geist Reservoir (ASD)
    - 2008-Morse Reservoir (Ocean Optics)
- AISA (9/6/2005)->Morse and Geist
  - Spectral range (392-981nm), 62 bands, 10 nm, 1 m
  - Calibrated with the empirical line method
- Hyperion (6/9/2007)->Eagle Creek
  - Spectral range (426-2396 nm), 242 bands, 10 nm, 30 m
  - Radiomtrically calibrate with ACORN

4. Methods-Spectral Modeling Approach

- Correlation Analysis
  - Selecting the most sensitive spectral variables to water quality parameters
    - In situ and imaging spectral data
    - Reflectance derivative
    - Band ratio (all about 300,000 combinations)
  - High correlation coefficients indicate sensitive spectral variables
- Linear and non-linear empirical models were built based on optimal band ratios
  - TP, Chl-a and SDT

4. Methods-Spectral Modeling Approach

- Genetic Algorithms (GA)-Partial Least Square (PLS)
  - GA for selecting optimal spectral parameters
  - PLS as the spectral-compositional model

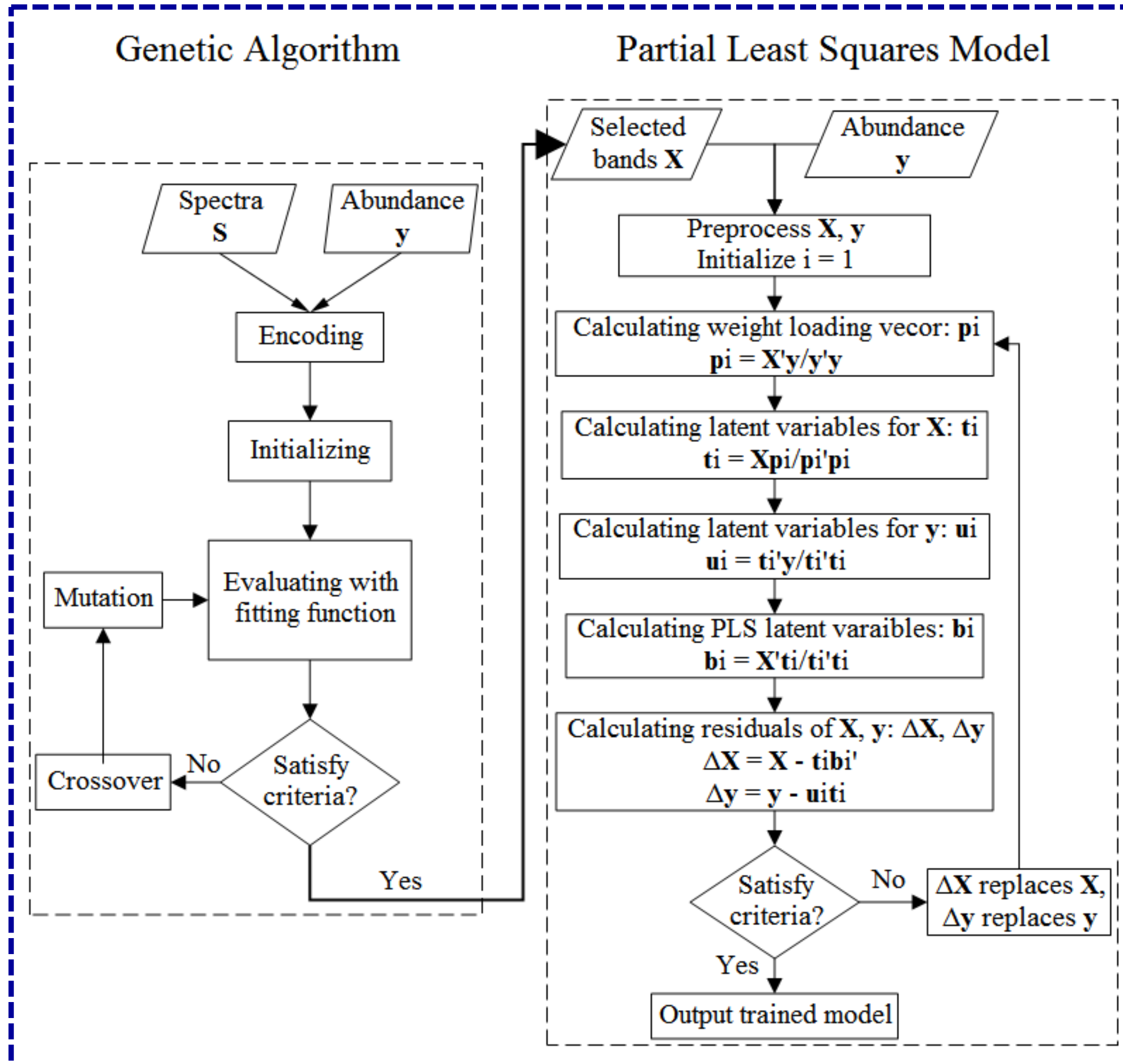

4. Methods-Spectral Modeling Approach

- Back-Propagation Neural Network (BPNN)-PLS
  - PLS provides the input variables for BPNN
  - BPNN accommodates nonlinearity

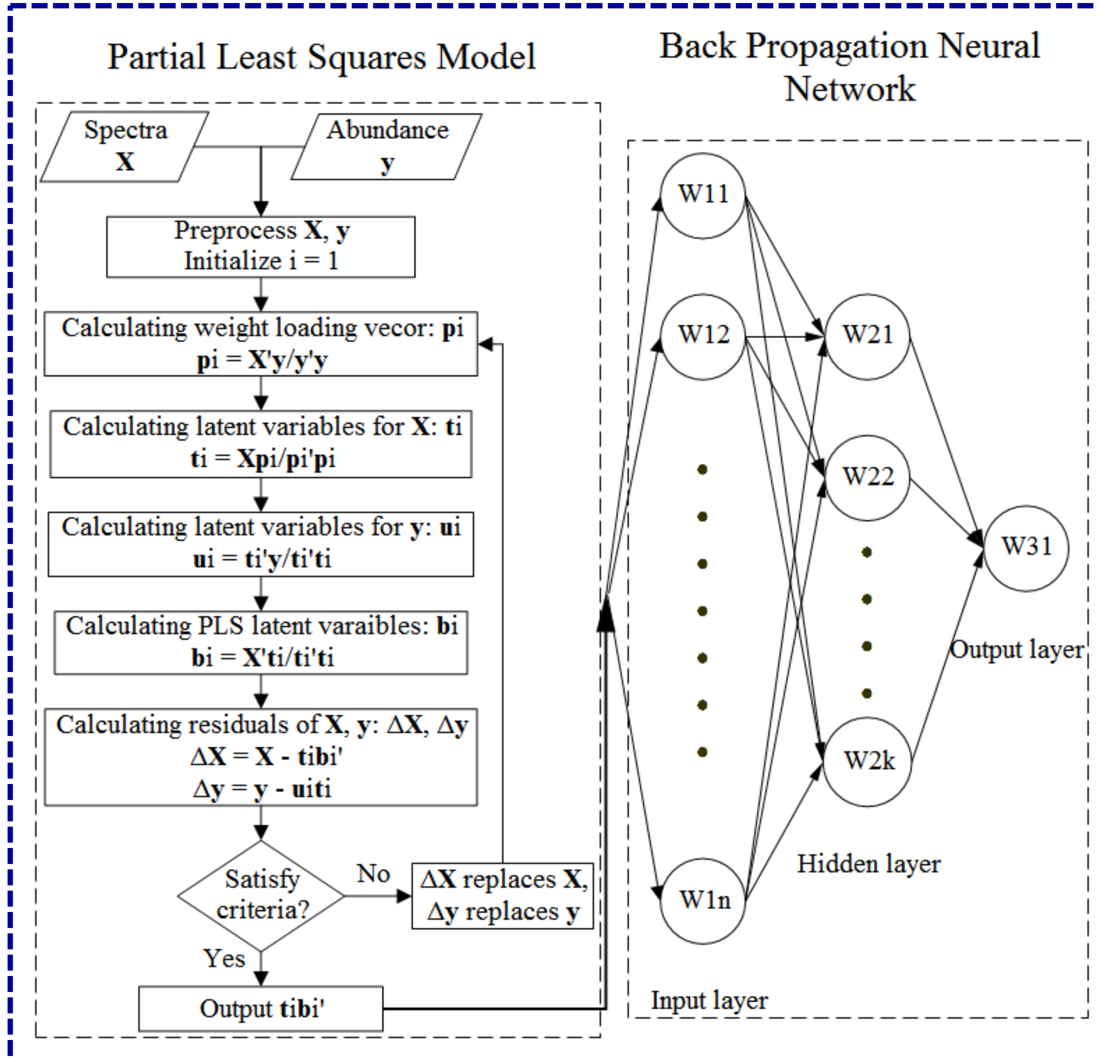

4. Methods-Eutrophic assessment

Carlson trophic index

$$\mathrm{TSI(TP)} = 10\left(6 - \frac{\ln(\frac{48}{\mathrm{TP}})}{\ln(2)}\right)$$

$$\mathrm{TSI(Chl-a)} = 10\left(6 - \frac{2.04 - 0.68\ln(\mathrm{Chl-a})}{\ln(2)}\right)$$

$$\mathrm{TSI(SDD)} = 10\left(6 - \frac{\ln(\mathrm{SDD})}{\ln(2)}\right)$$

TSI (average)= [TSI(TP)+TSI (Chl-a)+TSI (SDD)]/3

5. Results and Discussion-In Situ Data (2005)

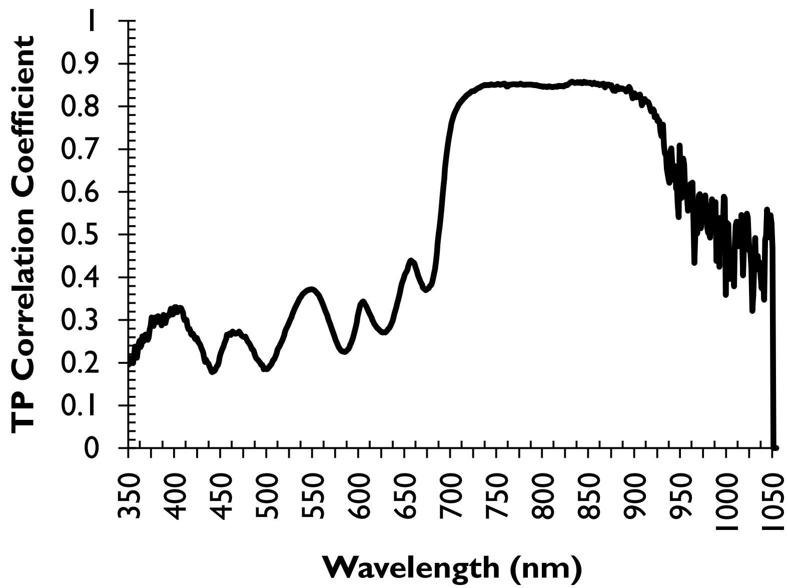

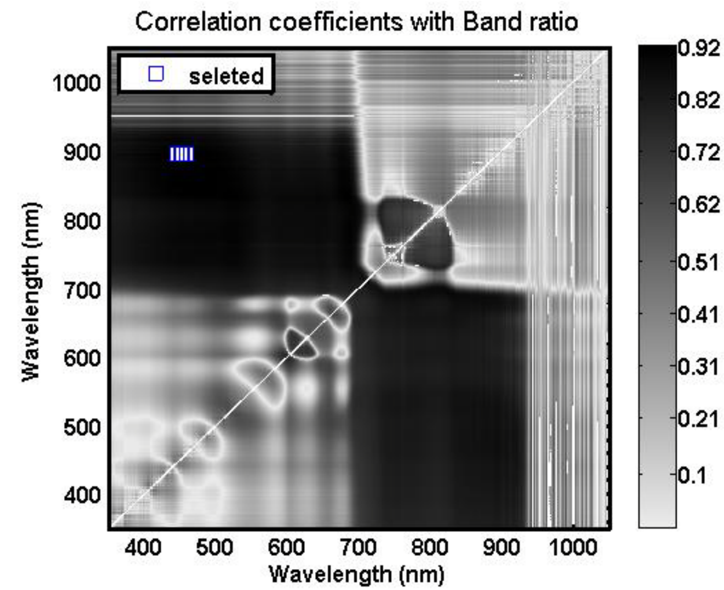

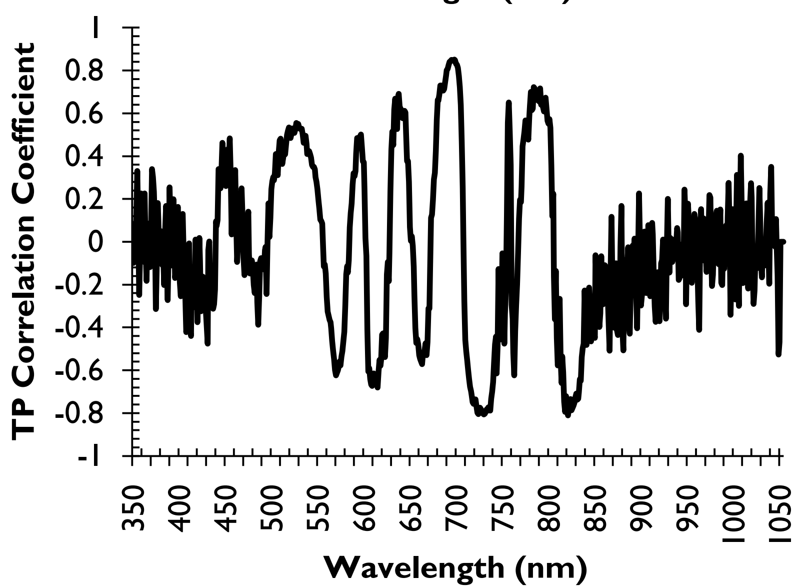

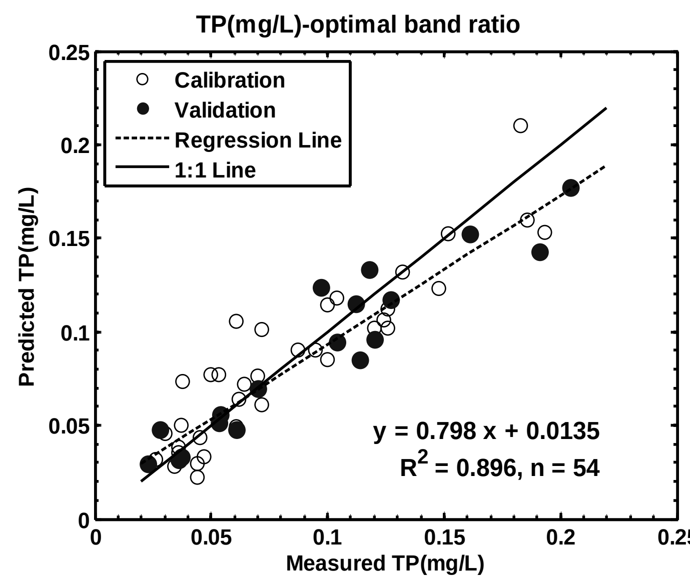

5. Results and Discussion-In Situ Data (2005)

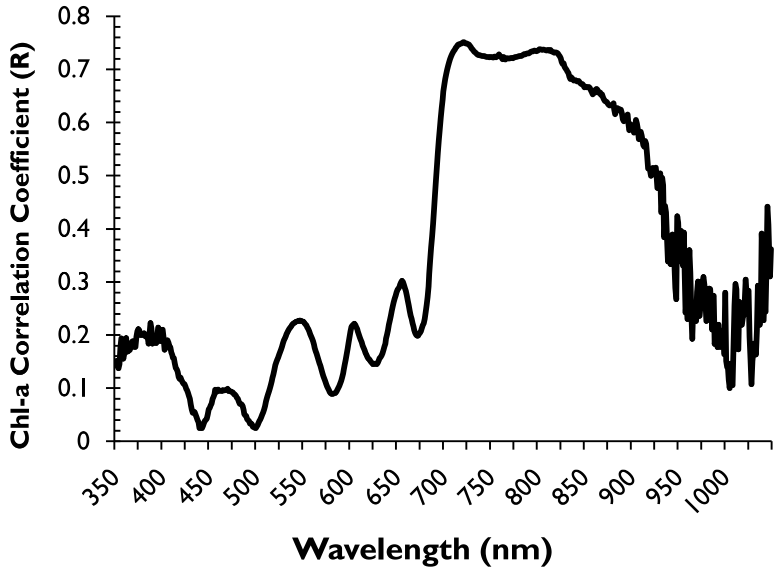

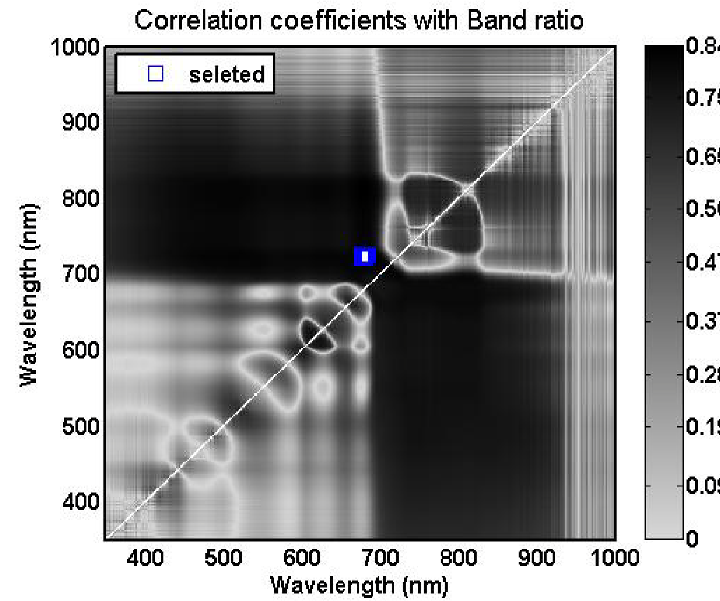

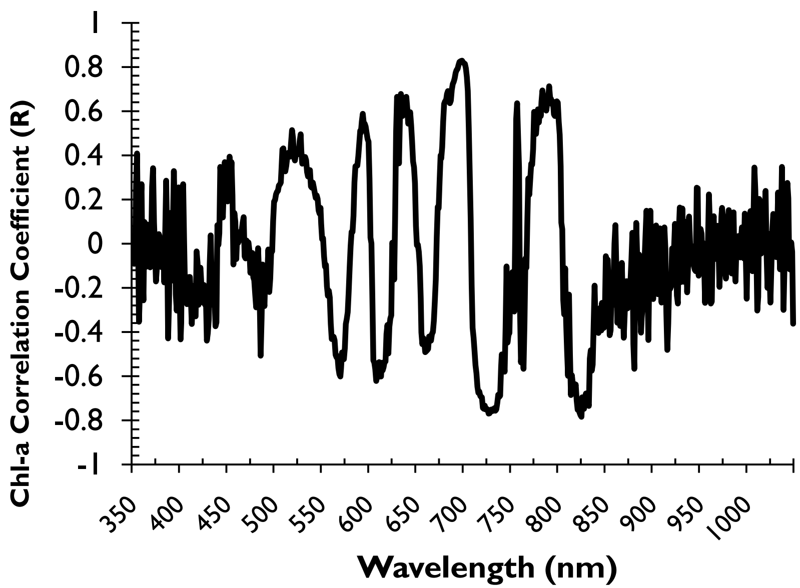

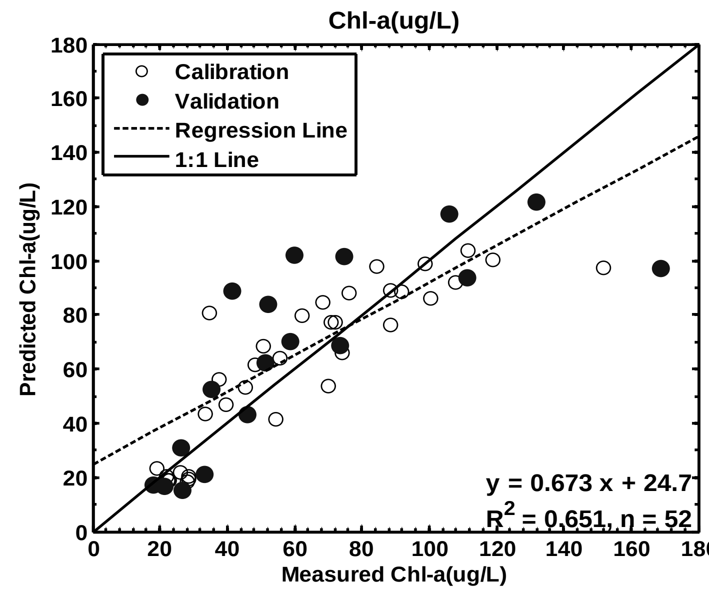

5. Results and Discussion-In Situ Data (2005)

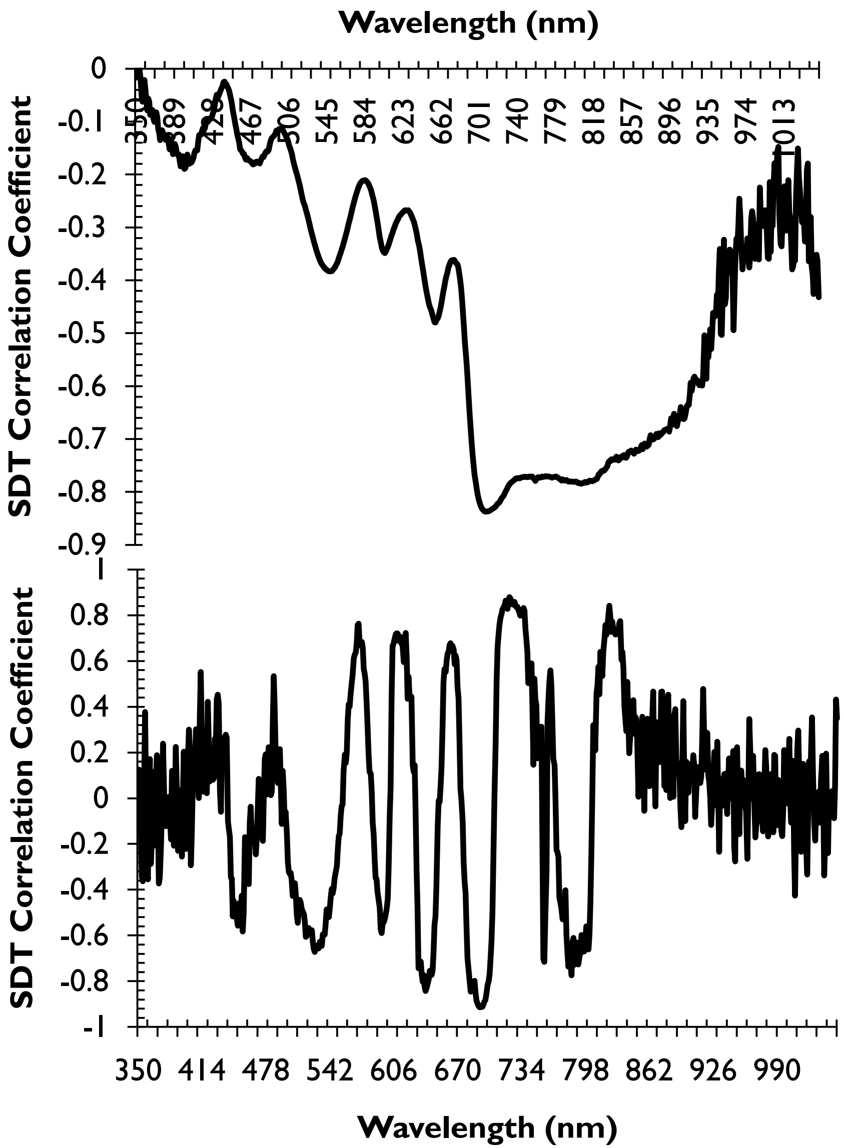

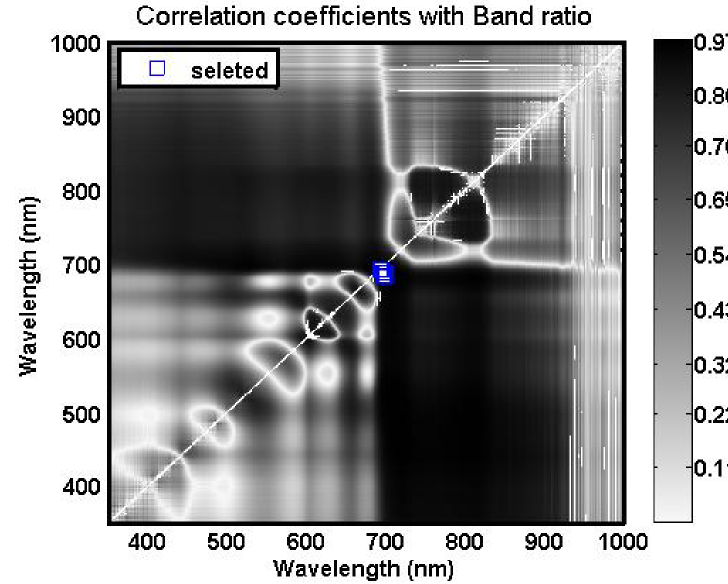

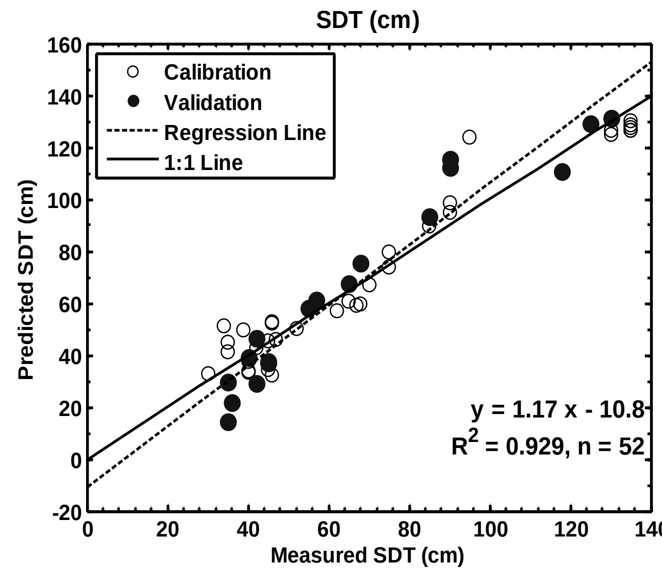

5. Results and Discussion-In Situ Data (2005)

GA-PLS

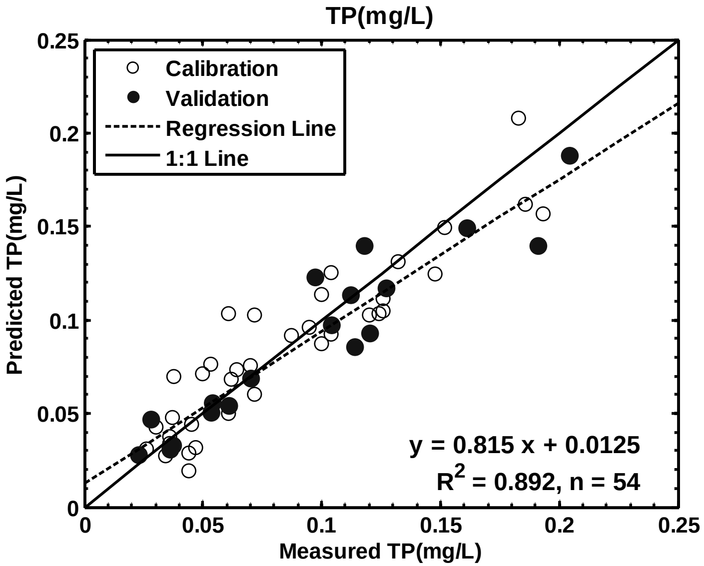

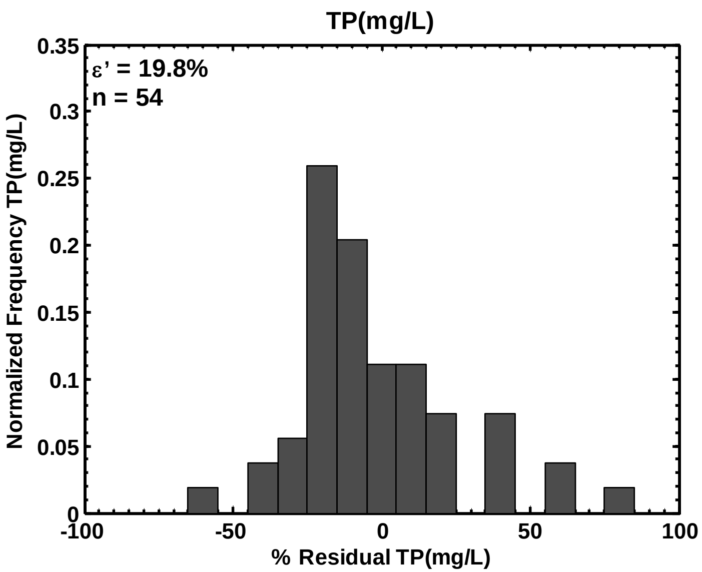

BPNN-PLS

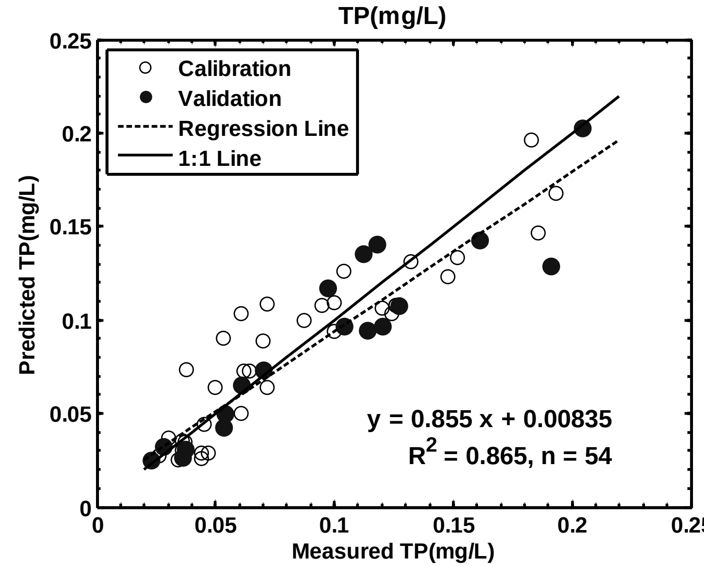

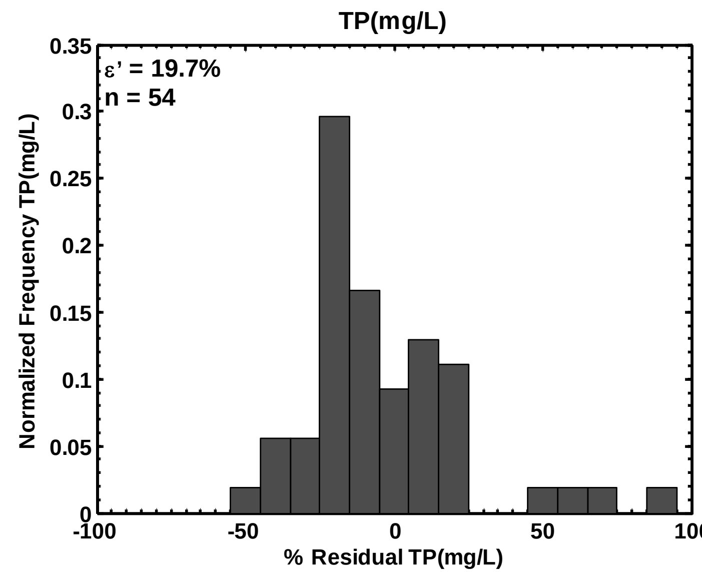

Error = (Predicted-measured)/measured

5. Results and Discussion-In Situ Data (2005)

GA-PLS

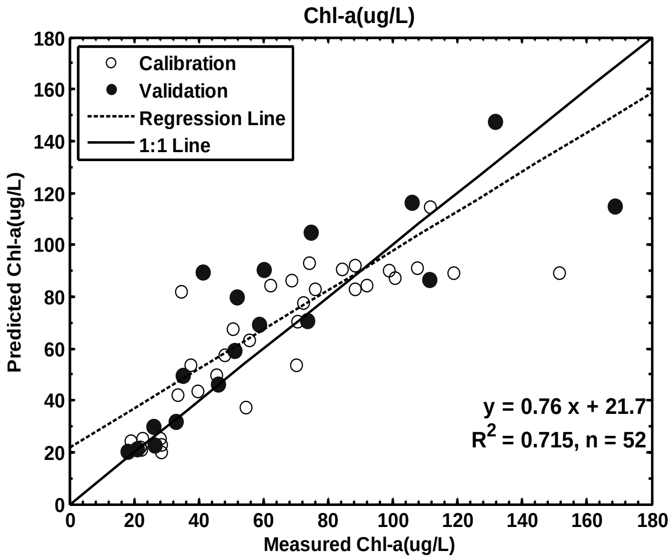

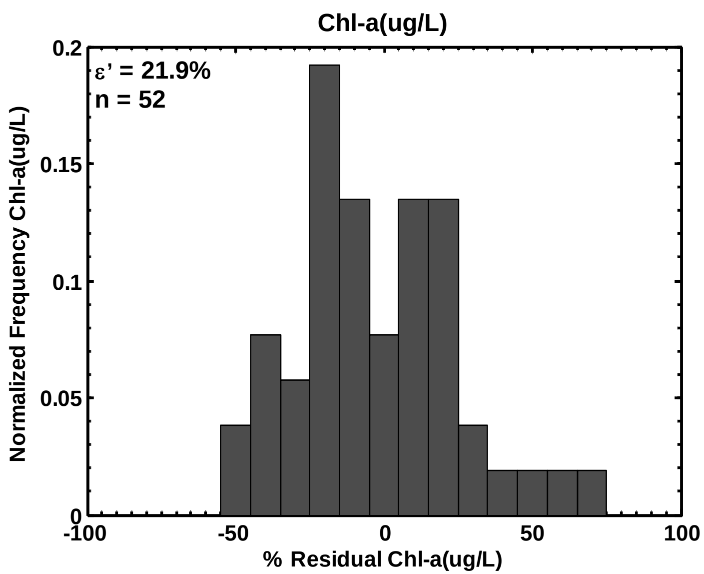

BPNN-PLS

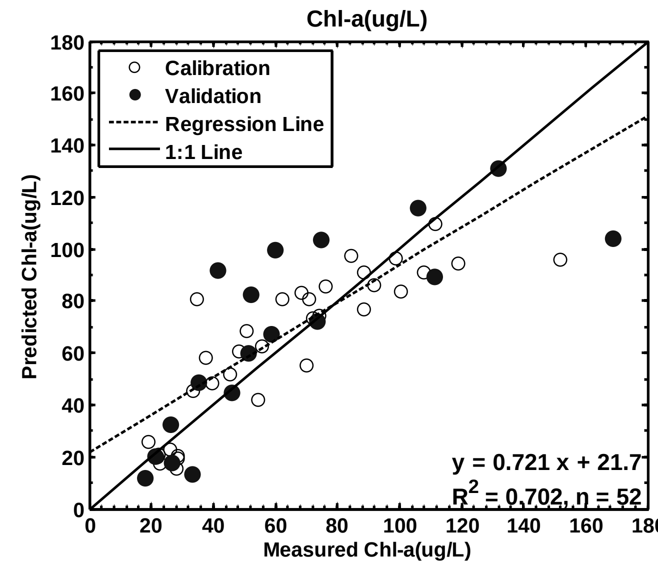

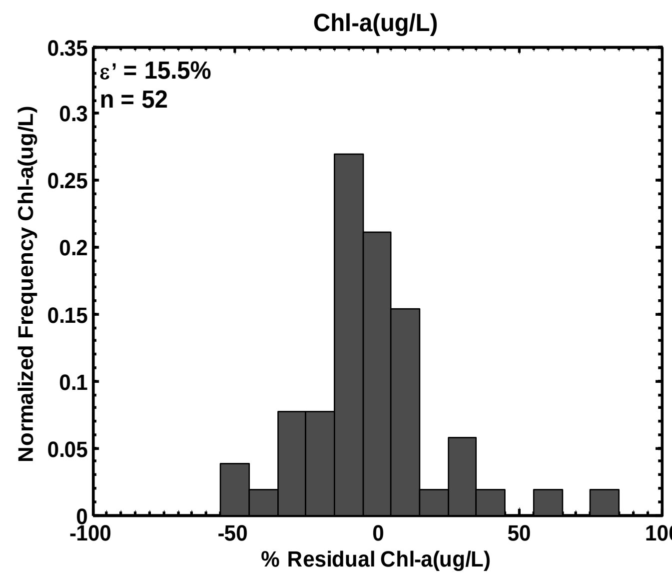

5. Results and Discussion-In Situ Data (2005)

GA-PLS

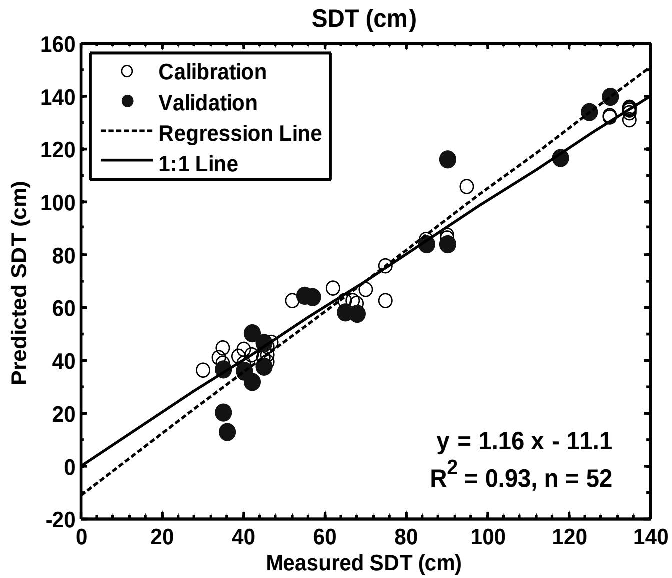

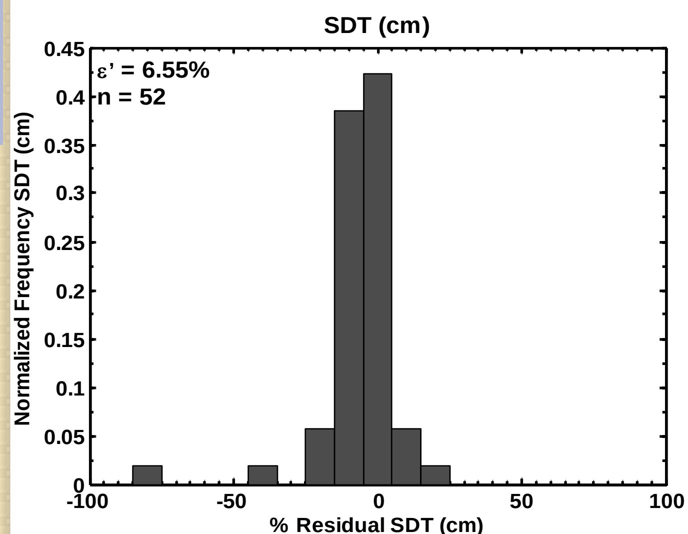

BPNN-PLS

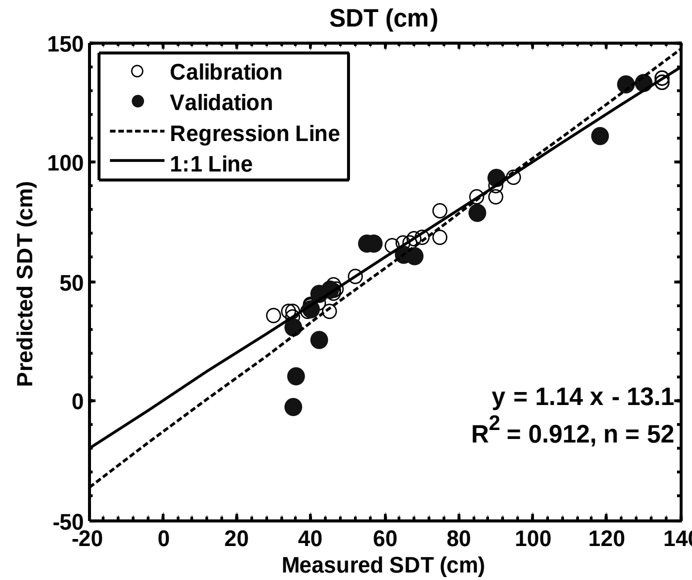

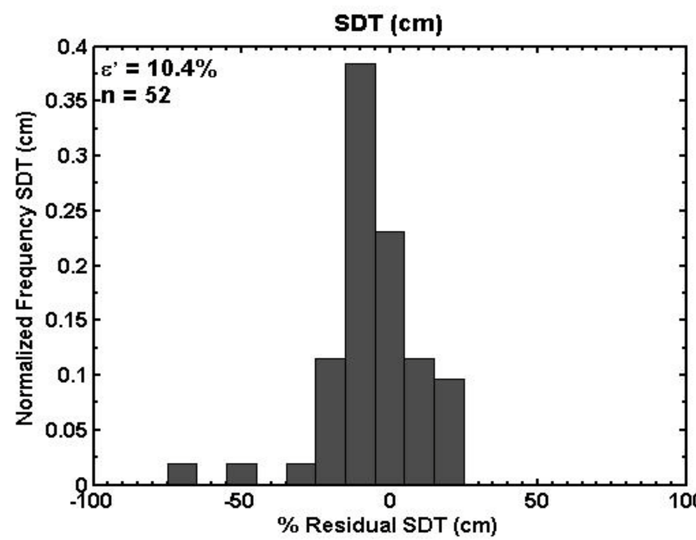

5. Results and Discussion-In Situ Data (2006)

GA-PLS

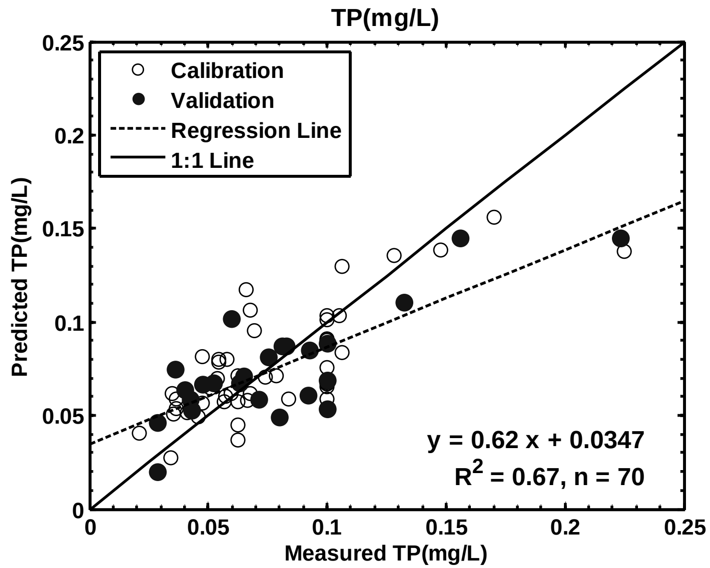

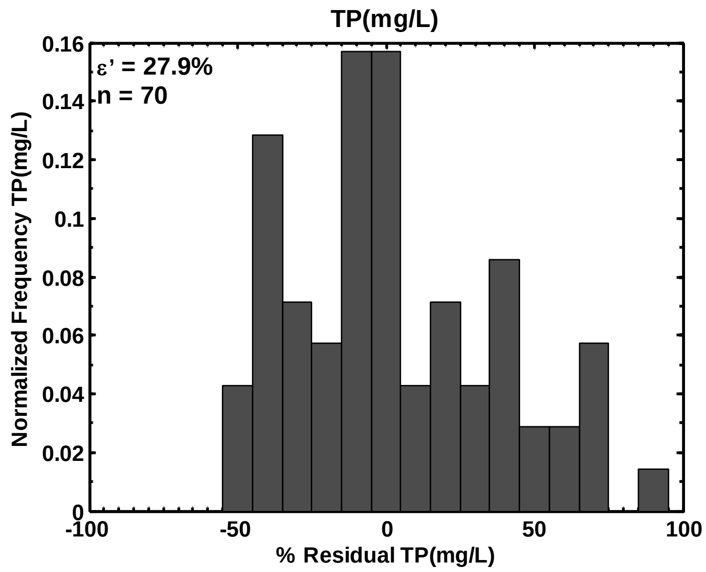

BPNN-PLS

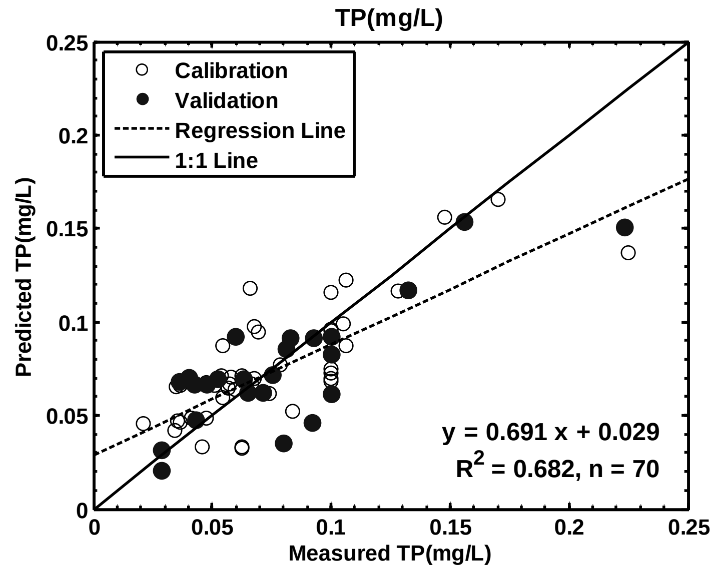

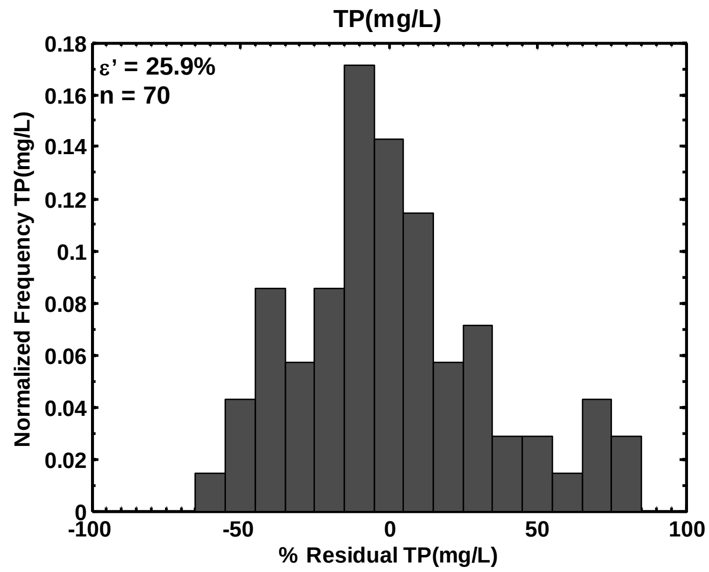

5. Results and Discussion-In Situ Data (2006)

GA-PLS

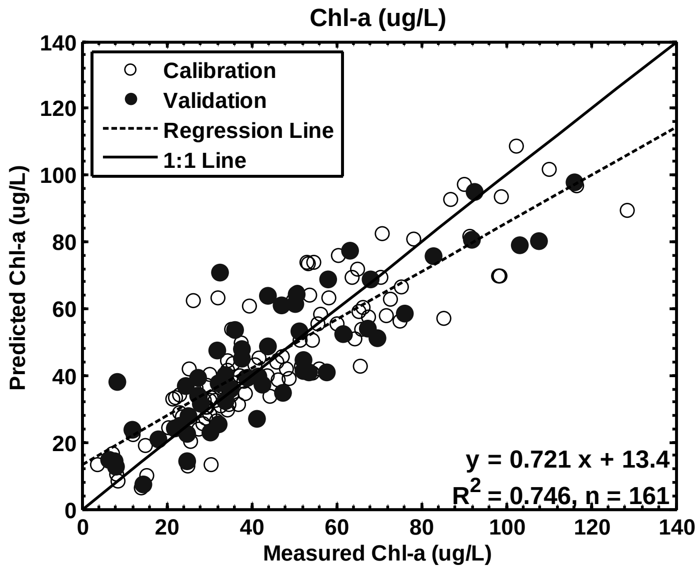

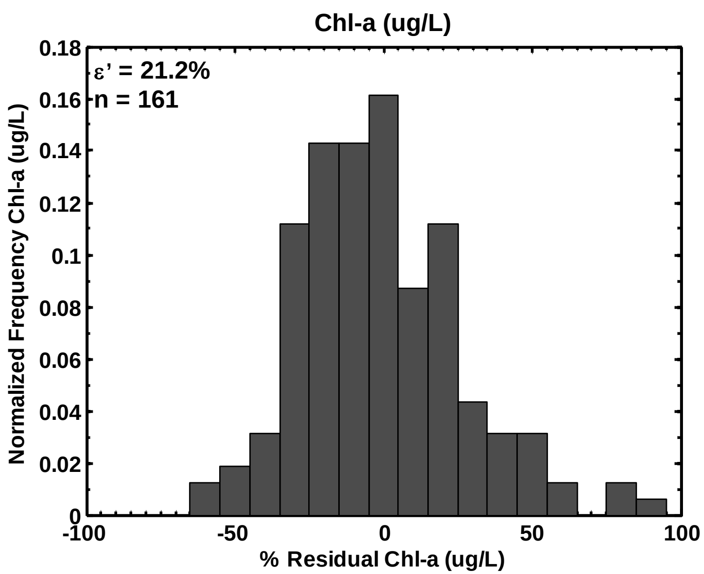

BPNN-PLS

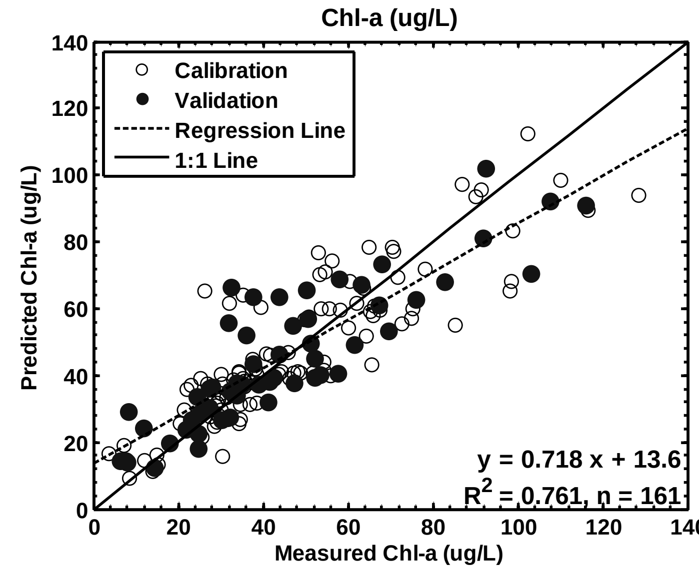

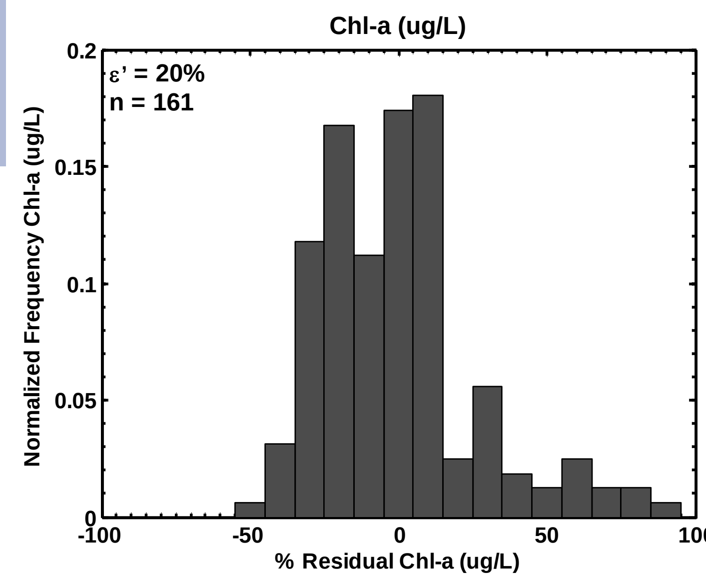

5. Results and Discussion-In Situ Data (2006)

GA-PLS

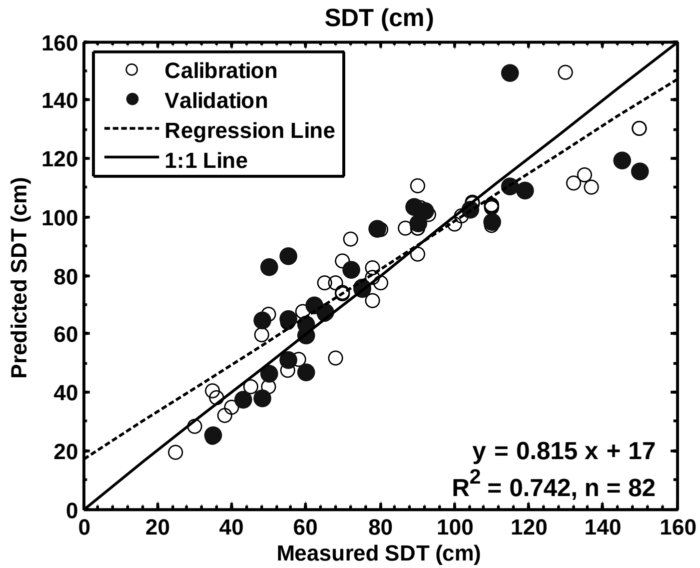

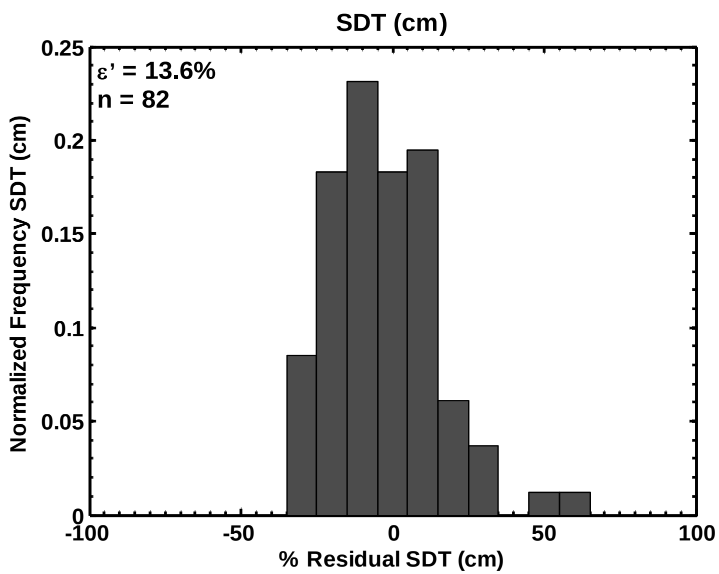

BPNN-PLS

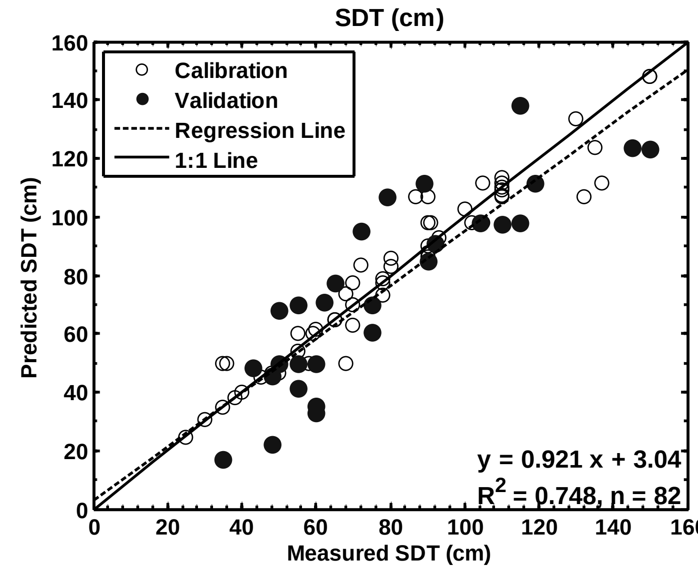

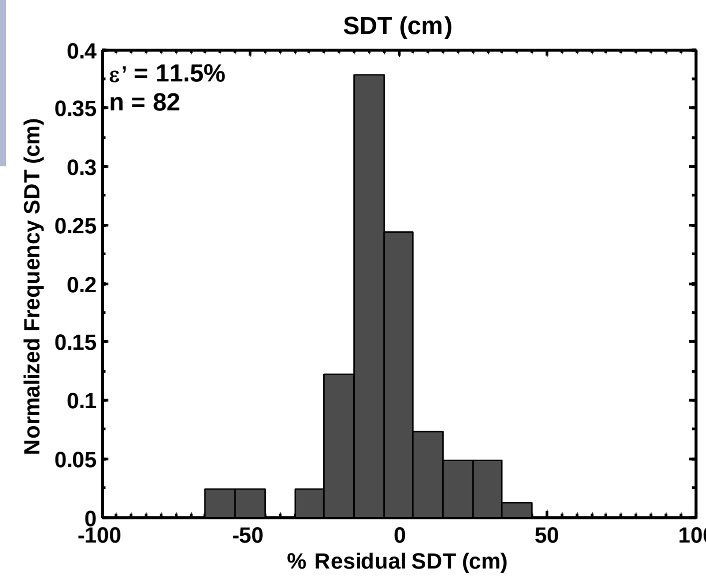

5. Results and Discussion-In Situ Data (2008)

GA-PLS

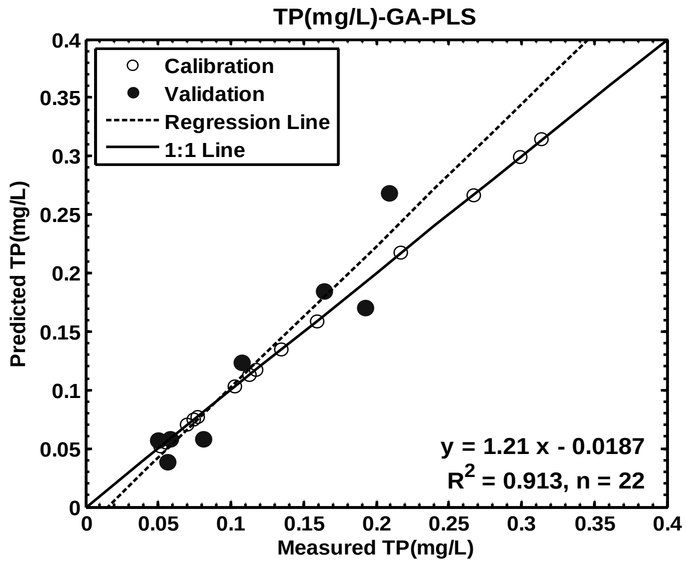

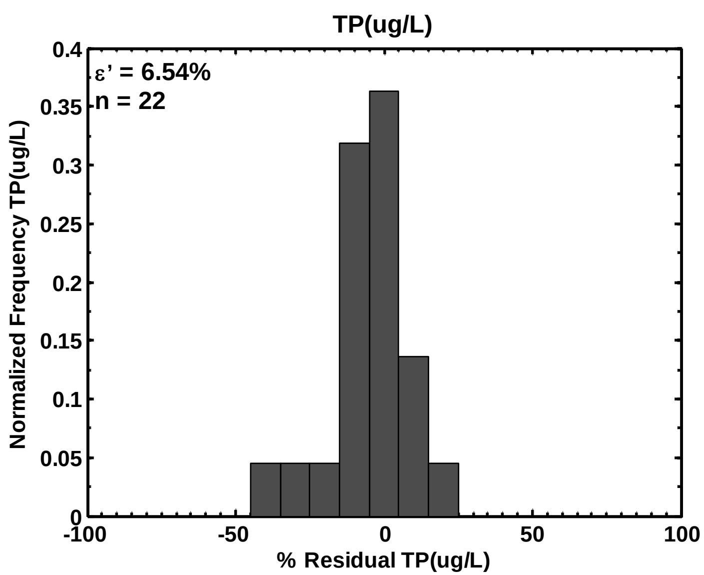

GA-PLS

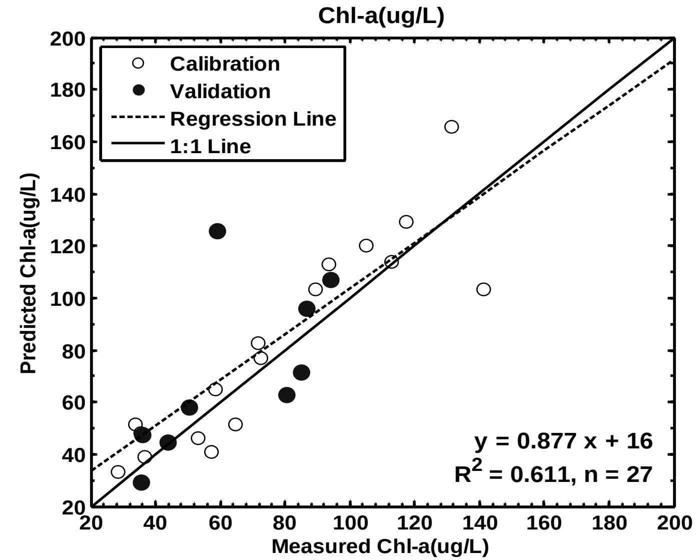

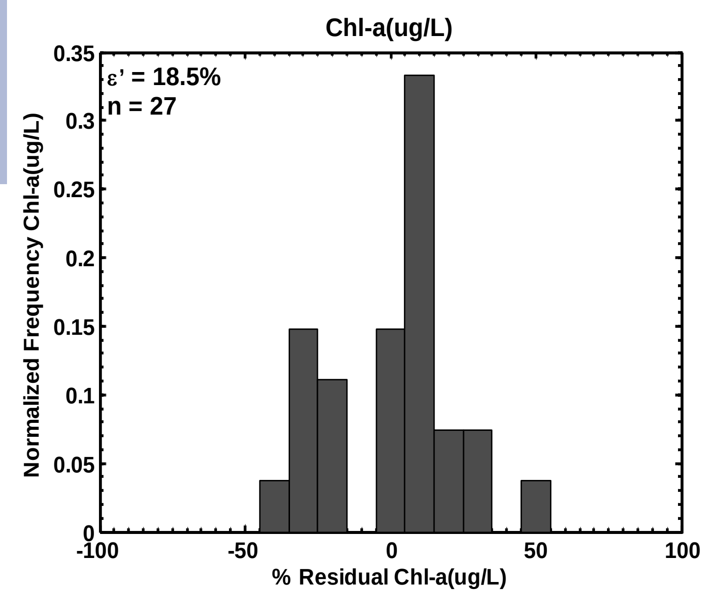

5. Results and Discussion- AISA Image Data

Analysis Result of the Morse Reservoir

GA-PLS

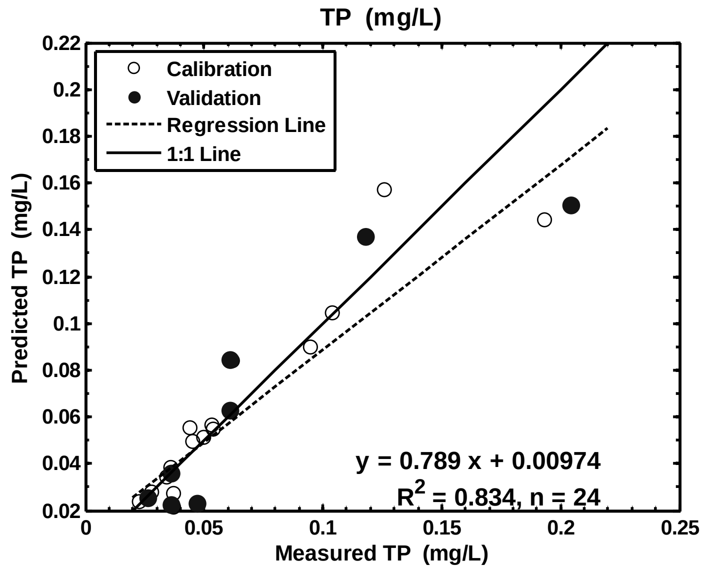

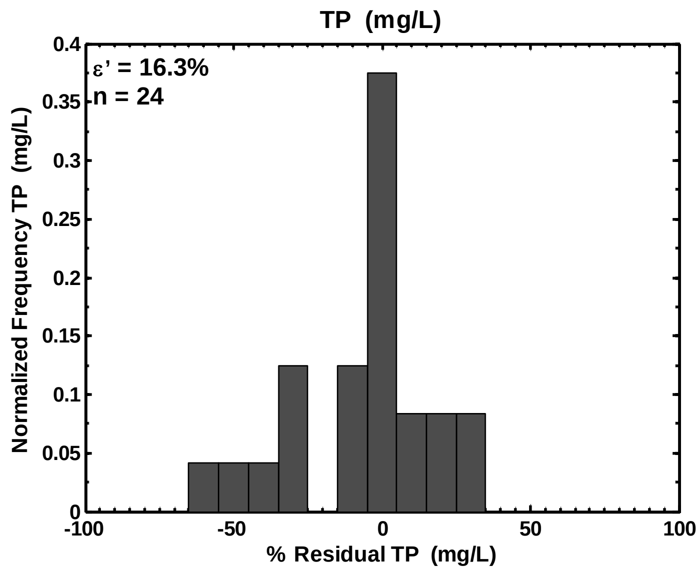

BPNN-PLS

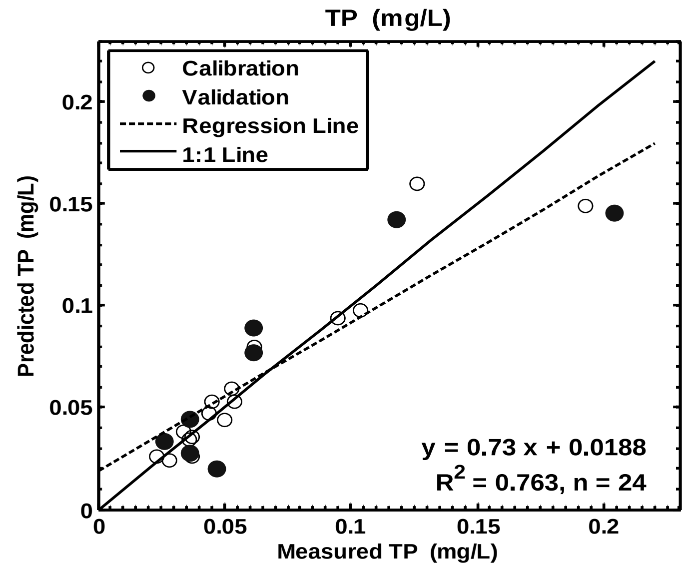

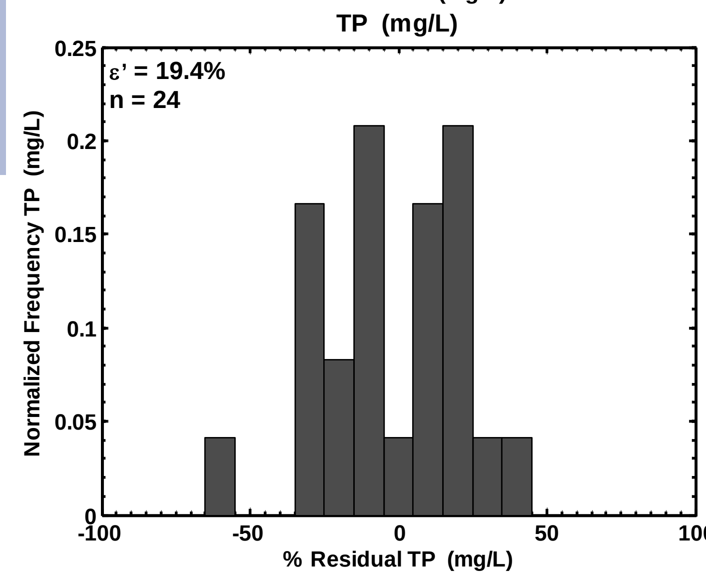

5. Results and Discussion- AISA Image Data

Analysis Result of the Morse Reservoir

GA-PLS

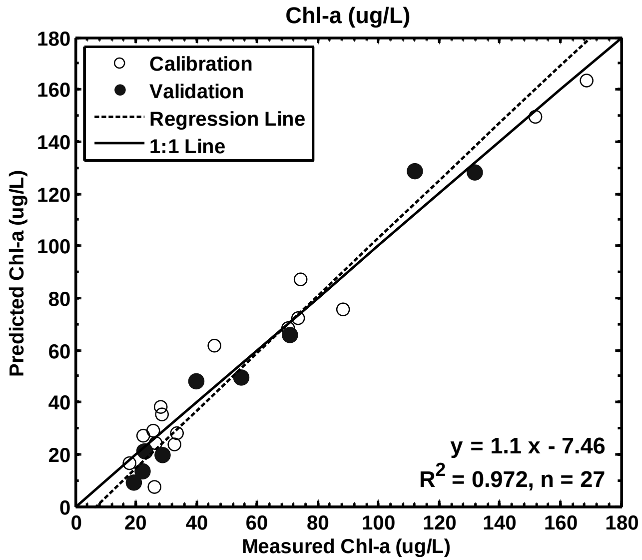

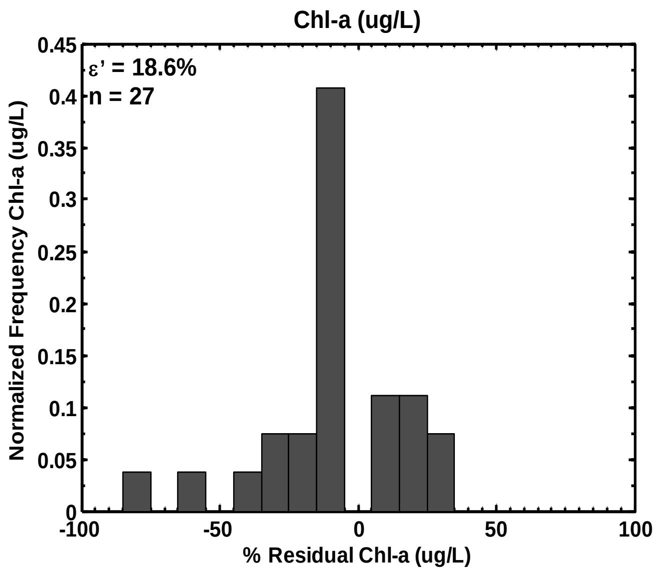

BPNN-PLS

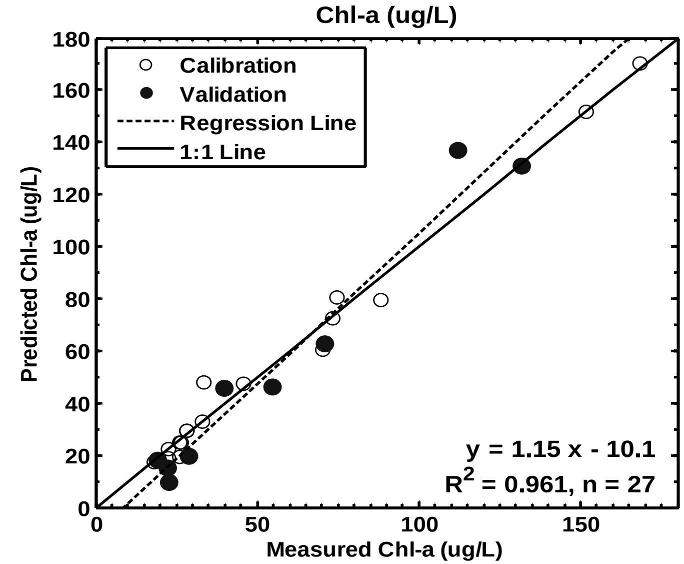

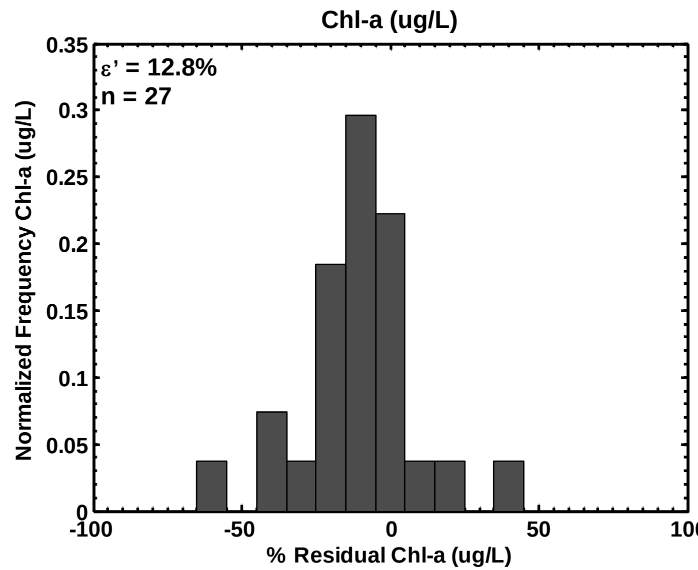

5. Results and Discussion- AISA Image Data

Analysis Result of the Morse Reservoir

GA-PLS

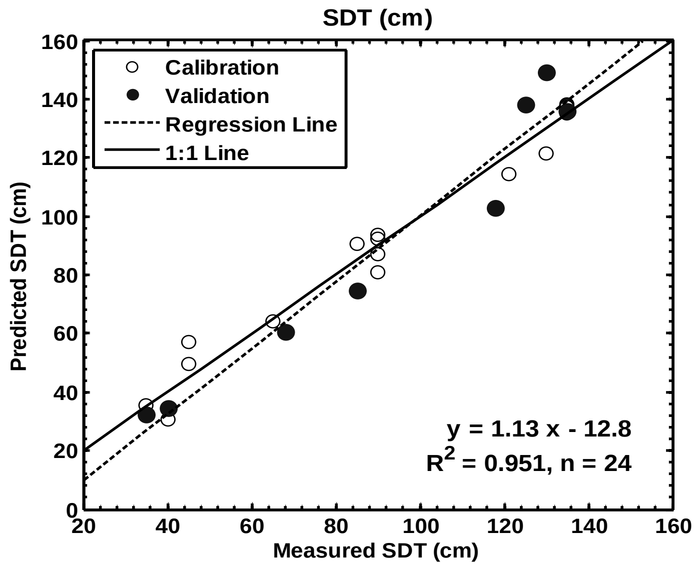

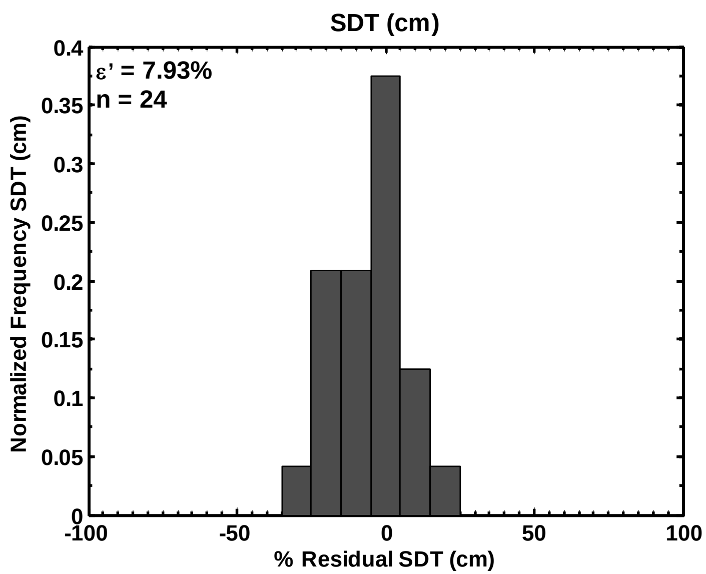

BPNN-PLS

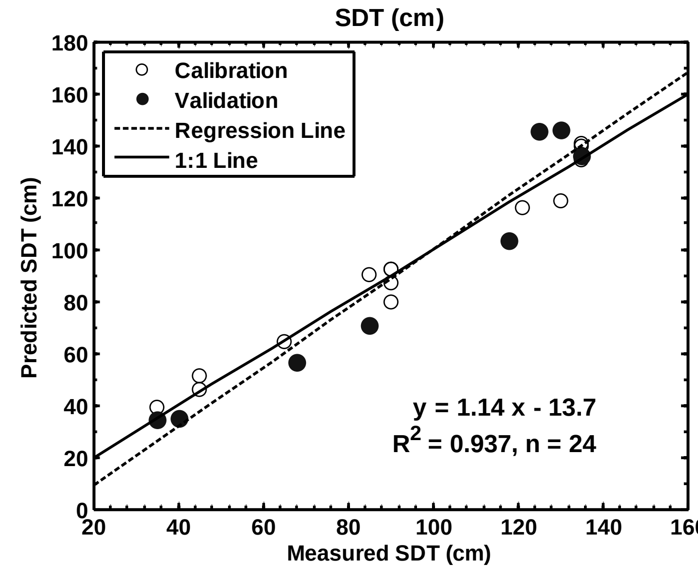

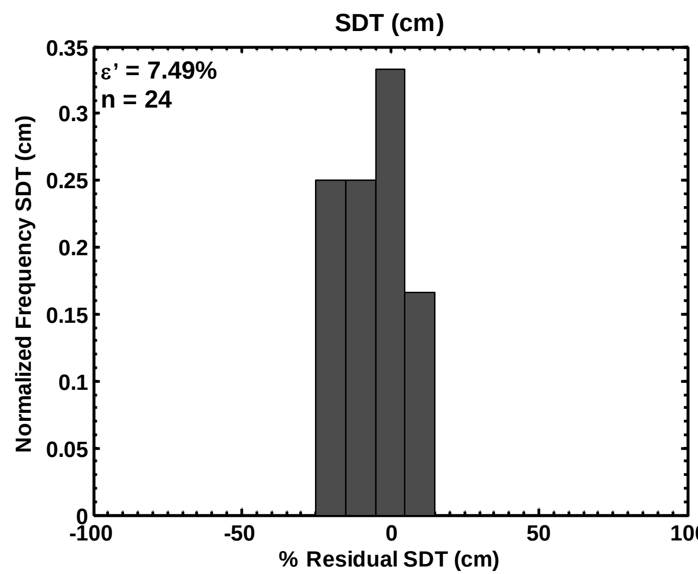

5. Results and Discussion- AISA Image Data

Analysis Result of the Morse Reservoir

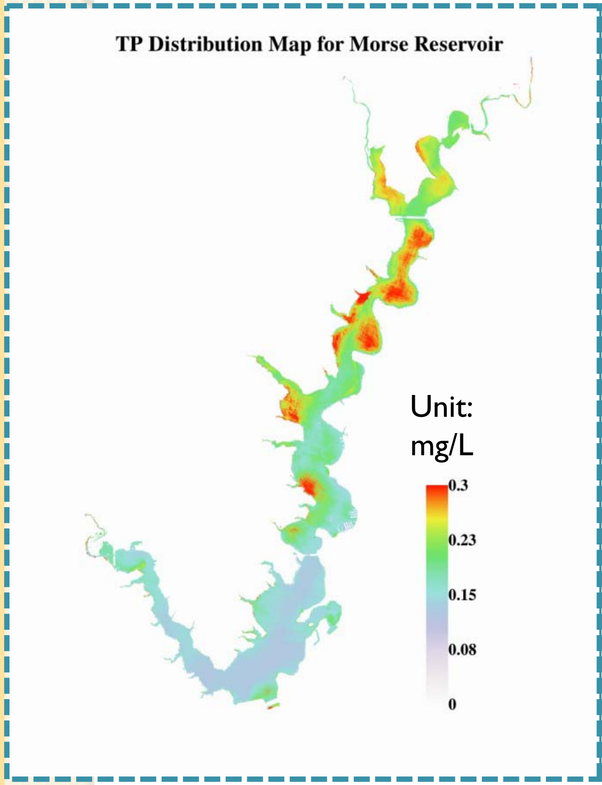

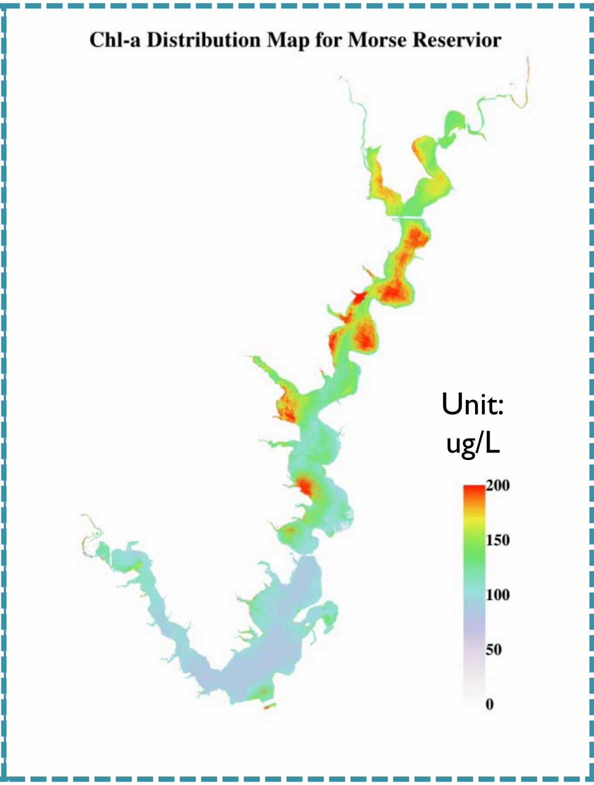

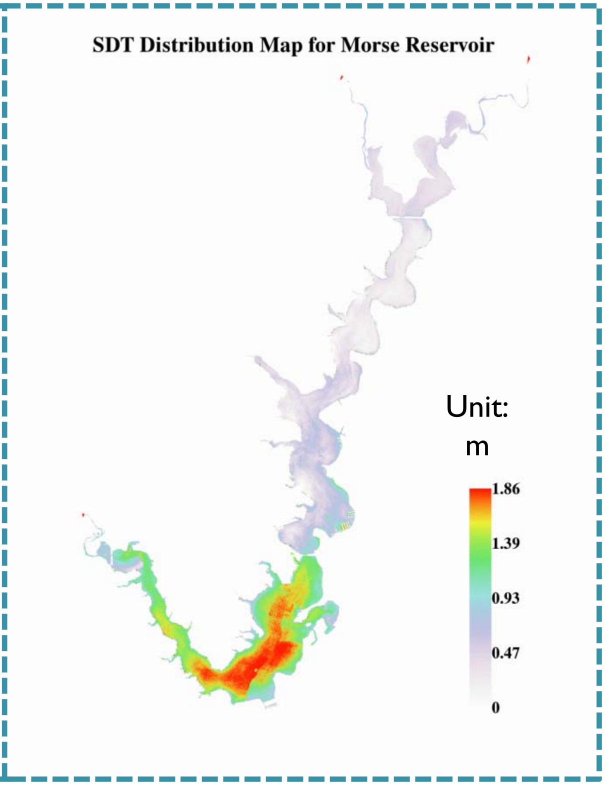

P (ug/L)	Chl (ug/L)	SD (m)	Trophic Class
0—12	0—2.6	>8—4	Oligotrophic
12—24	2.6—7.3	4—2	Mesotrophic
24—96	7.3—56	2—0.5	Eutrophic
96—384+	56—155+	0.5—<0.25	Hypereutrophic

5. Results and Discussion- AISA Image Data

Final Trophic Status Distribution Map for Morse Reservoir

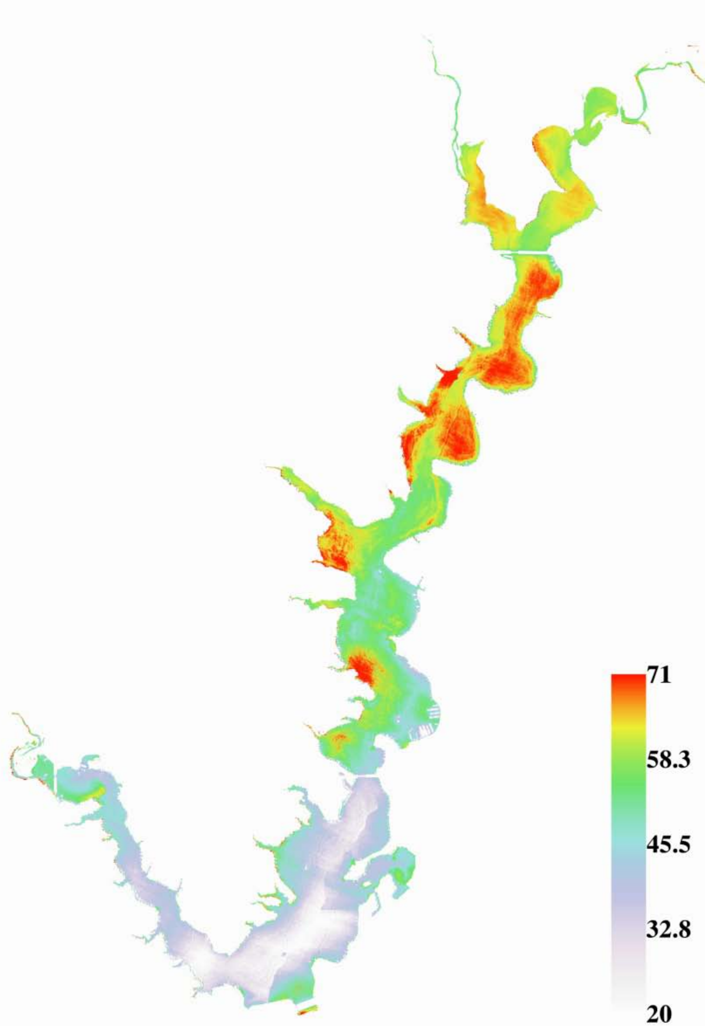

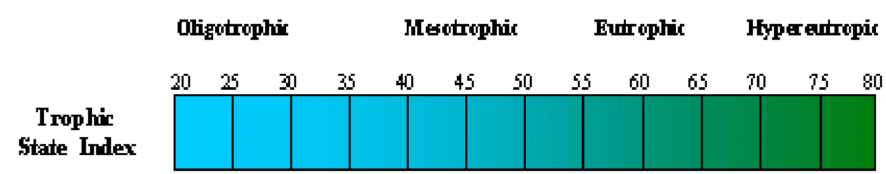

5. Results and Discussion- AISA Image Data

Analysis Result of the Geist Reservoir

GA-PLS

BPNN-PLS

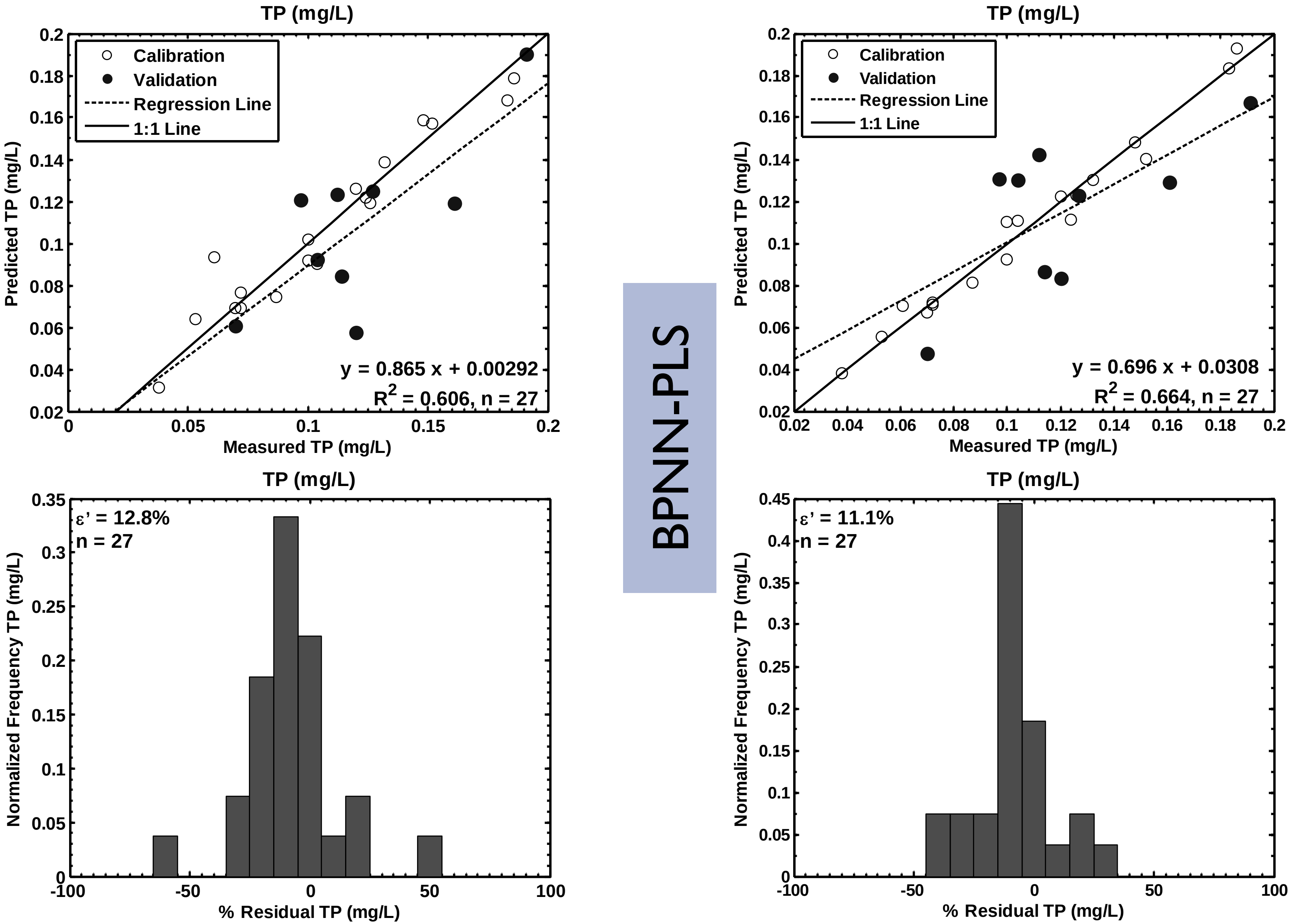

5. Results and Discussion- AISA Image Data

Analysis Result of the Geist Reservoir

GA-PLS

BPNN-PLS

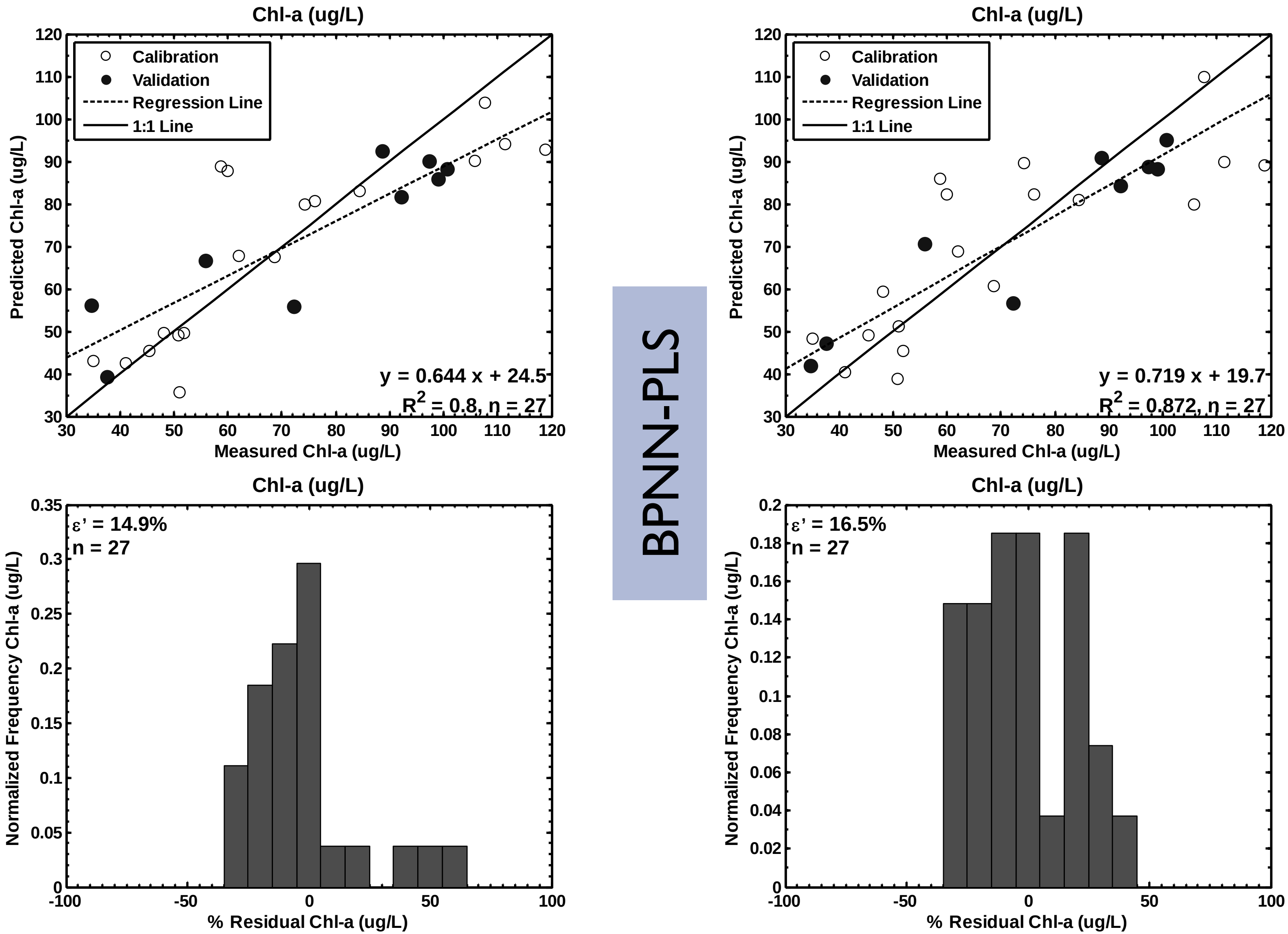

5. Results and Discussion- AISA Image Data

Analysis Result of the Geist Reservoir

GA-PLS

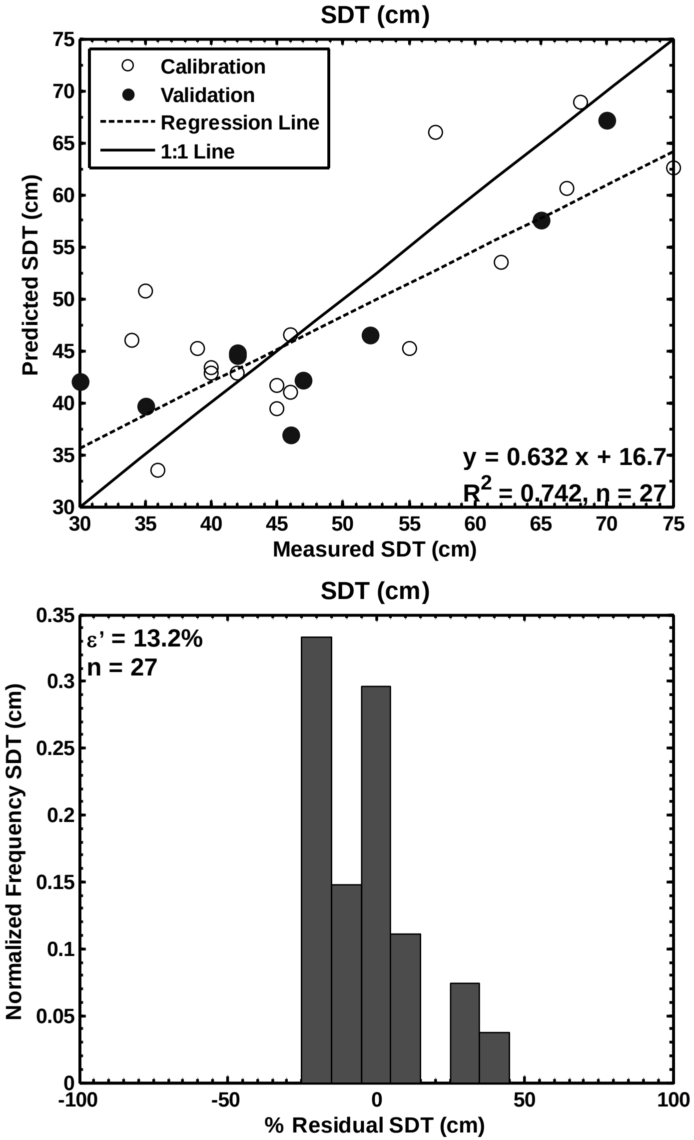

BPNN-PLS

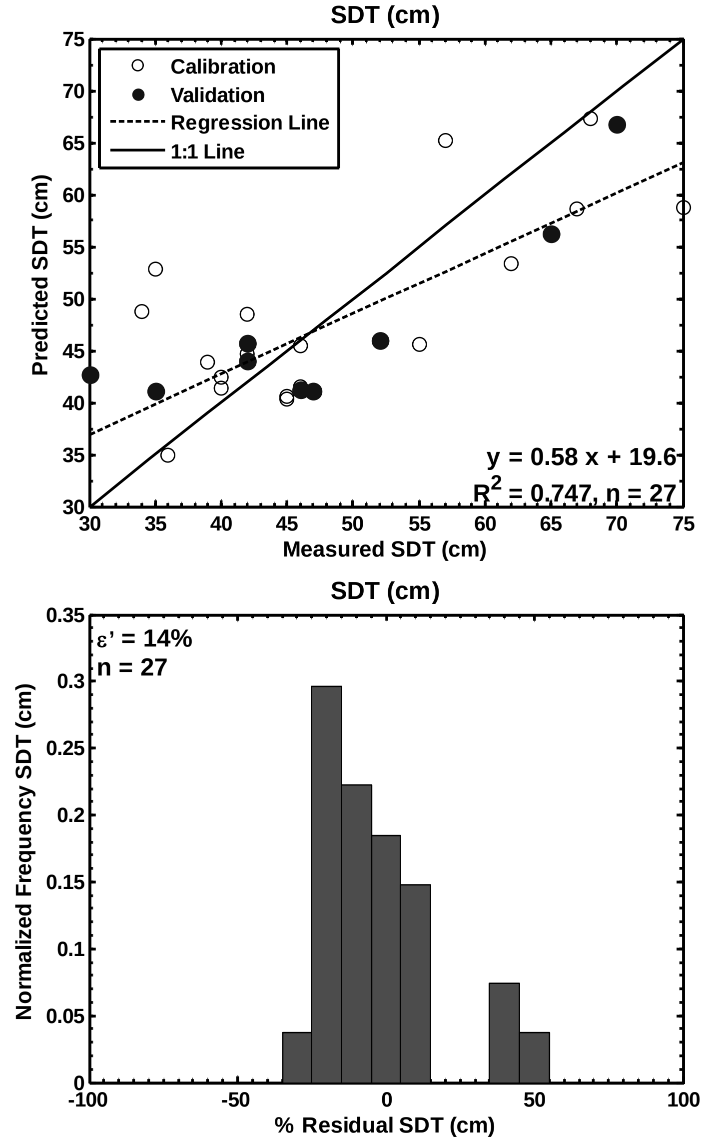

5. Results and Discussion- AISA Image Data

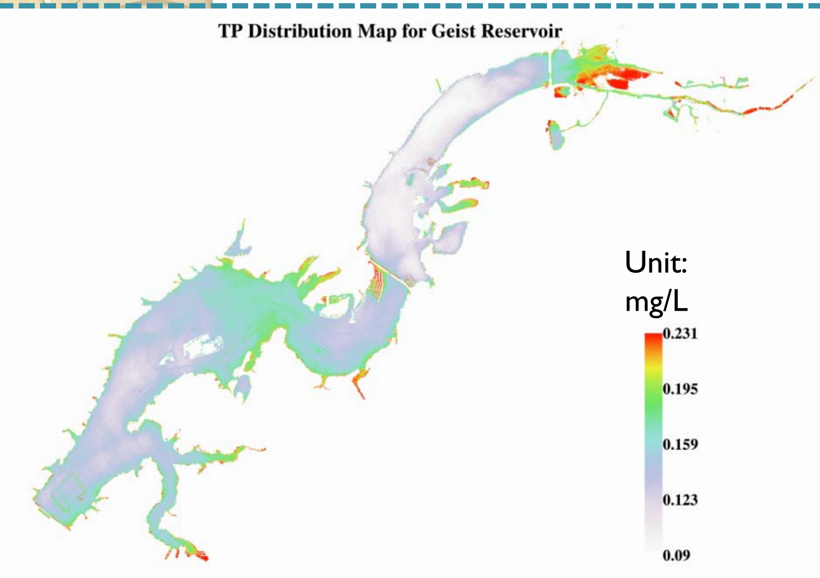

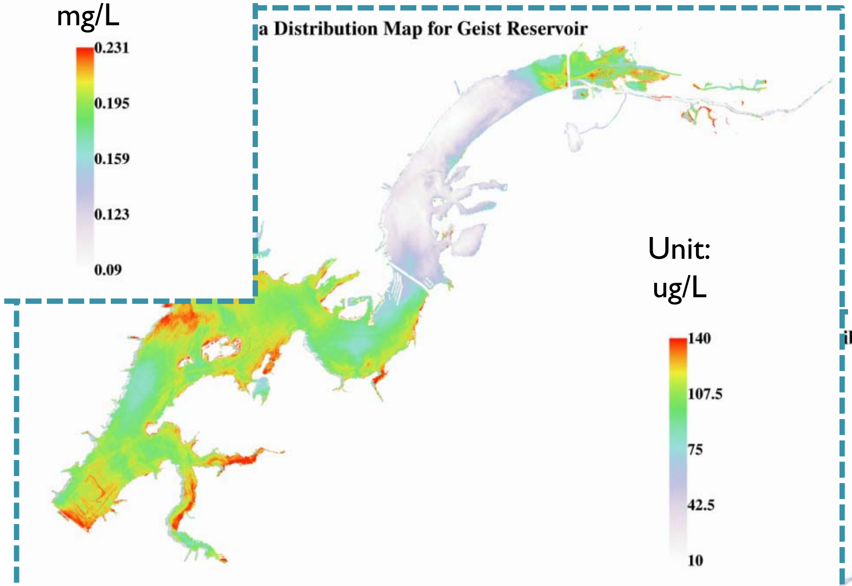

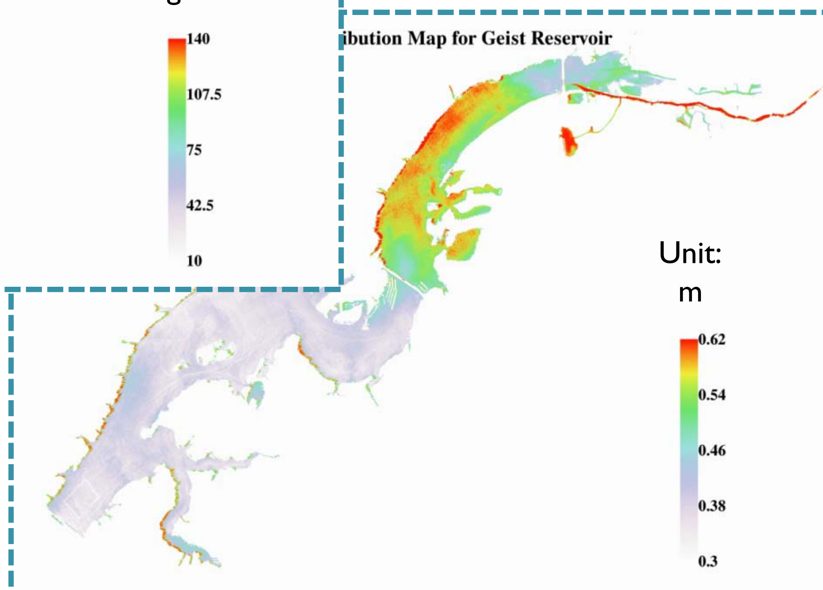

5. Results and Discussion- AISA Image Data

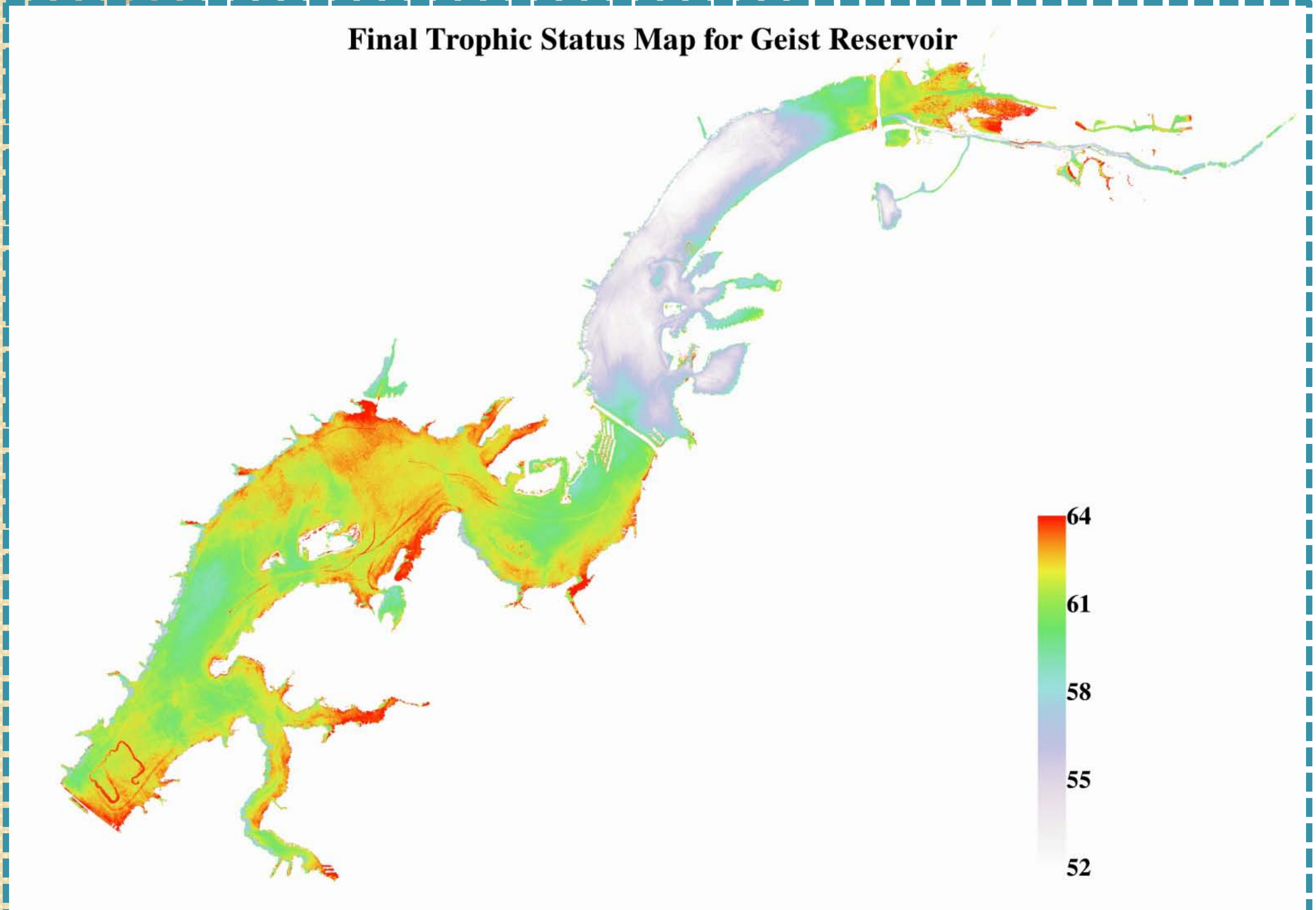

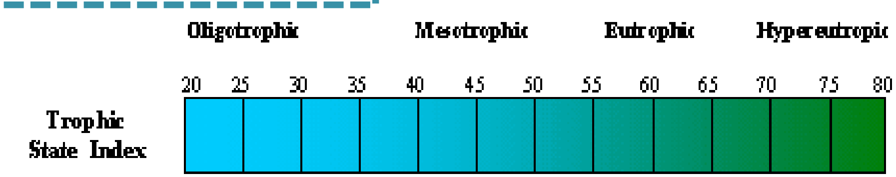

5. Results and Discussion-Hyperion Image Data

GA-PLS

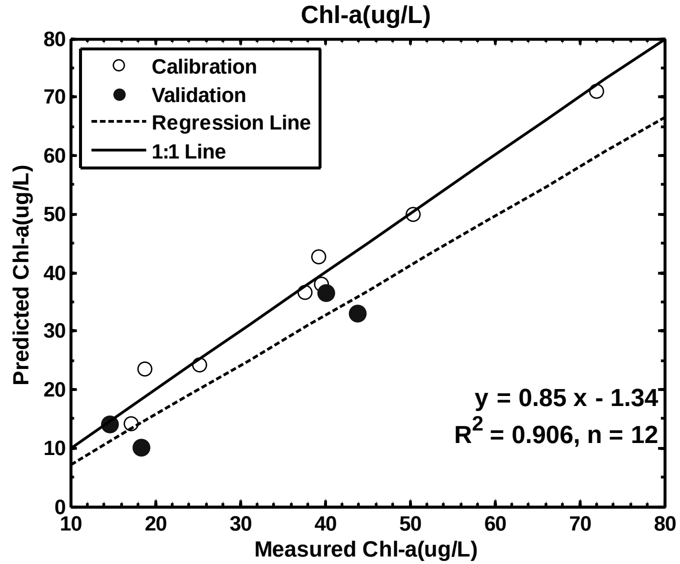

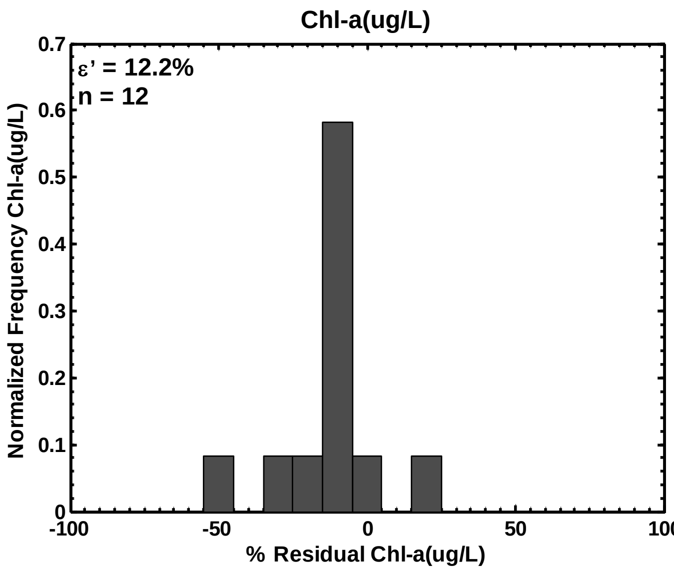

BPNN-PLS

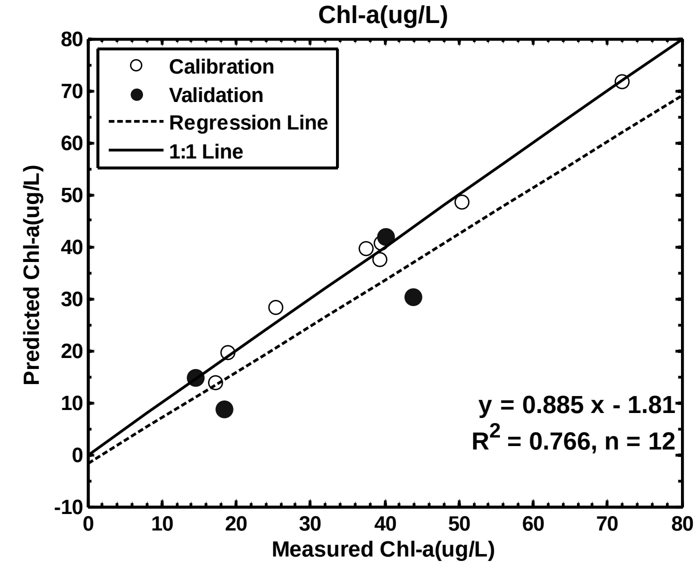

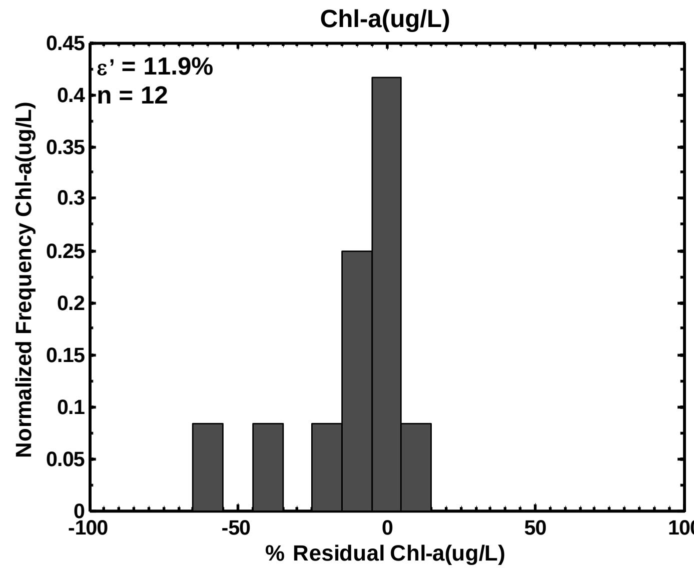

5. Results and Discussion-Hyperion Image Data

GA-PLS

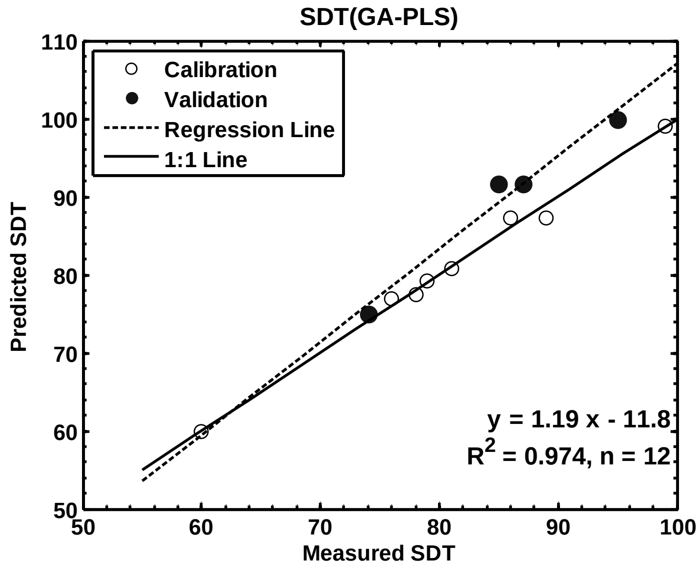

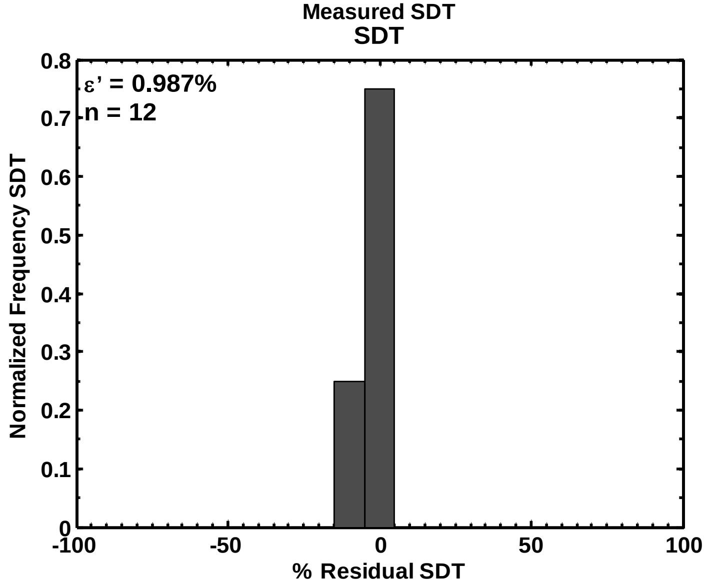

BPNN-PLS

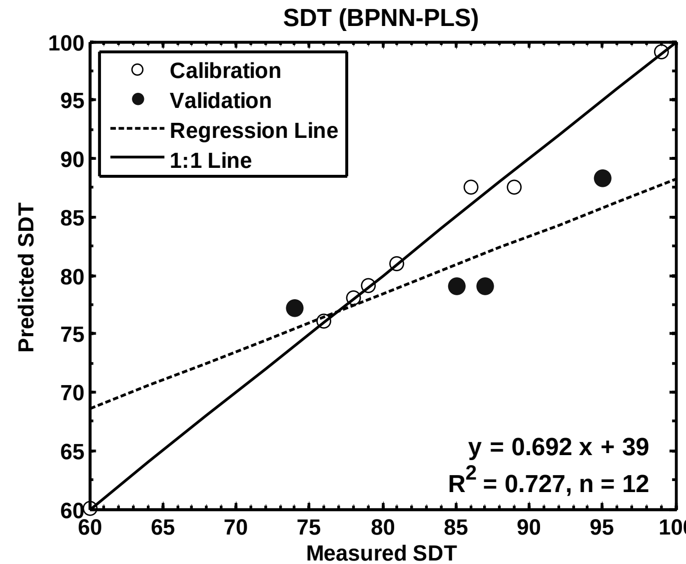

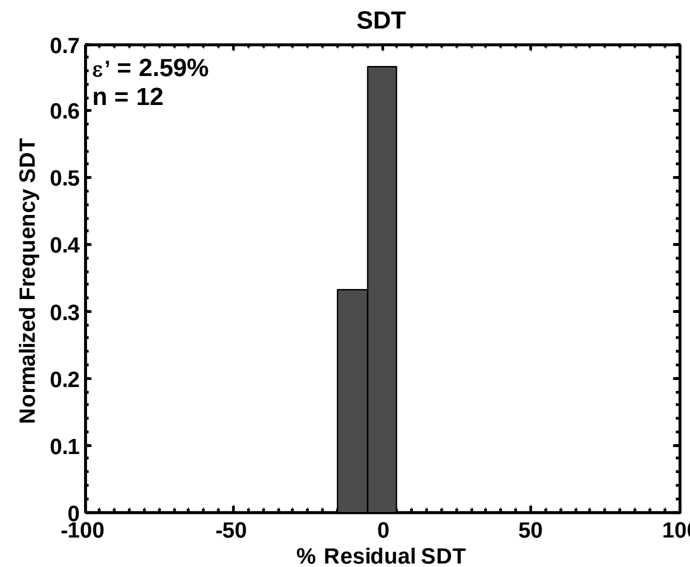

5. Results and Discussion-Hyperion Image Data

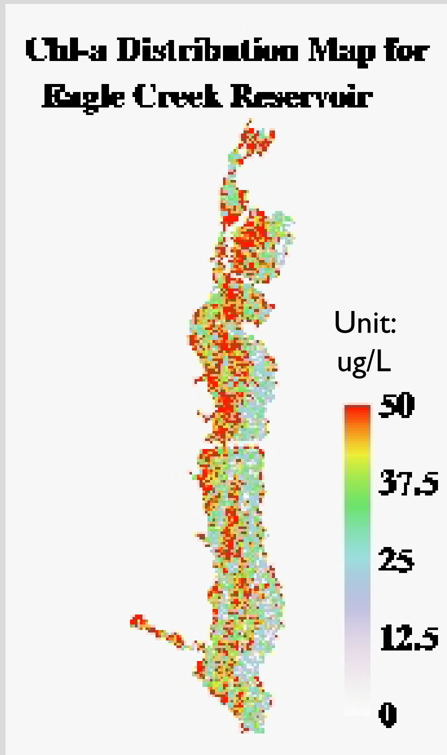

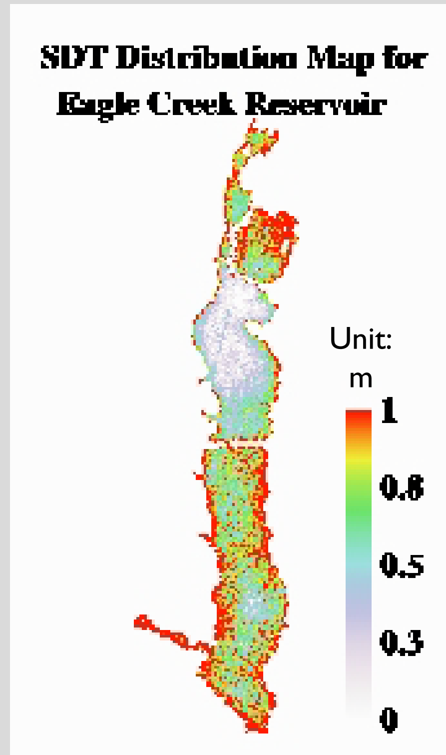

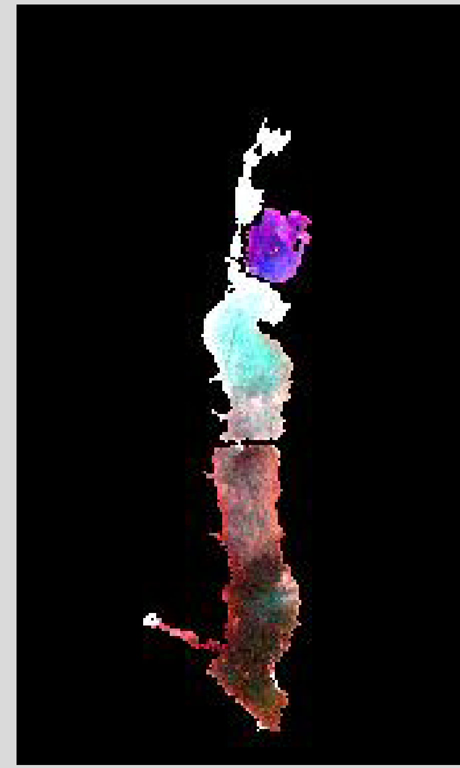

Low spatial resolution is a challenge when the image is used for water quality monitoring of small water bodies

6. Conclusions

- For the three investigated reservoirs, TP can be estimated with remote sensing data due to its close association with Chl-a, SDT, TSS and turbidity;
- GA-PLS has stable performances in our study, and BPNN-PLS did not outperform GA-PLS significantly in terms of accommodating non-linearity;
- If the same approach is applied for TP estimation of other case-II waters, correlation of TP to water compositional and physical parameters needs to be analyzed;
- Combining remotely estimated Chl-a, TP and SDT can be effective for assessment of trophic status of case-II waters.

Future Work

- Test these models with 2010 data sets;
- Conduct spatial correlation analyses of water nutrients, algae blooms, and temperature to determine potential relationships among these parameters;
- Use remote sensing mapping results to improve water quality models.

SWAT Hydrologic Model

EFDC Hydrodynamic Model

↓

HEM3D Water Quality and Algal Model

Climate Data, USGS Flow data, Water quality data, Etc.

Forecasting of spatial and temporal distribution of Cyanobacteria and Nutrients (N, P, C) in the reservoir

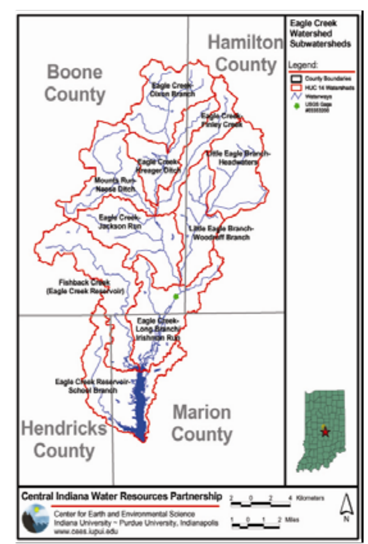

Acknowledgement

This work is supported by:

- National Aeronautics Space Administration (NASA) HyspIRI preparatory activities using existing imagery (HPAUEI) program;
- NASA Energy and Water Cycle program(grant No. NNX09AU87G).

Giant Kelp Forests and their Responses to Climate Variability

Kyle Cavanaugh, Dave Siegel, Dan Reed
University of California Santa Barbara

Macrocystis pyrifera – Giant Kelp

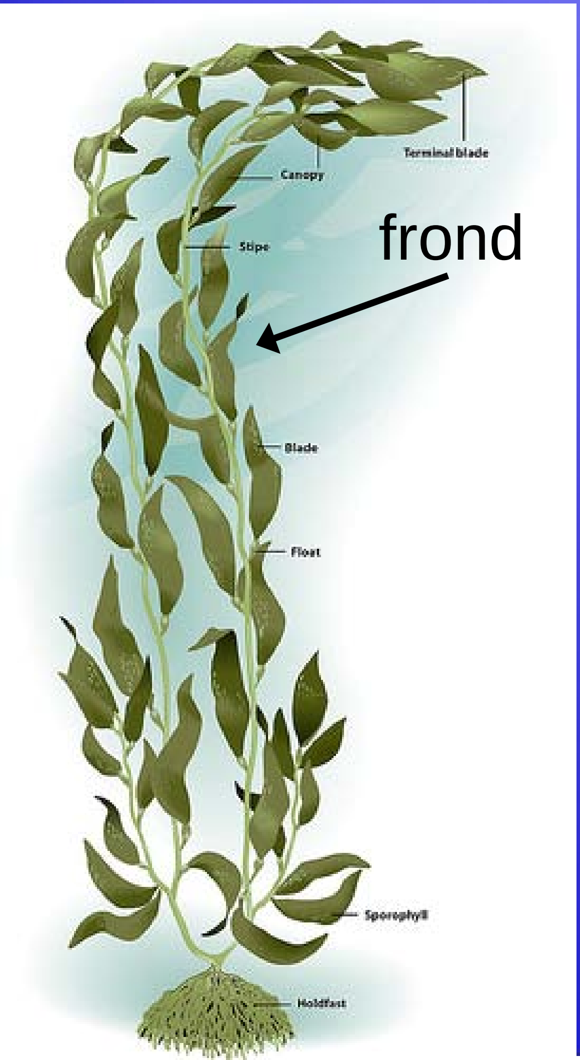

- Plant life spans:
  ~ 2.5 years
- Frond life spans:
  ~ 4 months
- Frond growth can be 0.5 m/day

What controls kelp populations?

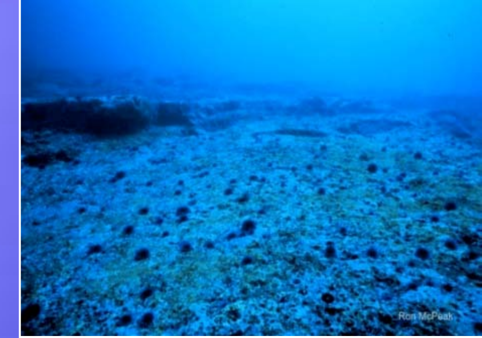

<u>NUTRIENTS</u>: "our most lasting effects result from very large scale, low-frequency episodic changes in nutrients" (Dayton et al. 1999)

<u>PHYSICAL DISTURBANCE</u>: Work in Southern and Central California found that wave driven disturbance explained more variability in biomass and production than nutrients or grazing (Reed et al. 2008; Reed et al. *in prep)*

Goal

- Characterize the controls of giant kelp dynamics across a wide range of spatial and temporal scales
  - by combining diver and satellite data

+

LANDSAT 5

- 30 m resolution multispectral imagery
- Imagery available from 1984-present with a 16 day repeat cycle
  - Cloud free image available approx. every 1-2 months

Spatial scaling issues

- Last year Phil Dennison and Dick Zimmerman presented results examining feasibility of mapping kelp at 60 m resolution
- Good agreement in kelp fractions when scaling up
- Bias in area estimates increases (nonlinearly) when resolution decreases
  - Depends on shape of kelp beds

LANDSAT Spectral Unmixing

- Model every pixel as a linear combination of water and kelp endmembers

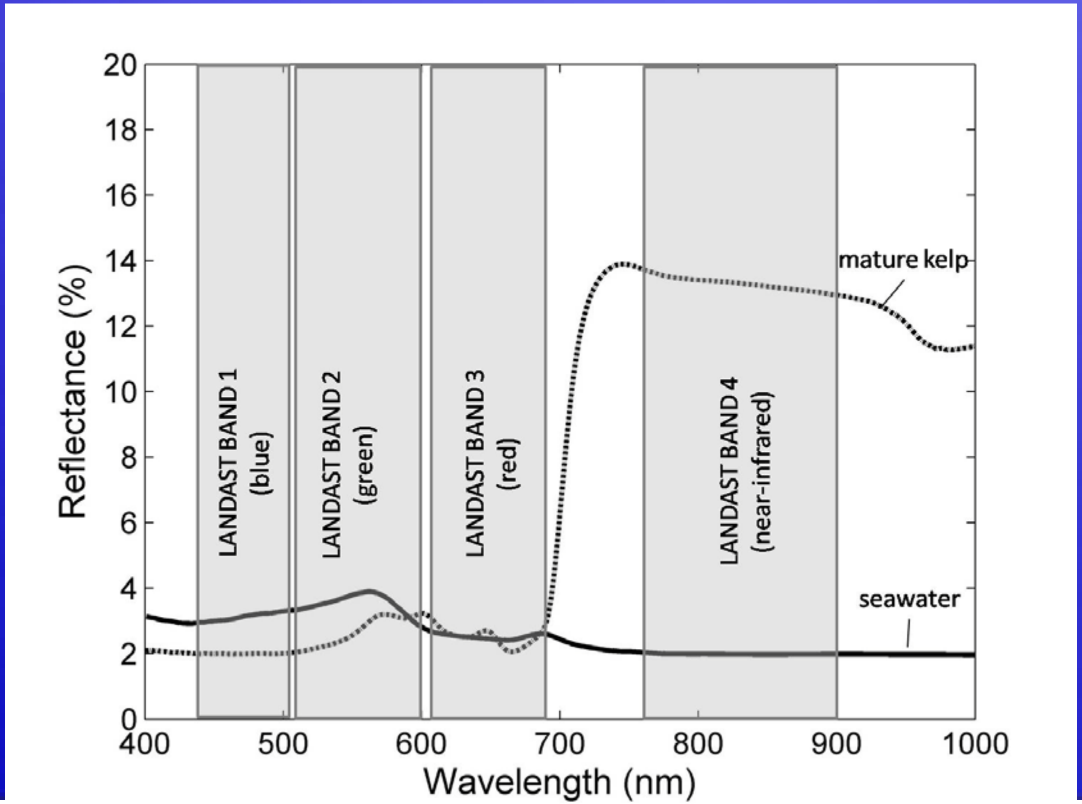

LANDSAT Spectral Unmixing

- Model every pixel as a linear combination of water and kelp endmembers

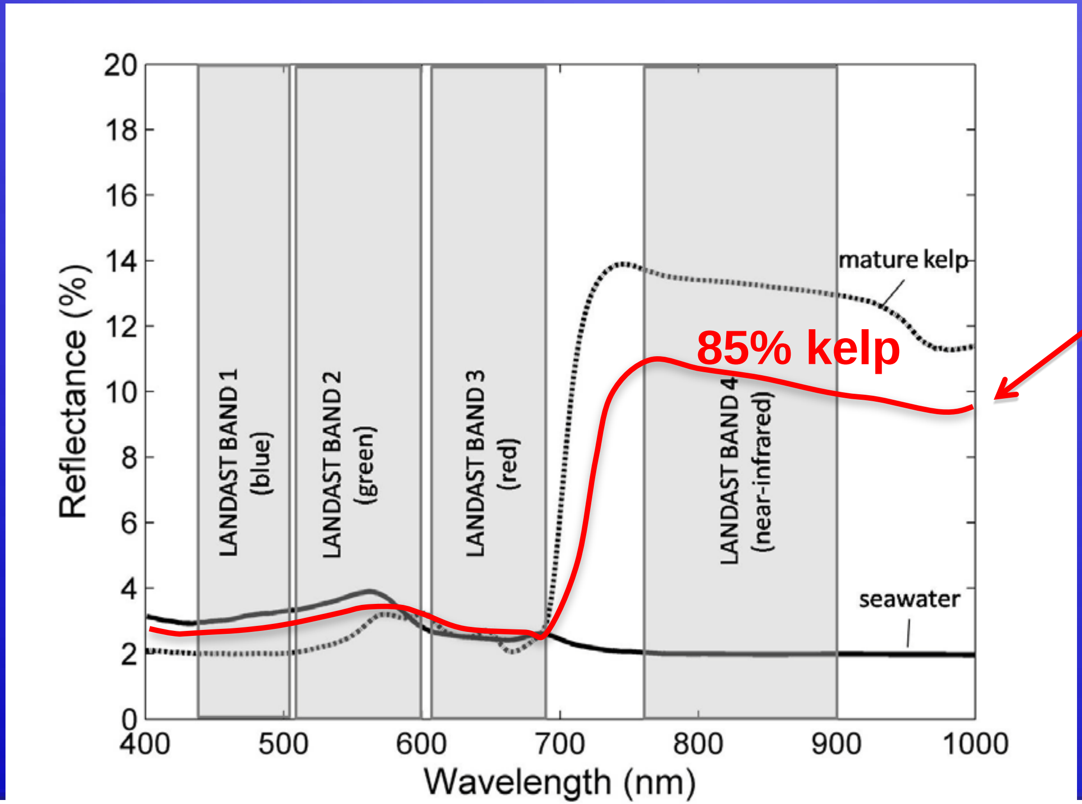

LANDSAT Spectral Unmixing

- Model every pixel as a linear combination of water and kelp endmembers

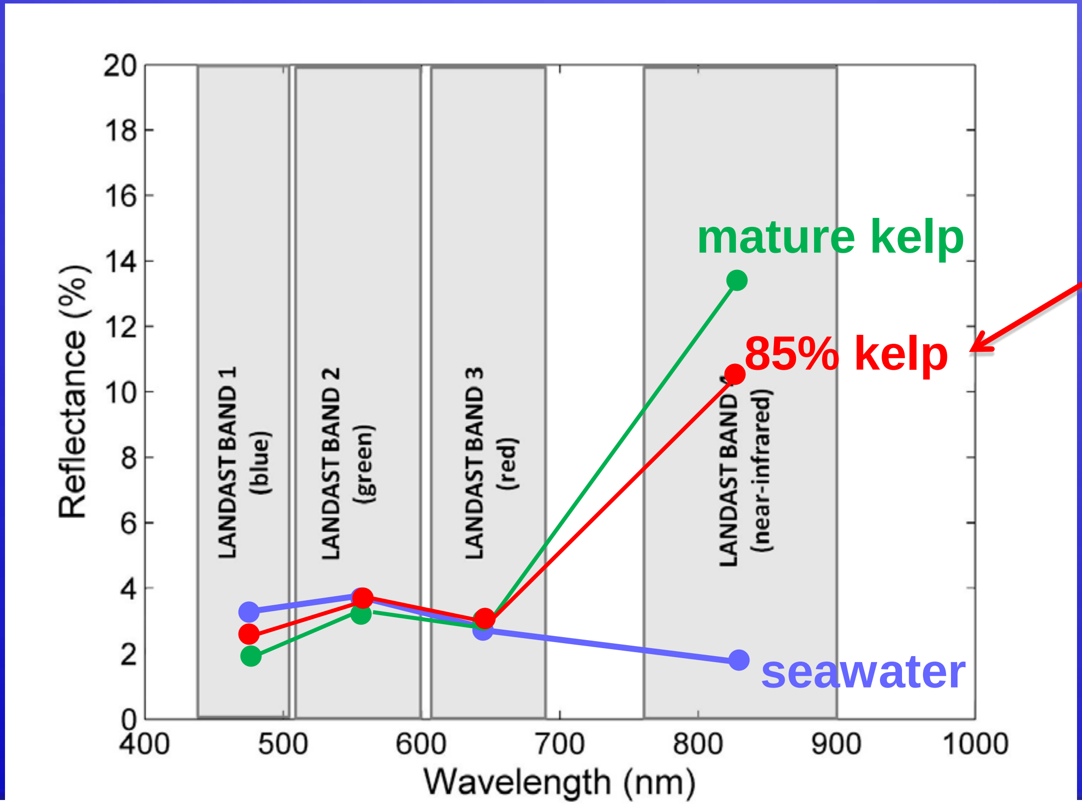

Endmember selection

- Single kelp spectra chosen from multitemporal spectral library (using EAR; Dennison and Roberts, 2003)
- Multiple water endmembers to account for water variability (sediment, glint, phytoplankton, etc.)

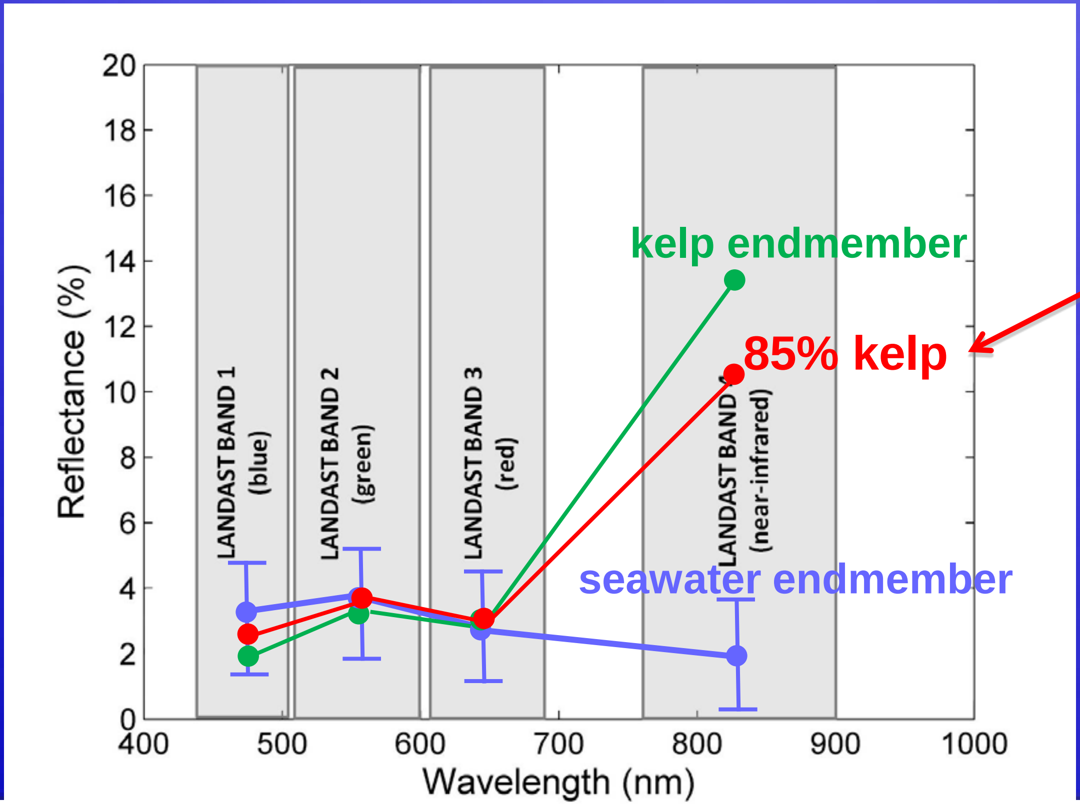

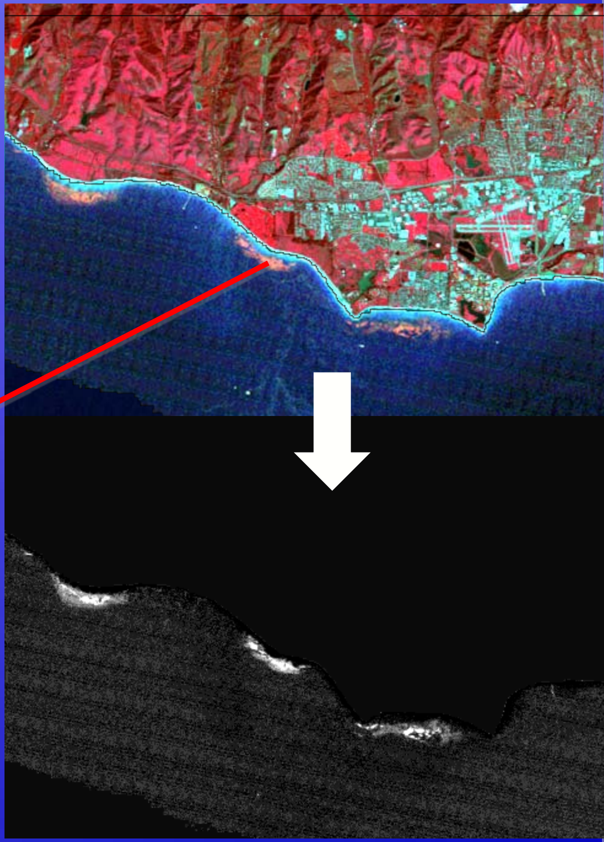

LANDSAT Spectral Unmixing

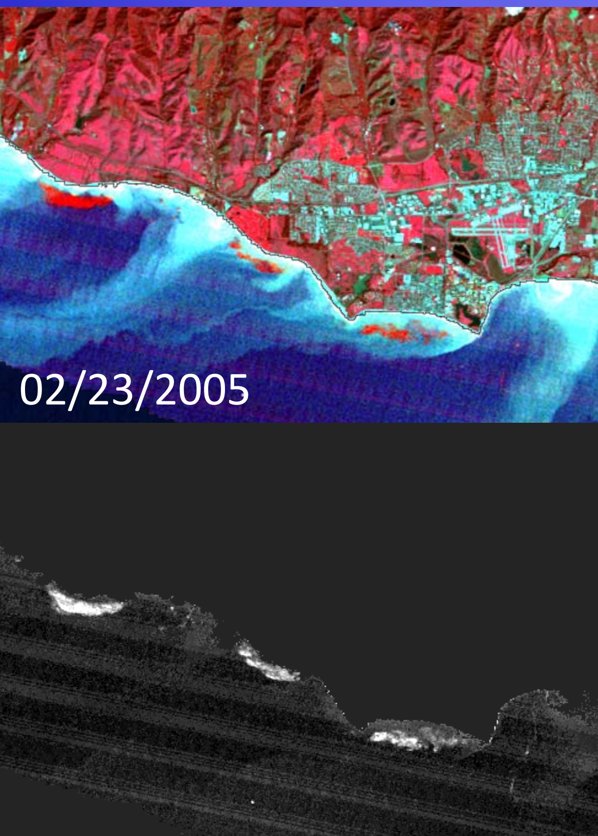

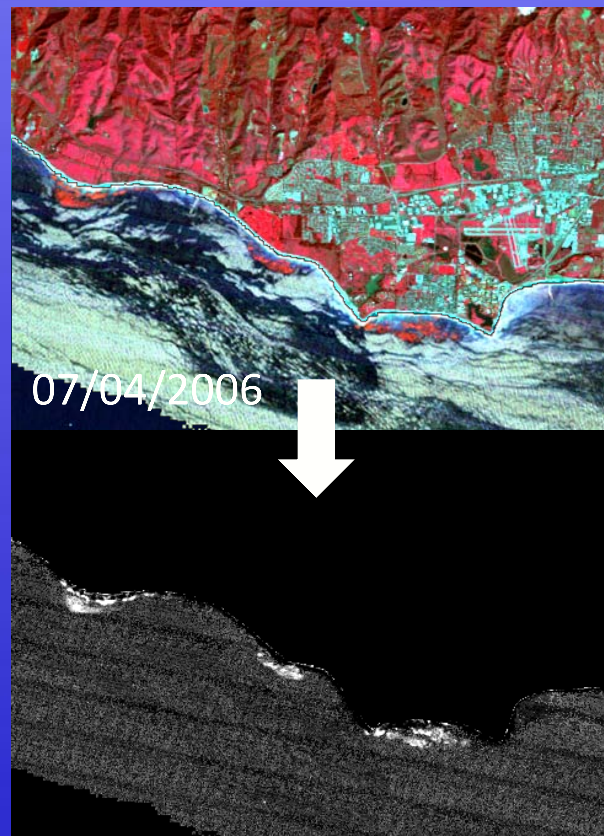

False Color Image

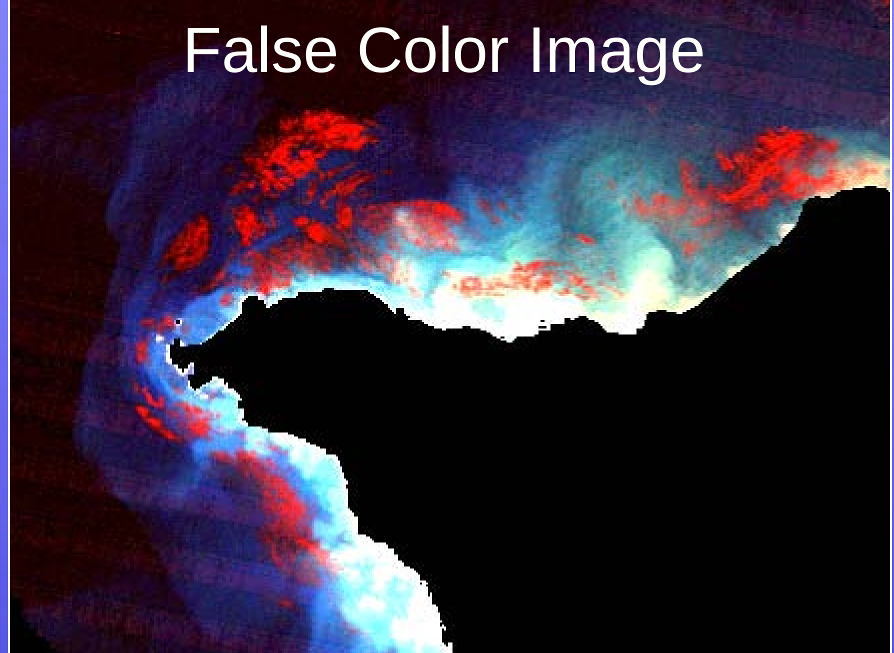

Kelp Fraction

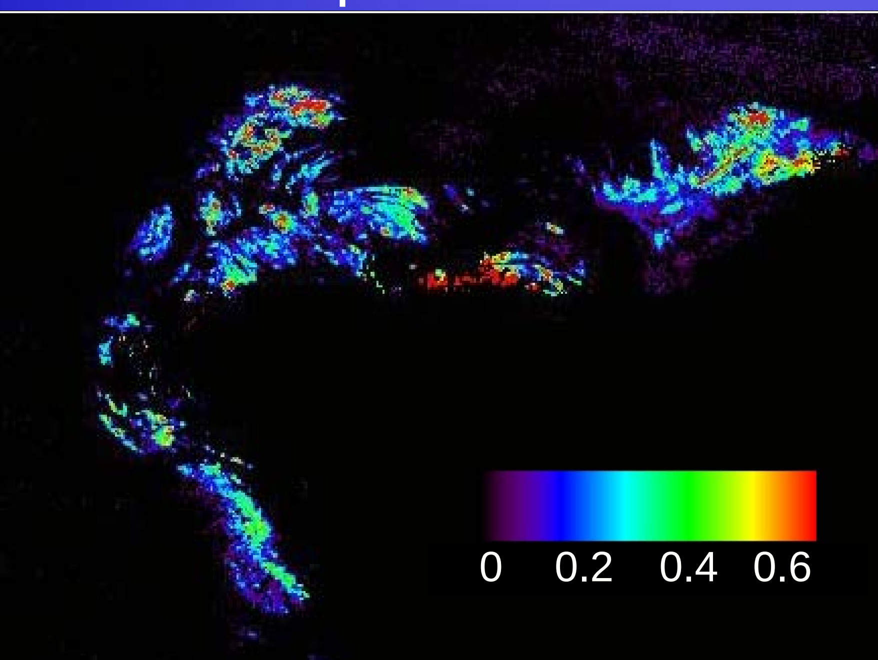

NDVI

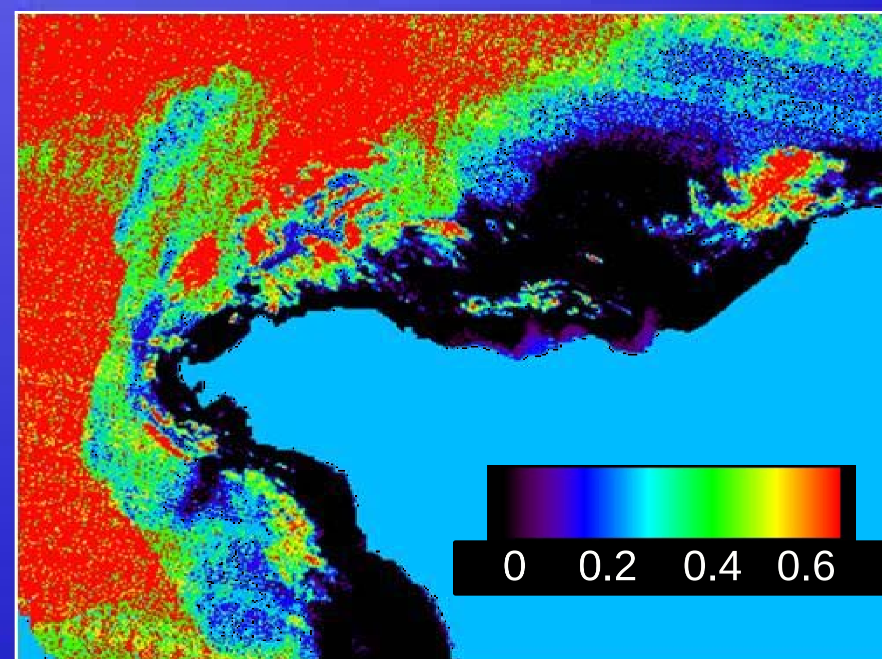

SBC-LTER Diver Surveys

- Turn fractions into canopy biomass
- Monthly non-destructive allometric biomass surveys from 2002-present

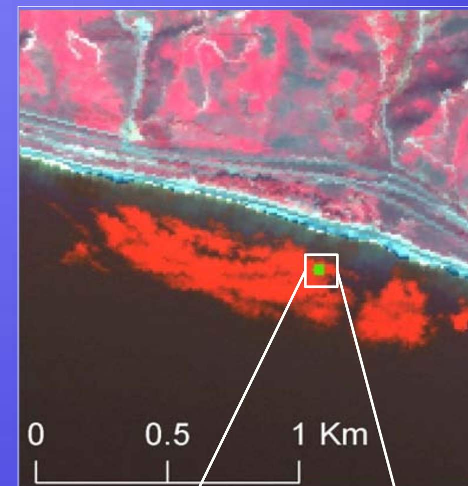

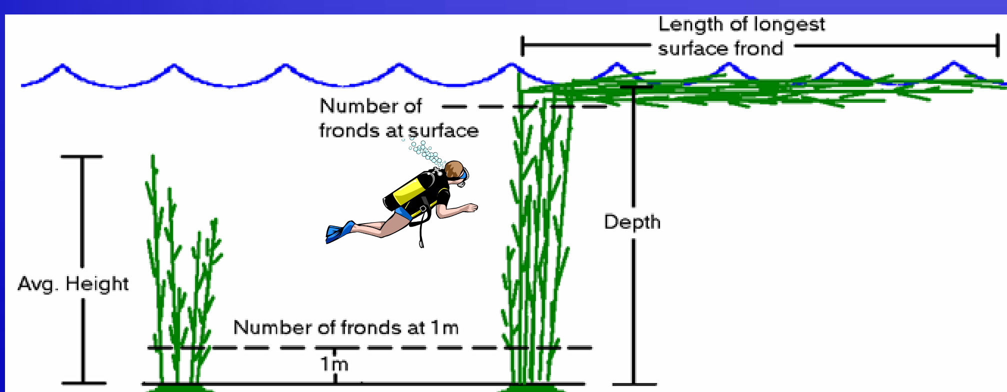

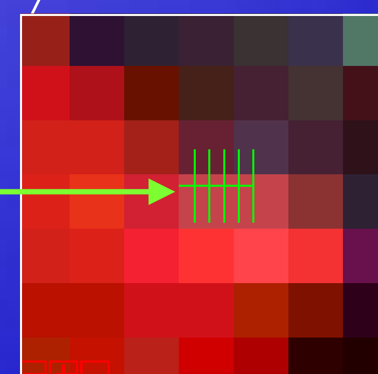

Biomass from LANDSAT

Strong relationship between kelp fraction and diver measured canopy biomass

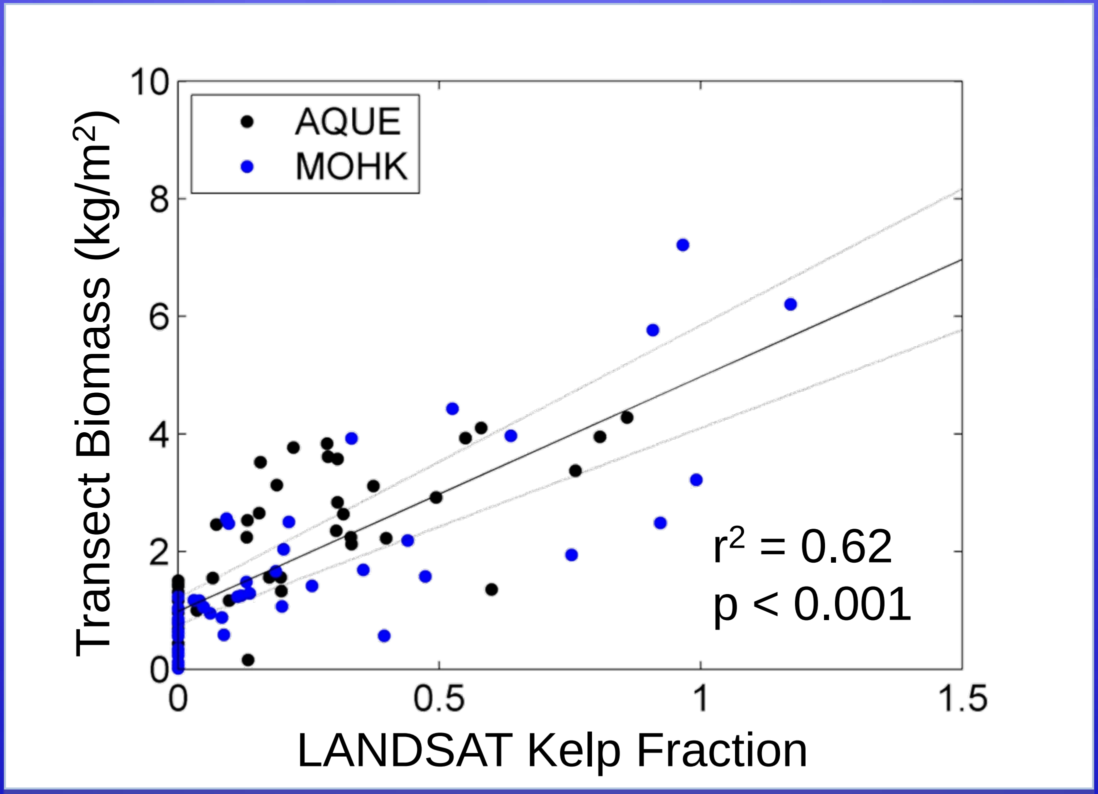

Biomass from LANDSAT

- Canopy biomass is better correlated to kelp fraction than NDVI

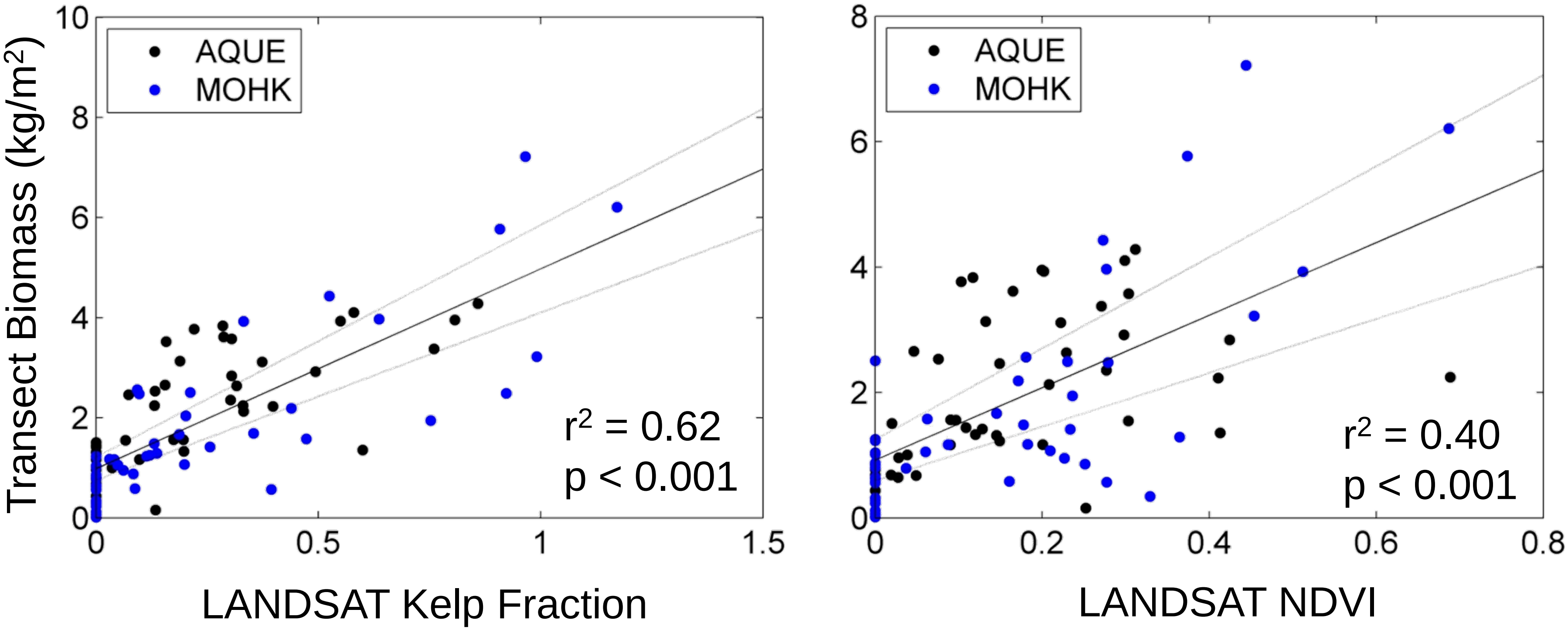

Temporal kelp dynamics in the Santa Barbara Channel (1984-2009)

Temporal kelp dynamics in the Santa Barbara Channel (1984-2009)

- Regional mean: 41500 metric tons of kelp canopy

  Equals mass of ~400 blue whales

- Low in winter, high in summer/fall
- Seasonal cycle superimposed on a 5-7 year cycle

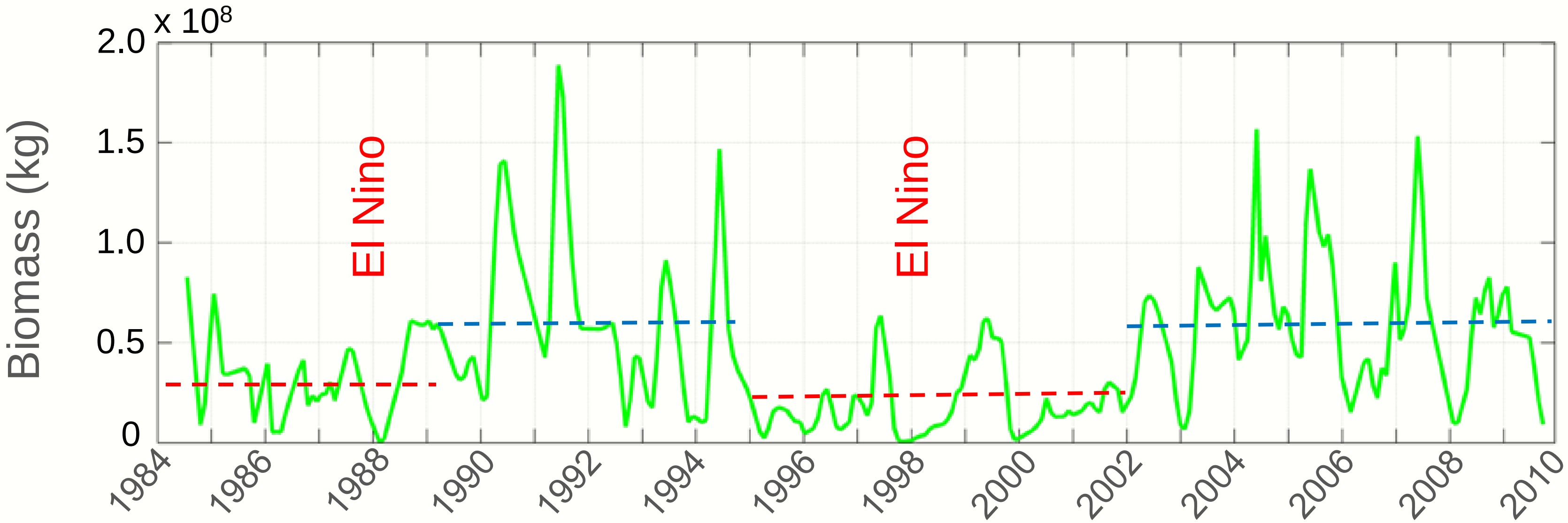

Physical Data

- Significant wave height from Harvest buoy (1987-2009)
- Sea surface temperature (SST) from Pt. Arguello buoy (1984-2009)

SST is a good proxy for nutrients

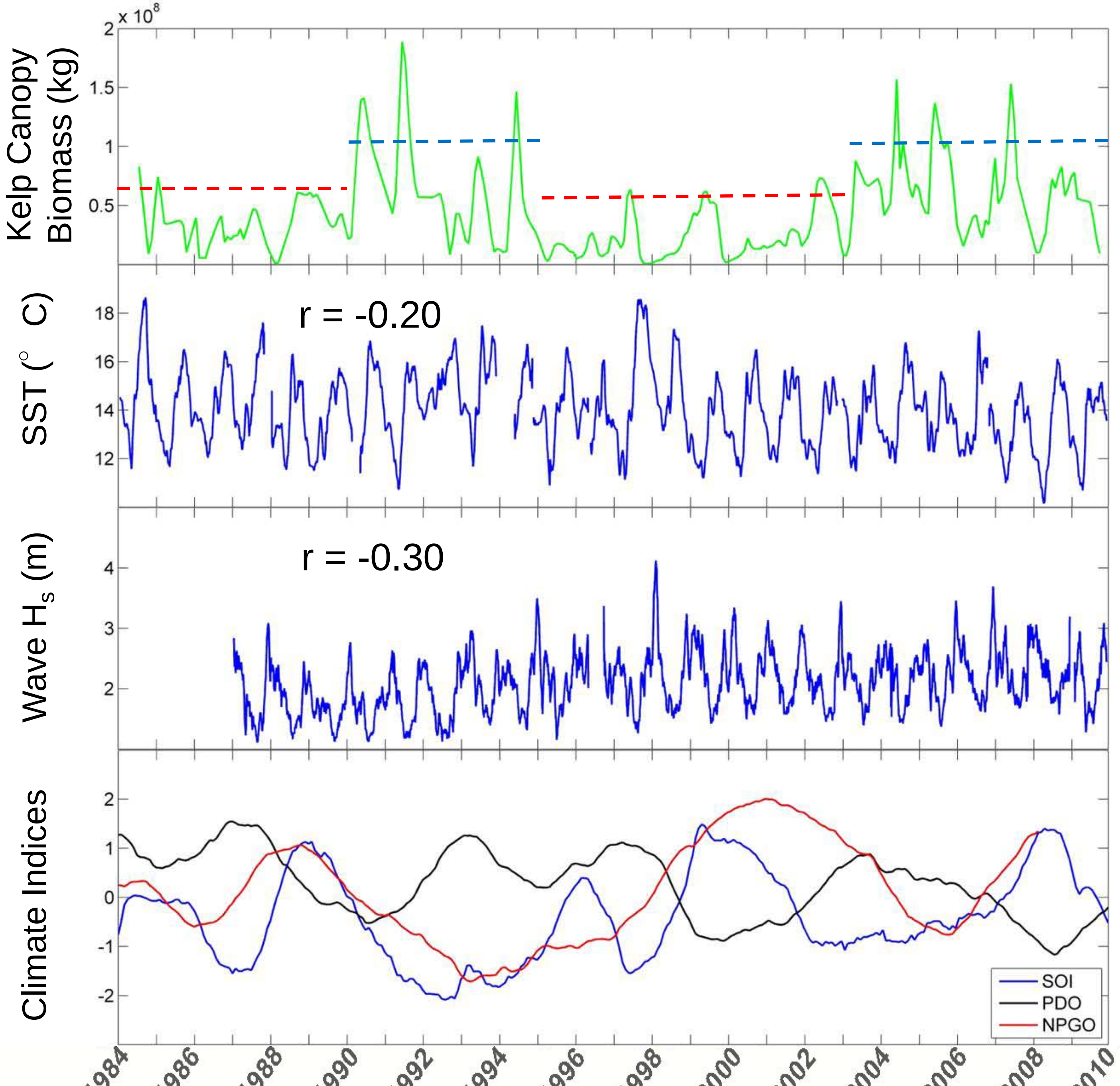

Kelp Canopy Biomass (kg)
x 10^8
2
1.5
1
0.5
SST (° C)
r = -0.20
18
16
14
12
Wave H_s (m)
r = -0.30
4
3
2
Climate Indices
2
1
0
-1
-2
SOI
PDO
NPGO
1984
1986
1988
1990
1992
1994
1996
1998
2000
2002
2004
2006
2008
2010

Seasonal Forcings

- Wave induced mortality is direct and immediate
- Effect of SST/nutrients is delayed and complicated by other factors

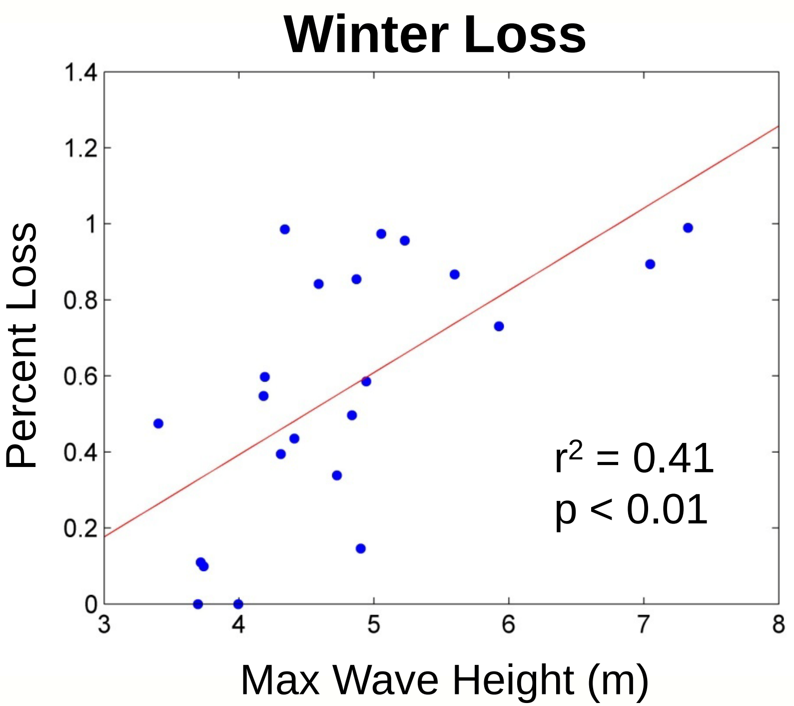

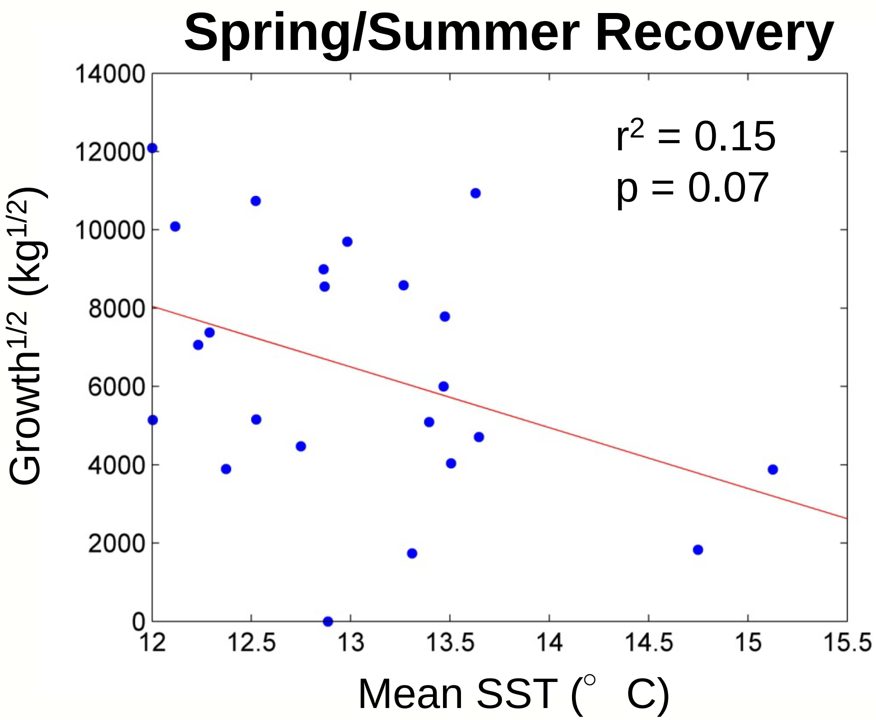

Inter-annual Forcings

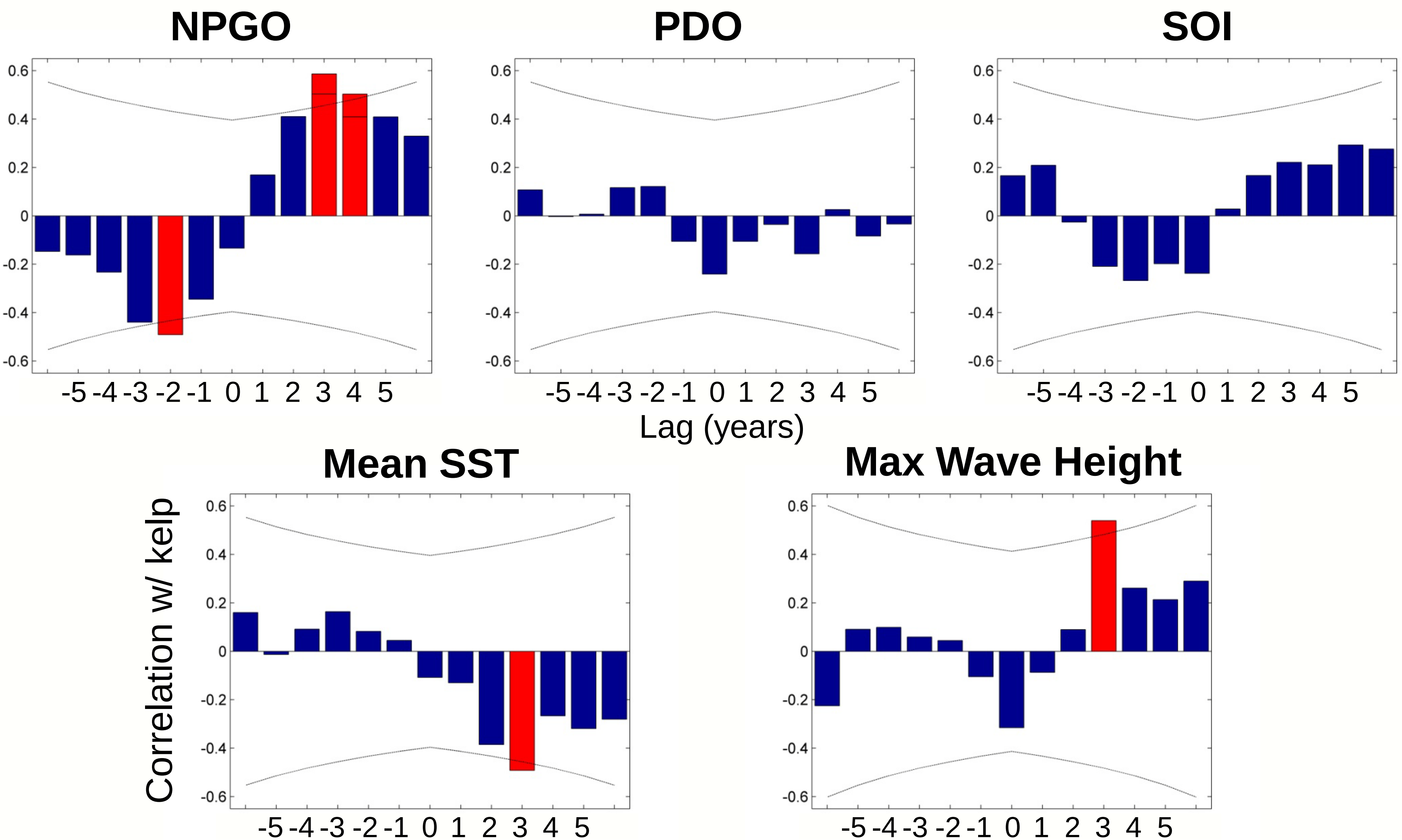

Kelp population controls

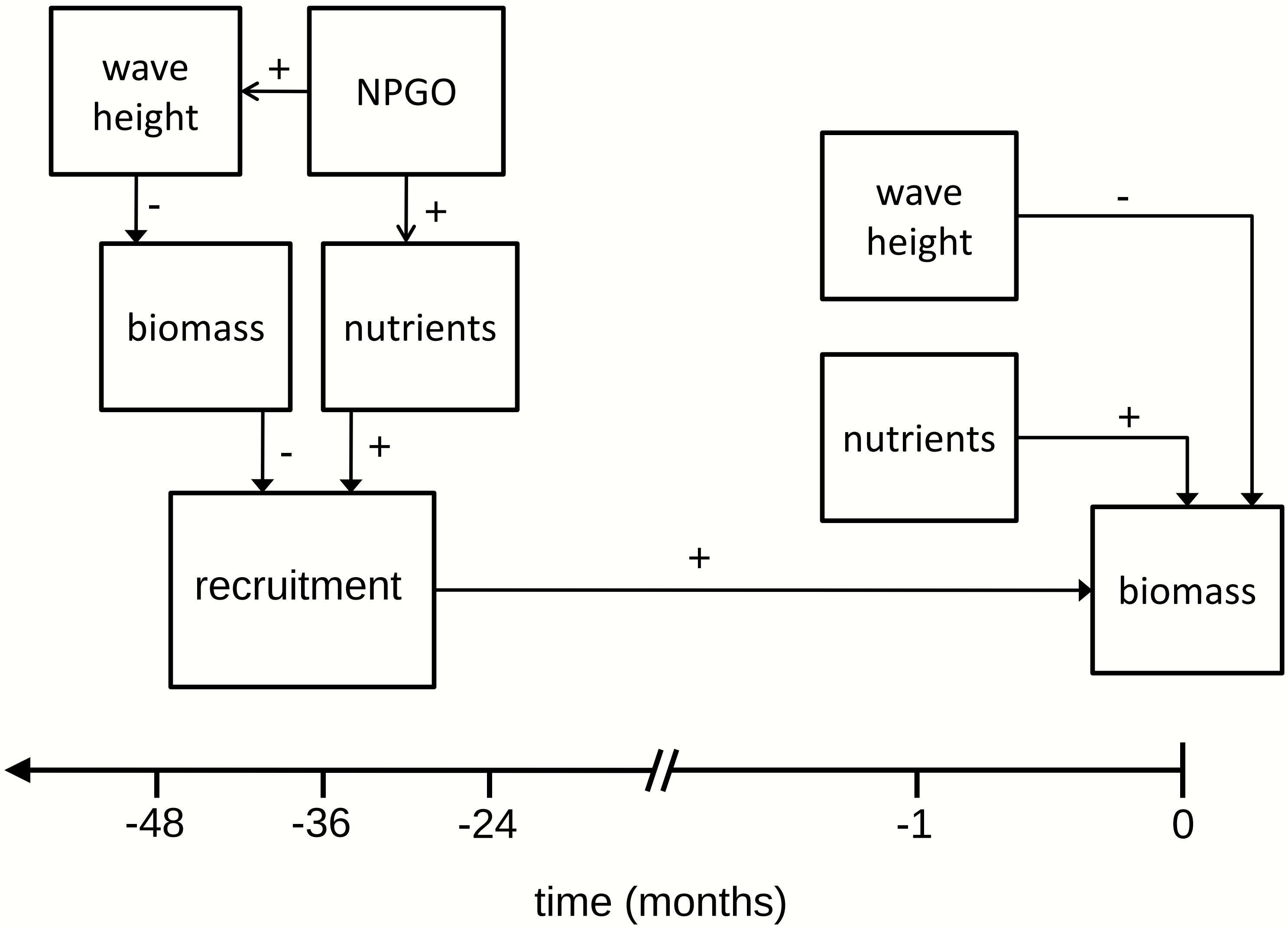

Spatial kelp dynamics in the Santa Barbara Channel (1984-2009)

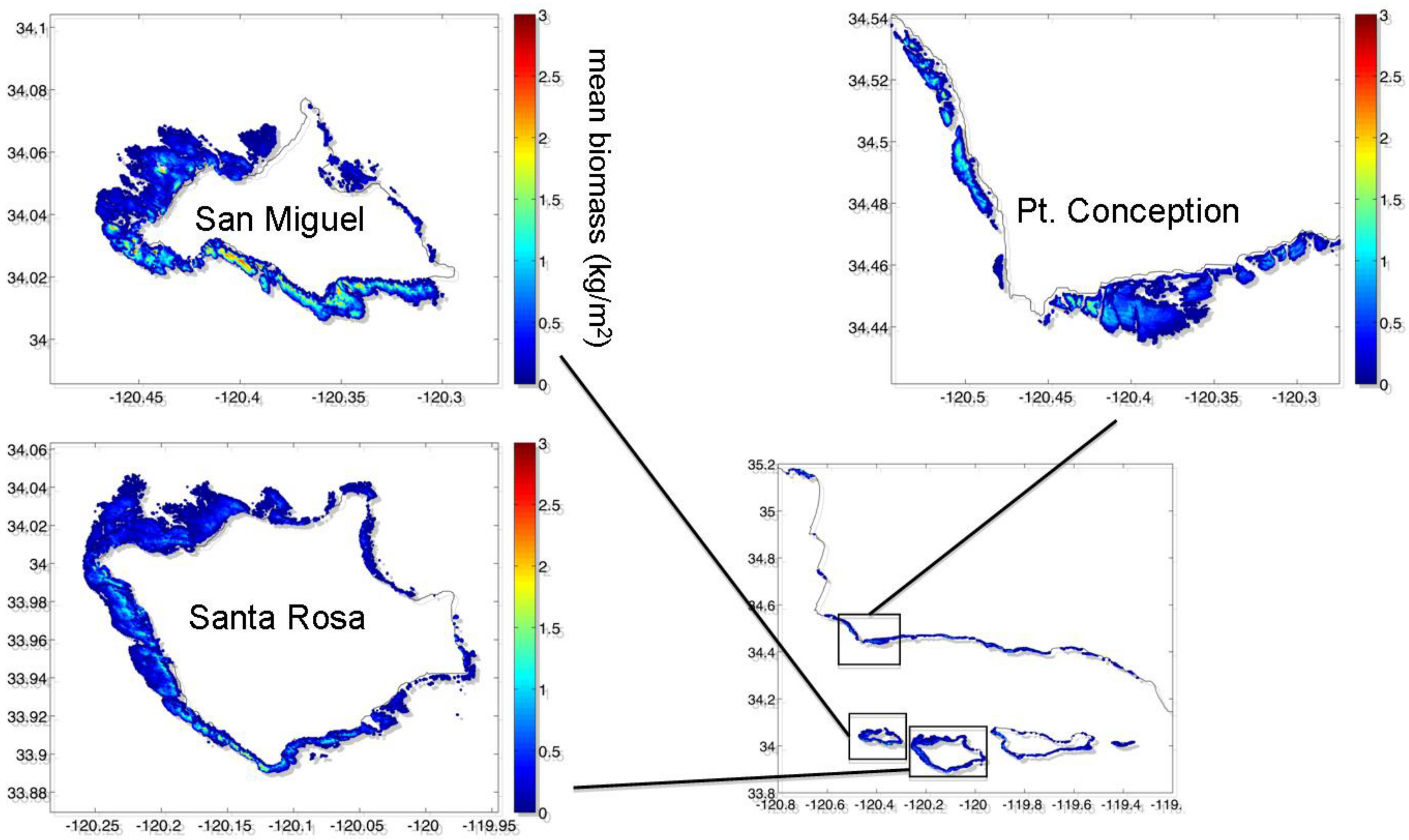

Cluster Analysis

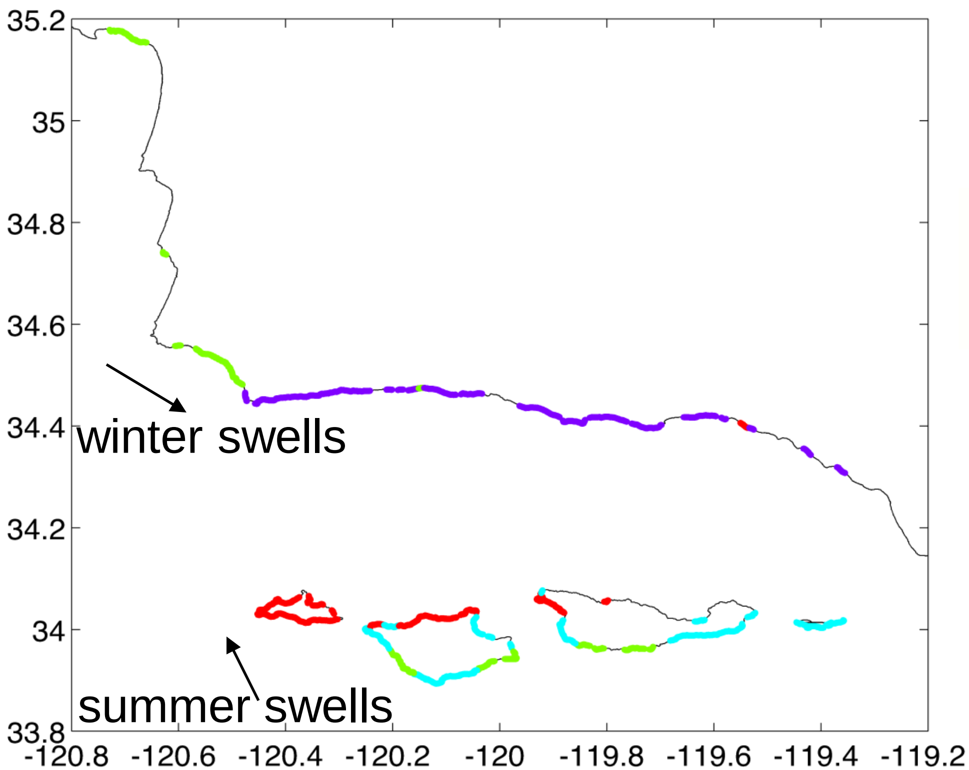

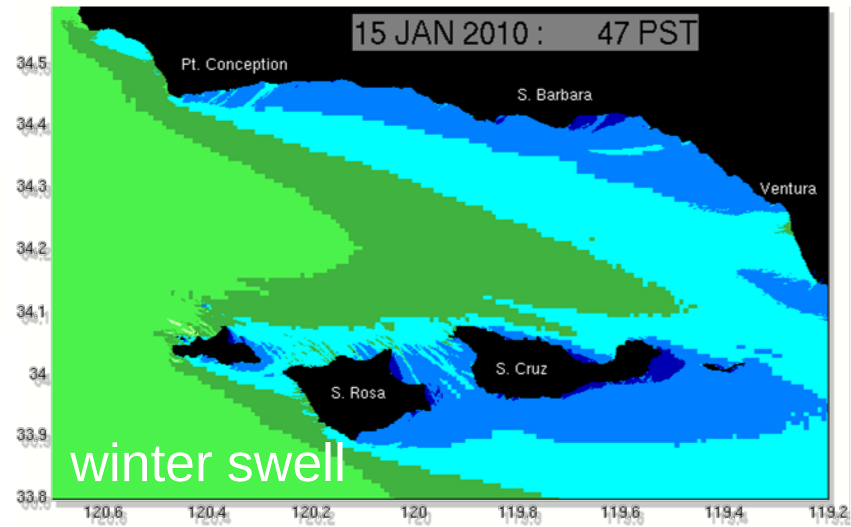

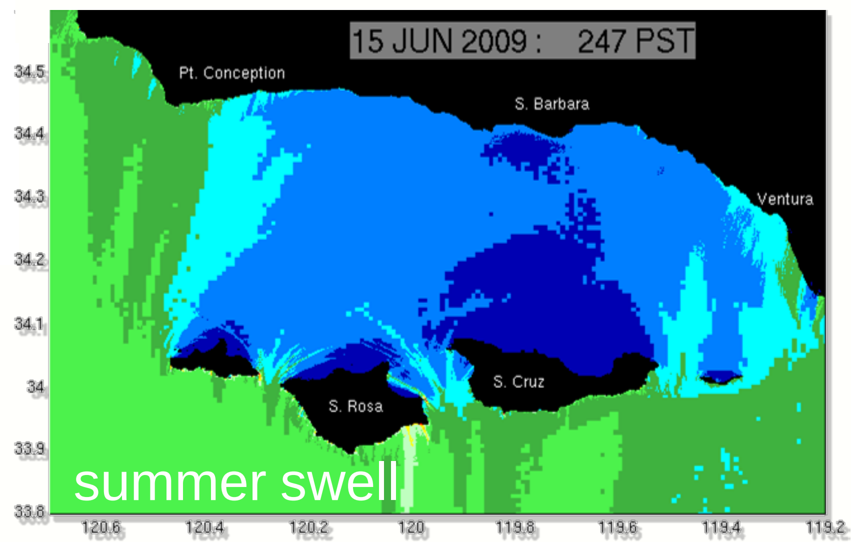

Correlation with physical variables

	kelp biomass			
sst	-0.05	**-0.32**	-0.05	**-0.26**
waves	**-0.52**	-0.13	**-0.32**	-0.15

Summary

- We have created a time series of giant kelp biomass in the Santa Barbara Channel between 1984-2010 with unprecedented spatial and temporal resolution from LANDSAT imagery
- Region-wide monthly kelp dynamics are negatively correlated with max wave height, annual kelp biomass lags SST, waves and the NPGO by 3 years
- Sub-regional dynamics cluster along wave exposure gradients

Moving forward (on to hyperspectral imagery)

- Spectral unmixing will be much more accurate
- Allows us to get at age structure, senescence, species differentiation
- Potential to combine LDCM & HyspIRI

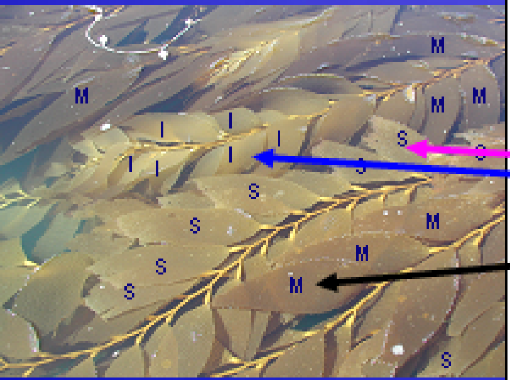

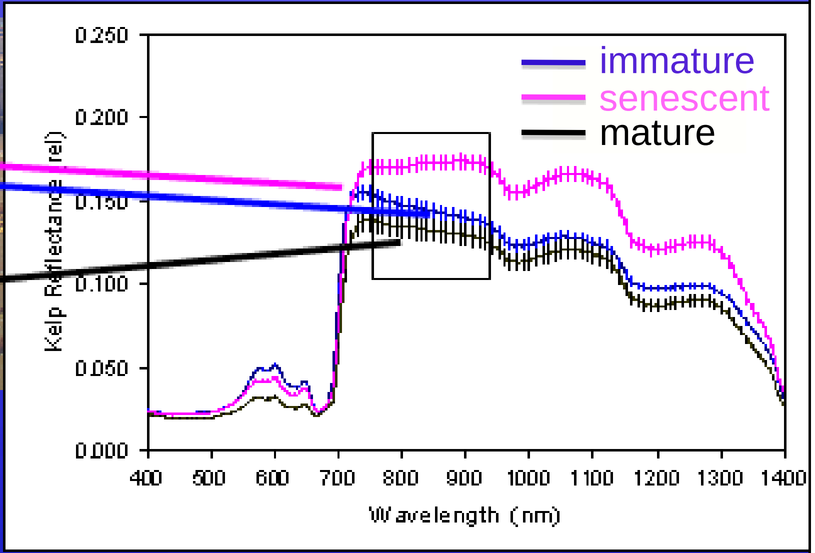

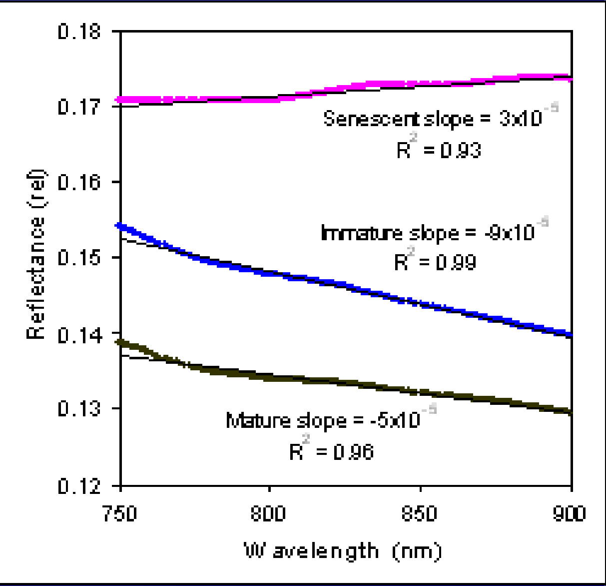

(data from Richard Zimmerman)

Thank You!!


NASA
NSF
Santa Barbara Coastal
Long Term Ecological Research

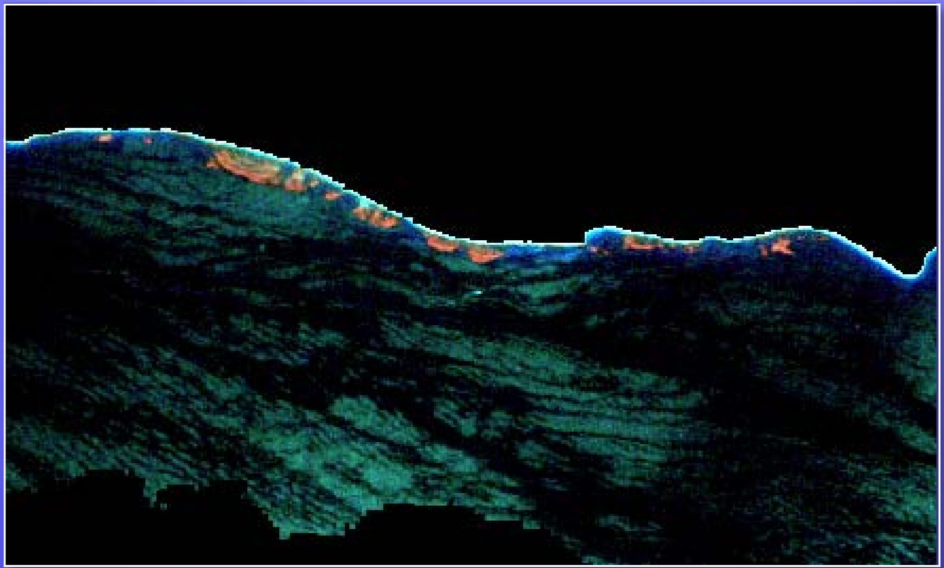

Kelp Fraction

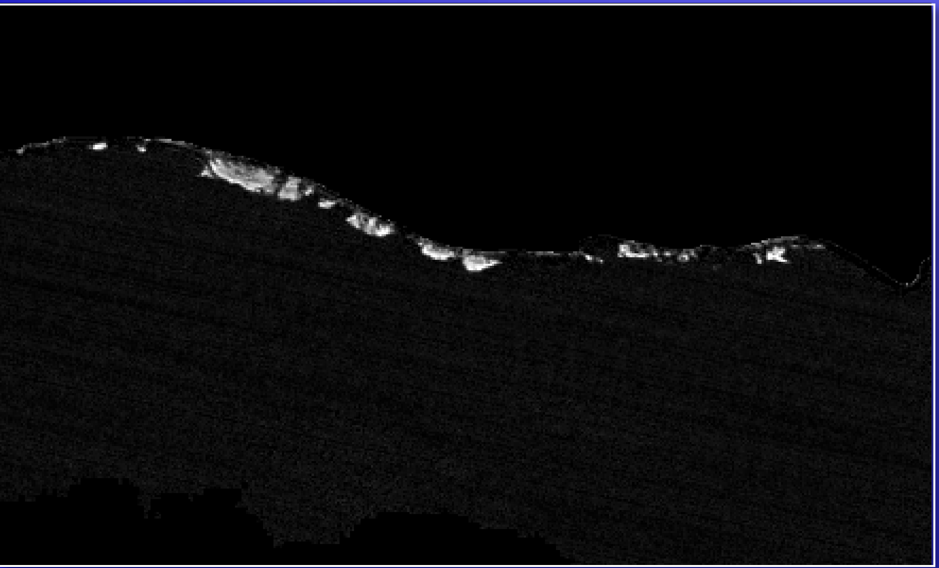

NDVI

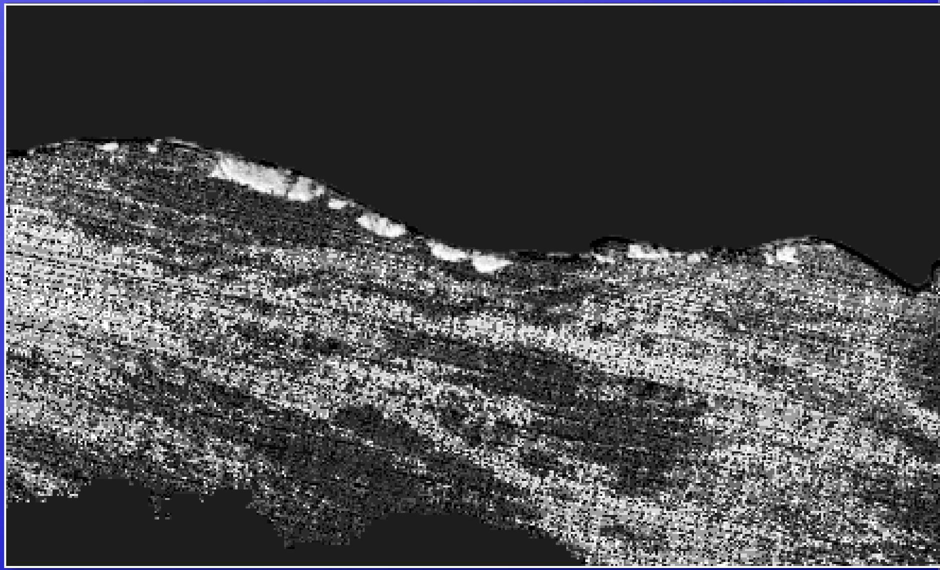

Seasonal Forcings

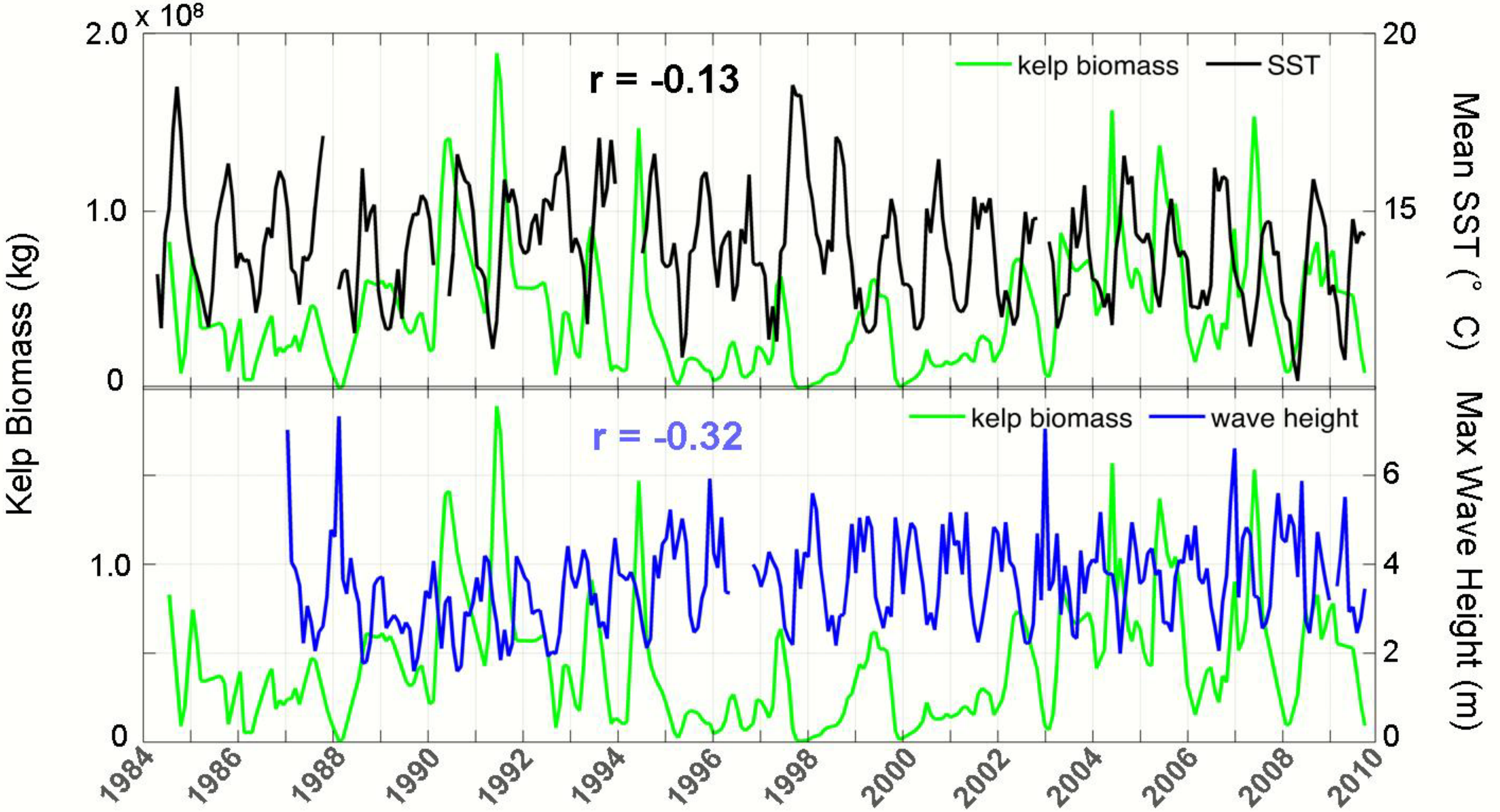

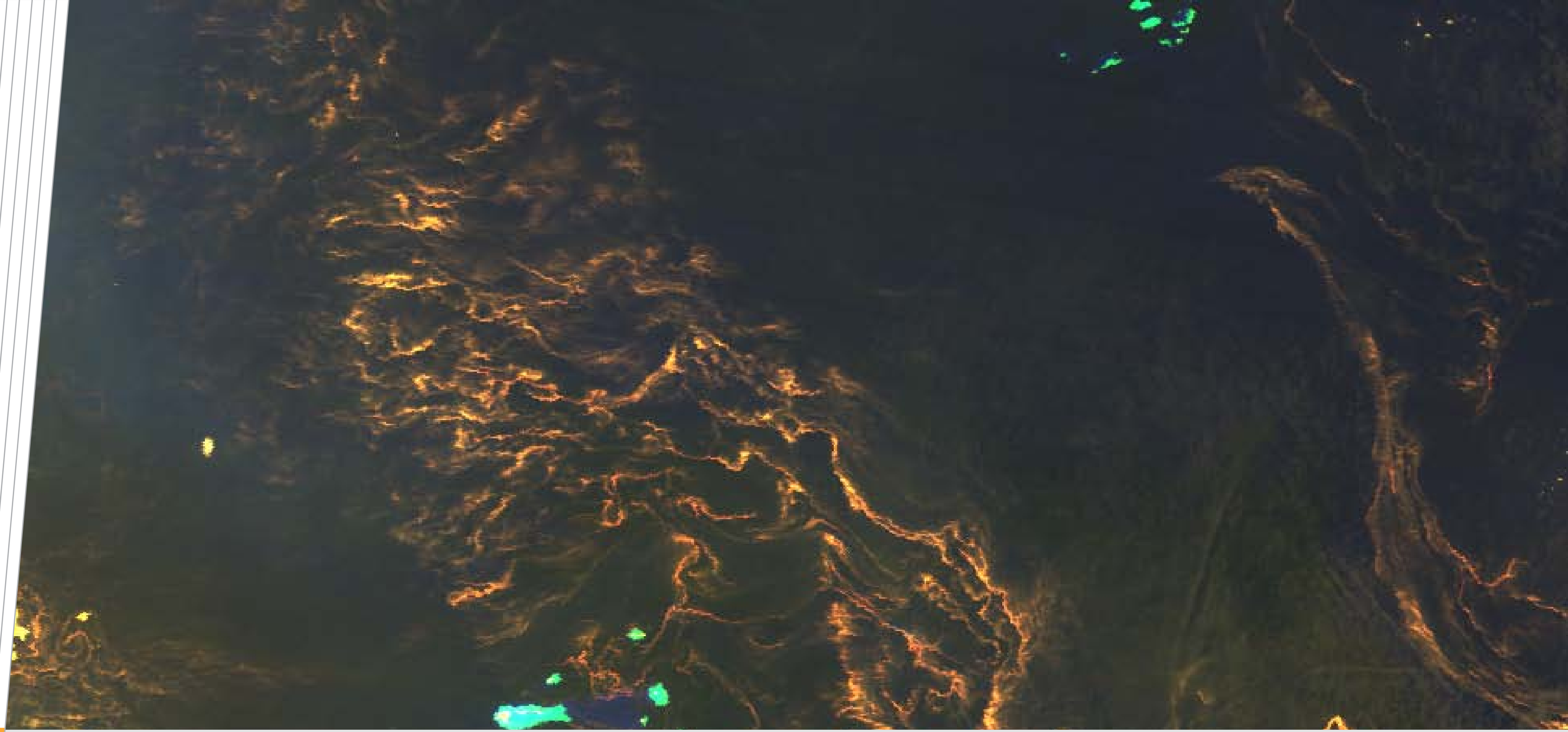

www.csiro.au

Glint-aerosol discrimination using NIR-SWIR wavelengths

Young-Je Park[1], Arnold Dekker, Eric Hochberg and HyspIRI Sun Glint Subgroup

24-26 Aug 2010 HyspIRI Science Workshop

National Research FLAGSHIPS
Wealth from Oceans

CSIRO

Outline

- HyspIRI glint compared to MODIS
- Existing glint correction techniques
- Aerosol and glint discrimination approach
- AVIRIS example
- Discussion
- Application to algal bloom monitoring

Introduction

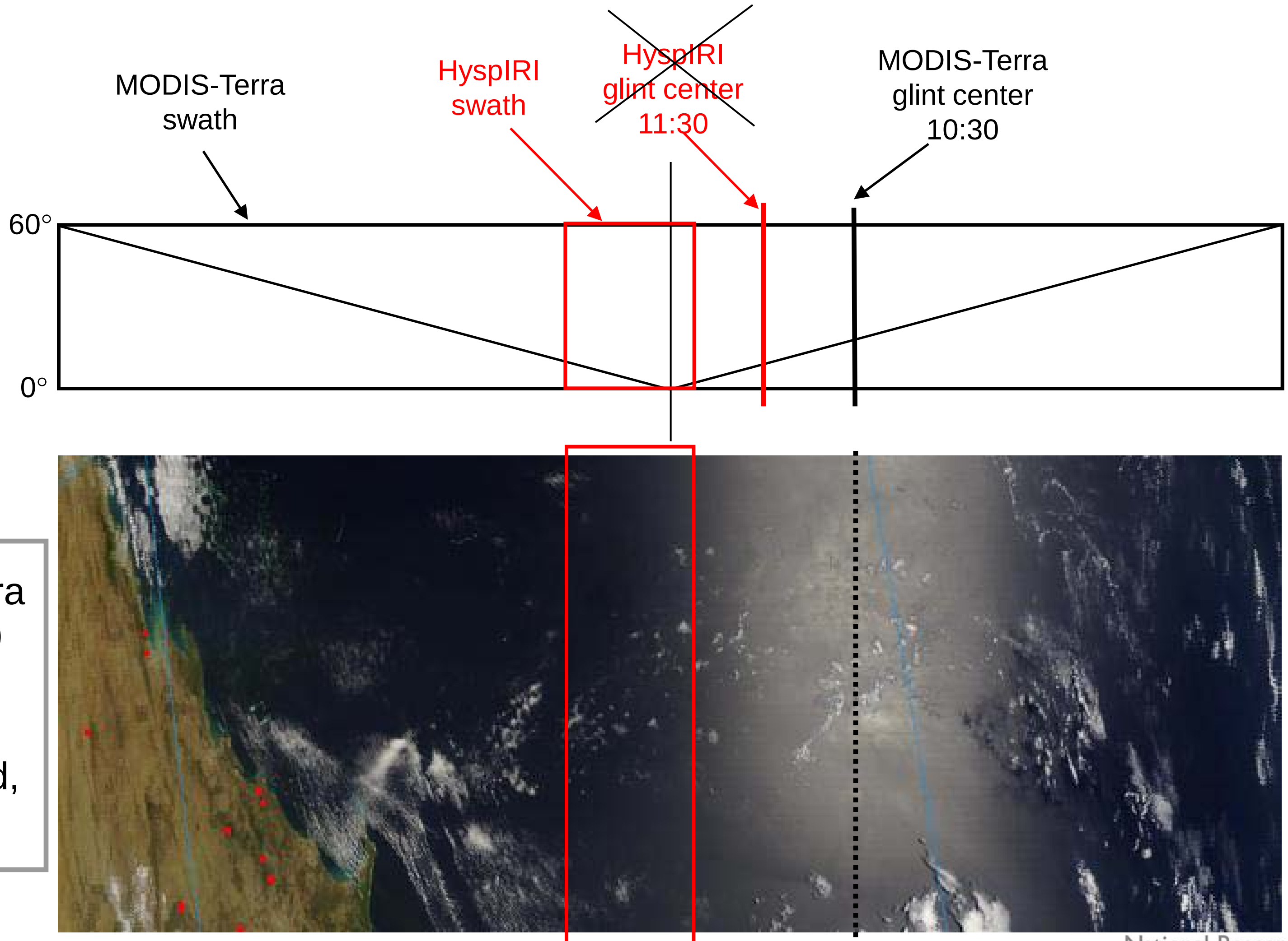

MODIS Terra image of 29 Nov 2006 over Queensland, Australia

Existing glint correction techniques

- For Medium-Coarse spatial resolution data (MODIS, MERIS)
  - Wind based surface slope model: Cox and Munk 1954
- High spatial resolution image
  - NIR-VIS linear relationship (Hochberg 2003)
  - NIR subtraction technique (Gao)
  - Uniform spectral offset approach (Goodman and Ustin, 2007)
- Why looking for new approach?
  - Use of adequate glint spectra normally decreasing to the blue
  - Automated processing

Glint-aerosol decoupling approach

- Top of atmosphere (at-sensor) reflectance

$$\rho_t = \underbrace{\rho_r}_{\text{Air molecules}} + \overbrace{\rho_a}^{\text{aerosol}} + \underbrace{\rho_g^{TOA}}_{\substack{\text{Glint} \\ \text{(sunglint + skyglint)}}} + \overbrace{\rho_w^{TOA}}^{\text{Water body}}$$

- Atmospheric-glint correction is meant to remove the reflectances due to air molecules, aerosols and glint from satellite measured reflectance.

- At wavelengths where water reflectance is zero

$$\rho_a + \rho_g^{TOA} = \rho_t - \rho_r$$

known

- Aerosol reflectance and glint reflectance can be decoupled
  - 1) using a spectral matching technique if we know the spectral shapes of aerosol and glint reflectances:

$$\rho_a(\lambda) = \rho_{a0} \cdot A(\lambda) \qquad \rho_g^{TOA}(\lambda) = \rho_{g0} \cdot G(\lambda)$$

OR

  - 2)Using a look-up table for $\rho_a + \rho_g^{TOA}$ as function of aerosol and wind speed as well as sun-sensor angles

Glint-aerosol discrimination approach

- RT (6S) simulations for HyspIRI east and west edges

$$\rho_a(\lambda) = \rho_{a0} \cdot A(\lambda)$$

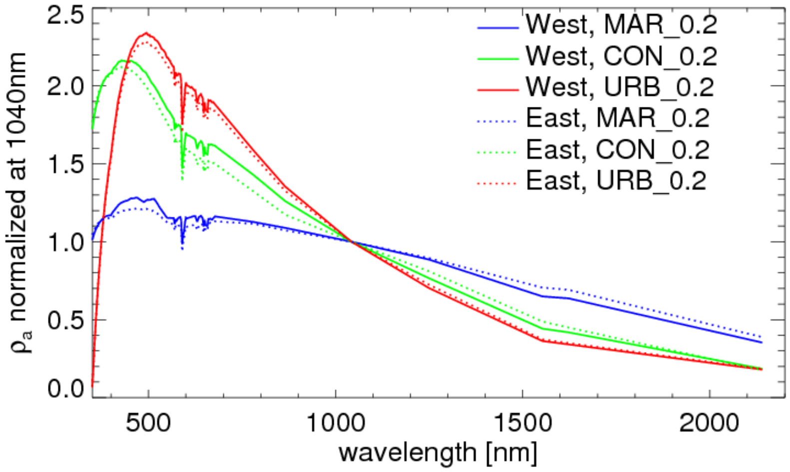

$$\rho_g^{TOA}(\lambda) = \rho_{g0} \cdot G(\lambda)$$

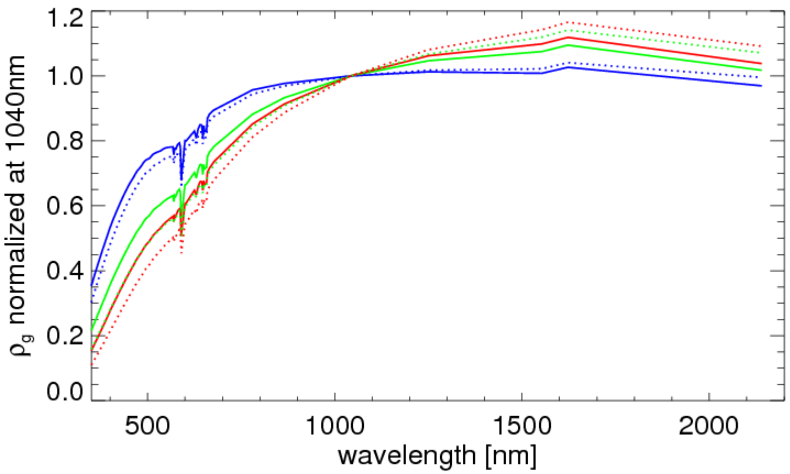

- Aerosol and glint reflectance have different spectral shapes
- TOA glint spectrum is the surface reflectance multiplied by a two-way atmospheric transmittance

Verification with HyspIRI simulation data

- ALOHA-East edge U=10m/s

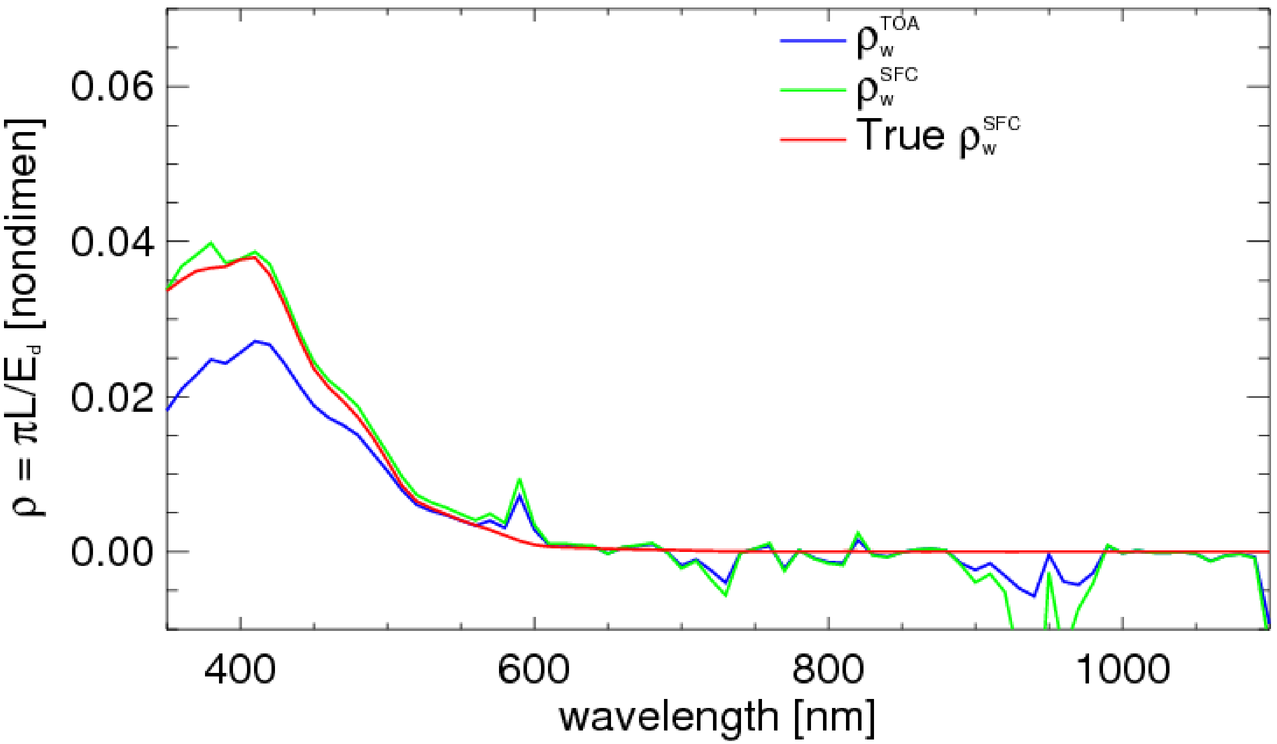

National Research FLAGSHIPS Wealth from Oceans CSIRO

AVIRIS example: French frigate shoals

- Apr. 18 2000 on French Frigate Shoals, Hawaii

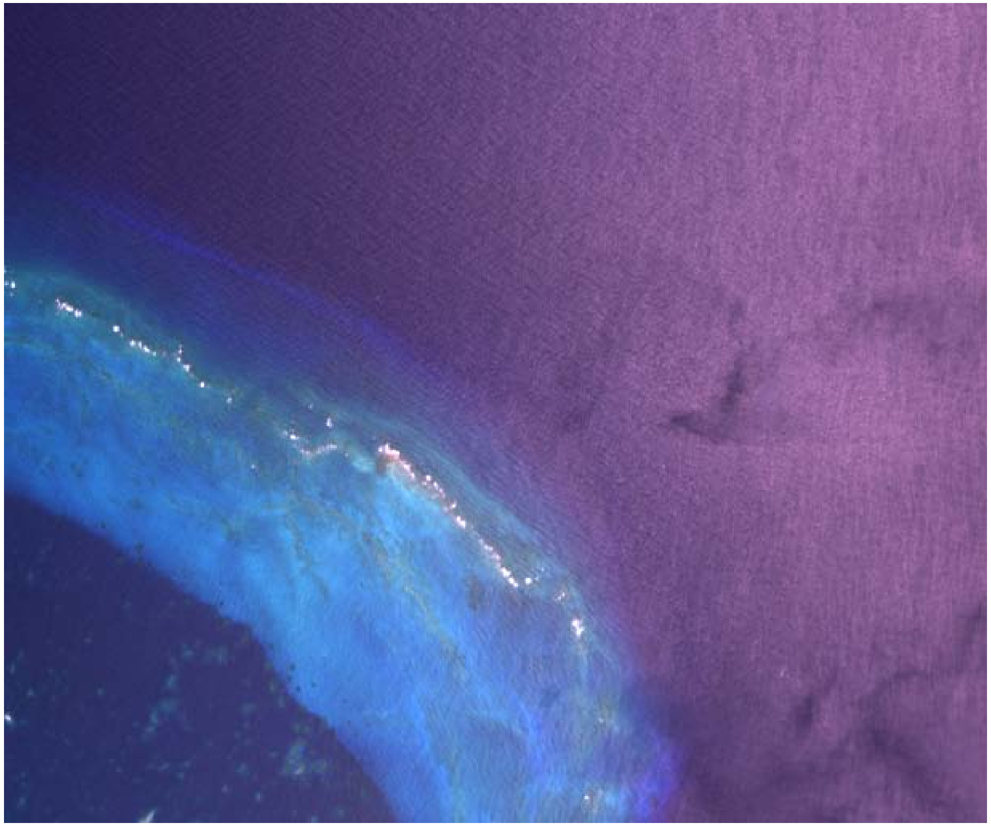

After correction

Before correction

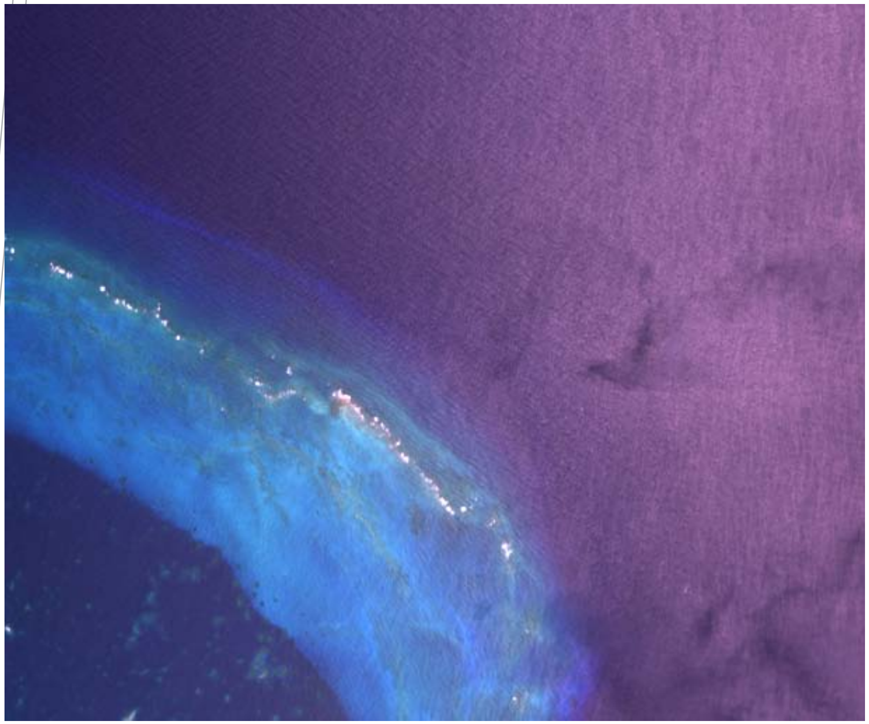

After correction

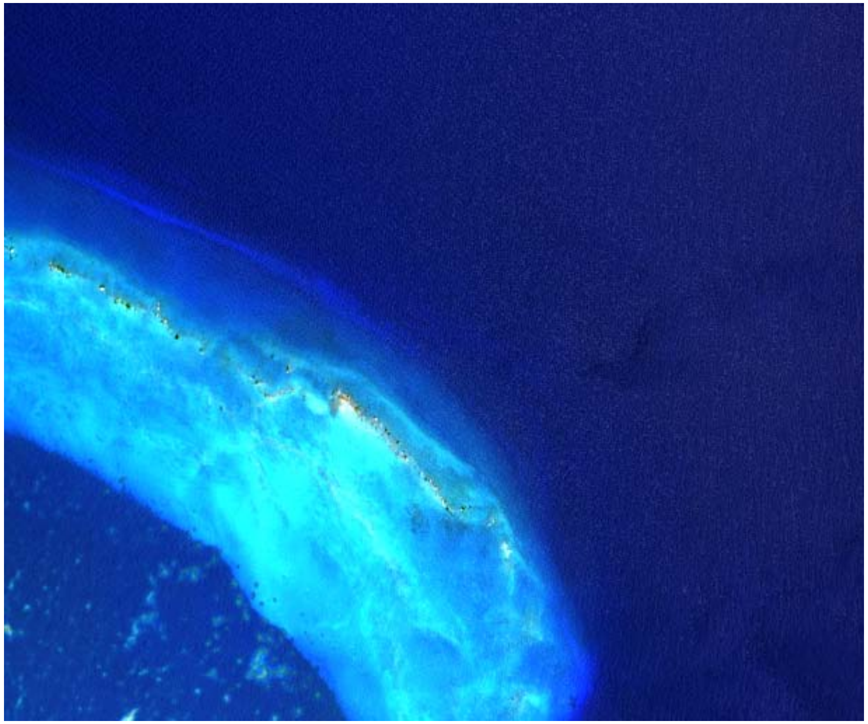

After correction with smoothed aerosol reflectance

Before correction

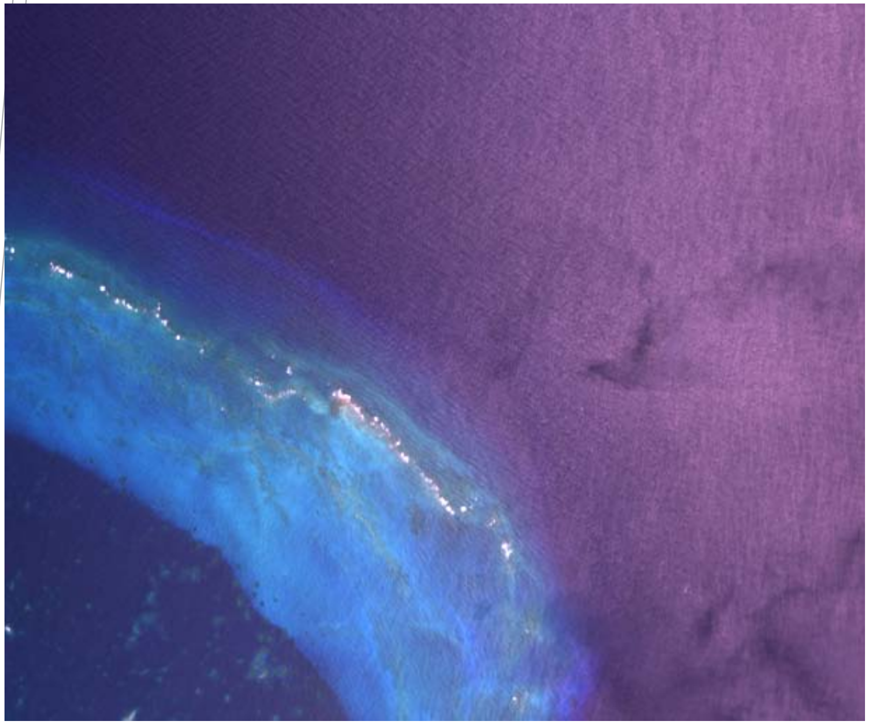

After correction

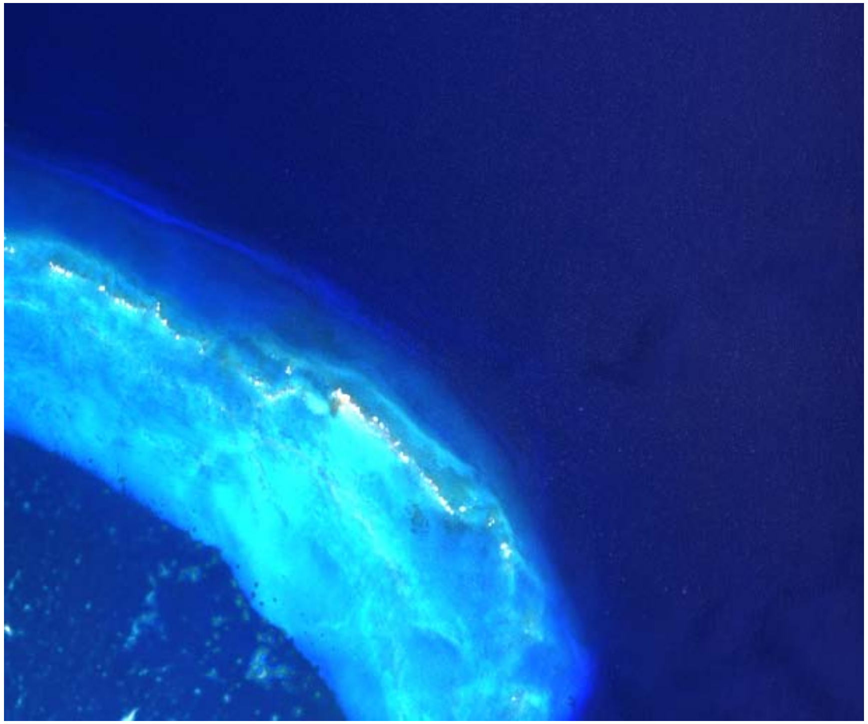

Transect

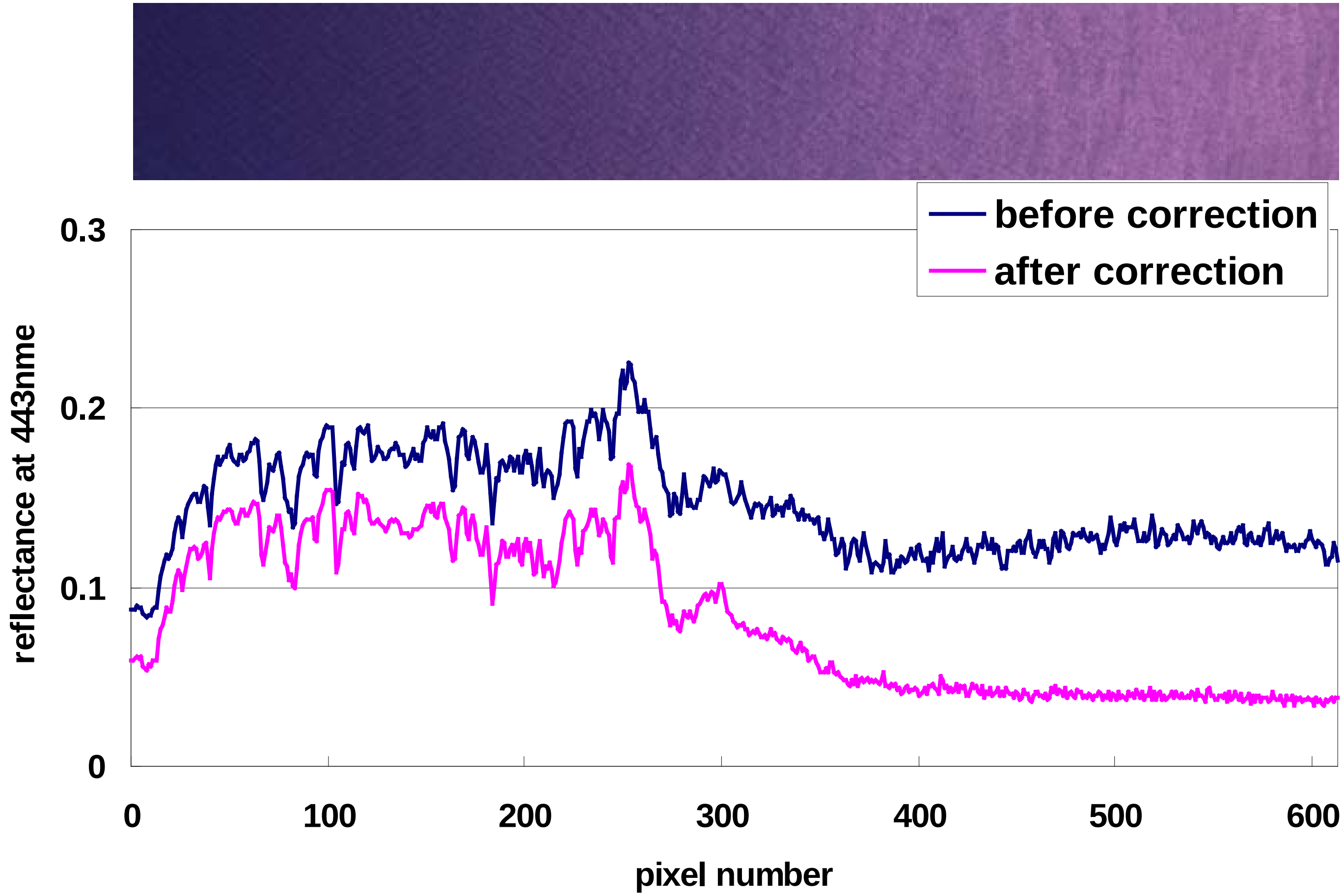

National Research
FLAGSHIPS
Wealth from Oceans
CSIRO

Spectra at a glint affected pixel

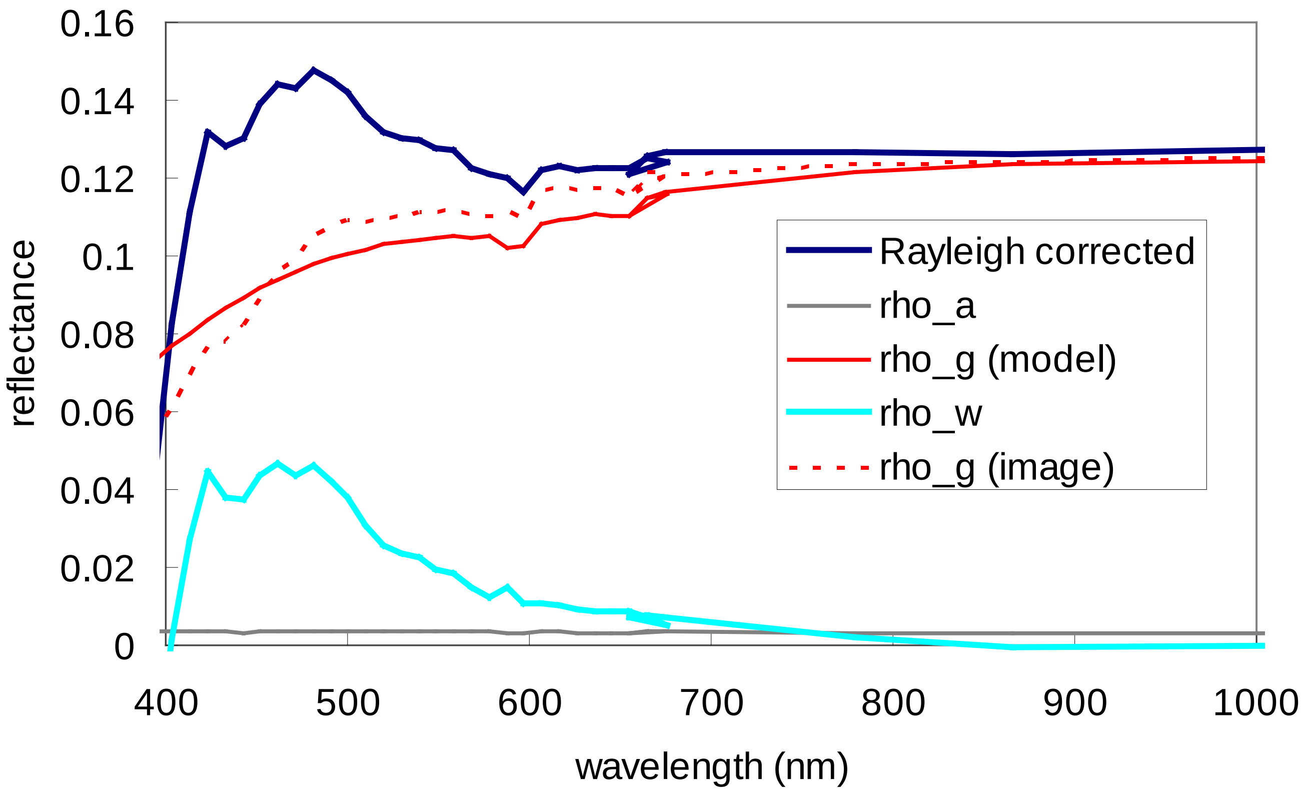

National Research FLAGSHIPS Wealth from Oceans

CSIRO

Discussion

- Aerosol optical properties = type and optical thickness
  - Suggested to apply a low pass spatial filter to the retrieved aerosol optical thickness
  - Can aerosol model (spectral slope) be derived? Difficult where sun glint is significant.
- For operational use, vicarious calibration of satellite data against model would be required for glint correction.

Glint correction for algal bloom detection

- Intense blooms of the brown algae, *Hincksia sordida* in Southeast Queensland recently have substantially reduced the recreational value. Wide spread algal blooms confirmed by aerial overflights and in situ observations were not visible in true colour image from the MODIS Rapidfire website.

Hincksia Sordida
Non-toxic filamentous brown algae
(E. Abal et al., 2006)

Top Of Atmosphere MODIS reflectance spectra for bloom and non-bloom (=ocean water) pixels

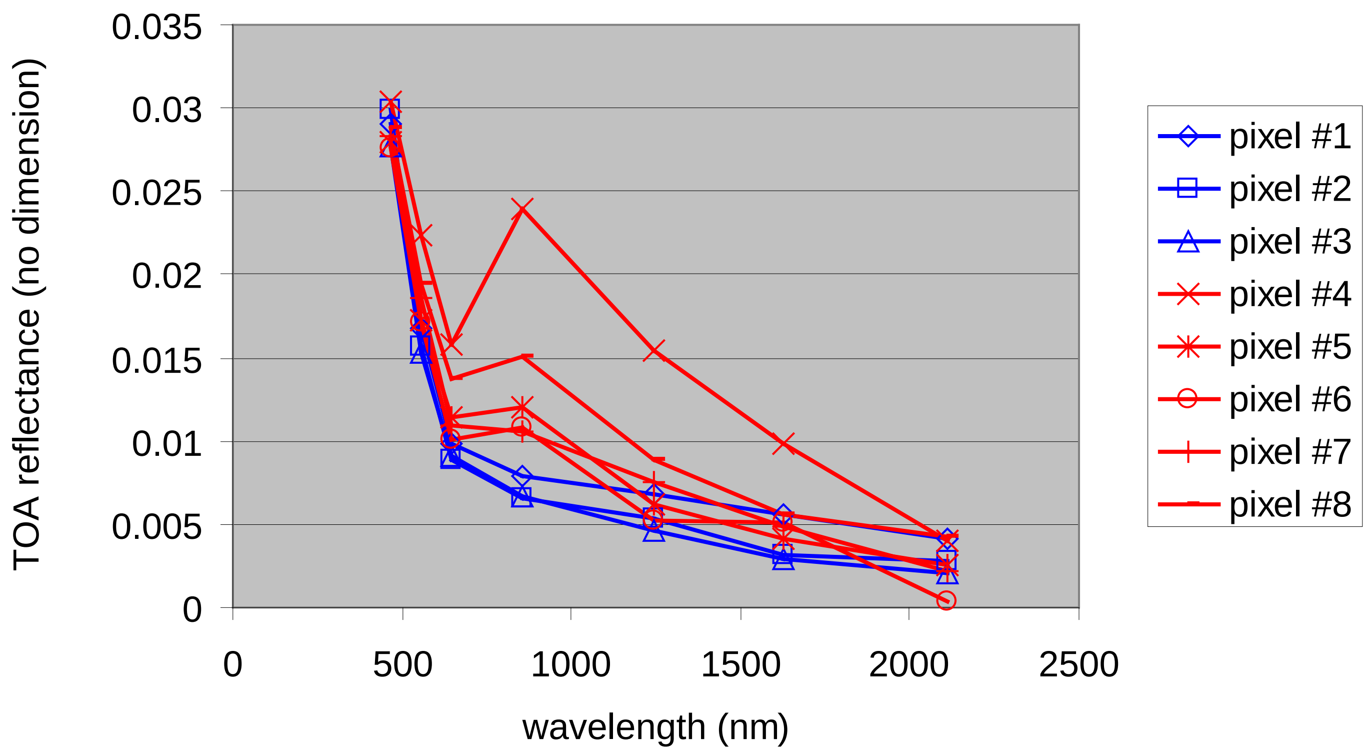

- Spectra from Terra image of Oct 3 2006
  - Blue curves for non-bloom pixels and red curves for bloom pixels.
  - Reflectance at 869nm should indicate the bloom intensity if the atmosphere and sea surface conditions are same

Satellite & Local Time

TOA RGB normal	TOA RGB FA	Rw RGB normal	Rw RGB FA
TOA RGB	Floating Algae (FA) enhanced TOA RGB	water reflectance (Rw) RGB	Floating Algae (FA) enhanced Rw RGB
R - 645nm G - 555nm B - 469nm	R - 859nm G - 645nm B - 469nm	R - 645nm G - 555nm B - 469nm	R - 859nm G - 645nm B - 469nm
(≈ NASA rapid response imagery)		*(TENTATIVE)*	*(TENTATIVE)*

Before atmospheric correction

After glint atmospheric correction

Aqua 2006 Oct 2 (275) 13:30

TOA RGB normal

TOA RGB FA

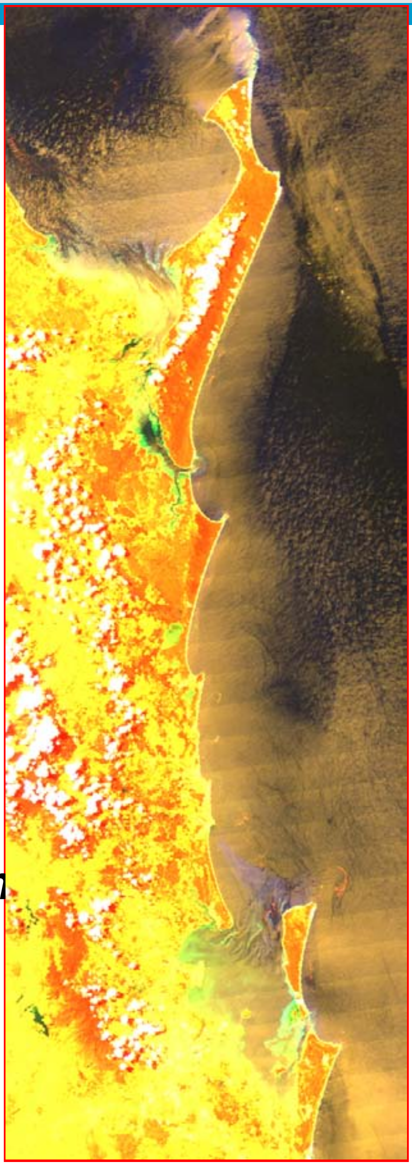

Rw RGB normal

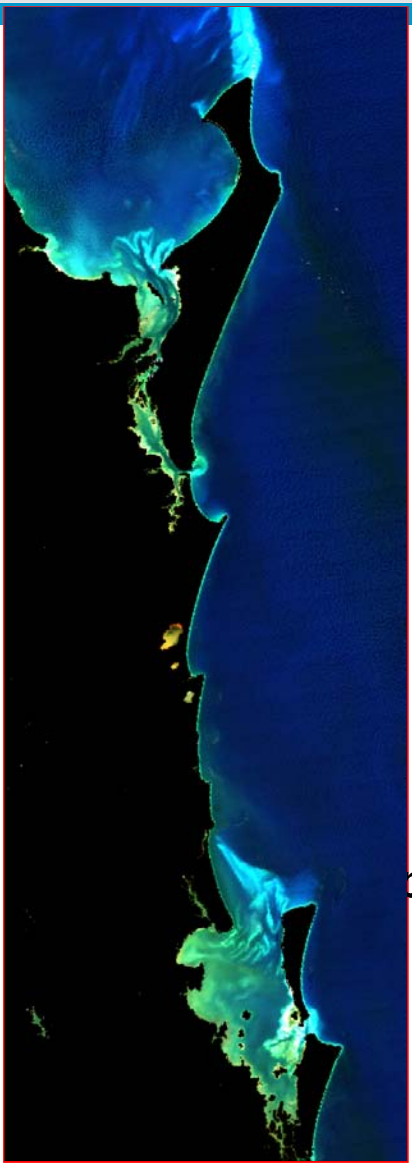

Rw RGB FA

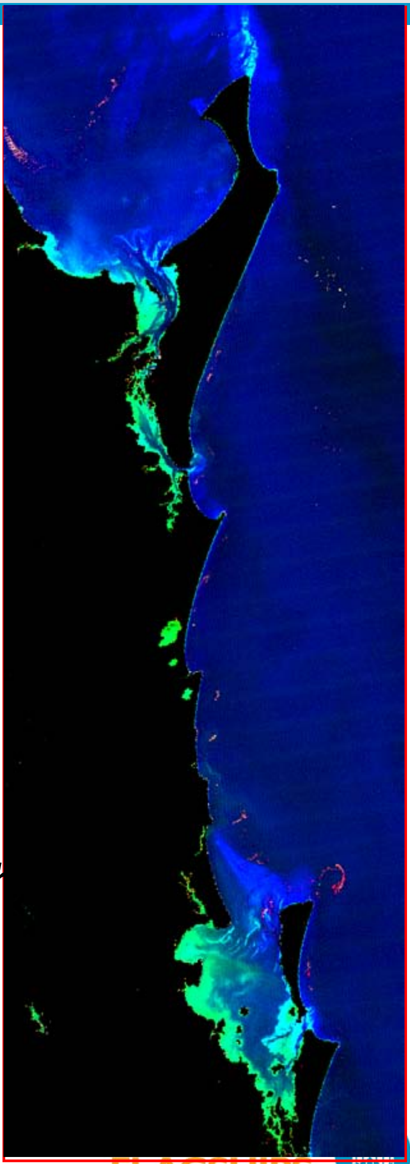

Summary

- HyspIRI sun glint should be substantially reduced by shifting the equator crossing time from 11.30 to 10.30 AM.
- Glint-aerosol discrimination algorithm has been verified with simulation data and the results from application to AVIRIS and MODIS images look promising.
- It will be important to make sure consistency between satellite data and radiative transfer model that will be used for atmospheric-glint correction. Need vicarious calibration or similar.

National Research FLAGSHIPS Wealth from Oceans CSIRO

Thank you

Environmental Earth Observation Group
CSIRO Land and Water
YoungJe Park
Email: young.park@csiro.au

CARIACO

CARBON RETENTION IN A COLORED OCEAN

Changes in community structure and productivity in a coastal upwelling system: The CARIACO ocean time-series and implications for future satellite measurements

Frank Muller-Karger

USF UNIVERSITY OF SOUTH FLORIDA COLLEGE OF MARINE SCIENCE

Institute for Marine Remote Sensing

CARIACO

Acknowledgements

- **_Colleagues and co-Investigators:_**
  - *Ramon Varela (FLASA)*
  - *Yrene Astor (FLASA)*
  - *Eduardo Klein (USB)*
  - *Robert Thunell (USC)*
  - *Mary Scranton (SUNY)*
  - *Gordon Taylor (SUNY)*
  - *Robert Weisberg (USF)*
  - *Kent Fanning (USF)*
  - *Laura Lorenzoni*
  - *[AND MANY OTHERS]*
- **_Funding and support:_**
  - *NSF*
  - *FONACIT*
  - *FLASA*
  - *USB*
  - *UCV*
  - *UDO*

FUNDACIÓN LA SALLE de Ciencias Naturales

USF UNIVERSITY OF SOUTH FLORIDA

Department of Geological Sciences UNIVERSITY OF SOUTH CAROLINA

STONY BROOK STATE UNIVERSITY OF NEW YORK

UNIVERSITY OF LOUISIANA Lafayette

IVIC

Northeastern UNIVERSITY

WOODS HOLE OCEANOGRAPHIC INSTITUTION 1930

Location

Cariaco Basin

Southeastern Caribbean

Time series station:
LAT 10.5° N
LON 64.65° W

~1400 m

CARIACO

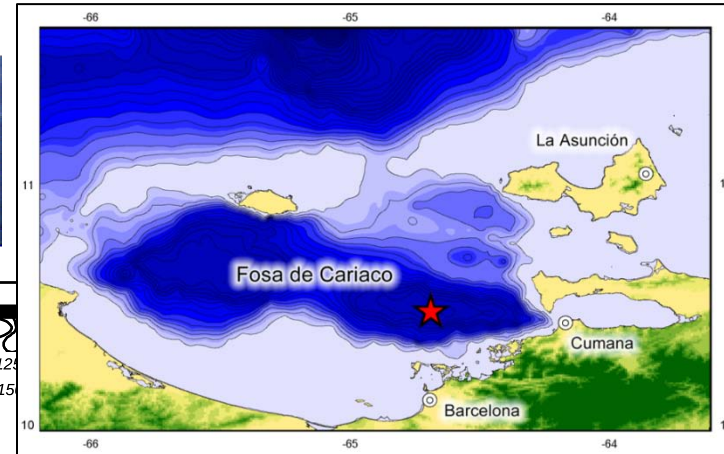

La Asunción
Fosa de Cariaco
Cumana
Barcelona
-66
-65
-64
11
10

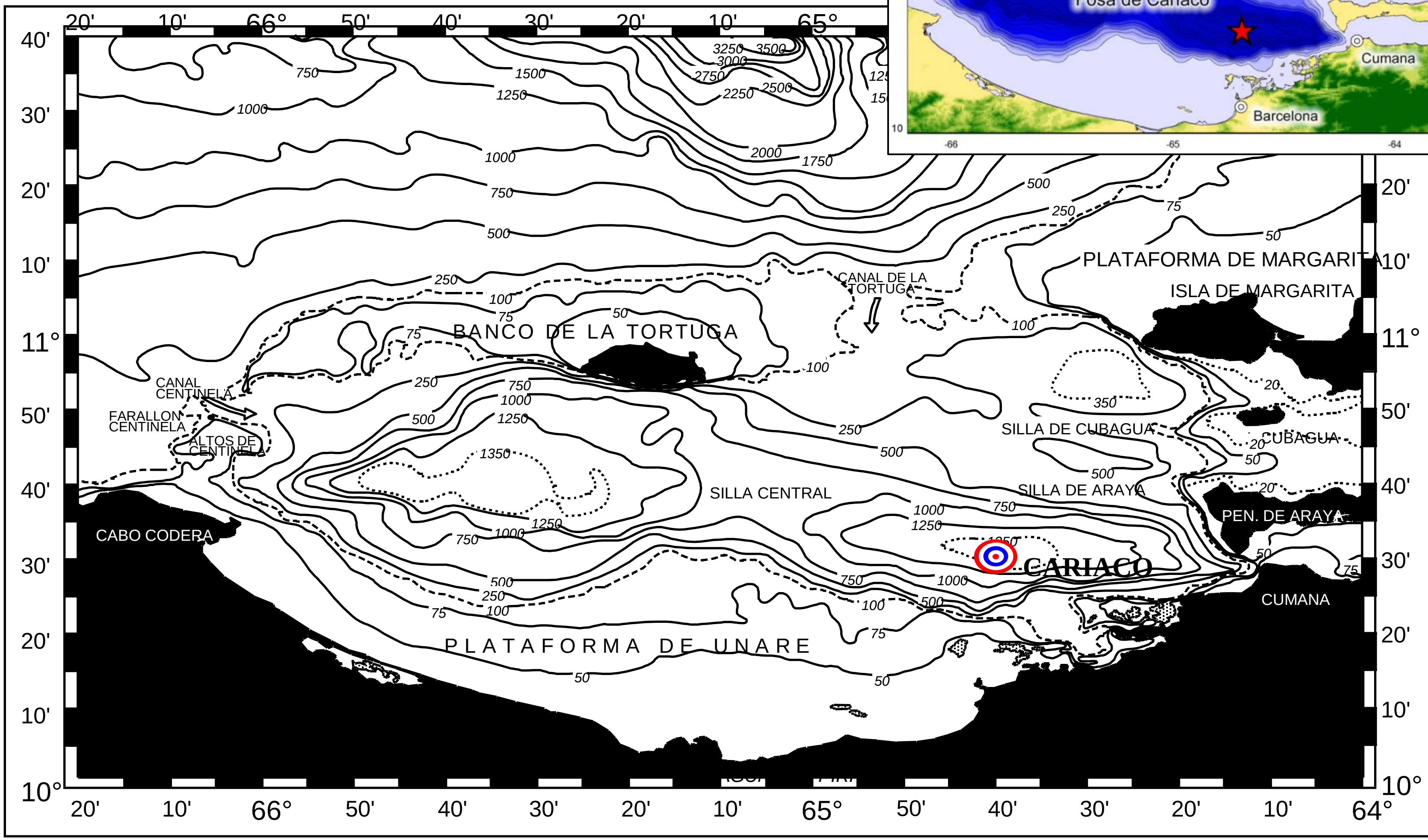

BANCO DE LA TORTUGA
CANAL DE LA TORTUGA
CANAL CENTINELA
FARALLON CENTINELA
ALTOS DE CENTINELA
PLATAFORMA DE MARGARITA
ISLA DE MARGARITA
SILLA DE CUBAGUA
CUBAGUA
SILLA DE ARAYA
SILLA CENTRAL
PEN. DE ARAYA
CABO CODERA
CARIACO
CUMANA
PLATAFORMA DE UNARE
66°
65°
64°
11°
10°

Cariaco Basin Characteristics

Tropical climate

Basin embedded in the continental shelf.

High primary production (~500 gC/m2/y)

<u>Alternating</u> seasonal upwelling and river discharge

Permanent **anoxia** below ~250m: undisturbed sediments.

Local **river inputs** (Minimal Orinoco and Amazon river influence)

High **Secondary production**: Sardine, demersal and other pelagic fisheries (~500Ktm/y).

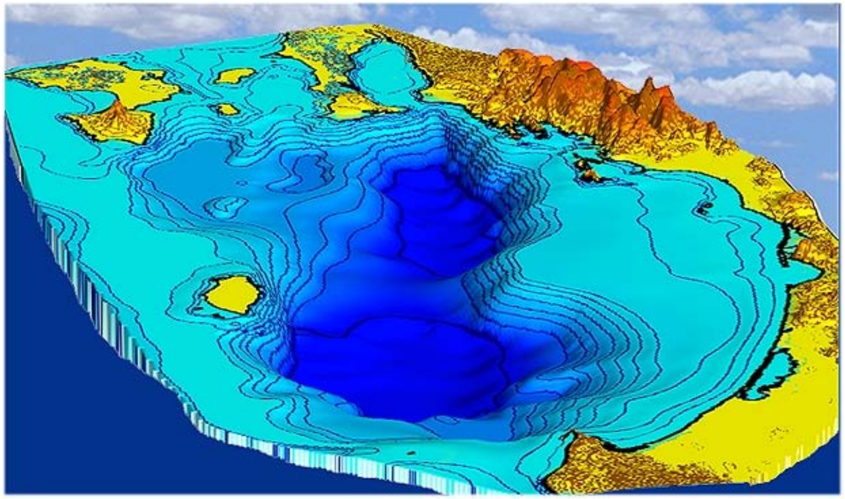

CARIACO

SeaWiFS satellite-derived
Chlorophyll-a and
other “pigments”

Mar 5, ’03

First half of year:
Windy / dry
High coastal upwelling
High primary production
Low river discharge

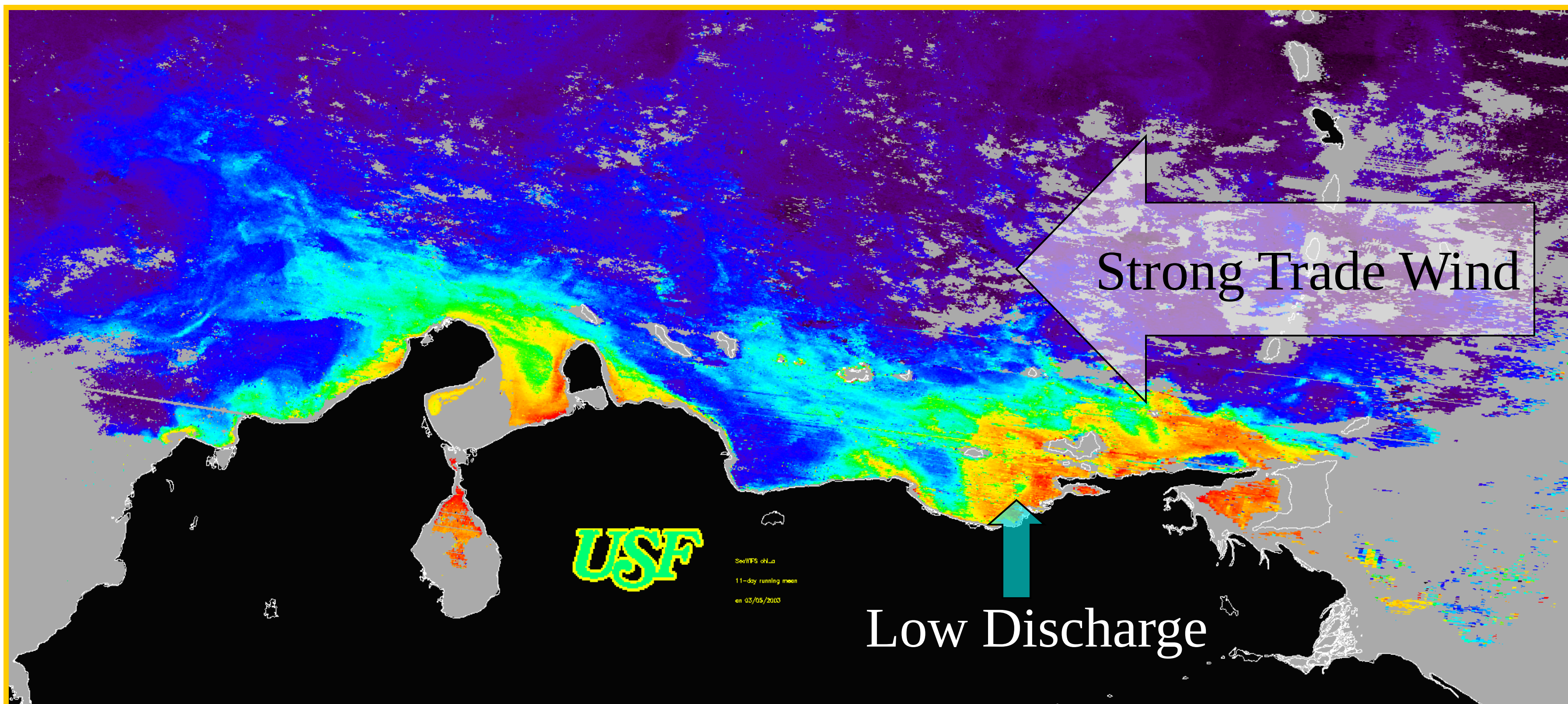

SeaWiFS satellite-derived Chlorophyll-a and other “pigments”

Oct 17, ‘03

Second half of year:
Less wind / wet
Low upwelling
Low primary production
High river discharge

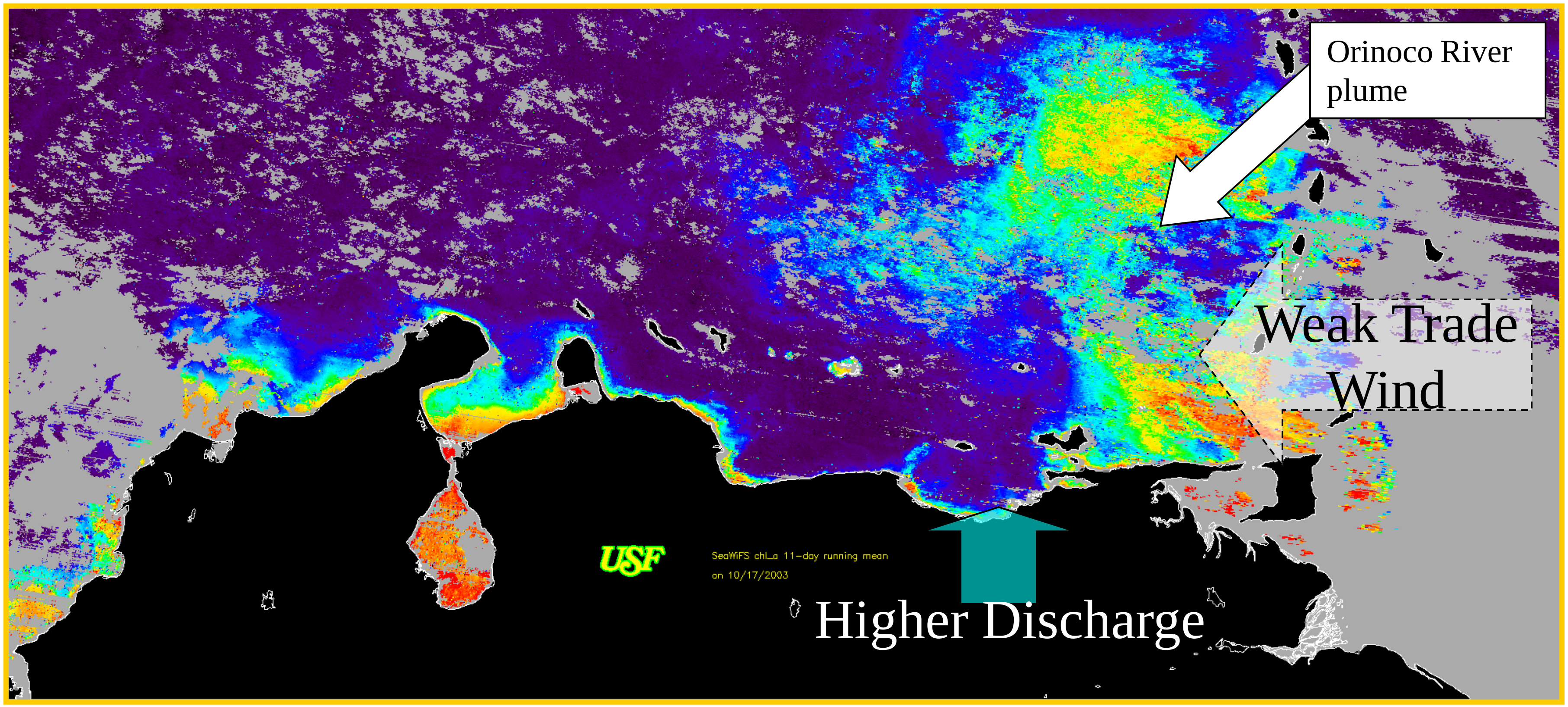

CARIACO

No benthic organisms

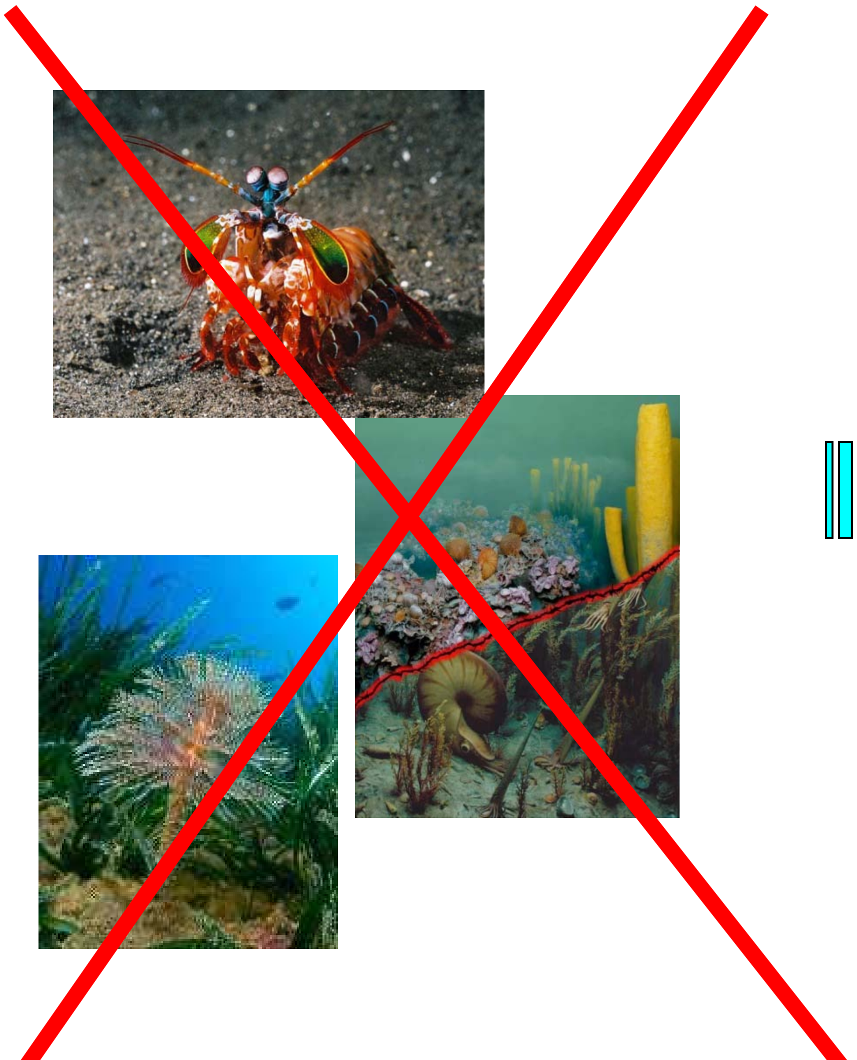

Laminated (“varved”) sediments

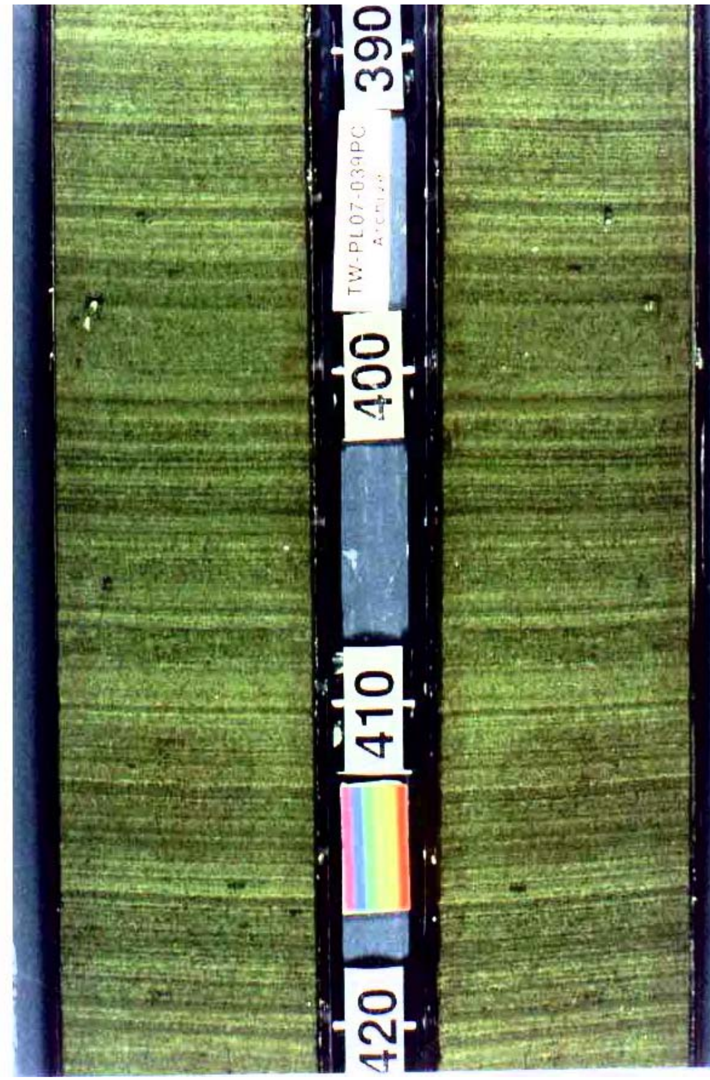

CARIACO

Sediment varves:

- *Lighter color laminae:*
  - *rich in plankton*
  - *(upwelling period)*
- *Dark laminae:*
  - *Riverine*
  - *detrital minerals*
  - *(rainy season)*

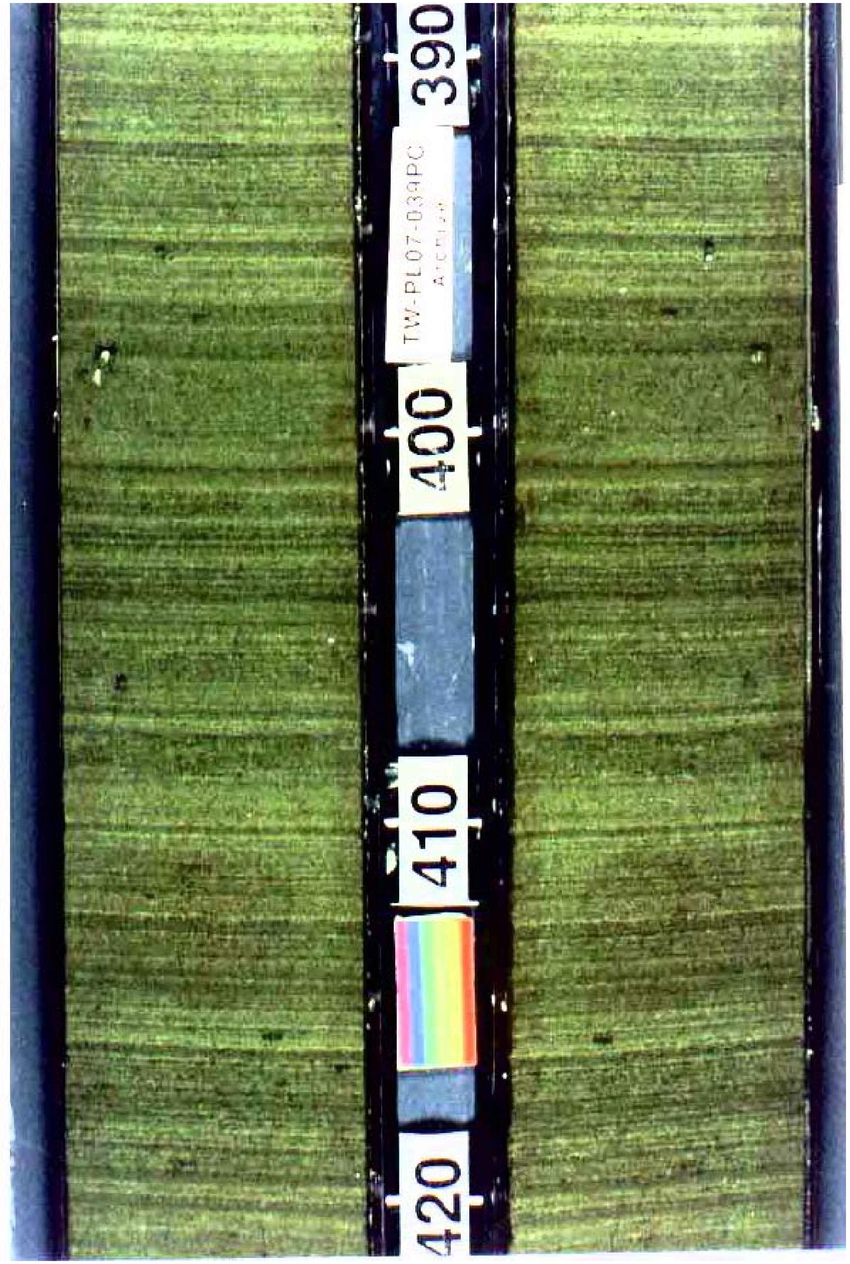

ODP Core Site 1002C.
Lea et al., 2003

CARIACO

Significance of basin

- *Continental margin / upwelling processes*
- *Oxic/anoxic oceanographic processes*
- *Sediment climate record (natural sediment trap)*
  - *anoxic bottom and absence of bioturbation lead to sediment varves*

TIME SERIES PROJECT
Scientific Objectives

- *Understand linkages between oceanographic processes and the production and sinking flux of particulate matter in the Cariaco Basin*
- *Explain climate / paleoclimate changes in the region (including Atlantic Ocean)*

Objectives of bio-optical research

Assess fundamental ecological characteristics of the system rapidly, repeatedly, over large scales and long times, and economically (e.g. use of remote sensing). Specifically:

- *Phytoplankton concentration*
- *Primary productivity*
- *Functional groups and community structure*

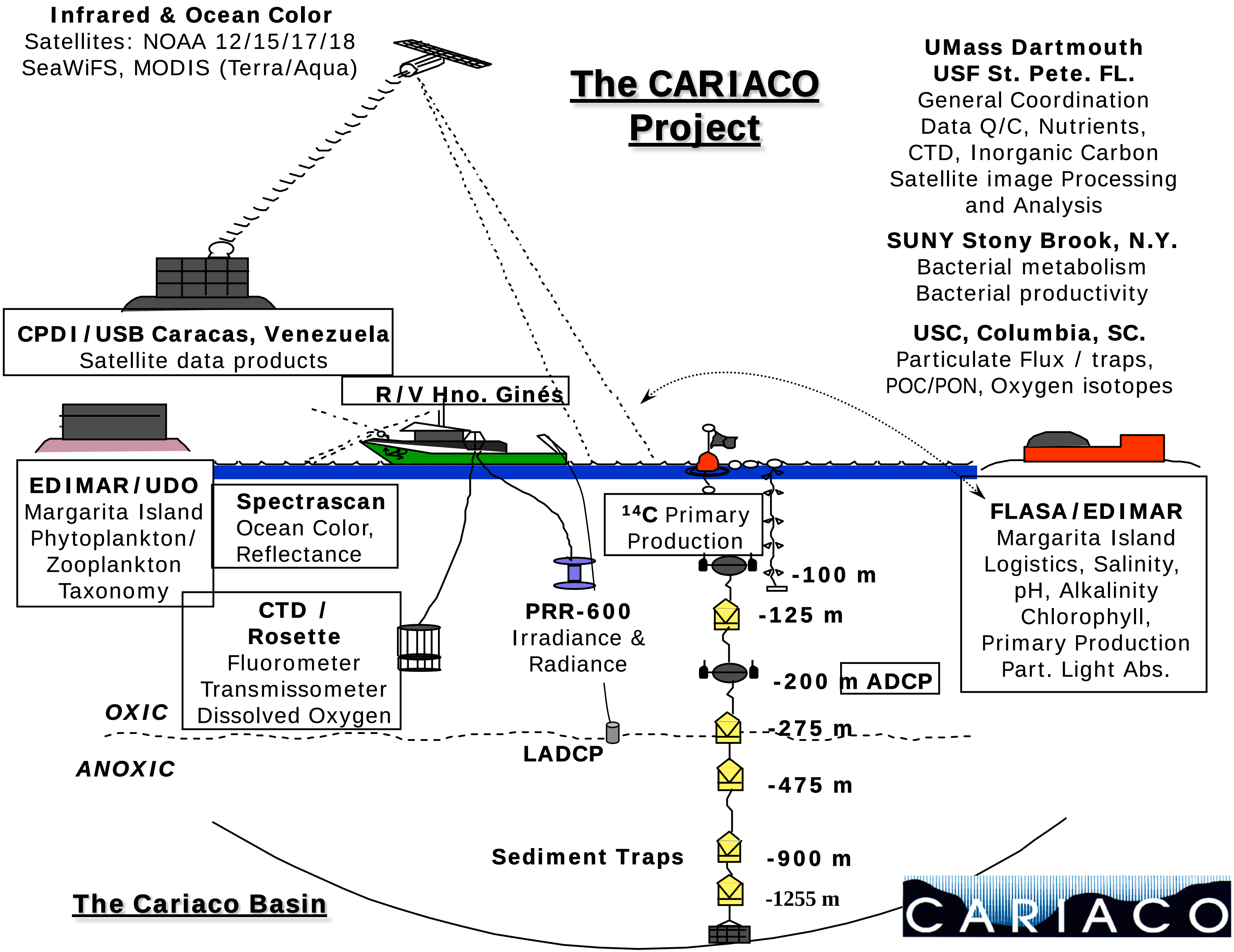

Infrared & Ocean Color
Satellites: NOAA 12/15/17/18
SeaWiFS, MODIS (Terra/Aqua)
The CARIACO Project
UMass Dartmouth
USF St. Pete. FL.
General Coordination
Data Q/C, Nutrients,
CTD, Inorganic Carbon
Satellite image Processing
and Analysis
SUNY Stony Brook, N.Y.
Bacterial metabolism
Bacterial productivity
USC, Columbia, SC.
Particulate Flux / traps,
POC/PON, Oxygen isotopes
CPDI / USB Caracas, Venezuela
Satellite data products
R/V Hno. Ginés
EDIMAR/UDO
Margarita Island
Phytoplankton/
Zooplankton
Taxonomy
Spectrascan
Ocean Color,
Reflectance
14C Primary
Production
FLASA/EDIMAR
Margarita Island
Logistics, Salinity,
pH, Alkalinity
Chlorophyll,
Primary Production
Part. Light Abs.
CTD /
Rosette
Fluorometer
Transmissometer
Dissolved Oxygen
PRR-600
Irradiance &
Radiance
-100 m
-125 m
-200 m ADCP
-275 m
-475 m
-900 m
-1255 m
OXIC
ANOXIC
LADCP
Sediment Traps
The Cariaco Basin
CARIACO

CARIACO
CARBON RETENTION IN A COLORED OCEAN

TIME SERIES DETAILS

- 10º30’N, 64º40’W (Venezuela)
- Operation: since November ’95 (monthly cruises, moorings)
  -hydrography / sediment traps
  -bio-optical /biogeochemical::
  * Phytoplankton concentration
  * HPLC pigment composition
  * Taxonomy
  * Primary productivity
  * Reflectance profiles
  * Hypersperspectral reflectance

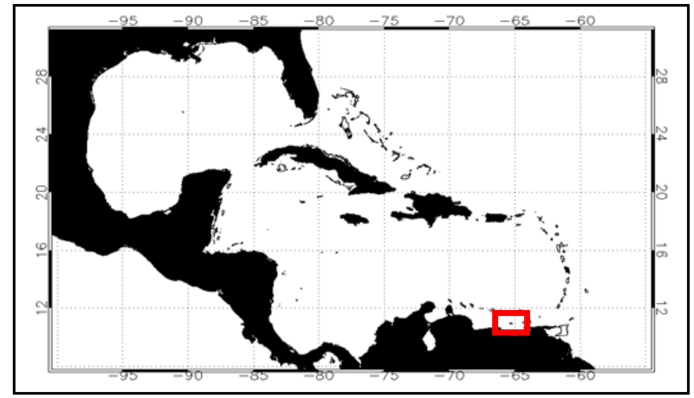

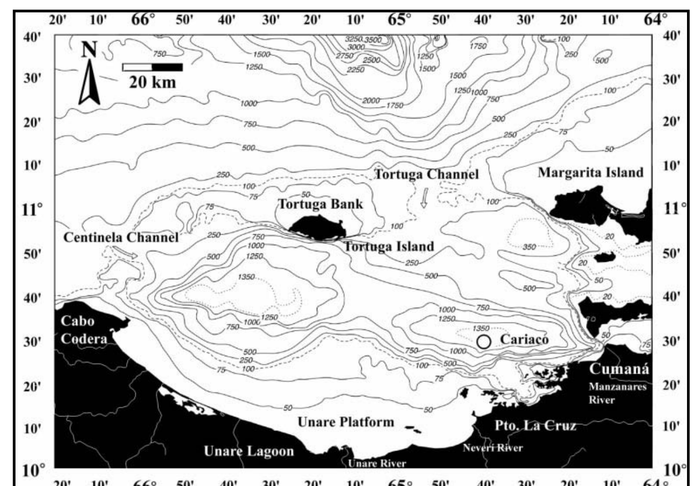

CARIACO

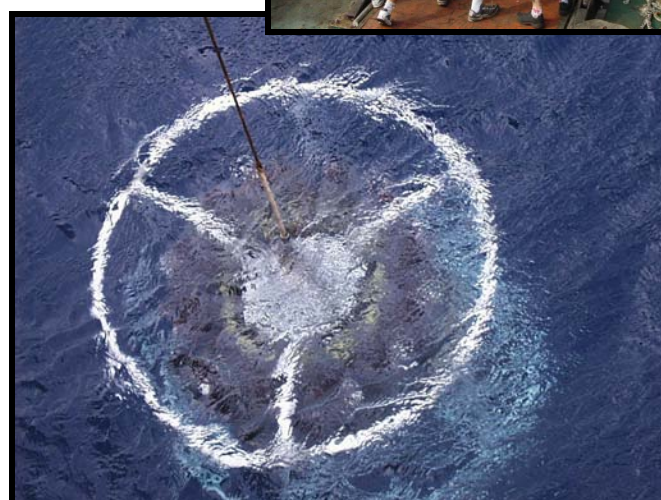

<u>R/V Hermano Gines</u>

25 m (~80 ft)

116 metric Ton

13 crew

8 science party

~$4,000/day

Sampling and keeping records…

Filtering…filtering…24 h a day…

Yrene Astor
Keeps us in line

CTD/rosette
hydrography

Sediment traps

Zooplankton

Primary
productivity

Bio-optics
(ocean color)

CARIACO cruises and data policy

Since Nov 1995:
172 core cruises (August 2010)
29 sediment trap and current meter recovery-redeployment cruises
30 biogeochemical and microbial process cruises
6 regional cruises

Implemented a policy for open and public sharing of samples, data, and information

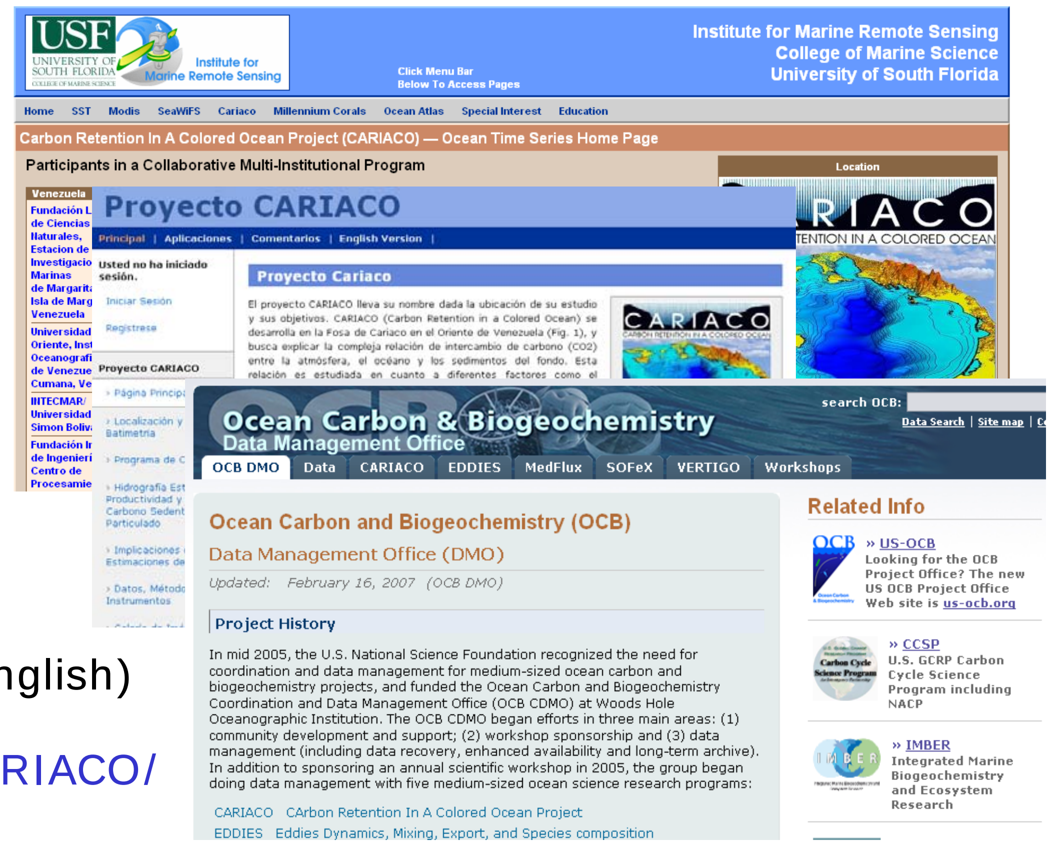

http://cariaco.ws (Spanish)

http://www.imars.usf.edu/CAR/ (English)

http://ocb.whoi.edu/jg/dir/OCB/CARIACO/

Temperature

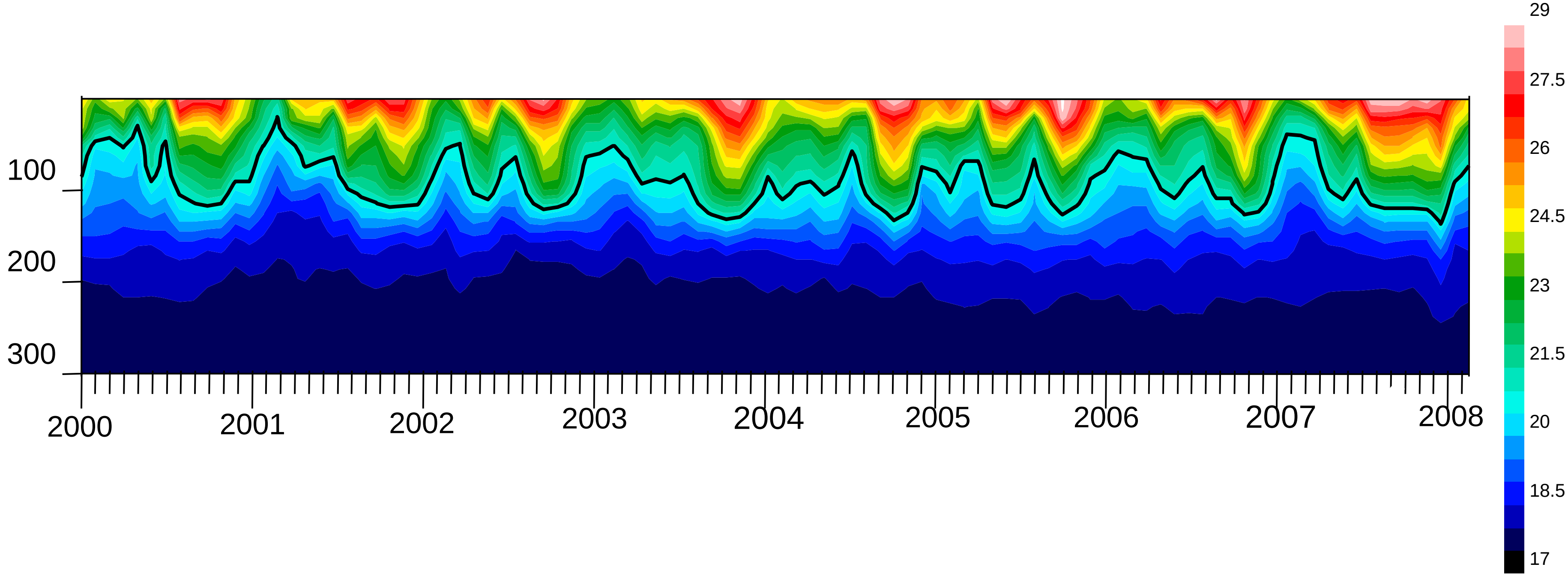

Upwelling intensity has decreased since we started the series

CARIACO

Long Term Changes in SST: Reduction in Annual Range

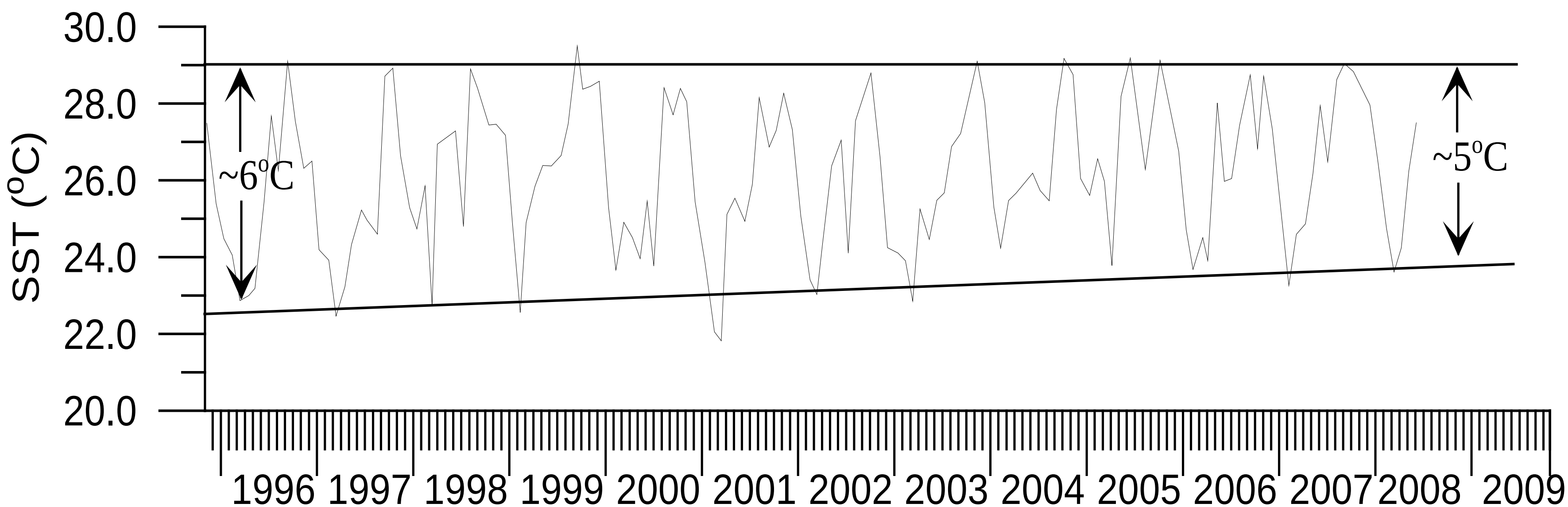

Contributed by
R. Thunell, USC

Primary Production

- *Chlorophyll and primary production highest in Jan-Apr*
- *A secondary peak seen during the summer upwelling*
- *Shift in phytoplankton community since ~2001 (now smaller cells)*
- *Amplitude of PP decreased since ~2000, with broader peaks*
- *Total annual production remains similar (~500 gC/m2/y)*

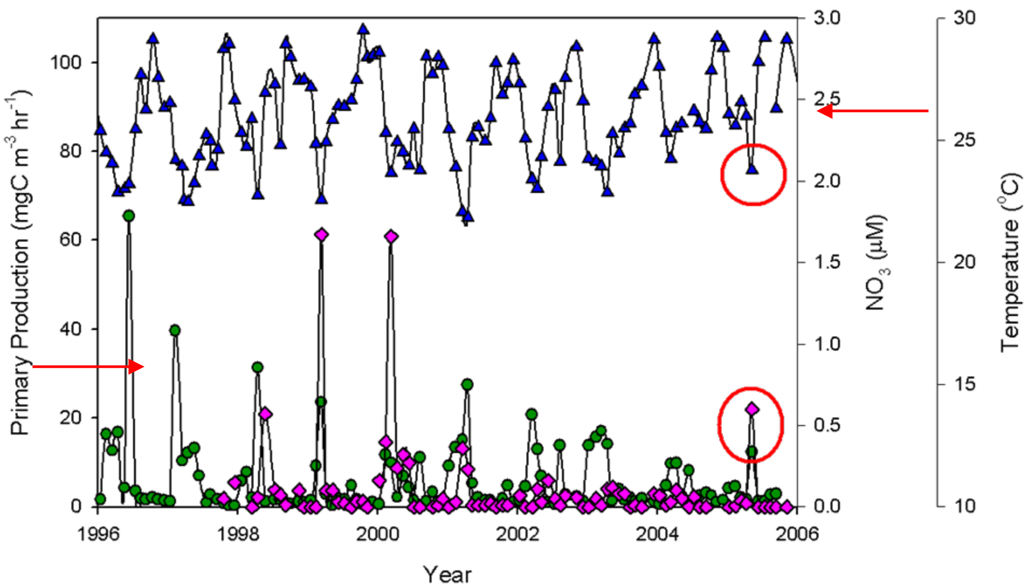

Trend in CO2 fugacity: fCO2 Increasing?

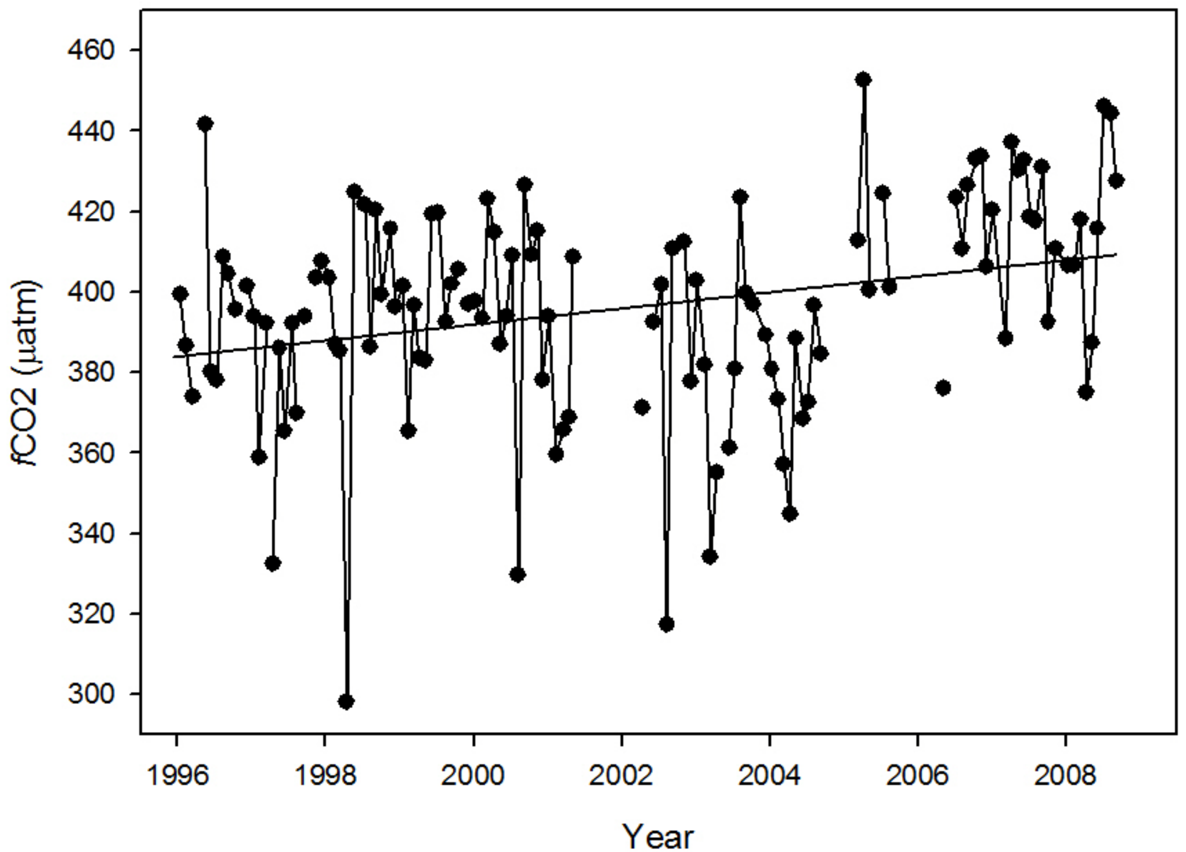

	Temperature	Δ	Salinity	Δ	fCO2	Δ
Max 1996-2001	29.50	**7.68**	37.00	**0.92**	441.70	**143.40**
min 1996-2001	21.82		36.07		298.30	
max 2002-2009	30.00	**7.15**	37.06	**1.22**	452.60	**135.30**
min 2002-2009	22.85		35.84		317.30	

CARIACO

Sediment trap samples

CARIACO

Particulate organic carbon flux

- Organic particle flux at 1300 m is:
  ~5x10^{-3} mol C m^{-2}d^{-1} or
  ~0.074 g m^{-2}d^{-1}
  (Thunell et al., 2007)
  - ~1.3% of primary productivity reaches the bottom

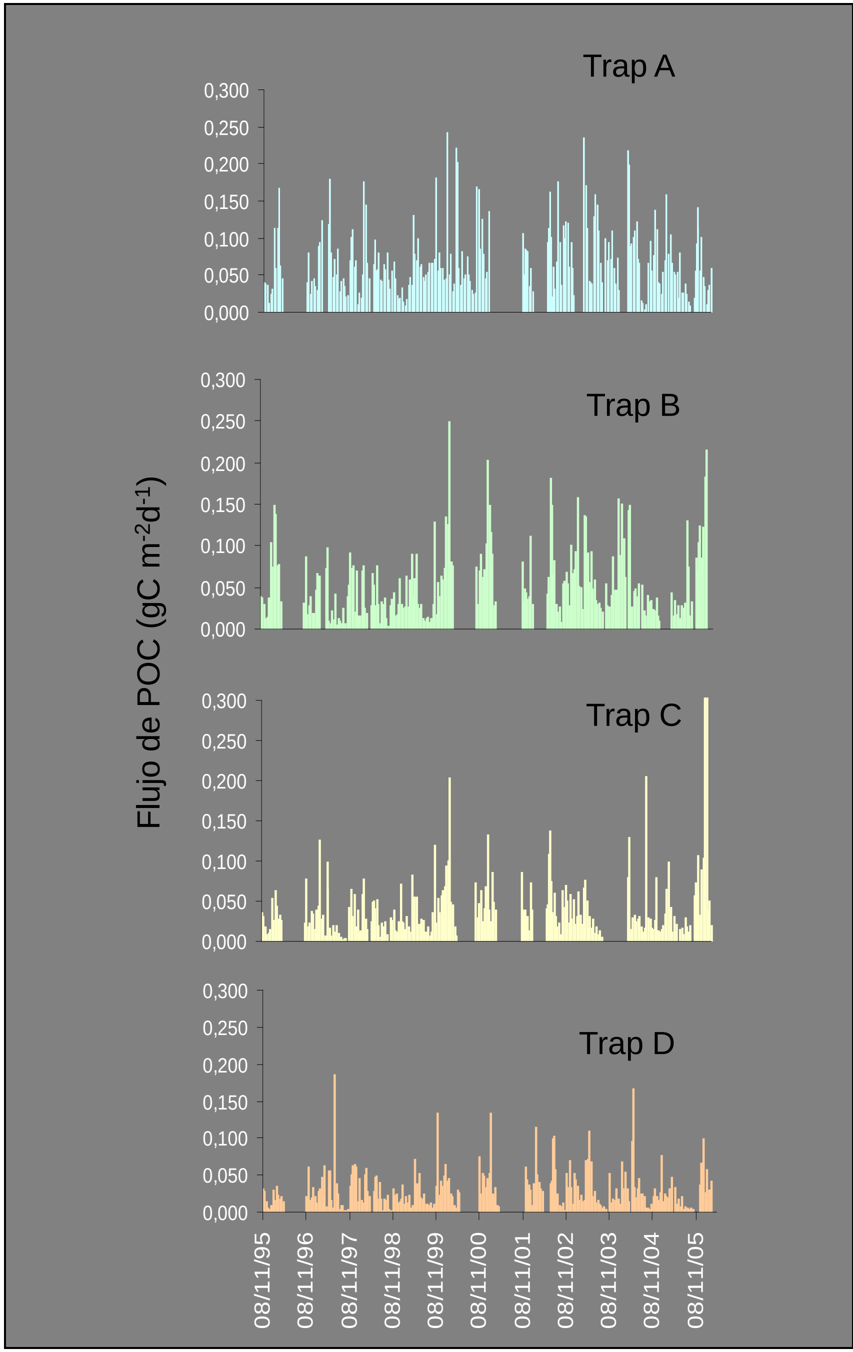

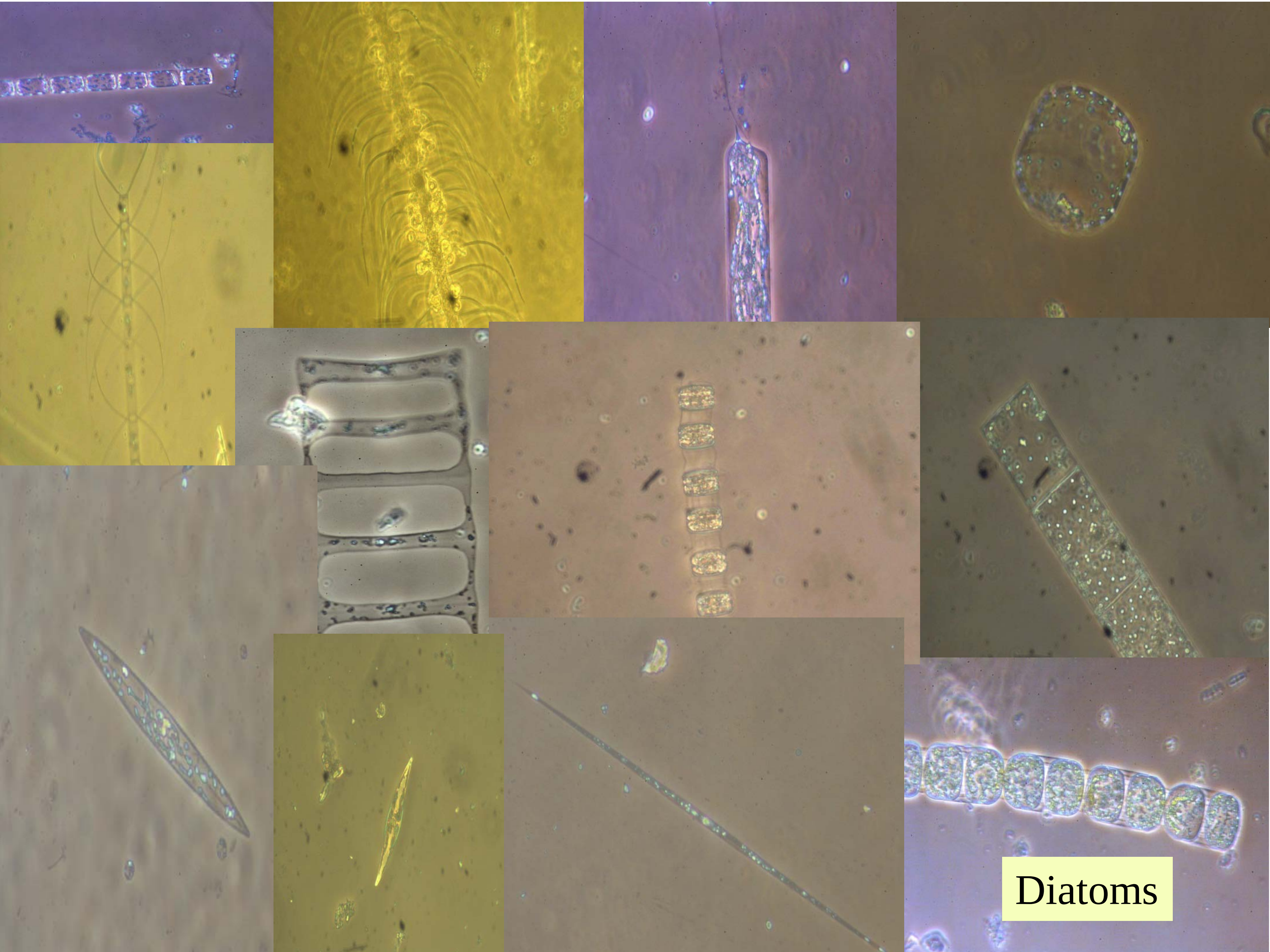
Diatoms

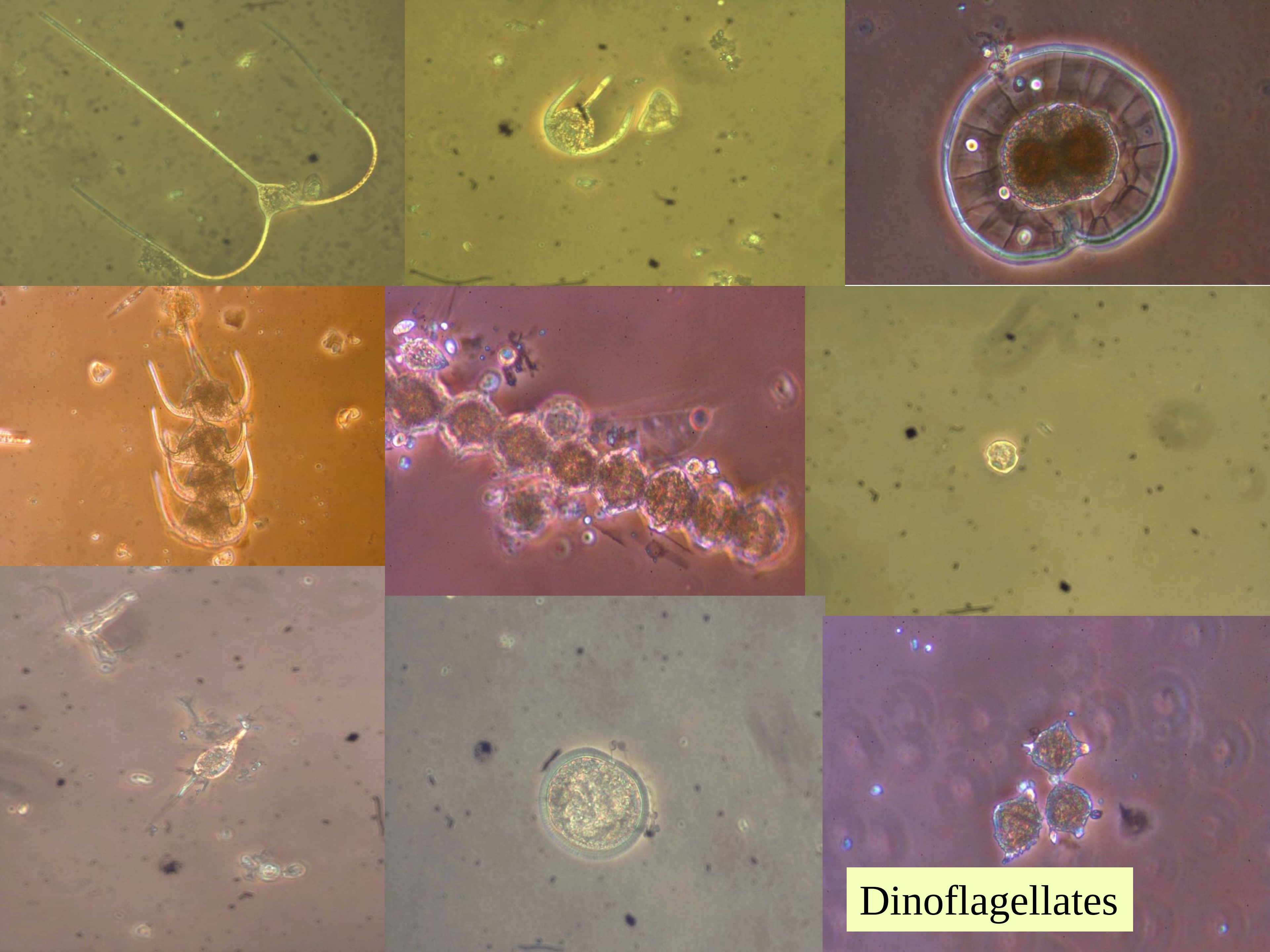

Dinoflagellates

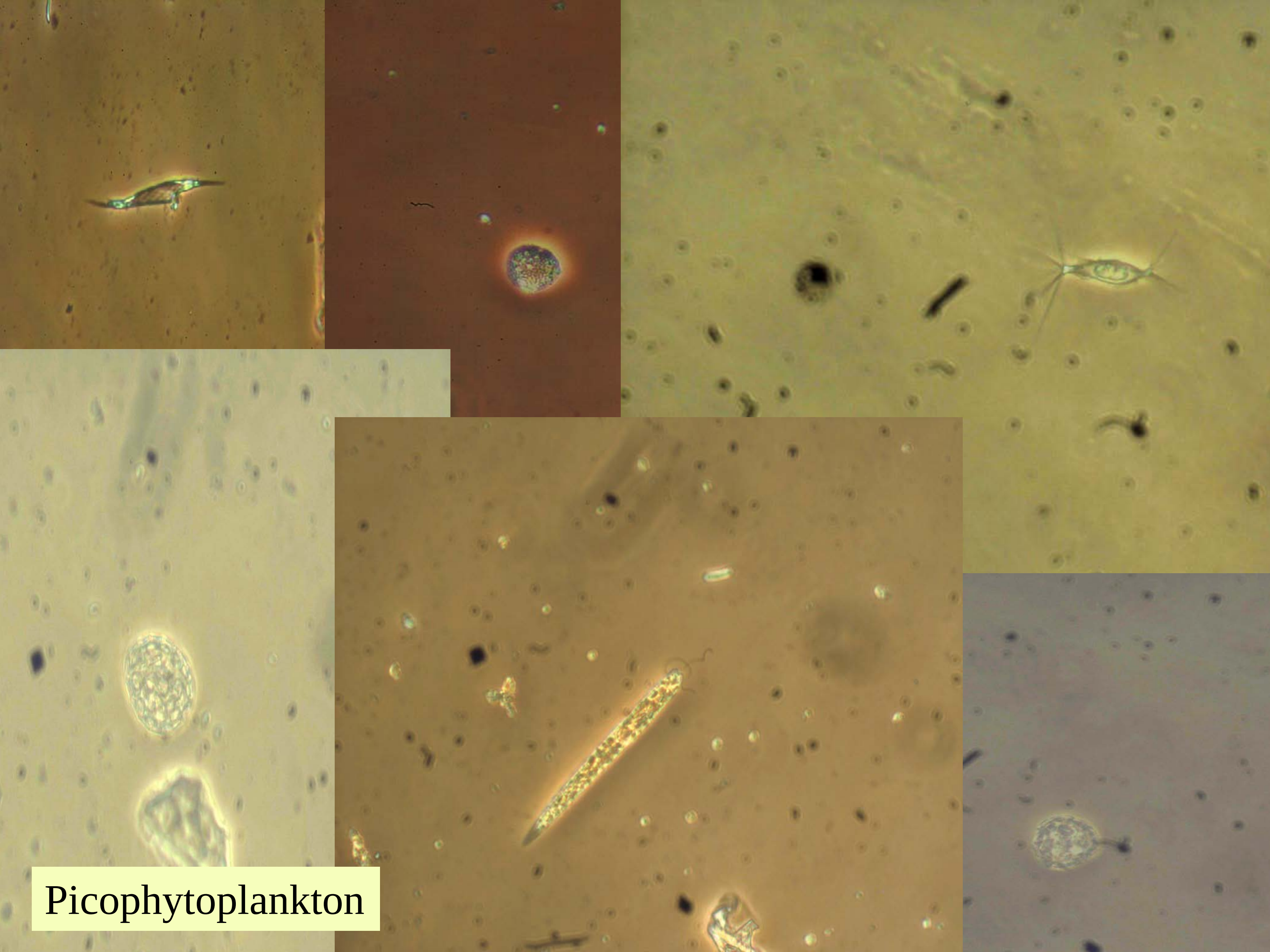
Picophytoplankton

Trichodesmium (N-fixer)

Pytoplankton pigments: HPLC

Pigment	Abbre.	Phytoplankton group/division/class
Chlorophyll c_3	Chl c_3	Prymnesiophyceae, Chrysophyceae
Chlorophyll $c_{1\text{-}2}$	Chl $c_{1\text{-}2}$	Chl c_1: Bacillariophyta, Prymnesiophyceae, Raphidophyceae Chl c_2: Cryptophyta, Bacillariophyta, Prymnesiophyceae, Raphidophyceae, Dinophyta, Chrysophyceae
Peridinin	per	Dinophyta
19'-Butanoyloxyfucoxanthin	19'-but	Prymnesiophyceae, Chrysophyceae
Fucoxanthin	fuco	Bacillariophyta, Prymnesiophyceae, Raphidophyceae, Chrysophyceae
19'-Hexanoyloxyfucoxanthin	19'-hex	Prymnesiophyceae
Prasinoxanthin	pras	Prasinophyceae
Alloxanthin	allo	Cryptophyta
Diatoxanthin+Diadinoxanthin	diat+diad	diat: trace pigment in Euglenophyta, Bacillariophyta, Prymnesiophyceae, Chrysophyceae, Raphidophyceae diad: Euglenophyta, Bacillariophyta, Prymnesiophyceae, Chrysophyceae, Raphidophyceae
Zeaxanthin	zea	Cyanobacteria, Rhodophyta, minor pigment in Chlorophyceae
Chlorophyll *b*	Chl*b*	Chlorophyceae, Prasinophyceae, Euglenophyta
Neoxanthin	neo	Chlorophyceae, Prasinophyceae
Divinyl chlorophyll *b*		Cyanobacteria (formerly Prochlorophyta)

Table 2.2. Phytoplankton signature pigments used to infer phytoplankton community composition. Based on literature review by Jeffrey and Vesk (1997).

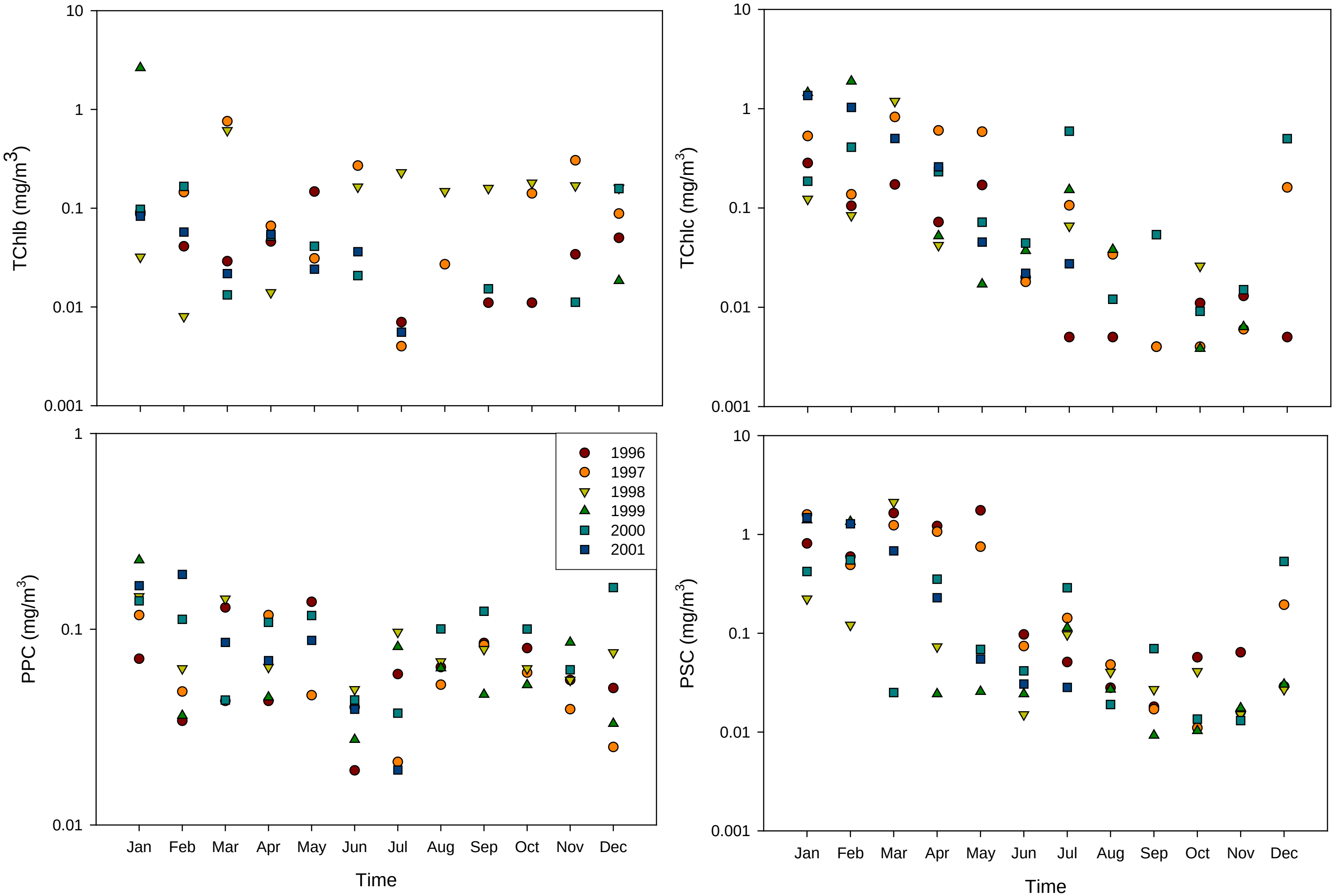

Variations in the concentration of phytoplankton accessory pigments at the CARIACO time-series station (1996 to 2001). A) Total chlorophyll-*b*, B) Photoprotective Carotenoids (PPC), C) Total Chlorophyll-*c*, D) Photosynthetic Carotenoids (PSC).

Mean (1996-2001) Seasonal Distribution of Phytoplankton Pigments with Depth (HPLC samples)

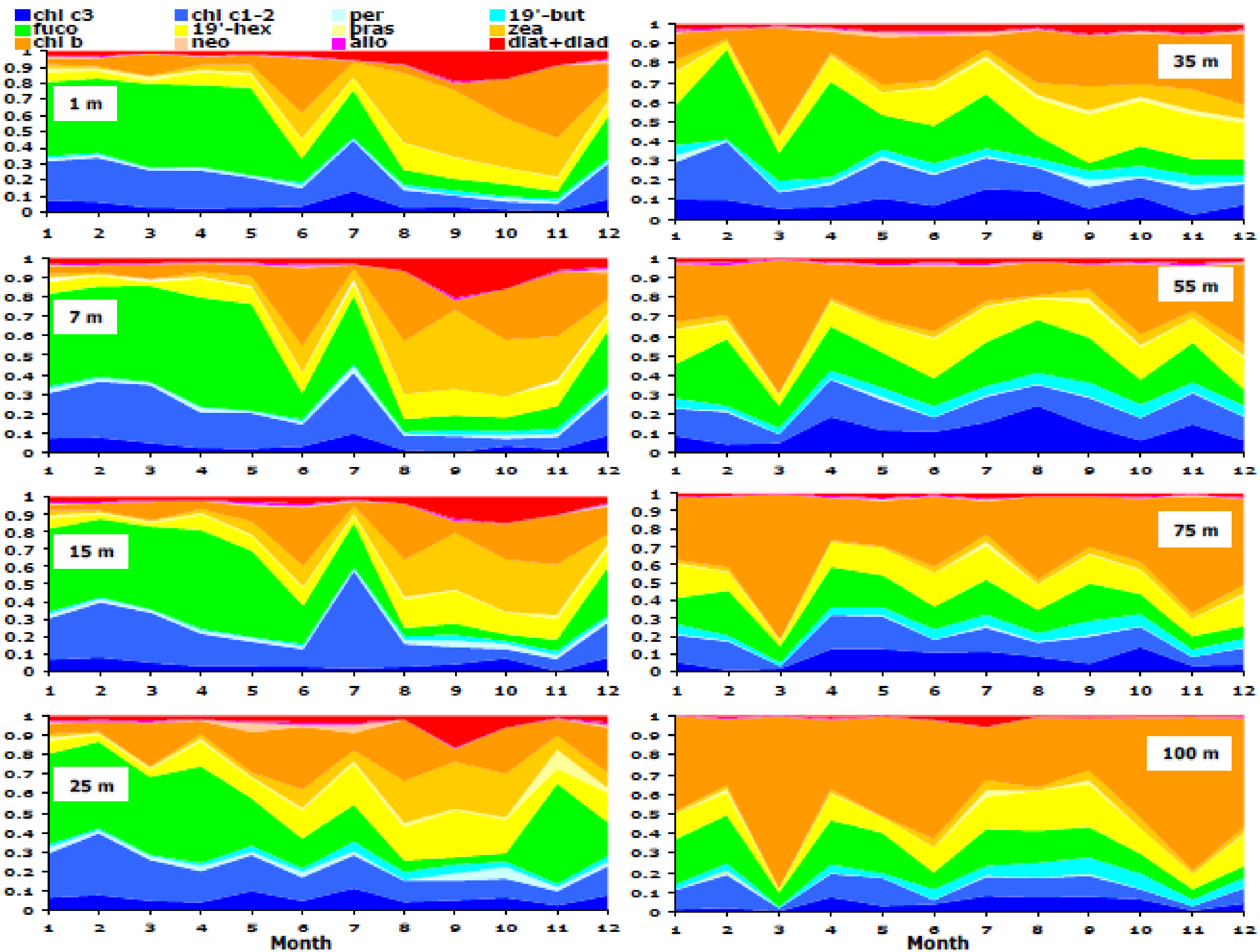

From: Natasha Rondon, MS Thesis, U Dalhousie

Mean (1996-2001) Seasonal Distribution of Phytoplankton Groups with Depth (taxonomic samples)

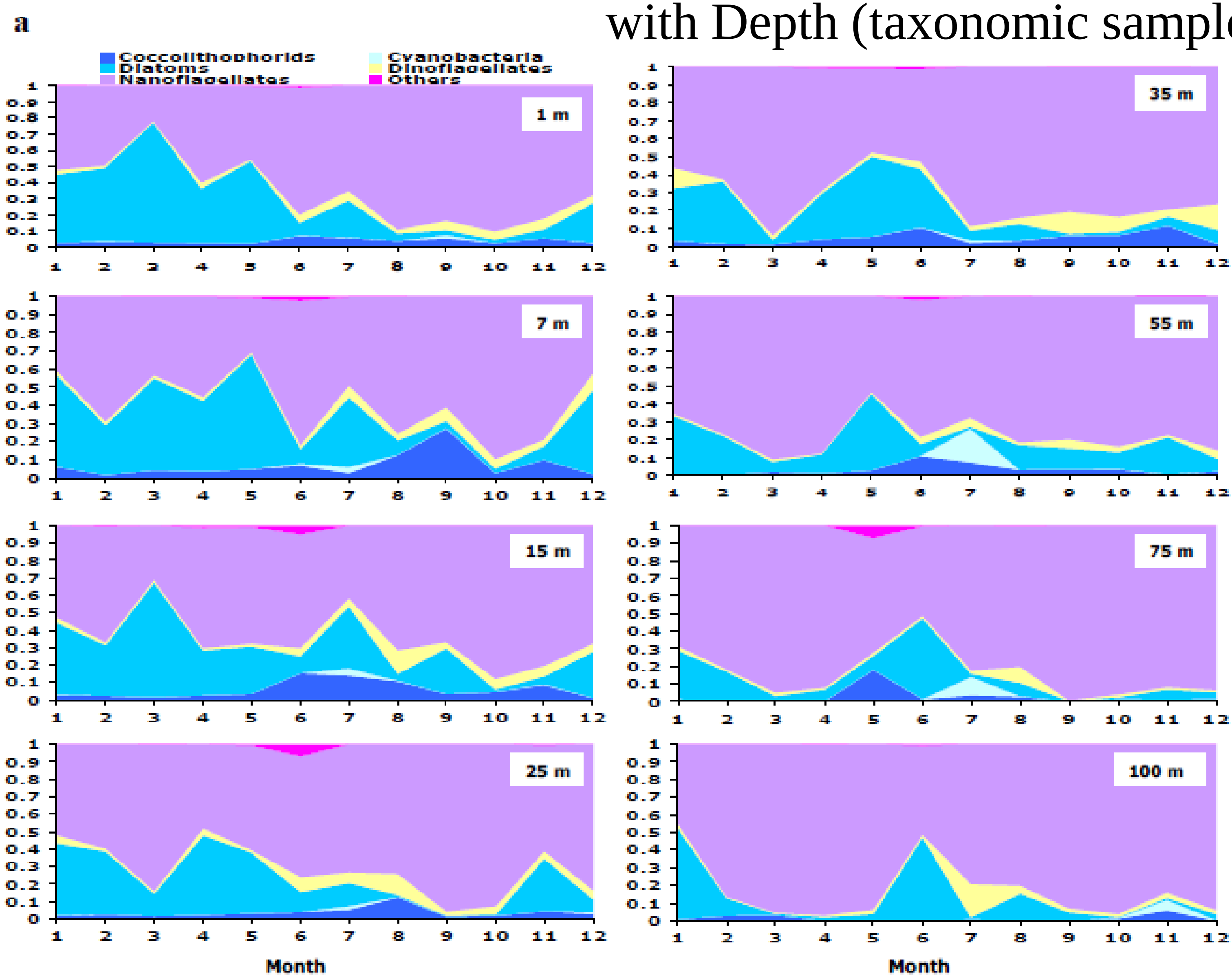

From: Natasha Rondon, MS Thesis, U Dalhousie

Interannual variability of phytoplankton groups (surface taxonomic samples)

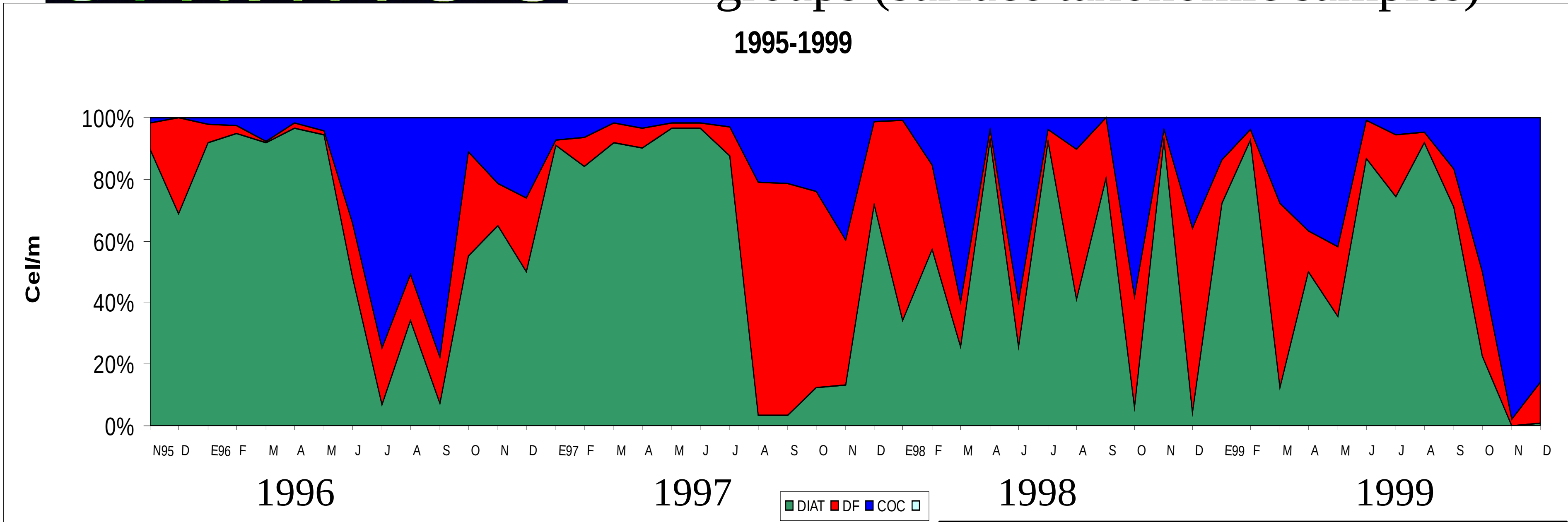

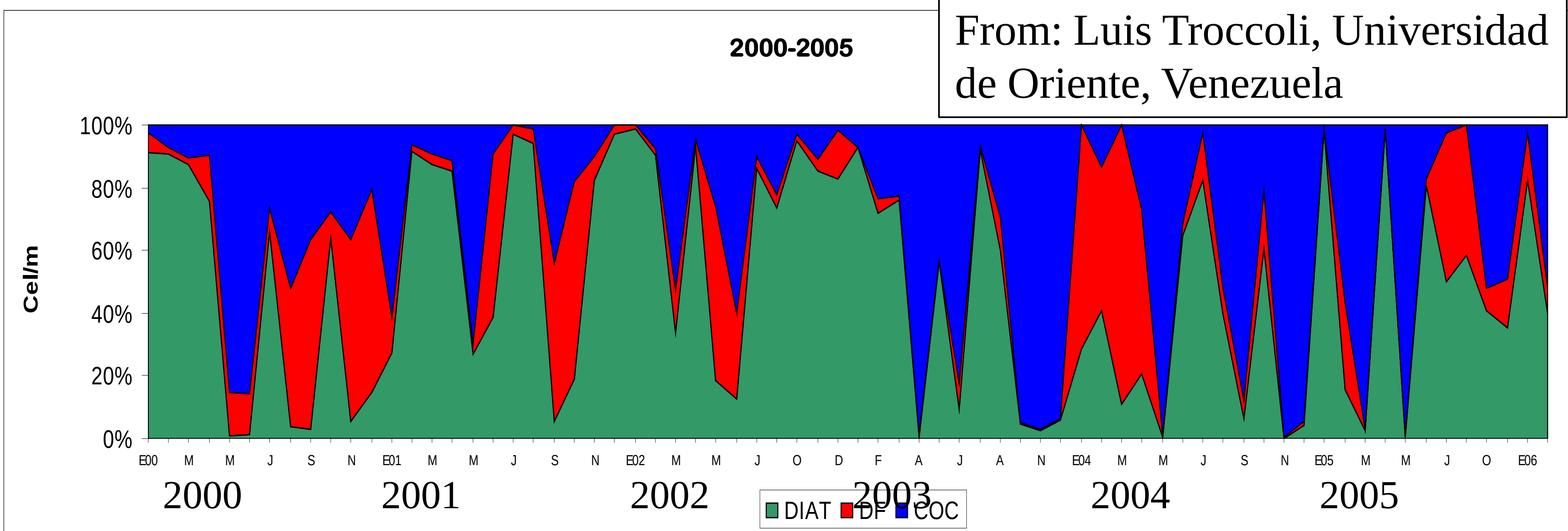

From: Luis Troccoli, Universidad de Oriente, Venezuela

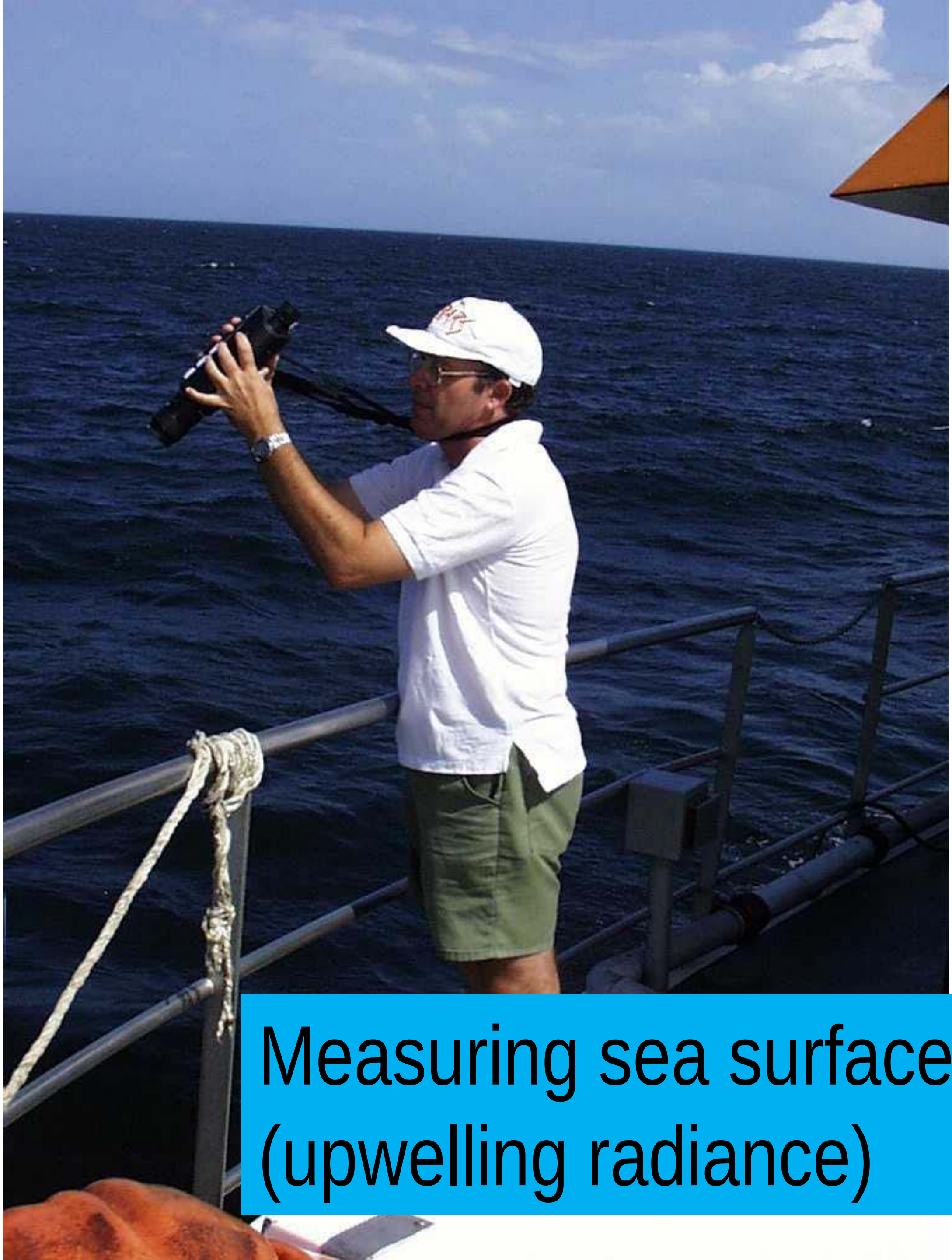

Measuring sea surface reflectance (upwelling radiance)

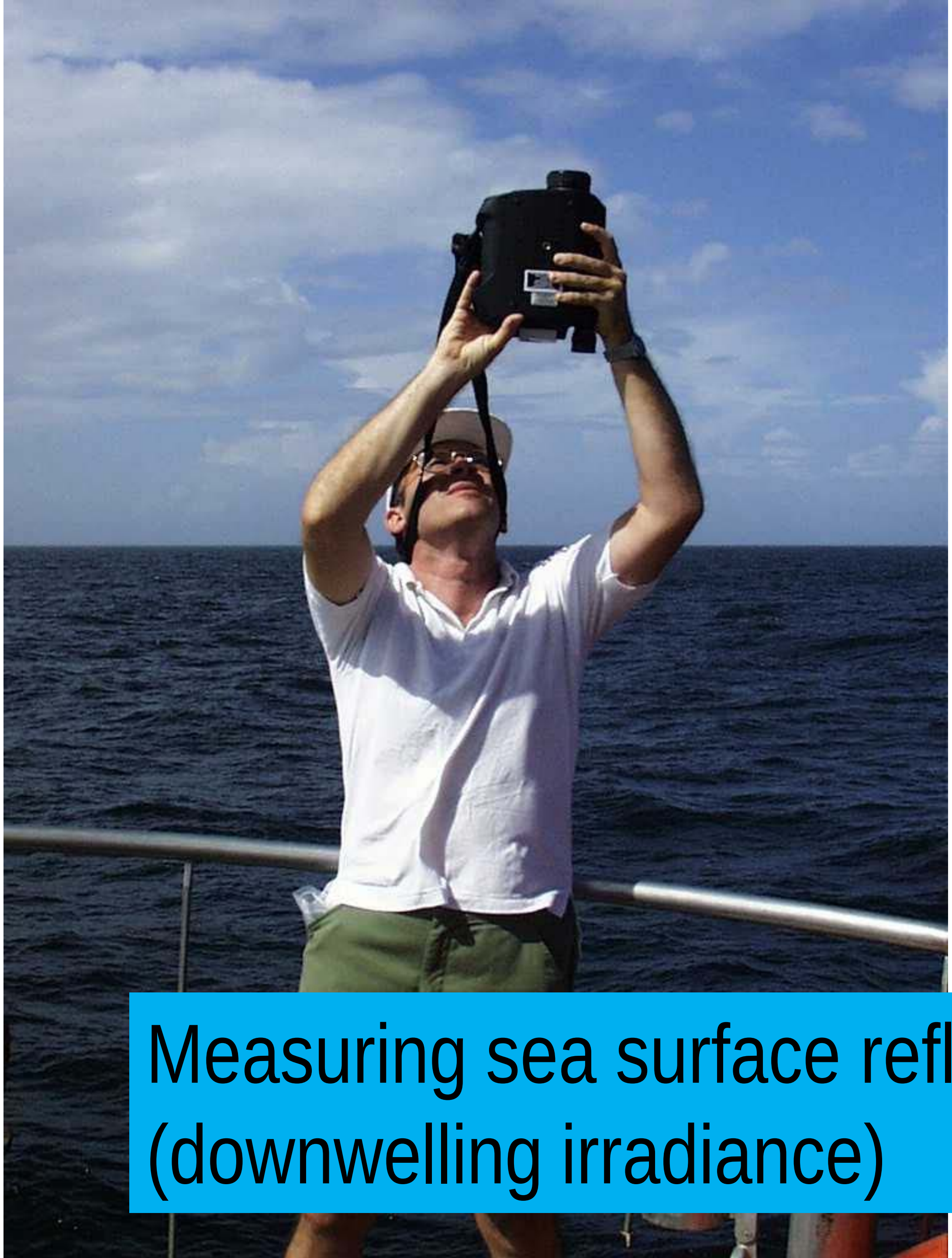

Measuring sea surface reflectance
(downwelling irradiance)

Seasonal cycle in reflectance

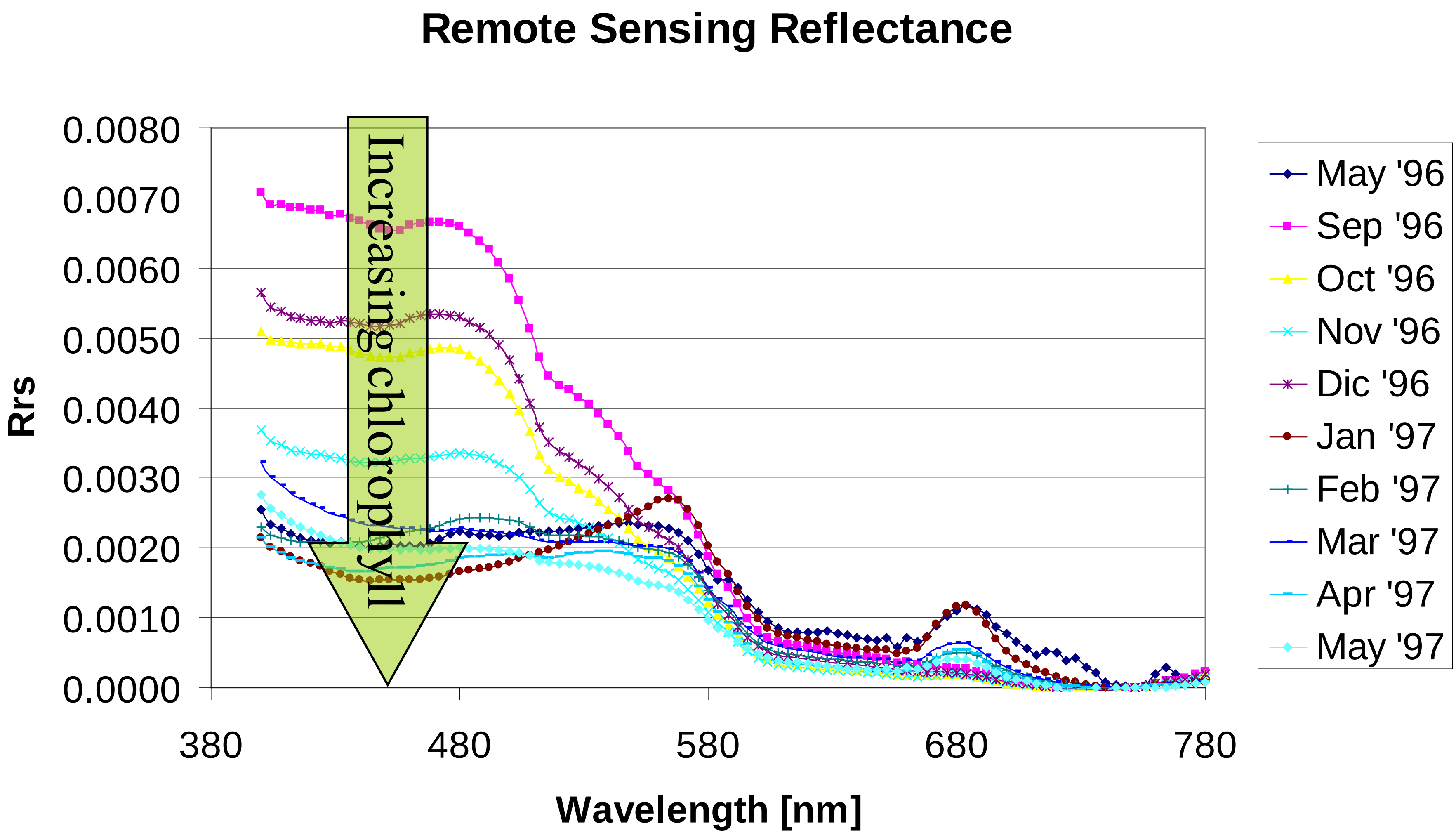

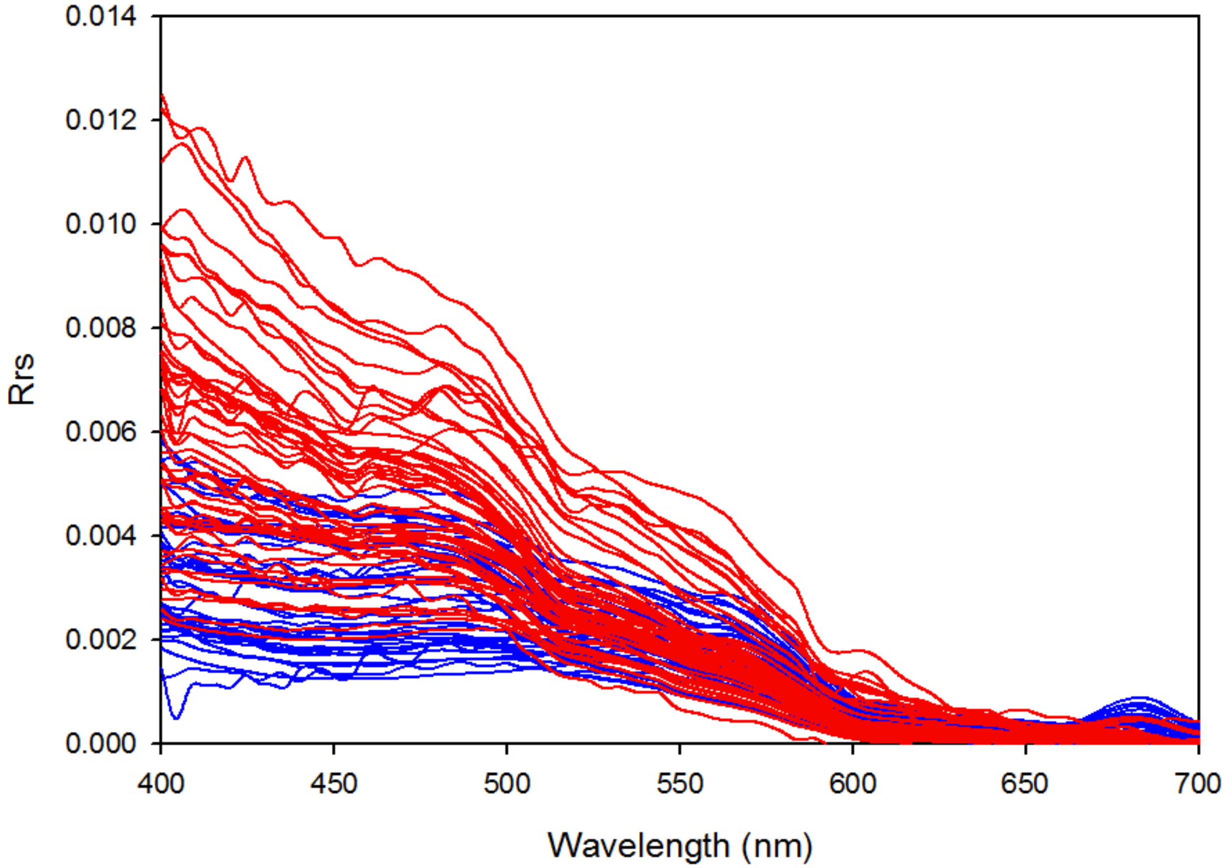

Remote sensing reflectance:

Blue: upwelling

Red: rainy season

CARIACO

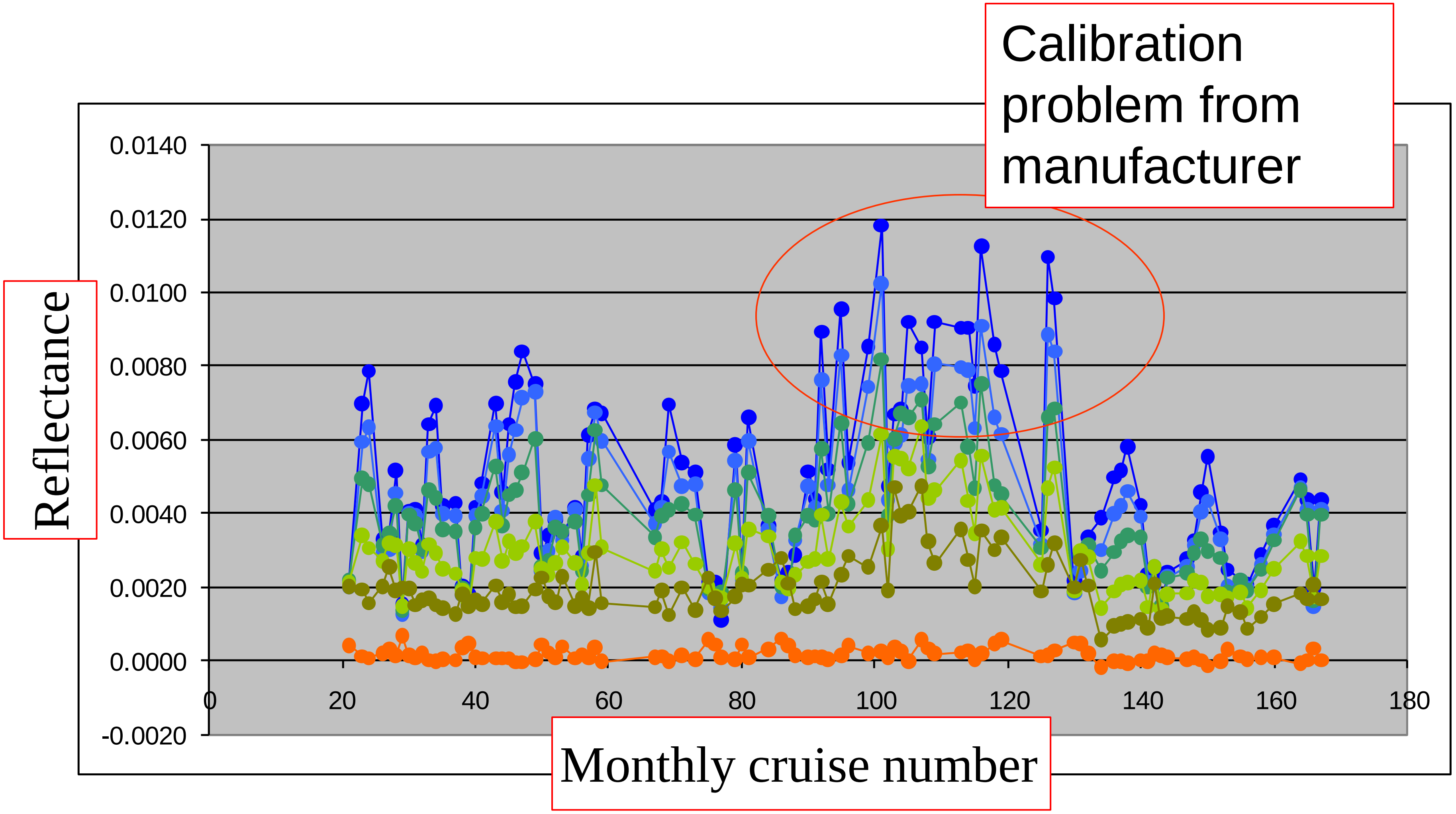

Calibration problem from manufacturer
Reflectance
0.0140
0.0120
0.0100
0.0080
0.0060
0.0040
0.0020
0.0000
-0.0020
0
20
40
60
80
100
120
140
160
180
Monthly cruise number

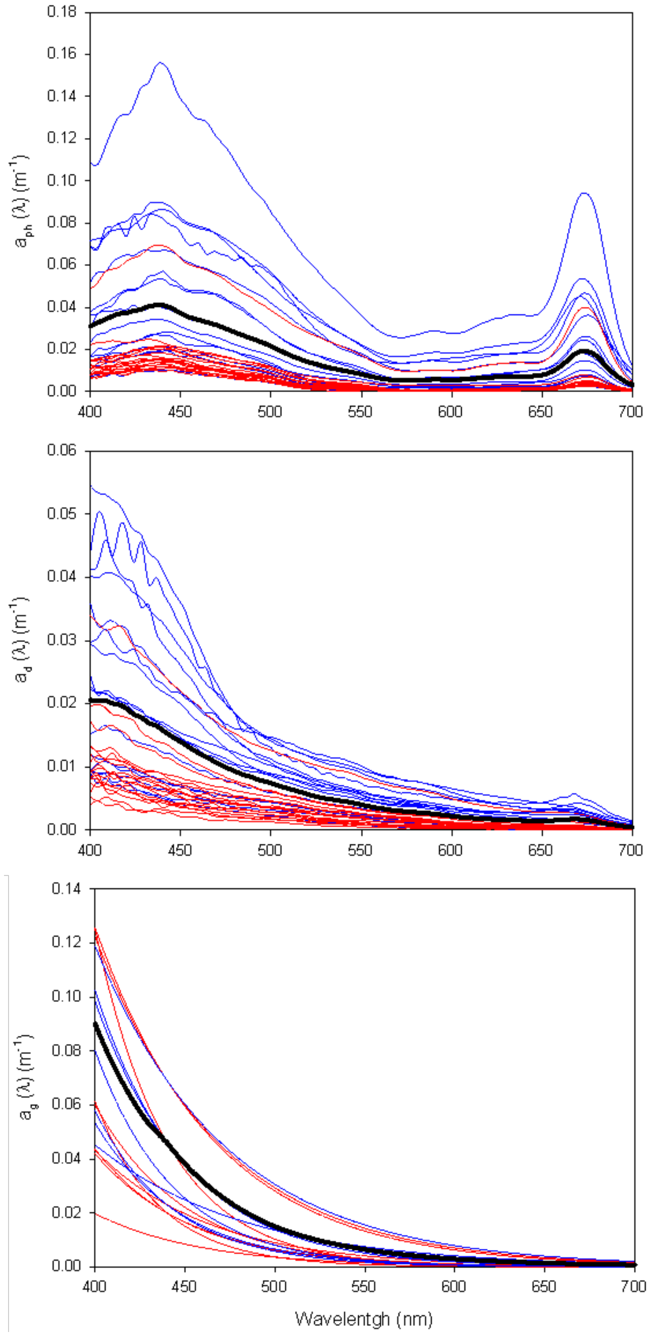

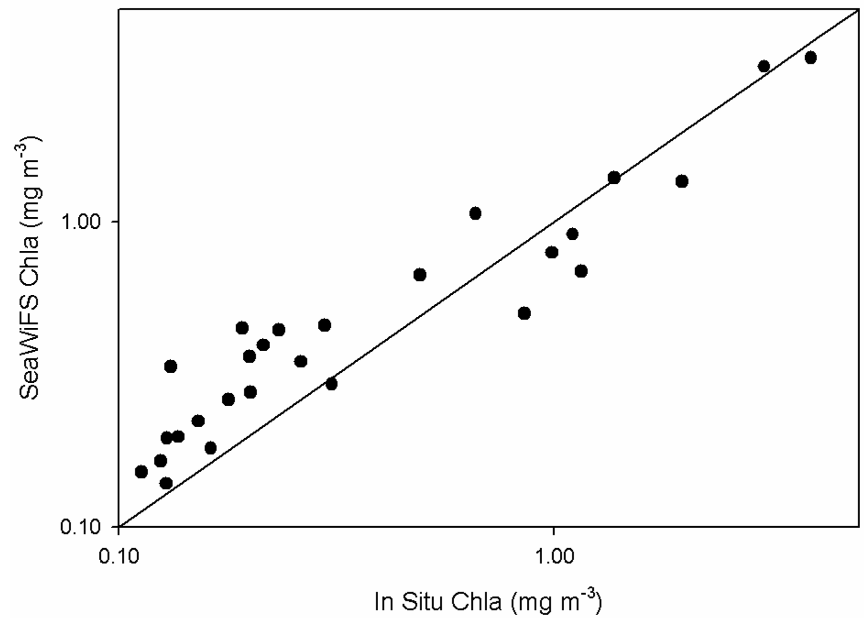

Concurrent 1 km2 SeaWiFS-derived chlorophyll-*a* estimates compared to *in situ* Chlorophyll *a* observations between January 1998 and December 2005 at the Cariaco time-series station (N = 29, R2=0.84, RMSE=57%). Solid line is the 1:1 relationship.

Absorption spectra
(a) phytoplankton,
(b) detrital material and
(c) CDOM
Blue: upwelling / Red: rainy season
Black: average values.

Much work to be done:

Post-doc wanted!

Some Key Findings

Community shifts:

Trade Winds decreased between 2001-2005 relative to 1996-2000:
-seasonal upwelling intensity decreased
-waters have become warmer
-annual PP remains about the same
-phytoplankton community shift from large diatoms to smaller cells
-coincides with regional fishery collapse (sardine)

2006-2008 upwelling seems to have increased, but not sardine fisheries

We should expect similar cases of interannual variability and long-term trends everywhere around the world – at this time we are unable to assess these changes or their impacts on either foodwebs, biogeochemistry or climate

Observations

Implications for future satellite programs / HyspIRI:

-Initiate planning for a comprehensive cal/val program, building on NASA SIMBIOS/SeaBASS experience
-Initiate planning for ecosystem assessments: land-ocean interactions
-Include time series efforts with relevant observations
-Coordinate with PACE/ACE, Geo-Cape teams

This will lead to:

-Interdisciplinary scientific understanding of the coastal zone including human activities.
-A practical classification for coastal habitats and the valuation of ecosystems services
-Quantify the distributions and biological diversity of coastal habitats and their changes
-Better assessment of carbon and nutrient cycling and sequestration in coastal habitats
-Identification of hot-spots of habitat diversity for use in setting priorities for restoration and conservation

CARIACO

<u>CARIACO and its people</u>

FLASA/EDIMAR

FONACIT

NSF

Many others

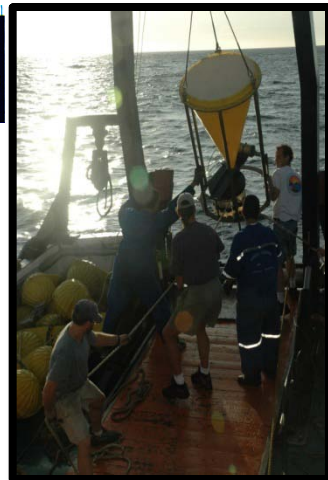

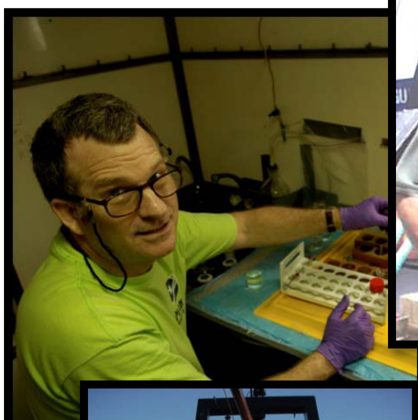

Hot Target Saturation Report

Vincent J. Realmuto

Jet Propulsion Laboratory

26 August 2010

Acknowledgements

Hot Target Saturation Subgroup
Airborne Sensor Facility/Ames Research Center

Contributors: Robert Wright, Mike Ramsey
Gregg Vaughan, Louis Giglio
Mark Foote

Instrument	Central Wavelength	Spatial Resolution (at nadir)	Temporal Coverage (daytime)	Saturation Temperature
AVHRR	3.7 μm	1.1 km	Daily (NOAA 18 + 19)	~ 321.5 K
VIRS (TRMM)	3.75 μm	2.4 km	2 day revisit	321K
ATSR/AATSR	3.7 μm	1 km /1.5 x 2 km	3 day revisit	311 K
MODIS	3.95 μm	1 km	Daily (Terra + Aqua)	478 K /506 K (Ch. 21) 330 K (Ch. 22)
GOES Imager	3.9 μm	2.3 x 4 km	3 hr/15-30 min	335 K
SEVIRI (MSG)	3.9 μm	3 km	15 min	335 K
HSRS (BIRD)	3.4 – 4.2 μm	370 m	Targeted	600 K

Heritage for HyspIRI 4-μm Channel

~ 30 Year Record of Measurements at 4-μm

Data Used in Fire and Hot Spot Detection Programs

HyspIRI Spatial Resolution (60 m) is Unprecedented

Why Do We Want a 4-μm Channel?

Planck's Law: Radiance as a Function of Temperature and Wavelength

$$B_\lambda(T) = \frac{C_1}{\pi\lambda^5\,[exp(C_2/\lambda T) - 1]}$$

$C_1 = 3.74151 \times 10^8$ W m^2 μm^4

$C_2 = 1.43879 \times 104$ μm K

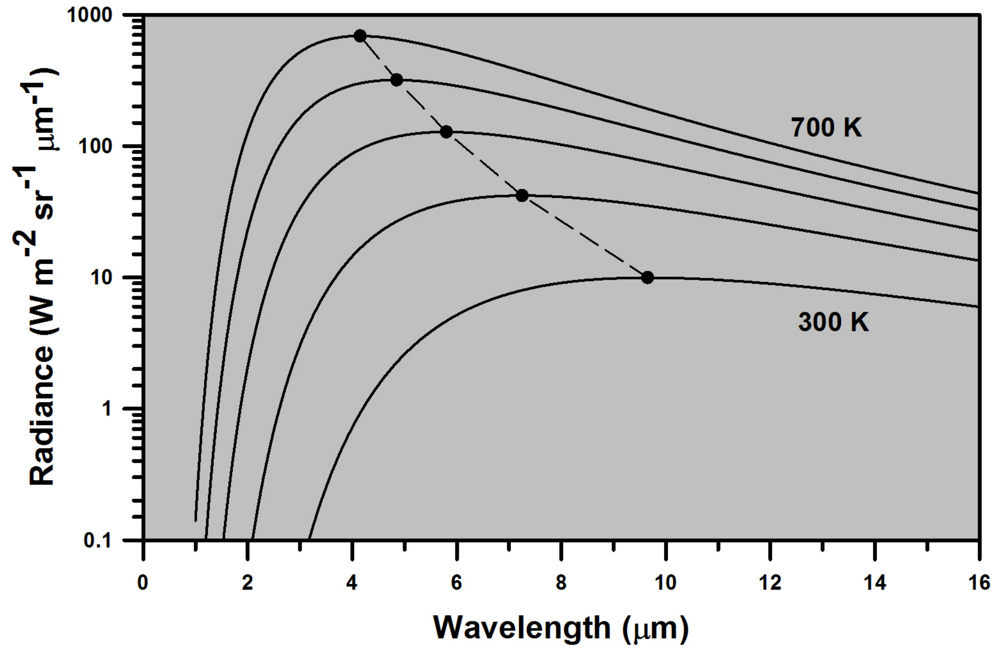

Wien's Displacement Law: Position of Peak Radiance is Inversely Proportional to Temperature

$\lambda_{max} = b/T$

$b \sim 3 \times 10^{-3}$ m K

High-Temperature Targets – Peak Radiance near 4 μm

Why Do We Want a 4-μm Channel?

Sub-Pixel Temperature Mix:
Presence of Hot Fraction Increases Radiance Near 4 μm

Need Multispectral Data to Recognize Sub-Pixel T Mixing

Two-Component Model:

$B_\lambda(T_{app})$ =
$B_\lambda(T_{bg})\,[1 - f\,] + B_\lambda(T_h)\,[\,f\,]$

f = Fractional Area of Hot Comp
T_{app} = Apparent Temperature
T_h = High Temperature
T_{bg} = Background Temperature

(modified from Wright et al., 2002)

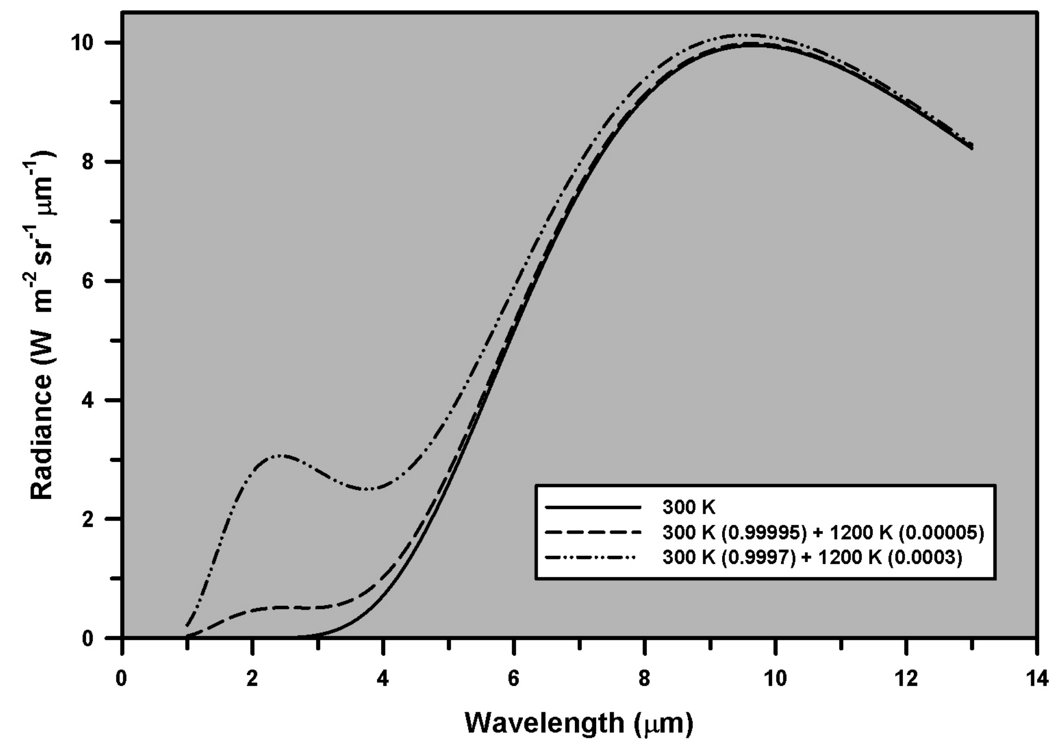

Increase in 4-μm Radiance Relative to 11-μm Radiance is the Foundation of:

- Estimation of Sub-Pixel Temperature (Dozier Method)
  - a) Inversion of Two-Component Model
  - b) Conservative Estimate When We Ignore Surface Emissivity and Atmospheric Transmission
- Automated Detection of Hot Spots
  - a) MODIS Fire Algorithm
  - b) MODVOLC Hot Spot Algorithm

Why Do We Want 60-m Spatial Resolution?

Sub-Pixel Mixing Decreases with Decrease in Pixel Size (IFOV)

HyspIRI:
Temp Distribution Retained

Apparent Temp Decrease ~25 K

MODIS:
Apparent Temp Decrease ~100 K

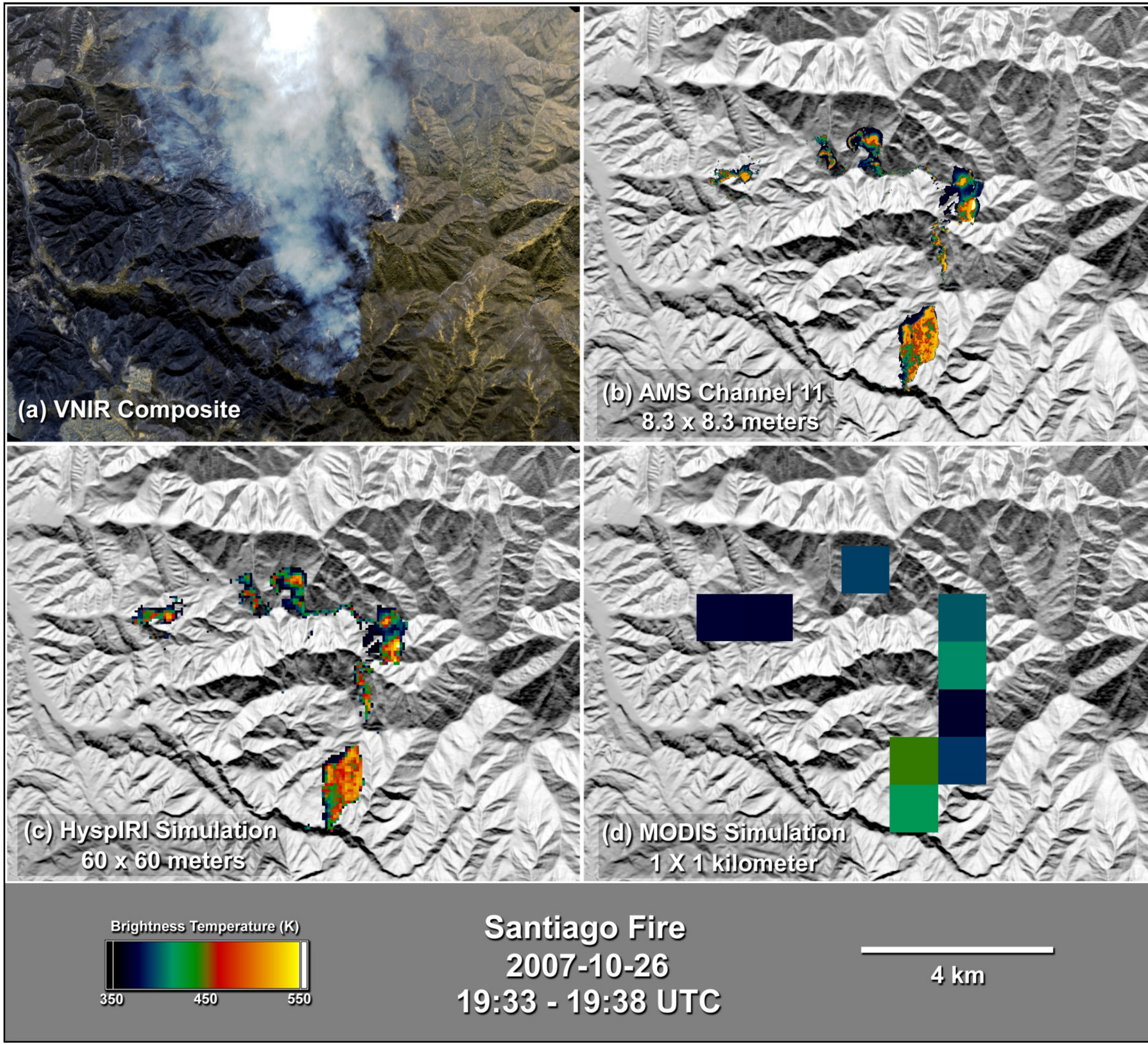

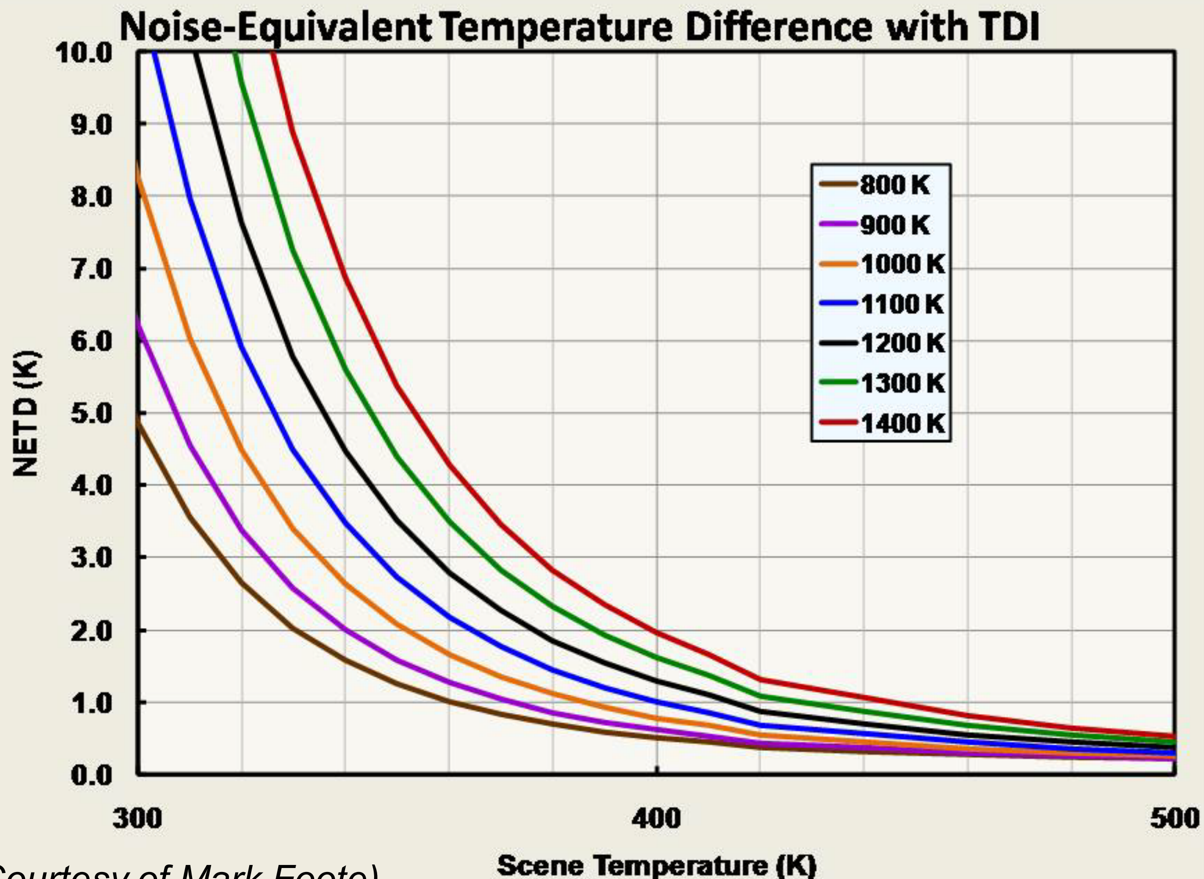

(Courtesy of Mark Foote)

Sensitivity vs. Saturation Temperature

Sensitivity Decreases With Increase in Saturation Temperature

Low Sensitivity of MODIS Ch. 21 (NEΔT = 3 K @ 330 K) Precluded Use in an Operational Sub-Pixel Temperature Estimation

Saturation Temperature ≤ 450 K for 1-km IFOV Based on Study of Fire Pixels from 40 MODIS Scenes [*Gao et al.*, 2007]

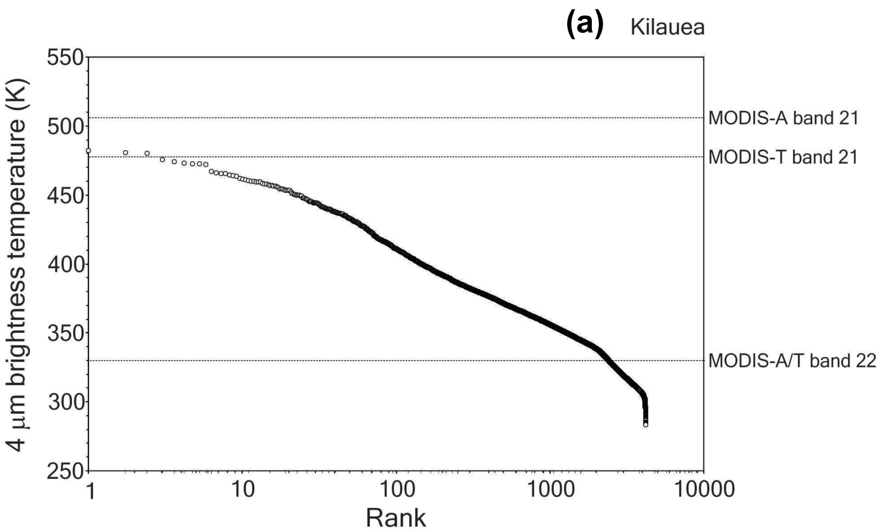

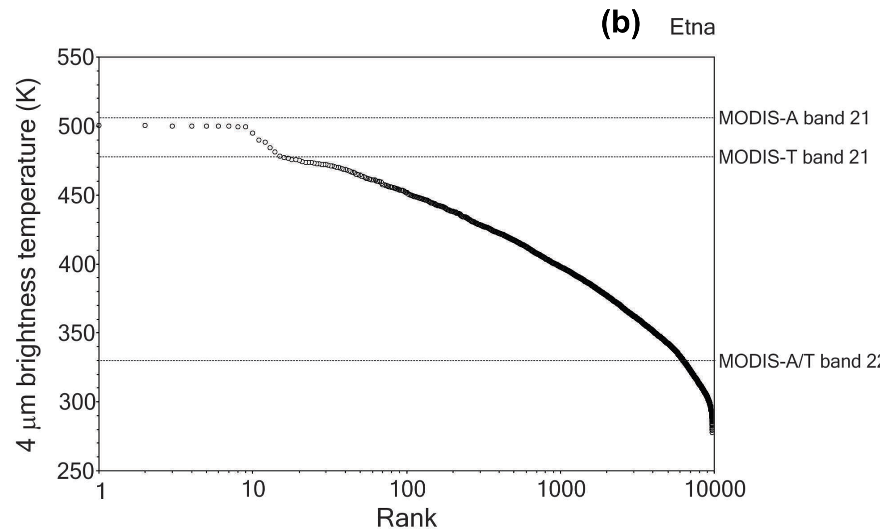

MODVOLC Record (2000 – 2009)

Ch. 21 Brightness Temperatures Corresponding to MODVOLC Hot Spots: (a) Kilauea, (b) Etna, and (c) Nyamuragira

Temperatures > 450 K Recorded for Each Volcano

High-Temperature Events are Rare (Over Time) – Very Low Probability in Statistical Analysis

HyspIRI Science Questions Require Estimates of High Temperatures

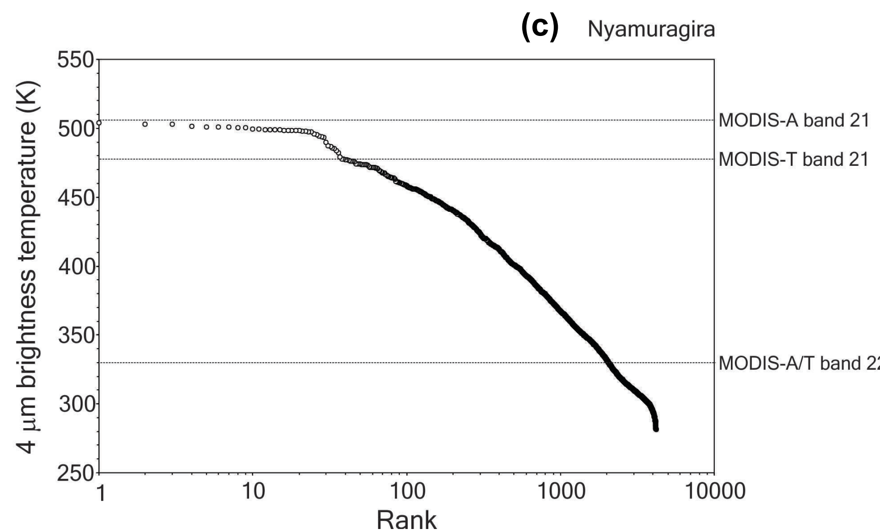

(Courtesy of Rob Wright)

Precursor Data Sets

Ground Rules:

(1) Sub-Pixel Temperature: Need to Know Sub-Pixel Area

(2) Spatial Resolution Better than 60 m

Minimize Sub-Pixel Mixing

Critical for Single-Channel Temperature Estimates

(3) Single-Channel MIR (3 – 5 μm) Data Preferable to Single-Channel TIR (8 – 12 μm) Data

(4) SWIR (~ 2 μm) Data from Night-Time Acquisitions

AMS Wildfire Sensor

Band	Wavelength µm	
1	0.42- 0.45	
2	0.45- 0.52	(TM1)
3	0.52- 0.60	(TM2)
4	0.60- 0.62	
5	0.63- 0.69	(TM3)
6	0.69- 0.75	
7	0.76- 0.90	(TM4)
8	0.91- 1.05	
9	1.55- 1.75	(TM5)
10	2.08- 2.35	(TM7)
11	3.60- 3.79	(VIIRS M12)
12	10.26-11.26	(VIIRS M15)

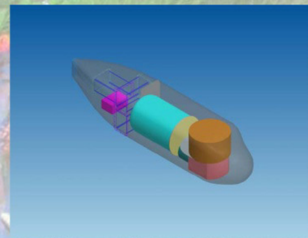

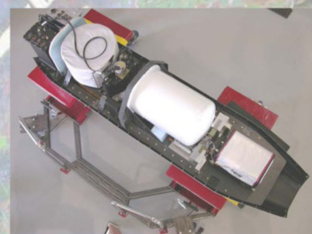

Total Field of View: 85.9 degrees
IFOV: 2.5mrad
Altitude: 25000'
Spatial Resolution: 20m (at sea level)

Flights Conducted Between 24 – 28 October 2007

Flight Line Count:

Grass Valley Fire:	25
Poomacha Fire:	19
Harris Fire:	15
Witch Fire:	26
Santiago Fire:	9

SOUTHERN CALIFORNIA WILDFIRES
as of 11/09/07 - 0600 Hours PST
with Start Dates - Chronologically

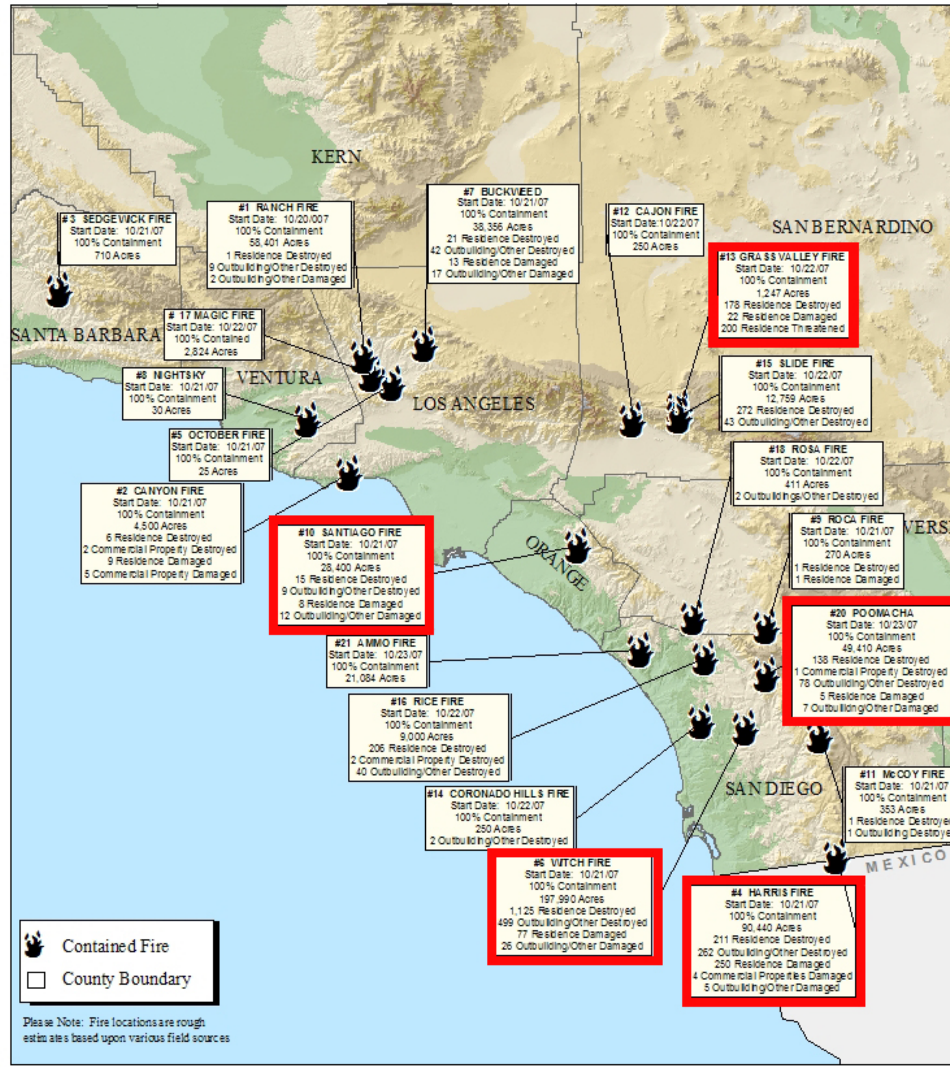

FEMA

Created by OES- GIS, D. Hula

Saturation of Band 11

No Data on Temperatures > 530 K

Aggregation to HyspIRI Resolution Mitigates Saturation

Band 11 Radiance is Good Proxy for HyspIRI at Temperatures Below 530 K

Band 11 Temps > Band 12 Temps: Indication of Sub-Pixel Mixing

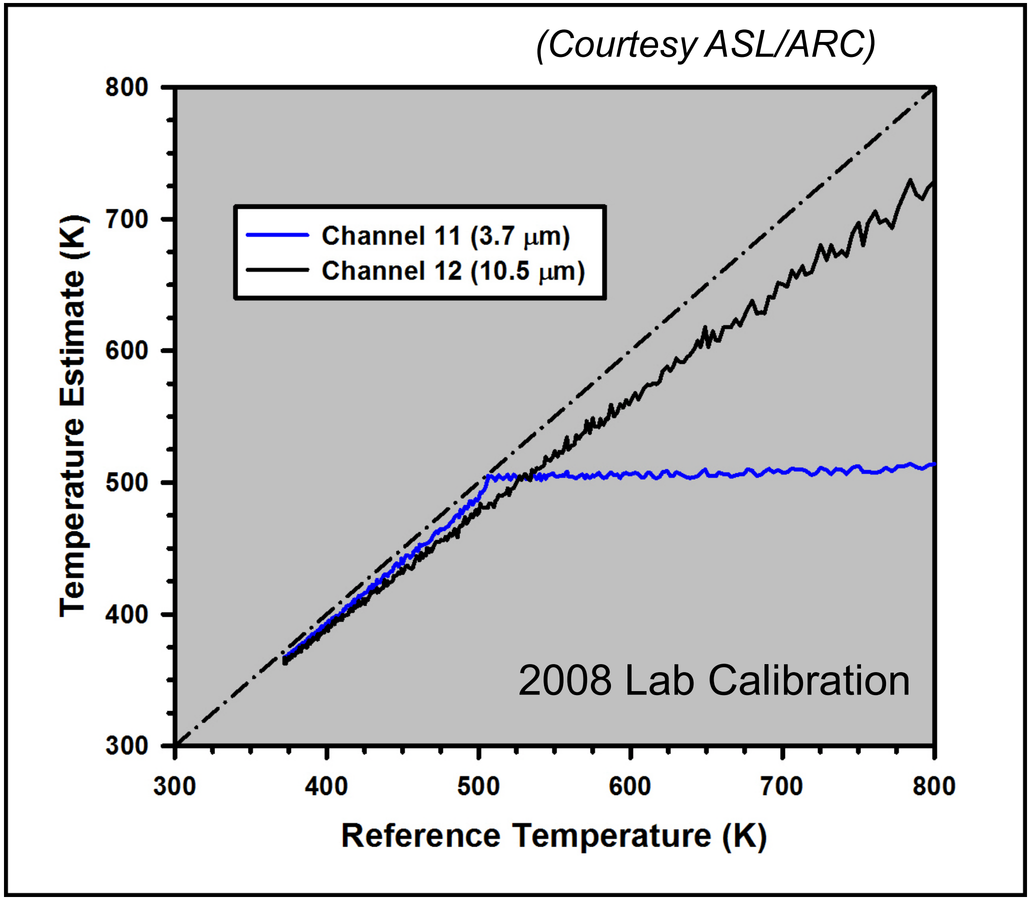

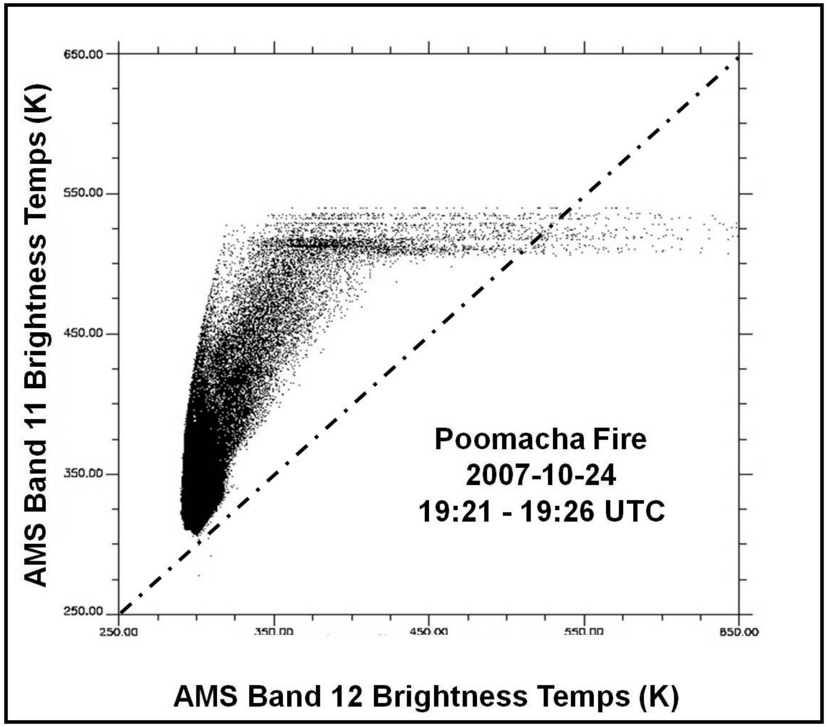

Can We Use Band 12?

Lab Cal: Band 12 Good to ~ 800 K

Lower Bound on Saturation Temperature

Systematic Under-Estimation of T:

~2 K @ 400 K; 75 K @ 800 K

$$T_{true} = (T_{est} - 71\ K)/0.8175$$

Band 12 Histograms

All Radiance Data Aggregated to 60-m HyspIRI Resolution

Temp Range 330 – 730 K to Isolate High-T Pixels

Statistics for All Fires Dominated by Poomacha (Contributed ~ 60 % of Hot Pixels)

Poomacha Fire Source of Hot Pixels ~ 720 K

Witch vs. Poomacha:

- Poomacha Burn Area 25% of Witch Burn Area
- Witch Fire Hot Pixels 12.5% of Poomacha Hot Pixels
- Temperature Alone Provides Little Info on Consumption of Biomass

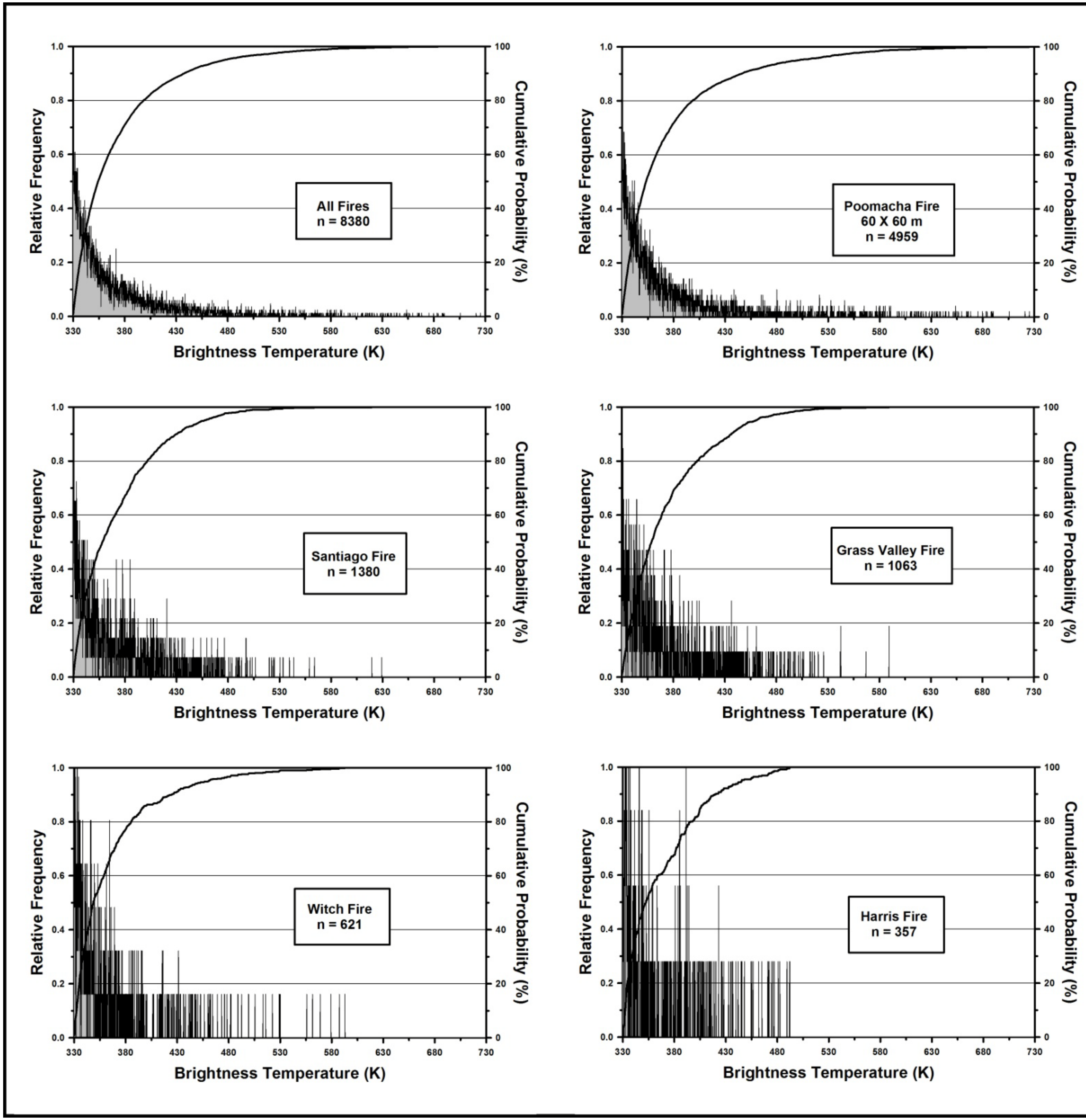

Effects of Sub-Pixel Mixing

Compare Temperatures at Native and Aggregated (60 m) Resolution

Temp Range 330 – 730 K to Isolate High-T Pixels

Cumulative Histograms Deviate for Temperatures > 380 K

Cumulative Probabilities Within 5 % for Entire Range of Temperature

Spatial Distribution of Poomacha Fire Temperatures Uniform to 60 m?

Caveats Aside:

Recommended <u>Lower</u> Bound on Saturation Temperature: 795 K

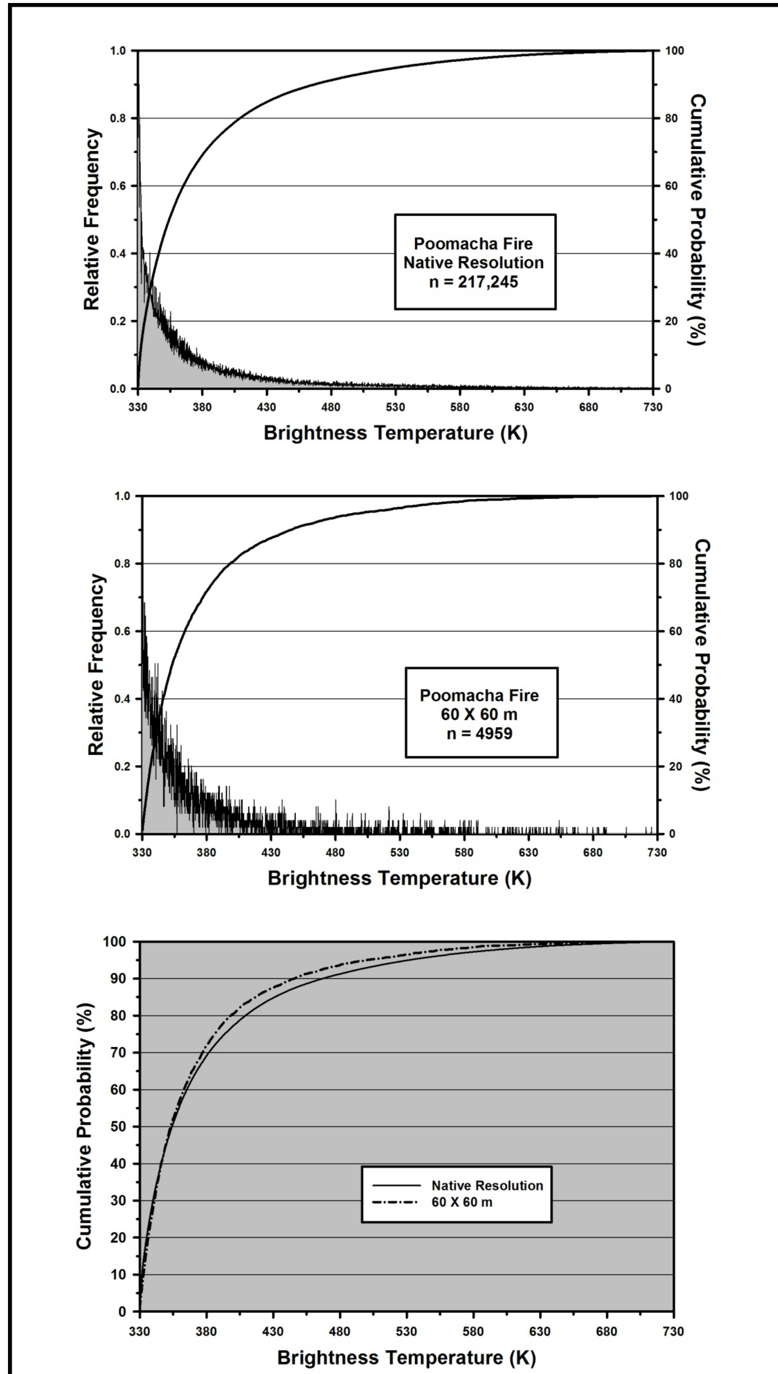

Realistic Saturation Limit for Wildfires?

Compare with BIRD/HSRS Estimates of Fire Temperature and Area

Confine Comparison to Fire Areas ≥ HyspIRI pixel

HyspIRI Pixel (60 X 60 M) = 0.36 Hectares

Highlighted Temperatures Would be Lost with Sat. Temp of 795 K

Kalimantan Peat Fire Yielded Lower Temperatures than “Open Flames” in Australia and Russia

Australia 2002-01-05		Kalimantan 2002-08-24/25		Lake Baikal 2003-06-16		Etna Lava Flow 2002-11-02	
T_f (K)	A_f (Ha)	T_f (K)	A_f (Ha)	T_f (K)	A_f (Ha)	T_f (K)	A_f (Ha)
815	0.48	860	2.5	800 - 920	4.4 - 8.4	540	25
715	2.3	740	1.9	668 – 771	0.7 – 1.5		
893	0.59	650	4.6	716 – 868	1.2 – 3.1		
852	0.92	520	2.1	740 - 839	0.38 – 0.71		
957	1.0	720	1.1	771 – 988	0.23 – 0.70		
796	0.39	690	3.0	819 – 913	1.4 – 2.3		
		590	3.3	694 – 882	0.36 – 1.21		
		560	0.7				

References: Briess et al.,2003; Oertel et al., 2004; Siegert et al, 2005; Zhukov et al., 2006

Volcanic Targets

ASTER Data from Hawaii: Aggregate to HyspIRI 60-m Resolution

Special Night-time Acquisition of VNIR and SWIR

No Solar Component – Radiance from Geothermal Sources

Saturation of TIR and SWIR (Despite Low Gain Setting for SWIR)

No Saturation in VNIR (with High Gain Setting)

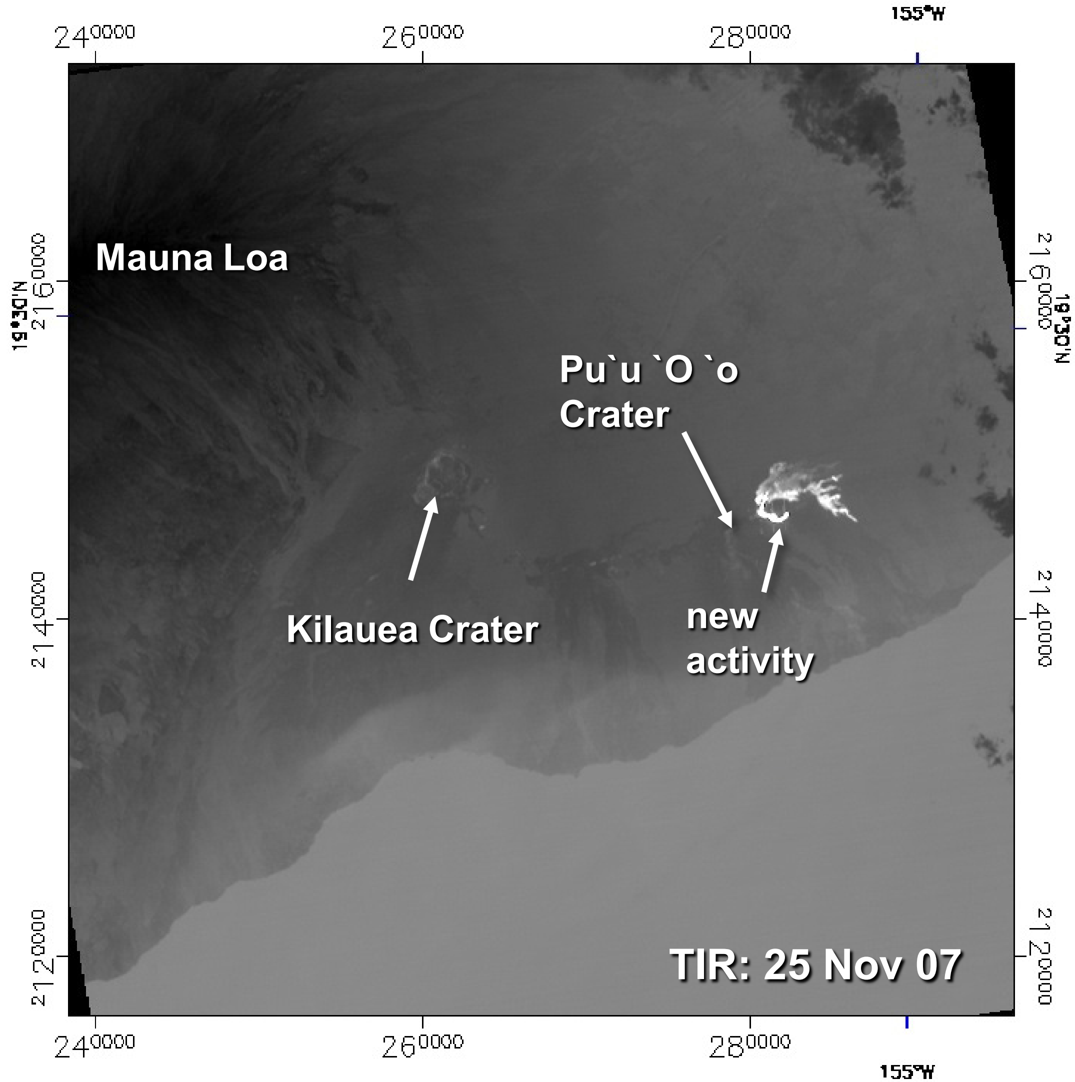

(Courtesy of Mike Ramsey)

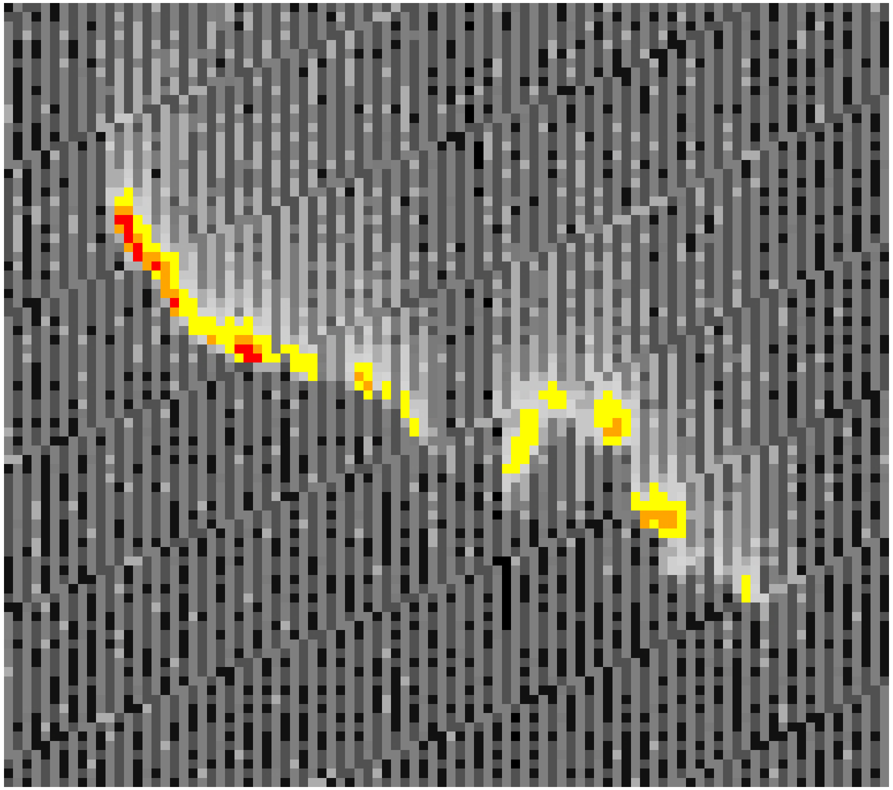

Band 3 at 15 m (ASTER)

Max. Temperature Detected: 1122 K

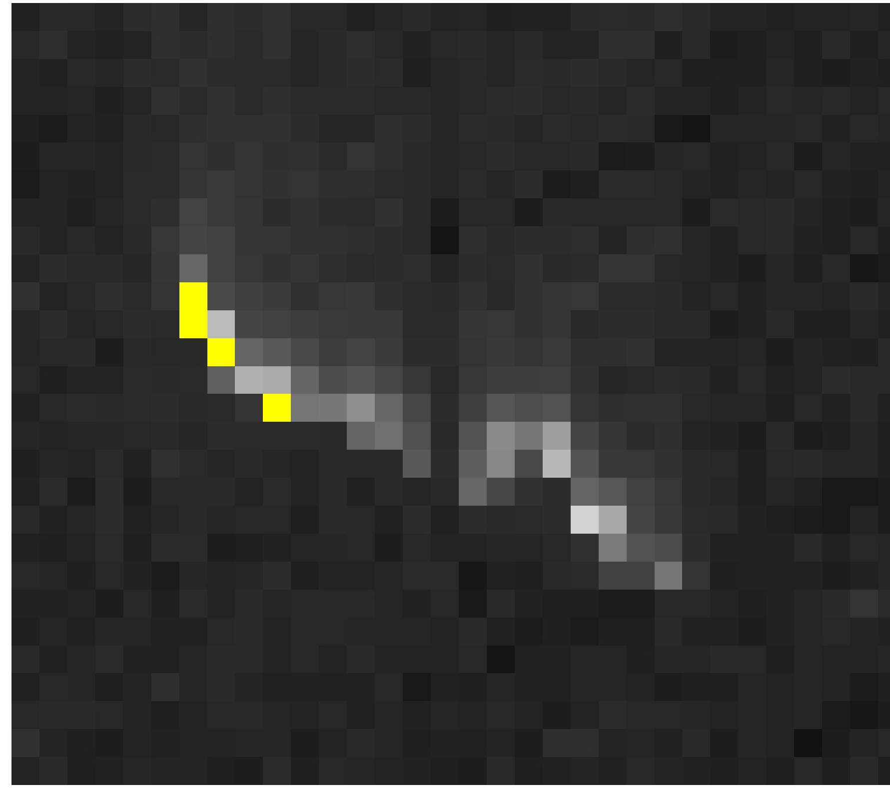

Band 3 at 60 m (HyspIRI)

Max. Temperature Detected: 993 K

Color Code for Temperature

Red:	1073 – 1123 K
Orange:	1023 – 1073 K
Yellow:	973 – 1023 K

(Courtesy of Mike Ramsey)

Volcanic Targets

ASTER Data from Kamchatka: Aggregate to HyspIRI 60-m Resolution

Lava Flow in Shadow of Cone – Decrease Solar Component in VNIR and SWIR

Solar Correction Applied for Remainder

Saturation of TIR and SWIR (Despite Low Gain Setting for SWIR)

No Saturation in VNIR (with Normal Gain Setting)

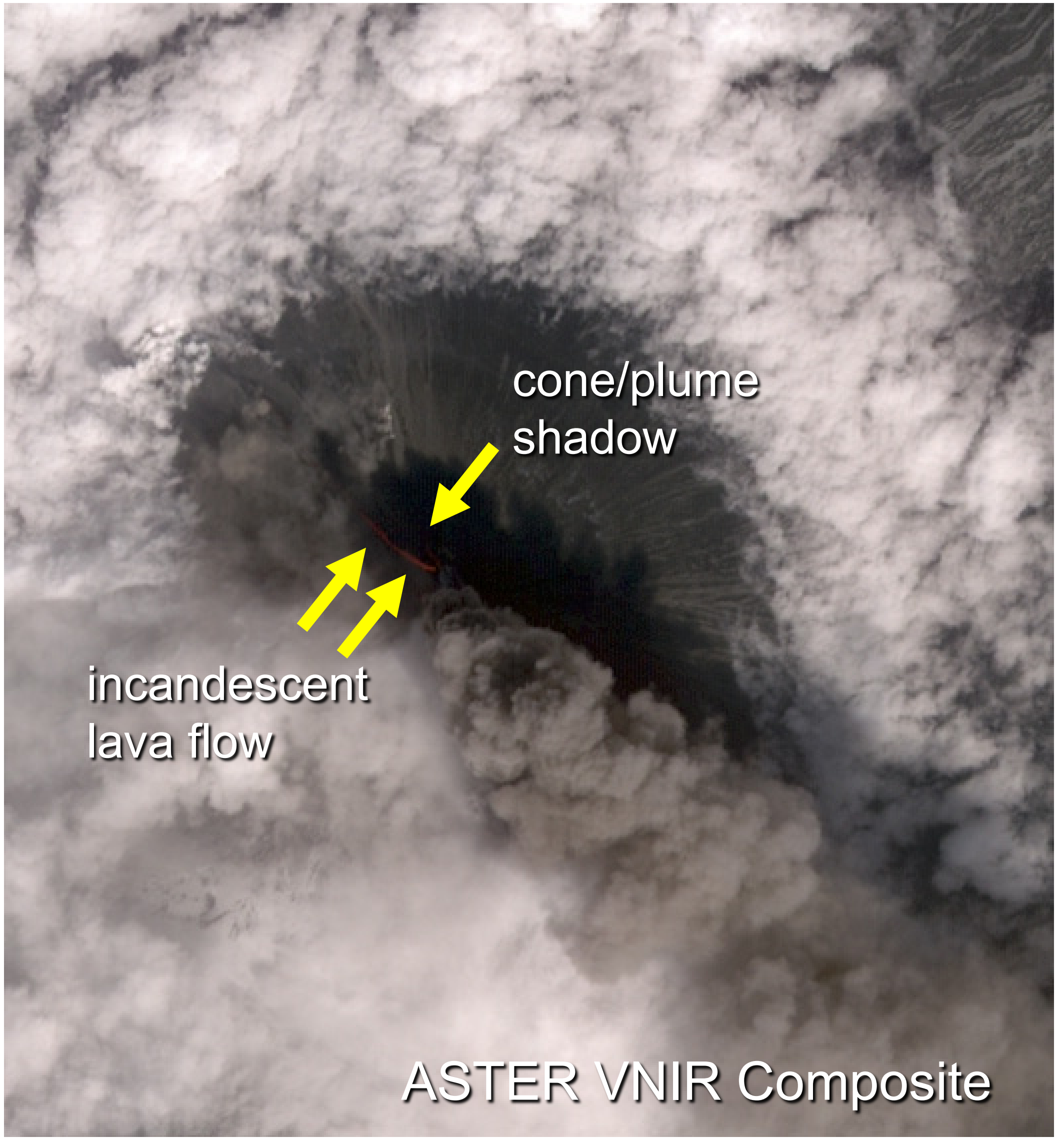

(Courtesy of Mike Ramsey)

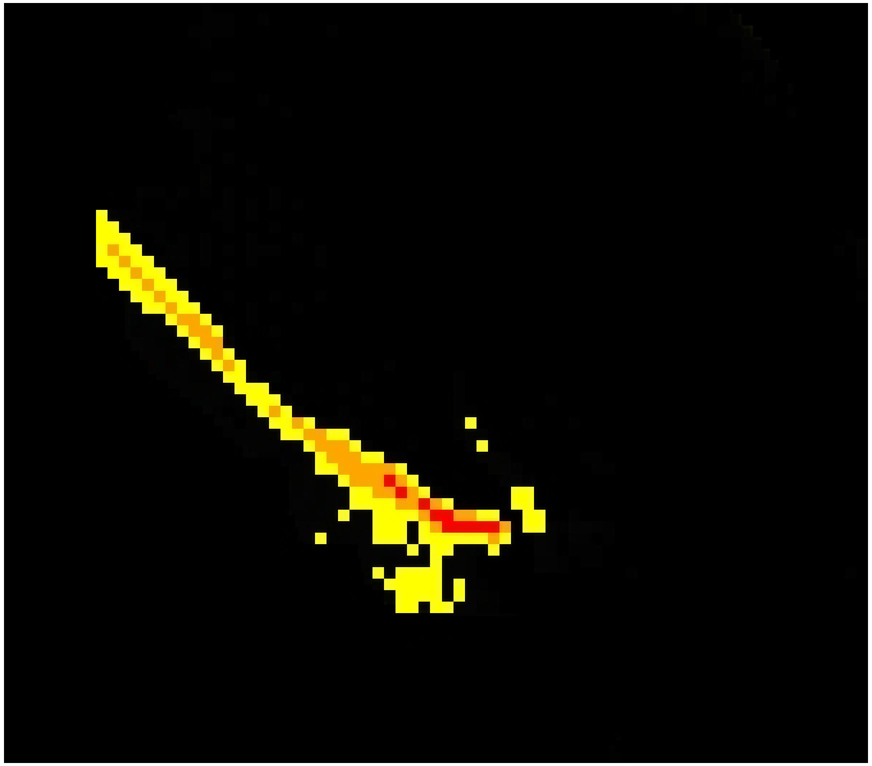

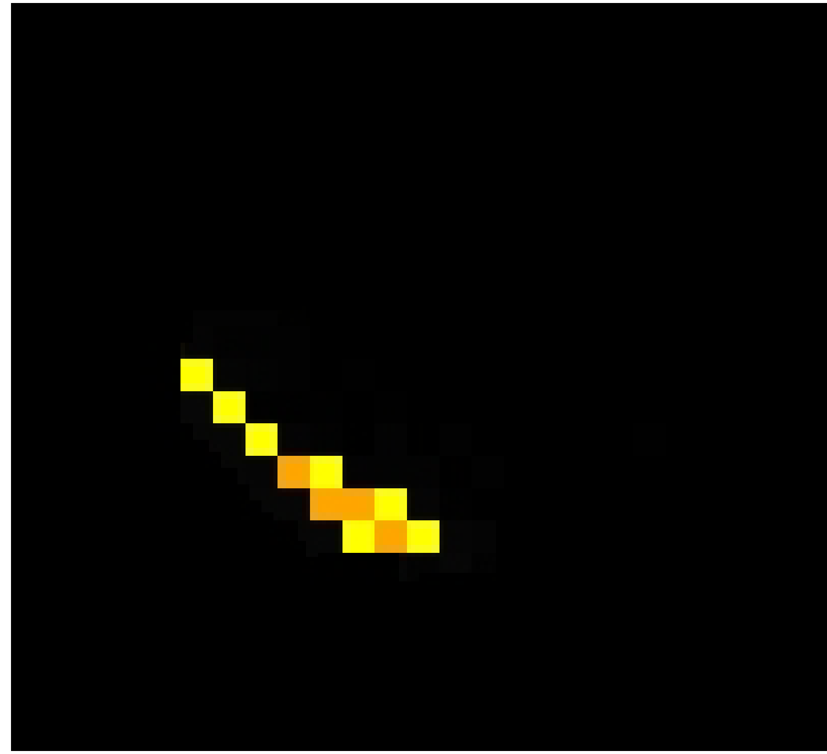

Band 3 at 15 m (ASTER)

Max. Temperature Detected: 1101 K

Band 3 at 60 m (HyspIRI)

Max. Temperature Detected: 1043 K

Color Code for Temperature

Red: 1073 – 1123 K

Orange: 1023 – 1073 K

Yellow: 973 – 1023 K

(Courtesy of Mike Ramsey)

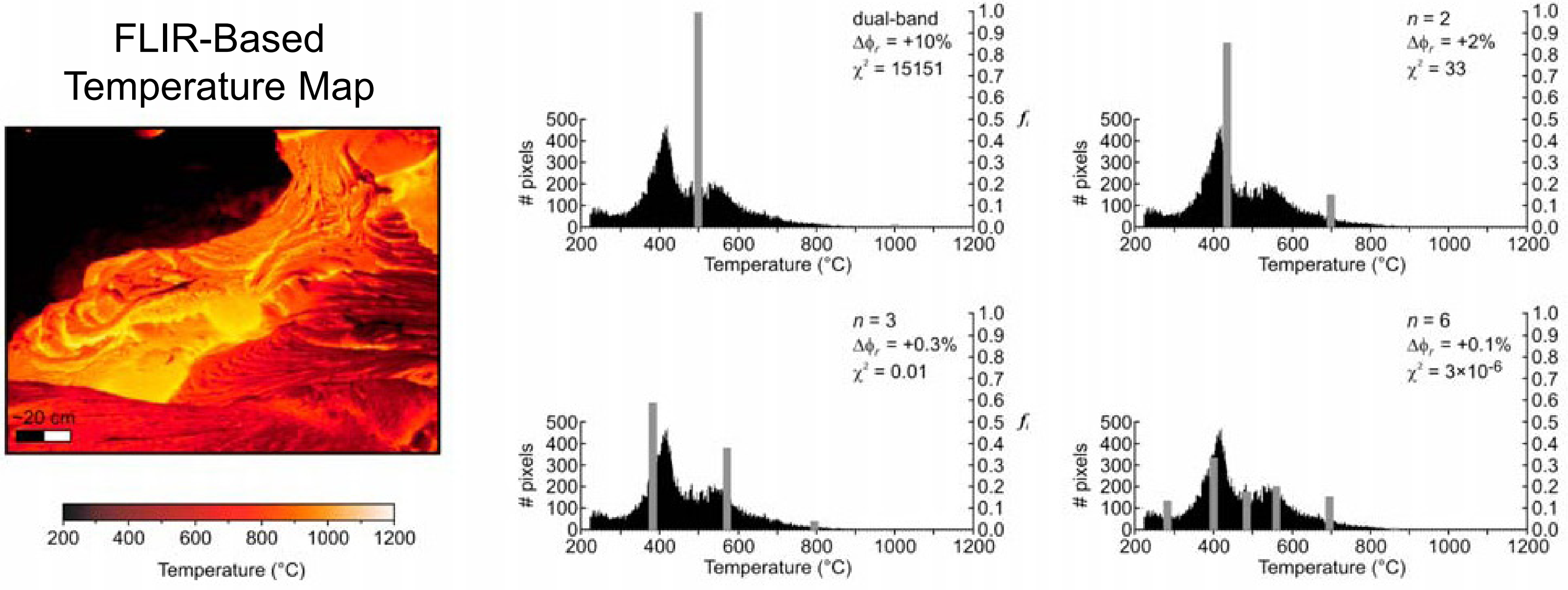

(Wright et al., 2010)

Hyperspectral VSWIR Imaging of Lava Flows

Temperature Distribution w/in Pixel Involves More than Two Components

Multi-Component Models Require Additional Spectral Information

Analyze Hyperion Data (196 Unique Bands between 0.4 – 2.5 μm);

Determine the Minimum Number of Components Needed to Fit Observed Spectrum

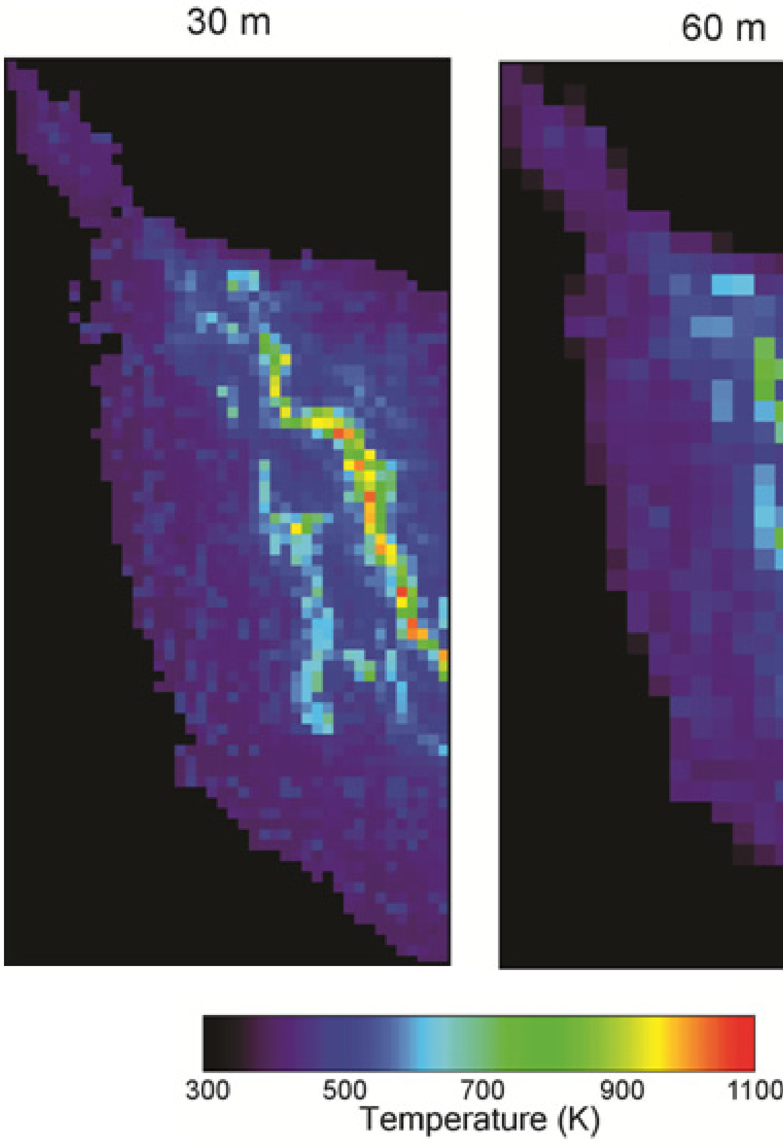

Application to Nyamuragira Lava Flow

Night-time Hyperion: 21 May 2004

Multi-Component Model Run for Each Pixel:

- Resulting Temperature Distribution Used to Generate Synthetic Radiance Spectrum Covering 0.4 – 14 μm
- Convolved With Spectral Response of HyspIRI 4-μm Channel

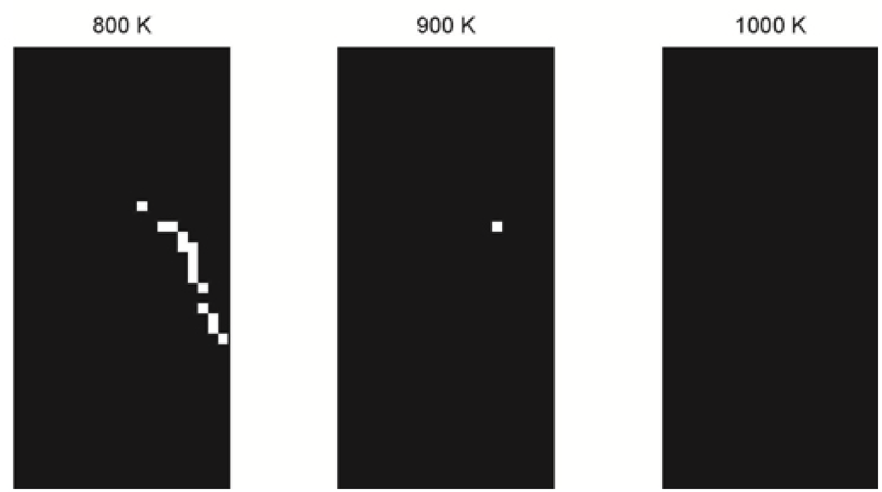

Sat. Temp. of 1000 K Needed to Avoid All Saturation

(Courtesy of Rob Wright)

Conclusion

Recommend Saturation Temperature of <u>1100 K</u>

Case Studies and Literature Search Found Temps ~ 1000 K

NEΔT of 1 K at 400 K: 0.25% Uncertainty

High Spatial Resolution: Increase Apparent Temperatures of Hot Spot Pixels

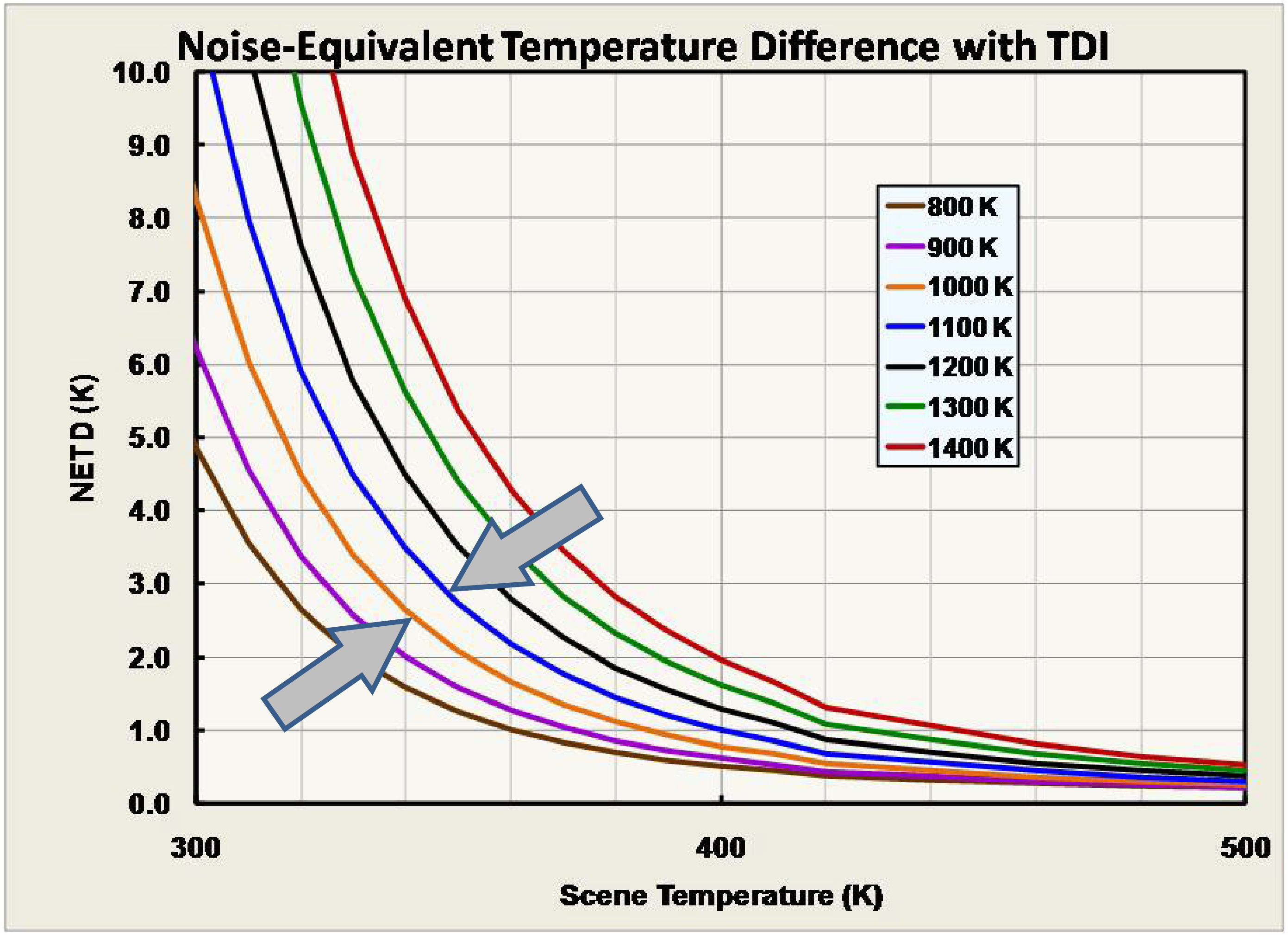

(Courtesy of Mark Foote)

HyspIRI Science Symposium on Ecosystem Data Products

NASA/GSFC, May 4 and 5, 2010
Building 33, Room H114

GSFC EO-1/HyspIRI Team

Betsy Middleton, NASA
Bob Knox, NASA
Steve Ungar, UMBC

Petya Campbell, UMBC
Qingyuan Zhang, UMBC
Fred Huemmrich, UMBC
Ben Cheng, ERT
Larry Corp, Sigma Space

Other Assistants for Symposium:
Hank Margolis, Laval University [TIMEKEEPER]
Sandi Bussard, Jacob Gude, Sheila Humke & Carla Evans
Sigma Space

look for flags on their name tags

HyspIRI Science Symposium on Ecosystem Data Products

Sponsor: NASA/Goddard Space Flight Center

May 4 & 5, 2010

Building 33, Conference Room H114 (and H118, H120)

Focus: Identifying Potential Higher Level Products for Climate/Carbon End Users

Objectives:

Identify science/application data products to be derived from HyspIRI measurements *by users*;

Discover/Discuss issues underlying data product processing/integration/fusion;

Prioritize the development of product prototypes.

Science Discipline Areas to be addressed: Terrestrial Ecosystems, Agriculture

Participants: 67 Active; 25 part-time

Science Questions for the HyspIRI Mission (http://hyspIRI.jpl.nasa.gov)

HyspIRI has three top-level science questions [identified in the NRC Decadal Survey] related to:

1) Ecosystem function and composition,

What is the global distribution and status of terrestrial and coastal-aquatic ecosystems and how are they changing?

2) Volcanoes and natural hazards,

How do volcanoes, fires and other natural hazards behave and do they provide precursor signals that can be used to predict future activity?

3) Surface composition and the sustainable management of natural resources.

What is the composition of the land surface and coastal shallow water regions and how can they be managed to support natural and human-induced change?

6 over-arching VSWIR questions. *VQ1-6 (with 35 sub-questions)*
5 over-arching TIR questions, *TQ1-5 (with 23 sub-questions)*
6 over-arching Combined VSWIR&TIR questions, *CQ1-6 (with 32 sub-questions)*

Terrestrial Ecosystems: *HyspIRI Science Questions for Symposium*

VQ1: Ecosystem Pattern, Spatial Distribution and Components

What is the global spatial pattern of ecosystem and diversity distributions and how do ecosystems differ in their composition or biodiversity?

VQ2: Ecosystem Function, Physiology and Seasonal Activity

What are the seasonal expressions and cycles for terrestrial and aquatic ecosystems, functional groups, and diagnostic species? How are these being altered by changes in climate, land use, and disturbance?

VQ3: Biogeochemical Cycles

How are the biogeochemical cycles that sustain life on Earth being altered/disrupted by natural and human-induced environmental change? How do these changes affect the composition and health of ecosystems and what are the feedbacks with other components of the Earth system?

VQ4: Disturbance Regimes

How are disturbance regimes changing and how do these changes affect the ecosystem processes that support life on Earth?

TQ2 and CQ2: Wildfires

TQ2: What is the impact of global biomass burning on the terrestrial biosphere and atmosphere, and how is this impact changing over time? CQ2: How are fires and vegetation composition coupled?

TQ3. Water Use and Availability:

How is consumptive use of global freshwater supplies responding to climate changes and demand, and what are the implications for sustainable management of water resources?

CQ4: Ecosystem Function and Diversity

How do species, functional type, and biodiversity composition within ecosystems influence the energy, water and biogeochemical cycles under varying climatic conditions?

Determine the global distribution, composition, and condition of ecosystems, including agricultural lands

Tree species mapping, Bartlett Forest, NH

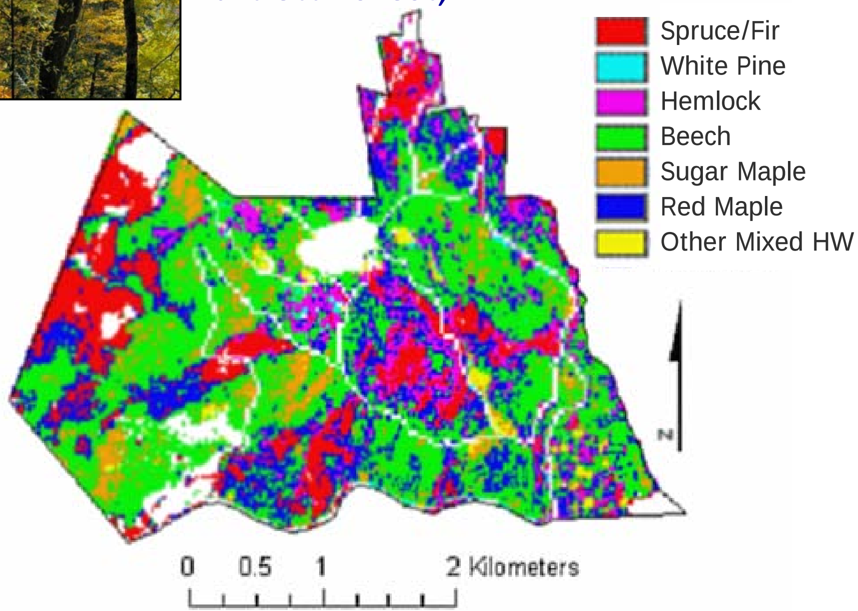

HyspIRI Airborne Simulator Data Set

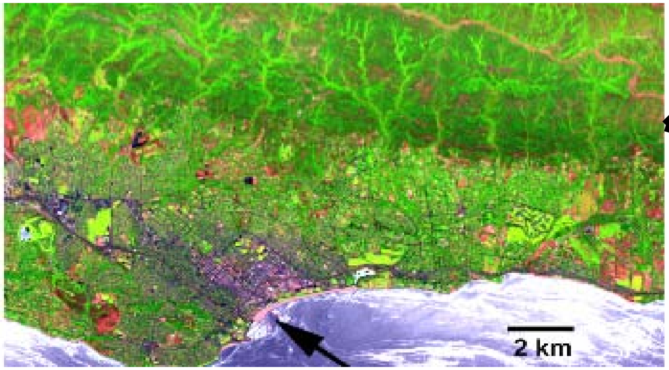

Societal Issue:

- Forests, farmlands and a variety of other ecosystems are critical to life on the Earth. Many ecosystems are changing in ways that are poorly understood.

Scientific Issue:

- Understanding the distribution, diversity and status of ecosystems is necessary for understanding how they function and for predicting future changes.

Approach (Why we need HyspIRI):

- HyspIRI will provide an important new capability to detect & monitor ecosystem composition and condition globally, with spectroscopic and thermal measurements.

Species Type Determination

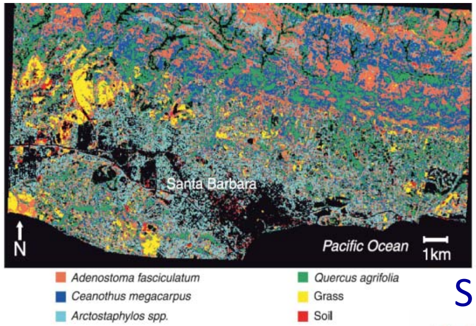

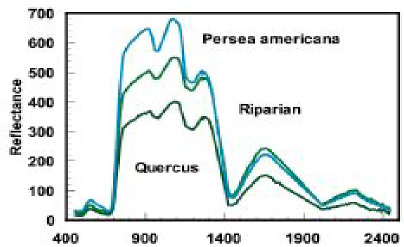

Species Fractional Cover

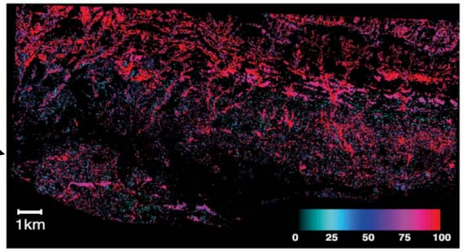

VSWIR Spectrometer (212 contiguous channels)

Level 0: Digital Numbers

Level 1: 1A - Level 0 reconstructed, time-referenced and annotated with ancillary information,
L1B : surface radiance spectra & water leaving radiance spectra at TOA. Cloud screened images.

Level 2: *Description* - Swath data. ***Products*** - TOA and Surface Reflectance (%) Spectra
.
==

User-Derived Products

Level 3: *Description* - Swath *and* Gridded data, Terrain corrected products.
Products: Albedo, Land cover classifications, Composites (seasonal, regional and global composites), Spectral indices for vegetation function/health, Spectral indicators for canopy contents (pigments, nitrogen, water, Maps of end-member abundance.

VSWIR Spectrometer (212 contiguous channels)

==

User-Derived Products-- Continued

Level 3: *Description* - Swath *and* Gridded data, Terrain corrected products.

Products: Albedo, Land cover classifications, Composites (seasonal, regional and global composites), Spectral indices for vegetation function/health, Spectral indicators for canopy contents (pigments, nitrogen, water, Maps of end-member abundance.

Level 4: *Description* – Time series, Model outputs, Multi-sensor data fusion, Assimilation with other data types (e.g., ET, Fire fuel & fuel moisture).

Products – Regional Scale (60m-1km): *For specific sites, watersheds, geographical units or global samples of ecosystems, but potentially for global maps:* Gross Primary or Ecosystem Production (GPP, GEP); Net Primary or Ecosystem Production (NPP, NEP); Fractional land cover; Fractional vegetation cover (FVC), based on: photosynthetic vegetation (PV) and non-photosynthetic vegetation (NPV), Soil, Water, Snow, Ice; Fractional PAR absorption (*f*APAR); Leaf area index (LAI); Water Content; Plant functional types (PFT); Fractional vegetation cover by PFT(FVC); Light-use efficiency (LUE); Canopy stress and Physiology (combining PFT, LAI, canopy water, nutrients, pigments); Ecological disturbance (>10% change); Susceptibility to fires (fire fuels & fuel moisture, FVC, canopy water); Susceptibility to hazards (e.g., landslides).

Products -Global Scale (gridded, ¼-1 deg+): *For modeling ecosystems/general cover categories:* GPP, GEP; NPP, NEP; Fractional land cover (Veg., Soil, Water, Snow, Ice); *f*APAR; LAI; Water Content; Disturbance (>10% change).

TIR Multiband Sensor (8 discrete bands)

Level 0: Digital Numbers
Level 1: 1A - Level 0, reconstructed, time-referenced and annotated with ancillary information; 1B – surface band radiances at TOA, Cloud screened images. ***Products*** – Brightness temperature.

Level 2: *Description* - Swath data. ***Products*** – Land Surface Temperature, LST (day or night); Surface Spectral Emissivity (day or night); Detection of fire events.

==

Level 3: *Description* – Day or night swath and gridded data, Terrain corrected, Day or Night Composites (seasonal, regional and global).

Products – Distribution and variation in land surface temperature, surface spectral emissivity maps, Water stress indicators; Fire severity, directions and associated risks.

Level 4: *Description* - Time series, Model outputs, Multi-sensor data fusion, Assimilation with other data types.

Products - Regional (60m-1km): *For specific sites, watersheds, geographical units, agricultural fields, or global samples of ecosystems, but potentially for global maps:* LST (from temperature/emissivity separation) by functional groups and ecosystem types, LST urban/sub-urban, Evapotranspiration (ET).

Products - Global (gridded, ¼-1 deg+): *For modeling ecosystems/general cover categories:* LST and emissions by Fractional land cover (Vegetation, Soil, Water, Snow, Ice), ET, Increase in sensible heat due to Urban Heat Islands (anthropogenic heat).

Synergy between TIR Day & Night and VSWIR & TIR

Level 4 Products: Time series, Model outputs, Multi-sensor data fusion, Assimilation with other data types.

TIR, day and night - ***Products - Regional (60m-1km)*** **&** ***Global (1-5 deg. grids)***:

Bi-weekly, monthly and/or seasonal averages for day-night temperature & emissivity differences per geographic study unit (watershed, etc.).

VSWIR and TIR – ***Products - Regional (60m-1km) & Global (1-5 deg. grids)***:

- Day-night temperature & emissivity differences according to vegetation/ecosystem type,
- LST (from day/night pairs) by functional groups and ecosystem types,
- Water/land boundaries defined,
- Ecosystem & Agricultural Crop Classifications, using both VSWIR & TIR,
- ET per ecosystem or agricultural type, using both VSWIR & TIR,
- Assess fire severity and available fuel by vegetation type,
- Develop spectral Reflectance & Emission libraries by land cover types and/or vegetation functional groups (at regional and global scales),
- Develop *high spectral resolution indicators of ecosystem/crop health,* by combining VSWIR indices and TIR indices; Construct spectral indicators of ecosystem function, disturbance, diversity, maturity to improve modeled predictions.
- Compare high spectral resolution indicators to currently used broadband indicators of ecosystem/crop function.

Expected Outcomes of Symposium

Goal: To Identify and Evaluate Potential Higher Level Products for Climate/Carbon End Users, in Terrestrial Ecosystem & Agriculture Science/Applications.

Objectives/Outcomes:

1] Identify science/application data products that could be derived from HyspIRI measurements ***by users***;

2] Prioritize the development of product prototypes.

3] Discover issues underlying data product processing and related to data integration/fusion.

4] Address the case for relevance of HyspIRI to climate change studies.

5] Develop a report on the community consensus for **1-4** above.

DAY 1 (May 4): Morning Agenda

I. Establish Background

8:30 am: Welcome-- HQ on the HyspIRI mission concept and Decadal Survey status [**Woody Turner**]

8:45 am: Objectives and Outline of the Symposium & Expected Results [**Betsy Middleton**]

8:55 am: Overview of the Mission: Description of the VSWIR and TIR instruments [**Rob Green & Simon Hook**]

9:15 am: Relevance of HyspIRI to Carbon and Climate [**Susan Ustin**]

9:30 am: Orbit & Platform Information, update from Team X [**Bogdan Oaida**]

9:45 am: Description and Examples of Typical VSWIR and TIR Image Collections [**Bob Knox**]

10:00 am: **Questions/Answers** (10 minutes)

10:10 -10:30 am: Coffee Break & Posters

II. Science & Application Products from the User Community: VSWIR & TIR

10:30 am –noon: Proposed VSWIR and TIR High Level Products [7 speakers, 10 min each]

[**Phil Townsend, John Gamon, Anatoly Gitelson, Mary Martin, Ben Cheng, Simon Hook, Martha Anderson, Susan Ustin**]

Noon - 1:00 pm: Lunch and Poster Session (Sandwiches/Drinks in conference serving area)

Plans for HyspIRI

Woody Turner

- Stay the course

- Continue to mature our technology and operations

- Strengthen the scientific case for the program

- Focus on the climate-relevance of our mission science

- Explore the potential to build the scientific basis for HyspIRI through utilization of products from airborne systems and upcoming spacecraft missions carrying spectrometers and TIR sensors
  (doing so will require additional funding)

- Look at results of HyspIRI preparatory activities solicitations

- Be ready!

Daylight side of a sun-synchronous reference orbit, with 10:30 AM equatorial crossing (mean local time) at a descending orbit node. The sub-solar point (yellow) shows the location on Earth where the Sun is directly overhead, east of the ground track.

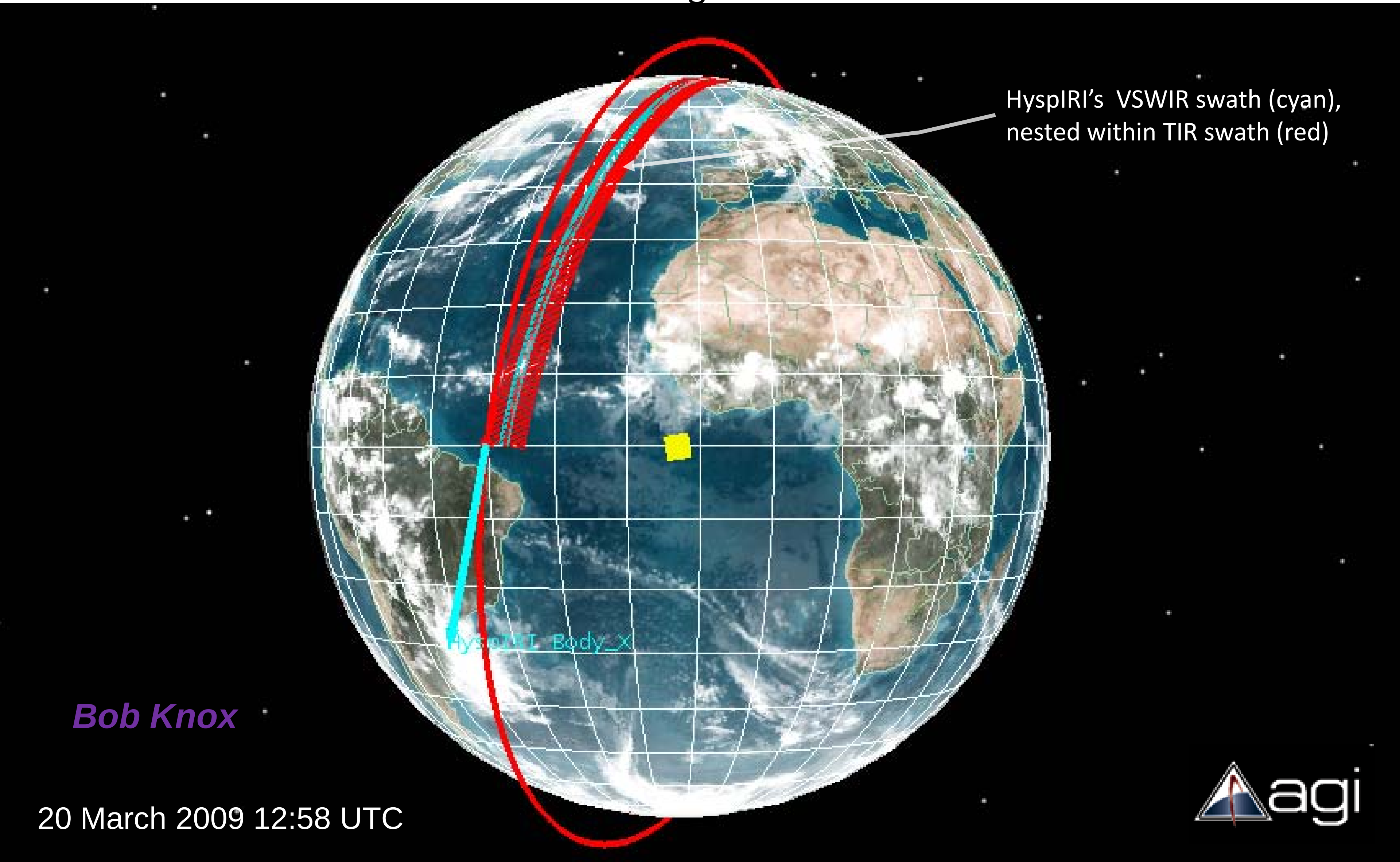

14 potential image collects for 1 simulated month (equatorial site)

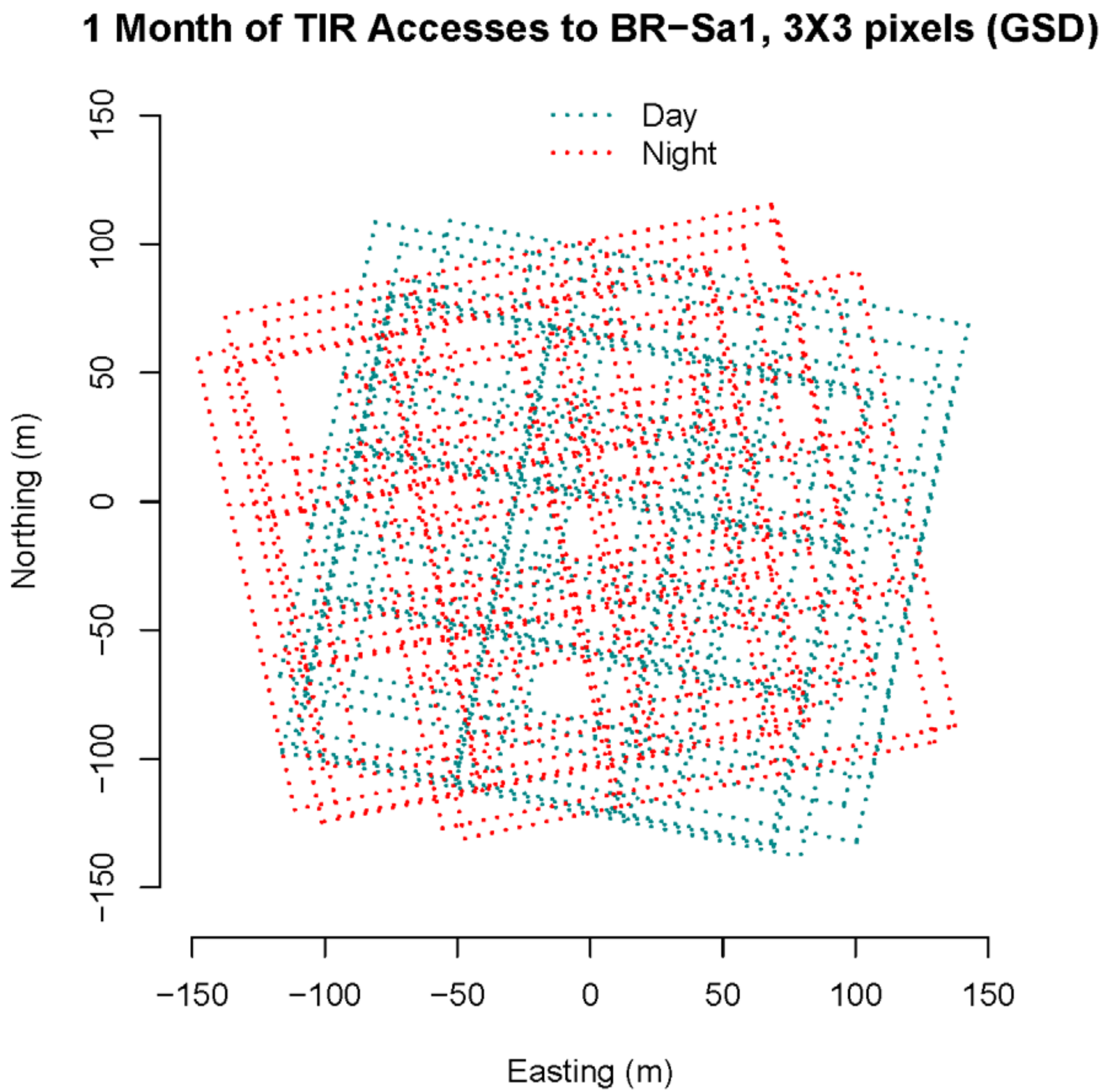

Bob Knox

Local time of TIR overpasses of 5 FLUXNET sites, simulated for 1 year

Near the equator, overpass times are separated by 12 hours, on average.

As the N latitude of the site increases, potential TIR collects are more frequent and less tightly clustered in local time.

When moving toward the North orbit pole (82.1 N), daytime collects are later and night collects earlier.

The reverse is true (not shown) when moving South.

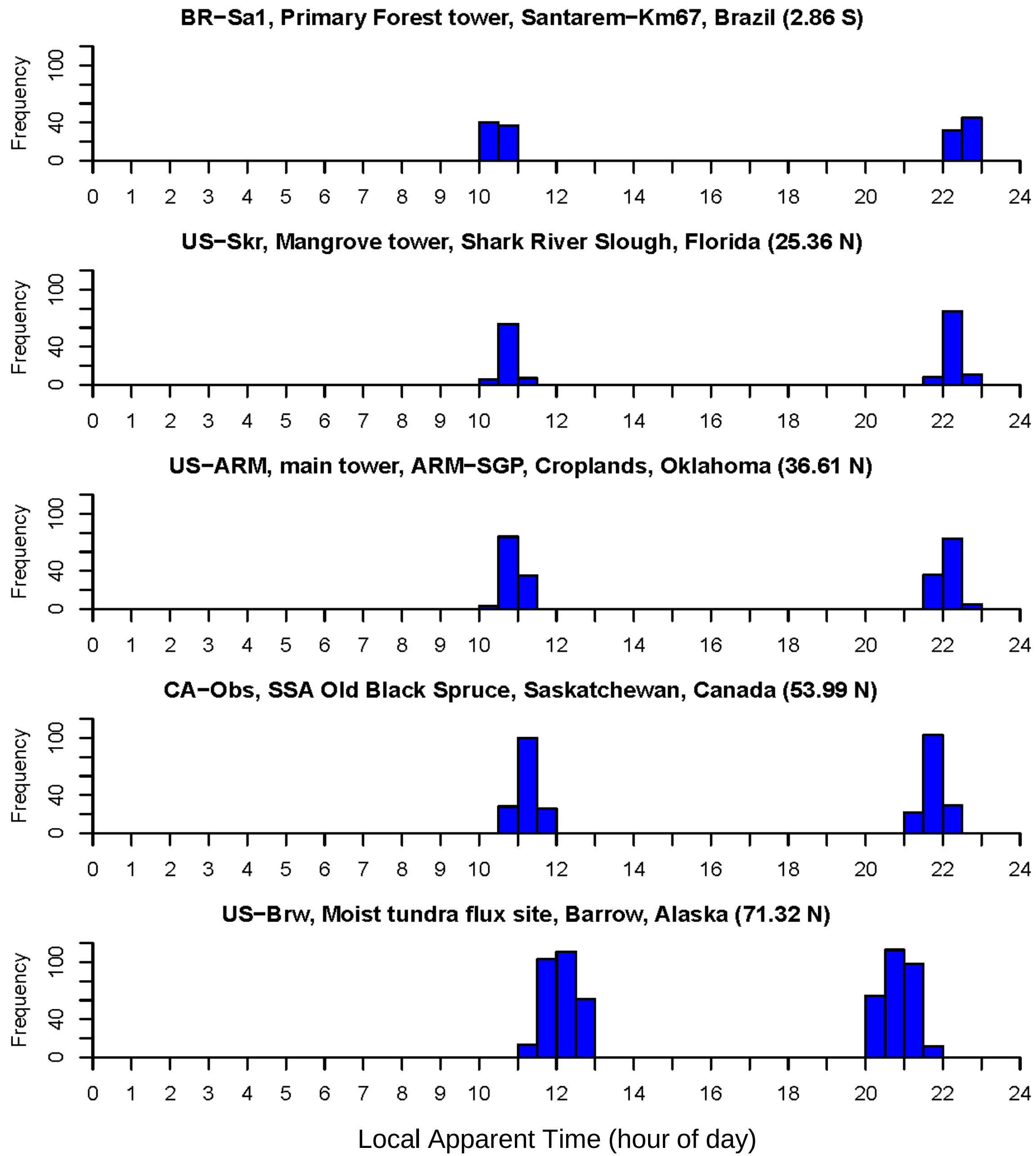

Bob Knox

TIR accesses for 1 simulated year

Bob Knox

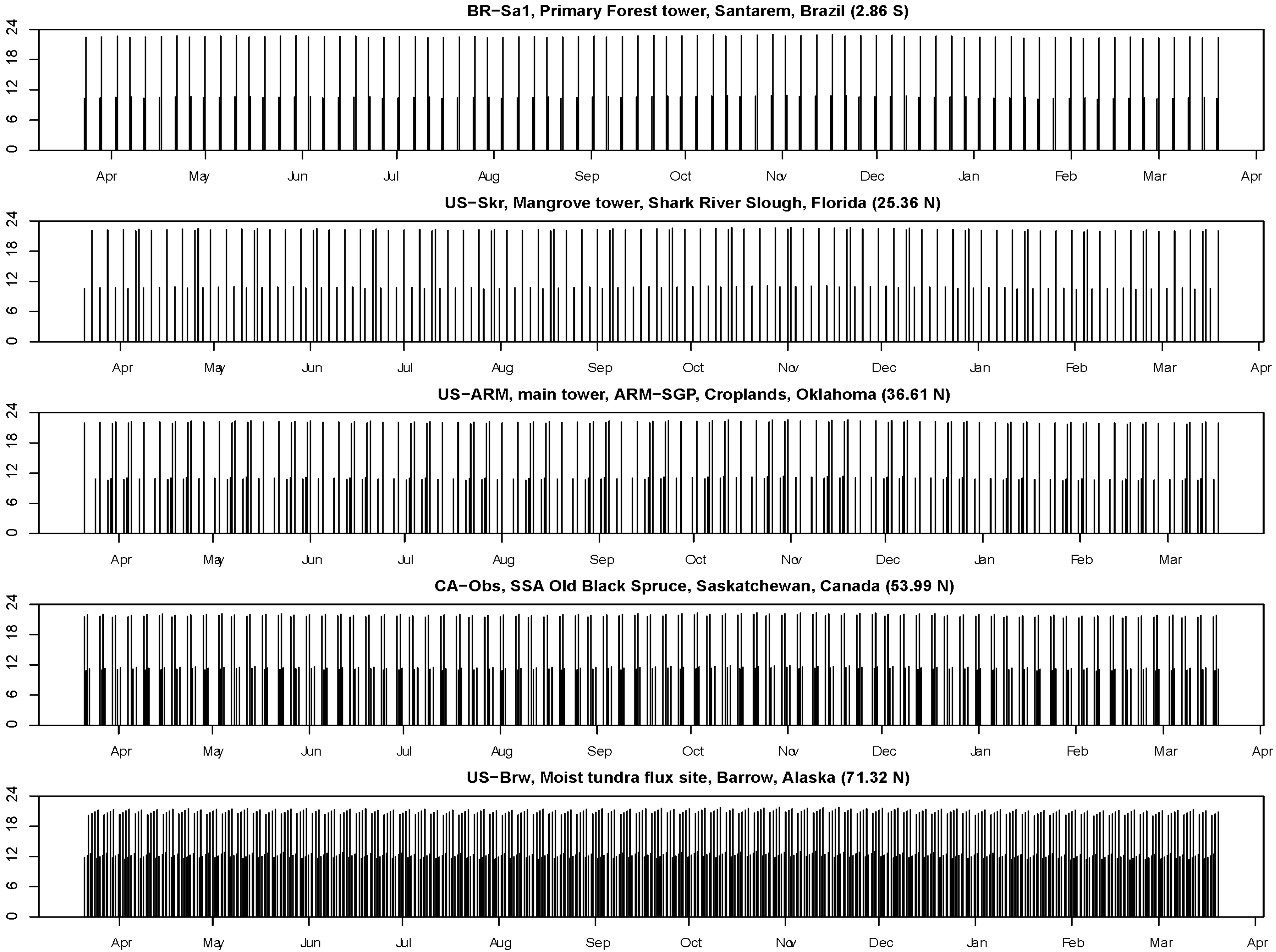

19 potential image collects for 1 simulated year (equatorial site)

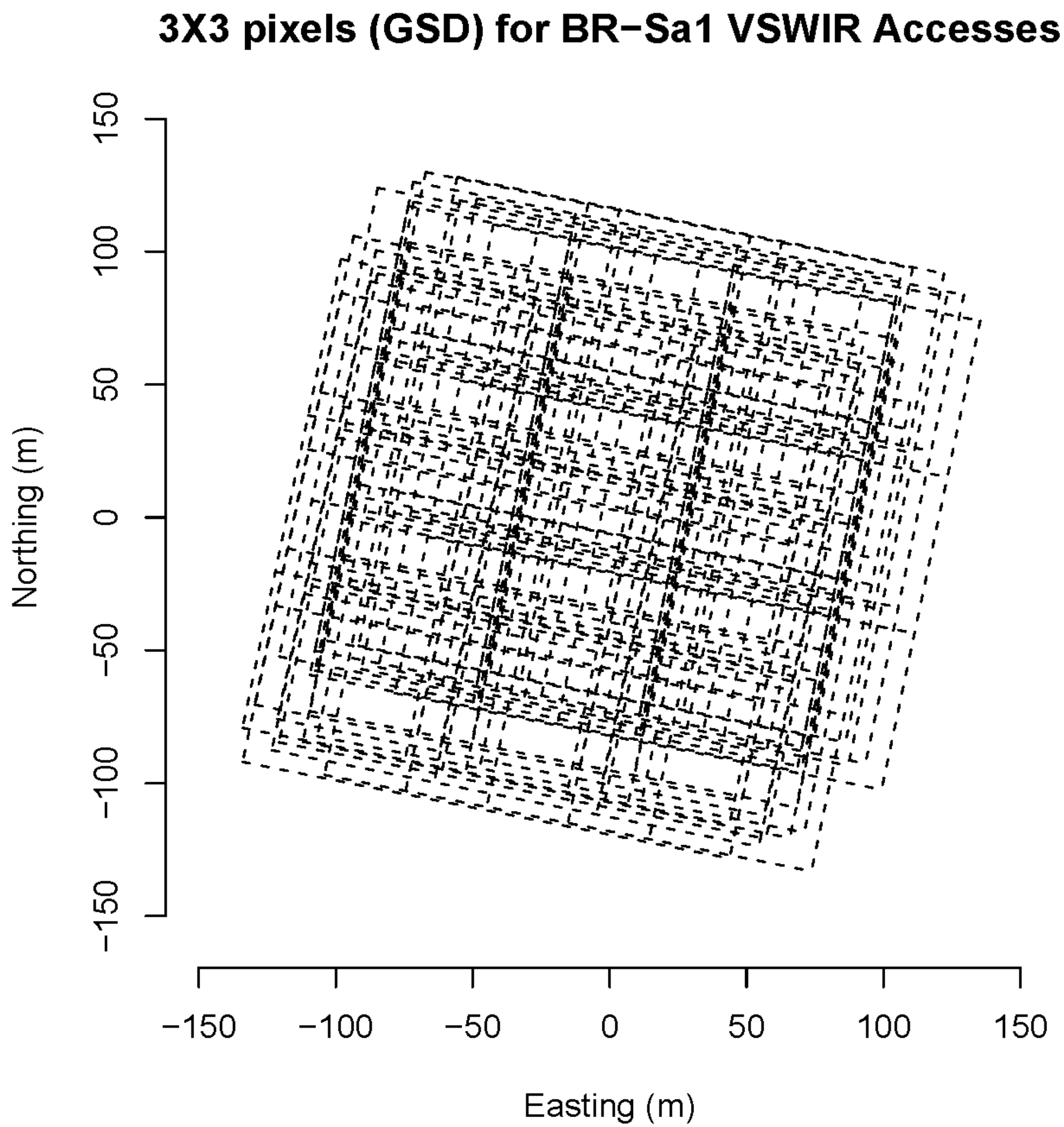

Bob Knox

Local time of VSWIR overpasses of 5 FLUXNET sites, simulated for 1 year

Local apparent time, for a fixed mean local time, varies with the Earth's orbit.

As the N latitude of the site increases, the local apparent time of potential VSWIR accesses also increase.

Near the North orbit pole (82.1 N) the local time may be nearly 6 hours later than when crossing the equator (not shown).

Moving toward the South orbit pole, local times are progressively earlier in the morning (not shown).

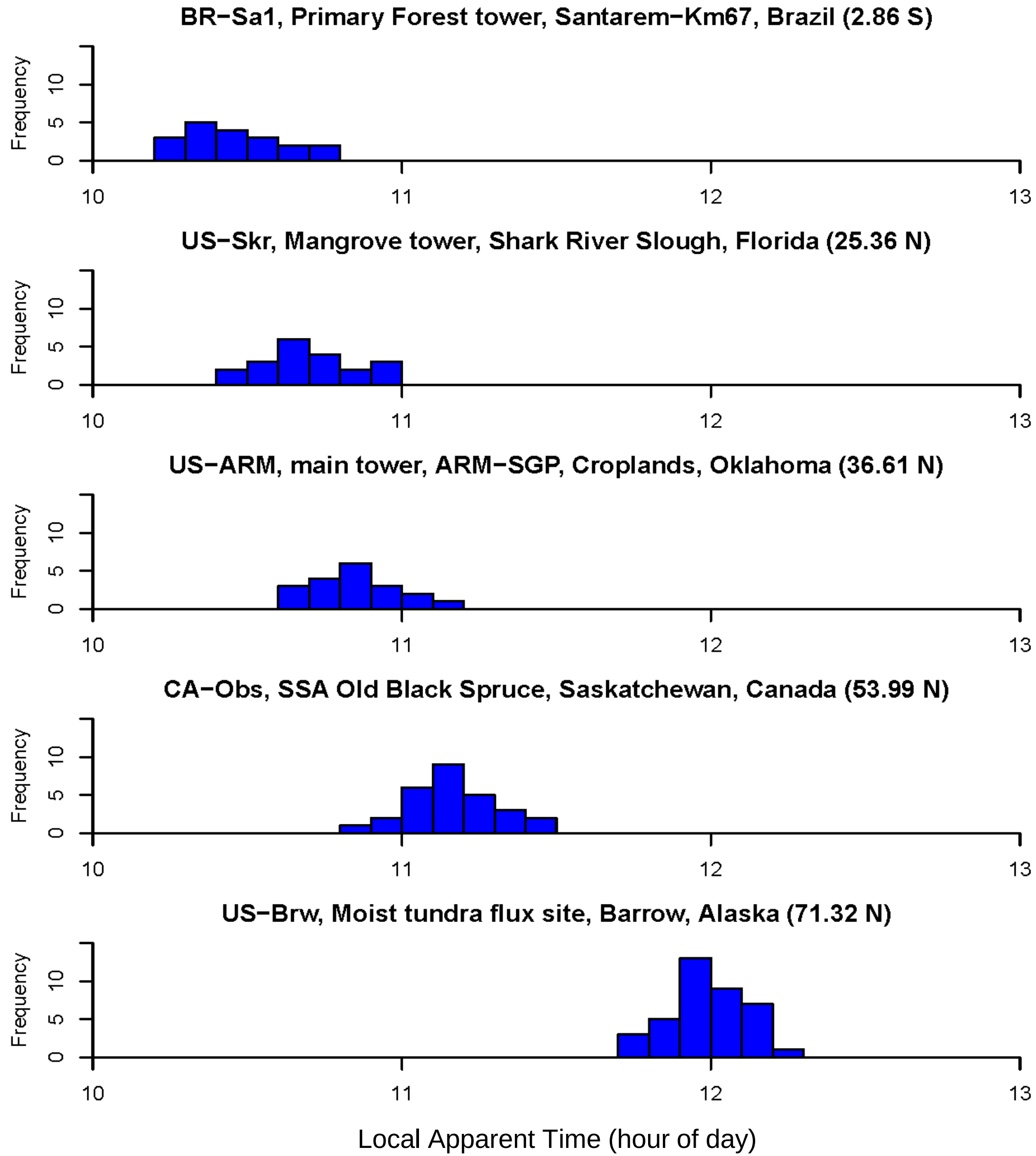

Bob Knox

VSWIR spectrometer accesses to three selected FLUXNET sites
1 simulated mission year: date & local apparent time

BR-Sa1: Brazil - Santarem km 67, Primary Forest (2.86 S)

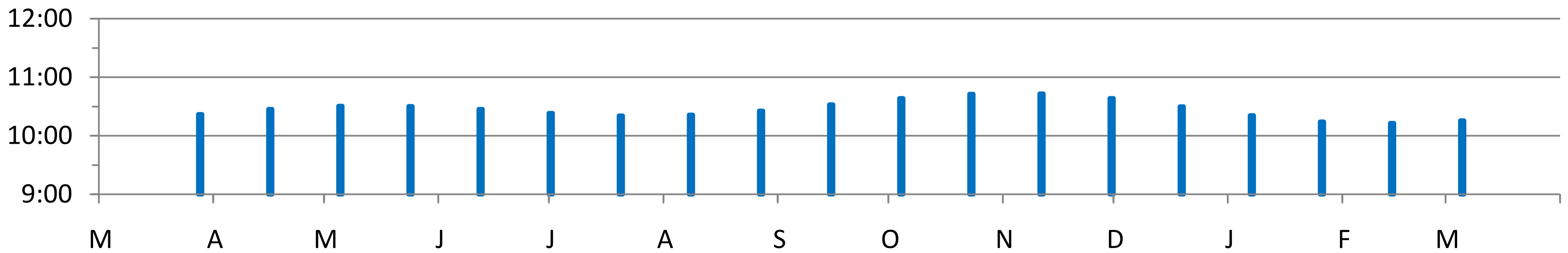

US-ARM: Southern Great Plains, Oklahoma, Main Tower, Croplands (36.6 N)

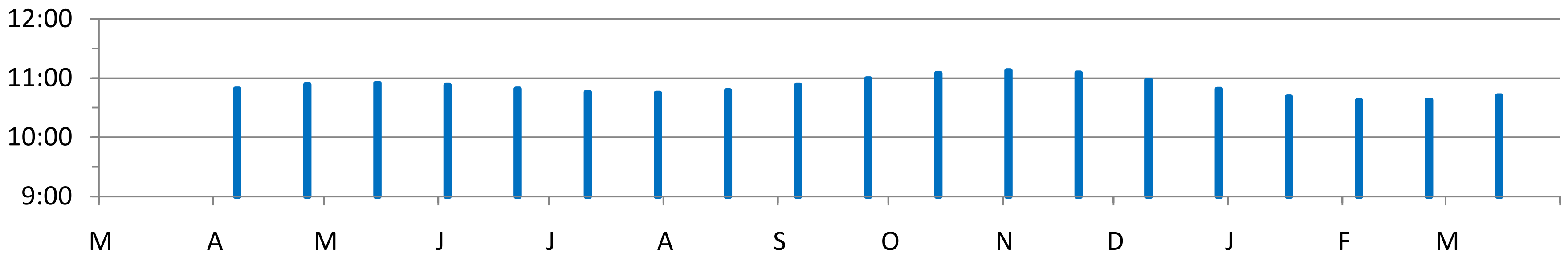

CA-Obs: Canada, Saskatchewan, BOREAS SSA - Old Black Spruce (53.99 N)

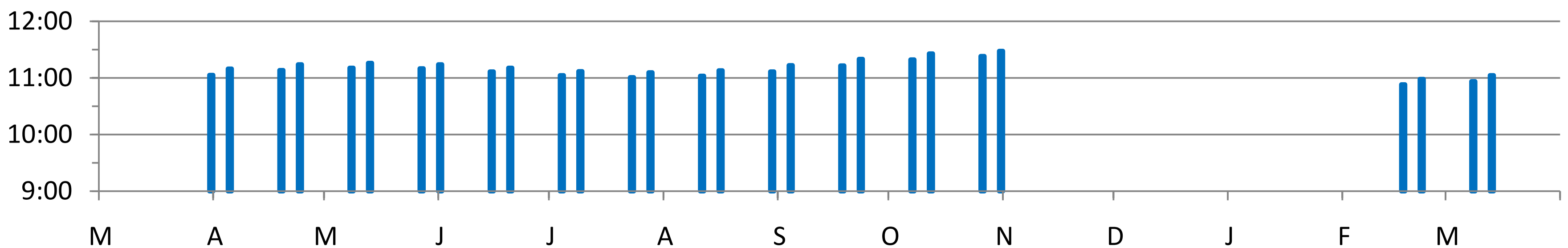

R.G. Knox, NASA GSFC, Biospheric Sciences Branch, Code 614.4. Simulated with STK v8.1.3, March 8, 2010.

DAY 1 (May 4): Afternoon Agenda

III. Factors Affecting Product Integrity and Availability **1:00 – 2:30 pm (10 min each)**

* Atmospheric Correction [**Rob Green**]
* Data volume/compression, SpaceCube [**Tom Flatley**]
* Intelligent Payload Module (IPM) & algorithms for upload [**Vuong Ly/Dan Mandl**]
* Low-latency Applications, Science, and Operations for HyspIRI [**Steve Chien**]
* On-line tools to facilitate HyspIRI products and analysis [**Petya Campbell**]
* Hyperspectral Input to models [**Fred Huemmrich**]
* Calibration/Validation & CEOS/GEO [**Joanne Nightingale**]
* Impact of Spectral-Spatial Misalignment on Measurement Accuracy [**Steve Ungar**]

IV. Science & Application Products from the User Community: Combined VSWIR & TIR

2:30 -2:50 pm: Combined VSWIR/TIR Products Overview: Issues & Examples
[**Bob Knox/Betsy Middleton**]

2:50-3:00 pm: **Questions/Answers** (10 minutes)

3:00-3:20 pm – Coffee Break & Posters

3:20- 4:30 pm: Proposed Combined Products (7 speakers, 10 min each)

[**Rasmus Houborg, Louis Giglio, Dar Roberts, Dale Quattrochi, Ben Cheng, Ray Kokaly, Craig Daughtry**]

DAY 1 (May 4): Afternoon Agenda Con't

<u>V. Special & Potential Observation Capabilities</u>

4:30-4:40 pm: Special Opportunities for Highly Sampled Areas
(orbit overlaps, high latitudes etc.) [**Bob Knox**]

4:40-4:50 pm: Synergy of VSWIR and Lidar for Ecosystem Biodiversity
[**Bruce Cook/Greg Asner**]

<u>VI. Break-Out Discussions</u> (Guidelines, **Betsy)**

4:55 -6:15 pm: Three Simultaneous Break-Out Discussions
(H114, H118, H120)
VSWIR Products [**Phil Townsend/John Gamon**]
TIR Products [**Simon Hook/Kurt Thome**]
Combined Products [**Dar Roberts/Susan Ustin**]

6:20 pm – Adjourn, Dinner at Chevy's Restaurant, Carpools Organized

The Break-Out Group Discussions

[Topics for consideration]

How important is HyspIRI to the User Community, for TE and climate?

What are the most important Products for Terrestrial Ecology?

What are the Tools needed to produce these Products?

What are the road-blocks to having Products that users want?

AGENDA – DAY 2 (May 5) Con't

<u>VIII. Building a Team Consensus</u>

10:30 – 11:00 am: Plenary Discussion, Aligning HyspIRI with Climate Observations [**Susan Ustin/Dar Roberts**]

11:00 – 11:30 am: Plenary Discussion on Priority Products, [**led by Betsy, Rob & Simon**]

11:30 am – Noon: Consensus on Draft Products for HyspIRI, Outline of Symposium Report [**Betsy, Rob, Simon**]

Noon – 12:30 pm: Preparation Activities for 3rd Science Workshop [**Rob, Simon, Woody Turner**]

12:30 pm: Close General Meeting

Adjourn, or Lunch at Cafeteria

*1:30-3:00 pm: **<u>Optional</u>** Opportunity to show PI presentations in small conference rooms [H118]*

and

Steering Committee Meeting [H120]

LUE – Leaf chlorophyll inter-correlation
Thermal-based flux mapping

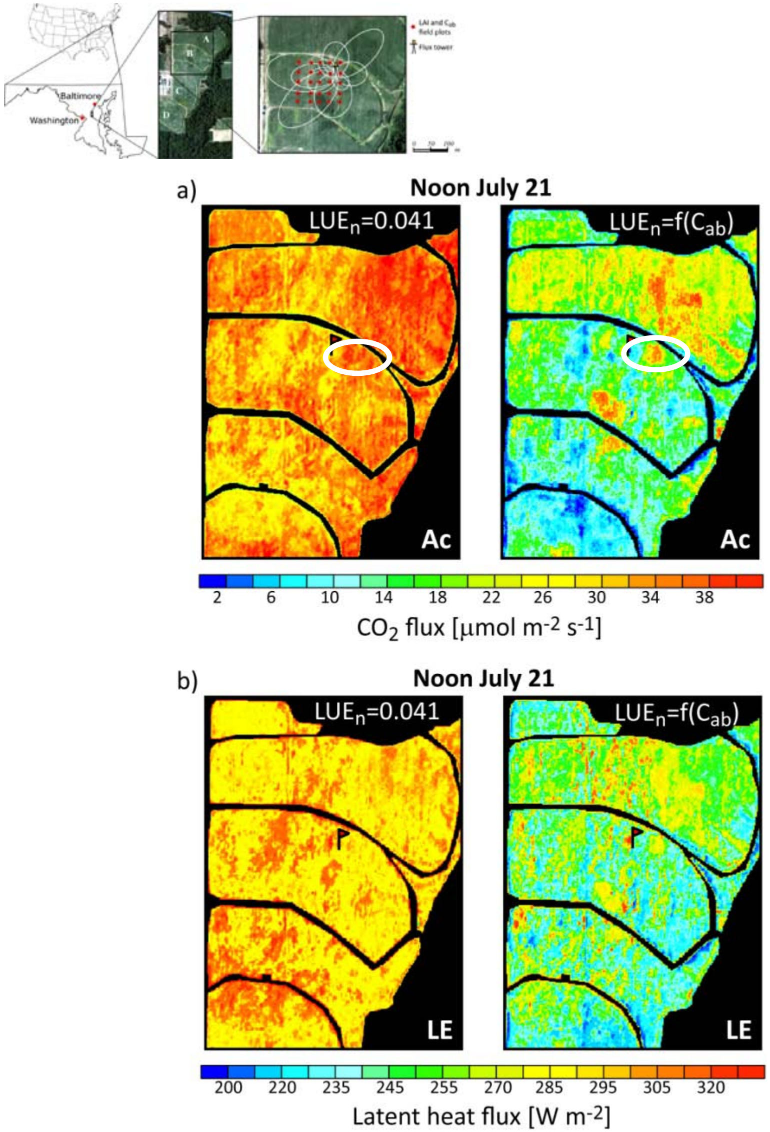

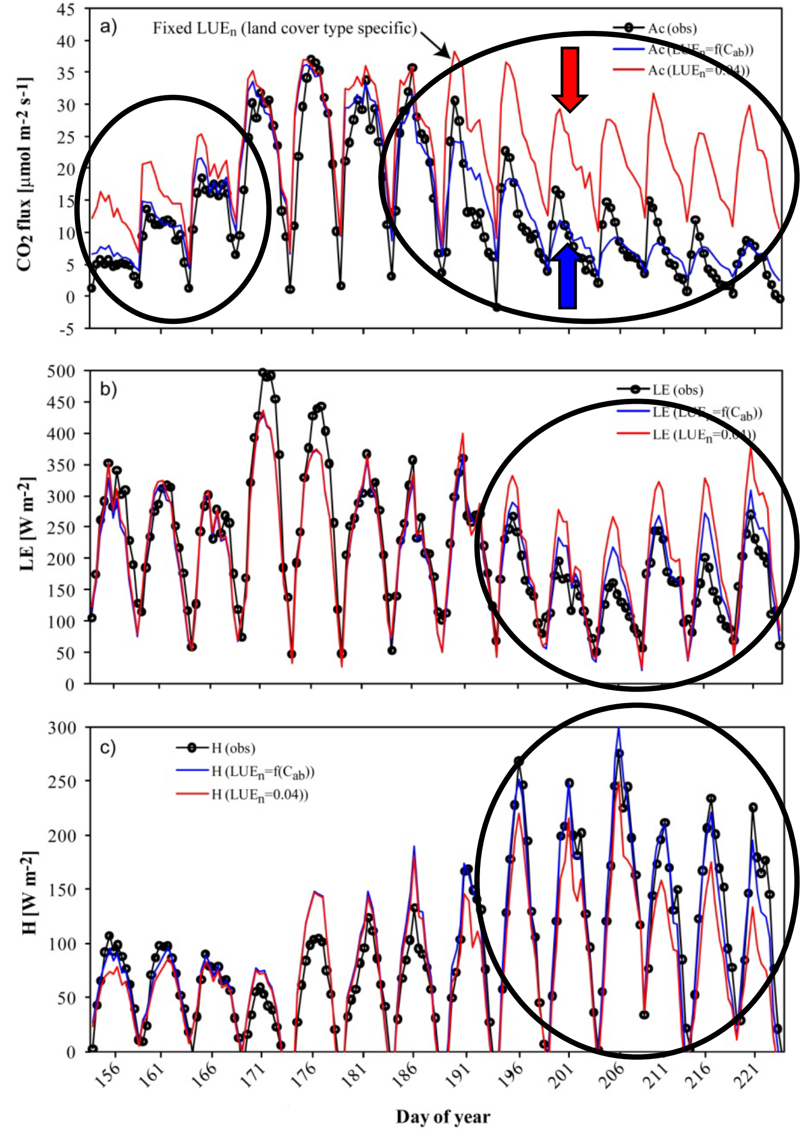

Rasmus Houborg

Iowa 2004

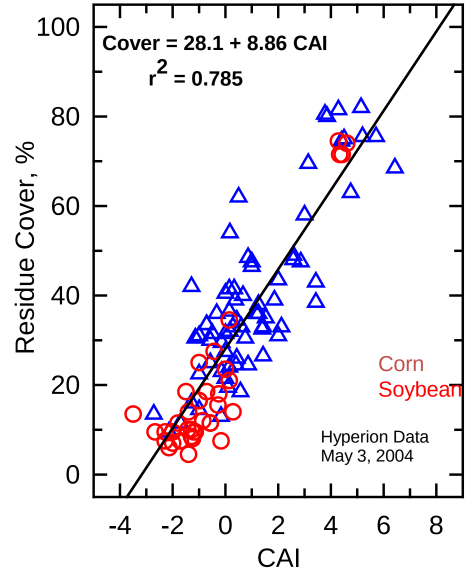

Slope of line is similar to ground-based (ASD) and aircraft (AVIRIS & AISA) data in MD, IN, and IA.

Residue cover was measured: May 10-12

Planting progress for May 9
(Iowa Crop & Weather, 2004)
Corn:
93% planted;39% emerged
Soybeans:
54% planted; 4% emerged

Hyperion Imagery was acquired: May 3

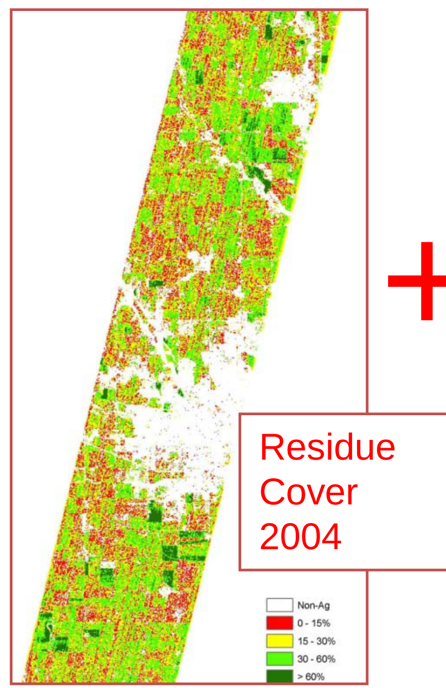

+

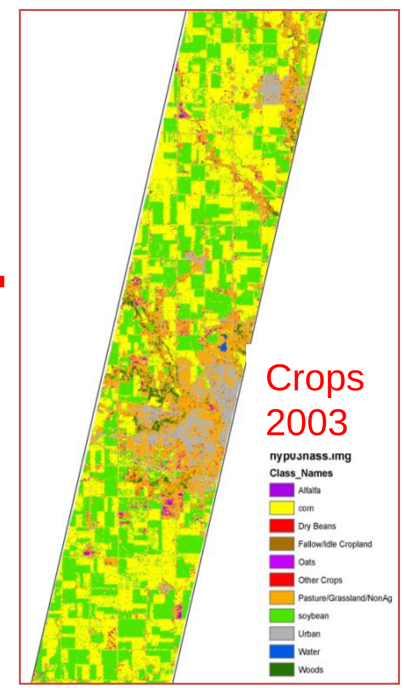

Daughtry

GPP estimation via Chl

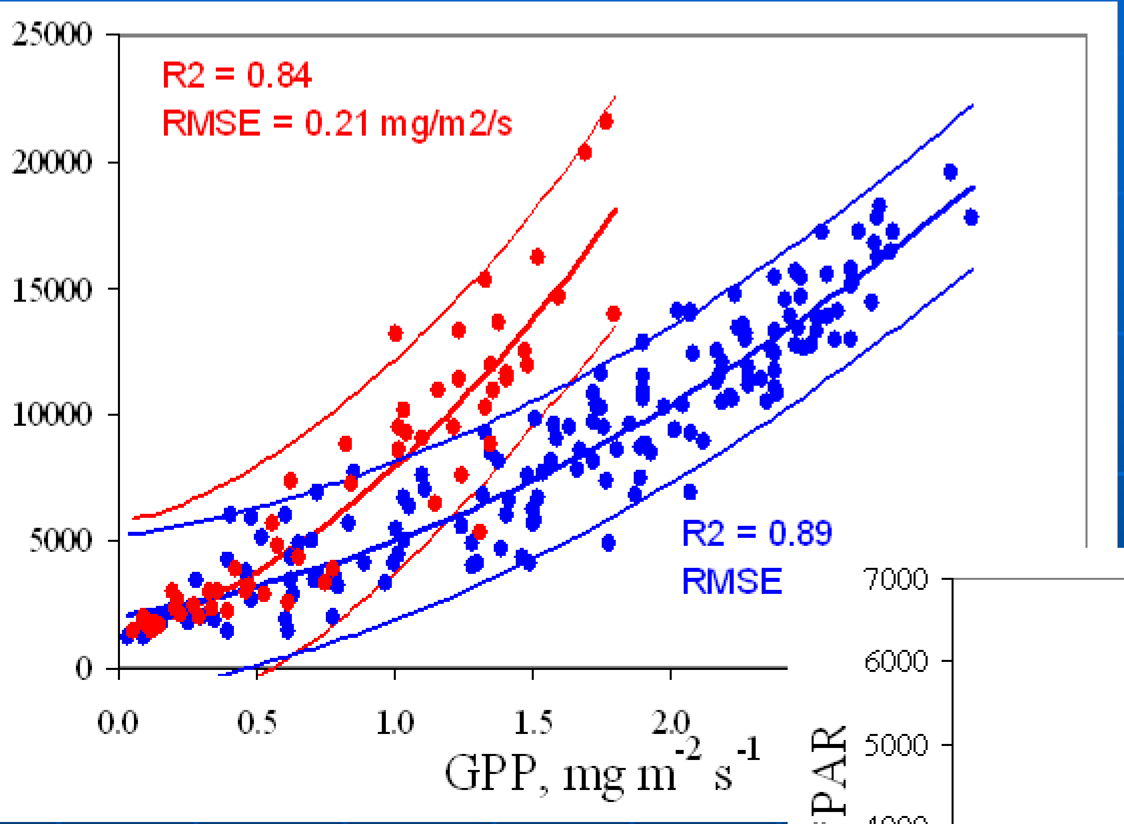

Maize
Soybeans

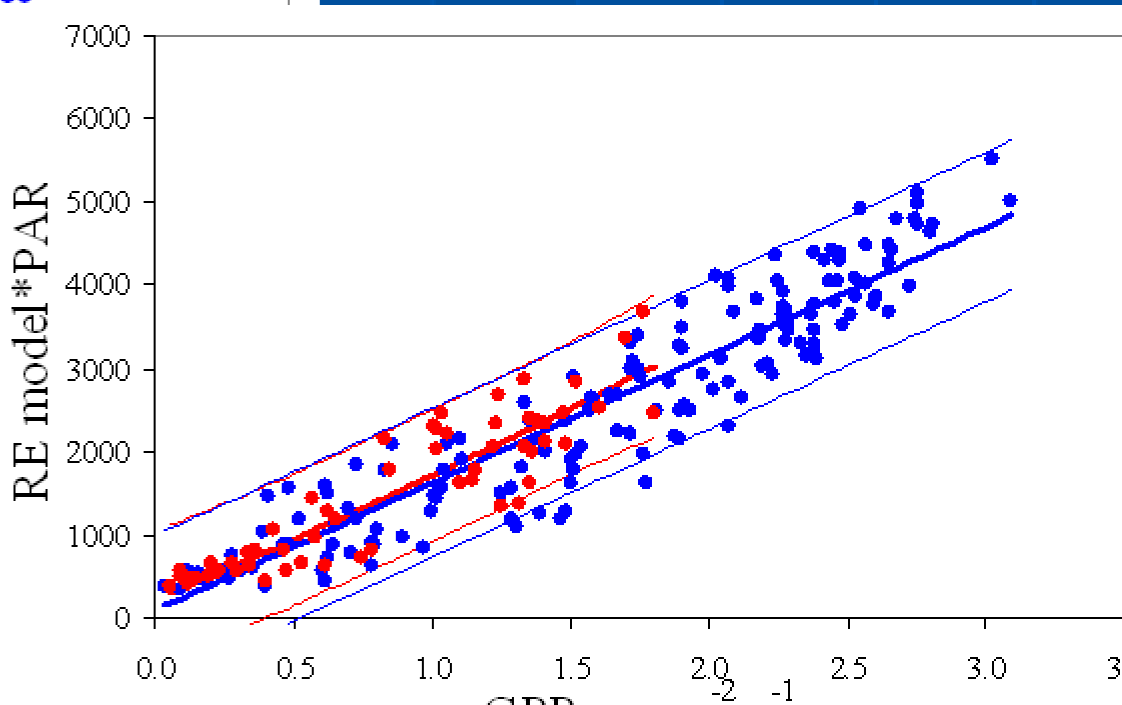

natoly Gitelson

USDA ARS United States Department Of Agriculture Agricultural Research Service

USDA-ARS HRSL Hydrology & Remote Sensing Lab Beltsville, Maryland, USA

OPE3 Optimizing Production Inputs for Economic and Environmental Enhancement (OPE3)

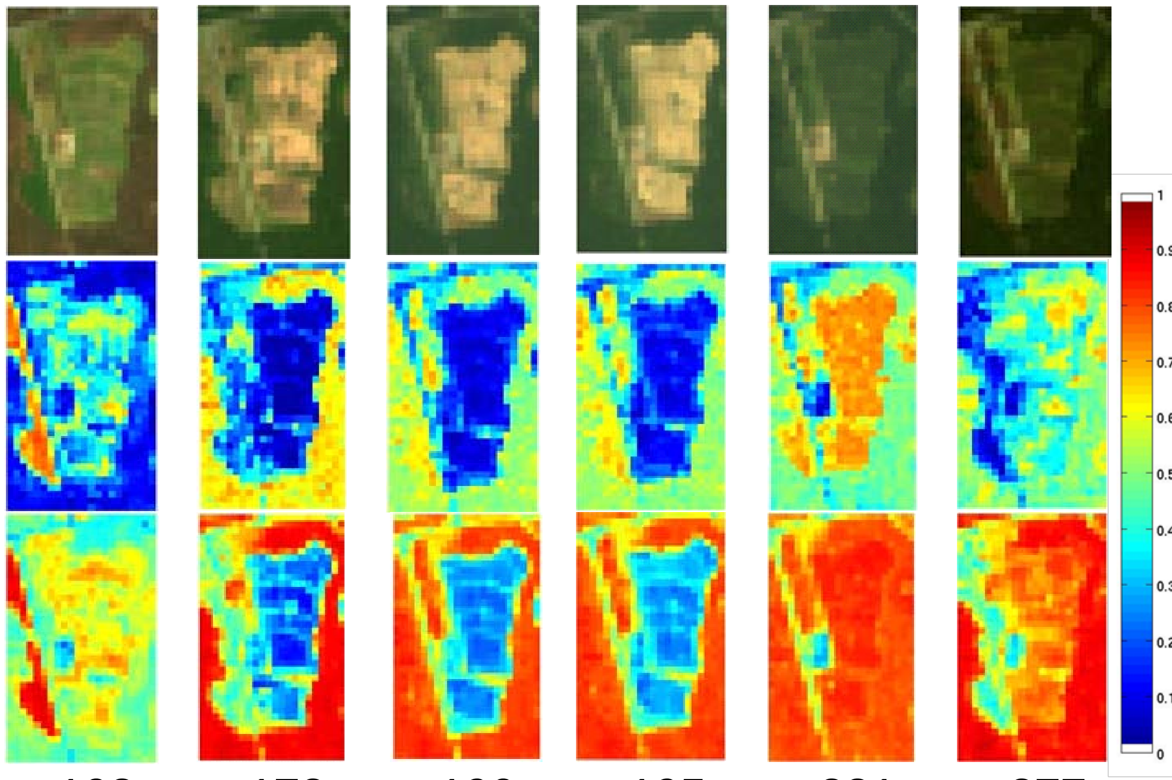

Qingyuan Zhang

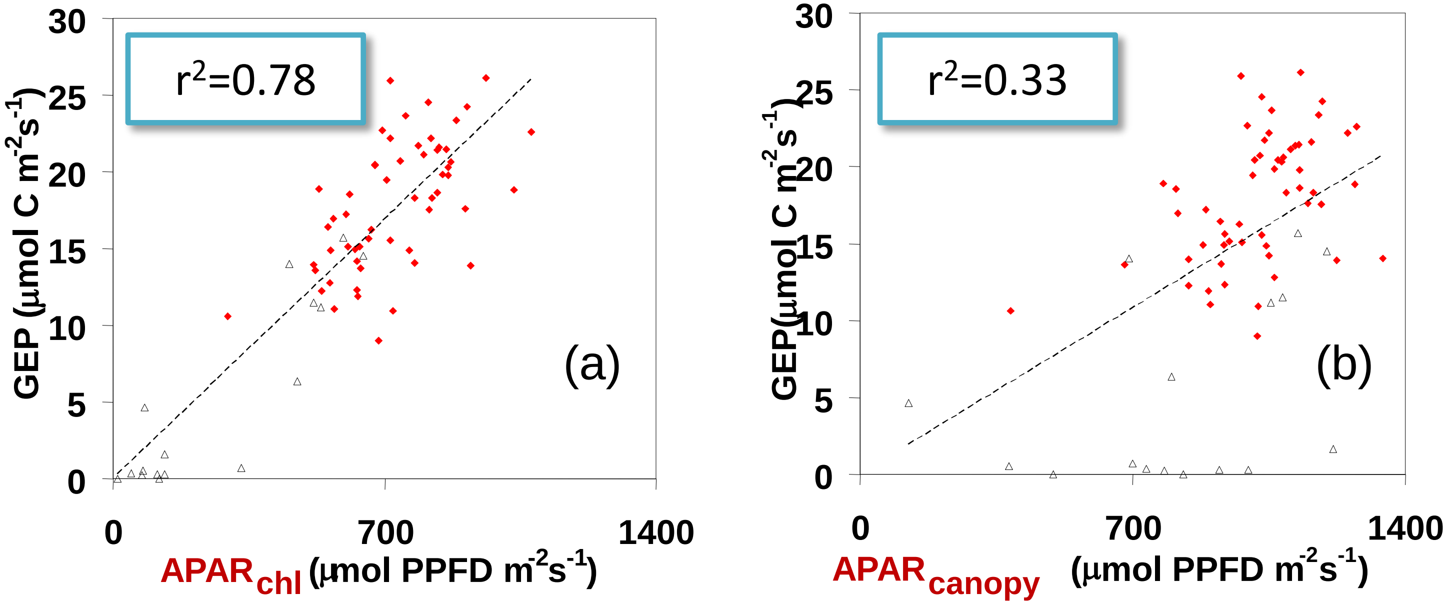

APARchl LUEchl Products

Qingyuan Zhang

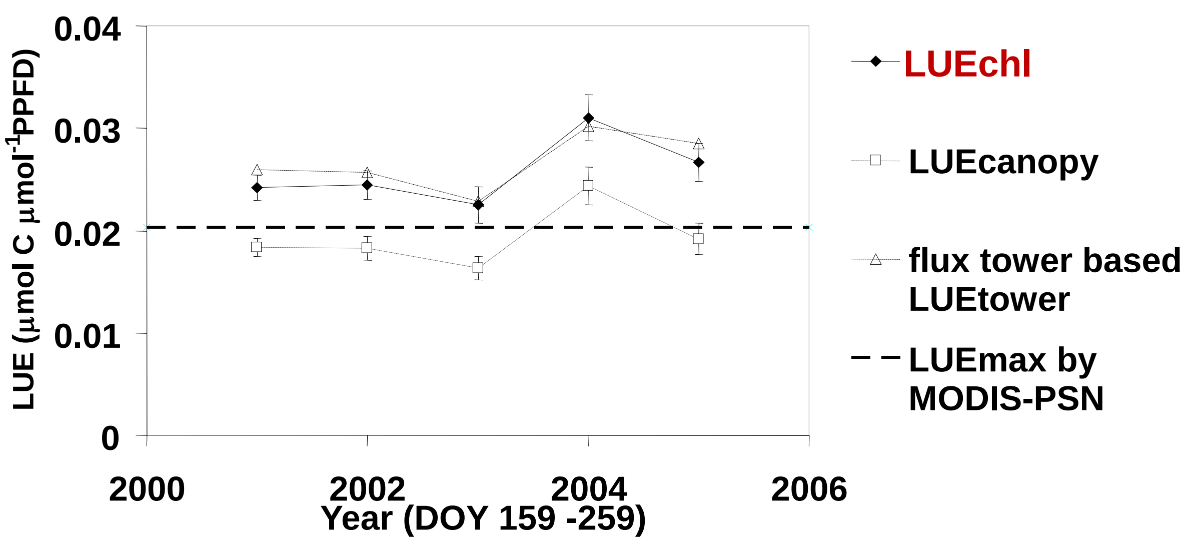

Zhang, Q., Middleton, E.M., Margolis, H.A., Drolet, G.G., Barrd, A.A., & Black, T.A. (2009). Can a satellite-derived estimate of the fraction of PAR absorbed by chlorophyll (FAPARchl) improve predictions of light-use efficiency and ecosystem photosynthesis for a boreal aspen forest? *Remote Sensing of Environment, 113, 880-888*

HyspIRI Combined “Integrated” Advanced Product for Urban Ecosystems Analysis

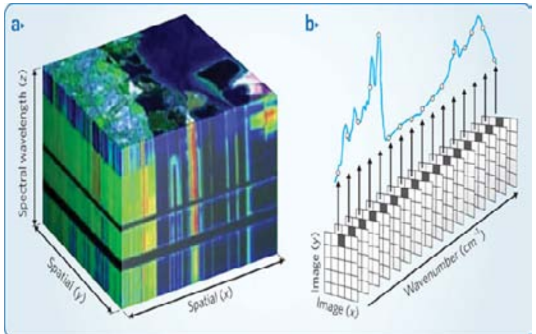

HyspIRI Hyperspectral VSWIR Level II Product
(NDVI, fPAR, surface reflectance characteristics)

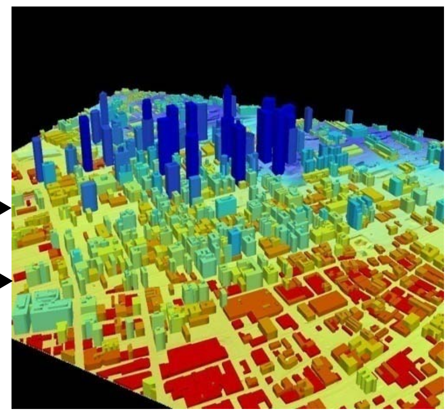

Lidar Data

=

HyspIRI VSWIR/TIR and Lidar composite data set
(X, y, z surface reflectance/thermal interactions of urban ecosystem processes)

HyspIRI TIR multispectral Level II product (8 TIR Bands)
(surface temperature, radiance, [day/night], emissivity)

Dale Quattrochi

JJJoanne Nightingale

HyspIRI Products

Existing Val Methods

Research Required

LPV Focus Group / Product	VSWIR L 2/ 3	VSWIR L4	VSWIR Global	TIR L4	SWIR / TIR
LAND COVER					
Fractional land cover / veg cover					
Disturbance, PFT, hazard susceptibility					
SURFACE RADIATION					
Surface Reflectance					
Albedo					
BIOPHYSICAL					
Gross / Net Primary Production					
fPAR					
LAI					
Water content, LUE, Pigments					
FIRE					
Detection of Fire events					
Fire fuel loads					
LAND SURFACE TEMPERATURE					
LST					
Emissivity					
Evapotranspiration					

Mature & Ready: *Proposed HyspIRI Terrestrial Ecology Products*

(* = Climate Variable; ** = Essential Climate Variables defined by CEOS/GEO)

(Green text items show significant enhancement over existing multi-spectral observations)

VSWIR Imaging Spectrometer ALONE

Level 4 Biophysical & Physiological Products

1 **Directional Canopy Albedo [**]**
2 Fractional Cover: Snow, Water and Ice [**]
3 Leaf Area Index, LAI [**]
4 Canopy fAPAR (PAR absorbed by vegetation) [**]
5 Canopy fAPARchl (PAR absorbed by chlorophyll-containing canopy only) [*]
6 **Total Canopy Chlorophyll Content [*]**
7 **Fractional Cover: Green Vegetation, Non-Photosynthetic Vegetation, impervious surfaces, soil [*]**
8 **Fractional Cover for Vegetation Classes: Coniferous, Deciduous, and Mixed Forests; Grasslands; Wetlands; Crops [*]**

Multi-Spectral TIR Imagery ALONE

Level 2 & 3 Products [Day or Night swath & gridded data] (Terrain corrected; Day/Night Seasonal Composites)

1 Soil Moisture [**]
2 Fire Severity & Direction & Fire Radiative Power [**]
3 Distribution and variation in land surface temperature [*]
4 Water Stress Indicators [*]
5 Emissivity-Based Land Surface Classification (e.g., pervious vs. impervious) [*]
6 Cloud Mask [*]

VSWIR + TIR Combined

Level 4 Combined Products

1 Biomass for Grasslands [**]
2 Diversity, Coastal Habitats [**]
3 Evapotransporation (ET) by Land Cover Type [*]
4 Functional Types/Species Composition [*]
5 Ecological Disturbance Area (logging, natural disasters, etc.) [*]
6 Drought Index (PET/AET) by Land Cover Type [*]

Proposed Terrestrial Ecology Products from HyspIRI

Potential Products Needing Further Validation (* = Climate Variable; ** = ECV defined by CEOS)

(Green text items show significant enhancement over existing multi-spectral observations)

VSWIR Imaging Spectrometer ALONE

Level 4 Biophysical & Physiological Products

1. **Photosynthetic Parameters (LUE, Jmax, Vcmax) [*]**
2. **Environmental Stress Measurements (response variables) [*]**
3. **Canopy N content (mass/area) [*]**
4. **Canopy Water Content [*]**
5. **Vegetation Pigment Content (Chl a, Chl b, Carotenoids, Anthocyanins)**
6. **Canopy Lignin and Cellulose**

Multi-Spectral TIR Imagery ALONE

L3 Products [Day or Night swath & gridded data]

1. Burn Area (experimental as TIR only)
2. Burn Severity (experimental as TIR only)

VSWIR + TIR Combined

L4 Products – Regional

1. **Surface Energy Flux [**]**
2. **Combusted Biomass [**]**
3. **Sensible Heat due to Urban Heat Islands (Anthropogenic Heat) [*]**
4. **LST: Day/Night Differences for Ecosystems & Urban Areas [*]**
5. **LST Urban/Suburban [*]**
6. **LST by Functional Groups and Ecosystem Types [*]**
7. **Surface Topographic Temperature Mapping [*]**

L4 Products – Global

1. **LST & Emissions by Fractional Land Cover (Vegetation, Soil, Water, Snow, Ice, etc.) [**]**
2. **Ecosystem/Crop Phenology with Fusion Approaches [*]**

The EO-1 Project is supporting HyspIRI:

1] with Hyperion Prototype Products;

2] with Technology development & Advances

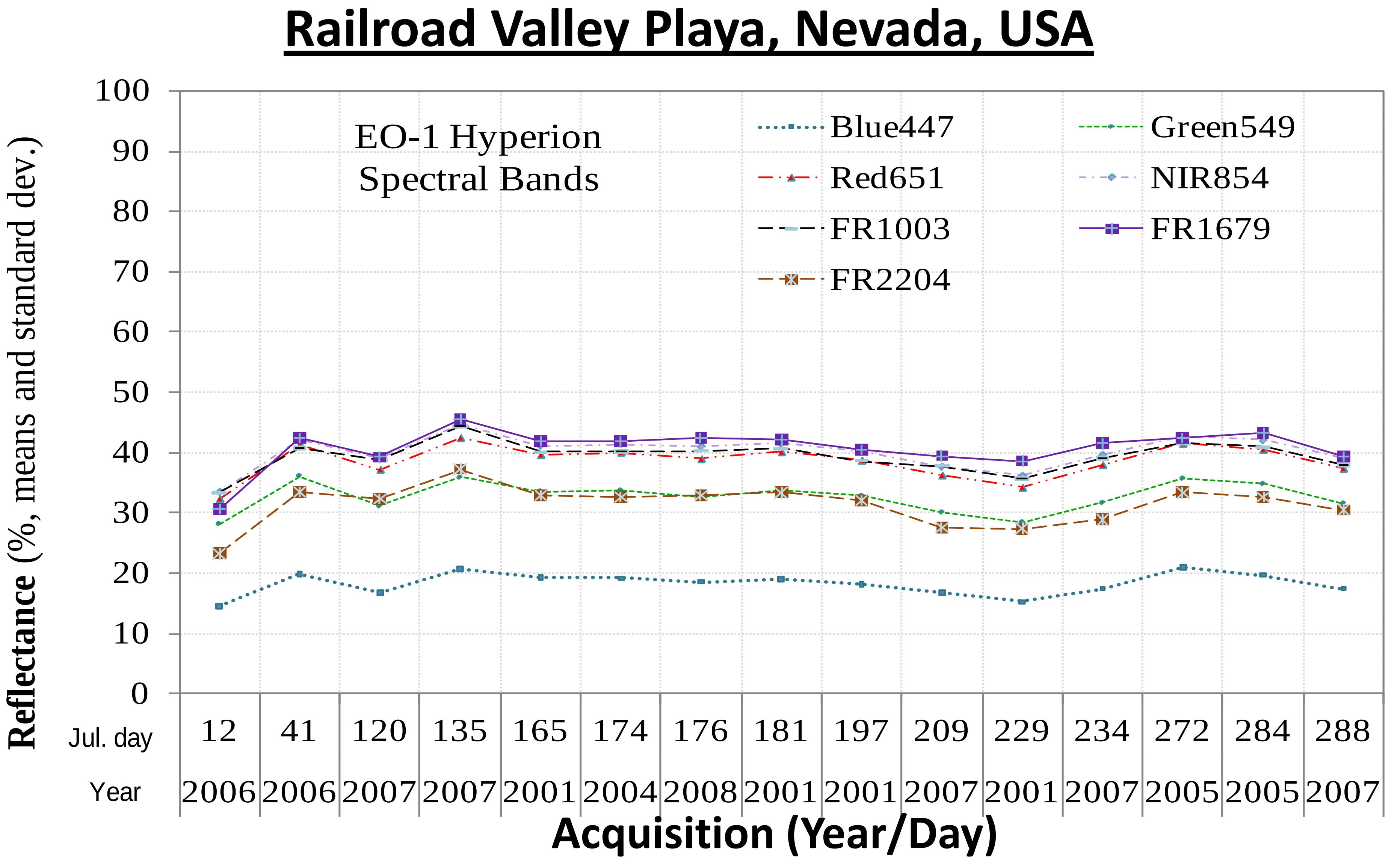

Railroad Valley Playa, Nevada, USA
EO-1 Hyperion
Spectral Bands
Blue447
Green549
Red651
NIR854
FR1003
FR1679
FR2204
Reflectance (%, means and standard dev.)
100
90
80
70
60
50
40
30
20
10
0
Jul. day
12
41
120
135
165
174
176
181
197
209
229
234
272
284
288
Year
2006
2006
2007
2007
2001
2004
2008
2001
2001
2007
2001
2007
2005
2005
2007
Acquisition (Year/Day)

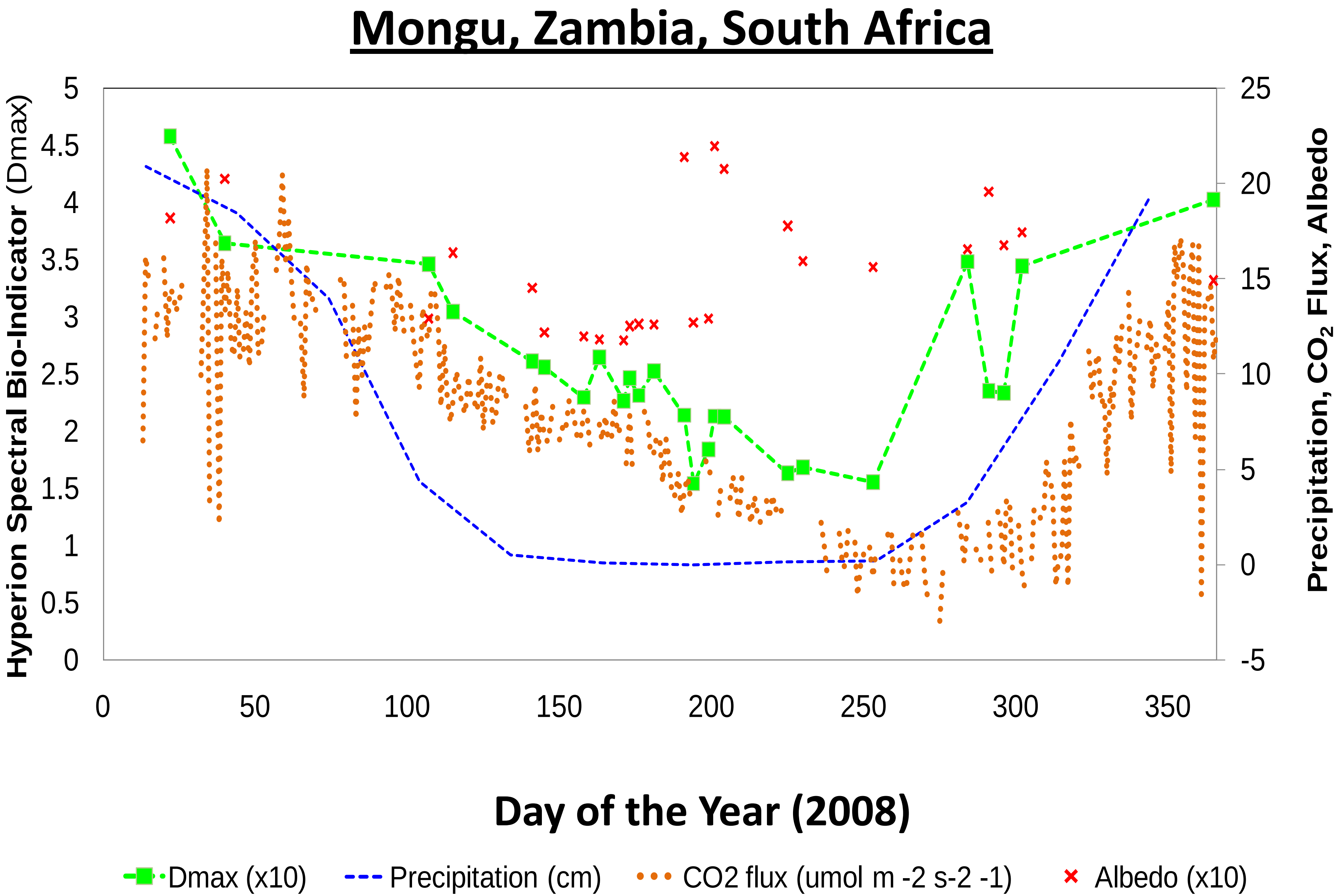

Mongu, Zambia, South Africa
Hyperion Spectral Bio-Indicator (Dmax)
Precipitation, CO_2 Flux, Albedo
5
4.5
4
3.5
3
2.5
2
1.5
1
0.5
0
25
20
15
10
5
0
-5
0
50
100
150
200
250
300
350
Day of the Year (2008)
Dmax (x10)
Precipitation (cm)
CO2 flux (umol m -2 s-2 -1)
Albedo (x10)

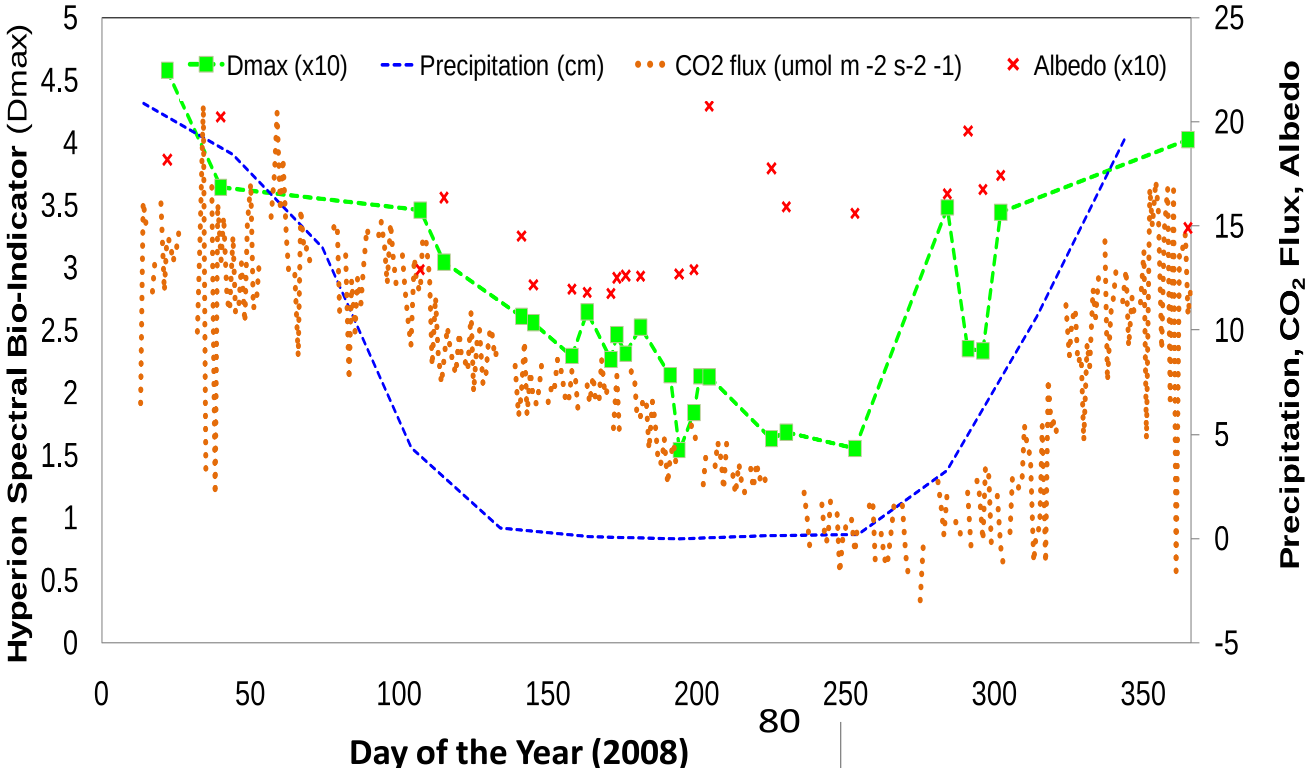

Mongu, Zambia
South Africa

Mongu, Konza, Duke, Barrow

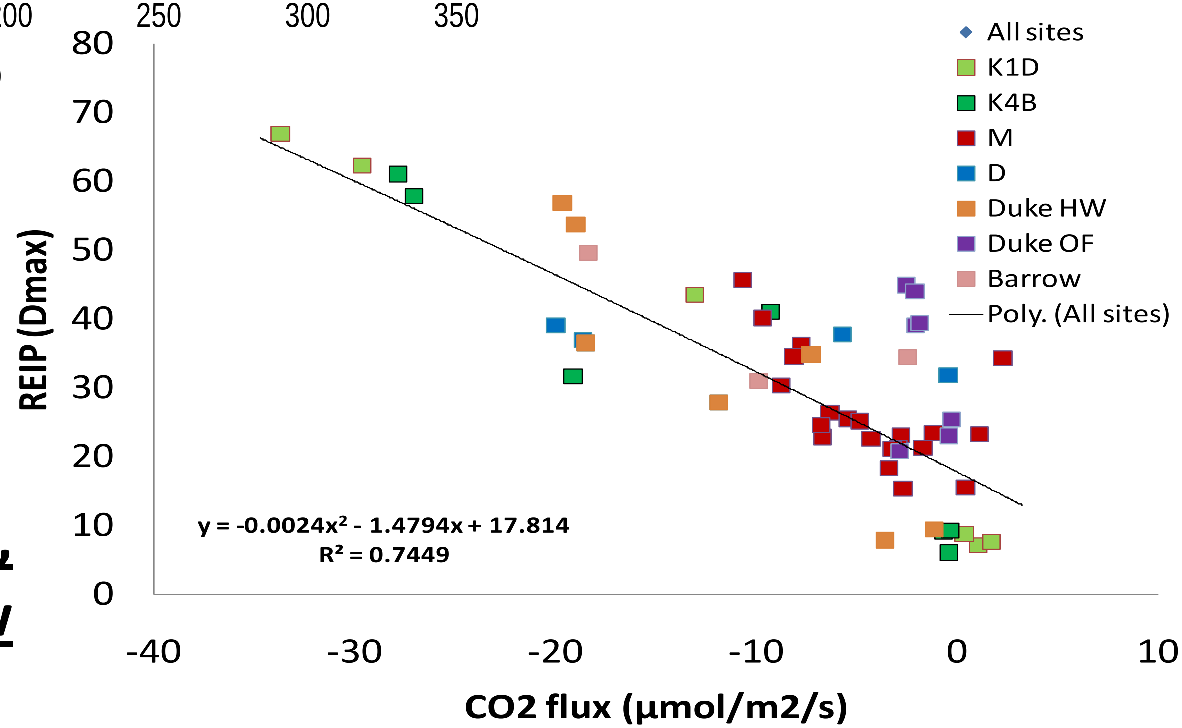

Earth Observing-1
10th anniversary

EO-1 Science Validation Meeting and an Evening of Celebration

The events will take place at NASA/GSFC, Greenbelt, MD
November 30 to December 2, 2010

Next GSFC Hosted Symosium
May 2011

Topics??

New Technology Developments– IPM, Low Latency?

More on Ecosystem Products– for Regional & Global?

Other Products?   Urban, Agriculture, Thermal Features & Events?

IPCC Climate Change 2007: Working

The Physical Science Basis

Chapter 7: Couplings Between Changes in the Climate System and Biogeochemistry: Executive Summary

The Land Surface and Climate

• Changes in the land surface (vegetation, soils, water) resulting from human activities can affect regional climate through shifts in radiation, cloudiness and surface temperature.

- ➢Changes in vegetation cover affect surface energy and water balances at the regional scale, from boreal to tropical forests.

- ➢The impact of land use change on the energy and water balance may be very significant for climate at regional scales over time periods of decades or longer.

Land Carbon. Understanding land carbon storage is a critical factor in predicting the growth of atmospheric CO_2 and subsequent global climate change. P. 273 , DS.

Susan Ustin

IPCC Climate Change 2007: Working The Physical Science Basis

2.5.8 Effects of Carbon Dioxide Changes on Climate via Plant Physiology: ‘Physiological Forcing’

Radiative Forcing and Physiological Forcing

Interactions bertween water and carbon

Spatial and temporal patterns of carbon and water vapor fluxes, Sky Oaks, CA

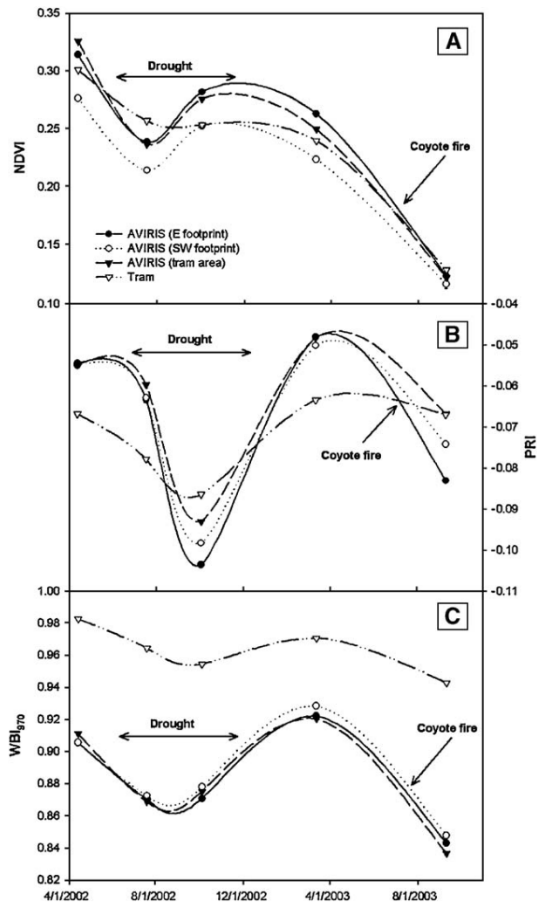

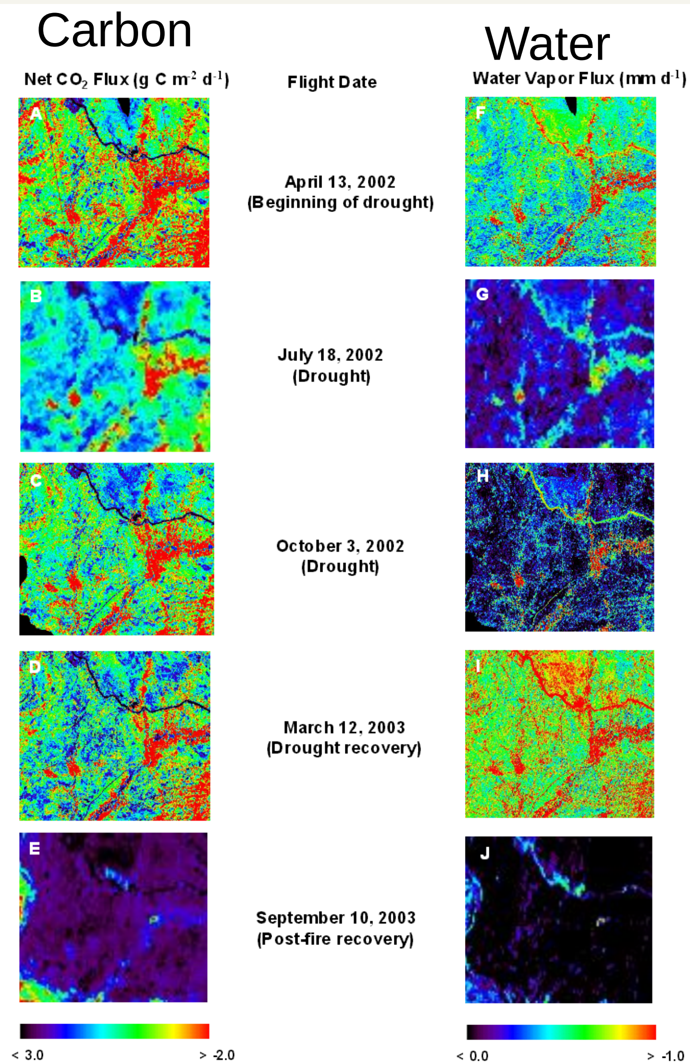

Susan Ustin

Fuentes et al. 2006

HyspIRI: Instruments, Platform, Observations

Rob Green (JPL)
Simon Hook (JPL)
Bogdan Oaida (JPL)
Bob Knox (GSFC)

HyspIRI - Imaging Spectroscopy (VSWIR) Science Measurements

Rob Green

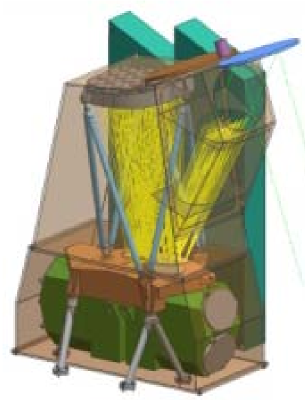

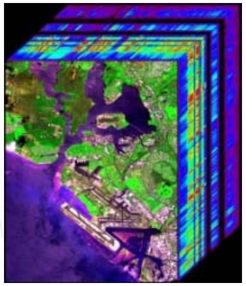

Mature Instrument concept: All components have flown in space.

Imaging spectrometer: 55kg / 41W

Schedule: 4 year phase A-D, 3 years operations (5 years consumables)

Full terrestrial coverage downlinked every 19 days

VQ1. Pattern and Spatial Distribution of Ecosystems and their Components

– What is the pattern of ecosystem distribution and how do ecosystems differ in their composition or biodiversity?

VQ2. Ecosystem Function, Physiology and Seasonal Activity

– What are the seasonal expressions and cycles for terrestrial and aquatic ecosystems, functional groups and diagnostic species? How are these being altered by changes in climate, land use, and disturbances?

VQ3. Biogeochemical Cycles

– How are biogeochemical cycles for carbon, water and nutrients being altered by natural and human-induced environmental changes?

VQ4. Changes in Disturbance Activity

– How are disturbance regimes changing and how do these changes affect the ecosystem processes that support life on Earth?

VQ5. Ecosystem and Human Health

– How do changes in ecosystem composition and function affect human health, resource use, and resource management?

VQ6. Land Surface and Shallow Water Substrate Composition

– What is the land surface soil/rock and shallow water substrate composition?

Measurement:

- 380 to 2500 nm at 10 nm
- Accurate 60 m resolution
- 19 days equatorial revisit
- Global land and shallow water

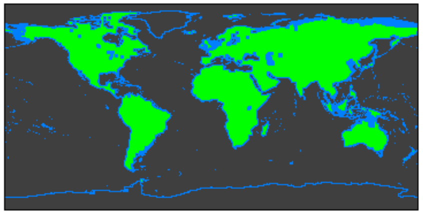

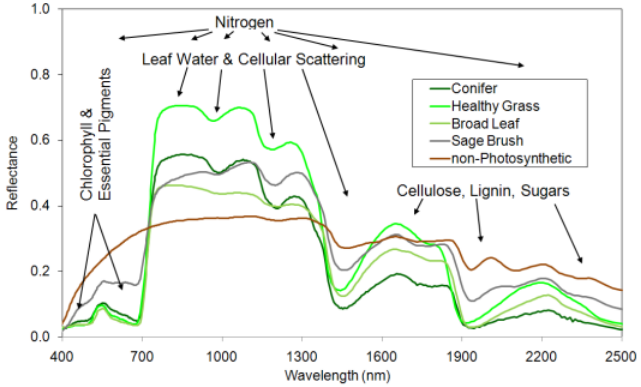

Map of dominant tree species, Bartlett Forest, NH

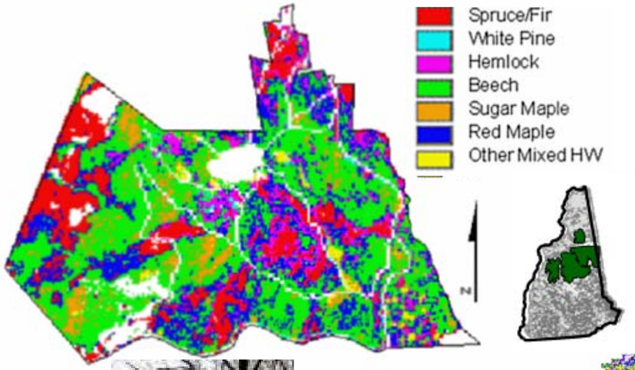

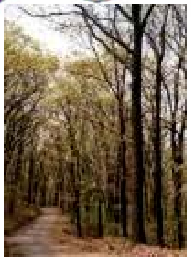

Soil C:N Ratio

White Mountain National Forest, NH

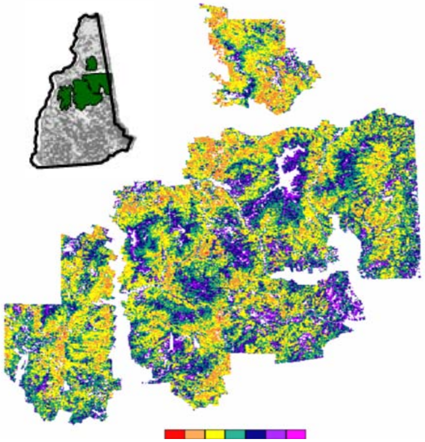

HyspIRI Thermal Infrared Multispectral (TIR) Science Measurements

Simon Hook

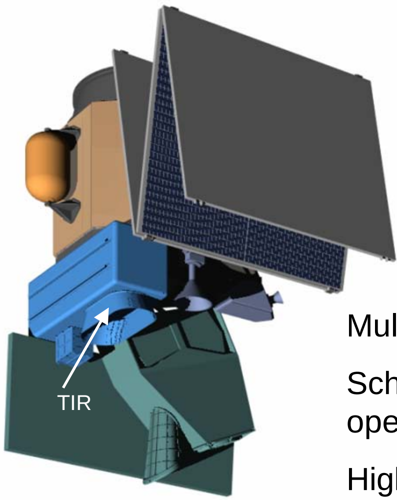

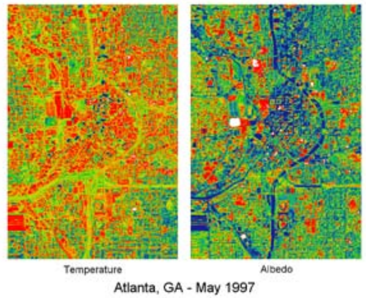

Multispectral Scanner

Schedule: 4 year phase A-D, 3 years operations

High Heritage

Science Questions:

TQ1. Volcanoes/Earthquakes (MA,FF)

– How can we help predict and mitigate earthquake and volcanic hazards through detection of transient thermal phenomena?

• TQ2. Wildfires (LG,DR)

– What is the impact of global biomass burning on the terrestrial biosphere and atmosphere, and how is this impact changing over time?

• TQ3. Water Use and Availability, (MA,RA)

– How is consumptive use of global freshwater supplies responding to changes in climate and demand, and what are the implications for sustainable management of water resources?

• TQ4. Urbanization/Human Health, (DQ,GG)

– How does urbanization affect the local, regional and global environment? Can we characterize this effect to help mitigate its impact on human health and welfare?

• TQ5. Earth surface composition and change, (AP,JC)

– What is the composition and temperature of the exposed surface of the Earth? How do these factors change over time and affect land use and habitability?

Measurement:

- 7 bands between 7.5-12 µm and 1 band at 4 µm
- 60 m resolution, 5 days revisit
- Global land and shallow water

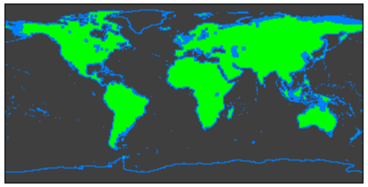

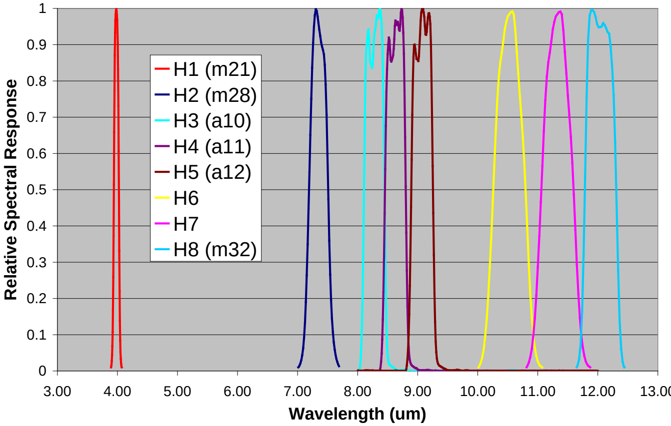

Andean volcano heats up

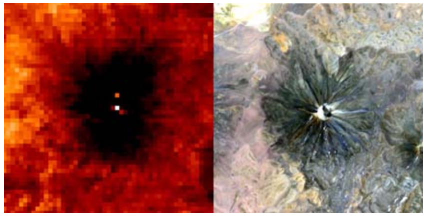

Urbanization

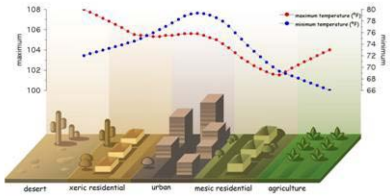

Volcanoes

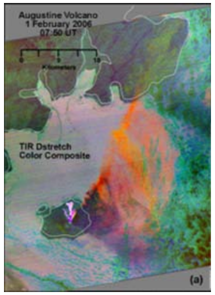

Water Use and Availability

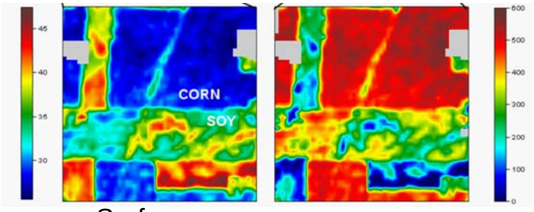

Surface Temperature

Evapotranspiration

Bogdan Oaida

Launch Vehicle Concept

- Taurus 3210 can meet the mission needs
  - Closest fit among currently NASA approved launchers
  - 30% margin (dry-mass CBE) with a Taurus-class launch vehicle
  - Fits dynamic volume envelope
  - 790 Kg launch capacity for HyspIRI Orbit
- Launch window
  - Mapping orbit reachable once per day

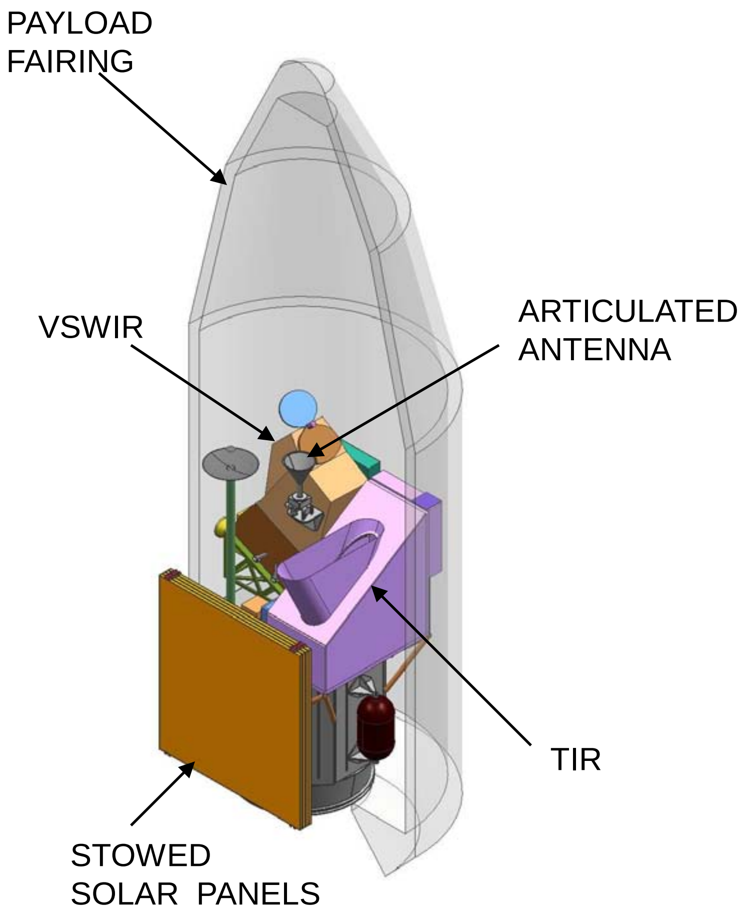

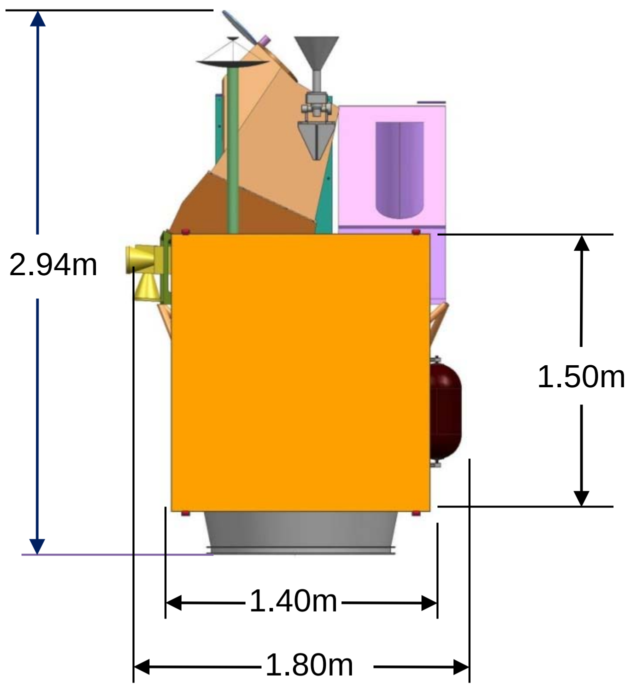

Proposed VSWIR and TIR Products

Phil Townsend (U WI)
John Gamon (U Alberta)
Anatoly Gitelson (U NE)
Mary Martin (U NH)
Qingyuan Zhang (GSFC)/Ben Cheng (GSFC)
Simon Hook (JPL)
Martha Anderson (USDA-Beltsville)
Susan Ustin (U California-Davis)

Phil Townsend

Examples: LMA – based on hypothesized relationships

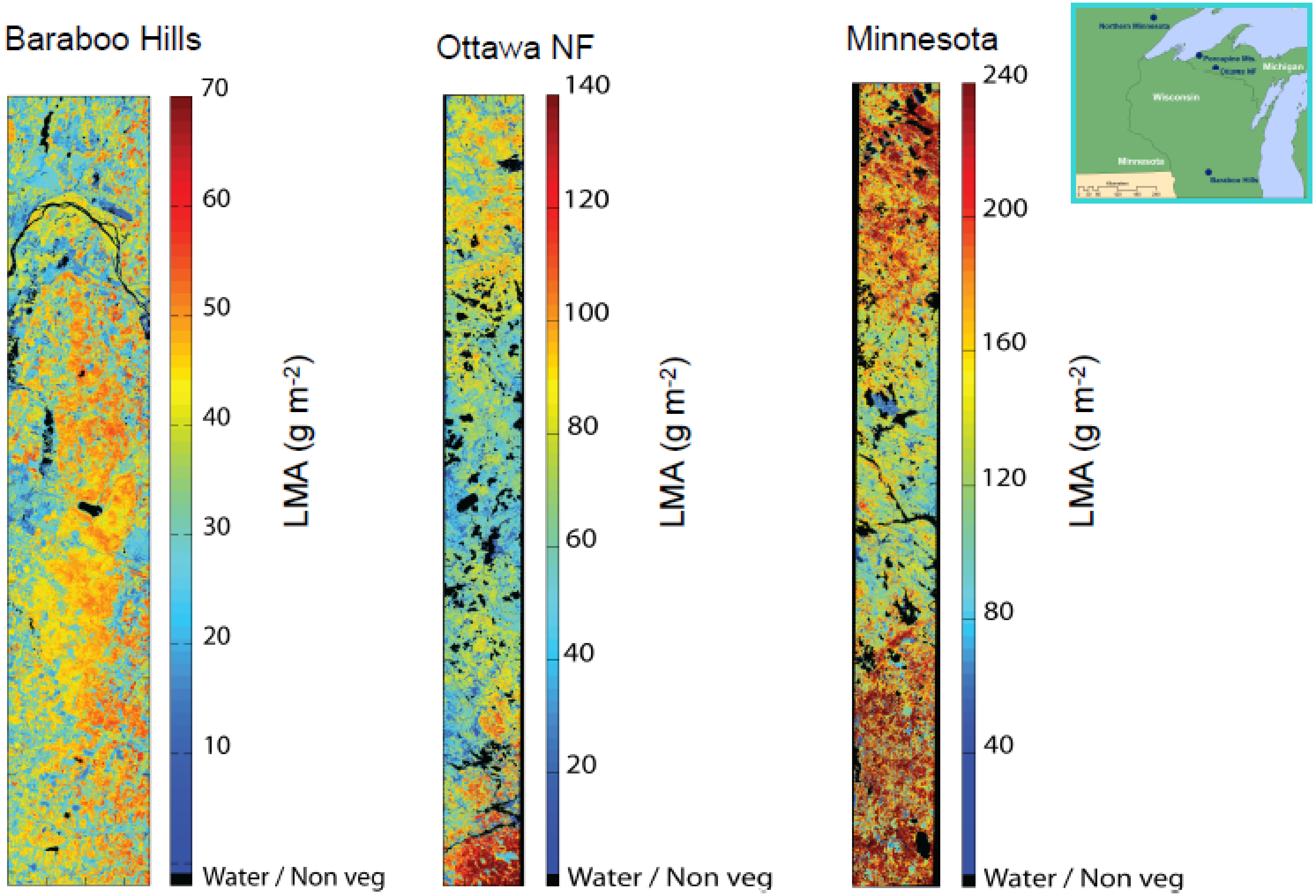

An operational PRI product could improve ecosystem carbon flux estimates, capturing physiological change under disturbance, stress, and changing vegetation composition

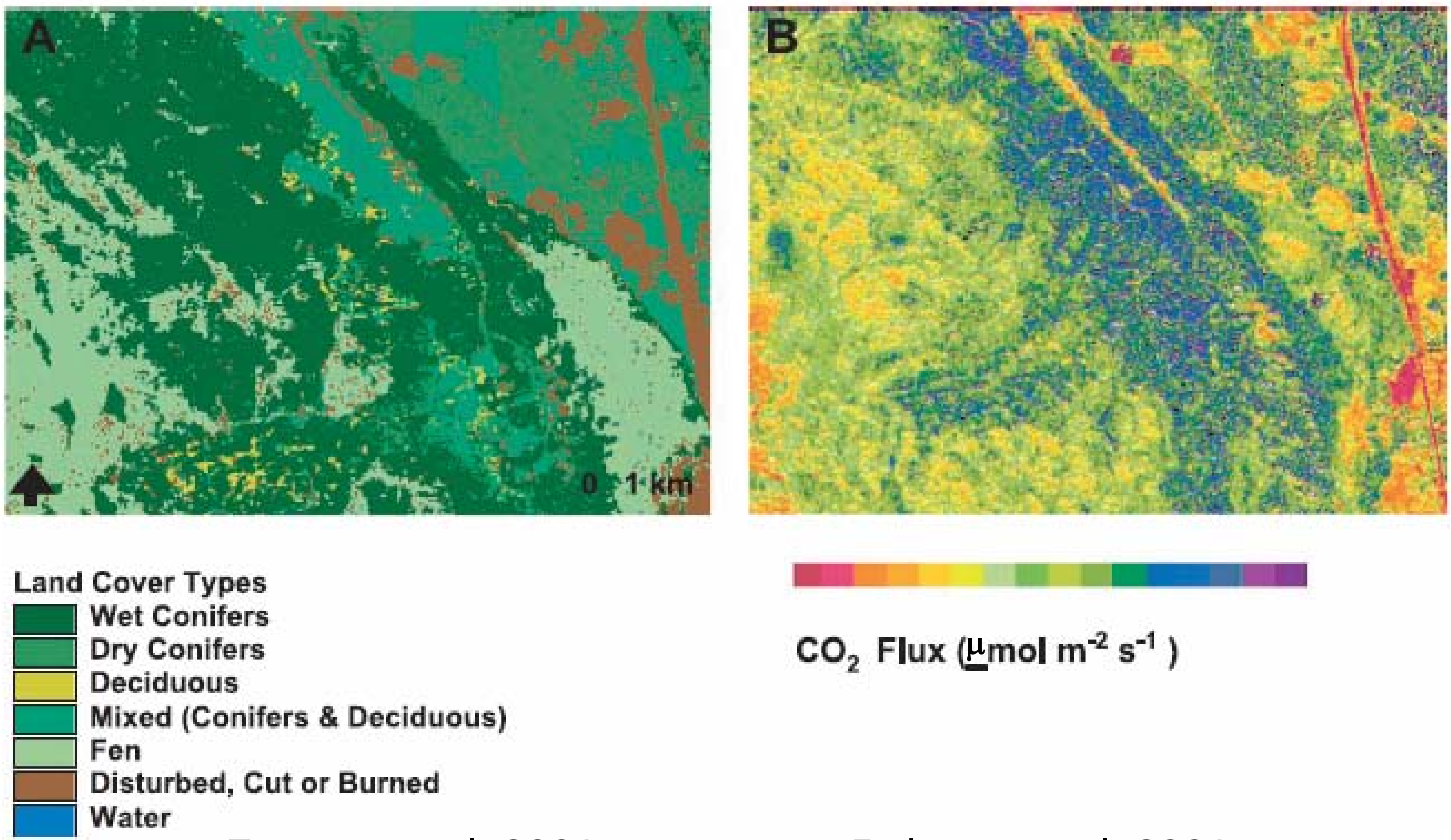

Fuentes et al. 2001 Rahman et al. 2001

John Gamon

GPP estimation via Chl

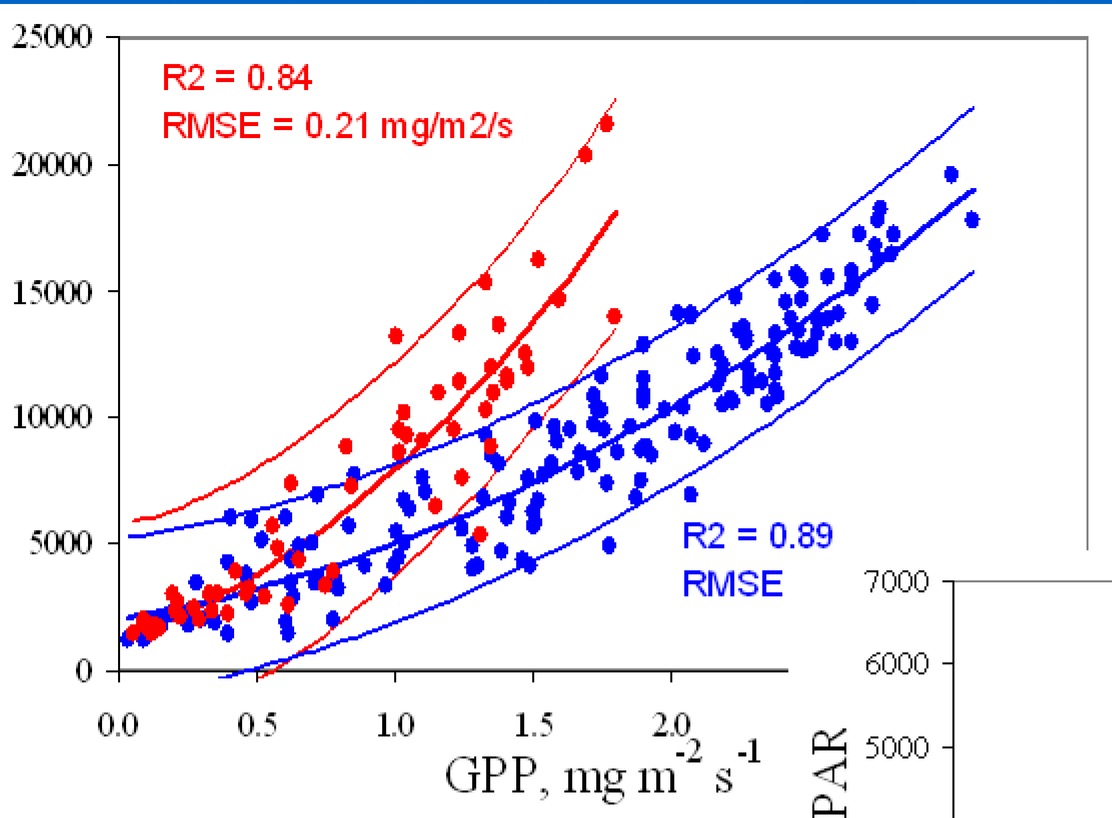

Maize
Soybeans

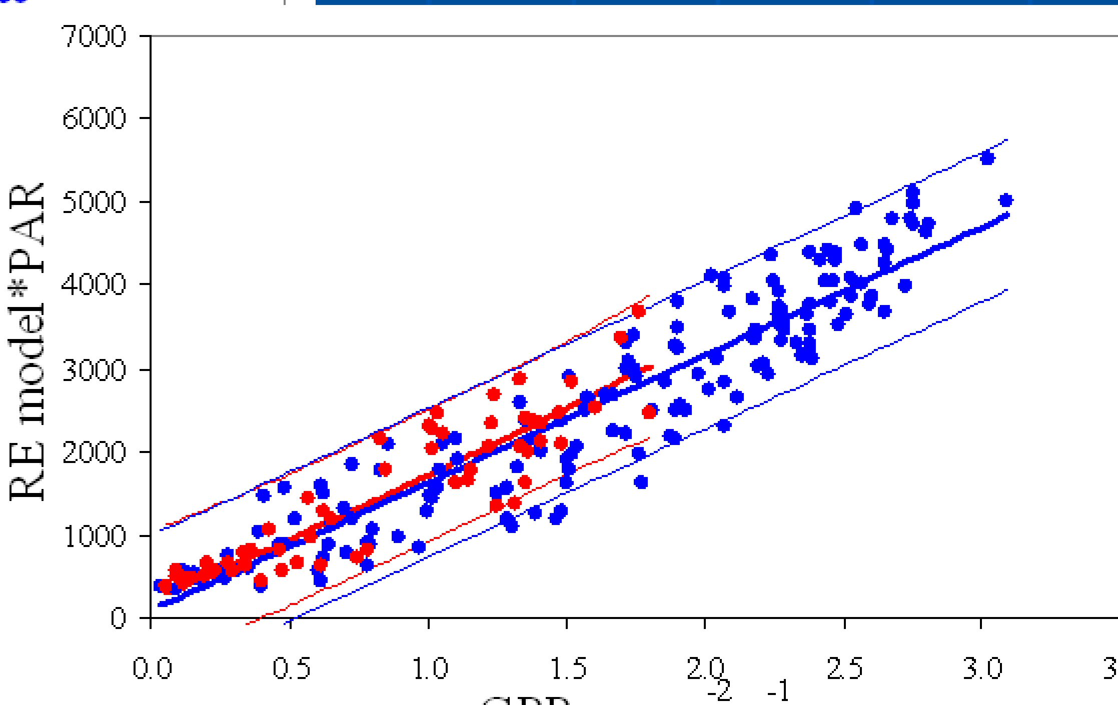

natoly Gitelson

AVIRIS-Predicted Foliar Chemistry Used to Estimate Soil Nitrogen Cycling

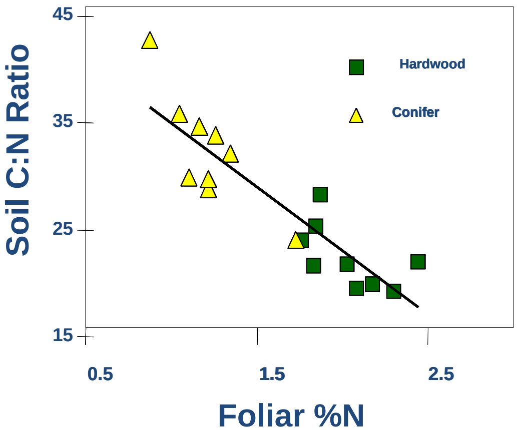

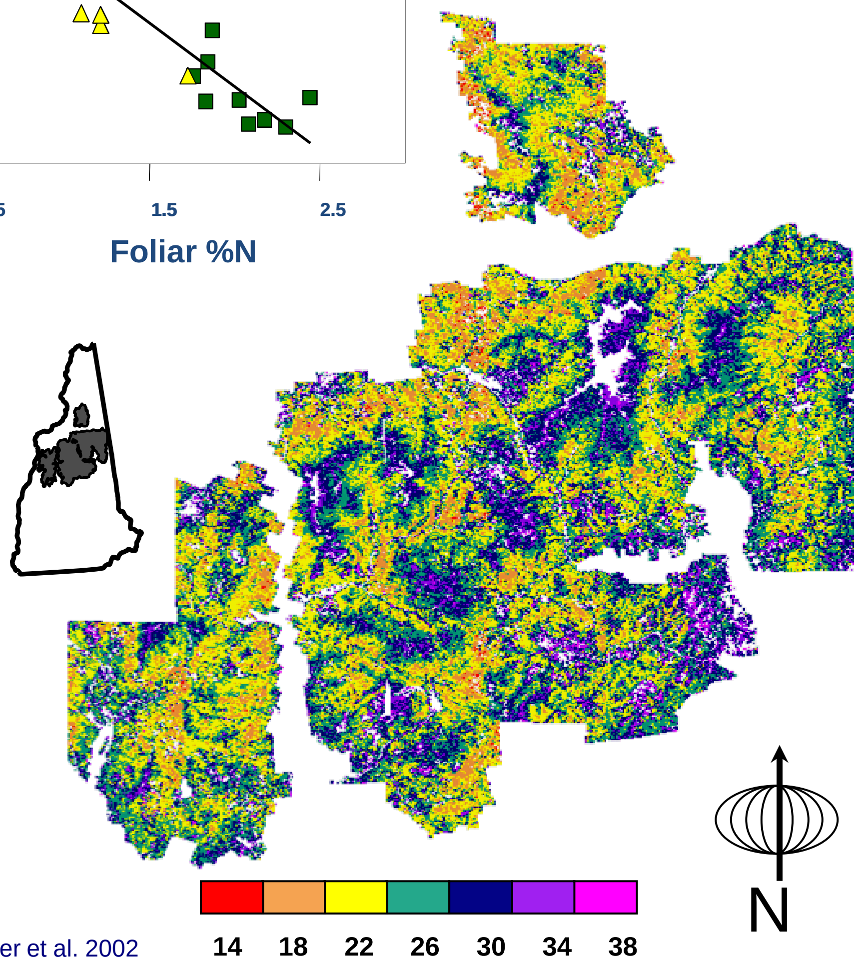

Ollinger et al. 2002

Predicted C:N versus Stream DOC

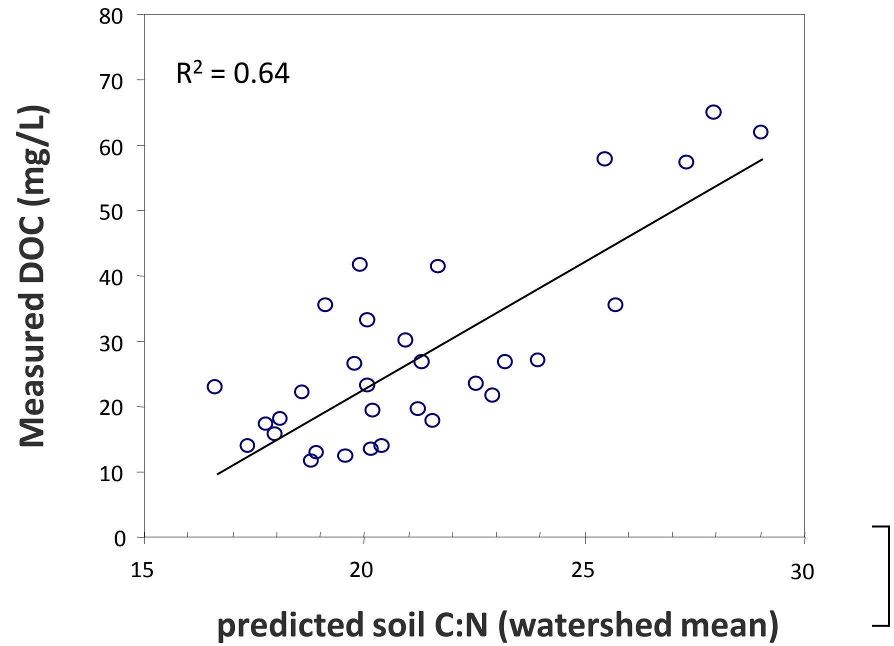

Mary Martin

Mary– her slide #5 Canopy N, Amax, and albedo…..

Death Valley - Mean Summer Emissivity - Band 10 (8.3μm)

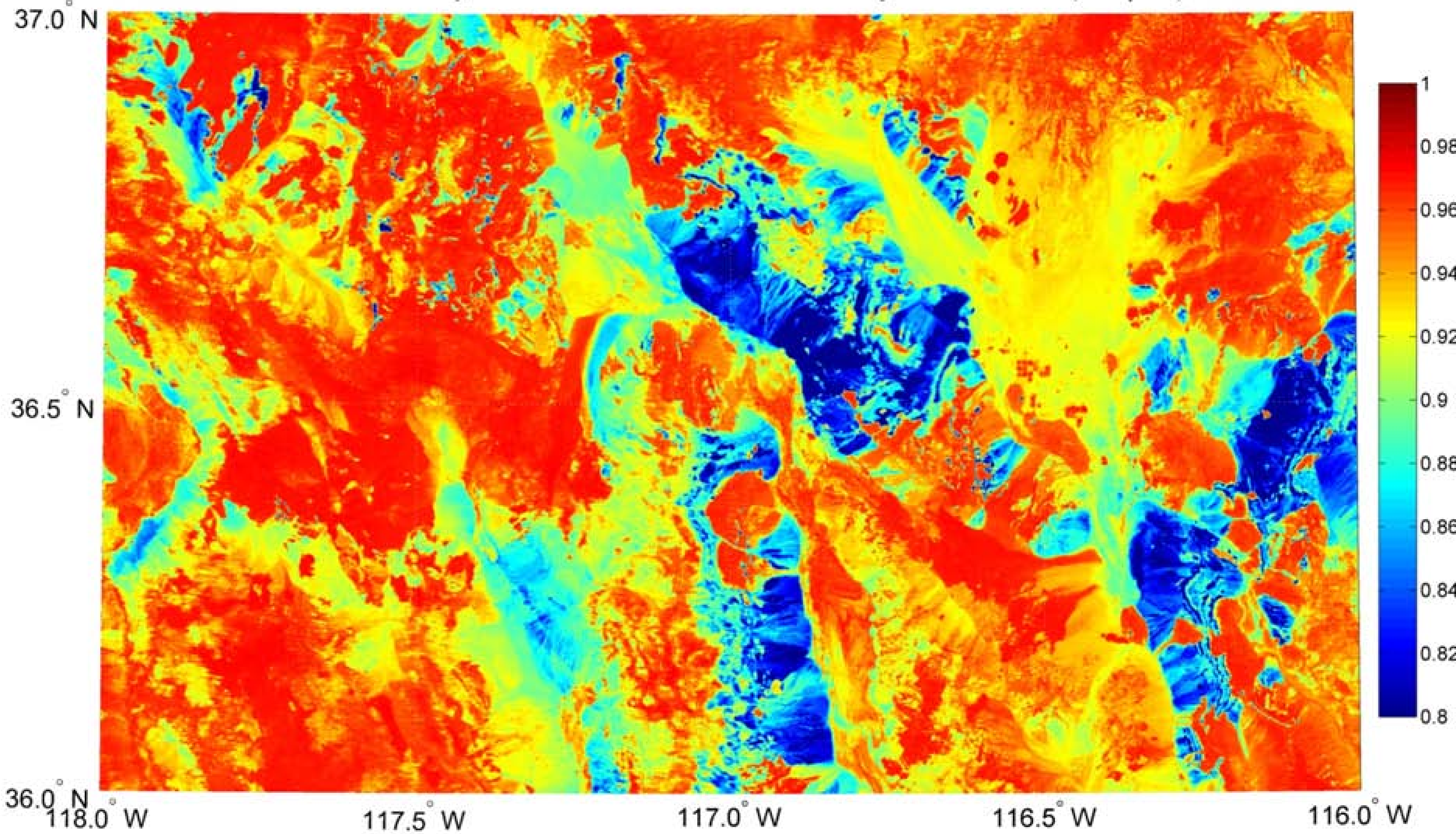

Simon Hook

Evapotranspiration: FORT PECK, MONTANA

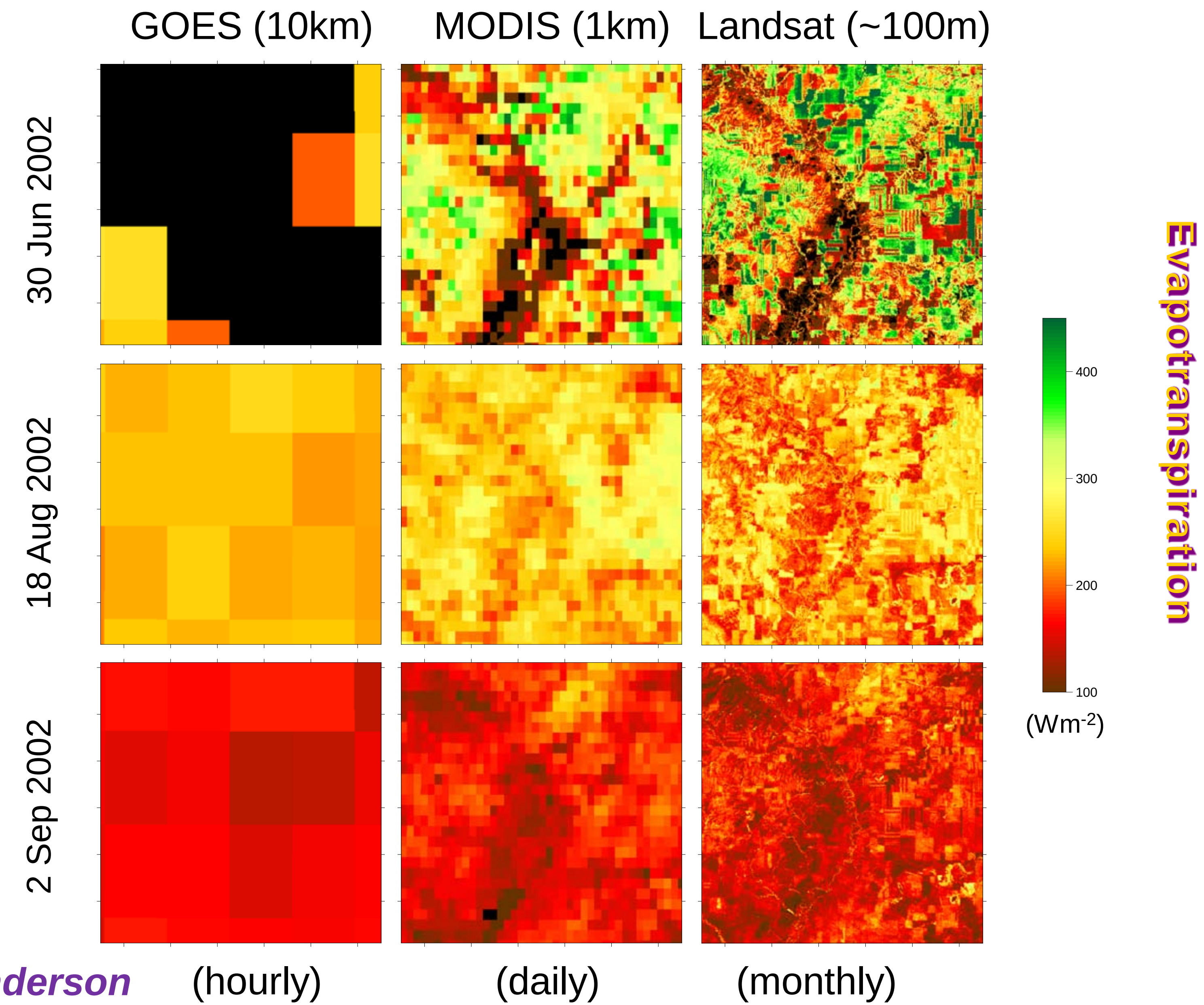

Martha Anderson

GOES/MODIS/Landsat FUSION

Martha Anderson

Daily Evapotranspiration – Reedy Lake, FL, 2002

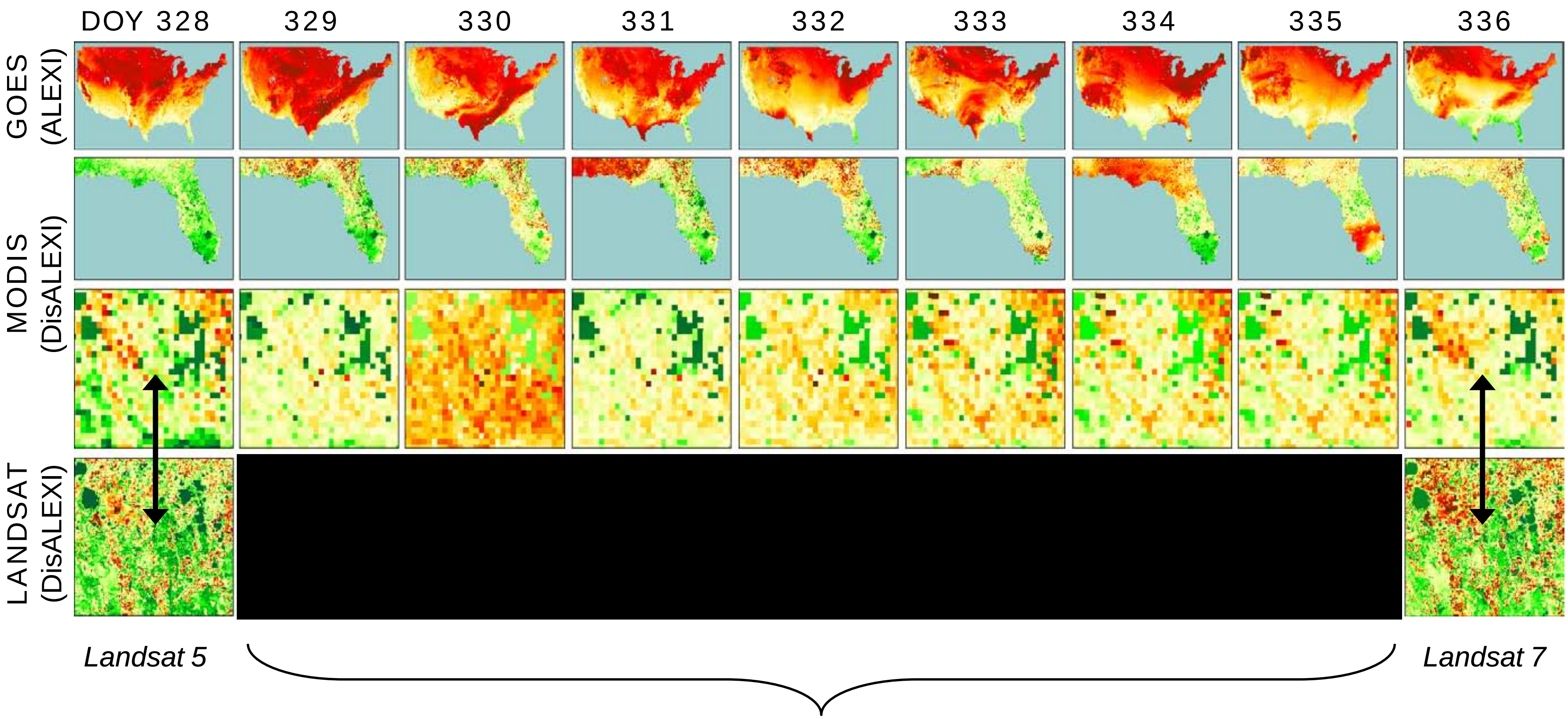

Spatial Temporal Adaptive Reflectance Fusion Model (STARFM) *(Gao et al, 2006)*

SMA Endmember Fraction Map Tracks Phenological Changes

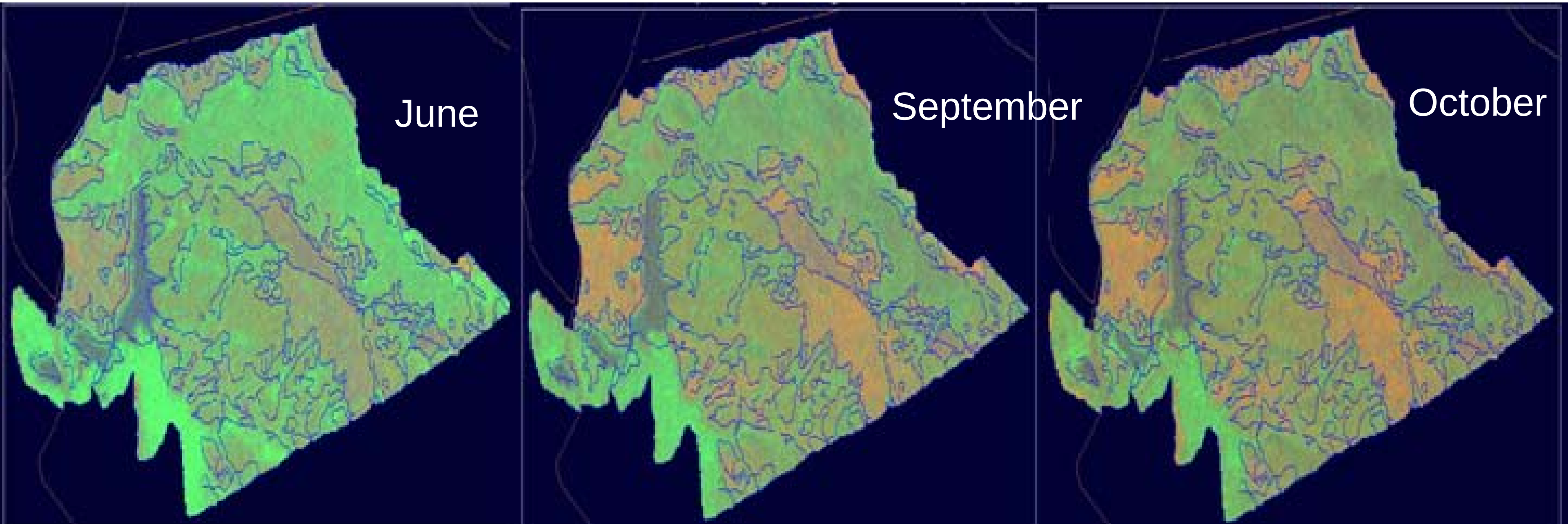

Endmembers:
Green vegetation
Dry vegetation
Soil

Independent Vegetation Map

Deciduous Forest
Mixed Evergreen Forest
Chaparral
Greenstone Grassland
Serpentine Grassland
Wetland
Lake

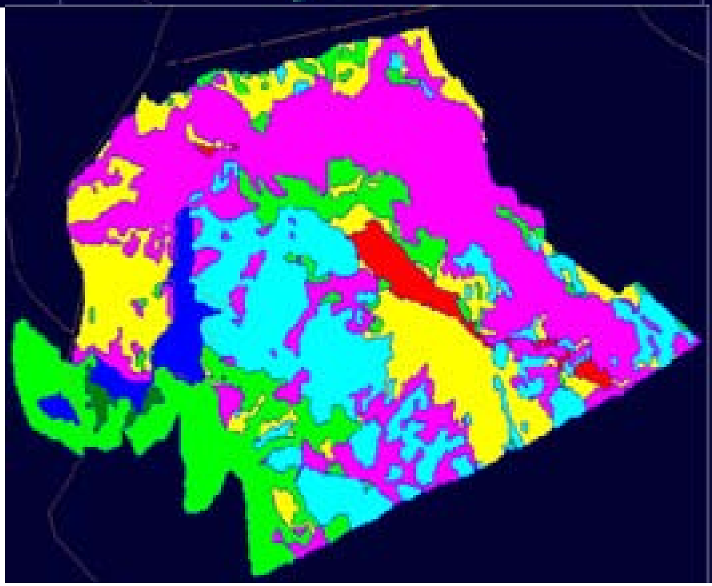

Susan Ustin

Ustin et al., 1999

Factors Affecting Product Integrity & Availability

Bo-Cai Gao (NRL)/Rob Green (JPL)
Tom Flately (GSFC)
Dan Mandl (GSFC)
Steve Chien (JPL)
Petya Campbell (GSFC)
Fred Huemmrich (GSFC)
Joanne Nightingale (GSFC)
Steve Ungar (GSFC)

Glint Removal Using AVIRIS Data Over Kaneohe Bay, HI

Bo-Cai Gao

Before

After

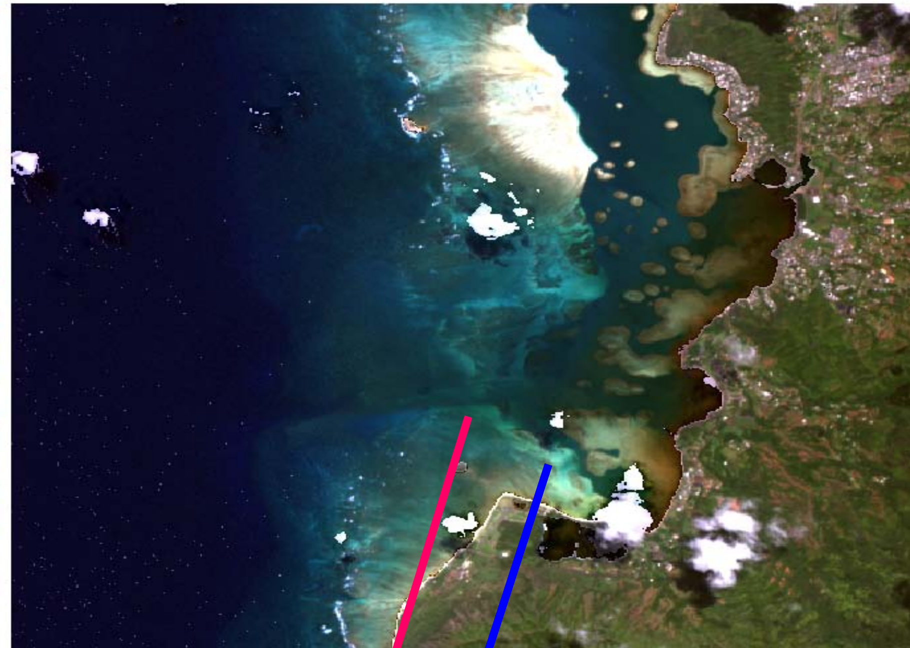

Sample Radiance Spectra

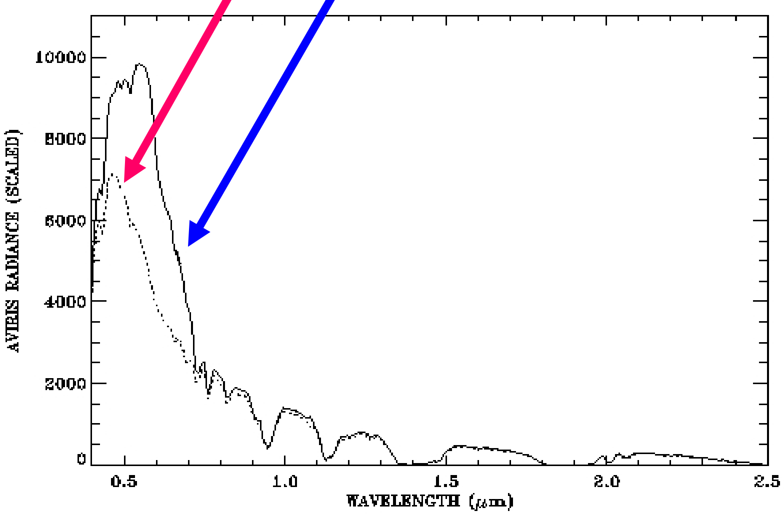

Sample Derived Reflectance Spectra

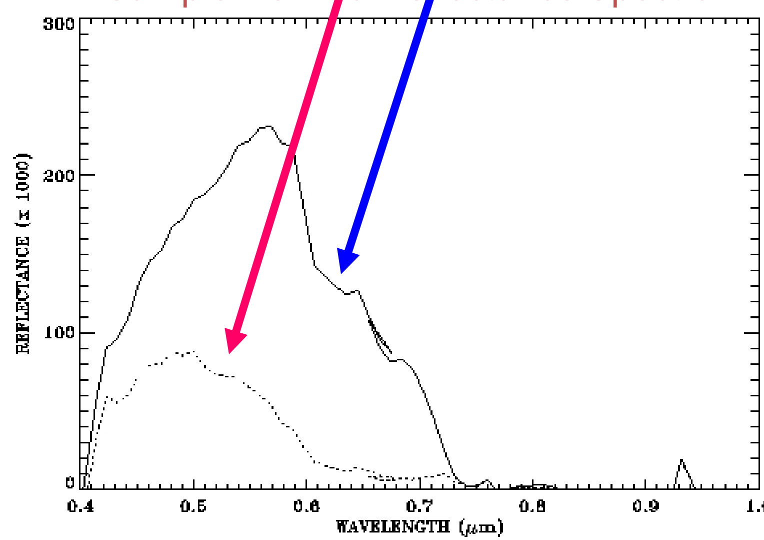

Tom Flately

Space Cube: On-Board Data Reduction

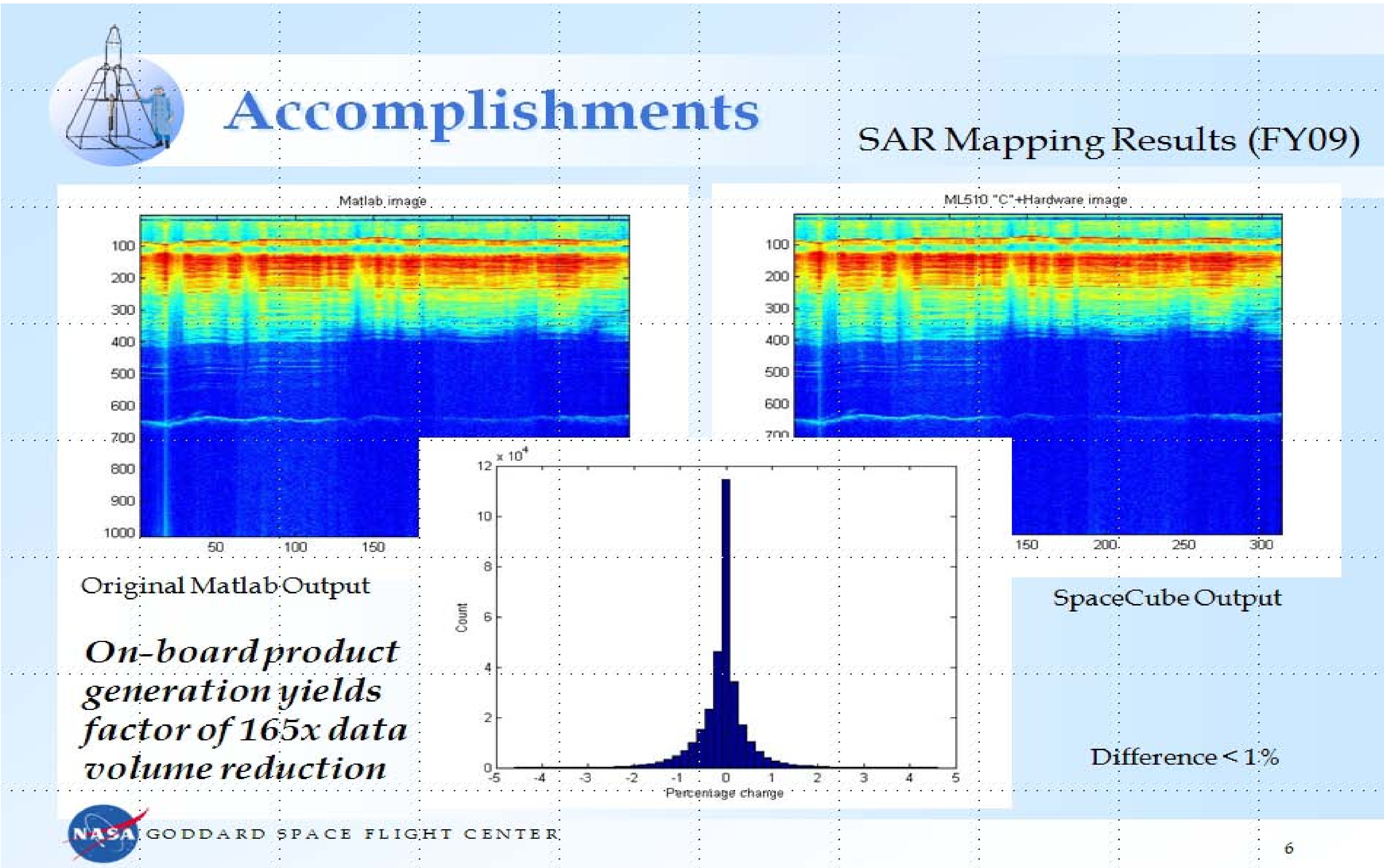

HyspIRI Data Flow

Dan Mandl

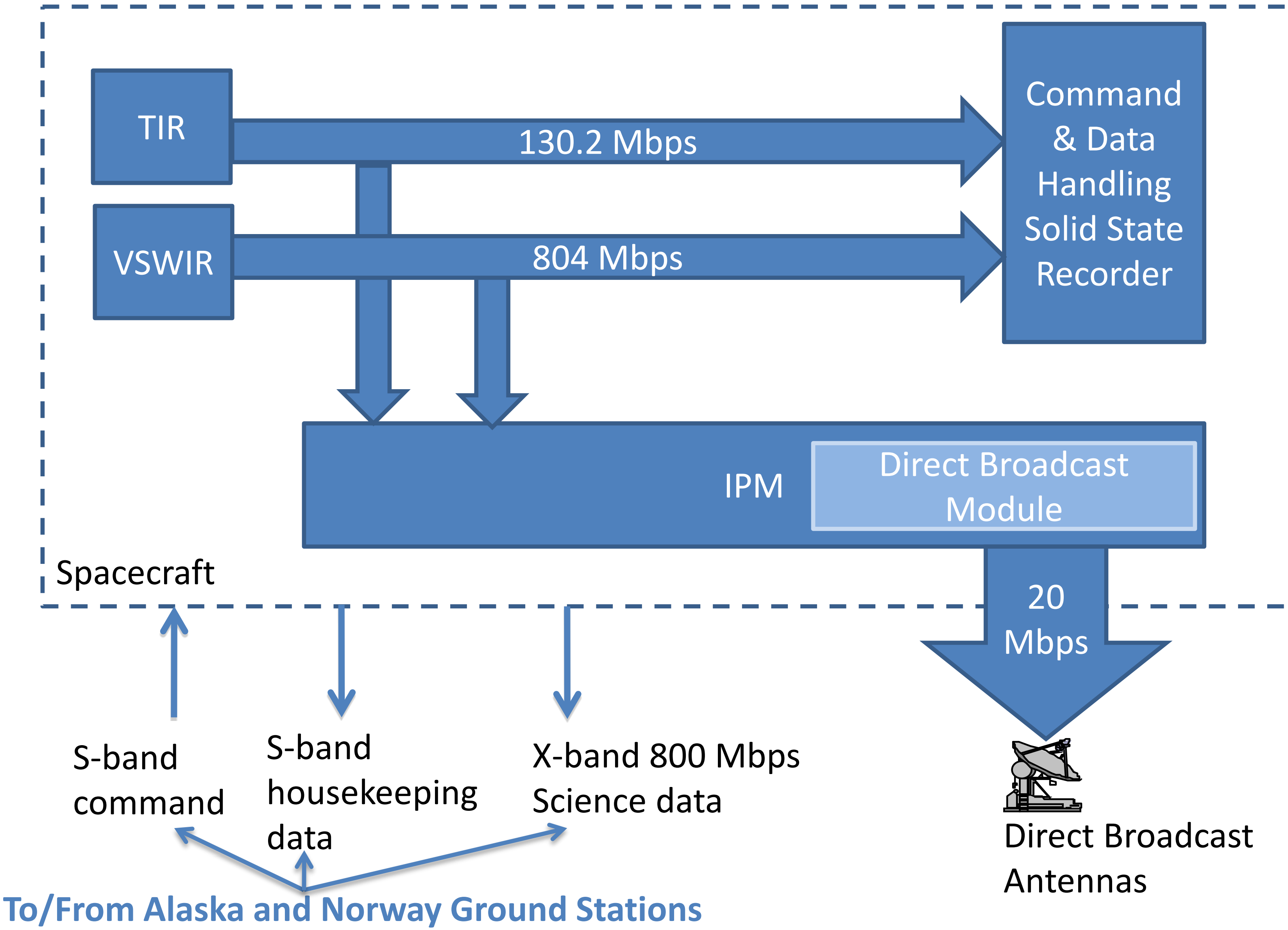

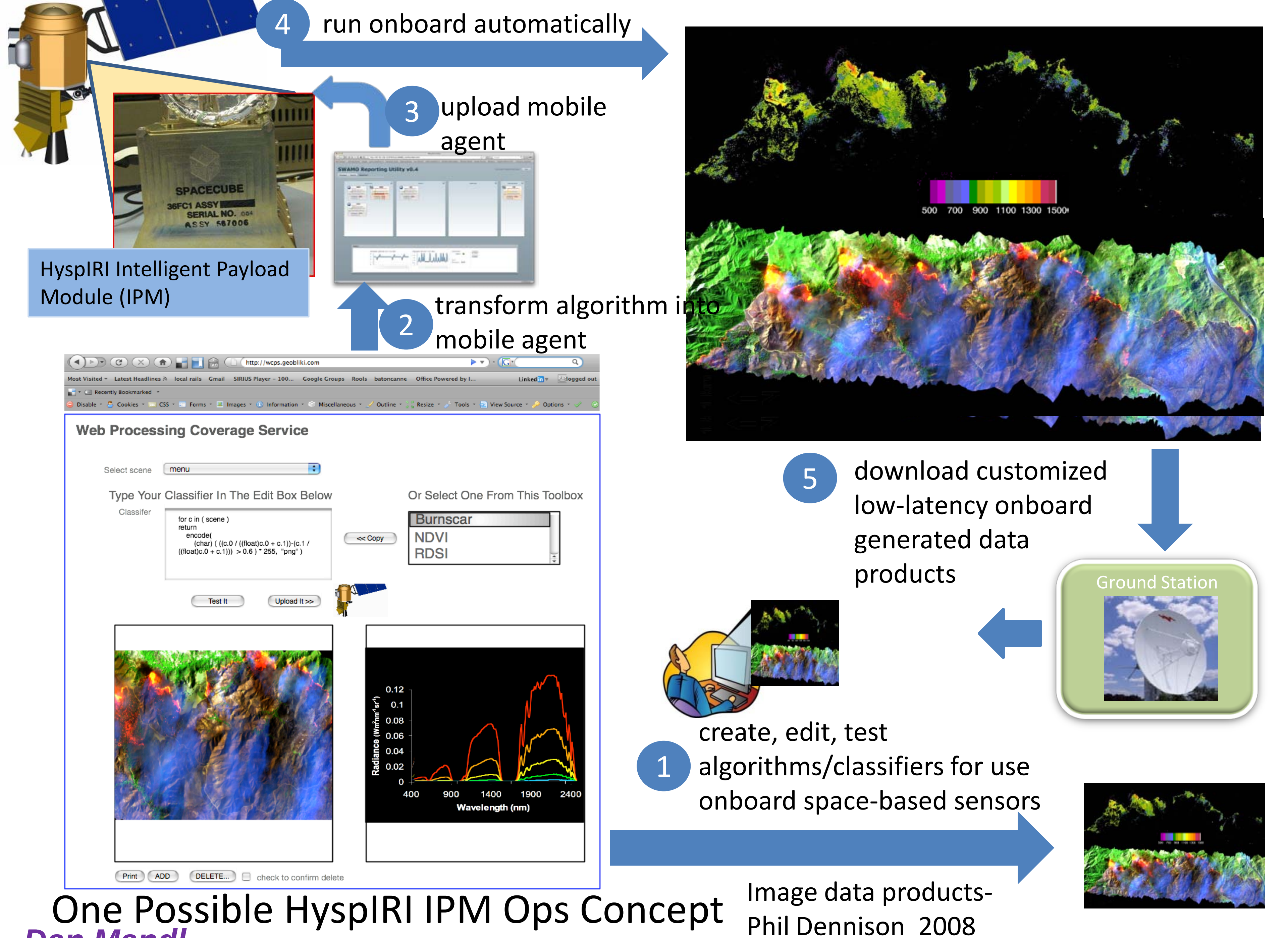

One Possible HyspIRI IPM Ops Concept

Dan Mandl

Rapid Data delivery:
02 May 2010 Hyperion Imagery

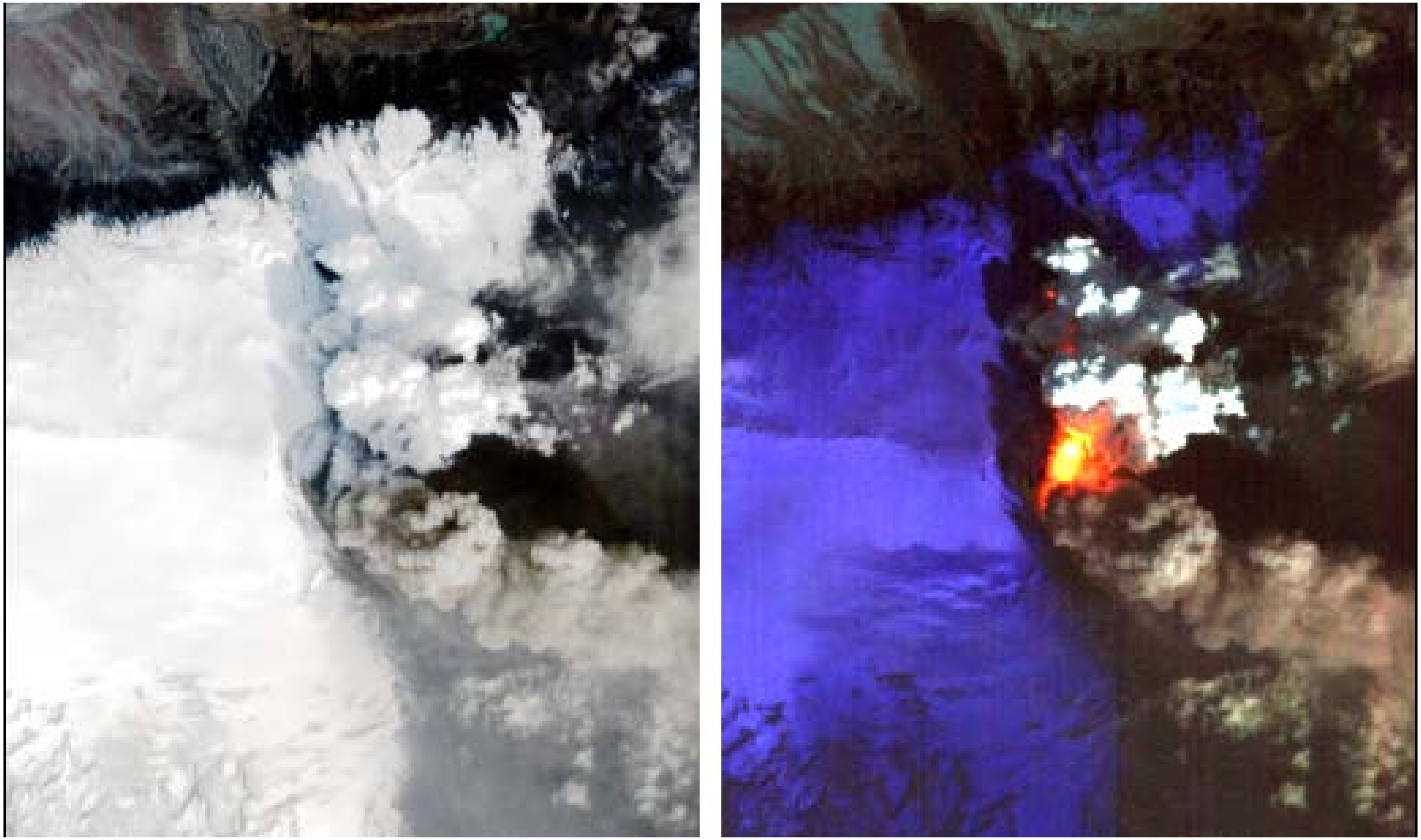

Left – True color   Right - thermal false color
Image courtesy EO-1 Mission/GSFC, Volcano Sensorweb/JPL A. Davies

Steve Chien

HyspIRI DB Concept

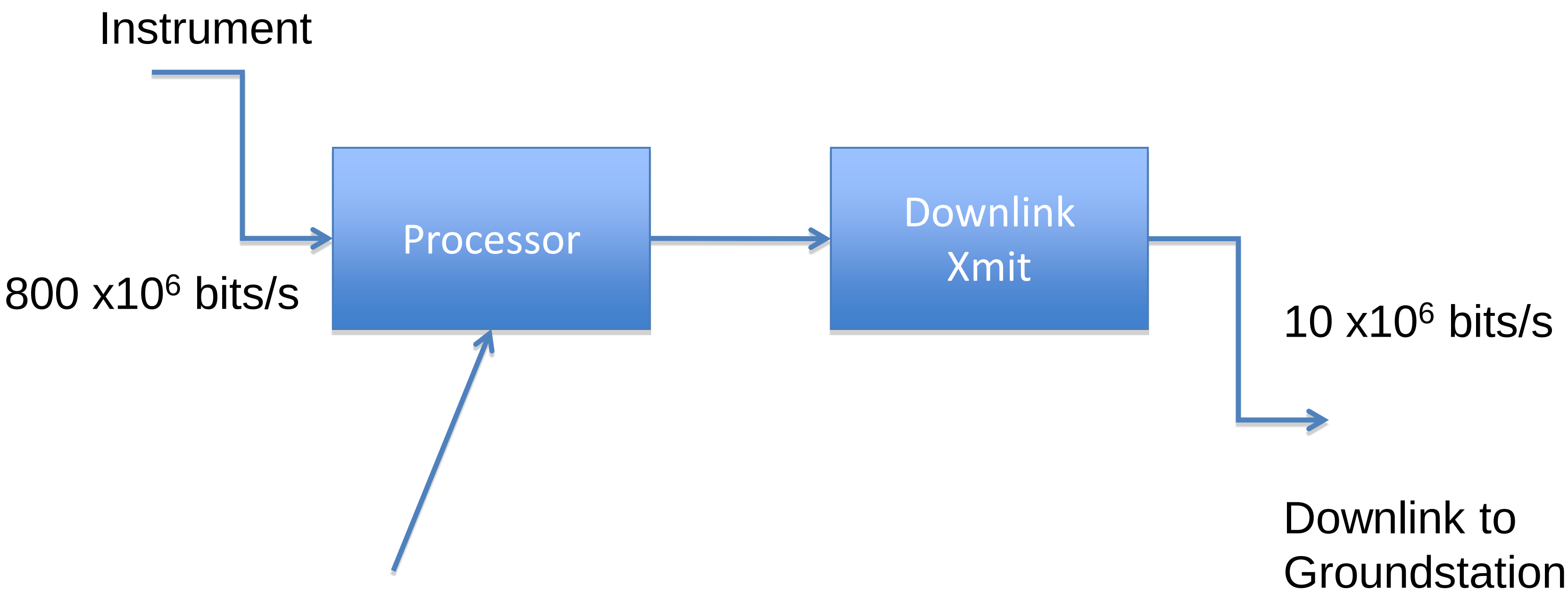

Powerful Space processor
currently evaluating
Spaceube 2.0, OPERA, I-Board

Steve Chien

Operations for HyspIRI DB

- Users specify “areas of interest” which are
  - geographical regions (polygon on surface of Earth)
  - product, (e.g. normalized burn index)
  - priority, (e.g. 50 on 1-100 scale)
  - Constraint (sun must be at least 20 degrees above horizon)
- In generic tool (e.g. Google Earth)
- DB can also be used to rapidly downlink “scenes”

Steve Chien

Climate – Ecosystem Feedbacks

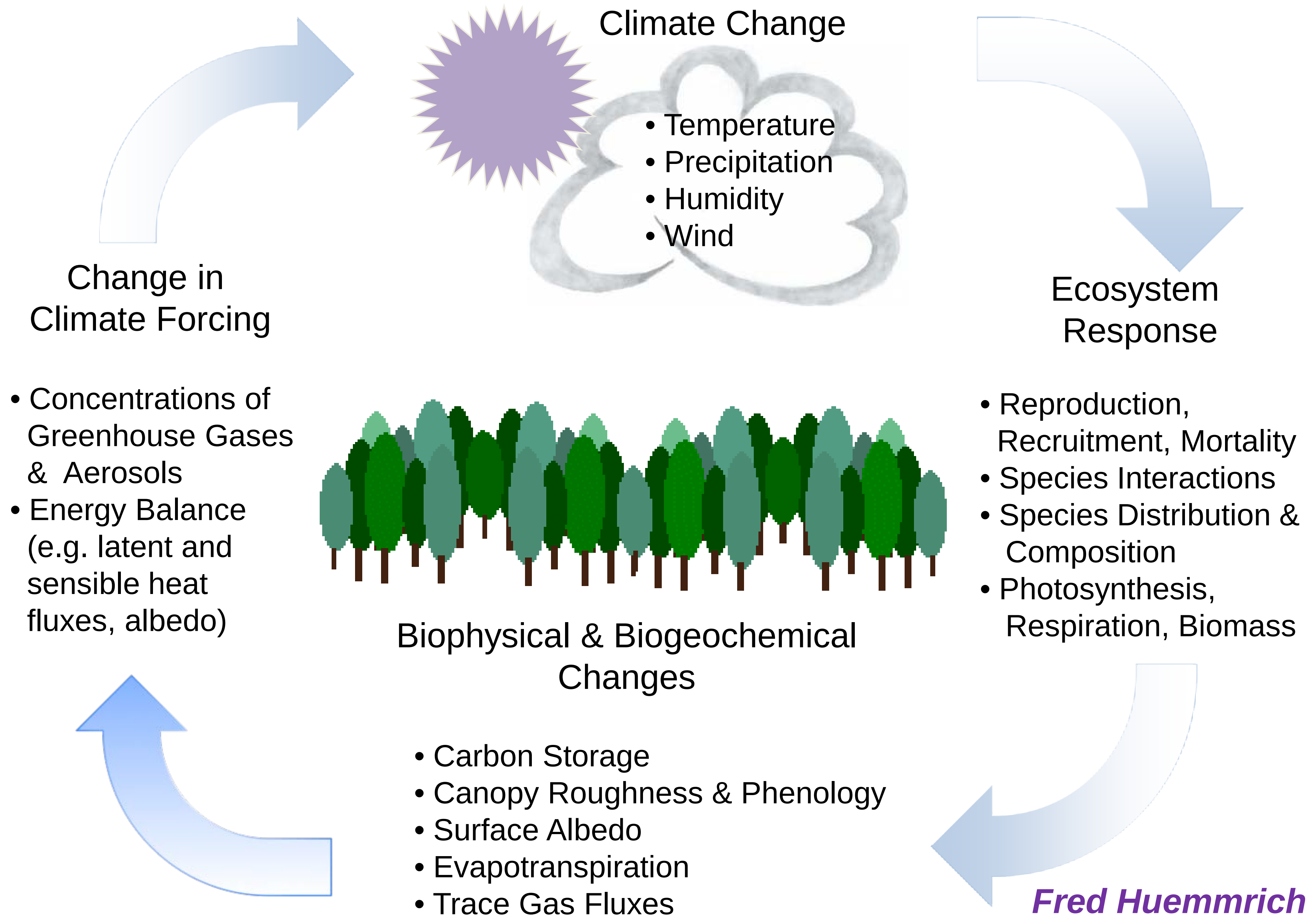

Conceptual Ecosystem Flux Model

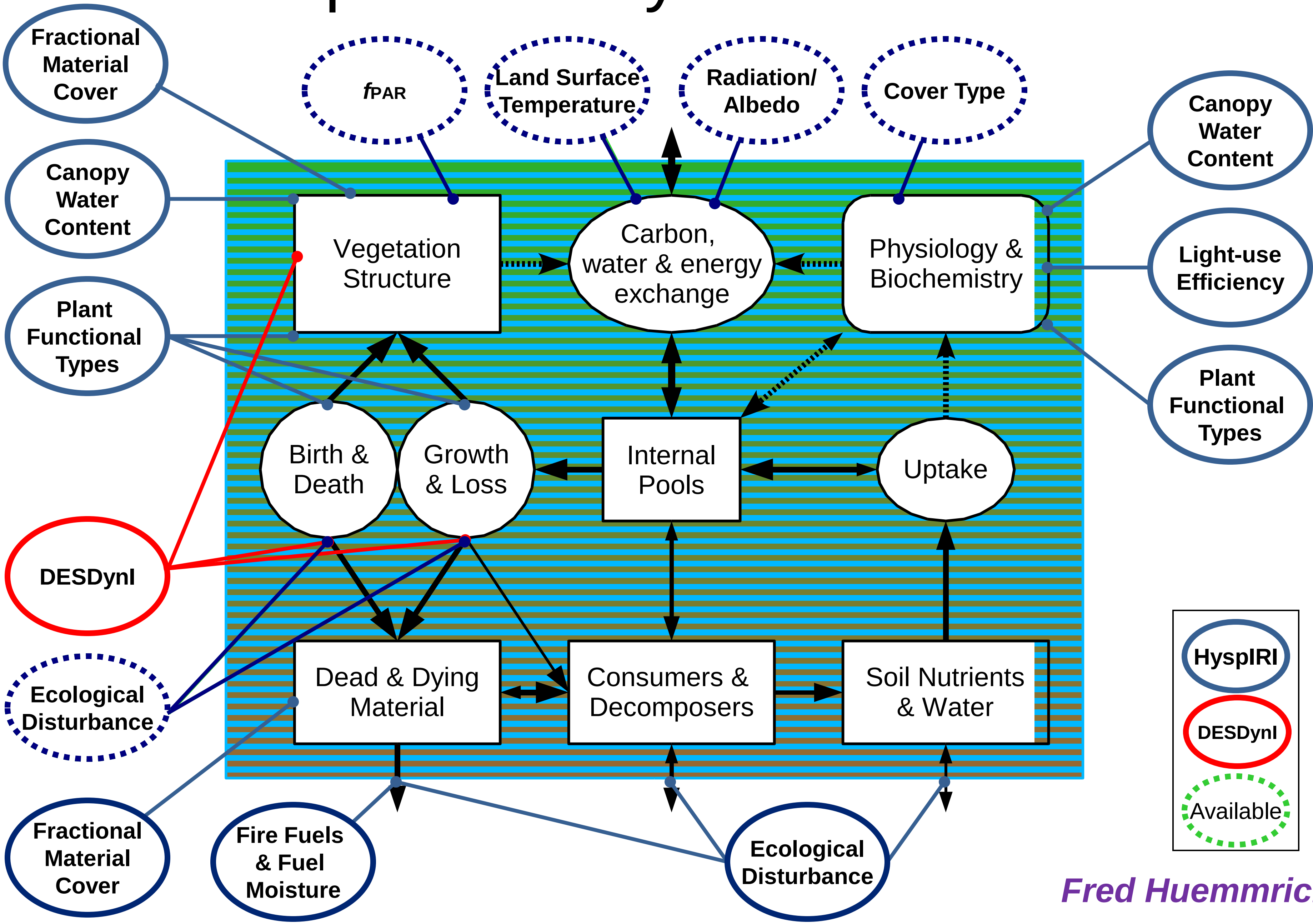

Fred Huemmrich

Petya Campbell

Current Tools - *Examples*

- Visualization and Image Processing of Environmental Resources (VIPER) - Advanced Spectral Mixture Analysis (UCSB, Roberts et al.)
- WINVICAR (JPL, Hook et al.) – work with thermal emissivity data from ASTER, MASTER, other EOS data as well
- Processing Routines in IDL for Spectroscopic Measurements (PRISM, USGS, Kokaly et al.)
- BEAM (C. Brockman/ESA) – data management, viewing and pre-processing for Envisat, PRISM, CHRIS/Proba, AVNIR, MO etc.

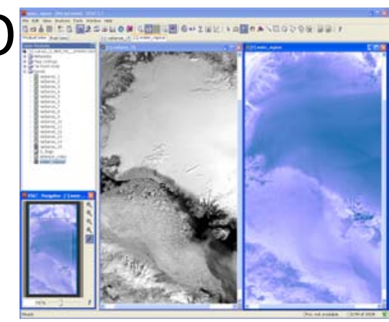

- Open Source Software Image Map (OSSIM, OSGeo)
- ENVI, ERDAS Imagine, PCI Geomatica, other …

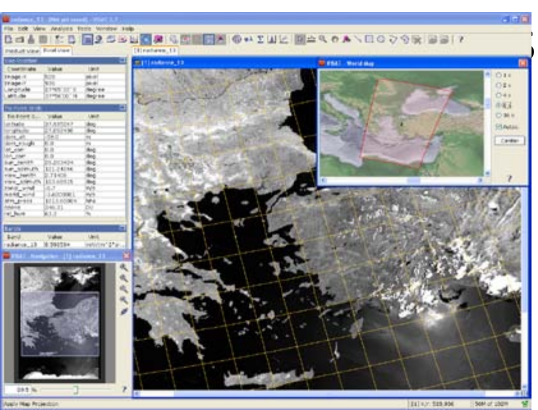

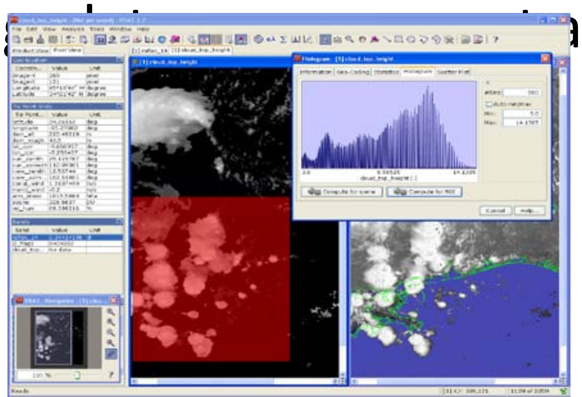

Time Series for CEOS Cal/Val Sites

Temporal variation in spectral characteristics

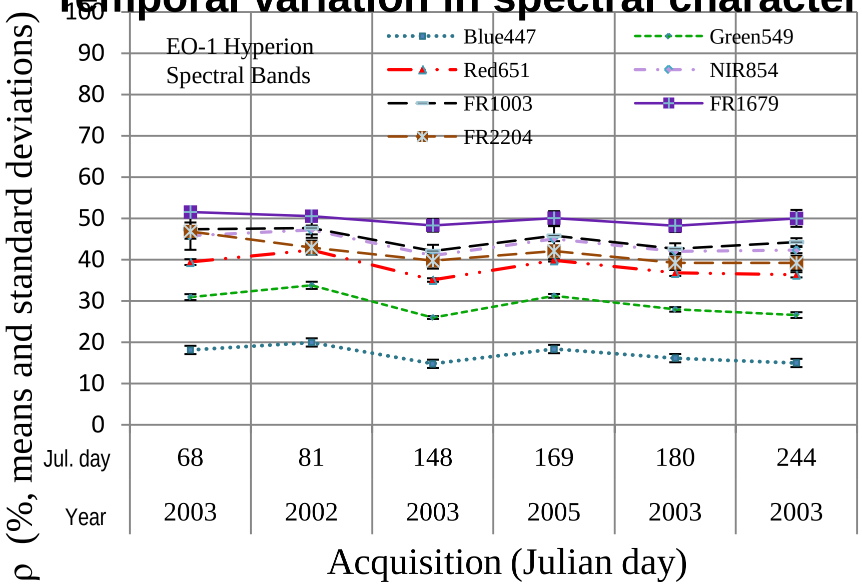

Reflectance differences

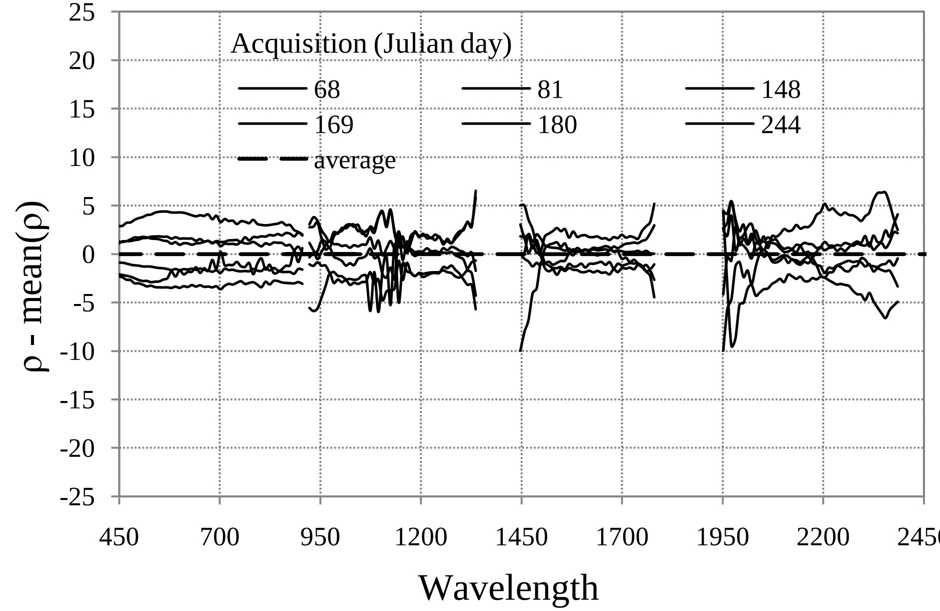

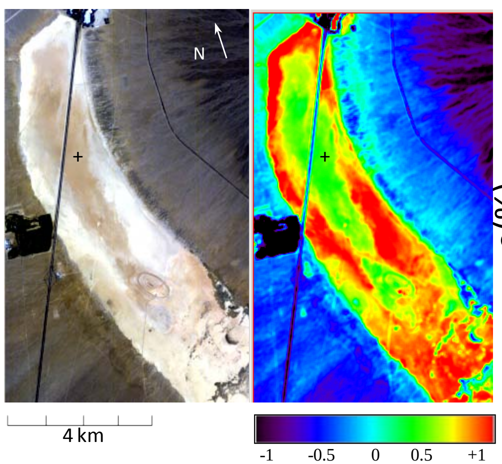

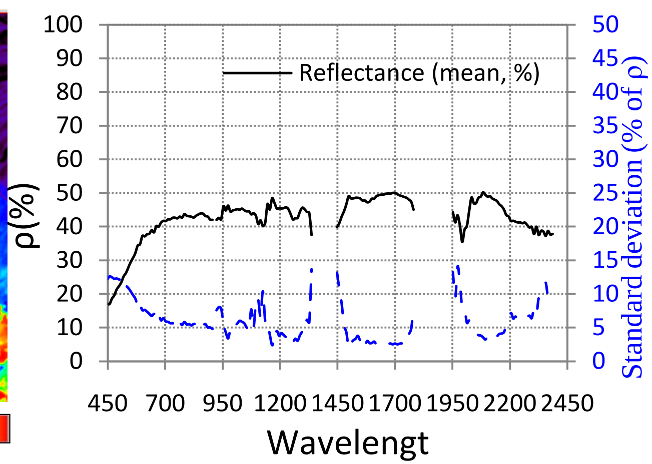

Example from Ivanpah playa: Natural color composite (RGB: 651, 549, 447), Getis Gi* statistics (band 549), Reflectance Mean and Standard Deviation

Petya Campbell

Scaling of Biophysical Products

- LAI, fPAR, GPP, NPP, Albedo
- Protocol for ground sampling, scaling and validation of LAI, fPAR and albedo products in preparation

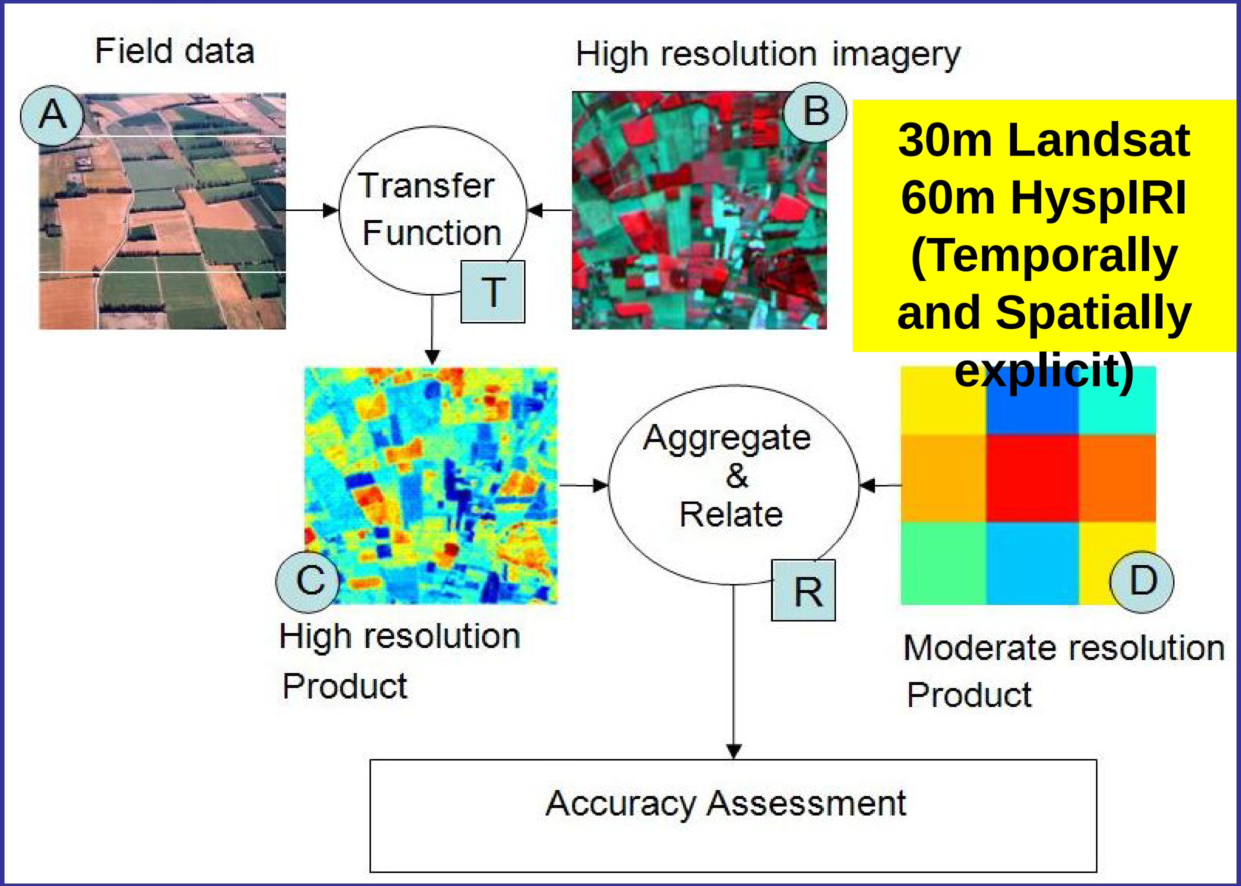

- HyspIRI will provide enhanced spatial / temporal capabilities for scaling activities (bridge 30m – 250m/1km+ gap)

Band-to-Band Registration
The Bottom Line

$$\left\langle \frac{R_{NIR}}{R_{VIS}} \right\rangle \neq \frac{\langle R_{NIR} \rangle}{\langle R_{VIS} \rangle}$$

Steve Ungar

Proposed Combined VSWIR /TIR Products

Rasmus Houborg (GSFC)
Louis Giglio (UMD)/ Ivan Csiszar (NOAA)
Dar Roberts (U California-Santa Barbara)
Dale Quattrochi (MSFC)
Ben Cheng (GSFC)
Ray Kokaly (USGS)
Craig Daughtry (USDA-Beltsville)
Bruce Cook (GSFC)/ Greg Asner (Carnegie Institute)

Sub-Pixel Fire Fraction

Louis Giglio

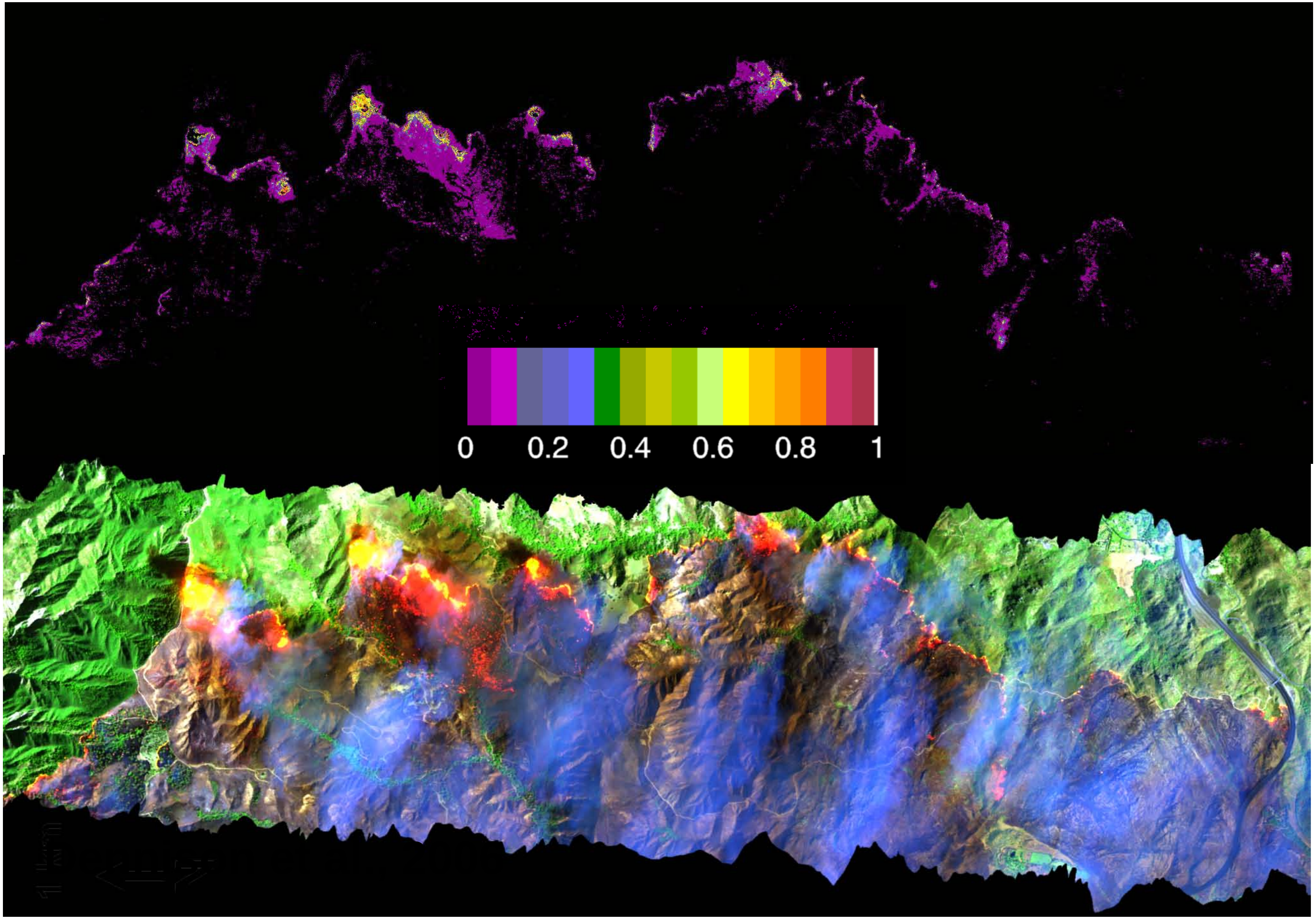

Dar Roberts

Combined VNIR-SWIR Physiological/Thermal Stress Measures

- **The ability to improve estimates of carbon uptake using PRI has been established using flux data and AVIRIS**
- **MODIS estimates of carbon uptake can be improved using LST and a vegetation index. What is the potential at 60 m with better indices?**

Plots of net and gross carbon dioxide flux measured at 7 Boreas flux tower sites compared to estimates of FPAR (NDVI) and quantum efficiency (PRI) from AVIRIS. From Rahman et al., 2001

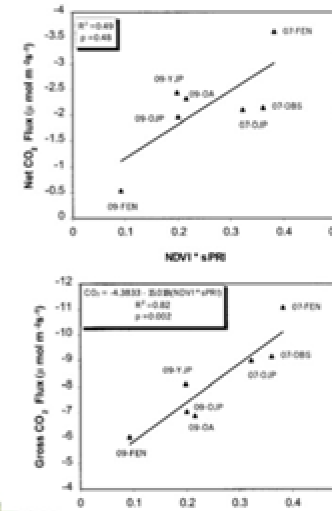

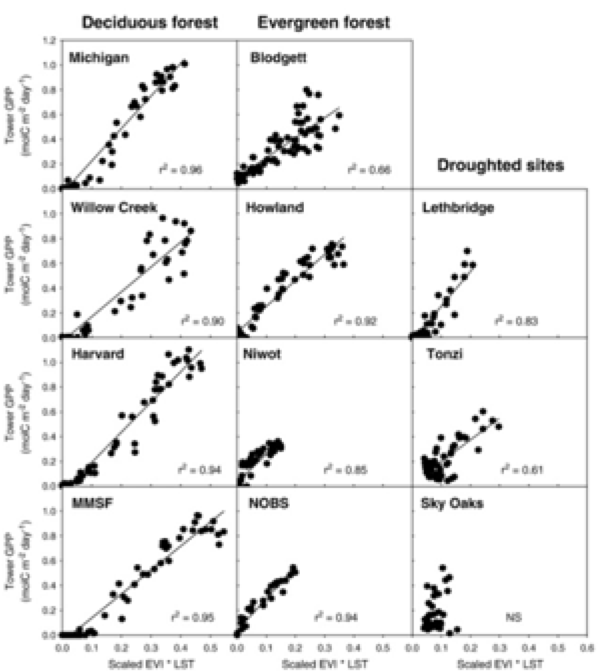

Plot of scaled EVI*LST compared to carbon uptake from flux towers.
Example derived from MODIS
From Sims et al., 2008

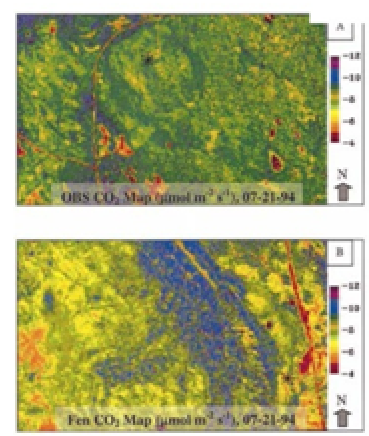

Maps of carbon dioxi uptake estimated from scaled PRI and NDVI calibrated to eddy flux data. From Rahman e al., 2001.

Production: Improved ASTER TES algorithm and suites of standard hyperspectr

HyspIRI Combined Composite Data Set Advanced Product for Urban Ecosystems Analysis

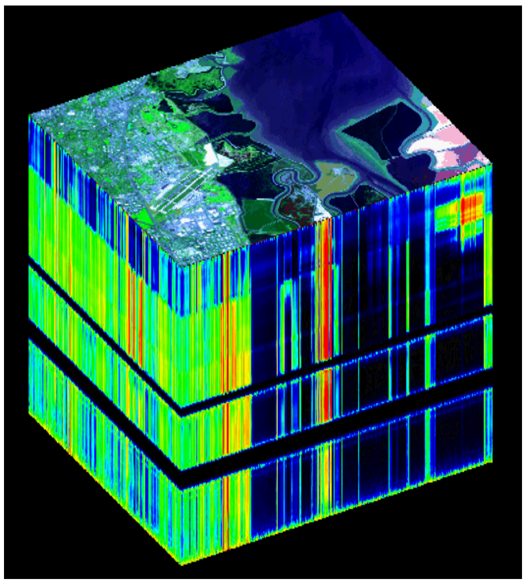

+

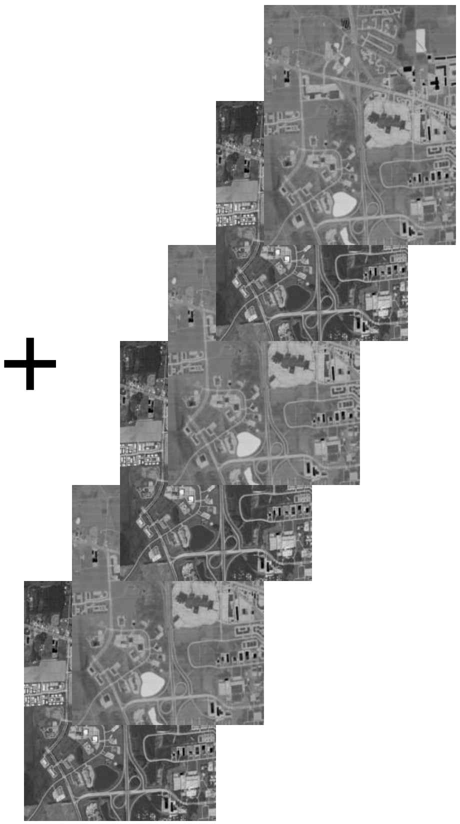

=

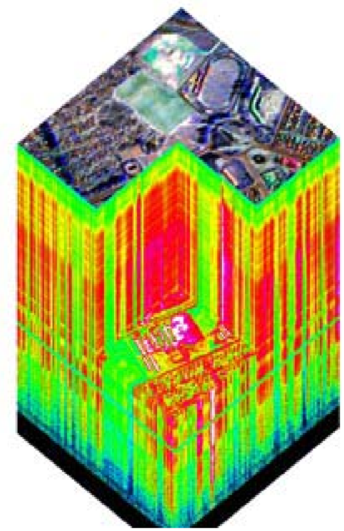

HyspIRI Hyperspectral VSWIR Level II Product
(NDVI, fPAR, surface reflectance characteristics)

HyspIRI TIR multispectral Level II product (8 TIR Bands)
(surface temperature, radiance, [day/night], emissivity)

HyspIRI VSWIR/TIR composite data set
(quantitative integrative measurement of urban surface reflectances, temperatures, and emissivity across the urban ecosystem)

Dale Quattrochi

Ben Cheng

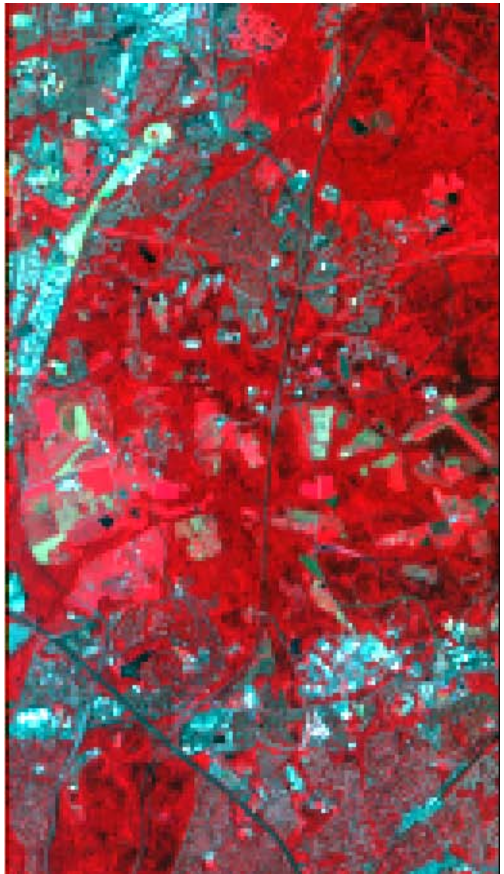

EO-1 Hyperion VSWIR

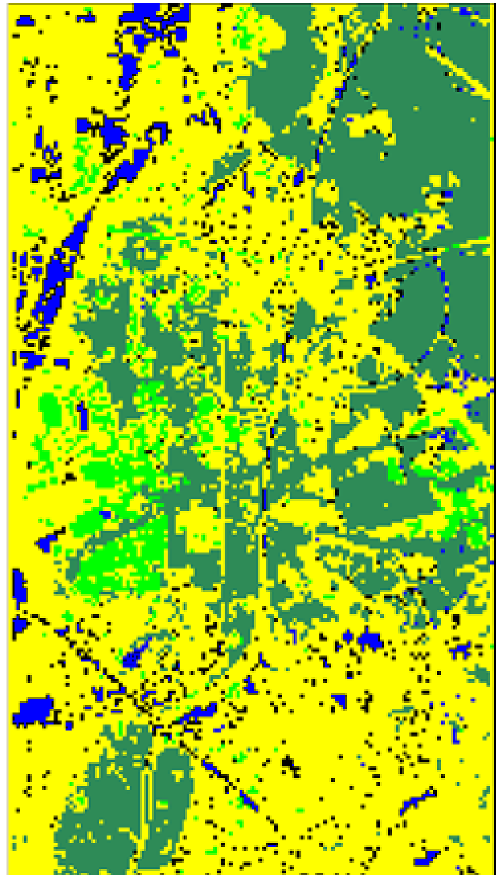

Greenbelt, MD

Mixed Forest

Crops

Residential / Grassland

Business / Industrial

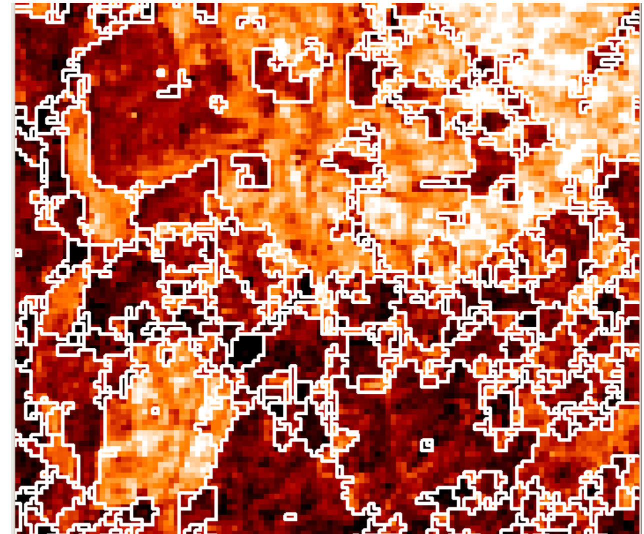

ASTER TIR 04/18/2009

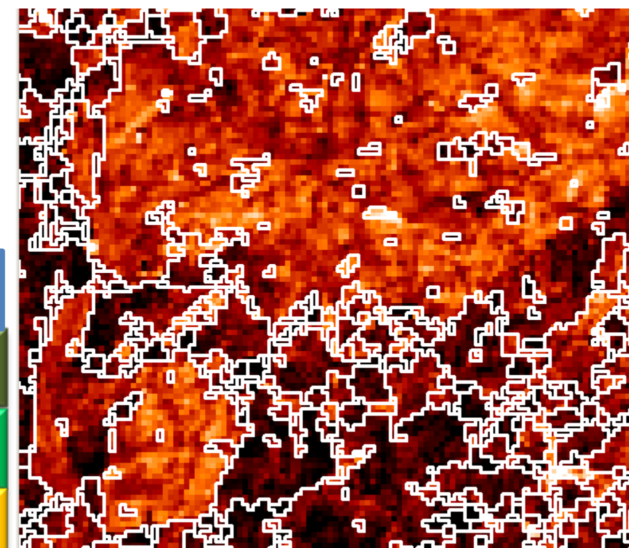

ASTER TIR 11/28/2009

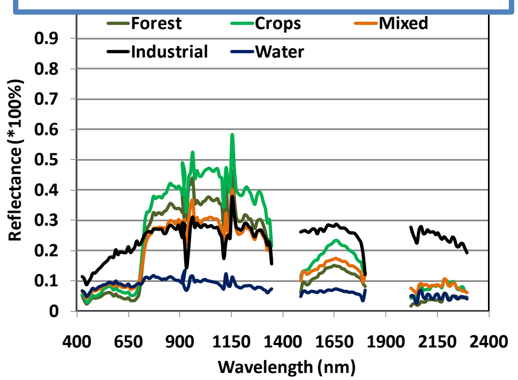

Spectroscopic Remote Sensing

- VSWIR: Detect patterns of pigment, water and cellulose/lignin content consistent with invasive plant and divergent from native plants
- TIR: Calculate land surface temperature, model evapotranspiration, compare to air temperature to reveal temporal patterns divergent from native plants

Spectroscopy and Invasive Plants

- Land management (treatment and evaluation)
- Shifts in plant composition (to non-woody)
- Soil composition (formation of caliche)
- Fire promotion (post-fire soil impact)
- Predictive modeling of expansion
- Climate change
- Identification of areas at risk for invasion

National-level detection, monitoring and early warning system for invasive plant species

Kokaly et al.

Carnegie Airborne Observatory (CAO)

3-D functional imaging of ecosystems

LiDAR for topography, canopy structure, LAI, etc.

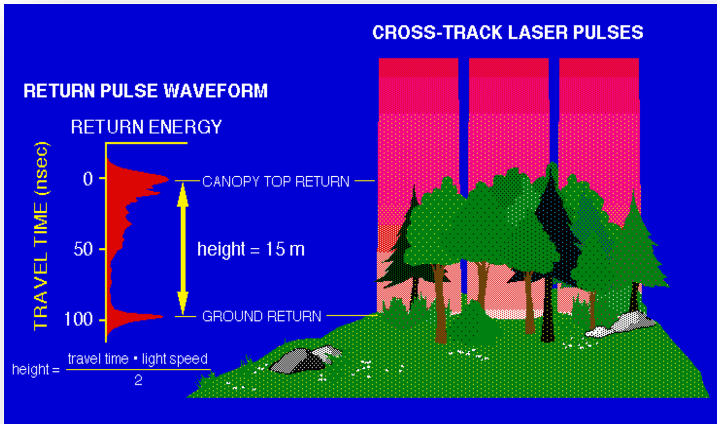

+

Hyperspectral for species, chemistry, etc.

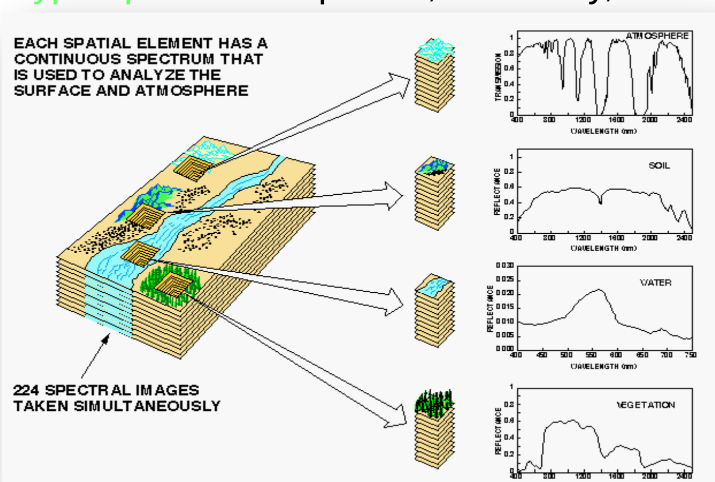

=

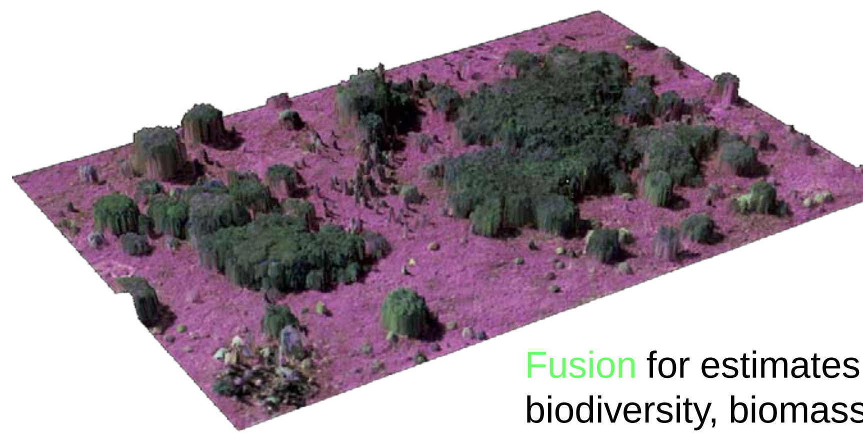

Fusion for estimates of biodiversity, biomass, sun/shade fraction, habitat suitability, etc.

Cook

Canopy chemistry and biodiversity in tropical forest canopies

Cook and Asner

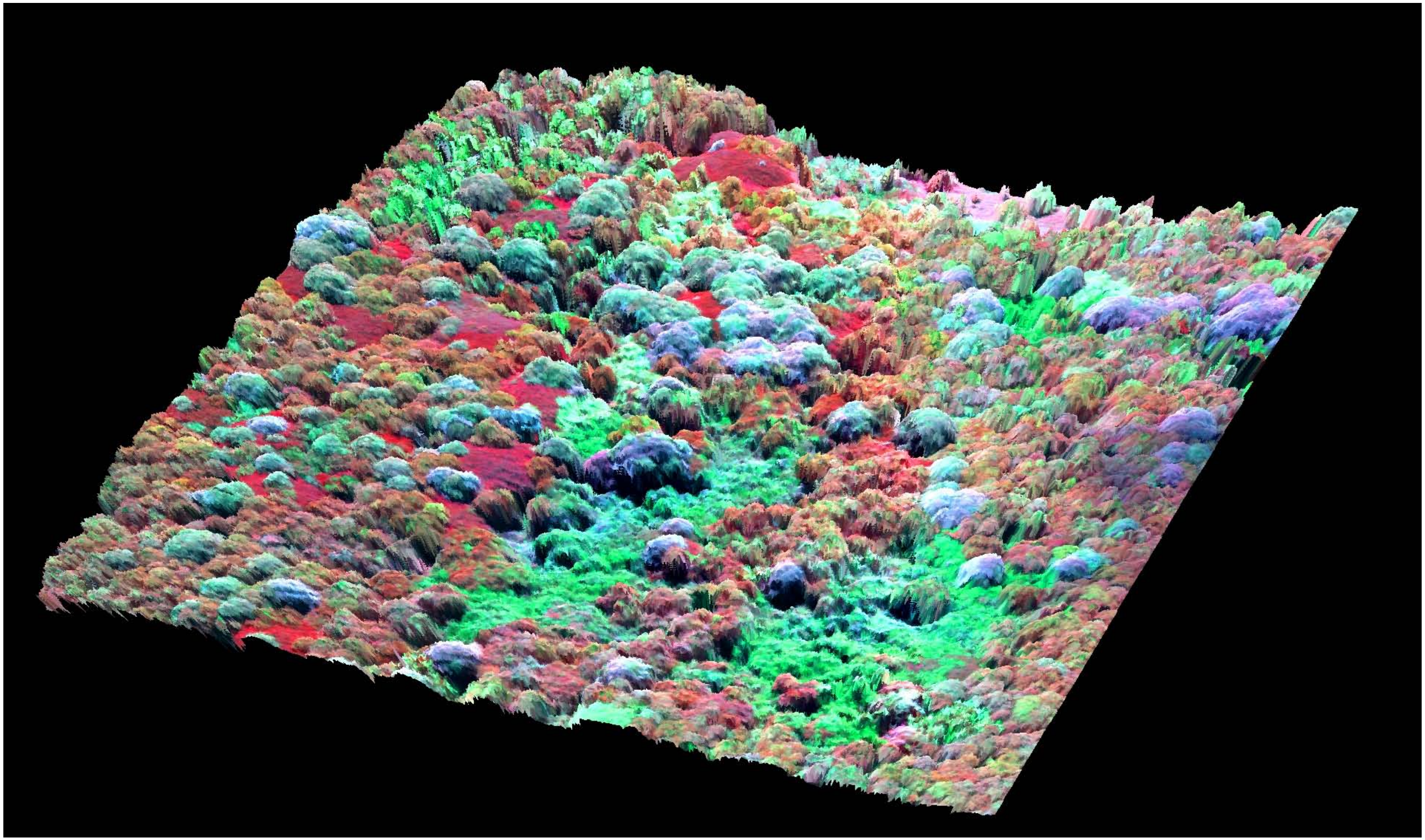

Cook

Study Sites

The study includes two independent locations with different regional climate and ecosystem types. Data aggregated to higher and lower spatial scales will be compared for the same locations.

Vancouver Island, Canada/Hoquiam, WA: includes portions of unique natural ecosystems such as the Olympic National Park, WA and the Great Victoria Watershed (GVWD) test site on Vancouver Island, BC and rural, sub-urban and urban environment associated with the city of Victoria, BC.

Jasper Ridge Biological Preserve (JRBP), CA: provides Mediterranean-type climate, with five major vegetation types: evergreen forest, deciduous forest, chaparral shrublands, herbaceous perennial wetlands, and annual grasslands

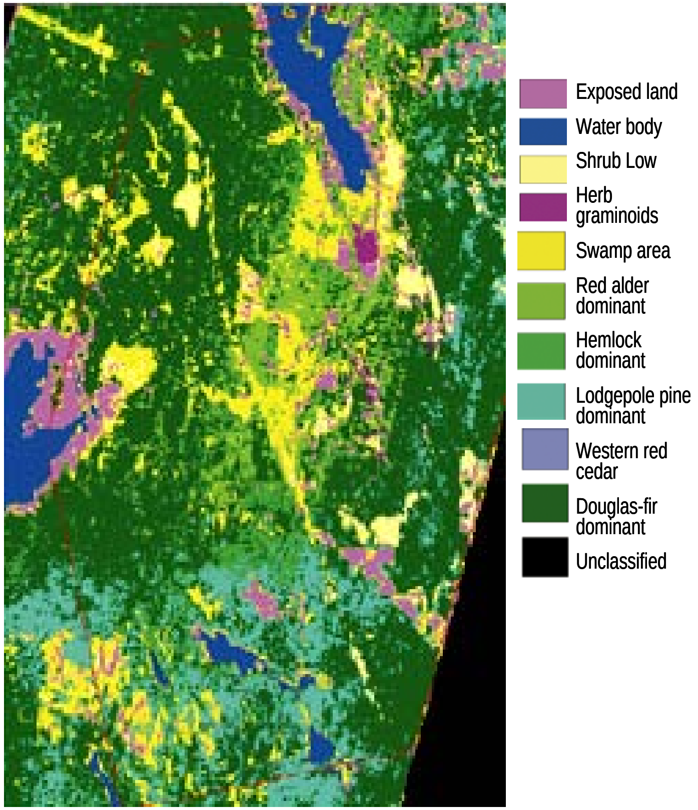

Hyperion land cover classification of the Greater Victoria Watershed (GVWD) test site on Vancouver Island (September 10 2001, Goodenough et al. 2003).

Campbell

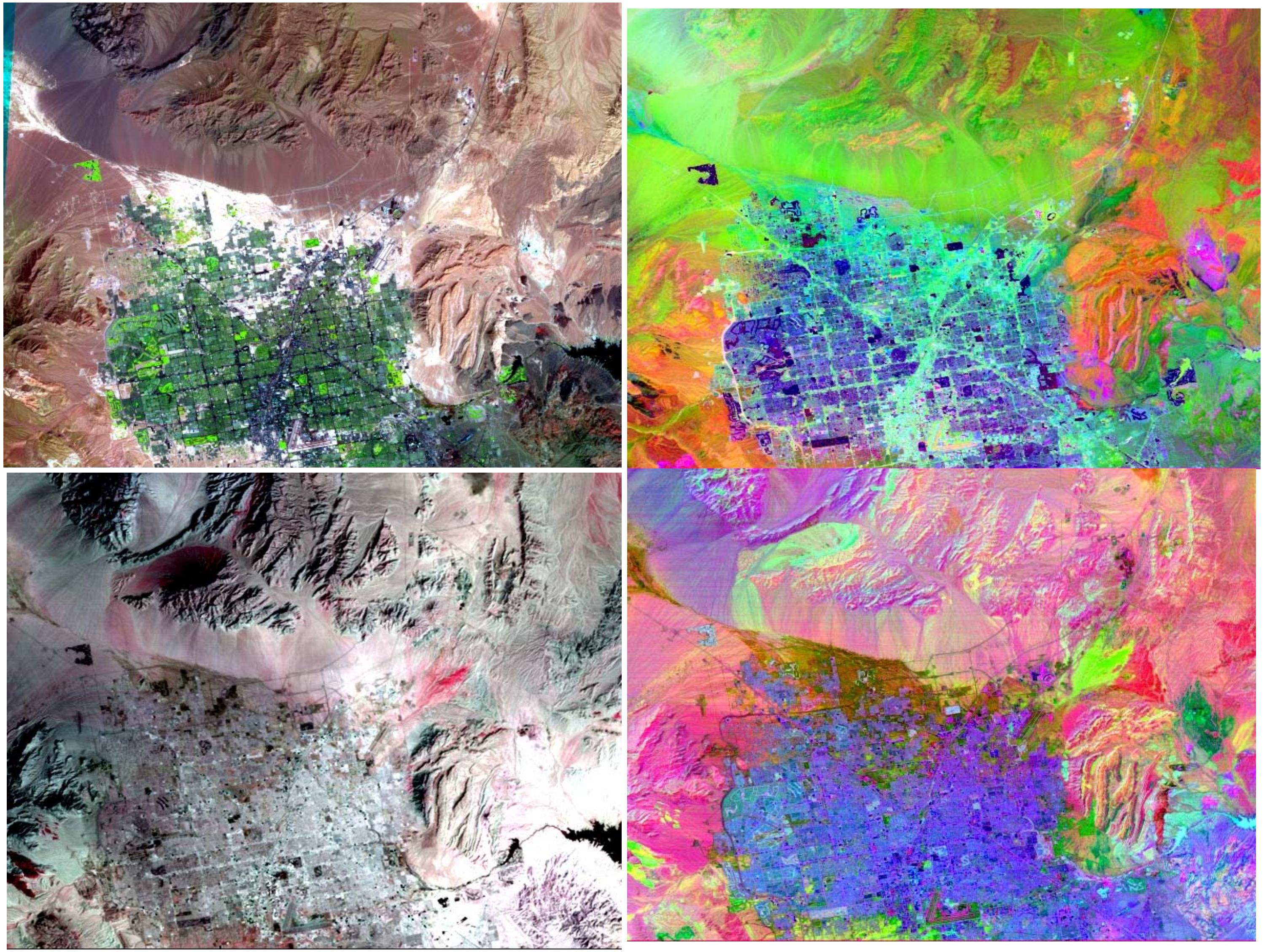

ASTER imagery, Las Vegas area: VSWIR aggregated to 90 m (upper left, vegetation in green) and TIR bands (lower left), principle components of reflective bands (upper right) and all VSWIR and TIR (lower right).

Campbell

Phil Townsend, slides 6, 12, 13

Green

Planned Civilian Satellite Missions

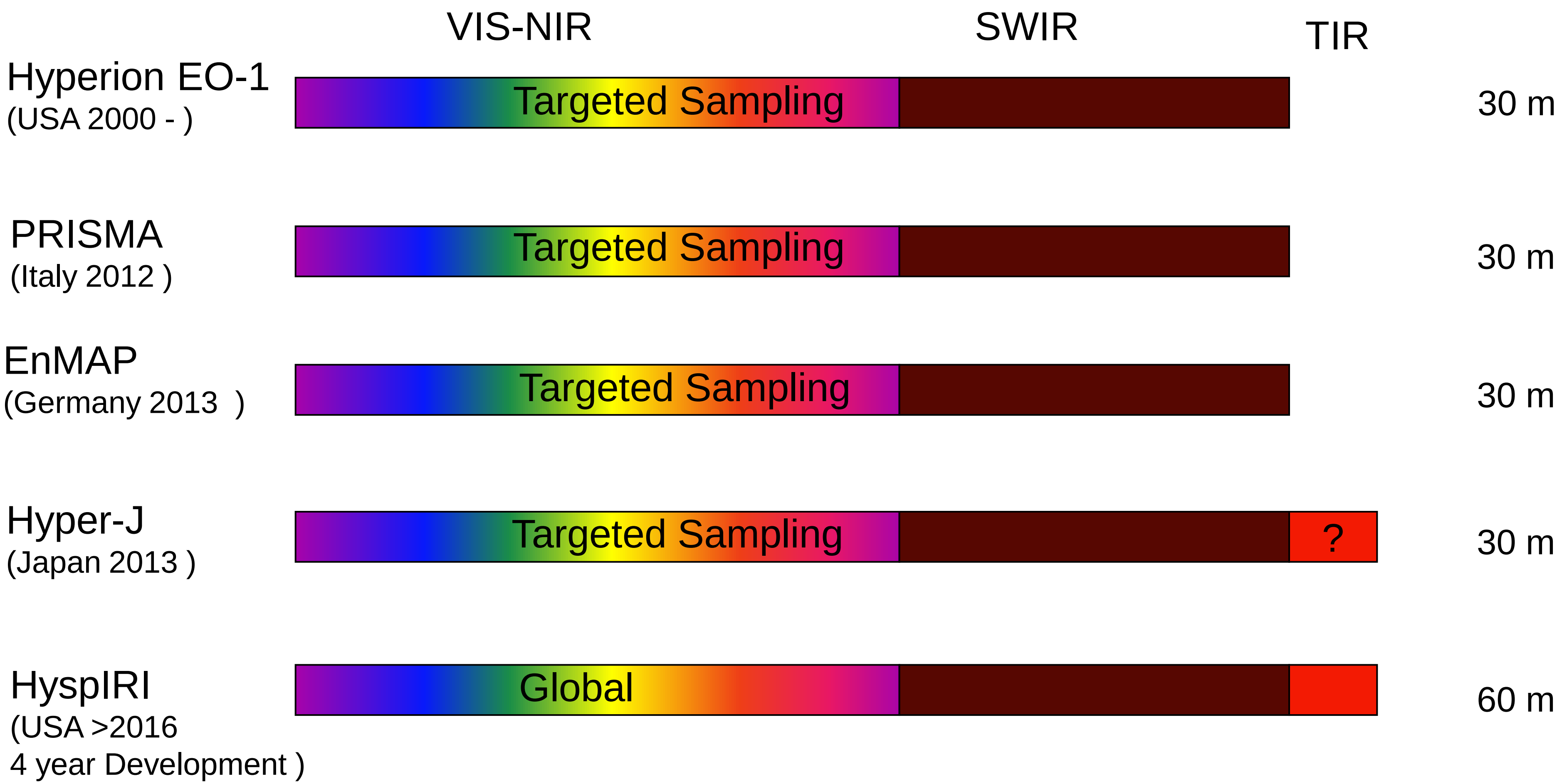

HyspIRI compared with possible International Imaging Spectroscopy Missions

Green

Only HyspIRI provides the full spectrum of data required to address climate-carbon cycle feedbacks articulated in the NRC Decadal Survey

HyspIRI Provides Seasonal and Annual Global Coverage that Uniquely Addresses Critical Gaps in Climate Research and Ecosystem Understanding.

>100 years for international mission to equal 1 year of HyspIRI

Country	Instrument	Swath km	Pixel Size, m	Terrestrial Coverage in 19 days	Repeat interval, days	TIR capability
USA	**HyspIRI**	**150**	**60**	**100%**	**19**	**8 TIR bands**
Germany	EnMAP	30	30	<1%	--	NO
Italy	PRISMA	30-60	20-30	<1%	--	NO
Japan?	ALOS3	30	30	<1%	--	NO
India?	IMS Resource Sat-3	25	25	<1%	--	1 TIR band

US, HyspIRI: a full spectral range (380 to 2500 at 10 nm), high SNR, uniform, 60m spatial with 150 km swath imaging spectrometer and multiband thermal imager (8 band thermal imager from 3-12 μm).

Other countries are occasionally mentioned (China, South Africa, South Korea, etc.). All are proposing first generation visible-only, small sample process/application missions with scattered terrestrial coverage and no TIR imager

Accuracy

Terms accuracy and precision can be sources of contention in discussions

- Accuracy is essentially how well the results agree to the actual value
- Precision is how well individual measurements agree with each other
- Repeatability is used interchangeably with precision

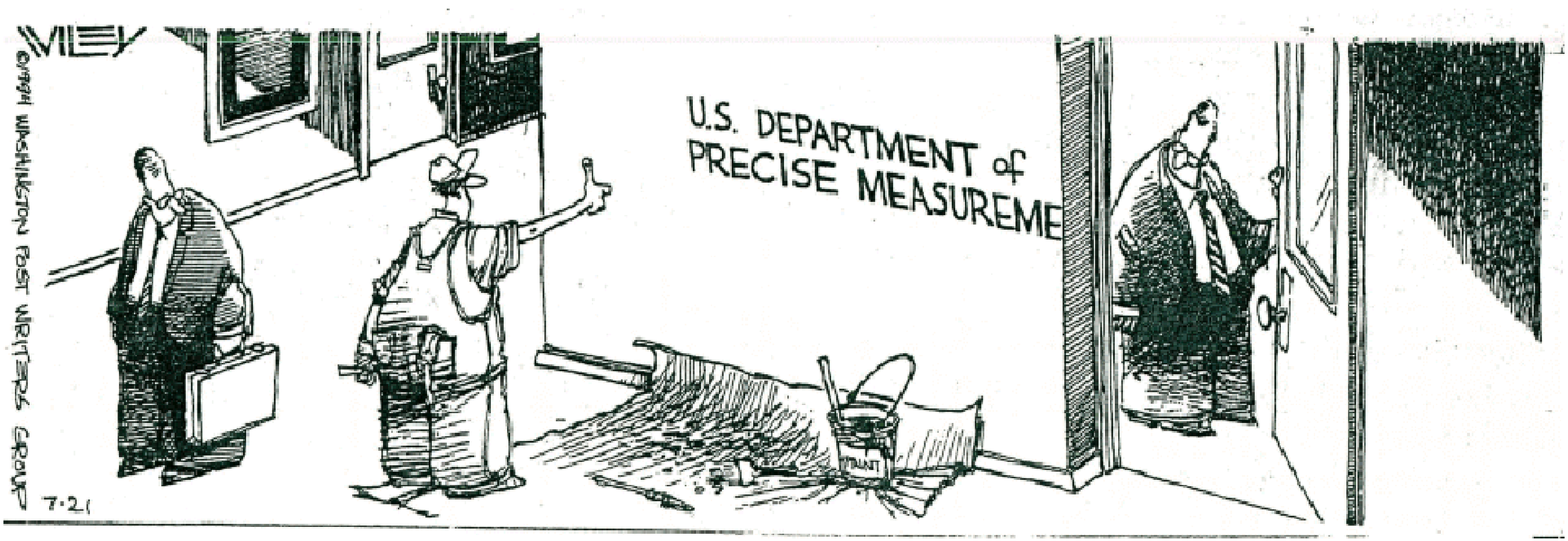

Thome

Spectral and Geometric calibration

Spectral and geometric calibration takes place prelaunch and on orbit as well

- Alignment between emissive and reflective bands
- Center wavelength and band shapes

1. Convolve SRF with High Resolution MODTRAN™ Model

2. Normalize Data (Green) to Model (Red)

3. Subtract Data from Model
Fit Straight Line
Compute Statistics

4. Shift Band Centers
Repeat Steps 1-4

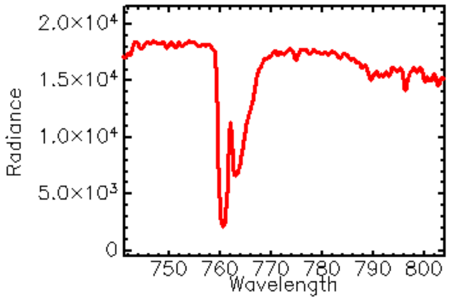

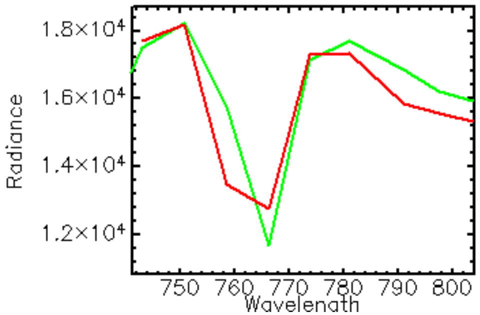

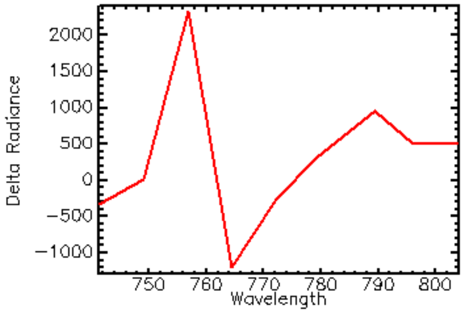

Thome

Back-Up Slides

Hyperion Imagery of Barrow, Alaska (July 2009)

July 20, 2009
False-Color and True-Color Images from Hyperion
Barrow, Alaska

Images are from NASA's Earth Observatory web site (http://earthobservatory.nasa.gov/)

Mapping Fuel Condition: Hyperion provides comparable measures to AVIRIS over a larger geographic region

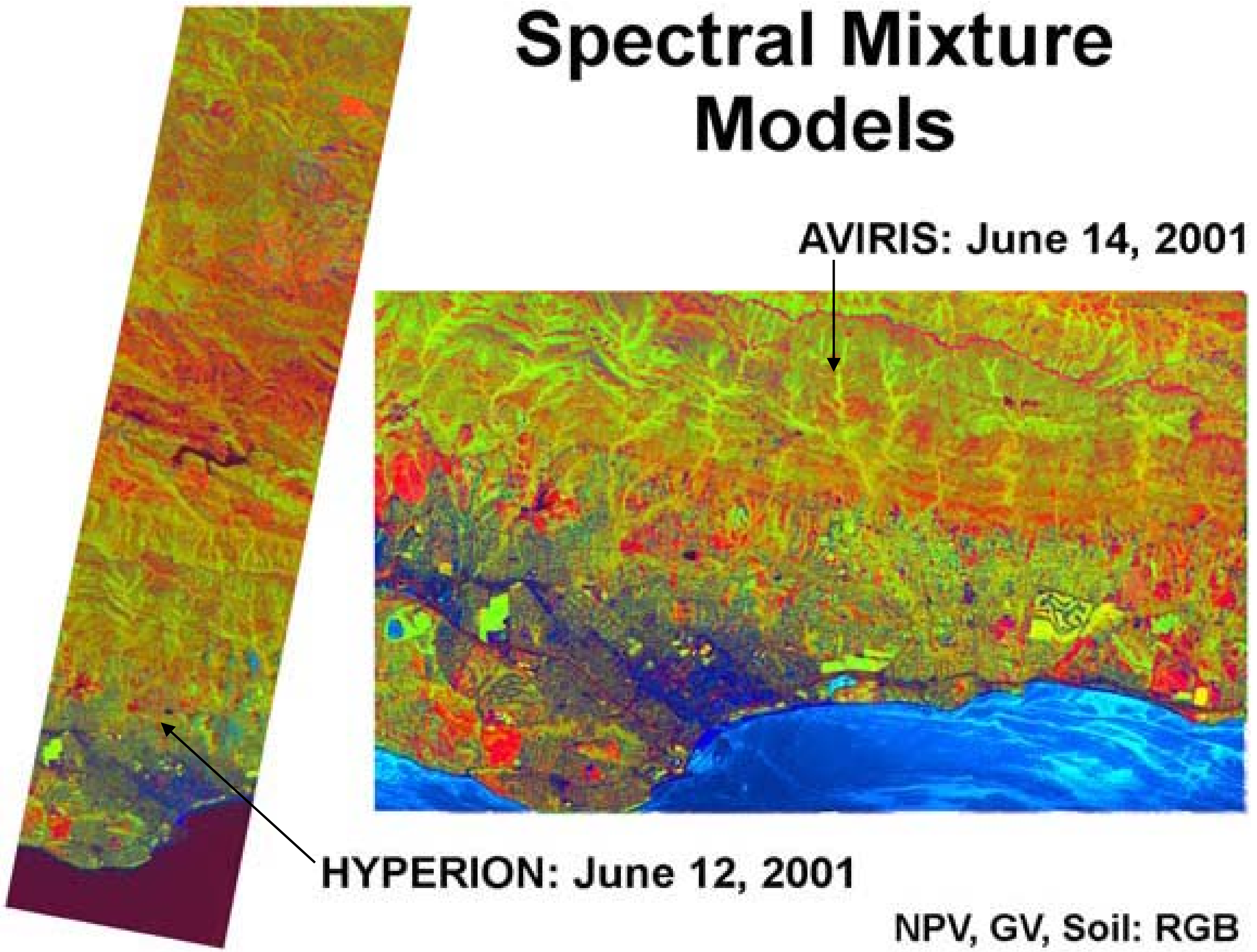

Roberts et al. (2003)

Science Measurements

Summary Measurement Characteristics

Spectral	
Bands (8) µm	3.98 µm, 7.35 µm, 8.28 µm, 8.63 µm, 9.07 µm, 10.53 µm, 11.33 µm, 12.05
Bandwidth	0.084 µm, 0.32 µm, 0.34 µm, 0.35 µm, 0.36 µm, 0.54 µm, 0.54 µm, 0.52 µm
Accuracy	<0.01 µm
Radiometric	
Range	Bands 2-8= 200K – 500K; Band 1= 1400K
Resolution	< 0.05 K, Linear Quantization to 14 bits
Accuracy	< 0.5 K 3-sigma at 250K
Precision (NEdT)	< 0.2K
Linearity	>99% characterized to 0.1 %
Spatial	
IFOV	60 m
MTF	>0.65 at FNy
Scan Type	Push-Whisk
Swath Width	600 km (±25.5° at 623 km altitude)
Cross-Track Samples	10,000
Swath Length	15.4 km (+/- 0.7-degrees at 623km altitude)
Down-Track Samples	256
Band-to-Band Co-registraion	0.2 pixels (12 m)
Pointing Knowledge	10 arcsec (50 microrad, 05 pixels, 30m on ground)

Status of Decadal Survey Missions

Woody Turner

- February 1, 2010: President's Budget released with a 5-year, $2.5 Billion total augmentation for NASA Earth Science
- March 18, 2010: NASA ESD sends Climate Augmentation Plan to OMB
- Plan calls for launch of all Tier 1 Missions by 2017 (also the launch of OCO reflight, GRACE follow-on, and SAGE III missions)
- Also, current plans are for Tier 2 missions to launch at the rate of 1 per year starting in 2019
- President's Budget direction requires NASA to obtain USGCRP Review of the Climate Augmentation Plan
- Review is taking place this month
- In the near-term, Tier 2 mission funding to continue; levels still TBD

IPCC Climate Change 2007: Working

The Physical Science Basis

Chapter 7: Couplings Between Changes in the Climate System and Biogeochemistry: Executive Summary

7.3.3 Terrestrial Carbon Cycle Processes and Feedbacks to Climate

To understand the reasons for CO_2 uptake and its likely future course, it is necessary to understand the underlying processes and their dependence on the key drivers of climate, atmospheric composition and human land management.

Drivers that affect the carbon cycle in terrestrial ecosystems can be classified as:

(1) direct climate effects (changes in precipitation, temperature and radiation regime);

(**2) atmospheric composition effects** (CO_2 fertilization, nutrient deposition, damage by pollution); and

(3) land use change effects (deforestation, afforestation, agricultural practices, and their legacies over time).

Susan Ustin

IPCC Climate Change 2007: Working Group The Physical Science Basis

Chapter 7: Couplings Between Changes in the Climate System and Biogeochemistry: Executive Summary

7.1.1 Terrestrial Ecosystems and Climate: Carbon Cycle Drivers

Changing Plant Functional Types in California from 1934 to 1996

Analyzed by James Thorne, UC Davis based on the Wieslander VTM Project, 1934

Grasslands
Mixed oak-pine savanna
Ponderosa pine forest
Mixed Montane Hardwod & Conifer
Mixed conifer
Lodgepole pine, red fir
Subalpine conifers

Historic WHR Types

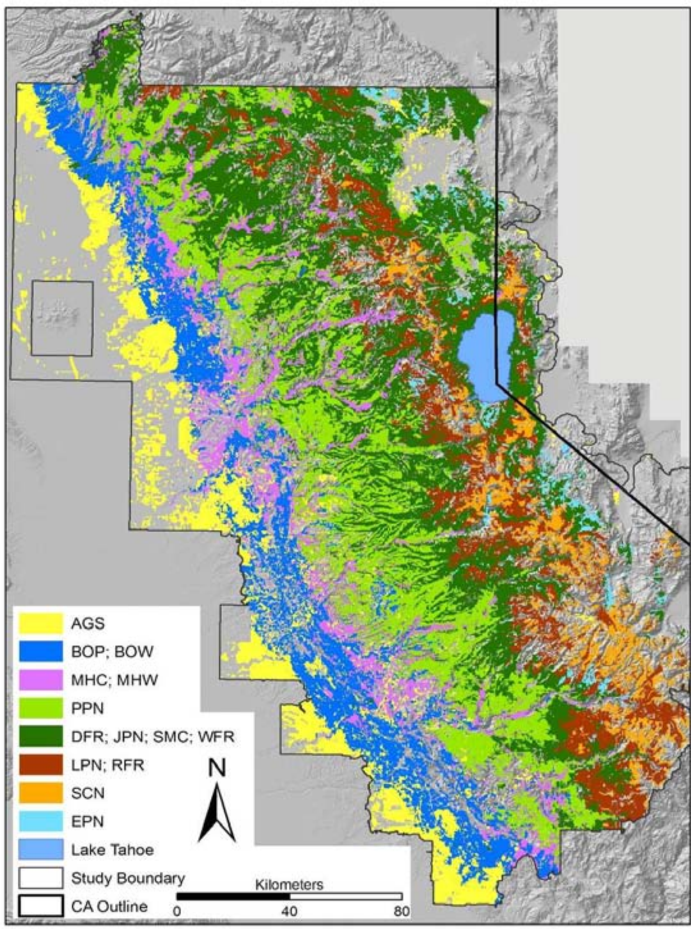

Current WHR Types

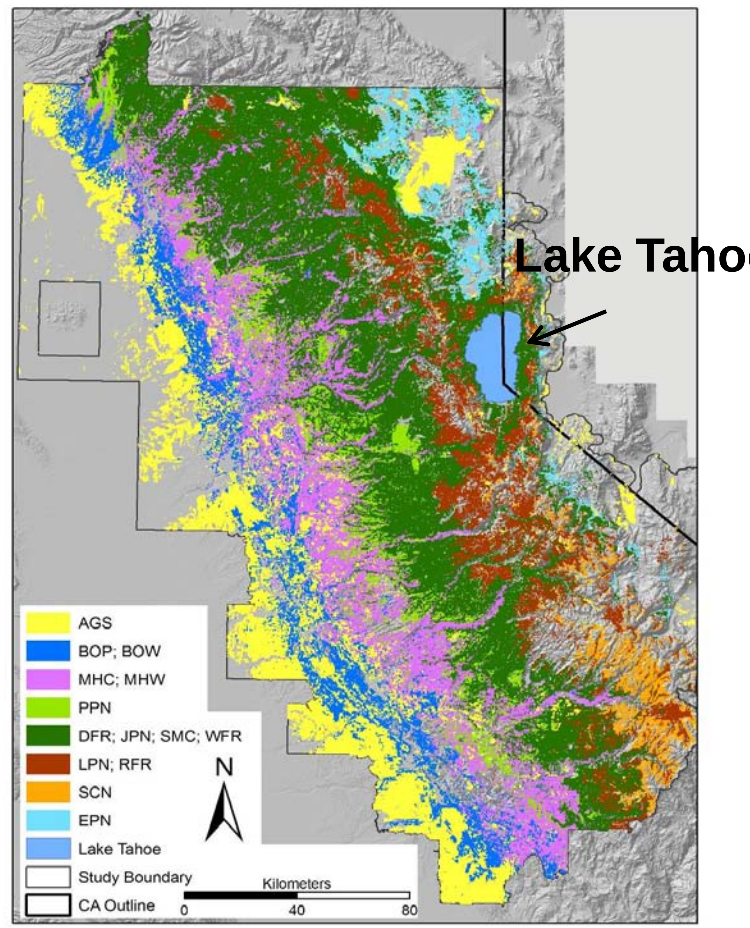

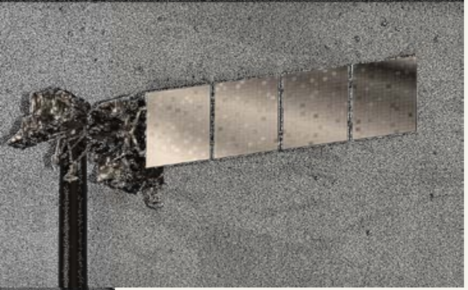

Susan Ustin

Relevance of HyspIRI to Carbon and Climate Science

Monitoring Vegetation Type and Functions

Global Land Cover Maps based on climate potential have biased Distributions

- ➢ Coarse Spatial Resolution data do not agree with actual land cover types

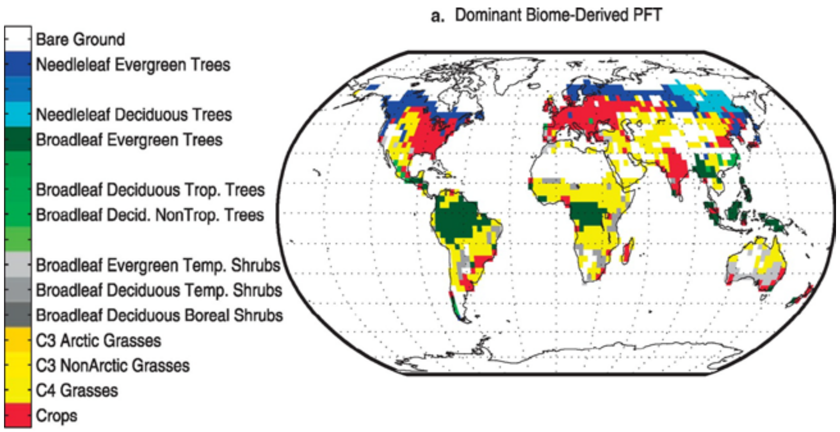

Satellite Based plant functional type maps have higher spatial resolution and are derived from actual measurements

- ➢ Maps remain too spatially coarse to monitor ecosystem changes
- ➢ Limited number of cover types; no subgrid elements

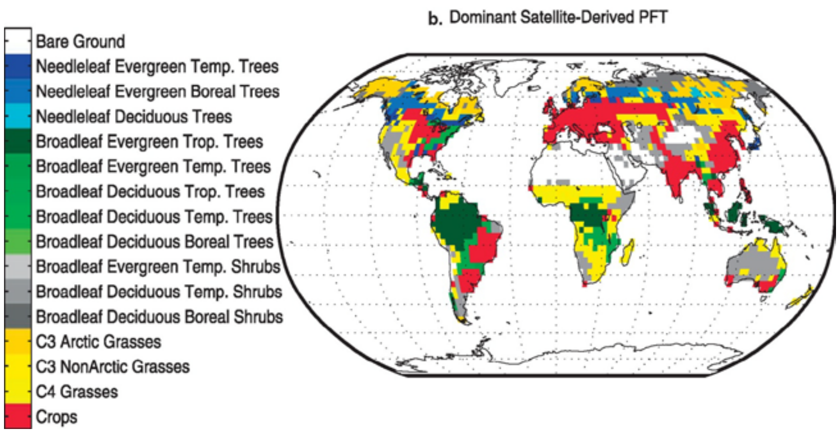

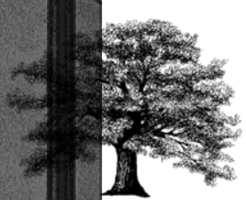

From: Bonan, GB, Levis S, Sitch S, Vertenstein M, Olson KW (2003). Global Change Biology 9: 1543-1556,
Figure b from: Ramankutty N. and Foley JA. (1999). Global Biogeochemical Cycles 13: 997-1027.

Measuring the Terrestrial Biosphere

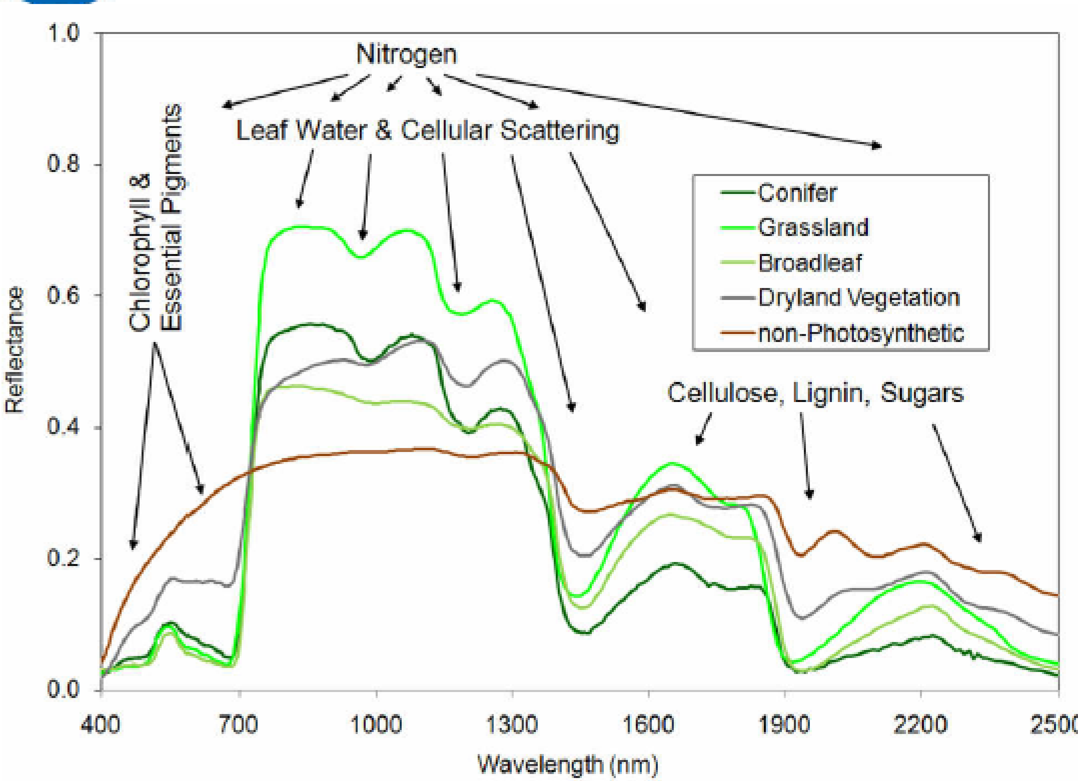

Imaging Spectroscopy is r
to measure critical variabl
terrestrial biosphere.

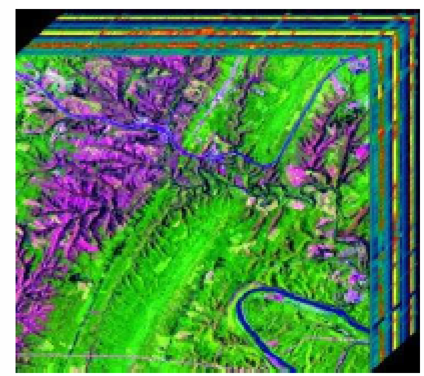

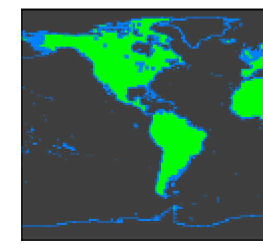

Multi-spectral imaging is insufficient

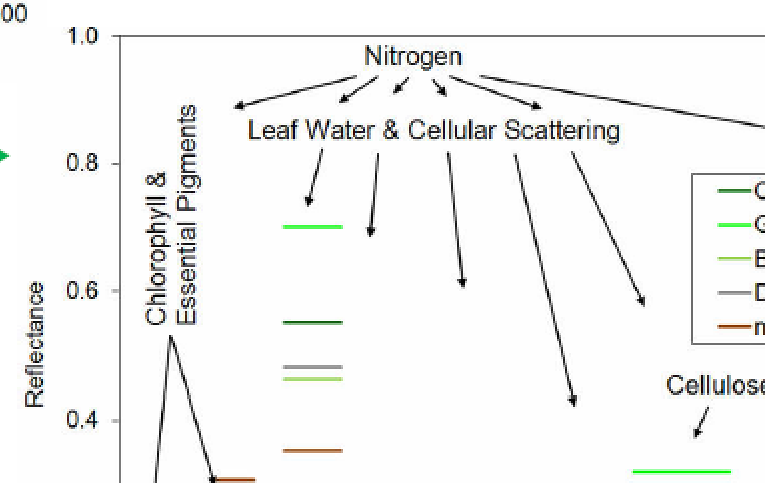

Mission Concept

TIR Overview

- Duration: 4 years development, 3 years science
- Coverage: Global land and shallow water every 5 days
- Day and Night imaging (1 day and night image at a given location obtained every 5 days)
- Data download using dual-polarization X-band at high-latitude stations
- Spacecraft: LEO RSDO bus (SA-200HP)
- Launch: Taurus-class launch vehicle

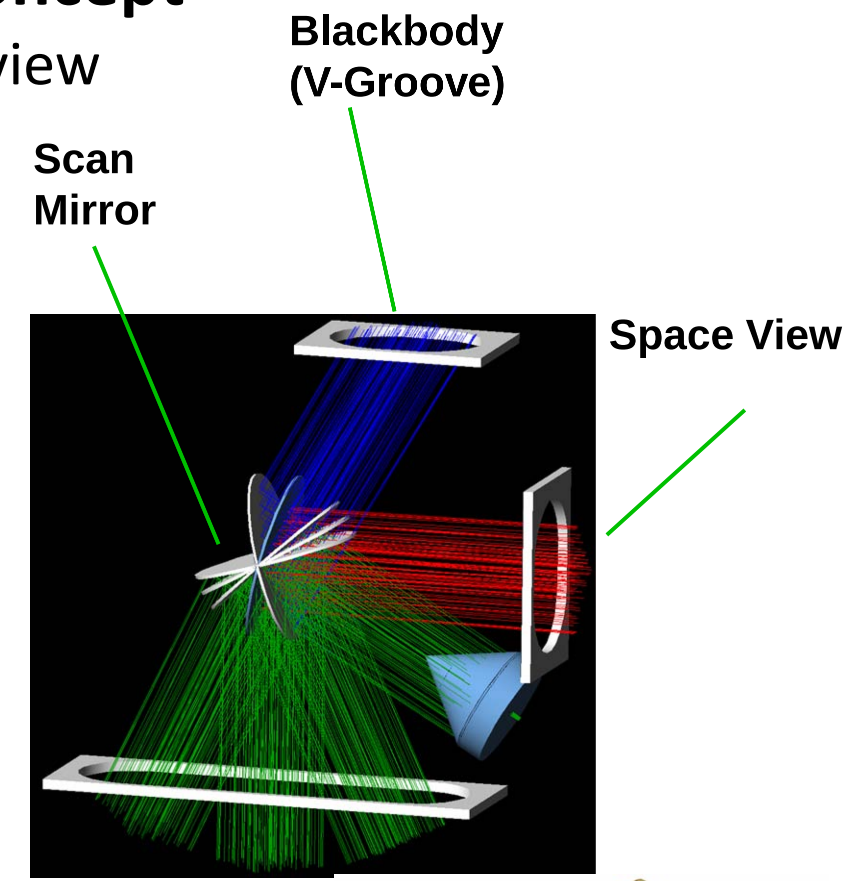

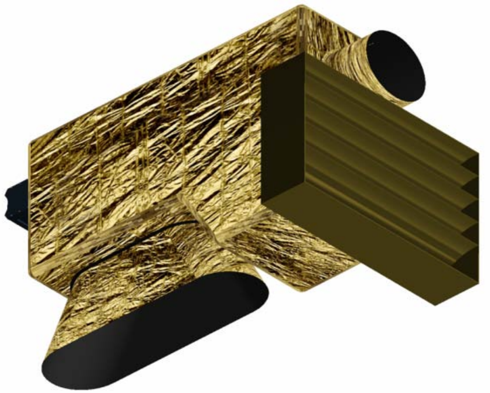

Simon Hook

Wildfires:

How are global fire regimes changing?

Simon Hook

High resolution thermal instrument can distinguish between the forest and non-forest parts of the flaming front allowing the fire type, intensity, etc., to be determined which indicates fire regime.

White squares show fire pixels detected by MODIS. Insufficient information to detect fire type

MIR band provides radiant flux to estimate rate at which biomass combusted and instantaneous emission estimate

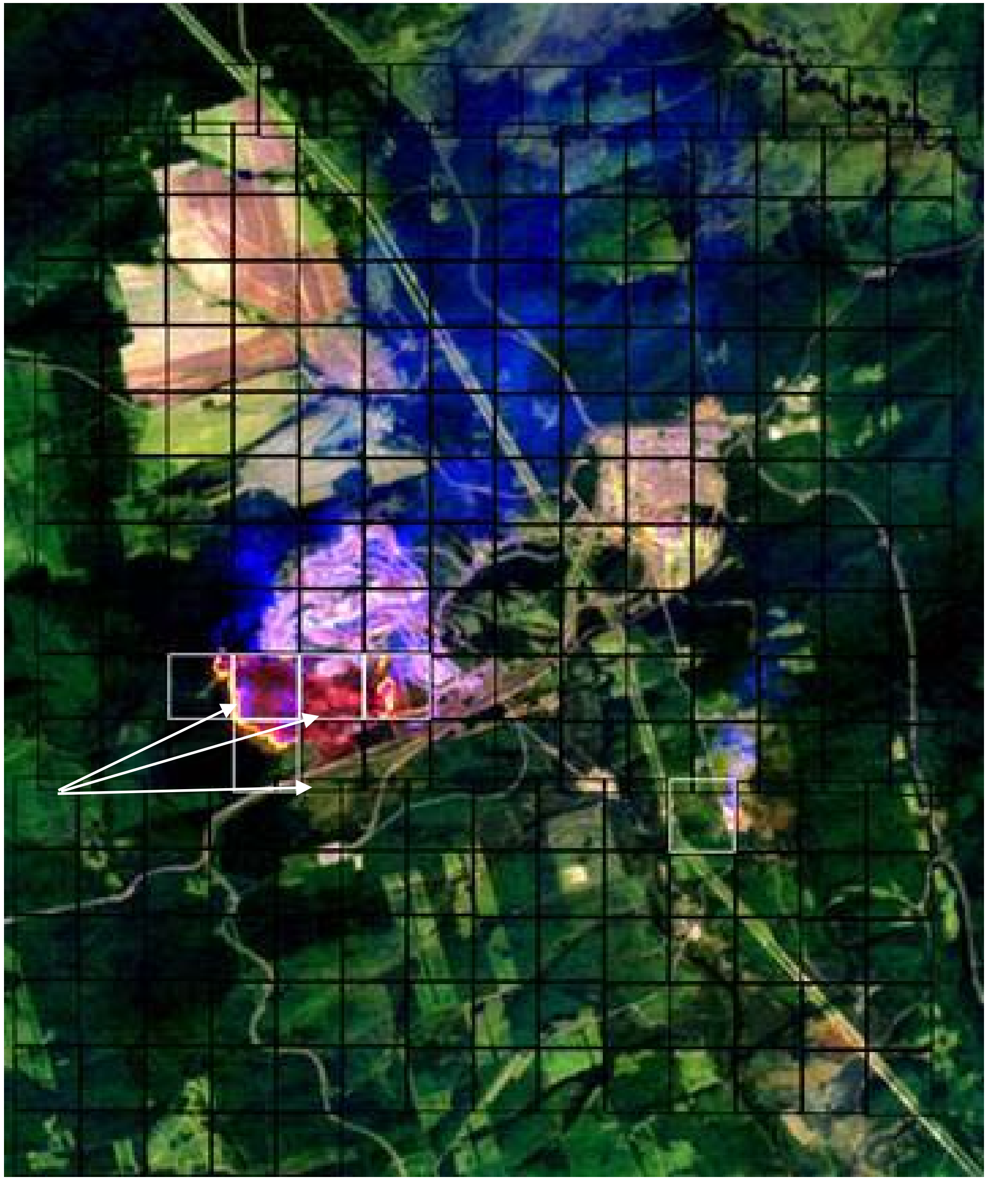

30 m ASTER scene with MODIS pixels superimposed (black squares)

Central Siberia

30 May 2001

HyspIRI will provide high spatial resolution mid to thermal infrared data for determining the fire regime and allowing flux estimation on a weekly basis

Bogdan Oaida

HyspIRI Mission Concept

Orbit Selection

- Key Orbit Design Considerations
  - Local time of observations
    - Sun-synchronous
    - 10:30 AM LTDN
  - Altitude
    - Low Earth Orbit
    - Repeating Ground track
  - Global coverage in a minimum number of days given the swath-width of each instrument.
    - VSWIR: 19 days revisit at the equator
    - TIR: 5 day revisit at the equator (1 day + 1 night)
- 626 km altitude at equator suits the needs of both instruments

Orbit selection and operations concept meet science requirements with very infrequent ground commanding or maintenance.

Operations Concept

- Systematic mapping vs. pointing capability
- Target map driven - No need for uploading acquisition sequences
- High resolution mode and Low resolution mode
- Direct Broadcast capability
  - Uses Intelligent Payload Module
  - Applications-driven

Operational Requirement	VSWIR	TIR
10:30 am sun-sync orbit	✓	✓
626 km altitude at equator	✓	✓
19 days revisit at the equator	✓	
5 day revisit at the equator		✓
Day Observation	✓	✓
Night Observation		✓
Pointing strategy to reduce sun glint	✓	
Surface reflectance in the solar reflected spectrum for elevation angles >20	✓	
Avoid terrestrial hot spot	✓	
Monthly Lunar View calibration	✓	✓
Weekly Solar View Calibration	✓	
Blackbody View Calibration		✓
Deep Space View Calibration		✓

Payload Accommodation and System Margins

Bogdan Oaida

Accommodations	VSWIR	TIR
Mass (CBE)	60 kg	64 kg
Volume	1.1 x 0.5 x 0.8 m	1.2 x 1.1 x 0.6 m
Power	41 W	103 W
FOV (crosstrack)	13.62 deg	50.7 deg
FOV (alongtrack)	95.9 microrad	95.9 microrad
Orientation	4 deg to starboard	nadir
Pointing		
Accuracy	165 arcsec (3σ/axis)	
Knowledge	2 arcsec (Pitch/Yaw axis 3σ); 8 arcsec (Roll axis 3σ)	
Stability	5 arcsec/sec (3σ)	

	Required	Design	Margin (D-R)/D
Swath width VSWIR	141km	151 km	6%
Swath width TIR	536km	600 km	11%
Recorder capacity	2.0 Tb	3.1 Tb	37%
Power	620 W (CBE)	965 W	36%
LV mass capability	530 (CBE, dry)	790 kg	32%

VSWIR's Local solar illumination constraint (SZA < 70 deg.)
Northern Hemisphere Winter Solstice

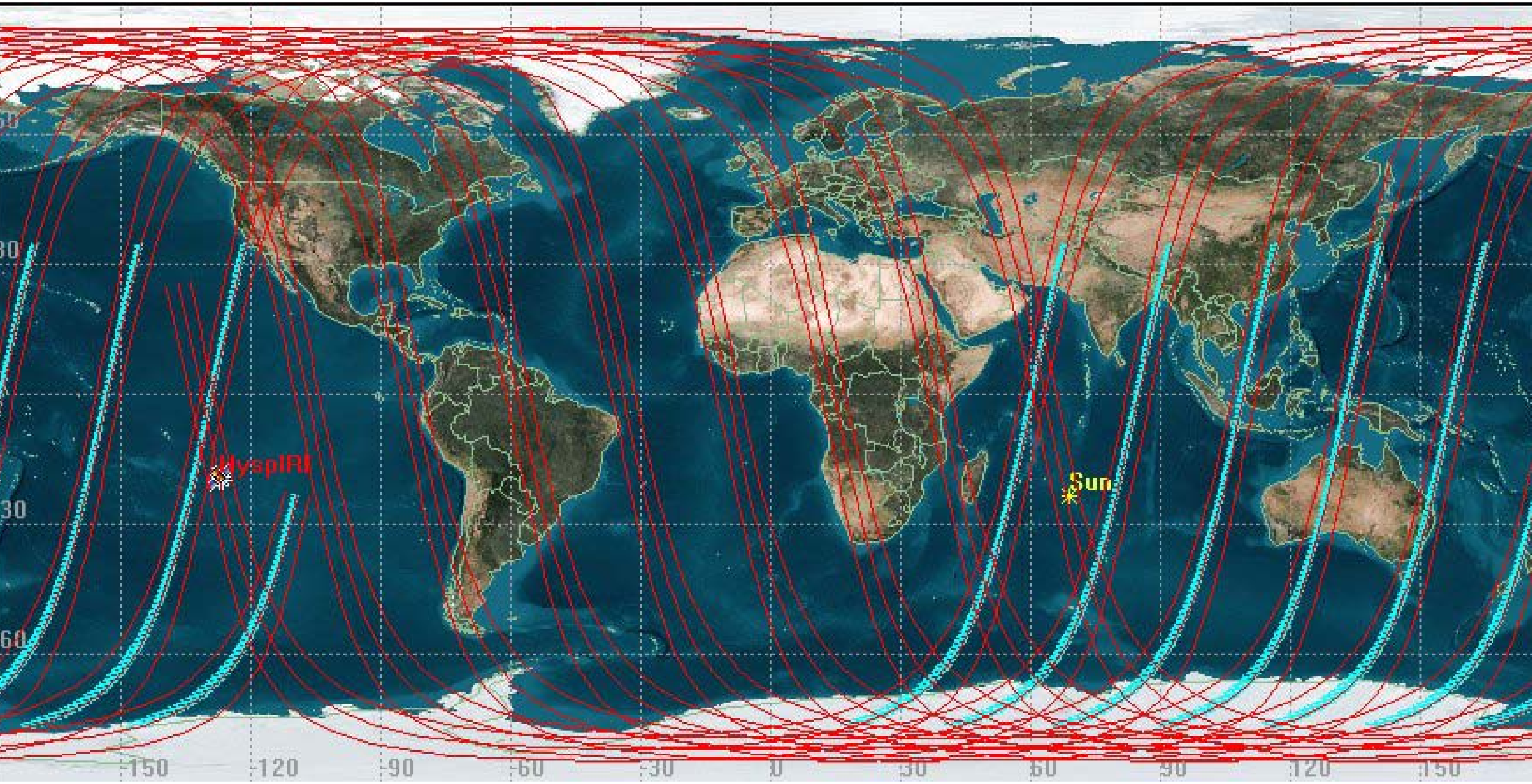

Bob Knox

Justification for PRI-type product

Amount of "Green stuff"

Physiological state (stress)

$$\text{Photosynthetic rate} = f(\underbrace{APAR}_{\text{NDVI}}) \times \varepsilon \begin{cases} \textbf{PRI – carotenoids} \\ \textbf{Canopy water} \\ \textbf{Temperature} \end{cases}$$

NDVI

Note synergy

Where:

APAR = Absorbed photosynthetically active radiation

ε = *Efficiency* with which absorbed radiation is converted to fixed carbon

***Determination of ε remains a primary challenge* (Field et al. 1998, Running et al. 2009)**

John Gamon

How does it work?

$$CI_{red\ edge} \propto [(\rho_{red\ edge})^{-1} - (\rho_{NIR})^{-1}]\ \ \rho_{NIR}$$

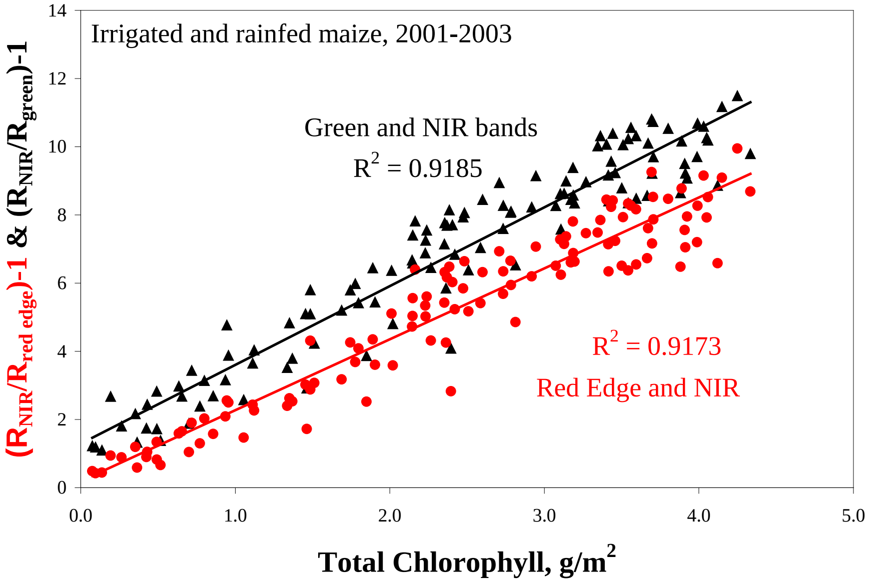

Gitelson et al., GRL, 2005

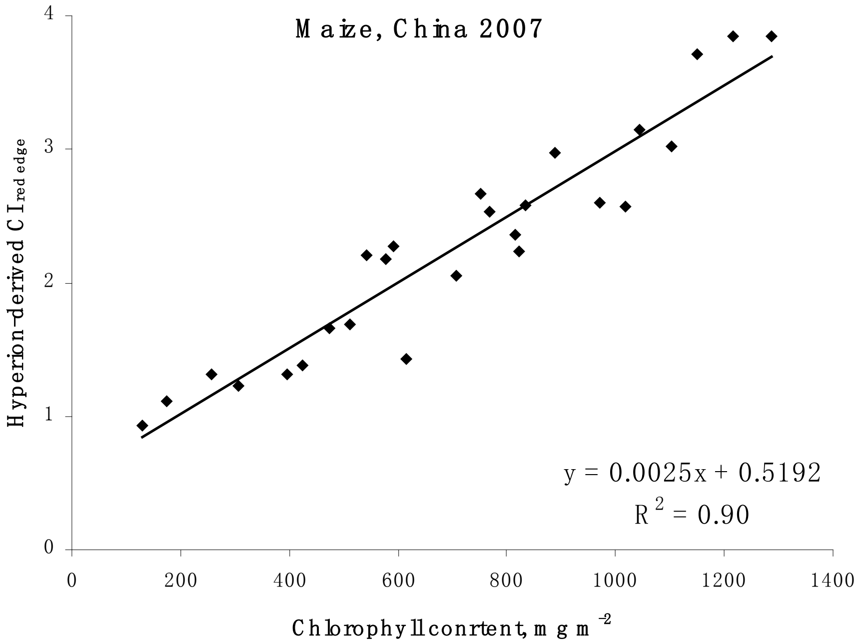

Wu et al., IJRS, 2010

Cloud Mask:
Cumulus + thin cirrus example

ASTER visible image

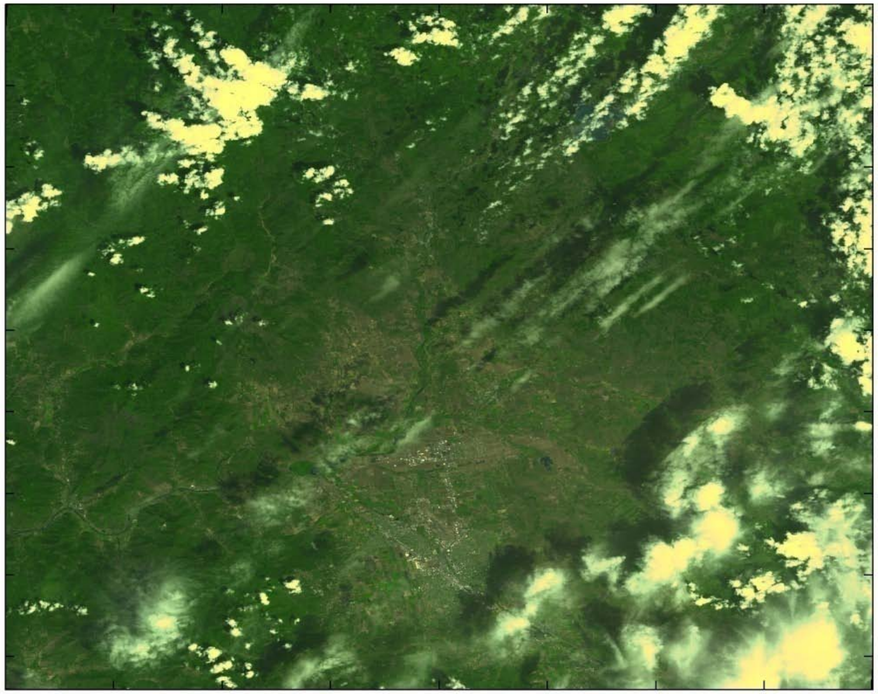

ASTER Cloud Mask + Fill

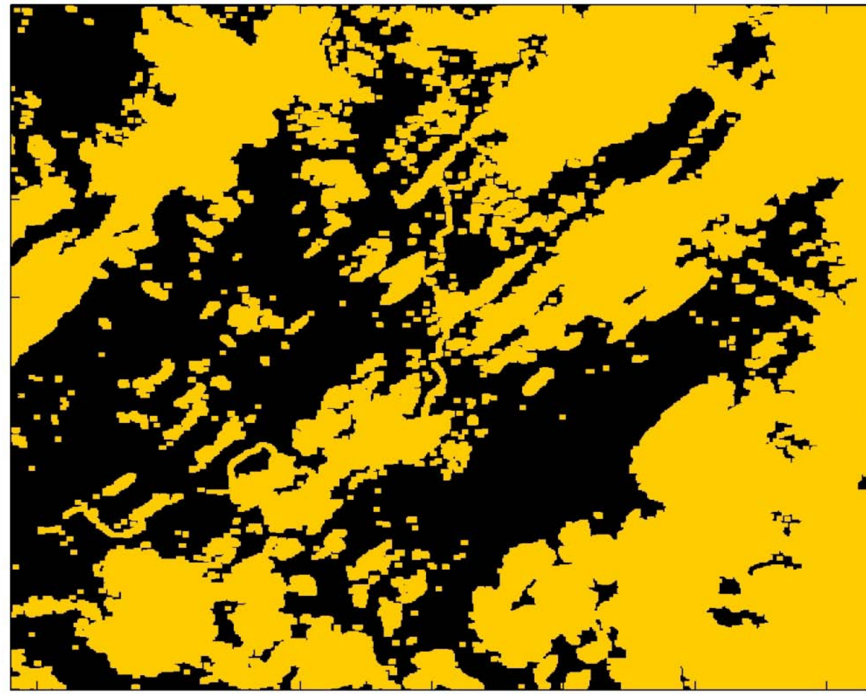

Shadow – **Cyan**

Cloud – **Gold**

Clear – **Black**

Simon Hook

Toxic Algae: Microcystis bloom

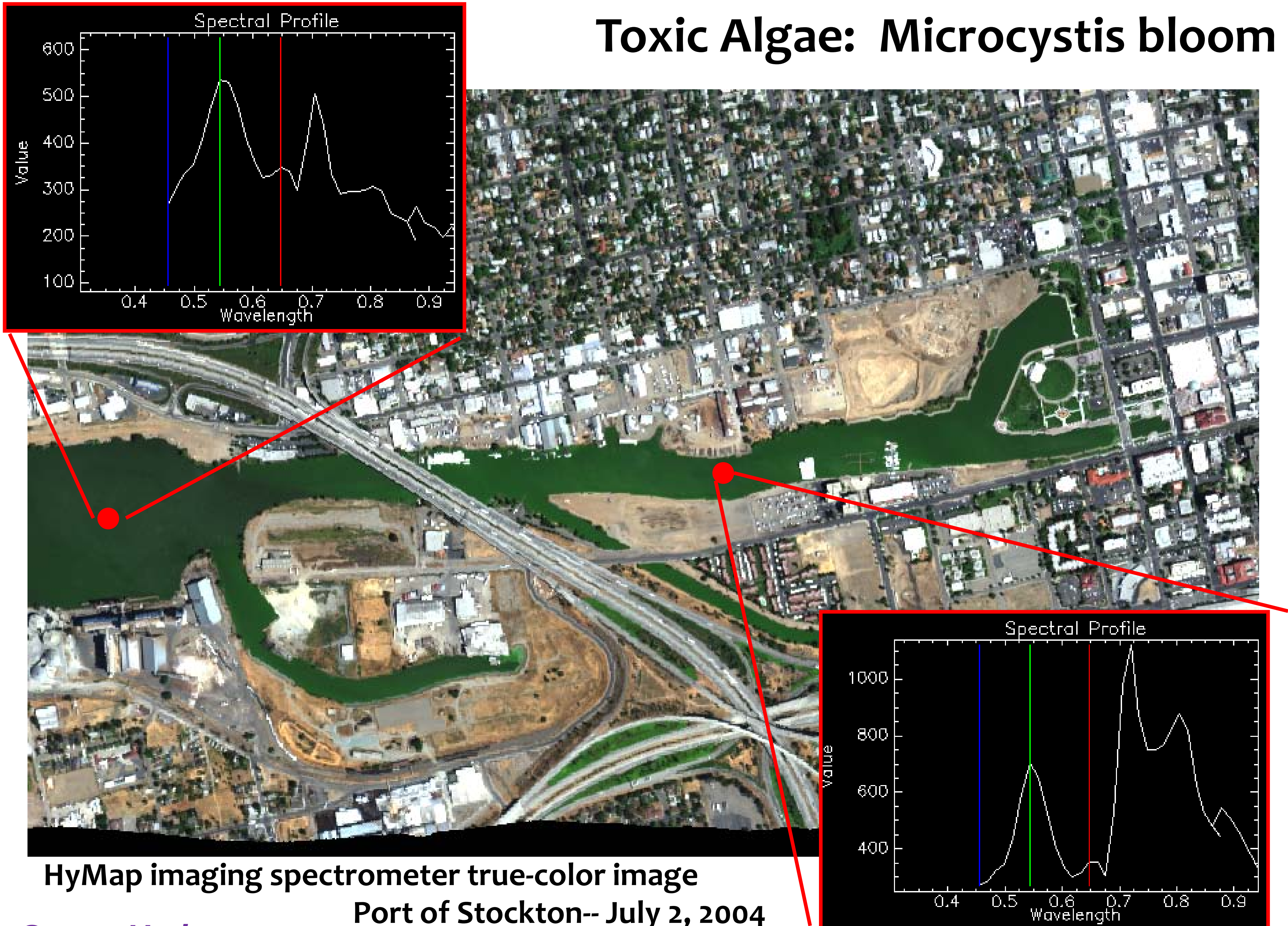

HyMap imaging spectrometer true-color image

Port of Stockton-- July 2, 2004

Susan Ustin

Atmospheric Correction

Bo-Cai Gao

MINERAL MAPPING USING ATREM OUTPUT

by Scientists at USGS in Denver, Colorado

RGB Image (Cuprite, NV)

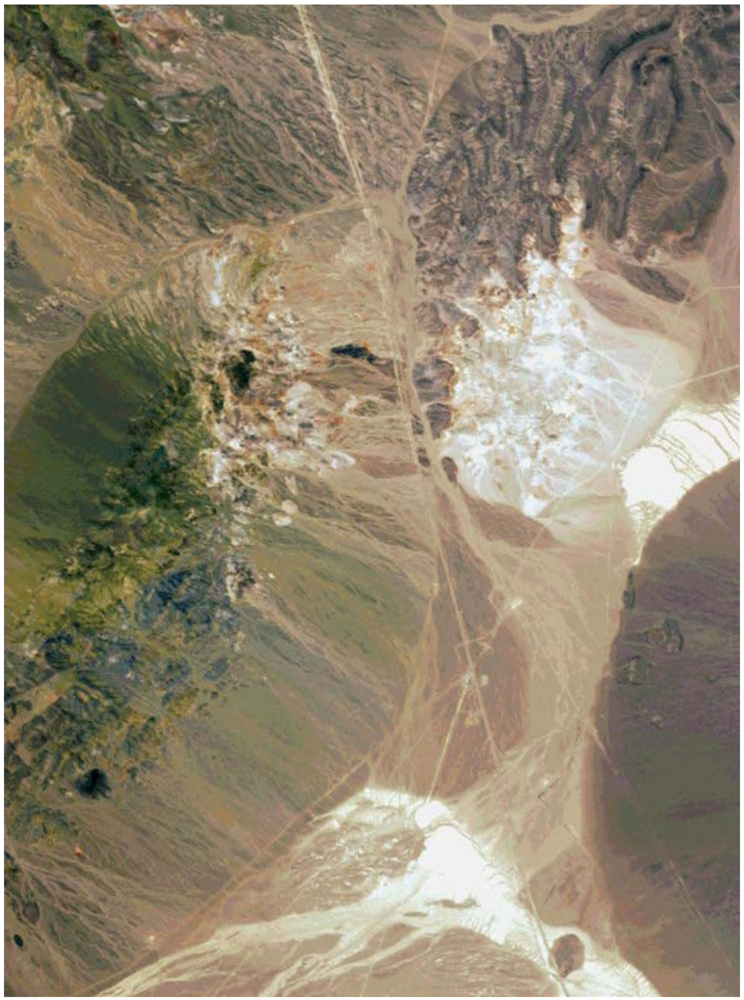

USGS Mineral Map, ~11x18 km

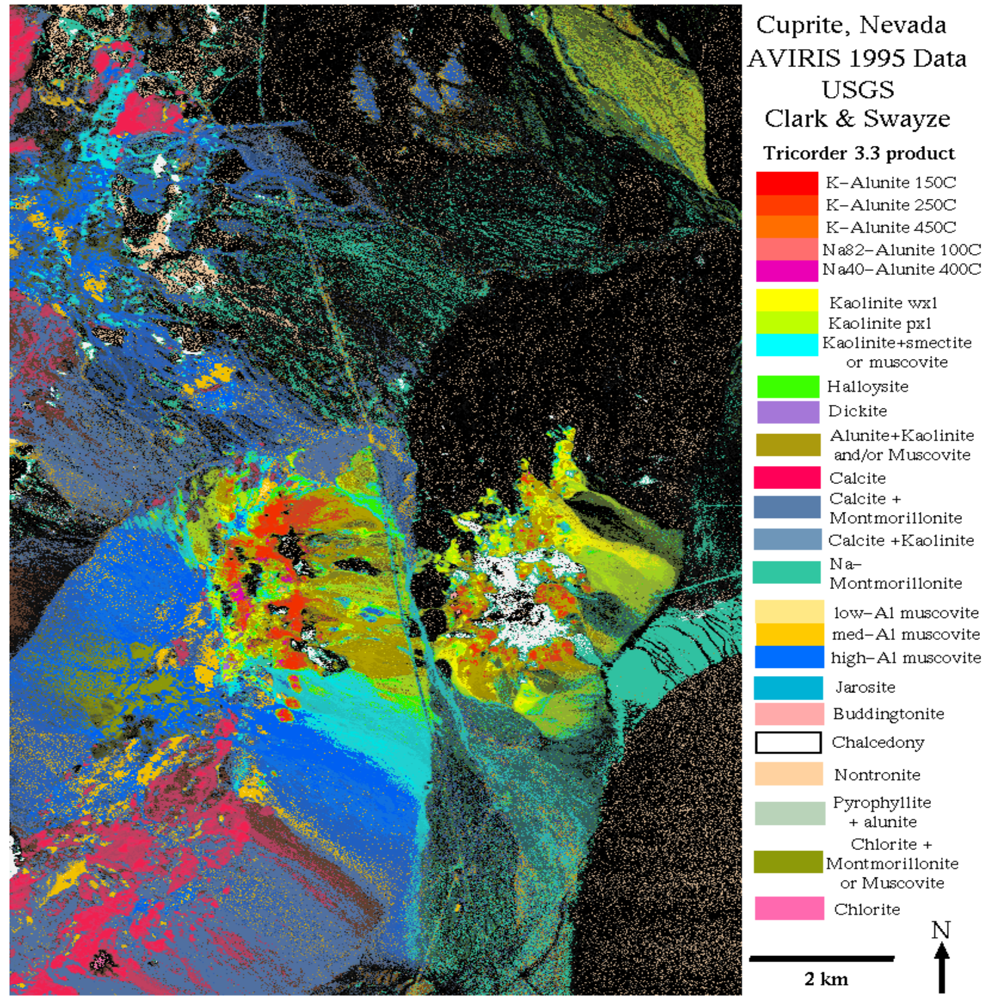

Processor Comparison

Tom Flately

	MIPS	Power	MIPS/ W
MIL-STD-1750A	3	15W	0.2
RAD6000	35	10-20W	2.33[1]
RAD750	300	10-20W	20[2]
SPARC V8	86	1W[3]	86[3]
LEON 3FT	60	3-5W[3]	15[3]
SpaceCube 1.0	3000	5-15W	400[4]
SpaceCube 2.0	5000	10-20W	500[5]

Notes:
1 – typical, 35 MIPS at 15 watts
2 – typical, 300 MIPS at 15 watts
3 – processor device only ... total board power TBD
4 – 3000 MIPS at 7.5 watts (measured)
5 – 5000 MIPS at 10 watts (calculated)

Results of half pixel misalignment and *"correction"* through linear re-sampling

Pixel Shift Scenario	Category 1 Ratio Value	Category 1 Discrepancy	Category 2 Ratio Value	Category 2 Discrepancy
VIS and NIR ½ pixel shift	*1.33*	*+33%*	*4.00*	*-20%*
VIS and NIR resampled	1.27	+27%	3.67	-26%
VIS and NIR unmixed	1.00	0%	5.00	0%

Inherent spectral/spatial integrity, required for HyspIRI, allows for substantially more accurate parameter determination than is possible with *currently planned* sequentially sampled pushbroom multispectral systems.

Unlike these multispectral systems, the rich spectral content offered by HyspIRI has the potential to mitigate the impact of temporal sampling offsets as well as to address mixed pixels.

Thermal-based flux mapping

Application to other regions

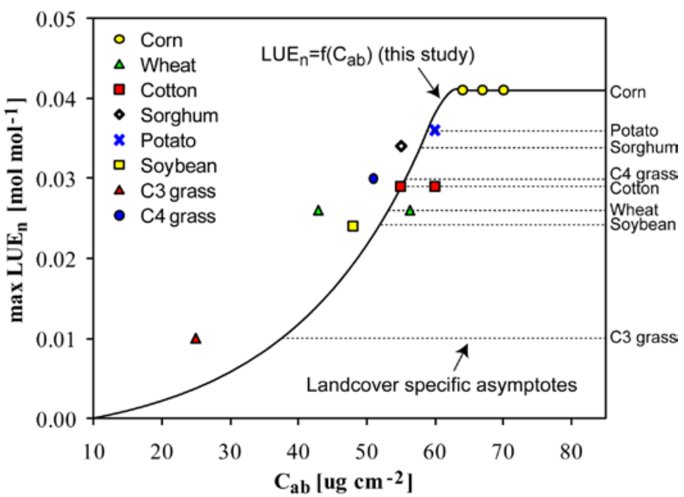

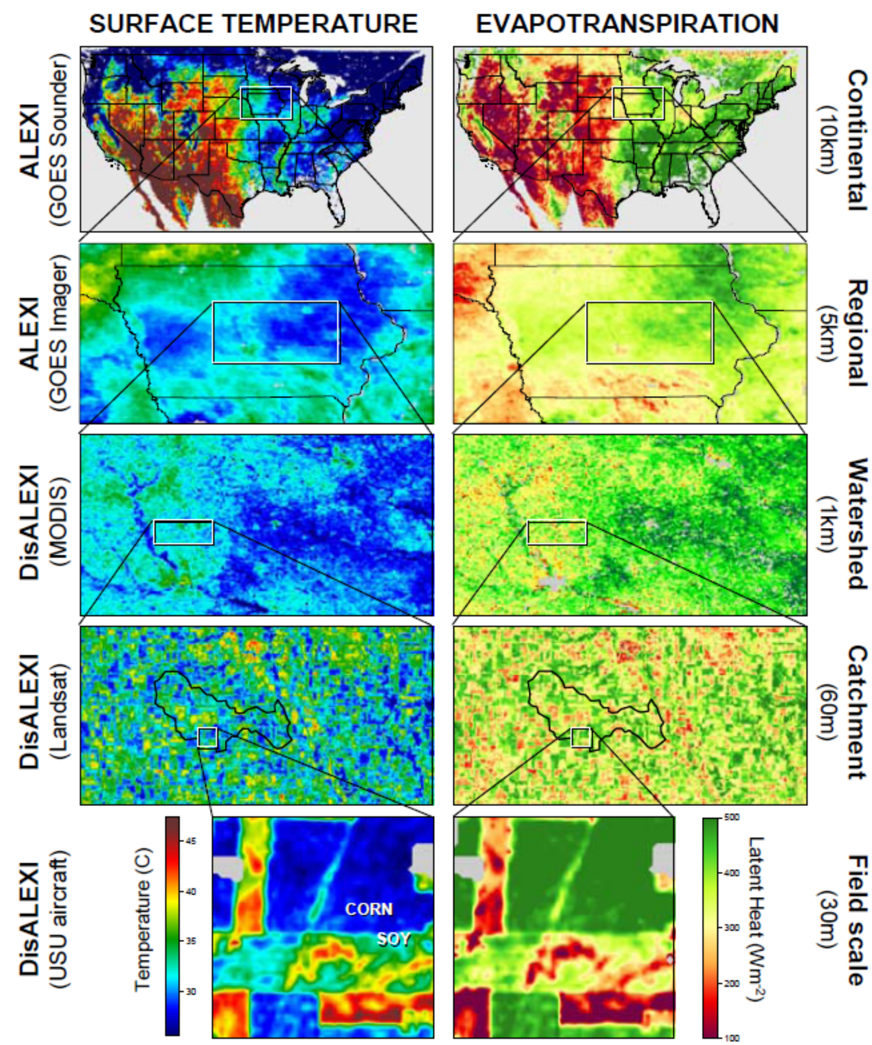

Rasmus Houborg

Fire Products: Benefits of HyspIRI

- Unprecedented sensitivity to flaming and smoldering fires
  - Can easily detect small agricultural fires (difficult with coarser resolution sensors)
- Fewer false alarms
- Straightforward retrieval of fire radiative power
  - Single band vs. three or more bands with existing sensors
- Greatly expanded spatial and temporal coverage
- Will provide large samples of detailed fire characteristics useful for statistically modeling fires and their behavior
- Calibrate and validate active fire observations derived from coarser resolution satellite data

Dar Roberts

Improved Temperature Emissivity Separation

- **Column water vapor is estimated using forward inversion as it varies spatially and with elevation**
- **Column water vapor is used to calculated downwelling radiance as a first step for emissivity estimation**

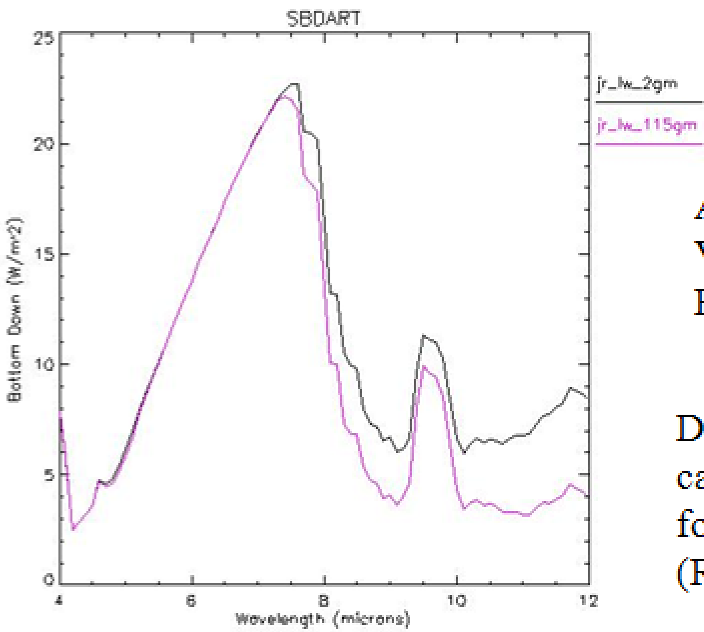

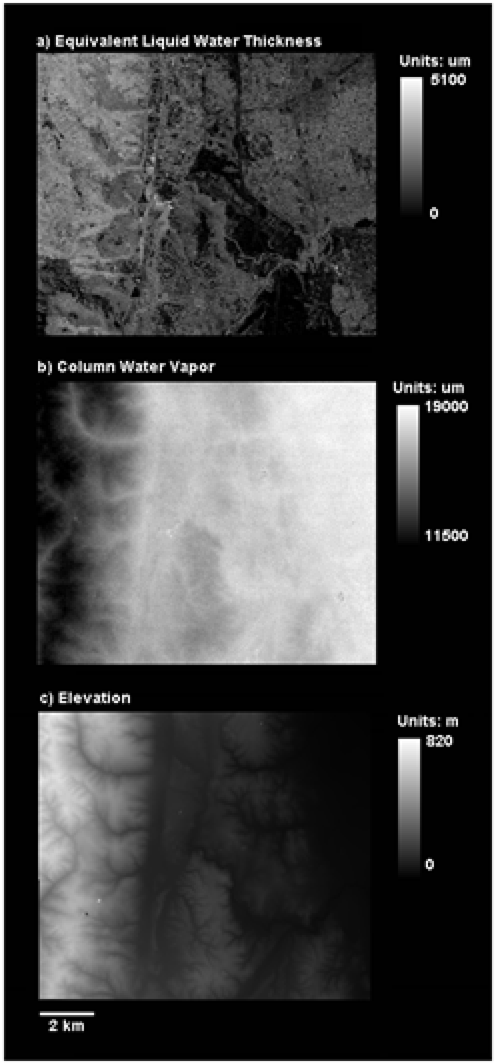

AVIRIS EWT, Column Water Vapor, and a DEM
From Roberts et al., 1997

Downwelling longwave calculated using SBDART for 1.15 and 2 g/m^2 water vapor (Richiazzi et al.)

Production: Standard ASTER TES Algorithm modified to include 60 m

Plant Functional Types

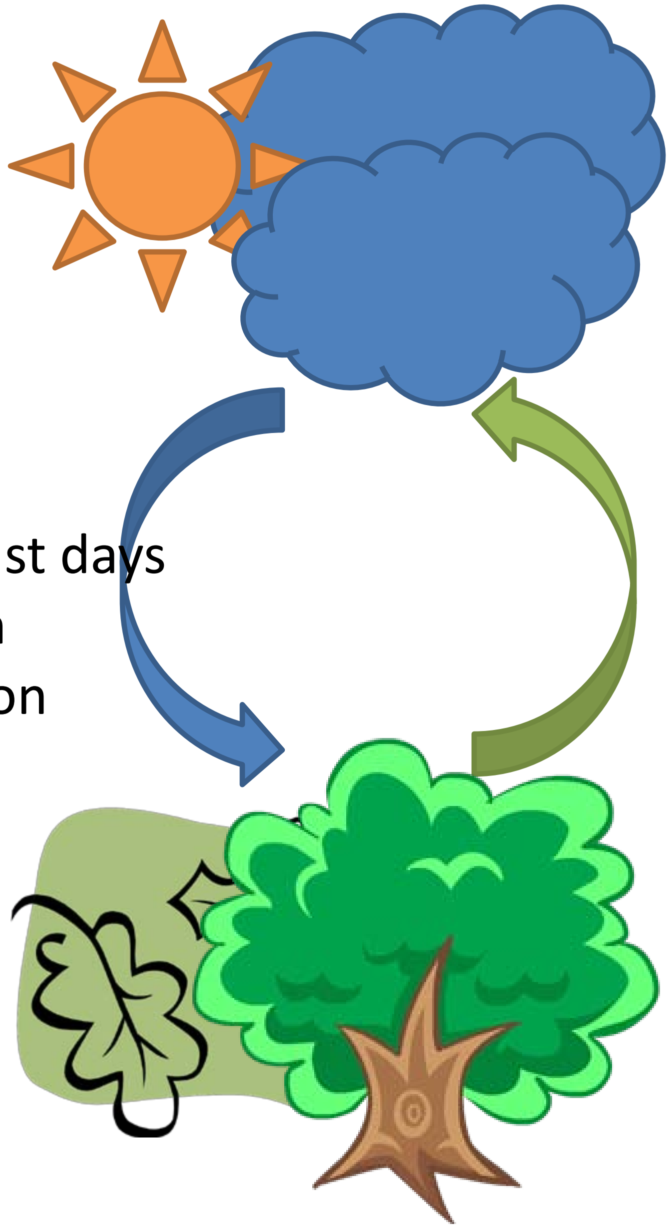

Changes in :

- Air temperature
- Precipitation
- # sunny vs. overcast days
- CO_2 concentration
- Nitrogen deposition

Changes in:

- Albedo
- Evapotranspiration
- Soil moisture
- Surface temperature

Changes in:

- Timing of greening
- Length of growing season
- Stomatal closure
- Balance among species
- PFTs, spatial & temporal

➢ Estimates of surface energy balance can be improved by better characterization of the surface.

- Cellulose Absorption Index (CAI) is a measure of the relative depth of the absorption feature near 2100 nm.
- Other features are associated with protein, lignin, and minerals.

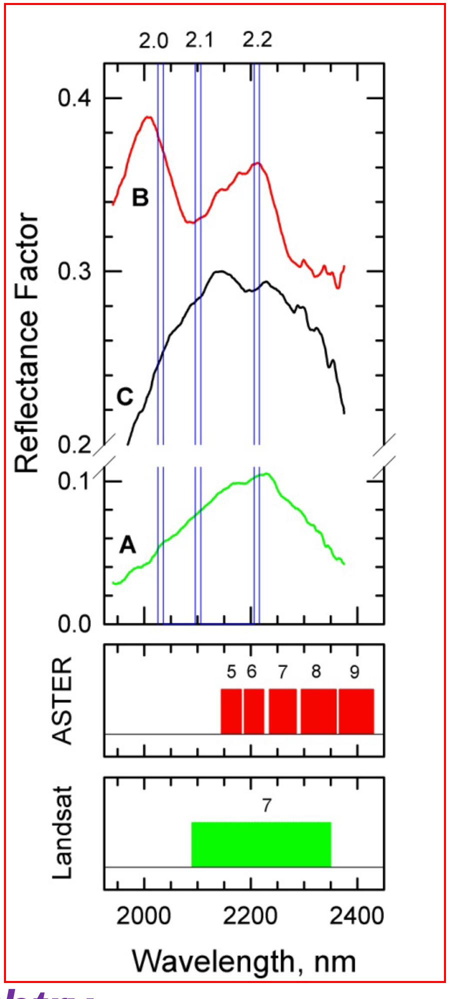

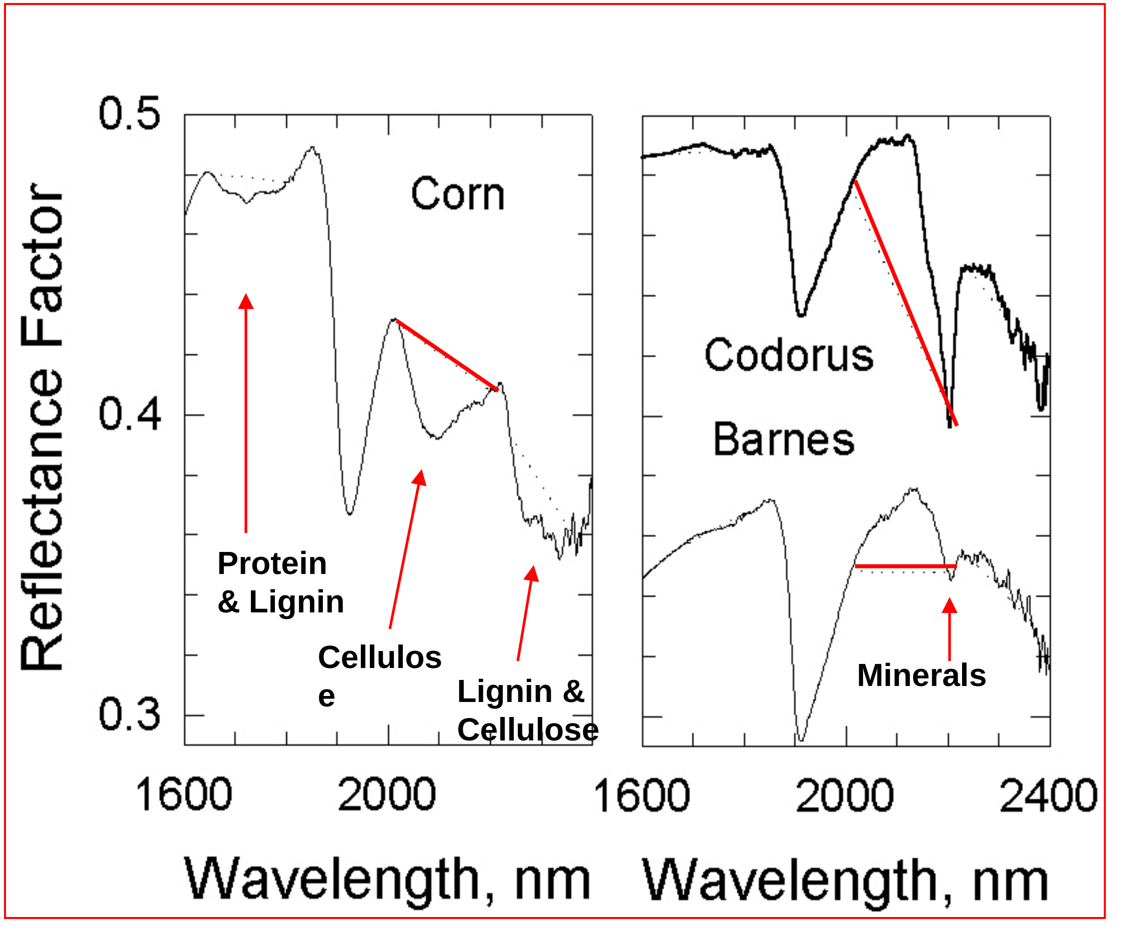

Daughtry

HyspIRI Example from Airborne-IS 2005

Green

- Airborne-IS example from Ivanpah Playa
- Solar reflected spectrum
- Offner spectrometer
- TCM6604a detector array
- HyspIRI calibration standards and approach

Level O

DN versus Band

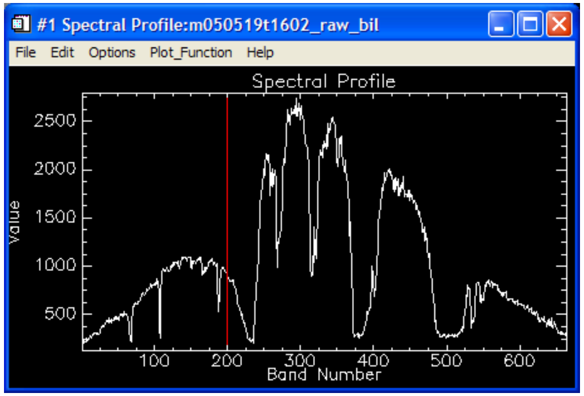

Level 1

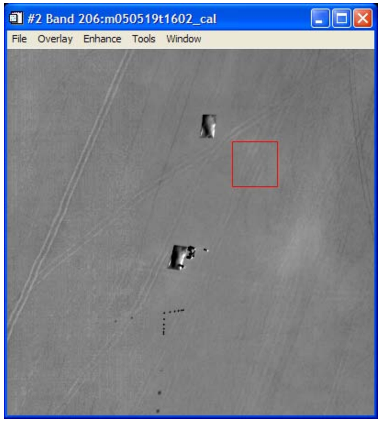

Radiance versus Wavelength

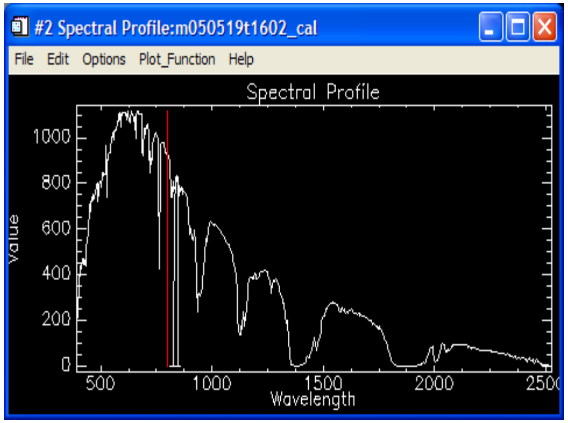

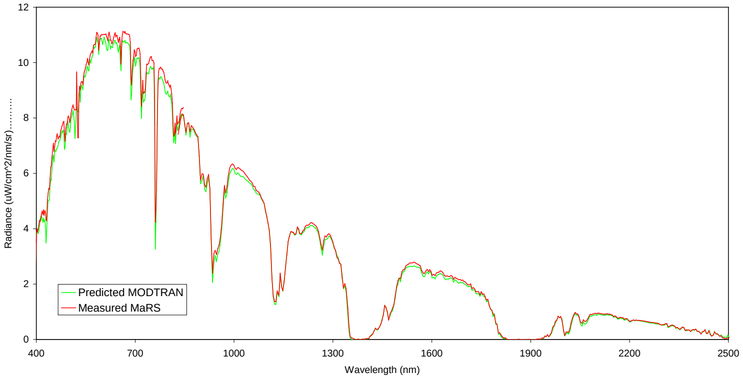

Hook

Radiometric Calibration

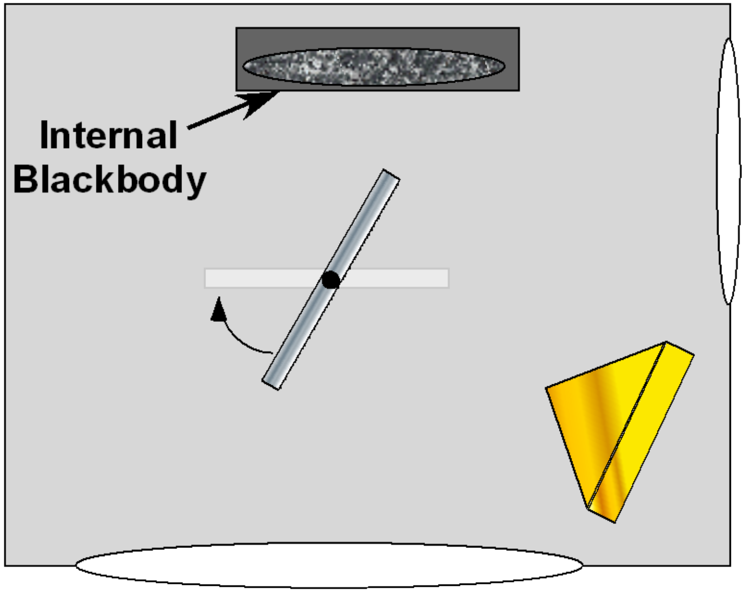

- Performed in vacuum to prevent condensation on cold blackbody surfaces.
- Scan mirror rotates to scan between internal blackbody, cold blackbody, and variable temperature blackbody.
- Variable temperature blackbody is stepped over entire scene temperature range.
- System nonlinearities can be determined using measured spectral response and blackbody response.
- NETD determined by temperature response and noise level.

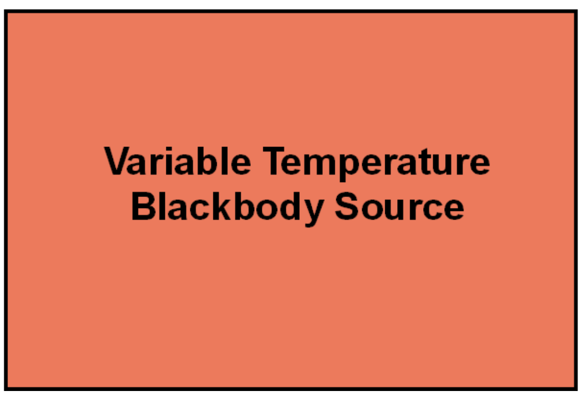

Hook

Large Area Coverage

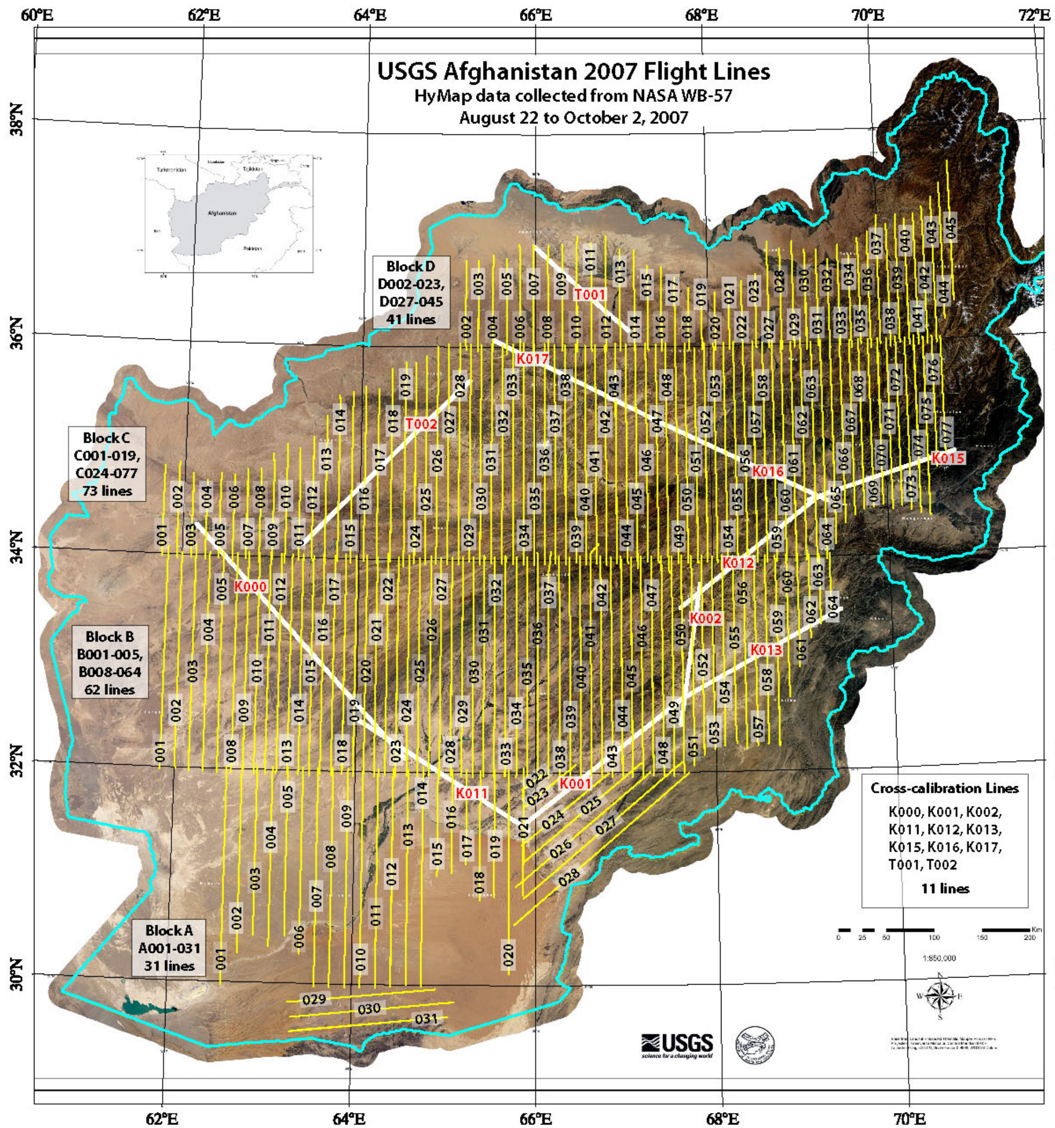

AGENDA – DAY 2 (May 5)

8:00 - 8:20 am: Coffee and donuts, Posters

8:30 -8:40 am: Review of Day 1 [**Betsy**]

VII. Related Activities to HyspIRI Mission

8:40 – 9:00 am: 2 Presentations on 2009 Funded HyspIRI Preparatory Studies
[**Petya Campbell, Phil Townsend**]

9:00 – 9:15 am: International collaborations, ISIS & WGCV [**Rob Green**]

9:15 – 9:35 am: A Mission Calibration Plan to support Products
[**Kurt Thome/Rob Green/Simon Hook**]

9:35 – 10:10 am: Synthesis of the Three Break-out Group Inputs (10 min each)
[**Phil/John, Simon/Kurt, Dar/Susan**]

10:10 -10:30 am: Coffee Break & Posters

HyspIRI VSWIR Science Measurements
Key SNR and Uniformity Requirements

Green

Benchmark Radiances

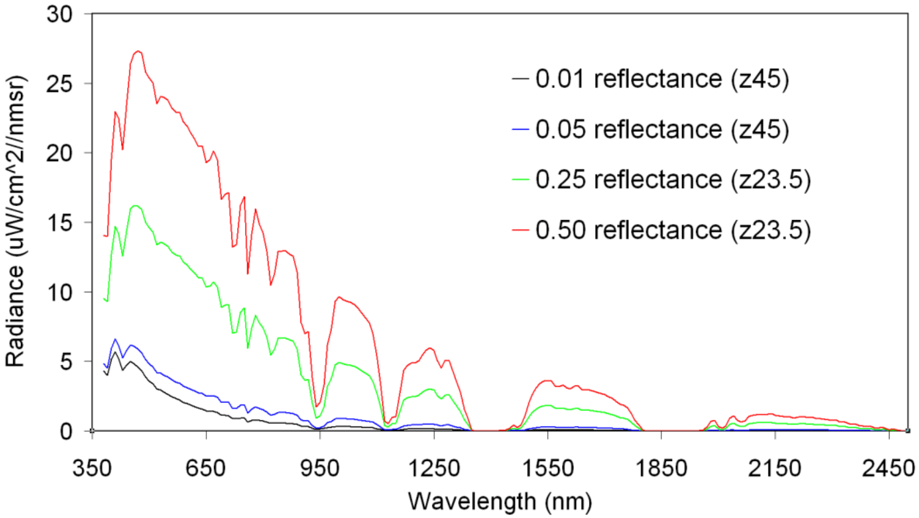

Required SNR

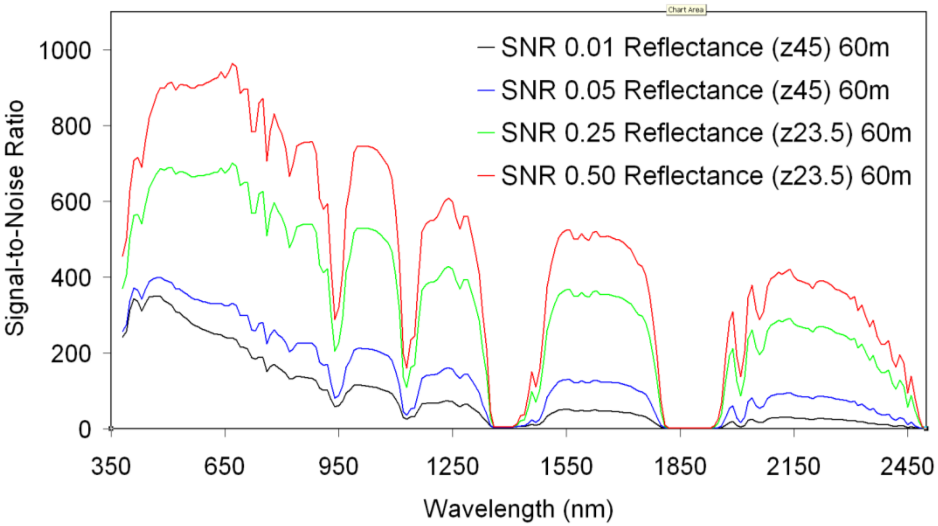

Uniformity Requirement

Cross Track Sample

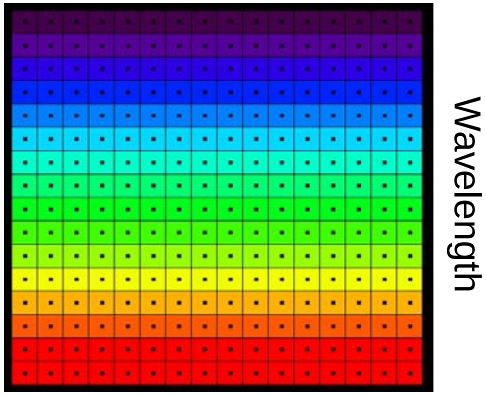

Depiction

-Grids are the detectors

-dots are the IFOV centers

-Colors are the wavelengths

Requirement

Spectral Cross-Track	>95% cross-track uniformity {<0.5 nm min-max over swath}
Spectral-IFOV-Variation	>95% spectral IFOV uniformity {<5% variation over spectral range}

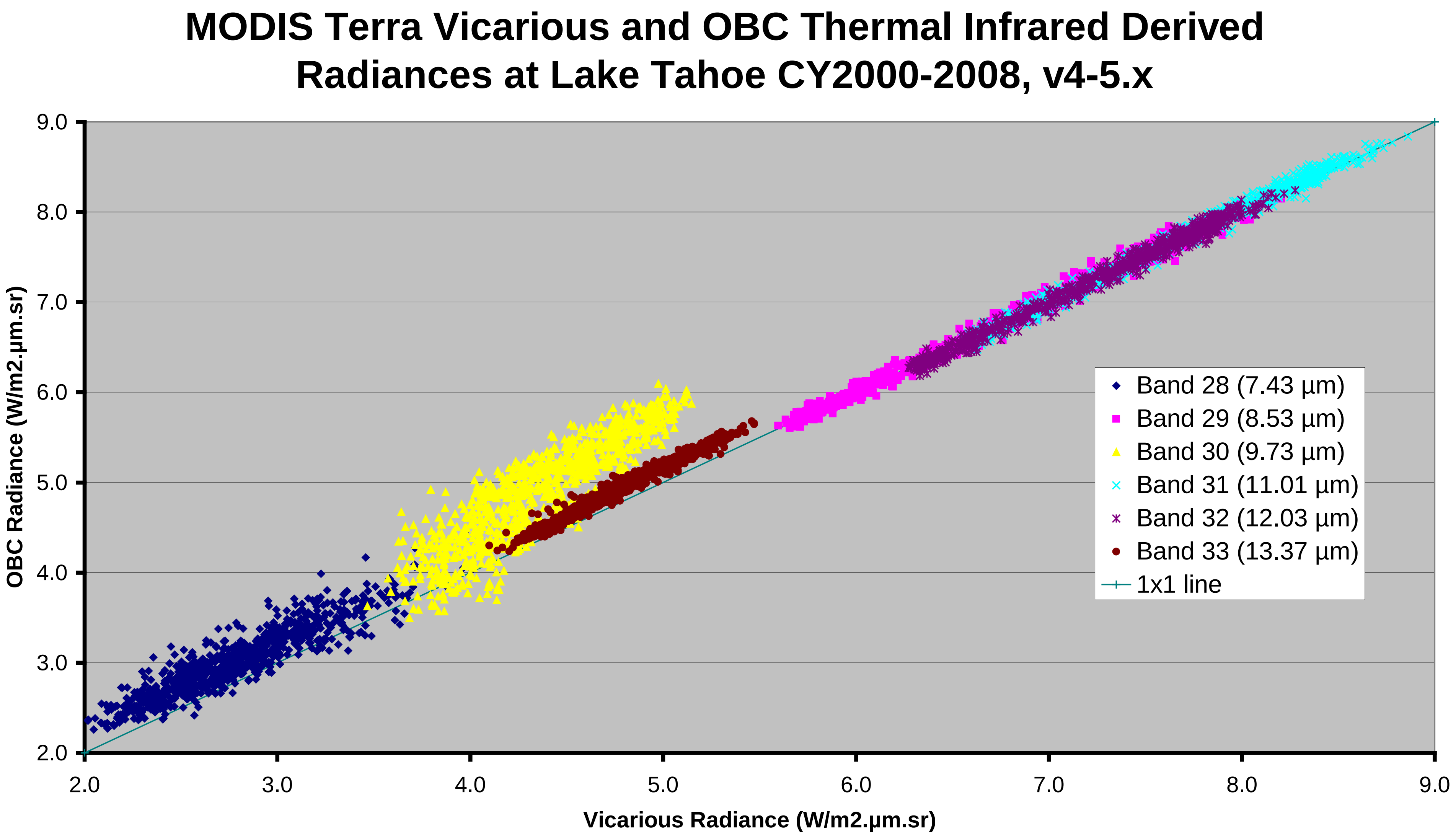
MODIS Terra Vicarious and OBC Thermal Infrared Derived Radiances at Lake Tahoe CY2000-2008, v4-5.x
OBC Radiance (W/m2.µm.sr)
Vicarious Radiance (W/m2.µm.sr)
2.0
3.0
4.0
5.0
6.0
7.0
8.0
9.0
Band 28 (7.43 µm)
Band 29 (8.53 µm)
Band 30 (9.73 µm)
Band 31 (11.01 µm)
Band 32 (12.03 µm)
Band 33 (13.37 µm)
1x1 line

Assessment of ecosystem diversity and urban boundaries:

Preliminary findings, exploring surface reflectance and emissivity

Petya K. E. Campbell*, **, Vanisha Bisnath☺, David Lagomasino☺☺ and Kurtis J. Thome**

* Joint Center for Earth Systems Technology (JCET), University of Maryland Baltimore County
☺ GSFC Summer Student Intern, Wesleyan University, Middletown, CT
☺☺ GSFC Summer Student Intern, Florida International University, Miami, FL
** NASA Goddard Space Flight Center , Greenbelt, MD

Background

Problem: With the increase in the population density, the effect of ever expanding conversion of land from rural to urban has become a problem of critical importance. *With increasing urbanization, land cover type and land surface temperature (LST) in urban and rural areas display significant differences, such as higher LST and lower moisture content.*

Hypotheses: The distribution, and spectral and spatial characteristics of optical and thermal data co-vary, in significantly different way in natural and anthropogenic environments; The combination of high spectral resolution optical and thermal infrared imagery will provide a powerful capability for more precise land cover type discrimination and ecosystem monitoring than possible using current satellite systems.

Science Questions

- How do natural environmental characteristics change under the effects of urbanization, affecting vegetation composition and function, and ecosystem health?

- How do natural vs. anthropogenic ecosystem compositions compare (similar environmental conditions) with regard to land cover types, diversity, function, and spectral properties?

- How do natural ecosystems respond to impinging environmental changes, particularly to urban growth and land cover change and the associated impacts of urbanization?

Goals

1. Using together VSWIR and TIR measurements, to assess the differences in natural and anthropogenic ecosystem composition and their vegetation bio-physical parameters.

2. Provide data that can elucidate how urbanization impacts the environment. Seeking common spectral trends associated with vegetation function, induced by natural and anthropogenic factors such as effects of urbanization and UHI, we would contribute toward improving the current capabilities for vegetation assessments.

3. Generate HyspIRI-like datasets and tools for work with the data.

Study Sites

The study includes two independent locations with different regional climate and ecosystem types. Data aggregated to higher and lower spatial scales will be compared for the same locations.

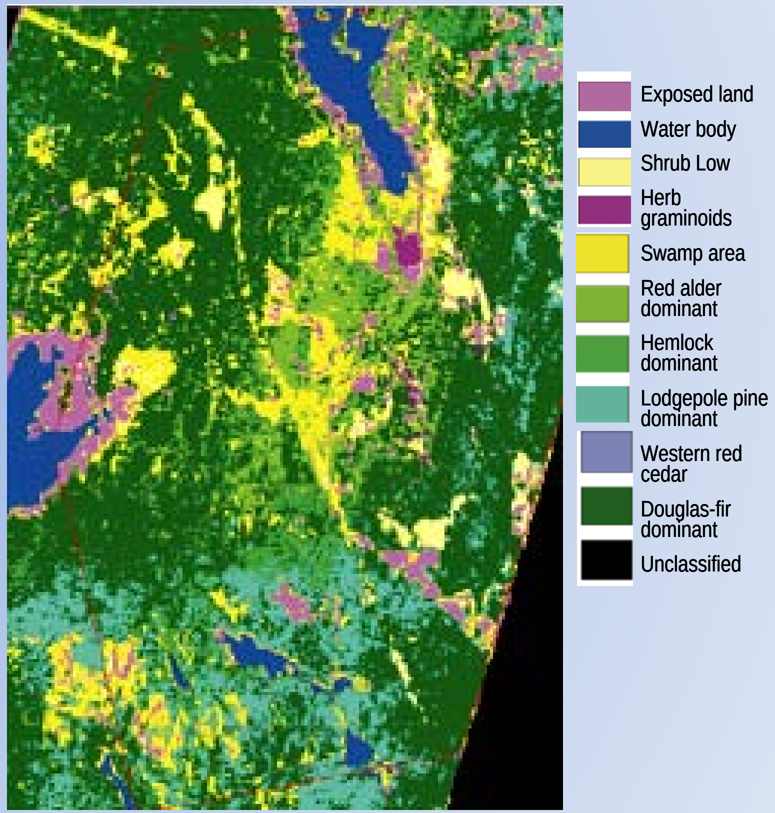

Hyperion land cover classification of the Greater Victoria Watershed (GVWD) test site on Vancouver Island (September 10 2001, Goodenough et al. 2003).

Vancouver Island, Canada/Hoquiam, WA: includes portions of unique natural ecosystems such as the Great Victoria Watershed (GVWD) test site on Vancouver Island, BC and rural, sub-urban and urban environment associated with the city of Victoria, BC.

Jasper Ridge Biological Preserve (JRBP), CA: provides Mediterranean-type climate, with five major vegetation types: evergreen forest, deciduous forest, chaparral shrublands, herbaceous perennial wetlands, and annual grasslands

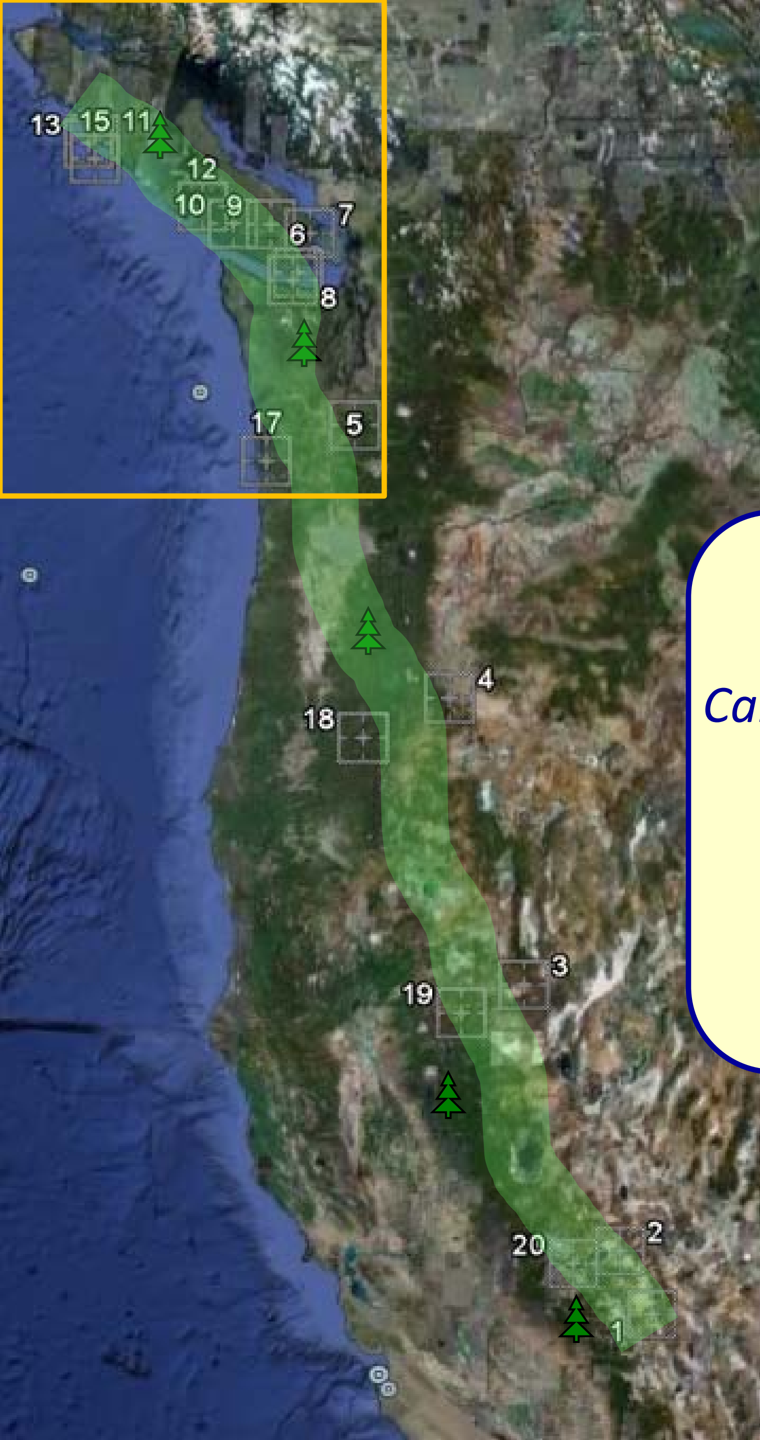

Area 1:

Vancouver Island
Canada/Hoquiam, WA

Data:

MASTER & AVIRIS

ASTER

EO-1 Hyperion

Area 2:
Jasper Ridge Biological Preserve (JRBP), CA

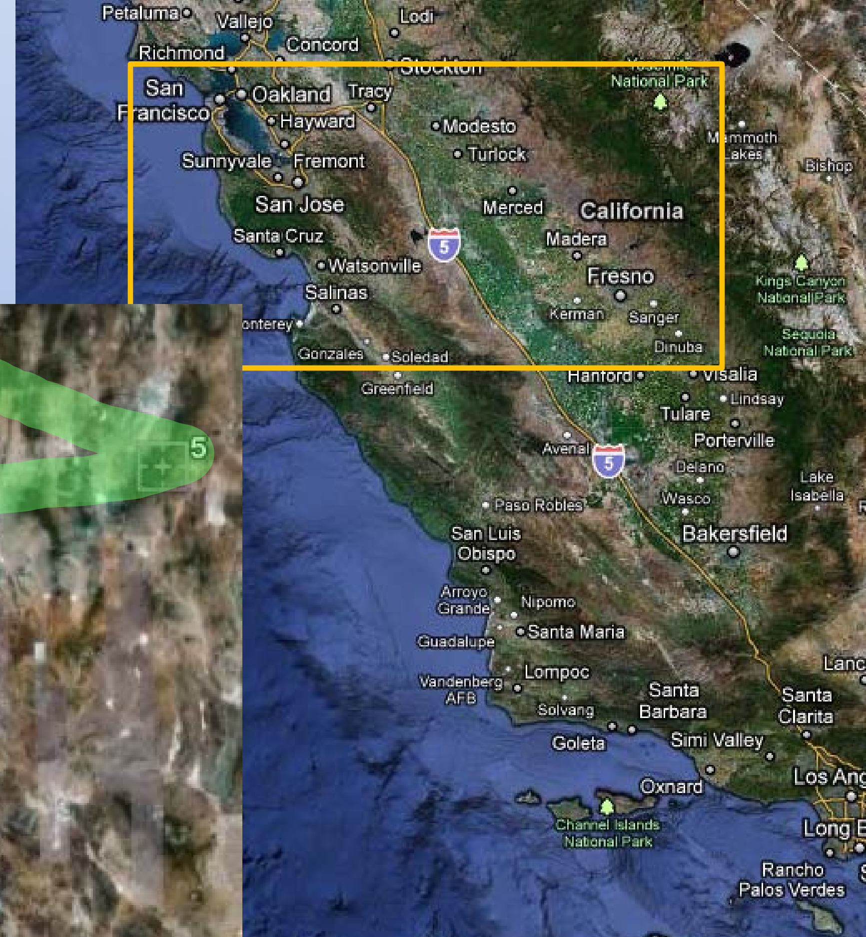

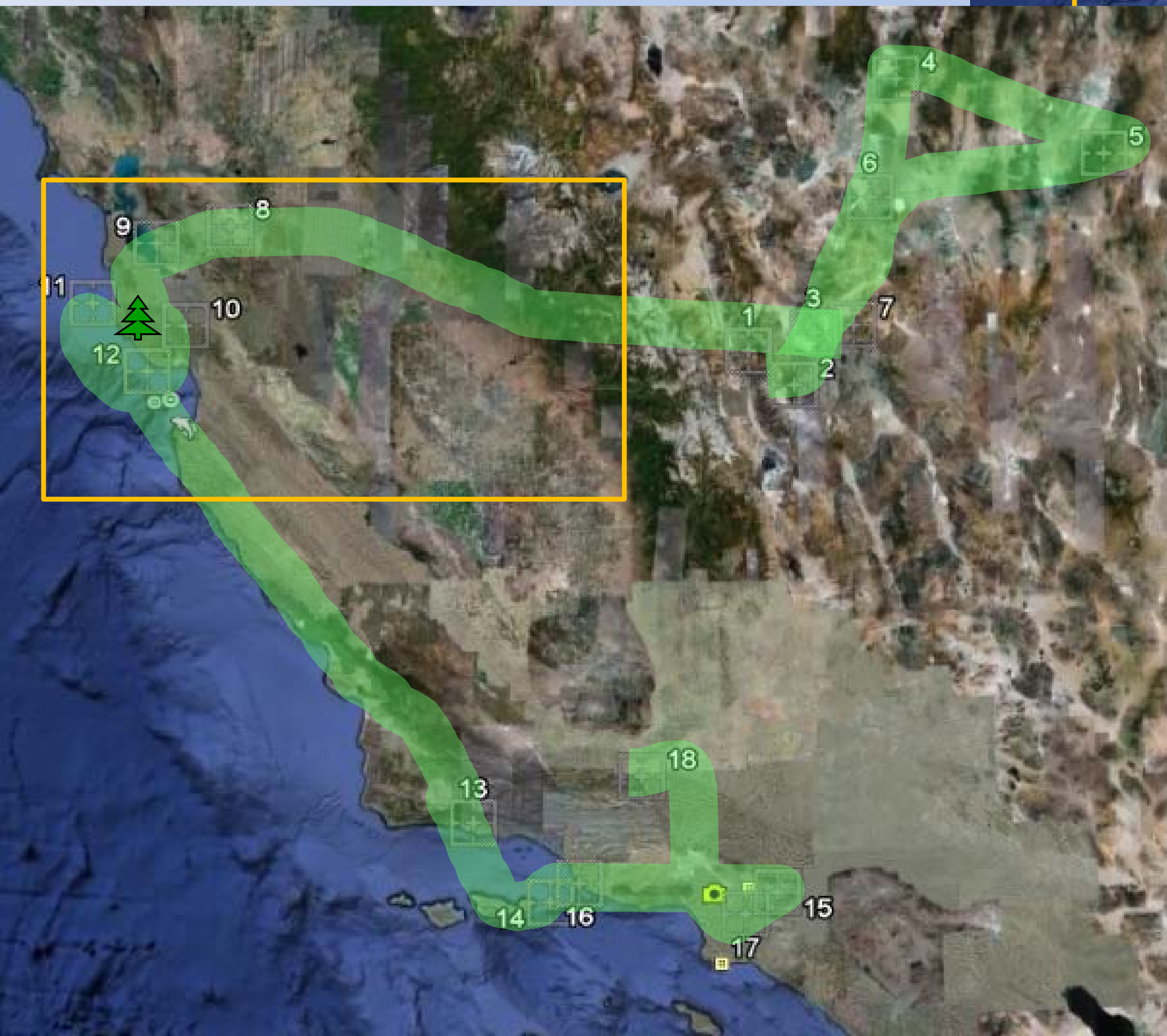

Data:

MASTER & AVIRIS

Hyperion

Calibration of TIR and VISWIR data

Lake Tahoe is a high-altitude, large-sized lake on the California-Nevada border near Reno, Nevada.

The *Ivanpah Playa* test site is approximately 3 km by 7 km in size with excellent spatial uniformity, hence its use for the vicarious calibration of reflective bands.

Sample MASTER imagery from the Ivanpah test site, reflectance (left), vegetation in green; thermal (right) side.

Capability of HyspIRI data for assessments of vegetation type and function

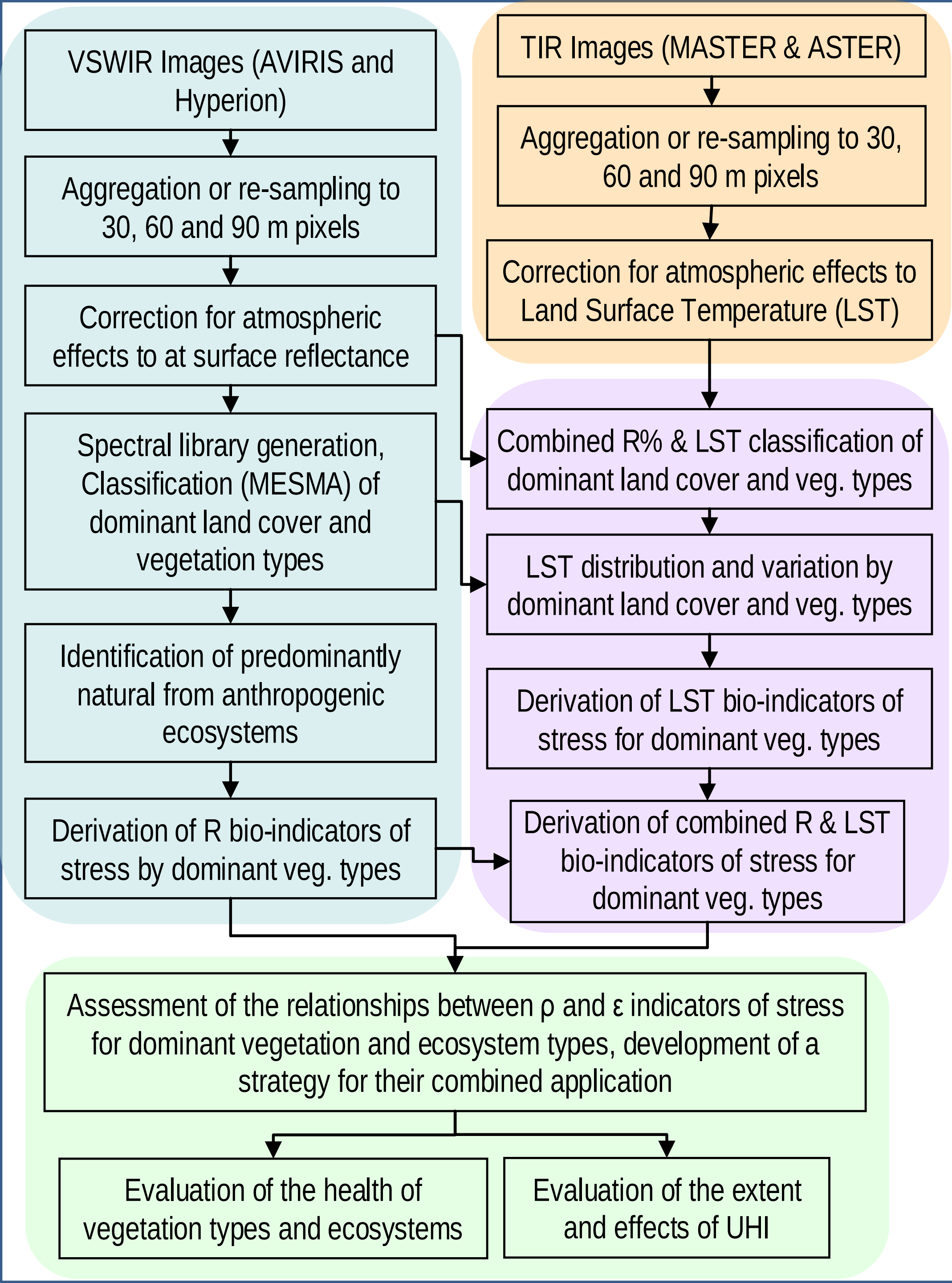

The analysis will be conducted using the native data resolution (~ 30 m), and aggregated to 60 and 90 m images, comparing the results.

Data

Parameters	HyspIRI VSWIR	AVIRIS	EO-1 Hyperion
Spectral range	*0.38 - 2.5 µm*	0.4 - 2.5 µm	0.4 - 2.5 µm
Band width	*10 nm*	10 nm	10 nm
number of bands	*~ 220*	224	220 (196 calibrated)
Spectral Coverage	*contiguous*	contiguous	contiguous
Spatial resolution	*60 m*	20 m	30 m
Swath width	*145 km*	11 km	7 km

Thermal infrared emission instruments and data characteristics (summary/overview)

HyspIRI TIR	Number of bands	Spectral bands (discrete)	Spatial resolution
TIR channel centers	*8*	*3.98, 7.35, 8.28, 8.63, 9.07, 10.53, 11.33, 12.05 µm*	*60 m*
Swath width	*600 km*		

MASTER	Number of bands	Spectral bands (discrete)	Spatial resolution
Spectral range 0.4 - 13 µm	50		5-25 m (B200) 10-30 m (DC-8) 50 m (ER-2)
0.45-2.39 µm	25	0.05 µm a part	
3.15-5.27 µm	15	0.15 µm a part	
7.75-12.87 µm	10	0.40-0.80 µm a part	
Total field of view	85.92°		

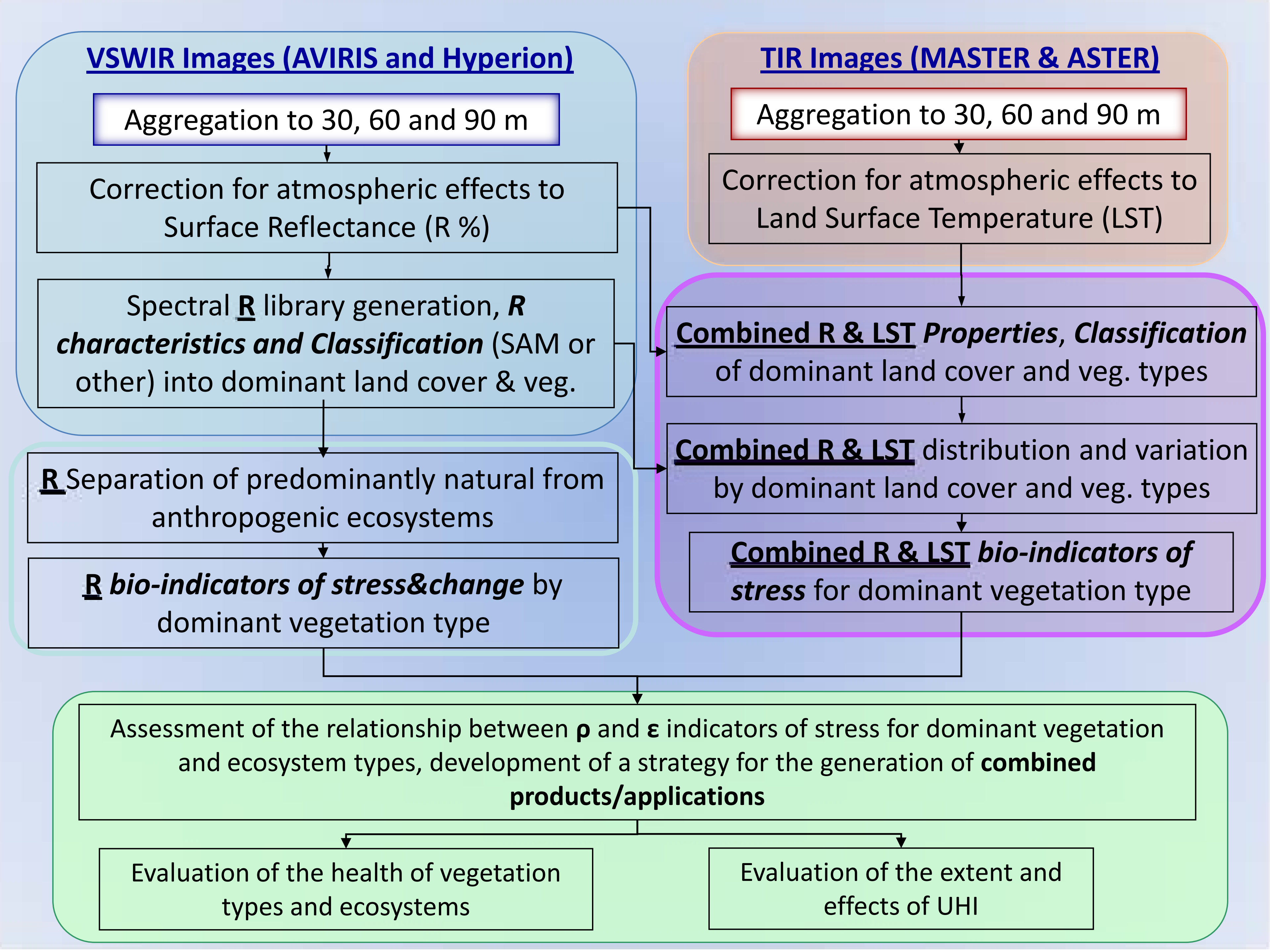
VSWIR Images (AVIRIS and Hyperion)
Aggregation to 30, 60 and 90 m
Correction for atmospheric effects to Surface Reflectance (R %)
Spectral R library generation, R characteristics and Classification (SAM or other) into dominant land cover & veg.
R Separation of predominantly natural from anthropogenic ecosystems
R bio-indicators of stress&change by dominant vegetation type
TIR Images (MASTER & ASTER)
Aggregation to 30, 60 and 90 m
Correction for atmospheric effects to Land Surface Temperature (LST)
Combined R & LST Properties, Classification of dominant land cover and veg. types
Combined R & LST distribution and variation by dominant land cover and veg. types
Combined R & LST bio-indicators of stress for dominant vegetation type
Assessment of the relationship between ρ and ε indicators of stress for dominant vegetation and ecosystem types, development of a strategy for the generation of combined products/applications
Evaluation of the health of vegetation types and ecosystems
Evaluation of the extent and effects of UHI

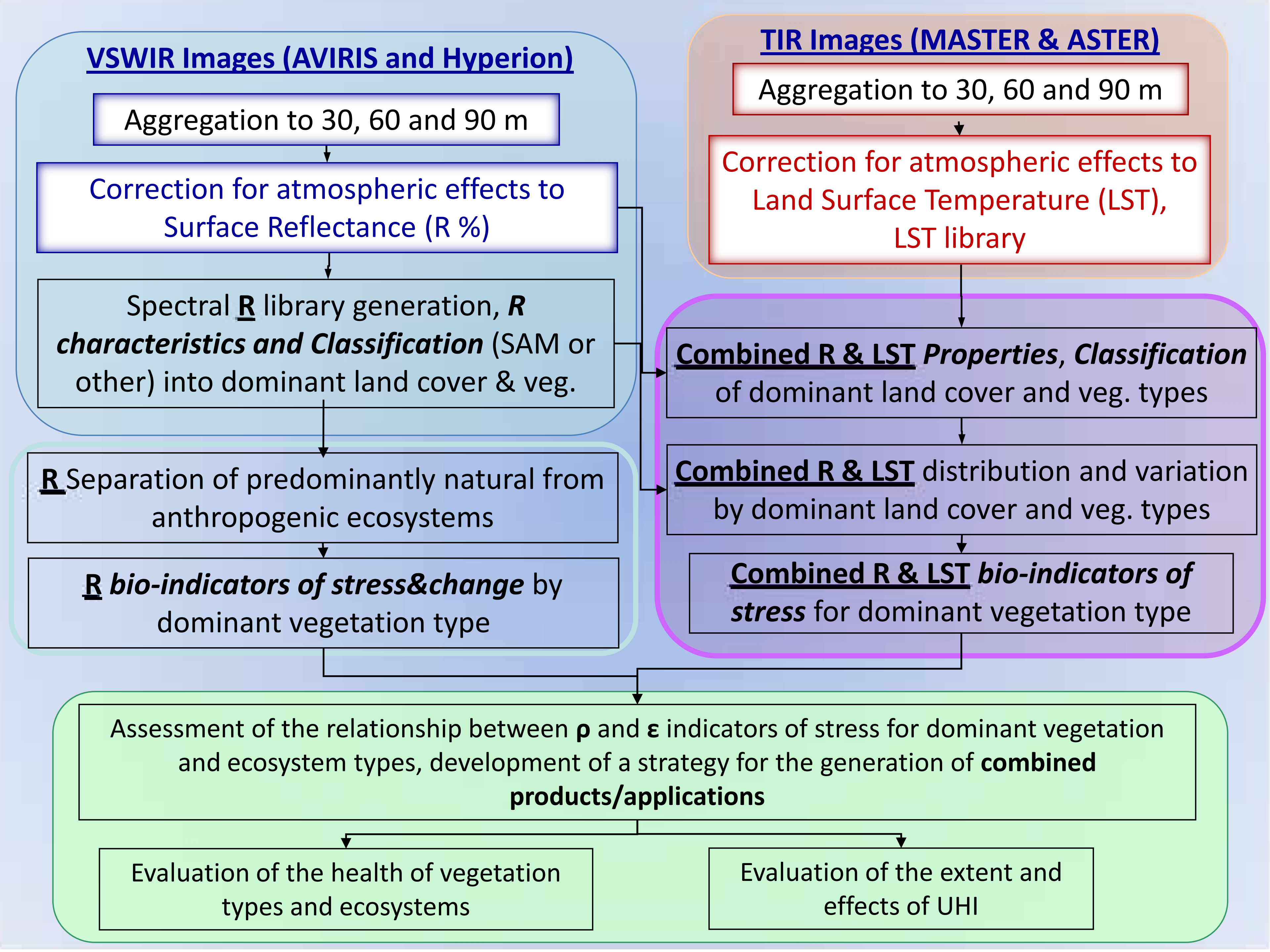

VSWIR Images (AVIRIS and Hyperion)
Aggregation to 30, 60 and 90 m
Correction for atmospheric effects to Surface Reflectance (R %)
Spectral R library generation, R characteristics and Classification (SAM or other) into dominant land cover & veg.
R Separation of predominantly natural from anthropogenic ecosystems
R bio-indicators of stress&change by dominant vegetation type
TIR Images (MASTER & ASTER)
Aggregation to 30, 60 and 90 m
Correction for atmospheric effects to Land Surface Temperature (LST), LST library
Combined R & LST Properties, Classification of dominant land cover and veg. types
Combined R & LST distribution and variation by dominant land cover and veg. types
Combined R & LST bio-indicators of stress for dominant vegetation type
Assessment of the relationship between ρ and ε indicators of stress for dominant vegetation and ecosystem types, development of a strategy for the generation of combined products/applications
Evaluation of the health of vegetation types and ecosystems
Evaluation of the extent and effects of UHI

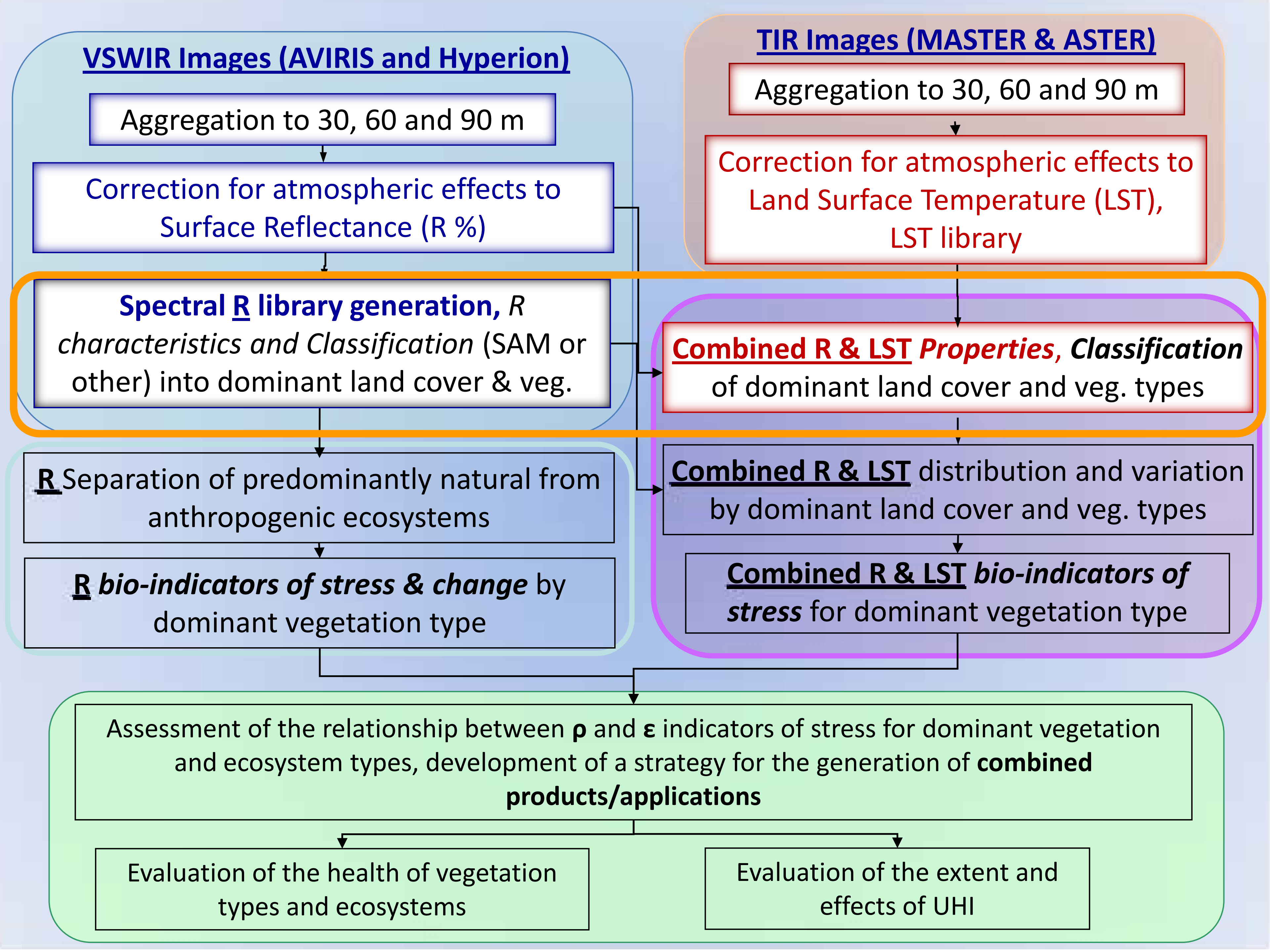

VSWIR Images (AVIRIS and Hyperion)
Aggregation to 30, 60 and 90 m
Correction for atmospheric effects to Surface Reflectance (R %)
Spectral R library generation, R characteristics and Classification (SAM or other) into dominant land cover & veg.
R Separation of predominantly natural from anthropogenic ecosystems
R bio-indicators of stress & change by dominant vegetation type
TIR Images (MASTER & ASTER)
Aggregation to 30, 60 and 90 m
Correction for atmospheric effects to Land Surface Temperature (LST), LST library
Combined R & LST Properties, Classification of dominant land cover and veg. types
Combined R & LST distribution and variation by dominant land cover and veg. types
Combined R & LST bio-indicators of stress for dominant vegetation type
Assessment of the relationship between ρ and ε indicators of stress for dominant vegetation and ecosystem types, development of a strategy for the generation of combined products/applications
Evaluation of the health of vegetation types and ecosystems
Evaluation of the extent and effects of UHI

HyspIRI Thermal Bands

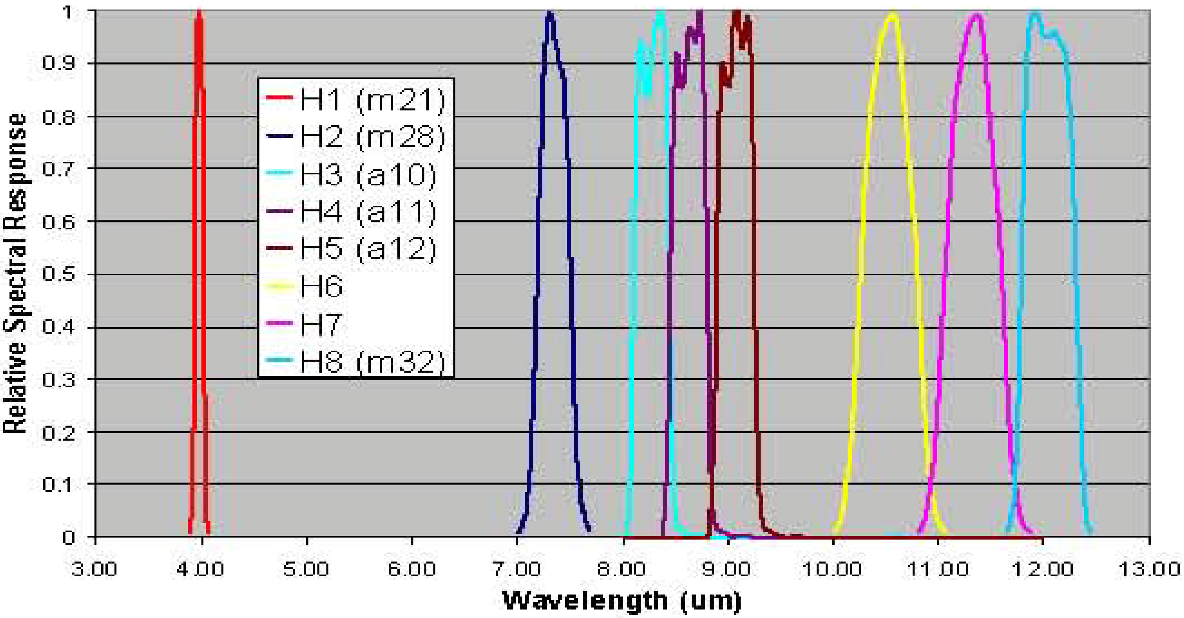

MASTER Thermal Bands

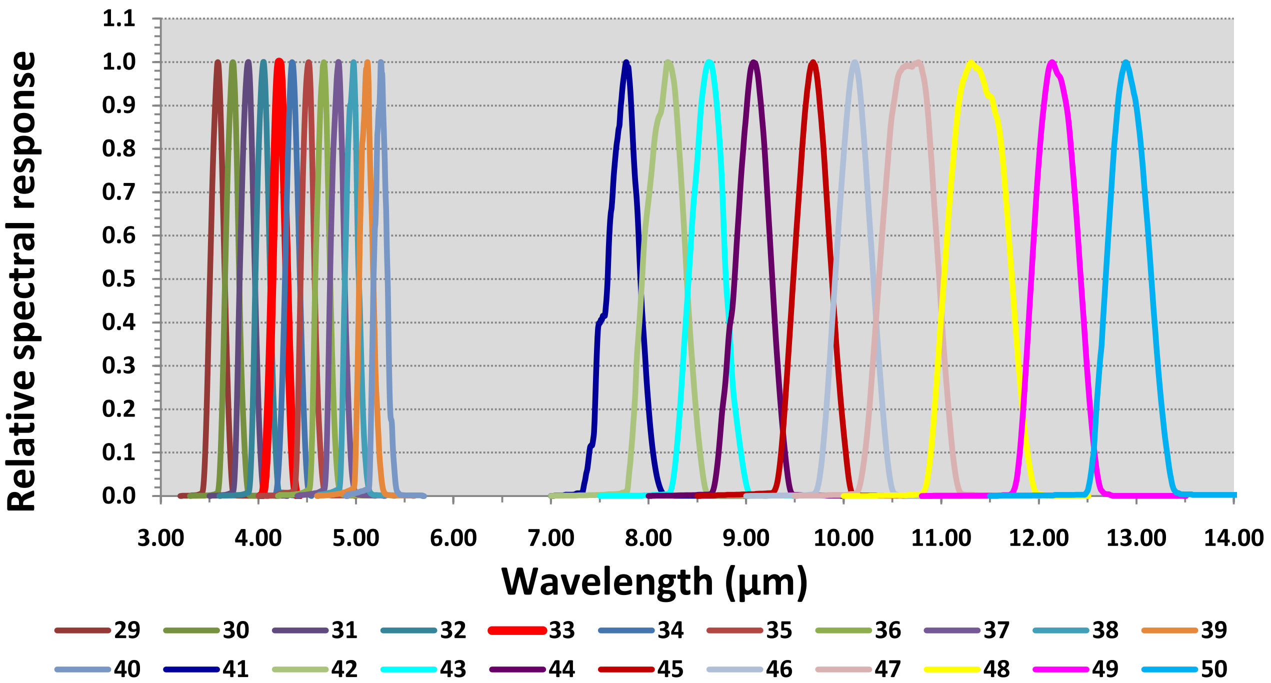

MASTER Thermal Bands Relative to HyspIRI

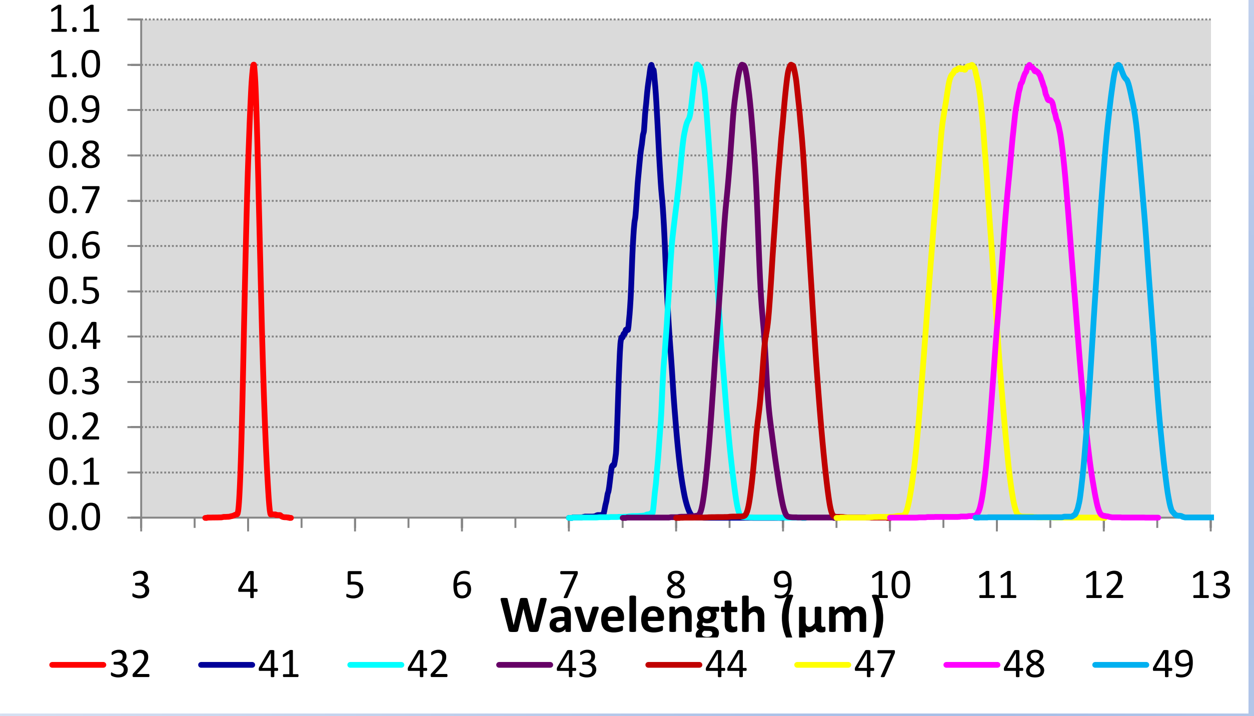

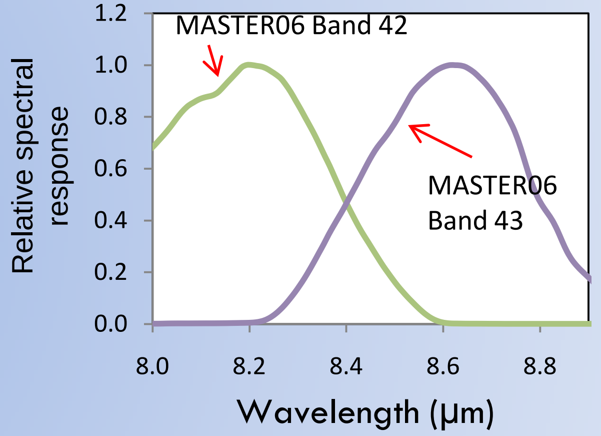

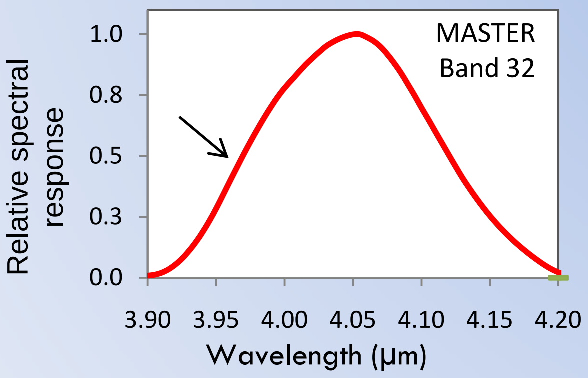

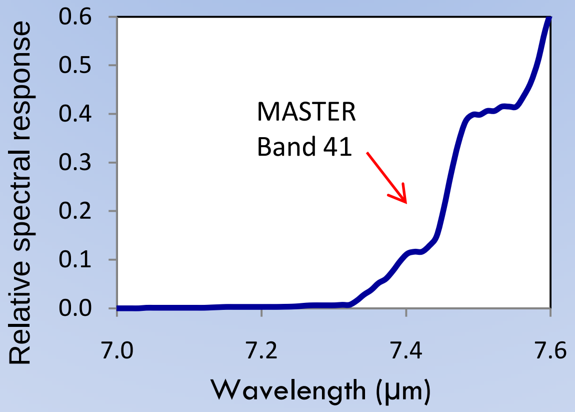

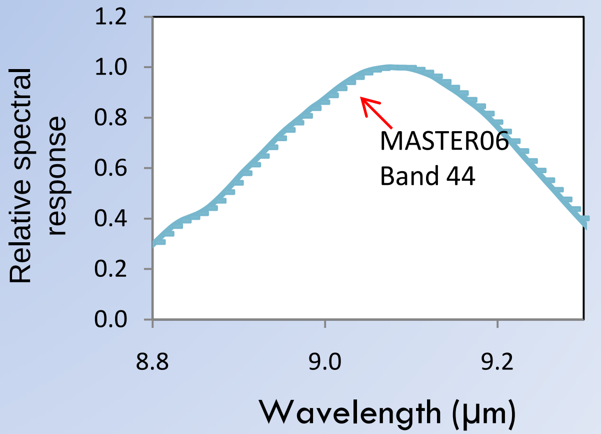

Spatial Aggregation of HyspIRI-like Thermal Bands

Original image pixel size varies (49.1 m, bands 32, 41, 42, 43, 44, 47, 48 and 49)

Aggregation to 60 m (MASTER, band 44)

Aggregation to 90 m (MASTER, band 44)

Atmospheric Correction of Thermal Data

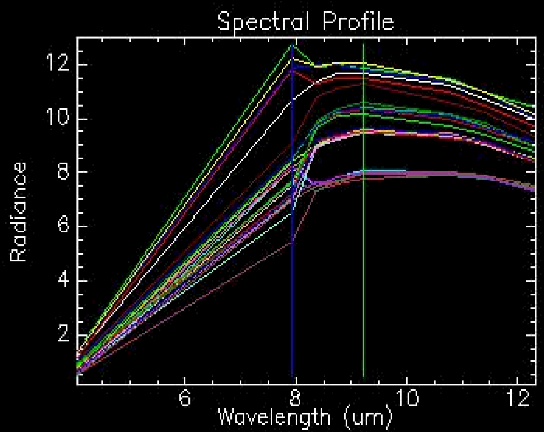

Max hit-normalized regression, 49.1 m resolution

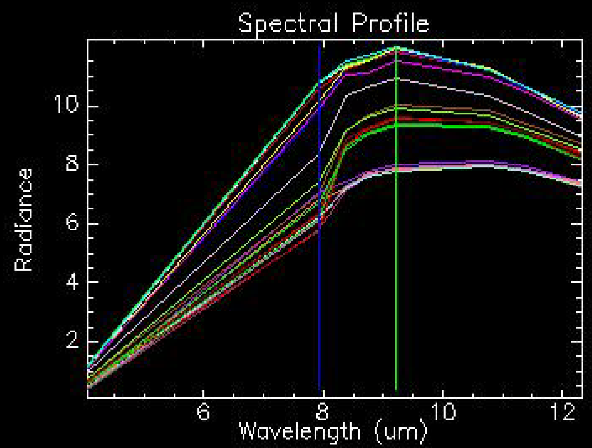

Max hit-top of bins, 60 m resolution

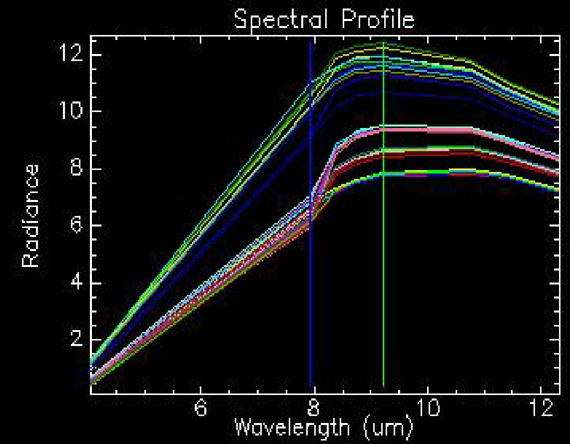

All-top of bins, 90 m aggregated image

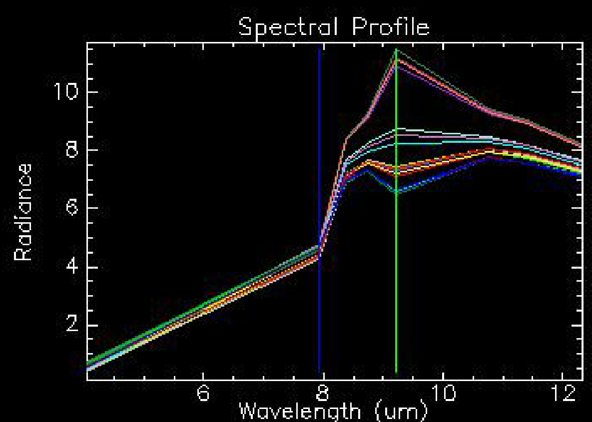

Ineffective atmospheric correction – images lacking contrasting cover types (e.g. large barren, or ocean cover, 60m)

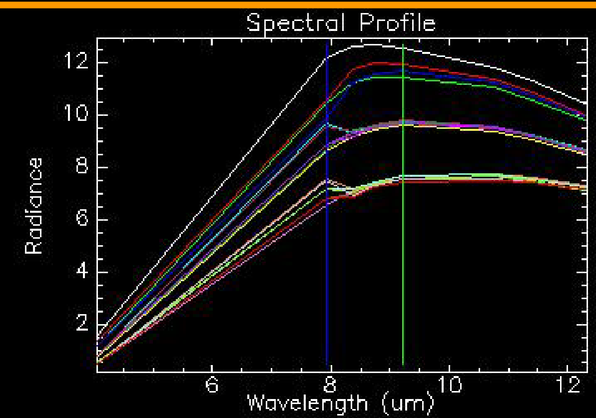

Effective atmospheric correction (60 m resolution, max hit-normalized regression)

Thermal Radiance of Rural Urban and Environments

- Assess the Variations in Thermal Radiance for ecosystems ranging from natural to urban
- Convert Radiance to Emissivity and Temperature to quantify the temperature and emissivity differences in ecosystems

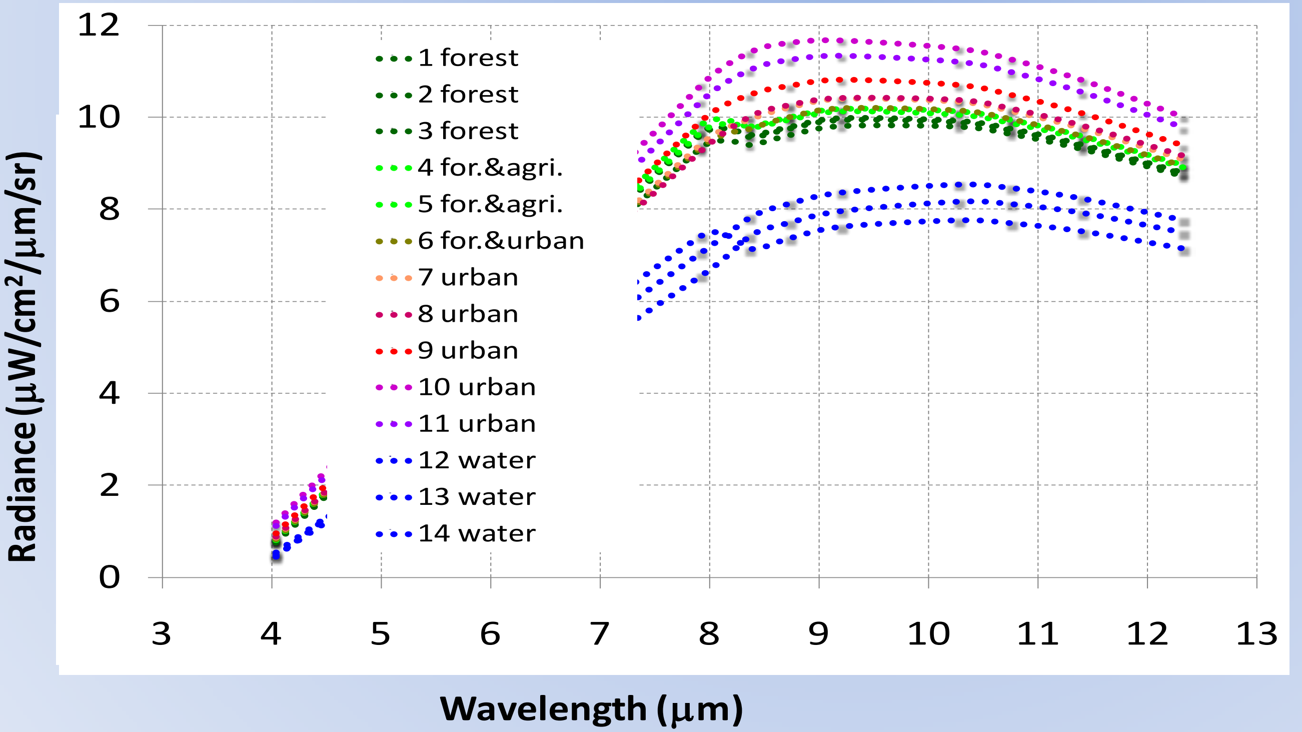

Temperature Gradient of Rural Urban and Environments

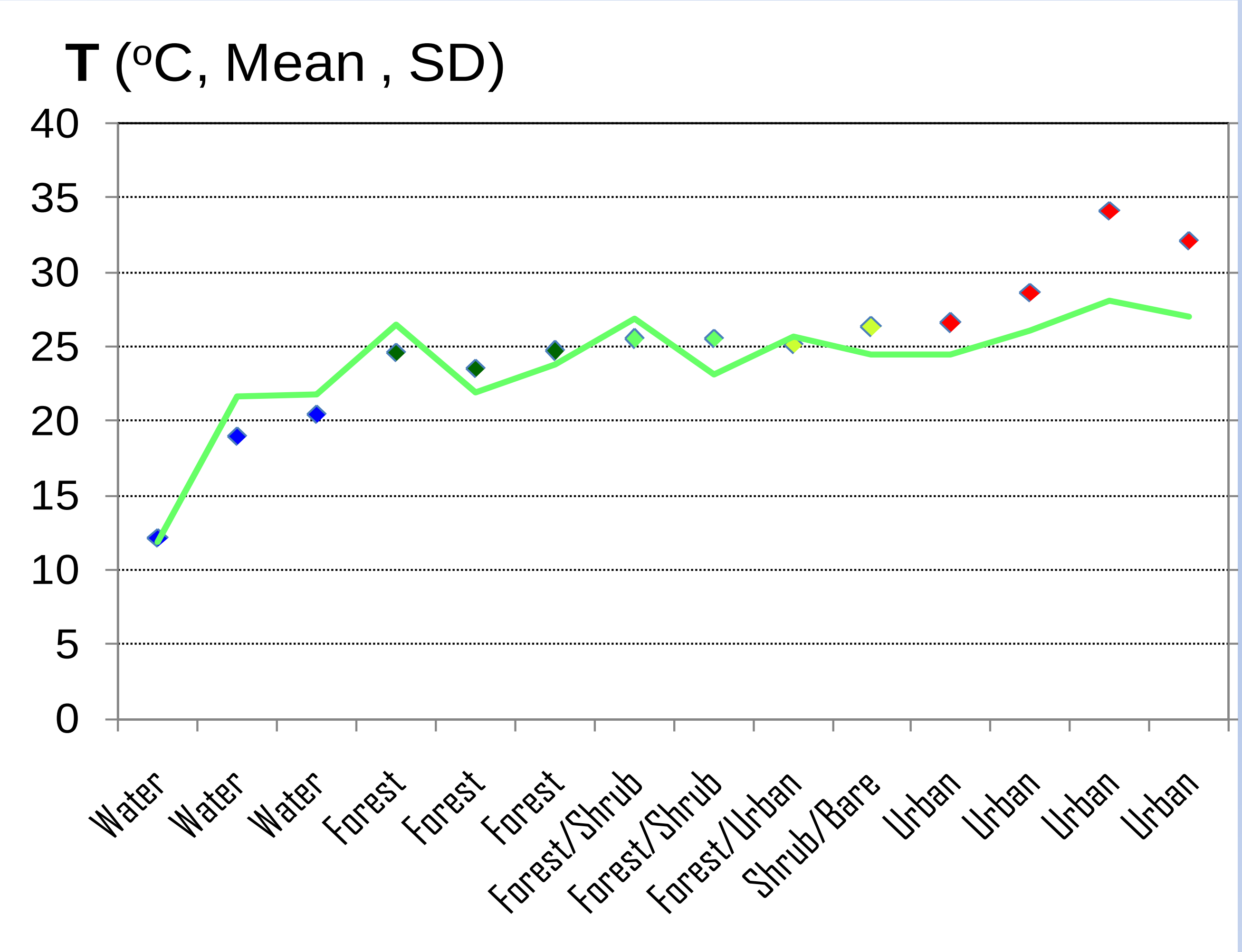

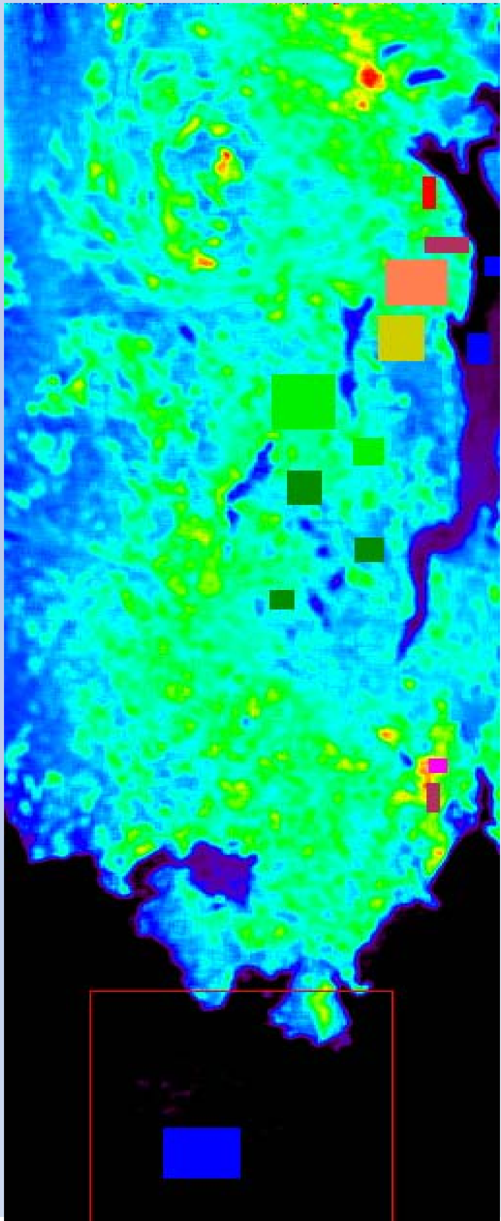

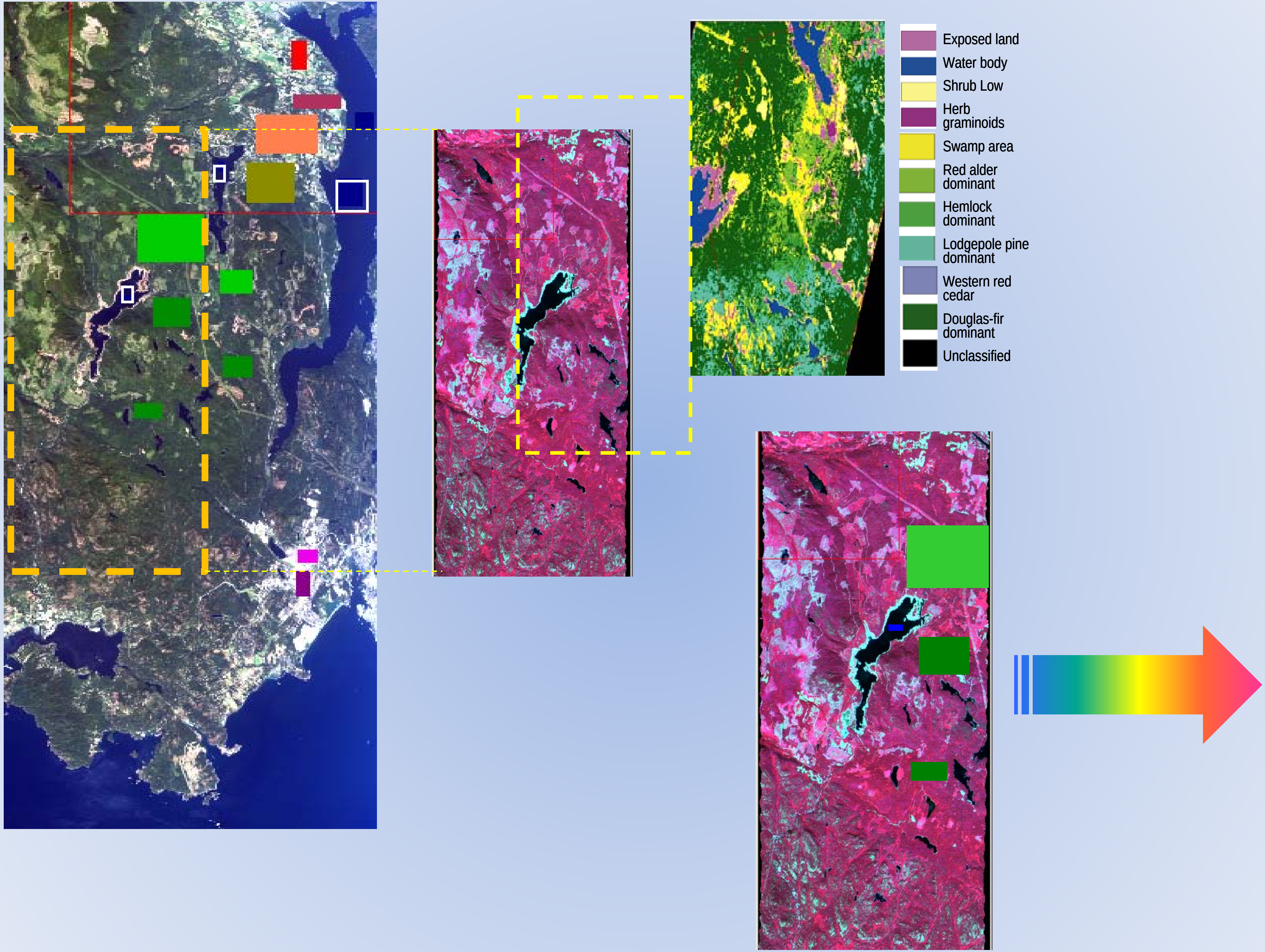
Exposed land
Water body
Shrub Low
Herb graminoids
Swamp area
Red alder dominant
Hemlock dominant
Lodgepole pine dominant
Western red cedar
Douglas-fir dominant
Unclassified

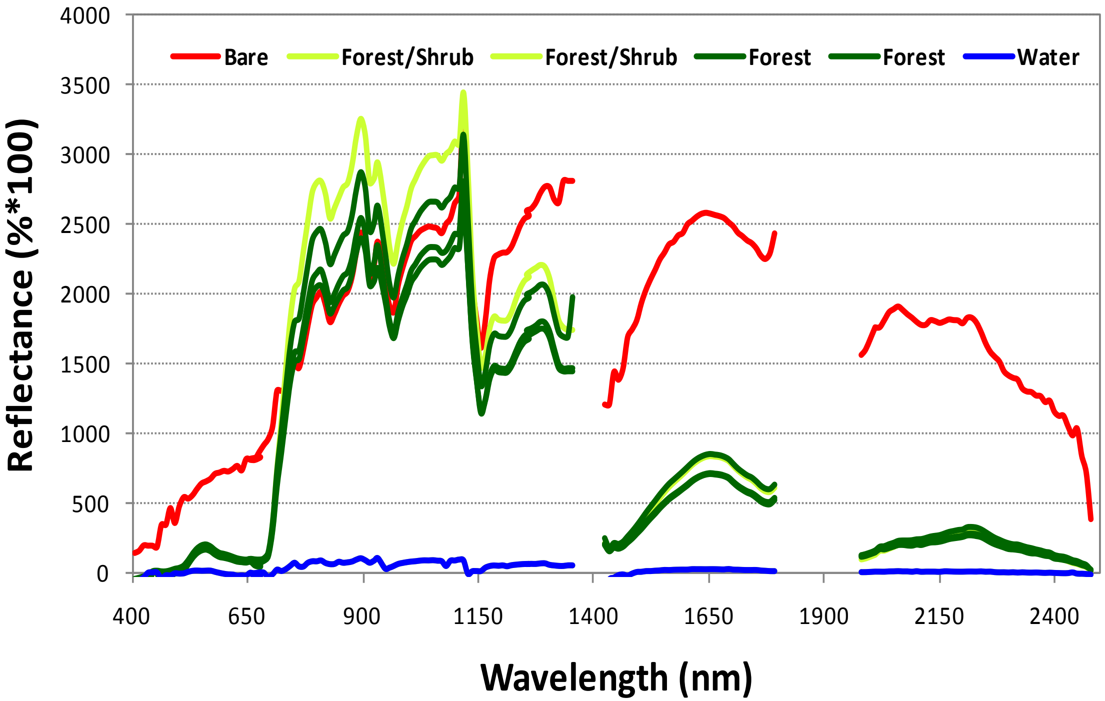
Bare
Forest/Shrub
Forest/Shrub
Forest
Forest
Water
Reflectance (%*100)
4000
3500
3000
2500
2000
1500
1000
500
0
400
650
900
1150
1400
1650
1900
2150
2400
Wavelength (nm)

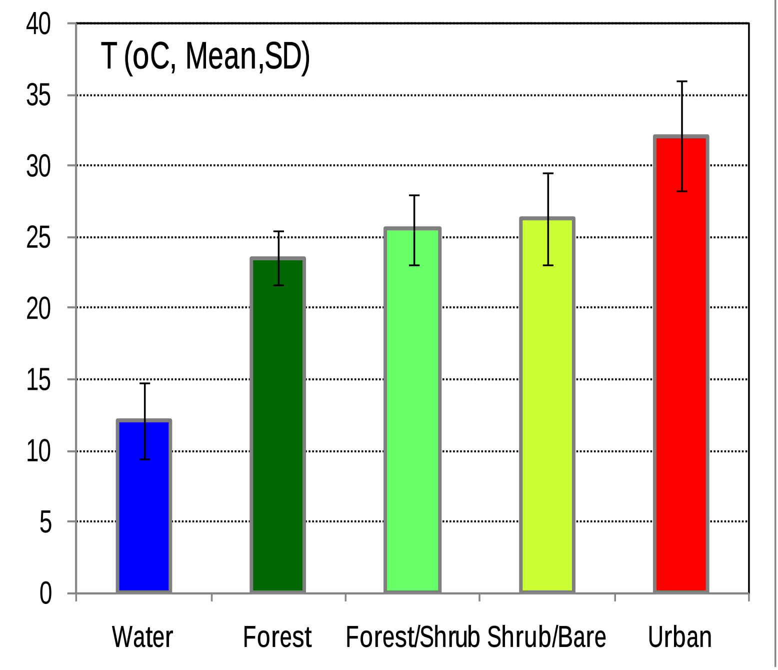
T (oC, Mean,SD)
40
35
30
25
20
15
10
5
0
Water
Forest
Forest/Shrub
Shrub/Bare
Urban

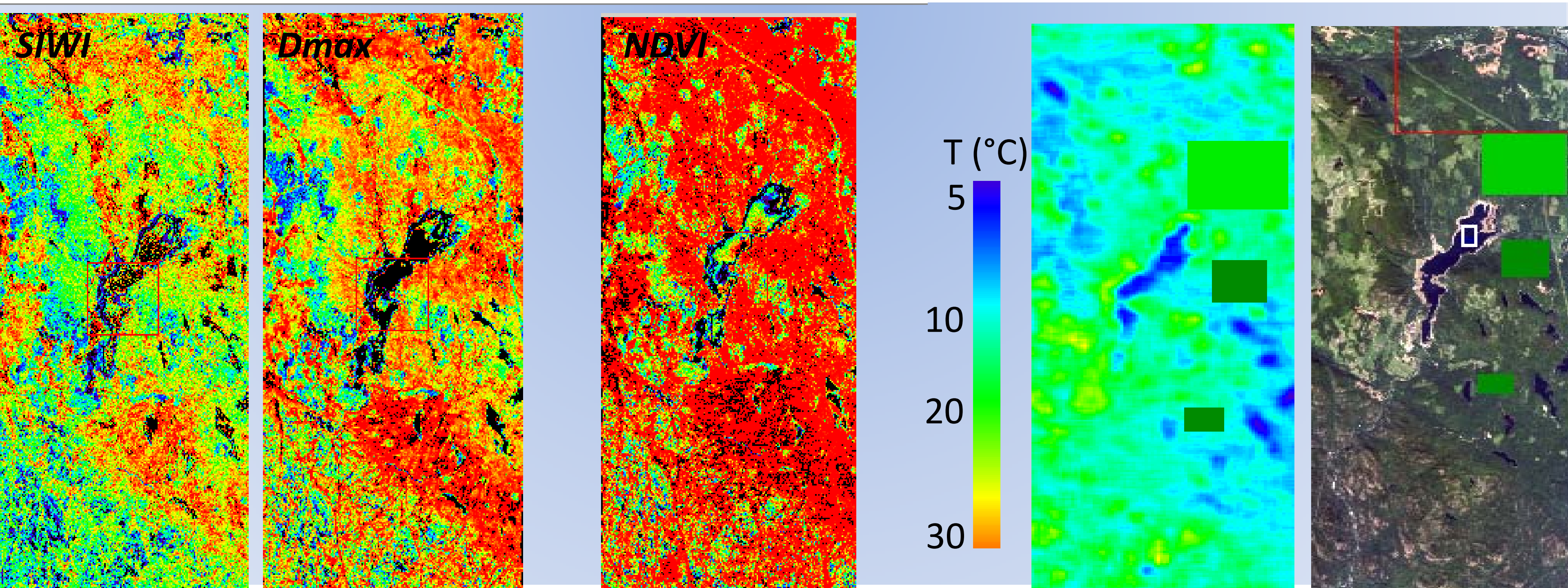
SIWI
Dmax
NDVI
T (°C)
5
10
20
30

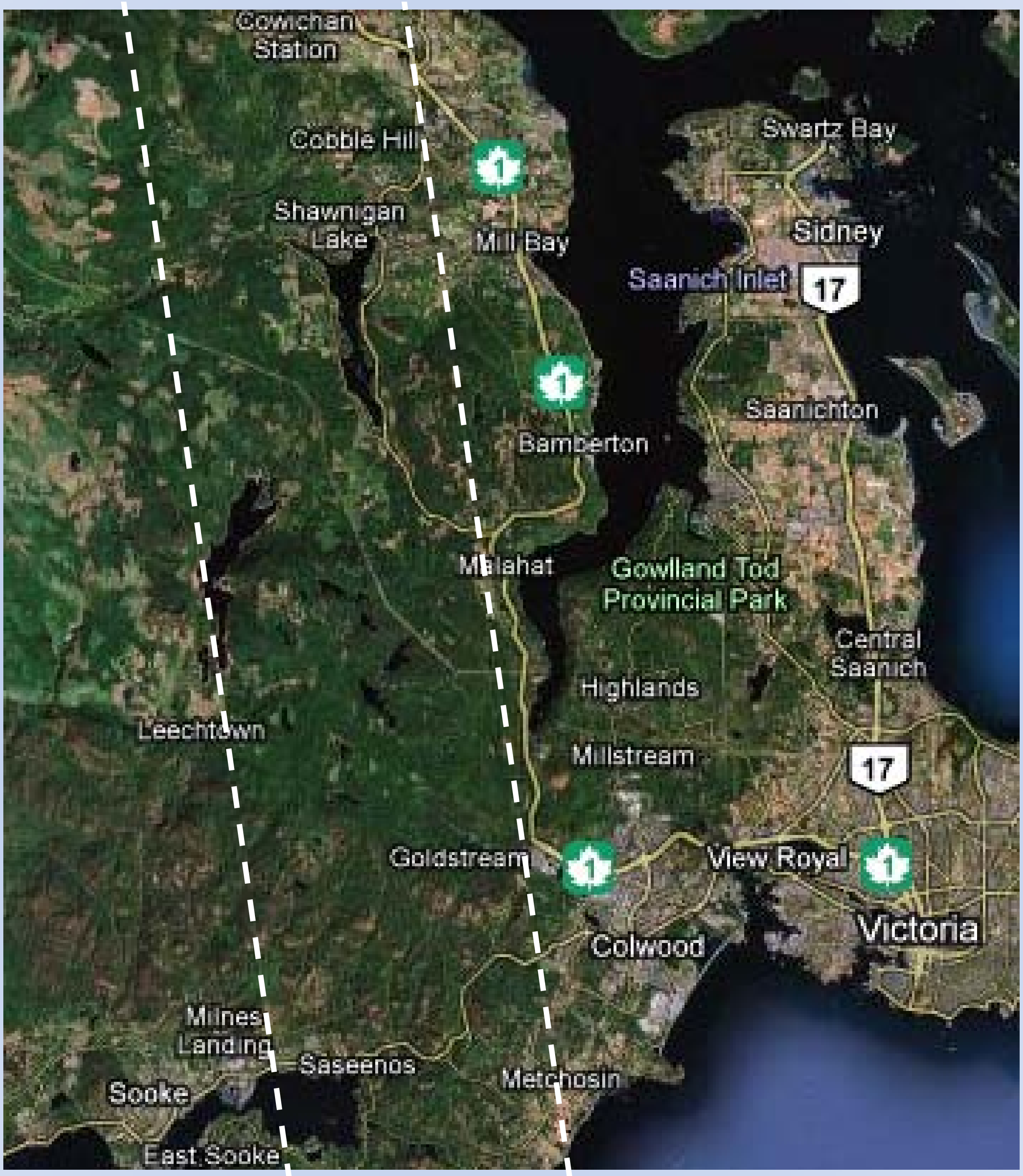

Cowichan Station
Cobble Hill
Shawnigan Lake
Mill Bay
Swartz Bay
Sidney
Saanich Inlet
17
1
Bamberton
Saanichton
Malahat
Gowlland Tod Provincial Park
Central Saanich
Highlands
Leechtown
Millstream
17
Goldstream
View Royal
1
Victoria
Colwood
Milnes Landing
Saseenos
Metchosin
Sooke
East Sooke

Site Spatial Uniformity / Spectral Variability

<u>Example from Ivanpah Playa, Hyperion</u>

A. Natural color composite (RGB: 651, 549, 447)

B. B. Getis Gi* statistics (band 549) calculated for 197 Jul day image

The Gi statistics calculated for G, R, NIR, SWIR bands produced similar results.

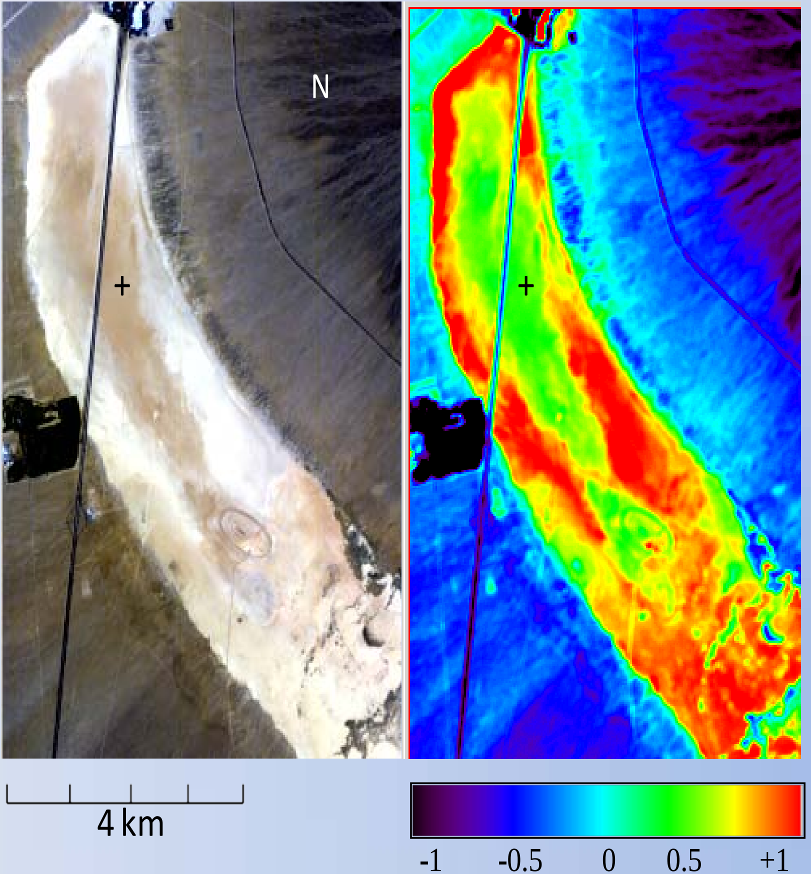

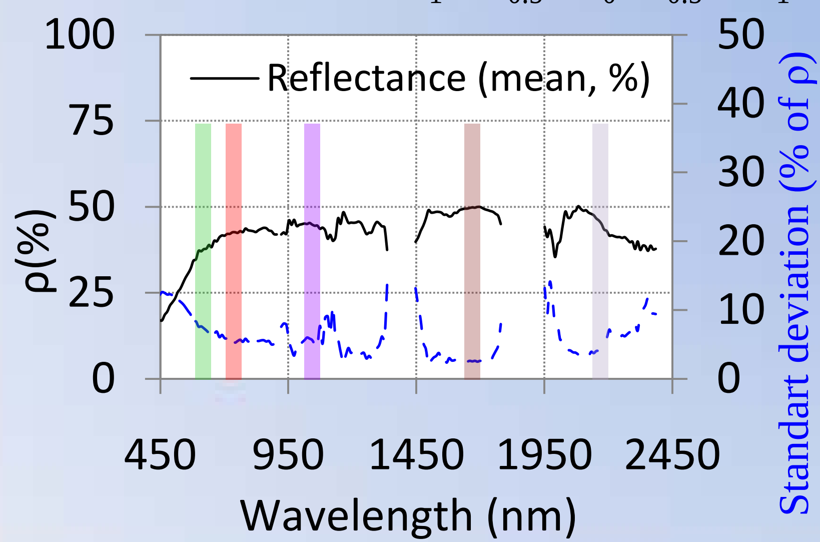

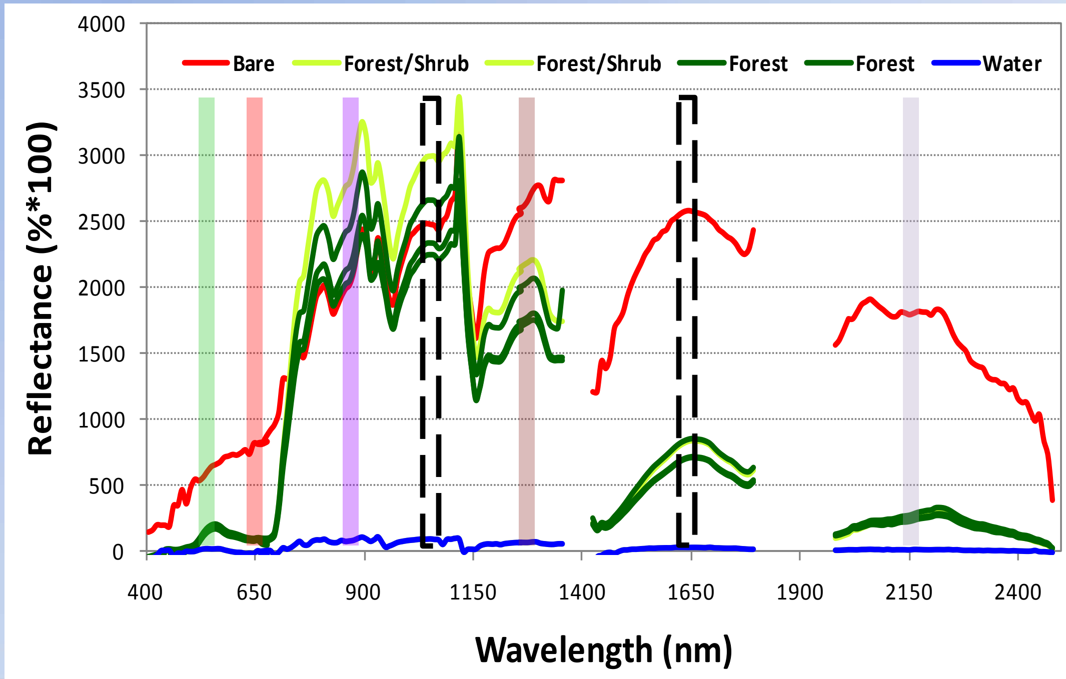

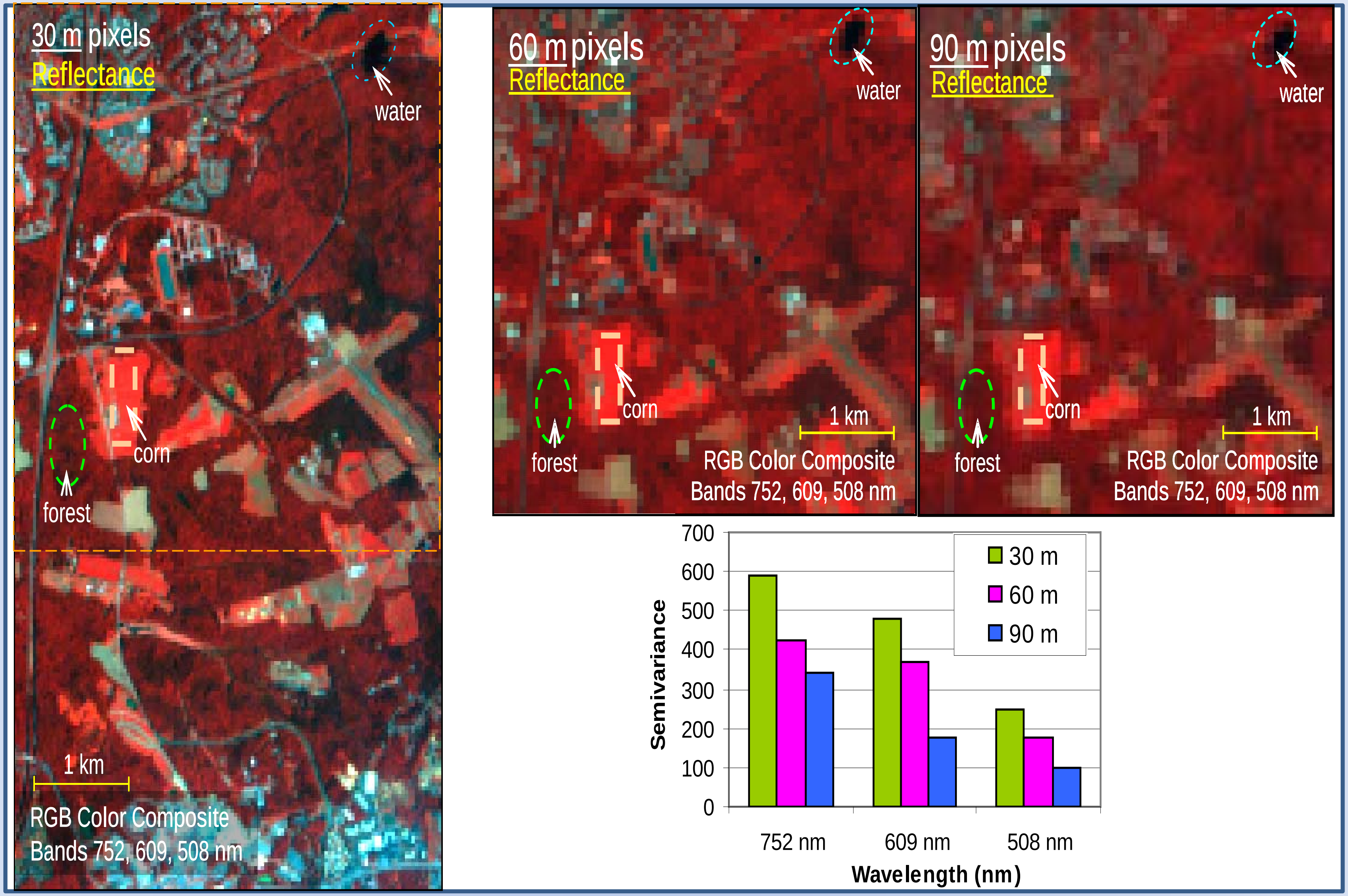

Examples of Hyperion reflectance image (30 m pixels) and the re-sampled to 60 and 90 m subset, demonstrate the spatial differences between HyspIRI-like data (60 m) and 30 and 90 m data.

30 m pixels

60 m pixels

Pixel size	Vegetation Indices:						Albedo		
	V1	PRI	REIP	Dmax	NDWI	NDVI	water	corn	forest
30 m	1.81	-0.14	721	0.749	0.14	0.81	0.03	0.20	0.14
60 m	1.88	-0.15	721	0.748	0.15	0.82	0.04	0.20	0.13

While there were significant differences in the spatial variability between the original 30 m and the aggregated to 60 and 90 m data, the spectral properties of the major land cover types did not significantly differ.

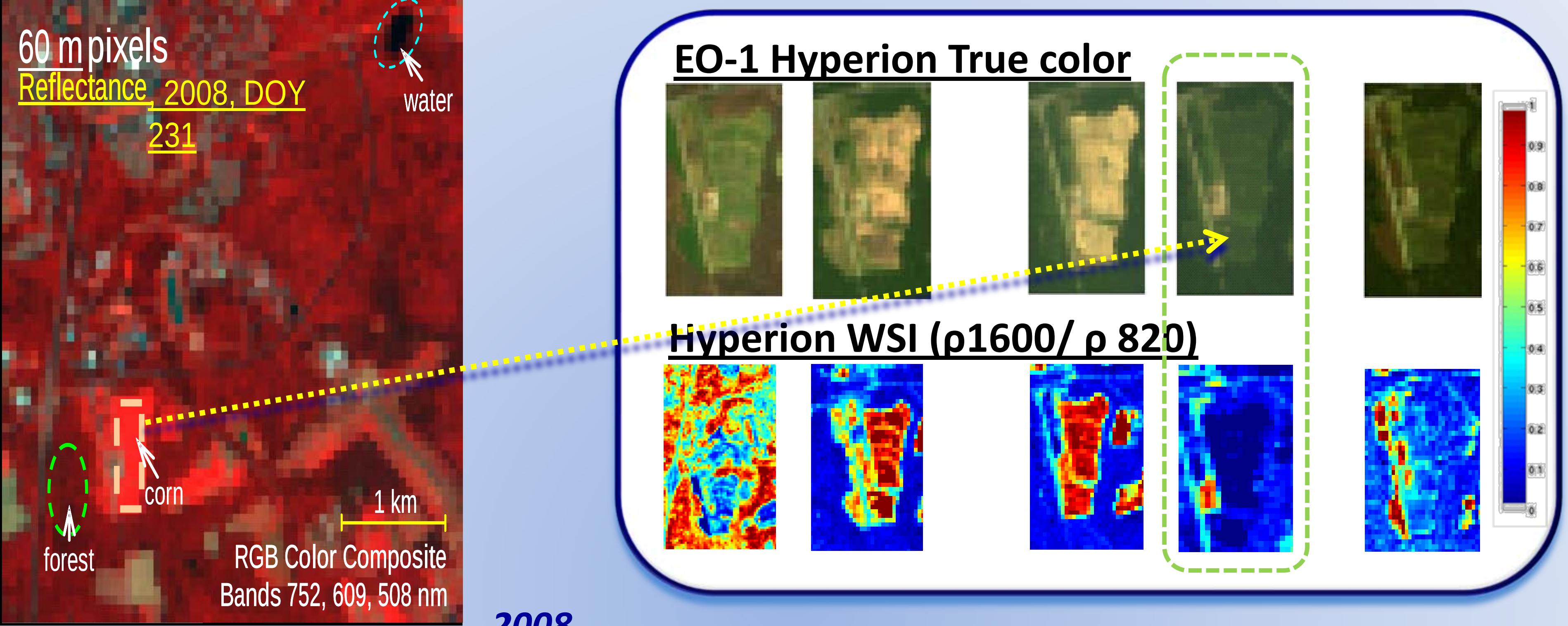

2008, DOY

108	172	195	231	277

Spring **Summer** **Fall**

Cover Type	Hyperion, 2008	V1	PRI	REIP	Dmax	WBI	Albedo
Corn	13-Jun	1.03	-0.04	712	0.36	0.96	0.461
	18-Aug	1.81	-0.06	722	0.75	1.09	0.197
	3-Oct	1.15	0.04	721	0.51	0.98	0.155
Forest	13-Jun	1.12	-0.06	712	0.89	1.00	0.257
	18-Aug	1.56	-0.03	722	0.51	1.01	0.140
	3-Oct	1.61	-0.10	712	0.42	0.94	0.127
Water	13-Jun	0.15	0.01	712	0.16	1.23	0.058
	18-Aug	0.52	0.02	712	0.10	1.46	0.031
	3-Oct	0.62	-0.07	712	0.08	0.93	0.036

Bio-physical parameter	Spectral bio-indicators *(examples)*	References
TIR indicators		
Water stress (100% vegetative cover)	CWSI = (ΔTcanopy – ΔTnws)/(ΔTmax – ΔTnws), where Tmax for non-transpiring and Tnws is "non-water-stressed" baseline temperature. 0 = no stress, 1 = maximal stress, Δ = (Tsurface - Tair)	Idso et al. 1981, Jackson, 1981
Irrigated vs. non-irrigated (100% veg.)	IG = (Tmax – Tcanopy)/(Tcanopy – Tnws),	Jones 1999
Increase in sensible heat due to UHI	Rn = G + LE + H, Rn + A = G + LE + H; where Rn is net radiation, G ground heat, LE latent heat, H sensible heat, A anthropogenic heat	Kato and Yamaguchi, 2005
Combined VSWIR & TIR indicators		
Relative water status (Veg. cover < 100%)	WDI trapezoid, defined by the fractional vegetation cover and Δ = (surface - air temperature); 0.0 well-watered (latent heat flux is limited only by atmospheric demand), 1.0 no available water	Moran et al. 1994
Water supply	WSVI=NDVI/Ts, where Ts is the brightness temperature at ~11 µm, the smaller this index is, the more severe the drought is	Hatfield et al. 2008
Temperature–vegetation dryness index	TVDI = (*T*s – *T*s_min)/(*a* + *b*NDVI – *T*s_min), where *T*s_min is the minimum temperature in the triangle; and *a* and *b* are the interception and slope of the dry edge, respectively	Wand et al. 2004
After WSVI and TDVI	Like WSVI and TVDI, but using VSWIR parameters sensitive to water stress, such as NDWI or SIWI.	New, to test

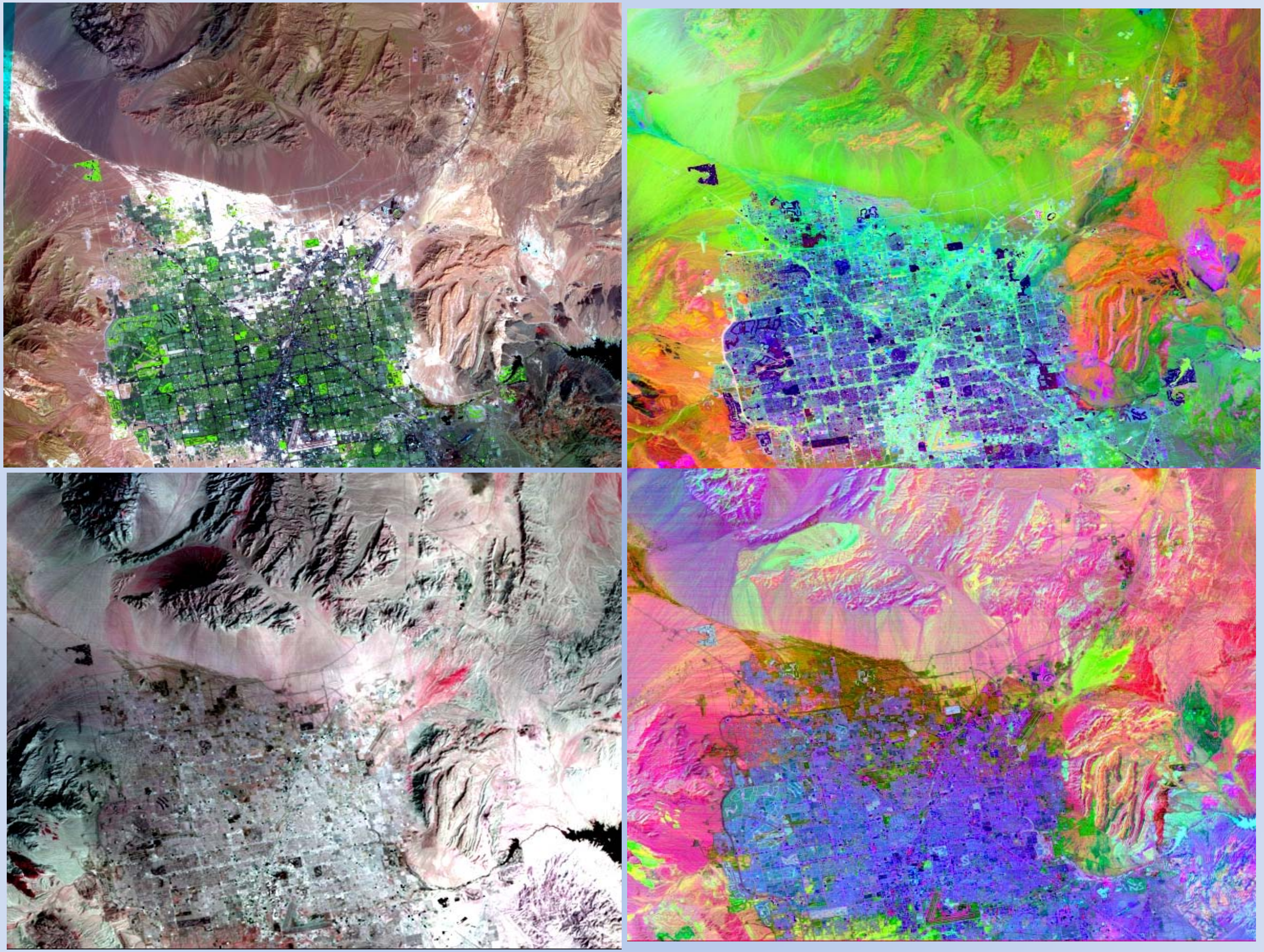

ASTER imagery, Las Vegas area: VSWIR aggregated to 90 m (upper left, vegetation in green) and TIR bands (lower left), principle components of reflective bands (upper right) and all VSWIR and TIR (lower right).

Deliverables and Milestones

- Best estimates of atmospheric properties needed to atmospherically correct the two HyspIRI-like data sets;
- Algorithm to spatially convolve the airborne or spaceborne imager data sets to 30, 60, and 90 m spatial resolution;
- Development of HyspIRI-like datasets;
- Development of HyspIRI-like spectral bio-indicators of ecosystem health;
- Classifications of HyspIRI-like data for a broad range of natural and anthropogenic ecosystems and vegetation functional types;
- Presentations at HyspIRI meetings, and final report.

Expected Results

- Through the combined use of reflective and emissive data, the proposed work will **evaluate the suitability of HyspIRI for delineating ecosystem functional types and tracking the conversion of land from rural to urban**.
- The research will produce two HyspIRI-like data sets combining reflectance and thermal data, which will be used to assess the **potential of HyspIRI data for delineating land cover and vegetation types**, discriminating natural versus urban ecosystems, and **assessing ecosystems diversity and health**.
- In addition, the work will produce methods and tools for work with the HyspIRI data.

Preliminary Findings

- MASTER's spectral bands 32 and 41 may not provide ideal simulation for HyspIRI
- Atmospheric correction of thermal images at 60m worked as well and better, than at the original resolution
- Thermal atmospheric correction was effective when playa, vegetation and water regions are present and well-delimited
- The 60m resolution can estimate differences in emissivity for urban and rural regions, and demonstrated higher temperatures in urban areas

Project Collaborators

- *Prof. David Goodenough (CFS Victoria, BC)*
- *Dr. Nicholas Coops (UBC, Vancouver, CA)*
- *Dr. Nona R. Chiariello (Stanford University, CA)*
- *Dr. Tony Trofymow (CFB Esquimalt, BC)*
- *Dr. Elizabeth Middleton (NASA/GSFC)*

Acknowledgments

The project provides research experience for graduate and undergraduate students, which participate through established programs, assisting with data processing, analysis and preparation of reports.

Temporal profile of Hyperion's Spectral Bio-indicators at CEOS/LPV Sites

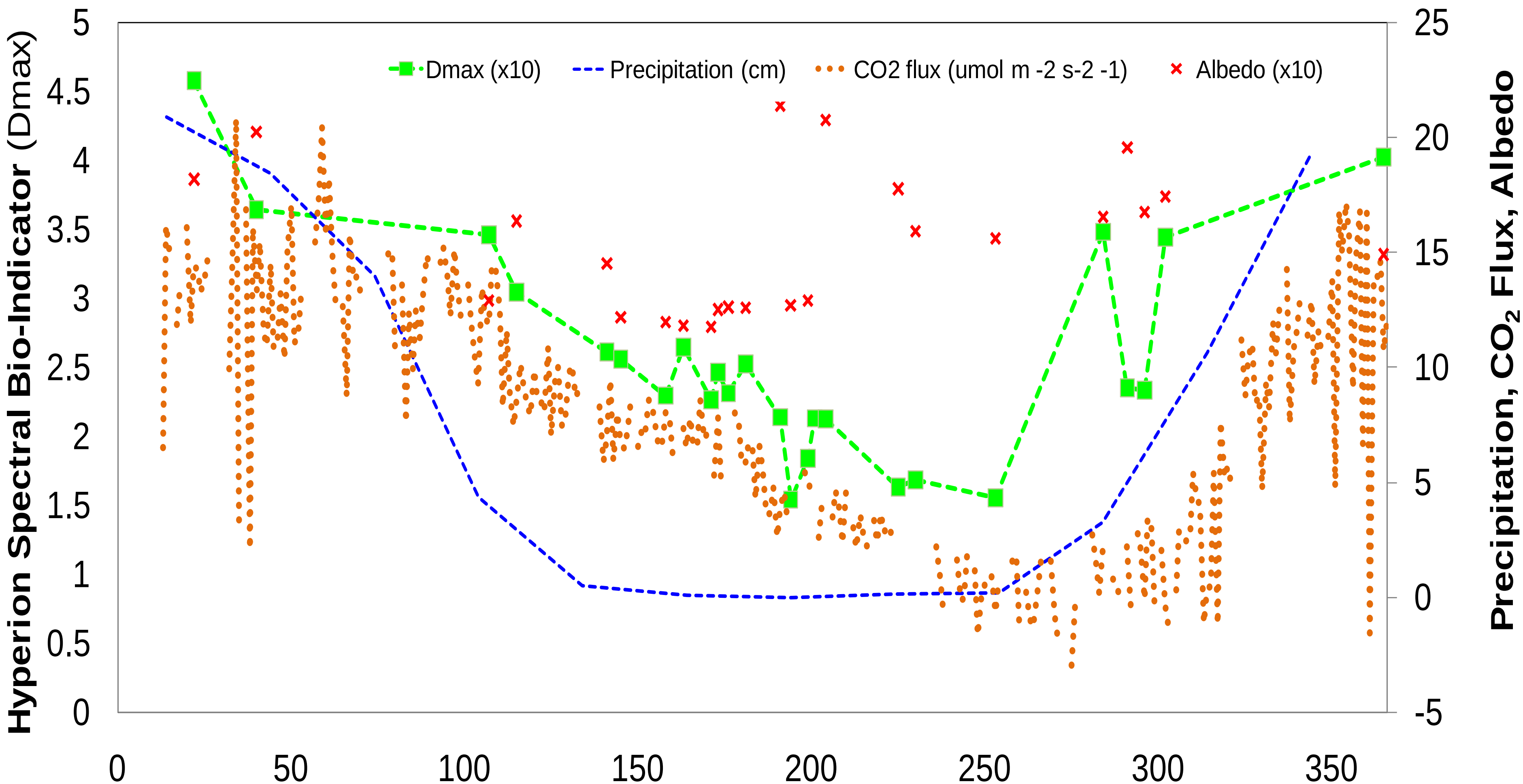

The temporal profile in the derivative spectral bio-indicator Dmax captures the dynamics in vegetation phenology at Mongu, Zambia

Thank You

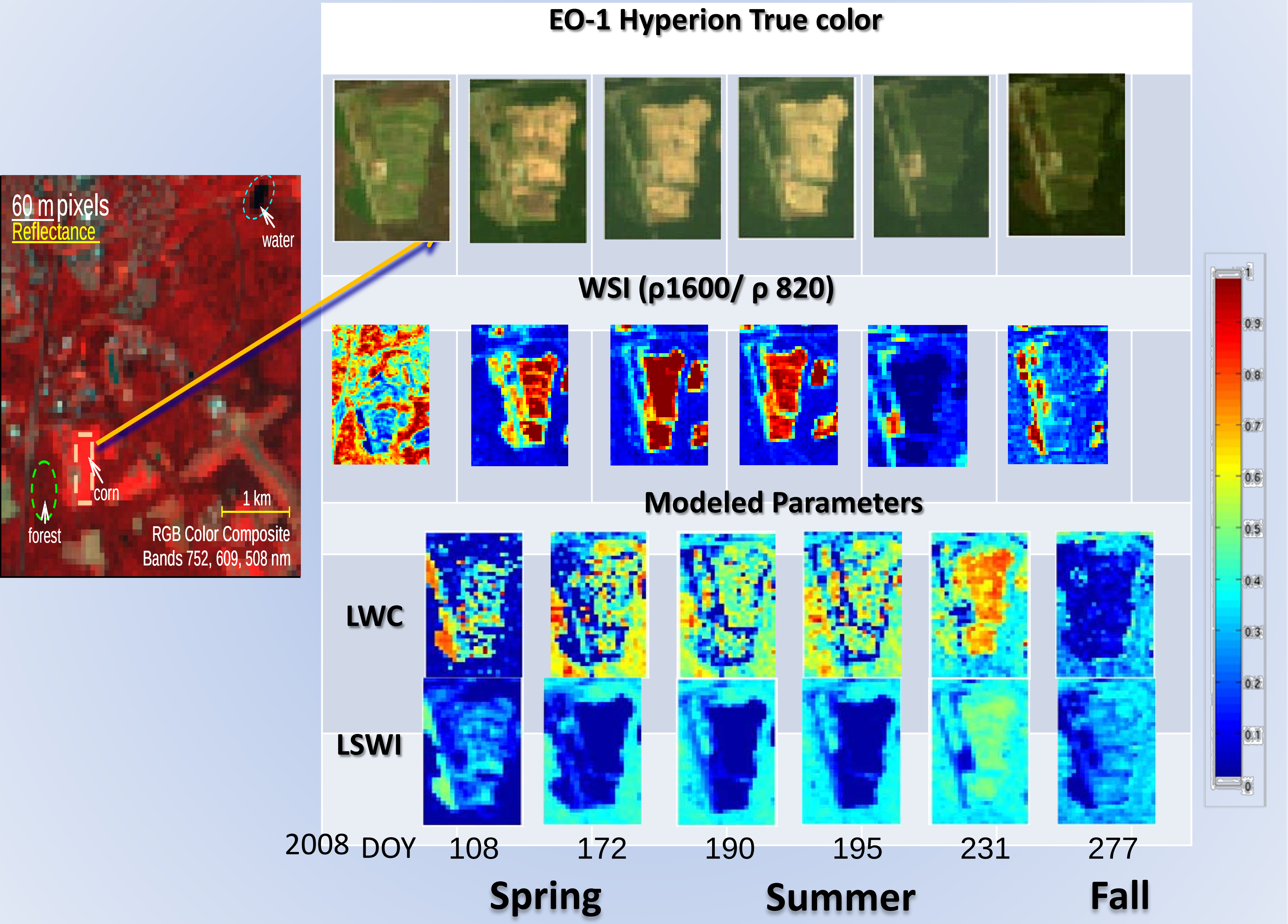

60 m pixels
Reflectance
water
corn
forest
1 km
RGB Color Composite
Bands 752, 609, 508 nm
EO-1 Hyperion True color
WSI (ρ1600/ ρ 820)
Modeled Parameters
LWC
LSWI
2008 DOY
108
172
190
195
231
277
Spring
Summer
Fall
1
0.9
0.8
0.7
0.6
0.5
0.4
0.3
0.2
0.1
0

Issues

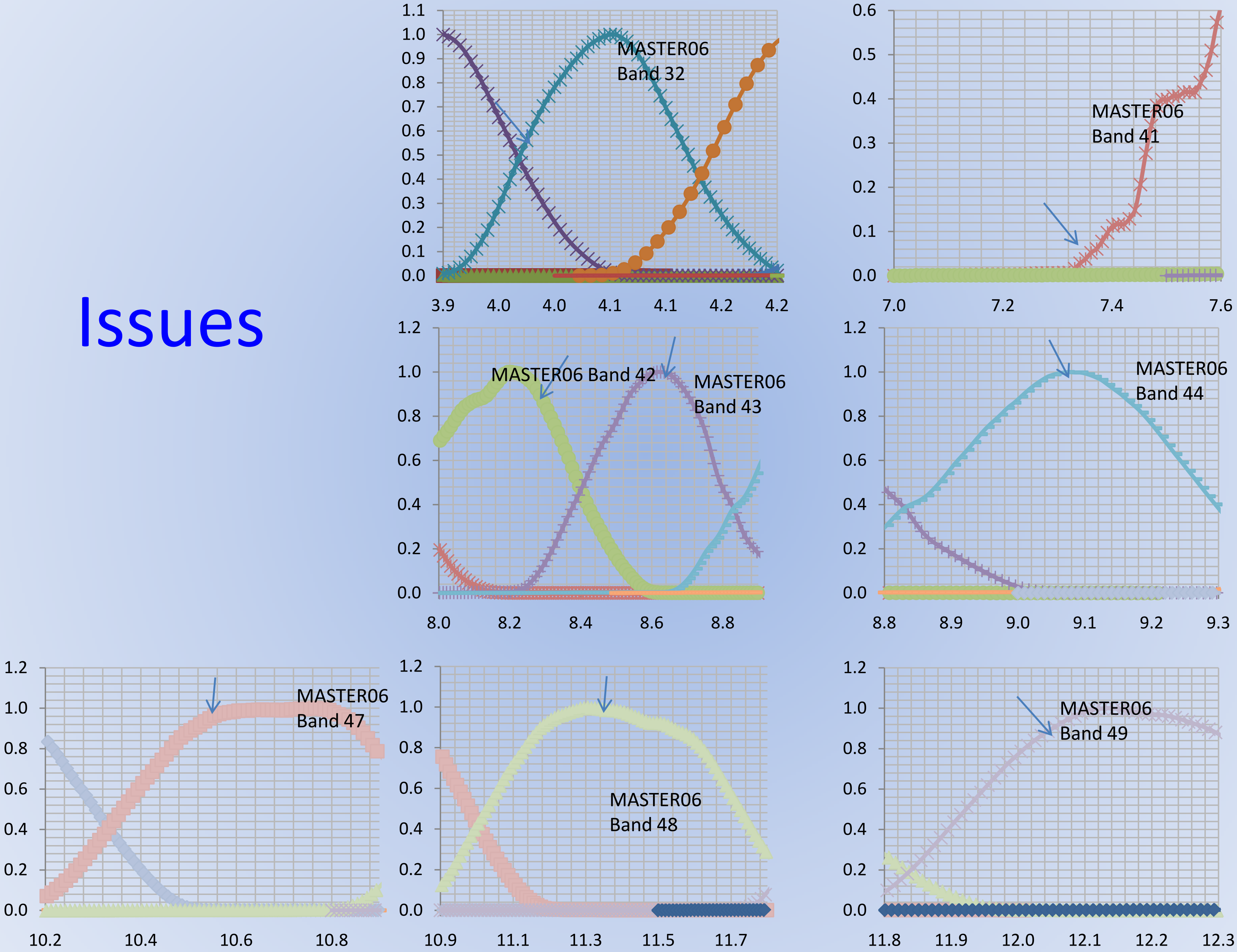

MASTER06 Band 32
MASTER06 Band 41
MASTER06 Band 42
MASTER06 Band 43
MASTER06 Band 44
MASTER06 Band 47
MASTER06 Band 48
MASTER06 Band 49

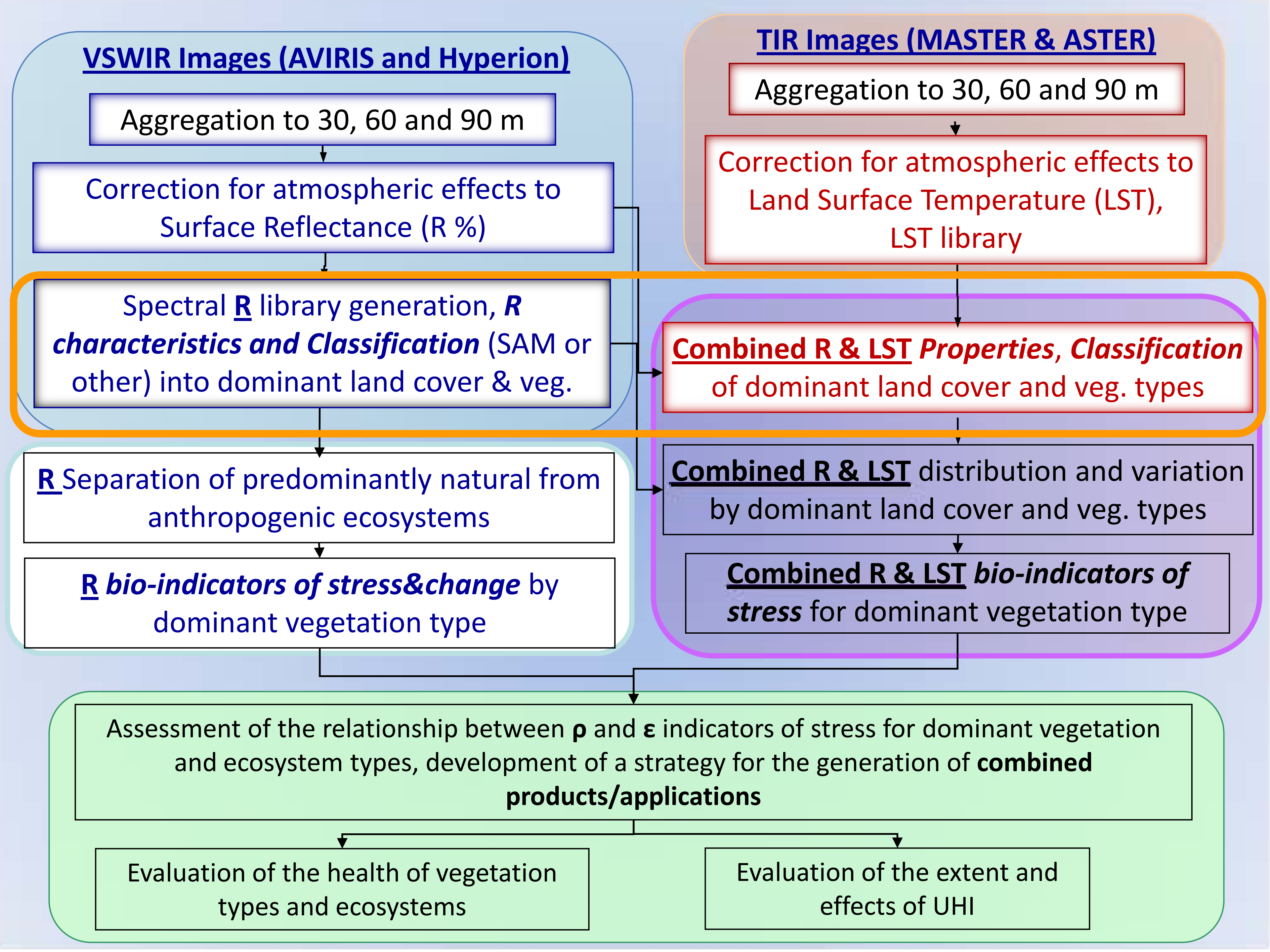
VSWIR Images (AVIRIS and Hyperion)
Aggregation to 30, 60 and 90 m
Correction for atmospheric effects to Surface Reflectance (R %)
Spectral R library generation, R characteristics and Classification (SAM or other) into dominant land cover & veg.
R Separation of predominantly natural from anthropogenic ecosystems
R bio-indicators of stress&change by dominant vegetation type
TIR Images (MASTER & ASTER)
Aggregation to 30, 60 and 90 m
Correction for atmospheric effects to Land Surface Temperature (LST), LST library
Combined R & LST Properties, Classification of dominant land cover and veg. types
Combined R & LST distribution and variation by dominant land cover and veg. types
Combined R & LST bio-indicators of stress for dominant vegetation type
Assessment of the relationship between ρ and ε indicators of stress for dominant vegetation and ecosystem types, development of a strategy for the generation of combined products/applications
Evaluation of the health of vegetation types and ecosystems
Evaluation of the extent and effects of UHI

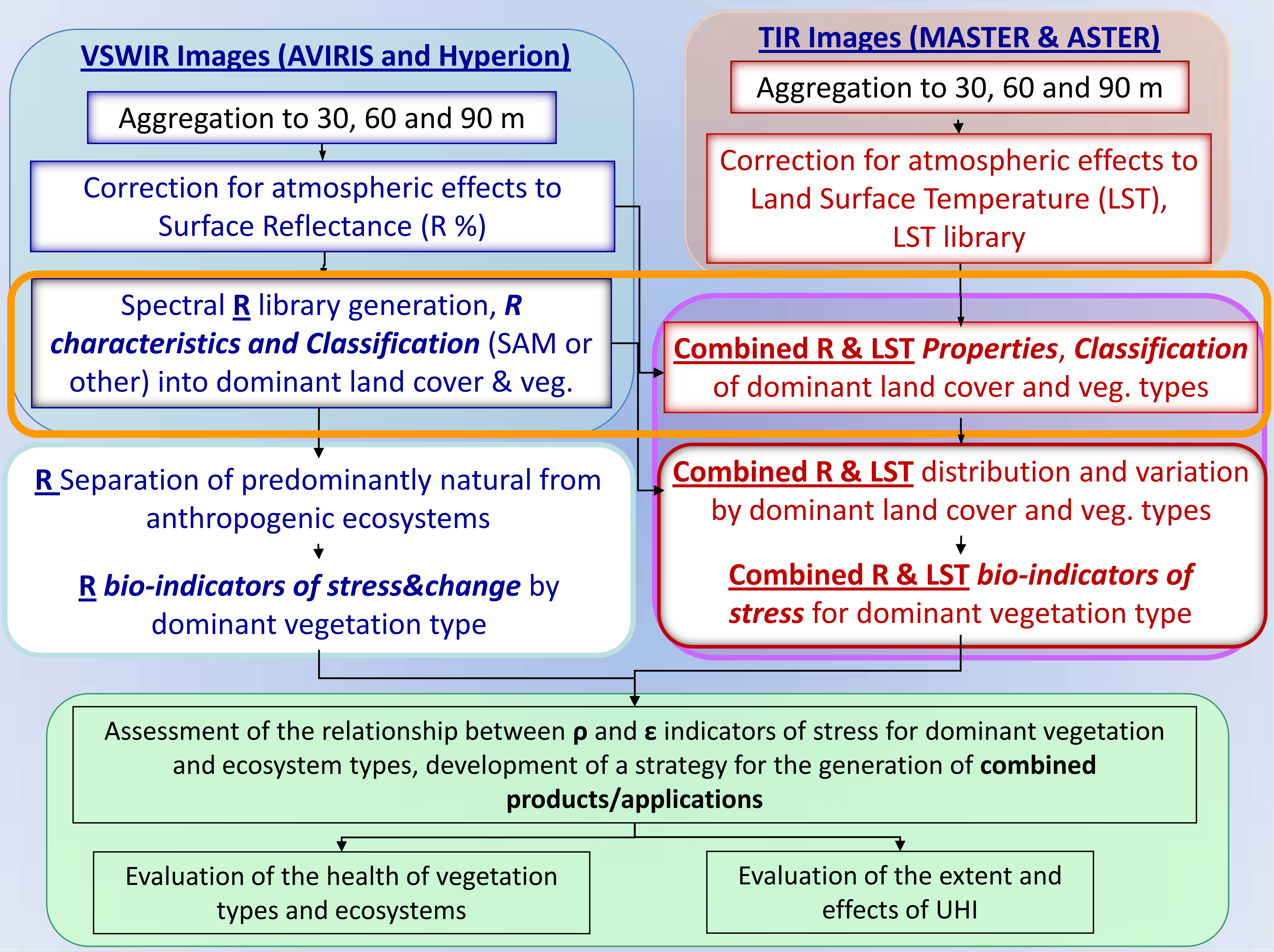
VSWIR Images (AVIRIS and Hyperion)
Aggregation to 30, 60 and 90 m
Correction for atmospheric effects to Surface Reflectance (R %)
Spectral R library generation, R characteristics and Classification (SAM or other) into dominant land cover & veg.
R Separation of predominantly natural from anthropogenic ecosystems
R bio-indicators of stress&change by dominant vegetation type
TIR Images (MASTER & ASTER)
Aggregation to 30, 60 and 90 m
Correction for atmospheric effects to Land Surface Temperature (LST), LST library
Combined R & LST Properties, Classification of dominant land cover and veg. types
Combined R & LST distribution and variation by dominant land cover and veg. types
Combined R & LST bio-indicators of stress for dominant vegetation type
Assessment of the relationship between ρ and ε indicators of stress for dominant vegetation and ecosystem types, development of a strategy for the generation of combined products/applications
Evaluation of the health of vegetation types and ecosystems
Evaluation of the extent and effects of UHI

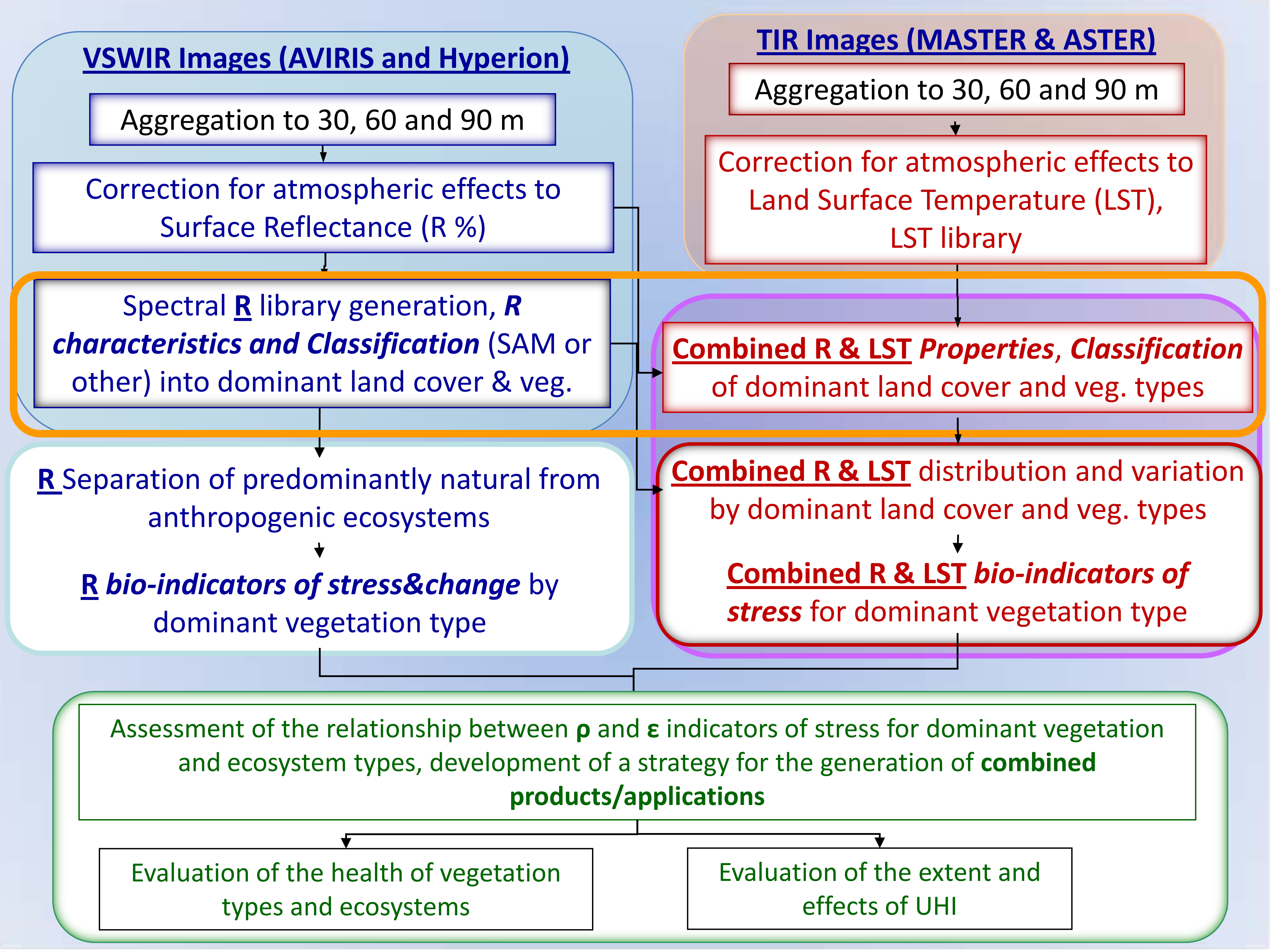
VSWIR Images (AVIRIS and Hyperion)
Aggregation to 30, 60 and 90 m
Correction for atmospheric effects to Surface Reflectance (R %)
Spectral R library generation, R characteristics and Classification (SAM or other) into dominant land cover & veg.
R Separation of predominantly natural from anthropogenic ecosystems
R bio-indicators of stress&change by dominant vegetation type
TIR Images (MASTER & ASTER)
Aggregation to 30, 60 and 90 m
Correction for atmospheric effects to Land Surface Temperature (LST), LST library
Combined R & LST Properties, Classification of dominant land cover and veg. types
Combined R & LST distribution and variation by dominant land cover and veg. types
Combined R & LST bio-indicators of stress for dominant vegetation type
Assessment of the relationship between ρ and ε indicators of stress for dominant vegetation and ecosystem types, development of a strategy for the generation of combined products/applications
Evaluation of the health of vegetation types and ecosystems
Evaluation of the extent and effects of UHI

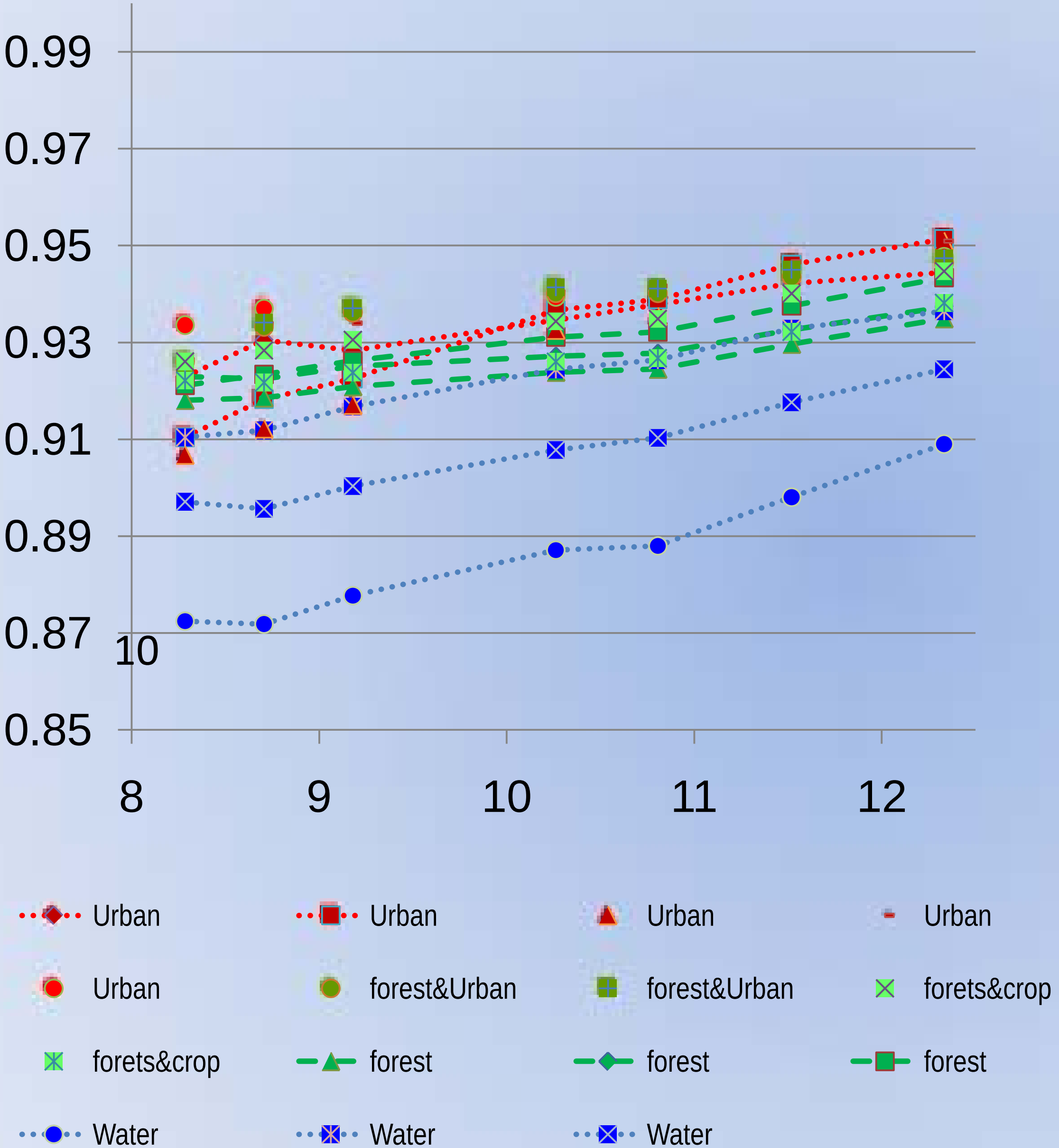

0.99
0.97
0.95
0.93
0.91
0.89
0.87
0.85
10
8
9
10
11
12
Urban
Urban
Urban
Urban
Urban
forest&Urban
forest&Urban
forets&crop
forets&crop
forest
forest
forest
Water
Water
Water

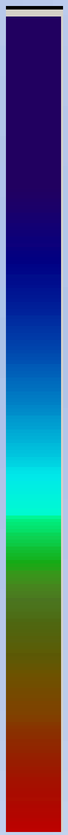

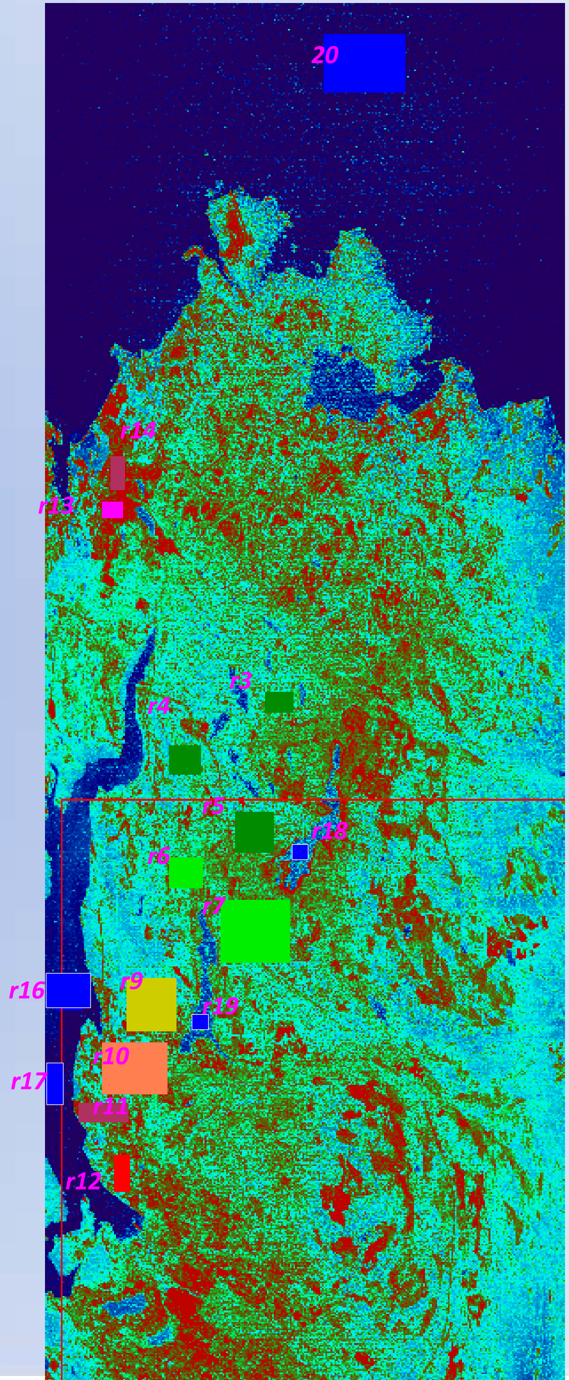

20
r14
r13
r3
r4
r5
r18
r6
r7
r9
r16
r19
r10
r17
r11
r12

Temporal profile of Hyperion at the CEOS Calibration site at Railroad Valley, NV

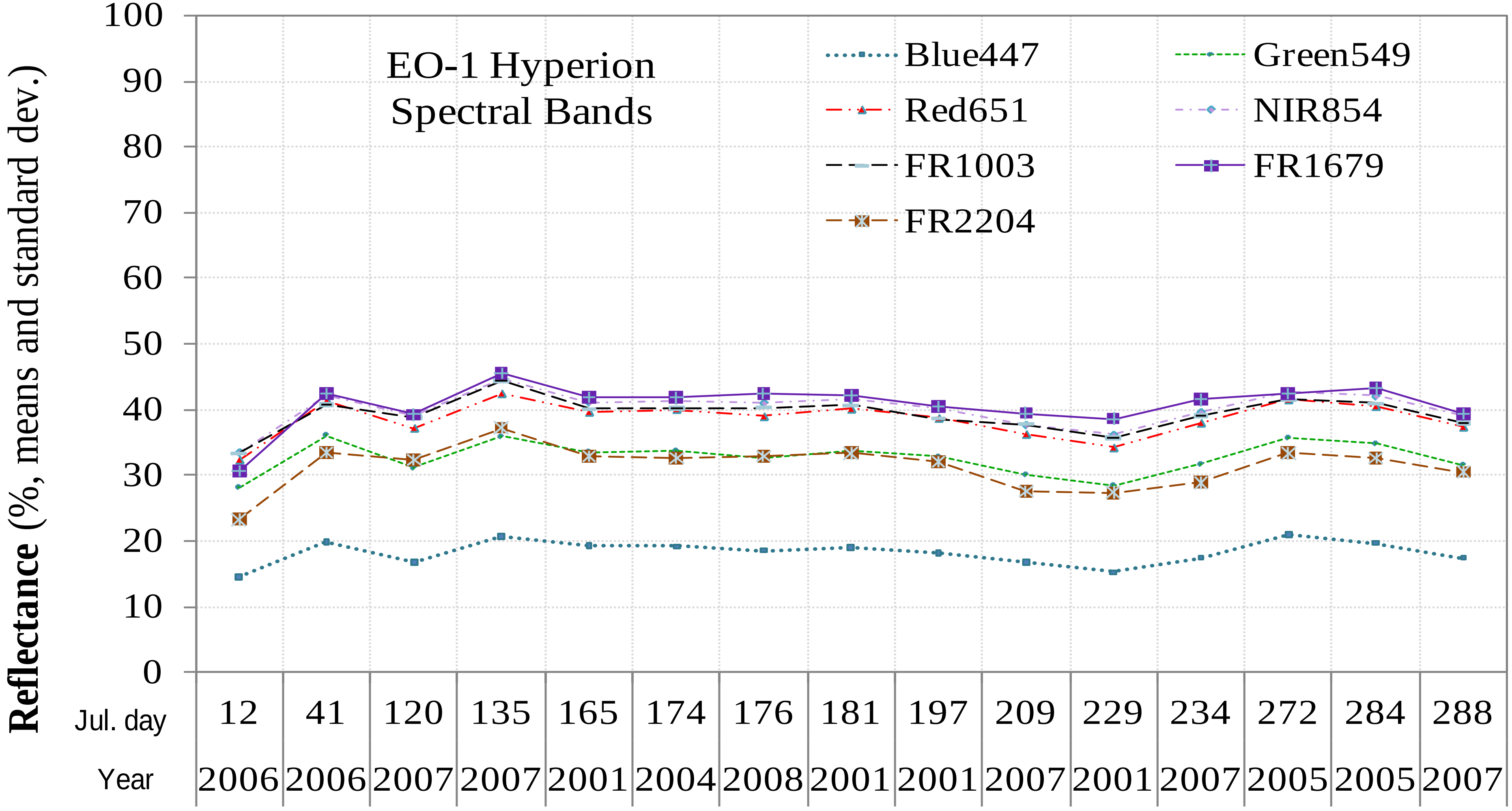

Linear temporal profile of the spectra demonstrates the relative stability of the spectral characteristics, as indicated for selected bands

Bio-physical parameter	Spectral bio-indicators *(examples)*	References
VSWIR indicators		
Chlorophyll in crops	$(R_{NIR}/ R^{-1}_{720\text{-}730}) - 1$	Gitelson et al., 2005
Canopy greenness	$EVI = G * \frac{R_{NIR} - R_{red}}{R_{NIR} + C_1 R_{red} - C_2 R_{blue} + L}$	Huete et al. 2002
Chlorophyll concentration estimation	$TCARI / OSAVI = \frac{3*[(R_{700} - R_{670}) - 0.2*(R_{700} - R_{550})*(R_{700} / R_{670})]}{(1+0.16)*(R_{800} - R_{700})/(R_{800} + R_{670} + 0.16)}$	Haboudane et al. 2002, Zarco-Tejada et al. 2004
Efficiency of photosynthesis	PRI=(R570-R531)/(R570+R531)	Gamon et al., 1992, Suarez et al. 2008
Canopy foliar water content	$NDWI = \frac{R_{NIR} - R_{1240}}{R_{NIR} + R_{1240}}$	Gao, 1996
Canopy foliar water content	$SIWI = \frac{R_{NIR} - R_{1640}}{R_{NIR} + R_{1640}}$	Fensholt and Sandholt, 2003
Vegetation stress	Average (R675…. R705)	Vogelman, 1993
Veg. structure and foliar biomass	NDVI = (R800-R670)/(R800+R670)	Deering, 1978
Stress/Chlorophyll	D714/D705, where D is product of first derivative transformation of R	Entcheva, 2004
Stress/ Chlorophyll	Dmax/D705, where Dmax is the maximum of D in the 670-730nm region	Entcheva, 2004

Remote Estimation of Pigment Content and Composition in Terrestrial Vegetation: Challenges and Solutions

Anatoly A. Gitelson

School of Natural Resources, University of Nebraska-Lincoln

26 August, 2010
HyspIRI

Goal: To develop techniques for estimating contents and composition of pigments in terrestrial vegetation

- Total chlorophyll content, chlorophyll-*a* and -*b*
- Total carotenoids content
- Total anthocyanins content

Chlorophylls

Chlorophylls relate to both the physiological status and the photosynthetic capacity of vegetation.

Chlorophylls absorb solar radiation and provide mechanisms for its utilization in photosynthetic reactions.

Total canopy chlorophyll content is objective quantitative measure of vegetation greenness.

Carotenoids and Anthocyanins

- Carotenoids contribute to light-harvesting and also play a photo-protective role, preventing damage to the photosynthetic apparatus in leaves.
- The induction of anthocyanins biosynthesis occurs as a result of <u>deficiencies</u> in nitrogen and phosphorus, wounding, pathogen infection, desiccation, low temperature, UV-irradiation etc. Anthocyanins fulfill important physiological functions by being involved in the <u>adaptation to numerous stresses</u> and environmental strain reduction.

Three-band model for pigment content estimation based on Kubelka-Munk remission function

$$f(\rho_\infty) = (1 - \rho_\infty^2)/2\rho_\infty = (a + b_b)/b_b \cong \rho_o^{-1}$$

ρ_∞ is reflectance of an ideal layer, in which a further increase in thickness results in no noticeable difference, ρ_o is reflectance measured against black background

$$\rho^{-1}(\lambda) \propto [a_{pigm}(\lambda) + a_0(\lambda) + b_b]/b_b$$

$$\text{Pigment Content} \propto [\underbrace{\rho^{-1}(\lambda_1)} - \underbrace{\rho^{-1}(\lambda_2)}]\ \underbrace{\rho(\lambda_3)}$$

Gitelson et al., GRL, 2003, 2006

Total canopy chlorophyll content

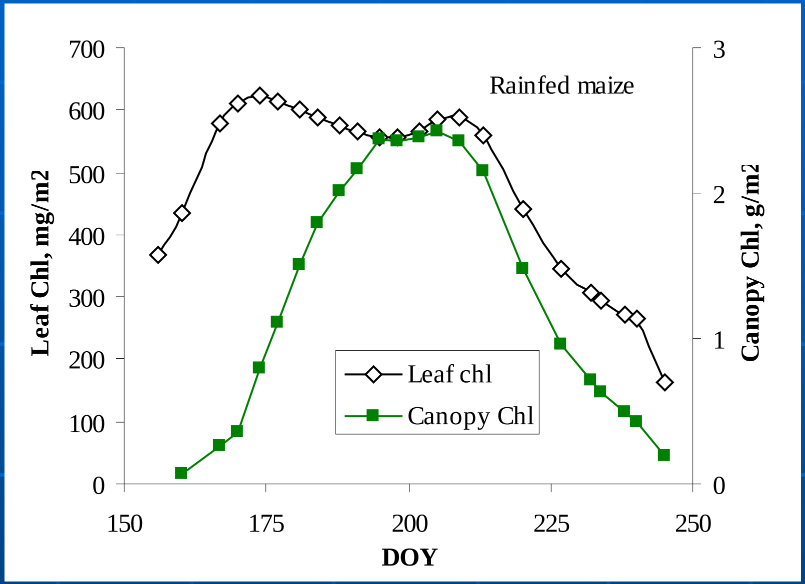

Total canopy Chl = total LAI Chl_{leaf}

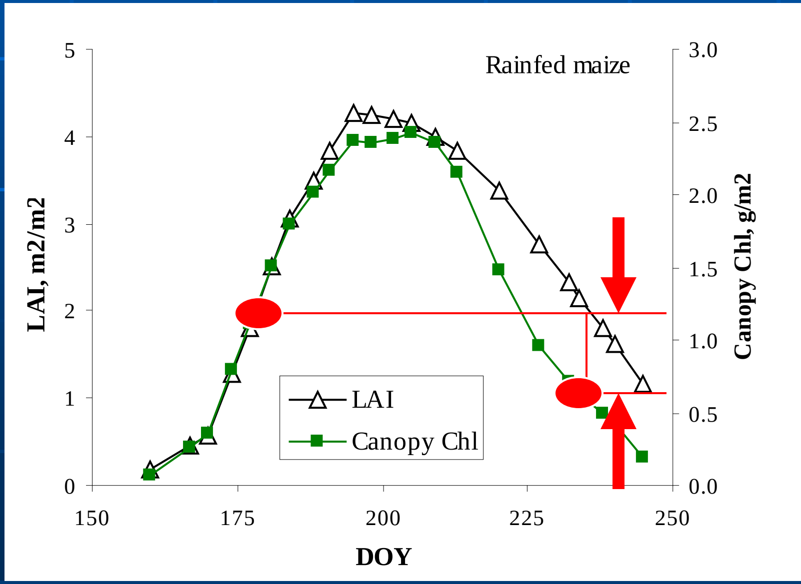

Chlorophyll content estimation

Only HyspIRI is able to uniquely provide it

$$\rho^{-1}(\lambda) \propto [a_{chl}(\lambda) + a_0(\lambda) + b_b]/b_b$$

Chlorophyll Index

$$CI \propto [\rho^{-1}(\lambda_1) - \rho^{-1}(\lambda_2)]\ \rho(\lambda_3)$$

Gitelson et al., GRL, 2003, 2006

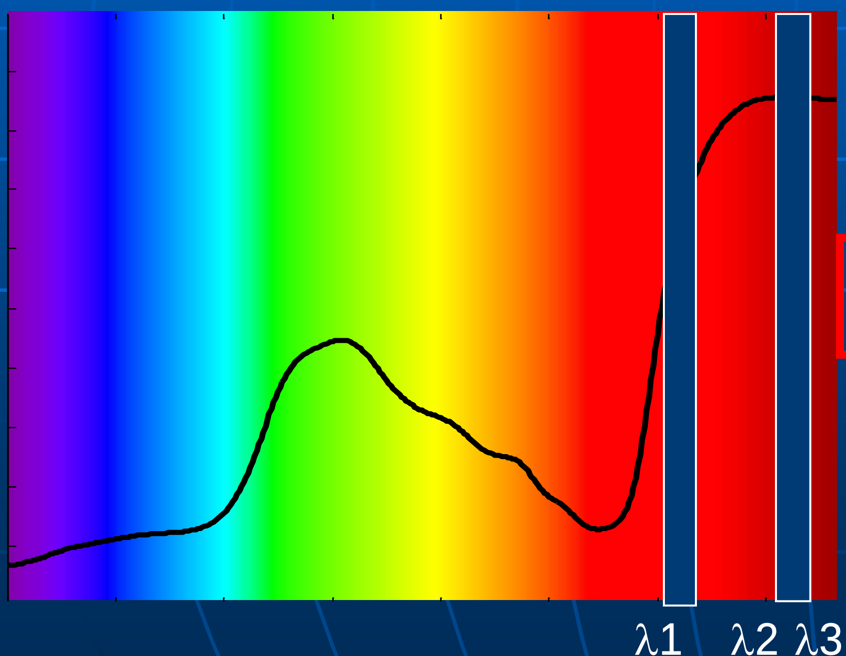

$$\boxed{\text{Total Chl} \propto CI = (\rho_{NIR}/\rho_{red\ edge}) - 1}$$

Gitelson et al., GRL, 2003

Only HyspIRI is able to uniquely provide it

$$\rho^{-1}(\lambda) \propto [a_{chl}(\lambda) + a_0(\lambda) + b_b]/b_b$$

Chlorophyll-*b* Index

$$CI_{chl\text{-}b} \propto \underbrace{[\rho^{-1}(\lambda_1)}_{a_{chl\text{-}a} + a_{chl\text{-}b}} - \underbrace{\rho^{-1}(\lambda_2)]}_{a_{chl\text{-}a}} \underbrace{\rho(\lambda_3)}_{b_b}$$

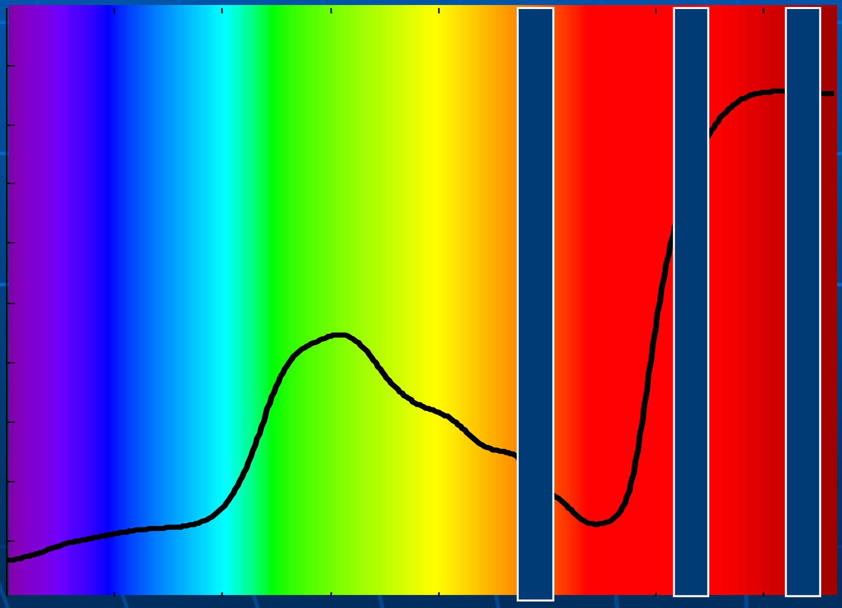

Chl-*b*

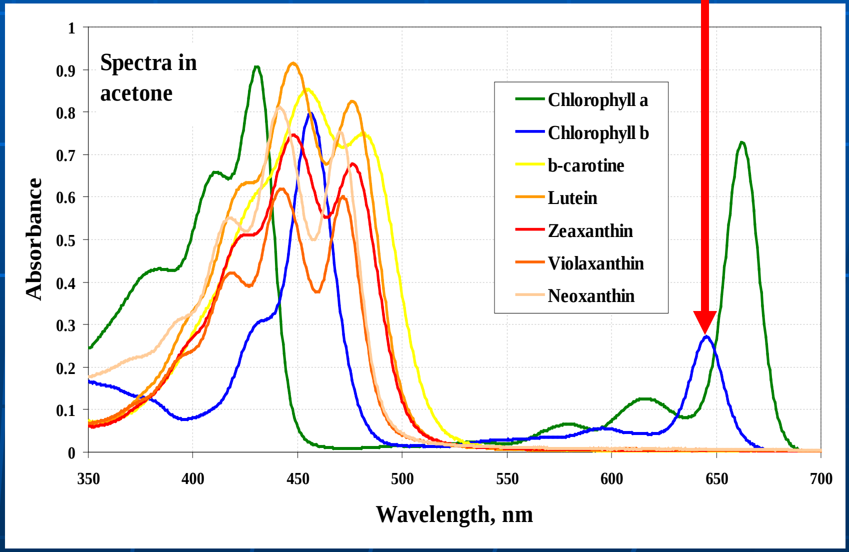

$$\boxed{Chl\text{-}b \propto CI_{chl\text{-}b} = (\rho^{-1}_{650} - \rho^{-1}_{red\ edge})\ \rho_{NIR}}$$

Performance of different methods to assess chlorophyll

Method	λ_1	λ_2	λ_3	Wavelength selection database	Relationship adjustment database	RMSE synthetic database ($\mu g.cm^{-2}$) N=2000	RMSE reduced database ($\mu g.cm^{-2}$) N=660	RMSE extended database ($\mu g.cm^{-2}$) N=1097
mSR	**405**	720	910	Synthetic	Experimental	12.80	5.64	*NA*
3BM	**700-730**	**755-800**	**765-800**	**Synthetic**	**Experimental**	**5.34**	**5.72**	**6.19**
SR	**713**	779		Synthetic	Experimental	10.88	5.74	6.15
ND	**711**	776		Synthetic	Experimental	10.41	5.81	6.39
3BM	**700-730**	755-800	765-800	Synthetic	Synthetic	6.27	6.07	6.53
$CI_{red\ edge}$	**690-720**	760-800		(1)	Experimental	5.33	6.11	6.87
mND	**410**	715	830	Synthetic	Experimental	12.28	6.26	*NA*
DDn	**711**	229		Synthetic	Experimental	12.48	6.29	*NA*
$NDVI_{red\ edge}$	**710**	**750**		**(3)**	**Experimental**	**12.20**	**6.34**	**7.42**
SR	**713**	779		Synthetic	Synthetic	9.20	6.44	6.75
RII	**705**	750		(3)	Experimental	47.42	6.47	7.66
$ND_{705,935}$	**705**	935		(2)	Experimental	12.35	6.70	*NA*
$ND_{705,935}$	**705**	935		(2)	(2)	13.60	6.71	*NA*
ND	**711**	776		Synthetic	Synthetic	9.54	6.78	7.27
mSR	**405**	720	910	Synthetic	Synthetic	11.04	6.85	*NA*
$SR_{710,970}$	**710**	970		(2)	Experimental	10.98	7.23	*NA*

Feret et al., 2010 submitted

Only HyspIRI is able to uniquely provide it

$$CI_{red\ edge} \propto [(\rho_{red\ edge})^{-1}-(\rho_{NIR})^{-1}]\ \ \rho_{NIR}$$

Leaf

Canopy

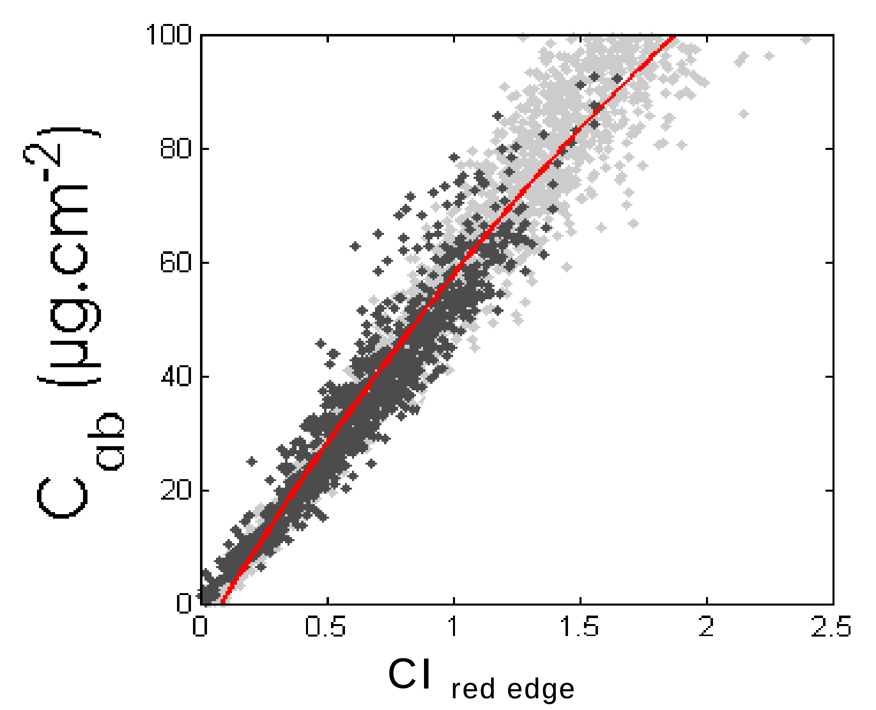

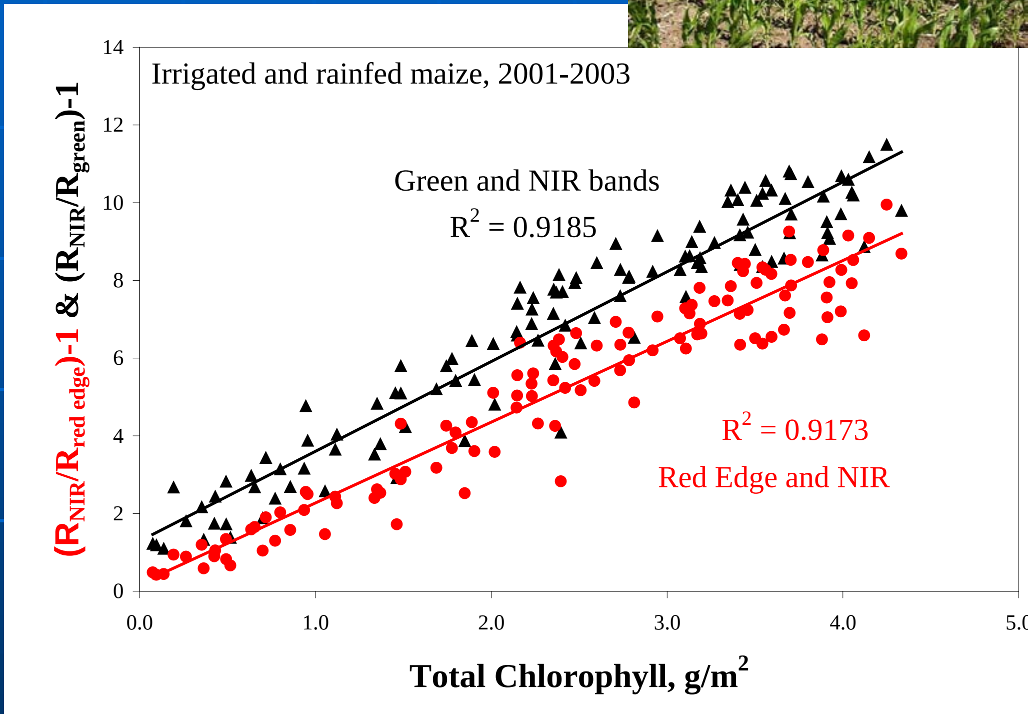

Feret et al., RSE, 2009

Gitelson et al., GRL, 2005

Only HyspIRI is able to uniquely provide it

$$CI_{red\ edge} \propto [(\rho_{red\ edge})^{-1}-(\rho_{NIR})^{-1}]\ \ \rho_{NIR}$$

Southern Old Aspen, the southern ecotone of the western boreal forests, Canada

Hyperion
Maize in China

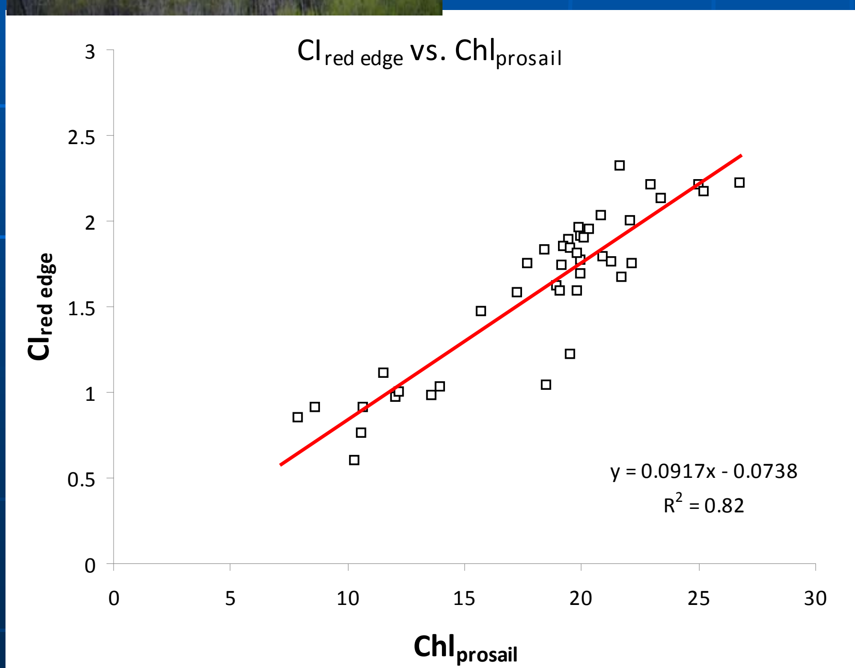

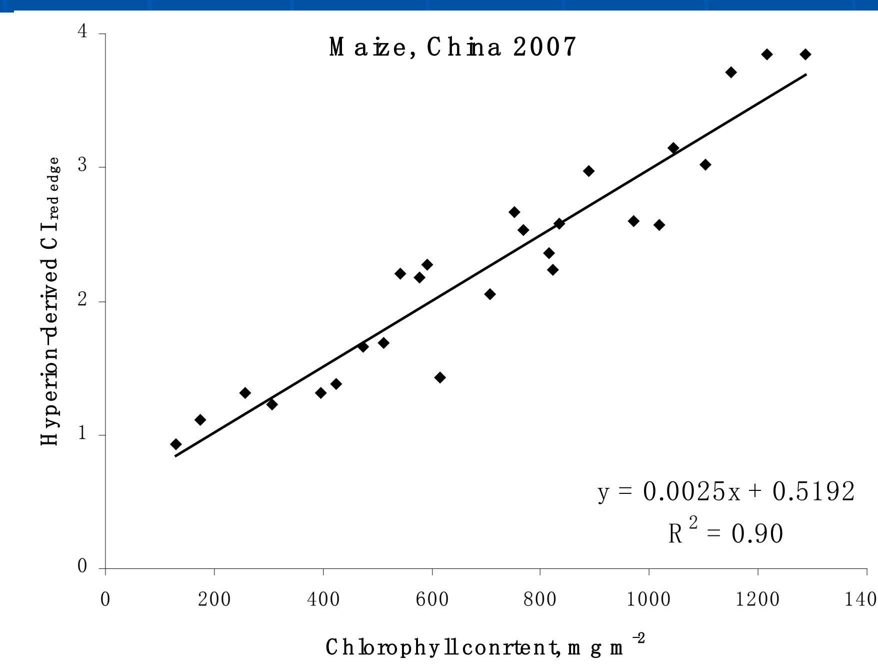

Hilker et al., 2010, submitted

Wu et al., IJRS, 2010

Carotenoids content estimation

Only HyspIRI is able to uniquely provide it

$$\rho^{-1}(\lambda) \propto [a_{chl}(\lambda) + a_0(\lambda) + b_b]/b_b$$

Carotenoids Reflectance Index

$$CRI \propto \underbrace{[\rho^{-1}(\lambda_1)}_{a_{car} + a_{chl}} - \underbrace{\rho^{-1}(\lambda_2)]}_{a_{chl}} \; \underbrace{\rho(\lambda_3)}_{b_b}$$

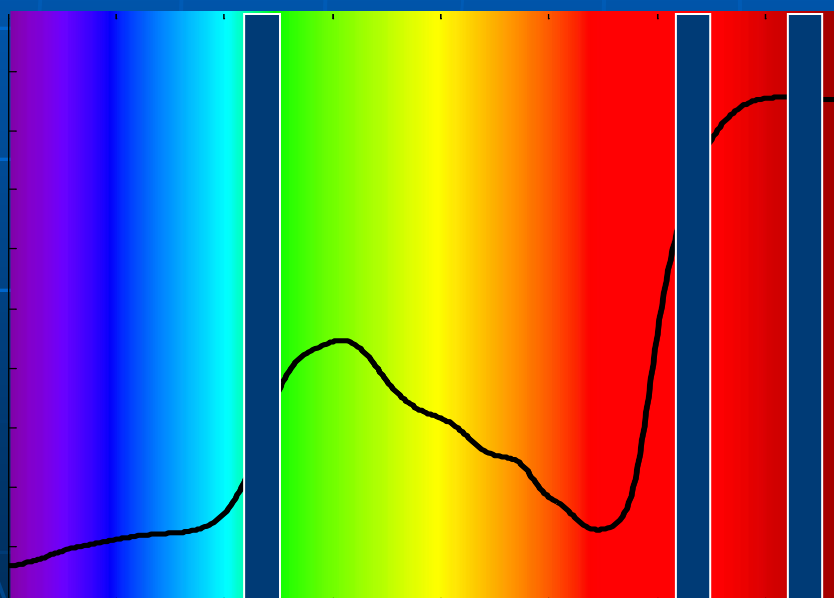

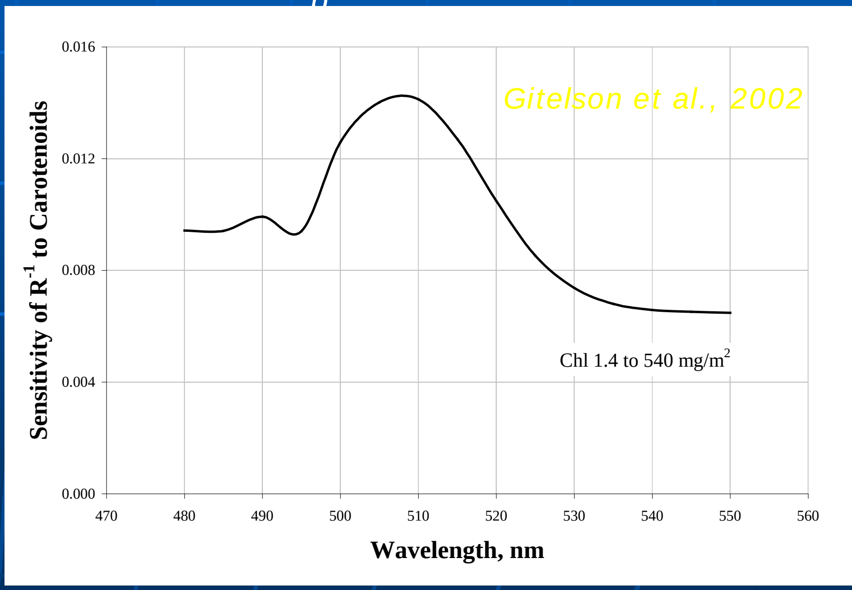

Gitelson et al., 2002

$$\boxed{Car \propto CRI = (\rho^{-1}_{515} - \rho^{-1}_{\text{red edge}})\ \rho_{NIR}}$$

Only HyspIRI is able to uniquely provide it

Carotenoids content estimation

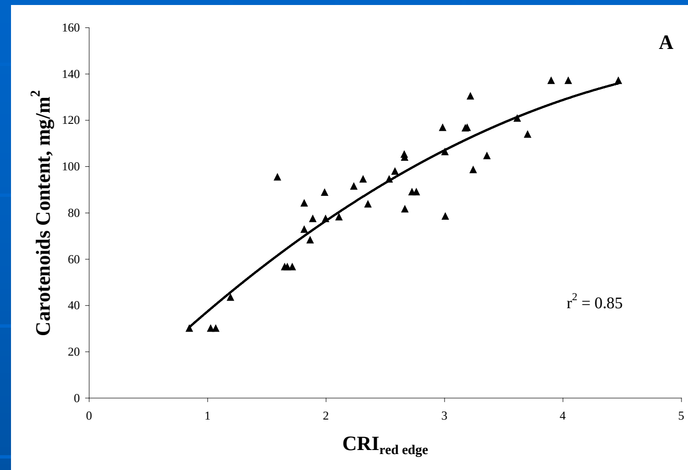

Gitelson et al., 2002

The Douglas-fir stand, Canada

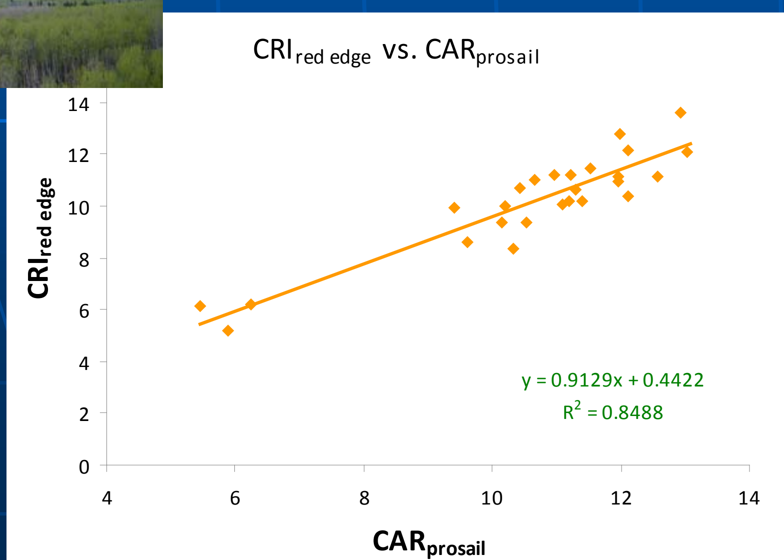

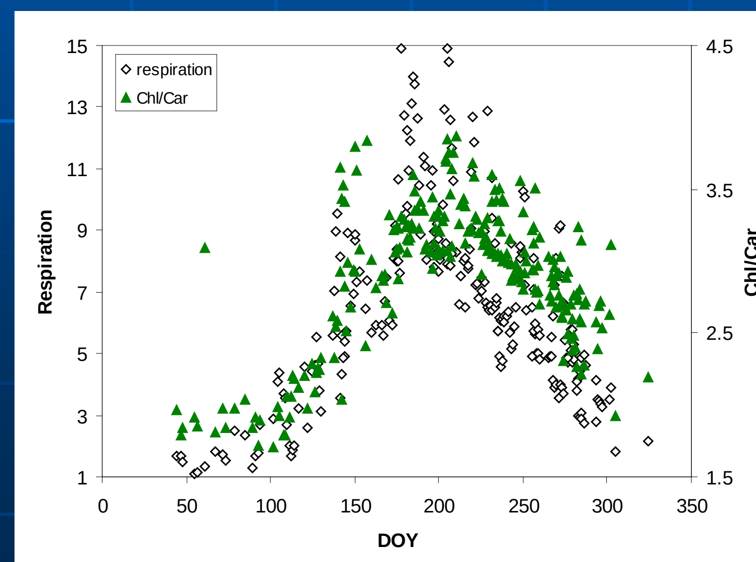

Hilker et al., 2010, submitted

Anthocyanins content estimation

Only HyspIRI is able to uniquely provide it

$$\rho^{-1}(\lambda) \propto [a_{chl}(\lambda) + a_0(\lambda) + b_b]/b_b$$

Anthocyanin Reflectance Index

$$ARI_{\text{red edge}} \propto \underbrace{[\rho^{-1}(\lambda_1)}_{a_{anth} + a_{chl}} - \underbrace{\rho^{-1}(\lambda_2)]}_{a_{chl}} \ \underbrace{\rho(\lambda_3)}_{b_b}$$

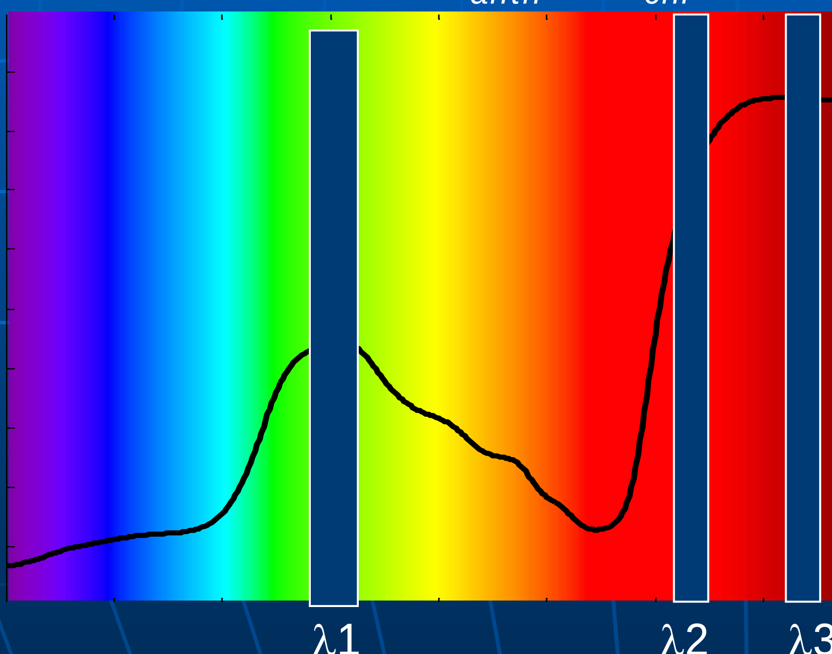

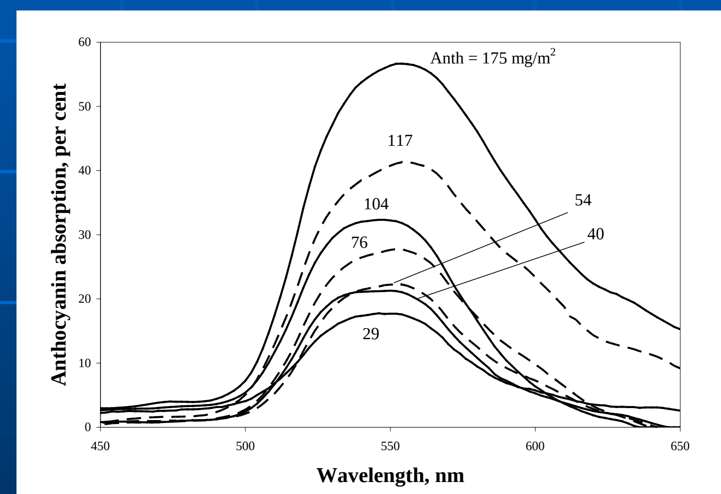

Gitelson et al., 2009

$$\boxed{Anth \propto ARI = (\rho^{-1}_{550} - \rho^{-1}_{\text{red edge}})\ \rho_{NIR}}$$

Gitelson et al., 2001

Only HyspIRI is able to uniquely provide it

Anthocyanins content estimation

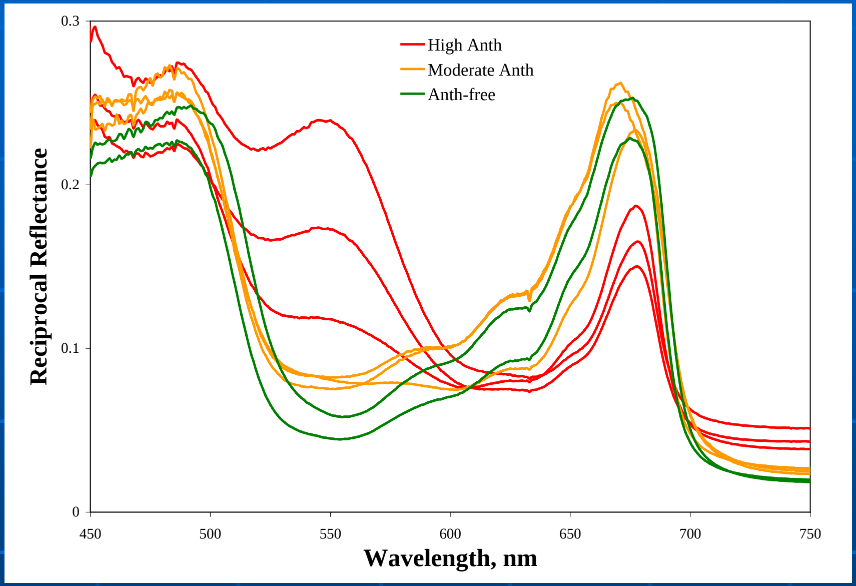

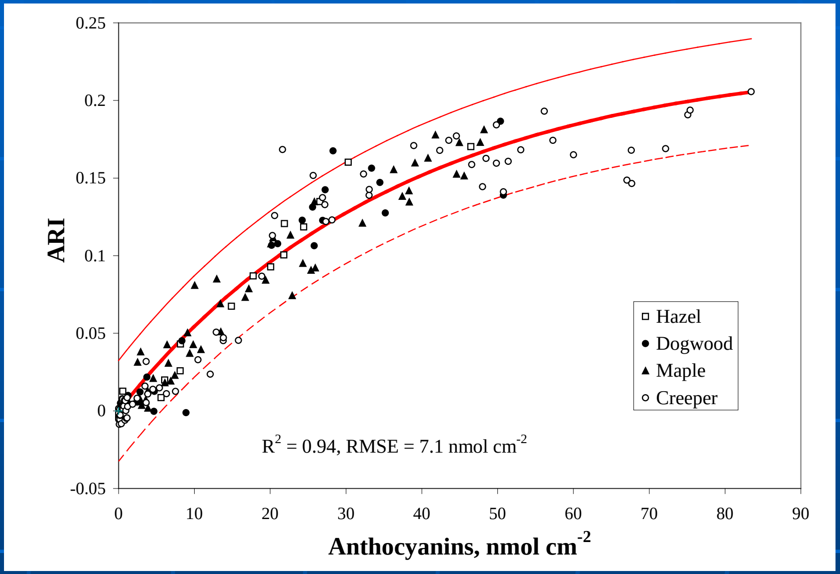

Gitelson et al., 2009

The induction of anthocyanins biosynthesis occurs as a result of deficiencies in nitrogen and phosphorus and other stresses

Anthocyanin levels (ARI) indicate physiological and biochemical changes from water stress (Asner, PNAS, 2004)

"...ARI showed high values for eucalypt as compared with other species. The differences were so amazing that I even used that as a classification algorithm and for tree delineation."

Jose A. Jimenez Berni, CSIRO

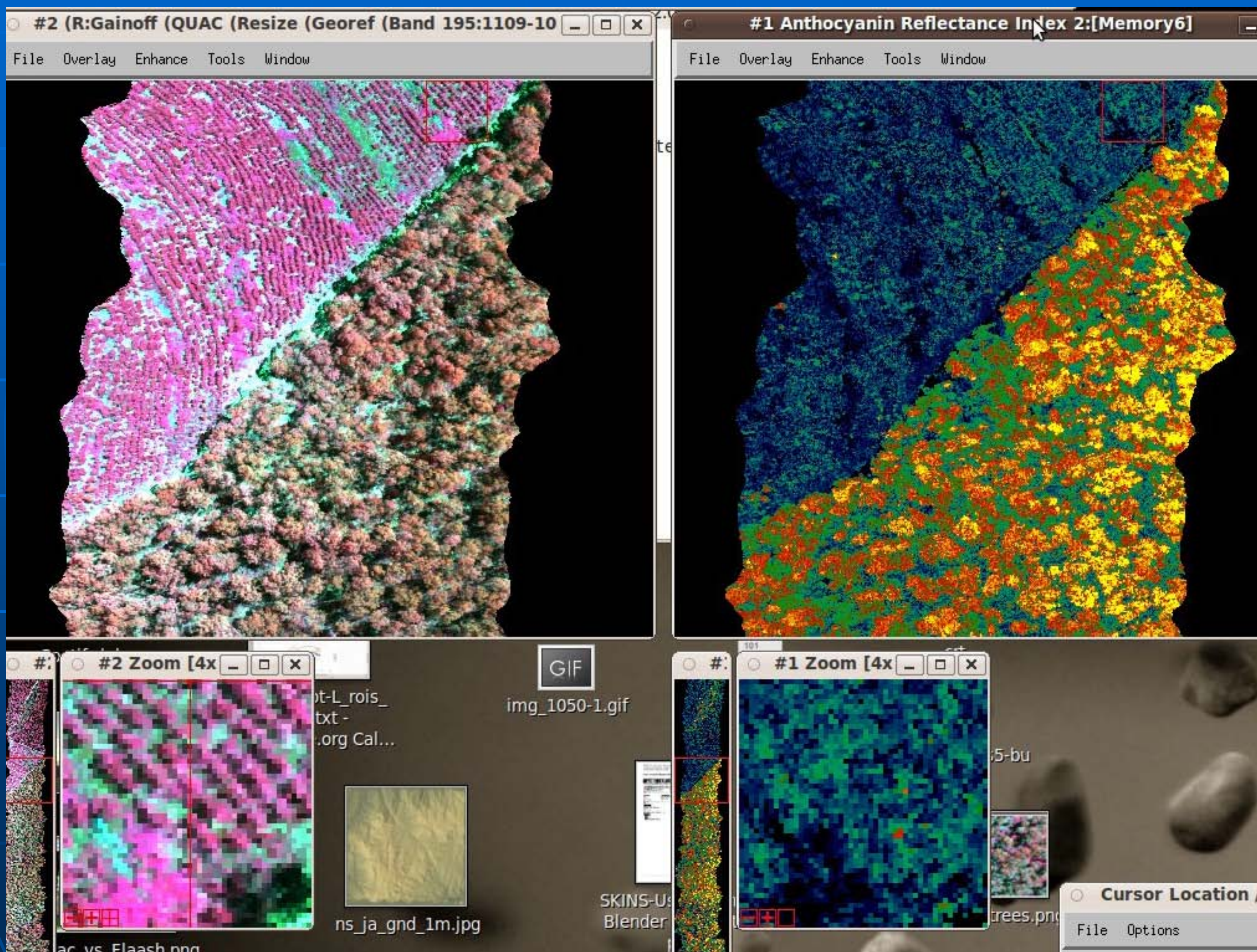

Vegetation Index Map: ARI = $(\rho^{-1}_{550}-\rho^{-1}_{710})\times\rho_{800}$

Only HyspIRI is able to <u>uniquely</u> provide it

Tree delineation based on Anthocyanin Reflectance Index

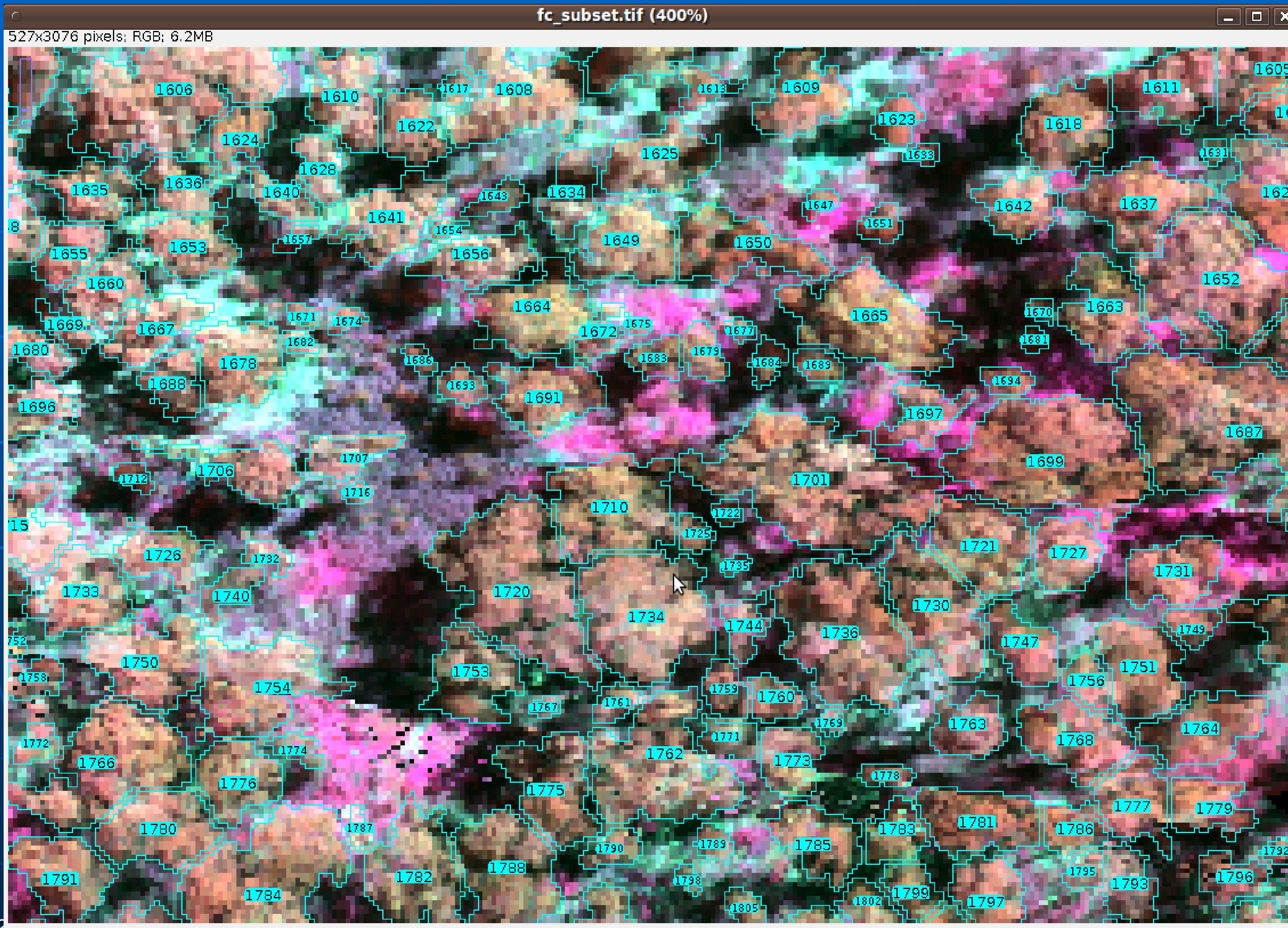

Courtesy: Jose A. Jimenez Berni, CSIRO

Relevance to carbon cycle science and climate science

GPP ∝ fAPAR×PAR×LUE

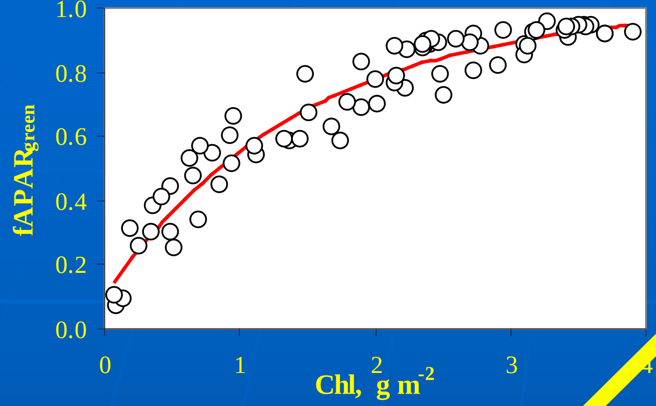

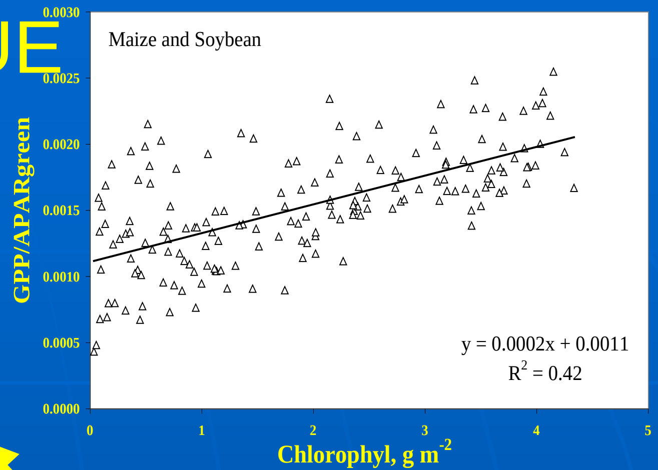

Chlorophyll

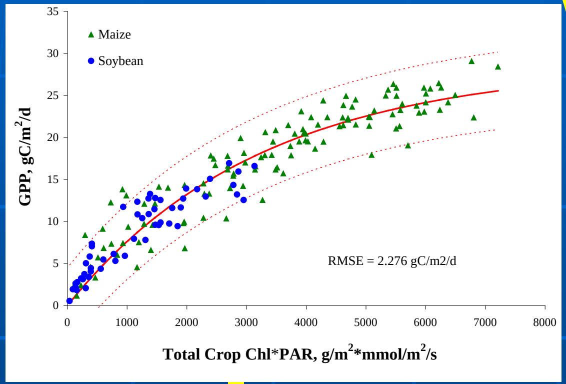

$fAPAR_{green}$

depends on amount of *chlorophyll*

LUE

chlorophyll is an indicator of efficiency of using fAPAR for photosynthesis

GPP = Chl×LUE×PAR

1. Production Efficiency Models

26 August, 2010
HyspIRI

$$GPP \propto LAI \times LUE \times PAR_{in}$$

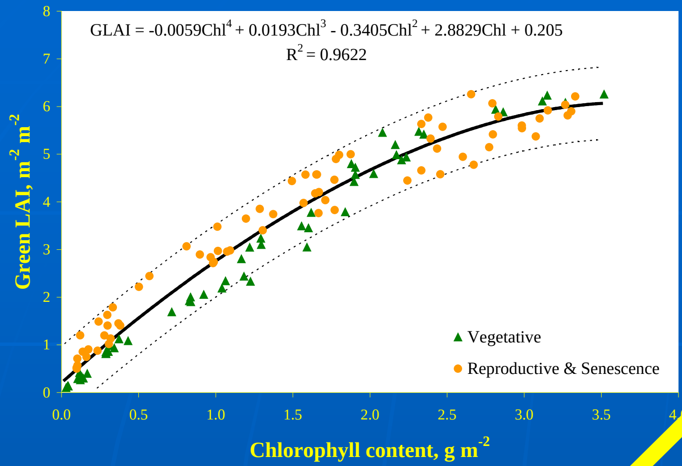

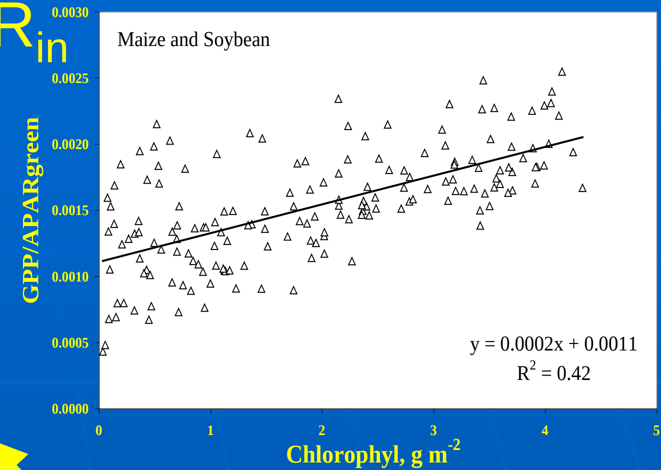

Chlorophyll

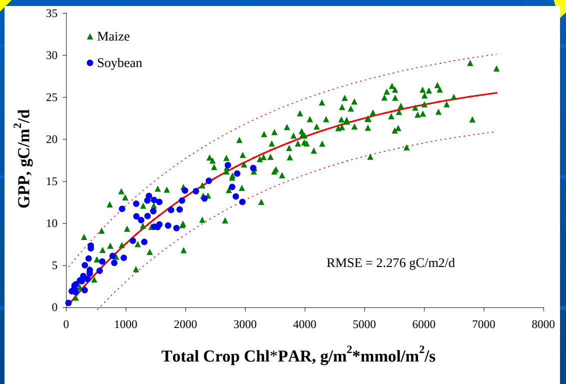

Green LAI

LUE

chlorophyll is an indicator of efficiency of using fAPAR for photosynthesis

Relates closely to *chlorophyll*

Chlorophyll is objective characteristic of plant greenness

$$GPP = Chl \times LUE \times PAR$$

2. Canopy Photosynthesis Models

Diagnosis of Maize N Status

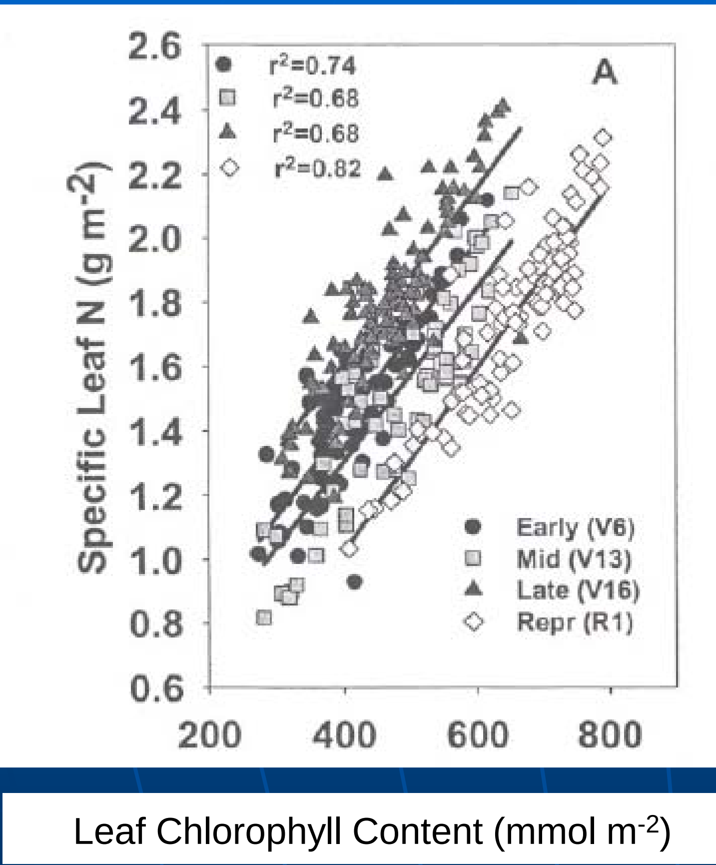

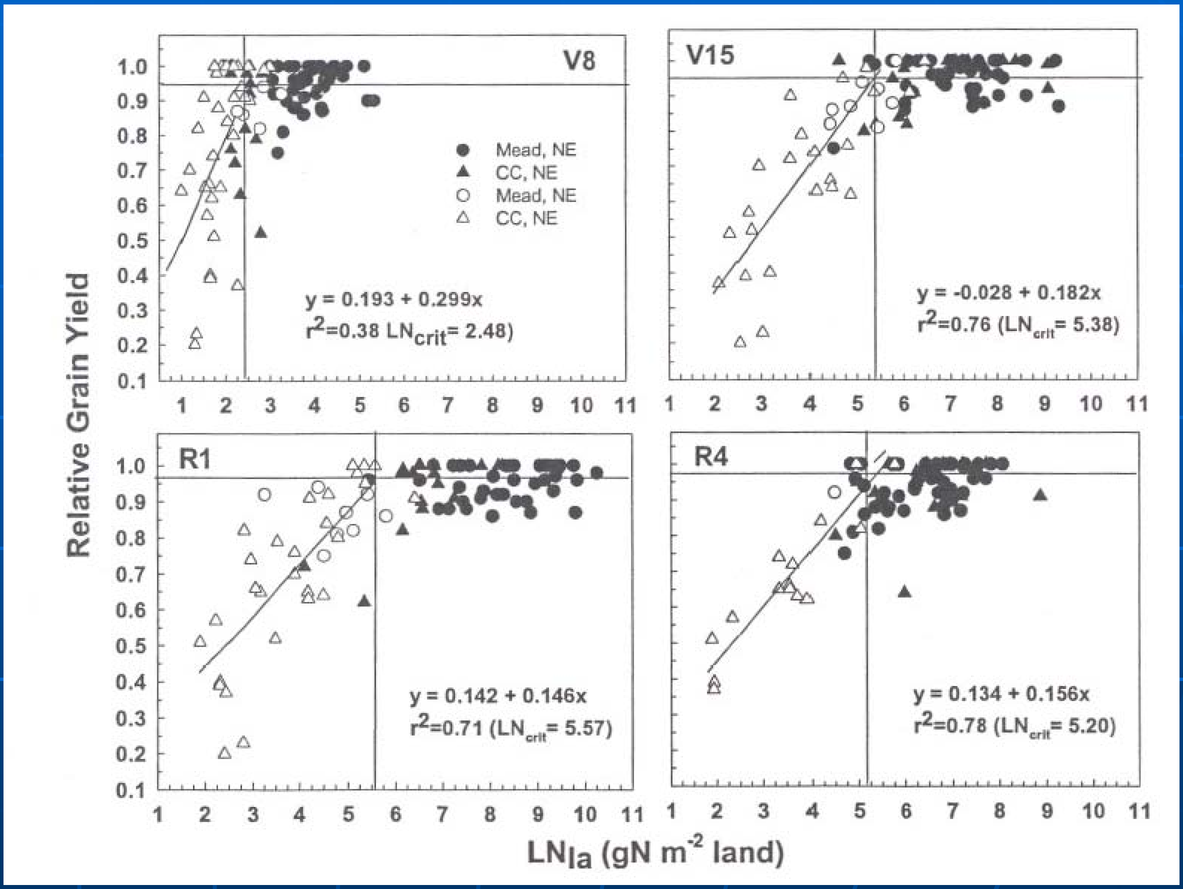

Specific leaf nitrogen (g N m^{-2} leaf) is closely related to leaf chlorophyll content

Walters, 2003

Leaf Nitrogen Per Unit Land Area is closely related to relative grain yield

Walters, 2003

Chlorophyll Content

GPP

N content

To estimate remotely *GPP*, one should find the way to accurately retrieve *chlorophyll content* from remotely sensed data

GPP and Canopy Chlorophyll

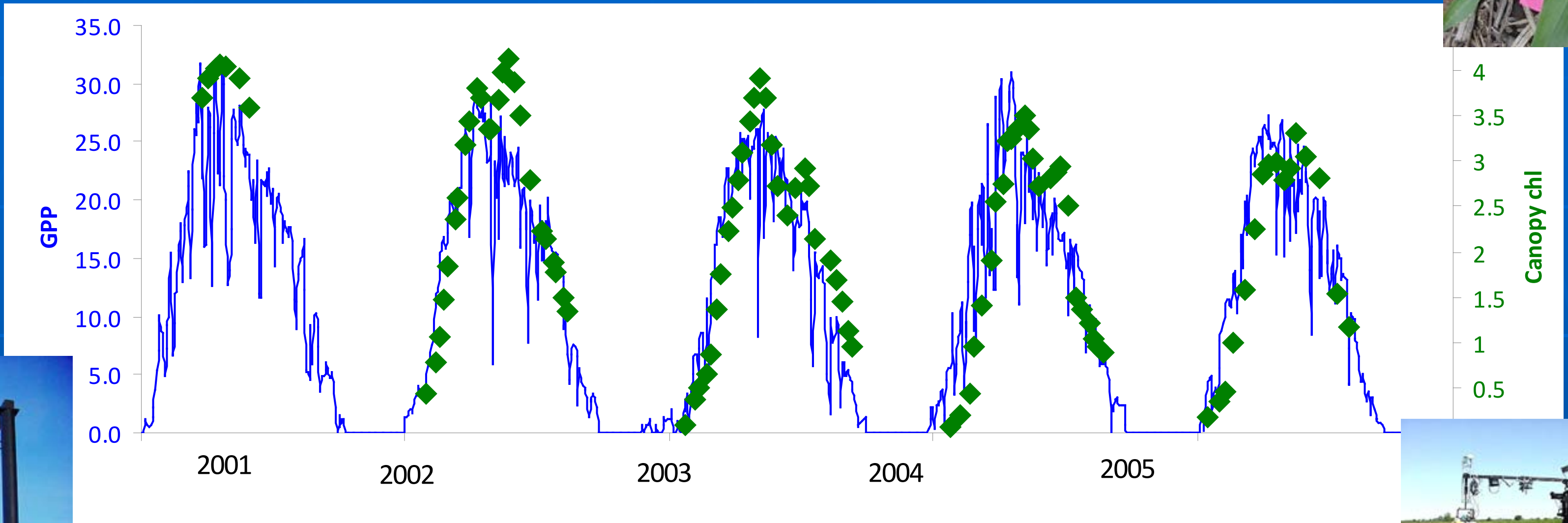

Proximal Sensing: GPP and Red edge Chlorophyll Index

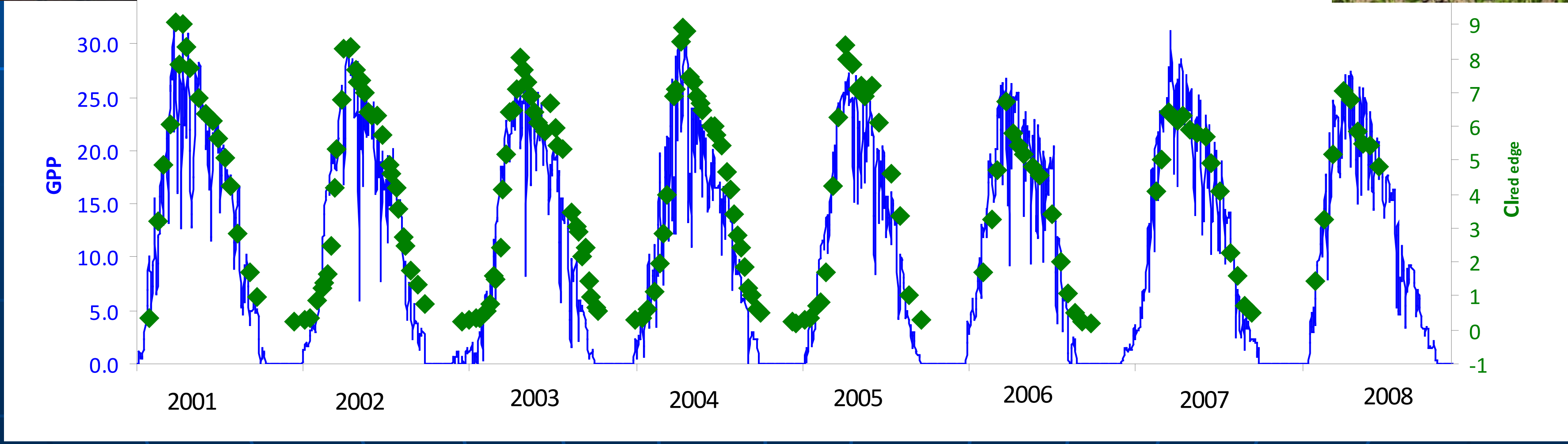

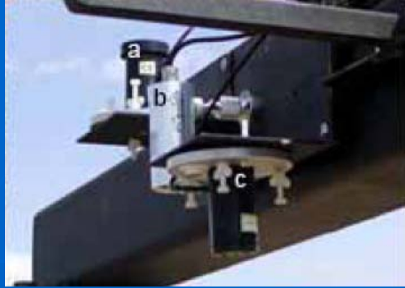

SKYE estimates of GPP

GPP & SKYE $CI_{red\ edge}$ vs. DOY

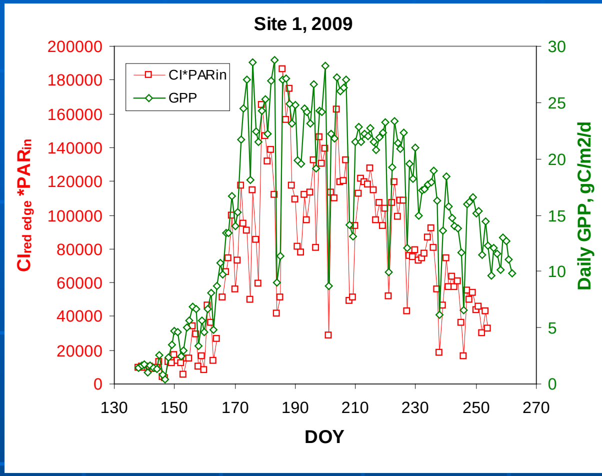

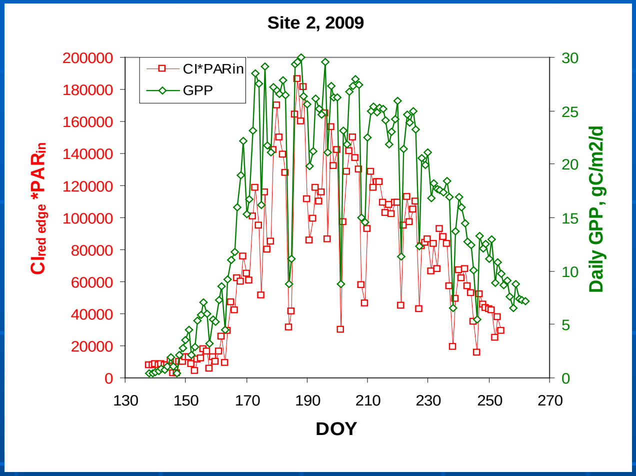

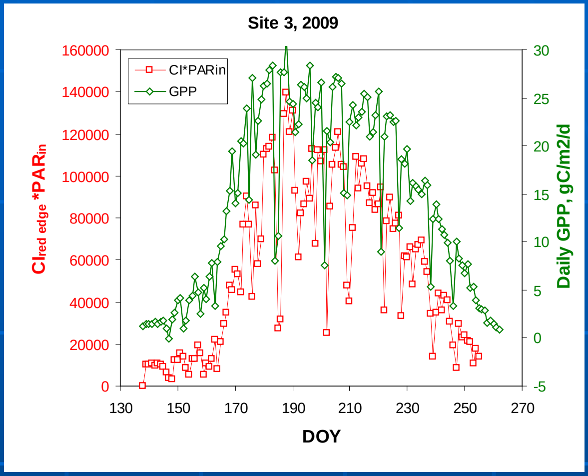

SKYE $CI_{red\ edge}$ vs. Maize GPP

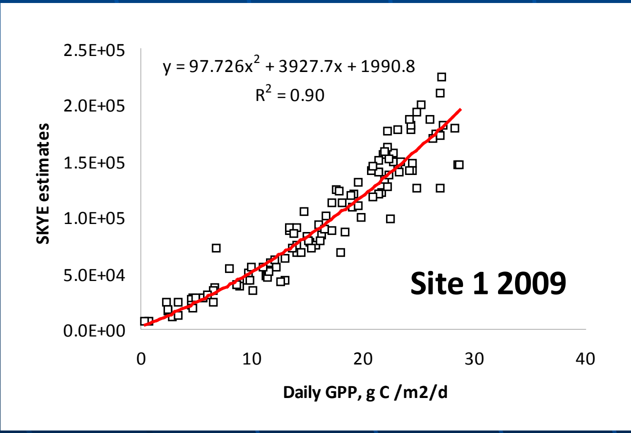

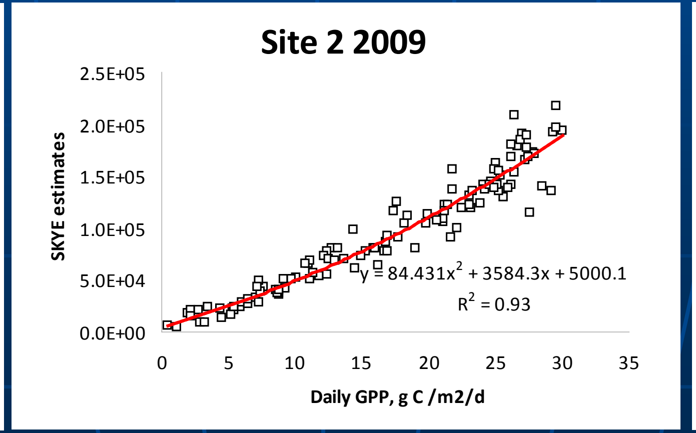

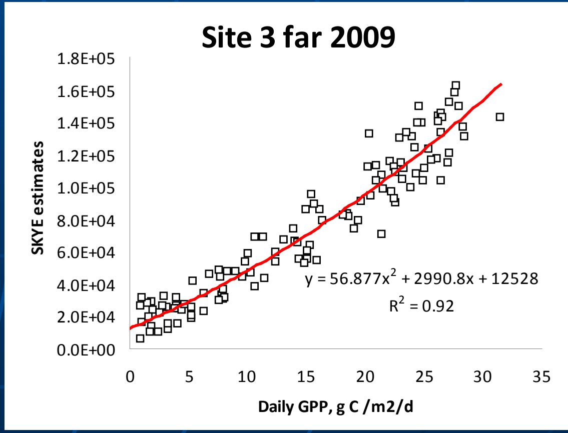

Species independent GPP estimation GPP vs. Red Edge NDVI and Chlorophyll Index

with red edge band 710-730 nm

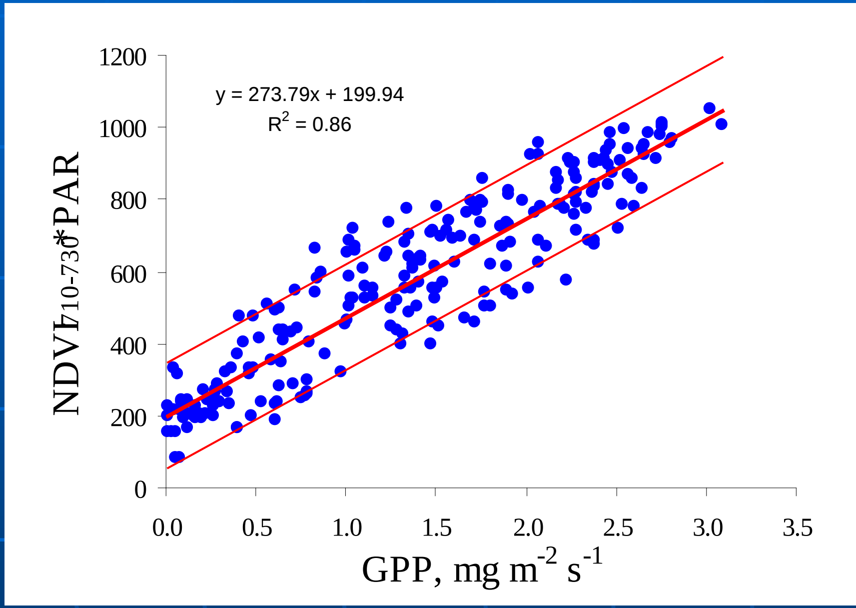

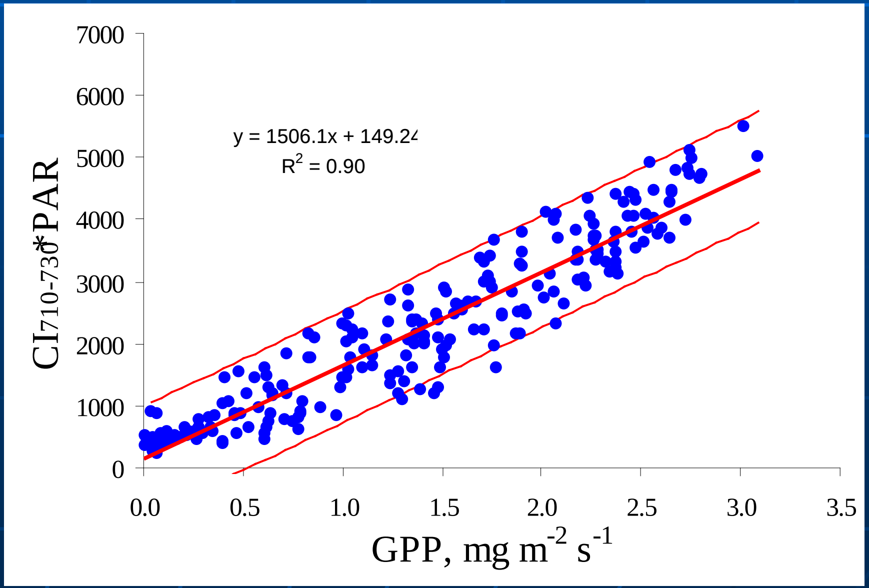

Chlorophyll vs. NEP and LUE

Southern Old Aspen, the southern ecotone of the western boreal forests, Canada

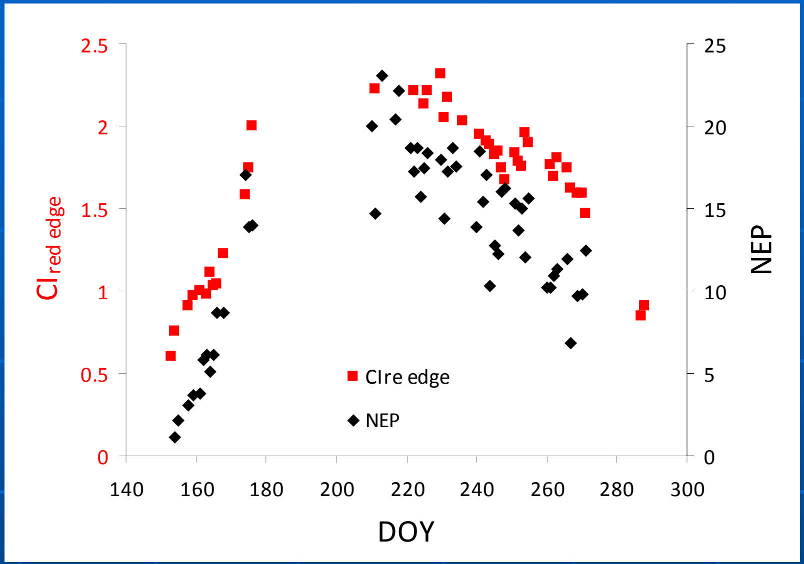

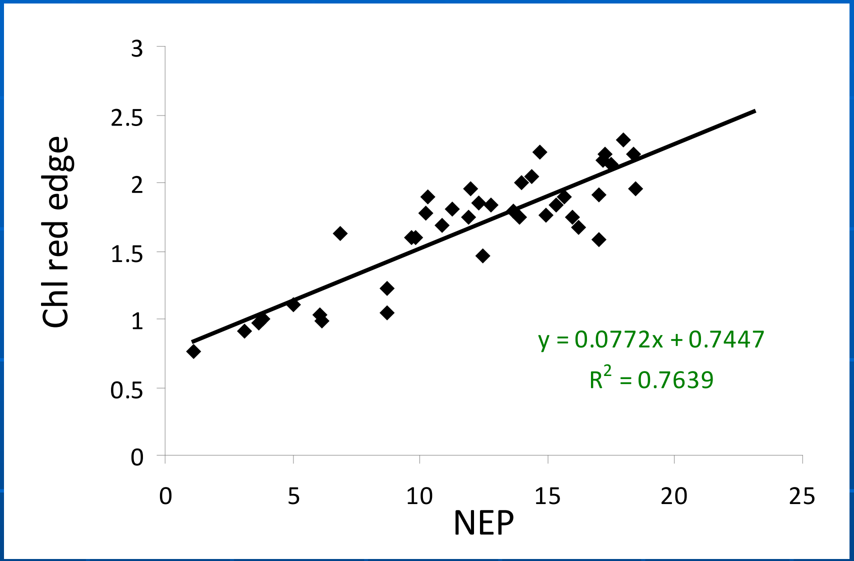

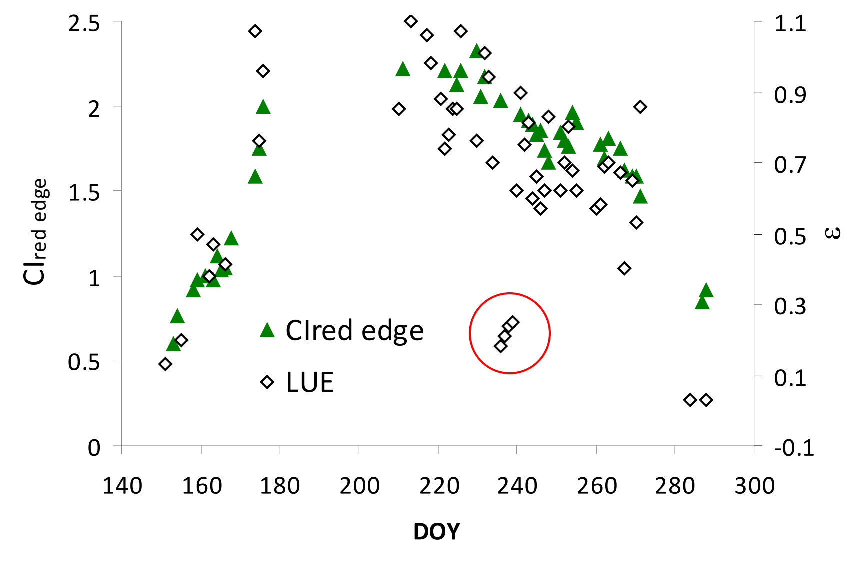

Hilker et al., 2010, submitted

Conclusions

- HyspIRI is unprecedented possibility to measure globally <u>spectrally, spatially and even temporally</u> pigment content and composition
  - in terrestrial vegetation
  - in inland and coastal waters (phytoplankton pigment concentrations)
- Pigment content and composition is a bridge between observations and models. It can be used for development of other HyspIRI products (e.g., LUE, GPP, LAI, $fAPAR_{green}$ among others)
- Main challenge is to calibrate and validate the products. To measure pigments analytically is labor intensive and time consuming. We developed reflectance-based techniques for pigment contents retrieval from radiometric data taken at leaf level and close range that can be used as ancillary data.

Thank you

agitelson2@unl.edu

An Investigation of Cloud Cover Probability for the HyspIRI Mission Using MODIS Cloud Mask Data

August 26th, 2010

Adam Gunderson, Montana State University

Mark Chodas, MIT

2010 NASA summer Space Grant worked performed at Jet Propulsion Laboratory, California Institute of Technology

Background

- Visible Shortwave Infrared Imager (VSWIR)
  - Specifications
    - 60 m spatial resolution
    - 145 km swath width
    - 380-2500 nm, 10 nm sampling
    - **19 day revisit**
      - **Global seasonal coverage**
      - **Allows for better knowledge of the planets ecosystem changes**

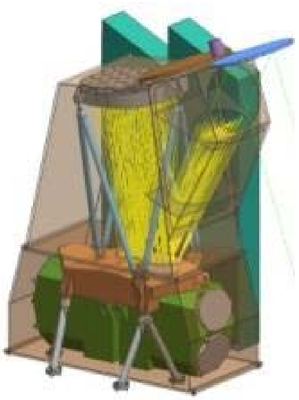

  - Current spacecraft orbit to fulfill coverage specifications
    - Sun Synchronous
    - 626 km LEO
    - 1030 UTCG Descending
    - 98° Inclination

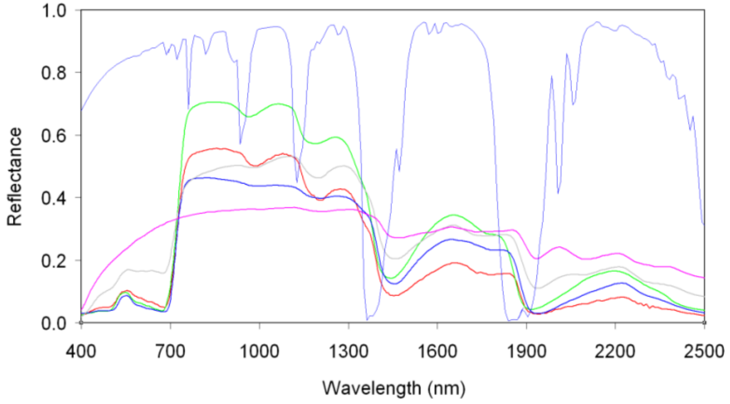

Objectives

- Data Sampling Requirements from the Whitepaper:
  - **Baseline**: <20 day revisit to provide >60% seasonal and >80% annual coverage of the terrestrial and shallow water regions of the Earth.
  - **Minimum**: <20 day revisit to provide >50% seasonal and >70% annual coverage of the terrestrial and shallow water regions of the Earth
- *A probability science retrieval model shall provide a better understanding of the feasibility regarding these requirements.*

Probability Science Collection

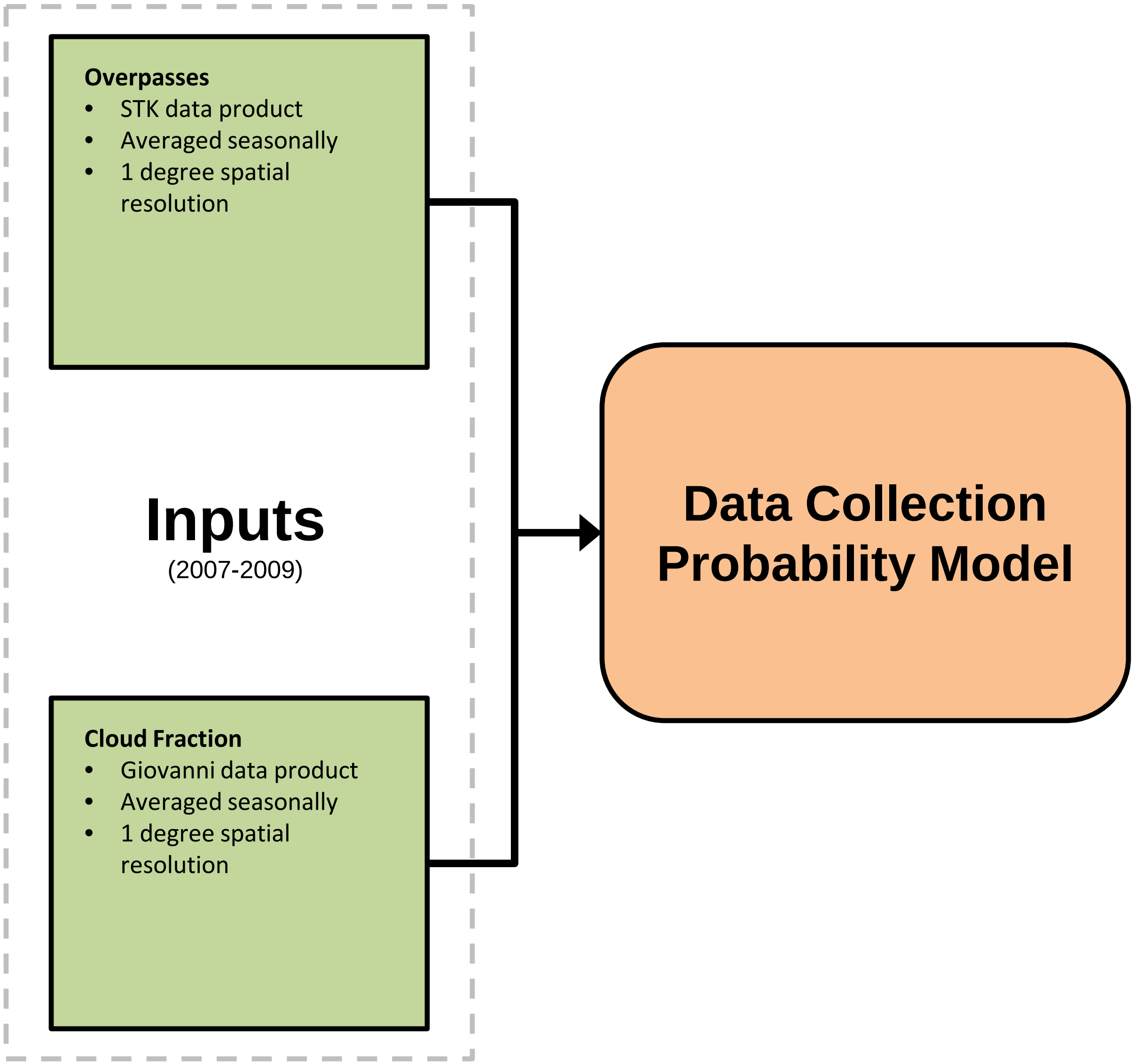

Overpasses

- Defined: The number of times VSWIR's swath comes in contact with the centroid of a 1x1 degree cell.
- Bounded -50m elevation map derived from NOAA ETOPO5 data

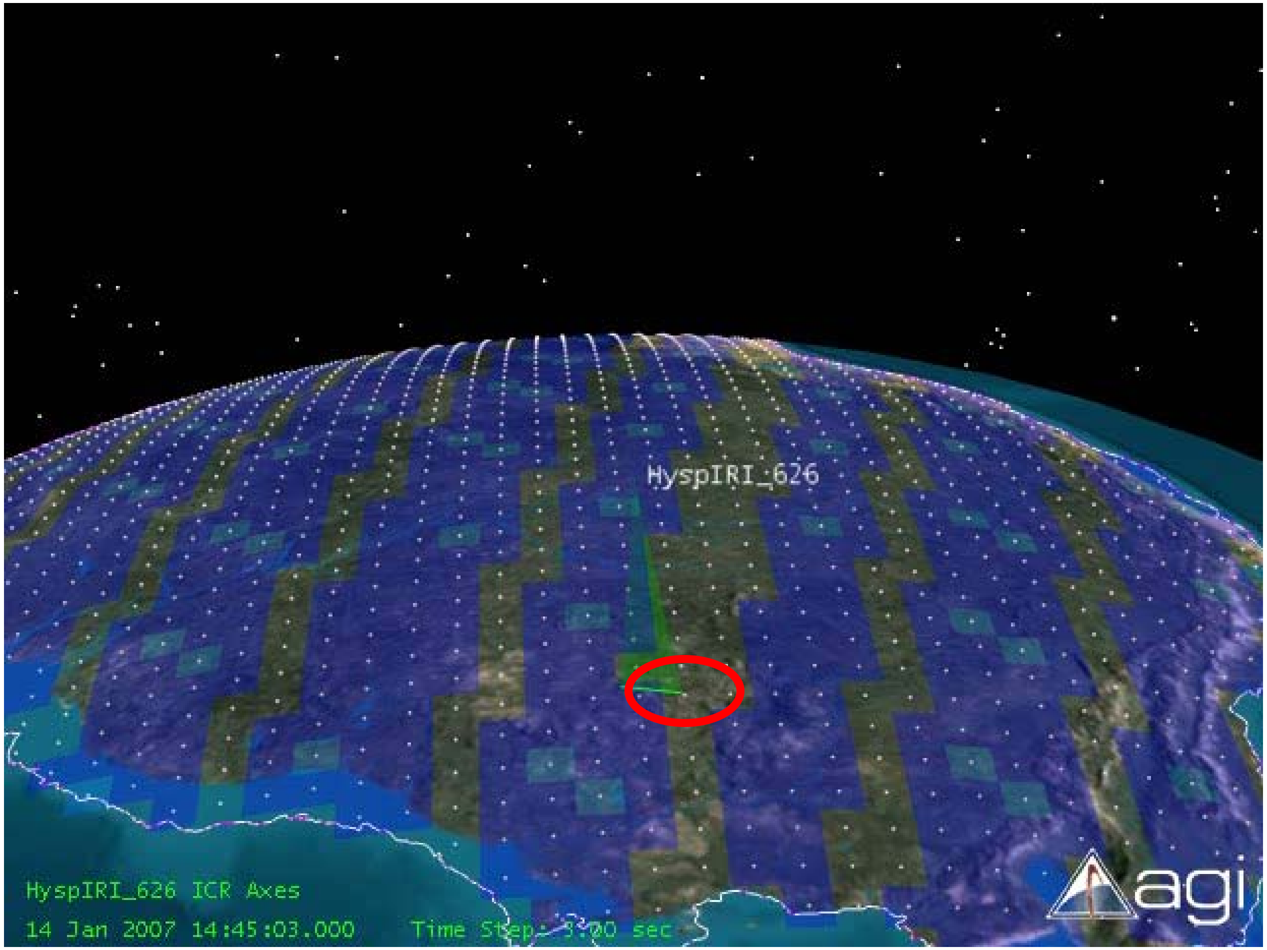

Example

- Uncolored: No overpasses
- **Blue: 1 overpass**
- **Aqua: 2 overpasses**

Limitations

- Partial swath-to-cell contacts not counted
- Produces artifacting in results.
- Remedied by increasing grid resolution at the cost of processing time.

Overpasses (2007)

Jan-Mar

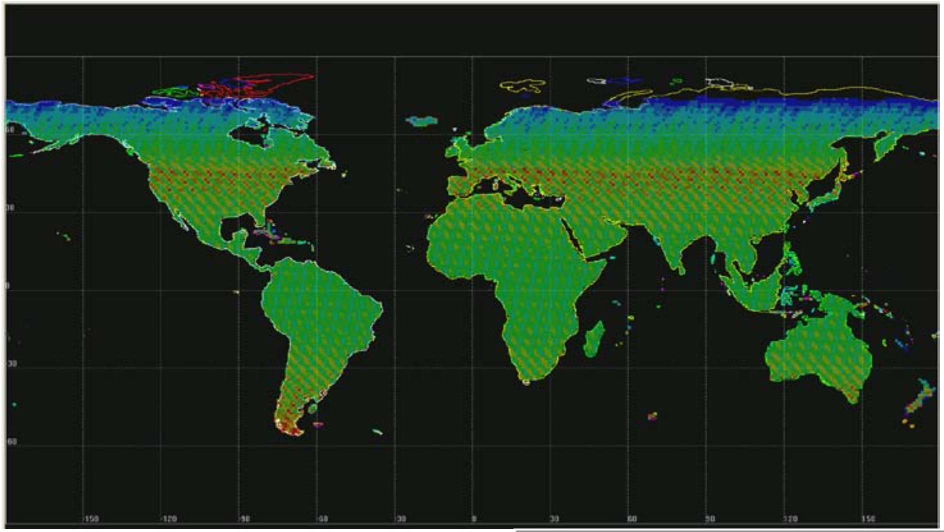

Apr-Jun

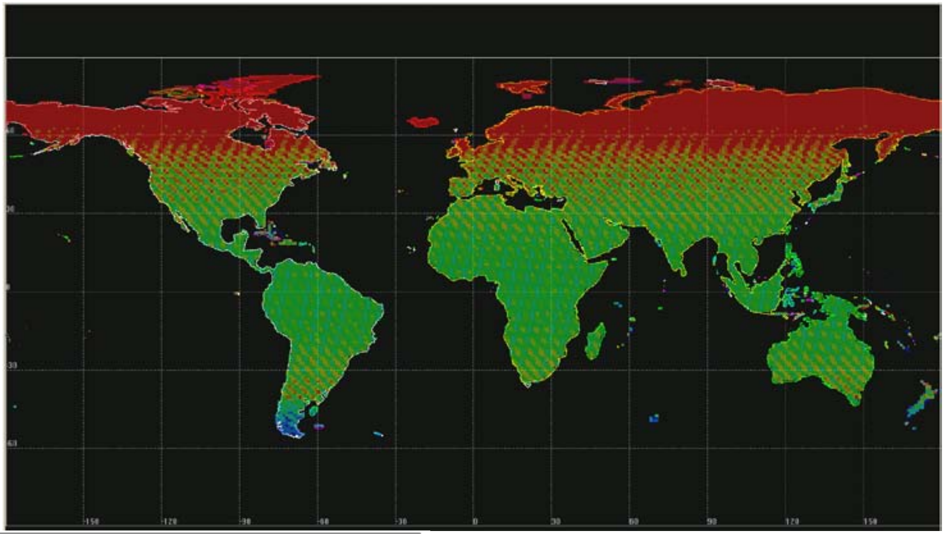

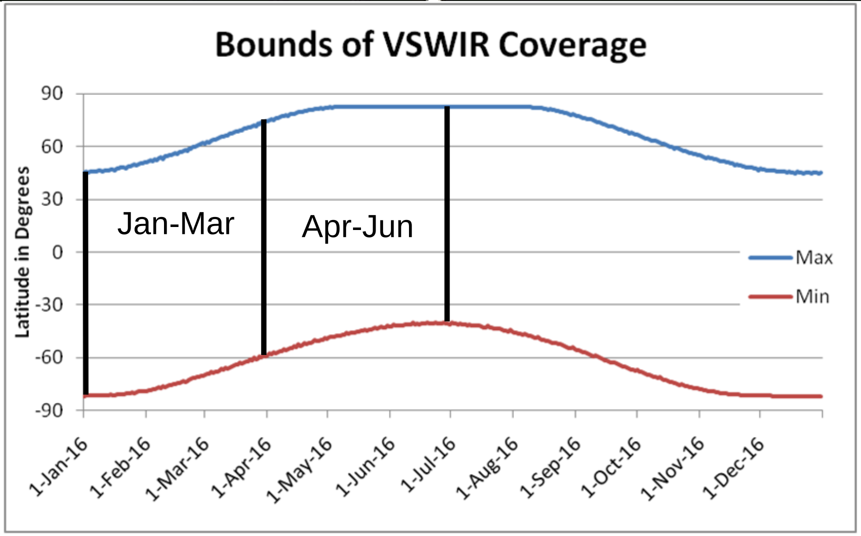

Plot Credit: Michael Mercury

Overpasses (2007)

Jul-Sep

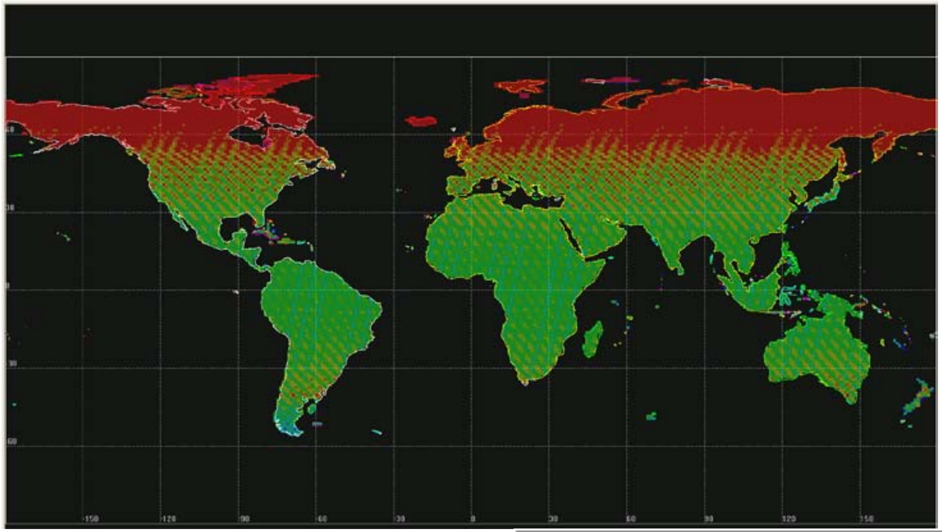

Oct-Dec

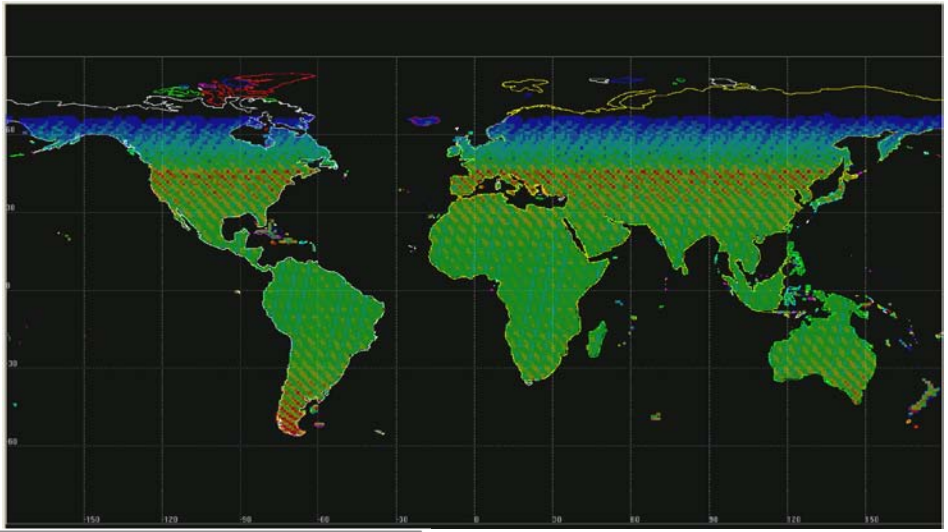

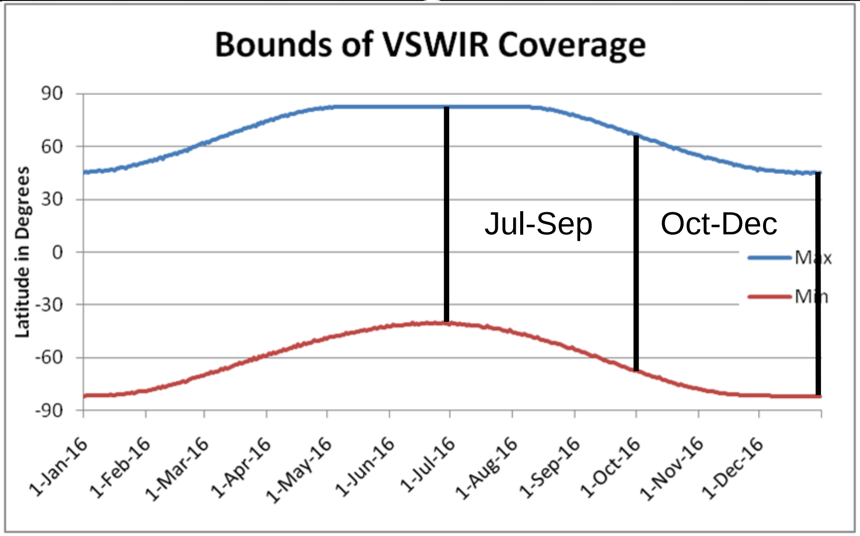

Plot Credit: Michael Mercury

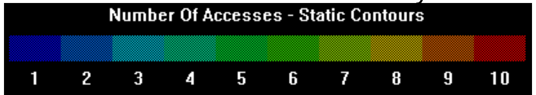

Cloud Fraction

- Defined:
  - Count of cloudy and probably cloudy pixels divided by the total number of pixels.
- Compiled using Giovanni
  - Web-based application developed by Goddard
    - http://disc.sci.gsfc.nasa.gov/giovanni
  - Uses MODIS-Terra monthly (L3 data product MOD_M3)
  - 1x1 degree pixels
  - Day pixels only, averaged seasonally

Cloud Fraction

(Blue denotes high cloud fraction)

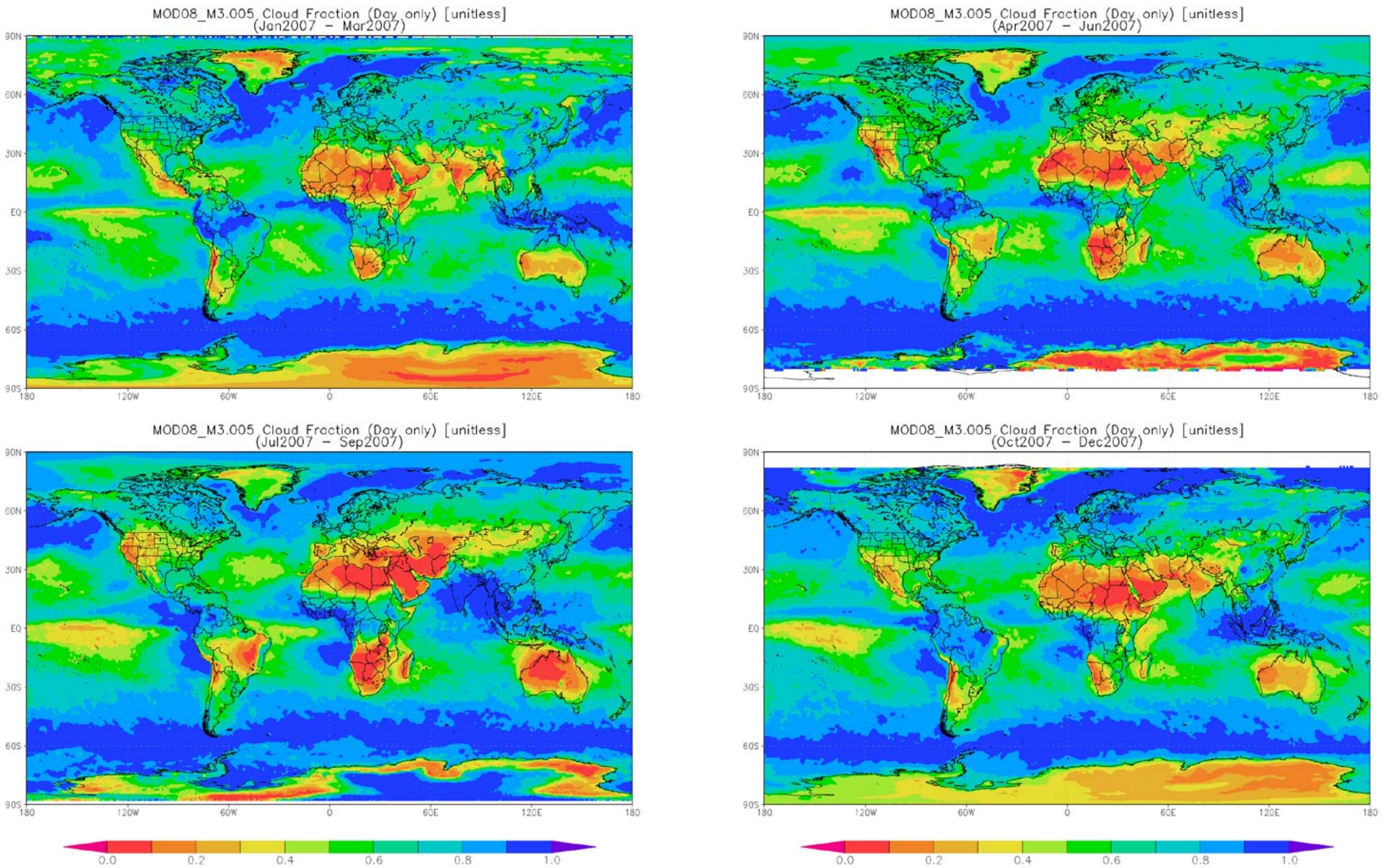

Probability Science Collection

Inputs

MATLAB Scripts
- Probability
  - Probability Calculations
  - Global Probability Map Creation
- Coverage
  - Surface Coverage Calculations
  - Distribution Plot Creation

Data Collection Probability Model

Outputs

Probability Maps
- Seasonal
- Averaged across 3 years

Coverage Plots
- Seasonal
- Averaged across 3 years

Probability Calculations

- Probability of Science Retrieval: P(s)
  - $P(s) = 1 - C^n$
    - C = Cloud Fraction (Giovanni Output)
    - n = Number of VSWIR overpasses (STK Output)
    - Example Calculation
      - 25% cloud fraction, 4 overpasses
      - 0.25*0.25*0.25*0.25 = 0.0039
      - P(s) = 1 – 0.0039 = 99.6%
- P(s) is calculated for each 1x1 degree cell
- Any missing "C" values from the MOD_08 dataset are ignored.

Probability Maps (2007-2009)

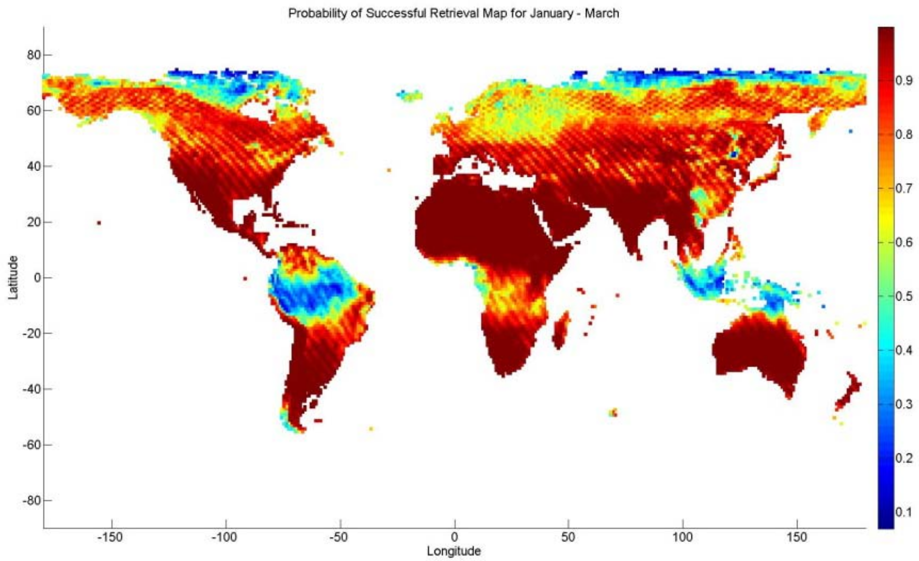

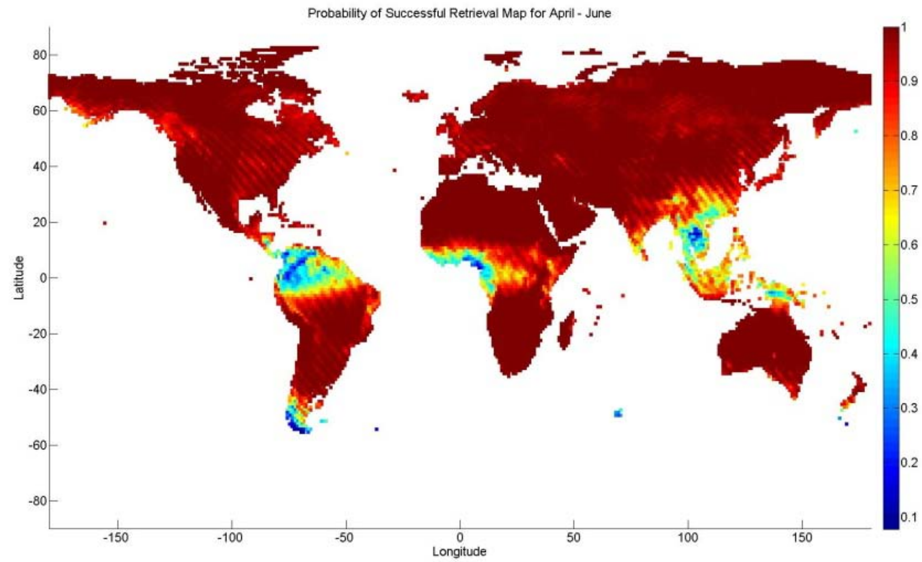

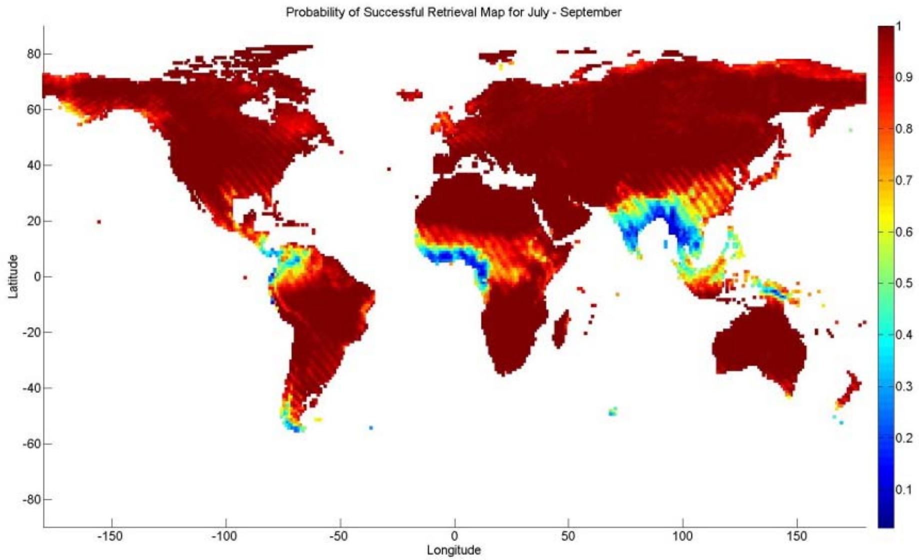

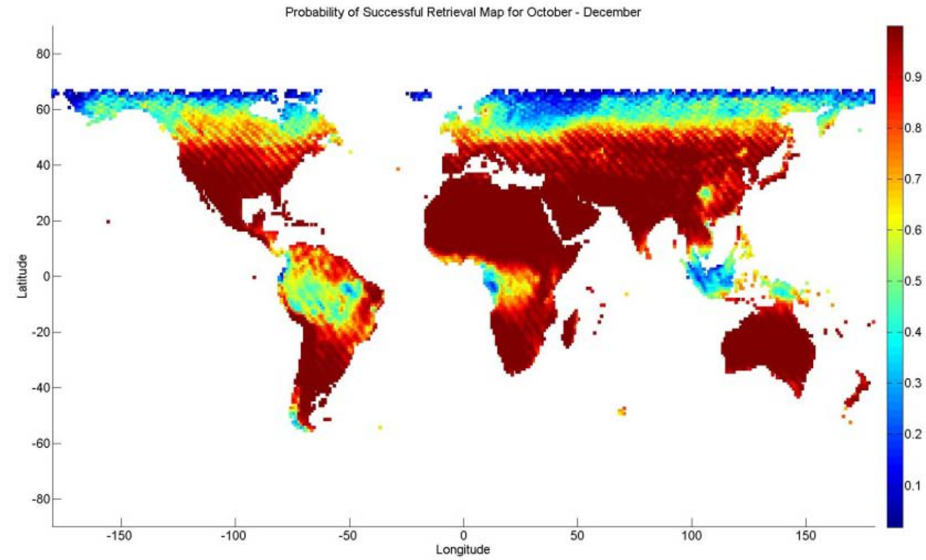

Surface Coverage Calculations

- Fraction of the terrestrial surface viewed by VSWIR: F(s)
  - Random number generator with a threshold based on P(s) to determine if a point is cloudy or not
  - Weighted each grid point by the associated block area
  - Divided the clear area by the total area
- Simulated the entire grid 5000 times to create the probability mass function of F(s)

Coverage Plots (2007-2009)

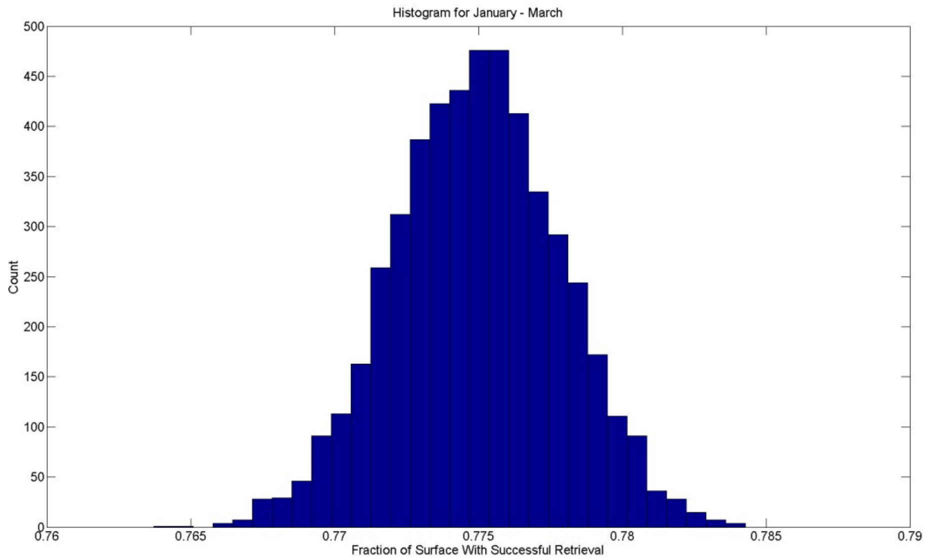

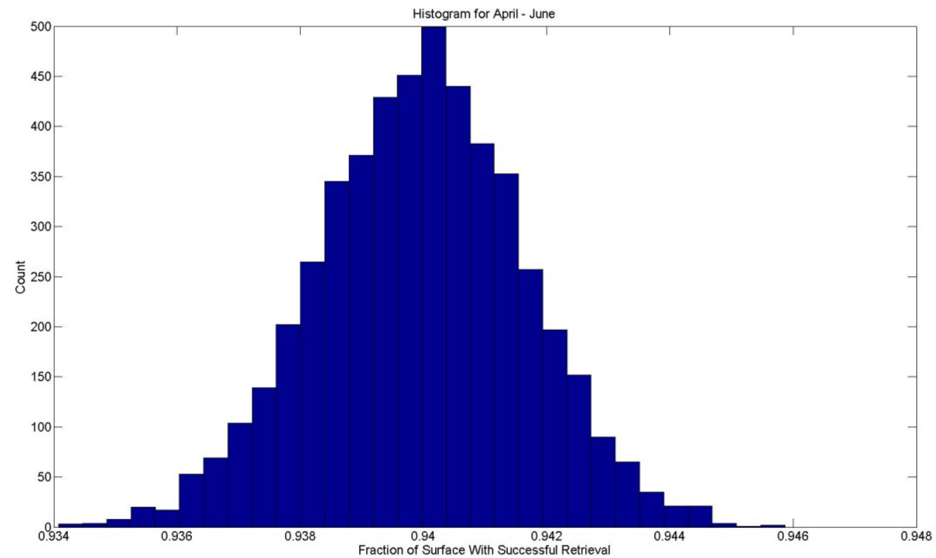

Seasonal coverage never drops below 60%

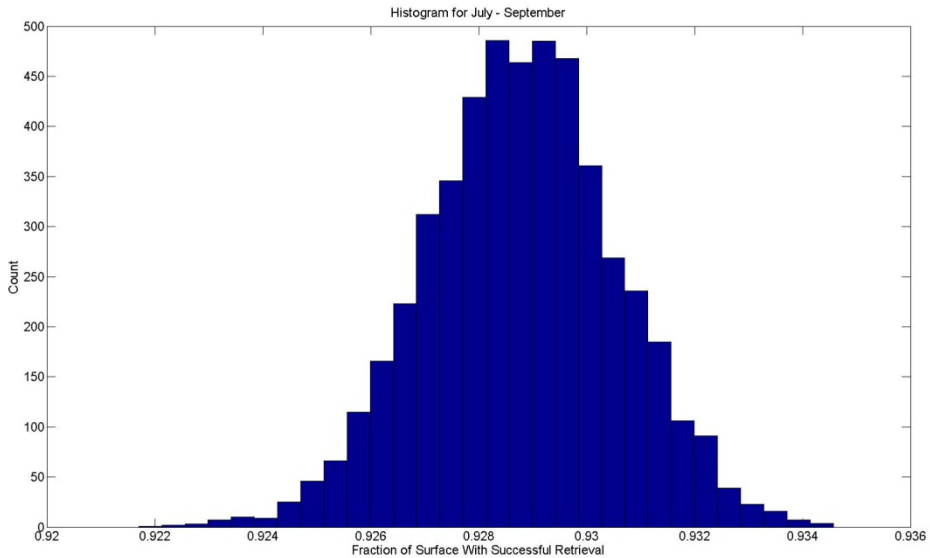

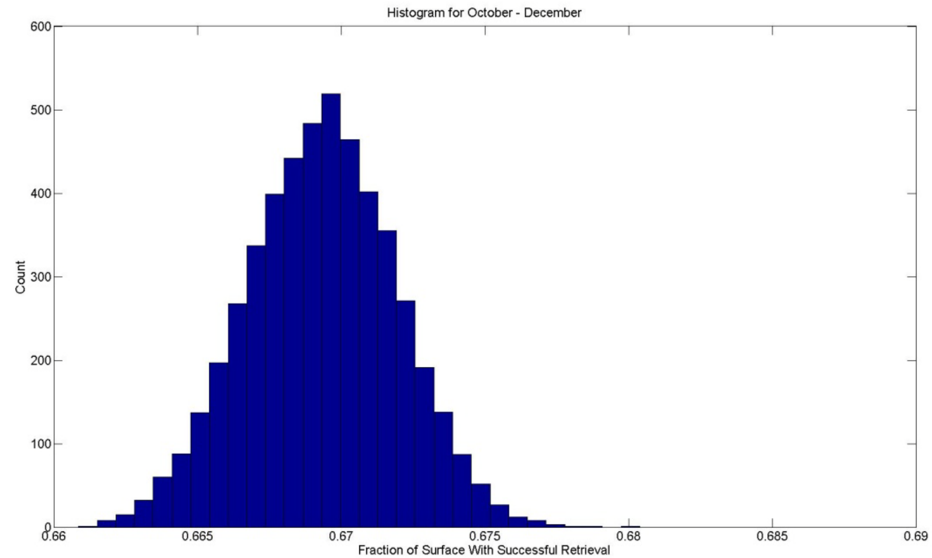

Brazilian Amazon

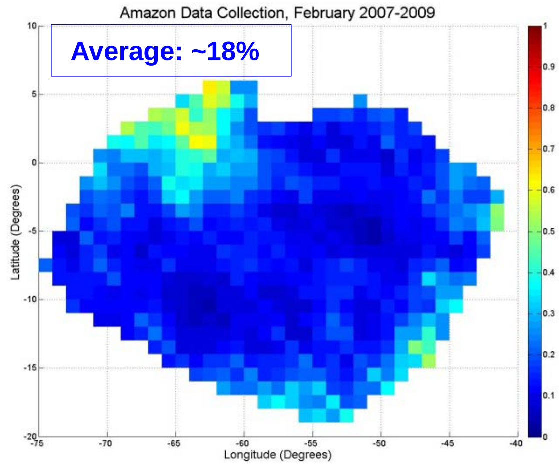

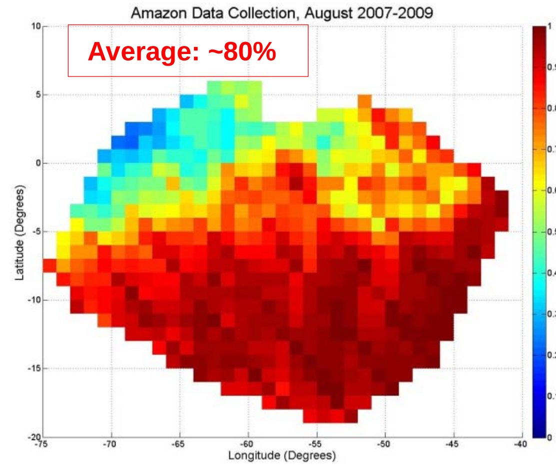

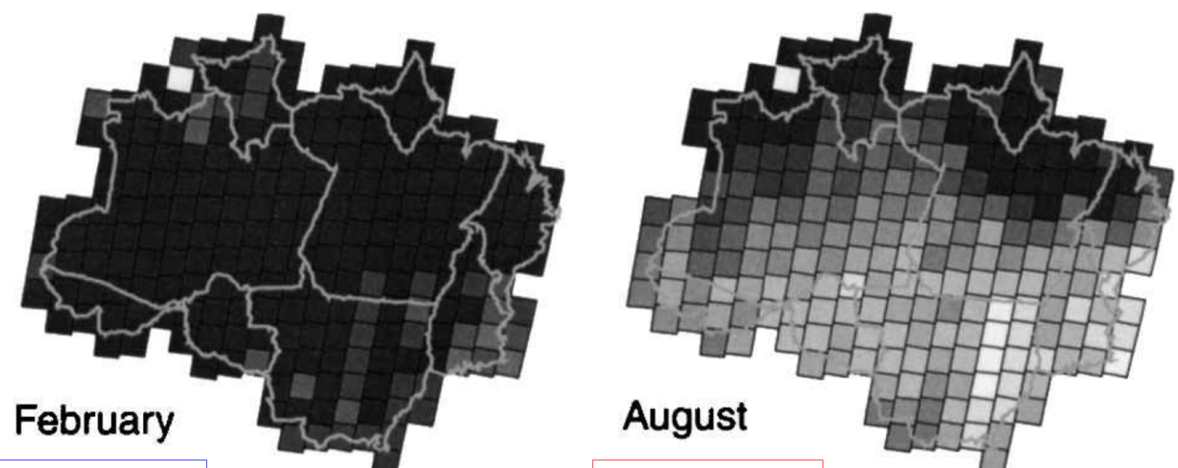

Average: ~10%

Average: ~65%

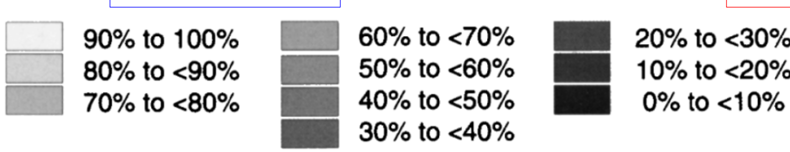

Asner, G. P.(2001) 'Cloud cover in Landsat observations of the Brazilian Amazon', International Journal of Remote Sensing, 22: 18, 3855 — 3862

Brazilian Amazon

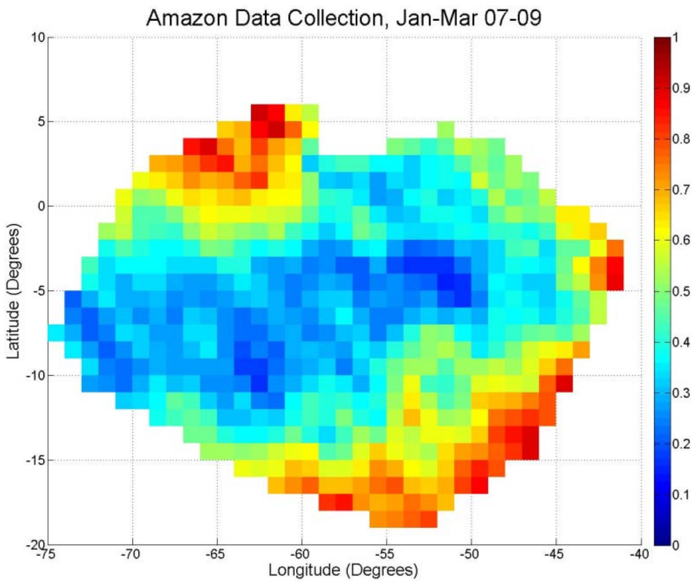

Brazilian Amazon

Seasonal View

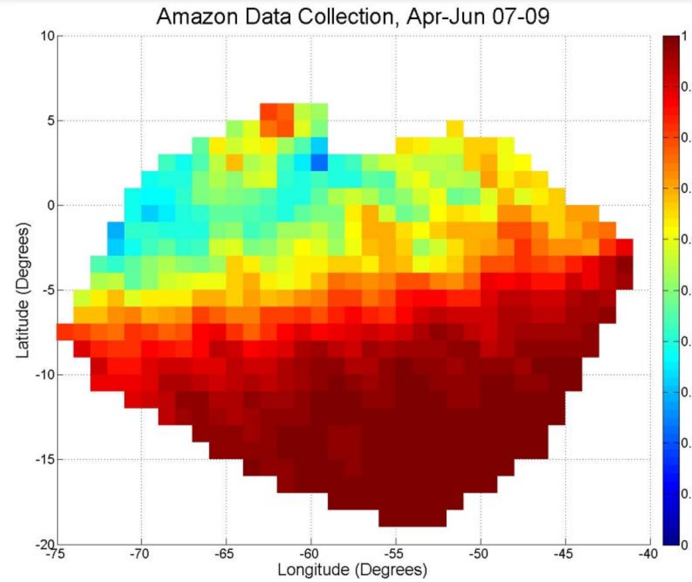

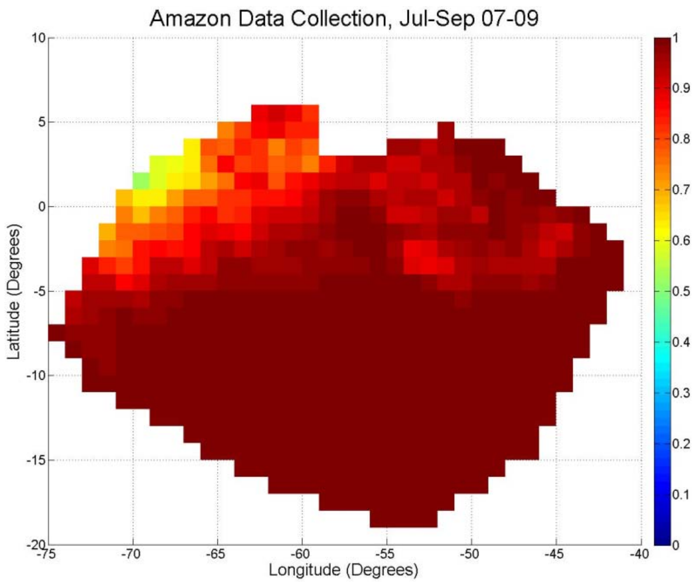

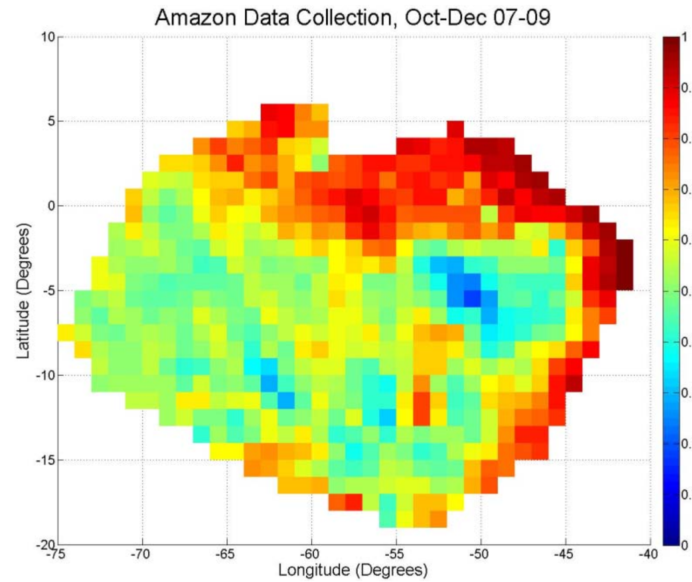

Conclusions

- Based on initial results VSWIR meets the current baseline requirements of >60% seasonal and >80% annual coverage of the terrestrial and shallow water regions of the Earth.
- Future Work
  - Similar analysis completed for TIR
  - Model with higher than one-degree resolution MODIS-Terra data.
  - Increase the resolution of the STK grid.

Acknowledgements

National Space Grant Consortium

JPL Education Office

Linda Rodgers
Robert Greene
Carl Bruce
Hannah Goldberg
Michael Mercury

Bogdan Oaida
Sarah Lundeen
Diane Evans
Danielle Nuding

The data used in this effort were acquired as part of the activities of NASA's Science Mission Directorate, and are archived and distributed by the Goddard Earth Sciences (GES) Data and Information Services Center (DISC).

Questions?

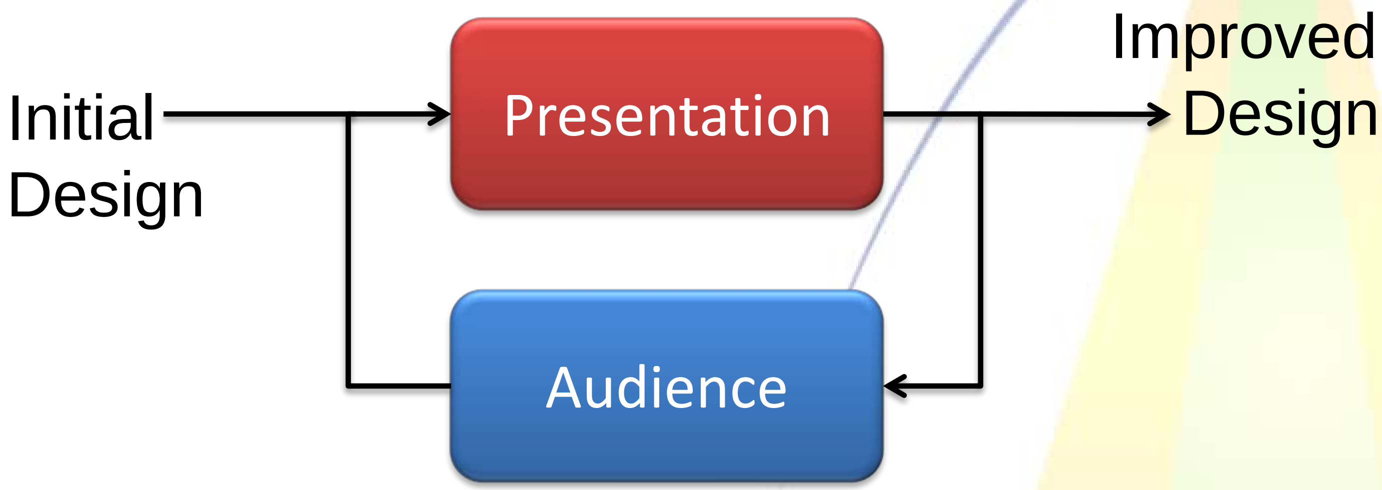

Back-up Slides

Probability.m

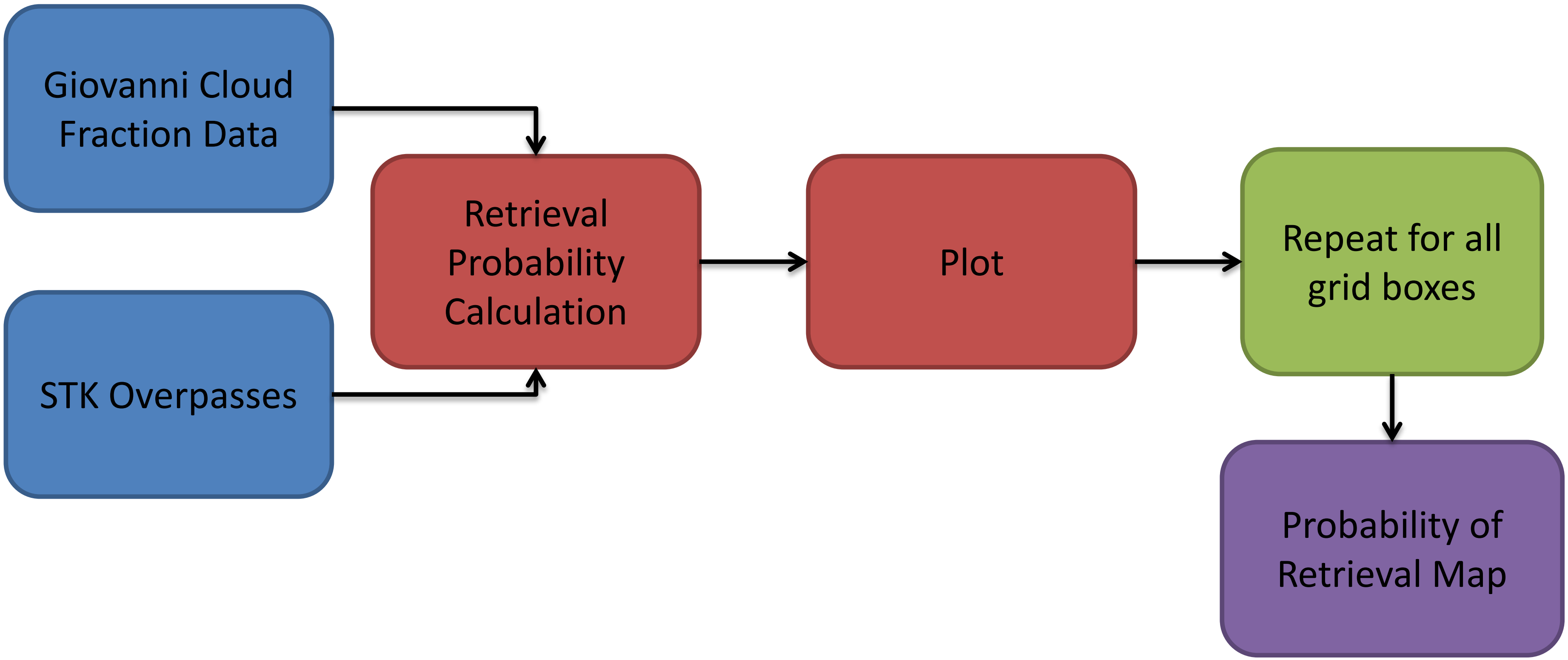

Coverage.m

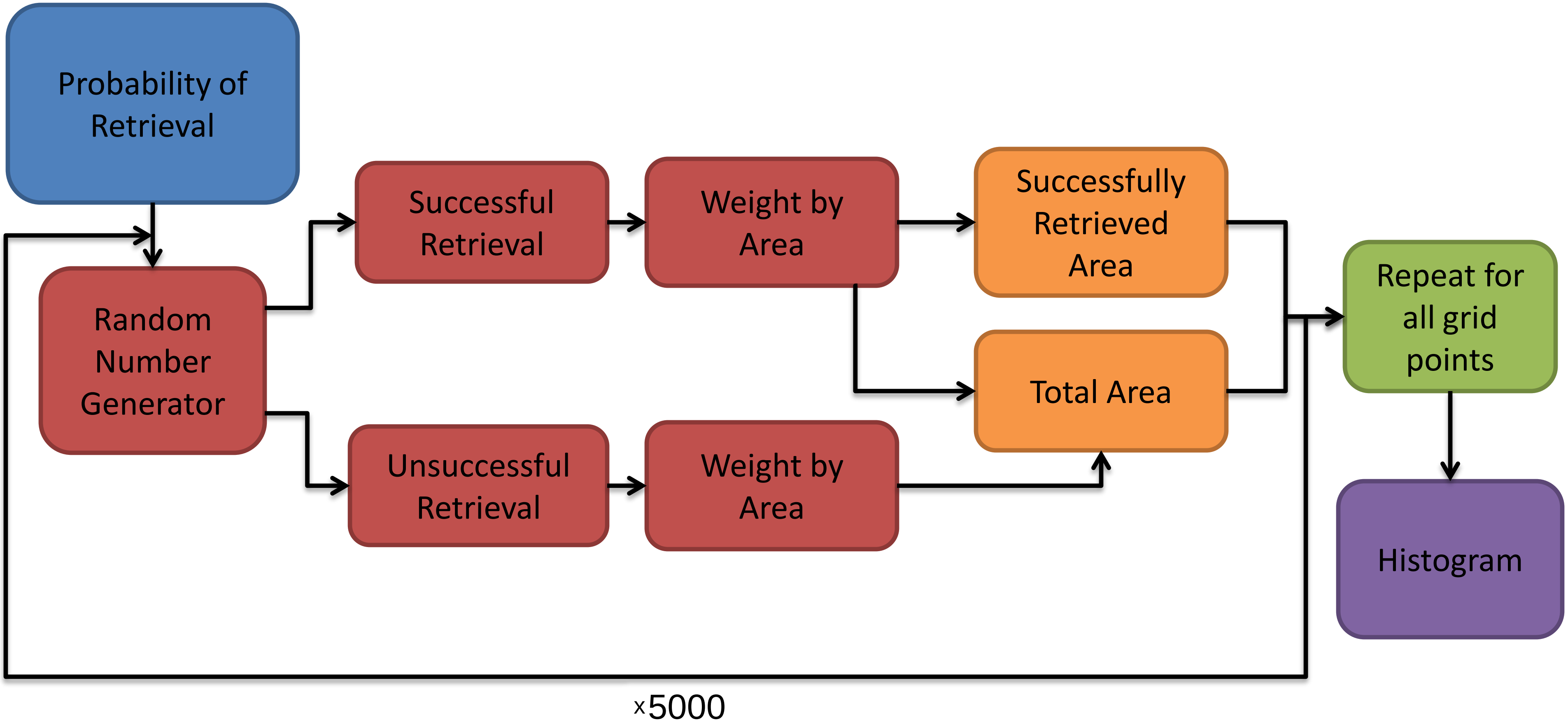

Probability of Retrieval
Random Number Generator
Successful Retrieval
Weight by Area
Unsuccessful Retrieval
Weight by Area
Successfully Retrieved Area
Total Area
Repeat for all grid points
Histogram
x5000

HyspIRI VSWIR Level 2 ATBDs and Sample Science Results from HICO on the International Space Station

Bo-Cai Gao

Remote Sensing Division,
Naval Research Laboratory, Washington, DC USA

OUTLINE

- VSWIR Level 2 ATBD for Land Surface Reflectance Retrievals
- VSWIR Level 2 ATBD for Water Leaving Reflectance Retrievals
- Preliminary Science Results from HICO on the International Space Station
- Summary

Atmospheric Correction Over Land

An AVIRIS Spectrum

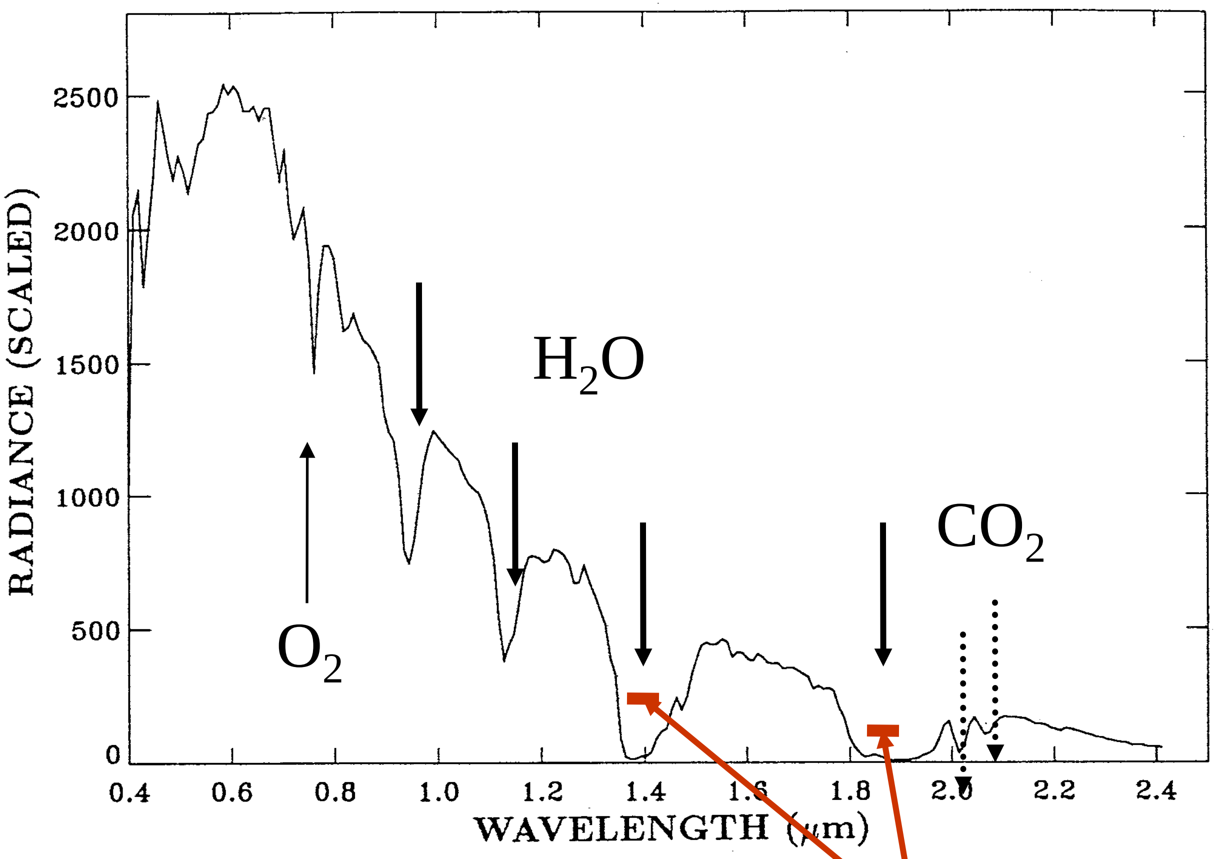

The AVIRIS spectrum is affected by atmospheric absorption and scattering effects. In order to obtain the surface reflectance spectrum, the atmospheric effects need to be removed.

Strong water vapor bands are located near 1.38 and 1.88 micron. No signals are detected under clear sky conditions.

Equations For Atmospheric Correction Over Land

The measured radiance at the satellite level can be expressed as:

$L_{obs} = L_a + L_{sun}\, t\, \rho$ (1)

L_a: path radiance;
ρ : surface reflectance;
L_{sun}: solar radiance above the atmosphere;
t: *2-way transmittance for the Sun-surface-sensor path*

Define the satellite apparent reflectance as

$\rho^*_{obs} = \pi\, L_{obs} / (\mu_0\, E_0)$ (2)

$\rho^*_{obs} = T_g\, [\, \rho_a + t\, \rho / (1 - \rho\, s)\,]$ (3)

By inverting Eq. (3) for ρ, we get:

$\rho = (\rho^*_{obs}/T_g - \rho^*_a) / [t + s\, (\rho^*_{obs}/T_g - \rho^*_a)\,]$ (4)

Gao, B.-C., K. H. Heidebrecht, and A. F. H. Goetz, Derivation of scaled surface reflectances from AVIRIS data, *Remote Sens. Env., 44*, 165-178, 1993.

SAMPLE REFLECTANCE RETRIEVALS WITH ATREM

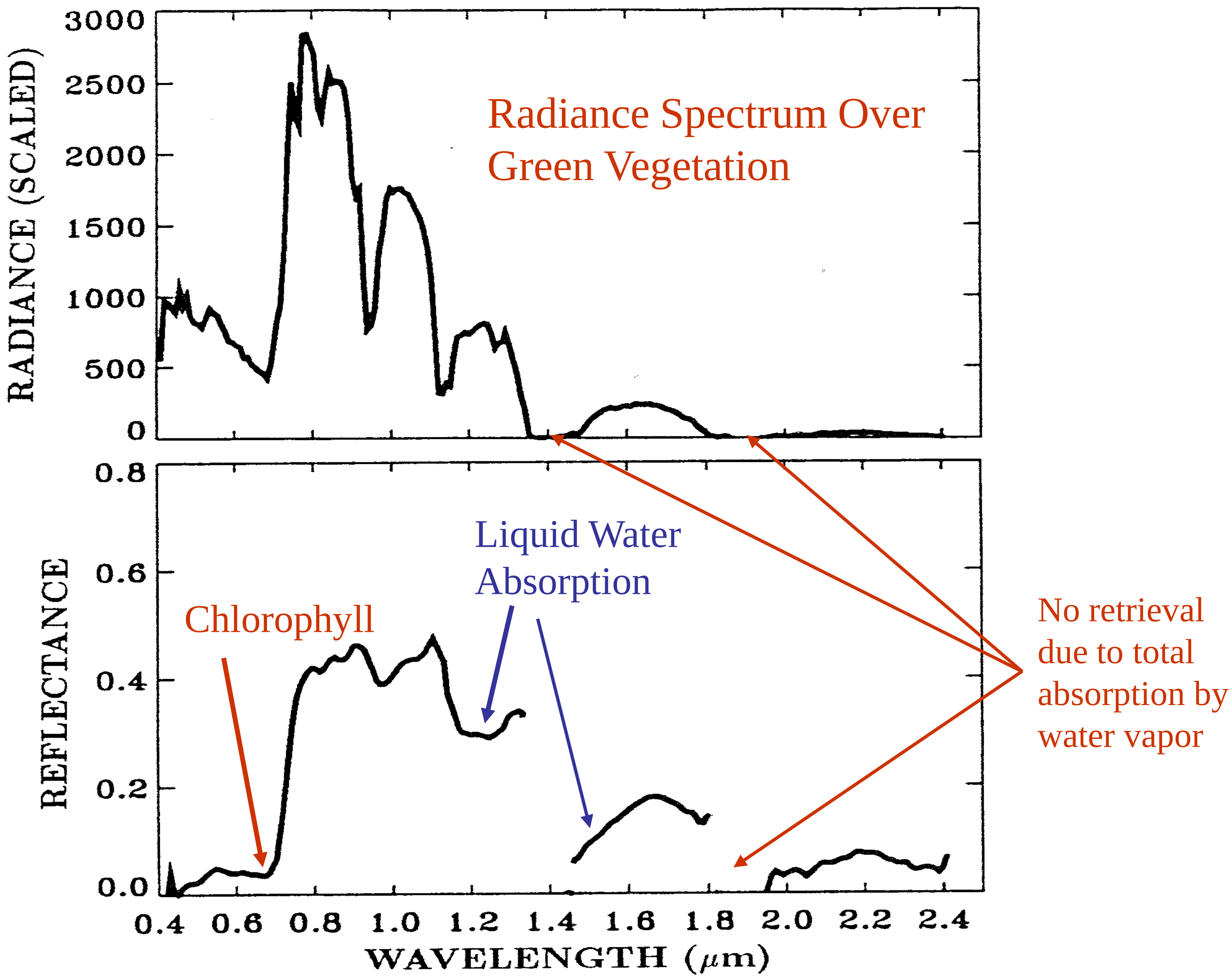

MINERAL MAPPING USING ATREM OUTPUT
by Scientists at USGS in Denver, Colorado

RGB Image (Cuprite, NV)

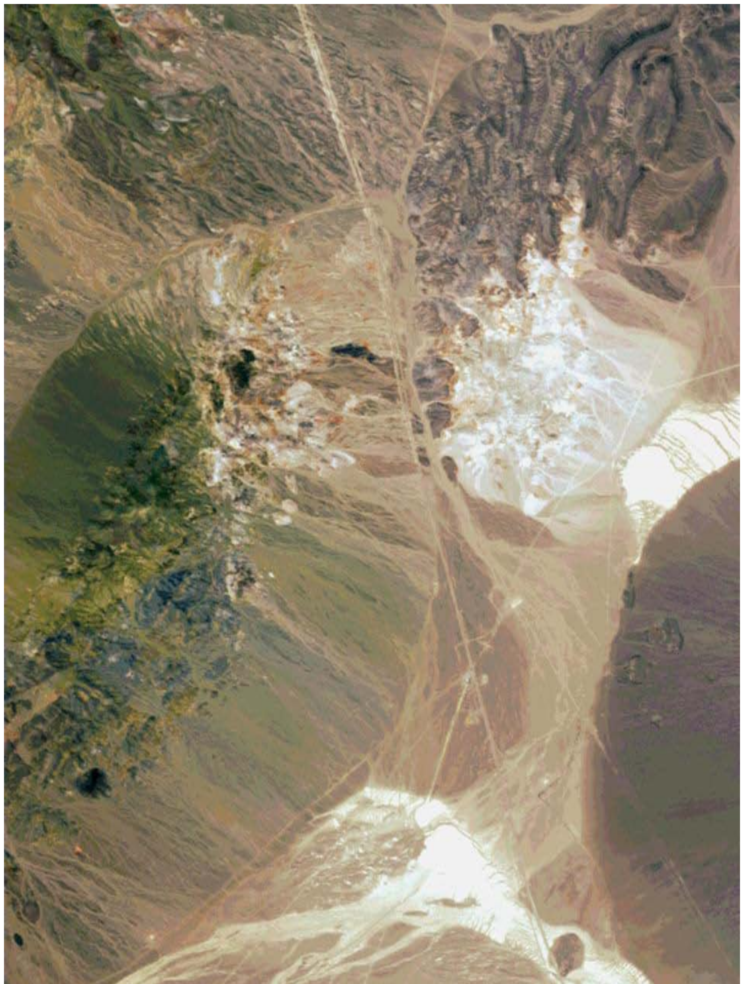

USGS Mineral Map, ~11x18 km

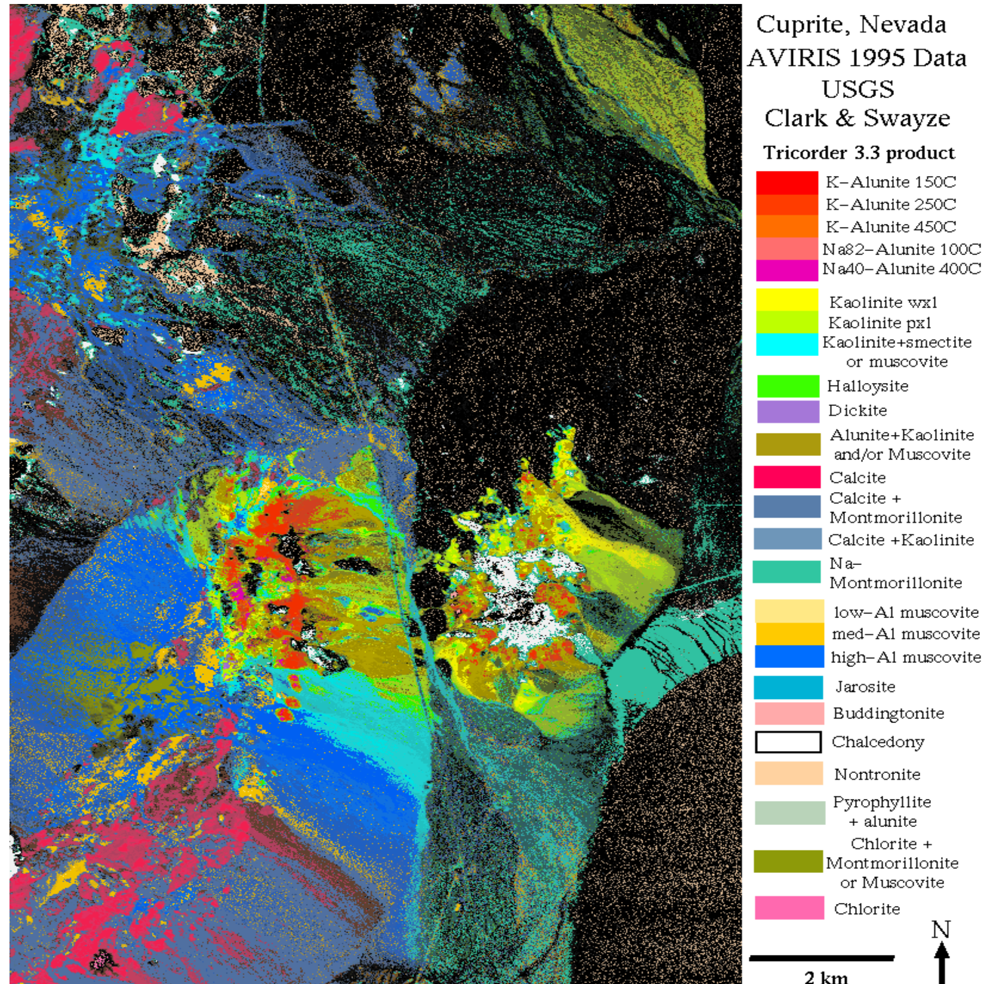

Atmospheric Correction Over Water

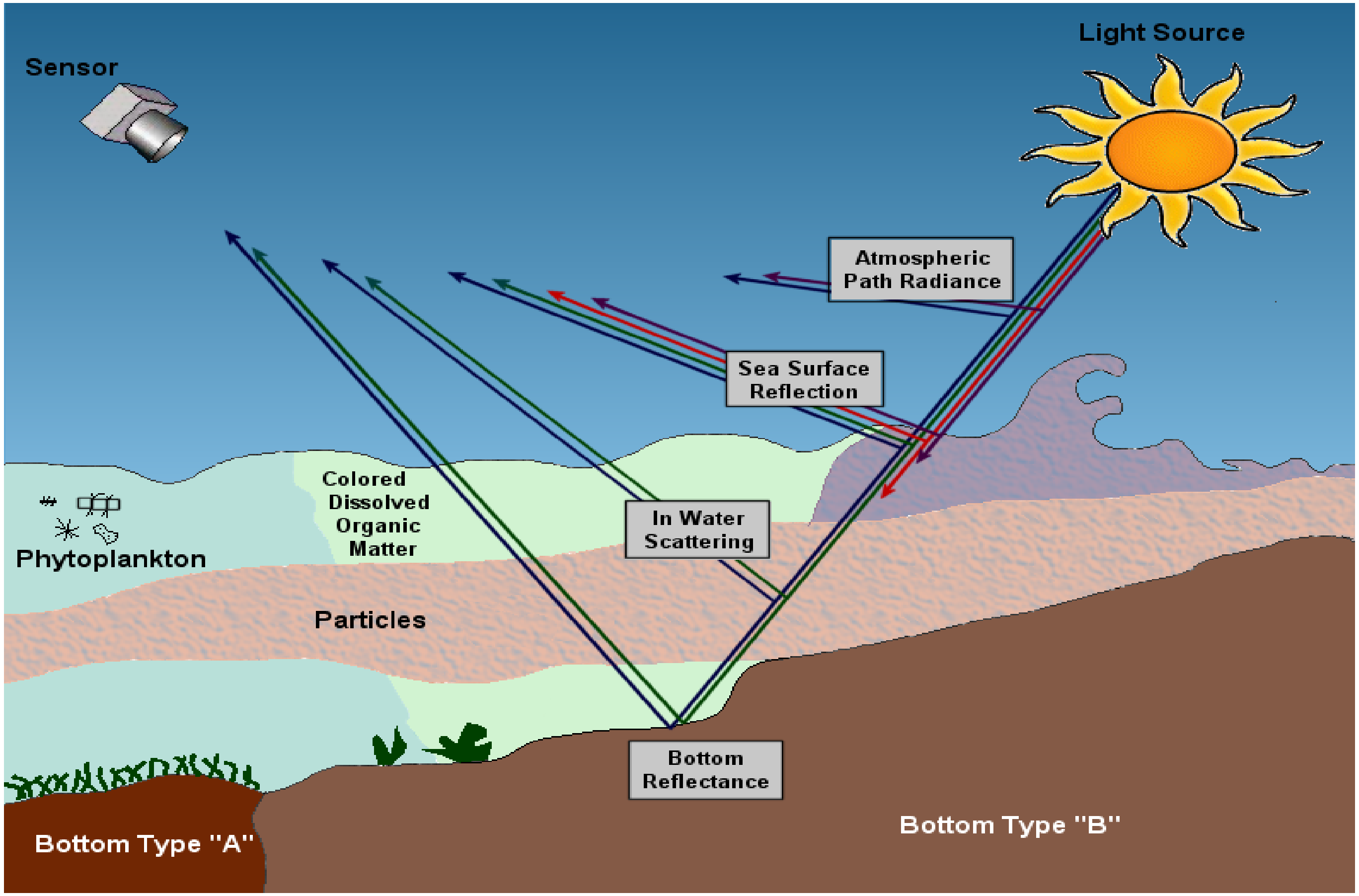

Over the dark water surfaces, ~90% of satellite radiances come from the atmosphere, and ~10% come from water. Very accurate atmospheric corrections are required in order to derive the useful water leaving reflectances. The specular reflection at the air/water interface introduces additional complications for modeling.

An AVIRIS Spectrum Over A Water Pixel

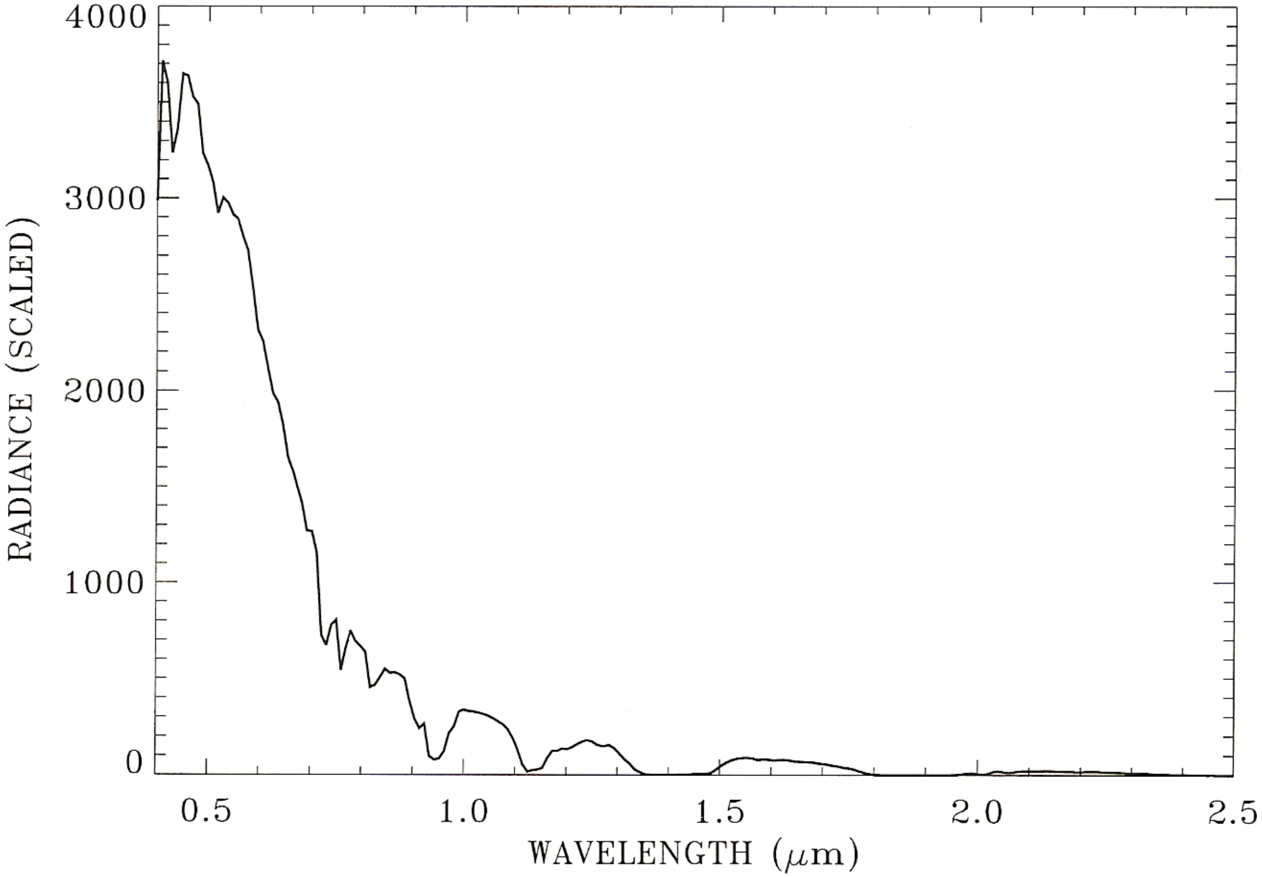

The radiances above one micron are very small.

Relevant Equations and Definitions

In the absence of gas absorption, the radiance at the satellite level is:

$L_{obs} = L_0 + L_{sfc}\, t'_u + L_w\, t_u,$ (1)

L_0: path radiance; L_w: water leaving radiance;

L_{sfc}: radiance reflected at water surface; t_u: *upward transmittance*

Define $L_{atm+sfc} = L_0 + L_{sfc}\, t'_u$ (2)

Eq. (1) becomes: $L_{obs} = L_{atm+sfc} + L_w\, t_u$ (3)

Multiply Eq. (3) by π and divide by ($\mu_0\, E_0$), Eq. (3) becomes:

$$\pi L_{obs} / (\mu_0\, E_0) = \pi L_{atm+sfc} / (\mu_0\, E_0) + \pi L_w\, t_d\, t_u / (\mu_0\, E_0\, t_d) \quad (4)$$

Several reflectances are defined as:

Satellite apparent reflectance: $\rho^*_{obs} = \pi L_{obs} / (\mu_0\, E_0),$ (5)

$$\rho^*_{atm+sfc} = \pi L_{atm+sfc} / (\mu_0\, E_0), \quad (6)$$

Water leaving reflectance: $\boldsymbol{\rho_w = \pi L_w / (\mu_0\, E_0\, t_d) = \pi L_w / E_d}$ (7)

Remote sensing reflectance: $\mathbf{R_{rs}} \boldsymbol{= \rho_w / \pi = L_w / E_d}$ (7')

Substitute Eqs (5) – (7) into Eq. (4): $\rho^*_{obs} = \rho^*_{atm+sfc} + \rho_w\, t_d\, t_u$ (8)

After consideration of gas absorption and multiple reflection between the atmosphere and surface and with further manipulation, we can get:

$$\rho_w = (\rho^*_{obs}/T_g - \rho^*_{atm+sfc}) / [t_d\, t_u + s\, (\rho^*_{obs}/T_g - \rho^*_{atm+sfc})\,] \quad (11)$$

Gao, B.-C., M. J. Montes, Z. Ahmad, and C. O. Davis, Atmospheric correction algorithm for hyperspectral remote sensing of ocean color from space, Appl. Opt., 39, 887-896, February 2000.

Atmospheric Correction for Water Surfaces

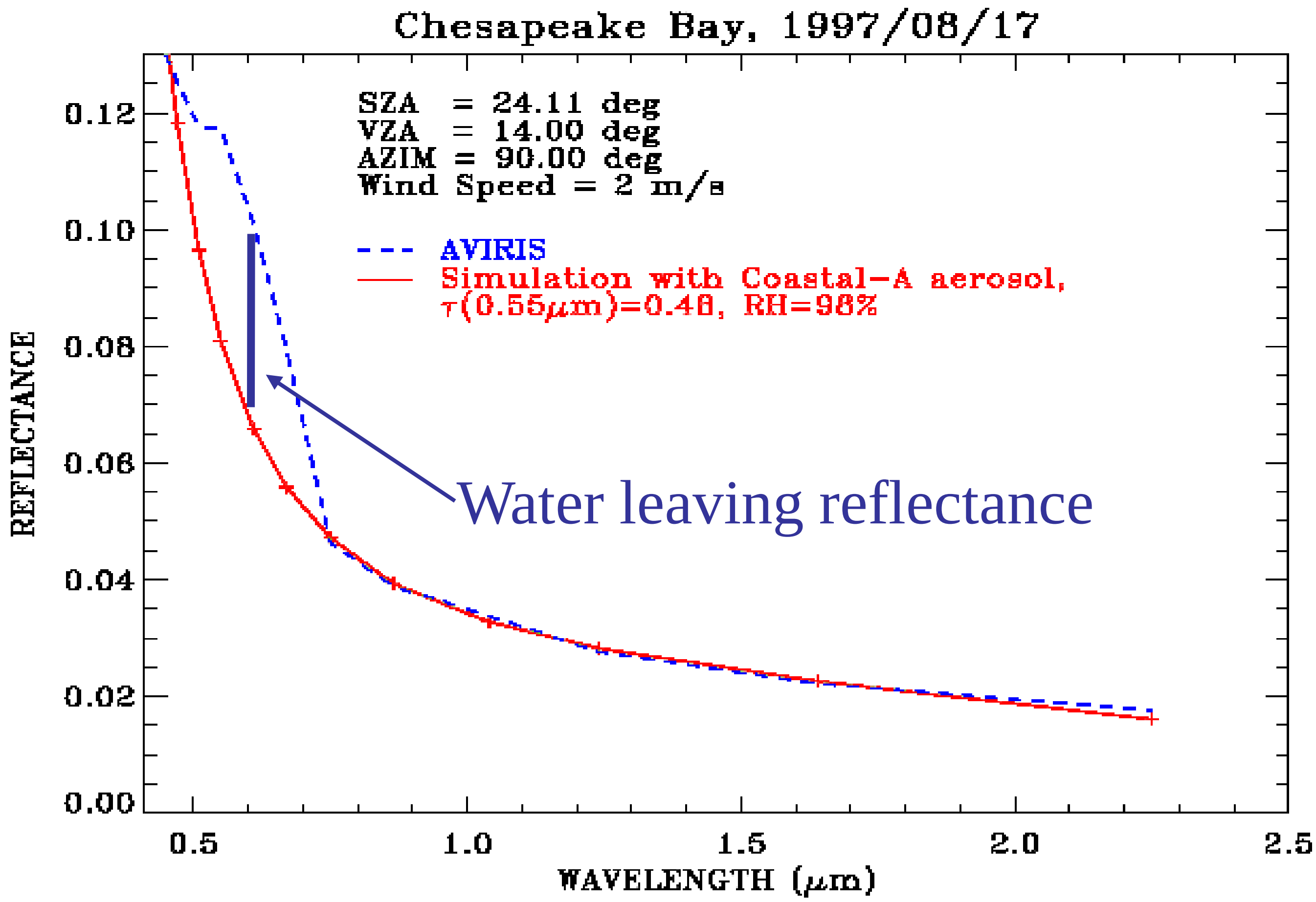

Channels at 0.86 and longer wavelengths are used to estimate atmospheric effects, and then extrapolate to the visible region. The differences between the two curves above are proportional to water leaving reflectances.

Glint Removal Using AVIRIS Data Over Kaneohe Bay, HI

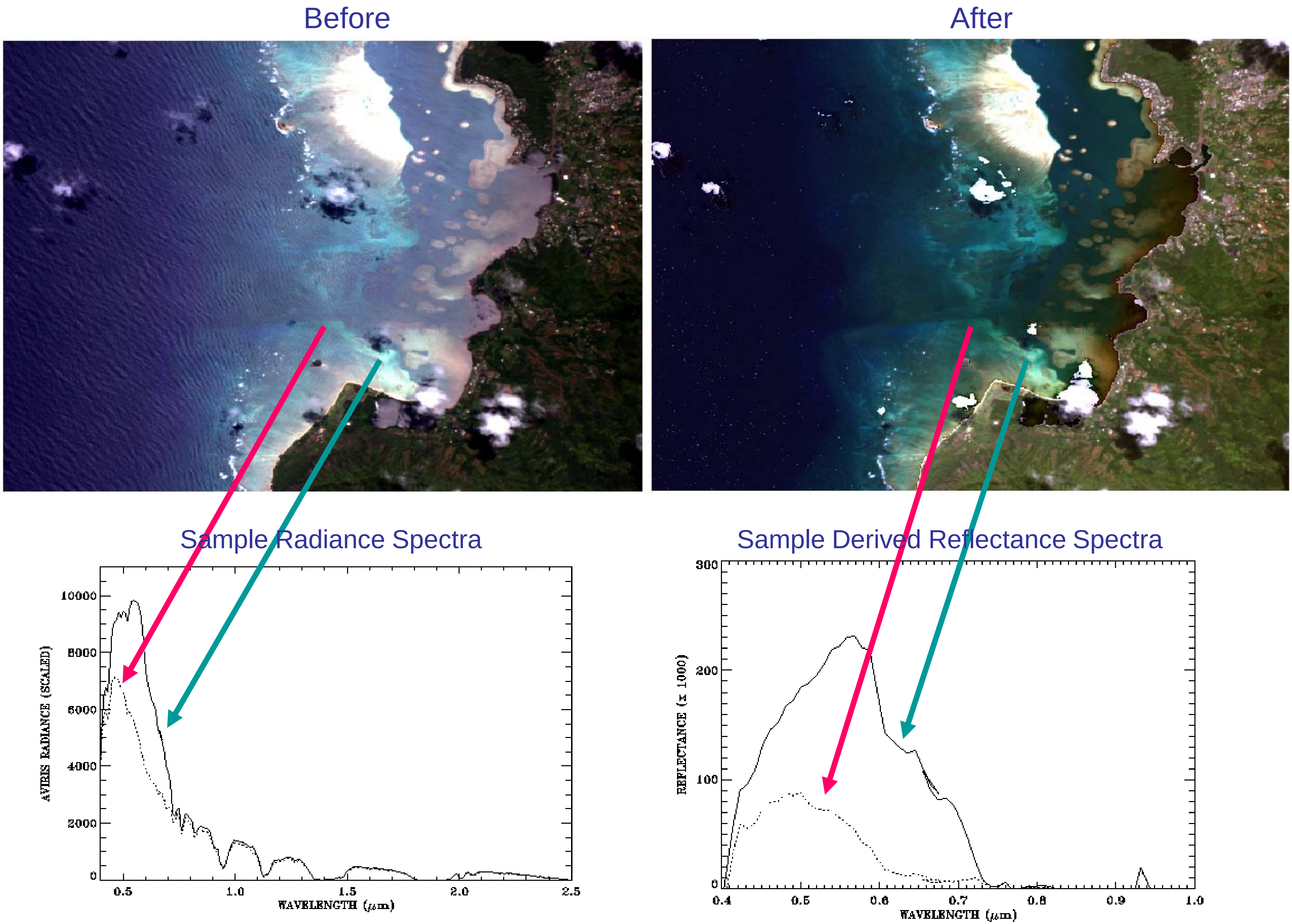

The HICO Instrument on The International Space Station

HICO as delivered

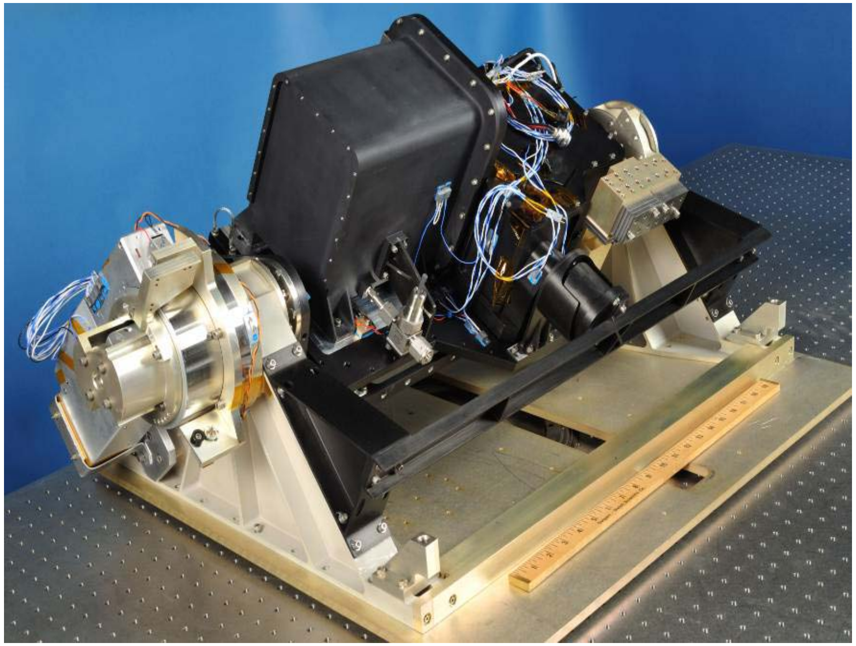

Optical diagram

Earth Surface Images from HICO

Images are about 43 km wide and 190 km long

Orientations are given below

Cape Town, South Africa, Oct. 3, 2009. Orientation is from NW at top to SE at bottom.

Lower Chesapeake Bay, Oct. 7, 2009. Orientation is from NW at top to SE at bottom.

Coast of South China Sea, near Hong Kong, China, Oct. 2, 2009. Orientation is from SW at bottom to NE at top.

Part of the Grand Canyon, Sept. 27, 2009. The center of the image is at 35° 50' N, 111° 23' W and the orientation is from SW at bottom to NE at top.

Florida Keys, over Key Largo, Sept. 27, 2009. Orientation is from SW at bottom to NE at top.

Sahara Desert over Egypt, Sept. 27, 2009. Orientation is from SW at bottom to NE at top.

Taken over the Bahamas, Oct. 2, 2009. Orientation is from NW at top to SE at bottom.

Gem of the Pacific. Midway Island, Sept. 27, 2009. Orientation is from NW at top to SE at bottom.

Spectral and Radiometrical Calibrations (Smear + 2nd Order Light Correction) Have Been Conducted to the HICO Data

Here, we illustrate the results of an empirical technique for correction of 2nd order light effect using shallow underwater features

HICO Images Over the Midway Island in the Pacific Ocean

RGB image

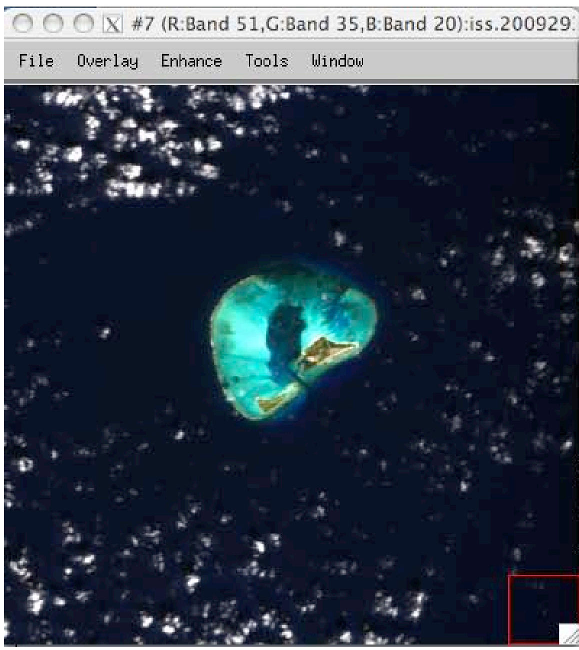

Before 2nd order correction (Band 105, 0.95 µm)

After 2nd order correction (Band 105, 0.95 µm)

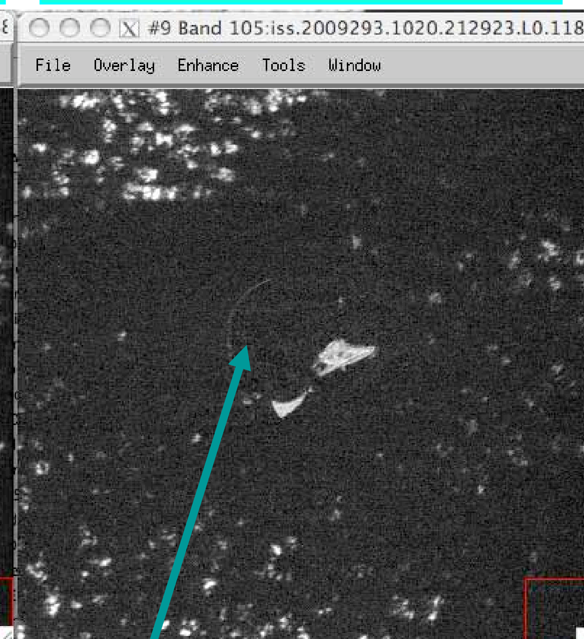

The bright features result from the 2nd order light of a visible channel

The bright features are removed

- Co-located HICO and MODIS Data Acquired Over Desert Areas Were Used to Adjust the HICO Gain Changes (from pre-launch lab-calibrations).
- After such adjustments, the radiances of HICO and MODIS data acquired over other surfaces, such as waters, agreed quite well.

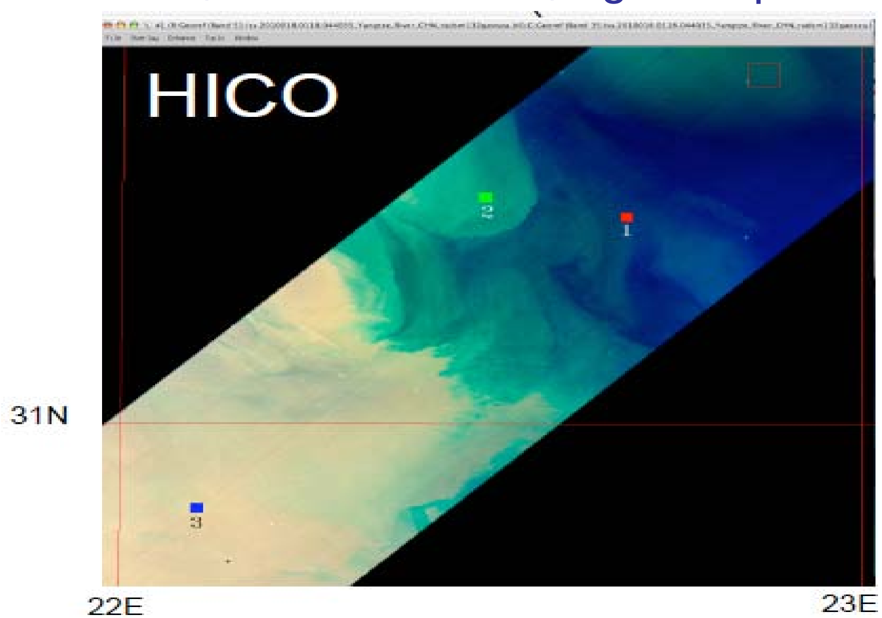

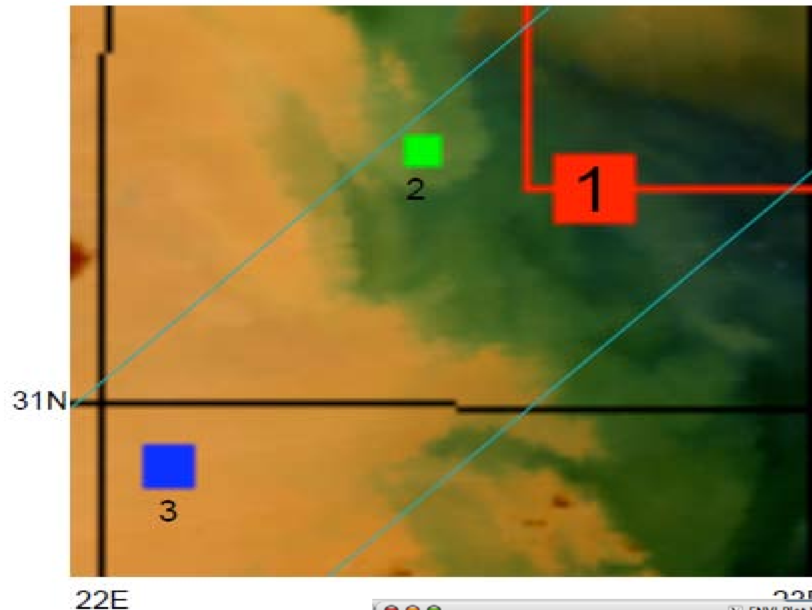

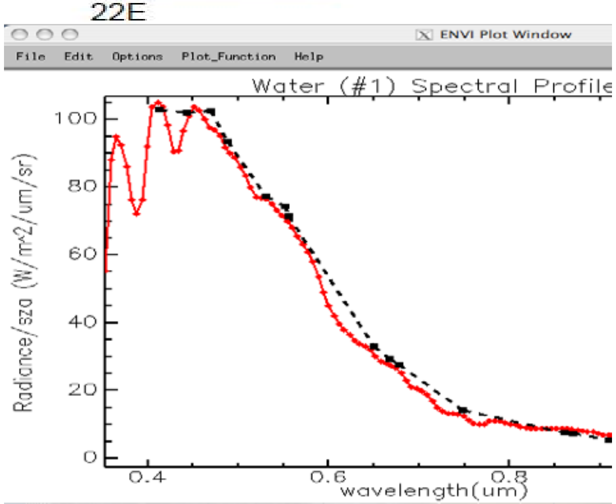

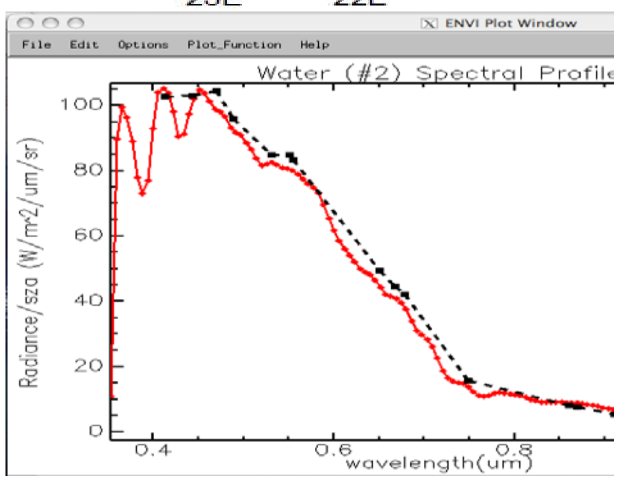

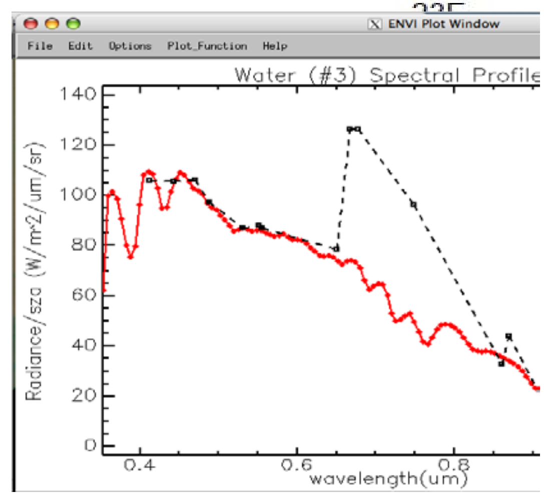

HICO Image Over The Gulf of Mexico (Oil Spill, 5/12/2010)

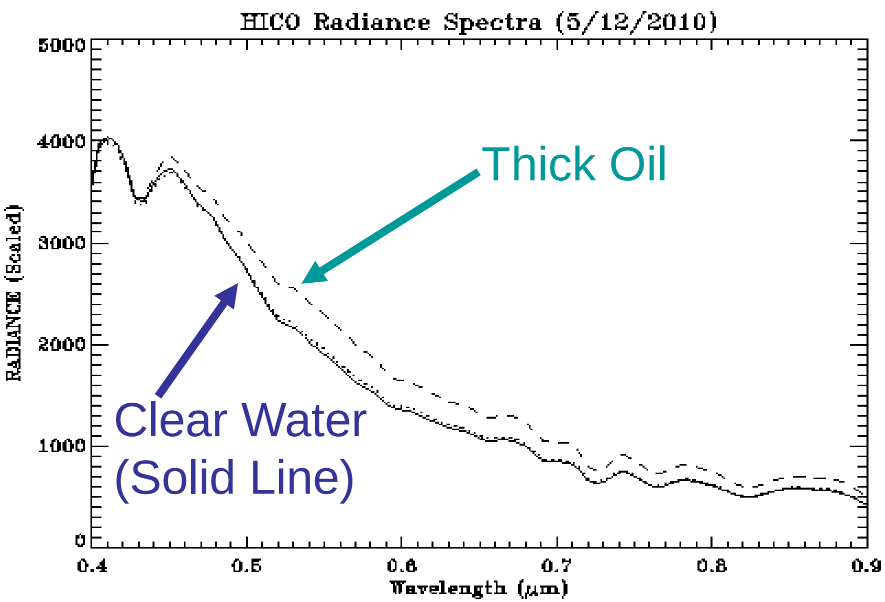

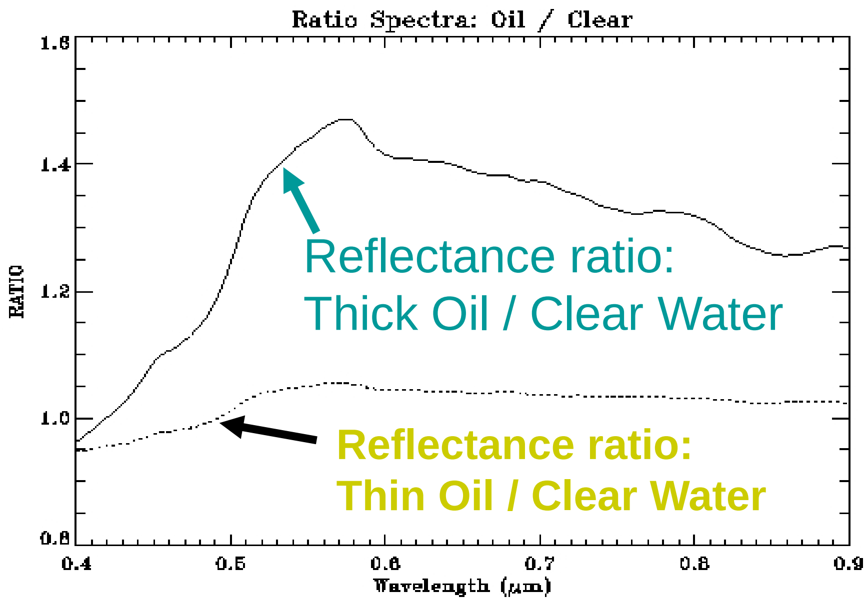

HICO RGB Image Over Gulf of Mexico, Chlorophyll & Kd_490 Images
(5/24/2010)

RGB

Chl (mg/m³)

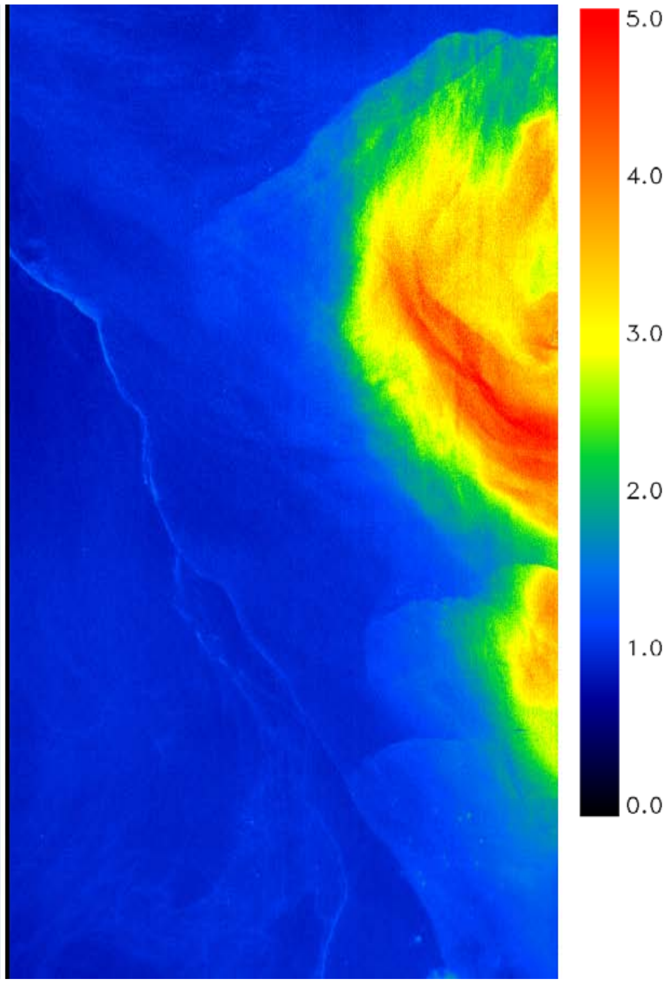

Kd_490 (m^{-1})

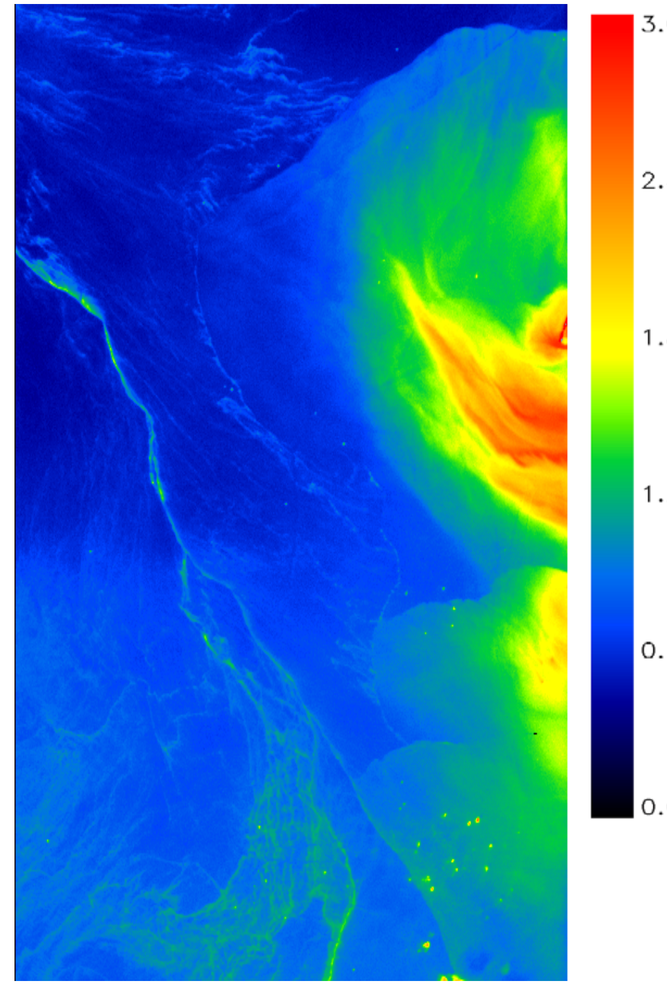

HICO RGB Image Over Gulf of California, Chlorophyll & Kd_490 Images

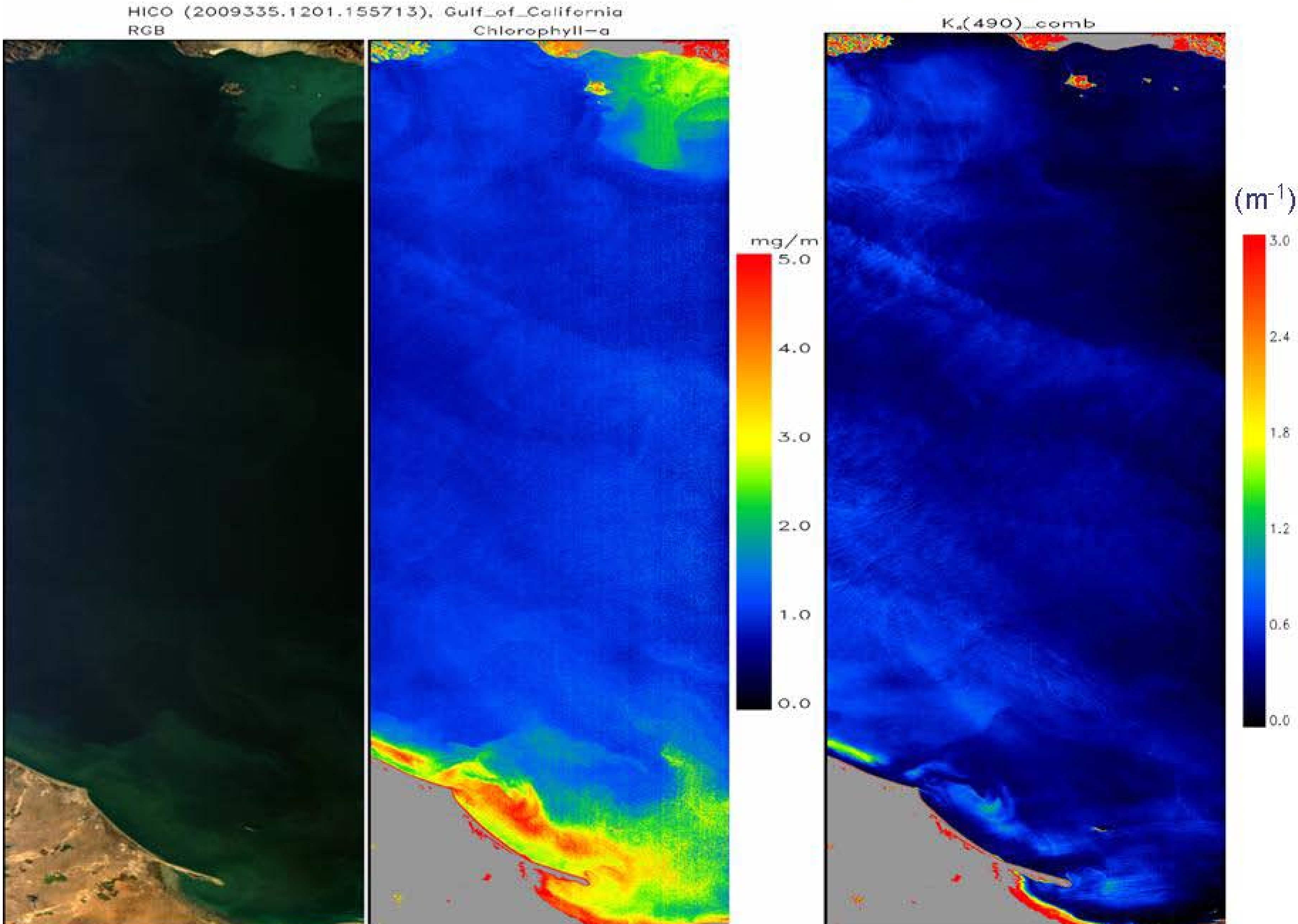

HICO RGB Image Over Tampa Bay, Chlorophyll & Kd_490 Images

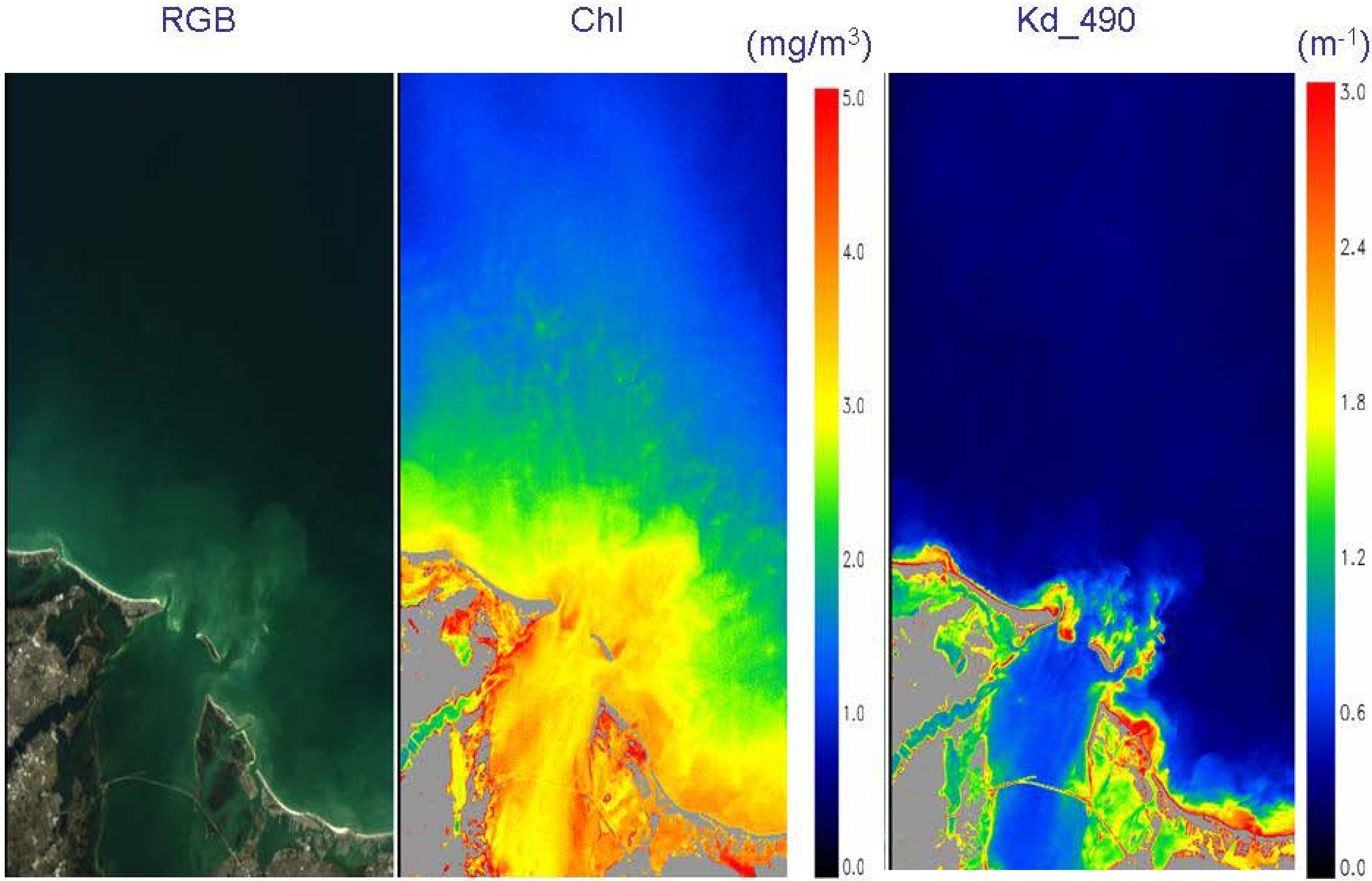

HICO RGB Image Over Chesapeake Bay, Chlorophyll & Kd_490 Images

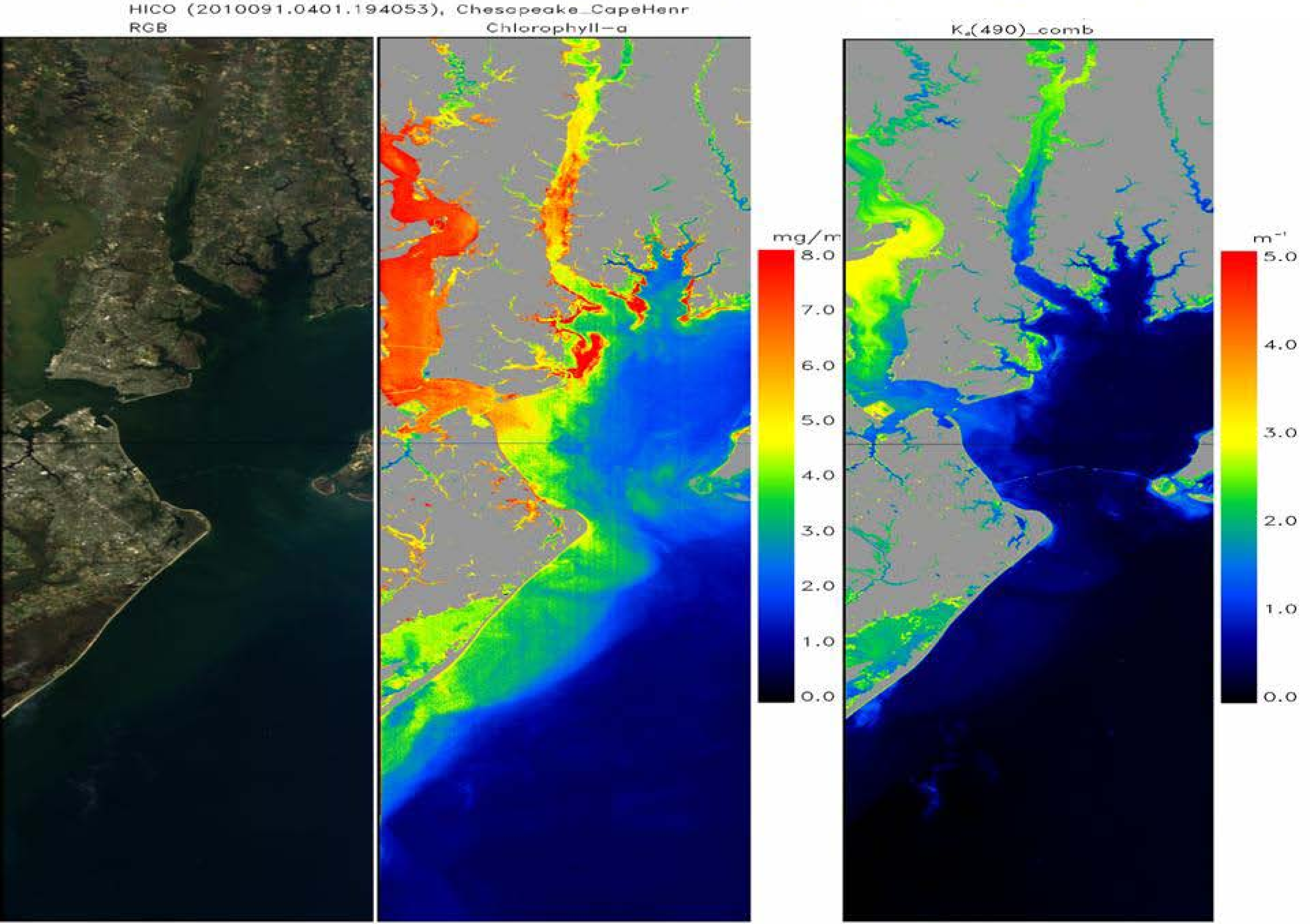

HICO RGB Image Over Persian Gulf, Chlorophyll & Kd_490 Images

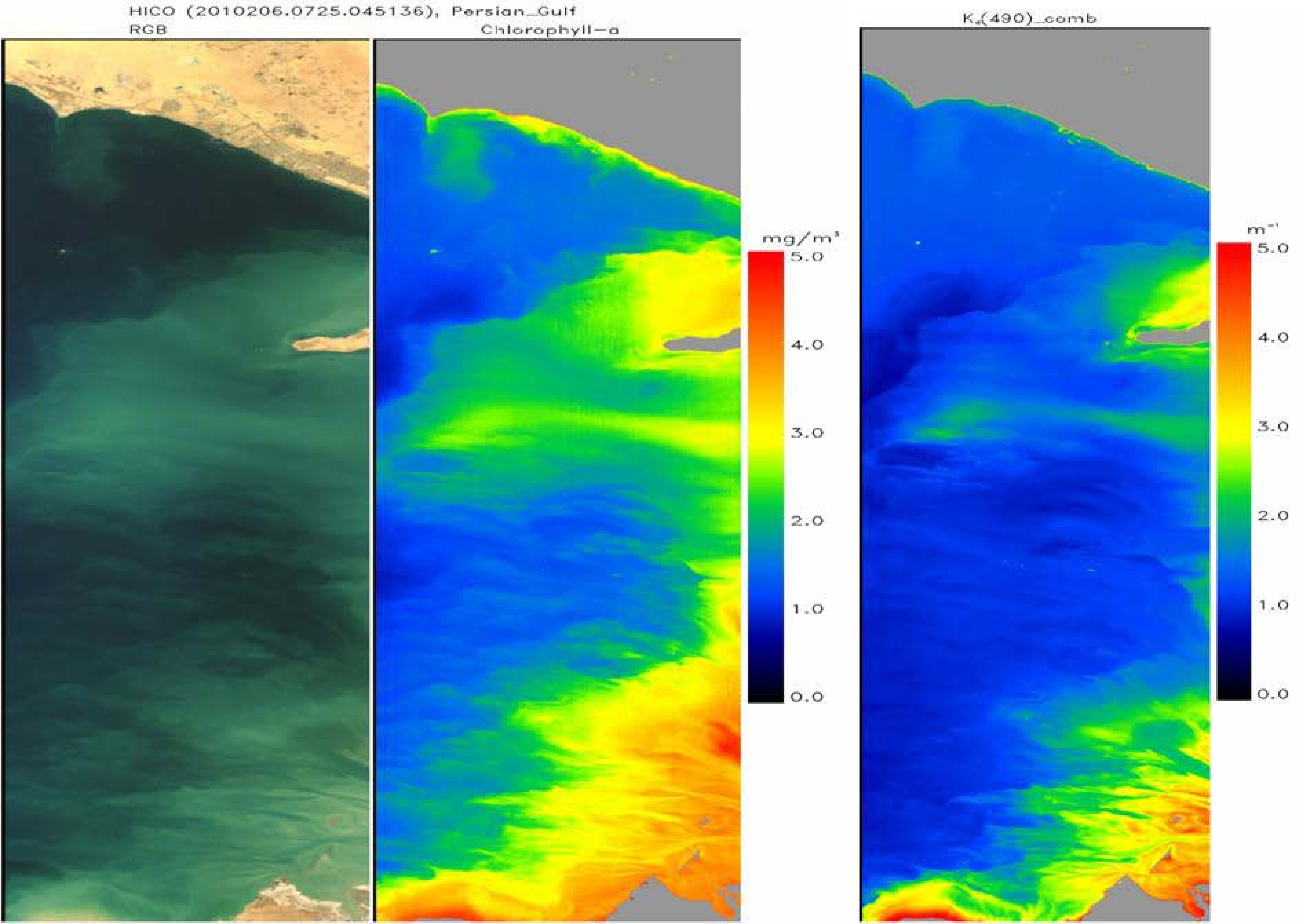

HICO RGB Image Over Olympic Beaches (WA), Chlorophyll & Kd_490 Images (7/9/2010)

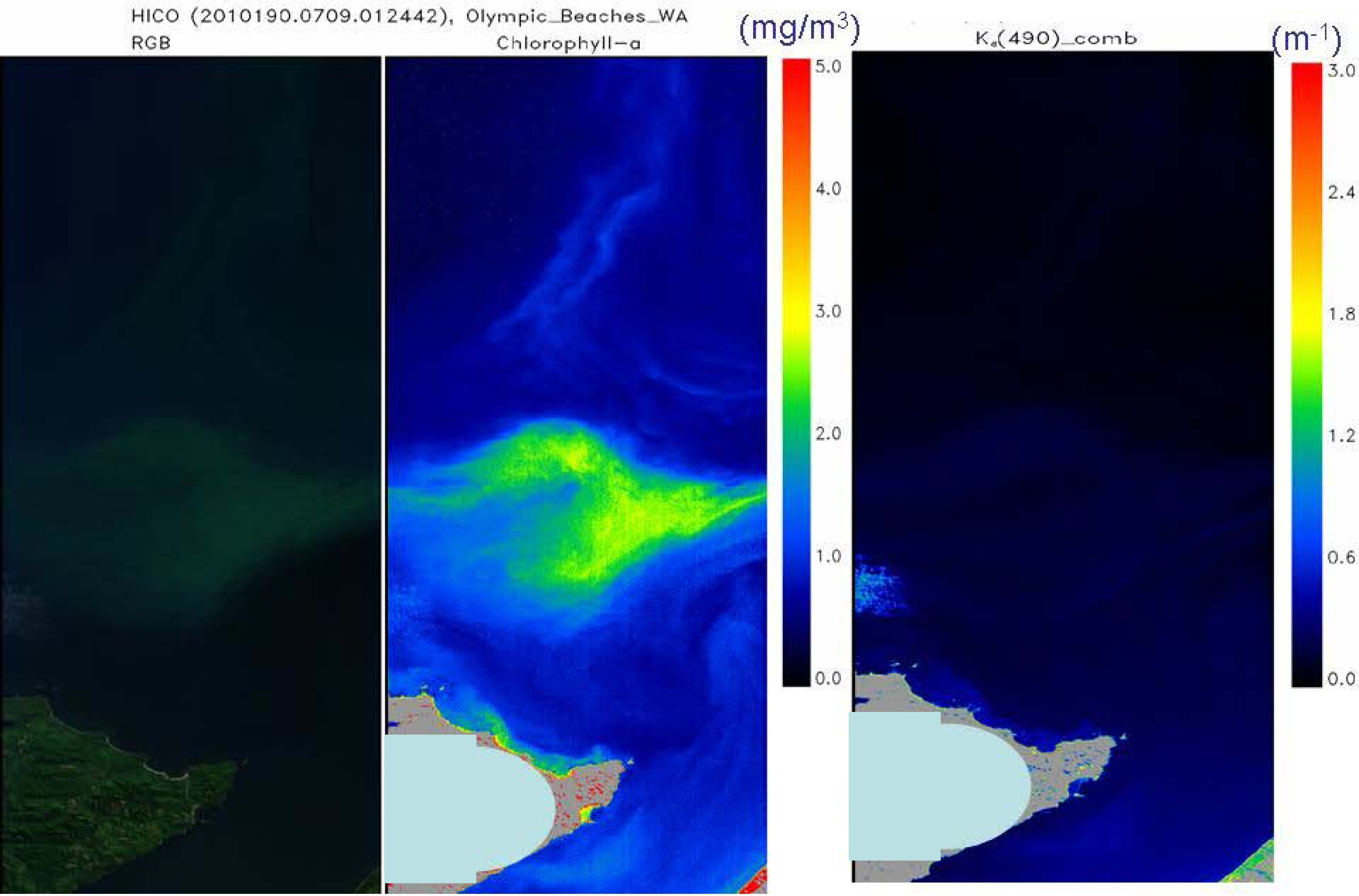

Summary

- At present, both the land and ocean version of the algorithms work reasonably well under typical atmospheric conditions.

- However, in the presence of absorbing aerosols, the model tends to overestimate the atmospheric contribution to the upwelling radiance, resulting in inferred surface reflectances which are biased low (even negative) in the blue region of the spectrum. Problem has been most prevalent in:
    - US east coastal areas in summer months
    - Desert regions

- Upgrades to the atmospheric correction algorithms are needed, particularly in view of major advances in aerosol models. Specific upgrades include:
    - Incorporation of absorbing aerosol models
    - Incorporation of UV channels (380 nm, 400 nm)

Backup Slides

SAMPLE REFLECTANCE RETRIEVALS WITH ATREM

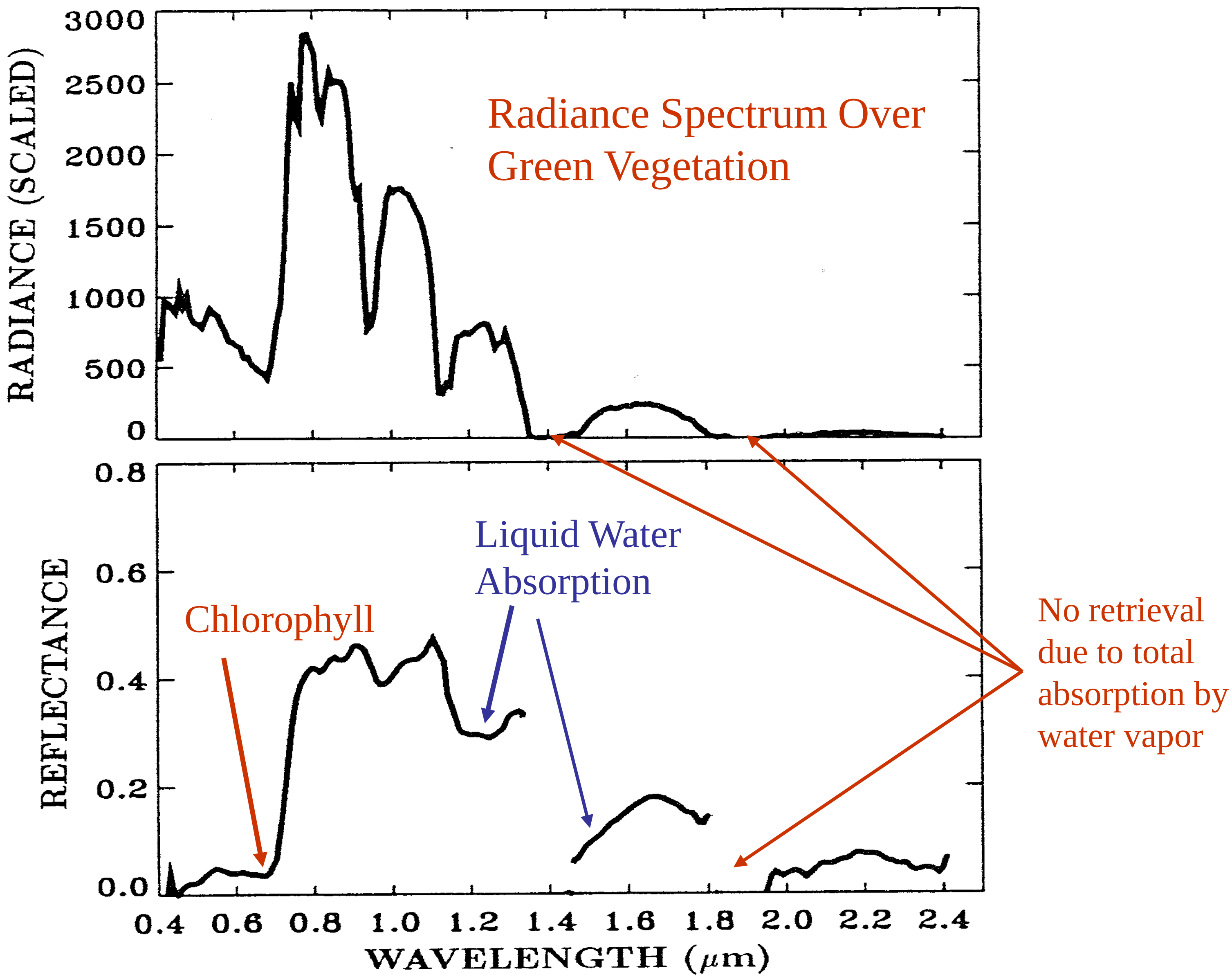

SAMPLE REFLECTANCE RETRIEVALS OVER MINERAL

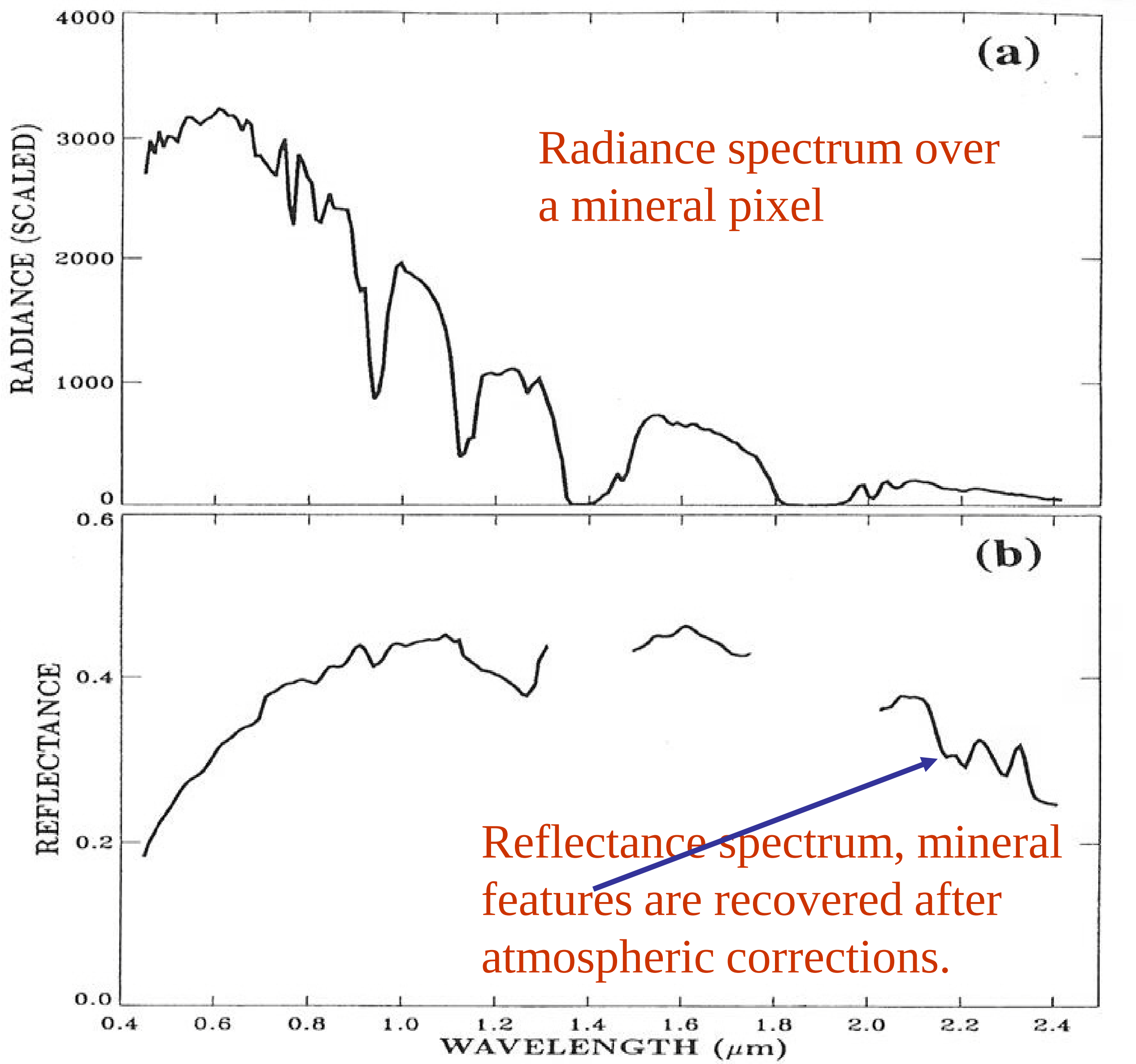

Examples of Cirrus Detection & Corrections

AVIRIS data acquired over Bowie, MD in summer 1997

E.

Hwy 50

CIRRUS IMAGE (1.38μm)

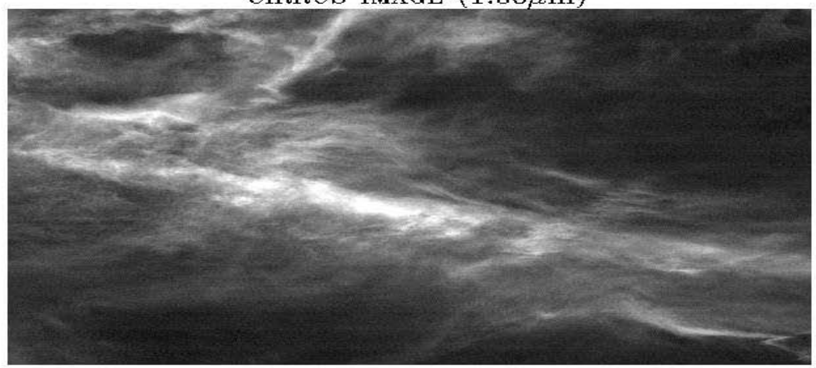

CIRRUS–CORRECTED IMAGE

An Example of Ocean Atmospheric Correction Including Surface Glint Correction

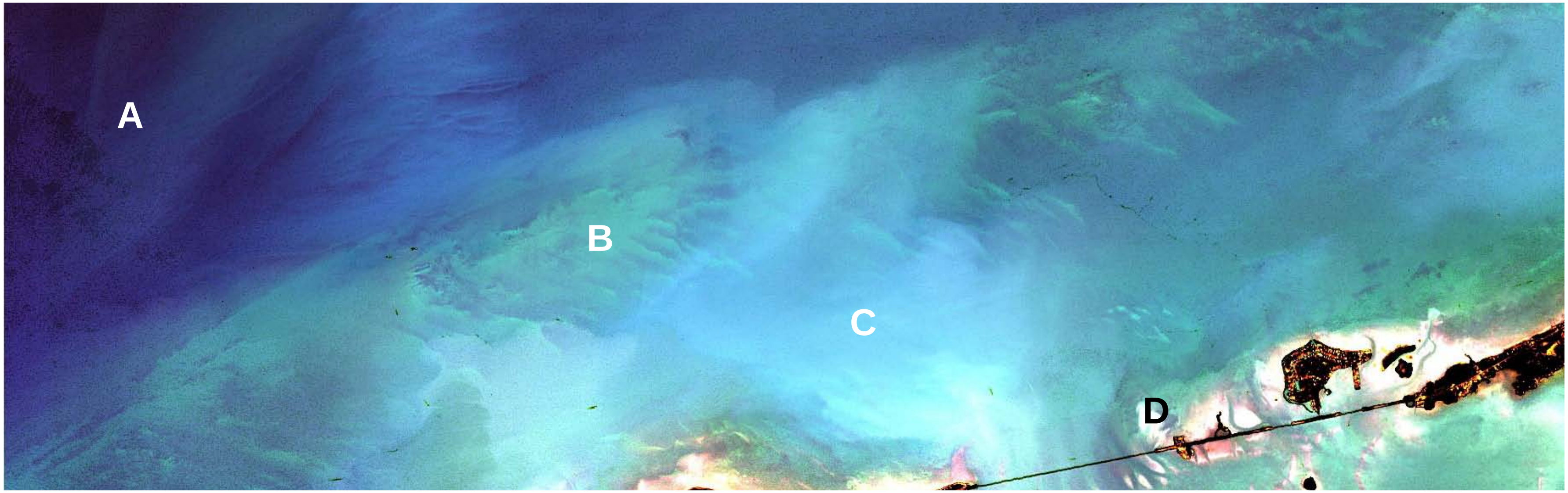

AVIRIS data were atmospherically corrected for ocean scenes. The data are corrected for skylight reflected off the sea surface. It is assumed that the water leaving radiance is 0 for wavelengths greater than 1.0 micron. Note how all of the spectra are 0 past 0.82 micron. (B.-C. Gao, M. J. Montes, Z. Ahmad, and C. O. Davis, *Appl. Opt.* 39, 887-896, 2000.)

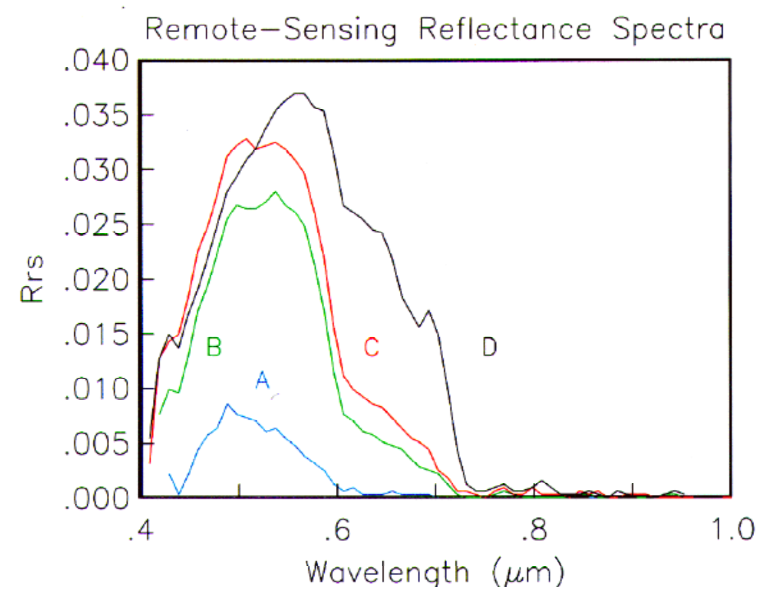

Sunglint Effect Removal With An Empirical Technique

Sunglint effect becomes stronger from left to right in an AVIRIS image. Individual wave facets are observed in the high spatial resolution AVIRIS image (20 m). It is not possible to use Cox & Munk model to predict sun glint effects in this case.

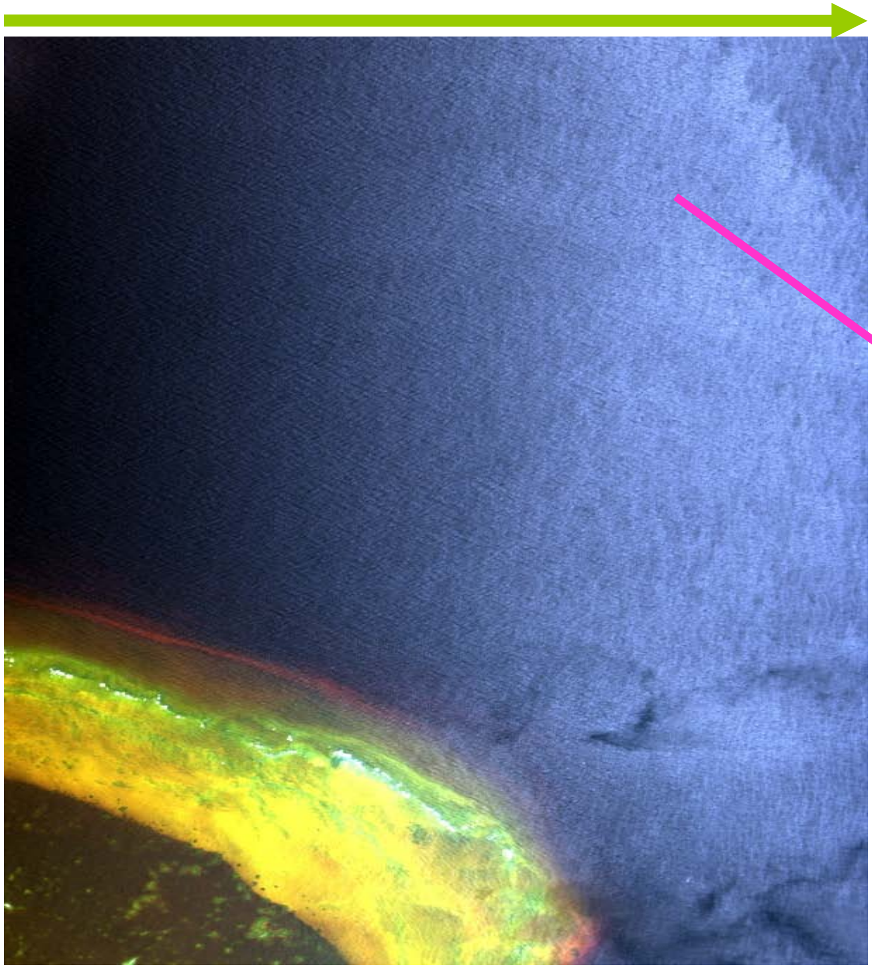

A sample sunglint apparent reflectance spectrum

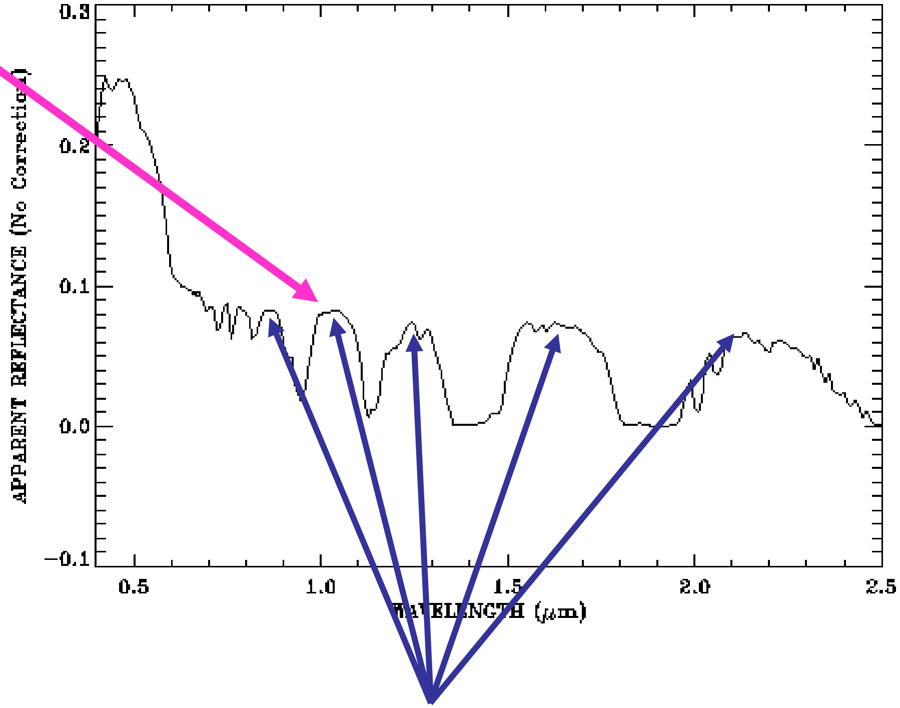

The sunglint reflectances for atmospheric window channels above 0.8 micron are almost constant. The empirical technique = ATREM (Land) reflectance minus 1.04 micron reflectance value on the pixel by pixel basis.

Images Before and After The Empirical Sunglint Correction

Before

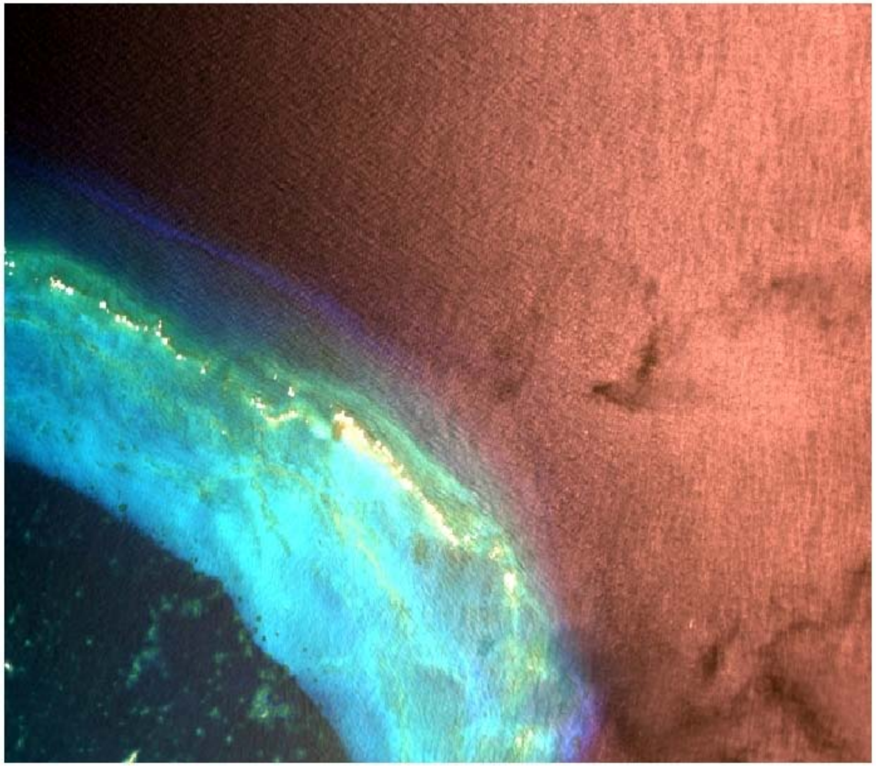

After

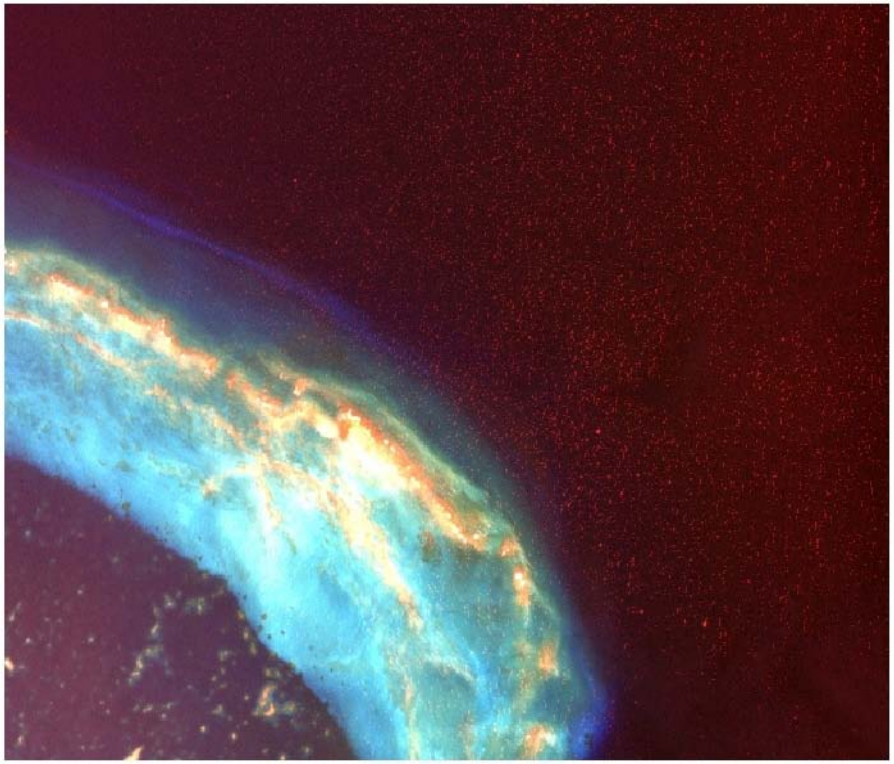

The image at right demonstrates that, after the empirical correction, the sunglint effects are mostly removed. The “contiguous” spatial features in the middle bottom portions of the image are seen much better. However, minor noise effects are seen in areas without bottom reflection.

HICO RGB Image & Sample Spectra of Florida Keys

Examples of an ASD Spectrum and a Water Leaving Reflectance Spectrum Retrieved From HICO Data Over Florida Keys

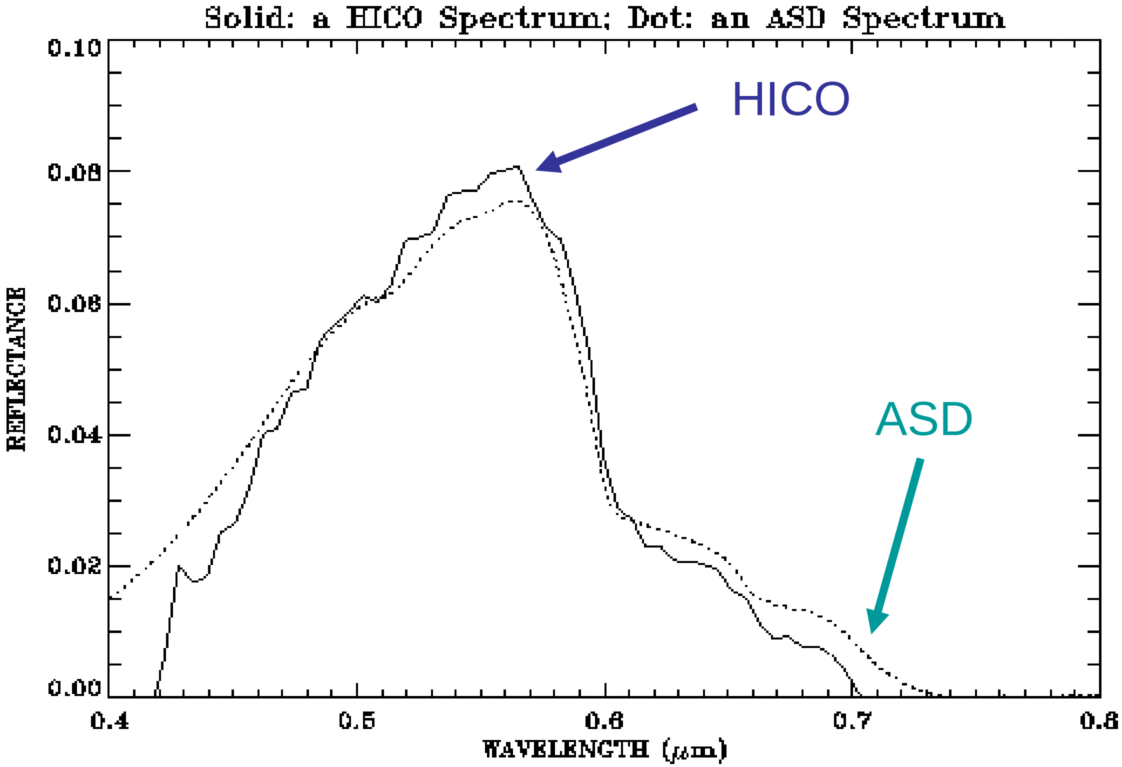

Please note that the shapes of the two spectra in the 0.45 – 0.8 micron wavelength Interval are very similar. The two spectra are not measured over the same time, nor over the same spatial location.

Spectral and Radiometrical Calibrations (Smear + 2nd Order Light Correction) Have Been Conducted to the HICO Data

Here, we illustrate the results of an empirical technique for correction of 2nd order light effect using shallow underwater features

HICO Images Over the Midway Island in the Pacific Ocean

RGB image

Before 2nd order correction (Band 105, 0.95 µm)

After 2nd order correction (Band 105, 0.95 µm)

The bright features result from the 2nd order light of a visible channel

The bright features are removed

HICO RGB Image Over Mekong Delta, Chlorophyll & Kd_490 Images

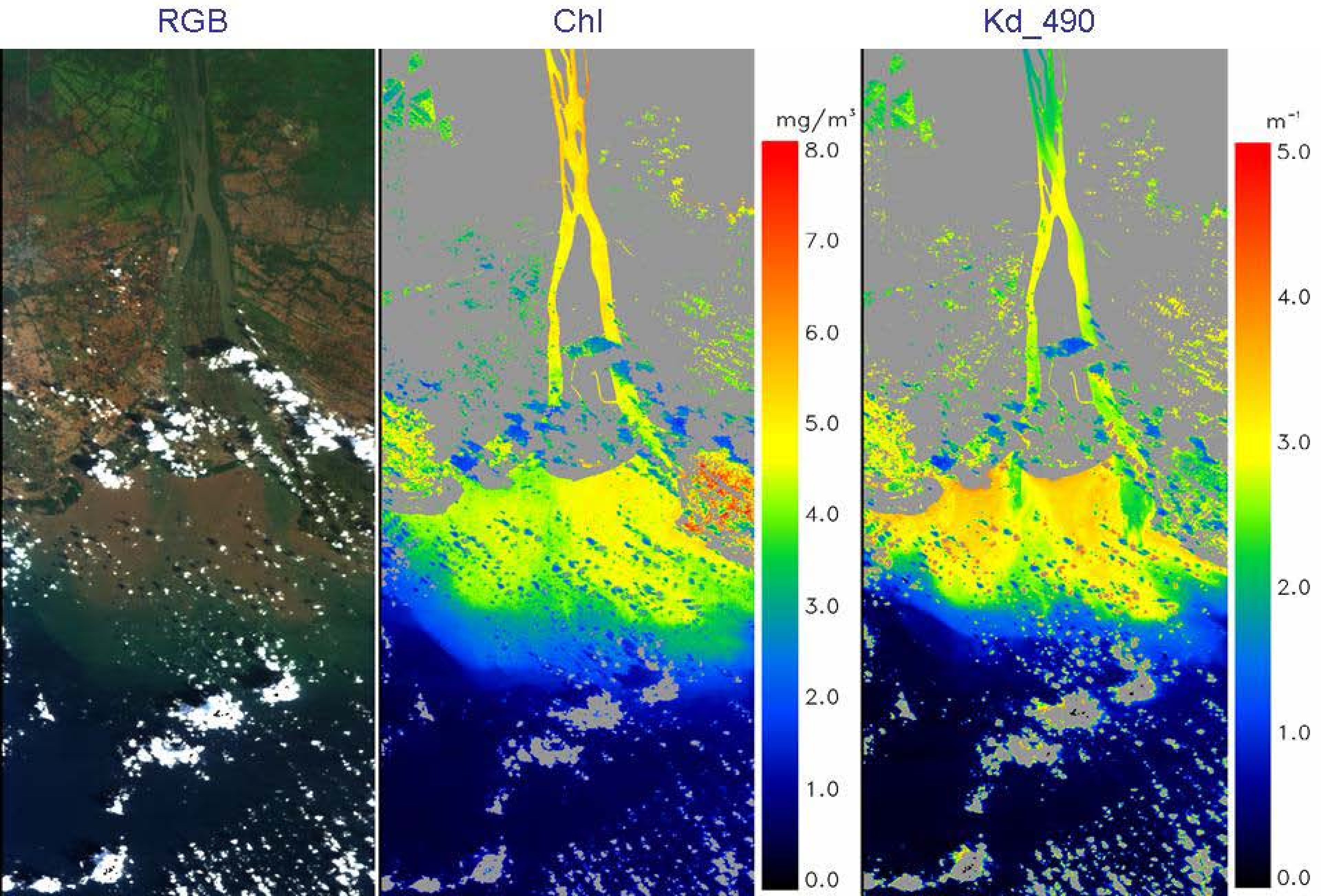

HICO RGB Image Over SE Caspian Sea, Chlorophyll & Kd_490 Images (5/9/2010)

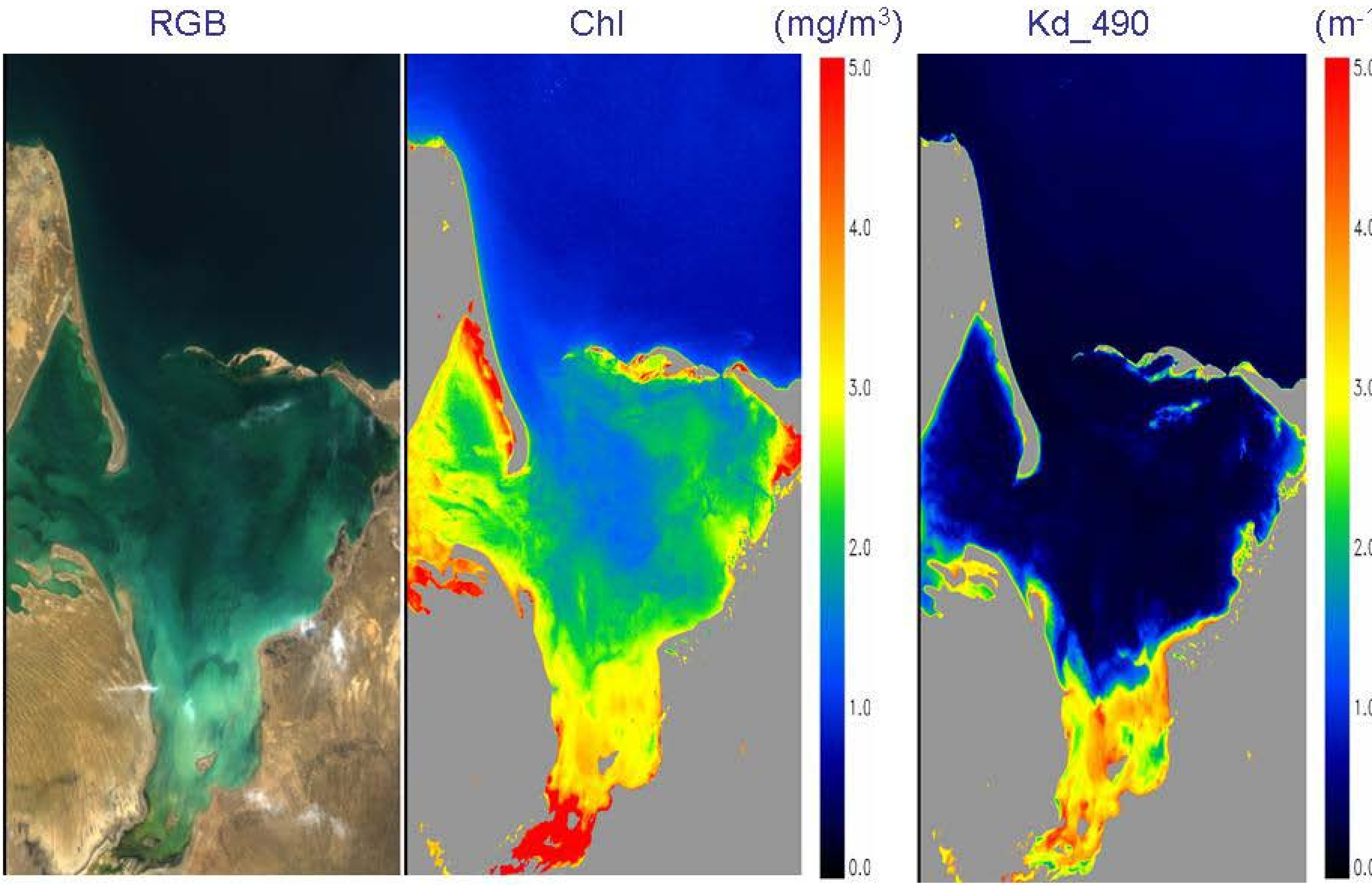

Vegetation Functional Type Analysis, Santa Barbara, CA

Dar Roberts, et al, UCSB

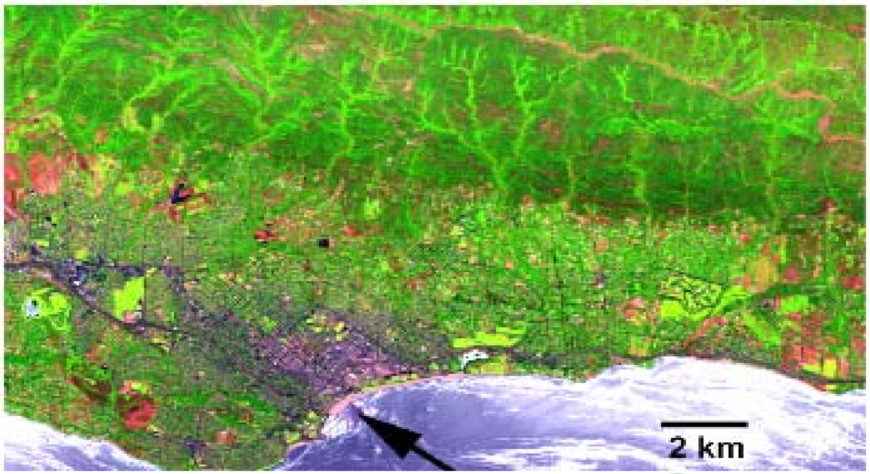

MESMA Species Type 90% accurate

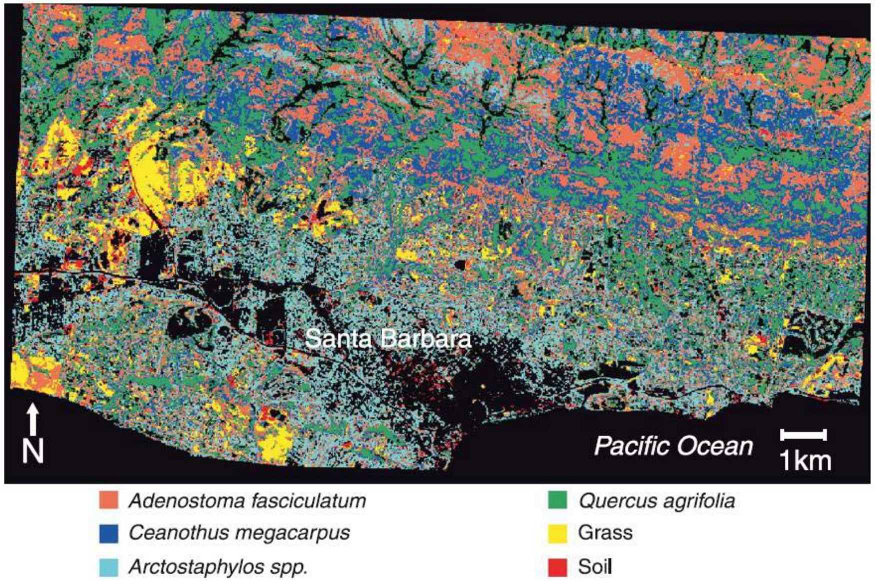

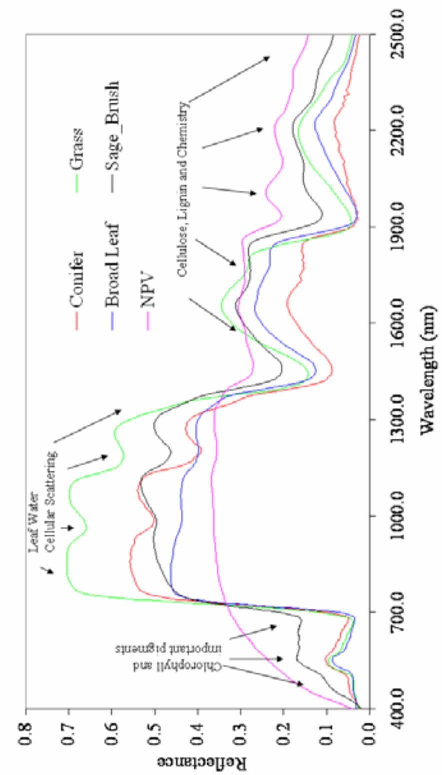

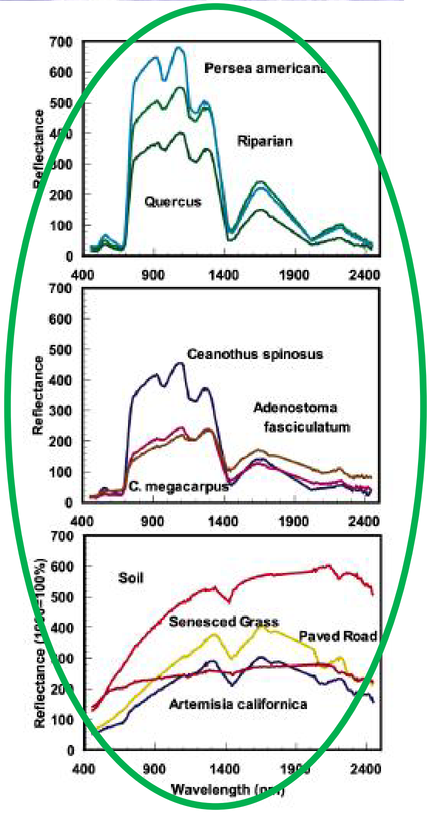

Species Fractional Cover

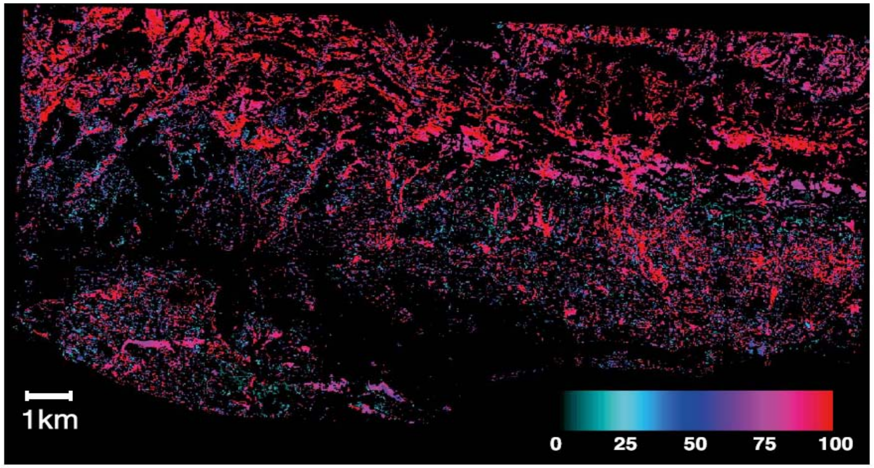

EnMAP and TES-GAP
Status of the Missions and Relevance to HyspIRI

A. Müller, H. Kaufmann T. Stuffler, S. Hofer, F. Buongiorno
and the EnMAP & TES-GAP Teams

EnMAP Overall Mission Goals

- An Imaging Spectrometer
- To provide high-spectral resolution observations of bio-geochemical and geophysical variables
- For Multipurpose Applications
- To observe and develop a wide range of ecosystem parameters encompassing agriculture, forestry, soil/geological environments and coastal zones/inland waters
- To Precisely Measure Ecosystem Parameters
- As Input to Ecosystem Models
- To enable the retrieval of presently undetectable, quantitative diagnostic parameters needed by the user community
- To Improve the Understanding of Land Surface Processes
- To provide high-quality calibrated data and data products to be used as inputs for improved modelling and understanding of biospheric/geospheric processes

Missionsparameter

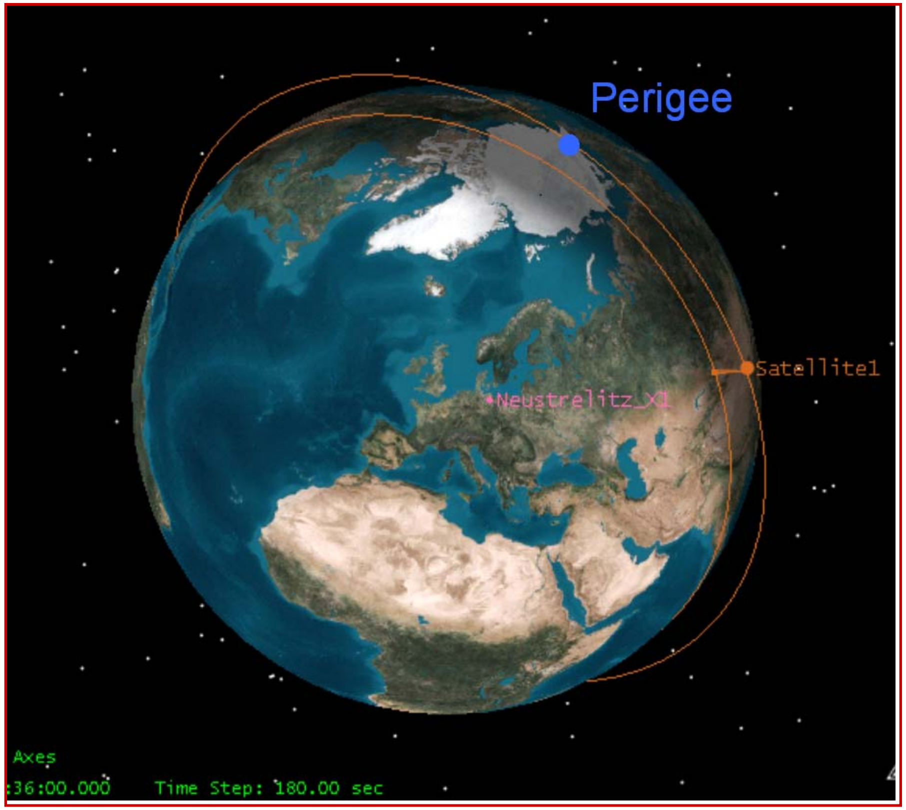

- Sun-synchronous, 11:00 LTDN LEO – reference altitude 653km
- 3 axis stabilized platform with OCS
- mass 850 kg / power 550 W avg.
- 512 Gbit mass memory / 320 Mbit/s X-band science data downlink
- 4 day global accessibility (±30° off-nadir)
- 4 day target revisit capability
- up to 50 data takes per day / total length 5000km

Sensor Parameter

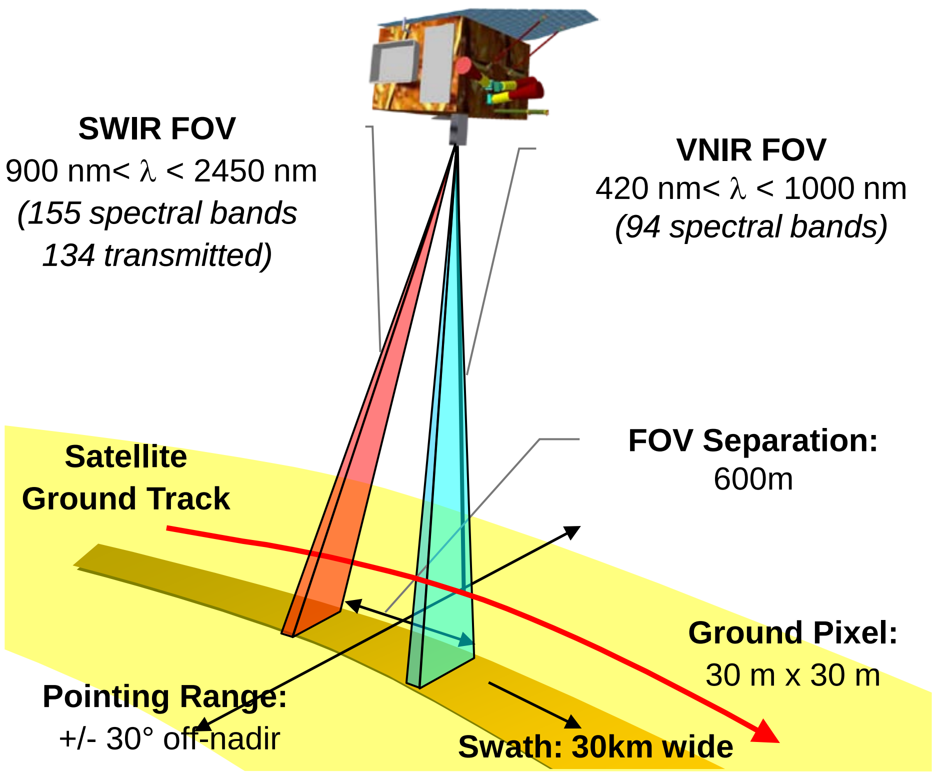

schlanke Kontur - Leitfarbe

- Pushbroom type hyper spectral imager
- Wavelength 420 - 2450 nm
- 30m GSD, 30 km swath (nadir)
- 228 spectral bands
- VNIR 6.5 nm sampling
- SWIR 10 nm sampling
- SNR > 150 @ 2200nm (ref. radiance)
- Polarization sensitivity < 5%
- Smile and Keystone < 0.2 pix
- Pointing knowledge 100m
- Radiometric accuracy 5%
- Radiometric stability 2.5%
- Response Linearity 0.5%
- Spectral accuracy 0.5nm / 1nm

Satellite Design

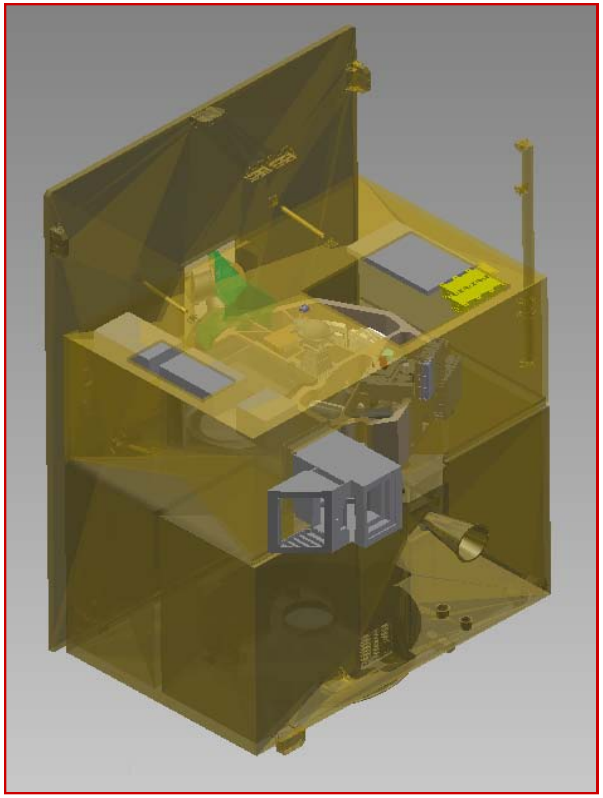

- Total Weight: ca. 850 kg
- Aver. Power: 450 W
- 512 Gbit mass memory
- 3 axis stabilized platform
- Pointing Stability: 1,5 m / 4 ms
- Pointing Knowledge: 100 m
- ± 30° off nadir pointing for observation
- Hydrazine propulsion system for orbit maintenance & disposal
- 320 Mbit/s X-Band science data downlink
- Lifetime in Orbit: > 5 years

Instrument Optik Unit Design

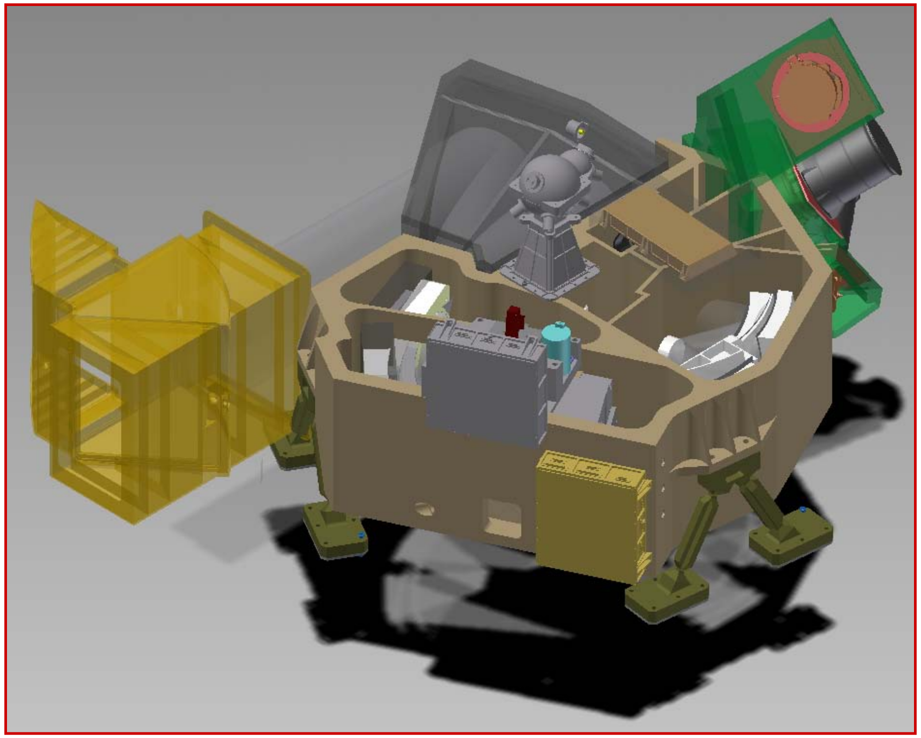

- Polished NiP coated Aluminum mirrors
- Monolithic Aluminum structure
- Quasi-isostatic mounting to platform
- Starcameras attached to IOU for pointing knowledge
- Redundant SWIR FPA due to cryocooler without flight heritage
- Gravity release < 5µm – opt. elements
- Eigenfreq. > 100 Hz
- Active thermal stabilization to 21°C ± 1K

Instrument Optik Design

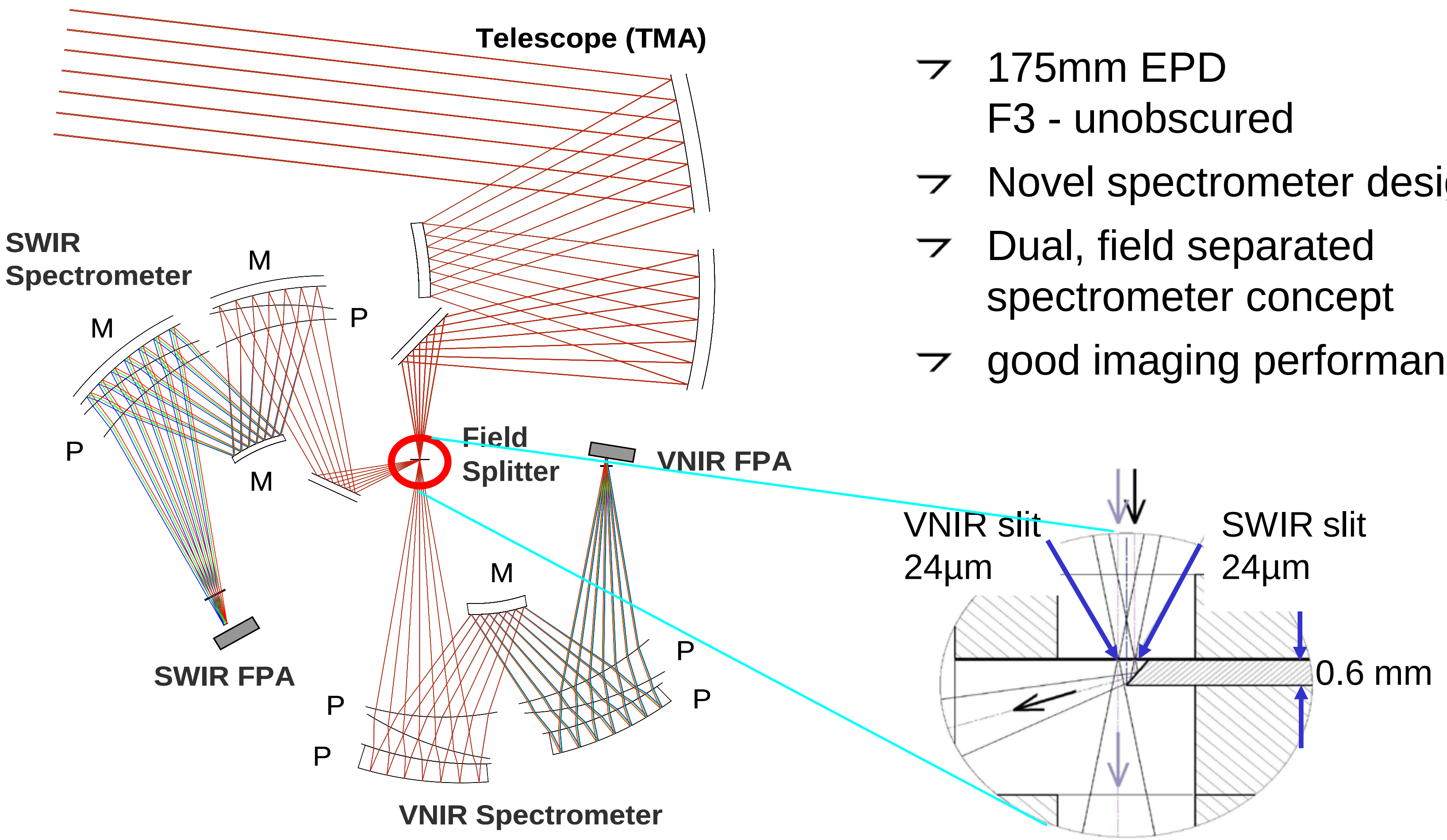

- 175mm EPD
  F3 - unobscured
- Novel spectrometer design
- Dual, field separated spectrometer concept
- good imaging performance

EnMAP Summary

- EnMAP primarily is considered as an environmental research satellite focusing on process oriented land surface dynamics
- PI: Charly Kaufmann, GFZ Potsdam
- Phase C/D in work, CDR of GS completed
- Launch scheduled for mid 2014
- 30 km Swath, 30m spatial resolution, 5-10 nm spectral bandwidth
- Level 2 Product: Ortho-rectified and atmospherically corrected data
- Strong scientific user support planned: Toolbox, Spectral Archive
- Open for international partnerships with respect to data utilization
- Information: http://www.enmap.org

TES GAP

Temperature Emissivity Signatures
for Geosphere and Pedosphere

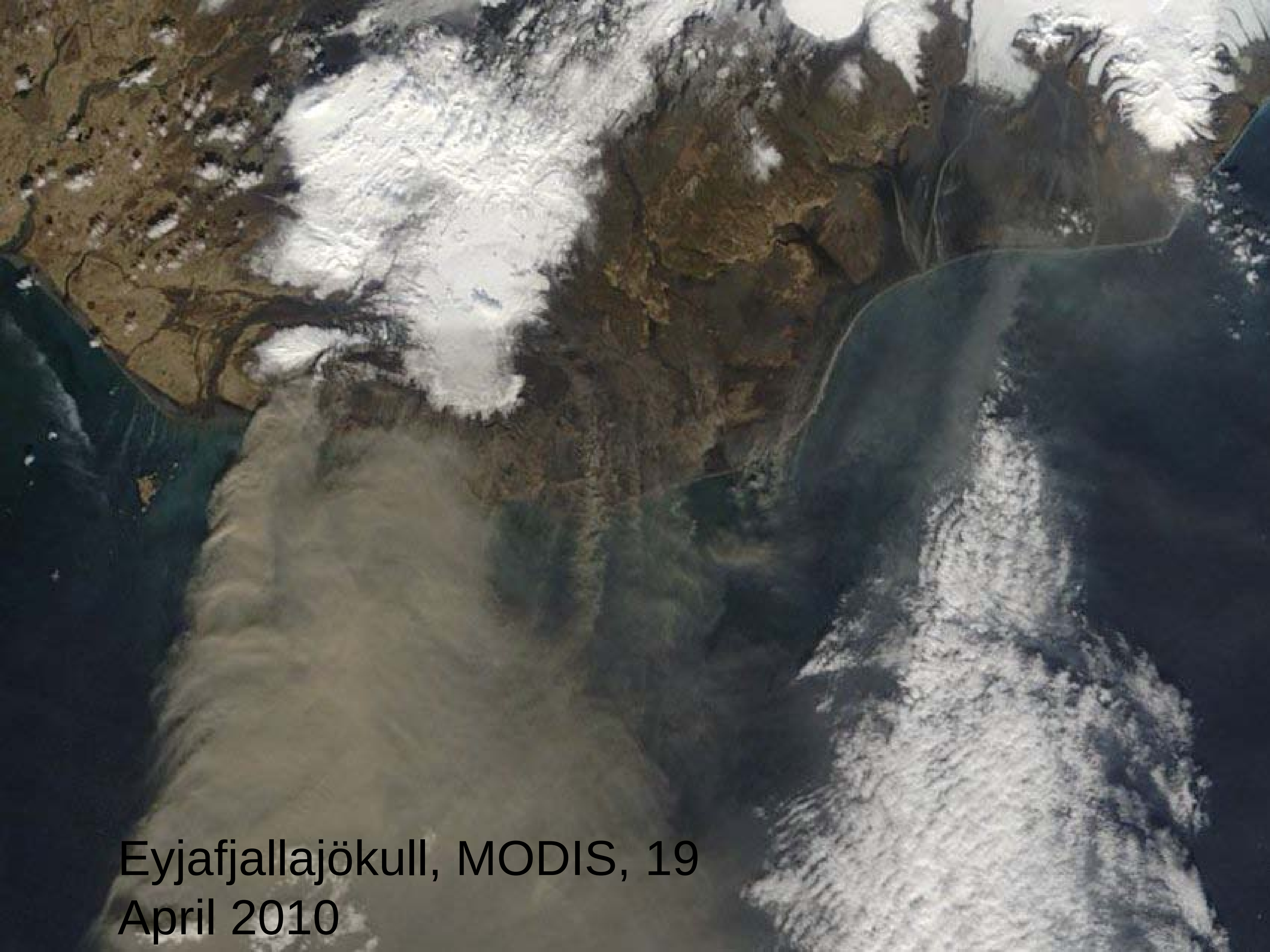

Eyjafjallajökull, MODIS, 19 April 2010

Monitoring of Precursor Indicators

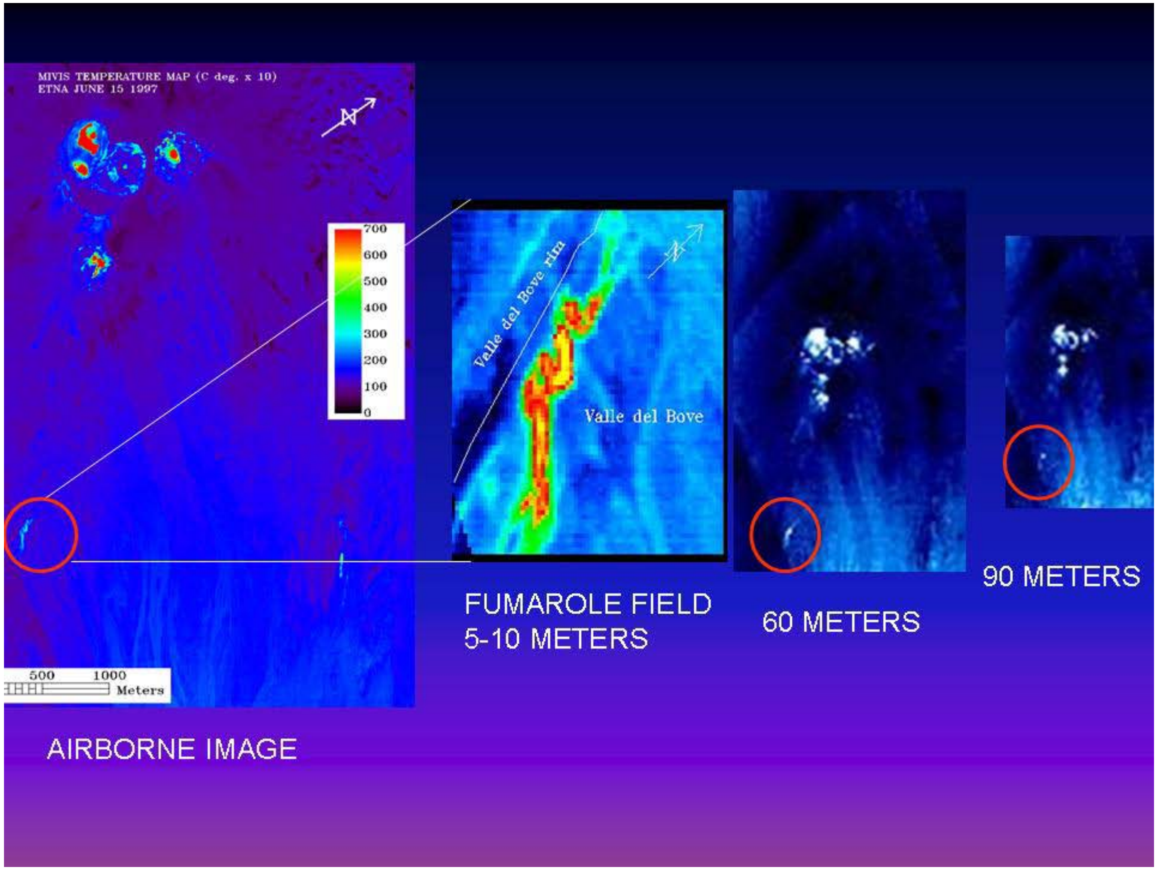

Characterisation of Soils

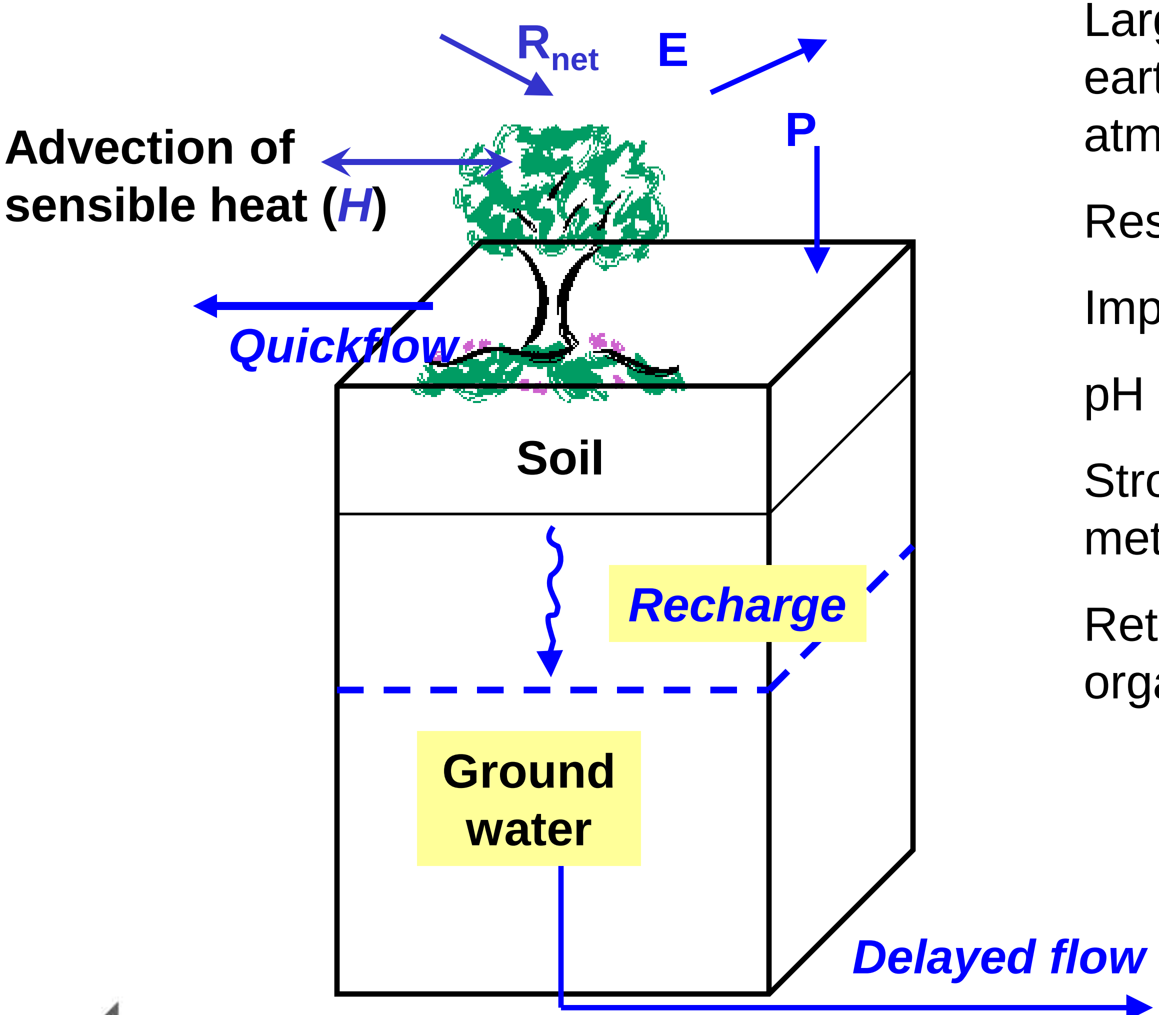

Largest pool of organic C on the earth's surface. 3x larger that atmospheric C

Reservoir of C, N, P, and S

Important role in C sequestration

pH buffering

Strong retention of Al and heavy metals

Retention of pesticides and other organic chemicals

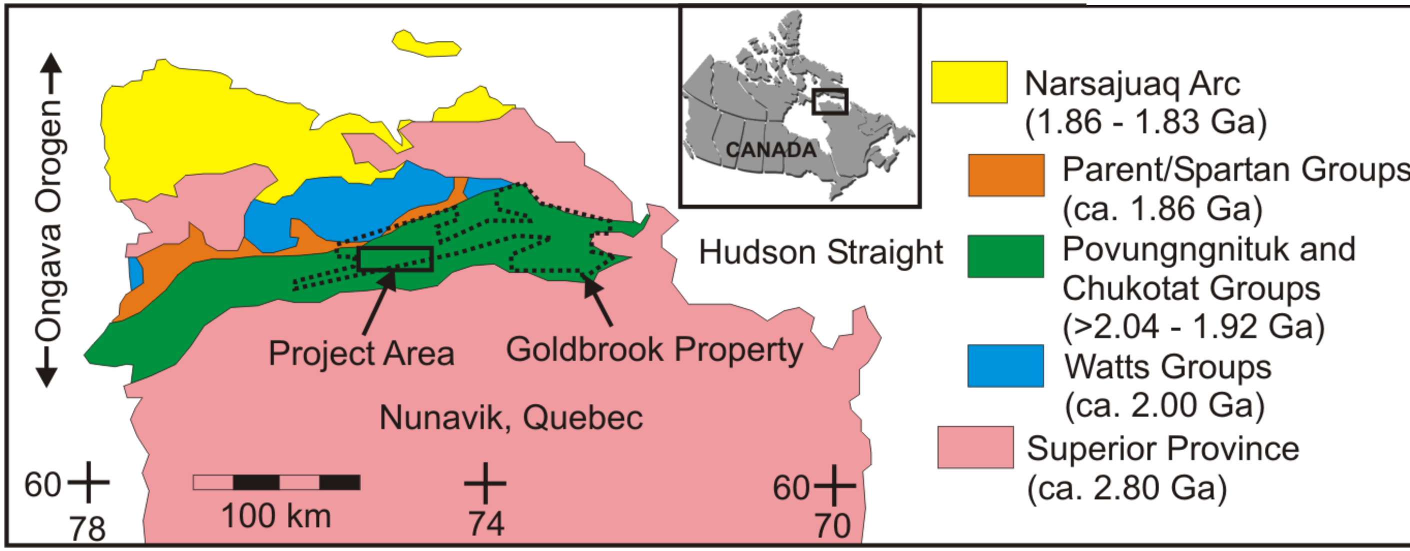
Ongava Orogen
CANADA
Narsajuaq Arc
(1.86 - 1.83 Ga)
Parent/Spartan Groups
(ca. 1.86 Ga)
Povungngnituk and
Chukotat Groups
(>2.04 - 1.92 Ga)
Watts Groups
(ca. 2.00 Ga)
Superior Province
(ca. 2.80 Ga)
Hudson Straight
Project Area
Goldbrook Property
Nunavik, Quebec
60
78
100 km
74
60
70

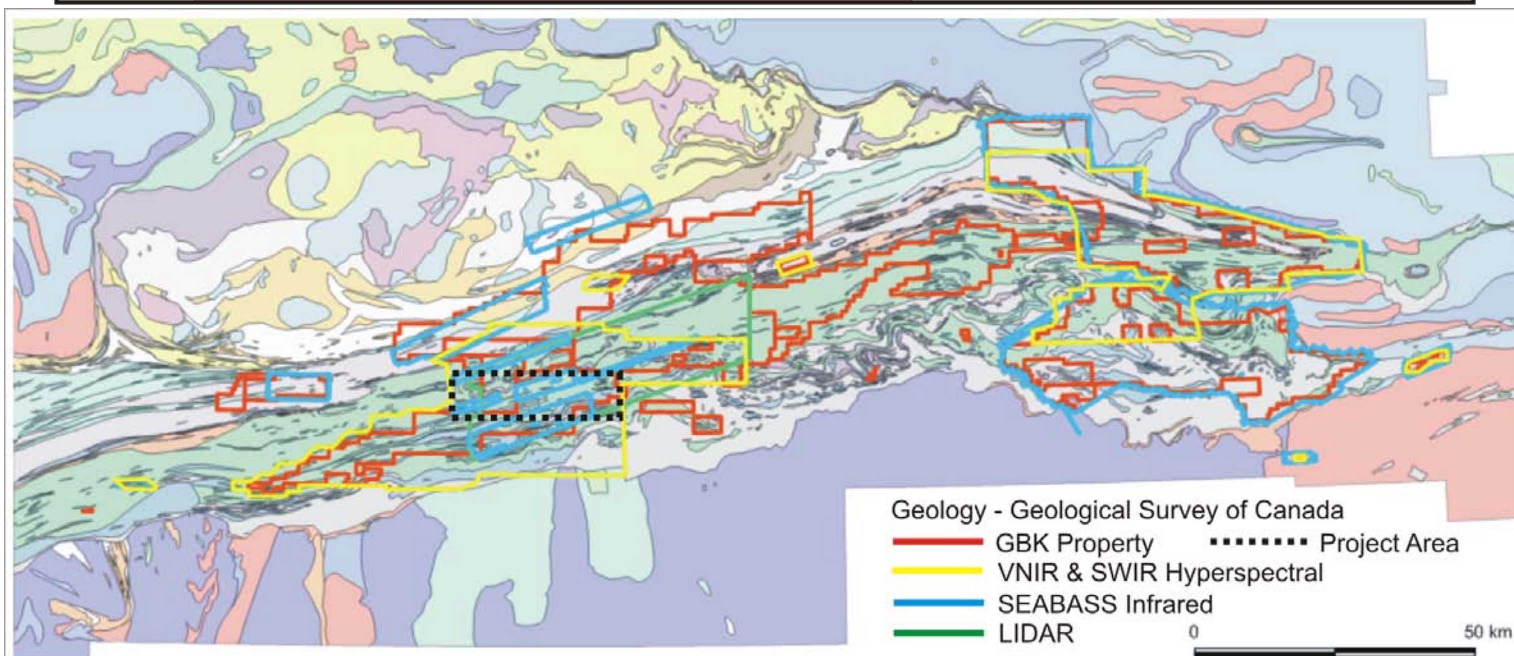
Geology - Geological Survey of Canada
GBK Property
Project Area
VNIR & SWIR Hyperspectral
SEABASS Infrared
LIDAR
0
50 km

Map Information Needs

- Mineral exploration requires detailed maps
- Ore bearing horizon is peridotite
- All rocks visibly dark but differing in mineralogical detail (type and abundance)

Regional map (1980's)

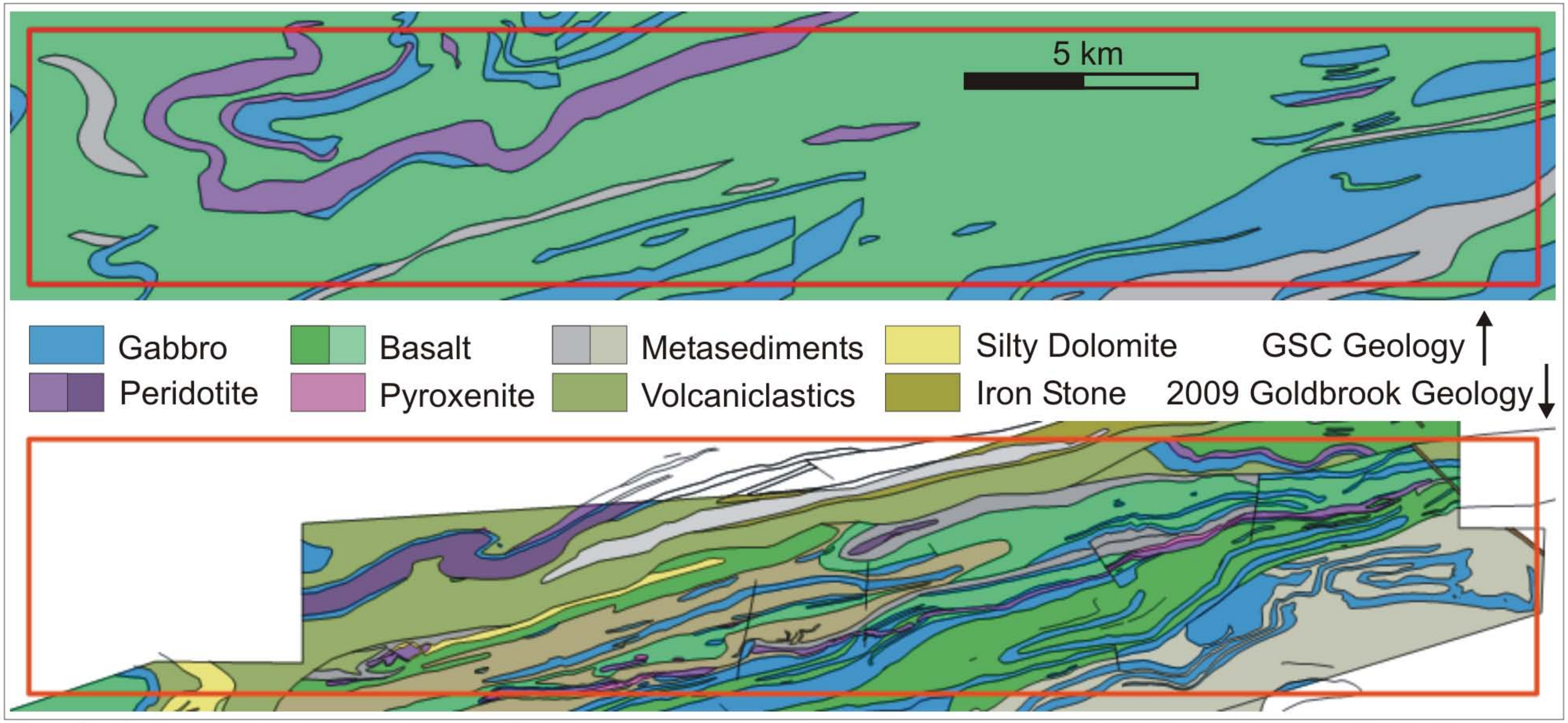

Detailed map (2009)

Terrane Characteristics

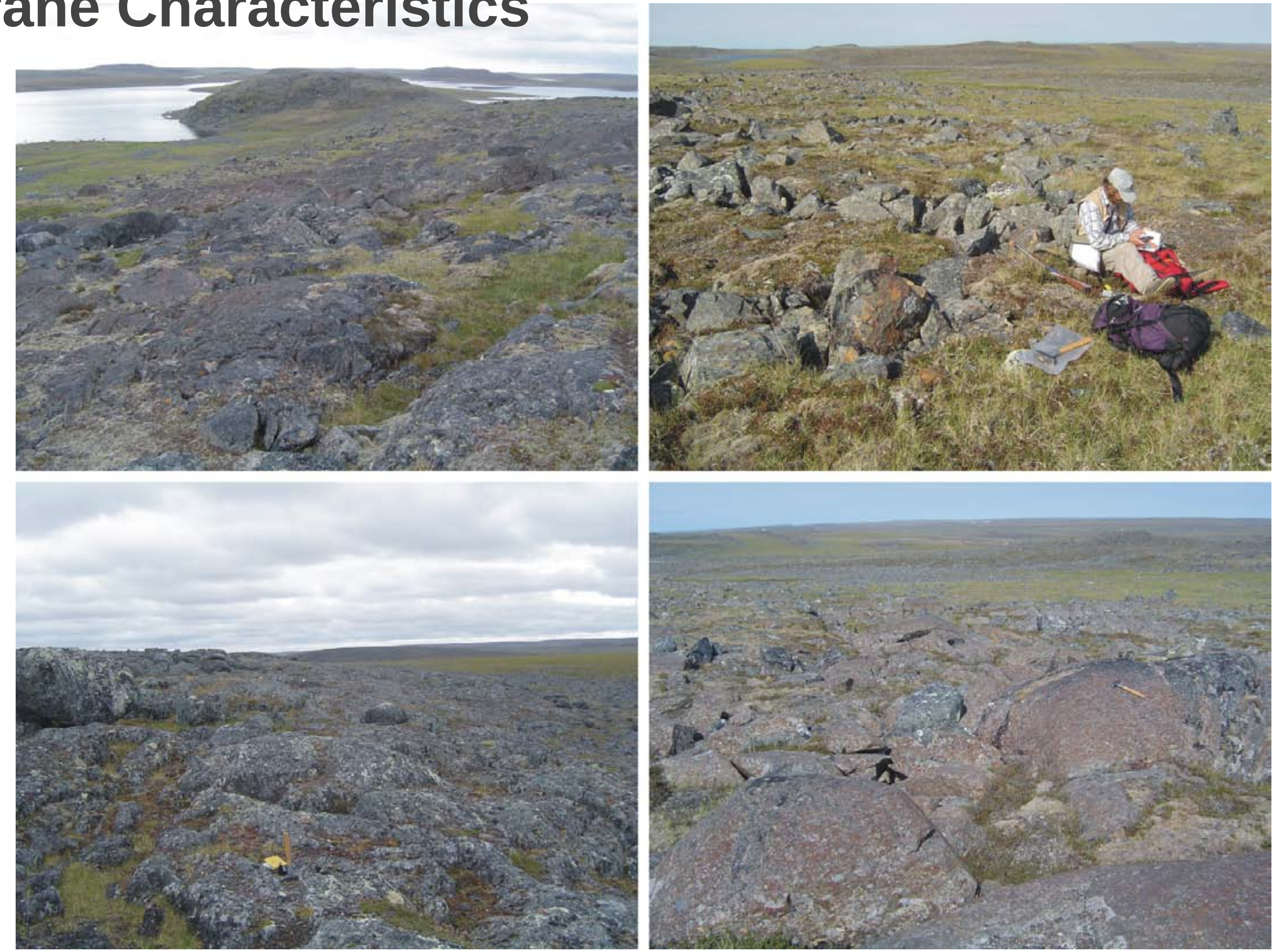

Frost heave, spatial continuity, lichen imparting color to bedrock

Mapping with SEBASS (4 meter data)

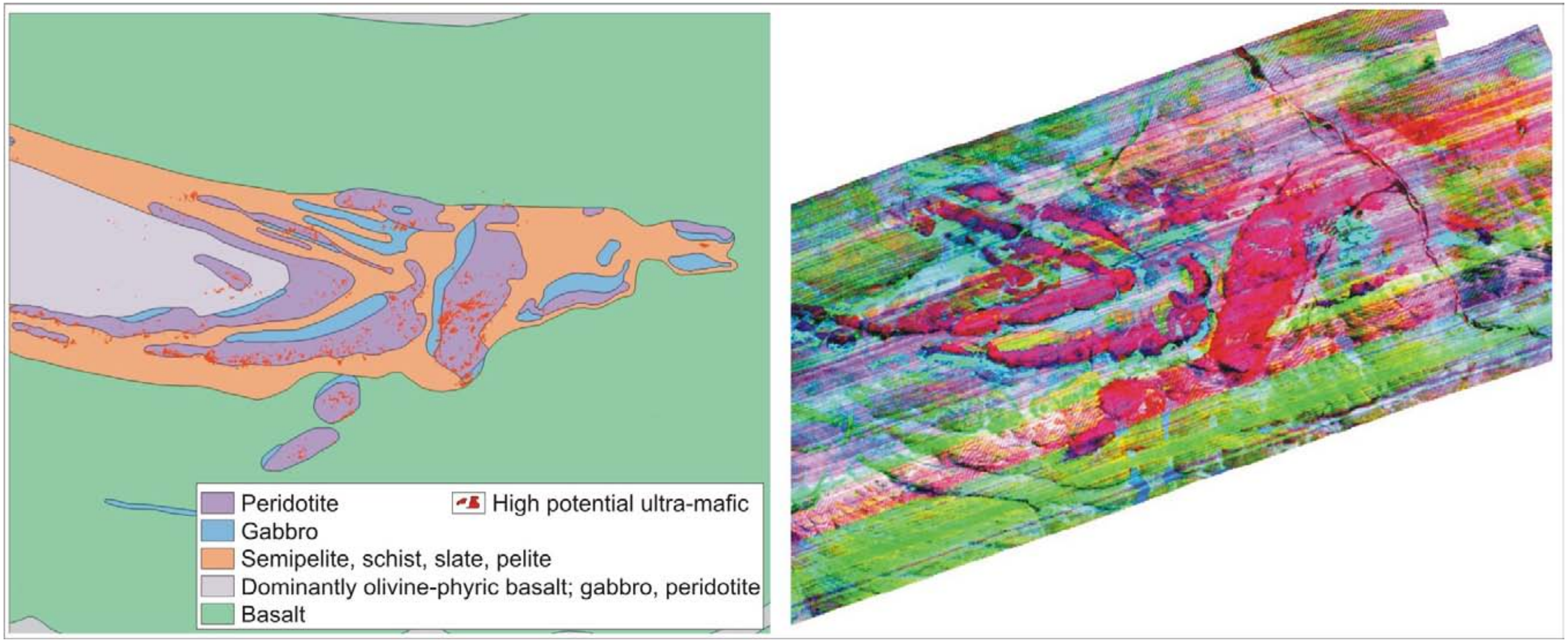

TES-GAP Science Objectives

- **Provide high precission emissivity and temperature measurements of land surfaces**
- **Measure soils surface composition and monitor soil dynamics**
  - determine SOM, soil mineralogy, moisture, roughness
  - monitor soil degradation and pedogenic processes
  - improve understanding of soil-atmosphere interaction
- **Measure volcanic thermal behaviour and gas emissions as precurser indicators to predict eruptions**
  - determine temperature of lava flows, craters and fumarol fields
  - quantitatively measure volcanic emission gases
- **Foster applications of thermal spectroscopy in other science areas**
  - Urban heat island
  - Biomass burning
  - Heat stress in inland and coastal waters

TES-GAP History & way forward

- ESA EEOM Call EE8 in 2009, Deadline for LoI: Dec 2009
- LoI from DLR & KT (TERM) and INGV & SelexGalileo (MARTHA)
- Decission on merge of both proposals in April 2010
- Submission of TES-GAP in June 2010
- ESA decission on Phase A studies (up to three) in Nov 2010
- ESA decission on implementation of one mission end of 2011
- Launch in 2018

TES-GAP - Proposal Team

- Andreas Müller, Dr. Tobias Storch, German Aerospace Center (DLR)
- Dr. Maria Fabrizia Buongiorno, Istituto Nazionale di Geofisica e Vulcanologia (INGV)
- Dr. Timo Stuffler, Markus Plattner, Kayser-Threde GmbH (KT)
- Tiziano Mazzoni, SelexGalileo
- Prof. Eyal Ben Dor, Tel Aviv University (TAU)
- Prof. Benoit Rivard, University of Alberta (UA)
- Prof. Jose Sobrino, University of Valencia (UV)
- Ivan Pippi, Istituto di Fisica “Nello Carrara” (IFAC)
- Dr. Martin Wooster, King’s College London (KCL)
- Prof. Sergio Teggi, Prof. Sergio Pugnaghi, University of Modena (UM)
- Dr. Stefania Amici, Dr. Stefano Corradini, Dr. Valerio Lombardo, Dr. C. Spinetti, INGV
- Dr. Simon Hook, Dr. Michael Abrams, Dr. Dave Pieri, NASA JPL

Proposed Mission Organisation

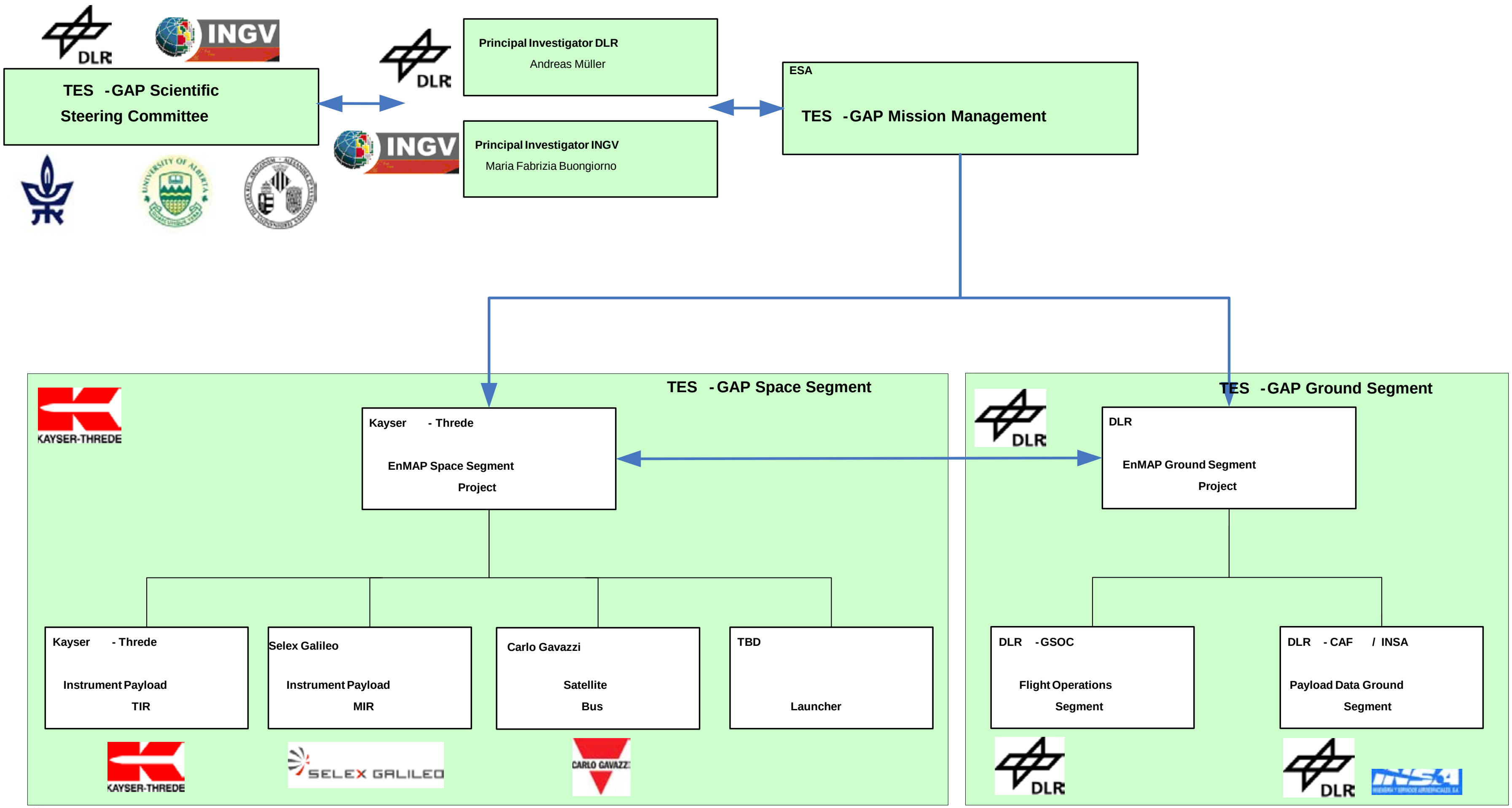

Thermal Signatures of Minerals

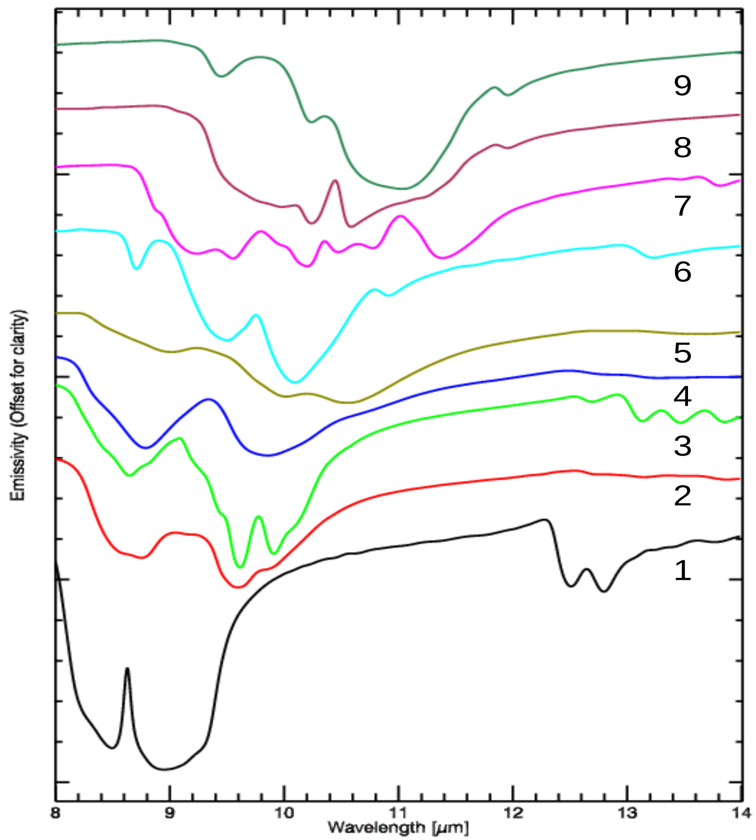

9) Forsterit

8) Olivin

7) Pyroxen

6) Hornblende

5) Labradorit

4) Oligoklas

3) Albit

2) Orthoklas

1) Quarz

Basalt

Granites

Rock forming Minerals

H. Kaufmann, GFZ

Instrument Requirements Simulations

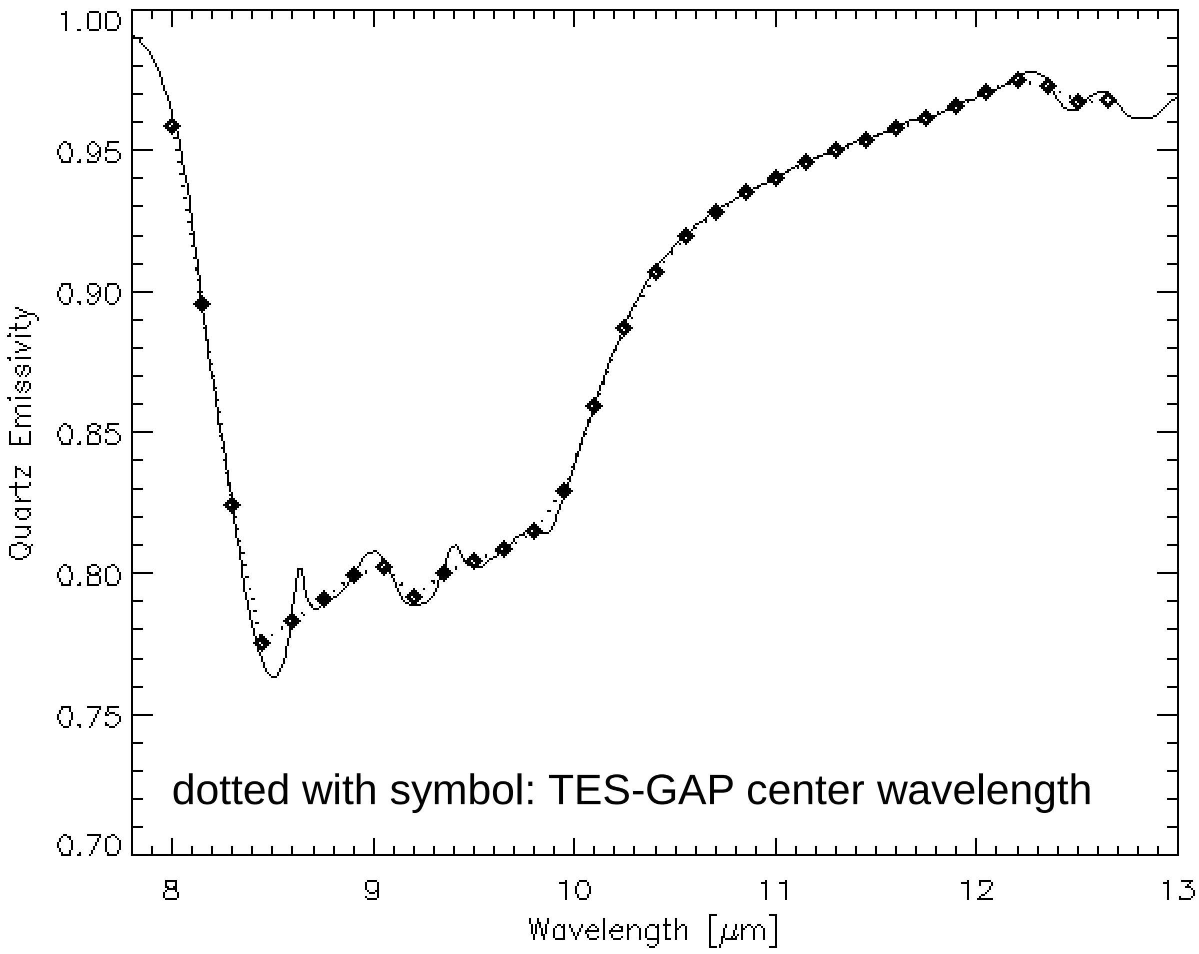

Spectral Coverage

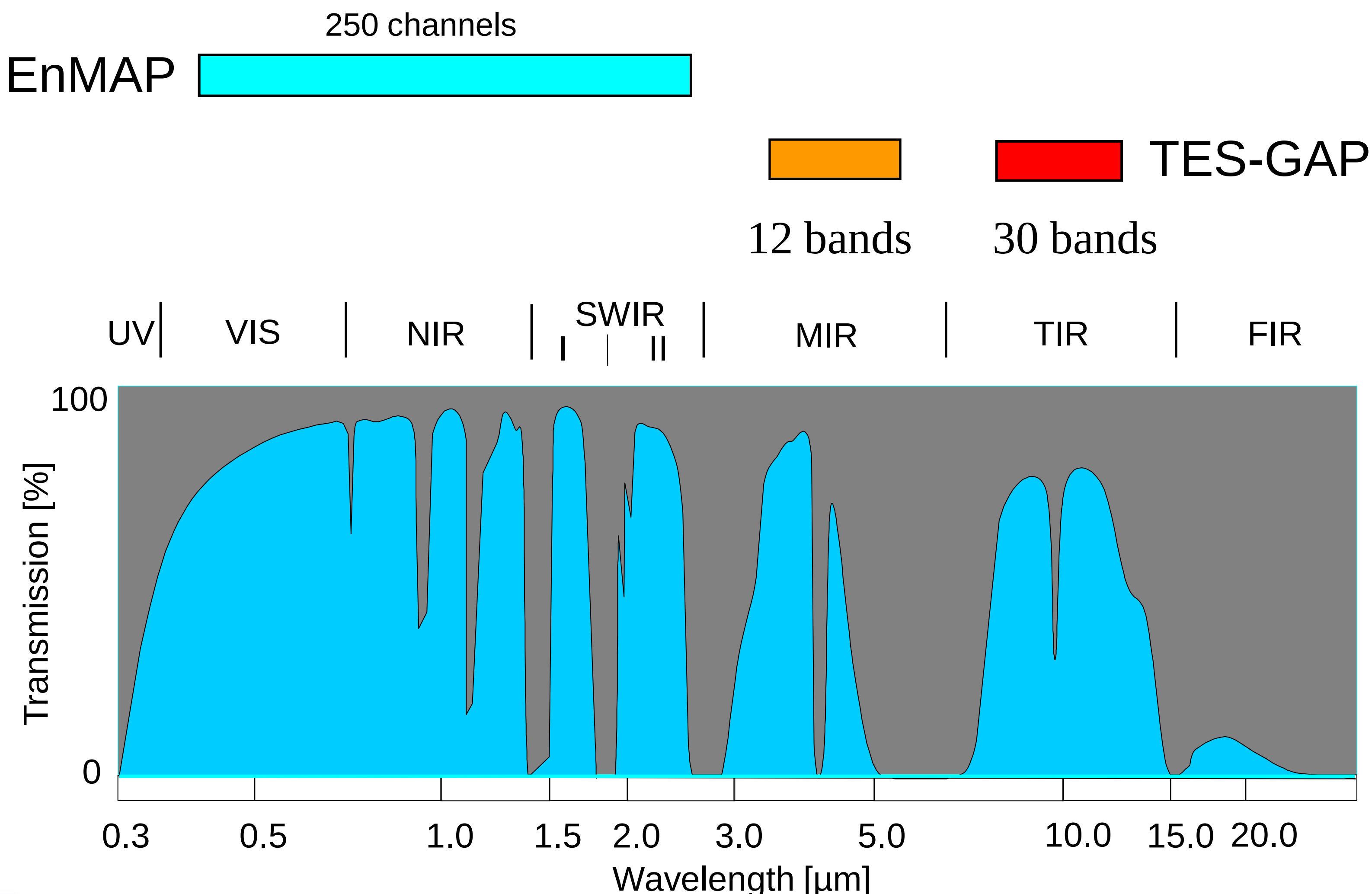

Preliminary TES-GAP Instrumentation / Mission Requirements

- MIR Radiometer Spectral and Radiometric Requirements
  - Coverage: 3-5 µm
  - No. of bands: ~12 , bandwith: ~150 nm
  - NEΔT: 0.05 K @ 300K & 0.1 K @ 1000K
- TIR Spectrometer Spectral and Radiometric Requirements
  - Coverage: 8-12.5 µm
  - No of bands: 30, bandwith: ~150 nm
  - NEΔT: 0.05 to 0.1 K @ 300K
- Geometric Requirements
  - Ground Sampling Distance: 60x60 m2
  - Swath width: 60-100 km
  - Repeat Cycle: tbd
  - Target Revisit: tbd (i.e. pointing)
  - Coverage: global access, regional coverage, focus on core test areas

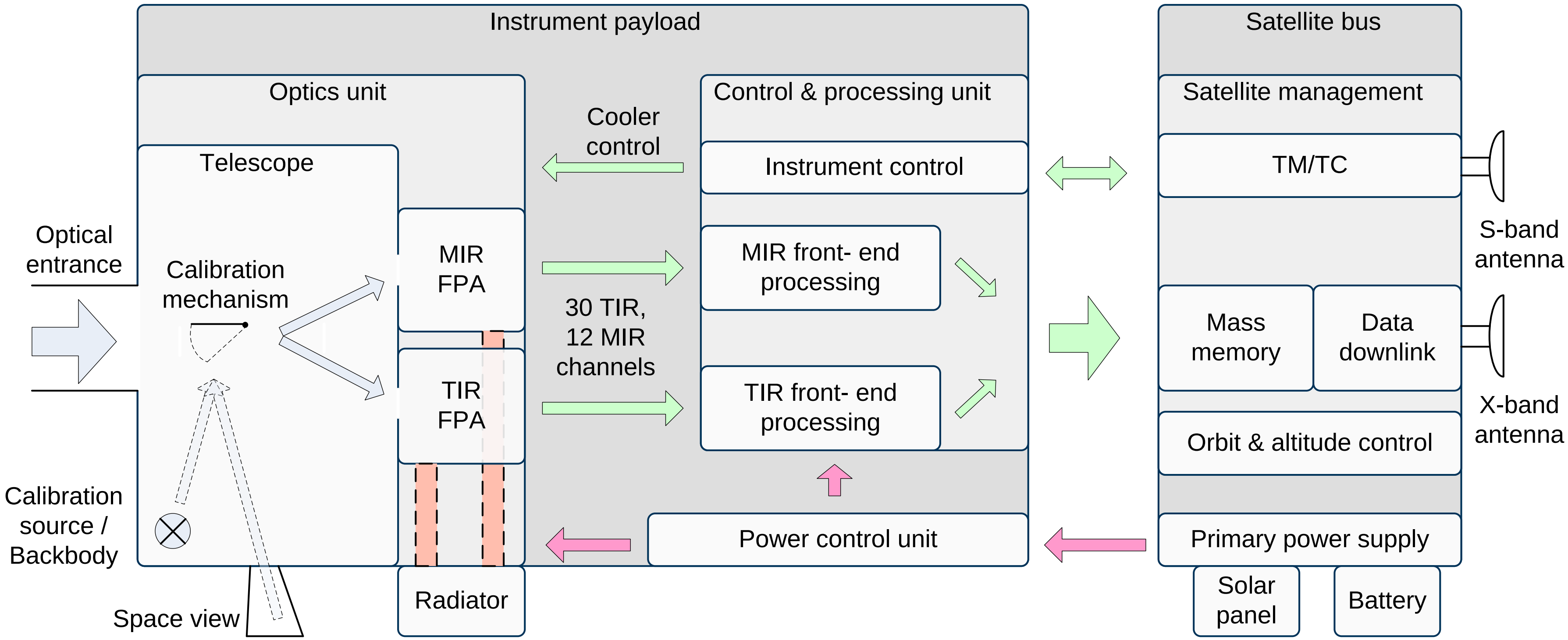
Instrument payload
Optics unit
Telescope
Optical entrance
Calibration mechanism
MIR FPA
TIR FPA
Calibration source / Backbody
Space view
Radiator
Cooler control
30 TIR, 12 MIR channels
Control & processing unit
Instrument control
MIR front- end processing
TIR front- end processing
Power control unit
Satellite bus
Satellite management
TM/TC
S-band antenna
Mass memory
Data downlink
X-band antenna
Orbit & altitude control
Primary power supply
Solar panel
Battery

TIR Instrument Design

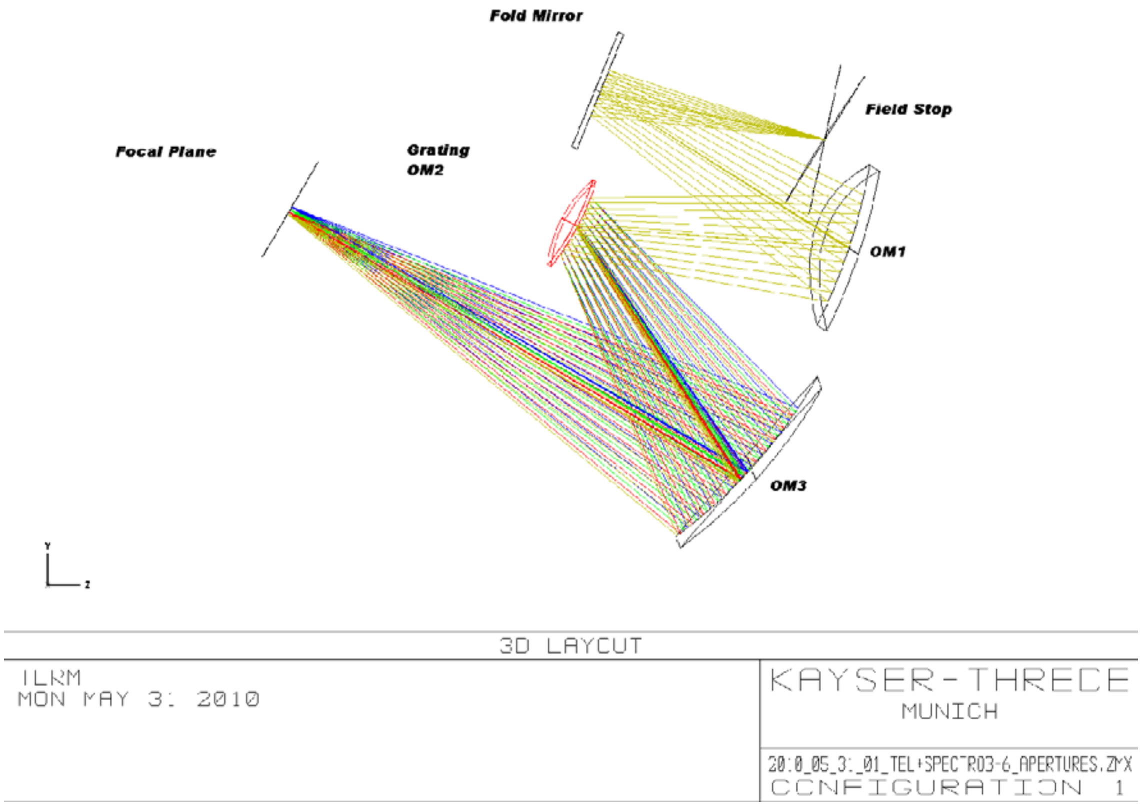

MIR Instrument design

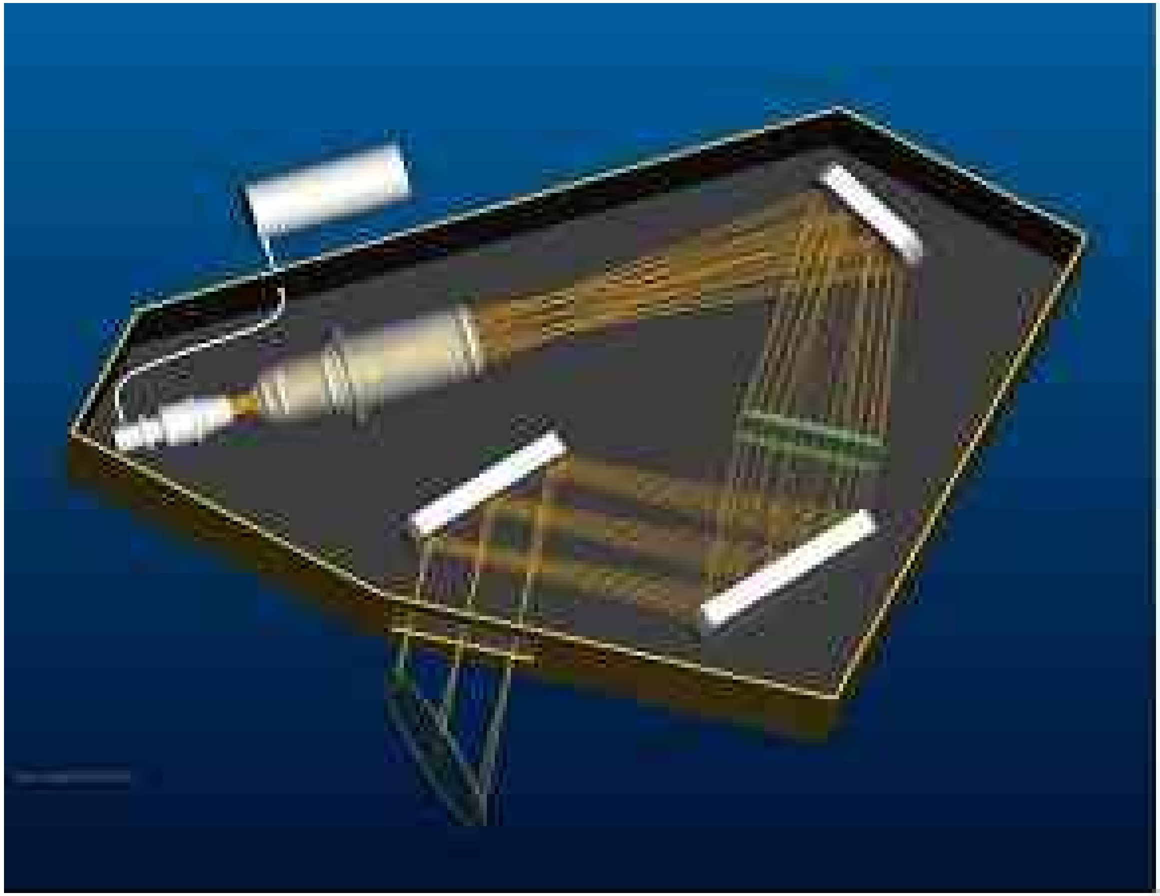

TES-GAP Bus & Orbit

- MITA (Carlo Cavazzi)
- 500 kg total mass
- lifetime of 3 to 5 years
- communication downlink in S- and X-band
- data rate 320 Mbit/s, X-Band
- 400 W electrical power (EOL)
- mass memory 512 Gbit

Orbit (identical to EnMAP)

- sunsynchroneous
- altitude of 640 km
- inclination angle 98°
- Equator crossing at 10:30 LTDN

Mission Schedule

TES-GAP	Start	End
Phase A	Sa 01.01.11	Mo 30.01.12
Phase B	Mi 01.02.12	Mo 30.09.13
Phase C	Di 01.10.13	Sa 28.02.15
Phase D	So 01.03.15	Mi 28.02.18
Phase E	Do 01.03.18	Di 28.02.23
Phase F	Mi 01.03.23	Fr 28.04.23

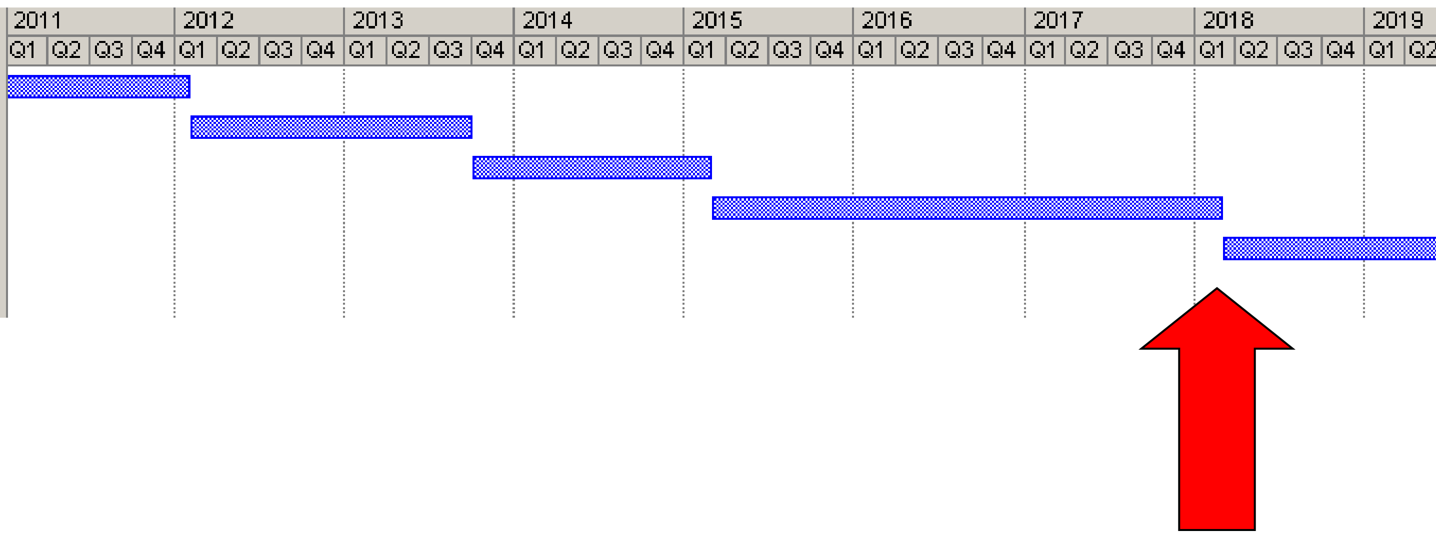

Launch 2018

Summary and Comparison to HyspIRI

	HyspIRI	EnMAP	TES-GAP
Specral Coverage	VSWIR/MIR/TIR	VSWIR	MIR/TIR
Spectral Bands	200+/1/7	200+	~12/30
Spatial Resolution	60 m2	30m2	60-90m2
Swath Width	150km/500km	30km	50-60km
Revisit Time	19 d	24d	~ 20 d
Coverage	Global	Regional	Regional
Purpose	Global Monitoring	Process Understanding	PU + Reginal Monitoring
Lifetime	3 years	5 years	5 years
Est. Launch Date	2021	2014	2018
Propability	-> HyspIRI Team	high	1:30

thank you for your attention!

Cost Estimate

ID	Mission Element	Costs [MEUR]	Comments
01	Satellite Bus	28	
02	Instrument Payload MIR/TIR	55	
03	Launcher	tbd	excluded
04	Ground Segment	12	operations and generic elements excluded
05	Margins	5	
Sum		100	

Processing Chain, Calibration and Data Quality Procedures of the Future Hyperspectral Satellite Mission EnMAP

DLR German Aerospace Centre

<u>M. Bachmann</u>, C. Makasy, A. de Miguel, A. Müller, R. Müller, A. Neumann, G. Palubinskas, R. Richter, M. Schneider, T. Storch, T. Walzel

GFZ Deutsches GeoForschungsZentrum

H. Kaufmann, L. Guanter, K. Segl

EOMAP GmbH&Co.KG

T.Heege, V.Kiselev

EnMAP Hyperspectral Imager

Deutsches Zentrum für Luft- und Raumfahrt e.V. in der Helmholtz-Gemeinschaft

… but first a few words on airborne hyperspectral in Europe:

EUFAR – European Facility for Airborne Research

EUFAR
European Facility For Airborne Research

http://www.eufar.net

- Objective: **Trans-national access to research infrastructure**
- Total of 33 European institutions, 22 instrumented aircrafts
- All major PAFs for airborne hyperspectral data in Europe & Israel included
  - PML/NERC, INTA, DLR, VITO/RSL, USBE, TAU, FUB (ONERA associated)
  - Access to 6+ hyperspectral instruments
- Flight hours, instrument & processing costs covered by European Commission (FP7)

- **Joint Research Activities** – for Hyperspectral:
- To develop **quality indicators and quality layers** for airborne hyperspectral imagery
  - Uncertainty propagation studies for pre-processing
  - Harmonization of data QIs
  - Recommendation on algorithms
- In addition: **Standards & Protocols** ("best practice") for airborne research

EnMAP (**En**vironmental **M**apping and **A**nalysis **P**rogram) is a German hyperspectral satellite mission providing high quality hyperspectral image data on a timely and frequent basis. Main objective is to investigate a wide range of ecosystem parameters encompassing agriculture, forestry, soil and geological environments, coastal zones and inland waters.

OUTLINE

- EnMAP mission (Characteristics, Elements)
- Automatic and operational processors for product generation
- Mission status

Mission and Instrument Characteristics

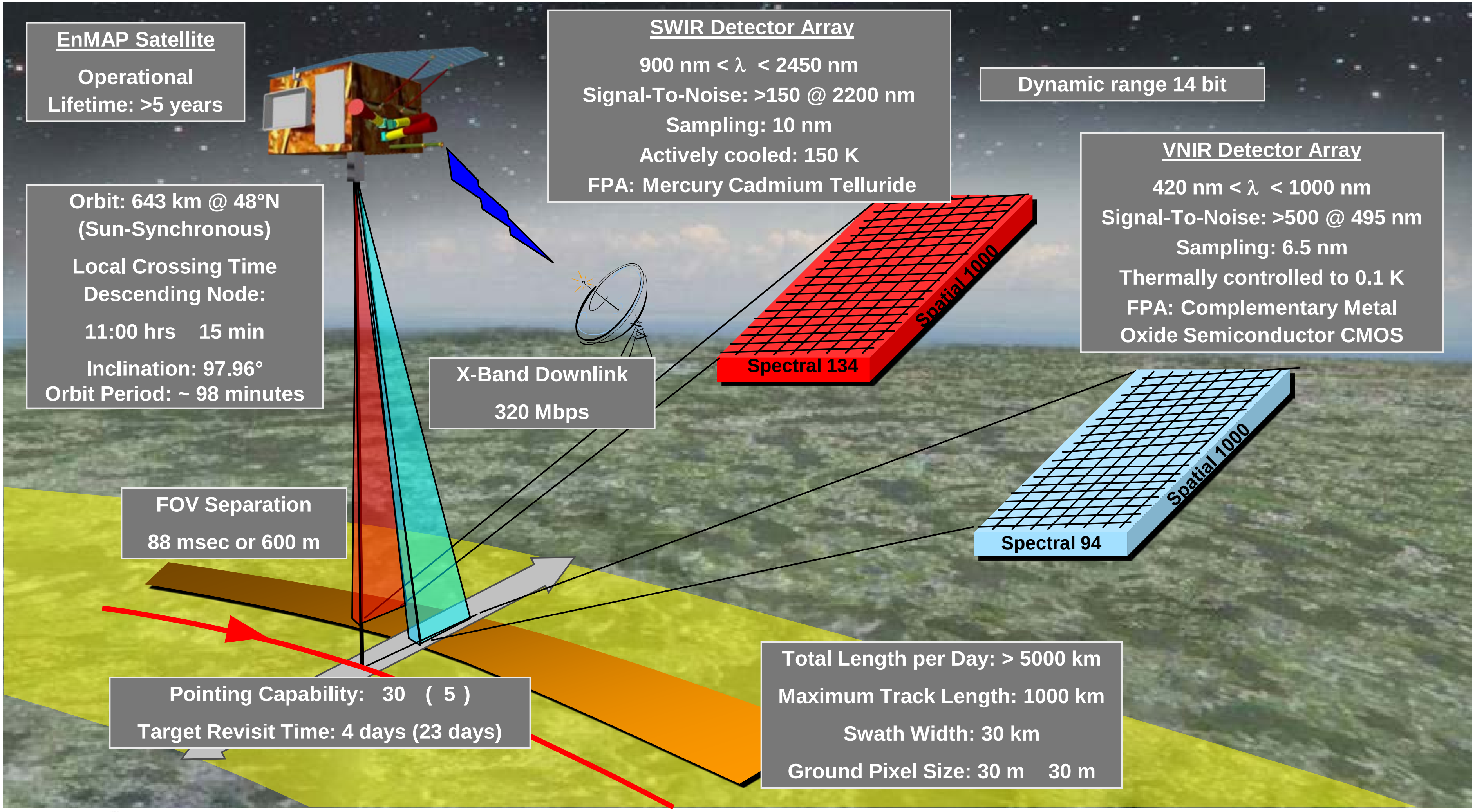

Overview Processing Chain

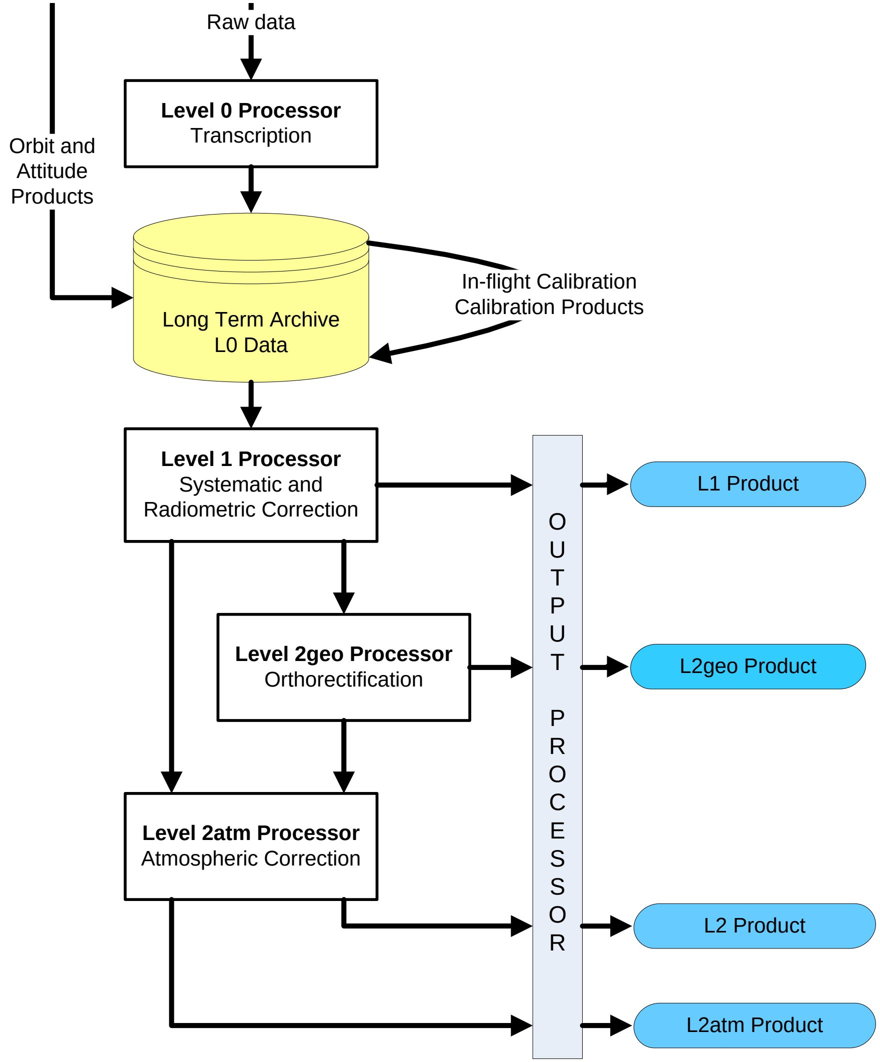

Level 0 Processor

The transcription processor de-compresses and collects information from different data streams, extracts and interprets information, performs screening, generates image tiles, adds data quality information

Level 1 Processor

The systematic/radiometric correction processor converts raw image pixels values to at-sensor radiance physical values

Level 2geo Processor

The geometric correction processor orthorectifies images using different methods (with and without automatically extracted GCPs)

Level 2atm Processor

The atmospheric correction processor produces reflectance values for land and water areas and generates cloud masks.

Output Processor

The output processor generates the product, the metadata and derives the log information from the information produced by the logging service.

Overview Processing Chain

Ensuring data quality:

- **Automated** within processors
- **Interactive** procedures
- **Independent** validation

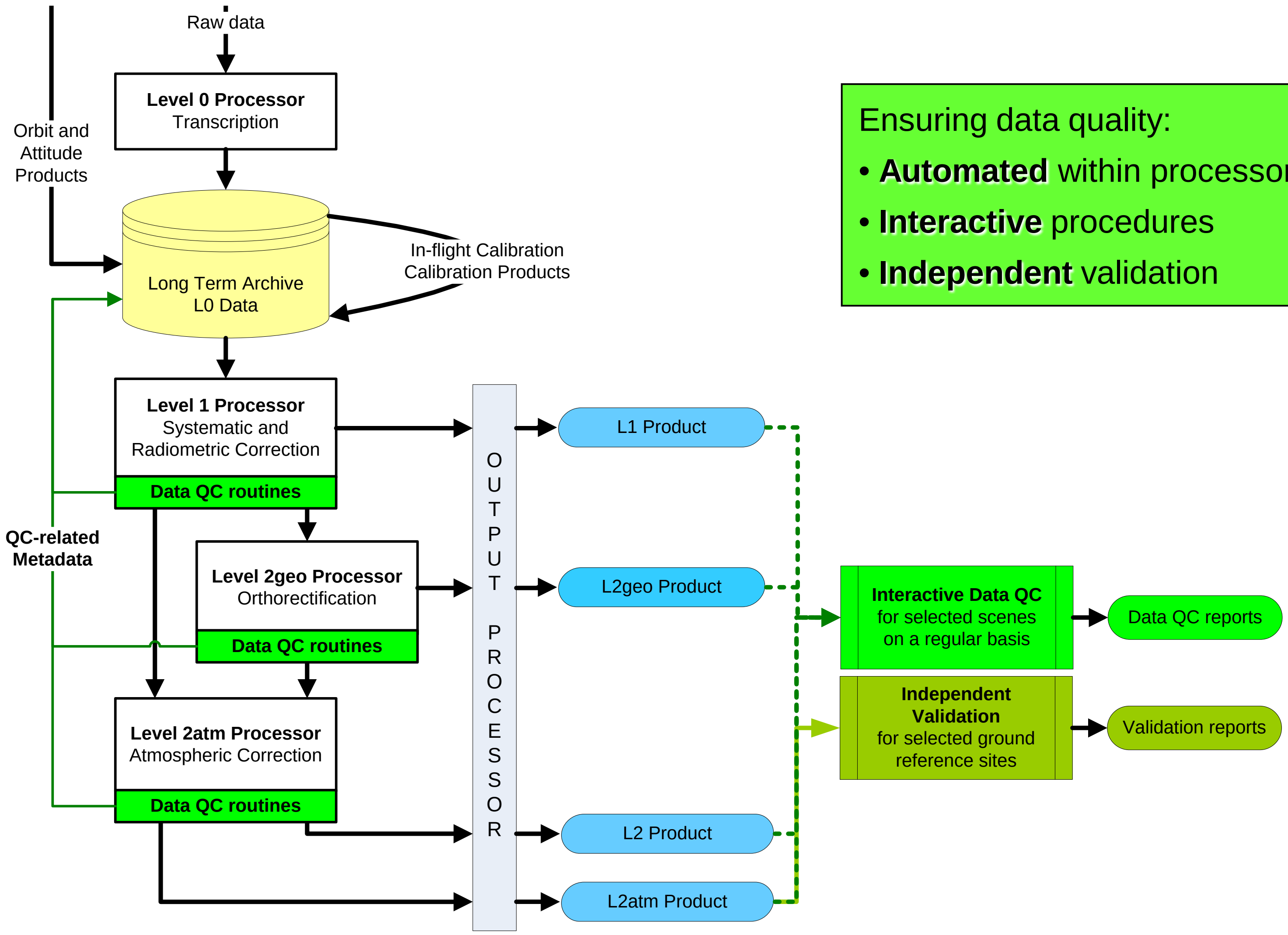

EnMAP Level 1 Processing

Performs:

Systematic Correction

Radiometric Correction

Creates:

At-sensor radiance

Metadata for further processing

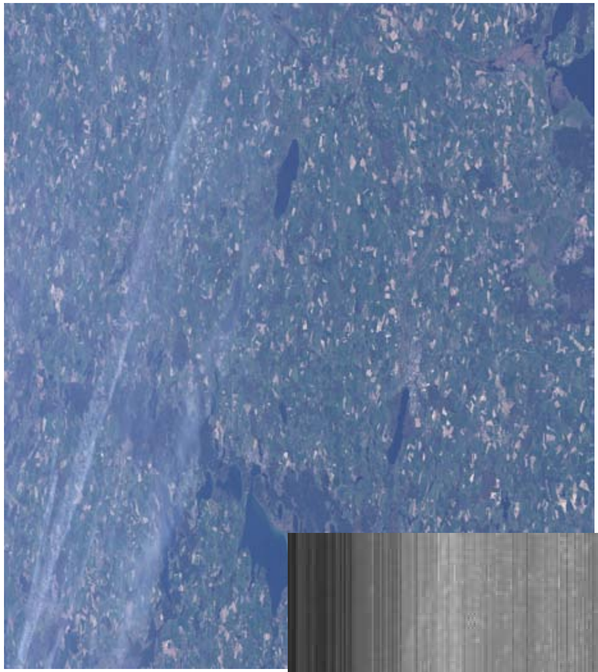

Example: ALOS Processor on behalf of ESA

EnMAP Level 1 Processing – detailed steps

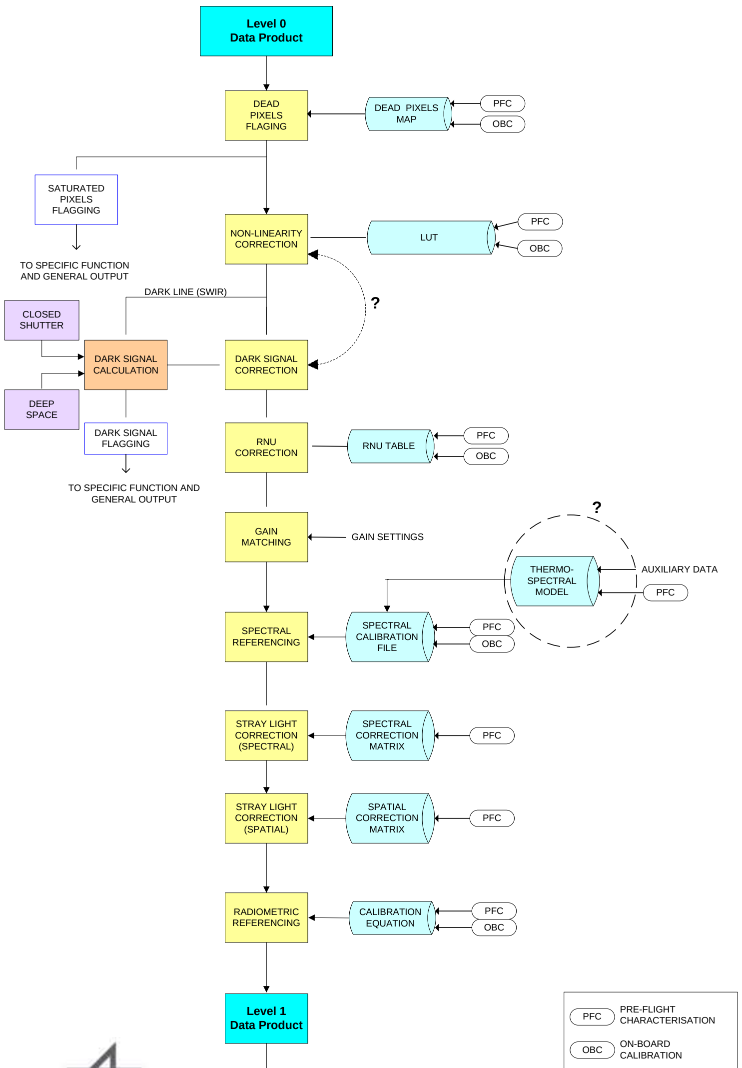

- Bad (dead & suspicious) pixel flaging
- Non-linearity correction
- Dark signal correction
- RNU correction
- Gain Matching (VNIR)
- Spectral referencing
- Spectral straylight correction
- Spatial straylight correction
- Radiometric referencing

EnMAP Level 2geo Processing

Performs
Geometric image corrections realized by different process flows

Creates
Orthoimages
Acc. < 3 GSD without Ref.
< 1 GSD with Ref.

Selectable Parameters
Projection:
UTM (Zone of center) (± 1 zone)
Geographic

Resampling:
Bi-cubic
Bi-linear
Nearest Neighbour

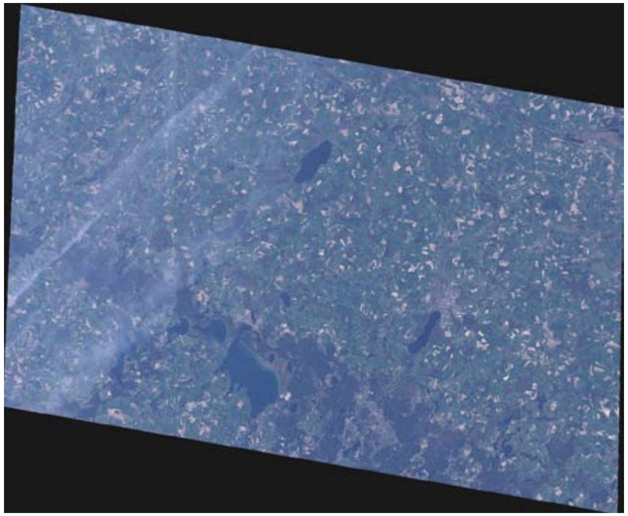

Example: ALOS Processor on behalf of ESA

EnMAP Level 2geo Processing using Reference Scenes

Original image

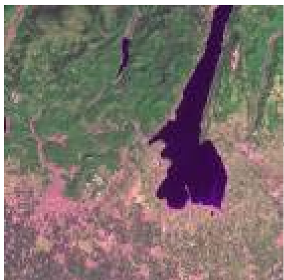

Global reference image database

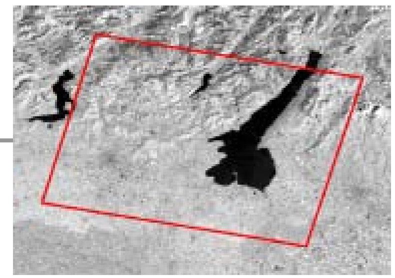

Reference image

Global DEM database

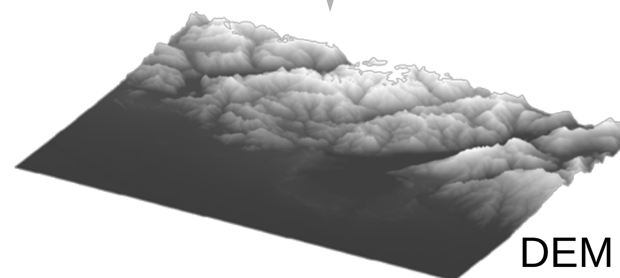

DEM

Matching

Tie points
GCP / ICP

Improvement
of Line-of-Sight Vectors

Generation of ortho image

Metadata
- **state vectors**
- **attitude**
- **sensor model**
- **time sync**
- **....**

Ortho image

Quality parameters derived from ICPs

EnMAP Level 2geo Processing
with automatic GCP extraction – heritage

European Mosaick (~3700 Scenes)

- IRS-P6 LISS III
- SPOT 4 HRVIR
- SPOT 5 HRG

Overall mean accuracy w.r.t. reference data set (~450 ICPs per 1000 km²)
RMSE$_{x/y}$ ~ 10 m (CE64 ~14m)

EnMAP Level 2atm Processing

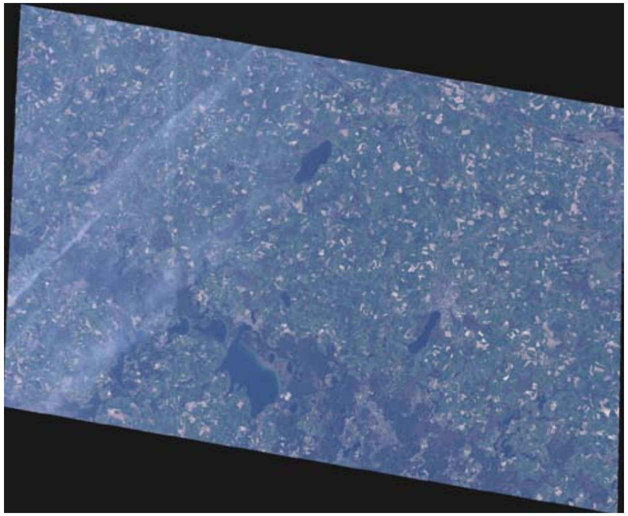

Performs
Atmospheric Correction
over land and water
Haze / Cirrus Removal
based on
  ATCOR (Land)
  MIP (Water)

Creates
Surface Reflectance
haze/cloud/water/land mask

Selectable Parameters
Only land / water
Combined product (if appl.)
Haze / cirrus removal
Flat / rugged terrain
Water type (clear / turbid)
…

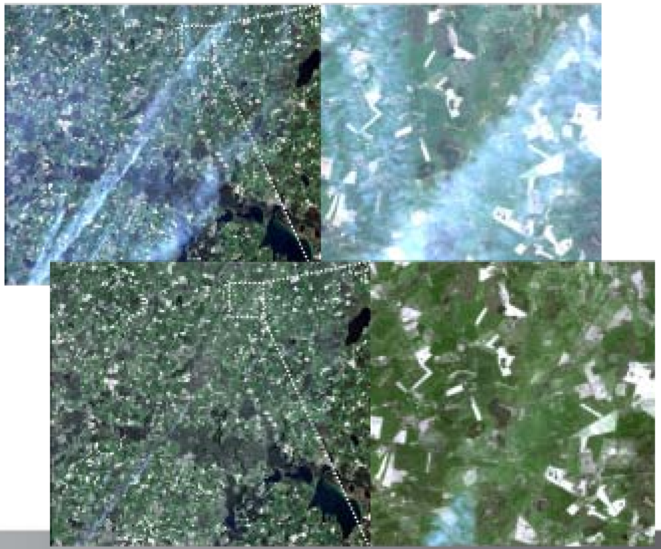

Example: ALOS Processor on behalf of ESA

Level 2atm Land Surface Processing

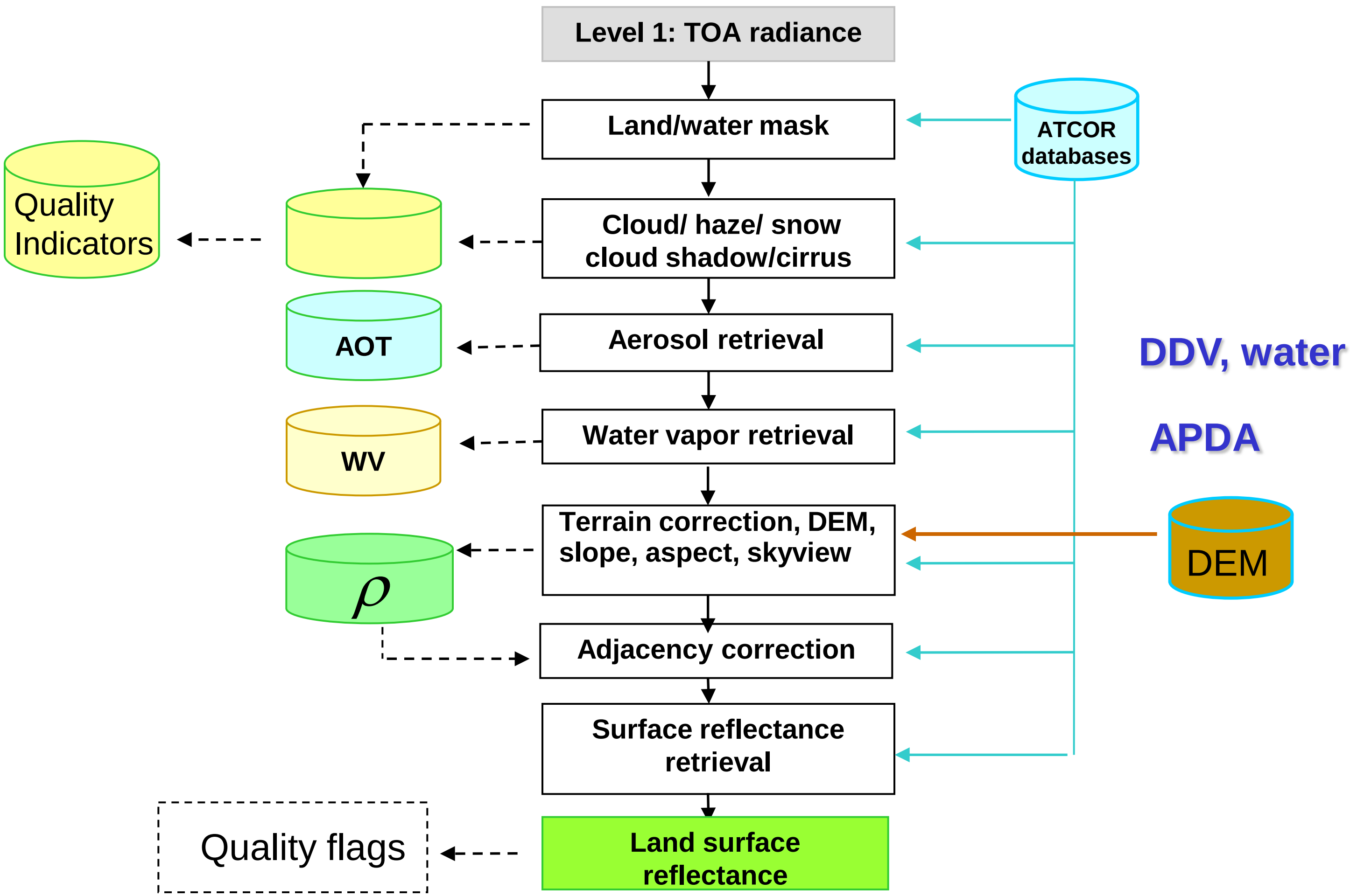

Level 2atm Water Surface Processing

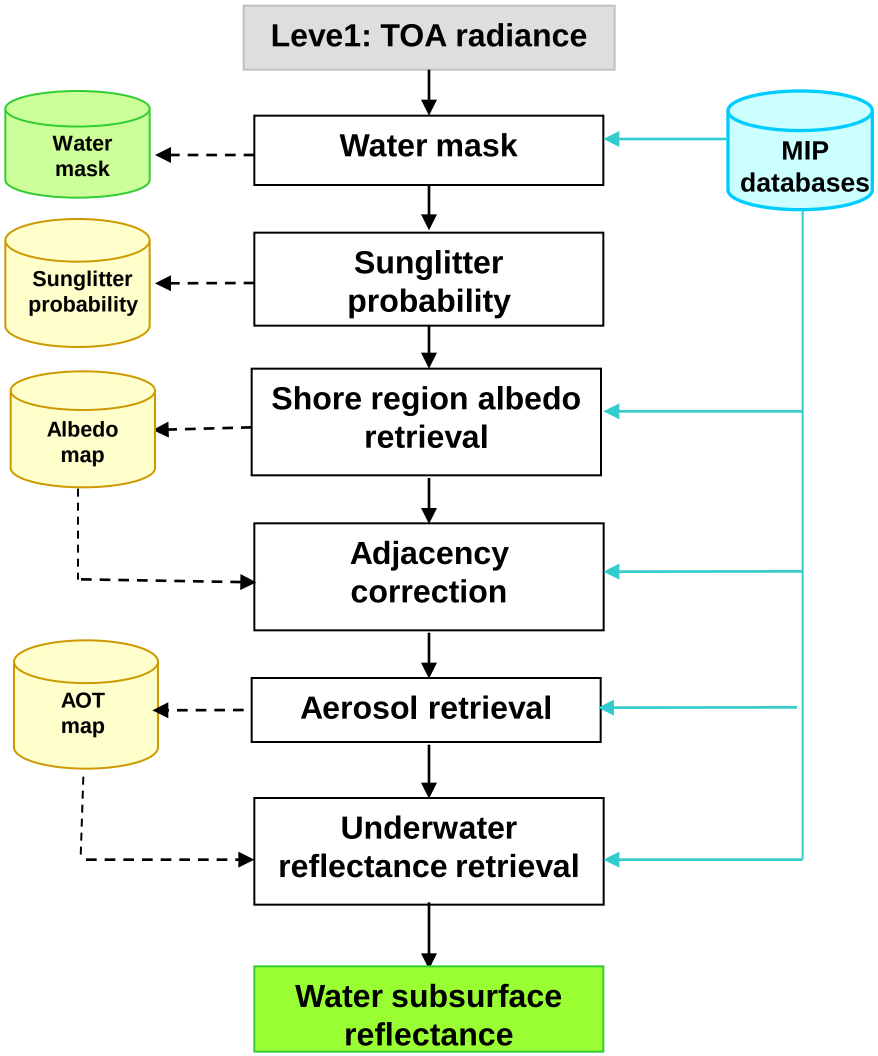

ATCOR : Example of Cloud Shadow Removal

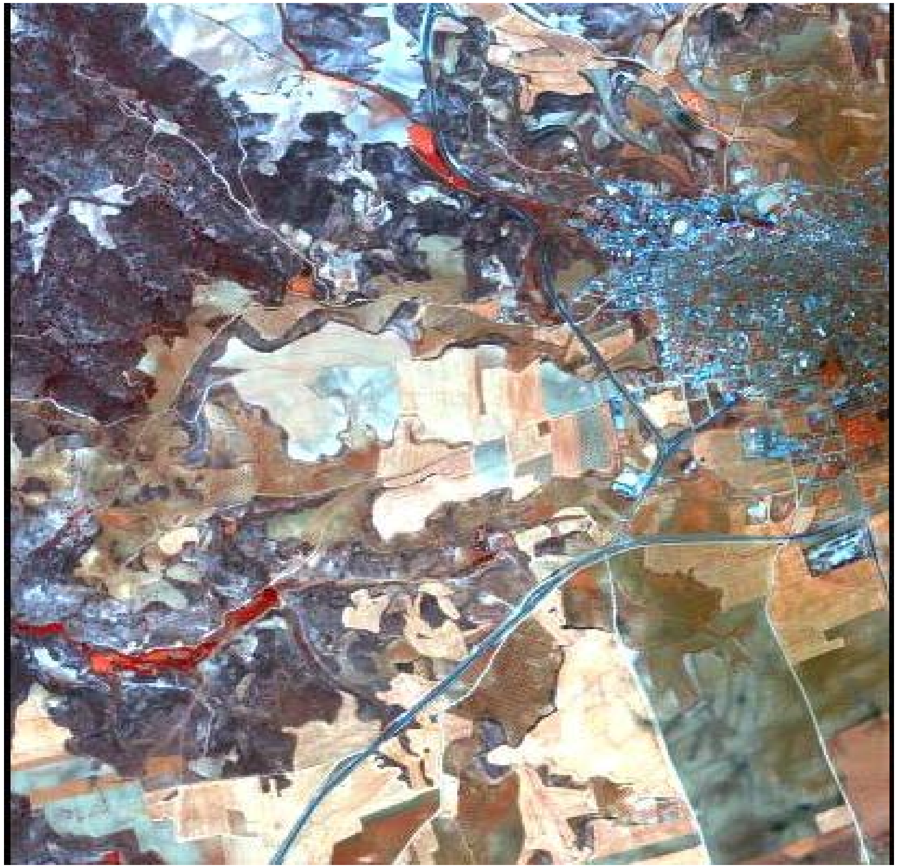

HyMap scene, Chinchon, Spain, 12 July 2003, RGB=878, 646, 462 nm

Ref: Richter & Mueller, 2005

ATCOR : Example of Cirrus Removal

AVIRIS scene, Bowie MD, 7 July 1996, RGB=634, 547, 458 nm

Ref: Gao et al., 2002

EnMAP Level 2atm Processing
flat terrain vs. rugged terrain atm. correction

Radiation components flat terrain

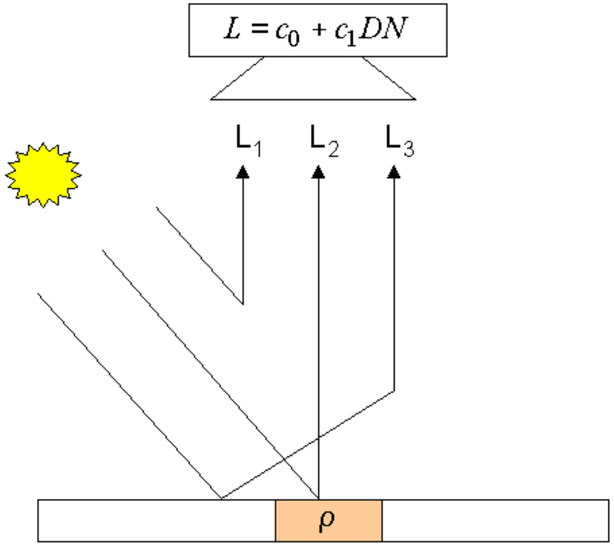

Surface reflectance

$$\rho = \frac{\pi\,(L - L_1)}{\tau\,(E_{dir}\,\cos\theta_s + E_{dif})}$$

Radiation components rugged terrain

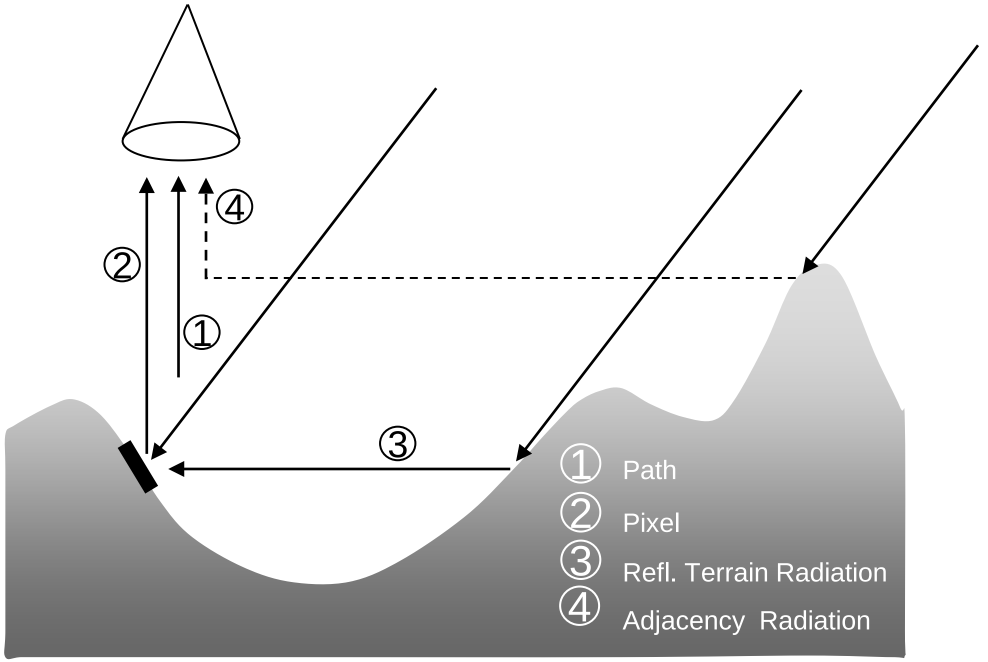

EnMAP Level 2atm Processing

high geometric accuracy necessary for topo correction

illumination map cos(local SZA)

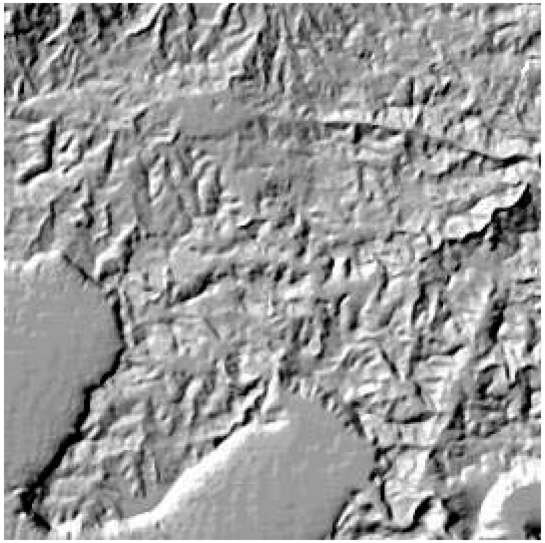

atm + topo corrected

Geom. Acc. < 1 pixel

atm + topo corrected
3 pixel shift →

Data QI Example: EnMAP L2_atm product

EnMAP Hyperspectral Imager

QC Entry	Parameter	Category	Report format	Metadata (DIMS IIF)	
				Internal	Public
			(**R**)eport (**L**)ayer		
overallQuality	**Overall data quality**	all	R	Y	Y
processorLog	Warning messages in processor log	IMG	R	Y	
sceneSZA	**Solar zenith angle**	IMG	R	Y	Y
sceneSunglint	Sun glint / sun glitter probability	IMG	R	Y	
cloudCover	**Percentage clouds**	ATM	R, L	Y	Y
hazeCover	Percentage haze	ATM	R, L	Y	Y
cirrusCover	Percentage cirrus	ATM	R, L	Y	Y
cloudShadow	Percentage cloud shadow	ATM	R, L	Y	Y
sceneWV	**Average scene WV**	ATM	R	Y	Y
sceneVIS	Average scene visibility / AOT	ATM	R	Y	Y
sceneAtmParam	**Validity of atm. correction**	ATM	R	Y	
sceneTerrain	DEM artifacts in terrain correction	ATM	R, L		
internalMasking	**Masks** generated during processing (cloud, shadow, haze, land / water)	ATM	R		
specCal	Artifacts related to spectral calibration / ATCOR LUTs	SPEC, ATM	R		

Blue: implemented in L2_atm land / L2_atm water processor

Mission Status

2003: Call for Proposals for a future Earth observation mission by DLR Agency

2004: EnMAP selected for Phase A study

2005: Phase A: study accomplished successfully (SRR)

2006: EnMAP selected for Phase B study

2007: Phase B: study accomplished successfully (PDR)

2008-2010: Phase C: Detailed Design (GS CDR passed in July ‘10) ✓

2010-2013: Phase D: Production, Test, Verification, Validation (ORR)

2014: EnMAP Launch with PSLV (LEOP & Commissioning Phase)

2014-2019: Operations Execution

2019- : De-orbiting

Thanks
for
your
attention

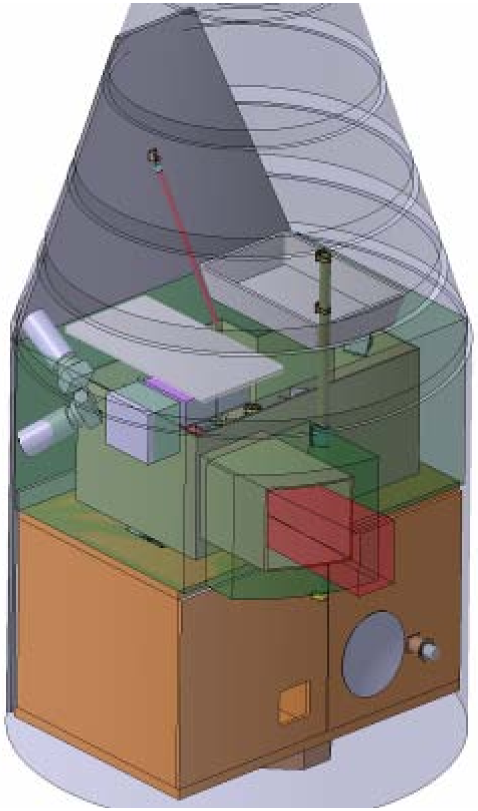

www.enmap.org

Backup Slides …

On-Board Calibration Means

Technical tools and operational modes to perform the necessary measurements for on-orbit calibration (and monitoring of instrument properties) throughout the mission:

- Shutter/calibration mechanism for dark value and calibration measurements
- Full aperture diffuser for Sun calibration (radiometric, absolute)
- Main integrating sphere (white Spectralon®) for relative radiometric assessment
- Secondary sphere (doped Spectralon®) for spectral calibration assessment
- Focal plane LEDs for linearity measurements

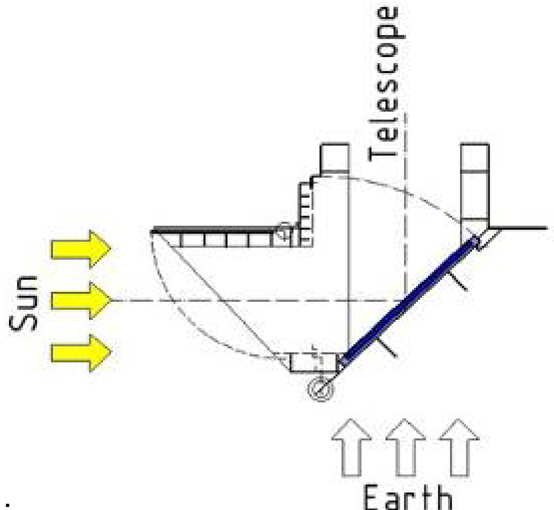

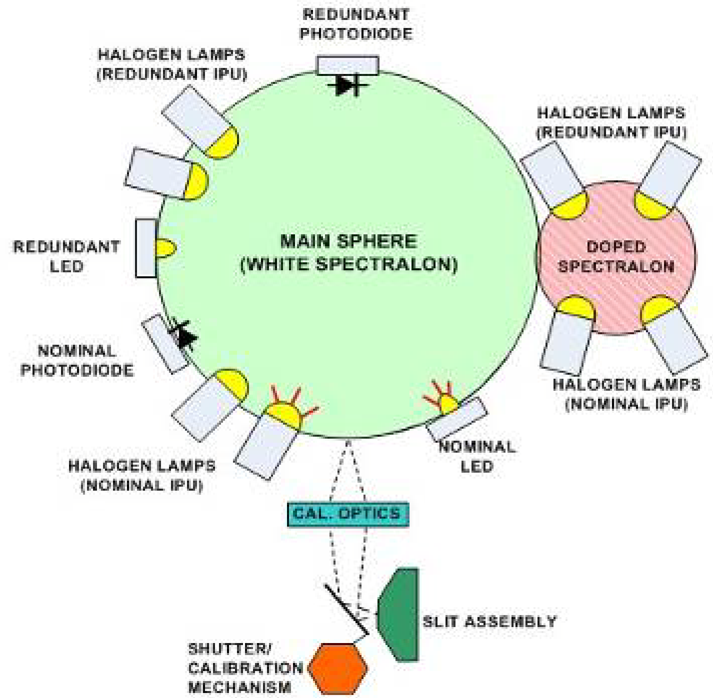

HSI in-flight calibration means except focal plane LEDs

(drawing © Kayser-Threde)

Calibration measurements

Summary of calibration measurements

Calibration type	Time	Frames	Data Volume	Frequency
Dark (shutter)	23 sec	2 * 128	0,27 GB	each datatake
Dark (deep space)	30 sec	1 * 1024	1,38 GB	every 3 months
Relative radiance calibration	17 min 13 sec	1 * 512 (5steps)	1,66 GB	weekly
Sun calibration	140 sec	2 * 1024	1,38 GB	monthly
Spectral calibration	5 min13 sec	1 * 1024	0,83 GB	monthly
Linearity measurement	< 5 min	2 * 128 * 40	5.8 GB	monthly

Data Quality Control

Including Quality Indicators (QI) for

General sensor characterization

(e.g., spectral smile)

Sensor calibration issues

(e.g., striping in pushbroom sensors)

Sensor performance during data acquisition

(e.g., data drops)

External conditions during overflight

(e.g., cloud coverage)

Processing

(e.g., uncertainty of geo-location)

Quality of auxiliary data used in processing

(e.g., DEM accuracy)

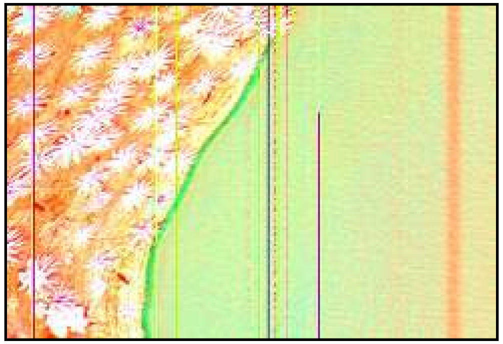

Addressing data QC related to radiometry

Tasks: assessment of **Data Properties** related to radiometry (**QC flag, QC report**),
indication to trigger on-board calibration (S-320) and instrument monitoring (S-340)

Issues: incorrect or instable radiometric calibration (gain & offset values),
contamination of detector elements

Approach for **automated** Data QC within L1 processor:

- Tests for scene / scene subset homogeneity
- Comparison with nominal values for:
- Difference in column mean DN / mean radiance and STDEV (=> **striping**)
- Correlation of neighboring bands within one column (=> **single detector failures**)
- Overall band-to-band correlation matrix (=> **stability of radiometric calibration**)

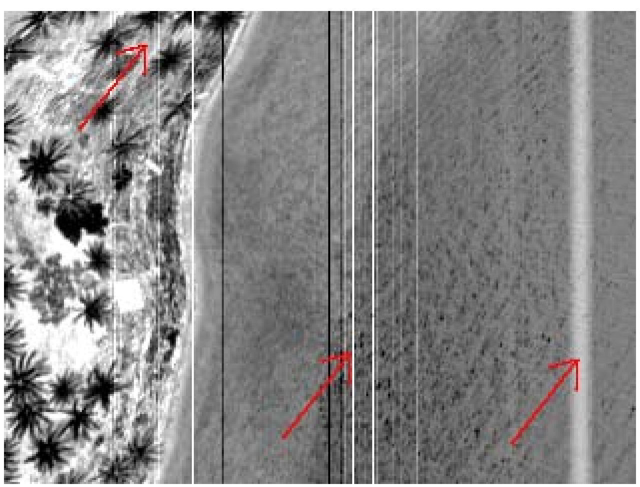

Striping in Pushbroom sensor data (MNF-transformed)

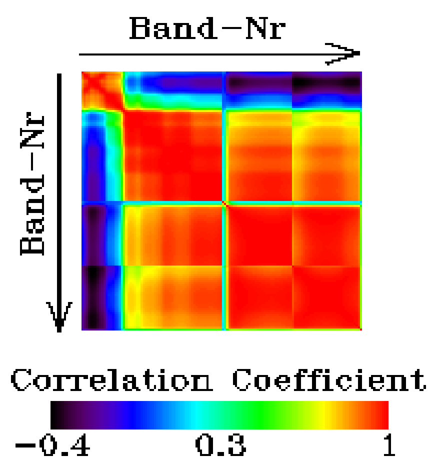

Band correlation matrix (no band defects)

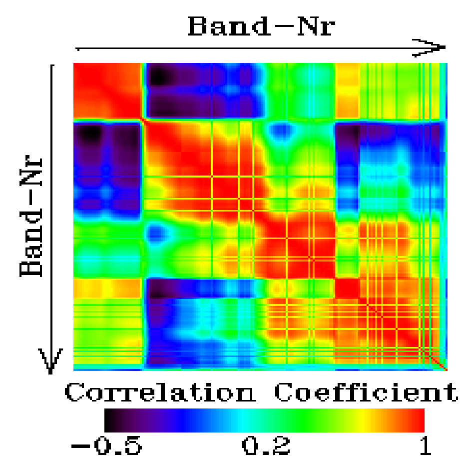

Band correlation matrix (known de-calibration issues)

QC Entry	Parameter	Category	Report format	Metadata (DIMS IIF)	
				Internal	Public
			(**R**)eport (**L**)ayer		
overallQuality	Overall data quality	all	R	Y	Y
stripingBanding	Artifacts related to **radiometric calibration**	RAD	R	Y	
dualGain	Artifacts related to dual gain	RAD	R, L		
saturationCrosstalk	Saturation, cross-talk, blooming	IMG	R, L	Y	Y
generalArtifacts	Other **artifacts** / suspicious pixel	IMG	R, L	Y	
sensorLog	Warning messages related to sensor	IMG	R	Y	
processorLog	Warning messages in processor log	IMG	R	Y	
internalMasking	**Masks** generated during processing (cloud, shadow, haze, land / water)	ATM	R		
specCal	Artifacts related to **spectral calibration**	SPEC	R		
signalToNoise	Signal-to-noise estimate	IMG	R		

Blue: implemented in L1 processor

EnMAP Data QC for L2_geo products

QC Entry	Parameter	Category	Report format	Metadata (DIMS IIF)	
				Internal	Public
			(**R**)eport (**L**)ayer		
orthoTerrain	DEM-related displacements	GEO	R	Y	
orthoRMSE	**Geometric accuracy** of the orthoimage (I)	GEO	R	Y	Y
orthoResidual	Geometric accuracy of the orthoimage (II)	GEO	R	Y	

Blue: implemented in L2_geo processor

Mission parameter

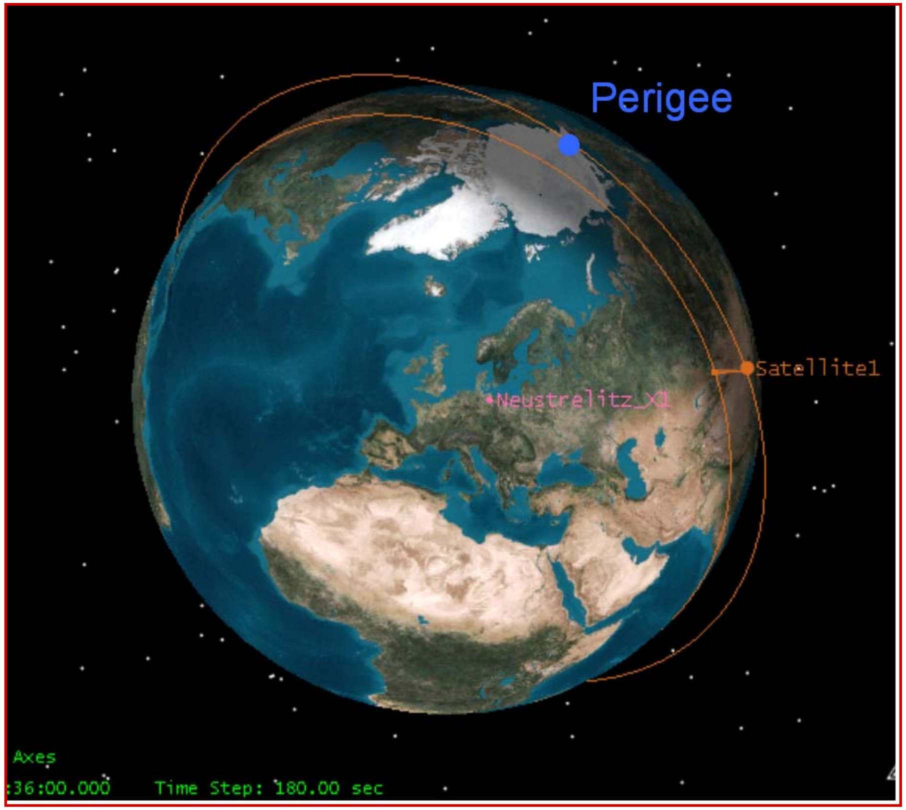

- Sun-synchronous, 11:00 LTDN LEO – reference altitude 653km
- 3 axis stabilized platform with OCS
- mass 850 kg / power 550 W avg.
- 512 Gbit mass memory / 320 Mbit/s X-band science data downlink
- 4 day global accessibility (30 off-nadir)
- 4 day target revisit capability
- up to 50 data takes per day / total length 5000km

Sensor Parameter

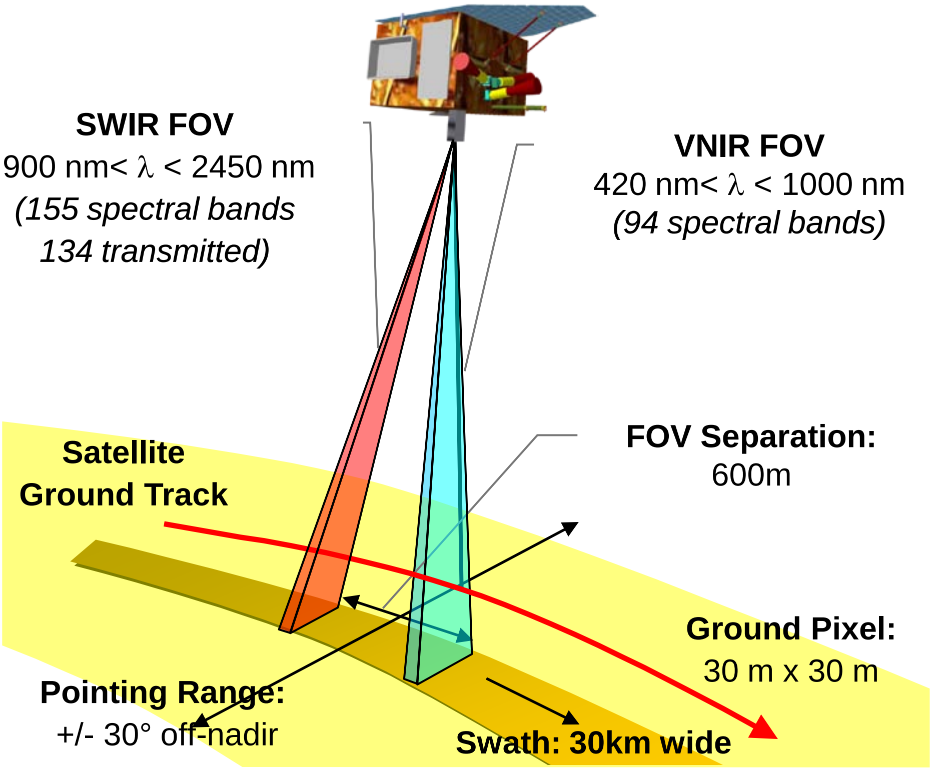

schlanke Kontur - Leitfarbe

- Pushbroom type hyper spectral imager
- Wavelength 420 - 2450 nm
- 30m GSD, 30 km swath (nadir)
- 228 spectral bands
- VNIR 6.5 nm sampling
- SWIR 10 nm sampling
- SNR > 150 @ 2200nm (ref. radiance)
- Polarization sensitivity < 5%
- Smile and Keystone < 0.2 pix
- Pointing knowledge 100m
- Radiometric accuracy 5%
- Radiometric stability 2.5%
- Response Linearity 0.5%
- Spectral accuracy 0.5nm / 1nm

Satellite Design

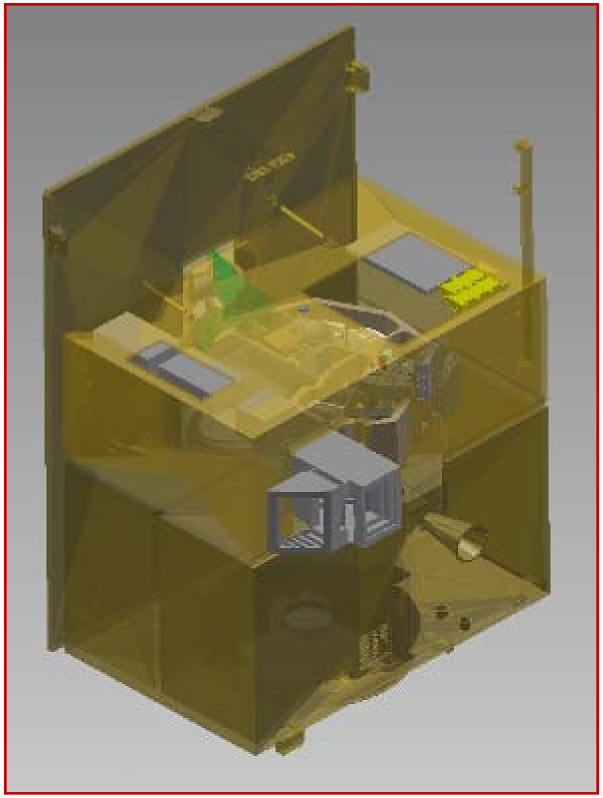

Total Weight: ca. 850 kg

Aver. Power: 450 W

512 Gbit mass memory

3 axis stabilized platform

Pointing Stability: 1,5 m / 4 ms

Pointing Knowledge: 100 m

30 off nadir pointing for observation

Hydrazine propulsion system for orbit maintenance & disposal

320 Mbit/s X-Band science data downlink

Lifetime in Orbit: > 5 years

Instrument Optic Unit Design

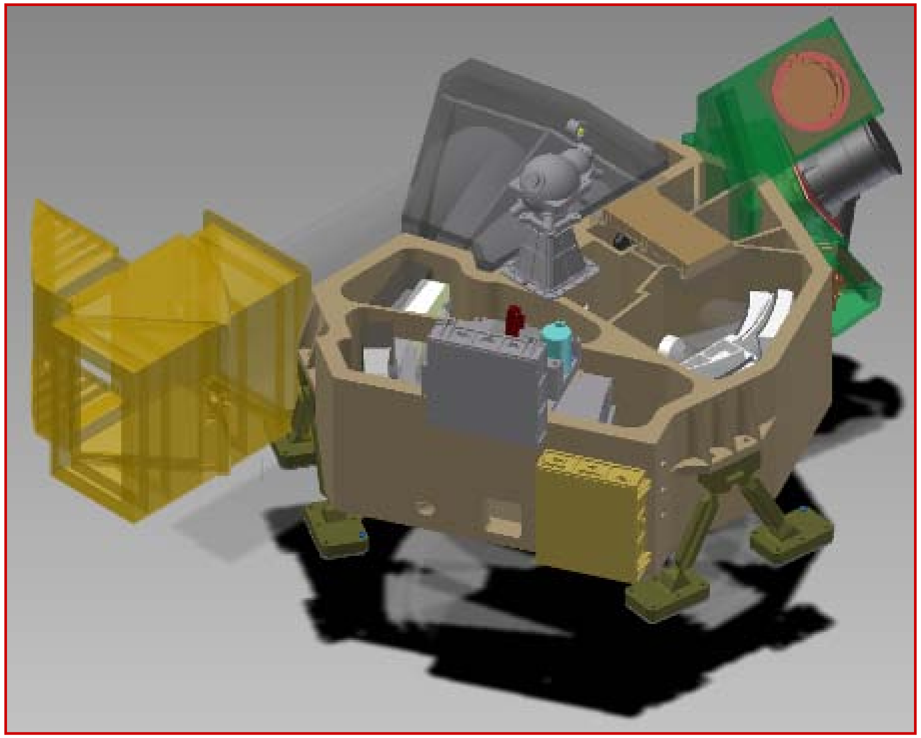

- Polished NiP coated Aluminum mirrors
- Monolithic Aluminum structure
- Quasi-isostatic mounting to platform
- Starcameras attached to IOU for pointing knowledge
- Redundant SWIR FPA due to cryocooler without flight heritage
- Gravity release < 5µm – opt. elements
- Eigenfreq. > 100 Hz
- Active thermal stabilization to 21 C ± 1K

Instrument Optic Design

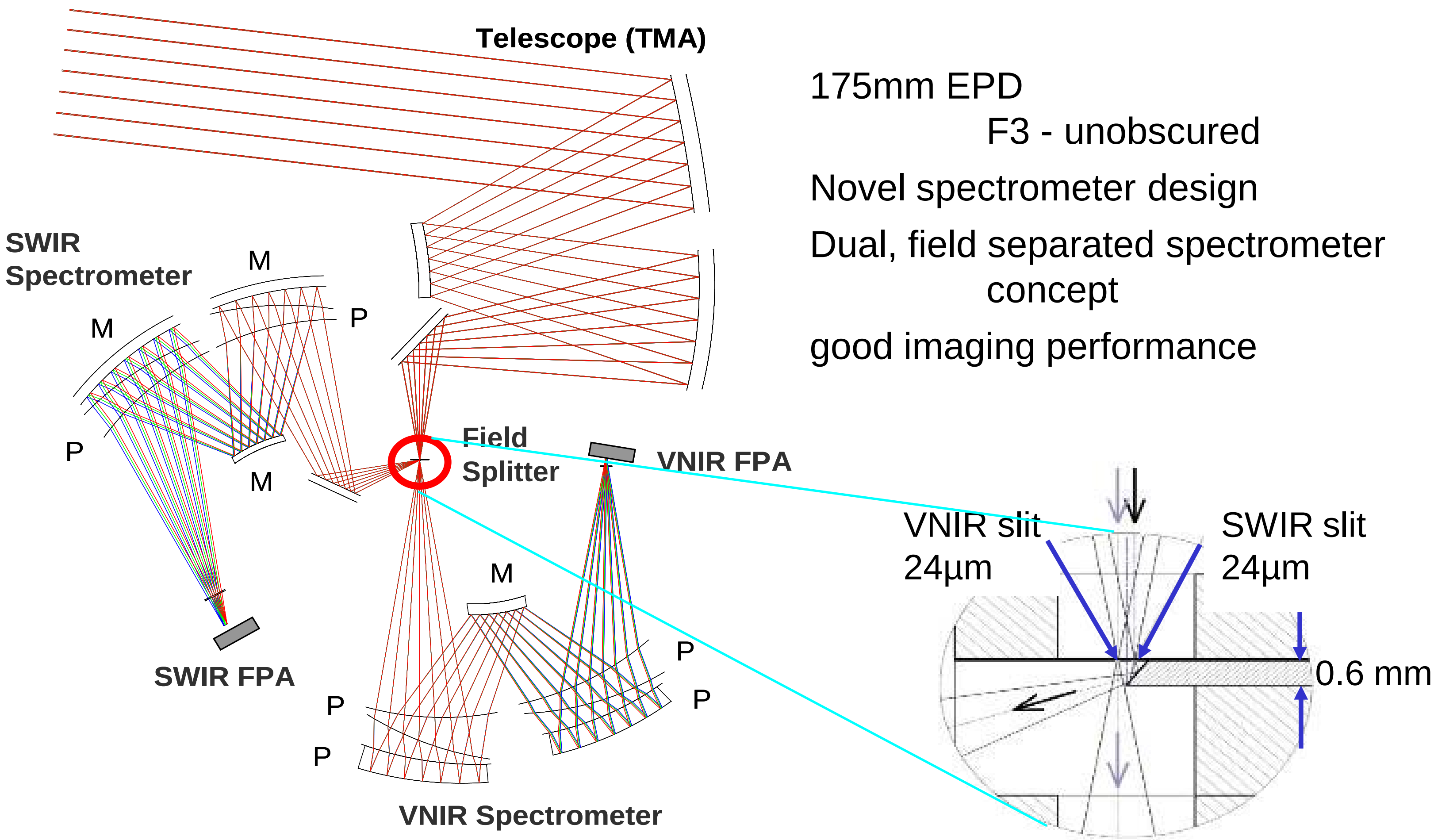

- 175mm EPD
  F3 - unobscured
- Novel spectrometer design
- Dual, field separated spectrometer concept
- good imaging performance

On-Board Calibration

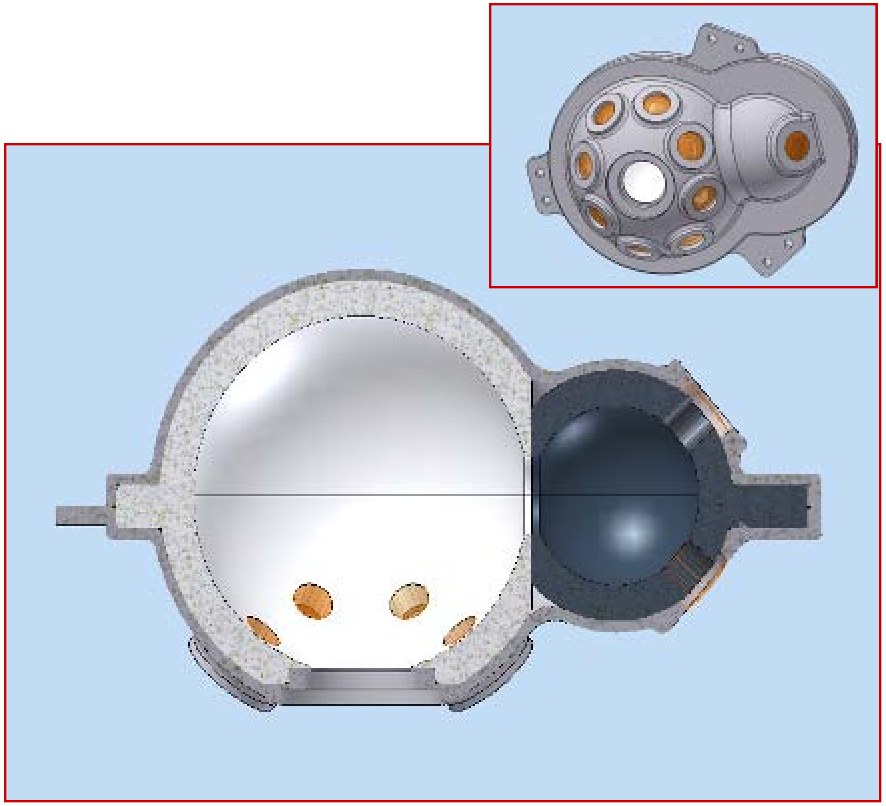

Integrating Sphere (KT design)

Radiometric stability check: “integrating sphere with sources at different levels”

Sources: 10W Halogen lamps
white high power LEDs

Coupling to spectrometers via imaging optics

Different levels by driving varying currents

………..

FAD?

Mission Elements

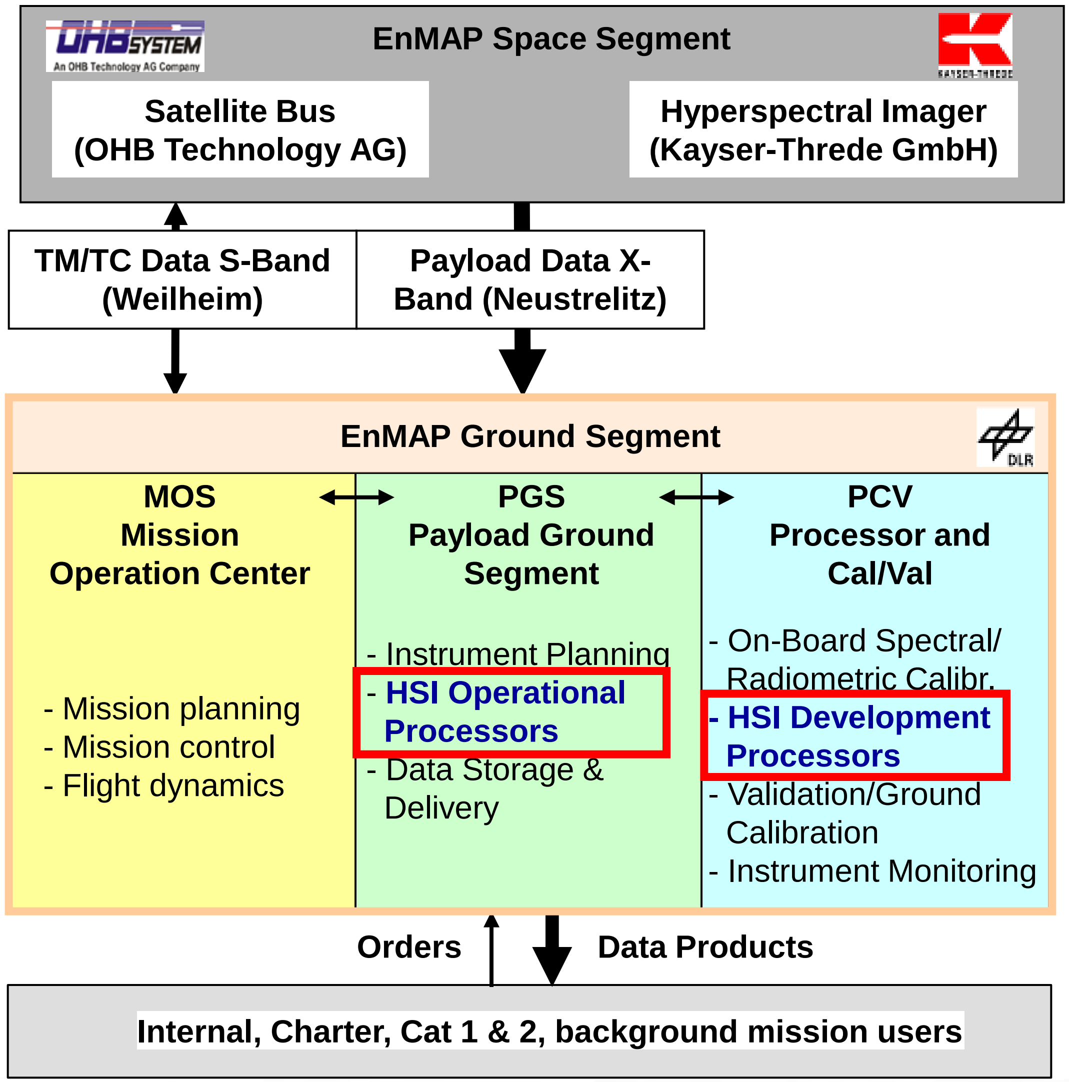

CAL/VAL ACTIVITIES ON EUROPEAN VOLCANOES TEST SITES IN THE VNIR-SWIR SPECTRAL RANGE.

Massimo Musacchio,
Maria Fabrizia Buongiorno, Stefania Amici, Stefano Corradini, Alessandro Piscini, Luca Merucci, Valerio Lombardo, Malvina Silvestri, Claudia Spinetti, Laura Colini.

Istituto Nazionale di Geofisica e Vulcanologia, Remote Sensing Unit, Rome Italy

Summary

- Topographic And Atmospheric Effects Removal Tool: Cirillo
- Test Sites Description and CAL/VAL activities on
  - Mt Etna
  - Pico de Teide
- PRISMA Mission and CAL/VaL test site

Introduction

- The accuracy of space measurements to monitor European active volcanoes (not only!) mainly depends on
  - The periodic validation of the data acquired by space
  - The effectiveness capability of atmospheric correction tool to remove Atmospheric and Topographic effects

TOPOGRAPHIC AND ATMOSPHERIC EFFECTS REMOVAL TOOL: CIRILLO

CIRILLO: basis

- CIRILLO is a procedure for the correction of spaceborne images acquired in the VIS-SWIR spectral range (0.40 μm 2.5 μm).

- The atmospheric terms needed by CIRILLO are computed by the well known radiative transfer models MODTRAN4.0 and 6S (adjacency effects).

CIRILLO: basis

- CIRILLO can produce the TOA ground reflectance that can be used as a first approximation of the actual ground reflectance. This option does not require any run of the radiative transfer models, hence the user has not to provide atmospheric data nor digital elevation models
- CIRILLO, starting from an at-the-sensor radiance image, produces a ground reflectance image corrected from atmospheric effects and from illumination changes due to tilted surfaces (**topographic effect**).
  - CIRILLO computes and corrects, starting from digital terrain models and solar position the illumination, changes due to relief.

Source-Target-Sensor schema

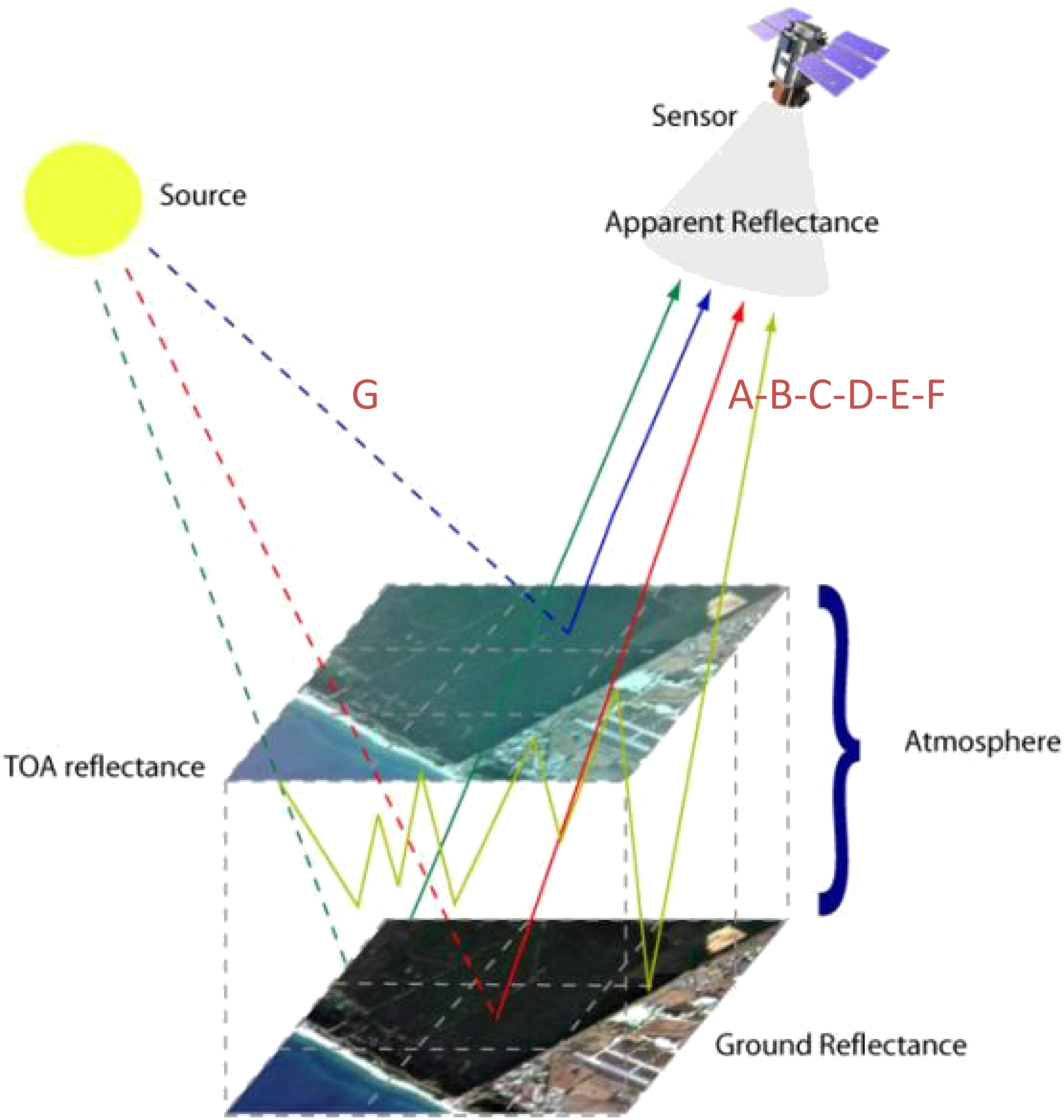

A. The sun radiance that reaches directly the pixel viewed by the sensor (target) and that is directly reflected by the target to the sensor;
B. The sun radiance that reaches directly the pixel viewed by the sensor (target) and that is reflected by the target to the sensor following a multiple scattering path;
C. The sun radiance that reaches the target following a multiple scattering path and that is directly reflected by the target to the sensor;
D. The sun radiance that reaches the target following a multiple scattering path and that is reflected by the target to the sensor following a multiple scattering path;
E. The sun radiance that directly reaches the surface surrounding the target and that is reflected by the surface to the sensor following a multiple scattering path;
F. The sun radiance that reaches the surface surrounding the target following a multiple scattering path and that is reflected by the surface to the sensor following a multiple scattering path;
G. The sun radiance that is directly scattered by the atmosphere to the sensor without reaching the ground.

All of these terms, with the exception of **G**), are also influenced by the orientation of the surface with respect to the sun illumination direction.

Radiative transfer model

$$\rho^{*} = Tg\left\{\rho_a + \frac{\rho}{1-\langle\rho_e\rangle s}\left[\beta\cdot\exp\left(-\frac{\tau}{\cos\theta_s}-\frac{\tau}{\cos\theta_v}\right)+t_{ds}\cdot\exp\left(-\frac{\tau}{\cos\theta_v}\right)\right] + \frac{\langle\rho_e\rangle}{1-\langle\rho_e\rangle s}\left[\exp\left(-\frac{\tau}{\cos\theta_s}\right)t_{dv}+t_{ds}\cdot t_{dv}\right]\right\}$$

$$\rho^{*} = (\pi\cdot L_m)/(E_s\cdot\cos\theta_s)$$

$$\beta = \cos\theta_n + \tan\theta_s \sin\theta_n \cos(\varphi_s - \varphi_n)$$

The slope is measured in degrees with the convention of 0 degrees for a horizontal plane.
The aspect angle is measured with the convention of 0 degrees to the north (up) and angles increasing clockwise.

ρ^{*} = (π·Lm)/(μs·Es): Top of Atmosphere reflectance);

ρ :	Corrected reflectance;
Lm :	Radiance measured by the sensor;
Es :	Esoatmospheric Solar flux;
θs , θv :	Solar zenith angle and view zenith angle;
ρa :	Atmospheric reflectance;
<ρe> :	Environmental reflectance;
Tg :	Atmospheric transmittance of the path sun-ground-sensor due to gas absorption;
τ :	Atmospherical Optical Thichkness;
S :	Downward spherical albedo of the atmosphere;
β :	Illumination factors for a tilted surface;
θn, φn :	Slope and the aspect angles of the target.

Improved topography modelling

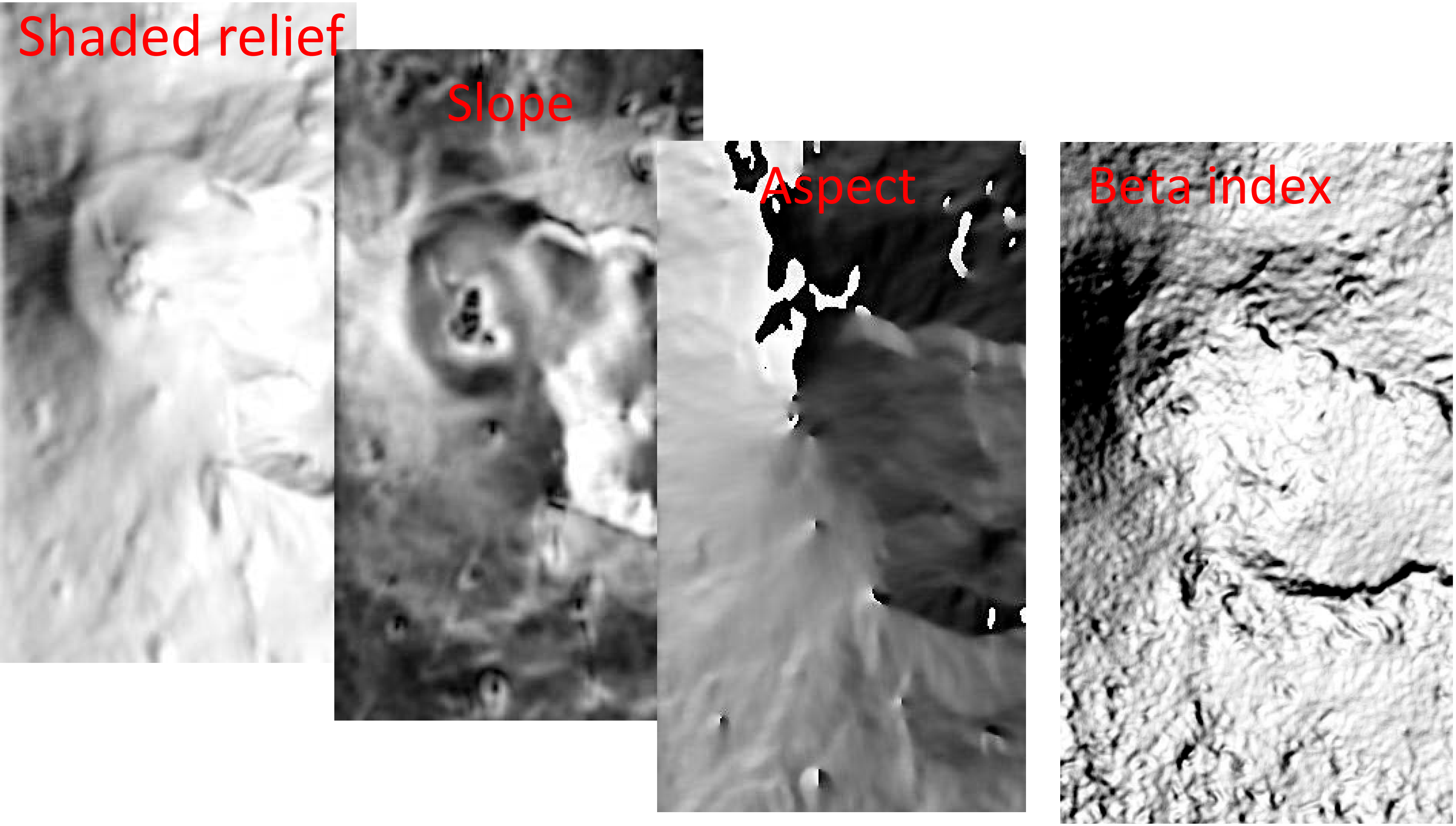

The atmospheric terms of Equation are extracted from each output run of MODTRAN4.0 and 6S in the electromagnetic range 400 nm to 2500 nm with a spectral step of 1 nm (6S has a spectral resolution of 2.5 nm, thus data are interpolated each nm) and convoluted with the response functions of the sensor to obtain in-band values

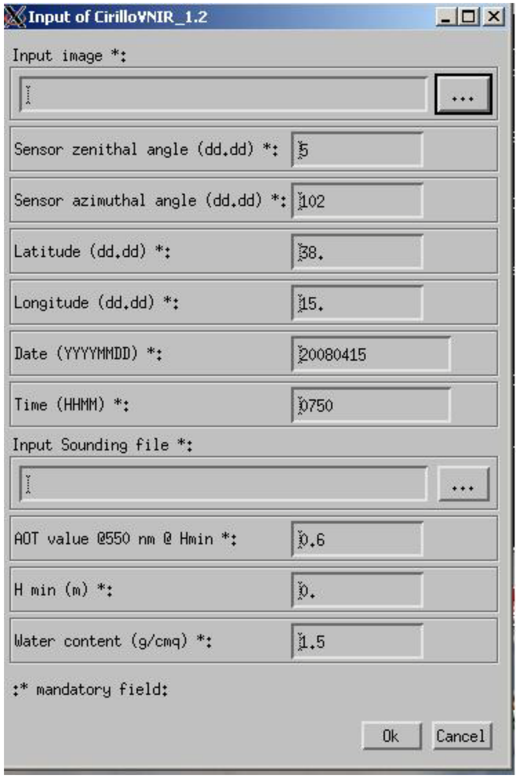

The environmental reflectance, that is the mean reflectance of the ground surrounding the pixel viewed by the sensor, is computed according the Richter method (Richter R., 1990, A fast atmospheric correction algorithm applied to Landsat TM images, Int. J. Remote Sensing, 11, pp. 159-166).

Mt. Etna – Diagala del Diavolo

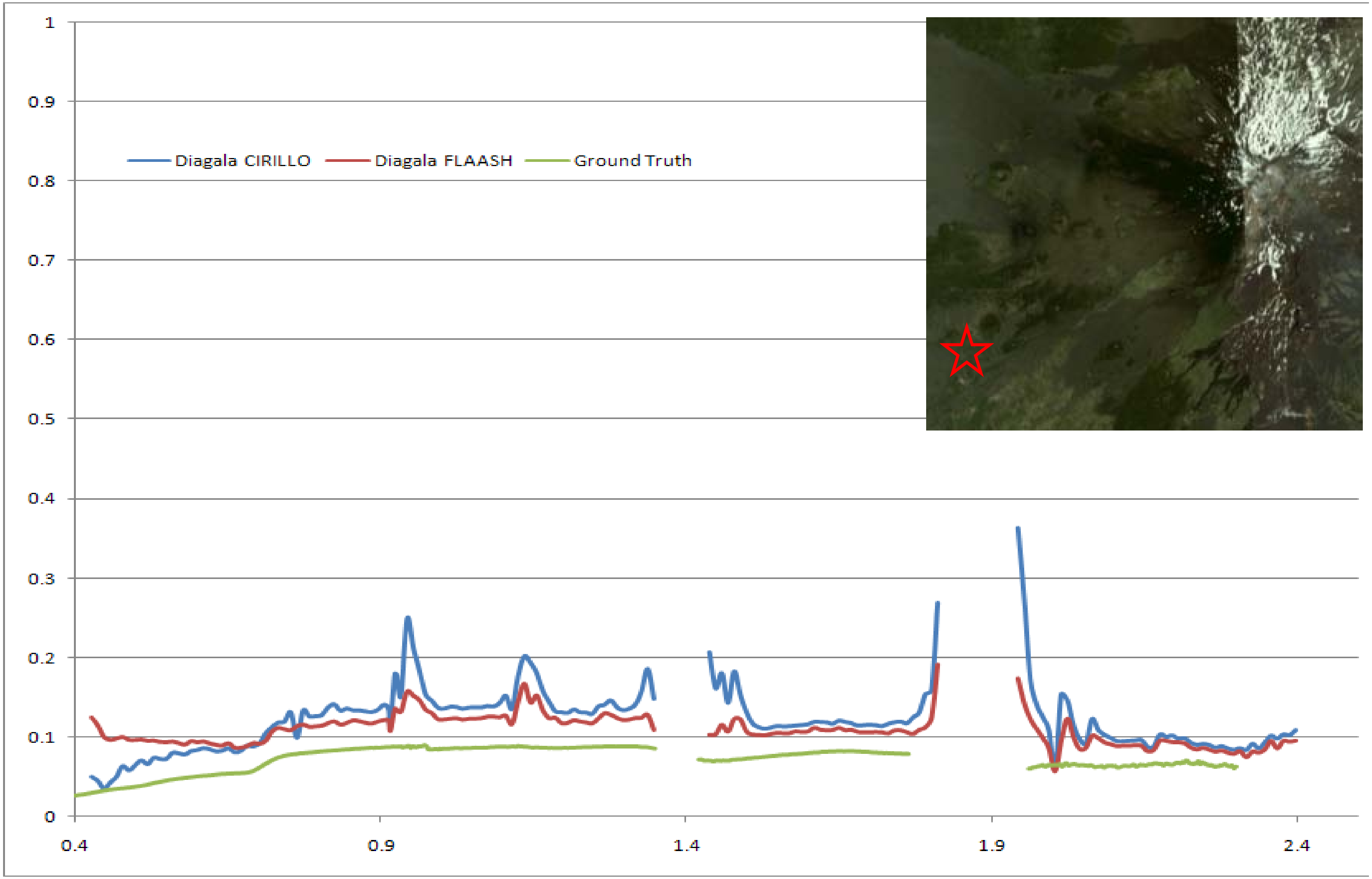

Example of Cirillo performance

MT. Etna:Belvedere

EUROPEAN VOLCANOES TEST SITES; CAL/VAL ACTIVITIES

Mt Etna CAL/VAL Site

Mt Etna

Etna summit area: Piano delle Concazze. This test site is covered by a homogeneous tephra (pyroclastic material from Central Crater, bombs, sansd, lapilli and ashs,) deposits characterized by a flat geometry with an area of approximately 12000 mq. The petrology of the outcropping rocks is quite constant: Hawaiiti/trachybasalt made of plagioclase (predominant) clinopyroxene, olivine. Rare brown amphibole

Reflectance and emissivity spectra have been measured with portable spectro-radiometers and FTIR instruments, temperature measurements have been acquired by using radiometers and thermal cameras. This test site shows a very low reflectance values (0.05) which provides information on the sensor performances on low albedo surfaces. The validation approach starts by removing atmospheric and topographic effects on the L1R Hyperion images and then compare the spectral response with the in situ data to evaluate the stability of the sensor radiometry versus time.

Volcanic activity

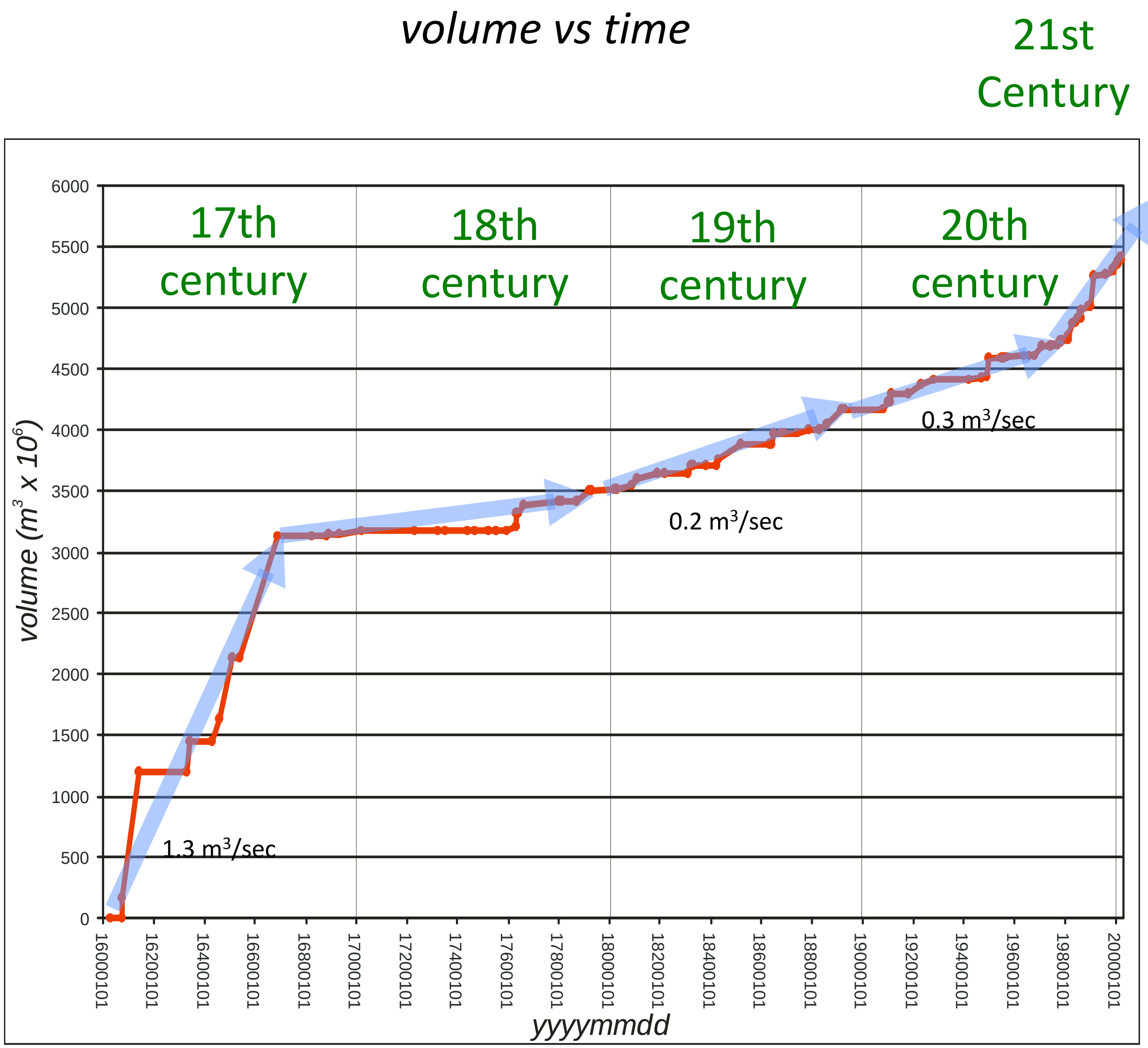

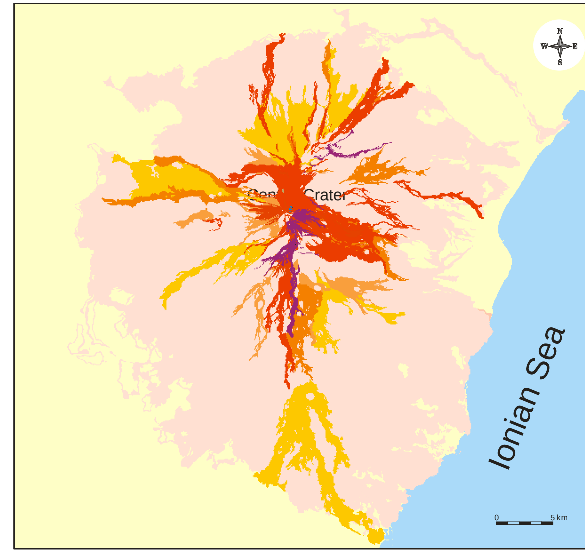

The volume of erupted products was very high during the 17th century, followed by a period of low activity lasted about 100 years.

Etna increased his effusive rate progressively between 18th and 19th centuries, culminating since 1950 in an significant increase of the volume of erupted products.

Mt. ETNA Test site: Ground data

- Discontinuous measurements
- Webcam network
- UV-scanner network for SO2 flux
- Seismic network
- GPS permanent network
- Gravimetric network
- Magnetic network

- Analysis of the erupted ash
- Analysis of the erupted products
- Geologic and structural surveys
- Thermal mapping from helicopter
- Thermal mapping from field

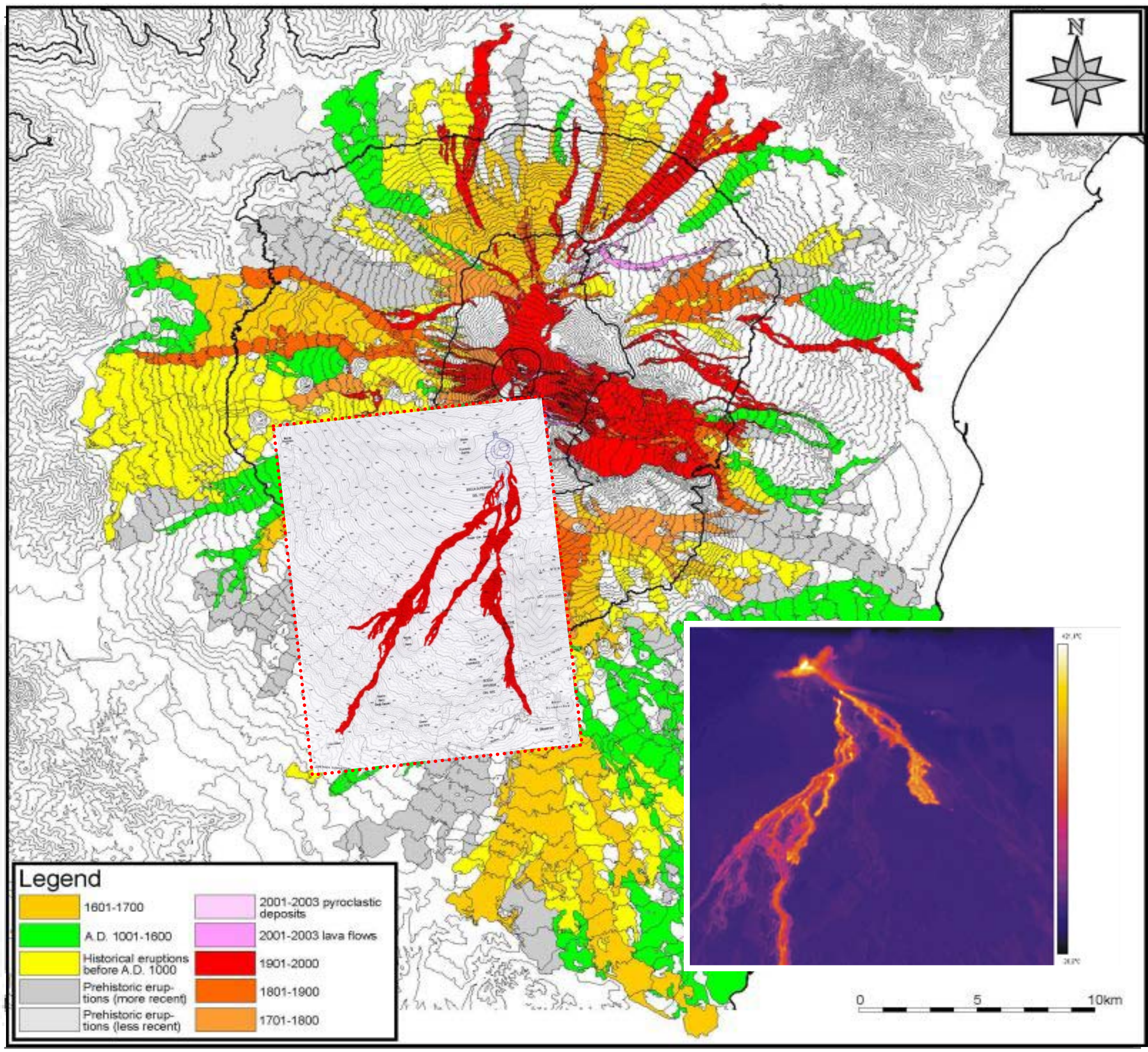

Mt Etna Field campaign: preliminary work

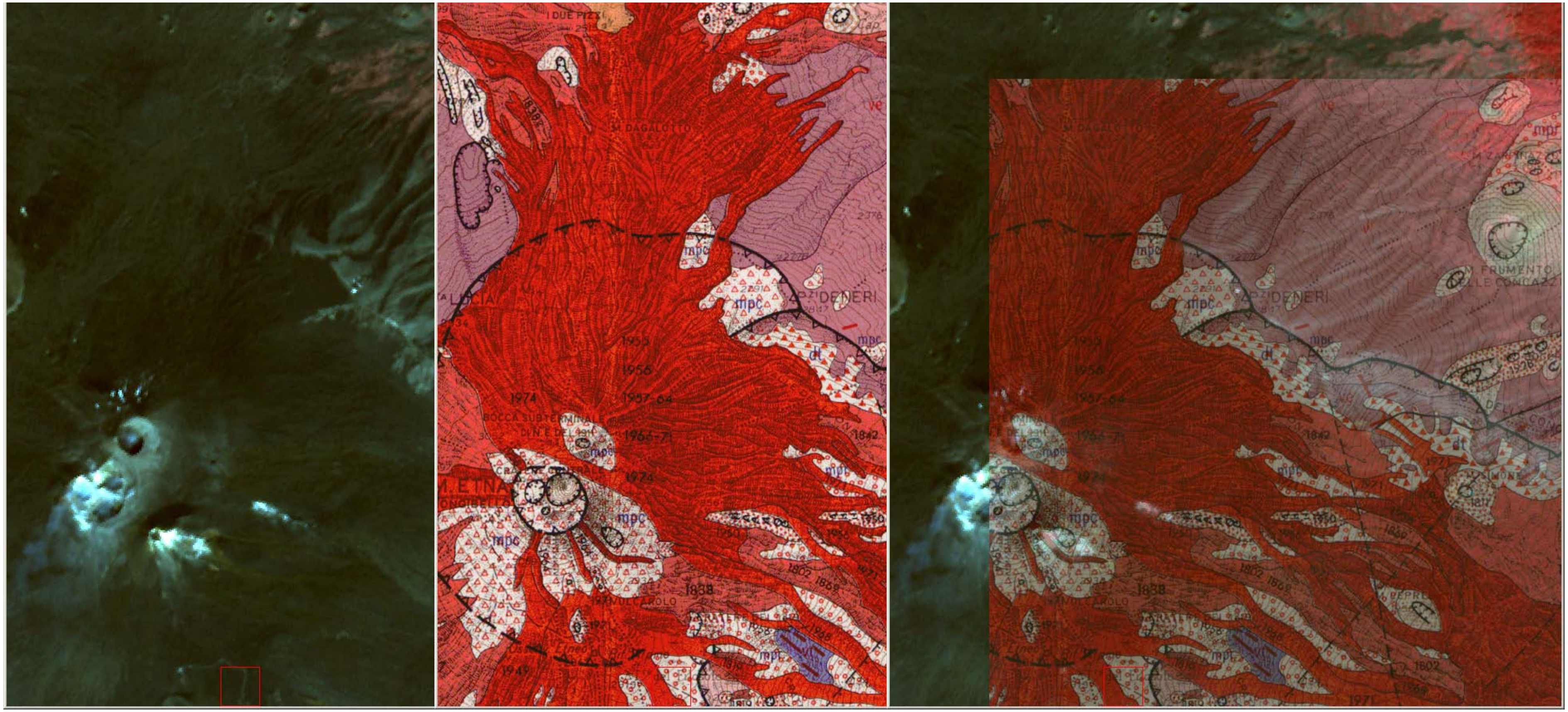

A preliminary identification of test sites was based on the following criteria:

They had to be as high as possible, wide, plane and open areas of homogenous surface material.

The have to be easy to reach on the field and easy to recognize and locate on the image.

Piano delle Concazze

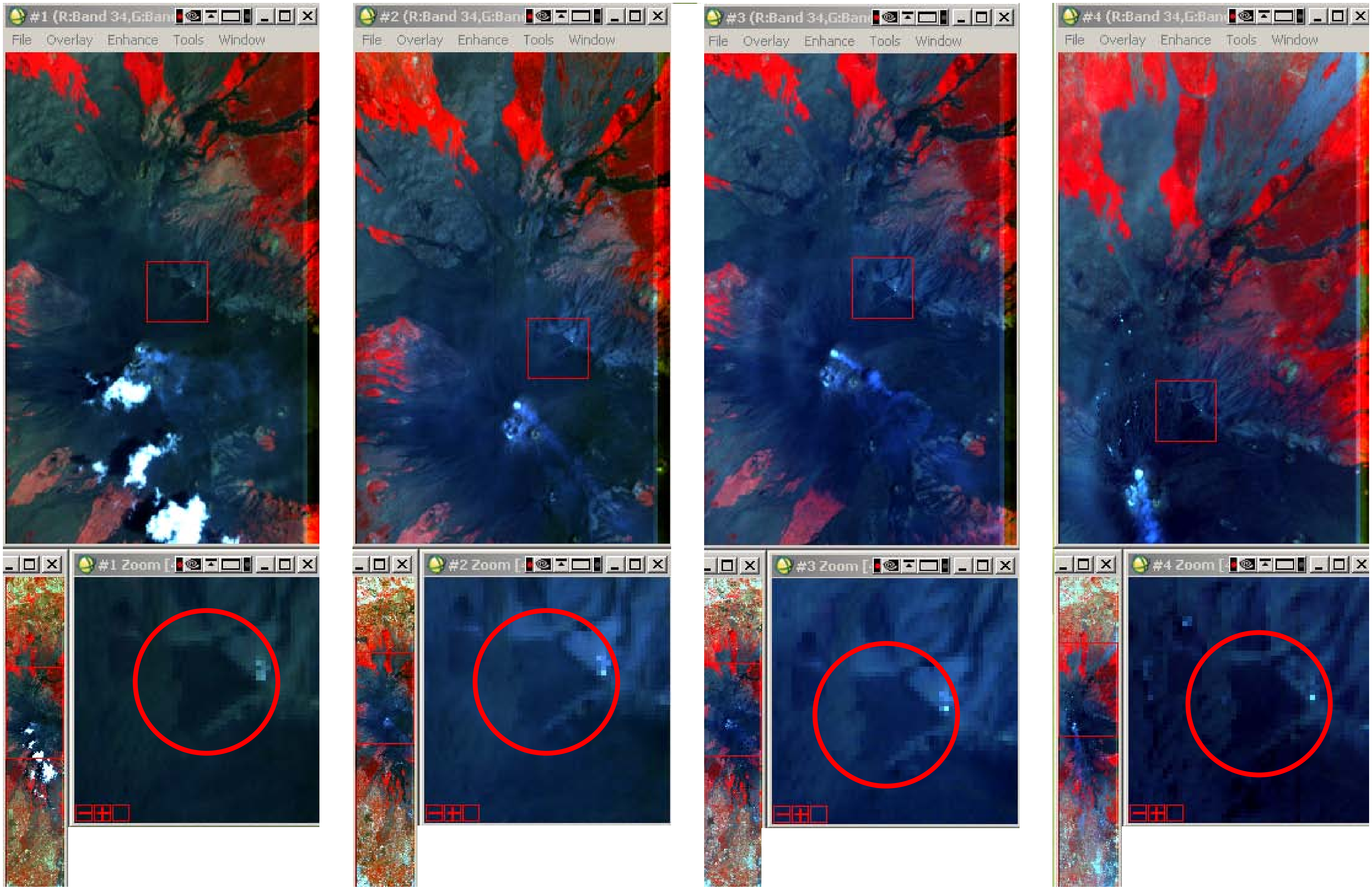

Mt. Etna – 2001-2009 sampled sites

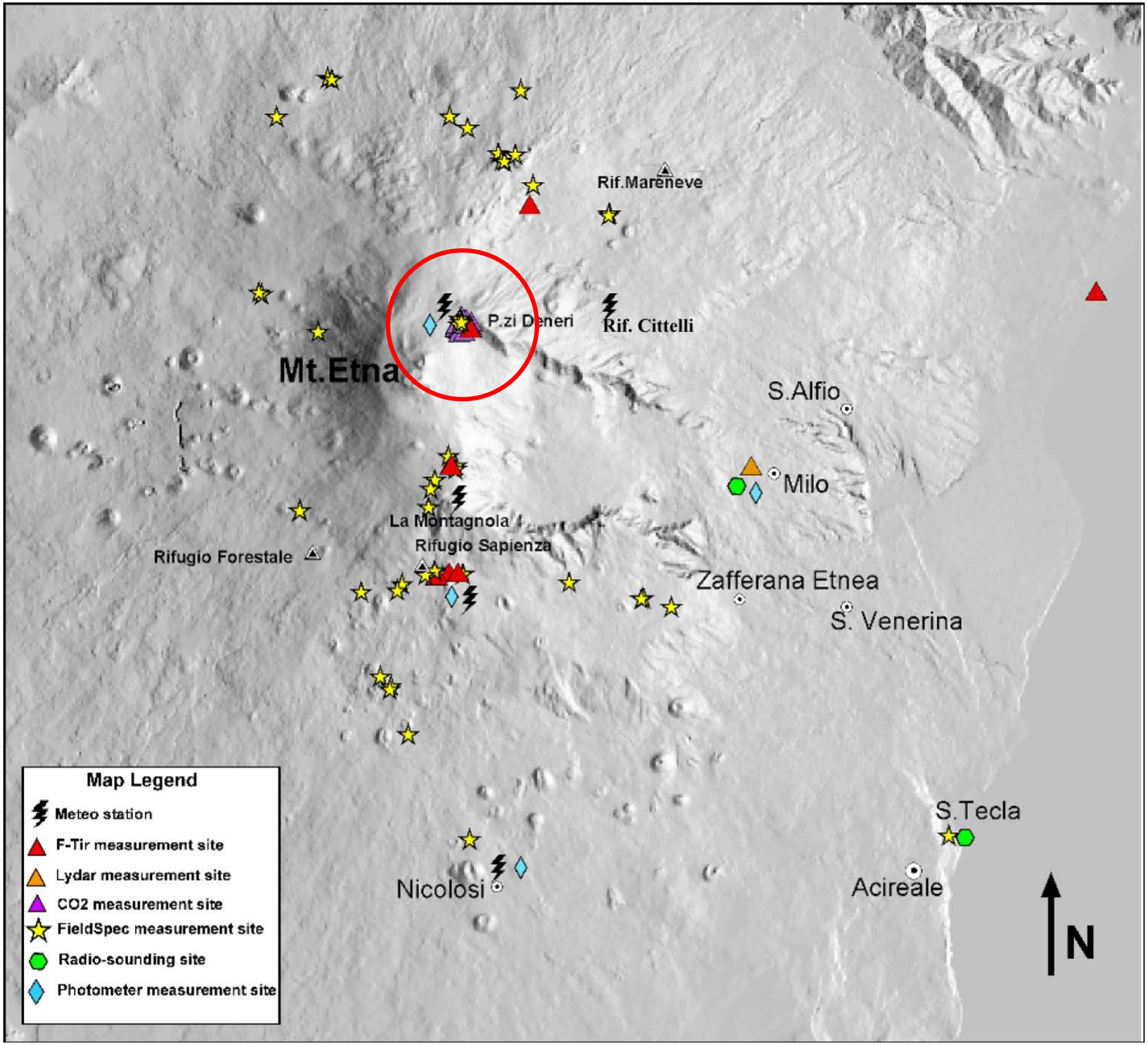

Mt. Etna – Piano delle Concazze 2001

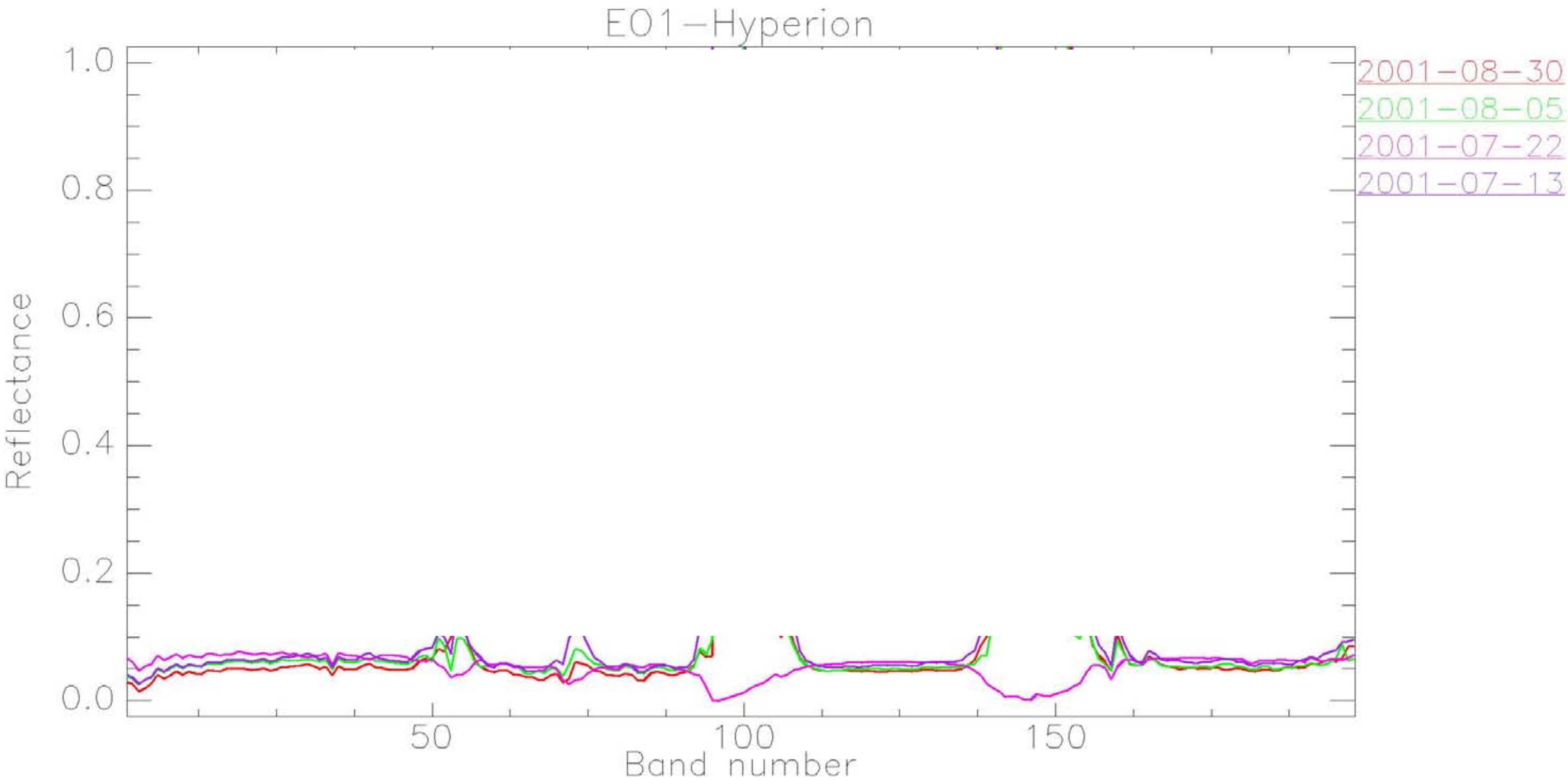

Mt. Etna – Piano delle Concazze 2003

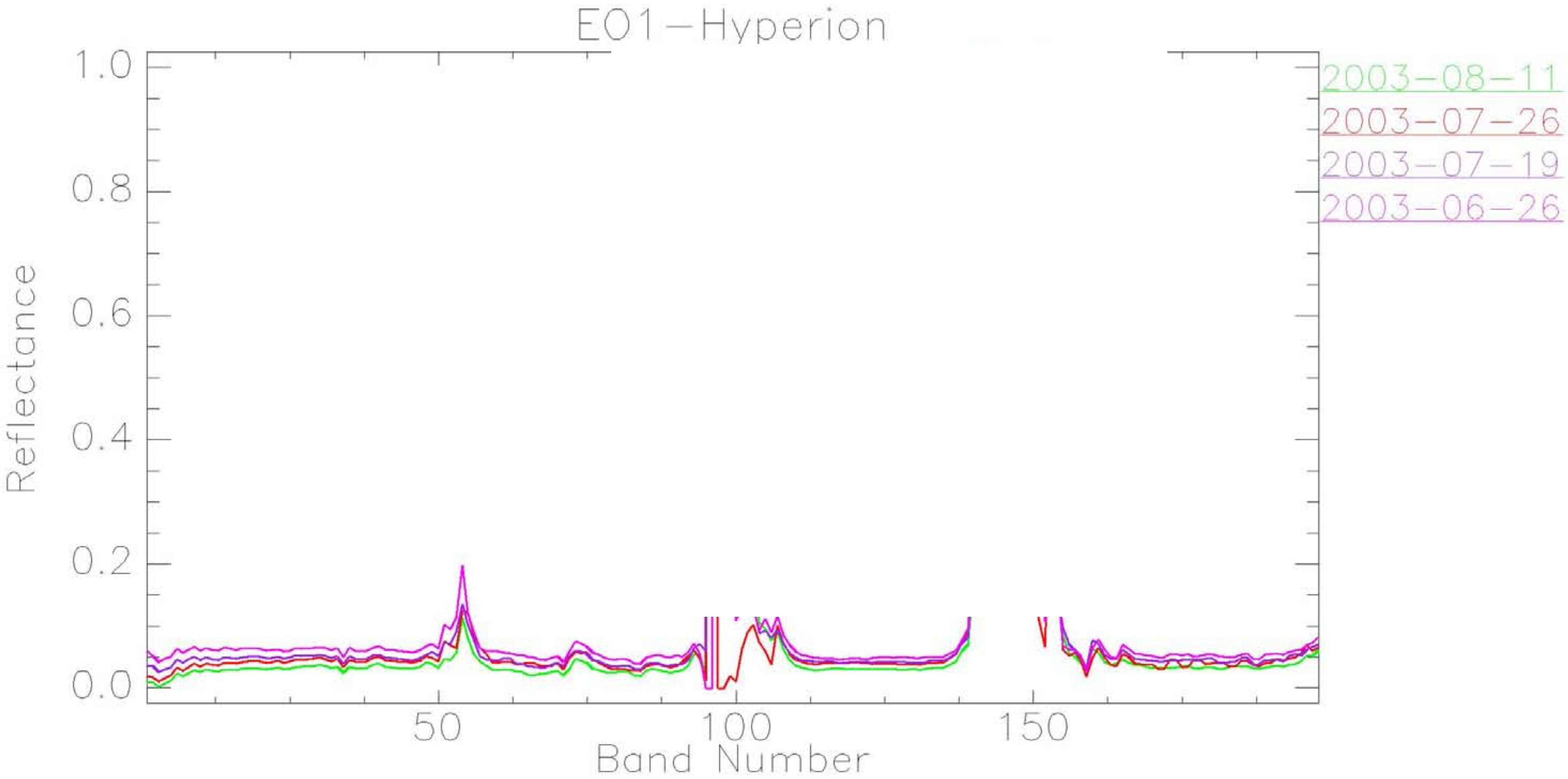

Mt. Etna – Piano delle Concazze 2004

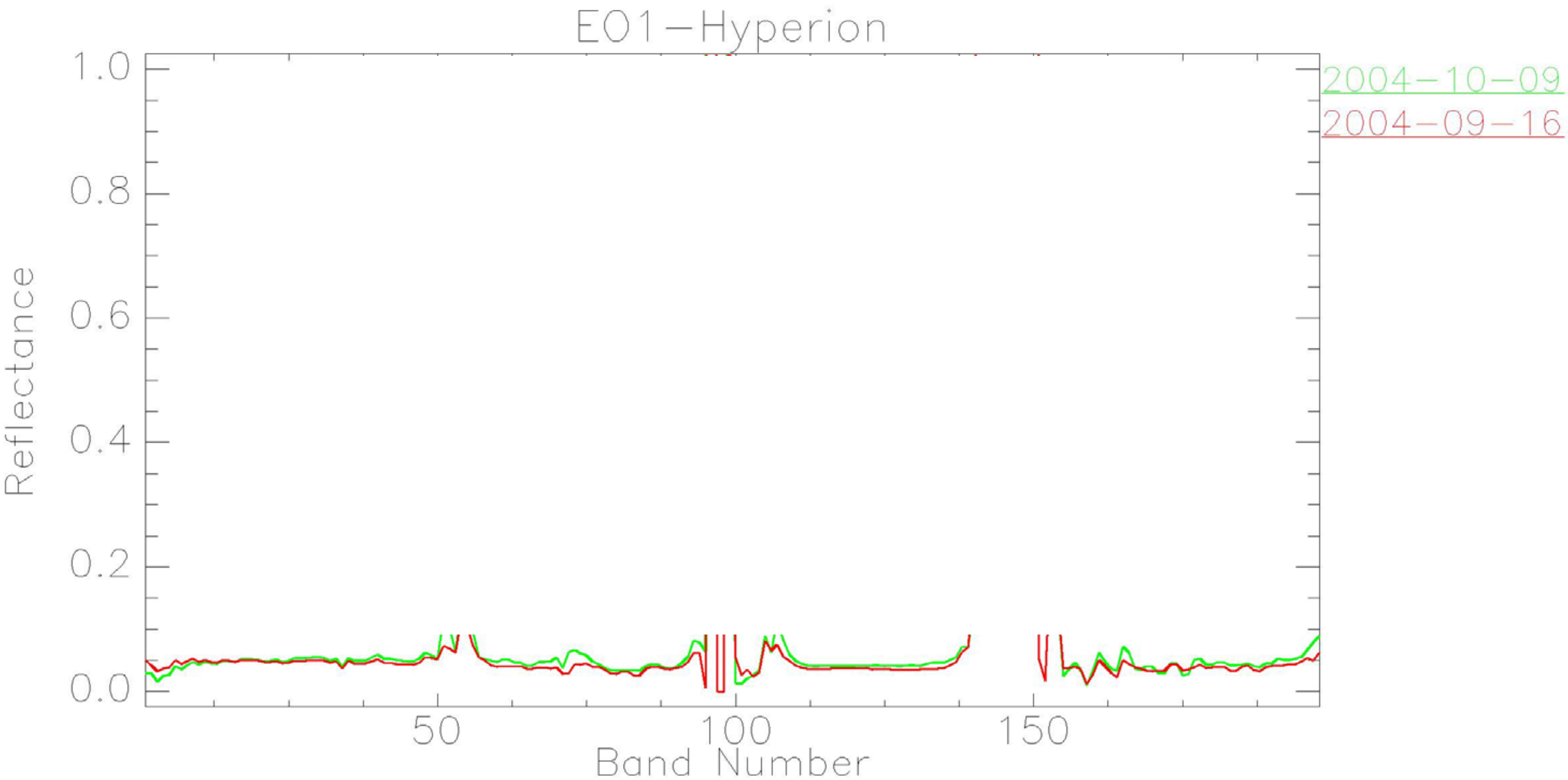

Mt. Etna – Piano delle Concazze 2005

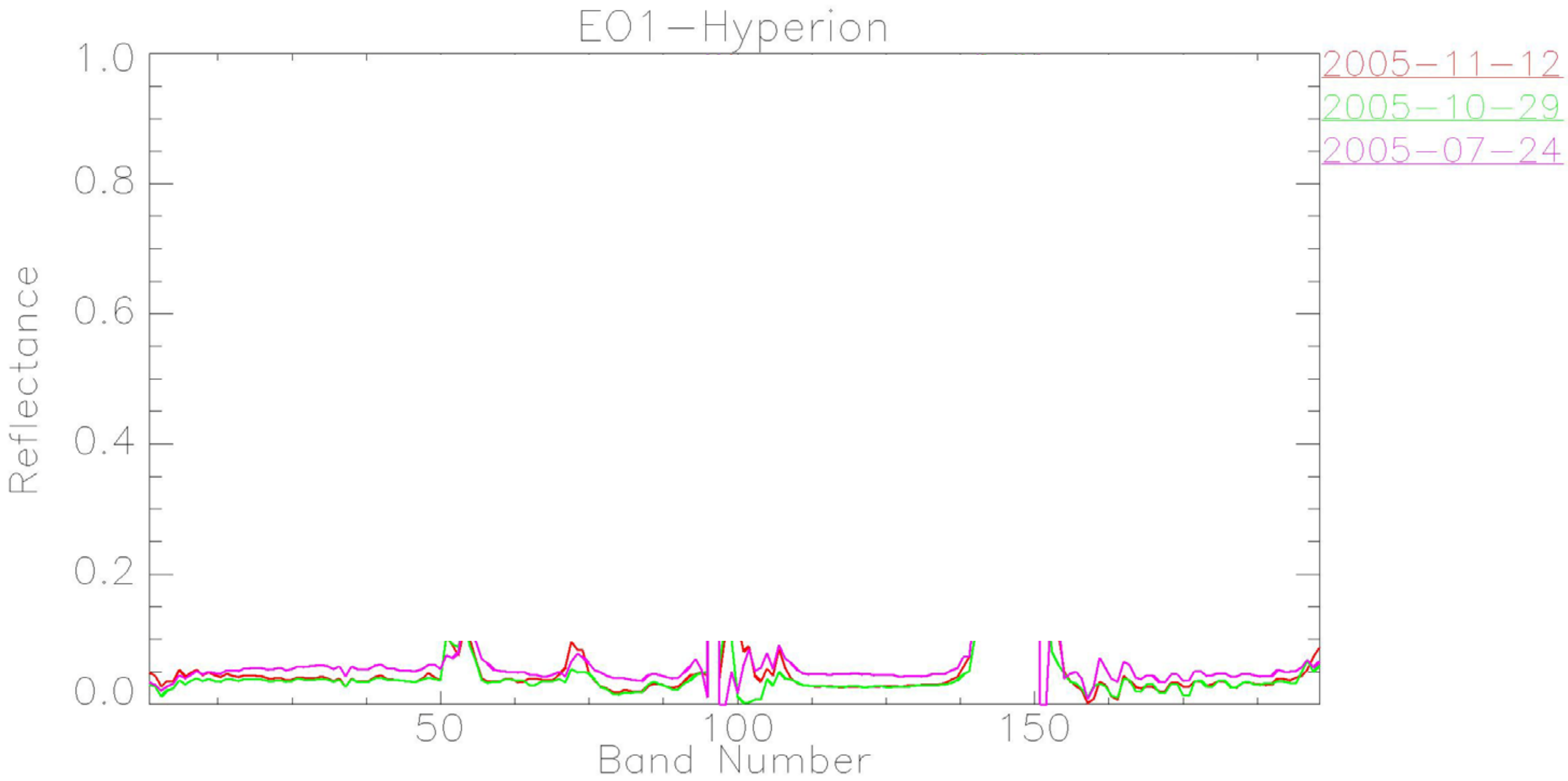

Mt. Etna – Piano delle Concazze 2006

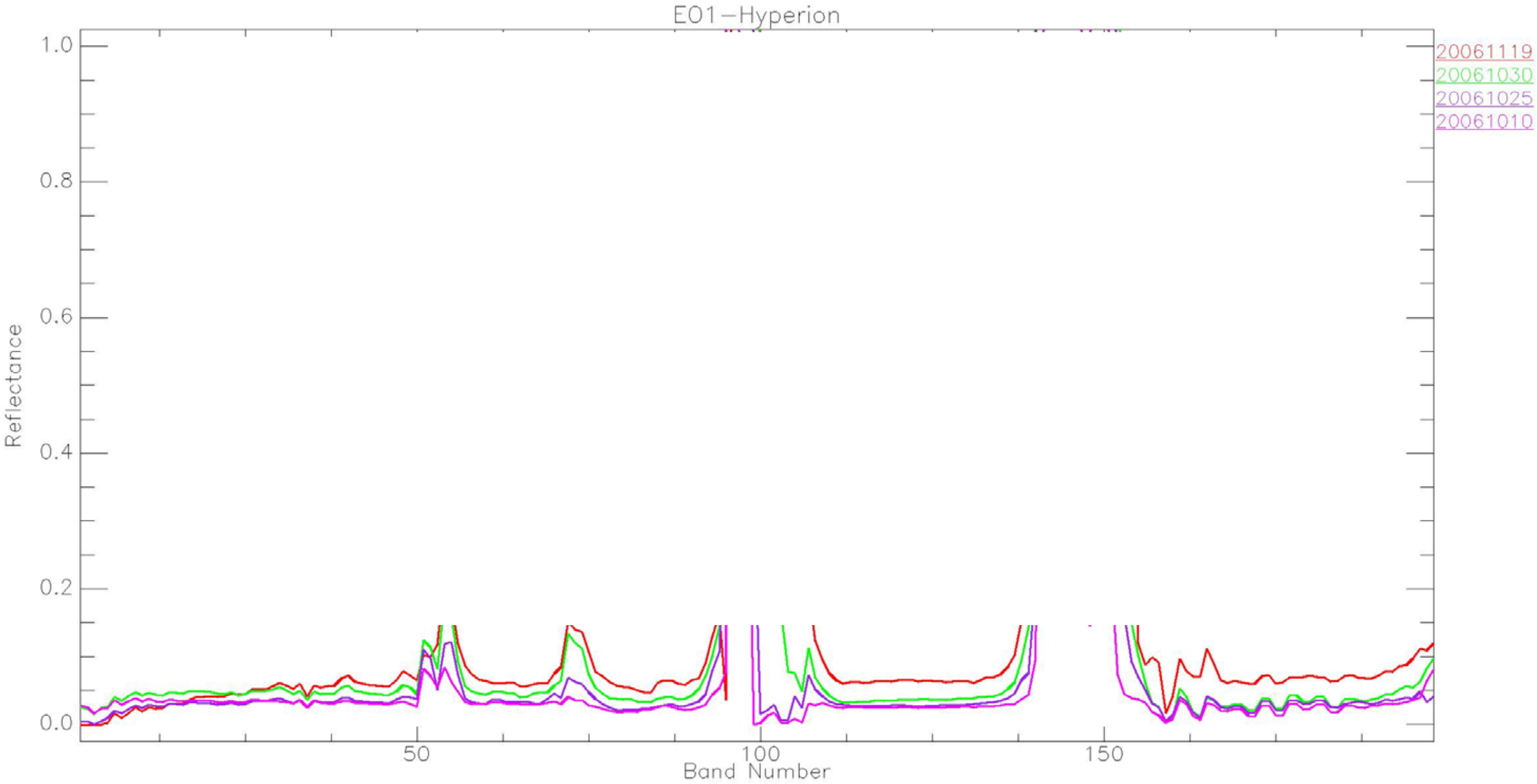

Mt. Etna – Piano delle Concazze 2007

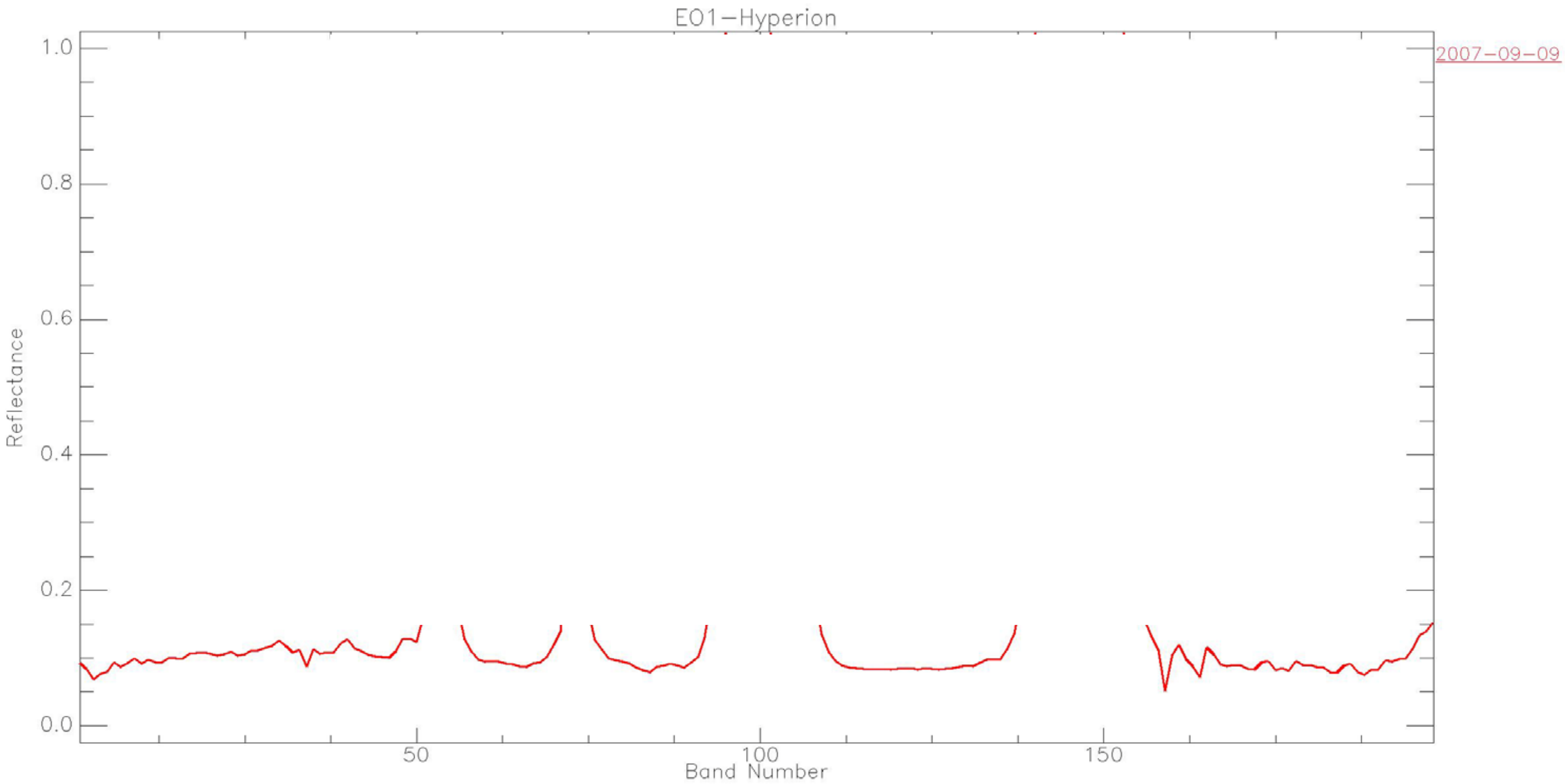

Mt. Etna – Piano delle Concazze 2008

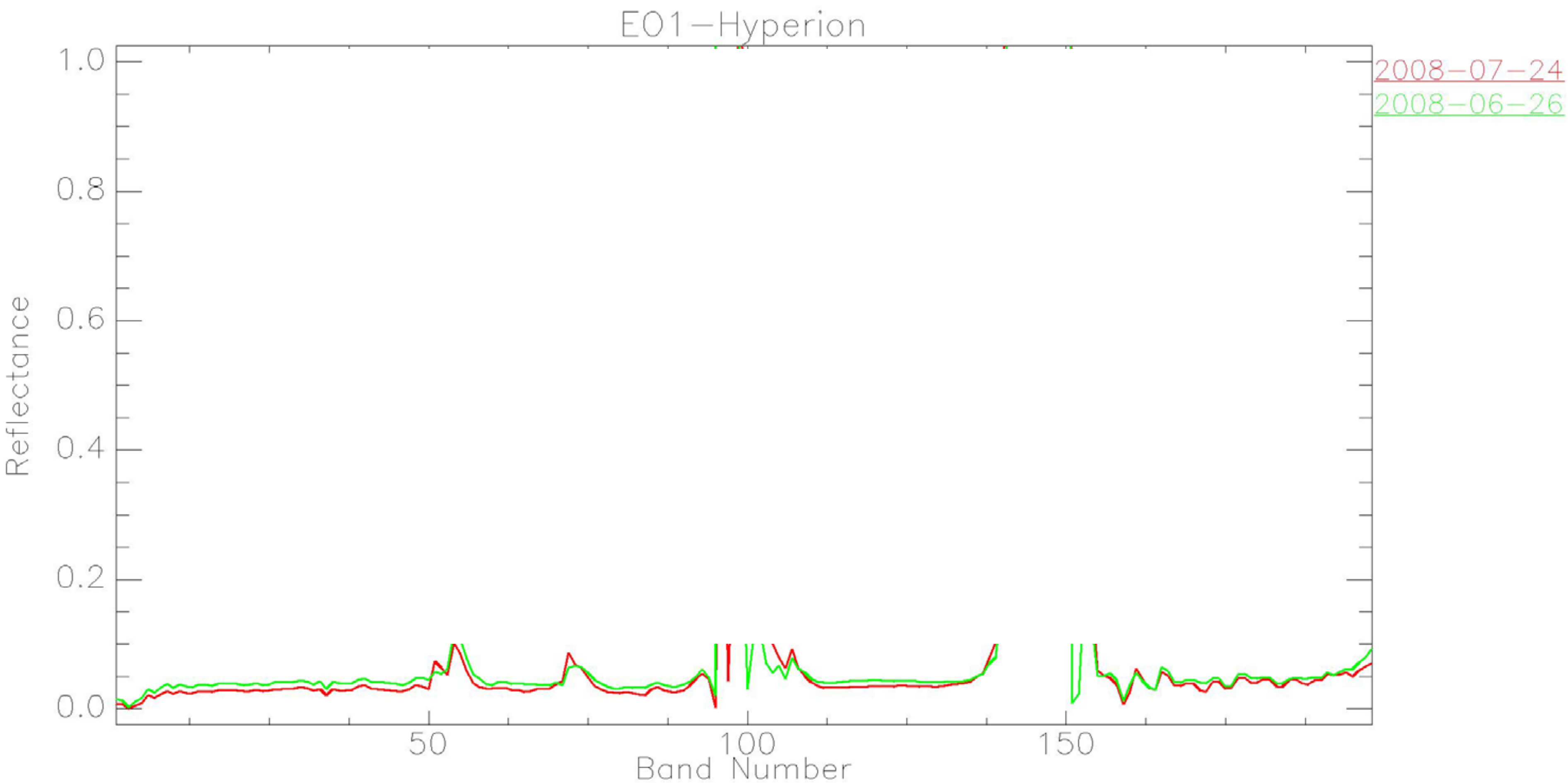

Mt. Etna – Piano delle Concazze 2009

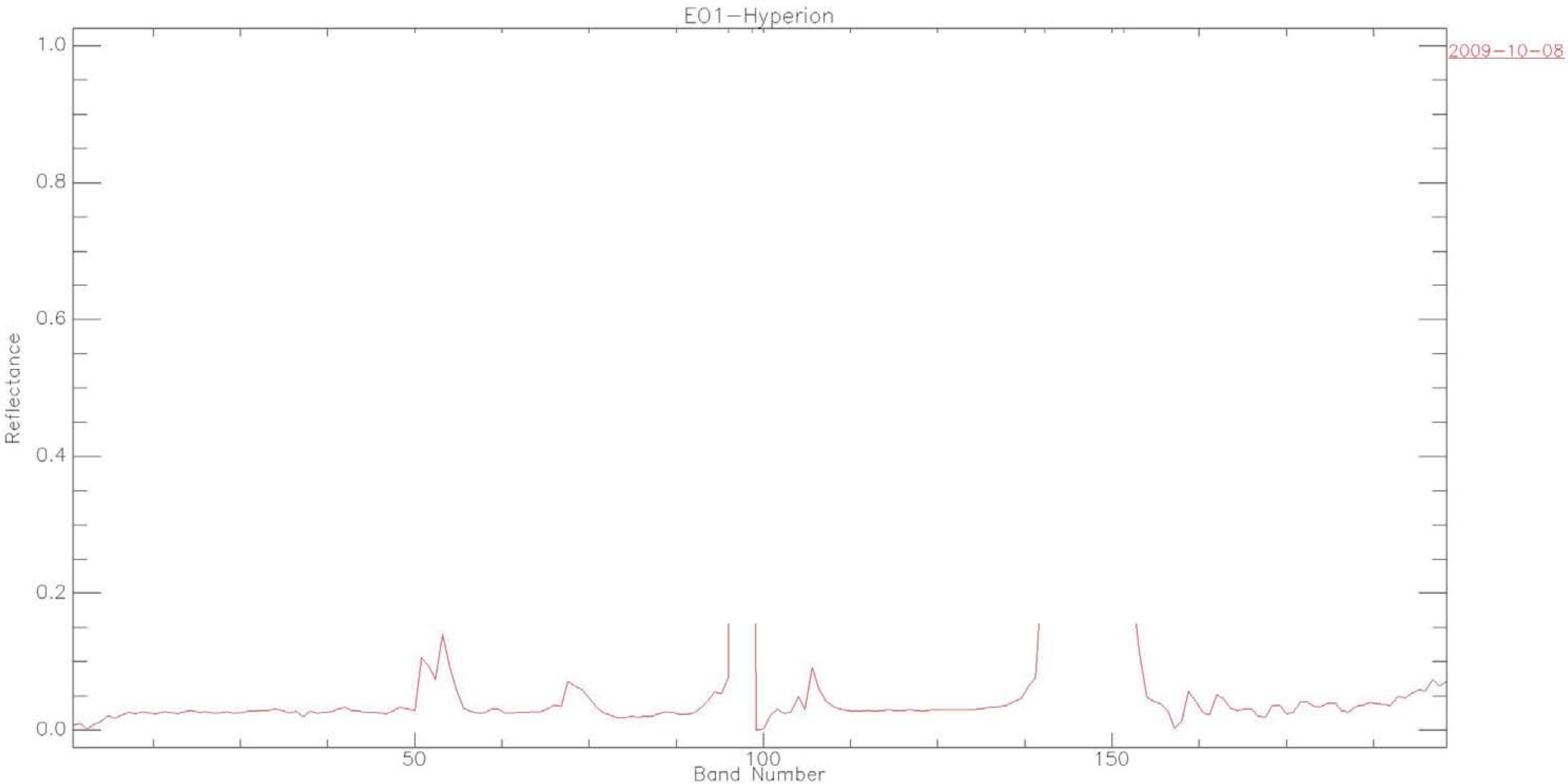

Piano delle Concazze, 9 years of measures

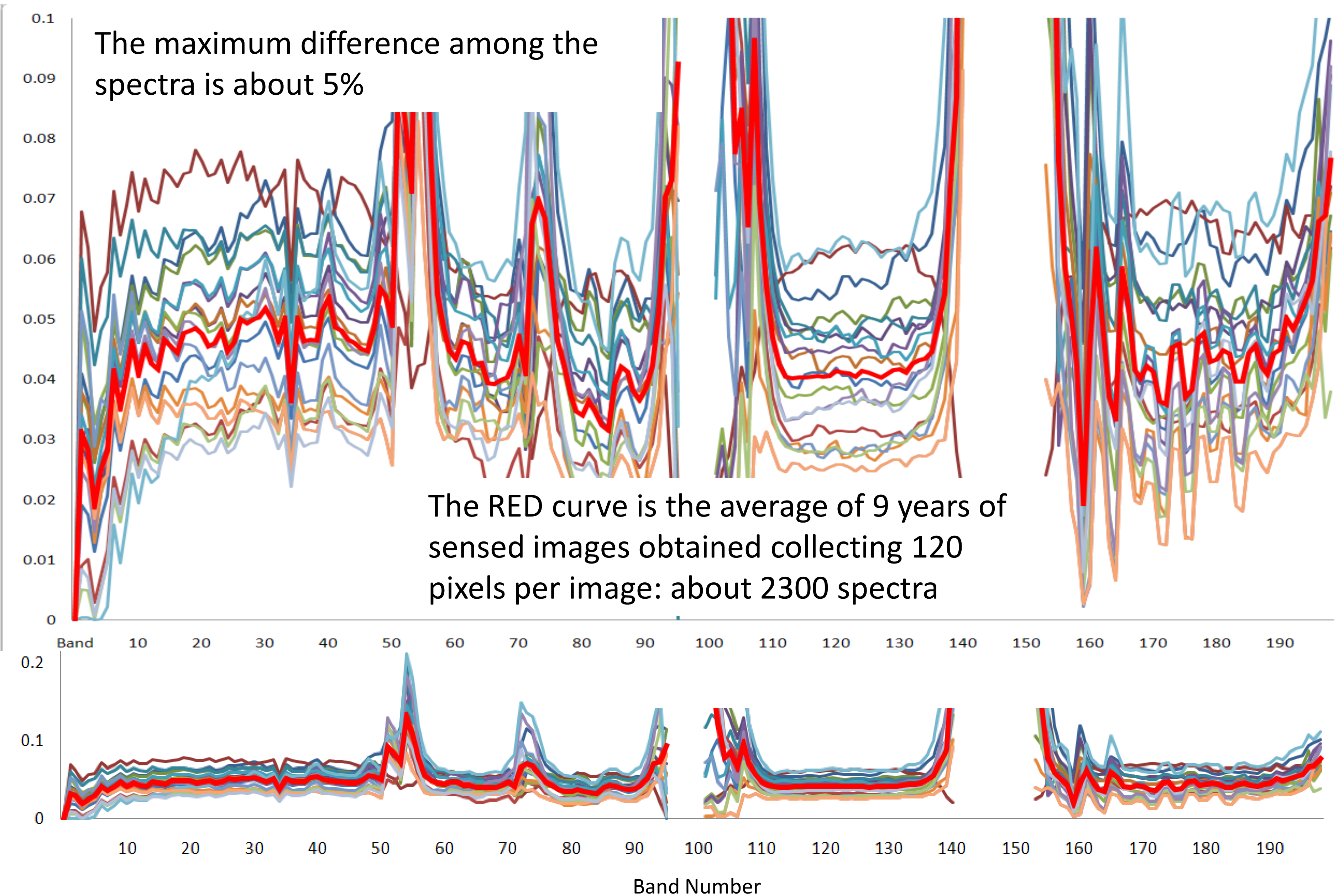

From Band Number to Wavelenght

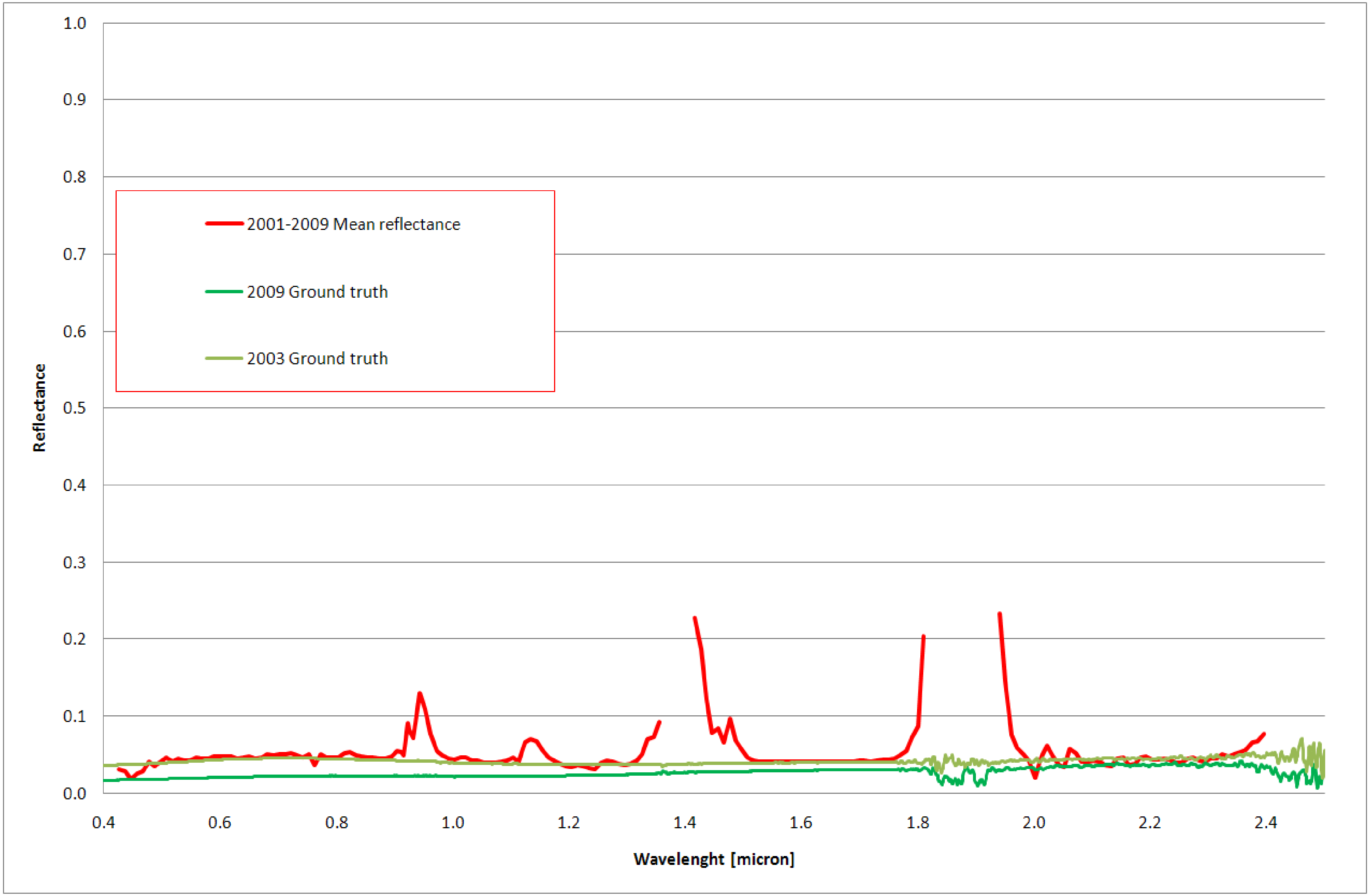

Conclusion

yyyy-mm-dd-hh-mm-ss	yyyy-mm-dd-hh-mm-ss
2001-05-26-09-26-04	2005-11-29-09-21-19
2001-06-20-09-19-37	2005-12-04-09-30-27
2001-07-13-09-25-32	2005-12-06-09-14-35
2001-07-22-09-19-25	2005-12-16-09-31-58

- Among 67 sensed images have been acquired over MT Etna by EO1-Hyperion
- Only 20 of them have been used in this analysis
- These images show that the Piano delle Concazze area represents a suitable site (in terms of constant spectral response) for VAL/CAL activities
- The used procedure for Atmospheric and Topographic removal effects well supports these VAL/CAL activities

2005-11-05-09-13-25	2009-10-03-09-25-40
2005-11-12-09-08-47	2009-10-08-09-19-58

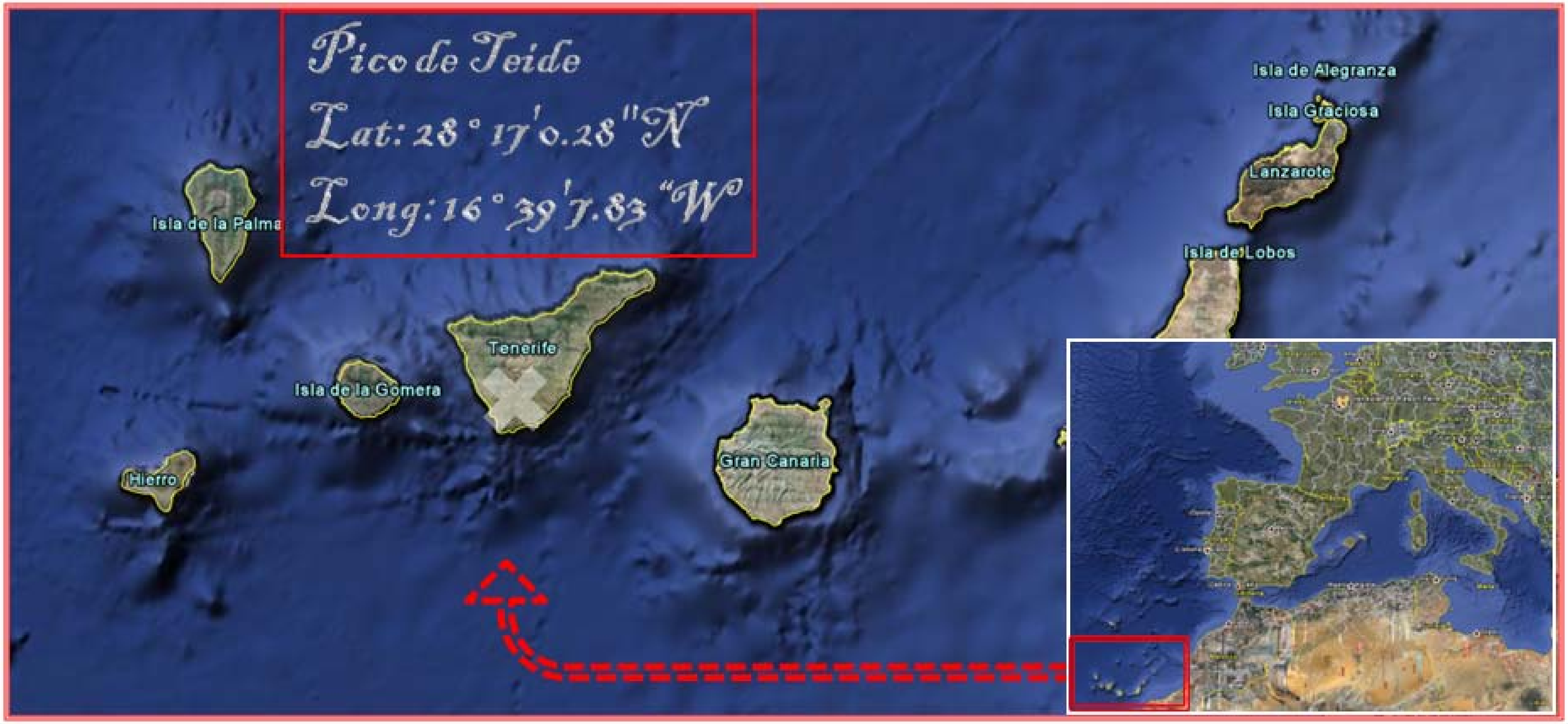

Pico de Teide CAL/VAL Site

Tenerife is the exposed part of a giant volcanic construct that extends from the floor of the eastern central Atlantic at 23700 m to 3718 m at the summit of Teide volcano. The subaerial history of the island began in the late Miocene

Plio-Quaternary, post-shield volcanism on Tenerife has been characterised by the cyclic development of petrologically evolved eruptive centres. The most recent eruptive cycle has produced the twin stratovolcanoes Pico de Teide (PT) and Pico Viejo (PV), and numerous flank-vent systems, whose products collectively form the PT/PV formation.

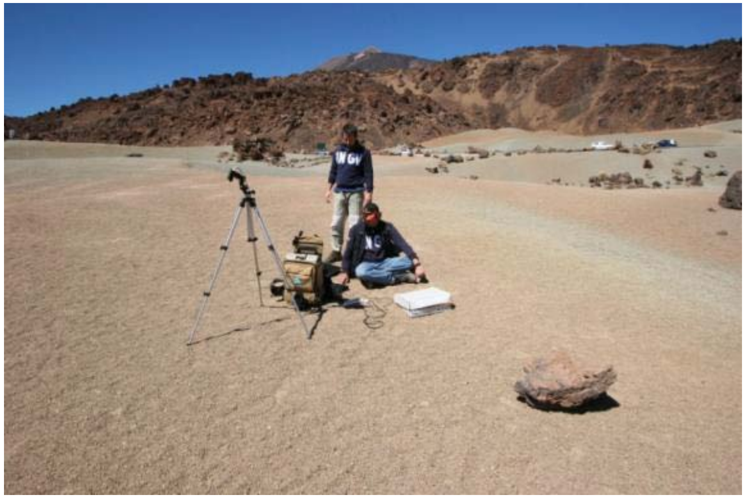

Pico de Teide Test site: Ground data

- Seismic Network
- Permanent GPS network
- Geochemical network
- Geodetic Network
- Geological Map

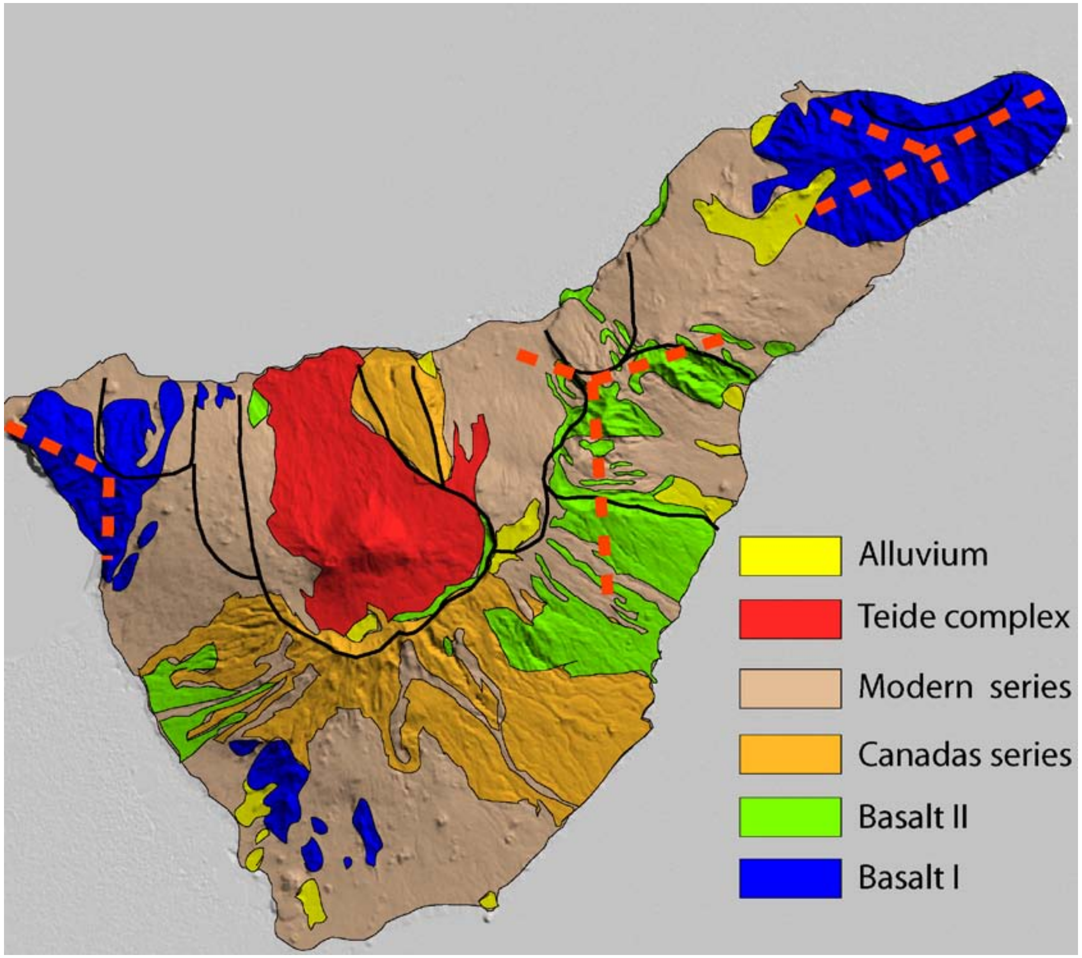

Available data frame

Hyperion (Red)

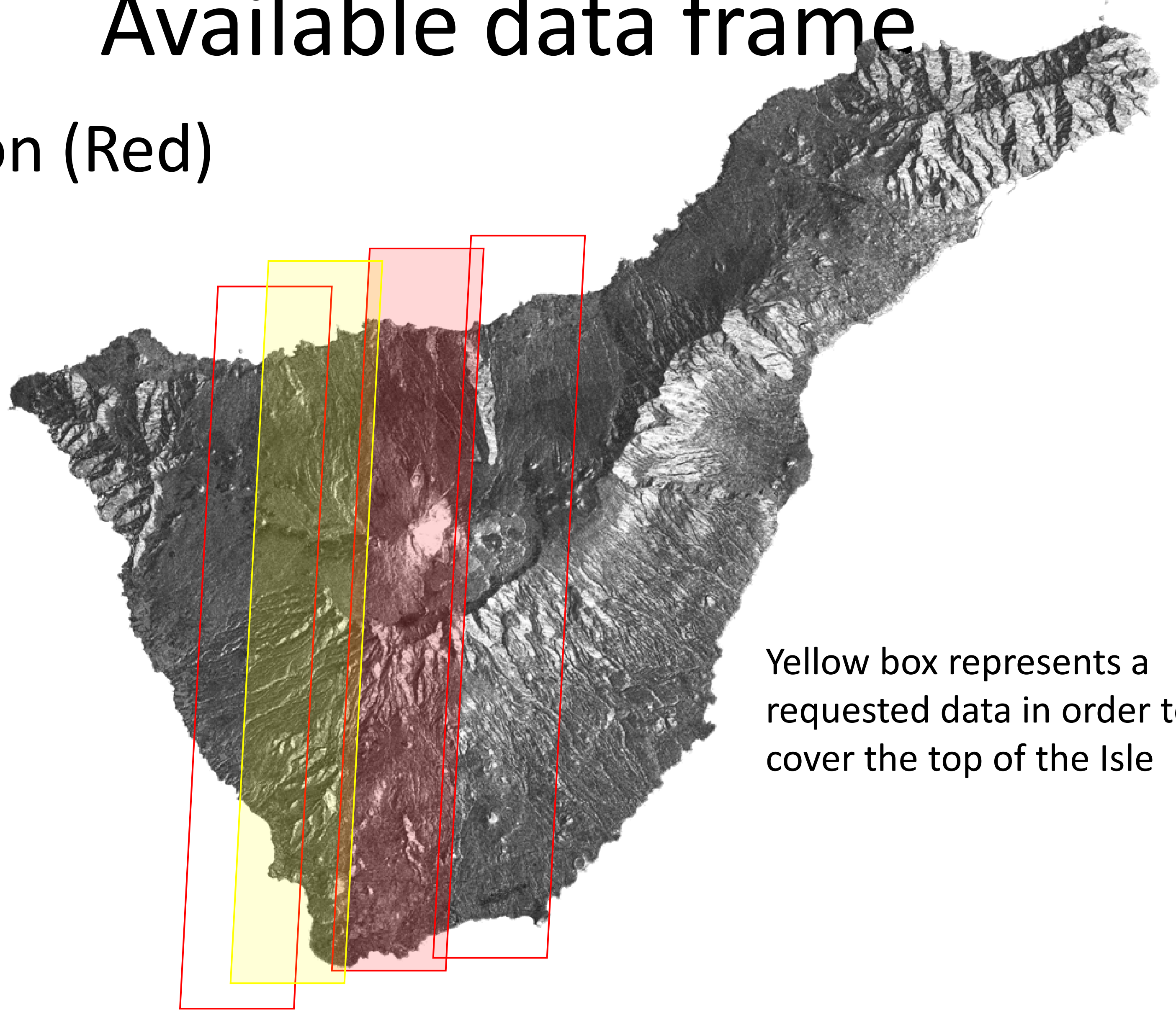

Yellow box represents a requested data in order to cover the top of the Isle

Pico de Teide Field campaign: preliminary work

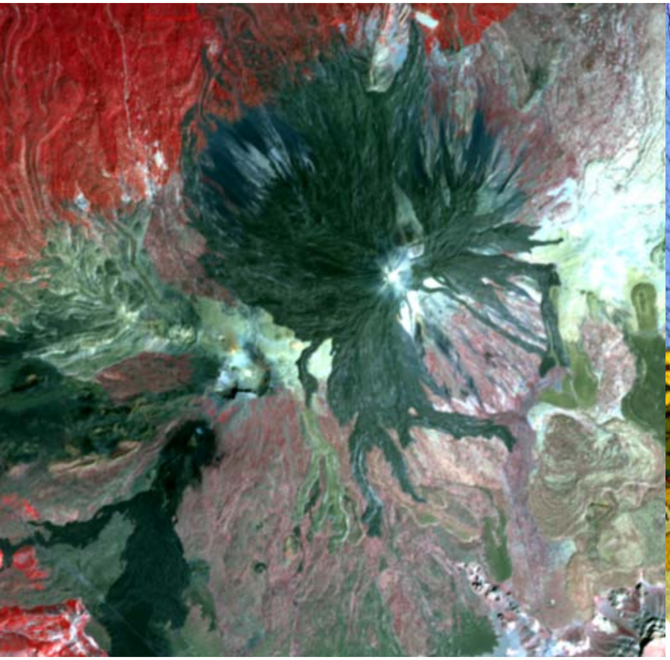

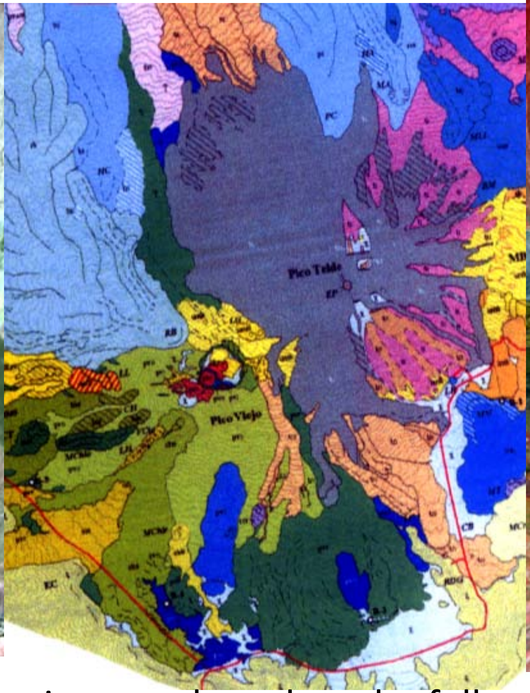

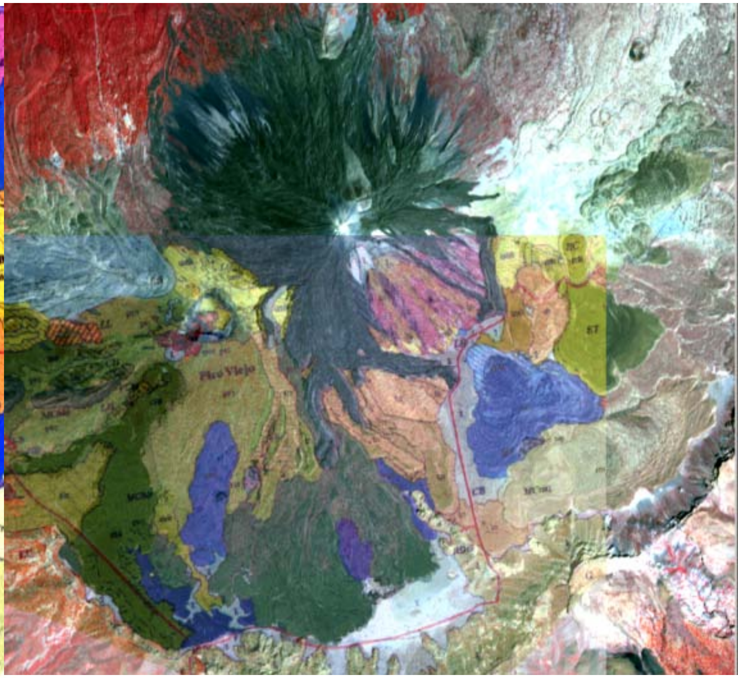

A preliminary identification of test sites was based on the following criteria:

They had to be as high as possible, wide, plane and open areas of homogenous surface material.

The have to be easy to reach on the field and easy to recognize and locate on the image.

Geological Map from “G.J. Ablay, J. Martì Journal of Volcanology and Geothermal Research 103 (2000)”

Geological Map

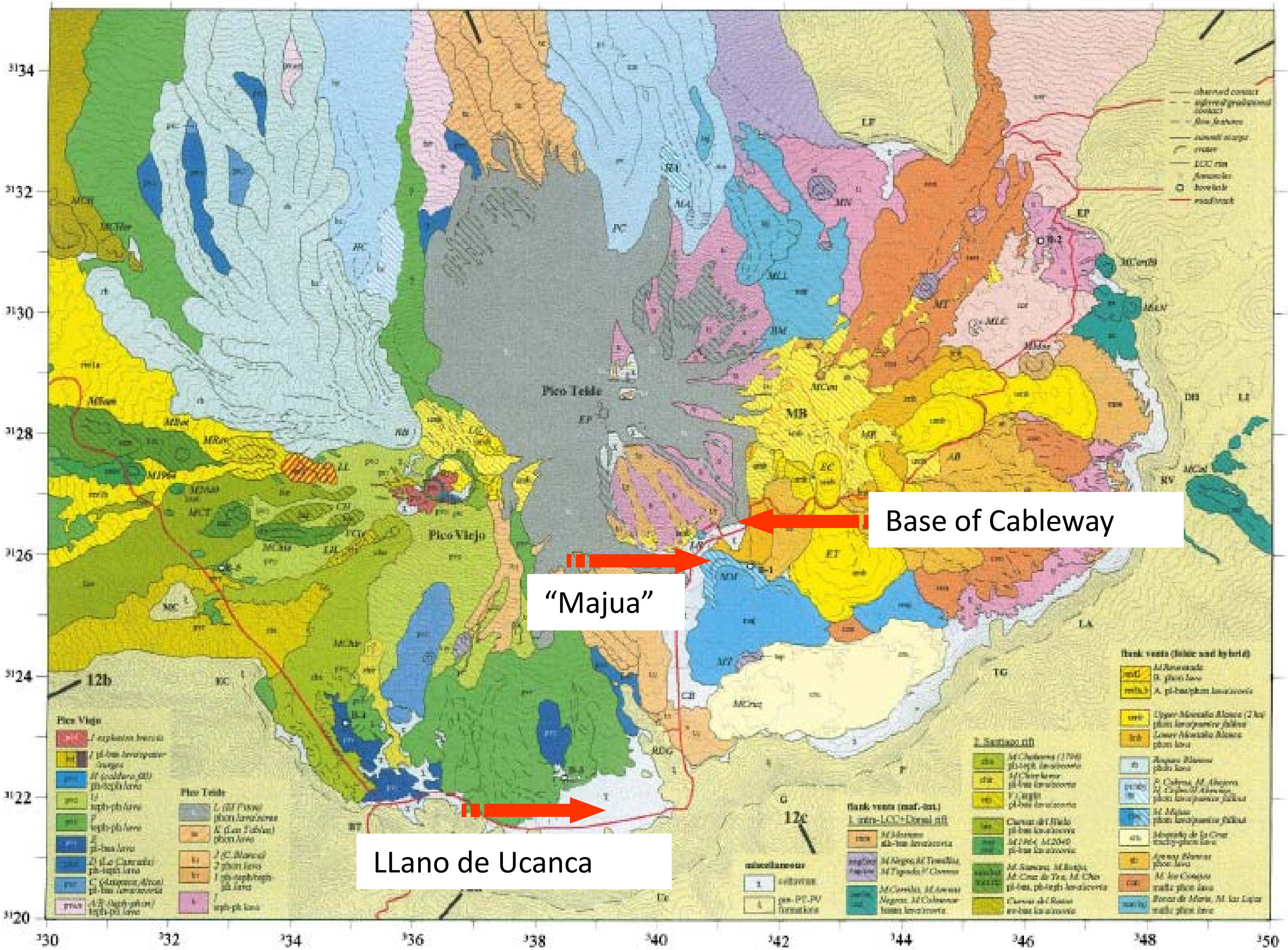

M. Majua

M. Majua

M. Majua is a strombolian pumice cone, 700 m in diameter and 55 m high, breached on its SE side by a wide, lobate, blocky flow of weakly evolved phonolite lava at least 30 m thick. On chemical grounds, the M. Majua member also comprises lava and spatter from Los Roques, which is a small vent on PT's lower S flank

Pico de Teide: M. Majua

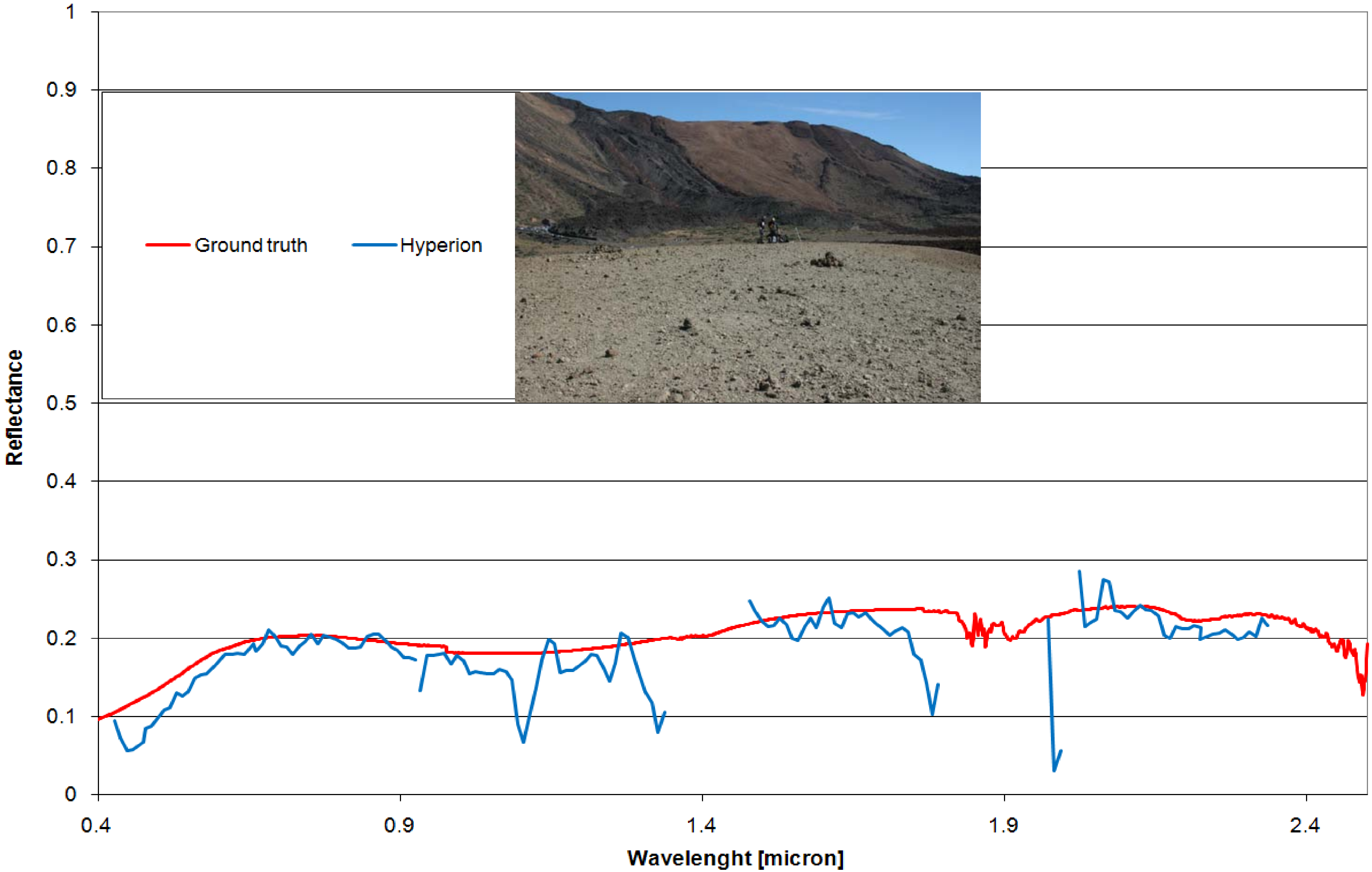

El Piton

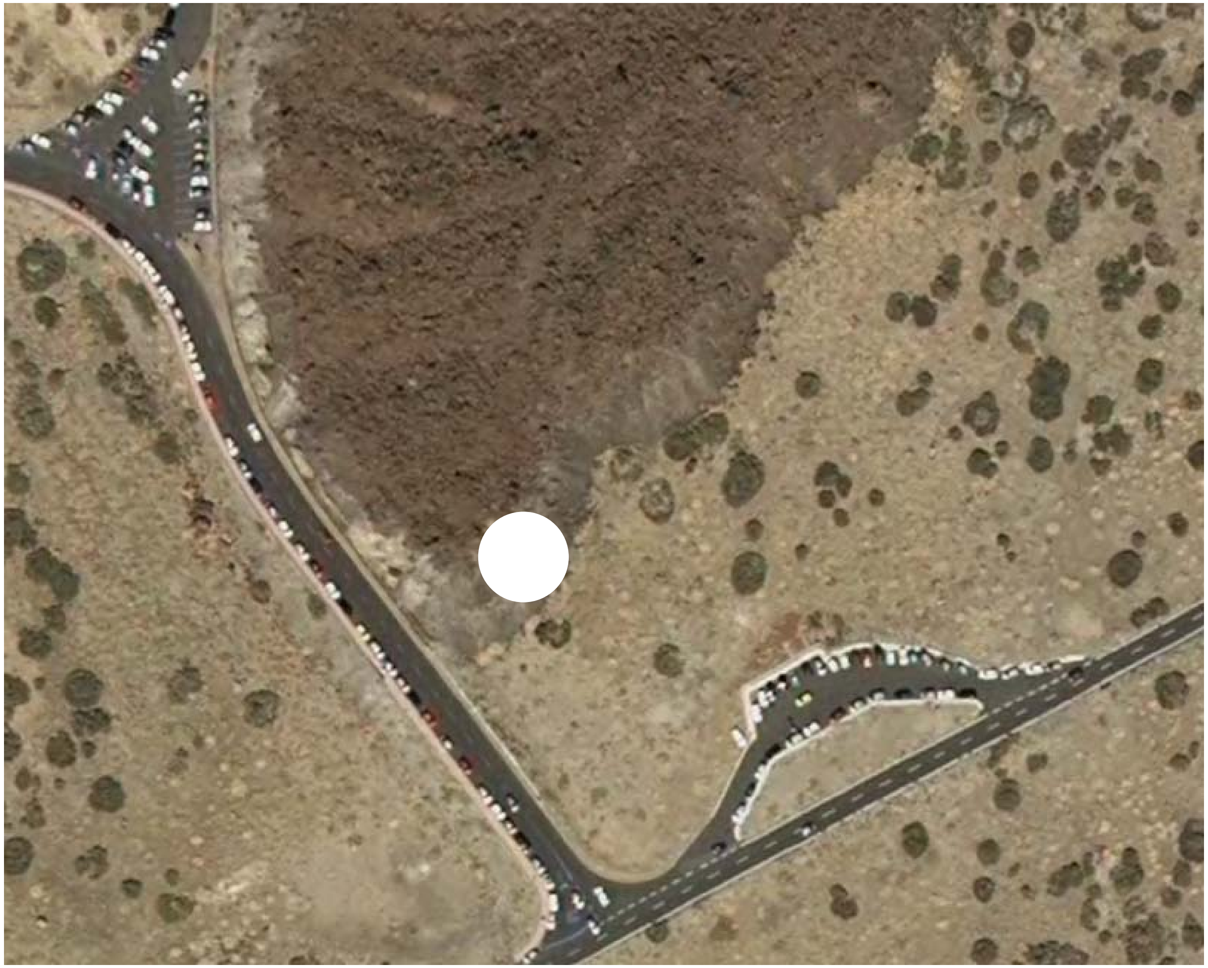

El Piton

El Piton "L" member comprises many thin, blocky flows of melanocratic, glassy, porphyritic phonolite lava derived from El Piton. Flows are steepsided with prominent channels and levees on the flanks, and lobate flow fronts at the cone base. The El Piton eruption is assigned a historic date of 1380 ad based on geomagnetic secular variation studies

Pico de Teide: El Piton

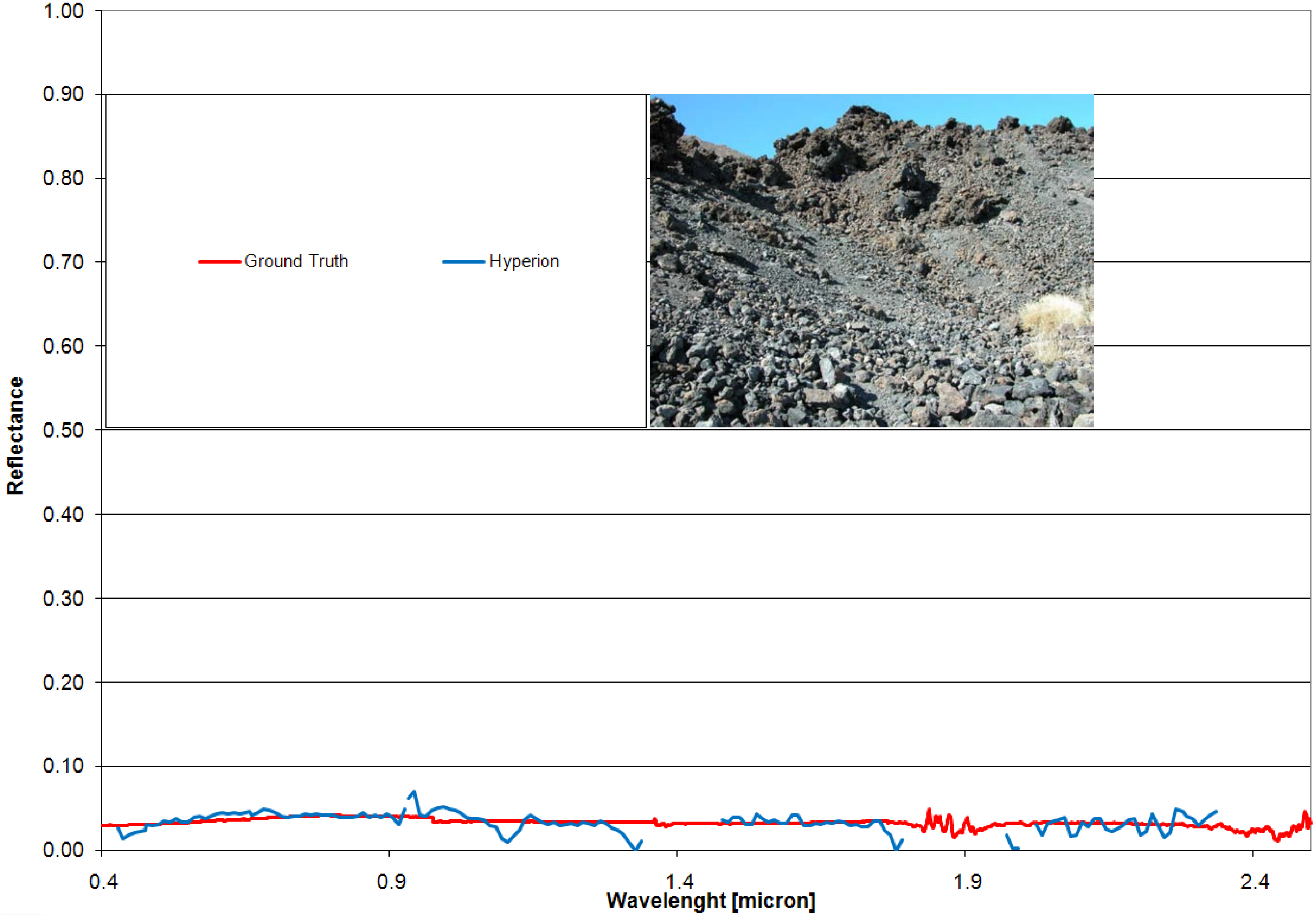

Colluvium deposit in Llano de Ucanca

Pico de Teide: Llano de Ucanca

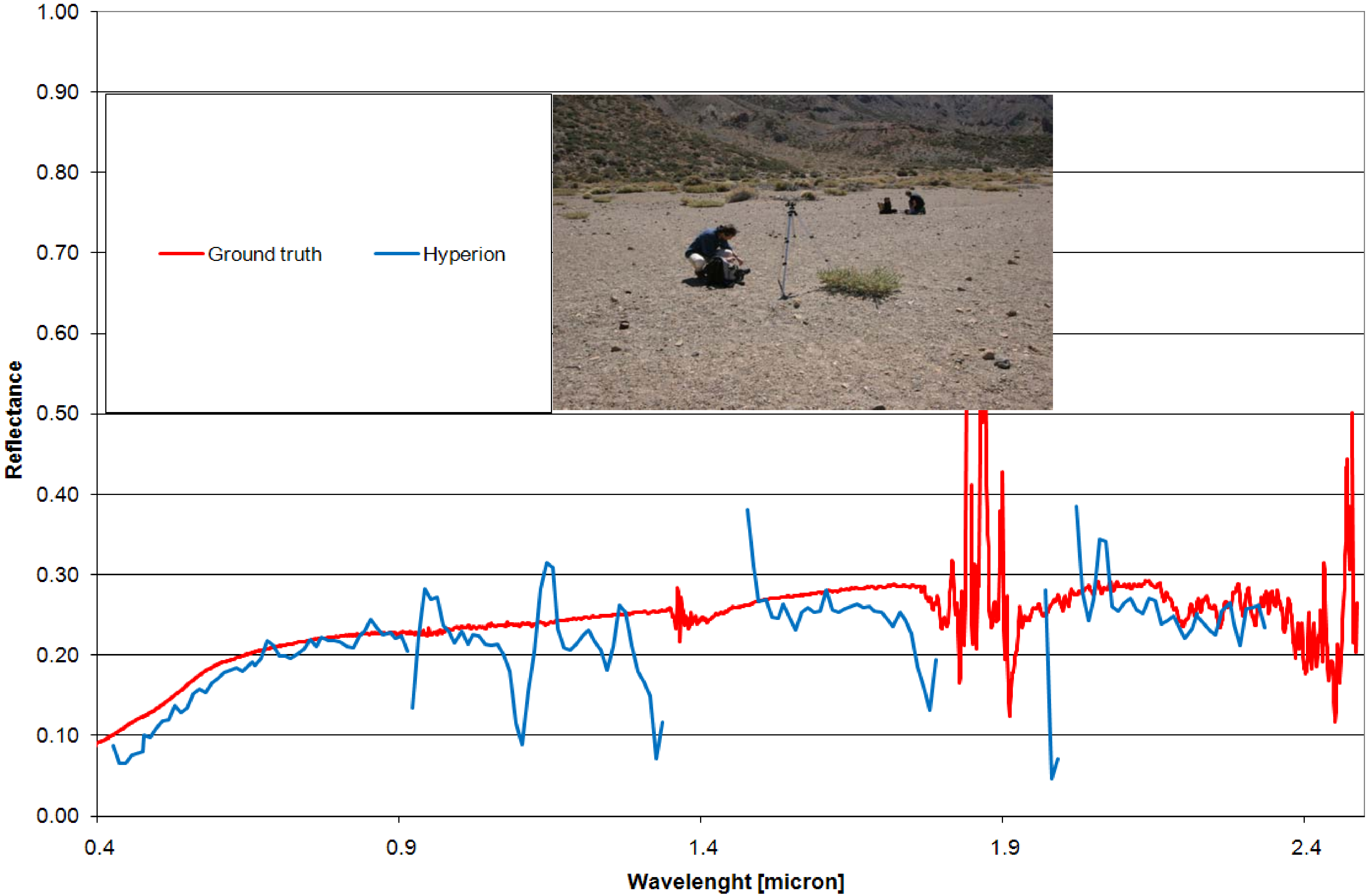

- The results of the val/cal activities on Etna and Teide are presented. The large availability of ground networks and the easy access to the summit areas make of these test sites very good references for the future vicarious calibration and validation activities for the HyspIRI Sensor and for the other planned hyperspectral missions in volcanic areas

Incoming hyperspecrtal ASI mission: PRISMA Precursore IperSpettrale (Hyperspectral Precursor) of the application mission

PRecursore IperSpettrale della Missione Applicativa

- PRISMA (PRecursore IperSpettrale of the application mission) is an earth observation system with electro-optical instrumentation which combines a hyperspectral sensor with a panchromatic, medium-resolution camera.

Objectives

- PRISMA is a "small" Italian mission of demonstrative/technological and pre-operational nature.
- The fundamental objectives are the following:
  - To develop a small mission entirely in Italy for monitoring natural resources and atmosphere characteristics, taking advantage of the prior developments carried out by ASI
  - Make available in a short period of time the data necessary to the scientific community for developing new applications for environmental risk management and observation of the territory, based on high-resolution spectral images
  - Test the hyperspectral payload in orbit - the first or among the first at the European level.

Technical aspects

Characteristics of the System:

- A satellite in LEO SSO (700 km) orbit with planned 5-year operational life
- Hyperspectral/Panchromatic Payload
  - Space resolution: 20-30 m (Hyp) / 2.5-5m (PAN)
  - Swath width: 30-60 km;
  - Spectral range: 0.4-2.5 mm (Hyp) / .4-.7 m (PAN)
  - Continuous coverage of spectral ranges with 10 nm bands

Algeria: Geo-morphology

The country is divided from north to south into four zones:

1. The Tellian Atlas (or the Tell) is made up of the northern-most steep relief flanked by rich coastal plains such as the Mitidja in the centre, the Chelif to the west and the Seybouse plains in the east;
2. The High Plateaus;
3. The Saharan Atlas as a succession of NE-SW oriented reliefs spreading from the Moroccan border to Tunisia;
4. The Sahara desert south of the Atlas yields most of Algeria's hydrocarbon resources. the desert is composed of large sand dunes (East and West Erg) and gravel plains (regs) with dispersed oases such as Ghardaia and Djanet .

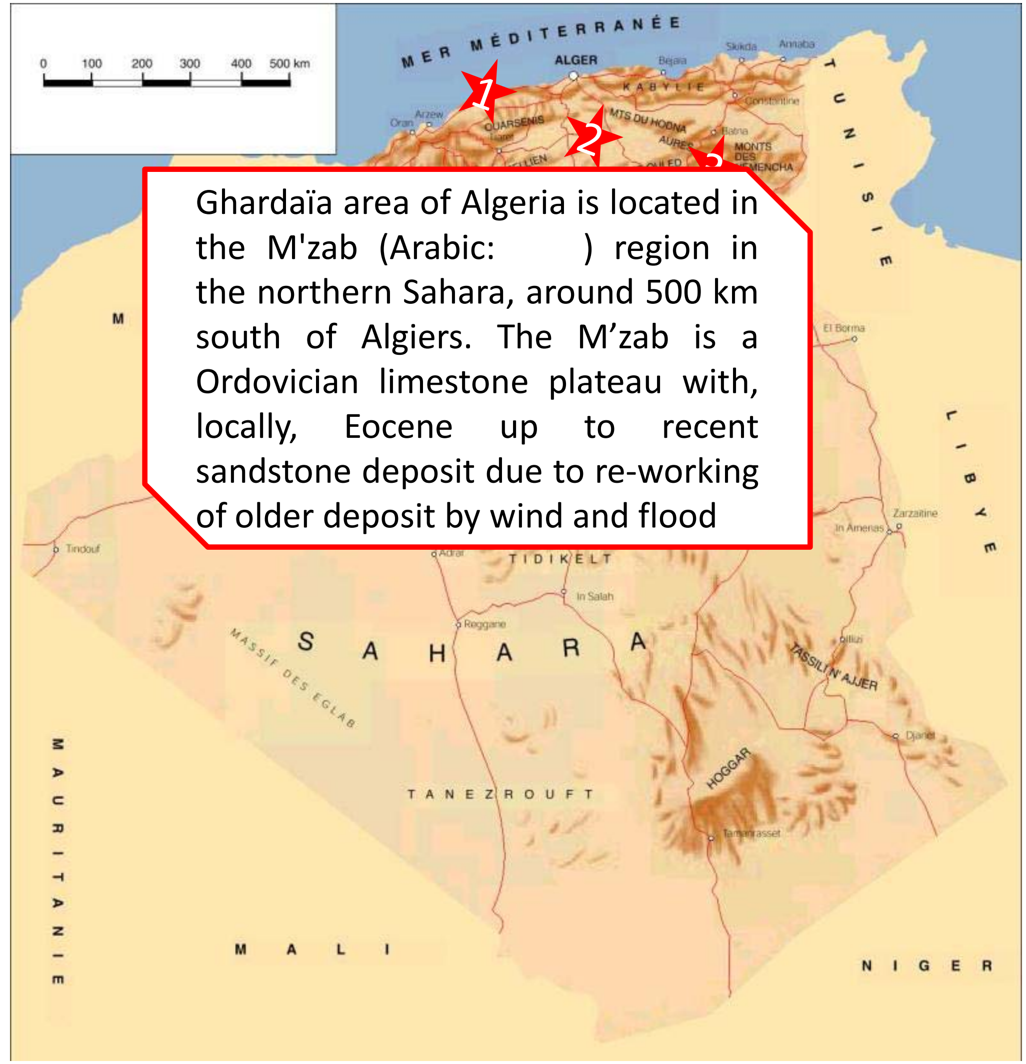

Ghardaïa area of Algeria is located in the M'zab (Arabic:) region in the northern Sahara, around 500 km south of Algiers. The M'zab is a Ordovician limestone plateau with, locally, Eocene up to recent sandstone deposit due to re-working of older deposit by wind and flood

Thank You!

For further information: Fabrizia Buongiorno, fabrizia.buongiorno@ingv.it

AQUARIUS/SAC-D

2010 HyspIRI Science Workshop

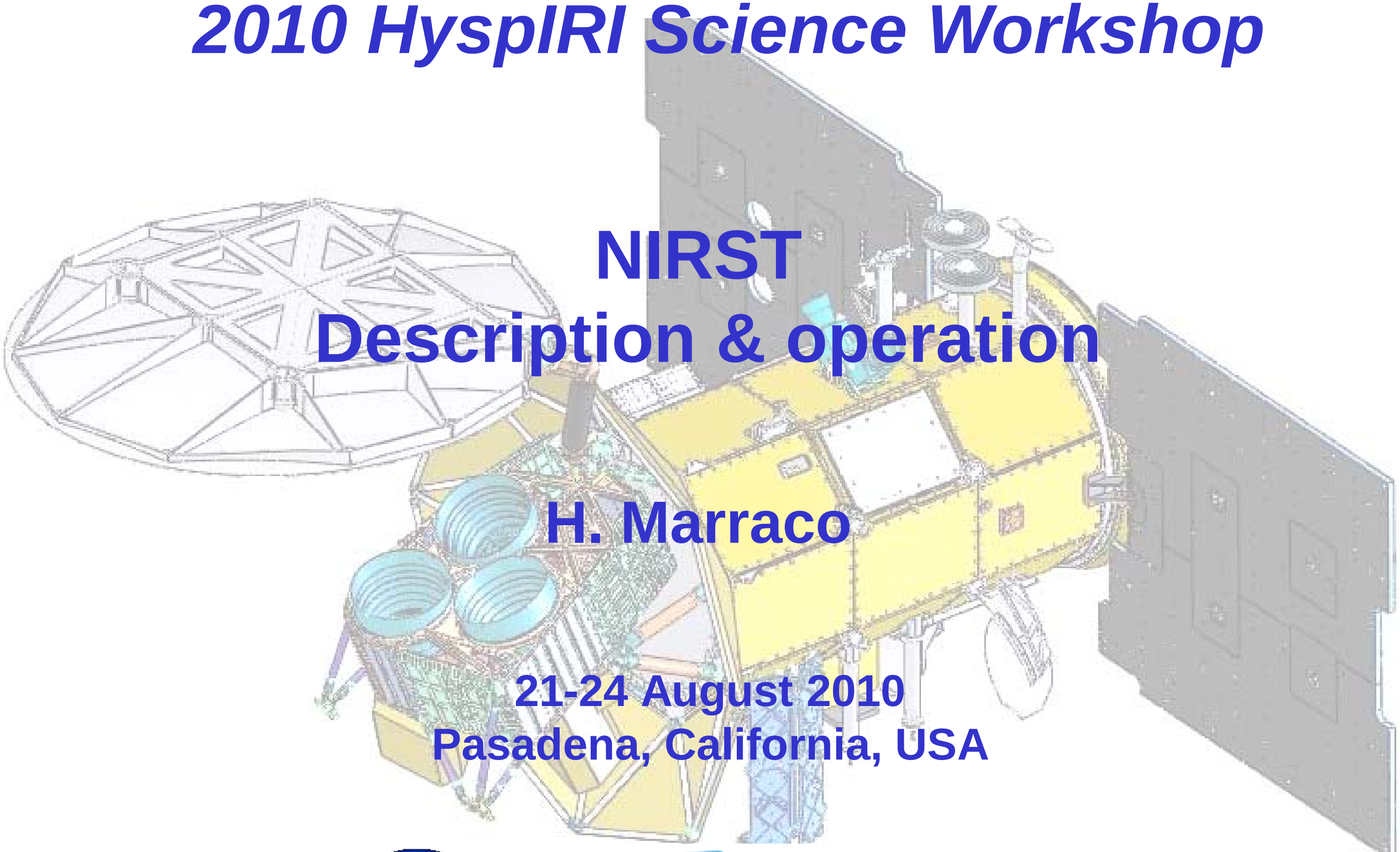

NIRST
Description & operation

H. Marraco

21-24 August 2010
Pasadena, California, USA

NASA

CONAE
COMISION NACIONAL DE ACTIVIDADES ESPACIALES

CSA ASC

BANDS

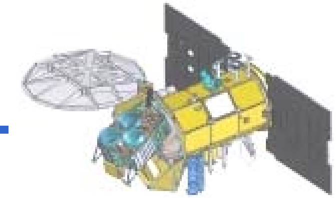

		MWIR2 (Band 1)	LWIR2 (Band 2)	LWIR3 (Band 3)
Central wavelength		3.8 µm	10.85 µm	11.85 µm
Band Limits		3.4 – 4.2 µm	10.4 – 11.3 µm	11.4 – 12.3 µm
Temperature	Min.	400K	250K	
	Max.	1000K	500K	
NEΔT		<1.5K @ 400K	<0.8K @ 300K	<0.4K @ 300K
Temp. accuracy		2.5K @ 400K	1.5K @ 300K	<2K @ 300K
Detectable size of fire event		$200m^2$ @ 1000K		

Conceptual design

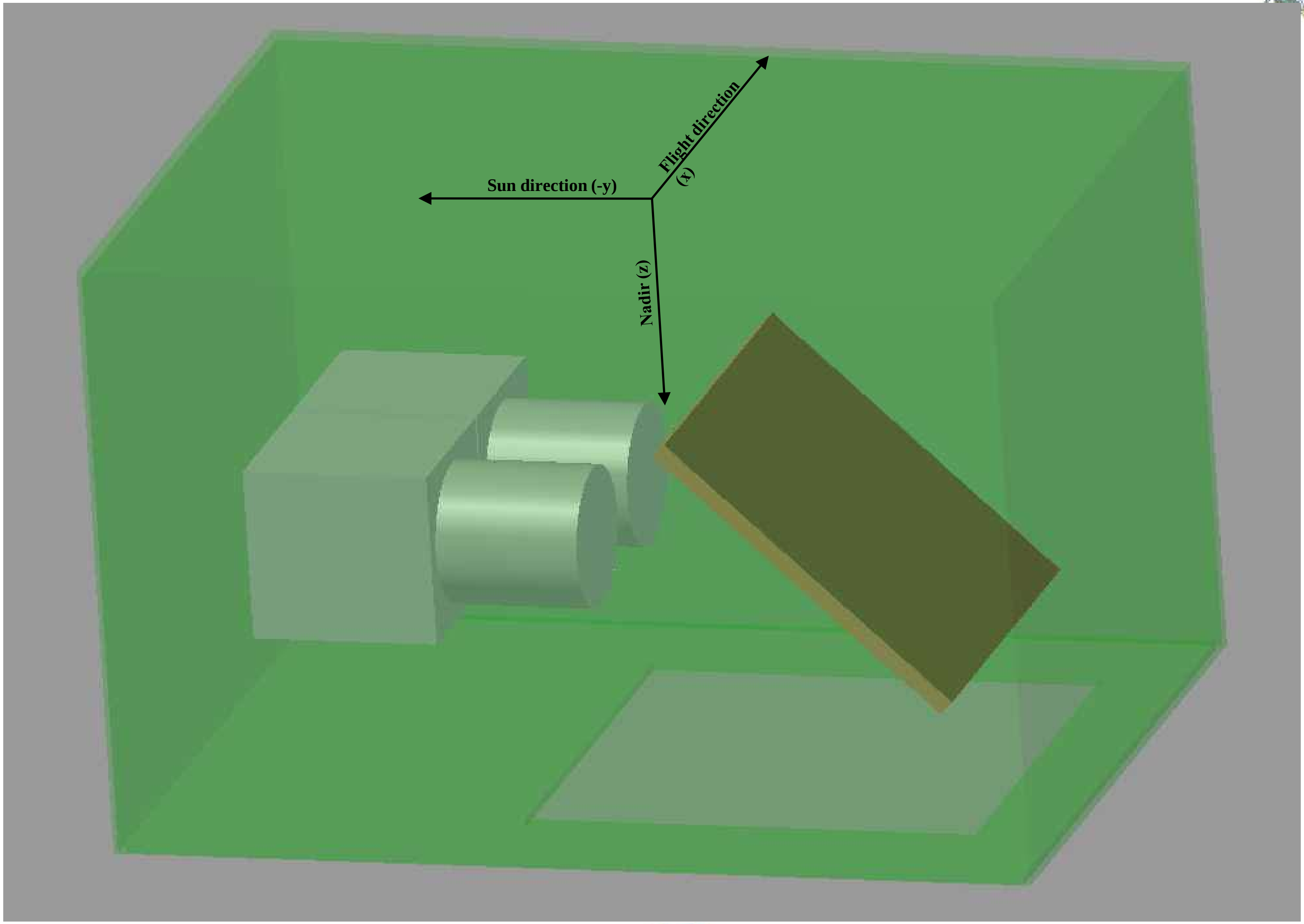

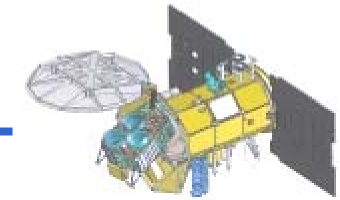

NIRST COMPONENTS

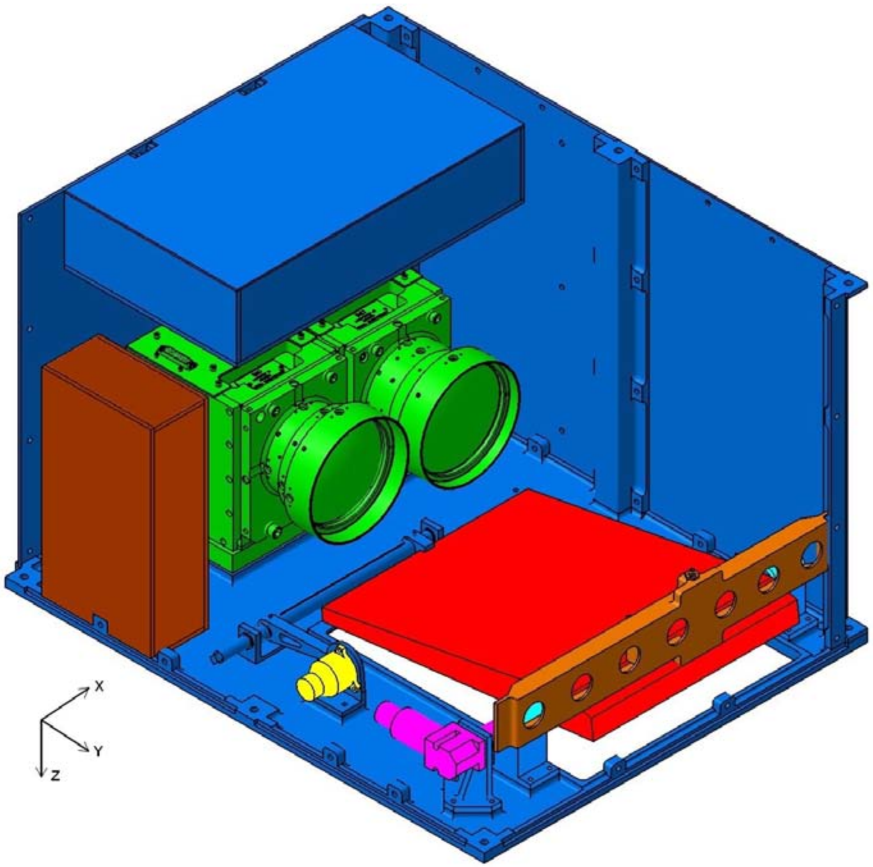

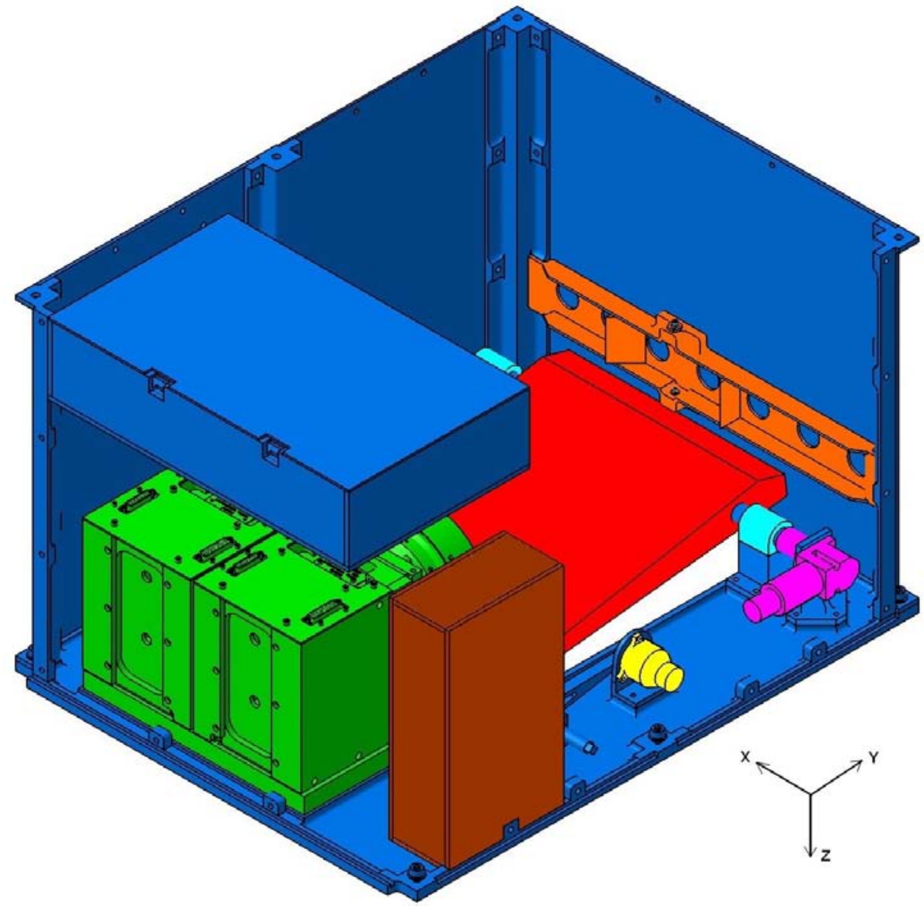

GREEN:	**INO-CSA**
BROWN:	**IAR**
YELLOW:	**TINI AEROSPACE**
BLUE:	**GEMA**
MAGENTA:	**CDA INTERCORP**
ORANGE:	**CIOP-GEMA**
LIGHT BLUE:	**SFK-AMPEP**
RED:	**AXSYS TECHNOLOGIES**

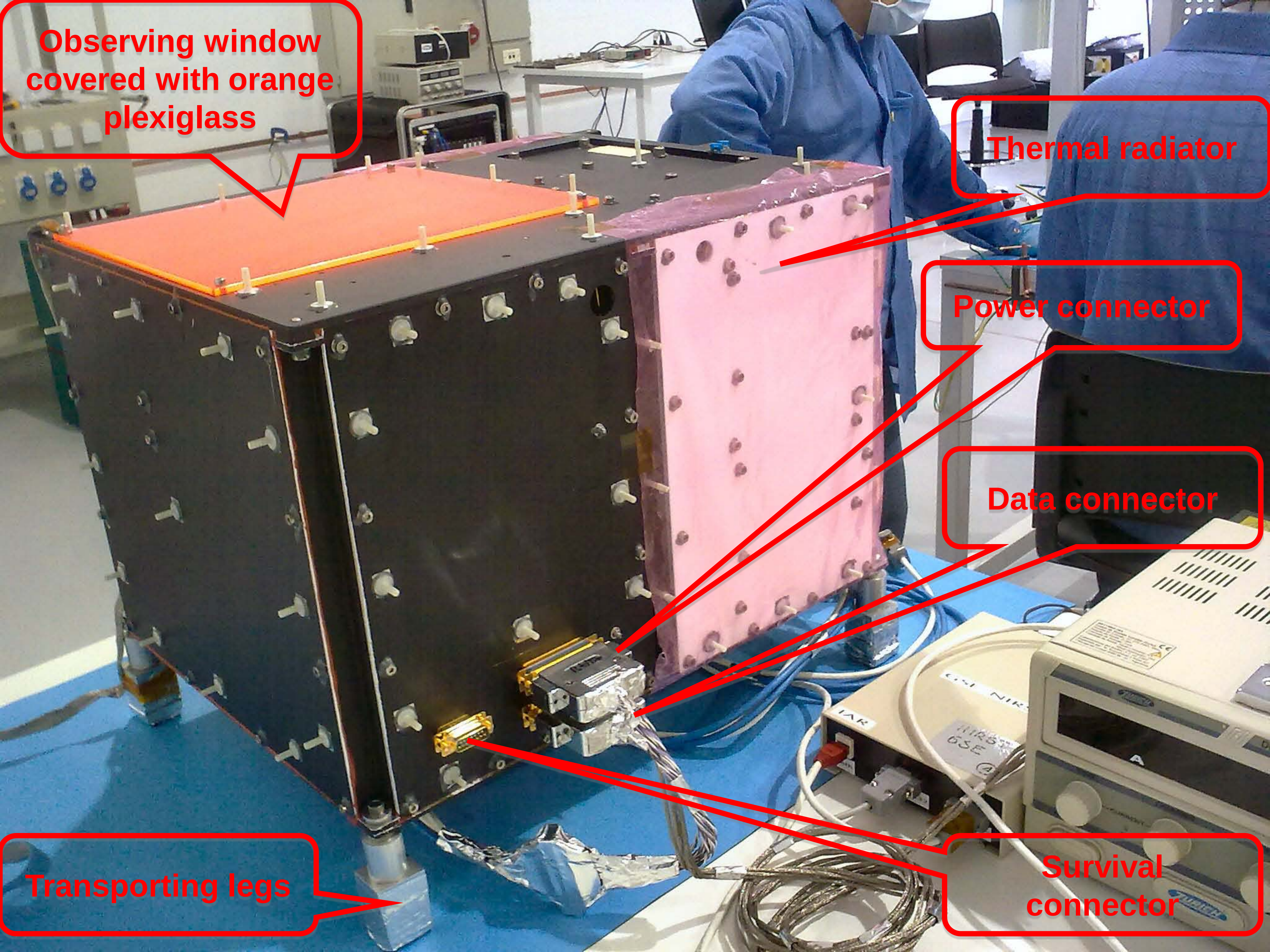
Observing window covered with orange plexiglass
Thermal radiator
Power connector
Data connector
Transporting legs
Survival connector

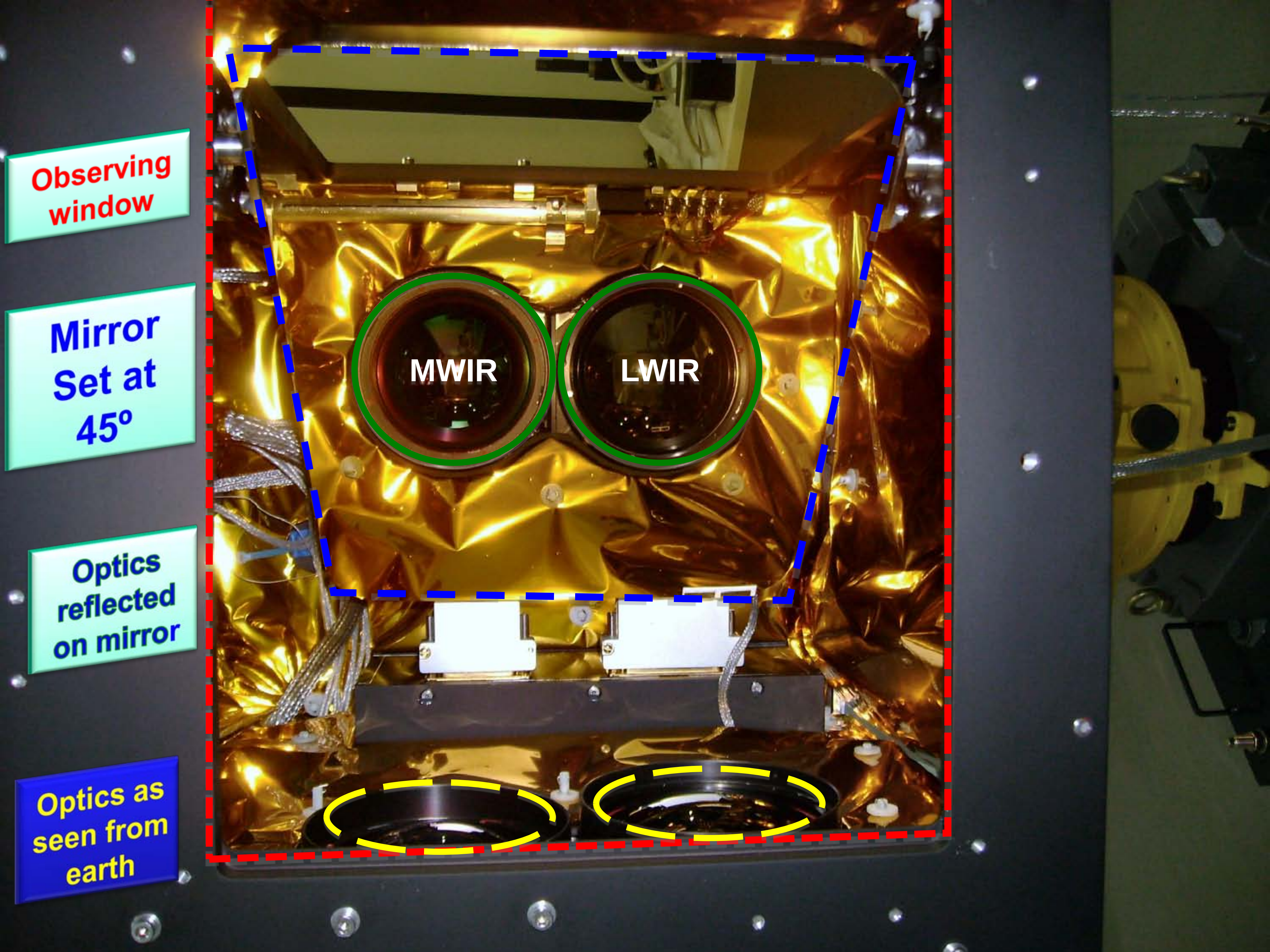
Observing window
Mirror Set at 45°
Optics reflected on mirror
Optics as seen from earth
MWIR
LWIR

FPA

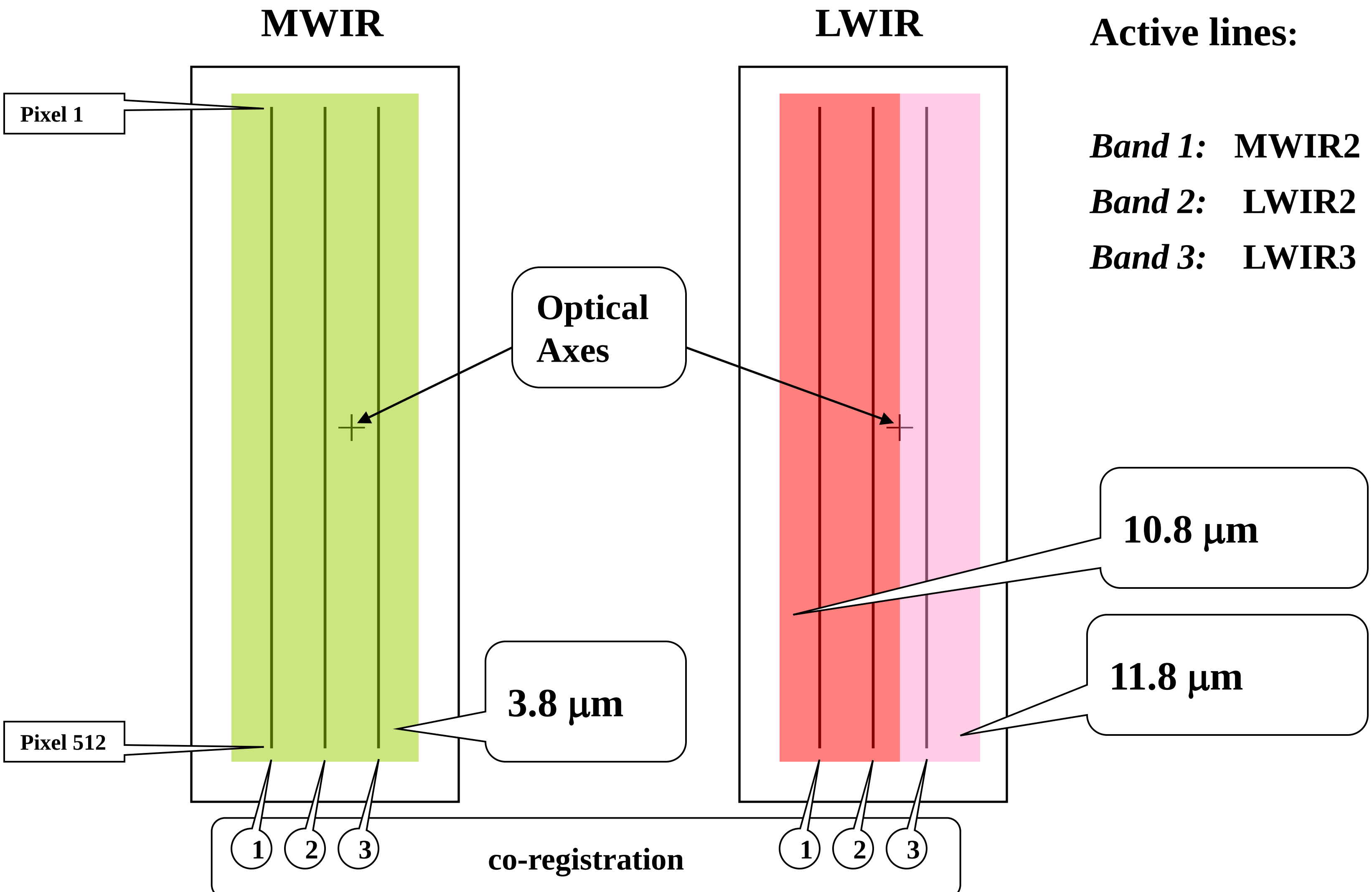

Active lines:

Band 1: **MWIR2**

Band 2: **LWIR2**

Band 3: **LWIR3**

AQUARIUS/SAC-D NIRST Fields of View

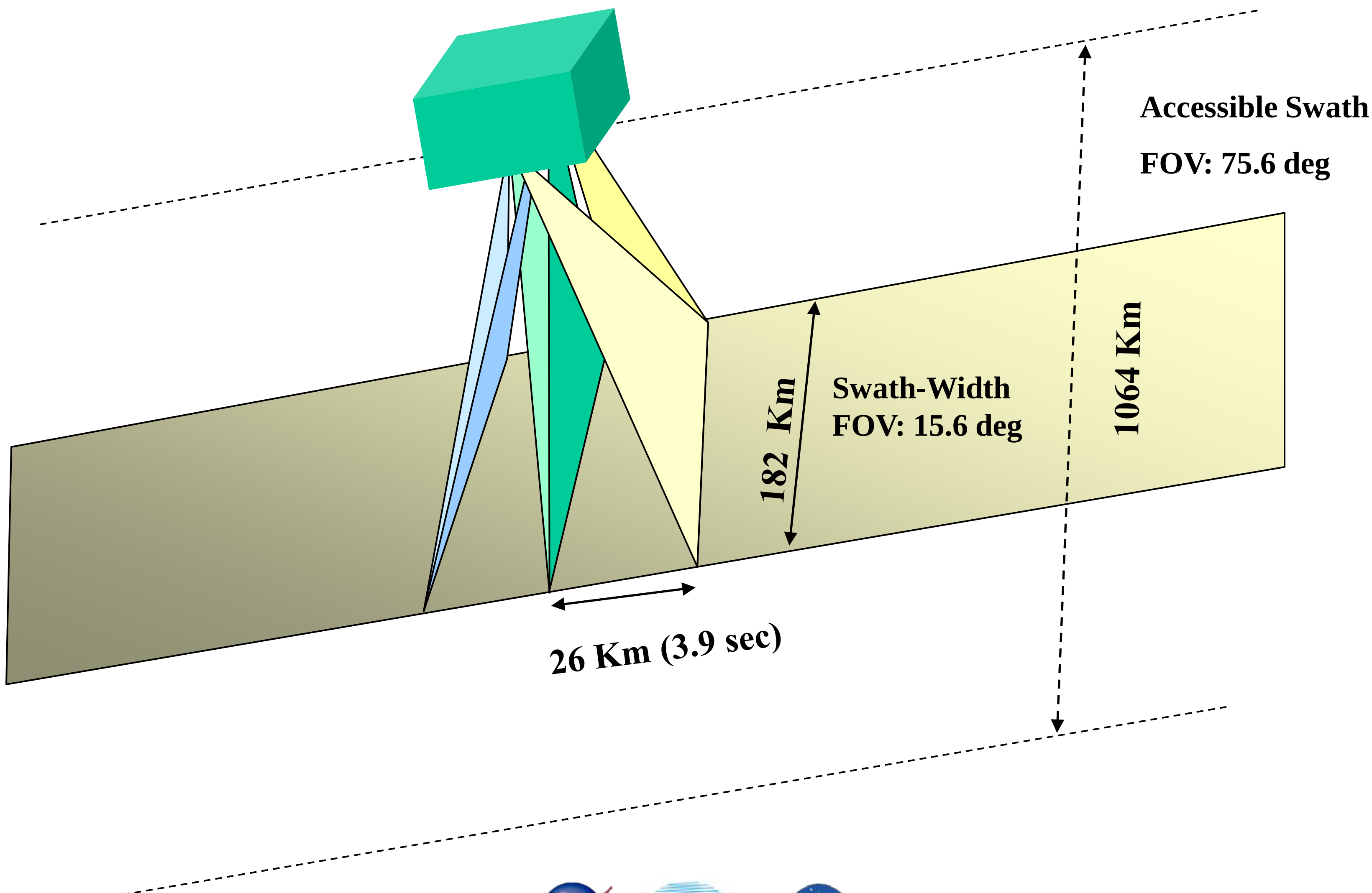

AQUARIUS/SAC-D

Revisit Scenario

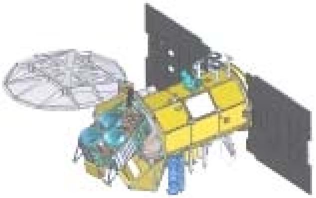

Virtual (1000 km swath)

Latitude	Example location	Average revisit interval (days)	Maximum missing days
±67º	Northern Canada	0.5	0
±55º	Tierra del Fuego, mid Canada	0.7	1
±23º	Jujuy	1.2	2

Nadir pointing (182 km swath)

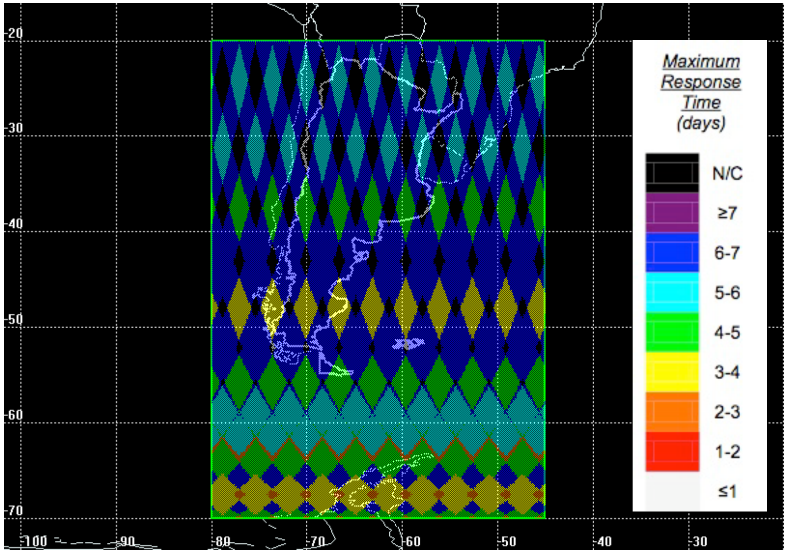

System Transfer Function

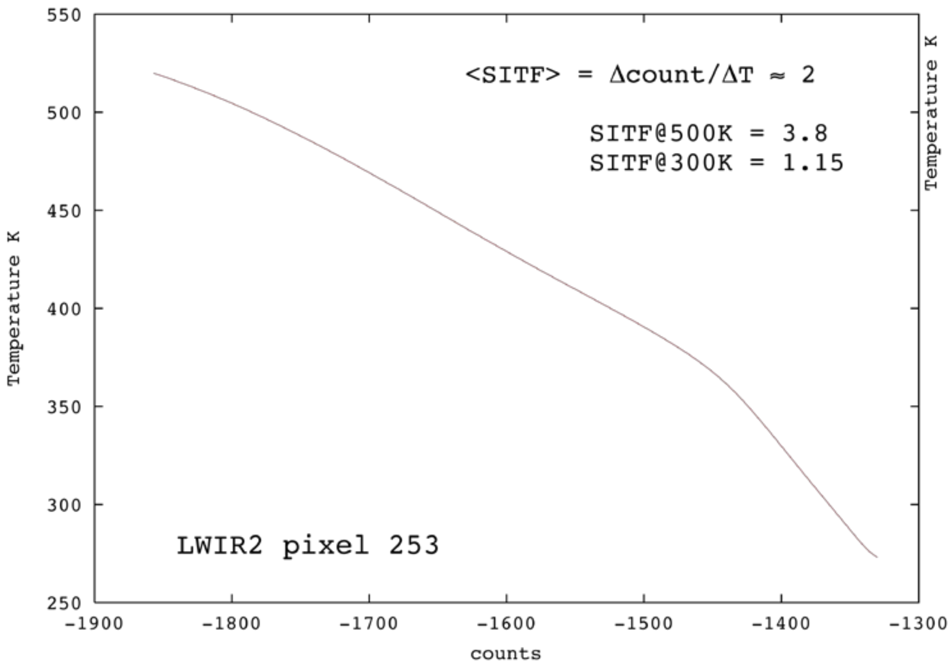

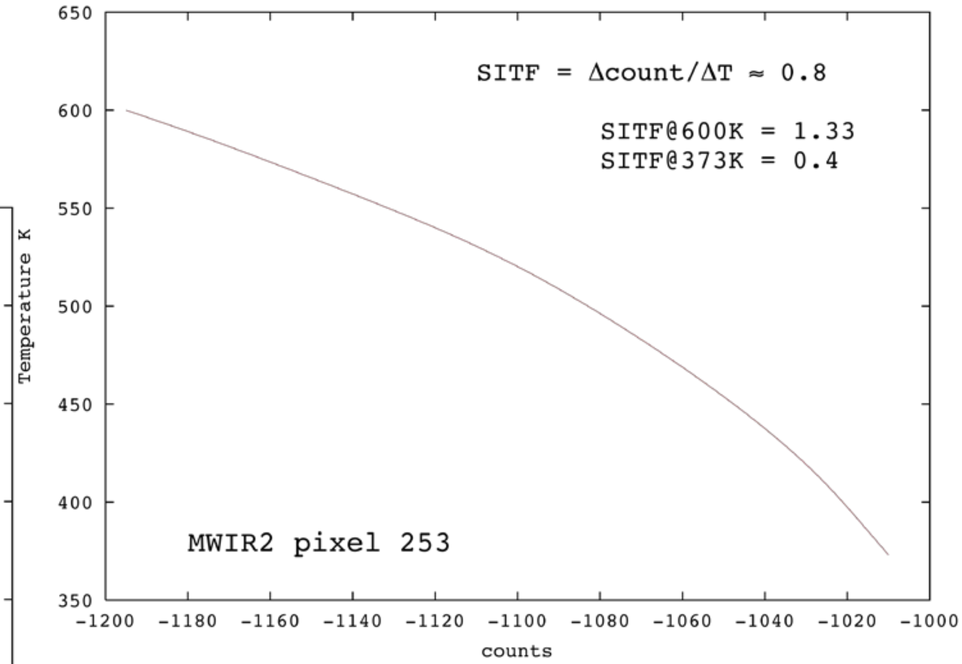

Power vs counts

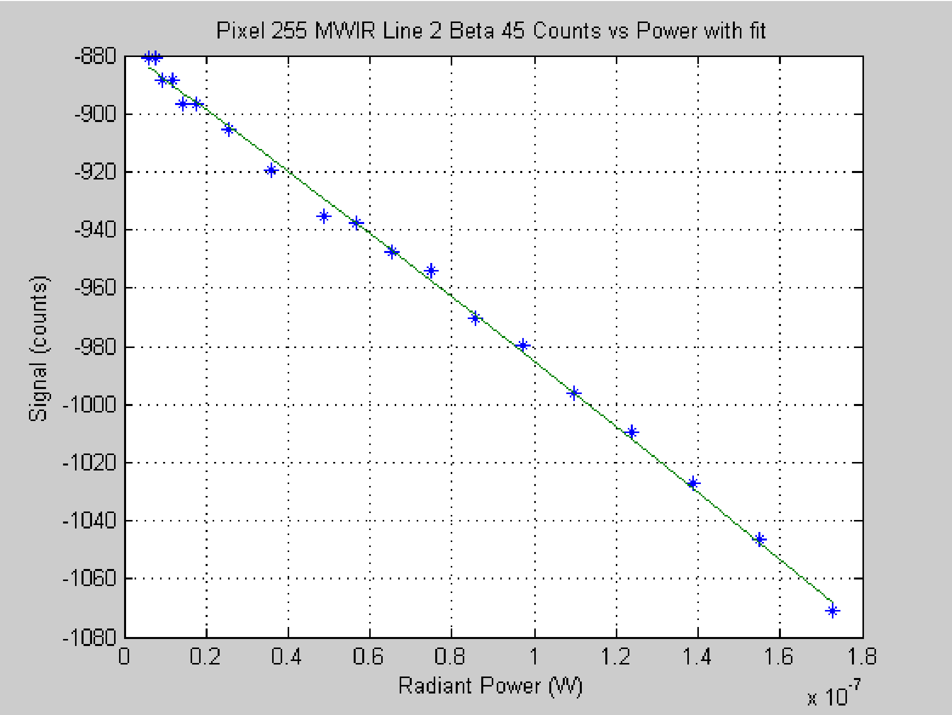

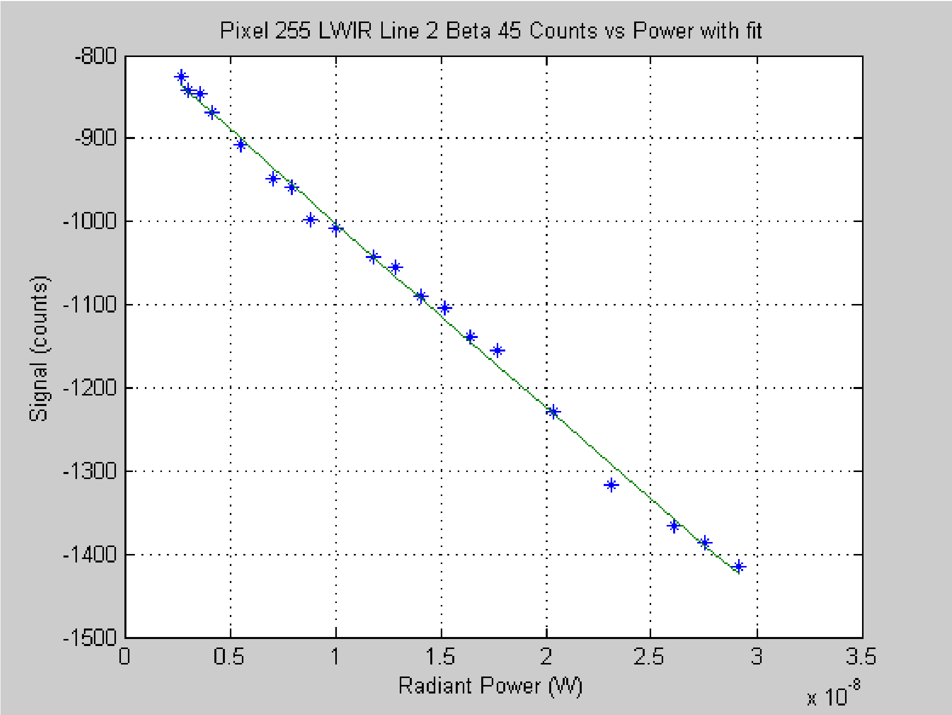

AQUARIUS/SAC-D

Observing Canada/Italy/Argentina

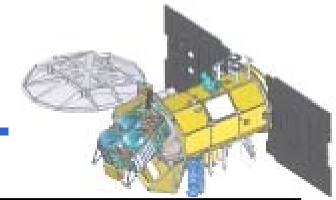

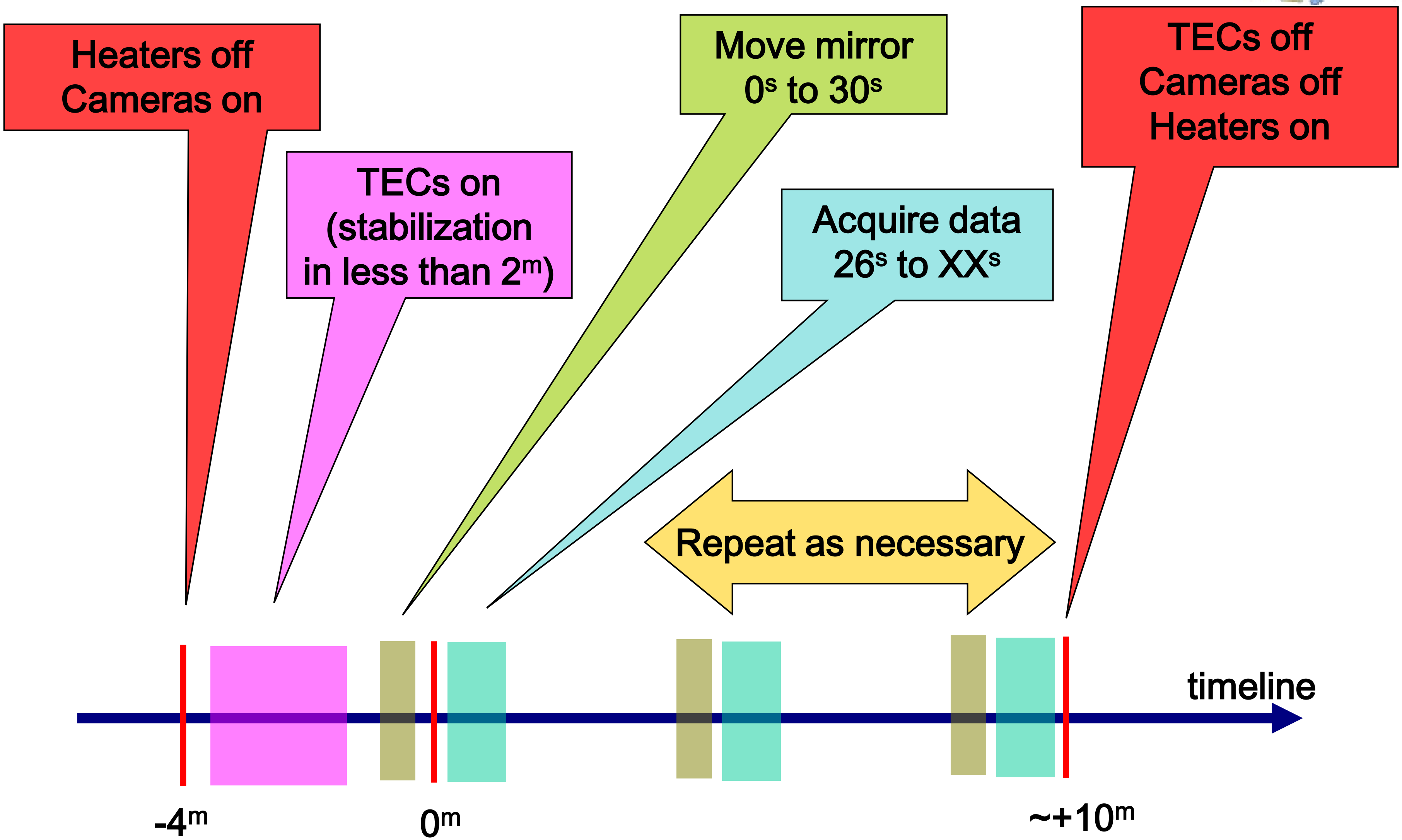

NIRST over Argentina & Canada

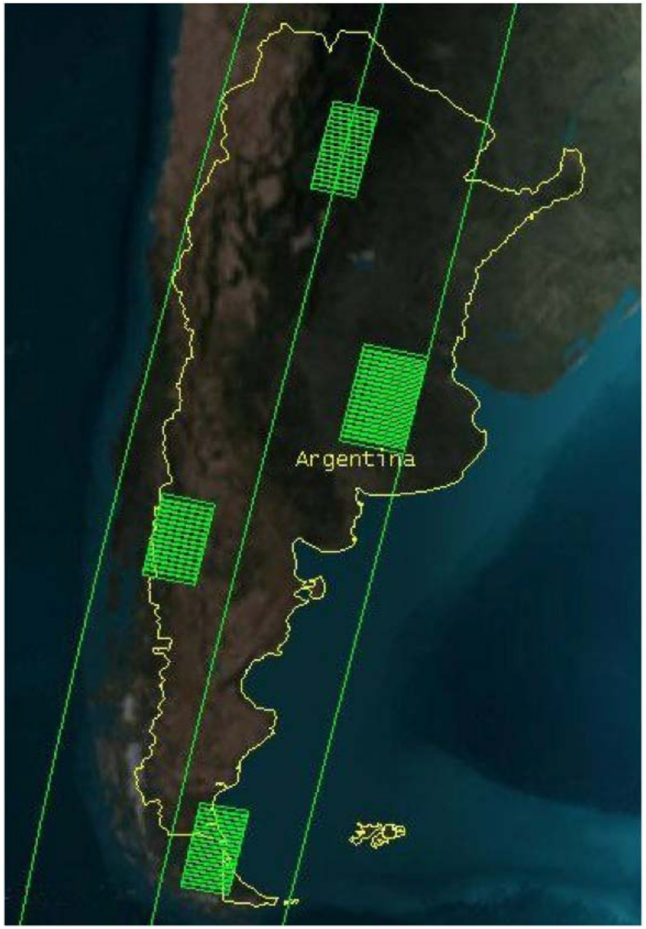

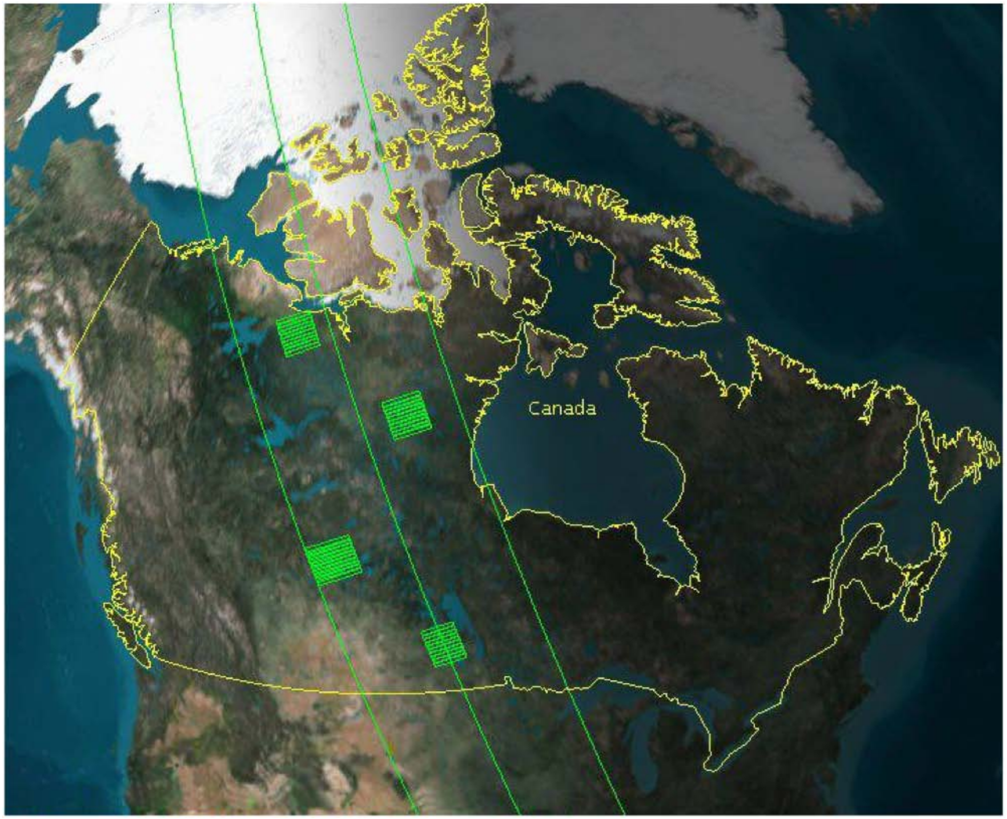

AQUARIUS/SAC-D

Inland waters

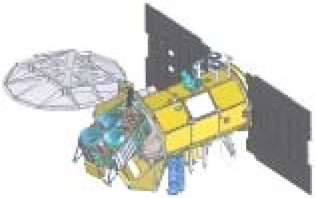

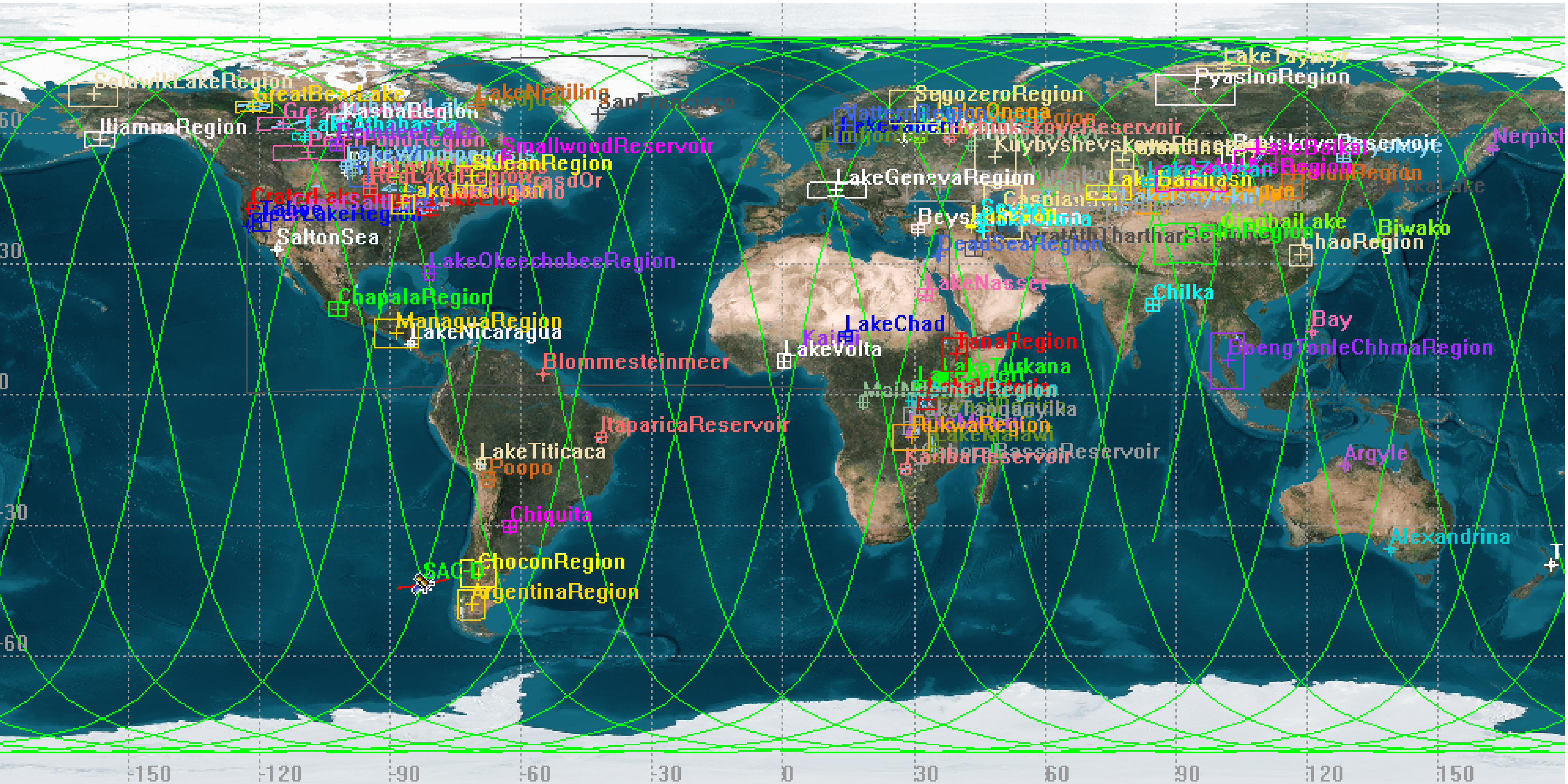

Weekly memory budget

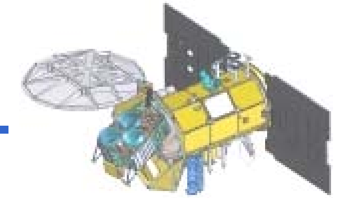

Data acquisition rate: 53 kbytes/sec

Weekly (103 rev.) statistics:

29 downloads when SAC-D is 5 over horizon at Córdoba Ground station.
92 virtual overflights of Canada and Italy.
185 possible inland waters acquisitions (only those necessary to get weekly complete data).

Assumptions:

1. All acquisitions over Argentina and inland waters in neighboring countries are downloaded in real time.
2. Data stored in mass memory is downloaded at 130 kbytes/sec.
3. Canada and Italy are covered in a TBD%.
4. Inland waters are covered in a TBD%.

Weekly memory budget

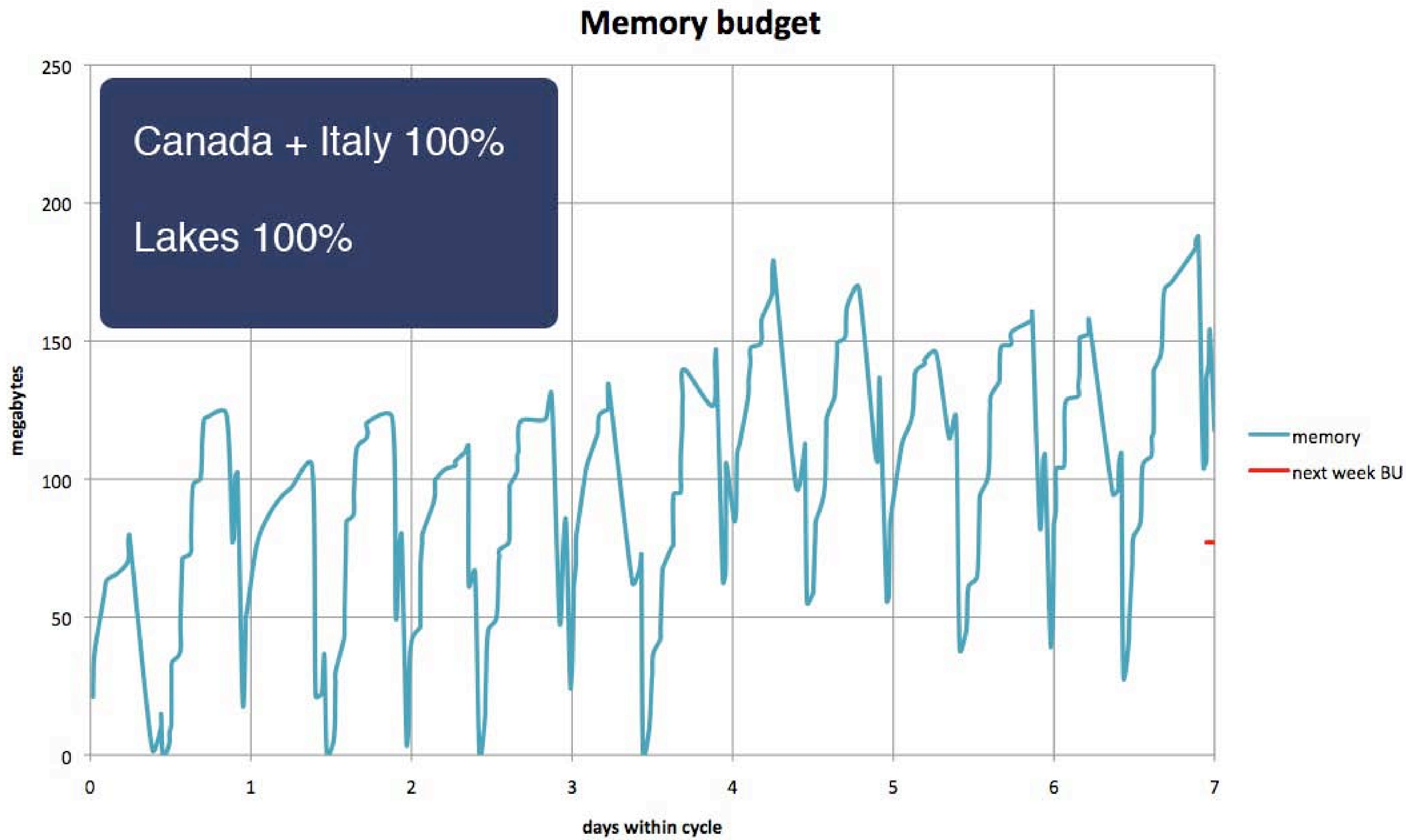

Weekly memory budget

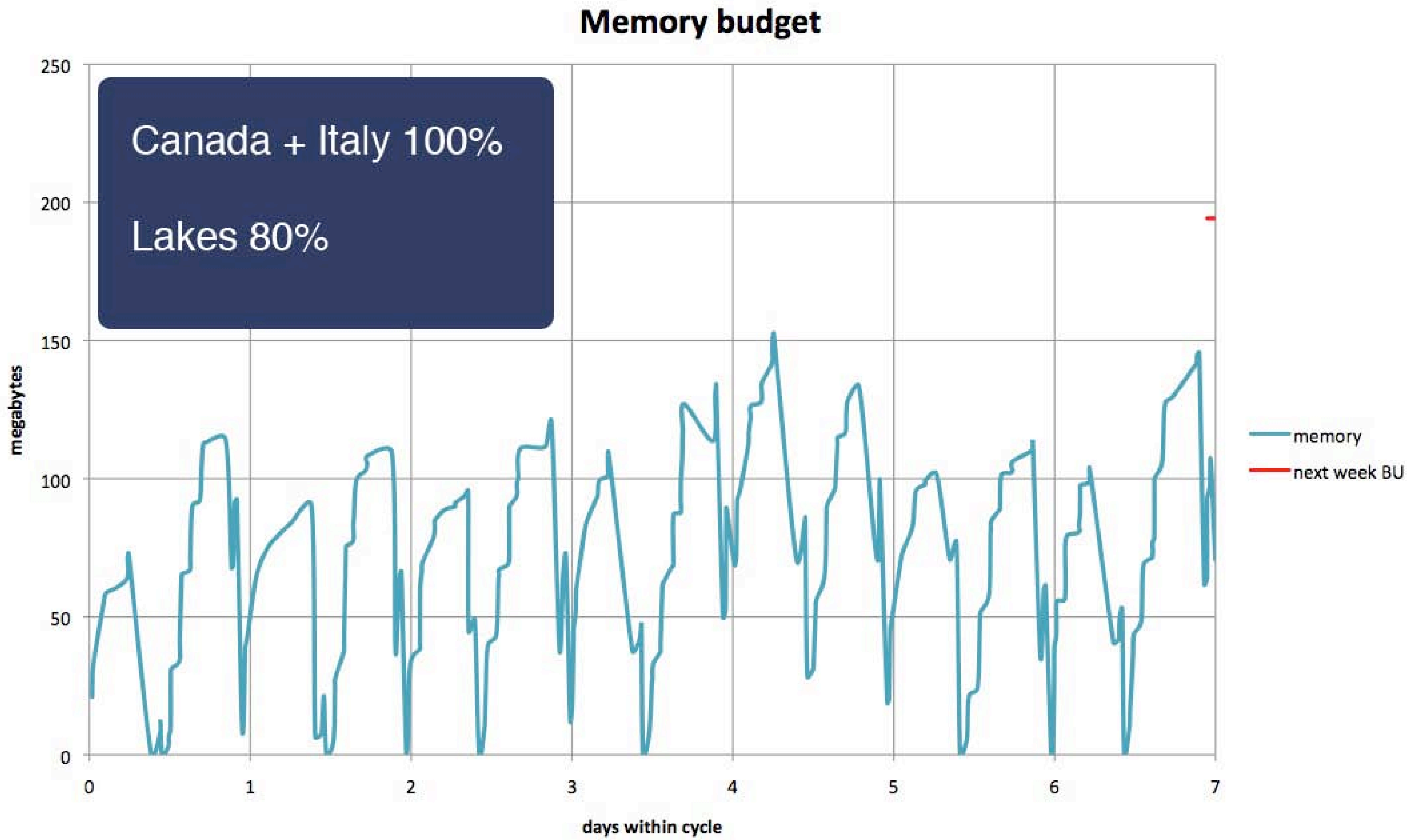

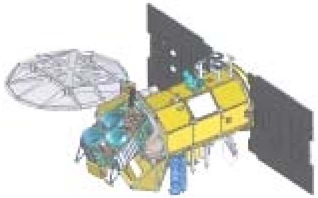

Back up slides

What we measure

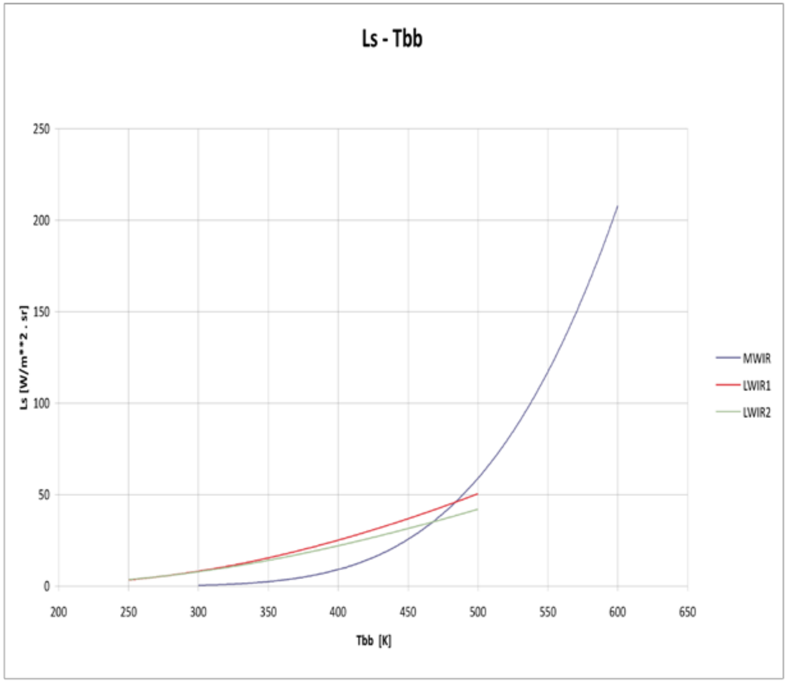

Steps in NIRST calibration

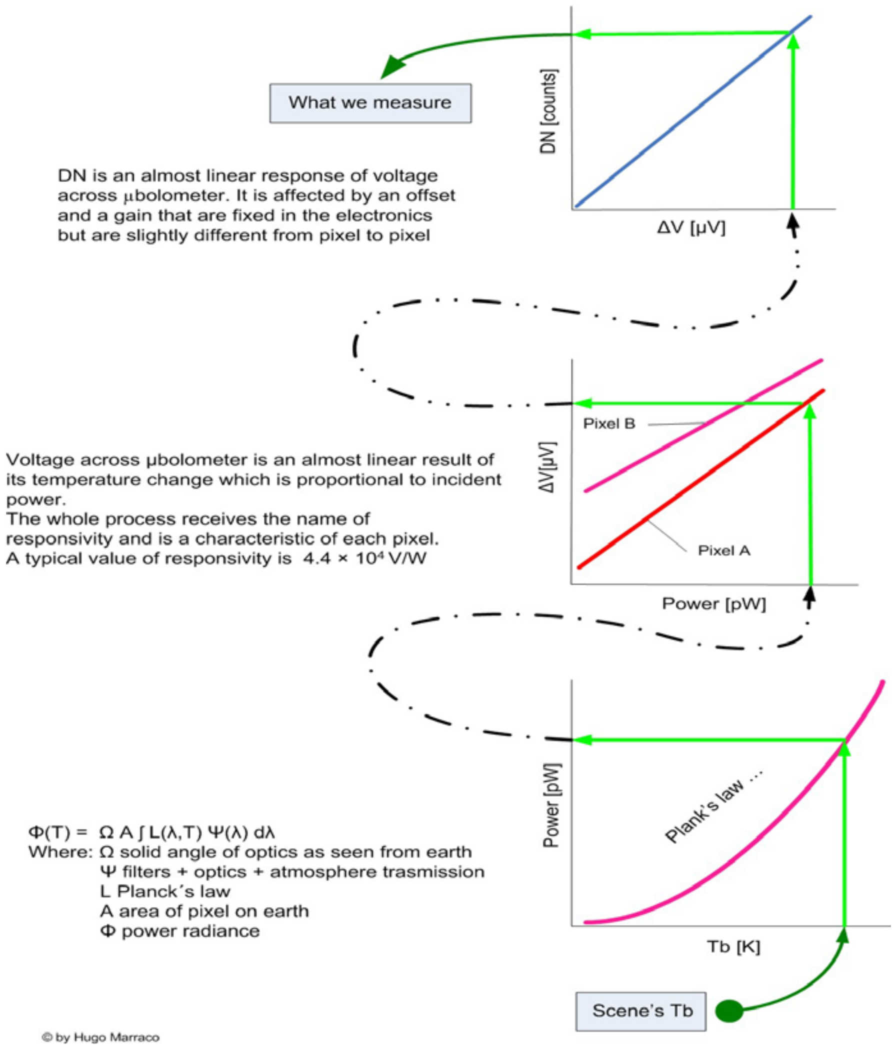

DVF (counts)

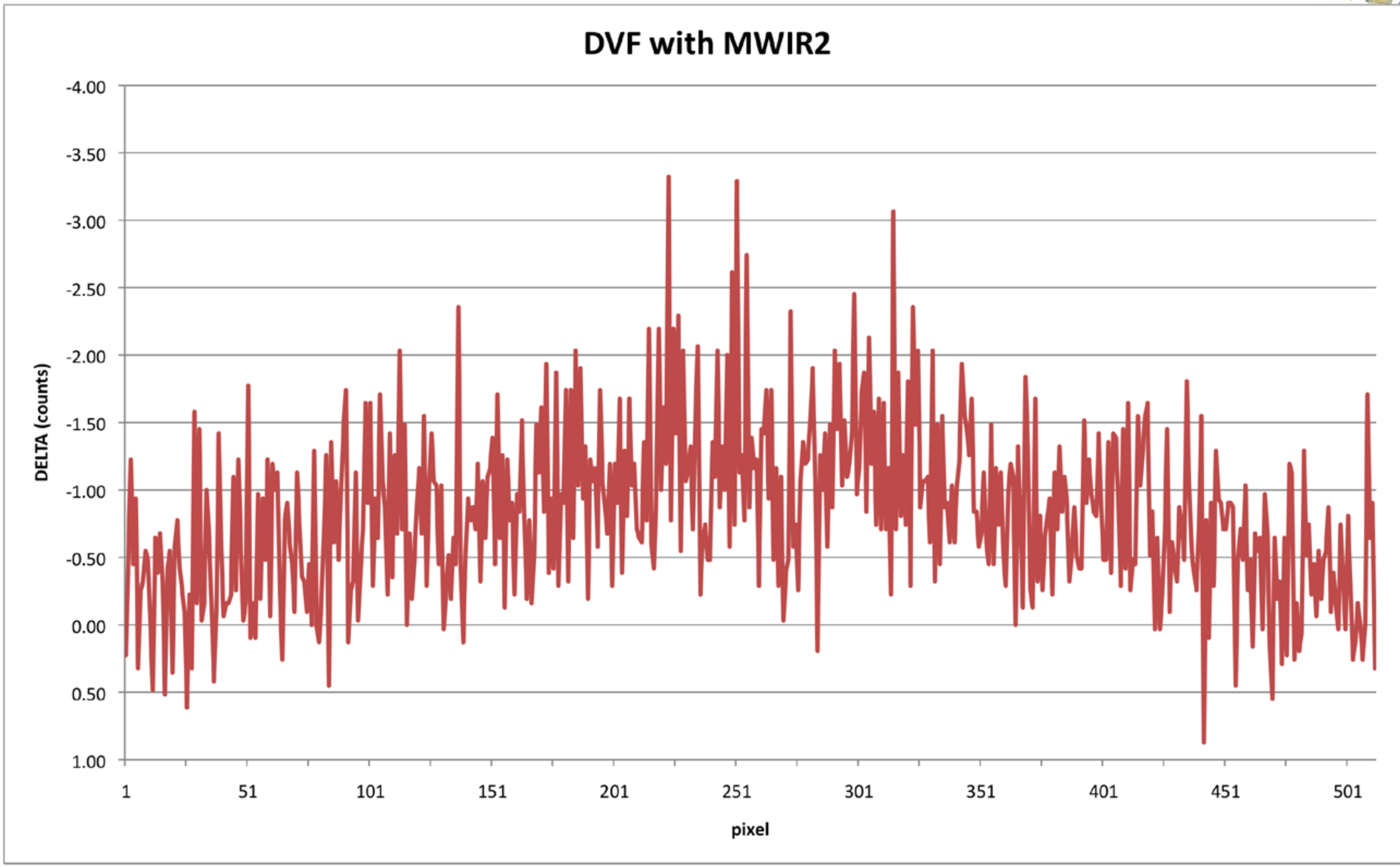
DVF with MWIR2
-4.00
-3.50
-3.00
-2.50
-2.00
-1.50
-1.00
-0.50
0.00
0.50
1.00
DELTA (counts)
1
51
101
151
201
251
301
351
401
451
501
pixel

DVF (power)

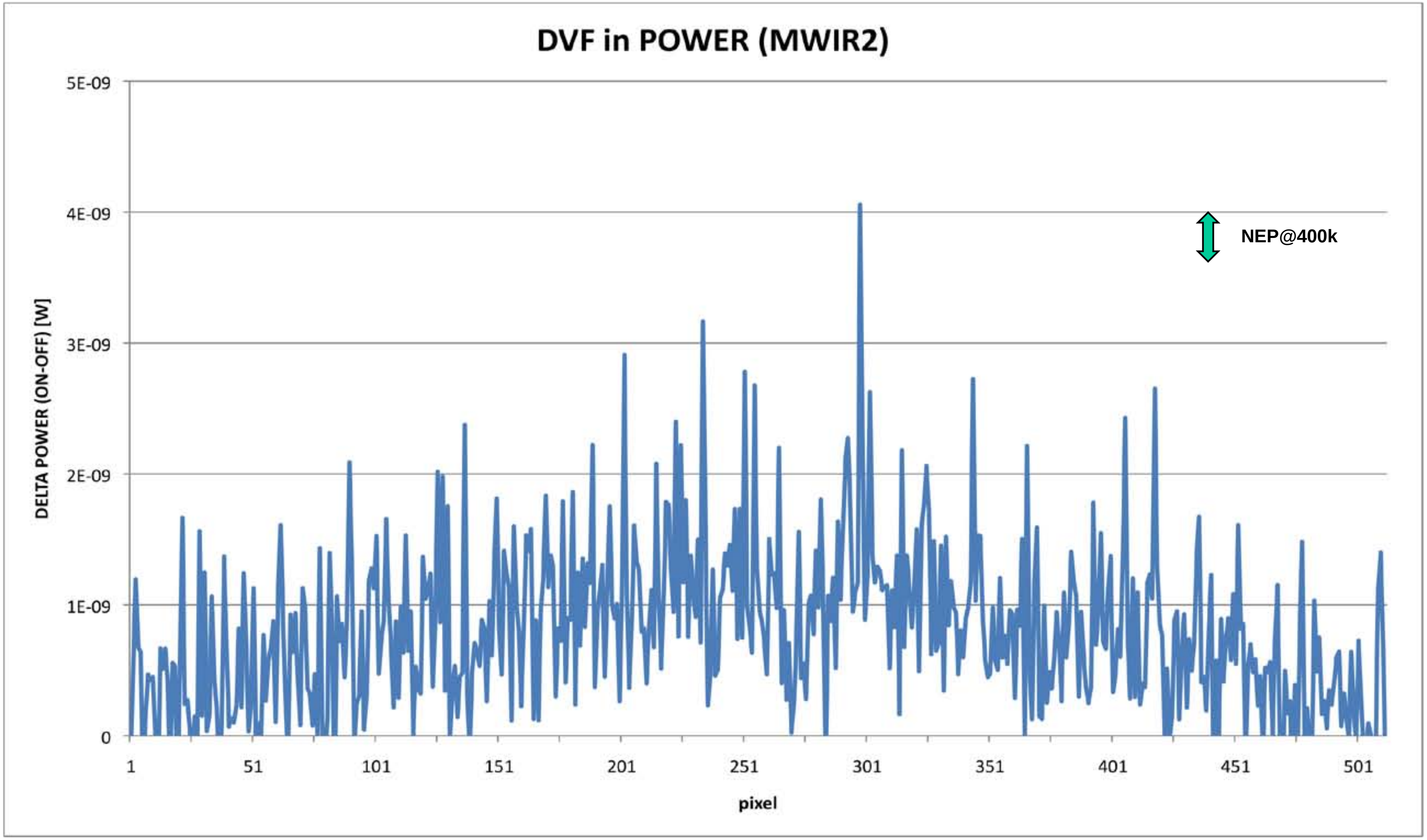
DVF in POWER (MWIR2)
5E-09
4E-09
3E-09
2E-09
1E-09
0
DELTA POWER (ON-OFF) [W]
1
51
101
151
201
251
301
351
401
451
501
pixel
NEP@400k

Pixel variety

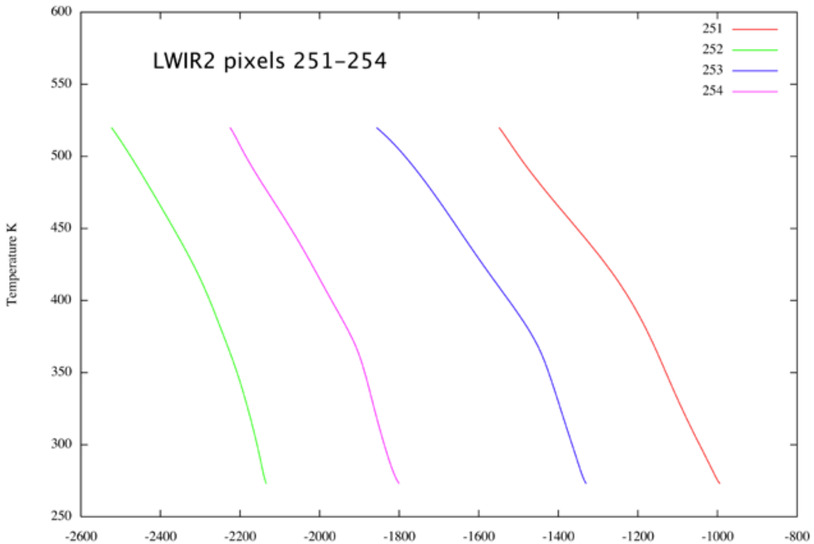

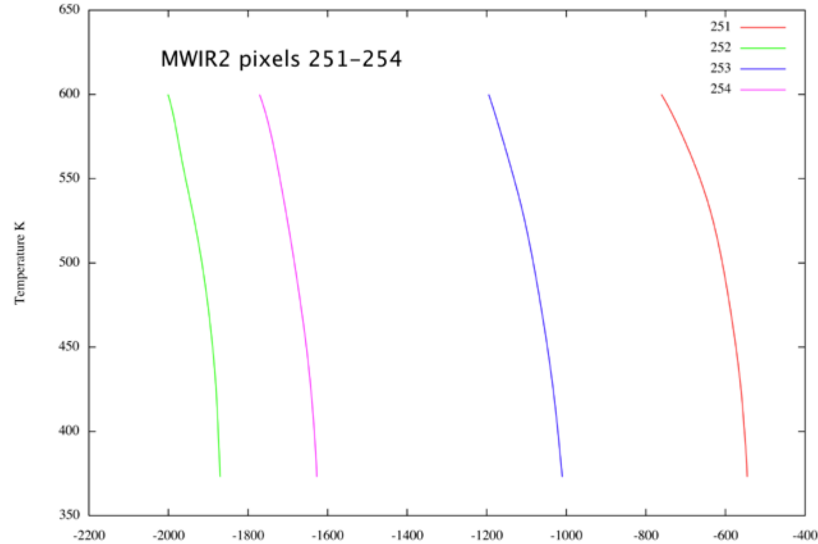

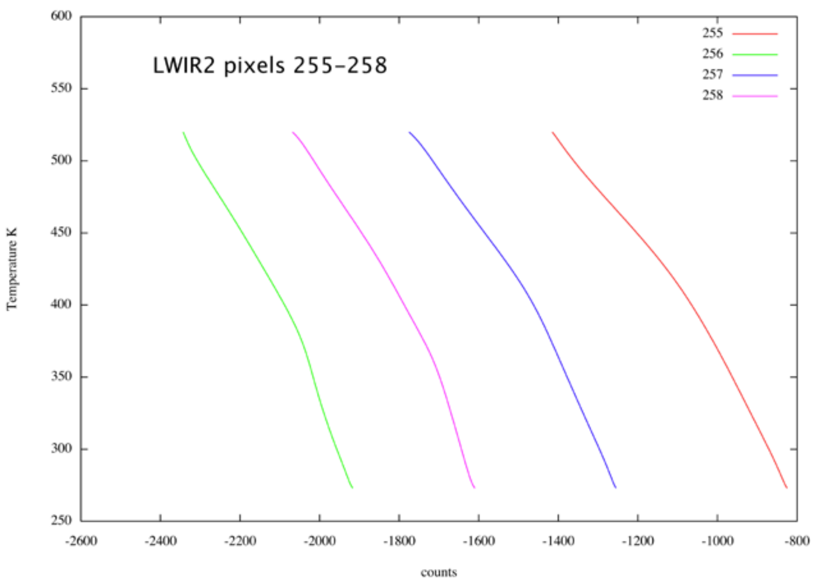

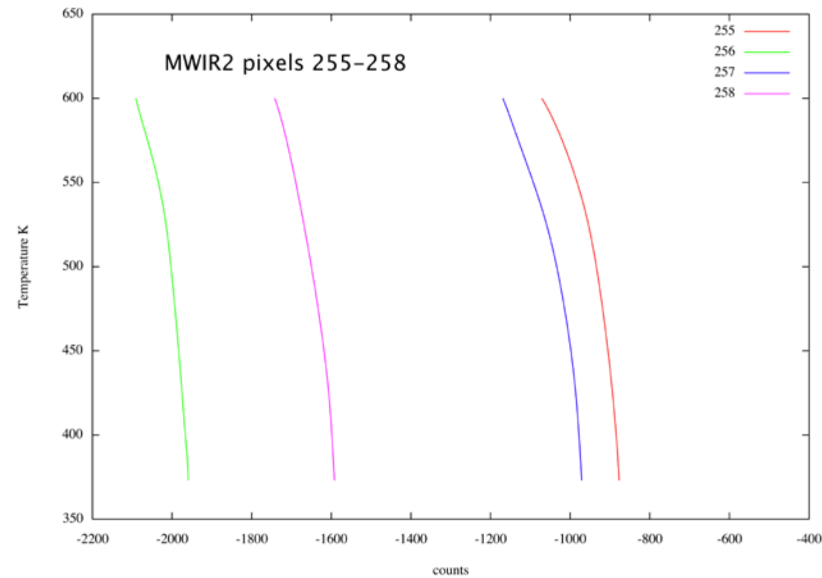

Active and reference (blind) pixels

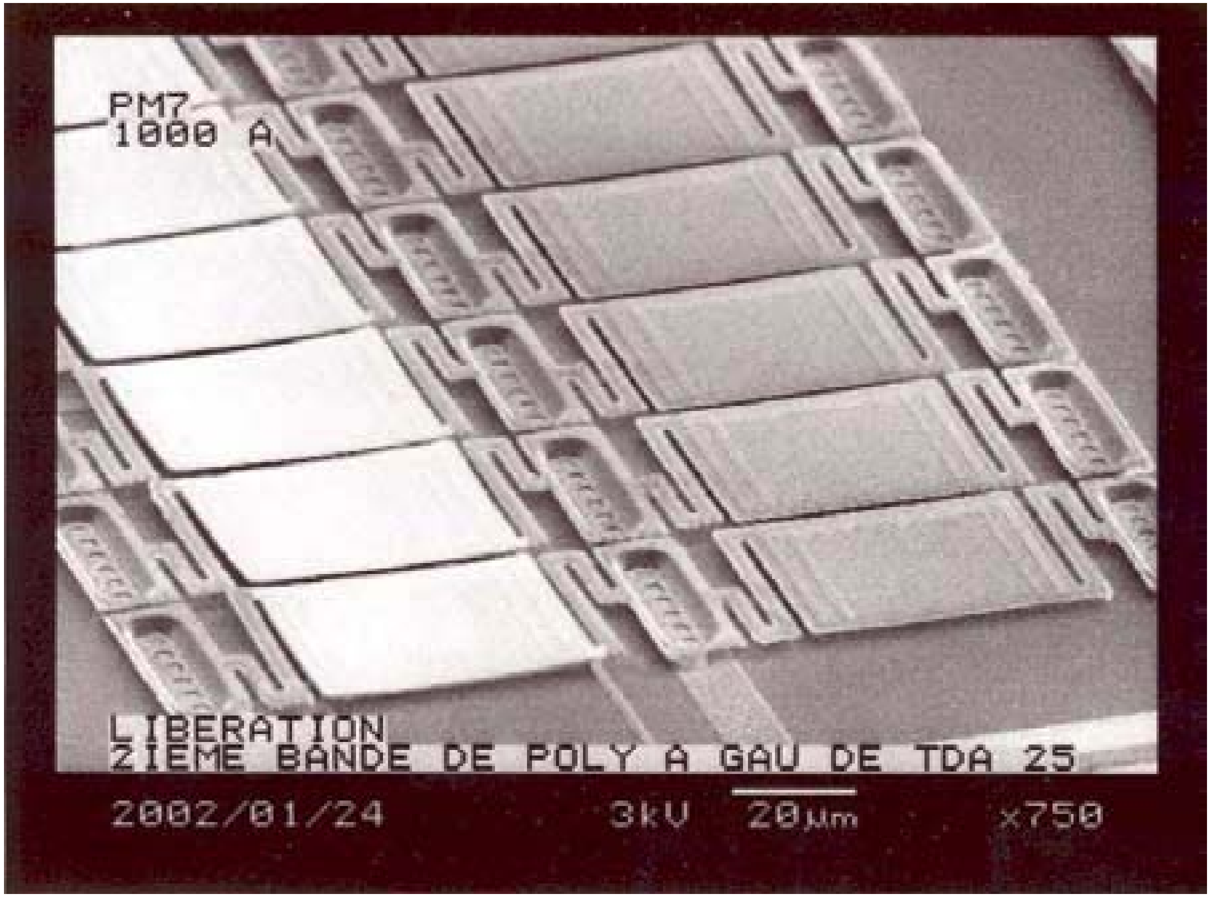

Blind pixel

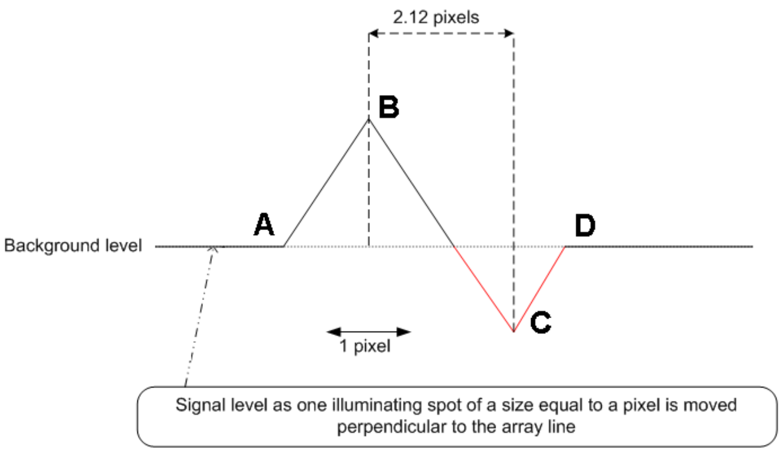

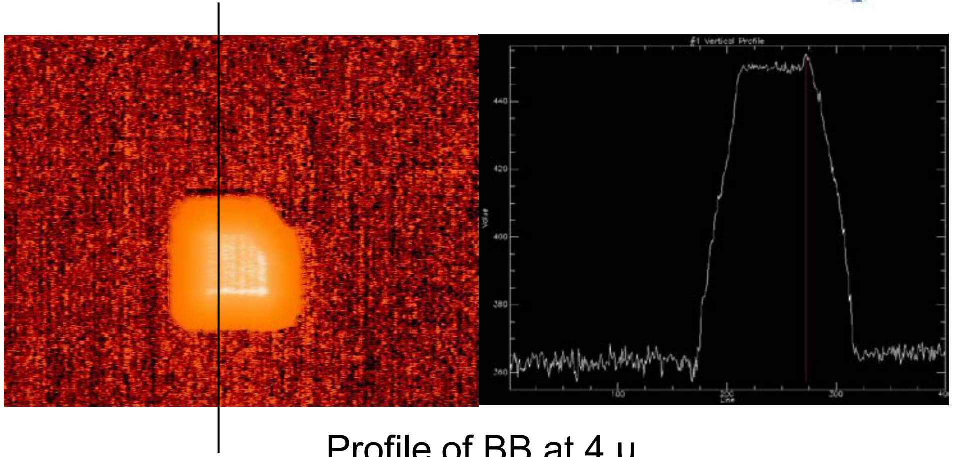

Profile of BB at 4 μ

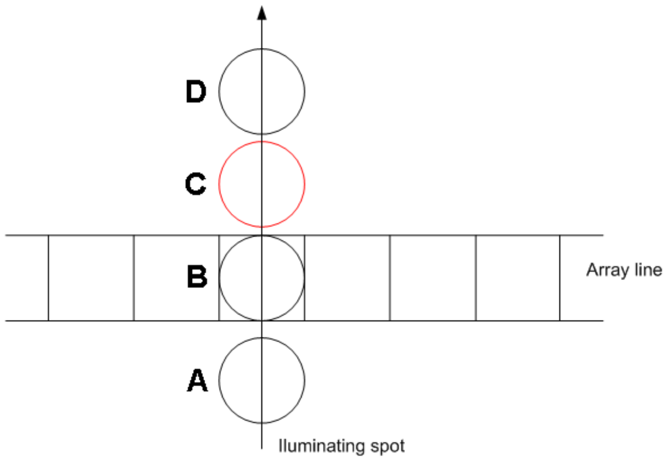

BAND	|Signal@C| / |signal@B| [%]
MWIR	51% 18%
LWIR	13% 2%

Blind pixel (MWIR)

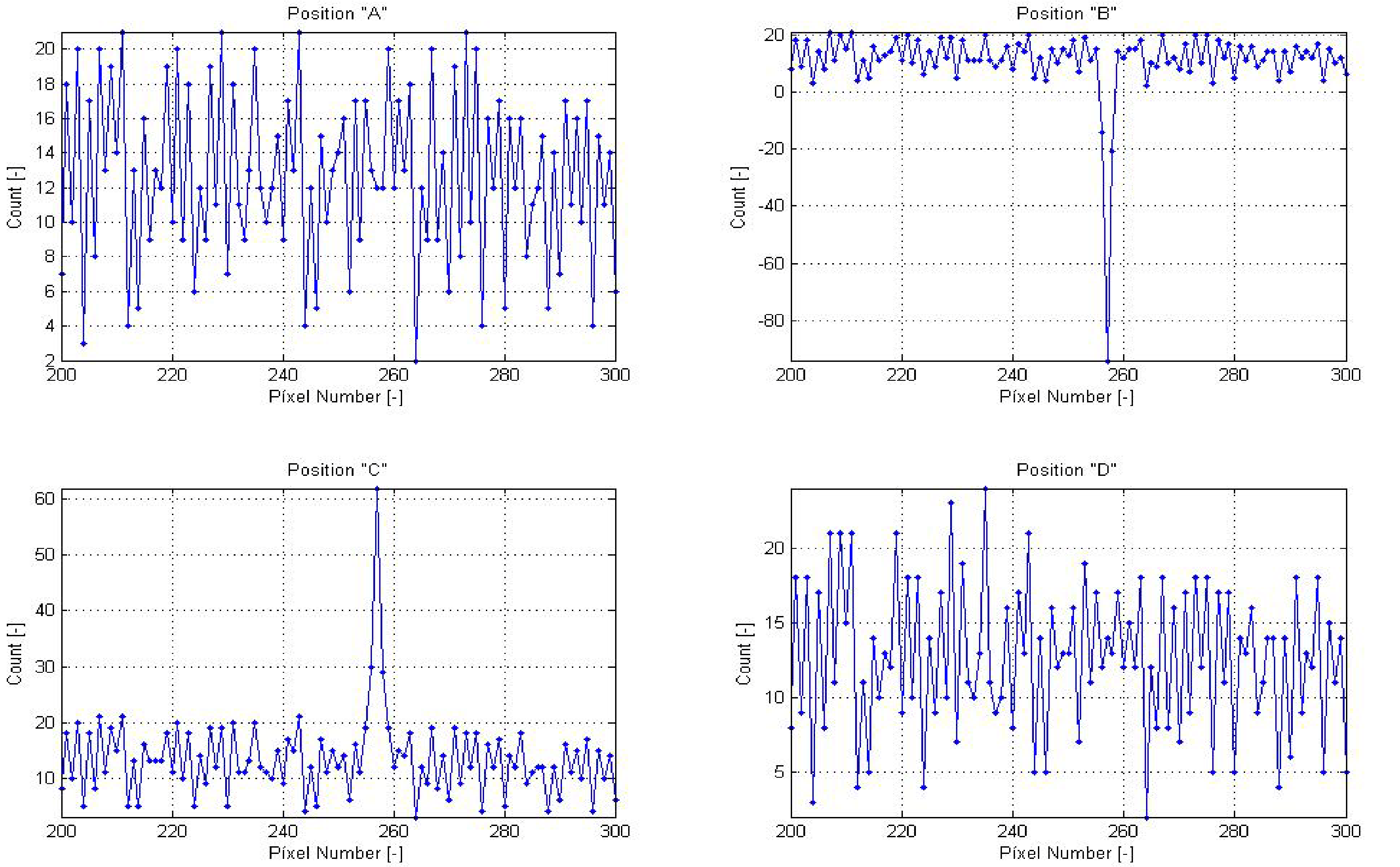

Priorities

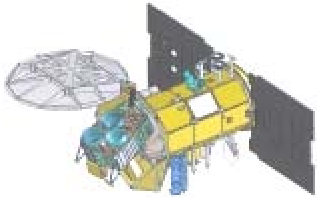

1. Emergencies
2. Instrument Health Care
3. Science Group & AOs
4. Common Users

Calibration setup

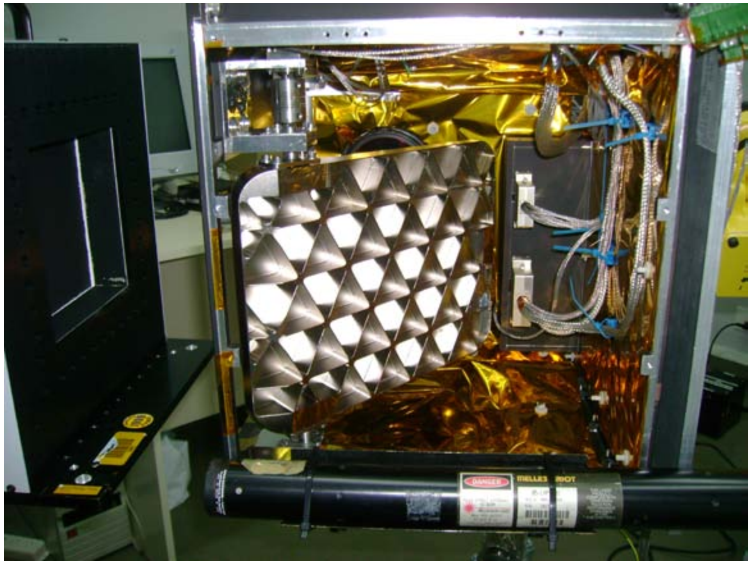

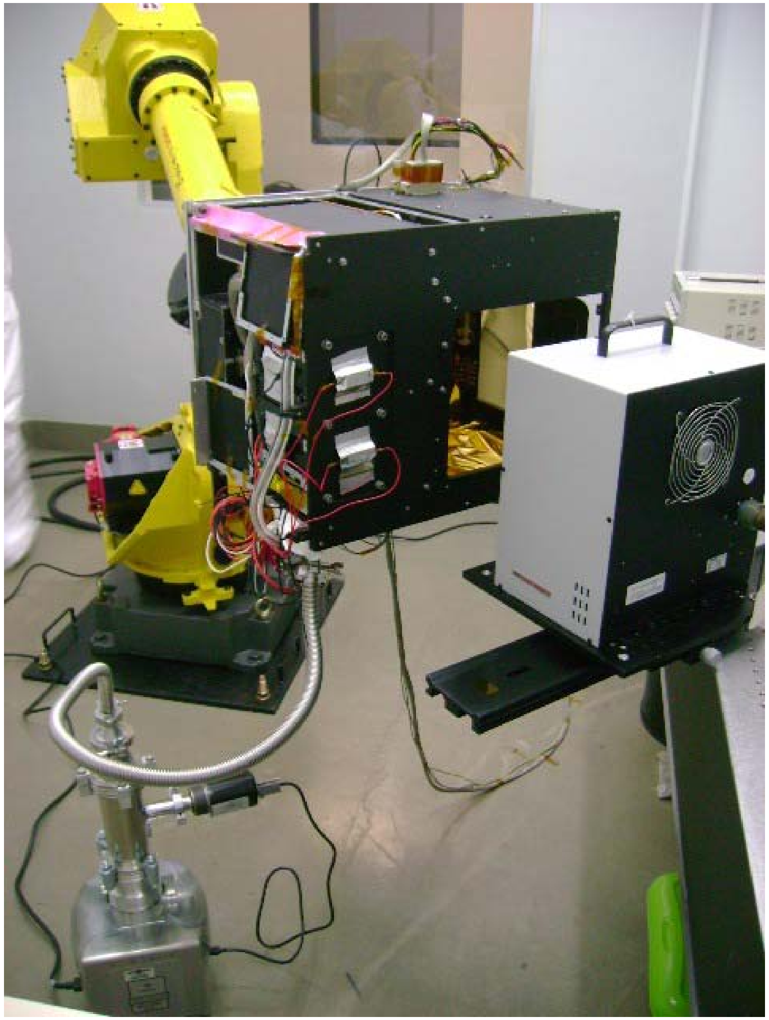

Scans at the optical lab

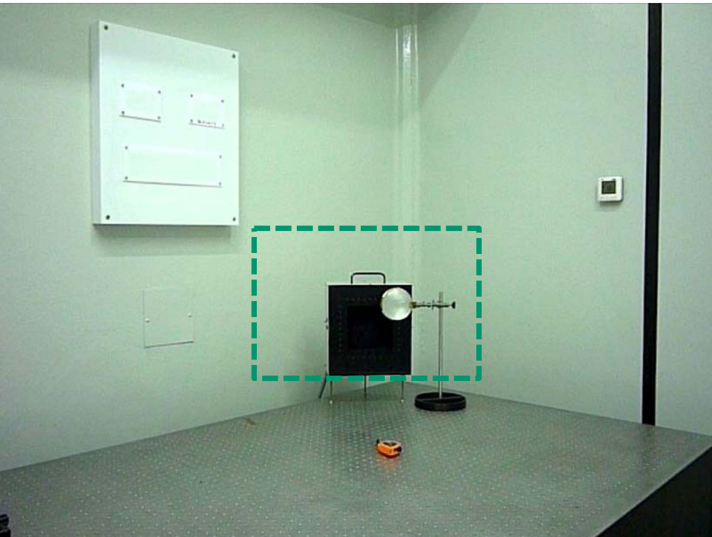

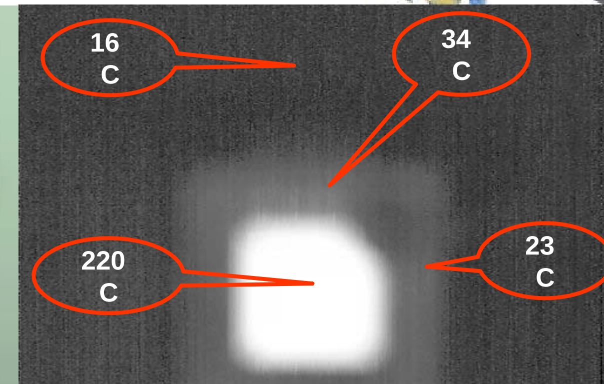

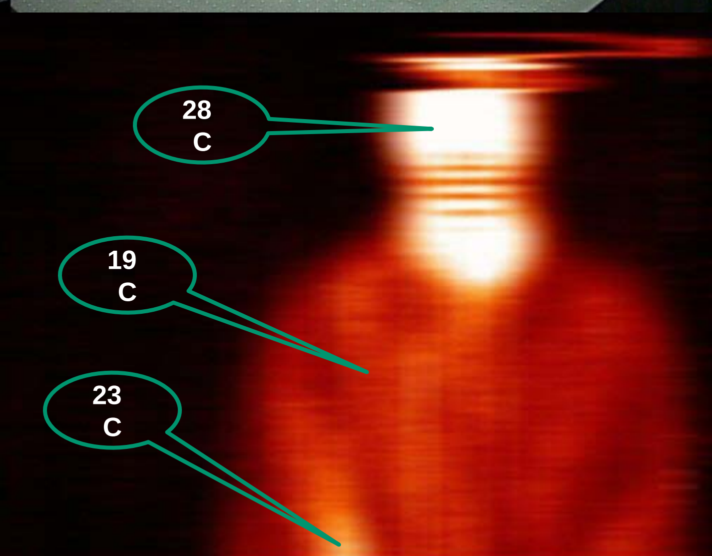

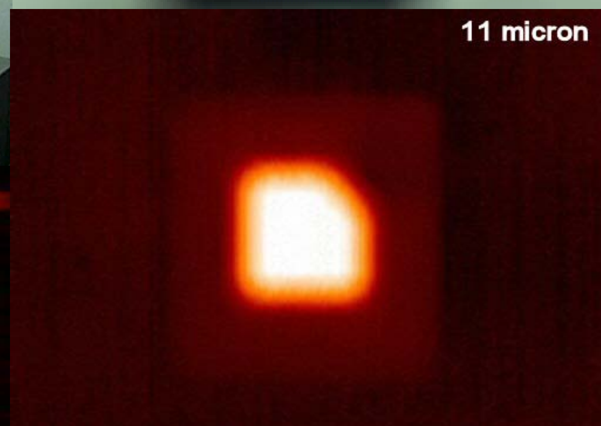

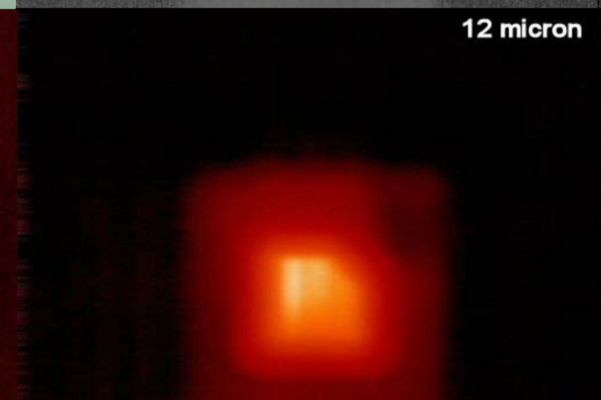

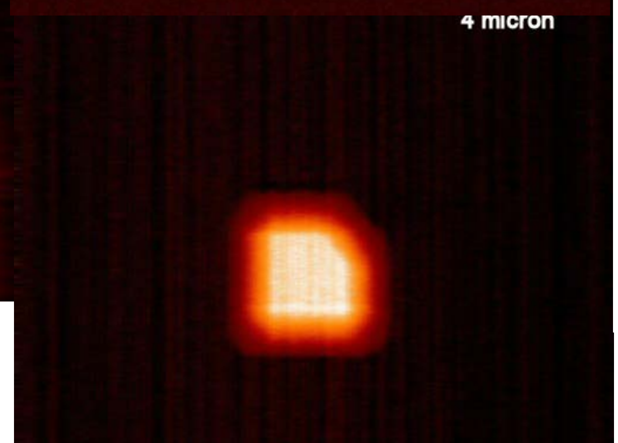

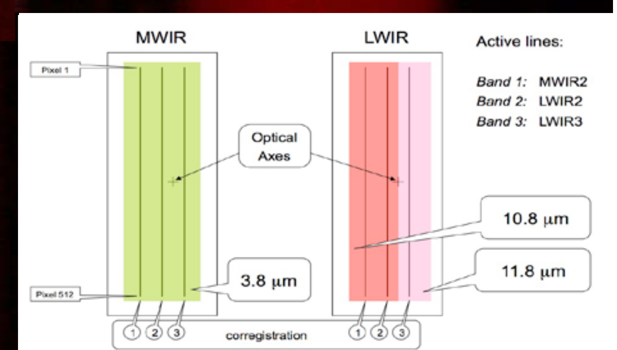

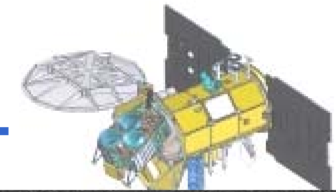

AQUARIUS/SAC-D

Pixel variety

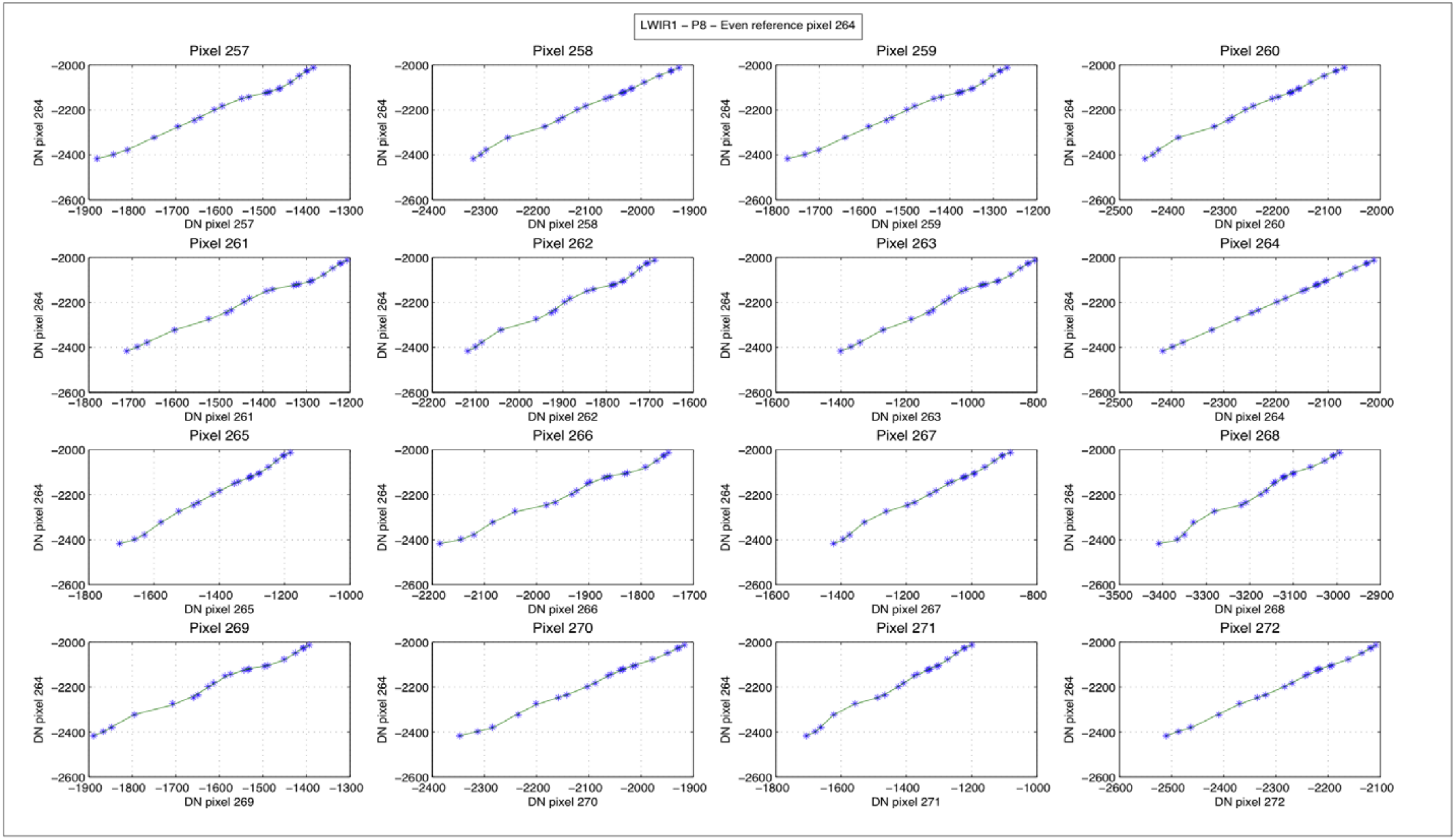

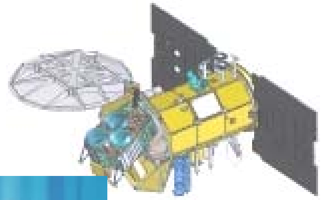

Design Overview

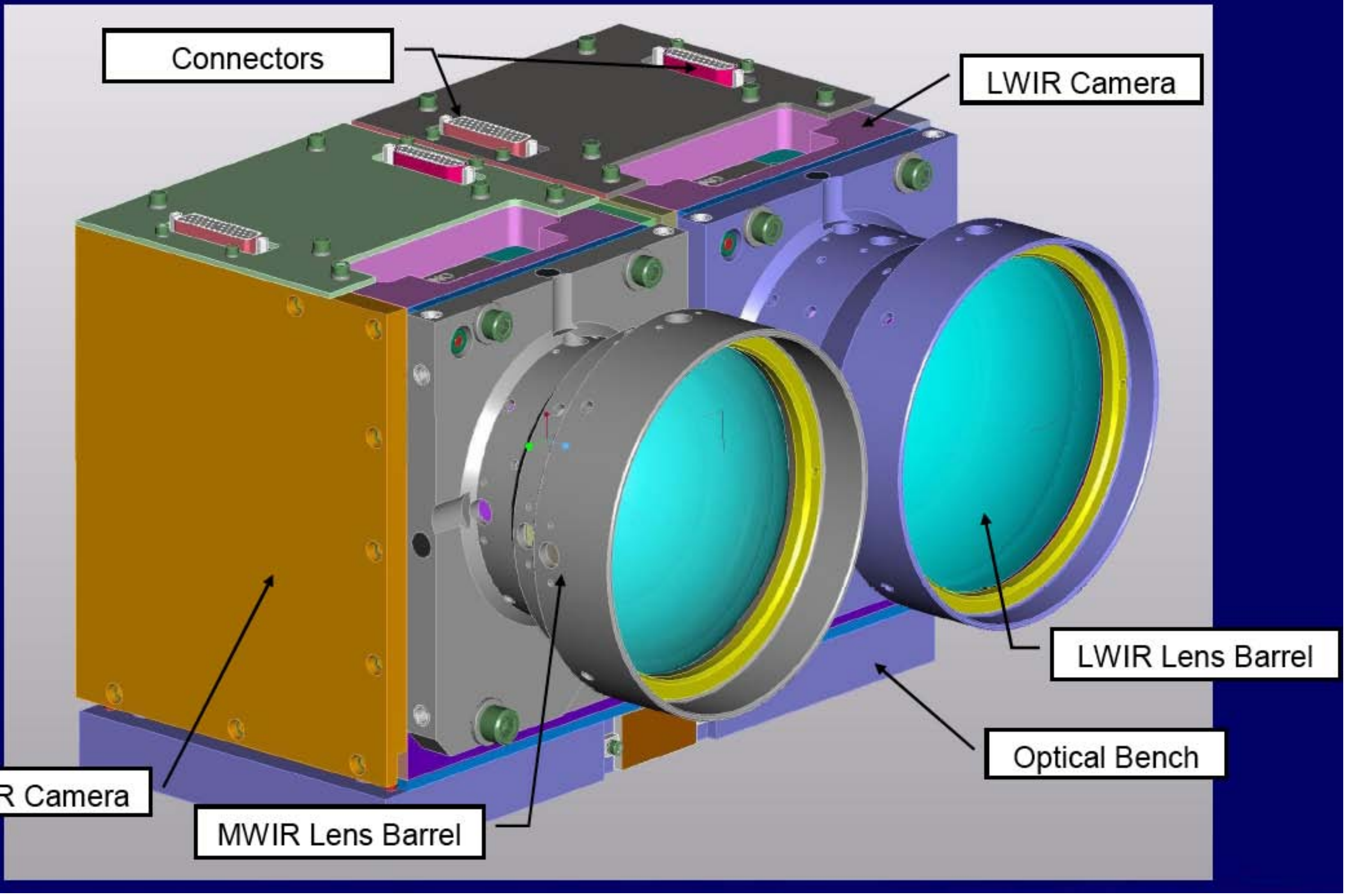

Mechanical Design – Overview Exploded

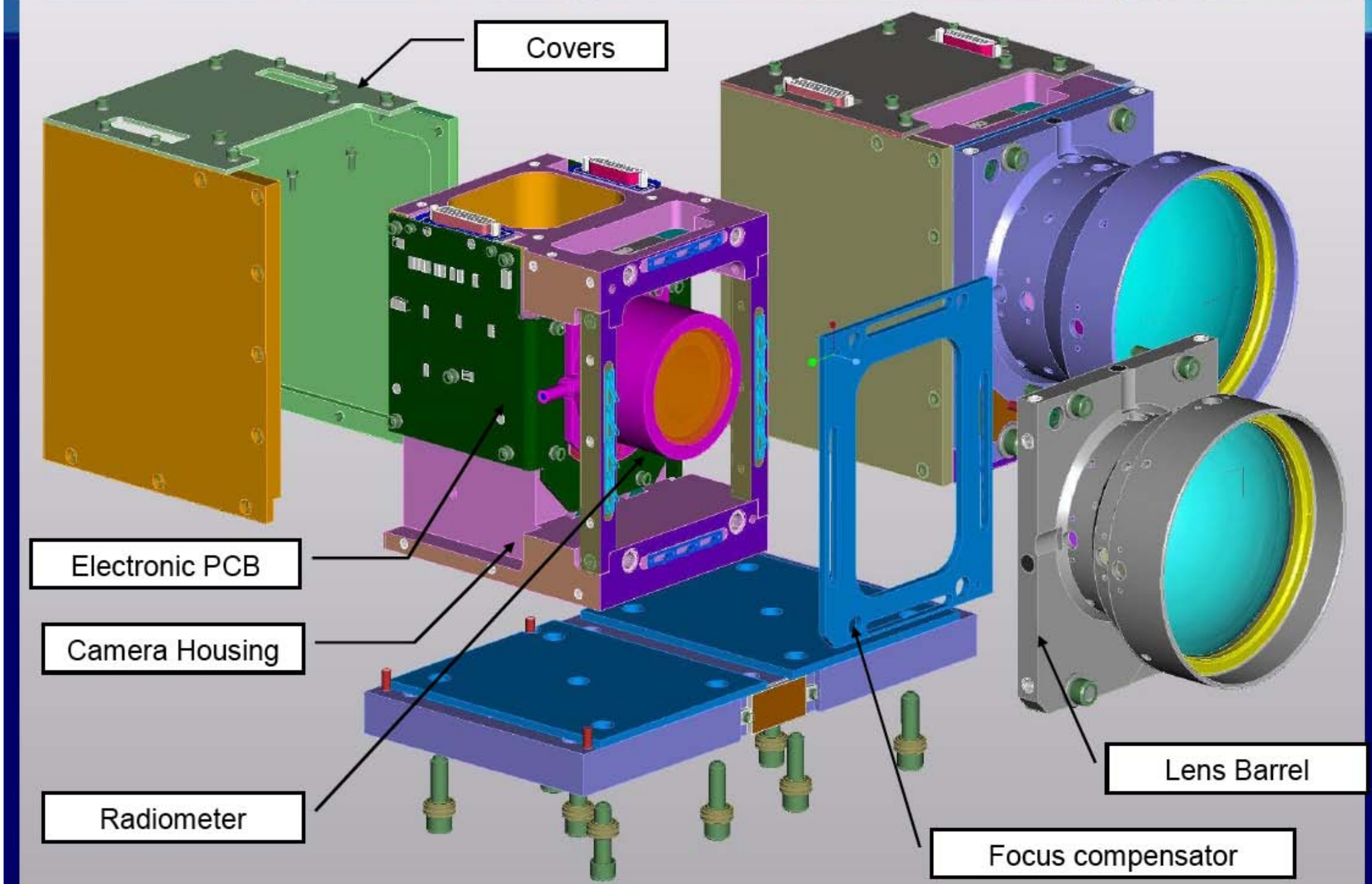

Pixels alongtrack (nadir)

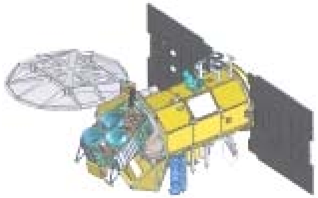

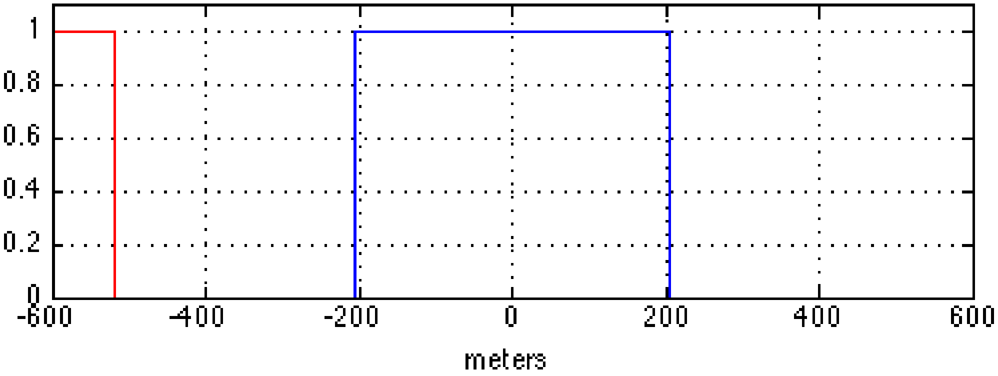

(59ms @ 6.9 km/s ≅ 410 m 0.53 mrad @ 657 km ≅ 350 m)

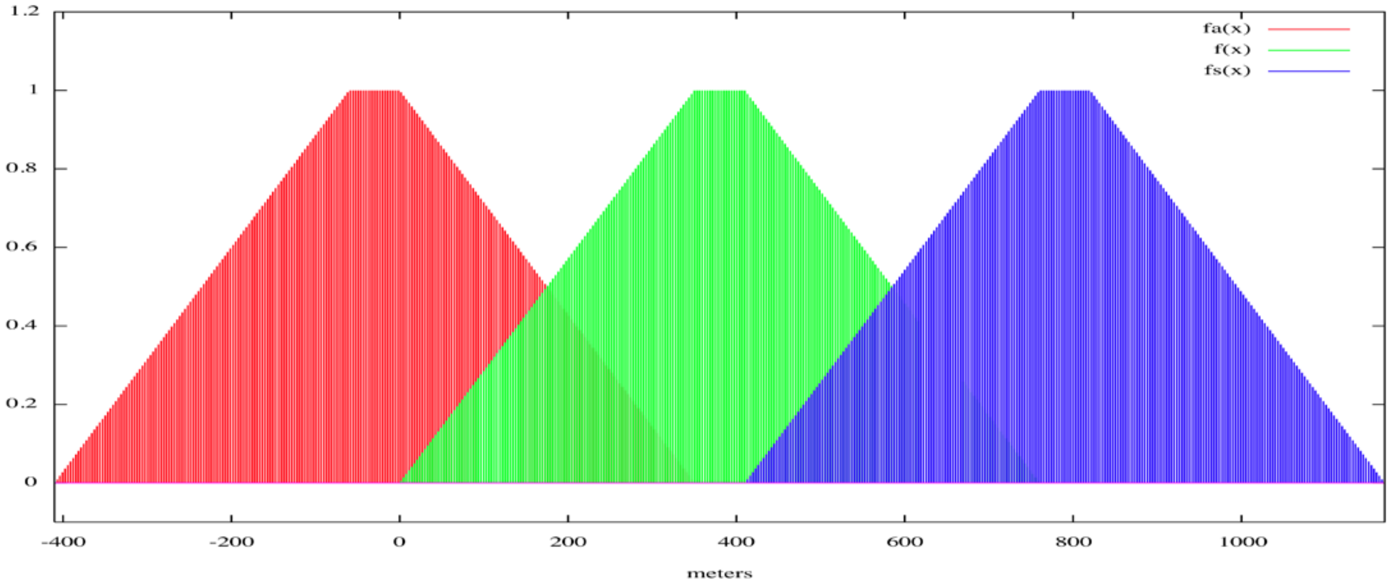

Integration

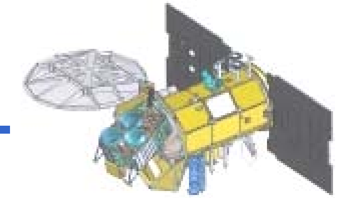

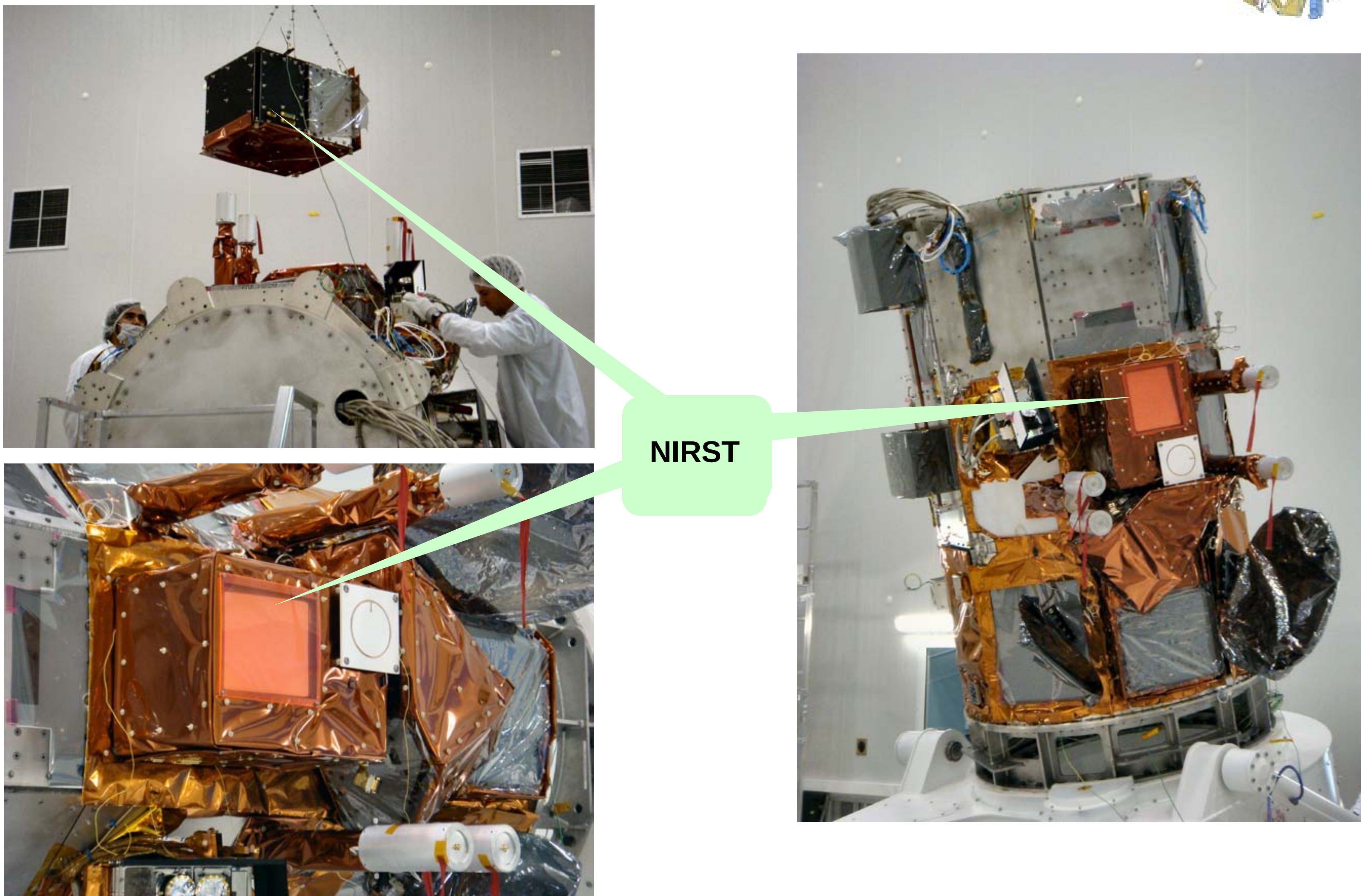

2010 HyspIRI Science Workshop
Aug 24-26, 2010 Pasadena

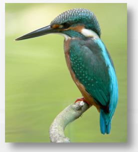

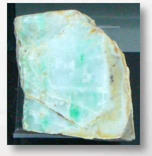

HISUI
Hyperspectal Imager Suite

A Japanese Spaceborne Hyperspectral and Multispectral Remote Sensing Mission

Tsuneo Matsunaga (National Institute for Environmental Studies)
and
Akira Iwasaki (University of Tokyo), Osamu Kahimura (ERSDAC),
Kenta Ogawa(Rakuno Gakune Univ.), Nagamitsu Ohgi (JAROS), and
Satoshi Tsuchida (AIST)

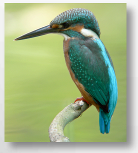

HISUI : Jade or Kingfisher(Kawasemi)

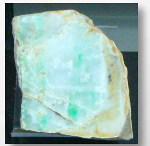

Jadeite from Geological Musium, AIST

翡　翠

www.moonmadness.jp/itoigawahisui.html

http://upload.wikimedia.org/wikipedia/commons/1/13/Alcedo_atthis_4_%28Lukasz_Lukasik%29.jpg

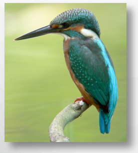

"What's new" since 2009 HyspIRI Workshop

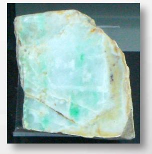

- Our mission was finally named!
- Calibration and ground data system studies were funded for FY 2010-2014.
- Working groups are being organized.
- Detailed design of the instrument is ongoing. CDR in FY2011
- Discussion with JAXA is ongoing.

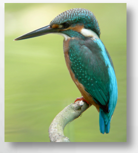

What is HISUI?
A Successor of ASTER and ALOS AVNIR-2

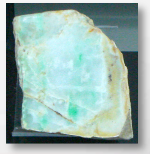

- **HISUI** is a spaceborne instrument suite which consists of hyperspectral and multispectral imagers.

- **HISUI** is being developed by Japanese Ministry of Economy, Trade, and Industry (METI) as its third spaceborne optical imager mission.

  1) OPS onboard JERS-1 satellite (1992 – 1998)
  2) ASTER onboard NASA's Terra satellite (1999 -)

- **HISUI** will be launched by H-IIA rocket in 2014 or later as one of mission instruments onboard JAXA's ALOS-3 satellite

  1) ALOS (2006 -) : Optical imagers (PRISM and AVNIR-2) and SAR
  2) ALOS-2 (2013 -) : SAR

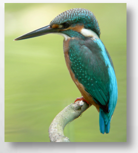

Targets / Objectives of HISUI Mission

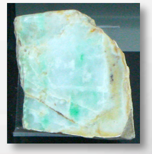

1) Global energy and resource related applications
   - Oil, gas, metal, ...
   - Observations for environmental assessments which are indispensable to resource developments

2) Other applications such as environmental monitoring, agriculture, and forestry

3) Promotion of domestic space and space utilization industry through wider applications of HISUI data

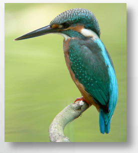

Ministry of Economy, Trade, and Industry's HISUI Mission Team

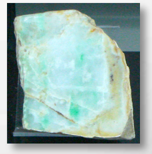

- Mission leader and three deputy leaders
- Instrument development — JAROS / NEC Corp.
- Calibration and data processing — AIST / ERSDAC
  - Calibration WG — Ishii, AIST
  - Level 1 WG — Iwasaki, UT
  - Level 2 WG — Yamamoto, AIST
  - Operation and Mission Planning WG — Matsunaga, NIES
  - Archive WG — Nakamura, AIST
- Application research — ERSDAC

AIST : Advanced Institute for Industril Science and Technology,
ERSDAC : Earth Remote Sensing Data Analysis Center,
JAROS: Japan Resources Observation System and Space Utilization Organization,
NIES: National Institute for Environmental Studies, UT : University of Tokyo

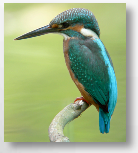

HISUI Mission Schedule

	FY2006	FY2007	FY2008	FY2009	FY2010	FY2011	FY2012	FY2013	FY2014
Instrument Development (JAROS, NEC)		*Conceptual Design*	*Preliminary Design*		*Detailed Design*	△ CDR			*Launch*
			Development Model			*Proto Flight Model*			
Calibration and Data Processing (AIST, ERSDAC)					*Calibration, Data processing, Ground data system, Operation mission planning, etc.*				
Application Research (ERSDAC)		*R&D for Data Utilization (oil&gas, mineral resources, agriculture, forest, environment, etc.)*							
		Design & Development of Spectral Database							

JAXA's ALOS-3 and HISUI

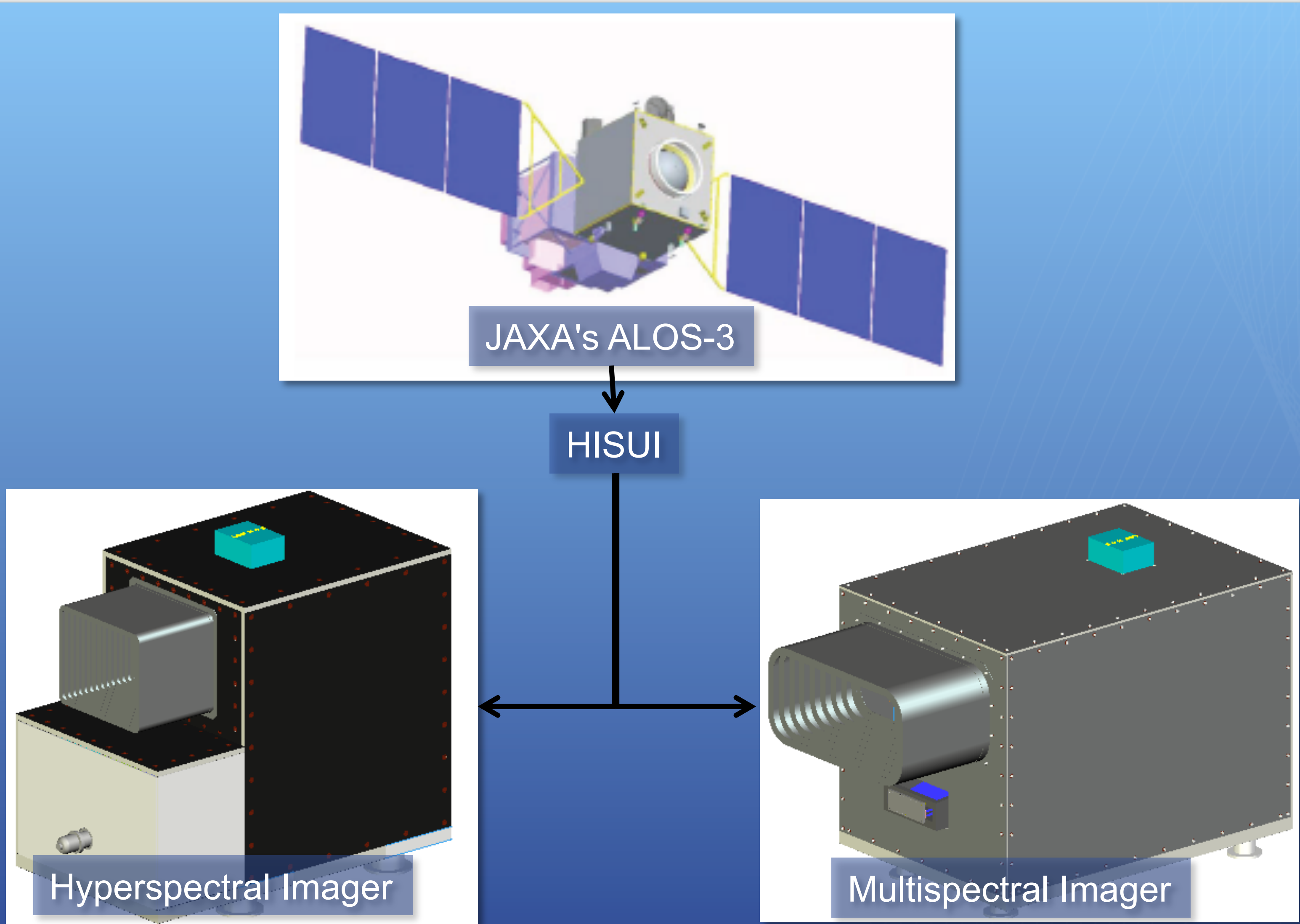

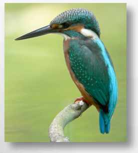

HISUI Requirements: Hyperspectral Imager

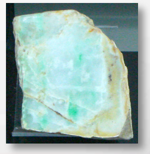

Parameter		Requirement
Spatial Resolution and Swath Width		30 m and 30 km
Spectral	Bands	185 (VNIR:57 SWIR:128)
	Range	0.4 - 2.5 μm VNIR:0.4-0.97 μm SWIR:0.9-2.5 μm
	Resolution	10 nm (VNIR), 12.5 nm (SWIR)
Signal to Noise Ratio (30% albedo)		≥ 450 @620 nm ≥ 300 @2100 nm
MTF		≥ 0.2
Dynamic Range		≥ 10 bits (current design=12bit)
Data Compression		Lossless (70%)
Pointing Capability		≈ ±3 ° (±30 km)

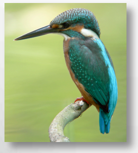

HISUI Requirements: Multispectral Imager

Parameter	Requirement
Spatial Resolution and Swath Width	5 m and 90 km
Number of Bands and Spectral Coverage	4 and 0.45 – 0.90 μm
Signal to Noise Ratio (30% albedo) and MTF	≥ 200 and ≥ 0.3
Dynamic Range	≥ 8 bits (current design = 12bits)
Data Compression	Lossless (70%)

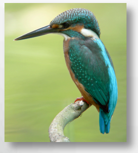

Specification of JAXA's ALOS-3 and Panchromatic Stereo Camera

Orbit Type and Altitude	Sun Synchronous, ≈ 620 km
Local Time At Descending Node	13:30 (TBD)
Orbits per Day	15 orbits/day (TBD)
Repeat Cycle and Interval between Orbits	60 days and 45 km(TBD)
Launch Vehicle	H II-A
Downlink Capability	800 Mbps (TBD)
Onboard Storage	> 200 GB (TBD)

Parameters of JAXA's Panchromatic Stereo Camera	Requirement
Spatial Resolution and Swath Width	0.8 m(nadir) and 50 km
Data Compression	Lossy (22%)

HISUI Functional Block Diagram

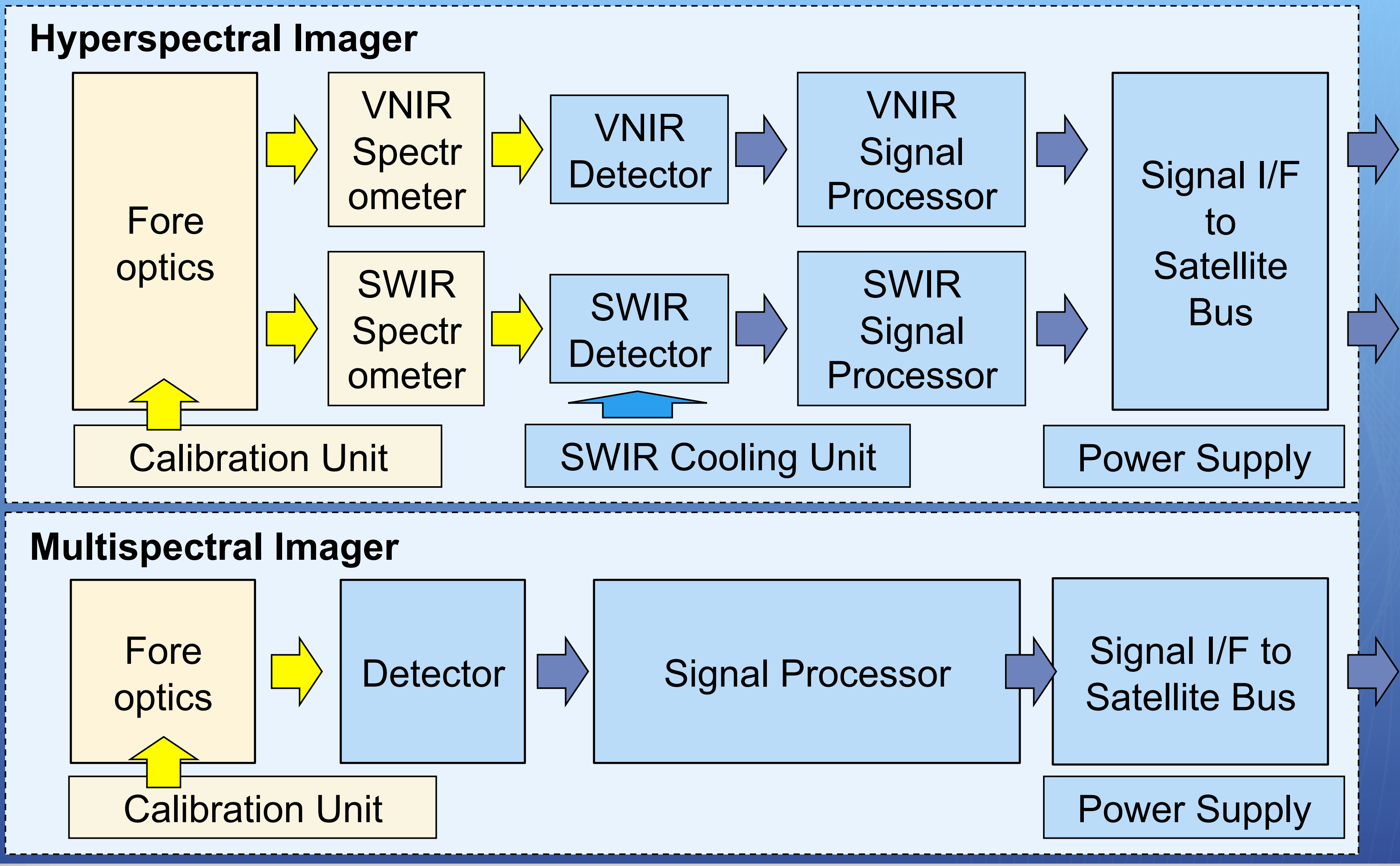

Optical Schematics of HISUI Hyperspectral Imager

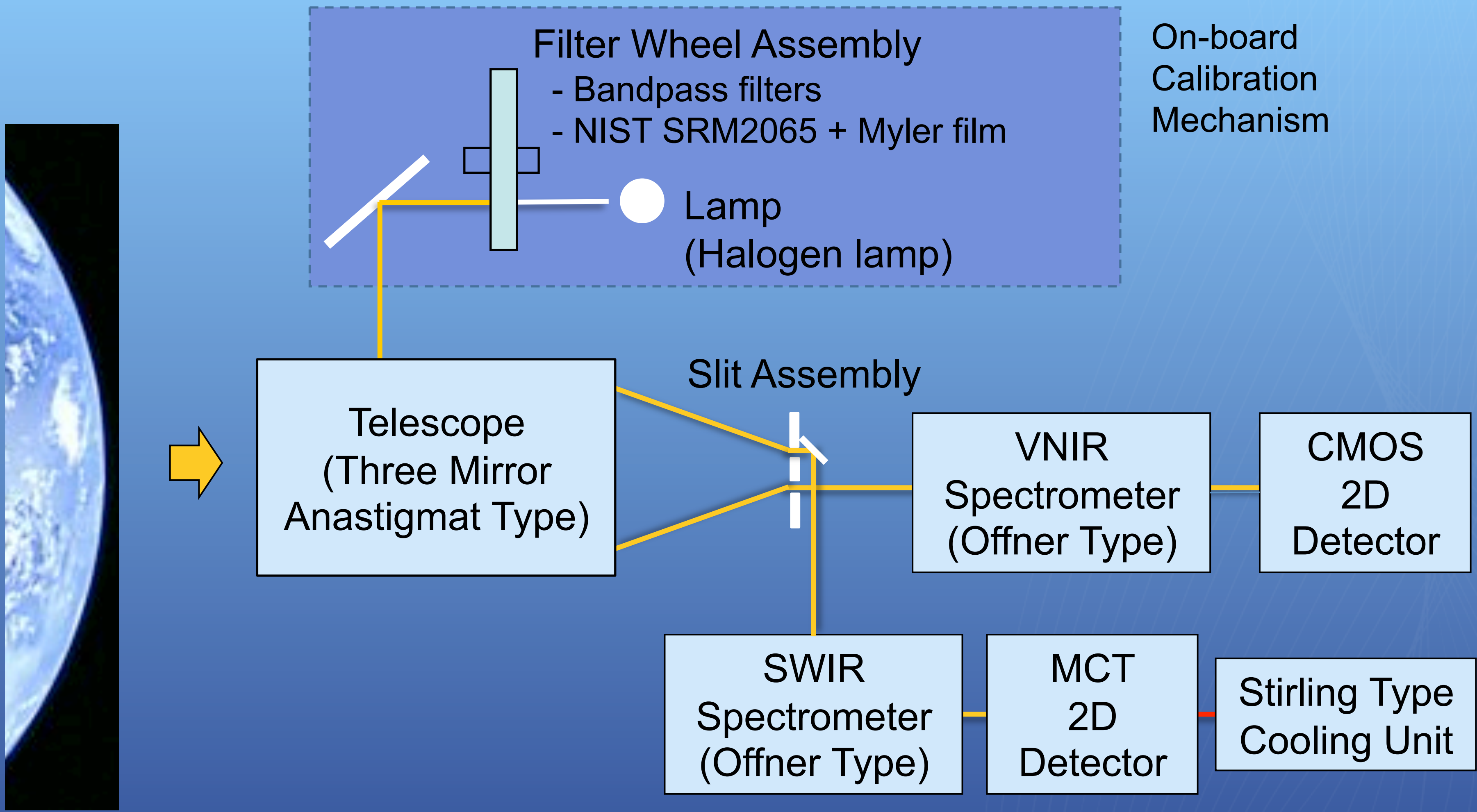

Optical Schematics of HISUI Multispectral Imager

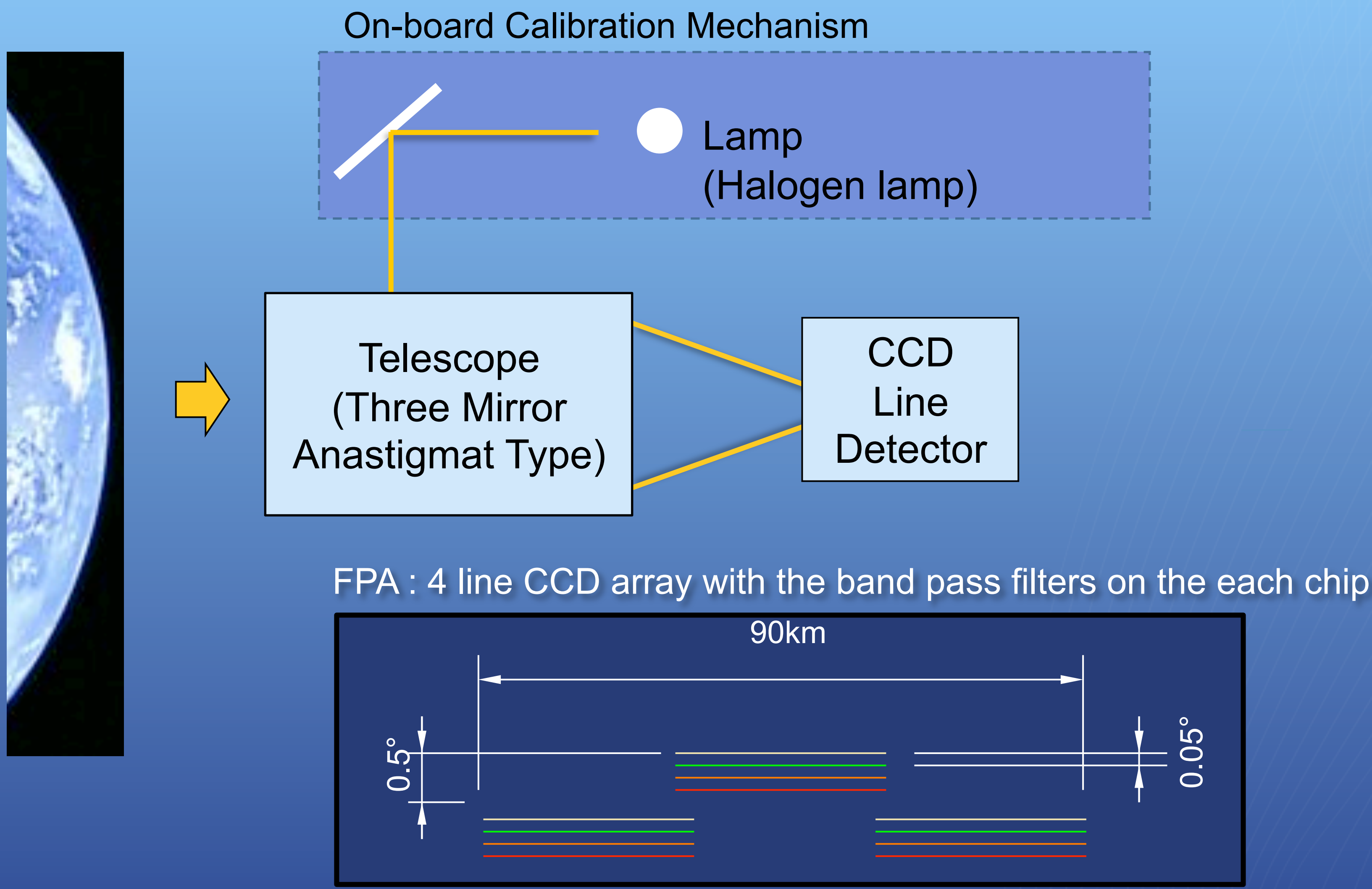

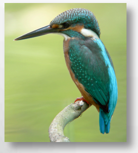

Operation of HISUI

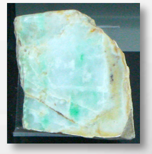

- Maximum operation time
  - 15 min / orbit and 15 orbits / days for each imagers
- Target observation + (semi) global mapping
  - Plus disaster mode and calibration mode
  - Nighttime hyperspectral SWIR observation
  - Area and frequency of (semi) global mapping depend on allocated downlink capability.
- Hyperspectral Imager and Multispectral Imager can be operated separately or simultaneously .
- Cross-track pointing for Hyperspectral Imager to fill gaps between orbits.

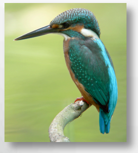

Cross-track Pointing of HISUI Hyperspectral Imager

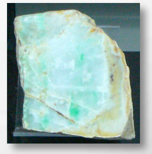

HISUI Hyperspectral Imager has a cross-track pointing mechanism to tilt the whole instrument and cover the eastern and the western parts of 90-km swath of HISUI Multispectral Imager.

Maximum Cross-track Pointing Angle
$\approx \pm \operatorname{atan}(30\text{ km} / 620\text{ km})$
$\approx \pm 3°$

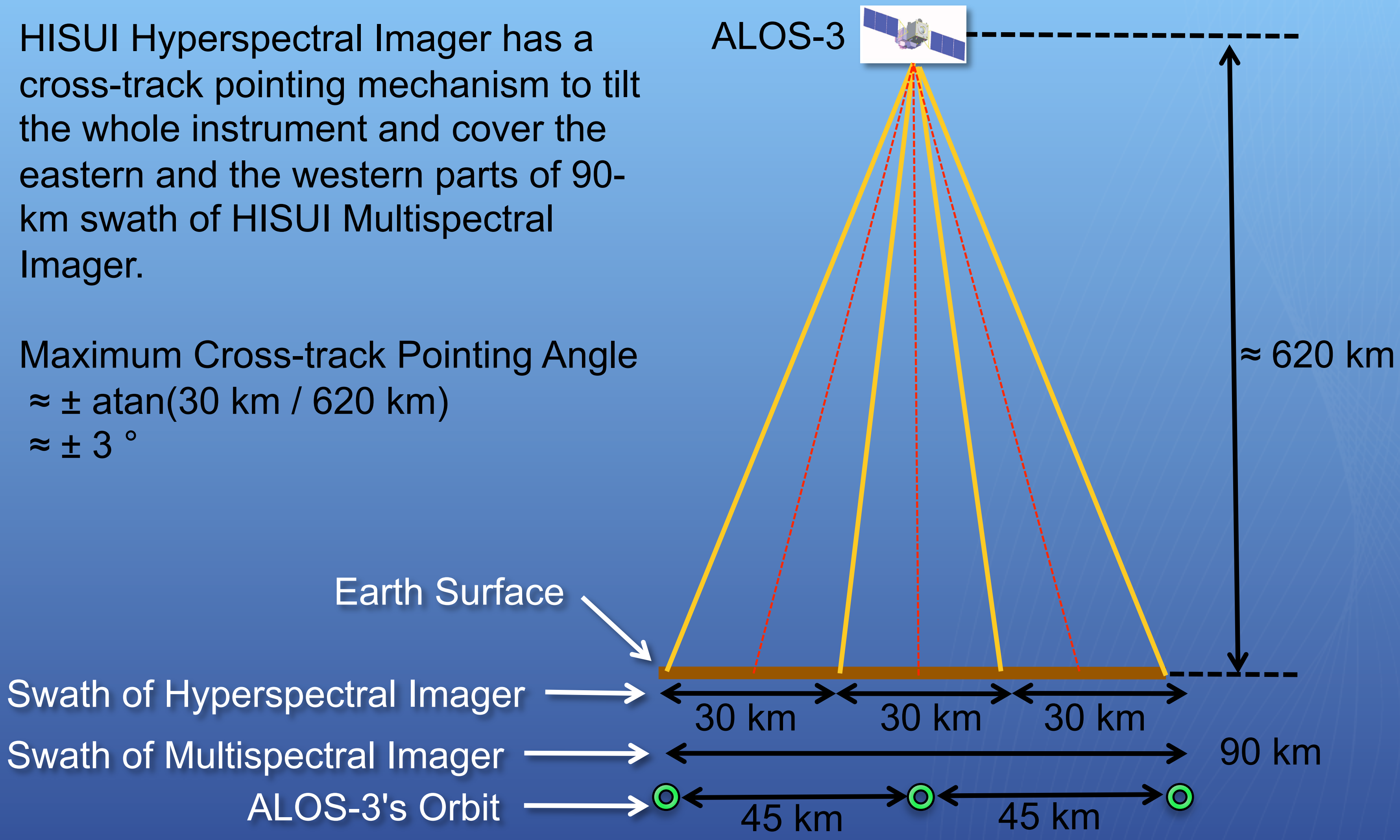

ALOS-3's Orbits and Land Observation

Blue and Red : maximum and minimum land fraction orbits
white : nightside

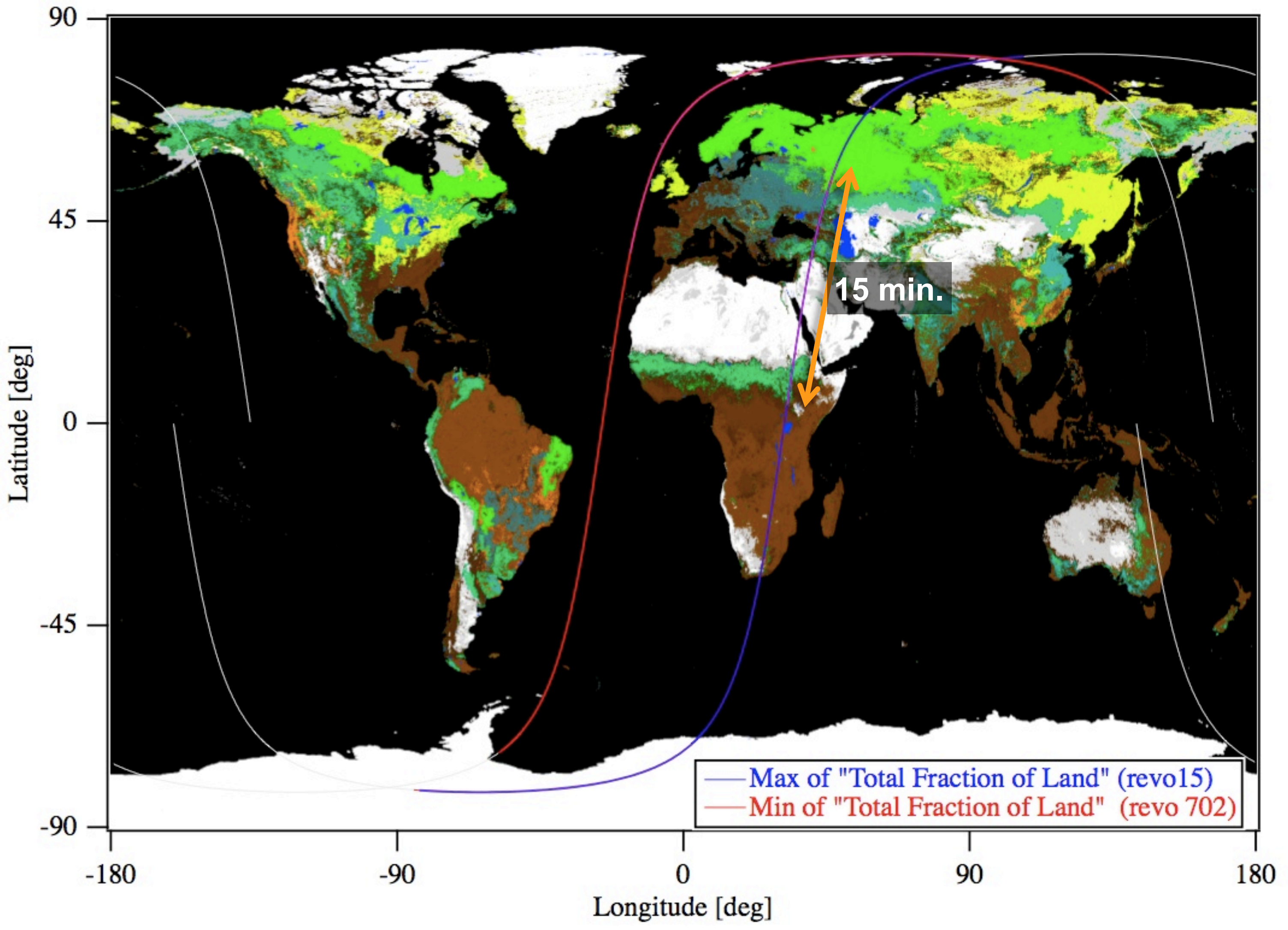

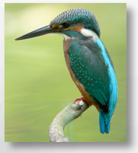

Cumulative Land Observation Time per Orbit of HISUI Hyperspectral Imager

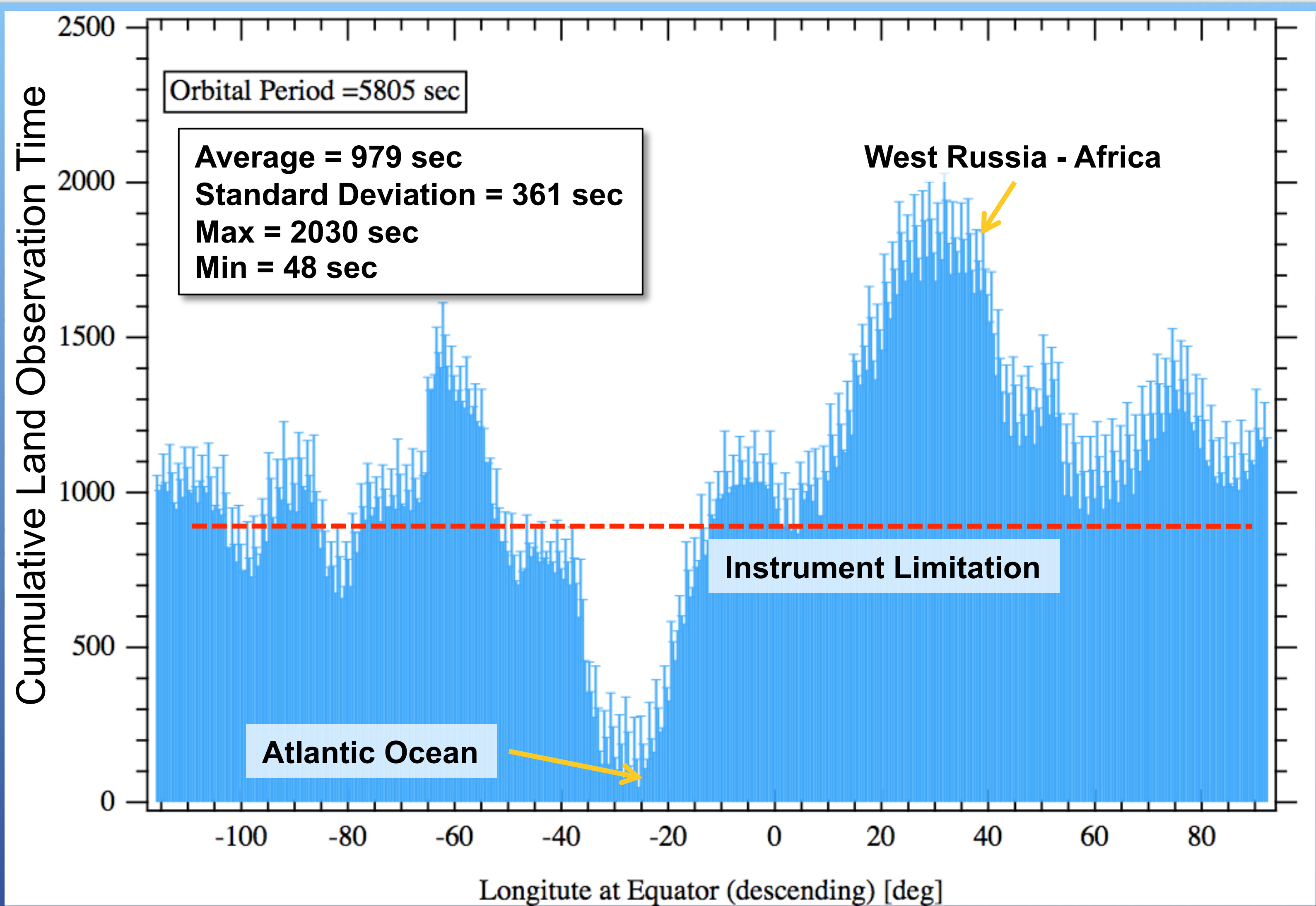

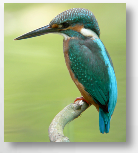

ALOS-3 and HISUI
Data Amount and Downlink

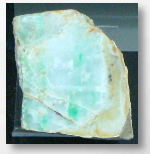

	Data Rate (70% Comp.)	Maximum Observation Time per Orbit	Maximum Data Amount per Orbit	Maximum Data Amount per Day
HISUI - Hyper	0.4 Gbps	15 min.	46 Gbyte	690 Gbyte
HISUI - Multi	1 Gbps	15 min.	110 Gbyte	1600 Gbyte

	Downlink Speed	Downlink Time per Day	Data Amount per Day
Ground Station	800 Mbps	20 min.	120 Gbyte
Relay Satellite	800 Mbps	220 min.	1320 Gbyte

- HISUI will share ALOS-3's downlink capability with JAXA's panchromatic camera.
- Discussion on downlink capability **allocation** is ongoing between METI and JAXA

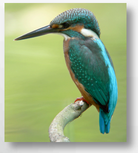

HISUI Product List (TBR)

Name	Description	
Level 1R	Raw DN product with all radiometric calibration coefficients. Spatial resampling is not applied. Smile properties and spectral continuity between VNIR and SWIR are considered.	
Level 1G	Geometrically corrected top-of-atmosphere spectral radiance product. Inter-telescope registration, parallax correction, and keystone property are considered. (Orthorectified product is under consideration)	
Level 2	Surface spectral reflectance product generated from L1R/G with QA information.	

*Definitions of products are common between hyperspectral and multispectral imagers

Brief Introduction of HISUI Working Groups

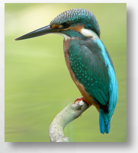

Calibration Working Group
Chair : Juntaro Ishii (AIST)

- Upgrading of the proven calibration system of ASTER
- Member: AIST, Univ. Tokyo, JAROS
- ***<u>Foremost tasks</u>***
  - Radiance scale based on standard blackbody sources traceable to the SI unit
  - Application of the newly developed M-C eutectic high temperature fixed point blackbody above 1100^{o}C
  - Effective calibration method for atmospheric absorption bands
  - Uncertainty analysis conformable to GUM
  - Reliable on-board radiometric / wavelength calibration methods

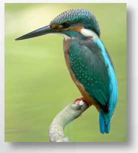

Calibration Working Group

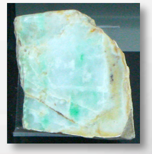

- Vicarious and cross calibration
  - New Approaches to vicarious calibration and cross calibration methodologies for HISUI
    - To revise the methodology for the large absorption region and high spectral resolution
  - Field survey of suitable test sites for VC in Australia
  - Field campaigns for VC at U.S. and Australia test sites
  - Strengthening of collaboration with foreign research institutes

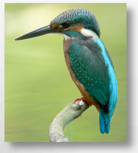

Level1 Working Group
Chair : Akira Iwasaki (Univ. Tokyo)

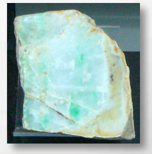

- Heritage of ASTER Level-1 Data Processing

- Member: AIST, ERSDAC, JAROS

- *Radiometric → Level-1R Product*
  Radiometric parameters are delivered by instrument team
  All radiometric coefficients are included in Level-1R data
  Smile properties must be considered
  Spectral continuity between VNIR and SWIR

- *Geometric → Level-1G Product*
  Data fusion of multi-telescope system
  Parallax correction for line sensor arranged in parallel
  Keystone properties must be considered
  Orthorectified data product is under consideration

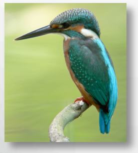

Level2 Working Group
Chair : Hirokazu Yamamoto (AIST)

- **Members:** AIST, Masao MORIYAMA (Nagasaki U.)

- ***Level-1R/Level-1G Product → Level-2 Product***
  - ✓ L2 algorithm will convert from L1R/L1G radiance to surface reflectance, which will be based on MODTRAN.
  - ✓ Irradiance model used in this module is TBD.
  - ✓ Terrain correction is TBD.
  - ✓ Products will include QA information
  - ✓ Orthorectified surface reflectance will be generated if Level-1G orthorectified radiance is available.

- ***L2 product validation***
  - ✓ Intercomparison among other satellite sensors by conversion from narrow bands to broad bands will be conducted.
  - ✓ Ground-based validation is TBD.

Operation and Mission Planning (OMP) WG
Chair : Tsuneo Matsunaga (NIES)

- Member : Matsunaga, Yamamoto (NIES)
  Kashimura, Kato, and Tachikawa (ERSDAC)
  Ogawa (Rakuno Gakuen Univ.)

- Missions of OMP WG
  1) Make long and short term observation and data processing plans
  2) Design HISUI's scheduling and mission achievement reporting system. ERSDAC will implement HISUI's OMP system based on the WG's design.

* Matsunaga, Kato, and Tachikawa are members of ASTER OMP WG.

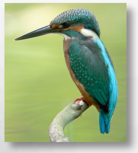

Archive Working Group
Chair : Ryosuke Nakamura (AIST)

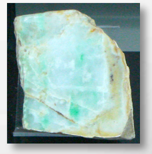

- Design versatile OGC standard framework for satellite data processing system (= GEO grid) http://www.geogrid.org/en/index.html
- Implementation of HISUI's ground system with GEO Grid
- Member: AIST, ERSDAC
- Prompt delivery of L1R , L1G and higher level products
- Possible data fusion with JAXA's panchromatic camera and other hyperspectral imagers

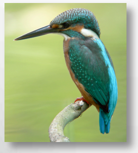

HISUI Frequently Asked Questions

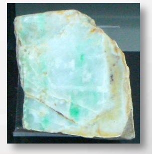

- **HISUI and Hyper-X**
  - Hyper-X is a project proposed by a group of private companies to operate a spaceborne hyperspectral imager transferred from Japanese government for commercial purposes.
  - No decisions have been made regarding full or partial privatization of HISUI yet.

- **Data Policy**
  - No decisions have been made yet.

- **Orbit of ALOS-3 satellite**
  - Discussion with JAXA is ongoing

- **International Collaboration**
  - METI/EnMAP telecon, AIST/CSIRO/ERSDAC joint vicarious calibration in west Australia ...

Wanted!
September 1987 Issue of National Geographic

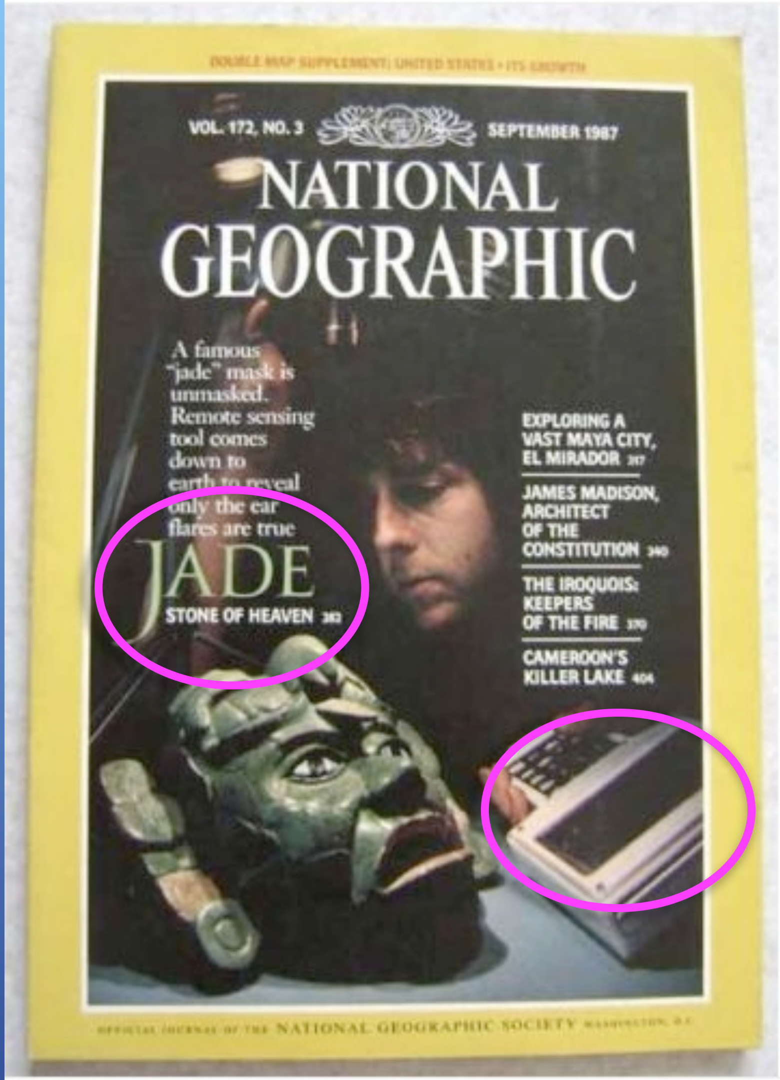

"Brian Curtiss, a geochemist who received his Ph.D. from University of Washington and a postdoctoral appointment at Caltech, joined CSES. He was featured on the cover of National Geographic for his work on identifying jade artifacts using reflectance spectroscopy."
(http://cires.colorado.edu/about/history/06.html)

Curtiss, Brian, "Visible and near-infrared spectroscopy for jade artifact analysis," in F.W. Lange (ed.) Precolumbian Jade: New Geological and Cultural Interpretations (Salt Lake City: University of Utah Press, 1993), pp. 73-81.

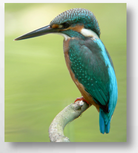

Thank you

AQUARIUS/SAC-D

2010 HyspIRI Science Workshop

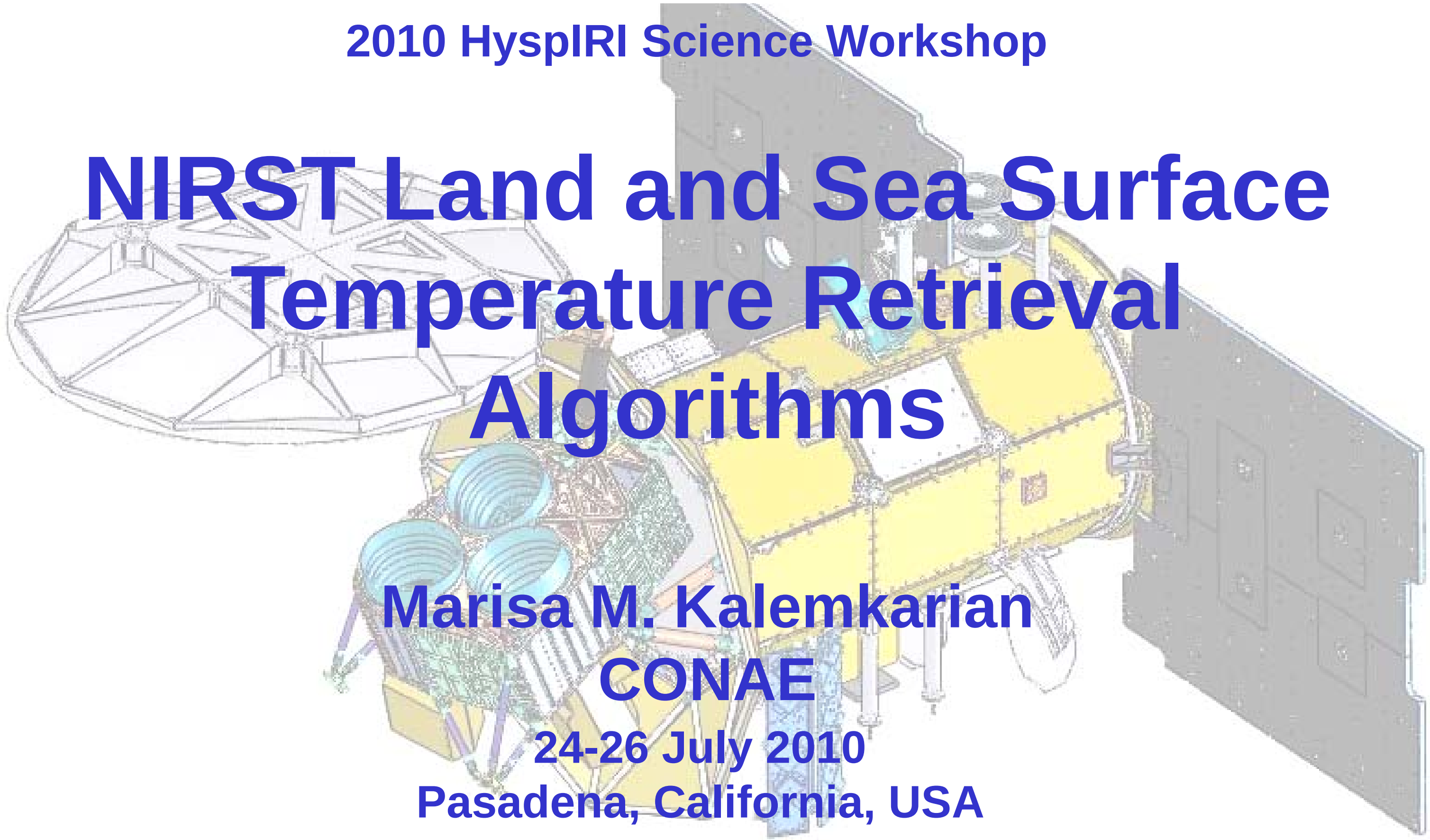

NIRST Land and Sea Surface Temperature Retrieval Algorithms

Marisa M. Kalemkarian
CONAE

24-26 July 2010
Pasadena, California, USA

NASA

CONAE
COMISION NACIONAL DE ACTIVIDADES ESPACIALES

ESR

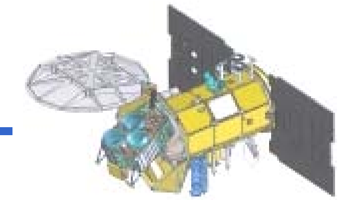

NIRST DERIVED PRODUCTS (Level 2)

- FIRE MAPPING AND FIRE RADIATIVE POWER
- VOLCANIC ACTIVITY MONITORING
- SEA SURFACE TEMPERATURE (SST)
- LAND SURFACE TEMPERATURE (LST)

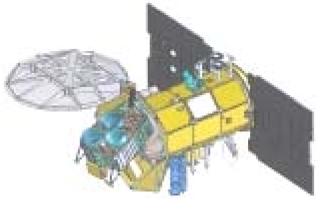

Summary of Processing Levels:

- L0A: No calibration or correction applied
- L1A: Relative Radiometric Calibration + Inter Band Co-registration
- L1B1: Relative Radiometric Calibration + Absolute Radiometric Calibration + Co-registration
- L1B2: Relative Radiometric Calibration + Absolute Radiometric Calibration + Geometric Correction (Map Projection – includes inter band co-registration).
- **L2: Geophysical Parameter**

NIRST Land and Sea Surface Temperature Retrieval Algorithms

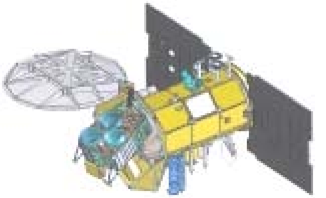

Product generation sequence:

• L1A is generated from L0 (+ Relat. Radiom. Calib. + Co-regist.)

• L1B1 is generated from L1A (+ Absol. Radiom. Calib.)

• L1B2 is generated from L0 (+ Relat. Radiom. Calib. + Absol. Radiom. Calib. + Geom. Calib. (Map Projection).

• L2 is generated from L1B1 (+ Retrieval Algorithms)

NIRST Land and Sea Surface Temperature Algorithms

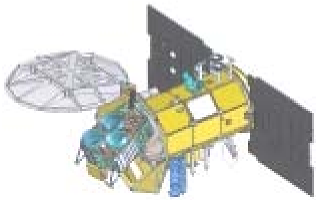

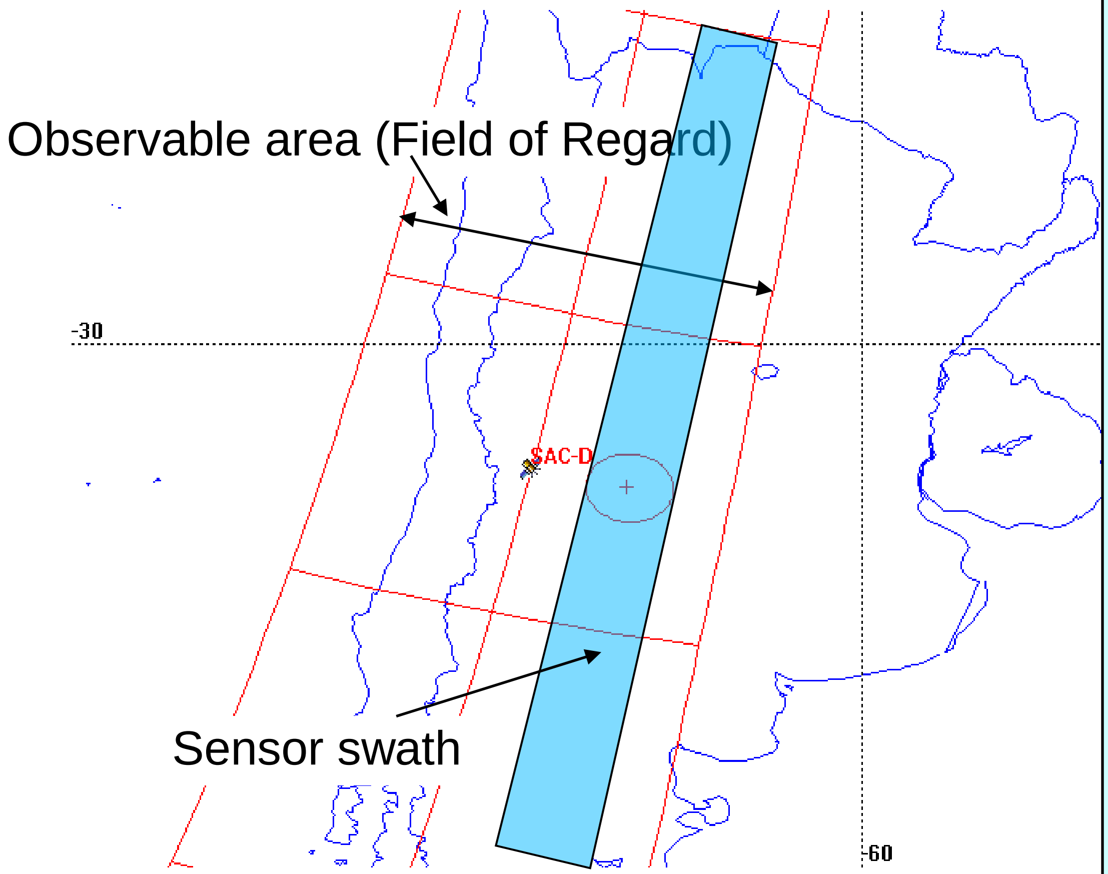

NIRST Bands and Geometry

- 3 Bands:
  - ✓ B1: 3.4 – 4.2 μm
  - ✓ B2: 10.4 – 11.3 μm
  - ✓ B3: 11.4 – 12.3 μm
- Swath: 180 Km at nadir
- Spatial resolution:
  - ✓ 350 m across track
  - ✓ 410 m along track
- Boresight pointing: +/-30° from nadir
- About 1000 km observable area across track

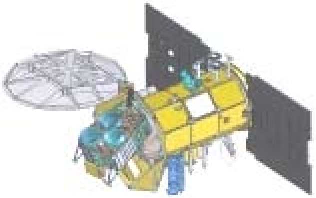

Fire Mapping
and
Fire Radiative Power

Fire Mapping and Fire Radiative Power

Examples of fires detected by MODIS algorithm in the Delta of Parana River - 2008

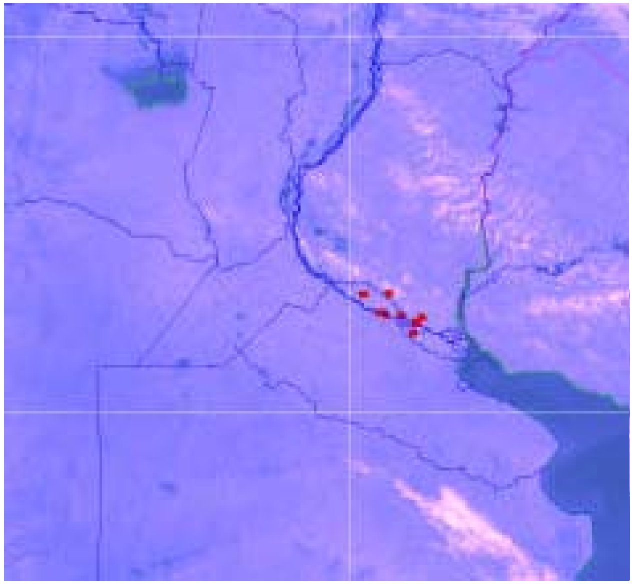

❖MODIS (Terra) sensor – April 15, 2008
Nighttime acquisition

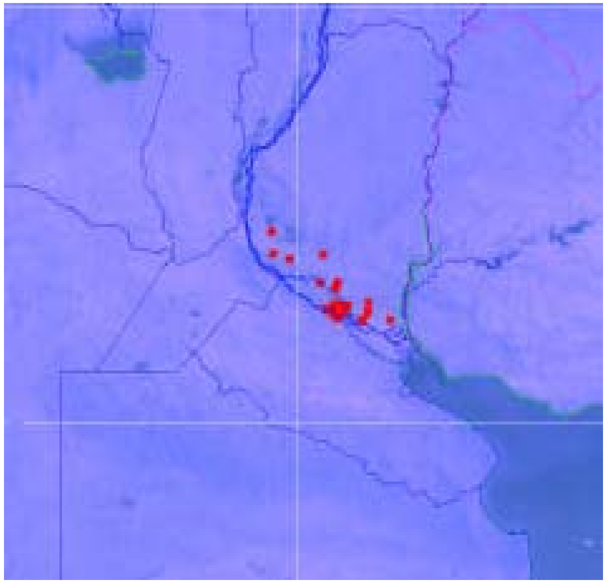

❖MODIS (Aqua) sensor – April 17, 2008
Nighttime acquisition

AQUARIUS/SAC-D

Fire Mapping and Fire Radiative Power

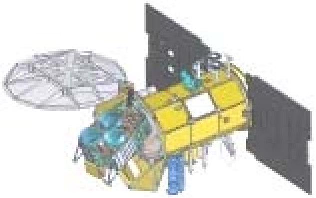

Example of MODIS resolution compared to BIRD resolution, which is similar to NIRST

MODIS data – 4µm band | BIRD data – 4µm band

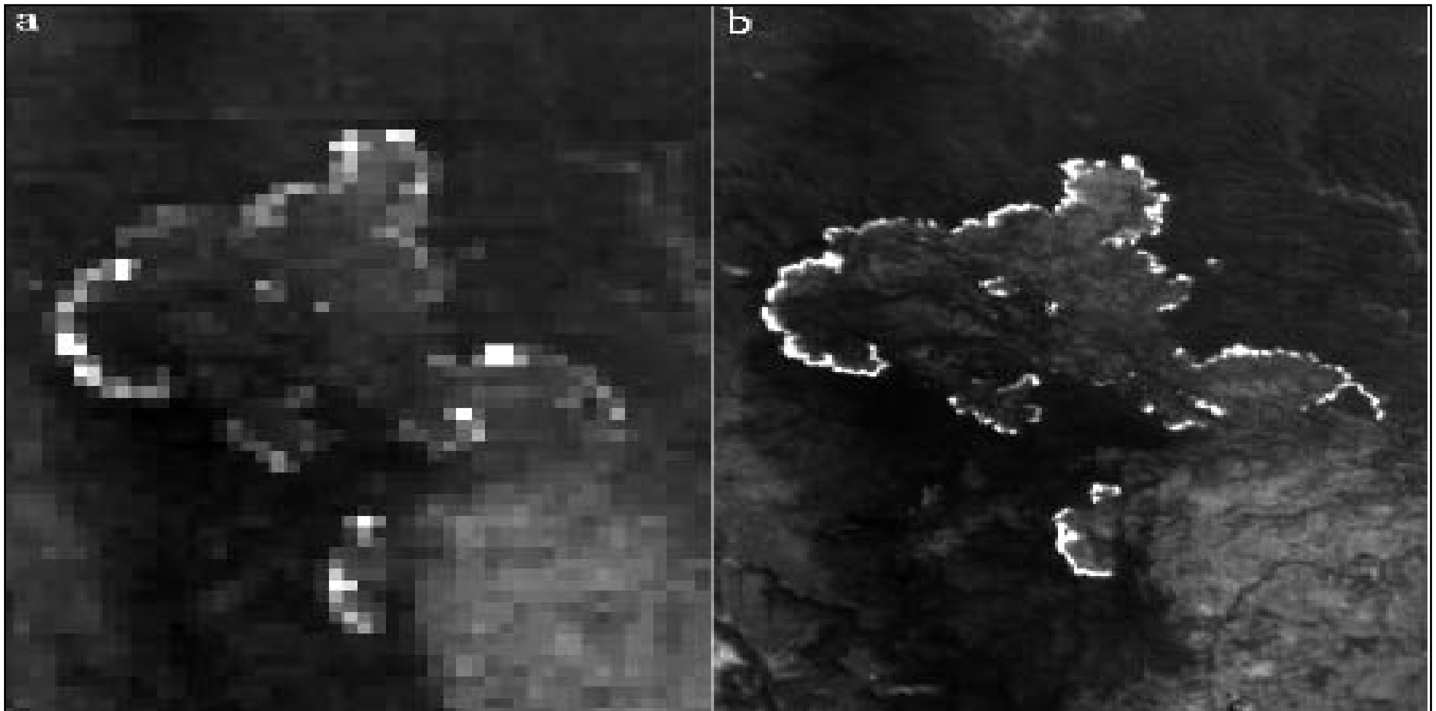

(From Wooster et al., 2003)

NIRST pixel size is similar to BIRD pixel size

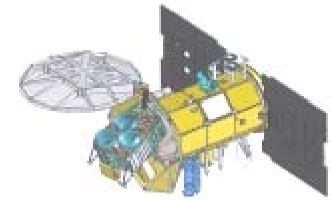

> FIRE DETECTION ALGORITHM FLOW CHART

FIRE Detection Algorithm (based on MODIS algorithm, Giglio 2003)

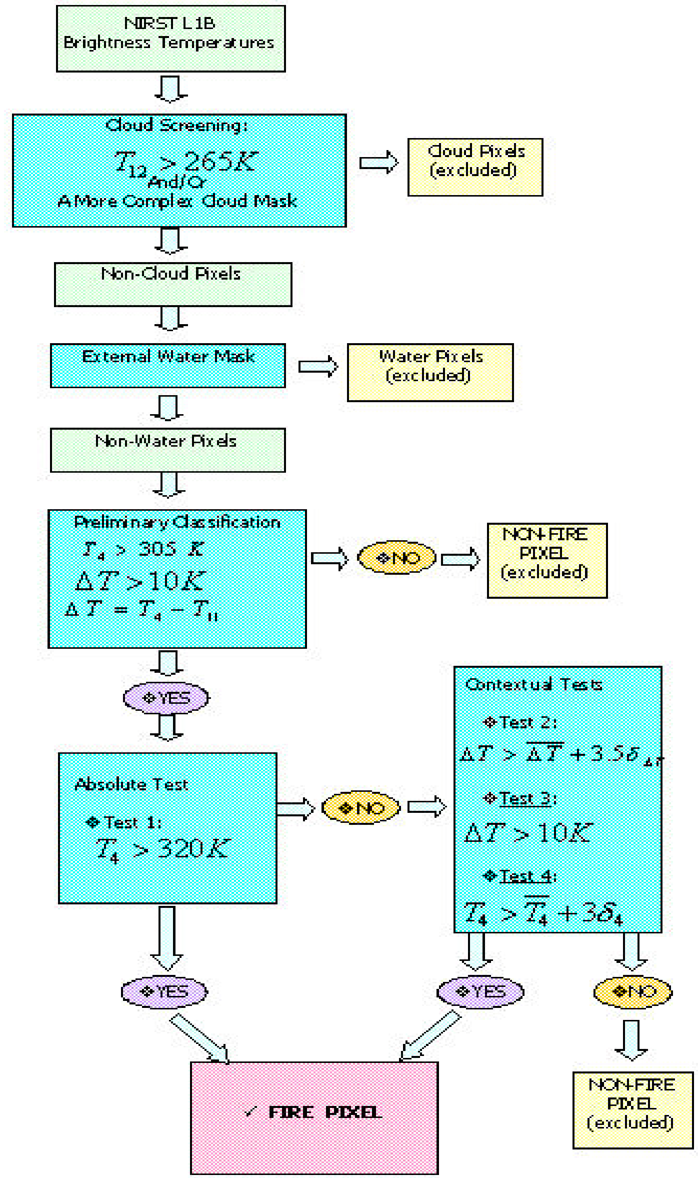

➢ FIRE DETECTION ALGORITHM FLOW CHART

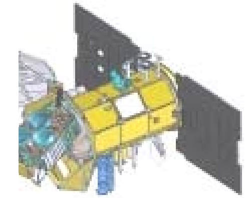

Flow chart of the
Fire Detection Algorithm:

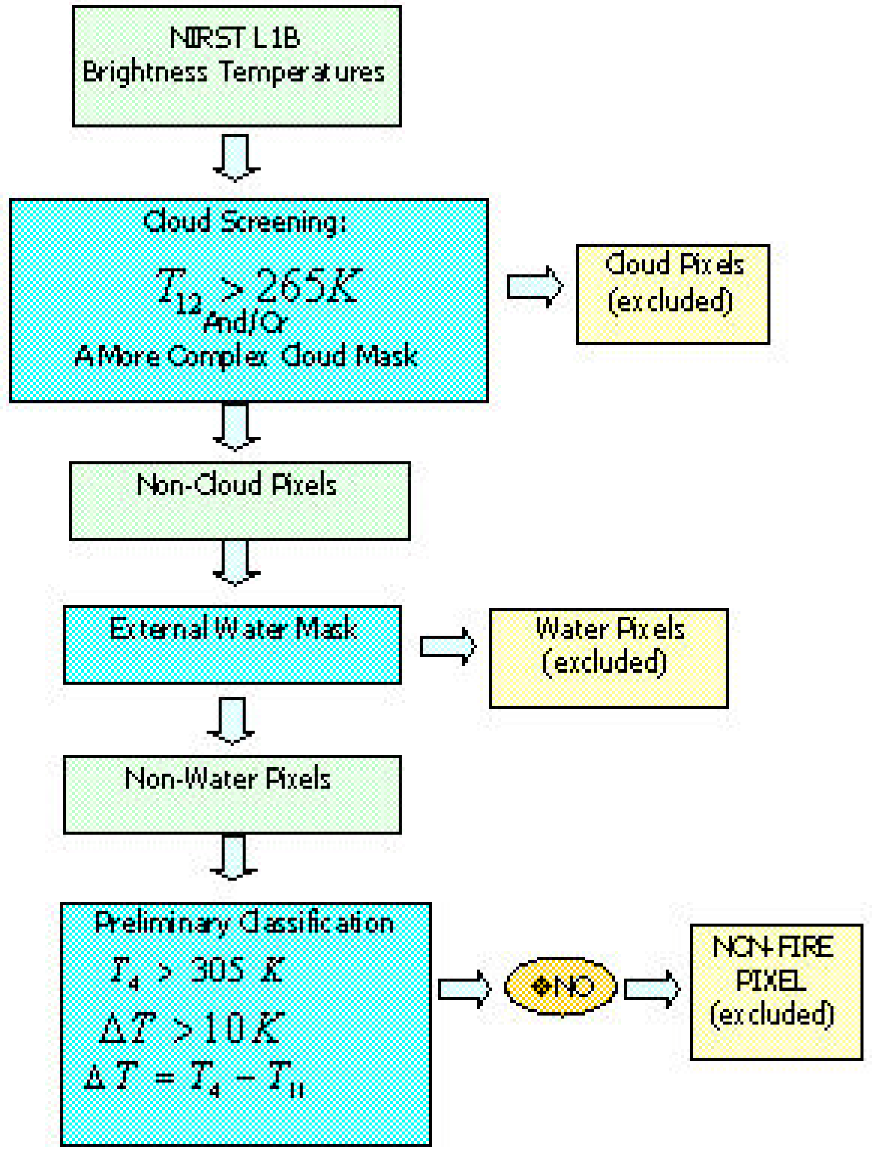

Continued…

Fire Mapping and Fire Radiative Power

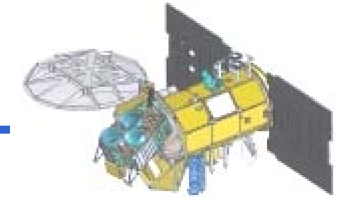

Flow chart of the
Fire Detection Algorithm:

Continued…

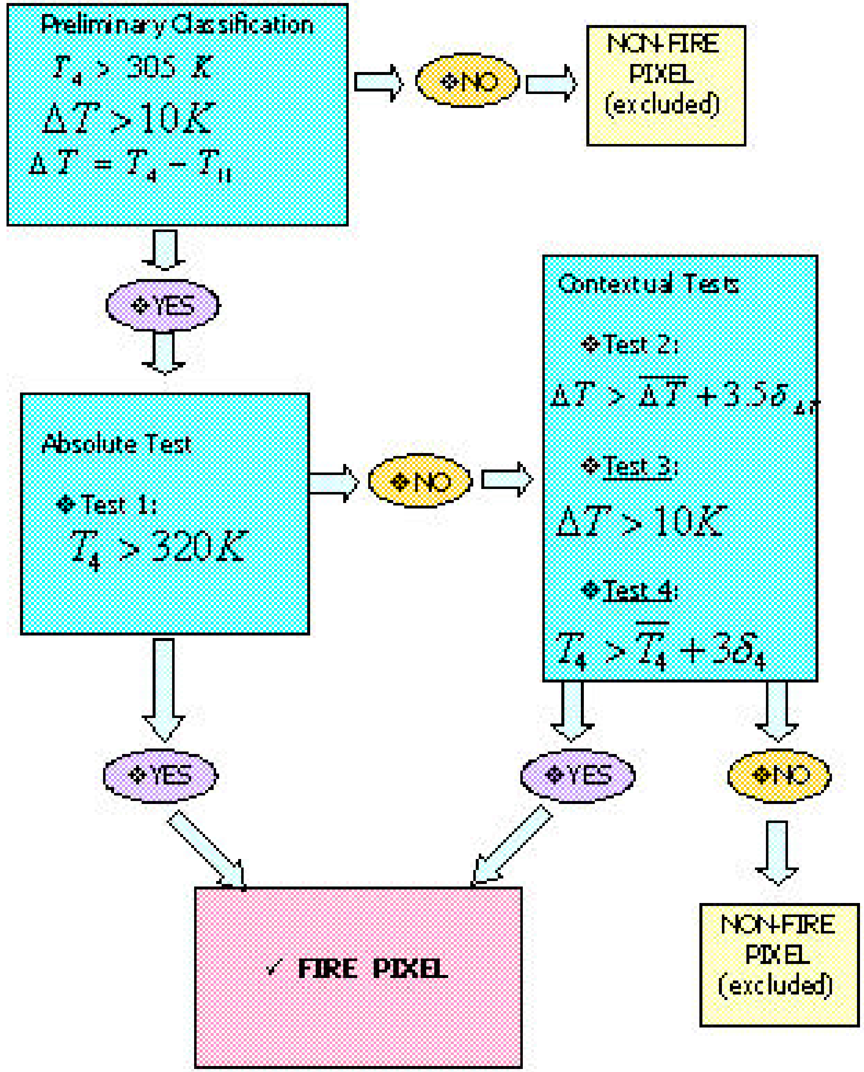

Fire Mapping and Fire Radiative Power

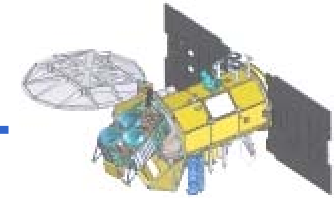

❖Fire Radiative Power (FRP)

Fires burn extensive areas in different vegetated landscapes across the globe, and constitute a major disturbance to land-based ecosystems.

By voraciously consuming biomass, releasing intense heat energy, and emitting thick plumes of smoke into the atmosphere, such large-scale fires exert several adverse effects on life, property, the environment, weather, and climate both directly and indirectly**.**

- **FRP is the amount of radiant heat energy liberated per unit time**
- **FRP** is related to the rate at which fuel is being consumed.

- Measuring **FRP** and integrating it over the lifetime of the fire provides an estimate of the **total Fire Radiative Energy (FRE),**

- **FRE,** for wildfires should be **proportional to the total mass of fuel biomass combusted.**

Fire Mapping and Fire Radiative Power

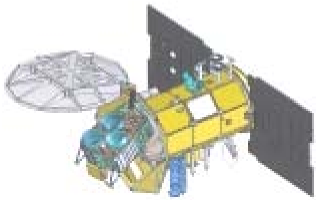

For each fire pixel detected, FRP is estimated using the empirical relationship of Kaufman et al. (1998),

$$\boxed{FRP = (\kappa_{sensor}\, 4.34\times 10^{-19}\, MWK^{-8} km^{-2})(T_4^8 - \overline{T}_4^{\,8}) A_{pix}}$$

where,

T_4 → 4-µm brightness temperature of the fire pixel

$\overline{T}_4$ → mean 4-µm brightness temperature of the non-fire background

A_{pix} → total area (in km2) of the pixel in which the fire was detected, taking into account its deformation due to projections and scan angles.

✓ The resulting value of the FRP is expressed in MW.

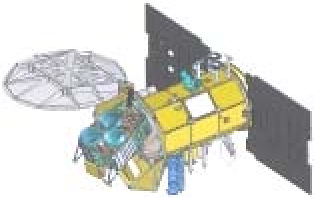

Sea Surface Temperature

Sea Surface Temperature

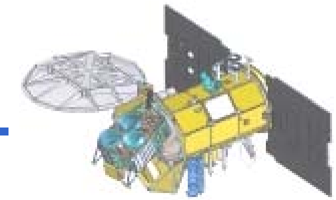

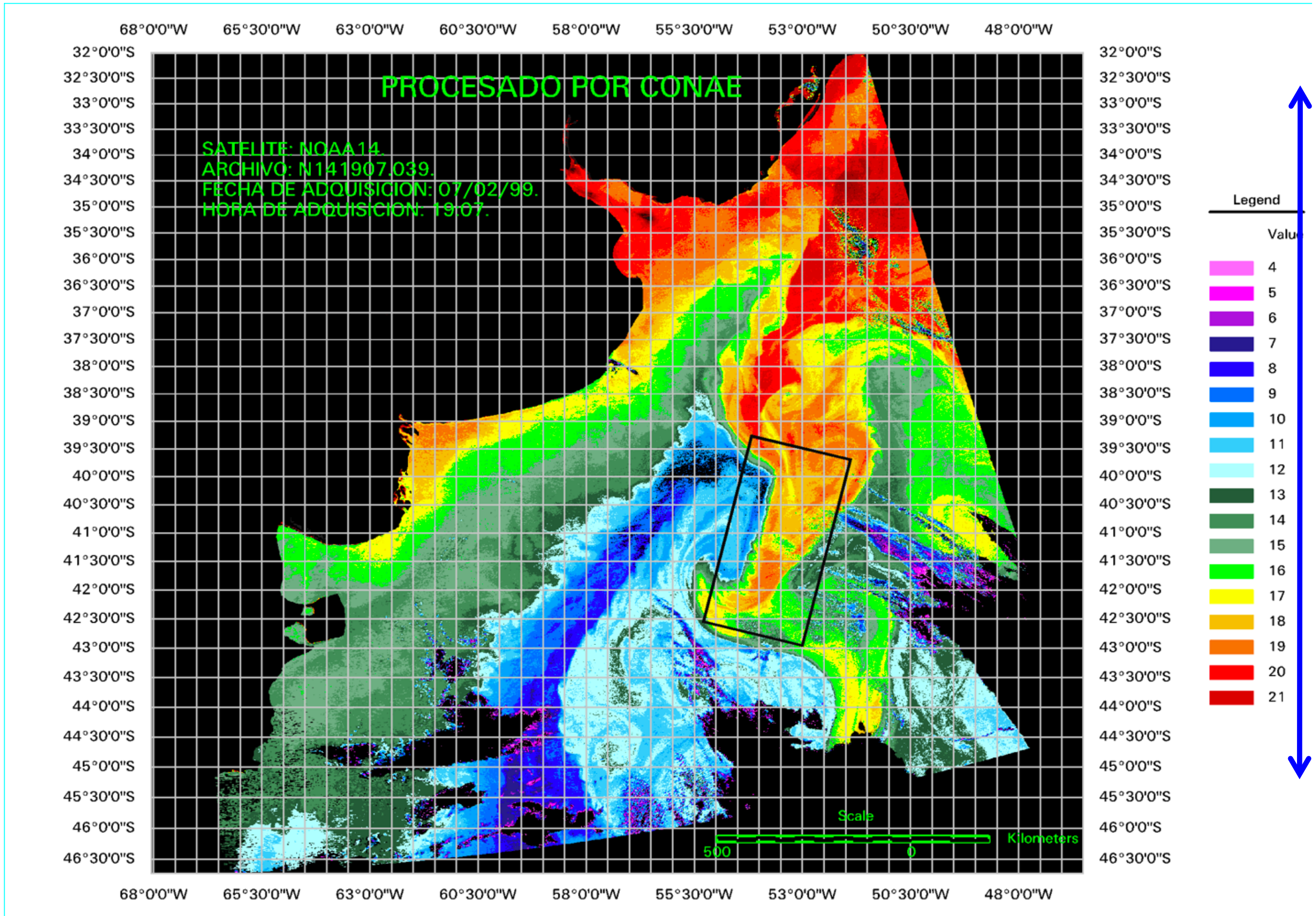

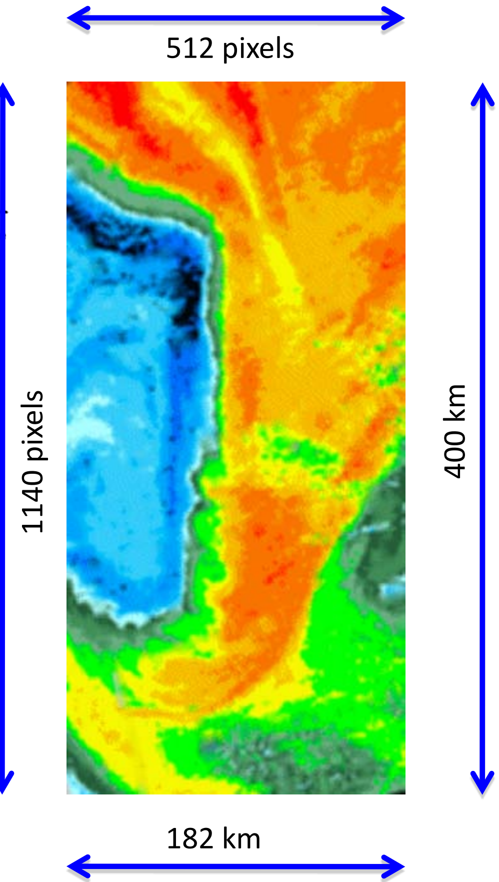

What a NIRST (almost 1 minute long) nadiral scan over the Malvinas-Brazil eddies would be

Sea Surface Temperature

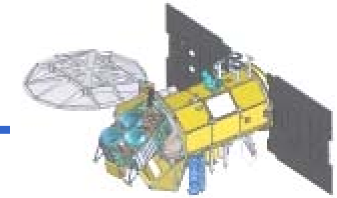

NIRST SST Algorithm will be based on the current algorithm that is used to calculate the AVHRR SST product, a non-linear split window equation:

$$\mathbf{SST = \alpha + \beta BT_{11} + \gamma(BT_{11} - BT_{12})T_{ref} + \delta[\sec(\Theta) - 1](BT_{11} - BT_{12})}$$

Where,

- T_{ref} is an estimated SST
- $\mathbf{BT_{11}}$ and $\mathbf{BT_{12}}$ are the brightness temperatures in bands 11 and 12 μm
- **α , β, γ and δ** *are* coefficients that should be **computed locally**
  (By regressing equations with in-situ data, plus either MODTRAN simulated BT_{11} and BT_{12}, or NIRST data once in orbit) and updated periodically.
- **ϴ** is the **viewing angle**

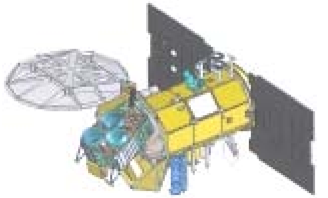

Land Surface Temperature

Land Surface Temperature

Example of ASTER LST compared to MODIS LST for the same area of study

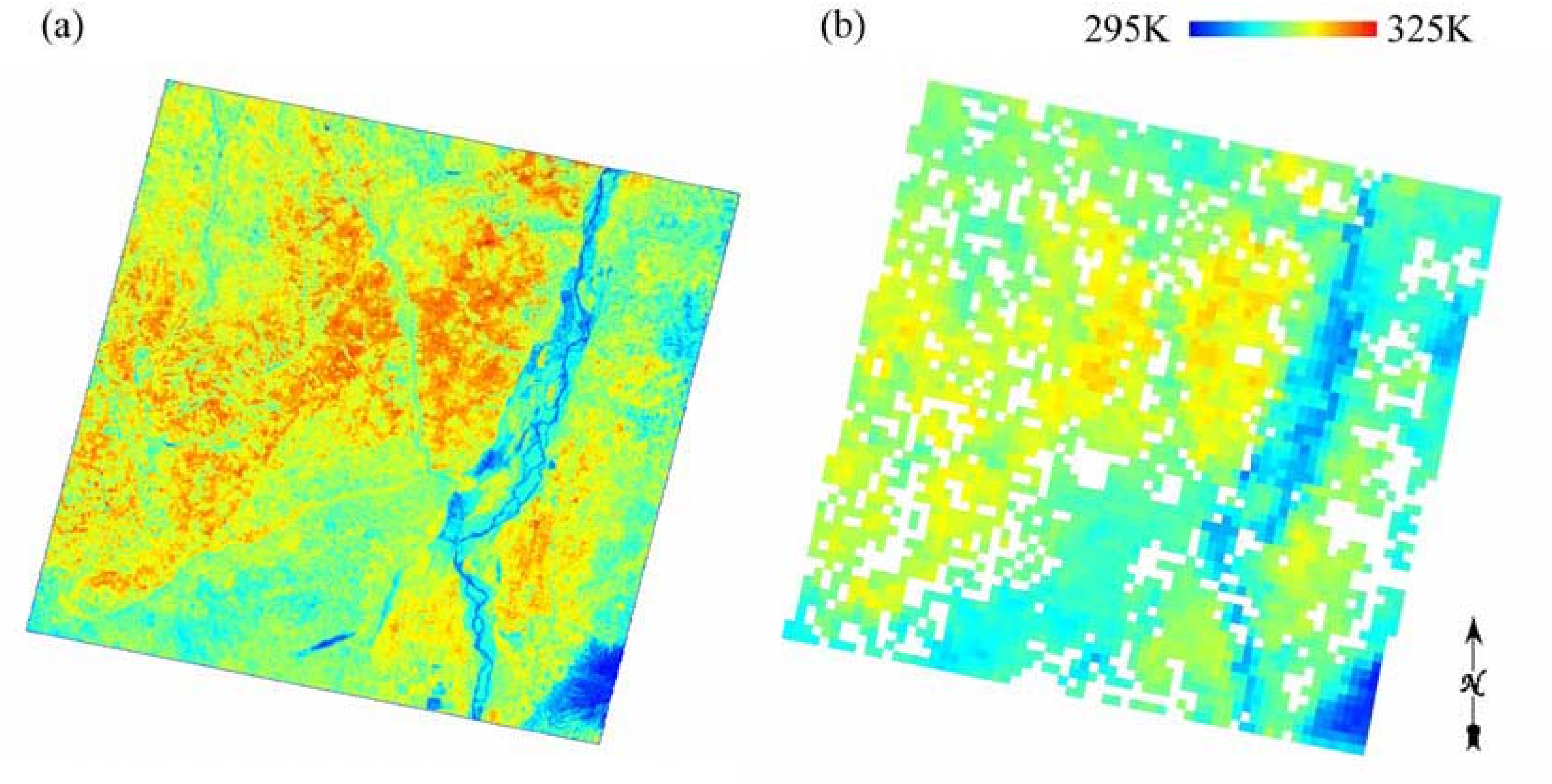

(From Liu et al., 2009)

Land Surface Temperature

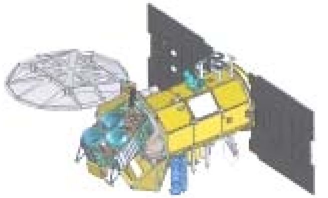

LST Algorithm

$$T_S = \left(A_1 + A_2 \frac{1-\varepsilon}{\varepsilon} + A_3 \frac{\Delta\varepsilon}{\varepsilon^2}\right)\frac{T_{11}+T_{12}}{2} + \left(B_1 + B_2 \frac{1-\varepsilon}{\varepsilon} + B_3 \frac{\Delta\varepsilon}{\varepsilon^2}\right)\frac{T_{11}-T_{12}}{2} + C$$

Where:

$$\Delta\varepsilon = (\varepsilon_{11} - \varepsilon_{12}) \qquad \varepsilon = \frac{(\varepsilon_{11} + \varepsilon_{12})}{2}$$

are the difference and mean of surface emissivities in bands 11 and 12 µm, which will be obtained with the MODIS 250m NDVI product,

T_{11} and T_{12} are the brightness temperatures in bands 11 and 12 µm,

A_1, A_2, A_3, B_1, B_2 and B_3 are coefficients that will be obtained by regressing equations with in situ data and MODTRAN simulated brightness temperatures.

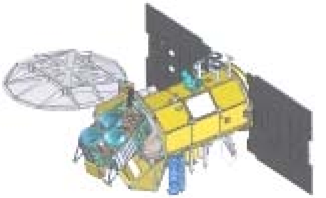

Volcanic Activity Monitoring

Volcanic Activity Monitoring

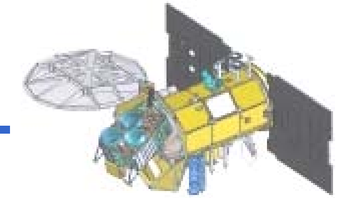

✓**Volcanic ash detection**

In standard visible and infrared satellite imagery volcanic ash clouds can resemble water-bearing clouds.

However, the radiative absorption properties of the silicate in the volcanic ash are different to those of water in the infrared wavelength range 11-12 microns.

An image showing the brightness temperature difference between channels at 11 and 12 microns (BT11 - BT12) can be used to **distinguish volcanic ash** from water-bearing clouds.

In general:

- BT11 - BT12 > 0 for water-bearing clouds
- BT11 - BT12 < 0 for volcanic ash clouds

Volcanic Activity Monitoring

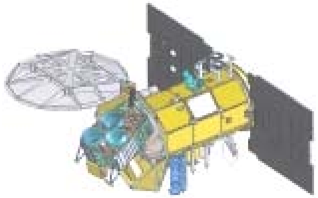

✓ **Hot Spot Detection -** Normalized Thermal Index Product (Wright et al., 2003)

$$NTI = \frac{B\ 4\ \mu m - B\ 12\ \mu m}{B\ 4\ \mu m + B\ 12\ \mu m} \quad (\text{Watt} / m^2\ \text{str}\ \mu m)$$

NTI > Threshold

✓ **Hot Spot Detection Product -** Average Zones. (Vicari et al., 2007)

Works with a difference image: **BTD (3.9 – 11) μm,**

and compares values between the zones containing the presumable hot spot and its neighbouring areas.

NIRST simulated data

Simulations shall be made by using the atmospheric **radiative transfer model MODTRAN** to simulate the TOA radiance with the appropriate thermal infrared channel **response function** of the NIRST sensor on board Aquarius/SAC-D.

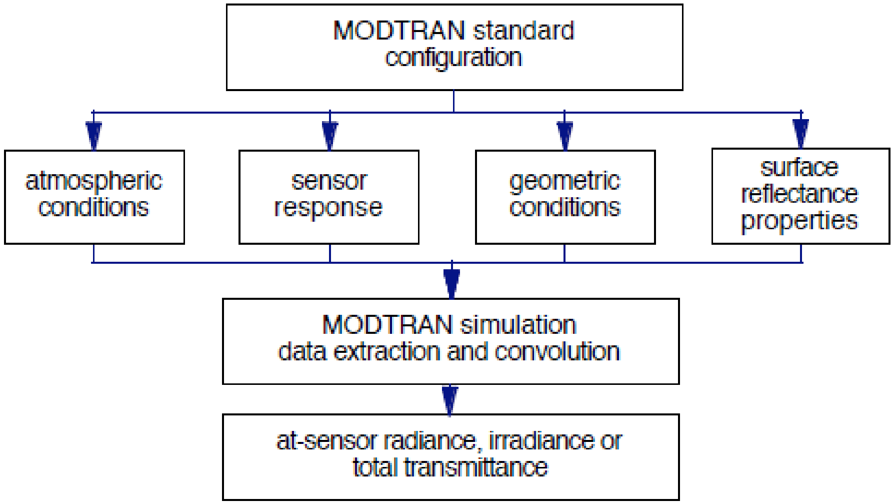

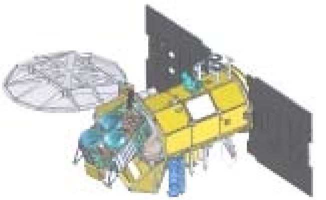

VALIDATION

- **Validation is a critical step in the quality control of products derived from Earth observation.**
- The main aim of a validation program is to assess whether the measurement processes are being achieved within the science requirements through validation of the final product.
- **Science** Validation **of NIRST derived products consists of** independent determination **of this products and** comparison **with the ones derived from NIRST processor.**
- **It may involve comparison of products with similar products derived by conventional means (in situ direct measurements of parameters such as wind, temperature, humidity, etc.). It is important that those products have themselves been validated and their accuracy and uncertainty established.**

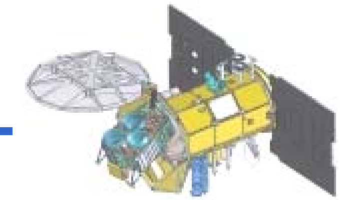

Validation outline

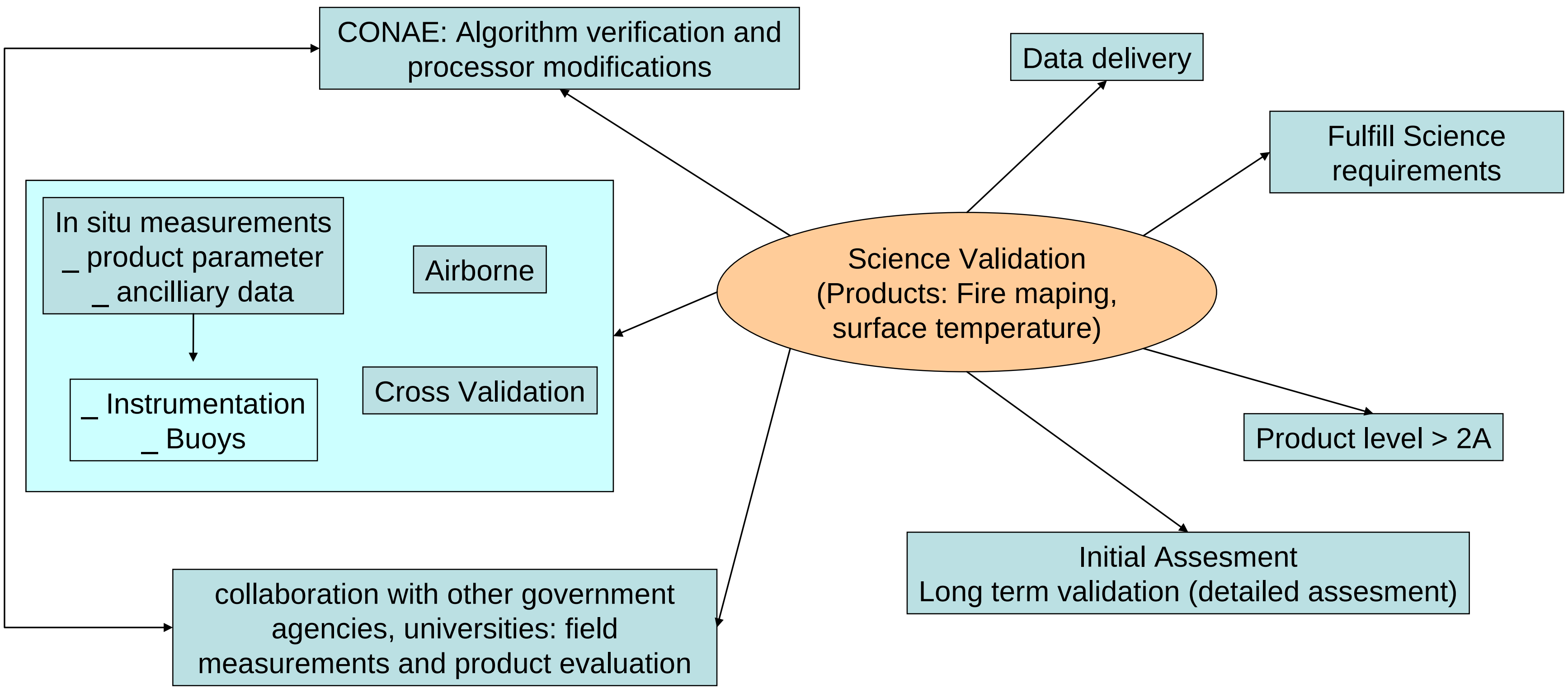

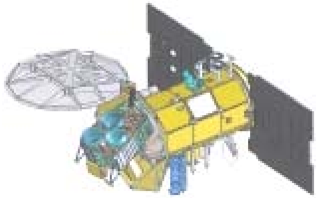

Thank you!

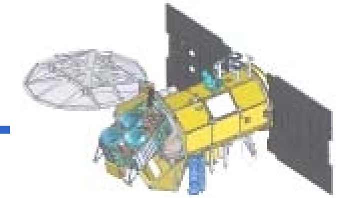

		MWIR2 (Band 1)	LWIR2 (Band 2)	LWIR3 (Band 3)
Central wavelength		3.8 µm	10.85 µm	11.85 µm
Band Limits		3.4 – 4.2 µm	10.4 – 11.3 µm	11.4 – 12.3 µm
Temperature	Min.	400K	250K	
	Max.	1000K	500K	
NEΔT		<1.5K @ 400K	<0.8K @ 300K	<0.4K @ 300K
Temp. accuracy		2.5K @ 400K	1.5K @ 300K	<2K @ 300K
Detectable size of fire event		200m^2 @ 1000K		

VALIDATION

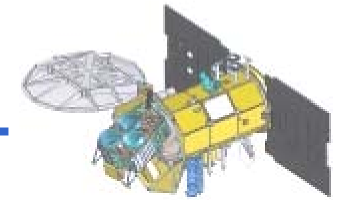

- **Validation is a critical step in the quality control of products derived from Earth observation.**

- The main aim of a validation program is to assess whether the measurement processes are being achieved within the science requirements through validation of the final product.

- **Science** Validation **of NIRST derived products consists of** independent determination **of this products and** comparison **with the ones derived from NIRST processor.**

- **It may involve comparison of products with similar products derived by conventional means (in situ direct measurements of parameters such as wind, temperature, humidity, etc.). It is important that those products have themselves been validated and their accuracy and uncertainty established.**

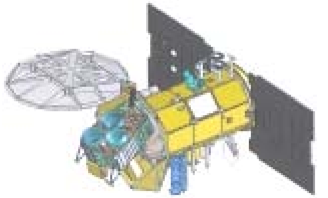

During the initial validation phase, the main objective is to make a first assessment of the quality of the NIRST derived data products, in a limited number of sites and seasons.

During the mission as a whole, the aims of the on-going validation program are:

- To make a detailed assessment of the quality of the NIRST data products in an increasing number of sites and seasons.
- To monitor the quality of the NIRST data products over the duration of the mission.

It shall be performed periodically to monitor the quality of the NIRST data products over the duration of the mission.

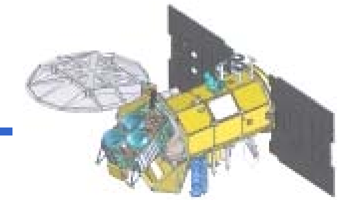

However data is acquired, an implementation for vicarious validation follows:

1- Site determination. The available ancillary data for the site should be taken into account. The extension of the area shall cover several NIRST pixels

2- Determination of necessary data as input to the process. This includes atmospheric and in-situ data from instrumentation or dependable sources.

3- Temperature retrieval from satellite. This will involve the algorithm, radiative transfer calculations (MODTRAN) with emissivity and atmospheric data as input**.**

4- Surface temperature determination:

4a- Through in-situ temperature measurements. Difference between bulk and skin temperature should be made.

4b- Through simulation with radiative transfer calculations (MODTRAN) with several temperatures and measured or simulated atmospheric conditions for the site of interest.

5- Derived product and measured/simulated product comparison

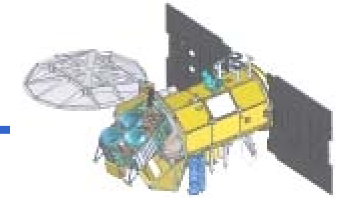

6- Evaluation of differences. This could involve a study of temperature as a function of meteorological conditions to determine whether differences can be attributed to a bad simulation or there is no possible match between both products after varying parameters among reasonable values for the site and season. This would require validation sites with equipment or buoys for time series evaluation, a global communication system could be used for this purpose to access the data. Wind speed, humidity and air temperature are some of the parameters needed to determine the boundary layer properties.

7- **Determination of causes of temperature retrieval error**. Must differentiate between:

- temperature retrieval
- model assumptions
- meteorological data

8- **Process (or algorithm) correction**.

Validation of active fire products has been recognized to be a difficult task which lacks well-established procedures.

Flagging pixels that contain burning as "fire", which yields "yes/no" binary fire maps, is commonly referred to as **"active fire detection."**

Independent information on fires can be obtained either by the **direct observation of fires** by alternative means or by **observing fire effects such as atmospheric emissions or land cover change**. For example, smoke plumes were used for the accuracy assessment of fire detections from the Advanced Very High Resolution Radiometer (AVHRR).

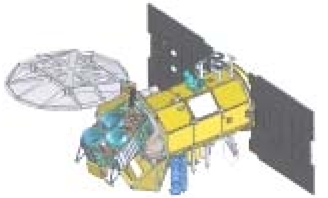

Geophysical parameters validation:

- Field work is needed to measure the geophysical parameters of interest, in specified locations, simultaneously with NIRST measurements
- The campaigns must be designed to collect a statistically significant number of samples
- Data for parameters validation could be obtained from DCPs, using the DCS instrument on board SAC-D
- The selected algorithms must be used for the retrieval of the specific parameters under evaluation from NIRST measurements
- A statistical analysis relating the field measurements and the parameter retrieved values must be carried out to obtain representative figures of the algorithms performance

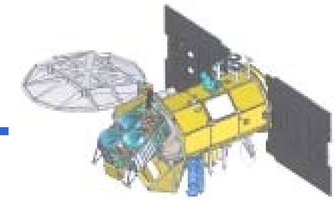

NIRST data Simulation:

At-sensor radiance simulation workflow with 4 input sections based on standard MODTRAN configurations.

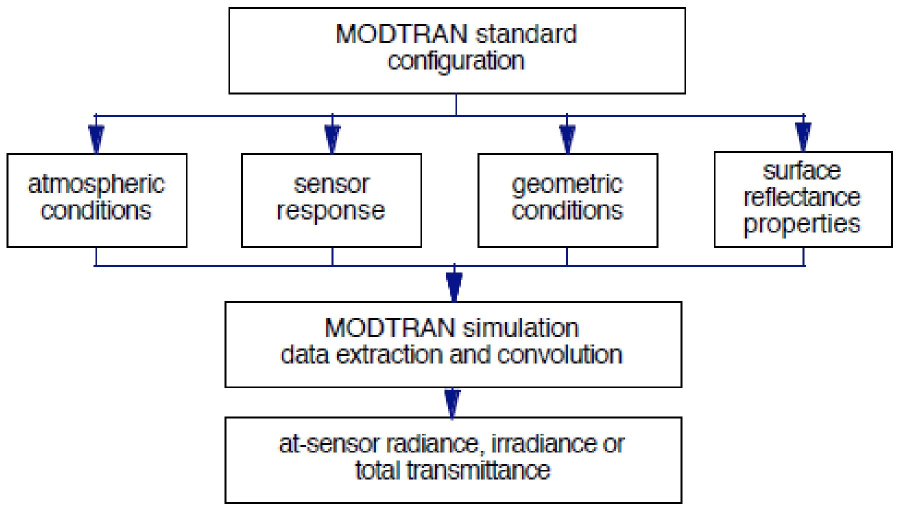

Australia – HyspIRI Partnerships

Alex Held, CSIRO

Australia and NASA HyspIRI

Our interests

CSIRO and Australian research community have an interest in future use of wall-to-wall, systematic data acquisitions of spaceborne imaging spectroscopy (hyperspectral) data for a wide range of national priority mapping and monitoring applications, which include:

- Geological Mapping and Exploration
- Coastal water quality monitoring
- Agricultural crop and condition monitoring
- Forest degradation monitoring
- Minesite and pollution monitoring
- Fuel type and fuel load mapping

New national programs such as projects under the ASRP, plus the "Terrestrial Ecosystem Research Network - TERN" (like the US NEON) and the "Integrated Marine Observing System – IMOS" provide excellent platforms for collaborations on improving ways to characterise land-surface dynamics and coastal & marine environments over Australian terrestrial and marine areas.

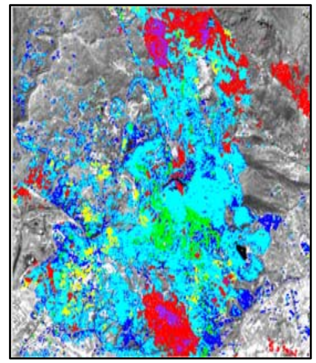

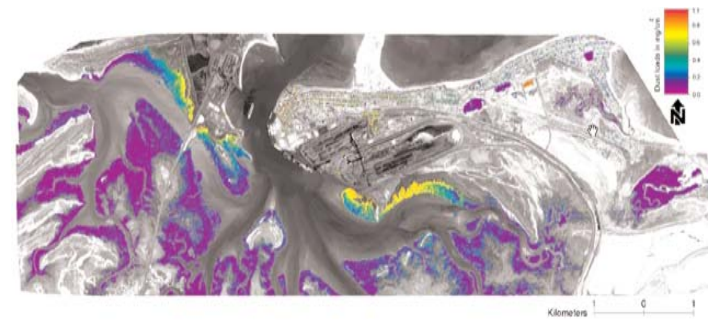

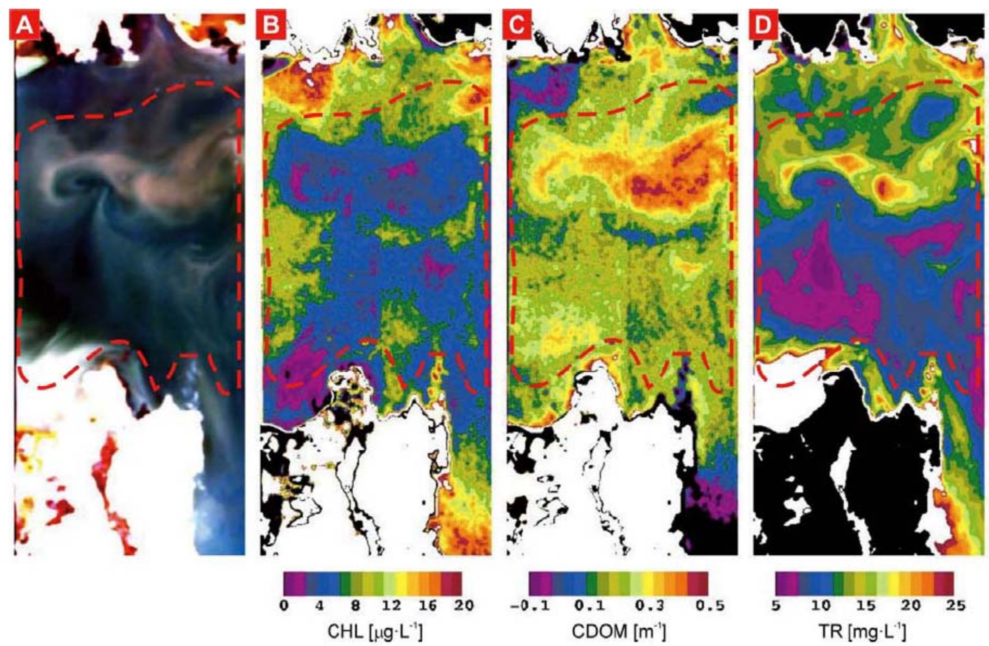

CSIRO

Multiple Uses for Imaging Spectroscopy Missions: Australian Context

Science ⟷ Management Support/Policy

Science Questions

- VQ1 - Pattern and Spatial Distribution of Ecosystems
- VQ2 - Ecosystem Function, Physiology and Seasonal Activity
- VQ3 - Biogeochemical Cycles
- VQ4 - Ecosystem Response to Disturbance
- VQ5 - Ecosystems and Human Well-being
- VQ6 - Surface and Shallow-Water Bottom Composition
- TQ1 - Volcanoes and Earthquakes
- TQ2 - Wildfires
- TQ3 - Water Use and Availability
- TQ4 - Human Health and Urbanization
- TQ5 - Earth Surface Composition and Change
- CQ1 - Coastal, Ocean, and Inland-Aquatic Environments
- CQ2 – Wildfires
- CQ3 - Volcanoes
- CQ4 - Ecosystem Function and Diversity
- CQ5 - Land Surface Composition and Change
- CQ6 - Human Health and Urbanization

- Calibration of Multi-spectral missions
- Wall-to-wall mapping every 19 days!

HyspIRI Standard Level 2, 3 Products

Key Government Needs

<u>Climate Change Monitoring/Modelling</u>:
- Derivation of Key Essential Climate Variables
- Improving Characterisation of Surface Emissivity Dynamics for new generation climate models
- Track changes in plant function and biodiversity

<u>National Priorities</u>
Economic Well-being: eg. Mineral Exploration
Food Security: Climate/Drought Impacts on Agriculture
Water Security: eg. Water Quality Monitoring
National Security
Etc.

<u>Policy-relevant Issues and International Obligations & Treaty Verification</u>:
- UN Climate Convention
- UN Desertification Convention
- UN Biodiversity Convention.

New Australian Space Research Program ($40+m)

- Started July 2009
- Includes a Space Policy Unit
- Funding Stream A: Space Education Development Grants
- Funding Stream B: Space Science and Innovation Project Grants

Among many others in Australia, CSIRO is proposing 3 ‘hyperspectral’ projects:

1. **Continental-scale hyperspectral terrestrial, coastal mapping and monitoring program**
2. **Development of a prototype thermal infrared (TIR) spectroscopy sensor**
3. **Continental Cal/Val Program**

CSIRO

Australia - US Collaborations/Partnerships

What can we offer:

•Extensive experience in Applications Development, as demonstrated during EO-1 Science Validation Team participation, and ongoing use of Hyperion data.

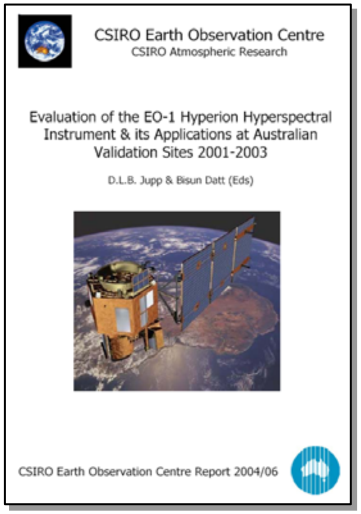
CSIRO Earth Observation Centre
CSIRO Atmospheric Research

Evaluation of the EO-1 Hyperion Hyperspectral Instrument & its Applications at Australian Validation Sites 2001-2003

D.L.B. Jupp & Bisun Datt (Eds)

CSIRO Earth Observation Centre Report 2004/06

•Radiometric calibration/validation: Part of large research infrastructure programs

Lake Frome, Lake Fefroy, Lake Argyle

•Access to airborne data from Hymap and other imaging spectrometer data sensors

• Future direct-readout capabilities, and processing via X-, Ka-band stations (Hobart & Darwin)

Australia hosts a large variety of sites and surface types for use in **Vicarious Radiometric Calibration** and for Level2, 3 **Product Validation**

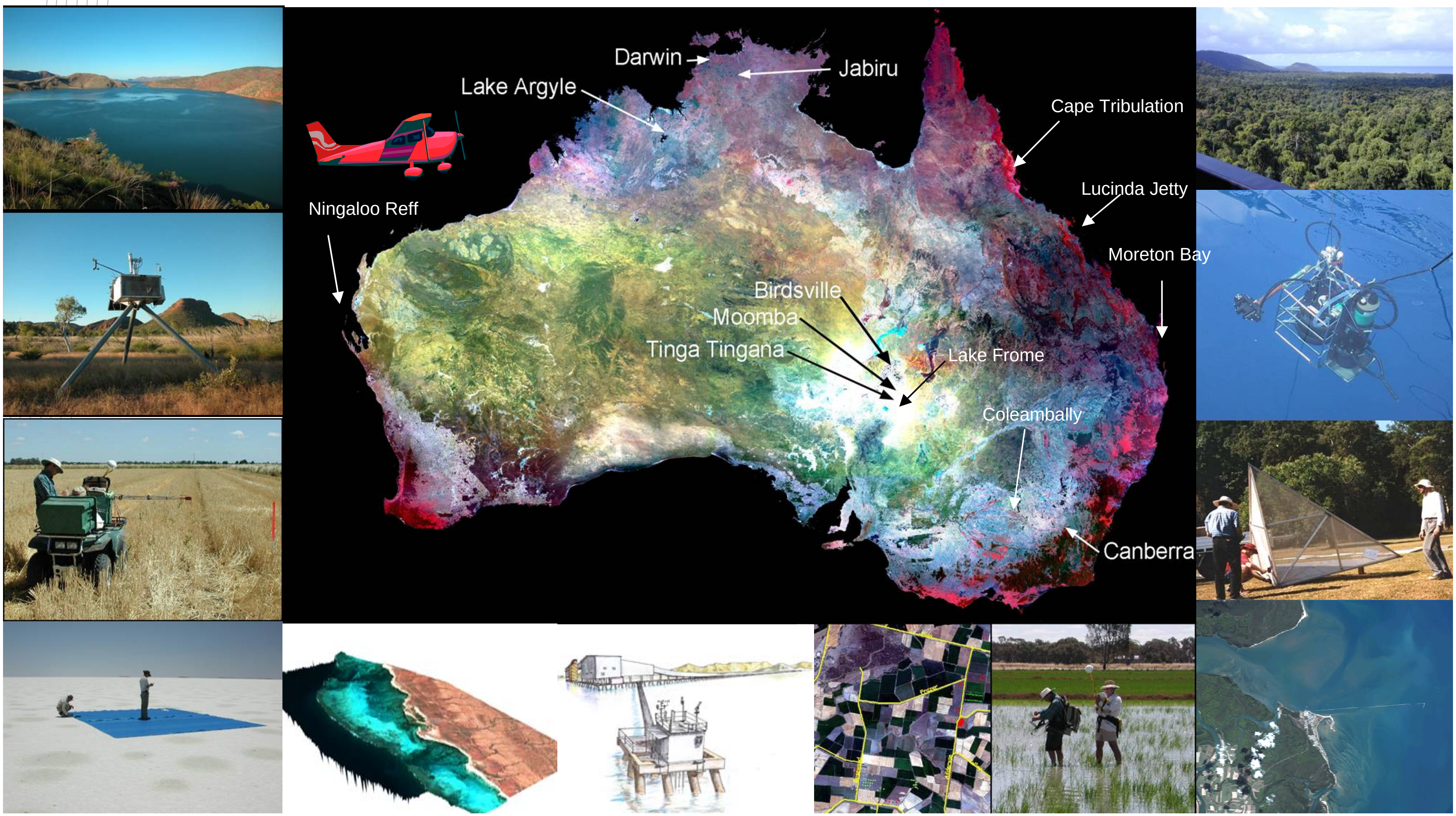

Sketch of LJCO facility

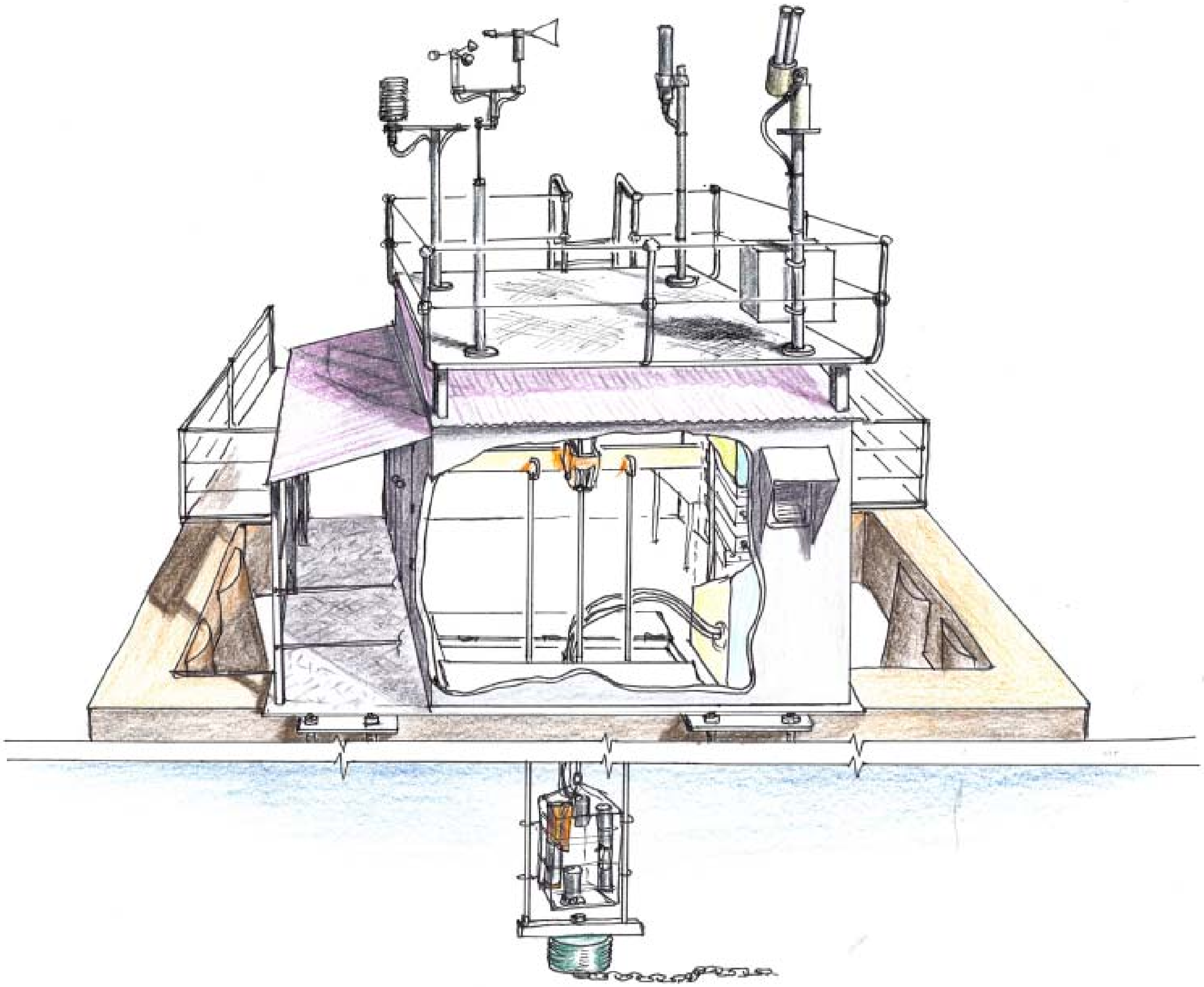

Establishment of Key Post-launch Spectroscopy Instrument Calibration & Validation Sites

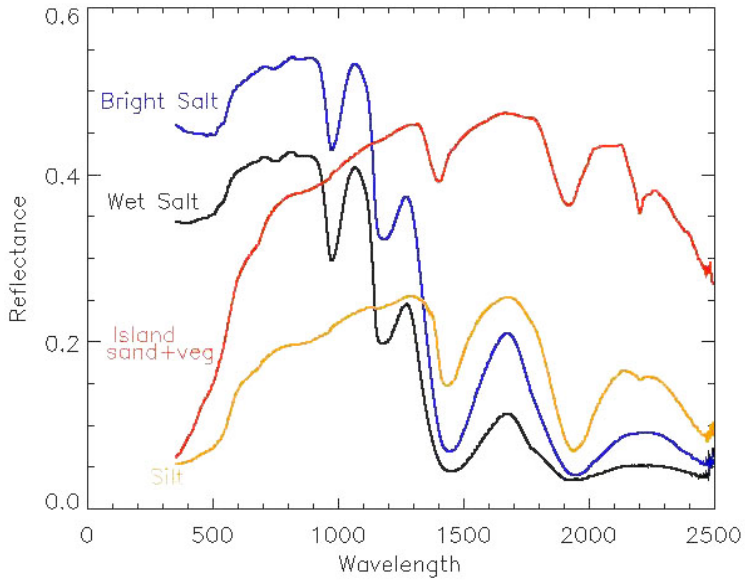

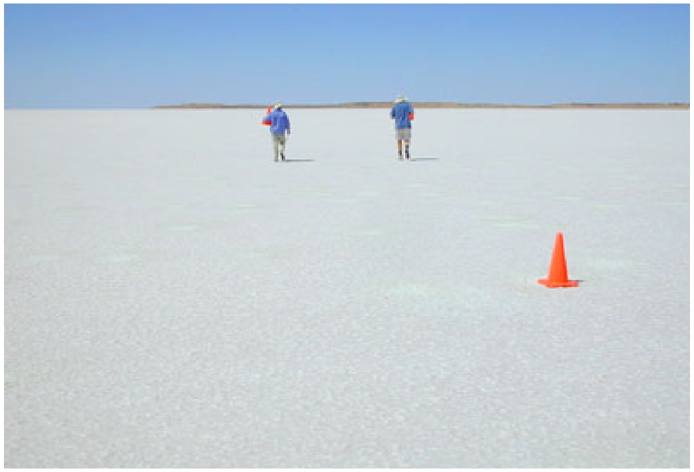

Upgrading Satellite Reception Facilities & National Data Networks

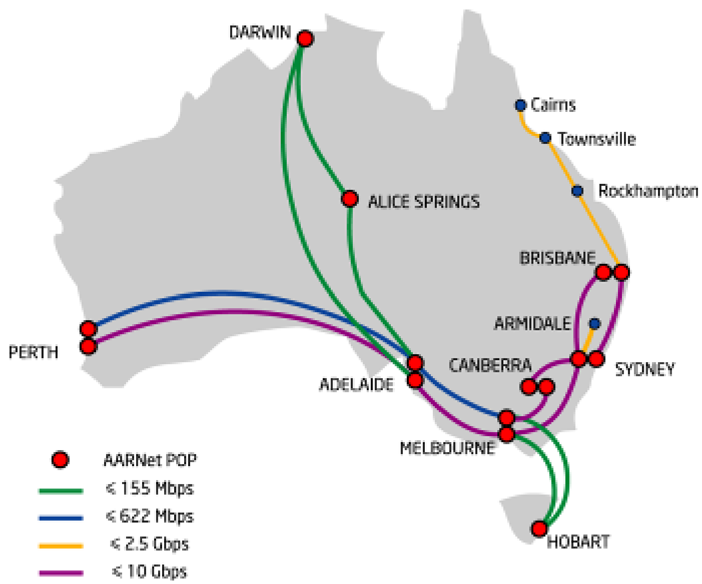

- Upgrading current facilities in <u>Darwin & Hobart</u> to dual-pol X-band and Ka-band downlink
- Science program on satellite – ground lidar communications
- Interconnected national broadband to international data centres
- Mass-data processing R&D

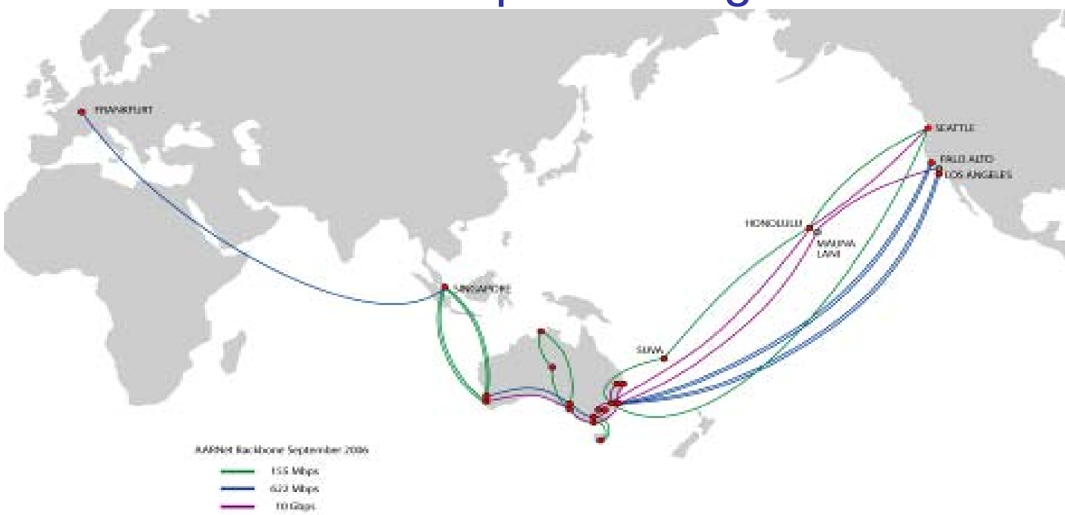

Simulating the response of the HyspIRI 4 μm channel to active lavas, using EO-1 Hyperion

Robert Wright

Hawai'i Institute of Geophysics and Planetology

University of Hawai'i Mānoa

Topics

- Data driven predictions of surface leaving radiance from active lavas based on non-linear unmixing of Hyperion data

- Simulating HyspIRI at-satellite radiance from these predictions

- The propensity of HyspIRI's 4 μm channel to saturate over terrestrial lavas: recommendation for setting L_{max}

- Some science results

What is the surface leaving radiance from Earth's active lavas?
a) simple modeling

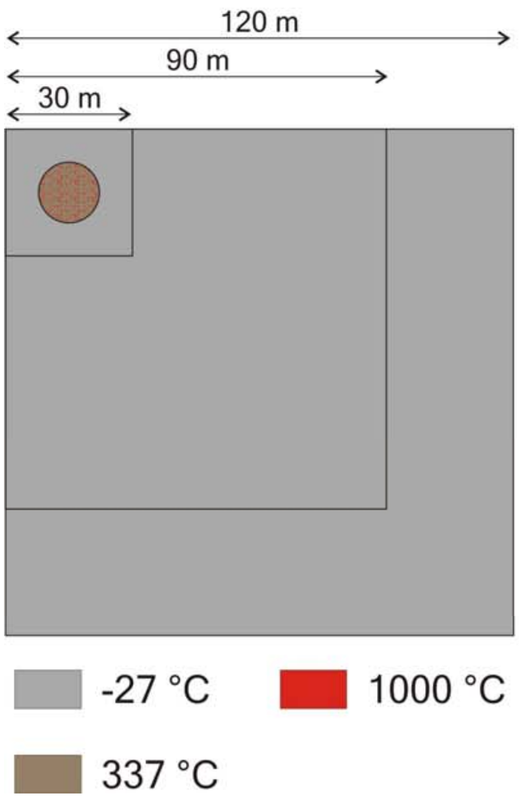

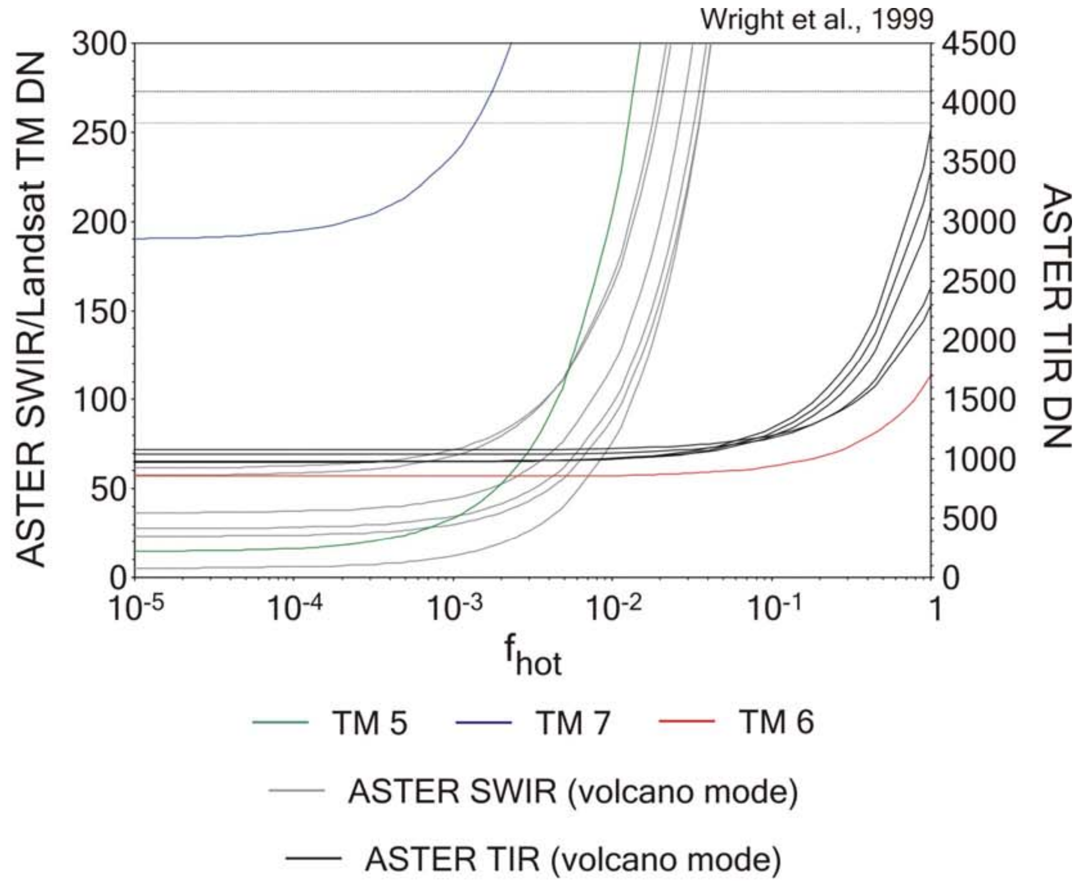

- Largely unconstrained by data
- How large? How hot? In what proportions?

What is the surface leaving radiance from Earth's active lavas?
b) combining modeling with real data

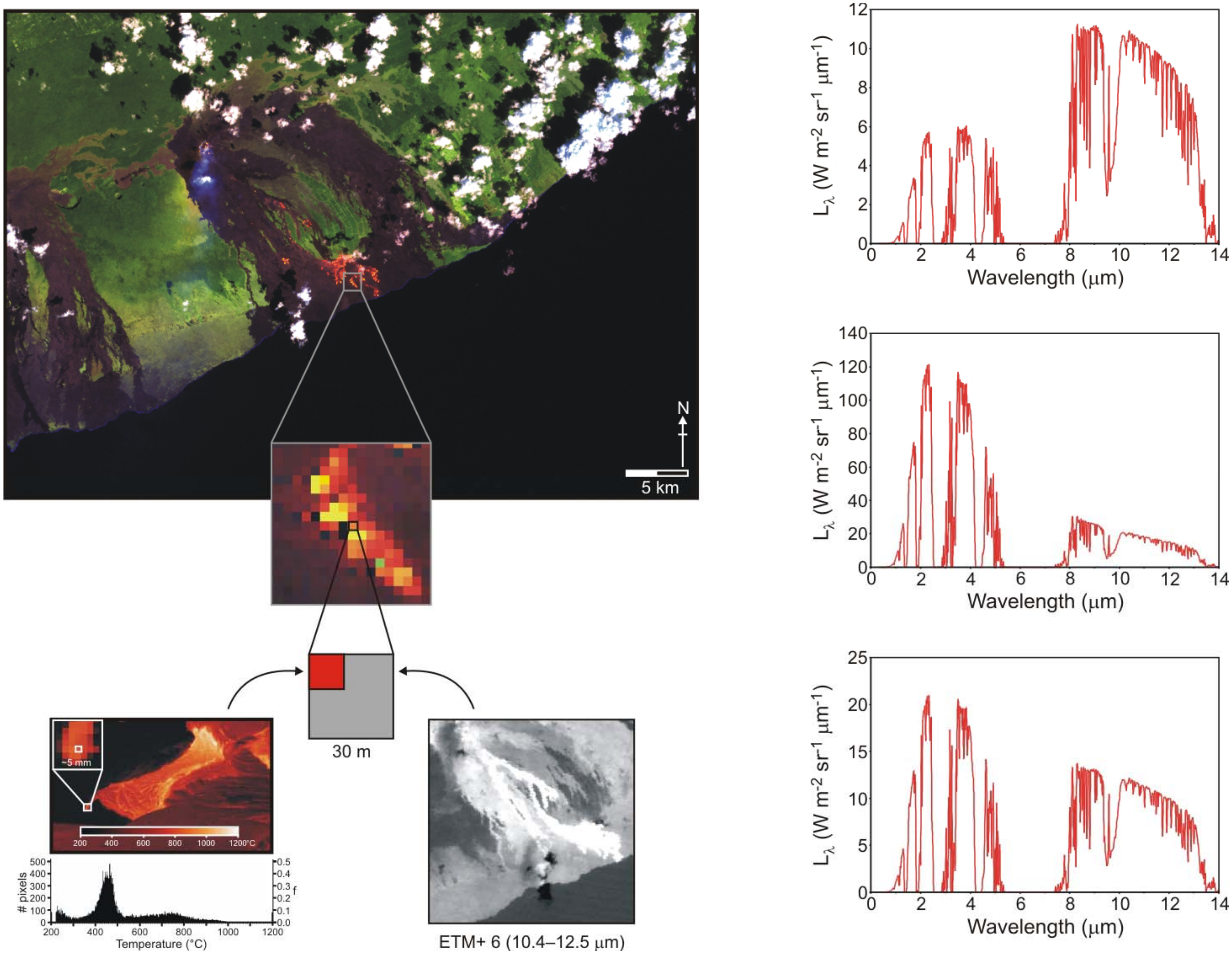

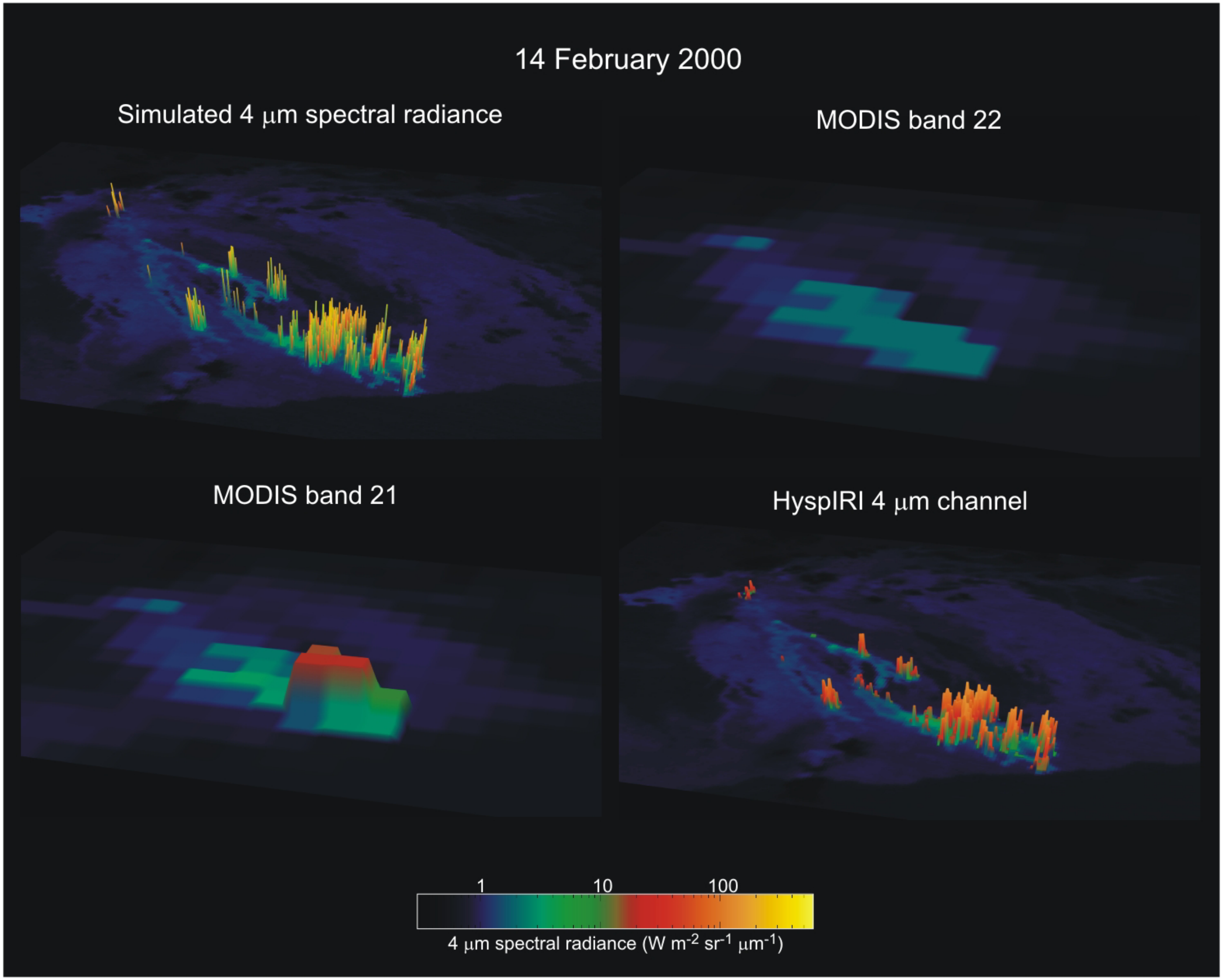

14 February 2000
Simulated 4 μm spectral radiance
MODIS band 22
MODIS band 21
HyspIRI 4 μm channel
1
10
100
4 μm spectral radiance (W m-2 sr-1 μm-1)

What is the surface leaving radiance from Earth’s active lavas?
c) simulating surface leaving radiance using real data

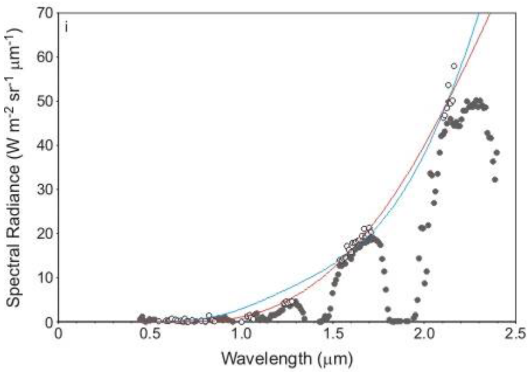

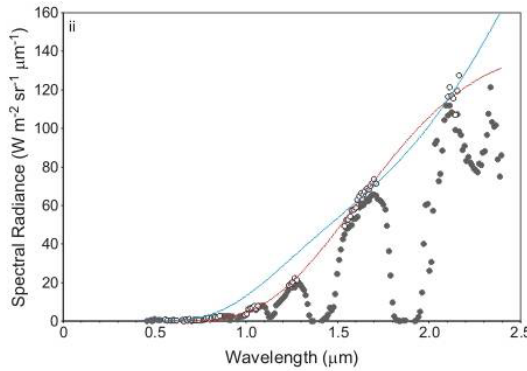

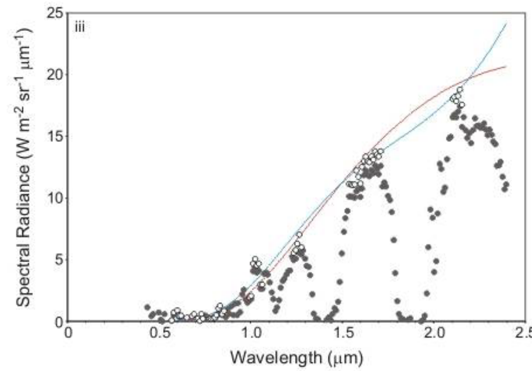

Wright et al., 2010

Pixel	i	ii	iii	iv	v	vi
Dual-band						
T_1	1150°C	1150°C	1150°C	1150°C	1150°C	1150°C
f_1	0.0006	0.0027	0.0006	0.0006	0.0035	0.0009
T_2	328°C	351°C	233°C	320 °C	328°C	254°C
f_2	0.9994	0.9973	0.9994	0.9994	0.9965	0.9991
rms	1.3	3.6	0.5	1.2	4.8	0.8
Unconstrained						
T_1	874°C	1067°C	1138°C	1001°C	920°C	963°C
f_1	0.003	0.0002	0.0005	0.0008	0.008	0.002
T_2	421°C	790°C	697°C	500°C	899°C	587°C
f_2	0.2	0.02	0.003	0.05	0.005	0.001
T_3	128°C	489°C	*	377°C	*	230°C
f_3	0.6	0.002	*	0.2	*	0.06
rms	0.7	1.2	0.4	0.7	1.8	0.7

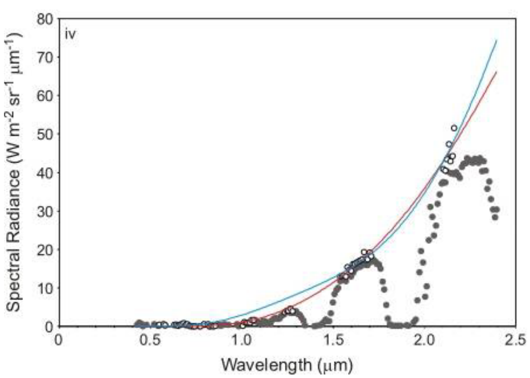

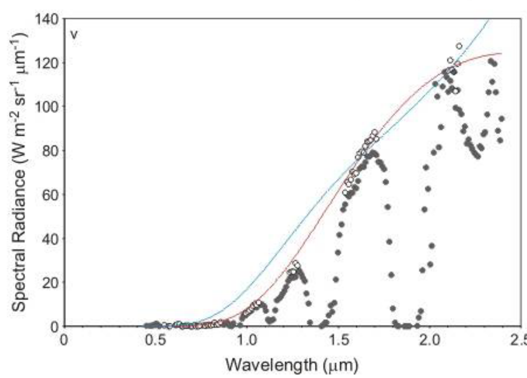

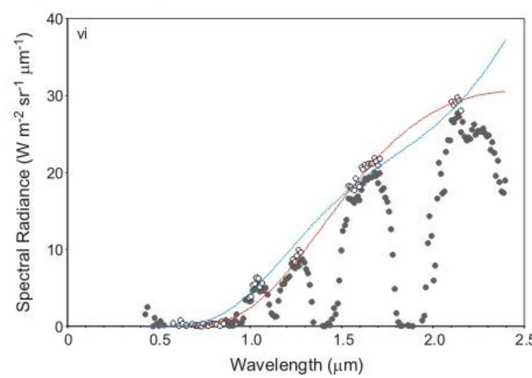

The ability to retrieve sub-pixel temperature characteristics using an imaging spectrometer

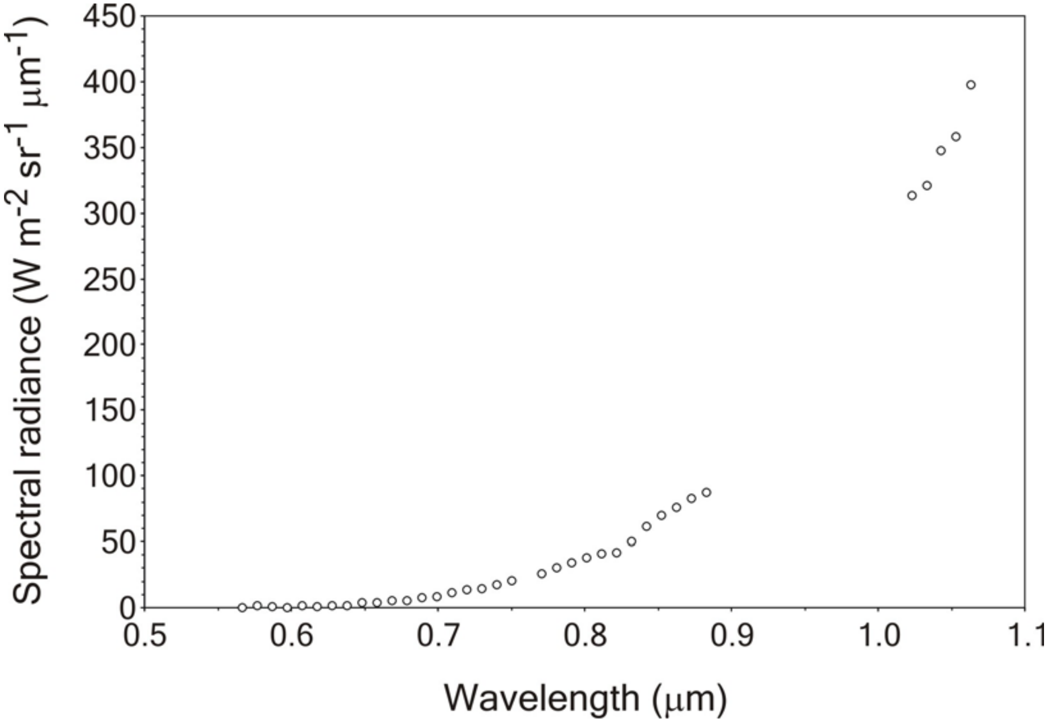

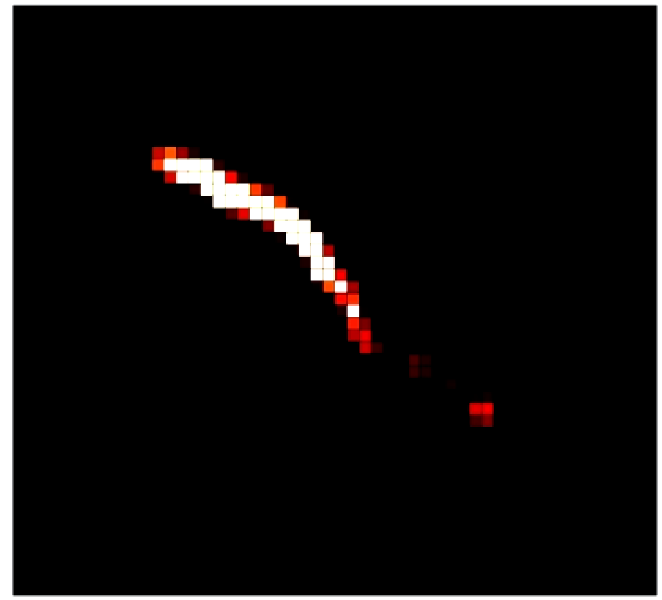

- Sub-pixel temperature characteristics can be determined for even the most radiant active lava surfaces

The desirability to quantify sub-pixel temperature mixing

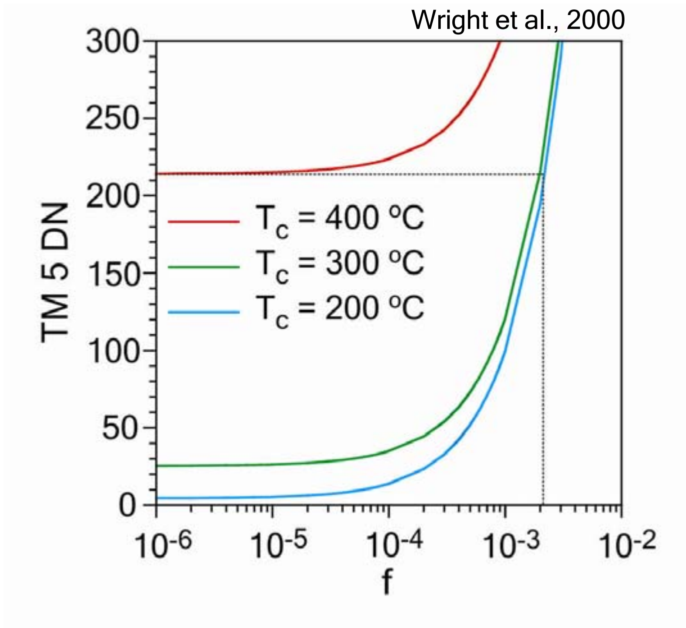

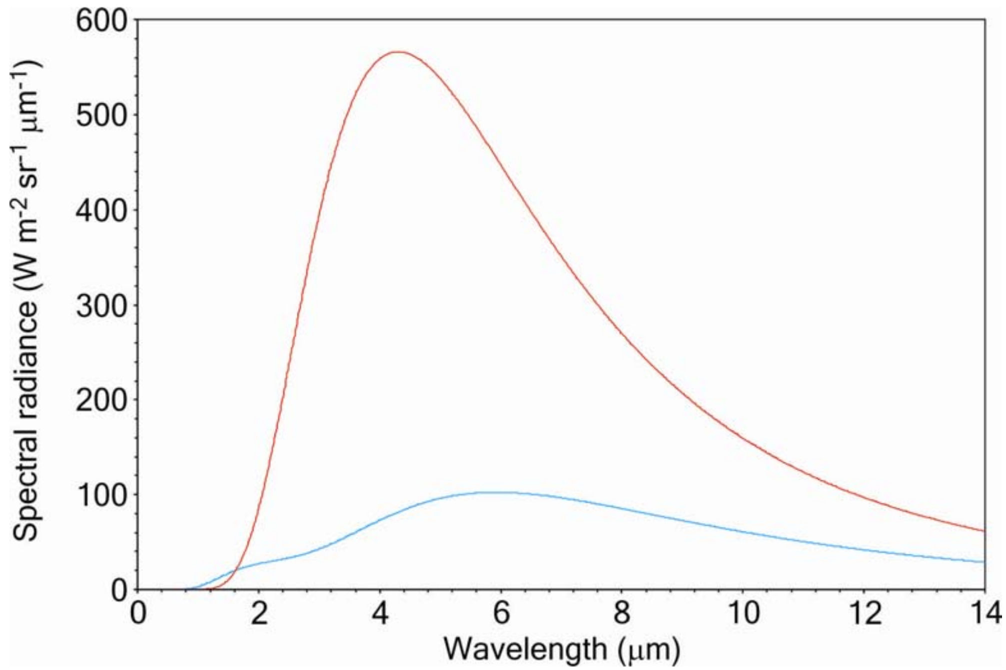

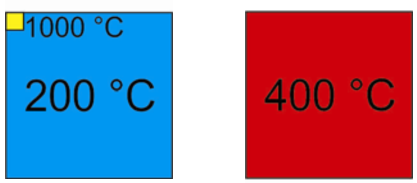

- Whole pixel/"Dozier" temperatures can easily misrepresent the nature of emitted spectral radiance from thermally complex active lava surfaces

Simulating HyspIRI data from Hyperion data

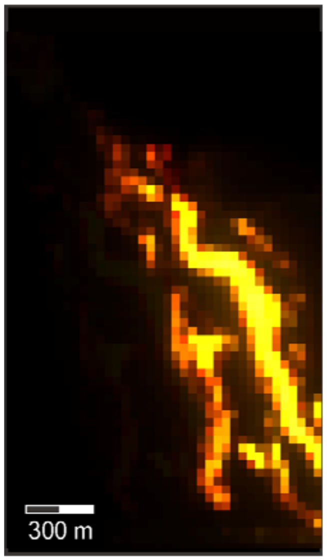

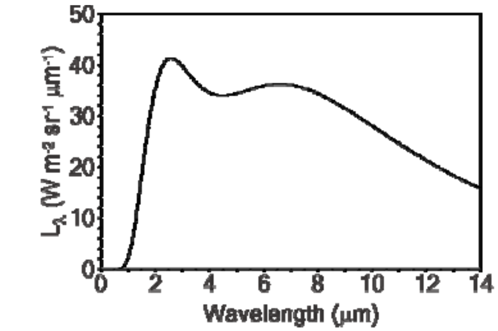

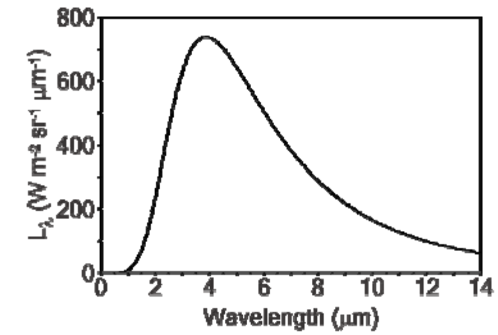

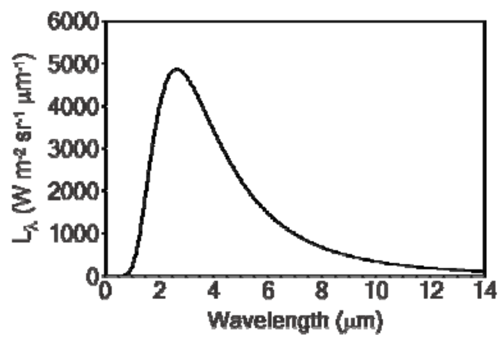

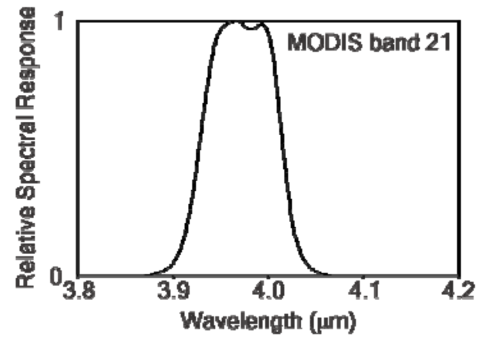

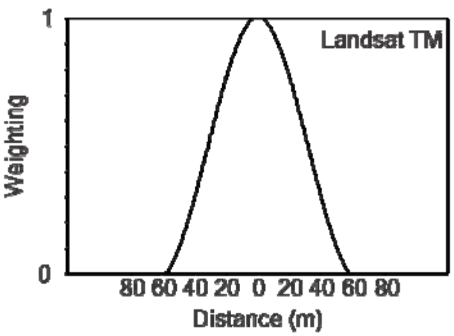

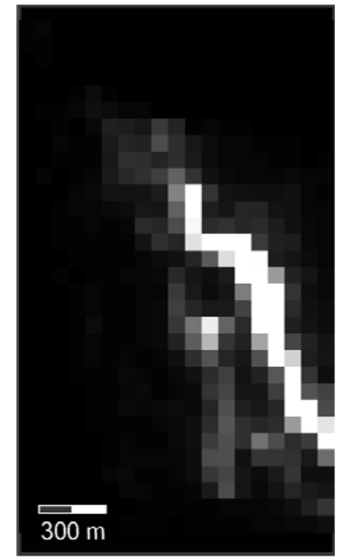

• Analyzed 60 Hyperion images encompassing the full spectrum of terrestrial active lava bodies


Photo: J. Durieux

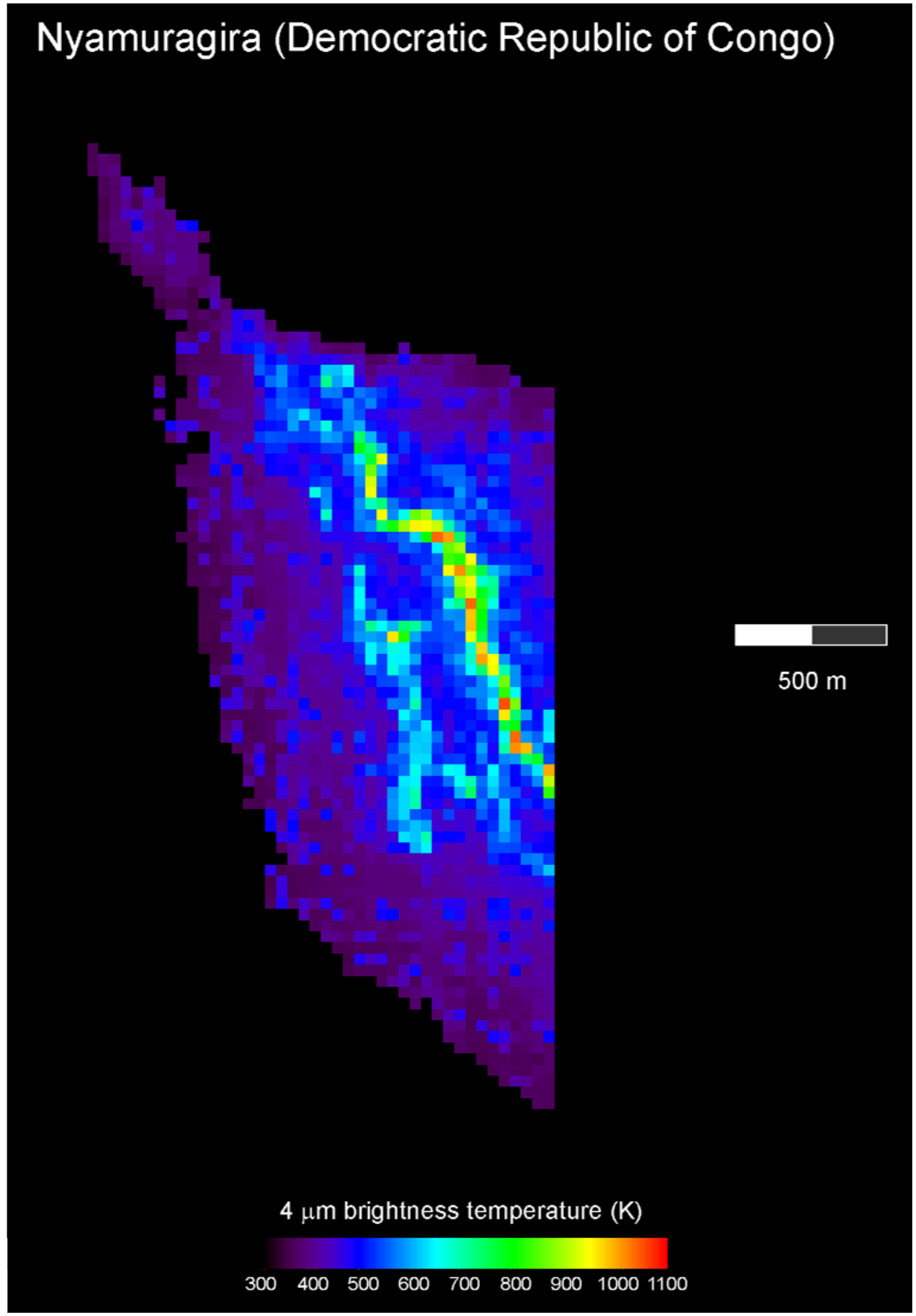
Nyamuragira (Democratic Republic of Congo)
500 m
4 µm brightness temperature (K)
300 400 500 600 700 800 900 1000 1100


Photo: M. Fulle

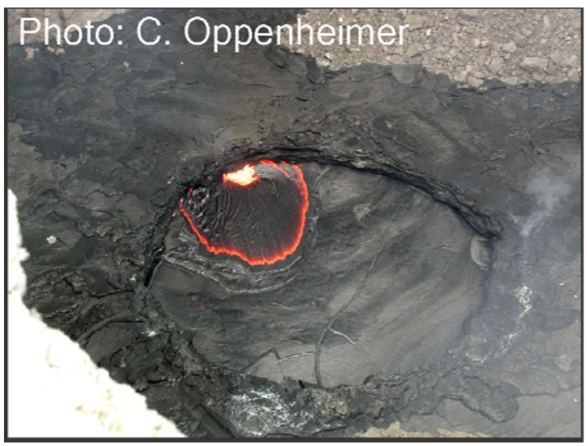
Photo: C. Oppenheimer

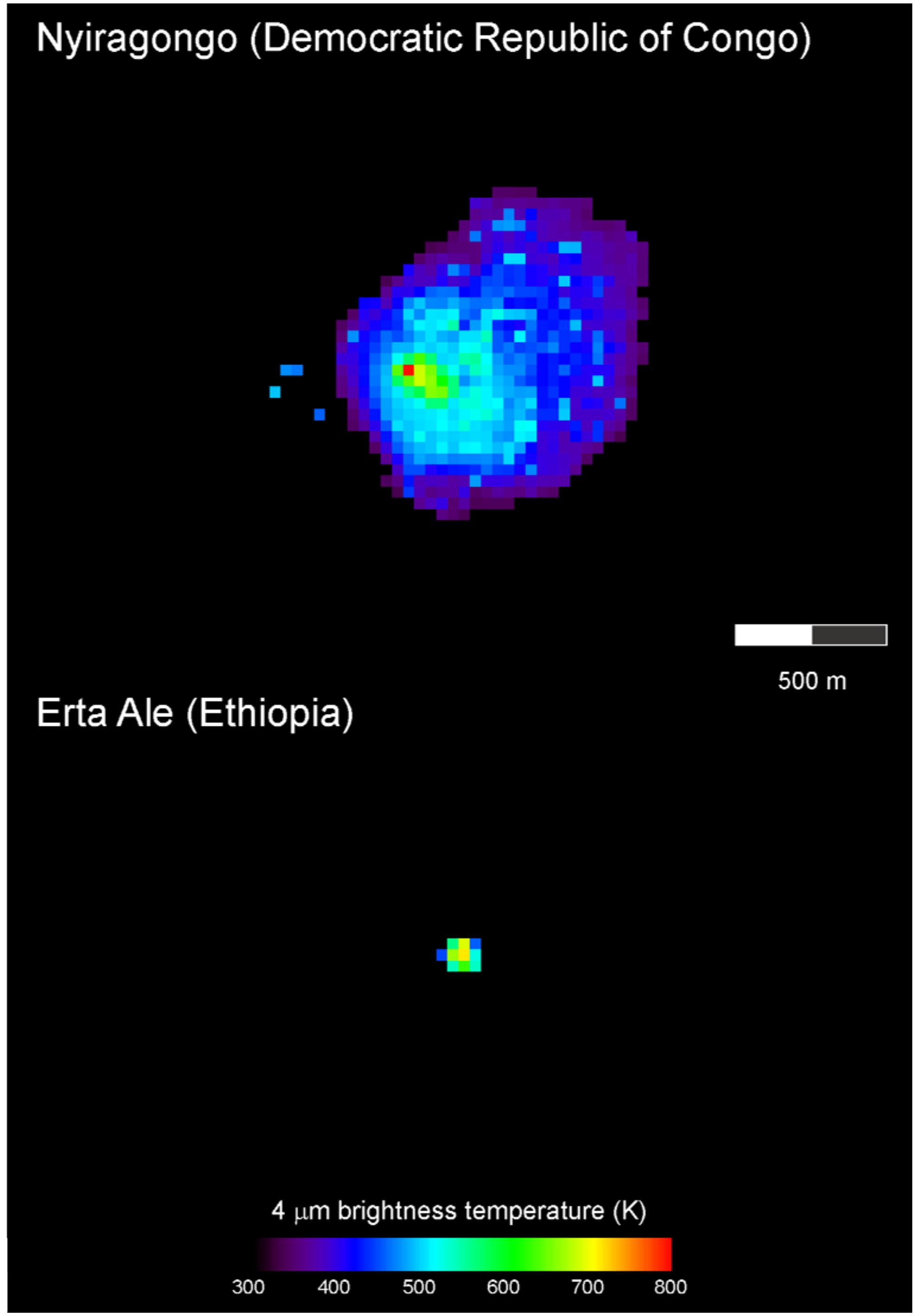
Nyiragongo (Democratic Republic of Congo)
500 m
Erta Ale (Ethiopia)
4 μm brightness temperature (K)
300
400
500
600
700
800


Photo: M. Wibe Lund

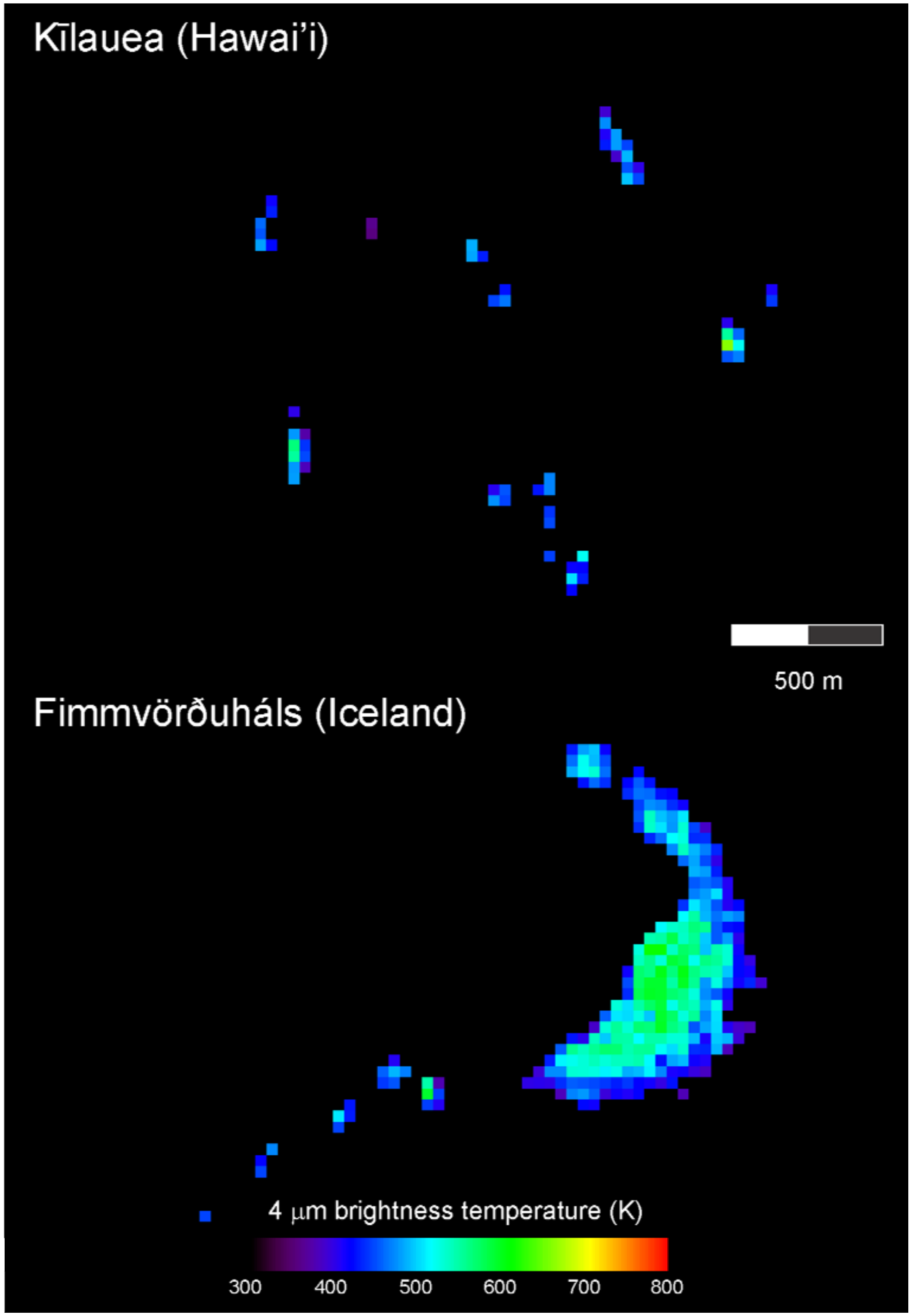
Kīlauea (Hawai'i)
500 m
Fimmvörðuháls (Iceland)
4 µm brightness temperature (K)
300
400
500
600
700
800

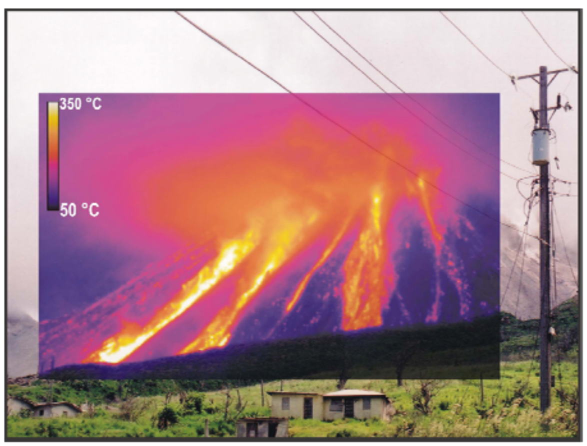

350 °C
50 °C

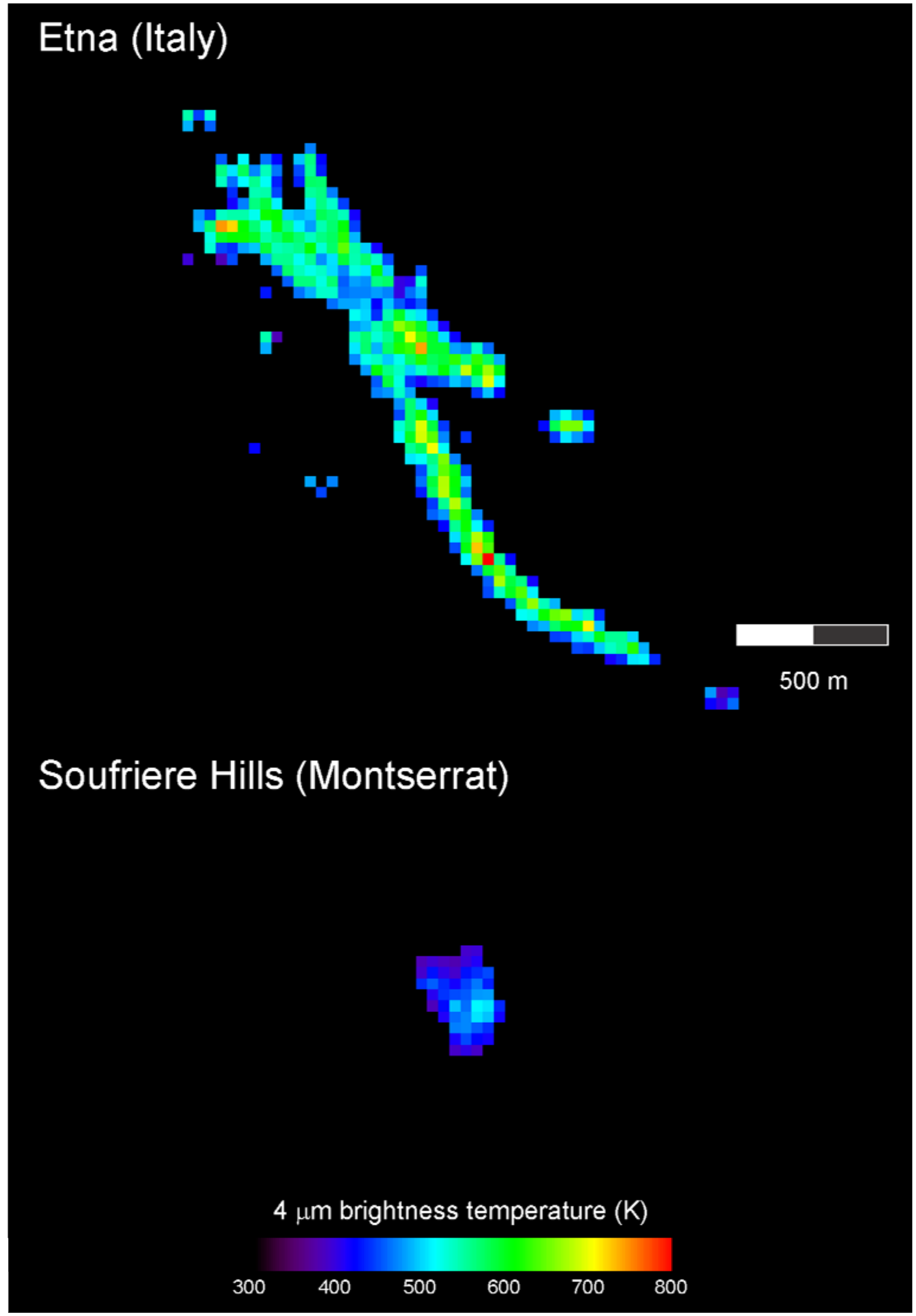

Etna (Italy)
500 m
Soufriere Hills (Montserrat)
4 µm brightness temperature (K)
300
400
500
600
700
800

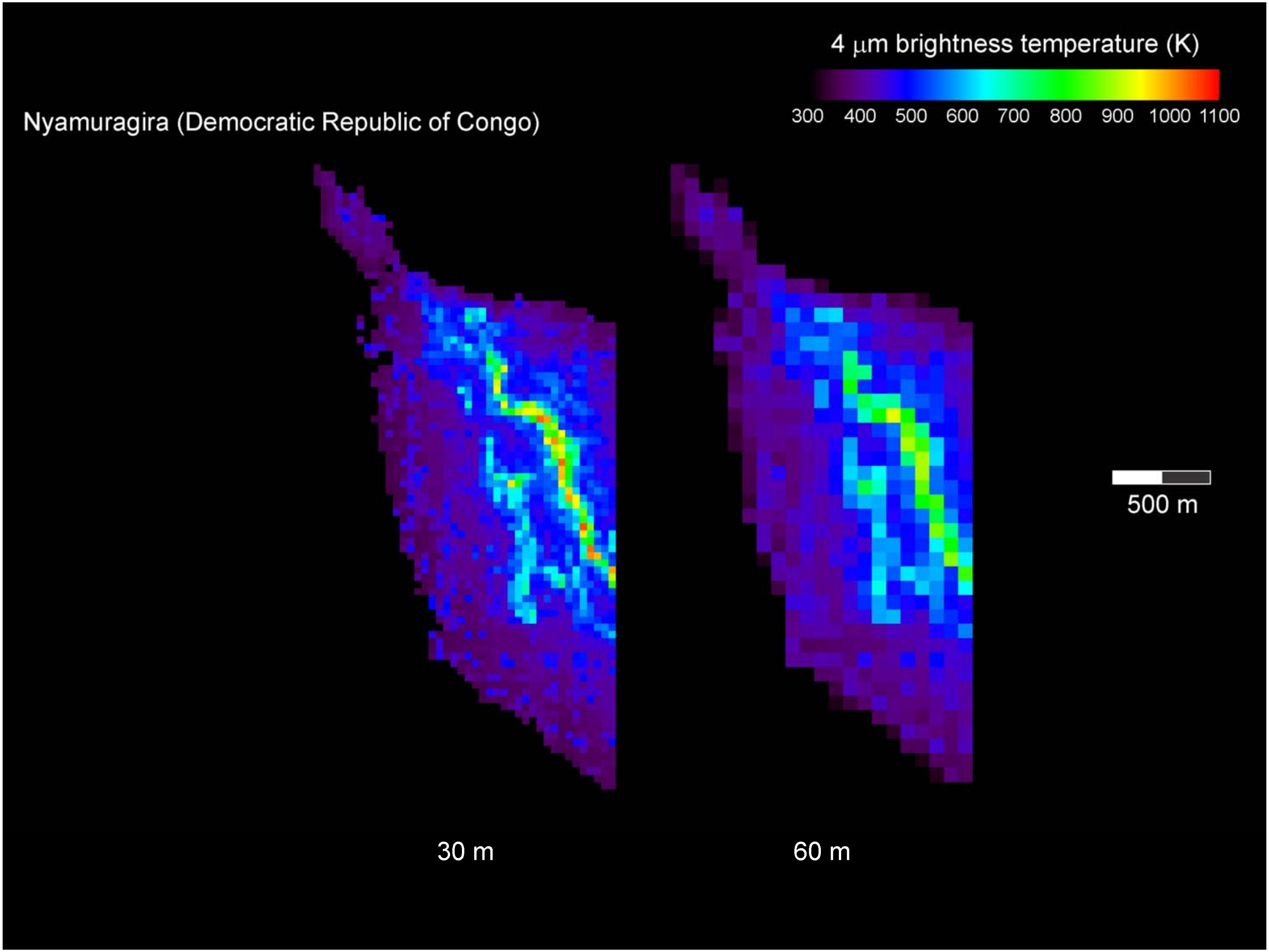

4 μm brightness temperature (K)
300 400 500 600 700 800 900 1000 1100
Nyamuragira (Democratic Republic of Congo)
500 m
30 m
60 m

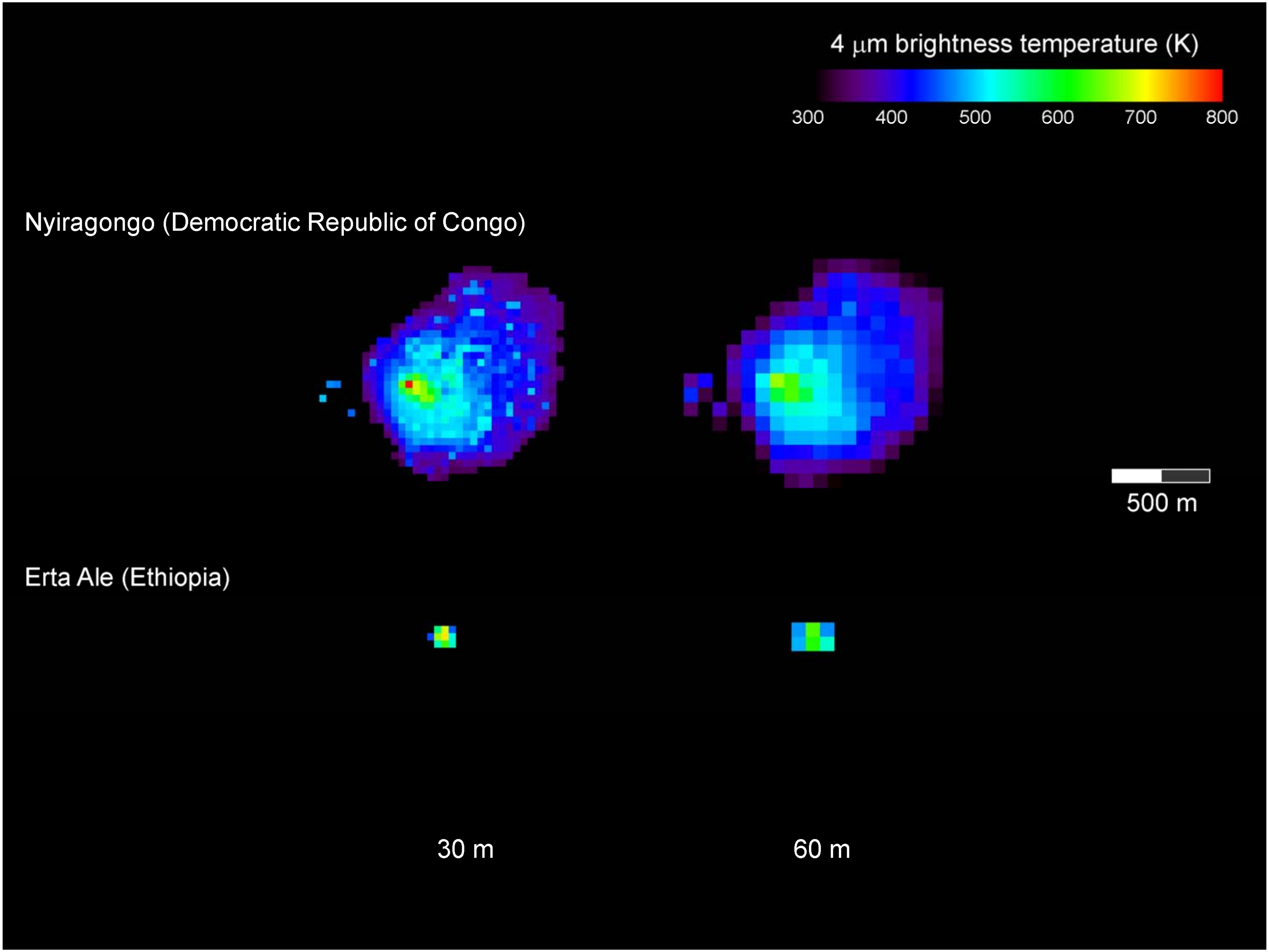
4 μm brightness temperature (K)
300
400
500
600
700
800
Nyiragongo (Democratic Republic of Congo)
500 m
Erta Ale (Ethiopia)
30 m
60 m

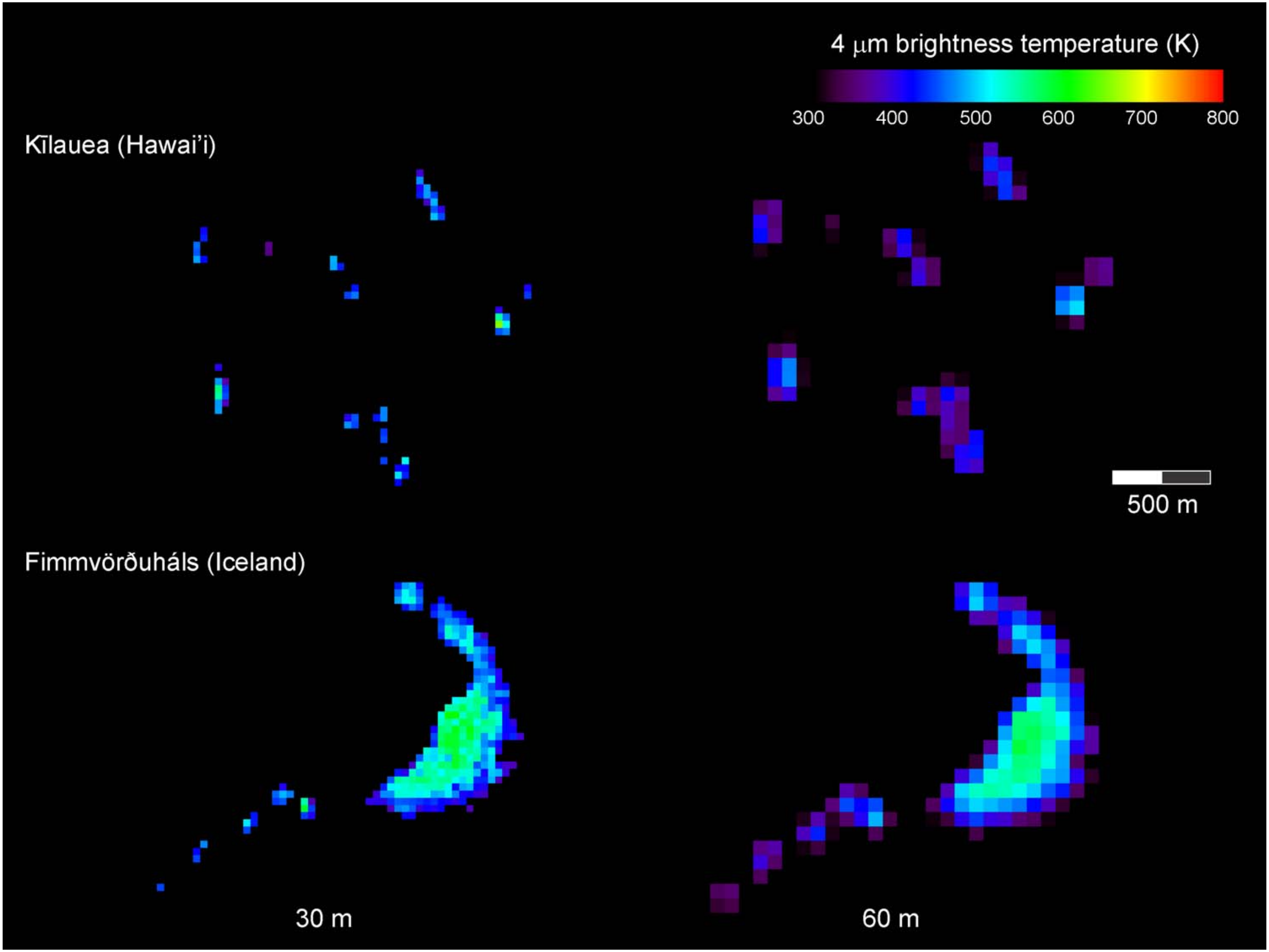
4 μm brightness temperature (K)
300
400
500
600
700
800
Kīlauea (Hawai'i)
500 m
Fimmvörðuháls (Iceland)
30 m
60 m

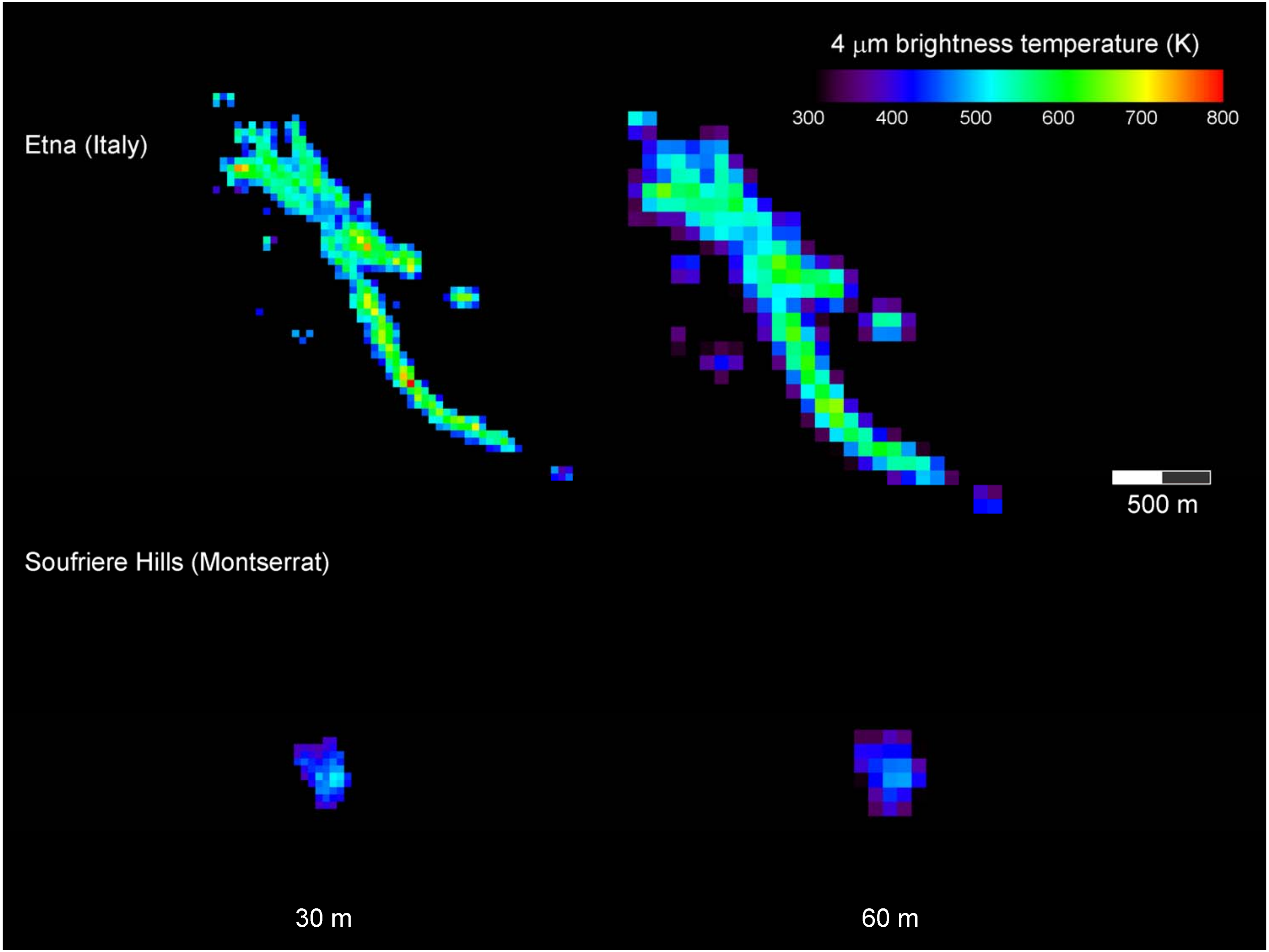
4 μm brightness temperature (K)
300
400
500
600
700
800
Etna (Italy)
500 m
Soufriere Hills (Montserrat)
30 m
60 m

T_{sat} for the HyspIRI 4 μm channel

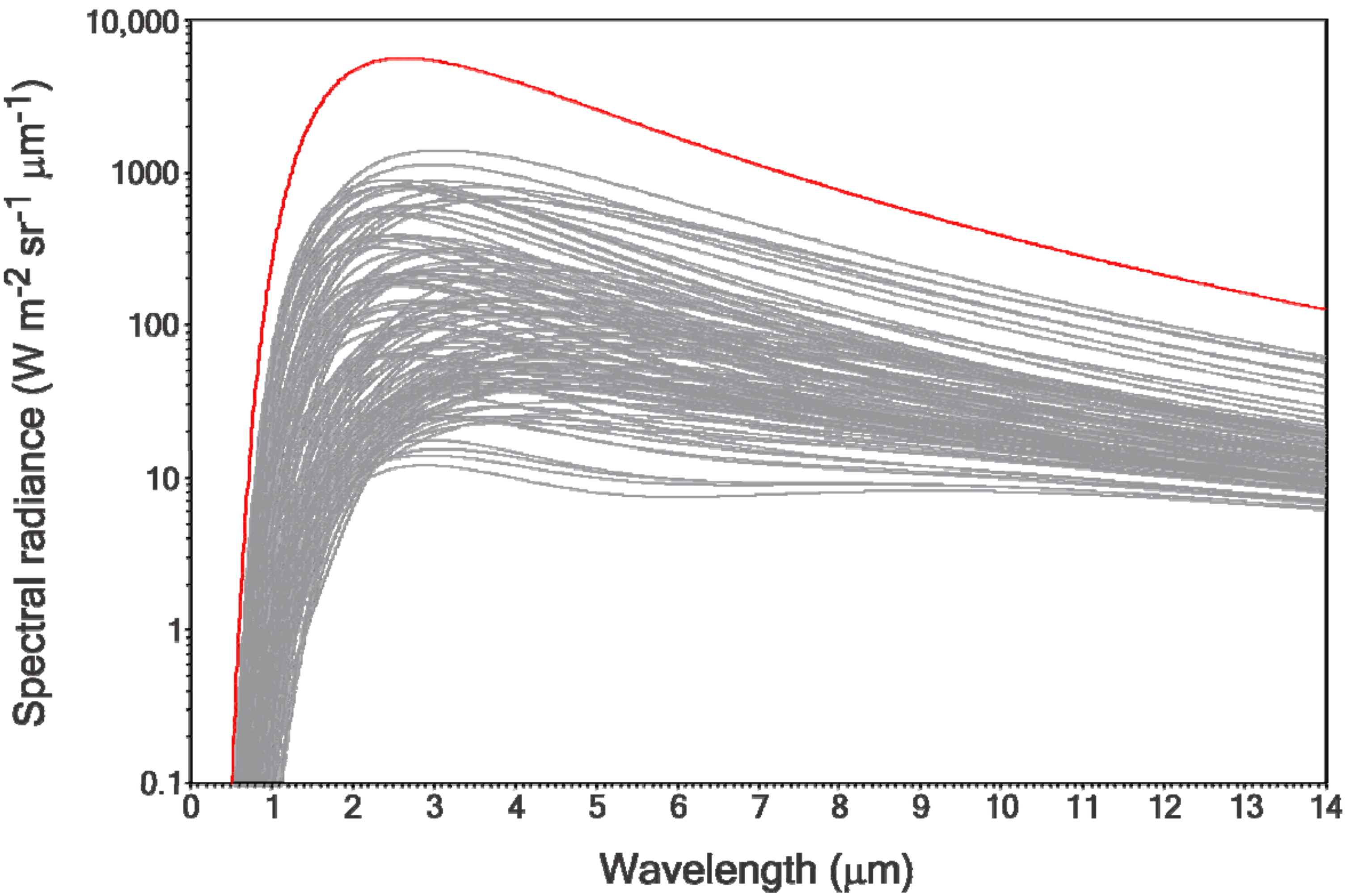

- What should the HyspIRI 4 μm channel saturation be set to?

Incidence of saturation as a function of assumed T_{sat}

T_{sat}(K)	$\#_{sat}$(i)	$\#_{sat}$(ii)
400	471	432
500	163	142
600	55	48
700	30	26
800	11	14
900	0	1
1000	0	0

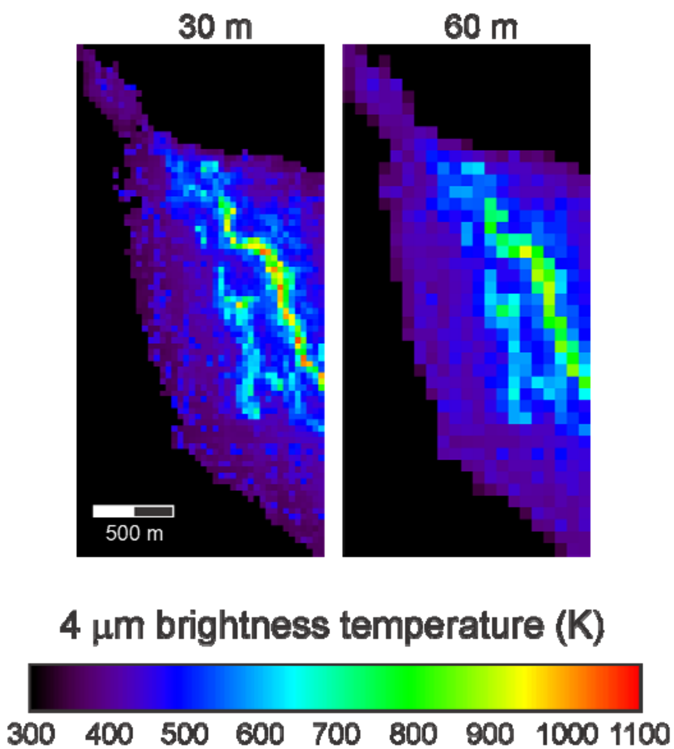

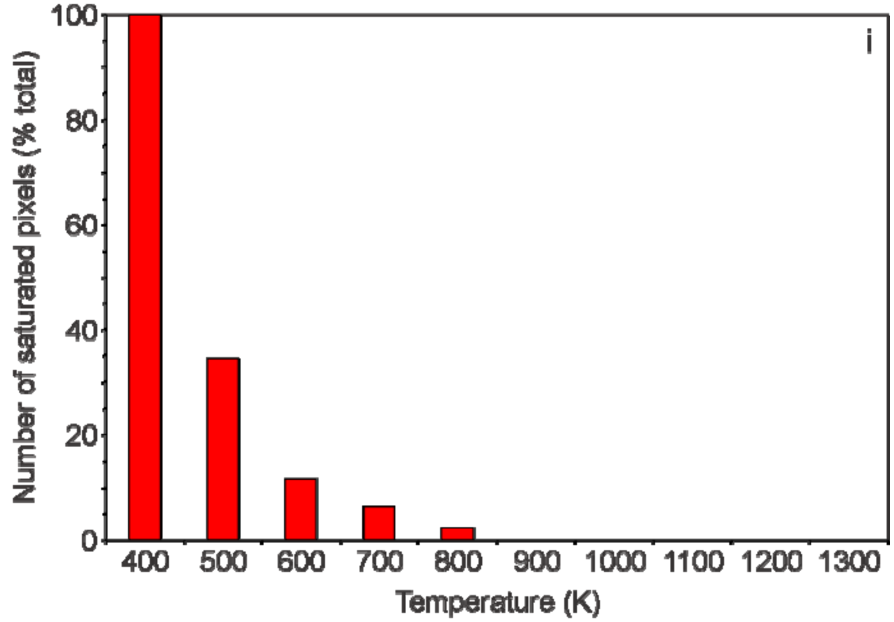

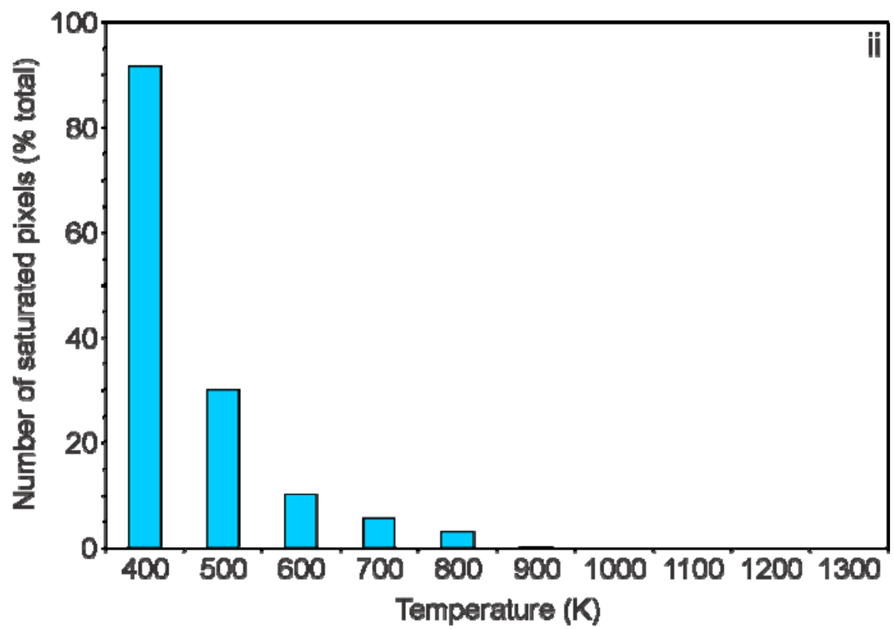

The important pixels are the ones which drive T_{sat} higher

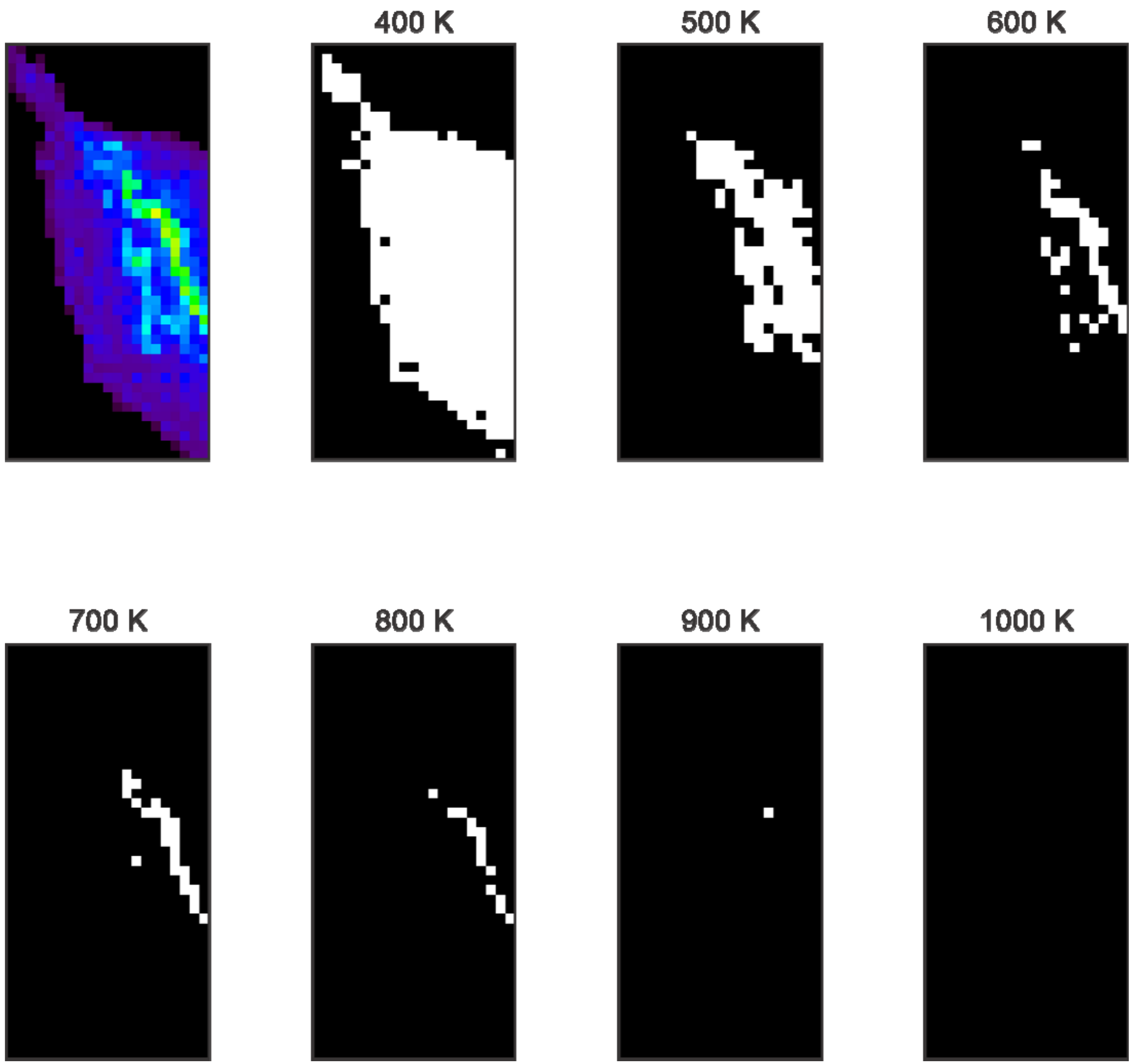

Recommendation: HyspIRI 4 μm T_{sat} not less than 1100 K

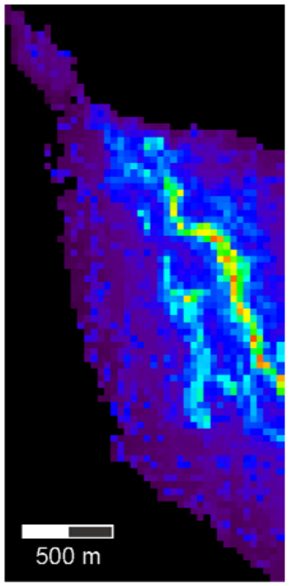

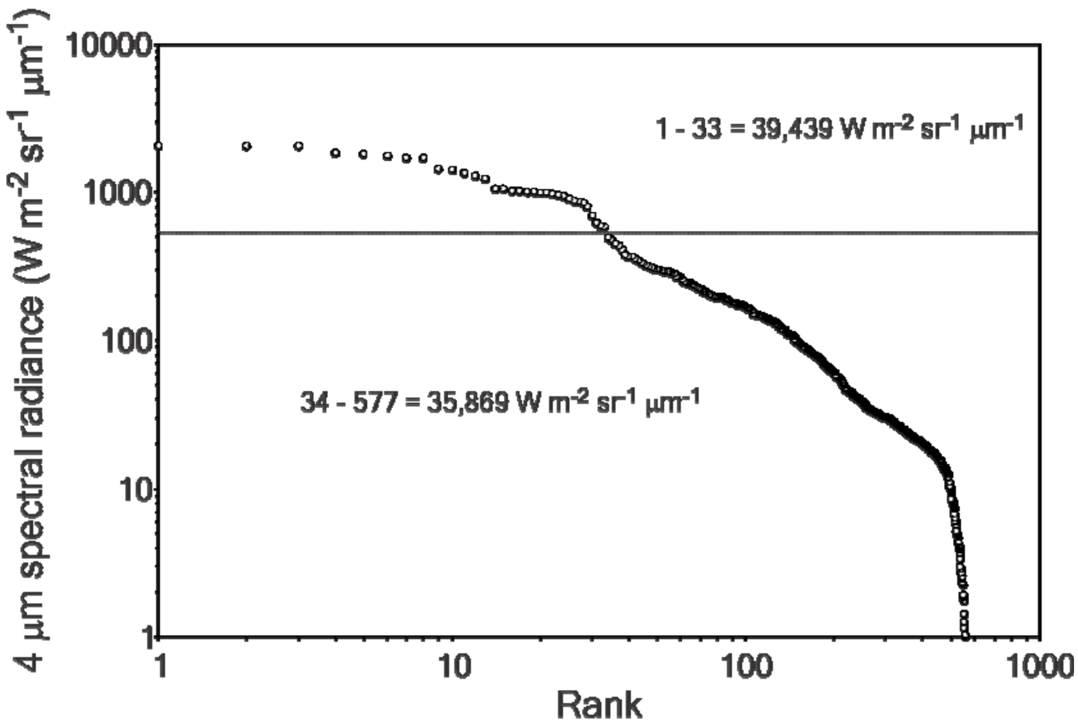

Aggregation of four most radiant pixels in simulated
30 m data set yields a maximum temperature of 1041 K at 60 m

Large lava-flow-forming eruptions are not uncommon

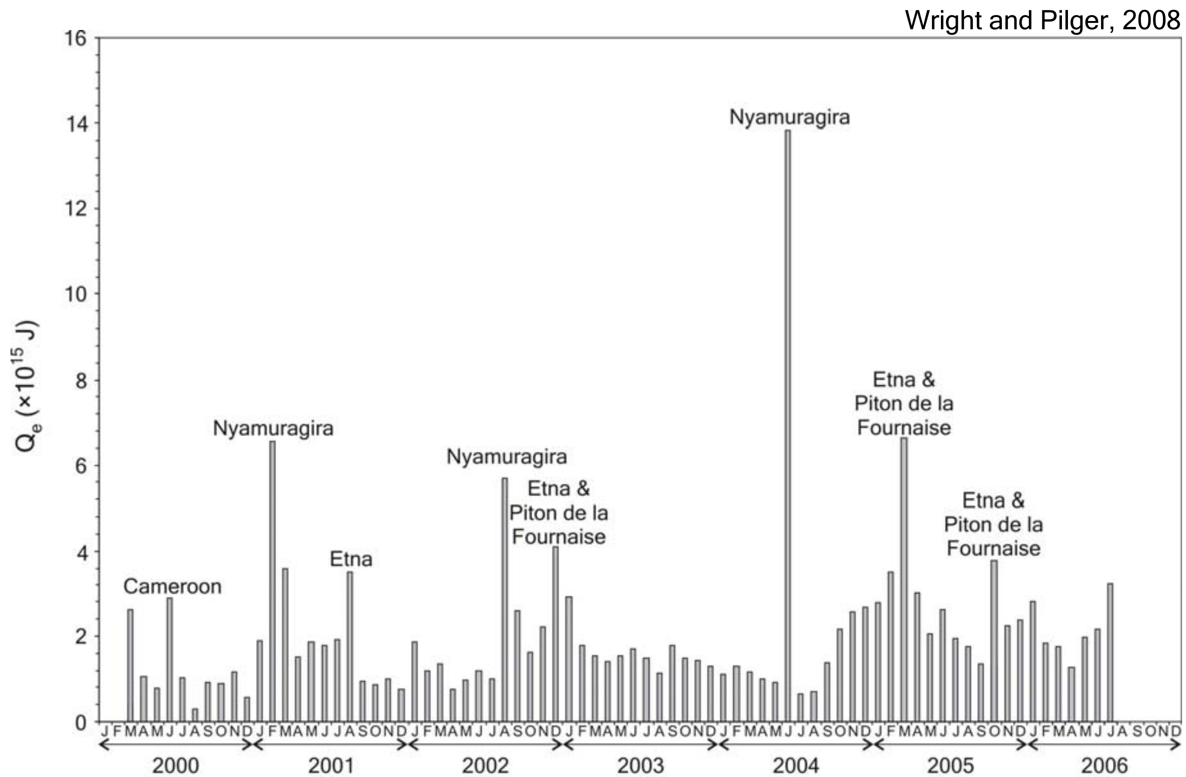

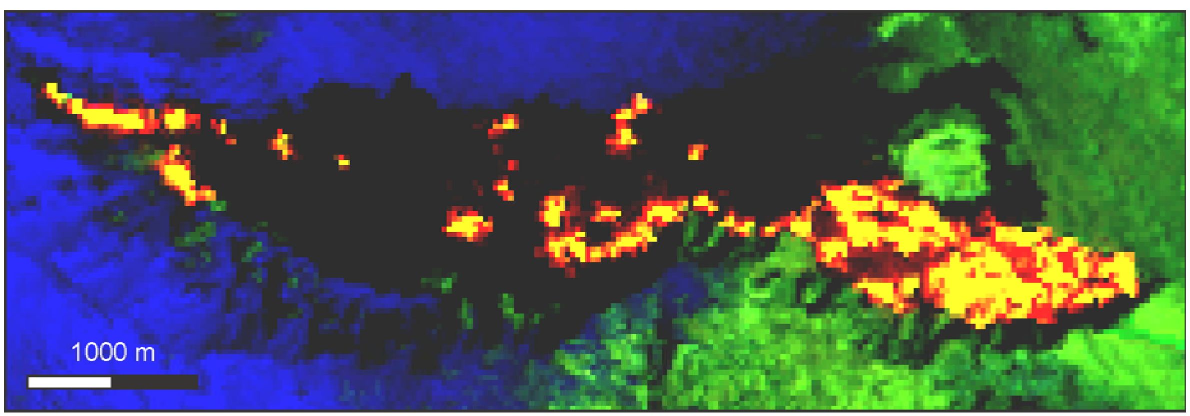

Mount Etna, 1991-1993 eruption

Lower predicted incidence of saturation over lava lakes and domes

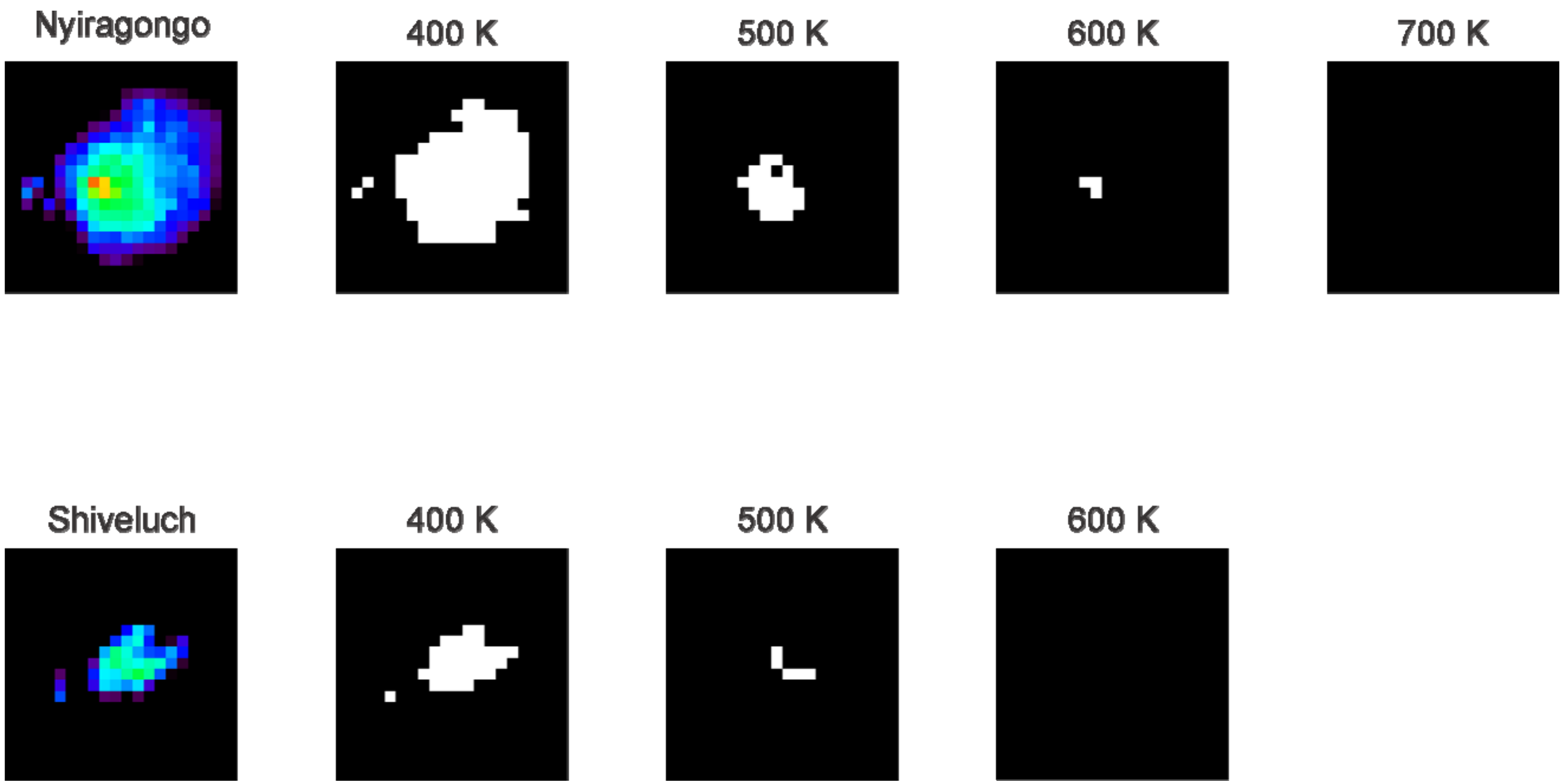

HyspIRI 11-14 μm data should prove useful for volcanologists

Mount Etna, Sicily

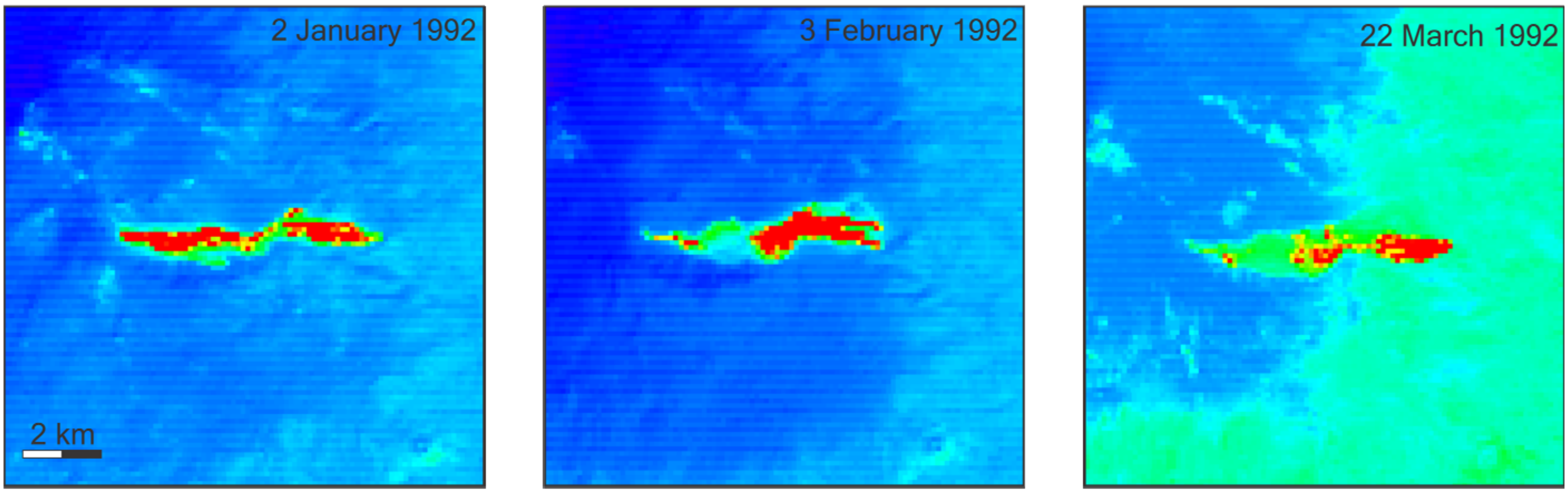

Red pixels are saturated in Landsat TM band 6, indicating a whole pixel temperature exceeding ~80 °C.

Temporal evolution of lava flow surface temperatures

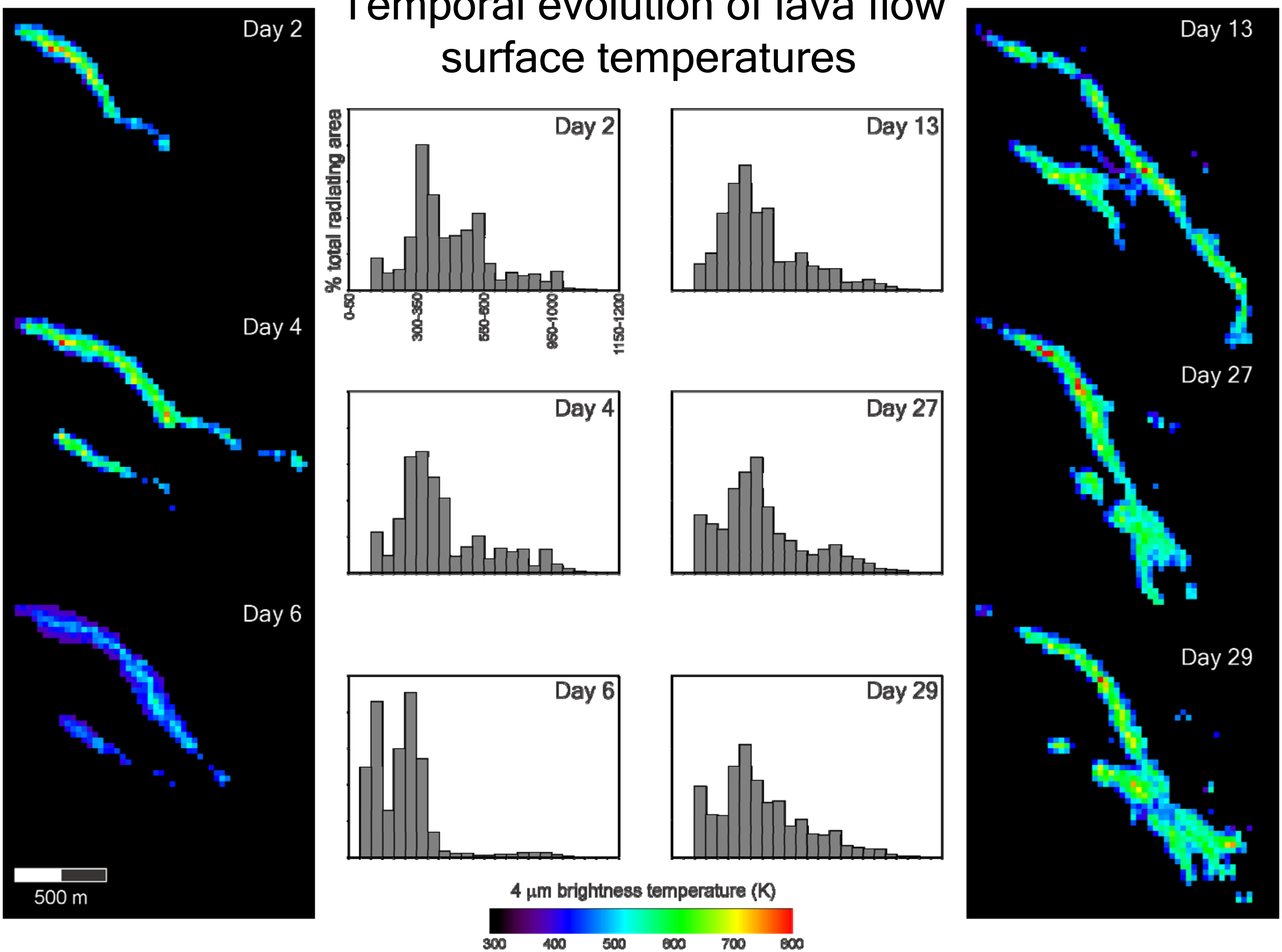

Lava temperature, age, and process that thermally renew active lava surfaces

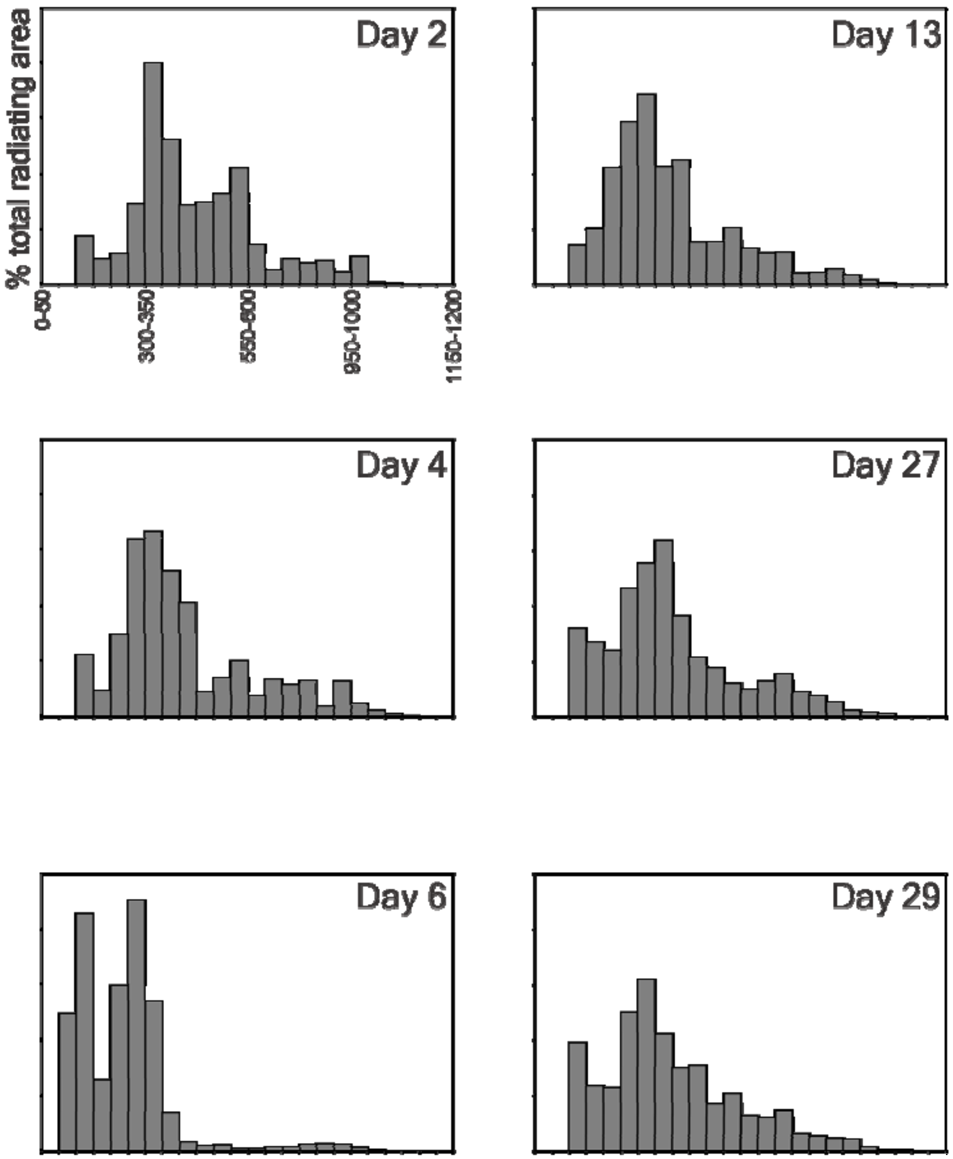

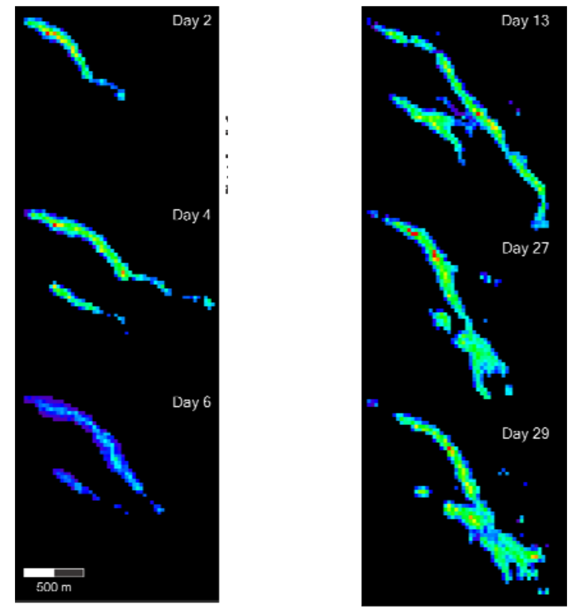

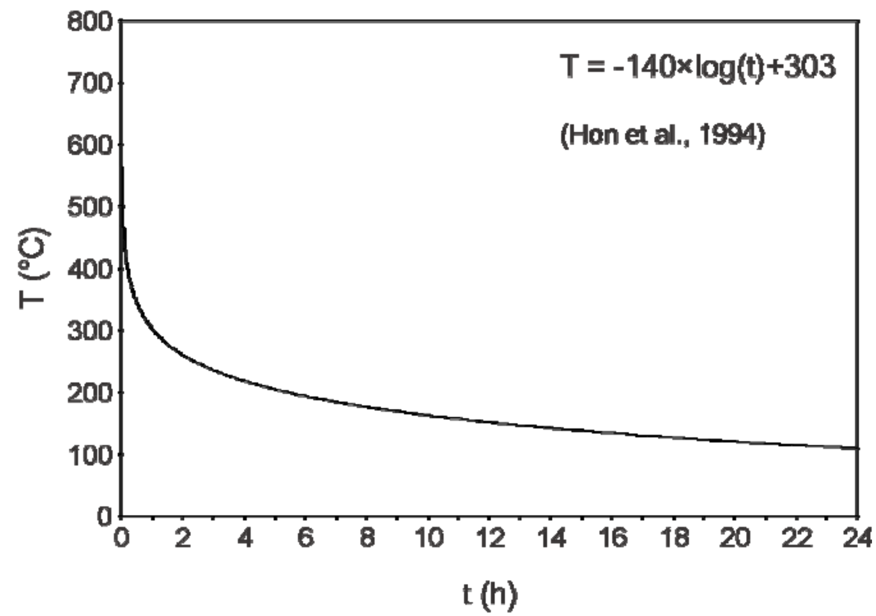

Driving numerical lava flow hazard predictions using satellite data

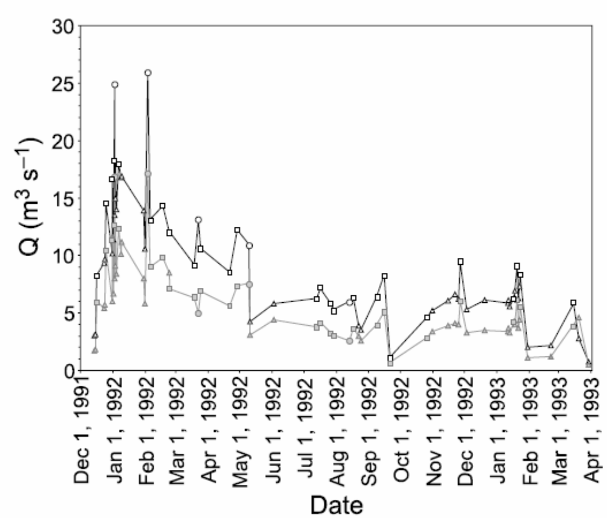

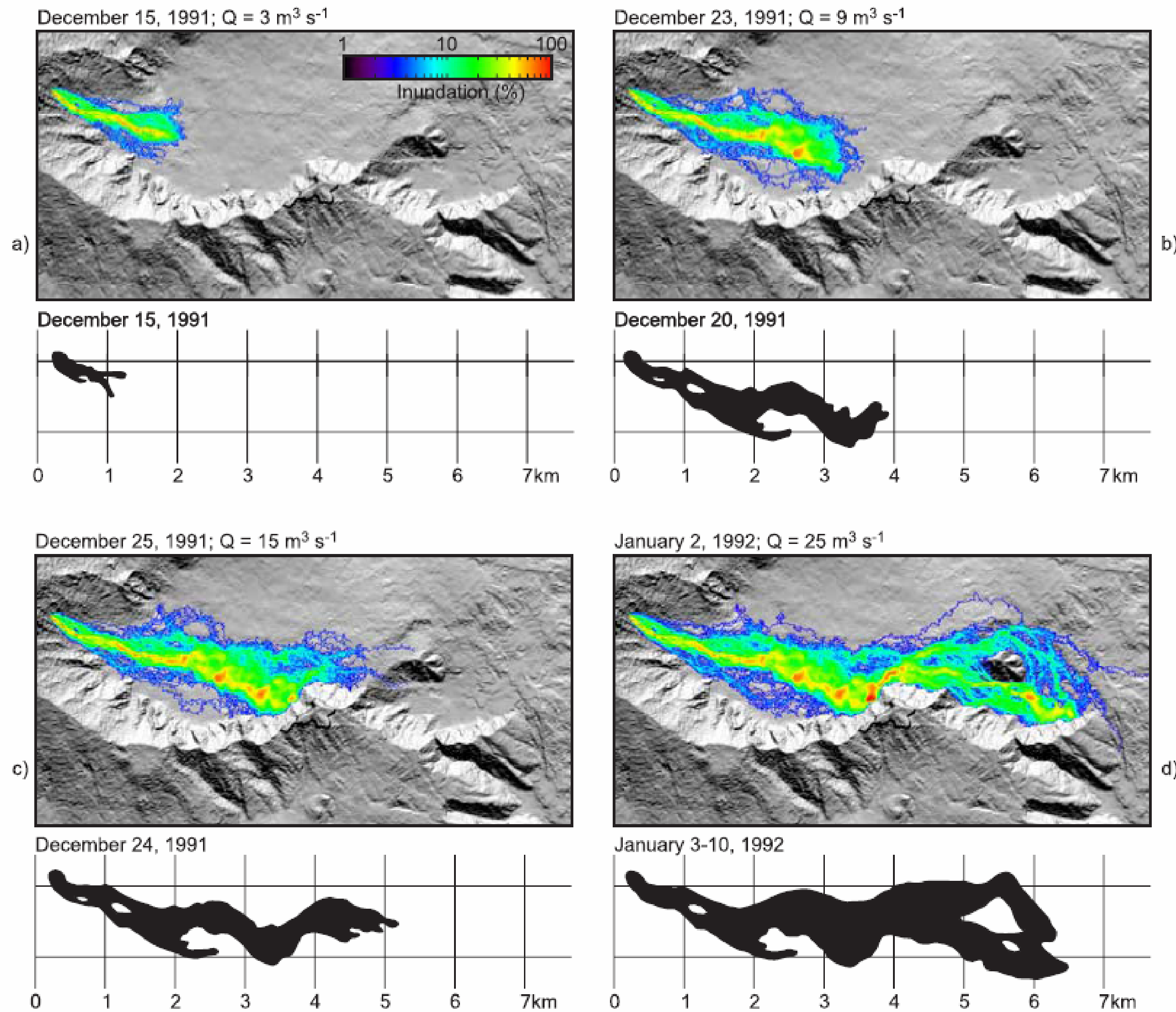

Wright et al., 2008

The temperature of Earth’s volcanoes

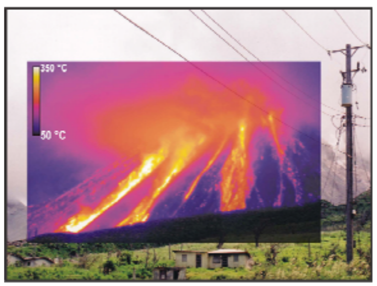

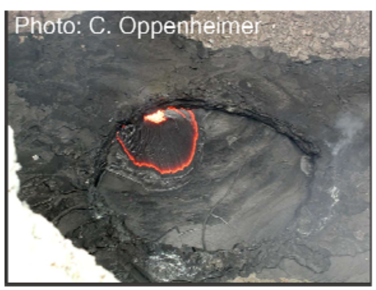

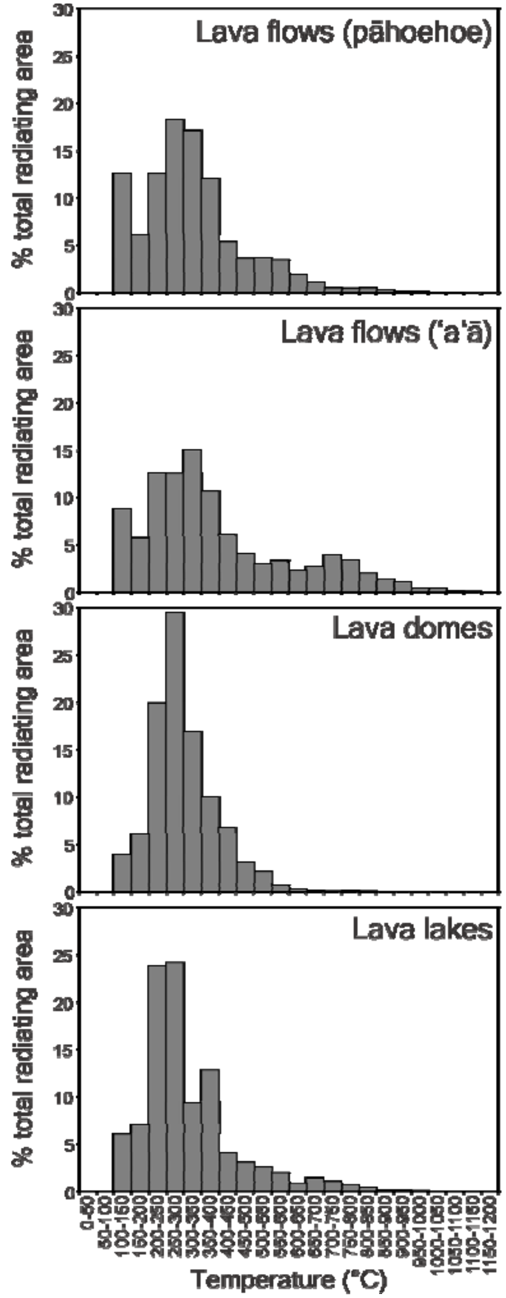

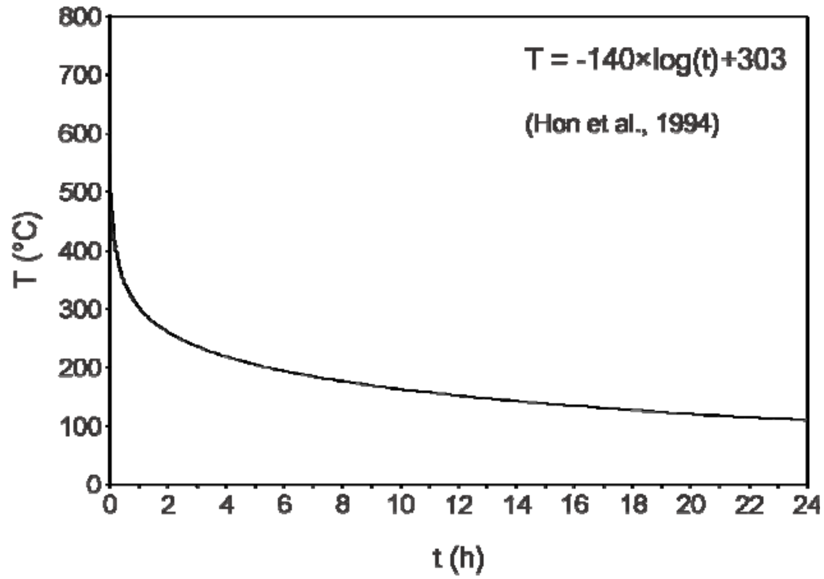

Simulating the performance of a detection algorithm

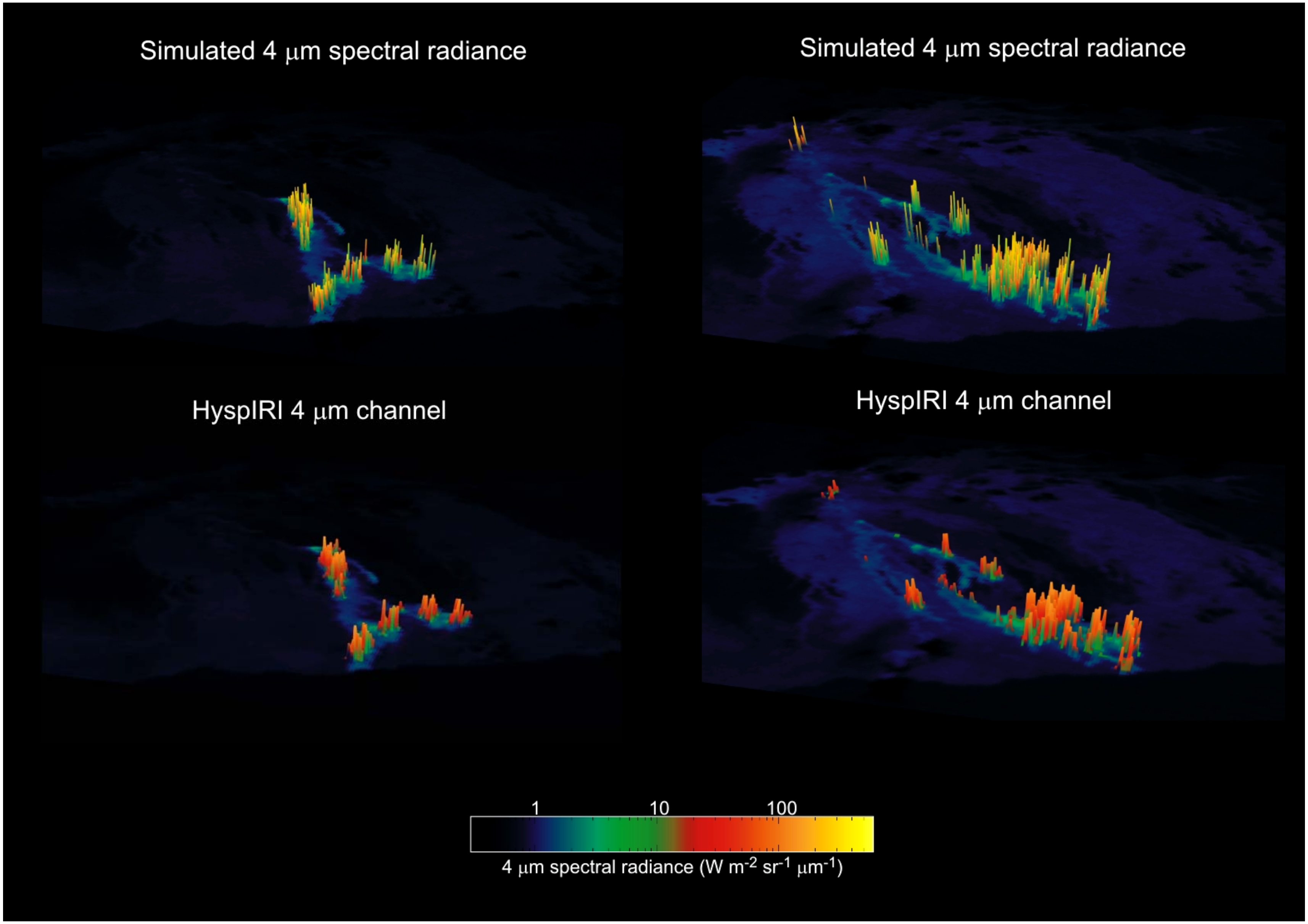

End

P. Izbekov (UAF/AVO)

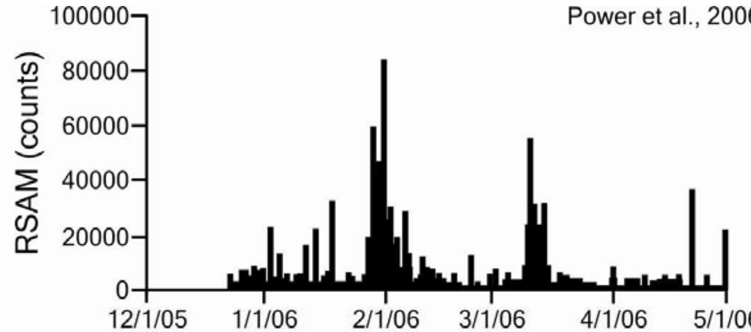

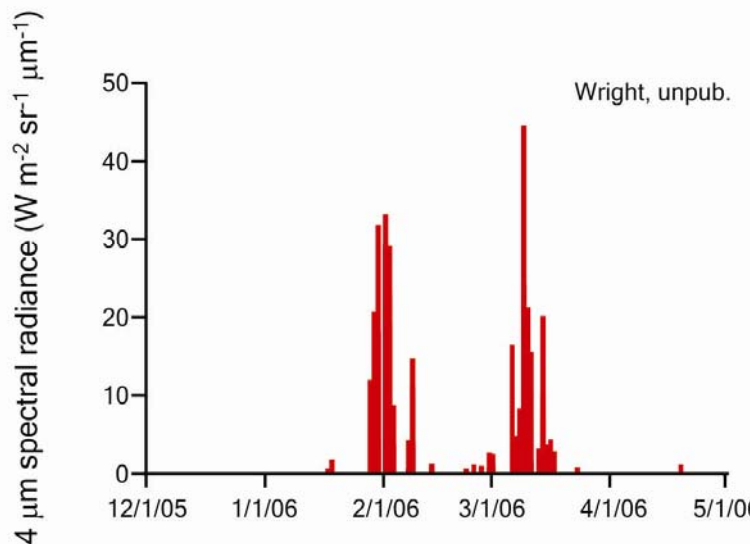

J. Durieux (©)

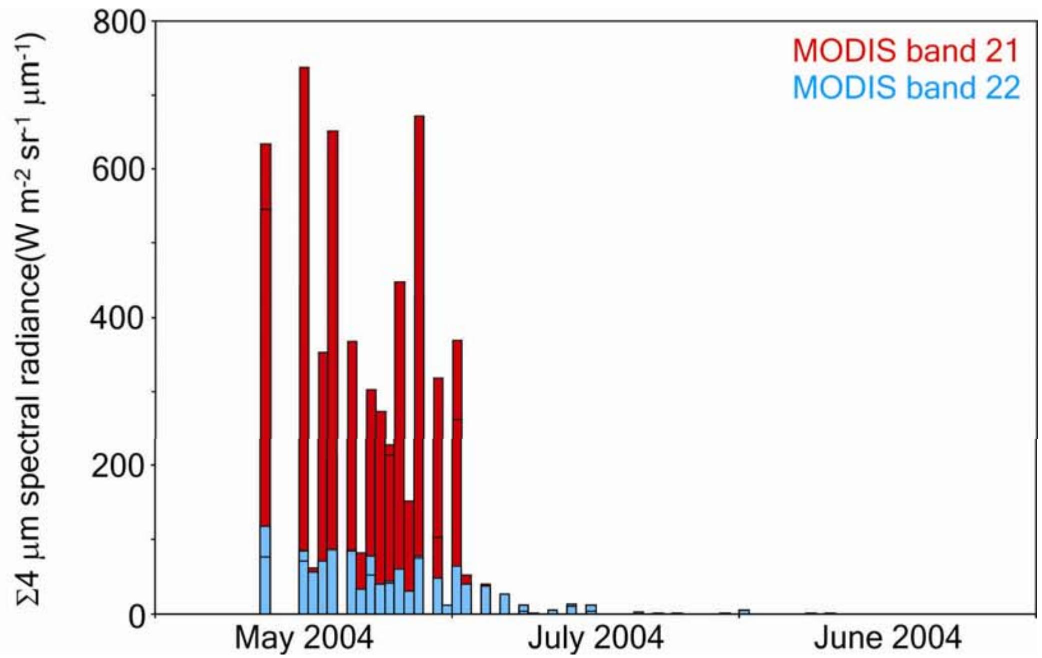

800
600
400
200
0
Σ4 μm spectral radiance(W m^{-2} sr^{-1} μm^{-1})
MODIS band 21
MODIS band 22
May 2004
July 2004
June 2004

ETM+ 4

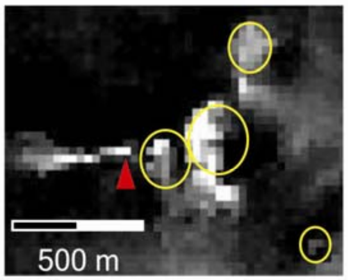

ETM+ 8

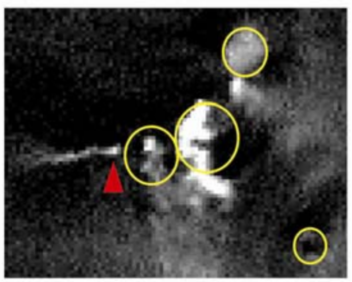

Mount Etna, 28 October 1999

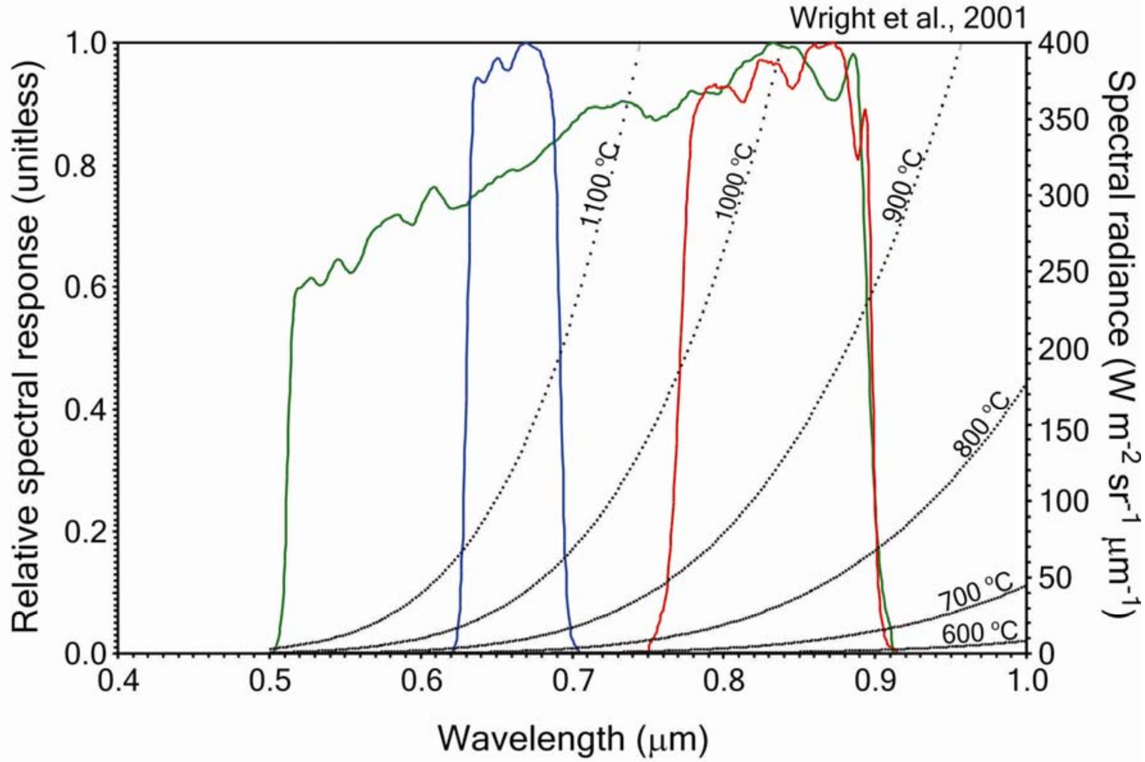

ETM+ 4 = 35.7 W m^{-2} sr^{-1} µm^{-1} = 819 °C
ETM+ 8 = 28.3 W m^{-2} sr^{-1} µm^{-1} = 922 °C

A difference in whole pixel temperature of 100 °C

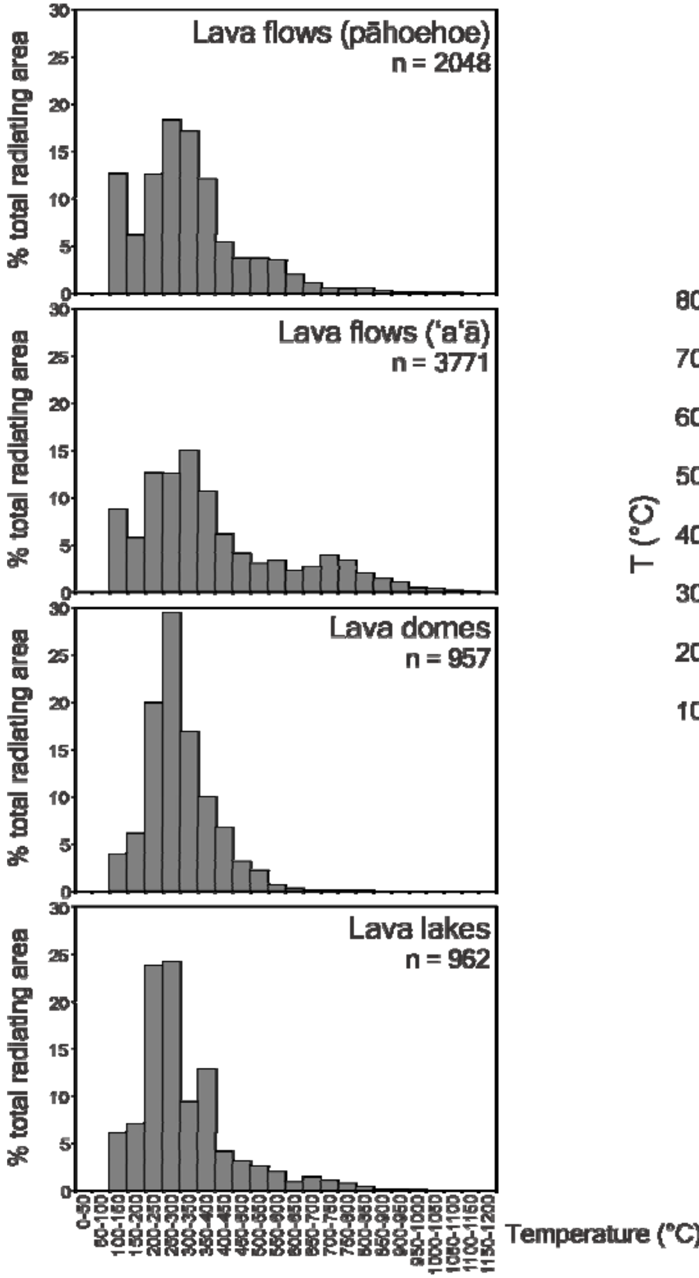
Lava flows (pāhoehoe)
n = 2048
Lava flows (ʻaʻā)
n = 3771
Lava domes
n = 957
Lava lakes
n = 962
% total radiating area
Temperature (°C)

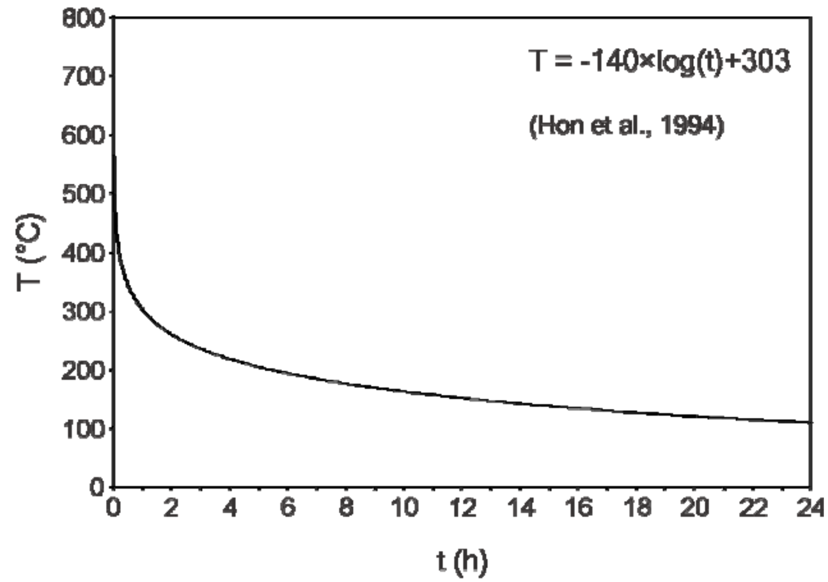
T = -140×log(t)+303
(Hon et al., 1994)
T (°C)
t (h)

MODTRAN®5.2 Radiative Transfer Model and Applications to HyspIRI

A. Berk, P.K. Acharya, S.M. Adler-Golden, L.S. Bernstein, M.J. Fox, R.G. Kennett, D.C. Robertson and R. Taylor
Spectral Sciences, Inc. (SSI), *Burlington, MA*
modtran@spectral.com (www.spectral.com)

G.P. Anderson and M.L. Hoke
Air Force Research Laboratory (AFRL), *Hanscom AFB, MA*

R.W. McMullen
Boston College, Chestnut Hill, MA

2010 HyspIRI Science Workshop
Pasadena, CA
24-26 August 2010

Acknowledgements

- Contract
  - Air Force Research Laboratory – BAA

    Development and Validation of Tools for Signature Exploitation Concepts

    Sandy Nierman
  - Department of Energy (NA-22) – Phase II SBIR

    Full Spectral Signature Simulation Models for Chemical Releases

    Victoria Franques
  - Spectral Sciences, Inc. – Phase II SBIR
- Technical
  - Vincent J. Realmuto
    Jet Propulsion Laboratory

Presentation Outline

- MODTRAN Overview

- A Localized Chemical Cloud Option

MODTRAN5
- General Description -

- Overview
  - 0.2 cm^{-1} IR/Vis/UV Transm., Rad. & Fluxes from 0.1 cm^{-1} Band Model

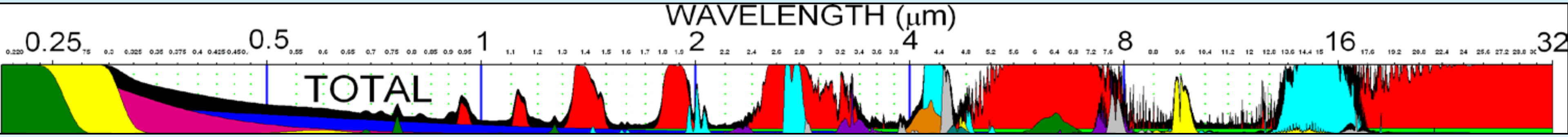

  - Stratified (1D) Molecular / Aerosol / Cloud Atmosphere
  - 2-Stream and DISORT Solar and Thermal Scattering
  - Spherical Refractive Geometry
- Many Applications Pertinent to HyspIRI
  - Sensor Design
  - Atmospheric Correction →
  - Measurement / Data Analyses
  - Scene Simulation
  - Algorithm Development
  - Today's focus:
    - *Localized chemical clouds*

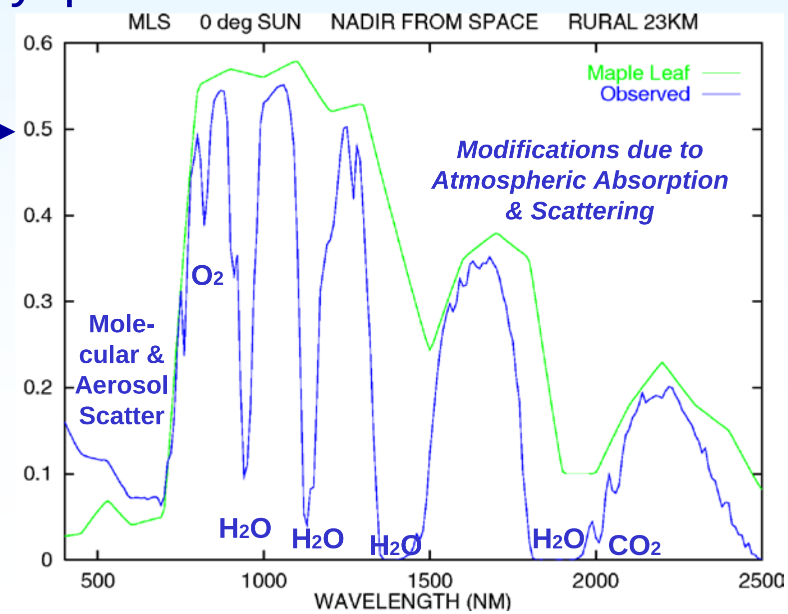

Sample MODTRAN Applications

- **FLAASH: *Fast Line-of-sight Atmospheric Analysis of Spectral Hypercubes***
  - **MODTRAN**-based atmospheric correction
  - SSI is lead developer with AFRL, NGA, NASA and SITAC collaboration & support
  - Retrieves scene visibility and pixel water vapor using 2-band methods
  - Compensates for atmospheric scattering (including adjacency effect) and absorption
  - Includes automated wavelength calibration, spectral polishing
- **PLANETS: *PLANETary Spectroscopy***
  - SSI planetary radiation transfer algorithm based on **MODTRAN5** band model
  - Validated against Jupiter, Saturn, Neptune and exoplanet spectra
    - Microwave through UV
    - Extended temperature range (5- 600K)
    - Planetary aerosol models
    - H_2-H_2, H_2-He, H_2-CH_4 and CH_4-CH_4 collision induced continua (CIA)

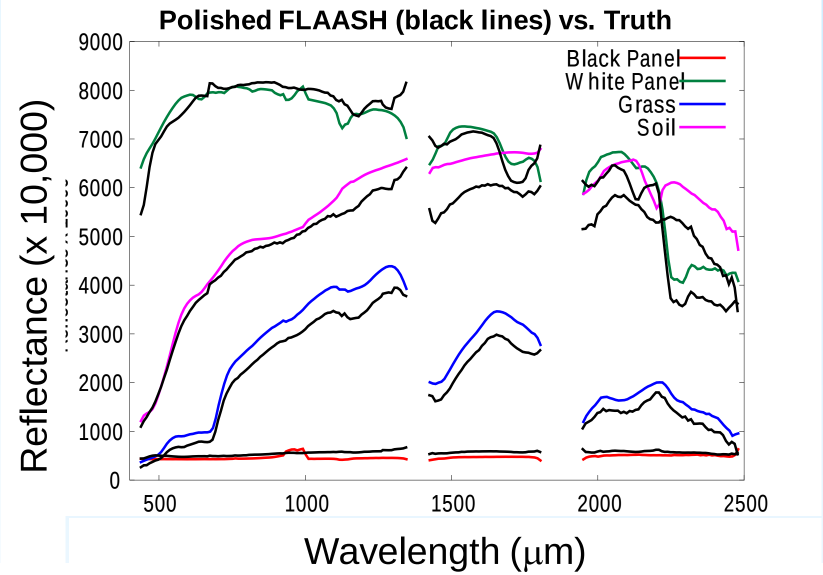

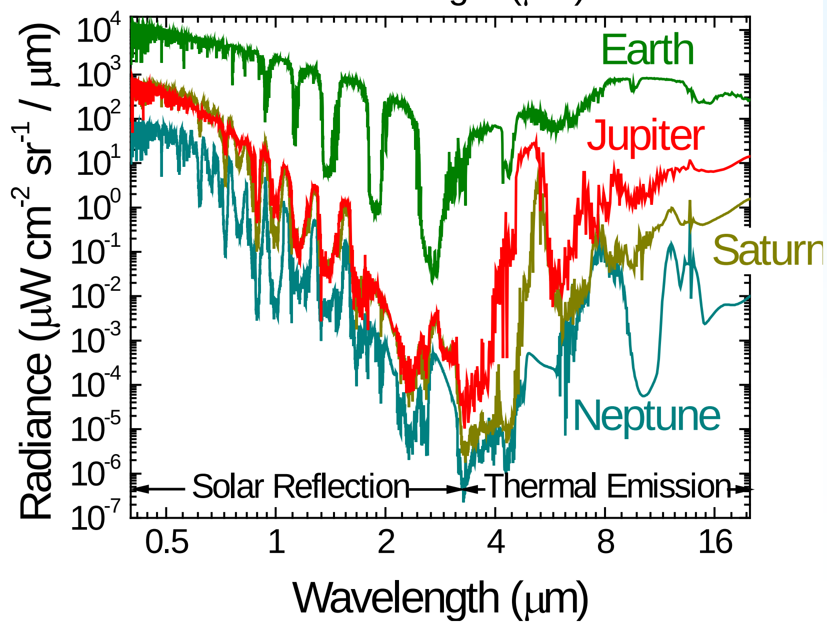

MODTRAN ®5 Overview
Absorbance = 1 – Transmittance

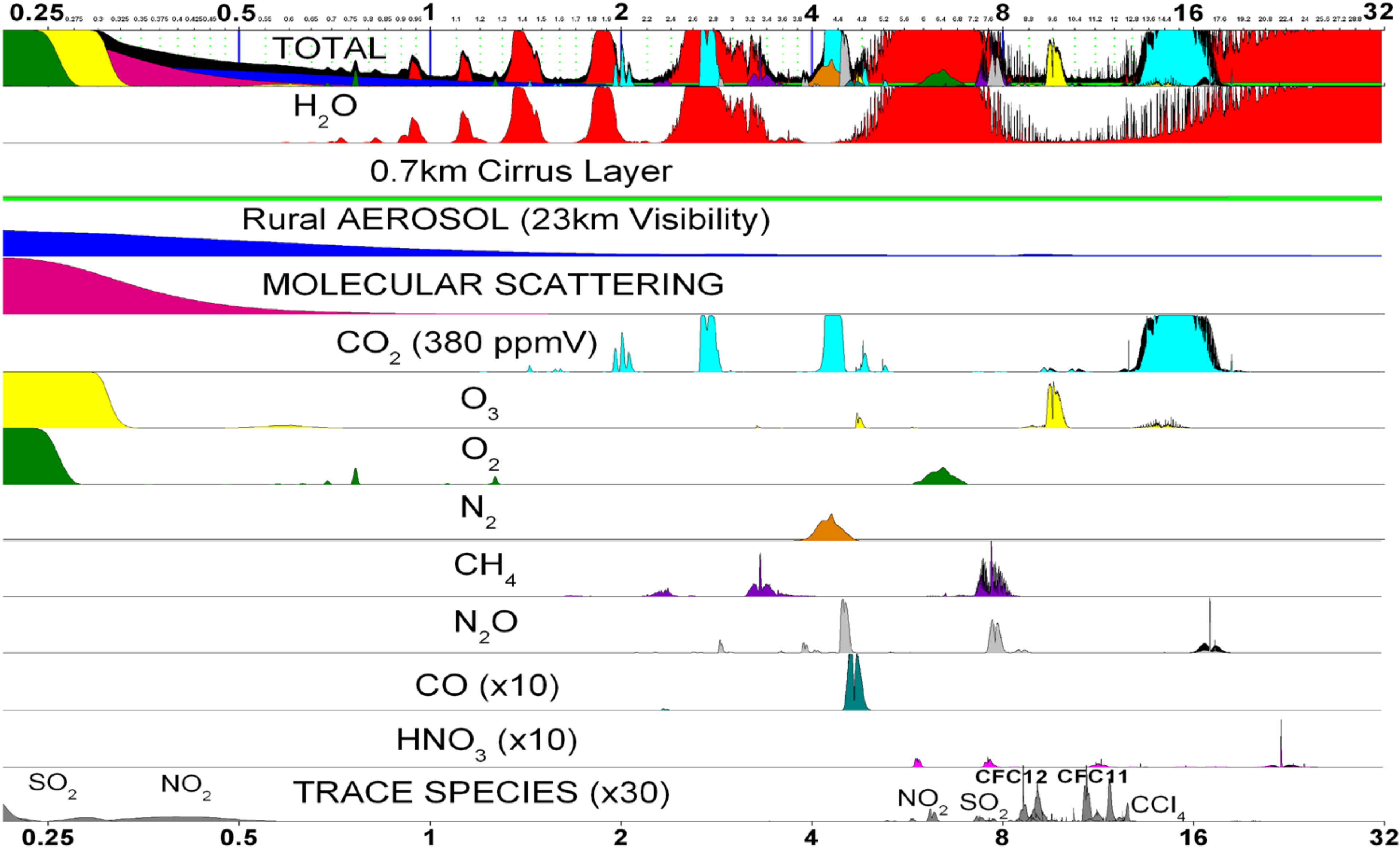

What's New
- Selected Upgrades -

	MODTRAN®4	MODTRAN®5.2.0.0 / 5.2.1.0
Band Model		
Spectral Resolutions	1.0, 5.0, 15.0 cm^{-1}	… + 0.1 cm^{-1}
Voigt Transmittance	Rogers-Williams interpolation	Exact expansion
HITRAN Data	Circa 2003	2008 with 2009 H_2O Update
Constituents	First 12 HITRAN molecules	39 HITRAN2008 molecules + Auxiliary Species Option
Inputs / Outputs		
Profile Scaling Input	CO_2, H_2O, O_3	All built-in molecular profiles
Spectral Data	Direct Transmittance, Flux, (Ir)Radiance, Cooling Rates	… + Diffuse Transmittances, Spherical Albedo
Spectral Channel (chn) File	Frequency, Wavelength, Transmittance, (Ir)Radiance	… + Component Transmittances, Component (Ir)Radiances, Brightness Temperature, Surface Directional Emissivity, Top-Of-Atmosphere Solar Irradiance
General		
Configuration Control	No	SVN w/ Configuration Control Board

HyspIRI Remote Sensing of Volcanic Plumes - Vincent J. Realmuto

TQ1: How can we help predict and mitigate earthquake and volcanic hazards through the detection of transient thermal phenomena?

Do volcanoes signal impending eruptions through changes in surface temperature and gas emission rates and are such changes unique to specific types of eruptions? **[DS 227]**

→ **Map SO_2 Content of Plumes**

What are the characteristic dispersal patterns and residence times for volcanic ash clouds and how long do such clouds remain a threat to aviation? **[DS 224]**

→ **Detect Plumes and Track Positions over Time**

3-Slab Radiative Transfer Model

Slab 2 Radiance $= \varepsilon_3(\lambda, x_3)\,B(\lambda, T_3) + \tau_3(\lambda, x_3)$[Plume Radiance]

Plume Radiance $= \varepsilon_2(\lambda, x_2)\,B(\lambda, T_2) + \tau_2(\lambda, x_2)$[Slab 1 Radiance]

Slab 1 Radiance $= \varepsilon_1(\lambda, x_1)\,B(\lambda, T_1) + \tau_1(\lambda, x_1)$[Ground Radiance]

Ground Radiance $= \varepsilon_o(\lambda, x_o)\,B(\lambda, T_o) + [1 - \varepsilon_o(\lambda, x_o)]\,\varepsilon_1(\lambda, x_1)\,B(\lambda, T_1)$

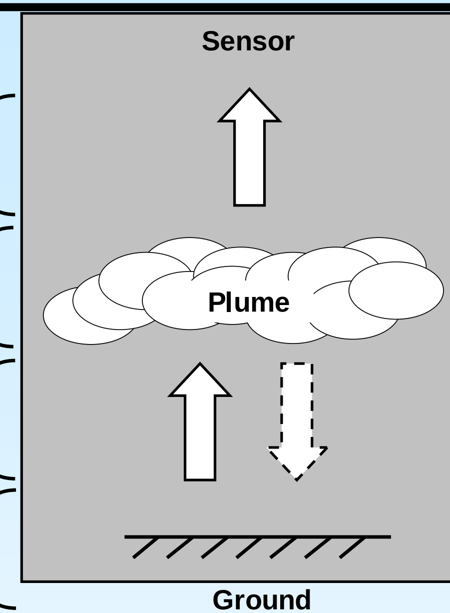

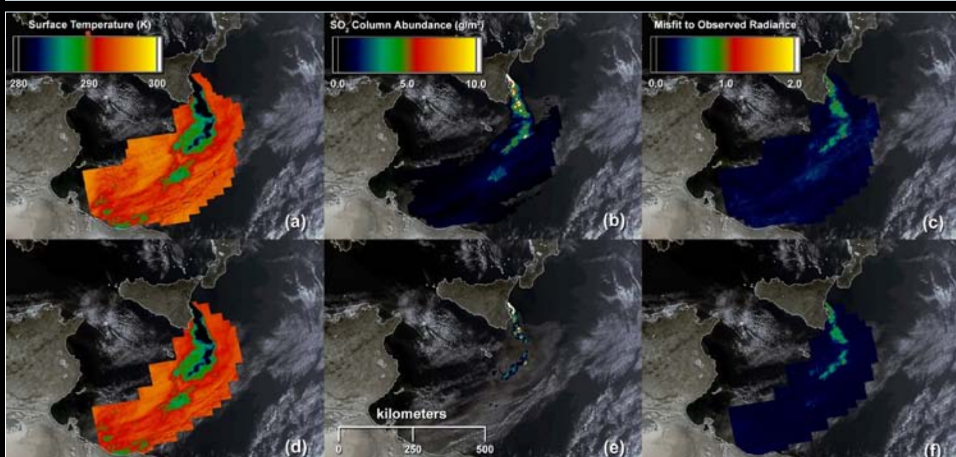

MODIS-Based SO_2 Retrievals: 28 October 2002

Comparison of Retrievals with 5-Band (Top Row) and 4-Band (Bottom Row) Surface Temperatures

Improved Sensitivity to Low Concentrations of SO_2

Increased Influence of Water Vapor on SO_2 Estimates – Requires Better Descriptions of Atm. Water Vapor (NCEP Reanalysis or AIRS L2?)

Summary Remarks

Inferior HyspIRI Results in Combined Retrieval are Counter-Intuitive

- HyspIRI Should Have More Leverage due to Higher Spectral Resolution
- More Analysis Necessary to Verify that Current Results are Repeatable

Success of H_2O Retrievals Bodes Well for Land Surface Products

In Practice, the Retrievals w/ 7.3 μm Channel have Been Problematic

- Technique Applied to MODIS and AIRS Data
- Too Much Variability in (Actual) Conditions within a Pixel? Need Increased Spatial Res?
- Restrict Application to Plumes at Altitudes >> 5 km?

Need Channels that will not Saturate in the Presence of H_2O and SO_2

- Additional Channel Between 7.5 and 8 μm(?)
- Shift the Positions of Bands 2 and 3 to Narrow the Intervening Gap

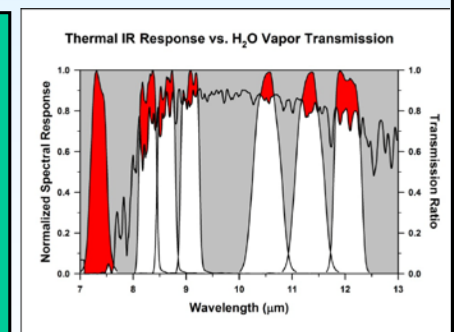

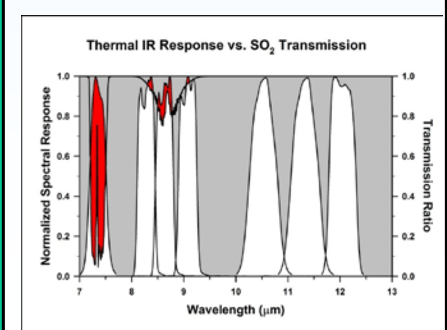

HyspIRI Channels with SO_2 Absorption

The 4μm channel, which is unaffected by H_2O absorption, contains a weak SO_2 band, and the solar scatter contribution to the radiance is significant

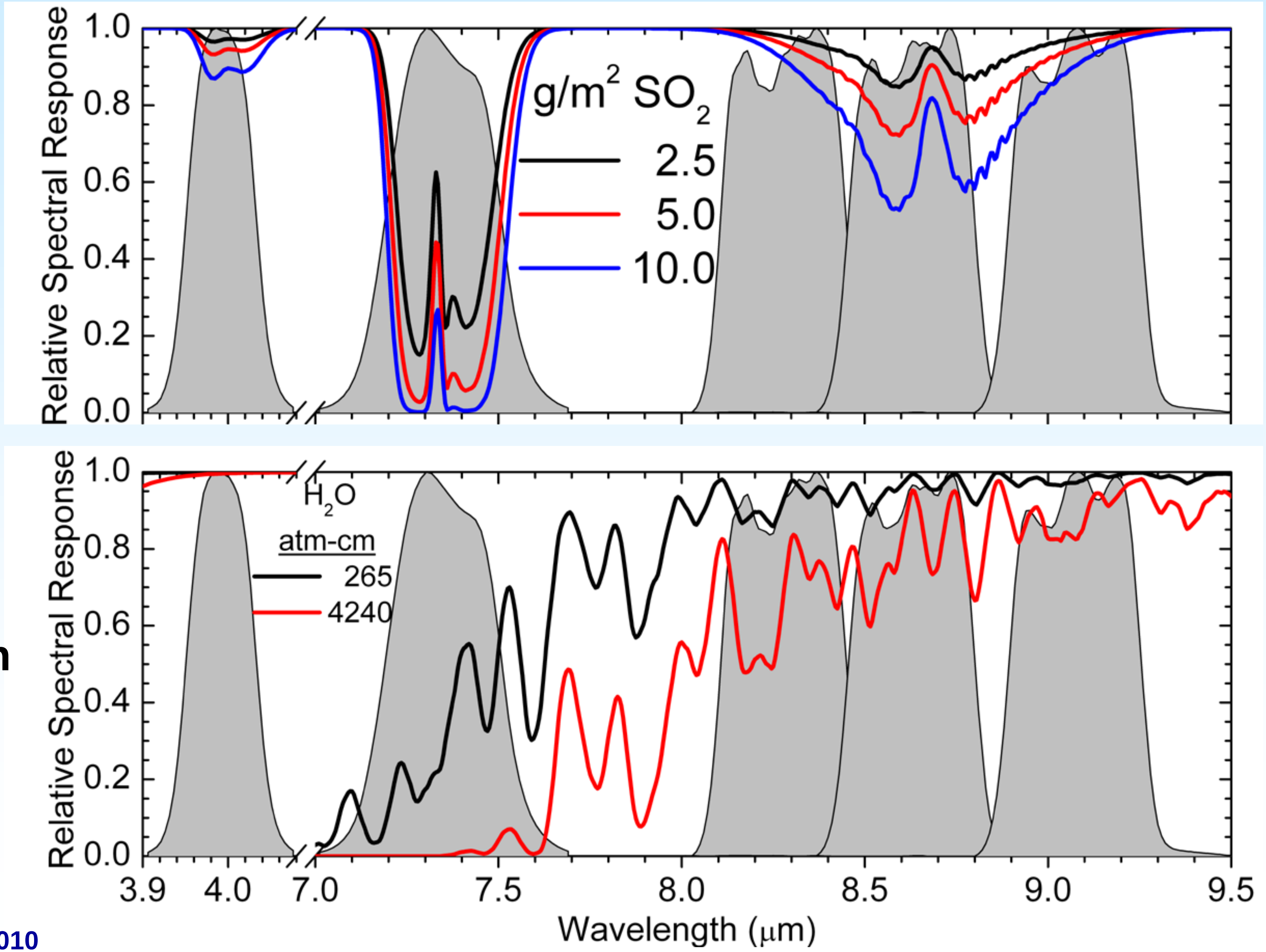

Modeling Chemical Clouds with MODTRAN
- Traditional Approaches -

1. Model chemical cloud externally

– MODTRAN cloud-free radiances

– Offline chemical cloud transmittances and source radiances

– Neglect finite cloud thickness, i.e., that the cloud and atmosphere actually coexist

– Sufficiently accurate for many applications

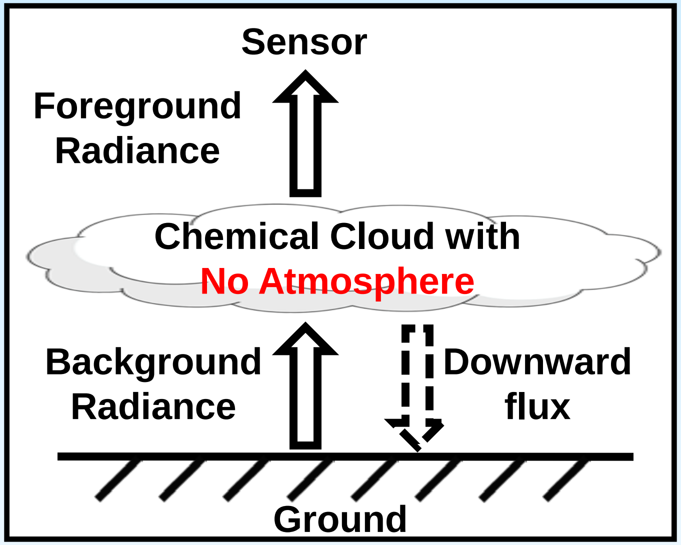

2. Embed cloud layer into atmosphere

– Cumbersome to implement

– Chemical cloud modeled as semi-infinite

- Adversely affects flux and scattered radiance calculations

– Transition region temperature gradients can cause failure of spherical refraction

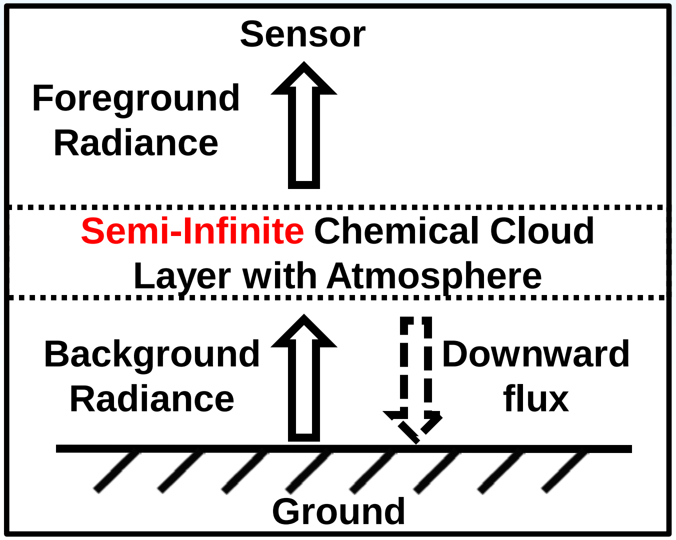

Modeling Chemical Clouds using MODTRAN
- New Local Cloud Approach -

3. Introduce a MODTRAN "*local*" chemical cloud option

- Band model data for 100's of molecules
- User-friendly cloud specification
- Line-of-sight (LOS) & solar geometries computed with cloud-free atmosphere to eliminate refractive path failures
- Radiative Transfer
  - ***Tailored treatment of chemical cloud single scatter solar radiation***
  - ***DISORT diffuse (scattered) radiance field determined from ambient atmosphere***
  - ***Chemical cloud absorption included in LOS scattered, $\Delta I'_{ms}$, and emitted, $\Delta I'_{emis}$, segment radiance calculations***
- Output cloud-free, cloud + atmosphere & contrast spectral signatures

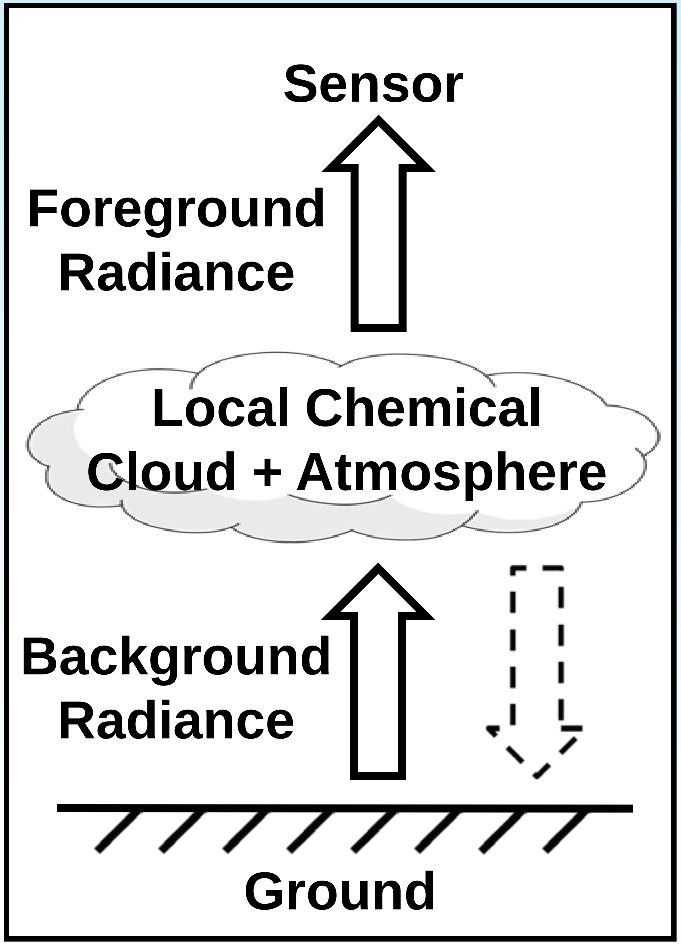

Single Layer Cloud Illustrations

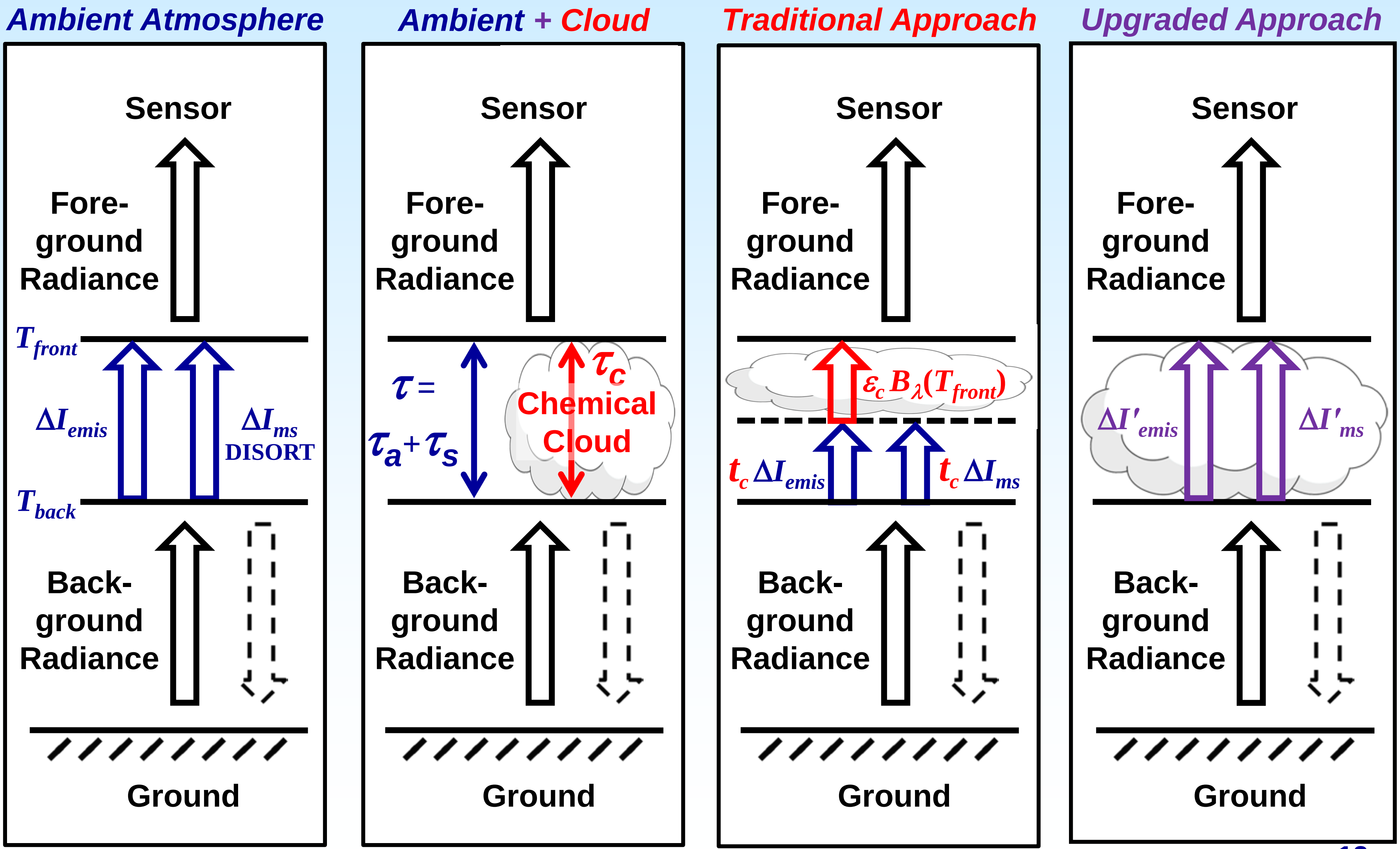

Chemical Cloud Effect on Segment Scattered Radiance

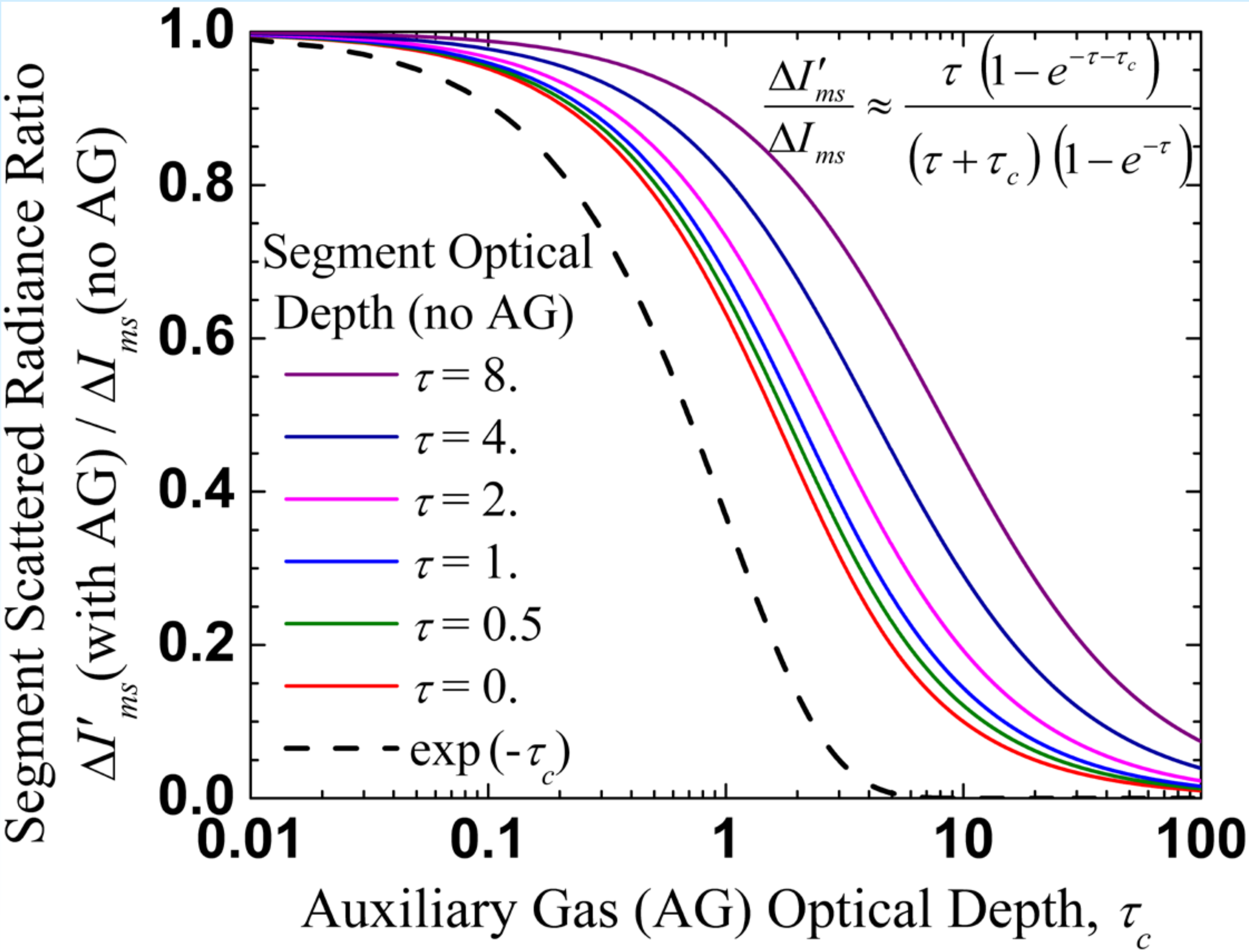

Upgraded Approach

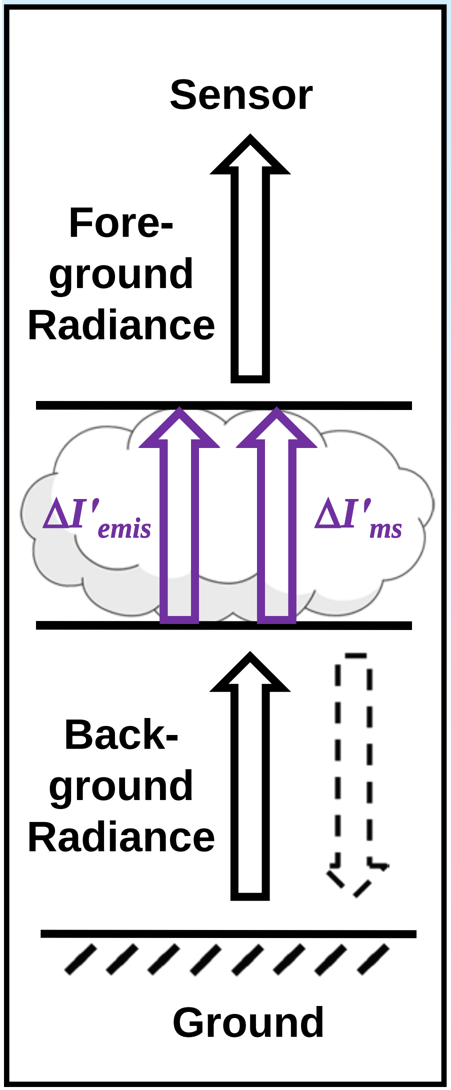

Chemical Cloud Effect on Segment Emitted Radiance

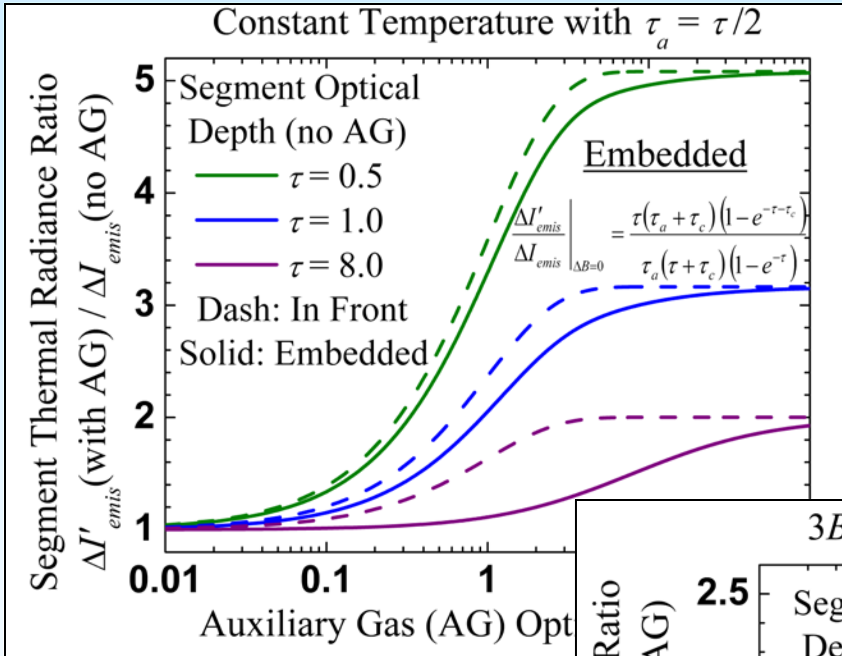

Utilize Linear-in-τ:

Linear variation of Planck emission with path absorption optical depth

← Isothermal Segment

Planck Emission increasing with Optical Depth, τ

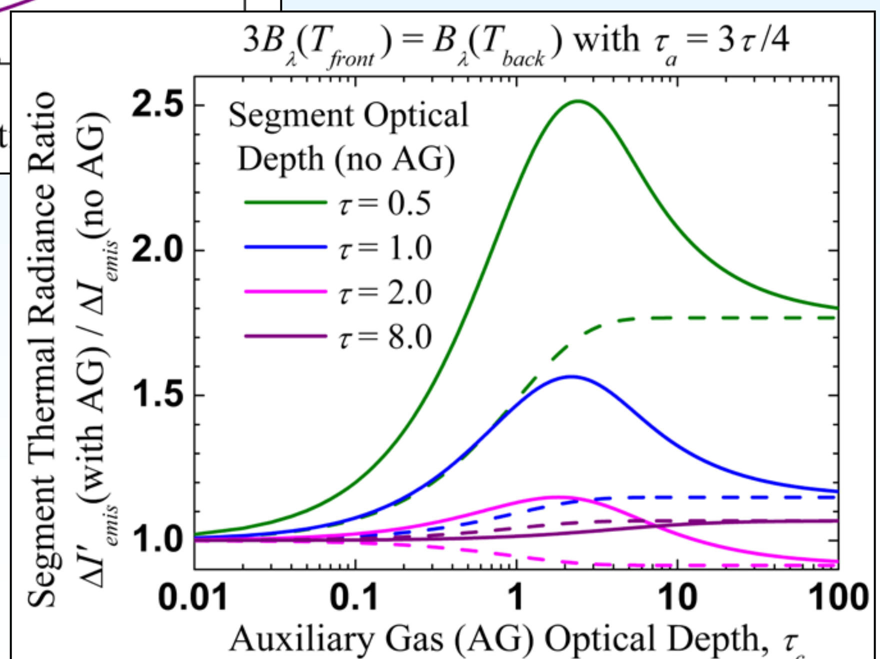

Upgraded Approach

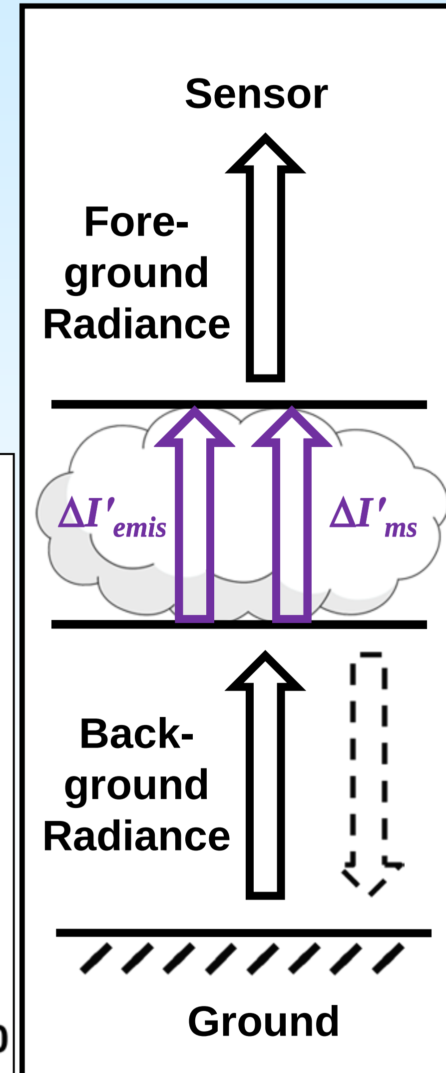

Summary

- MODTRAN®5.2 has been available since June 2009
  - The model provides major enhancements over MODTRAN4
  - Can serve as an important tool for NASA and HyspIRI program
- MODTRAN is designed for broad range of applications
  - Code developers (SSI / AFRL) provide support as needed
  - Presentation focused on modeling of local chemical cloud
    - New option includes radiative coupling of atmosphere + cloud
      - Being developed for DOE
      - Work in progress: MODTRAN upgrade will be complete by 30sep2010
    - Designed to provide user-friendly inputs, an extensive chemical database, and state-of-the-art radiative transfer
    - Year 2 will focus on verification (MCScene and DIRSIG 3D modeling) and validation (measurement comparisons)

MODTRAN5 Distribution

- MODTRAN®5.2 is available for license at **www.modtran.org**
  - Developed, maintained and validated by SSI and AFRL
  - Distributed for SSI by Ontar Corporation
  - Government Use ‘price’ covers code distribution, maintenance and limited customer support costs
- An End User License Agreement (EULA) is required
  - States license terms of use, limits on re-distribution (3 users at a single site)
  - A single copy EULA can be accepted electronically during online purchase
  - Many organization legal departments require review and minor modifications
- Customized license agreements can be developed with SSI for
  - Site licenses (>7 user group at a single location),
  - Enterprise/embedded code licenses,
  - Contractor operated Government facilities licenses,
  - University and State government agency licenses,
  - Educational classroom use licenses,
  - Etc.

Back ups

MODTRAN5 Overview
- General Description -

- IR / Vis / UV Transmittances, Radiances and Fluxes
  - Up to 0.2 cm^{-1} Spectral Resolution from 0.1 cm^{-1} Band Model

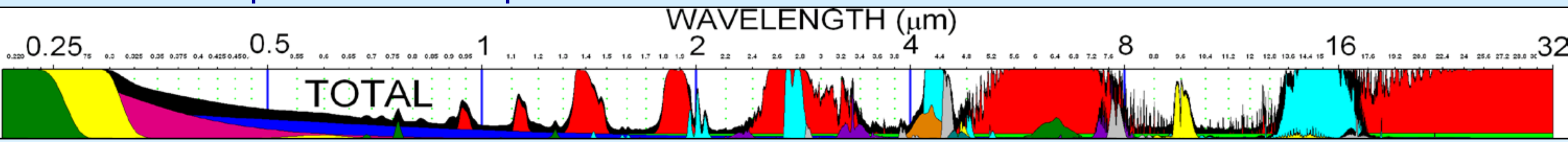

- Stratified Molecular / Aerosol / Cloud Atmosphere
  - Built-in, Auxiliary & User-Specified Molecules and Particulates
- 2-Stream and DISORT Solar and Thermal Scattering
  - Diffuse Transmittance and Spherical Albedo for Atmosphere Correction →

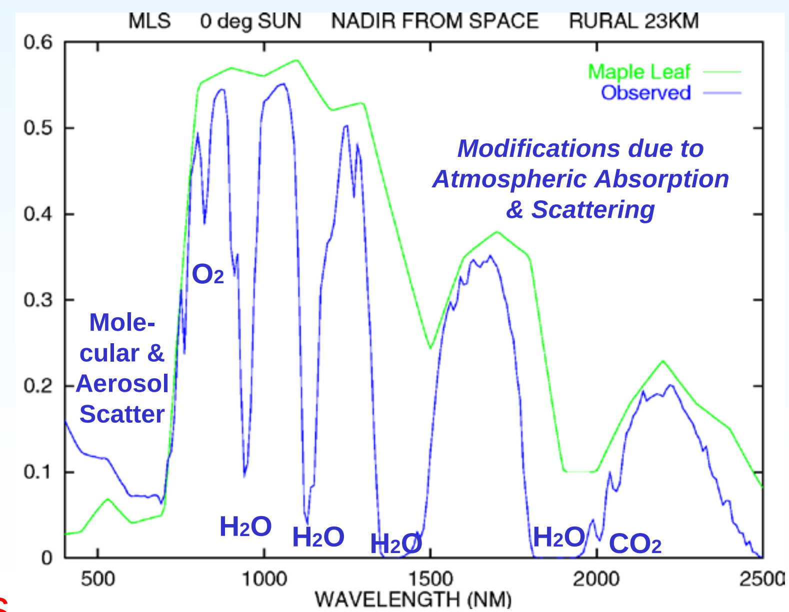

- Spherical Refractive Geometry
- Spectral Convolution & Filtering
- Many Applications Pertinent to HyspIRI
  - Sensor Design, Atmospheric Correction, Measurement / Data Analyses, Scene Simulation, Algorithm Development, …
  - Today's focus: Localized chemical clouds

What's New

	MODTRAN®4	MODTRAN®5.2.0.0 / 5.2.1.0
Band Model		
Spectral Resolutions	1.0, 5.0, 15.0 cm^{-1}	… + 0.1 cm^{-1}
Voigt Transmittance	Rogers-Williams interpolation	Exact expansion
Line Tail Model	Constant within spectral bin	Spectra fit to Padé Approximants
Line Center Model	One (S/d, 1/d) pair	… or Two (S/d, 1/d) pairs
HITRAN Data	Circa 2003	2008 with 2009 H_2O Update
Constituents	First 12 HITRAN molecules	39 HITRAN2008 molecules + Auxiliary Species Option
Temperature Range	180K to 305K	180K to 330K
Correlated-*k* Algorithm		
Number of *k*'s	33 (slow) or 17 (medium)	… w/ Adaptive Reduction to 4 or 1
Convergence	Rare Failures	No Failures (to date)
DISORT Scattering		
Max Streams No.	16	32 or Increase Parameter MI
Solar Zenith	Most Angles < 90°	Any Angles < 90°

What's New

	MODTRAN®4	MODTRAN®5.2.0.0 / 5.2.1.0
Inputs		
Temperature Profile	Model Atmosphere, User Defined	… **or** Model Atm. Perturbation
Water Profile	Model Atm. Density, User Defined	… **or** Model Atm. Relative Humidity
Profile Scaling	CO_2, H_2O, O_3	All built-in molecular profiles
Outputs		
Format	ASCII	… **or** Binary
Spectral Data	Direct Transmittance, Flux, (Ir)Radiance, Cooling Rates	… **+** Diffuse Transmittances, Spherical Albedo
Radiance Modes	Thermal only, Thermal and Solar	… **+** Solar Only
Primary (tp6) Output File	General Information, Spectral Data, and In-Band Cooling Rates	… **or** General Information Only **or** File Not Generated
Spectral Data (tp7,7sc) Files	Frequency, Wavelength, Component Transmittances, Component (Ir)Radiance	… **+** Brightness Temperature, Surface Directional Emissivity, Top-Of-Atmosphere Solar Irradiance
Spectral Channel (chn) File	Frequency, Wavelength, Transmittance, (Ir)Radiance	… **+** Component Transmittances, Component (Ir)Radiances, Brightness Temperature, Surface Directional Emissivity, Top-Of-Atmosphere Solar Irradiance

What's New

	MODTRAN®4	MODTRAN®5.2.0.0 / 5.2.1.0
Optical Data		
Molecular Cross-Sections	13 CFC species	… + O_2O_2 Visible Absorbance + Auxiliary Species Option
User Defined Aerosols	Spectral Tables (no data checking)	Spectral Tables (with data checking) or Angstrom Law Inputs
Cloud	Built in Model Clouds	… + Mie Water/Ice Data Table
Surface Reflectance	Spectral Albedo, Spectral BRDF	… **w/** Surface liquid water
Geometry		
Refraction	Based on Band Central Frequency	… **or** User-Defined Frequency
General		
Configuration Control	No	SVN w/ Configuration Control Board
Multiple Runs	Repeat Run from Single Input File	… + Multiple Input File Capability
Test Cases	27 sample inputs	58 sample inputs
Bug Fixes (See Readme)		

Modeling Chemical Clouds using MODTRAN

1. Model chemical cloud externally

- Cumbersome and Labor Intensive
  - Run MODTRAN to compute foreground + background and foreground radiances
  - Compute chemical cloud transmittance and source radiance offline
  - Spectrally combine components
- Neglects mixing of chemical cloud and atmosphere
  - Approximate treatment of radiative spectral correlations
  - Approximate treatment of emission and scattering radiance components
- Sufficiently Accurate for many applications

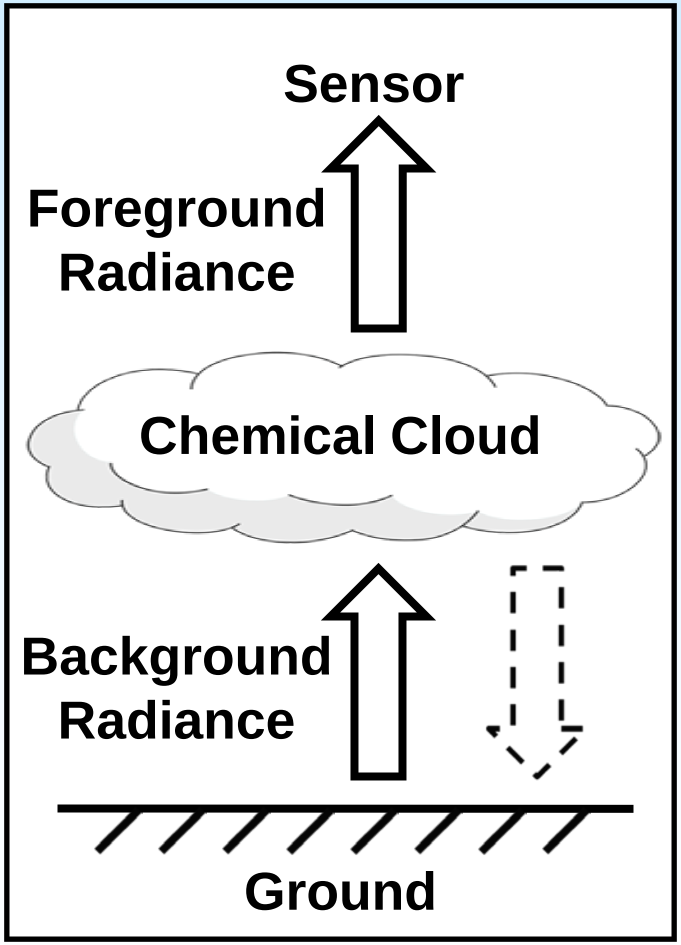

Modeling Chemical Clouds using MODTRAN

2. **Embed chemical cloud stratified layers into atmosphere**
   - Cumbersome to implement
     - Relaying often necessary for each LOS
     - Difficult to scale column densities
   - Chemical cloud modeled as semi-infinite
     - Unintended perturbation of scattered radiance calculations
     - Unintended perturbation of vertical flux calculations
   - Large vertical temperature gradients can arise within the chemical cloud to ambient atmosphere transition regions
     - *Spherical refraction geometry algorithm can fail*!

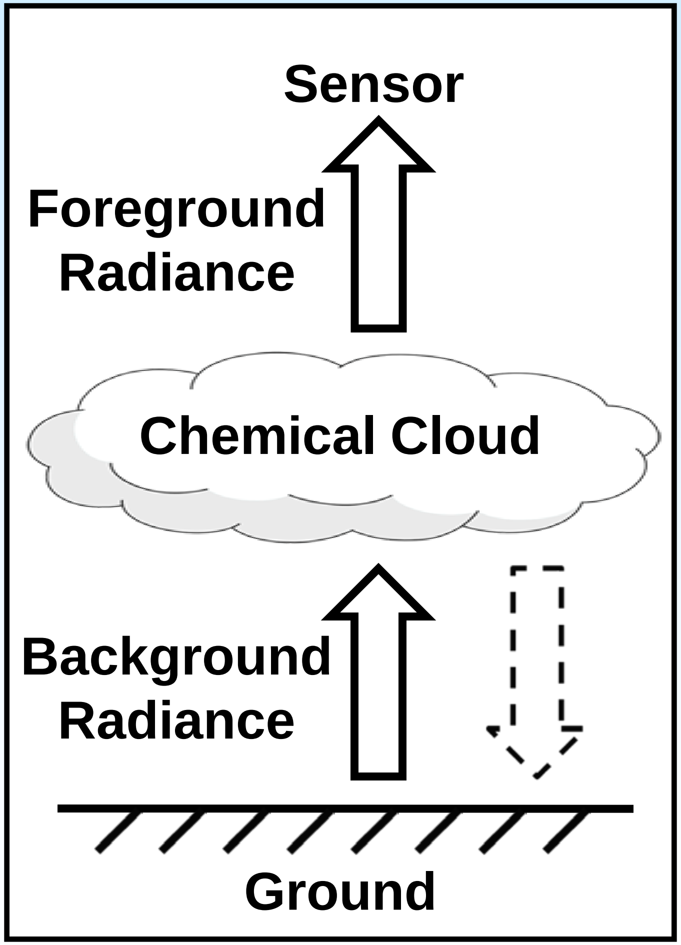

Modeling Chemical Clouds using MODTRAN

3. **Introduce a MODTRAN “*local* ” chemical cloud option**
   - Band model data for 100’s of molecules
   - User-friendly cloud specification
   - Path geometry without chemical cloud
     - Eliminates refractive algorithm failures
     - Insures contrast signature paths match
   - Radiative Transfer
     - Single scatter solar illumination paths attenuated by chemical cloud only for altitude levels containing cloud
     - ***Chemical cloud excluded from DISORT scattered radiance field calculation***
     - **Chemical cloud absorption effects on line-of-sight (LOS) radiance are modeled**
     - Output of cloud-free, cloud + atmosphere and contrast spectral signatures

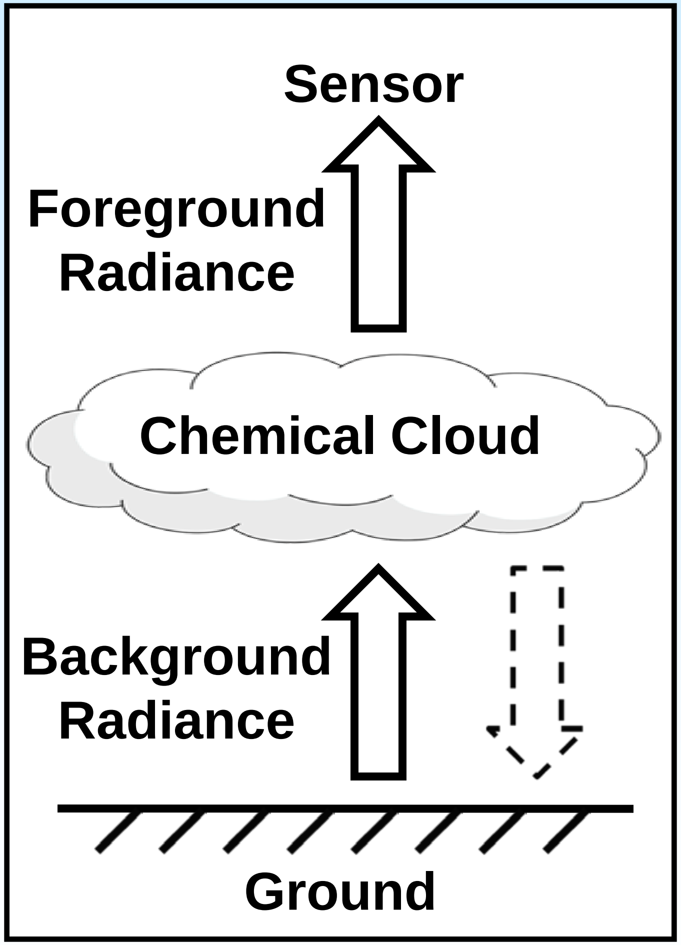

MODTRAN Local Chemical Cloud Option

User-friendly chemical cloud specification

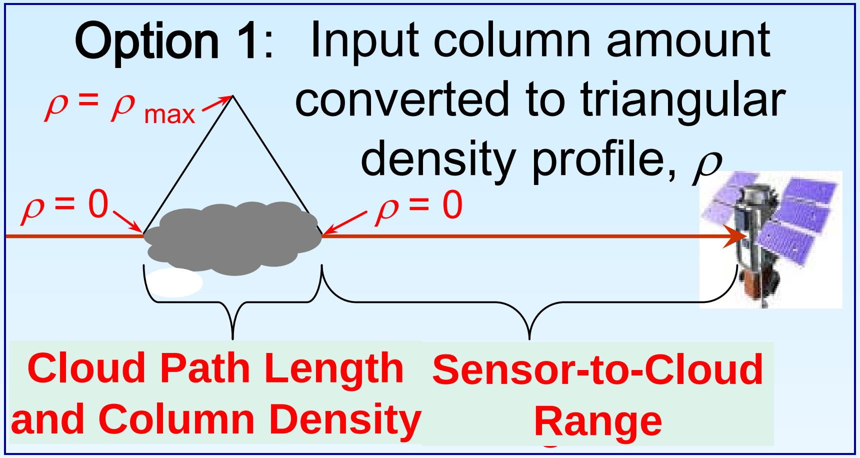

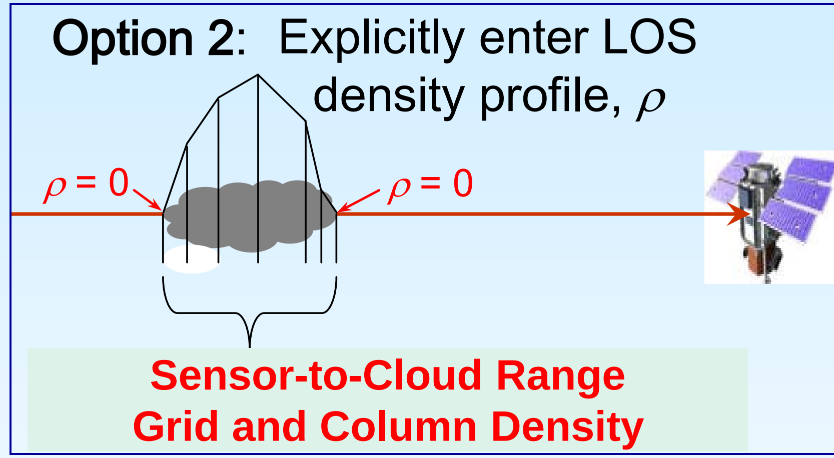

Single scatter solar illumination paths attenuated by chemical cloud only for altitude levels containing cloud

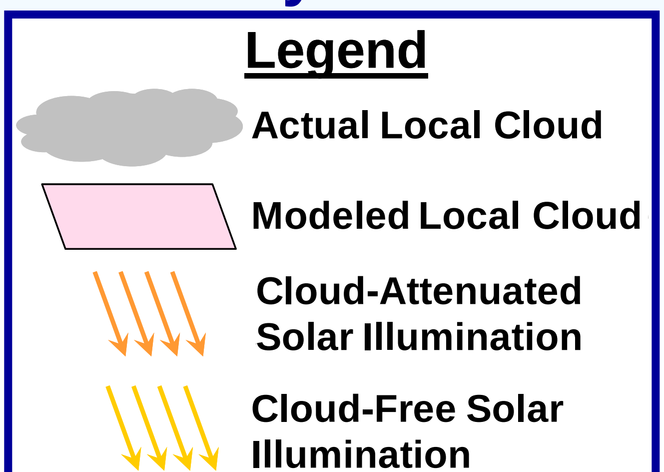

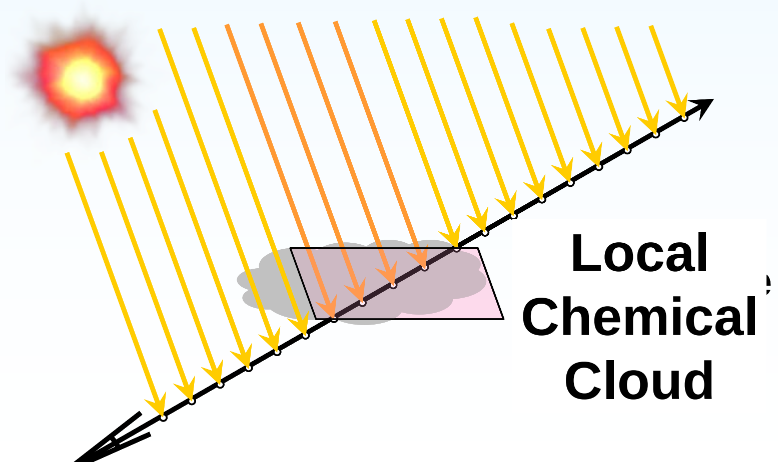

Single Layer Cloud Illustrations

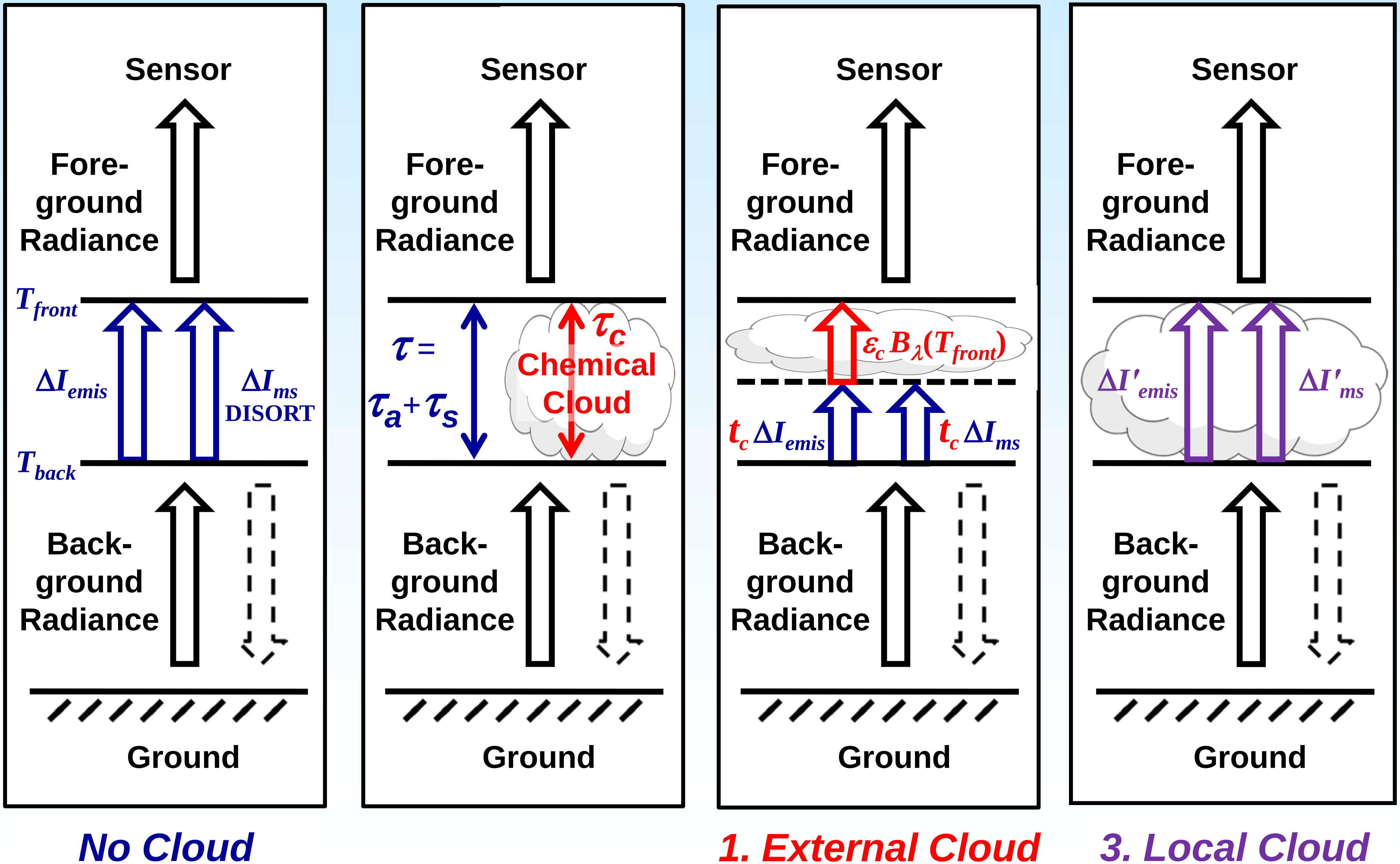

Chemical Cloud Effect on Segment Scattered Radiance

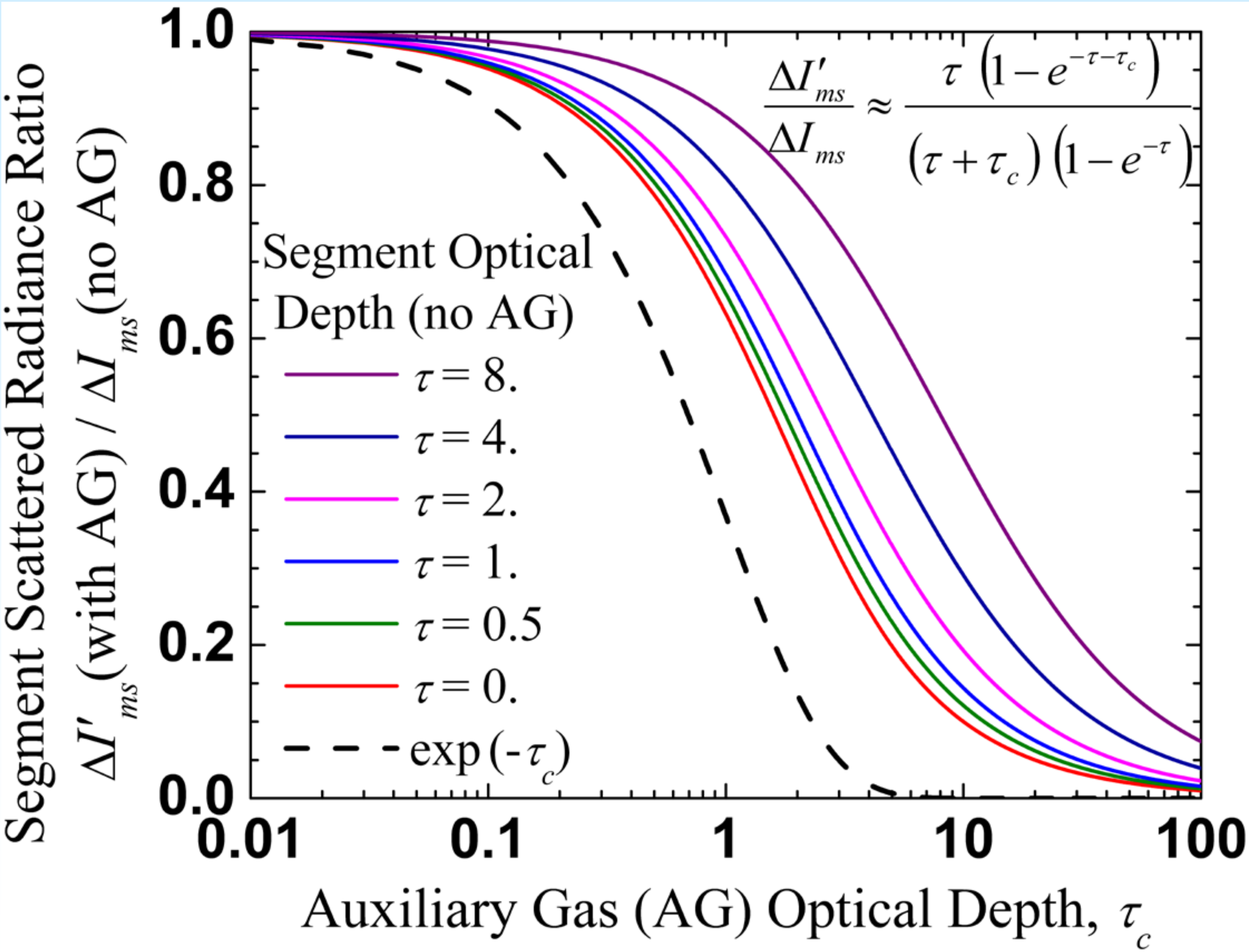

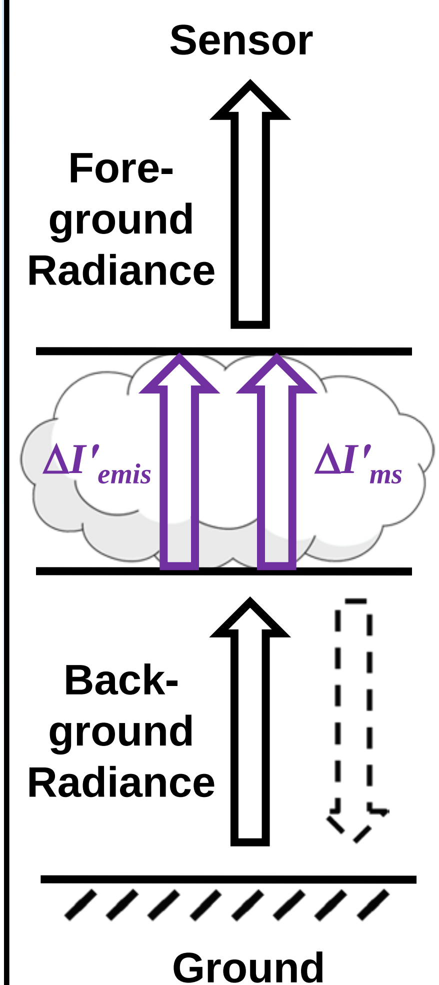

3. Embedded Local Cloud

Chemical Cloud Effect on Segment Emitted Radiance

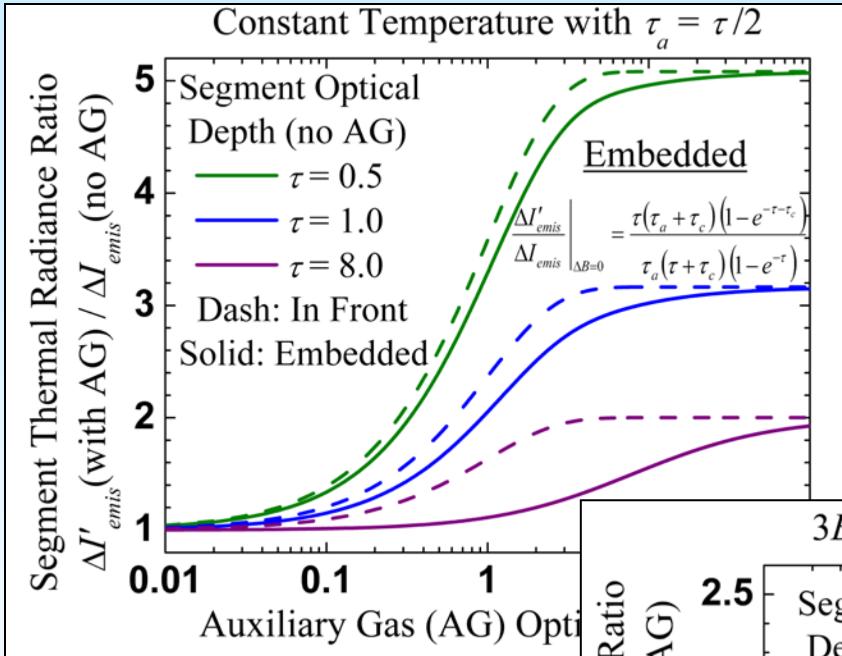

Utilizing Linear-in-τ Approach

Isothermal Segment

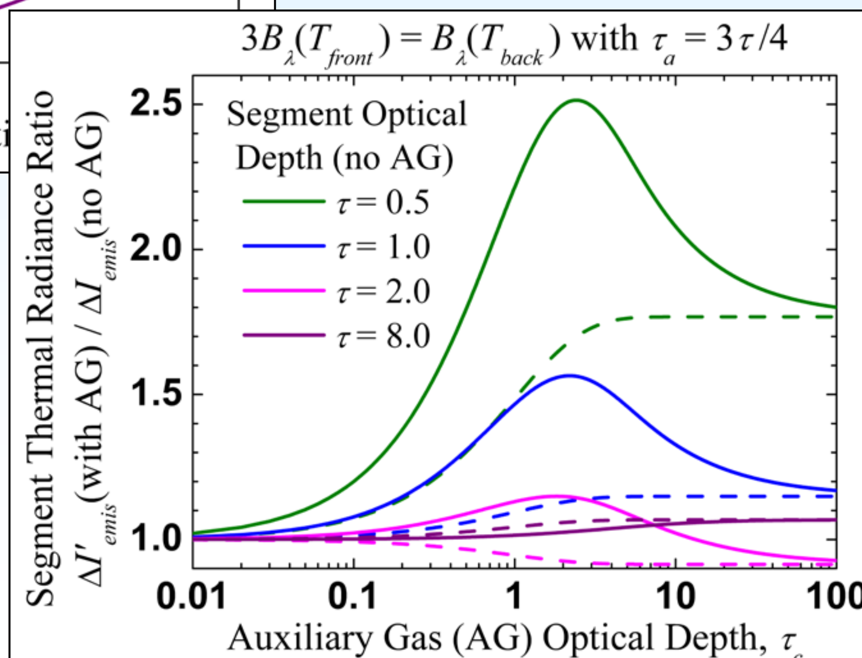

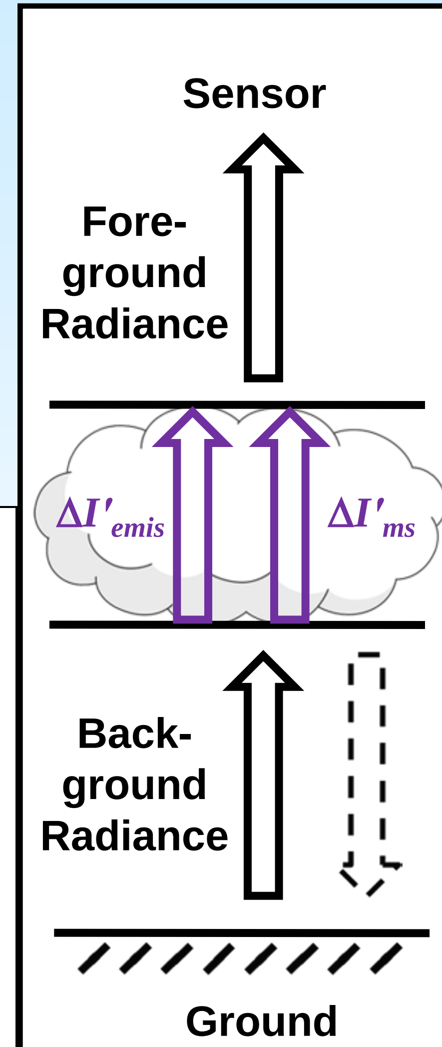

3. Embedded Local Cloud

Planck Emission Increasing with Optical Depth, τ

SIMULATED HYSPIRI DATA FOR MEASURING VOLCANIC THERMAL FEATURES

R. Greg Vaughan

USGS, Astrogeology Science Center, Flagstaff, AZ

August 26, 2010

HyspIRI Science Workshop , Pasadena, CA

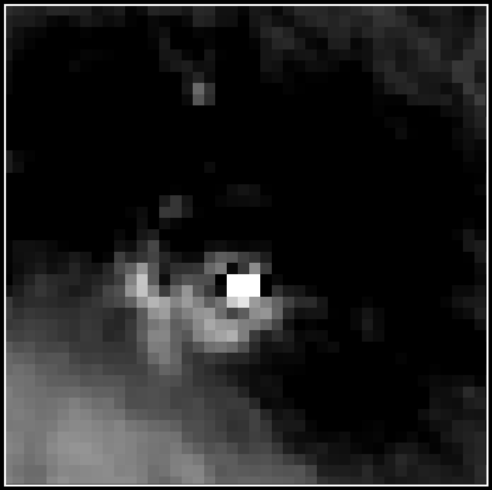

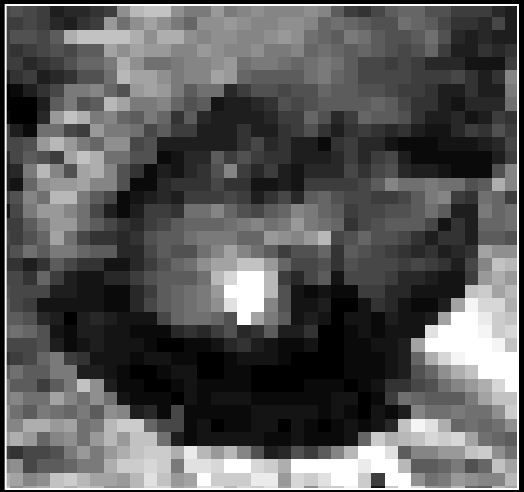

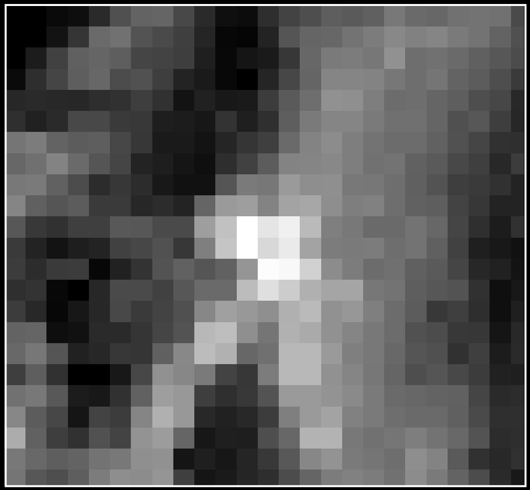

ACKNOWLEDGEMENTS

1) NASA ROSES (NNH09ZDA001N) HyspIRI Preparatory Activities Using Existing Imagery
2) USGS
3) National Park Service
4) NASA / Jet Propulsion Laboratory

HyspIRI Science Questions

1) How can we help predict and mitigate volcanic hazards through detection of transient thermal phenomena? (TQ1)

2) How do volcanoes signal impending eruptions through changes in surface temperature and thermal flux? (CQ3)

Outline

1) Simulated HyspIRI data over two different thermal targets with differing temperatures:
   - i) the 2004 Mount St. Helens dome, and
   - ii) hot springs in the Yellowstone geothermal area.

2) Analysis of the dynamic range of HyspIRI TIR (MIR and LWIR) channels.

Mount St. Helens dome eruption – Oct. 2004

MASTER
5 m pixels

9.1 um data

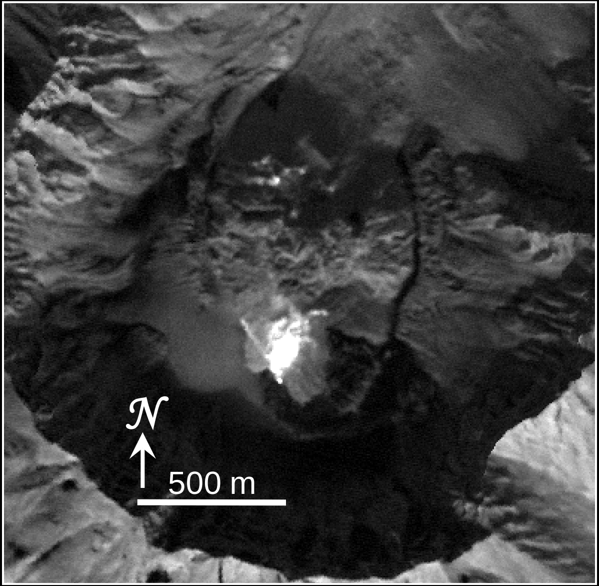

HyspIRI-sim
60 m pixels

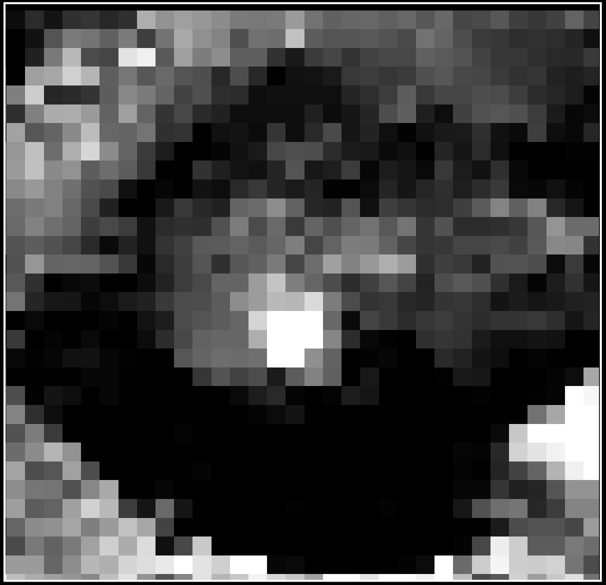

MASTER
5 m pixels

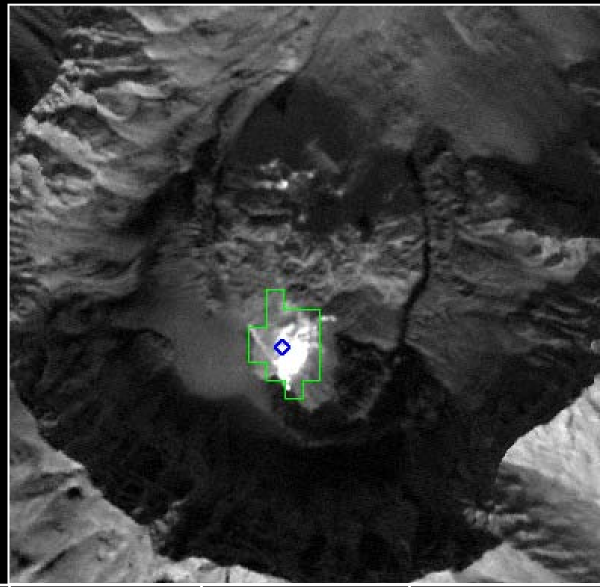

HyspIRI-sim
60 m pixels

ROI area: 57,600 m^2

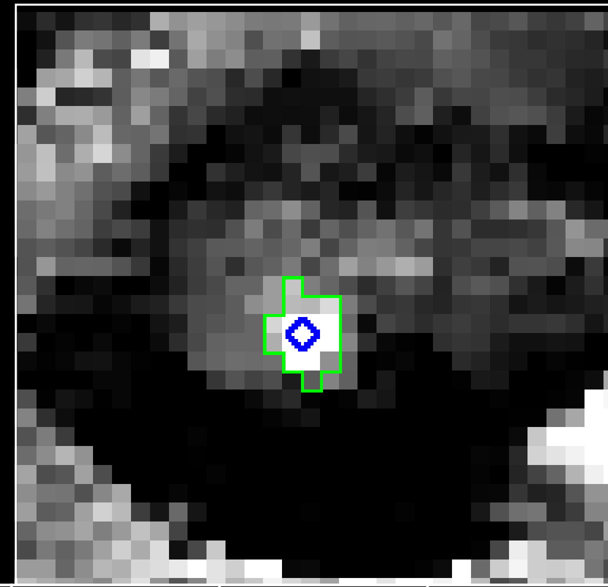

9.1 um	Min	Max	Mean		Min	Max	Mean
Radiance ($W/m^2/um/sr$)	7	119	12.5		8	47	14
Temp (C) $\varepsilon = 0.9$	10	305	47		20	164	55
Thermal Flux (MW)			SUM 31				SUM 34
4.0 um	Min	Max	Mean		Min	Max	Mean
Radiance ($W/m^2/um/sr$)	0.3	504	8.8		0.9	142	14
Temp (C) $\varepsilon = 0.9$	4	400	108		33	270	129
Thermal Flux (MW)			SUM 62				SUM 77

MASTER
5 m pixels

HyspIRI-sim
60 m pixels

ROI area: 57,600 m^2

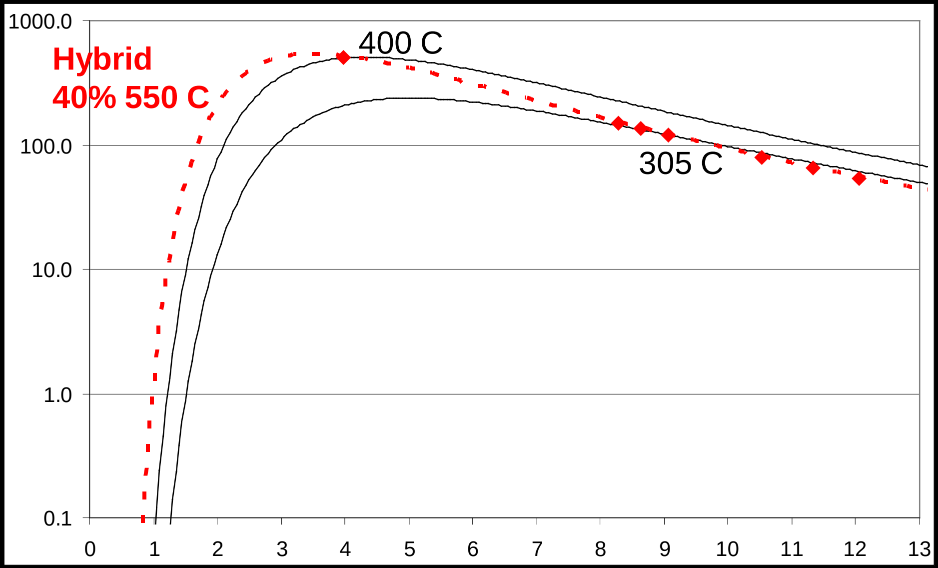

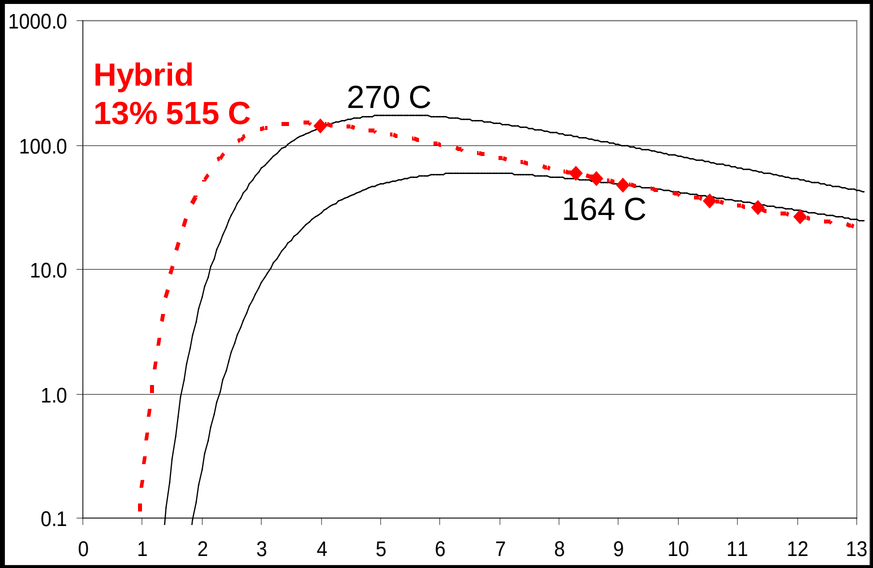

9.1 um	Min	Max	Mean		Min	Max	Mean
Radiance (W/m^2/um/sr)	7	119	12.5		8	47	14
Temp (C) $\varepsilon = 0.9$	10	305	47		20	164	55
Thermal Flux (MW)			SUM 31				SUM 34
4.0 um	Min	Max	Mean		Min	Max	Mean
Radiance (W/m^2/um/sr)	0.3	504	8.8		0.9	142	14
Temp (C) $\varepsilon = 0.9$	4	400	108		33	270	129
Thermal Flux (MW)			SUM 62				SUM 77

Yellowstone Geothermal Area

The Challenge of Thermal Monitoring

Over 10,000 individual thermal features, including fumaroles, mud pots, and the famous hot spring pools and geysers.

Most of these are clustered into about 80 unique thermal areas (thermal barrens).

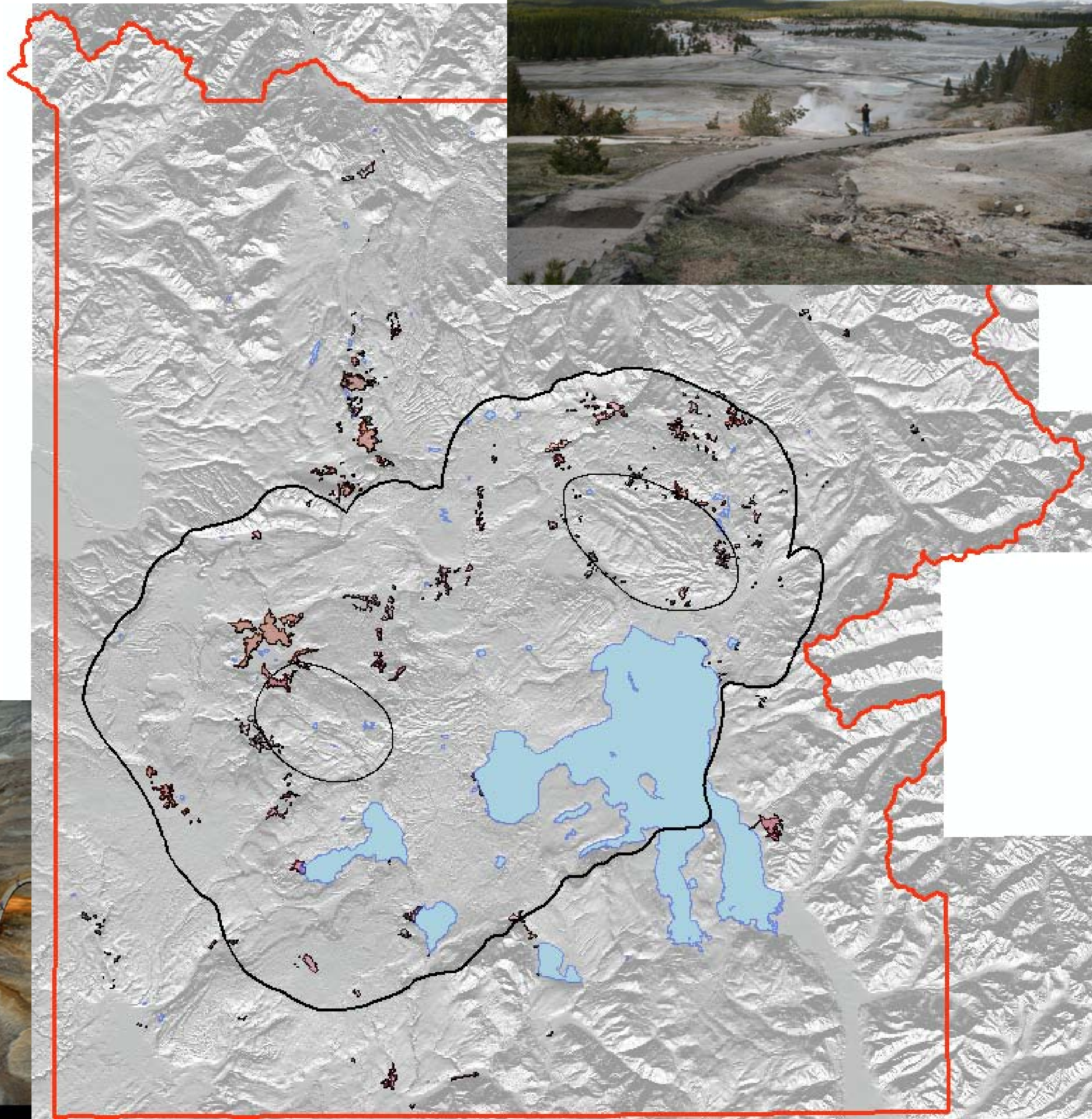

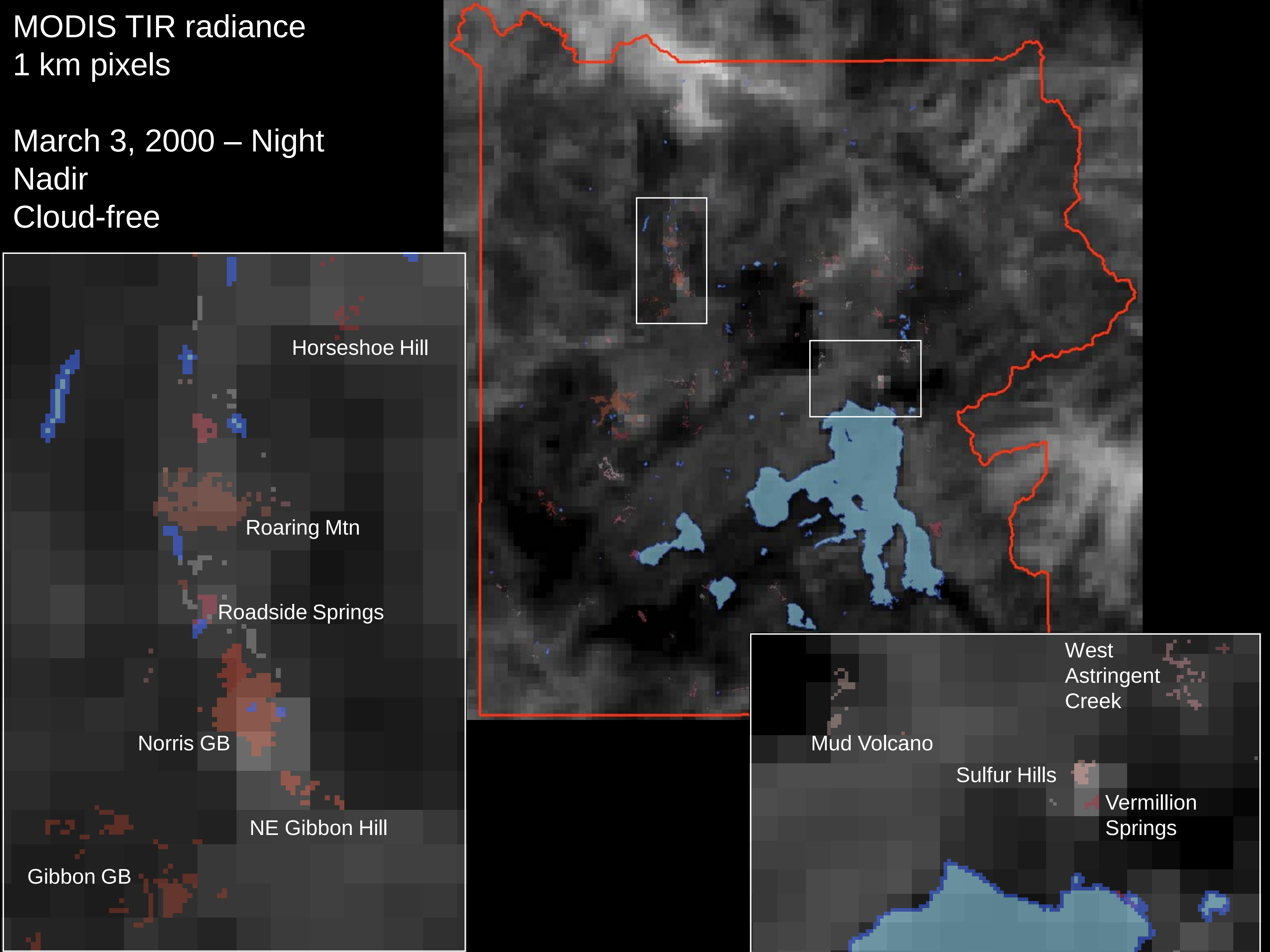
MODIS TIR radiance
1 km pixels
March 3, 2000 – Night
Nadir
Cloud-free
Horseshoe Hill
Roaring Mtn
Roadside Springs
Norris GB
NE Gibbon Hill
Gibbon GB
West
Astringent
Creek
Mud Volcano
Sulfur Hills
Vermillion
Springs

MODIS TIR radiance
1 km pixels

March 3, 2000 – Night
Nadir
Cloud-free

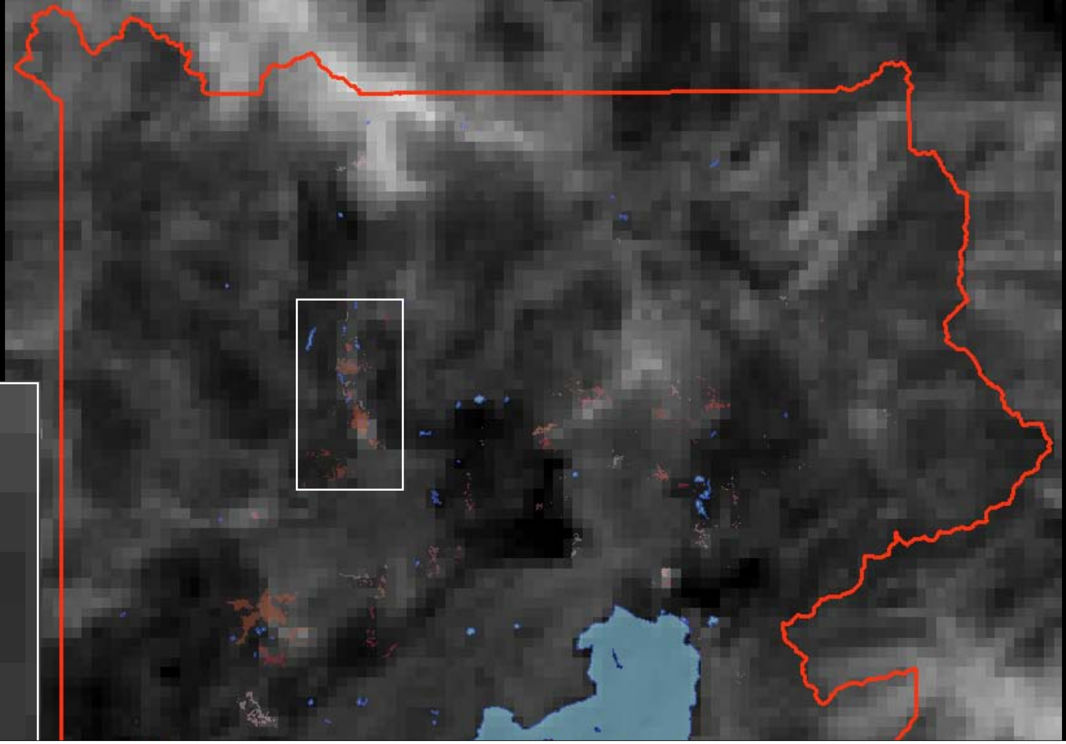

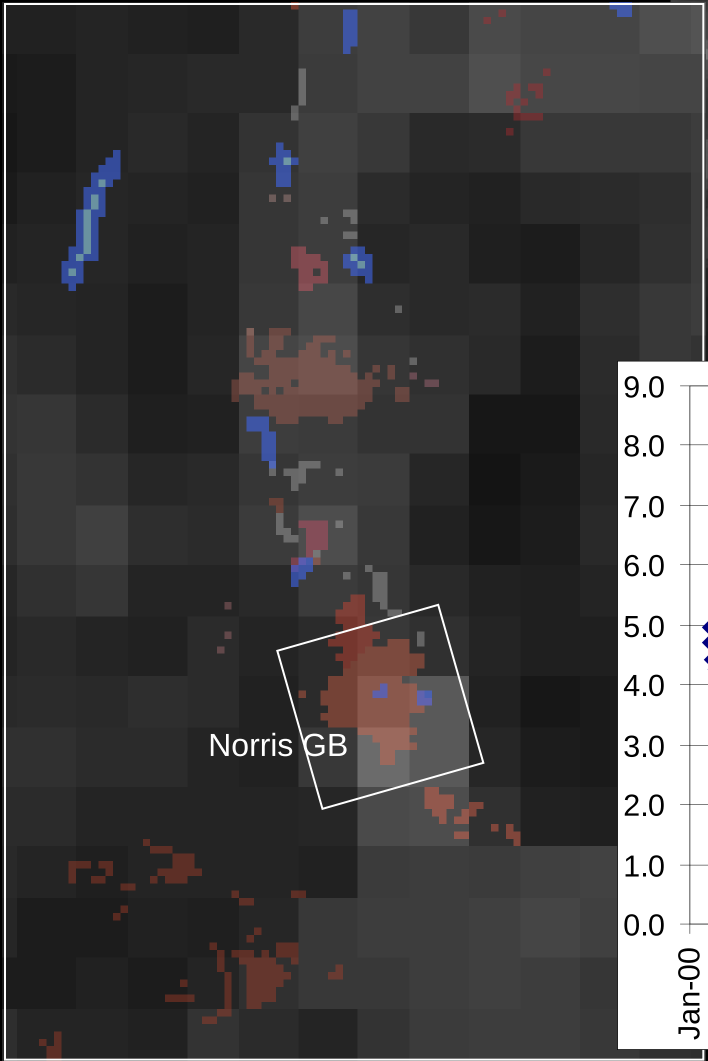

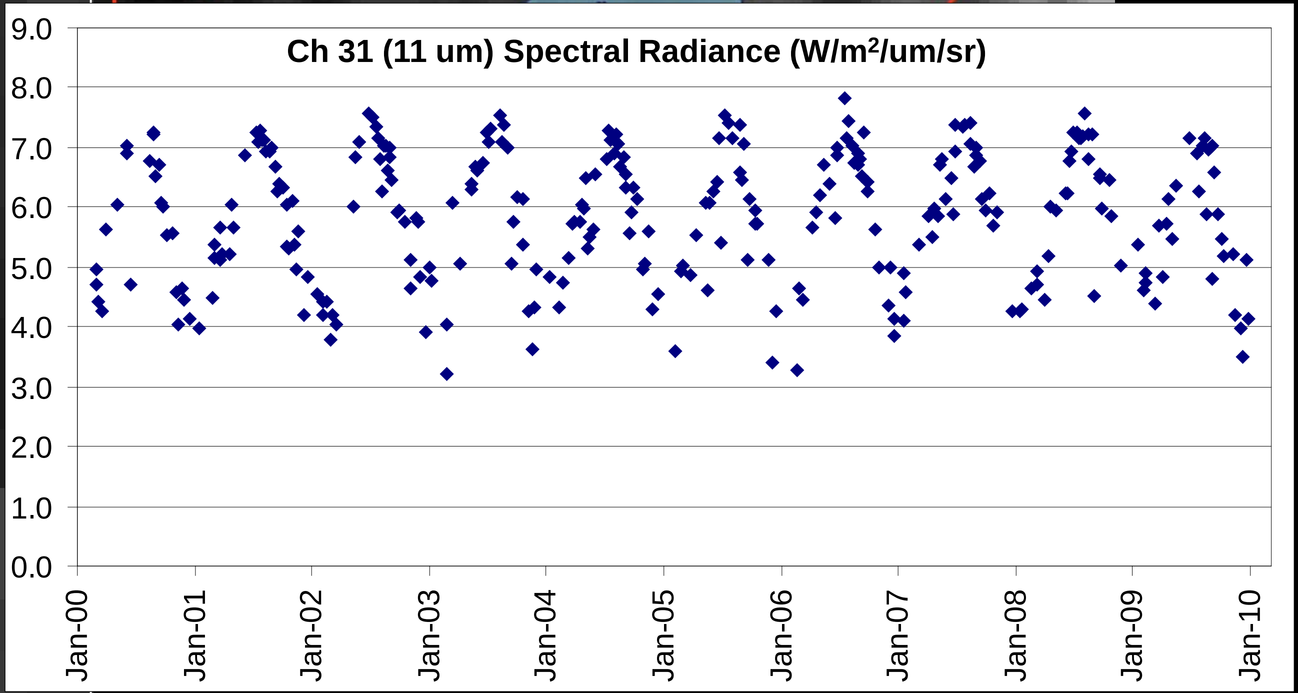

MODIS TIR radiance
1 km pixels

March 3, 2000 – Night
Nadir
Cloud-free

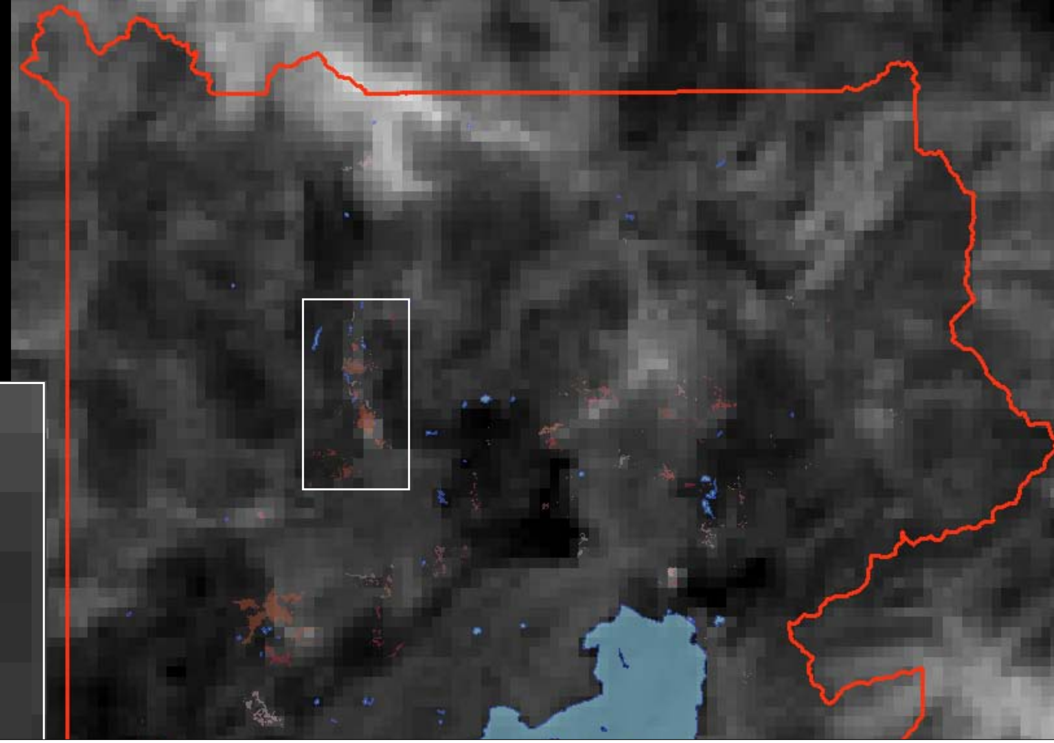

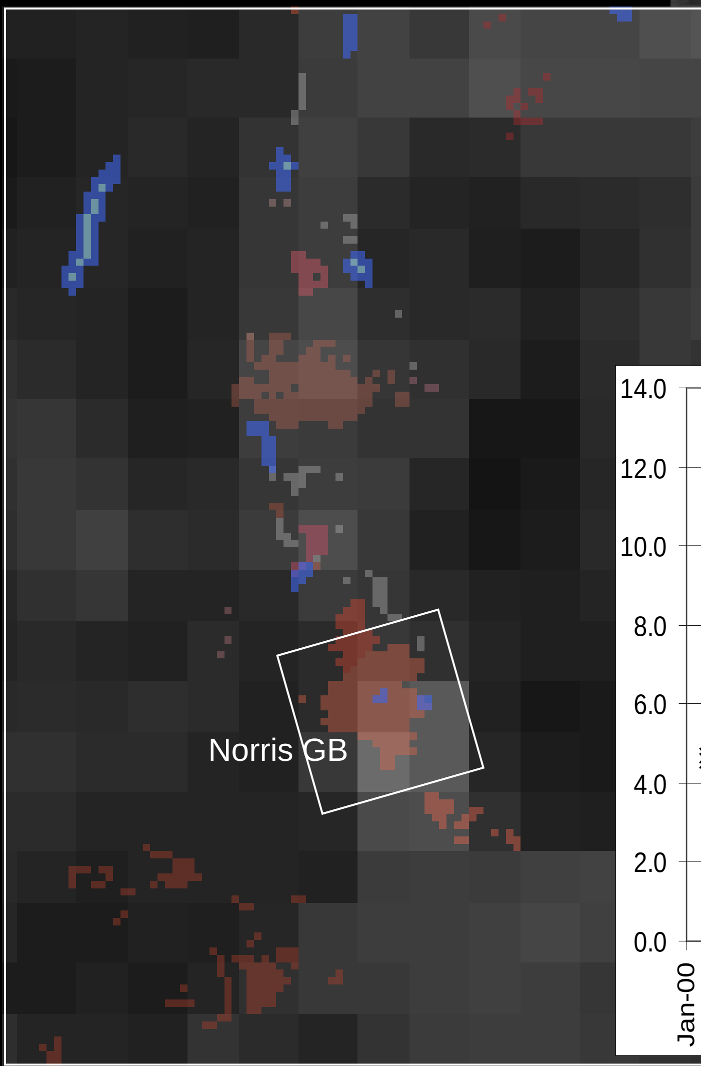

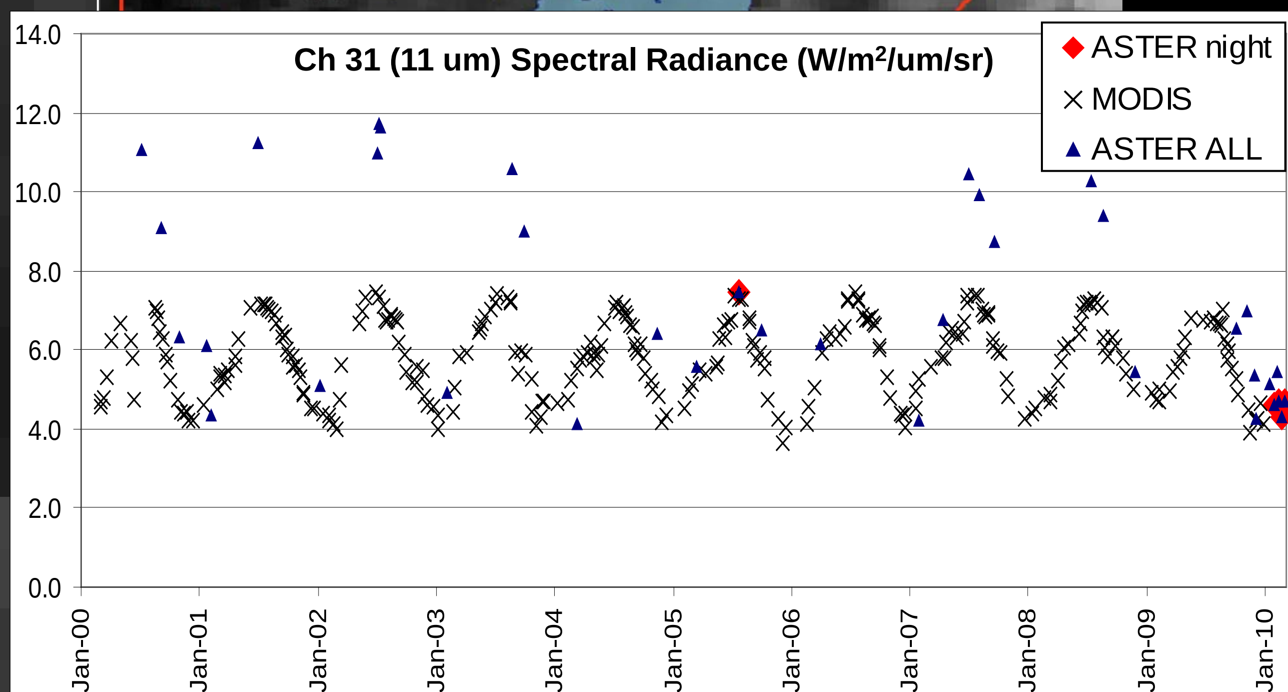

MODIS TIR radiance
1 km pixels

March 3, 2000 – Night
Nadir
Cloud-free

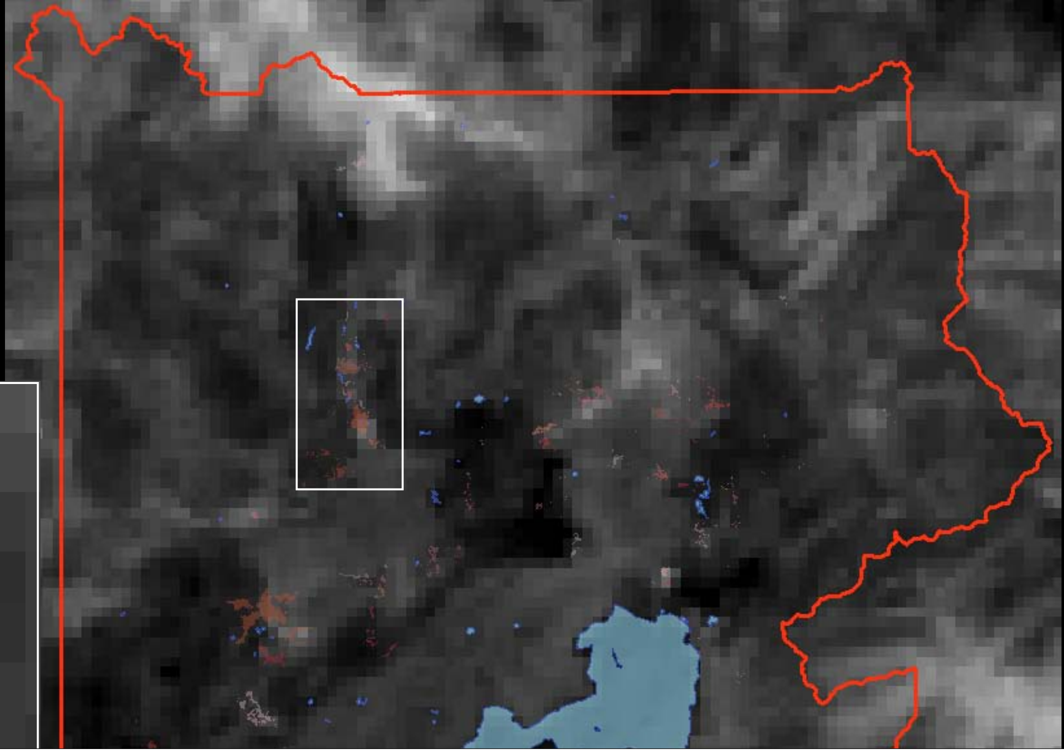

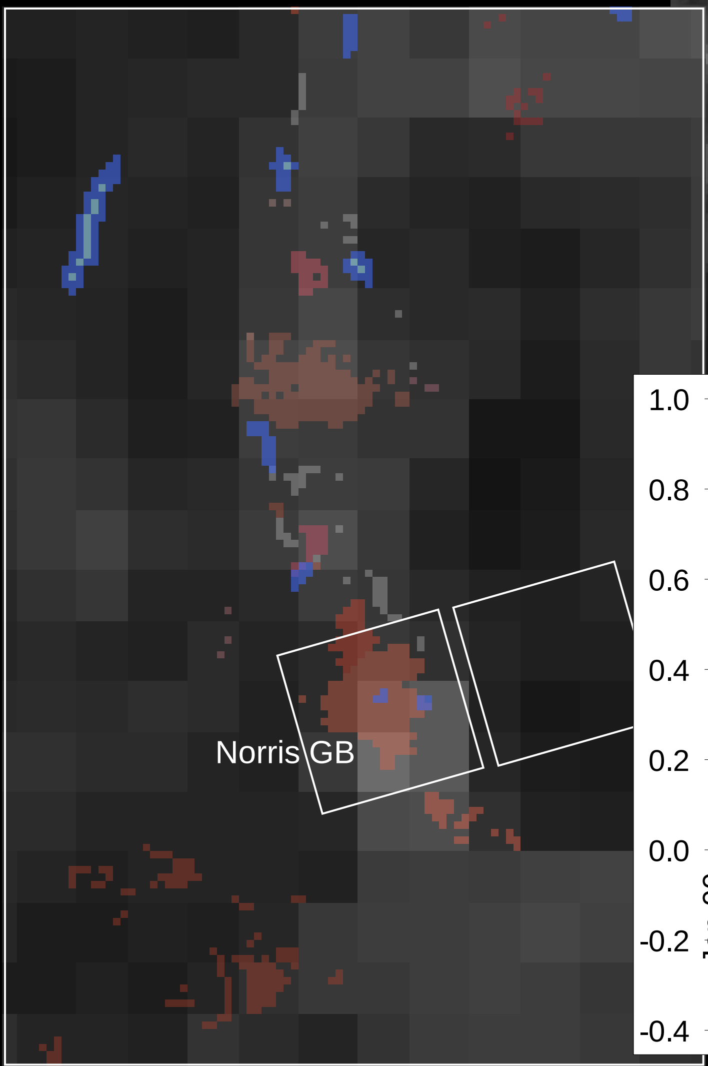

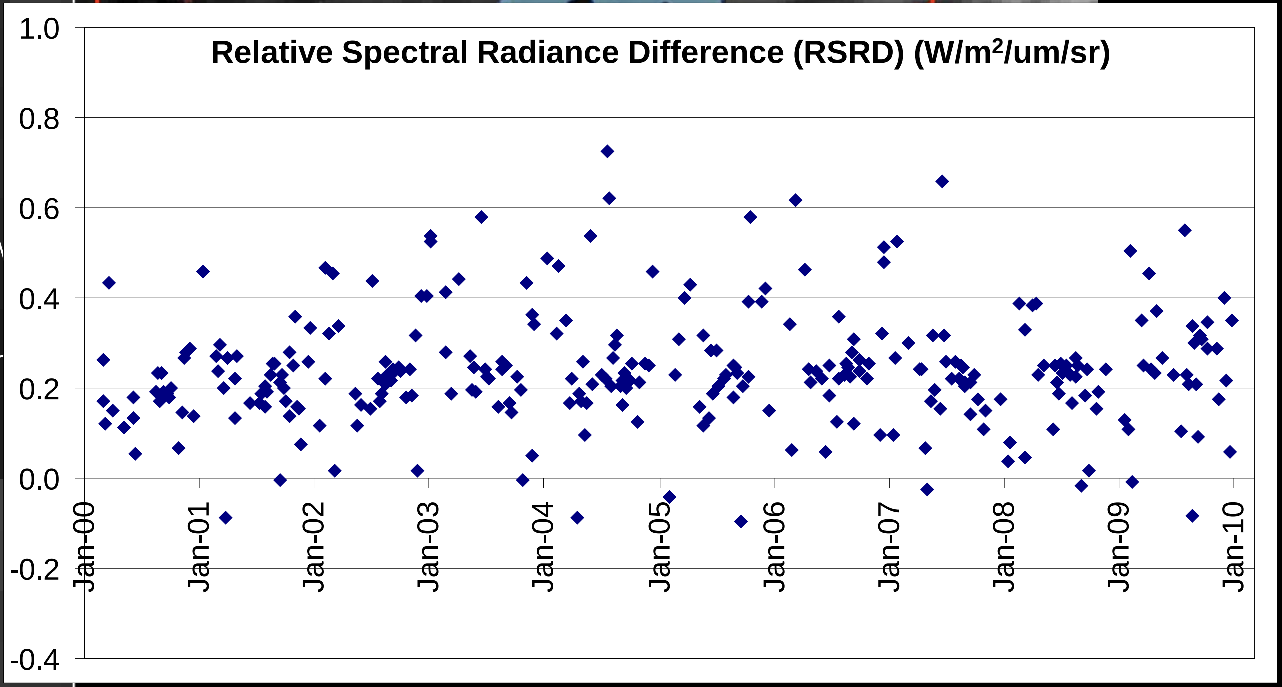

Yellowstone Geothermal Area

Midway Geyser Basin
Grand Prismatic
Spring & Excelsior
Geyser Crater

September 2006 – Day – 10.7 um

September 2007 – Day – 10.7 um

MASTER
45 m pixels

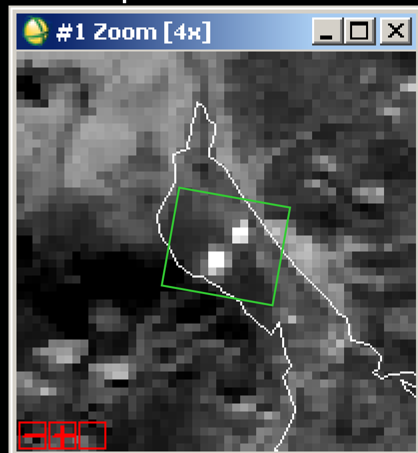

HyspIRI-sim
60 m pixels

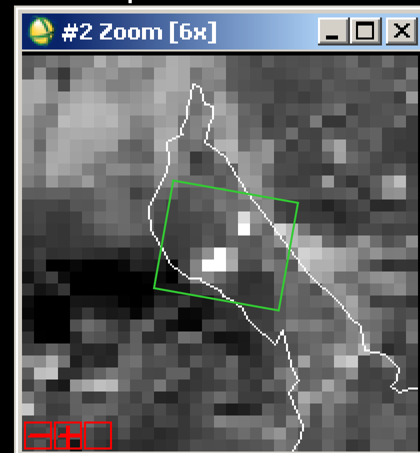

ASTER
90 m pixels

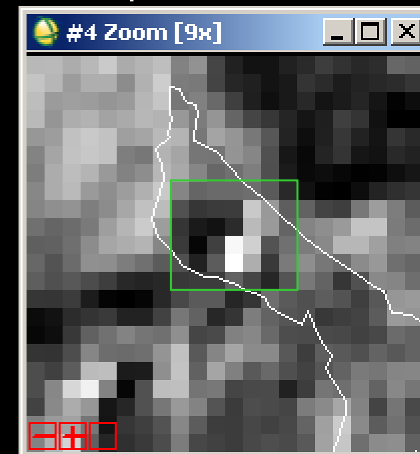

10.7 um	Max Temp (C)	Mean Temp (C)	Thermal Flux (MW)
MASTER 45-m	57	22	143
MASTER 60-m	56	21	142
ASTER 90-m	35	22	142

ROI area:
340,000 m^2

ASTER TIR radiance
90 m pixels

Mostly cloud-free
Night time Mosaic
Thermal areas in blue

<u>Total Geothermal Heat Flux</u>

From Cl^- flux measurements:
4.5 to 6.0 GW

From MODIS night time data:
1.7 to 2.2 GW

From ASTER night time data:
3.1 to 5.2 GW

From HyspIRI nighttime data:
I can't wait …

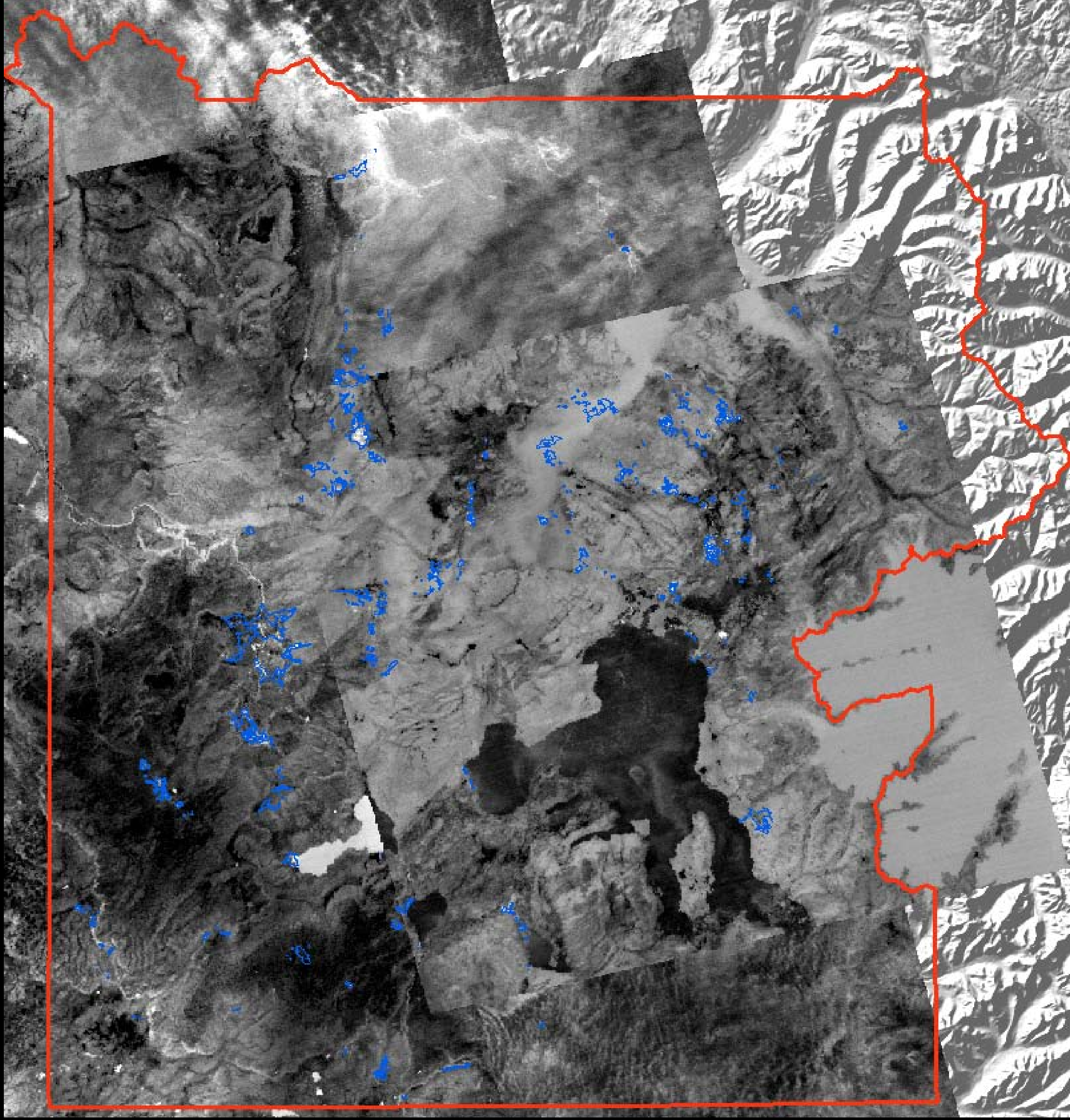

HyspIRI Dynamic Range

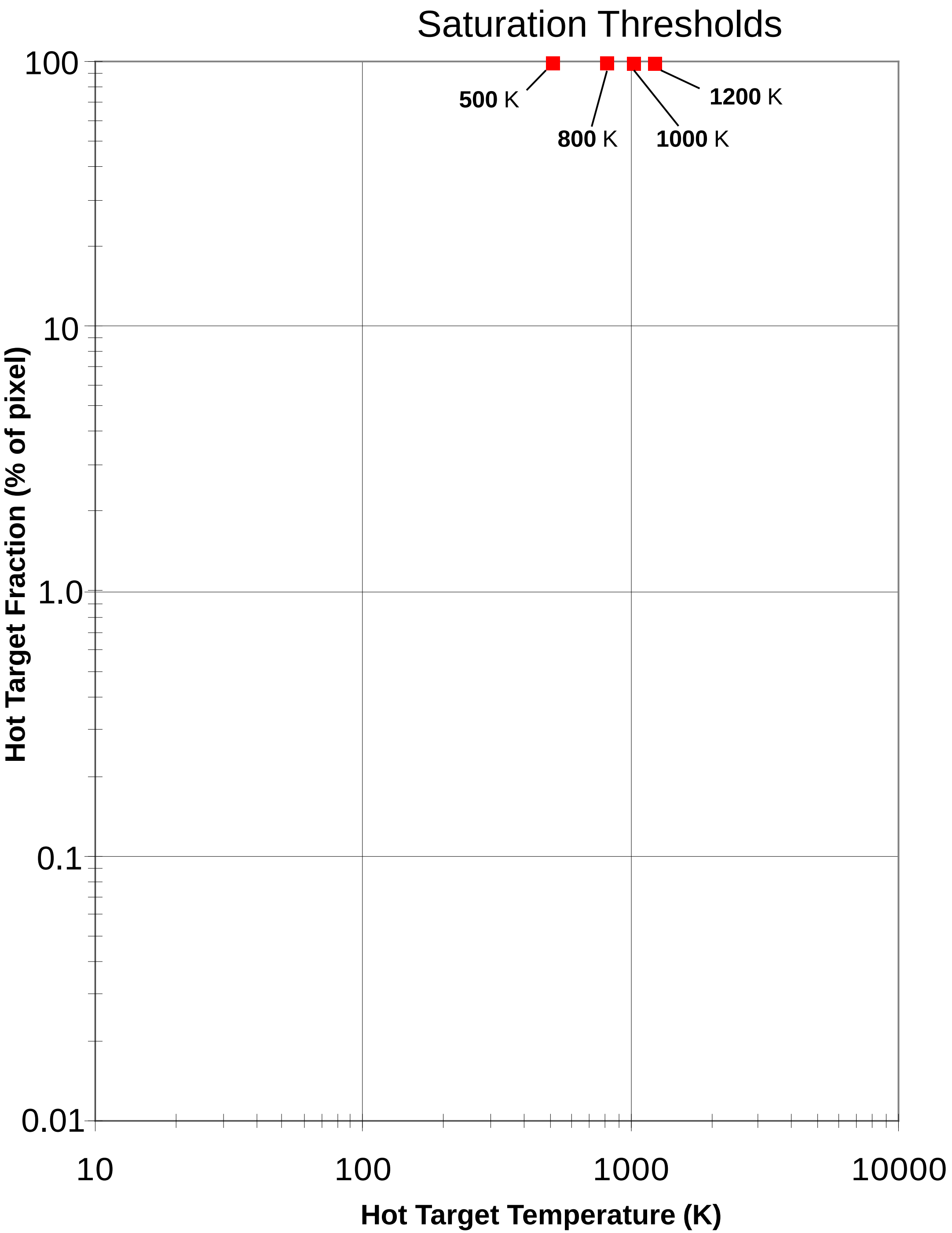

<u>Thermally Homogenous</u>
100% of pixel is a hot target. Obviously, in this case the saturation temperature will be the predefined maximum temperature.

If we set the max temperature of a certain TIR channel to a certain temperature, say 500 K, then if the total pixel integrated radiance corresponds to a temperature that exceeds this, you will have a saturated pixel.

HyspIRI Dynamic Range

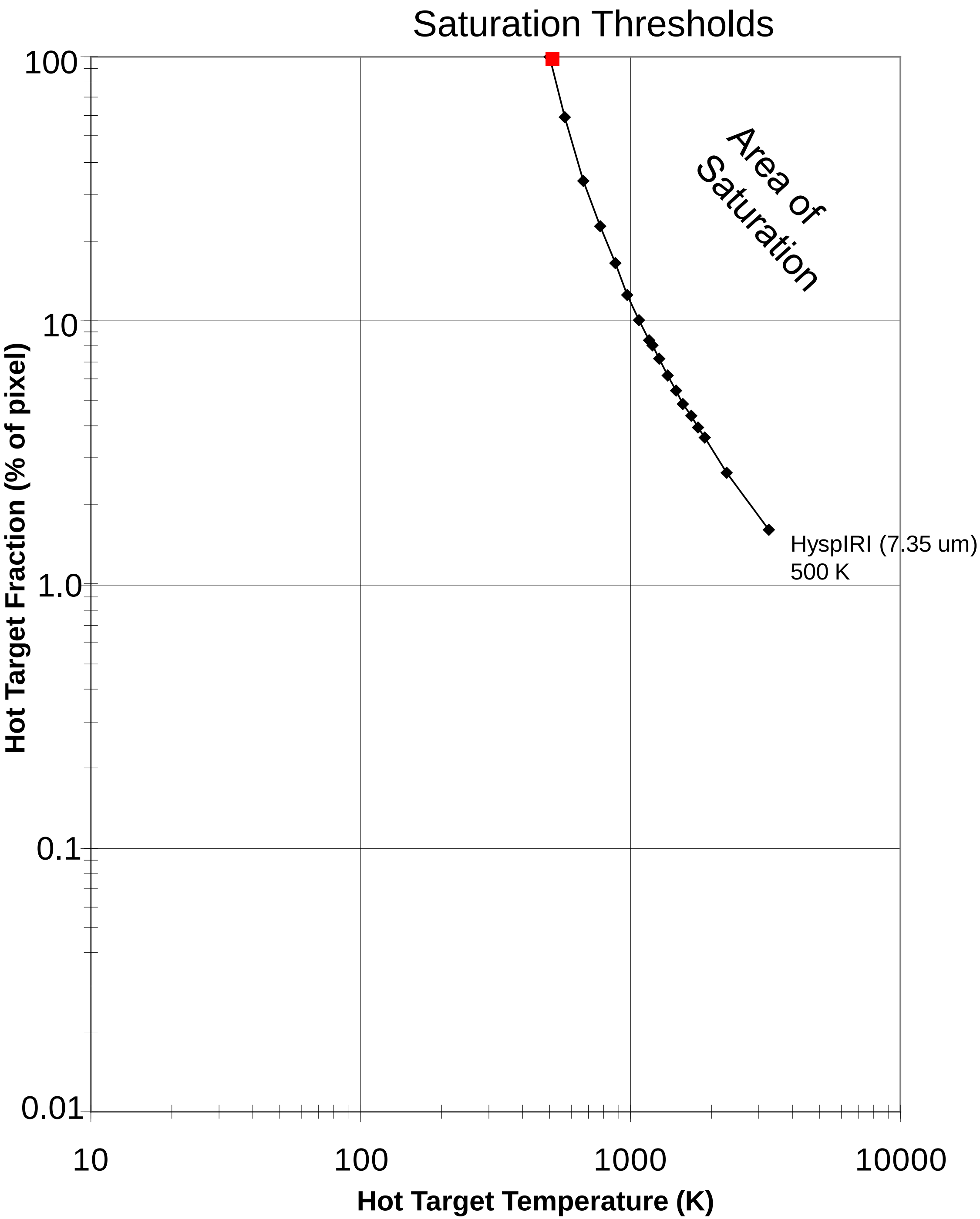

<u>Thermally Mixed</u>

if only a fraction of the pixel is hot target, and the rest is cooler background, then the saturation threshold will change.

<u>Saturation Thresholds</u>

For a range of hot target temps (with $T_{background}$=273 K) and target fractional areas, radiance values were calculated (ε=0.96) for each wavelength channel of interest.

For each Delta T ($T_{targ} – T_{bg}$), the % target area that resulted in a spectral radiance value corresponding to the saturation temperature for that channel defines the threshold curve.

HyspIRI Dynamic Range

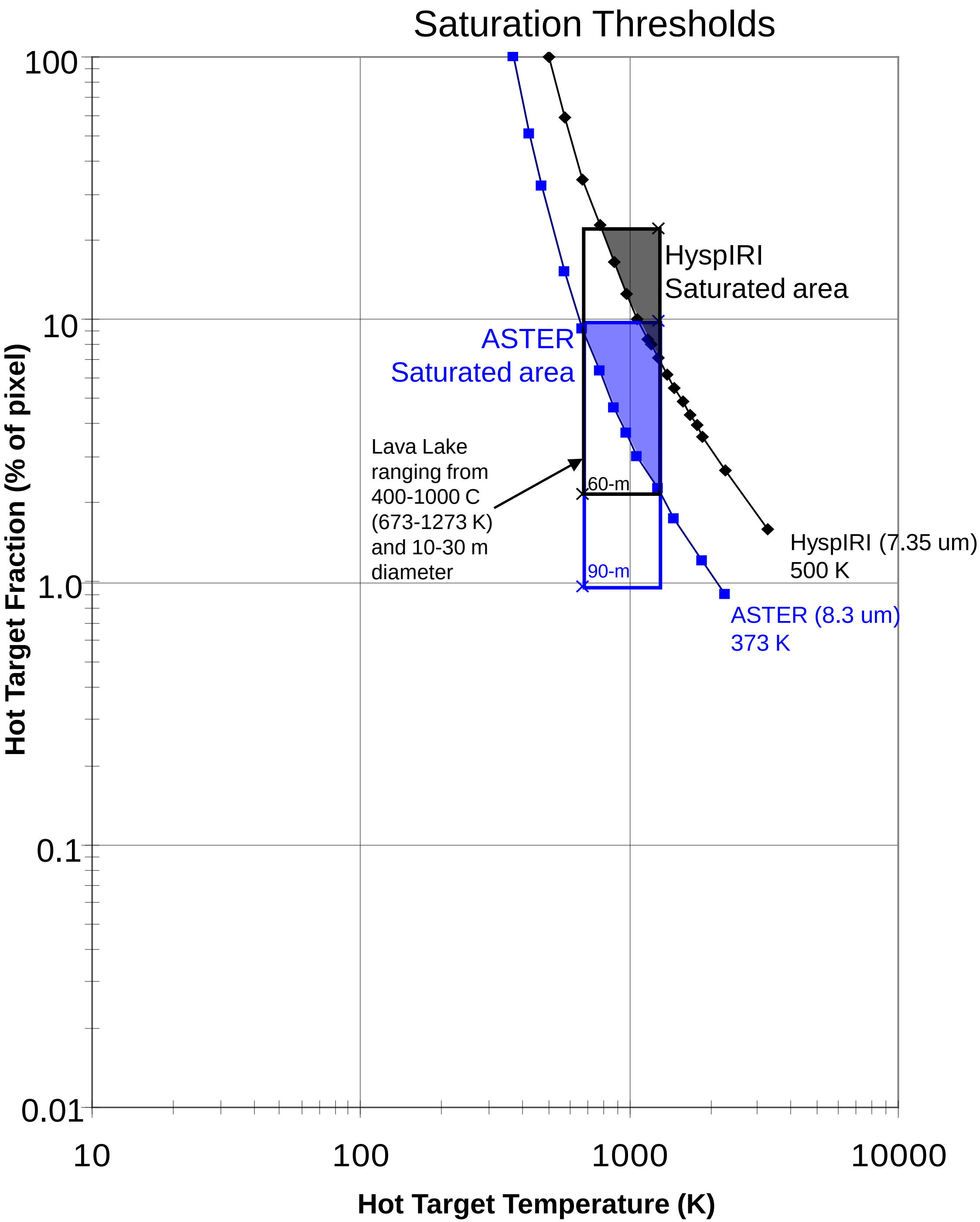

<u>Saturation Thresholds</u>

HyspIRI compared to ASTER

Trade-off between smaller pixels and higher saturation temperature

Overall improvement for HyspIRI

Less likely for HyspIRI to saturate over the same hot target than ASTER

HyspIRI Dynamic Range

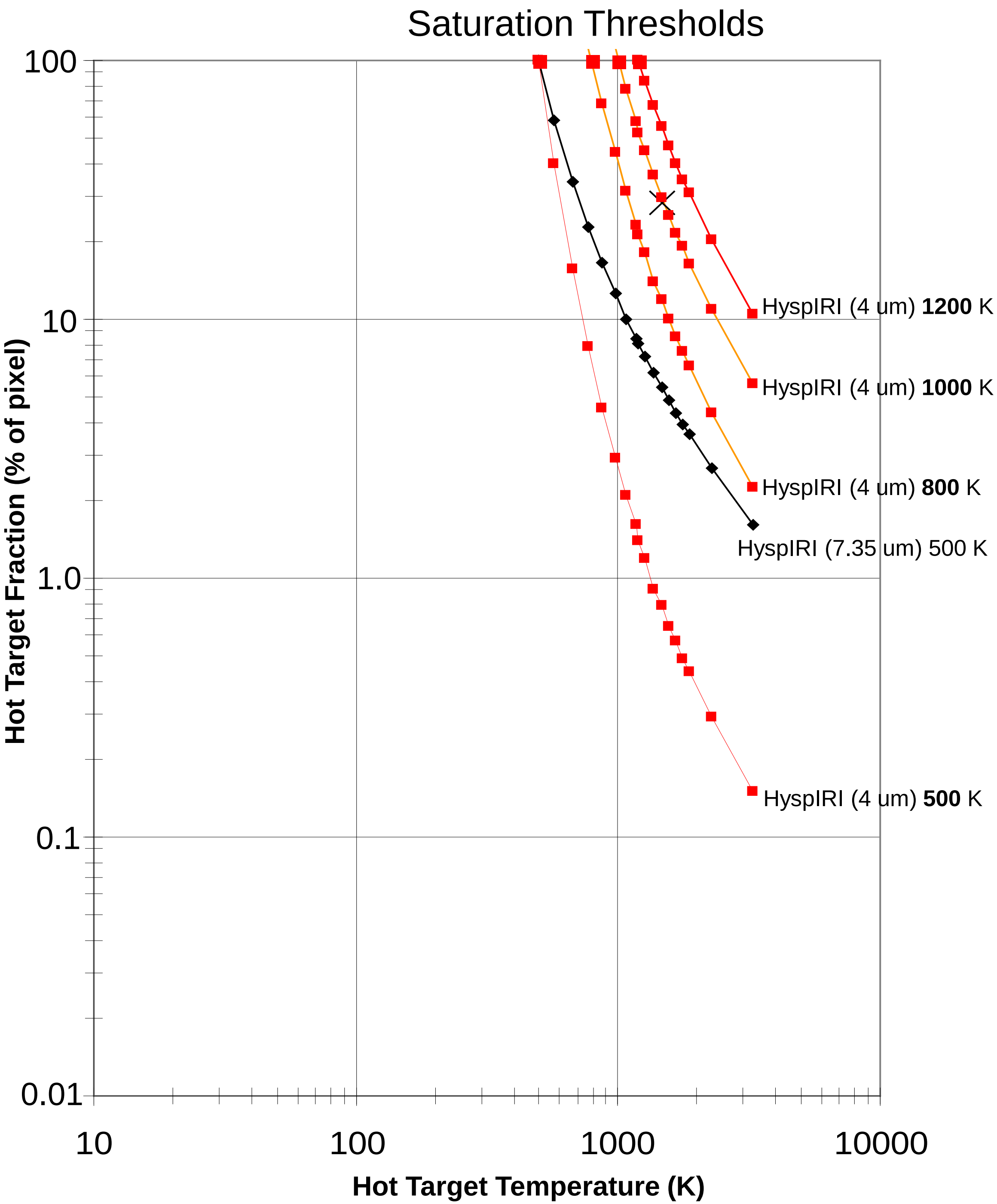

<u>Saturation Thresholds</u>

The MIR 4- um channel

At what temperature should the saturation be set?

If it’s too high (higher than any possible or expected temp / area conditions), then dynamic range is being wasted.

If it’s too low, then we will get saturated pixels over some very hot volcanic or fire targets, and the purpose of the 4-um channel is to characterize very hot targets, so saturation is to be avoided.

HyspIRI Dynamic Range

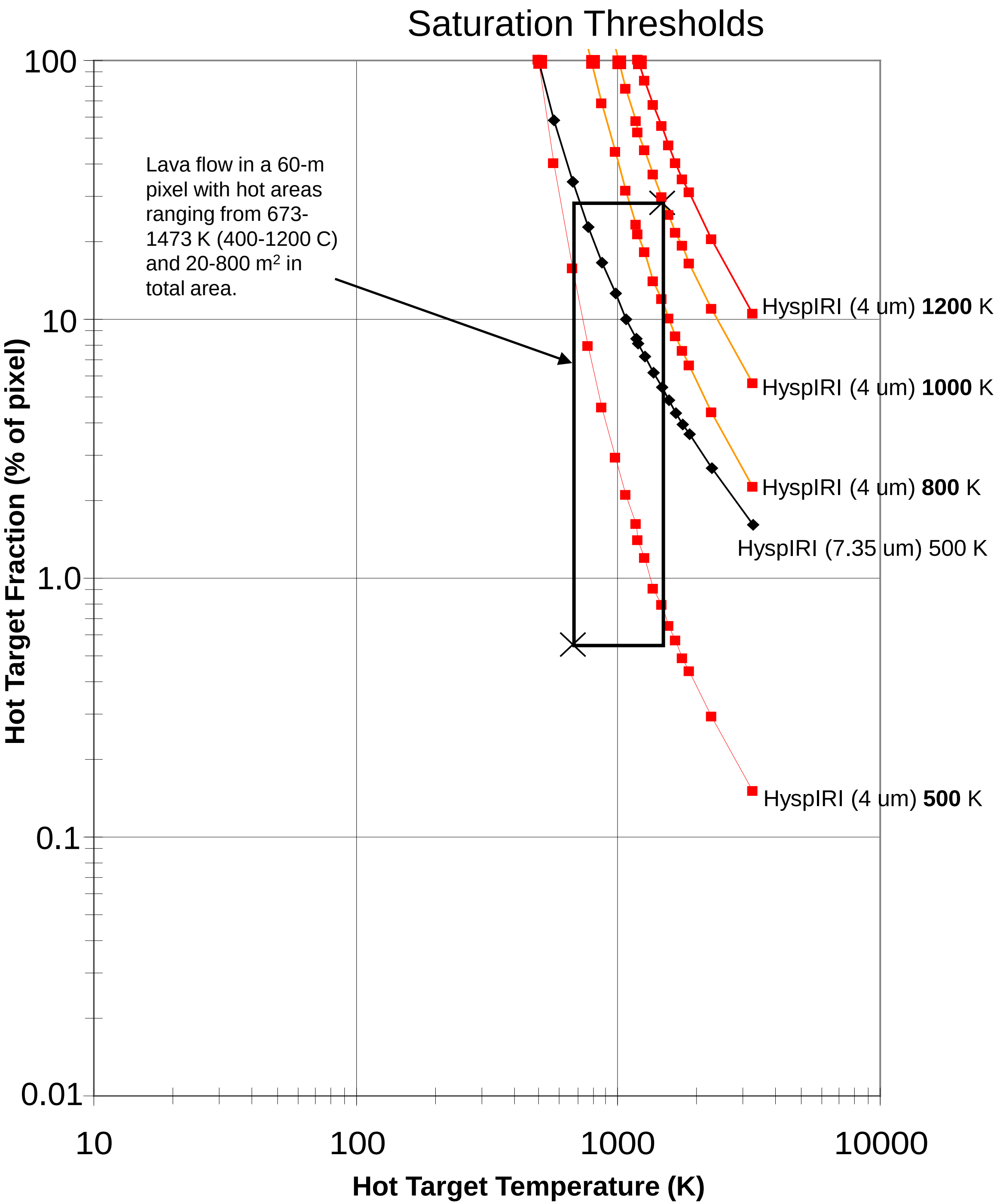

<u>Saturation Thresholds</u>

The MIR 4- um channel

At what temperature should the saturation be set?

Is a 1000-K saturation temperature good enough to cover the hottest likely volcanic features?

Some Concluding Thoughts

Pixel Size

The larger the pixels the less spatial information and the more sub-pixel thermal mixing. HyspIRI TIR data are comparable to ASTER TIR data, slightly better, but regardless of pixel size, you can model high temperature sub-pixel components very well with the wide wavelength separation of channels at the same spatial resolution.

Observation Frequency

Time series HyspIRI TIR data for continuous monitoring will be more like MODIS than ASTER, but with the sensitivity of ASTER – an important improvement.

Saturation

Compared to ASTER, HyspIRI TIR should be less likely to saturate over any given hot target. Having the 4-um channel with a saturation temperature of at least 1000 K to 1100K, a critical advantage.

Some Concluding Thoughts

1) How can we help predict and mitigate volcanic hazards through detection of transient thermal phenomena? (TQ1)

>> By the accurate characterization of transient thermal phenomenon (including spatial, temporal and thermal characteristics), which leads to hazard forecasting.

2) How do volcanoes signal impending eruptions through changes in surface temperature and thermal flux? (CQ3)

>> By exhibiting changes in surface temperature and thermal flux. And if we can measure these changes accurately in space, time, and magnitude, then we can use this information to help forecast volcanic hazards.

EXTRAS

HyspIRI Spectral Response

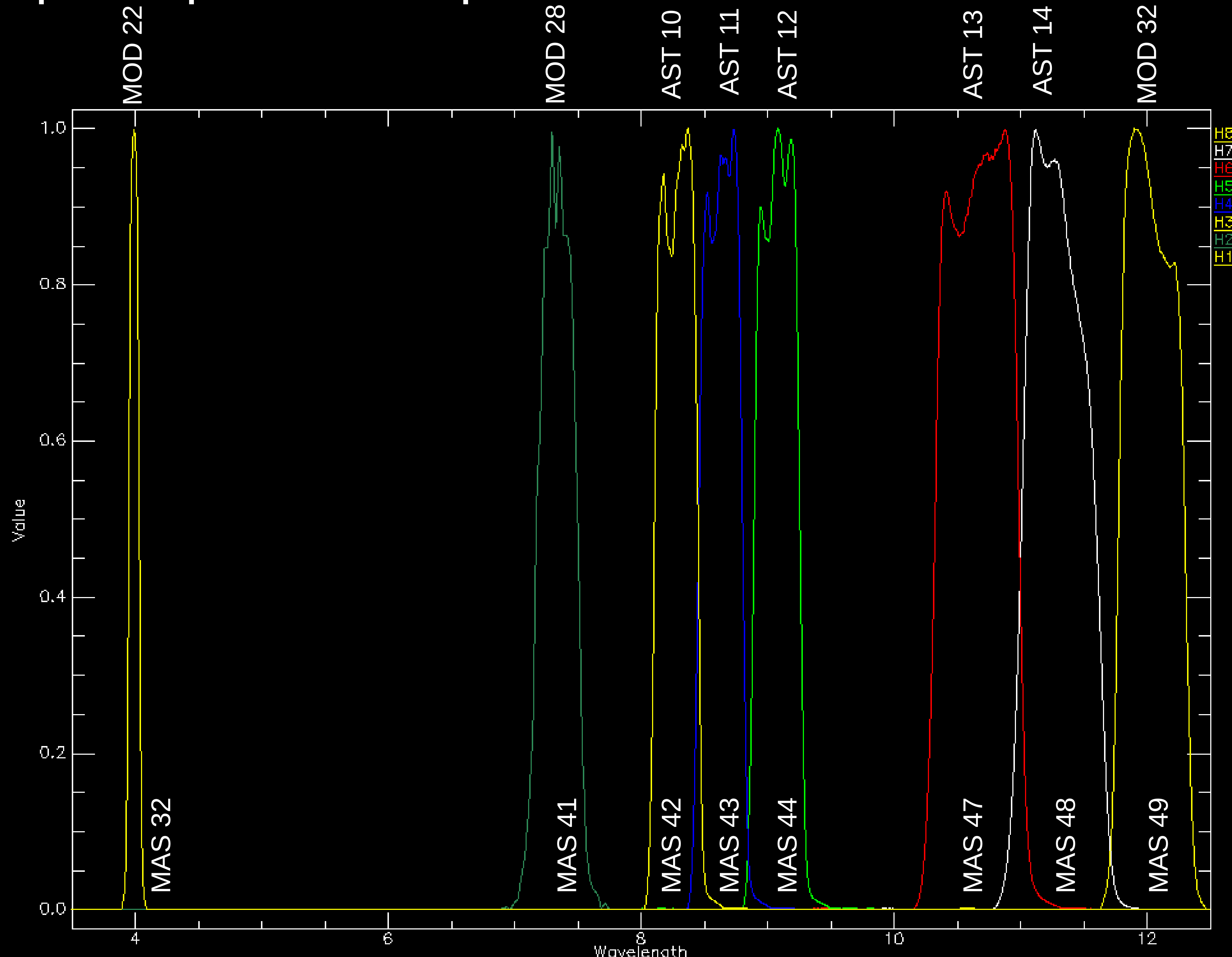

Hyperspectral – Infrared Imager (HyspIRI) Mission

Science Workshop 2010

HyspIRI Global Coverage, Data Management, and Downlink Approach

Michael Mercury
with contributions from the HyspIRI Team

National Aeronautics and Space Administration

Jet Propulsion Laboratory
California Institute of Technology
Pasadena, California

Ops Concept Overview

- Frequent Global Coverage:
  - VSWIR: 19 day global revisit
  - TIR: 5 day global revisit (1 day view + 1 night view)
  - 60 m resolution over land and shallow ocean
  - 1 km resolution over deep oceans, Greenland and Antarctica
- Tracking Network Meets Needs
  - Stations at Svalbard and Poker Flats
  - Existing capability for 800 Mbps dual-pol X band
  - Sufficient contacts to reduce SSR size to 1 Tb
- Regular On-Orbit Calibration of Instruments
  - VSWIR: Weekly Solar view + Monthly Lunar View
  - TIR: Monthly Lunar View + Black Body and Deep Space views
- Data Latency Does Not Drive System

VSWIR Ops:
- Pointing strategy to reduce sun glint
- Surface reflectance in the solar reflected spectrum for elevation angles >20
- Avoid terrestrial hot spots

National Aeronautics and Space Administration

Jet Propulsion Laboratory
California Institute of Technology
Pasadena, California

Key Requirements & Drivers

	Requirement	Status	Risk	Mitigation
Revisit	VSWIR: minimum every 19 days TIR: Minimum every 5 days	Met Met	None None	None None
Coverage	Global: TIR, VSWIR	Met	None	None
Data Rate	368 Mbps over land	Met	None	None
Data Volume	1.7 Pb per year	Met	None	None
SSR Size	Minimize it to reduce cost and risk.	Met with 1 Tb	Need to identify specific device	Identify specific device

All data and coverage requirements are met.

HyspIRI Global Coverage

- Due to the min 20 deg Sun elevation angle constraint on the VSWIR acquisition, the latitudes covered change with the seasons

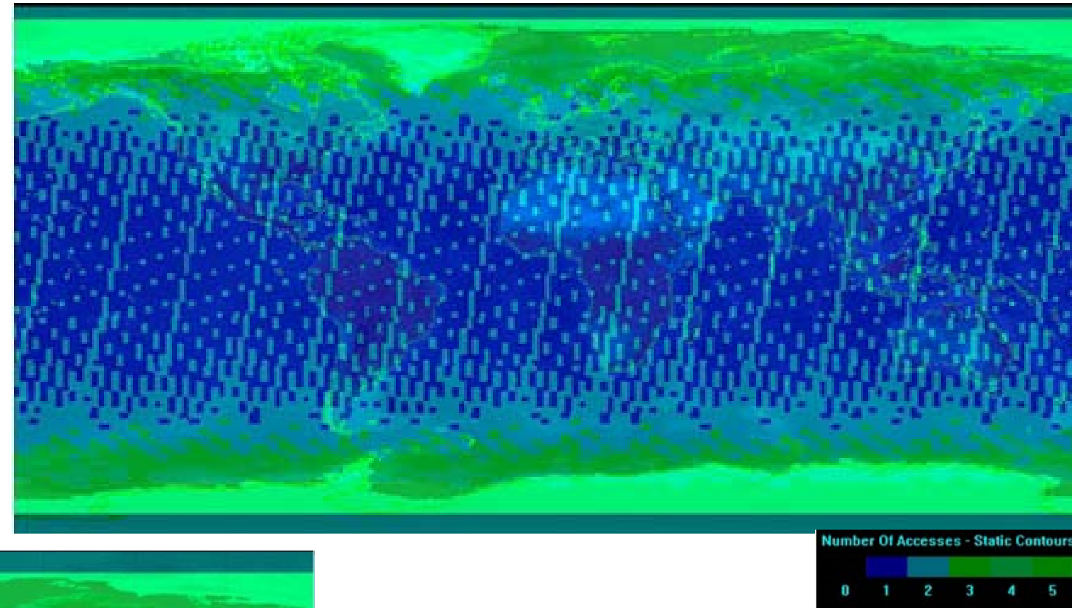

TIR Coverage after 5 days

VSWIR Coverage after 19 days

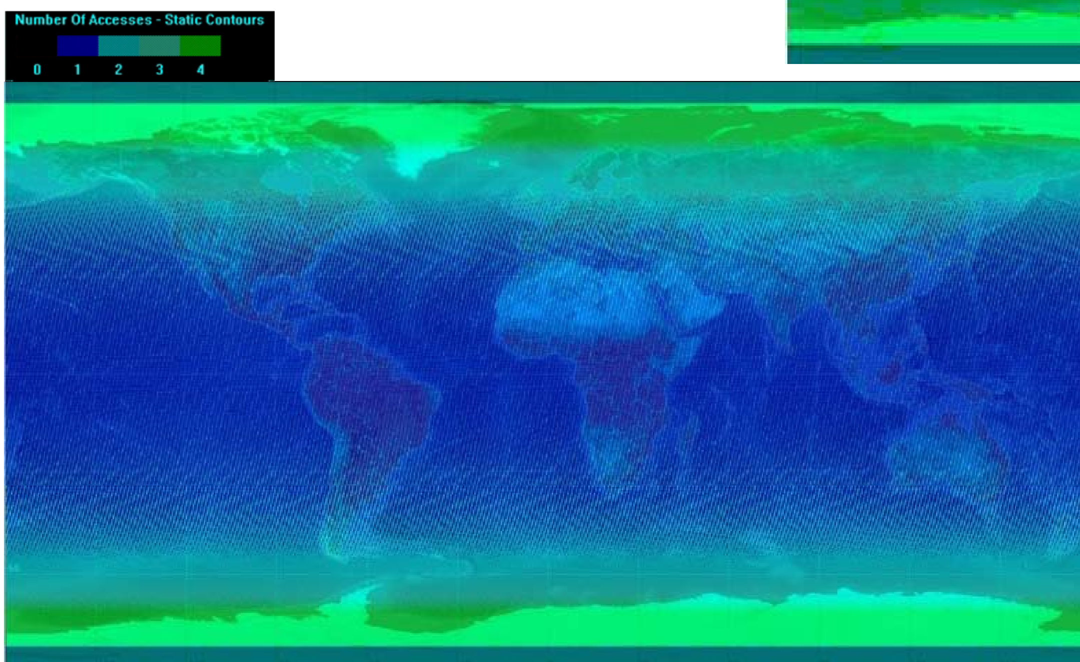

Swath Width Illustration

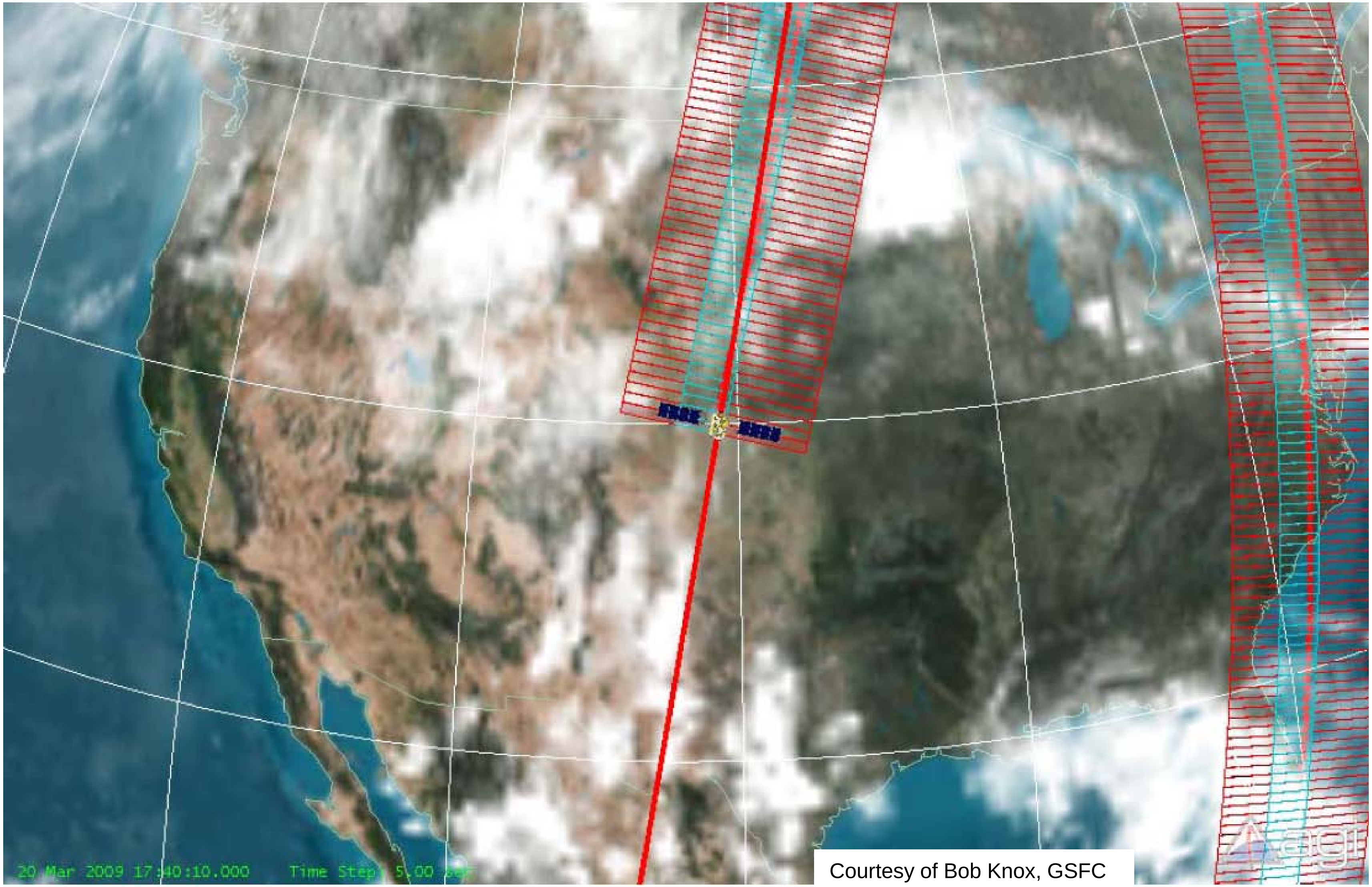

Courtesy of Bob Knox, GSFC

Coverage Video

Coverage Change with Seasons

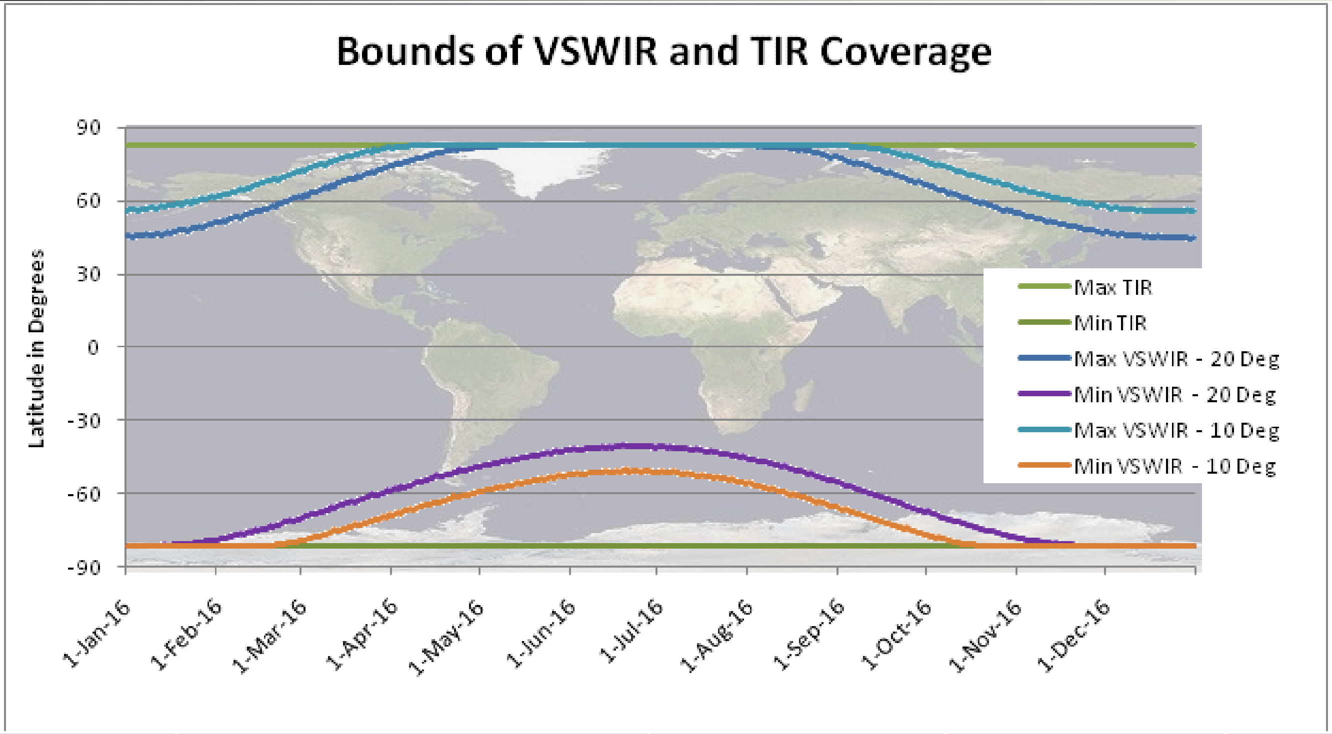

		VSWIR (20°)	VSWIR (10°)	TIR
Northern Hemisphere	Max Latitude [deg]	82.6	82.6	82.6
	Min Latitude [deg]	44.4	55.6	82.5
Southern Hemisphere	Max Latitude [deg]	-40.1	-50.1	-81.7
	Min Latitude [deg]	-81.8	-81.8	-81.8

Example Orbit

- Instrument modes change multiple times each orbit, but are clearly defined by geography and spacecraft location

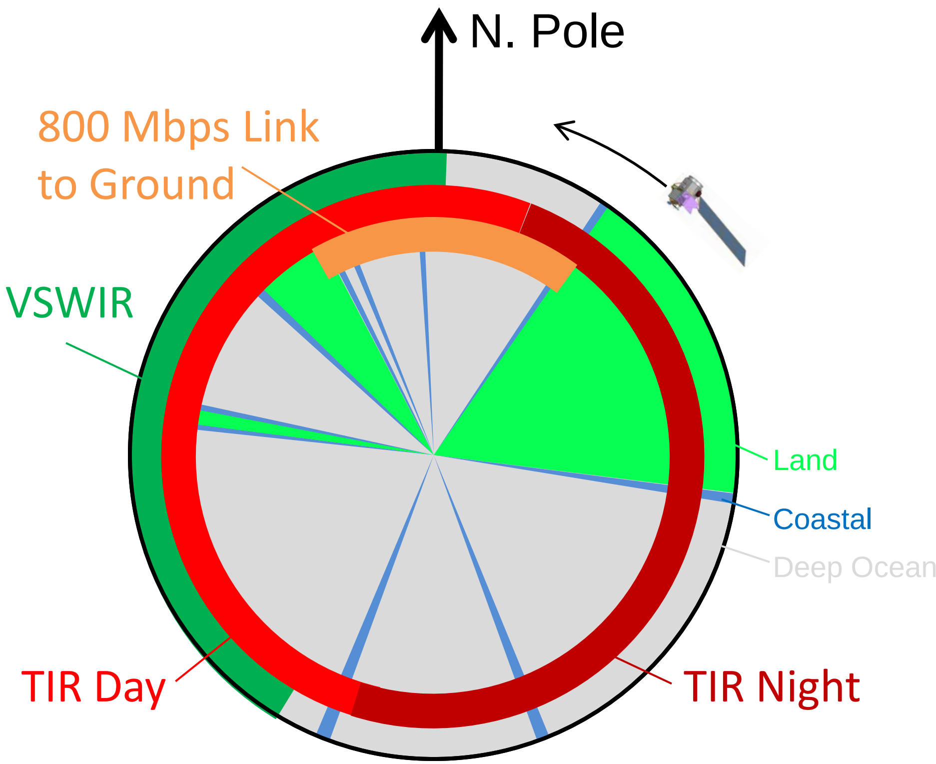

Cut away of earth with slice taken along plane of orbit

Imaging Mode

Instrument	Land	Coastal	Deep Ocean	Greenland	Antarctica
VSWIR	60 m	60 m	1 km	1 km	1 km
TIR	60 m	60 m	1 km	1 km	1 km

Target Map

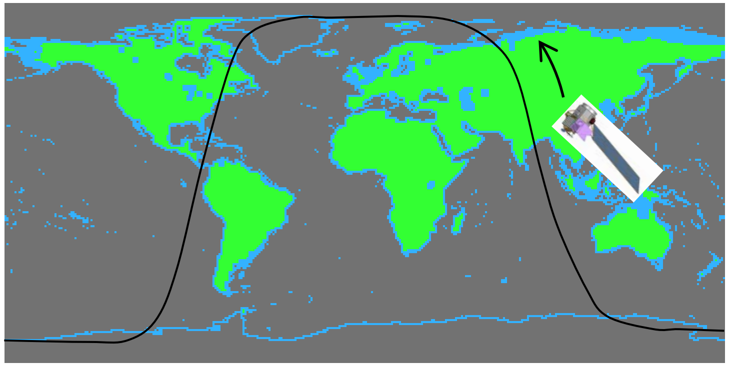

Duty Cycles

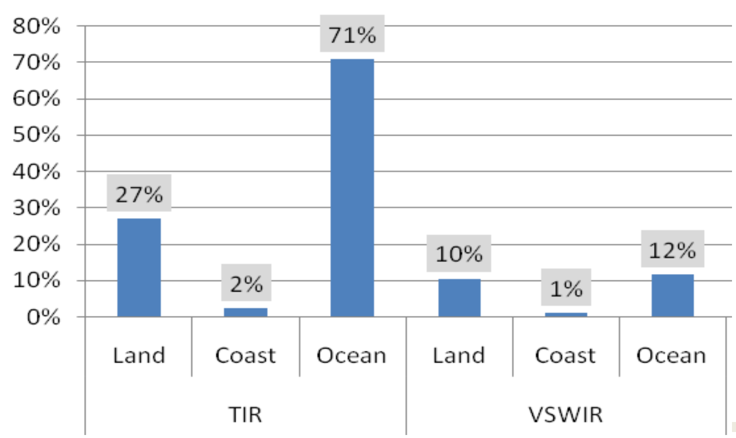

Data Volume Analysis

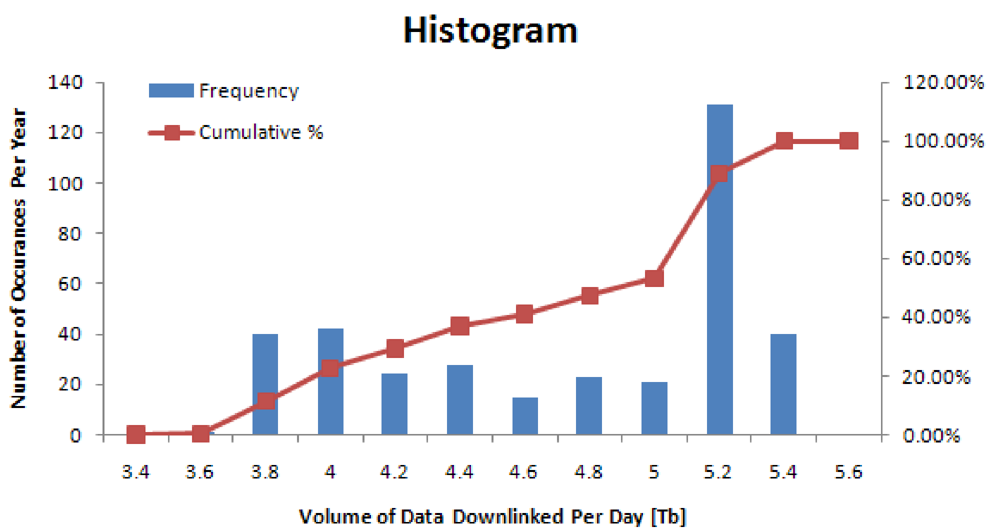

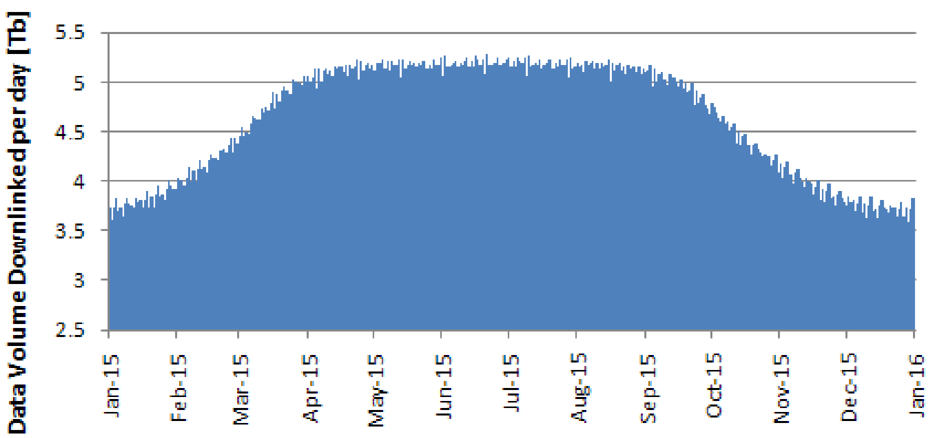

	Rate (Mbps)	On-board Compression
VSWIR: land	804.1	3:1
VSWIR: shallow	865.9	3:1
VSWIR: ocean	3.9	3:1
TIR: land	130.2	2:1
TIR: shallow	130.2	2:1
TIR: ocean	0.6	2:1

	Avg (Tb)	Min (Tb)	Max (Tb)
Per Day	4.64	3.59	5.29
Per Orbit	0.31	0.00	0.81

Total data volume for the 3 year mission: 5024 Tbits

SSR Sizing

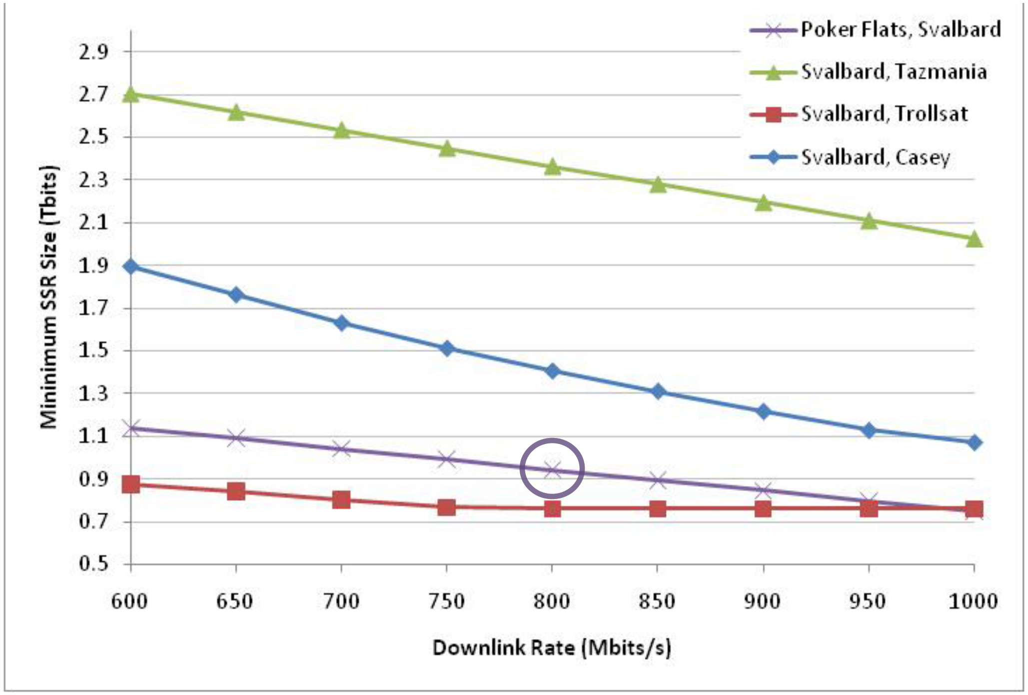

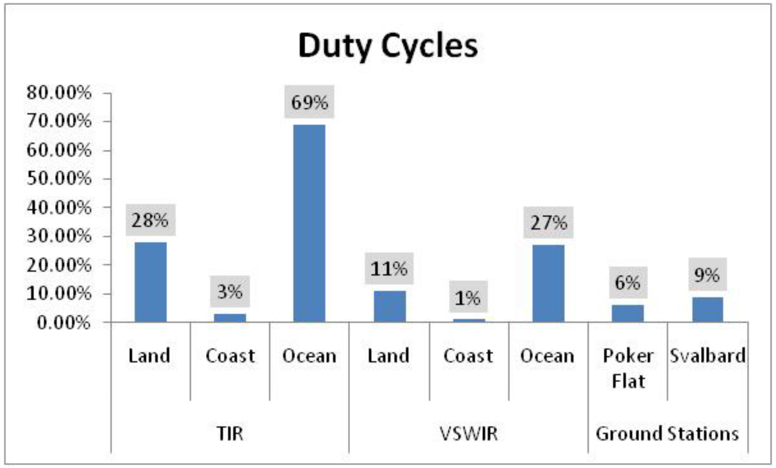

	Rate	On-board Compression
VSWIR_land	804.1 Mb/s	3:1
VSWIR_shallow	865.9 Mb/s	3:1
VSWIR_ocean	3.9 Mb/s	3:1
TIR_land	130.2 Mb/s	2:1
TIR_shallow	130.2 Mb/s	2:1
TIR_ocean	0.6 Mb/s	2:1

- 5° ground station mask
- 10 second acquisition time
- Any pass shorter than 250 seconds (incl. acquisition time) is not used
- 20 Deg VSWIR sun illumination angle constraint

Wrap Factors	
Contingency	30%
Overhead	10%

Ground Station Options

Stations (Dlink rate Mbps)	# passes per year	# of passes per day	SSR Size [Tb]	Minimum Pass Duration [min]
Svalbard (800)	4783	13.1	2.6	4
Svalbard (800)	5398	14.8	2.2	0.5
Svalbard (800) + Poker Flat (800)	5879	16.1	1.9	8
Svalbard (800) + Poker Flat (800)	7375	20.2	1.3	6
Svalbard (800) + Poker Flat (800)	8375	22.9	0.9	4
Svalbard (800) + Poker Flat (800)	9106	24.9	0.9	0.5

Link Assumptions

Spacecraft To Ground

- 800 Mbps dual-pol X band to Poker Flat and Svalbard
- Analysis performed over one year of data
  - Assumes a 5 degree elevation mask at each ground station
  - Assumptions for contact threshold
    - 10 s acquisition time subtracted from each access
    - Throw out any contacts that are shorter than 4 minutes (after 10 s acquisition is subtracted)
- 1.67 Petabits of data must be downlinked each year
- Require 8375 contacts per year of varying duration (in minutes)
  - Minimum: 4, Maximum: 10.5, Mean: 10.4

Ground to Ground

- All data needs to be transferred to a science data processing center at JPL within 2 weeks of downlink
- Occasional high priority requests for a limited volume of regional data to JPL within 6-48 hours of downlink

Managing Data Volume

Robust On-Board Storage

- On-board storage capacity
  - 1 Tb
    - 0.33 Tb/orbit
  - WorldView-1 and -2 have 2.2 Tb SSR
    - WorldView1: 0.33 Tb/orbit
    - WorldView2: 0.52 Tb/orbit
- 30% margin added to calculated required SSR size

Robust Downlink Design

- Downlink method
  - 800 Mbps, dual-pole X-band to Svalbard and Poker Flat (KSAT)
    - WorldView-1 and GeoEye-1 use similar downlink architecture
- Ground communications / latency
  - Back end infrastructure does not need upgrading to ensure timely delivery of data

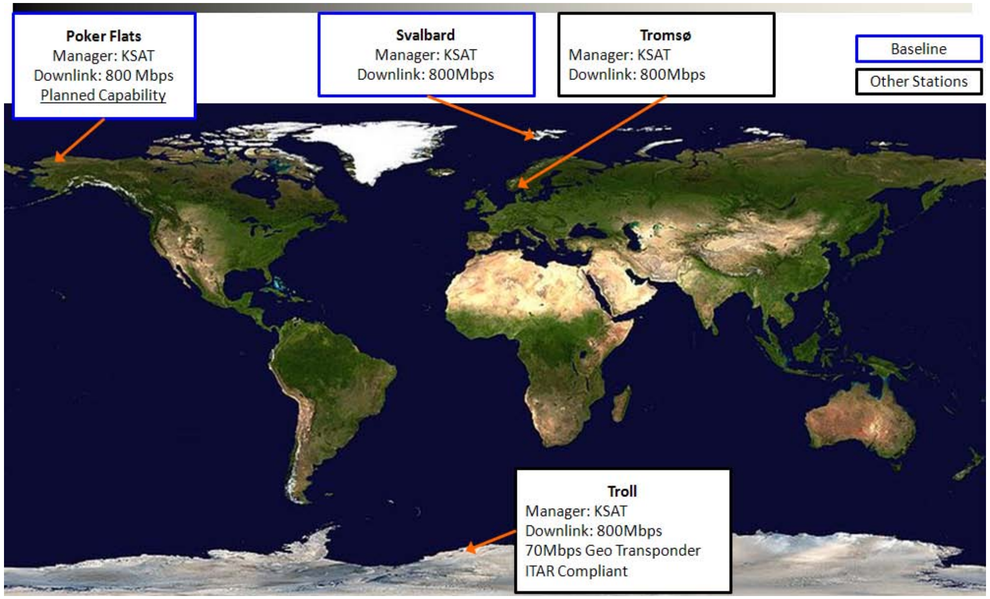

Summary

All Coverage, data management and downlink requirements met with baseline architecture:

- Revisit and Coverage:
  - 626 km altitude with VSWIR 150 km swath and TIR 600 km swath
- Data Rate / Data Volume / SSR Size
  - Svalbard and Poker Flat provide enough accesses to get down all 1674 Tb per year with a minimized SSR size

BACK UP

Crude Sanity Check on Data Volume

		VSWIR			TIR		
	Units	Land	Coast	Ocean	Land	Coast	Ocean
Uncompressed Data Rate	Mbps	804	866	4	130	130	1
Compression Factor		3	3	3	2	2	2
Compressed Data rate	Mbps	268	289	1	65	65	0.3
Duty Cycle	%	11%	1%	27%	28%	3%	69%
Data Volume Per Orbit	Tb	0.17	0.01	0.002	0.11	0.01	0.001
Total Data Volume Per Orbit	Tb	0.30					
Orbits Per Day		14.8					
Data Volume per Day	[Tb]	4.5					
Data Volume Per Year	[Tb]	1630					
Downlinks Per Year		8375					
Avg Downlinks Per Orbit		1.5					
Avg Downlink Duration	sec	621					
Downlink Rate	Mbps	800					
Available Downlink Vol.	Tb/year	4162.911					

VSWIR Solar Constraint

- 800 Mbps dlink to Troll and Poker Flat

VSWIR min Solar illumination angle [deg]	Mission Data Volume [Tb per year]	VSWIR Land Duty Cycle [%]	VSWIR Ocean Duty Cycle [%]	SSR Size for no missed ground stations [Tb]
10	1904	13	27	1.0
20	1675	11	25	1.0
Difference	**229 (12 %)**	**2 (15%)**	**2 (7%)**	**0 (0%)**

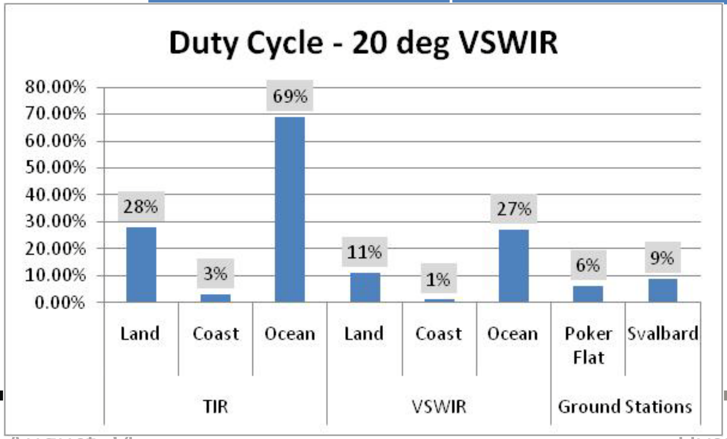

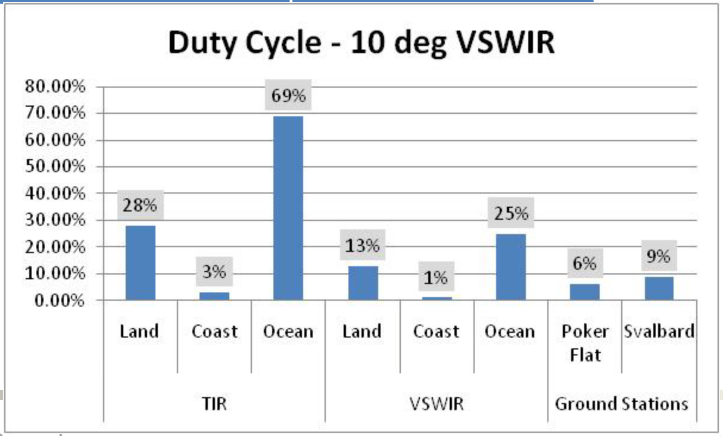

Swath Overlap Calculation

VSWIR

Calculation Direction

starting at repeat	starting at swath with			
140.9436506	150.5	km	swath width	crosstrack
142.2954768	151.9435	km	swath with along the equator	
6378	6378	km	radius of earth at equator	
40074.15589	40074.16	km	circumference at equator	
281.626351	263.7438	passes	number of passes to get full coverage	
5829	5829	sec per orbit		
86400	86400	sec per day		
14.82243953	14.82244	orbits per day		
14.82243953	14.82244	passes per day		
19	17.79355	days to cover (with one view of equator per orbit)		
Required to meet current requirements	Current Baseline			

6.35%of a swath Overlap between swaths

TIR

Calculation Direction

starting at repeat	starting at swath with			
535.5859	599.5	km	swath width	crosstrack
540.7228	605.25	km	swath with along the equator	
6378	6378	km	radius of earth at equator	
40074.16	40074.16	km	circumference at equator	
74.1122	66.21092	passes	number of passes to get full coverage	
5829	5829	sec per orbit		
86400	86400	sec per day		
14.82244	14.82244	orbits per day		
14.82244	14.82244	passes per day		
5	4.466938	days to cover (with one view of equator per orbit)		
Required to meet current requireme nts	Current Baseline			

10.66%of a swath Mean overlap between swaths

The North American ASTER Land Surface Emissivity Database (NAALSED) Version 3.0

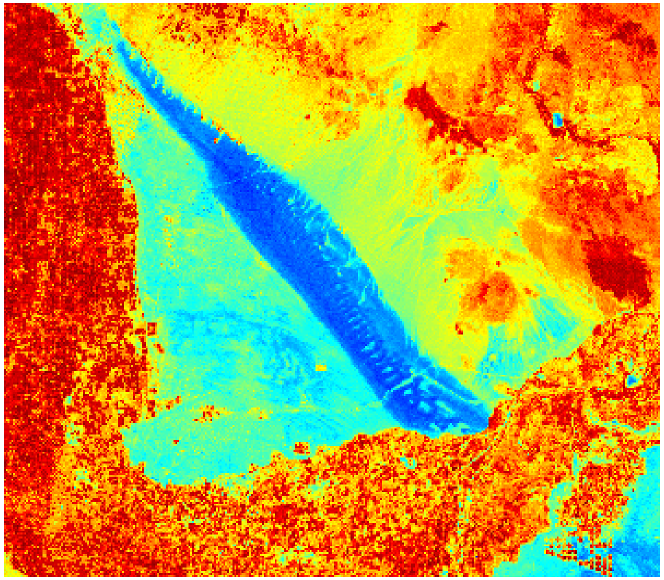

Glynn Hulley, Simon Hook

Jet Propulsion Laboratory, California Institute of Technology, Pasadena, CA

HyspIRI Science Workshop, Pasadena, CA, 24-26 August 2010

HyspIRI TIR Land Surface Temperature (LST) and Emissivity Relevance

- Physical: Emissivity error 1.5% = 1 K LST error
- Split-window: Emissivity error 0.5% = 1 K LST error
- LST Required for:
  - Measurements of fire parameters (Giglio, Csaszar)
  - Evapotranspiration models (Anderson)
  - Ecosystem function and Biodiversity (Asner, Townsend, Serbin, Roberts)
  - Modeling Urban heat islands (Weng)
  - Volcano monitoring, lava flows (Abrams, Realmuto, Vaughan, Wright)
  - Climate models (CDR’s) (Huemmrich, Minnett)
  - Surface composition, soil moisture (Ramsey, Scheidt)

Station Fire, Angeles National Forest, California

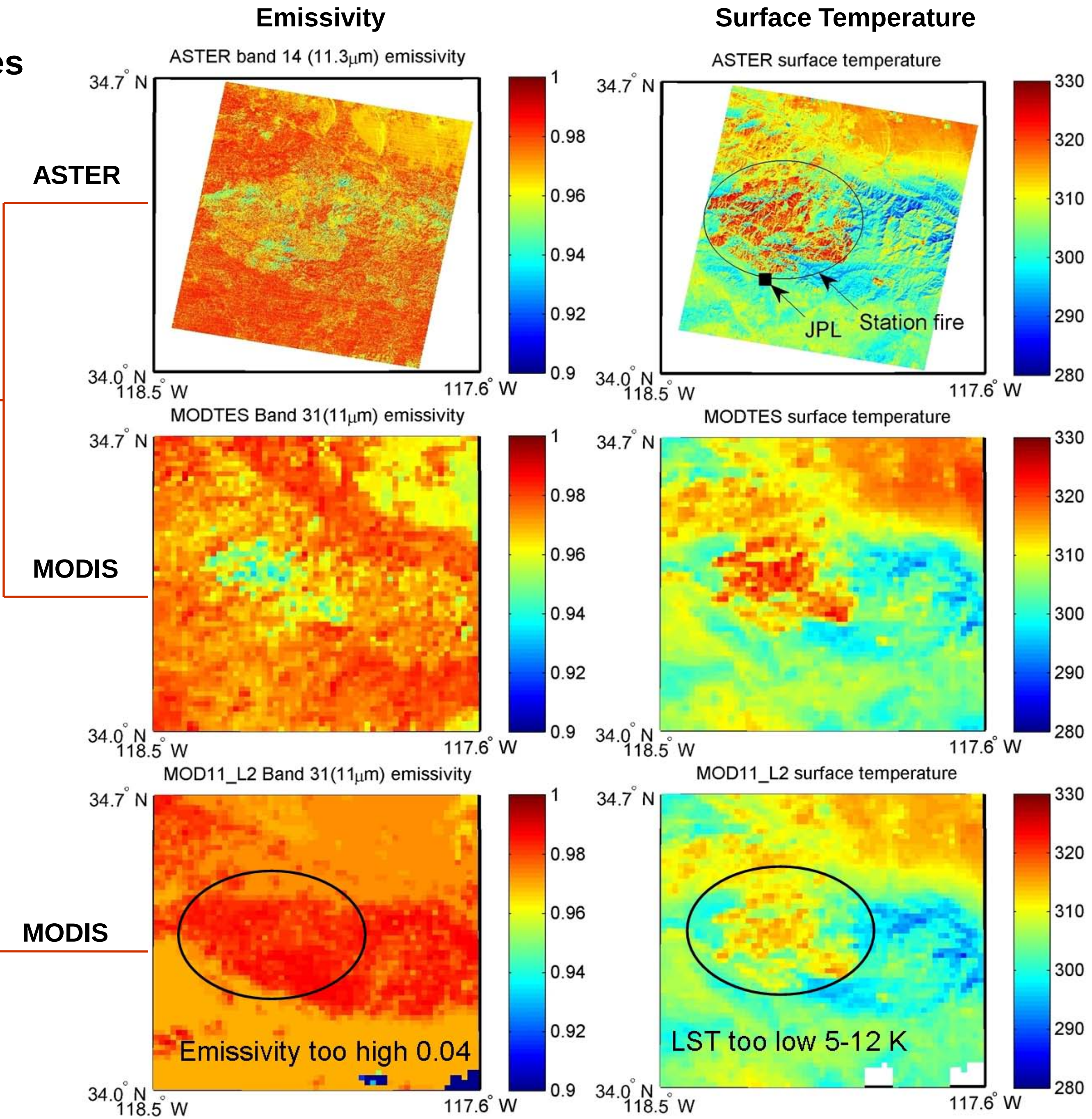

Temperature Emissivity Separation (TES) Algorithm

- Physical retrieval of LST and emissivity
- ASTER standard products

MODIS Split-window

- Emissivity assigned according to land cover classification
- Does not capture dynamic land cover changes

HyspIRI TIR Product ATBD’s

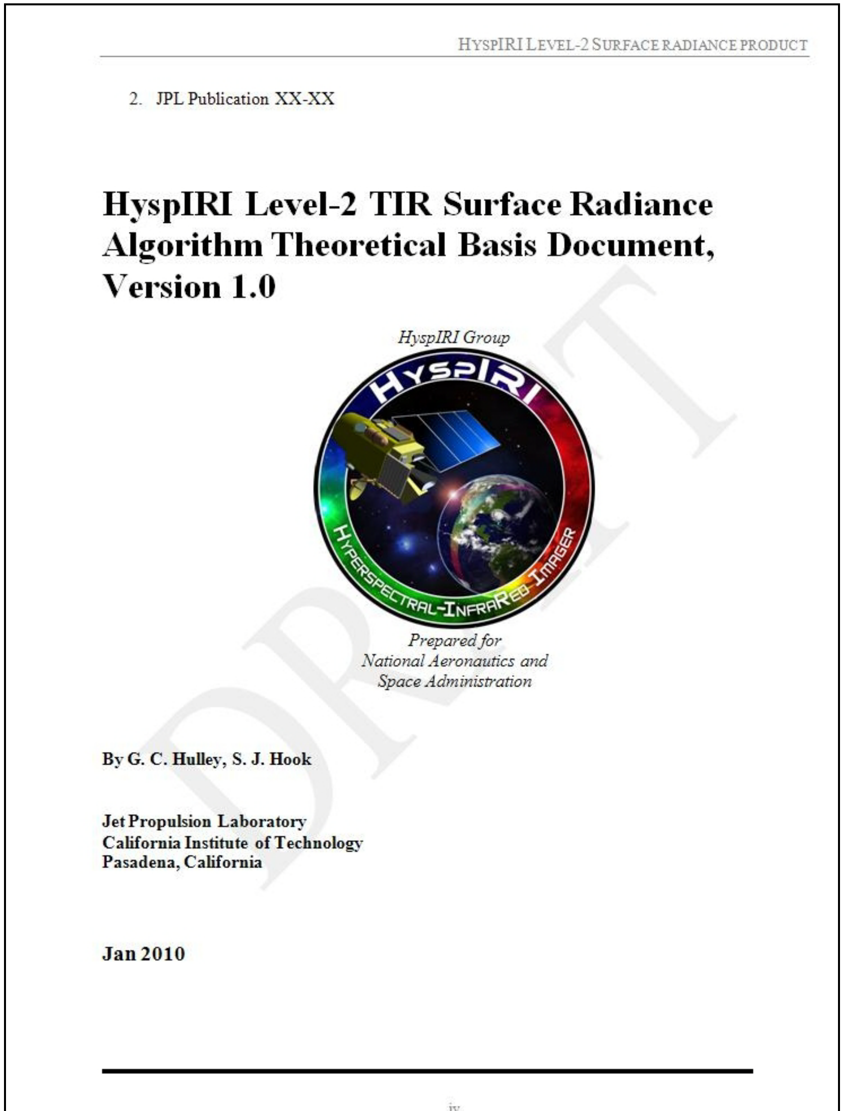

HYSPIRI LEVEL-2 SURFACE RADIANCE PRODUCT

2. JPL Publication XX-XX

HyspIRI Level-2 TIR Surface Radiance Algorithm Theoretical Basis Document, Version 1.0

HyspIRI Group

Prepared for
National Aeronautics and
Space Administration

By G. C. Hulley, S. J. Hook

Jet Propulsion Laboratory
California Institute of Technology
Pasadena, California

Jan 2010

iv

HYSPIRI LEVEL-2 SURFACE RADIANCE PRODUCT

2. JPL Publication XX-XX

HyspIRI Level-2 TIR Land Surface Temperature and Emissivity Algorithm Theoretical Basis Document, Version 1.0

HyspIRI Group

Prepared for
National Aeronautics and
Space Administration

By G. C. Hulley, S. J. Hook

Jet Propulsion Laboratory
California Institute of Technology
Pasadena, California

Jan 2010

iv

ASTER and HyspIRI TIR Product Characteristics

	ASTER	**HyspIRI**
Satellite	Terra (2000)	Expected launch: 2021+
Calibration	<0.3 K	<0.2 K
LST&E Algorithm	TES Calibration Curve	TES Calibration Curve
Atmospheric Correction	Water Vapor Scaling + MODTRAN	Water Vapor Scaling + MODTRAN
LST Product Accuracy	1.5 K	1 K
Product versions	Version 3	n/a
Temporal sampling	16 day repeat (1030 AM/PM)	5 day repeat (1030 AM/PM)
Spatial resolution	90 m	60 m
Spectral resolution	5 TIR bands (8-12 μm)	8 TIR bands (4-12 μm)
Swath Width	60 km	600 km

The North American ASTER Land Surface Emissivity Database (NAALSED)

Mapping Earth's emissivity at 100 m

- ASTER produces L-2 LST/emissivity products at 90m (AST 05, 08)
- Scenes (60 x 60 km) produced on demand, limited repeat (16 days) => no L-3 gridded datasets!
- **Solution:** Produce an ASTER seasonal surface emissivity map for North America (NAALSED) and extend to Global product
  - Summertime (Jul-Sep), 2000-2009
  - Wintertime (Jan-Mar), 2000-2009
- Applications:
  - ➢ Evaluating emissivity products from coarser resolution sensors: eg. MODIS (5 km), AIRS (45 km)
  - ➢ Geological mapping and resource exploration
  - ➢ Inputs to Climate and Ecology Models
  - ➢ Validation dataset and simulation of future sensors, eg. HyspIRI
  - ➢ Generate a long-term LST climate data record from Landsat

http://emissivity.jpl.nasa.gov

Jet Propulsion Laboratory
California Institute of Technology

+ View the NASA Portal

JPL HOME | EARTH | SOLAR SYSTEM | STARS & GALAXIES | TECHNOLOGY

North American Land Surface Emissivity Project

Home | Order | Publications | Validation | Examples | USCRN | Links

Log in

You are here: Home

Navigation

- Home
- Order
- Publications
- Validation
- Examples
- USCRN
- Links

« June 2010 »

Mo	Tu	We	Th	Fr	Sa	Su
	1	2	3	4	5	6
7	8	9	10	11	12	13
14	15	16	17	18	19	20
21	22	23	24	25	26	27
28	29	30				

North American Land Surface Emissivity Project

Welcome to the website for the North American Land Surface Emissivity Project. The goal of the project is to create a seamless database of emissivity from standard ASTER emissivity products for use in climate research. The Earth emits energy at wavelengths we cannot normally see, that energy is a function of the temperature and the emissivity of the surface. The surface emissivity primarily depends on the composition of the surface. Thus as the surface composition changes through, for example, land cover land use change, so does the surface emissivity. The land surface emissivity is measured by several instruments mounted on satellites and aircraft. Some of the most well known satellite sensors are AIRS, ASTER and MODIS.

Of these three satellite sensors, ASTER provides the most detailed emissivtiy images with a pixel spatial resolution of 90m. The image below was created by merging together all the ASTER emissivity data ever acquired over California, Nevada, Arizona and Utah under clear skies from 2000-2008 for the months July, August and September.

ASTER Mean Summer Emissivity - Band 12 (9.1 μm)

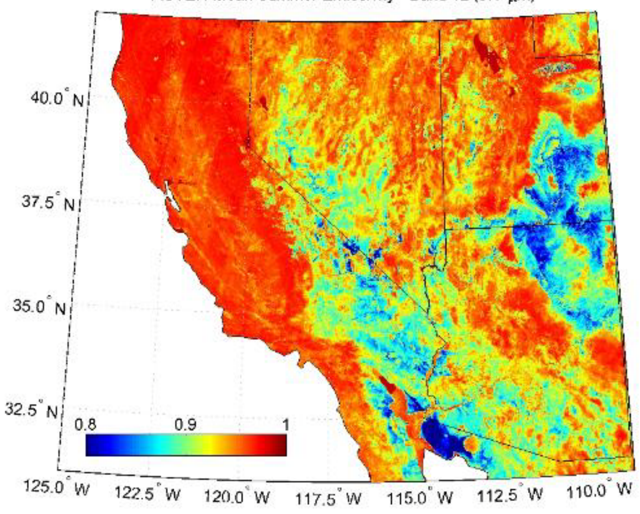

	NAALSED v2.0	NAALSED v3.0
Temporal coverage	2000-2008	2000-2010
Products	Emissivity Temperature NDVI Land/Water Map	Emissivity Temperature NDVI Land/Water Map DEM
Cloud mask	v1.0	v3.2
Atmospheric Profiles	NCEP GDAS - Temporal interpolation - 100 km - TOMS ozone	Terra MODIS (MOD07) - Coincident - 5 km - MOD07 ozone
Atmospheric Correction	Standard MODTRAN™3.5	Water Vapor Scaling (WVS) (Tonooka, 2005) MODTRAN™5.2 (Berk et al. 2005)
Temperature Emissivity Separation (TES) algorithm	Standard TES (Gillespie et al. 1998)	Standard TES (Gillespie et al. 1998)

NAALSED Summertime Emissivity (Jul-Sep 2000-2009), Band 12 (9.1 µm)
Degraded from 100 m to 5 km

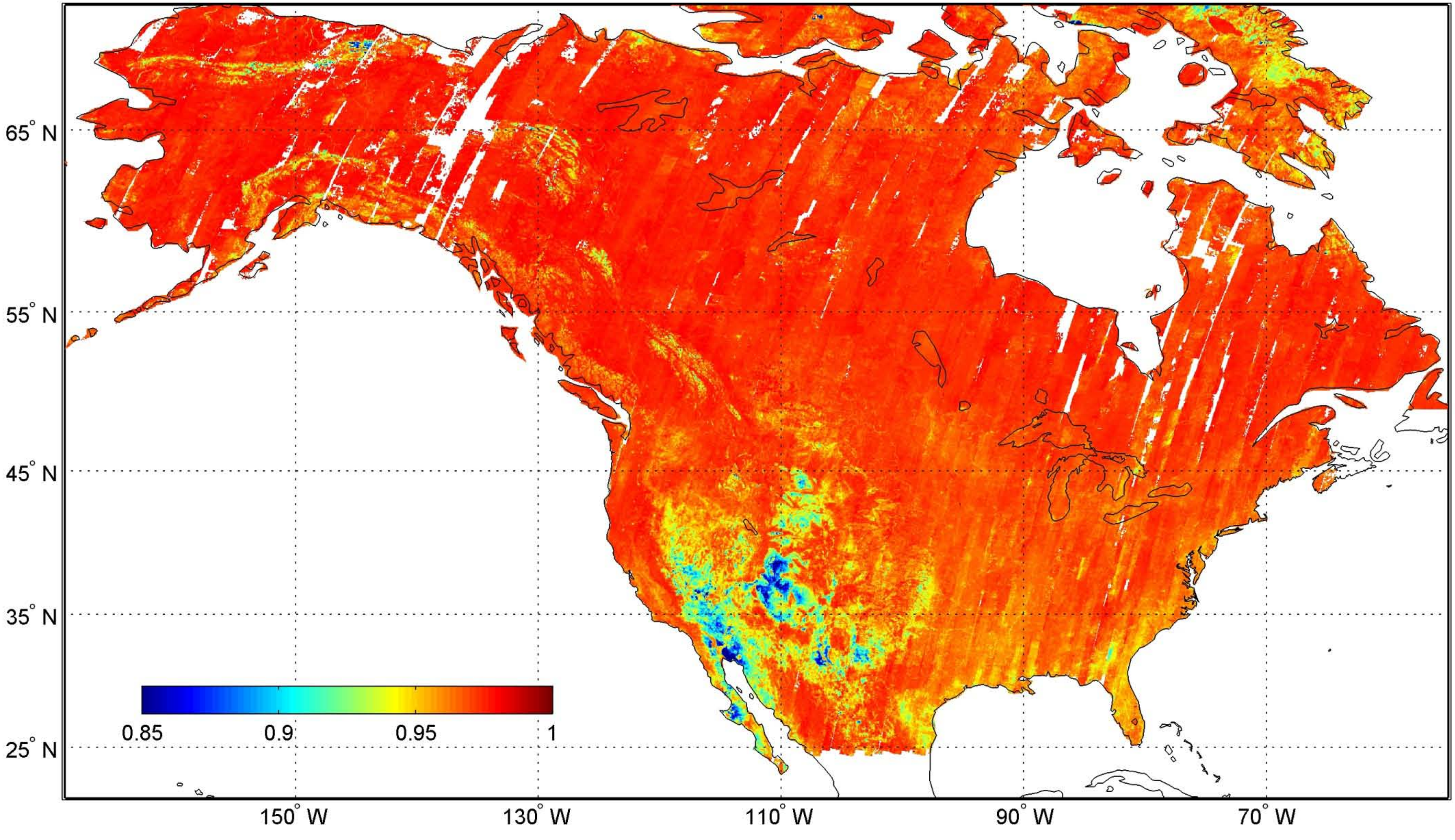

Total Scenes: 64,149
Usable: 39,848 (Cloud<80%)

NAALSED Summertime Emissivity (Jul-Sep 2000-2009), Band 14 (11.3 µm)

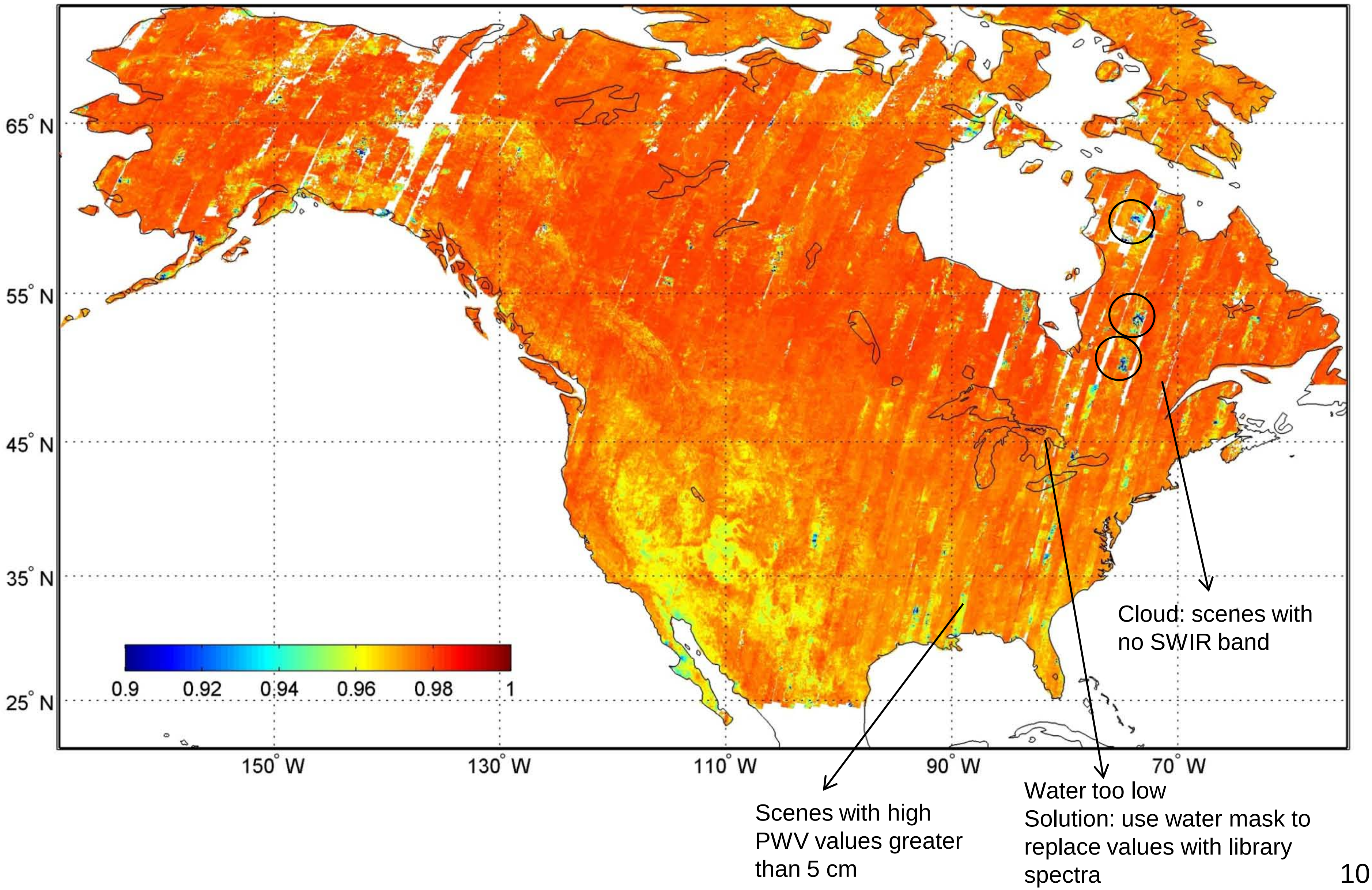

Death Valley - Decorrelation Stretch - RGB (Band 14,12,10)

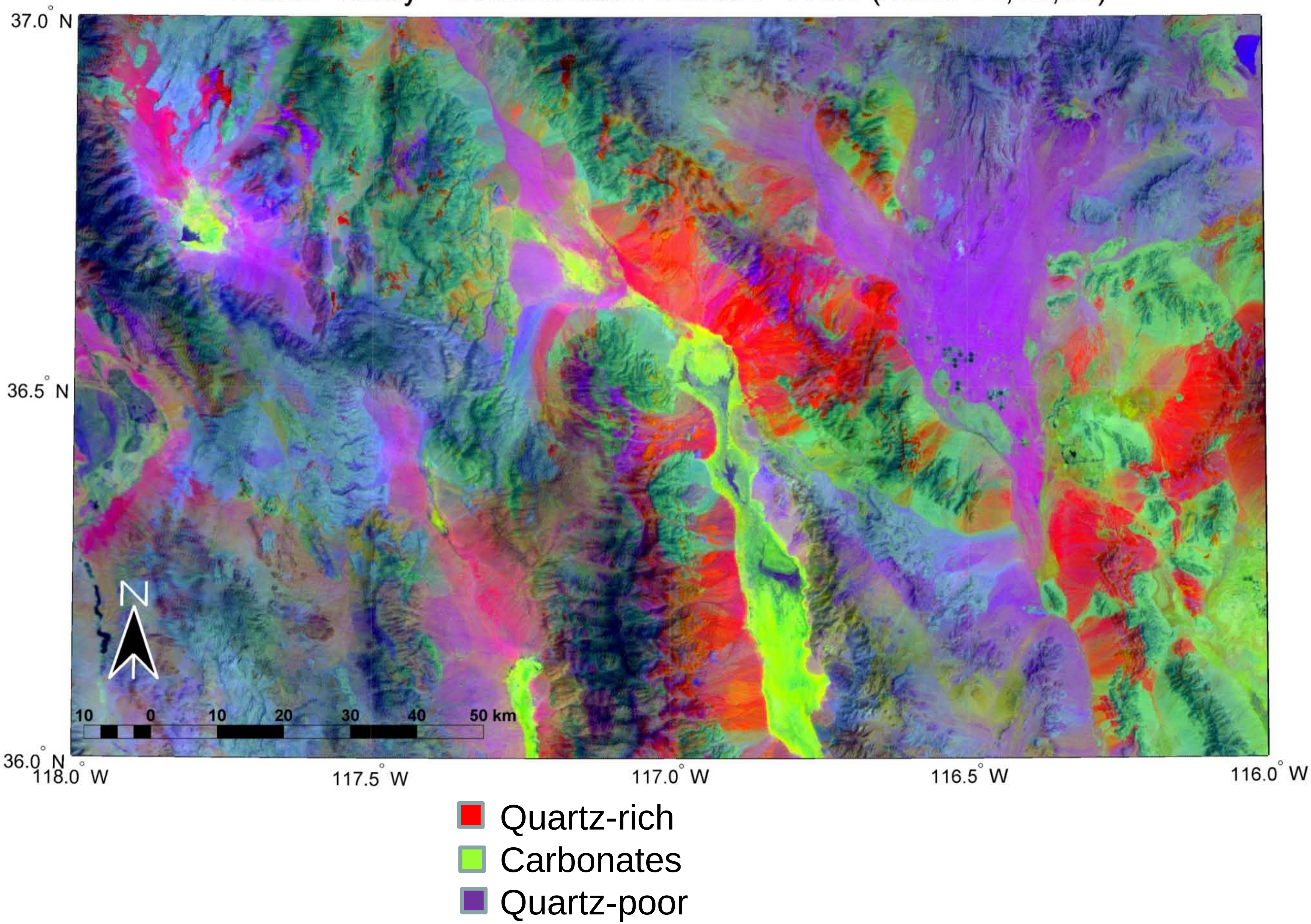

NAALSED Total Summertime Observations (Jul-Sep 2000-2009)

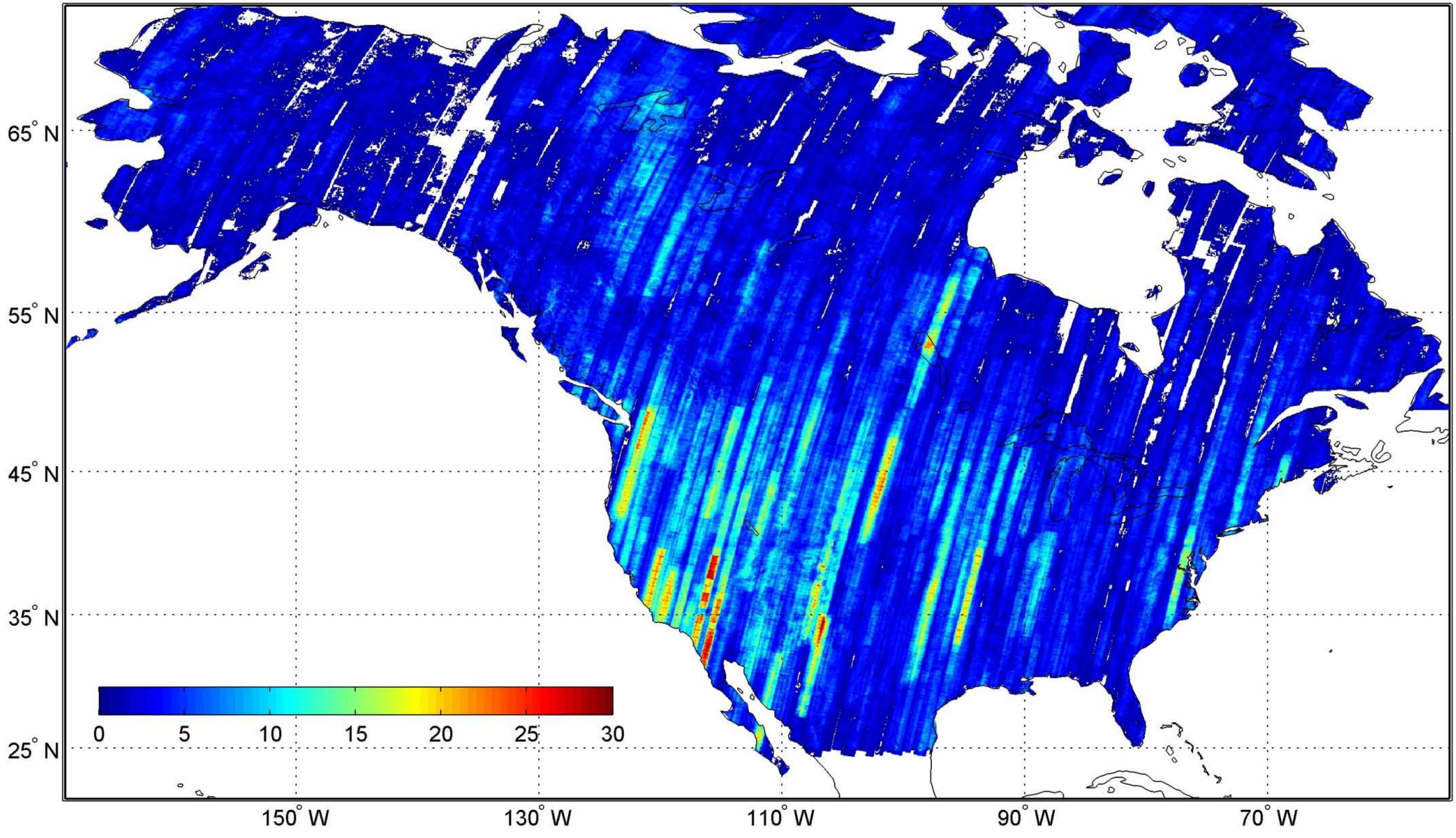

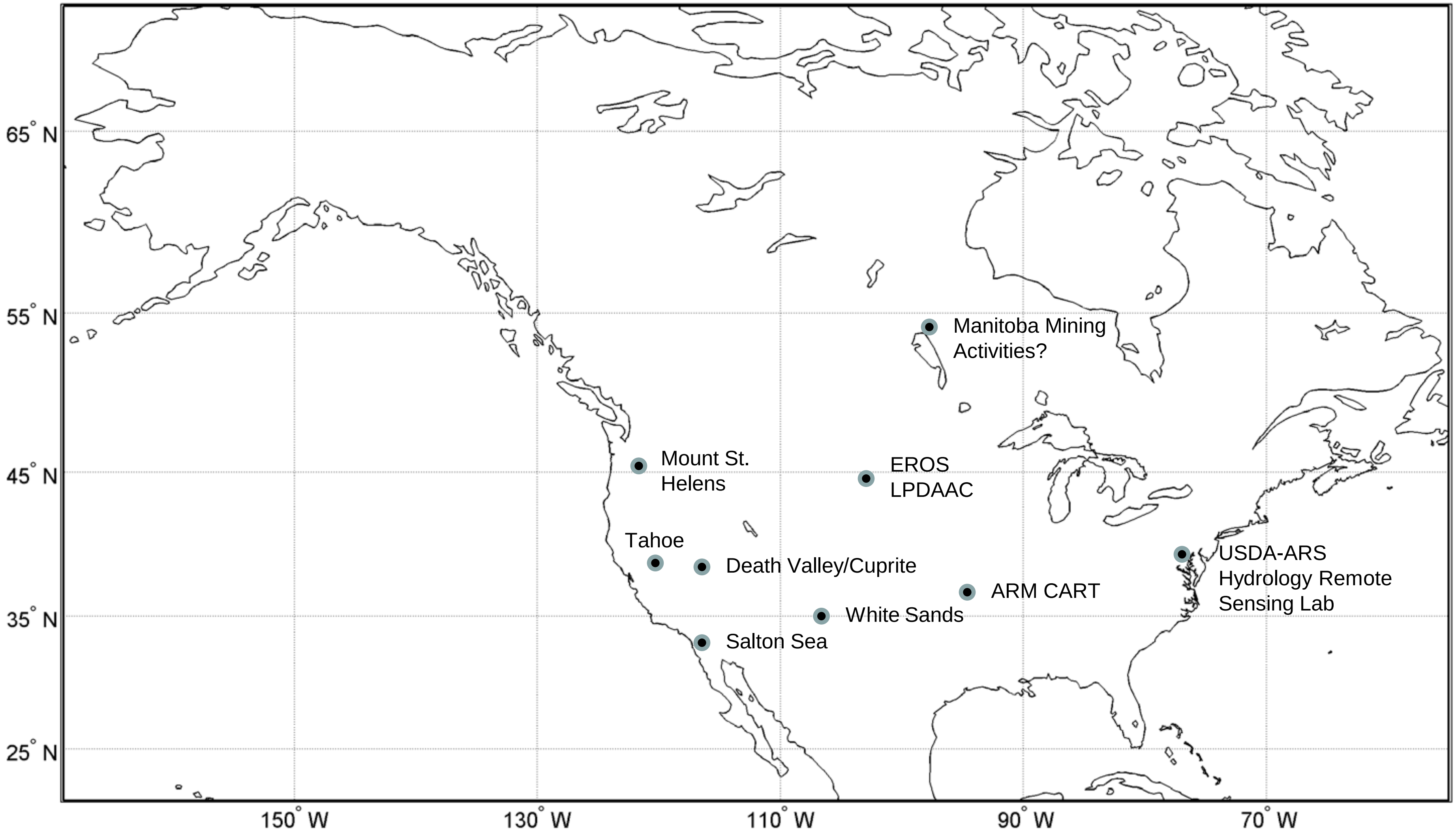
65° N
55° N
45° N
35° N
25° N
150° W
130° W
110° W
90° W
70° W
Manitoba Mining Activities?
Mount St. Helens
EROS LPDAAC
Tahoe
Death Valley/Cuprite
USDA-ARS Hydrology Remote Sensing Lab
ARM CART
White Sands
Salton Sea

Pseudo-invariant Sand Dune Emissivity Validation Results

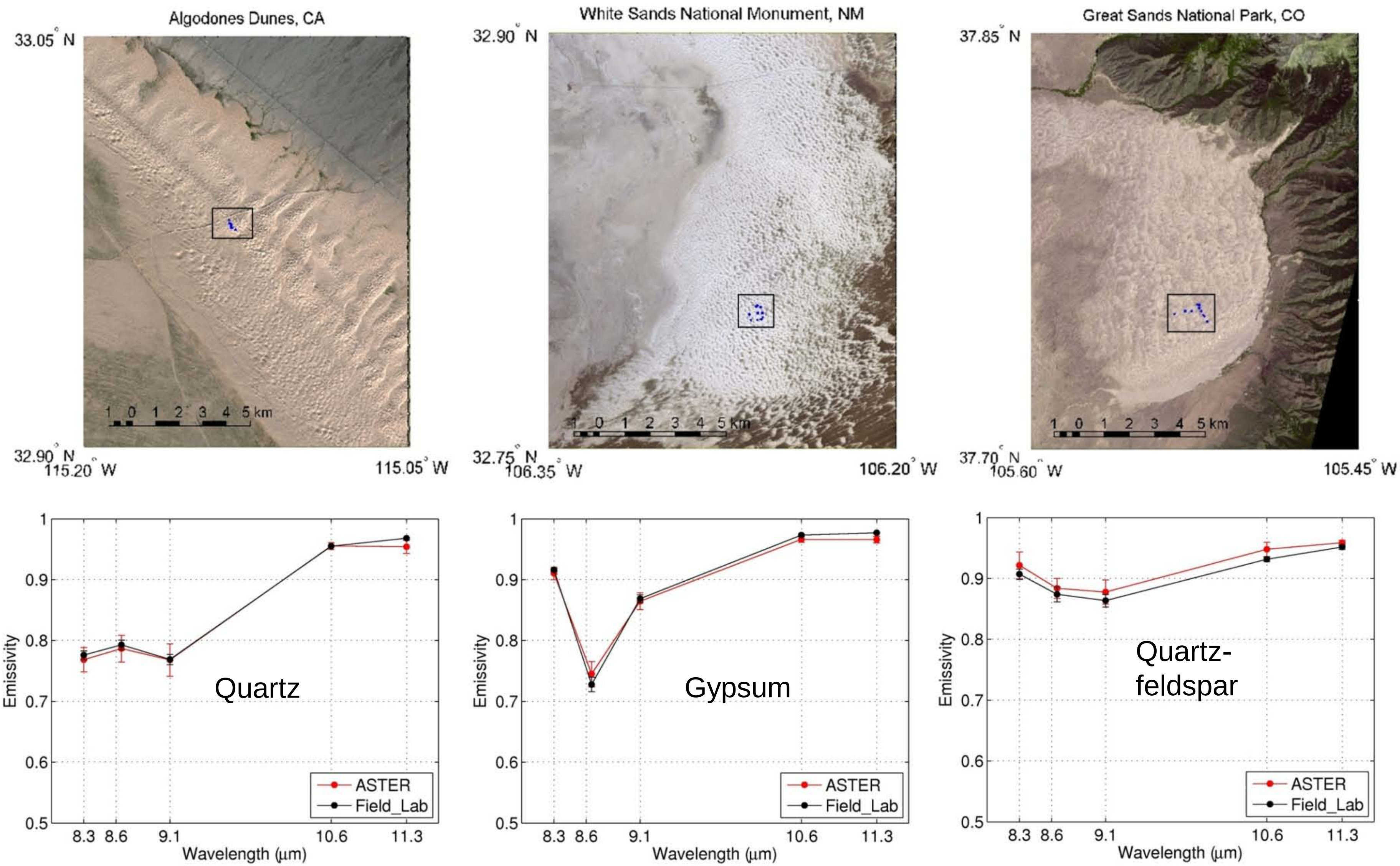

Hulley, G. C., Hook, S. J., and A.M. Baldridge, Validation of the North American ASTER Land Surface Emissivity Database (NAALSED) Version 2.0, *Remote Sensing of Environment* (2009), accepted

ASTER validation with pseudo-invariant sand dune sites

	ASTER MINUS LAB EMISSIVITY (%)					
Dune site	**Band 10**	**Band 11**	**Band 12**	**Band 13**	**Band 14**	**Mean**
Algodones	0.68	0.60	0.13	0.02	1.40	**0.57**
Stovepipe Wells	0.17	0.77	1.02	0.34	0.37	**0.53**
White Sands	0.34	2.76	0.16	0.92	1.08	**1.05**
Kelso Dunes	1.57	1.04	1.33	1.91	0.81	**1.33**
Great Sands	1.44	0.97	1.42	1.64	0.69	**1.23**
Moses Lake	0.69	0.52	0.42	0.61	1.01	**0.65**
~~Sand Mountain~~	~~7.74~~	~~6.47~~	~~9.01~~	~~1.82~~	~~1.10~~	~~**5.23**~~
Coral Pink	7.48	6.44	7.32	2.50	1.70	**4.90**
Little Sahara	3.55	2.39	2.60	0.96	0.19	**1.94**
Killpecker	2.34	1.99	2.26	1.33	0.81	**1.75**

< 1.6% (1 K)

NAALSED Band 14 (11.3 µm) minus MODIS Band 31 (10.8 µm)

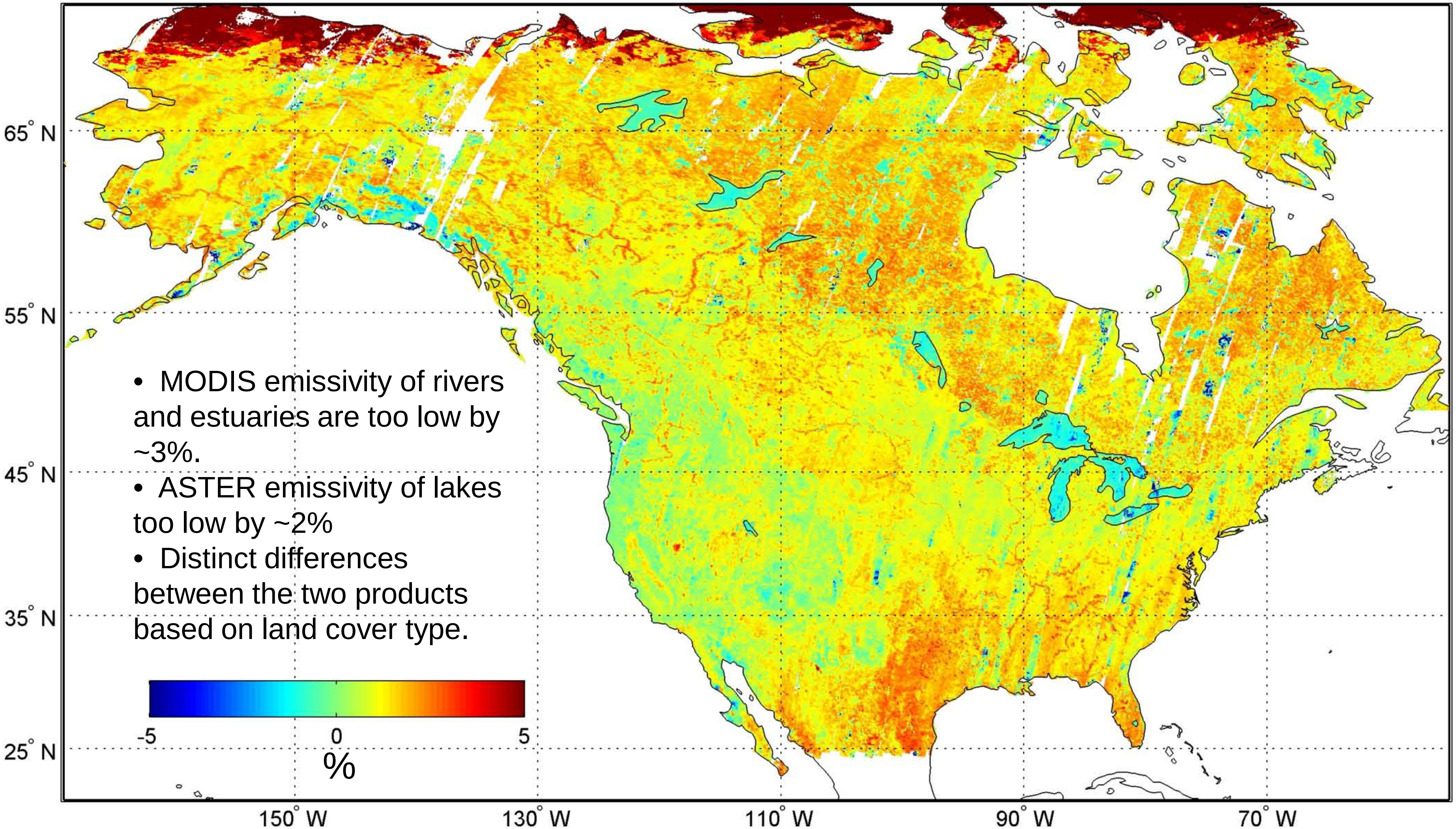

- MODIS emissivity of rivers and estuaries are too low by ~3%.
- ASTER emissivity of lakes too low by ~2%
- Distinct differences between the two products based on land cover type.

HyspIRI Cloud Detection Methodology

- Accurate and reliable cloud masking is critical for generating high quality HyspIRI Level-2 and Level-3 data products
- Daytime Cloud masking relies heavily on thresholding VSWIR reflectance tests
- HyspIRI VSWIR swath (150 km) and TIR swath (600 km) will not overlap
- HyspIRI Cloud Detection Options:
  - Generate separate VSWIR-only and TIR-only cloud masks?
  - Use external data source to fill in VSWIR gap in TIR swath?
  - Use NAALSED-based cloud detection (Landsat methodology)?
    - Pass-1: Uses combined VSWIR reflectances and TIR data to develop cloud signature
    - Pass-2: Use thermal classification to identify remaining clouds on TIR-only swath

NAALSED/Landsat Pass-1 Cloud Spectral Tests

Table 1. Pass-1 Filters and Threshold Tests Using Reflectance, r_i and Temperature, T_{sat}, Values From Equations (1) and (2)

Filter	Threshold Test	Function
1 Brightness Threshold	$r_2 > 0.08$	Eliminates low reflectance, dark pixels
2 Snow Threshold	$\mathrm{NDSI} = (r_1 - r_4)/(r_1 + r_4) < 0.7$	Eliminates snow
3 Temperature Threshold	$T_{sat} < 300$	Eliminates warm surface features
4 Band 4/5 Composite	$(1 - r_4)T_{sat} < 240 \Rightarrow$ snow present $(1 - r_4)T_{sat} < 250 \Rightarrow$ snow absent	Eliminates cold surfaces - snow, tundra
5 Growing vegetation	$\frac{r_3}{r_2} < 2$	Eliminates reflective growing vegetation
6 Senescing vegetation	$\frac{r_3}{r_1} < 2.3$	Eliminates reflective senescing vegetation
7 Rocks and Sand	$\frac{r_3}{r_4} > 0.83$	Eliminates reflective rocks and sand
8 Warm/Cold Cloud	$(1 - r_4)T_{sat} > 235 \Rightarrow$ warm cloud $(1 - r_4)T_{sat} < 235 \Rightarrow$ cold cloud	Warm and cold cloud classificiation
Cloud Shadow	$r_3 < 0.05$ and $\frac{r_3}{r_1} > 1.1$	Detects cloud shadows

NAALSED/Landsat Pass-2 Cloud Spectral Tests

- Pass-2 is applied to all ‘uncertain/ambiguous’ pixels identified from Pass-1 processing
- Thermal cloud signature is developed from Pass-1 clouds and new thermal thresholds determined based on statistical analysis (e.g. Max, min and mean cloud temperature, skewness etc.)

ASTER visible RGB

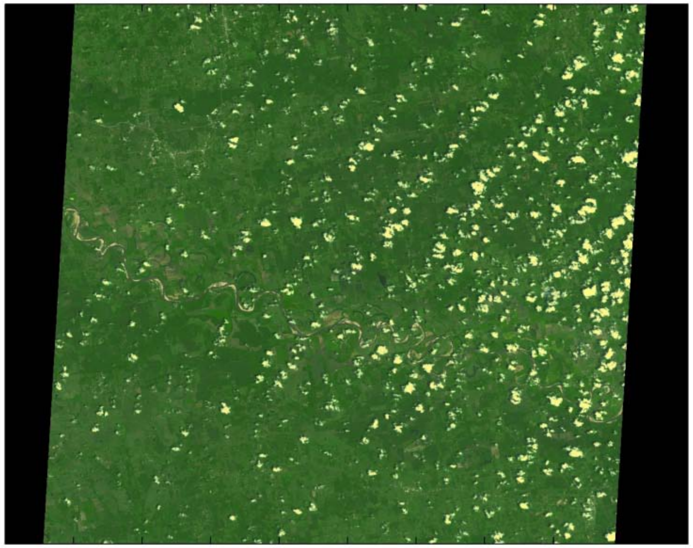

HyspIRI Simulated Pass-1

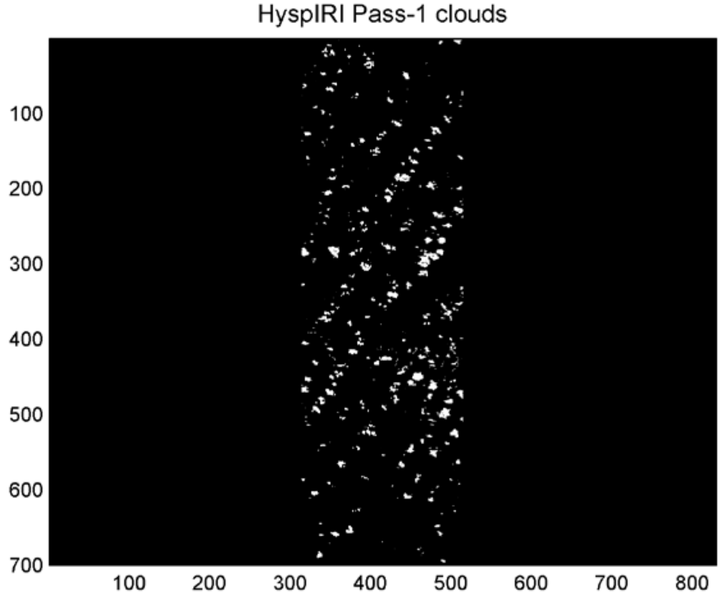

Mean Temperature: 292.22 K
Max Temperature: 299.96 K
Min Temperature: 287.89 K
Standard Deviation: 2.2 K
Skewness: 0.848

HyspIRI Simulated Pass-2

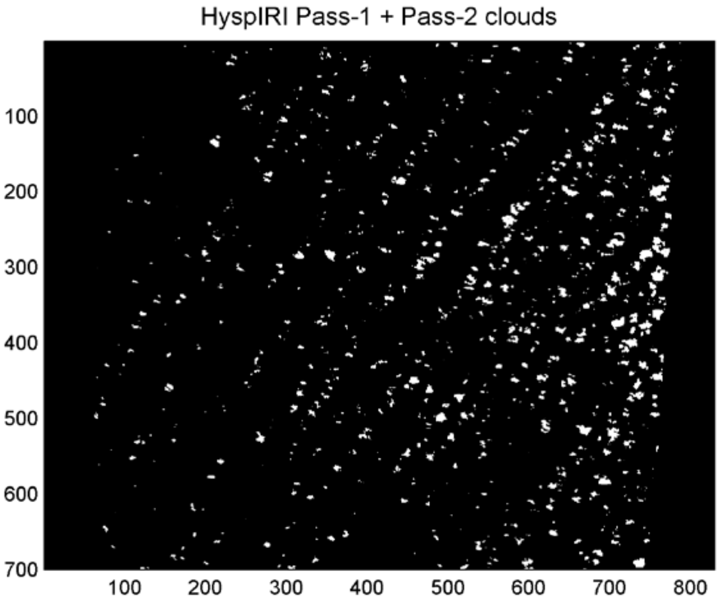

ASTER visible RGB

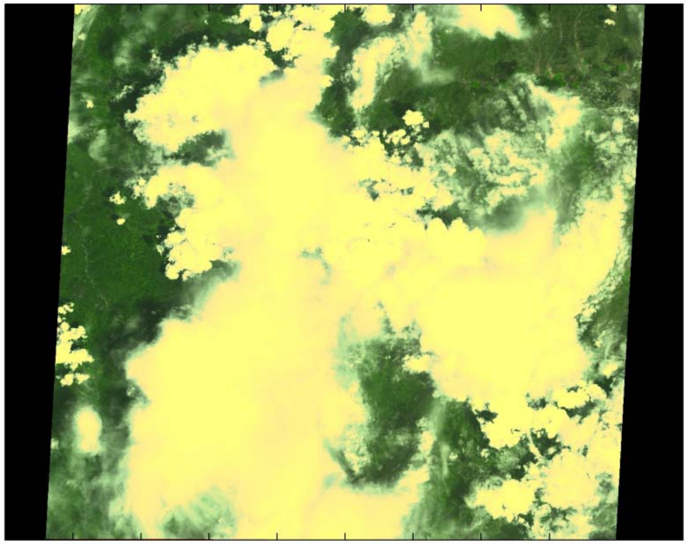

HyspIRI Simulated Pass-1

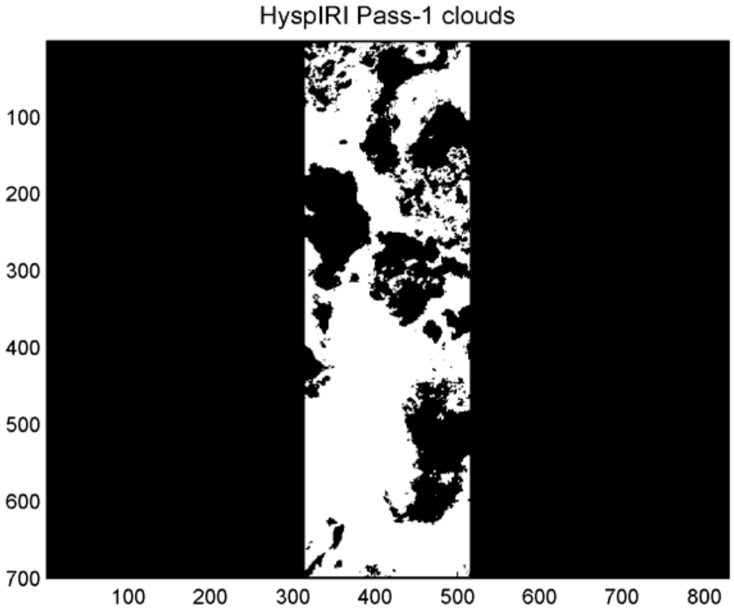

Mean Temperature: 252.42 K
Max Temperature: 299.88 K
Min Temperature: 231.52 K
Standard Deviation: 10.7 K
Skewness: 0.357

HyspIRI Simulated Pass-2

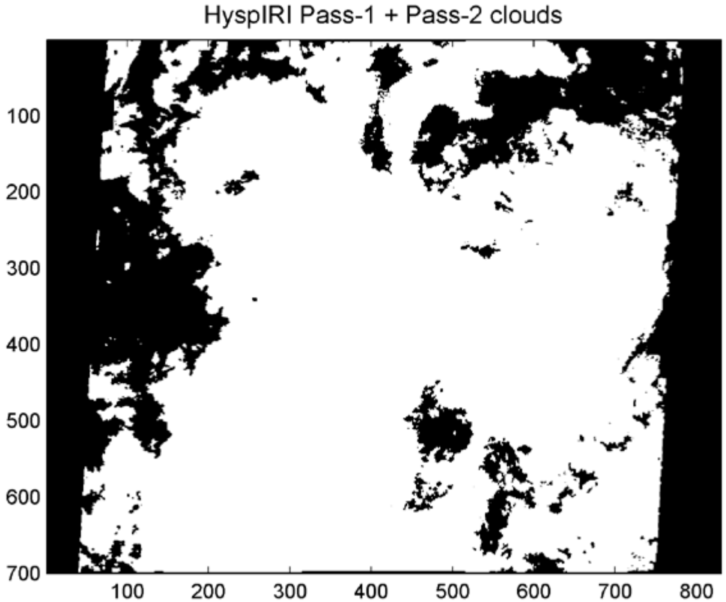

Future Work

- Acquire remaining scenes needed to fill gaps in NAALSED
- Release NAALSED v3.0 for North America
- Extend NAALSED to global coverage: North Africa – AIRS/IASI/MODIS products have large uncertainties in emissivity here
- Continue developing HyspIRI thermal infrared product ATBD’s
- Continue developing HyspIRI cloud detection methodology

The End

National Aeronautics and Space Administration

Jet Propulsion Laboratory
California Institute of Technology
Pasadena, California

www.nasa.gov

JPL 400-1278 7/06

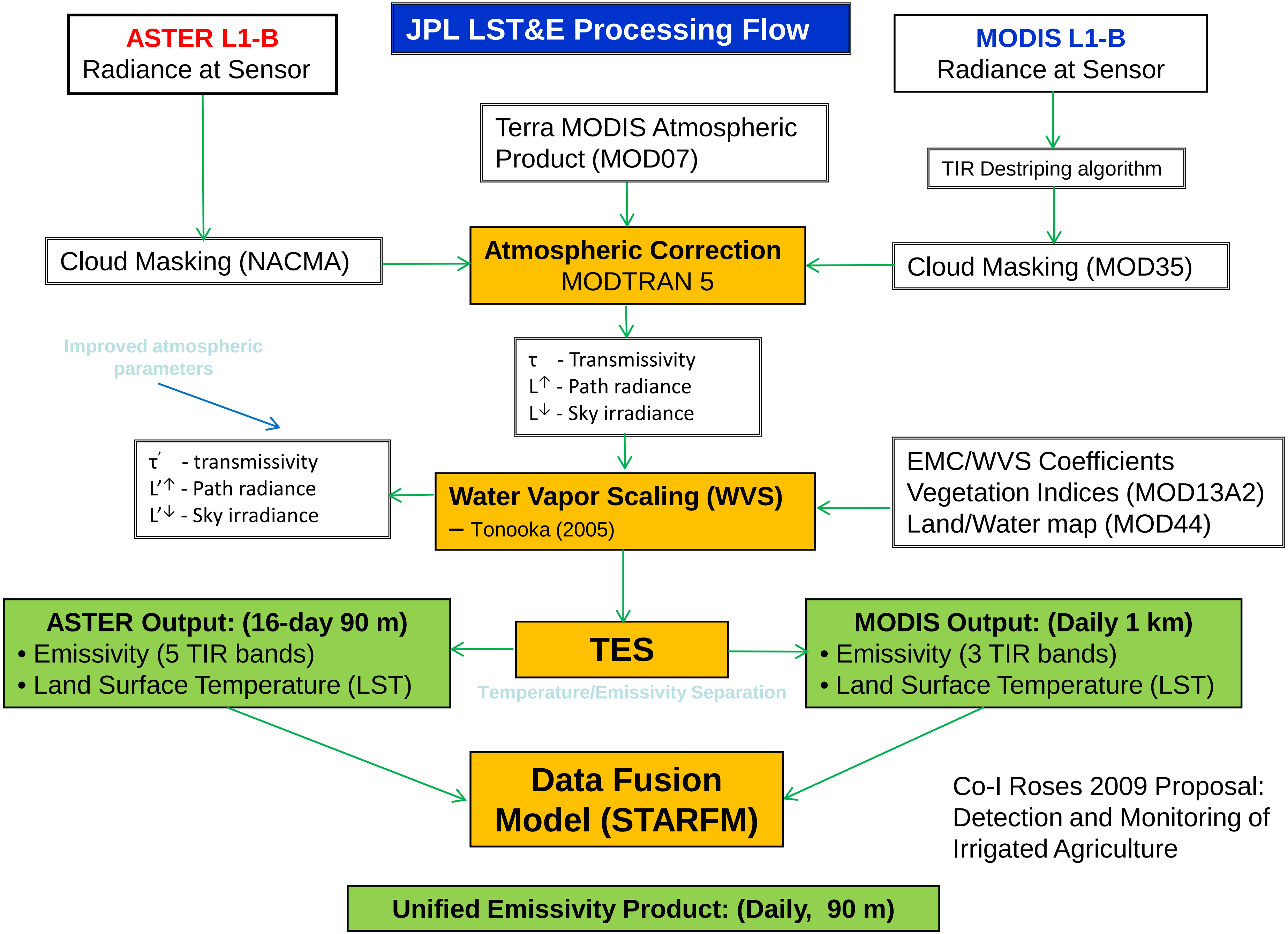
JPL LST&E Processing Flow
ASTER L1-B
Radiance at Sensor
MODIS L1-B
Radiance at Sensor
Terra MODIS Atmospheric Product (MOD07)
TIR Destriping algorithm
Cloud Masking (NACMA)
Atmospheric Correction
MODTRAN 5
Cloud Masking (MOD35)
Improved atmospheric parameters
τ - Transmissivity
L↑ - Path radiance
L↓ - Sky irradiance
τ′ - transmissivity
L′↑ - Path radiance
L′↓ - Sky irradiance
Water Vapor Scaling (WVS)
– Tonooka (2005)
EMC/WVS Coefficients
Vegetation Indices (MOD13A2)
Land/Water map (MOD44)
ASTER Output: (16-day 90 m)
• Emissivity (5 TIR bands)
• Land Surface Temperature (LST)
TES
Temperature/Emissivity Separation
MODIS Output: (Daily 1 km)
• Emissivity (3 TIR bands)
• Land Surface Temperature (LST)
Data Fusion
Model (STARFM)
Co-I Roses 2009 Proposal:
Detection and Monitoring of
Irrigated Agriculture
Unified Emissivity Product: (Daily, 90 m)

NAALSED Summertime Surface Temperature (Jul-Sep 2000-2009)

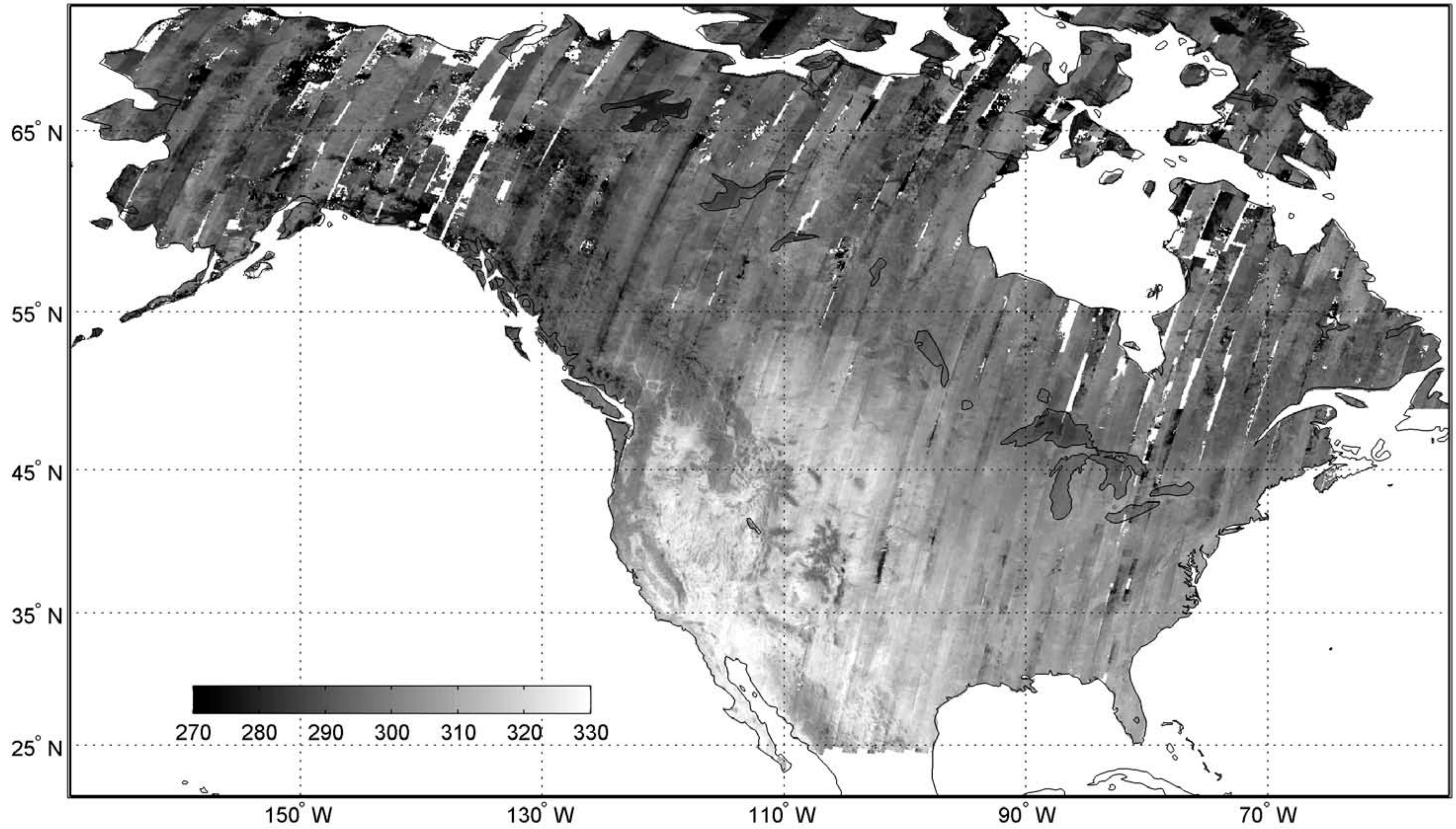

MODBF Summertime Emissivity (Jul-Sep 2003-2006), Band 29 (8.6 µm)

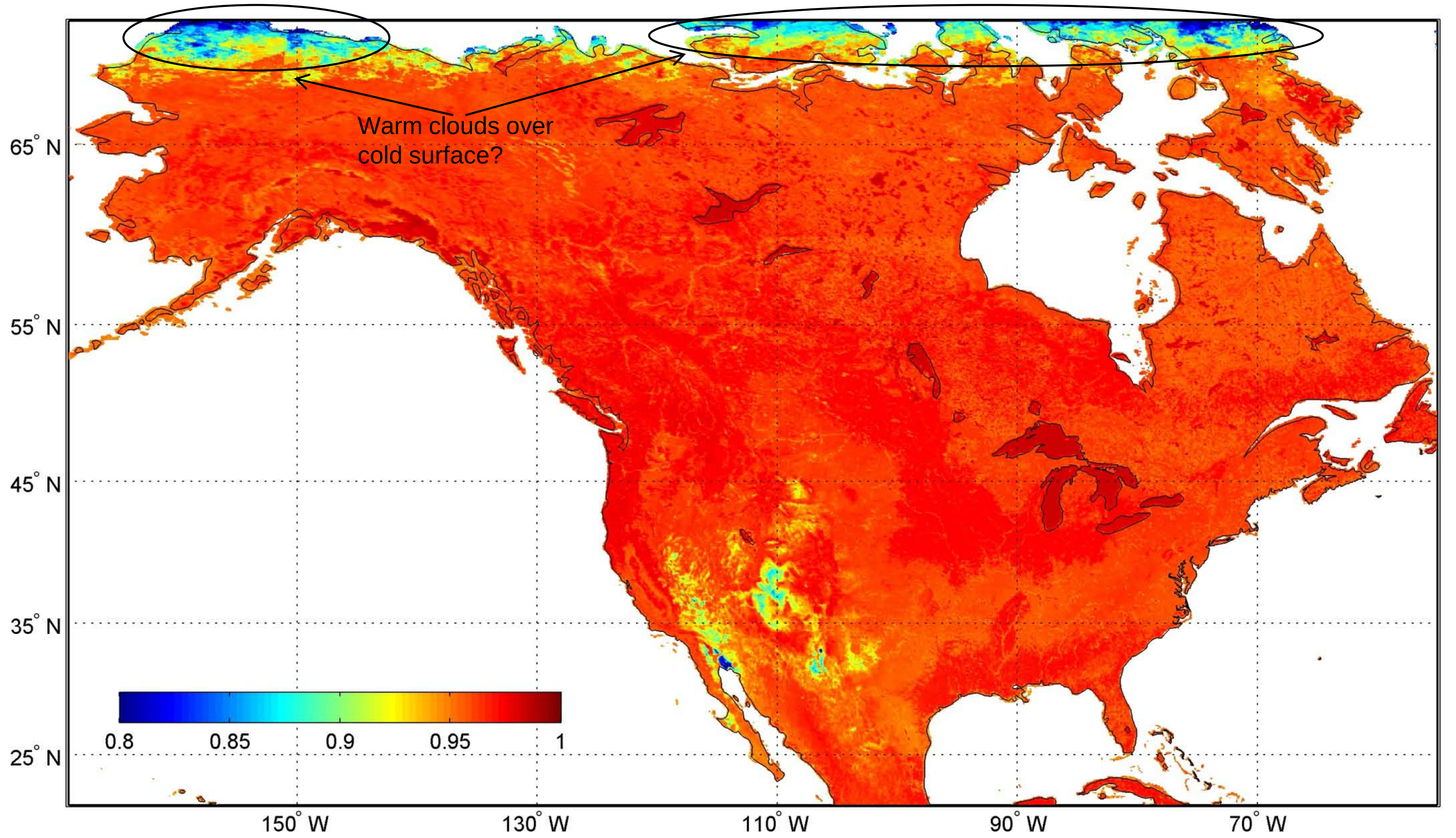

Pass-2 Processing (Landsat-7 Approach)

- Pass-2 involves using a thermal analysis to classify 'ambiguous' pixels from Pass-1 processing
- Thermal cloud signature is developed based on warm/cold cloud class identified in Pass-1 processing (eg. Max T, min T, mean T, skewness etc..)
- New temperature thresholds set for Pass-1 warm and cold cloud signatures based on statistical analysis (eg. Threshold adjusted for skewness)
- Decision tree used to accept one or both of cloud populations in final mask

- HyspIRI Cloud Processing Option:
  - Use VSWIR and TIR data to classify clouds using Pass-1 filters for VSWIR swath (150 km)
  - Set remaining pixels falling outside swath to ambiguous (600 km)
  - Use Pass-2 processing to classify remaining clouds on TIR swath

MODBF Summertime Emissivity (Jul-Sep 2003-2006), Band 31 (10.8 µm)

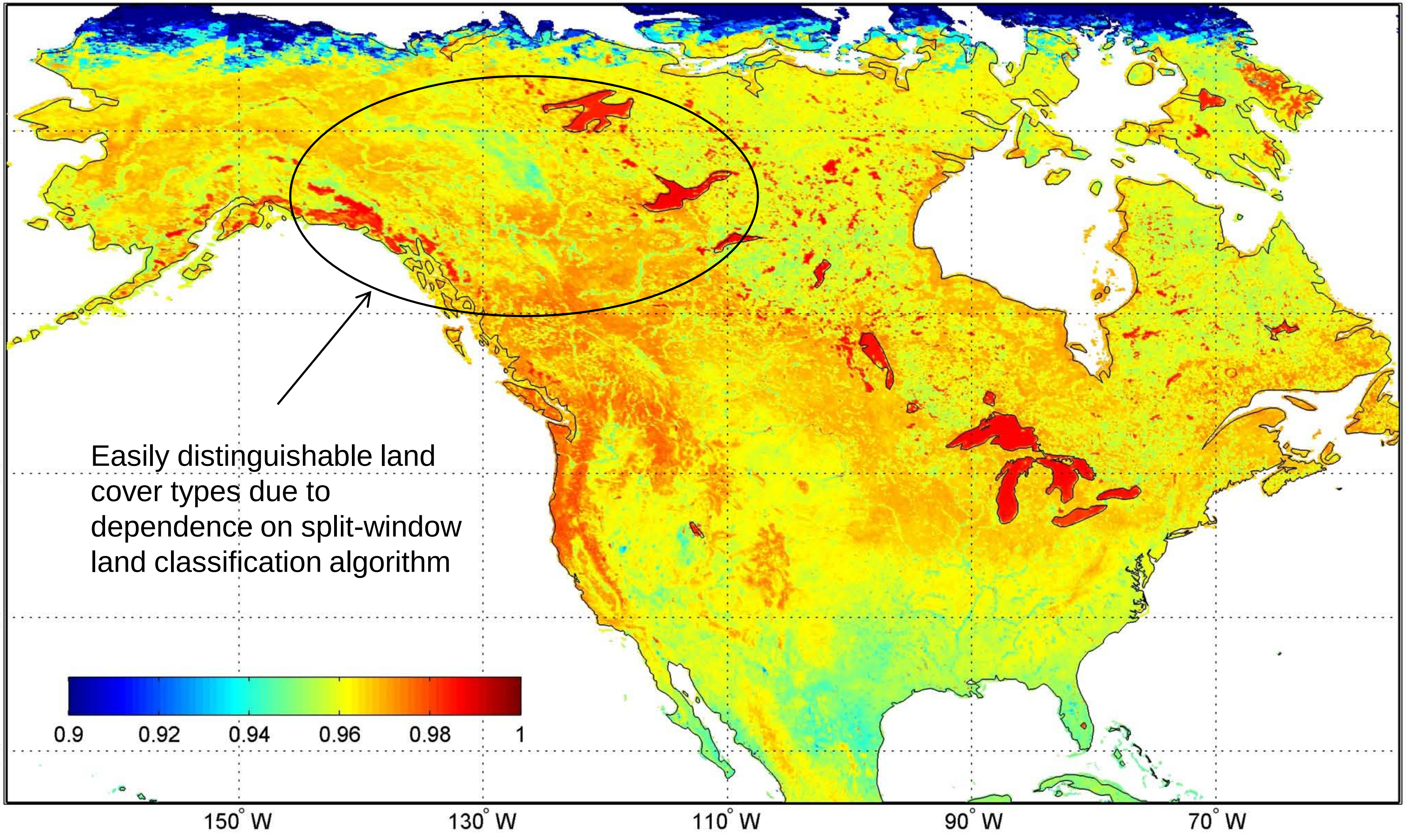

NAALSED Band 11(8.6 µm) minus MODBF Band 29 (8.6 µm)

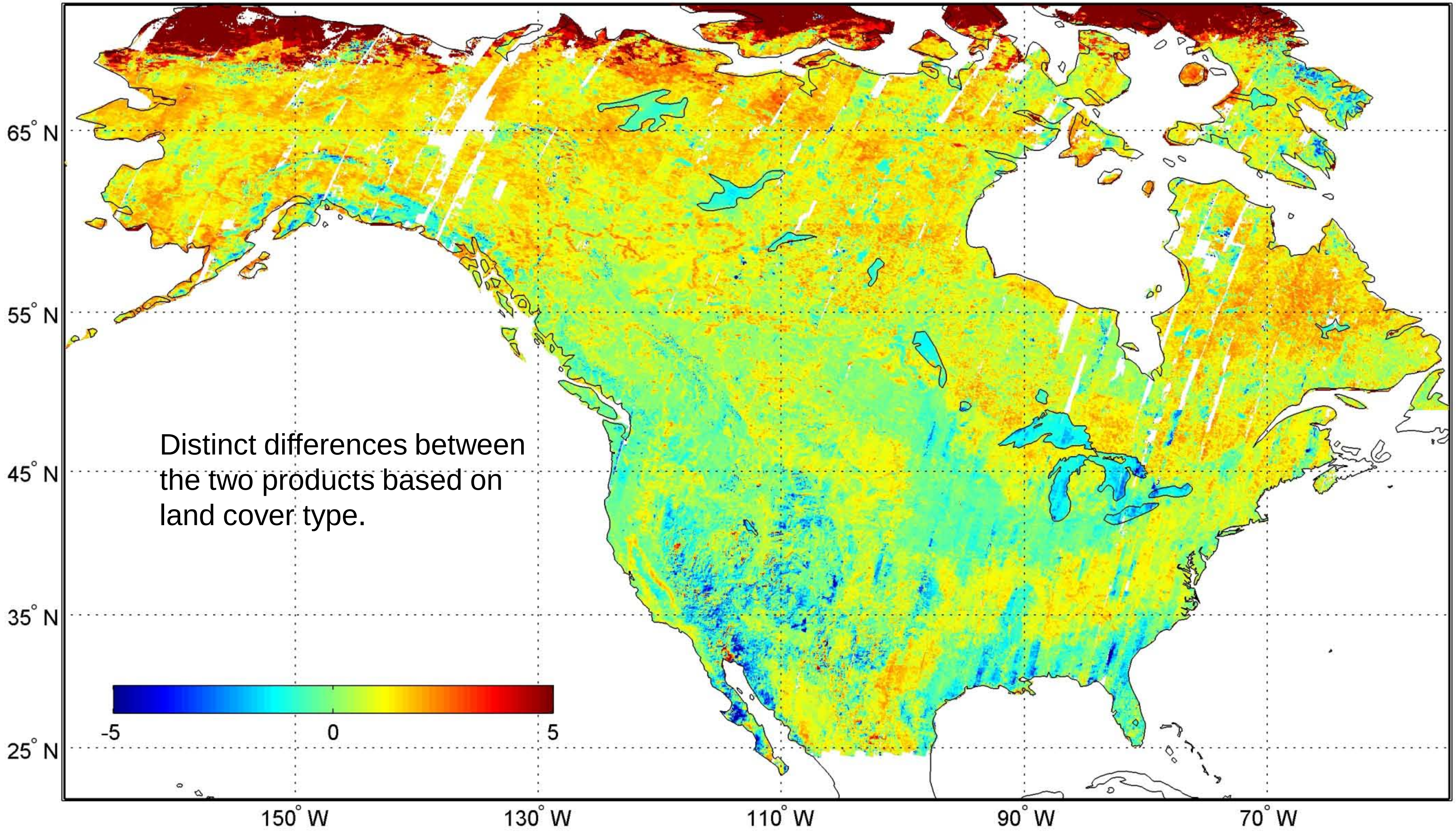

Distinct differences between the two products based on land cover type.

Relevance to Future JPL Missions

HyspIRI **– Tier 2 (2015-2020)**
Hyperspectral Infrared Imager

- Ecosystem response to natural and human-induced changes
- Monitoring natural hazards
- Land surface composition

- North American ASTER Land Surface Emissivity Database (NAALSED) – proxy HyspIRI dataset
- Algorithm development (thermal IR)
  - What is the appropriate temperature/emissivity separation algorithm for HyspIRI?
  - What atmospheric correction technique, and profiles to be used?
  - Cloud detection methodology?
- Level-2 Product Definition and ATBD's

Sand samples collected in field

Reflectance measured using Nicolet 520 FTIR spectrometer

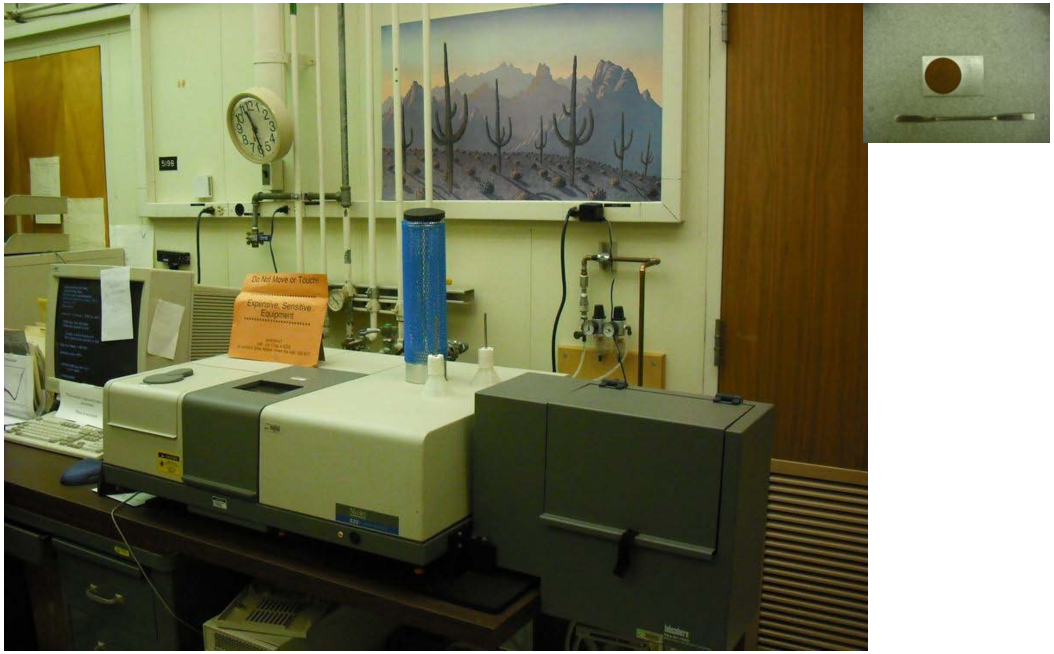

JPL

LAB MEASUREMENTS

spectral range: 2.5 – 15 µm

spectral resolution: 4 cm^{-1}

1000 scans in 10 minutes

$\varepsilon = 1 - r$

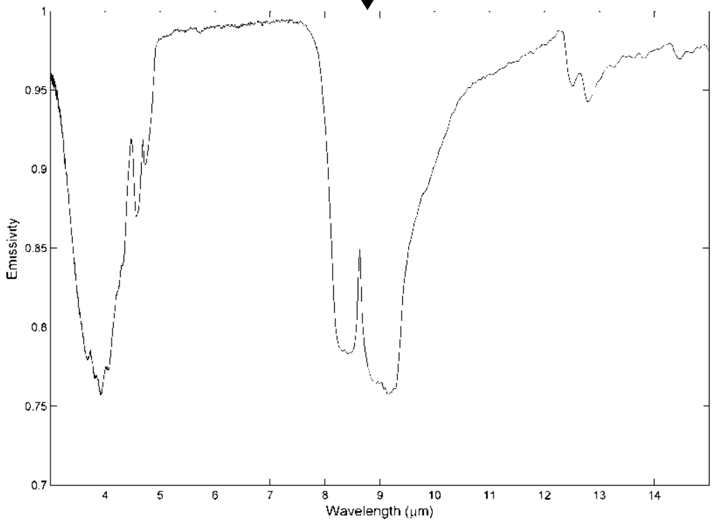

Pseudo-Invariant Sand Dune Sites

Table 1
Summary of the major characteristics of each dune site including locality, elevation, surface area, dune height, grain size, sand source and bulk mineralogy.

Dune site	Locality	Surface area (km^2)	Elevation/max dune height (m)	Grain size	Sand source	Mineralogy (XRD)
Algodones (32.95° N, 115.07° W)	Southeast CA, Eastern margin of the Salton Trough	720	94/80	Medium to coarse sand	Beach sand from Lake Cahuilla	Major: quartz
Coral Pink (37.04° N, 112.72° W)	Sand Valley, just north of UT–AZ border, west Kanab	13.6	1780/10	Medium sand	Navajo, Page and Estrada Jurassic sandstones of the Vermillion Cliffs	Major: quartz
Great Sands (37.77° N, 105.54° W)	San Luis Valley, CO, adjacent to Sangre de Cristo, NE of Alamosa	104	2560/230	Medium to coarse sand	Quartz and volcanic fragments derived from Santa Fe and Alamosa formations, recent fluvial (Rio Grande) deposits	Major: quartz Minor: potassium feldspar
Kelso (34.91° N 115.73° W)	Mojave Desert, CA, southeast of Baker	115	800/195	Medium sand	Derived from sedimentary, metamorphic, igneous terrains from Mojave River alluvial apron	Major: quartz Minor: potassium feldspar Trace: magnetite
Killpecker (41.98° N 109.10° W)	Southwest WY, from Eden across Rock Springs into Red Desert	550	2000/45	Medium sand	Sandstone and siltstone of the Laney member of the Green River Formation	Major: quartz Trace: magnetite Minor: plagioclase feldspar, epidote
Little Sahara/Lynndyl (39.7° N 112.39° W)	West-central UT, Sevier River drainage basin, west of Lynndyl	575	1560/200	Fine sand	Deltaic and shoreline sediments from the Provo shoreline of Lake Bonneville	Major: quartz Minor: plagioclase feldspar, pyroxene, carbonate, magnetite
Stovepipe Wells (36.62° N, 117.11° W)	Central Death Valley, CA, near Stovepipe Wells	7.7	−12/40	Medium sand	Mixed lithic fragments and quartz from Emigrant Pass to the west and Furnace Wash to the east	Major: quartz Minor: plagioclase feldspar, potassium feldspar
Moses Lake (47.05° N, 119.31° W)	Quincy Basin in central WA	40	345/18	Fine sand	Basaltic sand from the east bank of the Columbia River	Major: quartz, albite
White Sands (32.89° N, 106.33° W)	South-central NM, Tularosa Valley	704	1216/10	Fine sand	Paleo-lake Otero, present playa Lake Lucero to the southwest	Major: gypsum

Hulley, G. C., Hook, S. J., and A.M. Baldridge, (2009), Validation of the North American ASTER Land Surface Emissivity Database (NAALSED) Version 2.0, *Remote Sensing of Environment*, 113, 2224-2233

Thermal Infrared Radiative Transfer

$$\overset{\text{TOA Radiance}}{L_i(\theta)} = \overbrace{\underbrace{\tau_i(\theta)\cdot e_i\cdot B_i(T_S)}_{\text{Surface Emission}} + \underbrace{\tau_i(\theta)\cdot(1-e_i)\cdot\overline{L}_i^{\downarrow}}_{\text{Surface Reflection}}}^{\text{Surface Radiance}} + \underbrace{\int B_i(T(P))\,d\tau_i}_{\text{Atmospheric Emission}}$$

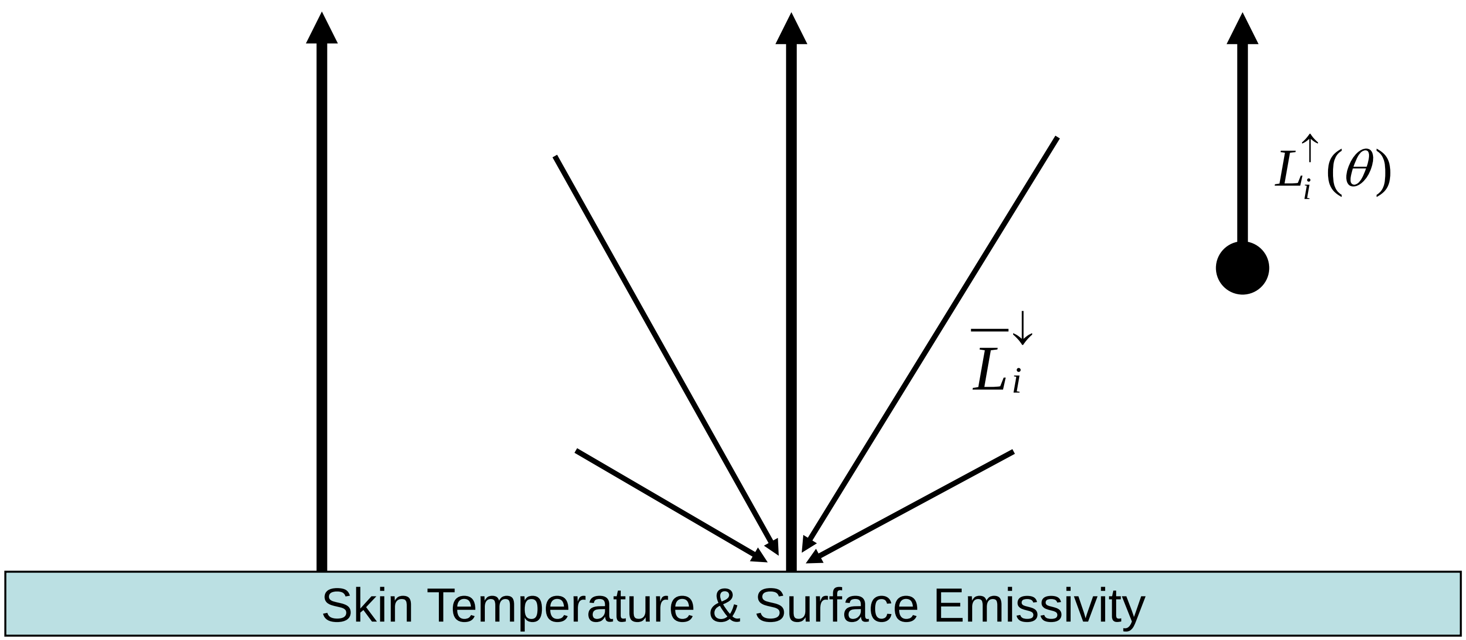

NAALSED Users and Applications

- ~100 registered NAALSED users *http://emissivity.jpl.nasa.gov*
- Current projects and applications:
  - **Arizona State University: JMARS (Java Mission-planning and Analysis for Remote Sensing) is a Java-based geospatial information system developed by Arizona State University**
  - **UW-Madison: NAALSED comparisons with MODIS baseline-fit emissivity product, used for retrieval of MOD07 profiles**
  - **JPL: AIRS (Atmospheric Infrared Sounder) and IASI (Infrared Atmospheric Sounding Interferometer) emissivity validation and intercomparison with NAALSED**
  - **JPL: Tropospheric Emission Spectrometer (TES) group will be using NAALSED as a first guess emissivity in retrieval of Ozone**
  - **Beijing Normal University: Developing an empirical relationship between NAALSED emissivity and NDVI products**
  - **JPL: Generate a land surface temperature product for Landsat**

Atmospheric Correction

Observed Radiance

Surface Radiance:

$$L_{surf,i} = e_i \cdot B_i(T_S) + (1 - e_i) \cdot \boxed{\overline{L}_i^{\downarrow}} = \frac{L_i(\theta) - \boxed{L_i^{\uparrow}(\theta)}}{\boxed{\tau_i(\theta)}}$$

- **Atmospheric Parameters:** $\tau_i(\theta)$, $L_i^{\uparrow}(\theta)$, $L_i^{\downarrow}(\theta)$

  Estimated using radiative transfer code such as MODTRAN with Atmospheric profiles and elevation data

- Derivation of e_i and T_s is an undetermined problem

  The number of parameters (T_s ,e_i in N channels) is always greater than the number of simultaneous equations needed to solve the problem (N)

  =>Additional, independent constraint is needed

MODIS Baseline-Fit (MODBF) Emissivity Product

- Input data: MODIS MYD11 (Aqua) Day-night emissivity retrieval with values at 8.6, 11 and 12 µm in TIR
- MODBF is characterized by model with inflection points at 8.3, 9.3, 10.8 and 12.1 µm in TIR
- MOD11 values at 8.6 um are assigned to inflection points at 8.3 and 9.3 µm , while MOD11 emissivity values at 11 and 12 µm are used to extend line from hinge points 10.8 and 12.1 µm.
- MODBF can be linearly interpolated between inflection points for comparisons with other instruments
- An eigenvector approach is used to produce emissivity at high spectral resolution from the inflection points for use with atmospheric retrieval algorithms

Motivation for Land Surface Temperature and Emissivity (LST&E) Products:

- Climate Modeling/Earth Surface Radiation Budget
  - Emissivity decrease of 0.1 results in 7 W/m^2 underestimation longwave radiation estimates (greenhouse gases, ~2 W/m^2)
- Atmospheric Retrievals
  - Emissivity error of 0.15 leads to more than 3º C error in boundary layer air temperature and up to 20% in boundary moisture profiles
- Land use, Land cover change (LCLUC)
  - Increased demand for agricultural land, and significant land cover changes from extreme climatic events => increased demand for high spatial and temporal resolution LST&E products for monitoring these events
- Soil Moisture Mapping
  - Evapotranspiration models require LST&E to characterize surface energy balance
  - LST will be critical input for NASA's future Soil Moisture Active & Passive (SMAP) mission

ASTER Temperature Emissivity Separation (TES) Algorithm

- Inversion of T and ε are underdetermined
- In TES, additional constraint arises from minimum emissivity (ε_{min}) vs spectral contrast (MMD) using calibration curve derived from lab results (see plot).
- Requires atmospherically corrected surface radiance, and downward sky irradiance as input
- Three error sources:
  - Reliance on empirical function
  - Atmospheric corrections
  - Radiometric calibration errors
- Reported accuracy:
  - T within 1.5 K and ε within 0.015 (1.5 %)

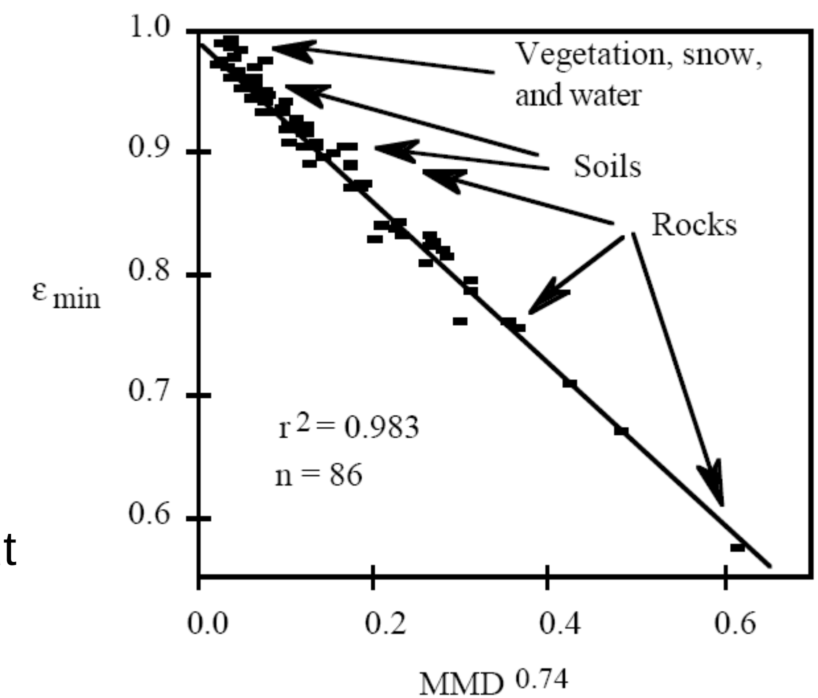

$$\varepsilon_{min} = 0.994 - 0.687 \cdot MMD^{0.74}$$

ASTER TIR Bands

Band 10	8.125 – 8.475 µm
Band 11	8.475 – 8.825 µm
Band 12	8.925 – 9.275 µm
Band 13	10.25 – 10.95 µm
Band 14	10.95 – 11.65 µm

NAALSED Status

- North America (22-71º N, 169-55° W) Summertime Product completed: (Jul- Aug) 2000-2009

- Products (100m):
  - Emissivity (5 TIR bands)
  - Surface Temperature
  - NDVI
  - Land/Water mask
  - DEM
  - Lat/Lon

	NAALSED v3.0
Temporal coverage	2000-2009
Total ASTER Summertime Scenes	64,149
Usable Scenes (Cloud <80%)	39,848
Cloud mask	v3.0 - Improved snow/cloud filter - Elevation dependent brightness temperature thresholding (GTOPO30) - Improved cirrus filter
Atmospheric Profiles	MODIS (MOD07) - 5 km Coincident Obs - MOD07 ozone
Atmospheric Correction	Water Vapor Scaling (Tonooka, 2005) MODTRAN 5
TES algorithm	Standard TES (Gillespie, 1998)

Orbit dynamics, overpass times and repeated sensor coverage: implications for seasonal measurements and change detection

Robert G. Knox and Elizabeth M. Middleton

NASA's Goddard Space Flight Center

Biospheric Sciences Branch, Code 614.4

Greenbelt, MD

Third HyspIRI Science Workshop, Pasadena, CA

August 26, 2010

Introduction

Context

- Mission requirements for 5-day and <20 day repeat overpasses.
- Sun-synchronous, repeating, low Earth orbit (LEO).
- Family of LEO reference concepts.
- HyspIRI concept was adjusted to reduce sun-glint in the VSWIR swath: Nominal mid-morning crossing time (10:30 AM) and 4° off-nadir pointing.

Outline

- Orbital geometry and repeat cycles for some suitable reference orbits.
- Imaging opportunities for each sensor (TIR & VSWIR)
  - Overpass times/dates for example sites
  - Variation in frequency with latitude
- View-illumination geometry variation and constraints.
- Observations at intervals shorter than 5-day or <20 day repeats.

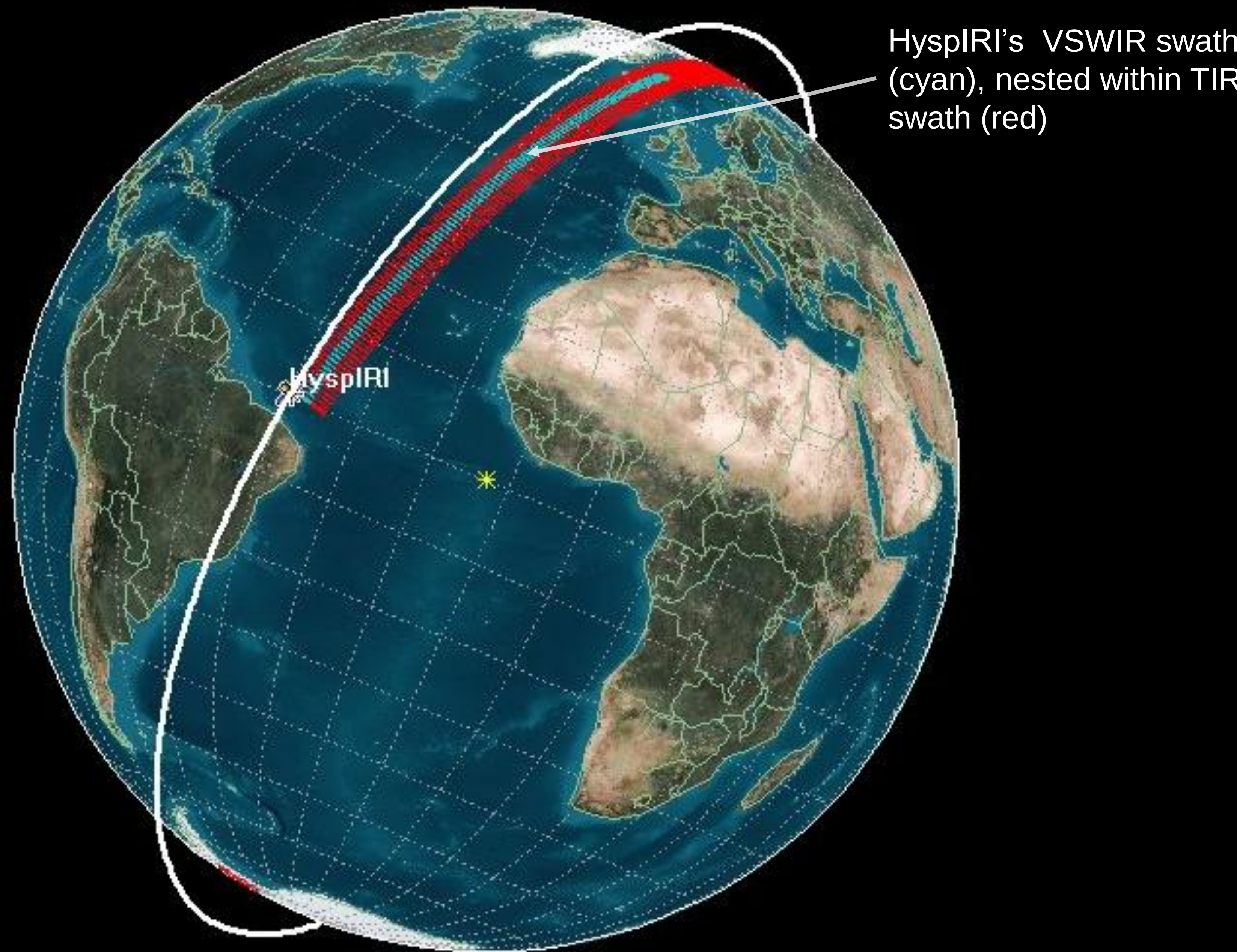

20 March 2009

Daylight side of a sun-synchronous reference orbit, with 10:30 AM equatorial crossing (mean local time) at a descending orbit node. The sub-solar point (yellow) shows the location on Earth where the Sun is directly overhead, east of the ground track. Green line shows the plane of the ecliptic. 3-D view shown in Earth Inertial Axes.

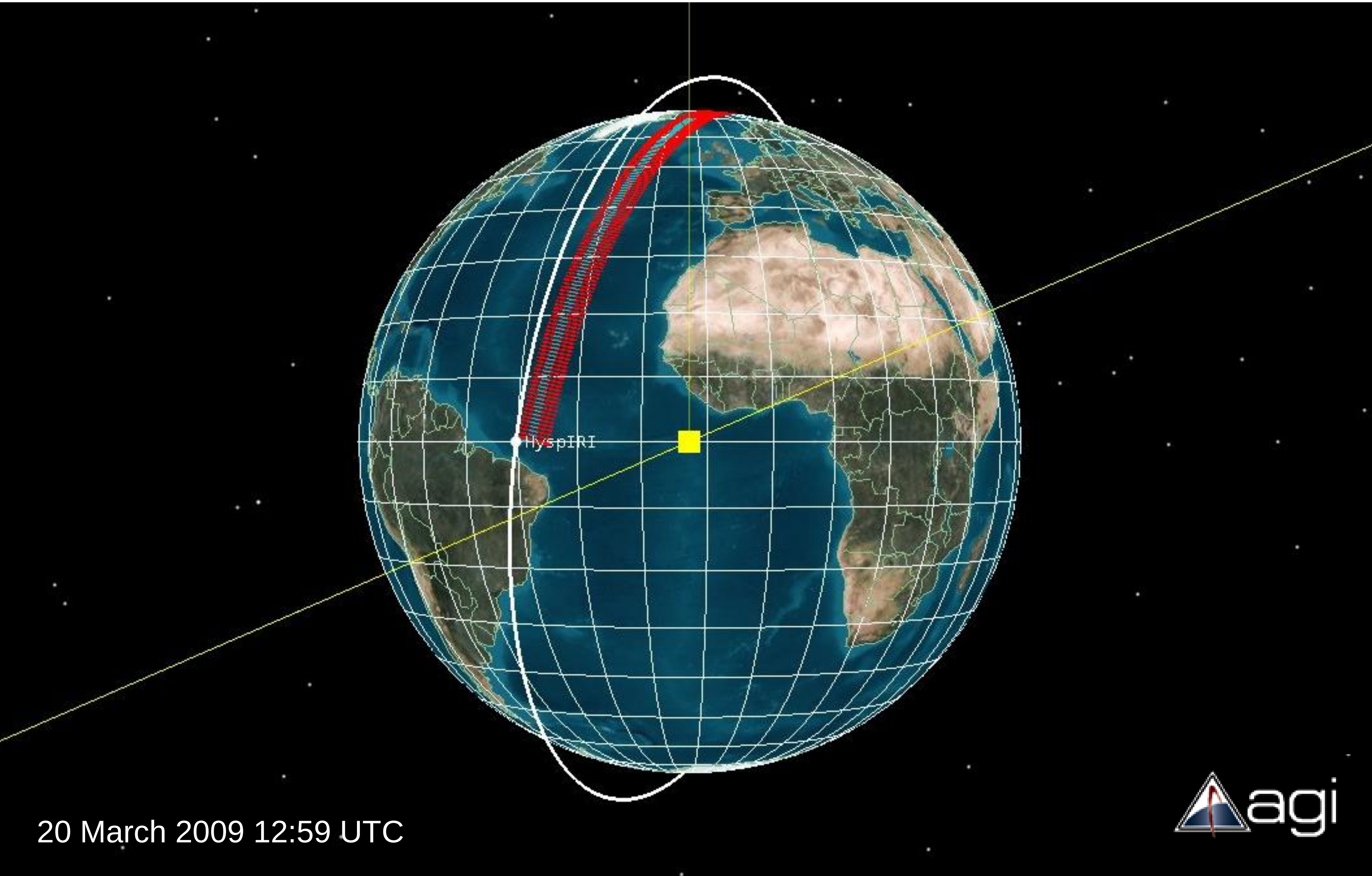

Orbital inclination (97.9) represents the angle between the Earth's equatorial plane, and the orbit plane, measured (by convention) at an ascending node.

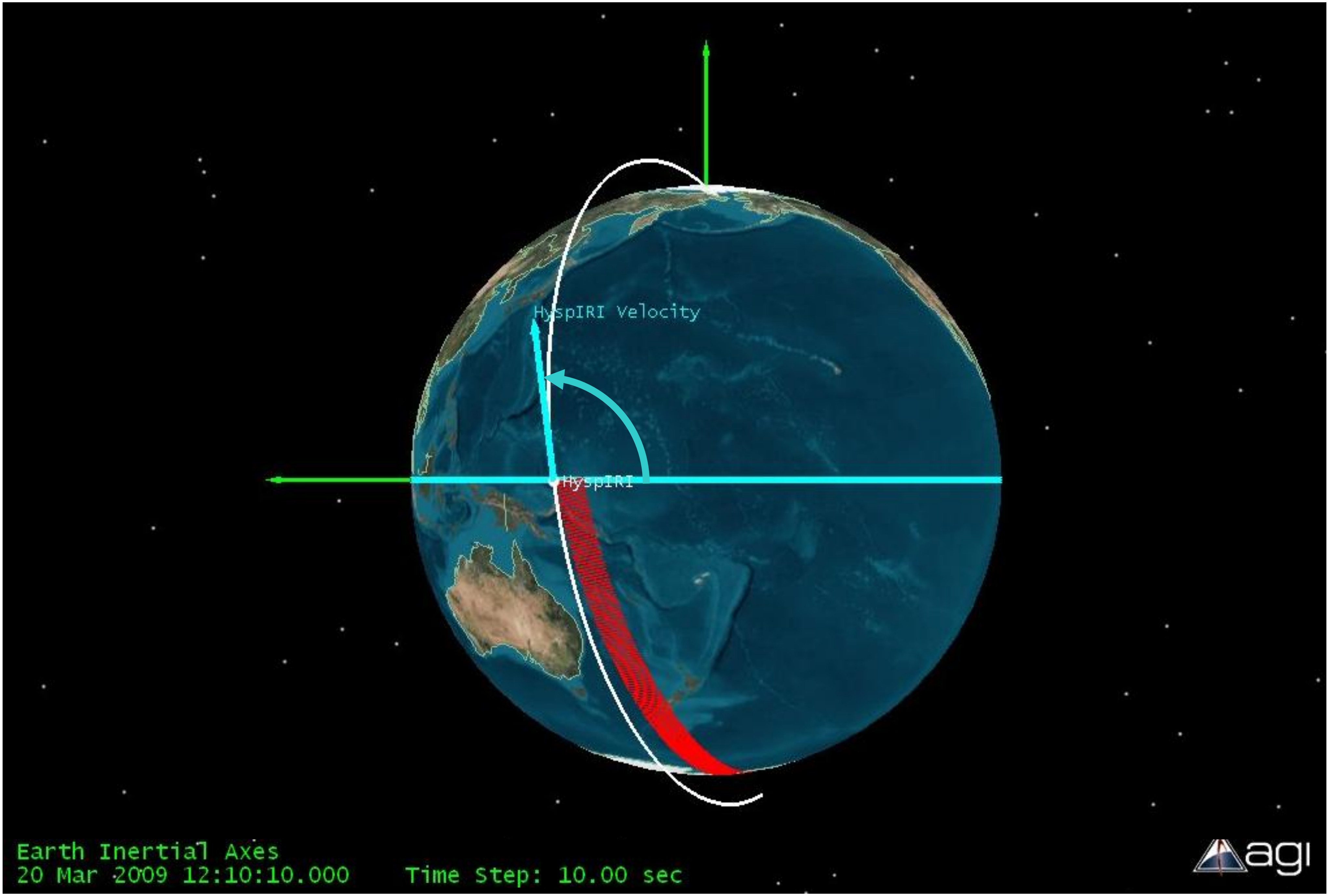

HyspIRI ground tracks shortly after completing a 5-day near repeat pattern:
(a) blue – descending (day) passes and orbit track;
(b) red – ascending (night) passes and orbit track.

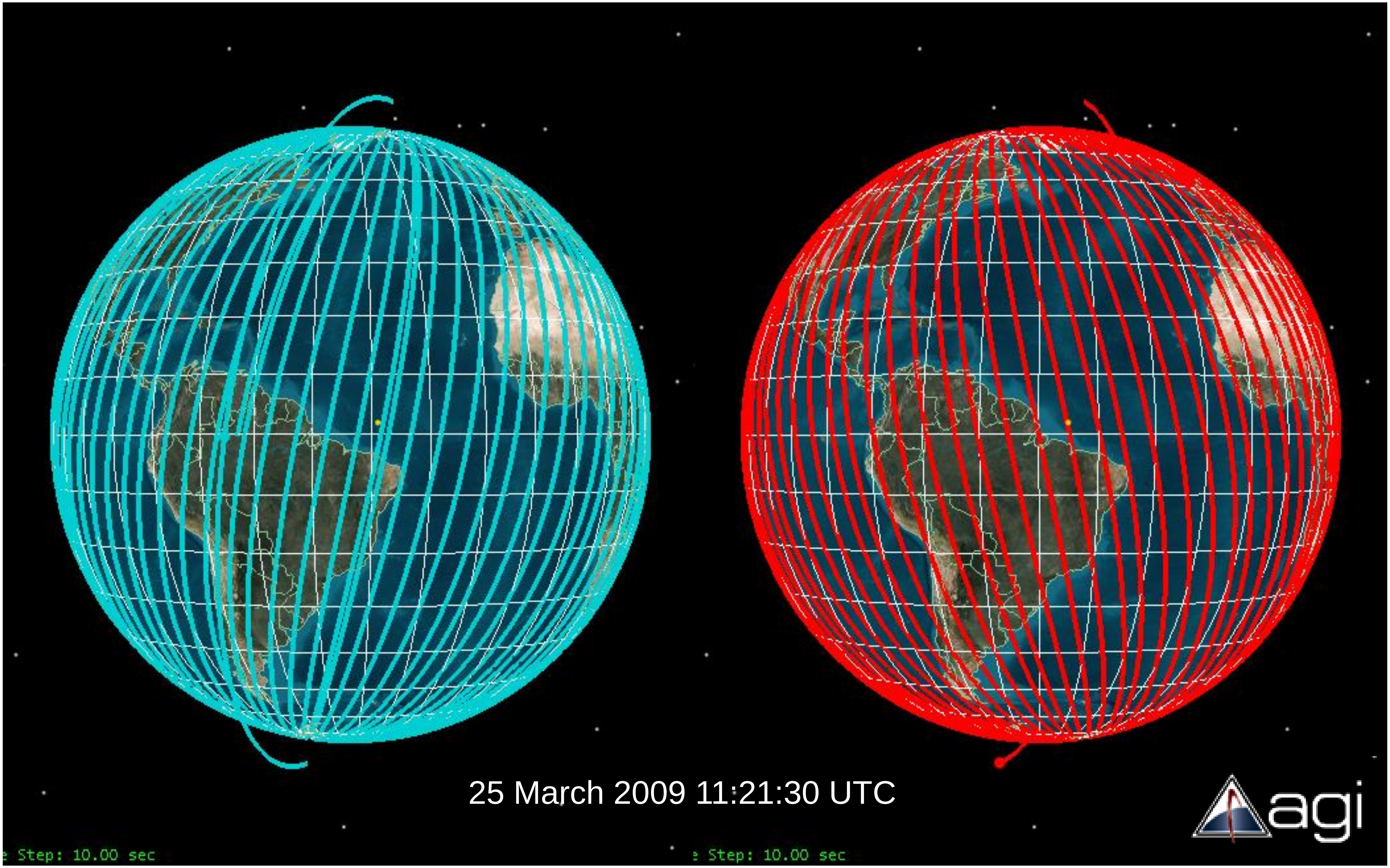

R.G. Knox simulation with STK v8.1.3. Orbit: alt. 626.8 km, inclination: 97.8°. Earth graphics courtesy of Analytical Graphics Inc.

Sampling pattern after 2 days, with instrument footprints at 30 second intervals

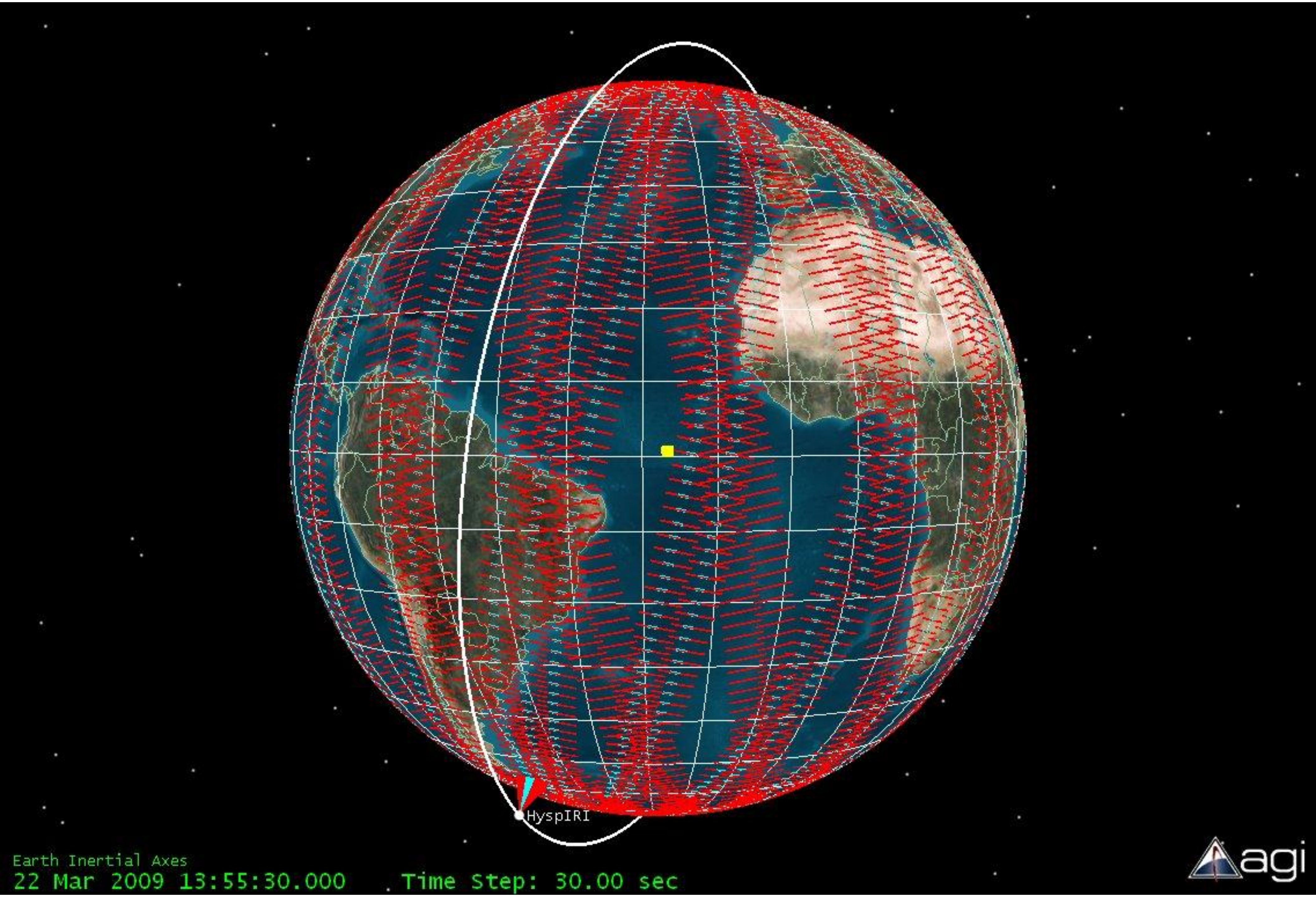

R.G. Knox simulation with STK v9.2. Orbit: alt. 626.8 km, inclination: 97.8°. Earth graphics courtesy of Analytical Graphics Inc.

Sampling pattern after 5 days, with instrument footprints at 30 second intervals

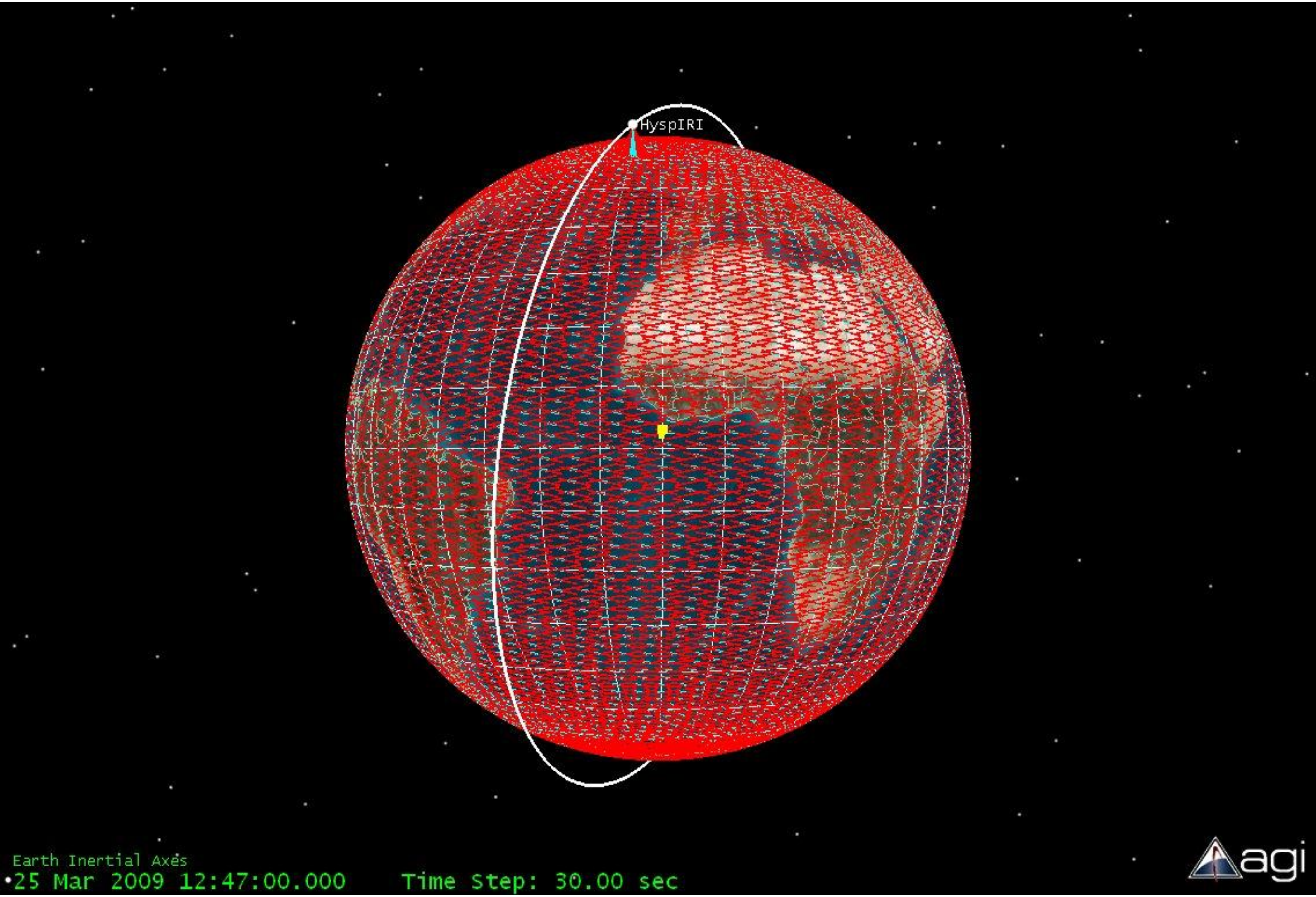

R.G. Knox simulation with STK v9.2. Orbit: alt. 626.8 km, inclination: 97.8°. Earth graphics courtesy of Analytical Graphics Inc.

HyspIRI sampling pattern after 5 days: Holes at N and S poles

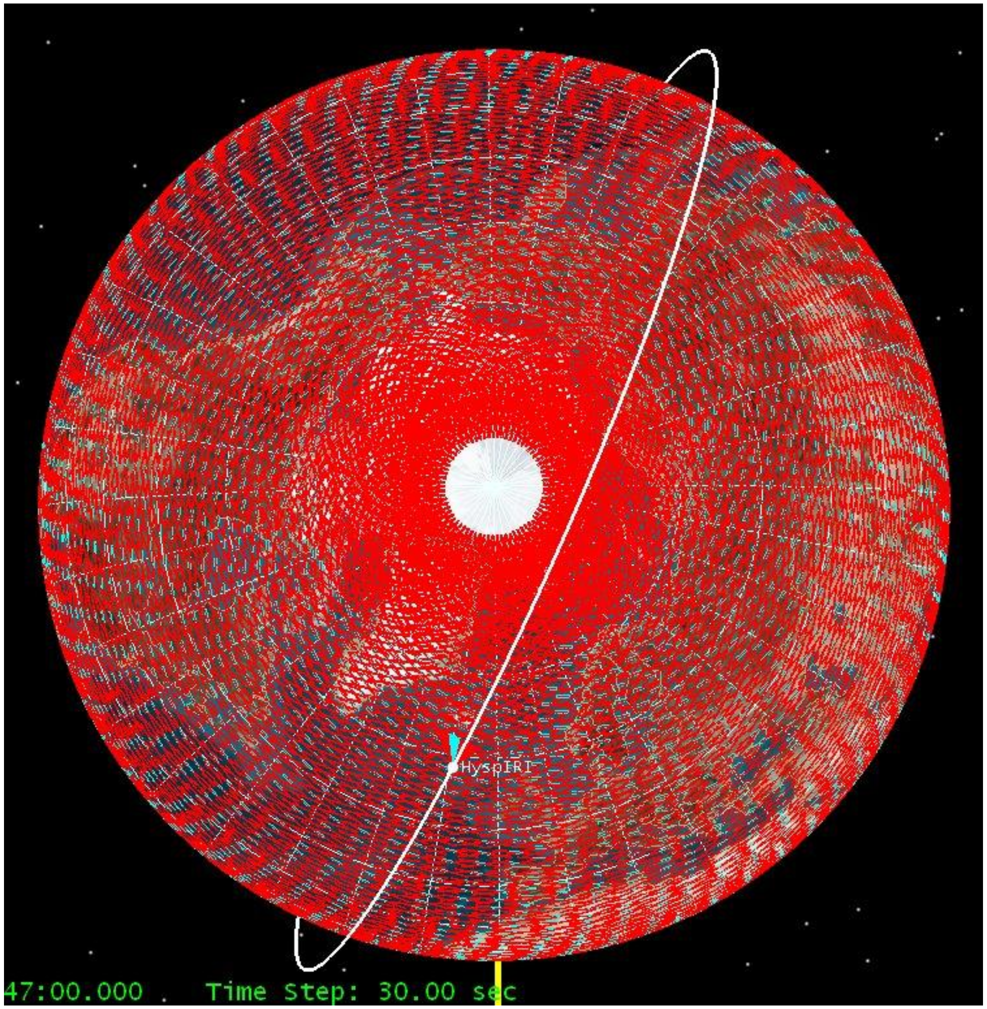

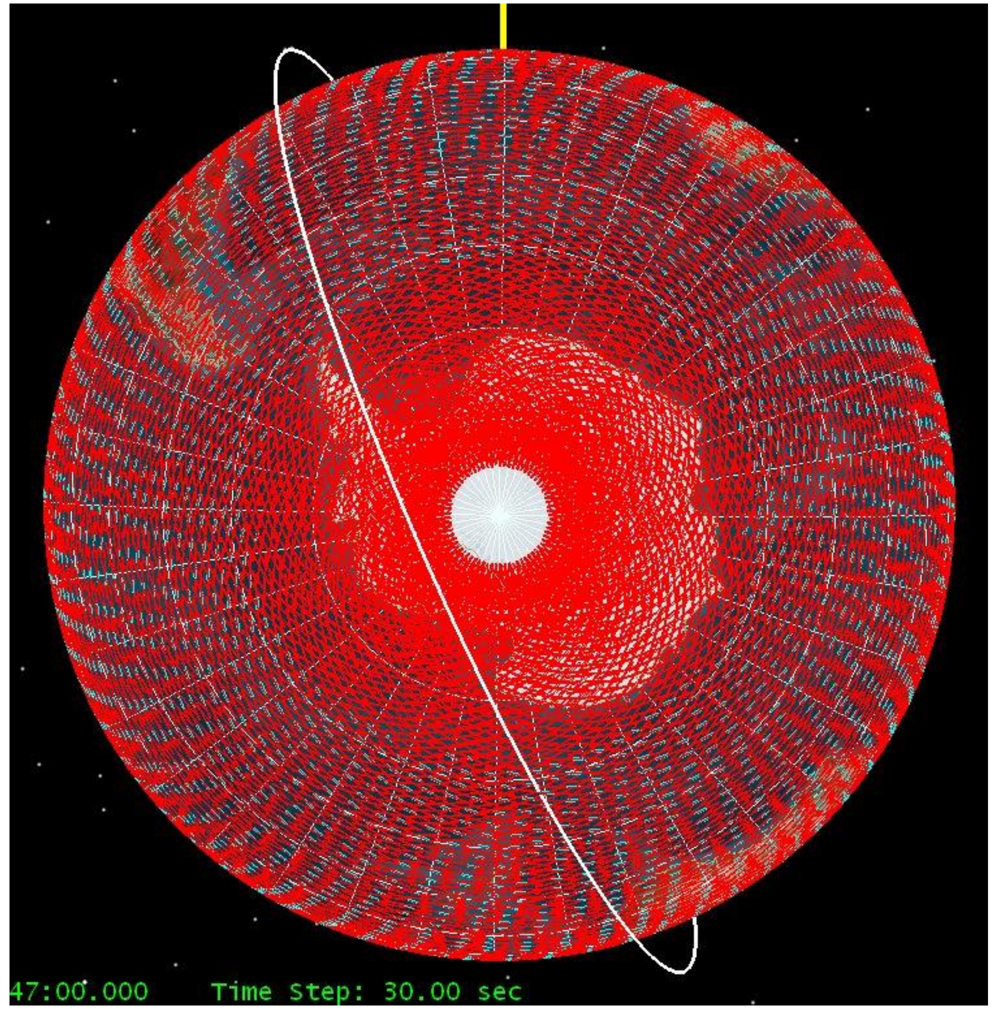

HyspIRI's nominal mid-morning (10:30 AM) crossing time is on a descending orbit (N-to-S) pass. Hence the observatory passes over sunlit terrain while descending east of the North Pole and while approaching west of the South Pole. TIR coverage is similar at both poles. (Ground tracks of sun-synch. orbits cannot pass directly over the poles.) Because the VSWIR sensor relies on reflected illumination, it can collect data from well-illuminated surfaces at higher latitudes in the north.

R.G. Knox simulation with STK v9.2. Orbit: alt. 626.8 km, inclination: 97.8°. Simulated mission days March 20-25, 2009. Nominal TIR & VSWIR FOV marked at 30 second intervals. Earth graphics courtesy of Analytical Graphics Inc.

Annual TIR imaging opportunities in a 5-day near-repeating orbit, 1 yr. simulation

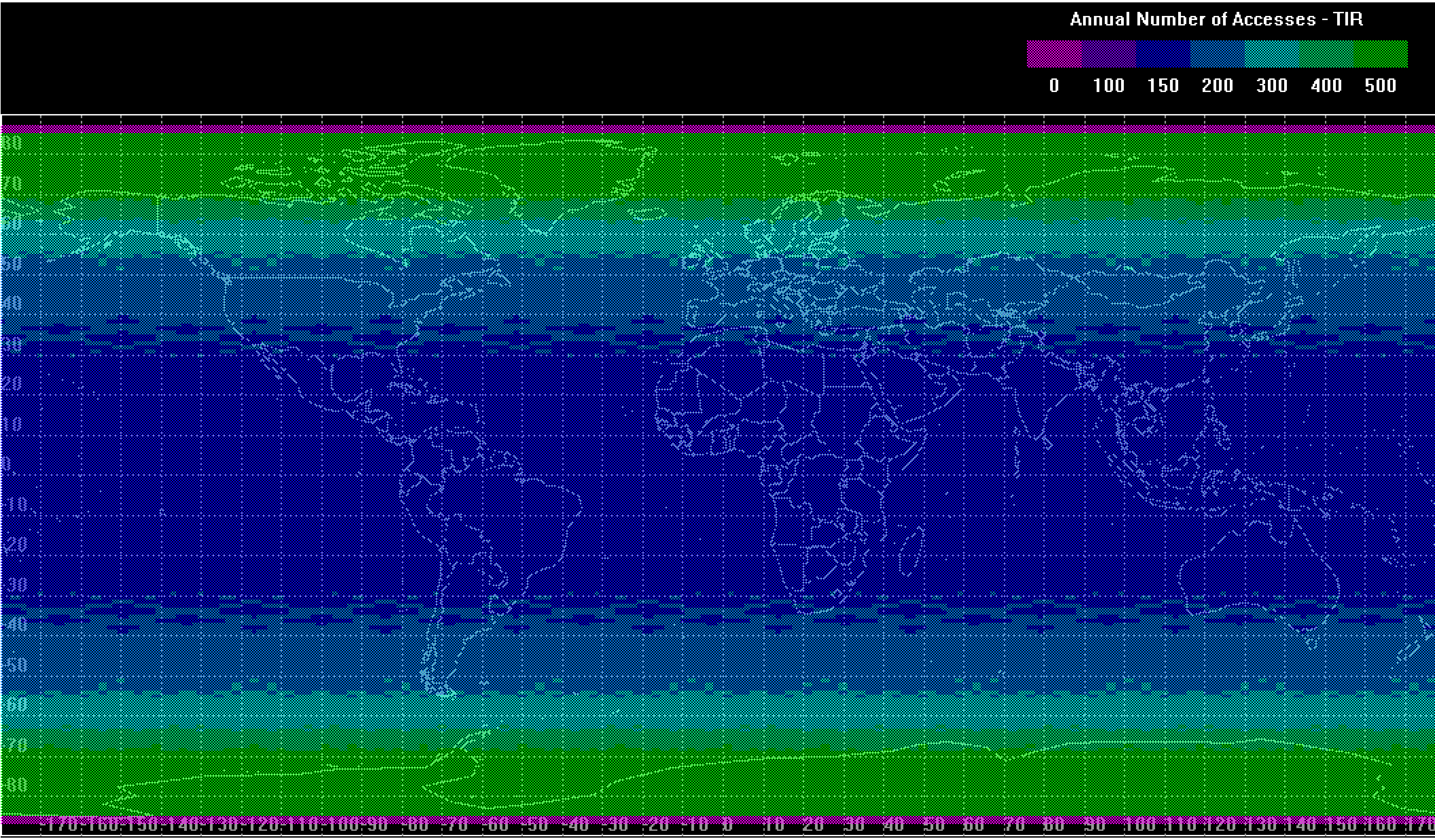

Nominal orbit: average alt. 626.8 km, inclination 97.8°. TIR imager FOV: +/- 25.46° (60 m pixel GSD at nadir, 9272 cross-track pixels).
R.G. Knox, NASA GSFC, Biospheric Sciences Branch, Code 614.4. Simulated with STK v8.1.3, March 7, 2010. Plotted May 3, 2010.

Annual TIR imaging opportunities in a 19/5-day repeat HyspIRI reference orbit
Swath: 50.92°, symmetric about nadir. Sampled using a 1 by 1 deg. coverage.

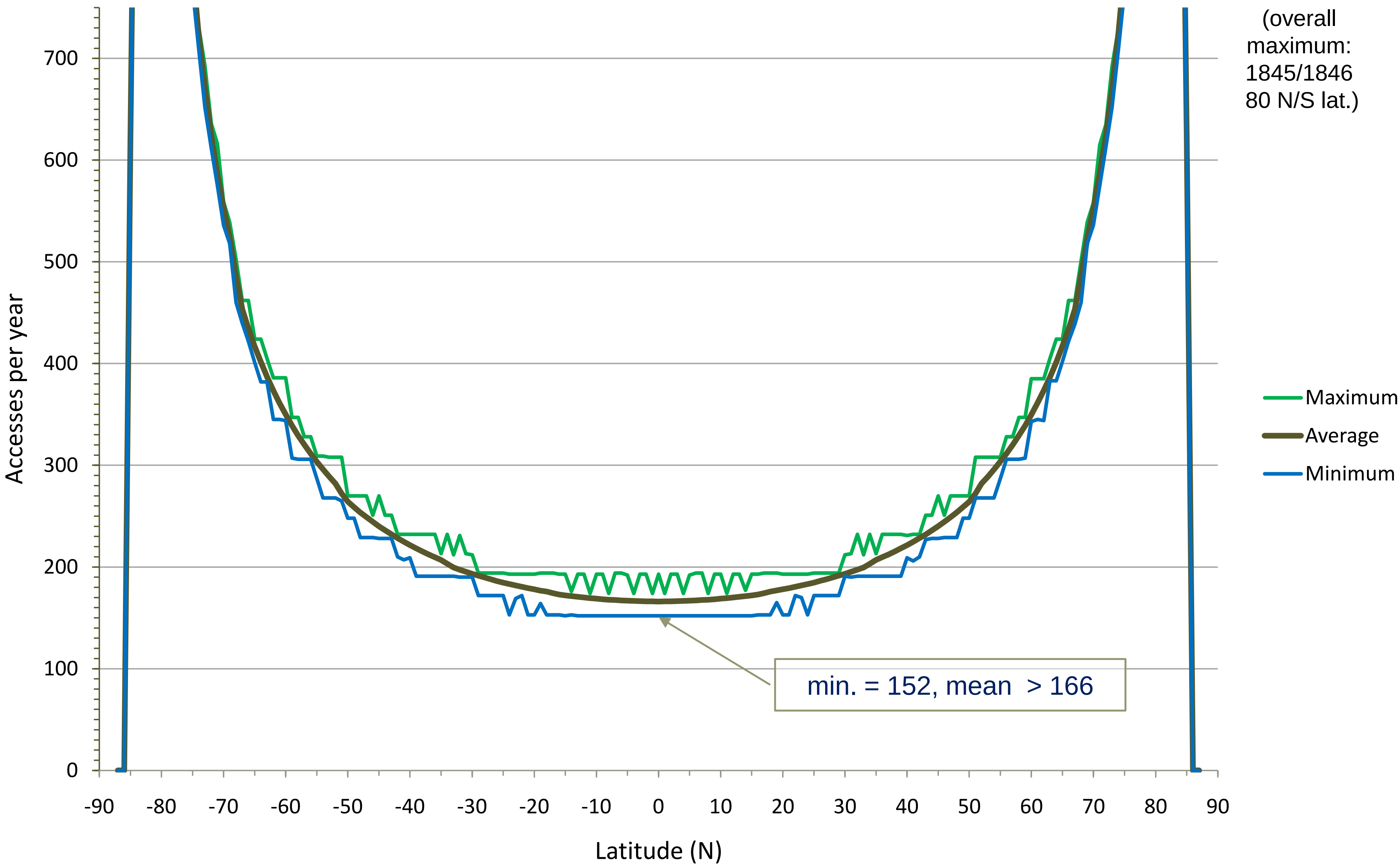

Nominal orbit: average alt. 626.8 km, inclination 97.8°. TIR imager FOV: +/- 25.46° (60 m pixel GSD at nadir, 9272 cross-track pixels).
R.G. Knox, NASA GSFC, Biospheric Sciences Branch, Code 614.4. Simulated with STK v8.1.3, March 7, 2010.

Annual VSWIR imaging opportunities in a 19-day repeating orbit, 1 yr. simulation, with a minimum solar elevation of 20°

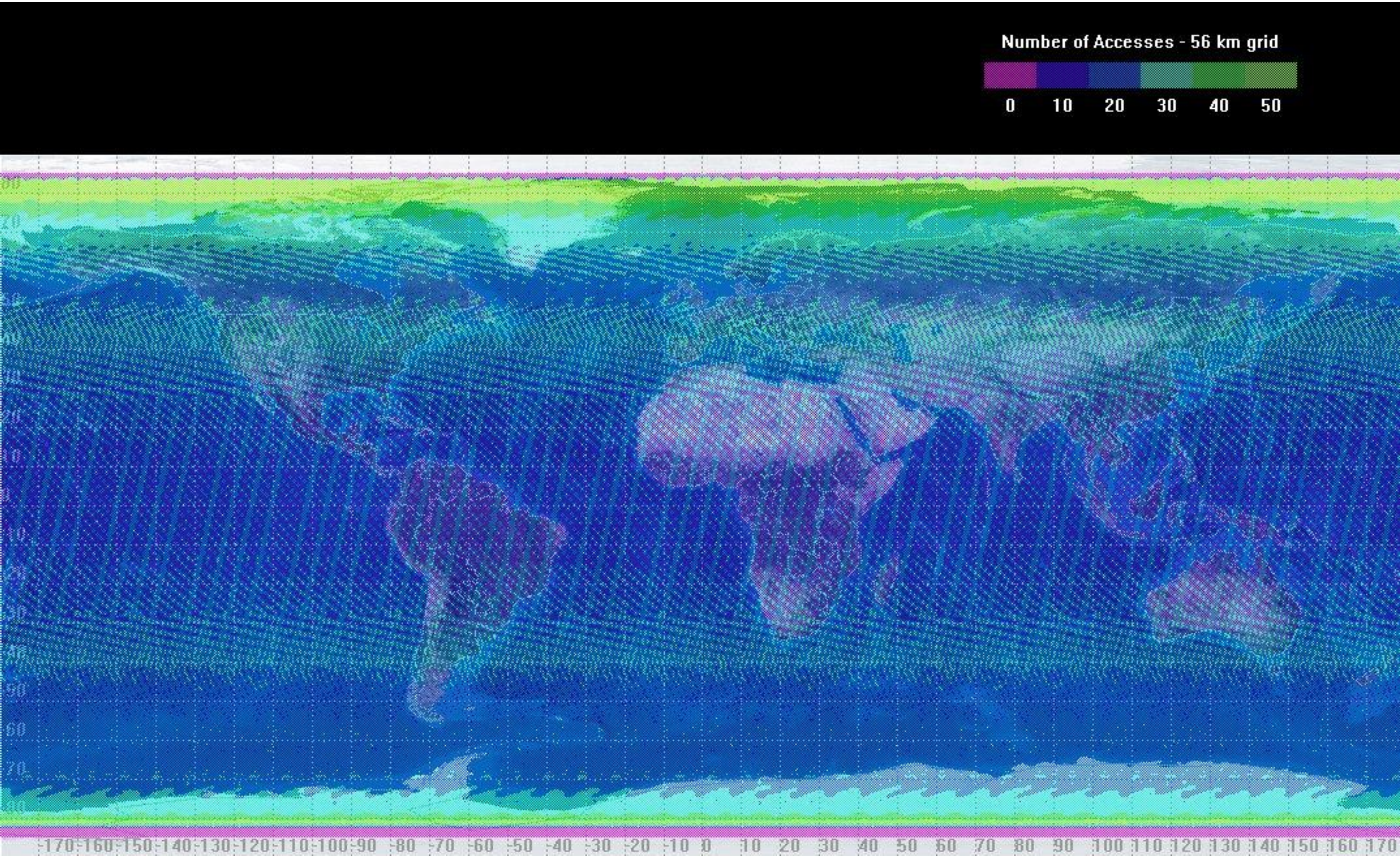

Nominal orbit: av. alt. 626.8 km, incl. 97.8°. VSWIR spectrometer FOV: 2.8° E, 10.8° W (60 m pixel GSD at nadir, 2480 cross-track pixels). R.G. Knox, NASA GSFC, Biospheric Sciences Branch, Code 614.4. Simulated with STK v9.2, August 20, 2010. Note aliasing with sample grid.

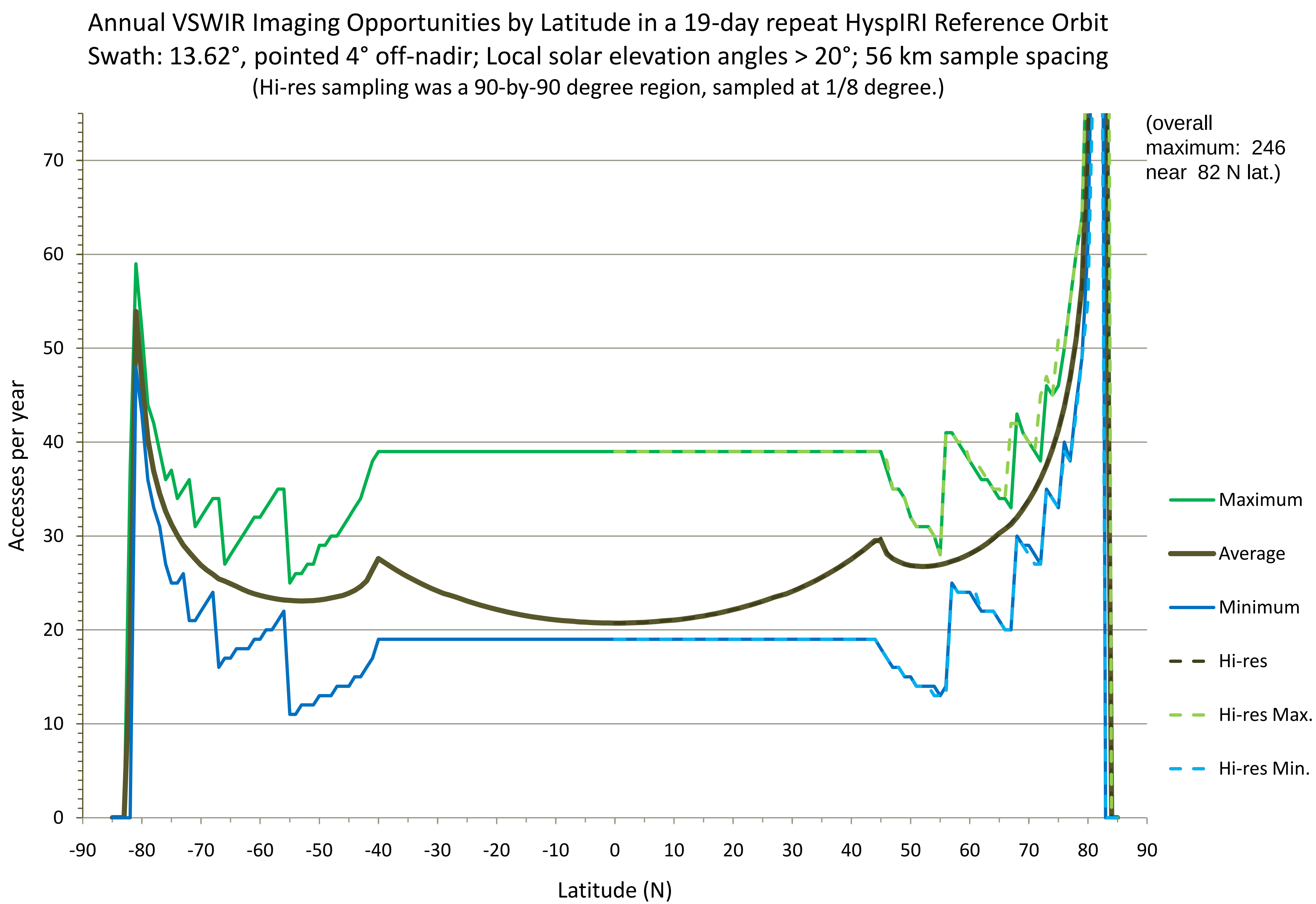

Nominal orbit: av. alt. 626.8 km, incl. 97.8°. VSWIR spectrometer FOV: 2.8° E, 10.8° W (60 m pixel GSD at nadir, 2480 cross-track pixels).
R.G. Knox, NASA GSFC, Biospheric Sciences Branch, Code 614.4. Simulated with STK v9.2, Aug. 20, 2010.; hi-res subset Aug. 17.

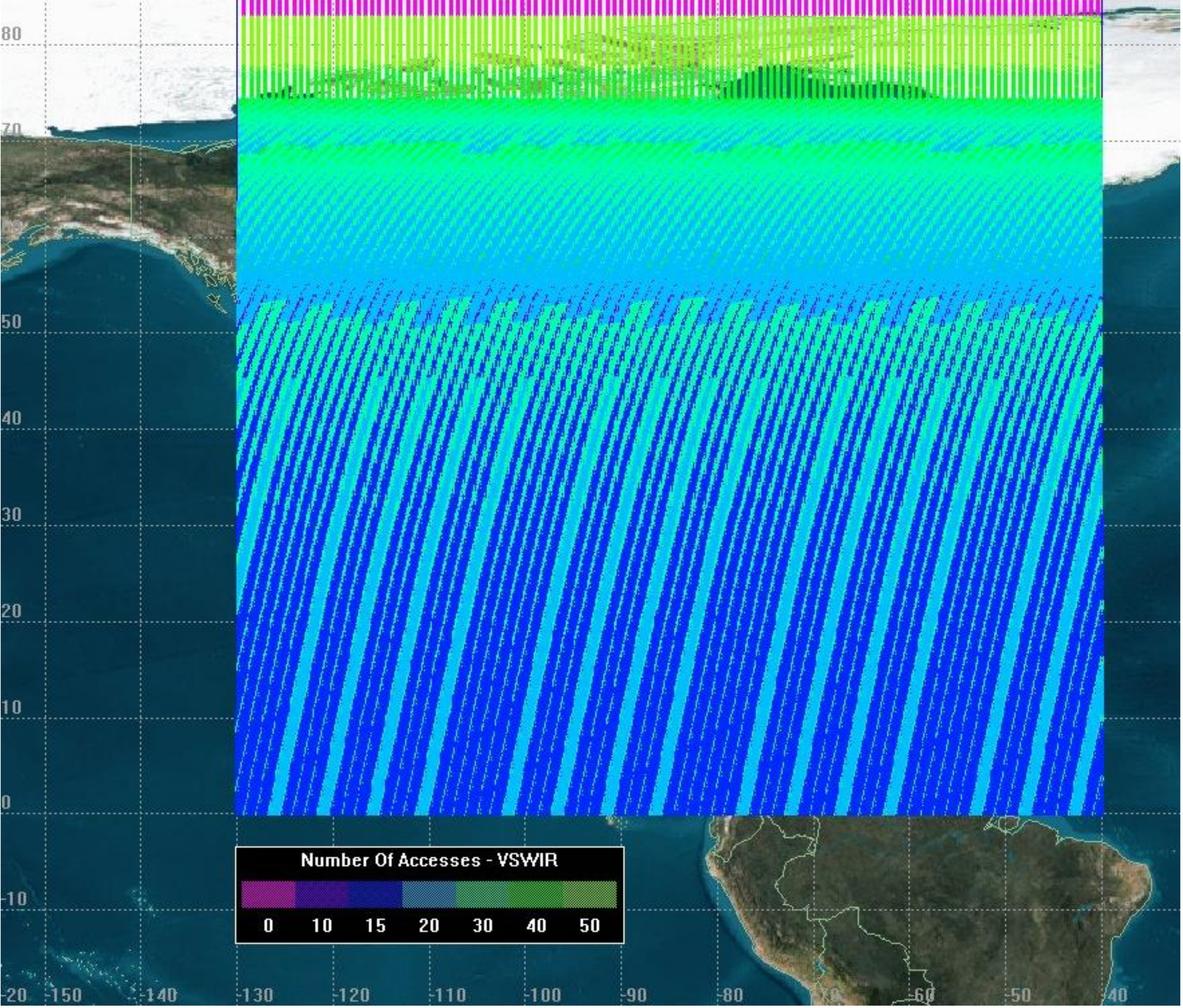

High resolution (1/8 degree) simulation of annual VSWIR coverage, 90 x 90 degree (lat, lon) region

Nominal orbit: av. alt. 626.8 km, incl. 97.8°. VSWIR spectrometer FOV: 2.8° E, 10.8° W (60 m pixel GSD at nadir, 2480 cross-track pixels).
R.G. Knox, NASA GSFC, Biospheric Sciences Branch, Code 614.4. Simulated with STK v9.2, August 17, 2010. Note aliasing at high latitudes.

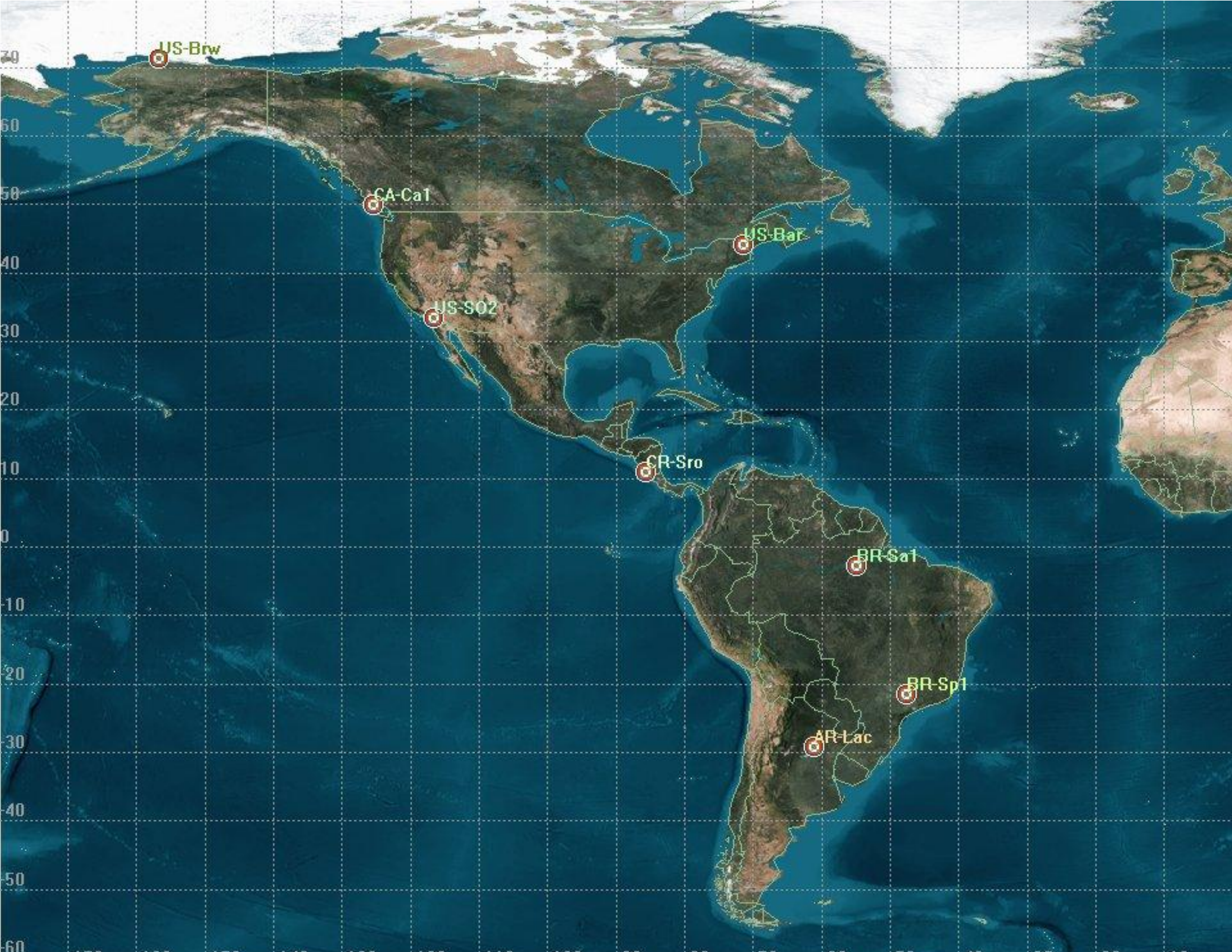
US-Brw
CA-Ca1
US-Bar
US-SO2
CR-Sro
BR-Sa1
BR-Sp1
AR-Lac
70
60
50
40
30
20
10
0
-10
-20
-30
-40
-50
-60

VSWIR accesses (SZA < 70°) for 1 simulated year

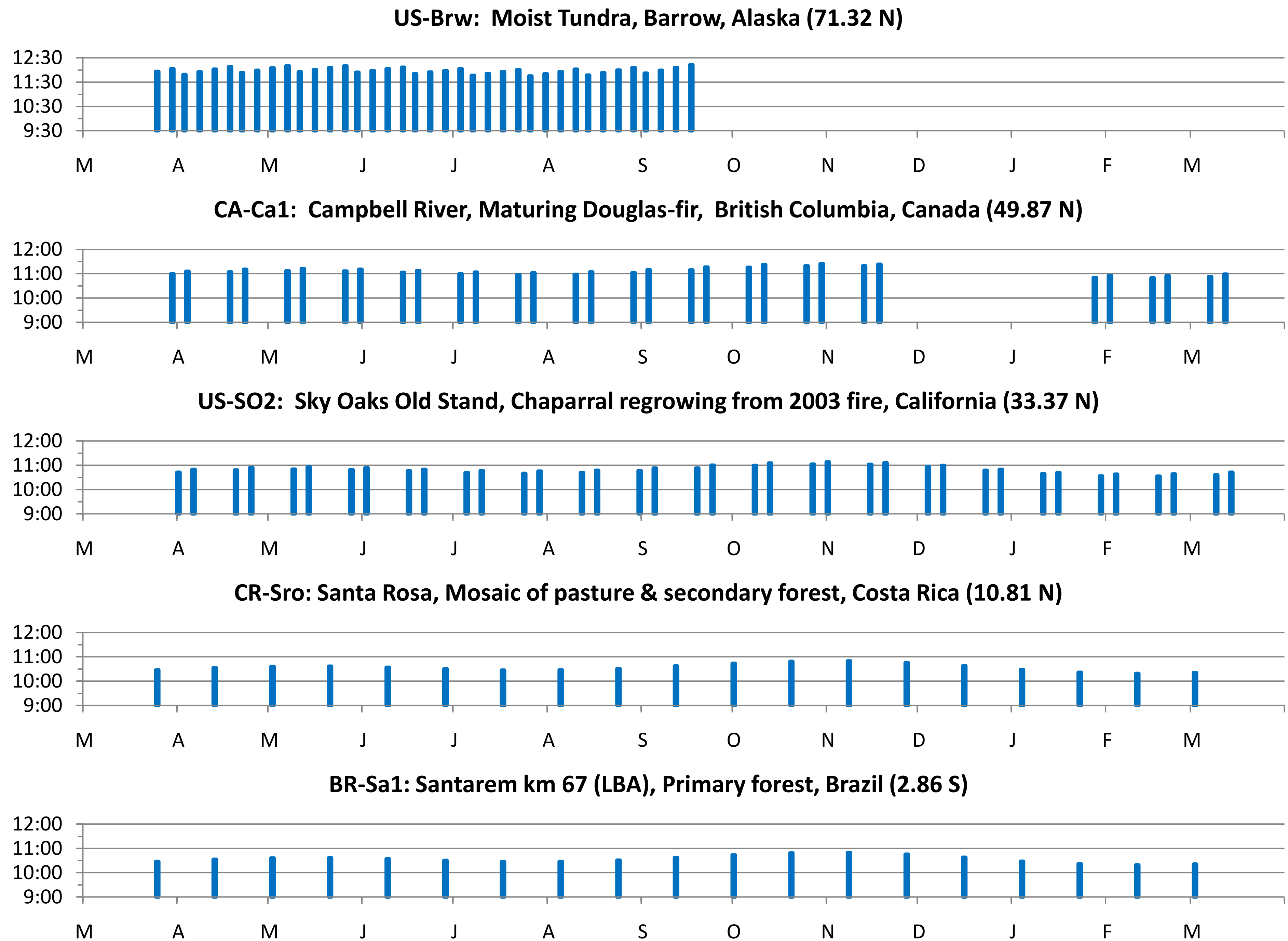

R.G. Knox & E.M. Middleton, NASA GSFC, Biospheric Sciences Branch, Code 614.4. Simulated with STK v9.2

VSWIR accesses for 1 simulated year

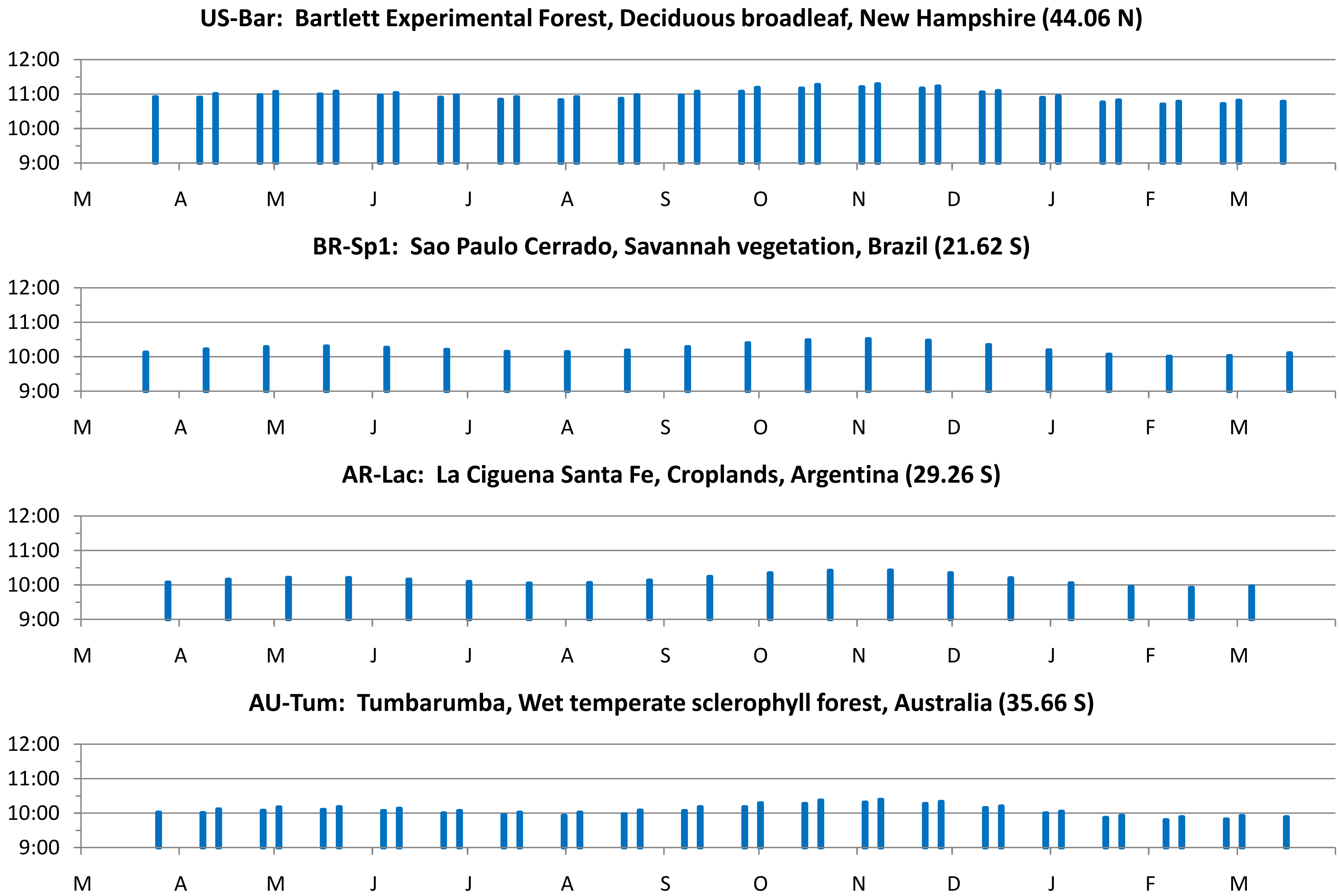

R.G. Knox & E.M. Middleton, NASA GSFC, Biospheric Sciences Branch, Code 614.4. Simulated with STK v9.2

Local time of VSWIR overpasses of 5 FLUXNET sites, simulated for 1 year

Local apparent time, for a fixed mean local time, varies with the Earth's orbit. (Blue bars are 6 minutes wide.)

As the N latitude of the site increases, the local apparent times of potential VSWIR accesses also increase.

Near the north orbit pole (82.1 N) the local time of potential accesses may be nearly 6 hours later than when crossing the equator (not shown).

Moving toward the south orbit pole local times are progressively earlier in the morning.

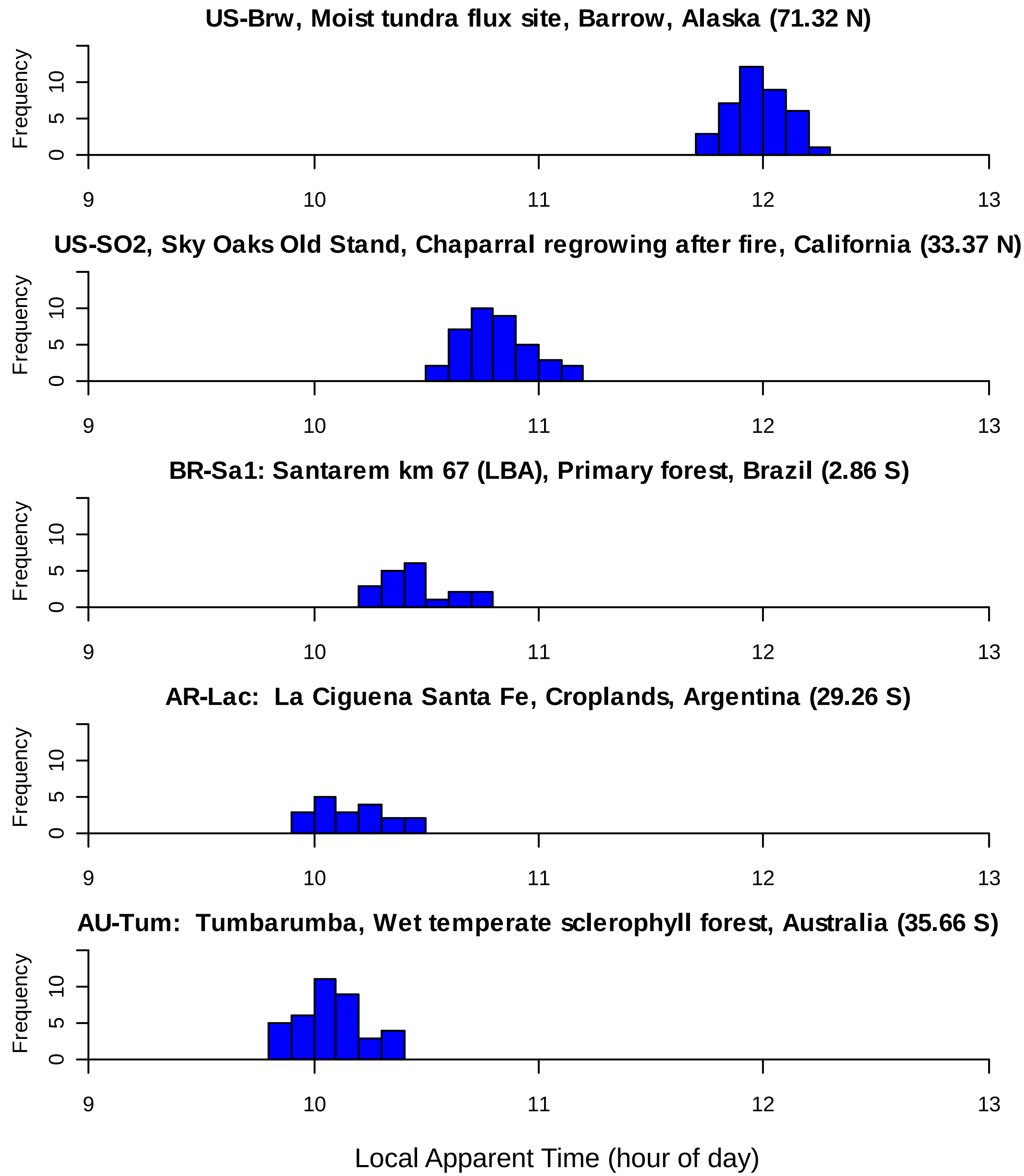

R.G. Knox & E.M. Middleton, NASA GSFC, Biospheric Sciences Branch, Code 614.4. Simulated with STK v9.2

Example HyspIRI access to Sky Oaks (US-SO2, Old Stand) flux site in southern California

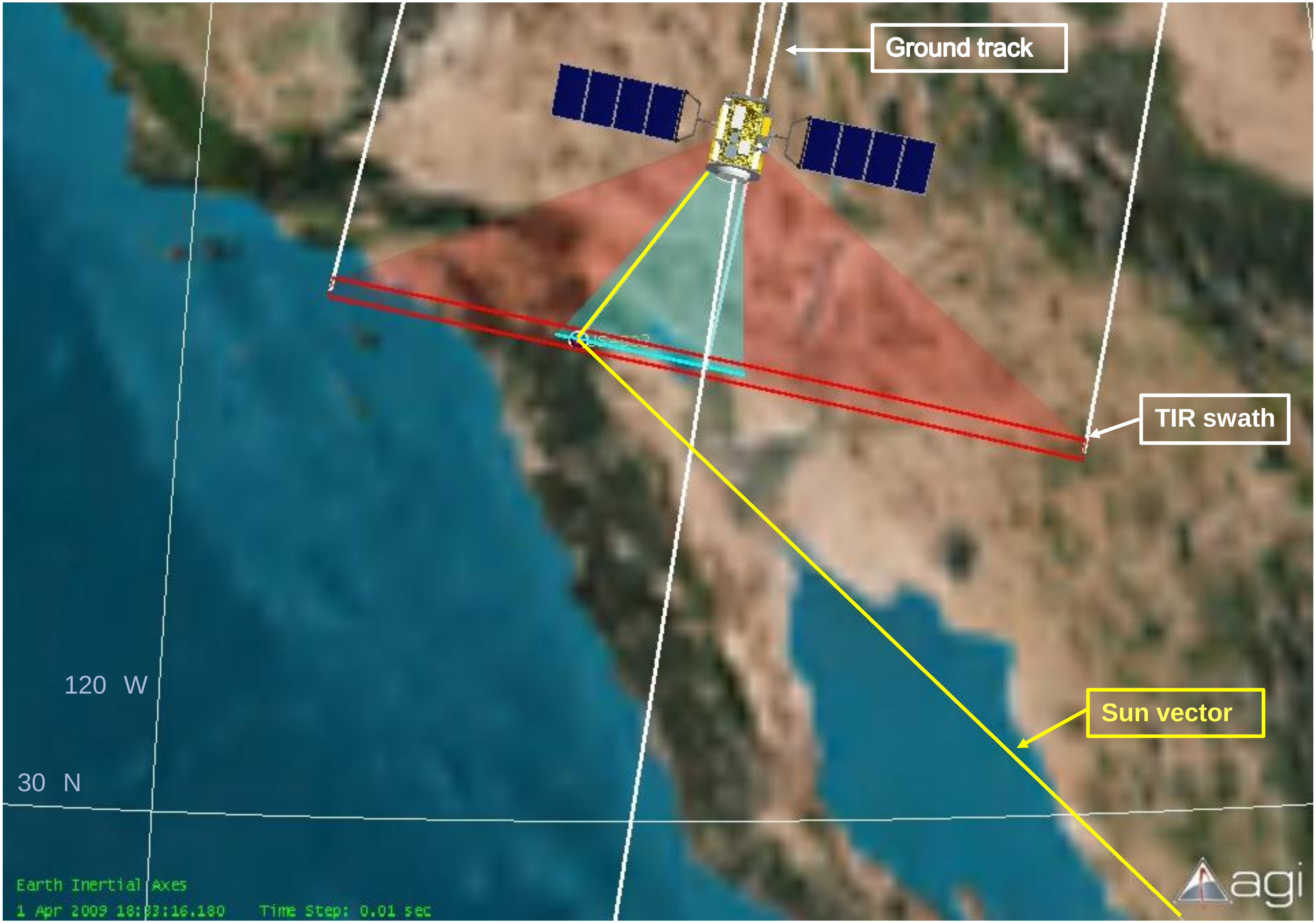

VSWIR swath (light blue) is nested within TIR cross-track scan pattern (red), with a swath center offset west of the satellite's ground track (white). Note view & illumination vectors (yellow). Access geometry simulated for 1 Apr 2009, 18:33:16.18 UTC, with STK v9.2.

Polar plots of illumination geometry for VSWIR and Daylight TIR accesses to Sky Oaks, Old stand, California (33.37 N)

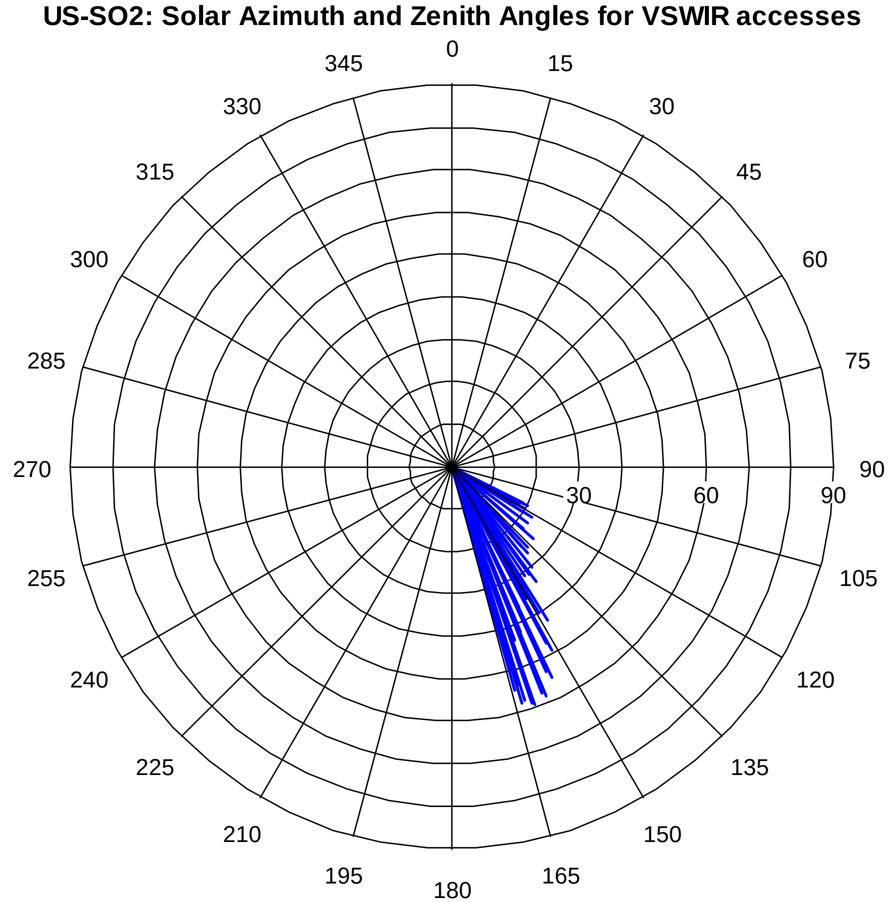

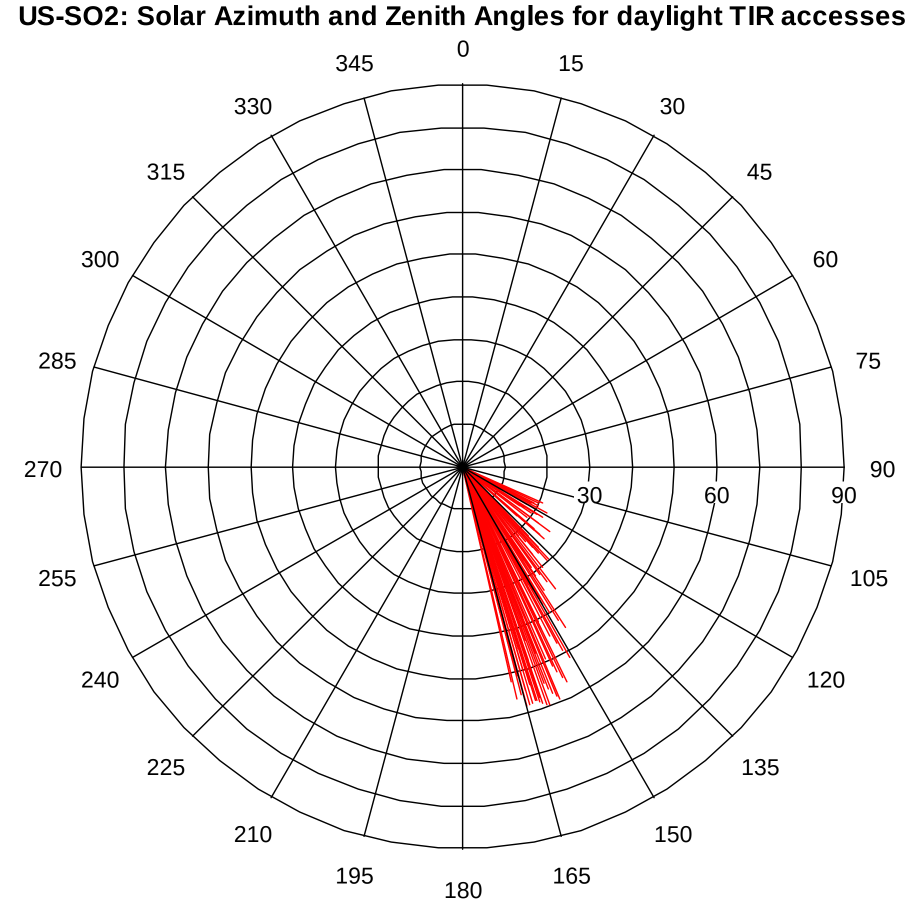

Solar Zenith Angle

Mean	37.75°
Std.dev.	14.69°

Solar Zenith Angle (daylight)

Mean	37.47°
Std.dev.	14.62°

R.G. Knox & E.M. Middleton, NASA GSFC, Biospheric Sciences Branch, Code 614.4. Simulated with STK v9.2

Polar plots of simulated illumination geometry for VSWIR accesses over 1 year, for 9 flux sites arranged by latitude.

Note that for clarity solar zenith angles were plotted from 0 to 80 degrees, and solar azimuths were marked in 30 degree increments.

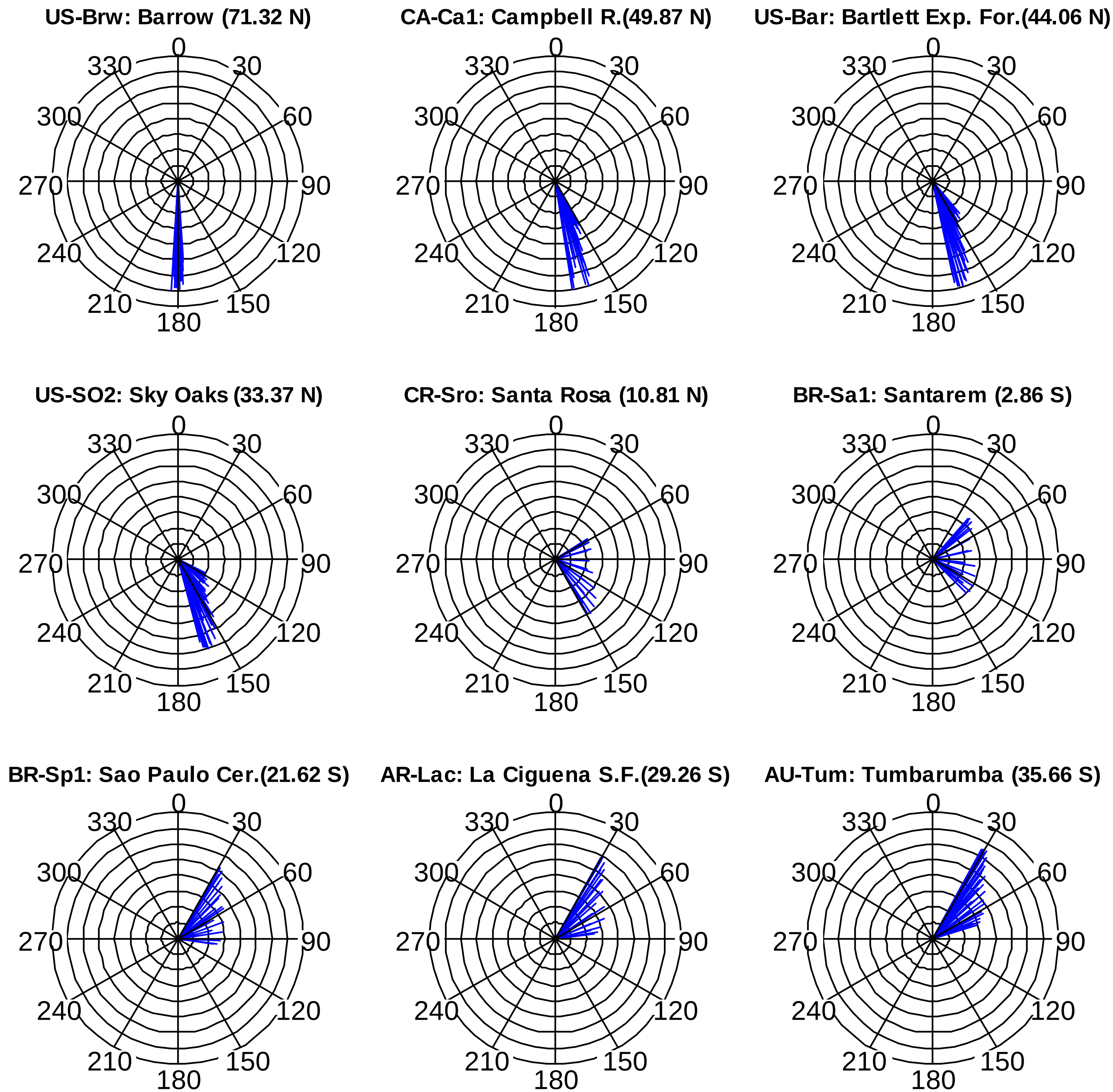

R.G. Knox & E.M. Middleton, NASA GSFC, Biospheric Sciences Branch, Code 614.4. Simulated with STK v9.2

Polar plots of simulated illumination geometry for daylight TIR accesses over 1 year, for 9 flux sites arranged by latitude.

Unlike VSWIR simulations, solar zenith angles exceed 70°, and above the Arctic circle solar azimuths include daylight observations on ascending orbit passes.

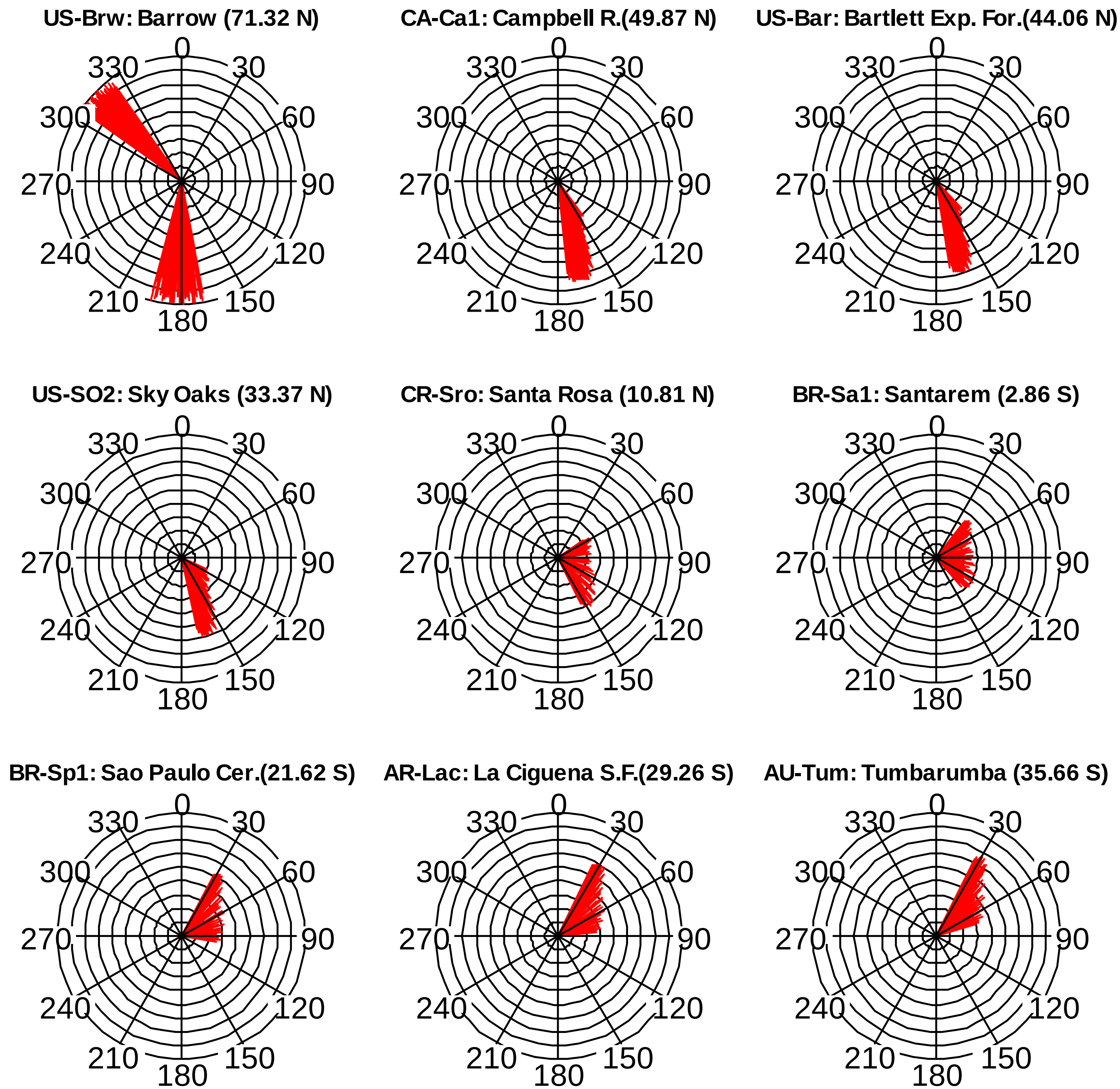

R.G. Knox & E.M. Middleton, NASA GSFC, Biospheric Sciences Branch, Code 614.4. Simulated with STK v9.2

Solar zenith angles (SZA) at times site viewed by HyspIRI instruments, over 1 simulated year

		VSWIR			Daylight TIR		
Flux Site	**Latitude**	**Mean SZA**	**Std. Dev.**	**n**	**Mean SZA**	**Std. Dev.**	**n**
US-Brw	71.3 N	56.0	6.9	38	70.5	14.1	322
CA-Ca1	49.9 N	46.7	14.3	32	50.9	16.1	135
US-Bar	44.1 N	46.0	16.0	38	47.3	16.0	104
US-SO2	33.4 N	37.8	14.7	38	37.5	14.6	96
CR-Sro	10.8 N	28.1	6.9	19	27.6	6.9	77
BR-Sa1	2.9 S	28.3	4.3	19	27.8	4.4	77
BR-Sp1	21.6 S	35.9	10.6	20	35.5	10.7	77
AR-Lac	29.3 S	41.0	12.8	19	40.2	12.7	96
AU-Tum	35.7 S	45.7	13.8	38	45.4	13.8	95

R.G. Knox & E.M. Middleton, NASA GSFC, Biospheric Sciences Branch, Code 614.4. Simulated with STK v9.2

Polar plots of simulated view geometry (red) for daylight TIR accesses over 1 year, for 9 flux sites arranged by latitude. Solar zenith angles (black) plotted in the principal plane.

At higher latitudes views are well outside the principal plane. With a mid-morning crossing time, some data will be collected near the principal plane at subtropical and tropical latitudes.

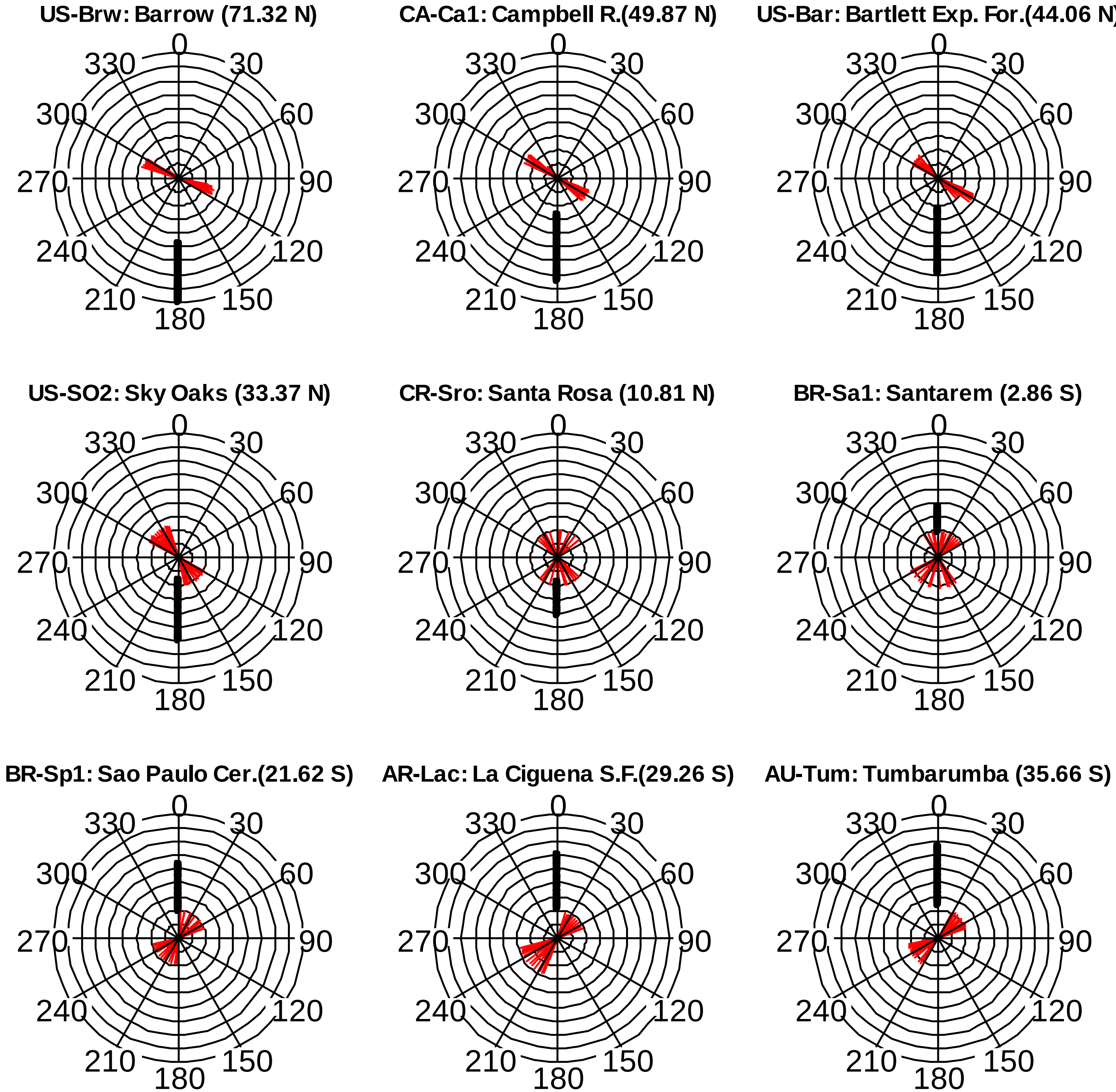

R.G. Knox & E.M. Middleton, NASA GSFC, Biospheric Sciences Branch, Code 614.4. Simulated with STK v9.2

TIR accesses for 1 simulated year

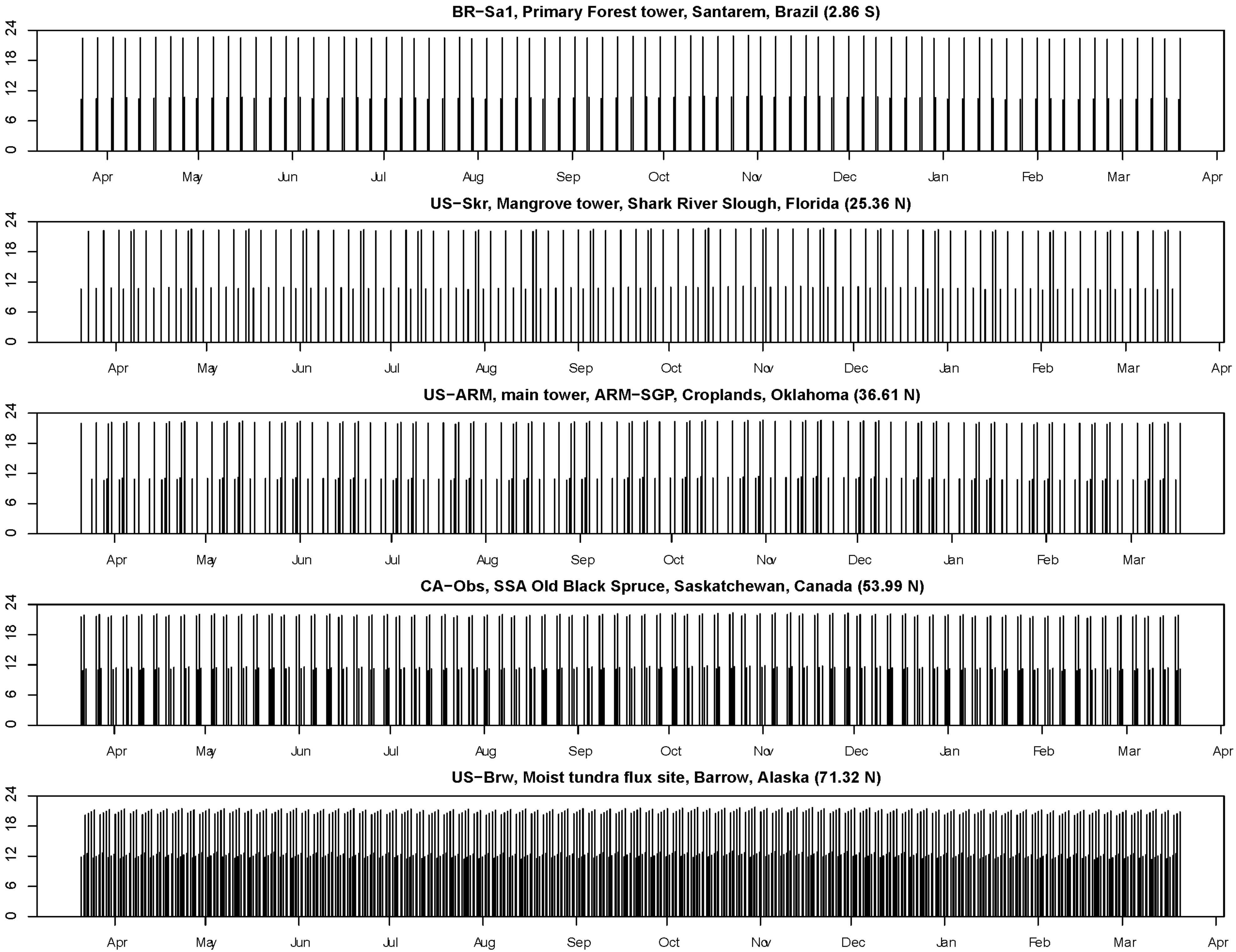

Minimum times between Multispectral Thermal (TIR) Imager accesses

Potential accesses simulated for 1 year, sampled over a 1 by 1 deg. grid

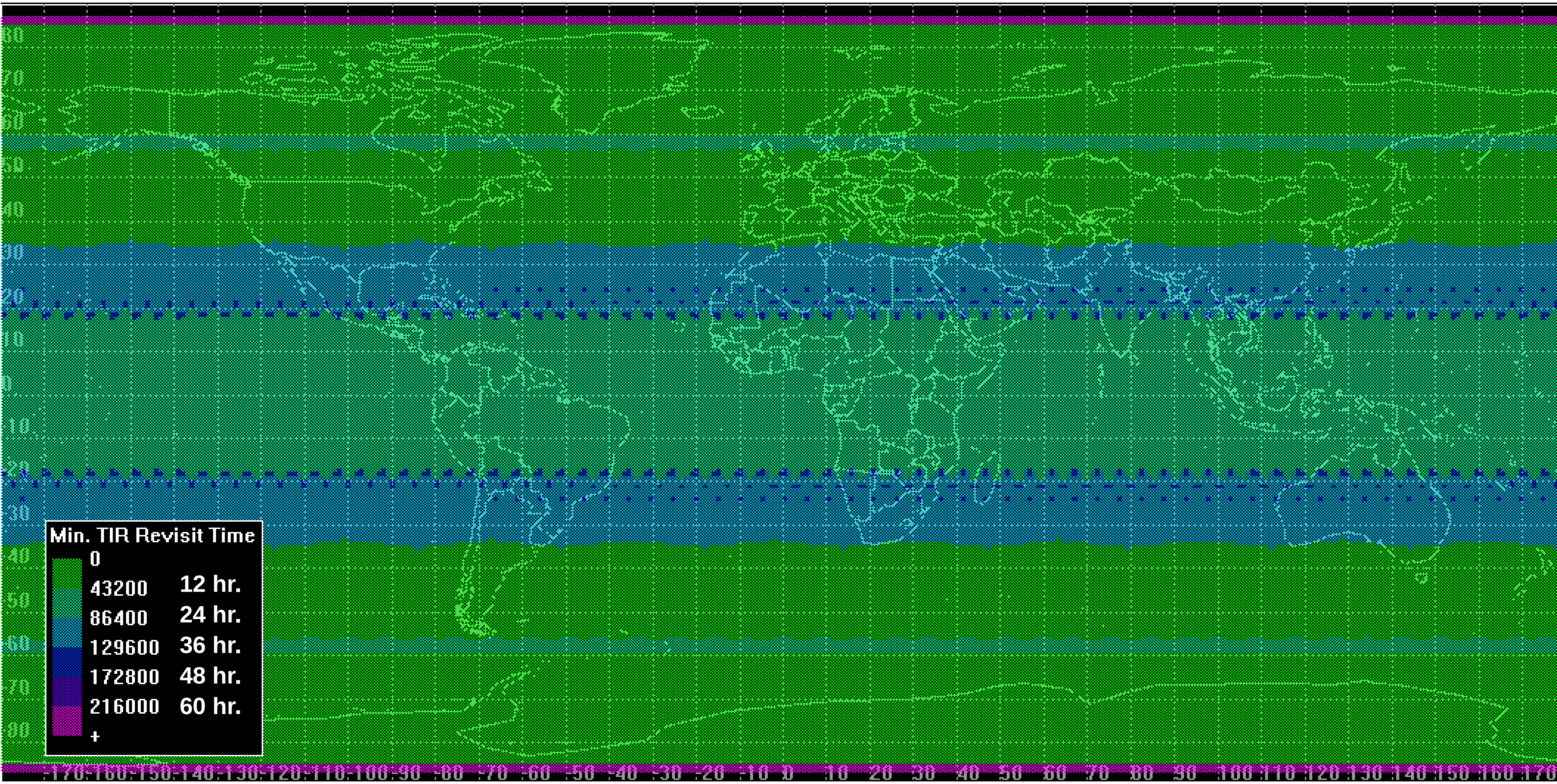

Nominal orbit: alt. 626.8 km, incl.: 97.8. TIR sensor FOV: +/- 25.46 (60 m pixel GSD at nadir, 9272 cross-track pixels).

R.G. Knox, NASA GSFC, Biospheric Sciences Branch, Code 614.4. Simulated with STK v8.1.3, March 20, 2010. Plotted May 3, 2010.

Some observations & conclusions

- The local apparent time for overpasses is usually **not** 10:30 AM.
- Viewing geometry is well-constrained in HyspIRI's reference design (*cf.* MODIS), but illumination geometry varies systematically with latitude. To produce consistent global data, algorithms will need to address this.
- A mid-morning orbit crossing time, for descending orbit passes, implies mid-day or later overpasses in the Arctic and progressively earlier morning overpasses in southern temperate to near-polar latitudes. This will reduce the quantity and/or quality of winter VSWIR data in the southern hemisphere. *(Glint reduction has trade-offs.)*
- A design concept to meet 5-day and < 20 day requirements (the reference orbit and instrument concepts) also provides highly sampled areas: e.g., high latitudes, overlapping swaths. (Longitudes with more frequent overlap might shift over the mission life—depending on specs. for maintaining orbit.)
- The reference orbit and TIR instrument swath provide day-night pairs—within 24 hours at most locations (not a mission requirement).

NASA

A Novel Approach to Report HyspIRI Location and Observation Information in a Compact Format for Data Distribution and Utilization

Joseph W. Boardman
Analytical Imaging and Geophysics, LLC
Boulder, CO
boardman@aigllc.com

Outline and Overview

- Some background on my biases
- AVIRIS, M3, CAO & ARTEMIS lessons
- Ray Tracing vs Rendering
- LOC and OBS files as backplanes
- HyspIRI Specifics
- Whole Earth is the Target
- >11 years to get ready?

Unique Spatial Aspects of Imaging Spectrometry Data

- It’s all about the spectra
- While map-projected products are the goal, the science must happen BEFORE the rendering/gridding
- Multi-temporal, multi-angle, BRDF, photometry, unmixing, etc all demand it
- Best-use of the data require supporting info regarding observation geometry
- Honor the spectral data, yet support the end users of products, with Pbytes...

Science THEN Rendering

NASA	CODMAC	Description
Packet Data	Raw - Level 1	Telemetry data stream as received at the ground station, with science and engineering data embedded.
Level 0	Edited - Level 2	Instrument science data (e.g., raw voltages, counts) at full resolution, time ordered, with duplicates and transmission errors removed.
Level 1-A	Calibrated - Level 3	Level 0 data that have been located in space and may have been transformed (e.g., calibrated, rearranged) in a reversible manner and packaged with needed ancillary and auxiliary data (e.g., radiances with the calibration equations applied).
Level 1-B	Resampled - Level 4	Irreversibly transformed (e.g., resampled, remapped, calibrated) values of the instrument measurements (e.g., radiances, magnetic field strength).
Level 2	Derived - Level 5	Geophysical parameters, generally derived from Level 1 data, and located in space and time commensurate with instrument location, pointing, and sampling.
Level 3	Derived - Level 5	Geophysical parameters mapped onto uniform space-time grids.

The IGM, GLT, GEO, ORT Model

example raw imagery

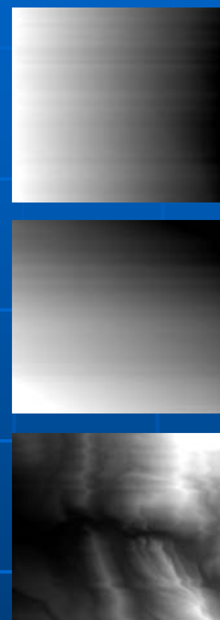

IGM products

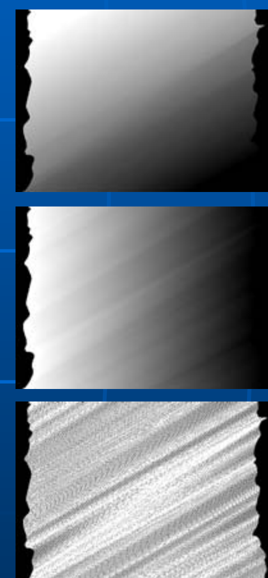

GLT products

3-d orthomosaic

AVIRIS Mosaic of Boulder

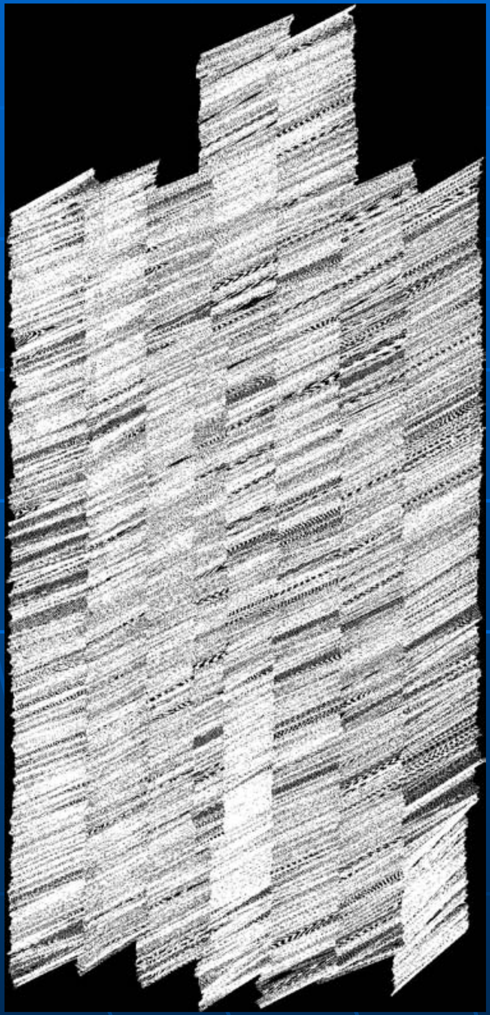

AVIRIS/CAO Fusion

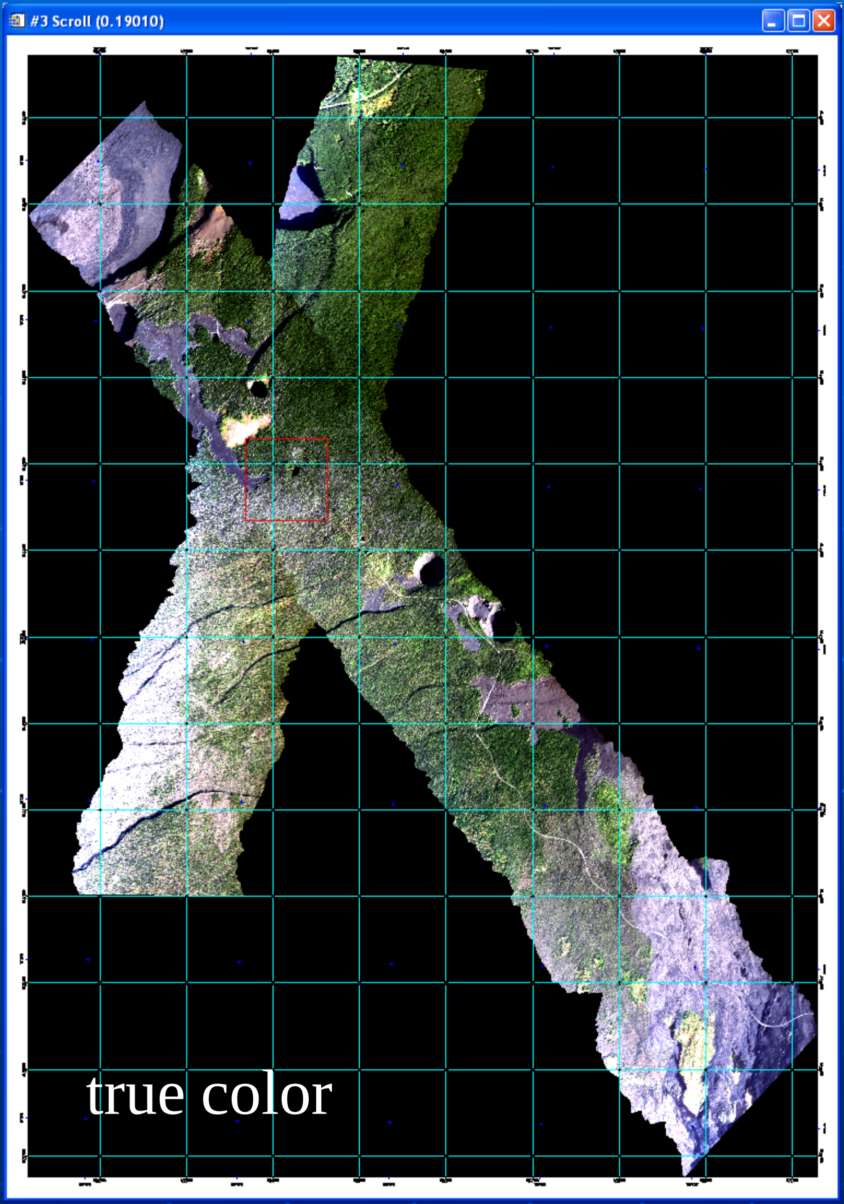

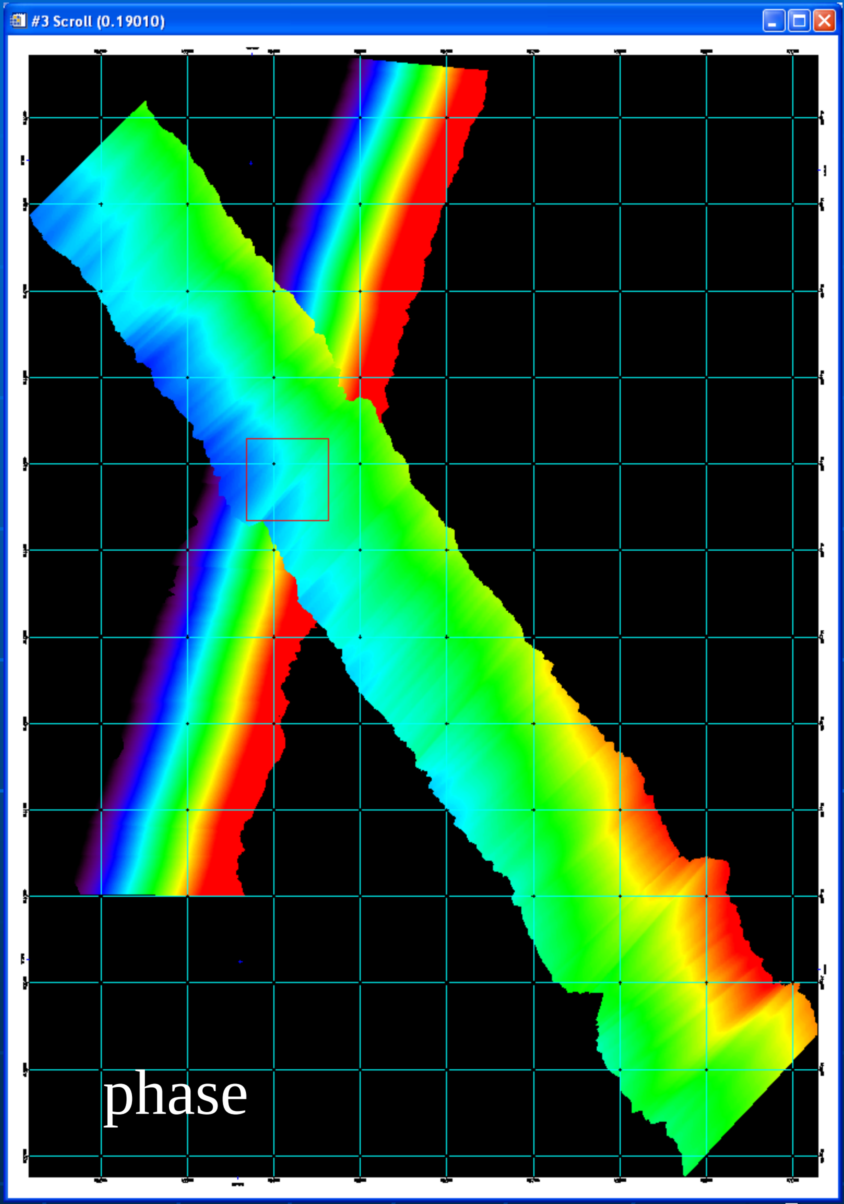

M3 on CH-1 at the Moon

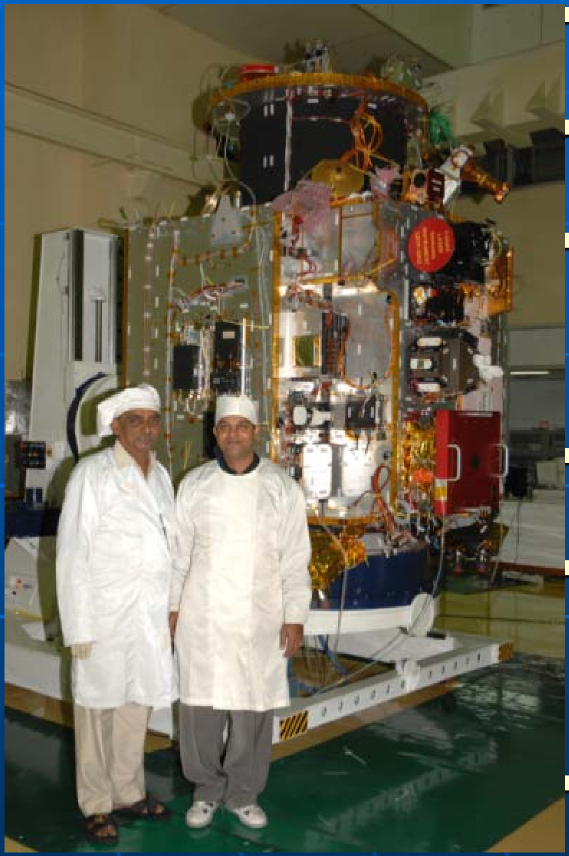

- Launched on PSLV October 22, 2008
- Lunar Orbit Insertion November 8, 2008
- Completed two of four planned Optical Periods (Nov08-Feb09 and Apr09-Aug09)
- CH-1 S/C comm. lost on August 29, 2009
- More than 90% of Moon covered with usable Global Mode data
- Minimal Target Mode collections

M3's Moon

PCs 7,8,9

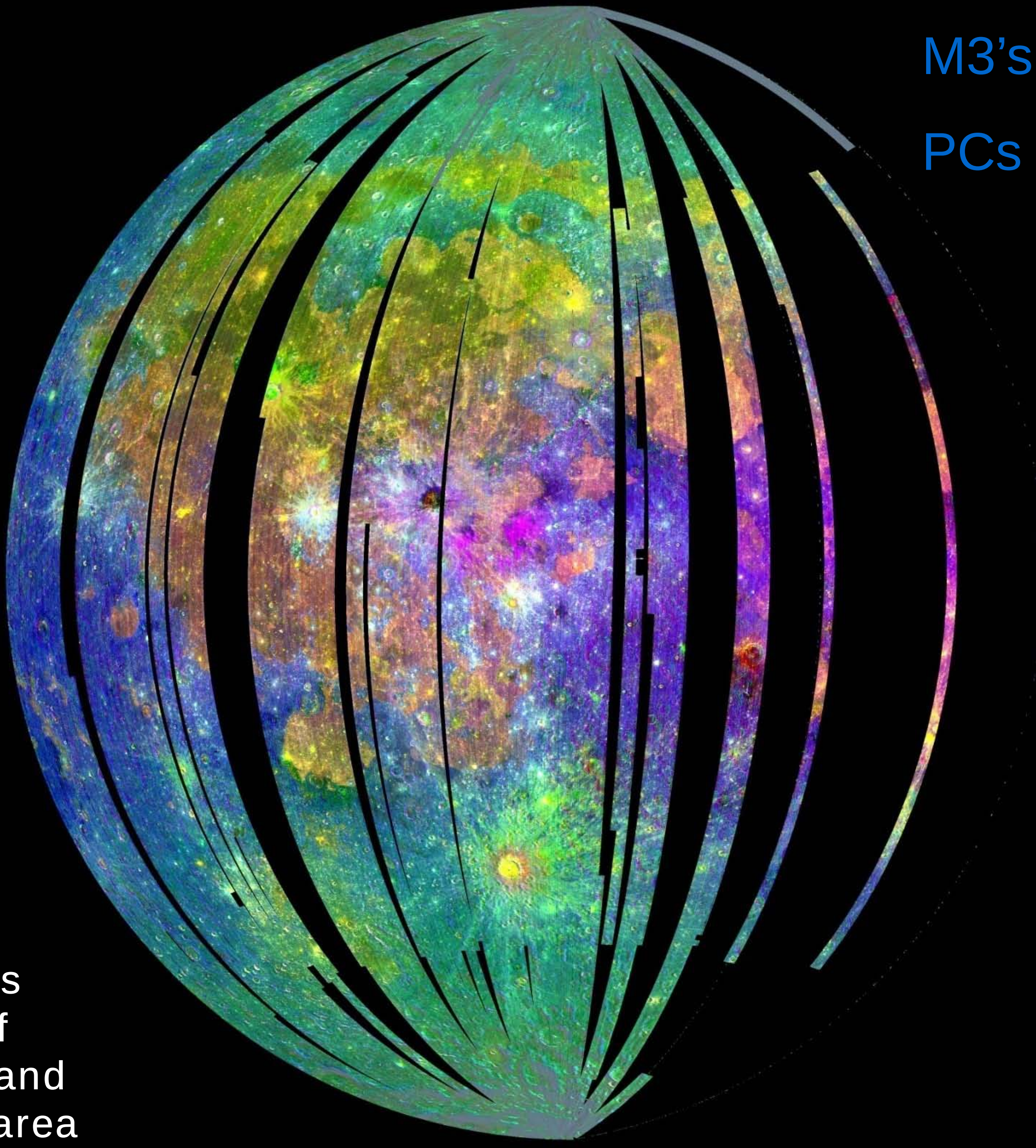

Moon has ~20% of Earth's land surface area

M3 Coverage Summary

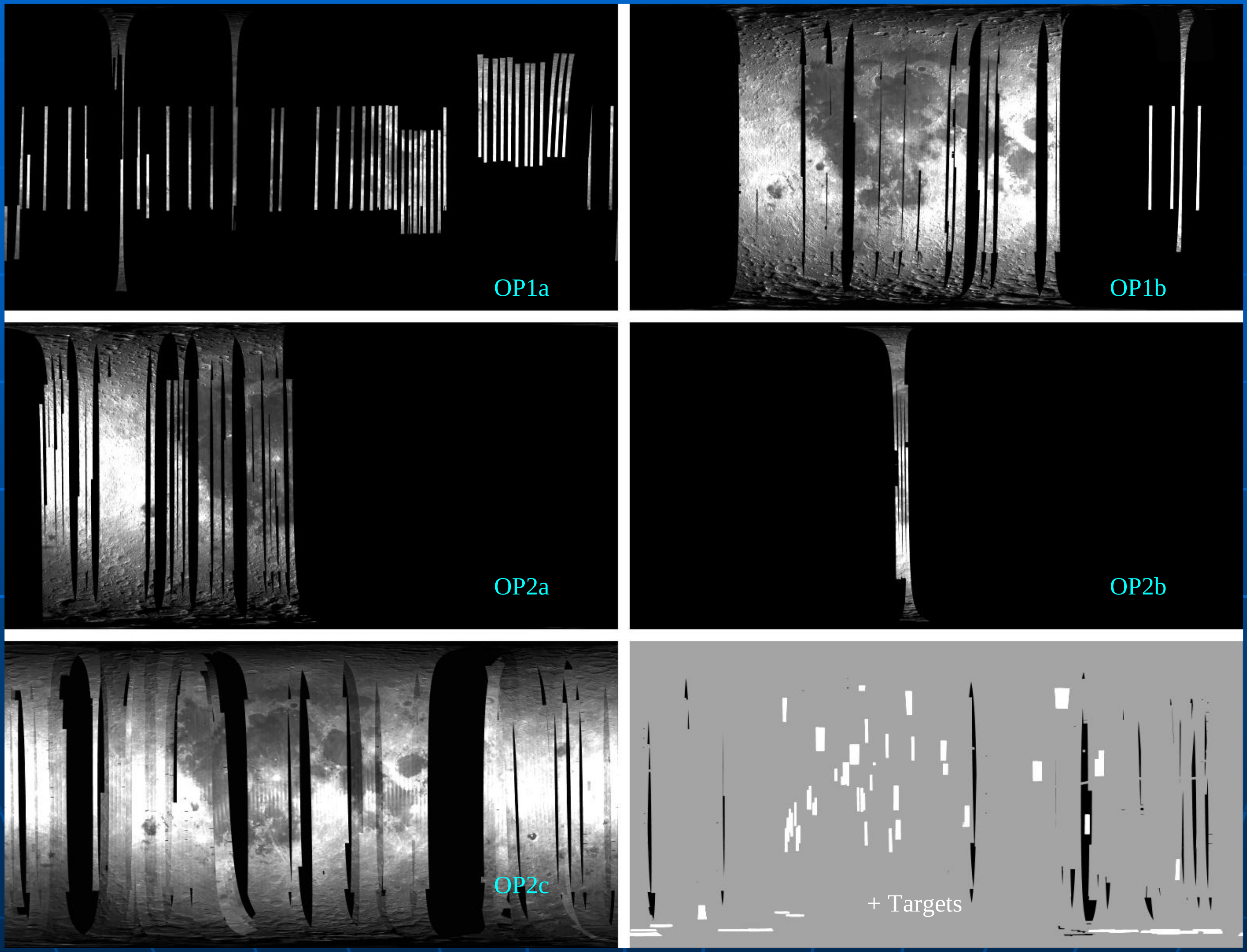

Ray Tracing

- Astrodynamics, geodesy, geometry, geophysics and photogrammetry (fun stuff)
- Timing, ephemeris, attitude and camera model (HyspIRI design requirements)
- ECI-to-ECEF: UT1 variations, nutation, precession, polar motion (operational)
- Refraction, velocity aberration, light time of flight (minor effects but well-modeled)
- Topographic model (adequate for 60m)
- Expect sub-pixel accuracy and stability

Observation Geometry

- 11 critical parameters on a per-pixel basis:
  - To-sun zenith angle (degrees)
  - To-sun azimuth angle (degrees)
  - To-sensor zenith angle (degrees)
  - To-sensor azimuth angle (degrees)
  - Phase angle (degrees)
  - To-sun path length (AU)
  - To-sensor path length (meters)
  - Local slope angle (meters)
  - Local aspect angle (meters)
  - Incidence angle wrt topo model (degrees)
  - Exitance angle wrt topo model (degrees)

Example M3 OBS Data

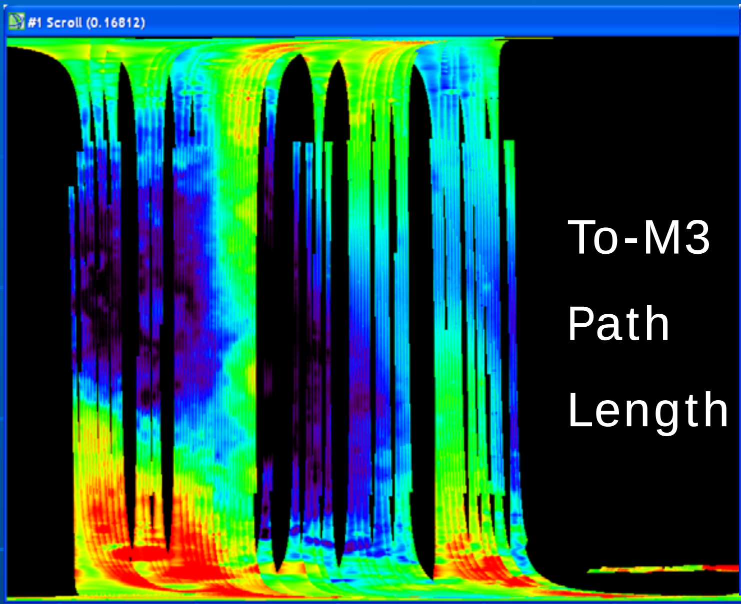

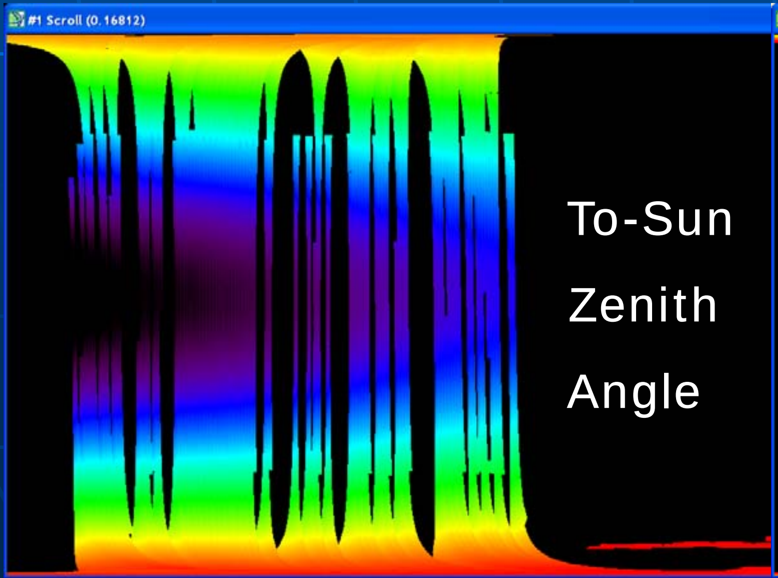

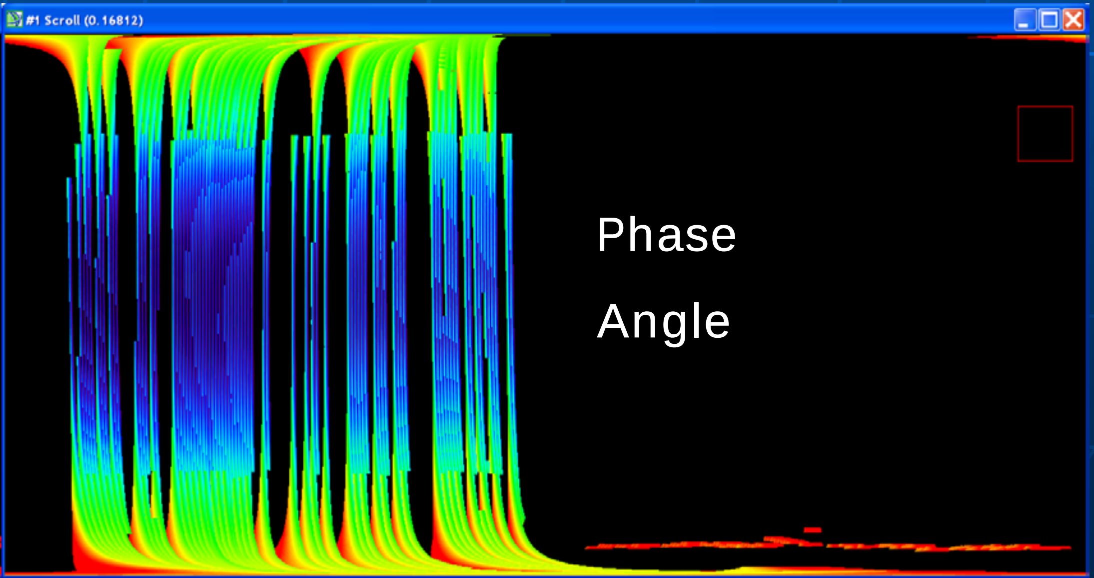

Image Cube + LOC and OBS Backplanes

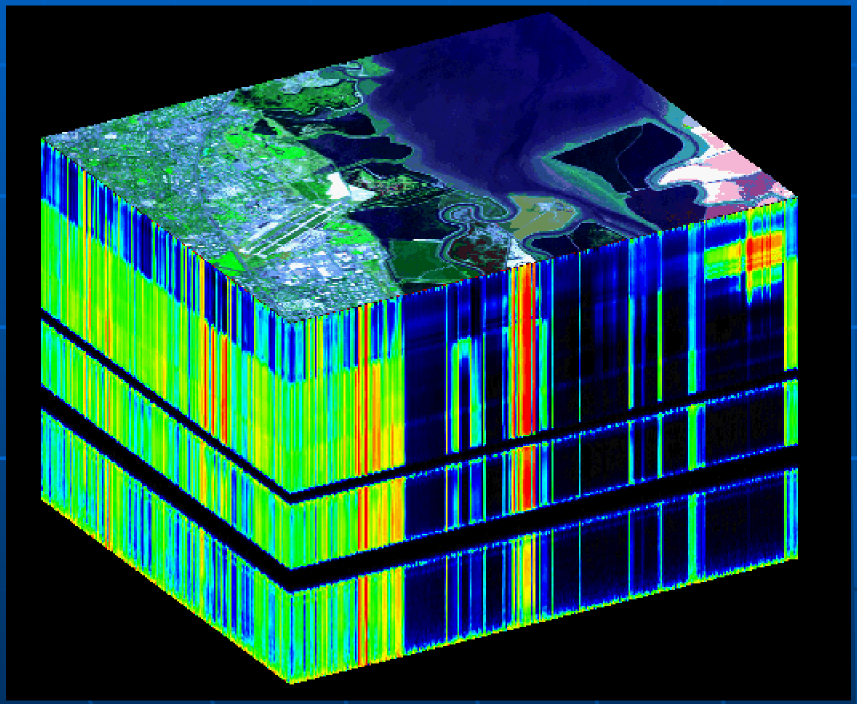

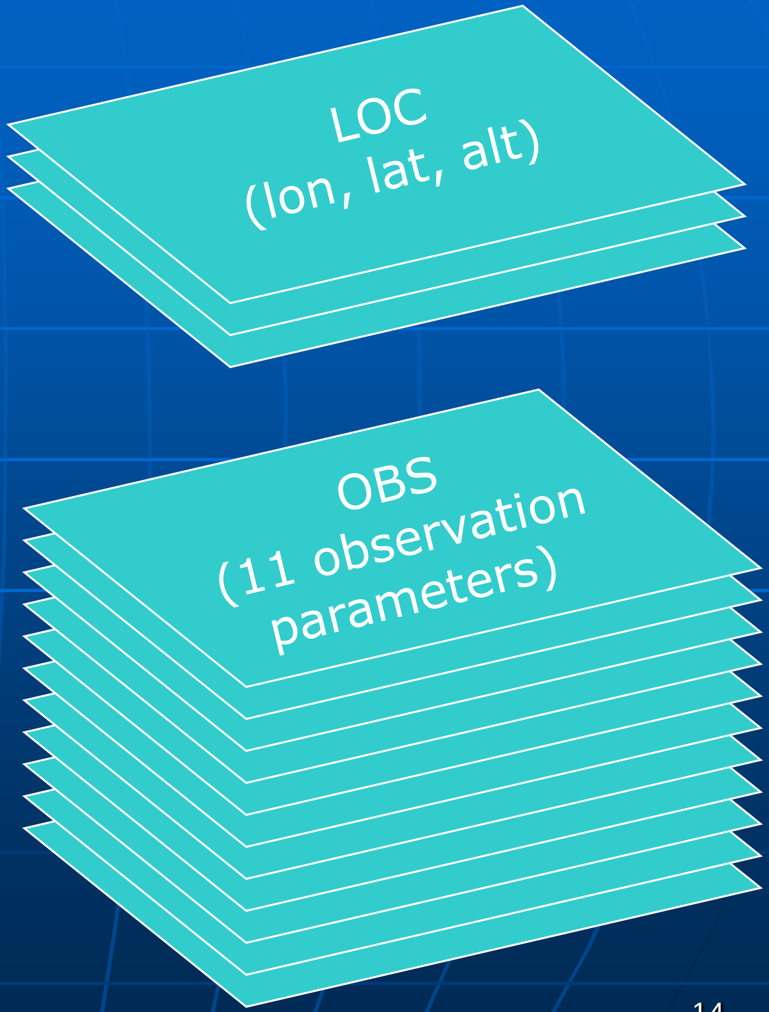

Some HyspIRI Specifics

- 626 km orbit -> 97.2 min period
- ~114 Hz frame rate, 2500 samples
- Avg. 35% of lit limb -> 292 M-pixels
- ~281 orbits / full Earth -> 19 days
- 82 G-pixels / 19 days
- 213 bands -> 426 bytes of radiance
- 20 bytes LOC, 44 bytes OBS
- Auxiliary data ~13% of combined
- 5.6 Tbytes of backplanes per 19-days
- 35.0 Tbytes of spectra per 19-days
- 2.3 Pbytes of combined result in 3 years

The Whole Earth is the “Target”

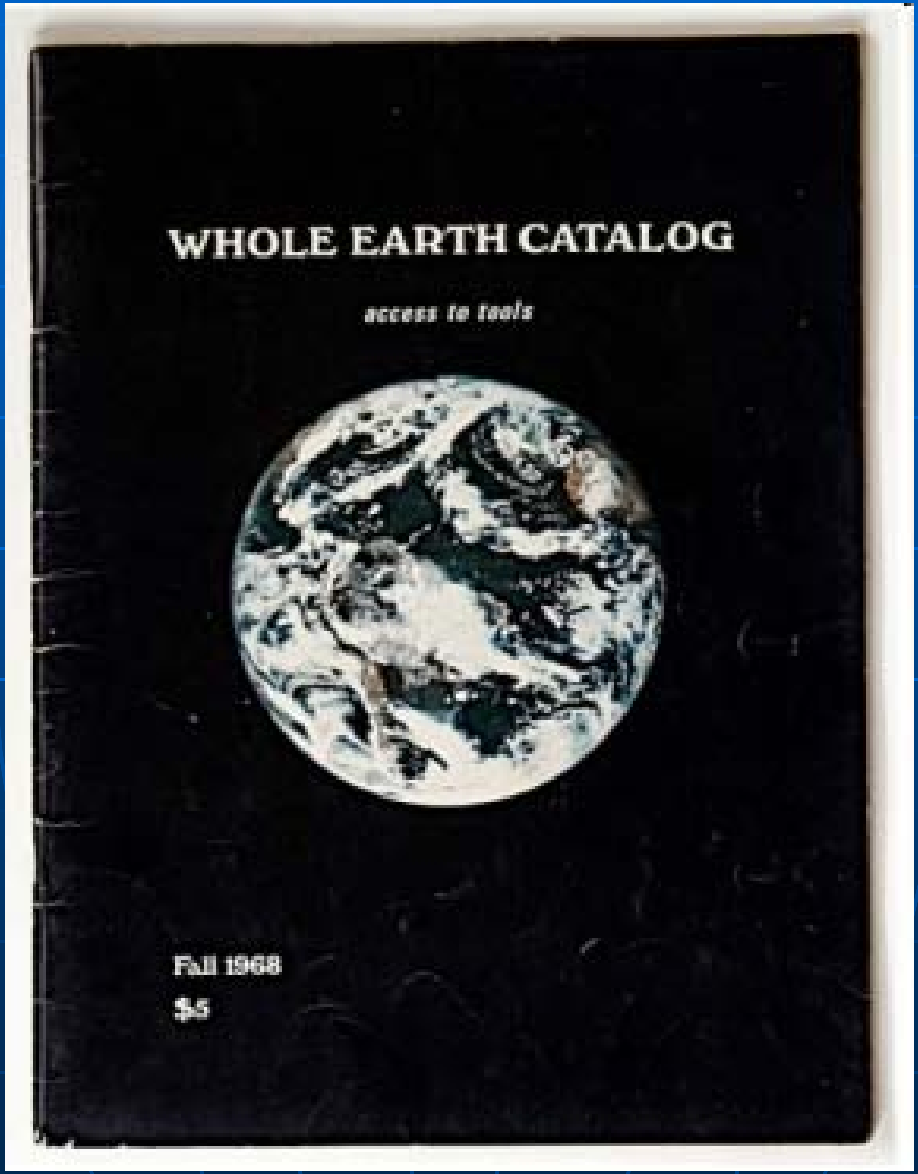

The Whole Earth is the "Target"

- Land surface of Earth ~50G 60m cells
- Perhaps the right approach is to pre-grid the whole planet in fixed 60m cells
- Global views, study sites, special projections pre-defined and gridded
- For 5 bytes/spectrum we could carry a "reverse GLT" index/lookup table
- For example, use UTM/UPS as a basis
- All spectra integer-coded to specific 60m cell

The Whole Earth is the “Target”

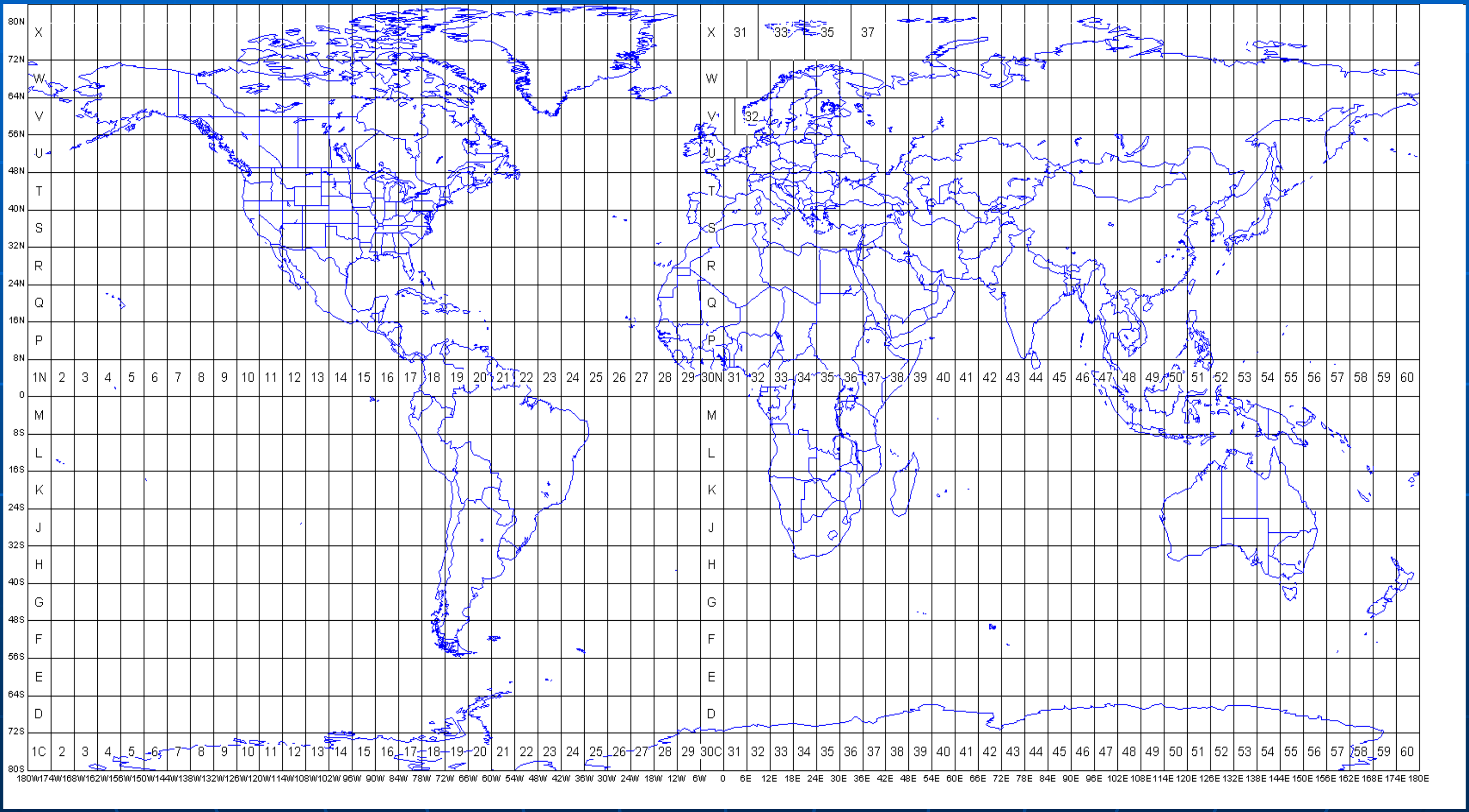

>11 Years to Get Ready?

- On one hand, certainly we'll benefit from computer/bandwidth/storage advances
- Other global missions will implement their own data models, may or may not support special needs of HyspIRI
- Clean slate, relevant heritage and plenty of time to implement the optimal system
- CAO, NEON, NGIS etc are valuable path finders and should be exploring this aspect of the HyspIRI model as test beds
- Jupiter, Saturn, Mars, Venus, Moon…Earth?

Baseline vs Minimum

Baseline	**Minimum**
380 to 2500 nm at ≤10 nm sampling at the specified signal-to-noise ratio and accuracy with >95% spectral/spatial uniformity at ≤60 m nadir spatial sampling with <20 day revisit to provide	380 to 2500 nm at ≤10 nm sampling at >80% of the specified signal-to-noise ratio and accuracy with >90% spectral/spatial uniformity at ≤60 m nadir spatial sampling with <20 day revisit to provide
>60% seasonal and >80% annual coverage of the terrestrial and shallow water regions of the Earth	> 50% seasonal and >70% annual coverage of the terrestrial and shallow water regions of the Earth
three years with a subset of measurements available near-real-time for designated science and applications.	two years.
8 spectral bands from the 3-5 micron and 8-12 micron regions of the spectrum at the specified noise-equivalent-delta-temperature and accuracy at ≤60 m nadir spatial sampling	8 spectral bands from the 3-5 micron and 8-12 micron regions of the spectrum at >80% the specified noise-equivalent-delta-temperature and accuracy at ≤60 m nadir spatial sampling with ≤5 day revisit
>60% Monthly, >70% seasonal and >85% annual coverage of the terrestrial and shallow water regions of the Earth	> 40% Monthly, > 60% seasonal and >70% annual coverage of the terrestrial and shallow water regions of the Earth

Note: We will keep you informed of any changes such as the change in the saturation limit of the MIR band to 1100K

HyspIRI

DRAFT PRELIMINARY

Level 1 Requirements and Mission Success Criteria

NASA Earth Science and Applications Decadal Survey

Robert O. Green, Simon Hook, Betsy Middleton, Stephen Ungar, Bob Knox, Woody Turner, John LaBrecque and the HyspIRI Team

Overview

Beginning in January 2007 a Mission Concept effort for HyspIRI Mission has been under way with involvement of NASA HQ, JPL, GSFC, and a broad Science Study Group and the 2008 workshop, 2009 workshop, 2010 symposium.

Beginning with the call of the NASA Earth Science and Applications Decadal Survey this team has worked to develop a end-to-end concept for implementation of the HyspIRI Mission.

Based on this effort and with input from SSG and the relevant communities a set of Level 1 Requirements and Success Criteria have been develop in accordance with the required NASA process.

In this presentation we are going to review key elements of the HyspIRI draft preliminary Level 1 Requirements and Success Criteria.

This is a required and enabling document for HyspIRI to proceed to the next step in the NASA Mission process.

Note: The HyspIRI Mission must remain appropriately aligned with the Decadal Survey.

HyspIRI Science Study Group

Mike Abrams	JPL	michael.j.abrams@jpl.nasa.gov	818-354-0937
Rick Allen	UID	rallen@kimberly.uidaho.edu	208-423-6601
Martha Anderson	USDA	Martha.Anderson@ars.usda.gov	301-504-6616
Greg Asner	Stanford	gpa@stanford.edu	650-462-1047
David Meyer	USGS EROS	dmeyer@usgs.gov	605-594-6046
Paul Bissett	FERI	pbissett@flenvironmental.org	813-866-3374 x102
Alex Chekalyuk	Lamont-Doh.	chekaluk@ldeo.columbia.edu	845-365-8552
James Crowley	USGS	jcrowley@usgs.gov	703-648-6356
Ivan Csiszar	UMD	icsiszar@hermes.geog.umd.edu	301-405-8696
Heidi Dierssen	U Conn.	heidi.dierssen@uconn.edu	860-405-9239
Friedmann Freund	Ames	friedemann.t.freund@nasa.gov	650 604-5183
John Gamon	U A	gamon@gmail.com	780-965-0345
Louis Giglio	UMD	louis_giglio@ssaihq.com	301 867-2030
Greg Glass	JHU	gglass@jhsph.edu	410-955-3708
Robert Green	JPL	rog@jpl.nasa.gov	818 354-9136
Simon Hook	JPL	simon.j.hook@jpl.nasa.gov	818-354-0974
James Irons	GSFC	James.R.Irons@nasa.gov	301-614-6657
Bob Knox	GSFC	Robert.G.Knox@nasa.gov	301-614-6656
John Mars	USGS	jmars@usgs.gov	703-648-6302
Betsy Middleton	GSFC	elizabeth.m.middleton@nasa.gov	301-614-6670
Peter Minnett	U. Miami	pminnett@rsmas.miami.edu	305-361-4104
Frank Muller Karger	U. MA Dart.	carib@marine.usf.edu	727-553-3335
Scott Ollinger	UNH	scott.ollinger@unh.edu	508 999 8193
Thomas Painter	U. of Utah	painter@geog.utah.edu	303.888.7119
Anupma Prakash	UAF	prakash@gi.alaska.edu	907-474-1897
Dale Quattrochi	MSFC	dale.quattrochi@nasa.gov	256-961-7887
Vince Realmuto	JPL	Vincent.J.Realmuto@jpl.nasa.gov	818-354-1824
Dar Roberts	UCSB	dar@geog.ucsb.edu	805-893-2276
Dave Siegel	UCSB	davey@icess.ucsb.edu	805-893-4547
Phil Townsend	U of Wisc.	ptownsend@wisc.edu	608-262-1669
Kevin Turpie	GSFC	kevin.r.turpie@nasa.gov	301-286-9996
Steve Ungar	GSFC	stephen.g.ungar@nasa.gov	301-614-6674
Susan Ustin	UC Davis	susan@cstars.ucdavis.edu	530-752-0621
Rob Wright	UHI	wright@higp.hawaii.edu	808-956 9194

Level 1 Requirements and Mission Success Criteria

Contents

Level 1 Requirements and Mission Success Criteria

4. Performance Requirements

4.1 Science Requirements

The science objectives in Section 2.2 can be achieved by either the baseline or minimum science mission requirements listed here, but the baseline mission provides substantially more value to NASA and the Earth Science Community.

- **4.1.1 Requirement: Baseline Science Mission**
- a) To address the Decadal Survey and community identified science and application questions related to terrestrial and coastal ocean ecosystem composition, function, and change as well as surface composition (DS113-115), the baseline science mission shall provide global mapping measurements of the surface reflectance or remote sensing reflectance for shallow water regions across the solar reflected spectrum from 380 to 2500 nm at ≤10 nm sampling at the specified signal-to-noise ratio and accuracy with >95% spectral/spatial uniformity at ≤60 m nadir spatial sampling with <20 day revisit to provide >60% seasonal and >80% annual coverage of the terrestrial and shallow water regions of the Earth for at least three years with a subset of measurements available near-real-time for designated science and applications.

Level 1 Requirements and Mission Success Criteria
VSWIR Benchmark Radiances

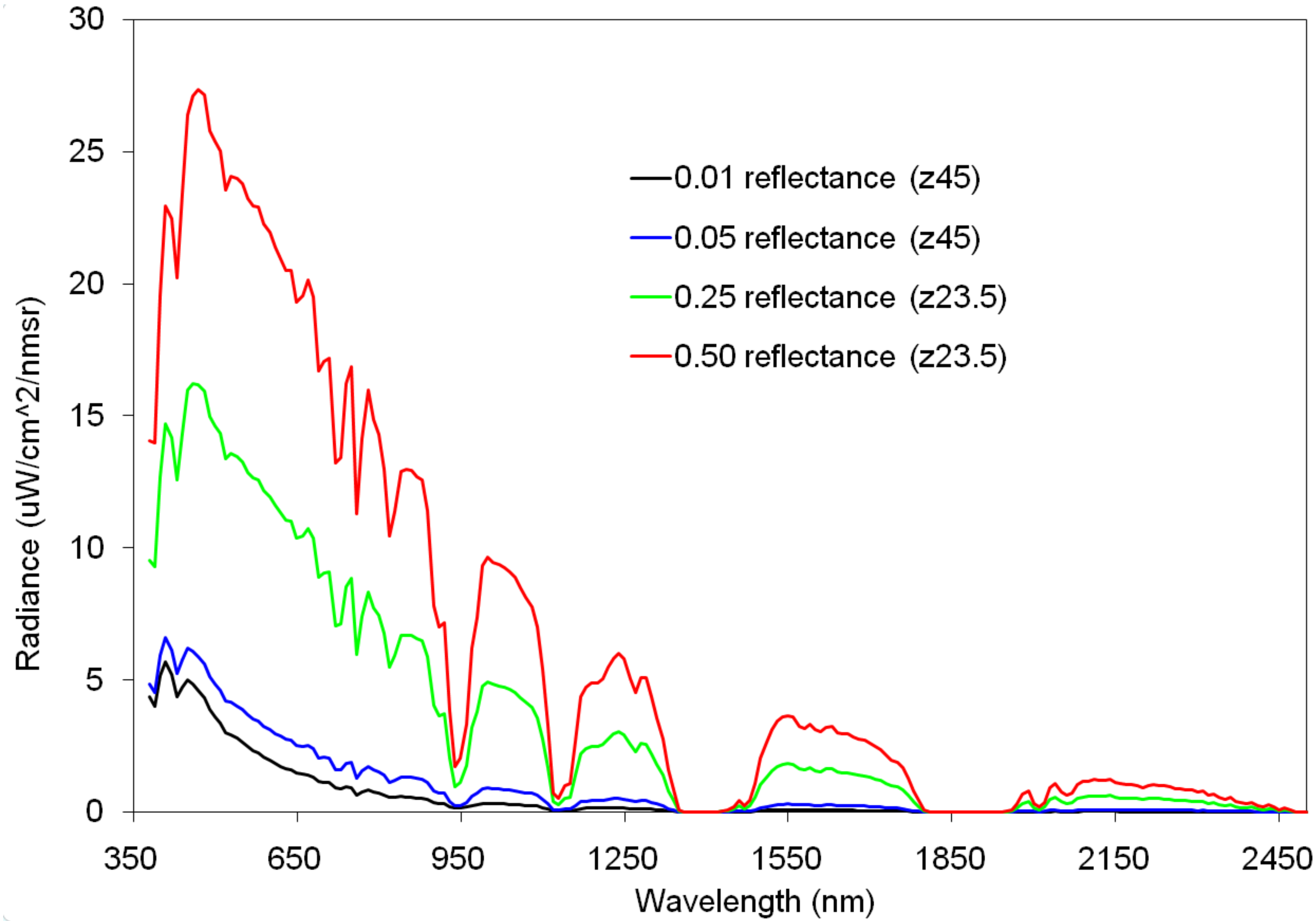

Level 1 Requirements and Mission Success Criteria VSWIR SNR

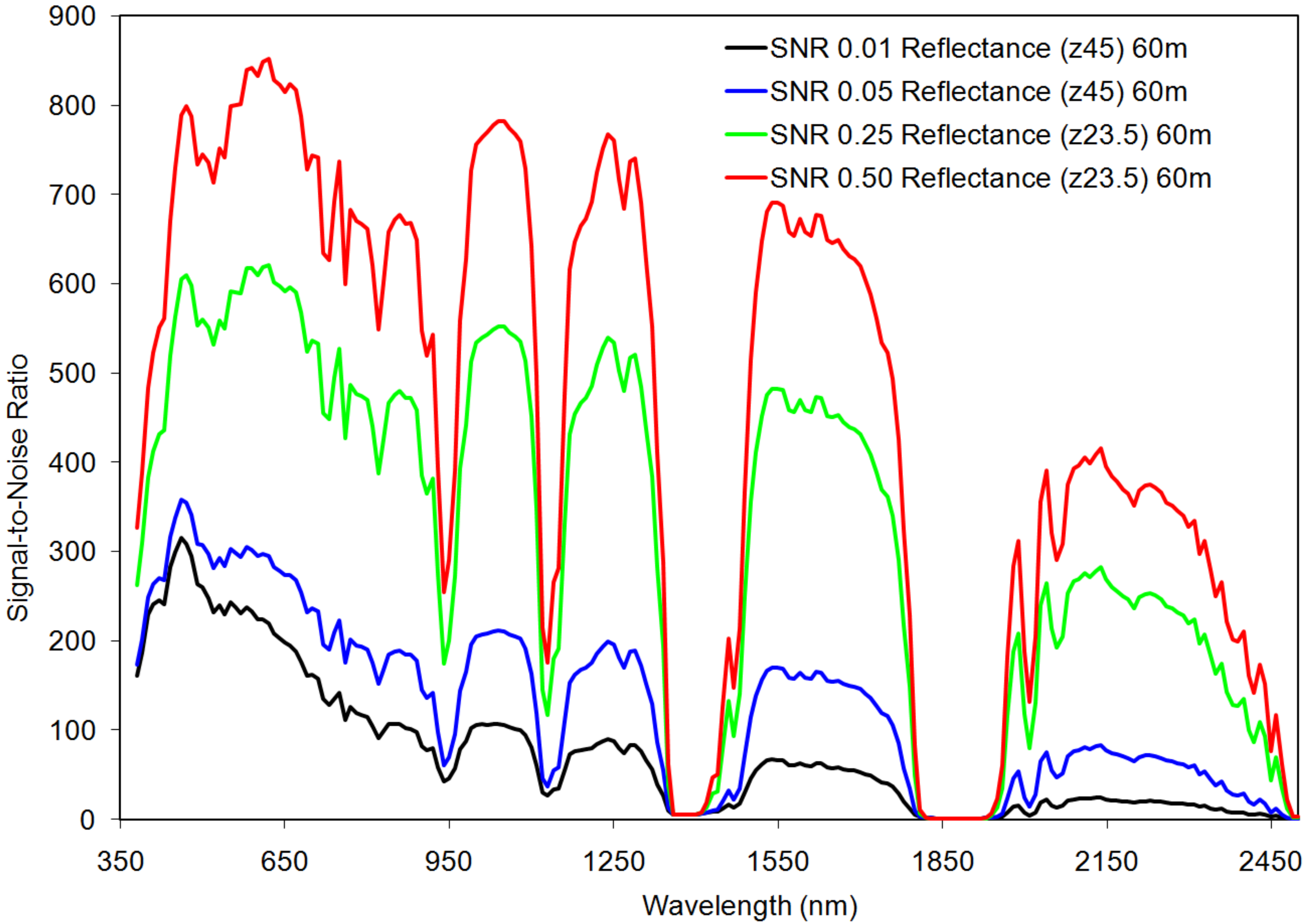

Level 1 Requirements and Mission Success Criteria (VSWIR Performance)

wavelength	0.01 reflectance (z45)	0.05 reflectance (z45)	0.25 reflectance (z23.5)	0.50 reflectance (z23.5)	wavelength	SNR 0.01 Reflectance (z45) 60m	SNR 0.05 Reflectance (z45) 60m	SNR 0.25 Reflectance (z23.5) 60m	SNR 0.50 Reflectance (z23.5) 60m	wavelength	Digitization Radiance (uW/ cm^2/nm/sr)
380	4.34E+00	4.84E+00	9.54E+00	1.41E+01	380	1.61E+02	1.73E+02	2.62E+02	3.27E+02	380	1.68E-02
390	3.99E+00	4.51E+00	9.28E+00	1.40E+01	390	1.87E+02	2.02E+02	3.09E+02	3.89E+02	390	1.22E-02
400	5.17E+00	5.93E+00	1.27E+01	1.95E+01	400	2.29E+02	2.49E+02	3.83E+02	4.83E+02	400	1.14E-02
410	5.69E+00	6.61E+00	1.47E+01	2.29E+01	410	2.41E+02	2.63E+02	4.12E+02	5.23E+02	410	1.15E-02
420	5.20E+00	6.14E+00	1.42E+01	2.25E+01	420	2.45E+02	2.70E+02	4.31E+02	5.51E+02	420	1.02E-02
430	4.37E+00	5.24E+00	1.26E+01	2.02E+01	430	2.40E+02	2.67E+02	4.36E+02	5.62E+02	430	8.88E-03
440	4.74E+00	5.77E+00	1.44E+01	2.34E+01	440	2.82E+02	3.16E+02	5.19E+02	6.70E+02	440	7.33E-03
450	5.01E+00	6.20E+00	1.60E+01	2.64E+01	450	2.99E+02	3.38E+02	5.63E+02	7.31E+02	450	6.99E-03
460	4.84E+00	6.09E+00	1.62E+01	2.71E+01	460	3.15E+02	3.58E+02	6.05E+02	7.89E+02	460	6.18E-03
470	4.60E+00	5.88E+00	1.62E+01	2.73E+01	470	3.08E+02	3.54E+02	6.09E+02	7.99E+02	470	6.09E-03
480	4.31E+00	5.61E+00	1.59E+01	2.72E+01	480	2.94E+02	3.41E+02	5.98E+02	7.88E+02	480	6.21E-03
490	3.87E+00	5.12E+00	1.50E+01	2.58E+01	490	2.63E+02	3.09E+02	5.53E+02	7.34E+02	490	6.77E-03
500	3.61E+00	4.86E+00	1.46E+01	2.54E+01	500	2.59E+02	3.07E+02	5.60E+02	7.45E+02	500	6.47E-03
510	3.38E+00	4.62E+00	1.43E+01	2.50E+01	510	2.47E+02	2.97E+02	5.50E+02	7.36E+02	510	6.54E-03
520	3.02E+00	4.20E+00	1.34E+01	2.35E+01	520	2.32E+02	2.81E+02	5.31E+02	7.13E+02	520	6.53E-03
530	2.94E+00	4.16E+00	1.36E+01	2.41E+01	530	2.39E+02	2.93E+02	5.59E+02	7.52E+02	530	6.02E-03
540	2.79E+00	4.02E+00	1.34E+01	2.40E+01	540	2.29E+02	2.84E+02	5.49E+02	7.42E+02	540	6.16E-03
550	2.65E+00	3.87E+00	1.33E+01	2.38E+01	550	2.43E+02	3.03E+02	5.91E+02	8.00E+02	550	5.28E-03
560	2.47E+00	3.67E+00	1.29E+01	2.32E+01	560	2.37E+02	2.98E+02	5.90E+02	8.00E+02	560	5.15E-03
570	2.33E+00	3.53E+00	1.27E+01	2.29E+01	570	2.31E+02	2.94E+02	5.89E+02	8.01E+02	570	5.07E-03
580	2.23E+00	3.43E+00	1.26E+01	2.29E+01	580	2.37E+02	3.05E+02	6.17E+02	8.40E+02	580	4.62E-03
590	2.08E+00	3.25E+00	1.22E+01	2.22E+01	590	2.32E+02	3.02E+02	6.17E+02	8.42E+02	590	4.47E-03
600	1.96E+00	3.13E+00	1.19E+01	2.19E+01	600	2.24E+02	2.94E+02	6.09E+02	8.33E+02	600	4.50E-03
610	1.84E+00	2.99E+00	1.16E+01	2.14E+01	610	2.23E+02	2.97E+02	6.19E+02	8.48E+02	610	4.23E-03
2200	1.72E-02	7.31E-02	4.71E-01	9.37E-01	2200	1.81E+01	6.44E+01	2.36E+02	3.51E+02	2200	9.85E-04
2210	1.87E-02	8.00E-02	5.10E-01	1.02E+00	2210	1.96E+01	6.96E+01	2.49E+02	3.68E+02	2210	9.79E-04
2220	1.89E-02	8.11E-02	5.16E-01	1.03E+00	2220	2.01E+01	7.12E+01	2.52E+02	3.74E+02	2220	9.65E-04
2230	1.88E-02	8.05E-02	5.12E-01	1.02E+00	2230	2.02E+01	7.15E+01	2.53E+02	3.75E+02	2230	9.52E-04
2240	1.82E-02	7.79E-02	4.97E-01	9.90E-01	2240	1.98E+01	7.05E+01	2.51E+02	3.72E+02	2240	9.39E-04
2250	1.74E-02	7.47E-02	4.78E-01	9.52E-01	2250	1.92E+01	6.87E+01	2.47E+02	3.66E+02	2250	9.30E-04
2260	1.64E-02	7.03E-02	4.52E-01	9.00E-01	2260	1.82E+01	6.55E+01	2.39E+02	3.55E+02	2260	9.28E-04
2270	1.60E-02	6.89E-02	4.43E-01	8.83E-01	2270	1.79E+01	6.45E+01	2.36E+02	3.51E+02	2270	9.26E-04
2280	1.55E-02	6.67E-02	4.30E-01	8.56E-01	2280	1.74E+01	6.31E+01	2.32E+02	3.46E+02	2280	9.23E-04
2290	1.50E-02	6.43E-02	4.15E-01	8.28E-01	2290	1.69E+01	6.14E+01	2.28E+02	3.41E+02	2290	9.19E-04
2300	1.39E-02	5.94E-02	3.87E-01	7.70E-01	2300	1.58E+01	5.79E+01	2.19E+02	3.28E+02	2300	9.14E-04
2310	1.44E-02	6.17E-02	3.98E-01	7.94E-01	2310	1.65E+01	5.99E+01	2.24E+02	3.35E+02	2310	9.09E-04
2320	1.16E-02	4.92E-02	3.23E-01	6.43E-01	2320	1.35E+01	4.98E+01	1.97E+02	2.98E+02	2320	9.06E-04
2330	1.26E-02	5.39E-02	3.51E-01	6.99E-01	2330	1.46E+01	5.37E+01	2.08E+02	3.12E+02	2330	9.07E-04
2340	1.04E-02	4.39E-02	2.90E-01	5.78E-01	2340	1.21E+01	4.50E+01	1.84E+02	2.79E+02	2340	9.11E-04
2350	8.65E-03	3.61E-02	2.42E-01	4.82E-01	2350	1.00E+01	3.77E+01	1.63E+02	2.50E+02	2350	9.18E-04
2360	9.78E-03	4.11E-02	2.72E-01	5.41E-01	2360	1.12E+01	4.19E+01	1.74E+02	2.66E+02	2360	9.27E-04
2370	7.28E-03	3.01E-02	2.02E-01	4.03E-01	2370	8.36E+00	3.16E+01	1.43E+02	2.22E+02	2370	9.33E-04
2380	6.32E-03	2.56E-02	1.74E-01	3.46E-01	2380	7.26E+00	2.72E+01	1.28E+02	2.02E+02	2380	9.36E-04
2390	6.21E-03	2.50E-02	1.71E-01	3.40E-01	2390	7.15E+00	2.68E+01	1.27E+02	2.00E+02	2390	9.36E-04
2400	6.71E-03	2.72E-02	1.85E-01	3.67E-01	2400	7.76E+00	2.91E+01	1.35E+02	2.11E+02	2400	9.29E-04
2410	4.50E-03	1.74E-02	1.20E-01	2.39E-01	2410	5.30E+00	1.94E+01	9.96E+01	1.61E+02	2410	9.21E-04
2420	3.75E-03	1.41E-02	9.89E-02	1.96E-01	2420	4.45E+00	1.60E+01	8.65E+01	1.42E+02	2420	9.16E-04
2430	4.95E-03	1.93E-02	1.34E-01	2.66E-01	2430	5.87E+00	2.16E+01	1.09E+02	1.74E+02	2430	9.12E-04
2440	4.13E-03	1.58E-02	1.10E-01	2.18E-01	2440	4.90E+00	1.78E+01	9.37E+01	1.52E+02	2440	9.14E-04
2450	1.85E-03	6.03E-03	4.28E-02	8.47E-02	2450	2.21E+00	7.07E+00	4.37E+01	7.65E+01	2450	9.19E-04
2460	3.00E-03	1.06E-02	7.60E-02	1.51E-01	2460	3.53E+00	1.21E+01	6.98E+01	1.17E+02	2460	9.27E-04
2470	1.58E-03	4.68E-03	3.39E-02	6.69E-02	2470	1.84E+00	5.38E+00	3.49E+01	6.21E+01	2470	9.43E-04
2480	7.80E-04	1.65E-03	1.07E-02	2.08E-02	2480	8.99E-01	1.89E+00	1.18E+01	2.21E+01	2480	9.57E-04
2490	4.00E-04	4.60E-04	1.39E-03	2.34E-03	2490	4.56E-01	5.24E-01	1.58E+00	2.64E+00	2490	9.69E-04
2500	4.30E-04	5.10E-04	1.68E-03	2.90E-03	2500	4.80E-01	5.70E-01	1.87E+00	3.21E+00	2500	9.88E-04

Level 1 Requirements and Mission Success Criteria

b) To address the Decadal Survey and community-identified science and application questions related to volcanoes, wild fires, water usage, urbanization and surface composition (DS113-115), the baseline science mission shall provide global mapping measurements of the surface radiance, temperature and emissivity with 8 spectral bands from the 3-5 micron and 8-12 micron regions of the spectrum at the specified noise-equivalent-delta-temperature and accuracy at ≤60 m nadir spatial sampling with ≤5 day revisit to provide >60% Monthly, >70% seasonal and >85% annual coverage of the terrestrial and shallow water regions of the Earth for at least three years with a subset of measurements available near-real-time for designated science and applications.

Specified NEdT

	Wavelength	Spectral Bandwidth	Min Nominal Radiance and Temperature	Max Nominal Radiance and Temperature	NEdT at Min nominal Temperature	NEdT at Max Nominal Temperature	NEdT at 300 K
	(microns)	(microns)	(W/m^2/micron/sr)	(W/m^2/micron/sr)	Kelvin	Kelvin	Kelvin
Band 1	3.98	0.08	14 (400 K)	9600 (1400 K)	1	0.12	11.2
Band 2	7.35	0.32	0.34 (200 K)	110 (500 K)	2.8	0.22	0.28
Band 3	8.28	0.34	0.45 (200 K)	100 (500 K)	2	0.22	0.24
Band 4	8.63	0.35	0.57 (200 K)	94 (560 K)	1.6	0.24	0.24
Band 5	9.07	0.36	0.68 (200 K)	86 (500 K)	1.2	0.24	0.22
Band 6	10.53	0.54	0.89 (200 K)	71 (500 K)	0.64	0.22	0.16
Band 7	11.33	0.54	1.1 (200 K)	58 (500 K)	0.56	0.26	0.16
Band 8	12.05	0.52	1.2 (200 K)	48 (500 K)	0.52	0.3	0.18

Digitization @ min radiance	Digitization @ max radiance	Digitization @ 300 K
(W/m^2/micron/sr)	(W/m^2/micron/sr)	(W/m^2/micron/sr)
4.0e-2 (0.12 K)	4.0e-2 (0.01 K)	5.0e-2 (1.4 K)
5.6e-3 (0.30 K)	5.6e-3 (0.009 K)	5.6e-3 (0.03 K)
4.8e-3 (0.23 K)	4.8e-3 (0.009 K)	4.8e-3 (0.03 K)
4.5e-3 (0.19 K)	4.5e-3 (0.009 K)	4.5e-3 (0.03 K)
4.1e-3 (0.15 K)	4.1e-3 (0.010 K)	4.1e-3 (0.03 K)
2.5e-3 (0.08 K)	2.5e-3 (0.008 K)	2.5e-3 (0.02 K)
2.2e-3 (0.07 K)	2.2e-3 (0.010 K)	2.2e-3 (0.02 K)
2.1e-3 (0.06 K)	2.1e-3 (0.012 K)	2.1e-3 (0.02 K)

Notes

Center wavelength is the average of the max and min wavelengths at the FWHM
Spectral bandwidth is the FWHM
Minimum nominal radiance is 200K except for 4 um band where it is 400K
Maximum nominal radiance is 500K except for 4 um band where it is 1400K

Level 1 Requirements and Mission Success Criteria

c) To address Decadal Survey and community-identified science and application questions (DS113-115), requiring combined reflectance, emissivity and temperature measurements, the baseline mission shall provide combined global mapping data sets.

Level 1 Requirements and Mission Success Criteria

<u>A termination review will be called if these requirements cannot be met</u>

4.1.2 Requirement: Minimum Science Mission

a) To address the Decadal Survey and community identified science and application questions related to terrestrial and coastal ocean ecosystem composition, function, and change as well as surface composition (DS113-115), the baseline science mission shall provide global global mapping measurements of the surface reflectance or remote sensing reflectance for shallow water regions across the solar reflected spectrum from 380 to 2500 nm at ≤10 nm sampling at >80% of the specified signal-to-noise ratio and accuracy with > 90% spectral/spatial uniformity at ≤60 m nadir spatial sampling with <20 day revisit to provide > 50% seasonal and >70% annual coverage of the terrestrial and shallow water regions of the Earth for at least two years.

Level 1 Requirements and Mission Success Criteria

b) To address the Decadal Survey and community identified science and application questions related to volcanoes, wild fires, water usage, urbanization and surface composition (DS113-115), the baseline science mission shall provide global mapping measurements of the surface temperature as well as emissivity and surface radiance in 8 spectral bands from the 3-5 micron and 8-12 micron regions of the spectrum at >80% the specified noise-equivalent-delta-temperature and accuracy at ≤60 m nadir spatial sampling with ≤5 day revisit to provide > 40% Monthly, > 60% seasonal and >70% annual coverage of the terrestrial and shallow water regions of the Earth for at least two years.

c) To address Decadal Survey and community identified science and application questions requiring combined reflectance, emissivity and temperature measurements, the threshold mission shall provide combined global mapping data sets.

Summary

Please keep these Level 1 Requirements and Success Criteria in mind as we proceed through the workshop.

We will review these Level 1 Requirements and Success Criteria at the end of the workshop.

Note: The HyspIRI Mission must remain appropriately aligned with the Decadal Survey.

NRC Decadal Survey - HyspIRI

Global vegetation species-type and physiological condition, including agricultural lands, for biosphere feedback and land-atmosphere interactions; Spectroscopically derived terrestrial land cover composition/albedo including snow, ice, dust climate interaction; Fire: fuel, occurrence, intensity and recovery globally, as well as volcano emissions; Fine spatial & temporal scale measures of surface temperature and energy balance, including urban heat Islands.

Visible ShortWave InfraRed (VSWIR) Imaging Spectrometer

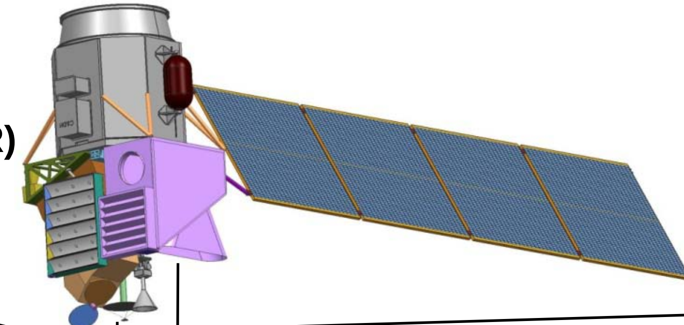

Multispectral Thermal InfraRed (TIR) Scanner

Map of dominant tree species, Bartlett Forest, NH

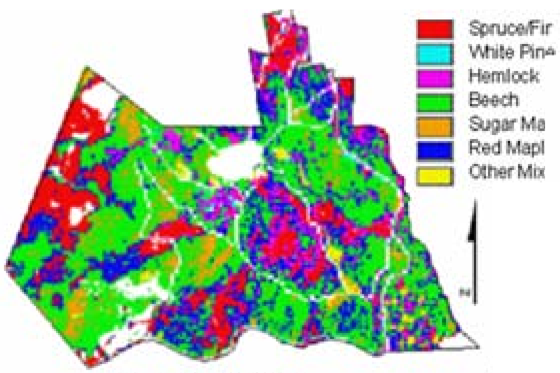

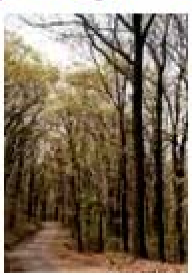

Soil C:N Ratio

White Mountain National Forest, NH

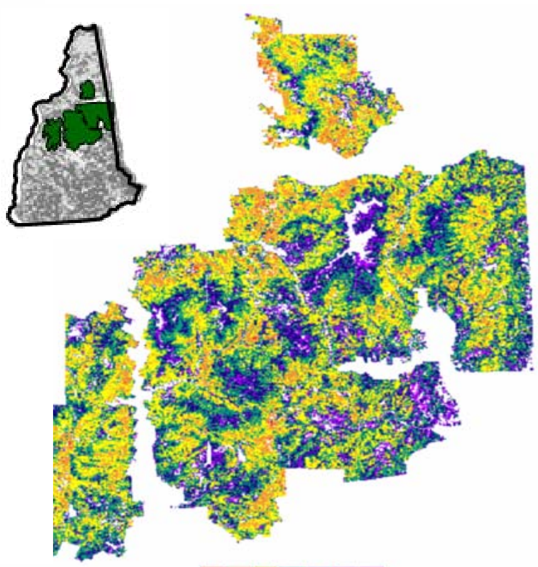

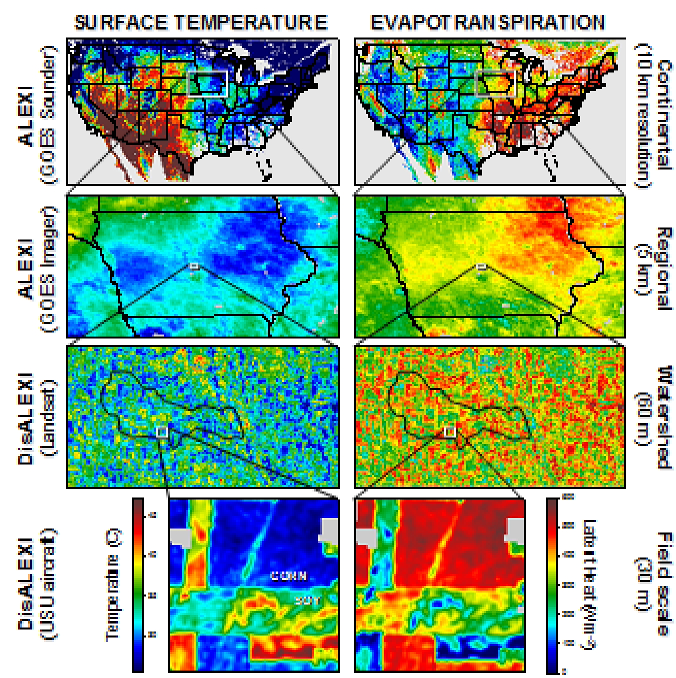

Workshop Review and Next Steps

- Workshop Review
  - Strong focus on climate relevance
  - Sunglint results indicated VSWIR data well suited for many inland water and coastal applications
  - Sunglint report in review
  - Baseline and minimum measurements concurred and refined. Refinements include change of TIR saturation to 1100K
  - Hot Target Saturation Report in draft
  - Workshop provides international forum for use of imaging spectrometer VSWIR and multispectral TIR data
  - No splinter group approach preferred
  - Need to better define products, especially Level 3,4 and identify which are Fundamental Climate Variables
  - Strong interest in large airborne campaign for product development and carbon assessment
  - Community felt that HyspIRI measurements would address HyspIRI science
  - Add time for discussion to avoid sequential presentations
  - Add evening slot for poster session with refreshments

- Next Steps
  - Continue to strengthen climate relevance and demonstrate applications as they occur e.g. volcanic ash cloud, Gulf oil spill
  - Refine product definitions and identify climate variables
  - Develop plan for large airborne campaign, identify what field data need to be acquired simultaneously
  - Develop international HyspIRI working group, focus on calval and developing measurement protocols
  - Strengthen domestic partnerships
  - Continue with Symposium – Workshop – Symposium sequence